

[Login/Register](#) | [Forgot your Password?](#) | [My Workspace](#) | [Shopping Cart](#)

[research + dekker.com -> results](#)

[Search](#) | [eBooks](#) | [Journals](#) | [Encyclopedias](#) | [Customer Service](#) | [Contact Us](#) | [Request Catalog](#) | [FAQs](#)

■ Brought to you by University of Toronto and Marcel Dekker, Inc.

Dekker is a digital publisher of authoritative scientific, technical, and medical content at the article level with links to full-text articles.

Products

[Table of Contents A-Z](#)

[FAQ: TOC A-Z](#)

[Description](#)

[Reviews](#)

[List of Contributors](#)

[Preface](#)

[Recent Updates](#)

[Upcoming Updates](#)

[Author Instructions](#)

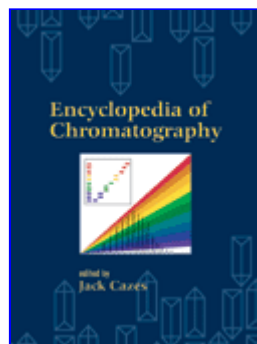
[Continue Shopping](#)

[Sales Reps & Booksellers](#)

 **Free TOC Alerts**

 **Recommend to your library**

To contact Dekker customer service by phone, please call 1-800-228-1160 (USA, Canada & South America) or +44 1264 343039 (Europe, Far East, Middle East & Africa).



Encyclopedia of Chromatography

You have Access to this item

■ To preview or view articles from this product, choose from the [Table of Contents](#)

■ [Search](#) for documents only within this product.

 **Save to My Workspace**

Edited by: [Jack Cazes](#) ¹

¹ *Florida Atlantic University, Boca Raton, U.S.A.*

Encyclopedia | Print Published: 06/29/2001 | Online Published: 06/29/2001
Hard Cover
927 pages | Illustrated
2nd Printing
ISBN: 0-8247-4123-4

Reviews

"The *Encyclopedia of Chromatography*, edited by Dr. Jack Cazes of Florida Atlantic University, is a welcome addition to the literature covering chromatography and methodologies....well-written and well-documented....easy reading....blend....should be seriously considered for inclusion in university, industrial, and government libraries."

—James T. Stewart, PhD

"...a wealth of information."

—*Journal of Planar Chromatography*

"Jack Cazes,... is the ideal person to edit this authoritative, up-to-date encyclopedia and provide[s] useful data..."

"This encyclopedia should become a first and frequently used source of information for chromatographers."

just about every conceivable chromatographic technique."
—*The Chemical Educator*

[Return to Top](#)

Description

New 2004 supplement now available! Please scroll down for more details.

Written by over 180 esteemed international authorities, and containing over 2600 cited works, and 1000 drawings, equations, tables, and photographs, the *Encyclopedia of Chromatography* covers high-performance liquid chromatography, gas chromatography, capillary electrophoresis, and thin-layer chromatography, field-flow fractionation, countercurrent chromatography, fluid chromatography, gel permeation chromatography, size exclusion chromatography, and hyphenated techniques.

Experts and novices will discover monumental advances in the field with updated chapters online

- | Antioxidant Activity: An Adaptation for Measurement by HPLC
- | Detection Principles
- | Enoxacin: Analysis by Capillary Electrophoresis and HPLC
- | Extra-Column Volume
- | Molecularly Imprinted Polymers for Affinity Chromatography

2004 Update Supplement

List Price: 2004 Update Supplement (0-8247-2153-5): \$150.00

In step with novel technologies and methodologies that have reshaped chromatography in recent years, this supplement reviews developments in HPLC, TLC, SFC, and other areas—presenting 50 authoritative entries filled with practical information and applications from biotechnology to environmental science to clinical pathology.

With **870** references plus over **150** tables and equations, the *2004 Update Supplement* encompasses

- | high speed SEC and CC methods
- | new technologies impacting LC-NMR and LC-MS-NMR
- | HPLC analysis of flavonoids and phenolic compounds and acids
- | the multicolumn gradient, or "walking column," technique
- | molecularly imprinted polymers and spacer groups for affinity chromatography
- | analysis of essential oils and steroids by GC
- | peak identification and purity determination with diode array detection

[Return to Top](#)



[Login/Register](#) | [Forgot your Password?](#) | [My Workspace](#) | [Shopping Cart](#)

[research + dekker.com -> results](#)

[Search](#) | [eBooks](#) | [Journals](#) | [Encyclopedias](#) | [Customer Service](#) | [Contact Us](#) | [Request Catalog](#) | [FAQs](#)

■ Brought to you by University of Toronto and Marcel Dekker, Inc.

Dekker is a digital publisher of authoritative scientific and medical content at the article level with full-text access.

Products

[Table of Contents A-Z](#)

[FAQ: TOC A-Z](#)

[Description](#)

[Reviews](#)

[List of Contributors](#)

[Preface](#)

[Recent Updates](#)

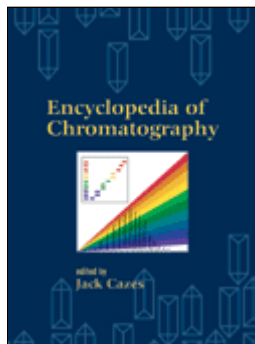
[Upcoming Updates](#)

[Back to Catalog page](#)

[Author Instructions](#)

[Continue Shopping](#)

[Sales Reps & Booksellers](#)



Encyclopedia of Chromatography

 [Free TOC Alerts](#)

 [Recommend to your library](#)

Table of Contents A-Z

■ [Search](#) for documents only within this product.

To contact Dekker customer service by phone, please call 1-800-228-1160 (USA, Canada & South America) or +44 1264 343039 (Europe, Far East, Middle East & Africa).



[A](#) [B](#) [C](#) [D](#) [E](#) [F](#) [G](#) [H](#) [I](#) [J](#) [K](#) [L](#) [M](#) [N](#) [O](#) [P](#) [Q](#) [R](#) [S](#) [T](#) [U](#)

416 articles

[β-Agonist Residues in Food, Analysis by LC](#)

Nikolaos A. Botsoglou

DOI: 10.1081/E-ECHR-120028860

[View HTML](#) [View PDF](#) [Order Reprints](#) [Save to My Workspace](#)

You have Access to this item

[Absorbance Detection in Capillary Electrophoresis](#)

Robert Weinberger

DOI: 10.1081/E-ECHR-120004560

[View HTML](#) [View PDF](#) [Order Reprints](#) [Save to My Workspace](#)

You have Access to this item

[Acoustic Field-Flow Fractionation for Particle Separation](#)

Niem Tri; Ronald Beckett

DOI: 10.1081/E-ECHR-120004561

[View HTML](#) [View PDF](#) [Order Reprints](#) [Save to My Workspace](#)

You have Access to this item

[Additives in Biopolymers, Analysis by Chromatographic Techniques](#)

Roxana A. Ruseckaite; Alfonso Jiménez

DOI: 10.1081/E-ECHR-120018660

[View HTML](#) [View PDF](#) [Order Reprints](#) [Save to My Workspace](#)

You have Access to this item

[Adhesion of Colloids on Solid Surfaces by Field-Flow Fractionation](#)

George Karaiskakis

DOI: 10.1081/E-ECHR-120004562

[View HTML](#) [View PDF](#) [Order Reprints](#) [Save to My Workspace](#)

You have Access to this item

[Adsorption Chromatography](#)

Robert J. Hurtubise

DOI: 10.1081/E-ECHR-120004563

[View HTML](#) [View PDF](#) [Order Reprints](#) [Save to My Workspace](#)

You have Access to this item

[Adsorption Studies by Field-Flow Fractionation](#)

Niem Tri; Ronald Beckett

DOI: 10.1081/E-ECHR-120004564

[View HTML](#) [View PDF](#) [Order Reprints](#) [Save to My Workspace](#)

You have Access to this item

[Advances in Chiral Pollutants Analysis by Capillary Electrophoresis](#)

Imran Ali; V. K. Gupta; Hassan Y. Aboul-Enein

DOI: 10.1081/E-ECHR-120027335

[View HTML](#) [View PDF](#) [Order Reprints](#) [Save to My Workspace](#)

You have Access to this item

[Affinity Chromatography of Cells](#)

Terry M. Phillips

DOI: 10.1081/E-ECHR-120004565

[View HTML](#) [View PDF](#) [Order Reprints](#) [Save to My Workspace](#)

You have Access to this item

[Affinity Chromatography with Immobilized Antibodies](#)

Monica J.S. Nadler; Tim Nadler
DOI: 10.1081/E-ECHR-120004566

[View HTML](#) [View PDF](#) [Order Reprints](#) [Save to My Workspace](#)

You have Access to this item

[Affinity Chromatography: An Overview](#)

David S. Hage; William Clarke
DOI: 10.1081/E-ECHR-120004567

[View HTML](#) [View PDF](#) [Order Reprints](#) [Save to My Workspace](#)

You have Access to this item

[Aggregation of Colloids by Field-Flow Fractionation](#)

Athanasia Koliadima
DOI: 10.1081/E-ECHR-120004568

[View HTML](#) [View PDF](#) [Order Reprints](#) [Save to My Workspace](#)

You have Access to this item

[Alumina-Based Supports for Liquid Chromatography](#)

Esther Forgács; Tibor Cserhádi
DOI: 10.1081/E-ECHR-120014245

[View HTML](#) [View PDF](#) [Order Reprints](#) [Save to My Workspace](#)

You have Access to this item

[Amino Acid Analysis by HPLC](#)

Susana Maria Halpine
DOI: 10.1081/E-ECHR-120004569

[View HTML](#) [View PDF](#) [Order Reprints](#) [Save to My Workspace](#)

You have Access to this item

[Amino Acids and Derivatives: Analysis by TLC](#)

Luciano Lepri; Alessandra Cincinelli
DOI: 10.1081/E-ECHR-120004570

[View HTML](#) [View PDF](#) [Order Reprints](#) [Save to My Workspace](#)

You have Access to this item

[Amino Acids, Peptides, and Proteins: Analysis by CE](#)

Danilo Corradini

DOI: 10.1081/E-ECHR-120004571

[View HTML](#) [View PDF](#) [Order Reprints](#) [Save to My Workspace](#)

You have Access to this item

[Analysis of Alcoholic Beverages by Gas Chromatography](#)

Fernando M. Lanças; M. de Moraes

DOI: 10.1081/E-ECHR-120004572

[View HTML](#) [View PDF](#) [Order Reprints](#) [Save to My Workspace](#)

You have Access to this item

[Analysis of Food Colors by Thin-Layer Chromatography/Scanning Densi-](#)

Hisao Oka; Yuko Ito; Tomomi Goto

DOI: 10.1081/E-ECHR-120014243

[View HTML](#) [View PDF](#) [Order Reprints](#) [Save to My Workspace](#)

You have Access to this item

[Analysis of Mycotoxins by TLC](#)

Philippe J. Berny

DOI: 10.1081/E-ECHR-120004573

[View HTML](#) [View PDF](#) [Order Reprints](#) [Save to My Workspace](#)

You have Access to this item

[Analysis of Plant Toxins by TLC](#)

Philippe J. Berny

DOI: 10.1081/E-ECHR-120004574

[View HTML](#) [View PDF](#) [Order Reprints](#) [Save to My Workspace](#)

You have Access to this item

[Analysis of Terpenoids by Thin-Layer Chromatography](#)

Simion Gocan

DOI: 10.1081/E-ECHR-120027339

[View HTML](#) [View PDF](#) [Order Reprints](#) [Save to My Workspace](#)

You have Access to this item

[Analyte–Analyte Interactions, Effect on TLC Band Formation](#)

Krzysztof Kaczmarek; Mieczysław Sajewicz; Wojciech Prus; Teresa Kov
DOI: 10.1081/E-ECHR-120028840

[View HTML](#) [View PDF](#) [Order Reprints](#) [Save to My Workspace](#)

You have Access to this item

[Antibiotics: Analysis by TLC](#)

Irena Choma
DOI: 10.1081/E-ECHR-120004575

[View HTML](#) [View PDF](#) [Order Reprints](#) [Save to My Workspace](#)

You have Access to this item

[Antioxidant Activity: An Adaptation for Measurement by HPLC](#)

Marino B. Arnao; Manuel Acosta; Antonio Cano
DOI: 10.1081/E-ECHR-120013365

[View HTML](#) [View PDF](#) [Order Reprints](#) [Save to My Workspace](#)

You have Access to this item

[Application of Capillary Electrochromatography to Biopolymers and Phar](#)

Ira S. Krull; Sarah Kazmi
DOI: 10.1081/E-ECHR-120004576

[View HTML](#) [View PDF](#) [Order Reprints](#) [Save to My Workspace](#)

You have Access to this item

[Applications of Evaporative Light-Scattering Detection in HPLC](#)

Juan G. Alvarez
DOI: 10.1081/E-ECHR-120004577

[View HTML](#) [View PDF](#) [Order Reprints](#) [Save to My Workspace](#)

You have Access to this item

[Applied Voltage: Effect on Mobility, Selectivity, and Resolution in Capilla](#)

Jetse C. Reijenga
DOI: 10.1081/E-ECHR-120004578

[View HTML](#) [View PDF](#) [Order Reprints](#) [Save to My Workspace](#)

You have Access to this item

[Aqueous Two-Phase Solvent Systems for Countercurrent Chromatograp](#)

Jean-Michel Menet

DOI: 10.1081/E-ECHR-120004579

[View HTML](#) [View PDF](#) [Order Reprints](#) [Save to My Workspace](#)

You have Access to this item

[Argon Detector](#)

Raymond P.W. Scott

DOI: 10.1081/E-ECHR-120004580

[View HTML](#) [View PDF](#) [Order Reprints](#) [Save to My Workspace](#)

You have Access to this item

[Assessment of Lipophilicity by Reversed-Phase TLC and HPLC](#)

Anna Tsantili-Kakoulidou

DOI: 10.1081/E-ECHR-120040663

World Price: *Not Yet Available*

[View HTML](#) [View PDF](#) [Order Reprints](#) [Save to My Workspace](#)

You have Access to this item

[Asymmetric Flow FFF in Biotechnology](#)

Thorsten Klein; Christine Hürzeler

DOI: 10.1081/E-ECHR-120004581

[View HTML](#) [View PDF](#) [Order Reprints](#) [Save to My Workspace](#)

You have Access to this item

[Automation and Robotics in Planar Chromatography](#)

Wojciech Markowski

DOI: 10.1081/E-ECHR-120004582

[View HTML](#) [View PDF](#) [Order Reprints](#) [Save to My Workspace](#)

You have Access to this item

[Axial Dispersion Correction Methods in GPC-SEC](#)

Gregorio R. Meira; Jorge R. Vega

DOI: 10.1081/E-ECHR-120004583

[View HTML](#) [View PDF](#) [Order Reprints](#) [Save to My Workspace](#)

You have Access to this item

[Band Broadening in Capillary Electrophoresis](#)

Jetse C. Reijenga

DOI: 10.1081/E-ECHR-120004584

[View HTML](#) [View PDF](#) [Order Reprints](#) [Save to My Workspace](#)

You have Access to this item

[Band Broadening in Size-Exclusion Chromatography](#)

Jean-Pierre Busnel

DOI: 10.1081/E-ECHR-120004585

[View HTML](#) [View PDF](#) [Order Reprints](#) [Save to My Workspace](#)

You have Access to this item

[Barbiturates, Analysis by Capillary Electrophoresis](#)

Chenchen Li; Huwei Liu

DOI: 10.1081/E-ECHR-120040662

World Price: *Not Yet Available*

[View HTML](#) [View PDF](#) [Order Reprints](#) [Save to My Workspace](#)

You have Access to this item

[Binding Constants: Determination by Affinity Chromatography](#)

David S. Hage; Sanjay Mukherjee

DOI: 10.1081/E-ECHR-120004586

[View HTML](#) [View PDF](#) [Order Reprints](#) [Save to My Workspace](#)

You have Access to this item

[Binding Molecules Via-SH Groups](#)

Terry M. Phillips

DOI: 10.1081/E-ECHR-120004587

[View HTML](#) [View PDF](#) [Order Reprints](#) [Save to My Workspace](#)

You have Access to this item

[Biopharmaceuticals by Capillary Electrophoresis](#)

Michel Girard
DOI: 10.1081/E-ECHR-120004588

[View HTML](#) [View PDF](#) [Order Reprints](#) [Save to My Workspace](#)

You have Access to this item

[Biopolymer Separations by Chromatographic Techniques](#)

Masayo Sakata; Chuichi Hirayama
DOI: 10.1081/E-ECHR-120038582

[View HTML](#) [View PDF](#) [Order Reprints](#) [Save to My Workspace](#)

You have Access to this item

[Biotic Dicarboxylic Acids, CCC Separation with Polar Two-Phase Solvent Cross-Axis Coil Planet Centrifuge](#)

Kazufusa Shinomiya; Yoichiro Ito
DOI: 10.1081/E-ECHR-120014224

[View HTML](#) [View PDF](#) [Order Reprints](#) [Save to My Workspace](#)

You have Access to this item

[Bonded Phases in HPLC](#)

Joseph J. Pesek; Maria T. Matyska
DOI: 10.1081/E-ECHR-120004589

[View HTML](#) [View PDF](#) [Order Reprints](#) [Save to My Workspace](#)

You have Access to this item

[Buffer Systems for Capillary Electrophoresis](#)

Robert Weinberger
DOI: 10.1081/E-ECHR-120004590

[View HTML](#) [View PDF](#) [Order Reprints](#) [Save to My Workspace](#)

You have Access to this item

[Buffer Type and Concentration, Effect on Mobility, Selectivity, and Resolution in Electrophoresis](#)

Ernst Kenndler
DOI: 10.1081/E-ECHR-120004591

[View HTML](#) [View PDF](#) [Order Reprints](#) [Save to My Workspace](#)

You have Access to this item

[Calibration of GPC-SEC with Narrow Molecular-Weight Distribution Standards](#)

Oscar Chiantore
DOI: 10.1081/E-ECHR-120004592

[View HTML](#) [View PDF](#) [Order Reprints](#) [Save to My Workspace](#)

You have Access to this item

[Calibration of GPC–SEC with Universal Calibration Techniques](#)

Oscar Chiantore
DOI: 10.1081/E-ECHR-120004593

[View HTML](#) [View PDF](#) [Order Reprints](#) [Save to My Workspace](#)

You have Access to this item

[Capacity](#)

M. Caude; A. Jardy
DOI: 10.1081/E-ECHR-120004594

[View HTML](#) [View PDF](#) [Order Reprints](#) [Save to My Workspace](#)

You have Access to this item

[Capillary Electrochromatography: An Introduction](#)

Michael P. Henry; Chitra K. Ratnayake
DOI: 10.1081/E-ECHR-120006099

[View HTML](#) [View PDF](#) [Order Reprints](#) [Save to My Workspace](#)

You have Access to this item

[Capillary Electrophoresis and HPLC for Analysis of Aromatic Diamidines,](#)

A. Negro; B. Rabanal
DOI: 10.1081/E-ECHR-120038594

[View HTML](#) [View PDF](#) [Order Reprints](#) [Save to My Workspace](#)

You have Access to this item

[Capillary Electrophoresis in Nonaqueous Media](#)

Ernst Kenndler
DOI: 10.1081/E-ECHR-120004598

[View HTML](#) [View PDF](#) [Order Reprints](#) [Save to My Workspace](#)

You have Access to this item

[Capillary Electrophoresis–Inductively Coupled Plasma–Mass Spectromet](#)

Clayton B'Hymer
DOI: 10.1081/E-ECHR-120028839

[View HTML](#) [View PDF](#) [Order Reprints](#) [Save to My Workspace](#)

You have Access to this item

[Capillary Electrophoresis on Chips](#)

Christa L. Colyer
DOI: 10.1081/E-ECHR-120004596

[View HTML](#) [View PDF](#) [Order Reprints](#) [Save to My Workspace](#)

You have Access to this item

[Capillary Electrophoresis: Introduction and Overview](#)

Joseph J. Pesek; Maria T. Matyska
DOI: 10.1081/E-ECHR-120004597

[View HTML](#) [View PDF](#) [Order Reprints](#) [Save to My Workspace](#)

You have Access to this item

[Capillary Isoelectric Focusing of Peptides, Proteins, and Antibodies](#)

Anders Palm
DOI: 10.1081/E-ECHR-120004604

[View HTML](#) [View PDF](#) [Order Reprints](#) [Save to My Workspace](#)

You have Access to this item

[Capillary Isoelectric Focusing: An Overview](#)

Robert Weinberger
DOI: 10.1081/E-ECHR-120005220

[View HTML](#) [View PDF](#) [Order Reprints](#) [Save to My Workspace](#)

You have Access to this item

[Capillary Isotachophoresis](#)

Ernst Kenndler
DOI: 10.1081/E-ECHR-120005219

[View HTML](#) [View PDF](#) [Order Reprints](#) [Save to My Workspace](#)

You have Access to this item

[Carbohydrates as Affinity Ligands](#)

I. Bataille; D. Muller

DOI: 10.1081/E-ECHR-120004605

[View HTML](#) [View PDF](#) [Order Reprints](#) [Save to My Workspace](#)

You have Access to this item

[Carbohydrates: Analysis by Capillary Electrophoresis](#)

Oliver Schmitz

DOI: 10.1081/E-ECHR-120004607

[View HTML](#) [View PDF](#) [Order Reprints](#) [Save to My Workspace](#)

You have Access to this item

[Carbohydrates: Analysis by HPLC](#)

Juan G. Alvarez

DOI: 10.1081/E-ECHR-120004606

[View HTML](#) [View PDF](#) [Order Reprints](#) [Save to My Workspace](#)

You have Access to this item

[Carbohydrates: Analysis by TLC—New Visualization](#)

N. Dimov

DOI: 10.1081/E-ECHR-120004608

[View HTML](#) [View PDF](#) [Order Reprints](#) [Save to My Workspace](#)

You have Access to this item

[Catalyst Characterization by Reversed Flow Gas Chromatography](#)

Dimitrios Gavril

DOI: 10.1081/E-ECHR-120041124

World Price: *Not Yet Available*

[View HTML](#) [View PDF](#) [Order Reprints](#) [Save to My Workspace](#)

You have Access to this item

[CCC Solvent Systems](#)

T. Maryutina; Boris Ya. Spivakov

DOI: 10.1081/E-ECHR-120004609

[View HTML](#) [View PDF](#) [Order Reprints](#) [Save to My Workspace](#)

You have Access to this item

[CE-MS: Large-Molecule Applications](#)

Ping Cao
DOI: 10.1081/E-ECHR-120004610

[View HTML](#) [View PDF](#) [Order Reprints](#) [Save to My Workspace](#)

You have Access to this item

[Cell Sorting Using Sedimentation Field Flow Fractionation: Methodologic Solutions—A “Cellulomics” Concept](#)

Philippe J. P. Cardot; Yves Denizot; Serge Battu
DOI: 10.1081/E-ECHR-120040664

World Price: *Not Yet Available*

[View HTML](#) [View PDF](#) [Order Reprints](#) [Save to My Workspace](#)

You have Access to this item

[Centrifugal Partition Chromatography: An Overview](#)

M.-C. Rolet-Menet
DOI: 10.1081/E-ECHR-120004611

[View HTML](#) [View PDF](#) [Order Reprints](#) [Save to My Workspace](#)

You have Access to this item

[Centrifugal Precipitation Chromatography](#)

Yoichiro Ito
DOI: 10.1081/E-ECHR-120004612

[View HTML](#) [View PDF](#) [Order Reprints](#) [Save to My Workspace](#)

You have Access to this item

[Ceramides: Analysis by Thin-Layer Chromatography](#)

Jacques Bodennec; Jacques Portoukalian
DOI: 10.1081/E-ECHR-120004613

[View HTML](#) [View PDF](#) [Order Reprints](#) [Save to My Workspace](#)

You have Access to this item

[Channeling and Column Voids](#)

Eileen Kennedy
DOI: 10.1081/E-ECHR-120004614

[View HTML](#) [View PDF](#) [Order Reprints](#) [Save to My Workspace](#)

You have Access to this item

[Characterization of Metalloproteins Using Capillary Electrophoresis](#)

Mark P. Richards

DOI: 10.1081/E-ECHR-120004615

[View HTML](#) [View PDF](#) [Order Reprints](#) [Save to My Workspace](#)[You have Access to this item](#)

[Chelating Sorbents for Affinity Chromatography \(IMAC\)](#)

Radovan Hynek; Anna Kozak; Jirí Sajdok; Jan Káň

DOI: 10.1081/E-ECHR-120004616

[View HTML](#) [View PDF](#) [Order Reprints](#) [Save to My Workspace](#)[You have Access to this item](#)

[Chemometrics in Chromatography](#)

Tibor Cserháti; Esther Forgács

DOI: 10.1081/E-ECHR-120014246

[View HTML](#) [View PDF](#) [Order Reprints](#) [Save to My Workspace](#)[You have Access to this item](#)

[Chiral Chromatography by Subcritical and Supercritical Fluid Chromatography](#)

Gerald J. Terfloth

DOI: 10.1081/E-ECHR-120005218

[View HTML](#) [View PDF](#) [Order Reprints](#) [Save to My Workspace](#)[You have Access to this item](#)

[Chiral Countercurrent Chromatography](#)

Ying Ma; Yoichiro Ito

DOI: 10.1081/E-ECHR-120004617

[View HTML](#) [View PDF](#) [Order Reprints](#) [Save to My Workspace](#)[You have Access to this item](#)

[Chiral Separations by Capillary Electrophoresis and Micellar Electrokinetic Chromatography with Cyclodextrins](#)

Paul K. Owens

DOI: 10.1081/E-ECHR-120004618

[View HTML](#) [View PDF](#) [Order Reprints](#) [Save to My Workspace](#)[You have Access to this item](#)

[Chiral Separations by GC](#)

Raymond P.W. Scott
DOI: 10.1081/E-ECHR-120004619

[View HTML](#) [View PDF](#) [Order Reprints](#) [Save to My Workspace](#)

You have Access to this item

[Chiral Separations by HPLC](#)

Nelu Grinberg; Richard Thompson
DOI: 10.1081/E-ECHR-120004620

[View HTML](#) [View PDF](#) [Order Reprints](#) [Save to My Workspace](#)

You have Access to this item

[Chiral Separations by Micellar Electrokinetic Chromatography with Chira](#)

Koji Otsuka; Shigeru Terabe
DOI: 10.1081/E-ECHR-120004621

[View HTML](#) [View PDF](#) [Order Reprints](#) [Save to My Workspace](#)

You have Access to this item

[Chromatographic Methods Used to Identify and Quantify Organic Polym](#)

Dennis Jenke
DOI: 10.1081/E-ECHR-120021147

[View HTML](#) [View PDF](#) [Order Reprints](#) [Save to My Workspace](#)

You have Access to this item

[Classification of Organic Solvents in Capillary Electrophoresis](#)

Ernst Kenndler
DOI: 10.1081/E-ECHR-120004622

[View HTML](#) [View PDF](#) [Order Reprints](#) [Save to My Workspace](#)

You have Access to this item

[Coil Planet Centrifuges](#)

Yoichiro Ito
DOI: 10.1081/E-ECHR-120014242

[View HTML](#) [View PDF](#) [Order Reprints](#) [Save to My Workspace](#)

You have Access to this item

[Cold-Wall Effects in Thermal FFF](#)

Martin E. Schimpf

DOI: 10.1081/E-ECHR-120004623

[View HTML](#) [View PDF](#) [Order Reprints](#) [Save to My Workspace](#)You have Access to this item

[Comprehensive Thermodynamic Approach to Ion Interaction Chromatography](#)

Teresa Cecchi

DOI: 10.1081/E-ECHR-120040673

World Price: *Not Yet Available*[View HTML](#) [View PDF](#) [Order Reprints](#) [Save to My Workspace](#)You have Access to this item

[Concentration Effects on Polymer Separation and Characterization by Thermal Field-Flow Fractionation](#)

Wenjie Cao; Mohan Gownder

DOI: 10.1081/E-ECHR-120004625

[View HTML](#) [View PDF](#) [Order Reprints](#) [Save to My Workspace](#)You have Access to this item

[Concentration of Dilute Colloidal Samples by Field-Flow Fractionation](#)

George Karaiskakis

DOI: 10.1081/E-ECHR-120004624

[View HTML](#) [View PDF](#) [Order Reprints](#) [Save to My Workspace](#)You have Access to this item

[Conductivity Detection in Capillary Electrophoresis](#)

Jetse C. Reijenga

DOI: 10.1081/E-ECHR-120004626

[View HTML](#) [View PDF](#) [Order Reprints](#) [Save to My Workspace](#)You have Access to this item

[Conductivity Detection in HPLC](#)

Ioannis N. Papadoyannis; Victoria F. Samanidou

DOI: 10.1081/E-ECHR-120004627

[View HTML](#) [View PDF](#) [Order Reprints](#) [Save to My Workspace](#)You have Access to this item

[Congener-Specific PCB Analysis](#)

George M. Frame, II

DOI: 10.1081/E-ECHR-120004628

[View HTML](#) [View PDF](#) [Order Reprints](#) [Save to My Workspace](#)[You have Access to this item](#)

[Copolymer Analysis by LC Methods, Including Two-Dimensional Chroma](#)

Peter Kilz

DOI: 10.1081/E-ECHR-120004629

[View HTML](#) [View PDF](#) [Order Reprints](#) [Save to My Workspace](#)[You have Access to this item](#)

[Copolymer Composition by GPC-SEC](#)

Sadao Mori

DOI: 10.1081/E-ECHR-120004630

[View HTML](#) [View PDF](#) [Order Reprints](#) [Save to My Workspace](#)[You have Access to this item](#)

[Copolymer Molecular Weights by GPC-SEC](#)

Sadao Mori

DOI: 10.1081/E-ECHR-120004631

[View HTML](#) [View PDF](#) [Order Reprints](#) [Save to My Workspace](#)[You have Access to this item](#)

[Coriolis Force in Countercurrent Chromatography](#)

Yoichiro Ito

DOI: 10.1081/E-ECHR-120004632

[View HTML](#) [View PDF](#) [Order Reprints](#) [Save to My Workspace](#)[You have Access to this item](#)

[Corrected Retention Time and Corrected Retention Volume](#)

Raymond P.W. Scott

DOI: 10.1081/E-ECHR-120004633

[View HTML](#) [View PDF](#) [Order Reprints](#) [Save to My Workspace](#)[You have Access to this item](#)

[Coumarins: Analysis by TLC](#)

Kazimierz Glowinski

DOI: 10.1081/E-ECHR-120004634

[View HTML](#) [View PDF](#) [Order Reprints](#) [Save to My Workspace](#)You have Access to this item

[Countercurrent Chromatographic Separation of Vitamins by Cross-Axis Centrifuge](#)

Kazufusa Shinomiya; Yoichiro Ito

DOI: 10.1081/E-ECHR-120014225

[View HTML](#) [View PDF](#) [Order Reprints](#) [Save to My Workspace](#)You have Access to this item

[Countercurrent Chromatography–Mass Spectrometry](#)

Hisao Oka; Yoichiro Ito

DOI: 10.1081/E-ECHR-120004635

[View HTML](#) [View PDF](#) [Order Reprints](#) [Save to My Workspace](#)You have Access to this item

[Creatinine and Purine Derivatives, Analysis by HPLC](#)

M.J. Arin; M. T. Diez; P. Garcia-del Moral; J. A. Resines

DOI: 10.1081/E-ECHR-120041122

World Price: *Not Yet Available*[View HTML](#) [View PDF](#) [Order Reprints](#) [Save to My Workspace](#)You have Access to this item

[Cross-Axis Coil Planet Centrifuge for the Separation of Proteins](#)

Yoichi Shibusawa; Yoichiro Ito

DOI: 10.1081/E-ECHR-120004636

[View HTML](#) [View PDF](#) [Order Reprints](#) [Save to My Workspace](#)You have Access to this item

[CZE of Biopolymers](#)

Feng Xu; Yoshinobu Baba

DOI: 10.1081/E-ECHR-120018663

[View HTML](#) [View PDF](#) [Order Reprints](#) [Save to My Workspace](#)You have Access to this item

[Dead Point \(Volume or Time\)](#)

Raymond P.W. Scott
DOI: 10.1081/E-ECHR-120004637

[View HTML](#) [View PDF](#) [Order Reprints](#) [Save to My Workspace](#)

You have Access to this item

[Degassing of Solvents](#)

Richard DeMuro
DOI: 10.1081/E-ECHR-120004638

[View HTML](#) [View PDF](#) [Order Reprints](#) [Save to My Workspace](#)

You have Access to this item

[Dendrimers and Hyperbranched Polymers: Analysis by GPC-SEC](#)

Nikolay Vladimirov
DOI: 10.1081/E-ECHR-120004639

[View HTML](#) [View PDF](#) [Order Reprints](#) [Save to My Workspace](#)

You have Access to this item

[Derivatization of Acids for GC Analysis](#)

Igor G. Zenkevich
DOI: 10.1081/E-ECHR-120004640

[View HTML](#) [View PDF](#) [Order Reprints](#) [Save to My Workspace](#)

You have Access to this item

[Derivatization of Amines, Amino Acids, Amides, and Imides for GC Anal](#)

Igor G. Zenkevich
DOI: 10.1081/E-ECHR-120004641

[View HTML](#) [View PDF](#) [Order Reprints](#) [Save to My Workspace](#)

You have Access to this item

[Derivatization of Analytes in Chromatography: General Aspects](#)

Igor G. Zenkevich
DOI: 10.1081/E-ECHR-120004642

[View HTML](#) [View PDF](#) [Order Reprints](#) [Save to My Workspace](#)

You have Access to this item

[Derivatization of Carbohydrates for GC Analysis](#)

Raymond P.W. Scott
DOI: 10.1081/E-ECHR-120004643

[View HTML](#) [View PDF](#) [Order Reprints](#) [Save to My Workspace](#)

You have Access to this item

[Derivatization of Carbonyls for GC Analysis](#)

Igor G. Zenkevich
DOI: 10.1081/E-ECHR-120004644

[View HTML](#) [View PDF](#) [Order Reprints](#) [Save to My Workspace](#)

You have Access to this item

[Derivatization of Hydroxy Compounds for GC Analysis](#)

Igor G. Zenkevich
DOI: 10.1081/E-ECHR-120004645

[View HTML](#) [View PDF](#) [Order Reprints](#) [Save to My Workspace](#)

You have Access to this item

[Derivatization of Steroids for GC Analysis](#)

Raymond P.W. Scott
DOI: 10.1081/E-ECHR-120004646

[View HTML](#) [View PDF](#) [Order Reprints](#) [Save to My Workspace](#)

You have Access to this item

[Detection \(Visualization\) of TLC Zones](#)

Joseph Sherma
DOI: 10.1081/E-ECHR-120004649

[View HTML](#) [View PDF](#) [Order Reprints](#) [Save to My Workspace](#)

You have Access to this item

[Detection in Countercurrent Chromatography](#)

M.-C. Rolet-Menet
DOI: 10.1081/E-ECHR-120004647

[View HTML](#) [View PDF](#) [Order Reprints](#) [Save to My Workspace](#)

You have Access to this item

[Detection Methods in Field-Flow Fractionation](#)

Martin Hassellöv

DOI: 10.1081/E-ECHR-120004648

[View HTML](#) [View PDF](#) [Order Reprints](#) [Save to My Workspace](#)[You have Access to this item](#)

[Detection Principles](#)

Kiyokatsu Jinno

DOI: 10.1081/E-ECHR-120013362

[View HTML](#) [View PDF](#) [Order Reprints](#) [Save to My Workspace](#)[You have Access to this item](#)

[Detector Linear Dynamic Range](#)

Raymond P.W. Scott

DOI: 10.1081/E-ECHR-120004650

[View HTML](#) [View PDF](#) [Order Reprints](#) [Save to My Workspace](#)[You have Access to this item](#)

[Detector Linearity and Response Index](#)

Raymond P.W. Scott

DOI: 10.1081/E-ECHR-120004651

[View HTML](#) [View PDF](#) [Order Reprints](#) [Save to My Workspace](#)[You have Access to this item](#)

[Detector Noise](#)

Raymond P.W. Scott

DOI: 10.1081/E-ECHR-120004652

[View HTML](#) [View PDF](#) [Order Reprints](#) [Save to My Workspace](#)[You have Access to this item](#)

[Displacement Chromatography](#)

John C. Ford

DOI: 10.1081/E-ECHR-120004653

[View HTML](#) [View PDF](#) [Order Reprints](#) [Save to My Workspace](#)[You have Access to this item](#)

[Displacement Thin-Layer Chromatography](#)

Mária Báthori

DOI: 10.1081/E-ECHR-120027006

[View HTML](#) [View PDF](#) [Order Reprints](#) [Save to My Workspace](#)

You have Access to this item

[Distribution Coefficient](#)

M. Caude; A. Jardy

DOI: 10.1081/E-ECHR-120004654

[View HTML](#) [View PDF](#) [Order Reprints](#) [Save to My Workspace](#)

You have Access to this item

[DNA Sequencing Studies by CE](#)

Yoshinobu Baba

DOI: 10.1081/E-ECHR-120004655

[View HTML](#) [View PDF](#) [Order Reprints](#) [Save to My Workspace](#)

You have Access to this item

[Drug Residues in Food, Detection/Confirmation by LC-MS](#)

Nikolaos A. Botsoglou

DOI: 10.1081/E-ECHR-120038629

[View HTML](#) [View PDF](#) [Order Reprints](#) [Save to My Workspace](#)

You have Access to this item

[Dry-Column Chromatography](#)

Mark Moskovitz

DOI: 10.1081/E-ECHR-120004656

[View HTML](#) [View PDF](#) [Order Reprints](#) [Save to My Workspace](#)

You have Access to this item

[Dual Countercurrent Chromatography](#)

David Y.W. Lee

DOI: 10.1081/E-ECHR-120004657

[View HTML](#) [View PDF](#) [Order Reprints](#) [Save to My Workspace](#)

You have Access to this item

[Dyes: Separation by Countercurrent Chromatography](#)

Adrian Weisz
DOI: 10.1081/E-ECHR-120004658

[View HTML](#) [View PDF](#) [Order Reprints](#) [Save to My Workspace](#)

You have Access to this item

[Eddy Diffusion in Liquid Chromatography](#)

J. E. Haky
DOI: 10.1081/E-ECHR-120004659

[View HTML](#) [View PDF](#) [Order Reprints](#) [Save to My Workspace](#)

You have Access to this item

[Effect of Organic Solvents on Ion Mobility](#)

Ernst Kenndler
DOI: 10.1081/E-ECHR-120004660

[View HTML](#) [View PDF](#) [Order Reprints](#) [Save to My Workspace](#)

You have Access to this item

[Effect of Temperature and Mobile Phase Composition on RP-HPLC Separation of Antibiotics](#)

J. Martín-Villacorta; R. Méndez; N. Montes; J. C. García-Glez
DOI: 10.1081/E-ECHR-120027336

[View HTML](#) [View PDF](#) [Order Reprints](#) [Save to My Workspace](#)

You have Access to this item

[Efficiency in Chromatography](#)

Nelu Grinberg; Rosario LoBrutto
DOI: 10.1081/E-ECHR-120004661

[View HTML](#) [View PDF](#) [Order Reprints](#) [Save to My Workspace](#)

You have Access to this item

[Efficiency of a Thin-Layer Chromatography Plate](#)

Wojciech Markowski
DOI: 10.1081/E-ECHR-120022515

[View HTML](#) [View PDF](#) [Order Reprints](#) [Save to My Workspace](#)

You have Access to this item

[Electro-osmotic Flow](#)

Danilo Corradini
DOI: 10.1081/E-ECHR-120004666

[View HTML](#) [View PDF](#) [Order Reprints](#) [Save to My Workspace](#)

You have Access to this item

[Electro-osmotic Flow in Capillary Tubes](#)

Danilo Corradini
DOI: 10.1081/E-ECHR-120004667

[View HTML](#) [View PDF](#) [Order Reprints](#) [Save to My Workspace](#)

You have Access to this item

[Electro-osmotic Flow Nonuniformity: Influence on Efficiency of Capillary](#)

Victor P. Andreev
DOI: 10.1081/E-ECHR-120004668

[View HTML](#) [View PDF](#) [Order Reprints](#) [Save to My Workspace](#)

You have Access to this item

[Electrochemical Detection](#)

Peter T. Kissinger
DOI: 10.1081/E-ECHR-120004662

[View HTML](#) [View PDF](#) [Order Reprints](#) [Save to My Workspace](#)

You have Access to this item

[Electrochemical Detection in CE](#)

Oliver Klett
DOI: 10.1081/E-ECHR-120004663

[View HTML](#) [View PDF](#) [Order Reprints](#) [Save to My Workspace](#)

You have Access to this item

[Electrokinetic Chromatography Including Micellar Electrokinetic Chroma](#)

Hassan Y. Aboul-Enein; Vince Serignese
DOI: 10.1081/E-ECHR-120004664

[View HTML](#) [View PDF](#) [Order Reprints](#) [Save to My Workspace](#)

You have Access to this item

[Electron-Capture Detector](#)

Raymond P.W. Scott
DOI: 10.1081/E-ECHR-120004665

[View HTML](#) [View PDF](#) [Order Reprints](#) [Save to My Workspace](#)

You have Access to this item

[Electrospray Ionization Interface for CE-MS](#)

Joanne Severs
DOI: 10.1081/E-ECHR-120004669

[View HTML](#) [View PDF](#) [Order Reprints](#) [Save to My Workspace](#)

You have Access to this item

[Elutropic Series of Solvents for Thin-Layer Chromatography](#)

Simion Gocan
DOI: 10.1081/E-ECHR-120027340

[View HTML](#) [View PDF](#) [Order Reprints](#) [Save to My Workspace](#)

You have Access to this item

[Elution Chromatography](#)

John C. Ford
DOI: 10.1081/E-ECHR-120004670

[View HTML](#) [View PDF](#) [Order Reprints](#) [Save to My Workspace](#)

You have Access to this item

[Elution Modes in Field-Flow Fractionation](#)

Josef Chmelík
DOI: 10.1081/E-ECHR-120004671

[View HTML](#) [View PDF](#) [Order Reprints](#) [Save to My Workspace](#)

You have Access to this item

[Enantiomer Separations by TLC](#)

Luciano Lepri; Alessandra Cincinelli
DOI: 10.1081/E-ECHR-120004672

[View HTML](#) [View PDF](#) [Order Reprints](#) [Save to My Workspace](#)

You have Access to this item

[Enantioseparation by Capillary Electrochromatography](#)

Yulin Deng

DOI: 10.1081/E-ECHR-120004673

[View HTML](#) [View PDF](#) [Order Reprints](#) [Save to My Workspace](#)

You have Access to this item

[End Capping](#)

Kiyokatsu Jinno

DOI: 10.1081/E-ECHR-120004674

[View HTML](#) [View PDF](#) [Order Reprints](#) [Save to My Workspace](#)

You have Access to this item

[Enoxacin: Analysis by Capillary Electrophoresis and HPLC](#)

Hassan Y. Aboul-Enein; Imran Ali

DOI: 10.1081/E-ECHR-120013364

[View HTML](#) [View PDF](#) [Order Reprints](#) [Save to My Workspace](#)

You have Access to this item

[Environmental Applications of SFC](#)

Yu Yang

DOI: 10.1081/E-ECHR-120004675

[View HTML](#) [View PDF](#) [Order Reprints](#) [Save to My Workspace](#)

You have Access to this item

[Environmental Pollutants Analysis by Capillary Electrophoresis](#)

Imran Ali; Hassan Y. Aboul-Enein

DOI: 10.1081/E-ECHR-120014229

[View HTML](#) [View PDF](#) [Order Reprints](#) [Save to My Workspace](#)

You have Access to this item

[Essential Oils Analysis by Gas Chromatography](#)

M. Soledad Prats; Alfonso Jiménez

DOI: 10.1081/E-ECHR-120018661

[View HTML](#) [View PDF](#) [Order Reprints](#) [Save to My Workspace](#)

You have Access to this item

[Evaporative Light Scattering Detection for Liquid Chromatography](#)

Sarah Chen

DOI: 10.1081/E-ECHR-120038633

[View HTML](#) [View PDF](#) [Order Reprints](#) [Save to My Workspace](#)

You have Access to this item

[Exclusion Limit in GPC-SEC](#)

Iwao Teraoka

DOI: 10.1081/E-ECHR-120004676

[View HTML](#) [View PDF](#) [Order Reprints](#) [Save to My Workspace](#)

You have Access to this item

[Extra-Column Dispersion](#)

Raymond P.W. Scott

DOI: 10.1081/E-ECHR-120004677

[View HTML](#) [View PDF](#) [Order Reprints](#) [Save to My Workspace](#)

You have Access to this item

[Extra-Column Volume](#)

Kiyokatsu Jinno

DOI: 10.1081/E-ECHR-120013345

[View HTML](#) [View PDF](#) [Order Reprints](#) [Save to My Workspace](#)

You have Access to this item

[Fast Gas Chromatography](#)

Richard C. Striebich

DOI: 10.1081/E-ECHR-120028084

[View HTML](#) [View PDF](#) [Order Reprints](#) [Save to My Workspace](#)

You have Access to this item

[Field-Flow Fractionation Data Treatment](#)

Josef Janča

DOI: 10.1081/E-ECHR-120004678

[View HTML](#) [View PDF](#) [Order Reprints](#) [Save to My Workspace](#)

You have Access to this item

[Field-Flow Fractionation Fundamentals](#)

Josef Janča

DOI: 10.1081/E-ECHR-120004680

[View HTML](#) [View PDF](#) [Order Reprints](#) [Save to My Workspace](#)

You have Access to this item

[Field-Flow Fractionation with Electro-osmotic Flow](#)

Victor P. Andreev

DOI: 10.1081/E-ECHR-120004679

[View HTML](#) [View PDF](#) [Order Reprints](#) [Save to My Workspace](#)

You have Access to this item

[Flame Ionization Detector for GC](#)

Raymond P.W. Scott

DOI: 10.1081/E-ECHR-120004681

[View HTML](#) [View PDF](#) [Order Reprints](#) [Save to My Workspace](#)

You have Access to this item

[Flavonoids, Analysis by Supercritical Fluid Chromatography](#)

Xia Yang; Huwei Liu

DOI: 10.1081/E-ECHR-120041126

World Price: *Not Yet Available*

[View HTML](#) [View PDF](#) [Order Reprints](#) [Save to My Workspace](#)

You have Access to this item

[Flow Field-Flow Fractionation: Introduction](#)

Myeong Hee Moon

DOI: 10.1081/E-ECHR-120004682

[View HTML](#) [View PDF](#) [Order Reprints](#) [Save to My Workspace](#)

You have Access to this item

[Fluorescence Detection in Capillary Electrophoresis](#)

Robert Weinberger

DOI: 10.1081/E-ECHR-120010668

[View HTML](#) [View PDF](#) [Order Reprints](#) [Save to My Workspace](#)

You have Access to this item

[Fluorescence Detection in HPLC](#)

Ioannis N. Papadoyannis; Anastasia Zotou

DOI: 10.1081/E-ECHR-120004683

[View HTML](#) [View PDF](#) [Order Reprints](#) [Save to My Workspace](#)

You have Access to this item

[Foam Countercurrent Chromatography](#)

Hisao Oka; Yoichiro Ito

DOI: 10.1081/E-ECHR-120004684

[View HTML](#) [View PDF](#) [Order Reprints](#) [Save to My Workspace](#)

You have Access to this item

[Focusing Field-Flow Fractionation of Particles and Macromolecules](#)

Josef Janča

DOI: 10.1081/E-ECHR-120004685

[View HTML](#) [View PDF](#) [Order Reprints](#) [Save to My Workspace](#)

You have Access to this item

[Forensic Applications of Capillary Electrophoresis](#)

Ivan Mikšik

DOI: 10.1081/E-ECHR-120004686

[View HTML](#) [View PDF](#) [Order Reprints](#) [Save to My Workspace](#)

You have Access to this item

[Forskolin Purification Using an Immunoaffinity Column Combined with a Monoclonal Antibody](#)

Hiroyuki Tanaka; Yukihiro Shoyama

DOI: 10.1081/E-ECHR-120004687

[View HTML](#) [View PDF](#) [Order Reprints](#) [Save to My Workspace](#)

You have Access to this item

[Fraction Collection Devices](#)

Gordon S. Hunter

DOI: 10.1081/E-ECHR-120004688

[View HTML](#) [View PDF](#) [Order Reprints](#) [Save to My Workspace](#)

You have Access to this item

[Frit-Inlet Asymmetrical Flow Field-Flow Fractionation](#)

Myeong Hee Moon
DOI: 10.1081/E-ECHR-120004689

[View HTML](#) [View PDF](#) [Order Reprints](#) [Save to My Workspace](#)

You have Access to this item

[Frontal Chromatography](#)

Peter Sajonz
DOI: 10.1081/E-ECHR-120004690

[View HTML](#) [View PDF](#) [Order Reprints](#) [Save to My Workspace](#)

You have Access to this item

[Fronting of Chromatographic Peaks: Causes](#)

Ioannis N. Papadoyannis; Anastasia Zotou
DOI: 10.1081/E-ECHR-120004691

[View HTML](#) [View PDF](#) [Order Reprints](#) [Save to My Workspace](#)

You have Access to this item

[Gas Chromatography System Instrumentation](#)

Mochammad Yuwono; Gunawan Indrayanto
DOI: 10.1081/E-ECHR-120040660

World Price: *Not Yet Available*

[View HTML](#) [View PDF](#) [Order Reprints](#) [Save to My Workspace](#)

You have Access to this item

[Gas Chromatography–Mass Spectrometry Systems](#)

Raymond P.W. Scott
DOI: 10.1081/E-ECHR-120004692

[View HTML](#) [View PDF](#) [Order Reprints](#) [Save to My Workspace](#)

You have Access to this item

[Golay Dispersion Equation for Open-Tubular Columns](#)

Raymond P.W. Scott
DOI: 10.1081/E-ECHR-120004694

[View HTML](#) [View PDF](#) [Order Reprints](#) [Save to My Workspace](#)

You have Access to this item

[GPC–SEC Analysis of Nonionic Surfactants](#)

Ivan Gitsov
DOI: 10.1081/E-ECHR-120004695

[View HTML](#) [View PDF](#) [Order Reprints](#) [Save to My Workspace](#)

You have Access to this item

[GPC-SEC Viscometry from Multiangle Light Scattering](#)

Philip J. Wyatt; Ron Myers
DOI: 10.1081/E-ECHR-120004698

[View HTML](#) [View PDF](#) [Order Reprints](#) [Save to My Workspace](#)

You have Access to this item

[GPC-SEC-HPLC Without Calibration: Multiangle Light Scattering Techni](#)

Philip J. Wyatt
DOI: 10.1081/E-ECHR-120004697

[View HTML](#) [View PDF](#) [Order Reprints](#) [Save to My Workspace](#)

You have Access to this item

[GPC-SEC: Effect of Experimental Conditions](#)

Sadao Mori
DOI: 10.1081/E-ECHR-120004696

[View HTML](#) [View PDF](#) [Order Reprints](#) [Save to My Workspace](#)

You have Access to this item

[GPC-SEC: Introduction and Principles](#)

Vaishali Soneji Lafita
DOI: 10.1081/E-ECHR-120004693

[View HTML](#) [View PDF](#) [Order Reprints](#) [Save to My Workspace](#)

You have Access to this item

[Gradient Development in Thin-Layer Chromatography](#)

Wojciech Markowski
DOI: 10.1081/E-ECHR-120004699

[View HTML](#) [View PDF](#) [Order Reprints](#) [Save to My Workspace](#)

You have Access to this item

[Gradient Elution](#)

J. E. Haky
DOI: 10.1081/E-ECHR-120004701

[View HTML](#) [View PDF](#) [Order Reprints](#) [Save to My Workspace](#)

You have Access to this item

[Gradient Elution in Capillary Electrophoresis](#)

Haleem J. Issaq
DOI: 10.1081/E-ECHR-120004702

[View HTML](#) [View PDF](#) [Order Reprints](#) [Save to My Workspace](#)

You have Access to this item

[Gradient Elution: Overview](#)

Ioannis N. Papadoyannis; Kalliopi A. Georga
DOI: 10.1081/E-ECHR-120004700

[View HTML](#) [View PDF](#) [Order Reprints](#) [Save to My Workspace](#)

You have Access to this item

[Gradient Generation Devices and Methods](#)

Miroslav Petro
DOI: 10.1081/E-ECHR-120004703

[View HTML](#) [View PDF](#) [Order Reprints](#) [Save to My Workspace](#)

You have Access to this item

[Headspace Sampling](#)

Raymond P.W. Scott
DOI: 10.1081/E-ECHR-120004704

[View HTML](#) [View PDF](#) [Order Reprints](#) [Save to My Workspace](#)

You have Access to this item

[Helium Detector](#)

Raymond P.W. Scott
DOI: 10.1081/E-ECHR-120004705

[View HTML](#) [View PDF](#) [Order Reprints](#) [Save to My Workspace](#)

You have Access to this item

[High-Speed SEC Methods](#)

Peter Kilz

DOI: 10.1081/E-ECHR-120014223

[View HTML](#) [View PDF](#) [Order Reprints](#) [Save to My Workspace](#)

You have Access to this item

[High-Temperature High-Resolution Gas Chromatography](#)

Fernando M. Lanças; J.J. S. Moreira

DOI: 10.1081/E-ECHR-120004706

[View HTML](#) [View PDF](#) [Order Reprints](#) [Save to My Workspace](#)

You have Access to this item

[Histidine in Body Fluids, Specific Determination by HPLC](#)

Toshiaki Miura; Naohiro Tateda; Kiichi Matsuhisa

DOI: 10.1081/E-ECHR-120025297

[View HTML](#) [View PDF](#) [Order Reprints](#) [Save to My Workspace](#)

You have Access to this item

[HPLC Analysis of Amino Acids](#)

Ioannis N. Papadoyannis; Georgios A. Theodoridis

DOI: 10.1081/E-ECHR-120004707

[View HTML](#) [View PDF](#) [Order Reprints](#) [Save to My Workspace](#)

You have Access to this item

[HPLC Analysis of Flavonoids](#)

Marina Stefova; Trajče Stafilov; Svetlana Kulevanova

DOI: 10.1081/E-ECHR-120016287

[View HTML](#) [View PDF](#) [Order Reprints](#) [Save to My Workspace](#)

You have Access to this item

[HPLC Column Maintenance](#)

Sarah Chen

DOI: 10.1081/E-ECHR-120038615

[View HTML](#) [View PDF](#) [Order Reprints](#) [Save to My Workspace](#)

You have Access to this item

[Hybrid Micellar Mobile Phases](#)

M. C. García-Alvarez-Coque; J. R. Torres-Lapasio

DOI: 10.1081/E-ECHR-120013363

[View HTML](#) [View PDF](#) [Order Reprints](#) [Save to My Workspace](#)

You have Access to this item

[Hydrodynamic Equilibrium in CCC](#)

Petr S. Fedotov; Boris Ya. Spivakov

DOI: 10.1081/E-ECHR-120004708

[View HTML](#) [View PDF](#) [Order Reprints](#) [Save to My Workspace](#)

You have Access to this item

[Hydrophilic Vitamins, Analysis by TLC](#)

Fumio Watanabe; Emi Miyamoto

DOI: 10.1081/E-ECHR-120028858

[View HTML](#) [View PDF](#) [Order Reprints](#) [Save to My Workspace](#)

You have Access to this item

[Hydrophobic Interaction Chromatography](#)

Karen M. Gooding

DOI: 10.1081/E-ECHR-120004709

[View HTML](#) [View PDF](#) [Order Reprints](#) [Save to My Workspace](#)

You have Access to this item

[Immobilized Metal Affinity Chromatography](#)

Roy A. Musil

DOI: 10.1081/E-ECHR-120004710

[View HTML](#) [View PDF](#) [Order Reprints](#) [Save to My Workspace](#)

You have Access to this item

[Immunoaffinity Chromatography](#)

David S. Hage; John Austin

DOI: 10.1081/E-ECHR-120004711

[View HTML](#) [View PDF](#) [Order Reprints](#) [Save to My Workspace](#)

You have Access to this item

[Immunodetection](#)

E. S.M. Lutz

DOI: 10.1081/E-ECHR-120004712

[View HTML](#) [View PDF](#) [Order Reprints](#) [Save to My Workspace](#)

You have Access to this item

[Industrial Applications of CCC](#)

Alain Berthod; Serge Alex; Sylvain Caravieilh; Claude De Bellefon
DOI: 10.1081/E-ECHR-120004713

[View HTML](#) [View PDF](#) [Order Reprints](#) [Save to My Workspace](#)

You have Access to this item

[Influence of Organic Solvents on \$pK_a\$](#)

Ernst Kenndler
DOI: 10.1081/E-ECHR-120004714

[View HTML](#) [View PDF](#) [Order Reprints](#) [Save to My Workspace](#)

You have Access to this item

[Injection Techniques for Capillary Electrophoresis](#)

Robert Weinberger
DOI: 10.1081/E-ECHR-120004715

[View HTML](#) [View PDF](#) [Order Reprints](#) [Save to My Workspace](#)

You have Access to this item

[Inorganic Analysis by CCC](#)

E. Kitazume
DOI: 10.1081/E-ECHR-120027337

[View HTML](#) [View PDF](#) [Order Reprints](#) [Save to My Workspace](#)

You have Access to this item

[Instrumentation of Countercurrent Chromatography](#)

Yoichiro Ito
DOI: 10.1081/E-ECHR-120004716

[View HTML](#) [View PDF](#) [Order Reprints](#) [Save to My Workspace](#)

You have Access to this item

[Intrinsic Viscosity of Polymers: Determination by GPC](#)

Yefim Brun
DOI: 10.1081/E-ECHR-120004717

[View HTML](#) [View PDF](#) [Order Reprints](#) [Save to My Workspace](#)

You have Access to this item

[Ion Chromatography Principles, Suppressed and Nonsuppressed](#)

Ioannis N. Papadoyannis; Victoria F. Samanidou

DOI: 10.1081/E-ECHR-120004718

[View HTML](#) [View PDF](#) [Order Reprints](#) [Save to My Workspace](#)

You have Access to this item

[Ion Exchange: Mechanism and Factors Affecting Separation](#)

Karen M. Gooding

DOI: 10.1081/E-ECHR-120004720

[View HTML](#) [View PDF](#) [Order Reprints](#) [Save to My Workspace](#)

You have Access to this item

[Ion-Exchange Buffers](#)

J. E. Haky

DOI: 10.1081/E-ECHR-120004719

[View HTML](#) [View PDF](#) [Order Reprints](#) [Save to My Workspace](#)

You have Access to this item

[Ion-Exchange Stationary Phases](#)

Karen M. Gooding

DOI: 10.1081/E-ECHR-120004721

[View HTML](#) [View PDF](#) [Order Reprints](#) [Save to My Workspace](#)

You have Access to this item

[Ion-Exclusion Chromatography](#)

Ioannis N. Papadoyannis; Victoria F. Samanidou

DOI: 10.1081/E-ECHR-120004722

[View HTML](#) [View PDF](#) [Order Reprints](#) [Save to My Workspace](#)

You have Access to this item

[Ion-Interaction Chromatography](#)

Teresa Cecchi

DOI: 10.1081/E-ECHR-120004723

[View HTML](#) [View PDF](#) [Order Reprints](#) [Save to My Workspace](#)

You have Access to this item

[Ion-Pairing Techniques](#)

Ioannis N. Papadoyannis; Anastasia Zotou

DOI: 10.1081/E-ECHR-120004724

[View HTML](#) [View PDF](#) [Order Reprints](#) [Save to My Workspace](#)

You have Access to this item

[Katharometer Detector for Gas Chromatography](#)

Raymond P.W. Scott

DOI: 10.1081/E-ECHR-120004725

[View HTML](#) [View PDF](#) [Order Reprints](#) [Save to My Workspace](#)

You have Access to this item

[Kovats Retention Index System](#)

Igor G. Zenkevich

DOI: 10.1081/E-ECHR-120004726

[View HTML](#) [View PDF](#) [Order Reprints](#) [Save to My Workspace](#)

You have Access to this item

[Large-Volume Injection for Gas Chromatography](#)

Yong Cai

DOI: 10.1081/E-ECHR-120004727

[View HTML](#) [View PDF](#) [Order Reprints](#) [Save to My Workspace](#)

You have Access to this item

[Large-Volume Sample Injection in FFF](#)

Martin Hassellöv

DOI: 10.1081/E-ECHR-120004728

[View HTML](#) [View PDF](#) [Order Reprints](#) [Save to My Workspace](#)

You have Access to this item

[Laser-Induced Fluorescence Detection for Capillary Electrophoresis](#)

Huan-Tsung Chang; Tai-Chia Chiu; Chih-Ching Huang

DOI: 10.1081/E-ECHR-120018658

[View HTML](#) [View PDF](#) [Order Reprints](#) [Save to My Workspace](#)

You have Access to this item

[LC-NMR and LC-MS-NMR: Recent Technological Advancements](#)

Maria Victoria Silva Elipe

DOI: 10.1081/E-ECHR-120014248

[View HTML](#) [View PDF](#) [Order Reprints](#) [Save to My Workspace](#)

You have Access to this item

[Lewis Base-Modified Zirconia as Stationary Phases for HPLC](#)

Y.-L. Hu; Y.-Q. Feng; S.-L. Da

DOI: 10.1081/E-ECHR-120014235

[View HTML](#) [View PDF](#) [Order Reprints](#) [Save to My Workspace](#)

You have Access to this item

[Lipid Analysis by HPLC](#)

Jahangir Emrani

DOI: 10.1081/E-ECHR-120004729

[View HTML](#) [View PDF](#) [Order Reprints](#) [Save to My Workspace](#)

You have Access to this item

[Lipid Classes: Purification by Solid-Phase Extraction](#)

Jacques Bodennec; Jacques Portoukalian

DOI: 10.1081/E-ECHR-120004730

[View HTML](#) [View PDF](#) [Order Reprints](#) [Save to My Workspace](#)

You have Access to this item

[Lipid Separation by Countercurrent Chromatography](#)

Kazuhiro Matsuda; Sachie Matsuda; Yoichiro Ito

DOI: 10.1081/E-ECHR-120022507

[View HTML](#) [View PDF](#) [Order Reprints](#) [Save to My Workspace](#)

You have Access to this item

[Lipids Analysis by Thin-Layer Chromatography](#)

Boryana Nikolova-Damyanova

DOI: 10.1081/E-ECHR-120004731

[View HTML](#) [View PDF](#) [Order Reprints](#) [Save to My Workspace](#)

You have Access to this item

[Lipids Analysis by TLC](#)

Boryana Nikolova-Damyanova

DOI: 10.1081/E-ECHR-120025293

[View HTML](#) [View PDF](#) [Order Reprints](#) [Save to My Workspace](#)

You have Access to this item

[Lipophilic Vitamins by Thin-Layer Chromatography](#)

Alina Pyka

DOI: 10.1081/E-ECHR-120004733

[View HTML](#) [View PDF](#) [Order Reprints](#) [Save to My Workspace](#)

You have Access to this item

[Lipophilicity Determination of Organic Substances by Reversed-Phase Thin-Layer Chromatography](#)

Gabriela Cimpan

DOI: 10.1081/E-ECHR-120004732

[View HTML](#) [View PDF](#) [Order Reprints](#) [Save to My Workspace](#)

You have Access to this item

[Lipoprotein Separation by Combined Use of Countercurrent Chromatography and Thin-Layer Chromatography](#)

Yoichi Shibusawa; Yoichiro Ito

DOI: 10.1081/E-ECHR-120025294

[View HTML](#) [View PDF](#) [Order Reprints](#) [Save to My Workspace](#)

You have Access to this item

[Liquid Chromatography–Mass Spectrometry](#)

Ioannis N. Papadoyannis; Georgios A. Theodoridis

DOI: 10.1081/E-ECHR-120004734

[View HTML](#) [View PDF](#) [Order Reprints](#) [Save to My Workspace](#)

You have Access to this item

[Liquid–Liquid Partition Chromatography](#)

Anant Vailaya

DOI: 10.1081/E-ECHR-120004735

[View HTML](#) [View PDF](#) [Order Reprints](#) [Save to My Workspace](#)

You have Access to this item

[Long-Chain Polymer Branching: Determination by GPC–SEC](#)

André M. Striegel

DOI: 10.1081/E-ECHR-120004736

[View HTML](#) [View PDF](#) [Order Reprints](#) [Save to My Workspace](#)

You have Access to this item

[Longitudinal Diffusion in Liquid Chromatography](#)

J. E. Haky

DOI: 10.1081/E-ECHR-120004737

[View HTML](#) [View PDF](#) [Order Reprints](#) [Save to My Workspace](#)

You have Access to this item

[Magnetic FFF and Magnetic SPLIT](#)

Maciej Zborowski; Jeffrey J. Chalmers; P. Stephen Williams

DOI: 10.1081/E-ECHR-120005221

[View HTML](#) [View PDF](#) [Order Reprints](#) [Save to My Workspace](#)

You have Access to this item

[Mark–Houwink Relationship](#)

Oscar Chiantore

DOI: 10.1081/E-ECHR-120005222

[View HTML](#) [View PDF](#) [Order Reprints](#) [Save to My Workspace](#)

You have Access to this item

[Mass Transfer Between Phases](#)

J. E. Haky

DOI: 10.1081/E-ECHR-120005223

[View HTML](#) [View PDF](#) [Order Reprints](#) [Save to My Workspace](#)

You have Access to this item

[Metal-Ion Enrichment by Countercurrent Chromatography](#)

Eiichi Kitazume

DOI: 10.1081/E-ECHR-120005224

[View HTML](#) [View PDF](#) [Order Reprints](#) [Save to My Workspace](#)

You have Access to this item

[Metal-Ion Separation by Micellar High Performance Liquid Chromatogra](#)

S. Muralidharan

DOI: 10.1081/E-ECHR-120005225

[View HTML](#) [View PDF](#) [Order Reprints](#) [Save to My Workspace](#)

You have Access to this item

[Metals and Organometallics: Gas Chromatography for Speciation and A](#)

Yong Cai; Weihua Zhang

DOI: 10.1081/E-ECHR-120005226

[View HTML](#) [View PDF](#) [Order Reprints](#) [Save to My Workspace](#)

You have Access to this item

[Metformin and Glibenclamide, Simultaneous Determination by HPLC](#)

B. L. Kolte; B. B. Raut; A. A. Deo; M. A. Bagool; D. B. Shinde

DOI: 10.1081/E-ECHR-120038482

[View HTML](#) [View PDF](#) [Order Reprints](#) [Save to My Workspace](#)

You have Access to this item

[Microcystin, Isolation by Supercritical Fluid Extraction](#)

Bing Yu; Huwei Liu

DOI: 10.1081/E-ECHR-120040661

World Price: *Not Yet Available*

[View HTML](#) [View PDF](#) [Order Reprints](#) [Save to My Workspace](#)

You have Access to this item

[Migration Behavior: Reproducibility in Capillary Electrophoresis](#)

Jetse C. Reijenga

DOI: 10.1081/E-ECHR-120005227

[View HTML](#) [View PDF](#) [Order Reprints](#) [Save to My Workspace](#)

You have Access to this item

[Minimum Detectable Concentration \(Sensitivity\)](#)

Raymond P.W. Scott

DOI: 10.1081/E-ECHR-120005228

[View HTML](#) [View PDF](#) [Order Reprints](#) [Save to My Workspace](#)

You have Access to this item

[Mixed Stationary Phases in GC](#)

Raymond P.W. Scott

DOI: 10.1081/E-ECHR-120005229

[View HTML](#) [View PDF](#) [Order Reprints](#) [Save to My Workspace](#)

You have Access to this item

[Mobile Phase Modifiers for SFC: Influence on Retention](#)

Yu Yang

DOI: 10.1081/E-ECHR-120005230

[View HTML](#) [View PDF](#) [Order Reprints](#) [Save to My Workspace](#)

You have Access to this item

[Molecular Interactions in GC](#)

Raymond P.W. Scott

DOI: 10.1081/E-ECHR-120005231

[View HTML](#) [View PDF](#) [Order Reprints](#) [Save to My Workspace](#)

You have Access to this item

[Molecular Weight and Molecular-Weight Distributions by Thermal FFF](#)

Martin E. Schimpf

DOI: 10.1081/E-ECHR-120005232

[View HTML](#) [View PDF](#) [Order Reprints](#) [Save to My Workspace](#)

You have Access to this item

[Molecularly Imprinted Polymers for Affinity Chromatography](#)

Georgios A. Theodoridis

DOI: 10.1081/E-ECHR-120013368

[View HTML](#) [View PDF](#) [Order Reprints](#) [Save to My Workspace](#)

You have Access to this item

[Monolithic Disk Supports for HPLC](#)

A. Podgornik; M. Barut; A. Strancar

DOI: 10.1081/E-ECHR-120016288

[View HTML](#) [View PDF](#) [Order Reprints](#) [Save to My Workspace](#)

You have Access to this item

[Multidimensional TLC](#)

Simion Gocan

DOI: 10.1081/E-ECHR-120005233

[View HTML](#) [View PDF](#) [Order Reprints](#) [Save to My Workspace](#)

You have Access to this item

[Natural Products Analysis by CE](#)

Noh-Hong Myoung

DOI: 10.1081/E-ECHR-120005234

[View HTML](#) [View PDF](#) [Order Reprints](#) [Save to My Workspace](#)

You have Access to this item

[Natural Rubber: GPC-SEC Analysis](#)

Frederic Bonfils

DOI: 10.1081/E-ECHR-120005235

[View HTML](#) [View PDF](#) [Order Reprints](#) [Save to My Workspace](#)

You have Access to this item

[Neuropeptides and Neuroproteins by Capillary Electrophoresis](#)

E.S. M. Lutz

DOI: 10.1081/E-ECHR-120005236

[View HTML](#) [View PDF](#) [Order Reprints](#) [Save to My Workspace](#)

You have Access to this item

[Neurotransmitter and Hormone Receptors: Purification by Affinity](#)

Terry M. Phillips

DOI: 10.1081/E-ECHR-120005237

[View HTML](#) [View PDF](#) [Order Reprints](#) [Save to My Workspace](#)

You have Access to this item

[Nitrogen/Phosphorus Detector](#)

Raymond P. W. Scott

DOI: 10.1081/E-ECHR-120005238

[View HTML](#) [View PDF](#) [Order Reprints](#) [Save to My Workspace](#)

You have Access to this item

[Nonionic Surfactants: GPC-SEC Analysis](#)

Ivan Gitsov

DOI: 10.1081/E-ECHR-120005239

[View HTML](#) [View PDF](#) [Order Reprints](#) [Save to My Workspace](#)

You have Access to this item

[Normal-Phase Chromatography](#)

Fred M. Rabel

DOI: 10.1081/E-ECHR-120005240

[View HTML](#) [View PDF](#) [Order Reprints](#) [Save to My Workspace](#)

You have Access to this item

[Normal-Phase Stationary Packings](#)

Rosario LoBrutto

DOI: 10.1081/E-ECHR-120005241

[View HTML](#) [View PDF](#) [Order Reprints](#) [Save to My Workspace](#)

You have Access to this item

[Nucleic Acids, Oligonucleotides, and DNA: Capillary Electrophoresis](#)

Yuriko Kiba; Yoshinobu Baba

DOI: 10.1081/E-ECHR-120005242

[View HTML](#) [View PDF](#) [Order Reprints](#) [Save to My Workspace](#)

You have Access to this item

[Octanol-Water Partition Coefficients by CCC](#)

Alain Berthod

DOI: 10.1081/E-ECHR-120005243

[View HTML](#) [View PDF](#) [Order Reprints](#) [Save to My Workspace](#)

You have Access to this item

[On-Column Injection for GC](#)

Mochammad Yuwono; Gunawan Indrayanto

DOI: 10.1081/E-ECHR-120040675

World Price: *Not Yet Available*

[View HTML](#) [View PDF](#) [Order Reprints](#) [Save to My Workspace](#)

You have Access to this item

[Open-Tubular \(Capillary\) Columns](#)

Raymond P.W. Scott

DOI: 10.1081/E-ECHR-120005244

[View HTML](#) [View PDF](#) [Order Reprints](#) [Save to My Workspace](#)

You have Access to this item

[Open-Tubular and Micropacked Columns for Supercritical Fluid Chromatography](#)

Brian Jones

DOI: 10.1081/E-ECHR-120005245

[View HTML](#) [View PDF](#) [Order Reprints](#) [Save to My Workspace](#)

You have Access to this item

[Optical Activity Detectors](#)

Hassan Y. Aboul-Enein; Ibrahim A. Al-Duraibi

DOI: 10.1081/E-ECHR-120005246

[View HTML](#) [View PDF](#) [Order Reprints](#) [Save to My Workspace](#)

You have Access to this item

[Optical Quantification \(Densitometry\) in TLC](#)

Joseph Sherma

DOI: 10.1081/E-ECHR-120005247

[View HTML](#) [View PDF](#) [Order Reprints](#) [Save to My Workspace](#)

You have Access to this item

[Optimization of Thin-Layer Chromatography](#)

Wojciech Prus; Teresa Kowalska

DOI: 10.1081/E-ECHR-120005248

[View HTML](#) [View PDF](#) [Order Reprints](#) [Save to My Workspace](#)

You have Access to this item

[Organic Acids, Analysis by Thin Layer Chromatography](#)

Nataša Brajenović

DOI: 10.1081/E-ECHR-120041125

World Price: *Not Yet Available*

[View HTML](#) [View PDF](#) [Order Reprints](#) [Save to My Workspace](#)

You have Access to this item

[Organic Extractables from Packaging Materials: Chromatographic Methods Identification and Quantification](#)

Dennis Jenke

DOI: 10.1081/E-ECHR-120018659

[View HTML](#) [View PDF](#) [Order Reprints](#) [Save to My Workspace](#)

You have Access to this item

[Overpressured Layer Chromatography](#)

Jan K. Różyło

DOI: 10.1081/E-ECHR-120005249

[View HTML](#) [View PDF](#) [Order Reprints](#) [Save to My Workspace](#)

You have Access to this item

[Packed Capillary Liquid Chromatography](#)

Fernando M. Lanças

DOI: 10.1081/E-ECHR-120005250

[View HTML](#) [View PDF](#) [Order Reprints](#) [Save to My Workspace](#)

You have Access to this item

[Particle Size Determination by Gravitational FFF](#)

Pierluigi Reschiglian

DOI: 10.1081/E-ECHR-120005251

[View HTML](#) [View PDF](#) [Order Reprints](#) [Save to My Workspace](#)

You have Access to this item

[Peak Identification with a Diode Array Detector](#)

Ioannis N. Papadoyannis; H. G. Gika

DOI: 10.1081/E-ECHR-120016289

[View HTML](#) [View PDF](#) [Order Reprints](#) [Save to My Workspace](#)

You have Access to this item

[Peak Purity Determination with a Diode Array Detector](#)

I. N. Papadoyannis; H. G. Gika
DOI: 10.1081/E-ECHR-120022509

[View HTML](#) [View PDF](#) [Order Reprints](#) [Save to My Workspace](#)

You have Access to this item

[Peak Skimming for Overlapping Peaks](#)

Wes Schafer
DOI: 10.1081/E-ECHR-120005252

[View HTML](#) [View PDF](#) [Order Reprints](#) [Save to My Workspace](#)

You have Access to this item

[Pellicular Supports for HPLC](#)

Danilo Corradini
DOI: 10.1081/E-ECHR-120005253

[View HTML](#) [View PDF](#) [Order Reprints](#) [Save to My Workspace](#)

You have Access to this item

[Penicillin Antibiotics in Food: Liquid Chromatographic Analysis](#)

Yuko Ito; Tomomi Goto; Hisao Oka
DOI: 10.1081/E-ECHR-120022511

[View HTML](#) [View PDF](#) [Order Reprints](#) [Save to My Workspace](#)

You have Access to this item

[Peptide Analysis by HPLC](#)

Karen M. Gooding
DOI: 10.1081/E-ECHR-120005254

[View HTML](#) [View PDF](#) [Order Reprints](#) [Save to My Workspace](#)

You have Access to this item

[Peptide Separation by Countercurrent Chromatography](#)

Ying Ma; Yoichiro Ito
DOI: 10.1081/E-ECHR-120038595

[View HTML](#) [View PDF](#) [Order Reprints](#) [Save to My Workspace](#)

You have Access to this item

[Pesticide Analysis by Gas Chromatography](#)

Fernando M. Lanças; M. A. Barbirato

DOI: 10.1081/E-ECHR-120005255

[View HTML](#) [View PDF](#) [Order Reprints](#) [Save to My Workspace](#)

You have Access to this item

[Pesticide Analysis by Thin-Layer Chromatography](#)

Joseph Sherma

DOI: 10.1081/E-ECHR-120005256

[View HTML](#) [View PDF](#) [Order Reprints](#) [Save to My Workspace](#)

You have Access to this item

[pH, Effect on MEKC Separation](#)

Koji Otsuka; Shigeru Terabe

DOI: 10.1081/E-ECHR-120005257

[View HTML](#) [View PDF](#) [Order Reprints](#) [Save to My Workspace](#)

You have Access to this item

[pH-Peak-Focusing and pH-Zone-Refining Countercurrent Chromatography](#)

Yoichiro Ito

DOI: 10.1081/E-ECHR-120005258

[View HTML](#) [View PDF](#) [Order Reprints](#) [Save to My Workspace](#)

You have Access to this item

[Pharmaceuticals: Analysis by TLC](#)

Philippe J. Berny

DOI: 10.1081/E-ECHR-120005259

[View HTML](#) [View PDF](#) [Order Reprints](#) [Save to My Workspace](#)

You have Access to this item

[Phenolic Acids in Natural Plants: Analysis by HPLC](#)

E. Brandšterová; A. Žiaková-Čaniová

DOI: 10.1081/E-ECHR-120013369

[View HTML](#) [View PDF](#) [Order Reprints](#) [Save to My Workspace](#)

You have Access to this item

[Phenolic Compounds, Analysis by HPLC](#)

P. B. Andrade; R. M. Seabra

DOI: 10.1081/E-ECHR-120016780

[View HTML](#) [View PDF](#) [Order Reprints](#) [Save to My Workspace](#)

You have Access to this item

[Phenolic Drugs, New Visualizing Reagents for Detection in TLC](#)

Alina Pyka

DOI: 10.1081/E-ECHR-120028856

[View HTML](#) [View PDF](#) [Order Reprints](#) [Save to My Workspace](#)

You have Access to this item

[Phenols and Acids: Analysis by TLC](#)

Luciano Lepri; Alessandra Cincinelli

DOI: 10.1081/E-ECHR-120005260

[View HTML](#) [View PDF](#) [Order Reprints](#) [Save to My Workspace](#)

You have Access to this item

[Photodiode-Array Detection](#)

Hassan Y. Aboul-Enein; Vince Serignese

DOI: 10.1081/E-ECHR-120005261

[View HTML](#) [View PDF](#) [Order Reprints](#) [Save to My Workspace](#)

You have Access to this item

[Photophoretic Effects in FFF of Particles](#)

Vadim L. Kononenko

DOI: 10.1081/E-ECHR-120005262

[View HTML](#) [View PDF](#) [Order Reprints](#) [Save to My Workspace](#)

You have Access to this item

[Plant Extracts: Analysis by TLC](#)

Gabriela Cimpan

DOI: 10.1081/E-ECHR-120005263

[View HTML](#) [View PDF](#) [Order Reprints](#) [Save to My Workspace](#)

You have Access to this item

[Plate Number, Effective](#)

Raymond P.W. Scott

DOI: 10.1081/E-ECHR-120005264

[View HTML](#) [View PDF](#) [Order Reprints](#) [Save to My Workspace](#)

You have Access to this item

[Plate Theory](#)

Raymond P.W. Scott

DOI: 10.1081/E-ECHR-120005265

[View HTML](#) [View PDF](#) [Order Reprints](#) [Save to My Workspace](#)

You have Access to this item

[Pollutant–Colloid Association by Field-Flow Fractionation](#)

Ronald Beckett; Bailin Chen; Niem Tri

DOI: 10.1081/E-ECHR-120005266

[View HTML](#) [View PDF](#) [Order Reprints](#) [Save to My Workspace](#)

You have Access to this item

[Pollutants in Water by HPLC](#)

Silvia Lacorte; Damià Barceló

DOI: 10.1081/E-ECHR-120005267

[View HTML](#) [View PDF](#) [Order Reprints](#) [Save to My Workspace](#)

You have Access to this item

[Polyamide Analysis by GPC–SEC](#)

Tuan Q. Nguyen

DOI: 10.1081/E-ECHR-120005268

[View HTML](#) [View PDF](#) [Order Reprints](#) [Save to My Workspace](#)

You have Access to this item

[Polycarbonates: GPC–SEC Analysis](#)

Nikolay Vladimirov

DOI: 10.1081/E-ECHR-120005269

[View HTML](#) [View PDF](#) [Order Reprints](#) [Save to My Workspace](#)

You have Access to this item

[Polyester Analysis by GPC–SEC](#)

Sam J. Ferrito

DOI: 10.1081/E-ECHR-120005270

[View HTML](#) [View PDF](#) [Order Reprints](#) [Save to My Workspace](#)

You have Access to this item

[Polymer Additives: Analysis by Chromatographic Techniques](#)

M. L. Marín; Alfonso Jiménez Migallon

DOI: 10.1081/E-ECHR-120005271

[View HTML](#) [View PDF](#) [Order Reprints](#) [Save to My Workspace](#)

You have Access to this item

[Polymer Degradation in GPC–SEC Columns](#)

Raniero Mendichi

DOI: 10.1081/E-ECHR-120005272

[View HTML](#) [View PDF](#) [Order Reprints](#) [Save to My Workspace](#)

You have Access to this item

[Polymerase Chain Reaction Products: Analysis Using Capillary Electroph](#)

Mark P. Richards

DOI: 10.1081/E-ECHR-120005273

[View HTML](#) [View PDF](#) [Order Reprints](#) [Save to My Workspace](#)

You have Access to this item

[Polynuclear Aromatic Hydrocarbons in Environmental Materials: Extract Supercritical Fluid Extraction](#)

Maria de Fatima Alpendurada

DOI: 10.1081/E-ECHR-120022514

[View HTML](#) [View PDF](#) [Order Reprints](#) [Save to My Workspace](#)

You have Access to this item

[Porous Graphitized Carbon Columns in Liquid Chromatography](#)

Irene Panderi

DOI: 10.1081/E-ECHR-120025298

[View HTML](#) [View PDF](#) [Order Reprints](#) [Save to My Workspace](#)

You have Access to this item

[Potential Barrier Field-Flow Fractionation](#)

George Karaiskakis

DOI: 10.1081/E-ECHR-120005274

[View HTML](#) [View PDF](#) [Order Reprints](#) [Save to My Workspace](#)

You have Access to this item

[Preparative HPLC Optimization](#)

Michael Breslav

DOI: 10.1081/E-ECHR-120005275

[View HTML](#) [View PDF](#) [Order Reprints](#) [Save to My Workspace](#)

You have Access to this item

[Preparative TLC](#)

Edward Soczewinski; Teresa Wawrzynowicz

DOI: 10.1081/E-ECHR-120005276

[View HTML](#) [View PDF](#) [Order Reprints](#) [Save to My Workspace](#)

You have Access to this item

[Procyanidin Separation by CCC with Hydrophilic Solvent Systems](#)

Yoichi Shibusawa; Yoichiro Ito

DOI: 10.1081/E-ECHR-120027338

[View HTML](#) [View PDF](#) [Order Reprints](#) [Save to My Workspace](#)

You have Access to this item

[Programmed Flow Gas Chromatography](#)

Raymond P.W. Scott

DOI: 10.1081/E-ECHR-120005277

[View HTML](#) [View PDF](#) [Order Reprints](#) [Save to My Workspace](#)

You have Access to this item

[Programmed Temperature Gas Chromatography](#)

Raymond P.W. Scott

DOI: 10.1081/E-ECHR-120005278

[View HTML](#) [View PDF](#) [Order Reprints](#) [Save to My Workspace](#)

You have Access to this item

[Prostaglandins: Analysis by HPLC](#)

Harald John

DOI: 10.1081/E-ECHR-120005279

[View HTML](#) [View PDF](#) [Order Reprints](#) [Save to My Workspace](#)

You have Access to this item

[Protein Analysis by HPLC](#)

Karen M. Gooding

DOI: 10.1081/E-ECHR-120005280

[View HTML](#) [View PDF](#) [Order Reprints](#) [Save to My Workspace](#)

You have Access to this item

[Protein Immobilization](#)

Jamel S. Hamada

DOI: 10.1081/E-ECHR-120005281

[View HTML](#) [View PDF](#) [Order Reprints](#) [Save to My Workspace](#)

You have Access to this item

[Protein Separations by Flow Field-Flow Fractionation](#)

Galina Kassalainen; S. Kim Ratanathanawongs Williams

DOI: 10.1081/E-ECHR-120005283

[View HTML](#) [View PDF](#) [Order Reprints](#) [Save to My Workspace](#)

You have Access to this item

[Proteins as Affinity Ligands](#)

Ji-Feng Zhang

DOI: 10.1081/E-ECHR-120005282

[View HTML](#) [View PDF](#) [Order Reprints](#) [Save to My Workspace](#)

You have Access to this item

[Purge-Backflushing Techniques in Gas Chromatography](#)

Silvia Lacorte; Anna Rigol

DOI: 10.1081/E-ECHR-120014247

[View HTML](#) [View PDF](#) [Order Reprints](#) [Save to My Workspace](#)

You have Access to this item

[Purification of Cyanobacterial Hepatotoxin Microcystins by Affinity Chromatography](#)

Fumio Kondo

DOI: 10.1081/E-ECHR-120016781

[View HTML](#) [View PDF](#) [Order Reprints](#) [Save to My Workspace](#)

You have Access to this item

[Purification of Peptides with Immobilized Enzymes](#)

Jamel S. Hamada

DOI: 10.1081/E-ECHR-120005284

[View HTML](#) [View PDF](#) [Order Reprints](#) [Save to My Workspace](#)

You have Access to this item

[Pyrolysis–Gas Chromatography–Mass Spectrometry Techniques for Poly Studies](#)

Alfonso Jiménez Migallon; M. L. Marín

DOI: 10.1081/E-ECHR-120005285

[View HTML](#) [View PDF](#) [Order Reprints](#) [Save to My Workspace](#)

You have Access to this item

[Quantitation by External Standard](#)

Tao Wang

DOI: 10.1081/E-ECHR-120005286

[View HTML](#) [View PDF](#) [Order Reprints](#) [Save to My Workspace](#)

You have Access to this item

[Quantitation by Internal Standard](#)

J. Vial; A. Jardy

DOI: 10.1081/E-ECHR-120005287

[View HTML](#) [View PDF](#) [Order Reprints](#) [Save to My Workspace](#)

You have Access to this item

[Quantitation by Normalization](#)

J. Vial; A. Jardy

DOI: 10.1081/E-ECHR-120005288

[View HTML](#) [View PDF](#) [Order Reprints](#) [Save to My Workspace](#)

You have Access to this item

[Quantitation by Standard Addition](#)

J. Vial; A. Jardy

DOI: 10.1081/E-ECHR-120010669

[View HTML](#) [View PDF](#) [Order Reprints](#) [Save to My Workspace](#)

You have Access to this item

[Quantitative Structure–Retention Relationship in Thin-Layer Chromatog](#)

N. Dimov

DOI: 10.1081/E-ECHR-120005289

[View HTML](#) [View PDF](#) [Order Reprints](#) [Save to My Workspace](#)

You have Access to this item

[Quinolone Antibiotics in Food, Analysis by LC](#)

Nikolaos A. Botsoglou

DOI: 10.1081/E-ECHR-120038631

[View HTML](#) [View PDF](#) [Order Reprints](#) [Save to My Workspace](#)

You have Access to this item

[Radiochemical Detection](#)

Eileen Kennedy

DOI: 10.1081/E-ECHR-120005291

[View HTML](#) [View PDF](#) [Order Reprints](#) [Save to My Workspace](#)

You have Access to this item

[Radius of Gyration Measurement by GPC-SEC](#)

Raniero Mendichi

DOI: 10.1081/E-ECHR-120005292

[View HTML](#) [View PDF](#) [Order Reprints](#) [Save to My Workspace](#)

You have Access to this item

[Rate Theory in Gas Chromatography](#)

Raymond P.W. Scott

DOI: 10.1081/E-ECHR-120005293

[View HTML](#) [View PDF](#) [Order Reprints](#) [Save to My Workspace](#)

You have Access to this item

[Refractive Index Detector](#)

Raymond P.W. Scott

DOI: 10.1081/E-ECHR-120005294

[View HTML](#) [View PDF](#) [Order Reprints](#) [Save to My Workspace](#)

You have Access to this item

[Resin Microspheres as Stationary Phase for Liquid Ligand Exchange Chr](#)

Zhikuan Chai

DOI: 10.1081/E-ECHR-120018657

[View HTML](#) [View PDF](#) [Order Reprints](#) [Save to My Workspace](#)

You have Access to this item

[Resolution in HPLC: Selectivity, Efficiency, and Capacity](#)

J. E. Haky

DOI: 10.1081/E-ECHR-120005295

[View HTML](#) [View PDF](#) [Order Reprints](#) [Save to My Workspace](#)

You have Access to this item

[Resolving Power of a Column](#)

Raymond P.W. Scott

DOI: 10.1081/E-ECHR-120005296

[View HTML](#) [View PDF](#) [Order Reprints](#) [Save to My Workspace](#)

You have Access to this item

[Response Spectrum in Chromatographic Analysis](#)

Dennis R. Jenke

DOI: 10.1081/E-ECHR-120038481

[View HTML](#) [View PDF](#) [Order Reprints](#) [Save to My Workspace](#)

You have Access to this item

[Retention Factor: Effect on MEKC Separation](#)

Koji Otsuka; Shigeru Terabe

DOI: 10.1081/E-ECHR-120005297

[View HTML](#) [View PDF](#) [Order Reprints](#) [Save to My Workspace](#)

You have Access to this item

[Retention Gap Injection Method](#)

Raymond P.W. Scott

DOI: 10.1081/E-ECHR-120005298

[View HTML](#) [View PDF](#) [Order Reprints](#) [Save to My Workspace](#)

You have Access to this item

[Retention Time and Retention Volume](#)

Raymond P.W. Scott

DOI: 10.1081/E-ECHR-120010670

[View HTML](#) [View PDF](#) [Order Reprints](#) [Save to My Workspace](#)

You have Access to this item

[Reversed-Phase Chromatography: Description and Applications](#)

Joseph J. Pesek; Maria T. Matyska

DOI: 10.1081/E-ECHR-120005299

[View HTML](#) [View PDF](#) [Order Reprints](#) [Save to My Workspace](#)

You have Access to this item

[Reversed-Phase Stationary Phases](#)

Joseph J. Pesek; Maria T. Matyska

DOI: 10.1081/E-ECHR-120005300

[View HTML](#) [View PDF](#) [Order Reprints](#) [Save to My Workspace](#)

You have Access to this item

[R_f](#)

Luciano Lepri; Alessandra Cincinelli

DOI: 10.1081/E-ECHR-120005290

[View HTML](#) [View PDF](#) [Order Reprints](#) [Save to My Workspace](#)

You have Access to this item

[Rotation Locular Countercurrent Chromatography](#)

Kazufusa Shinomiya

DOI: 10.1081/E-ECHR-120005301

[View HTML](#) [View PDF](#) [Order Reprints](#) [Save to My Workspace](#)

You have Access to this item

[Sample Application in TLC](#)

Simion Gocan

DOI: 10.1081/E-ECHR-120040674

World Price: *Not Yet Available*

[View HTML](#) [View PDF](#) [Order Reprints](#) [Save to My Workspace](#)

You have Access to this item

[Sample Preparation](#)

W. Jeffrey Hurst

DOI: 10.1081/E-ECHR-120005302

[View HTML](#) [View PDF](#) [Order Reprints](#) [Save to My Workspace](#)

You have Access to this item

[Sample Preparation and Stacking for Capillary Electrophoresis](#)

Zak K. Shihabi

DOI: 10.1081/E-ECHR-120005303

[View HTML](#) [View PDF](#) [Order Reprints](#) [Save to My Workspace](#)

You have Access to this item

[Sample Preparation Prior to HPLC](#)

Ioannis N. Papadoyannis; Victoria F. Samanidou

DOI: 10.1081/E-ECHR-120016782

[View HTML](#) [View PDF](#) [Order Reprints](#) [Save to My Workspace](#)

You have Access to this item

[Scale-up of Countercurrent Chromatography](#)

Ian A. Sutherland

DOI: 10.1081/E-ECHR-120005304

[View HTML](#) [View PDF](#) [Order Reprints](#) [Save to My Workspace](#)

You have Access to this item

[SEC with On-Line Triple Detection: Light Scattering, Viscometry, and Re](#)

Susan V. Greene

DOI: 10.1081/E-ECHR-120005305

[View HTML](#) [View PDF](#) [Order Reprints](#) [Save to My Workspace](#)

You have Access to this item

[Sedimentation Field-Flow Fractionation of Living Cells](#)

Philippe Cardot; T. Chianea; S. Battu

DOI: 10.1081/E-ECHR-120005306

[View HTML](#) [View PDF](#) [Order Reprints](#) [Save to My Workspace](#)

You have Access to this item

[Selection of a Gradient HPLC System](#)

Pavel Jandera

DOI: 10.1081/E-ECHR-120041120

World Price: *Not Yet Available*

[View HTML](#) [View PDF](#) [Order Reprints](#) [Save to My Workspace](#)

You have Access to this item

[Selection of an Isocratic HPLC System](#)

Pavel Jandera

DOI: 10.1081/E-ECHR-120041123

World Price: *Not Yet Available*

[View HTML](#) [View PDF](#) [Order Reprints](#) [Save to My Workspace](#)

You have Access to this item

[Selectivity](#)

Hassan Y. Aboul-Enein; Ibrahim A. Al-Duraibi

DOI: 10.1081/E-ECHR-120005307

[View HTML](#) [View PDF](#) [Order Reprints](#) [Save to My Workspace](#)

You have Access to this item

[Selectivity: Factors Affecting, in Supercritical Fluid Chromatography](#)

Kenneth G. Furton

DOI: 10.1081/E-ECHR-120005308

[View HTML](#) [View PDF](#) [Order Reprints](#) [Save to My Workspace](#)

You have Access to this item

[Separation of Alkaloids by Countercurrent Chromatography](#)

Fuquan Yang; Yoichiro Ito

DOI: 10.1081/E-ECHR-120016783

[View HTML](#) [View PDF](#) [Order Reprints](#) [Save to My Workspace](#)

You have Access to this item

[Separation of Antibiotics by Countercurrent Chromatography](#)

M.-C. Rolet-Menet
DOI: 10.1081/E-ECHR-120005309

[View HTML](#) [View PDF](#) [Order Reprints](#) [Save to My Workspace](#)

You have Access to this item

[Separation of Chiral Compounds by CE and MEKC with Cyclodextrins](#)

Bezhan Chankvetadze
DOI: 10.1081/E-ECHR-120005310

[View HTML](#) [View PDF](#) [Order Reprints](#) [Save to My Workspace](#)

You have Access to this item

[Separation of Flavonoids by Countercurrent Chromatography](#)

L. M. Yuan
DOI: 10.1081/E-ECHR-120041127

World Price: *Not Yet Available*

[View HTML](#) [View PDF](#) [Order Reprints](#) [Save to My Workspace](#)

You have Access to this item

[Separation of Metal Ions by Centrifugal Partition Chromatography](#)

S. Muralidharan
DOI: 10.1081/E-ECHR-120005311

[View HTML](#) [View PDF](#) [Order Reprints](#) [Save to My Workspace](#)

You have Access to this item

[Separation Ratio](#)

Raymond P.W. Scott
DOI: 10.1081/E-ECHR-120010671

[View HTML](#) [View PDF](#) [Order Reprints](#) [Save to My Workspace](#)

You have Access to this item

[Sequential Injection Analysis in HPLC](#)

Raluca-Ioana Stefan; Jacobus F. van Staden; Hassan Y. Aboul-Enein
DOI: 10.1081/E-ECHR-120005312

[View HTML](#) [View PDF](#) [Order Reprints](#) [Save to My Workspace](#)

You have Access to this item

[Settling Time of Two-Phase Solvent Systems in Countercurrent Chroma](#)

Jean-Michel Menet

DOI: 10.1081/E-ECHR-120005313

[View HTML](#) [View PDF](#) [Order Reprints](#) [Save to My Workspace](#)[You have Access to this item](#)

[Silica Capillaries: Chemical Derivatization](#)

Joseph J. Pesek; Maria T. Matyska

DOI: 10.1081/E-ECHR-120005314

[View HTML](#) [View PDF](#) [Order Reprints](#) [Save to My Workspace](#)[You have Access to this item](#)

[Silica Capillaries: Epoxy Coating](#)

James J. Bao

DOI: 10.1081/E-ECHR-120005315

[View HTML](#) [View PDF](#) [Order Reprints](#) [Save to My Workspace](#)[You have Access to this item](#)

[Silica Capillaries: Polymeric Coating for Capillary Electrophoresis](#)

Xi-Chun Zhou; Lifeng Zhang

DOI: 10.1081/E-ECHR-120005316

[View HTML](#) [View PDF](#) [Order Reprints](#) [Save to My Workspace](#)[You have Access to this item](#)

[Silver Ion TLC of Fatty Acids](#)

Boryana Nikolova-Damyanova

DOI: 10.1081/E-ECHR-120025292

[View HTML](#) [View PDF](#) [Order Reprints](#) [Save to My Workspace](#)[You have Access to this item](#)

[Size Separations by Capillary Electrophoresis](#)

Robert Weinberger

DOI: 10.1081/E-ECHR-120005317

[View HTML](#) [View PDF](#) [Order Reprints](#) [Save to My Workspace](#)[You have Access to this item](#)

[Solute Focusing Injection Method](#)

Raymond P.W. Scott
DOI: 10.1081/E-ECHR-120005318

[View HTML](#) [View PDF](#) [Order Reprints](#) [Save to My Workspace](#)

You have Access to this item

[Solute Identification in TLC](#)

Gabriela Cimpan
DOI: 10.1081/E-ECHR-120025296

[View HTML](#) [View PDF](#) [Order Reprints](#) [Save to My Workspace](#)

You have Access to this item

[Solvent Effects on Polymer Separation by ThFFF](#)

Wenjie Cao; Mohan Gownder
DOI: 10.1081/E-ECHR-120005319

[View HTML](#) [View PDF](#) [Order Reprints](#) [Save to My Workspace](#)

You have Access to this item

[Spacer Groups for Affinity Chromatography](#)

Terry M. Phillips
DOI: 10.1081/E-ECHR-120013343

[View HTML](#) [View PDF](#) [Order Reprints](#) [Save to My Workspace](#)

You have Access to this item

[Spiral Disk Assembly: An Improved Column Design for High-Speed Cou Chromatography \(HSCCC\)](#)

Yoichiro Ito; Fuquan Yang
DOI: 10.1081/E-ECHR-120022510

[View HTML](#) [View PDF](#) [Order Reprints](#) [Save to My Workspace](#)

You have Access to this item

[Split/Splitless Injector](#)

Raymond P.W. Scott
DOI: 10.1081/E-ECHR-120005320

[View HTML](#) [View PDF](#) [Order Reprints](#) [Save to My Workspace](#)

You have Access to this item

[Stationary Phases for Packed Column Supercritical Fluid Chromatograph](#)

Stephen L. Secreast
DOI: 10.1081/E-ECHR-120005321

[View HTML](#) [View PDF](#) [Order Reprints](#) [Save to My Workspace](#)

You have Access to this item

[Stationary-Phase Retention in Countercurrent Chromatography](#)

Jean-Michel Menet
DOI: 10.1081/E-ECHR-120005322

[View HTML](#) [View PDF](#) [Order Reprints](#) [Save to My Workspace](#)

You have Access to this item

[Steroid Analysis by Gas Chromatography](#)

Gunawan Indrayanto; Mochammad Yuwono
DOI: 10.1081/E-ECHR-120022512

[View HTML](#) [View PDF](#) [Order Reprints](#) [Save to My Workspace](#)

You have Access to this item

[Steroid Analysis by TLC](#)

Muhammad Mulja; Gunawan Indrayanto
DOI: 10.1081/E-ECHR-120005323

[View HTML](#) [View PDF](#) [Order Reprints](#) [Save to My Workspace](#)

You have Access to this item

[Supercritical Fluid Chromatography with Evaporative Light-Scattering D](#)

Christine M. Aurigemma; William P. Farrell
DOI: 10.1081/E-ECHR-120005325

[View HTML](#) [View PDF](#) [Order Reprints](#) [Save to My Workspace](#)

You have Access to this item

[Supercritical Fluid Chromatography with Mass Spectrometric Detection](#)

Manuel C. Ventura
DOI: 10.1081/E-ECHR-120005326

[View HTML](#) [View PDF](#) [Order Reprints](#) [Save to My Workspace](#)

You have Access to this item

[Supercritical Fluid Chromatography with Nitrogen Chemiluminescence C](#)

William P. Farrell
DOI: 10.1081/E-ECHR-120005327

[View HTML](#) [View PDF](#) [Order Reprints](#) [Save to My Workspace](#)

You have Access to this item

[Supercritical Fluid Chromatography: An Overview](#)

Fernando M. Lanas; M. C.H. Tavares
DOI: 10.1081/E-ECHR-120005324

[View HTML](#) [View PDF](#) [Order Reprints](#) [Save to My Workspace](#)

You have Access to this item

[Supercritical Fluid Extraction](#)

Christopher E. Bunker
DOI: 10.1081/E-ECHR-120027677

[View HTML](#) [View PDF](#) [Order Reprints](#) [Save to My Workspace](#)

You have Access to this item

[Surface Phenomena in Sedimentation FFF](#)

S. N. Semenov
DOI: 10.1081/E-ECHR-120005328

[View HTML](#) [View PDF](#) [Order Reprints](#) [Save to My Workspace](#)

You have Access to this item

[Surfactants: Analysis by HPLC](#)

Juan G. Alvarez
DOI: 10.1081/E-ECHR-120005329

[View HTML](#) [View PDF](#) [Order Reprints](#) [Save to My Workspace](#)

You have Access to this item

[Synergistic Effects of Mixed Stationary Phases in Gas Chromatography](#)

L. M. Yuan
DOI: 10.1081/E-ECHR-120016784

[View HTML](#) [View PDF](#) [Order Reprints](#) [Save to My Workspace](#)

You have Access to this item

[Systematic Selection of Solvent Systems for High Speed Countercurren](#)

Hisao Oka; Yoichiro Ito
DOI: 10.1081/E-ECHR-120016785

[View HTML](#) [View PDF](#) [Order Reprints](#) [Save to My Workspace](#)

You have Access to this item

[Taxanes Analysis by HPLC](#)

Georgios A. Theodoridis
DOI: 10.1081/E-ECHR-120013367

[View HTML](#) [View PDF](#) [Order Reprints](#) [Save to My Workspace](#)

You have Access to this item

[Taxines Analysis by HPLC](#)

Georgios Theodoridis
DOI: 10.1081/E-ECHR-120013366

[View HTML](#) [View PDF](#) [Order Reprints](#) [Save to My Workspace](#)

You have Access to this item

[Taxoids Analysis by TLC](#)

Tomasz Mroczek; Kazimierz Glowinski
DOI: 10.1081/E-ECHR-120005330

[View HTML](#) [View PDF](#) [Order Reprints](#) [Save to My Workspace](#)

You have Access to this item

[Temperature Program: Anatomy](#)

Raymond P.W. Scott
DOI: 10.1081/E-ECHR-120005333

[View HTML](#) [View PDF](#) [Order Reprints](#) [Save to My Workspace](#)

You have Access to this item

[Temperature: Effect on MEKC Separation](#)

Koji Otsuka; Shigeru Terabe
DOI: 10.1081/E-ECHR-120005331

[View HTML](#) [View PDF](#) [Order Reprints](#) [Save to My Workspace](#)

You have Access to this item

[Temperature: Effects on Mobility, Selectivity, and Resolution in Capillar](#)

Jetse C. Reijenga

DOI: 10.1081/E-ECHR-120005332

[View HTML](#) [View PDF](#) [Order Reprints](#) [Save to My Workspace](#)

You have Access to this item

[Terpenoids, Separation by HPLC](#)

Gabriela Cimpan

DOI: 10.1081/E-ECHR-120025295

[View HTML](#) [View PDF](#) [Order Reprints](#) [Save to My Workspace](#)

You have Access to this item

[Theory and Mechanism of Thin-Layer Chromatography](#)

Teresa Kowalska; Wojciech Prus

DOI: 10.1081/E-ECHR-120005334

[View HTML](#) [View PDF](#) [Order Reprints](#) [Save to My Workspace](#)

You have Access to this item

[Thermal FFF of Polymers and Particles](#)

Martin E. Schimpf

DOI: 10.1081/E-ECHR-120005336

[View HTML](#) [View PDF](#) [Order Reprints](#) [Save to My Workspace](#)

You have Access to this item

[Thermal FFF of Polystyrene](#)

Seungho Lee

DOI: 10.1081/E-ECHR-120005337

[View HTML](#) [View PDF](#) [Order Reprints](#) [Save to My Workspace](#)

You have Access to this item

[Thermal FFF: Basic Introduction and Overview](#)

Martin E. Schimpf

DOI: 10.1081/E-ECHR-120005335

[View HTML](#) [View PDF](#) [Order Reprints](#) [Save to My Workspace](#)

You have Access to this item

[Thermodynamics of GPC-SEC Separation](#)

Iwao Teraoka

DOI: 10.1081/E-ECHR-120005338

[View HTML](#) [View PDF](#) [Order Reprints](#) [Save to My Workspace](#)

You have Access to this item

[Thermodynamics of Retention in Gas Chromatography](#)

Raymond P.W. Scott

DOI: 10.1081/E-ECHR-120005339

[View HTML](#) [View PDF](#) [Order Reprints](#) [Save to My Workspace](#)

You have Access to this item

[Thin-Layer Chromatographic Study of Quantitative Structure–Retention](#)

L. Zhang; Qin-Sun Wang

DOI: 10.1081/E-ECHR-120005340

[View HTML](#) [View PDF](#) [Order Reprints](#) [Save to My Workspace](#)

You have Access to this item

[Thin-Layer Chromatography of Natural Pigments](#)

Tibor Cserhádi; Esther Forgács

DOI: 10.1081/E-ECHR-120005342

[View HTML](#) [View PDF](#) [Order Reprints](#) [Save to My Workspace](#)

You have Access to this item

[Thin-Layer Chromatography of Synthetic Dyes](#)

Tibor Cserhádi; Esther Forgács

DOI: 10.1081/E-ECHR-120005343

[View HTML](#) [View PDF](#) [Order Reprints](#) [Save to My Workspace](#)

You have Access to this item

[Thin-Layer Chromatography–Mass Spectrometry](#)

Jan K. Rózylo

DOI: 10.1081/E-ECHR-120005341

[View HTML](#) [View PDF](#) [Order Reprints](#) [Save to My Workspace](#)

You have Access to this item

[Three-Dimensional Effects in Field-Flow Fractionation: Theory](#)

Victor P. Andreev

DOI: 10.1081/E-ECHR-120005344

[View HTML](#) [View PDF](#) [Order Reprints](#) [Save to My Workspace](#)

You have Access to this item

[TLC Immunostaining of Steroidal Alkaloid Glycosides](#)

Waraporn Putalun; Hiroyuki Tanaka; Yukihiro Shoyama

DOI: 10.1081/E-ECHR-120005345

[View HTML](#) [View PDF](#) [Order Reprints](#) [Save to My Workspace](#)

You have Access to this item

[TLC Sandwich Chamber](#)

Simion Gocan

DOI: 10.1081/E-ECHR-120005346

[View HTML](#) [View PDF](#) [Order Reprints](#) [Save to My Workspace](#)

You have Access to this item

[TLC Sorbents](#)

Luciano Lepri; Alessandra Cincinelli

DOI: 10.1081/E-ECHR-120005347

[View HTML](#) [View PDF](#) [Order Reprints](#) [Save to My Workspace](#)

You have Access to this item

[Topological Indices, Use in HPLC](#)

Alina Pyka

DOI: 10.1081/E-ECHR-120041121

World Price: *Not Yet Available*

[View HTML](#) [View PDF](#) [Order Reprints](#) [Save to My Workspace](#)

You have Access to this item

[Trace Enrichment](#)

Fred M. Rabel

DOI: 10.1081/E-ECHR-120005348

[View HTML](#) [View PDF](#) [Order Reprints](#) [Save to My Workspace](#)

You have Access to this item

[Troubleshooting HPLC Instrumentation](#)

I. N. Papadoyannis; V. F. Samanidou

DOI: 10.1081/E-ECHR-120022508

[View HTML](#) [View PDF](#) [Order Reprints](#) [Save to My Workspace](#)

You have Access to this item

[Two-Dimensional Thin-Layer Chromatography](#)

Simion Gocan

DOI: 10.1081/E-ECHR-120022513

[View HTML](#) [View PDF](#) [Order Reprints](#) [Save to My Workspace](#)

You have Access to this item

[Ultrathin-Layer Gel Electrophoresis](#)

András Guttman; Csaba Barta; Árpád Gerstner; Huba Kalász; Mária Sas

DOI: 10.1081/E-ECHR-120005349

[View HTML](#) [View PDF](#) [Order Reprints](#) [Save to My Workspace](#)

You have Access to this item

[Unified Chromatography](#)

Fernando M. Lanças

DOI: 10.1081/E-ECHR-120005350

[View HTML](#) [View PDF](#) [Order Reprints](#) [Save to My Workspace](#)

You have Access to this item

[Uremic Toxins in Biofluids, Analysis by HPLC](#)

Ioannis N. Papadoyannis; Victoria F. Samanidou

DOI: 10.1081/E-ECHR-120025291

[View HTML](#) [View PDF](#) [Order Reprints](#) [Save to My Workspace](#)

You have Access to this item

[Validation of HPLC Instrumentation](#)

Ioannis N. Papadoyannis; Victoria F. Samanidou

DOI: 10.1081/E-ECHR-120018662

[View HTML](#) [View PDF](#) [Order Reprints](#) [Save to My Workspace](#)

You have Access to this item

[Validation of TLC Analyses](#)

Gunawan Indrayanto; Mochammad Yuwono

DOI: 10.1081/E-ECHR-120016786

[View HTML](#) [View PDF](#) [Order Reprints](#) [Save to My Workspace](#)

You have Access to this item

[van't Hoff Curves](#)

Raymond P.W. Scott

DOI: 10.1081/E-ECHR-120005351

[View HTML](#) [View PDF](#) [Order Reprints](#) [Save to My Workspace](#)

You have Access to this item

[Vinyl Pyrrolidone Homopolymer and Copolymers: SEC Analysis](#)

Chi-san Wu; Larry Senak; James Curry; Edward Malawer

DOI: 10.1081/E-ECHR-120005352

[View HTML](#) [View PDF](#) [Order Reprints](#) [Save to My Workspace](#)

You have Access to this item

[Viscometric Detection in GPC-SEC](#)

James Lesec

DOI: 10.1081/E-ECHR-120005353

[View HTML](#) [View PDF](#) [Order Reprints](#) [Save to My Workspace](#)

You have Access to this item

[Vitamin B₁₂ and Related Compounds in Food, Analysis by TLC](#)

Fumio Watanabe; Emi Miyamoto

DOI: 10.1081/E-ECHR-120028859

[View HTML](#) [View PDF](#) [Order Reprints](#) [Save to My Workspace](#)

You have Access to this item

[Void Volume in Liquid Chromatography](#)

Kiyokatsu Jinno

DOI: 10.1081/E-ECHR-120005354

[View HTML](#) [View PDF](#) [Order Reprints](#) [Save to My Workspace](#)

You have Access to this item

[Weak Affinity Chromatography](#)

David S. Hage

DOI: 10.1081/E-ECHR-120028855

[View HTML](#) [View PDF](#) [Order Reprints](#) [Save to My Workspace](#)

You have Access to this item

[Wheat Protein by Field-Flow Fractionation](#)

S. G. Stevenson; K. R. Preston
DOI: 10.1081/E-ECHR-120005355

[View HTML](#) [View PDF](#) [Order Reprints](#) [Save to My Workspace](#)

You have Access to this item

[Whey Proteins, Anion-Exchange Separation](#)

Kyung Ho Row; Du Young Choi
DOI: 10.1081/E-ECHR-120028857

[View HTML](#) [View PDF](#) [Order Reprints](#) [Save to My Workspace](#)

You have Access to this item

[Zeta-Potential](#)

Jetse C. Reijenga
DOI: 10.1081/E-ECHR-120010672

[View HTML](#) [View PDF](#) [Order Reprints](#) [Save to My Workspace](#)

You have Access to this item

[Zirconia-Silica Stationary Phases for HPLC: Overview and Applications](#)

R. Andrew Shalliker; Sindy Kayillo
DOI: 10.1081/E-ECHR-120013344

[View HTML](#) [View PDF](#) [Order Reprints](#) [Save to My Workspace](#)

You have Access to this item

[Zone Dispersion in Field-Flow Fractionation](#)

Josef Janča
DOI: 10.1081/E-ECHR-120005356

[View HTML](#) [View PDF](#) [Order Reprints](#) [Save to My Workspace](#)

You have Access to this item

[Return to top](#)



About Dekker | Author Services | Site Map

© Copyright 1997 - 2005, by Marcel Dekker

β -Agonist Residues in Food, Analysis by LC

Nikolaos A. Botsoglou

Aristotle University, Thessaloniki, Greece

INTRODUCTION

β -Agonists are synthetically produced compounds that, in addition to their regular therapeutic role in veterinary medicine as bronchodilatory and tocolytic agents, can promote live weight gain in food-producing animals. They are also referred to as repartitioning agents because their effect on carcass composition is to increase the deposition of protein while reducing fat accumulation. For use in lean-meat production, doses of 5 to 15 times greater than the recommended therapeutic dose would be required, together with a more prolonged period of in-feed administration, which is often quite near to slaughter to obviate the elimination problem. Such use would result in significant residue levels in edible tissues of treated animals, which might in turn exert adverse effects in the cardiovascular and central nervous systems of the consumers.^[1]

There are a number of well-documented cases where consumption of liver and meat from animals that have been illegally treated with these compounds, particularly clenbuterol, has resulted in massive human intoxication.^[1] In Spain, a foodborne clenbuterol poisoning outbreak occurred in 1989–1990, affecting 135 persons. Consumption of liver containing clenbuterol in the range 160–291 ppb was identified as the common point in the 43 families affected, while symptoms were observed in 97% of all family members who consumed liver. In 1992, another outbreak occurred in Spain, affecting this time 232 persons. Clinical signs of poisoning in more than half of the patients included muscle tremors and tachycardia, frequently accompanied by nervousness, headaches, and myalgia. Clenbuterol levels in the urine of the patients were found to range from 11 to 486 ppb. In addition, an incident of food poisoning by residues of clenbuterol in veal liver occurred in the fall of 1990 in the cities of Roanne and Clermont-Ferrand, France. Twenty-two persons from eight families were affected. Apart from the mentioned cases, two farmers in Ireland were also reported to have died while preparing clenbuterol for feeding to livestock.

Although, without exception, these incidents have all been caused by the toxicity of clenbuterol, the entire group of β -agonists are now treated with great suspicion by regulatory authorities, and use of all β -agonists in farm

animals for growth-promoting purposes has been prohibited by regulatory agencies in Europe, Asia, and the Americas. Clenbuterol, in particular, has been banned by the FDA for any animal application in the United States, whereas it is highly likely to be banned even for therapeutic use in the United States in the near future. However, veterinary use of some β -agonists, such as clenbuterol, cimaterol, and ractopamine, is still licensed in several parts of the world for therapeutic purposes.

MONITORING

Monitoring programs have shown that β -agonists have been used illegally in parts of Europe and United States by some livestock producers.^[1] In addition, newly developed analogues, often with modified structural properties, are continuously introduced in the illegal practice of application of growth-promoting β -agonists in cattle raising. As a result, specific knowledge of the target residues appropriate to surveillance is very limited for many of the β -agonists that have potential black market use.^[2] Hence, continuous improvement of detection methods is necessary to keep pace with the rapid development of these new, heretofore unknown β -agonists. Both gas and liquid chromatographic methods can be used for the determination of β -agonist residues in biological samples. However, LC methods are receiving wider acceptance because gas chromatographic methods are generally complicated by the necessity of derivatization of the polar hydroxyl and amino functional groups of β -agonists. In this article, an overview of the analytical methodology for the determination of β -agonist in food is provided.

ANALYSIS OF β -AGONISTS BY LC

Included in this group of drugs are certain synthetically produced phenethanolamines such as bambuterol, bromobuterol, carbuterol, cimaterol, clenbuterol, dobutamine, fenoterol, isoproterenol, mabuterol, mapenterol, metaproterenol, pirbuterol, ractopamine, reproterol, rimiterol, ritodrine, salbutamol, salmeterol, terbutaline, and

tulobuterol. These drugs fall into two major categories, i.e., substituted anilines, including clenbuterol, and substituted phenols, including salbutamol. This distinction is important because most methods for drugs in the former category depend on pH adjustment to partition the analytes between organic and aqueous phases. The pH dependence is not valid, however, for drugs within the latter category, because phenolic compounds are charged under all practical pH conditions.

EXTRACTION PROCEDURES

β -Agonists are relatively polar compounds that are soluble in methanol and ethanol, slightly soluble in chloroform, and almost insoluble in benzene. When analyzing liquid samples for residues of β -agonists, deconjugation of bound residues, using 2-glucuronidase/sulfatase enzyme hydrolysis prior to sample extraction, is often recommended.^[3,4] Semisolid samples, such as liver and muscle, require usually more intensive sample pretreatment for tissue breakup. The most popular approach is sample homogenization in dilute acids such as hydrochloric or perchloric acid or aqueous buffer.^[3-6] In general, dilute acids allow high extraction yields for all categories of β -agonists, because the aromatic moiety of these analytes is uncharged under acidic conditions, whereas their aliphatic amino group is positively ionized. Following centrifugation of the extract, the supernatant may be further treated with β -glucuronidase/sulfatase or subtilisin A to allow hydrolysis of the conjugated residues.

CLEANUP PROCEDURES

The primary sample extract is subsequently subjected to cleanup using several different approaches, including conventional liquid–liquid partitioning, diphasic dialysis, solid-phase extraction, and immunoaffinity chromatography cleanup. In some instances, more than one of these procedures is applied in combination to achieve better extract purification.

LIQUID–LIQUID PARTITION

Liquid–liquid partitioning cleanup is generally performed at alkaline conditions using ethyl acetate, ethyl acetate/*tert*-butanol mixture, diethyl ether, or *tert*-butylmethyl

ether/*n*-butanol as extraction solvents.^[5,7,8] The organic extracts are then either concentrated to dryness, or re-partitioned with dilute acid to facilitate back extraction of the analytes into the acidic solution. A literature survey shows that liquid–liquid partitioning cleanup resulted in good recoveries of substituted anilines such as clenbuterol,^[7,8] but it was less effective for more polar compounds such as salbutamol.^[5] Diphasic dialysis can also be used for purification of the primary sample extract. This procedure was only applied in the determination of clenbuterol residues in liver using *tert*-butylmethyl ether as the extraction solvent.^[6]

SOLID-PHASE EXTRACTION

Solid-phase extraction is, generally, better suited to the multiresidue analysis of β -agonists. This procedure has become the method of choice for the determination of β -agonists in biological matrices because it is not labor and material intensive. It is particularly advantageous because it allows better extraction of the more hydrophilic β -agonists, including salbutamol. β -Agonists are better suited to reversed-phase solid-phase extraction due, in part, to their relatively non-polar aliphatic moiety, which can interact with the hydrophobic octadecyl- and octyl-based sorbents of the cartridge.^[9-11] By adjusting the pH of the sample extracts at values greater than 10, optimum retention of the analytes can be achieved. Adsorption solid-phase extraction, using a neutral alumina sorbent, has also been recommended for improved cleanup of liver homogenates.^[5] Ion-exchange solid-phase extraction is another cleanup procedure that has been successfully used in the purification of liver and tissue homogenates.^[12] Because multiresidue solid-phase extraction procedures covering β -agonists of different types generally present analytical problems, mixed-phase solid-phase extraction sorbents, which contained a mixture of reversed-phase and ion-exchange material, were also used to improve the retention of the more polar compounds. Toward this goal, several different sorbents were designed, and procedures that utilized both interaction mechanisms have been described.^[5,9,13]

IMMUNOAFFINITY CHROMATOGRAPHY

Owing to its high specificity and sample cleanup efficiency, immunoaffinity chromatography has also received widespread acceptance for the determination of β -agonists in biological matrices.^[3,4,12,14] The potential



of online immunoaffinity extraction for the multiresidue determination of β -agonists in bovine urine was recently demonstrated, using an automated column switching system.^[14]

SEPARATION PROCEDURES

Following extraction and cleanup, β -agonist residues are analyzed by liquid chromatography. Gas chromatographic separation of β -agonists is generally complicated by the necessity of derivatization of their polar hydroxyl and amino functional groups. LC reversed-phase columns are commonly used for the separation of the various β -agonist residues due to their hydrophobic interaction with the C₁₈ sorbent. Efficient reversed-phase ion-pair separation of β -agonists has also been reported, using sodium dodecyl sulfate as the pairing counterion.^[15]

DETECTION PROCEDURES

Following LC separation, detection is often performed in the ultraviolet region at wavelengths of 245 or 260 nm. However, poor sensitivity and interference from coextractives may appear at these low detection wavelengths unless sample extracts are extensively cleaned up and concentrated. This problem may be overcome by post-column derivatization of the aromatic amino group of the β -agonist molecules to the corresponding diazo dyes through a Bratton-Marshall reaction, and subsequent detection at 494 nm.^[15] Although spectrophotometric detection is generally acceptable, electrochemical detection appears more appropriate for the analysis of β -agonists due to the presence on the aromatic part of their molecule of oxidizable hydroxyl and amino groups. This method of detection has been applied in the determination of clenbuterol residues in bovine retinal tissue with sufficient sensitivity for this tissue.^[8]

CONFIRMATION PROCEDURES

Confirmatory analysis of suspected liquid chromatographic peaks can be accomplished by coupling liquid chromatography with mass spectrometry. Ion spray LC-MS-MS has been used to monitor five β -agonists in bovine urine,^[14] whereas atmospheric-pressure chemical ionization LC-MS-MS has been used for the identification of ractopamine residues in bovine urine.^[9]

CONCLUSION

This literature overview shows that a wide range of efficient extraction, cleanup, separation, and detection procedures is available for the determination of β -agonists in food. However, continuous improvement of detection methods is necessary to keep pace with the ongoing introduction of new unknown β -agonists that have potential black market use, in the illegal practice.

REFERENCES

1. Botsoglou, N.A.; Fletouris, D.J. *Drug Residues in Food. Pharmacology, Food Safety, and Analysis*; Marcel Dekker: New York, 2001.
2. Kuiper, H.A.; Noordam, M.Y.; Van Dooren-Flipsen, M.M.H.; Schilt, R.; Roos, A.H. Illegal use of beta-adrenergic agonists—European Community. *J. Anim. Sci.* **1998**, *76*, 195–207.
3. Van Ginkel, L.A.; Stephany, R.W.; Van Rossum, H.J. Development and validation of a multiresidue method for beta-agonists in biological samples and animal feed. *J. AOAC Int.* **1992**, *75*, 554–560.
4. Visser, T.; Vredenburg, M.J.; De Jong, A.P.J.M.; Van Ginkel, L.A.; Van Rossum, H.J.; Stephany, R.W. Cryotrapping gas-chromatography Fourier-transform infrared spectrometry—A new technique to confirm the presence of beta-agonists in animal material. *Anal. Chim. Acta* **1993**, *275*, 205–214.
5. Leyssens, L.; Driessen, C.; Jacobs, A.; Czech, J.; Raus, J. Determination of beta-2-receptor agonists in bovine urine and liver by gas-chromatography tandem mass-spectrometry. *J. Chromatogr.* **1991**, *564*, 515–527.
6. Gonzalez, P.; Fente, C.A.; Franco, C.; Vazquez, B.; Quinto, E.; Cepeda, A. Determination of residues of the beta-agonist clenbuterol in liver of medicated farm-animals by gas-chromatography mass-spectrometry using diphasic dialysis as an extraction procedure. *J. Chromatogr.* **1997**, *693*, 321–326.
7. Wilson, R.T.; Groneck, J.M.; Holland, K.P.; Henry, A.C. Determination of clenbuterol in cattle, sheep, and swine tissues by electron ionization gas-chromatography mass-spectrometry. *J. AOAC Int.* **1994**, *77*, 917–924.
8. Lin, L.A.; Tomlinson, J.A.; Satzger, R.D. Detection of clenbuterol in bovine retinal tissue by high performance liquid-chromatography with electrochemical detection. *J. Chromatogr.* **1997**, *762*, 275–280.
9. Elliott, C.T.; Thompson, C.S.; Arts, C.J.M.; Crooks, S.R.H.; Van Baak, M.J.; Verheij, E.R.; Baxter, G.A. Screening and confirmatory determination of ractopamine residues in calves treated with growth-promoting doses of the beta-agonist. *Analyst* **1998**, *123*, 1103–1107.
10. Van Rhijn, J.A.; Heskamp, H.H.; Essers, M.L.; Van de Wetering, H.J.; Kleijnen, H.C.H.; Roos, A.H. Possibilities for confirmatory analysis of some beta-agonists using 2

- different derivatives simultaneously. *J. Chromatogr.* **1995**, *665*, 395–398.
11. Gaillard, Y.; Balland, A.; Doucet, F.; Pepin, G. Detection of illegal clenbuterol use in calves using hair analysis. *J. Chromatogr.* **1997**, *703*, 85–95.
12. Lawrence, J.F.; Menard, C. Determination of clenbuterol in beef-liver and muscle-tissue using immunoaffinity chromatographic cleanup and liquid-chromatography with ultraviolet absorbency detection. *J. Chromatogr.* **1997**, *696*, 291–297.
13. Ramos, F.; Santos, C.; Silva, A.; Da Silveira, M.I.N. Beta(2)-adrenergic agonist residues—Simultaneous methylboronic and butylboronic derivatization for confirmatory analysis by gas-chromatography mass-spectrometry. *J. Chromatogr.* **1998**, *716*, 366–370.
14. Cai, J.; Henion, J. Quantitative multi-residue determination of beta-agonists in bovine urine using online immunoaffinity extraction coupled-column packed capillary liquid-chromatography tandem mass-spectrometry. *J. Chromatogr.* **1997**, *691*, 357–370.
15. Courtheyn, D.; Desaeve, C.; Verhe, R. High-performance liquid-chromatographic determination of clenbuterol and cimaterol using postcolumn derivatization. *J. Chromatogr.* **1991**, *564*, 537–549.



Absorbance Detection in Capillary Electrophoresis

Robert Weinberger

CE Technologies, Inc., Chappaqua, New York, U.S.A.

Introduction

Most forms of detection in High-Performance Capillary Electrophoresis (HPCE) employ on-capillary detection. Exceptions are techniques that use a sheath flow such as laser-induced fluorescence [1] and electrospray ionization mass spectrometry [2].

In high-performance liquid chromatography (HPLC), postcolumn detection is generally used. This means that all solutes are traveling at the same velocity when they pass through the detector flow cell. In HPCE with on-capillary detection, the velocity of the solute determines the residence time in the flow cell. This means that slowly migrating solutes spend more time in the optical path and thus accumulate more area counts [3].

Because peak areas are used for quantitative determinations, the areas must be normalized when quantitating without standards. Quantitation without standards is often used when determining impurity profiles in pharmaceuticals, chiral impurities, and certain DNA applications. The correction is made by normalizing (dividing) the raw peak area by the migration time. When a matching standard is used, it is unnecessary to perform this correction. If the migration times are not reproducible, the correction may help, but it is better to correct the situation causing this problem.

Limits of Detection

The limit of detection (LOD) of a system can be defined in two ways: the concentration limit of detection (CLOD) and the mass limit of detection (MLOD). The CLOD of a typical peptide is about 1 $\mu\text{g/mL}$ using absorbance detection at 200 nm. If 10 nL are injected, this translates to an MLOD of 10 pg at three times the baseline noise. The MLOD illustrates the measuring capability of the instrument. The more important parameter is the CLOD, which relates to the sample itself. The CLOD for HPCE is relatively poor, whereas the MLOD is quite good, especially when compared to HPLC. In HPLC, the injection size can be 1000 times greater compared to HPCE.

The CLOD can be calculated using Beer's Law:

$$\text{CLOD} = \frac{A}{ab} = \frac{5 \times 10^{-5}}{(5000)(5 \times 10)^{-3}} = 2 \times 10^{-6} M \quad (1)$$

where A is the absorbance (AU), a is the molar absorptivity (AU/cm/M), b is the capillary diameter or optical path length (cm), and CLOD is the concentration (M). The noise of a good detector is typically 5×10^{-5} AU. A modest chromophore has a molar absorptivity of 5000. Then in a 50- μm -inner diameter (i.d.) capillary, a CLOD of $2 \times 10^{-6} M$ is obtained at a signal-to-noise ratio of 1, assuming no other sources of band broadening.

Detector Linear Dynamic Range

The noise level of the best detectors is about 5×10^{-5} AU. Using a 50- μm -i.d. capillary, the maximum signal that can be obtained while yielding reasonable peak shape is 5×10^{-1} AU. This provides a linear dynamic range of about 10^4 . This can be improved somewhat through the use of an extended path-length flow cell. In any event, if the background absorbance of the electrolyte is high, the noise of the system will increase regardless of the flow cell utilized.

Classes of Absorbance Detectors

Ultraviolet/visible absorption detection is the most common technique found in HPCE. Several types of absorption detectors are available on commercial instrumentation, including the following:

1. Fixed-wavelength detector using mercury, zinc, or cadmium lamps with wavelength selection by filters
2. Variable-wavelength detector using a deuterium or tungsten lamp with wavelength selection by a monochromator
3. Filter photometer using a deuterium lamp with wavelength selection by filters
4. Scanning ultraviolet (UV) detector
5. Photodiode array detector



Each of these absorption detectors have certain attributes that are useful in HPCE. Multiwavelength detectors such as the photodiode array or scanning UV detector are valuable because spectral as well as electrophoretic information can be displayed. The filter photometer is invaluable for low-UV detection. The use of the 185-nm mercury line becomes practical in HPCE with phosphate buffers because the short optical path length minimizes the background absorption.

Photoacoustic, thermo-optical, or photothermal detectors have been reported in the literature [4]. These detectors measure the nonradiative return of the excited molecule to the ground state. Although these can be quite sensitive, it is unlikely that they will be used in commercial instrumentation.

Optimization of Detector Wavelength

Because of the short optical path length defined by the capillary, the optimal detection wavelength is frequently much lower into the UV compared to HPLC. In HPCE with a variable-wavelength absorption detector, the optimal signal-to-noise (S/N) ratio for peptides is found at 200 nm. To optimize the detector wavelength, it is best to plot the S/N ratio at various wavelengths. The optimal S/N is then easily selected.

Extended Path-Length Capillaries

Increasing the optical path length of the capillary window should increase S/N simply as a result of Beer's Law. This has been achieved using a z cell (LC Packings, San Francisco CA) [5], bubble cell (Agilent Technologies, Wilmington, DE), or a high-sensitivity cell (Agilent Technologies). Both the z cell and bubble cell are integral to the capillary. The high-sensitivity cell comes in three parts: an inlet capillary, an outlet capillary, and the cell body. Careful assembly permits the use of this cell without current leakage. The bubble cell provides approximately a threefold improvement in sensitivity using a 50- μ m capillary, whereas the z cell or high-sensitivity cell improves things by an order of magnitude. This holds true only when the background electrolyte (BGE) has low absorbance at the monitoring wavelength.

Indirect Absorbance Detection

To determine ions that do not absorb in the UV, indirect detection is often utilized [6]. In this technique, a UV-absorbing reagent of the same charge (a co-ion) as the solutes is added to the BGE. The reagent elevates the baseline, and when nonabsorbing solute ions are present, they displace the additive. As the separated ions migrate past the detector window, they are measured as negative peaks relative to the high baseline. For anions, additives such as trimellitic acid, phthalic acid, or chromate ions are used at 2–10 mM concentrations. For cations, creatinine, imidazole, or copper(II) are often used. Other buffer materials are either not used or added in only small amounts to avoid interfering with the detection process.

It is best to match the mobility of the reagent to the average mobilities of the solutes to minimize electrodispersion, which causes band broadening [7]. When anions are determined, a cationic surfactant is added to the BGE to slow or even reverse the electroosmotic flow (EOF). When the EOF is reversed, both electrophoresis and electro-osmosis move in the same direction. Anion separations are performed using reversed polarity.

Indirect detection is used to determine simple ions such as chloride, sulfate, sodium, and potassium. The technique is also applicable to aliphatic amines, aliphatic carboxylic acids, and simple sugars [8].

References

1. Y. F. Cheng and N. J. Dovichi, *SPIE*, 910: 111 (1988).
2. E. C. Huang, T. Wachs, J. J. Conboy, and J. D. Henion, *Anal. Chem.* 62: 713 (1990).
3. X. Huang, W. F. Coleman, and R. N. Zare, *J. Chromatogr.* 480: 95 (1989).
4. J. M. Saz and J. C. Diez-Masa, *J. Liq. Chromatogr.* 17: 499 (1994).
5. J. P. Chervet, R. E. J. van Soest, and M. Ursem, *J. Chromatogr.* 543: 439 (1991).
6. P. Jandik, W. R. Jones, A. Weston, and P. R. Brown, *LC-GC* 9: 634 (1991).
7. R. Weinberger, *Am. Lab.* 28: 24 (1996).
8. X. Xu, W. T. Kok, and H. Poppe, *J. Chromatogr. A* 716: 231 (1995).



Acoustic Field-Flow Fractionation for Particle Separation

Niem Tri

Ronald Beckett

Monash University, Melbourne, Australia

Introduction

Field-flow fractionation (FFF) is a suite of elution methods suitable for the separation and sizing of macromolecules and particles [1]. It relies on the combined effects of an applied force interacting with sample components and the parabolic velocity profile of carrier fluid in the channel. For this to be effective, the channel is unpacked and the flow must be under laminar conditions. Field or gradients that are commonly used in generating the applied force are gravity, centrifugation, fluid flow, temperature gradient, and electrical and magnetic fields. Each field or gradient produces a different subtechnique of FFF, which separates samples on the basis of a particular property of the molecules or particles.

Research and Developments

The potential for using acoustic radiation forces generated by ultrasonic waves to extend the versatility of FFF seems very promising. Although only very preliminary experiments have been performed so far, the possibility of using such a gentle force would appear to have huge potential in biology, medicine, and environmental studies.

Acoustic radiation or ultrasonic waves are currently being exploited as a noncontact particle micromanipulation technique [2]. The main drive to develop such techniques comes from the desire to manipulate biological cells and blood constituents in biotechnology and fine powders in material engineering.

In a propagating wave, the acoustic force, F_{ac} , acting on a particle is a function of size given by [1]

$$F_{ac} = \pi r^2 E Y_p \quad (1)$$

where r is the particle radius, E is the sound energy density, and Y_p is a complicated function depending on the characteristics of the particle which approaches unity if the wavelength used is much smaller than the particle. Particles in a solution subjected to a propagat-

ing sound wave will be pushed in the direction of sound propagation. Therefore, sized-based separations may be possible if this force is applied to generate selective transport of different components in a mixture. In a FFF channel, it is likely that the receiving wall will reflect at least some of the emitted wave. If the channel thickness corresponds exactly to one-half wavelength, then a single standing wave will be created (see Fig. 1). For a single standing wave, it is interesting to note that three pressure (force) nodes are generated, one at each wall and one in the center of the channel.

Yasuda and Kamakura [3] and Mandralis and co-workers [4] have demonstrated that it is possible to generate standing-wave fields between a transducer and a reflecting wall, although of much larger dimensions (1–20 cm) than across a FFF channel. Sound travels at a velocity of 1500 m/s through water, which translates to a wave of frequency of approximately 6 MHz for a 120- μ m thick FFF channel.

The force experienced by a particle in a stationary acoustic wave was reported by Yosioka and Kawasima [5] to be

$$F_{ac} = 4\pi r^3 \kappa E_{ac} A \sin(2\kappa x) \quad (2)$$

where r is the particle radius, κ is the wave number, E_{ac} is the time-averaged acoustic energy density, and A is the acoustic contrast factor given by

$$A = \frac{1}{3} \left(\frac{5\rho_p - 2\rho_l}{\rho_l + 2\rho_p} - \frac{\gamma_p}{\gamma_l} \right) \quad (3)$$

where ρ_p and γ_p are the particle density and compressibility, respectively, and ρ_l and γ_l are the liquid density and compressibility, respectively. Thus, in a propagating wave, the force on a particle has a second-order dependence, and in a standing wave, the force is third order. This should give rise to increased selectivity for separations being carried out in a standing wave [6].

Due to the nature of the acoustic fields, the distribution of the particles will depend on the particle size and the compressibility and density of the particle rel-



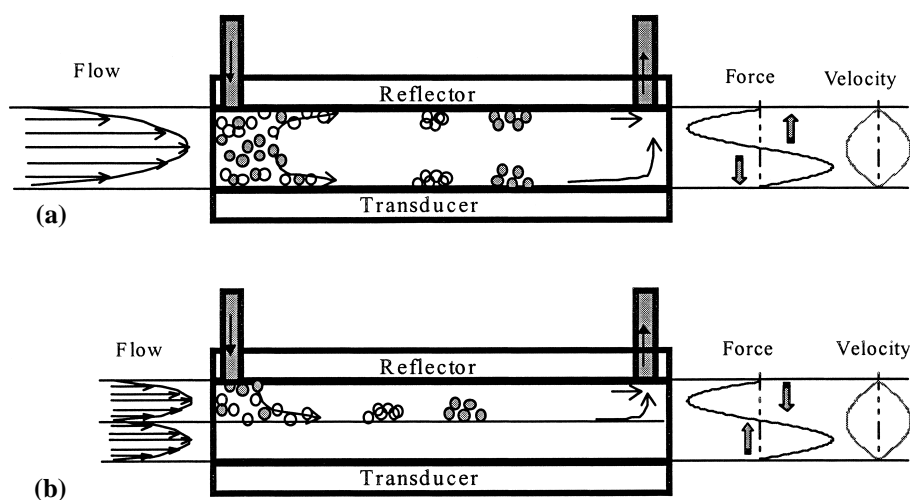


Fig. 1 Acoustic FFF channels suitable for particles with (a) $A > 0$ and (b) $A < 0$, utilizing a divided acoustic FFF channel.

ative to the fluid medium. Closer examination of the acoustic contrast factor shows that it may be negative (usually applicable to biological cells which are more compressible and less dense relative to the surrounding medium) or positive (as is in many inorganic and polymer colloids). Therefore, acoustic FFF (AcFFF) has tremendous potential in very clean separations of cells from other particles. One important application may be for the separation of bacterial and algal cells in soils and sediments.

If the acoustic contrast factor $A > 0$, then a conventional FFF channel will enable normal and steric mode FFF separations to be carried out (Fig. 1a).

However, if $A < 0$, then the particles will migrate toward the center of the channel. In this case, a divided FFF cell could be used as shown in Fig. 1b. This ensures that particles are driven to an accumulation wall rather than the center of the channel where the velocity profile is quite flat and selectivity would be minimal.

Johnson and Feke [7] effectively demonstrated that latex spheres migrate to the nodes (center of the cell) and Hawkes and co-workers [8] showed that yeast cells migrate to the antinodes (walls of the cell). These authors used a method similar to SPLITT, which is another technique closely related to FFF, also originally developed by Giddings [9]. Semyonov and Maslow [10] demonstrated that acoustic fields in a FFF channel af-

fected the retention time of a sphere of $3.8 \mu\text{m}$ diameter when subjected to varying acoustic fields. However, the high resolution inherent in FFF has not yet been exploited.

Naturally, with some design modifications to the FFF channel, SPLITT cells could be used for sample concentration or fluid clarification.

References

1. J. C. Giddings, *J. Chem. Phys.* 49: 81 (1968).
2. T. Kozuka, T. Tuziuti, H. Mitome, and T. Fukuda, *Proc. IEEE* 435 (1996).
3. K. Yasuda and T. Kamakura, *Appl. Phys. Lett.* 71: 1771 (1997).
4. Z. Mandralis, W. Bolek, W. Burger, E. Benes, and D. L. Feke, *Ultrasonics* 32: 113 (1994).
5. K. Yosioka and Y. Kawasima, *Acustica* 5: 167 (1955).
6. A. Berthod and D. W. Armstrong, *Anal. Chem.* 59: 2410 (1987).
7. D. A. Johnson and D. L. Feke, *Separ. Technol.* 5: 251 (1995).
8. J. J. Hawkes, D. Barrow, and W. T. Coakley, *Ultrasonics* 36: 925 (1998).
9. J. C. Giddings, *Anal. Chem.* 57: 945 (1985).
10. S. N. Semyonov and K. I. Maslow, *J. Chromatogr.* 446: 151 (1998).

Additives in Biopolymers, Analysis by Chromatographic Techniques

Roxana A. Ruseckaite

University of Mar del Plata, Mar del Plata, Argentina

Alfonso Jiménez

University of Alicante, Alicante, Spain

INTRODUCTION

Biopolymers are naturally occurring polymers that are formed in nature during the growth cycles of all organisms; they are also referred to as natural polymers.^[1] Their synthesis generally involves enzyme-catalyzed, chain growth polymerization reactions, typically performed within cells by metabolic processes.

Biodegradable polymers can be processed into useful plastic materials and used to supplement blends of the synthetic and microbial polymer.^[2] Among the polysaccharides, cellulose and starch have been the most extensively used. Cellulose represents an appreciable fraction of the waste products. The main source of cellulose is wood, but it can also be obtained from agricultural resources. Cellulose is used worldwide in the paper industry, and as a raw material to prepare a large variety of cellulose derivatives. Among all the cellulose derivatives, esters and ethers are the most important, mainly cellulose acetate, which is the most abundantly produced cellulose ester. They are usually applied as films (packaging), fibers (textile fibers, cigarette filters), and plastic molding compounds. Citric esters (triethyl and acetyl triethyl acetate) were recently introduced as biodegradable plasticizers in order to improve the rheological response of cellulose acetate.^[2]

Starch is an enormous source of biomass and most applications are based on this natural polymer. It has a semicrystalline structure in which their native granules are either destroyed or reorganized. Water and, recently, low-molecular-weight polyols,^[2] are frequently used to produce thermoplastic starches. Starch can be directly used as a biodegradable plastic for film production because of the increasing prices and decreasing availability of conventional film-forming materials. Starch can be incorporated into plastics as thermoplastic starch or in its granular form. Recently, starch has been used in various formulations based on biodegradable synthetic polymers in order to obtain totally biodegradable materials. Thermoplastic and granular starch was blended with polycaprolactone (PCL),^[3] polyvinyl alcohol and its co polymers,

and polyhydroxyalcanoates (PHAs).^[4] Many of these materials are commercially available, e.g., Ecostar (polyethylene/starch/unsaturated fatty acids), Mater Bi Z (polycaprolactone/starch/natural additives) and Mater Bi Y (polyvinylalcohol-co-ethylene/starch/natural additives). Natural additives are mainly polyols.

The proteins, which have found many applications, are, for the most part, neither soluble nor fusible without degradation. Therefore, they are used in the form in which they are found in nature.^[1] Gelatin, an animal protein, is a water-soluble and biodegradable polymer that is extensively used in industrial, pharmaceutical, and biomedical applications.^[2] A method to develop flexible gelatin films is by adding polyglycerols. Quite recently, gelatin was blended with poly(vinyl alcohol) and sugar cane bagasse in order to obtain films that can undergo biodegradation in soil. The results demonstrated the potential use of such films as self-fertilizing mulches.^[5]

Other kinds of natural polymers, which are produced by a wide variety of bacteria as intracellular reserve material, are receiving increasing scientific and industrial attention, for possible applications as melt processable polymers. The members of this family of thermoplastic biopolymers are the polyhydroxyalcanoates (PHAs). Poly-(3-hydroxy)butyrate (PHB), and poly(3-hydroxy)butyrate-hydroxyvalerate (PHBV) copolymers, which are microbial polyesters exhibiting useful mechanical properties, present the advantages of biodegradability and biocompatibility over other thermoplastics. Poly(3-hydroxy)butyrate has been blended with a variety of low- and high-cost polymers in order to apply PHB-based blends in packaging materials or agricultural foils. Blends with nonbiodegradable polymers, including poly(vinyl acetate) (PVAc), poly(vinyl chloride) (PVC), and poly(methylmethacrylate) (PMMA), are reported in the literature.^[4] Poly(3-hydroxy)butyrate has been also blended with synthetic biodegradable polyesters, such as poly(lactic acid) (PLA), poly(caprolactone), and natural polymers including cellulose and starch.^[2] Plasticizers are also included into the formulations in order to prevent degradation of the polymer during processing. Polyethylene glycol,



oxypropylated glycerol, dibutylsebacate (DBS), dioctylsebacate (DOS), and polyisobutylene (PIB) are commonly used as PHB plasticizers.^[6]

As was pointed out above, the processing and in-use biopolymer properties depend on the addition of other materials that provide a more convenient processing regime and stabilizing effects. Therefore the identification and further determination of these additives, as well as the separation from the biopolymer matrix, is necessary, and chromatographic techniques are a powerful tool to achieve this goal.

Many different compounds can be used as biopolymer additives, most of them are quite similar to those used in traditional polymer formulations. The use of various compounds as plasticizers, lubricants, and antioxidants has been recently reported.^[7-9] Antioxidants are normally used to avoid, or at least minimize, oxidation reactions, which normally lead to degradation and general loss of desirable properties. Phenol derivatives are mostly used in polymers, but vitamin E and α -tocopherols are those most commonly found in biopolymer formulation.^[10]

IDENTIFICATION AND DETERMINATION OF ADDITIVES IN BIOPOLYMERS

The modification and general improvement of properties caused by the addition of such compounds is a very interesting issue to be studied with a wide range of analytical techniques. Their identification and eventual determination is usually carried out by chromatographic techniques coupled to a variety of detection systems, most often mass spectrometry (MS). This powerful hyphenated technique, extensively used in many different analyses, combines the separation capabilities of chromatographic techniques with the potential use of MS to elucidate complicated structures and to identify many chemical compounds with low limits of detection and high sensitivities. The use of MS also permits the simultaneous detection and determination of several of those additives in a single analysis. This is especially valuable when only a small quantity of material is available, which is the usual case in some biopolymer formulations.

Some proposals have been recently reported to couple different chromatographic techniques with MS for the analysis of biopolymers and biocomposites, as well as additives used in such formulations. Gas chromatography-mass spectrometry (GC-MS) was used in some particular determinations, but always with the need for complicated extraction procedures. One example is the adaptation to biopolymers of a method for the simultaneous determination of diamines, polyamines, and aromatic amines in wines and other food samples.^[11] While this method was

successfully applied in such samples, it is not clear that its application to the determination of these additives in biopolymers will be easy, because of potential problems in the extraction of analytes prior to GC-MS. The proposed ion-pair extraction method is not always easily adaptable to solid samples. Therefore the potential application of this sensitive method to biopolymers is still under discussion.

Size-exclusion chromatography (SEC) coupled to MS is the most successful chromatographic technique applied in the field of biopolymers. As is well known, SEC is a powerful analytical technique that allows separation of analytes based on their different molecular sizes. Size-exclusion chromatography is a common step in the separation and further purification of biopolymers, and the coupling with MS was firstly proposed for proteins and other biological samples.^[12] One of the main drawbacks of traditional SEC, which was the limited range of molecular sizes to be measured, was recently overcome by the proposal of new columns with no limits in the molecular size of the species to be analyzed. This allows the possibility to separate and further analyze a large number of compounds, regardless of their chemical structures. The introduction of new packings and more stable columns allowed the development of high-performance size exclusion chromatography (HPSEC).

However, the on-line interfacing of HPSEC to MS for powerful detection is not as easy as in the case of conventional high-performance liquid chromatography (HPLC). A very promising possibility has been raised with the introduction of a new MS technique, which the authors named chemical reaction interface mass spectrometry (CRIMS).^[13] This new approach permits the monitoring of any organic molecules, even the most complicated, after their derivatization and transformation to low-molecular-weight products, which are amenable to easy MS detection. By determination of some structural and compositional parameters, the CRIMS response is proportional to the amount of specific organic elements present in biopolymers. This method has been recently applied to the analysis of biopolymers of different chemical nature, such as polysaccharides and proteins;^[14] its potential extension to other kinds of biopolymers is still under study.

Size-exclusion chromatography has been recently applied, with success, to the analysis of biopolymers derived from biomass, as it is used for the determination of molecular mass distributions of polymeric compounds in general, because of its short analysis time, high reproducibility, and accuracy.^[15] This application of SEC has permitted the separation and further detection of polymeric and monomeric residues of biopolymers, as well as the estimation of the degree of polymerization and eventual uses of natural products as additives, not only in

biocomposites, but in many industrial applications, e.g., food additives.

Another important development in the field of biopolymer analysis is the introduction of matrix-assisted laser desorption ionization (MALDI), which is a rather recent soft ionization technique that produces molecular ions of large organic molecules. In combination with time-of-flight (TOF) mass spectrometry, it was proposed as a valuable tool for the detection and characterization of biopolymers, such as proteins, peptides, and oligosaccharides, in many types of samples.^[16] The use of these recently developed techniques has not decreased the use of chromatography in determinations of biopolymers. Some efforts on the adaptation of the separation abilities of HPLC to the high potential of MALDI-TOF for the sensitive determination of additives in biocomposites are currently being carried out.

In all these applications, the separation step is one of the most critical during the whole analytical process. Solid phase extraction (SPE) and capillary electrophoresis (CE) were also proposed for high-resolution and quantitative separations of analytes. Therefore it is likely that the use of chromatographic techniques in this area will be increased in the near future. The development of adequate interfaces for such hyphenated techniques is the most important problem to be solved by researchers in the field of biopolymer analysis.

A recent study of separation and determination of antioxidants in polymers showed the potential use of HPLC for the separation and isolation of tocopherols in polymers and biopolymers.^[10] It was shown that although a large number of HPLC product peaks are formed, they corresponded to different stereoisomeric forms of only a small number of oxidative coupling products of tocopherol. The chromatographic parameters determined in this way, coupled to the study of spectral characteristics, allowed the complete identification of all antioxidants used in these polymers.

PYROLYSIS OF BIOPOLYMERS AND BIOCOMPOSITES

It is recognized that pyrolysis of biopolymers and biocomposites results in a large variety of primary and secondary products, such as carbon dioxide, methane, and other hydrocarbons. These low-molecular-mass products must be investigated to understand the behavior of biopolymers at high temperatures, under degradation conditions. All of these compounds are volatile and can be detected by GC^[17] or HPLC^[18] analysis. In the first study, a special two-stage GC system was used for the analysis of flash-pyrolysis products. With this system, the pyrolysis was directly conducted in inert carrier gas.

Two different columns coupled to an MS detector allowed the analysis of the resulting volatile products.

To obtain these results, it is usual to couple GC and MS. The pyrolysis products are first separated in the column and then immediately analyzed in the mass spectrometer. Therefore it is possible to obtain reliable and reproducible results in a single run with a relatively short time of analysis. Therefore high-resolution MS, in combination with pyrolysis and GC, is a unique approach to develop quantitative information in the analysis of biopolymers. Problems arising in high-resolution MS are the increased loss of sensitivity with increasing resolving power and, also, the decreased signal-to-noise ratio caused by the use of internal standards. In the case of biopolymers, it is usual to combine high-resolution MS with low-energy ionization modes, such as chemical ionization (CI) and field ionization (FI), in order to avoid high fragmentation, which could lead to information losses. Electron impact ionization (EI) at the normal ionizing voltage (70 eV) causes excessive fragmentation. Thus much information is lost by such MS detection, as many small additive fragments are not specific. Methods such as FI and CI are useful because of the difficulties arising from EI, such as the variation of fragmentation depending on instrumental conditions and the fact that only low-mass ions are observed. Soft ionization methods allow conservation of more information about structures and molecular identity. However, one problem with the soft ionization methods is the higher cost of instrumentation.

The identification of the degradation processes of additives in biopolymers was also studied by pyrolysis GC-MS (Pyr-GC-MS). However, direct additive analysis by flash-pyrolytic decomposition is usually not easy for this kind of sample. Therefore a prior separation of additives, or additive fragments contained in the polymer matrix, is usually necessary. A major advantage of pyrolysis GC-MS is the nonrequirement of pretreatment of the sample. The fragments formed in this way are then separated in the gas chromatograph and detected with the mass spectrometer. Additive detection in biopolymers with pyrolysis GC-MS is influenced by fragmentation, which is conditioned by the ionization mode, the concentration of the analyte, and the structures of the additive and biopolymer fragments. It is usual that polymer matrix fragments, at high concentrations, are superimposed on the additive fragments. Therefore it is necessary to filter additive fragments from the background of the biopolymer matrix to permit seeing a difference between them. The degree of fragmentation depends on the pyrolysis temperature. Thus pyrolysis GC-MS is of limited use for additive analysis in thermally labile and low-volatility products, which give a high fragmentation. For the same reason, it is also necessary to perform pyrolysis at temperatures that are not too high.



The use of pyrolysis GC-MS is still not common in the analysis of biopolymers and biocomposites because of the large quantity of parameters to be controlled for the development of a method. It is not easy, in a dynamic system, to transfer from a flow of inert gas (Pyr-GC) to vacuum conditions (MS). On the other hand, quantification is based on the fact that degradation is ion-specific, and that a given substance always produces the same fragments. This is not the case with biopolymer additives, especially in natural products, where fragmentation can proceed in several directions. This requires the use of internal standards and multiple measurements of each sample. Therefore a complete quantification requires considerable time and effort.

Despite all these drawbacks, the potential use of pyrolysis GC-MS in biopolymer analysis is quite promising when considering the latest developments in instrumentation. There is a current tendency in analytical Pyr-GC-MS to preserve and detect higher-molecular-weight fragments. This led to developments in instrumentation, such as improvement of the direct transfer of high-molecular-weight and polar products to the ion source of the mass spectrometer, the measurement of these compounds over extended mass ranges, and the use of soft ionization conditions. In addition, the potential of Pyr-GC-MS has been greatly enhanced by the use of high-resolution capillary columns combined with computer-assisted techniques.

CONCLUSION

The application of a wide variety of chromatographic techniques to the analysis of additives in biopolymers is a current tendency in many research laboratories around the world. The increasing interest in the use of biopolymers in many technological applications will raise the research in this field in the future. Therefore, the potential of chromatography for separation, identification, and quantification will be very important for the development of reliable and reproducible analytical methods.

REFERENCES

- Chandra, R.; Rustgi, R. Biodegradable polymers. *Prog. Polym. Sci.* **1998**, *23*, 1273–1335.
- Amass, W.; Amass, A.; Tighe, B. A review of biodegradable polymers: Uses, current developments in the synthesis and characterization of biodegradable polymers and recent advances in biodegradation studies. *Polym. Int.* **1998**, *47*, 89–144.
- Ishiaku, U.S.; Pang, K.W.; Lee, W.S.; Mohd-Ishak, Z.A. Mechanical properties and enzymatic degradation of thermoplastic and granular sago starch filled poly(epsilon-caprolactone). *Eur. Polym. J.* **2002**, *38*, 393–401.
- Avella, M.; Matuscelli, E.; Raimo, M. Properties of blends and composites based on poly(3-hydroxy)butyrate (PHB) and poly(3-hydroxybutyrate-hydroxyvalerate) (PHBV) copolymers. *J. Mater. Sci.* **2000**, *35*, 523–545.
- Chiellini, E.; Cinelli, P.; Corti, A.; Kenawy, E.R. Composite films based on waste gelatin: Thermal-mechanical properties and biodegradation testing. *Polym. Degrad. Stab.* **2001**, *73*, 549–555.
- Savenkova, L.; Gercberga, Z.; Nikolaeva, V.; Dzene, A.; Bibers, I.; Kalnin, M. Mechanical properties and biodegradation characteristics of PHB-based films. *Proc. Biochem.* **2000**, *35*, 573–579.
- Wang, F.C.Y. Polymer additive analysis by pyrolysis-gas chromatography I. Plasticizers. *J. Chromatogr., A* **2000**, *883*, 199–210.
- Wang, F.C.Y.; Buzanowski, W.C. Polymer additive analysis by pyrolysis-gas chromatography III. Lubricants. *J. Chromatogr., A* **2000**, *891*, 313–324.
- Wang, F.C.Y. Polymer additive analysis by pyrolysis-gas chromatography IV. Antioxidants. *J. Chromatogr., A* **2000**, *891*, 325–336.
- Al-Malaika, S.; Issenhuth, S.; Burdick, D. The antioxidant role of vitamin E in polymers. V. Separation of stereoisomers and characterization of other oxidation products of dl- α -tocopherol formed in polyolefins during melt processing. *J. Anal. Appl. Pyrolysis* **2001**, *73*, 491–503.
- Fernandes, J.O.; Ferreira, M.A. Combined ion-pair extraction and gas chromatography-mass spectrometry for the simultaneous determination of diamines, polyamines and aromatic amines in Port wine and grape juice. *J. Chromatogr., A* **2000**, *886*, 183–195.
- Kriwacki, R.W.; Wu, J.; Tennant, L.; Wright, P.E.; Siuzdak, G. Probing protein structure using biochemical and biophysical methods—Proteolysis, matrix-assisted laser desorption/ionization mass spectrometry, high-performance liquid chromatography and size-exclusion chromatography. *J. Chromatogr., A* **1997**, *777*, 23–30.
- Lecchi, P.; Abramson, F.P. Analysis of biopolymers by size exclusion chromatography–mass spectrometry. *J. Chromatogr., A* **1998**, *828*, 509–513.
- Lecchi, P.; Abramson, F.P. Size exclusion chromatography–chemical reaction interface mass spectrometry: “A perfect match”. *Anal. Chem.* **1999**, *71*, 2951–2955.
- Papageorgiou, V.P.; Assimopoulou, A.N.; Kyriacou, G. Determination of naturally occurring hydroxynaphthoquinone polymers by size-exclusion chromatography. *Chromatographia* **2002**, *55*, 423–430.
- Kaufmann, R. Matrix-assisted laser desorption ionization (MALDI) mass spectrometry: A novel analytical tool in molecular biology and biotechnology. *J. Biotechnol.* **1995**, *41*, 155–175.
- Pouwels, A.D.; Eijkel, G.B.; Boon, J.J. Curie-point pyrolysis–capillary gas chromatography–high resolution mass spectrometry of microcrystalline cellulose. *J. Anal. Appl. Pyrolysis* **1989**, *14*, 237–280.
- Radlein, A.G.; Grinshpun, A.; Piskorz, J.; Scott, D.S. On the presence of anhydro-oligosaccharides in the syrups from the fast pyrolysis of cellulose. *J. Anal. Appl. Pyrolysis* **1987**, *12*, 39–49.

Adhesion of Colloids on Solid Surfaces by Field-Flow Fractionation

George Karaiskakis

University of Patras, Patras, Greece

Introduction

The adhesion of colloids on solid surfaces, which is of great significance in filtration, corrosion, detergency, coatings, and so forth, depends on the total potential energy of interaction between the colloidal particles and the solid surfaces. The latter, which is the sum of the attraction potential energy and that of repulsion, depends on particle size, the Hamaker constant, the surface potential, and the Debye–Huckel reciprocal distance, which is immediately related to the ionic strength of carrier solution. With the aid of the field-flow fractionation technique, the adhesion and detachment processes of colloidal materials on and from solid surfaces can be studied. As model samples for the adhesion of colloids on solid surfaces (e.g., Hastelloy-C), hematite ($\alpha\text{-Fe}_2\text{O}_3$) and titanium dioxide (TiO_2) submicron spherical particles, as well as hydroxyapatite [$\text{Ca}_5(\text{PO}_4)_3\text{OH}$] submicron irregular particles were used. The experimental conditions favoring the adhesion process were those decreasing the surface potential of the particles through the pH and ionic-strength variation, as well as increasing the effective Hamaker constant between the particles and the solid surfaces through the surface-tension variation. On the other hand, the detachment of the same colloids from the solid surfaces can be favored under the experimental conditions decreasing the potential energy of attraction and increasing the repulsion potential energy.

Methodology

Field-flow fractionation (FFF) technology is applicable to the characterization and separation of particulate species and macromolecules. Separations in FFF take place in an open flow channel over which a field is applied perpendicular to the flow. Among the various FFF subtechniques, depending on the kind of the applied external fields, sedimentation FFF (SdFFF) is the most versatile and accurate, as it is based on simple physical phenomena that can be accurately described mathematically. SdFFF, which uses a centrifugal grav-

itational force field, is a flow-modified equilibrium sedimentation-separation method. Solute layers that are poorly resolved under static equilibrium sedimentation become well separated as they are eluted by the laminar flow profile in the SdFFF channel. In normal SdFFF, where the colloidal particles under study do not interact with the channel wall, the potential energy of a spherical particle, $\varphi(x)$, is related to the particle radius, a , to the density difference, $\Delta\rho$, between the particle (ρ_s) and the liquid phase (ρ), and to the sedimentation field strength expressed in acceleration, G :

$$\varphi(x) = \frac{4}{3}\pi a^3 \Delta\rho Gx \quad (1)$$

where x is the coordinate position of the center of particle mass.

When the colloidal particles interact with the SdFFF channel wall, the total potential energy, φ_{tot} , of a spherical particle is given by

$$\begin{aligned} \varphi_{\text{tot}} = & \frac{4}{3}\pi a^3 \Delta\rho Gx + \frac{A_{132}}{6} \left[\ln\left(\frac{h+2a}{h}\right) - \frac{2a(h+a)}{h(h+a)} \right] \\ & + 16\epsilon a \left(\frac{kT}{e}\right)^2 \tan h\left(\frac{e\psi_1}{4kT}\right) \tan h\left(\frac{e\psi_2}{4kT}\right) e^{-\kappa x} \end{aligned} \quad (2)$$

where the second and third terms of Eq. (2) accounts for the contribution of the van der Waals attraction potential and of the double-layer repulsion potential between the particle and the wall, respectively, A_{132} is the effective Hamaker constant for media 1 and 2 interacting across medium 3, h is the separation distance between the sphere and the channel wall, ϵ is the dielectric constant of the suspending medium, e is the electronic charge, ψ_1 and ψ_2 are the surface potentials of the particles and the solid wall, respectively, k is Boltzmann's constant, T is the absolute temperature, and κ is the Debye–Huckel reciprocal length, which is immediately related to the ionic strength, I , of the medium.

Equation (2) shows that the total potential energy of interaction between a colloidal particle and a solid



substrate is a function of the particle radius and surface potential, the ionic strength and dielectric constant of the suspending medium, the value of the effective Hamaker constant, and the temperature. Adhesion of colloidal particles on solid surfaces is increased by a decrease in the particle radius, surface potential, the dielectric constant of the medium and by an increase in the effective Hamaker constant, the ionic strength of the dispersing liquid, or the temperature. For a given particle and a medium with a known dielectric constant, the adhesion and detachment processes depend on the following three parameters:

1. The surface potential of the particles, which can be varied experimentally by various quantities one of which is the suspension pH
2. The ionic strength of the solution, which can be varied by adding to the suspension various amounts of an indifferent electrolyte
3. The Hamaker constant, which can be easily varied by adding to the suspending medium various amounts of a detergent. The later results in a variation of the medium surface tension.

Applications

The critical electrolyte (KNO_3) concentrations found by SdFFF for the adhesion of $\alpha\text{-Fe}_2\text{O}_3(\text{I})$ (with nominal diameter $0.148\ \mu\text{m}$), $\alpha\text{-Fe}_2\text{O}_3(\text{II})$ (with nominal diameter $0.248\ \mu\text{m}$), and TiO_2 (with nominal diameter $0.298\ \mu\text{m}$) monodisperse spherical particles on the Hastelloy-C channel wall were $8 \times 10^{-2}M$, $3 \times 10^{-2}M$, and $3 \times 10^{-2}M$, respectively. The values for the same sample ($\alpha\text{-Fe}_2\text{O}_3$) depend on the particle size, in accordance with the theoretical predictions, whereas the same values are identical for various samples [$\alpha\text{-Fe}_2\text{O}_3(\text{II})$ and TiO_2] having different particle diameters. The latter indicates that these values depend also, apart from the size, on the sample's physicochemical properties, as is predicted by Eq. (2). The detachment of the whole number of particles of the above samples from the channel wall was succeeded by decreasing the ionic strength of the carrier solution.

The critical KNO_3 concentration for the detachment process was $3 \times 10^{-2}M$ for the $\alpha\text{-Fe}_2\text{O}_3(\text{I})$ sample and $1 \times 10^{-3}M$ for the samples of $\alpha\text{-Fe}_2\text{O}_3(\text{II})$ and TiO_2 . Those obtained by SdFFF particle diameters after the detachment of the adherent particles [$0.148\ \mu\text{m}$ for $\alpha\text{-Fe}_2\text{O}_3(\text{I})$, $0.245\ \mu\text{m}$ for $\alpha\text{-Fe}_2\text{O}_3(\text{II})$,

and $0.302\ \mu\text{m}$ for TiO_2] are in excellent agreement with the corresponding nominal particle diameters obtained by transmission electron microscopy. The desorption of all of the adherent particles was verified by the fact that no elution peak was obtained, even when the field strength was reduced to zero. A second indication for the desorption of all of the adherent material was that the sample peaks after adsorption and desorption emerge intact and without degradation.

In a second series of experiments, the adhesion and detachment processes of hydroxyapatite (HAP) polydisperse particles with number average diameter of $0.261\ \mu\text{m}$ on and from the Hastelloy-C channel wall were succeeded by the variation of the suspension pH, whereas the medium's ionic strength was kept constant ($10^{-3}M\ \text{KNO}_3$). At a suspension pH of 6.8, the whole number of injected HAP particles was adhered at the beginning of the SdFFF channel wall, which was totally released when the pH increased to 9.7, showing that, except for the ionic strength, the pH of the suspending medium is also a principal quantity influencing the interaction energy between colloidal particles and solid surfaces. The number-average diameter of the HAP particles found by SdFFF after the detachment of the adherent particles ($d_N = 0.262\ \mu\text{m}$) was also in good agreement with that obtained when the particles were injected into the channel with a carrier solution in which no adhesion occurs ($d_N = 0.261\ \mu\text{m}$).

The variation of the potential energy of interaction between colloidal particles and solid surfaces can be also succeeded by the addition of a detergent to the suspending medium, which leads to a decrease in the Hamaker constant and, consequently, in the potential energy of attraction.

In conclusion, field-flow fractionation is a relatively simple technique for the study of adhesion and detachment of submicrometer or supramicrometer colloidal particles on and from solid surfaces.

Future Developments

Looking to the future, it is reasonable to expect more experimental and theoretical work in order to quantitatively investigate the adhesion/detachment phenomena of colloids on and from solid surfaces by measuring the corresponding rate constants with the aid of FFF.



Suggested Further Reading

- Athanasopoulou, A. and G. Karaiskakis, *Chromatographia* 43: 369 (1996).
- Giddings, J. C., M. N. Myers, K. D. Caldwell, and S. R. Fisher, in *Methods of Biochemical Analysis* Vol. 26, D. Glick (ed.), John Wiley & Sons, New York, 1980, p. 79.
- Giddings, J. C., G. Karaiskakis, K. D. Caldwell, and M. N. Myers, *J. Colloid Interf. Sci.* 92(1): 66 (1983).
- Hansen, M. E. and J. C. Giddings, *Anal. Chem.* 61: 811 (1989).
- Hiemenz, P. C., *Principles of Colloid and Surface Chemistry*, Marcel Dekker, Inc., New York, 1977.
- Karaiskakis, G. and J. Cazes (eds.), *J. Liq. Chromatogr. Rel. Technol.* 20 (16 & 17) (1997).
- Karaiskakis, G., A. Athanasopoulou, and A. Koliadima, *J. Micro. Separ.* 9: 275 (1997).
- Koliadima, A. and G. Karaiskakis, *J. Chromatogr.* 517: 345 (1990).
- Ruckenstein, E. and D. C. Prieve, *AIChE J.* 22(2): 276 (1976).



Adsorption Chromatography

Robert J. Hurtubise

University of Wyoming, Laramie, Wyoming, U.S.A.

Introduction

In essence, the original chromatographic technique was adsorption chromatography. It is frequently referred to as liquid–solid chromatography. Tswett developed the technique around 1900 and demonstrated its use by separating plant pigments. Open-column chromatography is a classical form of this type of chromatography, and the open-bed version is called thin-layer chromatography.

Adsorption chromatography is one of the more popular modern high-performance liquid chromatographic techniques today. However, open-column chromatography and thin-layer chromatography are still widely used [1]. The adsorbents (stationary phases) used are silica, alumina, and carbon. Although some bonded phases have been considered to come under adsorption chromatography, these bonded phases will not be discussed. By far, silica and alumina are more widely used than carbon. The mobile phases employed are less polar than the stationary phases, and they usually consist of a signal or binary solvent system. However, ternary and quaternary solvent combinations have been used.

Adsorption chromatography has been employed to separate a very wide range of samples. Most organic samples are readily handled by this form of chromatography. However, very polar samples and ionic samples usually do not give very good separation results. Nevertheless, some highly polar multifunctional compounds can be separated by adsorption chromatography. Compounds and materials that are not very soluble in water or water–organic solvents are usually more effectively separated by adsorption chromatography compared to reversed-phase liquid chromatography.

When one has an interest in the separation of different types of compound, silica or alumina, with the appropriate mobile phase, can readily accomplish this. Also, isomer separation frequently can easily be accomplished with adsorption chromatography; for example, 5,6-benzoquinoline can be separated from 7,8-benzoquinoline with silica as the stationary phase and

2-propanol:hexane (1:99). This separation is difficult with reversed-phase liquid chromatography [1].

Stationary Phases

Silica is the most widely used stationary phase in adsorption chromatography [2]. However, the extensive work of Snyder [3] involved investigations with both silica and alumina. Much of Snyder's earlier work was with alumina. Even though the surface structures of the two adsorbents have distinct differences, they are sufficiently similar. Thus, many of the fundamental principles developed for alumina are applicable to silica. The general elution order for these two adsorbents is as follows [1]: saturated hydrocarbons (small retention time), olefins, aromatic hydrocarbons, aromatic hydrocarbons < organic halides, sulfides, ethers, nitro-compounds, esters < aldehydes < ketones, alcohols < amines, sulfones, sulfoxides, amides, carboxylic acids (long retention time). There are several reasons why silica is more widely used than alumina. Some of these are that a higher sample loading is permitted, fewer unwanted reactions occur during separation, and a wider range of chromatographic forms of silica are available.

Chromatographic silicas are amorphous and porous and they can be prepared in a wide range of surface areas and average pore diameters. The hydroxyl groups in silica are attached to silicon, and the hydroxyl groups are mainly either free or hydrogen-bonded. To understand some of the details of the chromatographic processes with silica, it is necessary to have a good understanding of the different types of hydroxyl groups in the adsorbent [1,3]. Chromatographic alumina is usually γ -alumina. Three specific adsorption sites are found in alumina: (a) acidic, (b) basic, and (c) electron-acceptor sites. It is difficult to state specifically the exact nature of the adsorption sites. However, it has been postulated that the adsorption sites are exposed aluminum atoms, strained Al—O bonds, or cationic sites [4]. Table 1 gives some of the properties of silica and alumina.



Table 1 Some Adsorbents Used in Adsorption Chromatography

Type	Name	Form	Average particle size (μm)	Surface area (m^2/g)
Silica ^a	BioSil A	Bulk	2–10	400
	μ Porasil	Column	10	400+
Silica ^b	Hypersil	Bulk	5–7	200
	Zobax Sil	Bulk or column	6	350
Alumina ^a	ICN Al-N	Bulk	3–7, 7–12	200
	MicroPak Al	Bulk or column	5, 10	79
Alumina ^b	Spherisorb AY	—	5, 10, 20	95

^aIrregular^bSpherical

Source: Adapted from Ref. 1.

The adsorbent water content is particularly important in adsorption chromatography. Without the deactivation of strong adsorption sites with water, nonreproducible retention times will be obtained, or irreversible adsorption of solutes can occur. Prior to using an adsorbent for open-column chromatography, the adsorbent is dried, a specified amount of water is added to the adsorbent, and then the adsorbent is allowed to stand for 8–16 h to permit the equilibration of water [3,4]. If one is using a high-performance column, it is a good idea to consider adding water to the mobile phase to deactivate the stronger adsorption sites on the adsorbent. Some of the benefits are less variation in retention times, partial compensation for lot-to-lot differences in the adsorbent, and reduced band tailing [1]. However, there can be some problems in adding water to the mobile phase, such as how much water to add to the mobile phase for optimum performance. Snyder and Kirkland [1] have discussed several of these aspects in detail.

Table 2 Selected Solvents Used in Adsorption Chromatography

Solvent	Solvent strength (ϵ^0)	
	Silica	Alumina
<i>n</i> -Hexane	0.01	0.01
1-Chlorobutane	0.20	0.26
Chloroform	0.26	0.40
Isopropyl ether	0.34	0.28
Ethyl acetate	0.38	0.58
Tetrahydrofuran	0.44	0.57
Acetonitrile	0.50	0.65

Source: Adapted from Ref. 1.

Mobile Phases

To vary sample retention, it is necessary to change the mobile-phase composition. Thus, the mobile phase plays a major role in adsorption chromatography. In fact, the mobile phase can give tremendous changes in sample retention characteristics. Solvent strength controls the capacity factor's values of all the sample bands. A solvent strength parameter (ϵ^0), which has been widely used over the years, can be employed quantitatively for silica and alumina. The solvent strength parameter is defined as the adsorption energy of the solvent on the adsorbent per unit area of solvent [1,3]. Table 2 gives the solvent strength values for selected solvents that have been used in adsorption chromatography. The smaller values of ϵ^0 indicate weaker solvents, whereas the larger values of ϵ^0 indicate stronger solvents. The solvents listed in Table 2 are single solvents. Normally, solvents are selected by mixing two solvents with large differences in their ϵ^0 values, which would permit a continuous change in the solvent strength of the binary solvent mixture. Thus, some specific combination of the two solvents would provide the appropriate solvent strength. In adsorption chromatography, the solvent strength increases with solvent polarity, and the solvent strength is used to obtain the proper capacity factor values, usually in the range of 1–5 or 1–10. It should be realized that the solvent strength does not vary linearly over a wide range of solvent compositions, and several guidelines and equations that allow one to calculate the solvent strength of binary solvents have been developed for acquiring the correct solvent strength in adsorption chromatography [1,3]. However, it frequently happens that the solvent strength is such that all of the solutes are not separated



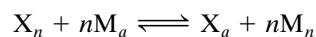
in a sample. Thus, one needs to consider solvent selectivity, which is discussed below.

To change the solvent selectivity, the solvent strength is held constant and the composition of the mobile phase is varied. It should be realized that because the solvent strength is directly related to the polarity of the solvent and polarity is the total of the dispersion, dipole, hydrogen-bonding, and dielectric interactions of the sample and solvent, one would not expect that solvent strength alone could be used to fine-tune a separation. A trial-and-error approach can be employed by using different solvents of equal ϵ^0 . However, there are some guidelines that have been developed that permit improved selectivity. These are the "B-concentration" rule and the "hydrogen-bonding" rule [1]. In general, with the B-concentration rule, the largest change in selectivity is obtained when a very dilute or a very concentrated solution of B (stronger solvent) in a weak solvent (A) is used. The hydrogen-bonding rule states that any change in the mobile phase that results in a change in hydrogen-bonding between sample and mobile-phase molecules usually results in a large change in selectivity. A more comprehensive means for improving selectivity is the solvent-selectivity triangle [1,5]. The solvent-selectivity triangle classifies solvents according to their relative dipole moments, basic properties, and acidic properties. For example, if an initial chromatographic experiment does not separate all the components with a binary mobile phase, then the solvent-selectivity triangle can be used to choose another solvent for the binary system that has properties that are very different than one of the solvents in the original solvent system. A useful publication that discusses the properties of numerous solvents and also considers many chromatographic applications is Ref. 6.

Mechanistic Aspects in Adsorption Chromatography

Models for the interactions of solutes in adsorption chromatography have been discussed extensively in the literature [7–9]. Only the interactions with silica and alumina will be considered here. However, various modifications to the models for the previous two adsorbents have been applied to modern high-performance columns (e.g., amino-silica and cyano-silica). The interactions in adsorption chromatography can be very complex. The model that has emerged which describes many of the interactions is the displacement model developed by Snyder [1,3,4,7,8]. Generally, retention is assumed to occur by a displacement process. For ex-

ample, an adsorbing solute molecule X displaces n molecules of previously adsorbed mobile-phase molecules M [8]:



The subscripts n and a in the above equation represent a molecule in a nonsorbed and adsorbed phase, respectively. In other words, retention in adsorption chromatography involves a competition between sample and solvent molecules for sites on the adsorbent surface. A variety of interaction energies are involved, and the various energy terms have been described in the literature [7,8]. One fundamental equation that has been derived from the displacement model is

$$\log\left(\frac{k_1}{k_2}\right) = \alpha' A_s (\epsilon_2 - \epsilon_1)$$

where k_1 and k_2 are the capacity factors of a solute in two different mobile phases, α' is the surface activity of the adsorbent (relative to a standard adsorbent), A_s is the cross-sectional area of the solute on the adsorbent surface, and ϵ_1 and ϵ_2 are the solvent strengths of the two different mobile phases. This equation is valid in situations where the solute and solvent molecules are considered nonlocalizing. This condition is fulfilled with nonpolar or moderately polar solutes and mobile phases. If one is dealing with multisolvent mobile phases, the solvent strength of those solvents can be related to the solvent strengths of the pure solvents in the solvent system. The equations for calculating solvent strengths for multisolvent mobile phases have been discussed in the literature [8].

As the polarities of the solute and solvent molecules increase, the interactions of these molecules become much stronger with the adsorbent, and they adsorb with localization. The net result is that the fundamental equation for adsorption chromatography with relatively nonpolar solutes and solvents has to be modified. Several localization effects have been elucidated, and the modified equations that take these factors into consideration are rather complex [7,8,10]. Nevertheless, the equations provide a very important framework in understanding the complexities of adsorption chromatography and in selecting mobile phases and stationary phases for the separation of solutes.

Applications

There have been thousands of articles published on the application of adsorption chromatography over the



decades. Today, adsorption chromatography is used around the world in all areas of chemistry, environmental problem solving, medical research, and so forth. Only a few examples will be discussed in this section. Gogou et al. [11] developed methods for the determination of organic molecular markers in marine aerosols and sediment. They used a one-step flash chromatography compound-class fractionation method to isolate compound-class fractions. Then, they employed gas chromatography/mass spectrometry and/or gas chromatography/flame ionization detection analysis of the fractions. The key adsorption chromatographic step prior to the gas chromatography was the one-step flash chromatography. For example, an organic extract of marine aerosol or sediment was applied on the top of a 30×0.7 -cm column containing 1.5 g of silica. The following solvent systems were used to elute the different compound classes: (a) 15 mL of n-hexane (aliphatics); (b) 15 mL toluene:n-hexane (5.6:9.4) (polycyclic aromatic hydrocarbons and nitro-polycyclic aromatic hydrocarbons); (c) 15 mL n-hexane:methylene chloride (7.5:7.5) (carbonyl compounds); (d) 20 mL ethyl acetate:n-hexane (8:12) (n-alkanols and sterols); (e) 20 mL (4%, v/v) pure formic acid in methanol (free fatty acids). This example illustrates very well how adsorption chromatography can be used for compound-class separation.

Hanson and Unger [12] have discussed the application of nonporous silica particles in high-performance liquid chromatography. Nonporous silica packings can be used for the rapid chromatographic analysis of biomolecules because the particles lack pore diffusion and have very effective mass-transfer capabilities. Several of the advantages of nonporous silica are maximum surface accessibility, controlled topography of ligands, better preservation of biological activity caused by shorter residence times on the column, fast column regeneration, less solvent consumption, and less susceptibility to compression during packing. The very low

external surface area of the nonporous supports is a disadvantage because it gives considerably lower capacity compared with porous materials. This drawback is counterbalanced partially by the high packing density compared to porous silica. The smooth surface of the nonporous silica offers better biocompatibility relative to porous silica. Well-defined nonporous silicas are now commercially available.

References

1. L. R. Snyder and J. J. Kirkland, *Introduction to Modern Liquid Chromatography*, 2nd ed., John Wiley & Sons, New York, 1979.
2. J. H. Knox (ed.), *High-Performance Liquid Chromatography*, Edinburgh University Press, Edinburgh, 1980.
3. L. R. Snyder, *Principles of Adsorption Chromatography*, Marcel Dekker, Inc., New York, 1968.
4. L. R. Snyder, in *Chromatography: A Laboratory Handbook of Chromatographic and Electrophoretic Methods*, 3rd ed., E. Heftmann (ed.), Van Nostrand Reinhold, New York, 1975, pp. 46–76.
5. L. R. Snyder, J. L. Glajch, and J. J. Kirkland, *Practical HPLC Method Development*, John Wiley & Sons, New York, 1988, pp. 36–39.
6. P. C. Sadek, *The HPLC Solvent Guide*, John Wiley & Sons, New York, 1996.
7. L. R. Snyder and H. Poppe, *J. Chromatogr.* 184: 363 (1980).
8. L. R. Snyder, in *High-Performance Liquid Chromatography, Vol. 3*, C. Horvath (ed.), Academic Press, New York, 1983, pp. 157–223.
9. R. P. W. Scott and P. Kucera, *J. Chromatogr.* 171: 37 (1979).
10. L. R. Snyder and J. L. Glajch, *J. Chromatogr.* 248: 165 (1982).
11. A. I. Gogou, M. Apostolaki, and E. G. Stephanou, *J. Chromatogr. A*, 799: 215 (1998).
12. M. Hanson and K. K. Unger, *LC-GC* 15: 364 (1997).



Adsorption Studies by Field-Flow Fractionation

Niem Tri

Ronald Beckett

Monash University, Melbourne, Australia

Introduction

Adsorption is an important process in many industrial, biological, and environmental systems. One compelling reason to study adsorption phenomena is because an understanding of colloid stability depends on the availability of adequate theories of adsorption from solution and of the structure and behavior of adsorbed layers. Another example is the adsorption of pollutants, such as metals, toxic organic compounds, and nutrients, onto fine particles and their consequent transport and fate, which has great environmental implications. Often, these systems are quite complex and it is often favorable to separate these into specific size for subsequent study.

Background Information

A new technique able to separate such complex mixtures is field-flow fractionation [1–3]. Field-flow fractionation (FFF) is easily adaptable to a large choice of field forces (such as gravitational, centrifugal, fluid cross-flows, electrical, magnetic and thermal fields or gradients) to effect high-resolution separations. Although the first uses for FFF were for sizing of polymer and colloidal samples, recent advances have demonstrated that well-designed FFF experiments can be used in adsorption studies [4,5].

Although the theory of FFF for the characterisation and fractionation of polymers and colloids has been outlined elsewhere, two important features of FFF need to be emphasized here. The first is the versatility of FFF, which is partly due to the diverse range of operating fields that may be used and the fact that each field is capable of delivering different information about a colloidal sample. For example, an electrical field separates particles on the basis of both size and charge, whereas a centrifugal field (sedimentation FFF) separates particles on the basis of buoyant mass (i.e. size and density). The second important feature is that this information can usually be measured directly from the retention data using rigorous theory. This is

in contrast to most forms of chromatography (size-exclusion chromatography exempted), where the retention time of a given component must be identified by running standards.

In 1991, both Beckett et al. [4] and Li and Caldwell [5] published articles demonstrating novel but powerful uses for sedimentation FFF in probing the characteristics of adsorbed layers or films on colloidal particles. Beckett et al.'s article demonstrated that it is possible to measure the mass of an adsorbed coating down to a few attograms (10^{-18} g), which translates to a mean coating thickness of human γ -globulin, ovalbumin, RNA, and cortisone ranging from 0.1 to 20 nm. A discussion of the theory and details of the experiment is beyond the scope of this article. However, it is possible to appreciate how such high sensitivities arise by considering the linear approximation of retention time, t_r , of an eluting particle in sedimentation FFF with the field-induced force on the particle, F .

$$t_r = t_0 \frac{Fw}{6kT} \quad (1)$$

where w is the thickness of the channel (typically 100–500 μm), k is the Boltzmann constant, and T is the temperature in Kelvin. F is the force on the individual particle and is the product of the applied field and the buoyant mass of the particle (relative mass of the particle in the surrounding liquid medium).

The highest sensitivity of retention time to changes in the surface coating was found to occur when the density of the core particle was equal to that of the surrounding medium (i.e., the buoyant mass diminishes to zero and no retention is observed for the bare particle). If a thin film of a much denser material is adsorbed onto the particles, then the small increment in mass due to the adsorbed film causes a significant change in the particle's buoyant mass (see Fig. 1a). Consequently, the force felt by the particle is now sufficient to effect retention by an observable amount. Incidentally, analogous behavior is also possible if the coatings are less dense than the carrier liquid. If the diameter of the bare particle is known (from independ-



ent experiments) so that the surface area can be estimated, then it is also possible to calculate the thickness of the adsorbed film, provided the density of the film is the same as the bulk density of the material being adsorbed (i.e., no solvation of the adsorbed layer). In some systems, it may be possible to alter the solvent density to match the core particle density by the addition of sucrose or other density modifiers to the FFF carrier solution.

Using the above approach with experimental results from centrifugal FFF, adsorption isotherms were constructed by directly measuring the mass of adsorbate deposited onto the polymer latex particle surface at different solution concentrations. It was found that for human globulin and ovalbumin adsorbates, Langmuir isotherms were obtained. The measured limiting adsorption density was found to agree with values measured using conventional solution uptake techniques.

The model used in the above studies ignores the departure from the bulk density of the adsorbate brought about by the interaction of the two interfaces. Li and Caldwell's article addresses this issue by introducing a three-component model consisting of a core particle, a flexible macromolecular substance with affinity toward the particle, and a solvation shell (see Fig. 1b).

In this model, the buoyant mass is then the sum of the buoyant mass of the three components, assuming that these are independent of the mass of solvent occupied in the solvation shell. Thus, the mass of the adsorbed shell can be calculated if information about the mass and density of the core particle and the density of the macromolecule and solvent are known. Photon correlation spectroscopy, electron microscopy, flow FFF, or other sizing techniques can readily provide some independent information on the physical or hydrodynamic particle size, and pycnometry can be used to measure the densities of the colloidal suspension, polymer solution, and pure liquid.

The above measurements were combined to estimate the mass of the polymer coating, a surface coverage density, and the solvated layer thickness. These results showed good agreement with the adsorption data derived from conventional polymer radiolabeling experiments.

Another approach for utilizing FFF techniques in the study of adsorption processes is to use the following general protocol:

1. Expose the suspension to the adsorbate
2. Run the sample through an FFF separation and collect fractions at designated elution volume intervals corresponding to specific size ranges

3. Analyze the size fractions for the amount of adsorbate

It must be emphasized that only strongly adsorbed material will be retained on the particles as the sample is constantly washed by the carrier solution during the FFF separation. Unless adsorbent is added to the carrier, these experiments will not represent the reversible equilibrium adsorption situation.

This approach was first outlined by Beckett et al. [6], where radiolabelled pollutants (^{32}P as orthophosphate, ^{14}C in atrazine, and glyphosate) were adsorbed to two Australian river colloid samples. Sedimentation FFF was used to fractionate the samples and the radioactivity of each fraction was measured. From this, it was possible to generate a surface adsorption density distribution (SADD) across the size range of the sample. The SADD is a plot of the amount of compound adsorbed per unit particle surface area as a

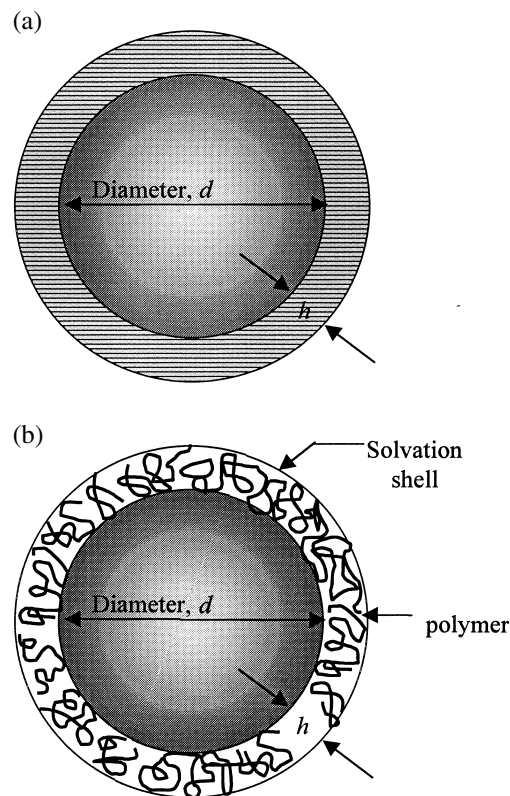


Fig. 1 Schematic representation of the adsorption complex proposed by (a) Beckett et al. [4] showing the core particle with a dense nonhydrated adsorbed film and by (b) Li and Caldwell [5] showing the core particle with an adsorbed polymer and the associated solvation shell.

function of the particle size. It was shown that the adsorption density was not always constant, indicating perhaps a change in particle mineralogy, surface chemistry, shape, or texture as a function of particle size.

The above method is currently being extended to use other sensitive analytical techniques such as inductively coupled plasma–mass spectrometry (ICP–MS), graphite furnace atomic absorption (GFAAS), and inductively coupled plasma–atomic emission spectrophotometry (ICP–AES). With multielement techniques, it is not only possible to measure the amount adsorbed but changes in the particle composition with size can be monitored [7], which is most useful in interpreting the adsorption results [8]. Hasselov et al. [9] showed that using sedimentation FFF coupled to ICP–MS, it was possible to study both the major elements Al, Si, Fe, and Mn but also the Cs, Cd, Cu, Pb, Zn, and La. It was shown that it was possible to distinguish between the weaker and stronger binding sites as well as between different adsorption and ion-exchange mechanisms.

In electrical FFF, samples are separated on the basis of surface charge and even minute amount of adsorbate will significantly be reflected in electrical FFF data, as demonstrated by Dunkel et al. [10]. However, this technique is severely limited by the generation of polarization products at the channel wall due to the applied voltages.

In conclusion, the versatility and power of FFF are not restricted to its ability to effect high-resolution separations and sizing of particles and macromolecules. FFF can also be used to probe the surface properties of colloidal samples. Such studies have great potential to provide detailed insight into the nature of adsorption phenomena.

References

1. K. D. Caldwell, *Anal. Chem.* 60: 959A (1988).
2. J. C. Giddings, *Science* 260: 1456 (1993).
3. R. Beckett and B. T. Hart, in *Environmental Particles*, J. Buffle and H. P. van Leeuwen (eds.), Lewis Publishers, 1993, Vol. 2, pp. 165–205.
4. R. Beckett, Y. Ho, Y. Jiang, and J. C. Giddings, *Langmuir* 7: 2040 (1991).
5. J.-T. Li and K. D. Caldwell, *Langmuir* 7: 2034 (1991).
6. R. Beckett, D. M. Hotchin, and B. T. Hart, *J. Chromatogr.* 517: 435 (1990).
7. J. F. Ranville, F. Shanks, R. J. F. Morrison, P. Harris, F. Doss, and R. Beckett, *Anal. Chem. Acta* 381: 315 (1999).
8. J. Vanberkel and R. Beckett, *J. Liq. Chromatogr. Related Technol.* 20: 2647 (1997).
9. M. Hasselov, B. Lyven, and R. Beckett, *Environ. Sci. Technol.* 33: 4528 (1999).
10. M. Dunkel, N. Tri, R. Beckett, and K. D. Caldwell, *J. Micro. Separ.* 9: 177 (1997).



Advances in Chiral Pollutants Analysis by Capillary Electrophoresis

Imran Ali

National Institute of Hydrology, Roorkee, India

V. K. Gupta

Indian Institute of Technology, Roorkee, India

Hassan Y. Aboul-Enein

King Faisal Specialist Hospital and Research Center, Riyadh, Saudi Arabia

INTRODUCTION

At present, about 60,000 organic substances are used by human beings and, presumably, some of these compounds are toxic and contaminate our environment. Some of the pesticides, phenols, plasticizers, and polynuclear aromatic hydrocarbons are chiral toxic pollutants. About 25% of agrochemicals are chiral and are sold as their mixtures. Recently, it has been observed that one of the two enantiomers of the chiral pollutant/xenobiotic may be more toxic than the other enantiomer.^[1] This is an important information to the environmental chemist when performing environmental analysis, as the data of simple, direct analysis do not distinguish which enantiomeric structure of a certain pollutant is present and which is harmful. Biological transformation of the chiral pollutants can be stereoselective; thus uptake, metabolism, and excretion of enantiomers may be very different.^[1] Therefore the enantiomeric composition of the chiral pollutants may be changed in these processes. Metabolites of the chiral pollutants are often chiral. Thus to obtain information on the toxicity and biotransformation of the chiral pollutants, it is essential to develop a suitable method for the analysis of the chiral pollutants. Therefore diverse groups of people, ranging from the regulators to the materials industries, clinicians and nutritional experts, agricultural scientists, and environmentalists are asking for data on the ratio of the enantiomers of the chiral pollutants. Chromatographic modalities, e.g., gas chromatography (GC) and high-performance liquid chromatography (HPLC), have been used for the chiral analysis of the pollutants. The high polarity, low vapor pressure, and the need for derivatization of some environmental pollutants make the GC method complicated. The inherent limited resolving power, complex procedures involved in the optimization of the chiral resolution of the pollutant, and the use of large amounts of solvents and sample volumes are the main drawbacks of HPLC. Conversely,

capillary electrophoresis (CE), a versatile technique of high speed and sensitivity, is a major trend in analytical science; some publications on the chiral analysis of pollutants have appeared in recent years. The high efficiency of CE is due to the flat flow profile originated and to a homogeneous partition of the chiral selector in the electrolyte which, in turn, minimizes the mass transfer. Recently, Ali et al.^[2] reviewed the chiral analysis of the environmental pollutants by CE. Therefore in this article, attempts have been made to explain the art of the enantiomeric resolution of the chiral environmental pollutants by CE.

CHIRAL SELECTORS

As in the case of chromatography, a chiral selector is also required in CE for enantiomeric resolution. Generally, suitable chiral compounds are used in the background electrolyte (BGE) as additives and hence are called chiral selectors or chiral BGE additives. There are only a few publications available that deal with the chiral resolution on a capillary coated with the chiral selector in CE.^[3] The analysis of the chiral pollutants discussed in this chapter is restricted only to using chiral selectors in the BGE. The most commonly used chiral BGE additives are cyclodextrins, macrocyclic glycopeptide antibiotics, proteins, crown ethers, ligand exchangers, and alkaloids.^[4,5] A list of these chiral BGE additives is presented in Table 1.

APPLICATIONS

Capillary electrophoresis has been used for the analysis of chiral pollutants, e.g., pesticides, polynuclear-aromatic hydrocarbons, amines, carbonyl compounds, surfactants, dyes, and other toxic compounds. Moreover, CE has also been utilized to separate the structural isomers of various

Table 1 Some of the most commonly used chiral selectors

Chiral selectors (chiral BGE additives)	Refs.
Cyclodextrins	[5,6]
Macrocyclic glycopeptide antibiotics	[6]
Proteins	[6,7]
Crown ethers	[6,8]
Alkaloids	[6]
Polysaccharides	[6,9]
Calixarenes	[6,9]
Imprinted polymers	[10]
Ligand exchangers	[10]

toxic pollutants such as phenols, polyaromatic hydrocarbons, etc. Sarac et al.^[11] resolved the enantiomers of 2-hydrazino-2-methyl-3-(3,4-dihydroxyphenyl) propionic acid using cyclodextrin as the BGE additive. The cyclodextrins used were native, neutral, and ionic in nature with phosphate buffer as BGE. Weseloh et al.^[12] investigated the CE method for the separation of biphenyls, using a phosphate buffer BGE with cyclodextrin as the chiral additive. Miura et al.^[13] used CE for the chiral resolution of seven phenoxy acid herbicides using methylated cyclodextrins as the BGE additives. Furthermore, the same group^[14] resolved MCP, DCP, 2,4-D, 2,4-CPA, 2,4,5-T, 2,3-CPA, 2,2-CPA, 2-PPA, and silvex pesticides using cyclodextrins, with negatively charged sulfonyl groups, as the chiral BGE additives. Gomez-Gomar et al.^[15] investigated the simultaneous enantioselective separation of (\pm)-cizolirine and its impurities, (\pm)-*N*-desmethylcizolirine, (\pm)-cizolirine-*N*-oxide, and (\pm)-5-(hydroxybenzyl)-1-methylpyrazole, by capillary electrophoresis. Otsuka et al.^[16] described the latest advancement by coupling capillary electrophoresis with mass spectrometry; this setup was used for the chiral analysis of phenoxy acid herbicides. The authors also described an electrospray ionization (ESI) method for the CE-MS interface. Generally, nonvolatile additives in sample solutions sometimes decrease the MS sensitivity and/or signal intensity. However, heptakis(2,3,6-tri-*O*-methyl)- β -cyclodextrin (TM- β -CD) was used as a chiral selector; it migrated directly into the ESI interface. Using the negative-ionization mode, along with a methanol-water-formic acid solution as a sheath liquid, and nitrogen as a sheath gas, stereoselective resolution and detection of three phenoxy acid herbicide enantiomers was successfully achieved with a 20-mM TM- β -CD in a 50-mM ammonium acetate buffer (pH 4.6).^[17] Zerbinati et al.^[18] resolved the four enantiomers of the herbicides mecoprop and dichlorprop using an ethylcarbonate derivative of β -CD with three substituents per molecule of hydroxypropyl- β -CD and native β -CD. The perform-

ances of these chiral selectors have been quantified by means of two-level full factorial designs and the inclusion constants were calculated from CE migration time data. The analysis of the chiral pollutants by CE is summarized in Table 2. To show the nature of the electropherograms, the chiral separation of dichlorprop enantiomers is shown in Fig. 1 with different concentrations of α -cyclodextrin.^[18]

OPTIMIZATION OF CE CONDITIONS

The analysis of the chiral pollutants by CE is very sensitive and hence is controlled by a number of experimental parameters. The optimization parameters may be categorized into two classes, i.e., the independent and dependent parameters. The independent parameters are under the direct control of the operator. These parameters include the choice of the buffer, pH of the buffer, ionic strength of the buffer, type of chiral selectors, voltage applied, temperature of the capillary, dimension of the capillary, BGE additives, and various other parameters. Conversely, the dependent parameters are those directly affected by the independent parameters and are not under the direct control of the operator. These types of parameters are field strength (V/m), EOF, Joule heating, BGE viscosity, sample diffusion, sample mobility, sample charge, sample size and shape, sample interaction with capillary and BGE, molar absorptivity, etc. Therefore the optimization of chiral resolution can be controlled by varying all of the parameters mentioned above. For detailed information on the optimization of chiral analysis, one should consult our review.^[2] However, a protocol for the optimization of the chiral analysis is given in Scheme 1.

DETECTION

Normally, the chiral pollutants in the environment occur at low concentrations and therefore a sensitive detection method is essential and is required in chiral CE. The most commonly used detectors in the chiral CE are UV, electrochemical, fluorescence, and mass spectrometry. Mostly, the detection of the chiral resolution of drugs and pharmaceutical in CE has been achieved by a UV mode^[13,27] and therefore the detection of the chiral pollutants may be achieved by the same method. The selection of the UV wavelength depends on the type of buffer, chiral selector, and the nature of the environmental pollutants. The concentration and sensitivity of UV detection are restricted insofar as the capillary diameter limits the optical path length. It has been observed that some pollutants, especially organochloro pesticides, are



Table 2 Chiral analysis of some pollutants by capillary electrophoresis

Chiral pollutants	Sample matrix	Electrolytes	Detection	Refs.
Fenoprop, mecoprop, and dichlorprop	–	20 mM tributyl- β -CD in 50 mM, ammonium acetate, pH 4.6	MS	[16]
Dichlorprop and 2-(2,4-dichlorophenoxy) propionic acid	–	100 mM acetic acid–sodium acetate buffer (pH 5.0) containing α -, β -, and γ -CDs	UV 206 nm	[18]
2-Phenoxypropionic acid, dichlorprop, fenoxaprop, fluzaziprop, haloxyfop, and diclofop enantiomers	–	75 mM Britton–Robinson buffer with 6 mM Vancomycin	–	[19]
Imazaquin isomer	–	50 mM sodium acetate, 10 mM dimethyl- β -CD, pH 4.6	–	[20]
Phenoxy acid herbicides	–	200 mM sodium phosphate, pH 6.5 with various concentrations of OG	–	[20]
Diclofop	–	50 mM sodium acetate, 10 mM trimethyl- β -CD, pH 3.6	–	[20]
Imazamethabenz isomers	–	50 mM sodium acetate, 10 mM dimethyl- β -CD, pH 4.6	–	[20]
2-(2-Methyl-4-chlorophenoxy) propionic acid	–	0.05 M lithium acetate containing α -cyclodextrins	UV 200 nm	[21]
2-(2-Methyl-4,6-dichlorophenoxy) propionic acid	–	0.05 M lithium acetate containing β -cyclodextrin	UV 200 nm	[21]
2-(2,4-Dichlorophenoxy) propionic acid	–	0.05 M lithium acetate containing heptakis-(2,6-di- <i>O</i> -methyl)- β -cyclodextrin	UV 200 nm	[21]
2-(2-Methyl-4-chlorophenoxy) propionic acid and 2-(2,4-dichlorophenoxy)-propionic acid	–	0.03 M lithium acetate containing heptakis-(2,6-di- <i>O</i> -methyl)- β -cyclodextrin	UV 200 nm	[22]
2-(2-Methyl-4-chlorophenoxy) propionic acid	–	0.05 M NaOAc, pH 4.5, with α -CD	UV 230	[23]
Phenoxy acid	–	0.1 M phosphate buffer, pH 6 with Vancomycin	–	[24]
		Ristocetin	–	[24,25]
		Teicoplanin	–	[24,26]
		0.1 M phosphate and acetate buffer containing OM	–	[27]
		OG	–	[28]
Phenoxy acid derivatives	–	β -CD and TM- β -CD	–	[23,29]
Silvex	–	0.4 M borate, pH 10 containing <i>N,N</i> -bis-(<i>D</i> -gluconamidopropyl)-cholamide (Big CHAP) and -deoxycholamide (Deoxy big CHAP)	–	[30]

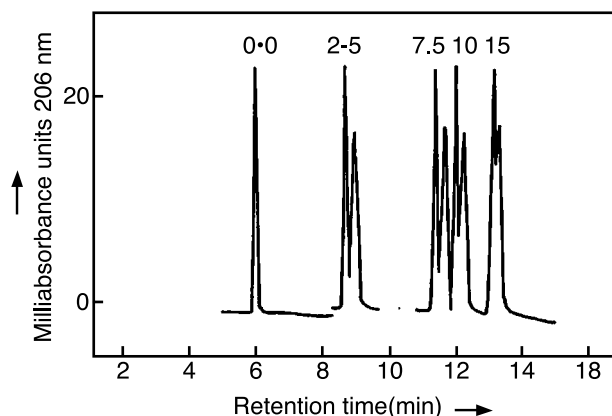


Fig. 1 Electropherograms of dichlorprop herbicide enantiomers with increasing concentrations of α -cyclodextrin. (From Ref. [18].)

UV transparent and therefore for such type of applications, electrochemical and mass spectrometry are the best detectors. Some of the chiral selectors, such as proteins and macrocyclic glycopeptide antibiotics, are UV-absorbing in nature and hence the detection of enantiomers becomes poor.

Only a few reports are available in the literature dealing with the limits of the detection for the chiral resolution of environmental pollutants by CE, indicating mg/L to $\mu\text{g/L}$ as the limits of the detection. Tsunoi et al.^[14] carried out an extensive study on the determination of the limits of the detection for the chiral resolution of herbicides. The authors used a 230-nm wavelength for the detection and the minimum limit of the detection achieved was 4.7×10^{-3} M for 2,4-dichlorophenoxy acetic acid. On the other hand, Mechref and El Rassi^[29] reported better detection limits, for herbicides, in the derivatized mode, in comparison to the underivatized mode. For example, the limit of the detection was enhanced by almost 1 order of magnitude from 1×10^{-4} M (10 pmol) to 3×10^{-5} M (0.36 pmol). In the same study, the authors reported 2.5×10^{-6} M and 1×10^{-9} M as the limits of detection for the herbicides by fluorescence and laser-induced fluorescence detectors, respectively.

SAMPLE PREPARATION

Many of the impurities are present in samples of environmental or biological origin. Therefore sample pretreatment is very important and a necessary step for reproducible chiral resolution. Real samples often require the application of simple procedures, such as filtration, extraction, dilution, etc. A search of the literature conducted and discussed herein (Table 2) indicates that all of the chiral

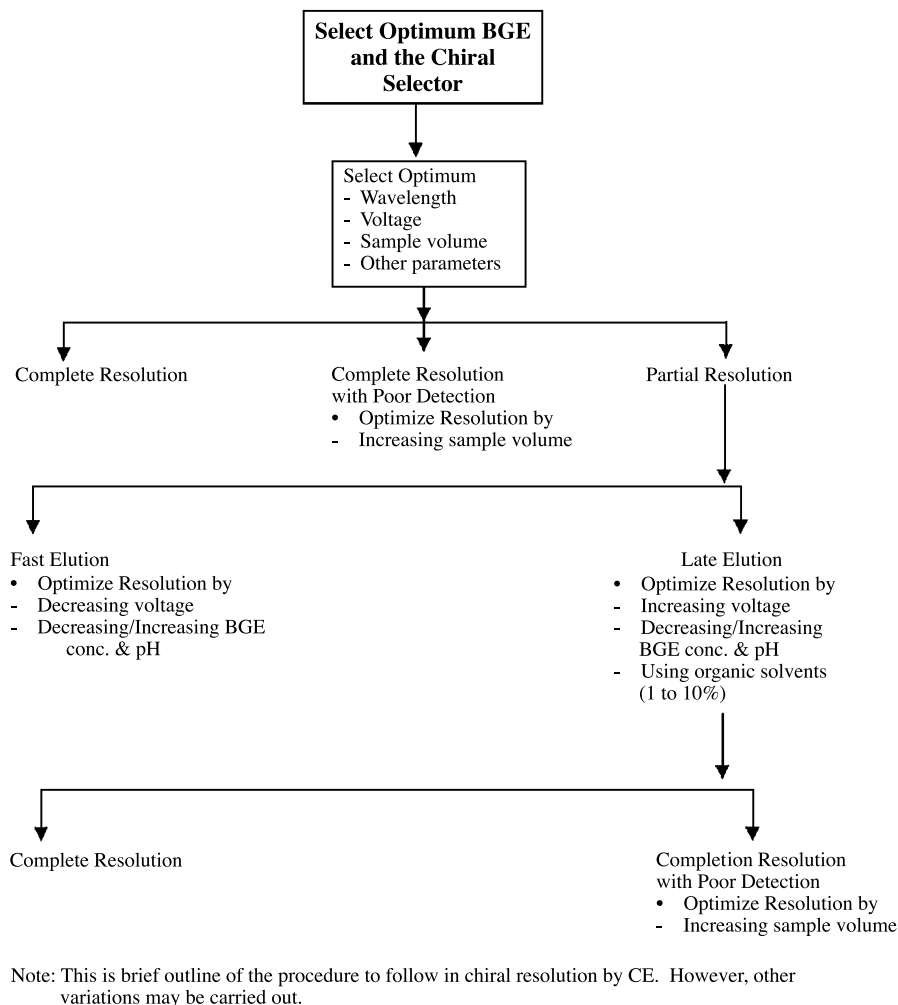
resolution of the environmental pollutants was carried out, by CE, in laboratory-synthesized samples only. Therefore no report is published on the sample pretreatment prior to the chiral resolution of the environmental pollutants by CE. Some reviews have been published, however, on the pretreatment and sample preparation methodologies for the achiral analysis of pollutants.^[31,32] Therefore these approaches may be utilized for the preconcentration and sample preparation in the chiral CE of the environmental pollutants. Dabek-Zlotorzynska et al.^[32] reviewed the sample pretreatment methodologies for environmental analysis before CE. Moreover, some reviews have also been published in the last few years on this issue.^[33–35] Whang and Pawliszyn^[36] designed an interface that enables the solid-phase microextraction (SPME) fiber hyphenation to CE. They prepared a semi-custom-made polyacrylate fiber to reach the SPME–CE interface. The authors tested the developed interface to analyze phenols in water and therefore the same may be used for the chiral resolution of the pollutants.

MECHANISMS OF THE CHIRAL SEPARATION

It is well known that a chiral environment is essential for the enantiomeric resolution of racemates. In CE, this situation is provided by the chiral compounds used in the BGE and is known as the chiral selector or chiral BGE additive. Basically, the chiral recognition mechanisms in CE are similar to those in chromatography using a chiral mobile-phase additive mode, except that the resolution occurred through different migration velocities of the diastereoisomeric complexes in CE. The chiral resolution occurred through diastereomeric complex formation between the enantiomers of the pollutants and the chiral selector. The formation of diastereomeric complexes depends on the type and nature of the chiral selectors used and the nature of the pollutants.

In the case of cyclodextrins, the inclusion complexes are formed and the formation of diastereomeric complexes is controlled by a number of interactions, such as π – π complexation, hydrogen bonding, dipole–dipole interaction, ionic binding, and steric effects. Zerbinati et al.^[17] used ethylcarbonate- β -CD, hydroxypropyl- β -CD, and native α -CD for the chiral resolution of mecoprop and dichlorprop. The authors calculated the performance of these chiral selectors by means of a two-level full factorial design and calculated inclusion constants from CE migration time data. Furthermore, they have proposed the possible structure of inclusion complexes on the basis of molecular mechanics simulations. Recently, Chankvetadze et al.^[37] explained the chiral recognition mechanisms in cyclodextrin-based CE using UV, NMR,





Scheme 1 The protocol for the development and optimization of CE conditions for the chiral resolution.

and electrospray ionization mass spectrometric methods. Furthermore, the authors determined the structures of the diastereomeric complexes by an X-ray crystallographic method.

The macrocyclic antibiotics have some similarities and differences with the cyclodextrins. Most of the macrocyclic antibiotics contain ionizable groups and, consequently, their charge and possibly their three-dimensional conformation can vary with the pH of the BGE. The complex structures of the antibiotics containing different chiral centers, inclusion cavities, aromatic rings, sugar moieties, and several hydrogen donor and acceptor sites are responsible for their surprising chiral selectivities. This allows for an excellent potential to resolve a greater variety of racemates. The possible interactions involved in the formation of diastereomeric complexes are π - π complexation, hydrogen bonding, inclusion complexation, dipole interactions, steric interactions, and anionic and

cationic binding. Similarly, the diastereomeric complexes are formed with other chiral selectors involving specific interactions. In this way, the diastereomeric complexes possessing different physical and chemical properties are separated on the capillary path (achiral phase). The different migration times of these formed diastereomeric complexes depend on their sizes, charges, and their interaction with the capillary wall and, as a result, these complexes are eluted at different time intervals.

CAPILLARY ELECTROPHORESIS VS. CHROMATOGRAPHY

Today, chromatographic modalities are used frequently for the analysis of chiral pollutants. The wide application of HPLC is due to the development of various chiral stationary phases and excellent reproducibility. However,

HPLC suffers from certain drawbacks, as the chiral selectors are fixed on the stationary phase and hence no variation in the concentrations of the chiral selectors can be carried out. Moreover, a large amount of the costly solvent is consumed to establish the chiral resolution procedure. Additionally, the poor efficiency in HPLC is due to the profile of the laminar flow, mass transfer term, and possible additional interactions of enantiomers with the residual silanol groups of the stationary phase. Gas chromatography also suffers from certain drawbacks as discussed in the "Introduction."

On the other hand, the chiral resolution in CE is achieved using the chiral selectors in the BGE. The chiral separation in CE is very fast and sensitive, involving the use of inexpensive buffers. In addition, the high efficiency of CE is due to the flat profile created and to a homogeneous partition of the chiral selector in the electrolyte which, in turn, minimizes the mass transfer. Generally, the theoretical plate number in CE is much higher in comparison to chromatography and thus a good resolution is achieved in CE. In addition, more than one chiral selector can be used simultaneously for optimizing the chiral analysis. However, reproducibility is the major problem in CE and therefore the technique is not popular for the routine chiral analysis. The other drawbacks of CE include the waste of the chiral selector as it is used in the BGE. In addition, chiroptical detectors, such as polarimetric and circular dichroism, cannot be used as detection devices because of the presence of the chiral selector in the BGE. Moreover, some of the well-known chiral selectors may not be soluble in the BGE and thus a stationary bed of a chiral selector may allow the transfer of the advantages of a stationary bed inherent in HPLC to electrically driven technique, i.e., CE. This will allow CE to be hyphenated with the mass spectrometer, polarimeter, circular dichroism, and UV detectors without any problem. Briefly, at present, CE is not a very popular technique as is chromatography for the chiral analysis of pollutants, but it will gain momentum in the near future.

CONCLUSION

Analysis of the chiral pollutants at trace levels is a very important and demanding field. In recent years, capillary electrophoresis has been gaining importance in the direction of chiral analysis of various racemates. A search of the literature cited herein indicates a few reports on the chiral resolution of environmental pollutants by CE. It has not achieved a respectable place in the routine chiral analysis of these pollutants due to its poor reproducibility and to the limitations of detection. Therefore many scientists have suggested various modifications to make CE a method of choice. To achieve good reproducibility,

the selection of the capillary wall chemistry, pH and ionic strength of the BGE, chiral selectors, detectors, and optimization of BGE have been described and suggested for the analysis of organic and inorganic pollutants.^[38–43] In addition, some other aspects should also be addressed so that CE can be used as a routine method in this field. The most important points related to this include the development of new and better chiral selectors, detector devices, and addition of a cooling device in the CE apparatus. In addition, chiral capillaries should be developed and the CE device should be hyphenated with mass spectrometer, polarimetric, and circular dichroism detectors, which may result in good reproducibility and improved limits of detection. The advancement of CE as a chiral analysis technique has not yet been fully explored and research in this direction is currently underway. In summary, there is much to be developed for the advancement of CE for the analysis of chiral pollutants. It is hoped that CE will be recognized as the technique of choice for chiral analysis of the environmental pollutants.

ABBREVIATIONS

BGE	Background electrolyte
CD	Cyclodextrin
CE	Capillary electrophoresis
2,2-CPPA	2-(2-Chlorophenoxy) propionic acid
2,3-CPPA	2-(3-Chlorophenoxy) propionic acid
2,4-CPPA	2-(4-Chlorophenoxy) propionic acid
2,4-D	(2,4-Dichlorophenoxy) acetic acid
DCPP	2-(2,4-Dichlorophenoxy) propionic acid
EOF	Electroosmotic flow
ESI	Electron spray ionization
GC	Gas chromatography
HPLC	High-performance liquid chromatography
MCPP	2-(4-Chlorophenoxy) propionic acid
MS	Mass spectrometer
NMR	Nuclear magnetic resonance
OG	<i>n</i> -Octyl- β -D-glucopyranoside
OM	<i>n</i> -Octyl- β -D-maltopyranoside
SPME	Solid-phase microextraction
SPME-CE	Solid-phase microextraction capillary electrophoresis
2,4,5-T	(2,4,5-Trichlorophenoxy) acetic acid
TM- β -CD	2,3,6-Tri- <i>O</i> -methyl- β -cyclodextrin
UV	Ultraviolet

REFERENCES

1. *Stereoselectivity of Pesticides, Biological and Chemical Problems: Chemicals in Agriculture*; Ariens, E.J., van



- Rensen, J.J.S., Welling, W., Eds.; Elsevier: Amsterdam, 1988; Vol. 1.
2. Ali, I.; Gupta, V.K.; Aboul-Enein, H.Y. Chiral resolution of the environmental pollutants by capillary electrophoresis. *Electrophoresis* **2003**, *24*, 1360–1374.
3. Jung, M.; Mayer, S.; Schurig, V. Enantiomer separations by GC, SFC and CE on immobilized polysiloxane bonded cyclodextrins. *LC GC* **1994**, *7*, 340–347.
4. Blaschke, G.; Chankvetadze, B. Enantiomer separation of drugs by capillary electromigration techniques. *J. Chromatogr., A* **2000**, *875*, 3–25.
5. Zaugg, S.; Thormann, W. Enantioselective determination of drugs in body fluids by capillary electrophoresis. *J. Chromatogr., A* **2000**, *875*, 27–41.
6. Chankvetadze, B. *Capillary Electrophoresis in Chiral Analysis*; John Wiley & Sons: New York, 1997.
7. Haginaka, J. Enantiomer separation of drugs by capillary electrophoresis using proteins as chiral selectors. *J. Chromatogr., A* **2000**, *875*, 235–254.
8. Tanaka, Y.; Otsuka, K.; Terabe, S. Separation of enantiomers by capillary electrophoresis-mass spectrometry employing a partial filling technique with a chiral crown ether. *J. Chromatogr., A* **2000**, *875*, 323–330.
9. *The Impact of Stereochemistry on Drug Development and Use*; Aboul-Enein, H.Y., Wainer, I.W., Eds.; John Wiley & Sons: New York, 1997; Vol. 142.
10. Gübitz, G.; Schmid, M.G. Chiral separation principles in capillary electrophoresis. *J. Chromatogr., A* **1997**, *792*, 179–225.
11. Sarac, S.; Chankvetadze, B.; Blaschke, G. Enantioseparation of 3,4-dihydroxyphenylalanine and 2-hydrazino-2-methyl-3-(3,4-dihydroxyphenyl)propanoic acid by capillary electrophoresis using cyclodextrins. *J. Chromatogr., A* **2000**, *875*, 379–387.
12. Welseloh, G.; Wolf, C.; König, W.A. New technique for the determination of interconversion processes based on capillary zone electrophoresis: Studies with axially chiral biphenyls. *Chirality* **1996**, *8*, 441–445.
13. Miura, M.; Terashita, Y.; Funazo, K.; Tanaka, M. Separation of phenoxy acid herbicides and their enantiomers in the presence of selectively methylated cyclodextrin derivatives by capillary zone electrophoresis. *J. Chromatogr., A* **1999**, *846*, 359–367.
14. Tsunoi, S.; Harino, H.; Miura, M.; Eguchi, M.; Tanaka, M. Separation of phenoxy acid herbicides by capillary electrophoresis using a mixture of hexakis(2,3-di-*O*-methyl)- and sulfopropylether- α -cyclodextrins. *Anal. Sci.* **2000**, *16*, 991–993.
15. Gomez-Gomar, A.; Ortega, E.; Calvet, C.; Merce, R.; Frigola, J. Simultaneous separation of the enantiomers of cizolirtine and its degradation products by capillary electrophoresis. *J. Chromatogr.* **2002**, *950*, 257–270.
16. Otsuka, K.; Smith, J.S.; Grainger, J.; Barr, J.R.; Patterson, D.G., Jr.; Tanaka, N.; Terabe, S. Stereoselective separation and detection of phenoxy acid herbicide enantiomers by cyclodextrin-modified capillary zone electrophoresis-electrospray ionization mass spectrometry. *J. Chromatogr., A* **1998**, *817*, 75–81.
17. Zerbinati, O.; Trotta, F.; Giovannoli, C. Optimization of the cyclodextrin-assisted capillary electrophoresis separation of the enantiomers of phenoxyacid herbicides. *J. Chromatogr., A* **2000**, *875*, 423–430.
18. Zerbinati, O.; Trotta, F.; Giovannoli, C.; Baggiani, C.; Giraudi, G.; Vanni, A. New derivatives of cyclodextrins as chiral selectors for the capillary electrophoretic separation of dichlorprop enantiomers. *J. Chromatogr., A* **1998**, *810*, 193–200.
19. Desiderio, C.; Polcaro, C.M.; Padiglioni, P.; Fanali, S. Enantiomeric separation of acidic herbicides by capillary electrophoresis using vancomycin as chiral selector. *J. Chromatogr., A* **1997**, *781*, 503–513.
20. Penmetsa, K.V.; Leidy, R.B.; Shea, D. Enantiomeric and isomeric separation of herbicides using cyclodextrin-modified capillary zone electrophoresis. *J. Chromatogr., A* **1997**, *790*, 225–234.
21. Nielsen, M.W.F. (Enantio-)separation of phenoxy acid herbicides using capillary zone electrophoresis. *J. Chromatogr., A* **1993**, *637*, 81–90.
22. Nielsen, M.W.F. LIMS: A report on the 7th International LIMS Conference held at Egham, UK, 8–11 June, 1993. *Trends Anal. Chem.* **1993**, *12*, 345–356.
23. Garrison, A.W.; Schmitt, P.; Ketrup, A. Separation of phenoxy acid herbicides and their enantiomers by high-performance capillary electrophoresis. *J. Chromatogr., A* **1994**, *688*, 317–327.
24. Gasper, M.P.; Berthod, A.; Nair, U.B.; Armstrong, D.W. Comparison and modeling of vancomycin, ristocetin A and teicoplanin for CE enantioseparations. *Anal. Chem.* **1996**, *68*, 2501–2514.
25. Armstrong, D.W.; Gasper, M.P.; Rundlet, K.L. Highly enantioselective capillary electrophoretic separations with dilute solutions of the macrocyclic antibiotic ristocetin A. *J. Chromatogr., A* **1995**, *689*, 285–304.
26. Rundlet, K.L.; Gasper, M.P.; Zhou, E.Y.; Armstrong, D.W. Capillary electrophoretic enantiomeric separations using the glycopeptide antibiotic, teicoplanin. *Chirality* **1996**, *8*, 88–107.
27. Mechref, Y.; El Rassi, Z. Capillary electrophoresis of herbicides: III. Evaluation of octylmaltopyranoside chiral surfactant in the enantiomeric separation of phenoxy acid herbicides. *Chirality* **1996**, *8*, 518–524.
28. Mechref, Y.; El Rassi, Z. Capillary electrophoresis of herbicides: II. Evaluation of alkylglucoside chiral surfactants in the enantiomeric separation of phenoxy acid herbicides. *J. Chromatogr., A* **1997**, *757*, 263–273.
29. Mechref, Y.; El Rassi, Z. Capillary electrophoresis of herbicides: I. Pre-column derivatization of chiral and achiral phenoxy acid herbicides with a fluorescent tag for electrophoretic separation in the presence of cyclodextrins and micellar phases. *Anal. Chem.* **1996**, *68*, 1771–1777.
30. Mechref, Y.; El Rassi, Z. Micellar electrokinetic capillary chromatography with in-situ charged micelles: VI. Evaluation of novel chiral micelles consisting of steroidal-glycoside surfactant-borate complexes. *J. Chromatogr., A* **1996**, *724*, 285–296.
31. Martinez, D.; Cugat, M.J.; Borrull, F.; Calull, M. Solid-phase extraction coupling to capillary electrophoresis with



- emphasis on environmental analysis. *J. Chromatogr., A* **2000**, 902, 65–89.
32. Dabek-Zlotorzynska, E.; Aranda-Rodriguez, R.; Keppel-Jones, K. Recent advances in capillary electrophoresis and capillary electrochromatography of pollutants. *Electrophoresis* **2001**, 22, 4262–4280.
33. Haddad, P.R.; Doble, P.; Macka, M. Developments in sample preparation and separation techniques for the determination of inorganic ions by ion chromatography and capillary electrophoresis. *J. Chromatogr., A* **1999**, 856, 145–177.
34. Fritz, J.S.; Macka, M. Solid-phase trapping of solutes for further chromatographic or electrophoretic analysis. *J. Chromatogr., A* **2000**, 902, 137–166.
35. Pedersen-Bjegaard, S.; Rasmussen, K.E.; Halvorsen, T.G. Liquid-liquid extraction procedures for sample enrichment in capillary zone electrophoresis. *J. Chromatogr., A* **2000**, 902, 91–105.
36. Whang, C.; Pawliszyn, J. Solid phase microextraction coupled to capillary electrophoresis. *Anal. Commun.* **1998**, 35, 353–356.
37. Chankvetadze, B.; Burjanadze, N.; Pintore, G.; Bergenthal, D.; Bergander, K.; Mühlenbrock, C.; Breitzkreuz, J.; Blaschke, G. Separation of brompheniramine enantiomers by capillary electrophoresis and study of chiral recognition mechanisms of cyclodextrins using NMR spectroscopy, UV spectrometry, electrospray ionization mass spectrometry and X-ray crystallography. *J. Chromatogr., A* **2000**, 875, 471–484.
38. Pacakova, V.; Coufal, P.; Stulik, K. Capillary electrophoresis of inorganic cations. *J. Chromatogr., A* **1999**, 834, 257–275.
39. Liu, B.F.; Liu, B.L.; Cheng, J.K. Analysis of inorganic cations as their complexes by capillary electrophoresis. *J. Chromatogr., A* **1999**, 834, 277–308.
40. Valsecchi, S.M.; Polesello, S. Analysis of inorganic species in environmental samples by capillary electrophoresis. *J. Chromatogr., A* **1999**, 834, 363–385.
41. Timerbaev, A.R.; Buchberger, W. Prospects for detection and sensitivity enhancement of inorganic ions in capillary electrophoresis. *J. Chromatogr., A* **1999**, 834, 117–132.
42. Horvath, J.; Dolnik, V. Polymer wall coatings for capillary electrophoresis. *Electrophoresis* **2001**, 22, 644–655.
43. Mayer, B.X. How to increase precision in capillary electrophoresis. *J. Chromatogr., A* **2001**, 907, 21–37.



Affinity Chromatography of Cells

Terry M. Phillips

Ultramicro Analytical Immunochemistry Resource, DBEPS, ORS, OD, NIH, Rockville, Maryland, U.S.A.

Introduction

Affinity cell separations techniques are based on principles similar to those described in procedures for the isolation of molecules and are used to quickly and efficiently isolate specific cell types from heterogeneous cellular suspensions. The procedure (Fig. 1) involves making a single-cell suspension and passing it through a column packed with a support to which a selective molecule (ligand) has been immobilized. As the cells pass over the immobilized ligand-coated support (Fig. 1a), the ligand interacts with specific molecules

on the cell surface, thus capturing the cell of interest (Fig. 1b). This cell is retained by the ligand-coated support while nonreactive cells are washed through the column. Finally, the captured cell is released (Fig. 1c) by disrupting the bond between the ligand and its selected molecule, allowing a homogeneous population of cells to be harvested.

Research and Developments

Although affinity chromatography of cells is essentially performed in a similar manner to other affinity techniques, it is commonly used for both negative and positive selection. Negative selection removes specific cell types from the sample population, whereas positive selection isolates a single cell type from the sample. In the latter situation, the selected cells are recovered by elution from the immobilized ligand, thus yielding an enriched population. However, unlike molecules, cells are often quite delicate and care must be exercised when choosing the chromatographic support and the method of retrieval. The support matrix must exhibit minimal nonspecific cell adhesion but be sufficiently porous to allow cells to pass through without physically trapping them or creating undue shear forces likely to cause cell injury or death. Usually, the support matrices of choice are loosely packed fibers, large-pore cross-linked dextrans or agarose, and large plastic or glass beads. The elution agent must also be carefully selected. It must be able to either disrupt the binding of the ligand to the cell surface molecule or it must be able to compete with the cell molecule for ligand binding. In many cases, such as lectin affinity chromatography, the elution agent is easy to select — it is usually a higher concentration of the sugar to which the ligand binds. Elution agents for other techniques, such as immunoaffinity, are harder to select. Harsh acid or alkaline conditions, although efficient at breaking antibody–antigen binding, are usually detrimental to cells. Elution in these cases is often achieved using mild acids, cell molecule competition (like the lectins), or mild chaotropic ion elution.

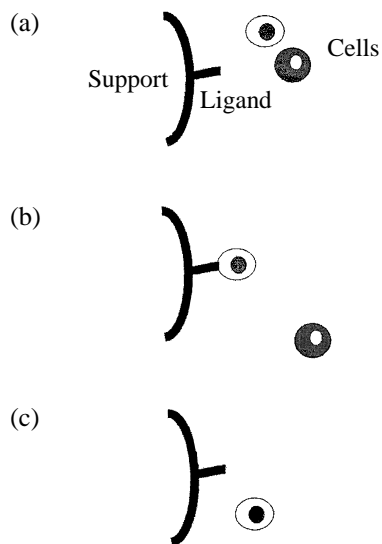


Fig. 1 Affinity isolation of specific cells. (a) The cell suspension containing the cell of interest (clear cytoplasm) and another cell type (dark cytoplasm) are passed over the support bearing a selective ligand immobilized to its surface. (b) The ligand interacts with its target molecule on the cell of interest, thus capturing it. The other cell type is not bound and passes through the column. (c) The bound cell is released by the addition of an elution agent to the running buffer of the column. This agent disrupts the binding between the ligand and the cell, thus releasing the cell. The free cell is now washed through the column and harvested as a homogeneous population.



Immunologists have long used the relatively non-specific affinity of charged nylon wool to fractionate lymphocytes into different subpopulations. Such separations are achieved because certain subpopulations of lymphocytes express an affinity for the charged fibers, whereas others do not. This negative selection process has been used to prepare pure suspensions of T-lymphocytes for many years but has recently been replaced by the more selective immunoaffinity procedures. A good review of the early history of affinity cell separation is provided by Sharma and Mahendroo [1]; however, the review focuses primarily on the application of lectins as the selective ligands for cell affinity chromatography. Tlaskalova-Hogenova et al. [2] demonstrated the usefulness of affinity cell chromatography to isolate T- and B-lymphocytes from human tissues. These authors describe comparative studies on three popular approaches to the isolation of lymphocyte subpopulations, namely nylon wool columns, immunoaffinity cell panning (a batch technique using antibodies immobilized to the bottom of culture dishes), and immunoaffinity using anti-human immunoglobulins attached to Sephron (hydroxyethyl methacrylate) or Sepharose supports. These studies clearly indicate that the selectiveness of immobilized antibodies were superior for isolating defined subpopulations of cells.

Current Applications

Immobilized antibody ligands or immunoaffinity chromatography is now the approach of choice for cell separation procedures. Kondorosi et al. [3] prepared columns packed with a support coated with nonimmune rat immunoglobulin and used these columns to isolate cells expressing surface Fc or immunoglobulin receptors, whereas van Overveld et al. [4] used anti-human IgE-coated Sepharose beads as an immunoaffinity chromatography step when fractionating human mast cells from lung tissue.

Plant lectins are one of the most popular ligands for affinity cell separations. These molecules express selective affinities for certain sugar moieties (Table 1), different lectins being used as selective agents for specific sugars. Whitehurst et al. [5] found that the lectin *Pisum sativum* agglutinin could bind feline B-lymphocytes much more readily than T-lymphocytes and used lectin-coated supports to obtain pure subpopulations of T-lymphocytes by negative selection. Additionally, the retained cells were recovered by elution from the immobilized lectin with a suitable sugar. Lectins are efficient ligands for cell selection, but, in many cases, their interaction with the selected cell surface molecule is highly stable and efficient, requiring mechanical agitation of the packing before recovery of the cells can be achieved. Pereira and Ka-

Table 1 Lectins and Their Reactive Sugar Moieties

Common name	Latin name	Reactive sugar residues
Castor bean RCA ₁₂₀	<i>Ricinus communis</i>	β-D-Galactosyl
Fava bean	<i>Vicia faba</i>	D-Mannose, D-Glucose
Gorse UEA I	<i>Ulex europaeus</i>	α-L-Fucose,
UEA II		N,N'-Diacetylchitobiose
Jacalin	<i>Artocarpus integrifolia</i>	α-D-Galactosyl, β-(1,3) <i>n</i> -Acetyl galactosamine
Concanavalin A	<i>Canavalia ensiformis</i>	α-D-Mannosyl, α-D-Glucosyl
Jequirity bean	<i>Abrus precatorius</i>	α-D-Galactose
Lentil	<i>Lens culinaris</i>	α-D-Mannosyl, α-D-Glucosyl
Mistletoe	<i>Viscum album</i>	β-D-Galactosyl
Mung bean	<i>Vigna radiata</i>	α-D-Galactosyl
Osage orange	<i>Maclura pomifera</i>	α-D-Galactosyl, <i>N</i> -Acetyl-D-galactosaminyl
Pea	<i>Pisum sativum</i>	α-D-Glucosyl,
		α-D-Mannosyl
Peanut	<i>Arachis hypogaea</i>	β-D-Galactosyl
Pokeweed	<i>Phytolacca americana</i>	<i>N</i> -acetyl-β-D-Glucosamine oligomers
Snowdrop	<i>Galanthus nivalis</i>	Nonreducing terminal end of α-D-mannosyl
Soybean	<i>Glycine max</i>	<i>N</i> -Acetyl-D-galactosamine
Wheatgerm	<i>Triticum vulgare</i>	<i>N</i> -Acetyl-β-D-glucosaminyl, <i>N</i> -Acetyl-β-D-glucosamine oligomers



bat [6] have reported the use of lectins immobilized to Sephadex or Sepharose beads for the isolation of erythrocytes.

Another useful ligand is protein A, which is a protein derived from the wall of certain *Staphylococcus* species of bacteria. This reagent binds selected classes of IgG immunoglobulin via their Fc or tail portion making it an excellent ligand for binding immunoglobulins attached to cell surfaces, making it an ideal general-purpose reagent. Ghetie et al. [7] demonstrated that protein A-coated Sepharose beads were useful for cell separations following initial incubation of the cells with IgG antibodies directed against specific cell surface markers. Surface IgG-bearing cells mouse spleen cells were pretreated with rabbit antibodies to mouse IgG prior to passage over the protein A-coated support. The cells of interest were then isolated by positive selection chromatography.

In addition to bacterial proteins, other binding proteins such as chicken egg white avidin have become popular reagents for affinity chromatography. These supports work on the principle that immobilized avidin binds biotin, which can be chemically attached to a variety of ligands including antibodies. Tassi et al. [8] used a column with an avidin-coated polyacrylamide support to bind and retain cells marked with biotinylated antibodies. Human bone marrow samples were incubated with monoclonal mouse antibodies directed against the surface marker CD34, followed by a second incubation with biotinylated goat anti-mouse immunoglobulins. Binding of the biotin to

the avidin support effectively isolated the antibody-coated cells.

Conclusion

A wide variety of immobilized antigens, chemicals, and receptor molecules have been used effectively for affinity cell chromatography. Sepharose beads coated with thyroglobulin have been used to separate thyroid follicular and para-follicular cells, and immobilized insulin on Sepharose beads has been used to isolate adipocytes by affinity chromatography. Dvorak et al. [9] reported the successful retrieval of a 95% pure fraction of chick embryonic neuronal cells using an affinity chromatography approach utilizing α -bungarotoxin immobilized to Sepharose beads.

References

1. S. K. Sharma and P. P. Mahendroo, *J. Chromatogr.* 184: 471 (1980).
2. H. Tlaskalova-Hogenova, V. Vetvicka, M. Pospisil, L. Fornusek, L. Prokesova, J. Coupek, A. Frydrychova, J. Kopecek, H. Fiebig, and J. Brochier, *J. Chromatogr.* 376: 401 (1986).
3. E. Kondorosi, J. Nagy, and G. Denes, *J. Immunol. Methods* 16: 1 (1977).
4. F. J. van Overveld, G. K. Terpstra, P. L. Bruijnzeel, J. A. Raaijmakers, and J. Kreukniet, *Scand. J. Immunol.* 27: 1 (1988).
5. C. E. Whitehurst, N. K. Day, and N. Gengozian, *J. Immunol. Methods* 175: 189 (1994).
6. M. E. Pereira and E. A. Kabat, *J. Cell Biol.* 82: 185 (1979).
7. V. Ghetie, G. Mota, and J. Sjoquist, *J. Immunol. Methods* 21: 133 (1978).
8. C. Tassi, A. Fortuna, A. Bontadini, R. M. Lemoli, M. Gobbi, and P. L. Tazzari, *Haematologica* 76(Suppl. 1): 41 (1991).
9. D. J. Dvorak, E. Gipps, and C. Kidson, *Nature* 271: 564 (1978).



Affinity Chromatography with Immobilized Antibodies

Monica J. S. Nadler

Beth Israel Deaconess Medical Center and Harvard Medical School, Boston, Massachusetts, U.S.A.

Tim Nadler

Applied Biosystems, Framingham, Massachusetts, U.S.A.

Introduction

Antibodies are serum proteins that are generated by the immune system which bind specifically to introduced antigens. The high degree of specificity of the antibody–antigen interaction plays a central role in an immune response, directing the removal of antigens in concert with complement lysis (humoral immunity). Importantly, this high degree of specific binding has been exploited as an analytical tool: Antigens can be detected, quantified, and purified from sources in which they are in low abundance with numerous contaminants. Examples include enzyme-linked immunosorbent assays (ELISAs), Ouchterlony assays, and Western blots. Antibodies that are specifically immobilized on high-performance chromatographic media offer a means of both detection and purification that is unparalleled in specificity, versatility, and speed.

We will focus, here, on the use of immobilized antibodies for analytical affinity chromatography, which offers a number of advantages over standard partition chromatography. The first advantage is the specificity imparted by the antibody itself, which allows an antigen to be completely separated from any contaminants. During a chromatographic run with an antibody affinity column, all of the contaminants wash through the column unbound, and the bound antigen is subsequently eluted, resulting in only two peaks generated in the chromatogram (contaminants in the flow-through step and antigen in the elution step). With antibodies which are immobilized on high-speed media such as perfusive media [1,2], typical analytical chromatograms can be generated in less than 5 min and columns can last for hundreds of analyses. In Fig. 1, an example of 5 consecutive analytical affinity chromatography assays are shown, followed by the results of the last 5 assays of a set of 5000. Note that, here, the cycle time for loading, washing out the unbound material, eluting the bound material, and reequilibration

of the affinity column is only 0.1 min (6 s). Also note that the calibration curve has changed little between the first analysis and after 5000 analyses, demonstrating both the durability and reproducibility of this analytical technique. Although many soft-gel media are also available for antibody immobilization, these media do not withstand high linear velocity and, therefore, are not suited for high-performance affinity chromatography.

Affinity chromatography using immobilized antibodies offers several advantages over conventional chromatographic assay development. First, assay development can be very rapid because specificity is an inherent property of antibody and solvent mobile-phase selection is limited to a capture buffer and an elution buffer, which is often the same from one antibody to the next. Therefore, there is less “column scouting” for appropriate conditions. In addition, the assays are fast (see above) and chromatograms yield only two peaks instead of multiple peaks. Furthermore, the two peaks in the affinity chromatogram indicate both antigen concentration (from the eluted peak) and purity (from the ratio of the eluted peak to the total peak area). Thus, affinity chromatography with immobilized antibodies allows both fast assay development and rapid analysis times.

The limitations of immobilized antibody affinity chromatography are few. First, plentiful amounts of antibody, usually milligram quantities, are required to get reasonable ligand density on a useful amount of chromatographic media. Also, it is optimal if the antibody is antigen affinity purified, so that when it is immobilized, no other contaminating proteins with competing specificity dilute the antibody's concentration. Finally, the antibody must be amenable to affinity chromatography such that it is not irreversibly denatured by the immobilization process and can withstand many cycles of antigen capture and elution. Both monoclonal and polyclonal antibodies have been used successfully.



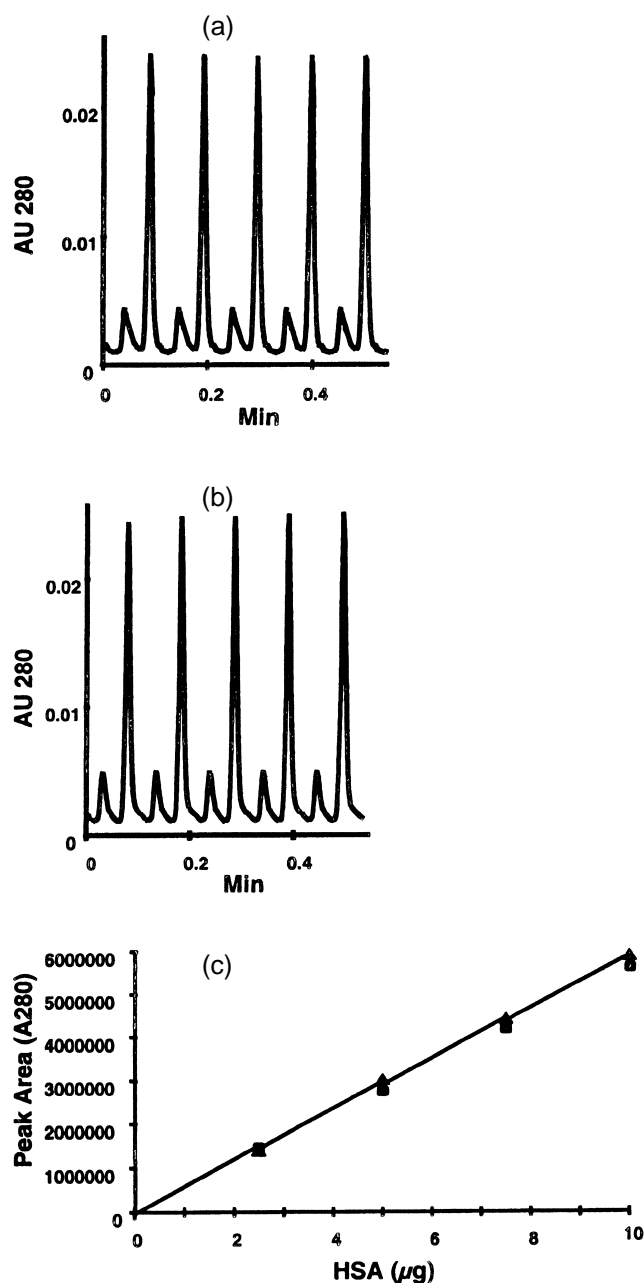


Fig. 1 Examples of affinity chromatography with an epoxy-immobilized polyclonal anti-human serum albumin (HSA) antibody in a 2.1-mm-inner diameter \times 30-mm POROS CO column run at 5 mL/min (8000 cm/h) using phosphate-buffered saline for loading and 12 mM HCl with 150 mM NaCl for elution. The sample was 10 μ g HSA at 1 mg/mL. (a) shows the first five analyses of a relatively pure sample of HSA, where the first small peak is the unbound contaminant and the larger peak is the elution of the HSA from the affinity column. (b) shows the results of the last 5 analyses from a set of 5000 and (c) shows the calibration curve before (squares) the 5000 analyses and after (triangles).

Immobilization Chemistries

Many different chemistries can be used to immobilize antibodies onto chromatographic media and only a few will be discussed. In most cases, the chromatographic media is coated with the active chemistry, which will then react with the antibody. These include amine reactive chemistries such as epoxide-, aldehyde-, and cyanogen bromide (CNBr)-activated media, carboxyl reactive chemistries such as carbodiimides, aldehyde-reactive chemistries such as amino and hydrazide, and thiol-reactive chemistries such as iodoacetyl and reduce thiol media. Although there are several antibody isotypes (IgA, IgE, IgG, IgM), the most common antibody immobilized for affinity chromatography is IgG, which is composed of four polypeptide chains (two heavy and two light) which are disulfide linked to form a Y-shaped structure capable of binding two antigens. For best results, it is also important to antigen affinity purify the antibody prior to immobilization to yield optimum binding capacity and a wider dynamic range for analytical work. Also note that the antibody may be digested with pepsin or papain to separate the constant region from the antigen-binding domains, which may then be immobilized.

Antibodies are very often immobilized through their amino groups either through the N-terminal amines or the epsilon amino groups of lysine. Reactions with epoxide-activated media are performed under alkaline conditions and lead to extremely stable linkages between the chromatographic support and the antibody. Similarly, immobilization using an aldehyde-activated media first proceeds through a Schiff base intermediate which must then be reduced (often by sodium cyanoborohydride) to yield a very stable carbon–nitrogen bond linking the antibody to the media. *N*-Hydroxy-succinimide-activated media also couples via primary amines and leads to a stable linkage in a single-step reaction. The major advantage of these chemistries is that they are extremely stable due to the formation of covalent bonds to the media. Although less stable but easy to use is CNBr-activated media, which also immobilizes antibodies through their primary amines.

Antibodies can also be immobilized through their carboxyl groups by first treating them with a carbodiimide such as EDC (1-ethyl-3-[3-dimethylamino-propyl]-carbodiimide) followed by immobilization on an amine-activated chromatographic resin. It is important to note that EDC does not add a linker chain between the antibody and the media, but simply facilitates the formation of an amide bond between the

antibody's carboxyl and the amine on the media. Coupling through sulfhydryls on free cysteines can be accomplished with thiol-activated media by formation of disulfide bonds between the media and the antibody. However, this coupling is not stable to reducing conditions and a more stable iodoacetyl-activated media is often preferred because the resulting carbon-sulfur bond is more stable. Free cysteines can be generated in the antibody by use of mild reducing agents (e.g., 2-mercaptoethylamine), which can selectively reduce disulfide bonds in the hinge region of the antibody. Alternatively, antibodies may also be immobilized through their carbohydrate moieties. One method involves oxidation of the carbohydrate with sodium periodate to generate two aldehydes in the place of vicinyl hydroxyls. These aldehydes may then be coupled either directly to hydrazide-activated media or through amine-activated media with the addition of sodium cyanoborohydride to reduce the Schiff base. The primary advantages of these chemistries is to offer alternative linkages to the antibody beyond primary amines.

In addition, antibodies may also be coupled to other previously immobilized proteins. For example, the antibody may be first captured on protein A or protein G media and then cross-linked to the immobilized protein A or G with reagents such as glutaraldehyde or dimethyl pimelimidate. The advantage here is that the antibody need not be pure prior to coupling because the protein A or protein G will selectively bind only antibody and none of the other serum proteins. The disadvantage is that free protein A or protein G will still be available to cross-react with any free antibody in samples to be analyzed, which will only be problematic with serum-based samples.

Antibody coupling does not need to be covalent to be effective. For example, biotinylated antibodies can be coupled to immobilized streptavidin. The avidin-biotin interaction is extremely strong and will not break under normal antigen elution conditions. The advantage of this immobilization protocol is that many different biotinylation reagents are available in a wide range of chemistries and linker chain lengths. Once biotinylated and free biotin are removed, the antibody is simply injected onto the streptavidin column and it is ready for use. Immobilization can be accomplished through hydrophobic interaction by simply injecting the antibody onto a reversed-phase column and then blocking with an appropriate protein solution such as albumin, gelatin, or milk. This is analogous to techniques used to coat ELISA plates and perform Western blots, and although this noncovalent coupling is

not stable to organic solvents and detergents, it can last for hundreds of analyses under the normal aqueous analysis conditions. The advantage of this immobilization is that it can be done very quickly (in several minutes) by simply injecting an antibody first and then a blocking agent.

Operation

A wide range of buffers can be used for loading the sample and eluting the bound antigen; however, for best analytical performance, a buffer system that has low a low ultraviolet (UV) cutoff and rapid reequilibration properties is desirable. One of the better examples is phosphate-buffered saline (PBS) for loading and 12 mM HCl with 150 mM NaCl. The NaCl is not required in the elution buffer but helps to minimize baseline disturbances due to the refractive index change between the PBS loading buffer and the elution buffer because both will contain about 150 mM NaCl. UV detection is well suited for these assays and wavelengths at 214 or 280 nm are commonly used.

For analytical work, large binding capacities are not required, but increased capacity does increase the dynamic range of the analysis. However, the dynamic range can be increased by injecting a smaller volume of sample onto the column at the expense of sensitivity at the low end of the calibration curve. Likewise, sensitivity can be increased by injecting more sample volume.

Application Examples

The most obvious way to use immobilized antibodies for analytical affinity chromatography is to simply use it in a traditional single-column method to determine an antigen's concentration and/or purity. However, there are a number of ways this technique can be advanced to more sophisticated analyses. For example, instead of immobilizing an antibody, the antigen may be immobilized to quantify the antibody as has been done with the Lewis Y antigen [3]. However, the analysis is still a single-column method.

Immobilized antibodies have also been used extensively in multidimensional liquid chromatography (MDLC) analyses. As shown in Fig. 2, an affinity column with immobilized anti-HSA is used to capture all of the human serum albumin in a sample, allowing all of the other components to flow through to waste. Then, the affinity chromatography column is eluted directly into a size-exclusion column where albumin



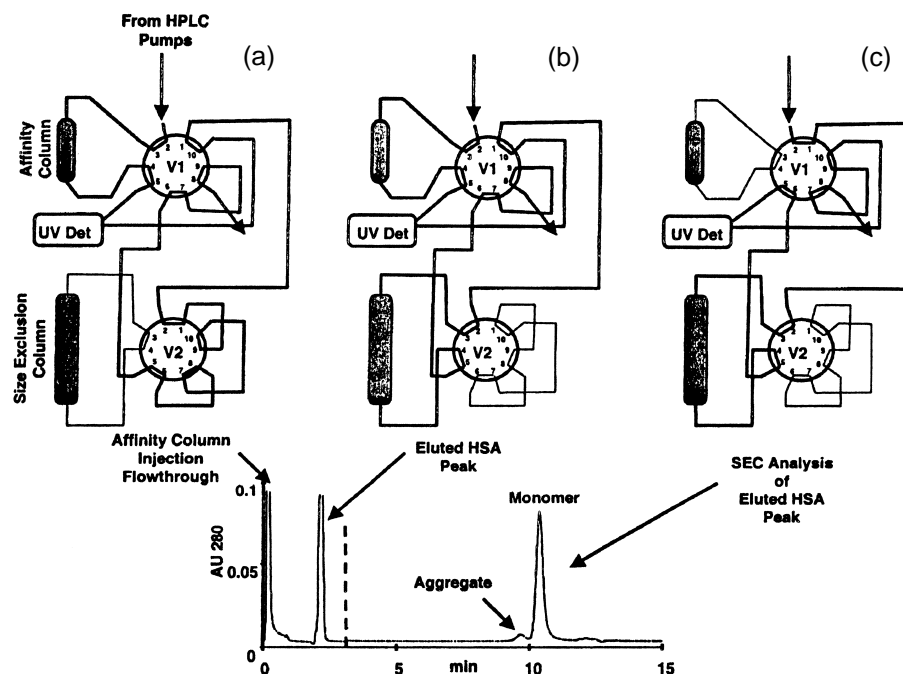


Fig. 2 Example of a multidimensional liquid chromatographic analysis for albumin aggregates using immobilized antibody affinity chromatography with size-exclusion chromatography. (a) Shows the flow path during the loading of the sample to capture the albumin monomer and aggregates while allowing all other proteins to elute to waste. (b) Shows the transfer of the albumin and its aggregates to the size-exclusion column. (c) Shows the flow path used to elute the size-exclusion column to separate the aggregate and monomer. (d) Shows the UV trace from this analysis. Note that in this plumbing configuration, the albumin passes through the detector twice, once as it is transferred from the affinity to the size-exclusion column and again as the albumin elutes from the size-exclusion column. The affinity column is a 2.1-mm-inner diameter (i.d.) \times 30 mm POROS XL column to which anti-human serum albumin has been covalently cross-linked, run at 1 mL/min, loaded in PBS, and eluted with 12 mM HCl. The size-exclusion column is a 7.5-mm-i.d. \times 300-mm Ultrasphere OG run at 1 mL/min with 100 mM potassium phosphate with 100 mM sodium phosphate, pH 7.0. The sample was 100 μ g heat-treated albumin.

monomers and aggregates are separated and quantified. In this example, neither mode of chromatography would be sufficient by itself. The affinity media does not distinguish between monomer and aggregate, and the size-exclusion column would not be able to discriminate between albumin and the other coeluting proteins in the sample. Other MDLC applications employing immobilized antibodies include an acetylcholine esterase assay utilizing size-exclusion chromatography [4], combinations of immobilized antibodies with reversed-phase analysis [5–7], protein variant determination using immobilized antibodies to select hemoglobin from a biological sample followed by on-column proteolytic digestion, and liquid chromatography–mass spectrometry peptide mapping [8].

There are many more examples of immobilized antibodies used for affinity chromatography which are not mentioned here, but it was the goal of this section

to present some of the capabilities of this technique for analytical chromatographic applications.

References

1. N. B. Afeyan, N. F. Gordon, I. Mazsaroff, L. Varady, S. P. Fulton, Y. B. Yang, and F. E. Regnier, Flow-through particles for the high-performance liquid chromatographic separation of biomolecules: Perfusion chromatography, *J. Chromatogr.* 519(1): 1 (1990).
2. N. B. Afeyan, N. F. Gordon, and F. E. Regnier, "Automated real-time immunoassay of biomolecules," *Nature* 358(6387): 603 (1992).
3. M. A. Schenerman and T. J. Collins, "Determination of a monoclonal antibody binding activity using immunodetection," *Anal. Biochem.* 217(2): 241 (1994).
4. M. Vanderlaan, R. Lotti, G. Siek, D. King, and M. Goldstein, Perfusion immunoassay for acetylcholinesterase: ana-

- lyte detection based on intrinsic activity, *J. Chromatogr. A* 711(1): 23 (1995).
5. B. Y. Cho, H. Zou, R. Strong, D. H. Fisher, J. Nappier, and I. S. Krull, Immunochromatographic analysis of bovine growth hormone releasing factor involving reversed-phase high-performance liquid chromatography-immunodetection, *J. Chromatogr. A* 743(1): 181 (1996).
 6. J. E. Battersby, M. Vanderlaan, and A. J. Jones, Purification and quantitation of tumor necrosis factor receptor immunoadhesin using a combination of immunoaffinity and reversed-phase chromatography, *J. Chromatogr. B* 728(1): 21 (1999).
 7. C. K. Holtzapple, S. A. Buckley, and L. H. Stanker, Determination of four fluoroquinolones in milk by on-line immunoaffinity capture coupled with reversed-phase liquid chromatography, *J. AOAC Int.* 82(3): 607 (1999).
 8. Y. L. Hsieh, H. Wang, C. Elicone, J. Mark, S. A. Martin, and F. Regnier, Automated analytical system for the examination of protein primary structure, *Anal. Chem.* 68(3): 455 (1996).



Affinity Chromatography: An Overview

David S. Hage
William Clarke

University of Nebraska, Lincoln, Nebraska, U.S.A.

Introduction

Affinity chromatography is a liquid chromatographic technique that uses a “biologically related” agent as a stationary phase for the purification or analysis of sample components [1–4]. The retention of solutes in this method is generally based on the same types of specific, reversible interactions that are found in biological systems, such as the binding of an enzyme with a substrate or an antibody with an antigen. These interactions are exploited in affinity chromatography by immobilizing (or adsorbing) one of a pair of interacting molecules onto a solid support and using this as a stationary phase. This immobilized molecule is known as the *affinity ligand* and is what gives an affinity column the ability to bind to particular compounds in a sample.

Affinity chromatography is a valuable tool in areas such as biochemistry, pharmaceutical science, clinical chemistry, and environmental testing, where it has been used for both the purification and analysis of compounds in complex sample mixtures [1–5]. The strong and relatively specific binding that characterizes many affinity ligands allows solutes that are quantitated or purified by these ligands to be separated with little or no interferences from other sample components. Often, the solute of interest can be isolated in one or two steps, with purification yields of 100-fold to several thousand-fold being common [2]. Similar selectivity has been observed when using affinity chromatography for compound quantitation in such samples as serum, plasma, urine, food, cell cultures, water, and soil extracts [3–5].

General Formats for Affinity Chromatography

The most common scheme for performing affinity chromatography is by using a step gradient for elution, as shown in Fig. 1. This involves injecting a sample onto the affinity column in the presence of a mobile phase that has the right pH and solvent composition for solute–ligand binding. This solvent, which repre-

sents the weak mobile phase of the affinity column, is called the application buffer. During the application phase of the separation, compounds which are complementary to the affinity ligand will bind as the sample is carried through the column by the application buffer. However, due to the high selectivity of the solute–ligand interaction, the remainder of the sample components will pass through the column nonretained. After the nonretained components have been completely washed from the column, the retained solutes can be eluted by applying a solvent that displaces them from the column or that promotes dissociation of the solute–ligand complex. This solvent represents the strong mobile phase for the column and is known as the elution buffer. As the solutes of interest elute from the column, they are either measured or collected for later use. The column is then regenerated by reequilibration with the application buffer prior to injection of the next sample [2–4].

Even though the step-gradient, or “on/off” elution method illustrated in Fig. 1 is the most common way of performing affinity chromatography, it is sometimes possible to use affinity methods under isocratic conditions. This can be done if a solute’s retention is sufficiently weak to allow elution on the minute-to-hour time scale and if the kinetics for its binding and dissociation are fast enough to allow a large number of solute–ligand interactions to occur as the analyte travels through the column. This approach is sometimes called weak-affinity chromatography and is best performed if a solute binds to the ligand with an association constant that is less than or equal to about 10^4 – $10^6 M^{-1}$ [3,6].

Types of Affinity Ligands

The most important factor in determining the success of any affinity separation is the type of ligand that is used within the column. A number of ligands that are commonly used in affinity chromatography are listed in Table 1. Most of these ligands are of biological origin, but a wide range of natural and synthetic mole-



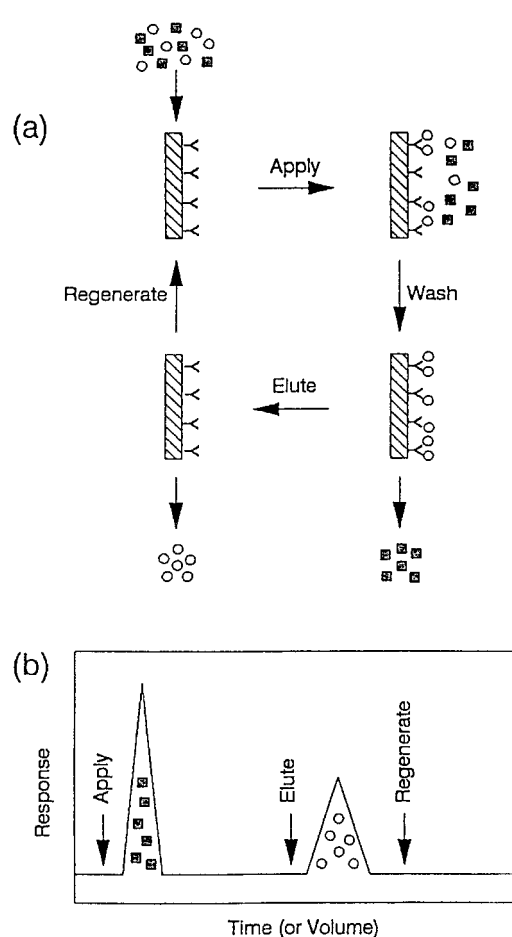


Fig. 1 (a) Typical separation scheme and (b) chromatogram for affinity chromatography. The open circles represent the test analyte and the squares represent other, nonretained sample components. [Reproduced with permission from the Clinical Ligand Assay Society from D. S. Hage, *J. Clin. Ligand Assay* 20: 293 (1998).]

cules of nonbiological origin can also be used. Regardless of their origin, all of these ligands can be placed into one of two categories: high-specificity ligands or general ligands [2–4].

The term *high-specificity ligand* refers to a compound which binds to only one or a few closely related molecules. This type of ligand is used in affinity systems where the goal is to analyze or purify a specific solute. Examples include antibodies (for binding antigens), substrates or inhibitors (for separating enzymes), and single-stranded nucleic acids (for the retention of a complementary sequence). As this list suggests, most high-specificity ligands tend to be of biological origin and often have large association constants for their particular analytes. *General*, or *group-*

specific, ligands are compounds which bind to a family or class of related molecules. These ligands are used when the goal is to isolate a class of structurally related compounds. General ligands can be of either biological or nonbiological origin and include compounds such as protein A or protein G, lectins, boronates, triazine dyes, and immobilized metal chelates. This class of ligands usually exhibits weaker binding for solutes than is seen with high-specificity ligands; however, some general ligands like protein A and protein G do have association constants that rival those of high-specificity ligands [7].

Support Materials

Another important factor to consider in affinity chromatography is the material used to hold the ligand within the column. Ideally, this support should have low nonspecific binding for sample components, it should be easy to modify for ligand attachment, and it should be stable under the flow-rate, pressure, and solvent conditions that will be employed in the analysis or purification of samples. Depending on what type of support material is being used, affinity chromatography can be characterized as being either a low- or high-performance technique [4].

In *low-performance* (or *column*) *affinity chromatography*, the support is usually a large-diameter, nonrigid

Table 1 Common Ligands Used in Affinity Chromatography

Type of ligand	Examples of retained compounds
<i>High-Specificity Ligands</i>	
Antibodies	Various agents (drugs, hormones, peptides, proteins, viruses, etc.)
Enzyme inhibitors and cofactors	Enzymes
Nucleic acids	Complementary nucleic acid strands and DNA/RNA-binding proteins
<i>General Ligands</i>	
Lectins	Small sugars, polysaccharides, glycoproteins, and glycolipids
Protein A and protein G	Intact antibodies and Fc fragments
Boronates	Catechols and compounds which contain sugar residues, such as polysaccharides and glycoproteins
Synthetic dyes	Dehydrogenases, kinases and other proteins
Metal chelates	Metal-binding amino acids, peptides, or proteins

material (e.g., a carbohydrate-based gel or one of several synthetic organic-based polymers). The low back pressures that are produced by these supports means that these materials can often be operated under gravity flow or with a peristaltic pump, making them relatively simple and inexpensive to use for affinity purifications or in sample pretreatment. Disadvantages of these materials include their slow mass-transfer properties and their limited stabilities at high flow rates and pressures. These factors tend to limit the direct use of these supports in analytical applications, where both rapid and efficient separations are usually desired [2,5].

High-performance affinity chromatography (HPAC) is characterized by a support which consists of small, rigid particles capable of withstanding high flow rates and/or pressures [2–4,8,9]. Examples of affinity supports that are suitable for work under these conditions include modified silica or glass, azalactone beads, and hydroxylated polystyrene media. The stability and efficiency of these supports allows them to be used with standard high-performance liquid chromatography (HPLC) equipment. Although the need for HPLC instrumentation does make HPAC more expensive to perform than low-performance affinity chromatography, the better speed and precision of HPAC makes it the affinity method of choice for many analytical applications.

Immobilization Methods

A third item to consider in affinity chromatography is the way in which the ligand is attached to the solid support, or the *immobilization method*. For a protein or peptide, this generally involves coupling the molecule through free amine, carboxylic acid, or sulfhydryl residues present in its structure. Immobilization of a ligand through other functional sites (e.g., aldehyde groups produced by carbohydrate oxidation) is also possible. All immobilization methods involve at least two steps: (a) an *activation step*, in which the support is converted to a form which can be chemically attached to the ligand, and (b) a *coupling step*, in which the affinity ligand is attached to the activated support. Occasionally, a third step is necessary to remove remaining activated groups.

The method by which an affinity ligand is immobilized is important because it can affect the actual or apparent activity of the final affinity column. If the correct procedure is not used, a decrease in ligand activity can result from multisite attachment, improper orientation, and/or steric hindrance. *Multisite attachment* refers to

the coupling of a ligand to the support through more than one functional group, which can lead to distortion of the ligand's active region and a loss of activity. This can be avoided by using a support with a limited number of activated sites or by using a method that couples through groups that occur only a few places in the structure of the ligand. *Improper orientation* can lead to a loss in activity by coupling the ligand to the support through its active region; this can be minimized by coupling through functional groups that are distant from this region. *Steric hindrance* refers to the loss of ligand activity due to the presence of a nearby support or neighboring ligand molecules that interfere with solute binding. This effect can be avoided through the use of a spacer arm or by using supports that contain a relatively low coverage of the ligand.

Application and Elution Conditions

Two other items that must be considered in affinity chromatography are the application and elution buffers. Most application buffers in affinity chromatography are solvents that mimic the pH, ionic strength, and polarity experienced by the solute and ligand in their natural environment. This gives the solute its highest association constant for the ligand and, thus, its highest degree of retention on the column. The application buffer should also be chosen so that it minimizes nonspecific binding due to undesired sample components.

Elution conditions in affinity chromatography are usually chosen so that they promote either the fast or gentle removal of solute from the column. The two approaches used for this are *nonspecific elution* and *biospecific elution*, respectively [2]. Biospecific elution is based on the addition of a competing agent that gently displaces a solute from the column. This is done by either adding an agent that competes with the ligand for solute (i.e., *normal-role elution*) or that competes with the solute for ligand-binding sites (i.e., *reversed-role elution*). Although it is a gentle method, biospecific elution does result in long elution times and broad solute peaks that are difficult to quantitate. Nonspecific elution uses a solvent that directly promotes weak solute–ligand binding. For instance, this is done by changing the pH, ionic strength or polarity of the mobile phase or by adding a denaturing agent or chaotropic substance to the elution buffer. Nonspecific elution tends to be much faster than biospecific elution and results in sharper peaks with lower limits of detection. However, care must be exercised in nonspecific



elution to avoid using a buffer which is too harsh and causes solute denaturation or a loss of ligand activity.

Types of Affinity Chromatography

There are many types of affinity chromatography that are in common use. *Bioaffinity chromatography* is probably the broadest category and includes any method that uses a biological molecule as the affinity ligand. *Immunoaffinity chromatography* (IAC) is a special category of bioaffinity chromatography in which the affinity ligand is an antibody or antibody-related agent [3,5,8,10]. This creates a highly specific method that is ideal for use in affinity purification or in analytical methods that involve complex samples. *Immunoextraction* is a subcategory of IAC in which an affinity column is used to isolate compounds from a sample prior to analysis by a second method. IAC can also be used to monitor the elution of analytes from other columns, giving rise to a scheme known as *postcolumn immunodetection*. Another common type of bioaffinity method is that which uses bacterial cell-wall proteins like protein A or protein G for antibody purification. In *lectin affinity chromatography*, immobilized lectins like concanavalin A or wheat germ agglutinin are used for binding to molecules which contain certain sugar residues. Additional types of bioaffinity chromatography are those that make use of ligands which are enzymes, inhibitors, cofactors, nucleic acids, hormones, or cell receptors [1–4].

There are also many types of affinity chromatography that use ligands which are of a nonbiological origin. One example is *dye-ligand affinity chromatography*, which uses an immobilized synthetic dye that mimics the active site of a protein or enzyme. This is a popular tool for enzyme and protein purification. *Immobilized metal-ion affinity chromatography* (IMAC) is an affinity technique in which the ligand is a metal ion which is complexed with an immobilized chelating agent. This is used to separate proteins and peptides that contain amino acids with electron-donor groups. *Boronate affinity chromatography* employs boronic acid or a boronate as the affinity ligand. These ligands are useful

in binding to compounds which contain *cis*-diol groups, such as catecholamines and glycoproteins [1–4].

There are a number of other chromatographic methods closely related to traditional affinity chromatography. For instance, affinity chromatography can be adapted as a tool for studying solute–ligand interactions. This application is known as *analytical*, or *quantitative*, *affinity chromatography* and can be used to acquire information regarding the equilibrium and rate constants for biological interactions, as well as the number and type of binding sites that are involved in these interactions [11]. Other methods that are related to affinity chromatography include *hydrophobic interaction chromatography* (HIC) and *thiophilic adsorption*. HIC is based on the interactions of proteins, peptides, and nucleic acids with short nonpolar chains, such as those that were originally used as spacer arms on affinity supports. Thiophilic adsorption, also known as *covalent* or *chemisorption chromatography*, makes use of immobilized thiol groups for solute retention. Applications of this method include the analysis of sulfhydryl-containing peptides or proteins and mercurated polynucleotides. Finally, many types of *chiral liquid chromatography* can be considered affinity methods because they are based on binding agents which are of a biological origin. Examples include columns which use cyclodextrins or immobilized proteins for chiral separations [4].

References

1. J. Turkova, *Affinity Chromatography*, Elsevier, Amsterdam, 1978.
2. R. R. Walters, *Anal. Chem.* 57: 1099A (1985).
3. D. S. Hage, *Handbook of HPLC*, E. Katz, R. Eksteen, and N. Miller (eds.), Marcel Dekker, Inc., New York, 1998, Chap. 13.
4. D. S. Hage, *Clin. Chem.* 45: 593 (1999).
5. D. S. Hage, *J. Chromatogr. B* 715: 3 (1998).
6. D. Zopf and S. Ohlson, *Nature* 346: 87 (1990).
7. R. Lindmark, C. Biriell, and J. Sjöquist, *Scand. J. Immunol.* 14: 409 (1981).
8. M. de Frutos and F. E. Regnier, *Anal. Chem.* 65: 17A (1993).
9. S. Ohlson, L. Hansson, P.-O. Larsson, and K. Mosbach, *FEBS Lett.* 93: 5 (1978).
10. G. J. Calton, *Methods Enzymol.* 104: 381 (1984).
11. I. M. Chaiken (ed.), *Analytical Affinity Chromatography*, CRC Press, Boca Raton, FL, 1987.



Aggregation of Colloids by Field-Flow Fractionation

Athanasia Koliadima

University of Patras, Patras, Greece

Introduction

The separation of the components of complex colloidal materials is one of the most difficult challenges in separation science. Most chromatographic methods fail in the colloidal size range or, if operable, they perform poorly in terms of resolution, recovery, and reproducibility. Therefore, it is desirable to examine alternate means that might solve important colloidal separation and characterization problems encountered in working with biological, industrial, environmental, and geological materials. One of the most important colloidal processes that is generally quite difficult to characterize is the aggregation of single particles to form complexes made up of multiples of the individual particles. Aggregation is a common phenomenon for both natural and industrial colloids. The high degree of stability, which is frequently observed in colloidal systems, is a kinetic phenomenon in that the rate of aggregation of such systems may be practically zero. Thus, in studies of the colloidal state, the kinetics of aggregation are of paramount importance. Although the kinetics of aggregation can be described easily by a bimolecular equation, it is not an easy thing to do experimentally.

One technique for doing this is to count the particles microscopically. In addition to particle size limitation, this is an extraordinarily tedious procedure. Light scattering can be also used for the kinetic study of aggregation, but experimental turbidities must be interpreted in terms of the number and size of the scattering particles.

In the present work, it is shown that the field-flow fractionation (FFF) technique can be used with success to study the aggregation phenomena of colloids.

The techniques of field-flow fractionation appear to be well suited to colloid analysis. The special subtechnique of sedimentation FFF (SdFFF) is particularly effective in dealing with colloidal particles in the diameter range from 0.02 to 1 μm , using the normal or Brownian mode of operation (up to 100 μm using the steric-hyperlayer mode). As a model sample for the observation of aggregate particles by SdFFF, of

poly(methyl methacrylate) was used, whereas for the kinetic study of aggregation by SdFFF, the hydroxyapatite sample $[\text{Ca}_5(\text{PO}_4)_3\text{OH}]$ consisting of submicron irregularly shaped particles was used. The stability of hydroxyapatite, which is of paramount importance in its applications, is dependent on the total potential energy of interaction between the hydroxyapatite particles. The latter, which is the sum of the attraction potential energy and that of repulsion, depends on particle size, the Hamaker constant, the surface potential, and the Debye–Hückel reciprocal distance, which is immediately related to the ionic strength of carrier solution.

Methodology

Field-flow fractionation is a highly promising tool for the characterization of colloidal materials. It is a dynamic separation technique based on differential elution of the sample constituents by a laminar flow in a flat, ribbonlike channel according to their sensitivity to an external field applied in the perpendicular direction to that of the flow.

The total potential energy of interaction between two colloidal particles, U_{tot} , is given by the sum of the energy of interaction of the double layers, U_R , and the energy of interaction of the particles themselves due to van der Waals forces, U_A . Consequently,

$$U_{\text{tot}} = U_R + U_A \quad (1)$$

For identical spherical particles U_R and U_A are defined as follows:

$$U_R = \frac{\epsilon r \psi_0^2}{2} \ln[1 + \exp(-\kappa H)] \quad (\kappa r \gg 1) \quad (2)$$

$$U_R = \frac{\epsilon r \psi_0^2}{R} \exp(-\kappa H) \quad (\kappa r \ll 1) \quad (3)$$

$$U_A = -\frac{A_{212}r}{12H} \quad (4)$$



where ϵ is the dielectric constant of the dispersing liquid, r is the radius of the particle, Ψ_0 is the particle's surface potential, κ is the reciprocal double-layer thickness, R is the distance of the centers of the two particles, A_{212} is the effective Hamaker constant of two particles of type 2 separated by the medium of type 1, and H is the nearest distance between the surfaces of the particles.

Equations (2)–(4) show that the total potential energy of interaction between two colloidal spherical particles depends on the surface potential of the particles, the effective Hamaker constant, and the ionic strength of the suspending medium. It is known that the addition of an indifferent electrolyte can cause a colloid to undergo aggregation. Furthermore, for a particular salt, a fairly sharply defined concentration, called “critical aggregation concentration” (CAC), is needed to induce aggregation.

The following equation gives the rate of diffusion-controlled aggregation, u_r , of spherical particles in a disperse system as a result of collisions in the absence of any energy barrier to aggregate:

$$u_r = -k_r N_0^2 \quad (5)$$

where k_r is the second-order rate constant for diffusion-controlled rapid aggregation and N_0 is the initial number of particles per unit volume.

In the presence of an energy barrier to aggregate, the rate of aggregation, u_s , is

$$u_s = -k_s N_0^2 \quad (6)$$

where k_s is the rate constant of slow aggregation in the presence of an energy barrier.

The stability ratio, w , of a dispersion is defined as the ratio of the rate constants for aggregation in the absence, k_r , and the presence, k_s , of an energy barrier, respectively:

$$w = \frac{k_r}{k_s} \quad (7)$$

The aggregation process is described by the bimolecular kinetic equation

$$\frac{1}{N_i} = \frac{1}{N_0} + k_{app} t_i \quad (8)$$

where N_i is the total number of particles per unit volume at time t_i and k_{app} is the apparent rate constant for the aggregation process. The measurement of the independent kinetic units per unit volume, N_i , at different times t_i can give the rate constant for the aggregation process.

Considering that d_{N_0} and d_{N_i} are the measured number-average diameters of the particles at times $t = 0$ and t_i , respectively, Eq. (8), for polydisperse samples, gives

$$d_{N_i}^3 = d_{N_0}^3 + d_{N_0}^3 N_0 k_{app} t_i \quad (9)$$

Equation (9) shows that from the slope of the linear plot of the $d_{N_i}^3$ versus t_i , the apparent rate constant k_{app} can be determined, as the N_0 values can be found from the ratio of the total volume of the injected sample to the volume of the particle, which can be determined from the diameter calculated from the intercept of the above plot.

Applications

The observation of a series of peaks (Fig. 1) while analyzing samples of poly(methyl methacrylate) (PMMA) colloidal latex spheres by SdFFF suggests that part of the latex population has aggregated into

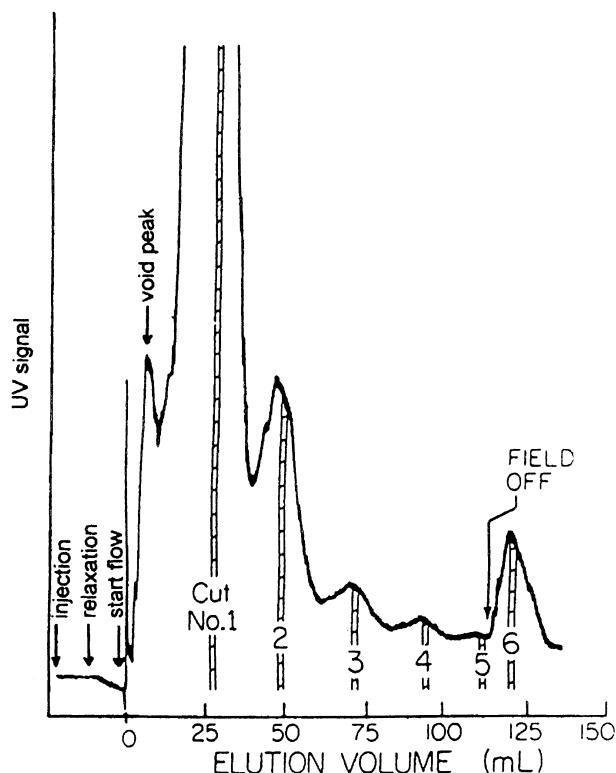


Fig. 1 Sedimentation field-flow fractionation fractogram of 0.207- μ m poly(methyl methacrylate) aggregate series from which six cuts were collected and analyzed by electron microscopy. Experimental conditions: field strength of 61.6 g and flow rate of 0.84 mL/min. [Reproduced with permission from H. K. Jones et. al. (1988) *J. Chromatogr.* 455: 1; Copyright Elsevier Science Publishers B. V.]

doublets, triplets, and higher-order particle clusters. The particle diameter of the latex spheres was given as $0.207\ \mu\text{m}$. The aggregation hypothesis is confirmed by retention calculations and by electron microscopy. For this purpose, narrow fractions or cuts were collected from the first five peaks as shown in Fig. 1. A fraction was also collected for the peak which appeared after the field was turned off. The individual fractions were subjected to electron microscopy and as expected, cut No. 1 yielded singlets, cut No. 2 yielded doublets, cut No. 3 yielded triplets, cut No. 4 yielded quads, cut No. 5 yielded quintets, and the cut after the field was turned off yielded clusters from six individual particles.

Sedimentation field-flow fractionation was used also for the kinetic study of hydroxyapatite (HAP) particles' aggregation in the presence of various electrolytes to determine the rate constants for the bimolecular process of aggregation and to investigate the possible aggregation mechanisms describing the experimental data. The HAP sample contained polydisperse, irregular colloidal particles with number-average diameter $d_N = 0.262 \pm 0.046\ \mu\text{m}$.

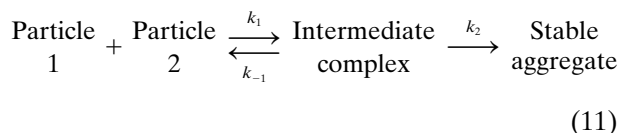
The number-average diameter, d_N , for the HAP particles increases with the electrolyte KNO_3 concentration until the critical aggregation concentration is reached, where the d_N value remains approximately constant. The starting point of the maximum d_N corresponds to the electrolyte concentration called CAC. The last value, which depends on the electrolyte used, was found to be $1.27 \times 10^{-2} M$ for the electrolyte KNO_3 .

According to Eq. (9), the plot of d_N^3 versus t_i at various electrolyte concentrations determines the apparent rate constant, k_{app} , of the HAP particles' aggregation. The found k_{app} value for the aggregation of the HAP particles in the presence of $1 \times 10^{-3} M$ KNO_3 is $2.5 \times 10^{-21}\ \text{cm}^3/\text{s}$. It is possible to make a calculation which shows whether the value of k_{app} is determined by the rate at which two HAP particles can diffuse up to each other (diffusion control) or whether the rate of reaction is limited by other slower processes. The rate constant for the bimolecular collision (k_1) of the HAP particles, can be calculated by the Stokes–Einstein equation:

$$k_1 = \frac{8kT}{3n} \text{cm}^3/\text{s} \quad (10)$$

where n is the viscosity of the medium. The calculated value of $k_1 = 1.1 \times 10^{-11}\ \text{cm}^3/\text{s}$ is about 10 orders of magnitude greater than the value of k_{app} actually measured. So, the aggregation rates are slower than those expected if the process was simply diffusion controlled

when electrostatic repulsion is absent. The latter indicates that the minimal mechanism for the aggregation process of the HAP particles would be



where k_{-1} is the rate constant for the dissociation of the intermediate aggregate and k_2 is the rate constant for the process representing the rate-determining step in the aggregation reaction. Because k_{app} , describing the overall process, is smaller than the calculated k_1 value, there must be rapid equilibration of the individual particles and their intermediate complexes followed by the slower step of irreversible aggregation. The stability factor, w , of HAP's particles found to be 4.4×10^9 is too high, indicating that the particles are very stable, even in the presence of significant quantity of the electrolyte KNO_3 .

As a general conclusion, the FFF method can be used with success to study the aggregation process of colloidal materials.

Future Developments

Looking to the future, it is reasonable to expect continuous efforts to improve the theoretical predictions and more experimental work to investigate the aggregation phenomena of natural and industrial colloids.

Suggested Further Reading

- Athanasopoulou, A., G. Karaiskakis, and A. Travlos, *J. Liq. Chromatogr. Related Technol.* 20 (16&17): 2525 (1997).
- Athanasopoulou, A., D. Gavril, A. Koliadima, and G. Karaiskakis, *J. Chromatogr. A* 845: 293 (1999).
- Caldwell, K. D., T. T. Nguyen, J. C. Giddings, and H. M. Mazzone, *J. Virol. Methods* 1: 241 (1980).
- Everett, D. H., *Basic Principles of Colloid Science*, Royal Society of Chemistry Paperbacks, London, 1988.
- Family, F. and D.P. Landan (eds.), *Kinetic of Aggregation and Gelation*, North-Holland, Amsterdam, 1984.
- Jones, H. K., B. N. Barman, and J. C. Giddings, *J. Chromatogr.* 455: 1 (1988).
- Koliadima, A., *J. Liq. Chromatogr. Related Technol.* 22(16): 2411 (1999).
- Wittgren, B., J. Borgström, L. Piculell, and K. G. Wahlund, *Biopolymers* 45: 85 (1998).



Alumina-Based Supports for Liquid Chromatography

Esther Forgács

Tibor Cserhádi

Institute of Chemistry, Hungarian Academy of Sciences, Budapest, Hungary

INTRODUCTION

Various liquid chromatographic techniques offer a unique possibility for the separation and quantitative determination of a large variety of organic, metalloorganic, and inorganic compounds with highly similar molecular structures. These methods are indispensable in medical practice and research, pharmaceutical chemistry, food science and technology, environmental pollution control, legislation procedures, etc. The rapid development of the theory of the retention processes in chromatography have made it obvious that the efficient separation of various compounds (selection of the best separation method, support and mobile phase, and any other parameter influencing the efficacy) requires a profound knowledge of the impact of molecular characteristics of solutes, stationary and mobile phases, and their interplay at the molecular level on retention. The expert application of such knowledge will highly facilitate the rational design of optimal separation methods. As the chemistry and physicochemistry of the surface of the support determines the retention characteristics of stationary phases, physical methods such as nuclear magnetic resonance (NMR), Fourier transform infrared (FTIR), etc., have been frequently used to study the stationary phases in liquid chromatography.

The overwhelming majority of liquid chromatographic separations are carried out in silica or in silica-based, reversed-phase (mainly octadecylsilica, ODS) stationary phases. Although the retention characteristics of silica and surface-modified silica supports are excellent, and they can be used for the successful separation of a wide variety of solutes, they also have some drawbacks. Thus, the acidic character of the free silanol groups exert a considerable impact on the retention behavior of both silica and silica-based supports; basic solutes are more strongly bonded onto the silica surface than neutral or acidic substances, resulting in unpredictable retention behavior. Moreover, silica and silica derivatives are not stable at alkaline pHs, making the separation of strongly basic compounds difficult. The objectives of the newest developments in liquid chromatography are the development and practical application of more stable supports than

silica and modified silicas, with different separation capacities (alumina, zirconia, titania, mixed oxides, and their modified derivatives, porous graphitized carbon, various polymer supports, etc.). Although these new supports show excellent separation characteristics, they are not well known, not frequently used, and the molecular basis of retention has not been elucidated in detail.

The objectives of this article are the enumeration and critical evaluation of the recent results obtained in the assessment of the relationship between the physicochemical characteristics and retention behavior of a wide variety of solutes on alumina stationary phases and the elucidation of the efficacy of various multivariate mathematical–statistical methods for the quantitative description of such relationships.

ALUMINA

Alumina offers another alternative to silica because of its inherent higher pH stability. However, in contrast to its extensive use as a medium in column chromatography for purification purposes, or for separations in the normal-phase mode, there are still relatively few reports concerning alumina-based materials in the reversed-phase mode.

The chromatographic aspects of the surface characteristics of alumina stationary phases have not been studied as profoundly as zirconia supports; however, the presence of hydroxyl and oxide ions on the surface has been reported.^[1]

Crystalline alumina may exist in various forms; the τ -form is generally used in chromatography. Alumina strongly adsorbs water molecules, as depicted in Fig. 1. The two different hydroxyl groups show acidic or alkaline properties, resulting in amphoteric characteristics and ion exchange behavior of the alumina surface, as demonstrated in Fig. 2.^[2] It has been further shown that the simultaneous interaction of pH, the composition of buffer and that of the mobile phase modifier governs the retention on alumina surfaces in ion exchange chromatography.^[3,4] The good separation characteristics of alumina stationary phase were exploited, not only in the ion-exchange mode, but also in the adsorption (direct phase)



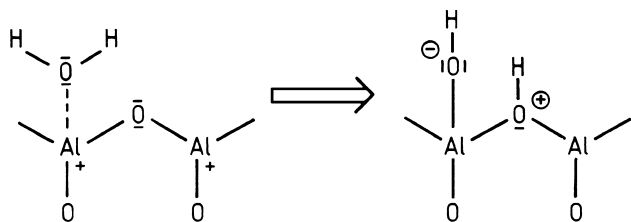


Fig. 1 Chemisorption of water on bare alumina. (From Ref. [2].)

chromatographic mode. Alumina supports have been frequently used in thin-layer chromatography (TLC), and the separation of inorganic and organometallic solutes on alumina layers was reviewed.^[5] Nonionic surfactants (α -(1,1,3,3-tetramethylbutyl)phenyl ethylene oxide oligomers) were also separated on alumina layers using *n*-hexane mixed with ethyl acetate, dioxane, and tetrahydrofuran (THF), and the data were evaluated by spectral mapping technique. Surfactants were separated according to the number of ethylene oxide groups in the molecule; surfactants with longer ethylene oxide chain were eluted later. This finding indicates that the polar ethylene oxide units turn toward the stationary phase and that they are bonded to the adsorption sites on the alumina surface. Calculations proved that the solvent strength of THF was the highest, followed by dioxane and ethyl acetate. The selectivity of ethyl acetate differed considerably from the selectivities of THF and dioxane.^[6] Other nonionic surfactants (nonylphenyl^[7] and tetrabutylphenyl^[8] ethylene-oxide oligomers) were successfully separated on an alumina high-performance liquid chromatography (HPLC) column using *n*-hexane-ethyl acetate mixtures as mobile phases. Significant linear correlations were found between the molecular parameters of the solutes and their retention characteristics:

$$\log k'_0 = 3.61 + (0.37 \pm 0.03)n_e \quad r = 0.9911 \quad (1)$$

$$b = 3.54 + (1.18 \pm 0.03)n_e \quad r = 0.9991 \quad (2)$$

where k'_0 is the capacity factor of nonylphenyl ethylene-oxide oligomer surfactants, extrapolated to zero concentration of ethyl acetate in the mobile phase; b is the slope value of the linear relationship between the $\log k'$ values of surfactants and the concentration of ethyl acetate in the eluent \pm standard deviation; and n_e is the number of ethylene oxide groups per molecule.

$$\log k'_0 = 3.41 + (0.36 \pm 0.01)n_e + (0.13 \pm 0.03)PI$$

$$F = 217.65 \quad (3)$$

$$b = 3.56 + (0.78 \pm 0.07)n_e + (0.52 \pm 0.13)PI$$

$$F = 64.65 \quad (4)$$

where PI characterizes the position of the butyl substituents, other symbols are the same as in Eqs. 1 and 2.

The data entirely support the previous conclusions concerning the retention mechanism of surfactants on alumina. Moreover, Eqs. 3 and 4 indicate that alumina is an excellent support for the separation of tetrabutylphenyl ethylene oxide oligomers according to the number of ethylene oxide groups and the position of the alkyl substituents in one run. The efficiency of alumina support for the separation of positional isomers was also established with HPLC-mass spectrometry (HPLC-MS).^[9]

MODIFIED ALUMINA

Polymers have also been used for the coating of alumina. Thus, maleic acid adsorbed onto the alumina surface was, in situ, polymerized with 1-octadecene and cross-linked with 1,4-divinylbenzene.^[10] It was assumed that the polymer forms a monolayer on the alumina, forming a reversed-phase surface. This assumption was substantiated by results showing that the retention order of model compounds was the same as on an ODS column. The lower separation capacity of the new stationary phase was tentatively explained by the lower surface porosity of alumina. Principal component analysis was employed for the elucidation of the relationship

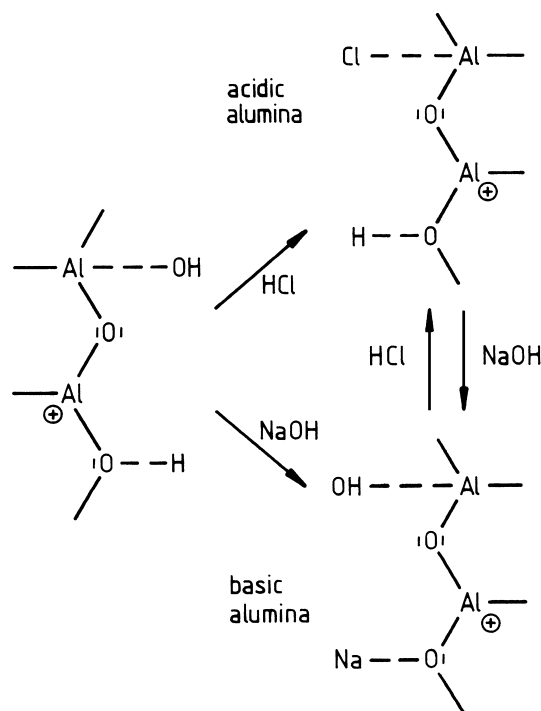


Fig. 2 Surface behavior of alumina in basic and acidic media, respectively. (From Ref. [2].)

between the retention behavior of nonhomologous series of solutes on polybutadiene (PBD)-coated alumina and their physicochemical parameters.^[11] Calculations revealed significant relationships between the capacity factor extrapolated to pure water (k'_w) and the physicochemical parameters:

$$\log k'_w = 0.052 + 0.208(\log P) \quad (5)$$

$$n = 21; s = 0.279; r = 0.9711; F = 314$$

$$\log k'_w = 1.618 + 0.089\text{bonrefr } 2.505\delta \quad (6)$$

$$n = 21; s = 0.500; r = 0.9090; F = 42.8$$

$$\log k'_w = 1.272 + 0.089\text{bonrefr } 2.648\delta + 0.598\text{ind} \quad (7)$$

$n = 21; s = 0.394; r = 0.9476; F = 49.8$ where $\log P$ is the hydrophobicity, “bonrefr” is the molecular refractivity, “delta” is the submolecular polarity parameter, “ind” indicator variable (0 for heterocyclics and 1 for benzene derivatives). Calculations indicated that PBD-coated alumina behaves as an RP stationary phase, the bulkiness and the polarity of the solute significantly influencing the retention. The separation efficiency of PBD-coated alumina was compared with those of other stationary phases for the analysis of *Catharanthus* alkaloids. It was established that the pH of the mobile phase, the concentration and type of the organic modifier, and the presence of salt simultaneously influence the retention. In this special case, the efficiency of PBD-coated alumina was inferior to that of ODS.^[12] The retention characteristics of polyethylene-coated alumina (PE-Alu) have been studied in detail using various nonionic surfactants as model compounds.^[13] It was found that PE-Alu behaves as an RP stationary phase and separates the surfactants according to the character of the hydrophobic moiety. The relationship between the physicochemical descriptors of 25 aromatic solutes and their retention on PE-coated silica (PE-Si) and PE-Alu was elucidated by stepwise regression analysis.^[14]

$$\log k'_{\text{PE-Alu}} = 0.144(\pm 0.092) + 0.9325(\pm 0.0505) \times \log k'_{\text{PE-Si}} \quad (8)$$

$$n = 25; r = 0.968; s = 0.333; F = 340$$

$$\log k'_{\text{PE-Alu}} = 1.474(\pm 0.376) + 0.5976(\pm 0.2990)R_2 + 0.9162(\pm 0.3025)\pi_2^* + 0.8279(\pm 0.2624) \times \sum \beta_2^H + 3.206(\pm 0.304)V_x \quad (9)$$

$$n = 24; r = 0.958; s = 0.397; F = 53$$

$$\log k'_{\text{PE-Si}} = 1.670(\pm 0.373) + 0.9167(\pm 0.2120)\pi_2^* + 3.842(\pm 0.267)V_x \quad (10)$$

$$n = 24; r = 0.956; s = 0.398$$

$$\log k'_{\text{PE-Alu}} = 2.122(\pm 0.549) + 2.068(\pm 0.798)\delta_{\text{max}} + 0.3283(\pm 0.0897)\mu + 0.00940(\pm 0.00111)V_{\text{aq}} \quad (11)$$

$$n = 25; r = 0.926; s = 0.525; F = 42$$

$$\log k'_{\text{PE-Si}} = 2.401(\pm 0.456) + 2.424(\pm 0.662)\delta_{\text{max}} + 0.2821(\pm 0.0746)\mu + 0.01057(\pm 0.00092)V_{\text{aq}} \quad (12)$$

$n = 25; r = 0.953; s = 0.436; F = 69$ where μ is the total dipole moment, δ_{max} is the maximum electron excess charge (electron deficiency) on an atom in the solute molecule, V_{aq} is the solvent (water) accessible molecular volume. Calculations proved that both stationary phases behave as RP supports, with the retention strength of PE-Si being higher. The retention can be successfully related to the molecular parameters included in the calculations.

The differences observed may be attributed to free silanol groups on the silica surface not covered by the polyethylene coating.

Various synthetic methods were developed for the covalent binding of hydrophobic ligands to the surface of

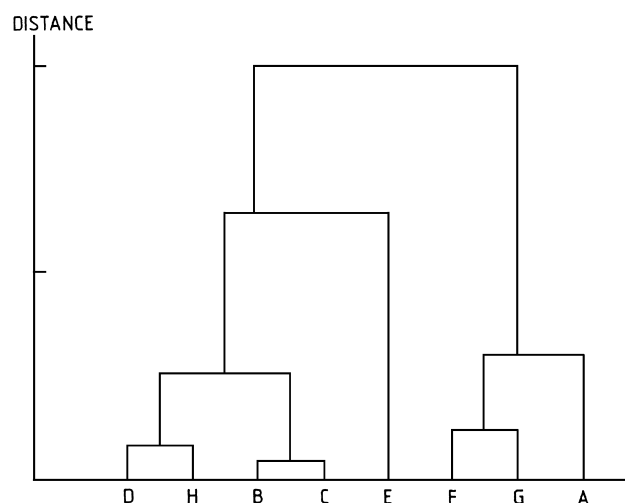


Fig. 3 Two-dimensional nonlinear selectivity map of reversed-phase HPLC columns. Number of iterations: 377. Maximum error: 2.1×10^{-3} . (A) C₁ silica; (B) C₂ silica; (C) C₆ silica; (D) C₈ silica; (E) C₁₈ silica; (F) polyethylene coated silica; (G) polyethylene-coated alumina; (H) C₁₈ alumina. (From Ref. [19].)



alumina.^[15,16] These methods generally resulted in real RP stationary phases with higher pH stability than the silica-based stationary phase. The retention of 33 commercial pesticides was determined on OD alumina, ODS, and on alumina support.^[17] Stepwise regression analysis proved that the retention of pesticides on OD alumina does not significantly depend on the lipophilicity of pesticides determined on a silica-based RP support. This discrepancy was tentatively explained by the different binding characteristics of the adsorption centers on the surfaces of silica and alumina not covered by the hydrophobic ligand. Using another set of solutes, the similarities of the retention order on both OD alumina and ODS was observed.^[18]

The spectral mapping technique, combined with cluster analysis and nonlinear mapping, was used for the comparison of the retention behaviors of RP silica and RP alumina columns using tributylphenol ethylene oxide oligomers as model compounds.^[19] The columns included in the experiments were C₁, C₂, C₆, C₈, and C₁₈ silica, PE-Si, alumina, and C₁₈ alumina. The retention strengths of RP-HPLC columns showed considerable variations, the strongest and the weakest being C₁₈ silica and PE-Si, respectively. The retention strength of alkyl-modified silicas depended linearly on the carbon load. The two-dimensional selectivity map and the cluster dendogram of the column selectivities are depicted in Figs. 3 and 4, respectively. From the results, it is clear that both the strength and the selectivity of retention show high variations. C₁, PE-Si, and PE-Alu exhibited similar retention selectivity.

This result may be attributed to the fact that polyethylene chains lie parallel to the surface of the support, with the end groups being anchored to the polar adsorption centers. According to this model, only the surface of the polyethylene coating pointing toward the mobile phase is available to the solutes in the mobile

phase. This apolar polymeric layer is similar in thickness to the C₁ coating but differs markedly from the longer alkyl chains that are more or less immersed in the mobile phase and are providing more CH₂ groups for the binding of apolar solutes. The conclusions drawn from the two-dimensional nonlinear mapping and cluster analysis are similar, suggesting that both methods can be used for the reduction of the dimensionality of a multidimensional spectral map.

CONCLUSIONS

The development of new nonsilica-based stationary phases was mainly motivated by the poor stability of silica and modified silicas at extreme pH values. It was shown that alumina supports can be used successfully for the solution of a wide variety of analytical problems concerning the separation of natural products, pharmaceuticals, and xenobiotics at any mobile phase pH. Moreover, alumina shows different retention characteristics than silica (i.e., it shows higher separation capacity for positional isomers). The data may facilitate not only the solution of various practical separation problems in liquid chromatography, but will also promote a better understanding of the underlying physicochemical principles governing retention.

REFERENCES

1. Snyder, L.R. Separability of aromatic isomers on alumina: Mechanism of adsorption. *J. Phys. Chem.* **1962**, 72, 489–492.
2. Laurent, C.; Billiet, H.A.H.; de Galan, L. The use of organic modifiers in ion exchange chromatography on alumina. The separation of basic drugs. *Chromatographia* **1983**, 17, 253–258.
3. Laurent, C.; Billiet, H.A.H.; de Galan, L. On the use of alumina in HPLC aqueous mobile phases at extreme pH. *Chromatographia* **1983**, 17, 394–398.
4. Laurent, C.; Billiet, H.A.H.; de Galan, L.; Byutenhuys, F.A.; van der Maeden, F.P.B. High-performance liquid chromatography of proteins on alumina. *J. Chromatogr.* **1984**, 287, 45–49.
5. Ahmad, J. The use of alumina as stationary phase for thin layer chromatography of inorganic and organometallic compounds. *JPC, J. Planar Chromatogr. Mod. TLC* **1996**, 9, 236–239.
6. Szilagyi, A.; Forgács, E.; Cserhádi, T. Separation of non-ionic surfactants according to the length of the ethylene oxide chain on alumina layers. *Toxicol. Environ. Chem.* **1998**, 65, 95–102.
7. Forgács, E.; Cserhádi, T. Retention behavior of nonylphe-

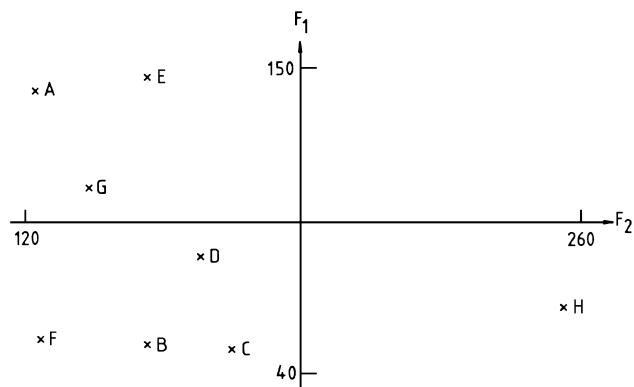


Fig. 4 Cluster dendrogram of RP-HPLC columns. For symbols, see Fig. 3. (From Ref. [19].)

- nyl ethyleneoxide oligomers on an alumina high-performance liquid chromatographic column. *Fresenius J. Anal. Chem.* **1995**, 351, 688–689.
8. Forgács, E.; Cserhádi, T. Retention behaviour of tributylphenol ethylene oxide oligomers on an alumina high performance liquid chromatographic column. *J. Chromatogr.* **1994**, 661, 239–243.
 9. Kősa, A.; Dőbo, A.; Vèkey, K.; Forgács, E. Separation and identification of nonylphenylethylene oxide oligomers by high-performance liquid chromatography with UV and mass spectrometric detection. *J. Chromatogr., A* **1998**, 819, 297–302.
 10. Mao, Y.; Fung, B.M. Use of alumina with anchored polymer coating as packing material for reversed-phase high performance liquid chromatography. *J. Chromatogr., A* **1997**, 790, 9–15.
 11. Kaliszan, R.; Osmialowski, K. Correlation between chemical structure of non-congeneric solutes and their retention on polybutadiene-coated alumina. *J. Chromatogr.* **1990**, 506, 3–16.
 12. Theodoridis, G.; Papadoyannis, I.N.; Hermans-Lokkerbol, A.; Verpoorte, R. A study of the behaviour of some new column materials in the chromatographic analysis of *Catharanthus* alkaloids. *Chromatographia* **1997**, 45, 52–57.
 13. Forgács, E. Comparison of reversed-phase chromatographic systems with principal component and cluster analysis. *Anal. Chim. Acta* **1994**, 296, 235.
 14. Cserhádi, T.; Forgács, E.; Payer, K.; Haber, P.; Kaliszan, R.; Nasal, A. Quantitative structure–retention relationships in separation mechanism studies on polyethylene-coated silica and alumina stationary phases. *LC GC Int.* **1998**, 11, 240.
 15. Pesek, J.J.; Lin, H.-D. Evaluation of synthetic procedures for the chemical modification of alumina for HPLC. *Chromatographia* **1989**, 28, 565–574.
 16. Pesek, J.J.; Sandoval, E., Jr.; Su, M. New alumina-based stationary phases for high-performance liquid chromatography. *J. Chromatogr.* **1993**, 630, 95–103.
 17. Cserhádi, T.; Forgács, E. Separation of pesticides on an octadecyl-coated alumina column. *Fresenius J. Anal. Chem.* **1997**, 358, 558–560.
 18. Haky, J.E.; Vemulapalli, S.; Wieserman, L.F. Comparison of octadecyl-bonded alumina and silica for reversed-phase high performance liquid chromatography. *J. Chromatogr.* **1990**, 505, 307–318.
 19. Forgács, E.; Cserhádi, T. Determination of retention behaviour of some non-ionic surfactants on reversed-phase high-performance liquid chromatography supports by spectral mapping in combination with cluster analysis or non-linear mapping. *J. Chromatogr., A* **1996**, 722, 281–287.

Amino Acid Analysis by HPLC

Susana Maria Halpine

Consultant, Playa Del Rey, California, U.S.A.

Introduction

Amino acid analysis (AAA) is a classic analytical technique that characterizes proteins and peptides based on the composition of their constituent amino acids. It provides qualitative identification and is essential for the accurate quantification of proteinaceous materials.

Amino acid analysis is widely applied in research, clinical facilities, and industry. It is a fundamental technique in biotechnology, used to determine the concentration of peptide solutions, to confirm protein binding in antibody conjugates, and for end-terminal analysis following enzymatic digestion. Clinical applications include diagnosing metabolic disorders in newborns. In industry, it is used for quality control of products ranging from animal feed to infant formula.

The analysis of a polypeptide typically involves four steps: hydrolysis (or deproteinization with physiological samples), separation, derivatization, and detection. Hydrolysis breaks the peptide bonds and releases free amino acids, which are then separated by side group using column chromatography. Derivatization with a chromogenic reagent enhances the separation and spectral properties of the amino acids and is required for sensitive detection. A data processing system compares the resulting chromatogram, based on peak area or peak height, to a calibrated standard (see Fig. 1a). The results, expressed as mole percent and microgram of residue per sample, determine the percent composition of each amino acid as well as the total amount of protein in the sample. Unknown proteins may be identified by comparing their amino acid composition with those in protein databases. Successful identification of unknown proteins may be achieved using Internet search programs.

Other techniques, such as capillary electrophoresis and [matrix-assisted laser desorption ionization] mass spectrometry, provide qualitative analyses, often with greater speed and sensitivity. Nevertheless, AAA by high-performance liquid chromatography (HPLC) complements other structural analysis techniques, such as peptide sequencing, and remains indispensable for quantifying proteinaceous materials.

Peptide Hydrolysis

Conventional hydrolysis exposes the polypeptide to 6M HCl acid under vacuum at 110°C for 20–24 h [1,2]. Protective agents, such as 0.1% phenol, are added to improve recovery. Gas-phase hydrolysis, in which the acid is delivered as a vapor, gives comparable results to the liquid phase. Additionally, the gas phase minimizes acid contaminants and allows parallel hydrolysis of standards and samples within the same chamber.

Acid hydrolysis yields 16 of the 20 coded amino acids; tryptophan is destroyed, cysteine recovery is unreliable, and asparagine and glutamine are converted to aspartic acid and glutamic acid, respectively. Furthermore, some side groups, such as the hydroxyl in serine, promote the breakdown of the residue, whereas aliphatic amino acids, protected by steric hindrance, require longer hydrolysis time. This variation in yield can be overcome by hydrolyzing samples for 24, 48, and 72 h and extrapolating the results to zero time point.

The reaction rate doubles with every 10°C increase, so that hydrolysis at 145°C for 4 h gives results comparable to the conventional method. Microwave hydrolysis reduces analysis time to 30–45 min. Alternative hydrolysis agents include sulfonic acid, which often gives better recovery but is nonvolatile, and alkaline hydrolysis, used in the analysis of tryptophan, proteoglycans, and proteolipids.

Careful sample preparation and handling during the hydrolysis step are critical for maintaining accurate and reproducible results. Salts, metal ions, and other buffer components remaining in a sample may accelerate hydrolysis, producing unreliable quantification. The Maillard reaction between amino acids and carbohydrates results in colored condensation products (humin) and decreased yield. Routine method calibration with proteins and amino acid standards, use of an internal standard (1 nmol norleucine is used for sensitive analysis), and control blanks are strongly recommended, along with steps to minimize background contaminants (see Fig. 1b). The practical limit for high-sensitivity hydrolysis is 10–50 ng of sample; be-



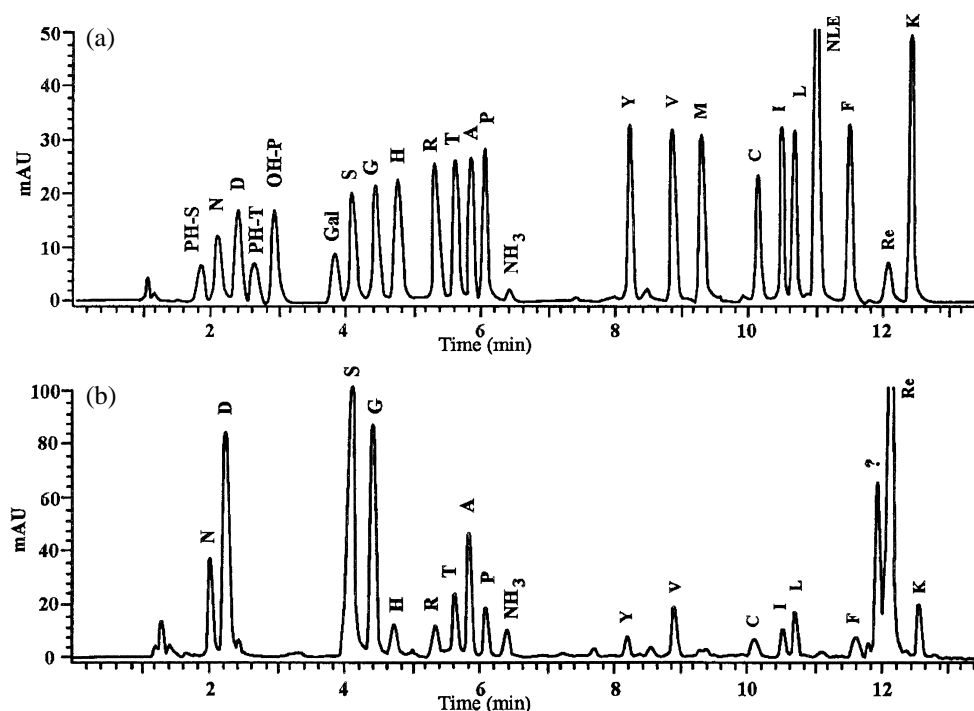


Fig. 1 (a) 200 pmol of PTC-amino acid standard, including phosphoserine (PH-S), aspartate (N), glutamate (D), phosphothreonine (PH-T), hydroxyproline (OH-P), galactosamine (Gal), serine (S), glycine (G), histidine (H), arginine (R), threonine (T), alanine (A), proline (P), tyrosine (Y), valine (V), methionine (M), cysteine (C), isoleucine (I), leucine (L), norleucine (NLE, 1 nmol internal standard), phenylalanine (F), excess reagent (Re), and lysine (K). (b) Analysis of a human fingerprint, taken up from watchglass using a mixture of water and ethanol. (Courtesy of National Gallery of Art and the Andrew W. Mellon Foundation.)

low this amount, background contaminants begin to play a larger role.

Derivatizing Reagents for Analysis of Amino Acids by HPLC

The first automated analyzer was developed by Moore, Stein, Spackman, and Hamilton in the 1950s. Hydrolysates were separated on an ion-exchange column, followed by postcolumn reaction with ninhydrin. Although this system remains the standard method, its major drawback is low sensitivity. Several methods have since been developed offering high sensitivity and faster analyses without sacrificing reproducibility [1–4].

Amino acids react with many reagents to form stable derivatives and strong chromophores (see Table 1). Derivatization can precede (precursor) or follow (in-line postcolumn) the chromatographic separation. Both precolumn and postcolumn systems are currently employed: ninhydrin and PTC analyzers are widely used, whereas AQC, OPA and OPA-FMOC systems provide the highest sensitivity.

Postcolumn systems typically use cation-exchange columns with either sodium citrate (for hydrolysates)

or lithium citrate (for physiological samples) as mobile phases. Contaminating salts and detergents are better tolerated because the samples are “cleaned up” before reaction with the reagent. The additional reagent pump, however, may lead to sample dilution, peak broadening, baseline fluctuations, and longer analysis time (30–90 min). Fluorescent reagents are compatible with a wider range of buffers, but the buffers must be amine-free if used with postcolumn methods.

Since the 1980s, precolumn derivatization methods have gained wider acceptance due to simpler preparation, faster analyses, and better resolution. The separation on reversed-phase C-8 or C-18 columns typically requires low-ultraviolet (UV) mobile phases, such as sodium phosphate or sodium acetate buffers, with acetonitrile or methanol as organic solvents. Separation times range from 15 to 50 min.

Improved Recovery of Sensitive Amino Acids

Cysteine and tryptophan require special treatment for quantitative analysis [5]. Cysteine/cysteine can be determined using three equally successful methods: oxidation, alkylation, and disulfide exchange. Oxidation to

Table 1 Amino Acid Derivatization Reagents

Reagent	Chromophore	Detection limit	Separation time	Drawbacks	Advantages
AQC (6-aminoquinolyl- <i>N</i> -hydroxysuccinimidyl carbamate)	Fluorescent (ex. 245 nm, em. 395 nm); UV 245 nm	160 fmol	35–50 min precolumn	Quaternary gradient elution required for complex, non-hydrolysate samples	Tolerates salts and detergents, rapid reaction, stable product, good reagent separation, high sensitivity and accuracy
Dabsyl chloride (4- <i>N,N</i> -dimethylaminoazobenzene-4'-sulfonyl chloride)	Visible 436 nm	Low fmol	18–44 min precolumn	Multiple products, critical concentration	Stable product, good separation, high sensitivity
Dansyl chloride (5- <i>N,N</i> -dimethylaminonaphthalene-1-sulfonyl chloride)	Fluorescent (ex. 360–385 nm, em. 460–495 nm); UV 254 nm	Low pmol	60–90 min precolumn	Multiple products, critical concentration, difficult separation leads to long separation time	Stable product
Fluorescamine (4-phenylspiro[furan-2(3H), 1'-phthalan]-3,3'-dione)	Fluorescent (ex. 390 nm, em. 475 nm)	20–100 pmol	30–90 min postcolumn	Secondary amine pretreatment, critical concentration, may give background interference	Rapid reaction, stable product, good reagent separation
FMOC (9-fluorenylmethylchloroformate)	Fluorescent (ex. 265 nm, em. 320 nm); UV 265 nm	1 pmol	20–45 min precolumn	Multiple products, extraction of excess reagent	Stable product, used with OPA for detection of secondary amine
Ninhydrin (triketohydrindene hydrate)	Primary amine (440 nm), secondary amine (570 nm)	100 pmol	30 min postcolumn	Low sensitivity and resolution	Good reproducibility
OPA (ortho-phthalaldehyde)	Fluorescent (ex. 340 nm, em. 455 nm)	50 fmol	90 min postcolumn, 17–35 pre-column	Secondary amine pretreatment, slow reaction, unstable derivative, background interference	Good reagent separation, high sensitivity and reproducibility with automated system
PITC (phenylisothiocyanate)	UV 254 nm	1 pmol	15–27 min precolumn	Salt interference, requires refrigeration, excess reagent removed under vacuum	Ease of use, flexibility, good separation, reproducibility enhanced with automation

Source: Refs. 1 and 2.

cysteic acid is commonly carried out by pretreatment with performic acid. Alkylation using pretreatment with 4-vinylpyridine or iodoacetate produces piridylethylcysteine (PEC) and carboxymethylcysteine (CMC), respectively. Disulfide exchange is achieved by adding reagents such as dithiodipropionic acid, dithiodiglycolic acid, or dimethylsulfoxide (DMSO) to the HCl acid during hydrolysis. The latter treatment offers both ease of use as well as accurate yields.

The superior approach to tryptophan analysis involves the addition of dodecanethiol to HCl acid, es-

pecially when combined with automatic vapor-phase hydrolysis. Alternative hydrolysis agents such as methane sulfonic acid, mercaptoethanesulfonic acid, or thioglycolic acid can produce 90% or greater yields. Acid hydrolysis additives and alkaline hydrolysis using 4.2M NaOH are also used with varying results.

Qualitative analysis of glycopeptides and phosphoamino acids is achieved through a separate, partial hydrolysis with 6N HCl acid at 110°C for 1 and 1.5 h, respectively. Separation of cysteine, tryptophan, and amino sugars requires minimal chromatographic ad-



justments; phosphoamino acid separation is straightforward using the reversed phase, but it is cumbersome using ion exchange.

Analysis of Free and Modified Amino Acids

Blood, urine, cerebrospinal, and other physiological fluids contain a great number of posttranslationally modified amino acids (approximately 170 have been studied to date) and in a wider range of concentrations than protein hydrolysates [6]. Additionally, plant sources produce about 500 nonprotein amino acids and, in geological samples, highly unusual amino acids may indicate extraterrestrial origin [7, 8].

Although the free amino acids in these samples do not require hydrolysis, blood plasma and cerebrospinal fluid must be deproteinized before analysis. Proteins may bind irreversibly to ion-exchange columns, resulting in loss of resolution. Furthermore, any peptide hydrolases must be inactivated. For ion-exchange analyses, a protein precipitant is added before centrifugation. Sulfosalicylic acid, a common precipitating agent, is added in solid form to avoid sample dilution. For reversed-phase analyses, ultrafiltration, size-exclusion chromatography, or organic solvent extraction is recommended. Samples with low protein and high amino acid concentrations, such as urine and amniotic fluid, need only to be diluted before analysis.

Precolumn derivatives are more tolerant to lipid-rich samples. Changing the guard-column routinely is recommended to avoid column buildup, especially for reversed-phase systems.

Amino Acid Racemization Analysis

Racemization, the interconversion of amino acid enantiomers, occurs slowly in biological and geological systems. Although the L-form is the most prevalent, D-amino acids are found in fossils and living organisms. The rate increases with extreme pH values, high temperature, and high ionic strength. Rates also vary among amino acids: at 25°C, the racemization half-life of serine is about 400 years, whereas that of isoleucine is 40,000. Enantiomer analysis is used to confirm the bioactivity of synthetic peptides and for geological dating [1,3,8].

Hydrolysis itself accelerates racemization. Shorter acid exposure at higher temperatures, such as 160°C for 1 h, decreases racemization by about 50% compared to conventional hydrolysis. Liquid-phase

methanesulfonic acid, conventional, and microwave hydrolysis produce progressively higher rates of racemization. Addition of phenol, however, significantly reduces racemization during microwave hydrolysis [1].

The three general approaches to enantiomer separation entail a chiral stationary phase, a chiral mobile phase, or a chiral reagent. Tandem columns, with reversed and chiral stationary phases, were used to separate 18 D-L pairs of PTC-amino acids in 150 min. OPA-amino acid enantiomers have been separated on both ion-exchange and reversed-phase columns using a sodium acetate buffer with a L-proline-cupric acetate additive. Chiral reagents, such as Marphay's reagent and OPA/IBLC (*N*-isobutiril-L cysteine), were successfully used for racemization analysis within 80 min.

Acknowledgments

The author would like to thank Dr. Steven Birken, Dr. Chun-Hsien Huang, Dr. Stacy C. Marsella, and Dr. Conceicao Minetti for their assistance in proofreading this article.

References

1. M. Fountoulakis and H.-W. Lahm, Hydrolysis and amino acid composition analysis of proteins, *J. Chromatogr. A* 826: 109 (1998).
2. C. Fini, A. Floridi, V. N. Finelli, and B. Wittman-Liebold (eds.), *Laboratory Methodology in Biochemistry, Amino Acid Analysis and Protein Sequencing*. CRC Press, Boca Raton, FL, 1990.
3. G. C. Barrett (ed.), *Chemistry and Biochemistry of Amino Acids*, Chapman and Hall, London, 1985.
4. W. S. Hancock (ed.), *CRC Handbook of HPLC for the Separation of Amino Acids, Peptides, and Proteins, Vol. I*, CRC Press, Boca Raton, FL, 1984.
5. D. J. Strydom, T. T. Andersen, I. Apostol, J. W. Fox, R. J. Paxton, and J. W. Crabb, Cysteine and tryptophan amino acid analysis of ABRF92-AAA, in *Techniques in Protein Chemistry IV*, R. Hogue Angeletti (ed.), Academic Press, San Diego, 1993, pp. 279–288.
6. P. A. Haynes, D. Sheumack, L. G. Greig, J. Kibby, and J. W. Redwood, Applications of automated amino acid analysis using 9-fluorenylmethyl chloroformate, *J. Chromatogr.* 588: 107 (1991).
7. G. Rosenthal, *Plant Nonprotein Amino and Imino Acids: Biological, Biochemical, and Toxicological Properties*, Academic Press, New York, 1982.
8. P. E. Hare, T. C. Hoering, and K. King (eds.), *Biogeochemistry of Amino Acids*, John Wiley & Sons, New York, 1980.



Amino Acids and Derivatives: Analysis by TLC

Luciano Lepri

Alessandra Cincinelli

Università degli Studi di Firenze, Firenze, Italy

Introduction

Amino acids are derivatives of the carboxylic acids in which a hydrogen atom in the side chain (usually on the alpha carbon) has been replaced by an amino group and, therefore, they are amphoteric.

In weak acid solution (about pH 5–6.0) the carboxyl group of a neutral amino acid (one amino group and one carboxyl group) is dissociated, and the amino group binds a proton to give a dipolar ion (zwitterion). The pH at which the concentration of the dipolar ion is a maximum is called the isoelectric point (pI) of that amino acid. The isoelectric point of an amino acid is calculated from the relationship

$$pI = \frac{1}{2}(pK_1 + pK_2)$$

where pK_1 and pK_2 refer to the dissociation of carboxyl group and protonated amino group, respectively.

Amino acids constitute the basic units of all proteins. The number of α -amino acids obtained from various proteins is about 40, but only 20 are present in all proteins in varying amounts.

Thin-layer chromatography (TLC) is one of the most promising separation methods for such compounds that are not amenable to gas chromatographic analysis.

Preparation of Test Solutions

Amino acids should be as free from impurities as possible because they also exhibit a pronounced capacity for binding metal ions. The analysis of amino acids in natural fluids or extracts requires the removal of interfering compounds prior to chromatographic separation, in order to prevent tailing and deformation of the spots (i.e., in urine samples and hydrolizates of proteins or peptides, high salt concentrations occur). Salts can be conveniently removed by passing the sample through a cation-exchange resin column.

Enrichment of amino acids in urine can be performed by extracting the lyophilized sample (10 mL) with 1 mL methanol–1 M HCl mixture (4:1 v/v) and applying an aliquot of supernatant liquid to the plate after centrifugation.

Chromatographic Techniques for Amino Acid Separation

Untreated Amino Acids

Standard solutions of amino acids have been prepared in aqueous–alcoholic solvents (e.g., 70% ethanol), with the addition of hydrochloric acid (0.1 M) for the dissolution of relatively insoluble amino acids (i.e., tyrosine and cystine). Detection is generally performed with a ninhydrin reagent. After color development with the ninhydrin reagent, the treatment of the layer with a complex-forming cation (e.g., Cu^{II} , Cd^{II} , Ni^{II}) changes the blue color to red and increases colorfastness considerably. More specific coloration of amino acids can be achieved by adding bases such as collidine and cyclohexylamine to the detecting agent solution.

Amino acids have been separated on layers of a wide variety of inorganic and organic adsorbents, ion exchangers, and impregnated plates. The two most commonly used adsorbents are silica gel and cellulose.

Separation on Silica Gel and Cellulose Layers

It is interesting to note that by using neutral eluents such as ethanol or n-propanol–water, the acidic amino acids (Glu, Asp) travel much faster on silica gel than basic amino acids (Lys, Arg, His), which, indeed, show very small R_f values. The difference is likely due to cation exchange between the protonated amino groups of basic amino acids (two or more amino groups and one carboxyl group) and the acidic groups present on silica gel. The strong retention observed for these compounds when eluting with acidic solvents (see Table 1) confirms such a



Table 1 R_f Values of the 20 Common Amino Acids in Different Experimental Conditions (Ascending Technique)

Amino acid and symbol	Silica gel G (A)	Micro-crystalline cellulose (B)	Fixion 50-X8 (Na ⁺) (C)	Silanized silica gel +4% HDBS (D)	pI
Glycine (Gly)	18	15	56	83	6.0
Alanine (Ala)	22	29	51	74	6.0
Serine (Ser)	18	16	67	85	5.7
Threonine (Thr)	20	21	67	83	6.5
Leucine (Leu)	44	64	22	26	6.0
Isoleucine (Ile)	43	60	28	31	6.1
Valine (Val)	32	48	43	54	6.0
Methionine (Met)	35	23	28	42	5.8
Cysteine (Cys)	7	3	56	—	5.0
Proline (Pro)	14	34	—	63	6.3
Phenylalanine (Phe)	43	55	14	21	5.5
Tyrosine (Tyr)	41	36	12	45	5.7
Tryptophan (Trp)	47	36	2	13	5.9
Aspartic acid (Asp)	17	15	72	86	3.0
Asparagine (Asn)	14	—	—	85	5.4
Glutamic acid (Glu)	24	27	35	83	3.2
Glutamine (Gln)	15	—	—	—	5.7
Arginine (Arg)	6	11	2	28	10.8
Histidine (His)	5	7	11	40	7.6
Lysine (Lys)	3	7	8	47	9.8

Note: Eluents: A = *n*-butanol–acetic acid–water (80 + 20 + 20 v/v/v); B = 2-butanol–acetic acid–water (3:1:1 v/v/v); C = 84 g citric acid + 16 g NaOH + 5.8 g NaCl + 54 g ethylene glycol + 4 mL conc. HCl (pH = 3.3); D = 0.5M HCl + 1M CH₃COOH in 30% methanol (pH = 0.7).

hypothesis. A similar phenomenon is also observed on cellulose plates and might be due to the cellulose carboxyl groups.

Furthermore, it is seen that a hydroxyl group in the molecule does not necessarily reduce the R_f value as the chromatographic behavior of serine with respect to glycine on both layers of silica gel and cellulose shows (see Table 1). Some of the numerous eluents that have been used for the separation of amino acids on silica gel are acetone–water–acetic acid–formic acid (50:15:12:3), ethylacetate–pyridine–acetic acid–water (30:20:6:11), 96% ethanol–water–diethylamine (70:29:1), chloroform–formic acid (20:1), chloroform–methanol (9:1), isopropanol–5% ammonia (7:3), and phenol–0.06M borate buffer pH 9.30 (9:1). On cellulose plates, ethylacetate–pyridine–acetic acid–water (5:5:1:3), *n*-butanol–acetic acid–water (4:1:1 and 10:3:9), *n*-butanol–acetone–ammonia–water (20:20:4:1), collidine–*n*-butanol–acetone–water (2:10:10:5), phenol–methanol–water (7:10:3), ethanol–acetic acid–water (2:1:2), and cyclohexanol–acetone–diethylamine–water

(10:5:2:5), have also been used as eluents. Separation efficiency can be increased by two-dimensional (TD) chromatography. Several solvent systems are suitable for TD separations and the combination of chloroform–methanol–17% ammonium hydroxide (40+40+20 v/v/v) and phenol–water (75 g+25 g) will separate all protein amino acids, except leucine and isoleucine, on silica plates.

Separation on Ion Exchangers and Impregnated Plates

Cellulose ion exchangers (e.g., diethylaminoethyl cellulose) and ion-exchange resins have been widely used as stationary phases for TLC separation of untreated amino acids.

Fixion 50-X8 commercial plates, which contain Dowex 50-X8 type resin, have been tested on both Na⁺ and H⁺ forms for 30 amino acids and the results obtained for the 20 common protein amino acids are reported in Table 1. The isomer pair leucine and isoleucine is well separated by this method. In addi-



tion, the hydroxyl group notably increases the R_f values owing to the hydrophobic properties of the resin and the pairs serine and glycine, and threonine and alanine can be resolved.

Many studies have been recently focused on impregnated plates. The methods used for impregnation depend on whether the plates are home-made or commercially available. In the first case, the impregnation reagent is usually added to a slurry of the adsorbent, whereas ready-to-use plates are dipped in the solution of the reagent.

The resolution of amino acids has been reported by using different metal ions as impregnating agents at various concentrations. On silica gel impregnated with Ni(II) salts, the results indicate a predominant role of partitioning phenomenon when eluting with acidic aqueous and nonaqueous solutions (e.g., *n*-butanol–acetic acid–water and *n*-butanol–acetic acid–chloroform in the 3:1:1 v/v/v ratio). The impregnation of silanized silica gel with 4% dodecylbenzenesulfonic acid (HDBS) solution on both home-made and ready-to-use plates is particularly useful in resolving amino acids [1,2]. The parameters affecting the retention of amino acids on these layers are type of adsorbent, concentration and properties of the impregnating agent, percentage and kind of organic modifier, pH, and ionic strength of the eluent.

The data of Table 1 show that complete resolution of basic amino acids (Arg, His, Lys) and of neutral amino acids which differ in their side-chain carbon atom number (e.g., Gly, Ala, Met, Val, Leu, or Ile) are possible on home-made plates of silanized silica gel (C_2) impregnated with a 4% solution of dodecylbenzenesulfonic acid in 95% ethanol. More compact spots can be obtained on RP-18 ready-to-use plates dipped in the same solution of the surfactant agent.

Resolution of Amino Acid Derivatives

The identification of N-terminal amino acids in peptides and proteins is of considerable practical importance because it constitutes an essential step in the process of sequential analysis of peptide structures.

Many N-amino acid derivatives have been proposed to this purpose and the most commonly studied by TLC are 2,4-dinitrophenyl (DNP)- and 5-dimethylamino-1-naphthalene-sulfonyl (Dansyl,Dns)-amino acids, and 3-phenyl-2-thiohydantoins (PTH-amino acids).

Recently, 4-(dimethylamino)azobenzene-4'-isothiocyanate (DABITC) derivatives of amino acids have been also investigated.

DNP-Amino Acids

The dinitrophenylation of amino acids, peptides, and proteins and their separation by one-dimensional and two-dimensional TLC have been reviewed by Rosmus and Deyl [3]. DNP-amino acids are divided into those which are ether extractable and those which remain in the aqueous phase.

Water-soluble α -DNP-Arg, α -DNP-His, ϵ -DNP-Lys, bis-DNP-His, O-DNP-Tyr, DNP-cysteic acid ($CySO_3H$), and DNP-cystine (Cys)₂ have been identified on silica gel plates in the *n*-propanol–34% ammonia (7:3 v/v) system. Although separation of DNP-Arg and ϵ -DNP-Lys is incomplete (R_f values of 0.43 and 0.44, respectively), both of them can be detected because of the color difference produced in the ninhydrin reaction.

Ether-soluble DNP-amino acids have been investigated by one-dimensional and TD chromatography. This last technique offers the possibility of almost complete separation of the two groups of derivatives.

The yellow color of DNP-amino acids deepens upon exposure to ammonia vapor and it is sufficiently intense that 0.1 μ g can be visualized. The detection limit is lower (about 0.02 μ g) under ultraviolet (UV) light (360 nm with dried plates and 254 nm with wet ones), but it increases for TD chromatography (about 0.5 μ g). At present, the applications of DNP-amino acids are limited.

PTH-Amino Acids

The formation of PTH-amino acids by the Edman degradation [4] of peptides and proteins or by successive modifications of the method constitutes the most commonly used technique for the study of the structure of biologically active polypeptides today. Identification of PTH-amino acids in mixtures may be successfully achieved by TLC. Quantitative determination is based on UV absorption (detection limit 0.1 μ g at 270 nm). An alternative is offered by the chlorine/tolidine test, which is very useful because the minimal amount required for detection is about 0.5 μ g.

Using one-dimensional chromatography on alumina, polyamide, and silica gel, difficulties are encountered in resolving Leu/Ile and Glu/Asp pairs as well as other combinations of PTH-amino acids (e.g., Phe/Val/Met/Thr). The most common solvents used on polyamide plates are *n*-heptane–*n*-butanol–acetic acid (40:30:9), toluene–*n*-pentane–acetic acid (60:30:35), ethylene chloride–acetic acid (90:16), and ethylacetate–*n*-butanol–acetic acid (35:10:1), and



those on silica gel are *n*-heptane–methylene chloride–propionic acid (45:25:30), xylene–methanol (80:10), chloroform–ethanol (98:2), chloroform–ethanol–methanol (89.25:0.75:10), chloroform–*n*-butylacetate (90:10), diisopropyl ether–ethanol (95:5), methylene chloride–ethanol–acetic acid (90:8:2), *n*-hexane–*n*-butanol (29:1); *n*-hexane–*n*-butylacetate (4:1), pyridine–benzene (2.5:20), methanol–carbon tetrachloride (1:20), and acetone–methylene dichloride (0.3:8). The complete resolution of specific mixtures is possible with TD chromatography by the use of certain solvent systems given above.

The characteristic colors of PTH-amino acids, following ninhydrin spray and the colored spots observed under UV light on polyamide plates containing fluorescent additives, are very useful in identifying those amino acids that have nearly identical R_f values.

Thin-layer chromatography of PTH-amino acids has been reviewed by Rosmus and Deyl [3].

Dns-Amino Acids

Dansylation reaction in bicarbonate buffer (pH = 9.5) is widely used for identification of N-terminal amino acids in proteins and it is the most sensitive method for quantitative determination of amino acids because dansyl derivatives are fluorescent under an UV lamp (254 nm).

Much research has been focused on silica gel and polyamide plates, using both one-dimensional and TD chromatography.

No solvent system resolves all the Dns-amino acids by one-dimensional chromatography and, also, TD chromatography requires more than two runs for a complete resolution. The most common used eluents on polyamide layers are benzene–acetic acid (9:1), toluene–acetic acid (9:1), toluene–ethanol–acetic acid (17:1:2), water–formic acid (200:3), water–ethanol–ammonium hydroxide (17:2:1 and 14:15:1), ethylacetate–ethanol–ammonium hydroxide (20:5:1), *n*-heptane–*n*-butanol–acetic acid (3:3:1), chlorobenzene–acetic acid (9:1), and ethylacetate–acetic acid–methanol (20:1:1).

A widely employed chromatographic system is based on polyamide plates eluted with water–formic acid (200:3 v/v) in the first direction and benzene–acetic acid (9:1 v/v) in the second direction.

A third run in 1M ammonia–ethanol (1:1, v/v) or ethylacetate–acetic acid–methanol (20:1:1, v/v/v) re-

solves especially basic Dns-amino acids or Glu/Asp and Thr/Ser pairs, respectively.

DABTH-Amino Acids

These derivatives are obtained in basic medium by the reaction of DABITC with the primary amino group of N-terminal amino acids in peptides. The color difference between DABITC (or its degradation products) and DABTH-amino acids facilitates identification on TLC. These derivatives are colored compounds and, because of their stability and sensitivity, are usually used for qualitative and quantitative analyses of amino compounds such as amino acids and amines.

All DABTH-amino acids except the Leu/Ile pair can be separated by TD chromatography on layers of polyamide, with water–acetic acid (2:1, v/v) and toluene–*n*-hexane–acetic acid (2:1:1, v/v/v) as solvents 1 and 2, respectively.

Resolution of the DABTH-Leu/DABTH-Ile pair on polyamide is possible with formic acid–ethanol (10:9, v/v) and on silica plates using chloroform–ethanol (100:3, v/v), as eluent.

Cbo- and BOC-Amino Acids

Carbobenzoxy (Cbo) and *tert*-butyloxycarbonyl (BOC) amino acids are very useful in the synthesis of peptides and, consequently, their separation from each other and from unreacted components used in their preparation is very important.

For this separation, various mixtures of *n*-butanol–acetic acid–5% ammonium hydroxide and of *n*-butanol–acetic acid–pyridine with or without the addition of water were used on silica gel.

The BOC-amino acids give a negative ninhydrin test; however, if the plates are heated at 130°C for 25 min and immediately sprayed with a 0.25% solution of ninhydrin in butanol, a positive test is obtained.

Resolution of Enantiomeric Amino Acids and Their Derivatives

Amino acids are optically active, and the separation of the enantiomeric pairs is an important task. The topic is discussed in the article Enantiomeric Separations by TLC.

References

1. L. Lepri, P. G. Desideri, and D. Heimler, Reversed-phase and soap-thin-layer chromatography of amino acids, *J. Chromatogr.* 195: 65 (1980).
2. L. Lepri, P. G. Desideri, and D. Heimler, Thin-layer chromatography of amino acids and dipeptides on RP-2, RP-8 and RP-18 plates impregnated with dodecylbenzenesulphonic acid, *J. Chromatogr.* 209: 312 (1981).
3. J. Rosmus and Z. Deyl, The methods for identification of N-terminal amino acids in peptides and proteins. Part B, *J. Chromatogr.* 70: 221 (1972).
4. P. Edman, Method for determination of the amino acid sequence in peptides, *Acta Chem. Scand.* 4: 283 (1950).

Suggested Further Reading

Bhushan, R. and J. Martens, Amino Acids and their Derivatives, in *Handbook of Thin-Layer Chromatography*, J. Sherma and B. Friend (eds.), Marcel Dekker, Inc., New York, 1996, Vol. 71, pp. 389–425.



Amino Acids, Peptides, and Proteins: Analysis by CE

Danilo Corradini

Institute of Chromatography, Rome, Italy

Introduction

Amino acids, peptides, and proteins are analyzed by a variety of modes of capillary electrophoresis (CE) which employ the same instrumentation, but are different in the mechanism of separation. A fundamental aspect of each mode of CE is the composition of the electrolyte solution. Depending on the specific mode of CE, the electrolyte solution can consist of either a continuous or a discontinuous system. In continuous systems, the composition of the electrolyte solution is constant along the capillary tube, whereas in discontinuous systems, it is varied along the migration path.

Capillary zone electrophoresis (CZE), micellar capillary electrokinetic chromatography (MECC), capillary gel electrophoresis (CGE), and affinity capillary electrophoresis (ACE) are CE modes using continuous electrolyte solution systems. In CZE, the velocity of migration is proportional to the electrophoretic mobilities of the analytes, which depends on their effective charge-to-hydrodynamic radius ratios. CZE appears to be the simplest and, probably, the most commonly employed mode of CE for the separation of amino acids, peptides, and proteins. Nevertheless, the molecular complexity of peptides and proteins and the multifunctional character of amino acids require particular attention in selecting the capillary tube and the composition of the electrolyte solution employed for the separations of these analytes by CZE.

Discussion

The various functional groups of amino acids, peptides, and proteins can interact with a variety of active sites on the inner surface of fused-silica capillaries, giving rise to peak broadening and asymmetry, irreproducible migration times, low mass recovery, and, in some cases, irreversible adsorption. The detrimental effects of these undesirable interactions are usually more challenging in analyzing proteins than peptides or amino acids, owing to the generally more complex molecular structures of the larger polypeptides. One of the earliest, and still more adopted, strategy to pre-

clude the interactions of peptides and proteins with the wall of bare fused-silica capillaries is the chemical coating of the inner surface of the capillary tube with neutral hydrophilic moieties [1]. The chemical coating has the effect of deactivating the silanol groups by either converting them to inert hydrophilic moieties or by shielding all the active interacting groups on the capillary wall. A variety of alkylsilane, carbohydrate, and neutral polymers can be covalently bonded to the silica capillary wall by silane derivatization [2]. Polyacrylamide (PA), poly(ethylene glycol) (PEG), poly(ethylene oxide) (PEO), and polyvinylpyrrolidone (PVP) can be successfully anchored onto the capillary surface treated with several different silanes, including 3-(methacryloxy)-propyltrimethoxysilane, 3-glycidoxypentyltrimethoxysilane, trimethoxyallylsilane, and chlorodimethyloctylsilane. Alternatively, a polymer can be adsorbed onto the capillary wall and then cross-linked *in situ*. Other procedures are based on simultaneous coupling and cross-linking. Alternative materials to fused silica such as polytetrafluoroethylene (Teflon) and poly(methyl methacrylate) (PMMA) hollow fibers has found limited application.

The deactivation of the silanol groups can also be achieved by the dynamic coating of the inner wall by flushing the capillary tube with a solution containing a coating agent. A number of neutral or charged polymers with the property of being strongly adsorbed at the interface between the capillary wall and the electrolyte solution are employed for the dynamic coating of bare fused-silica capillaries. Modified cellulose and other linear or branched neutral polymers may adsorb at the interface between the capillary wall and the electrolyte solution with the main consequence of increasing the local viscosity in the electric double layer and masking the silanol groups and other active sites on the capillary surface. This results in lowering or suppressing the electro-osmotic flow and in reducing the interactions with the capillary wall.

Polymeric polyamines are also strongly adsorbed in the compact region of the electric double layer as a combination of multisite electrostatic and hydrophobic interactions. The adsorption results in masking the silanol groups and the other adsorption active sites on



the capillary wall and in altering the electroosmotic flow, which is lowered and, in most cases, reversed from cathodic to anodic. One of the most widely employed polyamine coating agents is polybrene (or hexadimrine bromide), a linear hydrophobic polyquaternary amine polymer of the ionene type [3]. Alternative choices are polydimethyldiallylammonium chloride, another linear polyquaternary amine polymer, and polyethylenimine (PEI). Very promising is the efficient dynamic coating obtained with ethylenediamine-derivatized spherical polystyrene nanoparticles of 50–100 nm diameter, which can be successively converted to a more hydrophilic diol coating by *in situ* derivatization of the free amino groups with 2,3-epoxy-1-propanol [4].

In most cases, the electrolyte solution employed in CZE consists of a buffer in aqueous media. Although all buffers can maintain the pH of the electrolyte solution constant and can serve as background electrolytes, they are not equally meritorious in CZE. The chemical nature of the buffer system can be responsible for poor efficiency, asymmetric peaks, and other untoward phenomena arising from the interactions of its components with the sample. In addition, the composition of the electrolyte solution can strongly influence sample solubility and detection, native conformation, molecular aggregation, electrophoretic mobility, and electro-osmotic flow. Consequently, selecting the proper composition of the electrolyte solution is of paramount importance in optimizing the separation of amino acids, peptides, and proteins in CZE. The proper selection of a buffer requires evaluating the physical–chemical properties of all components of the buffer system, including buffering capacity, con-

ductivity, and compatibility with the detection system and with the sample.

Nonbuffering additives are currently incorporated into the electrolyte solution to enhance solubility, break aggregation, modulate selectivity, improve resolution, and allow detection, which is particularly challenging for amino acids and short peptides. In addition, a large number of amino compounds, including monovalent amines, amino sugars, diaminoalkanes, polyamines, and short-chain alkylammonio quaternary salts are successfully employed as additives for the electrolyte solution to aid in minimizing interactions of peptides and proteins with the capillary wall in bare fused-silica capillaries. Other additives effective at preventing the interactions of proteins, peptides, and amino acids with the capillary wall include neutral polymers, zwitterions, and a variety of ionic and non-ionic surfactants [5]. Less effective at preventing these untoward interactions are strategies using electrolyte solutions at extreme pH values, whether acidic, to suppress the silanol dissociation, or alkaline, to have both the analytes and the capillary wall negatively charged.

Selectivity in CZE is based on differences in the electrophoretic mobilities of the analytes, which depends on their effective charge-to-hydrodynamic radius ratios. This implies that selectivity is strongly affected by the pH of the electrolyte solution and by any interaction of the analyte with the components of the electrolyte solution which may affect its charge and/or hydrodynamic radius.

Additives can improve selectivity by interacting specifically, or to different extents, with the components of the sample. Most of the additives employed in amino acid, peptide, and protein CZE are amino modifiers,

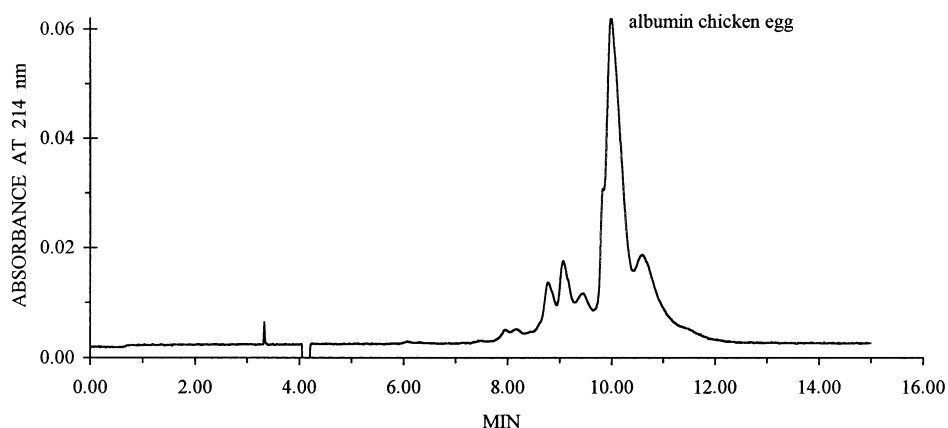


Fig. 1 Detection of microheterogeneity of albumin chicken egg by capillary zone electrophoresis. Capillary, bare fused-silica (50 μ m \times 37 cm, 30 cm to the detector); electrolyte solution, 25 mM Tris-glycine buffer containing 0.5% (v/v) Tween-20 and 2.0 mM putrescine; applied voltage, 20 kV; UV detection at the cathodic end.

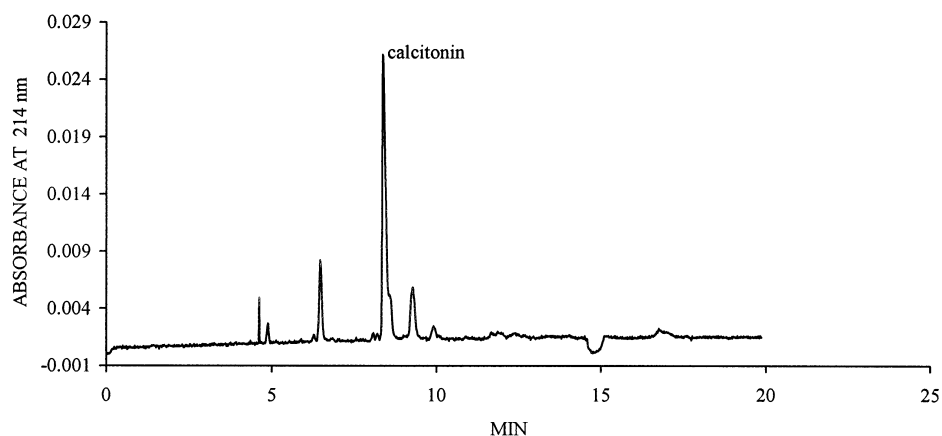


Fig. 2 Separation of impurities from a sample of synthetic human calcitonin for therapeutic use by CZE. Capillary, bare fused-silica (50 $\mu\text{m} \times 37$ cm, 30 cm to the detector); electrolyte solution, 40 mM N,N,N',N' -tetramethyl-1,3-butanediamine (TMBD), titrated to pH 6.5 with phosphoric acid; applied voltage, 15 kV; UV detection at the cathodic end.

zwitterions, anionic or cationic ion-pairing agents, inclusion complexants (only for amino acids and short peptides), organic solvents, and denaturing agents.

The capability of several compounds to ion-pair with amino acids, peptides, and proteins is the basis for their selection as effective additives for modulating the selectivities of these analytes in CZE [5]. Selective ion-pair formation is expected to enlarge differences in the effective charge-to-hydrodynamic radius ratio of these analytes, leading to enhanced differences in their electrophoretic mobilities, which determine improved selectivity. Several diaminoalkanes, including 1,4-diaminobutane (putrescine), 1,5-diaminopentane (cadaverine), 1,3-diaminopropane, and N,N,N',N' -tetramethyl-1,3-butanediamine (TMBD) can be successfully employed as additives for modulating the selectivity of peptides and proteins (see Figs. 1 and 2). Moreover, several anions, such as phosphate, citrate, and borate, which are components of the buffer solutions employed as the background electrolyte, may also act as ion-pairing agents influencing the electrophoretic mobilities of amino acids, peptides, and proteins and, hence, selectivity and resolution. Other cationic ion-pairing agents include the ionic polymers polydimethyldiallylammonium chloride and polybrene, whereas myo-inositol hexakis-(dihydrogen phosphate), commonly known as phytic acid, is an interesting example of a polyanionic ion-pairing agent.

Surfactants have been investigated extensively in CE for the separation of both charged and neutral molecules using a technique based on the partitioning of the analyte molecules between the hydrophobic micelles formed by the surfactant and the electrolyte solution, which is termed micellar electrokinetic capil-

lary chromatography (MECC or MEKC). This technique is widely used for the analysis of a variety of peptides and amino acids [6], but it is less popular for protein analysis [7]. The limited applications of MECC to protein analysis may be attributed to several factors, including the strong interactions between the hydrophobic moieties on the protein molecules and the micelles, the inability of large proteins to penetrate into the micelles, and the binding of the monomeric surfactant to the proteins. The result is that, even though the surfactant concentration in the electrolyte solution exceeds the critical micelle concentration, the protein-surfactant complexes are likely to be not subjected to partitioning in the micelles, as do amino acids, peptides, and other smaller molecules.

However, surfactants incorporated into the electrolyte solution at concentrations below their critical micelle concentration (CMC) may act as hydrophobic selectors to modulate the electrophoretic selectivity of hydrophobic peptides and proteins. The binding of ionic or zwitterionic surfactant molecules to peptides and proteins alters both the hydrodynamic (Stokes) radius and the effective charges of these analytes. This causes a variation in the electrophoretic mobility, which is directly proportional to the effective charge and inversely proportional to the Stokes radius. Variations of the charge-to-hydrodynamic radius ratios are also induced by the binding of nonionic surfactants to peptide or protein molecules. The binding of the surfactant molecules to peptides and proteins may vary with the surfactant species and its concentration, and it is influenced by the experimental conditions such as pH, ionic strength, and temperature of the electrolyte solution. Surfactants may bind to samples, either to the



same extent [e.g., protein–sodium dodecyl sulfate (SDS) complexes], or to a different degree, which can enlarge differences in the electrophoretic mobilities of the separands.

In CGE, the separation is based on a size-dependent mechanism similar to that operating in polyacrylamide gel electrophoresis (PAGE), employing as the sieving matrix either entangled polymer solutions or gel-filled capillaries [8]. This CE mode is particularly suitable for analyzing protein complexes with SDS. The separation mechanism is based on the assumption that fully denatured proteins hydrophobically bind a constant amount of SDS (1.4 g of SDS per 1 g of protein), resulting in complexes of approximately constant charge-to-mass ratios and, consequently, identical electrophoretic mobilities. Therefore, in a sieving medium, protein–SDS complexes migrate proportionally to their effective molecular radii and, thus, to the protein molecular weight. Consequently, SDS–CGE can be used to estimate the apparent molecular masses of proteins, using calibration procedures similar to those employed in SDS–PAGE.

Continuous electrolyte solution systems are also employed in ACE [9], where the separation depends on the biospecific interaction between the analyte of interest and a specific selector or ligand. The molecules with bioaffinity for the analyte (the selector or ligand) can be incorporated into the electrolyte solution or can be immobilized, either to an insoluble polymer filled into the capillary or to a portion of the capillary wall. ACE is a useful and sensitive tool for measuring the binding constant of ligands to proteins and characterizing molecular properties of peptides and proteins by analyzing biospecific interactions. Examples of biospecific interactions currently investigated by ACE include molecular recognition between proteins or peptides and low-molecular-mass receptors, antigen–antibody complexes, lectin–sugar interactions, and enzyme–substrate complexes. ACE is also employed for the chiral separation of amino acids using a protein as the chiral selector.

Enantiomeric separations of amino acids and short peptides are performed using either a direct or the indirect approach [10]. The indirect approach employs chiral reagents for diastereomer formation and their subsequent separation by various modes of CE. The direct approach uses a variety of chiral selectors that are incorporated into the electrolyte solution. Chiral selectors are optically pure compounds bearing at least one functional group with a chiral center (usually represented by an asymmetric carbon atom) which allows sterically selective interactions with the two enantiomers. Among others, cyclodextrins (CDs) are the

Amino Acids, Peptides, and Proteins: Analysis by CE

most widely chiral selectors used as additives in chiral CE. These are cyclic polysaccharides built up from D-(+)-glucopyranose units linked by α -(1,4) bonds, whose structure is similar to a truncated cone. Substitution of the hydroxyl groups of the CDs results in new chiral selectors which exhibit improved solubility in aqueous solutions and different chiral selectivity. Other chiral selectors include crown ethers, chiral dicarboxylic acids, macrocyclic antibiotics, chiral calixarenes, ligand-exchange complexes, and natural and semisynthetic linear polysaccharides. Chiral selectors are also commonly employed in combination with ionic and nonionic surfactants for enantiomeric separations of amino acids and peptides by MECC.

In discontinuous systems, the composition of the electrolyte solution is varied along the migration path with the purpose of changing one or more parameters responsible for the electrophoretic mobilities of the analytes. The discontinuous electrolyte solution systems employed in capillary isoelectric focusing (CIEF) have the function of generating a pH gradient inside the capillary tube in order to separate peptides and proteins according to their isoelectric points [11]. Each analyte migrates inside the capillary until it reaches the zone with the local pH value corresponding to its isoelectric point, where it stops moving as a result of the neutralized charge and consequent annihilated electrophoretic mobility. CIEF is successfully employed for the resolution of isoenzymes, to measure the isoelectric point (pI) of peptides and proteins, for the analysis of recombinant protein formulation, hemoglobins, human serum, and plasma proteins. Discontinuous electrolyte solution systems are also employed in capillary isotachopheresis (CITP), where the analytes migrate as discrete zones with an identical velocity between a leading and a terminating electrolyte solution having different electrophoretic mobilities. CITP finds large applications as an on-line preconcentration technique prior to CZE, MECC, and CGE. It is also employed for the analysis of serum and plasma proteins and amino acids [12].

The majority of amino acids and short peptides have no, or only negligible, UV absorbance. Detection of these analytes often requires chemical derivatization using reagents bearing UV or fluorescence chromophores. High detection sensitivity, reaching the attomolar (10^{-21}) mass detection limit can be obtained using fluorescence labeling procedures in combination with laser-induced fluorescence detection [13]. A variety of fluorescence and UV labeling reagents are currently employed, including *o*-phthaldehyde (OPA), fluorescein isothiocyanate (FITC), 1-dimethylaminonaphthalene-5-sulfonyl chloride (dansyl chloride), 4-



phenylspiro[furan-2(3H)-1'phthalene (fluorescamine), and naphthalene dicarboxaldehyde (NDA). However, derivatization may reduce the charge-to-hydrodynamic radius ratio differences between analytes, making separations difficult to achieve. In addition, precolumn derivatization is not suitable for large peptides and proteins, due to the formation of multilabeled products. These problems can be overcome using postcolumn derivatization procedures.

Another, very attractive alternative is indirect UV detection [14]. This indirect detection procedure makes use of a UV-absorbing compound (or "probe"), having the same charge as the analytes, that is incorporated into the electrolyte solution. Displacement of the probe by the migrating analyte generates a region where the concentration of the UV-absorbing species is less than that in the bulk electrolyte solution, causing a variation in the detector signal. In the indirect UV detection technique, the composition of the electrolyte solution is of critical importance, because it dictates separation performance and detection sensitivity.

Probes currently employed in the indirect UV detection of amino acids include *p*-aminosalicylic acid, benzoic acid, phthalic acid, sodium chromate, 4-(*N,N'*-dimethylamino)benzoic acid, 1,2,4-benzenetricarboxylic acid (trimellitic acid), 1,2,4,5-benzenetetracarboxylic acid (pyromellitic acid), and quinine sulfate. Several of these probes are employed in combination with metal cations and cationic surfactants, which are incorporated into the electrolyte solution as modifiers of the electro-osmotic flow.

Coupling mass spectrometry (MS) to capillary electrophoresis provides detection and identification of amino acids, peptides, and proteins based on the accurate determination of their molecular masses [15]. The most critical part of coupling MS to CE is the interface technique employed to transfer the sample components from the CE capillary column into the vacuum of the MS. Electrospray ionization (ESI) is the dominant interface which allows a direct coupling under atmospheric pressure conditions. Another distinguishing features of this "soft" ionization technique when applied to the analysis of peptides and proteins is the generation of a series of multiple charged, intact ions.

These ions are represented in the mass spectrum as a sequence of peaks, the ion of each peak differing by one unit of charge from those of adjacent neighbors in the sequence. The molecular mass is obtained by computation of the measured mass-to-charge ratios for the protonated proteins using a "deconvolution algorithm" that transforms the multiplicity of mass-to-charge ratio signals into a single peak on a real mass scale. Obtaining multiple charged ions is actually advantageous, as it allows the analysis of proteins up to 100–150 kDa using mass spectrometers with an upper mass limit of 1500–4000 amu.

Concentration detection limits in CE–MS with the ESI interface are similar to those with UV detection. Sample sensitivity can be improved by using ion-trapping or time-of-flight (TOF) mass spectrometers. MS analysis can also be performed off-line, after appropriate sample collection, using plasma desorption–mass spectrometry (PD–MS) or matrix-assisted laser desorption–mass spectrometry (MALDI–MS).

References

1. S. Hjerten, *Chromatogr. Rev.* 9: 122 (1967).
2. I. Rodriguez and S. F. Y. Li, *Anal. Chim. Acta* 383: 1 (1999).
3. J. E. Wiktorowicz and J. C. Colburn, *Electrophoresis* 11: 769 (1990).
4. Kleindiest, G., C. G. Huber, D. T. Gjerde, L. Yengoyan, and G. K. Bonn, *Electrophoresis* 19: 262 (1998).
5. D. Corradini, *J. Chromatogr. B* 699: 221 (1997).
6. P. G. Muijselaar, K. Otsuka, and S. Terabe, *J. Chromatogr. A* 780: 41 (1998).
7. M. A. Stregé and A. L. Lagu, *J. Chromatogr. A* 780: 285 (1997).
8. A. Guttman, *Electrophoresis* 17: 1333 (1996).
9. H. Kajiura, *Anal. Chim. Acta* 383: 61 (1999).
10. H. Wan and L. G. Blomberg, *J. Chromatogr. A* 875: 43 (2000).
11. R. Rodriguez-Diaz, T. Wehr, and M. Zhu, *Electrophoresis* 18: 2134 (1997).
12. P. Gebauer and P. Bocek, *Electrophoresis* 18: 2154 (1997).
13. K. Swinney and D. J. Bornhop, *Electrophoresis* 21: 1239 (2000).
14. S. Hjerten, K. Elenbring, F. Kilar, J.-L. Liao, A. J. C. Chen, C. J. Siebert, and M.-D. Zhu, *J. Chromatogr.* 403: 47 (1987).
15. R. D. Smith, J. A. Loo, C. J. Barinaga, C. G. Edmonds, and H. R. Udseth, *J. Chromatogr.* 480: 211 (1989).



Analysis of Alcoholic Beverages by Gas Chromatography

Fernando M. Lanças
M. de Moraes

Laboratório de Cromatografia, Instituto de Química de São Carlos, Universidade de São Paulo, São Carlos/SP, Brazil

Introduction

Alcoholic beverages have been consumed by a significant range of worldwide population since the beginning of civilization until the present time. Therefore, there should be a great interest on consumption of beverages quality and, consequently, the usage of a suitable analytical technique to verify and control this desirable quality.

Alcoholic beverages are classified, in a general way, in fermented beverages (such as beer, wine, sake, etc.) and distilled ones (vodka, whisky, aguardente, tequila, cognac, liquors, etc.). The main volatile substances present in most alcoholic beverages belongs to the following chemical classes: alcohols (including ethanol, methanol, isobutanol, 3-methyl butan-2-ol, etc.), esters (such as ethyl acetate, methyl acetate, ethyl isobutyrate, isoamyl acetate, etc.), aldehydes (propanal, isobutanal, acetal, furfural, etc.), acids (acetic acid, propionic acid, butyric acid, etc.) and ketones (acetone, diacetyl, etc.).

Some of the substances are of greater concern than the others due to its relative quantities or to its flavored characteristic [1]. As an example, ethanol is the major compound in the group of alcohols being responsible for the formation of various other substances, such as acetaldehyde, resulting from ethanol oxidation, and it is the most abundant of the carbonylic compounds in distilled beverages. For the same reason, acetic acid is the major compound within its group, the carboxylic acids.

Fusel alcohols (e.g., 1-propanol and 3-methyl butan-2-ol) as well as ethanol are also important substances in the alcohols group contributing to the flavor of distilled beverages because their odor is very distinctive and characteristic. There is an enormous variety of substances in small concentrations belonging to the esters group. Even so, ethyl acetate corresponds to more than 50% of the esters within this group.

These compounds are responsible to important characteristics as smell and taste, in which the large fraction of these substances originates from fermentation or during beverages storage [1].

Because gas chromatography (GC) is an analytical technique in which separation and identification of volatile compounds occurs, it might be considered the best technique for this kind of sample [2].

Analysis by Gas Chromatography

Analysis of alcoholic beverages by gas chromatography have as their main objectives to investigate flavoring compounds and contaminants which might be intentional or occasional. Whereas the former ones (the flavors) are analyzed to control their favorable characteristics to the beverage, the adulterants have to be controlled due to their deleterious contribution. Adulteration includes the addition of certain compounds to enhance a desirable flavor. Because these compounds are usually added as a racemic mixture, their presence can be verified using a suitable chiral column for enantiomer separation [3]. On the other hand, occasional contaminants are substances originating in small quantities during beverage production and might be carcinogenic. The main source might be raw materials like grape, sugar cane, and so forth contaminated with pesticides [4] or as a result of the fermentation process itself [5,6].

Comments in each major part of the GC instrumentation as used for beverage analysis are presented.

Sample Introduction

Distilled Beverages

Generally, samples are injected in the chromatographic system without any dilution or pretreatment step, using the split mode (i.e., with sample division), which is suitable for the analysis of the major compounds in beverages. When the objective of analysis is the determination of compounds present in small quantities ($\mu\text{g/L}$), some extraction and/or concentration step is necessary, followed by the sample injection in the splitless mode (without sample division). This last sample introduction mode is usually



combined with extraction techniques such as liquid–liquid extraction (LLE), solid-phase extraction (SPE) [4], and solid-phase microextraction (SPME) [7,8].

Fermented Beverages

Sample introduction is basically the same compared to the distilled one. Nevertheless, in many complex samples (i.e., some kind of wines), it is not advisable to inject them into the chromatograph without a pretreatment step.

Recently, SPME has provided many improvements as the cleanup step of complex samples, particularly for the analysis of volatile compounds by *headspace* techniques [8]. SPME is a solventless extraction and concentration technique which has advantages as a simple and economic technique that reduces health hazards and environmental issues.

Columns

Until 1960, all commercial chromatographic columns were packed in wide-bore tubing and separations had low resolution and low efficiency, taking a long time for a run to be completed. Since then, there have been significant improvements with the introduction of wall-coated open tubular (WCOT) columns, whose inner diameter was smaller than the packed ones are coated with a thin film of the liquid phase [9].

When capillary fused-silica columns arose, a large number of separations of complex samples have obtained success as a result of the higher number of plates (about 30 times over the packed columns in average).

Despite the efficient separations, it has been noticed that some low-boiling compounds of alcoholic beverages coeluted because of the use of a polar stationary phase. This column separates mainly based on the boiling temperatures of chemical substances, but separation becomes very difficult if there are some compounds with similar boiling temperatures. A polar stationary phase like poly(ethylene glycol) (PEG) is a better choice for this sort of problem because these separations are based on compound structures. In all cases, cross-linked or immobilized phases are recommended because they are more thermolabile and also resistant to most solvents. This is particularly important when splitless injection is used in combination with PEG-type phases because otherwise a severe column bleeding might be observed after $\sim 220^{\circ}\text{C}$.

Detection Systems

The flame ionization detector (FID) is one of the most commonly used detectors in beverage analysis by GC, as it is suitable to most groups of compounds investigated in alcoholic beverages [9]. This occurs because almost all compounds of interest in such samples are able to burn in the flame, forming ions and producing a potential difference measured by a collector electrode.

In trace analysis of contaminant substances, one can use specific detectors for certain compounds, such as a nitrogen–phosphorus detector (NPD), thus gaining detection ability for nitrogenated and phosphorylated compounds; the electron-capture detector (ECD) shows excellent performance for chlorinated substances and the flame photometric detector (FPD) is the most widely used for sulfur-containing compounds.

Gas chromatography–mass spectrometry (GC–MS) combination has become one of the most important coupling in analytical chemistry used for the confirmation of results obtained by other detectors [9]. This technique is based on the fragmentation of the molecules that arrives into the detector. Ion formation occurs and they are separated by the

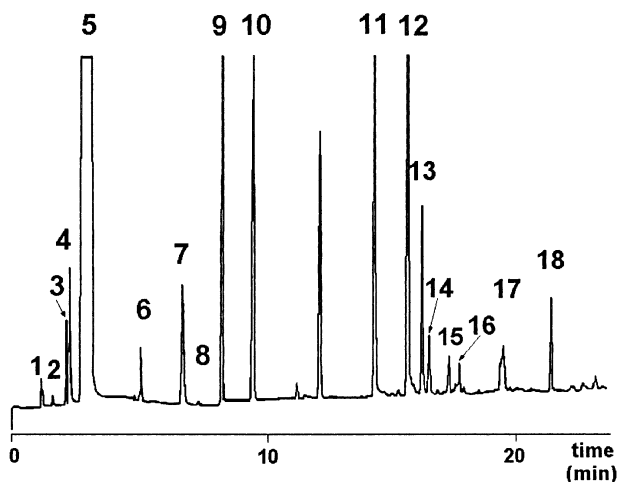


Fig. 1 Gas chromatographic analysis of white wine sample by fused-silica column poly(ethylene glycol) type (15.00 m \times 0.53 mm \times 1.00 μm). Chromatographic conditions: carrier gas: hydrogen (3.6 mL/min); column temperature: 40°C (4 min) \rightarrow $8^{\circ}\text{C}/\text{min} \rightarrow 270^{\circ}\text{C}$; injector port temperature: 250°C ; detector temperature: 300°C . Identity of the selected peaks: (1) acetaldehyde, (2) acetone, (3) ethyl acetate, (4) ethanol, (5) ethanol, (6) propanol, (7) isoamyl acetate, (8) *n*-butanol, (9) heptanone, (10) isoamyl alcohol, (11) acetic acid, (12) propionic acid, (13) isobutyric acid, (14) 2,3 butanediol, (15) 1,2 propanediol, (16) butyric acid, (17) isovaleric acid, (18) valeric acid.

mass/charge ratio (m/z) generally detected by a electron multiplier. Quantitative analysis can be realized through the single-ion monitoring (SIM) mode, where some characteristic ions are selected and monitored increasing the detection sensibility and selectivity. Another qualitative technique, gas chromatography–sniffing [10] is very much used for flavor analysis, despite discordance among researchers. In this case, the volatile substances from a extract are separated by GC, and as they leave the equipment through a specially designed orifice, a trained analyst is able to smell some of the substances and tentatively identify them.

More than 500 compounds have been found in concentrated flavor extracts in distilled beverages [1]. For this reason, there is an obvious necessity to find and optimize analytical techniques capable of investigating and to keep trading control of the alcoholic beverages. Among them, gas chromatography has been far from any other preferred tool for the analysis of alcoholic beverages.

Acknowledgments

Professor Lanças wishes to express his acknowledgments to FAPESP (Fundação de Amparo à Pesquisa do Estado de São Paulo), CNPQ (Conselho Nacional de Desenvolvimento Científico e Tecnológico), and CAPES (Coordenação de Aperfeiçoamento e Pessoal de Nível Superior) for financial support to our laboratory and a fellowship to Marcelo de Moraes.

References

1. L. Nykänen and I. Nykänen. Distilled beverages, in *Volatile Compounds in Foods and Beverages*, H. Maarse (ed.), Marcel Dekker, Inc., New York, 1991, pp. 547–580.
2. F. M. Lanças and M. S. Galhiane, Fast routine analysis of light components of alcoholic beverage using large bore open tubular fused silica column, *Bol. Soc. Chil. Quim.* 38: 177 (1993).
3. W. A. König, new developments in enantiomer separation by capillary gas chromatography, in *Analysis of Volatiles Methods, Applications*, P. Schreier (ed.), Berlin, 1984, pp. 77–91.
4. A. Kaufmann, fully automated determination of pesticides in wine, *J. AOAC Int.* 80(6): 1302 (1997).
5. J. F. Lawrence, B. D. Page, and B. S. Conacher, the formation and determination of ethyl carbamate in alcoholic beverages, *Adv. Environ. Sci. Technol.* 23: 457 (1990).
6. K. Shiomi, Determination of acetaldehyde, acetal and other volatile congeners in alcoholic beverages, *J. High Resol. Chromatogr.* 14(2): 136 (1991).
7. J. Pawliszyn, *Solid Phase Microextraction—Theory and Practice*, Wiley–VCH, New York, 1997, pp. 1–247.
8. D. de la C. Garcia, M. Reichenächer, K. Danzer, C. Hurlbeck, C. Bartsch, and K. H. Feller, analysis of wine bouquet components using headspace solid phase micro extraction–capillary gas chromatography, *J. High Resol. Chromatogr.* 21(7), 373 (1998).
9. R. M. Smith, *Gas and Liquid Chromatography in Analytical Chemistry*, John Wiley & Sons, London, 1988, pp. 1–401.
10. N. Abbott, P. Etievant, D. Langlois, I. Lesschaeve, and S. Issanchou, Evaluation of the representativeness of the odor of beer extracts prior to analysis by GC eluate sniffing, *J. Agric. Food Chem.* 41(5): 777 (1993).





Analysis of Food Colors by Thin-Layer Chromatography/Scanning Densitometry

Hisao Oka

Yuko Ito

Tomomi Goto

Aichi Prefectural Institute of Public Health, Nagoya, Japan

INTRODUCTION

Many synthetic and natural colors are used in foods all over the world. In Japan, 12 synthetic and 66 natural colors are generally permitted for use in foods. The Japanese government requires labeling on the package concerning kinds of colors that have been used in the contained foods. However, nonpermitted colors are also frequently detected in food, and also unlabeled foods are found in the market. Thus, the inspection of colors in foods has been performed by a public health agency.

The analyses of colors in foods have been mainly achieved by thin-layer chromatography (TLC), because TLC is a simple and effective technique for the separation of components in a mixture. However, the only useful information obtained from a TLC plate to identify a component is the R_f value; the identification of the separated components is difficult unless an appropriate spectrometric method, such as ultraviolet-visible absorption spectrometry, is used. A stepwise operation, including individual component separation by TLC and measurement of the spectrum, is laborious and time-consuming, because it requires extra steps such as extraction of the desired compound from the TLC plate and elimination of adsorbents.

TLC/scanning densitometry is a useful tool for the identification of the target compounds on a TLC plate, because the combined methods can separate and then directly measure ultraviolet-visible absorption spectra of the compounds without the laborious and time-consuming procedures described above. In this paper, we deal with the identification of synthetic and natural colors in foods using TLC/scanning densitometry.

SYNTHETIC COLORS

A simple and rapid identification method for synthetic colors in foods has been established, using TLC/scanning densitometry.^[1] Forty-five synthetic colors were able to be completely separated on a C18 TLC plate by complementary use of the following four solvent systems: 1) acetonitrile–methanol–5% sodium sulfate (3:3:10);

2) methyl ethyl ketone–methanol–5% sodium sulfate (1:1:1); 3) acetonitrile–methanol–5% sodium sulfate (1:1:1); and 4) acetonitrile–dichloromethane–5% sodium sulfate (10:1:5). We measured the visible absorption spectra of the synthetic colors on the developed C18 TLC plates by scanning densitometry to identify them. The spectra of the colors purified from foods were in close agreement with those of the standard colors, and the reliability of identification was established.

Next, we successfully applied this technique to the identification of an unknown synthetic color in a pickled vegetable.^[2] This color was suspected to be orange II (Or-II), which is not permitted for use in foods in Japan. It was difficult to identify Or-II by conventional analytical methods for food colors, including TLC and high-performance liquid chromatography (HPLC), because there are actually three isomers in total: orange I (Or-I), orange RN (Or-RN), and Or-II, due to differences in the positions of hydroxyl groups in the molecules. Under conventional TLC or HPLC conditions, it is hard to separate these isomers from each other. As shown in Fig. 1 (left), the unknown color showed the same R_f value as those of Or-II and Or-RN, although it showed a different R_f value from Or-I. In order to identify the unknown color, we measured the visible absorption spectrum of the color using TLC/scanning densitometry and compared it with those of Or-II and Or-RN. Both spectra of the unknown color and Or-II gave maximum absorption at only 485 nm; however, that of Or-RN showed maximum absorption at 485 and 400 nm. Therefore, we identified the unknown color in the pickled vegetable to be Or-II.

Thus, TLC/scanning densitometry is shown to be effective for the identification of an unknown synthetic color in foods.

NATURAL COLORS

Lac Color and Cochineal Color

Lac color is a natural food additive extracted from a stick lac, which is a secretion of the insect *Coccus laccae*

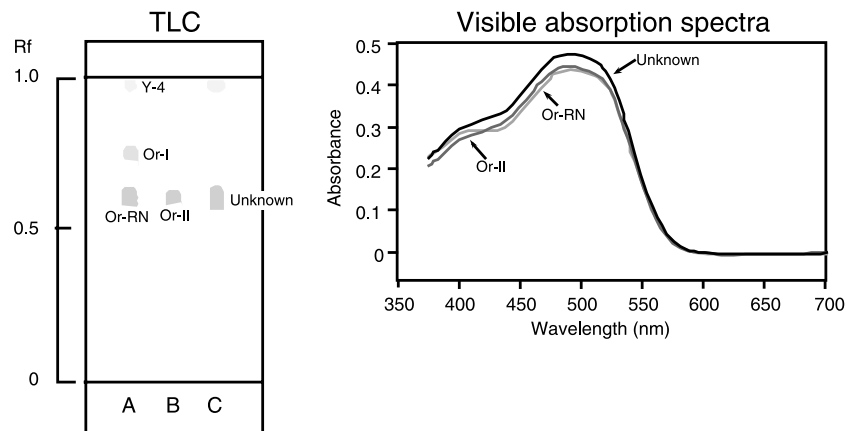


Fig. 1 Thin-layer chromatograms and visible absorption spectra of synthetic colors extracted from a pickled vegetable under TLC/scanning densitometry. (A) Standards of tartrazine (Y-4), orange I (Or-I), and orange RN (Or-RN). (B) Standard of orange II (Or-II). (C) Extract of the sample. TLC/scanning densitometric conditions. Plate: RP-18 (E. Merck). Solvent system: methyl ethyl ketone-methanol-5% sodium sulfate (1:1:1). Apparatus: Shimadzu CS-9000. Wavelength scanning range: 370–700 nm. Slit size: 0.4×0.4 mm. Measuring mode: reflecting absorption.

(*Laccifer lacca* Kerr), and is widely used for coloring food. It is known that the red color is derived from a water-soluble pigment including laccaic acids A, B, C, and E. Cochineal color extracted from the dried female bodies of the scale insect (*Coccus cacti* L.) is water-soluble and has a reddish color. The main coloring component is carmic acid.

Because these colors are frequently used in juice, jam, candy, jelly, etc., it is required to establish a simple and rapid analysis method using TLC. However, as described in the “Introduction,” the only useful information obtained from a TLC plate to identify a component is the Rf value. Therefore, we applied TLC/scanning densitometry to the identification of lac and cochineal colors in foods.^[3]

TLC conditions

After various experiments, the best results were obtained using methanol–0.5 mol/L oxalic acid (5:4.5) as the solvent system, with a C18 TLC plate. As shown in Fig. 2 (left), the lac color standard was separated into two spots at Rf values of 0.60 and 0.29, and cochineal color standard gave a spot at Rf value of 0.52. Anthraquinone compounds, such as lac and cochineal colors, showed extreme tailing on the C18 TLC plate using conventional TLC conditions. We have previously found that the use of a solvent system containing oxalic acid is effective for controlling the tailing of anthraquinone compounds. Therefore, we decided to use a solvent system containing oxalic acid and tried various TLC conditions. Finally, we found the best conditions described above.

Measurement of visible absorption spectrum by scanning densitometry

Reflection spectra of the spots of lac color standard at Rf values of 0.60 and 0.29 and cochineal color standard at Rf value of 0.52 on the TLC plate were taken under the conditions described above. The obtained spectra showed good agreement with the spectra obtained from methanol solutions. Therefore, we considered that TLC/scanning densitometry is effective for the identification of these natural colors.

Application to commercial food

Reproducibility of the Rf Value by Reversed Phase TLC. In order to examine the effects of the contaminants contained in the sample on the Rf value, 122 commercial foods (41 foods for lac color and 81 foods for cochineal color) were analyzed by C18 TLC as described above. The obtained Rf values of the spots were then compared. The difference between the Rf value of the standard color and the Rf value of the color in the sample was expressed as the ratio between the Rf value of the color in the sample (Ra) and the Rf value of the standard color (Rs); the reproducibility was evaluated according to the coefficient of variation of this ratio.^[4] With respect to lac color, the average Ra/Rs values were 0.99 with a coefficient of variation of 8.1% and 1.00 with 4.6% for spots at Rf values of 0.29 and 0.60, respectively. Cochineal color gave an average Ra/Rs value of 0.99 with a coefficient of variation of 5.9%. These results suggest that the spots extracted from the samples appear nearly at the same positions as those of

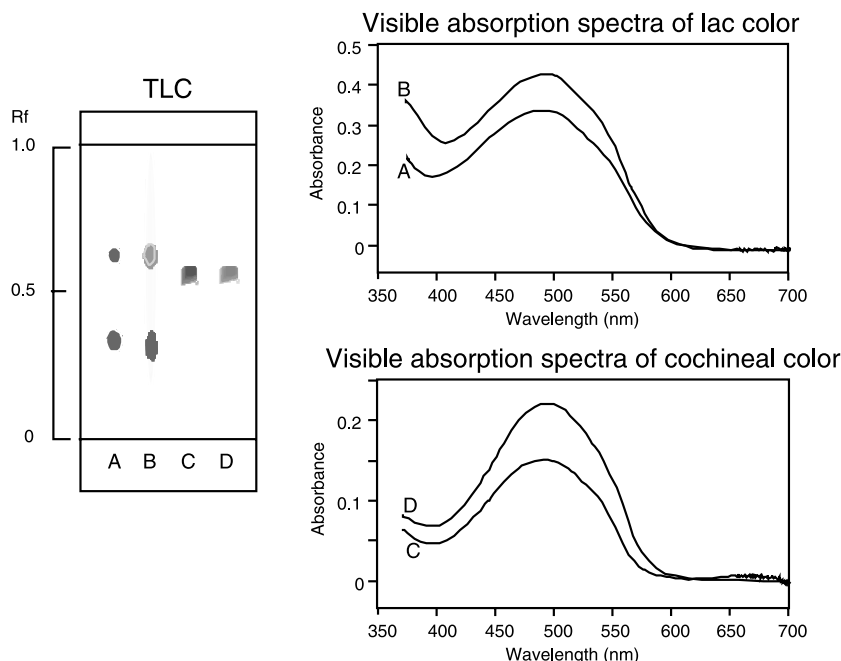


Fig. 2 Thin-layer chromatograms and visible absorption spectra of lac color and cochineal color extracted from commercial foods under TLC/scanning densitometric conditions. (A) Lac color standard. (B) Extract of jelly. (C) Cochineal color standard. (D) Extract of spaghetti sauce. Plate: RP-18 (E. Merck). Solvent system: methanol-0.5 mol/L oxalic acid (5.5:4.5). Other conditions: see Fig. 1.

the lac color and the cochineal color standard without being affected by contaminants in the sample, and that the identification of the color is reliable and reproducible.

Identification by TLC/Scanning Densitometry. The visible absorption spectra of the spots of the lac and cochineal colors on the C18 TLC plates, for which the reproducibility of the Rf value had been evaluated, were measured using a scanning densitometer. Fig. 2 shows the typically obtained TLC chromatograms and spectra obtained from the spots. The spectra of the colors purified from foods were in good agreement with those of the standard colors; thus, the reliability of identification was then established.

Paprika Color

Paprika color is obtained by extraction from the fruit of red peppers (*Capsicum annuum*) and contains capsanthin and its esters, formed from acids, such as lauric acid, myristic acid, and palmitic acid, in large amounts as its color components. Commercially available paprika colors are known to have different compositions of these color components, depending on the material from which the paprika color is extracted; this makes the identification of paprika color, based on the analysis of the color components, impossible, causing difficulty in developing a simple, rapid, and reliable identification method for the

paprika color in foods. Therefore, we investigated a TLC/scanning densitometric method for the identification of paprika color using capsanthin, which is a main product of saponification, as an indicator.^[5]

TLC conditions

When a paprika color standard, before saponification, was subjected to C18 TLC, a number of overlapping spots were observed, and a satisfactory separation could not be obtained. This was probably due to the paprika color containing a large number of esters. Paprika color is known to be hydrolyzed into a carotenoid and a fatty acid when saponified under mild conditions. Thus, a paprika color standard, after saponification, was subjected to TLC using a solvent system of acetonitrile–acetone–*n*-hexane (11:7:2) on a C18 plate. It was found that the paprika color standard, after saponification, was satisfactorily separated into a main spot having an Rf value of 0.50 and two subspots having Rf values of 0.60 and 0.75 (Fig. 3A). The main spot was identical with the spot of the capsanthin standard in terms of its Rf value, color, and shape (Fig. 3C).

As described above, it was suggested that the paprika color is hydrolyzed into a carotenoid and a fatty acid by saponification under mild conditions. Next, the saponification conditions were investigated; based on various experimental results, the following saponification condi-

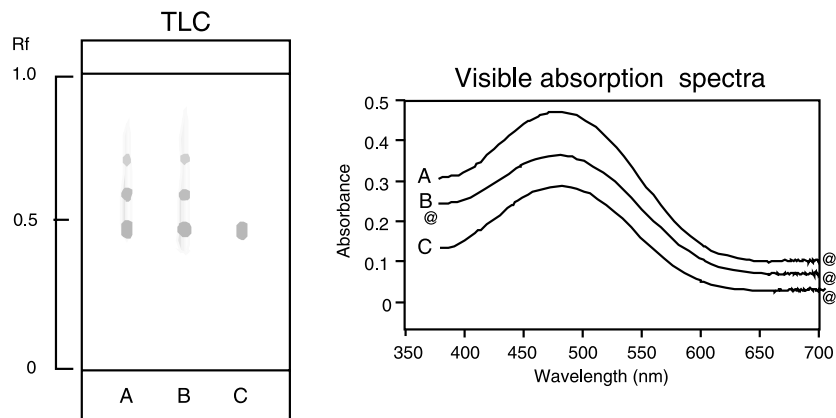


Fig. 3 Thin-layer chromatograms and visible absorption spectra of hydrolyzed paprika colors extracted from commercial foods under TLC/scanning densitometric conditions. (A) Hydrolyzed paprika color standard. (B) Hydrolyzed extract of rice-cracker. (C) Capsanthin. Plate: RP-18 (E. Merck). Solvent system: acetonitrile-acetone-*n*-hexane (11:7:2). Other conditions: see Fig. 1.

tions were selected: reaction time, 24 hr; amount of 5% sodium hydroxide-methanol solution, 2 mL.

Measurement of visible absorption spectrum by scanning densitometry

The separated spots, obtained by subjecting a paprika color standard, after saponification, to C18 TLC under the conditions described above, were then subjected to scanning densitometry. The visible absorption spectra were scanned in the wavelength range of 370–700 nm, and excellent visible absorption spectra were obtained (Fig. 3A). The spectrum of the main spot ($R_f=0.50$) of the paprika color, after saponification, showed its maximum absorption wavelength at 480 nm, which identically matches the spectrum of the capsanthin standard (Fig. 3C).

Application to commercial foods

Reproducibility of the R_f Value by Reversed-Phase TLC. The paprika color in 42 samples from commercially available foods, that had a label stating the use of paprika color, were analyzed by C18 TLC to examine the influence of the coexisting substances from the sample on the R_f value. The obtained R_f values of the main spot ($R_f=0.50$) of saponified paprika color were then compared, and R_a/R_s value was computed. The average R_a/R_s value was 1.01 with a coefficient of variation of 2.6%, suggesting that the spot extracted from the samples appear nearly at the same position as that of the paprika color standard without being affected by contaminants in the sample and that the identification of the color is reliable and reproducible.

Identification by Reversed-Phase TLC/Scanning Densitometry. The visible absorption spectra of the main spot of the saponified paprika color on the C18 TLC plates, for

which the reproducibility of the R_f value had been evaluated, were measured using a scanning densitometer. Fig. 3 shows the typically obtained TLC chromatograms and spectra obtained from the spots. The spectra of the colors purified from foods were in good agreement with those of the standard colors, and the identification reliability was then established.

Gardenia Yellow

Gardenia yellow is a yellow color obtained by extracting or hydrolyzing the fruit of the *Gardenia augusta* MERR. var. *gardiflora* HORT. with water or ethanol and is widely used for the coloring of noodles, candies, and candied chestnuts. The yellow color is derived from the carotenoids crocin and crocetin. Crocetin is the hydrolysis product of crocin. Gardenia yellow has been conventionally analyzed by a method based on reversed-phase chromatography/scanning densitometry using crocin as the indicator. However, when this method was applied to samples containing caramel or anthocyanins, their spots overlapped with that of crocin, which made it difficult to identify the gardenia yellow. Therefore, we evaluated an analytical method for gardenia yellow based on C18 TLC/scanning densitometry using crocetin as the indicator by hydrolyzing crocin, extracted from food samples, into crocetin.^[6]

Hydrolysis and TLC conditions

In order to examine the optimal hydrolysis conditions of crocin, a standard crocin solution was hydrolyzed by varying the pH of the solution, temperature, and incubation time; the degree of hydrolysis was followed by C18 TLC as described below. Samples of crocin were completely hydrolyzed to crocetin by adjusting the pH to 11 or above with 0.1 mol/L sodium hydroxide and incu-

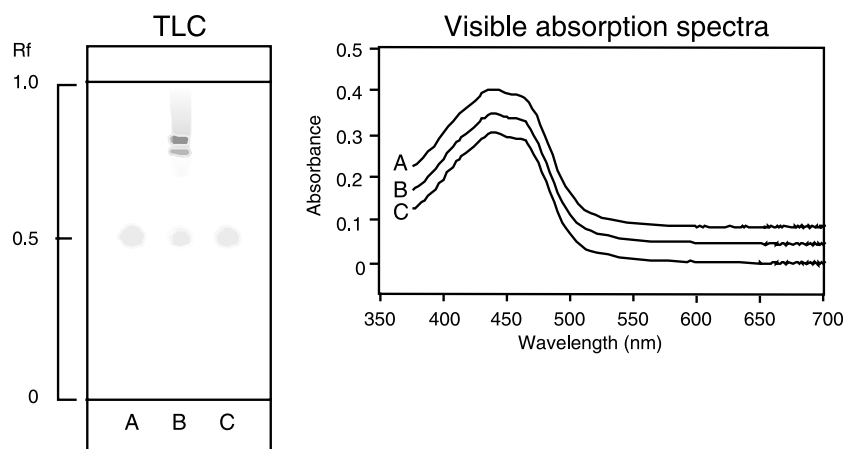


Fig. 4 Thin-layer chromatograms and visible absorption spectra of the hydrolyzed gardenia yellow extracted from commercial foods under TLC/scanning densitometry. (A) Hydrolyzed gardenia yellow standard. (B) Candy containing gardenia yellow and anthocyanin. (C) Crocetin. Plate: RP-18 (E. Merck). Solvent system: acetonitrile-tetrahydrofuran-0.1 mol/L oxalic acid (7:8:7). Other conditions: see Fig. 1.

bating them at 50°C for 30 min. Therefore, we applied these conditions to hydrolyze crocin to crocetin in the subsequent work.

Next, we investigated the optimal TLC conditions for the separation of crocin and crocetin and found that the combined use of a C18 TLC plate and solvent system of acetonitrile-tetrahydrofuran-0.1 mol/L oxalic acid (7:8:7) gave a satisfactory separation. Under these TLC conditions, crocin gives three spots at R_f values of 0.74, 0.79, and 0.83, and crocetin gives one spot at an R_f value of 0.51 (Fig. 4, left).

Measurement of visible absorption spectrum by scanning densitometry

Reflection spectra of the spots on the TLC plates separated under the conditions described above were measured at scanning wavelengths of 370–700 nm. Fig. 4 (right) shows the visible absorption spectra obtained; the maximum absorption wavelengths were 435 and 460 nm, being in complete agreement with the visible absorption spectrum for the standard preparation of crocetin.

Application to commercial foods

As described above, foods that contained caramel or anthocyanins, for which the identification of gardenia yellow was impossible by the analytical method using crocin as an indicator due to the appearance of interfering spots at the same positions as the spots of crocin on the C18 TLC plates, were analyzed by the present method. As shown in Fig. 4 (left), crocetin appeared as a clear spot on the plate, and the shape and R_f value of the spot were in

close agreement with those of the standard preparation. Hence, gardenia yellow can be identified using crocetin as the indicator.

Reproducibility of the R_f Value by Reversed-Phase TLC. To examine the influence of the contaminants contained in the sample on the R_f value, 37 commercial foods were analyzed by C18 TLC. The obtained R_f values of the spots were then compared. The mean value of R_a/R_s was 0.99, and the coefficient of variation was 2.5%. These results suggest that the spots of crocetin generated by hydrolysis appear nearly at the same positions as those of the standard color, without being affected by contaminants in the sample, and that the identification of the color is reliable and reproducible.

Identification by Reversed-Phase TLC/Scanning Densitometry. The visible absorption spectra of the crocetin spots on the reversed-phase TLC plates, for which the reproducibility of the R_f value had been evaluated, were measured using a scanning densitometer. Fig. 4 shows the typically obtained TLC chromatograms and spectra obtained. The spectra of the colors purified from foods were in close agreement with that of the standard dye, and the identification reliability was then established.

CONCLUSIONS

We introduced the identification of food colors in foods using TLC/scanning densitometry and consider the method to be sufficiently applicable to routine analyses at facilities such as the Centers of Public Health and the Food Inspection Office. Also, we consider that TLC/

scanning densitometry is applicable to the identification of various food additives, drugs, and pesticides in foods. However, TLC/scanning densitometry has a limitation: It can be applied only to samples which have chromophores in the molecules. Recently, applications of the TLC/matrix-assisted laser desorption ionization time-of-flight mass spectrometry (TOF MS),^[7] TLC/fast atom bombardment MS,^[7] and TLC/multiphoton ionization TOF MS^[8] have been reported. Combined uses of these techniques and TLC/scanning densitometry can develop further applications of TLC.

REFERENCES

1. Ohno, T.; Ito, Y.; Mikami, E.; Ikai, Y.; Oka, H.; Hayakawa, J.; Nakagawa, T. Identification of coal tar dyes in cosmetics and foods using reversed phase TLC/scanning densitometry. *Jpn. J. Toxicol. Environ. Health* **1996**, *42*, 53–59.
2. Ueno, E.; Ohno, T.; Oshima, H.; Saito, I.; Ito, Y.; Oka, H.; Kagami, T.; Kijima, H.; Okazaki, K. Identification of small amount of coal tar dyes in foods by reversed phase TLC/scanning densitometry with sample concentration techniques. *J. Food Hyg. Soc. Jpn.* **1998**, *39*, 286–291.
3. Itakura, Y.; Ueno, E.I.; Ito, Y.; Oka, H.; Ozeki, N.; Hayashi, T.; Yamada, S.; Kagami, T.; Miyazaki, Y.; Otsuji, Y.; Hatano, R.; Yamada, E.; Suzuki, R. Analysis of lac and cochineal colors in foods using reversed phase TLC/scanning densitometry. *J. Food Hyg. Soc. Jpn.* **1999**, *40*, 183–188.
4. Ozeki, N.; Oka, H.; Ikai, Y.; Ohno, T.I.; Hayakawa, J.; Sato, T.; Ito, M.; Ito, Y.; Hayashi, T.; Yamada, S.; Kagami, T.; Miyazaki, Y.; Otsuji, Y.; Hatano, R.; Yamada, E.; Suzuki, R.; Suzuki, R. Application of reversed phase TLC to the analysis of coal tar dyes in foods. *J. Food Hyg. Soc. Jpn.* **1993**, *34*, 542–545.
5. Hayashi, T.; Ueno, E.; Ito, Y.; Oka, H.; Ozeki, N.; Itakura, Y.; Yamada, S.; Kagami, T.; Miyazaki, Y. Analysis of β -carotene and paprika color in foods using reversed phase TLC/scanning densitometry. *J. Food Hyg. Soc. Jpn.* **1999**, *40*, 356–362.
6. Ozeki, N.; Oka, H.; Ito, Y.; Ueno, E.; Goto, T.; Hayashi, T.; Itakura, Y.; Ito, T.; Maruyama, T.; Tsuruta, M.; Miyazawa, T.; Matsumoto, H. A reversed-phase thin-layer chromatography/scanning densitometric method for the analysis of gardenia yellow in food using crocetin as an indicator. *J. Liq. Chromatogr.* **2001**, *24*, 2849–2860.
7. Wilson, I.D. The state-of-the-art in thin-layer chromatography–mass spectrometry: A critical appraisal. *J. Chromatogr., A* **1999**, *856*, 429–442.
8. Krutchinsky, A.N.; Dolgin, A.I.; Utsal, O.G.; Khodorovski, A.M. Thin-layer chromatography–laser desorption of peptides followed by multiphoton ionization time-of-flight mass spectrometry. *J. Mass Spectrom.* **1995**, *30*, 375–379.

Analysis of Mycotoxins by TLC

Philippe J. Berny

Unité de Toxicologie, Ecole Nationale Veterinaire de Lyon, Marcy l'Etoile, France

Introduction

Thin-layer chromatography (TLC) is a widely used analytical technique for many investigative purposes. Detection of mycotoxins by means of TLC has been in use for many years. Official methods of analysis often rely on these techniques for both identification and quantification of several mycotoxins [1].

Mycotoxins are natural toxins produced by fungi contaminating foods and feeds. They may be extremely toxic [e.g., aflatoxin (*Aspergillus flavus*), which is a potent carcinogen [2]. They may be found in plant-derived products, but also in the tissues of exposed animals, where they can accumulate and, thus, be a serious health hazard for human beings. Consequently, many analytical methods have been developed in order to assess the potential contamination of food derived either from plants or from food-producing animals. A third group of analytical techniques has been developed for diagnostic purposes in animals without any direct public health hazard. In this article, we will briefly review some of the techniques available to address these three goals.

Analysis of Plants and Plant-Derived Products for Mycotoxins

Analysis of plants may yield very interesting results, because they are the major carrier of fungi and of mycotoxins. The presence of a genus of fungus may or may not be associated with the production of mycotoxins, depending on the climatic conditions at the time of harvest, for instance [3]. Therefore, it is extremely interesting to have qualitative as well as quantitative methods for the determination of mycotoxins in these matrices. Numerous techniques have been developed to determine the nature and degree of contamination of plants with mycotoxins; it would not be possible to present all of them in a single article.

Extraction and cleanup procedures usually require solid-phase extraction based on commercially available C₁₈ cartridges, for instance, after liquid extraction with common organic solvents (methylene dichloride,

chloroform, acetonitrile [3–5]). This step appears to be necessary to remove most of the interfering components such as carotenoids or chlorophylls, which are highly abundant in plants. Table 1 gives a list of some of the mycotoxins which can be analyzed by TLC, together with analytical features (plate material, elution, detection/visualization, limit of detection). Of particular interest are the following products: aflatoxins B₁, B₂, G₁, and G₂, zearalenon, ochratoxin, and fumonisins B₁ and B₂ in maize. Recently, high-performance TLC (HPTLC) techniques have also been applied to forage samples commonly infected with an endophyte considered as symbiotic but responsible for disorders in animals [5]. These mycotoxins include lolitrems and ergot alkaloids.

Thin-layer chromatographic plates used are generally silica gel plates, although C₁₈ reversed-phase TLC plates may occasionally be used [4]. Elution may be monodimensional or bidimensional [3]. The former is more common. Recent automated gradient techniques appear promising for the simultaneous determination of several mycotoxins in a single sample. Solvents used for elution depend on the type of plate used. Most of the time, organic solvents (ethanol chloroform, acetone) are used. One feature of HPTLC is that it uses much less solvent than high-performance liquid chromatography (HPLC) and permits analysis of many samples in a very short time [5].

Detection may be based on several techniques; older systems used postelution derivatization [8] and observation of colored spots. It is more common now to use either ultraviolet (UV) [5] or even fluorescence [3, 4] because these techniques allow quantification of mycotoxin residues. More complex systems have been tested (computer imaging [7]) for particular applications, but these techniques are not applied to routine analysis of plants.

Analysis of Animal Tissues

Because animals may accumulate mycotoxins in their tissues, and considering the high toxicity of some products, it is a public health concern to have analytical



techniques available for routine detection and quantitation of residues of these compounds in edible tissues of food-producing animals. Analysis of animal tissues may be difficult for several reasons:

1. Mycotoxins are poorly concentrated in many tissues or biological fluids (e.g., muscle or milk) and the analytical method employed should be sensitive enough to detect down to a few micrograms mycotoxins per kilogram sample or even less (aflatoxins in muscle samples, for instance [2]).
2. Tissues and organs may contain interfering substances on chromatograms or densitograms.

For extremely toxic compounds like aflatoxins, acceptable daily intakes (ADI) have been defined and it is, therefore, necessary to check suspected tissues to monitor residues at this level.

Thin-layer chromatography and HPTLC offer many advantages over other conventional methods (gas chromatography, HPLC), such as rapidity, simplicity, and sensitivity. However, it is usually necessary to extract and purify samples before spraying them onto TLC plates. In the case of aflatoxins, for instance, a commonly employed technique is based on liquid extraction by an organic solvent (chloroform), followed by purification on a silica gel column. The column has to be washed to elute interfering substances (with hexane and ether) and aflatoxins are eluted individually or all together with a specific combination of solvents (chloroform and acetone) [2].

If the purpose of the TLC technology is only to screen samples, the results may be merely qualitative.

Older methods were usually based on the visual determination of dark spots on a bright fluorescent plate under UV light. Another use of TLC in the determination of mycotoxin residues is as preparative TLC, in which specific spots are visualized, scraped, and resublimized for further analysis (Association of Official Analytical Chemistry).

More and more, however, quantitative analysis can be performed by means of scanners (UV, fluorescence), and HPTLC does not need to be completed by another analytical technique for the precise determination of residues. Today, most official methods of analysis for the detection of mycotoxins in foods are based on TLC technology.

Diagnostic Purposes

Mycotoxicoses may induce various pathological disorders in animals as well as in human beings. Considering the poor specificity of the signs observed and the very low concentrations of the toxic compounds in most biological tissues or fluids, it is necessary to be able to analyze, promptly and efficiently, biological samples to evaluate the risk of mycotoxicosis. The most common mycotoxins involved include aflatoxins, fumonisins, ochratoxin, zearalenon, and T2 toxin [9]. Analysis is usually based on foods and feeds (cereals, etc.). In swine, for instance, an epidemiological study conducted on feed samples detected ochratoxin (mean 58.3 µg/kg) and zearalenon (mean 30.3 µg/kg) in corn. These concentrations were associated with respiratory disorders and also infertility [10]. The advantage of TLC/HPTLC in such a situa-

Table 1 Examples of HPTLC Methods for the Determination of Mycotoxins in Biological Samples

Mycotoxin	Plate	Matrix	Elution	Detection	Results	Ref.
Aflatoxins B1, G1, M1	Si60	Muscle, liver, kidney	1-Hexane/tetrahydrofuran/ethanol 2-CHCl ₃ /methanol	Fluorescence	LOD ^a : 0.01 µg/kg (B1, M1) LOD: 0.005 µg/kg (G1)	2
Fumonisin B1, B2	C18	Corn	Methanol/KCl 4% in water	Fluorescamin Fluorescence	LOD: 0.1 (B2), 0.5 (B1) µg/kg, re- covery > 80%	4
Lolitrems	Si60	Forage	CH ₂ Cl ₂ /acetonitrile	UV (268 nm)	LOD: 0.1 mg/kg, recovery > 90%	5
Patulin	Si60	Fruit	1-Hexane/diethylether, 2-diethylether	UV (273 nm)	LOD: 40–100 µg/kg	7
Zearalenon	Si60	Corn	Toluene/ethylacetate/formic acid	Fluorescence	LOD: 2.6 µg/kg, recovery > 63%	10

^aLOD = limit of detection.

tion is that it provides rapid and specific analysis of food samples at a low cost and, therefore, a reasonable cost/benefit ratio for breeders. If the diagnosis has to be confirmed on animal/human tissues or fluids, depending on the compound of interest, HPTLC techniques may also be available and convenient (see above).

Conclusion

Thin-layer chromatography and HPTLC offer many possibilities for the determination of mycotoxins in plant or animal samples. Plant samples usually contain higher concentrations of mycotoxins, but analysis of animal tissues may be necessary either to confirm a suspected mycotoxicosis or to detect potential residues for human food. Many official methods are available, based on TLC, and the recent development of HPTLC also offers many possibilities for the detection and quantitation of several mycotoxins in various biological samples.

References

1. R. Stubblefield, J. P. Honstead, and O. L. Shotwell, *J. Assoc. Off. Anal. Chem.* 74(6): 897 (1991).
2. A. Fernandez, R. Belio, J. J. Ramos, M. C. Sanz, and T. Saez, *J. Sci. Food Agric.* 74: 161 (1997).
3. S. I. Phillips, P. W. Wareing, A. Dutta, S. Panigrahi, and V. Medlock, *Mycopathology* 133: 15 (1996).
4. G. E. Rottinghaus, C. E. Coatney, and H. C. Minor, *J. Vet. Diagn. Invest.* 4(3): 326 (1992).
5. P. Berny, P. Jaussaud, A. Durix, C. Ravel, and S. Bony, *J. Chromol.* 769: 343 (1997).
6. Y. Liang, M. E. Baker, B. Todd Yeager, and M. Bonner Denton, *Anal. Chem.* 68: 3885 (1996).
7. P. F. Ross, L. G. Rice, R. D. Plattner, G. D. Osweiler, T. M. Wilson, D. L. Owens, H. A. Nelson, and J. L. Richard, *Mycopathology* 114(3): 129 (1991).
8. G. D. Osweiler, T. L. Carson, W. B. Buck, and G. A. Van Gelder, *Clinical and Diagnostic Veterinary Toxicology*, 3rd ed., Kendall/Hunt, Dubuque, 1988.
9. C. Ewald, A. Rehm, and C. Haupt, *Berlin. Münch. Tierärztlich. Wochen.* 104(5): 161 (1991).
10. M. Dawlatana, R. D. Coker, M. L. Nagler, G. Bluden, and G. W. O. Oliver, *Chromatographia* 47: 215 (1998).



Analysis of Plant Toxins by TLC

Philippe J. Berny

Unité de Toxicologie, Ecole Nationale Veterinaire de Lyon, Marcy l'Etoile, France

Introduction

Analysis of plants is a vast and complex field of analytical chemistry. There is a constant need for new compounds or active ingredients for pharmaceutical or other interesting properties. Plant chemistry is such that a wide variety of compounds may be produced within the different organs. Toxins usually represent only a small fraction of the total organic matter of the plant. It is important, however, to be able to analyze and detect those toxins, especially when poisoning cases are suspected. Although vegetal toxins are extremely diverse in nature, a common feature among them is that they are heatunstable. Consequently, standard gas chromatographic (GC) or GC-MS (mass spectrometric) procedures cannot be routinely used to detect them, and the use of liquid chromatography appears of benefit.

Analysis of plant toxins is required in the following circumstances:

1. When plant poisoning is suspected in human beings or in animals: In this situation, the analyst must be able to separate the plant toxin from its plant matrix and/or from an animal tissue of fluid. The toxin is also diluted as compared with the plant product.
2. For research or development purposes: when a family of plants is under investigation and the presence of a toxin is suspected and not expected (therapeutic use).
3. When a family of toxins is wellknown, like the pyrrolizidine alkaloids [1], it is highly interesting to screen suspected plants for their presence when poisoning is suspected in animals and there may be some residues in food, even in animals which did not present any disorder.

In this article, we will review some examples of these three areas of plant chemistry and see how thin-layer chromatography (TLC) or high-performance thin-layer chromatography (HPTLC) can fulfill the various requirements.

Investigation of Suspected Poisoning Cases

Poisoning by plants can occur with various animal species, including human beings. It obviously occurs most frequently in herbivores like cattle or sheep and examples of analytical investigation are more common in these species. Unfortunately, it is generally necessary to screen rumen content for plant toxins and this matrix is extremely rich in organic constituents, including natural pigments. Careful and adapted cleaning steps are necessary. When alkaline or acidic substances are to be determined, pH-based liquid-liquid separation may be used.

Our first example is based on a very severe acute poisoning case with yew trees (*Taxus* sp.). These trees contain a highly toxic group of toxins known as taxins. Cattle or sheep usually do not eat the leaves or branches of yew trees because of their bitter taste. Unfortunately, bitterness tends to disappear when the leaves are dessicated, but toxicity remains and animals may eat enough to become deadly sick. One published example mentioned poisoning in 43 cattle, with 17 dead before any treatment or diagnosis could be attempted [2]. Diagnosis may rely on the epidemiological evidence of poisoning (cut branches) or on necropsy (branches in the rumen), but these elements may not necessary be conclusive and analytical techniques may represent the only way of confirming a tentative diagnosis. The published method for yew tree analysis in cattle relied on the analysis of rumen contents and identification of taxol. This alcohol is specific of the *Taxus* genus, although it may not be the toxic substance, but it is easily obtained from commercial dealers, whereas taxins have to be extracted and purified.

The development of scanners for HPTLC also offers better potential and we have further developed the method of Panter et al. [2] with ultraviolet (UV) scanning (at 238 nm) and quantification prior to derivatization (confirmatory analysis). Eventually, diagnosis relies on the determination of Taxins (primarily taxin B) in the rumen content. As an example, Fig. 1 provides a densitogram of a rumen content with identification of



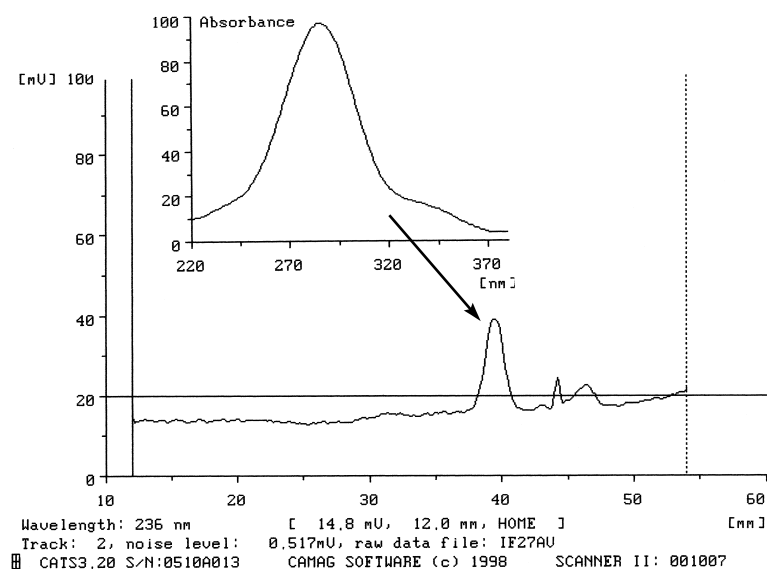


Fig. 1 Rumen content with taxin B (arrow) and its UV spectrum.

taxin peaks and the solid-phase UV spectrum of this compound in a case of confirmed yew tree poisoning. The same technique could be applied to determine the most toxic part of the plant, the effect of season on the toxin content, and so forth. For example, it was found that the leaves contained about 0.03% taxol, while the stem and twigs contained around 0.001% and 0.0006%, respectively [2].

Identification of Toxins in Plant Screenings for Research or Development Purposes

Some plants are famous for the presence of toxic substances. One major group of toxicants involved is the pyrrolizidine alkaloids. These substances induce severe poisoning manifested by emaciation, anemia, and skin lesions which may develop over months or years and may eventually result in the death of the poisoned animals. These compounds represent both a toxic and economic threat in some areas of the world, (e.g., in the Himalayans [1]). Screening of plants may be highly desirable to prevent these losses. Winter et al. [1] developed screening methods based either on high-performance liquid chromatography (HPLC) or on TLC. They used silica gel plates with a mixture of ethylacetate, acetone, ethanol, and ammonia (5/3/1/1) and postchromatographic derivatization with *o*-chloranil and Erlich's reagent. This technique was only qualitative but gave results in accordance with reference HPLC techniques. With these two techniques, the au-

thors analyzed over 350 samples (various plants, plant parts, and locations) to determine the presence and amount of alkaloids.

Another example of the use of TLC in research is given by Ma et al. [3], who used TLC as a taxonomic tool to classify plants. Their example was based on the lycopodium alkaloids of plants from the Lycopodiaceae family. The TLC technique used was qualitative and also relied on postchromatographic derivatization with Dragendorff's reagent [3]. It should be stated that plant toxins are usually recognized by means of qualitative TLC and visualization based on postchromatographic derivatization procedures. Common solutions rely on common reactions of alkaloids, and the use of Dragendorff's reagent is one of these solutions (combined mixture of tartaric acid, bismuth nitrate, and potassium iodide), and vanillin reagent enables the detection of amines and amino acids.

The Chinese pharmacopoea uses a wide range of plants and herbal medicines and Chinese scientists have been publishing methods and techniques for decades, identifying therapeutic substances or toxic ingredients of traditional remedies. The interested reader should refer preferentially to the *Journal of Chinese Herbal Medicine* to find analytical methods.

Identification of new compounds may start with TLC analysis of plant extracts. For instance, Jakupovic et al. [4] isolated and further identified several diterpenes from *Euphorbia segetalis*. Similarly, chamomile essential oil (*Chamomilla reticulata*) was analyzed with 11 different development systems and the authors discussed

both the most efficient (separation power) and the ideal way they are to be used to identify an unknown component in such a complex mixture, using the minimum number of TLC systems [5]. This area of work still has to be investigated, considering the wide variety of the vegetal reign and of potential plant toxins.

Detection of Residues in Food

This part is certainly the least developed, to our knowledge. It is important to remember, however, that an animal may ingest a toxic plant and may also survive. If this is the case, and provided this animal or its production are intended for human consumption, one should be able either to analyze tissues and fluids for toxin residues or to monitor fluids (plasma, milk, urine) to determine whether this animal or its productions can be considered safe for human consumption. There are very limited examples of such occurrences. In our laboratory, we analyzed muscular tissues after a confirmed yew tree poisoning case (*Taxus baccata*). Three animals did not display any significant trouble except for a transient depression, which resolved itself after 12 h. These animals were butchered and muscle samples were analyzed for taxin residues, as they were known to be exposed to it. Our analytical technique (extraction in alkalinized methylene dichloride) followed by TLC development based on a modification of a published technique (9685), showed that the muscle samples contained between 0.012 and 0.015 $\mu\text{g/g}$ taxin (wet weight). The presence of taxin in muscle tissues had never been previously reported in cattle after moderate poisoning. Based on this result, the meat was

not considered edible. This example is, simply, to illustrate that residues of plant toxins in food-producing animals should be part of a research or development protocol whenever possible.

Conclusion

Plant toxins represent one of the most important areas of analytical development and the few techniques related herein should only be considered as mere examples of the numerous possibilities of TLC in this field. With the development of densitometry and multiple development systems, the separation power of TLC and its quantitative potential are increasing as well. Considering the usual thermal instability of many plant toxins and their high polarity, HPTLC certainly offers one of the most powerful technologies for the detection, identification, and quantification of plant toxins.

References

1. H. Winter, A. A. Seawright, H. J. Noltie, A. R. Mattocks, R. Jukes, K. Wangdi, and J. B. Gurung, *Vet. Rec.* 134: 135 (1994).
2. K. E. Panter, R. J. Molyneux, R. A. Smart, L. Mitchell, and S. Hansen, *J. Amr. Vet. Med. Assoc.* 202: 1476 (1993).
3. X. Q. Ma, S. H. Jiang, and D. Y. Zhu, *Biochem. Syst. Ecol.* 26: 723 (1998).
4. J. Jakupovic, F. Jeske, T. Morgenstern, J. A. Marco, and W. Berendsohn, *Phytochemistry* 47: 1583 (1998).
5. M. Medic-Saric, G. Stanic, Z. Males, and S. Saric, *J. Chromatogr. A* 776: 355 (1997).



Analysis of Terpenoids by Thin-Layer Chromatography

Simion Gocan

"Babeş-Bolyai" University, Cluj-Napoca, Romania

INTRODUCTION

Terpenes are among the most widespread and chemically diverse groups of natural products. Fortunately, despite their structural diversity, they have a simple unifying feature by which they are defined and by which they may be easily classified. Terpenes are a unique group of hydrocarbons, based on isoprene or an isopentane structure.

Terpenes can be classified by the number of five-carbon units they contain: hemiterpene (C_5), monoterpene (C_{10}), sesquiterpene (C_{15}), diterpene (C_{20}), triterpene (C_{30}), and tetraterpene (C_{40}). Like the monoterpenes, most of the sesquiterpenes are considered to be essential oils because they belong to the steam distillable fraction. Diterpenes have higher boiling points; they are considered to be resins. Triterpenes include common triterpenes, steroids, saponins, sterolins, and cardiac glycosides. The most common tetraterpenoids are the carotenoids. Sesquiterpenes exist in a variety of forms, including linear, bicyclic, and ticyclic frameworks. The type of cyclization can be with open chain, mono-, bicyclic, etc. Also, the number and positions of the double bonds, the asymmetric centers, and the type and number of functional groups distinguish numerous components of each group.

Terpenoids can be classified also into hydrocarbons, alcohols, carbonyl compounds, phenols, acids, esters, oxides, and peroxides.

CHROMATOGRAPHIC SEPARATION

Hydrocarbons

Generally speaking, thin-layer chromatography (TLC) has a large number of applications. The first problem with which the analyst is confronted concerns gathering information regarding the mixture to be separated, in terms of mixture polarity and the range of molecular masses. In the case of hydrocarbons that have one nonpolar character, an adsorption separation technique is

recommended. Terpene hydrocarbons (mono- and sesquiterpene) can be conveniently separated on layers of silica gel or alumina. Moreover, highly active layers are necessary. After the usual drying, they have to be stored in a vacuum desiccator at 30 mm Hg, containing potassium hydroxide as a desiccant. Because of the weak polar nature of the compounds, solvents of low polarity must be used as mobile phases for the separation. The most frequently used solvents as the mobile phase are as follows: petroleum ether, hexane, isopentane, dimethylbutane, cyclohexane, methylcyclohexane, benzene, chloroform, benzene-acetone (95:5, v/v), benzene-ethyl acetate (2:1, v/v), and toluene. The choice of solvent depends upon the polarities of the components of the terpene hydrocarbon mixtures on the desired separation. For the detection (visualization) of the compounds after separation, the solvent will be evaporated from the plate and various zones will be indicated by spraying with suitable reagents. On spraying with a fluorescein solution and exposing to bromine vapor, compounds that absorb bromine faster than the fluorescein show up as yellow spots on a pink background. Other reagents can be used for detection with good results; they include iodine vapor, vanilin/ H_2SO_4 , or $KMnO_4/H_2SO_4$, and a chloroform solution of antimony pentachloride. Very unreactive compounds can be located by spraying with a concentrated sulfuric-nitric acid mixture and heating to cause charring of the compounds.^[1,2] Table 1 gives the hR_f values of some terpenes on silica gel and alumina in various solvents used as mobile phases.

A good separation of sesquiterpene hydrocarbons has been performed on alumina in combination with a perfluoroalkane (70°C to 80°C) mobile phase.^[3]

To increase the resolution in TLC separation of some monoterpenes, silver nitrate-impregnated silica gel, with benzene as the mobile phase, was used. Three conclusions were drawn from these studies:^[7] 1) cyclic terpenes with a single internal double bond did not readily form a π -complex; 2) cyclic or acyclic terpenes with two nonterminal double bonds do not readily form π -complexes unless the double bonds are *cis* conjugated; and 3) cyclic or acyclic terpenes with exocyclic or terminal double bonds do form π -complexes.

Table 1 R_f values of terpenes and color reaction with vanillin/ H_2SO_4 reagent

Compound	Silica gel					Alumina			Silica gel impregnated AgNO ₃		Vanillin/H ₂ SO ₄ color after 30 min
									25 %	3.125 %	
	S ₁	S ₂	S ₃	S ₄	S ₅	S ₁	S ₆	S ₇	S ₈		
<i>Monoterpenes</i>											
Camphene	83	84	79	94	79	95			53		Light orange
<i>p</i> -Cymene	67	38	62	95	60	89					None
Limonene	41	54	96	66					35	62.5	Bluish green
<i>d</i> -Limonene	76					93					Bluish green
β-Myrcene	74					92					Blue
Mircene									20	50.5	Blue
α-Ocimene	71					91					Blue
<i>t</i> -β-Ocimene	71					91					Blue
Ocimene									35	52.0	Blue
α-Phellandrene									41	63.0	Blue
β-Phellandrene	79					93			50		Blue
α-Pinene	90	83	84	96	83	96			67		Blue
β-Pinene	88	80	75			95			46		Blue
α-Pyronene	80					90					Blue
β-Pyronene	80					90					Blue
Sabinene	75					93			29		Blue
Terpinolene	75	64	60			92			62		Bluish green
α-Terpinene	76					93			49	70.5	Bluish green
γ-Terpinene	76					93			59		Bluish green
α-Thujene	80					95					Blue
Verbenene	81					95					Blue
<i>Sesquiterpenes</i>											
		F	G								
γ-Bisabolene	71	10	8			93	50	33			Brownish green
δ-Cadinene	72	20	12			93	71	35			Dark blue
β-Caryophyllene	74	30	16			94	65	44			Purple
α-Cedrene	89	44	36			96	73	56			Purple
α-Humulene	65	12	8			90	35	30			Lavender
β-Santalene	78	20	15			94	64	48			Dark blue
β-Selenene	78	17	13			94	41	33			Dark green
Valencene	76	21	17			93	51	32			Maroon
Yalangene	88	40	32			96	87	64			Lavender
β-Zingaberene	75	18	13			94	57	30			Dark green

S_1 =Skellysolve B (hexanes);^[3] S_2 =hexane;^[4] S_3 =cyclohexane;^[4] S_4 =benzene;^[5] S_5 =15% ethyl acetate in hexane;^[5] S_6 =perfluoroalkene, b.p. 70–80°C;^[3] S_7 =low boiling perfluokerosene;^[3] S_8 =benzene, 25% $AgNO_3$,^[6] and 3.125% $AgNO_3$.^[7] Vanillin/ H_2SO_4 .^[3]

The silver nitrate-impregnated silica gel (25%) was applied to the separation of some sesquiterpenes. It was found that a mixture of β -selinene and caryophyllene could be separated satisfactorily by development with *n*-hexane and benzene–acetone (95:5, v/v) as mobile phases.^[18] After the development, the plates are dried in air and then sprayed with a solution of chlorosulfonic acid in acetic acid (1:2) and heated at 130°C. Usually, different

colored spots are observed, e.g., humulene, brown; caryophyllene, blue; longifolene, pink.

Oxygenated Terpenes

The problem of identifying individual compounds from essential oils is often complicated by the similarities in

molecular structures and physical properties. In a very important instance, the R_f values serve as a means of distinguishing two classes of material-hydrocarbons from nonhydrocarbons. Hydrocarbons have an appreciable R_f

value with hexane as the mobile phase, whereas non-hydrocarbons have an R_f equal to zero (Table 2). By use of this property, it is possible to separate hydrocarbons from oxygenated compounds for the preparation of

Table 2 R_f values of some oxygenated terpenes and other essential oil constituents on silica gel in various eluent systems

Compound	Eluent system							Reagent
	S ₁	S ₂	S ₃	S ₄	S ₅	S ₆	S ₇	
<i>Alcohols</i>								
Citronellol	0	19	27	39	41	14		Yellow brown ^a
Nerol	0	14	26	38	42	16		Yellow brown ^a
Geraniol	0	12	20	40	43	15		Yellow brown ^a
Linaloo	0	15	36	47	45	25		Yellow brown ^a
α-Terpineol	0	8	29	34	36	16		Yellow brown ^a
Menthol						21		
<i>d</i> -Neomentol						29		Yellow brown ^a
Borneol						17		
<i>Aldehydes</i>								
Citral	0	15	45	64	57		10	Yellow brown ^b
Lauric aldehyde	4	50	58	72	67			
Cinnamaldehyde	0	9	31	70	68			Orange brown ^b
Vanillin						5		Yellow orange ^b
Asarylaldehyde						6		Orange ^b
Furfural	0	6	21	44	41	10		Violet ^b
Anisaldehyde						13		Yellow ^b
Cuminic aldehyde						25		Yellow ^b
Benzaldehyde						25		
<i>Ketones</i>								
Carvone	0	37	45	72	62		10	Gray brown ^b
Methyl heptenone	0	35	48	74	62		13	Gray brown ^b
Pulegone	0	60	58	65	76			
Camphor	0	28	56	39	55			
Fenchone							9	Gray brown ^b
Piperitone							8	Gray brown ^b
Menthone							20	Gray brown ^b
Methyl nonyl ketone							16	Gray brown ^b
<i>Esters</i>								
Geranyl acetate	0	27	69	66	52			Gray blue ^c
Neryl acetate	0	39	69	56	50			Gray blue ^c
Citronellyl acetate	0	35	68	66	57			
Octyl acetate	0	50	98	98	82			
Terpinyl acetate	0	42	66	61	55			Gray blue ^c
Methyl anthranilate	0	26	52	65	53			
Ethyl anthranilate	0	25	58	70	46			
Carvyl acetate	0	64	69	79	67			
<i>Oxides</i>								
1,8-Cineol	0	12	48	68	68			
Linaloöl monoxide	0	3	21	20	20			

S₁=hexane;^[4] S₂=chloroform (alcohol-free);^[4] S₃=ethyl acetate-hexane (15:85, v/v);^[4] S₄=ethyl acetate-chloroform (alcohol-free) (10:90, v/v);^[4] S₅=ethyl acetate-benzene (15:85, v/v);^[4] S₆=ethyl acetate-benzene (5:95, v/v);^[9] S₇=benzene.^[2]

^aAntimony pentachloride.

^b*o*-Dianisidine.

^cVanillin/H₂SO₄.

terpene oils. Table 2 contains the hR_f values of oxygenated terpenes on a silica gel thin-layer plate in different solvents that have been found useful for characterizing these types of materials.

Terpene Alcohols

The alcohols were chromatographed on silica gel using various eluent systems. The compounds were detected with the fluorescein–bromine reagent. The phosphomolybdenic acid reagent is very sensitive but nonspecific. The anisaldehyde–sulfuric acid reagent is of higher sensitivity and specificity.

It is possible to achieve a separation of the stereoisomeric menthols on silica gel G layers using chloroform and a series of solvents that are nearly isoelutotropic with chloroform.^[2] The following hR_f values were obtained: menthol, 32; isomenthol, 29; neomenthol, 40; and neoisomenthol, 36. With anisaldehyde–sulfuric acid, a blue violet color is obtained. Another example is the stereoisomeric separation of *trans*, *trans*-farnesol, and *cis*, *trans*-farnesol on silica gel using ethyl acetate–benzene (5:95, v/v) as the mobile phase, giving hR_f values of 27 and 36, respectively. For the detection of these substances, the vanillin/ H_2SO_4 reagent proved suitable.^[10] This system, slightly modified, which used benzene–ethyl acetate (80:20, v/v), gives a good separation of all the stereoisomers of farnesol present in a commercial mixture, as well as other terpene alcohols.^[11]

The silver nitrate-impregnated silica gel G was used to obtain a separation with a group of tetracyclic triterpene alcohols, which could not be separated on untreated silica gel. However, on silica gel G (Ag impregnated), the R_f values were sufficiently different so as to enable the substances to be identified separately. Chloroform was used as the mobile phase. The tetracyclic triterpenes were detected by spraying with one of the three reagents: 50% sulfuric acid in water or 10% phosphomolibdic acid in ethanol or chlorosulfonic and acetic acids (1:2) followed by heating in an oven at 150°C.^[12]

Besides normal-phase TLC, reversed-phase TLC was used by impregnating the silica gel layer with paraffin or silicone oil and using hydrophilic solvents as mobile phases. By this method, it is possible to achieve a good separation of alcohols belonging to groups with the same number of carbon atoms.

Acids and Esters

Essential oils often contain esters of terpene alcohols; the most common are the acetates, formates, propionates, etc. The separation of different esters was performed on silica

gel layers, using benzene, chloroform, and other similar solvents as mobile phases. All of the color reactions for terpene alcohols can be used for the detection of their esters. No differences have been observed in the color esters function as a result of their acid nature.

A group of triterpenic acids were found in *Bredemeyera floribunda*, *Alphitonia excelsa*, and *Crataegus oxyacantha*.^[13] The separation was carried out on silica gel layers using diisopropyl ether–acetone (5:2, v/v). In this case, oleanic, oleanonic, ursolic, and betulinic acids showed the same hR_f value, i.e., 68. As cochalic, bredemolic, and machaerinic acids gave tailings in this eluent, addition of 5% pyridine to the same solvent gave the following R_f values: 15, 62, and 27, respectively. The compounds were detected with chlorosulfonic acid.

Another example of applications concerning separation of piperonylic, 5-, 2-, and 6-methoxypiperonylic acids was performed on silica gel layers using ethyl acetate–hexane–acetic acid (50:50:0.5, v/v) as the mobile phase. Detection was performed by spraying with a chromotropic–sulfuric acid reagent. With these conditions the following hR_f values of 64, 54, 47, and 37 were obtained, respectively.^[14]

Aldehydes and Ketones

These compounds appear in various essential oils and are distinguished by characteristic odors. Some of them are easily produced by synthesis and are frequently used in the perfume industry. Aldehydes and ketones can be separated on silica gel thin-layer plates with solvents such as hexane, chloroform, and benzene in different proportions with ethyl acetate, or only in chloroform or benzene. The detection of the aldehydes can be performed by spraying with a solution of *o*-dianisidine in glacial acetic acid. Some ketones can be detected with the fluorescein–bromine spray, but compounds such as camphor, which are very unreactive, could be detected only by spraying with concentrated sulfuric acid containing nitric acid, followed by heat. A 5% solution of $AlCl_3$ in ethanol is specific for sesquiterpene lactones. Other terpenes, steroids, antrachinones, glycosides, and alkaloids do not interfere, nor do other types of lactones such as coumarins, cardenolides, and saturated or unsaturated γ -lactones. The reaction gives a violet or brown color on the layer, or yellow, brown, or green fluorescence under UV radiation at 366 nm, after spraying a plate with reagent solution and heating at 120°C for 10 to 15 min.^[15]

The 2,4-dinitrophenylhydrazones have also been used as a means of separating terpene carbonyl compounds. The oxo-terpene was separated by means of these derivatives using silica gel with chloroform–carbon



tetrachloride in various proportions (1:19, 1:9, 1:5.6 v/v) as well as petroleum ether-benzene (3:7, v/v). No spraying agent was used, as the spots themselves were distinctly colored.^[16]

The ionone derivatives and pseudoionones were separated on silica gel layers with benzene as the mobile phase. The compounds, after development, were detected by spraying with either 2,4-dinitrophenylhydrazine or a vanillin-sulfuric acid mixture. The following mean R_f values were obtained: pseudoionone, 0.384; α -ionone, 0.580; β -ionone, 0.505; α -methylionone, 0.756; and β -methylionone, 0.699.^[17] For improved separation, 14 terpenoids, e.g., α - and β -ionone, were subjected to TLC on silica gel impregnated with 15% AgIO_3 , with benzene-ethyl acetate (4:1, v/v) as the mobile phase. The spots were detected by spraying the dried plate with methanol-sulfuric acid and heated at 110°C. The R_f values obtained were approximately equal to or considerably higher than those obtained on AgNO_3 -impregnated plates.^[18]

Oxides and Peroxides

Oxides and peroxides can occur in many essential oils by a photochemical reaction. 1,8-Cineol and linalool monoxide can be readily separated on silica gel thin layers with 1-nitropropane-hexane (1:1, v/v), as the mobile phase.^[4] In this case, they have exhibited R_f values of 73 and 8, respectively.^[4] Another pair of compounds, ascaridole and 1,8-cineol, can be easily separated on a silica gel layer, obtaining a value for chloroform as the mobile phase of 63 and 54, respectively.^[2] The antimony chloride reagent gives a gray color. The potassium iodide-acetic acid-starch test is usually better than ferrous thiocyanate.

Phenylpropane and Phenol Derivatives

The separation of the hydroxyphenylpropane derivatives used in medicine and the perfume industry is of particular interest. Today, many useful drugs can be obtained from plants. Thin-layer chromatography is one of the most rapid methods for the identification of the active substances in medicinal plant extracts containing hydroxyphenyl propane derivatives. Using silica gel plates with benzene solvent as the mobile phase could separate a series of these compounds. Besides silica gel thin layers, alumina and polyamide layers were used in combination with different solvents as mobile phases, for instance, chloroform, petroleum ether-acetic acid (95:5, v/v), or petroleum ether-pyridine (95:5, v/v). There are many different color reagents that can be used for the detection of the spots. A blue coloration is obtained after spraying with the phosphomolybdic acid reagent. The clearest color

distinction is obtained by spraying a mixture of antimony tri- and penta-chloride (1:1), or anisaldehyde-sulfuric acid. Antimony trichloride solution makes the colors intense, but the spots do not show fluorescence immediately in long-wave UV light; but it does appear in about 1 day. Besides the R_f values, the colors of fluorescence can contribute to the identification of some compounds. For instance, eugenol methyl ether gives a greenish-yellow fluorescence, and isoeugenol methyl ether (*cis-trans* mixture) shows up reddish brown.^[1,2]

The following rules were obtained from the R_f values of a large group of phenylpropane and phenol derivatives under the conditions described above: 1) The polarity of the compound increases with increasing number of free phenol groups (OH). 2) Methylation of the hydroxyl group (OCH_3) decreases the polarity. The R_f values decrease with increasing of the methoxy number. For silica gel with benzene as the mobile phase in a saturation chamber: anethol, 1 OCH_3 , $hR_f=56$; eugenolmethyl ether, 2 OCH_3 , $hR_f=15$; and asarone, 3 OCH_3 , $hR_f=10$. 3) The effect of hydrogen bond formation between two adjacent phenolic groups and the consequent decrease in the polarity: *ortho*-compound < *p*-compound (safrol, $hR_f=57$, and catechol, $hR_f=0$). 4) Increase in the size of the alkylating group decreases the polarity: propenyl guaetol < benzyleugenol < methyleugenol. 5) When functional groups are situated closely together, the adsorption affinity of each is decreased and the R_f value of the compound increases. 6) The introduction of an aliphatic side chain on the nucleus has a negligible effect on the R_f values.^[1,2]

Phenylpropane derivatives (feluric, caffeic, and chlorogenic acids) and flavonoids were identified in a methanolic extract from flowers of *Sambuci nigra* by using TLC on silica gel 60 F₂₅₄. The efficiency of 10 TLC eluent systems was investigated by three mathematical techniques. It has been established that the favorable mobile phases for TLC of compounds investigated are ethyl acetate-methanol-water (100:13.5:2.5:10, v/v) and ethyl acetate-formic acid-water (8:1:1, v/v).^[19] In the same manner, there were selected optional solvent systems for the separation of caffeic acid, chlorogenic acid, and some flavonoids from methanolic extracts from *Lavandula flos*. It has been shown that the best eluent systems are ethyl acetate-formic acid acetic acid-water (100:11:11:27, v/v) and ethyl acetate formic acid-water (8:1:1, v/v).^[20] Also, for TLC separation of the methanolic extract from *Rosmarinus officinalis* L. the system ethyl acetate-formic acid-acetic acid-water (100:11:11:27, v/v) has been found.^[21] Detection of the phenolic acids and flavonoids was achieved by spraying the plates with 1% methanolic diphenylboryloxyethylamine, then 5% ethanolic polyethylene glycol 4000. The chromatograms were evaluated in UV light at 366 nm

(phenolic acids appeared as blue spots and flavonoids as orange-yellow fluorescent spots).^[22]

REFERENCES

1. Kirchner, J.G. *Thin-Layer Chromatography*, 2nd Ed.; John Wiley & Sons: New York, 1978; 897–923.
2. Stahl, E. *Thin-Layer Chromatography, A Laboratory Handbook*; Springer-Verlag: Berlin, 1965; 187–210.
3. Attaway, J.A.; Barabas, L.J.; Wolford, R.W. *Anal. Chem.* **1965**, *37*, 1289–1290.
4. Miller, J.M.; Kirchner, J.K. *Anal. Chem.* **1953**, *25*, 1107–1108.
5. Kirchner, J.G.; Miller, J.M.; Keller, G.J. *Anal. Chem.* **1951**, *23*, 420–425.
6. Schantz, M.V.; Juvonen, S.; Hemming, R. *J. Chromatogr.* **1965**, *20*, 618–620.
7. Lawrence, B.M. *J. Chromatogr.* **1968**, *38*, 535–537.
8. Gupta, A.S.; Dev, S. *J. Chromatogr.* **1963**, *12*, 189–195.
9. Schantz, M.V.; Juvonen, S.; Oksanen, A.; Hakamaa, I. *J. Chromatogr.* **1968**, *38*, 364–372.
10. Tyihák, E.; Vágújfalvi, D.V.; Hágony, P.L. *J. Chromatogr.* **1963**, *11*, 45–49.
11. McSweeney, G.P. *J. Chromatogr.* **1963**, *1*, 183–185.
12. Ikan, R. *J. Chromatogr.* **1965**, *17*, 591–593.
13. Tschesche, R.; Lampert, F.; Santzke, G. *J. Chromatogr.* **1961**, *5*, 217–224.
14. Beroza, M.; Jones, W.A. *Anal. Chem.* **1962**, *34*, 1029–1030.
15. Villar, A.; Rios, J.L.; Simeon, S.; Zafra-Polo, M.C. *J. Chromatogr.* **1984**, *303*, 306–308.
16. Vashist, V.N.; Handa, K.L. *J. Chromatogr.* **1965**, *8*, 412–413.
17. Dhont, J.H.; Dijkman, G.J. *Analyst (Lond.)* **1964**, *89*, 681–682.
18. Kohli, J.C.; Badaisha, K.K. *J. Chromatogr.* **1985**, *320*, 455–456.
19. Males, Z.; Medi-Šari, M. *J. Planar Chromatogr.* **1999**, *12*, 345–349.
20. Medi-Šari, M.; Males, Z. *Pharmazie* **1999**, *54*, 362–364.
21. Medi-Šari, M.; Males, Z. *J. Planar Chromatogr.* **1997**, *10*, 182–187.
22. Wagner, H.; Bladt, S.; Zainski, E.M. *Drogenanalyse*; Springer-Verlag: Berlin, 1983.



Analyte–Analyte Interactions, Effect on TLC Band Formation

Krzysztof Kaczmarek

Technical University of Rzeszów, Rzeszów, Poland

Mieczysław Sajewicz

Silesian University, Katowice, Poland

Wojciech Prus

School of Technology and the Arts in Bielsko-Biała, Bielsko-Biała, Poland

Teresa Kowalska

Silesian University, Katowice, Poland

INTRODUCTION

Chromatographic separations are mainly used for analytical purposes and, as such, are termed analytical chromatography. Chromatography, however, is gaining increasing importance as a tool that enables isolation of preparative amounts of the desired substances. Such “preparative chromatography” is usually achieved with LC and HPLC, but also occasionally with thin layer chromatography (TLC).

Each separation occurs because of the different interactions of each species with a sorbent. To describe the partitioning process, knowledge of the isotherm involved is needed. In analytical chromatography, the concentration of a species in an analyzed sample is very low, so description of the retention process typically requires knowledge of the slope of the isotherm when the concentration is zero.

When chromatography is used in the preparative mode, the entire dependence of the equilibrium on the concentrations of adsorbed and nonadsorbed solute must be established. The equilibrium isotherm is usually nonlinear and analysis of such isotherms is a necessary prerequisite to enable prediction of the retention mechanism.

OVERVIEW

Physicochemical description of retention processes in liquid chromatography (planar chromatography included) is far from complete and, therefore, new endeavors are regularly undertaken to improve existing retention models and/or to introduce the new ones. The excessive simplicity of already established retention models in planar chromatography is—among other reasons—because some types of intermolecular interaction in the chromatographic sys-

tems are disregarded. For example, none of the validated models focusing on prediction of solute retention takes into consideration so-called “lateral interactions,” the term used to denote self-association of solute molecules.

The aim of this report is to give insight into the role of lateral interactions in TLC band formation.

THEORY OF CHROMATOGRAPHIC BAND FORMATION

Study of the mechanism of adsorption in TLC is more difficult than in column liquid chromatography. The nonlinear isotherm model in TLC can be designed in a qualitative way only, after investigation of chromatographic band shape and of the concentration distribution within this band; phenomena characteristic of TLC band formation can also have a major effect on the mechanism of retention.

Transfer Mechanism in TLC

In TLC, as most frequently practiced, transfer of mobile phase through the thin layer is induced by capillary flow. Solvents or solvent mixtures contained in the chromatographic chamber enter capillaries in the solid bed, attempting to reduce both their free surface area and their free energy. The free-energy gain ΔE_m of a solvent entering a capillary is given by the relationship:

$$\Delta E_m = - \frac{2\gamma V_n}{r} \quad (1)$$

where γ is the free surface tension, V_n denotes the molar volume of the solvent, and r is the capillary radius.

From Eq. 1, it follows that the capillary radius r has a very important effect on capillary flow; a smaller radius

leads to more efficient flow. The methods used for preparation of commercial stationary phases and supports cannot ensure all pores are of equal, ideal diameter; this results in side effects that contribute to the broadening of chromatographic spots. Other mechanisms of spot broadening are described below.

Broadening of Chromatographic Bands as a Result of Eddy Diffusion and Resistance to Mass Transfer

The most characteristic feature of chromatographic bands is that the longer the development time and the greater the distance from the start, the greater become their surface areas. This phenomenon is not restricted to planar chromatography—it occurs in all chromatographic techniques. Band broadening arises as a result of eddy and molecular diffusion, the effects of mass transfer, and the mechanism of solute retention.

Eddy diffusion of solute molecules is induced by the uneven diameter of the stationary phase or support capillaries, which automatically results in uneven mobile phase flow rate through the solid bed. Some solute molecules are thus displaced more quickly than the average rate of displacement of the solute, whereas others are retarded.

Molecular diffusion is the regular diffusion in the mobile phase, the driving force of each dissolving process and, therefore, needs no further explanation.

The effects of mass transfer are different in the stationary and mobile phases. The resistance to mass transfer in the mobile phase varies with the reciprocals of mobile phase velocity and the diffusivity of the species. The resistance to mass transfer inside the stationary phase varies with the reciprocal of diffusivity and is proportional to the radius of the adsorbent granules attached to the chromatography plate, or the structural complexity of the internal pores in chromatographic paper. For both types of mass-transfer resistance, band stretching is proportional in each direction, as measured from the geometrical spot center, and increases in magnitude the greater the resistance.

All the aforementioned phenomena, which contribute jointly to spot broadening, are used to be described as the effective diffusion. Effective diffusion is a convenient notion, which, apart from being concise and informative, emphasizes that all the contributory phenomena occur simultaneously.

Broadening of Chromatographic Bands as a Result of the Mechanism of Retention

Mechanisms of solute retention, which are also responsible for spot broadening, differ from one chromatographic technique to another, and their role in this process is far

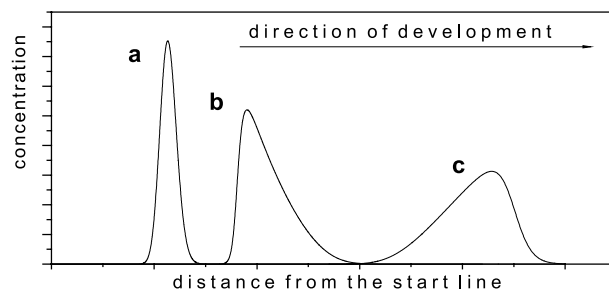


Fig. 1 Three examples of concentration profiles along the chromatographic stationary phase bed: (a) symmetrical without tailing, (b) skewed with tailing toward the mobile-phase front, and (c) skewed with tailing toward the origin.

less simple than that of diffusion and mass transfer. Use of densitometric detection has, however, furnished insight into concentration profiles across the chromatographic band, enabling estimation of the role of solute retention in peak broadening and prediction of the retention mechanism. Figure 1 shows three examples of such concentration profiles in the absence of mass overload.

Numerous efforts have been made to describe the band broadening effect and the formation of the concentration profiles. The most interesting models are those that consider band broadening as a two-dimensional process.

Two models of two-dimensional band broadening were established by Belenky et al.^[1,2] and by Mierzejewski.^[3] In these models, nonlinearity of the adsorption isotherm was neglected so that elliptical spots only, with symmetrically distributed concentration (as shown in Fig. 1a), could be modeled. We will now focus our attention on the effect of the adsorption mechanism on the concentration profiles of chromatographic bands.

ADSORPTION EQUILIBRIUM ISOTHERMS

Isotherm models reflect interactions between active sites on the sorbent surface and the adsorbed species and, simultaneously, interactions occurring exclusively among the adsorbed species. The dependence of isotherm shapes on concentration profiles in TLC is fully analogous to relationships between HPLC peak profiles and the isotherm models, which have been discussed in depth by Guiochon et al.^[4]

Let us briefly recall several chromatographic models and analyze the correspondence between concentration profiles and types of isotherm. The simplest isotherm model is furnished by Henry's law.

$$q = HC \quad (2)$$

where q is the concentration of the adsorbed species, H is Henry's constant, and C is the concentration in the mobile



phase. This isotherm is also called the linear isotherm, and concentration profiles obtained with its aid are similar to that shown in Fig. 1a. It should be stressed that, for the linear isotherm, peak broadening results from eddy diffusion and from resistance of the mass transfer only; it does not depend on Henry's constant. In practice, such concentration profiles are observed only for analyte concentrations that are low enough for the equilibrium isotherm to be regarded as linear.

One of the simplest nonlinear isotherm models is the Langmuir model.

$$q = \frac{q_s KC}{1 + KC} \quad (3)$$

where q_s is the saturation capacity and K the equilibrium constant. To make use of this isotherm, ideality of the liquid mixture and of the adsorbed phase must be assumed. Concentration profiles obtained with the aid of this isotherm are similar to that presented in Fig. 1c. The larger the equilibrium constant, the more stretched is the concentration tail (and the chromatographic band).

More complicated models take into account lateral interaction between the adsorbed molecules. One of these models was designed by Fowler and Guggenheim.^[5] It assumes ideal adsorption on a set of the localized sites, with weak interactions among molecules adsorbed on neighboring sites. It also assumes that the energy of interactions between two adsorbed molecules is so small that the principle of random distribution of the adsorbed molecules on the sorbent surface is not significantly affected. For liquid–solid equilibria, the Fowler and Guggenheim isotherm is empirically extended and written in the form:

$$KC = \frac{\theta}{1 - \theta} e^{-\chi\theta} \quad (4)$$

where χ denotes the empirical interaction energy between two molecules adsorbed on nearest-neighbor sites, and θ is the degree of the surface coverage. For $\chi=0$, the Fowler–Guggenheim isotherm simply becomes the Langmuir isotherm.

Another model, which takes into account lateral interaction and surface heterogeneity, is the Fowler–Guggenheim–Jovanovic isotherm.^[6]

$$\theta = 1 - e^{-(aCe^{\chi\theta})^v} \quad (5)$$

where a is a constant and χ a heterogeneity term.

The next model, which assumes single-component localized monolayer adsorption with specific lateral interactions among all the adsorbed molecules, is the Kiselev model.^[7–9] The final equation of this model is

$$\frac{\theta}{(1 - \theta)C} = \frac{K}{(1 - KK_a(1 - \theta)C)^2} \quad (6)$$

where $\theta=q/q_s$, K is the equilibrium constant for adsorption of analyte on active sites, and K_a is the association constant.

All these isotherms can generate the concentration profiles presented in Fig. 1b. The more pronounced the tailing, the stronger the lateral interactions. The concentration profiles presented in Fig. 1b could also be obtained if the adsorbed species formed multilayer structures.^[10,11]

Multilayer isotherm models can be derived from the equations:

$$K_1 C(q_s - q_1 - q_2 - q_3 - \dots - q_n) - q_1 = 0 \quad (7)$$

$$K_2 Cq_1 - q_2 = 0 \quad (8)$$

$$K_3 Cq_2 - q_3 = 0 \quad (9)$$

$$K_n Cq_{n-1} - q_n = 0 \quad (10)$$

where the first equation describes the equilibrium between free active sites and adsorbed species, and subsequent equations depict equilibria between adjacent analyte layers. It is usually assumed that $K_2=K_3=\dots=K_n=K_a$. This set of equations (i.e., Eqs. 7–10) results in the isotherm:

$$q = q_s \frac{KC(1 + 2K_p C + 3(K_p C)^2 \dots)}{1 + KC + KCK_p C + KC(K_p C)^2 \dots} \quad (11)$$

The Retention Model

Qualitative modeling of the experimentally observed densitometric profiles for any given adsorption isotherm has been presented in Refs. [11] and [12] on the basis of the model:

$$\frac{\partial C}{\partial t} + w \frac{\partial C}{\partial x} + \Phi \frac{\partial q}{\partial t} = D_x \frac{\partial^2 C}{\partial x^2} + D_y \frac{\partial^2 C}{\partial y^2} \quad (12)$$

with the assumed boundary conditions:

$$\left. \frac{\partial C}{\partial x} \right|_{x=0, x=x_1} = \left. \frac{\partial C}{\partial y} \right|_{y=0, y=y_1} = 0 \quad (13)$$

where Eq. 12 represents the differential mass balance for the mobile phase and the solid state, w is the average mobile-phase flow rate, C and q are, respectively, the concentrations (mol dm⁻³) of the analyte in the mobile phase and on the sorbent surface, D_x and D_y are, respectively, the effective diffusion coefficients lengthwise (x) and in the direction perpendicular to this direction (y), Φ is the so-called phase ratio, and x_1 and y_1 are the plate length and width, respectively. It was assumed



at time $t=0$, analyte is concentrated in a rectangular spot at the start of the chromatogram.

The Role of Intermolecular Interactions: Multilayer Adsorption

When low-molecular-weight carboxylic acids are chromatographed on cellulose powder with a nonpolar mobile phase, the densitograms obtained are similar to those presented in Fig. 2. Carboxylic acids form associative multimers by hydrogen bonding because of the presence of the negatively polarized oxygen atom from the carbonyl group and the positively polarized hydrogen atom from the hydroxyl group. Direct contact of these cyclic acidic dimers with a sorbent results in forced cleavage of most of the dimeric rings (e.g., because of inevitable intermolecular interactions by hydrogen bonding with hydroxyl groups of the cellulose), thus considerably shifting the equilibrium of self-association toward linear associative multimers.

The tendency of carboxylic acid analytes to form associative multimers can also be viewed as multilayer adsorption. Analysis of the concentration profiles presented in Fig. 2 reveals that for low concentrations of the analyte, peaks a and b are similar to the band profiles simulated by use of the Langmuir isotherm, whereas peaks c–f resemble profiles obtained by use of the anti-Langmuir isotherm (tailing toward the front of the chromatogram is more pronounced than tailing toward the start of the chromatogram.).

More spectacular results are obtained with some alcohols. Figures 3 and 4 depict the densitometric profiles for 5-phenyl-1-pentanol chromatographed on Whatman No. 3 and Whatman No. 1 chromatography papers.

In this instance, very steep concentration profiles toward the start of the chromatogram are obtained; this is

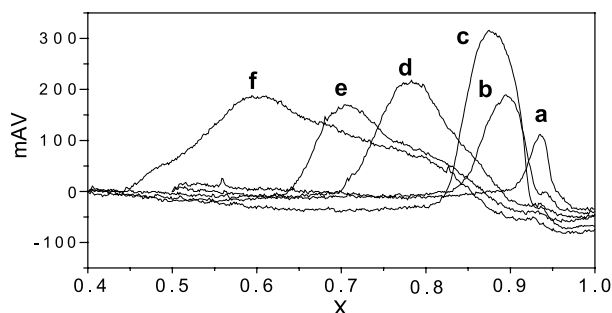


Fig. 2 Concentration profiles of 4-phenylbutyric acid on microcrystalline cellulose at 15°C with decalin as mobile phase. Concentrations of the analyte solutions in 2-propanol were (a) 0.1, (b) 0.2, (c) 0.3, (d) 0.4, (e) 0.5, and (f) 1.0 M. The volumes of sample applied were 3 μ L. (From Ref. [13].)

Analyte–Analyte Interactions, Effect on TLC Band Formation

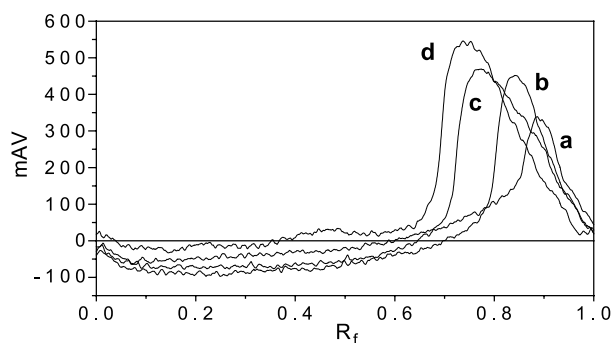


Fig. 3 Concentration profiles of 5-phenyl-1-pentanol obtained on Whatman No. 3 chromatography paper at ambient temperature with *n*-octane as mobile phase. Concentrations of the analyte solutions in 2-propanol were (a) 0.5, (b) 1.0, (c) 1.5, and (d) 2.0 M. The volumes of sample applied were 5 μ L. (From Ref. [14].)

indisputably indicative of some kind of interaction among the adsorbed molecules. The concentration profiles presented in Figs. 2–4 can be obtained theoretically from the model given by Eqs. 12 and 13 combined with the isotherm (Eq. 11), assuming three-layer adsorption as a maximum.

As an example, qualitative reproduction of the experimental concentration profiles shown in Figs. 3 and 4 is given in Fig. 5. The Eq. 11 constants of the adsorption isotherm, the mobile phase velocity, and effective diffusion coefficients were chosen to reproduce the shapes of the lengthwise cross sections of the chromatographic bands obtained in the experimental densitograms.

The calculations presented in graphical form in Fig. 5 were performed for $q_s=1.5$, $K=0.5$, $K_p=5$, $w=0.3$ cm min^{-1} , $D_x=0.007$ $\text{cm}^2 \text{min}^{-1}$, and an initial spot length of 0.06 cm. The phase ratio Φ was assumed to be 0.25.

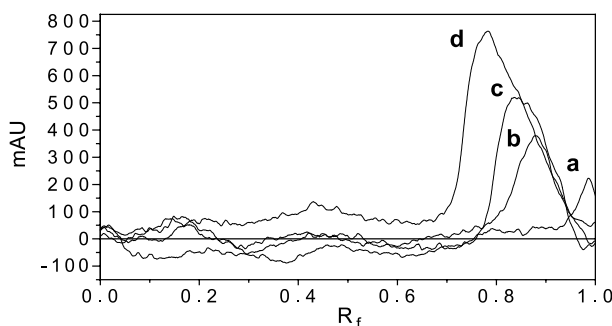


Fig. 4 Concentration profiles of 5-phenyl-1-pentanol obtained on Whatman No. 1 chromatography paper at ambient temperature with *n*-octane as mobile phase. Concentrations of the analyte solutions in 2-propanol were (a) 0.25, (b) 0.50, (c) 0.75, and (d) 1.0 M. The volumes of sample applied were 5 μ L. (From Ref. [14].)



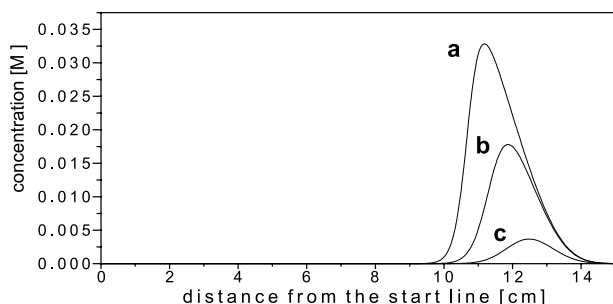


Fig. 5 The lengthwise cross section of the simulated chromatogram for a hypothetical alcohol or acid, according to the model given by Eqs. 12 and 13 in conjunction with the isotherm given by Eq. 11. Concentrations of the applied solutions were (a) 1.0, (b) 0.5, and (c) 0.1 M.

From Fig. 5, it is apparent that the adsorption fronts are considerably less steep than the desorption fronts, and that the adsorption fronts simulated for different initial concentrations of the spots overlap. Similar behavior is apparent in the typical experimental densitograms, given in Figs. 3 and 4. In all these densitograms, the adsorption fronts for the different concentrations of acid also overlap.

CONCLUSION

Satisfactory qualitative agreement between experimental and theoretical concentration profiles for polar analytes suggests their retention is substantially affected by lateral interactions, which are probably even more complex than is assumed in this isotherm model. Overlapping of the adsorption fronts can be explained solely on the basis of the lateral interactions among the adsorbed molecules.

REFERENCES

1. Belenky, B.G.; Nesterov, V.V.; Gankina, E.S.; Smirnov, M.M. A dynamic theory of thin layer chromatography. *J. Chromatogr.* **1967**, *31*, 360–368.
2. Belenky, B.G.; Nesterov, V.V.; Smirnov, M.M. Theory of thin-layer chromatography. I. Differential equation of thin-

- layer chromatography and its solution (in Russian). *Zh. Fiz. Khim.* **1968**, *42*, 1484–1489.
3. Mierzejewski, J.M. The mechanism of spot formation in flat chromatographic systems. I. Model of fluctuation of substance concentration on spots in paper and thin layer chromatography. *Chem. Anal. (Warsaw)* **1975**, *20*, 77–89.
4. Guiochon, G.; Shirazi, S.G.; Katti, A.M. *Fundamentals of Preparative and Nonlinear Chromatography*; Academic Press: Boston, MA, 1994.
5. Fowler, R.H.; Guggenheim, E.A. *Statistical Thermodynamics*; Cambridge University Press: Cambridge, UK, 1960.
6. Quinones, I.; Guiochon, G. Extension of a Jovanovic–Freundlich isotherm model to multicomponent adsorption on heterogeneous surfaces. *J. Chromatogr. A* **1998**, *796*, 15–40.
7. Berezin, G.I.; Kiselev, A.V. Adsorbate–adsorbate association on a homogenous surface of a nonspecific adsorbate. *J. Colloid Interface Sci.* **1972**, *38*, 227–233.
8. Berezin, G.I.; Kiselev, A.V.; Sagatelyan, R.T.; Sinitsyn, V.A. Thermodynamic evaluation of the state of the benzene and ethanol on a homogenous surface of a nonspecific adsorbent. *J. Colloid Interface Sci.* **1972**, *38*, 335–340.
9. Quinones, I.; Guiochon, G. Isotherm models for localized monolayers with lateral interactions. Application to single-component and competitive adsorption data obtained in RP-HPLC. *Langmuir* **1996**, *12*, 5433–5443.
10. Wang, C.-H.; Hwang, B.J. A general adsorption isotherm considering multi-layer adsorption and heterogeneity of adsorbent. *Chem. Eng. Sci.* **2000**, *55*, 4311–4321.
11. Kaczmariski, K.; Prus, W.; Dobosz, C.; Bojda, P.; Kowalska, T. The role of lateral analyte–analyte interactions in the process of TLC band formation. II. Dicarboxylic acids as the test analytes. *J. Liq. Chromatogr. Relat. Technol.* **2002**, *25*, 1469–1482.
12. Prus, W.; Kaczmariski, K.; Tyrpień, K.; Borys, M.; Kowalska, T. The role of the lateral analyte–analyte interactions in the process of TLC band formation. *J. Liq. Chromatogr. Relat. Technol.* **2001**, *24*, 1381–1396.
13. Kaczmariski, K.; Sajewicz, M.; Pieniak, A.; Piętka, R.; Kowalska, T. Densitometric acquisition of concentration profiles in planar chromatography and its possible shortcomings. Part 1. 4-Phenylbutyric acid as an analyte. *Acta Chromatogr.* **2004**, *14*, 5–15.
14. Sajewicz, M.; Pieniak, A.; Piętka, R.; Kaczmariski, K.; Kowalska, T. Densitometric comparison of the performance of Stahl-type and sandwich-type planar chromatographic chambers. *J. Liquid Chromatogr. Relat. Technol.* **2004**.



Antibiotics: Analysis by TLC

Irena Choma

Marie Curie Skłodowska University, Lublin, Poland

Introduction

Antibiotics are an extremely important class of human and veterinary drugs. Chemically, they constitute a widely diverse group with different functions and modes of operation. They can be derived from living organisms or obtained synthetically. However, all of them exhibit antibacterial properties (i.e., either inhibit the growth of, or kill, bacteria).

Background Information

Penicillin, the first natural antibiotic produced by genus *Penicillium*, discovered in 1928 by Fleming, as well as sulfonamides, the first chemotherapeutic agents discovered in the 1930s, lead a long list of currently known antibiotics. Besides β -lactams (penicillins and cephalosporins) and sulfonamides, the list includes aminoglycosides, macrolides, tetracyclines, quinolones, peptides, polyether ionophores, rifamycins, linkosamides, coumarins, nitrofurans, nitro heterocycles, chloramphenicol, and others.

In principle, antibiotics should eradicate pathogenic bacteria in the host organism without causing significant damage to it. Nevertheless, most antibiotics are toxic, some of them even highly. The toxicity of antibiotics for humans is not only due to medical treatment but also to absorption of those drugs along with contaminated food. In modern agricultural practice, antibiotics are administered to animals, both for treatment of diseases and for prophylaxis, as well as to promote growth as feed or water additives. When proper withdrawal periods are not observed, unsafe antibiotic residues or their metabolites may be present in edible products (e.g., in milk, eggs, and meat). Some of them, like penicillins, can cause allergic reactions in sensitive individuals. Therefore, monitoring antibiotic residues should be an important task for government authorities.

There are many analytical methods for determining antibiotics in body fluids and food. They can be based on microbiological, immunochemical, and physico-

chemical principles. The most popular methods belonging to the latter group are chromatographic ones, mainly liquid chromatography, including high-performance liquid chromatography (HPLC) and thin-layer chromatography (TLC).

High-performance liquid chromatography offers high sensitivity and separation efficiencies. However, it requires sophisticated equipment and is expensive. Usually, before HPLC analysis, tedious sample pretreatment is necessary, such as protein precipitation, ultrafiltration, partitioning, metal chelate affinity chromatography (MCAC), matrix solid-phase dispersion (MSPD), or solid-phase extraction (SPE). Generally, the sample cleanup procedures used before TLC separation are the same as for HPLC. Nevertheless, they can be strongly limited in the case of screening TLC or when the plates with a concentrating zone are applied.

Thin-layer chromatography is less expensive and less complicated than HPLC, provides high sample throughput, and usually requires limited sample pretreatment. However, the method is generally less sensitive and selective and offers poor resolution. Some of these problems can be solved by high-performance thin-layer chromatography (HPTLC) or forced-flow planar chromatography (FFPC). Lower detection limits can also be achieved using an autosampler for injection, applying special techniques of development and densitometry as a detection method, and/or spraying the plate after development with appropriate reagents.

There is also a possibility of coupling TLC with mass spectrometry (MS). Then, TLC can reach selectivity, sensitivity, and resolution close to those of HPLC.

Thin-layer chromatography stripped of the above-mentioned attributes may still serve as a screening method (i.e., one which establishes the presence or absence of antibiotics above a defined level of concentration). Screening TLC methods show sensitivity similar to microbiological assays, which are the most popular screening methods, applied for controlling antibiotic residues in food in many countries. Thin-layer chromatography–bioautography (TLC–B) is one of the TLC screening methods. The developed TLC plates



are placed on or immersed in a bacterial growth medium which has been seeded with an appropriate bacteria strain. The locations of zones of growth inhibition provides the information about antibiotic residues.

In relation to extremely diverse nature of antibiotics, a variety of different separation and detection modes is used in analytical practice. Short characteristics and some general rules of separation for the most popular classes of antibiotics are presented next.

Penicillins

The basic structure of penicillins is a thiazolidine ring linked to a β -lactam ring to form 6-aminopenicillanic acid, the so-called "penicillin nucleus." This acid, obtained from *Penicillium chrysogenum* cultures is a precursor for semisynthetic penicillins produced by attaching different side chains to the "nucleus." The most widely used stationary phase for analysis of penicillins is silica gel, but reversed-phase (RP) or cellulose plates have also been employed. It is advantageous to add acetic acid to the mobile phase and/or spotting acetic acid before the sample injection in order to avoid the decomposition of β -lactams on silica gel. RP phases usually contain pH 5–6 buffer and organic solvent(s). The most popular detection is bioautography and ultraviolet (UV) densitometry, often coupled with spraying with appropriate reagents.

Cephalosporines

Cephalosporines are derived from natural cephalosporin C produced by *Cephalosporium acremonium*. They possess a cephem nucleus (7-aminocephalosporanic acid) substituted with two side chains. They are commonly divided into three classes differing in their spectra and toxicity. Cephalosporines can be analyzed both by normal and reversed-phase TLC or HPTLC; hence, more efficient separation is obtained on silanized gel than on bare, untreated silica gel. Mobile phases are polar and similar to those used for penicillins. Acetic acid or acetates are very often components of solvents for normal phase (NP) TLC, the ammonium acetate–acetic acid buffer for RP TLC. All cephalosporines can be detected at 254 nm. The detection limit can be diminished by applying reagents such as ninhydrin, iodoplatinate, chloroplatinic acid, or iodine vapor. Alternative to UV detection is bioautography with, for instance, *Neisseria catarrhalis*.

Aminoglycosides

Aminoglycosides consist of two or more amino sugars joined via a glycoside linkage to a hexose nucleus. Streptomycin was isolated in 1943 from *Streptomyces griseus*, then others were discovered in different *Streptomyces* strains. Aminoglycosides are particularly active against aerobic microorganisms and against *Tubercle bacillus*, but because of their potential ototoxicity and nephrotoxicity, they should be carefully administered. Aminoglycosides, due to their extremely polar, hydrophilic character, are analyzed mostly on silica gel. Polar organic solvents (methanol, acetone, chloroform) mixed with 25% aqueous ammonia are the most popular mobile phases. Because the majority of aminoglycosides lack UV absorption, they must be derivatized by spraying or dipping after development with, for instance, fluram, vanillin, or ninhydrin solutions. Bioautography with *Bacillus subtilis*, *Sarcina lutea*, and *Mycobacterium phlei* is also possible.

Macrolides

Macrolides are bacteriostatic antibiotics composed of a macrocyclic lactone ring and one or more deoxy sugars attached to it. The main representative of the class, erythromycin, was discovered in 1952 as a metabolic product of *Streptomyces erythreus*. Now, erythromycin experiences its renaissance because of its high activity against many new, dangerous bacteria such as *Campylobacter* or *Legionella*. The macrolide antibiotics group is still being expanded due to the search for macrolides of pharmacokinetic properties better than erythromycin. Separation of macrolides is performed on silica gel, kieselguhr, cellulose, and reversed-phase layers. Silica gel and polar mobile phases are very frequently applied, usually with the addition of methanol, ethanol, ammonia, sodium, or ammonium acetate. Because of the absence of chromophore groups, bioautography or postchromatographic derivatization is used, mainly charring by spraying with acid solutions (e.g., anisaldehyde–sulfuric acid–ethanol) and heating.

Tetracyclines

Tetracyclines, consisting of a octahydronaphthacene skeleton, are "broad-spectrum" antibiotics produced by *Streptomyces* or obtained semisynthetically. They can be separated both by RP and NP TLC. Cellulose,



kieselguhr, or silica gel impregnated with EDTA or Na₂EDTA can be used. Impregnation is necessary due to the very strong interaction of tetracyclines with hydroxyl groups and with trace metals in the silica surface. Also, mobile phases, both for RP or NP TLC, should contain chelating agents such as Na₂EDTA, citric, or oxalic acid. Tetracyclines give fluorescent spots, which can be detected by UV lamp, fixed at 366 nm or by densitometry. Spraying with reagents, for instance with Fast Violet B Salt solution, provides lower detection levels. Tetracyclines can also be detected by fast-atom bombardment–mass spectrometry (FAB–MS) and bioautography.

Quinolones

Nalidixic acid, discovered casually in 1962, was the first member of this class, although of rather minor importance. In the 1980s, synthetic fluoroquinolones were developed and became valid antibiotics with broad spectra and of good tolerance. Quinolones may be analyzed on silica gel plates, preferably impregnated with Na₂EDTA or K₂HPO₄. Multicomponent organic mobile phases are employed, usually with the addition of aqueous solutions of ammonia or acids. Densitometry or fluorescence densitometry are preferred detection methods, sometimes preceded by postchromatographic derivatization.

Peptides

Peptide antibiotics are composed of the peptide chain of amino acids, D and L, covalently linked to other moieties. Most peptides are toxic and are poorly absorbed from the alimentary tract. Peptide antibiotics are difficult to analyze in biological and food samples, as they are similar to matrix components. They can be separated on silica gel, amino silica gel, and silanized silica gel plates. A variety of mobile phases are applied, from a simple one like chloroform–methanol to a multicomponent one like *n*-butanol–butyl acetate–

methanol–acetic acid–water. Bioautographic detection can be employed with *Bacillus subtilis* and *Mycobacterium smegmatis* or densitometry as well as fluorescence densitometry after spraying the plate with reagents such as ninhydrin or fluram.

Besides typical antibiotics analysis, focused on the separation of antibiotics belonging to one or different classes, there are many examples of diverse TLC applications such as the following:

1. Purity control of antibiotics
2. Purification of newly discovered antibiotics before further testing
3. Examining stability and breakdown products of antibiotics in solutions and dosage forms
4. Analysis of antibiotic metabolites
5. Studying interactions of antibiotics with cell membrane or human serum albumin
6. Examining reactions of antibiotics with different compounds
7. Separation of antibiotics derivatives, obtained in the process of searching for new antibiotics
8. Quantitation of antibiotics by densitometry without elution with a solvent
9. Thermodynamic study of the retention behavior of antibiotics
10. Determining hydrophobicity parameters of antibiotics by RP TLC
11. Applying some antibiotics as stationary or mobile-phase additives

Suggested Further Reading

- Barker, S. A., and C. C. Walker, *J. Chromatogr.* 624: 195 (1992).
Bobbitt, D. R. and K. W. Ng, *J. Chromatogr.* 624: 153 (1992).
Boison, J. O., *J. Chromatogr.* 624: 171 (1992).
Hoogmartens, J. (ed.), *J. Chromatogr. A* 812 (1998) (special issue).
Lambert, H. P. and F. W. O'Grady, *Antibiotics and Chemotherapy*, 6th ed., Longman Group UK Ltd., London, 1992.
Choma, I., in Sherma, J., and B. Fried (eds.), *Handbook of Thin-Layer Chromatography*, 3rd ed., Marcel Dekker, Inc., New York, 2003.





Antioxidant Activity: An Adaptation for Measurement by HPLC

Marino B. Arnao

Manuel Acosta

Antonio Cano

University of Murcia, Murcia, Spain

INTRODUCTION

The determination of antioxidant activity (capacity or potential) of diverse biological samples is generally based on the inhibition of a particular reaction in the presence of antioxidants. The most commonly used methods are those involving chromogenic compounds of a radical nature: the presence of antioxidant leads to the disappearance of these radical chromogens. They are either photometric or fluorimetric and can comprise kinetic or end-point measurements. Recently, there has been increasing interest in the adaptation of these methods for on-line determinations using liquid chromatography. In this article, we present the adaptation to high-performance liquid chromatography (HPLC) of our methods for the determination of the antioxidant activity in a range of samples. Advantages and disadvantages of these methods are discussed.

A biological antioxidant is a compound that protects biological systems against the potentially harmful effects of processes or reactions that cause excessive oxidation. Hydrophilic compounds, such as vitamin C, thiols, and flavonoids, as well as lipophilic compounds, such as vitamin E, vitamin A, carotenoids, and ubiquinols, are the best-known natural antioxidants. Many of these compounds are of special interest due to their ability to reduce the hazard caused by reactive oxygen and nitrogen species (ROS and RNS, some are free radicals), and have been associated with lowered risks of cardiovascular diseases and other illnesses related to oxidative stress.^[1] Practically all the above mentioned compounds are obtained through the ingestion of plant products such as fruits and vegetables, nuts, flours, vegetable oils, drinks, and infusions, taken fresh or as processed foodstuffs.^[2] A common property of these compounds is their antioxidant activity. The activity of an antioxidant is determined by:

1. Its chemical reactivity as an electron or hydrogen donor in reducing the free radical.
2. The fate of the resulting antioxidant-derived radical and its ability to stabilize and delocalize the unpaired electron.
3. Its reactivity with other antioxidants present.

Thus, antioxidant activity is a parameter that permits quantification of the capacity of a compound (natural or artificial) and/or a biological sample (from a wide range of sources) to scavenge free radicals in a specific reaction medium.^[1,3,4]

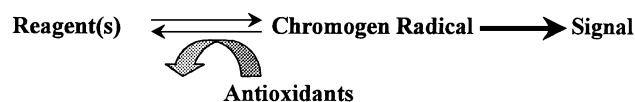
METHODS TO MEASURE ANTIOXIDANT ACTIVITY

Antioxidant activity can be measured in a number of different ways. The most commonly used methods are those in which a chromogenic radical compound is used to simulate ROS and RNS; it is the presence of antioxidants that provokes the disappearance of these chromogenic radicals, as shown in the reaction model given in Scheme 1. In order for this method to be effective, it is necessary to obtain synthetic metastable radicals that can easily be detected by photometric or fluorimetric techniques. Nevertheless, different strategies for the quantification of antioxidant activity have been utilized: e.g., decoloration or inhibition assays. Details of these strategies and commonly used methods have been presented and reviewed elsewhere.^[3,4]

When chromogenic radicals are used to determine antioxidant activity, the simplest method is to:

1. Dissolve the radical chromogen in the appropriate medium.
2. Add antioxidant.
3. Measure the loss of radical chromogen photometrically by observing the decrease in absorbance at a fixed time.
4. Correlate the decrease observed in a dose-response curve with a standard antioxidant (e.g., trolox, ascorbic acid), expressing the antioxidant activity as equivalents of standard antioxidant, a well-established parameter in this respect being Trolox Equivalent Antioxidant Capacity (TEAC).^[3]

2,2'-Azino-bis-(3-ethylbenzthiazoline-6-sulfonic acid (ABTS) (Fig. 1) and α,α' -diphenyl- β -picrylhydrazyl radi-



Scheme 1 Reaction model of antioxidant activity determination using chromogenic radicals.

cal (DPPH) are the two most commonly used synthetic compounds in antioxidant activity determinations. ABTS, when oxidized by the removal of one electron, generates a metastable radical. The ABTS radical cation ($\text{ABTS}^{\cdot+}$) has a characteristic absorption spectrum with maxima at 411, 414, 730, and 873 nm (Fig. 1), with extinction coefficients of 31 and $13 \text{ mM}^{-1} \text{ cm}^{-1}$ at 414 and 730 nm, respectively.^[5] In the reaction between $\text{ABTS}^{\cdot+}$ and antioxidants, the radical is neutralized by the addition of one electron (see the reaction presented in Scheme I). This leads to the disappearance of the $\text{ABTS}^{\cdot+}$, which can be estimated by the decrease in absorbance (virtually any wavelength between 400 and 900 nm can be selected to avoid exogenous absorption interferences). Generally, $\text{ABTS}^{\cdot+}$ is generated directly from its precursor in aqueous media by a chemical reaction (e.g., manganese dioxide, ABAP, potassium persulfate) or by an enzymatic reaction (e.g., peroxidase, hemoglobin, met-myoglobin) (see references in Ref. [5]).

Recently, we have developed a method based on $\text{ABTS}^{\cdot+}$ generated by horseradish peroxidase (HRP) that permits the evaluation of the antioxidant activity of pure compounds and plant-derived samples.^[6] The method is easy, accurate, and fast to apply and presents numerous advantages because it avoids undesirable side reactions, does not require high temperatures to generate ABTS radicals, and allows for antioxidant activity to be studied over a wide range of pH values. This method is capable of determining both hydrophilic (in buffered media) antioxidant activity (HAA) and lipophilic (in organic media) antioxidant activity (LAA).^[5] In the second case, $\text{ABTS}^{\cdot+}$ is generated directly in ethanolic medium by HRP, which is a powerful oxidizing biocatalyst that can act in nonaqueous media—a capacity that has been widely used in biotechnological applications. Thus, it is possible to estimate the antioxidant activity of both antioxidant types in the same sample (HAA and LAA). The antioxidant capacities of natural compounds, such as ascorbic acid, glutathione, cysteine, phenolic compounds (resveratrol, gallic acid, ferulic acid, quercetin, etc.), or synthetic antioxidants, such as BHT, BHA, or trolox (a structural analog of vitamin E), have been estimated, as well those of plant extracts or samples from other sources. Different applications of the method have determined antioxidant activity in a range of foodstuffs.^[7] The $\text{ABTS}^{\cdot+}$ chromogen used in our method

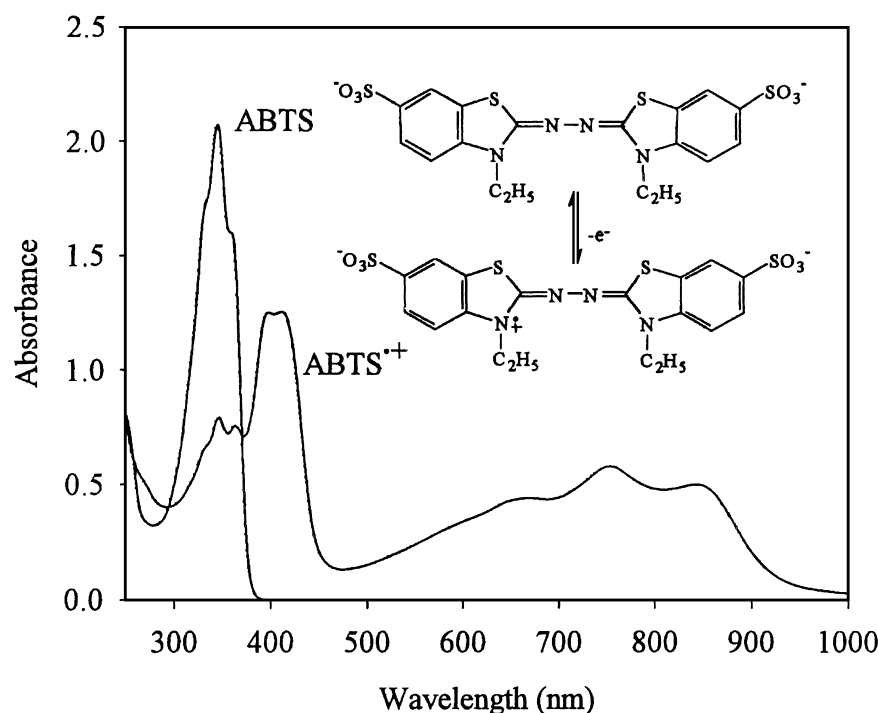


Fig. 1 Spectral characteristics of ABTS and its oxidation products, the ABTS radical ($\text{ABTS}^{\cdot+}$), showing absorbance of up to 1000 nm. The chemical structures show the nitrogen-centered radical cation of $\text{ABTS}^{\cdot+}$.

has been compared with another widely used radical chromogen, DPPH[•]; it was concluded that in the determination of the antioxidant potential of citrus and wine samples, the DPPH[•] method could significantly underestimate TEAC by up to 36% compared to ABTS^{•+}.^[8] Also, we have applied the method to study the total antioxidant activity of different vegetable soups, obtaining relevant data on the relative contribution of hydrophilic (ascorbic acid and phenols) and lipophilic (carotenoids) components to their total antioxidant activity.^[9] On the other hand, our methods have been used in animal physiological studies on changes in the plasma antioxidant status caused by the hormone melatonin in rats^[10] and by other authors on the effect of “in vivo” oxidant stress in the rat aorta.^[11]

Under our assay conditions, ABTS^{•+} generation progresses quickly and only 1–5 min is necessary to reach maximum absorbance. This is a decisive factor in the easy and rapid application of the assay with minimal reagent manipulation. In contrast, other assays that use ABTS^{•+} to measure the activity of lipophilic antioxidants have certain drawbacks, among which are: lengthy time (up to 16 hr) to chemically generate and stabilize ABTS^{•+} via potassium persulfate;^[12] a previous filtration step when manganese dioxide is used; or, in the case of the assay that uses ABAP, high temperatures (45–60°C) that tend to affect ABTS^{•+} stability. The advantage of enzymatic ABTS^{•+} generation, as opposed to chemical generation, is that the reaction can be controlled by the amount of H₂O₂ added, while the exceptional qualities of HRP in ABTS^{•+} generation is an important feature in both the aqueous and the organic system.^[5,6] The most significant limiting factor in this type of strategy is the fact that the ABTS^{•+} must be stable during the analysis; we were able to optimize the conditions to ensure >99% stability. During optimization, it was verified that the concentration ratio between radical (ABTS^{•+}) and substrate (ABTS) is a determining factor for the stability of ABTS^{•+}, although pH and temperature are also important elements. With respect to the sensitivity of these methods, the calibration using L-ascorbic acid presented a detection limit of 0.15 nmol and a quantification limit of 0.38 nmol. For lipophilic antioxidants, LOD of 0.08 and LOQ of 0.28 nmol of trolox were obtained. The LOD and LOQ of similar values were obtained for α -tocopherol and β -carotene.

ANTIOXIDANT ACTIVITY BY HPLC

The possibility of automating antioxidant activity determination and applying it to a large number of samples was an interesting objective. Previously, we have adapted our method as a microassay using a microplate reader to determine total antioxidant activity.^[5] Recently, other

authors have adapted radical chromogenic tests into methods that combine the advantages of rapid and sensitive chromogen radical assays with HPLC separation for the on-line determination of radical scavenging components in complex mixtures. Specifically, the DPPH[•] method and the method of Rice-Evans, which uses ABTS^{•+} generated chemically with potassium persulfate, have been adapted as such.^[13,14] Nonetheless, the chemical generation of ABTS^{•+} via potassium persulfate required 16–17 hr to complete. Our methods resulted in faster and better controlled generation of stable ABTS radical because ABTS^{•+} was generated enzymatically in only 2–5 min, with perfect control over the amount of ABTS^{•+} formed and its stability (ABTS/ABTS^{•+} ratios).^[6] The speedy generation of ABTS^{•+} permitted quick acquisition of the absorbance value desired in the detector by the addition of aliquots of H₂O₂ to the ABTS solution.

The adaptation of the ABTS^{•+} method as an on-line test required that the chromogen radical should be stable for sufficient time in different solvents to permit the utilization of isocratic or gradient elution programs. The on-line reaction time between ABTS^{•+} and potential antioxidants was an additional potential limiting factor.

For on-line measurement of the antioxidant activity of samples using liquid chromatography, it is first necessary to consider the basic equipment required. Thus, the determination of antioxidant activities in separate components of samples by HPLC in a postcolumn reaction of analytes with preformed ABTS^{•+} requires at least:

1. Two pumps, one for the mobile-phase solutions and another for the preformed ABTS^{•+} solution. A pulse dampener is recommended to minimize pulse oscillations.
2. A sample injector.
3. The chromatography column.
4. A reaction coil of adequate length to give the desired reaction time.
5. A UV–visible (UV–VIS) detector.
6. An integration system (software) for data analysis.

Fig. 2 shows a schematic diagram of the equipment used in this study. In this case, because only one diode array detector was available, two injections of the sample were necessary: one to obtain the UV profile (at 250 nm) and another for the antioxidant activity profile at 600 nm (negative peaks). If two UV–VIS detectors had been used, only one injection would have been required to obtain the dual-HPLC profile but the chromatograms must be time-normalized.

In this type of analysis, a dual-HPLC profile was obtained. The UV profile (injection one) was of interest because all the main components of biological samples

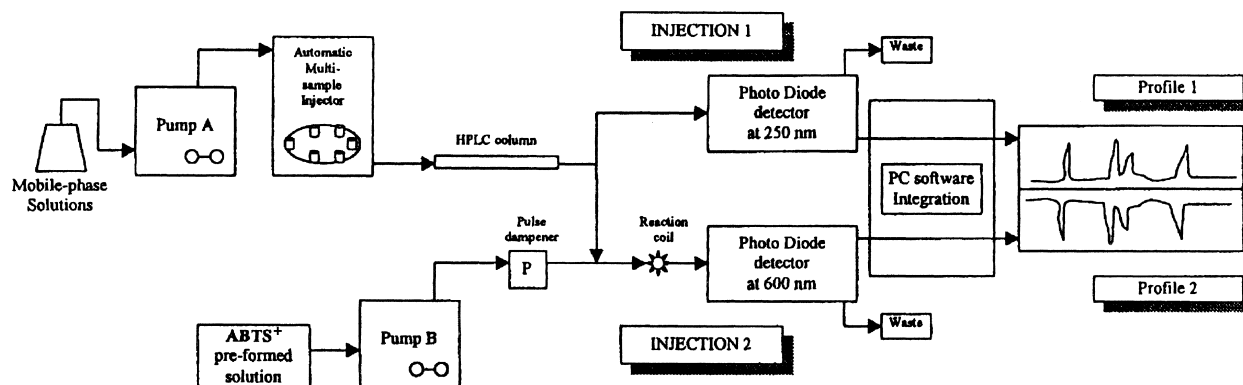


Fig. 2 Instrumental scheme for the determination of antioxidant activities by HPLC using $\text{ABTS}^{\bullet+}$ as chromogenic radical.

are absorbed in this wavelength range. The second injection detected absorbance changes at 600 nm or higher (see absorption spectrum of $\text{ABTS}^{\bullet+}$ in Fig. 1) to give the antioxidant activity profile. The photodiode array detector additionally recorded the absorption spectra of peaks and, consequently, could also provide data on the possible chemical nature of the analyzed compounds. The HPLC-ABTS method can be used to characterize hydrophilic (ascorbic acid, phenolic compounds, organic acids, etc.) or lipophilic antioxidants (trolox, a synthetic standard antioxidant analog of vitamin E or carotenoids such as β -carotene, lycopene, xanthophylls, etc.). Using standard antioxidants, the dual-HPLC profile as shown in Fig. 3 could be obtained. In Fig. 3A, the upper chromatogram (trolox detected at 250 nm) and the lower chromatogram (the scavenging activity of trolox vs. $\text{ABTS}^{\bullet+}$ measured at 600 nm) were correlated. A calibration curve relating the antioxidant concentration and the signal (600 nm, as peak areas) was obtained and used as standard to express all data as TEAC. Generally, a known amount of trolox was injected into HPLC in any chromatographic conditions (to analyze hydrophilic or lipophilic compounds) to quantify its antioxidant activity and obtain the calibration curve. Thus, antioxidant activity was calculated from the sum of the peak areas of the chromatogram profile at 600 nm (negative peaks) and expressed as trolox equivalents (TEAC) using the previously mentioned calibration curves. An example of another important antioxidant (resveratrol) is shown in Fig. 3B.

Another significant aspect was the stability of the radical chromogen $\text{ABTS}^{\bullet+}$ in different solvents, in isocratic or gradient elution programs. We found that in the mobile phases used in our determinations (saline solutions and mixtures of organic solvents in different proportions), the observed fall was less than 0.01 expressed as $-\Delta\text{Abs}_{730\text{nm}}/\text{min}$.^[15] This stability is high

enough to obtain accurate data, approximately 10 times greater than the data reported in Ref. [14].

It was very important to guarantee at least 1 min of on-line reaction time between $\text{ABTS}^{\bullet+}$ and the antioxidants because fast antioxidants, such as trolox or ascorbic acid, reacted with $\text{ABTS}^{\bullet+}$ almost immediately, but other antioxidants required more time. In our case, trolox and ascorbic acid presented TEAC values of 1.0

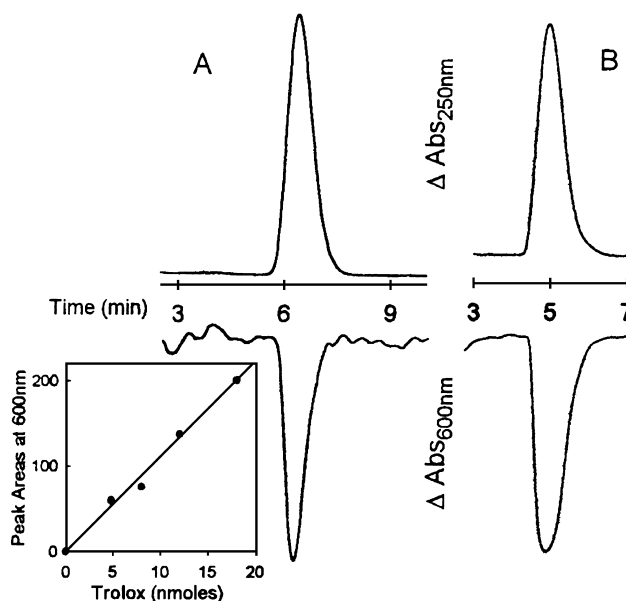


Fig. 3 Dual-HPLC plots of two antioxidants: trolox and resveratrol. Upper chromatograms show UV profiles registered at 250 nm and lower chromatograms $\text{ABTS}^{\bullet+}$ scavenging (antioxidant activity) profiles registered at 600 nm (negative peak). In (A), trolox was detected with a retention time of 6.2 min. Inset: Calibration curve of scavenging activity (peak areas at 600 nm) for different amounts of trolox. In (B), resveratrol was detected at 5.0 min.

Antioxidant Activity: An Adaptation for Measurement by HPLC

5

and 0.99, respectively, using the HPLC-ABTS method (Table 1); similar values were obtained using the ABTS end-point method or the method of Rice-Evans.^[3,6] In the method of Koleva et al.,^[14] ascorbic acid presented time dependence: at 30 s, 60% of TEAC was expressed. In our system, and to guarantee sufficient on-line reaction time, a stainless steel reaction coil of 1 mL volume (2.5 m × 0.7 mm i.d.) coupled to a pump was connected to the chromatographic system (between the column and the diode detector) (Fig. 2). Thus, using a suitable elution program (0.5–0.7 mL/min of mobile phases) and introducing between 0.3 and 0.5 mL/min of the preformed ABTS^{•+} (0.2 mM), a total on-line reaction time of 1 min was obtained.

Under these conditions, a study of the antioxidant potential of pure compounds could be carried out. Table 1 shows the values of antioxidant activity (expressed as TEAC) of different compounds of interest, determined by the on-line method (HPLC-ABTS method) and compared with the values obtained by our conventional photometric end-point method.^[6] As can be observed, the two most important standard antioxidants, trolox and ascorbic acid, presented similar TEAC using either method. Thus, either can be used as reference to express antioxidant activity, except that trolox has the advantage because it can be used in both hydrophilic and lipophilic assays. The TEAC values of phenolic compounds were underestimated by approximately half when the HPLC-ABTS method was used as compared to the end-point method. This was due to the different reactivities of antioxidants with ABTS^{•+}, and because, unfortunately, the time dependence of on-line scavenging activity determinations made it very difficult to obtain the total reaction for the slowest antioxidants, resulting in a partial estimation of this activity. Nevertheless, the HPLC-ABTS method provided important additional information in the form of correlation between the different peaks of a sample and their antioxidant activities.

The HPLC-ABTS has been used in a study on the HAA and the LAA of fresh citrus and tomato juices.^[15]

Table 1 Antioxidant activities of different compounds determined by the HPLC-ABTS and by the end-point method

Compound	Antioxidant activity (TEAC)	
	HPLC-ABTS method	End-point method ^a
L-Ascorbic acid	0.99	1.0
Trolox	1.0	1.0
Ferulic acid	0.87	1.94
Gallic acid	1.39	3.02
Resveratrol	1.32	2.34
Quercetin	2.83	4.30

^a(From Ref. [4].)

The data obtained showed a good correlation between vitamin C content and HAA and slight underestimations of LAA. We are currently applying this method to different plant materials with the aim of finding out which compounds apport significant antioxidant properties to the foodstuffs studied.

CONCLUSIONS

Determinations of antioxidant activity are widely used in phytochemistry, nutrition, food chemistry, clinical chemistry, as well as in human, animal, and plant physiology, etc. Methods adapted to HPLC have appeared only recently but can be expected to have multiple applications in the future. ABTS^{•+} is an excellent metastable chromogen for the detection and quantification of the HAA and LAA of biological samples. Thus, using a simple photometer (end-point method),^[6] a microplate reader (multisample titration method),^[5] or HPLC equipment, a broad range of possibilities are available for the characterization of diverse samples (animal- or plant-derived). Some applications of special interest could include:

1. Characterization of biological samples (e.g., plant extracts, foods).
2. Studies on the changes in the antioxidant activity of material during industrial or postharvest processing (e.g., thermal processes, Maillard reactions, and cold storage of foods, etc.).
3. The search for new natural antioxidants of vegetable or marine origin.
4. Clinical determinations.

ACKNOWLEDGMENTS

This work was supported by the Instituto Nacional de Investigación y Tecnología Agraria y Alimentaria (I.N.I.A., Ministerio de Ciencia y Tecnología, Spain) project CAL00-062 and by the project PI-9/00759/FS/01 (Fundación Séneca, Murcia, Spain). A. Cano has a grant from the Fundación Séneca of the Comunidad Autónoma de Murcia (Spain). The authors wish to thank A.N.P. Hiner for checking the draft of this manuscript.

REFERENCES

1. Halliwell, B.; Gutteridge, J.M.C. *Free Radicals in Biology and Medicine*, 3rd Ed.; Halliwell, B., Gutteridge, J.M.C., Eds.; Oxford Univ. Press: New York, 2000.
2. Mackerras, D. Antioxidants and health. Fruits and vegetables or supplements? *Food Aust.* **1995**, *47*, S3–S23.



3. Rice-Evans, C.A.; Miller, N.J. Total antioxidant status in plasma and body fluids. *Methods Enzymol.* **1994**, *234*, 279–293.
4. Arnao, M.B.; Cano, A.; Acosta, M. Methods to measure the antioxidant activity in plant material. A comparative discussion. *Free Radic. Res.* **1999**, *31*, S89–S96.
5. Cano, A.; Acosta, M.; Arnao, M.B. A method to measure antioxidant activity in organic media: Application to lipophilic vitamins. *Red. Rep.* **2000**, *5*, 365–370.
6. Cano, A.; Hernández-Ruiz, J.; García-Cánovas, F.; Acosta, M.; Arnao, M.B. An end-point method for estimation of the total antioxidant activity in plant material. *Phytochem. Anal.* **1998**, *9*, 196–202.
7. Arnao, M.B.; Cano, A.; Acosta, M. Total antioxidant activity in plant material and its interest in food technology. *Rec. Res. Dev. Agric. Food Chem.* **1998**, *2*, 893–905.
8. Arnao, M.B. Some methodological problems in the determination of antioxidant activity using chromogen radicals: A practical case. *Trends Food Sci. Technol.* **2000**, *11*, 419–421.
9. Arnao, M.B.; Cano, A.; Acosta, M. The hydrophilic and lipophilic contribution to total antioxidant activity. *Food Chem.* **2001**, *73*, 239–244.
10. Plaza, F.; Arnao, M.; Zamora, S.; Madrid, J.; Rol de Lama,

Antioxidant Activity: An Adaptation for Measurement by HPLC

- M. Validación de un microensayo con ABTS^{•+} para cuantificar la contribución de la melatonina al estatus antioxidante total del plasma de rata. *Nutr. Hosp.* **2001**, *16*, 202.
11. Laight, D.W.; Gunnarsson, P.T.; Kaw, A.V.; Anggard, E.E.; Carrier, M.J. Physiological microassay of plasma total antioxidant status in a model of endothelial dysfunction in the rat following experimental oxidant stress in vivo. *Environ. Toxicol. Pharmacol.* **1999**, *7*, 27–31.
12. Re, R.; Pellegrini, N.; Proteggente, A.; Pannala, A.; Yang, M.; Rice-Evans, C.A. Antioxidant activity applying an improved ABTS radical cation decolorization assay. *Free Radic. Biol. Med.* **1999**, *26*, 1231–1237.
13. Koleva, I.I.; Niederländer, H.A.G.; van Beek, T.A. An on-line HPLC method for detection of radical scavenging compounds in complex mixtures. *Anal. Chem.* **2000**, *72*, 2323–2328.
14. Koleva, I.I.; Niederlander, H.A.G.; van Beek, T.A. Application of ABTS radical cation for selective on-line detection of radical scavengers in HPLC eluates. *Anal. Chem.* **2001**, *73*, 3373–3381.
15. Cano, A.; Alcaraz, O.; Acosta, M.; Arnao, M. On-line antioxidant activity determination: Comparison of hydrophilic and lipophilic antioxidant activity using the ABTS^{•+} assay. *Red. Rep.* **2002**, *7*, 103–109.

Application of Capillary Electrochromatography to Biopolymers and Pharmaceuticals

Ira S. Krull
Sarah Kazmi

Northeastern University, Boston, Massachusetts, U.S.A.

Introduction

The Capillary Electrochromatography Technique

Capillary electrochromatography (CEC) has grown considerably over the past few years, due to the developments in column technology and the appearance of several articles demonstrating the high efficiencies possible with this technique [1]. The literature has shown that there can be numerous applications for this technology, which was not possible with the earlier separation methods. Tsuda published an article that discussed the CEC technique in detail [2]. The technique itself is a derivative of high-performance capillary electrophoresis (HPCE) and high-performance liquid chromatography (HPLC), where the separations are performed using fused-silica tubes of 50–100 μm inner diameter (i.d.), that are packed with either a monolithic packing or small (3 μm or smaller) silica-based particles [3–5]. The packing is similar to the conventional HPLC; however, the mobile phase is driven by electro-osmosis, which results from the electric field applied across the capillary rather than by pressurized flow. The mobile phase is made up of aqueous buffers and organic modifiers [e.g., acetonitrile, (ACN)]. An electro-osmotic flow (EOF) of up to 3 $\mu\text{m}/\text{s}$ can be generated. It is a plug flow, where the linear velocity is independent of the channel width and there is no column back-pressure [4]. Partitioning or adsorption of the neutral analyte occurs in the same way as in HPLC. The analytes are separated while moving through the column with the EOF. Charged solutes have additional electrophoretic mobility in the applied electric field; therefore, the separation occurs by electrophoresis and partitioning. The selectivity in analysis of the charged analytes is increased by electromigration of the sample molecules. The flat flow profile results in a more efficient radial mass transport compared to the parabolic laminar flow in pressure-driven liquid chromatography (LC), and this results in

a significant enhancement in separation performance and shorter analysis times [1,5,6]. The capillaries can be made shorter to offer the same plate count as HPLC, therefore reducing the back-pressure. The packing material is smaller compared to HPLC, so with the high electric fields, the efficiency of this technique is very high (up to about 500,000 plates/m) [1], the peaks are sharp, the resolution is high, and the process is highly selective. An article by Angus et al. [7] demonstrated the separation efficiencies of 200,000–260,000 plates/m that were obtained by CEC and were reproducible from column to column for structurally related, polar neutral compounds of pharmaceutical relevance. The sample capacity in CEC is 10–100 times higher than that of capillary electrophoresis (CE), and this means that more sample volume can be placed on the CEC column to give better sensitivity. The high capacity comes from the high column loadability that results from the stationary phase's retentive mechanism [8]. The absence of additives and predominantly organic mobile phases make CEC better suited for use in mass spectrometry (MS). In fact, nonaqueous CEC is already being practiced by analysts [8]. A recent article by Hansen and Helboe gives a detailed study of the possibility of using CEC to replace gradients or ion-pairing reagents. The group optimized the separation of six nucleotides using a background analyte consisting of 5 mM acetic acid, 3 mM triethylamine (TEA), and 98% acetonitrile and a C_{18} 3- μm column. This was accomplished in half the time taken for a similar separation in HPLC [9].

A variation of gradient CEC is pressurized-flow CEC or PEC (pressurized flow electrochromatography). A pump forms the gradient and then allows part of this pressurized flow to pump the mobile phase through the packed bed. In this way, one can perform isocratic or gradient CEC with part of the mobile-phase driving force being pumped, part electrophoretic and part electroosmotic flows [1,8,10].



Detection of Biomolecules and Pharmaceuticals in CEC

There are many different types of detectors used for pharmaceutical applications in CEC. They vary from indicating just the presence of a sample [fluorescence (FL)], to giving some qualitative information about a sample [photodiode array UV/vis detection (PDA)], to absolute sample determination of the analyte (MS). The methods can be on-column, off-column, and end-column. With on-column, the solutes are detected while still on the capillary, in off-column, the solute is transported from the outlet of the capillary to the detector, and end-column is done with the detector placed right at the end of the capillary. Some modes of detection used in CEC are as follows:

1. UV/vis absorbance detection is widely used in capillary electrophoresis. Absorptivity depends on the chromophore (light-absorbing part) of the solute, the wavelength of the incident light, and the pH and composition of the run buffer. A photodetector measures light intensities and the detector electronics convert this into absorbance [11].
2. Fluorescence detection. When light energy strikes a molecule, some of that energy may be given off as heat and some as light. Depending on the electronic transitions within a molecule, the light given off may be fluorescent or phosphorescent [12]. Fluorescence occurs when an electron drops from an excited singlet to the ground state, as opposed to phosphorescence, which occurs when an electron's transition is from an excited triplet to the ground state.
3. LIF detection, such as argon ion, helium-cadmium [5], and helium-argon lasers, can be used for this detection method. The criterion for choosing the laser is that the wavelength should be at or near the excitation maxima for the solute to be determined. The higher the power of the laser, the higher the intensity and the peak height and the laser's ability to focus the beam to a small spot.
4. MS detection [4]. This is the only detector that has high sensitivity and selectivity and can be used universally; therefore, the increased interest in interfacing this technology with CEC compared to other detection methods. It can detect all solutes that have a molecular weight within the mass range of the MS. In the selected ion-monitoring mode, it detects only solutes of a given mass, and in the total ion chromatogram mode, it detects all the solutes within a given mass range.

Current applications of CEC use on-column UV or laser-induced fluorescence detection; however, for UV, the path length is quite short, which limits sensitivity, although bubble, Z-shaped, and high-sensitivity cells have helped to improve detection limits. However, UV and fluorescence are only good for samples that fluoresce and absorb light or are amenable to derivatization with fluorescing or absorbing chromophores. These detectors impose difficult cell volumes and sample size limits if high separation efficiencies are to be realized, and they are very expensive. All of these drawbacks are nonexistent for MS techniques, which are expensive but provide more structural information and high sensitivity and appear to have the greatest overall potential [8].

According to an issue of *LC-GC* [8], combining CEC with detection techniques such as MS, MS-MS and inductively coupled plasma (ICP)-MS are easier to accomplish, as the flow rates are at nanoliter per minute levels. Analysts must add makeup solvent after the capillary separation for certain ionization methods, and, because it is added later, users can select solvents that are more compatible with the detection technique. CEC mobile phases have a high organic solvent content that is more amenable to MS. Also, the low CEC flow rates means less maintenance and downtime for MS source cleaning.

In the references to the application of CEC to biopolymers, most of the work discusses CEC-electrospray ionization (ESI)-MS, much less to direct CEC-UV/FL methods. However, much of the work has evolved from the use of commercially available, prepacked capillaries, such as C₁₈ or ion exchange or a mixed mode containing both ion exchange and reversed phase. There are very few articles that have actually attempted to develop new phases specifically for biopolymers.

When using MS, the actual CEC conditions never really need to be fully optimized because the MS accomplishes the additional resolution and specific identification, as needed. The specific mobile-phase conditions in CEC-MS may be quite different than for CEC-UV/FL or HPLC, and thus optimization of CEC-MS conditions will be somewhat different than for CEC-UV/FL. This would include, just as for LC-MS, the use of volatile organic solvents and organic buffers, low flow rates, no void volumes, or loss of resolution in the CEC-MS interface and the usual interfacing requirements already developed and optimized for CE-MS [10,13-23].

Few descriptions of quantitation have been reported so far. Most of the literature is qualitative by nature, simply demonstrating suitable, if not fully optimized, experimental conditions that provide evidence of the presence of certain biopolymers and their high resolution from other components in that particular sample. Absolute quantita-



tion and validation needs to be developed and fully optimized for CEC, to become a more valuable and applicable separation mode for biopolymers.

Separation of Proteins

Capillary electrochromatography can accomplish high plate counts, as mentioned earlier; this means a high peak capacity (number of peaks that can be fitted into a typical separation time for a given length of column), therefore highly complex materials can be separated. The implication of better peak capacities is a better resolution of the peaks in a complex analyte. Because of the frequent overlap of peaks due to components in a complex sample, it is difficult to demonstrate peak purity with other methods. It is possible in CEC to quantitatively determine the presence of a particular analyte. CEC techniques have produced the separation of the enantiomers of amino acids [24–27]. This is done with limited use of solvents, buffer additives, salts, organics, chiral species, packing materials, and total time of analysis. Other groups have successfully utilized gradient elution to separate mixtures of dansylated amino acid mixtures on the ODS (octadecylsilane) stationary phase [24]. Also, microprocessor control of pressure flow and voltage, automated sample injection, automated data collection, automated capillary switching, and the ability to interface with a variety of detection instrumentation make CEC an appealing technique for protein separation and peptide mapping.

Proteins and peptides are water-soluble complex molecules that are composed of amino acids linked by peptidic and disulfide bonds. Proteins are really just larger peptides of higher molecular weight, and antibodies are larger proteins of specific conformations, shape, size and immunogenicity, together with antigenic recognition properties [28–31]. The type, number, and sequence of amino acids in the chain determine the chemical characteristics of a peptide. The amino acid sequence determines the electrophoretic properties of the peptide. In addition to the amine terminus of the sequence, the amine and the guanidine residues of lysine and arginine are the main carriers of the positive charges, and the negative charge contribution is associated with the carboxylic acid terminus and the acidic groups of the aspartic and glutamic acids. The isoelectric and isoionic points of the peptide are their important characteristics in electrophoresis. These points are similar in peptides but not identical; the isoelectric point is determined by the given aqueous medium, whereas the isoionic point is related to the interactions with protons. The relation of the electrophoretic mobility of the peptides and their relative molecular weight is described by Offord's equation:

$$\mu_{\text{rel}} = \frac{Z}{[\sqrt[3]{(M^2)}]}$$

where μ_{rel} is the relative mobility, Z is the total net charge, and M is the molar mass in gram per mole. Calculation of the net charge cannot be done easily from the pK values of the acidic and basic groups for large peptides, but additional factors such as conformational differences, primary sequence, chirality, and so forth need to be considered.

The popular methods of analysis of proteins currently are HPLC, HPCE, and MS. However, due to the complexity of proteins, LC approaches show a single, broad, ragged peak, which indicates that the method is unable to resolve the individual species [1]. In CEC, the success of the protein separation requires that the capillary packing material meet certain properties. Depending on the ionic characteristics of the biopolymers, pH-dependent "ideal" packings would be either reversed-phase (RP) or ion-exchange chromatography (IEC) or a combination of both [1,32–46]. There are several references that detail the possible application of size-exclusion chromatographic (SEC) packings in CEC, but these have mainly been applied to synthetic organic polymers and much less to biopolymers [47–50]. Regardless of which packing is actually utilized, it should contain a stationary (bonded, not coated) phase that can successfully interact with the biopolymers, as in RP-HPLC, and prevent any unwanted silanol interactions with the underlying silica or ionic sites. It must also provide additional or programmable EOF, besides that from the uncoated fused-silica capillary walls. Perhaps an ideal packing would combine a cationic-exchange material (cationic-exchange chromatography (CIEC)) together with RP, in order to allow separations based on RP (hydrophobicity) alone, a combination of RP and IEC, or just IEC alone, mobile phase (buffer) dependent. Also, that packing, be it single or mixed mode, should prevent unwanted biopolymer (e.g., peptide amino groups) interaction with the support, such as amine-silanol hydrogen-bonding in RP-HPLC for amine containing analytes (e.g., pharmaceuticals, peptides, and proteins). Additional articles on open tubular CEC (OT-CEC) applications, where a coating is applied on the inner surface of the capillary as in capillary gas chromatography (GC) have appeared [51–54]. There are articles on packed-bed CEC, where there is a real packing in the capillary [55,56]. Also, then there are methods that employ just CEC, without any additional, pressure-driven flow [38,39], as well as pressurized CEC or PEC, with additional pressurized flow [4,51–53]. There is also electro-HPLC that utilizes gradient elution with an applied voltage, but it is mainly conventional HPLC with some voltage applied sporadically or continuously during the HPLC separation [54].



CEC of Biopolymers (Proteins, Peptides, and Antibodies)

The majority of the applications of CEC for biopolymers have dealt with peptides, of varying sizes and complexity, utilizing different modes of CEC (OT-CEC, conventional isocratic CEC, gradient CEC, PEC, and others). The following accounts are listed according to the work of different authors in the field.

Palm and Novotny applied the polymeric gel beds (monoliths) for peptide resolutions in CEC [5]. The peptide separation used the above packing beds with 29% C₁₂ as the ligand. Additional CEC conditions are indicated in Fig. 1, which depicts the separation of a series of tyrosine-containing peptides, with detection at 270–280 nm. In this particular study, peptide elution patterns were very sensitive to changes in pH and ACN concentrations. A gradient elution technique, not employed here, would have been more appropriate for such samples of peptides having small differences in their constitution. Attempts to elute protein samples were unsuccessful with these particular gel matrices, perhaps due to the high hydrophobicity of the packings [5].

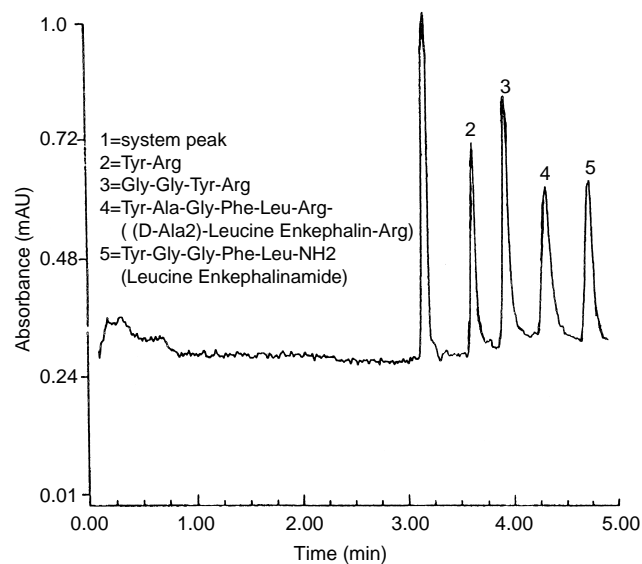


Fig. 1 Isocratic electrochromatography of peptides in a capillary filled with a macroporous polyacrylamide–polyethylene glycol matrix, derivatized with a C₁₂ ligand (29%) and containing acrylic acid. Conditions: mobile phase, 47% acetonitrile in a buffer; voltage, 22.5kV (900 V/cm), 7 μ m; sample concentration, 4–10 mg/mL; detection, UV absorbance at 270 nm; other conditions are described in Ref. 5. (From Ref. 5; reproduced with permission of the authors and the American Chemical Society.)

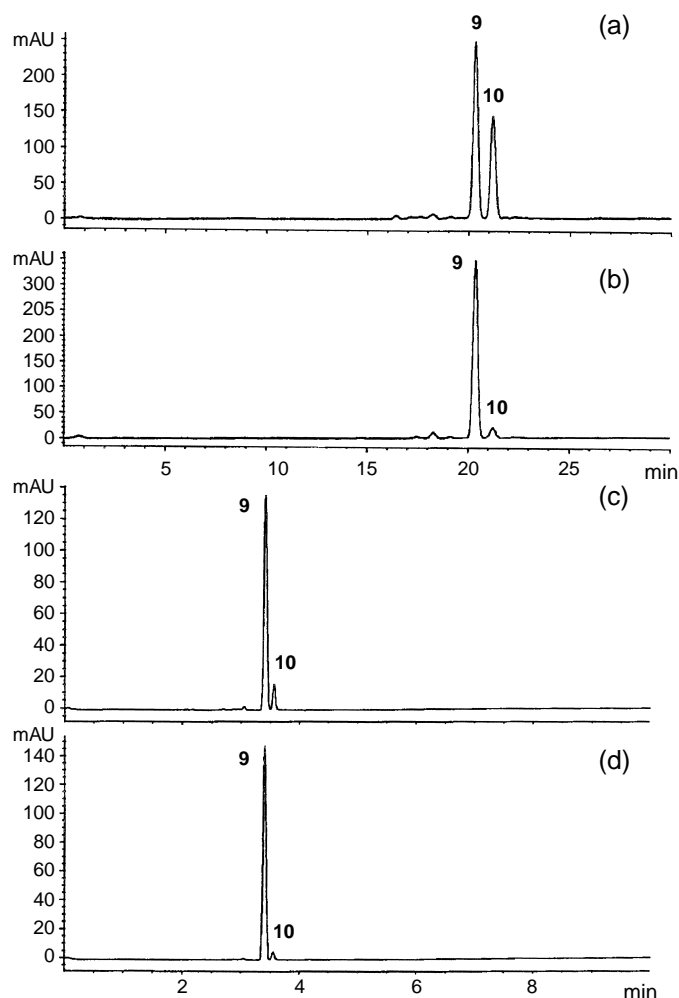


Fig. 2 Separation of synthetic, protected tetrapeptide intermediates: (9) *N*-methyl C- and N-protected tetrapeptide; (10) non-*N*-methyl C- and N-protected tetrapeptide. The structures of these compounds is proprietary information and consequently cannot be disclosed. Detection wavelength of 210 nm with a 10-nm bandwidth and a 1-s rise time. Electrochromatography was performed on a 250 mm \times 50 μ m i.d. spherisorb ODS-1 packed capillary using an acetonitrile-Tris (50 mmol/L, pH 7.8) buffer 80:20 v/v mobile phase, capillary temperature of 15°C, and an electrokinetic injection of 5 kV/15 s. (a) Synthetic mixture of protected tetrapeptides 9 and 10. Efficiency values of 124,000 and 131,000 plates/m were obtained for analytes 9 and 10, respectively. (b) Chromatogram of synthetically prepared 9, the presence of residual nonmethylated tetrapeptide (10) can be seen. (c) Chromatogram of synthetically prepared 9, spiked with 10% of the nonmethylated tetrapeptide (10). Efficiency values of 83,000 and 101,000 plates/m were obtained for analytes 9 and 10, respectively. (d) Chromatogram of synthetically prepared 9, the presence of residual nonmethylated tetrapeptide (10) can be clearly seen at the 3% level. Additional conditions are indicated in Ref. 38. (From Ref. 38; reproduced with permission of the authors and John Wiley and Sons, Inc.)

Euerby et al. reported the separation of an N-methylated, C- and N-protected tetrapeptide from its nonmethylated analog, (Fig. 2) [38]. These separations utilized a Spherisorb ODS-1, 3- μm packing material, without pressure-driven flow (true CEC using a commercially available CE instrument), and an ACN buffer. Using nonoptimized, nonpressurized CEC conditions (non-PEC, non-pressure-driven CEC), separation of the two tetrapeptides could be achieved in a run time of 21 min with efficiency values of 124,000 and 131,000 plates/m. In comparison, when a pressurized CE (buffer reservoirs and capillary were pressurized, with pressure-driven flow of buffer) system was used, separation of the components was achieved within 3.5 min. According to Euerby et al. the separation of these two peptides using a pressure-driven HPLC gradient analysis took 30 min and gave comparable peak area results. Although this study illustrated the improved efficiency of both nonpressurized CEC and pressurized CEC over HPLC, no reasonable conclusions can be drawn from this work.

The attempts that have been made to utilize true chemometric optimization of operating conditions in CEC are unclear in most of the studies done utilizing CEC. This has been done for many years in GC and HPLC, as well as in CE, but there are no obvious articles that have appeared which have utilized true chemometric software approaches to optimization in CEC [57–59]. It is not clear that any true method optimization has been performed or what analytical figures of merit were used to define an optimized set of conditions for biopolymer analysis by CEC. It is also unclear as to why a specific stationary phase (packing) was finally selected as the optimal support in these particular CEC applications for biopolymers. In the future, it is hoped that more sophisticated optimization routines, especially computerized chemometrics (expert systems, theoretical software, or simplex/optiplex routines) will be employed from start to finish.

The coupling of ESI and MS with a pressurized CEC system (PEC) has been shown to separate peptides [4]. This particular study of Schmeer et al. utilized a commercial reversed phase silica gel, Gromsil ODS-2, 1.5- μm packing material, already utilized in capillary HPLC for peptide separations. It was never made perfectly clear why this particular packing material was selected or why PEC was selected for MS interfacing over conventional, isocratic CEC conditions. It is possible that the EOF alone with this packing material was insufficient to elute all peptides in a reasonable time frame and, thus, pressurized flow was introduced. No gradient elution PEC was demonstrated in this particu-

lar study. A mixture of enkephalin methyl ester and enkephalin amide was separated using the packed capillary column (Fig. 3). The coupling of these two methods showed enhanced sensitivity and detectability. Like the Euerby study, this offered little insight into the capabilities of CEC to separate peptides; however, the study does provide a nice example of a peptide separation based on chromatographic and electrophoretic separation mechanisms, probably occurring simultaneously. This report also described the ability of easily interfacing CEC and PEC with ESI–MS.

The coupling of an MS with CEC or PEC provides several advantages. With the capillary columns of 100 μm inner-diameter (i.d.), flow rates of 1–2 L/min are obtained, which are ideal for electrospray MS [4]. No interface like a liquid sheath flow is required and the sintered silica gel frits allow direct coupling of the packed capillary columns without additional transfer capillaries. The spray is therefore formed directly at the outlet side of the column. Verheij et al. carried out the first coupling of a pseudoelectrochromatography system to a fast-atom bombardment (FAB)–MS in 1991 [6]. However, this required transfer capillaries that caused a loss in efficiency, which was also a problem with other experimentations with this technique.

Lubman's group published several papers on the PEC–MS system [51–54]. Reverse-phase open tubular columns (RP–OTC), which were prepared by a sol-gel process, were coated with an amine that enhanced the EOF in an acidic buffer solution and reduced the nonspecific adsorption between the peptides and the column wall. A six-peptide mixture was separated to baseline within 3 min using this system coupled to an on-line ion-trap storage–time-of-flight mass spectrometer (ITS–TOFMS). A full-range mass detection speed of 8 Hz was used in all these experiments, which was rapid to maintain the high efficiency and ultrafast separation. A high-quality total ion chromatogram could be obtained with only a couple of femtomoles of peptide samples, due to the high-duty cycle of the MS and the column path-length-independent and concentration-sensitive feature of the ESI process. The concentration limit of detection was also improved to about $1 \times 10^{-6}M$ because of the preconcentration capability of the reversed-phase CEC. A tryptic digest of horse myoglobin was successfully separated within 6 min on the gradient CEC system. The use of the MS increased the resolving power of this system by clearly identifying the coeluting components.

Another article by Wu et al. [52] dealt with a PEC coupled to an ion-trap storage/reflectron TOFMS (RTOFMS) for the analysis of peptide mixtures and



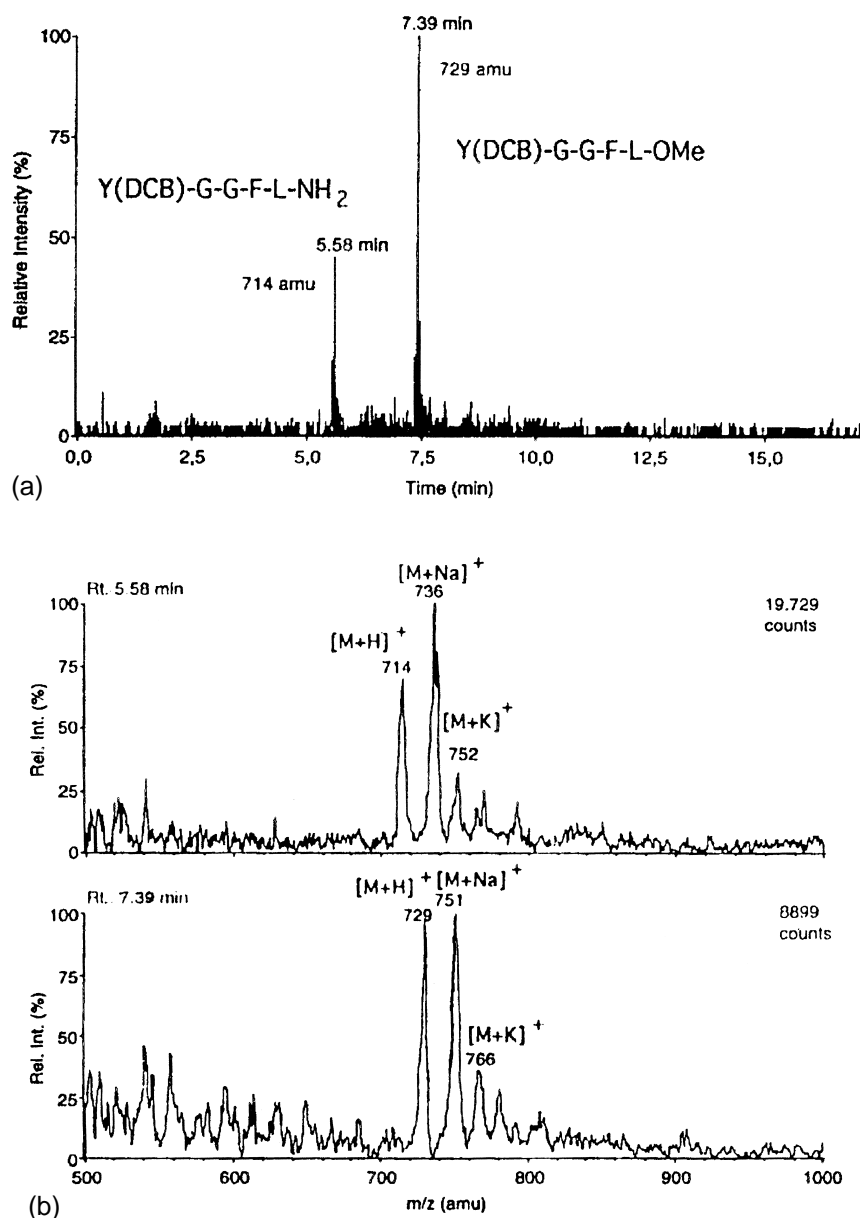


Fig. 3 Interfacing of pressure-driven CEC (PEC) for the separation of two simple peptides, enkephalin methyl ester (5.58 min) and enkephalin amide (7.39 min). (a) Extracted mass chromatogram of m/z 714 and 729 for the on-line peptide separation. Specific operating conditions are indicated in Ref. 4. (b) Mass spectra taken from the chromatographic peaks in (a), illustrating true M_r and the presence of $M+H$, $M+Na$, and $M+K$ cations at appropriate m/z (amu) values. (From Ref. 4; reproduced with permission of the authors and the American Chemical Society.)

protein digests. Taking advantage of the EOF, a high separation efficiency has been achieved in PEC due to a relatively flat flow profile and the use of smaller packing materials. With columns only 6 cm long, a tryptic digest of bovine cytochrome-c was successfully separated in about 14 min by properly tuning the applied voltage and the supplementary pressure. A relatively

complex protein digest (tryptic digest) of chicken albumin gave 20 peaks (resolved) in the total ion current chromatogram in 17 min (Fig. 4). The sample concentrations were also on the order of about $1 \times 10^{-5} M$. The detector increased the resolving power of PEC by unambiguously identifying coeluting components. The CEC was directly interfaced to the MS via an ESI,

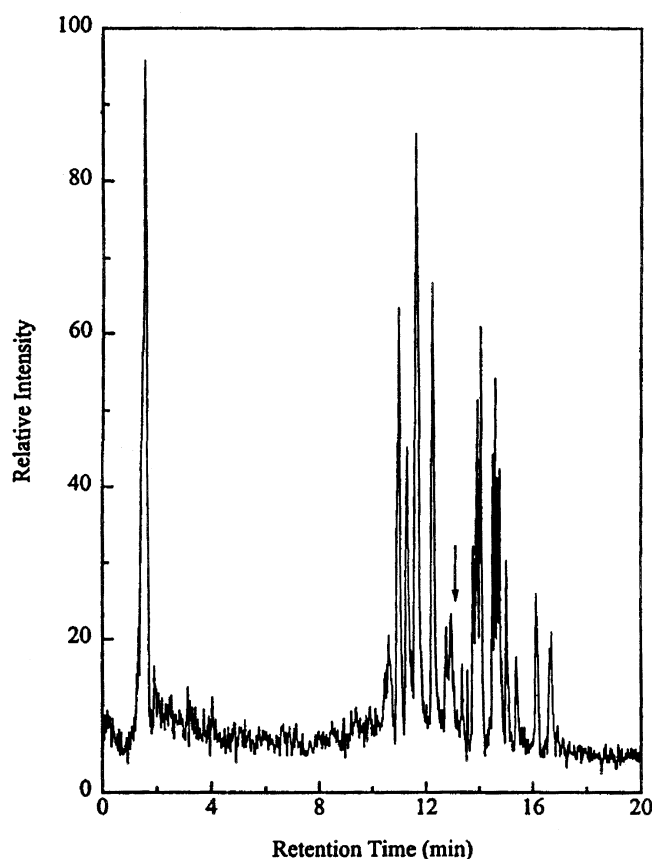


Fig. 4 The total ion chromatography (TIC) of the separation of a tryptic digest of chicken ovalbumin with a sample injection amount of 12 pmol corresponding to the original protein [52]. Column length, 6 cm. Conditions: 20 min, 0–40% acetonitrile gradient; 1000 V applied voltage with a 40-bar supplementary pressure. (From Ref. 52; reproduced with permission of the authors and the American Chemical Society.)

which provided the molecular-weight information of the protein digest products and structural information via MS–MS (Table 1). The device uses a quadrupole ion trap as a front-end storage device, which converts a continuous electrospray beam for TOF analysis. The storage property of the ion trap provides ion integration for low-intensity signals, whereas the nonscanning property of the TOFMS provides high sensitivity. A description of the MS is provided in an article by Wu et al. [54]. According to an article by Verheij et al., problems that were encountered earlier, like formation of bubbles, have been overcome by using liquid junctions to apply the electric field over the column [60].

A recent review article by the Lubman group points out that there are some serious advantages in using an

open tubular column (OTC) for CEC as compared with packed-bed CEC [54]. OTCs with inner diameters around 10 μm have been found to have a smaller plate height when compared to packed columns. This is due to the lack of band-broadening effects associated with the presence of packing materials and end-column frits. OTC capillaries do not require end frits. High concentration sensitivity is another advantage of OTCs, as columns with very small dimensions are used. The small diameters of OTCs allow for the use of a higher voltage in CEC, without significant Joule heating. OTCs can also often provide more rapid separations than packed columns, by eliminating intraparticle diffusion, which is an important elimination for ultrafast separations in packed columns. However, there are some grave difficulties involved in using OTCs, perhaps because of the real difficulties with sample injection and detection. The injection volume of OTCs is in the low nanoliter or even picoliter range. The very small inner diameters of most OTCs make optical detection difficult, but they are very compatible with a concentration-sensitive detection method, such as ESI–IT–TOFMS. With peptide mixtures, however, gradient elution CEC, with or without pressure-driven flow, is almost required over isocratic or step-gradient methods, because small changes in the mobile phase composition results in large changes in peptide retention times.

In a later study, Pesek et al. reported the separation of other proteins using a diol stationary phase [61–64]. The use of a diol stationary phase should result in a surface that is more hydrophilic than a typical alkyl-bonded moiety, like C_{18} or C_8 . The overall results showed significant variations in retention times due to differences in solute-bonded phase interactions. Other factors, such as pH, could also influence this interaction, due to its influence on charge and protein conformations. Combining all these factors in the separation of peptides and proteins provides an experimentalist with many decisions to be made in the optimized experimental conditions to be used. Other chemical modifications of etched fused silica need to be studied in order to provide a better understanding of their interactions with proteins and peptides, as well as other classes of biopolymers.

Conclusions

At the present time, although there are several applications of CEC–PEC to biopolymer classes, these are to be considered only preliminary and not necessarily fully optimized in all possible parameters. At times,



significant improvements in peak shape, plate counts, resolutions, efficiency, and the time of analysis can be realized. However, final optimizations of these separations have not been realized or possible. Some workers have utilized pressurized flow to solve the problems of obtaining reasonable EOF without silanol-analyte interaction; however, this does not solve the problem. It just forces the analyte to elute and approaches electro-HPLC, rather than true CEC. There are real differences between electro-HPLC, PEC and CEC that need to be recognized. There does not, in general,

seem to have been any serious attempt to utilize any chemometric software approaches in CEC-PEC for biopolymer separation optimizations or rationale for doing so. At this time, packings are simply used because they were on the shelf in a laboratory or commercially available and not necessarily because they were really the best for protein-peptide separations in PEC-CEC. There remains a need for research-oriented column choices from commercial vendors to avoid the need to pack capillaries in-house with commercial HPLC supports.

Table 1 Comparison of Calculated and Measured Tryptic Peptides of Chicken Ovalbumin from PEC-MS

No.	Tryptic peptides	Calculated mass ^a	Determined mass ^{a,b}	Sequence
1	1-16	1709.0	1709.6	GSIGAASMEFCFDVFK
4, 5	47-55	1080.2	1079.7	DSTRTQINK
5	51-55	602.7	602.9	TQINK
6, 7	56-61	781.0	781.4	VVRFDK
7	59-61	408.5	408.4	FDK
10	105-110	779.8	780.1	IYAEER
11	111-122	1465.8	1466.3	YPILPEYLQCVK
12	123-126	579.7	579.7	ELYR
13	127-142	1687.8	1687.5	GGLEPINFQTAADQAR
16	182-186	631.7	631.6	GLWEK
16, 17	182-189	996.1	995.9	GLWEKAFK
17	187-189	364.4	364.5	AFK
18	190-199	1209.3	1209.0	DEDTQAMPFR
20	219-226	821.9	821.7	VASMASEK
21	227-228	277.4	277.6	MK
23	264-276	1581.7	1581.3	LTEWTSSNVMEER
24, 25	277-279	405.5	405.4	KIK
26	280-284	646.8	646.8	VYLPR
26, 27	280-286	924.2	924.4	VYLPRMK
27, 28	285-290	813.0	813.1	MKMEEK
28	287-290	535.6	535.5	MEEK
30	323-339	1773.9	1774.2	ISQAVHAAHAEINEAGR
31	340-359	2009.1	2008.5	EVVGSAAEAGVDAASVSEEFR
32	360-369	1190.4	1190.2	ADHPFLFCIK
33	370-381	1345.6	1345.3	HIATNAVLFFFGR
33, 34	370-385	1750.1	1749.5	HIATNAVLFFFGRCSVSP
34	382-385	404.5	404.4	CVSP

^a Average masses.

^b Average of all charge states observed.

Source: Ref. 52; reproduced with permission of the authors and the American Chemical Society.



References

1. I. S. Krull, K. Mistry, and R. Stevenson, *Am. Lab.* 16A (August 1998).
2. T. Tsuda, *Anal. Chem.* 59: 521 (1987).
3. J. A. Olivares, N. T. Nguyen, C. R. Yonker, and R. D. Smith, *Anal. Chem.* 59: 1230 (1987).
4. K. Schmeer, B. Behnke, and E. Bayer, *Anal. Chem.* 67: 3656 (1995).
5. A. Palm and M. V. Novotny, *Anal. Chem.* 69: 4499 (1997).
6. E. R. Verheij, U. R. Tjaden, W. A. M. Niessen, and J. van der Greef, *J. Chromatogr.* 554: 339 (1991).
7. P. D. A. Angus, E. Victorino, K. M. Payne, C. W. Demarest, T. Catalano, and J. F. Stobaugh, *Electrophoresis* 19: 2073 (1998).
8. R. E. Majors, *LC-GC Magazine* 16(2): 96 (1998).
9. S. H. Hansen and T. Helboe, *J. Chromatogr. A* 836: 315 (1999).
10. J. P. Landers (ed.), *CRC Handbook of Capillary Electrophoresis—Principles, Methods, and Applications*, 2nd ed., CRC Press, Boca Raton, FL, 1997.
11. D. R. Baker, *Capillary Electrophoresis*, Techniques in Analytical Chemistry Series, John Wiley & Sons, New York, 1995.
12. D. M. Hercules, *Fluorescence and Phosphorescence Analysis: Principles and Applications*, Interscience, New York, 1966, p. 19.
13. R. L. Cunico, K. M. Gooding, and T. Wehr, *Basic HPLC and CE of Biomolecules*, Bay Bioanalytical Laboratory, Richmond, CA, 1998.
14. Cs. Horvath and J. G. Nikelly (eds.), *Analytical Biotechnology: Capillary Electrophoresis and Chromatography*, ACS Symposium Series Vol. 434, American Chemical Society, Washington, DC, 1990.
15. S. F. Y. Li, *Capillary Electrophoresis: Principles, Practice and Applications*, Elsevier Science, Amsterdam, 1992.
16. P. D. Grossman and J. C. Colburn (eds.), *Capillary Electrophoresis—Theory and Practice*, Academic Press, San Diego, CA, 1992.
17. P. G. Righetti (ed.), *Capillary Electrophoresis in Analytical Biotechnology*, CRC Series in Analytical Biotechnology, CRC Press, Boca Raton, FL, 1996.
18. P. Camilleri (ed.), *Capillary Electrophoresis: Theory and Practice*, CRC Press, Boca Raton, FL, 1993.
19. R. A. Mosher and W. Thormann, *The Dynamics of Electrophoresis*, VCH, Weinheim, 1992, Chap. 7.
20. K. D. Altria and M. M. Rogan, *Introduction to Quantitative Applications of Capillary Electrophoresis in Pharmaceutical Analysis, A Primer*, Beckman Instruments, Inc., Fullerton, CA, 1995.
21. R. Weinberger and R. Lombardi, *Method Development, Optimization and Troubleshooting for High Performance Capillary Electrophoresis*, Simon and Schuster Custom Publishing, Needham Heights, MA, 1997.
22. B. L. Karger and Wm. Hancock (eds.), *High Resolution Separation and Analysis of Biological Macromolecules*, Methods in Enzymology Series Vol. 270, Part A, Fundamentals, Academic Press, San Diego, CA, 1996.
23. K. D. Altria (ed.), *Capillary Electrophoresis Guidebook, Principles, Operation and Applications*, Methods in Molecular Biology, Humana Press, Totowa, NJ, 1996.
24. I. S. Lurie, R. P. Meyers, and T. S. Conver, *Anal. Chem.* 70: 3255 (1998).
25. P. Sandra, A. Dermaux, V. Ferraz, M. M. Dittman, and G. Rozing, *J. Micro. Separ.* 9: 409 (1997).
26. A. Dermaux, P. Sandra, M. Ksir, and K. F. F. Zarrouck, *J. High Resolut. Chromatogr.* 21: 545 (1998).
27. D. Li, H. H. Knobel, S. Kitagawa, A. Tsuji, H. Watanabe, M. Nakshima, and T. Tsuda, *J. Micro. Separ.* 9: 347 (1997).
28. J. R. Mazzeo and I. S. Krull, *Capillary Electrophoresis—Technology*, N. Guzman (ed.), Marcel Dekker, Inc., New York, 1993, Chap. 29.
29. J. R. Mazzeo, J. Martineau, and I. S. Krull, *CRC Handbook of Capillary Electrophoresis: Principles, Methods, and Applications*, J. P. Landers, (ed.), CRC Press, Boca Raton, FL, 1994, Chap. 18.
30. X. Liu, Z. Sosic, and I. S. Krull, *J. Chromatogr. B* 735: 165 (1996).
31. I. S. Krull, J. Dai, C. Gendreau, and G. Li, *J. Pharm. Biomed. Anal.* 16: 377 (1997).
32. Capillary Electrochromatography, Symposium, San Francisco, CA, organized by the California Separations Science Society, San Francisco, August 1997.
33. Royal Society of Chemistry Analytical Division, Northeast Region, Chromatography and Electrophoresis Group, Symposium on New Developments and Applications in Electrochromatography, University of Bradford, Bradford, U.K. December 3, 1997.
34. T. Tsuda (ed.), *Electric Field Applications in Chromatography, Industrial and Chemical Processes*, VCH, Weinheim, 1995.
35. M. M. Dittmann, K. Weinand, F. Bek, and G. P. Rozing, *LC/GC Mag.* 13(10): 800 (1995).
36. M. M. Dittmann and G. P. Rozing, *J. Chromatogr. A* 744: 63 (1996).
37. G. Ross, M. Dittmann, F. Bek, and G. Rozing, *Am. Lab.* (March 1996), p. 34.
38. M. R. Euerby, D. Gilligan, C. M. Johnson, S. C. P. Roulin, P. Myers, and K. D. Bartle, *J. Micro. Separ.* 9: 373 (1997).
39. M. R. Euerby, C. M. Johnson, K. D. Bartle, P. Myers, and S. C. P. Roulin, *Anal. Commun.* 33: 403 (1996).
40. M. M. Robson, M. G. Cikalo, P. Myers, M. R. Euerby, and K. D. Bartle, *J. Micro. Separ.* 9: 357 (1997).
41. J. H. Miwaya and M. S. Alesandro, *LC/GC Mag.* 16(1): 36 (1998).
42. R. E. Majors, *LC/GC Mag.* 16(1): 12 (1998).
43. I. H. Grant, *Capillary Electrochromatography*, K. D. Altria (ed.), Methods in Molecular Biology Vol. 52, Humana Press, Totowa, NJ, 1996, Chap. 15.
44. M. R. Euerby, C. M. Johnson, and K. D. Bartle, *LC/GC Int.* (January 1998), p. 39.
45. M. G. Cikalo, K. D. Bartle, M. M. Robson, P. Myers, and



- M. R. Euerby, *Analyst* 123: 87R (1998).
46. W. Wei, G. Luo, and C. Yan, *Am. Lab.* 20C (January 1998).
47. E. C. Peters, K. Lewandowski, M. Petro, J. M. J. Frechet, and F. Svec, IN HPLC 98, St. Louis, MO, May 1998.
48. E. C. Peters, K. Lewandowski, M. Petro, F. Svec, and J. M. J. Frechet, *Anal. Commun.* 35: 83 (1998).
49. E. C. Peters, M. Petro, F. Svec, and J. M. J. Frechet, *Anal. Chem.* 69: 3646 (1997).
50. E. Venema, J. C. Kraak, H. Poppe, and R. Tijssen, *Chromatographia* 48(5/6): 347 (1998).
51. J. T. Wu, P. Huang, M. X. Li, M. G. Qian, and D. M. Lubman, *Anal. Chem.* 69: 320 (1997).
52. J. T. Wu, P. Huang, M. X. Li, M. G. Qian, and D. M. Lubman, *Anal. Chem.* 69: 2908 (1997).
53. J. T. Wu, P. Huang, M. X. Li, M. G. Qian, and D. M. Lubman, *Anal. Chem.* 69: 2870 (1997).
54. J. T. Wu, P. Huang, M. X. Li, M. G. Qian, and D. M. Lubman, *J. Chromatogr. A* 794: 377 (1998).
55. C. Yang and Z. El Rassi, *Electrophoresis* 19: 2061 (1998).
56. M. Zhang and Z. El Rassi, *Electrophoresis* 19: 2068 (1998).
57. R. J. Bopp, T. J. Wozniak, S. L. Anliker, and J. Palmer, *Pharmaceutical and Biomedical Applications of Liquid Chromatography*, C. M. Riley, W. J. Lough, and I. W. Wainer (eds.), Progress in Pharmaceutical and Biomedical Analysis Vol. 1, Pergamon/Elsevier Science, Amsterdam, 1994, Chap. 10.
58. J. W. Dolan and L. R. Snyder, *Am. Lab.* 50 (May 1990).
59. L. R. Snyder, J. J. Kirkland, and J. L. Glajch, *Practical HPLC Method Development*, 2nd ed., John Wiley & Sons, New York, 1997, Chap. 10.
60. E. R. Verheij, U. R. Tjaden, W. A. M. Niessen, and J. van der Greef, *J. Chromatogr.* 712: 201 (1995).
61. J. J. Pesek, M. T. Matyska, J. E. Sandoval, and E. J. Williamsen, *J. Liq. Chromatogr. Related Technol.* 19(17/18): 2843 (1996).
62. J. J. Pesek, M. T. Matyska, and L. Mauskar, *J. Chromatogr. A* 763: 307 (1997).
63. J. J. Pesek and M. T. Matyska, *J. Chromatogr. A* 736: 255 (1996).
64. J. J. Pesek and M. T. Matyska, *J. Chromatogr. A* 736: 313 (1996).



Applications of Evaporative Light-Scattering Detection in HPLC

Juan G. Alvarez

Beth Israel Deaconess Medical Center, Harvard Medical School, Boston, Massachusetts, U.S.A.

Introduction

High-performance liquid chromatography (HPLC) is mainly carried out using light absorption detectors as ultraviolet (UV) photometers and spectrophotometers (UVD) and, to a lesser extent, refractive index detectors (RID). These detectors constitute the main workhorses in the field [1]. The sensitive detection of compounds having weak absorption bands in the range 200–400 nm, such as sugars and lipids is, however, very difficult with absorption detectors. The use of the more universal RID is also restricted in practice because of its poor detection limit and its high sensitivity to small fluctuations of chromatographic experimental conditions, such as flow rate, solvent composition, and temperature [2]. Moreover, if the separation of complex samples requires the use of gradient elution, the application of RID becomes almost impossible. Although for some solutes the use of either a reaction detector (RD) or a fluorescence detector (FD) is possible, this is not a general solution. In this regard, the analysis of complex mixtures of lipids or sugars by HPLC remains difficult owing to the lack of a suitable detector.

The miniaturization of detector cells is also extremely difficult and the technological problems have not yet been solved because the detection limit should also be decreased or, at least, kept constant [2–6]. Some progress in the design of very small cells for UVD and FD has been reported [3–7], but the miniaturization of RD and RID seems much more difficult in spite of some suggestions [8]. Similarly, the development of open tubular columns is plagued by the lack of a suitable detector with a small contribution to band broadening.

A nonselective detector more sensitive than the RID and easier to use with a small contribution to band broadening is thus desirable in HPLC. The mass spectrometer would be a good solution if it were not so complex [10] and expensive. The electron-capture detector (ECD) [11] and flame-based detectors have been suggested [12]. Both are very sensitive and could be made with very small volumes. Unfortunately, the

ECD can be used only with volatile analytes and it is very selective. Both ECD and flame-based detectors are very sensitive to the solvent flow rate, and noisy signals are often produced. The adaptability of these detectors to packed columns is thus difficult. This probably explains why the ECD has been all but abandoned.

The evaporative light-scattering analyzer [13–14], on the other hand, is an alternative solution which seems very attractive for a number of reasons. As most analytes in HPLC have a very low vapor pressure at room temperature and the solvents used as the mobile phase have a significant vapor pressure, some kind of phase separation is conceivable.

Evaporative Light-Scattering Detector

Principle of Operation

The unique detection principle of evaporative light-scattering detectors involves nebulization of the column effluent to form an aerosol, followed by solvent vaporization in the drift tube to produce a cloud of solute droplets (or particles), and then detection of the solute droplets (or particles) in the light-scattering cell.

Detector Components

Nebulizer: The nebulizer is connected directly to the analytical column outlet. In the nebulizer, the column effluent is mixed with a steady stream of nebulizing gas, usually nitrogen, to form an aerosol. The aerosol consists of a uniform dispersion of droplets. Two nebulization properties can be adjusted to regulate the droplet size of the analysis. These properties are gas and mobile-phase flow rates. The lower the mobile-phase flow rate, the less gas and heat are needed to nebulize and evaporate it. Reduction of flow rate by using a 2.1- μm -inner diameter column should be considered when sensitivity is important. The gas flow rate will also regulate the size of the droplets in the aerosol. Larger droplets will scatter more light and increase the



sensitivity of the analysis. The lower the gas flow rate, the larger the droplets. It is also important to remember that the larger the droplet, the more difficult it will be to vaporize in the drift tube. An unvaporized mobile phase will increase the baseline noise. There will be an optimum gas flow rate for each method which will produce the highest signal-to-noise ratio.

Drift tube: In the drift tube, volatile components of the aerosol are evaporated. The nonvolatile particles in the mobile phase are not evaporated and continue down the drift tube to the light-scattering cell to be detected. Nonvolatile impurities in the mobile phase or nebulizing gas will produce noise. Using the highest-quality gas, solvents, and volatile buffers, preferably a filter, will greatly reduce the baseline noise. Detector noise will also increase if the mobile phase is not completely evaporated. The sample may also be volatilized if the drift-tube temperature is too high or the sample is too volatile. The optimal temperature in the drift tube should be determined by observing the signal-to-noise ratio with respect to temperature.

Light-scattering cell: The nebulized column effluent enters the light-scattering cell. In the cell, the sample particles scatter the laser light, but the evaporated mobile phase does not. The scattered light is detected by a silicone photodiode located at a 90° from the laser. The photodiode produces a signal which is sent to the analog outputs for collection. A light trap is located 180° from the laser to collect any light not scattered by particles in the aerosol stream.

The signal is related to the solute concentration by the function $A = am^x$, where x is the slope of the response line, m is the mass of the solute injected in the column, and a is the response factor.

Applications

Evaporative light-scattering detection finds wide applicability in the analysis of lipids and sugars. The analysis of lipids and sugars by HPLC has classically been hampered due to the lack of absorbing chromophores in these molecules. Accordingly, most analyses are carried out by gas chromatography, requiring derivatization in the case of the sugars or being especially difficult like the separation of the high-molecular-weight triglycerides, or even impossible for the important class of phospholipids, which cannot withstand high temperatures. Specific applications are as follows:

1. Use of evaporative light scattering detector in reversed-phase chromatography of oligomeric surfactants. Y. Mengerink, H. C. De Man, and S. J. Van Der Wal, *J. Chromatogr.* 552: 593 (1991)

2. A rapid method for phospholipid separation by HPLC using a light-scattering detector: W. S. Letter, *J. Liq. Chromatogr.* 15: 253 (1992)
3. Detection of HPLC separation of glycopospholipids: J. V. Amari, P. R. Brown, and J. G. Turcotte, *Am. Lab.* 23 (Feb. 1992)
4. Analysis of fatty acid methyl esters by using supercritical fluid chromatography with mass evaporative light-scattering detection: S. Cooks and R. Smith, *Anal. Proc.* 28, 11 (1991)
5. HPLC analysis of phospholipids by evaporative light-scattering detection: T. L. Mounts, S. L. Abidi, and K. A. Rennick, *J. AOCS* 69: 438 (1992)
6. Determination of cholesterol in milk fat by reversed-phase high-performance liquid chromatography and evaporative light-scattering detection: G. A. Spanos and S. J. Schwartz, *LC-GC* 10(10): 774 (19XX)
7. A qualitative method for triglyceride analysis by HPLC using ELSD: W. S. Letter, *J. Liq. Chromatogr.* 16: 225 (1993)
8. Detect anything your LC separates, P. A. Asmus, *Res. Dev.* 2: 96 (1986).
9. Rapid separation and quantification of lipid classes by HPLC and mass (light scattering) detection: W. H. Christie, *J. Lipid Res.* 26: 507 (1985)

References

1. R. P. W. Scott, *Liquid Chromatography Detectors*, Elsevier, Amsterdam, 1977.
2. H. Colin, A. Krstulovic, and G. Guiochon, *Analysis* 11: 155 (1983).
3. R. P. W. Scott and P. Kucera, *J. Chromatogr.* 169: 155 (1979).
4. H. Knox and M. T. Gilbert, *J. Chromatogr.* 186: 405 (1979).
5. G. Guiochon, *Anal. Chem.* 53: 1318 (1981).
6. G. Guiochon, in *Miniaturization of LC Equipment*, P. Kucera (ed.), Elsevier, Amsterdam, 1983.
7. P. Kucera and H. Umagat, *J. Chromatogr.* 255: 563 (1983).
8. J. W. Jorgensen and E. J. Guthrie, *J. Chromatogr.* 255: 335 (1983).
9. J. W. Jorgensen, S. L. Smiths, and M. Novotny, *J. Chromatogr.* 142: 233 (1977).
10. P. J. Arpino and G. Guiochon, *Anal. Chem.* 51: 682A (1979).
11. F. W. Willmont and R. J. Dolphin, *J. Chromatogr. Sci.* 12: 695 (1974).
12. V. L. McGuffin and M. Novotny, *J. Chromatogr.* 218: 179 (1981).
13. J. H. Charlesworth, *Anal. Chem.* 50: 1414 (1978).
14. R. Macrae and J. Dick, *J. Chromatogr.* 210: 138 (1981).



Applied Voltage: Effect on Mobility, Selectivity, and Resolution in Capillary Electrophoresis

Jetse C. Reijenga

University of Technology, Eindhoven, The Netherlands

Introduction

Generally, migration times t_m in capillary electrophoresis (CE) are inversely proportional to the applied voltage; in terms of analysis time, the voltage should, therefore, be as large as possible:

$$t_m \propto \frac{1}{V}$$

Under conditions optimized for limited power dissipation, effective mobilities and selectivities (defined as effective mobility ratios) are independent of the applied voltage.

Efficiency is also determined by the applied voltage, but in a much more complicated manner (see Band

Broadening in Capillary Electrophoresis). If efficiency is limited by diffusion, a higher voltage also leads to a higher efficiency. Limitations are due to insulation properties and heat dissipation. Voltages larger than 30 kV should always be avoided because of danger of sparking and leaking currents, even more so in cases of significant atmospheric humidity. Excessive heat dissipation leads to an average temperature increase inside the capillary, which can be reduced by forced cooling. What cannot be reduced is the contribution of heat dissipation to band broadening. This can only be reduced by a lower conductivity, a lower current density, or a smaller inner diameter (see Band Broadening in Capillary Electrophoresis). In the case of diffusion-limited efficiency, the efficiency (as given by the plate number) is directly proportional to the applied voltage:

$$N \propto V$$

The ultimate criterion for quality of separation is the resolution R , given by the following relationship:

$$R = \frac{\Delta t_m}{4\sigma}$$

With the definition of plate number, it follows that $R \propto \sqrt{V}$.

Figure 1 shows a computer simulation of the resolution and analysis time of a mixture of anions at 5, 10, and 25 kV. In order to better visualize the effect on resolution, a logarithmic x axis was chosen.

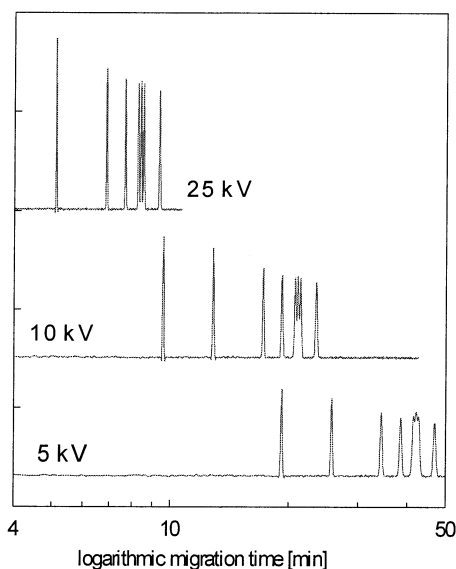


Fig. 1 Analysis of a mixture of weak anions at three different voltages. Suppressed EOF in a 400-mm capillary with negative inlet polarity. *Note:* The time axis is logarithmic.

Suggested Further Reading

- Hjertén, S., *Chromatogr. Rev.* 9: 122 (1967).
Jorgenson, J. W. and K. D. Lucaks, *Science* 222: 266 (1983).
Li, S. F. Y., *Capillary Electrophoresis – Principles, Practice and Applications*, Elsevier, Amsterdam, 1992.
Reijenga, J. C. and E. Kenndler, *J. Chromatogr. A* 659: 403 (1994).
Reijenga, J. C. and E. Kenndler, *J. Chromatogr. A* 659: 417 (1994).



Aqueous Two-Phase Solvent Systems for Countercurrent Chromatography

Jean-Michel Menet

Process Development Chemistry, Aventis Pharma, Vitry-sur-Seine, France

Introduction

Aqueous two-phase solvent (ATPS) systems are made of two aqueous liquid phases containing various polymers. Such systems are gentle toward biological materials and they can be used for the partition of biomolecules, membrane vesicles, cellular organites, and whole cells. They are characterized by a high content of water in each phase, by very close densities and refraction indices of the two phases, by a very low interfacial tension, and by high viscosities of the phases. As a result, settling times are particularly long and may last up to 1 h or longer.

The partition of a substance between the two phases depends on many factors. Theoretical studies have been carried out in order to better understand the reasons for the separation in two aqueous phases, thanks to the introduction of various polymers, and the role of various factors on the partition of the substances. However, no global theory is available to predict the observed behaviors. Hopefully, some empirical knowledge has been acquired which will help in the use of these unique solvent systems.

Various devices have been used for the partition of substances in ATPS systems. Countercurrent chromatography (CCC) has again revealed its unique features, because it has enabled the use of such very viscous systems at relatively high flow rates while obtaining a satisfactory efficiency and a good resolution for the separation. Many applications have been described in the literature for the use of ATPS systems with CCC devices.

ATPS Systems

For further information on ATPS systems and the partitioning, we strongly recommend the books by Albertsson [1] and Walter et al. [2], which are reference books in this area.

Polymers Used for ATPS Systems

Many ATPS systems contain a polymer which is sugar based and a second one which is of hydrocarbon ether type. Sugar-based polymers include dextran (Dx), hydroxy propyl dextran (HPDx), Ficoll (Fi) (a polysaccharide), methyl cellulose (MC), or ethylhydroxyethyl cellulose (EHEC). Hydrocarbon ether-type polymers include poly(ethylene glycol) (PEG), poly(propylene glycol) (PPG), or the copolymer of PEG and PPG. Derivatized polymers can also be useful, such as PEG-fatty acids or di-ethylaminoethyl-dextran (Dx-DEAE).

Dextran, or α -1,6-glucose, is available in a mass range from 10,000 to 2,000,000. Dx T500 fractions, also called Dx 48 from Pharmacia (Uppsala, Sweden), are among the best known: their weight-average molecular weight (M_w) varies from 450,000 to 500,000. These white powders contain about 5–10% of water. PEG is a linear synthetic polymer which is available in many molecular weights, the most common being between 300 and 20,000.

Physical Properties of the ATPS Phases

Common characteristics of ATPS phases are their high content of water for both phases, typically 85–99% by weight and very close densities and refraction indices for the two phases. Moreover, both phases are viscous and the interfacial tension is low, from 0.1 to 0.001 dynes/cm. The settling times in the Earth's gravitational field range from 5 min to 1 h.

Practical Use of ATPS

Because ATPS systems are particularly suited for protein separations, many research workers have worked in this area and have tried to model their behavior when varying the composition of these systems. However, there are still no theoretical models to calculate,



a priori, the partition coefficient of a protein for a wide range of molecular weights of polymers and concentrations in salts and polymers. However, it remains possible to have qualitative explanations of the role of key factors on the partition of the substances.

Choice of the ATPS System

The general principle for designing an ATPS system is to try various systems, either made from two phases containing polymers or from one phase containing a polymer and the other component a salt. The nature of the substances to be separated shall be taken into account: Fragile solutes may be denaturated by a too high interfacial tension, as encountered in aqueous polymer-salt systems. Some substances may even aggregate in an irreversible way, or be altered in other ways by their contact with some polymers or salts. Moreover, some substances can require the specific use of given salts, or pH, or temperature. When all the previous considerations have been taken into account, the partition coefficients can then be determined in test-tube experiments. Afterward, the composition of the phases can be adjusted.

Systems Suited for the Separation of Molecules

A simple way consists in testing two ATPS systems, dextran 40/PEG-8000 and dextran 500/PEG-8000, which lead to a relatively quick settling and allow reproducible results. For charged macromolecules, the two key parameters are the pH with regard to the isoelectric point of the product and the nature and concentration of the chosen salt. The composition in polymer has a smaller influence, except for some neutral compounds.

Systems Suited for the Separation of Cells and Particles

The main parameter for such separations is the difference of concentrations of each polymer between the two phases. If the concentrations in polymer are quite high, particles tend to adsorb at the interface of the two phases, without any specificity. For instance, all human erythrocytes adsorb at the interface of the dextran 500/PEG-8000 systems with respective concentrations higher than 7.0% and 4.4% (w/w).

The goal is to find a system close to the critical point (in the phase diagram) to achieve the separation, as the partition coefficients all become close to 1. However, this requires an increased attention to the experimen-

tal conditions in order to obtain reproducible results. If necessary, a change in the molecular weight of one of the polymers allows one to choose the aqueous phase in which the particle tends to accumulate. For instance, most mammalian cells partition between the interface and the upper phase rich in PEG in dextran 500/PEG-8000 systems, whereas they partition between the interface and the lower phase rich in dextran in dextran 40/PEG-8000 systems.

Adjustment of the Partition Coefficient

We note that the partition coefficient K is defined as the ratio of the concentration of the substance in the upper phase to its concentration in the lower phase. As cells and particles tend to partition between one phase and the interface, only molecules, such as proteins, are the subject of this section.

First, the partition coefficient of the substance should be determined in a standard system, such as dextran 500 (7.0%, w/w)/PEG-8000 (5.0%, w/w) with 5–10 mM of buffer added. Then, the following empirical laws can be used for the adjustment:

1. K is increased by diminishing the molecular weight of the polymer which is predominant in the upper phase (e.g., PEG) or by increasing the molecular weight of the polymer which is predominant in the lower phase (e.g., dextran). Reversing these changes decreases K .
2. K is significantly different than the unit value only if the concentrations of the polymers are high. K tends to the unit value when the concentrations of the polymers are decreased.
3. K can be adjusted by the addition of a salt, as long as the proteins are not close to their isoelectric points. For a negatively charged protein, K is decreased by following the series: phosphate < sulfate < acetate < chloride < thiocyanate < perchlorate and lithium < ammonium < sodium < potassium (for instance, lithium decreases K by a smaller amount than sodium). The influence of the nature of the salt may be amplified by an increase of the pH, which increases the negative net charge of the molecule. Positively charged proteins exhibit the opposite behavior. All these rules apply only for low concentrations of salts. Higher concentrations could, however, be used to favor the partition of the molecules in the upper phase.
4. Charged polymers can also be used; their influence is greater than that of the salts. The



most common include charged polymers derived from PEG, such as PEG-TMA (trimethylamino) or PEG-S (sulfonate). Dextran can also be modified.

5. The derivatization by hydrophobic groups can also facilitate the extraction of molecules containing hydrophobic sites. The most common polymer is PEG-P (PEG-palmitate).

K depends on the temperature, but in a complex way, so that its use is difficult for common cases.

Optimization of the Selectivity

Some general rules apply to proteins in PEG/dextran systems and are summarized as follows:

1. The concentration of the polymer is important: Decreasing the concentrations brings the system closer to the critical point (in the phase diagram), smoothing K values toward the unit value and finally decreasing the selectivity.
2. The nature of the salt is important. The most important effects are encountered for NaClO_4 , which extracts positively charged molecules in the upper phase, and tetrabutyl ammonium phosphate, which extracts negatively charged proteins in the upper phase.

Applications

These aqueous two-phase solvent systems are more difficult to handle than organic-based solvent systems, so that the number of applications in the literature is quite small as compared to the other systems. However, these applications are really specific, quite often striking in their separation power, and they truly reveal some unique features of countercurrent chromatography.

Former applications of ATPS systems on CCC devices were gathered by Sutherland et al. [3]. For instance, both toroidal and type J [also called a high-speed countercurrent chromatograph (HSCCC)] countercurrent chromatographs were successfully applied for the fractionation of subcellular particles. Using standard rat liver homogenates, plasma membranes, lysosomes, and endoplasmic reticulum were separated by a 3.3% (w/w) dextran T500, 5.4% PEG-6000, 10 mM sodium phosphate-phosphoric acid buffer (pH 7.4), 0.26M sucrose, 0.05 mM Na_2EDTA , and 1 mM ethanol. Purification of torpedo electroplax membranes were also carried out, and the separation of various bacterial cells were also described, including the purification of different strains of *Escherichia coli*

and the separation of *Salmonella typhirum* cells, using PEG-dextran ATPS systems. Moreover, these CCC devices were also applied to larger cells, such as the separation of various species of red blood cells.

In the same way, the separation of cytochrome-c and lysozyme was achieved in 1988 by Ito and Oka [4] using the type J (or HSCCC) device. The chosen ATPS system consisted of 12.5% (w/w) PEG-1000 and 12.5% (w/w) dibasic potassium phosphate in water. The two peaks were resolved in 5 h using a 1-mL/min flow rate, but the retention of the stationary phase was as low as 26%. The limitation of this type of apparatus is definitely the low retention of the stationary phase for ATPS systems.

Several ATPS systems were also used with a centrifugal partition chromatograph (also called Sanki-type from the name of its unique manufacturer). Foucault and Nakanishi [5] tested PEG-1000/ammonium sulfate, PEG-8000/dextran, and other PEG-8000/hydroxypropylated starch on a test separation of crude albumin using a model LLN centrifugal partition chromatograph (CPC) containing six partition cartridges. They demonstrated that the systems could be used with the CPC apparatus, but the efficiency was particularly low (due to very poor mass transfer) and the flow rate was quickly limited by a strong decrease in the retention of the stationary phase (and not by the back-pressure). Afterward, CPC was then not considered as really suited for ATPS systems.

The third type, which is close in principle to the type J high-speed countercurrent chromatograph, was designed in the early eighties and is named "cross-axis coil planet centrifuge." Such a new design has led to successful results with highly viscous polymer phase systems [6]. Indeed, it allows satisfactory retention of the stationary phase of ATPS systems, either in the polymer-salt form or the polymer-polymer form. Such an apparatus eliminates the main drawback of the previous CCC devices, as it allows one to maintain a good retention of the stationary phase with a sufficient flow rate to ensure an acceptable separation or purification time. Using such solvent systems, it has been applied to the separation and purification of various protein samples:

- Mixture of cytochrome-c, myoglobin, ovalbumin and hemoglobin [7]
- Histones and serum proteins [8]
- Recombinant uridine phosphorylase from *E. coli* lysate [9]
- Human lipoproteins from serum [10]
- Lactic acid dehydrogenase from a crude bovine heat extract [11]



- Profilin–actin complex from *Acanthamoeba* extract [12]
- Lysozyme, ovalbumin, and ovotransferrin from chicken egg white [13]
- Acidic fibroblast growth factor from *E. coli* lysate [14]

The cross-axis coil planet centrifuge has, consequently, has been demonstrated to be particularly suited for the use of ATPS systems, leading to satisfactory retention of the stationary phase while keeping a sufficient flow rate of the mobile phase to limit the duration of the experiments.

References

1. P.-A. Albertson, *Partition of Cell Particles and Macromolecules*, 3rd ed., John Wiley & Sons, New York, 1986.
2. H. Walter, D. E. Brooks, and D. Fisher, *Partitioning in Aqueous Two-Phase Systems*, Academic Press, New York, 1985.
3. I. A. Sutherland, D. Heywood-Waddington, and Y. Ito, *J. Chromatogr.* 384: 197 (1987).
4. Y. Ito and H. Oka, *J. Chromatogr.* 457: 393 (1988).
5. A. P. Foucault and K. Nakanishi, *J. Liq. Chromatogr.* 13(12): 2421 (1990).
6. M. Bhatnagar, H. Oka, and Y. Ito, *J. Chromatogr.* 463: 317 (1989).
7. Y. Shibusawa and Y. Ito, *J. Chromatogr.* 550: 695 (1991).
8. Y. Shibusawa and Y. Ito, *J. Liq. Chromatogr.* 15: 2787 (1992).
9. Y. W. Lee, Y. Shibusawa, F. T. Chen, J. Myers, J. M. Schooler, and Y. Ito, *J. Liq. Chromatogr.* 15: 2831 (1992).
10. Y. Shibusawa, Y. Ito, K. Ikewaki, D. J. Rader, and J. Bryan Brewer, Jr. *J. Chromatogr.* 596: 118 (1992).
11. Y. Shibusawa, Y. Eriguchi, and Y. Ito, *J. Chromatogr. B* 696: 25 (1997).
12. Y. Shibusawa and Y. Ito, *Am. Biotechnol. Lab.* 15: 8 (1997).
13. Y. Shibusawa, S. Kihira, and Y. Ito, *J. Chromatogr. B* 709: 301 (1998).
14. J. M. Menet, Thèse de Doctorat de l'Université Paris 6 (1995).



Argon Detector

Raymond P. W. Scott

Scientific Detectors Ltd., Banbury, Oxfordshire, England

Introduction

The argon detector was the first of a family of detectors developed by Lovelock [1] in the late 1950s; its function is quite unique. The outer octet of electrons in the noble gases is complete and, as a consequence, collisions between argon atoms and electrons are perfectly elastic. Thus, if a high potential is set up between two electrodes in argon and ionization is initiated by a suitable radioactive source, electrons will be accelerated toward the anode and will not be impeded by energy absorbed from collisions with argon atoms. However, if the potential of the anode is high enough, the electrons will eventually develop sufficient kinetic energy that, on collision with an argon atom, energy can be absorbed and a *metastable* atom can be produced. A metastable atom carries *no* charge but adsorbs its energy from collision with a high-energy electron by the displacement of an electron to an outer orbit. This gives the metastable atom an energy of about 11.6 electron volts. Now 11.6 V is sufficient to ionize most organic molecules. Hence, collision between a metastable argon atom and an organic molecule will result in the outer electron of the metastable atom collapsing back to its original orbit, followed by the expulsion of an electron from the organic molecule. The electrons produced by this process are collected at the anode, generating a large increase in anode current. However, when an ion is produced by collision between a metastable atom and an organic molecule, the electron, simultaneously produced, is immediately accelerated toward the anode. This results in a further increase in metastable atoms and a consequent increase in the ionization of the organic molecules. This cascade effect, unless controlled, results in an exponential increase in ion current with solute concentration.

The relationship between the ionization current and the concentration of vapor was deduced by Lovelock [2,3] to be

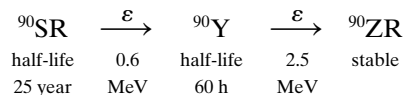
$$I = \frac{CA(x + y) + Bx}{CA\{1 - a \exp[b(V - 1)]\} + B}$$

where A , B , a , and b are constants, V is the applied potential, x is the primary electron concentration, and y is the initial concentration of metastable atoms. The rapid increase in current with increasing vapor concentration, as predicted by the equation, is controlled by the use of a high impedance in series with detector power supply. As the current increases, more volts are dropped across the resistance, and less are applied to the detector electrodes.

The Simple or Macro Argon Detector Sensor

A diagram of the macro argon detector sensor is shown in Fig. 1. The cylindrical body is usually made of stainless steel and the insulator made of PTFE or for high-temperature operation, a suitable ceramic. The very first argon detector sensors used a tractor sparking plug as the electrode, the ceramic seal being a very efficient insulator at high temperatures.

Inside the main cavity of the original sensor was a strontium-90 source contained in silver foil. The surface layer on the foil that contained the radioactive material had to be very thin or the β particles would not be able to leave the surface. This tenuous layer protecting the radioactive material is rather vulnerable to mechanical abrasion, which could result in radioactive contamination (strontium-90 has now been replaced by ^{63}Ni). The radioactive strength of the source was about 10 mCu which for strontium-90 can be considered a *hot* source. The source had to be inserted under properly protected conditions. The decay of strontium-90 occurs in two stages, each stage emitting a β particle producing the stable atom of zirconium-90:



The electrons produced by the radioactive source were accelerated under a potential that ranged from 800 to 2000 V, depending on the size of the sensor and the position of the electrodes. The signal is taken across a $1 \times 10^8\text{-}\Omega$ resistor, and as the standing current from the ionization of the argon is about $2 \times 10^{-8}\text{ A}$,



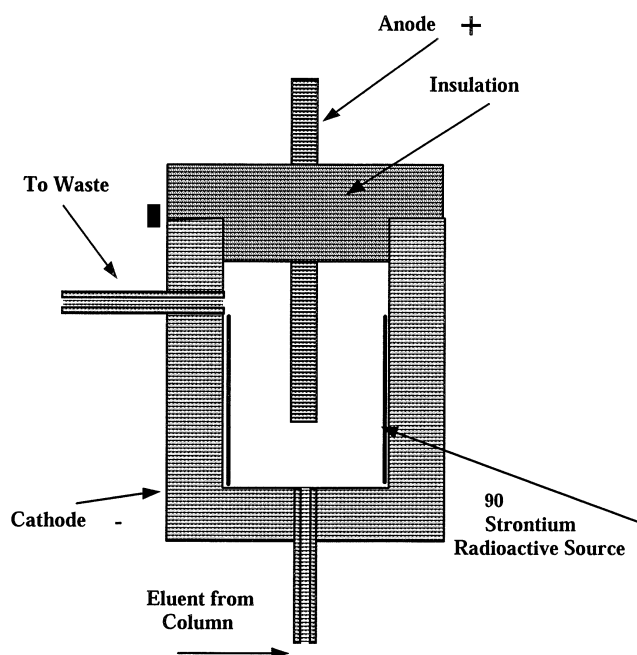


Fig. 1 The macro argon detector.

there is a standing voltage of 2 V across it that requires “backing off.”

In a typical detector, the primary current is about 10^{11} electrons/s. Taking the charge on the electron as 1.6×10^{-19} C, this gives a current of 1.6×10^{-8} A. According to Lovelock [1], if each of these electrons can generate 10,000 metastables on the way to the electrode, the steady-state concentration of metastables will be about 10^{10} per milliliter (this assumes a life span for the metastables of about 10^{-5} s at NTP). From the kinetic theory of gases, it can be calculated that the probability of collision between a metastable atom and an organic molecule will be about 1.6:1. This would lead to a very high ionization efficiency and Lovelock claims that in the more advanced sensors ionization efficiencies of 10% have been achieved.

The minimum detectable concentration of a well-designed argon detector is about an order of magni-

tude higher than the FID (i.e., 4×10^{-13} g/mL). Although the argon detector is a very sensitive detector and can achieve ionization efficiencies of greater than 0.5%, the detector was not popular, largely because it was not linear over more than two orders of magnitude of concentration ($0.98 < r > 1.02$) and its response was not predictable. In practice, nearly all organic vapors and most inorganic vapors have ionization potentials of less than 11.6 eV and thus are detected. The short list of substances that are not detected include H_2 , N_2 , O_2 , CO_2 , $(CN)_2$, H_2O , and fluorocarbons. The compounds methane, ethane, acetonitrile, and propionitrile have ionization potentials well above 11.6 eV; nevertheless, they do provide a slight response between 1% and 10% of that for other compounds. The poor response to acetonitrile makes this substance a convenient solvent in which to dissolve the sample before injection on the column. It is also interesting to note that the inorganic gases H_2S , NO , NO_2 , NH_3 , PH_3 , BF_3 , and many others respond normally in the argon detector. As these are the type of substances that are important in environmental contamination, it is surprising that the argon detector, with its very high sensitivity for these substances, has not been reexamined for use in environmental analysis.

References

1. J. E. Lovelock, *Gas Chromatography* 1960, R. P. W. Scott (ed.), Butterworths Scientific, London 1960, p. 9.
2. J. E. Lovelock, *J. Chromatogr.* 1: 35 (1958).
3. J. E. Lovelock, *Nature* (London) 181: 1460 (1958).

Suggested Further Reading

- R. P. W. Scott, *Chromatographic Detectors*, Marcel Dekker, Inc., New York, 1996.
 R. P. W. Scott, *Introduction to Gas Chromatography*, Marcel Dekker, Inc., New York, 1998.



Assessment of Lipophilicity by Reversed-Phase TLC and HPLC

Anna Tsantili-Kakoulidou

University of Athens, Athens, Greece

INTRODUCTION

The purpose of this review is to summarize the conditions used to derive chromatographic lipophilicity indices, to appraise associated difficulties, and to provide an overview of their relation with octanol–water partition coefficients. In this aspect, both techniques will be discussed in parallel.

LIPOPHILICITY

The major importance of lipophilicity in drug design has been well established since the pioneering work of Hansch in the 1960s. Penetration across biological membranes during drug transport, hydrophobic interactions with receptors, as well as toxic aspects of drug actions are governed, to a great extent, by this property.^[1,2] The most widely accepted measure of lipophilicity is the octanol–water partition coefficient, which is expressed in its logarithmic form as $\log P$. A variety of experimental protocols for the determination of $\log P$ are reported in the literature.^[3,4] The classical shaking flask method, via direct partition experiments, is tedious and time-consuming, while presenting limitations concerning the $\log P$ range, which can be reliably measured. Partition chromatographic techniques, in particular high-performance liquid chromatography (HPLC) and reversed-phase thin layer chromatography (RP-TLC), permit an easy and rapid measurement of various indices that provide information on the lipophilic behavior of chemicals and offer a popular alternative, combining the possibility of automation, high dynamic range, and low sensitivity to impurities, while being compound-sparing.^[5,6] Extrapolated capacity factors to pure water as mobile phase, expressed as $\log k_w$ and R_{Mw} , are considered as more representative lipophilicity indices compared to isocratic $\log k$ and R_M .^[5–8] Literature is rich in research articles investigating similarities/dissimilarities between octanol–water partitioning and chromatographic retention. The selection of either technique is associated with the state of the art concerning their technology. Moreover, all assumptions dealing with the complex nature of lipo-

philicity as the outcome of intermolecular and intramolecular interactions, involving electronic, steric, or conformational effects, embrace chromatographic retention as well.^[9,10]

STATIONARY PHASES IN PARTITION CHROMATOGRAPHY

In RP-TLC, silica gel plates impregnated with a strong hydrophobic agent (paraffin oil or silicone oil, usually 5%) have been extensively used in the past as nonpolar stationary phases. Nowadays, plates covered with octadecyl-silanized (ODS) silica gel are available. In this material, the silanol groups are etherified with alkyls containing 8 (C_8) or 18 (C_{18}) carbon atoms. The low wettability of HPTLC plates coated with highly etherified silica gel poses limitations in the water content of the mobile phase. This problem is circumvented by the use of RP- C_{18} plates with 50% etherification. However, the presence of free silanol groups may lead to undesirable silanophilic interactions, especially with low water content in the mobile phase.^[11]

ODS silica gel is, in most cases, the filling material in HPLC columns. Because the columns in HPLC are not disposable, one should take into account the pH limitations of this material (i.e., outside the pH range 2–7.5). The second problem is associated with the presence of free silanol groups, which may be responsible for silanophilic interactions, as already mentioned.^[5,12–14] Nowadays, end-capped BDS or ABZ columns are available, which are treated with secondary silanization using small alkyls or zwitterionic fragments to bind the free silanol groups, thus suppressing their contribution to retention.^[13]

Octadecyl–polyvinylalcohol copolymer gel, ODP, offers an alternative as a nonpolar stationary phase in HPLC.^[12,13] With this material, no silanophilic interactions take place and there are no pH limitations. Drawbacks of ODP columns are the large retention times observed and the longer equilibration time required.

Octanol-coated ODS columns have also been used in an effort to better simulate octanol–water partitioning.

However, retention times were less reproducible due to instability and column bleeding.^[13]

Recently, immobilized artificial membrane (IAM) stationary phases are becoming more popular for membrane simulation.^[15] In IAM columns, silica gel is chemically bonded to phospholipids. There are various types of IAM columns. Among them, the most frequently used is IAMPC, which contains phosphatidylcholine.

MOBILE PHASES USED IN PARTITION CHROMATOGRAPHY

The mobile phases in RP-TLC and HPLC are mixtures of water or buffer with organic modifiers. With an octanol-coated stationary phase, no organic modifier is added to the mobile phase, whereas in IAM chromatography, the organic modifier is necessary only in the case of highly retained solutes.^[13,15]

The most common organic modifiers are methanol, acetonitrile, and tetrahydrofuran. Acetonitrile may not be suitable for use with an ODP stationary phase,^[12] whereas this solvent is the modifier of choice in IAM chromatography.^[15]

The buffer composition of the aqueous component may affect the retention of ionizable solutes. Some authors suggest the use of morpholinepropanesulfonic acid (MOPS). The zwitterionic nature of this buffer offers the advantage that it does not lead to any interactions with the solutes.^[12,13]

The addition of a masking agent to the mobile phase may be necessary when silanophilic interactions interfere with the partition mechanism. Silanophilic interactions are important in the case of protonated amines, or with solutes containing strong hydrogen bond acceptor groups, especially when mobile phases poor in water content are used.^[12,14] Hydrophobic amines (e.g., *n*-decylamine) are suitable masking agents; however, their addition to the mobile phase adds an extra component to chromatographic conditions.

CAPACITY FACTORS AS LIPOPHILICITY INDICES

The lipophilicity indices measured by RP-TLC and HPLC are derived from the retardation factor R_f and the retention time t_r , respectively. R_f and t_r are converted to the logarithm of the capacity factor ($R_M/\log k'$) via Eqs. 1 and 2:

$$R_M = \log(1/R_f - 1) \quad (1)$$

$$\log k = [\log(t_r - t_o)/t_o] \quad (2)$$

where t_o is the retention time of an unretained compound, usually the solvent front or an inorganic salt such as potassium bichromate.

The less polar a solute is, the stronger will be its interaction with the stationary phase, which is expressed by decreasing R_f values and increasing R_M values in RP-TLC and by increasing retention times and $\log k'$ values in HPLC. Thus R_M and $\log k'$ values are directly correlated to octanol–water $\log P$ via Collander-type equations:

$$\log P = aR_M + b \quad (3)$$

$$\log P = a' \log k' + b' \quad (4)$$

where the coefficients a, b , and a', b' are derived by regression analysis. The quality of the equations depends on the chromatographic conditions and the solutes.

For lipophilicity assessment, calibration equations with types similar to Eqs. 3 and 4 should be constructed using compounds with known $\log P$ values. These calibration equations are applied for further $\log P$ calculations. According to the author, it is recommended to measure more than one set of isocratic R_M or $\log k'$ values to construct the corresponding calibration equations and to calculate the average $\log P$.^[16]

Instead of isocratic capacity factors derived for a selected mobile phase composition, one can use extrapolated R_{Mw} and $\log k'_w$ values, which correspond to 100% aqueous mobile phase.^[5–8,11–13]

Equations 5 and 6 describe the relationship between retention and fraction ϕ of the organic modifier present in the mobile phase:

$$R_M = A\phi^2 - B\phi + C \quad (5)$$

$$\log k' = A'\phi^2 - B'\phi + C' \quad (6)$$

The intercepts C and C' correspond to R_{Mw} and $\log k'_w$, respectively.

For a certain ϕ range, the quadratic term in Eqs. 5 and 6 may not be significant. In that case, R_{Mw} and $\log k'_w$ are obtained by linear extrapolation according to Eqs. 7 and 8:

$$R_M = -S\phi + R_{Mw} \quad (7)$$

$$\log k' = -S'\phi + \log k'_w \quad (8)$$

Linearly extrapolated capacity factors should be preferred because quadratic extrapolation may lead to erroneous overestimated values. The linearity range depends on the organic modifier as well as on the solutes. Methanol does not disrupt, substantially, the hydrogen bonding network of water and, usually, a wide linearity range is achieved relative to acetonitrile or tetrahydrofuran.

However, in the case of protonated amines, quadratic relationships were obtained with MeOH.^[17] In general, for polar solutes, linearity holds within a limited range using mobile phases rich in aqueous component. In contrast, for



more hydrophobic solutes, linear extrapolation is still possible with mobile phases rich in organic modifier. It has been suggested that linearity holds better for modifier concentrations that produce $0 < \log k' < 1$.^[18]

ISOCRATIC VS. EXTRAPOLATED CAPACITY FACTORS

Extrapolated capacity factors, R_{Mw} and $\log k'_w$, are in the same order as the octanol–water $\log P$ values and are considered as more general lipophilicity indices. Because the slopes in Eqs. 7 and 8 may vary considerably, the extrapolation lines may intersect each other, thereby leading to an inversion of lipophilicity in a higher percentage of organic modifiers (Fig. 1). In this aspect, a proper expression of the lipophilicity actually is found only at 100% aqueous phase composition. However, some authors argue that extrapolated capacity factors can predict $\log P$ only for compounds that do not contain strong hydrogen bond acceptor substituents.^[19] Nevertheless, the problem of nonhydrophobic interactions can be faced by the proper selection of the stationary phase and the protection of the silanophilic sites.

However, extrapolated capacity factors may be affected by the nature of the organic modifier. In a study concerning the measurement of lipophilicity indices for monosubstituted benzenes by HPLC, the $\log k'_w$ values of the more polar derivatives appeared to be lower when methanol was used as an organic modifier, compared to the $\log k_w$ values obtained with acetonitrile.^[12] In contrast, for nonpolar derivatives, acetonitrile led to lower $\log k'_w$ values. An analogous decrease in the $\log k_w$ values for a series of lipophilic 9*H*-xanthene and 9*H*-thioxanthene derivatives was observed when tetrahydrofuran was

used instead of methanol.^[20] The differences in the extrapolated capacity factors described above may be attributed to changes in the hydrophobic character of the stationary phase caused by organic modifiers and water molecules dragged onto the reversed-phase material during equilibration.

It is the opinion of the author that the best simulation of the octanol–water system is achieved with (end-capped) silanized octadecylsilica gel stationary phase, methanol as the organic modifier, and a masking agent, if necessary. Depending on the structure of the solutes, in many such cases, a good correlation between the chromatographic data and $\log P$ is obtained with the coefficients a, a' and b, b' close to 1 and 0, respectively.

$$\log P = aR_{Mw} + b \quad (9)$$

$$\log P = a' \log k'_w + b' \quad (10)$$

Far from being a general rule, Eqs. 11–13 represent three examples of 1:1 correlation between $\log P$ and extrapolated capacity factors obtained under the above-recommended conditions:

$$R_{Mw} = 0.959(\pm 0.011) \log P + 0.067(\pm 0.147) \quad (11)$$

[$n=121$, $r=0.967$, $s=0.353$, $F=1703$ (RP-18 plates; from Ref. [11])]

$$\log P = 1.01(\pm 0.08) \log k_w - 0.43(\pm 0.25) \quad (12)$$

[$n=19$, $r=0.947$ (ABZ column; from Ref. [13])]

$$\log P = 0.91(\pm 0.03) \log k_w + 0.18(\pm 0.12) \quad (13)$$

[$n=28$, $r=0.983$, $s=0.181$, $F=763$ (ODS column + *n*-decylamine as masking agent; from Ref. [12])].

EFFECT OF IONIZATION ON RETENTION

To correct capacity factors for ionization, the same equations are used as for the corresponding correction of the apparent partition coefficients. Thus for monoprotic acids and bases, Eqs. 13 and 14 are suggested for extrapolated, as well as isocratic, capacity factors derived from HPLC and RP-TLC:

$$\log k_w = \log k_{w(\text{app})} + \log(1 + 10^{\text{pH} - \text{p}K_a}) \quad \text{acids} \quad (14)$$

$$\log k_w = \log k_{w(\text{app})} + \log(1 + 10^{\text{p}K_a - \text{pH}}) \quad \text{bases} \quad (15)$$

However, whether the effects of ionization in the octanol–water partition systems in HPLC and TLC are similar remains to be clarified. The stationary phase material, and, especially the presence of the acidic silanol sites, may have an active role. Moreover, concerning the two

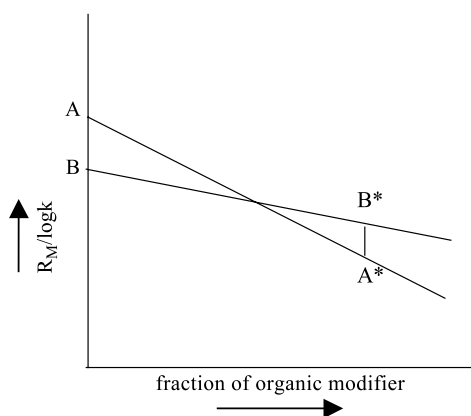


Fig. 1 Plot of $R_M / \log k$ vs. fraction of organic modifier. Inversion of lipophilicity occurs for organic modifier concentrations higher than the intersection point of the lines.

chromatographic techniques, even in the case of identical stationary phases, an essential difference between HPLC and TLC is the fact that, in HPLC, the column is equilibrated with the mobile phase before runs are conducted. Thus the stationary phase is adjusted to the mobile phase pH, whereas on a TLC plate, a pH gradient is formed.

EFFECT OF CONFORMATION IN RETENTION

Conformational effects in lipophilicity have been well established.^[9] Analogous effects, although not necessarily to the same extent, may be expected in retention. In such cases, differences in the partitioning behavior in the octanol–water system and the chromatographic system may be manifested, thus affecting the quality of equations.

OTHER CHROMATOGRAPHIC DATA AS LIPOPHILICITY-RELEVANT EXPRESSIONS

The slope S of the regression curve used to obtain $\log k'_w$ or R_{Mw} (Eqs. 7 and 8) and (Eqs. 7 and 8) is considered to encode significant information on the lipophilic behavior of the solute. In a simplified aspect, the slope is thought to express, mainly, the solute/solvent interactions, whereas the intercept value is rather associated with solute stationary phase interactions. Some authors relate the slope S to the specific hydrophobic surface area.^[21] Basically, the retention mechanism consists of two components: the size of the solute (reflected by its volume or surface area), and its hydrogen-bonding capacity. If there are no considerable differences in hydrogen-bonding capacity within a series of compounds, a good relationship between the slope and the intercept is anticipated:

$$S = aR_{Mw} + b$$

$$S' = a' \log k_w + b'$$

Thus slope analysis may unravel differences in hydrogen bonding within a series of compounds.^[13]

The organic modifier concentration ϕ_o , which produces an equal molar distribution between the stationary phase and the mobile phase, leading to $\log k=0$, has also been proposed as a measure to rank lipophilicity.^[22] ϕ_o indices have been mainly developed for HPLC. They correspond to the quotient:

$$\phi_o = \log k_w / S$$

Based on the ϕ_o concept, a fast gradient method RP-HPLC has been proposed to determine the chromatographic hydrophobicity index (CHI) as a high-throughput alternative to other lipophilicity measures.^[23] For this

purpose, gradient retention times (t_g) are measured and converted to CHI values by means of a calibration equation, derived by a set of standards with well-determined CHI (ϕ_o) values:

$$CHI = \text{slope} \times t_g + \text{intercept}$$

The absolute magnitude of the CHI parameter depends on the values assigned to the set of standards. The method has the advantage that, once the calibration equation has been established, the retention parameter is obtained from a single fast gradient run, thus saving time and solvents. The CHI parameter has been reported to correlate satisfactorily with $\log P$.

CONCLUSION

RP-TLC and HPLC provide a variety of descriptors that can be used as lipophilicity indices. Among them, extrapolated capacity factors often lead to 1:1 correlation with octanol–water $\log P$. On the other hand, isocratic capacity factors need fewer experiments to be determined; however, they depend strongly on chromatographic conditions. The CHI combines easy and rapid measurements with a uniform lipophilicity scale. However, both lipophilicity and reversed-phase chromatographic retention are composite phenomena and, consequently, their resemblance cannot always be anticipated. Because standard reference sets cannot be available for all structurally diverse compounds, a comparison between chromatographic indices and octanol–water $\log P$ within the series of the investigated compounds is still indispensable.

REFERENCES

1. van de Waterbeemd, H.; Testa, B. The Parameterization of Lipophilicity and Other Structural Properties in Drug Design. In *Advances in Drug Research*; Testa, B., Ed.; Academic Press: New York, 1987; Vol. 16, 85–227.
2. Conradi, R.A.; Burton, P.S.; Borchard, R.T. Physico-Chemical and Biological Factors That Influence a Drug's Cellular Permeability by Passive Diffusion. In *Lipophilicity in Drug Action and Toxicology*; Pliska, V., Testa, B., van de Waterbeemd, H., Eds.; VCH: Weinheim, 1996; 233–252.
3. Leo, A.; Hansch, C.; Elkins, D. Partition coefficients and their uses. *Chem. Rev.* **1973**, *71*, 525–616.
4. Hersey, A.; Hill, A.P.; Hyde, R.M.; Livingstone, J. Principles of method selection in partition studies. *Quant. Struct.-Act. Relatsh.* **1989**, *8*, 288–296.
5. Kaliszan, R. High performance liquid chromatographic methods and procedures of hydrophobicity determination. *Quant. Struct.-Act. Relatsh.* **1990**, *9*, 83–87.



6. Dross, K.P.; Mannhold, R.; Rekker, R.F. Drug lipophilicity in QSAR practice: II. Aspects of R_M -determinations; critics of R_M -corrections; interrelations with partition coefficients. *Quant. Struct.-Act. Relatsh.* **1992**, *11*, 36–44.
7. Tsantili-Kakoulidou, A.; El Tayar, N.; van de Waterbeemd, H.; Testa, B. Structural effects in the lipophilicity of di- and poly-substituted benzenes as measured by reversed phase high-performance liquid chromatography. *J. Chromatogr.* **1987**, *389*, 33–45.
8. Biagi, G.L.; Barbaro, A.M.; Recanatini, M. Determination of lipophilicity by means of reversed-phase thin layer chromatography: 3. Study for the TLC equations for a series of ionizable quinolone derivatives. *J. Chromatogr., A* **1994**, *678*, 127–137.
9. Testa, B.; Carrupt, P.-A.; Gaillard, P.; Tsai, R.-S. Intramolecular Interactions Encoded in Lipophilicity: Their Nature and Significance. In *Lipophilicity in Drug Action and Toxicology*; Pliška, V., Testa, B., van de Waterbeemd, H., Eds.; VCH: Weinheim, 1996; 49–71.
10. Tsantili-Kakoulidou, A.; Varvaresou, A.; Siatra-Papastaikoudi, Th.; Raevsky, O. A comprehensive investigation of the partitioning and hydrogen bonding behavior of indole containing derivatives of 1,3,4-thiadiazole and 1,2,4-triazole by means of experimental and calculative approaches. *Quant. Struct.-Act. Relatsh.* **1999**, *18*, 482–489.
11. Mannhold, R.; Dross, K.; Sonntag, C. Estimation of Lipophilicity by Reversed-Phase Thin-Layer Chromatography. In *Lipophilicity in Drug Action and Toxicology*; Pliška, V., Testa, B., van de Waterbeemd, H., Eds.; VCH: Weinheim, 1996; 141–156.
12. Bechalany, A.; Tsantili-Kakoulidou, A.; El Tayar, N.; Testa, B. Measurement of lipophilicity indices by reversed-phase high-performance liquid chromatography: Comparison of two stationary phases and various eluents. *J. Chromatogr.* **1991**, *541*, 221–229.
13. van Waterbeemd, H.; Kansy, M.; Wagner, B.; Fischer, H. Lipophilicity Measurement by Reversed-Phase High-Performance Liquid Chromatography (RP-HPLC). In *Lipophilicity in Drug Action and Toxicology*; Pliška, V., Testa, B., van de Waterbeemd, H., Eds.; VCH: Weinheim, 1996; 73–87.
14. El Tayar, N.; Tsantili-Kakoulidou, A.; Roethlisberger, T.; Testa, B.; Gal, J. Different partitioning behavior of sulphonyl-containing compounds in reversed-phase high-performance liquid chromatography and octanol–water systems. *J. Chromatogr.* **1988**, *439*, 237–244.
15. Geetha, T.; Singh, S. Applications of immobilized stationary-phase liquid chromatography: A potential in vitro technique. *PSTT* **2000**, *3*, 406–416.
16. Tsantili-Kakoulidou, A.; Antoniadou-Vyza, A. Determination of the Partition Coefficients of Adamantyl Derivatives by Reversed Phase TLC and HPLC. In *QSAR: Quantitative Structure–Activity Relationships in Drug Design*; Alan R. Liss, Inc., 1989; 71–74.
17. El Tayar, N.; van de Waterbeemd, H.; Testa, B. Measurements of protonated basic compounds by reversed-phase high-performance liquid chromatography: II. Procedure for the determination of a lipophilic index by reversed-phase high-performance liquid chromatography. *J. Chromatogr.* **1985**, *320*, 305–312.
18. Schoenmakers, P.J.; Billiet, H.A.H.; de Galan, L. Influence of organic modifiers on the retention behavior in reversed-phase liquid chromatography and its consequences for gradient elution. *J. Chromatogr.* **1979**, *185*, 179–195.
19. Yamagami, C.; Yokota, M.; Takao, N. Hydrophobicity parameters determined by reversed-phase liquid chromatography: 9. Relationship between capacity factor and water–octanol partition coefficient of monosubstituted pyrimidines. *J. Chromatogr., A* **1994**, *662*, 49–60.
20. Tsantili-Kakoulidou, A.; Filippatos, E.; Todoulou, O.; Papadaki-Valiraki, A. Use of reversed phase high-performance liquid chromatography in lipophilicity studies of 9H-xanthene and 9H-thioxanthene derivatives containing an aminoalkanamide or a nitrosoureido group. Comparison between capacity factors and calculated octanol–water partition coefficients. *J. Chromatogr., A* **1993**, *654*, 43–52.
21. Horvath, C.; Melander, W.; Molnar, I. Solvophobic interactions in liquid chromatography with non polar stationary phases. *J. Chromatogr.* **1976**, *125*, 129–156.
22. Perišić-Janjić, N.U.; Acanski, M.M.; Janjić, N.J.; Lazarević, M.D.; Dimova, V. Study of the lipophilicity of some 1,2,4-triazole derivatives by RP-HPLC and TLC. *JPC, J. Planar Chromatogr.* **2000**, *13*, 281–284.
23. Valko, K.; Bevan, C.; Reynolds, D. Chromatographic hydrophobicity index by fast-gradient RP-HPLC: A high-throughput alternative to log P /log D . *Anal. Chem.* **1997**, *69*, 2022–2029.



Asymmetric Flow FFF in Biotechnology

Thorsten Klein

Christine Hürzeler

Postnova Analytics, Munich, Germany

Introduction

The research and development in the fields of biochemistry, biotechnology, microbiology, and genetic engineering are fast-growing areas in science and industry. Chromatography, electrophoresis, and ultracentrifugation are the most common separation methods used in these fields. However, even these efficient and widespread analytical methods cannot cover all applications. In this article, asymmetric flow field-flow fractionation (AF4) is introduced as a powerful analytical separation technique for the characterization of biopolymers and bioparticles. Asymmetric flow field-flow fractionation can close the gap between analyzing small and medium-sized molecules/particles [analytical methods: high-performance liquid chromatography (HPLC), GFC, etc.] on the one hand and large particles (analytical methods: sedimentation, centrifugation) on the other hand [1,2], whereas HPLC and GFC are overlapping with asymmetric field-flow fractionation in the lower separation ranges.

First publications about field-flow fractionation (FFF) by Giddings et al. [3] appeared in 1966. From this point, FFF was developed in different directions and, in the following years, various subtechniques of FFF emerged. Well-known FFF subtechniques are sedimentation FFF, thermal FFF, electric FFF, and flow FFF. Each method has its own advantages and gives a different point of view of the examined sample systems. Using sedimentation FFF shows new insights about the size and density of the analytes, thermal FFF gives new information about the chemical composition and the size of the polymers/particles, and electric FFF separates on the basis of different charges. Flow FFF, and especially asymmetric flow FFF (the most powerful version of flow FFF) is the most universal FFF method, because it separates strictly on the basis of the diffusion coefficient (size or molecular weight) 2. and it has the broadest separation range of all the FFF methods. It is usable for a large number of applications in the fields of biotechnology, pharmacology, and genetic engineering.

Separation Principle of Asymmetric Flow Field-Flow Fractionation

All FFF methods work on the same principle and use a special, very flat separation channel without a stationary phase. The separation channel is used instead of the column, which is needed in chromatography. Inside the channel, a parabolic flow is generated, and perpendicular to this parabolic flow, another force is created. In principle, the FFF methods only differ in the nature of this perpendicular force.

The separation channel in asymmetrical flow FFF (AF4) is approximately 30 cm long, 2 cm wide, and between 100 and 500 μm thick. A carrier flow which forms a laminar flow profile streams through the channel. In contrast to the other FFF methods, there is no external force, but the carrier flow is split into two partial flows inside the channel. One partial flow is led to the channel outlet and, afterward, to the detection systems. The other partial flow, called the cross-flow, is pumped out of the channel through the bottom of the channel. In the AF4, the bottom of the separation channel is limited through a special membrane and the top is made of an impermeable plate (glass, stainless steel, etc.). The separation force, therefore, is generated internally, directly inside the channel, and not by an externally applied force.

Under the impact of the cross-flow, the biopolymers/particles are forced in the direction of the membrane. To ensure that the analytes do not pass through the membrane, different pore sizes can be used. In this way, the analytes can be selectively rejected and it is possible to remove low-molecular compounds before the separation. The analytes' diffusion back from this membrane is counteracted by the cross-flow, where, after a time, a dynamic equilibrium is established. The medium equilibrium height for smaller sized analytes is located higher in the channel than for the larger analytes. The smaller sized analytes are traveling in the faster velocity lines of the laminar channel flow and will be eluted first. As a result, fractograms, which



show size separation of the fractions, are obtained as an analog to the chromatograms from HPLC or GFC.

Applications of AF4 in Biotechnology

In addition to widespread applications in the field of polymer and material science or environmental research, AF4 can be used in bioanalytics, especially for the characterization of proteins, protein aggregates, polymeric proteins, cells, cell organelles, viruses, liposomes, and various other bioparticles and biopolymers.

Cells and Viruses

The advantage of AF4, in contrast to chromatography, is the capability to separate bioparticles and biopolymers which usually stick onto chromatography columns. They are more or less filtered out (removed) by the stationary phase. Various applications using AF4 for the separation of shear-force sensitive bioparticles with high molecular weight and size have been reported in the literature. They deal with the efficient and fast separation of viruses [4,5] and bacteria [5]. Reference 4 discusses the investigation of a virus (STNV) with AF4 and the separation of the viral aggregates. In Reference 5, Litzen Wahlund report the separation of a virus (CPMV) together with different other proteins (BSA, Mab). They also present the characterization of bacillus streptococcus faecalis and its aggregates using AF4.

Proteins/Antibodies/DNA

The separation of proteins with AF4 has been demonstrated a number of times. For example, the fractionation of ferritin [7], of HSA and BSA [8], and of monoclonal antibodies [8], including their various aggregates, were published. AF4 is especially suitable for the separation and characterization of large and sensitive proteins and their aggregates because it is fast and gentle and aqueous solvents can be used that achieve maximum bioactivity of the isolated proteins and antibodies. Furthermore, even very large and sticky proteins can be analyzed because of the relatively low surface area and the separation in the absence a stationary phase. Nearly independent of the nature of the bioparticles, AF4 separates by size (diffusion coefficient). Therefore, DNA, RNA, and plasmids can be separated quickly and gently, together with proteins. Reference 6 deals with this issue and presents the AF4 separation of a mixture of cytochrome-c, BSA, ferritin, and plasmid DNA.

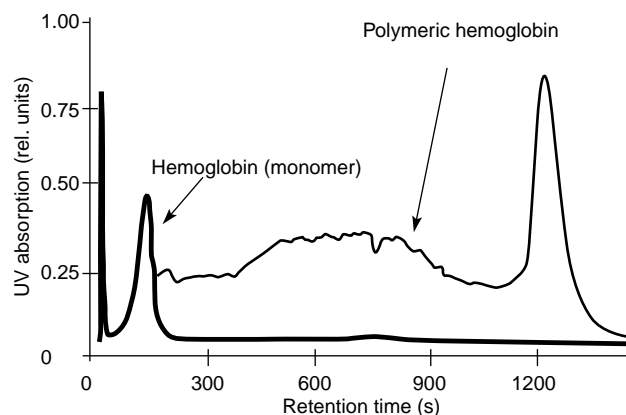


Fig. 1 Pig hemoglobin separated with AF4 and UV detection.

Artificial Polymeric Proteins

In addition to the characterization of well-known protein substances (serum proteins, aggregates, antibodies, etc.), AF4 is also a very promising separation/characterization technique for a new class of artificially made polymeric proteins from therapeutic/diagnostic applications, such as poly-streptavidin and polymeric hemoglobin [personal communication of the authors]. These proteins usually have very high molecular weights and huge molecular sizes, and they are difficult to analyze by conventional GFC and related techniques. Very often, these proteins are also sticky and show adsorptive effects on the column material. Using AF4 without a stationary phase and without size-exclusion limit, these polymeric proteins can be readily separated and characterized. The application shown in Fig. 1 was done using an AF4 system (HRFFF 10.000 series, Postnova Analytics) and ultraviolet (UV) detection at 210 nm.

Summary

Asymmetric flow FFF is a new member in the FFF family of separation technologies; it is a powerful characterization technique, especially suited for the separation of large and complex biopolymers and bioparticles. AF4 has many of the general benefits of FFF; it adds on several additional characteristics. In particular, these characteristics are as follows:

1. No sample preparation, or only limited sample preparation necessary.
2. Possibility of direct injection of unprepared samples.

3. Large accessible size molecular-weight range, no size-exclusion limit.
4. Very gentle separation conditions in the absence of a stationary phase.
5. Weak or no shear forces inside the flow channel.
6. Rapid analysis times, generally faster than GFC.
7. Fewer sample interactions during separation because of small surface area.
8. On-line sample concentration/large volume injection possible.
9. Gentle and flexible because it uses a wide range of eluents/buffers/detectors.
10. AF4 is a useful analytical tool, and when the limitations of the technology (e.g., sample interactions with membrane or the sample dilution during separation) are carefully observed, samples can be characterized where other analytical technologies fail or only yield limited information.

References

1. T. Klein, Chemisch-physikalische Charakterisierung von schwermetallhaltigen Hydrokolloiden in natürlichen aquatischen Systemen mit Ultrafiltration und Flow-FFF. Diploma thesis, TU-Munich (1995).
2. T. Klein, Entwicklung und Anwendung einer Asymmetrischen Fluß-Feldflußfraktionierung zur Charakterisierung von Hydrosolen, Ph.D. thesis, TU-Munich (1998).
3. J. C. Giddings, A new separation concept based on a coupling of concentration and flow nonuniformities, *Separ. Sci. I*: 123 (1966).
4. A. Litzen and K. G. Wahlund. Zone broadening and dilution in rectangular and trapezoidal asymmetrical flow field-flow fractionation channels, *Anal. Chem.* 63: 1001 (1991).
5. A. Litzen and K. G. Wahlund. Effects of temperature, carrier composition and sample load in asymmetrical flow field-flow fractionation, *J. Chromatogr.* 548: 393 (1991).
6. J. J. Kirkland, C. H. Dilks, S. W. Rementer, and W. W. Yau. Asymmetric-channel flow field-flow fractionation with exponential force-field programming. *J. Chromatogr.* 593: 339 (1992).
7. C. Tank and M. Antonietti. Characterization of water-soluble polymers and aqueous colloids with asymmetrical flow field-flow fractionation, *Macromol. Chem. Phys.* 197: 2943 (1996).
8. A. Litzen, J. K. Walter, H. Krischollek, and K. G. Wahlund. Separation and quantitation of monoclonal antibody aggregates by asymmetrical flow field-flow fractionation and comparison to gel permeation chromatography, *Anal. Biochem.* 212: 169 (1993).



Automation and Robotics in Planar Chromatography

Wojciech Markowski

Medical University, Lublin, Poland

Introduction

Automation involves the use of systems (instruments) in which an element of nonhuman decision has been interpolated. It is defined as the use of combinations of mechanical and instrumental devices to replace, refine, extend, or supplement human effect and faculties in the performance of a given process, in which at least one major operation is controlled, without human intervention, by a feedback system. A feedback system is defined as an instrumental device combining sensing and commanding elements which can modify the performance of a given act [1].

Three approaches to the automation process can be distinguished, taking into account the criterion of the flexibility of the automation device [2]. The first, denoted as flexible, is characterized by the possibility of adaptation of the instruments to new and varying demands required from the laboratory; examples of these instruments are robots. The second approach, denoted as semiflexible, involves some restrictions for the tasks executed by the instrument; the tasks are controlled by a computer program and its menu. As examples, autosamplers or robots of limited moves can be given. In the third approach, the instruments can execute one or two tasks, without feasibility of new requirements; as examples, supercritical fluid extractors or equipment for dissolution of samples can be given.

Automation processes have several advantages: better reproducibility, increase of the number of samples which can be analyzed, personnel can be utilized for more creative tasks (e.g., planning of experiments and interpretation of results). Harmful conditions in the workplace can be avoided and the equipment of the laboratory can be more effectively utilized.

To illustrate the feasibility of automation in thin-layer chromatography (TLC), the fundamental operations of the chromatographic process are given in Fig. 1 [3].

The first and basic stage of the process, not limited to TLC, but also occurring in other chromatographic techniques, is the preparation of samples. This is the most tedious, time-consuming and error-generating process in the whole analytical cycle which can be fully

automated, or the automated stations may be complementary to operations or tasks executed individually. For instance, in a station, a volume of liquid is transferred from the first to a second container, an internal standard is added, and the solution is diluted and mixed. Further actions may be executed manually. Another, more advanced, solution consists in automated execution of the tasks by the station and the sample is transferred from one station to the other by a robot or another transport device.

In a limited version, only the most critical stages are automated by the use of robots with limited, strictly defined movements; examples are automated processes of solid-phase extraction (SPE), heating, and mixing. The robots are controlled by a computer and the operator chooses the suitable values of the parameters from given ranges (e.g., autosampler).

Sample Application

The application of the sample onto the thin layer is a critical moment, owing to later localization by the scanner (densitometer) and the beginning of the chromatographic process at the moment of contact of the liquid sample with the chromatographic bed. Therefore, the applicator must warrant the precise localization of the sample and uniform compact cross-section of the starting band. Semiautomatic applicators presently available have the volume range of 20 nL to 10 μ L. The sample is delivered from 0.5-, 1.0-, and 10- μ L syringes. The piston stroke can be set in a continuous manner. To apply the sample, the piston is stopped and the solution is injected from the end of the capillary; the whole volume of the sample is displaced from the capillary. The position of the end of the capillary is adapted to the layer thickness, the spring-relieved syringe guide warrants that the capillary needle only lightly touches the adsorbent layer, thereby avoiding its damage. The change of position is automatic. The device permits application of spots or streaks at a distance of 5 mm from the edge of the plate; the syringe can be washed twice. A more advanced version is a



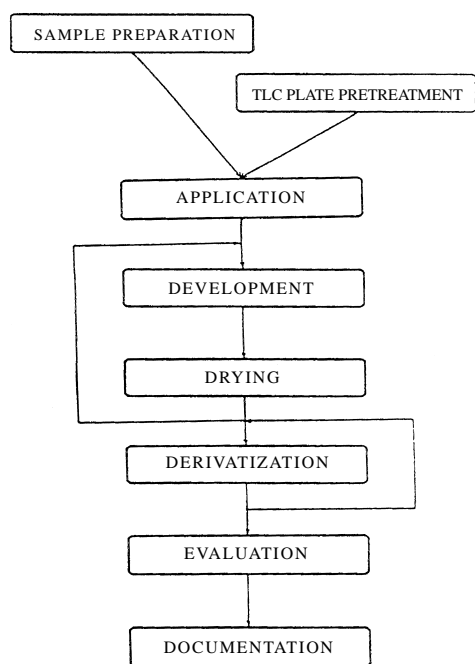


Fig. 1 Survey on operation succession in QTLC.

computer-controlled applicator (e.g., Desaga TLC Applicator AS 30 or Camag Automatic TLC System) composed of an application module, interface, software, and an IBM PC-AT.

The application module dispenses samples from a stainless-steel capillary which is connected to a dosage syringe operated by a stepping motor. Samples can be applied as spots or bands onto TLC plates or sheets up to 20×20 cm. Bandwise sample application uses the spray-on technique; for spotwise application, either contact transfer or spraying may be selected. The samples are contained in vials, which may be sealed with regular septa. The vials are arranged in racks with 16 positions; two racks may be inserted per application program. The application pattern can be selected for normal development, for development from both sides, and for circular and anticircular chromatography.

Development of the Chromatogram

The next important stage is the chromatogram development. ADC chambers (Automatic Developing Chamber, Camag), DC-MAT (Byron), TLC-MAT (Desaga) are automatically operating development systems. They increase the reproducibility of the chromatographic results because the development is carried out under controlled conditions. The progress of the solvent front is monitored by a sensor. The devel-

opment process is terminated as soon as the mobile phase has traveled the programmed distance. Preconditioning, tank or sandwich configuration, solvent migration distance, and the drying conditions are selectable. All relevant parameters are entered via a keypad. The AMD system (Automated Multiple Development, Camag) is a fully automated version of multiple development and stepwise technique with a free choice of mobile-phase gradient. Because the chromatogram is developed repeatedly in the same direction and each individual run is somewhat farther than the last, a focusing of the separated substance zones takes place in the direction of development. The chromatography is reproducible because the mobile phase is removed from the separation chamber after each step and the layer is completely freed from the mobile phase, in vacuum. Then, a fresh mobile phase is introduced for the next run. Provided all parameters, including solvent migration increments, are properly maintained, which is only possible with a fully automatic system, the densitogram of a chromatogram track can be superimposed with a matched-scale diagram of the gradient.

Another device for automated development is the chamber constructed by Tyihak [4], in which the adsorbent layer is placed between two plates and the mobile phase flows under increased applied pressure. It can be operated in the linear or radial mode. Another automated device is the UMRC (Ultra Micro Rotation Chromatograph), where the eluent is delivered to the center of a rotating TLC plate [5]. A simple device was constructed by Delvorde and Postaire [6] in which the liquid is pumped out (by vacuum) which causes the flow of the mobile phase and decreases the vapor pressure.

Derivatization

Derivatization can be carried out both before and after development of the plate. In the latter case, it may be applied before detection or after scanning densitometry. Derivatization may be carried out using the device constructed by Kruzic (Anton Paar KG), where the sprayer moves along a vertical guide while the plate moves horizontally [7]. Another method of derivatization consists in immersion of the plate into a suitable reagent solution. For this purpose, the device available from Camag can be used (Camag Chromatogram Immersion Device III), in which a low velocity motor causes the immersion and removal of the plate from the reagent solution.



Evaluation

Thin-film chromatographic detection, contrary to other chromatographic techniques, requires stopping development, drying of the layer, and scanning with an appropriate detector. There are basically two alternatives for the evaluation of thin-layer chromatograms: elution of the separated substance from the layer, followed by photometric determination (indirect determination), and *in situ* evaluation (scanning) directly on the TLC plate. The *in situ* evaluation of the chromatogram is carried out using a high-resolution chromatogram spectrophotometer (densitometer) to scan each chromatogram track, from start to solvent front in the direction of development, by means of a slit. The measurements are carried out either in the visible-light range for colored or fluorescent substances or in the ultraviolet (UV) range for UV-light-absorbing solutes. The wavelength of maximum absorption is generally selected as measurement wavelength. The scanning process yields absorption or fluorescence scans (peaks) which are also used to assess the quality of chromatographic separation. TLC plates are generally scanned in the reflectance mode (diffuse reflectance), meaning that the monochromatic light is directed by a mirror to the layer surface at 90° and the diffuse reflectance is measured at 45° by means of a detector. The optical pathways used for absorption and fluorescence measurements are identical in commercially available scanners. The only difference is the light source: Visible-light measurements are performed using tungsten lamps, whereas high-pressure mercury lamps are used for fluorescence measurements and deuterium lamps for absorption measurements in the UV range. In the case of fluorometric detection, it is also necessary to place a cutoff filter in front of the detector to prevent the comeasurement of the short-wavelength excitation radiation. All functions of the scanner are controlled from a personal computer that is linked via an RS232 interface. The scanner transmits all measurement data, in digital form, to the computer for processing with the specific software. The final report is based in the following sequence: raw data acquisition–integration–calibration, and calculation. Integration is performed, *postrun*, from the raw data gathered during scanning (i.e., after all tracks of a chromatogram plate have been measured). Integration results can be influenced by selecting appropriate integration parameters. As all measured raw data remain stored on a disk, reintegration with other parameters is possible at any time. The system auto-

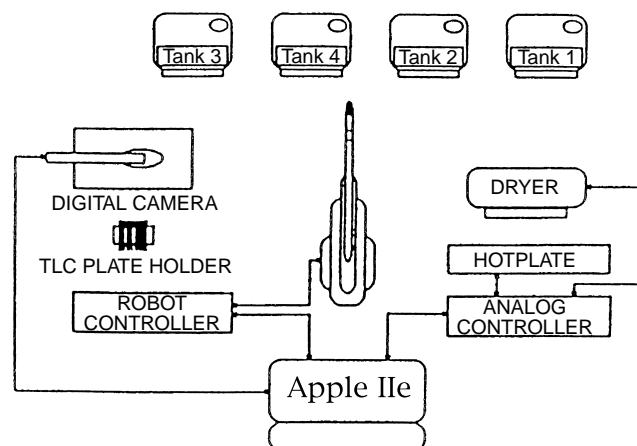


Fig. 2 Prosek robotic TLC apparatus.

and possible breakdowns. A robotics system allows space saving and easier integration of equipment in the laboratory. Today, a conventional robot has a movable arm. The purpose of the arm is to extend the capabilities of the human arm. There are five basic parts to every robotic arm: controller, arm, drive, end effector, and sensor. There are also five basic functions: base, shoulder, elbow, pitch, and roll. Most modern robots belong to one of four categories: Cartesian, spherical and cylindrical robots, and revolute arms [8]. In 1989, Prosek et al. [3] developed a planar chromatography robot (Fig. 2). Its arm, supported by a rotating base, executed four degrees of freedom movements. Its work envelope comprised four tanks: the first for cleaning, the second for development, and the last two for derivatization by dipping. Also required was a hot plate, a drying system, and a digital camera for evaluation of the derivatized plate. The system was controlled by an Apple IIe computer.

The planar chromatography automaton was designed by Delvordre and Postaire with the objective of reducing the number of human movements required for the handling of precoated plates [8]. This device uses a conveyor-belt-like system to sustain all the chromatographic steps along with their own supply of reagents and tools. The procedure comprises six stages. Using this method, qualitative and quantitative data are obtained 50–150 min after starting the procedure.

Technological progress has enabled automation of planar chromatography and will provide users with a greatly improved technique. Such improvements will now meet requirements of the industrial sector, not only in terms of productivity, effectiveness, reduced



cost, GLP, and environmental quality, but also on the technical side (validation, flexibility, evolution). Complete chromatographic automation will bring planar chromatography to the same level as other chromatographic methods.

References

1. *IUPAC Compendium of Analytical Literature*, Pergamon Press, Oxford, 1978, pp. 22–23.
2. R. E. Majors and B. D. Holden, *LC-GC Int.* 6(9): 530 (1993).
3. M. Prošek, M. Pukl, A. Smidownik, and A. Medja, *J. Planar Chromatogr.* 2(6): 244 (1989).
4. E. Tyihak and E. Mincsovics, *LC-GC Int.* 4: 24 (1991).
5. S. Nyiredy, L. Batz, and O. Sticcer, *J. Planar Chromatogr.* 2: 53 (1989).
6. P. Delvordre, C. Reynault, and E. Postaire, *J. Liq. Chromatogr.* 15: 1673 (1992).
7. F. Kreuzig, *Chromatographia* 13: 238 (1980).
8. E. P. R. Postaire, P. Delvordre, and Ch. Sarbach, in *Handbook of Thin-Layer Chromatography*, 2nd ed., J. Sherma and B. Fried (eds.), Marcel Dekker, Inc., New York, 1997, pp. 373–385.

Automation and Robotics in Planar Chromatography



Axial Dispersion Correction Methods in GPC–SEC

Gregorio R. Meira

Jorge R. Vega

INTEC, Universidad Nacional del Litoral and CONICET, Santa Fe, Argentina

Introduction

In ideal size-exclusion chromatography (SEC), fractionation is exclusively by hydrodynamic volume. Due to axial dispersion, however, a whole distribution of hydrodynamic volumes (and, therefore, of molecular weights) is instantaneously present in the detector cell. Under these conditions, it is assumed that the mass chromatogram $w(V)$ (i.e., the instantaneous mass w versus the elution time or elution volume V) is a broadened version of a true (or corrected) mass chromatogram $w^c(V)$, as follows [1]:

$$w(V) = \int_{-\infty}^{\infty} g(V, V_0) w^c(V_0) dV_0 \quad (1)$$

where $g(V, V_0)$ is the (in general, nonuniform and skewed) spreading function and V_0 is a dummy integration variable that also represents the average retention volumes. At each V_0 , an (in principle, different) individual $g(V)$ function must be defined. The determination of $g(V, V_0)$ is still a matter of controversy that is outside the scope of the present article.

With narrow standards of known molecular weights, a calibration $\log M(V)$ can be obtained; such a calibration is assumed to be unaffected by axial dispersion. If the chromatogram $w(V)$ is combined with the molecular-weight calibration, a broadened molecular weight distribution (MWD) $w(M)$ will be estimated. The corresponding number-average molecular weight \bar{M}_n will result underestimated, and the weight-average molecular weight \bar{M}_w and the polydispersity \bar{M}_w/\bar{M}_n will both be overestimated. If a broad and smooth chromatogram is obtained with a modern high-resolution column set, the axial dispersion effect is expected to be negligible, and no specific corrections will be required. In contrast, axial dispersion correction may be important in the cases of (a) a narrow chromatogram with a width that is close to that of the broadening functions in the same elution volume range and (b) a wide chromatogram, but containing sharp elbows and/or narrow peaks. Equation (1) has been extended

to other detectors such as molar mass or specific group sensors. In all cases, the same function $g(V, V_0)$ is applicable; this is because the broadening is assumed independent of the polymer chemical nature. For example, calling $s_w(V)$ the chromatogram obtained from a light-scattering detector, the following may be written [2]:

$$s_w(V) = \int_{-\infty}^{\infty} g(V, V_0) s_w^c(V_0) dV_0 \quad (2)$$

where $s_w^c(V)$ is the corrected molar mass chromatogram and $s_w(V)$ is proportional to $[w(V)M_w(V)]$, where $M_w(V)$ is the instantaneous weight-average molecular weight. Even with perfectly accurate sensors, a distorted MWD $w(M_w)$ will be estimated from $s_w(V)$ and $w(V)$. However, in that case, the \bar{M}_w estimate will still be exact, whereas \bar{M}_n and therefore the polydispersity will be both underestimated [3].

Correction Methods for Mass Chromatograms

Consider the numerical inversion of Eq. (1), that is, the calculation of $w^c(V)$ from the knowledge of $w(V)$ and $g(V, V_0)$. To this effect, let us first transform the continuous model of Eq. (1) into the following equivalent discrete model:

$$\mathbf{w} = \mathbf{G} \mathbf{w}^c \quad (3a)$$

with

$$\mathbf{G} = \begin{bmatrix} g(1, 1) & \cdots & g(1, j) & \cdots & g(1, p) \\ \vdots & & g(j, j) & & \vdots \\ g(n, 1) & \cdots & & & g(n, p) \end{bmatrix}, \quad (n > p) \quad (3b)$$

where \mathbf{w} is a $(n \times 1)$ -column vector containing only the nonzero heights of $w(V)$ sampled at regular ΔV intervals, \mathbf{w}^c is a $(p \times 1)$ -column vector containing only the nonzero heights of $w^c(V)$, and \mathbf{G} is a rectangular matrix



that represents $g(V, V_0)$. Each column of \mathbf{G} contains the heights of the successive (discrete) broadening functions, with the average retention volume heights at $(c + j, j)$. The following is verified: (a) the p elements of \mathbf{w}^c correspond to the central elements of \mathbf{w} ; (b) $n - p + 1$ is equal to the number of nonzero elements of the discrete version of $g(V)$; and (c) the largest elements of \mathbf{G} are located c rows below the main diagonal, and the elements on the top-right hand corner and bottom-left hand corner are all zeros.

Were it not for the ill-conditioned nature of the problem, \mathbf{w}^c could be simply estimated from $\hat{\mathbf{w}}^c = [\mathbf{G}^T \mathbf{G}]^{-1} \mathbf{G}^T \mathbf{w}$; where the “hat” indicates the estimated value. Unfortunately, $[\mathbf{G}^T \mathbf{G}]^{-1}$ is almost singular; therefore, such a solution is highly oscillatory with negative peaks.

In what follows, several correction techniques originally developed for mass chromatograms are described. Such techniques are (a) the “phenomenological” Methods I–III that consider the system as a “black box” and numerically invert Eq. (1) prior to calculating the MWD, and (b) the more specific Methods IV–V that (avoiding the ill-conditioned nature of the numerical inversion) require an independent molecular-weight calibration and calculate the MWD in a single step. Methods I–III are, in general, suitable for nonuniform and skewed broadening functions.

Method I: The Difference Function [4]

Consider the iterative procedure presented as Method 1 in Ref. 4. The following set of difference equations must be first calculated:

$$\Delta_i \mathbf{w} = \Delta_{i-1} \mathbf{w} - \mathbf{G} \Delta_{i-1} \mathbf{w}, \quad \text{with} \quad \Delta_0 \mathbf{w} = \mathbf{w}, \quad (i = 1, 2, \dots) \quad (4)$$

where i is the iteration step. Then, as $i \rightarrow \infty$, it is expected that $\Delta_i \mathbf{w} \rightarrow 0$, and the corrected chromatogram is given by $\hat{\mathbf{w}}^c = \sum_{i=1}^{\infty} \Delta_i \mathbf{w}$. In practice, the best solution is obtained in a generally small number of iterations.

Method II: Singular Value Decomposition [5]

The final expression for this least-squares estimation procedure is

$$\hat{\mathbf{w}}^c = \sum_{k=1}^r \frac{\mathbf{u}_k^T \mathbf{w}}{\sigma_k} \mathbf{v}_k \quad r \leq p, \quad \sigma_1 \geq \sigma_2 \geq \dots \geq \sigma_r \dots \geq \sigma_p \geq 0 \quad (5)$$

where \mathbf{u}_k and \mathbf{v}_k are the eigenvectors of $\mathbf{G}\mathbf{G}^T$ and $\mathbf{G}^T\mathbf{G}$, respectively, σ_k are the singular values [5] of \mathbf{G} , and p

Axial Dispersion Correction Methods in GPC–SEC

is the full rank of \mathbf{G} . In Eq. (5), the number of “effective” terms is limited to r because the lower σ_k ’s excessively amplify the measurement noise. The lowest admissible σ_r must be larger than the inverse of the lowest signal-to-noise ratio. The lowest signal-to-noise ratio is, in turn, normally found at the chromatogram tails.

Method III: The Kalman Filter [6]

This fast and effective digital algorithm is based on a linear stochastic model that is equivalent to Eq. (1). The theoretical background is beyond the scope of the present article; unfortunately, some knowledge of the basic Kalman filtering theory [5,7] is necessary for an adequate algorithm adjustment. The adjustment requires estimating the variances of the measurement noise and of the expected solution.

In all direct-inversion methods, the best adjustment normally involves a trade-off between an excessively “rich” solution that may contain spurious high-frequency oscillations and negative peaks, and an excessively smoothed solution where the high-frequency information is lost, but it is otherwise acceptable. Consider now some methods that avoid the direct chromatogram inversion.

Method IV: Rotation of the Calibration Curve [8,9]

This method aims at obtaining the corrected MWD in a single step, by simply rotating the linear calibration $\log M(V)$ counterclockwise around some selected midpivoting point. In this way, the effective molecular-weight range is reduced with respect to that obtained from the original calibration. The technique is numerically robust, but, unfortunately, it is based on the following rather strong assumptions: (a) the axial dispersion must be uniform and Gaussian; (b) the chromatogram itself must be Gaussian or Wesslau [9]; and (c) the original molecular-weight calibration must be linear and of the form $M = D_1 \exp(-D_2 V)$. The rotated calibration $M = D'_1 \exp(-D'_2 V)$ is obtained from

$$D'_1 = D_1 \exp \left\{ \frac{D_2 \sigma_g^2 [D_2 (\sigma_w^2 - \sigma_g^2) - 2\bar{V}]}{2\sigma_w^2} \right\} \quad (6a)$$

$$D'_2 = D_2 \exp \left(1 - \frac{\sigma_g^2}{\sigma_w^2} \right) \quad (6b)$$

where σ_g^2 and σ_w^2 are the variances of $g(V)$ and $w(V)$, respectively, and the pivoting abscissa \bar{V} is the number-average retention volume of the chromatogram.



Method V: The Approximate “Analytical” Solution [10]

This approach is based on assuming (a) a Gaussian (but nonuniform) axial dispersion with a variance $\sigma_g^2(V)$; (b) a Gaussian (but nonuniform) instantaneous MWD of variance $\sigma_0^2(V)$ and average retention volume $V_0(V)$; and (c) an (in general nonlinear) calibration $M = D_1(V) \exp[-D_2(V)V]$. The corrected chromatogram is obtained from

$$\hat{w}^c(V) = w(V) \left(\frac{\sigma_g^2(V)}{\sigma_0^2(V)} \right) \exp \left(- \frac{(V - V_0(V))^2}{2\sigma_0^2(V)} \right) \quad (7a)$$

with:

$$V_0(V) = V + \frac{1}{D_2(V)} \cdot \ln \left(\frac{w(V + D_2(V)\sigma_g^2(V))}{\sqrt{w(V - D_2(V)\sigma_g^2(V))w(V + D_2(V)\sigma_g^2(V))}} \right) \quad (7b)$$

$$\sigma_0^2(V) = \sigma^2(V) + \frac{1}{D_2^2(V)} \cdot \ln \left(\frac{w(V - D_2(V)\sigma_g^2(V))w(V + D_2(V)\sigma_g^2(V))}{w^2(V)} \right) \quad (7c)$$

Method V assumes that the instantaneous MWDs are Gaussian. However, the instantaneous MWDs are never truly Gaussian, even for Gaussian broadening functions, thus reducing the precision of the approach. (For example, it can be shown that at the chromatogram tails, the instantaneous distributions are always highly skewed with the concavities facing toward the mid-chromatogram section [3].)

An Evaluation Example

Correction methods are best evaluated through synthetic (or numerical) examples. The reason for this is that only in numerical examples, the true solution is a priori known, and therefore the quality of the different estimation algorithms can be adequately compared. (In contrast, in a real SEC measurement, the true corrected chromatogram or MWD are never accurately known.) In what follows, Methods I–V are evaluated on the basis of a synthetic example that has been previously investigated in several occasions. [6,11–13]

The basic data consist of the corrected chromatogram $w^c(V)$ and the (uniform) broadening function $g(V)$ presented in Fig. 1a. The proposed example is particularly demanding because (a) $w^c(V)$ is multi-peaked and (b) the variance of $w^c(V)$ is comparable to

the variance of $g(V)$. For a uniform broadening, Eq. (1) reduces to a simple convolution integral. By convolution of $w^c(V)$ and $g(V)$, a noise-free “measurement” was first obtained. Then, this function was rounded to the last integer. [13] This procedure is equivalent to adding a zero-mean white noise (with a rectangular probability distribution in the range ± 0.5) to the noise-free measurement. The resulting “chromatogram” is $w(V)$ in Fig. 1a. Note that the multimodality of $w^c(V)$ is lost in $w(V)$.

In the cited works [6,11–13], only the ability of several numerical inversion algorithms for recuperating $w^c(V)$ was evaluated, and the MWD calculation was not considered. In the present article, the purely numerical Methods I–III are compared with Methods IV and V, which require a linear molecular-weight calibration. For this reason, the calibration $\log M(V)$ is included in Fig. 1b. From that calibration and $w^c(V)$, the “true” MWD $w^c(\log M)$ of Figs. 1c–1f was obtained. Note that the selection of a uniform and Gaussian broadening is not a limitation for an adequate evaluation of the (more general) Methods I–III.

In Figs. 1c–1f, the MWDs recuperated through Methods I–V are compared with the real distribution. In Table 1, the real and estimated average molecular weights and polydispersities are presented. In Method I, the best results were found when limiting the procedure to only four iterations (Fig. 1c). In Method II, the full rank of \mathbf{G} was $p = 61$, and the signal-to-noise ratio at the chromatogram tails suggested truncating the summation of Eq. (5) at $r = 16$. The obtained solution exhibits a negative peak (Fig. 1d). For comparison, the less “rich” solution with $r = 9$ is also shown in Fig. 1d. In Method III, a (time-invariant) measurement noise variance was estimated from the baseline noise, and a (time-varying) solution variance was estimated by simply squaring the raw chromatogram heights (Fig. 1e). In Method IV, the rotated calibration is shown in Fig. 1b, and the recuperated distribution is given in Fig. 1f. In Method V, it was numerically observed that (for the adopted linear calibration) the solution becomes almost independent of $D_2(V)$ (Fig. 1f).

To verify the validity of Method IV, the real instantaneous MWDs were simulated. From such distributions, the true instantaneous averages $M_n(V)$ and $M_w(V)$ were calculated and represented in Fig. 1b using a logarithmic scale. Clearly, $\log M_n(V)$ and $\log M_w(V)$ differ from the (linear) rotated calibration. The differences occur because the original chromatogram is non-Gaussian. This illustrates the limitations of applying the technique to a chromatogram of an arbitrary shape.

The following comments can be made. Only Method II [5] (with $r = 16$) and Method III [6] were



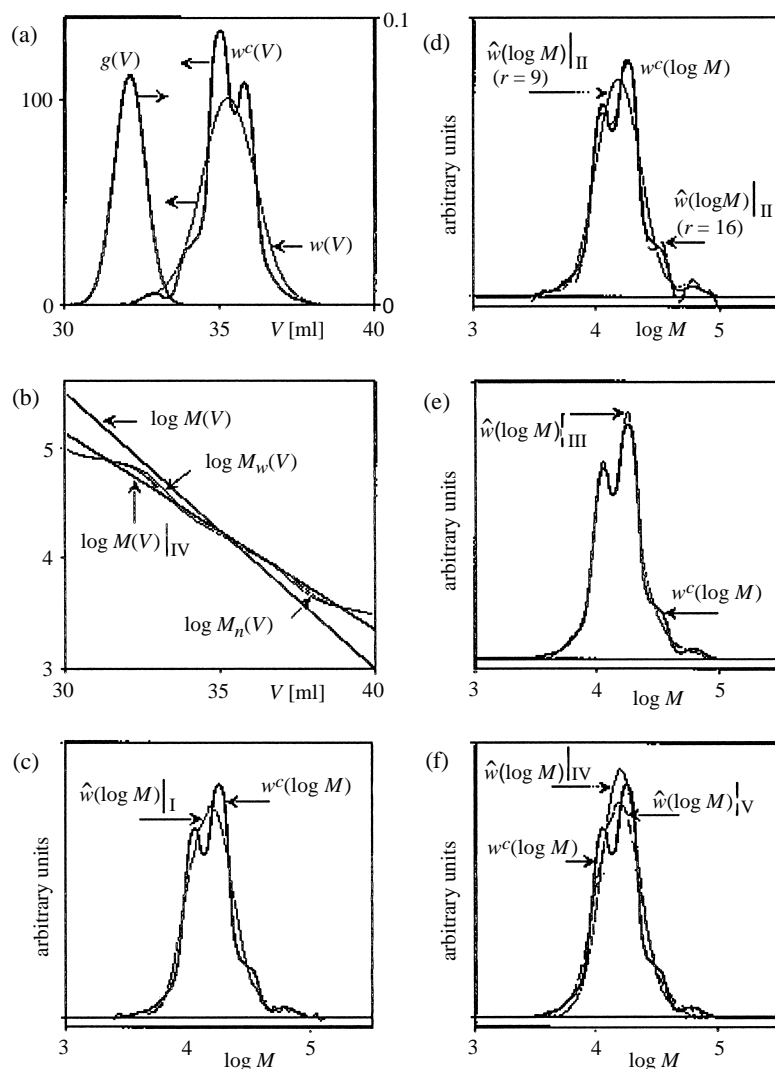


Fig. 1 The numerical example [6,11–13]. (a) "True" mass chromatogram $w^c(V)$, uniform broadening $g(V)$, and resulting "measured" chromatogram $w(V)$. (b) Molecular-weight calibration $\log M(V)$, "rotated" calibration according to Method IV [8,9] $\log M(V)|_{IV}$, and calibrations assuming ideal molar mass sensors $\log M_n(V)$ and $\log M_w(V)$. (c–f) Comparison between the true MWD $w^c(\log M)$ and the MWD estimates $\hat{w}^c(\log M)$ obtained from Methods I[4], II[5], III[6], IV[8,9], and V[10].

capable of recuperating the details of the true MWD; all others produce unimodal solutions. In general, the more sophisticated correction techniques such as Methods II and III require a priori information on the measurement noise and/or on the expected solution. This generally yields better estimations, but at the cost of complicating the adjustment procedure. The recuperated average molecular weights presented in Table 1 are, in all cases, quite acceptable.

Correction Methods for Multidetector SEC

A difficulty with multidetector SEC is that downstream chromatograms are shifted (and eventually distorted) with respect to the first-emerging chromatogram. This is a consequence of the interdetector capillaries and the (downstream) detector cell volumes. Such corrections are outside the scope of the present article.

Table 1 The Numerical Example^a: “True” versus Recuperated Average Molecular Weights

	“True” values	Without correct.	Method I ($i = 4$)	Method II ($r = 9$)	Method II ($r = 16$)	Method III	Method IV	Method V
\overline{M}_n	13,975	13,464	14,029	13,993	14,033	14,084	14,871	14,038
\overline{M}_w	17,342	18,041	17,315	17,310	17,313	17,156	17,224	17,335
$\overline{M}_w/\overline{M}_n$	1.241	1.340	1.234	1.237	1.234	1.218	1.158	1.235

^aFrom Refs. 6 and 11–13.

Methods I–III are clearly applicable to chromatograms produced by any SEC sensor. As we have seen, all chromatograms are distorted in a similar fashion through a common broadening function $g(V, V_0)$. For this reason, similar difficulties in their individual numerical inversions are to be expected.

Many problems remain still unsolved in relation to axial dispersion correction in multidetection SEC. For example, when an on-line light-scattering detector is used, the instantaneous weight-average molecular weight is obtained from the ratio between the light scattering and the mass signals. Unfortunately, the measurement errors makes it unfeasible to independently invert each raw chromatogram prior to performing the signals ratio. Furthermore, even the direct signals ratio is only feasible in the mid-chromatogram section. A similar problem is presented when analyzing a linear copolymer by standard dual detection (i.e., employing a UV spectrophotometer and a differential refractometer). In this case, it seems preferable to first calculate the instantaneous mass and copolymer composition directly from the raw chromatograms, and then correct such derived variables for axial dispersion. [14] (The more obvious alternative procedure of first correcting the individual chromatograms for axial dispersion and then calculating the derived variables is not recommendable due to the propagation of errors [14].)

References

1. L. H. Tung, Method of calculating molecular weight distribution function from gel permeation chromatograms. III. Application of the method, *J. Appl. Polym. Sci.* 10: 1271 (1966).
2. M. Netopilik, Correction for axial dispersion in gel permeation chromatography with a detector of molar masses, *Polym. Bull.* 7: 575 (1982).
3. P. I. Prougenes, D. Berek, and G. R. Meira, Size exclusion chromatography of polymers with molar mass detection. Computer simulation study on instrumental broadening biases and proposed correction method, *Polymer* 40: 117 (1998).
4. T. Ishige, S. I. Lee, and A. E. Hamielec, Solution of Tung's axial dispersion equation by numerical techniques, *J. Appl. Polym. Sci.* 15: 1607 (1971).
5. J. M. Mendel, *Lessons in Estimation Theory for Signal Processing, Communications, and Control*, Prentice-Hall, Englewood Cliffs, NJ, 1995.
6. D. Alba and G. R. Meira, Inverse optimal filtering method for the instrumental broadening in SEC, *J. Liq. Chromatogr.* 7: 2833 (1984).
7. A. Felinger, *Data Analysis and Signal Processing in Chromatography*, Data Handling in Science and Technology Vol. 21, Elsevier, Amsterdam, 1998.
8. W. W. Yau, H. J. Stoklosa, and D. D. Bly, Calibration and molecular weight calculations in GPC using a new practical method for dispersion correction-GPCV2, *J. Appl. Polym. Sci.* 21: 1911 (1977).
9. C. Jackson and W. W. Yau, Computer simulation study of size exclusion chromatography with simultaneous viscometry and light scattering measurements, *J. Chromatogr.* 645: 209 (1993).
10. A. E. Hamielec, H. J. Ederer, and K. H. Ebert, Size exclusion chromatography of complex polymers. Generalized analytical corrections for imperfect resolution, *J. Liq. Chromatogr.* 4: 1697 (1981).
11. K. S. Chang and R. Y. M. Huang, A new method for calculating and correcting molecular weight distributions from permeation chromatography, *J. Appl. Polym. Sci.* 13: 1459 (1969).
12. L. M. Gugliotta, D. Alba, and G. R. Meira, Correction for instrumental broadening in SEC through a stochastic matrix approach based on Wiener filtering theory, *ACS Symp. Ser.* 352: 287 (1987).
13. L. M. Gugliotta, J. R. Vega, and G. R. Meira, Instrumental broadening correction in size exclusion chromatography. Comparison of several deconvolution techniques, *J. Liq. Chromatogr.* 13: 1671 (1990).
14. R. O. Bielsa and G. R. Meira, Linear copolymer analysis with dual-detection size exclusion chromatography: Correction for instrumental broadening, *J. Appl. Polym. Sci.* 46: 835 (1992).



Band Broadening in Capillary Electrophoresis

Jetse C. Reijenga

University of Technology, Eindhoven, The Netherlands

Introduction

As in chromatography, band broadening in capillary electrophoresis (CE) is determined by a number of instrumental and sample parameters and has a negative effect on detectability, due to dilution. Also, as in chromatographic techniques, the user can minimize some, but not all, of the parameters contributing to band broadening. In capillary electrophoresis, injection and detection are generally on-column, so that band broadening is limited to on-column effects. As will be shown, several effects are similar in chromatography; others are specific for CE and, in particular, for the potential gradient as a driving force. General equations for CE in open systems are given where the relative contribution of electro-osmosis is given by the electromigration factor f_{em} , given by

$$f_{em} = \frac{\mu_{eff}}{\mu_{eff} + \mu_{EOF}}$$

in which μ_{eff} is the effective mobility and μ_{EOF} is the electro-osmotic flow mobility. This electromigration factor is unity for systems with suppressed EOF.

The band-broadening contributions can be described in the form of a plate-height equation, where one usually assumes, as in chromatography, mutual independence of terms.

Injection

Band broadening due to injection is naturally proportional to the injection volume, relative to the capillary volume, but, in contrast to chromatography, sample stacking or destacking may decrease or respectively increase the injection band broadening thus defined. Without stacking or destacking, the following plate-height term can be used:

$$H_{inj} = \frac{\delta_{inj}^2}{12L_d}$$

in which δ_{inj} is the length in the capillary of the sample plug and L_d is the length of the capillary to the detector.

Naturally, the above relationship can be rewritten in terms of sample and capillary volume, which are in the order of 10 nL and 1 μ L, respectively.

Diffusion

As in chromatography, the effect of diffusion on band broadening is generally pronounced. It is directly proportional to the diffusion coefficient and the residence time between injection and detection. This effect can, consequently, be reduced by increasing the voltage, or by increasing the electro-osmotic flow, in cases where cations are analyzed at positive inlet polarity, where it further shortens the analysis times. The effect is less at lower temperatures (as the diffusion coefficient decreases approximately 2.5% per degree Celsius of temperature drop), but most significantly decreases with increasing molecular mass of the sample component.

$$H_{diff} = \frac{2Dt_m}{L_d}$$

in which L_d is the capillary length to the detector, D is the diffusion coefficient, and t_m is the migration time. Substituting the diffusion coefficient, using the Nernst–Einstein relation, yields

$$H_{diff} = \frac{2RTf_{em}}{z_{eff}EF}$$

in which R is the gas constant, T is the temperature, z_{eff} is the overall effective charge of the sample ion, E is the electric field strength, and F is the Faraday constant. In this relationship, z_{eff} and E , by definition, have opposite signs for negative values of f_{em} only.

Detection

The detector time constant and detector cell volume are both involved. The slit width along the length of the capillary is proportional to the latter. A value of



200 μm for the slit width in the case of 10^5 plates in a 370-mm capillary has negligible contribution to band broadening:

$$H_{\text{slit}} = \frac{\delta_{\text{det}}^2}{12L_d}$$

where δ_{det} is the detector slit width along the capillary axis. In cases of diode array detection, larger slit widths are usually applied; this reduces the noise level but may affect the peak shape at high plate numbers ($>10^5$).

The contribution of the detector time constant τ is modeled by the following relation:

$$H_\tau = L_d \left(\frac{\tau}{t_m} \right)^2$$

A detector time constant τ of 0.2 s is generally safe.

Thermal Effects

In cases of a relatively high current density, power dissipation in the capillary may result in significant radial temperature profiles. The plate-height contribution is given by

$$H_{\text{ther}} = \frac{f_T^2 \kappa^2 E^5 R_i^6 z_{\text{eff}} F f_{\text{em}}}{1536 R T \lambda_s^2}$$

where f_T is the temperature coefficient for conductivity, κ is the specific conductivity of the buffer, E is the electric field strength, R_i is the capillary inner diameter, and λ_s is the thermal conductivity of the solution.

As the effective mobility increases with the temperature at approximately 2.5% per degree, radial mobility differences may accumulate to significant band-broadening effects. The effect increases with increasing current density and capillary inner diameter. In a 75- μm -inner diameter capillary, a power dissipation of 1–2 W/m is generally safe. This value is calculated by multiplying the voltage and the current and dividing by the capillary length. Under these conditions, the radial temperature profile in the capillary is less than 0.5°C and the contribution to peak broadening negligible. In the case of higher conductivity buffers (e.g., a pH 3 phosphate buffer), the power dissipation and temperature profile can be 10 times higher and the effect on peak broadening significant. It should be emphasized that more effective cooling has

Band Broadening in Capillary Electrophoresis

no effect on thermal band broadening; the only effect is decreased averaged temperature inside the capillary.

Electro-osmotic Effects

Electro-osmosis in open systems is generally considered not to contribute to peak broadening. In hydrodynamically closed systems with nonsuppressed electro-osmosis, or in cases of axially different electro-osmotic regimes, however, a considerable contribution may result. The corresponding plate-height term is

$$H_{\text{EOF}} = \frac{R_i^2 \zeta^2 \varepsilon^2 z_{\text{eff}} E F}{24 R T \eta^2 \mu_{\text{eff}}^2}$$

where ε is the dielectric constant and η is the local viscosity of the buffer at the plane of shear. This relationship shows that, in closed systems, the ζ -potential should be close to zero and that a viscosity increase near the capillary wall will be advantageous.

Electrophoretic Effects

Peak broadening due to electrophoretic effects are generally proportional to the conductivity (and thus the ionic strength) of the sample solution, relative to that of the buffer. This effect is readily understood when considering that in the case of a high sample concentration, the electric field strength (and, consequently, the linear velocities) in the sample plug are much lower than in the adjacent buffer. Due to this, a dilution (destacking) of the sample occurs. This is illustrated in curve a in Fig. 1 — the separation of a concentrated 1 mM solution benzenesulfonic, *p*-toluene sulfonic, and benzoic acid, dissolved in a buffer of 1 mM propionic acid/Tris to pH 8.

Alternatively, when injecting a low-conductivity (diluted, 0.01 mM) sample in a 25-mM buffer of same composition (curve b in Fig. 1 — 100 times amplified with respect to the others), the local field strength in the sample compartment is higher than in the adjacent buffer, resulting in a rapid focusing of ionic material at the sample–buffer interface (stacking), and resulting in very sharp sample injection plugs and high plate counts. This stacking takes place during the first second after switching on the high voltage. It may thus be advantageous to inject a larger volume of a more diluted sample for better efficiency. Choosing a higher-conductivity buffer also enhances the effect, where one has to consider that this may result in more pronounced band broadening due to other effects. Curve



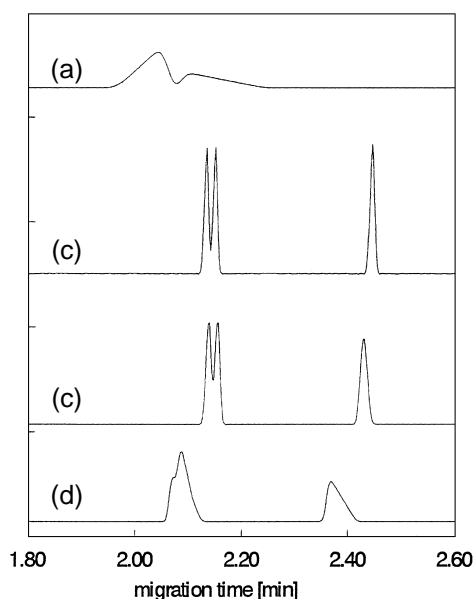


Fig. 1 Electrophoretic bandbroadening effects of benzoates as sample. Destacking trace a (1-mM sample in 1-mM buffer), stacking trace b (0.01-mM sample in 25-mM buffer), and trace c (1-mM sample in 25-mM buffer) and peak triangulation trace d (1-mM sample in 25-mM chloride buffer).

c in Fig. 1 shows that in such a high-conductivity buffer, even the 1-mM sample is separated to reasonable extent.

Peak symmetry is another important issue. Generally, capillary zone electrophoresis peaks are non-Gaussian and show nonsymmetry. This peak triangulation increases with increasing concentration overload. It is also proportional to the difference in effective mobility of the sample ion and the co-ion in the buffer. For instance, analyzing the same 1-mM sample mixture in a buffer consisting of, for example, 25 mM chloride/Tris to pH 8 will give triangular peaks (curve d in Fig. 1) because the effective mobility of benzoic acid is much lower than that of the buffer anion chloride: The buffer co-ion is not properly tuned to the sample component mobilities.

Suggested Further Reading

- Giddings, J. C., in *Treatise on Analytical Chemistry*, I. M. Kolthoff and P. J. Elving (eds.), John Wiley & Sons, New York, 1981, Part I, Vol. 5.
- Hjertén, S., *Chromatogr. Rev.* 9: 122 (1967).
- Jorgenson, J. W., and K. D. Lucaks, *Science* 222: 266 (1983).
- Kenndler, E., *J. Capillary Electrophoresis* 3(4): 191 (1996).
- Reijenga, J. C. and E. Kenndler, *J. Chromatogr. A* 659: 403 (1994).
- Reijenga, J. C. and E. Kenndler, *J. Chromatogr. A* 659: 417 (1994).
- Virtanen, R., *Acta Polytech. Scand.* 123: 1 (1974).



Band Broadening in Size-Exclusion Chromatography

Jean-Pierre Busnel

Université Du Maine, U.M.R. 6120/CNRS, Le Mans, France

Introduction

In classical chromatography, band broadening (BB), which defines the shape of the chromatogram of a pure solute, is one of the factors limiting the resolution, but individual peaks are generally observable and the discussion of BB extent is direct. In size-exclusion chromatography (SEC), the situation is more complex, as we observe, generally, only the envelope of a large number of individual peaks (Fig. 1). Imperfect resolution and its consequences on results cannot be directly observed. A few years after the pioneer publication on SEC by Moore [1], Tung [2] presented the general mathematical problem of band-broadening correction (BBC). Until 1975, a number of simplified procedures have been proposed in order to compensate for the limited resolution of columns. After 1975, a spectacular increase in column resolution rendered the problem less important, but, recently, there is a growing interest in BBC as SEC users intend to obtain more and more detailed information on molecular-weight distributions (MWDs) and not only average MW values. For this reason, this discussion is separated into three parts:

- Experimental determination of extent of BB
- Interpretation of BB processes
- Correction methods for BB

Experimental Determination of the Extent of Broad-Banding

It is useful to choose a solute which is really eluted by a size-exclusion process, without adsorption or any additional interaction phenomena which might modify the shape of the peak. The most trivial method is to analyze the shape of a low-MW pure substance. This is usually used to determine the number of theoretical plates, $N = (V_r/\sigma)^2$, where V_r is the retention volume (volume at peak top) and σ is the standard deviation. σ can be computed from the weighing of each data point of the peak or can be estimated from the width at 10% maximum height ($\sigma = W_{0.1}/4.3$).

For this reason, when using THF as eluent and styrene/DVB gels, methanol or toluene are not good candidates; octadecane is preferred. For aqueous SEC, saccharose is the classical standard.

For polymers, a number of authors have claimed that the peak width increases as the MW increases, but to discuss band broadening for polymers, several precautions are required. First, it is necessary to be sure that the injected solution is sufficiently dilute to prevent any viscous effect. (Practically no viscous effect is observable, even for narrow standards when $[\eta]C < 0.1$; for flexible polymers, this corresponds roughly to a concentration < 1 mg/mL for MWs up to 500,000; for a higher MW, it is necessary to reduce the concentration.) Then, the real difficulty is to analyze very narrow standards for which polymolecularity is sufficiently low, so as not to participate in the peak width, or at least which polymolecularity is very precisely known.

Commercial indications on standards are in progress, but suppliers rarely guarantee the exact value for $I_p = M_w/M_n$. A tendency is to guarantee that I_p is lower than a given value, but that is not sufficient for precise BB study. Usual values for medium MW standards are $I_p < 1.03$ and $I_p < 1.05$ for high MW standards; the situation is worse for aqueous SEC with values around 1.1.

Recently, possibilities appeared with the results from thermal gradient interaction chromatography (TGIC) [3]. That method has a much better resolution than SEC and allows a very precise determination of I_p . It is even possible to use it for a preparative scale to obtain extremely narrow standards, but, until now, it is only available for organic-soluble standards.

With all these precautions and when using modern columns, it clearly appears that peaks are not Gaussian, but systematically skewed. New computing facilities allow one to analyze more precisely such peaks by various functions. The best results seems to be obtained by exponentially modified gaussian (EMG) functions [4], which are the convolution of a Gaussian dispersion and an exponential decay. In that case, two parameters define the shape of the peak σ and τ , which allow quantitative mapping of BB characteris-



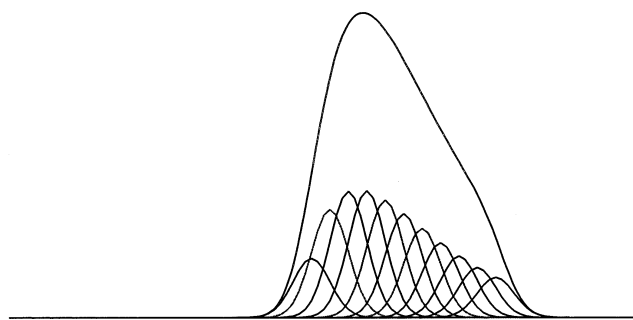


Fig. 1 Example of imperfect resolution: 10 peaks, $R = 0.25$ between neighbors.

tics for further correction. Generally, σ and τ are constant or admit a limited increase with MW for samples eluted well after the void volume. However, a dramatic increase of σ and τ occurs near the total exclusion volume [5].

Band-Broadening Interpretation

As previously indicated, this discussion is organized for chromatograms from very narrow polymer standards for which we can consider that the effect of molecular weight distribution is negligible and for which the unique separation process is size exclusion. With these limitations, the contribution to band broadening is conveniently separated into extra column effects, eddy dispersion, static dispersion, and mass transfer. In the most classical chromatographic interpretation, extra-column effects are not discussed and the three other contributions are considered as Gaussian, so there is simply the addition of their variances. The number of theoretical plates is defined as $N = (V_e/\sigma)^2$ and the influence of v , the linear velocity of the eluent, is summarized by the so-called Van Deemter equation:

$$H = \frac{L}{N} = a + \frac{b}{v} + cv$$

This classical interpretation is not sufficient, as experimental results clearly indicate that there is peak skewing; for this reason, it is useful to study each contribution separately.

Static Dispersion

This classical contribution corresponds to the diffusion of the sample along the axis of the column by Brownian motion during the time t_0 spent in the interstitial volume. That spreading effect is Gaussian and its standard deviation σ is related to D , the diffusion

Band Broadening in Size-Exclusion Chromatography

coefficient of the solute: $\sigma = (2Dt_0)^{1/2}$. In classical operating conditions in modern liquid chromatography, that contribution is generally a minor one, due to the use of relatively high flow rate. In SEC, the diffusion coefficients of polymers are very low and that contribution becomes negligible.

Extra-Column Effects

Generally, these effects are not discussed in detail, considering it is only necessary to select a chromatographic apparatus with a proper design to render these effects negligible. Recent results indicate that this situation tends to be different for macromolecular solutes. Using a chromatographic apparatus for which the column is replaced by tubings of various lengths, the end of elution is characterized by an exponential decay, the time of which is dependent not only on geometry but also strongly increases for high-MW solutes. The explanation is related to the more or less rapid averaging of radial positions of the solute in a cylindrical tube. In the case of high-molecular-weight solutes, the diffusion coefficient is small. Solute molecules which enter near the center of the tube stay in the high-velocity zone and those which enter near the walls stay in low-velocity zones; this introduces skewing which is much more important than for low-molecular-weight solutes.

Eddy Dispersion

This contribution is related to the variety of channels available for any solute molecule throughout the elution process. These channels are defined by the interstitial volume between the beads of the column package, so they correspond to a variety of shapes and flow velocities. This produces a distribution in elution time which is classically considered as Gaussian and weakly depends on flow rate. As a rule of thumb, the theoretical plate height corresponding to this effect can be considered as being equal to the bead diameter of the packing for well-packed columns.

More detailed results take into account a “wall effect” to explain why elution profiles are skewed, even for nonretained solutes in modern columns. Detailed experimental results were recently presented by Farkas and Guiochon [6] on the radial distribution of flow velocity using local multichannel detection devices. On average, the flow velocity is very homogeneous in the center of the column, but, inevitably, it becomes lower near the walls. Similarly, the peak shape from a local microdetector situated near the wall is

clearly distorted and skewed compared with that of a similar detector situated near the center of the column.

Mass Transfer

The simple model of a theoretical plate, which is simply the affirmation of the existence of N successive equilibrium steps, is not satisfactory, as it assumes a Gaussian spreading.

To obtain more realistic information, it is necessary to discuss the rate of exchange between the interstitial volume and pores [7]. Potschka [8] proposed taking into account the competition between diffusion and convection in the special situation of “perfusion chromatography,” where very large pores exist inside the beads, which allow some distribution of the solute by convection.

Recently, a model has been proposed for which pores are simply long cylinders and time of residence corresponds to a one-dimension Brownian motion [5]. Exact mathematical expressions are available for describing that process [9] and the distribution of such time of residence is highly skewed. Additionally, for each solute molecule, the number of visited pores obeys a Poisson distribution, and when the average number of visits becomes small, the distribution of elution time becomes wider and more skewed. That explains, precisely, why strong peak distortion is observed for samples eluted near the total exclusion limit.

Band-Broadening Correction

As first stated by Tung, the general starting point is that the experimental chromatogram $H(V)$ (from a concentration detector) is the convolution of $g(V, V_r)$, the spreading function defining the elution of a single species with a peak apex position of V_r , and $w(V_r) dV_r$, the weight fraction of species which peak apex, is between V_r and $V_r + dV_r$:

$$H(V) = \int_{V_1}^{V_2} g(V, V_r) w(V_r) dV_r$$

In any case, a second step consists of converting $w(V_r)$ into $w(M)$ by defining a calibration curve which correlates M and V_r .

As there is only a finite number of data points and, with some instrumental noise, generally such an inversion problem is ill-defined, the stability of the values of $w(V_r)$ depends on the algorithm which is used. Among

the huge number of articles treating such problems, a review by Meira and co-workers [10] gives useful information on the mathematical aspects and a detailed review by Hamielec [11] presents a variety of instrumental situations, from the simplest one (constant Gaussian spreading function and simple concentration detector) to the most complex (general spreading function, multidetection).

To take into account experimental evidence which clearly indicates systematic skewing, this discussion will no longer concern methods limited to Gaussian spreading functions.

Simplest Situation: Constant Spreading Function, Linear Calibration Curve, Single Concentration Detector

This situation corresponds to a useful approximation in many cases, and it is almost strictly exact when the sample has a narrow MWD. From the chromatogram of an ideal isomolecular sample, considering that it is defined by a set of h_i values equidistant on the elution volume axis, classical summations give the uncorrected molecular-weight values:

$$M_{n_{\text{uncorrected}}} = \frac{\sum h_i}{\sum (h_i/M_i)} \quad \text{and} \quad M_{w_{\text{uncorrected}}} = \frac{\sum (h_i M_i)}{\sum h_i}$$

and the peak apex position gives the real molecular weight: M_{peak} .

Therefore, two correction factors exist for M_n and M_w :

$$K_n = \frac{M_{\text{peak}}}{M_{n_{\text{uncorrected}}}} \quad \text{and} \quad K_w = \frac{M_{\text{peak}}}{M_{w_{\text{uncorrected}}}}$$

For any other isomolecular sample analyzed on the same system, the change is simply a shift along the elution volume axis and each M_i value is multiplied by the same factor. Thus, the correction factors are unchanged. Finally, any broad MW sample analyzed on the same system is the addition of a set of isomolecular species; therefore, when summing, there is factorization of the correction factors and

$$M_{n_{\text{corrected}}} = K_n M_{n_{\text{uncorrected}}} \\ M_{w_{\text{corrected}}} = K_w M_{w_{\text{uncorrected}}}$$

This very simple BBC can always be used, at least to give a preliminary indication of the extent of BB. When using extremely narrow standards, as obtained by preparative TGIC, the result is accurate; more easily, it is possible to set the correction factors between



two limits: lower one using data from a low-MW pure chemical and a higher limit using data from an imperfect narrow standard.

General Situation: Spreading Function Depends on Elution Volume and Calibration Curve Is Not Linear, Single Concentration Detector

In such cases, as stated by Meira and co-workers [10], the quality of results depends on computational refinements. It is necessary to add specific constraints related to the chromatographic problem: rejection of negative values or unrealistic fluctuations in the weight distribution. The normal way is to invert the large matrix defining the spreading function for any position on the elution volume scale. With modern computational facilities, that becomes easy, but it is still not trivial to obtain stable results, and proper filtering processes are useful.

Good results can be obtained by using a more direct iterative method which can be briefly presented: n equidistant values are chosen on the elution volume scale; let us note these values as V_i (typically, n can be 200). Any sample is arbitrarily defined as the sum of n isomolecular species, whose positions at the peak apex are V_j . For each peak j , n values of heights h_{ij} for each V_i value are computed, normalizing the surface (the peak shape is defined by interpolation from experimental BB data).

The chromatogram corresponding to the sample is defined by a set of n H_i values at positions V_i .

To define the weight distribution of the sample, it is simply necessary to adjust a set of w_i values until the summation converges toward the experimental H_i values. For the first attempt, $w_i = H_i$: This gives, by addition, a chromatogram ($H1_i$). Then, $w_i = w_i * H_i / H1_i$; that gives $H2_i$, and so on until convergence.

The method is reasonably efficient. Stable convergence is observed except for very large samples for which the problem is too severely ill-conditioned. Applying it to narrow PS standards allows one to find, again, the true polymolecularity index.

Multidetetection Problem

The aim of multidetection, especially LS/DRI coupling, is to find a useful calibration curve directly from the sample data and without external information from standards. A crude calibration curve is obtained by plotting, on a semilogarithmic scale, the instantaneous weight average M_{wi} values for each data point at elution volume V_i . At this point, correction for BB is rarely

Band Broadening in Size-Exclusion Chromatography

used, as the accuracy of the calibration curve is generally poor and does not justify sophisticated corrections. Additionally, for complex polymers (blends, copolymers, branched polymers, etc.), a variety of molecular weights are eluted at the same position, even in the absence of band broadening [12], so it is still very difficult to propose a general solution for the problem and results are available only for simplified situations. Normally, it would be necessary to find the exact weight distribution w_i , as in the preceding paragraph, simply using the DRI signal; then, it becomes possible to adjust the calibration curve until the calculated M_{wi} values converge toward the experimental set of M_{wi} values.

Conclusion

Band broadening in SEC has several specific aspects, compared with other chromatographic processes. Solutes may have very low diffusion coefficients and that introduces additional tailing due the imperfect averaging of radial positions all along the tubing. Mass transfer can be described from Brownian motion properties, and for samples eluted near total exclusion volume, as the number of visited pores become small, this introduces a significant increase of skewing and a very important loss of resolution.

For correcting band broadening, the main difficulty is in obtaining precise mapping of the spreading function of the system. Normally, this needs very high quality standards and TGIC offers new possibilities in that area. Computational techniques are now sufficiently efficient to solve the general inversion problem associated with band-broadening correction, but it still needs some precautions to obtain stable results without artificial oscillations. Finally, as corrections become very important and unstable near total exclusion volume, it remains very imprudent to interpret data when part of the sample is totally excluded. It is better to first find a well-adapted column set, able to efficiently fractionate the whole sample.

References

1. J. C. Moore, *J. Polym. Sci. A-2* 835 (1964).
2. L. H. Tung, *J. Appl. Polym. Sci.* 10: 375 (1966).
3. W. Lee, H. C. Lee, T. Park, T. Chang, and J. Y. Chang, *Polymer* 40: 7227 (1999).
4. M. S. Jeansonne and J. P. Foley, *J. Chromatogr. Sci.* 29: 258 (1991).
5. J.-P. Busnel, F. Foucault, L. Denis, W. Lee, and T. Chang, *J. Chromatogr. A* 930: 61 (2001).



6. T. Farkas and G. Guiochon, *Anal. Chem* 69: 4592 (1997).
7. D. H. Kim and A. F. Johnson, in *Size Exclusion Chromatography*, T. Provder (ed.), ACS Symposium Series 245, American Chemical Society, Washington, DC, 1984.
8. M. Potschka, *J. Chromatogr* 648: 41 (1993).
9. I. Karatzas and S. Shreve, in *Brownian Motion and Stochastic Calculus*, Springer-Verlag, New York, 1991.
10. L. M. Gugliotta, J. R. Vega, and G. R. Meira, *J. Liq. Chromatogr.* 13: 1671 (1990).
11. A. E. Hamielec, in *Steric Exclusion Liquid Chromatography of Polymers*, J. Janca (ed.), Marcel Dekker, Inc., New York, 1984, pp. 117–160.
12. W. Radke, P. F. W. Simon, and A. H. E. Muller, *Macromolecules* 29: 4926 (1996).



Barbiturates, Analysis by Capillary Electrophoresis

Chenchen Li

Huwei Liu

Peking University, Beijing, P.R. China

INTRODUCTION

Capillary electrophoresis (CE) is becoming a popular analytical tool for determining drugs because of its simplicity, high speed, and high efficiency. The present review studies different modes of CE used in the determination and chiral separation of barbiturates, as well as current developments in sample preparation for barbiturates in biological fluids. The comparison of different modes of CE with other separation approaches is also discussed.

BARBITURATES

Barbiturates, derivatives of barbituric acid, are found in a variety of pharmaceuticals, such as sedatives, hypnotics, and antiepileptics. However, their levels in body fluids have to be regulated within a narrow therapeutic window to avoid toxicity. Therefore determination of barbiturates in serum, plasma, and urine is important for investigation of intoxication, therapeutic drug monitoring, and pharmacokinetic and metabolic studies. Hence, many instrumental approaches for the analysis of barbiturates in body fluids, including immunoassays^[1] and chromatographic methods, such as gas chromatography (GC),^[2] gas chromatography–mass spectrometry (GC-MS),^[3] and high-performance liquid chromatography (HPLC),^[4–6] have been developed. Immunological techniques offer high performance, speed of analysis, and sensitivity. However, they are not specific enough to distinguish a single compound because barbiturates interfere with each other. Chromatographic methods have been applied for the determination of all common barbiturates, even while they require time-consuming sample pretreatment and are characterized by a low sample throughput.^[7]

In recent years, CE has been successfully applied in the field of biochemical and analytical chemistry. It has been found to be attractive for pharmaceutical analysis because of its advantages related to excellent separation efficiency, high mass sensitivity, minimal use of samples and solvents, and the possibility of using different direct and indirect detection systems. This review focuses on analytical assays for barbiturates by CE.

SAMPLE PREPARATION FOR BARBITURATES IN BODY FLUIDS

Sample preparation is important here because matrices of biological fluids are so complicated that interfering signals are likely to appear in typical separation-based determinations. Among various sample preparation techniques, there are two major approaches combined with CE: liquid–liquid extraction (LLE) and solid-phase extraction (SPE) [or solid-phase microextraction (SPME)].

LLE

LLE with chloroform from acidified serum is widely executed^[7–11] after the method of Shiu and Nemoto.^[12] However, chloroform is of great toxicity and is not suitable for routine use. LLE with pentane at pH 6.4^[7] was investigated for feasibility with seven barbiturates and was found to be specific for thiopental—an important barbiturate being used for anaesthetic medication and treatment of head trauma with severe brain injury. Comparing acetonitrile deproteinization with chloroform deproteinization, Shihabi demonstrated the feasibility of acetonitrile for extraction of pentobarbital. However, electropherograms obtained by extraction with chloroform are more sensitive and cleaner.^[9] Wu et al.^[10] used LLE with ether for extraction from serum, and chloroform for extraction from urine. They obtained recoveries of six barbiturates from 86.6% to 118%.

SPE and SPME

Although LLE is useful, it is being replaced by SPE or SPME because LLE is a time-consuming and laborious process that involves consumption of large volumes of organic solvents. The use of SPE for subsequent analysis is achieved in one step, and the results have shown that this is a reproducible, safe, convenient, and time-saving alternative to LLE. Most SPE applications use disposable cartridges or columns packed with C₁₈-bonded silica, which is the most classic packing for this technique.^[7,10,11,13,15] Moreover, SPME is based on partition equilibrium of target compounds between the sample

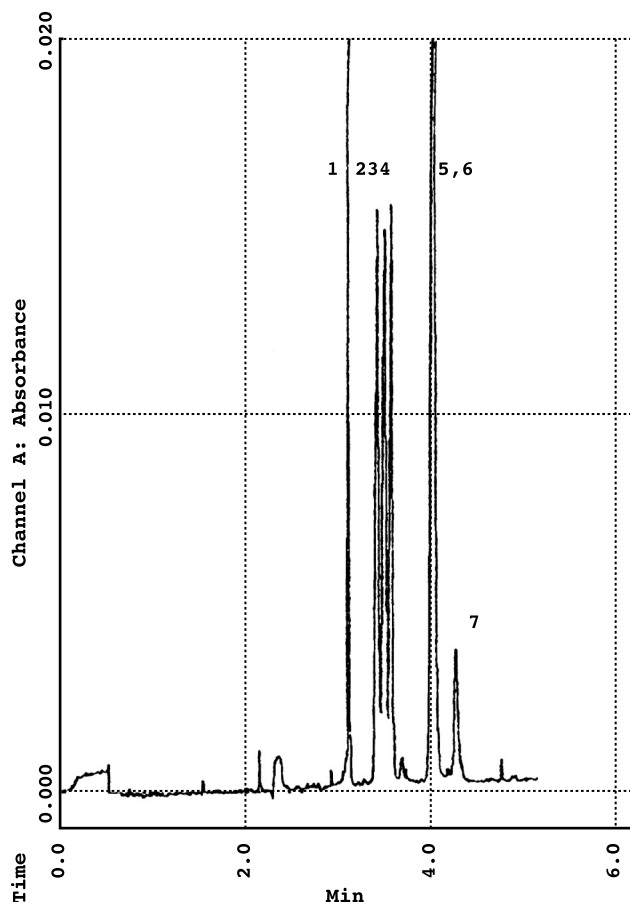


Fig. 1 Separation of different barbiturates using a 500-mmol/L borate buffer, pH 8.5. (1) Internal standard; (2) pentobarbital; (3) secobarbital; (4) amobarbital; (5) phenobarbital; (6) butabarbital; and (7) contamination.

matrices and a polymeric stationary phase, such as plasticized poly(vinyl chloride) (PVC),^[14] which is coated onto a fused silica fiber.

Among these techniques, the SMPE device is reported to be the easiest to construct and it performs very reliably.

Thus alkaline or neutral compounds are expected not to be extracted or backextracted, and will not interfere with analysis of barbiturates. Barbiturate concentrations of 0.1–0.3 ppm in urine and about 1 ppm in serum can be determined.^[14,16]

CE MODES OF OPERATION

Capillary zone electrophoresis (CZE) and micellar electrokinetic capillary chromatography (MEKC) are the most common CE modes used in determining barbiturates. We will discuss them separately.

Analysis by CZE

In CZE, the separation mechanism is based on differences in the charge/mass ratios of ionic analytes. An electric field is applied to the capillary filled with a running buffer, and cations go to the cathode, whereas anions migrate to the anode. But because of the electroosmotic flow (EOF) of the buffer, which is the driving force of CE, all analytes will move in the direction of EOF (usually toward the negative electrode as the inner surface of fused silica capillary is negatively charged). Although barbiturates are negatively charged at high pH, their migration velocities are close to each other and their separations by CZE are more or less insufficient. A separation of some common barbiturates using a 500 mmol/L borate buffer (pH 8.5) and an applied voltage of 11 kV is illustrated in Fig. 1.^[9] The phenobarbital peak was not resolved from butabarbital. Boone et al.^[17] improved separation performance by using a 90 mmol/L borate buffer (pH 8.5) and an applied voltage of 30 kV. It was found that an applied voltage of 30 kV resulted in faster separations and a better resolution compared to lower voltages. In addition, the Tapso–Tris buffer has a higher buffering capacity but lower conductivity. Baseline

Table 1 Running conditions of MEKC for determination of barbiturates

Analytes	Running buffer	Reference
Barbital, allobarbital, phenobarbital, butalbital, thiopental, amobarbital, and pentobarbital	50 mM SDS, 9 mM Na ₂ B ₄ O ₇ , 15 mM Na ₂ H ₂ PO ₄ (pH 7.8)	[7]
Barbital, phenobarbital, methyl phenobarbital, amobarbital, thiopental, pentobarbital, and secobarbital	100 mmol/L SDS:100 mmol/L Na ₂ H ₂ PO ₄ :MeOH:H ₂ O (70:15:5:10)	[10]
Seven barbiturates and 14 benzodiazepines	100 mM borate, 10 mM SDS, and 5 M urea (pH 8.5)	[11]
Heptabarbital, hexobarbital, pentobarbital, butalbital, and phenobarbital	30 mmol/L SDS, 30 mmol/L borate (pH 9.3), with 200 mL/L acetonitrile	[13]
Twenty-five barbiturates	50 mM SDS, 20 mM phosphate (pH 8.4)	[17]

Table 2 Comparison of CZE and MEKC for determining barbiturates

	CZE	MEKC
Total analysis time	No more than 10 min	About 15 min
Separation efficiencies	High	High
Analytical window	Relatively small window because of the resemblance of the chemical structures and the pK values of the barbiturates ^[17]	Provides a significantly increased analytical window
Resolution	Some barbiturates interfere with each other	Improved
Pretreatment process	Complex and time-consuming (unsatisfied resolution with LLE)	Both LLE and SPE produce good results

separation of 10 barbiturates and eight benzoates was achieved in a 50-mM Tapso-Tris buffer system.^[14] Recently, Delinsky et al.^[15] completely resolved barbiturates from meconium in a 150-mM Tris running buffer after sample preparation by SPE.

Analysis by MEKC

MEKC is another CE method based on the differences between interactions of analytes with micelles present in the separation buffer, which can easily separate both

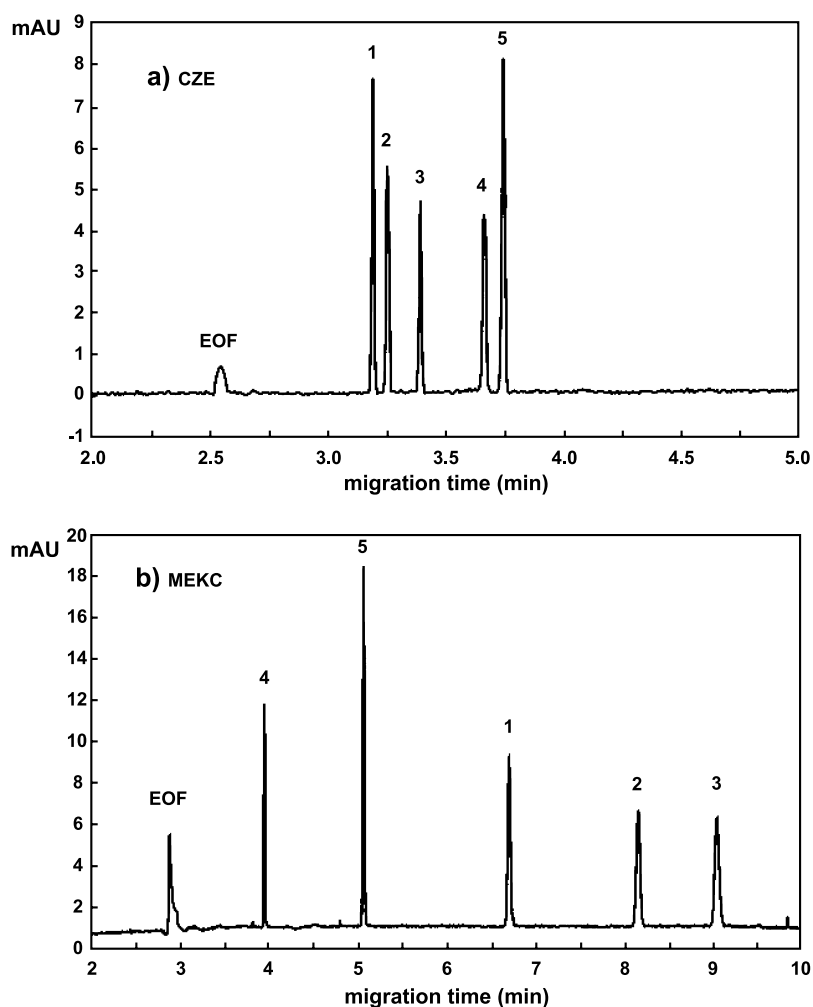


Fig. 2 Electropherograms of the separation of five barbiturate standards using CZE (a) and MEKC (b). Peaks: (1) hexobarbital; (2) methohexital; (3) secobarbital; (4) barbital; and (5) phenobarbital.

charged solutes and neutral solutes with either hydrophobic or hydrophilic properties. Micelles are formed by adding a surfactant [at a concentration above its critical micelle concentration (CMC)] to the separation buffer, and act as the so-called pseudo-stationary phase. The most striking observation is the resolution of MEKC, which is more likely to separate complex mixtures than CZE. Because of their similar migration velocities, barbiturates are most commonly investigated in the MEKC mode.^[7,8,10–13,16–19]

There are various buffers and modifiers that can be selected and combined in MEKC to optimize separation; some typical examples are summarized in Table 1.

COMPARISON OF CZE AND MEKC

A comparison of the CZE and MEKC modes for determining barbiturates is summarized in Table 2.

Figure 2^[17] shows electropherograms of a mixture of five barbiturate standards; it can be observed that the addition of micelles in MEKC clearly resulted in a different separation mechanism, reflected in various changes in elution order, compared to CZE. The migration behavior in MEKC depends largely on the hydrophobic interaction of the analytes with the micelles. Hydrophobic components are more solubilized in the micelles, resulting in a slower migration compared to less hydrophobic compounds.

OPTIMIZATION OF SEPARATION

Various types of coated capillaries have been applied to the CE separation of barbiturates for improvement of separation selectivity and efficiency.^[11,20,21] Jinno et al. reported a series of investigations on PAA and AA-co-IPAAM-coated columns in both CZE and MEKC modes.

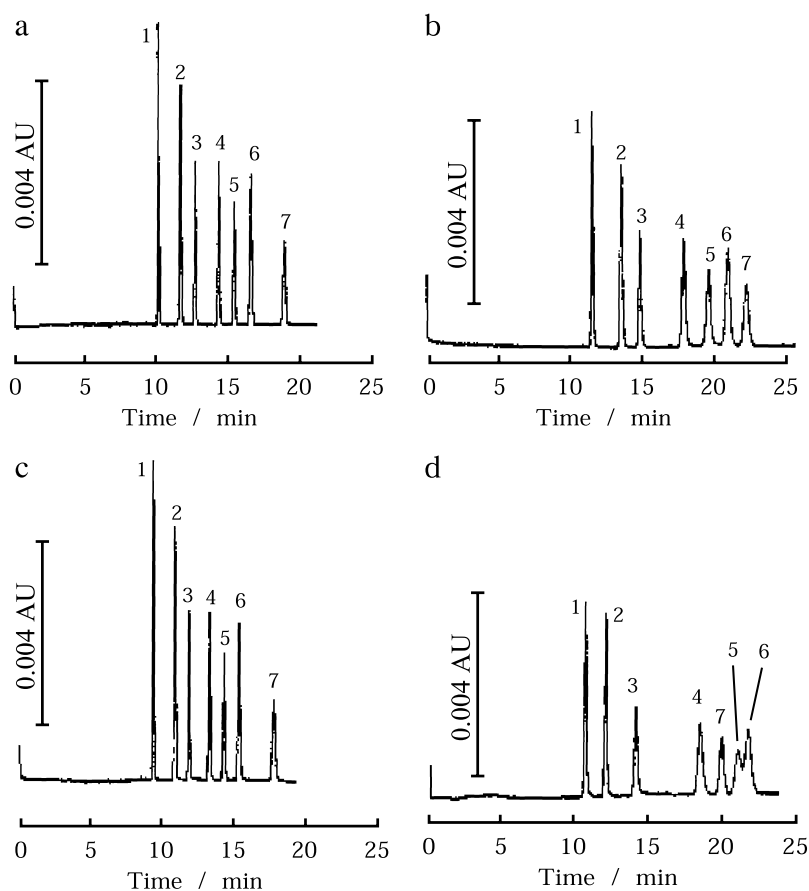


Fig. 3 Separation of barbital by the use of a capillary coated with (a and c) 10% T PAA and (b and d) 10% T poly(AA-co-IPAAM) containing 85% IPAAM. Experiments were carried out at (a and b) ambient temperature or (c and d) elevated temperature. Conditions: capillary column, 50 cm \times 0.075 mm ID (25 cm effective length); buffer, 100 mM Tris–150 mM boric acid (pH 8.3); field strength, 300 V/cm; injection, electromigration for 5 sec at the side of cathode. Peak identification: (1) phenobarbital; (2) barbital; (3) mephobarbital; (4) amobarbital; (5) secobarbital; (6) pentobarbital; (7) metharbital.



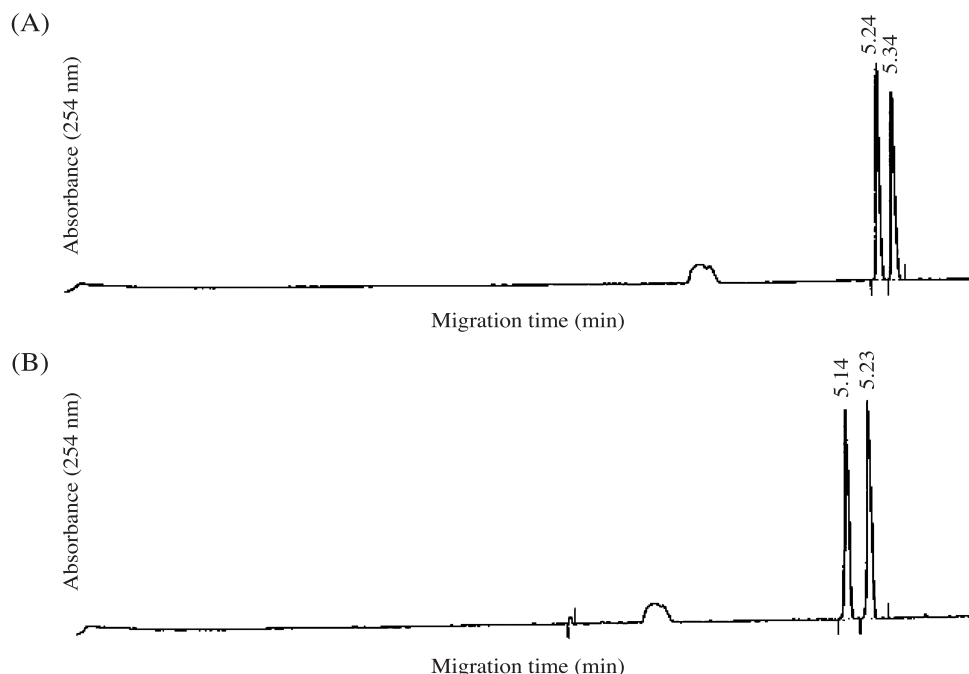


Fig. 4 Typical electropherograms of enantiomers of (A) pentobarbital and (B) secobarbital on a 57 cm \times 75 μ m ID fused silica capillary. The run buffer contained 40 mM HPBCD in 20 mM ammonium acetate buffer (pH 9.0) with detection at 254 nm. The capillary was thermostated at 25°C and the run voltage was set to 15 kV.

By the use of polyacrylamide (PAA) coating for the capillary, EOF was sufficiently eliminated, leading to a shorter analysis time and better resolution.^[11,20] In addition, the elution order of barbiturates partly changed because of the hydrophobic nature of PAA. It must be noted that a noncross-linked copolymer containing IPAAM had thermosensitive properties, and elution order was different at elevated temperatures when compared with that at ambient temperature,^[21] as illustrated in Fig. 3.

In CE, the use of a reproducible identification parameter is very important because it influences identifi-

cation power (IP). Boone et al.^[17] used μ_{eff} and μ_{eff}^c instead of migration times to enhance reproducibility, to reduce the upward trend of RSD with increasing migration time, and to correct for outliers.

CHIRAL SEPARATION OF BARBITURATES

Chiral separation is one of the major outstanding advantages for CE compared to other separation techniques. As enantiomers have identical electrophoretic

Table 3 Comparative study of three techniques to determine barbiturates

Techniques	Advantages	Disadvantages
GC	High sensitivity and selectivity Coupled with mass spectrometry for the identification of unknowns	Inadequate for polar, thermolabile, and low-volatility analytes
LC	Application to all organic solutes in spite of volatility or thermal stability Both mobile and stationary phase compositions are variables	High consumption of expensive, high-purity gases Insufficient separation selectivity and efficiency Related long analysis time Large amounts of expensive and toxic organic solvents used as mobile phase, such as acetonitrile ^[5] and methanol. ^[6]
CE	High separation efficiency Small consumption of expensive reagents and toxic solvents	Inadequate detection limit Lack of highly selective detectors

Copyright © Marcel Dekker, Inc. All rights reserved.



mobilities, some chiral complexing reagents, called chiral selectors, must be added to the separation buffer to form diastomeric complexes in dynamic equilibrium. One of the most versatile techniques for achieving chiral recognition is the addition of cyclodextrins (CDs). It is reported that determination of (*R*)-secobabital and (*S*)-secobabital from serum was achieved by addition of hydroxypropyl- γ -cyclodextrin (HPGCD)^[16] or hydroxypropyl- β -cyclodextrin (HPBCD)^[18] in the running buffer. Figure 4 illustrates a typical electropherogram of pentobarbital and secobabital enantiomers, separated by HPBCD. Conradl and Vogt et al.^[22] investigated the separation of (*R*)-thiopental and (*S*)-thiopental, and (*R*)-phenobarbital and (*S*)-phenobarbital by using α -CD and β -CD as chiral selectors, separately. They found out that the enantiomers of thiopental were not separated by β -CD, whereas cyclobarbitol enantiomers were separated by both α -CD and β -CD. It is assumed that the size of the cavity of β -CD allows the side chain of thiopental, with the asymmetric carbon atom, to penetrate completely. Therefore the formation of stereoselective complexes is unlikely. In the case of α -CD, the C₅ substituents of thiopental are optimal in size and structure to fit into the cavity whereas; for cyclobarbitol, a partial inclusion of the cyclohexene ring or the methyl group at the C₅ of the heterocycle into the cavity is probable. However, the separation of cyclobarbitol with low α -CD concentration was less efficient.

COMPARISON OF CE, GC, AND LC

LC, GC, and CE are three typical analytical separation approaches used to determine barbiturates. The advantages and disadvantages of the three techniques are summarized in Table 3.

CONCLUSION

CE offers fast analysis, low consumable expenses, ease of operation, high separation efficiency, and selectivity. Now, CE has undoubtedly become an attractive technique for the determination and therapeutic monitoring of barbiturates and other drugs, and it is becoming more and more important in biological and toxicological analyses. It was also indicated that CE has a good potential for systematic toxicological analysis (STA).^[17]

At present, the coupling of CE to MS is attractive because it facilitates the identification of analytes and improves detection sensitivity. Combining CE with fluorescence detection greatly improves the sensitivity and selectivity for determining proteins and other biological molecules. Future trends of CE will be used to develop

more coupling methods to combine CE with highly selective detectors and to achieve miniaturization and automation for extremely fast, easy, and real-time determination in pharmaceutical and biological analyses.

REFERENCES

- Colbert, D.L.; Smith, D.S.; Landon, J.; Sidki, A.M. Single-reagent polarization fluoroimmunoassay for barbiturates in urine. *Clin. Chem.* **1984**, *30*, 1765.
- Berry, D.J. Gas chromatography analysis of the commonly prescribed barbiturates at therapeutic and overdose levels in plasma and urine. *J. Chromatogr.* **1973**, *86*, 89.
- Soo, V.A.; Bergert, R.J.; Deutsch, D.G. Screening and quantification of hypnotic sedatives in serum by capillary gas chromatography with a nitrogen-phosphorus detector, and confirmation by capillary gas chromatography-mass spectrometry. *Clin. Chem.* **1986**, *32*, 325.
- Elisabeth, I.; Rene, S.; Dieter, J. Screening for drugs in clinical toxicology by high-performance liquid chromatography: Identification of barbiturates by post-column ionization and detection by a multiplex photodiode array spectrophotometer. *J. Chromatogr.* **1988**, *428*, 369.
- Feng, C.L.; Liu, Y.T.; Luo, Y. HPLC-DAD analysis of thirteen soporific sedative drugs in human blood. *Acta Pharm. Sin.* **1995**, *30* (12), 914-919.
- Coppa, G.; Testa, R.; Gambini, A.M.; Testa, I.; Tocchini, M.; Bonfigli, A.R. Fast, simple and cost-effective determination of thiopental in human plasma by a new HPLC technique. *Clin. Chim. Acta* **2001**, *305*, 41-45.
- Thormann, W.; Meier, P.; Marcolli, C.; Binder, F. Analysis of barbiturates in human serum and urine by high-performance capillary electrophoresis-micellar electrokinetic capillary chromatography with on-column multi-wavelength detection. *J. Chromatogr.* **1991**, *545*, 445-460.
- Meier, P.; Thormann, W. Determination of thiopental in human serum and plasma by high-performance capillary electrophoresis-micellar electrokinetic chromatography. *J. Chromatogr.* **1991**, *559*, 505-513.
- Shihabi, Z.K. Serum pentobarbitol assay by capillary electrophoresis. *J. Liq. Chromatogr.* **1993**, *16* (9/10), 2059-2068.
- Wu, H.; Guan, F.; Luo, Y. Determination of barbiturates in human plasma and urine by high performance capillary electrophoresis. *Yaowu Fenxi Zazhi* **1996**, *16* (5), 316-321.
- Jinno, K.; Han, Y.; Sawada, H.; Taniguchi, M. Capillary electrophoretic separation of toxic drugs using a polyacrylamide-coated capillary. *Chromatographia* **1997**, *46* (5/6), 309.
- Shiu, G.K.; Nemoto, E.M. Simple, rapid and sensitive reversed-phase high-performance liquid chromatographic method for thiopental and pentobarbital determination in plasma and brain tissue. *J. Chromatogr.* **1982**, *227*, 207.
- Evenson, M.A.; Wilktorowicz, J.E. Automated capillary electrophoresis applied to therapeutic drug monitoring. *Clin. Chem.* **1992**, *38* (9), 1847-1852.



14. Li, S.; Weber, S.G. Determination of barbiturates by solid-phase microextraction and capillary electrophoresis. *Anal. Chem.* **1997**, *69*, 1217–1222.
15. Delinsky, D.C.; Srinivasan, K.; Solomon, H.M.; Bartlett, M.G. Simultaneous capillary electrophoresis determination of barbiturates from meconium. *J. Liq. Chromatogr. Relat. Technol.* **2002**, *25* (1), 113–123.
16. Srinivasan, K.; Zhang, W.; Bartlett, M.G. Rapid simultaneous capillary electrophoretic determination of (R)- and (S)-secobarbital from serum and prediction of hydroxypropyl- γ -cyclodextrin—secobarbital stereoselective interaction using molecular mechanics simulation. *J. Chromatogr. Sci.* **1998**, *36*, 85–90.
17. Boone, C.M.; Franke, J.-P.; de Zeeuw, R.A.; Ensing, K. Evaluation of capillary electrophoretic techniques towards systematic toxicological analysis. *J. Chromatogr., A* **1999**, *838*, 259–272.
18. Srinivasan, K.; Bartlett, M.G. Comparison of cyclodextrin-barbiturate noncovalent complexes using electrospray ionization mass spectrometry and capillary electrophoresis. *Rapid Commun. Mass Spectrom.* **2000**, *14*, 624–632.
19. Wu, H.; Guan, F.; Luo, Y. A universal strategy for systematic optimization of high performance capillary electrophoretic separation. *Chin. J. Anal. Chem.* **1996**, *24* (10), 1117–1122.
20. Jinno, K.; Han, Y.; Hirokazu, S. Analysis of toxic drugs by capillary electrophoresis using polyacrylamide-coated columns. *Electrophoresis* **1997**, *18* (2), 284–286.
21. Sawada, H.; Jinno, K. Capillary electrophoretic separation of structurally similar solutes in noncross-linked poly(acrylamide-*co*-*N*-isopropylacrylamide) solution. *Electrophoresis* **1997**, *18* (11), 2030–2035.
22. Conradl, S.; Vogt, C. Separation of enantiomeric barbiturates by capillary electrophoresis using a cyclodextrin-containing run buffer. *J. Chem. Educ.* **1997**, *74* (9), 1122–1125.



Binding Constants: Determination by Affinity Chromatography

David S. Hage
Sanjay Mukherjee

University of Nebraska, Lincoln, Nebraska, U.S.A.

Introduction

Numerous interactions within cells and the body are characterized by the specific binding that occurs between two or more molecules. Examples include the binding of hormones with hormone receptors, drugs with target enzymes or receptors, antibodies with antigens, and small solutes with transport proteins. The study of these interactions is important in determining the role they play in biological systems. Because of this, there have been numerous methods developed to characterize such reactions. One of these approaches is that of affinity chromatography.

Affinity chromatography is a liquid-chromatographic technique that makes use of an immobilized ligand, usually of biological origin, for the separation and analysis of analytes within a sample. However, it is also possible to use affinity chromatography as a tool for studying the interactions that take place between the ligand and injected solutes. This application is known as *quantitative* or *analytical affinity chromatography*. Some attractive features of this approach include its relative simplicity, good precision and accuracy, and ability to use the same ligand for multiple studies. There are various techniques that are employed for such studies. These include methods for measuring both equilibrium constants and rate constants for biological processes, thus giving data on the thermodynamics and kinetics of these reactions.

Zonal Elution

The method of *zonal elution* is one of the most common techniques used in affinity chromatography to examine biological interactions. An example of this type of experiment is shown in Fig. 1a. In its usual form, zonal elution involves the application of a small amount of analyte (in the absence or presence of a competing agent) to a column that contains an immobilized ligand. The retention of the analyte in this case will depend on how strongly the

analyte and competing agent bind to the ligand and on the amount of ligand that is in the column. This makes it possible to measure the equilibrium constants for these binding processes by examining the change in analyte retention as the competing agent's concentration is varied. Zonal elution has been used to examine numerous biological systems, including the binding of drugs with transport proteins, lectins with sugars, enzymes with inhibitors, and hormones with hormone-binding proteins.

Equation (1) represents one specific type of zonal elution study, in which the injected analyte and competing agent bind at a single common site on the immobilized ligand:

$$k = \frac{\{K_{a,A}m_L\}}{\{V_M(1 + K_{a,I}[I])\}} \quad (1)$$

Similar equations can be derived for other systems, such as those involving multiple types of binding sites or the presence of both soluble and immobilized forms of the ligand. In Eq. (1), $K_{a,A}$ and $K_{a,I}$ are the association equilibrium constants for the binding of the ligand to the analyte (A) and competing agent (I) at their site of competition. The term $[I]$ is the concentration of I that is being applied to the column, m_L is the moles of common ligand sites for A and I, and V_M is the void volume of column. The term k is the retention factor (or capacity factor) that is measured for A, as given by the relationship $k = (t_R/t_M) - 1$, where t_R is the retention time for A and t_M is the column void time. In this case, the values of the association constants $K_{a,A}$ and/or $K_{a,I}$ can be obtained by examining how the retention factor for A changes with $[I]$. If these studies are performed at several temperatures, thermodynamic values can also be obtained for the changes in enthalpy and entropy that occur during these binding processes.

Frontal Analysis

An alternative approach for equilibrium constant measurements is to use the method of *frontal analysis*. In this



technique, a solution containing a known concentration of the analyte is continuously applied to an affinity column at a fixed flow rate (see Fig. 1b). As the solute/analyte binds to the immobilized ligand, the ligand becomes saturated with the analyte and the amount of analyte eluting from the column gradually increases. This forms a characteristic breakthrough curve. The

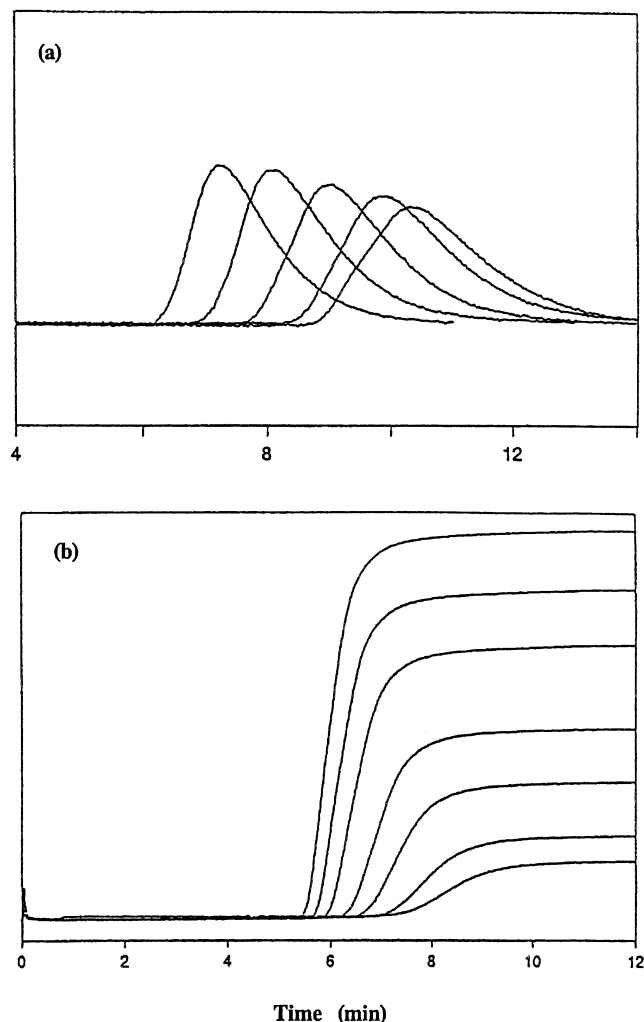


Fig. 1 (a) Zonal elution studies for the injection of *R*-warfarin onto an immobilized human serum albumin column in the presence (left to right) of $1.90\text{--}0 \cdot 10^{-6}$ M L-reverse triiodothyronine as a competing agent. (b) Frontal analysis studies for the binding of *R*-warfarin to immobilized human serum albumin at applied analyte concentrations (left to right) of $1.50\text{--}0.22 \cdot 10^{-6}$ M. [Reproduced with permission from Elsevier from B. Loun and D. S. Hage, *J. Chromatogr. B* 665: 303 (1995) and the American Chemical Society from B. Loun and D. S. Hage, *Anal. Chem.* 66: 3814 (1994).]

volume of the analyte solution required to reach the mean position of this curve is measured. If the association and the dissociation kinetics are fast, the mean position of the breakthrough curve will be related to the concentration of the applied solute, the amount of ligand in the column, and the association equilibrium constants for solute–ligand binding. Frontal analysis experiments have been used to examine such systems as drug–protein binding, antibody–antigen interactions, and enzyme–inhibitor interactions.

A simple example of a frontal analysis system is one where an applied analyte binds to a single type of immobilized ligand site. In this situation, the following equation can be used to relate the true number of active binding sites in the column (m_L) to the apparent moles of analyte ($m_{L,\text{app}}$) required to reach the mean position of the breakthrough curve:

$$\frac{1}{m_{L,\text{app}}} = \frac{1}{K_{a,A}m_L[A]} + \frac{1}{m_L} \quad (2)$$

As defined earlier, $K_{a,A}$ is the association constant for the binding of A to L, and [A] is the molar concentration of analyte applied to the column. Equation (2) predicts that a plot of $1/m_{L,\text{app}}$ versus $1/[A]$ for a system with single-site binding will give a straight line with a slope of $1/(K_{a,A}m_L)$ and an intercept of $1/m_L$. The value of $K_{a,A}$ can be determined by calculating the ratio of the intercept to the slope, and $1/m_L$ is obtained from the inverse of the intercept. Similar relationships can be derived for cases in which there is more than one type of binding site or in which both a competing agent and solute are applied simultaneously to the column.

One disadvantage of frontal analysis is that it requires a relatively large amount of analyte for study. However, frontal analysis does provide information on both the association constant for a solute and its total number of binding sites in a column. This feature makes frontal analysis the method of choice for high accuracy in equilibrium measurements, because the resulting association constants are essentially independent of the number of binding sites in the column.

Band-Broadening Measurements

Another group of methods in analytical affinity chromatography are those that examine the kinetics of biological interactions. *Band-broadening measurements* (also known as the *isocratic method*) represent one such approach. This is really a modification of the zonal elution method in which the widths of the eluting peaks are measured along with their retention times.

Systems that have been studied with this method include the binding of lectins with sugars, the interactions of drugs and amino acids with serum albumin, and the kinetics of protein-based chiral stationary phases.

This type of experiment involves injecting a small amount of an analyte onto an affinity column while carefully monitoring the retention time and width of the eluting peak. These injections are performed at several flow rates on both the affinity column and on a column of the same size which contains an identical support but with no immobilized ligand being present. This control column is needed to help correct for any band broadening that occurs due to processes other than the binding and dissociation of the analyte from the immobilized ligand. By comparing plots of the peak widths (or plate heights) for the affinity and control columns, it is possible to determine the value of the dissociation rate constant for the analyte–ligand interaction.

Split-Peak Effect

Another way in which kinetic information can be obtained by affinity chromatography is to use the *split-peak effect*. This effect occurs when the injection of a single solute gives rise to two peaks: the first representing a nonretained fraction and the second representing the retained solute. This effect can be observed even when only a small amount of analyte is injected and is the result of slow adsorption kinetics and/or the slow mass transfer of the analyte within the column. Such an effect can occur in any type of chromatography, but it is most common in affinity columns because of their smaller size, their lower amount of binding sites, and the slower association rates of affinity ligands compared to other types of stationary phases.

One way in split-peak measurements can be performed is by injecting a small amount of analyte onto an affinity column at various flow rates. A plot of the inverse negative log of the measured free fraction is then made versus the flow rate. The slope of this graph is related to the adsorption kinetics and mass-transfer rates within the column. If the system is known to have adsorption-limited retention or if the mass-transfer rates are known, then the association rate constant for ana-

lyte binding can be determined. This approach has the advantages of being fast to perform and potentially has greater accuracy and precision than band-broadening measurements. Its disadvantages are that it requires fairly specialized operating conditions that may not be suitable for all analytes. Examples of biological systems that have been examined by the split-peak method include the binding of protein A and protein G to immunoglobulins, and the binding of antibodies with both high- and low-molecular-weight antigens.

Peak-Decay Method

The peak-decay method is a third approach that can be used in affinity chromatography to examine the kinetics of an analyte–ligand interaction. This technique is performed by first equilibrating and saturating a small affinity column with a solution that contains the analyte of interest or an easily detected analog of this analyte. The column is then quickly switched to a mobile phase in which the analyte is not present. The release of the bound analyte is then monitored over time, resulting in a decay curve. This decay is related to the dissociation rate of the analyte and the mass-transfer kinetics within the column. If the mass-transfer rate is known or is fast compared to analyte dissociation, then the decay curve can be used to provide the dissociation rate constant for the analyte from the immobilized ligand. Systems which have been studied with this approach include the dissociation of drugs from transport proteins and the dissociation of sugars from immobilized lectins.

Suggested Further Reading

- Chaiken, I. M. (ed.), *Analytical Affinity Chromatography*, CRC Press, Boca Raton, FL, 1987.
Dunn, B. M. and I. M. Chaiken, *Proc. Natl. Acad. Sci. USA* 71: 2372 (1974).
Hage, D. S. and S. A. Tweed, *J. Chromatogr. B* 699: 499 (1997).
Hage, D. S., R. R. Walters, and H. W. Hethcote, *Anal. Chem.* 58: 274 (1986).
Kasai, K.-I. and S.-I. Ishii, *J. Biochem.* 78: 653 (1975).
Loun, B. and D. S. Hage, *Anal. Chem.* 68: 1218 (1996).
Wainer, I. W., *J. Chromatogr. A* 666: 221 (1994).



Binding Molecules Via —SH Groups

Terry M. Phillips

Ultramicro Analytical Immunochemistry Resource, DBEPS, ORS, OD, NIH, Rockville, Maryland, U.S.A.

Introduction

A prerequisite for producing a good affinity support is a firm, stable attachment of the ligand to the surface of the support. There are numerous linkage chemistries available for performing this task, and although the most popular approach is a reaction between the reactive side groups on the support with a primary amine on the ligand, there are a number of supports that can perform similar attachments through free thiol or sulfhydryl groups.

Discussion

Supports containing maleimide reactive side groups are specific for free sulfhydryl groups present in the ligand when the reaction is performed at pH 6.5–7.0. At pH 7.0, the interaction of maleimides with sulfhydryl groups is approximately 1000-fold faster than with amine groups. The stable thioether linkage formed between the maleimide support and the sulfhydryl group on the ligand cannot be easily cleaved under physiological conditions, therefore ensuring a stable affinity matrix. Immobilization of sulfhydryl-containing molecules can also be achieved using either α -haloacetyl or pyridyl sulfide cross-linking agents. The α -haloacetyl cross-linkers [i.e., *N*-succinimidyl(4-iodoacetyl) aminobenzoate)] contain a iodoacetyl group that is able to react with sulfhydryl groups present in the ligand at physiological pH. During this reaction, the nucleophilic substitution of iodine with a thiol takes place, producing a stable thioether linkage. However, a shortcoming of this approach is that the α -haloacetyls interact with other amino acids, especially when a shortage or absence of free sulfhydryl groups exists. Linkage of pyridyl disulfides with aliphatic thiols at pH 4.0–5.0 produces a disulfide bond with the release of pyridine-2-thione as a by-product of the reaction. A disadvantage of this approach is the acidic pH of the reaction, which is essential for optimal linkage. The reaction can be performed at physiological pH, but under these conditions, the reaction is extremely slow.

Ligand immobilization through sulfhydryl groups can be advantageous due to its ability to be site directed. Additionally, depending on the linkage, the ligand and support can be cleavable, allowing the same support to be reused. However, many useful affinity ligands do not possess free sulfhydryl groups, and in such cases, free sulfhydryl groups can be engineered into the ligand via a series of commercially available reagents. Traut's reagent (2-iminothiolane) is the most common, although *N*-succinimidyl *S*-acetylthioacetate (SATA) and *N*-succinimidyl-3-(2-pyridyldithio)propionate (SPDP) can also be used (Fig. 1). Traut's reagent reacts with primary amines present in the ligand and introducing exposed sulfhydryl groups for further coupling reactions.

Chrissey et al. [1] described an interesting use of sulfhydryl-mediated immobilization for immobilizing thiol-modified DNA. A hetero-bifunctional cross-

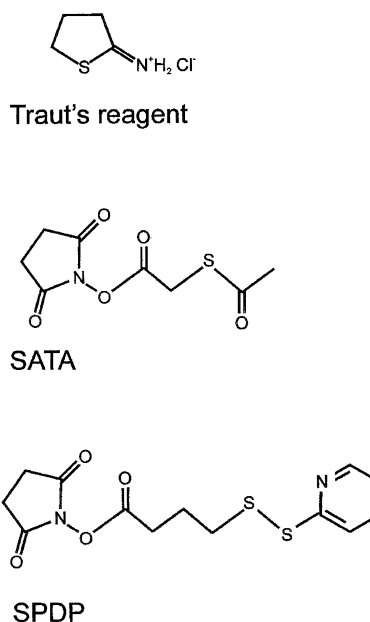


Fig. 1 Chemical structures of commercially available reagents for introducing sulfhydryl groups into molecules.



linker bearing both thiol and amino reactive groups was used to immobilize thiol-modified DNA oligomers to self-assembled monolayer silane films on fused-silica and oxidized silicon substrates. The advantage of this approach was to use site-directed immobilization to ensure the correct orientation of the DNA molecule.

Cleaving disulfide bonds already present in the ligand can also generate free sulfhydryl groups. The classic example of this approach is the digestion of the IgG antibody molecule to produce two monovalent, reactive FAb fragments, each containing a free sulfhydryl group. In this case, reduction of the disulfide bridge (holding the two FAb arms together) is achieved using Cleland's reagent (DTT: dithiothreitol). The FAb is then attached to free thiol groups present on the support by reforming a disulfide bond [2]. The advantage of this approach is that not only is a covalent linkage formed but also the linkage helps to orient the antigen receptor of the FAb away from the support matrix.

References

1. L. A. Chrisey, G. U. Lee, and C. E. O'Ferrall, *Nucleic Acids Res.* 24: 3031 (1996).
2. T. M. Phillips, *Anal. Chim. Acta* 372: 209 (1998).

Suggested Further Reading

- Hermanson, G. T., A. K. Mallia, and P. K. Smith, *Immobilized Affinity Ligand Techniques*, Academic Press, New York, 1992.
- Lundblad, R. L., *Techniques in Protein Modification*, CRC Press, Boca Raton, FL, 1995.
- Wong, S. S., *Chemistry of Protein Conjugation and Cross-linking*, CRC Press, Boca Raton, FL, 1991.



Biopharmaceuticals by Capillary Electrophoresis

Michel Girard

Bureau of Biologics and Radiopharmaceuticals, Health Canada, F.G. Banting Research Centre, Ottawa, Ontario, Canada

Introduction

In the relatively short period of time since the introduction of the first commercial instruments in the late 1980s, capillary electrophoresis (CE) has established itself as one of the most versatile analytical techniques. In addition to providing exceptional separation efficiencies, it offers substantial advantages over conventional slab-gel electrophoretic techniques, namely fast separation times, automation, reproducibility, and quantitative capabilities. Furthermore, owing to the different mechanisms by which products are separated in CE, data generated are generally complementary to those obtained by high-performance liquid chromatography (HPLC), thus allowing for more complete product characterization. CE methods have also been successfully validated with respect to well-established analytical criteria (e.g., precision, accuracy, reproducibility, and linearity), making them a source of reliable information. These considerations are of key importance to the pharmaceutical industry in adopting CE as a front-line analytical technique for product characterization to meet the specific requirements associated with the manufacturing and testing of biopharmaceuticals [1].

Historical Perspective in the Development of Biopharmaceuticals

Therapeutic products consisting of biopolymers (e.g., proteins) are generally referred to as biopharmaceuticals. Although, to date, most products on the market are proteins and polypeptides, new therapeutics based on antisense oligonucleotides or DNA fragments are being developed. Traditionally, biopharmaceuticals were obtained from biological sources (e.g., human, animal, plant, or cellular origin) in the form of crude extracts or partially purified components of extracts. Because of the highly complex nature of these mixtures, only minimal physicochemical characterization could be carried out and product evaluation was generally based on a biological response or surrogate bioassays. Although a few traditional products remain

in use today, newer production methods based on recombinant DNA or hybridoma technology are now being used for the large-scale production of biopharmaceuticals. These developments have been paralleled by major advances in biomolecular separation techniques and, consequently, have resulted in improvements in product development leading to the preparation of more consistent products with purity levels approaching those of conventional, small-molecule pharmaceuticals. A number of important therapeutic proteins such as human growth hormone (hGH), insulin, interferons (IFN- α , β , and γ), tissue plasminogen activator (tPA), erythropoietin (EPO), and hepatitis B vaccine have been produced in this manner and their approval for human use has been based on a comprehensive chemistry and manufacturing submission with a strong emphasis on high-resolution analytical methodologies including CE.

Application of Capillary Electrophoresis to Biopharmaceuticals

Capillary electrophoresis has widespread applications in the field of biopharmaceuticals, particularly for product characterization. It is a technique particularly well suited for assessing product heterogeneity arising from posttranslational modifications, degradation, or genetic variation. There are several CE modes, based on different separation mechanisms, which, alone or in combination, can be used (Table 1). The choice of the most appropriate CE separation mode, or combination thereof, will depend on the nature of the product under study and the type of information required. In the following sections, a brief overview of the use of CE for the characterization of biopharmaceuticals with respect to product identity and purity will be presented.

Product Identity

One of the critical aspects to be considered during the manufacturing of any drug is product identity. Although, in itself, it does not fulfill all of the requirements for a safe and effective drug, product identity



testing provides assurance that the product generated is that which is intended and offers a measure of the consistency of the manufacturing process. CE-based methods have been widely applied to confirm product identity of biopharmaceuticals. Approaches usually involve the comparison of the property of the substrate to that of a preestablished, well-characterized reference standard with demonstrated efficacy and safety. Aside from performing a simple identity test involving comigration of the substrate with the reference standard, a number of methods have been devised to provide qualitative and quantitative information with respect to specific structural features of the molecule (e.g., primary sequence, molecular weight/size, and carbohydrate profile).

Peptide mapping is one of the most powerful tools for the identification of proteins and it has been successfully adapted to CE [2]. It involves the cleavage of the amino acid chain at specific sites, using proteases or chemicals, to generate a mixture of smaller peptides. The analysis of the resulting peptide digest is generally carried out by capillary zone electrophoresis (CZE), where products are separated based on differences in charge-to-mass ratios. Methods using capillary isoelectric focusing (CIEF) or micellar electrokinetic chromatography (MEKC) have also been reported. The peptide map serves as a fingerprint of the substrate which, when compared to a reference standard, enables the confirmation of the identity and allows the detection and identification of amino acid and peptide modifications. In addition, it may be used to confirm the presence and position of disulfide bridges and glycosylation sites. When linked to mass spectrometry (MS), peptide mapping by CZE can also be used as an effective replacement for pro-

tein sequencing. Besides its application to simple proteins, peptide mapping by CZE has been particularly useful for the characterization of monoclonal antibodies (MAbs) [3]. Peptide mapping by CZE is usually faster than by high-performance liquid chromatography (HPLC) and typically provides greater resolution of a larger number of peptides.

Several important therapeutic proteins are glycoproteins (e.g., EPO and tPA) which exist as mixtures of closely related species that differ in their glycosylation patterns (glycoforms). These differences are often the result of both compositional and sequence variations. Moreover the biological activity of glycoproteins is frequently linked to the presence of these carbohydrates and, consequently, the characterization of glycoprotein microheterogeneity represents one of the more challenging tasks in identity testing. Several CE approaches, based mostly on CZE and CIEF, have been devised [4]. For the frequently encountered sialoglycoproteins (i.e., sialic acid-containing glycoproteins), the analysis of the glycoform profile can be performed on intact glycoproteins. Alternatively, an analysis of the oligosaccharide profile may be performed following chemical or enzymatic release from the polypeptide. In both cases, the profile obtained is an indication of the varying number of sialic acid residues on the oligosaccharide chains. Methods have also been developed for the analysis of the monosaccharide composition resulting from hydrolysis. In such a case, the monosaccharides must be derivatized with reagents such as 1-aminopyrene-3,6,8-trisulfonate, which provides both a readily ionizable group and a detectable chromophore. Finally, CE is a valuable tool for the confirmation of the structural integrity of glycoproteins in final drug formulations [5].

Table 1 Common Capillary Electrophoresis Separation Modes for the Characterization of Biopharmaceuticals

Mode	Separation mechanism	Application
Capillary zone electrophoresis (CZE),	Charge-to-size ratio	Proteins and peptides, peptide mapping, glycoproteins, monoclonal antibodies, carbohydrates and oligosaccharides
Capillary isoelectric focusing (CIEF),	Isoelectric point (pI)	Proteins and peptides, glycoproteins, monoclonal antibodies, isoelectric point determination, peptide mapping
Capillary gel electrophoresis (CGE),	Size determination	Protein molecular weight determination, aggregates, oligonucleotides, DNA fragments, polysaccharides
Micellar electrokinetic chromatography (MEKC),	Partition based on hydrophobicity	Peptide mapping, carbohydrates

Other useful identity tests that may be adequately performed by CE include protein molecular-weight (or DNA size) determination using capillary gel electrophoresis (CGE) [6] and isoelectric point (pI) determination using CIEF [7]. Typically, a protein molecular-weight determination is performed under denaturing conditions where sodium dodecyl sulfate (SDS)–protein complexes are formed with net negative charges that are proportional to their masses. These complexes migrate through the gel-filled capillary, acting as a sieving medium, in order of increasing molecular weight. The mobility of the substrate is used to estimate the molecular weight from a preestablished calibration plot of log molecular mass versus mobility prepared from a series of protein standards of known molecular mass. CGE separation of SDS–proteins has the advantage over SDS–polyacrylamide gel electrophoresis (PAGE) of giving higher resolution and requiring shorter analysis time. Similarly, using appropriate standards, CIEF can be used to determine the pI of a protein. Product identity techniques such as CGE and CIEF can be of great value to biopharmaceutical manufacturers because they can be incorporated into in-process controls as was recently demonstrated for two recombinant proteins [8].

Several monoclonal antibodies (MAbs) have been prepared for therapeutic purposes. They are among the most complex protein-based molecules, consisting of several light and heavy polypeptide chains, joined by multiple disulfide bridges, and containing a number of glycosylation sites of varying sequences and arrangements. Typically, MAbs are very large molecules with molecular weights around 150,000 Da, a feature that, when combined with their structural complexity, makes high-resolution chromatographic methods for the analysis of the intact molecule of little value. However, CE approaches have been highly successful for the characterization of MAbs [9]. Although all of the major CE separation modes have been applied, CIEF and CGE are particularly useful techniques. For instance, the high resolution achieved in CIEF allows monitoring of the profile of charge isoforms resulting from differential C-terminal processing (at lysine or arginine), a situation that frequently occurs in mammalian cell-derived products. CGE analysis under denaturing conditions has been used to estimate MAbs molecular weight as well as the presence of aggregates. When performed under denaturing and reducing conditions, CGE provides an effective way to monitor the light and heavy chains that make up the typical antibody structure.

Product Purity

Purity determination is an essential component of the assessment of the quality of any drug. However, the purity determination of biopharmaceuticals is not as straightforward as for small-molecule pharmaceuticals because biopharmaceuticals are structurally complex and have a wide range of potential impurities. Approaches usually involve the judicious choice of a combination of methods that will enable the detection and quantitation of impurities from which an overall purity assessment can be made. CE-generated data now play a significant role in such purity assessments.

Proteins are inherently labile molecules, especially when placed under non-physiological conditions, and, consequently, the formation of impurities may occur throughout their manufacturing process. Common protein degradation pathways leading to the formation of several types of impurities have been identified (Table 2) and most of these impurities can be detected by CE [10]. For instance, CE can be used successfully for the separation and detection of low levels of charge variants such as deamidation products of asparagine or glutamine residues as well as clipped forms resulting from proteolytic cleavage of the polypeptide chain. In particular, CZE has proven to be highly effective for simple proteins having no carbohydrate-mediated heterogeneity present. The high efficiency of CZE, in some cases, allows the resolution of multiple-charge variants, such as occur in hGH [11], to be accomplished in a single run. The high resolving power and quantitative properties of CGE can be used to detect nondissociable aggregates and clipped forms in proteins as well as deletion sequence in antisense oligonucleotides.

The coupling of CE to high-sensitivity detection devices such as laser-induced fluorescence (LIF) detectors provides substantial enhancement of the detection limits of impurities [12].

Table 2 Typical Impurities in Protein Biopharmaceuticals

Deamidation products
Oxidation products
Disulfide interchange
Proteolytic cleavage products
Aggregates
Amino acid substitutions
N-, C-terminal truncated product



Conclusion

The use of capillary electrophoresis has become an integral part of the study of biopharmaceuticals, especially for the monitoring of product identity and purity. It is a powerful technique that, in many instances, has been shown to be superior to the more conventional electrophoretic techniques and complementary to the widely used high-resolution chromatographic techniques. It is particularly well suited to the study of complex mixtures such as glycoproteins and monoclonal antibodies.

References

1. M. Richardson, Biopharmaceutical regulation and product analysis: Origin, reform and the well-characterised product, *J. Biotechnol. Healthcare* 3: 36 (1996).
2. E. C. Rickard and J. K. Towns, The use of capillary electrophoresis for peptide mapping of proteins, in *New Methods in Peptide Mapping for the Characterization of Proteins*, W. S. Hancock (ed.), CRC Press, Boca Raton, FL 1996, pp. 97–118.
3. J. Liu, H. Zhao, K. J. Volk, S. E. Klohr, E. H. Kerns, and M. S. Lee, Analysis of monoclonal antibody and immunoconjugate digests by capillary electrophoresis and capillary liquid chromatography, *J. Chromatogr. A* 735: 357 (1996).
4. K. Takechi and S. Honda, Analysis of glycoproteins, glycopeptides and glycoprotein-derived oligosaccharides by high performance capillary electrophoresis, *J. Chromatogr. A* 220: 377 (1996).
5. H. P. Bietlot and M. Girard, Analysis of recombinant human erythropoietin in drug formulations by high performance capillary electrophoresis, *J. Chromatogr. A* 759: 177 (1997).
6. B. L. Karger, F. Foret, and J. Berka, Capillary electrophoresis with polymer matrices: DNA and protein separation and analysis, *Methods Enzymol.* 271: 293 (1996).
7. T. Wehr, M. Zhu, and R. Rodriguez-Diaz, Capillary isoelectric focusing, *Methods Enzymol.* 270: 358 (1996).
8. A. Buchacher, P. Schulz, J. Choromanski, H. Schwinn, and D. Josic, High performance capillary electrophoresis for in-process control in the production of antithrombin III and human clotting factor IX, *J. Chromatogr. A* 802: 355 (1998).
9. I. S. Krull, X. Liu, J. Dai, C. Gendreau, and G. Li, HPCE methods for the identification and quantitation of antibodies, their conjugates and complexes, *J. Pharm. Biomed. Anal.* 16: 377 (1997).
10. G. Teshima and S.-L. Wu, Capillary electrophoresis analysis of recombinant proteins, *Methods Enzymol.* 271: 264 (1996).
11. P. Dupin, F. Galinou, and A. Bayol, Analysis of recombinant human growth hormone and its related impurities by capillary electrophoresis, *J. Chromatogr. A* 707: 396 (1995).
12. T. T. Lee, S. J. Lillard and E. S. Yeung, Screening and characterization of biopharmaceuticals by high performance capillary electrophoresis with laser-induced native fluorescence detection, *Electrophoresis* 14: 429 (1993).



Biopolymer Separations by Chromatographic Techniques

Masayo Sakata

Chuichi Hirayama

Kumamoto University, Kumamoto, Japan

INTRODUCTION

Endotoxin (lipopolysaccharides; LPS) is an integral part of the outer cellular membrane of Gram-negative bacteria and is responsible for organization and stability. In the biotechnology industry, Gram-negative bacteria are widely used to produce recombinant DNA products such as peptides and proteins. Thus these products are always contaminated with LPS. Such contaminants have to be removed from drugs and fluids before use in injections, because their potent biological activities cause pyrogenic reactions.

To achieve selective removal of LPS from final biological products, such as proteins and protective antigens, it is necessary to consider not only the chemical and physical structures of LPS, but also those of the adsorbents and proteins, as well as the solution conditions. In physiological solutions, LPS aggregates form supramolecular assemblies (M_w : 4×10^5 to 1×10^6) with phosphate groups as the head group and exhibit a net-negative charge because of their phosphate groups. However, as proteins may release LPS monomers from the aggregates, we assume that LPS aggregates comprise a wide range of molecular sizes, with M_w from 2×10^4 to 1×10^6 in physiological solutions. On the other hand, the molecular weights of proteins are generally about 1×10^4 to 5×10^5 . Therefore it is extremely difficult to separate LPS from protein solely by size-separation methods, such as size-exclusion chromatography and ultrafiltration. Various procedures of LPS removal, such as ion exchange membrane, ultrafiltration, and extraction, have been developed for pharmaproteins. These procedures, however, are unsatisfactory with respect to selectivity, adsorption capacity, and protein recovery.

For the removal of LPS from final solutions of bioproducts, selective adsorption has proven to be the most effective technique. Therefore considerable effort is being put into the development of adsorbents capable of retaining high LPS selectivity under physiological conditions (ionic strength of $\mu=0.05$ – 0.2 , neutral pH). Recently, numerous cationic polymer adsorbents have been developed for removing LPS from protein solutions. This article will elucidate the chromatographic properties

of various LPS adsorbents and will describe recent findings concerning methods for eliminating LPS from protein solutions using the adsorption technique.

CHROMATOGRAPHIC MATRICES WITH POLYCATIONIC LIGANDS

Lipopolysaccharide is an amphipathic substance^[1–3] that has both an anionic region (the phosphoric acid groups) and a hydrophobic region (the lipophilic groups). From this point of view, an LPS-selective ligand should have, not only cationic properties, but also hydrophobic properties.^[4–6] Figure 1 shows structures of various cationic substances that are suitable as LPS-selective ligands. Through immobilization of polymyxin B on CNBr-activated Sepharose, Issekutz^[7] created a polymyxin–Sepharose adsorbent for selective removal of LPS. This adsorbent is now commercially available. Although the polymyxin–Sepharose columns showed high LPS-adsorbing activity, protein losses during passage through the column have been noted (20% loss of BSA in Ref. [8]). This is due to the ionic interaction between the cationic region of the polymyxin B and the net-negatively charged proteins at low ionic strengths. Furthermore, polymyxin B is not suitable as a ligand for LPS removal from a solution for intravenous injection because it could escape from the column and would be physiologically active in solution. If any polymyxin is to be released into a solution, it would be physiologically active. Poly(ethyleneimine) (PEI)-immobilized cellulose fibers have been prepared by Morimoto et al.^[9] and the PEI fibers showed significant LPS-adsorbing capacity under physiological conditions (neutral and ionic strength of $\mu=0.1$ – 0.2). In a more recent publication, poly(ϵ -lysine) (PL) was covalently immobilized onto cellulose spherical particles and used for selective adsorption of LPS from protein solutions.^[10] In addition, the PL (degree of polymerization: 35, pK_a : 7.6) (Chisso)^[11] produced by *Streptomyces albulus*, which has become commercially available as a safe food preservative, is more suitable as a ligand than is polymyxin B. The high LPS adsorption of chromatographic matrices having

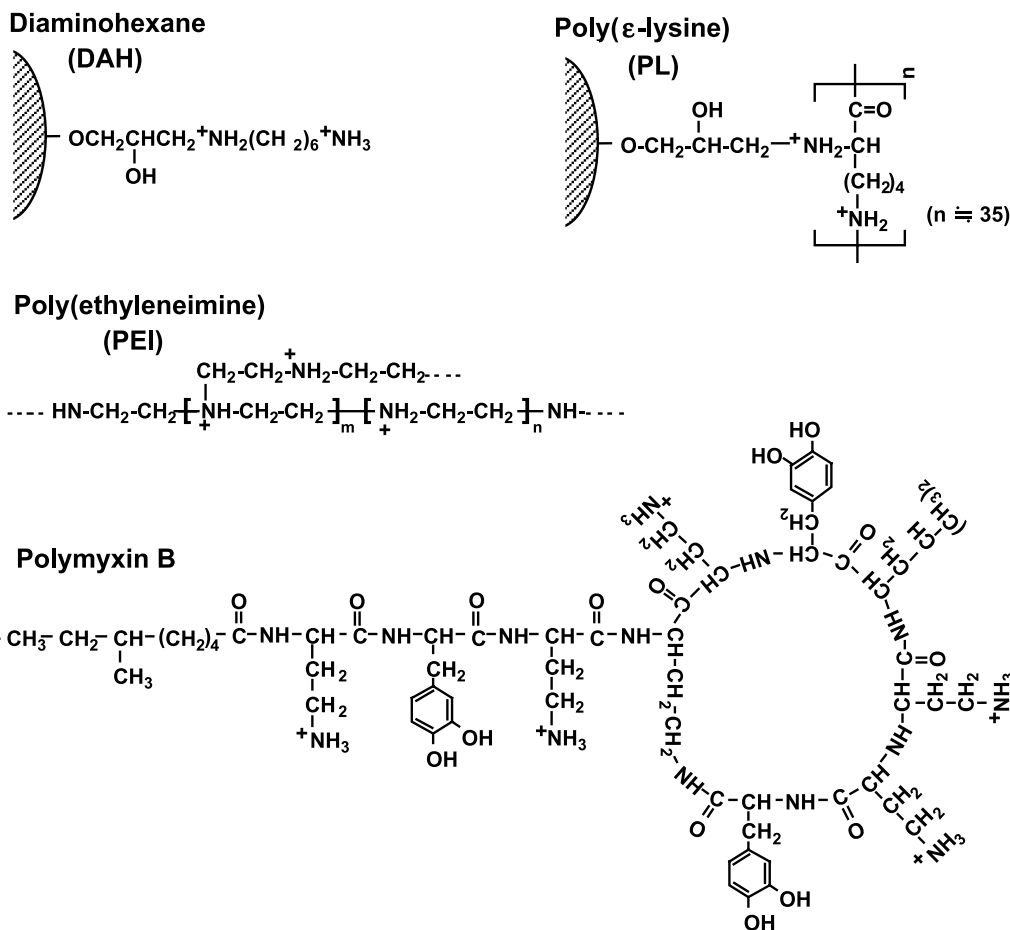


Fig. 1 Structure of LPS-selective ligands. Sepharose and cellulose particles are used as the matrix.

polycationic ligands, such as polymyxin B, PEI, or PL, is possibly due to the simultaneous effects of the cationic properties of the ligand and its hydrophobic properties.

EFFECTS OF VARIOUS FACTORS ON THE SEPARATION OF BIOPOLYMERS BY POLYCATIONIC ADSORBENTS

Effect of Pore Size of the Adsorbent on LPS Selectivity

To achieve the selective removal of LPS, it is important to determine the adsorbing activity of proteins. Table 1 shows the effect of the adsorbent pore size (molecular mass exclusion of polysaccharide, M_{lim})^[12] on the adsorption of cellular products (biorelated polymers). The various PL-immobilized cellulose particles (PL cellulose) with pore sizes of $M_{\text{lim}} \times 10^3$ to $>2 \times 10^6$ were used as adsorbents. Lipopolysaccharide, DNA, and

RNA, which are anionic biorelated polymers with phosphoric acid groups, were adsorbed very well by all the adsorbents. By contrast, the adsorption of protein was more dependent on the M_{lim} of the adsorbent than its anion-exchange capacity (AEC). The adsorption of BSA (M_w 6.9×10^4), an acidic protein, increased from 5% to 68% with an increase in the M_{lim} from 2×10^3 to 1×10^4 . The adsorption of γ -globulin (M_w 1.6×10^5), a hydrophobic protein, increased from 2% to 22% with an increase in the M_{lim} from 1×10^4 to $>2 \times 10^6$. Polymyxin–Sephacrose with large pore size ($M_{lim} > 2 \times 10^6$) also adsorbed BSA (78%) and γ -globulin (26%), as shown in Table 1. Very little of the other neutral or basic proteins adsorbed onto the adsorbents under similar conditions. As a result, only when the PL cellulose (10^3), with a M_{lim} of 2×10^3 and AEC of 0.6 meq/g, was used as the adsorbent at pH 7.0 and ionic strength of $\mu=0.05$ were LPS and DNA selectively well adsorbed.

The results reported in Table 1 show that the adsorption of protein was caused, mainly, by the entry of the protein



Table 1 Effect of adsorbent's pore size on adsorption of a bio-related polymer

Cellular product	(pI)	Adsorption ^a (%)				
		AEC ^f (meq/g)	PL-cellulose (10 ³) ^b	PL-cellulose (10 ⁴) ^c	PL-cellulose (10 ⁶) ^d	Polymyxin- sepharose ^e
			0.6	0.8	0.6	0.2
		Pore size (M_{lim}) ^g	2×10^3	1×10^4	$> 2 \times 10^6$	$> 2 \times 10^6$
Ovalbumin	4.6		2	65	85	75
BSA	4.9		5	68	82	78
Myoglobin	6.8		<1	<1	<1	<1
γ -Globulin	7.4		2	2	22	26
Lysozyme	11.0		<1	<1	<1	<1
DNA (salmon spermary)			99	99	99	99
RNA (yeast)			98	99	99	99
LPS (<i>E. coli</i> O111:B4)			91	98	99	99
LPS (<i>E. coli</i> UKT-B)			89	96	99	99

^aThe adsorption of a cellular product was determined using a batchwise method with 0.3 mL of wet adsorbent and 2 mL of a sample solution (100 μ g/mL, pH 7.0, ionic strength of $\mu=0.05$).

^bPoly(ϵ -lysine)-immobilized Cellfine-GC-15.^[10]

^cPoly(ϵ -lysine)-immobilized Cellfine-GC-700.^[10]

^dPoly(ϵ -lysine)-immobilized Cellfine-CPC.^[10]

^eDetixi-Gel.^[7]

^fAnion-exchange capacity of the adsorbent.

^gValue deduced as molecular weight of polysaccharide.^[12]

into the pores of the adsorbent. This indicates that both BSA and γ -globulin can readily penetrate into a particle with an M_{lim} of $>2 \times 10^6$, but cannot penetrate into a particle with 2×10^3 (M_{lim}). On the other hand, it would also appear that LPS aggregates are not able to enter the pores of the adsorbents with 2×10^3 (M_{lim}) because their molecular weights (4×10^5 to 1×10^6)^[13] are significantly larger than the M_{lim} of the adsorbent. Many of the standard LPS molecules (*Escherichia coli* O111:B4 and UKT-B), however, were well adsorbed even by the adsorbent with an M_{lim} of 2×10^3 , as shown in Table 1. We previously reported^[13] that the LPS molecules were adsorbed by aminated poly(γ -methyl L-glutamate) particles not only into the pores of the particles but also on their surfaces. Poly(ϵ -lysine)-immobilized cellulose particles have similar characteristics.

Effect of Degree of Ligand Polymerization on Adsorption of Biopolymer

For selective removal of LPS from a protein solution, it is also necessary to select the ligand of the adsorbent. Figure 2 shows the effects of a buffer's ionic strength and pH on the adsorption of LPS by diamino-hexane- (DAH), PL-, or PEI-immobilized cellulose particles. Diamino-hexane monomer (M_w : 116), PL (degree of polymerization: 35, M_w :

4.0×10^3), and PEI (degree of polymerization: 1600, M_w : 7×10^4) were used respectively as adsorbent ligands, and cellulose particles with M_{lim} 2×10^3 (Cellufine GC-15) were used as the matrix. As shown in Fig. 2a, the higher the

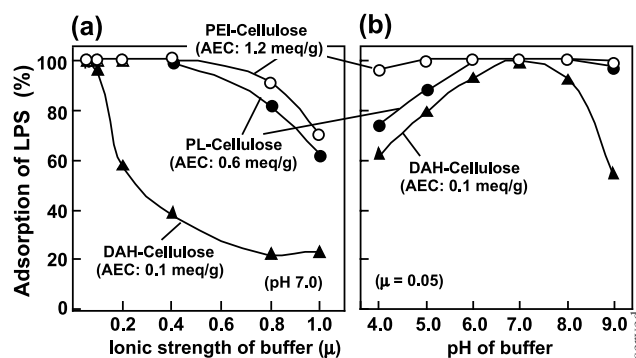


Fig. 2 Effects of a buffer's (a) ionic strength and (b) pH on the adsorption of LPS by various aminated cellulose adsorbents. The adsorption of LPS was determined using a batchwise method with 0.2 g of the wet adsorbent and 2 mL of a LPS (*E. coli* O111:B4, 1000 ng/mL) solution. Adsorbent and AEC of adsorbent: PEI-cellulose=poly(ethyleneimine)-immobilized Cellufine-GC15 (AEC: 1.2 meq/g); PL-cellulose=poly(ϵ -lysine)-immobilized Cellufine-GC15 (AEC: 0.6 meq/g); DAH-cellulose=diamino-hexane-immobilized Cellufine-GC15 (AEC: 0.2 meq/g). M_{lim} of adsorbent: 2×10^3 .



ionic strength of the buffer the lower the LPS-adsorbing activity of the adsorbent. Both PEI cellulose and PL cellulose always showed a greater LPS-adsorbing activity (99% to 82%) at a wide range of ionic strengths ($\mu=0.05$ –0.8). The adsorbing activity of DAH cellulose decreased markedly when the ionic strength was increased to 0.2 or higher. Figure 2b shows the effect of pH on the adsorption of LPS by various aminated cellulose adsorbents. The larger the molecular weight (polymerization degree) of an adsorbent's ligand the higher the LPS-adsorbing activity of the adsorbent. Over a wide pH range of 4.0–9.0 and at an ionic strength of $\mu=0.05$, PEI cellulose (AEC: 1.2 meq/g), with the largest polymerization degree of ligand, always showed the highest LPS-adsorbing activity (>98%). Poly(ϵ -lysine)-immobilized cellulose (AEC: 0.6 meq/g) also showed a high activity (>97%) over a pH range from 6.0 to 9.0, although it decreased from 99% to 75% as the pH decreased from 6.0 to 4.0. On the other hand, DAH cellulose (AEC: 0.1 meq/g) showed high adsorbing activity only at pH 7.0.

Figure 3a and b shows the effect of a buffer's ionic strength on adsorption of BSA and γ -globulin, respectively, by aminated cellulose adsorbents. The stronger the ionic strength the lower the BSA-adsorbing activity of the adsorbent (Fig. 3a). By contrast, adsorption of BSA and γ -globulin is independent of ionic strength (Fig. 3b). Poly(ethyleneimine)-immobilized cellulose showed the highest adsorption of each protein among the three adsorbents.

From these results (Table 1, Figs. 2 and 3), we assumed that the adsorbing activity of aminated-cellulose adsorbents for biopolymers was induced by the simultaneous effects of their cationic properties and hydrophobic or other properties. The charge of LPS is anionic at pH

values greater than its pK_a ($pK_1=1.3$ ^[14]). The charge of BSA is also anionic at pH values greater than 4.9 (its pI). The adsorption of LPS and BSA increased with increasing AEC content of the adsorbent (Figs. 2 and 3). It is also dependent on the ionic strength and pH values (Fig. 2a and b, respectively). These results suggest that aminated-cellulose adsorbents adsorb LPS and BSA mainly by ionic interaction. On the other hand, the ionic interaction of the adsorbent with γ -globulin (pI : 7.4) is not induced at pH 7.0, as the charge of the protein is cationic at a pH under its pI value. γ -Globulin is a weakly hydrophobic protein. Its adsorption was independent of ionic strength and increased with an increase in the hydrophobicity (ligand-polymerization degree) of the adsorbent (Fig. 3b). Hou and Zaniewski^[15] also reported that a hydrophobic bond was formed between LPS and the polymeric affinity matrix. These findings suggest the participation of hydrophobic binding. Furthermore, as shown in Table 1, polycation-immobilized cellulose adsorbents bind more strongly with LPS than protein. This is because the pK_a of the phosphate residues of LPS is lower than the pI of protein (pI : 4.6–11.0), and, probably, because the LPS is adsorbed by the adsorbent through its multipoint attachment onto the polycation chain of the adsorbent surface.

CHROMATOGRAPHIC RESULTS FOR SELECTIVE LPS REMOVAL

For selective LPS removal, it is necessary not only to select the ligand of the adsorbent, but also to control the conditions of the buffer (pH and ionic strength). The effect of ionic strength on the selective adsorption of LPS from a BSA-containing solution by various aminated cellulose adsorbents ($M_{lim} 2 \times 10^3$) was examined (results are shown in Fig. 4a–c). A BSA solution, 500 μ g/mL of BSA and 100 ng/mL of standard LPS, was used as a sample solution. The LPS-adsorbing activity of DAH cellulose decreased remarkably with an increase in the ionic strength. The DAH cellulose selectively adsorbed LPS only at $\mu=0.05$ (Fig. 4a). Poly(ethyleneimine)-immobilized cellulose showed adsorbing activities for both LPS and BSA over a wide ionic strength, from $\mu=0.05$ to 0.8 (Fig. 4c). It cannot therefore selectively adsorb LPS from the BSA solution at all ionic strengths. By contrast, PL cellulose selectively adsorbed LPS in the solution at ionic strengths of $\mu=0.05$ to 0.4 and pH 7.0, without adsorption of BSA (Fig. 4b). The residual concentrations of LPS after treatment were less than 100 pg/mL [1 endotoxin unit (EU)/mL] and each BSA recovery was over 95%.^[10] The threshold level for

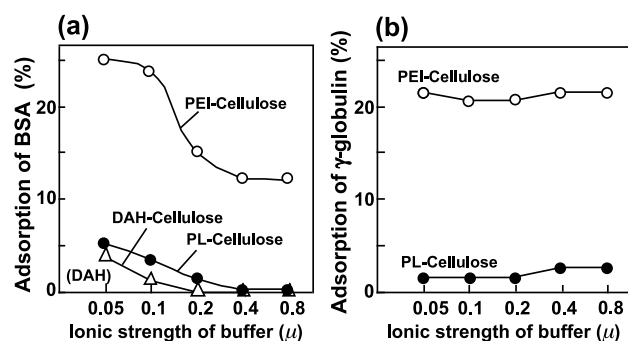


Fig. 3 Effect of a buffer's ionic strength on the adsorption of (a) BSA and (b) γ -globulin by various aminated cellulose adsorbents reported in Fig. 2. The adsorption of protein was determined using a batchwise method with 0.2 g of the wet adsorbent and 2 mL of a protein (100 μ g/mL) solution.

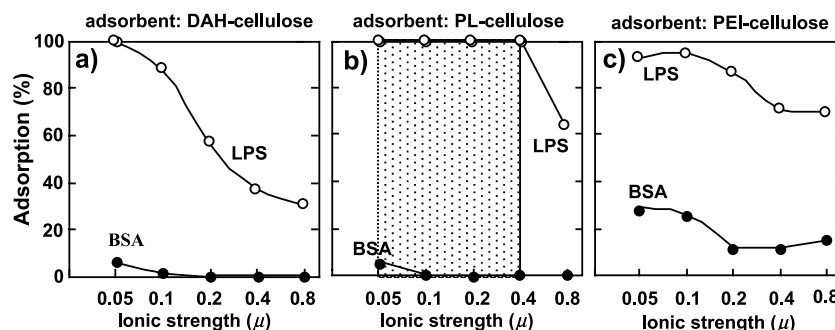


Fig. 4 Effects of ionic strength on selective adsorption of LPS from a BSA solution containing LPS by the various aminated cellulose adsorbents reported in Fig. 2. The selective adsorption of LPS was determined by a batchwise method with 0.2 g of the wet adsorbent and 2 mL of a sample solution [BSA: 500 μg/mL, LPS (*E. coli* O111:B4): 100 ng/mL, pH 7.0, and ionic strength of $\mu=0.05\text{--}0.8$].

intravenous application is set to 5 EU per kg body weight per hour by all pharmacopoeias.^[2] The PL-cellulose adsorbent was able to remove LPS from a BSA solution to a level below 1 EU/mL.

As regards the adsorbing capacity of LPS, the cationic polymers with large pore sizes show a greater capacity, because of the entry of LPS molecules into the large pores. We have already reported^[10] that PL cellulose with $M_{lim}>2\times10^6$ can reduce the concentration of LPS to 0.1 EU/mL or under in a LPS solution, at a neutral pH and $\mu=0.05\text{--}0.4$. As shown in Table 1, Polymyxin B-Sepharose ($M_{lim}>2\times10^6$) and PL cellulose (10^6) ($M_{lim}>2\times10^6$) readily removed LPS from lysozyme and myoglobin solutions at pH 7 without a loss of protein. This is because the ionic interaction of the adsorbent with lysozyme (pI 11.0) and myoglobin (pI 6.8) is not induced at pH 7.0. Thus the cationic polymer particles having a large pore size are suitable as an adsorbent for removal of LPS from bioproducts (pI : 7.0–11.0) containing large quantities of LPS, such as a crude antigen solution originating from a Gram-negative bacterium.

CONCLUSION

The present results suggest that PL-cellulose spherical particles can reduce the concentrations of natural LPS to 1 EU/mL or lower in drugs and fluids used for intravenous injection, at a neutral pH and ionic strengths of $\mu=0.05\text{--}0.4$. These processes did not affect the recovery, even of acidic proteins such as BSA. The high LPS-adsorbing activity of the PL cellulose is possibly due to the cationic properties of the ligand and its suitable hydrophobic properties. The high LPS selectivity of the particles with small pore size is due to the size-exclusion effects on protein molecules. By contrast, that of the particles with

large pore sizes is due to the decreases in ionic interactions for net-negative charged proteins, which arise when the buffer's ionic strength is adjusted to 0.2 or stronger.

For practical application, ease of regeneration is very important. The PL-cellulose spherical particles can be completely regenerated by frontal chromatography with 0.2 M sodium hydroxide followed by 2.0 M sodium chloride.^[10] Their stable structures, even under extreme pH values, are due to their $-\text{CHNH}-$ bonds. Of course, the development of even better adsorbents should be pursued, by continuing this search for materials. To achieve selective removal of LPS, it is important to not only select a suitable ligand, but also to adjust the pore size of the matrix.

REFERENCES

1. Vaara, M.; Nikaido, H. Outer Membrane Organization. In *Handbook of Endotoxin*; Rietschel, E.T., Ed.; Elsevier: Amsterdam, 1984; Vol. 1, 1–45.
2. Hirayama, C.; Sakata, M.; Ihara, H.; Ohkuma, K.; Iwatsuki, M. Effect of the pore size of an animated poly(γ -methyl L-glutamate) adsorbent on selective removal of endotoxin. *Anal. Sci.* **1992**, 8, 805–810.
3. Li, L.; Luo, R.G. Protein concentration effect on protein-lipopolysaccharide (LPS) binding and endotoxin removal. *Biotechnol. Lett.* **1997**, 19, 135–138.
4. Petsch, D.; Anspach, F.B. Endotoxin removal from protein solutions. *J. Biotechnol.* **2000**, 79, 97–119.
5. Minobe, S.; Watanabe, T.; Sato, T.; Tosa, T.; Chibata, I. Preparation of adsorbents for pyrogen adsorption. *J. Chromatogr.* **1982**, 248, 401–408.
6. Matsumae, H.; Minobe, S.; Kindan, K.; Watanabe, T.; Tosa, T. Specific removal of endotoxin from protein solutions by immobilized histidine. *Biotechnol. Appl. Biochem.* **1990**, 12, 129–140.
7. Issekutz, A.C. Removal of Gram-negative endotoxin



- from solutions by affinity chromatography. *J. Immunol. Methods* **1983**, *61*, 275–281.
8. Anspach, F.B.; Kilbeck, O. Removal of endotoxins by affinity sorbents. *J. Chromatogr., A* **1995**, *711*, 81–92.
9. Morimoto, S.; Sakata, M.; Iwata, T.; Esaki, A.; Hirayama, C. Preparations and applications of polyethyleneimine-immobilized cellulose fibers for endotoxin removal. *Polym. J.* **1995**, *27*, 831–839.
10. Todokoro, M.; Sakata, M.; Matama, S.; Kunitake, M.; Ohkuma, K.; Hirayama, C. Pore-size controlled and poly(ϵ -lysine)-immobilized cellulose spherical particles for removal of lipopolysaccharides. *J. Liq. Chromatogr. Relat. Technol.* **2002**, *25* (4), 601–614.
11. Shima, S.; Sakaki, H. Poly-L-lysine produced by *Streptomyces*: Part III. Chemical studies. *Agric. Biol. Chem.* **1981**, *45* (11), 2503–2508.
12. Hirayama, C.; Ihara, H.; Nagaoka, S.; Furusawa, H.; Tsuruta, S. Regulation of pore-size distribution of poly-(γ -methyl L-glutamate) spheres as a gel permeation chromatography packings. *Polym. J.* **1990**, *22* (7), 614–619.
13. Hirayama, C.; Sakata, M.; Ihara, H.; Ohkuma, K.; Iwatsuki, M. Effect of pore size of an aminated poly (γ -methyl L-glutamate) adsorbent on the selective removal of endotoxin. *Anal. Sci.* **1992**, *8*, 805–810.
14. Hou, K.C.; Zaniwski, R. Depyrogenation by endotoxin removal with positively charged depth filter cartridge. *J. Parenter. Sci. Technol.* **1990**, *44*, 204–209.
15. Hou, K.C.; Zaniwski, R. The effect of hydrophobic interaction on endotoxin adsorption by polymeric affinity matrix. *Biochem. Biophys. Acta* **1991**, *1073*, 149–154.



Biotic Dicarboxylic Acids, CCC Separation with Polar Two-Phase Solvent Systems Using a Cross-Axis Coil Planet Centrifuge

Kazufusa Shinomiya

Nihon University, Chiba, Japan

Yoichiro Ito

National Institutes of Health, Bethesda, Maryland, U.S.A.

INTRODUCTION

Among various types of countercurrent chromatographic instruments developed in the past, the cross-axis coil planet centrifuge (cross-axis CPC) is one of the most useful systems for separation of numerous kinds of natural and synthetic products.^[1-3]

The cross-axis CPC produces a unique mode of planetary motion, such that the column holder rotates about its horizontal axis while revolving around the vertical axis of the centrifuge.^[4,5] This motion provides satisfactory retention of the stationary phase for viscous, low-interfacial tension, two-phase solvent systems, such as aqueous-aqueous polymer phase systems. Our previous studies demonstrated that the cross-axis CPC equipped with a pair of multiplayer coils or eccentric coil assemblies in the off-center position was very useful for the separation of proteins with polyethylene glycol-potassium phosphate solvent systems.^[6-8] The apparatus is also useful for the separation of highly polar compounds such as sugars,^[9] hippuric acid, and related compounds,^[10] which require the use of polar two-phase solvent systems.

This article illustrates the separation of biotic dicarboxylic acids using the cross-axis CPC with eccentric coil assemblies.^[11]

CCC APPARATUS AND SEPARATION COLUMNS

The cross-axis CPC produces a synchronous planetary motion of the column holder, which rotates about its horizontal axis and simultaneously revolves around the vertical axis of the apparatus at the same angular velocity. In the $X-1.5L$ type of the apparatus, the column holder

was mounted at an off-center position ($X=10$ cm and $L=15$ cm), which provides efficient mixing of the two-phase solvent systems and stable retention of the stationary phase in the coiled column.

The separation column was prepared using a pair of eccentric coil assemblies, which were made by winding a 1 mm-ID PTFE (polytetrafluoroethylene) tubing onto 7.6 cm long, 5 mm-OD nylon pipes forming a series of tight left-handed coils. A set of these coil units was symmetrically arranged around the holder hub of 7.6 cm diameter in such a way that the axis of each coil unit is parallel to the axis of the holder. A pair of eccentric coil assemblies was mounted on the rotary

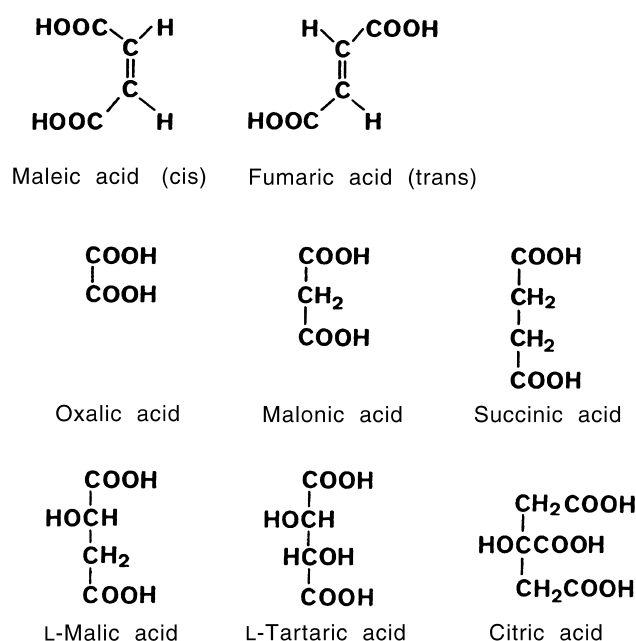


Fig. 1 Chemical structures of polar organic acids.

frame, one on each side, and serially connected with a flow tube.

CCC SEPARATION OF DICARBOXYLIC ACIDS

The chemical structures of eight typical biotic dicarboxylic acids are shown in Fig. 1. They are extremely hydrophilic and require a specific reaction for detection using the color-producing reagent such as 2-nitrophenylhydrazine hydrochloride.^[12,13]

Fig. 2 illustrates the partition coefficient (K) values for these dicarboxylic acid samples in the polar two-phase solvent systems composed of methyl *t*-butyl ether (MBE)/1-butanol/acetonitrile (AcN)/aqueous 0.1% trifluoroacetic acid (TFA), at various volume ratios. K

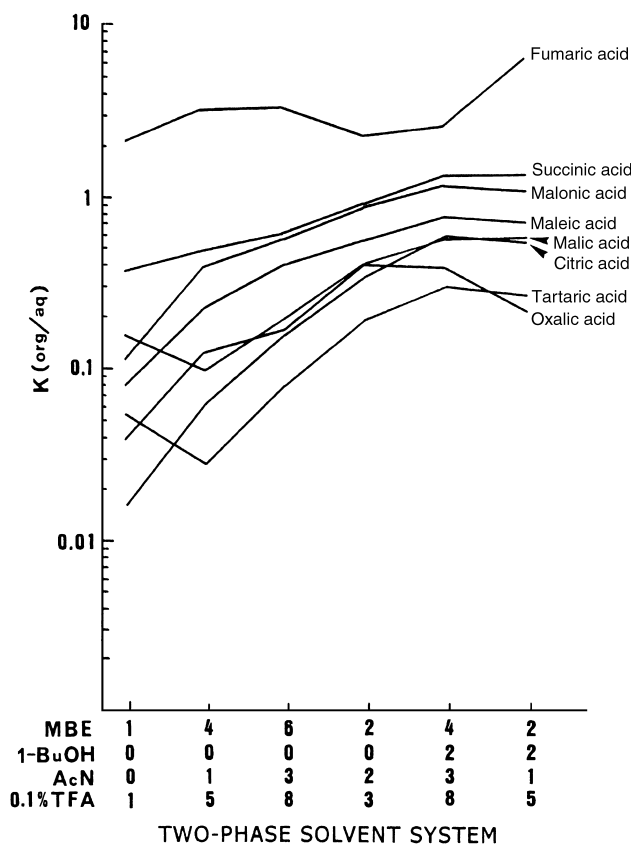


Fig. 2 Partition coefficients (K org/aq) of polar organic acids in methyl *t*-butyl ether/1-butanol/acetonitrile/aqueous 0.1% trifluoroacetic acid system. K is expressed by solute concentration in the organic phase divided by that in the aqueous phase. MBE = methyl *t*-butyl ether; 1-BuOH = 1-butanol; AcN = acetonitrile; TFA = trifluoroacetic acid.

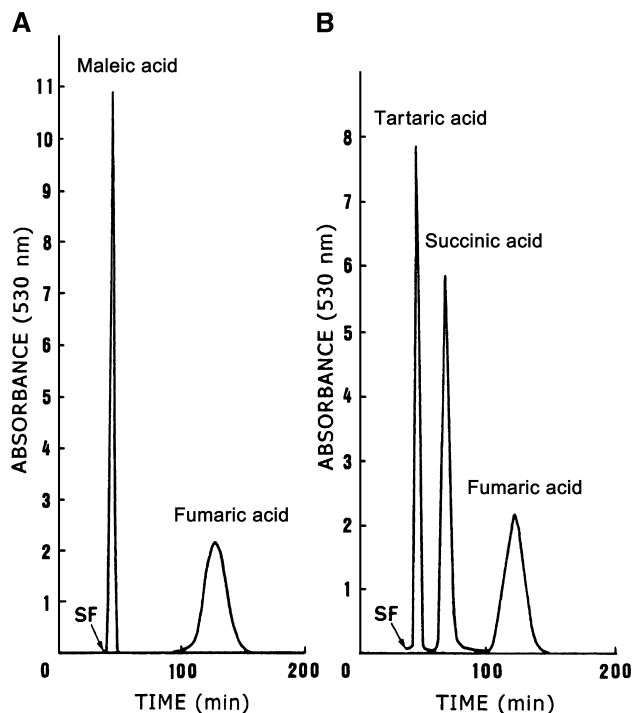


Fig. 3 CCC separation of polar organic acids by cross-axis CPC. Experimental conditions: apparatus, cross-axis CPC equipped with a pair of eccentric coil assemblies, 1 mm ID and 26.5 mL total column capacity; sample, (A) maleic acid (3 mg) and fumaric acid (3 mg); (B) tartaric acid (5 mg), succinic acid (5 mg) and fumaric acid (2.5 mg); solvent system, methyl *t*-butyl ether/1-butanol/acetonitrile/aqueous 0.1% trifluoroacetic acid (A) (1:0:0:1); (B) (2:0:2:3); mobile phase, lower phase; flow rate, 0.4 mL/min; revolution, 800 rpm. SF = solvent front.

values of the organic acids decreased as the hydrophobicity of the solvent system was increased, except for fumaric acid, which showed high K values regardless of the phase composition.

Fig. 3 illustrates the CCC chromatograms of dicarboxylic acids obtained with the above solvent system. In Fig. 3A, maleic acid and fumaric acid are separated at a volume ratio of 1:0:0:1, which is used for the separation of aromatic acids such as hippuric acid.^[10] Using a more polar solvent system, at a volume ratio of 2:0:2:3, tartaric acid, succinic acid, and fumaric acid were well resolved by the lower aqueous mobile phase, as shown in Fig. 3B.

Fig. 4 illustrates a chromatogram of oxalic acid, malonic acid, and succinic acid obtained using the most polar binary solvent system, composed of 1-butanol/water. All components were well resolved from each other and eluted within 2.3 h, using the lower aqueous phase as the mobile phase.

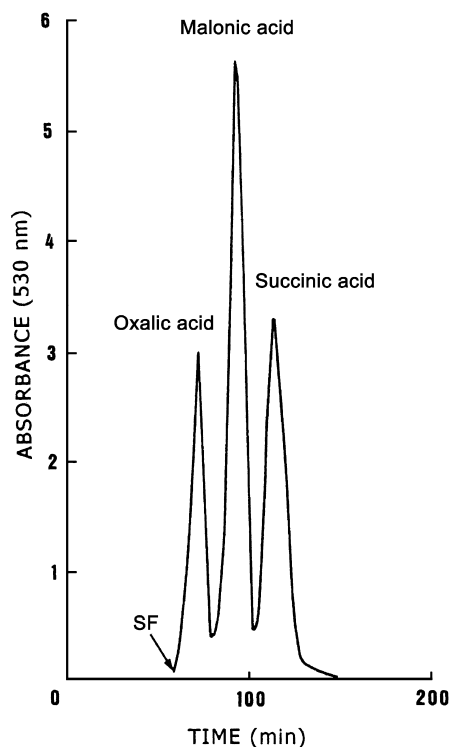


Fig. 4 CCC separation of oxalic acid, malonic acid, and succinic acid by cross-axis CPC. Experimental conditions: sample, 3 mg each; solvent system, 1-butanol/water; flow rate, 0.25 mL/min. For other experimental conditions, see the Fig. 3 caption. SF=solvent front.

As described above, various polar organic acids, such as dicarboxylic acids, can be separated with polar two-phase solvent systems, using the cross-axis CPC equipped with a pair of eccentric coil assemblies mounted in the off-center position.

REFERENCES

1. *Countercurrent Chromatography: Theory and Practice*; Mandava, N.B., Ito, Y., Eds.; Marcel Dekker: New York, 1988.
2. Conway, W.D. *Countercurrent Chromatography: Apparatus, Theory, and Applications*; VCH: New York, 1990.
3. *High-Speed Countercurrent Chromatography*; Ito, Y., Conway, W.D., Eds.; Wiley-Interscience: New York, 1996.
4. Ito, Y. Cross-axis synchronous flow-through coil planet centrifuge free of rotary seals for preparative countercurrent chromatography. Part I: Apparatus and analysis of acceleration. *Sep. Sci. Technol.* **1987**, 22, 1971.
5. Ito, Y. Cross-axis synchronous flow-through coil planet centrifuge free of rotary seals for preparative countercurrent chromatography. Part II: Studies on phase distribution and partition efficiency in coaxial coils. *Sep. Sci. Technol.* **1987**, 22, 1989.
6. Shinomiya, K.; Menet, J.-M.; Fales, H.M.; Ito, Y. Studies on a new cross-axis coil planet centrifuge for performing counter-current chromatography. I. Design of the apparatus, retention of the stationary phase, and efficiency in the separation of proteins with polymer phase systems. *J. Chromatogr.* **1993**, 644, 215.
7. Shinomiya, K.; Inokuchi, N.; Gnabre, J.N.; Muto, M.; Kabasawa, Y.; Fales, H.M.; Ito, Y. Countercurrent chromatographic analysis of ovalbumin obtained from various sources using the cross-axis coil planet centrifuge. *J. Chromatogr., A* **1996**, 724, 179.
8. Shinomiya, K.; Muto, M.; Kabasawa, Y.; Fales, H.M.; Ito, Y. Protein separation by improved cross-axis coil planet centrifuge with eccentric coil assemblies. *J. Liq. Chromatogr. Relat. Technol.* **1996**, 19, 415.
9. Shinomiya, K.; Kabasawa, Y.; Ito, Y. Countercurrent chromatographic separation of sugars and their p-nitrophenyl derivatives by cross-axis coil planet centrifuge. *J. Liq. Chromatogr. Relat. Technol.* **1999**, 22, 579.
10. Shinomiya, K.; Sasaki, Y.; Shibusawa, Y.; Kishinami, K.; Kabasawa, Y.; Ito, Y. Countercurrent chromatographic separation of hippuric acid and related compounds using cross-axis coil planet centrifuge with eccentric coil assemblies. *J. Liq. Chromatogr. Relat. Technol.* **2000**, 23, 1575.
11. Shinomiya, K.; Kabasawa, Y.; Ito, Y. Countercurrent chromatographic separation of biotic dicarboxylic acids with polar two-phase solvent systems using cross-axis coil planet centrifuge. *J. Liq. Chromatogr. Relat. Technol.* **2001**, 24, 2625.
12. Horikawa, R.; Tanimura, T. Spectrophotometric determination of carboxylic acids with 2-nitrophenylhydrazine in aqueous solution. *Anal. Lett.* **1982**, 15, 1629.
13. Shinomiya, K.; Ochiai, H.; Suzuki, H.; Koshiishi, I.; Imanari, T. Simple method for determination of urinary mucopolysaccharides. *Bunseki Kagaku* **1986**, 35, T29.

Bonded Phases in HPLC

Joseph J. Pesek
Maria T. Matyska

San Jose State University, San Jose, California, U.S.A.

Introduction

The development of chemically bonded stationary phases is one of the major factors that lead to the growth of high-performance liquid chromatography (HPLC) and is responsible for its importance as a separation technique.

Historical Background

In its earliest form, gravity flow moved the mobile phase through the column which was generally packed with a solid adsorbent such as silica or alumina. In a few instances, a high-molecular-weight liquid was coated on the solid particle to provide different types of selectivity. Under these circumstances, the column was similar to those used in gas chromatography (GC), where a liquid stationary phase was held in place by physical forces alone. In GC, the requirement for the stationary phase to remain in place for a long time is low volatility. In liquid chromatography, the requirement for durability is insolubility in the mobile phase. However, with the development of reliable high-pressure pumps that could produce stable flow rates for long periods of time, immiscibility with the mobile phase is not sufficient. At the pressures used to force solvents through most packed HPLC columns (from tens to a few hundred atmospheres), the shear forces developed at the interface between the stationary and the mobile phases are high enough to remove even insoluble liquids from the surface of the solid support. The stationary phase then is forced out of the column as an insoluble droplet. Removal of the stationary phase from a chromatography column is usually referred to as "column bleed." Therefore, it was necessary to develop a means of fixing the stationary phase on the solid support through a chemical bond. If the chemical bond between the surface of the solid support and the compound used as the stationary phase is stable under the experimental conditions of the HPLC

experiment (temperature and mobile-phase composition), then column bleed will be avoided.

Fortunately, the most common support material used in liquid-chromatography experiments was silica. The chemistry of silica had been investigated for many years so a considerable amount of information was available about possible reactions on its surface. Silica can be considered as a polymer of silicic acid (H_2SiO_3). The terminal groups of the polymer located on the surface of the solid are hydroxide groups. These $\text{Si}-\text{OH}$ functions are referred to as silanols. Because they come from an acid precursor, they are acidic themselves and generally have a $\text{p}K_a$ near 5. This value is variable, depending on other constituents in the silica matrix such as metals. The structure of silica, including its major chemical features, are shown in Fig. 1. The polymeric unit consists of a series of siloxane bonds ($-\text{Si}-\text{O}-\text{Si}-$) that are slightly hydrophobic in nature. What is generally regarded as the most prominent feature on the surface is the silanol group, as indicated earlier. In a few cases, a single silicon atom will have two hydroxyl groups, which is called a geminal silanol. The silanols exist in two forms. First, they can be independent of other entities around them and are thus referred to as free or isolated silanols. If they are

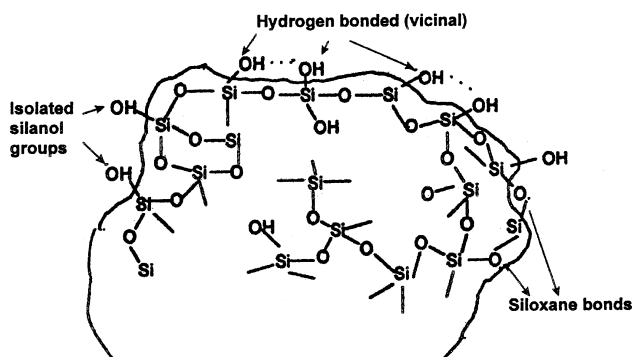


Fig. 1 Structure of silica showing the surface chemical features.



close enough to interact with a neighboring silanol, then these moieties become hydrogen-bonded or associated silanols. All forms of silanol are polar hydrophilic species. The relative number of free versus hydrogen-bonded silanols also has an influence on the pK_a value of the silica. Finally, because of the polar and hydrogen-bonding characteristics of the silanols, water is strongly adsorbed to the surface. This water is not easily removed, even at prolonged heating above 100°C. It is this complex matrix that must undergo a chemical reaction in order to attach a moiety to the surface as a stationary phase. According to the findings of early investigations on the reactivity of silica, it was determined that the silanol groups were the site of chemical modification on the surface.

The concept of attaching an organic moiety as a stationary phase to a silica surface was first applied in packed-column gas chromatography. The rationale for developing these materials was to prevent column bleed at the high temperatures required for some separations in GC. As long as the chemical bond was stable, the organic moiety would remain fixed to the surface. Some of the reactions utilized for the attachment of organic compounds in the synthesis of bonded sta-

tionary phases were originally developed for the modification of ordinary glass surfaces. Therefore, it was known that most of these modified surfaces were reasonably temperature stable and should be applicable to the bonding of organic groups onto the porous silica particles used as supports in chromatography.

The first reaction used for the modification of porous silica in chromatography involves an alcohol as the organic species. This process is referred to as an esterification reaction. This may seem like incorrect nomenclature in order to describe the chemical process taking place between the silanol ($\text{Si}-\text{OH}$) and the organic compound ($\text{R}-\text{OH}$). However, the OH of the silanol is an acidic species, so the reaction taking place involves an acid and an alcohol, which, in typical organic chemistry nomenclature, is an esterification. The chemical reaction is illustrated in Fig. 2. The product of this reaction can be used as a stationary phase in gas chromatography because the material is thermally stable up to temperatures of approximately 300°C. However, the $\text{Si}-\text{O}-\text{C}$ bond that exists between the surface and the bonded moiety is hydrolytically unstable in the presence of relatively small amounts of water. Therefore, these materials

REACTION TYPE	REACTION	SURFACE LINKAGES
ESTERIFICATION	$\text{Si}-\text{OH} + \text{R}-\text{OH} \rightarrow \text{Si}-\text{OR} + \text{H}_2\text{O}$	$\text{Si}-\text{O}-\text{C}$
ORGANOSILANE	$\text{Si}-\text{OH} + \text{X}-\text{SiR}'_2\text{R} \rightarrow \text{Si}-\text{O}-\text{SiR}'_2\text{R} + \text{HX}$ $\begin{array}{c} \text{O} \\ \\ \text{Si}-\text{OH} \\ \\ \text{O} \end{array} + \text{X}_2\text{Si}-\text{R} \rightarrow \begin{array}{c} \text{O} \\ \\ \text{Si}-\text{O}-\text{Si}-\text{R} \\ \quad \\ \text{O} \quad \text{O} \end{array} + 3\text{HX}$	$\text{Si}-\text{O}-\text{Si}-\text{C}$
CHLORINATION FOLLOWED BY REACTION OF GRIGNARD REAGENTS OR ORGANOLITHIUM COMPOUNDS	$\text{Si}-\text{OH} + \text{SOCl}_2 \xrightarrow{\text{Toluene}} \text{Si}-\text{Cl} + \text{SO}_2 + \text{HCl}$ a). $\text{Si}-\text{Cl} + \text{BrMgR} \rightarrow \text{Si}-\text{R} + \text{MgClBr}$ or b). $\text{Si}-\text{Cl} + \text{Li}-\text{R} \rightarrow \text{Si}-\text{R} + \text{LiCl}$	$\text{Si}-\text{C}$
a). TES SILANIZATION	$\begin{array}{c} \text{O} \\ \\ \text{Si}-\text{OH} \\ \\ \text{O} \end{array} \rightarrow \begin{array}{c} \text{O} \quad \text{O} \\ \quad \\ \text{Si}-\text{O}-\text{Si}-\text{H} \\ \quad \\ \text{O} \quad \text{O} \end{array}$ $\begin{array}{c} \text{O} \\ \\ \text{Si}-\text{OH} \\ \\ \text{O} \end{array} \rightarrow \begin{array}{c} \text{O} \quad \text{O} \\ \quad \\ \text{Si}-\text{O}-\text{Si}-\text{H} \\ \quad \\ \text{O} \quad \text{O} \end{array}$ $\begin{array}{c} \text{O} \\ \\ \text{Si}-\text{OH} \\ \\ \text{O} \end{array} \rightarrow \begin{array}{c} \text{O} \quad \text{O} \\ \quad \\ \text{Si}-\text{O}-\text{Si}-\text{H} \\ \quad \\ \text{O} \quad \text{O} \end{array}$	a). $\text{Si}-\text{H}$ monolayer
b). HYDROSILATION	b). $\text{Si}-\text{H} + \text{CH}_2 = \text{CH}-\text{R} \xrightarrow{\text{Catalyst}} \text{Si}-\text{CH}_2-\text{CH}_2-\text{R}$	b). $\text{Si}-\text{C}$

Fig. 2 Reactions for the modification of silica surfaces.

cannot be used for stationary phases in liquid chromatography, where water comprises even a small fraction of the mobile phase.

The second reaction shown in Fig. 2 is the most common means used for the modification of silica surfaces. This method is referred to as organosilanization. Within this general reaction scheme, there are two possible approaches, as shown in Fig. 2. The first possibility involves the use of an organosilane reagent ($\text{RR}'\text{R}'\text{SiX}$) with only a single reactive group (X). The substituents on the silicon atom are as follows: X is a halide, most often Cl, methoxy or ethoxy; R is the organic moiety giving the surface the desired properties (i.e., hydrophobic, hydrophilic, ionic, etc.), and R' is a small organic group, typically methyl. This reaction leads to a single siloxane bond between the reagent and the surface. Because of the single point of attachment of the reagent, the resulting bonded material is referred to as a monomeric phase. The second approach to organosilanization involves a reagent with the general formula RSiX_3 . The substituents on the silicon atom in this reagent are defined as above. The basic difference between the approaches (as shown in Fig. 2) is that the reagent with three reactive groups results in bonding to the surface as well as cross-linking among adjacent bonded moieties and is referred to as a polymeric phase. This cross-linking effect provides extra stability to the bonded moiety but is less reproducible than the monomeric method. The one-step organosilanization procedure is relatively easy and the modification of the surface can be done by stirring the reagent continuously with the porous silica support. The reaction mixture is heated for about 1–2 h, then the reagent solution is removed, usually by centrifugation and/or filtration. The bonded phase is then washed with several solvents and dried under vacuum to remove as much of the rinse solutions as possible. Organosilanization accounts for virtually all of the commercially available chemically bonded stationary phases.

Another method that has been reported for the modification of silica supports is based on a chlorination/organometalation two-step reaction sequence. This process is also depicted in Fig. 2. In the first step, the silanols on the porous silica surface are converted to chlorides via a reaction with thionyl chloride. This step must be done under extremely dry conditions because the presence of any water results in the reversal of the reaction with hydroxyl replacing the chloride ($\text{Si}-\text{Cl}$), resulting in the regeneration of silanols ($\text{Si}-\text{OH}$). If the chlorinated material can be preserved (usually done in a closed vessel purged with a dry gas like nitrogen), then an organic group can be at-

tached to the surface via a Grignard reaction or an organolithium reaction. The main advantage of this process is that it produces a very stable silicon–carbon linkage at the surface. However, the stringent reaction conditions for the first step and the possibility of forming salts that could affect chromatographic properties as by-products in the second reaction have resulted in relatively little commercial use of this process.

The final method shown in Fig. 2 involves, first, silanization of the silica surface, followed by attachment of the organic group through a hydrosilation reaction. In the first step, the use of triethoxysilane under controlled conditions results in a monolayer of the cross-linked reagent being deposited on the surface. This reaction results in the replacement of hydroxides by hydrides. In the second step, an organic moiety is attached to the surface via the hydride moiety by a hydrosilation reaction using a catalyst such as hexachloroplatinic acid (Speier's catalyst), but other transition metal complexes or a free-radical initiator have been reported as well. This process also results in a silicon–carbon bond at the surface, does not require dry conditions (water is required as a catalyst in the first step), and is applicable to a variety of unsaturated functional groups in the hydrosilation reaction, although terminal olefins are the most common. The silanization/hydrosilation method also has seen limited commercial utilization to date.

In all of the reactions described, the choice of the organic moiety on the reagent (R group) determines the properties of the material as a stationary phase. Therefore, selection of a hydrophobic moiety where R is typically an alkyl group leads to a stationary phase that selectively retains nonpolar analytes. These materials are typically used in reversed-phase chromatography. If the organic moiety contains a polar functional group such as amine, cyano, or diol, then the stationary phase selectively retains polar compounds. These materials are typically used in normal-phase chromatography.

The bonding of the organic group on the surface results in the replacement of silanols whose adsorptive properties are strong, especially for bases, and often nonreproducible. Although it is impossible to replace all silanols, the remaining $\text{Si}-\text{OH}$ groups are often shielded from solutes by the steric hindrance of the bonded organic moiety. In many cases though, some silanols are accessible to typical solutes. In order to inhibit the interaction between analytes and residual silanols, the bonded phase is subjected to an additional reaction referred to as endcapping. In this case, a small organosilane, often trimethylchlorosilane, penetrates into the spaces between the bonded groups to react



with the most accessible silanols. This process generally greatly reduces or eliminates solute interactions with silanols.

After the bonded phase is prepared, it must be packed into a column, usually a stainless-steel tube. In order for the material to form a uniform bed of high density that will not form voids after prolonged use, the packing process must be done under high pressure (> 500 atm). The stationary phase is mixed with a solvent of approximately the same density as silica, so that a slurry is formed. This slurry is then forced into the column at high pressure with another solvent, usually methanol. After packing, most stationary phases require several hours of conditioning, with the mobile phase passing through the column at normal flow rates, before actual chromatographic analysis can begin.

Suggested Further Reading

- Iler, R. K., *The Chemistry of Silica*, John Wiley & Sons, New York, 1979.
- Marciniec, B., *Comprehensive Handbook on Hydrosilylation*, Pergamon Press, Oxford, 1992.
- Nawrocki, J., *Chromatographia* 31: 177 (1991).
- Nawrocki, J., *Chromatographia*, 31: 193 (1991).
- Pesek, J. J. and M. T. Matyska, *Interf. Sci.* 5: 103 (1997).
- Pesek, J. J., M. T. Matyska, J. E. Sandoval, and E. J. Williamsen, *J. Liq. Chromatogr. Related Technol.* 19: 2843 (1996).
- Unger, K. K., *Porous Silica*, Elsevier, Amsterdam, 1979.
- Vansant, E. F., P. Van Der Voort and K. C. Vrancken, *Characterization and Chemical Modification of Silica*, Elsevier, Amsterdam, 1995.



Buffer Systems for Capillary Electrophoresis

Robert Weinberger

CE Technologies, Inc., Chappaqua, New York, U.S.A.

Introduction

The solution contained within the capillary in which the separation occurs is known as the background electrolyte (BGE), carrier electrolyte, or, simply, the buffer. The BGE always contains a buffer because pH control is the most important parameter in electrophoresis. The pH may affect the charge and thus the mobility of an ionizable solute. The electro-osmotic flow (EOF) is also affected by the buffer pH. Table 1 contains a list of buffers that may prove useful in high-performance capillary electrophoresis (HPCE). As will be seen later, only a few of these buffers are necessary for most separations.

Other reagents, known as additives, are often added to the BGE to adjust selectivity (secondary equilibrium), modify the EOF, maintain solubility, and reduce the adherence of the solute or sample matrix components to the capillary wall. Table 2 provides these applications, along with some of the commonly used reagents.

Buffers

The selection of the appropriate buffer is usually straightforward. For acids, start with a borate buffer (pH 9.3), and for bases, a phosphate buffer (pH 2.5). These two buffer systems, along with the appropriate additives will work well for most applications. Both buffers have good buffer capacity and the ultraviolet (UV) absorbance of each is low. If bases are not soluble in phosphate buffer, acetate buffer (pH 4) may be more effective. Higher pHs may be required for basic proteins to avoid solute adherence to the capillary wall. If pH 7 is desired, the phosphate buffer works well at that pH. If necessary, the buffer pH can be fine-tuned using a mobility plot.

Alternative buffer systems include zwitterions and dual-buffering reagents. Zwitterionic buffers such as bicine, tricine, CAPS, MES, and Tris may be useful for protein and peptide separations. An advantage of a zwitterionic buffer is low conductivity when the buffer pH is adjusted to its pI . There is little buffer capacity when the pK_a and pI are separated by more than 2 pH

units. When the pI and pK_a are close together, the buffer is known as an isoelectric buffer [1].

Selection of the appropriate counterion is also important. Lithium ion has the lowest mobility of the alkali earth metals. Its use provides for a low-conductivity buffer. Sodium salts are used more frequently due to purity and availability. It makes little sense to ever use a potassium salt. Dual-buffering systems with low-mobility ions and counterions (Tris-phosphate, Tris-borate, aminomethylpropanediol-cacodylic acid) are effective in minimizing buffer conductivity. These buffers are often used in the slab-gel, where low conductivity is particularly important.

The buffer concentration plays an important role in the separation. Typical buffer concentrations range from 20 to 150 mM. At the higher buffer concentrations, the production of heat may require the use of lower field strength or smaller-diameter capillaries (25 μm instead of 50 μm). An Ohm's law plot is used to select the appropriate voltage. The advantages of high-concentration buffers include improved peak shape, fewer wall effects, and increased sample stacking.

Low-concentration buffers (less than 20 mM) provide the fastest separations because solute mobility and EOF is inversely proportional to the square root of the buffer concentration. Because the conductivity of a dilute buffer is low, a high electric field strength can be used as well. Problems with low-concentration buffers are loading capacity, wall effects, and poor stacking. Sawtooth-shaped peaks from a process known as electrodispersion may occur whenever the solute concentration approaches the BGE concentration. It also becomes more likely that proteins will adhere to the capillary wall when the buffer concentration is low. Ionic-strength-mediated sample stacking relies on a high-conductivity BGE and a low-conductivity sample [2]. This important process is less effective at low buffer concentrations. When indirect detection is employed, the buffer (indirect detection reagent) concentration must be kept low to optimize sensitivity [3]. Sawtooth peaks are often observed when this technique is used.

It is important to refresh the BGE reservoirs frequently to avoid a process known as buffer depletion



Table 1 Buffers for HPCE

Buffer	p <i>K_a</i>	Buffer	p <i>K_a</i>
Aspartate	1.99	DIPSO	7.5
Phosphate	2.14, 7.10, 13.3	HEPES	7.51
Citrate	3.12, 4.76, 6.40	TAPSO	7.58
β-Alanine	3.55	HEPPSO	7.9
Formate	3.75	EPPS	7.9
Lactate	3.85	POPSO	7.9
Acetate	4.76	DEB	7.91
Creatinine	4.89	Tricine	8.05
MES	6.13	GLYGLY	8.2
ACES	6.75	Bicine	8.25
MOPSO	6.79	TAPS	8.4
BES	7.16	Borate	9.14
MOPS	7.2	CHES	9.55
TES	7.45	CAPS	10.4

[4]. Electrolysis at the respective electrodes produces protons and hydroxide ions. This can cause pH changes in the buffer reservoirs.

High-pH buffers (>pH 11) are used for certain small ion separations and for the separation of carbohydrates using indirect detection. Adsorption of carbon dioxide can cause the buffer pH to decline. It is best to use small containers filled to the top when storing these buffers.

Buffer Additives

Secondary Equilibrium

If two solutes are inseparable based on pH alone, secondary equilibrium can be employed to effect a separation. The following equilibrium expressions can be written [5].

**Table 2** Buffer additives

Purpose	Reagent	Mechanism
Modify mobility	Borate	Complex with carbohydrates, diols
	Calixarenes	Inclusion complex
	Chelating agents	Complex formation with metals
	Crown ethers	Inclusion complex
	Cyclodextrins	Inclusion complex
	Dendrimers	Inclusion complex
	Macrocyclic antibiotics	Inclusion complex
	Organic solvents	Solvation
	Sulfonic acids	Ion-pair formation
	Surfactants	Micelle interaction
	Transition metals	Complex formation
	Quaternary amines	Ion-pair formation
Modify EOF	Cationic surfactant	Dynamic coating, EOF reversal
	Linear polymers	Dynamic coating
	Organic solvents	Affects viscosity
	Cationic surfactant	Dynamic coating, EOF reversal
Reduce wall effects	Linear polymers	Dynamic coating
		Covers silanols
Polyamines		Hydrophobicity
Maintain solubility	Organic solvents	"Iceberg effect"
	Urea	





If the equilibrium is pushed too far to the left, no separation can occur because A^+ and B^+ are inseparable. When the reagent interacts with the solute, the mobility decreases because the neutral reagent contributes mass without charge. However, if the equilibrium is pushed too far to the right, no separation occurs because A^+R and B^+R are inseparable. Separation only occurs when two conditions are met:

1. K_A does not equal K_B .
2. The equilibrium is not pushed to either extreme.

The next feature to consider is the charge of the reagent and solute. To separate charged solutes, the reagent can be charged or neutral. When the solute is neutral, the reagent must be charged.

Micelles and cyclodextrins are the most common reagents used for this technique. Micellar electrokinetic capillary chromatography (MECC or MEKC) is generally used for the separation of small molecules [6]. Sodium dodecyl sulfate at concentrations from 20 to 150 mM in conjunction with 20 mM borate buffer (pH 9.3) or phosphate buffer (pH 7.0) represent the most common operating conditions. The mechanism of separation is related to reversed-phase liquid chromatography, at least for neutral solutes. Organic solvents such as 5–20% methanol or acetonitrile are useful to modify selectivity when there is too much “retention” in the system. Alternative surfactants such as bile salts (sodium cholate), cationic surfactants (cetyltrimethylammonium bromide), nonionic surfactants (polyoxyethylene-23-lauryl ether), and alkyl glucosides can be used as well.

Cyclodextrins (CD) are frequently used for chiral recognition [7], although they are quite useful for achiral applications as well. Many classes have been used including native, functionalized, sulfobutylether, and highly sulfated CDs. The latter two are generally most effective for chiral and structural isomer separations. The typical CD concentrations range from 1 to 20 mM in 20–50 mM of borate (pH 9.3) or phosphate buffer (pH 2.5). Other reagents useful for chiral recognition include macrocyclic antibiotics, bile salts, chiral surfactants, noncyclic oligosaccharides and polysaccharides, and crown ethers.

Additional reagents useful for secondary equilibrium include borate buffer for carbohydrates, chelating agents for transition metals, ion-pair reagents for acids and bases, transition metals for proteins and peptides, silver ion for alkenes, and Mg^{2+} for nucleosides.

Electro-osmotic Flow Control

The control of EOF is critical to the migration time precision of the separation. Among the factors affecting the EOF are buffer pH, buffer concentration, buffer viscosity, temperature, organic modifiers, cationic surfactants or protonated amines, polymer additives, field strength, and the nature of the capillary surface.

At pH 2.5, the EOF is approximately 10^{-5} cm²/V/s in 50 mM buffer. At pH 7, it is an order of magnitude higher. The EOF is inversely proportional to BGE viscosity and is proportional to temperature, up until the point where heat dissipation is inadequate. Organic modifiers such as methanol decrease the EOF because hydro-organic mixtures have higher viscosity compared to water alone. Acetonitrile does not strongly affect the EOF. Polymer additives such as methylcellulose derivatives increase viscosity as well as coat the capillary wall.

Cationic surfactants and protonated polyamines may reverse the direction of the EOF as they impart a positive charge on the capillary wall. This technique is used to prevent wall interactions with cationic proteins. Changing the direction of the EOF is important in anion analysis where comigration of anions and the EOF is required. Otherwise, highly mobile anions such as chloride migrate toward the anode, whereas lower mobility anions are swept by the EOF toward the cathode.

A new series of reagents (CElixir, MicroSOLV, Long Branch, NJ) have been shown to dramatically stabilize the EOF, resulting in highly reproducible run-to-run and capillary-to-capillary migration times [8]. First, a capillary is treated as usual with 0.1N sodium hydroxide, followed by a rinse with a polycation solution. Then, a second layer consisting of a polyanion in a buffer at the desired pH is flushed through the capillary. Replicate runs are virtually superimposable, yielding reproducibility seldom found in HPCE. The reagents have been shown to work best for bases below at a pH below the pK_a .

Maintaining Solubility

All solutes and matrix components must remain in solution for an effective separation to occur. In aqueous systems, surfactants and urea are the most useful reagents. Organic solvents can be used as well, but this is less desirable because of evaporation. It can be difficult to separate solutes with widely different solubilities in a single run. In some cases, nonaqueous separations are necessary.



Reducing Wall Effects

Wall effects, or the adherence of material to the bare silica capillary wall, has been a difficult problem since the early days of HPCE, particularly for large molecules such as proteins. Small molecules can have, at most, one point of attachment to the wall and the kinetics of adsorption/desorption are rapid. Large molecules can have multiple points of attachment resulting in slow kinetics. Several solutions have been proposed, including the use of (a) extreme-pH buffers, (b) high-concentration buffers, (c) amine modifiers, (d) dynamically coated capillaries, and (e) treated or functionalized capillaries.

In the first case, it was recognized that if the buffer pH is greater than 2 units above the protein pK_a , the anionic protein would be repelled from the anionic capillary wall [9]. At a $pH < 2$, the capillary wall is neutral and does not attract the cationic protein. The problem with this approach is that a wide range of pHs are not available for use and separations of similar proteins may not occur. For high- pI proteins such as histones, a buffer pH of 13 is required. The conductivity and UV background of such an electrolyte is too high to be generally applicable.

The use of high-concentration buffers is effective in reducing wall effects. This includes electrolytes containing up to 250 mM added salt. The problem with this approach is the high conductivity of the BGE. This requires a reduction in field strength resulting in lengthy separations. Zwitterionic buffers titrated to their pI can be used as well at concentrations approaching 1M. At that concentration, it is important to select a reagent with low UV absorption.

The latter three cases are most commonly employed to reduce wall effects. In the third case, amine modifiers such as polyamines are added to the BGE at concentrations ranging from 1 to 60 mM [10]. These reagents coat the free silanols and reduce wall interactions. Now, any pH electrolyte can be employed. Diaminobutane, otherwise known as putrescine, is the preferred reagent because it is less volatile compared to diaminopropane. Monovalent amines such as triethanolamine are not as effective in this regard.

Dynamically coated capillaries (case d) are often used to reduce wall effects [11]. The mechanism of

charge reversal is as follows. Ion-pair formation between the cationic head group of the surfactant and the anionic silanol group naturally occurs. The hydrophobic surfactant tail extending into the bulk solution is poorly solvated by water. The molecular need for solvation is satisfied by binding to the tail of another surfactant molecule. The cationic head group of the second surfactant molecule now extends into the bulk solution. The capillary wall becomes positively charged and the EOF is directed toward the anode. Separations are performed using the reversed-polarity mode (inlet side negative). Following this approach, a buffer pH is selected that is below the pI of the target protein. The cationic protein is now repelled from the cationic wall.

When coated capillaries are employed (case e), conventional buffers without additives to reduce wall effects are used. Urea and/or organic solvents can be added to aid solubility. Reagents for secondary equilibrium can be used as well. It is best to operate at a pH below 8 to maximize the stability of the often labile coating material. Coated capillaries are also used simply to eliminate the EOF in some applications.

References

1. P. G. Righetti, C. Gelfi, M. Perego, A. V. Stoyanov, and A. Bossi, *Electrophoresis*, 18: 2145 (1997).
2. D. Burgi and R.-L. Chien, *Anal. Chem.* 63: 2042 (1991).
3. P. Jandik, W. R. Jones, A. Weston, and P. R. Brown, *LC-GC* 9: 634 (1991).
4. M. Macka, P. Andersson, and P. R. Haddad, *Anal. Chem.* 70: 743 (1998).
5. S. A. C. Wren and R. C. Rowe, *J. Chromatogr.* 603: 235 (1992).
6. H. Nishi and S. Terabe, *J. Chromatogr. A* 735: 3 (1996).
7. B. Chankvetadze, *Capillary Electrophoresis in Chiral Analysis*, John Wiley & Sons, Chichester, 1997.
8. R. Weinberger, *Am. Lab.* 31: 59 (1999).
9. H. H. Lauer and D. McManigill, *Anal. Chem.* 58: 166 (1986).
10. J. A. Bullock and L.-C. Yuan, *J. Microcol. Separ.* 3: 241 (1991).
11. J. E. Wiktorowicz and J. C. Colburn, *Electrophoresis* 11: 769 (1990).



Buffer Type and Concentration, Effect on Mobility, Selectivity, and Resolution in Capillary Electrophoresis

Ernst Kenndler

Institute for Analytical Chemistry, University of Vienna, Vienna, Austria

Introduction

Resolution in capillary zone electrophoresis (CZE) is, as in elution chromatography, a quantity that describes the extent of the separation of two consecutively migrating compounds, i and j . It is the result of the counterplay of two effects: migration and zone dispersion. The different migration velocities of the two separands lead (at least potentially) to the separation of the sample zones. The simultaneous mixing of the samples with the background electrolyte (BGE), caused by a number of processes, results in zone broadening and counteracts separation. Both effects determine the overall degree of separation. A quantitative measure that describes this degree is the resolution R_{ji} , a dimensionless number. It is expressed by the difference of the apex of the two peaks, on the one hand. It is of advantage not to measure this difference in an absolute scale (e.g., in seconds when the electropherogram is depicted in the time domain). In fact, a relative scale is taken, which is based on the widths of the peaks. We define the resolution as the difference in migration times, t , related to the peak width, taken, for example, by the mean standard deviation of the Gaussian peaks, as the scaling unit:

$$R_{ji} \equiv \frac{t_j - t_i}{2(\sigma_{t,i} + \sigma_{t,j})} \quad (1)$$

Baseline separation is achieved for two peaks with the same area when the resolution is 1.5. For peak area ratios larger than unity, the resolution must be larger.

Selectivity and Efficiency

This definitional equation (1) is not very operative and is, thus, transformed to an expression which more clearly visualizes the dependence of the resolution on sample properties and experimental variables. The migration times are substituted for by the mobilities of the separands, and the standard deviations by the plate

height, H , or the plate number, N , respectively. The resulting resolution is then

$$R_{ji} = \frac{1}{4} \frac{\mu_i - \mu_j}{\bar{\mu}} \sqrt{\frac{L}{\bar{H}}} = \frac{1}{4} \frac{\Delta\mu}{\bar{\mu}} \sqrt{\bar{N}} \quad (2)$$

where $\bar{\mu}$, \bar{H} , and \bar{N} are the average values; L is the migration distance.

The resolution consists of two terms, the selectivity term, $\Delta\mu/\bar{\mu}$, with the relative difference of the mobilities, and the efficiency term, the square root of the mean plate number. It must be pointed out that the plate height, \bar{H} , on which this plate number is based consists of all the contributions to peak broadening.

At this point, a differentiation should be made between two cases: the simple one, where migration is only caused by the electric force on the ionic separands, and the second, where an additional migration due to the occurrence of an electro-osmotic flow (EOF) takes place.

Resolution in Absence of EOF

Two main parameters determine the resolution: the effective mobility and the plate number. The effective mobility of a simple ion (e.g., the anion from a monovalent weak acid) is given by

$$\mu_{\text{eff}} = \frac{\mu_{\text{act}}}{1 + 10^{\text{p}K_a - \text{pH}}} \quad (3)$$

We take, here, only protolysis into consideration and do not discuss such important other equilibria such as complexation or interactions with pseudo-stationary phases. It follows from Eq. (3) that the effective mobility depends on the actual mobility (that of the fully charged particle at the ionic strength of the experiment), on the $\text{p}K_a$ value of the analyte, and on the pH of the BGE. It follows that all these properties determine the selectivity term in the resolution.

The actual mobility depends on the following:

1. *The solvent.* There is a more or less pronounced influence of the solvent viscosity, reflected by



Walden's rule. However, this rule is obeyed in rare cases; mainly in some mixed aqueous–organic solutions is an acceptable agreement found. On the other hand, in very viscous aqueous solutions of water-soluble polymers, such as poly(ethylene glycol), it was found that the actual mobility is independent of the viscosity.

2. *The size of the solvated ion.* Here, we must note that water is an excellent solvent for anions and cations as well, compared to most organic solvents. Only few exceptions for preferred solvation of the organic solvents are found (e.g., for Ag^+ and acetonitrile).
3. *The ionic strength of the BGE.* The dependence of the mobility on the ionic strength is expressed for simple systems (and simple ions) by the theory of Debye, Hückel, and Onsager. Without going into detail, we can state that the mobility decreases, in all cases, with increasing ionic strength of the BGE, and the decrease is more pronounced the higher the charge number of the ion.
4. *On the temperature.* In aqueous solutions, the mobility increases with temperature roughly by about 3% per degree. This is a strong effect as, for example, a temperature difference of only 5K between the center and the wall of the separation capillary leads to a mobility difference of about 15%.

The $\text{p}K_a$ value is also a function, mainly, of the solvent. Note that the pH scale is strongly dependent on the kind of solvent. Restricting the discussion to protolysis, it can be followed that the pH of the buffer has the most pronounced effect on the effective mobility, because the other effects change the mobility roughly in parallel for all separands. Again, it must be pointed out that other equilibria have an enormous potential to affect the effective mobility (cf. e.g., the use of cyclodextrins to introduce selectivity for the separation of enantiomers).

How is the efficiency influenced by the BGE? Peak broadening is the result of different processes in CZE occurring during migration [in addition, extracolumn effects contribute to peak width (e.g., that stemming from the width and shape of the injection zone, or the aperture of the detector cell)]. If the system behaves linearly, the individual peak variances (the second moments), σ_{ind}^2 , are additive according to

$$\sigma_{\text{tot}}^2 = \Sigma \sigma_{\text{ind}}^2 = \sigma_{\text{extr}}^2 + \sigma_{\text{dif}}^2 + \sigma_{\text{Joule}}^2 + \sigma_{\text{conc}}^2 + \sigma_{\text{ads}}^2 \quad (4)$$

where the subscripts extr, dif, Joule, conc, and ads indicate the contributions from extracolumn dispersion, longitudinal diffusion, Joule self-heating, concentration

overload, and wall adsorption, respectively. All but one effect might be eliminated: The longitudinal diffusion is inevitable. Plate number expressing this contribution is dependent on the voltage, U , applied and on the charge number, z_i , of the analytes according to

$$N_i \approx 20z_i U \quad (5)$$

at 20°C. It is obvious that the charge number depends on the pH of the BGE, as it is related to the degree of ionization. It follows that the plate number is a function of the pH as well. Thus, the resolution is influenced by the pH of the BGE twofold: via the selectivity, on the one hand, and via the plate number, on the other hand.

In conclusion, it follows for the limiting case of longitudinal diffusion as the only peak-broadening effect, that the resolution depends on the following:

- Instrumental variables: U and T
- Analyte parameters: μ_{act} and $\text{p}K_a$
- Chemical conditions determining the degree of ionization, α , or charge number z .

Resolution in Presence of EOF

The EOF brings an additional, unspecific velocity vector to the electrophoretic migration of the separands. The total migration velocity of the analyte, i , is then

$$v_{i,\text{tot}} = (\mu_{i,\text{eff}} + \mu_{\text{EOF}})E \quad (6)$$

Note that the mobilities are taken as signed quantities. By convention, cations have positive electrophoretic mobilities and those of anions are negative. The mobility of the EOF when directed toward the cathode has positive sign, and vice versa.

The effect of the EOF on migration time and selectivity depends on the mutual signs of the mobilities of analytes and EOF, respectively. Concerning the change in separation selectivity, we refer to the expression of the selectivity term in the resolution equation. The difference between the mobilities of the two separands, i and j , will not be influenced by the EOF. However, the mean mobility is larger for the case of comigration. This means that the selectivity term in the expression for the resolution is always reduced in this case. In practice, selectivity is lost for cation separation when the EOF is directed, as is usual in uncoated fused-silica capillaries, toward the cathode. For this reason, cationic additives are applied in the BGE to reverse the EOF direction.

The effect of the EOF on separation selectivity (in comparison with the situation without EOF) can be

quantified by the so-called electromigration factor, or reduced mobility, μ_i^* , defined as

$$\mu_i^* = \frac{\mu_{i,\text{eff}}}{\mu_{i,\text{eff}} + \mu_{\text{EOF}}} \quad (7)$$

The change of the selectivity term in the resolution is directly expressible by μ_j^* . Interestingly, the effect of the EOF on the dispersion effects, expressed by the plate height H , also depends directly on μ^* . For longitudinal diffusion, Joule self-heating, and concentration overload, the variation of the plate height in the presence of the EOF is directly dependent upon this reduced mobility according to

$$H^{\text{EOF}} = H^0 \mu^* \quad (8)$$

where the superscript 0 indicates the system without EOF. For wall adsorption, the corresponding effect is related to the reciprocal of μ^* .

An analysis of the effect of the EOF on the resolution brings the following result: For comigration of the analyte and EOF, the efficiency always increases and the selectivity term always decreases. As the decrease is directly proportional to μ^* but the gain in plate number is only increasing with the square root of μ^* , the resolution is always worse than without comigrating EOF.

For the case of counter migration, the situation is more complicated, because the overall effect depends on the magnitude of the mobility of analyte and that of the EOF. Roughly, it can be concluded that the res-

olution is increased for a given pair of analytes when the EOF is counterdirected, and it has a lower mobility than the analytes. Here, efficiency is lost, but selectivity is gained overproportionally. When the EOF mobility reaches a value that is twice as large as the analyte mobility (note that the signs of the mobilities are different), an analogous situation is found as without EOF. At mobilities of the EOF larger than twice the analyte mobility (conditions not impossible for high pH values of the BGE), resolution is worse here than without EOF, but the analysis time is shorter than in all other cases. It should be pointed out that all of these effects can be quantified by the reduced mobility defined in Eq. (7).

Suggested Further Readings

- Camillieri, P., *Capillary Electrophoresis, Theory and Practice*, CRC Press, Boca Raton, FL, 1998.
- Giddings, J. C., *J. Chromatogr.* 480: 21 (1989).
- Guzman, N. A., *Capillary Electrophoresis Technology*, Marcel Dekker, Inc., New York, 1993.
- Kenndler, E., *J. Microcol. Separ.* 10: 273 (1998).
- Kenndler, E., in *High Performance Capillary Electrophoresis, Theory, Techniques and Applications*, M. G. Khaledi (ed.), John Wiley & Sons, New York, 1998, Vol. 146, pp. 25–76.
- Landers, J. P., *Handbook of Capillary Electrophoresis*, 2nd ed. CRC Press, Boca Raton, FL, 1997.
- Reijenga, J. C., and E. Kenndler, *J. Chromatogr. A* 659: 403 (1994).



Calibration of GPC–SEC with Narrow Molecular-Weight Distribution Standards

Oscar Chiantore

Università degli Studi di Torino, Torino, Italy

Introduction

In size-exclusion chromatography (SEC), polymer solutions are injected into one or more columns in series, packed with microparticulate porous packings. The packing pores have sizes in the range between ~ 5 and 10^5 nm, and during elution, the polymer molecules may or may not, depending on their size in the chromatographic eluent, penetrate into the pores. Therefore, smaller molecules have access to a larger fraction of pores compared to the larger ones, and the macromolecules elute in a decreasing order of molecular weights. For each type of polymer dissolved in the chromatographic eluent, and eluting through the given set of columns with a pure exclusion mechanism, a precise empirical correlation exists between molecular weights and elution volumes. This relationship constitutes the calibration of the SEC system, which allows the evaluation of average molecular weights (MWs) and molecular-weight distributions (MWDs) of the polymer under examination.

Direct column calibration for a given polymer requires the use of narrow MWD samples of that polymer, with molecular weights covering the whole range of interest. The polydispersity of the calibration standards must be less than 1.05, except for the very low and very high MWs ($< 10^3$ and $> 10^6$), for which polydispersity can reach 1.20. The chromatograms of such standards give narrow peaks and to each standard is associated the retention volume of the peak maximum.

There is a limited number of polymers for which narrow MWD standards are commercially available: polystyrene, poly(methyl methacrylate), poly(α -methyl styrene), polyisoprene, polybutadiene, polyethylene, poly(dimethyl siloxane), polyethyleneoxide, pullulan, dextran, polystyrene sulfonate sodium salt, and globular proteins. In some cases, the standards available cover a limited molecular weight range, so it may be impossible to construct the calibration curve over the complete column pore volume.

Standard methods for calibration of SEC columns with narrow MWD samples have been published by the American Society for Testing and Materials (ASTM

D2596-97) and the Deutsches Institut for Normung (DIN 55672-1).

Procedure

Fresh solutions of the standards are prepared in the solvent used as chromatographic eluent. Calibration solutions should be as dilute as possible, in order to avoid any concentration dependence of sample retention volumes. The concentration effect causes an increase of retention volumes with increased sample concentration. As a rule of thumb, when high efficiency microparticulate packings are used, the concentration of narrow standards should be $\leq 0.025\%$ (w/v) for MW over 10^6 , $\leq 0.05\%$ for MW between 10^6 and 2×10^5 , and $\leq 0.1\%$ for MW down to 10^4 . With a lower MW and in the oligomer range, the sample concentration can be higher than the previously suggested values.

Two or more standards may be dissolved and injected together to determine several retention volumes with a single injection. In such a case, the MW difference between the samples in the mixture should be sufficient to give peaks with baseline resolution. A sufficient number of narrow MWD standards, with different MWs, are required for establishing the calibration of a SEC column system. At least two standards per MW decade should be injected, and a minimum of five calibration points should be obtained in the

MW Fractionation Range of the Column Set

The maximum injection volume depends from column size and packing pore volumes, and for high-efficiency 300×8 -mm columns, it is generally recommended not to exceed $100 \mu\text{L}$ per column.

The flow rate of the chromatographic apparatus must be extremely stable and reproducible: Flow rate fluctuations about the specified value should be lower than 3%, and long-term drift lower than 1%. Repeatability of flow rate setting is extremely important, as a 1% constant deviation of the actual flow rate from the



required value may give 20% differences in calculated MW averages.

The systematic errors introduced by flow rate differences may be avoided by adding to the solutions a minimum amount of a low-molecular-weight internal standard (*o*-dichloro benzene, toluene, acetone, sulfur) which must not interfere with the polymer peaks. Flow rate is monitored in each chromatogram by measuring the retention time of the internal standard, and eventual variations may be corrected accordingly.

The peak retention times for the narrow polymer standards are measured from the chromatograms and transformed into retention volumes according to the real flow rate. For each standard, the logarithm of nominal molecular weight is plotted against its peak elution volume. Often, retention times are directly employed and plotted as the measured variable, and in this case, the condition of equal flow rate elutions for all the standards and for any subsequent sample analysis is achieved by means of the internal standard elution.

The molecular weight of the standards is supplied by the producers, either with a single value which should correspond to that of peak maximum, or with a complete characterization data sheet containing the values of M_n and M_w determined by osmometry and light scattering. In the latter case, the peak molecular weight to be inserted in the calibration plot is the mean value $(M_n M_w)^{1/2}$. A typical calibration curve for a three-column set, $300 \times 7.5 \mu\text{m}$, packed with a mixture of individual pore sizes is shown in Fig. 1. The calibration curve has a central part which is essentially linear and becomes curved at the two extremes: on the high-MW side when it approaches the retention value of totally excluded samples; on the low-MW side with a downward curvature until it reaches the retention time of total pore permeation.

The calibration curve, therefore, defines the extremes of retention times (or volumes) for the specific column system, the useful retention interval for sample analysis, and the related MW range. Columns packed with a balanced mixture of different pore sizes are capable of giving linear calibrations over the whole MW range of practical interest, from the oligomer region to more than 10^6 .

The plot of $\log M$ versus peak retention volumes of narrow standards is represented in the more general form by a n th-order polynomial of the type

$$\log M = A + BV_r + CV_r^2 + DV_r^3 + \dots$$

the coefficients of which are determined by regression on the experimental data. Most usually, when the lin-

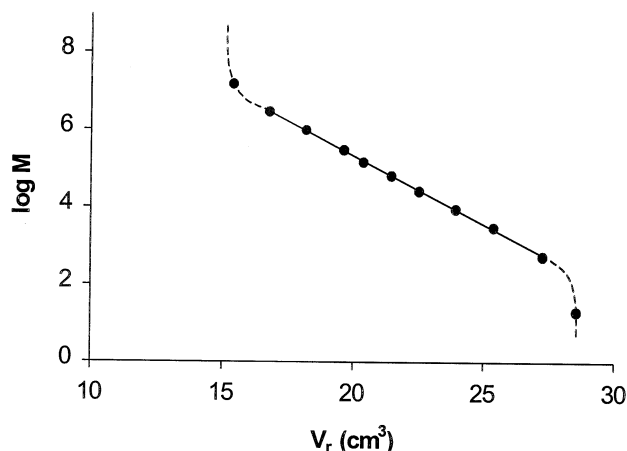


Fig. 1 Example of calibration curve with narrow MWD standards.

ear plot is not sufficient to fit the points, a third-order polynomial will be adequate to represent the curve. Higher-order equations, although improving the fit, should be used with great care, as they can lead to unrealistic oscillations of the function.

The goodness of different equations fitted to the experimental data points is assessed by the results of statistical analysis or by simply considering the standard error of the estimate. It should be also considered that the adequacy of the calibration function for the determination of correct MW values is also dependent on the quality of the narrow MWD standards. Their nominal MWs are determined with independent absolute methods and are affected by experimental errors which may be different between samples with different MWs, or coming from different producers. A check of the quality of the narrow standards may be obtained by calculating the percent MW deviation of each standard from the calibration curve:

$$\Delta M(V_i) \% = \frac{M_{\text{peak}}(V_i) - M_{\text{calc}}(V_i)}{M_{\text{peak}}(V_i)} \times 100$$

A plot of $\Delta M(V_i) \%$ versus $\log M$ results in positive and negative values scattered around the MW axis, which allows one to visualize the limits of percent error into which the MW of standards are estimated by the calibration curve. If the MW error of some standard is found to be significantly larger than all the others, it is likely that its nominal MW is incorrect. The point of such sample should be removed from the calibration and the regression recalculated.

The calibration curve should always cover the MW of the samples that must be analyzed. Extrapolation of

the calibration outside the range of injected polymer standards should be avoided in MW determinations.

From the calibration curve, the resolution power of the column set may also be evaluated. Resolution between two adjacent peaks, 1 and 2, is defined in terms of their retention volumes, V_r , and peak widths, w :

$$R_s = \frac{2(V_{r2} - V_{r1})}{w_1 + w_2}$$

The calibration is often expressed in the form of $\ln M$ versus V_r , and assuming a linear function, it may be written as

$$\ln M = \ln D_1 - D_2 V_r$$

By solving for V_r and substituting into the relationship for R_s , we obtain

$$R_s = \frac{\ln(M_1/M_2)}{wD_2} = \frac{\ln(M_1/M_2)}{4\sigma D_2}$$

valid for peaks of similar width or standard deviation σ , where $w_1 \approx w_2 = w = 4\sigma$. The above equation

shows that the MW fractionation of SEC columns is linked to both their useful pore volume (slope D_2 of the calibration curve) and to packing quality (column efficiency or number of plate heights, determining peak widths). Working with columns having linear calibration in their whole fractionation range guarantees equal resolution power over several MW decades.

Suggested Further Readings

- ASTM D 5296-97, Standard Test Method for Molecular Weight Averages and Molecular Weight Distribution of Polystyrene by High Performance Size-Exclusion Chromatography (1997).
- DIN 55672-1, Gelpermeationschromatographie Teil 1: Tetrahydrofuran als Elutionsmittel (1995–02) (1995).
- Janca, J. (ed.), *Steric Exclusion Liquid Chromatography of Polymers*, Marcel Dekker, Inc., New York, 1984.
- Mori, S. and H. Barth, *Size Exclusion Chromatography*, Springer-Verlag, Berlin, 1999.
- Yau, W. W., J. J. Kirkland, and D. D. Bly, *Modern Size-Exclusion Liquid Chromatography*, John Wiley & Sons, New York, 1979.



Calibration of GPC–SEC with Universal Calibration Techniques

Oscar Chiantore

Università degli Studi di Torino, Torino, Italy

Introduction

Direct calibration of GPC–SEC columns requires well-characterized polymer standards of the same type of polymer one has to analyze. However, narrow molecular-weight distribution (MWD) standards are available for a limited number of polymers only, and well-characterized broad MWD standards are not always accessible. The parameter controlling separation in GPC–SEC is the size of solute in the chromatographic eluent. Therefore, if different polymer solutes are eluted in the same chromatographic system with a pure exclusion mechanism, at the same retention volume, molecules with the same size will be found.

Discussion

By plotting the logarithm of solute size versus retention volume, the points of all different polymers will be represented by a unique curve – a universal calibration curve. Thus, by application of the universal calibration, average molecular weights (MWs) and MWDs of any type of polymer may be evaluated from the size-exclusion chromatograms, provided that the relationship between molecular size and polymer molecular weight is known.

Several size parameters can be used to describe the dimensions of polymer molecules: radius of gyration, end-to-end distance, mean external length, and so forth. In the case of SEC analysis, it must be considered that the polymer molecular size is influenced by the interactions of chain segments with the solvent. As a consequence, polymer molecules in solution can be represented as equivalent hydrodynamic spheres [1], to which the Einstein equation for viscosity may be applied:

$$\eta = \eta_0(1 + 2.5\phi_s) \quad (1)$$

η and η_0 are the viscosities of solution and solvent, respectively, and ϕ_s is the volume fraction of solute particles in the solution.

By expressing the solute concentration c in grams per cubic centimeter, the relationship holds:

$$\phi_s = \frac{cN_A V_h}{M} \quad (2)$$

where N_A is Avogadro's number and V_h and M are the hydrodynamic volume and the molecular weight of the solute, respectively. Substituting in Eq. (1) and taking into account that

$$[\eta] = \lim_{c \rightarrow 0} \left(\frac{(\eta - \eta_0)/\eta_0}{c} \right) \quad (3)$$

we obtain

$$[\eta]M = 2.5N_A V_h \quad (4)$$

Equation (4) states that the hydrodynamic volume of a polymer molecule is proportional to the product of its intrinsic viscosity times the molecular weight.

The use of $[\eta]M$ as size parameter for GPC–SEC universal calibration was first proposed by Benoit and co-workers [2] and shown to be valid for homopolymers and copolymers with various chemical and geometrical structures. Their data are reported in the semilogarithmic plot of Fig. 1.

The hydrodynamic volume parameter $[\eta]M$ has been proven to be applicable also to the cases of rod-like polymers [3] and to separations in aqueous solvents [4] where, however, secondary nonexclusion mechanisms often superimpose and affect the sample elution behavior. In the latter situation, careful choice of eluent composition must be made in order to avoid any possible polymer-packing interaction.

The application of universal calibration requires a primary column calibration with elution of narrow MWD standards. For SEC in tetrahydrofuran, polystyrene (PS) standards are generally used. Intrinsic viscosities of the standards are either known or calculated from the proper Mark–Houwink equation, so that the plot of $\log[\eta]_{\text{PS}}M_{\text{PS}}$ values versus retention vol-



umes V_r may be created. The universal calibration equation is obtained by polynomial regression, in the same way described for the calibration with narrow MWD standards.

Average molecular weights and MWDs of any polymer sample eluted on the same columns with pure exclusion mechanism may be calculated by considering that, at any retention volume, the following relationship holds:

$$[\eta]_i M_i = [\eta]_{PS,i} M_{PS,i} \quad (5)$$

from which

$$M_i = \frac{[\eta]_{PS,i} M_{PS,i}}{[\eta]_i} \quad (6)$$

To solve Eq. (6), the denominator must be known. Substituting into the denominator the Mark–Houwink expression $[\eta] = KM^a$ for the investigated polymer and rearranging, we obtain

$$M_i = \left(\frac{[\eta]_{PS,i} M_{PS,i}}{K} \right)^{1/1+a} \quad (7)$$

where K and a are the constants of the viscosimetric equation for that polymer, dissolved in the chromatographic eluent and at the temperature of analysis.

From Eq. (7), the molecular weight of each fraction in the chromatogram is obtained and average molecular weights may be calculated by application of the appropriate summations. The numerator in Eq. (7) is the value of the universal calibration at each retention volume.

The necessary conditions for application of the universal calibration method and for calculation of molecular weights through Eq. (6) is the knowledge of the $[\eta]_i$ values, which are obtained from the Mark–Houwink equations when the pertinent values of K and a constants are known. An alternative way is to make a continuous measurement of $[\eta]_i$ at the different elution volumes with an on-line viscometer detector coupled to the usual concentration detector system.

Methods for application of the universal calibration have been developed also for cases where K and a of the polymer of interest are not known and neither $[\eta]_i$ values are measured. Such methods are based on the availability of two broad MWD standards, having different molecular weights, of the polymer under examination [5].

One important property of the universal calibration concept is that, in the SEC separation of complex polymers (i.e., polymers with different architectures or copolymers with nonconstant chemical composition), at

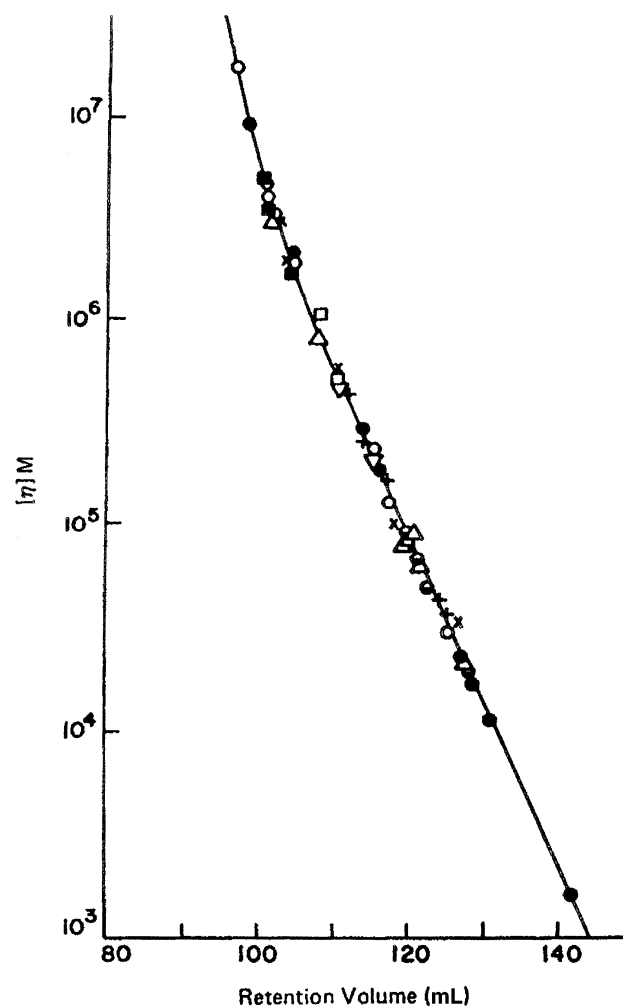


Fig. 1 Retention volume versus $[\eta]M$. (From Ref. 2, © J. Wiley & Sons, Inc.)

each retention volume, $V_{r,i}$, molecules with same hydrodynamic volume but possibly different molecular weights will elute. It has been demonstrated that, in such a case, the application of the hydrodynamic volume parameter, $[\eta]M$ gives the number-average molecular weight, M_n , of the polymer [6]. In fact, at each retention volume, the intrinsic viscosity of the eluted fraction is given by the weight average over the n different molecular species present:

$$[\eta]_i = w_1[\eta]_1 + w_2[\eta]_2 + \dots + w_n[\eta]_n \quad (8)$$

Equation (8) may be written as

$$[\eta]_i = \frac{[\eta]_1 M_1 w_1}{M_1} + \frac{[\eta]_2 M_2 w_2}{M_2} + \dots + \frac{[\eta]_n M_n w_n}{M_n} \quad (9)$$

As the condition holds, at each retention volume

$$[\eta]_1 M_1 = [\eta]_2 M_2 = \cdots = [\eta]_{PS} M_{PS} \quad (10)$$

Equation (9) becomes

$$[\eta]_i = [\eta]_{PS} M_{PS} \sum \left(\frac{w_i}{M_i} \right) = \frac{[\eta]_{PS} M_{PS}}{M_{n,i}} \quad (11)$$

$$[\eta]_i M_{n,i} = [\eta]_{PS} M_{PS} \quad (12)$$

By considering all the fractions of the chromatogram, the M_n value of the whole sample may be then calculated.

Experimental aspects for the determination of molecular weight averages and MWD distributions by GPC–SEC using universal calibration are described in a standard ASTM method [7]. Detailed discussion on the validity and limitations of the method may be also found in Ref. 8.

References

1. P. J. Flory, *Principles of Polymer Chemistry*, Cornell University Press, Ithaca, NY, 1953.
2. Z. Grubisic, P. Rempp, and H. Benoit, *J. Polym. Sci. B* 5:753 (1967).
3. J. V. Dawkins and M. Hemming, *Polymer* 16:554 (1975).
4. P. L. Dubin, *Aqueous Size Exclusion Chromatography*, Elsevier, Amsterdam, 1988.
5. H. Coll and D. K. Gilding, *J. Polym. Sci. A-2*, 8:89 (1970).
6. A. E. Hamielec, A. C. Ouano, and L. L. Nebenzahl, *J. Liquid Chromatogr. I*:111 (1978).
7. ASTM D 3593-80, Standard Test Method for Molecular Weight Averages and Molecular Weight Distribution of Certain Polymers by Liquid Size-Exclusion Chromatography (Gel Permeation Chromatography – GPC) Using Universal Calibration (1980).
8. J. V. Dawkins, in *Steric Exclusion Liquid Chromatography of Polymers* (J. Janca ed.), Marcel Dekker, Inc., New York, 1984.



Capacity

M. Caude

A. Jardy

ESPCI, Paris, France

Introduction

The capacity is closely related to the number of active sites of the stationary phase per volume or mass unit. Practically, there are two definitions corresponding to two different approaches to the problem. On the one hand, there is the linear capacity and, on the other, the maximum available capacity.

Discussion

It is well known that when increasing the injected sample quantity, whether in volume or in concentration, peaks are distorted and/or shifted beyond a cer-

tain limit; the column is said to be overloaded. To quantify how much sample can be injected into a column without altering the resolution, it is convenient to define the column linear capacity. It is well known, for small injected quantities, that solute retention times and column efficiency are not affected by the sample size. However, above a critical sample size, a noticeable decrease in retention time and column efficiency are always observed.

Snyder has defined [1] the adsorbent linear capacity as the ratio (weight sample)/(weight stationary phase) giving a value of k' (or V_R) reduced by 10% relative to the constant k' values measured for smaller samples (Fig. 1). In Figure 1, the adsorbent (Silica Davison) has a linear capacity close to 0.5 mg of dibenzyl per gram of silica. When the linear capacity of the column is exceeded, qualitative and quantitative analyses become much more complicated. Retention factors vary according to the injected solute quantity and the column efficiency can be tremendously decreased, entailing a degradation of resolution. Therefore, for analytical separations, it is always preferable to choose operating conditions corresponding to the linear capacity (k' and N values are constant whatever the injected sample sizes).

However, the practical interest of column linear capacity is very limited because its value varies according to various parameters: solute nature and retention and, even for the same quantity of injected solute, both the injected volume and the solute concentration of the injected solution. Thus, although widely accepted, the column linear capacity is misleading because it characterizes not only the thermodynamic nature of the chromatographic system but also the kinetic conditions (in term of column efficiency).

Consequently, it is preferable, according to Gareil et al. [2], to define the concept of maximum available capacity C_D for a stationary phase:mass of solute Q_s entailing the saturation of the mass m of stationary phase contained in the column for given operating conditions:

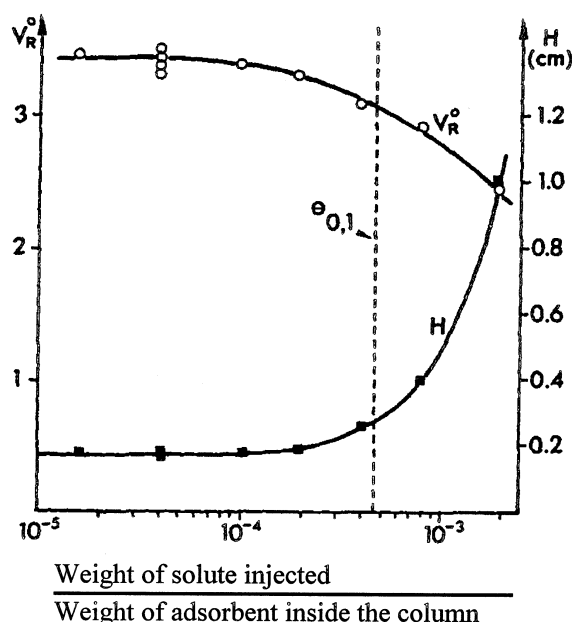


Fig. 1 Variation of the specific retention volume V_R^0 and of the height equivalent to a theoretical plate H as a function of the weight of injected solute (dibenzyl) related to the weight of adsorbent inside the column. (From Ref. 1.)



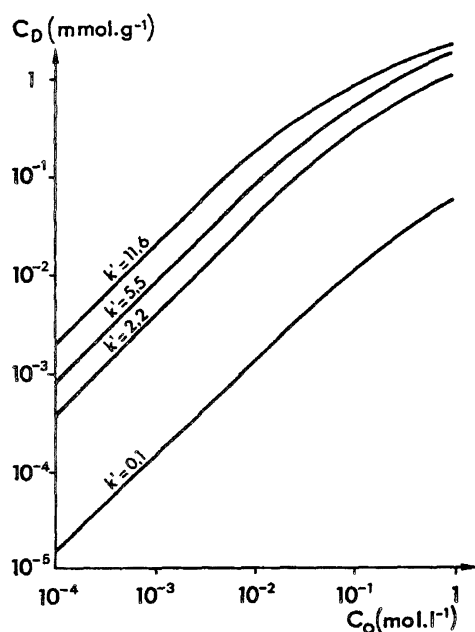


Fig. 2 Variation of the available capacity C_D as a function of the solute concentration in the mobile-phase C_0 (logarithm scales). In the case of reversed-phase chromatography, the stationary phase is *n*-octyl-bonded silica Lichroprep R.P.8 with 11.6% of carbon, the mobile phases are water–methanol mixtures, and the solute is phenol.

$$C_D = \frac{Q_s}{m} \quad (1)$$

with

$$k' = \frac{Q_s}{Q_m} = \frac{Q_s}{V_m C_0} \quad (2)$$

The combination of Eqs. (1) and (2) gives

$$C_D = \frac{k' V_m C_0}{m}$$

where k' is the solute retention factor measured for an analytical injection, V_m is the mobile-phase volume

contained in the column, and C_0 is the solute concentration in the mobile phase.

Figure 2 shows, for various retention factors, the available capacity variation versus the solution concentration in the mobile phase in reversed-phase chromatography. These curves, called distribution isotherms, can be divided into two parts. In the first part, a linear variation of C_D versus C_0 is observed (bilogarithm scale); in the second part, a plateau is reached. In the first part and for the same retention (k' constant), the available capacity is independent of the solute nature.

The maximum available capacity is defined as the C_D limit value when both C_0 and k' are high ($C_0 \cong 1 \text{ mol/L}$, $k' \geq 10$). This value does not vary either with C_0 , or k' , or the solute nature (for the same family).

The maximum available capacity depends on the nature of the stationary phase: specific area for adsorption, the ion-exchange capacity for ion-exchange capacity, and the bonded rate for partition chromatography.

As a general rule, the maximum values of available capacity vary from 1.2 mmol/g (silica having a specific area close to 400 m²/g) to 5 mEq/g for the cation exchanger (sulfonate groups).

References

1. L. R. Snyder, *Anal Chem.* 39:698 (1967).
2. P. Gareil, L. Semerdjian, M. Caude, and R. Rosset, J. High. Resolut. Chromatogr. Chromatogr. Commun. 7:123 (1984).

Suggested Further Reading

- Knox, J. H. (ed.), *High Performance Liquid Chromatography*, Edinburgh University Press, Edinburgh, 1978, pp. 27–28, 50.
- Rosset, R., Caude, M., and Jardy, A., *Chromatographies en phases liquide et supercritique*, Masson, Paris, 1991, pp. 32–37.

Capillary Electrochromatography: An Introduction

Michael P. Henry

Advanced Technology Center, Beckman Coulter, Inc., Fullerton, California, U.S.A.

Chitra K. Ratnayake

Bioresearch Systems Development Center, Beckman Coulter, Inc., Fullerton, California, U.S.A.

Introduction

In 1998, Dadoo et al. [1] succeeded in achieving near-baseline resolution of five polynuclear aromatic hydrocarbons in less than 5 s by capillary electrochromatography (CEC) (see Fig. 1). These high speeds were obtained from a combination of factors, including a modest column length (6.5 cm), a high column plate number (13,000 plates) associated with 1.5- μm non-porous C_{18} particles, and a high voltage (28 kV). Although this separation is one of the fastest achieved in a liquid phase, higher column plate numbers have been obtained. Smith and Evans [2] report values of greater than 8 million plates per meter for the analysis of tricyclic antidepressants on a 3- μm sulfopropyl-bonded silica. These values are clearly due to a focusing effect within the column, whose reproducibility has not entirely withstood close scrutiny. Dadoo et al. [1] has produced CEC columns which generate plate numbers of about 700,000 per meter when peaks were detected before they passed through the outlet column frit. These results illustrate how closely practical achievements in CEC have now approached predicted theoretical performance maxima. The technique has not always been such a high performer.

History

Pretorius et al. [3] were among the first investigators to carry out packed column liquid chromatography in a tangential electric field (capillary electrochromatography) as a feasible alternative to using pressure. Their 1- μm -i.d. (inner diameter) quartz columns filled with 75–125- μm silica particles gave reduced plate heights of about 3 by CEC versus the pressure mode values of about 8. This improvement in column efficiency was qualitatively predicted from the fact that the driving force in CEC — electro-osmotic flow — originates from the double electrical layer on the surface of the capil-

lary and sorbent particles and, therefore, generates a relatively flat flow profile across the tube. This has the fundamental effect of producing sharper peaks and, ultimately, higher resolution in a shorter time. Because there are few or no pressure gradients generated within a CEC column, long packed capillaries containing very small particles are possible.

As the mobile phase moves through the capillary containing the sorbent under the effect of this electro-osmotic flow (EOF), sample components partition between the two phases in sorption and diffusive mechanisms characteristic of liquid chromatography. Ions in the sample move both under the influence of EOF and by their added attraction toward the oppositely charged electrode (electrophoresis). Uncharged components, on the other hand, move only under the influence of EOF. Thus, sample components, in general, separate by chromatographic and, sometimes, electrophoretic processes.

The full advantages of electrochromatography were not to be realized until the technology needed to create narrow capillaries (<200 μm i.d.) stable frits and sensitive detection systems had matured. Small-diameter tubes are necessary in order to reduce Joule heating due to the effect of electrical current generated by high voltage.

Thus, in 1981, Jorgenson and Lukacs [4] carried out experiments in CEC using an instrument (see Fig. 2) whose basic design is still used today. In addition to acting as a combined injector, separation medium, and flow cell, their column could also be used in the capillary electrophoresis (CE), CEC, and micro-LC (liquid chromatographic) modes. However, the fused-silica capillaries (170 μm i.d.) drawn in their labs, packed with 10- μm particles and operated in neat acetonitrile, gave rather modest improvements in efficiency over standard liquid chromatographic techniques, with reduced plate heights of no less than 1.9. These disappointing results, coupled with an admission of the technical difficulty of using this technique, led these authors



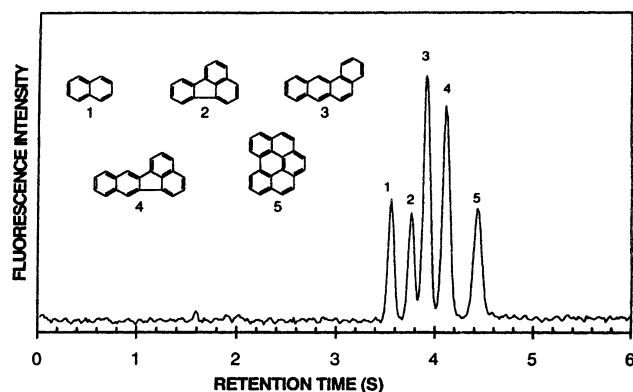


Fig. 1 Electrochromatogram of naphthalene (1), fluoranthene (2), benz[*a*]anthracene (3), benzo[*k*]fluoranthene (4), and benzo[*ghi*]perylene (5), using 1.5- μm nonporous octadecylsilyl bonded (ODS) particles. Column dimensions: 100- μm i.d. \times 6.5-cm packed length (10 cm total length). Mobile phase: 70% acetonitrile in a 2-mM Tris solution; applied voltage for separation: 28 kV; injection: electrokinetic at 5 kV for 2 s. (Reprinted with permission from Ref. 1.)

to conclude that CEC would only be useful in wider-bore (several centimeters) preparative scale processes; a suggestion also made by Pretorius et al. [3].

Then, in 1991, Knox and Grant [5], working carefully with 3- and 5- μm particles, showed that it was practical to achieve dimensionless property of less than 1 in the CEC mode. These results confirmed their strongly optimistic view of the future of this technique, and a few years later, interest in CEC rapidly accelerated.

Operational Limits

Knox and Grant [5] have placed a general maximum limit of 200 μm on the inner diameter of capillaries used in CEC in order to avoid problems with excessive internal heating that harms column efficiency in aqueous/organic solutions. In principle, however, wider-bore tubes can be used, provided the current and field strength are kept low or the thermal conductivity of the system is kept high. In general, currents should be kept below 50 μA and field strengths held below 1000 V/cm.

Capillary electrochromatography in nonaqueous mobile phases is possible provided that the electrical double layer is formed with appropriate dissolved salts [3].

The ionic strength of most conventional buffers, such as phosphate, acetate, or borate, needs to be kept within the range 0.002M to 0.05M, but care needs to be

Capillary Electrochromatography: An Introduction

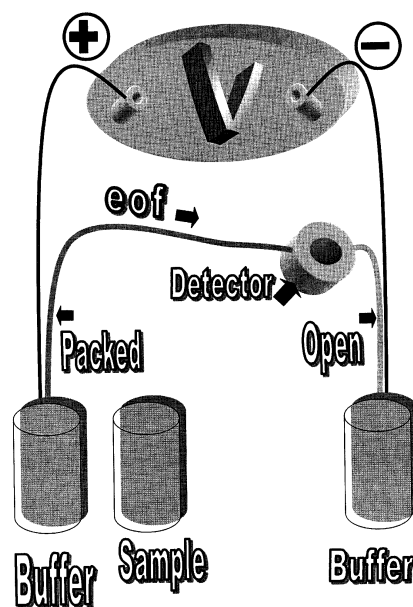


Fig. 2 Schematic of a typical electrochromatograph.

taken with the lower concentration to avoid buffer capacity depletion due to hydrolysis. Zwitterionic buffers such as morpholino ethanesulfonic acid (MES) (whose electrical conductivity is low) can be used in the range 0.010M to 0.1M without undue heating problems, provided the field strength and aqueous content are kept low and the capillary is cooled.

Unlike high-performance liquid chromatography (HPLC), there is no maximum length for capillaries in CEC, but the longer columns mean slower chromatography and equilibration. Generally, columns in CEC are no longer than 60 cm.

Instrumentation

Creative solutions to practical problems abound in the evolution of instruments designed to carry out CEC. Pretorius and co-workers' [3] graphite electrodes, quartz tubing, glass wool frits, and on-column pressure injection gave way to Jorgenson and Lukacs' [4] fused-silica tubing, sintered frits, and electrokinetic injection (see Fig. 2). Commercially developed automated instruments designed for CE, whose appearance in 1988 followed these last authors' breakthrough research, have been used for most applications in CEC. Modern instruments therefore consist of the column, a cooling system, detector, voltage controller, autosampler, and data processor. In-capillary optical focusing of ultraviolet, visible, and laser radiation has largely solved the

problems of detection [1]. In-column (through the packing) detection of appropriate analytes by laser-induced fluorescence has improved the general efficiency by avoiding the deterioration of the peak shape that often occurs as the analyte zone passes through the outlet frit [1].

Columns for modern CEC have been prepared using standard HPLC particles, from 0.5 to 10 μm in diameter, bearing C_{18} , phenyl, C_8 , C_6 , C_4 , CN, amino, sulfo, and other functional groups and a variety of chiral polymers such as proteins and polysaccharides [6]. *In situ* sintered silica-based frits are most often used in these columns [7] which are generally slurry packed at high pressures. Several types of so-called monolithic (single piece) columns have been developed [8] which dispense with frits while generally maintaining high efficiency.

Applications

Most chemical classes have been separated and analyzed by CEC [6]. These include many classes of pharmaceuticals, environmental chemicals, explosives, natural products, drugs of abuse, polypeptides, oligosaccharides, nucleosides, and their bases and polynucleotides. Applications of CEC are readily found in *Analytical Abstracts* for example, a publication of the American Chemical Society, or the indexes of journals such as the *Journal of Chromatography*.

Euerby et al. [9] have systematically investigated the effects of the bonded phase, mobile phase, buffer type, field strength, pH, and temperature on the resolution of specific substituted barbiturates. Critical parameters for the optimization of efficiency of basic drugs by CEC (as for HPLC) include the nature of the sample solvent, pH, and concentration of ion-pair reagents, for example.

Typical buffers include alkali metal and ammonium phosphates and acetates, morpholino ethanesulfonic acid and Tris. Silica-based packings are used in the pH range 2–9. Methanol and acetonitrile are the two most commonly used organic solvents. Ion-pair reagents such as hexylamine and trifluoroacetic acid have been employed for basic compounds.

Problems, Issues, and Future Prospects

A fundamental theory of CEC that will provide a better understanding of mechanisms of separation is being developed. In particular, the work of Rathore and Horváth [10] in elucidating electrical properties of packed is particularly interesting. Technological issues

that remain to be addressed include the difficulty of dealing with bubble formation and the fragility of conventional columns due to the aggressive frit-forming methods currently used. Monolithic columns [8,11,12] appear to have advantages in this regard.

Majors [13] has compiled the results of his perspectives survey of 14 leading separation scientists with an interest in CEC. As expected, there is a wide divergence in the opinions of these leaders with regard to current issues and future prospects for CEC. However, few underestimated the current technological difficulties of column manufacture, reproducibility of chromatographic and electro-osmotic properties of the packed capillary, and the short-term problems of competing with HPLC or CE, but the majority of scientists interviewed believe that like any new technique, these problems will be overcome and that CEC will become a routine method of analysis in time.

On the other hand, the future of CEC may lie with the exciting developments in microfabrication [14], where capillaries are open channels 1.5 μm wide and 4.5 cm long and can achieve efficiencies of 800,000 plates per meter.

References

1. R. Dadoo, R. N. Zare, C. Yan, and D. S. Anex, *Anal. Chem.* 70:4787 (1998).
2. N. W. Smith and M. B. Evans, *Chromatographia* 41:197 (1995).
3. V. Pretorius, B. J. Hopkins, and J. D. Schieke, *J. Chromatogr.* 99:23 (1974).
4. J. W. Jorgenson and K. D. Lukacs, *J. Chromatogr.* 218:209 (1981).
5. J. H. Knox and I. H. Grant, *Chromatographia* 32:317 (1991).
6. K. D. Altria, N. W. Smith, and C. H. Turnbull, *Chromatographia* 46:664 (1997).
7. M. M. Dittman, G. R. Rozing, G. Ross, T. Adam, and K. K. Unger, *J. Capillary Electrophoresis* 5:201 (1997).
8. E. C. Peters, M. Petro, F. Svec, and J. M. J. Freché, *Anal. Chem.* 70:2296 (1998).
9. M. R. Euerby, C. M. Johnson, S. F. Smyth, N. Gillot, D. A. Barrett, and P. N. Shaw, *J. Microcolumn Separ.* 11:305 (1999).
10. A. S. Rathore and Cs. Horváth, *Anal. Chem.* 70:3069 (1998).
11. C. K. Ratnayake, C. S. Oh, and M. P. Henry, *J. Chromatogr. A* 887:277 (2000).
12. C. K. Ratnayake, C. S. Oh, and M. P. Henry, *J. High Resol. Chromatogr.* 23:81 (2000).
13. R. E. Majors, *LC-GC* 16:96 (1998).
14. B. He, N. Tait, and F. Regnier, *Anal. Chem.* 70:3790 (1998).



Capillary Electrophoresis and HPLC for Analysis of Aromatic Diamidines, Comparison of

A. Negro

B. Rabanal

University of León, Leon, Spain

INTRODUCTION

High-performance liquid chromatography (HPLC) can be considered to have been established by Ettre and Horvath. The popularity of HPLC may be explained by the versatility of this technique, which can be used to separate and quantify large or small; polar, nonpolar, or inorganic; and chiral or achiral molecules. In addition, its methods are easily automated, increasing the number of analyses that can be performed in a given time, improving accuracy and precision, as well as reducing costs. It was around 1960 that HPLC achieved its peak growth. This can be attributed, in large part, to its widespread acceptance by the pharmaceutical industry.

Electrophoresis is an analytical technique that was first introduced by Tiselius^[2] in 1937. Thirty-five years ago, Hjertén^[3] showed that it was possible to carry out electrophoretic separations in a 300.0- μ m glass tube and to detect the separation of compounds by ultraviolet absorption. Capillary electrophoresis (CE) did not become popular until 1981, when Jorgenson and Lukacs^[4] published work in which they demonstrated the simplicity of the instrumental setup required and the high resolving power of CE. The results shown were astonishing: sharp narrow peaks, 400,000 theoretical plates per meter (compared with 10,000 theoretical plates per meter of HPLC), and short analysis times. Galery introduced the first commercial instrument in 1988. There are excellent reviews of CE, among which should be mentioned are the ones done by Kuhr, Isaaq or Camilleri. These look at the increasing number of applications and future prospects.

CAPILLARY ELECTROPHORESIS

CE has had considerable success over the last 20 years. Gas chromatography and HPLC^[1] are still the dominant techniques. However, CE has several distinct advantages over other separation techniques.^[5–7] One advantage CE has, relative to HPLC, is its simplicity and applicability for the separation of widely differing substances, such as organic molecules, inorganic ions, and so on, using the same instrument and, in most cases, the same capillary, while

changing only the composition of the buffer used. This cannot be said with regard to any other separation techniques. In addition, CE offers the highest resolving power.

The aim of the work reported here was to study how changes in the principal parameters for each technique affect the separation processes when analyzing a series of aromatic diamidines, and, based on the results obtained, to establish comparisons between the two analytical techniques.

The aromatic diamidines are compounds of considerable pharmaceutical interest. This is, among others, for the following reasons: they have a strong antiprotozoan action and participate in the metabolism and transport of polyamines, inhibiting, for instance, *S*-adenosyl-L-methionine decarboxylase (SAMDC). Therefore, because this route is closely linked to cell proliferation processes, aromatic diamidines can slow down or prevent the growth of tumors.^[8–10] The substances used in this work are as follows:^[11,12]

1. Pentamidine: 4,4'-[1,5-pentanediy] *bis*(oxy)]*bis*-benzenecarboximidamide
2. Stilbamidine: 4,4'-(1,2-ethenediy)]*bis*-benzenecarboximidamide
3. DAPI: 4',6-diamidino-2-(4-amidinophenyl)indole dilactate
4. Propamidine: 4,4'-[1,3-propanediy]bis(oxy)]*bis*-benzenecarboximidamide
5. Hydroxystilbamidine: 4-[2-[4-(aminoiminomethyl)-phenyl]ethenyl]-3-hydroxybenzene-carboximidamide
6. Phenamidine: 4,4'-diamidinodiphenylether
7. Diampron: 3,3'-diamidinocarbanilide
8. Berenil: 4,4'-diamidinodiazamino benzene
9. Dibromopropamidine: 2',2''-dibromo-4',4''-diamidino-1,3-diphenoxypropane.

EXPERIMENTAL TECHNIQUES

Chemicals and Reagents

Pentamidine isethionate salt, berenil diacetate salt, and DAPI dihydrochloride salt were obtained from

Sigma-Aldrich Química SA (Madrid, Spain). Diampron isethionate salt, hydroxystilbamidine isethionate salt, propamidine isethionate salt, dibromopropamidine isethionate salt, phenamidine isethionate salt, and stilbamidine isethionate salt were generously donated by Rhône Poulenc Rorer (Dagenham, UK). The ion-pairing reagents, pentane sulphonate, hexane sulphonate, heptane sulphonate, octane sulphonate, and decane sulphonate sodium salts were supplied by Sigma-Aldrich Química SA. Methanol of HPLC grade and other chemicals of analytical grade were supplied by Merck (Darmstadt, Germany). The water used was purified with a Milli-Q system purchased from Millipore (Bedford, MA).

Chromatographic System

The HPLC system comprised a Beckman 116 programmable solvent pump with a Beckman 168 photodiode detector—this was checked and data were processed with the Gold Nouveau software system (Beckman Coulter, Palo Alto, CA) and a Beckman 507 automatic injector with a 100.0- μ L loop and a heating chamber for the columns. Analyses were carried out with an Ultrasphere ODS column (5.00- μ m particle size, 15.0 cm \times 4.60 mm internal diameter) purchased from Beckman Coulter. A guard column (2.00 cm \times 2.00 mm internal diameter), packed with Spherisorb RP-18 (30.0–40.0 μ m pellicular), was supplied by Upchurch Scientific (Oak Harbor, WA).

Electrophoretic System

The CE system consisted of a P/ACE System 2100 high-performance CE apparatus (Beckman Coulter, Fullerton, CA). An untreated, fused silica capillary tube (Beckman Coulter) was used, with dimensions of 75.0- μ m ID, L_t =57.0 cm, and L_d =50.0 cm, enclosed in a liquid-cooled cassette. Detection was performed with a UV-VIS detector (λ =200.0 nm). Equipment was checked and data were processed with the Beckman P/ACE Station V 1.2 software (Beckman Coulter).

RESULTS AND DISCUSSION

To carry out a comparison of HPLC and CE, the effects of varying the parameters common to the two techniques with the greatest impact on the separation processes were evaluated. These were: pH of the mobile phase and electrolytes, buffer concentration, and temperature, with the gathered data compared in each case.

As these are separation techniques based on radically differing physical principles, it is evident that there are certain parameters, specific to a given technique, that have a strong influence over the separation process in only one

of the two and are not comparable. In HPLC, there is the influence of concentration and chain length of the ion-pairing reagent and the methanol percentage; in CE, there is influence of the choice of electrolyte, length of the capillary, and voltage applied. Variations in these parameters were also taken into account because they provide extremely useful information for making an overall comparison of the two techniques.

Parameters Common to HPLC and CE

Influence of pH in the mobile phase

The pH value is the parameter with the greatest impact on the separation of ionizable molecules. To keep aromatic diamidines ionized, it is necessary to work at very low pH levels, in the range 3.00–4.50, as the diamidine groups twice present in each molecule confer on them a strongly basic character (pK_a =13.86).^[13] To determine the influence of pH in HPLC, five diamidines were analyzed using a mobile phase consisting of 25.0 mM citrate buffer, 45.0% methanol, and 4.00 mM octane sulphonate sodium salt, at a temperature (T) of 30.0°C and at pH values of 3.00, 3.25, and 3.70. The chromatograms obtained are shown in Fig. 1. It can be observed that, as pH increases, retention times are noticeably shortened for all the substances, with no significant variations being noted in resolution. The influence of pH in CE^[14] was studied by using 25.0 mM citrate buffer at T =30.0°C, 14.0 kV voltage, and pH levels of 3.50, 3.70, and 4.25. Figure 1 shows that a drop in pH does not bring with it any large change in migration times, but it does produce a significant variation in resolution. It may be observed that a good separation of all nine diamidines is possible only at pH=3.70. For all the substances, it can be noted that the times required for analyses using CE are around half those in HPLC and that efficiency is much greater in all cases with CE than it is with HPLC, with good resolution. The most appropriate pH levels for the analyses of these substances in aqueous solutions and in the serum and urine are very similar with the two techniques because both require the molecules to be strongly ionized.

Influence of buffer concentration

For HPLC, it has been decided that the preferred buffer is citrate; it was necessary to establish the most suitable concentration. To study this influence, five diamidines were analyzed using a mobile phase consisting of 45.0% methanol, 4.00 mM octane sulphonate, and citrate buffer at various concentrations of 15.0, 25.0, and 35.0 mM, with T =30.0°C and pH=3.25 in all cases. In Fig. 2, we see the results obtained. A change from 25.0 to 35.0 mM barely



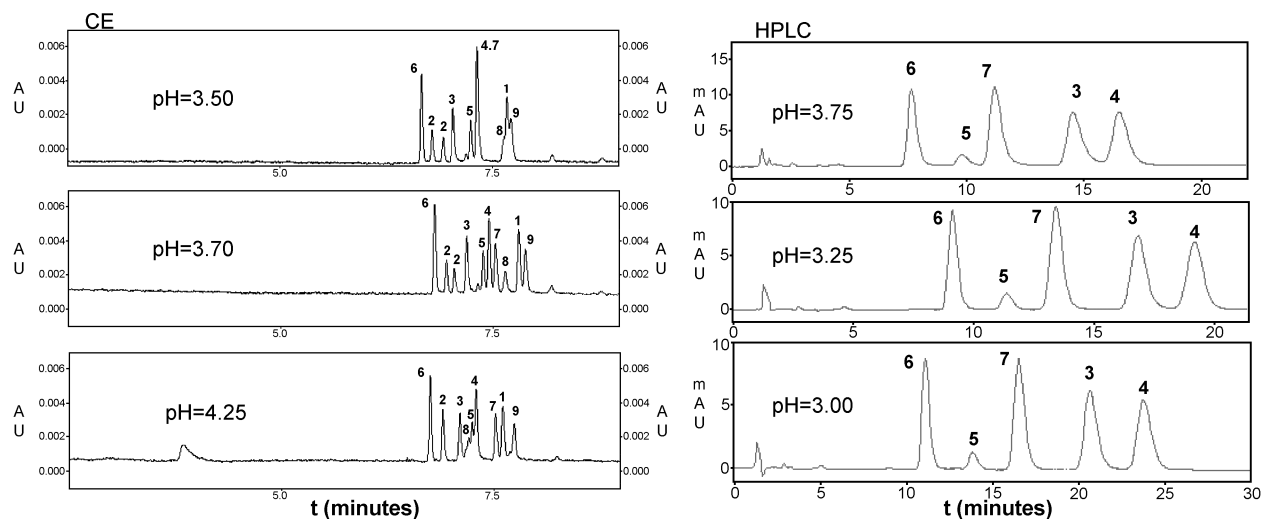


Fig. 1 Influence of pH in HPLC and CE. In HPLC, this effect was studied using a mobile phase consisting of 25.0 mM citrate buffer, 45.0% methanol, $T=30.0^{\circ}\text{C}$, 4.00 mM sodium octane sulphonate, and pH levels of 3.00, 3.25, and 3.75. In CE, a 25.0-mM citrate buffer electrolyte was used; pH values were 3.50, 3.70, and 4.25, and the voltage was 14.0 kV. (View this art in color at www.dekker.com.)

affects retention times for any of the substances, but a drop from 25.0 to 15.0 mM decreases retention times by almost 30.0% in every case.

With CE, citrate buffer was also selected as the electrolyte for the study, and all nine diamidines were analyzed by using an electrolyte composed of citrate buffer at pH=3.70, $T=30.0^{\circ}\text{C}$, and 14.0 kV voltage, at various concentrations (10.0, 25.0, and 40.0 mM), to determine which was the most appropriate. The results obtained are presented in Fig. 2. It can be seen that when

concentrations go down to 10.0 mM, migration times are greatly reduced, but resolution also falls considerably; at 25.0 mM, resolution starts to be acceptable, and, at 40.0 mM, a good compromise between migration times and resolution is achieved. Comparison of the variations in buffer concentration in HPLC and CE allows one to conclude that, in both cases, a decrease in the concentration of the buffer reduces the time required for analyses. This reduction is much more striking in the case of CE and, in every instance, analysis times with CE are on the

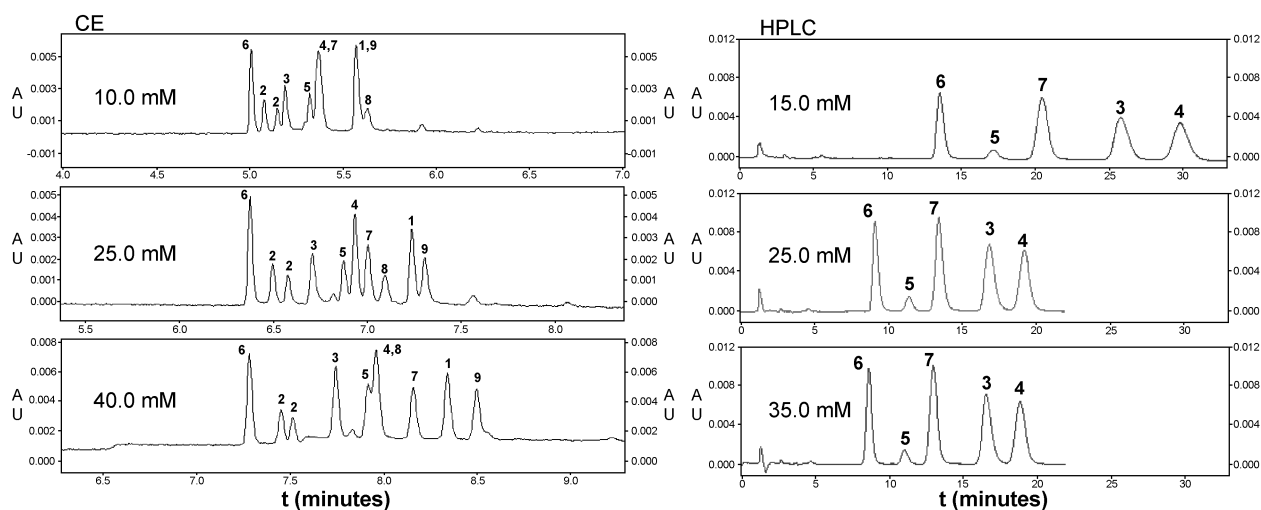


Fig. 2 Influence of buffer concentration in HPLC and CE. In HPLC, this effect was studied using a mobile phase consisting of citrate buffer at concentrations of 15.0, 25.0, and 35.0 mM, with 45.0% methanol, 4.00 mM sodium octane sulphonate, and pH=3.25. In CE, a citrate buffer electrolyte was used at concentrations of 10.0, 25.0, and 40.0 mM, with pH=3.70, voltage, 14.0 kV; and $T=30.0^{\circ}\text{C}$. (View this art in color at www.dekker.com.)

order of half of what they are with HPLC. Consequently, efficiency is much higher for all the compounds with CE than with HPLC, whereas resolution is good in both.

Influence of temperature

To study the effects of temperature in the analysis of these diamidines by means of HPLC, we used a mobile phase composed of 25.0 mM citrate buffer, with pH=3.25, 45.0% methanol, and 4.00 mM octane sulphonate, at three different temperatures: 24.0°C, 30.0°C, and 39.0°C. It may be noted in Fig. 3 that increasing the temperature causes a notable drop in retention times, whereas resolution remains at very good levels.

The temperature at which CE is carried out has to be selected carefully because this is one of the most influential parameters in the CE process.^[15] Precise temperature control during the CE process is of great importance in achieving good separation selectivity and, above all, good reproducibility.^[16,17] To study temperature variation in CE, an electrolyte composed of 25.0 mM citrate buffer, with pH=3.70 and 14.0 kV voltage, was used at temperatures of 25.0°C, 30.0°C, and 40.0°C. Figure 3 shows that an increase in temperature causes a drastic reduction in migration times, but also reduces resolution excessively, causing serious problems for separation from 30.0°C onward.

If CE and HPLC at 30.0°C are compared, it will be noted, as in all previous cases, that CE has much shorter analysis times than HPLC and that efficiency is much higher with CE than with HPLC, with good resolution being attained in both.

Parameters Exclusive to HPLC

Influence of concentration and chain length of the ion pair-forming agent

A technique often used in the analysis of ionic molecules is the formation of ion pairs^[18] because this permits the separation of substances that are too ionized to separate by means of adsorption-partition methods, but are too insoluble in water to be analyzed through ion exchange techniques.^[19] The pH of the mobile phase must be adjusted to ensure that the molecules are totally ionized and can combine with the ion pair-forming agent through the counterion. The substances most often used to form ion pairs are alkyl-sulphonate salts of varying chain length. In this work, several reagents of this type were evaluated, having chain lengths ranging from 5 to 10 carbons; the influence of the concentration of each was also investigated to determine which was the most suitable.

The effects of sulphonate salt concentration and chain length on the retention factor (k') were studied by measuring k' , using only berenil as the diamidine, with a mobile phase consisting of 25.0 mM citrate buffer, pH=3.25, 45.0% methanol, $T=30.0^\circ\text{C}$, with pentane sulphonate, hexane sulphonate, heptane sulphonate, octane sulphonate, and decane sulphonate sodium salts at concentrations of 0.00, 1.00, 2.00, 3.00, 4.00, 5.00, 6.00, 9.00, and 12.00 mM. The resultant data are shown in Fig. 4, where it may be observed that retention times and hence k' increase as the concentration of the ion pair-forming agent increases. This increase is much more

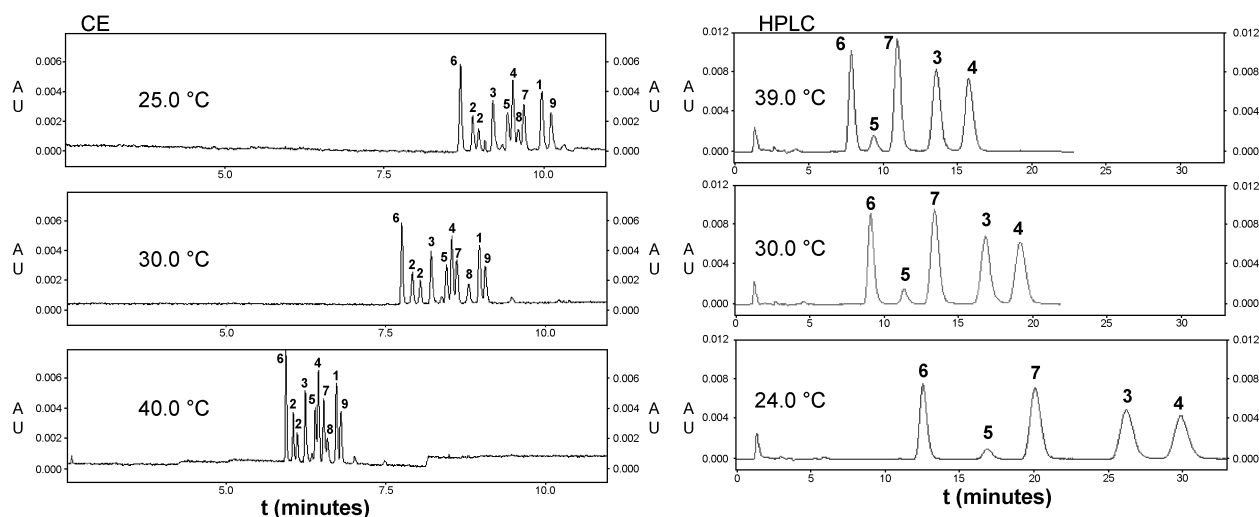


Fig. 3 Influence of temperature in HPLC and CE. In HPLC, this effect was studied using a mobile phase consisting of 25.0 mM citrate buffer, 45.0% methanol, 4.00 mM sodium octane sulphonate, pH=3.25, and $T=24.0^\circ\text{C}$, 30.0°C , and 39.0°C . In CE, the electrolyte used was 25.0 mM citrate buffer, with pH=3.70, 14.0 kV voltage, and $T=25.0^\circ\text{C}$, 30.0°C , and 40.0°C . (View this art in color at www.dekker.com.)

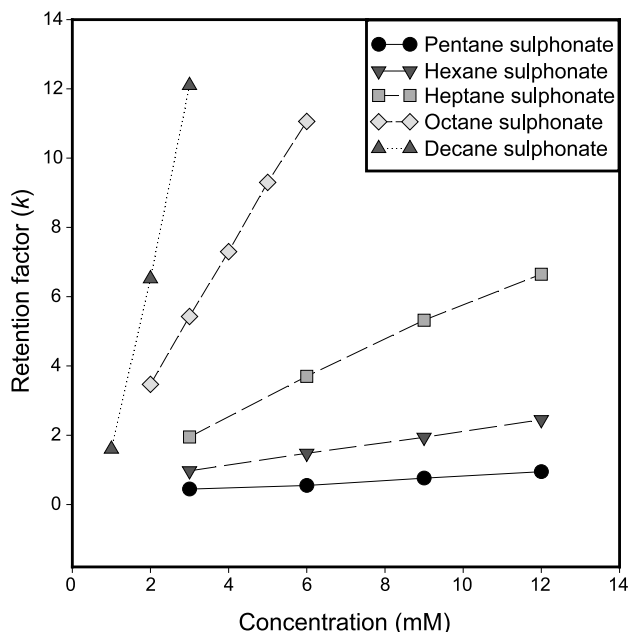


Fig. 4 Influence of concentration and chain length of the ion pair-forming agent in HPLC. This effect was studied using a mobile phase consisting of 25.0 mM citrate buffer, 45.0% methanol, and pH=3.25, containing pentane sulphonate, hexane sulphonate, heptane sulphonate, octane sulphonate, and decane sulphonate sodium salts at concentrations of 0.00, 1.00, 2.00, 3.00, 4.00, 5.00, 6.00, 9.00, and 12.0 mM. (View this art in color at www.dekker.com.)

pronounced when reagents with longer chain lengths are used.

Influence of methanol content

Two solvents were initially evaluated as organic modifiers for the mobile phase, these being acetonitrile and methanol. Methanol was finally selected, principally because of its greater solubility with respect to ion-forming reagents.

The effect of methanol percentage in the mobile phase on retention times was studied by using a mobile phase consisting of 25.0 mM citrate buffer, pH=3.25, $T=30.0^{\circ}\text{C}$, and 4.00 mM octane sulphonate and methanol at 42.0%, 45.0%, and 50.0%. Figure 5 shows that, with increasing percentages of methanol, retention times drop considerably and resolution decreases, but up to 50.0% methanol, this remains within acceptable limits.

Parameters Exclusive to CE

Selection of electrolyte

With a view to selecting the most suitable electrolyte for CE,^[20,21] all the diamidines under study were analyzed by

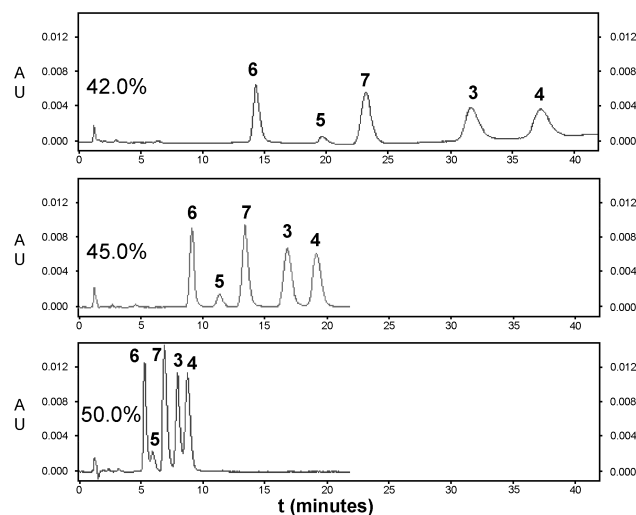


Fig. 5 Influence of methanol content in HPLC. This effect was studied using a mobile phase consisting of 25.0 mM citrate buffer, pH=3.25, $T=30.0^{\circ}\text{C}$, 4.00 mM octane sulphonate, and 42.0%, 45.0%, and 50.0% methanol. (View this art in color at www.dekker.com.)

using various buffers (phosphate, acetate, and citrate), all at 25.0 mM, pH=3.70, $T=30.0^{\circ}\text{C}$, and 14.0 kV voltage, as shown in Fig. 6. Only citrate gave useful values of resolution and efficiency for all the diamidines, together with migration times that were adequate for the kind of analysis they intended to optimize. Hence, citrate was also chosen for all the CE works.

Length of capillary

The length of the capillary is directly related to the electric field, efficiency, resolution,^[22] and amount of

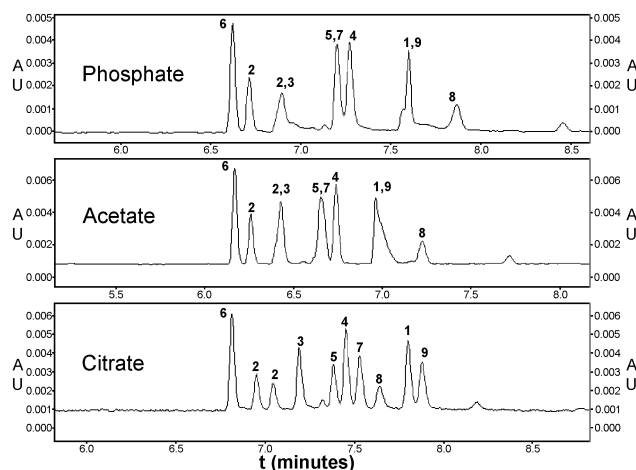


Fig. 6 Selection of electrolyte in CE. Electropherograms of nine diamidines using phosphate, acetate, and citrate electrolytes (25.0 mM), pH=3.70, $T=30.0^{\circ}\text{C}$, and 14.0 kV voltage.



Table 1 Effect of capillary length on the volume of sample loaded and strength of the electric field

Length of capillary (cm)	Volume injected (nL)	Capillary occupied by the injection (mm)	Percentage of capillary occupied	Analyte loaded (ng)	Strength of electric field (V/cm)
77.0	21.77	4.92	0.70	8.80	181.0
57.0	29.41	6.65	1.33	147.0	245.0

Capillary, 75.0- μ m ID; overall lengths, 77.0 and 57.0 cm (70.0 and 50.0 cm to the detector); electrolyte, 25.0 mM citrate buffer; pH=3.70; voltage, 14.0 kV; $T=30.0^{\circ}\text{C}$; injection under pressure for 5.00 sec.

sample loaded. An increase from 50.0 to 70.0 cm, up to the detector (from 57.0 to 77.0 cm overall dimension) in the length of the capillary, causes the quantity of sample loaded to be reduced by approximately 26.0% and the strength of the field to be generated when applying the same potential drops by approximately the same amount (Table 1). To study the influence of the length of the capillary on migration times, the following conditions were used: capillary, 75.0- μ m ID; lengths, 50.0 and 70.0 cm to the detector (57.0 and 77.0 cm overall length); electrolyte, 25.0 mM citrate buffer; pH=3.70; $T=30.0^{\circ}\text{C}$; and voltage, 14.0 kV. Figure 7 shows that as the length is increased from 50.0 to 70.0 cm, migration times are virtually doubled and a striking improvement in efficiency is achieved (i.e., an increase of between 10.0% and 15.0% in the number of theoretical plates), with good resolution.

Voltage applied

The voltage applied is one of the factors of greatest influence in a CE experiment because almost all the parameters governing separation are related to this voltage. The analysis time is inversely proportional to the applied voltage because of, among other things, the higher electrosomotic flow. An increase in the voltage

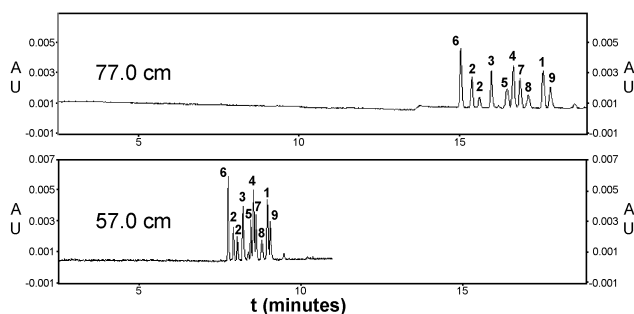


Fig. 7 Influence of capillary length in CE. Capillary, 75.0- μ m ID; lengths, 50.0 and 70.0 cm to detector (57.0 and 77.0 cm overall); electrolyte, 25.0 mM citrate buffer; pH=3.70; $T=30.0^{\circ}\text{C}$; and voltage, 14.0 kV.

also brings with it a growth in Joule heating^[15,16] and, if this is not effectively eliminated, it may cause variations in resistance, pH, viscosity of the electrolyte, and so on, thus rendering the analysis impossible to reproduce. With a view to optimizing the voltage, the Ohm's law plot of intensity against voltage must be kept in mind. The maximum efficiency in electrophoretic separation is attained at the point where this plot begins to deviate from linearity.^[23] In the work reported here, this occurred from 24.0 kV upward, and, when this value was exceeded, a pronounced decrease in efficiency occurred.^[24] In Fig. 8, the effects mentioned above can be readily seen; between the electropherogram at 8.00 kV and its counterpart at 14.0 kV, a clear increase in efficiency is observed, with resolution remaining at acceptable levels. On the other hand, in the electropherogram taken at 26.0 kV, outside the limits of linearity under Ohm's law, there is a complete loss of the improvements in both resolution and efficiency produced by higher voltage. This work was carried out using 25.0 mM citrate electrolyte, pH=3.70, and $T=30.0^{\circ}\text{C}$, at voltages of 8.00, 14.0, and 26.0 kV.

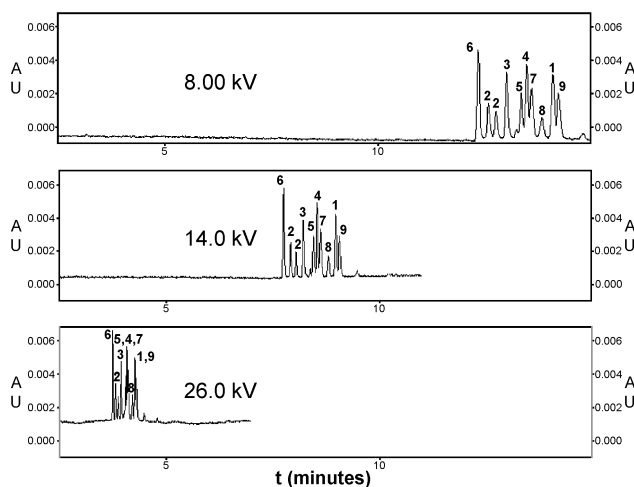


Fig. 8 Influence of variations in voltage in CE. Electrolyte, 25.0 mM citrate buffer; pH=3.70; $T=30.0^{\circ}\text{C}$, and voltages, 8.00, 14.0, and 26.0 kV.

Table 2 Performance of HPLC and CE in separation of aromatic diamidines

	HPLC	CE
<i>Detection limit (ng/mL)</i>		
Pentamidine	20.00	300.0
Stilbamidine	10.00	300.0
DAPI	5.00	300.0
Propamidine	30.00	200.0
Hydroxystilbamidine	15.00	400.0
Phenamidine	20.00	150.0
Diampron	10.00	300.0
Berenil	60.00	500.0
Dibromopropamidine	40.00	600.0
<i>Precision (% CV)</i>		
Pentamidine	1.09	3.04
Stilbamidine	1.03	1.68
DAPI	1.16	2.88
Propamidine	1.53	2.37
Hydroxystilbamidine	0.70	3.73
Phenamidine	0.70	3.52
Diampron	0.97	2.43
Berenil	0.85	1.55
Dibromopropamidine	1.36	5.30
<i>Efficiency (theoretical plates)</i>		
Pentamidine	2.22×10^3	2.92×10^5
Stilbamidine	3.91×10^3	3.04×10^5
DAPI	4.60×10^3	2.93×10^5
Propamidine	3.19×10^3	2.92×10^5
Hydroxystilbamidine	3.87×10^3	2.79×10^5
Phenamidine	3.65×10^3	3.06×10^5
Diampron	4.57×10^3	2.78×10^5
Berenil	3.17×10^3	2.43×10^5
Dibromopropamidine	2.63×10^3	2.46×10^5

CONCLUSION

A detailed study was undertaken of each of the parameters affecting the process of separation analysis in HPLC and

CE for nine aromatic diamidines. The results obtained are noted and discussed; in the tables, comparative features of the two techniques that emerge from the data collected are recorded.

Performance of HPLC and CE in the Separation of Aromatic Diamidines

The data emerging from this work allow the selection of the optimum conditions for the analysis of each substance in aqueous solution, serum, and urine. For HPLC, they are: 25.0 mM citrate buffer, pH=3.25, 45.0% methanol, column Ultrasphere ODS (5.00- μ m particle size, 15.0 cm \times 4.60 mm ID), 1.00 mL/min flow, and $T=30.0^\circ\text{C}$. The following features depend on the specific substance under analysis: pentamidine, 4.00 mM hexane sulphonate, $\lambda=265.0$ nm; stilbamidine, 4.00 mM octane sulphonate, $\lambda=330.0$ nm; DAPI, 8.00 mM heptane sulphonate, $\lambda=350.0$ nm; propamidine, 6.00 mM heptane sulphonate, $\lambda=265.0$ nm; hydroxystilbamidine, 4.00 mM octane sulphonate, $\lambda=350.0$ nm; phenamidine, 4.00 mM octane sulphonate, $\lambda=265.0$ nm; diampron, 4.00 mM octane sulphonate, $\lambda=254.0$ nm; berenil, 4.00 mM octane sulphonate, $\lambda=370.0$ nm; and dibromopropamidine, 3.00 mM hexane sulphonate, $\lambda=265.0$ nm.

For CE, the optimum values were: overall length of capillary, 57.0 cm (50.0 cm to the detector); 75.0- μ m ID; electrolyte, 25.0 mM citrate; pH=3.70, injection under pressure for 5.00 sec; voltage, 14.0 kV; $T=30.0^\circ\text{C}$; and $\lambda=200.0$ nm.

Analyses by means of HPLC and CE were carried out under these conditions for all the compounds, and comparative data for the two techniques are summarized in Table 2. The efficiency of CE is two orders of magnitude greater than HPLC for all the substances analyzed. The limits of detection for HPLC are much lower than in CE, there being some cases, such as DAPI,

Table 3 Operational differences between HPLC and CE

	HPLC	CE
Quantity of sample introduced into the system	10.0–1000.0 μL	1.00–50.0 nL
Size of the detector cell	8.00–12.0 mm^3	0.015 mm^3
Detection wavelength	Generally from 230.0 nm upwards	Possible to use wavelengths down to 185.0 nm
Interference	All components of the sample must pass through the detector	Possible to stop the analysis once the substance of interest has been detected
Flow	0.50–2.00 mL/min	Few microliters per minute
Equipment stabilization time	Requires balancing of the column with different timings before reliable results are obtained	Analysis can be carried out almost immediately after connection of equipment

Copyright © Marcel Dekker, Inc. All rights reserved.



Table 4 Schematic table of the advantages of HPLC and CE

	HPLC	CE
Versatility	+++	++++
Speed of optimization of methods	++	++++
Stabilization time	++	++++
Analysis time	++	+++
Sensitivity	+++	++
Reproducibility of times	+++	++
Reproducibility of areas	+++	++
Precision	+++	++
Efficiency	++	++++
Amplitude of linear range	++++	++
Resolution capacity	++	++++
Interferences in complex samples	++	++++
Sample preparation	++	++++
Sample volume	++	++++
Application at pilot scale	++++	+
Automatization	+++	++++
Price of reagents and other consumables	++	++++

where the detection limit is 60 times lower with HPLC than with CE. Values for precision are significantly better with HPLC than with CE.

Operational Differences Between HPLC and CE

Table 3 shows some of the differences in working practices between HPLC and CE.

Advantages of HPLC and CE

To summarize the work reported here, there is a schematic presentation of views on the advantages and drawbacks of each technique in Table 4.

REFERENCES

1. Ettre, L.S.; Horvath, C. Foundations of modern liquid chromatography. *Anal. Chem.* **1975**, *47*, 422A.
2. Tiselius, A. A new apparatus for electrophoretic analysis of colloidal mixtures. *Faraday Soc.* **1937**, *33*, 524–531.
3. Hjertén, S. Free zone electrophoresis. *Chromatogr. Rev.* **1967**, *9*, 122–239.
4. Jorgenson, J.; Lukacs, K.D. Zone electrophoresis in open tubular glass capillaries. *Anal. Chem.* **1981**, *53*, 1298–1302.
5. Kuhr, W.G. Capillary electrophoresis. *Anal. Chem. (Fund. Rev.)* **1990**, *62*, 403R.
6. Issaq, H.J. Thirty-five years of capillary electrophoresis: Advances and perspectives. *J. Liq. Chromatogr. Relat. Technol.* **2002**, *25* (8), 1153–1170.
7. Camilleri, P. *Capillary Electrophoresis, Theories and Practice*, 2nd Ed.; Camollari, P., Ed.; CRC Press: Boca Raton, FL, 1997; 1–22.
8. Grasilli, E.; Bettuzzi, S.; Monti, D.; Ingletti, M.C.; Franceschi, C.; Corty, A. Studies on the relationship between cell proliferation and cell death: Opposite patterns of SGP-2 and ornithine decarboxylase mRNA accumulation in PHA-stimulated human lymphocytes. *Biochem. Biophys. Res. Commun.* **1991**, *59*, 180.
9. Pegg, A.E. Recent advances in the biochemistry of polyamines in eukaryotes. *Biochem. J.* **1986**, *234*, 249.
10. Pegg, A.E. Polyamine metabolism and its importance in neoplastic growth and a target for chemotherapy. *Cancer Res.* **1988**, *48*, 759.
11. Rabanal, B.; Merino, G.; Negro, A. Determination by capillary zone electrophoresis of berenil, phenamidine, diampron and dibromopropamide in serum and urine. *J. Chromatogr., B* **2000**, *738*, 293–303.
12. Rabanal, B.; Negro, A. Study of nine aromatic diamidines designed to optimize their analysis by HPLC. *J. Liq. Chromatogr.* **2003**, *26* (20), 3499–3512.
13. Charton, M. The application of the Hammett equation to amidines. *J. Org. Chem.* **1965**, *30*, 969.
14. Bocek, P.; Deml, M.; Gebauer, P.; Dolnik, V. *Analytical Isotachophoresis*; VCH: Weinheim, 1988.
15. Rush, R.S.; Cohen, A.S.; Karger, B.L. Influence of column temperature on the electrophoretic behavior of myoglobin and α -lactalbumin in high-performance capillary electrophoresis. *Anal. Chem.* **1991**, *63*, 1346–1350.
16. Nelson, R.J.; Paulus, A.; Cohen, A.S.; Guttman, A.; Karger, B.L. Use of Peltier thermoelectric devices control column temperature in high performance capillary electrophoresis. *J. Chromatogr., B* **1989**, *480*, 111–127.
17. Sepaniak, M.J.; Cole, R.O. Column efficiency in micellar electrokinetic chromatography. *Anal. Chem.* **1987**, *59*, 472–476.
18. Eksborg, S.; Lagerstrom, P.; Modin, R.; Schill, G. Ion pair chromatography of organic compounds. *J. Chromatogr., A* **1973**, *83*, 99–110.
19. Braithwaite, A.; Smith, F.J. *Chromatographic Methods*, 5th Ed.; Blackie Academic and Professional, 1996.
20. Issaq, H.J.; Atamna, I.Z.; Muschik, G.M.; Janini, G.M. The effect of electric field strength, buffer type and concentration on separation parameters in capillary zone electrophoresis. *Chromatographia* **1991**, *32*, 155–161.
21. Nashabeh, W.; El Rassi, Z. Capillary zone electrophoresis of pyridylamino derivatives of maltooligosaccharides. *J. Chromatogr.* **1990**, *514*, 57–64.
22. Cohen, A.S.; Paulus, A.; Karger, B.L. High performance capillary electrophoresis using open tubes and gels. *Chromatographia* **1987**, *24*, 15–24.
23. Beckers, J.L.; Everaests, F.M. Isotachophoresis with two leading ions and migration behaviour in capillary zone electrophoresis: II. Migration behaviour in capillary zone electrophoresis. *J. Chromatogr., A* **1990**, *508*, 19–26.
24. McLaughlin, G.M.; Nolau, J.A.; Lindahl, J.L.; Palmieri, R.H.; Anderson, K.N.; Morris, S.C.; Morrison, J.A.; Bronzert, T.J. Pharmaceutical drug separations by HPCE: Practical guidelines. *J. Chromatogr.* **1992**, *15* (6&7), 961–1021.



Capillary Electrophoresis in Nonaqueous Media

Ernst Kenndler

Institute for Analytical Chemistry, University of Vienna, Vienna, Austria

Introduction

Organic solvents are used in capillary electrophoresis (CE) for several reasons:

1. To increase the solubility of lipophilic analytes.
2. To affect the actual mobilities of the analytes (those of the fully charged species at the ionic strength of the solution).
3. To change the pK values of the analytes.
4. To influence the magnitude of the electro-osmotic flow.
5. To influence the equilibrium constant of association reactions between analytes and additives (e.g., for the adjustment of the degree of complexation; an important example is the separation of chiral compounds by the use of cyclodextrins).
6. In some rare cases, to allow homoconjugation or heteroconjugation of the analytes with other species present and, thus, enable separation. For such interactions, a low dielectric constant of the solvent is a prerequisite.

Application of Nonaqueous Solvents

The organic solvents are applied in many cases in order to enhance the separation selectivity by changing the effective mobilities of the analytes. They are either applied as pure solvents, or as nonaqueous mixtures, or as constituents of mixed aqueous–organic systems. Solvents used for CE, as described in the literature, are methanol, ethanol, propanol, acetonitrile, tetrahydrofuran, formamide, *N*-methylformamide, *N,N*-dimethylformamide, *N,N*-dimethylacetamide, dimethylsulfoxide, acetone, ethylacetate, and 2,2,2-trifluoroethanol.

Organic solvents have relevance in many fields of application: for the separation of inorganic ions, organic anions and cations, pharmaceuticals and drugs, amino acids, peptides, and proteins.

There are some practical restrictions for the use of organic solvents:

1. Many organic solvents have a significant ultraviolet (UV) absorbance in the range of wavelengths that are normally also used for the detection of the analytes. This property leads to a poor signal-to-noise ratio or limits the applicability to solutes with UV absorbances at a higher wavelength.
2. Many electrolytes cannot be used as buffers, due to their low solubilities in organic solvents.
3. The low dielectric constant of solvents suppresses ion dissociation and favors ion-pair formation.
4. Important physicochemical properties (e.g., ionization constants of weak acids and bases) are often not known, which leads to a more or less random experimental approach for the optimization of the resolution.
5. In this context, it should be mentioned that the clear determination of the pH scale in these solvents is not a straightforward task, which may introduce a certain inaccuracy for the description of the experimental conditions. As this aspect is not adequately considered in many articles on CE in nonaqueous solvents, it is discussed here in more detail.

Acidity Scales in Organic Solvents

When investigating the effect of organic solvents on the pK_a of an acid, the significance of the pH scale in this solvent must be questioned. We base such scales on the measurement of the activity of the solvated proton. We define the activity, a_i , of a particle, i , the proton in the case of interest, by the difference between the chemical potential, ω_i , in the given and in a standard state (indicated by superscript 0)

$$\omega_i = \omega_i^0 + RT \ln a_i$$



In practice, we therefore differentiate a number of acidity scales: the standard, the conventional, the operational, and the absolute (thermodynamic) scale.

Standard Acidity Scale

The standard state might be chosen in various ways (e.g., as the state at infinitely diluted solution). The resulting standard acidity scale is characterized by the activity of the proton solvated by the given solvent, HS, according to

$$\text{pH} = -\log a_{\text{SH}_2^+} \quad (1)$$

The range of this scale is defined by the ionic product of the solvent, pK_{HS} .

Measurements in the standard acidity scale are carried out in cells without liquid junctions (e.g., with the following setup: Pt/H₂/HCl in SH/AgCl/Ag). It is assumed, here, that the activities of the solvated proton and the counterion, chloride, are equal. In this case, the electromotive force (emf) of the cell can be expressed by

$$E = E_{\text{S}}^0 - \frac{RT}{F} \ln a_{\text{SH}_2^+} a_{\text{Cl}^-} = E_{\text{S}}^0 - \frac{2RT}{F} \ln (c_{\text{HCl}} \gamma_{\text{HCl}}) \quad (2)$$

where c_{HCl} is the concentration and γ_{HCl} is the mean activity coefficient of HCl. E_{S}^0 is the standard potential of the silver chloride electrode in the given solvent, S, after extrapolation of the measured emf to zero ionic strength. Rearrangement leads to the expression of the pH in the standard scale:

$$\text{pH} = -\frac{(E - E_{\text{S}}^0)F}{2.3RT} + \log c_{\text{Cl}^-} + \log \gamma_{\text{Cl}^-} \quad (3)$$

Conventional Acidity Scale

The standard acidity scale, although well defined theoretically, has the limitation in practice that only the mean activity coefficient, but not the single-ion activity coefficient, is thermodynamically assessable. The single-ion coefficient depends on the composition of the solution as well. One way to circumvent this problem would be to have a defined value of the activity coefficient for one selected ion. Given that, all other activity coefficients could be obtained from the activity coefficients of the particular electrolytes and that special single-ion coefficient. The value of this selected

coefficient could be used, then, as the base of the conventional acidity scale. This single-ion activity coefficient is derived for chloride by the Debye-Hückel theory. This choice is made by convention, initially proposed for aqueous solutions; it is accepted also for other amphiprotic, polar solvents. Note that the measurements of the proton activity are carried out in cells without liquid junction.

Operational Acidity Scale

Due to the disadvantage of working with cells without liquid junctions, in practice the operational scale uses buffer solutions with known conventional pH for the calibration of cells with liquid junction [e.g., the convenient glass electrode (with the calomel or silver electrode, respectively, as reference)]. After calibration of the measuring cell (with a buffer of known conventional pH), the acidities of unknown samples can be measured in the same solvent. It is clear that for the standard buffers used, the conventional and the operational pH are identical. However, we cannot assume such an identity for the unknown samples. This is because the activities and the mobilities of the different ionic species might change the potential on the boundary with all liquid junctions (even without taking effect of the nonelectrolytes into account).

Absolute (Thermodynamic) Scale and Medium Effect

This scale, in fact, would allow comparing the basicities of the different solvents in a general way. It is based on the question of the chemical potential of the proton (as a single-ion species) in water, W, and the organic solvent, S. Taking the hypothetical 1M solution as the standard state, the chemical potential is given, according to Eq. (1), as

$$\omega_{\text{H}^+} = \omega_{\text{H}^+}^0 + RT \ln m_{\text{H}^+} + RT \ln \gamma_{\text{H}^+} \quad (4)$$

where m is the molal concentration. The so-called medium effect on the proton is given by

$$\begin{aligned} \ln {}_{\text{W}}\gamma_{\text{H}^+} - \ln {}_{\text{S}}\gamma_{\text{H}^+} &= \ln \left(\frac{{}_{\text{W}}\gamma_{\text{H}^+}}{{}_{\text{S}}\gamma_{\text{H}^+}} \right) \\ &= \ln {}_m\gamma_{\text{H}^+} = \frac{{}_{\text{S}}\omega_{\text{H}^+}^0 - {}_{\text{W}}\omega_{\text{H}^+}^0}{RT} \end{aligned} \quad (5)$$

${}_m\gamma_{\text{H}^+}$ is named the transfer activity coefficient. The medium effect is proportional to the reversible work of

transfer of 1 mol of protons in water to the solvent, S (in both solutions at infinite dilution). If the medium effect is negative, the proton is more stable in the solvent, S. It is, thus, an unequivocal measure of the basicity of the solvent, compared to water, as it allows us to establish a universal pH scale due to

$$-\log w_{\text{aH}^+} = -\log s_{\text{aH}^+} - \log m\gamma_{\text{H}^+} \quad (6)$$

It is a serious drawback that it is not possible to determine the transfer activity coefficient of the proton (or of any other single-ion species) directly by thermodynamic methods, because only the values for both the proton and its counterion are obtained. Therefore, approximation methods are used to separate the medium effect on the proton. One is based on the simple *sphere-in-continuum* model of Born, calculating the electrostatic contribution of the Gibb's free energy of transfer. This approach is clearly too weak, because it does not consider solvation effects. Different extrathermodynamic approximation methods, unfortunately, lead not only to different values of the medium effect but also to different signs in some cases. Some examples are given in the following: $\log m\gamma_{\text{H}^+}$ for methanol +1.7 (standard deviation 0.4); ethanol +2.5 (1.8), *n*-butanol +2.3 (2.0), dimethyl sulfoxide -3.6 (2.0), acetonitrile +4.3 (1.5), formic acid +7.9 (1.7), NH_3 -16. From these data, it can be seen that methanol has about the same basicity as water; the other alcohols are less basic, as is acetonitrile. Di-

methyl sulfoxide, on the other hand, is more basic than water. However, the basicity of the solvent is not the only property that is important for the change of the pK values of weak acids in comparison to water. The stabilization of the other particles that are present in the acido-basic equilibrium is decisive as well.

Suggested Further Readings

- Bates, R. G., Medium effect and pH in nonaqueous and mixed solvents, in *Determination of pH, Theory and Practice*, John Wiley & Sons, New York, 1973, pp. 211–253.
- Covington, A. K. and T. Dickinson, Introduction and solvent properties, in *Physical Chemistry of Organic Solvents Systems* (A. K. Covington and T. Dickinson, eds.), Plenum Press, London, 1973, pp. 1–23.
- Kolthoff, I. M. and M. K. Chantooni, General introduction to acid–base equilibria in nonaqueous organic solvents, in *Treatise on Analytical Chemistry, Part I, Theory and Practice* (I. M. Kolthoff and P. J. Elving, eds.), John Wiley & Sons, New York, 1979, pp. 239–301.
- Popov, A. P. and H. Caruso, Amphiprotic solvents, in *Treatise on Analytical Chemistry, Part I, Theory and Practice* (I. M. Kolthoff and P. J. Elving, eds.), John Wiley & Sons, New York, 1979, pp. 303–347.
- Sarmini, K. and E. Kenndler, Ionization constants of weak acids and bases in organic solvents, *J. Biophys. Biochem. Methods* 38:123 (1999).
- Sarmini, K. and E. Kenndler, Influence of organic solvents on the separation selectivity of capillary electrophoresis, *J. Chromatogr. A* 792:3 (1997).



Capillary Electrophoresis–Inductively Coupled Plasma–Mass Spectrometry

Clayton B'Hymer

University of Cincinnati, Cincinnati, Ohio, U.S.A.

INTRODUCTION

Capillary electrophoresis (CE) has many well-known advantages including low sample-volume requirements, high plate number (i.e., peak efficiency), the ability to separate positive, neutral, and negatively charged species in a single run, and, when properly developed, relatively short analysis times. The ability of CE to separate ionic multispecies and to have low operational costs makes the technique superior in certain specific applications to conventional high-performance liquid chromatography (HPLC). The inductively coupled plasma-mass spectrometer (ICP-MS) has the advantages of possessing low detection limits for the majority of the chemical elements. The ICP-MS detector has other additional positive attributes including linearity over a wide dynamic range, multielement detection capability, and the ability to perform isotopic analysis. Also, the ICP-MS is known to have minimal matrix-effect problems when compared to other detection systems. Sample matrix-effect problems are further reduced in CE–ICP-MS analysis owing to the small sample size and flow rates associated with CE. With all of these strong points, CE–ICP-MS is a rapidly growing hyphenated technique; the separation capability of CE is combined with the highly sensitive, element-specific detection system of ICP-MS.

HISTORICAL BACKGROUND AND USE

The first research papers describing CE–ICP-MS were written in 1995 by the Olesik, Lopez-Avila, and Barnes research groups.^[1–3] The coupling of the ICP-MS detector with CE and HPLC has become the dominant analysis technique for elemental speciation analysis. Elemental speciation analysis is defined as the separation, identification, and quantification of the different chemical forms (organometallic and inorganic) and oxidation states of specific elements in a given sample. Information on elemental speciation in clinical and environmental material is vital in the study of mechanisms of element transport within living as well as environmental systems,

elemental bioavailability, metabolic pathways within living organisms, and toxicology.

THE FUNDAMENTALS OF CAPILLARY ELECTROPHORESIS–INDUCTIVELY COUPLED PLASMA–MASS SPECTROMETRY

The Inductively Coupled Plasma–Mass Spectrometry Detector

Mass spectrometry (MS) has established itself as the detection system of choice for CE of trace metals and metalloids, as well as their chemical species. The inductively coupled plasma-mass spectrometer (ICP-MS) has dominated CE analysis methods in recent years. The ICP-MS differs from the more commonly used electrospray or ion-spray mass spectrometer method of ion generation. The electrospray MS can be described as using a “soft” ion source; that is, structural information can be obtained from molecular fragments. The ICP-MS is a “hard” ion source; that is, the plasma generally operates at an approximate temperature of 8000 K. Under these conditions, the ICP generates ions of elements and a few polyatomic ions. The ICP-MS has been well documented since its early development by both the Houk^[4] and Gray^[5] research groups over 20 years ago. A diagram of a typical commercial ICP-MS detector is shown in Fig. 1. The inductively coupled plasma is formed from a flow of gas, typically argon, through a series of concentric tubes made of quartz called the torch. The ICP torch is surrounded by a copper load coil. The load coil is connected to a radio-frequency generator, which operates between 27 and 40 MHz at a power of 700–1500 W.^[6] This induces an oscillating magnetic field near the exit of the torch. A plasma is formed while a spark is applied to the flowing gas stream to form gaseous ions. The free electrons created during this process are accelerated by the magnetic field and bombard other gas atoms; this causes further ionization and produces the plasma. Sample introduction into the plasma is via a carrier argon gas flow through the central tube of the ICP torch. Liquid samples are nebulized into an aerosol before being carried

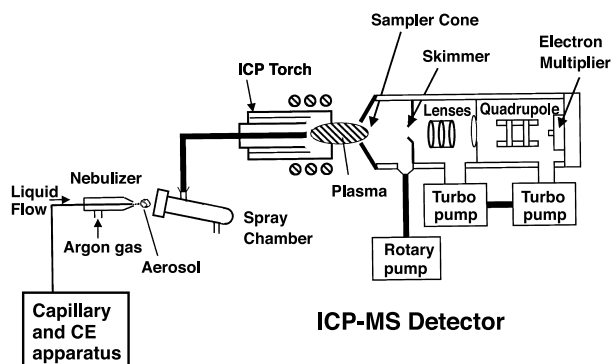


Fig. 1 The inductively coupled plasma-mass spectrometer (ICP-MS) used as a detector for high-performance liquid chromatography (HPLC). The liquid sample passes through the capillary into a nebulizer where it is changed into an aerosol. The aerosol passes through a spray chamber and into the plasma. The analytes pass into the mass spectrometer. The CE interface is not in detail in this figure.

into the ICP torch, a function performed by a nebulizer and spray chamber. The nebulizer produces the aerosol, and the spray chamber separates and removes the large droplets from the aerosol to form a more uniform mist. Once the fine aerosol sample reaches the plasma, vaporization, atomization, and ionization of the analyte to element ions occur almost simultaneously. Coolant and auxiliary gas are added to the ICP torch to keep the quartz from melting and to provide a tangential flow of gas, which serves to center and stabilize the plasma.

Beyond the ICP torch are the sampler and skimmer cones of a typical mass spectrometer (Fig. 1). Ions generated from the sample pass through the aperture of the cones into low-pressure chambers. Ion lenses, which are actually a series of electrodes, are used to “focus” the ion path, before reaching the quadrupole mass analyzer. Ions of only one mass-to-charge ratio are transmitted at a time and impacted onto an electron multiplier detector. The electron pulse is amplified and this signal is then recorded by the instrument’s data system. The diagram in Fig. 1 displays a quadrupole mass analyzer, but other spectrometers have been used with CE including scanning instruments such as the double-focusing and sector-field mass detectors, and for fast separations of multielement mixtures of chemical species, the time-of-flight (TOF) MS.

Alternative plasmas have been occasionally used for elemental speciation analysis, including the microwave-induced plasma (MIP), which has been reviewed in Ref. [7] and the low-power helium plasma. Both of these plasma sources have the advantage of reduced gas and power consumption over the traditional ICP; however, the use of these plasmas with interfaces with CE has been

very infrequent and does not warrant further discussion in this article. The MIP has been occasionally used with low flow rate liquid sample introduction. The low-power helium plasma has generally only been used with gas chromatographic (GC) interfaces; their low-power levels are generally not capable of properly vaporizing and ionizing a liquid aerosol.

Interfacing Capillary Electrophoresis to the Inductively Coupled Plasma–Mass Spectrometer

Overview of design considerations

The main design challenge of CE–ICP-MS is in the actual interface. In the typical practice of CE, a fused silica capillary filled with a buffer has both ends submerged or in physical contact with two buffer reservoirs. Electrodes placed in the buffer reservoir provide the application of a high electrical potential through the capillary. When attempting to interface CE to an ICP-MS, several problems need to be overcome. One is that CE has an extremely low flow rate (approximately $1 \mu\text{L min}^{-1}$ or less). This requires the use of a low liquid flow nebulizer to be used in the interface. A low liquid flow rate nebulizer is required that maintains a high transport efficiency and delivers a large quantity of analyte to the plasma. The ICP-MS detector sensitivity is based on mass of the analytes, not concentration of the solution. Because CE injection volumes are low, high transport efficiency by the nebulizer is vital to reduce analyte loss to the MS detector. The second problem with CE–ICP-MS interfacing is that an electrical connection must be maintained to the end of the fused silica capillary, yet the capillary must still introduce the CE buffer flow into the nebulizer and produce a uniform aerosol for the analysis system. This problem has been solved by various designs, which usually involves the addition of a “make-up” buffer or sheath electrolyte added near the end of the fused silica capillary. Interfacing CE with ICP-MS has the advantage of requiring a low liquid flow rate, and therefore places a small demand on the desolvation and solvent load capacity of the inductively coupled plasma. This makes a more stable plasma less subject to long-term signal drift over the course of several CE runs. Two other design considerations of a CE–ICP-MS interface are countering or minimizing laminar flow through the capillary generated by the operation of the nebulizer^[8] and minimizing band broadening for the separation of analytes. There are various strategies in reducing laminar flow through the electrophoretic capillary, and band broadening is minimized through geometry considerations in the design of the CE–ICP-MS



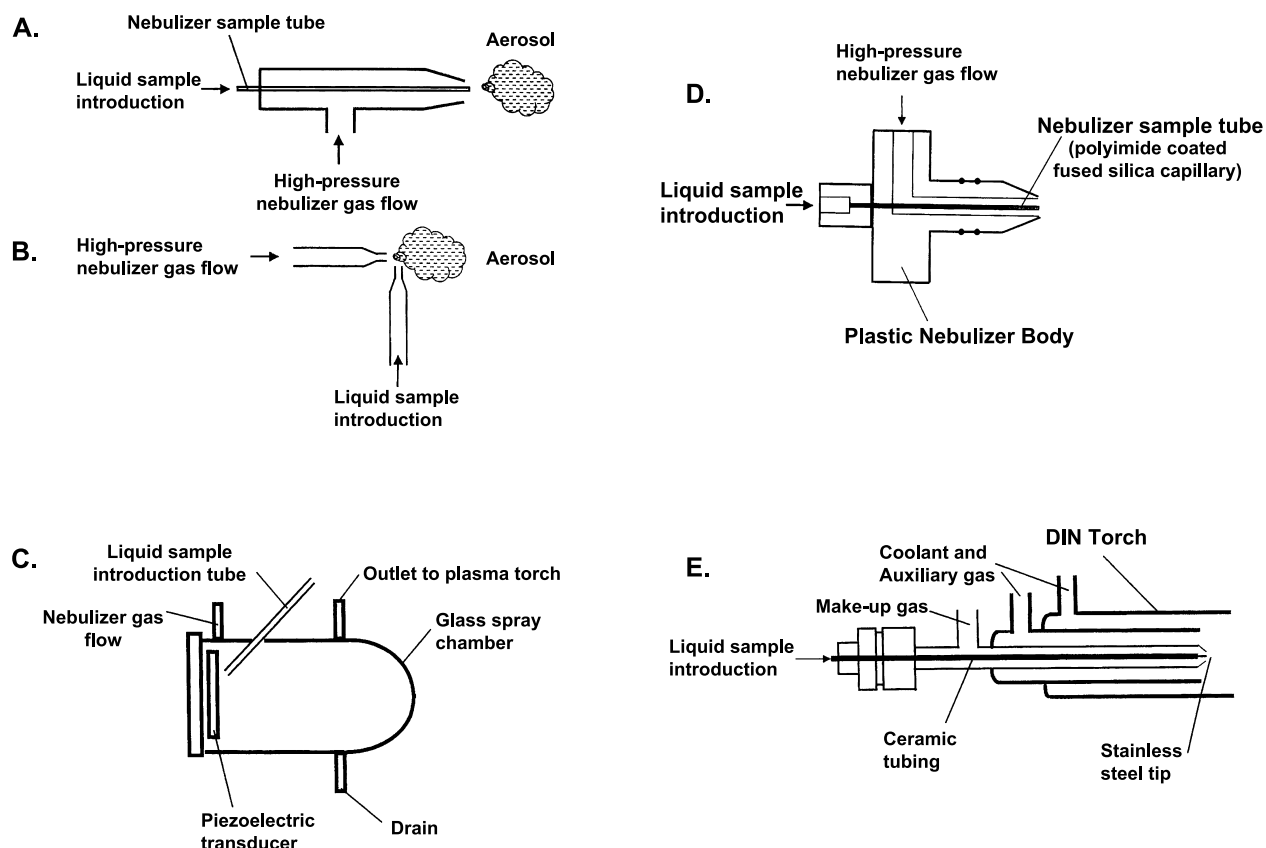


Fig. 2 (A) The concentric nebulizer; (B) The cross-flow nebulizer; (C) The ultrasonic nebulizer (USN); (D) The microconcentric nebulizer (MCN) by CETAC. The body of this nebulizer is made of plastic; (E) The direct injection nebulizer (DIN).

interface. These points will be discussed in further detail in this article.

The nebulizer

A basic understanding of the nebulizer function and the types of nebulizers is necessary to successfully interface CE to the ICP-MS. Nebulization, as previously described, is the process to form an aerosol, i.e., to suspend a liquid sample into a gas in the form of a cloud of droplets. The quality of any nebulizer is based on many different parameters including mean droplet diameter, droplet size distribution, span of droplet size distribution, droplet number density, and droplet mean velocity. There are numerous nebulizers commercially available for the use with ICP-MS systems, and their detailed description can be found elsewhere.^[9,10] Pneumatic designs, both concentric and cross flow, are the most popular for CE interfaces with the occasional use of the ultrasonic nebulizer (USN). Figure 2 shows some typical nebulizers. The pneumatic nebulizer is either a concentric design (Fig. 2A), where both the gas stream and the liquid flow in

the same direction or the cross-flow design (Fig. 2B), where the gas stream is at a right angle to liquid flow. Gas flowing past the tip of the liquid sample introduction tube generates the aerosol. The ultrasonic nebulizer (Fig. 2C) consists of a piezoelectric transducer and a liquid sample introduction tube. Liquid flow over the transducer plate forms a thin film and is nebulized by the high-frequency mechanical vibrations from the transducer.

There are several concentric-like pneumatic low liquid flow nebulizers commercially available that are often used in the construction of CE-ICP-MS interfaces. The Meinhard high-efficiency nebulizer (HEN) (Meinhard Glass Products, Golden, Colorado) is a variation of the concentric nebulizer that has smaller internal dimensions and is specifically designed to operate at low liquid flow rates. A very similar nebulizer is also commercially available and is known as the MicroMist nebulizer (Glass Expansion Pty. Ltd., Victoria, Australia). Another low-flow commercial nebulizer, the Microconcentric Nebulizer (MCN) (CETAC Technologies, Inc., Omaha, Nebraska) has been used with liquid flow rates down to 10–30 $\mu\text{L min}^{-1}$. The MCN is also concentric in nature, but it

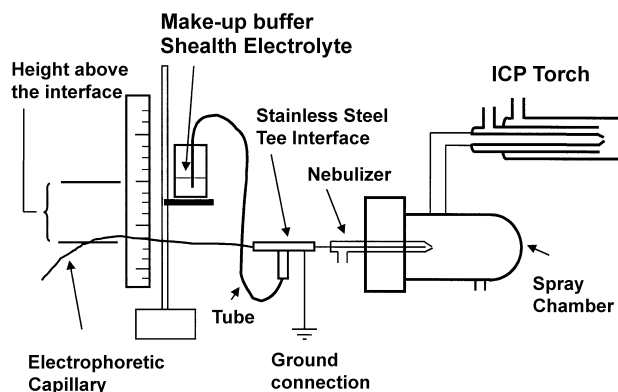


Fig. 3 A typical self-aspirating CE–ICP–MS interface. The make-up buffer/sheath electrolyte reservoir is positioned above the interface to provide the correct pressure and flow of buffer to the pneumatic nebulizer.

differs from both the Meinhard and MicroMist in having its outer body constructed of plastic instead of glass. Also, the MCN has its inner sample tube made of fused silica capillary tube, not drawn glass (Fig. 2D). All three of these commercial nebulizers have comparable analyte transport efficiencies.

Although there has been limited use with CE interfaces, the direct injection nebulizer (DIN) was first described by Shum et al.^[11] and later used by Liu et al.^[12] for CE (Fig. 2E). In this design, the nebulizer introduces the sample very near the plasma inside the ICP torch and eliminates the spray chamber assembly. Close to 100% analyte transport efficiency can theoretically be obtained with the DIN, but the nebulizer is restricted to very low liquid flow rate and thus is well matched to CE interfacing. This design does induce local plasma cooling due the lack of desolvation and detection limits are only slightly improved over other nebulizer designs.^[12]

Specific capillary electrophoresis interface designs

The CE–ICP–MS interface based on the sheath-flow (make-up buffer) and pneumatic concentric nebulizers described by Lu et al.^[3] is the most widely used CE–ICP–MS interface, and it has also been applied to electrospray MS interfaces.^[13] The sheath-flow or make-up buffer acts to complete electrical connection to the exit end of the electrophoretic capillary; grounding is achieved by having a metal tube or metal “tee” near the connection to the nebulizer (Fig. 3) or by coating the capillary with silver^[1] (Fig. 4). The second function of the sheath flow is to compensate for the suction effect. Low pressure created near the tip of the pneumatic nebulizer by the flow gas of the operating nebulizer can induce laminar flow through

the electrophoretic capillary. This can impair separation of analytes. Sheath flow can be introduced into the nebulizers by either self-aspiration with gravity siphoning control or by a pumping system. These strategies involve the precise addition of a sheath or make-up buffer to the nebulizer to prevent the degradation of the CE separation profile of the analytes. In the self-aspiration designs, the sheath flow is automatic, although adjustments to height of the sheath buffer reservoir (Fig. 3) can be used to optimize flow and separation to the nebulizer–CE interface. When a pumping system is used, the flow rate must be optimized to obtain the desired separation by reducing laminar flow through the capillary.

The use of controlled sheath-flow/make-up buffer rates to give equivalent CE–MS and CE–UV electropherograms was reported by Day et al.^[14] It has also been reported that the sheath flow should be kept low and just compensate for laminar flow through the electrophoretic capillary.^[8] This minimizes dead volume and band broadening of the CE separation. Precise pumping of a make-up buffer was demonstrated by Kinzer et al.^[8] and later by Sutton et al.^[15] The use of sol–gel frits near the exit tip of the electrophoretic capillary has been reported to reduce laminar flow effects and reduce the sheath flow.^[16] Other important design and optimization considerations exit for the sheath-flow/make-up buffer interfaces. The positioning of the electrophoretic capillary into a concentric nebulizer is critical in these designs. Placement of the exit tip of the capillary close to the tip of the nebulizer can increase the “suction effect” and cause greater laminar flow to be generated through the capillary. Placement too far back from the tip of the nebulizer may induce greater band broadening from the extra dead volume. There has been some arguments about dilution effects of the sheath

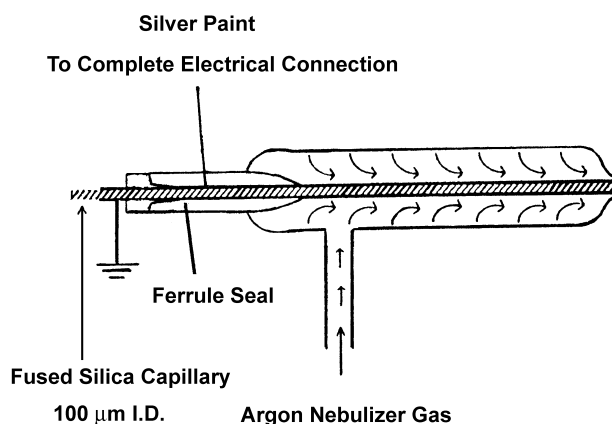


Fig. 4 Interface of an electrophoresis capillary and the concentric nebulizer. Silver paint was used to complete the electrical connection. (Reproduced from Ref. [1] with permission of the American Chemical Society, copyright 1995.)



flow; that is, the sheath-flow lowers sensitivity of the MS detector from dilution of the analytes. The use of a sheath flow does not cause a decrease in sensitivity because of dilution, but actually because of a decrease in analyte transport efficiency through the spray chamber to the plasma. Large liquid flow rates generally have less-efficient analyte transport, droplet sizes, and distribution change so that the analyte loss is greater out the spray chamber drain. Generally, the sheath flow rate can be kept low and the low liquid flow nebulizers commercially available have high analyte transport efficiency, making loss of sensitivity minimal. Finally, if the sheath-flow/make-up buffer is different from the run buffer, changes to the separation will obviously occur. Creation of a pH gradient across the electrophoretic capillary or isoelectric focusing from the use of a mismatch of the run and make-up buffer may cause undesirable results with the analyte separation.

Another less often used, but successful, technique to counter laminar flow in pneumatic-based nebulizer CE-ICP-MS interfaces is by the application of negative buffer reservoir pressure. This approach was first demonstrated by Lu et al.^[3] and later by Taylor et al.^[17] A matching mechanical counterbalance to the pneumatic nebulizer's suction was used in both of these interfaces. The theoretical advantage of non-sheath-flow system is that sensitivity of the CE-ICP-MS system is not reduced by dilution by the make-up buffer. Olesik et al.^[1] originally described a sheathless pneumatic interface, but the main flaw in the design was the increased liquid flow through the electrophoretic capillary owing to the suction or Bernoulli effect of the operating nebulizer. The electro-osmotic flow of this CE system was measured at $0.05 \mu\text{L min}^{-1}$, while the natural aspiration rate of the nebulizer vacuum was measured to be $2 \mu\text{L min}^{-1}$. Some degradation of the separation of analytes was noted, but the high plate number of CE and the selective detection capability of MS allowed this to be a useful separation. Another problem encountered in some sheathless interfaces is the loss of electrical connectivity of the electrophoretic capillary.

Finally, other nebulizers have been used in CE-ICP-MS interfaces. In an interface developed by the Barnes research group^[18] using the ultrasonic nebulizer (USN), the ground connection was provided by a make-up buffer/sheath-flow electrolyte. The separations obtained with the USN were demonstrated by Barnes' group to be superior to those obtained using a concentric pneumatic nebulizer in their study. Kirlew et al.^[19] reported the comparison of a "home-made" ultrasonic nebulizer and a CETAC USN in CE-ICP-MS interfaces. Again, a make-up buffer was used, added to the system via a concentric capillary outside the electrophoretic capillary. In another work by Kirlew and Caruso,^[20] an oscillating capillary nebulizer

(OCN), which is a variation of the pneumatic concentric nebulizer built from flexible capillary tubes, was used in an interface. The OCN has had little application in CE interfaces, owing to its generally lower sensitivity performance when compared to other pneumatic nebulizers used with ICP-MS detection.^[21] The direct injection nebulizer (DIN), previously described in "The Nebulizer," was used by Liu et al.^[2] in a CE interface. The electrophoretic capillary was directly inserted through the central sample introduction capillary of the DIN. A platinum grounding electrode was positioned into a three-port connector. This connector contained the DIN sample introduction capillary as well as a make-up buffer flow. These alternative nebulizers have been successfully used in CE interfaces, but the pneumatic designs dominate the interface systems reported in the literature.

One last CE-ICP interface worthy of mention that is specific for the determination of elements capable of forming volatile compounds is by the use of a hydride generation system. Hydride generation followed by a gas-liquid separator in CE interfaces has been reviewed.^[22] This technique has a drawback, because only arsenic, tin, lead, antimony, bismuth, germanium, selenium, and tellurium are capable of forming gaseous hydrides at room temperature. Hydride generation allows for the introduction of analyte species into the inductively coupled plasma nearly quantitatively; that is, the transport efficiency is nearly 100% percent less some loss by venting in the gas-liquid separator or other inefficiencies within the interface/sampling tube design to the plasma. In theory, detection limits are lower. In practice, hydride generation of the analytes may occur at different rates and the extra complexity and expense of the interface make these systems less useful as compared to the direct sample introduction systems previously described.

APPLICATIONS IN SAMPLE ANALYSIS

As mentioned in the "Introduction," the main application of CE-ICP-MS is in the field generally known as elemental speciation analysis. There are a number of good reviews on elemental speciation CE advances including use MS detection; the two most recent were by Kannamkumarath et al.^[23] and Timerbaev.^[24] Work performed in this relatively young technique is very extensive, and only a few examples will be cited in this article.

Speciation analysis of arsenic and selenium is very active in the recent literature. The toxicity of arsenic varies widely and is dependent on the specific compound present. Arsenic in its various forms is also widely distributed in the environment and the food that humans eat. Speciation of arsenic in human depends both on the

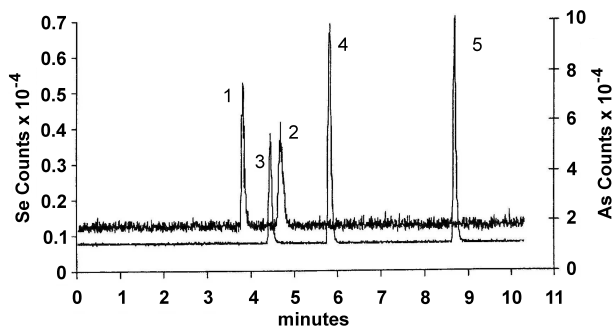


Fig. 5 Electropherogram of a mixed anion standard. Hydrodynamic injection (15 cm, 120 sec, 39.1 nL) with sodium borate buffer at pH 8. Peak 1: 3.2 ppm selenate; peak 2: 3.6 ppm selenite; peak 3: 1.9 ppm arsenate; peak 4: 4.4 ppm DMA; peak 5: 4.7 ppm arsenite. (Reproduced from Ref. [19] with permission of Elsevier Science, copyright 1998.)

form of the arsenic taken in and the metabolism within the body. Inorganic arsenic, in the forms of arsenite (As^{III}) and arsenate (As^{V}), is highly toxic. The common organic forms of arsenic have varying degrees of toxicity. Monomethylarsonic acid [MMA^{V} , $\text{CH}_3\text{AsO}(\text{OH})_2$] and

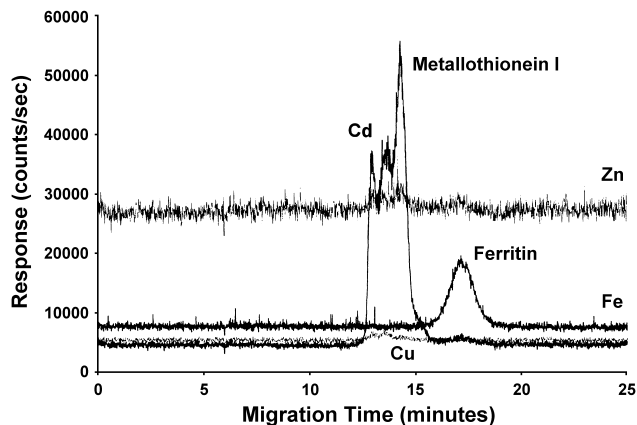


Fig. 7 Electropherogram showing separation of metallothionein I and ferritin. Zinc (mass 64) response at top and copper (mass 65) showed low signals for metallothionein. Cadmium (mass 114) showed a good response for metallothionein, and iron (mass 54) showed a good response for ferritin. This electropherogram was run using a run buffer of 15 mM Tris (hydroxymethyl) aminoethane (pH 6.8) at 15 kV, and the make-up buffer reservoir was positioned 2.5 cm above the MicroMist nebulizer. (Conditions are from Ref. [16].)

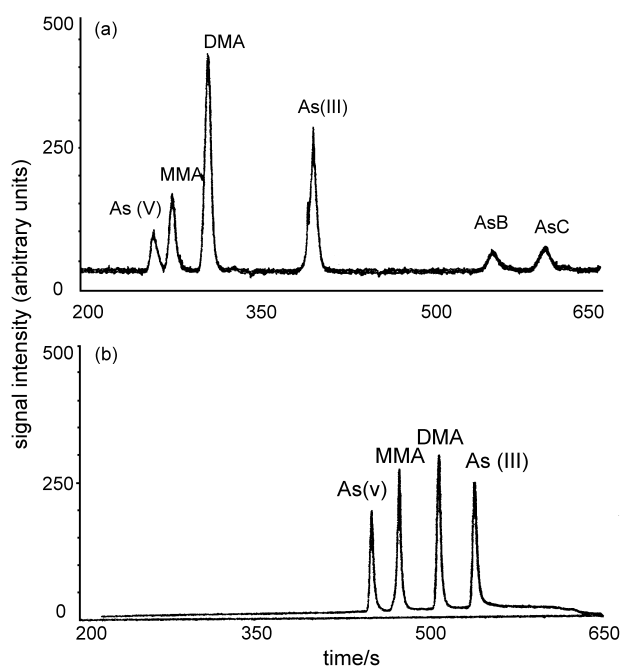


Fig. 6 (a) Electropherogram showing the separation of As^{V} , MMA, DMA, As^{III} , AsB, and AsC, obtained with CE-ICP-MS before optimization. (b) Electropherogram of approximately 20 $\mu\text{g/L}$ As^{V} , MMA, DMA, and As^{III} obtained after optimization of the CE-ICP-MS system. Conditions: 20 mM borate (pH 9.4), 2% OFM, 75 μm (id) capillary, total length 88 cm, 5 kPa for 40 sec plus 5 sec post injection, -25 kV. (Reproduced from Ref. [25] with permission of the Royal Society of Chemistry, copyright 1999.)

dimethylarsinic acid [DMA^{V} , $(\text{CH}_3)_2\text{AsO}(\text{OH})$] exhibit a toxicity factor of 1 in 400 that of the inorganic forms. Arsenobetaine [$(\text{CH}_3)_3\text{As}^+\text{CH}_2\text{COO}^-$] and arsenocholine [$(\text{CH}_3)_3\text{As}^+\text{CH}_2\text{CH}_2\text{O}^-$] are commonly found in seafood and are relatively nontoxic. A variety of arsenic compounds are currently used as antifungal agents, herbicides, and pharmaceuticals; they are also used in semiconductor processing and there was an extensive use in pesticides before the invention of the more advanced organophosphorus compounds. Thus the literature is filled with arsenic speciation analysis of food, the environment, and biological systems. Selenium has also been widely studied for many of the same reasons. Selenium intake in the human diet is essential, but excess intake can cause toxic reactions. A variety of selenium-containing species are present in the environment, natural foods, and food supplements.

In a previously mentioned work by Kirlow et al.,^[19] electrophoretic separations of Se^{IV} , Se^{VI} , As^{III} , As^{V} , and dimethylarsinic acid were performed using various ultrasonic nebulizer (USN) interfaces. Using the optimized CE interface conditions and a borate run buffer at pH 8, a separation was accomplished within 10 min. Electrokinetic injections gave better sensitivities for the analytes as compared to hydrostatic sample injection. In the Kirlow study, arsenate and selenite ions had very similar migration times, but these analytes were easily resolved by the multielement capability of the ICP-MS detector. An electropherogram of this work is shown in Fig. 5. In an application to field samples, Van Holderbek

et al.^[25] investigated arsenic speciation in three different sample matrices: drinking water, human urine, and soil leachate. All were run under basic conditions with 20 mM borate buffer (pH 9.40) and in the presence of cationic surfactant as the osmotic flow modifier (OFM) supplied by Waters Associates (Milford, Massachusetts). The separation of As^v, monomethylarsonic acid, dimethylarsinic acid, monomethylarsonic acid, arsenite As^{III}, arsenobetaine, and arsenocholine was obtained. Electropherograms from the Van Holderbeke study are shown in Fig. 6.

Capillary electrophoresis has been extensively used to separate biological molecules. Therefore it was only a natural extension that CE has been used for the analysis of metalloproteins and metal binding with other macromolecules. Also, the use of CE with the ICP-MS detector has been used in many studies reported in the literature. Metallothioneins are involved in metabolism and detoxification of several trace metals; thus the ability to monitor metallothioneins by CE-ICP-MS is of great importance. In a study of standard solutions of metallothionein I and ferritin, B'Hymer et al.^[16] used various geometrical configurations of a microconcentric nebulizer to obtain different electropherograms. A run buffer of 15 mM Tris (hydroxymethyl) aminomethane adjusted to pH 6.8 by the addition of HCl was used at a potential of 15 kV. An example electropherogram is shown in Fig. 7. The MS detector has the advantage of being capable of simultaneous monitoring of various elements, thus resolving the relative quantities of cadmium, copper, and zinc bound to the metallothionein. Ferritin was clearly resolved from the iron signal.

CONCLUSION AND FURTHER READING

The advantages of CE coupled with those of the ICP-MS detector will certainly allow this relatively young hyphenated technique to grow in the areas of elemental speciation and the analysis of environmental and biological samples. It is doubtful that CE will replace HPLC; however, CE will certainly compliment the other more traditional separation techniques owing to its separation being based on a physical rather than chemical partitioning. The ability of CE to use an extensive variety of electrolyte/buffer solutions so that specific chemical species of interest can be maintained during the course of a separation is another advantage. The improvement in the mass spectrometer will of course lead to better detection limits and capabilities. Again, the low-flow pneumatic nebulizer will probably continue to lead the work performed in building CE-ICP-MS interfaces. Also, the current selection of commercial low-flow nebulizer will aid in the construction and use of interfaces. Finally,

two books worthy of further reading are Akbar Montaser's *Inductively Coupled Plasma Mass Spectrometry* (Wiley-VCH, New York, 1998) and Joseph A. Caruso et al.'s *Elemental Speciation—New Approaches for Trace Elemental Analysis, Comprehensive Analytical Chemistry XXXIII* (Elsevier Science, Amsterdam, The Netherlands, 2000). Specific chapters were cited in this article, but both books comprise other chapters containing a wealth of information about capillary electrophoresis-inductively coupled plasma-mass spectrometry.

REFERENCES

- Olesik, J.W.; Kinzer, J.A.; Olesik, S.V. Capillary electrophoresis inductively-coupled plasma spectrometry for rapid elemental speciation. *Anal. Chem.* **1995**, *67*, 1–12.
- Liu, Y.; Lopez-Avila, V.; Zhu, J.J.; Weiderin, D.R.; Beckert, W.F. Capillary electrophoresis coupled online with inductively-coupled plasma-mass spectrometry for elemental speciation. *Anal. Chem.* **1995**, *67*, 2020–2025.
- Lu, Q.; Bird, S.M.; Barnes, R.M. Interface for capillary electrophoresis and inductively-coupled plasma-mass spectrometry. *Anal. Chem.* **1995**, *67*, 2949–2956.
- Houk, R.S.; Fassel, V.A.; Flesch, G.D.; Svec, H.L.; Gray, L.A.; Taylor, C.E. Inductively coupled argon plasma as an ion-source for mass-spectrometric determination of trace-elements. *Anal. Chem.* **1980**, *52*, 2283–2289.
- Date, A.R.; Gray, A.L. Plasma source-mass spectrometry using an inductively coupled plasma and a high-resolution quadrupole mass filter. *Analyst* **1981**, *106*, 1255–1267.
- Inductively Coupled Plasma Spectroscopy and Its Applications*; Hill, S.J., Ed.; Sheffield Academic Press: Sheffield, England, 1999.
- Olson, L.K.; Caruso, J.A. The helium microwave-induced plasma—An alternative ion-source for plasma-mass spectrometry. *Spectrochim. Acta, Part B* **1994**, *49*, 7–30.
- Kinzer, J.A.; Olesik, J.W.; Olesik, S.V. Effect of laminar flow in capillary electrophoresis: Model and experimental results on controlling analysis time and resolution with inductively coupled plasma mass spectrometry detection. *Anal. Chem.* **1996**, *68*, 3250–3257.
- Montaser, A.; Minich, M.G.; McLean, J.A.; Liu, H.; Caruso, J.A.; McLeod, C.W. Sample Introduction in ICPMS. In *Inductively Coupled Plasma Mass Spectrometry*; Montaser, A., Ed.; Wiley-VCH: New York, 1998; 1–47.
- B'Hymer, C.; Caruso, J.A. Nebulizer Sample Introduction for Elemental Speciation. In *Elemental Speciation—New Approaches for Trace Elemental Analysis, Comprehensive Analytical Chemistry XXXIII*; Caruso, J.A., Sutton, K.L.M., Ackley, K.L., Eds.; Elsevier Science: Amsterdam, The Netherlands, 2000; 211–224.
- Shum, S.C.K.; Nedderson, R.; Houk, R.S. Elemental speciation by liquid chromatography inductively coupled plasma mass-spectrometry with direct injection nebulization. *Analyst* **1992**, *117*, 577–582.
- Shum, S.C.K.; Pang, H-M.; Houk, R.S. Speciation of mercury and lead compounds by microbore column



- chromatography inductively coupled plasma-mass spectrometry with direct injection nebulization. *Anal. Chem.* **1992**, *64*, 2444–2450.
13. Smith, R.D.; Barinaga, C.J.; Udseth, H.R. Improved electrospray ionization interface for capillary zone electrophoresis-mass spectrometry. *Anal. Chem.* **1988**, *60*, 1948–1952.
14. Day, J.A.; Sutton, K.L.; Soman, R.S.; Caruso, J.A. A comparison of capillary electrophoresis using indirect UV absorbance and ICP-MS detection with a self-aspirating nebulizer interface. *Analyst* **2000**, *125*, 819–823.
15. Sutton, K.L.; B'Hymer, C.; Caruso, J.A. UV absorbance and inductively coupled plasma spectrometric detection for capillary electrophoresis—A comparison of detection modes and interface designs. *J. Anal. At. Spectrom.* **1998**, *13*, 885–891.
16. B'Hymer; Day, J.A.; Caruso, J.A. Evaluation of a microconcentric nebulizer and its suction effect in a capillary electrophoresis interface with inductively coupled plasma-mass spectrometry. *Appl. Spectrosc.* **2000**, *54*, 1040–1046.
17. Taylor, K.A.; Sharp, B.L.; Lewis, D.J.; Crews, H.M. Design and characterisation of a microconcentric nebuliser interface for capillary electrophoresis—Inductively coupled plasma mass spectrometry. *J. Anal. At. Spectrom.* **1998**, *13*, 1095–1100.
18. Lu, Q.; Barnes, R.M. Evaluation of an ultrasonic nebulizer interface for capillary electrophoresis and inductively coupled plasma mass spectrometry. *Microchem. J.* **1996**, *54*, 129–143.
19. Kirlew, P.W.; Caruso, J.A.; Castellano, M.T.M. An evaluation of ultrasonic nebulizers as interfaces for capillary electrophoresis of inorganic anions and cations with inductively coupled plasma mass spectrometric detection. *Spectrochim. Acta, Part B* **1998**, *53*, 221–237.
20. Kirlew, P.W.; Caruso, J.A. Investigation of a modified oscillating capillary nebulizer design as an interface for CE-ICP-MS. *Appl. Spectrosc.* **1998**, *52*, 770–772.
21. B'Hymer, C.; Sutton, K.L.; Caruso, J.A. A comparison of four nebulizer/spray chamber interfaces for the high performance liquid chromatographic separation of arsenic compounds using ICP-MS detection. *J. Anal. At. Spectrom.* **1998**, *13*, 855–858.
22. Taylor, A.; Branch, S.; Fisher, A.; Halls, D.; White, M. Atomic spectrometry update. Clinical and biological materials, foods and beverages. *J. Anal. At. Spectrom.* **2001**, *16*, 421–446.
23. Kannamkumarath, S.; Wrobel, K.; Wrobel, K.; B'Hymer, C.; Caruso, J.A. Capillary electrophoresis-inductively coupled plasma-mass spectrometry: An attractive complementary technique for elemental speciation analysis. *J. Chromatogr. A* **2002**, *975*, 245.
24. Timerbaev, A.R. Recent advances in capillary electrophoresis of inorganic ions. *Electrophoresis* **2002**, *23*, 3884–3906.
25. Van Hoderbeke, M.; Zhao, Y.; Vanhaecke, F.; Moens, L.; Dams, R.; Sndra, P. Speciation of six arsenic compounds using capillary electrophoresis inductively coupled plasma mass spectrometry. *J. Anal. At. Spectrom.* **1999**, *14*, 229–234.



Capillary Electrophoresis on Chips

Christa L. Colyer

Wake Forest University, Winston-Salem, North Carolina, U.S.A.

Introduction

It is no wonder that capillary electrophoresis (CE) has evolved into one of the premier separation techniques in use today, due to its extremely high efficiencies, fast analysis times, reduced sample and reagent consumption, and vast array of operating modes. The transposition of CE methods from conventional capillaries to channels on planar chip substrates is a more recent phenomenon and has been driven by several factors, including, but not limited to, the need for ever-more sensitive and selective assays, the need to manipulate increasingly smaller samples, and the desire to process many samples in parallel [1]. Perhaps of greater significance to the rapid development of this important field, however, is its amenability to the assimilation of multiple components of an assay — beyond simple separation of analytes — into a single, fully integrated device. The promise of the “lab-on-a-chip,” although seemingly ambitious in concept, is clearly attainable, and microchip capillary electrophoresis (μ -chip CE) has quickly established itself as one of the most fundamental constituents of such systems.

One of the first published demonstrations of capillary electrophoresis on a chip appeared in 1992, when Harrison et al. separated a mixture of fluorescein and calcein [2]. Although separation efficiencies and analysis times in this pioneering work did not represent significant improvements over those achievable by way of conventional CE, this work demonstrated the feasibility of miniaturizing a chemical analysis system involving electrokinetic phenomena for sample injection, separation, and solvent pumping. Within 2 years of the appearance of this seminal paper, analysis times on the order of seconds and even milliseconds had been demonstrated with similar μ -chip systems, and efficiencies in excess of 100,000 theoretical plates were routinely obtained. Subsequently, the integration of other functionalities, such as sample manipulations and chemical reactions, alongside the CE separation, has vaulted CE-on-a-chip to new heights.

Chip Fabrication Technology

The evolution of CE on a chip has directly benefited from the tremendous advances in semiconductor microfabrication technologies that have taken place over the past two decades. Although semiconducting substrates are not ideally suited to CE applications due to the high voltages applied for separation and fluid manipulation, many of the established semiconductor microfabrication techniques can be modified for the insulating glass or quartz substrates most commonly encountered in μ -chip CE. Here, the name μ -chip refers to the channel dimensions as opposed to the actual substrate dimensions, which commonly are on the order of 0.5 mm thick and anywhere from 3 to 10 cm in length and width (or diameter for circular substrates).

In many cases, standard photolithographic and wet-etching techniques are employed in the manufacture of CE chips. To begin, the clean glass or quartz substrate is uniformly coated with sequential thin layers of chromium/gold and positive photoresist by sputter-coating and spin-coating methods, respectively. The design for the CE channel structure is then transferred to the substrate by exposure of the photoresist to ultraviolet (UV) light through a photomask of the channel pattern. After photoresist development, a series of wet etches are employed, first to remove the metal etch mask and, second, to etch the channels into the substrate. Channels created in this fashion are trapezoidal in profile due to the isotropic etching of amorphous materials. Typical channel dimensions range from 5 to 40 μ m deep and 20 to 100 μ m wide (at half the channel depth). Residual photoresist and metal film are stripped from the etched substrate prior to thermal bonding of a cover plate, thereby forming closed channels suitable for electrophoresis. Access to the channels is most commonly gained through holes drilled in the cover plate prior to bonding.

Capillary electrophoresis chips so created are quite rugged due to the monolithic nature of their structure, and they can withstand applied voltages in the same range (up to 30 kV) as those commonly encountered in conventional CE. In addition, they offer greater heat



dissipation than conventional CE capillaries, thereby allowing for operation under conditions of higher power. Although quartz substrates have superior optical properties relative to their glass counterparts, both present an optically flat surface for detection schemes, which is a definite advantage over the curvature inherent to conventional capillary walls. As well, the void volumes associated with channel intersections on-chip are virtually nonexistent. Despite their many advantages, these chips are time-consuming and expensive to fabricate. As such, alternative methods for CE chip fabrication are being developed, such as the creation of channels in polymeric materials by casting, molding, and imprinting techniques. The success of these methods will rely, in part, on the concomitant development of suitable surface modification procedures to successfully manage channel wall properties.

Injection on Chips

Clever chip design permits the integration of the sample injector directly on the chip, thereby combining injection and separation functions by default on a single substrate. Most commonly, the injector is fashioned as a simple cross or "double-T" arrangement of etched channels, as shown in Fig. 1. One branch of this cross serves as the sample channel, and the other serves as the separation channel. Fluid flow is manipulated through this cross, just as with all other fluid manipulations on chip, by control of electrokinetic phenomena: electrophoresis and electro-osmosis. By first applying the appropriate voltage between the sample and sample waste reservoirs (Fig. 1a), the sample solution crosses the separation channel, filling the double-T intersection. Consequently, injection volumes are defined by the injector geometry. Typical sample plug volumes and lengths are on the order of about 10–100 pL and 50–200 μm , respectively. Provided the injection field strength and time are sufficient to ensure that the least mobile sample component has moved through the channel intersection, this method results in an unbiased injection, with all sample components represented in the intersection volume according to their original proportions. Having thus formed a sample plug, the voltage is switched so as to generate electro-osmotic flow along the separation channel (Fig. 1b), sweeping the sample plug out of the double-T injector and initiating separation along the second branch of the injector. This branch—the separation channel—typically ranges from 1 to 10 cm in length. Further control of sample plug size and shape and prevention of sample leakage

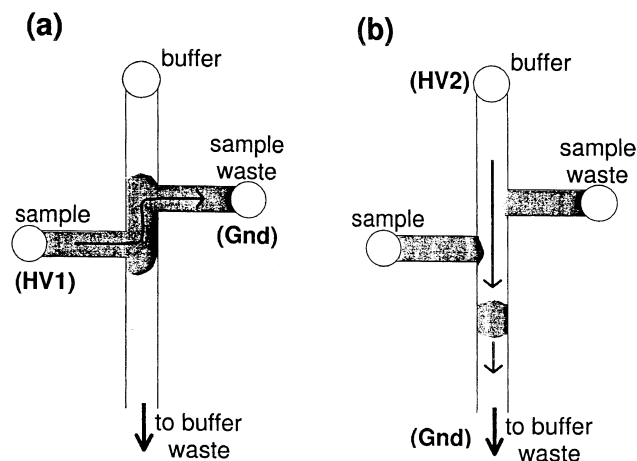


Fig. 1 Illustration of a microchip CE sample injector. Injection consists of (a) sample loading across the separation channel by application of a high voltage (HV1) across the sample and sample waste reservoirs, followed by (b) mobilization of the sample plug along the separation channel by application of HV2 across the buffer and buffer waste reservoirs.

can be effected by carefully controlling voltages applied to all four arms of the cross simultaneously during injection and separation phases.

Detection on Chips

It is not surprising that the requirements for detection on chips are very stringent, especially given the extremely small sample sizes discussed earlier. This need for sensitivity, along with the optically flat chip surface, makes laser-induced fluorescence (LIF) detection a natural choice; consequently, LIF detection on chips is the most widespread of all detection types. However, because relatively few analytes are natively fluorescent, LIF detection necessitates the development of selective and sensitive labeling strategies for each assay. Other detection methods, such as UV-vis absorption, chemiluminescence, and electrochemical, are less commonly encountered in chip CE, but they have been successfully demonstrated. Recently, the ability to generate an electrospray from the edge of a CE chip [3] has spawned a flurry of additional work in the area of electrospray ionization–mass spectrometry (ESI–MS) detection for CE chips. This promises to be a particularly powerful and exciting advance, as both quantitative and qualitative information can be provided simultaneously by this method of detection.

Beyond CE: Sample Manipulations

The most fundamental purpose of a CE chip is, of course, the separation and subsequent detection of analytes within a manifold of micromachined channels on a miniaturized substrate. This separation may take place as a result of basic electrokinetic phenomena or it may be enhanced or assisted by implementation of any one of various other separation techniques, such as isotachopheresis, micellar electrokinetic chromatography, isoelectric focusing, or capillary gel electrophoresis, all of which have been successfully demonstrated on-chip. However, the feature that truly distinguishes μ -chip CE from its conventional capillary counterpart is not its separative ability but, rather, its facility to integrate other functions onto the chip alongside the separation. This has already been discussed with respect to the sample injector and it is equally applicable to various sample preparation techniques. For example, controlled sample dilution, achieved by mixing buffer and sample streams directly on-chip, was first shown by Harrison et al. [4]. By increasing the voltage applied to a buffer reservoir while holding the voltage applied to a fluorescein dye sample reservoir constant, a controlled decrease in fluorescence intensity, corresponding to increasingly greater dilutions of the fluorescein, was observed downstream at the detector.

Preconcentration is another commonly encountered sample pretreatment method that has been successfully integrated onto a CE chip. Ramsey and co-workers incorporated a porous membrane structure into a microfabricated injection valve, enabling electrokinetic concentration of DNA samples using homogeneous buffer conditions [5]. Sample preconcentration in nonhomogeneous buffer systems—a technique known as sample stacking—has also been achieved on-chip [6].

Filtration is yet another pretreatment technique commonly encountered in CE. The reduced dimensions of fluid channels on chip substrates make the need for solution filtration all the more critical in this work. Until very recently, filtration was exclusively conducted “off-line” (i.e., before the sample and/or buffer solution was ever introduced to the chip). However, Regnier and co-workers recently micromachined solvent and reagent filters into quartz substrates using deep reactive ion etching [7]. Flow through these microfabricated lateral percolation filters was driven by electro-osmotic flow, thus making them compatible with other fluidic processes in a chip CE system. The on-chip filters were shown to be capable of removing a variety of particulate materials, ranging from dust to

cells. Surface fouling and loss of cationic proteins from analyte streams were minimized by applying a polyacrylamide coating to the filter surfaces. Hence, these selected examples of the transposition of some traditional sample pretreatment methods onto chip substrates and their compatibility with on-chip CE separations illustrate the potential for achieving a fully integrated lab-on-a-chip.

Beyond CE: Chemical Reactions on Chip

Full functionality of these chips cannot be realized by the integration of sample pretreatment, injection, and separation methods alone. Additionally, the ability to

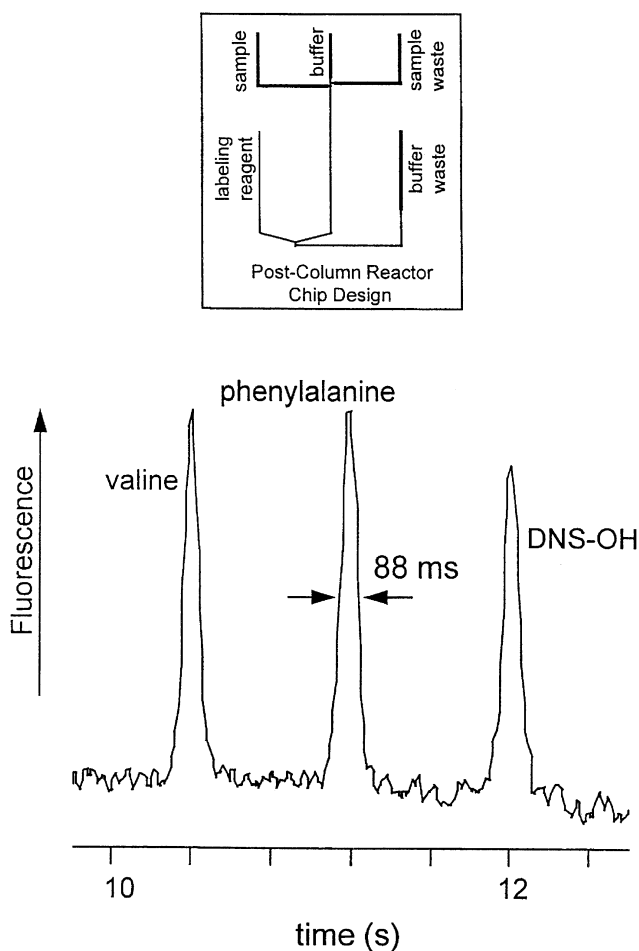


Fig. 2 Electrokinetically driven on-chip reaction in a CE-based system. Postseparation labeling of amino acids with OPA. Sample contained 200 μ M each of phenylalanine and valine, and 10 μ M of hydrolyzed dansyl chloride. The postcolumn reactor chip design is shown in the inset. [Reproduced from *Electrophoresis* 18:1733 (1997), with permission.]



carry out chemical reactions on-chip must be included in the list of integrated functions in order to extend the utility of these systems. Indeed, a wide variety of on-chip chemical reactions coupled to CE separations have been successfully demonstrated, including fluorescent derivatization, digestion of DNA and proteins, affinity-type reactions, and the polymerase chain reaction (PCR) for DNA amplification. The first of these reactions is necessitated by the laser-induced fluorescence detection schemes commonly used with CE chips. Because few analytes are natively fluorescent, it is often necessary to either (a) react the analyte with a fluorescent tag prior to separation (preseparation or precolumn labeling) or (b) separate the analyte first, followed by reaction of the separated zones with a derivatizing agent (postseparation or postcolumn labeling). The former, although leading to greater sensitivity, often suffers from increased band broadening and reduced separation efficiencies. The latter, although leading to higher efficiencies, offers reduced sensitivity and requires very fast labeling kinetics. Preseparation and postseparation labeling schemes were the first reactions demonstrated in conjunction with CE separations on chip substrates. Although the initial on-chip reactors suffered from inefficient mixing, and therefore inefficient reactions, improvements in channel structures and geometries along with optimization of solution conditions soon led to satisfactory results. The geometry of one such "second-generation" CE reactor chip is shown in Fig. 2, along with the electropherogram generated by postseparation labeling of amino acids with *o*-phthaldialdehyde (OPA). Despite the fact that the amino acids, once separated, had to mix and react with OPA in order to be rendered fluorescent, their corresponding peaks remained as sharp and well-defined as the peak obtained for hydrolyzed dansylchloride (DNS-OH), which did not react with OPA [8].

The products of digestion reactions involving either protein or DNA substrates are conveniently separated and detected by CE on a chip. Improvements in digestion product assays should, therefore, be realized by marrying the digestion reaction and separation on a single chip. Jacobson and Ramsey demonstrated one such marriage by fabricating a chip device capable of both digesting a DNA sample with a restriction enzyme and separating the resulting DNA fragments using electrophoresis in a sieving matrix. Subsequent detection of the DNA restriction fragments was achieved by way of LIF using an intercalating dye that was introduced to the fragments on-chip [9]. In some cases, the products of a digestion reaction may not, in themselves, be of interest, but, rather, they may be used to

determine information about the digestion enzyme itself. In one such chip assay, the reaction kinetics for the enzyme β -galactosidase were determined using resorufin β -D-galactopyranoside, a substrate that is hydrolyzed to resorufin, a fluorescent product [10]. Precise concentrations of substrate, enzyme, and inhibitor (phenylethyl β -D-thiogalactoside) were mixed on-chip, and the entire integrated assay was conducted in a 20-min period using only 120 pg of enzyme and 7.5 ng of substrate. Thus, the facility to perform digestion reactions directly on chip prior to separation and detection of digestion products necessarily improves the efficiency of these assay methods and represents a powerful new tool in the area of biochemical analysis.

Affinity-type reactions, which involve an analyte's affinity for a conjugate molecule, such as antibody-antigen interactions, form an important part of biochemical research. CE on a chip provides for the separation of complexes of the analyte with its conjugate from uncomplexed reagents. However, the ability to carry out the reaction between the analyte and its conjugate to form a complex directly on-chip, in conjunction with electrophoretic separation, is an important advance, and many examples of such on-chip affinity reactions exist. In one such example, Chiem and Harrison presented a μ -chip CE device capable of functioning as a complete immunoreactor for the determination of serum theophylline, a therapeutic drug for asthma treatment [11]. In this competitive immunoassay, a serum sample containing theophylline was mixed, directly on the chip, with fluorescently labeled theophylline tracer prior to introducing a limited amount of anti-theophylline antibody, also on-chip. The products of this immunoassay were subsequently separated by electrophoresis and detected by LIF on-chip. As the concentration of theophylline in the serum increased, this competitive assay led to an increase in signal for free, labeled theophylline and a corresponding decrease in signal for the labeled theophylline-antibody complex. Total analysis time, including on-chip reagent mixing, reaction, separation, and detection, was 150 s per sample, demonstrating one of the obvious advantages (along with reduced reagent consumption and increased sensitivity) of being able to conduct reactions on-chip alongside CE separations and other functions.

Another important reaction that has found a place on CE chips is the PCR, which is used to amplify DNA and which is critical to high-throughput genetic analyses. With the demonstrated ability of CE chips to integrate chemical reactions alongside high-speed separations, it is perhaps not surprising that μ -chip devices capable of genetic analysis would be fabricated. For

example, a single monolithic chip capable of PCR amplification of up to four DNA samples, followed by product analysis has been demonstrated [12]. Integrated onto this chip are the facilities to thermally lyse cells to release DNA, standard PCR protocols to amplify DNA, gel electrophoresis to separate PCR products, intercalation of a fluorescent dye into PCR products, and detection of labeled products by LIF. The level of sophistication in a device such as this clearly illustrates the reality of the lab-on-a-chip concept: A concept that is founded upon the many advantages of μ -chip CE.

Conclusions and Future Directions

The advantages typically associated with capillary electrophoresis, such as reduced sample and reagent consumption, reduced analysis time, and increased separation efficiency, are augmented when the CE system is transposed to a chip substrate. More importantly, however, μ -chip CE offers the further advantage of integrating analytical processes beyond separation. Sample preparation, injection, reaction, and detection can be seamlessly tied to the electrophoretic separation stage of the analysis. The monolithic CE chips capable of separation coupled to some of these other analytical steps are precursors to the ultimate "lab-on-a-chip," which promises high-throughput sensitive analyses with minimal user intervention. Applications of such devices in biochemical, clinical, forensic, and environmental analyses are seemingly unlimited. However, several challenges remain despite the great promise of these devices. In order to fully realize the advantages offered by the microfluidics regime of the chip, methods of addressing these microvolumes and of interfacing them to the macroscale world beyond the chip must be carefully managed. Although chip fabrication techniques are now well established, they are by no means accessible to the majority of analysts. Fabrication processes that rely less heavily on high-tech processing facilities must

be developed or, more realistically, the chips themselves must be made available inexpensively and in a variety of application designs for all potential users. Miniaturization or careful arrangement of the apparatus accompanying the CE chip, including power supplies, detection components, and computer controllers, into a compact and robust system must be considered in order to take full advantage of the chip's inherently small size. Finally, true parallel processing facilities must be routinely developed on single chips in order to increase sample throughput and increase the applicability of these systems to large-scale analytical problems. These challenges, although formidable, are worthy of solutions in order to successfully build lab-on-a-chip around the cornerstone of CE on a chip.

References

1. S. C. Jacobson and J. M. Ramsey, in *High-Performance Capillary Electrophoresis* (M. Khaledi, ed.), John Wiley & Sons, New York, 1998, pp. 613–633.
2. D. J. Harrison, A. Manz, Z. Fan, H. Lüdi, and H. M. Widmer, *Anal. Chem.* 64:1926 (1992).
3. R. S. Ramsey and J. M. Ramsey, *Anal. Chem.* 69:1174 (1997).
4. D. J. Harrison, K. Fluri, K. Seiler, Z. Fan, C. S. Effenhauser, and A. Manz, *Science* 261:895 (1993).
5. J. Khandurina, S. C. Jacobson, L. C. Waters, R. S. Foote, and J. M. Ramsey, *Anal. Chem.* 71:1815 (1999).
6. S. C. Jacobson and J. M. Ramsey, *Electrophoresis* 16:481 (1995).
7. B. He, L. Tan, and F. Regnier, *Anal. Chem.* 71:1464 (1999).
8. K. Fluri, G. Fitzpatrick, N. Chiem, and D. J. Harrison, *Anal. Chem.* 68:4285 (1996).
9. S. C. Jacobson and J. M. Ramsey, *Anal. Chem.* 68:720 (1996).
10. A. G. Hadd, D. E. Raymond, J. W. Halliwell, S. C. Jacobson, and J. M. Ramsey, *Anal. Chem.* 69:3407 (1997).
11. N. H. Chiem and D. J. Harrison, *Clin. Chem.* 44:591 (1998).
12. L. C. Waters, S. C. Jacobson, N. Kroutchinina, J. Khandurina, R. S. Foote, and J. M. Ramsey, *Anal. Chem.* 70:5172 (1998).



Capillary Electrophoresis: Introduction and Overview

Joseph J. Pesek
Maria T. Matyska

San Jose State University, San Jose, California, U.S.A.

Introduction

Electrophoresis has been used as a separation technique for decades, particularly by biochemists, in the open-bed format. In this mode, a layer of a gel is formed on a flat-bed support which is in contact with an electrolyte and two electrodes are situated at either end of the open slab. The sample is placed at one end of the separation medium, and when voltage is applied, the molecules migrate through the gel by electrophoresis. The components in the sample are separated based on their differences in electrophoretic mobility. The electrophoretic mobility is controlled by molecular parameters such as charge, size, and shape. After the electric field is turned off, the separation is evaluated by spraying the plate with a dye and the bands of the sample components become visible, similar to the detection format used in paper or thin-layer chromatography.

Discussion

Although the basic principle was conceived many years ago, the practical development of electrophoresis experiments in a closed or tubular format was only begun a little more than a decade ago. The main problem of the closed system is that the application of high voltages leads to the generation of Joule heat as current flows through the electrolyte solution. The heat generated can often cause sample decomposition or, more frequently, result in a large increase in molecular diffusion, leading to zone broadening that obliterates the separation between adjacent bands. Therefore, for these experiments to work in a tubular format, it is necessary to use capillary tubes with diameters of 100 μm or less in most cases. The answer to overcoming the Joule heat problem is to use fused-silica tubes, similar to those developed for capillary gas chromatography but having a smaller internal diameter. A second advantage of the fused-silica capillary is that it is suitable for direct on-line detection because it is optically trans-

parent to ultraviolet (UV) and visible light. Typical dimensions for the capillary under experimental conditions are an outer diameter (o.d.) of $\sim 375 \mu\text{m}$, an inner diameter (i.d.) of 50–100 μm , and an overall length of 50–100 cm. To protect the fragile fused-silica tube, the capillary is coated with an external layer of polyimide, allowing it to be flexible and manipulated into a variety of instrumental geometries. A detection window can be made by removing a small amount of the protective coating.

The fused-silica surface also provides another mechanism, electro-osmosis, which drives solutes through the tube under the influence of an electric field. The principle of electro-osmotic flow (EOF) is illustrated in Fig. 1. The inner wall of the capillary contains silanol groups on the surface that become ionized as the pH is raised above about 3.0. This creates an electrical double layer in the presence of an applied electric field so that the positively charged species of the buffer which are surrounded by a hydrated layer carry solvent toward the cathode (negatively charged electrode). This results in a net movement of solvent toward the cathode that will carry solutes in the same direction as if the solvent were pumped through the capillary. This electrically driven solvent pumping mechanism results in a flat flow profile in contrast to

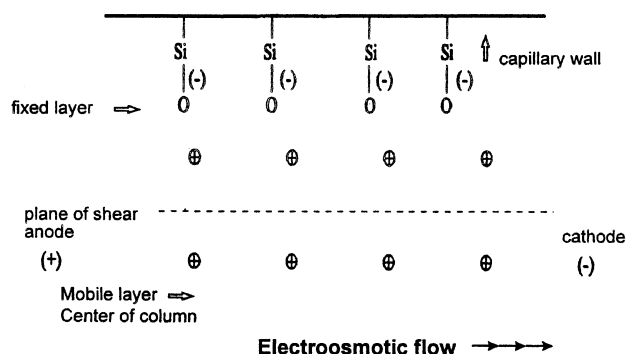


Fig. 1 Principle of electro-osmotic flow.



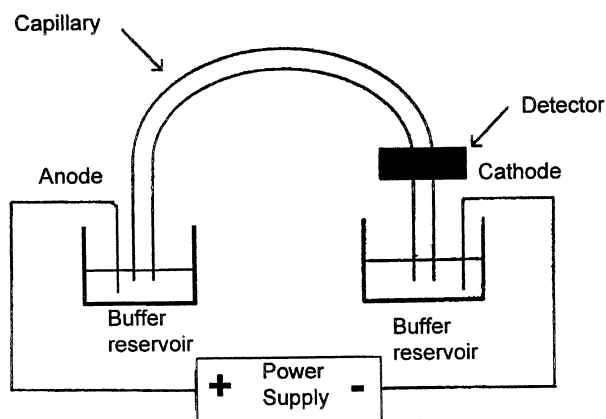


Fig. 2 Basic apparatus for capillary electrophoresis.

the laminar one (parabolic) obtained from mechanical pumps such as those used in high-performance liquid chromatography (HPLC). However, electro-osmotic flow is uniform throughout the capillary and does not depend on any solute properties. All solutes are affected by EOF uniformly and this process does not contribute to the separation mechanism. Therefore, only differences in electrophoretic velocity are responsible for the separation of charged compounds in a fused-silica capillary in the presence of an applied electric field. In fact, EOF is detrimental to the separation process because it moves positively charged species through the capillary faster, thus allowing less time for differences in electrophoretic velocity to separate two species with similar mobilities. This effect can be described mathematically by the following equation:

$$v_{\text{tot}} = v_{\text{ep}} + v_{\text{EOF}}$$

where v_{tot} is the total velocity of the charged species, v_{ep} is the electrophoretic velocity of that species, and v_{EOF} is the electro-osmotic velocity. In a typical experiment, sample migration rates through the capillary are as follows: cationic species > neutral compounds > anionic species. Because both cationic and anionic compounds can have different electrophoretic mobilities, they can be separated within the capillary. However, neutral species are carried through the capillary only by electro-osmotic flow, so these compounds will all migrate at the same rate and, therefore, cannot be separated by capillary electrophoresis (CE).

The basic apparatus necessary for a capillary electrophoresis system is shown in Fig. 2. The instrument must have the following components: power supply, electrodes (anode and cathode), vials for electrodes and buffers, separation capillary, detector, and data

Capillary Electrophoresis: Introduction and Overview

system or recorder (not shown). The function of each of these components is as follows:

Power Supply. This device supplies the high voltage to the system. Typically, experiments are run at several kilovolts up to 30 kV or more. Most power supplies will also have an ammeter to measure the current flowing through the system.

Electrodes. These components are generally platinum wires which serve as the contact point between the liquid (buffer solutions) in the system and the high-voltage power supply. An inert metal is desirable to avoid an electrochemical reaction or excessive fouling of the electrode surface that would disrupt current flow in the system.

Buffer Reservoirs. These containers hold the buffer solution that provides for a complete electrical circuit through the capillary and connection to the high-voltage supply. Due to electro-osmotic flow as described earlier, the vials also serve as reservoirs to maintain electroneutrality in the system.

Separation Capillary. The fused-silica capillary tube is the focal point in the instrument because sample separation takes place here. The length is typically 50–100 cm and the ends are placed in the buffer reservoirs. The capillary is filled with the running buffer before the analysis begins.

Detector. This device measures a property of the solute in order to determine when each compound has passed through a significant portion of the capillary to the detection window. The detector is not placed at the end of the capillary, as this part of the tube must be in the buffer solution. Solute properties most often used for detection are absorbance and fluorescence, although CE can also be coupled to a mass spectrometer.

Data System/Recorder. The simplest device for output is an ordinary recorder. However, an integrator will provide more information about the peaks (time and area). The most sophisticated apparatus is a computer, which can be used to process and evaluate the data. The computer can also be used to control the operations of the instrument.

The sample can be introduced into the capillary by several methods. The simplest approach is to remove the end of the capillary from the anode buffer reservoir and place it in the sample vial that has been elevated slightly above the level of the cathode buffer container. Gravity flow for several seconds will move some of the sample in the separation capillary. Another approach

is to place the anode end of the capillary into the sample vial and apply pressure to the analyte solution. The next method involves placing the anode end of the capillary in the sample vial and applying a vacuum to the cathodic side of the capillary to draw solution into the tube. The previous three means of sample introduction are referred to as hydrodynamic modes of injection. The last method involves placing the anodic end of the capillary in the sample vial and applying a low voltage for several seconds. This approach is referred to as electrokinetic injection.

Information about the analyte can be qualitative and/or quantitative, with the data resembling a chromatogram. The output from the recorder/integrator/data system is in the form of peaks which are indicated by a time (migration time) from the start of the experiment. The migration time is analogous to the retention time in a chromatographic separation and provides qualitative information by comparison to a known compound under identical experimental conditions. Because the majority of detection in CE is by spectroscopic means, the area under the peak is proportional to the concentration. Therefore, quantitative information can be obtained by making a calibration curve from a plot of peak area versus concentration.

Even though capillary electrophoresis is a relatively simple method, several formats exist that allow for analyses of different types of samples or to take advantage of certain solute properties. The primary modes of capillary electrophoresis are as follows:

Capillary Zone Electrophoresis. The most fundamental approach that involves the use of a fused-silica capillary placed between the two buffer vials so that separation of the sample component occurs after an electric field (voltage) is applied to the system. Separation of the analytes is based on differences in electrophoretic mobility. Only charged compounds, both large and small, can be separated in this format.

Capillary Gel Electrophoresis. In this mode, molecules are separated according to size as they migrate through a polymer matrix. The polymer can be in solution, physically coated on the capillary wall, or chemically bonded to the capillary wall. This mode is primarily used for the separation of large molecules like proteins, peptides, and DNA species.

Capillary Isoelectric Focusing. In this approach, the capillary contains a pH gradient. When the sample is introduced and voltage is applied, it mi-

grates to the point in the capillary where it has zero net charge (isoelectric point). The analytes are removed from the capillary by adding a salt to one of the reservoirs and then applying voltage again. The solutes will then migrate past the detector, with the time being related to its position in the capillary.

Capillary Isotachopheresis. In isotachopheresis, the capillary is first filled with a buffer of higher mobility than any of the solutes, then the sample, and, finally, a second buffer with lower mobility than any of the analytes. Separation occurs in the zone formed between the two electrolytes.

Micellar Electrokinetic Capillary Chromatography. Surfactants that form micelles in solution are added to the buffer in the capillary. When the solute is injected, it partitions itself between the buffer and the micelle. Migration of the solute depends on the amount of time it spends in the micelle versus the time it spends in the buffer. Therefore, the separation of analytes occurs due to differences in the partition coefficient between the two phases, much like in a chromatographic process.

Conclusion

Capillary electrophoresis is still an emerging technology. Rapid development is occurring in separation capillaries, detector technology, and applications.

Suggested Further Reading

- Altria, K. D., *Capillary Electrophoresis Guidebook: Principles, Operation and Applications*, Humana Press, Totowa, NJ, 1996.
- Camilleri, P., *Capillary Electrophoresis: Theory and Practice*, CRC Press, Boca Raton, FL, 1998.
- Hjerten, S., *Methods Enzymol.* 270:296 (1996).
- Landers, J. P., *Handbook of Capillary Electrophoresis*, 2nd ed., CRC Press, Boca Raton, FL, 1997.
- Lunte, S. M. and D. M. Radzik, *Pharmaceutical and Biomedical Applications of Capillary Electrophoresis*, Pergamon, Oxford, 1996.
- Parves, H., P. Candy, S. Parvez, and P. Roland-Gosselin, *Capillary Electrophoresis in Biotechnology and Environmental Analysis*, VSP, Utrecht, 1997.
- Righetti, P. G., *Capillary Electrophoresis in Analytical Biotechnology*, CRC Press, Boca Raton, FL, 1996.



Capillary Isoelectric Focusing of Peptides, Proteins, and Antibodies

Anders Palm

Cell and Molecular Biology, AstraZeneca, Lund, Sweden

Introduction

Capillary isoelectric focusing (CIEF) is a high-resolution technique for protein and peptide separation performed at academic sites and in the biotechnology and pharmaceutical industries for the analysis and characterization of, for example, recombinant antibodies and other recombinant proteins, isoforms of glycoproteins, point mutations in hemoglobin, and peptide mapping. Also, hyphenation to mass spectrometry and chip-based CIEF (microfabrication) have shown promise. CIEF kits and specific recipes/application notes are available from vendors of capillary electrophoresis (CE) equipment, as are a vast amount of publications and handbooks of CE published over recent years.

Capillary isoelectric focusing is a rapid analysis technique with typical run times of 5–30 min, fully automated with on-line detection and real-time data acquisition, and minute sample consumption (a few microliters is enough for repetitive injections). A linear dynamic range over one order of magnitude is achievable, and a detectability down to 5–10 $\mu\text{g/mL}$. A resolution of ΔpI -0.01 is possible under optimized conditions. Reproducibility of pI determination is typically <0.5% (RSD) using internal standards.

Sample Salt Content

For high-performance analysis, it is important that the sample applied has a low salt content [1]. Salt concentrations below 10 mM is preferable; concentrations above 40–50 mM should be desalted. The salt will compress the pH gradient so that it will occupy only some part of the capillary. Hereby, the resolution will decrease and the risk for protein precipitation will increase (see the section on Focusing, below). Also, focusing time will have to be increased as well as focusing/mobilization time being less reproducible.

Ampholytes

Several commercial ampholytes are available covering broad-range (pH 3–10) and narrow-range pH gradients (e.g., pH 6–8). Broad-range gradients are suitable for analysis of proteins covering a wide spectrum of isoelectric points, whereas narrow-range gradients are preferable for high-resolution separations where only minor differences in protein pI 's are expected [2]. Tailor-made gradients can easily be made by mixing ampholytes of different pH ranges or by adding ampholyte spacers [3]. It is preferable, also, to mix ampholytes (with a similar pH interval) from different suppliers so as to create a smoother gradient. Typical concentrations of ampholytes used are 1–5% (v/v); the concentration employed will affect, for example, the protein load, resolution, and focusing/mobilization voltage and time.

Additives

Additives are used in the sample–ampholyte solution either (a) to suppress protein aggregation/precipitation or (b) to decrease the electro-osmotic flow (EOF) velocity and/or protein adsorption to the capillary surface. Protein precipitation is often a major problem in CIEF due to a highly concentrated protein band, and because electrostatic repulsion is minimal at the pI , proteins interact strongly by hydrophobic interactions (also hydrogen-bonding) causing irreproducible migration time and peak area quantification and sometimes capillary clogging [1,2]. Precipitates are often seen as “spikes” in the electropherogram. Strategies to minimize precipitation include reducing the protein concentration and focusing time, applying a lower field strength, and/or using various additives. Because as high a resolution and detection sensitivity as possible are strived for, additives are often the first choice. Many such additives are used to enhance the solubility of proteins like (a) nonionic detergents (e.g., reduced



Triton X-100 and Brij-35), (b) zwitterions (e.g., CAPS and sulfobetain), (c) carbohydrates (e.g., sucrose, sorbitol, and cellulose derivatives), (d) urea, and (e) organic modifiers (e.g., ethylene glycol and glycerol). It is also common to mix different additives [3]. There seems to be no universal solubilization recipe covering all sorts of proteins. Instead, tailor-made recipes often must be worked out whenever precipitates are encountered. The commonly used mixture of 8M urea and 2% detergents, as employed in the first dimension in two-dimensional gel electrophoresis, often performs well, although attention must be paid to protein modification causing artifacts in the electropherogram [1]. Because urea also denatures proteins (in contrast to the other, more mildly, solubilizers), a shift in *pI* might be expected. See Ref. 3 for new types of solubilizers used in CIEF.

Additives used for decreasing the EOF and/or protein adsorption are often cellulose derivatives [e.g., hydroxypropylmethylcellulose (HPMC)]. The cellulose adsorbs to the capillary surface. Hereby, the viscosity will increase at the capillary surface (more than in bulk solution), causing a reduction in EOF as well as a decrease in protein adsorption to the capillary wall. The tendency for protein precipitation will also decrease by addition of cellulose derivatives.

Focusing

Focusing is the process where ampholytes and proteins migrate to their respective *pI* positions in the capillary. During focusing, current will decrease, as the current carrier ampholytes cease to migrate, and finally reach a constant value when the pH gradient is fully developed and the steady state has been attained (certain gradient drifts are often observed in CIEF whose presence will affect performance and reproducibility [2]). Normally, focusing is considered complete when current has decreased to 10% of its original value; a longer focusing time increases the risk for protein precipitation.

Resolution in CIEF is described by the following formula:

$$\Delta pI = 3 \left(\frac{D(dpH/dx)}{E(d\mu/dpH)} \right)^{1/2}$$

where *D* is the diffusion coefficient, *dpH/dx* is the change of pH with distance *x*, *E* is the electric field strength, and *dμ/dpH* is the change of mobility with pH [2]. The importance of the applied voltage is clearly

seen, as a higher field strength gives a better resolution and shorter focusing time. Field strengths between 300 and 700 V/cm are normally used. The optimal voltage may be determined experimentally from a series of runs with different voltages. The formula also reveals that proteins attain a higher resolution than peptides because their *D* values are lower and *dμ/dpH* is higher.

Mobilization

Single-Step CIEF

In single-step (electro-osmotic displacement) CIEF, focusing and mobilization take place simultaneously [1,2]. Here, a dynamically coated (or static coated with reasonably high EOF) capillary is used where the EOF is fast enough to sweep all proteins by the detector in a reasonable time frame and slow enough to simultaneously allow the protein zones to focus. Additives are used to manipulate the velocity of the EOF as well as to decrease protein adsorption. The single-step method benefits from short analysis times and an extended capillary lifetime but suffers from lower detectability (due to lower protein load), compromised resolution, and nonlinearity of the *pI* calibration curve [4]. A variant of the single-step CIEF is to use whole-column imaging detection where all the focused bands in the capillary are detected simultaneously without any need for mobilization [5].

Two-Step CIEF

Two-step CIEF is used when EOF in the capillary is strongly reduced. After focusing is complete, a separate mobilization step is applied where the protein bands are transported past the fixed detector. Mobilization can be achieved either by chemical means [for cathodic (anodic) mobilization, the composition of the catholyte (anolyte) is changed; thereby the pH gradient will change], or by applying a positive/negative pressure, or by a mixture of both [1,2]. A pressure will induce zone broadening due to the parabolic flow profile; a modest pressure in combination with high-voltage will preserve the high-resolution pattern 4. Pressure mobilization offers good reproducibility (migration times and *pI* values) and a linear *pI* calibration curve. Chemical mobilization shows the same performance and also exhibits the highest resolution, at the expense of longer migration times. Anodic mobilization affords a better resolution of the acidic region, whereas cathodic mobilization is preferable for the basic region [4].



Detection

Absorbance detection at 280 nm is mostly used. Below 220 nm is preferable for sensitive protein/peptide detection but is not possible because of background-absorbing ampholytes [2]. Proteins with chromophores (e.g., hemoglobins) can be detected at visual wavelengths. However, because CIEF is a concentrating technique (the protein bands will be concentrated about 100-fold during focusing), a fairly good sensitivity for most proteins is still attainable at 280 nm. For high-sensitivity analysis, laser-induced fluorescence detection might be an alternative, but it requires a labeling procedure [5,6]. By labeling, a change in intrinsic pI might occur and the same analyte might be subjected to multiple labeling sites showing several peaks in the electropherogram (especially proteins). This might, however, be the only choice for peptides lacking tyrosine and tryptophan. Whole-column imaging detection (no mobilization step needed) with different detection schemes is also possible for proteins and peptides [5].

Capillary isoelectric focusing coupled to mass spectrometry has gained popularity in recent years (by analogy to two-dimensional gel electrophoresis). Additional information obtained from mass spectrometry includes not only precise molecular-weight determination but also the possibility for peptide sequencing. Analysis of hemoglobin variants, recombinant proteins, and monoclonal antibodies have been demonstrated [1,7,8].

Application of CIEF to Peptides, Proteins, and Antibodies

Peptides

Peptides are not as commonly analyzed by CIEF as are proteins; one reason is their lower resolution, another their lower (or lack of) detectability at 280 nm (the wavelength mostly used). The separation of tryptic digests (peptide mapping) of proteins have been performed by using absorption detection at 280 nm and refractive index gradient imaging detection; no exact correlations were observed between measured and calculated pI values [1,5]. Refractive index detection is a universal detection method (i.e., independent of chromophores like tyrosine and tryptophan) but suffers from low sensitivity. Assays of trypsin activity have also been performed with laser-induced fluorescence detection for enhanced sensitivity, with detectability down to picomolar concentrations [5,6].

Hemoglobins

Analysis of hemoglobin (Hb) variants are of major clinical importance. Many hematological disorders exist where the globin chains have been subjected to alterations (e.g., point mutations or deletion of gene sequence). Four hemoglobin variants (A, F, S, and C) having very close pI values (from 7 to 7.40) are often employed as standards to demonstrate the high resolving power of CIEF [2]. Several other variants are possible to resolve (e.g., the separation of Hb A from its glycosylated form Hb A_{1c} whose pI 's differ only by 0.01 or less) [1,3]. Quantitative determination of Hb A_{1c} is routinely used for assessing the degree of diabetes. To improve the resolution between Hb A and Hb A_{1c}, spacers (β -alanine and 6-aminocaproic acid) were added to a mixture of pH 3–10 and pH 6–8 ampholytes in a coated capillary [3]. The spacers flatten the pH gradient in the pI region of the Hb's, thus allowing full separation.

Antibodies

Analysis of microheterogeneity in natural and recombinant monoclonal antibodies is a challenge where CIEF seems to be particularly well suited (see Fig. 1 [4]). Minor modifications (e.g., deamidation, improper folding, and a change in glycosylation pattern) arising from protein synthesis or posttranslational modifications are often detected by CIEF [1,2,9]. The use of CIEF and comparison to flat-bed IEF for routine analysis of recombinant immunoglobulins have been demonstrated with a coated capillary, methylcellulose, and a two-step mobilization procedure. The performance of the analysis and coating stability were constant for over 150 analyses with qualitatively and quantitatively equivalent immunoglobulin focusing profiles obtained via CIEF and IEF. Intra-assay reproducibility was less than 2% RSD for peak areas and 1% RSD for migration time. Interassay (72 h) reproducibility was less than 8% RSD for peak areas and 3% for migration time [10].

Glycoproteins

Applications of CIEF for the separation of isoforms of transferrin have been reported by several groups [1,2,5]. Transferrin contains different number of sialic acid residues, with an additional -1 charge added per residue. Also, transferrin bound to different amount of iron atoms has been separated by CIEF [1,2,5]. Glycoforms of recombinant tissue-type plasminogen activa-



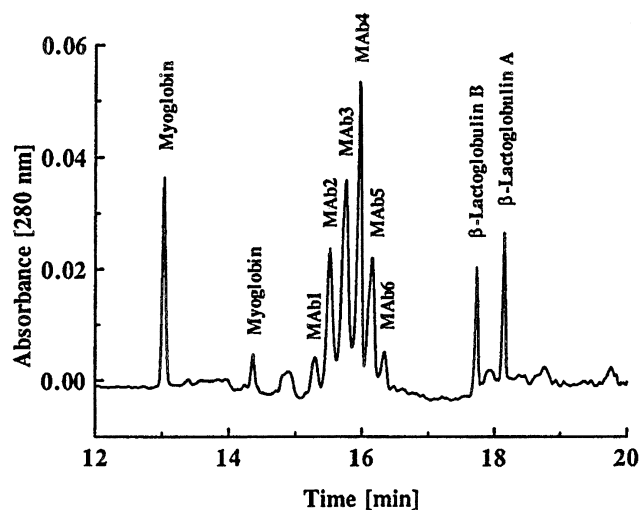


Fig. 1 CIEF of a mouse monoclonal antibody (MAb). Antibody concentration: 0.5 mg/mL; concentration of the marker proteins (myoglobin and β -lactoglobulin): 0.05 mg/mL; capillary: μ -SIL DB-1, 27 cm total length (20 cm to detector); carrier ampholytes: 4% Pharmalyte pH 3–10 including 1% TEMED and 0.8% methylcellulose (MC); anolyte: 10 mM H_3PO_4 in 0.4% MC; catholyte: 20 mM NaOH. Focusing for 2 min at 20 kV, followed by mobilization at low pressure (0.5 psi) at 20 kV. (From Ref. 4.)

tor (rtPA) is another sialic acid containing protein which has been the subject of analysis by CIEF [1,2,11]. A rapid (<10 min) one-step method was de-

veloped using a coated capillary, HPMC, and urea in a mixture of pH 3–10 and pH 5–8 ampholytes. Ten species could be detected. Intra-assay precision was less than 5% for peak migration times and 10% for normalized peak areas [11].

References

1. R. Rodriguez-Diaz, T. Wehr, and M. Zhu, *Electrophoresis* 18:2134 (1997).
2. X. Liu, Z. Sosic, and I. S. Krull, *J. Chromatogr. A* 735:165 (1996).
3. P. G. Righetti, A. Bossi, and C. Gelfi, *J. Capillary Electrophoresis* 4(2), 47 (1997).
4. C. Schwer, *Electrophoresis* 16:2121 (1995).
5. X. Fang, C. Tragas, J. Wu, Q. Mao, and J. Pawliszyn, *Electrophoresis* 19:2290 (1998).
6. K. Shimura, H. Matsumoto, and K. Kasai, *Electrophoresis* 19:2296 (1998).
7. J. Wei, C. S. Lee, I. M. Lazar, and M. L. Lee, *J. Microcol. Separ.* 11(3):193 (1999).
8. M-L Hagmann, C. Kionka, M. Schreiner, and C. Schwer, *J. Chromatogr. A* 816:49 (1998).
9. I. S. Krull, X. Liu, J. Dai, C. Gendreau, and G. Li, *J. Pharm. Biomed. Anal.* 16:377 (1997).
10. S. Tang, D. P. Nesta, L.R. Maneri, and K. R. Anumula, *J. Pharm. Biomed. Anal.* 19:569 (1999).
11. K. G. Moorhouse, C. A. Eusebio, G. Hunt, and A. B. Chen, *J. Chromatogr. A* 717:61 (1995).

Capillary Isoelectric Focusing: An Overview

Robert Weinberger

CE Technologies, Inc., Chappaqua, New York, U.S.A.

Introduction

Capillary isoelectric focusing (CIEF) employs a pH gradient developed within the capillary to separate zwitterions, usually proteins and peptides, based on each solute's pI . The technique is analogous to slab-gel CIEF [1] with several important differences: (a) Slab-gel IEF is a nonelution process. After running the electrophoretic step, the proteins are detected by staining. CIEF is usually an elution technique. The contents of the capillary are mobilized to pass through the detector region. (b) In the slab-gel, detection is by Commassie or silver staining. In CIEF, detection is by ultraviolet (UV) absorbance at 280 nm. (c) In the capillary format, no gel is required because mechanical stability is provided by the rigid capillary walls. (d) The field strength is at least an order of magnitude higher in the capillary format compared to the slab-gel.

The usual advantages of capillary electrophoresis apply equally to CIEF. Slab-gel IEF is extremely labor intensive and time-consuming. CIEF is simple to run, fully automated, and high speed and provides improved quantitative results compared to slab-gel IEF. This topic has been recently reviewed [2,3], as is usually covered as a chapter in many high-performance capillary electrophoresis textbooks.

pH Gradient Formation

A solution containing 0.5–2.0% carrier ampholytes and 0.1–0.4% methylcellulose (1500 cP for a 2% solution) is filled into the capillary. A coated capillary is used to suppress the electro-osmotic flow in conjunction with the methylcellulose solution. The sample (protein) concentration in the ampholyte blend is usually between 50 and 200 $\mu\text{g/mL}$. The inlet reservoir (anolyte) is filled with 10 mM phosphoric acid in methylcellulose solution. The outlet reservoir (catholyte) contains 20 mM sodium hydroxide.

The condition of the capillary immediately upon activation of the voltage is illustrated at the top of Fig. 1. In this case, the capillary is filled with a pI 3–10

mixture of ampholytes. Assuming the pH of the solution is 7, charges have been assigned to the individual ampholytes. The ampholyte charge dictates the direction of migration. Should any ampholytes migrate into a reservoir, the extreme pH conditions cause immediate charge reversal. Likewise, as the steady state is approached, should an ampholyte migrate into a more acidic or basic zone, charge reversal occurs as well. The result is the formation of a pH gradient as indicated at the bottom of Fig. 1. As each ampholyte approaches a pH equal to its individual pI , migration slows and then ceases. Because overlapping Gaussian zones of each ampholyte are formed, the gradient is smooth and linear.

The conventional pH range for CIEF is pH 3–10. Narrow-range gradients can be created by selecting custom ampholyte blends (e.g., pH 6–8). To avoid problems such as a step-gradient or the creation of water zones, the narrow-range ampholyte solution is usually supplemented with 20% pH 3–10 ampholytes. This ensures that there are sufficient ampholyte species to produce Gaussian overlaps.

The focusing step takes 2–5 min. at a field strength of 500–1000 V/cm. Overfocusing causes precipitation

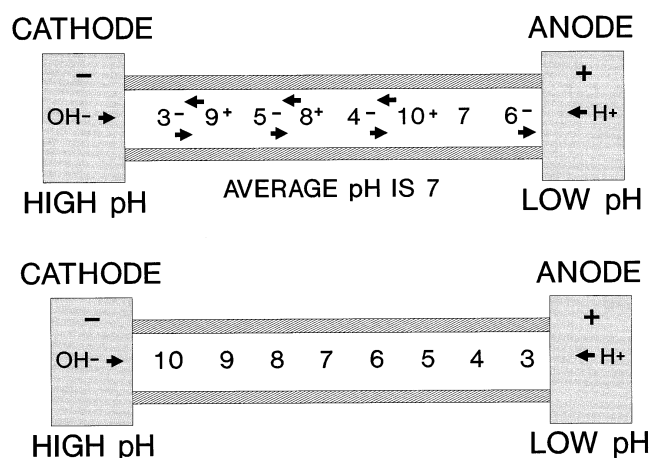


Fig. 1 Illustration of the process of pH gradient formation.



of proteins and can damage the capillary as well. Initially, the current is high as ampholytes and proteins are highly charged. As their pI 's are approached, the current declines and reaches 1–4 μA when focusing is complete.

The 2:1 ratio of base:acid in the reservoirs is not coincidental. It is selected to minimize drift of the pH gradient. The pH of the anolyte must be lower than that of the most acidic ampholyte; likewise, the pH of the catholyte must be higher than the most basic ampholyte. Otherwise, ampholytes will migrate into the reservoirs and cause gradient drift. If the EOF is not reduced, a form of cathodic drift occurs as well. An exception to this is when one-step mobilization is employed.

Internal standards are always used to calibrate the pH gradient. This is important because the salt content of the sample can compress the gradient. The ideal internal standard absorbs at a wavelength other than 280 nm. It can then be added to the ampholytes and monitored without producing interference. In this case, photodiode array detection is used for multiwavelength monitoring. Methyl red, pI 3.8, is ideal in this regard, but other such markers have not been identified. Aminomethylphenyl dyes are often used with monitoring at 400 nm, but they have some absorbance at 280 nm.

To prevent focused zones from reaching the blind side of the capillary past the detector, the ampholytes are either filled just prior to the detector or the reagent TEMED (*N,N,N,N*-tetramethylenediamine) is added to the blend at the appropriate concentration (0.5–2.0%). TEMED, a basic amine, then occupies that space past the detector window.

Resolving Power

The resolving power, ΔpI , of CIEF is described by

$$\Delta pI = 3\sqrt{\frac{D(dpH/dx)}{E(d\mu/dpH)}} \quad (1)$$

where D is the diffusion coefficient, E is the field strength, μ is the mobility of the protein, and $d\mu/dpH$ describes the mobility–pH relationship. The term dpH/dx represents the change in the buffer pH per unit of capillary length. This adjustable parameter is controlled by selecting an appropriate ampholyte pH range as well as the capillary length. Under optimal conditions, a resolution of 0.02 pH units is possible.

Mobilization

There are three ways of mobilizing the contents of the capillary: (a) chemical (salt) mobilization, (b) electroosmotic (one-step) mobilization, and (c) hydrodynamic mobilization. Hydrodynamic mobilization is the simplest and most widely used method. Low pressure is used to evacuate the capillary with the voltage activated. Laminar band broadening is minimized by simultaneous focusing. In one-step mobilization, the EOF is reduced but not absent. If done correctly, focusing occurs prior to any proteins reaching the detector. This is the fastest method but has lower resolution and linearity compared to hydrodynamic mobilization. Salt mobilization is infrequently used today, but it produces the highest resolution at the expense of run time and gradient linearity.

Detection

Because the ampholytes absorb below 250 nm, 280-nm detection is required. It is critical to run ampholyte blanks because the reagents are not checked by the manufacturers for UV absorption at 280 nm. The limit of detection is a few micrograms per milliliter of protein and this is usually limited by the UV reagent background. Proteins that are deficient in aromatic amino acids are poorly detected. Different lots of ampholytes from various manufacturers show variation in the UV background.

The combination of CIEF and mass spectrometry is analogous to two-dimensional electrophoresis [4]. In this case, the mass spectrometer provides the molecular-weight information instead of sodium dodecyl sulfate–polyacrylamide gel electrophoresis. This information can be obtained by on-line CIEF–MS [5] or by using CIEF as a micropreparative technique [6].

For the on-line system, CIEF is performed conventionally in a 20-cm capillary mounted inside an electrospray probe. After focusing, the outlet reservoir (catholyte) is removed and the capillary tip set to 0.5 μm outside of the probe. A sheath liquid of 50% methanol, 49% water, and 1% acetic acid (pH 2.6) pumped with a syringe pump at 3 $\mu L/min$ produces a stable electrospray. Cathodic mobilization is produced by changing the anolyte to the sheath liquid. The ampholyte ions were observed up to m/z 800 and thus did not interfere with the protein signals.

Additives for Hydrophobic Proteins

The tendency of hydrophobic proteins to aggregate and precipitate is a major problem in IEF whether in the slab-gel or capillary format. The focusing power of CIEF produces an increase in solute concentration by a factor of over 200 [7]. Proteins also readily precipitate as the pI is approached because their charge and, thus, electrostatic repulsion approach zero.

Protein precipitation is indicated first by spikes in the electropherogram followed by clogging of the capillary. Additives are required to suppress the aggregation of hydrophobic proteins to keep them in solution. Two excellent review articles describe this in detail [8,9].

Among the reagents used to prevent aggregation are urea, nonionic surfactants such as Brij-35, zwitterionic detergents such as sulfobetains, polyols such as ethylene glycol, glycerol, and sorbitol or nonreducing sugars. A strategy of mixing polyols and zwitterions is often successful in dealing with solubility problems.

Applications

Capillary isoelectric focusing has been employed for separations of many proteins, recombinant proteins, monoclonal antibodies, and protein glycoforms. The most widely used method employing CIEF is the determination of hemoglobin variants for the screening of genetic disorders, including sickle cell anemia, thalassemias, and other hemoglobinopathies. Figure 2 illustrates the separation of hemoglobins in a patient with Hb S/ β^+ thalassemia.

References

1. P. G. Righetti, *Isoelectric focusing: Theory, Methodology and Applications*, Elsevier Biomedical Press, Amsterdam, 1983.

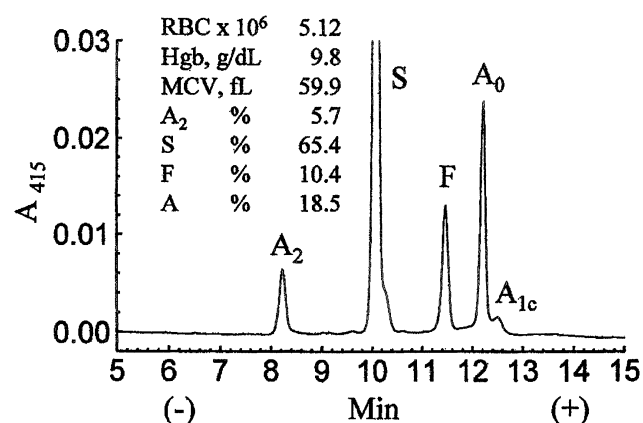


Fig. 2 Separation of hemoglobins by CIEF in blood from a patient suffering from Hb S/ β^+ thalassemia. Capillary: 27 cm (20 cm to detector) \times 50 μ m i.d. DB-1 (J & W Scientific); ampholytes: 2% pH 6–8:10–3 (10:1) Pharmalytes (Pharmacia Biotech) and 0.375% methylcellulose; catholyte: 20 mM sodium hydroxide; anolyte: 100 mM phosphoric acid in 0.375% methylcellulose; focusing: 5 min at –30 kV; mobilization: low pressure (0.5 psi) for 10 min at –30 kV; detection: UV, 415 nm. [Reprinted from *Electrophoresis* 18:1785 (1997), copyright (1997) Wiley-VCH.]

2. P. G. Righetti and A. Bossi, *Anal. Chim. Acta* 372:1 (1998).
3. T. J. Pritchett, *Electrophoresis* 17:1195 (1996).
4. Q. Tang, A. K. Harrata, and C. S. Lee, *Anal. Chem.* 69:3177 (1997).
5. Q. Tang, A. Kamel Harrata, and C. S. Lee, *Anal. Chem.* 67:3515 (1995).
6. F. Foret, O. Muller, J. Thorne, W. Gotzinger, and B. L. Karger, *J. Chromatogr. A* 716:157 (1995).
7. G. G. Yowell, S. D. Fazio, and R. V. Vivilechia, *J. Chromatogr.* 652:215 (1993).
8. T. Rabilloud, *Electrophoresis* 17:813 (1996).
9. R. Rodriguez-Diaz, T. Wehr, and N. Zhu, *Electrophoresis* 18:2134 (1997).



Capillary Isotachopheresis

Ernst Kenndler

Institute for Analytical Chemistry, University of Vienna, Vienna, Austria

Introduction

Three analytical electrophoretic techniques can be distinguished. They differ in the kind of background electrolyte (BGE) and in its arrangements. Zone electrophoresis has a uniform BGE without a gradient; in isoelectric focusing, the separation is established by the aid of a BGE forming a continuous (linear) pH gradient. In contrast, isotachopheresis (ITP) is an electrophoretic method with a stepwise gradient of the background electrolyte.

Isotachopheresis

In ITP, samples of only one charge type are separated in the same run (i.e., either anions or cations). The BGE in ITP is selected in the way that (the anion or cation of) the leading (L) and the terminating (T) electrolyte will have a higher and a lower mobility, μ , respectively, than the analytes of interest. Thus, the prerequisite for separation by ITP is that $\mu_L > \mu_{\text{analytes}} > \mu_T$.

Consider the case that the sample ions are anions (consisting of analytes A^- and B^-), and that the ions exhibit mobilities in the sequence $\mu_L > \mu_A > \mu_B > \mu_T$. The capillary is filled with L^- and T^- , separated by a sharp boundary, and the sample is injected between the two electrolyte zones (for simplicity, it is assumed that the counterions, Q^+ , are all the same). After application of an electric field, a certain field strength is established in the zones as depicted in Fig. 1 (it is assumed that the capillary has uniform diameter). Across the individual zone, the field strength is constant, but it increases due to the decreasing mobility (and increasing electrical resistance) from L to T. Across the zone of the mixed sample (A 1 B) it is constant as well, with strength E_{mix} . In this zone, the two analytes A and B are moving with different migration velocities, n , according to $v_A = \mu_A E_{\text{mix}}$ and $v_B = \mu_B E_{\text{mix}}$. Due to the higher mobility of A, this analyte moves faster here than B: $\mu_A E_{\text{mix}} > \mu_B E_{\text{mix}}$. This effect leads to the migration of ions A^- out of the mixed zone, forming a separate zone in front with pure

A^- (which is always placed behind the zone of the leading electrolyte). For B^- , the analogous situation occurs; it is moving slower in the mixed zone and forms a separate zone at the rear side (but in front of T). The formation of zones of pure analyte ions (obviously with counterions, Q^+ , the counter ions of the leading electrolyte) is, therefore, observed. Five zones can be differentiated in this transient state: L^- , pure A^- , mixed $A^- + B^-$, pure B^- , and T^- . Due to the different mobilities, the field strength increases in this sequence. Separation takes place as long as the mixed zone exists. Finally, this zone disappears and the isotachophoretic condition is established: All zones and zone boundaries migrate with the same mean velocity ("isotachopheresis"); consequently,

$$\mu_L E_L = \mu_A E_A = \mu_B E_B = \mu_T E_T \quad (1)$$

This is the isotachophoretic condition. The conditions of electroneutrality must be fulfilled as well, which means, in the case considered, that in each zone the concentration of ions and counterions is equal. The third condition is Ohm's law, stating that (for given constant current) the product of electrical conductivity and field strength in each zone is equal. The combina-

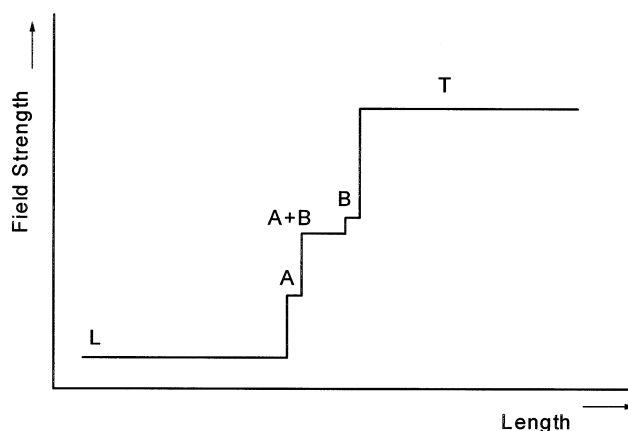


Fig. 1 Electrical field strength in the zones of the leading electrolyte, L, the sample consisting of A and B, and the termination electrolyte, T. For details, see the text.



tion of these conditions leads to the so-called regulation function (Kohlrausch), which reads in a simplified form (for monovalent strong electrolytes):

$$c_A = c_L \frac{\mu_A(\mu_L + \mu_Q)}{\mu_L(\mu_A + \mu_Q)} \quad (2)$$

It relates the concentration of a species in its own zone to the concentration of the species in the subsequent zone and, as a consequence, to the concentration of the first zone, the leading ion. It is also a function of the mobility of the ions involved: the analyte, the leading ion, and the counterion. This function allows two conclusions as follows.

As for given conditions, the mobilities in Eq. (2) are constant under ITP conditions; the concentration of the sample in its zone is constant as well. The concentration distribution is, therefore, given by a rectangular function. It follows that the temperature and the pH within the particular zone is constant, too, and changes stepwise at the boundary to the neighboring zone.

The concentration depends only on that of the leading ion; it is independent of the initial concentration in the sample. Therefore, ITP can act as an enrichment method, analogous to displacement chromatography and in contrast to zone electrophoresis and elution chromatography. The concentration in the steady state is adjusted to the value given in Eq. (2). If the concentration of the analyte species is lower in the initial sample, the higher steady-state concentration is established. This concentration is independent of the migration distance: there is no dilution with a BGE as there is in capillary zone electrophoresis (CZE).

The adjustment of the steady-state concentration to a certain constant value has the consequence that the zone length of an analyte depends on the amount present in the sample. Increasing the amount results in an increase of the zone length under ITP conditions. The

length is, therefore, the parameter for quantitative analysis.

The stepwise gradient of the electrical field at the zone boundary is the source of the “self-sharpening” effect in ITP. When, by diffusion, an ion migrates out of its own zone, into a neighboring zone (where the field strength is higher or lower, respectively), the condition given in Eq. (1) is not fulfilled any more. Therefore, the velocity of the considered ion is either accelerated or retarded, and the ion is pushed back into its initial zone. As a consequence, the boundary between the zones remains sharp and its shape is not dependent on the migration distance.

Isotachophoresis might have several advantages compared to zone electrophoresis. The adaptation to a considerably high concentration of the sample components in their own zones in the absence of further BGE favors the use of the electrical conductivity detector. The high concentration and the long sample zone have also some advantage in combining capillary electrophoresis with, for example, mass spectrometry. Also, ITP can be used as an enrichment technique prior to zone electrophoretic separation, a phenomenon that is applied routinely in sodium dodecyl sulfate–polyacrylamide gel electrophoresis using a discontinuous buffer for sample introduction, and a technique called sample stacking in CZE. In fact, both methods rely on an isotachophoretic principle.

Suggested Further Readings

- Bocek, P., M. Deml, P. Gebauer, and V. Dolnik, *Analytical Isotachophoresis*. VCH, Weinheim, 1988.
- Everaerts, F. M., J. L. Beckers, and T. P. E. M. Verheggen, *Isotachophoresis: Theory, Instrumentation, and Applications*, Elsevier, Amsterdam, 1976.
- Mosher, R. A., D. A. Saville, and W. Thormann, *The Dynamics of Electrophoresis*, VCH, Weinheim, 1992.



Carbohydrates as Affinity Ligands

I. Bataille

D. Muller

Institut Galilee, Université Paris Nord, Villetaneuse, France

Introduction

Since its conception 30 years ago, affinity chromatography has been a powerful technique to separate or purify biological compounds, but also a method to study the interactions between living systems and molecules of biological or therapeutical interest. Among these molecules, oses, polysaccharides, or more complex molecules such as glycosaminoglycans constitute a family of potential ligands.

Discussion

The majority of applications of affinity chromatography has been, for a long time, in the field of protein purification. For example, some of the most rewarding applications of affinity chromatography have been in the area of purification of hormone and drug receptors. Among these drugs, carbohydrate-based structures are well known for their biological activity (e.g., their anticoagulant or antiproliferative properties). Although some of these biological properties are widely used in medical applications, the mechanisms of action at the molecular level is not accurately determined.

An example of the use of carbohydrate-based affinity chromatography is, thus, the separation of proteins which are responsible for the action of bioactive polysaccharides or oses. The strategy consists in the immobilization of these carbohydrates on classical low- or high-pressure affinity phases. We will distinguish two types of ligands: those based on osidic structures and those prepared from glycosaminoglycans or polysaccharides.

Osidic Ligands

All osidic structures which can interact with proteins implicated in biological responses or phenomenons are, a priori, candidates as ligands in affinity chromatography. Here, we give some examples of oses

which have been successfully immobilized to make selective chromatographic supports.

Sialic Acid (N-Acetylneuraminic Acid)

Purification of immunoglobulins G is of great interest in biological science. Among other separation methods, affinity chromatography has been used in different ways. Affinity supports were first prepared using protein A or protein G, whose affinity constants take different values according to the IgG subclasses (IgG1, 2, 3, or 4). Among interesting carbohydrates, sialic acid is known to specifically interact with IgGs. Indeed, immunoglobulins are able to react to the presence of tumoral cells. The antigens which are suspected to promote this reaction are gangliosids. Beyond a ceramide molecule, some oses are present in gangliosids, among which are included between 1 and 3 sialic acids.

The hypothesis has been made that sialic acid may lead to the formation of specific interactions with immunoglobulins G. Some workers have, thus, developed affinity supports bearing sialic acid, in order to purify IgGs. Sialic acid can be extracted from swallow nests and coupled on activated coated silica. This support has been found to possess a good specificity for IgGs, in particular for the subclass IgG3 [1].

Supports prepared with sialic acid have also been used in the purification of insulin, as this sugar and N-acetylglucosamine have been found to take part in the interaction between insulin and its glycosylated receptor. The affinity between insulin and sialic acid-bearing supports has been found rather strong ($K_a \sim 10^9 M^{-1}$) and the system allows the separation of beef and pig insulins [2], which differ by only two amino acids.

N-Acetylglucosamine

N-Acetylglucosamine also shows a specific interaction with insulin. Affinity chromatography experiments have evidenced results very close to those observed in the case of sialic acid. An interesting result

Encyclopedia of Chromatography

DOI: 10.1081/E-Echr 120004605

Copyright © 2002 by Marcel Dekker, Inc. All rights reserved.



is that the improvement of both affinity and capacity of supports bearing both sugars [3]. These supports are supposed to more accurately mimic the structure of insulin receptor.

Mannose and Derivatives

Mannose has been immobilized in order to separate mannose-binding proteins such as mannose-binding lectin. When grafted onto agarose, it constitutes a purification step of a specific lectin which does not bind to DEAE-cellulose or Affi-gel Blue gel [4]. Another way to obtain mannose-binding lectin is to perform expanded-bed affinity chromatography by immobilizing mannose on a DEAE Streamline support [5]. Affinity agarose supports, grafted with pentamannosyl phosphate, allowed the testing of the functionality (in terms of ligand binding) of truncated and glycosylation-deficient forms of the mannose 6-phosphate receptor from insect cells [6]. Phosphomannan affinity chromatography has been used to purify a human insulin-like growth factor II mannose 6-phosphate receptor [7].

Glycosaminoglycans and Polysaccharides

Certainly, one of the most used glycosaminoglycans is heparin, because of its anticoagulant properties. Other glycosaminoglycans or polysaccharides have shown such properties; among them, sulfated dextran derivatives and naturally sulfated polysaccharides extracted from algae (fucans) will be discussed further.

Heparin

Anticoagulant properties are due to the formation of a complex between heparin and antithrombin (ATIII); heparin increases ATIII activity, inhibiting thrombin, which is responsible for the formation of the clot [8]. Although this complex is already characterized by a weak affinity, the exact mechanism of association between heparin and antithrombin is not exactly known. A multistep protocol of immobilization of heparin on silica beads permitted high-performance chromatographic phases to be obtained. Thus, it has been possible to evidence a slightly stronger affinity of heparin for antithrombin than for thrombin.

ATIII has been also used as a model protein to test a novel affinity chromatographic system: capillary affinity chromatography [9]. Separation quality has been found equivalent to that observed with classical affinity chromatography, whereas the necessary protein amount is strongly reduced to the nanogram level.

Heparin possesses an affinity for many molecules, among which is a phospholipid-binding protein, annexin V. Affinity chromatography evidenced the Ca^{2+} dependence of the binding mechanism [10]; von Willebrand factors with high and low molecular weights have been separated using their different affinities toward heparin [11].

Heparin has been used in enzyme purification such as recombinant human mast cell tryptase. The purified enzyme is fully active [12]. Heparin-based affinity chromatography also permitted the isolation of growth factors such as basic fibroblast growth factor (bFGF). The affinity is lower when bFGF is complexed with acidic gelatin [13]. The elution of synthetic TFPI (tissue factor pathway inhibitor) peptidic fragments on immobilized heparin has allowed one to find the peptidic sequence responsible for the TFPI-heparin interaction [14].

Heparin is able to inhibit smooth-muscle cells (SMCs) proliferation in vitro. SMCs are present in blood vessel walls and may proliferate in the case of an internal injury. The antiproliferative action of heparin is due to its internalization in SMCs, which is probably mediated by membrane receptors. Heparin-based affinity chromatography of SMCs membrane extracts allowed the separation of a few proteins, which could be implicated in the growth inhibition [15].

The different actions taking place in the overall affinity mechanism of immobilized heparin for different biological compounds is not yet elucidated, but the influence of ionic strength demonstrates the important contribution of ionic interactions in this mechanism. However, the large spectrum of biological activities of heparin is also a limit for its specificity.

Other Glycosaminoglycans

Dermatan sulfate is known to specifically catalyze thrombin inhibition by the plasmatic inhibitor heparin cofactor II (HCII). Dermatan sulfate has been immobilized on a dextran- or agarose-coated silica matrix. These systems were tested as high-performance chromatographic supports for the purification of HCII from human plasma. The eluted HCII was obtained with no contamination of ATIII, the other main thrombin inhibitor [16].

Dextran Derivatives

Phosphorylated dextran derivatives, called phosphodextrans, possess a strong affinity for K-vitamin-dependent coagulation factors, like factor II or pro-



thrombin. This property was used to separate them by affinity chromatography on phosphodextrans, which interact in a similar way as phospholipids from the cell membrane [17].

Heparinlike sulfated dextran derivatives, like carboxymethyldextran benzylamide sulfonates (CMDBS), have been immobilized on silica beads. By high-performance liquid affinity chromatography (HPLAC), they allow a good recovery of thrombin, with a yield of 80%. The affinity constant was estimated ($K_a \sim 10^5 M^{-1}$) and was found superior to the value obtained between thrombin and heparin. On the contrary, the affinity of dextran derivatives for ATIII is estimated at a lower value than that of heparin [17].

Fucans

Fucan is a sulfated polysaccharide, naturally present in algae such as *Fucus vesiculosus* or *Ascophyllum nodosum*. Fucan is a general name for a mixture of three polysaccharides, and among them, fucoidan (or homofucan) can be theoretically considered as an homopolymer of α -1,2 L-fucose-4-sulfate and has been studied as a ligand in the same way as fucan himself. Their interaction with two proteins implicated in the coagulation process (thrombin and antithrombin) has been studied and is at least partially ionic. However, the dissociation of the complex fucan–antithrombin seems to include a slower step which could be attributed to a conformation change of the fucan [18].

Fucan was also used as ligand for high-performance liquid affinity chromatography. In the same way as dextran derivatives, a good separation was obtained for thrombin, with a yield of 80%. The affinity constant was estimated in the same order as that obtained for CMDBS ($K_a \sim 10^5 M^{-1}$) and superior to the value obtained for heparin [17].

Conclusion

In this article, we have described several uses of carbohydrate compounds as affinity ligands. These few examples clearly demonstrate the importance of such affinity supports in the separation of biological products. Affinity chromatography is also able to help in the determination of the interaction mechanisms of carbohydrate derivatives in biological reactions. This developing field of research will lead to improved quality and specificity of affinity-chromatographic phases.

References

1. A. Serres, E. Legendre, J. Jozefonvicz, and D. Muller, Affinity of mouse immunoglobulin G subclasses for sialic acid derivatives immobilized on dextran-coated supports, *J. Chromatogr. B* 681:219 (1996).
2. H. Lakhari, J. Jozefonvicz, and D. Muller, Separation and purification of insulins on coated silica support functionalized with sialic acid by affinity chromatography, *J. Liquid Chromatogr. Related Technol.* 19:2423 (1996).
3. H. Lakhari, Supports de silice enrobée à ligands bio-spécifiques: Synthèse, caractérisation et relations structure-propriétés de séparation. Application à la purification de l'insuline et des immunoglobulines G. Thesis, University Paris 13, 1996.
4. L. S. M. Ooi, H. X. Wang, T. B. Ng, and V. E. C. Ooi, Isolation and characterization of a mannose-binding lectin from leaves of the chinese daffodil *Narcissus tazetta*, *Biochem. Cell Biol.* 76:601 (1998).
5. O. Bertrand, S. Cochet, and J. P. Cartron, Expanded bed chromatography for one-step purification of mannose binding lectin from tulip bulbs using mannose immobilized on DEAE Streamline, *J. Chromatogr. A* 822:19 (1998).
6. P. G. Marron-Terada, K. E. Bollinger, and N. M. Dahms, Characterization of truncated and glycosylation-deficient forms of the cation-dependent mannose 6-phosphate receptor expressed in baculovirus-infected insect cells, *Biochemistry* 37:17,223 (1998).
7. M. Costello, R. C. Baxter, and C. D. Scott, Regulation of soluble insulin-like growth factor II mannose 6-phosphate receptor in human serum: Measurement by enzyme-linked immunosorbent assay, *J. Clin. Endocrinol. Metab.* 84:611 (1999).
8. I. Björk, S. T. Olson, and J. D. Shore, Molecular mechanisms of the accelerating effect of heparin on the reactions between antithrombin and clotting proteinases, in *Heparin, Chemical and Biological Properties, Clinical Applications* (D. A. Lane and U. Lindahl, eds.), Edward Arnold, London, 1989, pp. 229–255.
9. X. J. Wu and R. J. Linhardt, Capillary affinity chromatography and affinity capillary electrophoresis of heparin binding proteins, *Electrophoresis* 19:2650 (1998).
10. I. Capila, V. A. Van der Noot, T. R. Mealy, B. A. Seaton, et al., Interaction of heparin with annexin V, *FEBS Lett.* 446:327 (1999).
11. B. E. Fischer, K. B. Thomas, U. Schlokot, and F. Dorner, Selectivity of von Willebrand factor triplet bands towards heparin binding supports structural model, *Eur. J. Haematol.* 62:169 (1999).
12. A. L. Niles, M. Maffit, M. Haak-Frendscho, C. J. Wheelless, et al., Recombinant mast cell tryptase: Stable expression in *Pichia pastoris* and purification of fully active enzyme, *Biotechnol. Appl. Biochem.* 28:125 (1998).
13. M. Muniruzzaman, Y. Tabata, and Y. Ikada, Complexation of basic fibroblast growth factor with gelatin, *J. Biomater. Sci. Polym. Ed.* 9:459 (1998).



14. Z. Y. Ye, R. Takano, K. Hayashi, T. V. Ta, et al., Structural requirements of human tissue factor pathway inhibitor (TFPI) and heparin for TFPI-heparin interaction, *Throm. Res.* 89:263 (1998).
15. A. S. Clairbois, D. Letourneur, D. Muller, and J. Joze-fonvicz, High-performance affinity chromatography for the purification of heparin-binding proteins from detergent-solubilized smooth muscle cell membranes, *J. Chromatogr. B* 706:55 (1998).
16. V. Sinniger, J. Tapon-Bretaudière, F. L. Zhou, A. Bros, et al., Immobilization of dermatan sulphate on a silica matrix and its possible use as an affinity chromatography support for heparin cofactor II purification, *J. Chromatogr.* 539:289 (1991).
17. F. L. Zhou, Supports à base de silice enrobée par des polysaccharides pour chromatographie d'affinité haute performance: Préparation, caractérisation et application dans la purification de protéines, thesis, University Paris 13, 1990.
18. E. Legendre, Etude par chromatographie d'affinité liquide haute performance des interactions entre des protéines de la coagulation et des polysaccharides sulfatés à activité anticoagulante immobilisés sur des supports de silice enrobée, thesis, University Paris 13, 1996.



Carbohydrates: Analysis by Capillary Electrophoresis

Oliver Schmitz

Division of Molecular Toxicology, German Cancer Research Center, Heidelberg, Germany

Introduction

Carbohydrates play an important role in many research and industrial domains. The huge number of stereoisomers, the immense combination possibilities of carbohydrate monomers in oligosaccharides, and the lack of chromophores are the major problems in the analysis of carbohydrates. Capillary electrophoresis (CE), in its various modes of operation, has been developed as a very useful tool in the analysis of carbohydrate species such as monosaccharides and oligosaccharides, glycoproteins, and glycopeptides.

Discussion

Some simple sugar mixtures, such as monosaccharides and oligosaccharides, consisting of not more than about 15 monomer units, can be separated in free solution due to their mass-to-charge ratio (m/z). For an increase in selectivity or for analyzing neutral carbohydrates, micellar electrokinetic chromatography (MEKC) can be used for analysis. In this case, charged amphiphilic molecules containing both hydrophilic and hydrophobic regions (e.g., sodium dodecyl sulfate) are used as buffer surfactants.

Higher oligosaccharides or polysaccharides possess unfavorable mass-to-charge ratios, preventing their effective resolution in open tubes. The separation of these carbohydrates is possible with capillary gel electrophoresis (CGE). The analytes are selectively retarded by a sieving network (gel or polymer matrix) due to differences in their sizes and structural conformations.

Complex carbohydrates (in particular, glycoproteins) play an important role in various biological processes and in biotechnological production of glycoproteinaceous pharmaceuticals. To elucidate the relationship between bioactivity and structures of complex carbohydrates, it is necessary to determine the sites of attachment of the oligosaccharide chains to the polypeptide backbone and to characterize the

oligosaccharide class (N- or O-linked, high mannose, hybrid, etc.).

For this reason, glycoproteins must first be isolated from the biological matrix by dialysis, preparative chromatography, isoelectric focusing, and so forth or by a combination of several methods. For a structural determination, degradation steps such as a site-specific proteolysis (e.g., with trypsin), removal of oligosaccharides from the polypeptide (by an enzymatic hydrolysis or hydrazine treatment), or chemical hydrolysis, yielding a monosaccharide mixture may be applied. Then, the CE can function as a powerful end method in analytical and structural glycobiology. Due to the complexity of the carbohydrate-dependent microheterogeneity of glycoproteins, several electrophoretic techniques are usually needed, in concert, to characterize the various glycoforms of a given glycoprotein.

For detection of carbohydrates in principle, ultraviolet (UV), laser-induced fluorescence, refractive index, electrochemical, amperometric, and mass spectrometric detection can be used. Mass spectrometry, with its various ionization methods, has traditionally been one of the key techniques for the structural determination of proteins and carbohydrates. Fast-atom bombardment (FAB) and electrospray ionization (ESI) are the two on-line ionization methods used for carbohydrate analysis. The ESI principle has truly revolutionized the modern mass spectrometry of biological molecules, due to its high sensitivity and ability to record large-molecule entities within a relatively small-mass scale.

The refractive index detection (RID), often used in high-performance liquid chromatography, is an interesting detection method in CE with a laser light source and a limit of detection (LOD) in the micromolar range. Electrochemical detection (ECD) and pulsed amperometric detection (PAD) of sugars are common and effective methods used in HPLC. Some recent communications show that the sensitivity of these detection methods in CE have an approximately 1000-fold better LOD than RID. Unfortunately, these de-



tectors (RID, ECD, and PAD) are not commercially available for capillary electrophoresis at the moment.

Indirect detection methods are a viable alternative for compounds lacking a chromophoric or a fluorophoric group. An electrolyte containing a chromophore or fluorophore allows the indirect detection

of carbohydrates. This method is based on the displacement of the background electrolyte (BGE) by carbohydrates, which are dissociated in strongly alkaline electrolytes. The LOD with indirect LIF detection is in the nanometer range, but the lack of any specificity is a great disadvantage of this detection

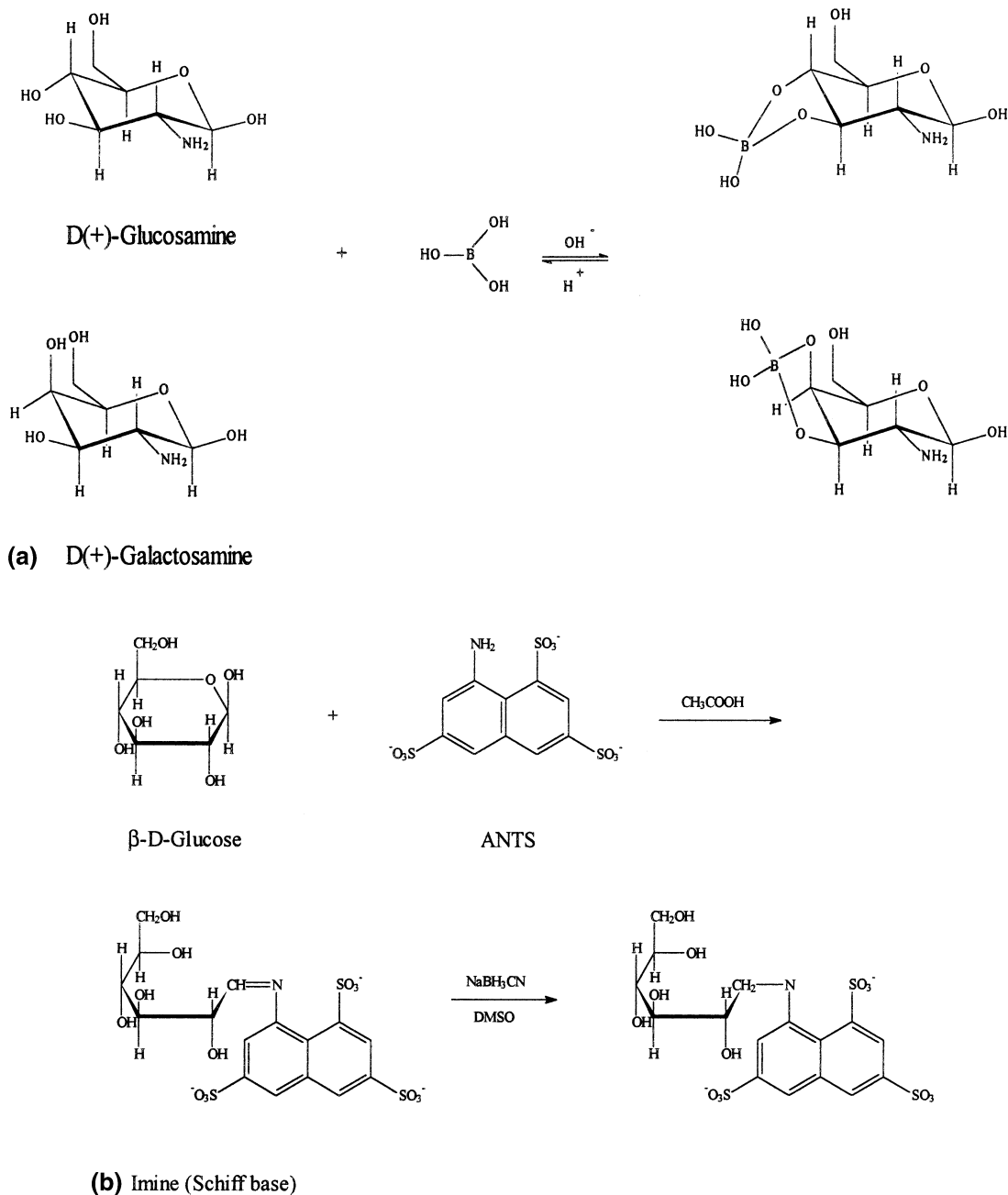


Fig. 1

method, because all sample compounds displace the BGE and the peak identification is only possible by the migration time.

Direct UV detection is the most versatile detection method in CE and is implemented in every commercial CE system. Unfortunately, its use for carbohydrates detection is restricted, because of their lack of conjugated π -electron systems and, consequently, the relatively low extinction coefficients. Despite this fact, it is possible to detect carbohydrates with UV detection without any derivatization at 200 nm. Sensitivity and selectivity can be increased by the use of an alkaline borate buffer as the electrolyte by *in situ* complexation with the tetrahydroxyborate ion rather than the boric acid (Fig. 1a). The LOD is between micromolar and nanomolar. A further advantage of very high pH values (>10) is the negative charge of the carbohydrates, which are repelled by the negatively charged surface. Consequently, the surface problems in high-performance capillary electrophoresis are much lower in carbohydrate analysis than in the analysis of proteins. Therefore, simple carbohydrates are often analyzed in uncoated fused-silica capillaries. Unlike the analysis of simple carbohydrates, for glycopeptides and glycoproteins, the use of coated capillaries such as hydroxypropylcellulose, hydroxyethylmethacrylate, polyether, or other commercially available coated fused-silica capillaries is necessary to achieve high resolution and reproducibility.

In complex matrices, the insufficient specificity at 200 nm and the low sensitivity of direct UV detection make the analysis of carbohydrates more difficult. Therefore, derivatization of carbohydrates with suitable agents is still a preferred approach for the detection of monosaccharides and oligosaccharides. Derivatization agents like 2-aminopyridine, 8-aminonaphthalein-1,3,6-trisulfonate (ANTS) or 8-aminopyren-1,3,6-trisulfonate

(APTS) can be introduced mostly by reductive amination. This reaction is based on imine formation (Schiff base) by the condensation of the aldehyde group in a carbohydrate with the amino group in a primary amine (fluorescent tag), followed by reduction to an N-substituted glycamine with a reductant like sodium cyanoborohydride (see Fig. 1b). Selection of the suitable derivatization reagent is important, because the electrophoretic migration of the carbohydrates and, therefore, the separation power is influenced by the properties of the tags. Fluorescent dyes are better suitable than UV-active derivatization reagents, because CE analysis permits the use of laser-induced-fluorescence (LIF) detection with excellent sensitivity up to the femtomolar-level.

In conclusion, capillary electrophoresis in carbohydrate analysis has advantages in both separation and detection over other techniques of electrophoresis, as well as chromatography. It allows high efficiency (up to a few million plate numbers) and very good sensitivities (up to femtomolar). In addition, CE permits analysis by a variety of separation modes simply by changing the electrolyte (capillary zone electrophoresis, MEKC, CGE).

Suggested Further Reading

- El Rassi, Z., *Electrophoresis* 18:2400 (1997).
Grimshaw, J., *Electrophoresis* 18:2408 (1997).
Linhardt, R. J. and A. Pervin, *J. Chromatogr. A* 720:323 (1996).
Novotny, M. V., Capillary electrophoresis of carbohydrates, in *High-Performance Capillary Electrophoresis* (M. G. Khaledi, ed.), John Wiley & Sons, New York, 1998, pp. 729–765.
Paulus, A. and A. Klockow, *J. Chromatogr. A* 720:353 (1996).
Suzuki, S. and S. Honda, *Electrophoresis* 19:2539 (1998).



Carbohydrates: Analysis by HPLC

Juan G. Alvarez

Beth Israel Deaconess Medical Center, Harvard Medical School, Boston, Massachusetts, U.S.A.

Introduction

Carbohydrates are widely distributed molecules in biological systems and pharmaceutical products, not only in free form but also in conjugated form. Because they are present in various forms and there are isomers and analogs, the separation of carbohydrates involves more difficult problems than those of proteins or nucleic acids. Difficulties are also found in detection, especially in biochemical and biomedical analyses due to their low abundance and the fact that photometric and fluorimetric methods cannot be applied directly because of the lack of chromophores and fluorophores.

Analysis of carbohydrates in body fluids by high-performance liquid chromatography (HPLC) using anion-exchange columns was first reported in the 1970s [1–5]. This method has been greatly improved by the use of packing materials of fine, spherical particles and by the development of photometric and fluorimetric postcolumn labeling systems for sensitive detection. Honda et al. established rapid automated methods for microanalysis of aldoses [6], uronic acids [7], and sialic acids using a Hitachi 2633 anion-exchange resin and a photometric and fluorimetric postcolumn labeling system with 2-cyanoacetamide. Alditols [8] were fluorescence labeled by the use of sequential periodate oxidation and the Hantzsch reaction. Microanalysis of aminosugars was successful when their borate complexes were separated in the cation-exchange mode and detected by fluorescence generated either by the reaction with 2-cyanoacetamide [9] or by the Hantzsch reaction [10]. All these methods are suitable for routine analysis of clinical samples because of their speed of analysis and high sensitivity.

The United States Food and Drug Administration and the regulatory agencies in other countries require that pharmaceutical products be tested for composition to verify their identity, strength, quality, and purity. Recently, attention has been given to inactive ingredients as well as active ingredients. Some of these ingredients are nonchromophoric and cannot be detected by absorbance. Some nonchromophoric ingredients, such as carbohydrates, glycols, sugar, alcohols,

amines, and sulfur-containing compounds, can be oxidized and, therefore, can be detected using amperometric detection. This detection method is specific for those analytes that can be oxidized at the selected potential, leaving all other nonoxidizable compounds transparent [11]. Amperometric detection is a powerful detection technique with a broad linear range and very low detection limits.

This review outlines current chromatographic methods utilized in the analysis of carbohydrates in biological systems and pharmaceutical products.

Analysis of Carbohydrates by Partition HPLC

Partition HPLC is an important type of chromatography for the analysis of monosaccharides and oligosaccharides. Analysis in this mode has the advantages that it requires a shorter analysis time and gives sharper peaks than anion-exchange chromatography of borate complexes, although it has the drawback of low sensitivity, as detection is usually performed by refractometry. Generally, silica gel whose silanol groups are substituted by alkyl or aminoalkyl groups is used as the stationary phase. HPLC separations using such a stationary phase has been applied successfully to separate oligosaccharides liberated from glycoproteins with hydrazine or borohydride in alkali, permitting quick separation within 60 min [12–14]. Previously, such oligosaccharides were separated and purified by tedious procedures involving gel permeation chromatography on Bio-Gel P-2 or P-4, paper chromatography, and paper electrophoresis. However, modified silica, especially amine-modified silica, has difficulties in durability, being unsuitable for routine analysis.

Analysis of Carbohydrates by Anion-Exchange HPLC

The introduction in the 1980s by Honda and Suzuki [15] of the anion-exchange resin resulted in a significant improvement in the separation of carbohydrates by HPLC using the partition mode. Honda



and Suzuki, using this mode, established analytical conditions common to aldoses, amino sugars, and sialic acids. Aldoses in the intact state, amino acids as their *N*-acetates, and sialic acids as *N*-acetylmannosamines were separated on a column of a proton-formed, sulfonated styrene–divinylbenzene copolymer and detected by measuring absorption at 280 nm after post-column labeling with 2-cyanoacetamide.

Postcolumn labeling is a characteristic feature of carbohydrate analysis in which no direct physical methods are available for sensitive detection. Many labeling methods have hitherto been developed. The methods with phenol in sulfuric acid [16], orcinol in sulfuric acid [17], anthrone in sulfuric acid [18], tetrazolium blue in alkali [19], copper(II)-2-2'-bicinchonitate [20], and 2-cyanoacetamide [21] are used for photometric detection. The methods with 2-cyanoacetamide [6], ethylenediamine [22], ethanolamine [23], taurine [24], and arginine [25] are used for fluorimetric detection. Some labeling methods for electrochemical detection were reported by Honda and Suzuki in 1984 [26,27].

Quantification of Carbohydrates by Anion-Exchange HPLC and Amperometric Detection

Two main columns are used in the analysis of carbohydrates by amperometric detection: the CarboPac™ PA10 and the CarboPac MA1 anion-exchange columns. The CarboPac PA10 column packing consists of a nonporous, highly cross-linked polystyrene–divinylbenzene substrate agglomerated with 460-nm-diameter latex. The MicroBead™ latex is functionalized with quaternary ammonium ions, which create a thin surface-rich anion-exchange site. The packing is specifically designed to have a high selectivity for carbohydrates. The PA10 has an anion-exchange capacity of approximately 100 $\mu\text{Eq}/\text{column}$.

The CarboPac MA1 resin is composed of a polystyrene–divinylbenzene polymeric core. The surface is grafted with quaternary ammonium anion-exchange functional groups. Its macroporous structure provides an extremely high anion-exchange capacity of 1450 $\mu\text{Eq}/\text{column}$. The CarboPac MA1 column is designed specifically for sugar alcohol and glycol separations. The PA10 but not the MA1 is compatible with eluents containing organic solvents, which can be used to clean these columns.

The equipment used for the analysis of carbohydrates by anion exchange and amperometric detection include a Dionex DX-500 system consisting of a GP40

Table 1 Separation of Carbohydrates, Alditols, Alcohols, and Glycols using a CarboPac MA1 Column and Pulsed Amperometry

Analyte	Retention time (min)
2,3-Butanediol	7.4
Ethanol	7.6
Methanol	7.8
Glycerol	9.0
Erythritol	10.1
Rhamnose	13.4
Arabitrol	14.2
Sorbitol	16.3
Galactitol	18.0
Mannitol	19.5
Arabinose	21.8
Glucose	23.3
Galactose	27.4
Lactose	29.7
Ribose	32.0
Sucrose	46.5
Raffinose	52.9
Maltose	61.2

gradient pump, an ED40 electrochemical detector, a LC30 chromatography oven, and a PeakNet chromatography workstation. A gold electrode is used for both column applications. The flow rate used for the PA10 column is 1.5 mL/min and 0.4 mL/min for the MA1. Injection volumes are typically 10 μL and the oven temperature 30°C. Eluent components include water and 200 mM sodium hydroxide for the PA10 column and water and 480 mM sodium hydroxide for the MA1 column. Eluent concentration for the PA10 column starts at 91% water/9% 200 mM sodium hydroxide for up to 11 min, 100% 200 mM sodium hydroxide from 11.1 to 17.6 min, and 91% water/9% 200 mM sodium hydroxide from 17.7 to 40.0 min. Eluent concentration for the MA1 column system starts at 52% water/48% 480 mM sodium hydroxide and is maintained for up to 60 min [28].

Table 1 shows the separation of alcohols (2,3-butanediol, ethanol, methanol), glycols (glycerol), alditols (erythritol, arabitrol, sorbitol, galactitol, mannitol), and carbohydrates (rhamnose, arabinose, glucose, galactose, lactose, sucrose, raffinose, maltose) using a CarboPac MA1 column set with 480 mM sodium hydroxide eluent flowing at 0.4 mL/min. The alcohols, sugar alcohols (alditols), glycols, and carbohydrates are well resolved. Maltose elutes at about 60 min.



References

1. R. L. Jolley and C. D. Scott, *Clin. Chem.* 16:687 (1970).
2. W. C. Butts and R. L. Jolley, *Clin. Chem.* 16:722 (1970).
3. S. Katz, S. R. Dinsmore, and W. W. Pitt, Jr., *Clin. Chem.* 17:731 (1971).
4. C. D. Scott, D. D. Chilcote, S. Katz, and W. W. Pitt, Jr., *J. Chromatogr. Sci.* 11:96 (1973).
5. D. S. Young, J. A. Epley, and P. Goldman, *Clin. Chem.* 17:765 (1971).
6. S. Honda, M. Takahashi, K. Kakehi, and S. Ganno, *Anal. Biochem.* 112:130 (1981).
7. S. Honda, S. Suzuki, M. Takahashi, K. Kakehi, and S. Ganno, *Anal. Biochem.* 134:34 (1983).
8. S. Honda, M. Takahashi, S. Shimada, K. Kakehi, and S. Ganno, *Anal. Biochem.* 128:429 (1983).
9. S. Honda, T. Konishi, S. Suzuki, M. Takahashi, K. Kakehi, and S. Ganno, *Anal. Biochem.* 134:483 (1983).
10. S. Honda, T. Konishi, S. Suzuki, K. Kakehi, and S. Ganno, *J. Chromatogr.* 281:340 (1983).
11. R. D. Rocklin, *J. Chromatogr.* 546:175 (1991).
12. S. J. Mellis and J. U. Baenziger, *Anal. Biochem.* 114:276 (1981).
13. V. K. Dua and C. A. Bush, *Anal. Biochem.* 133:1 (1983).
14. V. K. Dua and C. A. Bush, *Anal. Biochem.* 137:33 (1984).
15. S. Honda and S. Suzuki, *Anal. Biochem.* 142:167 (1984).
16. M. H. Simatupang, *J. Chromatogr.* 180:177 (1979).
17. D. F. Smith, D. A. Zopf, and V. Ginsburg, *Anal. Biochem.* 85:602 (1978).
18. K. J. Kramer, R. D. Speirs, and C. N. Childs, *Anal. Biochem.* 86:692 (1978).
19. K. Mopper and E. T. Degens, *Anal. Biochem.* 45:147 (1972).
20. K. Mopper and E. M. Gindler, *Anal. Biochem.* 56:440 (1973).
21. S. Honda, Y. Matsuda, M. Takahashi, K. Kakehi, and S. Ganno, *Anal. Chem.* 55:1079 (1980).
22. K. Mopper, R. Dawson, G. Liebezeit, and H. P. Hansen, *Anal. Chem.* 52:2018 (1980).
23. T. Kato and T. Kinoshita, *Anal. Biochem.* 106:238 (1980).
24. T. Kato and T. Kinoshita, *Chem. Pharm. Bull.* 26:1291 (1978).
25. H. Mikami and Y. Ishida, *Bunseki Kagaku* 32:E207 (1983).
26. R. D. Rocklin and C. A. Pohl, *J. Liquid Chromatogr.* 6:1577 (1983).
27. S. Honda, T. Konishi, and S. Suzuki, *J. Chromatogr.* 299:245 (1984).



Carbohydrates: Analysis by TLC—New Visualization

N. Dimov

Analytical Department, NIHFI, Sofia, Bulgaria

Introduction

There are many publications and comprehensive handbooks on the thin-layer chromatography (TLC) of carbohydrates (e.g., Refs. 1 and 2). The reason is their great importance in life science and the great diversity of cases: monosaccharide, disaccharide, trisaccharide, oligosaccharide, polysaccharide, aldose, ketose, triose, tetrose, pentose, hexose, as well as reducing and nonreducing sugars. In addition, when extracted from natural products or produced by fermentation, carbohydrates are accompanied by many impurities. That is why separation methods are used predominantly for their analysis.

Carbohydrates are polyhydroxy compounds (i.e., very polar compounds) with low volatility; a gas chromatographic (GC) analysis, therefore, will not be the best choice. GC methods continue to be applied in the cases when low concentrations have to be determined (e.g., in clinical analyses).

Due to high water solubility of monosaccharides, the use of the most routine high-performance liquid chromatography (HPLC) reversed-phase columns is also not suitable for their analysis. Extremely pure solvents have to be used if ultraviolet (UV) detection is applied. If a refractometer is used as the detector (RD), extremely steady chromatographic conditions are necessary. Nevertheless, HPLC is applied in the practice. The modern approach involves the use of propylamino columns (e.g., Refs. 3 and 4).

The best choice remains the TLC method. The impurities can be left on the start or eluted to the front; TLC can be used for qualitative and quantitative analyses, for screening, and so forth. Simultaneous analysis of several samples is possible. TLC affords an opportunity for a broad range of choices (more than 30) of visualizing agents. Most of them are chromogenic agents [1,2] with a mean sensitivity of 500–100 ng. The Stahl reagent — anisaldehyd/ H_2SO_4 — has a limit of detection (LOD) of 50 ng, but this reagent is not suitable for carbohydrate alcohols [3]. In a series of articles [5], Alperin et al. proposed the so-called thermal-UV detection of sugars but, again, with

low sensitivity (about 200 ng). The great number of reagents has also one disadvantage — lack of a firm visualization agent which answers the higher daily requirements for LOD.

More than eight types of stationary phases have been mentioned in Ref. 1 for the separation of carbohydrates, but the most popular is pure silica or impregnated with various inorganic ions silica gel G, because the separation is faster and provides more compact spots [2]. A modern stationary phase has become propylamino TLC plates. On both silica and amino plates, the separation is satisfactory (e.g., Refs. 2, 4, 6, and 7).

The remaining problems are (a) sensitivity (kind of visualization) and (b) quantitative analysis. Although the second problem has found its solution through the use of densitometers, the choice of visualization reagent remains a subject of individual personal decision. Klaus et al. [6] proposed a reagent-free visualization by heating propylamino stationary-phase plates. Sugars give fluorescent spots after heating at 120–150°C [8]. The sensitivity remains in the limits of micrograms.

The present article describes how fluorescent spots of carbohydrates can be achieved after heating, using common silica plates, applying the already accepted laboratory mobile phases.

Procedure

The well-known and widely applied TLC silica gel G plates 20 × 20 cm from Merck (Darmstadt, FRG) is used. Stock solutions from the compounds given in Table 1 were prepared. After corresponding dilution, a 1- μL sample is applied and the plate is developed for a distance of 10 cm using *n*-propanol–water, 8:2 (v/v), as the mobile phase. Densitometric evaluation is performed at 365 nm with a Camag TLC Scanner II in absorbance reflection mode. The plate is first air-dried and then heated in an oven for 5 min at 100°C. Immediately after drying, the plate is inserted in a tank saturated with ammonia atmosphere (ammonia solution in



Table 1 Behavior of 10 Carbohydrates, 2 Sugar Alcohols, and 1 Glycoside After Heating the Saturated-with-Ammonia Silica Plate at 160°C

Compound	Fluorescence at ng ^a		
Monosaccharides	50	10	1
Rhamnose	+	—	n
Ribose	—	n	n
Arabinose	+	—	n
Xylose	+	+	—
Glucose	+	—	—
Manose	—	n	n
Galactose	+	—	n
Disaccharides			
Saccharose	+	—	n
Trehalose	+	+	—
Maltose	+	—	n
Lactose	+	—	n
Sorbose	+	—	n
Trisaccharide			
Raphinose	+	—	n
Alcohol			
Mannitol	+	—	n
Sorbitol	+	—	n

^a+: well-observed spot suitable for quantitation; —: LOD; n: no observation.

a vessel). After 10 min, the plate is pulled out, covered tightly with another plate (which can be preliminarily placed in the tank or can be another spotted plate), and both are heated for 5 min at 160°C. The spots are observed under UV light at 365 nm. The behavior of all studied compounds is presented in Table 1. All studied carbohydrates as well as the sugar alcohols mannitol and sorbitol give orange fluorescence spots. The fluorescence remains stable for more than 1 week (which is less than the stability cited in Ref. 8, but enough for practical use).

The linear range is small — to about 100 ng. For an extended range of application (over the range to 1000 nm), a nonlinear relationship between peak area (*A*) and the quantity (ng) has been tested. For example, the equation for D-glucose is

$$\ln A = 7.722 - \frac{30.5}{\text{ng}} \quad (1)$$

with a correlation coefficient 0.993 and maximum error at the 1000-ng level — less than 10%. The area precision (intraplate repeatability) from six peaks of D-glucose at the 500-ng level is 4.1% and the height precision is 1.8%. The calculated (twice the noise of densitogram baseline) limit of detection (LOD) is 10-ng.

The proposed visualization procedure possesses good intraplate repeatability, the limit of detection is satisfactorily low, and it is more ecological than spraying with sulfuric acid-containing sprays (which also have poor reproducibility). The disadvantages of the proposed visualization procedure are poor reproducibility from plate to plate (interplate repeatability), dependence of the spot intensity both on structure and the extent of saturation with ammonia and heating, and lack of a wider linear range. The mentioned disadvantages can be overcome with a thorough validation and verification of the particular method. The proposed approach is an easy transferable one and can be applied directly to routine work.

Thus, it is anticipated that this little variation in every-day routine work in laboratories analyzing carbohydrates can be easily adapted and will contribute to a better Good Laboratory Practice (GLP).

References

1. E. Stahl, *Duenschicht-chromatography*, Springer-Verlag, Berlin, 1967.
2. B. Fried and J. Sherma, *Thin-Layer Chromatography. Techniques and Applications*, Marcel Dekker, Inc., New York, 1982; B. Fried and J. Sherma, *Thin-Layer Chromatography*, 4th ed., Marcel Dekker, Inc., New York, 1999.
3. G. W. Hay, B. A. Lewis, and F. Smith, *J. Chromatogr.* 11:479 (1963).
4. M. Okamoto, F. Yamada, and T. Omori, *J. High Resolut. Chromatogr. Chromatogr. Commun.* 5:163 (1982).
5. D. M. Alpein et al., *J. Chromatogr.* 242:299 (1982); 250:124 (1982); 265:193 (1983).
6. R. Klaus, W. Fischer, and H. E. Hauck, *Chromatographia* 28:364 (1989).
7. R. Klaus, W. Fischer, and H. E. Hauck, *Chromatographia* 39:97 (1994).
8. R. Klaus, W. Fischer, and H. E. Hauck, *LC-GC Int.* 8:151 (1995).



Catalyst Characterization by Reversed Flow Gas Chromatography

Dimitrios Gavril

University of Patras, Patras, Greece

INTRODUCTION

Reversed-flow gas chromatography (RF-GC) has been used to study the kinetics of surface-catalyzed reactions and the nature of the active sites. Reversed-flow gas chromatography is technically very simple, and it is combined with a mathematical analysis that gives the possibility for the estimation of various physicochemical parameters related to catalyst characterization, in a simple experiment, under conditions compatible with the operation of real catalysts. The experimental findings of RF-GC for the oxidation of CO over well-studied, silica-supported, platinum–rhodium bimetallic catalysts are in agreement with the results of other workers using different techniques, ascertaining that RF-GC methodologies can be used for the characterization of various solids with simplicity and accuracy.

OVERVIEW

During the last four decades, various chemical reactions concerning processes of technological and environmental interest have been related to the development of catalysts. Catalyst characterization is a necessary step, and it usually involves activity tests and investigation of the kinetics of the related reactions, as well as of the nature of the active sites.

Diffusion, adsorption, and surface reaction are closely interconnected in heterogeneous catalysis characterization studies. Chromatographic separation is a physicochemical process based also on diffusion, adsorption, as well as liquid dissolution. Based on the broadening factors embraced by the van Deemter equation, precise and accurate physicochemical measurements have been made by GC, using relatively low-cost instrumentation and a very simple experimental setup.

Reversed-flow gas chromatography is another gas chromatographic technique based on the perturbation of the carrier gas flow, which has been utilized for the measurement of physicochemical parameters. The fundamental difference of RF-GC from classical GC is the use of a T-form system of chromatographic columns (sampling and diffusion columns) placed perpendicularly, one

in the middle of the other. The carrier gas flows continuously through the sampling column, while it is stagnant into the diffusion column. The solid catalyst under study is placed either near the injection point at the closed end of the diffusion column, for experiments under non-steady-state conditions, or at the middle of the sampling column, for experiments under steady-state conditions, as shown in Fig. 1. The fact that the solid material is under investigation also classifies RF-GC in inverse gas chromatographic (IGC) methodologies. The reversing of the carrier gas flow for short time intervals results in extra chromatographic peaks on the continuous concentration–time curve. Thus repeated sampling of the physicochemical phenomena occurring in the diffusion column is achieved, and, by using the appropriate mathematical analysis, the values of the relevant physicochemical quantities are determined.

EXPERIMENTAL APPROACH

The experimental setup of RF-GC for the study of catalytic processes has been presented elsewhere;^[1–13] it is very simple. It comprises the following:

1. A conventional gas chromatograph equipped with the appropriate detector (e.g., flame ionization, thermal conductivity, etc.) depending on the reactant(s) and product(s). A separation column, L' , may also be incorporated in the GC oven. The separation column can be filled with the appropriate material for the separation of the reactants and products, and it can be heated in the same or at a different temperature from the sampling cell.
2. The “sampling cell” is formed by the sampling column $l' + l$ and the diffusion column L , which is connected perpendicularly to the middle of the sampling column. The ends, D_1 and D_2 , of the sampling column are connected through a four-port valve to the carrier gas inlet and the detector, as shown in Fig. 1.

Performing flow perturbations, negative and positive abrupt fronts are made to appear in the chromatogram,

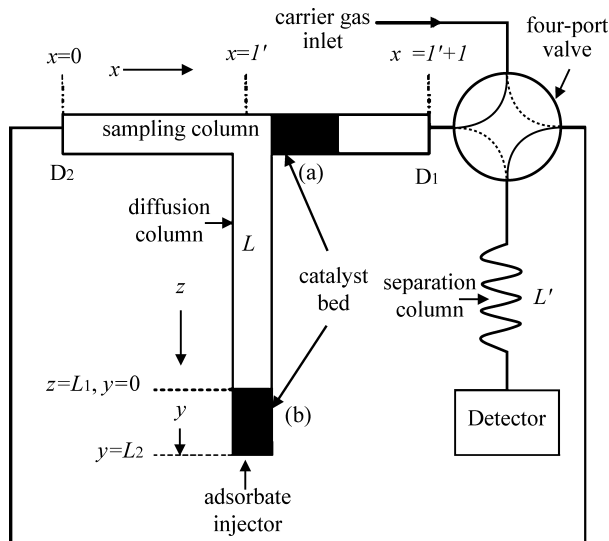


Fig. 1 Experimental setup used from RF-GC for the characterization of solid catalysts: (a) under steady-state conditions, with catalyst bed being put at a short length of sampling column l , near the junction of diffusion and sampling columns; (b) under non-steady-state conditions, with catalytic bed being put at the top of diffusion column L .

forming the so-called sampling peaks like those shown in Fig. 2 of Ref. [1]. The volumetric carrier gas flow rate does not affect the physicochemical phenomena occurring in the diffusion column, but only the speed of the sampling procedure.

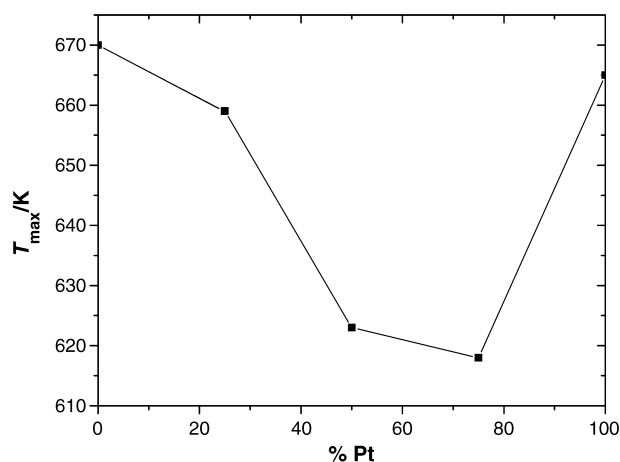


Fig. 2 Characteristic temperatures of maximum activity, T_{\max} (K), for the oxidation of CO, over Pt-Rh alloy catalysts against the catalyst Pt content (% Pt). (From Ref. [3].)

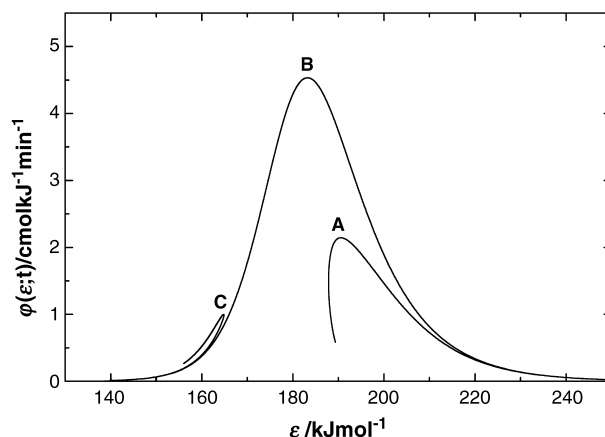


Fig. 3 Variation of the energy distribution function, $\phi(\epsilon; t)$ ($\text{cmol kJ}^{-1} \text{mol}^{-1}$), vs. the local adsorption energy, ϵ (kJ mol^{-1}), for the adsorption of carbon monoxide on a bimetallic silica-supported $\text{Pt}_{0.25}\text{-Rh}_{0.75}$ catalyst, at 698 K. (From Ref. [12].)

THEORETICAL

The sampling peaks are predicted theoretically by the “chromatographic sampling equation,” describing the concentration–time curve of the sampling peaks created by the flow reversals. The area or the height, H , of the sampling peaks is proportional to the concentration of the substance under study, at the junction, $x=l'$, of the sampling cell, at time t from the beginning of the experiment. If $\ln H$ is plotted against time, t , for each solute, the so-called diffusion band is obtained. An example is shown in Fig. 3 of Ref. [1].

Under Steady-State Conditions

Having placed the catalyst bed at a short length of the sampling column l near the junction of the diffusion and sampling column (Fig. 1), the catalytic behavior under steady-state conditions can be studied. In that case, time-dependent fractional conversions X_i , are determined from the heights or the areas of the sampling peaks obtained after each flow reversal, and overall conversions X can be calculated from the total areas of the “diffusion bands” corresponding to reactants and products.^[1]

Under Non-Steady-State Conditions

Having placed the catalyst bed at a short length from the entrance of the diffusion column L (Fig. 1), the catalytic behavior under non-steady-state conditions can be studied. In that case, not only conversions but also a large number



of physicochemical parameters related to the interaction of the studied catalyst with the injected adsorbate can be determined. The whole treatment of experimental data is based on the fact that the heights of the "sampling peaks" are described by a clear function of time comprising the sum of two to four exponentials.

$$H^{1/M} = \sum_i A_i \exp(B_i t) \quad (1)$$

where H are the heights of the experimentally obtained chromatographic peaks, M the response factor of the detector, and t the time from the beginning of the experiment. Eq. 1 is not an a priori assumption but results from the solution of the mathematical model. The values of the pre-exponential factors A_i and the corresponding coefficients of time B_i are easily and accurately determined from the chromatogram by PC programs of nonlinear least-squares regression (c.f. Appendix of Ref. [9]).

The experimental pairs H and t are the variables of Eq. 1. By introducing them into the data lines of the GWBASIC program, such as given in the Appendix of Ref. [9] together with other easily obtained quantities required by the input lines (such as the geometric details of the diffusion column, mass and porosity of the catalyst bed, solute amount, as well as its diffusion coefficient in the carrier gas, and the carrier gas flow rate), the various physicochemical parameters related to the studied catalyst are calculated.

POTENTIAL OF THE METHODOLOGY AND INDICATIVE RESULTS

Reversed-flow gas chromatography methodologies have been utilized for the investigation of various catalytic processes, and a large number of physicochemical quantities related to the kinetics of the elementary steps (adsorption, desorption, surface reaction) and the nature of the active sites have been determined. These parameters are summarized as follows:

1. Time dependent, X_t , and overall, X , conversions, either under steady- or non-steady-state conditions.^[1,2]
2. Adsorption, k_1 , desorption, k_{-1} , and surface reaction, k_2 , rate constants, and the respective activation energies, E_a .^[3-5]
3. Local adsorption energies, ε , local adsorption isotherms, $\theta(p, T, \varepsilon)$, local monolayer capacities, c_{\max}^* , and adsorption energy distribution functions, $f(\varepsilon)$, for

the adsorption of gases on heterogeneous surfaces circumventing altogether the integral equation:^[6,7]

$$\Theta(p, T) = \int_0^\infty \theta(\varepsilon, p, T) f(\varepsilon) d\varepsilon \quad (2)$$

where $\Theta(p, T)$ is the overall experimental adsorption isotherm.

4. The energy of the lateral molecular interactions on heterogeneous surfaces in a time-resolved procedure.^[8]
5. Surface diffusion coefficients for physically adsorbed or chemisorbed species on heterogeneous surfaces in a time-resolved procedure.^[9]
6. Standard free energy of adsorption and its probability density function over time, together with the geometrical mean of the London parts of the total surface free energy $(\gamma_1^L \gamma_2^L)^{1/2}$ of the adsorbed probe and the solid surface, accompanied by the relevant probability density functions over time.^[10,11]
7. Investigation of the nature of the various groups of active sites of solid catalysts.^[12]

The question naturally arising is how reliable are the physicochemical quantities determined by means of RF-GC. For this reason, the adsorption of CO, O₂, and CO₂, as well as the oxidation of CO, has been studied over well-studied, silica-supported, Pt-Rh bimetallic catalysts. The following are indicative conclusions extracted by using RF-GC, which are in agreement with the observations of other techniques:

1. The experimental data for carbon monoxide adsorption over the studied catalysts (in the absence of oxygen in the carrier gas), at temperatures higher than 300°C, suggest that the adsorption of CO is a dissociative process.^[2,4]
2. There is a characteristic temperature of maximum catalytic activity, T_{\max} , for every bimetallic catalyst. The temperatures found by RF-GC are very close to those found, for the same catalysts, by using different techniques.^[1-4]
3. The bimetallic catalysts exhibit higher catalytic activity at lower temperatures in comparison with pure Pt and Rh ones, as shown in Fig. 2. Other workers have also observed this synergism for Pt-Rh bimetallic catalysts.^[1-4]
4. The rate constants found by the RF-GC technique, such as those in Table 1, are very close to those determined experimentally by the frequency response method^[2,4,5] for the adsorption of CO on Pt/SiO₂.
5. The values of the estimated activation energies for CO dissociative adsorption, given in Table 2, are low.

Table 1 Rate constants for the adsorption (k_1), desorption (k_{-1}), and disproportionation reaction (k_2) of carbon monoxide over a Pt-SiO₂ catalyst, determined by RF-GC, at various temperatures

T (K)	$10^1 k_1$ (sec ⁻¹)	$10^4 k_{-1}$ (sec ⁻¹)	$10^4 k_2$ (sec ⁻¹)
555.0	1.33	6.09	2.80
573.6	1.41	6.48	2.91
595.7	1.59	6.76	3.62
615.6	1.63	6.85	4.04
633.6	1.86	7.34	4.13
643.2	1.84	7.63	3.78
657.7	1.83	7.82	3.95
673.2	1.98	8.23	4.00
692.3	2.13	8.74	4.15
707.5	2.27	9.29	4.58
723.7	2.68	9.62	4.53

Source: From Ref. [5].

Low activation energy values are indicative of corrugated surfaces. From the difference in the found energy barriers, it is also concluded that CO adsorption is the rate-determining step for CO dissociative adsorption, followed by the dissociation step. These findings suggest a precursor-mediated mechanism for CO dissociative adsorption.^[2]

- The nature of the different groups of active sites, for the catalytic oxidation of CO, has also been investigated from the experimentally determined energy distribution functions. The existence of three groups of active sites is observed as shown in Figs. 3 and 4,^[12] which is also expected from thermal desorption spectroscopy (TDS) for the adsorption of CO over group VIII noble metals.

Group A active sites correspond to the β states of TDS, arising from CO dissociative adsorption. The topography of these active sites is random, as the values of the lateral interaction energy, β , are negative. The B and C groups of active sites shown in our plots correspond to the α states of TDS. They are characterized

Table 2 Activation energies (kJ mol⁻¹) corresponding to the adsorption, E_{a1} , desorption, E_{a-1} , and disproportionation reaction, E_{a2} , of carbon monoxide over silica-supported Pt, Rh, and Pt_{0.50}-Rh_{0.50} alloy catalysts

% Rh	E_{a1} (kJ mol ⁻¹)	E_{a-1} (kJ mol ⁻¹)	E_{a2} (kJ mol ⁻¹)
0	13.1 ± 1.2	9.4 ± 0.6	8.4 ± 1.3
50	18.2 ± 2.6	12.6 ± 1.7	—
100	19.4 ± 6.5	11.9 ± 2.2	3.8 ± 1.0

Source: From Ref. [2].

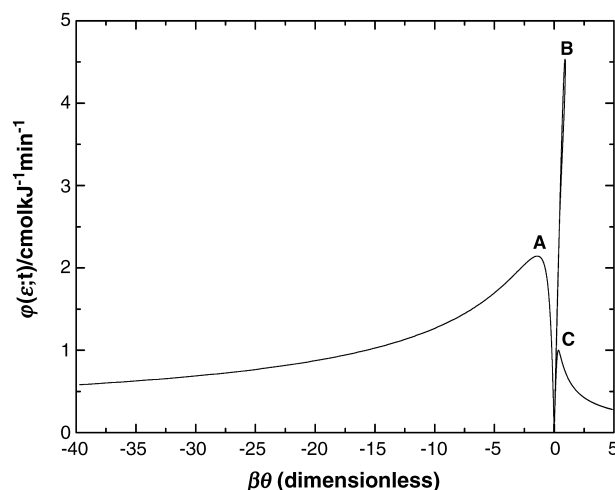


Fig. 4 Energy distribution function, $\phi(\epsilon;t)$ (cmol kJ⁻¹ mol⁻¹), against the dimensionless product of the lateral interaction energy (β) and the local isotherm (θ) $\beta\theta$, for carbon monoxide adsorption over a bimetallic Pt_{0.25}-Rh_{0.75} silica-supported catalyst, at 698 K. (From Ref. [12].)

by the positive values of β , which means that they have a patchwise topography. Group C active sites correspond to higher β values, in comparison with B group active sites. They are indicative of CO island formation. The experimentally found results also explain the superior activity of Pt_{0.25}+Rh_{0.75} alloy catalyst (synergism) as a result not only of its capacity to adsorb a higher amount of carbon monoxide, at lower temperatures, but also because this catalyst is characterized by a more random topography in contrast with the other studied silica-supported pure Pt and Rh catalysts.

The utilization of RF-GC methodologies can be extended in the study of the surface properties of various solids and related processes. Thus, in a recent work, the effect of the presence of hydrogen in the adsorptive behavior of a Rh/SiO₂ catalyst was studied, as the selective oxidation of CO in a rich hydrogen atmosphere is a process of great technological and environmental interest, because it is related to the development of proton exchange membrane fuel cells.^[13]

CONCLUSION

The usual inverse gas chromatography, in which the stationary phase is the main object of investigation, is a classical elution method that neglects the mass transfer phenomena; it does not take into account the sorption effect and it is also influenced by the carrier gas flow. In contrast to the integration method, the new methodology



of reversed-flow gas chromatography (RF-GC), although being an inverse gas chromatographic technique, is a differential method not depending either on retention times and net retention volumes or on broadening factors and statistical moments of the elution bands.

The RF-GC methodology is technically very simple and it is combined with a mathematical analysis that gives the possibility for the estimation of various physicochemical parameters related to solid catalysts characterization in a simple experiment under conditions compatible with the operation of real catalysts. The experimentally determined kinetic quantities are not only consistent with the results of other techniques, but, moreover, they can give important information about the mechanism of the relevant processes, the nature of the active sites, and the topography of the heterogeneous surfaces.

The utilization of RF-GC methodologies can be extended in the study of the surface properties of various solids of technological and environmental interest.

REFERENCES

1. Gavril, D. Reversed flow gas chromatography: A tool for instantaneous monitoring of the concentrations of reactants and products in heterogeneous catalytic processes. *J. Liq. Chromatogr. Relat. Technol.* **2002**, *25* (13–15), 2079–2099.
2. Gavril, D.; Loukopoulos, V.; Karaiskakis, G. Study of CO dissociative adsorption over Pt and Rh catalysts by inverse gas chromatography. *Chromatographia* **2004**, *59* (11), 721–729.
3. Gavril, D.; Katsanos, N.A.; Karaiskakis, G. Gas chromatographic kinetic study of carbon monoxide oxidation over platinum–rhodium catalysts. *J. Chromatogr., A* **1999**, *852*, 507–523.
4. Gavril, D.; Koliadima, A.; Karaiskakis, G. Adsorption studies of gases on Pt–Rh bimetallic catalysts by reversed flow gas chromatography. *Langmuir* **1999**, *15*, 3798–3806.
5. Gavril, D.; Karaiskakis, G. Study of the sorption of carbon monoxide, oxygen and carbon dioxide on Pt–Rh alloy catalysts by a new gas chromatographic methodology. *J. Chromatogr., A* **1999**, *845*, 67–83.
6. Katsanos, N.A.; Iliopoulou, E.; Roubani-Kalantzopoulou, F.; Kalogirou, E. Probability density function for adsorption energies over time on heterogeneous surfaces by inverse gas chromatography. *J. Phys. Chem., B* **1999**, *103* (46), 10228–10233.
7. Gavril, D. An inverse gas chromatographic tool for the experimental measurement of local adsorption isotherms. *Instrum. Sci. Technol.* **2002**, *30* (4), 397–413.
8. Katsanos, N.A.; Roubani-Kalantzopoulou, F.; Iliopoulou, E.; Vassiotis, I.; Siokos, V.; Vrahatis, M.N.; Plagianakos, V.P. Lateral molecular interaction on heterogeneous surfaces experimentally measured. *Colloids Surf., A* **2002**, *201*, 173–180.
9. Katsanos, N.A.; Gavril, D.; Karaiskakis, G. Time-resolved determination of surface diffusion coefficients for physically adsorbed or chemisorbed species on heterogeneous surfaces, by inverse gas chromatography. *J. Chromatogr., A* **2003**, *983* (1–2), 177–193.
10. Katsanos, N.A.; Gavril, D.; Kapolos, J.; Karaiskakis, G. Surface energy of solid catalysts measured by inverse gas chromatography. *J. Colloid Interface Sci.* **2003**, *270* (2), 455–461.
11. Margariti, S.; Katsanos, N.A.; Roubani-Kalantzopoulou, F. Time distribution of surface energy on heterogeneous surfaces by inverse gas chromatography. *Colloids Surf., A* **2003**, *226*, 55–67.
12. Gavril, D.; Nieuwenhuys, B.E. Investigation of the surface heterogeneity of solids from reversed flow inverse gas chromatography. *J. Chromatogr., A* **2004**, *1045* (1–2), 161–172.
13. Loukopoulos, V.; Gavril, D.; Karaiskakis, G. An inverse gas chromatographic instrumentation for the study of carbon monoxide's adsorption on Rh/SiO₂, under hydrogen-rich conditions. *Instrum. Sci. Technol.* **2003**, *31* (2), 165–181.



CCC Solvent Systems

T. Maryutina

Boris Ya. Spivakov

Vernadsky Institute of Geochemistry and Analytical Chemistry, Russian Academy of Sciences, Moscow, Russia

Introduction

Countercurrent chromatography has been mainly developed and used for preparative and analytical separations of organic and bio-organic substances [1]. The studies of the last several years have shown that the technique can be applied to analytical and radiochemical separation, preconcentration, and purification of inorganic substances in solutions on a laboratory scale by the use of various two-phase liquid systems [2]. Success in CCC separation depends on choosing a two-phase solvent system that provides the proper partition coefficient values for the compounds to be separated and satisfactory retention of the stationary phase. The number of potentially suitable CCC solvent systems can be so great that it may be difficult to select the most proper one.

Discussion

Recent studies have made it possible to classify water-organic solvent systems in CCC for separation of organic substances on the basis of the liquid-phase density difference, the solvent polarity, and other parameters from the point of view of stationary-phase retention in a CCC column [1,3–9]. Ito [1] classified some liquid systems as hydrophobic (such as heptane–water or chloroform–water), intermediate (chloroform–acetic acid–water and *n*-butanol–water) and hydrophilic (such as *n*-butanol–acetic acid–water) according to the hydrophobicity of the nonaqueous phase. Thirteen two-phase solvent systems were evaluated for relative polarity by using Reichardt's dye to measure solvachromatic shifts and using the solubility of index compounds [6].

However, the systems for inorganic separations are very different from those for organic separations, as, in most cases, they contain a complexing (extracting) reagent (ligand) in the organic phase and mineral salts and/or acids or bases in the aqueous phase. Thus, the complexation process, its rate, and the mass-transfer rate can play a significant role in the separation process [9]. There are three important criteria for choosing a two-phase liquid system.

First, the systems must be composed of two immiscible phases. Each solvent mixture should be thoroughly equilibrated in a separatory funnel at room temperature and the two phases separated after the clear two phases have been formed. When the nature of the organic sample to be separated is known, one may find a suitable solvent system by searching the literature for solvent systems that have been successfully applied to similar compounds [1,3–8]. In the case of organic–aqueous two-phase systems, the organic phase consists of one solvent or of a mixture of different solvents. Various nonaqueous–nonaqueous two-phase solvent systems have been used for separation of nonpolar compounds and/or compounds that are unstable in aqueous solutions. Separation of macromolecules and cell particles can be performed with a variety of aqueous–aqueous polymer–phase systems. Among the various polymer–phase systems available, the following two types are the most versatile for performing CCC [1,8]. Poly(ethylene glycol) (PEG)–potassium phosphate systems provide a convenient means of adjusting the partition coefficient of macromolecules by changing the molecular weight of PEG and/or the pH of the phosphate buffer. The PEG 6000–Dextran 500 systems provide a physiological environment, suitable for separation of mammalian cells by optimizing osmolarity and pH with electrolytes.

For preconcentration and separation of inorganic species, a stationary phase containing extracting reagents of different types (cation-exchange, anion-exchange, and neutral) in an organic solvent should be usually applied [2,9–12]. The mobile-phase components should not interfere with the subsequent analysis. Solutions of inorganic acids and their salts are most often used. The mobile phase may also contain specific complexing agents, which can bind one or several elements under separation.

Second, one of the phases (stationary one) must be retained in the rotating column to a required extent. The most important factor, which determines the separation efficiency and peak resolution for both organic and inorganic compounds, is the ratio of the stationary-phase volume retained in a column to the total col-



umn volume. The volume of the stationary phase V_s retained in the column depends on various factors, such as the physical properties of the two-phase solvent system, flow rate of the mobile phase, and applied centrifugal force field. In droplet CCC, where the separation is performed in a stationary column, a large density difference between the stationary solvent phases becomes the predominant factor for the retention of the stationary phase. In other CCC schemes, various types of two-phase solvent systems can be used under optimized experimental conditions. The influence of planetary centrifuge parameters and operation conditions on the stationary-phase retention have been well studied for some simple two-phase liquid systems consisting of water and one or two organic solvents [1,3–8].

According to Ito's classifications [1,3], hydrophobic organic phases are easily retained by all types of CCC apparatus. Intermediate solvent systems involve a more hydrophilic organic phase. Their tendency to evolve, after mixing, to a more stable emulsion than the hydrophobic systems decreases the retention of stationary phase. The hydrophilic two-phase systems containing a polar phase are even less retained in the column.

However, the addition of extracting reagents and mineral salts to a two-phase system (in case of inorganic separations) can strongly affect the physicochemical properties of liquid systems and, consequently, their hydrodynamic behavior and S_f value. Varying concentrations of the system constituents used for inorganic separation allows selective changing of a certain physicochemical parameter (interfacial tension γ , density difference between two liquid phases $\Delta\rho$, and viscosity of the organic stationary phase η_{org}). The type of the solvent may often have a great effect on the stationary-phase retention and, consequently, on the chromatographic process. The correlations between the physicochemical parameters of the complex liquid systems under investigation and their behavior in coiled columns are described in detail [10]. The composition and physicochemical properties of the organic phase in inorganic analysis were modified by adding an extracting reagent [e.g., di-2-ethylhexylphosphoric acid (D2EHPA), tri-*n*-butyl phosphate, trioctylamine] [2,10]. The density and viscosity of the organic phase were varied by changing the amount of reagents in the stationary phase. For example, a small addition (5%) of D2EHPA in an organic solvent (*n*-decane, *n*-hexane, chloroform, and carbon tetrachloride) leads to a considerable increase in the factor S_f in the organic solvent— $(\text{NH}_4)_2\text{SO}_4$ —water

systems (from 0 to 0.73 in the case of carbon tetrachloride) [10].

Third, the stationary phase should permit separate elution of the substances into the mobile phase and the selectivity toward samples of interest has to be sufficient to lead to separations with good resolution. The selectivity of solvent systems can be estimated by determination of the partition coefficients for each substance. The batch partition coefficients D^{bat} are calculated as the ratio of the component concentration in the organic phase to that in the aqueous phase. The dynamic partition coefficients of compounds D^{dyn} are determined from an experimental elution curve [7]. Several solvent systems for organic separation were investigated [4–8]. The most efficient evolution usually occurs when the value of the partition coefficient is equal 1. However, in some CCC schemes, the best results are obtained with lower partition coefficient values of 0.3–0.5 [1,4].

Conclusions

In inorganic analysis with the use of CCC, the stationary phase should provide preconcentration of the elements to be determined, if necessary. It should be noted that the element elution depends on the operation conditions for the planetary centrifuge, which influence the quantity of the stationary phase in the column. A chromatographic peak shifts to left and narrows if the volume of the stationary phase lowers (all the other factors being the same) [2]. The reagent concentration in the organic solvent also affects the elution curve shape and, therefore, the dynamic partition coefficient values. An increase of the reagent concentration in the organic phase leads to higher partition coefficients for the elements, and a better separation is achieved. However, a rather large volume of the mobile phase can be required for the elution of elements from the column.

The composition of the mobile phase also has an influence on the partition coefficients of inorganic substances and the separation efficiency. Concentrations of the mobile-phase constituents should provide partition coefficient values needed for the enrichment or separation of components under investigation. If a step-elution mode is used, partition coefficients higher than 10 and less than 0.1 are favorable for the enrichment of components into the stationary phase and their recovery into the mobile phase, respectively. Chemical kinetics factors may also play an important role in the separation of inorganic species by CCC [9]. It has been shown that the values of mass-transfer coefficients determine the



type of elution (isocratic or step), which is necessary for the element separation. The data on batch extraction (mass-transfer coefficients and partition coefficients) and parameters of chromatographic peaks (half-widths) can be interrelated by some empirical expressions [9]. The application of CCC in inorganic analysis looks promising because various two-phase liquid systems, providing the separation of a variety of inorganic species, may be used for the separation of trace elements.

References

1. Y. Ito, in *Countercurrent Chromatography. Theory and Practice* (N. B. Mandava and Y. Ito, eds.), Marcel Dekker, Inc., New York, 1988.
2. B. Ya. Spivakov, T. A. Maryutina, P. S. Fedotov, and S. N. Ignatova, in *Metal-Ion Separation and Preconcentration: Progress and Opportunities* (A. N. Bond, M. L. Dietz, and R. D. Rodgers, eds.), American Chemical Society, Washington, DC, 1999, pp. 333–347.
3. W. D. Conway, *Countercurrent Chromatography. Apparatus, Theory and Applications*, VCH, New York, 1990.
4. A. Berthod and N. Schmitt, *Talanta* 40:1489 (1993).
5. J.-M. Menet, D. Thiebaut, R. Rosset, J. E. Wesfreid, and M. Martin, *Anal. Chem.* 66:168 (1994).
6. T. P. Abbott and R. Kleiman, *J. Chromatogr.* 538:109 (1991).
7. S. Drogue, M.-C. Rolet, D. Thiebaut, and R. Rosset, *J. Chromatogr.* 593:363 (1992).
8. A. P. Foucault and L. Chevolot, *J. Chromatogr. A* 808:3 (1998).
9. P. S. Fedotov, T. A. Maryutina, A. A. Pichugin, and B. Ya. Spivakov, *Russ. J. Inorg. Chem.* 38:1878 (1993).
10. T. A. Matyutina, S. N. Ignatova, P. S. Fedotov, B. Ya. Spivakov, and D. Thiebaut, *J. Liquid Chromatogr. Related Technol.* 21:19 (1998).
11. E. Kitazume, M. Bhatnagar, and Y. Ito, *J. Chromatogr.* 538:133 (1991).
12. Yu. A. Zolotov, B. Ya. Spivakov, T. A. Maryutina, V. L. Bashlov, and I. V. Pavlenko, *Fresenius Z. Anal. Chem.* 35:938 (1989).



CE-MS: Large-Molecule Applications

Ping Cao

Tularik, Inc., South San Francisco, California, U.S.A.

Introduction

Capillary electrophoresis (CE) is a modern analytical technique which permits rapid and efficient separation of charged components present in small-sample volumes. Separation occurs due to differences in electrophoretic mobilities of ions inside small capillaries. The impetus for CE method developments focused primarily on the separation of larger biopolymers such as polypeptides, proteins, oligonucleotides, DNA, RNA, and oligosaccharides [1]. Mass spectrometry (MS) has long been recognized as the most selective and broadly applicable detector for analytical separations. Currently, electrospray ionization (ESI) serves as the most common interface between CE and MS. Generation of multiply-charged species with an ESI extends the applicability of conventional mass analyzers of limited mass-to-charge (m/z) ranges to molecular mass and structure determination of larger biopolymers. CE-MS combines the advantages of CE and MS so that information on both high efficiency and molecular masses and/or fragmentation can be obtained in one analysis. This article focuses on larger-molecular analysis by on-line CE-MS interfaced via ESI sources [2,3]. However, CE-MS using continuous-flow fast-atom bombardment (CF-FAB) sources employing either "liquid-junction" or "coaxial" interfaces and several off-line CE-MS combination should be noted.

When ESI-MS is employed as detector, the proper choice of a suitable electrolyte system is essential to both a successful CE separation and good quality ESI mass spectra. Even though a wide range of CE buffers were successfully electrosprayed when the liquid-junction and sheath flow CE-MS interfaces were employed since the low CE effluent flow is effectively diluted by a much large volume of sheath liquid [4]; the best detector response is produced by volatile electrolyte systems at the lowest practical concentration and ion strength and by minimizing other nonvolatile and charge-carrying components. Volatile reagents like ammonium acetate (pH 3.5–5.5) or formate (pH 2.5–5; both adjustable to high pH) and ammonium bi-

carbonate have been proven to be well suited for CE-ESI-MS.

Due to the inherent tendency to adsorb strongly to the inner walls of the fused-silica capillary, the analysis of proteins and peptides by CE has presented unique challenges to the analyst because this phenomenon gives rise to substantial peak broadening and loss of separation efficiency. Successful separations of proteins and peptides by CE involve efficient suppression of adsorption to the fused-silica wall. Basically, there are two approaches to prevent protein adsorption: modification of the fused-silica surface by dynamic or static coating or by performing analysis under experimental conditions that minimize adsorption [5]. The static coating capillary is preferred under CE-ESI-MS analysis of large molecules because the CE buffer composition is simplified. This article is meant only to provide the reader with a description of most common approaches taken to analyze large molecules, especially polypeptides and proteins, by CE-ESI-MS.

Large-Molecule Analysis of CE-MS by Neutral Capillary

Because there is no ionizable groups of the coating in the neutral capillary, the interaction between charged molecules with ionic capillary surface is eliminated. Also, the electro-osmotic flow (EOF) of a neutral capillary is eliminated. However, a continuous and adequate flow of the buffer solution toward the CE capillary outlet is an important factor for routine and reproducible CE-ESI-MS analysis; in order to maintain a stable ESI operation, some low pressure applied to the CE capillary inlet is usually needed, especially when the sheathless interface is employed. The disadvantage of the pressure-assisted CE-ESI-MS is the loss of some resolution because the flat flow profile of the EOF is partially replaced by the laminar flow profile of the pressure-driven system. A typical neutral capillary is a LPA (linear polyacrylamide)-treated capillary. Karger and co-workers [6] used mixtures of model proteins, a coaxial sheath flow ESI interface,



and a 75- μm -inner diameter (i.d.), 360- μm -outer diameter (o.d.), 50-cm-long LPA-coated capillary to evaluate CE-MS, CITP (capillary isotachopheresis)-MS, and the on-column combination of CITP-CE-MS. In the CE-MS experimental, 0.02M 6-amino-hexanoic acid + acetic acid (pH 4.4) was employed and a 18-kV constant voltage was applied during the experiment. Seven model proteins were well resolved. They showed that the sample concentration necessary to obtain a reliable full-scan spectrum was in the range of 10^{-5}M . However, by proper selection of the running buffers, they demonstrated that the on-column combination of both CITP and capillary zone electrophoresis (CZE) can improve the concentration detection limits for a full-scan CE-MS analysis to approximately 10^{-7}M .

Large-Molecule Analysis of CE-MS by a Positively Charged Capillary

To help overcome adsorption, positively charged coatings have been employed for the separation of positively charged solutes. In this approach, positively charged proteins are electrostatically repelled from the positively charged capillary inner wall. Two examples of such coatings are aminopropyltrimethoxysilane (APS) and polybrene, a cationic polymer. These coatings reverse the charge at the column-buffer interface and, thus, the direction of the EOF compared to uncoated capillaries.

The CE-MS analysis of the venom of the snake *Dendroaspis polylepis polylepis*, the black mamba, is reported by Tomer and co-workers [7]. A VG 12-250 quadrupole equipped with a Vestec ESI source (coaxial sheath flow interface) was employed for this experiment. The sheath fluid was a 50:50 methanol:3% aqueous acetic acid solution. The CE voltage was set at -30 kV during the analysis and the ESI needle was held at +3 kV. The CE running buffer used was 0.01M acetic acid at pH 3.5. The APS column was flushed with buffer solution for 10 min prior to sample analysis. The snake venom was dissolved in water at a concentration of 1 mg/mL and 50 nL of the analyte solution was injected into the column. They demonstrated the existence of at least 70 proteins from this venom.

One interesting example of intact protein analysis was described by Smith and co-workers [8]. They used the high sensitivity and mass accuracy of a Fourier transform ion cyclotron resonance (FTICR) MS detector to analyze hemoglobin α and β in a single human erythrocyte. Human erythrocytes were obtained from the plasma of a healthy adult male. A small drop

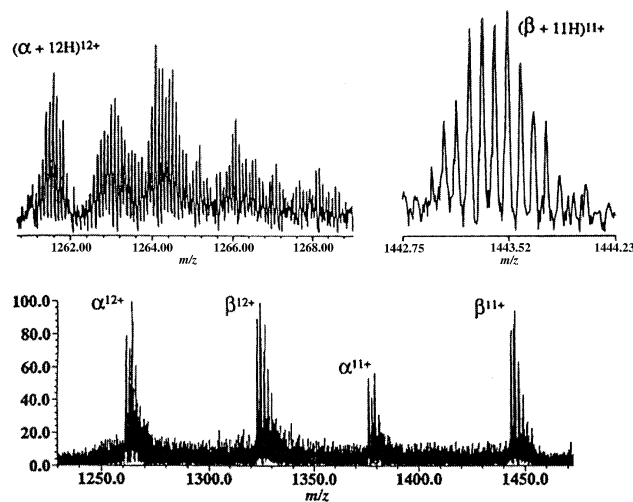


Fig. 1 Mass spectra obtained from CE-MS analysis of a single human erythrocyte using an FTICR mass analyzer. (Reproduced from Ref. 7, with permission).

of blood diluted with saline solution (pH 7.4) was placed on a microscope slide. With the help of a stereomicroscope and a micromanipulator, the etched terminus of the CE capillary was positioned within a few microns of the cell to be injected. Following electro-osmotic injection of the cell, the end of the CE capillary was placed in a vial containing the CE running buffer (10 mM acetic acid, pH 3.4), and the cell membrane was lysed via osmotic shock from the running buffer and the cellular contents of the cell released for subsequent CE separation and mass analysis. A 1-m APS column and a sheathless interface employing a gold-coated capillary with -30 kV CE separation and +3.8 kV ESI voltage were used for this study. They demonstrated that adequate sensitivity needed to characterize the hemoglobin from a single human erythrocyte ($\sim 450\ \mu\text{mol}$) and mass spectra with average mass resolution in excess of 45,000 (full width at half-maximum) were obtained for both the α - and β -chain of hemoglobin. Figure 1 shows the mass spectra obtained from this experiment.

In order to overcome the bubble formation associated with the sheathless CE-MS interface and quick degradation of the coated capillary, Moini et al. [9] introduced hydroquinone (HQ) as a buffer additive to suppress the bubbles formed due to the electrochemical oxidation of the CE buffer at the outlet electrode. The oxidation of water ($2\text{H}_2\text{O}(\text{l}) \leftrightarrow \text{O}_2(\text{g}) + 4\text{H}^+ + 4\text{e}^-$) was replaced with that of more easily oxidized HQ (hydroquinone $\leftrightarrow p$ -benzoquinone + $2\text{H}^+ + 2\text{e}^-$). Formation of p -benzoquinone, other than

the formation of oxygen gas, effectively suppresses gas bubble formation. The APS-coated capillaries and 10 mM acetic acid CE running buffer containing 10 or 20 mM HQ were used for the experiments. The CE outlet/ESI electrode was maintained at +2 kV and the CE inlet electrode was held at -30 kV. Tryptic digest of cytochrome-*c* and hemoglobin were used as model proteins. They demonstrated that the combination of the in-capillary electrode sheathless interface using a platinum wire, HQ as a buffer additive, and pressure programming at the CE inlet provides a rugged high-efficiency setup for analysis of peptide mixtures.

Because the concentration limits of detection of CE are often inadequate for most practical applications (approximately $10^{-6}M$), several analyte concentration techniques have been developed, including combining capillary isotachopheresis (CITP) with CE, transient isotachopheresis (tITP) in a single capillary, analyte stacking, and field amplification. Such electrophoretic techniques have extended the applicability of CE for the analysis of dilute analyte solutions. Chromatographic on-line sample concentration has been achieved by using an extraction cartridge which contains a bed of reversed-phase packing [10] or a membrane [11] with reversed-phase properties. Accumulated analyte on the cartridge can be prewashed to remove salts and buffers that are not suited for CE separation or ESI operation. Figeys and Aebersold [12] designed the solid-phase extraction (SPE)-CE-MS-MS system which consists of a small cartridge of C_{18} reverse-phase extraction material immobilized in a Teflon sleeve. Solutions of peptide mixtures typically derived by proteolysis of gel-separated proteins were forced through the capillary by applying positive pressure at the inlet and the peptides were concentrated on the SPE device. After equilibration with an electrophoresis buffer compatible with ESI, eluted peptides were separated by CE and analyzed by ESI-MS. A detection limit of 400 aM tryptic digest of bovine serum albumin (20 μ L of solution at a concentration of 20 aM/ μ L was applied) was achieved in the ion trap mass spectrometer-based system. This method was successfully applied to the identification

of yeast proteins separated by two-dimensional gel electrophoresis.

Applications of CE-MS to large molecules are progressing rapidly. As biology enters an era of large-scale systematic analysis of biological systems as a consequence of genome sequencing projects, rapid and sensitive identifications of large-scale (proteomewide) proteins that constitute a biological system is essential. CE-MS with its high separation efficiency, rapid separation, and economy of sample size is complementary to microcolumn high-performance liquid chromatography (μ HPLC)-MS. In addition, high-resolution, multiple-dimensional separations become increasingly attractive. HPLC-CE-MS, affinity CE-MS, capillary microreactor on line with CE-MS, and microchip-based separations will be used in a broad range of future applications.

References

1. W. G. Kuhr and C. A. Monnig, *Anal. Chem.* 64:389R (1992).
2. R. D. Smith and H. R. Udseth, *Pharmaceutical and Biomedical Applications of Capillary Electrophoresis*, Elsevier Science, New York, 1996, pp. 229-276.
3. J. F. Banks, *Electrophoresis* 18:2255 (1997).
4. R. D. Smith, J. A. Loo, C. G. Edmonds, C. J. Barinaga, and H. R. Udseth, *Anal. Chem.* 62:882 (1992).
5. P. Thibault and N. J. Dovichi, *Capillary Electrophoresis (Theory and Practice)*, 2nd ed., CRC Press, Boca Raton, FL, 1998, pp. 23-90.
6. T. J. Thompson, F. Foret, P. Vouros, and B. L. Karger, *Anal. Chem.* 65:900 (1993).
7. J. R. Perkins, C. E. Parker, and K. B. Tomer, *Electrophoresis* 14:458 (1993).
8. S. A. Hofstadler, J. C. Severs, and R. D. Smith, *Rapid Commun. Mass Spectros.* 10:919 (1996).
9. M. Moini, P. Cao, and A. J. Bard, *Anal. Chem.* 71:1658 (1999).
10. D. Figeys, and R. Aebersold, *Electrophoresis* 19:885 (1998).
11. A. J. Tomlinson, L. M. Benson, N. A. Guzman, and S. Naylor, *J. Chromatogr.* 744:3 (1996).
12. D. Figeys and R. Aebersold, *Electrophoresis* 18:360 (1997).



Cell Sorting Using Sedimentation Field Flow Fractionation: Methodologies, Problems, and Solutions—A “Cellulomics” Concept

Philippe J. P. Cardot

Yves Denizot

Serge Battu

Université de Limoges, Limoges, France

INTRODUCTION

Sedimentation field flow fractionation (SdFFF) is an efficient, analytical/preparative-scale, cell sorting device, in particular, if coupled with sophisticated cellular characterization techniques, devices, or methods, including flow cytometry (FC). Cell population, by analogy with “polymers,” appears very polydisperse and disperses in many dimensions, which may not be essentially biophysical (size, shape, density, and rigidity), but also functional (cell cycle, protein expression, and differentiation stage). Cell sample pretreatment has a unique goal, which is to provide a sterile and viable cell suspension at an appropriate concentration (1–10 million cells/mL). A particular elution mode, made possible in cell purification by exploiting complex hydrodynamic forces, is usually described as a “Hyperlayer.” This elution mode exploits slight differences in physical characteristics of the cell (size, shape, density, rigidity, and surface characteristics); trends are opened to their association with complete functional cell characteristics analyses. It is shown that cells can be eluted, in some examples, according to functional parameters (cell cycle and differentiation stage), and that correlations may exist between functional parameters and the physical ones. If a given cell population is considered, considerable information provided by the separation and the complete physical and functional analyses allows one to define, characterize, and produce a new type of cell subpopulation. Such separation/characterization process for cells can be described as “cellulomics,” by analogy with what is done for proteins of gene systems, keeping in mind the concept that the cell is the “fundamental and unique” localization and production factory of any gene and protein.

BACKGROUND

The last decades have shown considerable development of a large panel of cell sorting techniques.^[1–5] SdFFF, such

as elutriation or centrifugation methods, belongs to the group of “physical methods,” comparisons of which have already been assessed.^[1] In the present report, we will focus on the specific features of cell elution in FFF and on the necessity of coupling such a physical separation/purification system with detectors of high functional specificity. Cell sorting with FFF emerged in the scientific literature in the early 1980s of the last century. A pioneering report was published in 1984 by Caldwell et al.^[6] in which most of the separation rules and methodologies were described. At difference with all other species, cell sorting with FFF success was proved essential by using sedimentation subtechniques that required specific instrumentation and methodological setups. Systematic instrumentation development, allowing separation of living species in sterile conditions for further use, was initiated in the late 1990s in our laboratory.^[7,8]

It must be noted here that the main objective of cell separation in FFF is not only analytical, but also preparative. The main goal is strongly linked to the possibility not only to characterize as completely as possible the cell subpopulation, but to provide or produce new living cell subpopulations for any use. It is essential to keep these cells in surviving condition. Therefore considerable attention must be given to characterize a potential subpopulation, and to define and control their survival. However, if nonstable subpopulations are recovered, cinematic studies of their properties must be developed in terms of “time or age”-dependent characteristic modifications. To be clear, cells are eluted at a given stage; they are characterized or used at that stage, in whatever way they can be cultivated, maintained in survival, and evolved to other critical stages (the must be characterized) where they can be functionally used. Such complex receiver-oriented characteristic (ROC) separation/characterization step can be described as “cellulomics.”

In this report, specific instrumentation of SdFFF for cell sorting will be described. The interest and potential of the “Steric Hyperlayer”^[6,9] elution mode for cell sorting

will be discussed, keeping in mind basic rules for physically or functionally oriented separation development. By analogy with polymers, experimentally driven definitions, descriptions, and characterizations of cell populations will be provided, leading to an information matrix described as "cell population multipolydispersity."^[1]

A particular paragraph is devoted to some specific requirements for FFF cell sorting, such as sample preparation or separator poisoning. The battery of cell population or cell subpopulation characterization methods will be described with an FFF-dependent classification: physical methods compared to functional ones. Finally, experimental correlations between functional and physical cell characteristics lead to the isolation of very specific populations, thereby opening the field of "cellulomics." In this report, it is assumed that readers have a basic knowledge of separation sciences, in particular, in chromatography and FFF.

PRINCIPLE OF SdFFF AND INSTRUMENTATION

The FFF family encompasses a broad array of subtechniques; however, FFF techniques have in common the design of a channel, generally parallelepiped and often described as "ribbonlike," in which the critical dimensions are: 1) thickness, usually lower than 300 μm ; 2) length, between 20 and 100 cm; and 3) breadth, from 0.5 to 2 cm; with 4) tapered channel ends. An external field acts on the great surface of the ribbon to achieve flow rate-dependent separations (Hyperlayer elution mode for micron-sized species). SdFFF techniques can be divided into two groups. The first uses simple gravity or gravity fractions [i.e., gravitational/subgravitational FFF (GrFFF/GFFF)]; the second uses the multigravity field created by centrifugation generically described as SdFFF. With common associated devices (injection, flow, and detection devices), their instrumental design and setup are completely different. The GFFF separator is very simple to set up and does not require more specific skills than a simple "exploration desire," whereas SdFFF is much more complex to set up and requires long-term know-how in the absence of commercially available devices devoted to cell sorting.

INSTRUMENTATION

Instrumentation for cell sorting can be very simple, using gravitational FFF devices as described by our group,^[10–13] or by others.^[14–16] A complete technical instrumentation has been also described.^[17] The key parameter is the

material used to construct the channel walls, which must be as "inert" as possible if considered against the cellular materials or their media (protein clotting). Media or sample-derived wall treatment may occur when changing, considerably, elution conditions. Such goal is empirically well assessed in the biological technology using materials of various "biocompatible" polymers. Therefore it is only necessary to choose as an appropriate material the one compatible with FFF instrumentation (low deformation under sealing pressure). It must be noticed here that some materials can be appropriate for some cell groups and be completely unusable for others, which requires a versatile instrumentation.

In SdFFF, the same strategy is employed with materials tested in GFFF, with the only price that sealing and deformability linked with centrifugation rate must be controlled. However, one particular point must be taken into account in SdFFF; long connection tubings are necessary and they must be chosen to be "biocompatible" and with appropriate inner diameter. This point is highly critical. Diameters that are too narrow may induce shear forces, destroying selective parts of the sample; too large diameters induce noncolumn band spreading, thereby limiting resolution. Channel dimensions and tubing choices must be chosen in the light of the sample and of the separation goals. Unfortunately, only a few laboratories exert an instrumental effort to define and construct biocompatible SdFFF systems.^[18–20]

ELUTION MODE

Cells are in the 3–40 μm diameter range; channel thicknesses ranging from 70 to 250 μm are commonly used, depending on elution selectivity requirements. Therefore cell size cannot be ignored in the light of the channel thickness leading to an experimentally developed elution mode described as "Steric Hyperlayer."^[6,9] Again, in the light of the preceding paragraph, a "pure steric elution mode" must be avoided as possibly generating high particle–wall interactions, these being so far determined essentially on an experimental basis. Therefore elution conditions must meet the hypotheses developed in the Hyperlayer condition. As such, model cells are focused on different stream lines by the double and opposite actions of the external field and of forces generated by the cell in motion and described generically under the term of lift forces, driving the cell into an equilibrium position in the channel thickness. The lifting force characteristics are complex, were described for the first time by Ho and Leal,^[21] and were developed on a theoretical basis for FFF by Martin and Williams.^[22] Experimental proofs were given for cell sorting by Caldwell et al.^[6] If little is known about the kinetics of this focusing process using retention



ratio analysis, it is simplified in the determination of an average “equilibrium” position in the channel thickness of the cells eluted at a given retention ratio by a position(s) in the channel thickness given by the following equation:

$$R = \frac{3s}{w} \quad (1)$$

where R is the measured retention ratio, s is the distance between the average particle gravity center and the accumulation wall, and w is the channel thickness. The calculated s value does not describe the real distance at equilibrium, but can be considered an accurate evaluation of it, assuming that: 1) in identical experimental conditions, kinematics in the channel thickness of particles of analogous size, shape, and density is analogous; 2) flow injection reduces particle–wall interactions that are negligible; and 3) lifting forces are so intense that no particle–wall retardation effects occur. If s is greater than the cell greater radius, then elution is considered as a Hyperlayer. Therefore it is essential to obtain for cells an average position that is much larger than the cell radius; this ensures that cells have a low probability to interact with channel walls. Such considerations lead to a concept applied by Battu et al.^[19,20] for cell sorting—the “safety Hyperlayer” elution mode in which cell recovery is maximum in the case of flow-established injections. Depending on the elution conditions (channel dimensions, external field intensity, and flow rate), it is, so far, possible to state that, for spherical particles of identical density, the elution order is size-dependent, with the larger ones being eluted first. It is also, so far, possible to assess that, at identical sizes, spherical particles are eluted according to their mass, with the least dense being eluted first. More complex situations arise if, as in the case of cells, the population presents independent size and density distributions.

There is a particular injection mode, described often as “stop flow” or primary relaxation step, in FFF. Suspensions are inserted in the channel under an external field, then the flow is stopped for a given time (stop flow time and primary relaxation time) and flow is reestablished for elution. This particular injection procedure is specific for FFF separations^[6,23] and increases selectivity considerably, even in the case of the “Hyperlayer” elution mode. Historically, this was set up because of instrumental considerations, where the inlet tubing emerged at the depletion wall.^[6,10,23] Simple instrumentation modification involving, in contrast, the accumulation wall made it possible to avoid such procedure driving the species into a geometric location in the channel thickness close to the accumulation wall.^[7,8,11–13,18–20] If, experimentally, such modification was successful using a channel of reduced thickness, complex injection hydrodynamics occurs if the channels are thicker than 100 μm . Considerably reducing the “stop flow time,” or even avoiding it, is essential if cell sorting

strategies are considered. Very little is known in terms of cell–channel interactions (even with biocompatible materials) and the stop flow procedure may be at the origin of (reversible or not) cell sticking, leading either to cell destruction (which may be selective) or cell differentiation by simple contact (stem cells). From injection to injection, the wall structure at the injection zone may be completely altered (modified), leading to analysis or separation biases. Therefore a price must be paid in terms of separation power to reduce these possible interactions. Limiting separation power by using systematic flow-established injections is essential if cell subpopulation integrity maintenance is required (cell differentiation process); in these conditions, the probability that any cell of the sample will interact with the walls is reduced—a process also limited by the kinetics (whose characteristics are not known) of the Hyperlayer focalization. As collateral consequences of flow injection, separation times are considerably reduced, recovery is enhanced, and channel poisoning is reduced. Figure 1 shows the fractograms obtained in such conditions in the case of a mixture of ES cells and fibroblasts whose biological properties were analyzed.^[7] Low-intensity spikes at the end of every fractogram signifies field stop and a low reversible release of trapped material, which may not necessarily be made of cells only.

Mouse E14 ES cells were routinely grown onto a monolayer of mitomycin-treated primary embryonic mouse fibroblasts as a source of cytokines and growth factors. The medium consisted of DMEM with 15% fetal calf serum (Gibco, Cergy Pontoise, France), 100 U/mL penicillin, 100 $\mu\text{g/mL}$ streptomycin, 1 μM α -mercaptoethanol, and 10^3 U/mL leukemia-inhibitory factor (LIF; Gibco). ES cells were grown at 37°C in a humidified chamber with 10% CO_2 . ES cells were recovered with trypsin treatment for SdFFF experiments or subcultures. The SdFFF separation device used in this study includes a separation channel, which consisted of two $870 \times 30 \times$

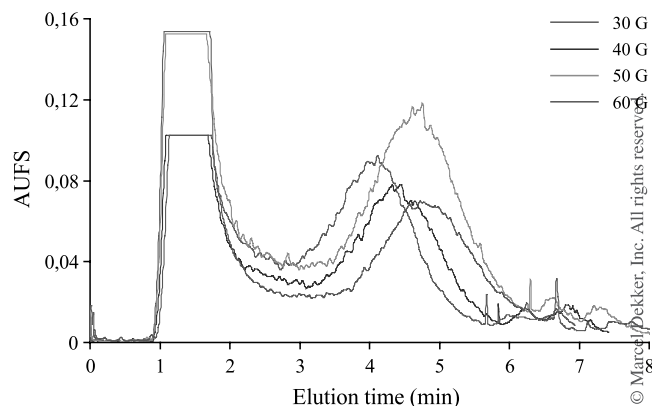


Fig. 1 Cell sorting with FFF. (View this art in color at www.dekker.com.)

2-mm polystyrene plates, separated by a Mylar spacer in which the channel ($785 \times 10 \times 0.125$ mm with two V-shaped ends of 70 mm) was carved. Inlet and outlet were 0.254 mm ID. Peek tubing (Upchurch Scientific, Oak Harbour, WA) was directly screwed into the accumulation wall. Then, polystyrene plates and Mylar spacers were sealed onto a centrifuge basket. The channel–rotor axis distance was measured at r (13.8 cm). Cleaning and decontamination procedures have been described in a previous report.^[3] The elution signal was recorded at 254 nm.

MULTIPOLYDISPERSITY: PHYSICAL/FUNCTIONAL AND DETECTION REQUIREMENTS

A First-Order Definition of Multipolydispersity: Example of Mass Distribution

This concept has already been defined for cell sorting.^[1] To precisely know the physical characteristics of cell

populations, let us imagine a simple bidimensional one where cells are spherical and rigid, and show independent size and density distribution. According to the Steric Hyperlayer mode, with some subpopulations, coelution is possible, generating a need for size or mass detectors. Therefore granulometric or mass measurements appearing at the outlet (online/offline) are essential in terms of separation developments.

Figure 2 shows a theoretical bidimensional polydispersity (size and density). The bidimensional Gaussian distribution is shown in Fig. 2A, where (S) is the size axis, (D) is the density, and C represents the number of particles. If such a sample is eluted according to the Hyperlayer elution mode, a broad fractogram is observed, as shown in Fig. 2B. From such a fractogram, every fraction corresponds to particles of different sizes and densities, as qualitatively shown in Fig. 2C. The front of the peak is associated with particles that are very different from the ones at the tail. It is possible to imagine granulometric detection all along the fractogram profile, as shown in Fig. 2D. If the density distribution coincided with the size distribution is considered, every fraction is

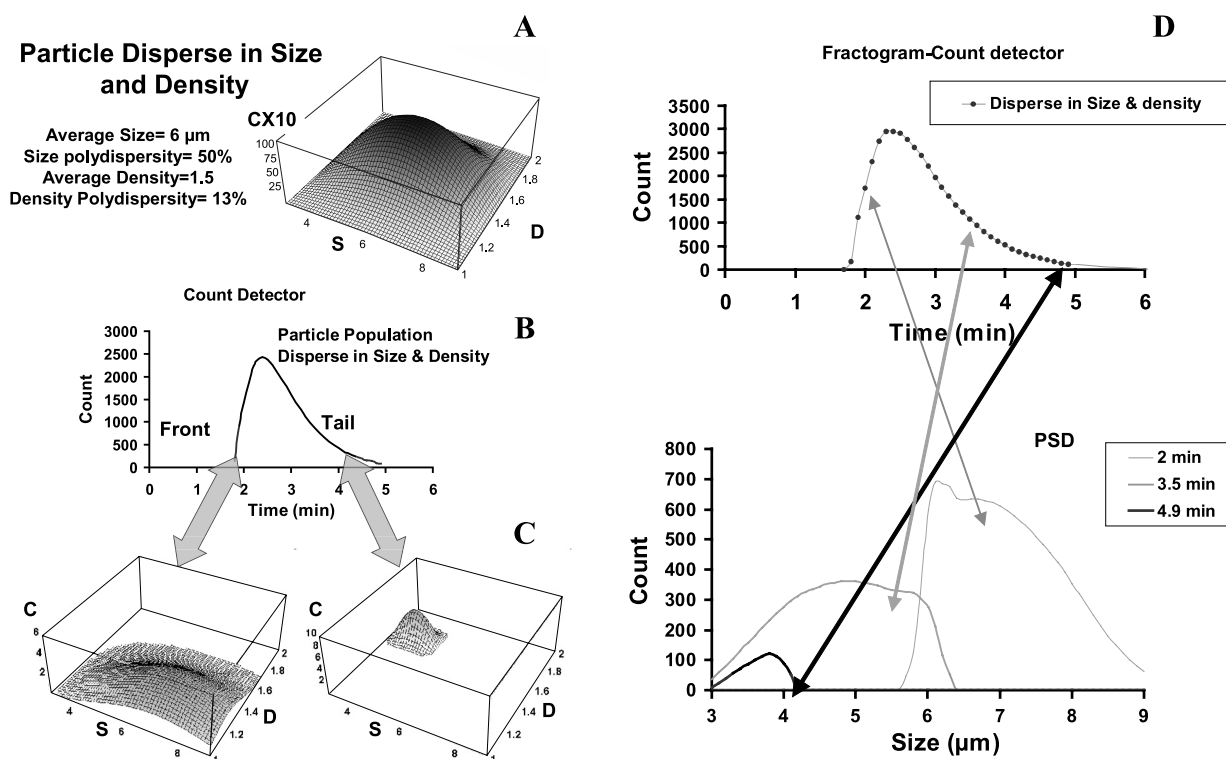


Fig. 2 The multipolydispersity concept: a bidimensional example (size and density distribution). Graph A represents the convolution if size and density distribution simulated by a bidimensional Gaussian. Fractogram B shows the elution profile obtained in the use of an ideal Steric Hyperlayer elution mode whose channel dimensions, external field, and carrier flow rate are chosen to produce discriminating separations on both size and density. Graph C shows bidimensional population pattern composing the fronting and tailing zones of the fractogram. The same fractogram is shown on graph D, with simulation of fraction collection or granulometric detector time constant with three examples of PSD obtained.



associated with a particular particle size distribution (PSD). It is essential to note that, in the simulation considered here, density distribution is not disperse enough to invert or modify the “size-dependent Hyperlayer elution order,” where the biggest and most polydisperse particles elute first. It is now interesting to determine this PSD in the density distributions.

GRANULOMETRIC PATTERNS AND DENSITY DISTRIBUTION

It may be possible to discriminate density vs. size if a single particle mass detector were available for micron-sized species. In the absence of such a detector, only indirect information is affordable, exploring the consequences of the Hyperlayer elution mode. From the abovedescribed bidimensional population (size and den-

ty), the Hyperlayer mode allows us to draw isodensity and isosize retention patterns. Such information coinvolved with the PSD permits the determination of the density distribution envelope of the fractions considered, as shown in Fig. 3. Graph A shows the isoretention pattern of the population. It is observed that, at the peak front, a PSD ranging from 5 to 9 μm is obtained, with light small particles (5 μm , 1.2 density) and heavy big ones (9 μm , 1.6 density). It is tempting to complicate such a chart in three dimensions, as shown in Fig. 3B, to draw an isosize retention chart as a function of density, whose bidimensional projection may be easier to read. Therefore it is observed that 3- μm particles (as well as 9- μm ones) are eluted at very different retention times, depending on their densities. It can be concluded that, in the light of what is known so far from the “Hyperlayer” elution mode, PSD obtained during elution can be linked to other dimensions (density, shape, and rigidity). Therefore it appears that

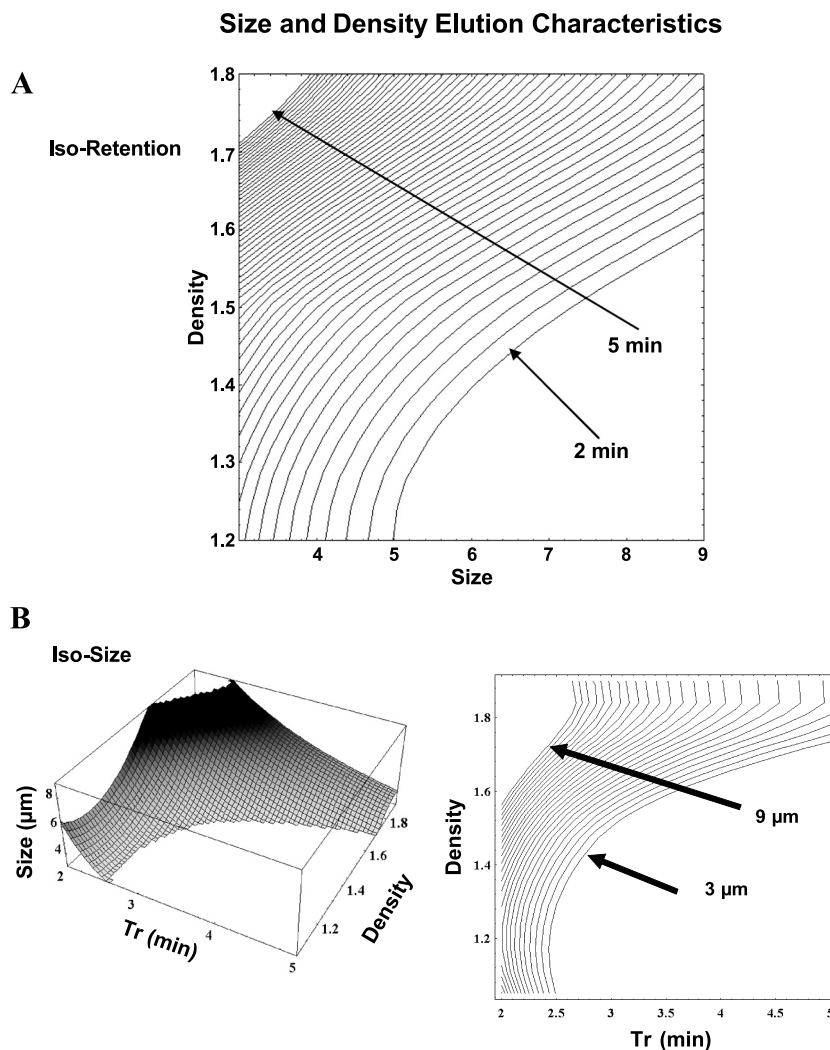


Fig. 3 (A) Granulometric pattern and (B) density distribution. Particle characteristics are described in Fig. 2.

large optimization processes are opened to understand the discriminating effects of channel dimensions, fields, and flow rates on a multipolydisperse population.

HIGHER ORDERS: PHYSICAL AND FUNCTIONAL

If it is relatively easy to adapt offline/online granulometric detectors allowing PSD at every retention time; only very few cell-specific characterization devices are available, with the preferred one being FC.^[24] FC’s versatility is impressive, allowing particle counting as well as a series of particle characteristics and distribution measurements using light diffusion principles and/or fluorescence.^[24] If used in its simplest mode, count histogram vs. diffused light leads to sophisticated information. When a single particle passes in front of a laser beam, the scattered (or emitted fluorescence) light generates a signal proportional to the studied parameter of that particle. If the collected light is at a large angle [90°, side scattering (SS)] from the incident laser beam, the signal is a complex function of the particle refractive index, composition, and surface characteristics.^[24,25] If the diffused light is collected at low angles^[24–26] [10, forward scattering (FS)], diffraction predominates and the signal is a function of the particle volume described by the Mie law.^[27] Therefore a multidimensional detection allowing population or subpopulation discrimination, whose pattern (fingerprint) can be associated with FFF retention properties, is made possible. Other detection methods can be used with specific functional properties (surface receptors and cell content), as already described by our group.^[7,28,29] Every sample or collected fraction (during FFF elution) can be, as a consequence, described by a battery of information—some being possibly calibrated, and some others looked at only from a qualitative or comparative point of view.

SPECIFIC REQUIREMENTS

Suspension

It is essential to prepare single cell suspensions, which exist naturally in very few cases (cultured cells such as HeLa, HeL, and blood cells). In most critical cases (solid tumors, tissues, and neural cells), a preliminary step is necessary and classically requires transformation of the tissue in suspension. Two methods are used: the first is mechanical,^[30] whereas the second requires enzymatic action.^[30] It is essential to obtain a monocell suspension, whose characteristics have to be controlled by FC. Once this suspension is obtained, another critical parameter is

its concentration; blood cells can be injected in a highly concentrated suspension, whereas neural ones must be inserted into the FFF system highly diluted, requiring large injection volumes. So far, no prediction rules have been established and the technique requires experience-based empirical knowledge.

FFF Device

Channel walls are assumed to be biocompatible, but so is the carrier phase, which can be added with specific surfactants to avoid aggregation during separations: so far, bovine serum albumin (BSA)^[11–13] (and, recently, cholic acid) appeared to be more stable and at least as efficient.^[31] Such precautions must be associated with systematic recovery measurements—a multidimensional concept associated with the detector pattern, and a comparison of the crude sample with every collected fraction.

Operating Conditions

A flow injection of appropriate cell number sometimes requires adapting the injection volume. In terms of elution, it is essential to observe or follow the safety Hyperlayer requirements that have been already defined. In this order, with the help of the granulometric detector, it is possible to determine the average sizes of cells eluting in the front and the tail of the fractogram, and to calculate, by means of the (*S*) position, their average position in the channel thickness; by experience, a useful recovery is found if the elution conditions (field and flow) drive to an average position in the channel thickness (*s*) at, at least, 0.75 times the diameter.

Poisoning/Cleaning

Cell suspensions are often introduced into the SdFFF separator in their cultivation media; these complex solutions encompass proteinaceous hydrophilic compounds as well as hydrophobic ones. It has been also observed that cell recovery may reach 90% in optimized conditions with either a reversible trapping (released at field stopped) or an irreversible one, leading to the release of cellular material that may interact irreversibly with channel walls, thereby leading to surface modifications. Using a biocompatible carrier phase may generate local bacterial growth, either at the channel surface or within the channel; some workers use some toxic cellular killing compounds (e.g., sodium azide).^[32] The experimenter must be warned about the toxicity, even at low concentration, of such compounds not only as far as the sample is concerned, but also the experimenter. With experience, it appears that channel poisoning is progressive,



with constant recovery reduction, as well as baseline and noise evolution. Therefore there is a need to regularly clean the channel over the life of the separator. This procedure is relatively easy and must be performed in three steps: channel wall regeneration, which destroys sorbed proteins or biological compounds such as membranes or genetic materials; sterilization of the channel by means of an appropriate cocktail involving hypochlorite and ethanol; and rinsing of the separator with sterile mobile phase to completely wash the channel.

The effectiveness of instrument design and setup to reduce cell-accumulation wall interactions was demonstrated, first, by the recovery of cells in the corresponding elution peak (>70%). Second, it was shown by conservation of cell viability, which was, after SdFFF elution, similar to that of the control population. Finally, reduction of interactions was partially demonstrated by a very low cell release peak, which was observed at the end of the fractogram when channel rotation was stopped and the mean gravity was equal to zero (external field applied=1g; Fig. 4); such procedure is not possible in GFFF. This residual signal corresponded to reversible cell sticking due to weak interactions between cells and the accumulation wall.^[7,11–14] Cells or cellular materials can be released from the accumulation wall under the effect of the mobile phase flowing in the absence of channel rotation. However, irreversible cell trapping is due to strong cell-channel interaction and cannot be reversed under these conditions. This phenomenon cannot be

observed on the fractogram and leads to channel poisoning, requiring routine channel wall regeneration procedures. For this purpose, cleaning cocktails used in FC or clinical instrumentation appear to be very effective.

These poisonings can be overcome by systematically performed cleaning and decontamination procedures.^[19,20,28,29] Some experiments (not published) have shown that the absence of effective and systematic channel cleaning has led to many problems, in particular, an increase in apoptosis of separated cells, even though elution conditions were set up to enhance the “Hyperlayer” mode because the small portion of definitively trapped cell die released apoptotic signals into the separator, which could activate apoptosis in freshly separated cells.

The different steps and instrument setups used for cleaning and decontamination have been extensively described.^[19,20,28,29] The cleaning procedure is based on the use of osmotic shock and injection of deproteinizing agent. The use of polystyrene plates and BSA-free mobile phase has simplified the previous steps,^[10–13] it is now performed as an end-of-day cleaning–decontamination procedure. First, phosphate-buffered saline (PBS; pH 7.4) was replaced by flushing the entire system with sterile distilled water at a high flow rate. Second, the entire SdFFF device was flushed at 0.8 mL/min for 30 min with a protein cleaning agent (CLENZ; Beckman Coulter, Fullerton, CA). The system was rinsed with sterile distilled water for 1 hr at 0.8 mL/min. Then, the entire SdFFF device was flushed at 0.8 mL/min for 30 min with a 3–4°C sodium hypochlorite solution. The system was rinsed with sterile distilled water for 2 hr at 1 mL/min. The system was then ready to use by replacing the sterile water with sterile PBS. By implementing this cleaning–decontamination procedure, the same channel can be used for analysis of various cell populations without sample cross-contamination and microorganism proliferation.

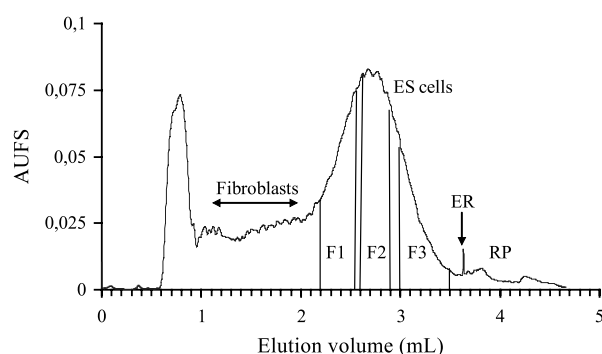


Fig. 4 Optimized SdFFF fractogram of ES Cells. Representative fractogram of ES cell suspensions after SdFFF elution. Elution conditions: Flow injection of 100 μ L of ES suspension; flow rate, 0.6 mL/min (sterile PBS, pH 7.4); and external multigravitational field, 40 (0.1g; spectrophotometric detection at 254 nm). Fractions were collected as follows: PF1, 3 min 40 sec/4 min 15 sec; PF2, 4 min 20 sec/4 min 50 sec; PF3, 5 min 0 sec/5 min 50 sec. ER corresponds to the end of channel rotation. In this case, the mean externally applied field strength was equal to zero gravity; thus RP, a residual signal, corresponds to the release peak of reversible cell accumulation wall sticking. (View this art in color at www.dekker.com.)

FROM PHYSICAL/FUNCTIONAL TO BIOLOGICAL, AN EMPIRICAL EXPERIENCE: THE CONCEPT OF “CELLULOMICS”

ES mice embryonic stem cells are an important tool for the generation of transgenic and gene modified mice. We report the effectiveness of an SdFFF cell sorter to provide, from a crude ES cell preparation, a purified ES cell fraction with the highest in vivo developmental potential, to prepare mice chimeras having a high percentage of chimerism.

By taking advantage of biophysical properties (size, density, and shape), SdFFF sorts viable cells without labeling of any kind. SdFFF has a great potential with major biomedical applications, including hematology,



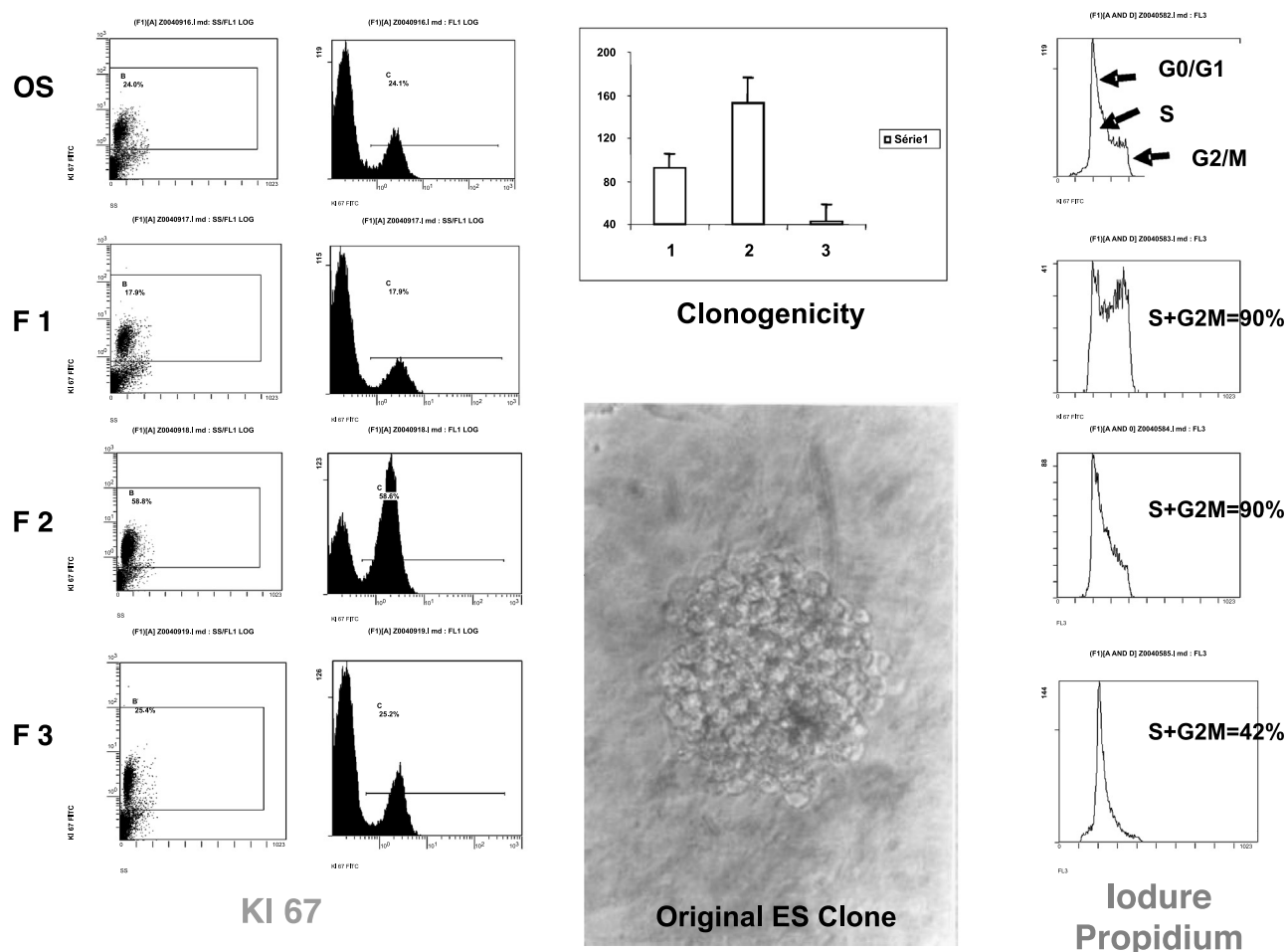


Fig. 5 ES cells, eluted as shown in Fig. 4, are characterized according to functional parameters described in the text: Bidimensional cytometric map of FS and fluorescence (Ki67). Right: Monodimensional propidium iodine fluorescence. Up center: Clonogenicity activities of the three collected fractions of Fig. 4. Down center: Microscopic image of ES cell clone.

neuroscience, cancer research, microorganism analysis, and molecular biology.^[8,19,20,30] Embryonic stem cells are used in studies of gene disruption and transgenesis by using their ability to colonize the germline after introduction into blastocysts. Major limitations are the time required to obtain germline transmission, which sometimes required numerous experiments. ES cell suspensions are a mixture of cells at various stages of proliferation; heterogeneity within cells arises during culture with respect to their in vivo developmental potential. We tested the effectiveness of SdFFF to provide, from crude ES cells, an enriched cell fraction with the highest in vivo developmental potential, to prepare chimeras having a high percentage of chimerism,^[7] as shown in Fig. 5.

E14 ES cell cultures and the SdFFF device were used as previously described.^[7,34] The optimal elution conditions (Hyperlayer mode^[35]) were: flow injection

1.5×10^5 cells/0.1 mL, flow rate 0.6 mL/min, mobile phase PBS pH 7.4, external multigravitational field strength 40.0 ± 0.1 g, and spectrophotometric detection $\lambda = 254$ nm. Three cell fractions were collected as shown in Fig. 4: F₁: 3 min 40 sec/4 min 15 sec; F₂: 4 min 20 sec/4 min 50 sec; F₃: 5 min/5 min 50 sec. Fractionated ES cells were stained with propidium iodide and analyzed for DNA cell status using an XL.2 flow cytometer (Beckman Coulter). The percentage of G₀/G₁ cells was higher in F₃ as compared with F₁ and F₂. The percentage of Ki67⁺ cells (a protein expressed in all phases of the cell cycle, except G₀ and early G₁)^[5] confirmed results with propidium iodide. Thus because F₂ and F₃ cells had the highest and lowest in vitro clonogenicity, respectively, 10 cells from these fractions were injected into C57 Bl/6 blastocysts to derive somatic chimeras. The frequency of chimeras obtained was similar (9 of 37 injected blastocysts). In

contrast, a higher degree ($p < 0.02$, Mann–Whitney U -test) of color coat chimerism was obtained with F_3 ($87 \pm 5\%$) compared to F_2 ($63 \pm 9\%$). A germline transmission was obtained for all four F_3 males within 3 months as compared with one of four F_2 males after 6 months.

These results clearly show that SdFFF can sort, in a few minutes, the most convenient ES cell population to generate chimeras having the highest ability to colonize the germline. This result is, in particular, based on its newly described capacity to sort cells by their position in the cell cycle. In conclusion, SdFFF is of great interest to improve transgenesis and might also have further interesting applications for human gene therapy.

CONCLUSION

The major difficulty in the development of FFF methodologies and instrumentations is linked to the complexity of correlating elution mode hypotheses (Hyperlayer) with experimental proofs, which depends essentially upon physical properties of the cellular material, such as size, density, shape, rigidity, and cellular viscosity, which are of greatest interest if the "physical point of view" is considered. This point of view is historical and is linked to the wide experience of FFF practitioners with latex or silica, micron-sized species, or starch granules, or others. There are some examples dealing with cellular materials (e.g., red blood cells or yeast) where elution is correlated with the abovedescribed physical properties; in these cases, "cellulomics" concepts are relatively simple.

More delicate are the situations where experimentally obtained functional properties, such as specific receptor presence or cell-dependent cycle elution, are the essential ROC and define the goal or the results of the separations. There is, as a consequence, a considerable task in understanding the very different origins of such links, where physics meets or generates biological results of interest, leading to the wide domain of "cellulomics."

The main general consideration that can be stated so far is: 1) the smoothness of the separations; 2) the absence of cell prelabeling; and 3) the development of biocompatible instrumentation, which allows subpopulation lineage to be produced, which are not only usable for fundamental studies such as differentiation pathways or apoptosis studies, but also for transplantation or genetic engineering. One must have in mind that the cell is definitively the place, home, and native localization of genes and proteins. The possibility of rapid, nondestructive separation, purification, and characterization of cells (cellulomics) opens fabulous dimensions for proteomics and genomics.

REFERENCES

- Lucas, A.; Lepage, F.; Cardot, Ph. *Field Flow Fractionation Handbook*; Shimpf, M.E., Caldwell, K., Giddings, J.C., Eds.; Wiley-Interscience: New York, 2000; 471.
- Lutz, M.P.; Geadick, G.; Hartmann, W. *Anal. Biochem.* **1992**, *200*, 376.
- Axen, R.; Porath, J.; Ernback, S. *Nature* **1967**, *214*, 1302.
- Hansen, E.; Hanning, K. *Methods Enzymol.* **1984**, *108*, 180.
- Sharpe, P.T. *Laboratory Techniques in Biochemistry and Molecular Biology*; Burdon, R.H., Knippenberg, P.H., Eds.; Elsevier: Amsterdam, 1988; Vol. 18, 208.
- Caldwell, K.D.; Cheng, Z.Q.; Hradecky, P.; Giddings, J.C. *Cell Biophys.* **1984**, *6*, 233.
- Guglielmi, L.; Battu, S.; Le Bert, M.; Faucher, J.L.; Cardot, P.J.P.; Denizot, Y. *Anal. Chem.* **2004**, *76* (6), 1580.
- Lautrette, C.; Cardot, P.J.P.; Vermot-Desroches, C.; Wijdenes, J.; Jauberteau, M.O.; Battu, S. *J. Chromatogr., B* **2003**, *791* (1–2), 149.
- Williams, P.S.; Koch, T.; Giddings, J.C. *Chem. Eng. Commun.* **1992**, *111*, 121.
- Cardot, P.J.; Gerota, J.; Martin, M. *J. Chromatogr.* **1991**, *568* (1), 93.
- Merino-Dugay, A.; Cardot, P.J.; Czok, M.; Guernet, M.; Andreux, J.P. *J. Chromatogr.* **August 7, 1992**, *579* (1), 73–83.
- Andreux, J.P.; Merino, A.; Renard, M.; Forestier, F.; Cardot, P. *Exp. Hematol.* **1993 Feb**, *21* (2), 326–330.
- Bernard, A.; Paulet, B.; Colin, V.; Cardot, P.J.P. *TrAC, Trends Anal. Chem.* **1995**, *14* (6), 266–273.
- Sanz, R.; Galceran, M.T.; Puignou, L. Determination of viable yeast cells by gravitational field-flow fractionation with fluorescence detection. *Biotechnol. Prog.* **2004**, *20* (2), 613–618.
- Urbankova, E.; Vacek, A.; Novakova, N.; Matulik, F.; Chmelik, J. Investigation of red blood cell fractionation by gravitational field-flow fractionation. *J. Chromatogr.* **1992 Nov 27**, *583* (1), 27–34.
- Urbankova, E.; Vacek, A.; Chmelik, J. Micropreparation of hemopoietic stem cells from the mouse bone marrow suspension by gravitational field-flow fractionation. *J. Chromatogr., B, Biomed. Sci. Appl.* **December 13, 1996**, *687* (2), 449–452.
- Cardot, Ph.; Chianea, T.; Battu, S. *SdFFF of Living Cells in Encyclopedia of Chromatography*; Cazes, J., Ed.; Marcel Dekker, Inc.: New York, 2002; 742.
- Metreau, J.M.; Gallet, S.; Cardot, P.J.; Le Maire, V.; Dumas, F.; Hervann, A.; Loric, S. *Anal. Biochem.* **1997**, *251* (2), 178.
- Battu, S.; Delebasse, S.; Bosgiraud, C.; Cardot, P.J. *J. Chromatogr., B* **2001**, *751* (1), 131.
- Battu, S.; Cook-Moreau, J.; Cardot, P.J.P. *J. Liq. Chromatogr. Relat. Technol.* **2002**, *25* (13–15), 2193–2210.
- Ho, P.B.; Leal, L.G. *J. Fluid Mech.* **1974**, *65*, 365.
- Martin, M.; Williams, P.S. *Theoretical Advances in*



- Chromatography and Related Separation Techniques*; Dondi, F., Guiochon, G., Eds.; NATO ASI Series, Kluwer Academic Publishers: London, 1991; Vol. 383, 513.
23. Lee, S.H.; Myers, M.N.; Giddings, J.C. Hydrodynamic relaxation using stopless flow injection in split inlet sedimentation field-flow fractionation. *Anal. Chem.* **November 1, 1989**, *61* (21), 2439–2444.
 24. Cram, L. Flow cytometry, an overview. *Methods Cell Sci.* **2002**, *24* (1–3), 1.
 25. Papa, S.; Zamaï, L.; Cecchini, T.; Del Grande, P.; Vitale, M. Cell cycle analysis in flow cytometry: Use of BrdU labelling and side scatter for the detection of the different cell cycle phases. *Cytotechnology* **1991**, *5* (Suppl. 1), 103–106.
 26. Petriz, J.; Tugues, D.; Garcia-Lopez, J. Relevance of forward scatter and side scatter in aneuploidy detection by flow cytometry. *J. Eur. Soc. Anal. Cell. Pathol.* **May 1996**, *10* (3).
 27. Adams, J.M. Light extinction photometer for measurement of particle sizes in polydispersions. *Rev. Sci. Instrum.* **1968**, *39* (11), 1748–1751.
 28. Cardot, P.; Battu, S.; Simon, A.; Delage, C. J. *Chromatogr., B* **2002**, *768* (2), 285–295.
 29. Sanz, R.; Cardot, P.; Battu, S.; Galceran, M.T. *Anal. Chem.* **September 1, 2002**, *74* (17), 4496–4504.
 30. Battu, S.; Elyaman, W.; Hugon, J.; Cardot, P.J. *Biochim. Biophys. Acta* **2001**, *1528* (2–3), 89.
 31. Reschiglian, P.; Zattoni, A.; Roda, B.; Cinque, L.; Melucci, D.; Min, B.R.; Moon, M.H. *J. Chromatogr., A* **2003**, *985*, 519–529.
 32. Hofstetter-Kuhn, S.; Rosler, T.; Ehrat, M.; Widmer, H.M. *Anal. Biochem.* **1992**, *206*, 300–308.
 33. Sanz, R.; Puignou, L.; Reschiglian, P.; Galceran, M.T. *J. Chromatogr., A* **2001**, *919* (2), 339–347.
 34. Giddings, J.C. *Field-Flow Fractionation Handbook*; Schimpf, M.E., Caldwell, K., Giddings, J.C., Eds.; Wiley-Interscience: New York, 2000.
 35. Pinaud, E. *Immunity* **2001**, *15*, 187–199.



Centrifugal Partition Chromatography: An Overview

M.-C. Rolet-Menet

Laboratoire de Chimie Analytique, UFR des Sciences Pharmacochimie et Biologie, Paris, France

Introduction

Centrifugal partition chromatography (CPC) belongs to the methods based on counter current chromatography (CCC). Separation is based on the differences in partitioning behavior of components between two immiscible liquids. Like high-performance liquid chromatography (HPLC), the phase retained in the column is called the stationary phase, the other one is called the mobile phase. In CCC, there are two modes to equilibrate the two immiscible phases. They depend on the characteristics of the centrifugal force field which permits retention of the stationary phase inside the column. Devices which equilibrate the phases according to the so-called “hydrodynamic mode” were developed by Ito [1]. They use a centrifugal force which is variable in intensity and direction. Alternated zones of agitation and settling of both phases take place along the column. By contrast, CPC uses a so-called “hydrostatic mode,” owing to a centrifugal force which is constant in intensity and direction. Therefore, the mobile phase penetrates the stationary phase by forming either droplets or jets or sprays. The more or less vigorous agitation of both phases depends on the intensity of the centrifugal force, the flow rate of the mobile phase, and the physical properties of the solvent system. Chromatographic separations obtained in hydrostatic mode are less efficient than in the hydrodynamic mode. However, the retention of the stationary phase is less sensitive to the physical properties of solvent systems, such as viscosity, density, and interfacial tension. This justifies the wide application field of CPC.

Apparatus

The CPC column is made of channels engraved in plates of an inert polymer (Fig. 1) and they are connected by narrow ducts. Several plates are put together to form a cartridge. The cartridges are placed in the rotor of a centrifuge and are connected to form the chromatographic column. The mobile phase enters and

leaves the column via rotary seals. Because two immiscible liquids are present in the channel, the denser liquid moves away from the axis because of the centrifugal force. The less dense liquid is pushed toward the axis. The mobile phase can be either the lighter or the denser phase. In the latter case, the mobile phase flows through the channels from the axis to the outside of the rotor. This is called the descending mode. The other case, the mobile phase flowing toward the axis, is called the ascending mode.

Hydrostatic apparatuses are manufactured by Sanki Engineering Limited (Kyoto, Japan). They include two types of device; the first is designed for analytical or semipreparative scale applications, and the second one for the scale-up at a industrial scale. CPC type LLN was introduced in 1984 but is no longer available since 1992. It can be thermostated from 15°C to 35°C in an ambient temperature of 25°C. Type HPCPC or Series 1000 supersedes type LLN. The HPCPC main frame is a 31 × 47 × 50-cm centrifuge operating in the range 0–2000 rpm; it cannot be thermoregulated. The rotor consist of two packs of six disks each, connected through a 1/16-in. tubing and easily removable. Larger instruments have internal volumes from 1.4 to 30 L and can be used with flow rates ranging from 20 to 700 mL/min and are custom designed for specific separation processes at a small industrial scale.

Retention of Stationary Phase

Before use, the column is first filled with a stationary phase and, afterward, rotated at the desired rotational speed. The mobile phase is then pumped into the cartridge at the desired flow rate and pushes a certain volume of stationary phase out of the column. Hydrostatic equilibrium is reached when the mobile phase is expelled out at the column outlet. The retention of stationary phase, designated S_F , is defined as

$$S_F = \frac{V_s}{V_t}$$

Encyclopedia of Chromatography

DOI: 10.1081/E-Echr 120004611

Copyright © 2002 by Marcel Dekker, Inc. All rights reserved.



where V_s is the stationary-phase volume in the column after equilibrium and V_t is the total volume of the column.

The value of S_F depends on several parameters, including the hydrodynamic properties of the channels, the centrifugal force (S_F increases to reach a maximum with the centrifugal force), the mobile-phase flow rate (S_F decreases linearly with the mobile-phase flow rate), the physical properties of the solvent system (such as viscosity, density, interfacial tension), the sample volume, the sample concentration, and the tensioactive properties of solutes to separate [2,3]. It is necessary to precisely monitor S_F because various chromatographic parameters depend on it, in particular the efficiency, the retention factor, and the resolution. Foucault proposed an explanation for the variation of S_F with the various parameters previously described. He modeled the mobile phase in a channel as a droplet and applied the Stokes' law which relies on the density difference between the two phases, the viscosity of the stationary phase, and the centrifugal force. Then, he applied the Bond number, derived from the capillary wavelength which was formerly introduced for the hydrodynamic mode [4] and which relies on the density difference between the two phases: the interfacial tension and the centrifugal force [3].

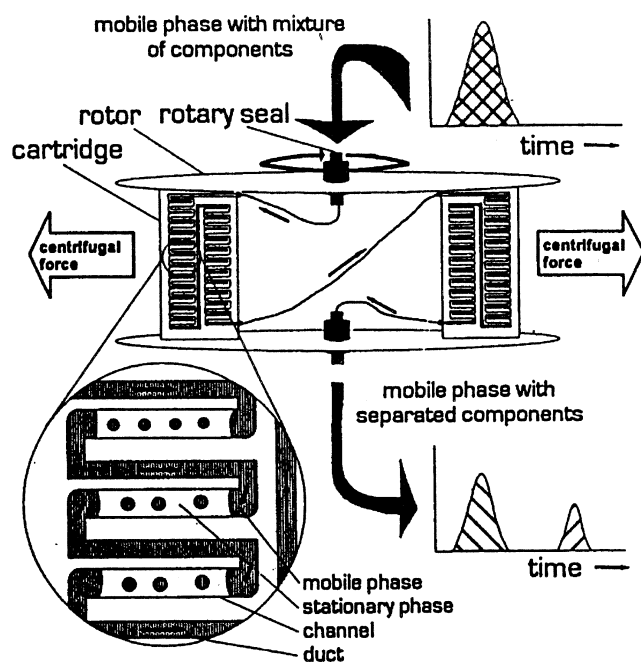


Fig. 1 Schematic representation of the CPC apparatus. (Reproduced with permission from Ref. 5.)

Centrifugal Partition Chromatography: An Overview

Pressure Drop

Van Buel et al. [5] have proposed a model to explain the considerable pressure drop arising in the column during CPC separation. The overall pressure drop is the sum of the hydrostatic pressure-drop term and of the hydrodynamic pressure-drop term over the individual parts of the system. The hydrostatic contribution is caused by the difference in density between the liquids in the ducts and in the channels ($\Delta P_{\text{stat}} = n l \Delta \rho \omega^2 R$, where n is the number of channels, l is the height of stationary phase in the channel, $\Delta \rho$ is the density difference of the both phases, ω is the rotational speed, and R is the average rotational radius of the cartridge). The hydrodynamic contribution (ΔP_{hydr}) is caused by the friction of the mobile phase with the walls of the channels and ducts. This latter, in a channel and a duct, is proportional to the mobile-phase density, the square of its linear velocity, the lengths of the channel and duct, the reverse of channel, and the duct diameter. Consequently, the overall pressure drop depends on the flow rate and rotational speed (input variables), on the physical properties of the two-phase solvent system (variables), on the geometry of the channels and ducts, on the number of channel-duct combinations (apparatus variables), and on the holdup of the stationary phase in the channel. The maximum pressure is limited by the rotary seals, which can support about 60 bars before leaking. Resolution and efficiency depend on the same variables as the pressure drop. Therefore, it is important to determine which combinations of input variables and liquid two-phase systems can be applied, with respect to the maximum pressure that can be supported by the rotary seal.

Efficiency

The efficiency (N) in CCC can be defined as in HPLC by

$$N = 16 \left(\frac{V_r}{\omega} \right)^2$$

where V_r is retention volume of the solute, ω is the peak base width expressed in volume unity as V_r , or for an asymmetrical peak according to the Foley-Dorsey formula

$$N = 41.7 \left(\frac{(t_r/\omega_{0.1})^2}{A/B + 1.25} \right)$$

where $\omega_{0.1}$ is the peak width at 10% of the peak height and A/B is the asymmetry factor with $A + B = \omega_{0.1}$.

The efficiency variation shows a minimum when the flow rate of the mobile phase is increased, which is the opposite of the usual HPLC Van Deemter plot. This observation has been modeled by Armonstrong et al. [6]. The mobile phase, when it comes out of the duct, flows very quickly to reach an intermediate emulsified layer and then settles in a third step before being transferred to another channel. In these conditions

$$\ln(1 - E) = \frac{A}{F} - BF^b$$

where

$$E = \frac{C_{m,t} - C_{m,0}}{C_{m,eq} - C_{m,0}}$$

($C_{m,t}$, $C_{m,0}$, and $C_{m,eq}$ are the solute concentrations in the mobile phase at a moment t , before equilibrium and after equilibrium, respectively), A depends on S_F , B on the physical properties of the solvent system, and b on solutes and solvent system. This variation is very interesting, because it shows that a high mobile-phase flow rate decreases the retention time without decreasing efficiency. However, it was observed that S_F decreases with the flow rate and the resolution R_s also decreases as described in the following section. The flow rate of the mobile phase may be increased to decrease the separation time, but, at the condition that S_F remain satisfactory to maintain a sufficient R_s [2]. Finally, it has been shown that N increases with the centrifugal force field [2].

Resolution

The resolution (R_s) in CCC can be defined as in HPLC by

$$R_s = 2 \left(\frac{V_{r2} - V_{r1}}{\omega_1 + \omega_2} \right) = 2V_s \left(\frac{K_2 - K_1}{\omega_1 + \omega_2} \right)$$

where V_{r1} and V_{r2} , ω_1 and ω_2 , and K_1 and K_2 are respectively the retention volumes, the peak base widths expressed in volume unity as V_r , and the partition coefficients of the first and second eluted solutes. R_s is directly proportional to volume V_s of the stationary phase, and, hence, on the flow rate of the mobile phase and the centrifugal force [2,7].

The resolution in CCC as in HPLC is governed by the Purnell relation

$$R_s = \frac{\sqrt{N}}{4} \left(\frac{k'_2}{1 + k'_2} \right) \left(\frac{1 - \alpha}{\alpha} \right)$$

where k'_2 is the retention factor of the second solute and α is the separation factor. N is controlled by F , the centrifugal force, S_F , and physical properties of the solvent system, and k' is controlled by the nature of the solvent system (through the partition coefficient K and S_F); α is controlled mainly by the solvent system. This relationship shows that it is essential, in CCC, to control technical parameters and to choose, judiciously, the solvent system to separate the products.

Solvent Systems

The choice of the solvent system is the key parameter to a good separation. On one hand, its physical properties define S_F , N , and R_s ; on the other hand, the relative polarities of its two phases define the partition coefficients of the solutes and, as a result, the selectivities and the retention factors. Usually, solvent systems are biphasic and made of three solvents, two of which are immiscible.

We only give basic directions for the choice of a solvent system. If the polarities of the solutes are known, the classification established by Ito [1] can be taken as a first approach. He classified the solvent systems into three groups, according to their suitability for apolar molecules ("apolar" systems), for intermediary polarity molecules ("intermediary" system), and for polar molecules ("polar" system). The molecule must have a high solubility in one of the two immiscible solvents. The addition of a third solvent enables a better adjustment of the partition coefficients. When the polarities of the solutes are not known, Oka's [8] approach uses mixtures of *n*-hexane (HEX), ethyl acetate (EtOAc), *n*-butanol (*n*-ButOH), methanol (MeOH), and water (W) ranging from the HEX-MeOH-W, 2:1:1 (v/v/v) to the *n*-BuOH-W, 1:1 (v/v) systems and mixtures of chloroform, methanol, and water. These solvent series cover a wide range of hydrophobicities from the nonpolar *n*-hexane-methanol-water system to the polar *n*-butanol-water system. Moreover, all these solvent systems are volatile and yield a desirable two-phase volume ratio of about 1. The solvent system leading to partition coefficients close to the unit value will be selected.



Applications

Numerous applications using CPC are described in reference books [1,3]. We will only give key examples extracted from the CPC literature (Table 1).

Polyphenols and Tannins

Open-column chromatography with silica gel and alumina is not applicable to the fractionation of tanins because of their strong binding to these adsorbents, which induces extensive loss of tannins. Such losses do not occur with countercurrent chromatography, as it does not use a solid stationary phase. Such molecules are very polar, so butanol-based solvent systems can be used. Centrifugal partition chromatography is more adequate in this case, as compared to hydrodynamic CCC, because of the good retention of the stationary phase of a such solvent system.

Okuda et al. [9] separated castalagin from vescalagin by using the solvent system *n*-butanol–*n*-propanol–water (4:1:5, v/v/v). They are diastereoisomers which differ only in the configuration of the hydroxyl group of the central carbohydrate moiety. In the same way, they have separated oligomeric hydrolyzable macrocyclic tannins, Oenothien B and Woodfordins by using *n*-butanol–*n*-propanol–water (4:1:5, v/v/v). In spite of a small structural difference (presence or absence of a galloyl group), these dimers showed a considerable difference of the partition coefficients in this solvent system (0.36 for Woodfordin C and 0.19 for Oenothien B).

Preparative Separation of Raw Materials

One of the major applications of CPC is the purification of natural products from vegetal extracts (flowers, roots, etc.) or crude extracts from fermenta-

tion broths without previous sample preparation. Hostettman et al. [10] have described many examples of the isolation of natural products by CPC. Some flavonoids are, for instance, purified by using solvent systems containing chloroform, some coumarins by using solvent systems containing *n*-hexane and ethyl acetate, and more polar products such as tannins by butanol based systems. The main interest of this technique lies, however, in the possibility of overloading its column so that all the applications of semi-preparative chromatography are available. For instance, Menet and Thiebaut [11] have separated 140 mg of an antibiotic from a crude extract of a fermentation broth. Some fractions up to a 95% purity were collected, whereas the original extract contained only 7% of the molecule of interest. They have also compared the performance of CPC, preparative liquid chromatography, and hydrodynamic mode CCC. They finally showed that the solvent consumption is the lowest for CPC and the enrichment is the best.

Measurement of log $K_{\text{oct-Water}}$ [12]

Octanol–water partition coefficients (K_{ow}) have been established as the most relevant quantitative physical property correlated with biological activity. CPC, using octanol and water as the two phases, is a useful alternative for providing octanol–water partition coefficients (K_{ow}). It offers the automation advantages as compared to HPLC and the classical shake flask method. Three approaches for determining K_{ow} by CPC have been described. The normal mode consists in equilibrating the CPC column according to a normal equilibrium or an overloading mode by artificially decreasing the volume of the stationary phase. K_{ow} is calculated according to the classic formula $K = k'(V_t - V_s)/V_s$. The second procedure is the dual-mode method, which is based on the exchange of the role of

Table 1 Applications of CPC

Species [Ref.]	Solvents system
Polyphenols tannins [3]	CHCl_3 –MeOH–water (7:13:8; v/v/v), CHCl_3 –MeOH– <i>n</i> -ProOH–water (9:12:2:8; v/v/v/v), <i>n</i> -ButOH– <i>n</i> -ProOH–water (4:1:5; v/v/v)
Triptolide and triptolide [3]	Hexane–EtOAc– CH_2Cl_2 –MeCN–MeOH– H_2O (12:10:3:10:5:6; v/v/v/v/v/v)
Lanthanoids [3]	Hexane containing bis(2-ethylhexyl) phosphoric/0.1 mol/L (H ₂ Na) Cl ₂ CHCOO to an appropriate pH
Flavonoids [10]	CHCl_3 –MeOH– H_2O (5:6:4; v/v/v)
Polyphenols [10]	C_6H_{12} –EtOAc–MeOH– H_2O (7:8:6:6; v/v/v/v)
Tannins [10]	<i>n</i> -ButOH– <i>n</i> -ProOH– H_2O (2:1:3; v/v/v)
Naphthoquinones [10]	<i>n</i> - C_6H_{14} –MeCN–MeOH (8:5:2; v/v/v)
Retinals [10]	C_6H_6 – <i>n</i> - C_5H_{12} –MeCN–MeOH (500:200:200:11; v/v/v/v)



the mobile and stationary phases during experiment. Therefore, the determination range of partition coefficients can be extended. The third procedure, the cocurrent mode, relies on the simultaneous pumping of a ratio of a small flow of octanol and a larger flow of water to elute strongly retained compounds.

References

1. B. N. Mandava and Y. Ito, Principles and instrumentation of counter current chromatography, in Counter Current Chromatography. Theory and Practice (B. N. Mandava and Y. Ito, eds.), Chromatographic Science Series Vol. 44 Marcel Dekker, Inc., New York, 1988, pp. 79–442.
2. J.-M. Menet, M.-C. Rolet, D. Thiébaud, R. Rosset, and Y. Ito, *J. Liquid Chromatogr.* 15:2883 (1992).
3. A. P. Foucault, Theory of Centrifugal Partition Chromatography, in Centrifugal Partition Chromatography (A. P. Foucault, ed.), Chromatographic Science Series Vol. 68 Marcel Dekker Inc., New York, 1995, pp. 25–50.
4. J.-M. Menet, D. Thiébaud, R. Rosset, J. E. Wesfreid, and M. Martin, *Anal. Chem.* 66:168 (1994).
5. M. J. van Buel, L. A. van der Wielen, and K. Ch. A. M. Luyben, Pressure drop in centrifugal partition chromatography, in Centrifugal Partition Chromatography (A. P. Foucault, ed.), Chromatographic Science Series Vol. 68 Marcel Dekker, Inc., New York, 1995, pp. 51–70.
6. D. W. Armstrong, G. L. Bertrand, and A. Berthod, *Anal. Chem.* 60:2513 (1988).
7. W. Murayama, T. Kobayashi, Y. Kosuge, H. Yano, Y. Nunogaki, and K. Nunogaki, *J. Chromatogr.* 239:643 (1982).
8. H. Oka, K.-I. Harada, and Y. Ito, *J. Chromatogr.* 812:35 (1998).
9. T. Okuda, T. Yoshida, and T. Hatano, Fractionation of plant polyphenols, in Centrifugal Partition Chromatography (A. P. Foucault, ed.), Chromatographic Science Series Vol. 68 Marcel Dekker, Inc., New York, 1995, pp. 99–132.
10. M. Maillard, A. Marston, and K. Hostettmann, High speed counter current chromatography of natural products, in High-Speed Counter Current Chromatography (Y. Ito and W. D. Conway, eds.), Chemical Analysis Series Vol. 32 John Wiley & Sons, New York, 1995, pp. 179–218.
11. M.-C. Menet and D. Thiebaut, *J. Chromatogr.* 831:203 (1999).
12. A. Berthod and K. Talabardon, Operating parameters and partition coefficient determination, in Counter Current Chromatography, in Counter Current Chromatography (J.-M. Menet and D. Thiébaud, eds.), Marcel Dekker, Inc., New York, 1999, pp. 121–148.



Centrifugal Precipitation Chromatography

Yoichiro Ito

National Heart, Lung, and Blood Institute, National Institutes of Health, Bethesda, Maryland, U.S.A.

Introduction

For many years, proteins have been fractionated with ammonium sulfate (AS) by stepwise precipitation. In this conventional procedure, an increasing amount of AS is added to the protein solution and the precipitates are removed by centrifugation in each step. Recently, "centrifugal precipitation chromatography" [1,2] has been developed to replace the tedious manual procedure. This novel chromatographic system is capable of internally generating a concentration gradient of AS through a long separation channel under a centrifugal force field. Proteins introduced into the channel are exposed to a gradually increasing AS concentration and finally precipitated at different locations according to their solubility in the AS solution. Then, the AS concentration in the upper channel is gradually reduced so that the AS concentration gradient in the lower channel is proportionally decreased. This manipulation causes the precipitated proteins to be redissolved and eluted out by repeating precipitation and dissolution along the channel. As in liquid chromatography, the effluent is continuously monitored with an ultraviolet (UV) monitor and fractionated into test tubes using a fraction collector.

The principle and unique design of the separation column is shown in Figs. 1a and 1b, respectively. In Fig. 1a, a pair of separation channels is partitioned by a dialysis membrane. A concentrated (C) AS solution is introduced through the upper channel at a high flow rate (V) from the right, whereas water is fed into the lower channel from the left at a much lower rate (v). This countercurrent flow of the two liquids through the channel results in AS transfer from the upper channel to the lower channel at every point, as shown by arrows across the membrane. Because the AS transfer rate through the membrane is proportional to the difference in AS concentration between the two channels, an exponential gradient of AS concentration (c) is formed through the lower channel. The system allows manipulation of the AS concentration in this gradient by modifying the AS concentration in the upper channel, as described earlier. The separation column is fabricated from a pair of plastic disks (high-density polyethylene,

13.5 cm in diameter and 1.5 cm thick) equipped with mutually mirror-imaged spiral grooves (1.5 mm wide, 2 mm deep, and ~ 200 cm long), as shown in Fig. 1b. A regenerated cellulose membrane with a desirable pore size (6000–8000 or 12,000–14,000) is sandwiched between these two disks which are, in turn, tightly pressed between two metal plates with a number of screws. The capacity of each channel is about 5 mL. This column assembly is mounted on the sealless continuous-flow centrifuge that allows continuous elution through the rotating column without the use of a conventional rotary seal device. The principle of this sealless flow centrifuge system is described in the entry Countercurrent Chromatography Instrumentation. Figure 1c schematically illustrates an entire elution system of the present chromatographic system. Two sets of pumps are used, one (upper right) for pumping AS solution at a high rate and the other (upper right) for eluting buffer solution and protein samples at a lower rate. The total of four flow tubes led from these two pumps are bundled together and clamped at the top of the sealless continuous-flow centrifuge to reach the column assembly as illustrated. As mentioned earlier, these flow lines are twist-free as the column rotates around the central axis of the centrifuge. Consequently, the system eliminates various complications such as leakage, clogging, and cross-contamination, often arising from the use of the conventional rotary seal device for multiple flow lines.

A series of experiments was conducted to study the AS transfer rate through the dialysis membrane by pumping a concentrated AS solution into the upper channel at 1 mL/min and water into the lower channel at varied flow rates ranging from 1 to 0.1 mL/min without sample injection. In these experiments, the AS input concentration into the upper channel and the AS output concentration from the lower channel were compared. The rate of the AS transfer rose, as expected, with the decreased flow rate through the water channel, and at a flow rate of 0.1 mL/min, the AS concentration collected through the lower channel reached nearly 100% that of the AS input in the upper channel. Whereas AS diffuses from the upper channel toward the lower channel, water in the lower channel is



absorbed into the upper channel. This water transfer rate is estimated by comparing input and output flow rates through the water channel. At an input rate of 0.1 mL/min, the outlet flow was decreased to one-fourth of the input rate, indicating that the separated fractions would be eluted in a highly concentrated state. Generating an AS concentration gradient and concentrating fractions are the two unique capabilities of the present system, which can be effectively utilized for fractionation of proteins.

Figure 2 illustrates serum protein separation by centrifugal precipitation chromatography: the chromatographic tracing of the elution curve in Fig. 2a and sodium dodecyl sulfate–polyacrylamide gel electrophoresis (SDS-PAGE) analysis of separated fractions in Fig. 2b. In this example, 100mL of normal human serum (pooled) was diluted to 1 mL and introduced into the separation channel. The experiment was initiated by filling both upper and lower channel with 75% AS solution followed by sample

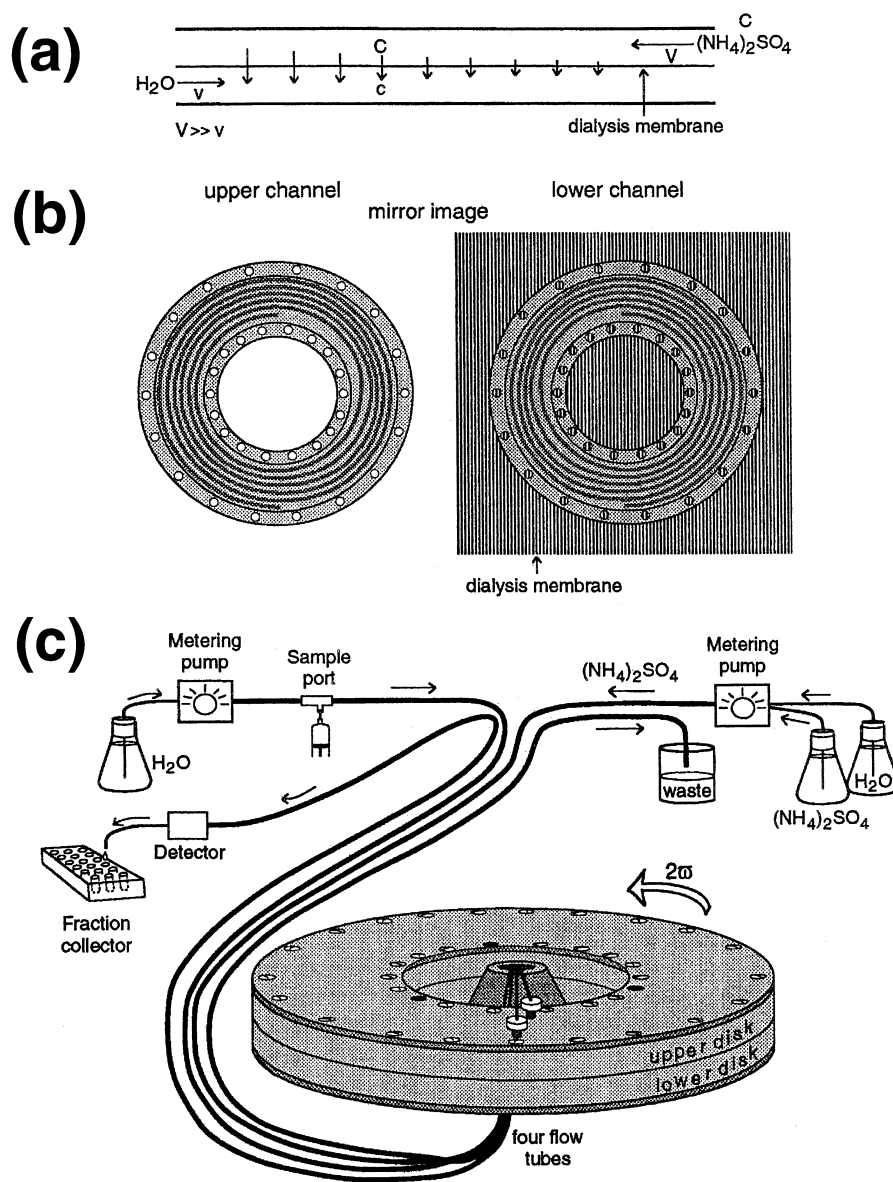


Fig. 1 (a) Principle of the present method; (b) design of the separation column assembly; (c) schematic illustration of the entire elution system of centrifugal precipitation chromatography.

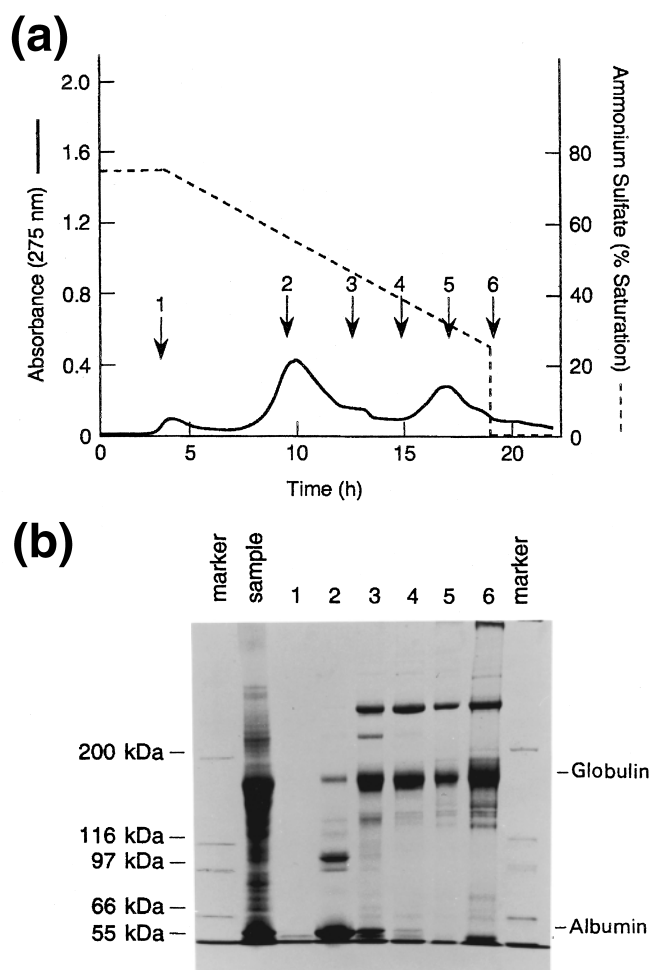


Fig. 2 Separation of human serum proteins by centrifugal precipitation chromatography: (a) Elution curve; (b) SDS-PAGE analysis of separated fractions.

charge into the lower channel through the sample loop. After the separation column assembly was rotated at 2000 rpm, the upper channel was eluted 75% AS solution at a flow rate of 1 mL/min while the lower channel was eluted with 50 mM potassium phosphate at 0.06 mL/min. After 4 h of elution, the AS concentration in the upper channel was linearly decreased down to 25%, as indicated in the chromatogram. The effluent from the lower channel was continuously monitored with an UV monitor (LKB Uvicord S) at 275 nm and fractionated into test tubes using a fraction collector (LKB Ultrac), and the AS solution eluted from the upper channel was discarded. The chromatogram (Fig. 2a) produced two major peaks, one at AS saturation at 60–50% and the other at 35–30%. The SDS-

PAGE analysis of peak fractions (Fig. 2b) revealed that the first peak represents albumin (MW 68,000) and the second peak, γ -globulin (MW 160,000).

Centrifugal precipitation chromatography can produce highly purified protein fractions because the proteins are refined by repetitive precipitation and dissolution. The method has the following advantages over the conventional manual procedure: The method is programmed and automated; the fractions are almost free of small molecules that are dialyzed through the membrane or otherwise quickly eluted out from the channel; noncharged macromolecules such as polysaccharides are washed out, whereas charged biopolymers such as DNA and RNA may also be separated according to their solubility in AS solution; and the method may be amenable for microscale to large-scale fractionation by designing the separation column in suitable dimensions.

The present system has been successfully applied to fractionation of various protein samples, including serum proteins, monoclonal antibodies (IgM against mast cells) from hybridoma culture supernatant, and minor protein components (less than 1% of total proteins) from a crude rabbit reticulocyte lysate containing a large amount of hemoglobin and protein-poly(ethylene glycol) conjugates. One important application of the present method is affinity separation using a ligand that can specifically bind to the target protein to substantially lower its solubility in the AS solution. This ligand-protein complex is then eluted out much later than most of other proteins. This affinity precipitation method has been demonstrated in the purification of recombinant proteins such as ketosteroid isomerase from a crude *Escherichia coli* lysate by adding an affinity ligand (17-estradiol-methyl-polyethylene-glycol-5,000) to the sample solution. The application of the present method may be extended to fractionation of other biopolymers such as DNA and RNA using a pH gradient.

References

1. Y. Ito, Centrifugal precipitation chromatography applied to fractionation of proteins with ammonium sulfate, *J. Liquid Chromatogr. Related Technol.* 22(18):2825 (1999).
2. Y. Ito, Centrifugal precipitation chromatography: Principle, apparatus, and optimization of key parameters for protein fractionation by ammonium sulfate precipitation, *Anal. Biochem.* 277:143 (2000).



Ceramides: Analysis by Thin-Layer Chromatography

Jacques Bodennec
Jacques Portoukalian

Laboratory of Tumor Glycobiology, Université Claude Bernard Lyon I, Oullins, France

Introduction

Thin-layer chromatography (TLC) is widely used in all chemical and biochemical disciplines for preparative as well as analytical purposes. TLC has been thoroughly used in lipid biochemistry and the number of applications is still growing, as more and more laboratories are using this method due to its low cost and ease of use and because new developments in TLC techniques allow better performance [1]. Ceramides are molecules of growing interest, because they are key intermediates in sphingolipid metabolism and they are involved in numerous cellular signal transduction processes [2]. Purification or isolation of these molecules is often carried out by liquid chromatography or TLC prior to further analysis by GLC or high-performance liquid chromatography (HPLC) and mass spectrometry. The aim of the present article is to describe the possibilities offered by TLC in the analysis and purification of ceramides on silica gel TLC and high-performance TLC (HPTLC) plates.

Separation of Ceramides Into Group Species

Thin-layer chromatography has been widely used in the separation of free ceramides into different groups. Indeed, ceramides constitute a class of molecules with a large number of molecular species differing in the constituting sphingoid base and in the species of fatty acids linked as amides (see Fig. 1). Despite the great number of molecular species that can be found in a tissue, the different ceramides can be efficiently separated into defined groups of species according to some structural criteria and to their chromatographic behavior on silica gel TLC plates [3]. The presence of hydroxyl groups at various positions in the ceramide molecule can be utilized to separate the species into groups of compounds with structural homology [3,4].

Separation of Ceramides into Groups with Respect to the Position and Number of Hydroxyl Groups

A systematic study by Karlsson and Pascher showed the thin-layer chromatographic behavior of ceramides species [3]. In that study, separation of molecular species onto silica gel plates was made possible according to the number and position of hydroxyls on ceramides by using chloroform-methanol, 95:5 (v/v), as the solvent system. The procedure was applied to separate ceramides of sphingomyelin isolated from bovine kidney and intestine for further analysis of their trimethylsilyl derivatives by gas chromatography-mass spectrometry (GC-MS) [5]. Separation of ceramide species according to the position and number of hydroxyl groups was also efficiently achieved by Motta et al. using chloroform-methanol-acetic acid, 190:9:1 (v/v) [4]. These authors proposed a designation of free ceramides based on the number and positions of hydroxyl groups in the ceramide molecule (Fig. 1). The migration rate of the molecule will be lowered by the presence of hydroxyl groups. This is due to enhanced interactions between the molecule and the silica gel, because hydrogen-bonding can occur between the hydroxyls of ceramide and silanols. Thus, ceramides containing phytosphingosine, a sphingoid base with three hydroxyl groups, linked to hydroxy fatty acids will have a lower R_f than ceramide containing sphingosine, a dihydroxy long-chain base, linked to a normal nonhydroxy fatty acid [3-7]. Such a separation of ceramide species into defined groups of relative structural homology can be obtained on silica gel plates when using solvent systems consisting of chloroform and methanol mixtures ranging from 50:2 to 50:5 by volume [7].

When the proportion of methanol is enhanced, free ceramides will tend to migrate close to the solvent front line, making the separation from other neutral lipids difficult, particularly with free fatty acids and cholesterol, which tend to tail in these solvent systems as compared to other neutral lipids. This

Encyclopedia of Chromatography
DOI: 10.1081/E-Echr 120004613

Copyright © 2002 by Marcel Dekker, Inc. All rights reserved.



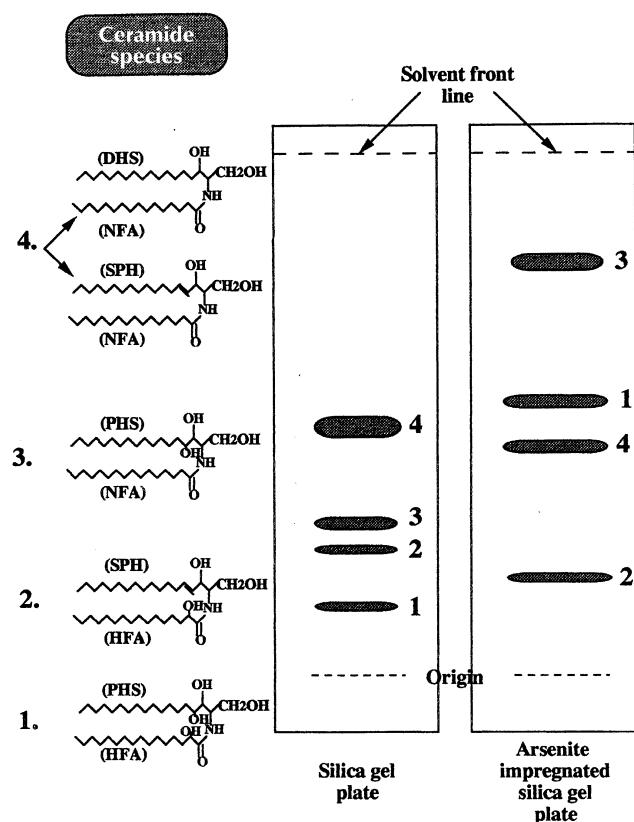


Fig. 1 Schematic representation of ceramide species separation into groups differing in position and number of hydroxyls, after migration onto silica gel or onto an arsenite-impregnated silica gel TLC plate. The plate is developed in chloroform–methanol 50:3.5, (v/v) as the solvent system. The ceramide structure is shown and the numbers refer to those reported close to the ceramide spot on the TLC plates. NFA: normal (nonhydroxy) fatty acid; HFA: hydroxy fatty acid; DHS: dihydrosphingosine; SPH: sphingosine; PHS: phytosphingosine.

problem can be minimized with prior purification of ceramide fraction by liquid chromatography or preparative TLC. Moreover, with the higher proportion of methanol in chloroform, some groups of ceramide species will tend to overlap. This is particularly true with ceramides containing three hydroxyl groups, such as ceramides containing sphingosine linked to hydroxy fatty acids and ceramides containing phytosphingosine linked to nonhydroxy fatty acids. With a greater proportion of methanol in chloroform (5 volumes of methanol to 50 volumes of chloroform), these last species will mix together, whereas if the methanol proportion in chloroform is lowered (2 volumes of methanol to 50 volumes of chloro-

Ceramides: Analysis by Thin-Layer Chromatography

form), these two homologous ceramide groups will be efficiently resolved from each other [6].

Little attention has been given to the possible overlapping of some of the separated ceramide groups with monoacylglycerols. In the solvent systems previously mentioned, these latter migrate very close to free ceramides, particularly ceramide containing phytosphingosine linked to normal fatty acids. Although their acyl or alkenyl bond can be removed easily by chemical treatment (alkaline methanolysis and mild acidic hydrolysis), this is not the case if the fatty acid is bound with an ether linkage. One way to prevent such a possible contamination of ceramide spots by monoacylglycerols is to further separate these glycerolipids from ceramides in a second direction perpendicular to the direction followed by the first solvent system.

Better separation of molecules will, indeed, be obtained with multidimensional TLC, because it allows the use of different solvent systems in each direction, so that the resolution of molecules which can overlap each other in one of the solvent systems can be achieved in the second one. This can be done by running the plate in diethyl ether, as monoacylglycerols will tend to migrate in this solvent, whereas ceramides do it poorly. In fact, the resolution of monoacylglycerols from free-ceramide group species can be obtained by a single run of the silica gel plate in chloroform–methanol 50:3.5 (v/v) [7]. This solvent mixture was shown to be optimal for the resolution of monoacylglycerols from ceramides while giving a good separation of ceramide species into groups of homologous compounds. Multidimensional TLC allows the separation of these compounds while preserving the other neutral lipids of interest whose structures can be altered by chemical treatment.

Effect of Carbon Chain Length and Unsaturation

Ceramide species do not only differ by the position and the number of their constituting hydroxyl groups. The carbon chain length and the degree of unsaturation of the sphingoid bases and fatty acids may also affect the chromatographic behavior of ceramides. It has been shown that on silica gel plates, an increase in unsaturation of the fatty acid constituting the ceramide will result in a slight increase in mobility [3]. Conversely, the presence of a 4-5 *trans* double bond in the sphingoid base does not seem to alter the migration of ceramides on a silica gel plate. Hence, ceramides containing sphinganine (dihydrosphingosine) instead of sphingosine linked to normal fatty acids will tend to migrate as

a unique spot under the solvent conditions previously cited. The ceramide spot number 2 (see Fig. 1) will be a mixture of ceramides containing sphinganine or sphingosine linked to normal fatty acids.

The chain length of the amide-linked fatty acid must also be considered. This was studied by Karlsson and Pascher, who compared the chromatographic behavior of synthetic ceramides with increasing fatty acid chain length [3]. The general feature is that, with increasing the fatty acid chain length, the ceramides migrate faster. Motta et al. reported the separation of ceramides containing phytosphingosine linked to C₂₄–C₂₆ fatty acids from ceramides with phytosphingosine linked to shorter fatty acids ranging from C₁₆ to C₁₈ [4]. They also succeeded in separating ceramides containing phytosphingosine and alpha-hydroxy fatty acids into two groups according to the chain length of fatty acids. This was possible along with a good resolution of ceramides according to the position and the number of hydroxyl groups [4].

Resolution of Ceramide Group Species onto Arsenite-Impregnated Silica Gel TLC Plates

Separation of ceramides into group species is also possible after impregnation of the silica gel layer with sodium arsenite. This glycol-complexing agent can be added directly into the silica gel mixture when preparing the TLC layer [3] or by spraying a solution of 1% sodium *meta* arsenite in methanol (w/v) onto precoated silica gel plates. Karlsson and Pascher recommended the use of arsenite-impregnated TLC plates for the separation of ceramides because of the better resolution than that which was obtained with plain silica gel plates [3]. When the arsenite-impregnated layer is used, ceramides are also separated according to the number and positions of hydroxyl groups. This separation is efficient using the system chloroform–methanol 95:5 (v/v) as the solvent. However, the chromatographic behavior of ceramide species is different on arsenite-impregnated layers as compared to plain silica gel. Hence, on arsenite silica gel layers, ceramides containing the trihydroxy base phytosphingosine migrate with a higher *R_f* than ceramides containing dihydroxy bases such as sphingosine and sphinganine linked to nonhydroxy fatty acids. This is not the case with plain silica gel, as shown in Fig. 1. The effect of a long-chain-base unsaturation is negligible when running ceramide mixtures on arsenite silica gel TLC. Hence, homologous ceramides containing either sphinganine or sphingosine will be mixed together at the end of migration.

The use of silica gel TLC plates (impregnated or not with arsenite) allows the separation of ceramide species into different groups of relative structural homology. This is based on the position and numbers of hydroxyl groups on the ceramide molecules. However, TLC allows a possible further fractionation of ceramide species according to the unsaturation of sphingoid bases or fatty acids. This is made possible by the impregnation of the silica gel plates with borate and silver nitrate.

Separation of Ceramides Species on Borate and Silver Nitrate TLC Plates

Ordinary silica gel TLC plates can be impregnated with sodium borate for the separation of ceramides. This is particularly suitable for the separation of ceramides containing saturated sphingoid base (sphinganine) from ceramide containing monounsaturated sphingoid base, such as sphingosine [3]. Resolution of such ceramide species is not really possible on ordinary or arsenite-impregnated silica gel plates. Boration of the TLC plate can circumvent such a challenge, because resolution of ceramides according to the presence or not of the sphingoid 4-5 *trans* double bond is efficiently achieved [3]. Moreover, the effect of borate as a complexing agent on fatty acid unsaturation was shown not to be significant, so that groups of ceramides could be separated with respect to the unsaturation of their sphingoid bases but not to the unsaturation of the N-linked fatty acids. This chromatographic tool has been used to study the bioconversion of dihydroceramide to ceramide [8].

The separation of ceramide species according to fatty acid unsaturation is, however, possible by using silver-ion-containing silica layers. In such conditions, ceramide species will migrate faster when decreasing the fatty acid unsaturation degree. Moreover, the degree of unsaturation of the sphingoid base is of significant importance, because the *R_f* of ceramide species will decrease by increasing the unsaturation of the sphingoid base. This can result in difficulties for the accurate separation and identification of some ceramide species differing in unsaturation of sphingoid bases or fatty acids [3]. Although such a separation of ceramide molecular species is possible, it is, in fact, seldom used. When a detailed analysis is needed, TLC shows its limits, as other analytical tools give more information. Gas chromatography or HPLC, either alone or coupled with mass spectrometry, are the best tools for the determination of ceramide molecular



species. However, TLC represents a reliable chromatographic technique which can be efficiently used for ceramide separation and purification into groups of compounds of relative structural homology. This is often based on the presence of different hydroxyl groups at different locations of the ceramide molecules. The separation scheme can be efficiently performed by running ceramide samples in a single direction on ordinary silica gel or arsenite-impregnated silica gel TLC plates. Potentiation of this separation scheme could be accomplished by running the plate in a second direction, perpendicular to the first one, after boration of the migration field so that further separation of sphinganine-containing ceramides from sphingosine-containing ceramides can simultaneously be achieved with the separation of groups with different hydroxyls. Such preparative and analytical use makes TLC an interesting tool for the investigation of ceramide biochemistry.

Ceramides: Analysis by Thin-Layer Chromatography

References

1. H. Kalasz and M. Bathori, *LC-GC Int.* 440 (1997).
2. D. K. Perry and Y. A. Hannun, *Biochim. Biophys. Acta* 1436:233 (1998).
3. K. A. Karlsson and I. Pascher, *J. Lipid Res.* 12:466 (1971).
4. S. Motta, M. Monti, S. Sesana, R. Caputo, S. Carelli, and R. Ghidoni, *Biochim. Biophys. Acta* 1182:147 (1993).
5. M. E. Breimer, K. A. Karlsson, and B. E. Samuelsson, *Lipids* 10:17 (1974).
6. J. Bodennec, G. Brichon, O. Koul, M. El Babili, and G. Zwingelstein, *J. Lipid Res.* 38:1702 (1997).
7. J. Bodennec, G. Brichon, J. Portoukalian, and G. Zwingelstein, *J. Liquid Chromatogr. Related Technol.* 22:1493 (1999).
8. L. Geeraert, G. P. Mannaerts, and P. P. Van Veldoven, *Biochem. J.* 327:125 (1997).



Channeling and Column Voids

Eileen Kennedy

Novartis Crop Protection, Inc., Greensboro, North Carolina, U.S.A.

Introduction

Channeling can occur when voids that are created in the packing material of a column cause the mobile phase and accompanying solutes to move more rapidly than the average flow velocity. The most common result of channeling is band broadening and, occasionally, elution of peak doublets.

Discussion

Column voids can develop in a poorly packed column from settling of the packing material or by erosion of the packed bed. In a properly packed column, voids can develop gradually over time or suddenly as the result of pressure surges. A void that forms in the inlet of a column may lead to poor peak shape, including severe band tailing, band fronting, or even peak doubling for every peak in the chromatogram. Filling the column inlet with the same or equivalent column packing can sometimes reduce voids. For this type of repair, the column should be held in a vertical position while the inlet frit is removed. The void will be evident as either settling of the packing material or as holes in the column surface. The new pack-

ing should be slurried with an appropriate mobile phase and packed into the column void with a flat spatula. Once the top of the new packing is level with the column end, a new inlet frit can be added and the end fitting reinstalled. The column should then be reconnected to the LC system and conditioned with the mobile phase at a fairly high flow rate to help settle the new column bed. After filling the void, the packing bed will generally be more stable if the repaired column is operated with the direction of flow reversed from the original direction. This repair procedure can be used to extend column life; however, it should be noted that the plate number of the repaired column would be, at best, only 80–90% of the original column. Columns that develop voids over time are often near the end of their useful life spans and in some cases it may be more cost efficient to discard such a column rather than to repair it.

Suggested Further Reading

- Dolan, J. W. and L. R. Snyder, *Troubleshooting LC Systems*, Humana Press, Totowa, NJ, 1989.
- Majors, R. E., The care and feeding of modern HPLC columns, *LC-GC* 16:900 (1998).



Characterization of Metalloproteins Using Capillary Electrophoresis

Mark P. Richards

Growth Biology Laboratory, USDA-ARS-ANRI, Beltsville, Maryland, U.S.A.

Introduction

Metalloproteins constitute a distinct subclass of proteins that are characterized by the presence of single or multiple metal ions bound to the protein by interactions with nitrogen, sulfur, or oxygen atoms of available amino acid residues or are complexed by prosthetic groups, such as heme, that are covalently linked to the protein. These metals function either as catalysts for chemical reactions or as stabilizers of the protein tertiary structure. Protein-bound metals may also be labile and, as such, be subject to transport, transient storage, and donation to other molecular sites of requirement within tissues and cells.

Background Information

Metalloproteins play critical roles in a wide variety of basic cellular functions, including respiration, gene expression, reproduction, and metabolism. Isolation, characterization, and quantification of individual metalloproteins are each necessary and important steps toward understanding their unique biological functions. Alone or in combination, various types of chromatography, electrophoresis, and spectrometric techniques have been employed to study many unique aspects of metalloprotein structure and function. However, no one technique currently offers the ability to isolate, characterize, and quantify individual metalloproteins in a single step from complex matrices such as tissue extracts or physiological fluids. Therefore, there is an ongoing need for new and more capable methodologies. Because of the small-sample volume requirement, high degree of resolution, and advanced instrument automation capabilities, capillary electrophoresis (CE) has gained increasing popularity in the analysis of proteins [1,2]. In fact, many of the CE-based techniques developed for general protein separations are directly applicable to metalloprotein analyses [2,3]. This article will emphasize some recent applications of CE and CE-related methodologies and their utility in providing new insight into the structure and function of a variety of metalloproteins.

Table 1 summarizes some of the ways CE has been applied to metalloprotein characterization. Altering capillary temperature, buffer ionic strength and pH, electric field strength (i.e., voltage), and capillary internal surface coating are but a few of the ways that CE conditions can be varied to influence the efficiency and selectivity of metalloprotein separations. Furthermore, different CE separation modes can be applied to gain new information about a specific metalloprotein [3]. For instance, capillary zone electrophoresis (CZE) can indicate a protein's net charge at a given pH; capillary isoelectric focusing (CIEF) gives a rapid estimate of its isoelectric point (pI); capillary gel electrophoresis (CGE), in the presence of sodium dodecyl sulfate (SDS), can be used to estimate its apparent molecular mass; and micellar electrokinetic capillary chromatography (MEKC) can be useful in characterizing its surface hydrophobicity.

Procedures

Varying CE separation conditions has been shown to be a particularly effective approach for improving the isolation and characterization of metallothioneins, a heterogeneous family of low-molecular-weight, cysteine-rich, heavy-metal-binding proteins [4]. It was found that (a) phosphate and borate buffers enhanced the sensitivity of detection at 200 nm by significantly reducing ultraviolet (UV) absorption of the background electrolyte, (b) the alkaline borate buffer (pH 8.4) gave rapid analysis times with reasonably high resolution, (c) the acidic phosphate buffer (pH 2.5) completely stripped zinc and cadmium from the proteins, yielding higher resolution and more reproducible separations of the apothioneins (metal-free proteins), (d) capillaries coated on their inner surface with a polyamine polymer that reversed electro-osmotic flow (EOF) or polyacrylamide that greatly suppressed EOF significantly improved resolution, (e) the MEKC mode of CE improved separation selectivity, and (f) photodiode array scanning detection to monitor UV absorption spectra of individual protein peaks separated at



Table 1 Characterization of Metalloproteins Using Capillary Electrophoresis

Identification and Purity Assessments
General characteristics (i.e., net charge, molecular weight, isoelectric point, etc.)
Monitoring purification steps
Separation of impurities or degradation products
Detection of unique UV/visible absorbance (chromophore)
Structural Information
Separation of molecular forms (i.e., isoforms, metalloforms, glycoforms, etc.)
Study of macromolecular assembly
Determination of metal-binding sites
Peptide mapping
Stability Determinations
Effects of temperature and pH
Buffer additives (i.e., metals and metal chelators)
Activity Measurements
Enzymatic activity
Electrophoretically mediated microassay (EMMA)
Isozyme profiling
Metal-Binding/Electrophoretic Mobility Shift
Affinity CE (ACE)
Immobilized metal-ion affinity CE (IMACE)
Metal-chelate coated capillaries
REDOX
oxidation state of protein-bound metal
Elemental Analyses
Indirect Detection Methods
Unique UV/visible absorbance spectra (chromophore)
Mass spectrometry (CE-MS)
Direct (Element-Specific) Detection Methods
Inductively coupled plasma–mass spectrometry (CE–ICP–MS)
Proton-induced x-ray emission (PIXE)

neutral pH was useful in determining both the presence and the type of metal associated with each.

Capillary electrophoresis is a useful tool for monitoring the purity of metalloproteins isolated from either natural or recombinant sources [3]. CZE was used to follow the purification progress of metallothioneins in samples subjected to gel filtration chromatography and reversed-phase high-performance liquid chromatography (HPLC) [3,4]. Detection of a unique chromophore arising from the interaction of metal ions and specific amino acid residues in the protein or with a prosthetic group attached to the protein can be useful. The selectivity achieved under such conditions can greatly reduce or even eliminate the need to purify metalloproteins prior to their analysis by CE. Two good examples of this are the detection of hemoglobin variants separated from red blood cell lysates by monitoring absorbance at 415 nm and the detection of transferrin in serum at 460 nm [3]. Absorbance at these characteristic wavelengths reflects the pres-

ence of iron atoms complexed by the heme moiety (hemoglobin) or by iron-binding sites located at the amino and carboxyl ends of the transferrin protein molecule. CE has also been used to characterize surface metal-binding sites on cytochrome-*c* and myoglobin modified with ruthenium-bis(bipyridine)imidazole, which imparts a strong absorbance at 292 nm to the modified proteins or peptides derived from a tryptic digest of the modified proteins [3].

Capillary electrophoresis has proven to be useful in characterizing different molecular forms of various metalloproteins like metallothionein, transferrin, and conalbumin [2–5]. Molecular forms arise from differences in the amino acid sequence of proteins (isoforms), differences in the amount or type of metal bound (metalloforms), or from differences in the type and amount of carbohydrate side chains linked to the protein (glycoforms). CZE was used to follow the formation of the oligomeric iron core and its incorpora-

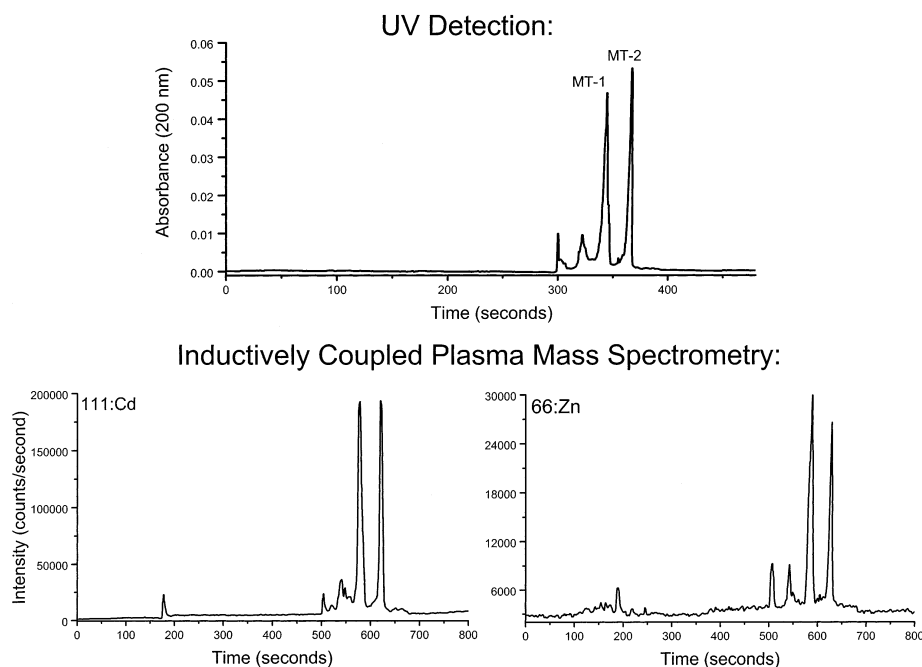


Fig. 1 Separation of rabbit liver metallothionein using CE-ICP-MS. The protein sample (1 mg/mL dissolved in deionized water) was first subjected to CZE with UV detection to optimize CE separation parameters for the major metallothionein isoforms (MT-1 and MT-2) shown in the upper panel. The CE instrument was then coupled to an ICP-MS instrument using a specially modified direct injection nebulizer (CETAC Technologies Inc., Omaha, NB) which enabled the entire capillary effluent from the CE to be directly injected into the ICP plasma torch, thus avoiding postcolumn dilution and band-broadening effects of conventional spray chamber nebulizers. Specific isotopes of cadmium (^{111}Cd) and zinc (^{66}Zn) associated with each isoform peak were monitored as shown by the figures in the lower panel.

tion into ferritin, to detect and quantify ferritin species or ferritin subunit proteins in purified or partially purified states, and to study the interaction of different metal ions with ferritin [2,3].

Structural stability of metalloproteins can be quickly assessed by CE under different conditions [2,3]. For example, thermally induced conformational changes in calcium-depleted α -lactalbumin and urea-induced unfolding of serum albumin were studied using CZE. The oxidation state of cysteine sulfhydryl groups in the zinc-containing protein, ribonuclease A, has been assessed using CZE to determine the presence or absence of a disulfide bond. Elevated capillary temperature altered the structure of myoglobin, which, in turn, resulted in reduction of the valence state of the iron atom bound to heme associated with this protein. Similarly, CIEF was used to separate and characterize different heme-iron valence hybrids of hemoglobin [6].

Buffer additives, especially metals and metal chelators, can have dramatic effects on CE-based separations of metalloproteins by causing shifts in their elec-

trophoretic mobility [3]. This observation forms the basis for a unique CE method referred to as affinity capillary electrophoresis or ACE. When a protein forms a complex with a charged metal-ion ligand, there can be a resulting change in electrophoretic mobility of the complexed protein relative to that of the metal-free protein. Scatchard analysis of the change in electrophoretic mobility of the protein as a function of the metal ion concentration in the separation buffer allows for the calculation of a metal-binding constant (K_b). ACE has been used to characterize K_b values for several metalloproteins, including (a) calcium affinity for calmodulin and C-reactive protein [3] and (b) the binding affinity of zinc for two separate sites in a highly basic, zinc-finger protein (NCp7) from the human immunodeficiency virus [7]. Haupt et al. [8] reported the development of an alternative CE affinity method based on immobilized metal affinity chromatography, which they called immobilized metal-ion affinity capillary electrophoresis or IMACE. In IMACE, metal ions (e.g., Cu^{2+}) are fixed to a soluble polyethylene glycol replaceable polymer matrix support added to the



CE separation buffer. IMACE was used to study surface-related affinity characteristics (number and accessibility of histidine residues and histidine microenvironment) for particular immobilized metal-ion chelate ligands in such proteins as cytochrome-*c*, ribonucleases A and B, chymotrypsin, and kallikrein [8].

Some of the most promising advances in our understanding of unique characteristics of metalloprotein structure and function come from continuing developments in detection methodologies and from further development and refinement of coupled (hyphenated) systems such as CE-mass spectrometry (CE-MS) and CE-inductively coupled plasma-mass spectrometry (CE-ICP-MS). The major difficulties restraining the routine use of such systems, aside from cost, arise from problems in interfacing the CE instrument with MS and ICP-MS instrumentation, although much progress is being made in this area [9]. CE-MS has been used to characterize metallothionein isoforms and metalloforms, the structures of which were deduced from discrete differences detected in molecular mass of the species separated by CE [10]. Using molecular masses calculated from the amino acid sequence and the type and amount of associated metals, it was possible to unequivocally identify distinct molecular forms.

The most definitive assessment of the metal composition of metalloproteins comes from the application of element-specific detection methods. CE-ICP-MS provides information not only about the type and quantity of individual metals bound to the proteins but also about the isotopes of each element as well [11,12]. Elemental speciation has become increasingly important to the areas of toxicology and environmental chemistry. Such analytical capability also opens up important possibilities for trace element metabolism studies. Figure 1 depicts the separation of rabbit liver metallothionein containing zinc, copper, and cadmium (the predominant metal) using CE-ICP-MS with a high-sensitivity, direct injection nebulizer (DIN) interface. UV detection (200 nm) was used to monitor the efficiency of the CE separation of the protein isoforms (MT-1 and MT-2), whereas ICP-MS detection made it possible to detect and quantify specific zinc, copper (not shown), and cadmium isotopes associated with the individual isoform peaks.

There are a number of emerging CE-based techniques that will greatly benefit the field of metallopro-

tein analysis in the near future. Major advances in interfacing instrumentation that will result in more efficient separations and more sensitive detection in coupled systems, especially for CE-MS and CE-ICP-MS, are occurring now [9]. Further development of capillary electrochromatography (CEC), new column packing materials, and commercial systems that allow for gradient elution CEC will have a major impact on improving CE separations of metalloproteins. Moreover, coupling CEC to MS or ICP-MS detectors will offer new and more powerful ways to isolate and characterize metalloproteins. The ability to accurately detect and quantify elemental isotopes offers the promise of being able to conduct isotope dilution experiments involving human and animal subjects in which metal metabolism will be studied and the molecular (metalloprotein) level. Finally, the push toward miniaturization of CE instrumentation (CE on a chip) will find increasing application in the analysis of metalloproteins. This will be especially true in clinical/diagnostic laboratories, where sample size may be severely limited.

References

1. J. P. Landers (ed.), *Handbook of Capillary Electrophoresis*, 2nd ed., CRC Press, Boca Raton, FL, 1997.
2. T. Wehr, R. Rodriguez-Diaz, and M. Zhu, *Capillary Electrophoresis of Proteins* (J. Cazes, ed.), Chromatographic Science Series Vol. 80, Marcel Dekker, Inc., New York, 1999.
3. M. P. Richards and J. H. Beattie, *J. Capillary Electrophoresis* 1:196 (1994).
4. M. P. Richards and J. H. Beattie, *J. Chromatogr. B* 669:27 (1995).
5. M. P. Richards and T.-L. Huang, *J. Chromatogr. B* 690:43 (1997).
6. M. L. Shih and W. D. Korte, *Anal. Biochem.* 238:137 (1996).
7. T. Guszczynski and T. D. Copeland, *Anal. Biochem.* 260:212 (1998).
8. K. Haupt, F. Roy, and M. A. Vijayalakshmi, *Anal. Biochem.* 234:149 (1996).
9. K. L. Sutton and J. A. Caruso, *LC-GC* 17:36 (1999).
10. C. B. Knudsen, I. Bjornsdottir, O. Jons, and S. H. Hansen, *Anal. Biochem.* 265:167 (1998).
11. Q. Lu, S. M. Bird, and R. M. Barnes, *Anal. Chem.* 67:2949 (1995).
12. B. Michalke and P. Schramel, *J. Chromatogr. A* 750:51 (1996).



Chelating Sorbents for Affinity Chromatography (IMAC)

Radovan Hynek

Anna Kozak

Jirí Sajdok

Jan Káš

Department of Biochemistry and Microbiology, Institute of Chemical Technology, Prague, Czech Republic

Introduction

Immobilized metal-ion affinity chromatography (IMAC) is a collective term that includes all kinds of affinity chromatography, where metal atoms or ions immobilized on polymer cause or dominate the interaction at the sorption site.

Discussion

Metal-chelate affinity chromatography was introduced as a specific method for fractionation of proteins by Porath et al. in 1975 [1]. The principle of this type of chromatographic method is that certain amino acid residues, such as histidine, cysteine, lysine, tryptophan, aspartic acid, glutamic acid, or phosphorylated amino acids, which are accessible on the protein surface, can interact through nonbonding lone-pair electron coordination with some metal ions. Metal cations Cu^{2+} , Ni^{2+} , Zn^{2+} , Co^{2+} , Fe^{3+} , Al^{3+} , and Cr^{3+} , which have been chelated to ligands immobilized on support material, have already been used for such specific interactions [2,3]. The most widely used chelating ligands for the isolation of proteins are iminodiacetic acid (IDA) and its analogs, such as tricarboxyethylenediamine (TED). IDA is covalently coupled to an insoluble matrix (e.g., agarose or Sepharose) and forms stable coordinate compounds with a variety of divalent metal ions. These chelates create bases for the above-mentioned specific adsorption. Elution of adsorbed solutes from immobilized metal-ion affinity adsorbents can be provided by changing the pH of the elution buffer or by a specific competing solute, such as histidine, imidazole, or sodium phosphate, depending on the interaction types involved.

Ligands coupled to agarose gels were commonly used at the beginning of IMAC application; however, these sorbents were not suitable for high-performance liquid chromatography (HPLC). Then, Small et al. [4]

used a silica-based matrix and demonstrated that such IMA sorbents can be used in HPLC techniques. The metal-chelate adsorbent “TSK gel chelate-5PW,” suitable for HPLC, which was prepared by coupling IDA to a hydrophilic resin-based matrix (TSK gel G 5000 PW), later became commercially available (Fig. 1).

Since the introduction of metal-ion affinity sorbents for the fractionation of proteins [1], the method became popular for the purification of a wide variety of biomolecules. Metal-ion affinity sorbents are also widely used for the immobilization of enzymes. At present, IMAC is a powerful method for separation of phosphorylated macromolecules, particularly proteins and peptides. The significance of techniques for separation and characterization of phosphorylated biomolecules is now increasing, because phosphorylation modulates enzyme activities and mediates cell membrane permeability, molecular transport, and secretion. Phosphorylated peptides can be separated from a peptide mixture on IDA-Sepharose with Fe^{3+} ions (Fig. 2). The majority of peptides pass freely through an IMAC column, whereas acidic peptides, including phosphorylated ones, are retained and can be released by a pH gradient.

Acidic peptides are released in the pH range 5.5–6.2 and phosphorylated peptides are eluted in the pH range 6.9–7.5 [5]. Elution of retained peptides can also be performed with sodium phosphate. IMAC has been

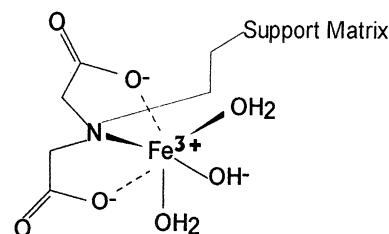


Fig. 1 Complex of water with IDA- Fe^{3+} .

Encyclopedia of Chromatography

DOI: 10.1081/E-Echr 120004616

Copyright © 2002 by Marcel Dekker, Inc. All rights reserved.



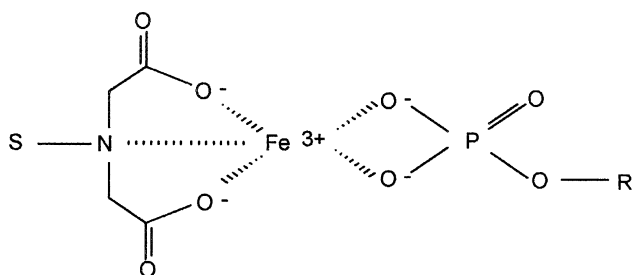


Fig. 2 Interaction of phosphate group with Fe^{3+} ion on IDA-Sepharese.

successfully used for the characterization of casein phosphopeptides in cheese extracts [6]. Phosphoproteins can be separated under very similar conditions as phosphopeptides. IMA sorbents were already used for fractionation of proteins according to the number of phosphate groups contained in their molecules.

Separations of biomolecules on IMA sorbents achieved significant advances in the past few years, but

detailed analyses of the mechanism of adsorption of molecules should be completed. Various factors, such as support matrix, chelating ligands, buffer composition, temperature, and so forth should be investigated in order to optimize analysis on metal-chelate ion affinity sorbents.

References

1. J. Porath, J. Carlsson, I. Olson, and G. Belfrage, *Nature* 258:598 (1975).
2. E. Sulkowski, *Trends Biotechnol.* 3:1 (1985).
3. E. S. Hemdan, Y. J. Zhao, E. Sulkowski, and J. Porath, *Proc. Natl. Acad. Sci. USA* 86:1811 (1989).
4. D. A. P. Small, T. Atkinson, and C. R. Lowe, in *Affinity Chromatography and Biological Recognition* (I. M. Chaiken, M. Wilchek, and I. Parikh, eds.), Academic Press, New York, 1983, p. 267.
5. G. Muszynska, G. Dobrorowolska, A. Medin, P. Ekman, and J. O. Porath, *J. Chromatogr.* 604:19 (1992).
6. R. Hynek, A. Kozak, V. Dráb, J. Sajdok, and J. Kás, *Adv. Food Sci. (CMTL)* 21(5/6):192 (1999).



Chemometrics in Chromatography

Tibor Cserhádi

Esther Forgács

Hungarian Academy of Sciences, Budapest, Hungary

INTRODUCTION

During the last few decades, one of the major advances in chromatography has been the development and commercialization of automated chromatographic instruments. The output of retention data per unit of time has been considerably increased, and the evaluation of large data matrices, containing large amounts of chromatographic information (i.e., retention parameters of a homologous or nonhomologous series of solutes, measured on various stationary and mobile phases), is no longer possible without the application of high-speed computers and a wide variety of chemometric techniques. These methods allow the simultaneous evaluation of an almost unlimited amount of data, highly facilitating the clarification of both practical and theoretical problems. These chemometric procedures have been extensively employed in chromatography for the identification of the basic factors influencing retention and separation; for the comparison of various stationary and mobile phases; for the assessment of the relationship between molecular structure and retention behavior (quantitative structure–retention relationship, QSRR); for the elucidation of correlations between retention behavior and biological activity; etc. As each chemometric procedure generally highlights only one, or only a few features of the chromatographic problem under analysis, the concurrent application of more than one technique is rather a rule than an exception.

The objectives of this article are the enumeration, brief description, and critical evaluation of the recent results obtained in the application of various chemometric techniques in chromatography, and the comparison of the efficacy of various methods for the quantitative description of a wide variety of chromatographic processes. Fundamentals of chemometrics are discussed to an extent to facilitate the understanding of the principles at the application level.^[1]

CHEMOMETRIC METHODS IN CHROMATOGRAPHY

Linear Regression Analyses

Linear and various multiple linear regression analysis techniques have been developed for the elucidation of the

relationship between one dependent and one or more independent variables.^[2] Because of their simplicity and excellent predictive power, they have been successfully applied in various fields of chromatography, such as gas–liquid (GLC), thin-layer (TLC), and high-performance liquid (HPLC) chromatography.

Linear regression analysis with one independent variable

This simple technique can be employed in the case when the dependence of one parameter (dependent variable, Y) on another parameter (independent variable, X) has to be verified:

$$Y = a + bX \quad (1)$$

The result contains the intercept (a) values, an indicator of the amount of Y when X is equal to zero; slope (b) values measuring the change of Y at unit change of X ; and the regression coefficient (r), an indicator of the extent of fit of equation to the experimental data, which serves for the determination of the significance level of the correlation and for the calculation of the variance of Y explained by X . Because of the restricted number of independent variables, the method found is only limited in applications in chromatography. It has been employed for the calculation of the dependence of the retention of one solute and the temperature of a column in GLC, and the concentration of one component in the mobile phase in TLC and HPLC. Furthermore, it can be used for the comparison of the separation characteristics of two (and no more) chromatographic systems. The $\log k'_o$ values of commercial pesticides, measured on alumina and on octadecyl-coated alumina columns, have been compared with this technique. They have been used for the calculation of the dependence of retention on the number of ethylenoxide groups of oligomeric nonionic surfactants on a porous graphitized carbon column; for the study of the effect of salt and pH on the hydrophobicity parameters of surfactant; for the assessment of the relationship between the retention and the hydrophobic surface area of nonylphenyl ethylene oxide oligomers on a polyethylene-coated zirconia HPLC column; for the determination of congenicity of a set of 2,4-dihydroxythiobenzanilide derivatives by reversed-phase (RP) HPLC; etc.

Linear regression analysis with more than one independent variable (multiple linear regression analysis)

When the relationship between one dependent variable and more than one independent variables has to be calculated, Eq. 1 must be modified accordingly:

$$Y = a + b_1X_1 \dots + b_iX_i \dots + b_kX_k \quad (2)$$

In this instance, the r value is suitable only for the calculation of the variance of Y , explained by the X values; consequently, for the establishment of the significance level of the correlation, the F value has to be calculated and compared with the tabulated data. The path coefficients (normalized slope values) indicate the relative impact of the individual X values independent of their original dimensions. Because of the possibility to include more variables in the equation, the application field of multiple linear regression is more extended than that of simple linear regression analysis. Thus, it has been recently employed for the investigation of the molecular mechanism of separation, for the classification of modern stationary phases, for structure–retention relationship study in HPLC and in GLC, for the elucidation of the correlation between retention and biological activity, and for the study of the retention mechanism in adsorption and RP TLC. The method found further applications in the study of the effect of cyclodextrins and cyclodextrin derivatives on the retention characteristics of a wide variety of bioactive compounds such as steroidal drugs, in the prediction of chromatographic properties of organophosphorous insecticides, and those of polychlorinated biphenyls in GLC.

Stepwise Regression Analysis

Stepwise regression analysis can be also used when the relationship between one dependent variable and more than one independent variables has to be assessed. In the common multiple linear regression analysis, the presence of independent variables exerting no significant influence on the change of dependent variable considerably decreases the significance level of the equation. Stepwise regression analysis automatically eliminates from the selected equation the dependent variables having no significant impact on the dependent variable, thereby increasing the reliability of calculation. The final form of the results of stepwise regression analysis is similar to Eqs. 1 or 2, depending on the number of independent variables selected by the method. Because of its versatility and simplicity, the method has been frequently

used in chromatography. It has found application in the study of the retention behavior of ethylene oxide surfactants and dansylated amino acids in adsorption and RP TLC, in the elucidation of the relative impact of various molecular parameters on the retention in adsorption and RP HPLC and GLC, in the determination of the molecular parameters significantly influencing the interaction of antibiotics with sodium dodecylsulfate measured by TLC, in the evaluation of the stability of pigments of paprika (*Capsicum annuum*) measured by HPLC, and in the determination of the relative impact of HPLC conditions on the retention behavior.

Partial Least Squares Regression (PLS)

When the independent variables are highly interrelated, the application of traditional methods for the calculation of linear regressions may cause biased and unreliable results. PLS has been developed for the prevention of errors originating from such intercorrelations. PLS has not been frequently employed in the analysis of chromatographic retention data; it has been only used in GLC for the study of the retention behavior of oxo compounds, in HPLC for the QSRR of chalcones, and in RP HPLC for the QSRR study of antimicrobial hydrazides.

Free–Wilson and Fujita–Ban Analysis

These special cases of multiple linear regression analysis have been developed for the determination of the impact of individual molecular substructures (independent variables) on one dependent variable. Both techniques are similar; yet, the Free–Wilson method considers the retention of the unsubstituted analyte as base, while Fujita–Ban analysis uses the less substituted molecule as reference. These procedures have not been frequently employed in chromatography; only their application in QSRR studies in RP TLC and HPLC have been reported.

Canonical Correlation Analysis (CCA)

CCA can be considered as a special case of multiple linear regression analysis, when the relationship between minimally more than one dependent variable (matrix I) and minimally more than one independent variable (matrix II) has to be elucidated. CCA calculates the relationships between matrices I and II by extracting theoretical factors which explain the maximum of variance of the matrix with the lower number of variables. However, it can be employed only in the instances when the number of de-

pendent variables is lower than that of independent variables. The maximal number of equations selected by CCA is equal to the number of columns in the smaller set of data. The results consist of the standard and weighted canonical coefficients (they are similar to the b values and path coefficients of Eq. 2), of the r values related to the ratio of variance explained by the equations, and of the X (Greek Chi) value, indicating the fitness of equation to the experimental data. Despite its evident benefits, the technique has not been frequently employed for the analysis of chromatographic data. It has been applied for the elucidation of the relationship between the retention parameters of ring-substituted aniline derivatives determined on various HPLC columns (smaller matrix) and their calculated physicochemical parameters (larger matrix), for the study of the relationship between the physicochemical parameters of steroidal drugs and their retention characteristics in HPLC, and for the assessment of the correlation between the physicochemical parameters of tetrazolium salts and their retention behavior in various TLC systems.

Multivariate Mathematical–Statistical Methods

The prerequisite of the application of the regression analytical methods discussed above is that one or more chromatographic parameters have to be considered as being the dependent variables. However, when the simultaneous relationships among more retention parameters, or more retention parameters and more physicochemical parameters of a given set of analytes have to be elucidated, the linear regression methods cannot be employed. A considerable number of multivariate methods have been developed to overcome the disadvantages of regression analyses.^[3] Various multivariate mathematical–statistical methods have been successfully employed for the elucidation of the relationship between the retention parameters and the structural descriptors of solutes for the comparison of more than two stationary phases, for the prediction of solute retention, for the assessment of the correlation between retention characteristics and biological activity, etc. As the information content of the mathematical–statistical methods considerably depends on the mode of calculation, the character of the problem to be elucidated limits, to some extent, the choice of the method.

Principal Component Analysis (PCA)

PCA can be used when the inherent relationships between the columns and rows of a data matrix have to be de-

termined without one (stepwise regression analysis) or more (CCA) being the selected dependent variables. PCA is a versatile and easy-to-use multivariate mathematical–statistical method. It has been developed to contribute to the extraction of maximal information from large data matrices containing numerous columns and rows. PCA makes possible the elucidation of the relationship between the columns and rows of any data matrix without being one the dependent variable. PCA is a so-called projection method representing the original data in smaller dimensions. It calculates the correlations between the columns of the data matrix and classifies the variables according to the coefficients of correlation. The results of PCA generally contain the so-called eigenvalues which are related to the relative importance of the principal components calculated by PCA, the variance explained by the individual PCs, and the contributions (impacts) of the columns and rows of the original matrix to the principal component loadings and variables, respectively. Unfortunately, PCA does not define the principal components as concrete physical or physicochemical entities; it only indicates its mathematical possibility. Calculating linear regression between the principal component loadings and the chromatographic parameters and physicochemical characteristics may help the determination of the concrete constitution of principal components. Stepwise regression analysis is especially adequate to carry out such types of calculations.

Because of its simplicity, PCA has been frequently used in many fields of up-to-date chromatographic research. Thus, PCA has been employed for the evaluation of molecular lipophilicity, for QSRR studies, for the testing of the authenticity of edible oils, for the determination of the botanical origin of cinnamon, for the differentiation of Spanish white wines, for the characterization of RP supports, for the assessment of the relationship between molecular structure and retention behavior, etc. The method has found further applications in the classification of chili powders according to the distribution of pigments separated by TLC, in the determination of the molecular parameters of peptides and barbituric acid derivatives showing a significant impact on their retention on porous graphitized carbon column, in QSRR study of pesticide retention on polyethylene-coated silica column, in the study of the retention characteristics of titanium dioxide and polyethylene-coated titanium dioxide stationary phases, in the comparison of alumina stationary phases in TLC and HPLC, in the elucidation of the relationship between the retention of environmental pollutants on an alumina HPLC column and their physicochemical parameters, and in the study of the energy of interaction between commercial pesticides and a nonionic surfactant by GLC.

Spectral Mapping Technique (SPM)

The calculation methods discussed above classify the chromatographic systems (stationary and mobile phases) or solute molecules while simultaneously taking into consideration the retention strength and retention selectivity; thus, it cannot be applied when the separation of the strength and selectivity of the effect is required. SPM, another multivariate mathematical–statistical method, overcomes this difficulty.^[4]

The SPM divides the information into two matrices using the logarithm of the data in the original matrix. The first one is a vector containing so-called potency values proportional to the overall effect; that is, it is a quantitative measure of the effect. The second matrix (selectivity map) contains the information related to the spectrum of activity, i.e., the qualitative characteristics of the effect. SPM first calculates the logarithm of the members of the original data matrix, facilitating the evaluation of the final plots in terms of log ratios. Subsequently, SPM subtracts the corresponding column-mean and row-mean from each logarithmic element of the matrix calculating potency values. The source of variation remaining in the centered data set can be evaluated graphically (selectivity map). This elegant and versatile calculation method has been used in chromatography for the characterization of stationary phases in TLC and HPLC, for the separation of the solvent strength and selectivity on a cyclodextrin-coated HPLC column using monoamine oxidase inhibitory drugs as solutes, for the investigation of the complex interaction between anticancer drugs and cyclodextrin derivatives, for the determination of the influence of storage conditions on pigments analyzed by HPLC, for the comparison of polymer-coated HPLC columns, and for the optimization of the microwave-assisted extraction of pigments for HPLC analysis.

Cluster Analysis (CA) and Nonlinear Mapping Technique (NLM)

Although both the PCA and the SPM techniques reduce the number of variables, the resulting matrices of PC loadings and variables and the spectral map are still multidimensional. The plot of PC loadings in the first vs. the second principal component has been frequently used for the evaluation of the similarities and differences among the observations. This method takes into consideration only the variance explained in the first two principal components and entirely ignores the impact of variances explained by the other principal com-

ponents on the distribution of the matrix elements. The use of this approximation is only justified when the first two principal components explain the overwhelming majority of variance, which is not probable in the case of large original data matrices. As the evaluation of the distribution of data points in the multidimensional space is extremely difficult, calculation methods were developed for the reduction of the dimensionality of the matrices to one (CA) or to two (NLM). These methods can also be employed for the reduction of the dimensionality of the original data matrices before any other mathematical–statistical evaluation. CA has been employed for the elucidation of the retention behavior of anti-hypoxia drugs in adsorption TLC, that of barbituric acid derivatives and anti-inflammatory drugs in HPLC, for the classification of pharmaceutical substances according to their retention data, for the prediction of retention of phosphoramidate derivatives, etc.

However, both CA and NLM take into consideration the positive and negative sign of the coefficient of correlation and carry out the calculation accordingly. Therefore, the highly but negatively correlated points are far away on the maps and on the cluster dendograms in the same manner as the points that are not correlated. This procedure leads to correct assumptions in the case when the scientist is interested only in the positive correlations among variables and observations. To evaluate precisely the relationships between the points without taking into consideration the positive or negative character of the correlation, it is advisable to carry out the calculations with the absolute values of PC loadings and variables. The validity of this experimental approximation has been proven in the evaluation of the interaction of nonsteroidal anti-inflammatory drugs with a model protein studied by HPLC, and the parallel application of the original PC loadings and their absolute values in the data reduction techniques has been proposed. This procedure has been successfully used for the study of the effect of carboxymethyl- β -cyclodextrin on the hydrophobicity parameters of steroidal drugs measured by TLC, and for the assessment of the binding characteristics of environmental pollutants to the wheat protein, gliadin, investigated by HPLC.

The distances between the elements on the cluster dendograms and NL maps are a quantitative measure of similarity: Smaller distances indicate greater similarity. However, the fact that the differences among the elements are significant or not cannot be established on the traditional NL map or on the cluster dendogram. A graphical approximation has been developed for the inclusion of standard deviation in the NL maps and cluster



dendograms. The data matrix for PCA has been composed from the main values of the matrix elements, the mean values minus twice their standard deviation, and the mean values plus twice their standard deviation. PCA has been carried out, and the cluster dendograms and NL maps have been calculated. A circle can be formed from the mean values and the mean value \pm two standard deviations on the NL map, the center of the circle being the mean, and the radius of the circle being represented by the mean \pm two standard deviations. It was assumed that the differences between the elements on the map are significant at the 95% significance level when the circles do not overlap. It was further assumed that the mean value and mean value \pm two standard deviations of the matrix elements are close to each other (form a triad) on the cluster dendogram when they significantly differ from the others. The method has been employed for the classification of paprika (*C. annuum*) powders according to their pigment composition as determined by HPLC and for the comparison of HPLC and TLC systems.

Miscellaneous Multivariate Methods

The chemometric methods discussed above have found widespread applications in chromatography, and many theoretical and practical chromatographers have become familiar with these techniques and have applied them successfully. However, other less well-known methods have also found applicability in the analysis of chromatographic retention data. Thus, canonical variate analysis has been applied in pyrolysis GC-MS,^[5] artificial neural network for the prediction of GLC retention indices, and factor analysis for the study of the retention behavior of *N*-benzylideneaniline derivatives.^[6]

CONCLUSIONS

The examples enumerated above prove conclusively that chemometric techniques can be effectively employed for the elucidation of a large number of problems in chromatography, connected with the accurate and precise evaluation of large data matrices.

These methods allow not only the classification and clustering of any set of chromatographic systems but also exact determination of the relationship between the characteristics (physicochemical parameters or molecular substructures) of solutes and their retention behavior. It can be further concluded that chemometry considerably

promotes a more profound understanding of the basic processes underlying chromatographic separations, increasing, in this manner, the efficiency (reliability, rapidity, etc.) of the methods.

REFERENCES

1. Cserhádi, T.; Forgács, E. Use of Multivariate Mathematical Statistical Methods for the Evaluation of Retention Data Matrices. In *Advances in Chromatography*; Brown, P.R., Grushka, E., Eds.; Marcel Dekker, Inc.: New York, 1996; Vol. 36, 1–63.
2. Mager, H. *Moderne Regressionsanalyse*; Salle, Sauerlander: Frankfurt am Main, Germany, 1982.
3. Mardia, K.V.; Kent, J.T.; Bibby, J.M. *Multivariate Analysis*; Academic Press: London, 1979.
4. Levi, P.J. Spectral map analysis. Factorial analysis of contrast, especially from log ratios. *Chemometr. Intell. Lab. Syst.* **1989**, 5, 105–116.
5. Kochanowski, B.K.; Morgan, S.L. Forensic discrimination of automotive paint samples using pyrolysis–gas chromatography–mass spectrometry with multivariate statistics. *J. Chromatogr. Sci.* **2000**, 38, 100–108.
6. Ounnar, S.; Righezza, M.; Chretien, J.R. Factor analysis in normal phase liquid chromatography of *N*-benzylideneanilides. *J. Liq. Chromatogr. Relat. Technol.* **1998**, 20, 2017–2037.

SUGGESTED FURTHER READING

- Acuna-Cueva, R.; Hueso-Urena, F.; Cabeza, N.A.J.; Jimenez-Pulido, S.B.; Moreno-Carretero, M.N.; Martos, J.M.M. Quantitative structure–capillary column gas chromatographic retention time relationships for natural sterols (trimethylsilyl esters) from olive oil. *J. Am. Chem. Soc.* **2000**, 77, 627–630.
- Al-Haj, M.A.; Kaliszan, R.; Nasal, A. Test analytes for studies of the molecular mechanism of chromatographic separations by quantitative structure–retention relationships. *Anal. Chem.* **1999**, 71, 2976–2985.
- Andrisano, V.; Bertucci, C.; Cavrini, V.; Recatini, M.; Cavalli, A.; Veroli, L.; Felix, G.; Wainer, I.W. Stereoselective binding of 2,3-substituted 3-hydroxypropionic acids on an immobilized human serum albumin chiral stationary phase. Stereo-chemical characterisation and quantitative structure–retention relationship study. *J. Chromatogr., A* **2000**, 876, 75–86.
- Dillon, W.R. *Multivariate Analysis*; John Wiley and Sons: New York, 1984; 213–254.
- Geladi, P.; Kowalski, B.R. Partial least-squares regression: A tutorial. *Anal. Chim. Acta* **1986**, 185, 1–17.
- Gozalbes, R.; de Julián-Ortiz, J.; Antón-Fos, G.M.; Galvez-



- Alvarez, J.; Garcia-Domenech, R. Prediction of chromatographic properties of organophosphorous insecticides by molecular connectivity. *Chromatographia* **2000**, *51*, 331–337.
- Hamoir, T.; Cuaste Sanchez, F.; Bourguignon, B.; Massart, D.L. Spectral mapping analysis: A method for the characterization of stationary phases. *J. Chromatogr. Sci.* **1994**, *32*, 488–498.
- Heberger, K.; Gorgenyi, M. Principal component analysis of Kovats indices for carbonyl compounds in capillary gas chromatography. *J. Chromatogr., A* **1999**, *845*, 21–31.
- Ivaniuc, O.; Ivanciuc, T.; Cabrol-Bass, D.; Balaban, A.T.; Com, D.L. Spectral mapping analysis: A method for the comparison of weighting schemes for molecular graph descriptors. Application in quantitative structure–retention relationship models for alkylphenols in gas–liquid chromatography. *J. Chem. Inf. Comput. Sci.* **2000**, *40*, 732–743.
- Jozwiak, K.; Szumilo, H.; Senczyna, B.; Niewiadomy, A. RP-HPLC as a tool for determining the congenericity of a set of 2,4-dihydroxythiobenzanilide derivatives. *Chromatographia* **2000**, *52*, 159–161.
- Kaliszan, R.; van Straaten, M.A.; Markuszewski, M.; Cramers, C.A.; Claessens, H.A. Molecular mechanism of retention in reversed-phase high-performance liquid chromatography and classification of modern stationary phases by using quantitative structure–retention relationships. *J. Chromatogr., A* **1999**, *855*, 455–480.
- Monatana, M.P.; Pappano, N.B.; Debattista, N.B.; Raba, J.; Lucio, J.M. High-performance liquid chromatography of chalcones. Quantitative structure–activity relationship using partial least squares (PLS) modeling. *Chromatographia* **2000**, *51*, 727–735.
- Sammon, J.W., Jr. A nonlinear mapping for data structure analysis. *IEEE Trans. Comput.* **1969**, *C18*, 401–407.

Chiral Chromatography by Subcritical and Supercritical Fluid Chromatography

Gerald J. Terfloth

Research and Development Division, SmithKline Beecham Pharmaceuticals, King of Prussia, Pennsylvania, U.S.A.

Introduction

The intrinsic physical properties of supercritical fluids — increased diffusivity and reduced viscosity — when compared to “normal” liquid phases, make subcritical/supercritical fluid chromatography a very attractive technology when short cycle times are required. Chiral subcritical/supercritical fluid chromatography typically is carried out using packed columns (pSFC) that are frequently identical in mechanical construction to the ones used in traditional high-performance liquid chromatography (HPLC). It should be noted, though, that capillary columns coated or packed with a chiral stationary phase have been used for the separation of racemic mixtures. The direct separation of racemic mixtures by chromatographic means can be effected by using chiral stationary-phase or chiral mobile-phase additives. Both techniques have been used successfully in HPLC and pSFC. The use of chiral pSFC is not limited to analytical applications. The relative ease of solvent removal and recycling, typically carbon dioxide modified with a polar organic solvent such as methanol, makes pSFC a very attractive tool for preparative separations. Equipment for laboratory- and industrial-scale pSFC in traditional discontinuous batch-chromatography mode, as well as in continuous simulated moving-bed (SMB) mode, has been developed and is commercially available. pSFC can be used as an orthogonal method when techniques such as reversed-phase HPLC, capillary electrophoresis, or capillary electrochromatography provide insufficient or ambiguous results.

Characteristics and Advantages of Subcritical and Supercritical Fluids

The advantages of using supercritical mobile phases in chromatography were recognized in the 1950s by Klesper et al. [1], among others. Carbon dioxide is the most frequently used supercritical mobile phase, due to its moderate critical temperature and pressure, almost

complete chemical inertness, safety, and cost. Virtually all published chiral pSFC separations have used carbon dioxide as the primary mobile-phase component. Compared to most commonly used organic solvents, it is environmentally friendly. The reduced viscosity of carbon dioxide-based mobile phases, typically one order of magnitude less than water (0.93 cP at 20°C), allows for efficient chromatography at higher flow rates. In addition, diffusion coefficients of compounds dissolved in supercritical mobile phases are about one order of magnitude larger than in traditional aqueous and organic mobile phases [$D_M(\text{naphthalene})$: $0.97 \times 10^{-4} \text{ cm}^2/\text{s}$ in CO_2 at 25°C, 171 bar, 0.90 g/cm^3]. This directly translates to higher efficiency of the separation due to improved mass transfer.

The first chiral separation using pSFC was published by Caude and co-workers in 1985 [3]. pSFC resembles HPLC. Selectivity in a chromatographic system stems from different interactions of the components of a mixture with the mobile phase and the stationary phase. Characteristics and choice of the stationary phase are described in the method development section. In pSFC, the composition of the mobile phase, especially for chiral separations, is almost always more important than its density for controlling retention and selectivity. Chiral separations are often carried out at $T < T_c$ using liquid-modified carbon dioxide. However, a high linear velocity and a low pressure drop typically associated with supercritical fluids are retained with near-critical liquids. Adjusting pressure and temperature can control the density of the subcritical/supercritical mobile phase. Binary or ternary mobile phases are commonly used. Modifiers, such as alcohols, and additives, such as acids and bases, extend the polarity range available to the practitioner.

A typical pSFC instrument, at first glance, is designed like an HPLC system. The major differences are encountered at the pump, the column oven, and downstream of the column. pSFC is best carried out using pumps in a flow-control mode. A regulator mounted downstream of the column and ultraviolet-visible detector (UV) controls the pressure drop in the chro-

Encyclopedia of Chromatography

DOI: 10.1081/E-Echr 120005218

Copyright © 2002 by Marcel Dekker, Inc. All rights reserved.



matographic system. Detection is not limited to UV. If pure carbon dioxide is used as the mobile phase, an easy-to-use, sensitive, and stable universal detector such as the flame ionization detector (FID) can be employed. Other detection techniques are Fourier-transform infrared (FTIR) and evaporative light-scattering detection (ELSD), or hyphenated techniques such as pSFC–MS (mass spectrometry) and pSFC–NMR (nuclear magnetic resonance). Temperature control of the mobile phase and column is achieved by a column oven allowing for operation under cryogenic conditions and/or from ambient temperature to 150°C.

CSFC, although, resembles gas chromatography (GC) at high pressures, with the pressure (density) programming taking the place of temperature programming used in GC. Typical operating temperatures are up to 100°C.

Method Development

Mechanistic considerations (e.g., the extensive work published on brush-type phases) or the practitioner's experience might help to select a chiral stationary phase (CSP) for initial work. Scouting for the best CSP/mobile phase combination can be automated by using automated solvent and column switching. More than 100 different CSPs have been reported in the literature to date. Stationary phases for chiral pSFC have been prepared from the chiral pool by modifying small molecules, like amino acids or alkaloids, by the derivatization of polymers such as carbohydrates, or by bonding of macrocycles. Also, synthetic selectors such as the brush-type ("Pirkle") phases, helical poly(meth)acrylates, polysiloxanes and polysiloxane copolymers, and chiral selectors physically coated onto graphite surfaces have been used as stationary phases.

Generally accepted starting conditions are summarized in Table 1. Typically, 5–15% of alkanol-modified

carbon dioxide is used as the mobile phase. Depending on the nature of the analyte, acids or bases can be added to the modifier for controlling ionization of the stationary phase and analyte. If partial selectivity is observed after the first injection, it is advisable to first adjust the modifier concentration. If the peak shape is not satisfactory, then the addition of 0.1% trifluoroacetic acid or acetic acid for acidic compounds or 0.1% diethyl amine or triethyl amine for basic compounds to the modifier can bring an improvement. In case the selectivity cannot be improved by the previous measures, decreasing the operating temperature can result in the desired separation. Although many chiral separations improve as the temperature is reduced, this does not occur in all cases. The temperature dependence of the selectivity does not necessarily follow the van't Hoff equation ($\ln \alpha \sim 1/T$), as one might expect, based on experience with other chromatographic techniques. Stringham and Blackwell [7], who have reported several examples of entropically driven separations, studied the effects of temperature in detail. In the temperature range between –10°C, 70°C (T_{iso}), and 190°C, a reversal of elution order for the enantiomers of a chlorophenylamide was observed on a (*S,S*)-Whelk-O 1 chiral stationary phase using 10% ethanol in carbon dioxide, at a pressure of 300 bar. The potential for reversing the elution order can be valuable if just one enantiomer of the CSP affecting the separation is available. If all of the above adjustments should fail, a different CSP should be investigated. Due to the low viscosity of carbon dioxide-based mobile phases, multiple columns can be coupled. This provides the opportunity to increase chemical selectivity for the analysis of complex samples by coupling an initial achiral column with a chiral column. Also, the successful coupling of multiple different chiral columns has been reported.

Applications

Analytical applications of chiral pSFC in chemical and pharmaceutical research, development, and manufacturing comprise the screening of combinatorial libraries, monitoring chemical and biological transformations from the laboratory to the process scale, following stereochemical preferences of drug metabolism and pharmacokinetics, and assessing toxicology and stability of drug substance and dosage form. Preparative applications are of considerable interest because of the relative ease with which the mobile phase can be removed and recycled. This is of particular interest in the pharmaceutical environment, be-

Table 1 Initial Conditions for Chiral Method Development Using Modified Carbon Dioxide as the Mobile Phase

Parameter	Unit	Value
Flow rate	mL/min	2.0
Pressure	bar	200
Temperature	°C	30
Methanol	%	10
Injection volume	μL	5
Sample concentration	mg/mL	1
Detection	Diode array detector, 190–320 nm	



cause a small amount of the desired product can be obtained, almost free of solvent, quite rapidly. Recent advances in automation and separation technology now allow for a predictable scale-up of the separation from a laboratory to a production scale.

References

1. E. Klesper, A. H. Corwin, and D. A. Turner, *J. Org. Chem.* 27:700 (1960).
2. D. R. Gere, *Science* 222:253 (1983).
3. P. A. Mourier, E. Eliot, M. H. Caude, and R. H. Rosset, *Anal. Chem.* 57:2819 (1985).
4. F. J. Ruffing, J. A. Lux, and G. Schomburg, *Chromatographia* 26:19 (1988).
5. K. Anton, J. Eppinger, L. Fredriksen, E. Francotte, T. A. Berger, and W. H. Wilson, *J. Chromatogr.* 666:395 (1994).
6. G. J. Terfloth, W. H. Pirkle, K. G. Lynam, and E. C. Nicolas, *J. Chromatogr.* 705:185 (1995).
7. R. W. Stringham and J. A. Blackwell, *Anal. Chem.* 68:2179 (1996).
8. K. W. Phinney, L. C. Sander, and S. A. Wise, *Anal. Chem.* 70:2331 (1998).

Suggested Further Reading

- Anton, K. and C. Berger, *Supercritical Fluid Chromatography with Packed Columns*, Marcel Dekker, Inc., New York, 1998.
- Berger, T. A., *Packed Column SFC*, The Royal Society of Chemistry, Cambridge, 1995.
- Chester, T. L., J. D. Pinkston, and D. E. Raynie, *Anal. Chem.* 68:487 (1996).



Chiral Countercurrent Chromatography

Ying Ma
Yoichiro Ito

National Heart, Lung, and Blood Institutes, National Institutes of Health, Bethesda, Maryland, U.S.A.

Introduction

Countercurrent chromatography (CCC) can be used for the separation of a variety of enantiomers by adding a chiral selector to the liquid stationary phase [1,2]. The method is free of complications arising from the use of a solid support and also eliminates the procedure of chemically bonding the chiral selector to a solid support as in conventional chiral chromatography.

In the past, various CCC systems, such as droplet CCC, rotation locular CCC (RLCCC), and centrifugal partition chromatography (CPC), have been used for the separation of chiral compounds. None of those techniques, however, is considered satisfactory for preparative purposes in terms of sample size, resolution, and/or separation time. In the early 1980s, the high-speed CCC (HSCCC) technique improved both the partition efficiency and separation time and has been successfully applied to the separation of racemates using a Pirkle-type chiral selector. Both analytical (milligram) and preparative (gram) separations can be performed simply by adjusting the amount of chiral selector in the liquid stationary phase in the standard separation column. A large-scale separation of enantiomers can also be performed by pH-zone-refining CCC, a recently developed preparative CCC technique for the separation of ionized compounds [3]. One of the important advantages of the CCC technique over the conventional chiral chromatography is that the method allows computation of the formation constant of the chiral-selector complex, one of the most important parameters for studies of the mechanism of enantioselectivity [4].

Standard High-Speed CCC Technique in Chiral Separation

The separations are performed using a commercial high-speed CCC centrifuge equipped with a multilayer coil separation column(s). The column is first entirely filled with the stationary phase that contains the desired amount of chiral selector (CS). In order to prevent the contamination of CS in the eluted fractions, some amount of the CS-free stationary phase should

be left at the end of the column, typically at about 10% of the total column capacity. After the sample solution is injected through the sample port, the mobile phase is pumped into the column while the column is rotated. Separation can be carried out by the successive injection of samples without renewing the stationary phase containing the chiral selector in the column.

Figure 1 shows the separation of four pairs of DNB-amino acid enantiomers by the standard CCC technique using a two-phase solvent system composed of hexane-ethyl acetate-methanol-10 mM HCl and *N*-dodecanoyl-L-3,5-dimethylanilide as a CS which is almost entirely partitioned into the organic stationary phase ($K > 100$) due to its high hydrophobicity. All analytes are well resolved in 1–3 h. The CS used in this separation is similar to the chiral stationary phase which has been introduced by Pirkle et al. for the high-performance liquid chromatography (HPLC) separation of racemic DNB-amino acid *t*-butylamide. A hydrophobic *N*-dodecanoyl group is connected to the CS molecule for retaining the CS in the organic stationary phase.

The effect of CS concentration in the stationary phase was investigated [1]. As the CS concentration is increased, the separation factor and peak resolution are also increased [5]. The result clearly indicates an important technical strategy: The best peak resolution is attained by saturating the CS in the stationary phase in a given column, where the resolution is further improved by using a longer and/or wider-bore coiled column, which can hold greater amounts of CS in the stationary phase.

The preparative capability of the present system is demonstrated in the separation of DNB-leucine enantiomers by varying the CS concentration in the stationary phase. The sample loading capacity is found to be determined mainly by the CS concentration or total amount of CS in the stationary phase; that is, the higher the CS concentration in the stationary phase, the greater the peak resolution and sample loading capacity. Consequently, the standard HSCCC column can be used for both analytical and preparative separations simply by adjusting the amount of CS in the stationary phase.



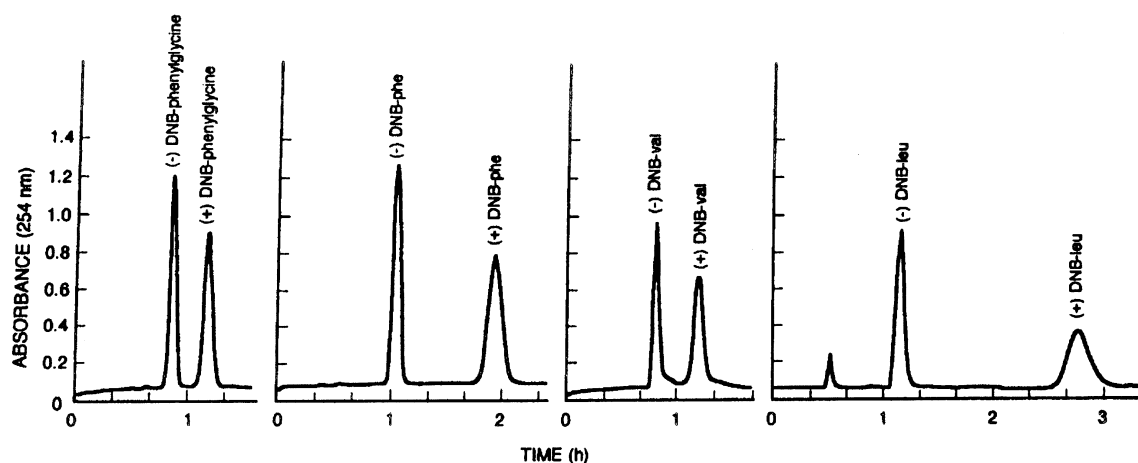


Fig. 1 Separation of four pairs of (\pm)-DNB-amino acids by the standard analytical HSCCC technique with a CS (*N*-dodecanoyl-L-proline-3,5-dimethylanilide) in the stationary phase.

pH-Zone-Refining CCC for Chiral Separation

pH-Zone-refining CCC is a powerful preparative technique that yields a succession of highly concentrated rectangular solute peaks with minimum overlap where impurities are concentrated at the peak boundaries

(see the entry pH Peak Focusing pH-Zone-Refining CCC). This technique was applied to the resolution of DNB-amino acid racemates using a binary two-phase solvent system composed of methyl *t*-butyl ether–water where trifluoroacetic acid (retainer) and CS were added to the organic stationary phase and ammonia

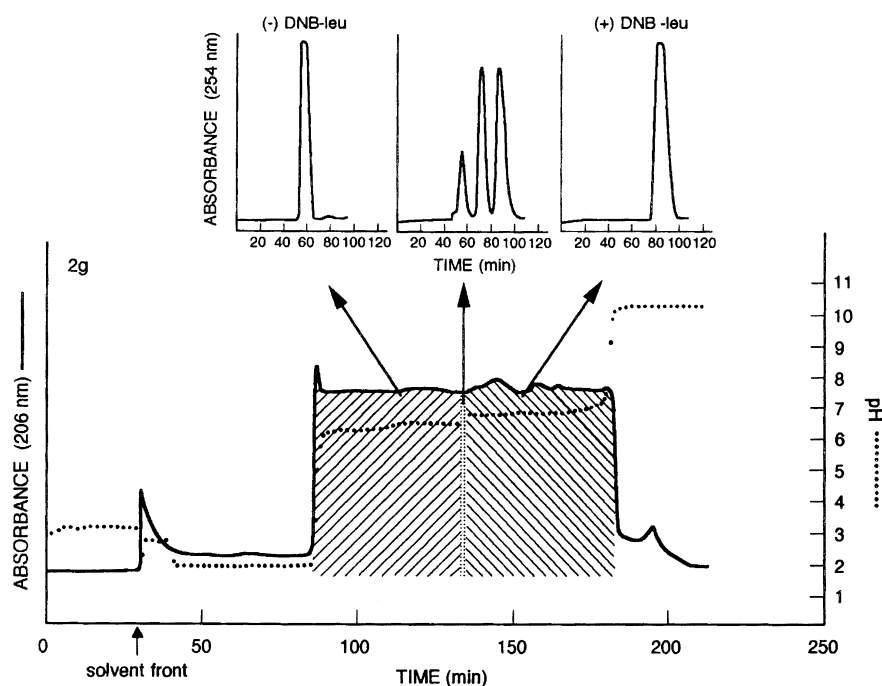


Fig. 2 pH-Zone-refining CCC separation of 2 g (\pm) DNB-leucine using the same HSCCC centrifuge with a CS (*N*-dodecanoyl-L-proline-3,5-dimethylanilide) in the stationary phase.

(eluter) to the aqueous mobile phase. Figure 2 shows a typical chromatogram obtained by pH-zone-refining CCC. The pH of the fraction (dotted line) revealed that the peak was evenly divided into two pH zones, each corresponding to a pure enantiomeric species with a sharp transition. Compared with the standard CCC technique, the pH-zone-refining CCC technique allows separation of large amounts in a shorter elution time.

In both techniques, leakage of the chiral selector into the elute can be completely eliminated by filling the outlet of the column with a proper amount of the CS-free stationary phase so as to absorb the chiral selector leaking into the flowing mobile phase.

Advantages

Countercurrent chromatography can be applied to the separation of enantiomers by adding a suitable chiral selector to the liquid stationary phase by analogy to binding the CS to the solid support in conventional chiral chromatography. The HSCCC technique has the following advantages over the conventional chromatography technique:

1. The method permits repetitive use of the same column for a variety of chiral separations by choosing appropriate CSs.
2. Both analytical and preparative separations can be performed with a standard CCC column by

adjusting the amount of CS in the liquid stationary phase, and the method is cost-effective, especially for large-scale preparative separations.

3. The separation factor and peak resolution can be improved simply by increasing the concentration of CS in the stationary phase.
4. The method is very useful for the investigation of the enantioselectivity of CS including determination of the formation constant and separation factor.
5. pH-Zone-refining CCC can be applied for gram-quantity separation in a short elution time.

References

1. Y. Ma and Y. Ito, Chiral separation by high-speed countercurrent chromatography, *Anal. Chem.* 67:3069 (1995).
2. Y. Ma, Y. Ito, and A. Foucault, Resolution of gram quantities of racemates by high-speed CCC, *J. Chromatogr. A* 704:75 (1995).
3. Y. Ito and Y. Ma, pH-Zone-refining countercurrent chromatography, *J. Chromatogr. A* 753:1 (1996).
4. Y. Ma, Y. Ito, and A. Berthod, A chromatographic method for measuring K_f of enantiomer-chiral selector complexes, *J. Liquid Chromatogr.* 22(19):2945 (1999).
5. Y. Ma and Y. Ito, Affinity CCC using a ligand in the stationary phase, *Anal. Chem.* 68:1207 (1996).



Chiral Separations by Capillary Electrophoresis and Micellar Electrokinetic Chromatography with Cyclodextrins

Paul K. Owens

Pharmaceutical Research and Development, AstraZeneca R&D Mölndal, Mölndal, Sweden

Introduction

In the area of pharmaceutical research, drug enantiomers are now recognized as potentially different drug entities which may have synergistic, similar, or antagonistic pharmacological properties to those of the desired effect. The pharmaceutical industry and the drug regulatory bodies, therefore, require high resolution, robust, fully validated, and highly selective analytical methodology that can discriminate drug enantiomeric substances for every stage of research and development, from drug discovery to clinical testing [1]. The aim of this brief review is to introduce the use of capillary electrophoresis (CE) and micellar electrokinetic chromatography (MEKC) as chiral separation techniques that employ cyclodextrin (CD) molecules as enantiomeric discriminating agents.

The use of CDs for chiral separations has, to date, been the most common approach when using CE or MEKC, so it would be difficult to discuss and detail every aspect relating to their chemistry, effects on separation, and application in this field. The emphasis will, thus, be placed on a short description of the principle and mechanism of chiral separation, typical method development procedures, and an outline of the influential experimental parameters using CE and MEKC. References to recent published review and research literature will enable the reader to explore this vast area further. It is also beyond the scope of this short introductory review to actually outline the actual CE or MEKC separation principles in detail, but an in-depth discussion can be found in this encyclopedia and references to recent textbooks and can be readily found elsewhere. It must, of course, be pointed out that CDs are not the only useful chiral selectors that can be employed using electrophoretic techniques. The use of chiral surfactants (bile salts), crown ethers, metal-chelation agents, carbohydrates, proteins, and glycopeptides have all been used effectively [2].

Capillary electrophoresis and micellar electrokinetic chromatography are fast, offer high resolution, and are cost-effective separation techniques that have been applied extensively for the discrimination of enantiomers using CDs, resulting in a number of review articles [2–6] and, recently, a book [7]. The separation principle in CE is based on differential migration of ionic solutes according to the mass/charge ratio through an electrolytic solution which is also moving by electro-osmosis under an applied electric field. MEKC is an extension of this technique originally developed for the separation of achiral neutral analytes by the incorporation of hydrophobic micelles to the background electrolyte. This allowed separation according to hydrophobic interactions, in addition to discrimination through differential mobility according to the mass/charge ratio. Fanali [8] and Ueda et al. [9] were among the earlier researchers to report the use of CDs for chiral discrimination by CE and MEKC, respectively. Since that earlier work, a vast number of racemic mixtures have been separated by many groups [2–7], whereas other groups have carried out useful theoretical and practical studies on the chiral mechanism taking place and parameters affecting enantioselectivity in CE [10,11].

Theory

Cyclodextrins are a family of three well-known, nonreducing cyclic oligosaccharides consisting of D-glucopyranose units bonded through α -1,4-linkages. The smallest is α -CD, followed by β -CD and γ -CD, which have six, seven, and eight D-glucopyranose units, respectively. In CDs, the D-glucopyranose units adopt a 4C_1 chair confirmation and orient themselves so that the overall molecule forms a toroid/hollow truncated cone structure, much like a doughnut. As a consequence of the CD conformation, all the primary hydroxyl groups are situated at the smaller edge of the truncated cone, whereas the chiral secondary hydroxyl

Encyclopedia of Chromatography

DOI: 10.1081/E-Echr 120004618

Copyright © 2002 by Marcel Dekker, Inc. All rights reserved.



groups are situated at the larger edge of the cone. The primary and secondary hydroxyl groups on the outside of the CD toroid give them a hydrophilic exterior, whereas the electron-rich glucosidic oxygen bridges inside the toroidal cavity result in a hydrophobic interior. These are two aspects that make them attractive chiral-discriminating molecules for CE and MEKC, because they are soluble in aqueous media while being capable of forming strong complexes with analyte molecules typically via hydrophobic insertion of an aromatic ring into the cavity.

Other favorable aspects include ultraviolet (UV) transparency, which allows their incorporation into the electrolyte, and the fact that they are relatively inexpensive. A more complete description of the chemical and physical properties of CDs, together with a schematic of their structure and shape, can be found in Fanali's review [5].

The β -CD molecule contains 35 asymmetric centers and guest racemic compounds can interact with this chiral environment. The interaction is normally governed by the size of the racemic guest molecule and, thus, its ability to form an inclusion complex. The possibility for additional interaction with the chiral secondary hydroxyl groups (at the large opening of the cone) is normally crucial and is considered to occur through hydrogen-bonding. The CD hydroxyl groups, 21 on the β -CD molecule, can also be modified chemically, thereby altering those CDs physical and chemical properties and, thus, the potential nature of interaction with a guest molecule. Derivatives used to date include alkyl-, hydroxyalkyl-, glucosyl-, maltosyl-, methyl-, hydroxyethyl-, hydroxypropyl-, acetyl-, and a range of chargeable functionalities. The aim of this derivatization may be (a) to improve the solubility of the CD, (b) to improve the fit and/or the degree or strength of association between a CD and its guest, or (c) to give the CD and/or the CD–guest complex enhanced or decreased mobility through greater size or by a charged functionality.

The enantioselective mechanism of CDs in CE and MEKC is similar to that in liquid chromatography (LC). Enantioselective interaction is thought to occur through the inclusion complex formation between a hydrophobic group of the analyte and the relatively hydrophobic interior of the CD cavity. As a result of the different three-dimensional spatial arrangement of each enantiomer, they may have a different binding constant with a particular CD. Just as in LC, this is a prerequisite to actually obtaining a chiral separation in CE or MEKC. When a charged enantiomer forms a complex with a CD, its charge/mass ratio and, thus, its

mobility decrease. The free or uncomplexed charged enantiomer migrates as it would in the absence of a CD. Therefore, differences in the binding constants determine the ratio of free/complexed enantiomers, and if the binding constants are sufficiently different for the two enantiomers, a chiral separation will occur. Theoretical aspects, including the relevant equations pertaining to the resolution of enantiomers and practical considerations for CE and MEKC when using CDs, can be found in Refs 2–10 and in the references therein.

The application of MEKC for chiral separation is primarily used when the enantiomers of interest are neutral. In conventional CE without micelles, neutral enantiomers will be swept along with the electro-osmotic flow (EOF) because they carry no ionic charge. If a neutral CD is present and forms a complex with these CDs, they will still move with the EOF. Thus, it is necessary for neutral enantiomers to create the potential for differential migration so that the overall complexes and free enantiomers will not just be swept along with the EOF. For this reason, the use of MEKC which utilizes ionic micelles for differential migration (through hydrophobic interaction) modified with CDs for enantioselectivity was applied [9]. The mechanism is as outlined for MEKC; however, because there are hydrophobic micelles inherently present in the electrolyte, additional interactions between the enantiomers and the micelle over those with just a CD may, of course, occur which will normally influence any observed separation.

Another approach may also be adopted for separating neutral enantiomers; the use of CDs that carry an overall anionic or cationic charge, sulfobutylether-, carboxymethyl-, sulfated-, phosphated-, or methylamino- are a few examples. If complexation occurs between neutral enantiomers and an ionic CD, the enantiomer–CD complex will carry an effective charge and will thus migrate to a greater or lesser extent than the EOF, thus creating the opportunity for a chiral separation. In conventional CE, where the EOF is in the cathodic direction, a CD carrying an overall cationic charge will result in the neutral drug enantiomers migrating before the EOF if complexation takes place; conversely, a CD carrying an anionic charge will result in the neutral drug enantiomers migrating after the EOF. Thus, it is not necessary to use a micellar system for the separation of neutral drug enantiomers when utilizing a CD that carries an overall cationic or anionic charge. The results, from theoretical aspects and practical applications of this type of chiral separation, have been reviewed [12].

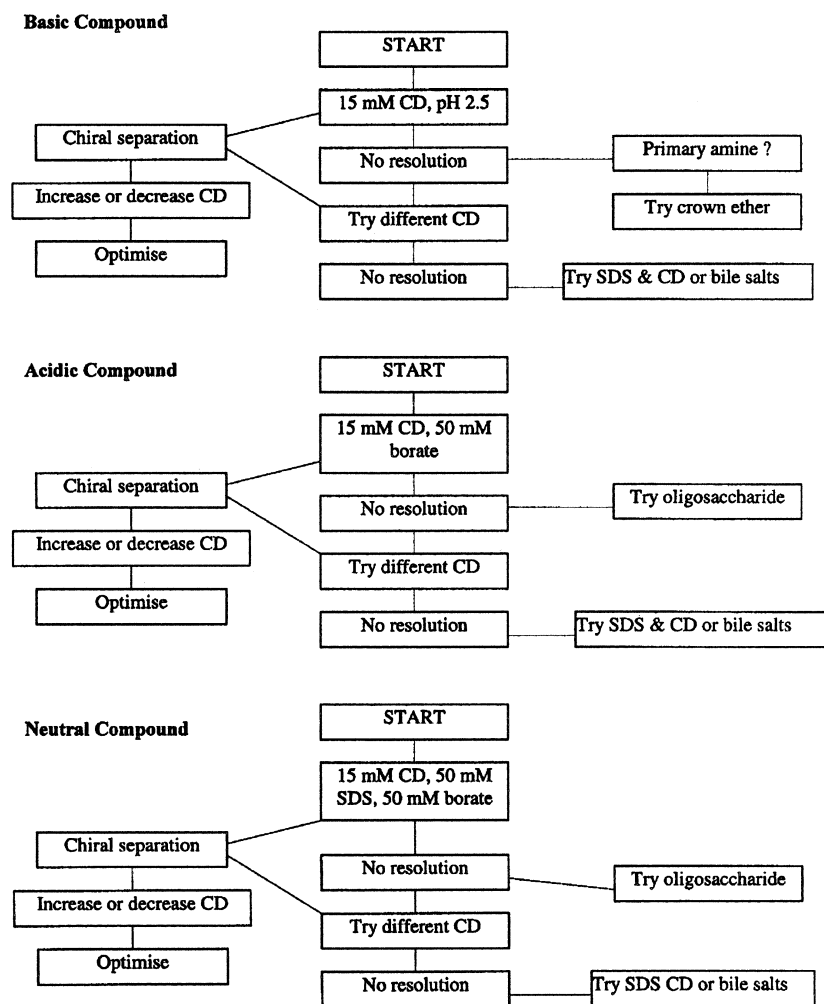


Fig. 1 Flow diagram indicating starting point and optimization procedure for enantiomeric separation of basic, acidic, and neutral compounds. [Adopted with kind permission from M. M. Rogan and K. D. Altria, Introduction to the theory and applications of chiral capillary electrophoresis, Beckman primer Vol. IV, p. 22, Part No. 726388.]

Obtaining Enantioselectivity in CE and MEKC

A flow diagram outlining possible starting points for obtaining a chiral separation for basic, acidic, and neutral compounds is shown in Fig. 1. A suitable starting point may be a low- and high-pH buffering system for basic and acidic compounds, respectively, with typically 15 mM of the medium-sized β -CD present in the electrolyte. It is necessary, as outlined earlier, to use a micellar system for the separation of neutral compounds and the most common surfactant is sodium dodecyl sulfate. In CE or MEKC, it is the background electrolyte that is necessary and responsible for any observed enantioselectivity. As a consequence, the simplest procedure to initially obtain and/or improve

any chiral resolution is to modify or control the parameters of that electrolyte. If no resolution is obtained from the initial result or it needs to be improved, many parameters can be modified, including the CD type, CD concentration, operating pH, buffer concentration, temperature, and the use of electrolyte additives like organic solvents or ion-pair reagents. The experimental variables for a chiral separation, including those that are not electrolyte based, and their typical influence are shown in Table 1. The most influential parameters are the nature and concentration of the CD. This is not surprising because these parameters will strongly influence the chiral recognition mechanism, which is based on complexation and interaction. This has been studied, in detail, through theo-



Table 1 Table of the Effects of Operating Parameters

Variable	Range	Effect of increasing variable
CD type and size		Large impact on chiral selectivity
CD concentration	1–100 mM	Increased viscosity, reduced EOF, increased solute migration if complexation occurs
Voltage	5–30 kV	Reduced analysis time; some loss in resolution
Current	5–250 μ A	Reduced analysis time; some loss in resolution
Capillary length	20–100 cm	Increased analysis time; gain in resolution
Capillary bore	25–100 μ m	Increased current; some loss in resolution
pH	1.5–11.5	Increased EOF; increased ionization of acids, reduced ionization of bases
Organic solvents	1–30% v/v	Gain or loss of resolution
Urea	1–7 M	Increased ionization of hydrophobic solutes (and CDs)
Ion-pair reagent	1–20 mM	Can reduce or increase resolution
Amine modifiers	1–50 mM	Reduced surface charge, reduced peak tailing
Viscosity	Various	Reduced EOF, longer migration times
Electrolyte concentration	5–200 mM	Increased resolution, increased current, lower EOF, solute ionization, reduced tailing
Cationic surfactant	1–20 mM	Reversal of EOF, increased solubilization, longer migration times
Injection time	1–20 s	Improved signal, some loss in resolution
Cellulose or polymer derivatives	0.1–0.5%	Can improve resolution
Bile salt type	10–50 mM	Choice has a large impact on chiral selectivity

Source: Adopted with kind permission from M. M. Rogan and K. D. Altria, Introduction to the theory and applications of chiral capillary electrophoresis, Beckman primer Vol. IV, p. 24 (Part No. 726388).

retical and practical studies by Wren and Rowe [10]. The chiral separations of the basic drug tocinide and related analogs using reasonably typical conditions is shown in Fig. 2, where the choice of CD is shown to strongly influence the enantioselectivity.

In addition to CD-modified MEKC, the use of mixed micelles incorporating CDs, CDs together with other chiral selectors (bile salts, ligand exchangers, crown ethers, etc. [5]), or mixed CD systems, neutral with neutral or neutral with charged CDs can also be extremely useful. A very attractive feature of the latter approach is the ability to control the enantiomeric migration order, an aspect that may be extremely useful if quantitation at low levels is required. Details of this technique are available in the review of Chankvetadze et al. [12].

Conclusions

It is hoped that the aim of this very short review article, to entice the reader into the world of chiral CE and MEKC using CDs, has been fulfilled. A brief description of the importance, historical background, method development, and theoretical and practical aspects concerning this approach is given. Additionally, possible alternative chiral selectors that can be applied in

order to achieve enantioselectivity in CE and MEKC are also mentioned.

References

1. W. H. De Camp, The FDA perspective on the development of stereoisomers, *Chirality* 1:2 (1989).
2. M. M. Rogan, K. D. Altria, and D. M. Goodall, Enantioselective separations using capillary electrophoresis, *Chirality* 6:25 (1994).
3. F. Bressolle, M. Audran, T.-N. Pham, and J.-J. Vallon, Cyclodextrins and enantiomeric separations of drugs by liquid chromatography and capillary electrophoresis: Basic principles and new developments, *J. Chromatogr. B* 687:303 (1996).
4. H. Nishi and S. Terabe, Micellar electrokinetic chromatography perspectives in drug analysis, *J. Chromatogr. A* 735(1–2):3 (1996).
5. S. Fanali, Controlling enantioselectivity in chiral capillary electrophoresis with inclusion complexation, *J. Chromatogr. A* 792:227 (1997).
6. H. Nishi, Enantioselectivity in chiral capillary electrophoresis with polysaccharides, *J. Chromatogr. A* 792(1–2):327 (1997).
7. B. Chankvetadze, *Capillary Electrophoresis in Chiral Analysis*, John Wiley & Sons, New York, 1997.
8. S. Fanali, Separation of optical isomers by capillary zone electrophoresis based on host–guest complexation with cyclodextrins, *J. Chromatogr.* 474:441 (1989).



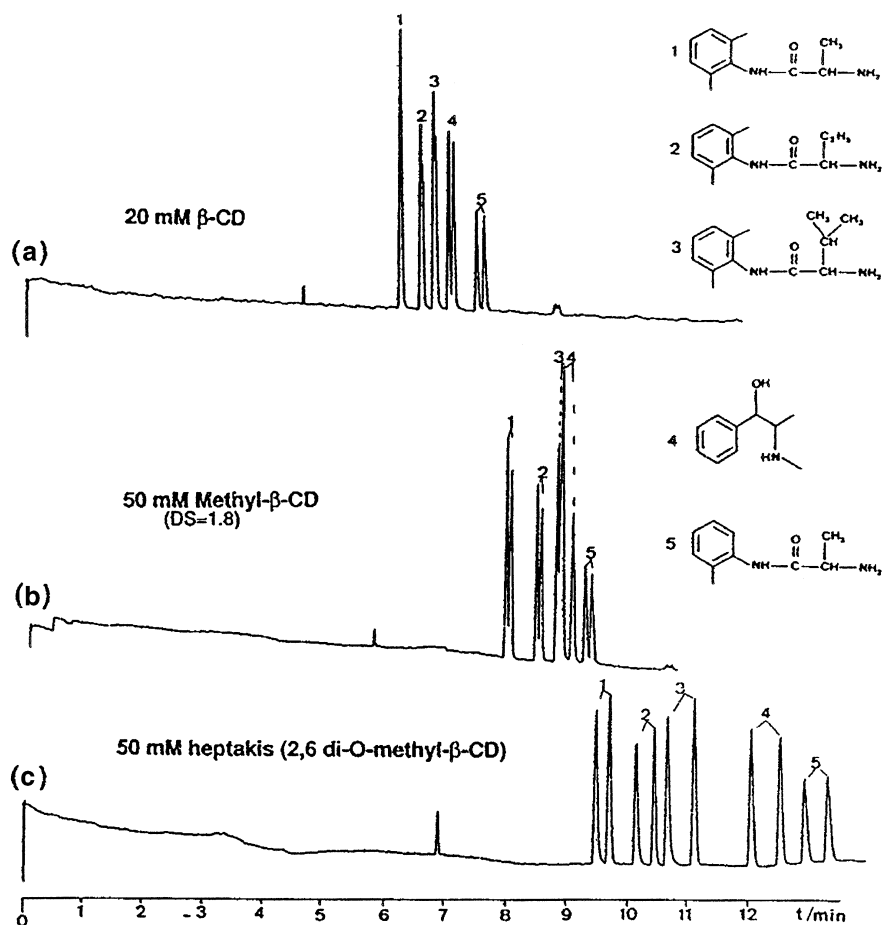


Fig. 2 Influence of cyclodextrin type on the chiral resolution of the basic drug tocainide and related substances using 40 mM sodium phosphate (pH 3.0) containing (a) 20 mM β -CD and (b) 50 mM methyl- β -CD and 50 mM heptakis (2,6 di-O-methyl- β -CD). [Adopted with kind permission from D. Belder and G. Schomburg, Chiral separations of basic and acidic compounds in modified capillaries using cyclodextrin-modified capillary zone electrophoresis, *J. Chromatogr. A* 666:351 (1994).]

9. T. Ueda, F. Kitamura, R. Mitchell, T. Metcalf, T. Kuwana, and A. Nakamoto, Chiral separation of naphthalene-2,3-dicarboxaldehyde-labeled amino-acid enantiomers by cyclodextrin-modified micellar electrokinetic chromatography with laser-induced fluorescence detection, *Anal. Chem.* 63:2979 (1991).
10. S. A. C. Wren and R. C. Rowe, Theoretical aspects of chiral separation in capillary electrophoresis. 3. Application to beta-blockers, *J. Chromatogr.* 635:113 (1993).
11. S. M., Branch, U., Holzgrabe, T. M., Jefferies, H. Mallwitz, and M. W., Matchett, Chiral discrimination of phenethylamines with β -cyclodextrin and heptakis (2,3-di-O-acetyl- β -cyclodextrin) by capillary electrophoresis and NMR spectroscopy, *J. Pharm. Biomed. Anal.* 12:1507 (1994).
12. B. Chankvetadze, G. Endresz, and G. Blaschke, Charged cyclodextrin derivatives as chiral selectors in capillary electrophoresis. *Chem. Soc. Rev.* 25:141 (1996).



Chiral Separations by GC

Raymond P. W. Scott

Scientific Detectors Ltd., Banbury, Oxfordshire, England

Introduction

In gas chromatography (GC), chiral selectivity is controlled solely by the choice of the stationary phase and the operating temperature. Thermodynamically, it is achieved by introducing an additional entropic component to the standard free energy of distribution. This is accomplished by employing a chiral stationary phase which will have unique spatially oriented groups or atoms that allow one enantiomer to interact more closely with the molecules of the stationary phase than the other. The enantiomer that can approach more closely to the stationary phase molecules will interact more strongly (the dispersive or polar charges being nearer) and, thus, the standard enthalpy of distribution of the two enantiomers will also differ. Consequently, the Van't Hoff curves will have different slopes and intersect at a particular temperature (see the entries Thermodynamics of Retention in GC and Van't Hoff Curves). At this temperature, the two enantiomers will co-elute and, hence, temperature is an important variable that must be used to control chiral selectivity. The farther the operating temperature of the column is away from the temperature of co-elution, the greater the separation ratio and the easier will be the separation (less theoretical plates, shorter column, faster analysis).

Historical Background

The first effective chiral stationary phases for GC were the derivatized amino acids [1], which, however, had very limited temperature stability. The first reliable GC stationary phase was introduced by Bayer and co-workers [2], who synthesized a thermally stable, low-volatility polymer by attaching L-valine-*t*-butylamide to the carboxyl group of dimethylsiloxane or (2-carboxypropyl)-methylsiloxane with an amide linkage. This stationary phase was eventually made available commercially as Chirasil-Val and could be used over the temperature range of 30°C to 230°C. OV-225 (a well-established polar GC stationary phase) has also been used for the synthesis of chiral

polysiloxanes, which, in this case, possess more polar characteristics than the (2-carboxypropyl)-methylsiloxane derivatives.

Although the polysiloxane phases carrying chiral peptides are still used in contemporary chiral GC, the presently popular phases are based on cyclodextrins. These materials are formed by the partial degradation of starch followed by the enzymatic coupling of the glucose units into crystalline, homogeneous, toroidal structures of different molecular sizes. The best known are the α -, β -, and γ -cyclodextrins which contain six (cyclohexamylose), seven (cycloheptamylose), and eight (cyclooctamylose) glucose units, respectively. The cyclodextrins are torus shaped macromolecules which incorporate the D(+)-glucose residues joined by α -(1-4)glycosidic linkages. The opening at the top of the torus-shaped cyclodextrin molecule has a larger circumference than that at the base. The primary hydroxyl groups are situated at the base of the torus, attached to the C₆ atoms. As they are free to rotate, they partly hinder the entrance to the base opening. The cavity size becomes larger as the number of glucose units increases. The secondary hydroxyl groups can also be derivatized to insert different interactive groups into the stationary phase. Due to the many chiral centers the cyclodextrins contain (e.g., β -cyclodextrin has 35 stereogenic centers), they exhibit high chiral selectivity and, as a consequence, are probably the most effective GC chiral stationary phases presently available.

Discussion

The α -, β -, or γ -cyclodextrins that have been permethylated do not coat well onto the walls of quartz capillaries and must be dissolved in appropriate polysiloxane mixtures for stable films to be produced. In contrast, underivatized cyclodextrins can be coated directly onto the walls of the column with the usual techniques. The thermal stability of a mixed stationary phase can be improved by including some phenylpolysiloxane in the coating material. Phenylpolysiloxane also significantly inhibits any oxidation that might

Encyclopedia of Chromatography

DOI: 10.1081/E-Echr 120004619

Copyright © 2002 by Marcel Dekker, Inc. All rights reserved.



take place at elevated temperatures. However, unless some methylsiloxane is present the cyclodextrin may not be sufficiently soluble in the polymer matrix for successful coating.

The inherent chiral activity of the cyclodextrins can be strengthened by bonding other chirally active groups to the secondary hydroxyl groups of the cyclodextrin. Certain derivatized cyclodextrins are susceptible to degradation, on contact with water or water vapor. Consequently, all carrier gases must be completely dry and all samples that are placed on the column must also be dry.

Derivatized cyclodextrins can interact with chiral substances in a number of different ways. If, the positions 2 and 6 are alkylated (pentylated), very dispersive (hydrophobic) centers are introduced that can strongly interact with any alkyl chains contained by the solutes. After pentylation of the 2 and 6 positions has been accomplished, the 3-position hydroxyl group can then be trifluoroacetylated. This stationary phase is widely used and it has been found that the derivatized γ -cyclodextrin is more chirally selective than the β material. It has been successfully used for the separation of both very small and very large chiral molecules. The cyclodextrin hydroxyl groups can also be made to react with pure "S" hydroxypropyl groups and then per-

methyated. As a result, the size selectivity of the stationary phase is reduced, but its interactive character is made more polar (hydrophilic). In general, the α or γ phases have less chiral selectivity than the β material. There are a considerable number of cyclodextrin-based chiral stationary phases commercially available and, without doubt, there will be many more introduced in the future.

References

1. D. Gil-Av, B. Feibush, and R. Charles-Sigler, *Tetrahedron Lett.* 1009 (1988).
2. H. Frank, G. J. Nicholson, and E. Bayer, *J. Chromatogr. Sci.* 15:174 (1974).

Suggested Further Reading

- Beesley, T. E. and R. P. W. Scott, *Chiral Chromatography*, John Wiley & Sons, Chichester, 1998.
- Scott, R. P. W., *Introduction to Gas Chromatography*, Marcel Dekker, Inc., New York, 1998.
- Scott, R. P. W., *Techniques of Chromatography*, Marcel Dekker, Inc., New York, 1995.



Chiral Separations by HPLC

Nelu Grinberg
Richard Thompson

Merck Research Laboratories, Rahway, New Jersey, U.S.A.

Introduction

Chirality arises in many molecules from the presence of a tetrahedral carbon with four different substituents. However, the presence of such atoms in a molecule is not a necessary condition for chirality. An object is said to be chiral if it is not superposable with its mirror image and achiral when the object and its mirror image are superposable. A chiral pair can be distinguished through their interaction with other chiral molecules to form either long-lived or transient diastereomers. Diastereomers are molecules containing two or more stereogenic (chiral) centers and having the same chemical composition and bond connectivity. They differ in stereochemistry about one or more of the chiral centers.

Long-Lived Diastereomers

Long-lived diastereomers are generated by chemical derivatization of the enantiomers with a chiral reagent. They may be separated subsequently by achiral means. Their formation energies have no relevance to their chromatographic separation; it is, rather, due to the difference in their solvation energies. Differences in their shape, size, or polarity will affect the energy needed to displace solvent molecules from the stationary phase [1].

There are several characteristics of diastereomeric chiral separations (also known as indirect enantiomeric separations) that are worth mentioning. Achiral phases that are cheaper, more rugged, and widely commercially available are used. The elution order can be controlled by choice of the chirality of the derivatizing agent. This feature is useful for the analysis of trace levels of enantiomers. The separation can be designed such that the minor enantiomer is eluted first, allowing for more accurate quantitation.

Derivatization requires that the species of interest must contain a functional group that can be chemically modified. There should be no enantioselectivity of the

rate of the derivatization [2]. There are several disadvantages to an indirect chromatographic chiral separation. The derivatization procedure may be complex and time-consuming and there is always a possibility of racemization during the derivatization procedure. In the case of preparative chromatography of the diastereomeric species, they have to be chemically reversed to the initial enantiomers. Figure 1 shows the main types of derivatives formed from amines, carboxylic acids, and alcohols in reaction with chiral reagents [3].

There are several structural considerations to achieving a diastereomeric separation. The diastereomers should possess a degree of conformational rigidity in order to maximize their physical differences. Large size differences between the groups attached to the chiral center enhance the separation in most cases. The distance between the asymmetric centers should be minimal and ideally less than three bonds. The presence of polar or polarizable groups can enhance hydrogen-bonding, interactions with the stationary phase, resulting in increased resolution.

Transient Diastereomers

Objects that can distinguish between enantiomers are chiral receptors. Nature gives us plenty of examples of chiral receptors, such as enzymes and nucleic acids. There are also man-made chiral receptors such as chiral phases (CP) used in gas chromatography, high-performance liquid chromatography (HPLC), supercritical fluid chromatography (SFC), and capillary electrophoresis (CE). The operation of a CP involves the formation of transient diastereomeric complexes between the enantiomer (selectand) and the CP (selector). They must be energetically nondegenerate in order to effect a separation. Because of their transient nature, it is usually not possible to isolate them.

There are specific criteria for the interaction between the selectand and the selector which leads to separation on a particular column [4]:



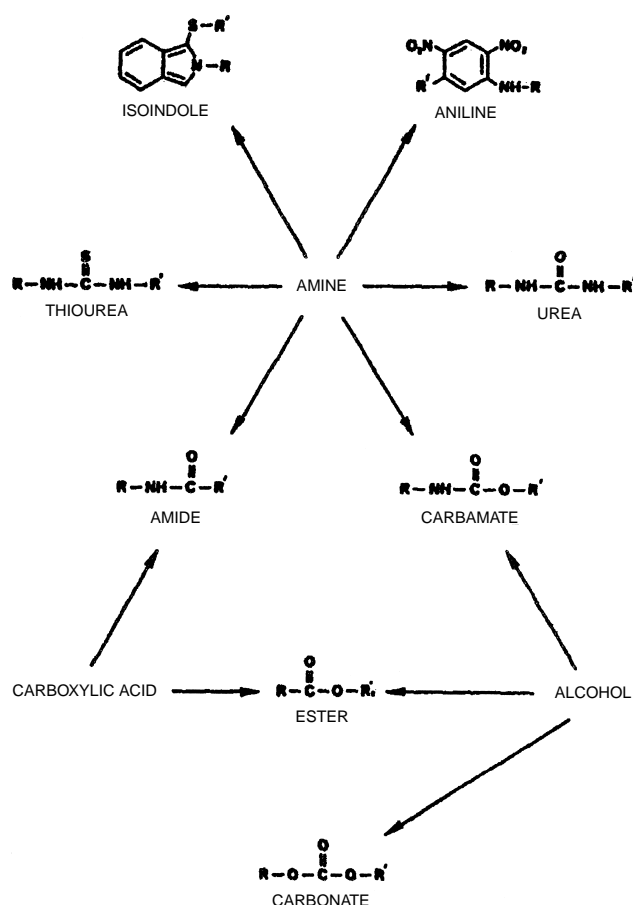


Fig. 1 Main types of derivatives formed from amines, carboxylic acids, and alcohols in reactions with chiral derivatizing reagents. (From Ref. 3.)

1. Strong interactions, such as p-p interactions, coordinative bonds, and hydrogen bonds between the selector and selectand
2. Close proximity of the transient bonds to the respective asymmetric carbons
3. Inhibition of free rotation of the transient bonds
4. Minimal noncontributing associative forms that do not bring the respective asymmetric centers to proximity

The diastereomeric associate between selectand and selector is formed through bonds between one or more substituents of the asymmetric carbon. These bonds are the leading selectand-selector interactions. Only when the leading bonds are formed and the asymmetric moieties of the two molecules are brought to close proximity do the secondary interactions (e.g.,

van der Waals, steric hindrance, dipole-dipole) become effectively involved (Fig. 2). The secondary interactions can affect the conformation and the formation energy of the diastereomeric associates. In Fig. 2a, the size, shape and polarity of the unbounded B, C, and D substituents of the selectand and their positions to the groups F, G, and H of the selector will determine the enantioselectivity of the system. One particular enantiomer of the selectands will interact more strongly with a particular selector. When the selective associate is formed through interactions A-E and B-F (Fig. 2b), enantioselectivity and elution order are determined by the effective size of unbounded groups C and D their relative positions, syn or anti, to groups G and H of the selector. In most of the cases that include hydrogen-bonding or ligand-metal complexes, the enantiomer with the larger nonbonded groups positioned syn to the selector's larger nonbonded group will elute last from the chiral column. When the selective association is formed through three leading inter-

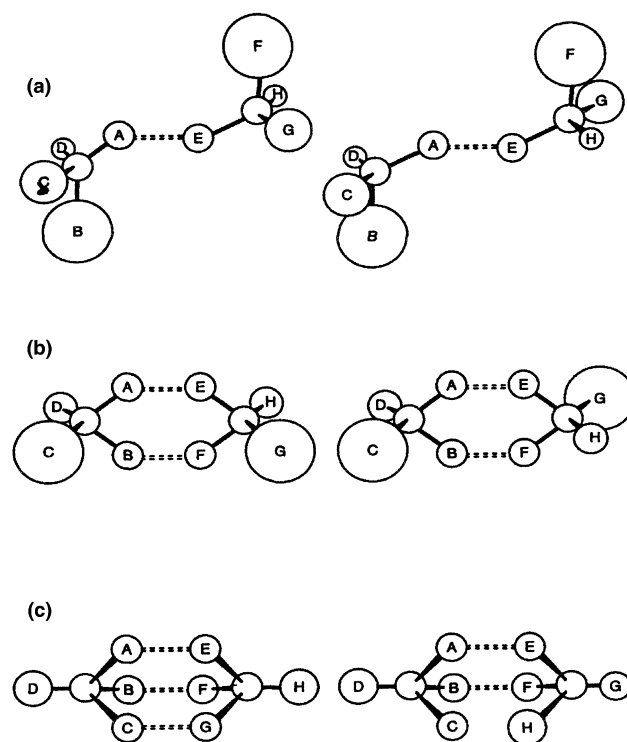


Fig. 2 Schematic representation of selectand-selector association. A dotted line represents a leading interaction between the two molecules. (a) The selectand forms a bond that involves only one substituent of its asymmetric carbon; (b) the selectand binds through two of its substituents; (c) the selectand binds through three substituents. (From Ref. 1.)

actions (Fig. 2c), the enantioselectivity is determined by the stereochemistry of the two enantiomers. One enantiomer in one configuration will establish three leading bonds (H bonds or a combination of H bonds and π - π interactions), whereas the other one will not [1].

In chromatographic systems, the selectors are either added to the mobile phase [chiral mobile phases (CMP)] or are bonded to a stationary phase (e.g., silica gel) as chiral stationary phases (CSP).

Chiral Mobile Phases

In this mode of separation, active compounds that form ion pairs, metal complexes, inclusion complexes, or affinity complexes are added to the mobile phase to induce enantioselectivity to an achiral column. The addition of an active compound into the mobile phase contributes to a specific secondary chemical equilibrium with the target analyte. This affects the overall distribution of the analyte between the stationary and the mobile phases, affecting its retention and separation at the same time. The chiral mobile phase approach utilizes achiral stationary phases for the separation. Table 1 lists several common chiral additives and applications.

Chiral Stationary Phases

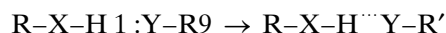
Compared to CMP, the mechanism of separation on a chiral stationary phase is easier to predict, due to a much simpler system. Because the ligand is immobilized to a matrix and is not constantly pumped through the system, the detection limits for the enantiomers are much lower. Depending on the ligand immobilized to the matrix, one can have different types of interactions between the selectand and selector: metal complexes, hydrogen-bonding, inclusion, π - π interactions, and dipole interactions, as well as a combination thereof.

Chiral Separation Where the Leading Interaction Is Established Through Metal Complexes (Ligand Exchange)

Chiral separation using ligand-exchange chromatography involves the reversible complexation of metal ions and chiral complexing agents. The central ion, usually Cu^{2+} or Ni^{2+} forms a bis complex with bidentates ligands. If one of the chelating ligands is anchored to a support, the CSP can form diastereomeric adsorbates with the bidentate selectand. The metal ion is held by the stationary phase through coordination to the bound ligand. If the coordination sphere of the metal is unsaturated or is occupied by weakly bound solvent molecules, it can reversibly attach different solute ligands from the mobile phase. The solute ligands are then resolved according to differences in their binding constants. Ligand exchange is possible only in systems where the interaction of the mobile ligand with the stationary phase is reversible. The coordination bonds must be kinetically labile. If the chelating ligands are amino acids and the metal is copper(II), the amine and carboxylate groups of the ligands are arranged around the metal ion in a trans configuration, forming a square planar complex. A third interaction should take place to ensure enantioselectivity. The third interaction may arise through steric hindrance or attractive or repulsive interactions between the selector and the selectand [15,16].

Chiral Separation Where the Leading Interaction Is Established Through Hydrogen-Bonding

A hydrogen bond is formed by the interaction between the partners $\text{R}-\text{X}-\text{H}$ and $:\text{Y}-\text{R}'$ according to



$\text{R}-\text{X}-\text{H}$ is the proton donor and $:\text{Y}-\text{R}$ makes an electron pair available for the bridging bond. X and Y are

Table 1 Main Classes of Chiral Additives and Their Applications

Mechanism	Additive	Application	Mode of separation	Ref.
Ion pair	(+)-10-camphorsulfonic acid	Aminoalcohols, alkaloids	HPLC	5, 6
Ion pair	Quinines	Carboxylic acids	HPLC	7, 8
Inclusion	Dimethyl β -cyclodextrin	Aminoalcohols, carboxylic acids	CE	9, 10
Inclusion	Crown ether	Primary amines	CE	11
Ligand exchange	L-Proline/ Cu^{2+}	Amino acids	HPLC	12
Proteins	α_1 -Acid glycoprotein	Hexobarbitone	CE	13
Antibiotics	Rifamycin	Amino acids	CE	14



atoms of higher electronegativity than hydrogen (e.g., C, N, P, O, S, F, Cl, Br, I). Hydrogen-bonding acceptors are the oxygen atoms in alcohols, ethers, and carbonyl compounds, as well as nitrogen atoms in amines and N-heterocycles. Hydrogen-bonding donors are hydroxy, carboxyl, and amide protons. Interactions can be modified by changing the elution conditions. The more nonpolar the elution conditions, the stronger the H-bond interactions. Enantioselectivity is determined by the strength of the hydrogen bonds, which is, in turn, affected by secondary interactions such as steric hindrance or attractive or repulsive interactions between the selector and the selectand.

Chiral Separation Through Charge Transfer

Complexes formed by weak interactions of electron donors with electron-acceptor compounds are known as charge-transfer complexes. The necessary condition for the formation of a charge transfer complex is the presence of an occupied molecular orbital of sufficiently high energy in the electron-donor molecule, and the presence of a sufficiently low unoccupied orbital in the electron-acceptor molecule. Small unsaturated hydrocarbons are usually weak donors or weak acceptors. Polynuclear aromatic hydrocarbons are efficient π -donor molecules. Replacement of a hydrogen atom in the parent molecule with an electron-releasing substituent such as alkyl, alkoxy, or amino, increases the capability of the molecule to donate π electrons. Aromatic molecules containing groups such as NO_2 , Cl, $\text{C}\equiv\text{N}$ are efficient electron acceptors. Carbonyl compounds are acceptors to aromatic hydrocarbons but are donors to bromine.

The overlapping and the orientation of the molecules in the crystal correspond to parallel planes if the bonding occurs only through π orbitals. π -donor– π -donor interactions do not occur in the same fashion because of repulsion between the π clouds. This repulsion leads to edge-to-face interactions, where weakly positive H atoms at the edge of the molecule point toward negatively charged C atoms on the faces of adjacent molecule. The dihedral ring planes are often close to perpendicular. Aromatic rings can act as hydrogen-bond acceptors for the amidic proton [17].

In general, the stability of a charge-transfer complex increases with the increase in the polarity of the solvent. To establish the enantiomeric separation under such conditions, secondary interactions must occur: namely the charge-transfer interactions have to be accompanied by hydrogen bonds and/or steric hindrance. Under these conditions, the mobile-phase con-

ditions should be adjusted such that these interactions are achieved. Figure 3 presents an example of a chiral stationary phase designed by Pirkle's group. This CSP allows for charge-transfer interaction with secondary interactions such as hydrogen-bonding and steric hindrance [18].

Chiral Separation Through Host–Guest Complexation

Cyclodextrins and crown ethers are the main classes of compounds able to undergo host–guest complexes with a particular pair of enantiomers. Cyclodextrins (CD) are natural macrocyclic polymers of glucose that contain 6–12 D-(+)-glucopyranose units which are bound through α -1,4-glucopyranose linkages. The number of glucose units per CD is denoted by a Greek letter: α for six, β for seven, and γ for eight (Fig. 4) [19]. The inherent chirality of the CD renders them useful for chromatographic enantioseparations. In most cases, an inclusion complex is formed between the solute and the cyclodextrin cavity. The host–guest complexation is dependent on the polarity, hydrophobicity, size, and geometry of the guest, as well as the size of the internal cavity of the CD. Enantioselectivity is then determined by the fit in the cavity and by the interactions between substituents attached to or near the chiral center of the analyte and the unidirectional secondary hydroxyl groups at the mouth of the cavity. The temperature, pH, and the composition of the mobile phase influence the complexation.

Under reversed-phase conditions, the presence of an organic modifier affects the binding of the guest molecule in the CD's cavity. The inclusion complex is usually strongest in water and decreases upon addition of organic modifiers. The modifier competes with the guest analyte for the cavity. Under normal-phase conditions, apolar solvents such as hexane and chloroform occupy the CD's cavity and cannot be easily displaced by the solute molecules. In these circumstances, the solute is usually restricted to interactions with the ex-

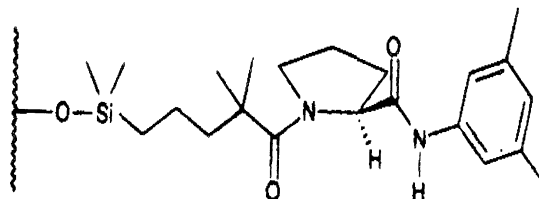


Fig. 3 The structure of the (*S*)-proline derivative chiral stationary phase. (From Ref. 18.)

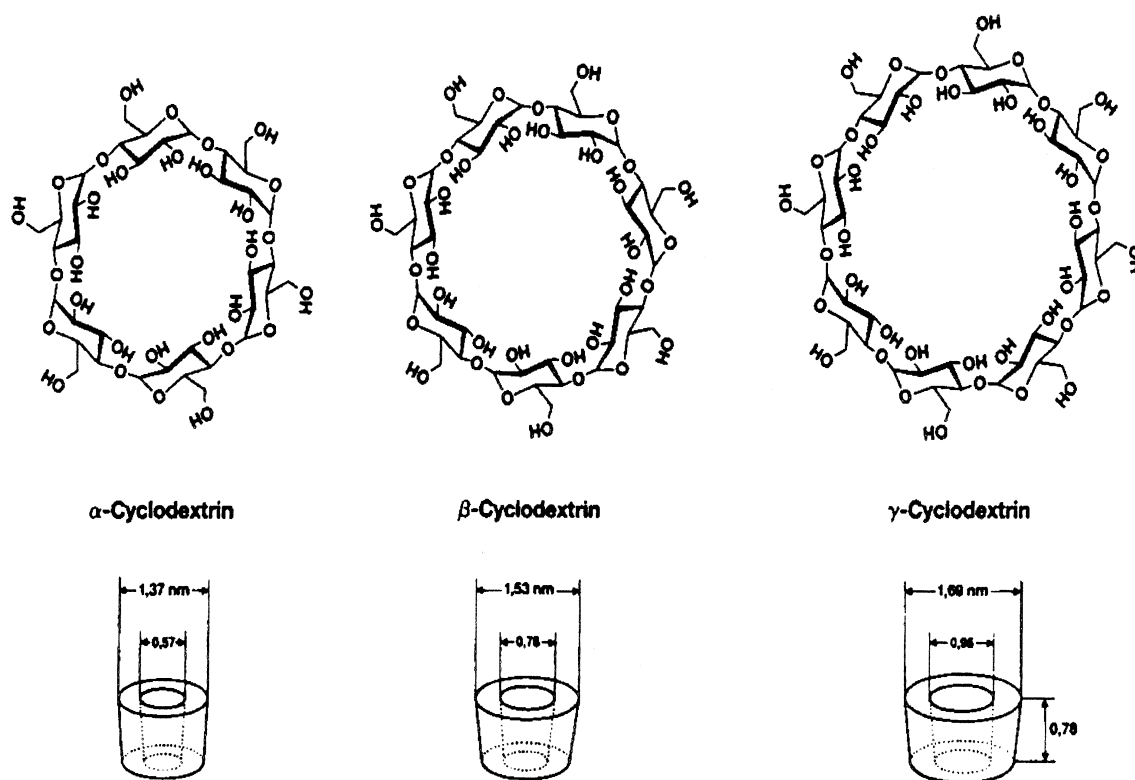


Fig. 4 Schematic representation of α -CD, β -CD, and γ -CD. (From Ref. 19.)

terior of the CD. Chemical modifications of CD has opened new possibilities for enantiorecognition, widening the range of compounds that can be separated into enantiomers [20].

Crown ethers, especially 18-crown-6 ethers, can complex not only inorganic cations but also alkylammonium compounds. The primary interactions occur between the hydrogens of the ammonium group and the oxygens of the crown ether. The introduction of bulky groups such as binaphthyl onto the exterior of the crown ether provides steric barriers and induces enantioselective interactions with the guest molecule.

The rigid binaphthyl units occupy planes that are perpendicular to the plane of the cyclic ether. One of the naphthalene rings forms a wall that extends along the sides and outward from the other face of the cyclic ether. The substituents attached at the 3-position of the naphthalene rings extend along the side or over the face of the cyclic ether. In the presence of a chiral primary amine, it forms a triple hydrogen bond with the primary ammonium cation. The same complex is formed whether the guest approaches from the top or from the bottom of the crown ether, as the crown ether

has a C_2 axis of symmetry. In the complex, the large (L), medium (M), and small (S) groups attached to the asymmetric carbon of the guest must adjust themselves into two identical cavities. The L is placed in one cavity and the M and S into the other cavity. M will reside in the pocket with S against the wall for the more stable diastereomeric complex (Fig. 5) [21].

Chiral Separation Through Combination of Interactions

Included in this category are stationary phases such as biopolymers (e.g., celluloses and cellulose derivatives, proteins) [22,23], as well as macrocyclic antibiotics [24]. These stationary phases exhibit interactions with a particular enantiomer through hydrogen-bonding, charge transfer, and inclusion interactions. They proved to be very effective in resolving a wide class of racemates encompassing a variety of structures. Describing the mechanism of such separation is very challenging due to the complexity of these stationary phases. Such stationary phases can be operated under reversed-phase conditions (protein phases, cellulose



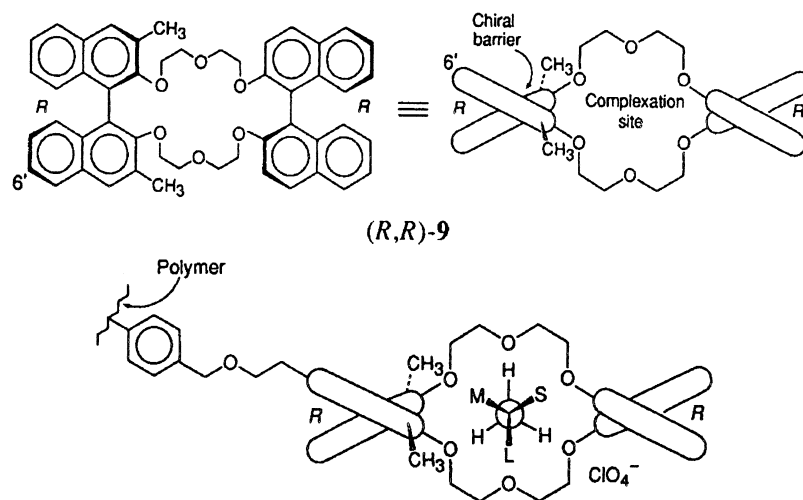


Fig. 5 Structure of the crown ether and the most stable complex. (From Ref. 21.)

phases, and macrocyclic antibiotics), as well as in the normal-phase conditions (cellulose phases and macrocyclic antibiotics). Conformational changes of biopolymers under the temperature and mobile-phase conditions can occur and they should be controlled such that the separation can be maximized [25,26].

References

1. B. Feisbush, *Chirality* 10:382 (1998).
2. W. Lindner, in *Chromatographic Chiral Separation* (M. Zieff and L. J. Crane, eds.), Marcel Dekker, Inc., New York, 1988, p. 91.
3. M. Ahnoff and S. Einarsson, in *Chiral Liquid Chromatography* (W. J. Lough, ed.), Blackie and Son, Glasgow, 1989, p. 39.
4. B. Feibush and N. Grinberg, in *Chromatographic Chiral Separation* (M. Zieff and L. J. Crane, eds.), Marcel Dekker, Inc., New York, 1988, p. 1.
5. C. Pettersson and G. Schill, *J. Chromatogr.* 204:179 (1981).
6. C. Pettersson and G. Schill, *Chromatographia* 16:192 (1982).
7. A. Karlsson and C. Pettersson, *Chirality* 4:323 (1992).
8. C. Pettersson and K. No, *J. Chromatogr.* 316:553 (1984).
9. A. Guttman, *Electrophoresis* 16:1900 (1995).
10. A. Guttman and N. Cooke, *J. Chromatogr.* 685:155 (1994).
11. J.-M. Lin, T. Nakagama, and T. Hobo, *Chromatographia* 42:559 (1996).
12. E. Gil-Av and S. Tishbee, *J. Am. Chem. Soc.* 102:5115 (1980).
13. B. Clar and J. Mame, *J. Pharm. Biomed. Anal.* 7:1883 (1989).
14. D. Armstrong, *Anal. Chem.* 66:1690 (1994).
15. V. A. Davankov, in *Advances in Chromatography* (J. C. Giddings, E. Grushka, J. Cazes, and P. R. Brown, eds.), Marcel Dekker, Inc., New York, 1980, Vol. 18, p. 139.
16. V. A. Davankov, A. A. Kurganov, and A. S. Bochkov, in *Advances in Chromatography* (J. C. Giddings, E. Grushka, J. Cazes, and P. R. Brown, eds.), Marcel Dekker, Inc., New York, 1983, Vol. 22, p. 71.
17. R. Foster, *Organic Charge-Transfer Complexes*, Academic Press, London, 1969, p. 217.
18. W. H. Pirkle and S. R. Selness, *J. Org. Chem.* 60:3252 (1995).
19. W. L. Konig, *Gas Chromatographic Enantiomer Separation with Modified Cyclodextrins*, Hüthig Buch Verlag, Heidelberg, 1992, p. 4.
20. A. M. Stalcup, in *A Practical Approach to Chiral Separations by Liquid Chromatography*, VCH, Weinheim, 1994, p. 1994.
21. D. J. Cram and J. M. Cram, *Container Molecules and Their Guests*, Royal Society of Chemistry, London, 1994, p. 56.
22. Y. Okamoto and Y. Kaida, *J. Chromatogr.* 666:403 (1994).
23. S. G. Allenmark and S. Anderson, *J. Chromatogr.* 666:167 (1994).
24. K. H. Ekborg-Ott, L. Youbang, and D. W. Armstrong, *Chirality* 10:434 (1998).
25. M. Waters, D. R. Sidler, A. J. Simon, C. R. Middaugh, R. Thompson, L. J. August, G. Bicker, H. J. Perpall, and N. Grinberg, *Chirality* 11:224 (1999).
26. T. O'Brien, L. Crocker, R. Thompson, K. Thomson, P. H. Toma, D. A. Conlon, B. Feibush, C. Moeder, G. Bocker, and N. Grinberg, *Anal. Chem.* 69:1999 (1997).

Chiral Separations by Micellar Electrokinetic Chromatography with Chiral Micelles

Koji Otsuka

Shigeru Terabe

Himeji Institute of Technology, Hyogo, Japan

Introduction

Since micellar electrokinetic chromatography (MEKC) was first introduced in 1984, it has become one of major separation modes in capillary electrophoresis (CE), especially owing to its applicability to the separation of neutral compounds as well as charged ones. Chiral separation is one of the major objectives of CE, as well as MEKC, and a number of successful reports on enantiomer separations by CE and MEKC has been published. In chiral separations by MEKC, the following two modes are normally employed: (a) MEKC using chiral micelles and (b) cyclodextrin (CD)-modified MEKC (CD-MEKC).

MEKC Using Chiral Micelles

An ionic chiral micelle is used as a pseudo-stationary phase; it works as a chiral selector. When a pair of enantiomers is injected to the MEKC system, each enantiomer is incorporated into the chiral micelle at a certain extent determined by the micellar solubilization equilibrium. The equilibrium constant for each enantiomer is expected to be different more or less among the enantiomeric pair; that is, the degree of solubilization of each enantiomer into the chiral micelle would be different for each. Thus, the difference in the retention factor would be obtained and different migration times would occur.

CD-MEKC

An ionic achiral micelle [e.g., sodium dodecyl sulfate (SDS)] and a neutral CD are typically used as a pseudo-stationary phase and a chiral selector, respectively. When a pair of enantiomers is injected into this system, two major distribution equilibria can be considered for the solutes or enantiomers: (a) the equilibrium between the aqueous phase and the micelle (i.e.,

micellar solubilization) and (b) the equilibrium between the aqueous phase and CD (i.e., inclusion complex formation). Each enantiomer may have a different equilibrium constant for the inclusion complex formation among the enantiomeric pairs due to the enantioselectivity of the CD. As a result, each enantiomer exists in the aqueous phase at a different time among the enantiomeric pairs; hence, the time spent in the micelle would be varied.

In some cases, an ionic chiral micelle (e.g., a bile salt) is also used as a chiral pseudo-stationary phase with a CD. Moreover, cyclodextrin electrokinetic chromatography (CDEKC), where a CD derivative having an ionizable group is used as a chiral pseudo-stationary phase, has become popular recently since several commercially available ionic CD derivatives have appeared. Although the CDEKC technique is actually beyond the field of MEKC, it is an important method for enantiomer separation by CE.

In this section, chiral separation by MEKC with chiral micelles is mainly treated. The development of novel chiral surfactants adaptable to pseudo-stationary phases in MEKC for enantiomer separation is continuously progressing. It seems somewhat difficult for a researcher to find an appropriate mode of CE when one wants to achieve a specific enantioseparation. However, nowadays, various method development kits for chiral separation have been commercially available and some literature on the topic is also available, so that helpful information may be obtained without difficulty.

MEKC Using Natural Chiral Surfactants

Bile Salts

Bile salts are natural and chiral anionic surfactants which form helical micelles of reversed micelle conformation. The first report on enantiomer separation by MEKC using bile salts was the enantioseparation of

Encyclopedia of Chromatography

DOI: 10.1081/E-Echr 120004621

Copyright © 2002 by Marcel Dekker, Inc. All rights reserved.



dansylated DL-amino acids (Dns-DL-AAs) and, since then, numerous papers have been available. Nonconjugated bile salts, such as sodium cholate (SC) and sodium deoxycholate (SDC), can be used at pH > 5, whereas taurine-conjugated forms, such as sodium taurocholate (STC) and sodium taurodeoxycholate (STDC), can be used under more acidic conditions (i.e., pH > 3). Several enantiomers, such as diltiazem hydrochloride and related compounds, carboline derivatives, trimetoquinol and related compounds, binaphthyl derivatives, Dns-DL-AAs, mephénytoin and its metabolites, and 3-hydroxy-1,4-benzodiazepins have been successfully separated by MEKC with bile salts. In general, STDC is considered as the most effective chiral selector among the bile salts used in MEKC.

The use of CDs with bile salt micelles has been also successful for enantiomer separations. For example, Dns-DL-AAs, baclofen and its analogs, mephénytoin and fenoldopam, naphthalene-2,3-dicarboxaldehyde derivatized DL-AAs (CBI-DL-AAs), diclofenac, ephedrine, nadolol, and other β -blockers, and binaphthyl-related compounds were enantioseparated by CD-MEKC with bile salts.

Digitonin and Saponins

Digitonin, which is a glycoside of digitogenin and used for the determination of cholesterol, is a naturally occurring chiral surfactant. By using digitonin with ionic micelles, such as SDS or STDC as pseudo-stationary phases, some phenylthiohydantoin-DL-AAs (PTH-DL-AAs) were enantioseparated.

On the other hand, glycyrrhizic acid (GRA) and β -escin can be employed as chiral pseudo-stationary phases in MEKC. Chiral separations of some Dns-DL-AAs and PTH-DL-AAs were achieved.

MEKC Using Synthetic Chiral Surfactants

N-Alkanoyl-L-Amino Acids

Various *N*-alkanoyl-L-amino acids, such as sodium *N*-dodecanoyl-L-valinate (SDVal), sodium *N*-dodecanoyl-L-alaninate (SDAla), sodium *N*-dodecanoyl-L-glutamate (SDGlu), *N*-dodecanoyl-L-serine (DSer), *N*-dodecanoyl-L-aspartic acid (DAsp), sodium *N*-tetradecanoyl-L-glutamate (STGlu), and sodium *N*-dodecanoyl-L-threoninate (SDThr) have been employed as synthetic chiral micelles in MEKC; several enantiomers have been successfully separated (Fig. 1). In each case, the addition of SDS, urea, and organic modifiers such as methanol or 2-propanol were essen-

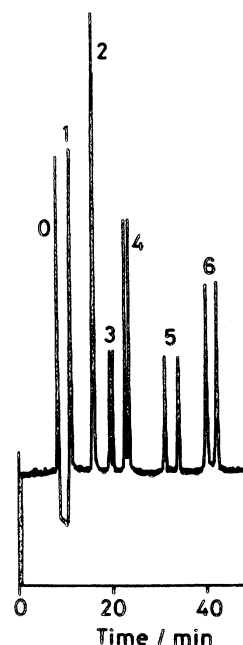


Fig. 1 Chiral separation of six PTH-DL-AAs by MEKC with SDVal. Corresponding AAs: (1) Ser, (2) Aba, (3) Nva, (4) Val, (5) Trp, (6) Nle; (0) acetonitrile. Micellar solution: 50 mM SDVal–30 mM SDS–0.5M urea (pH 9.0) containing 10% (v/v) methanol; separation column: 50 μ m inner diameter \times 65 cm, 50 cm effective; applied voltage, 20 kV; current, 17 μ A; detection wavelength, 260 nm; temperature, ambient. [Reprinted from K. Otsuka et al., *J. Chromatogr.* 559:209 (1991) with permission.]

tial to obtain improved peak shapes and enhanced enantioselectivity.

N-Dodecoxycarbonyl Amino Acids

Chiral surfactants of amino acid derivatives, such as (*S*)- and (*R*)-*N*-dodecoxycarbonylvaline (DDCV) and *N*-dodecoxycarbonylproline (DDCP) are available for enantiomer separation by MEKC: Several pharmaceutical amines, benzoylated amino acid methyl ester derivatives, piperidine-2,6-dione enantiomers, and aldose enantiomers were successfully resolved. Because both enantiomeric forms of DDCV or (*S*)- and (*R*)-forms are available, we can expect that the migration order of an enantiomeric pair would be reversed.

Alkylglucoside Chiral Surfactants

Anionic alkylglucoside chiral surfactants, such as dodecyl β -D-glucopyranoside monophosphate and

monosulfate, and sodium hexadecyl D-glucopyranoside 6-hydrogen sulfate, were used as chiral pseudo-stationary phases in MEKC, where several enantiomers (e.g., PTH-DL-AAs and binaphthol) were resolved.

Several neutral alkylglucoside surfactants, such as heptyl-, octyl-, nonyl-, and decyl- β -D-glucopyranosides and octylmaltopyranoside, were also employed for the enantiomer separation of phenoxy acid herbicides, Dns-DL-AAs, 1,1'-bi-2-naphthyl-2,2'-diyl hydrogen phosphate (BNP), warfarin, bupivacaine, and so forth.

Tartaric Acid-Based Surfactants

A synthesized chiral surfactant based on (*R,R*)-tartaric acid was used for the enantiomer separation in MEKC, where enantiomers having fused polyaromatic rings were separated easier than those having only a single aryl group.

Some PTH-DL-AAs and drug enantiomers were successfully resolved by using tartaric acid-based chiral surfactants.

Steroidal Glucoside Surfactants

Neutral steroidal glucoside surfactants, such as *N,N*-bis-(3-D-gluconamidopropyl)-cholamide (Big CHAP) and *N,N*-bis-(3-D-gluconamidopropyl)-deoxycholamide (Deoxy Big CHAP), which contain a cholic or deoxycholic acid moiety, respectively, have been introduced for use as chiral pseudo-stationary phases in MEKC. By using a borate buffer under basic conditions, these surfactant micelles could be charged via borate complexation. Some binaphthyl enantiomers, Tröger's base, phenoxy acid herbicide, and Dns-DL-AAs were enantioseparated.

MEKC Using High-Molecular-Mass Surfactants

The use of a high-molecular-mass surfactant (HMMS) or polymerized surfactant has been recently investigated as a pseudo-stationary phase in MEKC. Because a HMMS forms a micelle with one molecule, enhanced stability and rigidity of the micelle can be obtained.

Also, it is expected that the micellar size is controlled easier than with a conventional low-molecular-mass surfactant (LMMS). The first report on enantiomer separation by MEKC using a chiral HMMS appeared in 1994, where poly(sodium *N*-undecylenyl-L-valinate) [poly(L-SUV)] was used as a chiral micelle and binaphthol and laudanoline were enantioseparated. The optical resolution of 3,5-dinitrobenzoylated amino acid isopropyl esters by MEKC with poly(sodium (10-undecenoyl)-L-valinate) as well as with SDVal, SDAla, and SDThr was also reported.

As for the use of monomeric and polymeric chiral surfactants as pseudo-stationary phases for enantiomer separations in MEKC, a review article has been available.

The use of an achiral HMMS butyl acrylate–butyl methacrylate–methacrylic acid copolymer (BBMA) sodium salt was also investigated for enantiomer separations with CDs or as a CD–MEKC mode. A better enantiomeric resolution of Dns-DL-AAs was obtained by a β -CD–BBMA–MEKC system than an β -CD–SDS–MEKC system.

Polymerized dipeptide surfactants, which are derived from sodium *N*-undecylenyl-L-valine-L-leucine (L-SUVL), sodium *N*-undecylenyl-L-leucine-L-valine (L-SULV), sodium *N*-undecylenyl-L-leucine-L-leucine (L-SULL), and sodium *N*-undecylenyl-L-valine-L-valine (L-SUVV), were employed. Among these dipeptides, poly(L-SULV) showed the best enantioselectivity for the separation of 1,1'-bi-2-naphthol (BN).

Suggested Further Reading

- Camilleri, P., Chiral surfactants in micellar electrokinetic capillary chromatography, *Electrophoresis* 18:2332 (1997).
- Chankvetadze, B., *Capillary Electrophoresis in Chiral Analysis*, John Wiley & Sons, New York, 1997.
- Otsuka, K. and S. Terabe, Micellar electrokinetic chromatography, *Bull. Chem. Soc. Jpn.* 71:2465 (1998).
- Otsuka, K. and S. Terabe, Enantiomer separation of drugs by micellar electrokinetic chromatography using chiral surfactants, *J. Chromatogr. A* 875:163 (2000).
- Terabe, S., K. Otsuka, and H. Nishi, Separation of enantiomers by capillary electrophoretic techniques, *J. Chromatogr. A* 666:295 (1994).



Chromatographic Methods Used to Identify and Quantify Organic Polymer Additives

Dennis Jenke

Baxter Healthcare Corporation, Round Lake, Illinois, U.S.A.

INTRODUCTION

Plastic materials are widely used in numerous industries. The physiochemical nature of these materials provides a multitude of diverse products with their necessary, desirable performance characteristics. Commercial plastics are very complex materials. In addition to the various base polymers, commercially viable plastics contain a number of compounding ingredients (additives) whose purpose is to give the material its desired physical and/or chemical properties. Table 1 provides a brief summary of the types of additives typically encountered in commercial polymer systems.

Polymers and polymer systems are characterized for many reasons including the development of new materials or material sources, the end-use applications, the life test studies, the manufacturing control and troubleshooting, and the material or vendor identification. As it is typically the additive package that establishes the performance and processing properties of the commercial polymer, characterization of a polymer system for its additive package is essential in terms of material development, manufacturing, use, reuse, and, ultimately, disposal. A complete polymer characterization includes both the identities of the additives and their levels in the product. The identification and the quantification of additives in compounded polymers is generally a difficult task for the following reasons:

1. There is a wide variety of chemically diverse additive types. Literally, thousands of additives are commercially available, ranging from pure compounds, with molecular weights that vary from approximately 100 up to a few thousand mass units, to oligomers with up to 50 (or more) components.
2. Many additives are labile; thus, they are difficult to analyze without decomposition.
3. Complex mixtures of additives will normally be present in a commercial formulation.
4. Separation of the base polymer and the fillers from the organic additives are often required prior to additive analysis.

5. The levels of the organic additives in a commercial polymer may be quite low (and variable) compared to the base polymer and its associated fillers.

It is for these reasons that chromatographic methods of analysis have been widely employed in polymer characterization. In this paper, a review related to the chromatographic methods used to assess the identity and level of additives in polymer systems is provided.

DISCUSSION

Given the variety of additives used in commercial polymers, the task of characterizing such multicomponent systems for their additive packages can be daunting. While an analytical chemist has a multitude of chromatographic tools with which to perform an additive characterization, some guidance in terms of successfully applied strategies and methods can greatly facilitate the assessment. Thus this manuscript contains a general compilation of published chromatographic methods and strategies that have been successfully applied to the identification and the quantification of a large number of the more commonly encountered packaging material additives (Table 2 shows a listing of additives considered in this work's cited references). Examples are provided for each major separation strategy [e.g., high-performance liquid chromatography (HPLC), gas chromatography (GC), thin-layer chromatography (TLC), supercritical fluid chromatography (SFC)] and for most commonly employed detection methods [e.g., ultraviolet (UV), mass spectrometry (MS), flame ionization detector (FID)]. While the compilations in Tables 3–10 are by no means exhaustive or comprehensive, they are sufficiently broad in scope to provide the investigator with a general overview of the ways in which chromatography has been applied to meet the objectives of a polymer's characterization.

Tables 3–10 provide general method details, such as separation medium, elution, and detection conditions, and



Table 1 Common additives and fillers

Classification	Purpose	Examples
Antioxidants	Prevent thermal and/or oxidative degradation during processing, handling, and use. Typically are radical scavengers which interrupt the chain propagation steps of polymer autooxidation	Irganox 1010, Irgafos 168, BHT
Light stabilizers	Absorb UV light to prevent photooxidation	Tinuvin 327, 328, 384, 440, etc. (derivatives of 2-hydroxy-benzophenone)
Heat stabilizers	Protect polymers during thermal processing	Metallic salts, especially of weak fatty acids (e.g., zinc stearate)
Plasticizers	Increase the workability, flexibility or distensibility of polymer	Derivatives of organic acids such as adipic, azelic, citric, phosphoric, phthalic, trimellitic acids
Lubricants (slip agent)	Reduce polymer adhesion to metal surfaces during processing	Derivatives of fatty acids (esters, amides, metal salts, Erucamide, silicones)
Viscosity improvers	Control the flow and the sagging of prepolymers	Ethoxylated fatty acids
Accelerators, activators	Compounds that control the rate or the nature of cure of elastomers	Zinc oxide, stearic acid, 2-2'-dithiobis-benzothiazole, zinc dialkyldithio-carbamate
Mold release agents	Prevent adhesion between two surfaces (e.g., sticking of polymer and metal mold)	Derivatives of fatty acids, Montan wax, silicones, diethylene glycol monostearate, ethylene bis(stearamide)
Fillers (extenders)	Finely dissolved solids added to polymer systems to improve properties or to reduce cost	Calcium carbonate, kaolin, talc, alumina trihydrate
Flame retardants	Decrease flammability	Alumina trihydrate, mixtures of halogenated organics and antimony oxide
Antistatic agents	Dissipate electrostatic surface charge on polymer surfaces	Quaternary ammonium compounds, long-chain derivatives of glycols and polyhydric compounds, Atmos 150, <i>N,N</i> -bis (2-hydroxy-ethyl)alkyl-amine
Colorants	Improve the appearance of polymers, mask discoloration due to processing	Carbon black, titanium dioxide, azo-type dyes
Antimicrobial agents (biocides)	Reduce growth of microbes on polymer surfaces	Copper 8-hydroxyquinolate, <i>n</i> -(trichloromethylthio)phthalate
Cross-linking agents	Molecules that have two or more groups capable of reacting with the functional groups of polymer chains, where such a reaction connects or links the chains	2-mercaptobenzothiazole, benzoyl peroxide, dicumyl peroxide, sulfur, toluene diisocyanate
Blowing agents	Gas-forming agents that facilitate the expansion of the polymer during processing	Nitrogen, toluenesulfonyl semicarbazide, 1,1'-azobisforamide, phenyltetrazole

other operating conditions. The level of detail associated with each citation reflects the level of detail provided by the citation's author(s). The materials investigated, as well as the specific additives examined, are also indicated. General comments are provided in terms of sample preparation. Given the number of methods cited, it is not possible to provide chromatographic profiles which are readily available in the cited references.

In generating this review, the author balanced two objectives. The first objective was to summarize the most

current technologies that are utilized for the task of polymer characterization, thus providing the researcher with the most relevant and state-of-the-art tools for the task at hand. Thus emerging automated and hyphenated techniques, coupled with on-line sample preparation, high-efficiency separations, and selective and sensitive detection (e.g., supercritical fluid extraction (SFE)/HPLC/MS), have a prominent place in this review. However, this author also notes that more historically relevant methods, such as GC and HPLC with UV detection,

Table 2 Chemical names for the additives cited in this manuscript

Trade name	Chemical name	CAS RN
AcraWax C	<i>N,N'</i> -ethylenebistearamide	110-30-5
Adkstab PEP-24G	Cyclinepentan tetraol bis(2,4-di- <i>tert</i> -butylphenyl) phosphite	29741-53-7
AM340		
ATBC	<i>o</i> -Acetyl-tri- <i>n</i> -butyl citrate (see Citroflex A-4)	—
Atmos 150	A mixture of glycerol mono- and distearate	11099-07-3
BAC-E	2,6-bis[(Azidophenyl)methylene]-4-ethylcyclohexanone	
BBP	Benzyl <i>n</i> -butyl phthalate	85-68-7
Benzoflex-2860	A mixture of 19% di(2-ethylhexyl)adipate, 57% diethyleneglycol dibenzoate, 24% triethyleneglycol dibenzoate	400609-45-2
BEHB	Butylated hydroxyethylbenzene	
Behenamide	Docosanoic acid amide	3061-75-4
BHA	2- <i>tert</i> -Butyl-4-hydroxyanisole	25013-16-5
BHT	2,6-Di- <i>tert</i> -butyl- <i>p</i> -cresol	128-37-0
BHET	bis(2-Hydroxyethyl)terephthalate	
Bis-A-bis azide	1,1'-(1-Methylethylidene)-bis[4-(4-azidophenoxybenzene)]	
Bisphenol A	2,2'-bis(4-Hydroxyphenyl)propane	80-05-7
Brominated bisphenol A		
Brominated phenol		
Butyl oleate	9-Octadecanoic acid, butyl ester	142-77-8
Butyl palmitate	Hexadecanoic acid, butyl ester	111-06-8
Butyl stearate	Octadecanoic acid, butyl ester	123-95-5
Calcium stearate	Stearic acid, calcium salt	1592-23-0
Caprolactam	2-Oxohexamethyleneimine	105-60-2
Chimasorb 81	2-Hydroxy-4- <i>n</i> -octyloxybenzophenone	1843-05-6
Chimassorb 119 FL		
Chimassorb 944	Poly-[[6-[1,1,3,3,-tetramethylbutyl)amino]-1,3,5-triazine-2,4-diyl] [2,2,6,6-tetramethyl-4-piperidiny]imino]-1,6-hexanediyl[2,2,6,6-tetramethyl-4-piperidiny]imino]	71878-19-8
Citroflex A-4	2-Acetoxy-1,2,3-propanetricarboxylic acid tributyl ester	77-90-7
Cyanox 425	2,2'-Methylenebis(6- <i>tert</i> -butyl-4-ethylphenol)	88-24-4
Cyanox 1790	1,3,5-tris(4- <i>tert</i> -Butyl-3-hydroxy-2,6-dimethylbenzyl)-1,3,5-triazine-(1 <i>H</i> ,3 <i>H</i> ,5 <i>H</i>) trione	40601-76-1
Cyanox 2246	See Irganox 2246	—
Cyasorb UV 9		
Cyasorb UV-24	2,2'-Dihydroxy-4-methoxybenzophenone	131-53-3
Cyasorb UV 531	2-Hydroxy-4-(octyloxy)benzophenone	1843-05-6
Cyasorb UV 1084	2,2'-Thiobis(4- <i>tert</i> -octylphenoxy)(nibutylamine)nickel	14516-71-3
Cyasorb UV 1164	2,4-bis(2,4-Dimethylphenyl)-6-(2-hydroxy-4-octyloxyphenyl)-1,3,5-triazine	2725-22-6
Cyasorb 2908	3,5-di- <i>tert</i> -butyl-4-hydroxybenzoate	67845-93-6
Dechlorane Plus	1,2,3,4,7,8,9,10,13,14,14-Dodecachloro-1,4,4a,5,6,6a,7,10,10a,11,12, 12a-dodecahydro-1,4,7,10-dimethanodibenzo [<i>a,e</i>] cyclooctene	13560-89-9
DEHA	Di-(2-ethylhexyl) adipate, dioctyl adipate	103-23-1
Di-Cup	Dicumyl peroxide	80-43-3
Dibutyl sebacate		109-43-3
DEG	Diethylene glycol	111-46-6
DBP	Di- <i>n</i> -butyl phthalate	84-74-2
DEHP, DOP	Di(2-ethylhexyl) phthalate	117-81-7
Dinonyl phthalate	1,2-Benzenedicarboxylic acid, dinonyl ester	84-76-4
DMTDP	3,3'-Thiodipropionic acid di- <i>n</i> -tetradecyl ester	16545-54-3
DSTDP	Dioctadecyl 3,3'-thiodipropionate	693-36-7
DLTDP	Dilauryl 3,3'-thiodipropionate	123-28-4
Docosane		629-97-0
Eicosane		112-95-8

(Continued)



Table 2 Chemical names for the additives cited in this manuscript (*Continued*)

Trade name	Chemical name	CAS RN
Epoxol 9.5	Epoxidized linseed oil	8016-11-3
EG	Ethylene glycol	107-21-1
Erucamide	<i>cis</i> -13-Docosenamide	112-84-5
Ethyl palmitate	Hexadecanoic acid ethyl ester	628-97-7
Ethyl linoleate	9,12-Octadecanoic acid ethyl ester	544-35-4
Ethyl oleate	9-Octadecanoic acid ethyl ester	111-62-6
Ethyl stearate	Octadecanoic acid ethyl ester	111-61-5
Ethanox 330	See Irganox 1330	—
Hexadecane		544-76-3
Hexacosane		630-01-3
Hostanox O3	bis[3,3-bis(4-Hydroxy-3- <i>tert</i> -butylphenyl)butanoic acid] ethylene glycol ester	32509-66-3
Hostavin TMN 20	2,2,4,4-Tetramethyl-21-oxo-7-oxa-3,20-diazadispiro[5.1.11.2]heneicosane	64338-16-5
Ionol 220	2,6-Di(<i>tert</i> -butyl)-4-methylphenol (see Topanol OC)	—
Ionox 100	4-Hydroxymethyl-2,6-di- <i>tert</i> -butylphenol	88-26-6
Ionox 129	2,2'-Ethylidenebis(4,6-di- <i>tert</i> -butylphenol)	35958-30-6
Ionox 220	4,4-Methylenebis(2,6-di- <i>tert</i> -butylphenol)	118-82-2
Irgafos 168	tris(2,4-Di- <i>tert</i> -butylphenyl)phosphite	31570-04-4
Irgafos P-EPQ	Tetrakis(2,4-di- <i>tert</i> -butylphenyl)-4,4'-biphenylene diphosphonite	38613-77-3
Irganox 245	Triethylene glycol bis-3-(3- <i>tert</i> -butyl-4-hydroxy-5-methyl)propionate	36443-68-2
Irganox 259	1,6-bis[3-(3,5-Di- <i>tert</i> -butyl-4-hydroxyphenyl)propionyloxy]hexane	35074-77-2
Irganox 565	2,4-bis(Octylthio)-6-(3,5-di- <i>tert</i> -butyl-4-hydroxyanilino)-1,3,5-triazine	991-84-4
Irganox 1010	Tetrakis-methylene-(3,5-di- <i>tert</i> -butyl-4-hydroxyhydrocinnamate)-methane	6683-19-8
Irganox 1035	2,2'-Thiodiethylene bis[3-(3,5-di- <i>tert</i> -butyl-4-hydroxyphenyl)propionate]	41484-35-9
Irganox 1076	Octadecyl-3-(3',5'-di(<i>tert</i> -butyl)-4'-hydroxyphenyl)propionate	2082-79-3
Irganox 1098	<i>N,N</i> -bis[3-(3,5-di- <i>tert</i> -butyl-4-hydroxyphenyl)propionyl]hexamethylene-diamine	23128-74-7
Irganox 1222	Diethyl (3,5-di- <i>tert</i> -butyl-4-hydroxybenzyl)phosphonate	976-56-7
Irganox 1330	1,3,5-Trimethyl-2,4,6-tris(3,5-di- <i>t</i> -butyl-4-hydroxy-benzyl)-benzene	1709-70-2
Irganox 1425	Calcium bis(ethyl 3,5-di- <i>tert</i> -butyl-4-hydroxybenzylphosphonate)	65140-91-2
Irganox 2246	2,2'-Methylene-bis(4-methyl-6- <i>tert</i> -butylphenol)	119-47-1
Irganox 3052 FF	2,2'-Methylenebis(6- <i>tert</i> -butyl-4-methylphenol) monoacrylate	61167-58-6
Irganox 3114	1,3,5-tris(3,5-Di- <i>t</i> -butyl-4-hydroxybenzyl)- <i>s</i> -triazine-2,4,6-(1 <i>H</i> ,3 <i>H</i> ,5 <i>H</i>)trione	27676-62-6
Irganox MD1024	3,5-bis(1,1-Dimethylethyl)-4-hydroxybenzenepropionic acid	32687-78-8
Irganox MD1025	<i>N,N</i> -bis[1-oxo-3(3,5-di- <i>tert</i> -butyl-4-hydroxyphenyl)propane]hydrazine	
Irganox PS800	Di-lauryl thio-dipropionate	123-28-4
Irganox PS802	Di-stearyl thio-dipropionate	693-36-7
Isonox 129	2,2'-Ethylidenebis[4,6-di- <i>tert</i> -butylphenol]	35958-30-6
Kemamide U	See Oleamide	—
Lauric acid	Dodecanoic acid	143-07-7
Lowinox 22M46	See Irganox 2246	—
MHET	Mono-(2-hydroxyethyl)terephthalate	155603-50-2
Myristic acid	Tetradecanoic acid	544-63-8
	<i>N,N</i> -bis(2-hydroxyethyl)alkyl-amine	
Naugard SP		94765-89-6
Naugard XL-1	2,2'-Oxamidobis[ethyl 3-(3,5-di- <i>tert</i> -butyl-4-hydroxyphenyl)propionate]	70331-94-1
Naugawhite	2,2'-Methylenebis(4-methyl-6-nonylphenol)	7786-17-6
NC-4	1-(2,6-Dimethylphenylimino)imidazolidine	4859-06-7
Nonflex CBP	2,2'-Methylenebis(6-(1-methylcyclohexyl)- <i>p</i> -cresol)	77-62-3
Noclizer M-17	2,6-Di- <i>tert</i> -butyl-4-ethylphenol	4130-42-1
Octadecane		593-45-3
ODO	Octabromodiphenyl oxide	32536-52-0
Oleamide	9-Octadecenamide	301-02-0
Palmitic acid	Hexadecanoic acid	57-10-3
Palmitamide	Hexadecanoic acid amide	629-54-9

(Continued)

Table 2 Chemical names for the additives cited in this manuscript (*Continued*)

Trade name	Chemical name	CAS RN
Permanax WSP	2,2'-Methylenebis[4-methyl-6-(1-methylcyclohexyl)phenol]	77-62-3
Sanol LS744		
Sanol LS770		
Santonox	See Yoshinox SR	—
Santowhite	4,4'-Butylidenebis(3-methyl-6- <i>tert</i> -butylphenol)	85-60-9
Seesorb 101	2-Hydroxy-4-methylbenzophenone	131-57-7
Seesorb 202	4- <i>tert</i> -Butylphenylsalicylate	87-18-3
Seenox DM	3,3'-Thio-dipropionic acid dimyristyl ester	16545-54-3
Sodium benzoate	Benzoic acid, sodium salt	532-32-1
Stearamide	Octadecanamide	124-26-5
Stearic acid	Octadecanoic acid	57-11-4
Synprolam	Quaternary ammonium compounds, di-C13–C15-alkylmethyl, chlorides	308074-61-5
Terephthalic acid		100-21-0
TETO	Glyceryl tri-epoxyoleate	
Tetradecane		629-59-4
Tetracosane		646-31-1
Tinuvin 120	2',4'-Di- <i>tert</i> -butylphenyl-3,5-Di- <i>tert</i> -butyl-4-hydroxybenzoate	4221-80-1
Tinuvin 144	2- <i>tert</i> -Butyl-2-(4-hydroxy-3,5-di- <i>tert</i> -butylbenzyl)[bis(methyl,2,2,6,6-tetramethyl-4-piperidinyl)] dipropionate	63843-89-0
Tinuvin 234	2[2'-Hydroxy-3,5-di(1,1-dimethylbenzyl)phenyl]-2 <i>H</i> -benzotriazole	70321-86-7
Tinuvin 292	bis(1-Methyl-2,2,6,6-tetramethylpiperidinyl) sebacate	41556-26-7
Tinuvin 312	<i>N</i> -(2-ethoxyphenyl)- <i>N'</i> -(2-ethylphenyl)-ethanediamine	23949-66-8
Tinuvin 320	2-(2-Hydroxy-3,5-di- <i>tert</i> -butylphenyl)-2 <i>H</i> -benzotriazole	3846-71-7
Tinuvin 326	2-(3- <i>tert</i> -Butyl-2-hydroxy-5-methylphenyl)-2 <i>H</i> -5-chlorobenzotriazole	3896-11-5
Tinuvin 327	2-(2'-Hydroxy-3',5'-di(<i>tert</i> butyl)phenyl)-2 <i>H</i> -5-chlorobenzotriazole	3864-99-1
Tinuvin 328	2-(2'-Hydroxy-3',5'-di(<i>tert</i> butyl)phenyl)-2 <i>H</i> -chlorobenzotriazole	25973-55-1
Tinuvin 329	2-(2'-Hydroxy-5'- <i>tert</i> -octylphenyl)benzotriazole	3147-75-9
Tinuvin 350	2-(2 <i>H</i> -benzotriazol-2-yl)-4-(1,1-dimethylethyl)-6-(2-methylpropyl)phenol	134440-54-3
Tinuvin 384	Octyl 3-[3-(2 <i>H</i> -benzotriazol-2-yl)-5- <i>tert</i> -butyl-4-hydroxyphenyl]propionate	84268-23-5
Tinuvin 662		
Tinuvin 770	(2-(2-Hydroxy-3,5-bis(1-methyl-1-phenylether)phenyl)benzotriazole)	52829-07-9
Tinuvin 1130	α -[3-[2-(2 <i>H</i> -benzotriazol-2-yl)-5-(1,1,-dimethylethyl)-4-hydroxyphenyl]-1-oxopropyl-hydroxy-poly(oxy-1,2-ethanediyl)]	194810-48-2
Tinuvin P	2-(2-Hydroxy-5-methylphenyl)-2 <i>H</i> -benzotriazole	2440-22-4
TNPP	tris(Nonylphenyl) phosphite	26523-78-4
Topanol CA	1,1,3-tri(3- <i>tert</i> -butyl-4-hydroxy-6-methylphenyl)butane	1843-03-4
Topanol OC	2,4,6-tri- <i>tert</i> -butylphenol	128-37-0
TPP	Triphenyl phosphate	115-86-6
Tributylacetylcitrate	See Citroflex A-4	—
Ultrinox 626	bis(2,4-Di- <i>t</i> -butylphenyl)-pentaerythritol-diphosphite	26741-53-7
Uvitex OB	2,5-bis(5'- <i>tert</i> -Butyl-2'-benzoazolyl) thiophene	7128-64-5
Vulkanox CS		94766-18-4
Wingstay T		12674-05-4
Yoshinox 425	2,2'-Methylenebis(4-ethyl-6- <i>tert</i> -butylphenol)	88-24-4
Yoshinox BB	See Santowhite	—
Yoshinox SR	4,4'-Thiobis[3-methyl-6- <i>tert</i> -butylphenol]	96-69-5
Zinc stearate	Stearic acid, zinc salt	557-05-1



Table 3 Examples of HPLC methods (UV detection) used to identify and/or quantify packaging system additives

Material	Additive(s)	Sample preparation	Column	Mobile phase	λ (nm)	Other	Ref.
PE	Dicumyl peroxide, Santonox [®]	Extract with methanol, concentrate (evaporative)	Lichrosorb RP 18, 250 \times 4.6 mm, 10 μ m	Methanol/water, 80/20	254	1 mL/min	[1]
PVC	Di-(2-ethylhexyl) phthalate (DEHP), epoxidized linseed oil, tris(nonylphenyl) phosphite (TNPP)	Dissolve in tetrahydrofuran (THF), precipitate polymer with methanol, dry and dissolve residue	μ Porasil C ₁₈	Carbon tetrachloride-dichloromethane (65/35)	280	1 mL/min	[2]
LDPE, PP	BHT, Cyasorb 531, Tinuvin 327, Irganox 1076	Reflux with CCl ₄ or THF, filter, concentrate	μ Bondapak C ₁₈ , 60 \times 0.39 cm	Methanol/water/THF, 63/7/30	254	2 mL/min	[3]
LDPE, HDPE	Tinuvin P, BHT, BEHB, Oleamide, Cyasorb UV 531, Isonox 129, AM340, Irganox 1010, Irganox 3114, Erucamide	Soxhlet, ultrasonic or microwave extraction with various solvent systems	Nova-Pak C ₁₈ , 150 \times 3.9 mm, 4 μ m	A = water; B = acetonitrile; 3/2 initial, linear gradient to 100% B in 5 min	200	1.5 mL/min, T = 50°C	[4]
PP	Irgafos 168, Irganox 1076, Irganox 3114, Irganox 1010, Tinuvin P, Irgafos PEP-Q	Microwave extraction with 98/2 methylene chloride/2-propanol	Nova-Pak silica (150 \times 3.9 mm, 4 μ m) or resolve silica (150 \times 3.9 mm, 5 μ m)	70/30 <i>n</i> -butyl chloride/methylene chloride	225	1.5 mL/min, T = 30°C	[4]
Polyolefin	Irganox (245, 259, 565, 1010, 1035, 3114); Tinuvin (P, 234, 320, 326, 327, 328)	N/A ^a	Capcell Pak C ₁₈ , 250 \times 4.6 mm	Methanol/water mixtures (95/5, 90/10, 88/12, 85/15)	multiple	1 mL/min, T = 45°C, 20 μ L	[5]
Polyolefin	BHT, BHA, Irganox 1010, Irganox 565, Tinuvin 327, Tinuvin P	N/A ^a	Licrosphere 100 RP 18, 250 \times 4.6 mm, 5 μ m	Various binary and tertiary mixtures of methanol, water, and acetonitrile	multiple	20 μ L	[6]
General	BHT, Irganox antioxidants (245, 259, 565, 1010, 1035, 1076, 1098, 1222, 1330, etc.); UV absorbers (Tinuvin P, 312, 320, 327, 328, etc.)	N/A ^a	Ultrabase UB225, 250 \times 4.6 mm, 5 μ m; LiChrospher 100 RP 18e, 250 \times 4.6 mm, 5 μ m; Sphert 5-ODS, 250 \times 4.6 mm, 5 μ m	Quaternary gradient of THF, water, methanol, acetonitrile	Multiple wavelength UV and laser light scattering ^b	1 mL/min, 20 μ L, ambient temperature	[7] ^c

General	BHT, BHA	N/A ^a	Whatman Partisil PXS 10/25 ODS-2	0.05 M LiClO ₄ in 85% methanol	UV-electrochemical fluorescence	1 mL/min, 20 μ L, <i>T</i> = 40°C	[8] ^d
PP, ABS	Numerous ^e	Dissolve in MeCl ₂ , precipitate polymer with methanol	Spherisorb S30DS2, 150 \times 4.6 mm, 3 μ m	A = Acetonitrile; B = water; Initial = 40% A, ramped to 100% A in 15 min, maintained at 100% for 17 min	210, 280	1 mL/min (2 mL/min after 22 min); 10 μ L	[9]
PE	Topanol OC; Cyasorb UV 531; Irganox 1010, 1076, 1330	SFE contrasted to Soxhlet extraction with dichloromethane	Kaseisorb ODS-5, 550 \times 0.53 mm	Methanol	254 nm	Column pressure = 100 atm	[54]
PP	Irganox 1010, Irgafos 168	SFE	Licrosorb RP-18, 200 \times 4.6 mm, 5 μ m	Gradient from methanol/water (95/5) to 100% methanol in 17 min	280 nm	1.5 mL/min, 20 μ L	[11]
Polyolefin	Irganox PS802, 1010, 1076, 1425; calcium stearate; sodium benzoate	Microwave-assisted solvent extraction	Various; e.g., Microsper C ₁₈ , 250 \times 4.6 mm, 5 μ m	Water/acetonitrile/ <i>iso</i> -propanol; Start = 12/88/0; 0.1 min = 5/65/ 30; 10 min = 0/ 65/30; 18 min = 0/65/30	273 nm, light scattering	2 mL/min, 10 μ L, <i>T</i> = 50°C	[12]
PMMA	Irganox 1010, 1076; Irgafos 168	SFE	Nova-Pack C ₁₈ , 5 μ m	Acetonitrile/water gradient; start at 80/20, change to 100/0 in 5 min	254 nm	50 μ L	[13]
Dielectric resins	BAC-E, bis-A-bis- azide	Dissolution in THF	Zorbax RX C8, 100 \times 4.5 mm, 5 μ m ^f	A = 50/50 acetonitrile/ water; B = 90/10 mixture. Gradient was start ramp form 0% A to 100% B in 5 min, hold at 100% B for 5 min	254 nm (380 nm for internal standard)	3 mL/min	[14]

ABS = acrylonitrile-butadiene-styrene; HDPE = high-density polyethylene; LDPE = low-density polyethylene; PC = polycarbonate; PE = polyethylene; PMMA = polymethylmethacrylate; PP = polypropylene; PS = polystyrene; PVC = polyvinyl chloride.

^aThis reference examined the elution characteristics of the cited additives as a function of mobile phase and, thus, did not characterize actual polymers.

^bThese authors report that the UV response for the analytes is typically 5 to 50 times greater than the light-scattering response.

^cNumerous other examples of separations provided.

^dFor BHA, the sensitivity was EC > UV (230 nm) > FI. For BHT, the sensitivity was UV (280 nm) > EC > FI.

^eThis study examined the elution characteristics, sensitivity, and analytical recoveries of over 25 additives.

^fPreanalytical column sample cleanup was achieved on-line by SEC. This preanalytical processing was accomplished with a 25 cm \times 250 μ m i.d. fused silica capillary column (PL-Gel 50 Å, 5 μ m) and a THF mobile phase at 1.3 μ L/min.

Table 4 Examples of HPLC methods [infrared (IR) detection] used to identify and/or quantify packaging system additives

Material	Additive(s)	Sample preparation	Column	Mobile phase	λ (nm)	Other	Ref.
Polyurethane	Irganox 1010	Extraction with <i>n</i> -hexane	μ -Porasil C ₁₈	<i>n</i> -hexane/dichloromethane, 80/20	254 ^a	1 mL/min	[15]
PVC, PP, PE	Ionol 220, Irganox 1076, Tinuvin 327, Tinuvin 328, Cyasorb UV 531	Extraction with acetonitrile or methanol, evaporative concentration	RP: Spherisorb ODS-2, 100 \times 1.0 mm, 3 μ m; SEC: PL-Gel, 250 \times 4.6 mm, 5 μ m, 500 Å	RP = methanol/water (95./5); SEC = Dichloromethane	280 ^b	0.1–0.2 mL/min	[16]
PP	Irganox 1010, 3114; Tinuvin 326, 327	N/A ^c	Zorbax ODS, 250 \times 4.6 mm		N/A ^d	0.5 mL/min, 20 μ L	[17]
PP, PE	Irganox 245, 259, 1010, 1076, 1098, 3114; Irgafos 168; Tinuvin 234, 327, 328, 350; Sanowwhite, Ethanox 330; Lowinox 22M46; Kemamide U; Naugard; BHT; Ultrinox 626; Cyasorb 2908; Cyasorb UV 531	N/A ^c	Spherisorb ODS-2, 250 \times 4.6 mm, 5 μ m	Several cited ^e	280 nm and evaporative light scattering ^f	1 mL/min, 50 μ L, ambient temperature	[18] ^g

PE = polyethylene; PP = polypropylene; PVC = polyvinyl chloride.

^aPeak collected on potassium bromide powder and an IR spectrum obtained off-line.

^bOn-line Fourier transform infrared spectroscopy (FTIR) with spray-jet interface, deposition on a moving zinc selenide substrate. UV for quantitation, IR for identification.

^cThis reference examined the detection characteristics of the cited additives and, thus, did not characterize actual polymers.

^dUsed surface-enhanced infrared spectroscopy with effluent deposition on an Ag metal film (BaF₂ substrate). Reported a detection limit of 10 ng.

^eSeveral separations are cited in this manuscript. A gradient using methanol and water was used for the separation of nine additives. Initial composition, 94/6 methanol/water for 7 min, change immediately to 100% methanol, hold for 14 min.

^fPortion of column effluent deposited on a rotating germanium disk via drying nebulization.

^gDetection limits by IR were generally near 0.2 μ g, with quantities needed for accurate identification in the 0.5–1.0 μ g range.

Table 5 Examples of HPLC methods (MS detection) used to identify and/or quantify packaging system additives

Material	Additive(s)	Sample Preparation	Column	Mobile Phase	Detection	Other	Ref.
General (PP)	BHT, Irganox 1010, Irganox 1076, Irganox 1330, Santowhite	N/A ^a	ODS, 250 × 2.1 mm, 5 μm	A = 75/25 acetonitrile/water; B = 50/50 THF/acetonitrile; 0 min = 100% A, 10 min = 60% A, 20 min = 100% B, 30 min = 100% B, 32 min = 100% A	UV, 280 nm. Moving belt MS interface, chemical ionization (CI) and electron input ionization (EI) spectra obtained	0.2 mL/min, 10 μL	[19]
PVC	Mono-alkyl esters and di-alkyl phthalates	N/A ^a	Symmetry C-8, 150 × 3.9 mm, 5 μm	A = 0.1 M ammonium acetate in 10/90 methanol/water; B = 0.1 M ammonium acetate in methanol 0% to 100% B over 25 min, hold for 5 min	UV, 277 nm. Thermospray MS, + ions	1 mL/min	[20]
PP	NC-4, Naugard-XL, Irganox 1076	Extract with acetonitrile at 60°C for 72 hr	Symmetry C8, 150 × 3.9 mm, 3 μm	A = acetonitrile; B = water; 0 = 30% A, 10 min = 100% A, 30 min = 30% A, 40 min = 30% A	Multiple λ UV. MS = EI and atmospheric pressure chemical ionization (APCI) [positive ion, single ion monitoring (SIM)]		[21]
PP	Irganox 245, BHA, BHT, Bisphenol A, Topanol CA	N/A	Hypersil H5ODS, 100 × 4.6 mm, 5 μm	80/20 deuterated acetonitrile/water	UV, IR, MS, nuclear magnetic resonance (NMR) ^b	1 mL/min	[55]

PP = polypropylene; PVC = polyvinyl chloride.

^aThis reference examined the elution characteristics of the cited additives as a function of mobile phase and thus did not characterize actual polymers.^bThe column effluent was split after the column (95/5) between the FTIR flowcell [attenuated total reflection (ATR) used] and the MS detector (single quad, positive ions). The effluent from the FTIR cell was directed through the UV and ultimately NMR detectors.

Table 6 Examples of SFC methods used to identify and/or quantify packaging system additives

Material	Additive(s)	Sample preparation	Column	Mobile phase	Detection	Other	Ref.
General (PE)	Numerous ^a	N/A ^b ; SFE	C ₁₈ , 250 × 4.6 mm	CO ₂ with methanol modifier; 2% methanol for 1 min, linear to 10% after 10 min, hold for 5 min	APCI-MS (+ and – ionization), UV	2 mL/min, 10 µL	[22] ^c
PE	BHT, Tinuvin 326	SFE with various traps	Fused silica capillary (10 m × 0.1 mm i.d.) with octyl phase, 0.5-µm film	CO ₂ , pressure program (100 atm for 10 min, increased at 5 atm/min for 20 min)	FID	Column T = 90°C	[23]
Polyolefin (PP, PE)	BHT; Irganox PS800, PS802, 1010, 1076, 1330, 2246; Tinuvin P, 320, 326; Irgafos 168; Atmos 150	Soxhlet extraction with chloroform	Fused silica capillary (10 m × 0.05 mm i.d.) with 5% phenyl-polymethylsiloxane, 0.4-µm film	Various pressure and temperature programs with CO ₂ were reported	MS, EI	1 µL injection	[24, 25] ^{d,e}
PP	Numerous ^f	Soxhlet extraction with diethyl ether for 15 hr, precipitate polymer with ethanol	Fused silica capillary (15 m × 0.1 mm i.d.) with 5% phenyl-polymethylsiloxane, 0.5-µm film	CO ₂ at 140°C; pressure = 150 atm for 12 min, ramp to 350 atm at 3 atm/min	FID, FTIR microscope	2 µL split injection, T = 150°C	[26]
PE	BHT, Irganox 1010, Irgafos 168	SFE (contrasted to Soxhlet extraction)	Fused silica capillary (15 m × 0.1 mm i.d.) with SB-Biphenyl-30, 0.5-µm film	CO ₂ at 140°C; pressure = 100 atm, ramp to 200 atm at 3 atm/min, ramp at 10 atm/min to 400 atm	IR (flow through cell)	–	[27]
General	Tinuvin P, 326, 234, 770; Chimasorb 81, Irganox 1010, 1076, 1330; Irgafos 168, Irgafos P-EPQ, N,N-bis (2-hydroxyethyl) alkyl-amine	N/A ^b	Fused silica capillary (20 m × 0.1 mm i.d.) with DB-5, 0.4-µm film	CO ₂ ; pressure = 10.6 MPa for 10 min, ramp to 15 MPa in 3.5 min, hold for 5 min; ramp at 0.5 MPa/min to 35 MPa, hold for 10 min	FID and MS (EI, 70 eV)	2 mL/min, T = 140°C	[10]

LDPE	BHT, BHEB, Isonox 129, Irganox 1010, 1076	On-line SFE	Deltabond cyano, 100 × 1.0 mm i.d., 5 µm	100 atm for 3 min, 100–330 atm for 7 min, 330–450 atm for 1.5 min	FID	Column T = 100°C	[28] ^g
Polyurethane	BHT, Irganox 1010, Irganox 1076, dimonyl phthalate ^h	On-line SFE	30% biphenyl polysiloxane, 10 m × 50 µm i.d., 0.25-µm film	CO ₂ ; hold at 100 atm for 5 min, ramp at 5 atm/min to 300 atm, ramp at 20 atm/min to 400 atm	MS (EI)	Column T = 100°C	[29]
Nylon, polystyrene	Caprolactam and oligomers, stearic acid, Irganox 1076	On-line SFE	Deltabond cyano, 100 cm × 1 mm, 5 µm	CO ₂ ; hold at 100 atm for 2 min, ramp at 15 atm/min	FTIR	Column T = 100°C	[30]
PE, PP	BHT; Erucamide; Irgafos 168, Irganox 1010, 1076; Tinuvin 326, 770; Isonox 19; DLTDP	On-line SFE	Deltabond 300 Octyl, 250 cm × 1 mm	CO ₂ ; hold at 1500 psi for 6 min, ramp at 200 psi/min to 6000 psi	FID	FID T = 350°C; Column T = 150°C	[31]

LDPE = low-density polyethylene; PE = polyethylene; PP = polypropylene.

^aAdditives examined included: BHT; Irganox 245, 1010, 1035, 1076, 1330, 1425, PS802; Irgafos 168; Tinuvin 327, 328, 384 440, 622, 770, 1130; Topanol CA; Cyasorb UV1164; Oleamide; Erucamide; Synprolam; Chimassorb 944.

^bThis reference examined the elution characteristics of the cited additives as a function of mobile phase and, thus, did not characterize actual polymers.

^cThis reference provides elution characteristics and relative intensities for specific positive and negative ions.

^dThe performance of the SFC method was compared to that of an isocratic reversed phase (RP)-HPLC method (UV detection).

^eGC/MS was also used for compound identification.

^fAdditives included: Topanol OC; Tinuvin P, 292, 320, 326, 328, 770, 440, 144; Chimassorb 81; Erucamide; Irganox PS800, PS802, 245, 1010, 1035; MD1025, 1076, 1330, 3114.

^gThe SFE extraction was also coupled with HPLC separation and detection of the analytes.

^hThis method produced other additive peaks whose parent compound could not be identified.

Table 7 Examples of size exclusion chromatography (SEC)/gel permeation chromatography (GPC) methods used to identify and/or quantify packaging system additives

Material	Additive(s)	Sample preparation	Column	Mobile phase	Detection	Other	Ref.
PP	General ^a	Extraction with THF	Porogel A-1 (slurry-packed)	THF	Refractive index (RI) (collected fraction tested via IR for identification) UV	2 mL/min, column <i>T</i> = 30°C	[32]
PS, PVC	Tinuvin P, TNPP, TETO	Solvent extraction	500 Å, 100 Å and 50 Å PL-Gel (poly(styrene- divinylbenzene) 30 × 0.77 cm, 10 µm SEC (PL-Gel, 50 Å, 300 × 7.5 mm) coupled with normal phase (Nucleosil 100- 7 OH, 250 × 4.6 mm, 7 µm)	THF	UV	2 mL/min, column <i>T</i> = 30°C	[33]
Polyolefin (PP, PE)	BHT; Cyasorb UV 9; Cyasorb UV 1084; Tinuvin 326, 327; Irganox 1076	General ^b		<i>n</i> -hexane/ dichloromethane (73/27)	UV at 254 and 280 nm	0.9 mL/min, column <i>T</i> = 35°C	[34]
Polyolefin copolymers	Numerous ^c	Dissolution in THF	SEC (Ultrastaygel 10 ⁴ , 50 Å, 300 × 0.25 mm, 10 µm) coupled with GC (DB-1, 15 m × 0.32 mm i.d., 0.25-µm film)	SEC; THF mobile phase. GC; 100°C for 6 min, ramp at 16°C/min to 350°C	UV at 254 nm for SEC, MS (EI) for GC	For SEC: 3.0 µL/min, 0.2 mL injected	[35]

PE = polyethylene; PP = polypropylene; PS = polystyrene; PVC = polyvinyl chloride.

^aThis reference generated additive profiles for various test materials but did not specify the individual additives found.^bThis reference examined the chromatographic characteristics of the cited additives as a function of mobile phase and, thus, did not characterize actual polymers.^cThis reference documented chromatographic characteristics for many individual additives including plasticizers (phthalates, Citroflex A-4, TNPP); amides; Irganox and Irgafos antioxidants; UV absorbers (Tinuvin, Cyasorb); fatty acids (palmitic, stearic); Naugard XL-1; etc.

Table 8 Examples of TLC methods used to identify and/or quantify packaging system additives

Material	Additive(s)	Sample preparation	Plate	Mobile phase	Detection	Other	Ref.
Rubber	Numerous ^a	N/A ^b	Silica gel G, thickness of 250–300 µm	Numerous solvent systems examined vs. compound class	Various UV and visible developing reagents	Sample size: 3–5 µL	[36]
Polyolefin	Tinuvin 144, 770; Hostavin TMN 20	Extraction with chloroform, polymer precipitation, evaporative concentration	Alumina F254, 20 × 20 cm plate, 0.25-mm thickness	88/12, <i>n</i> -hexane/ <i>iso</i> -propanol	Chlorination with chlorine gas, sprayed with potassium iodide starch solution	Sample size: 10 µL	[37]
Elastomers	BHT, Cyanox 2246, Cyanox 425, Permanax WSP, Naugawhite, Wingstay T, Naugard SP, Vulkanox CS	Soxhlet extraction with acetone, evaporative concentration	Merck 11845 silica gel	Benzene	Sprayed with 2.34% sodium tetraborate, 0.33% sodium hydroxide, and 0.1% methanolic solution of <i>N</i> -chlorodichloro-2,6- <i>p</i> -benzoquinone monoimine	Sample size: 20 µL	[38]
PP, PVC	Irganox 1010, Tinuvin 770, Chimassorb 119 FL, DEHP	N/A ^b	Silica gel 60 F254, 5 × 10 cm plate, 250-µm thickness	Toluene-diethyl ether (10/1) on first plate, acetone-formic acid (4/6) on second plate	UV for plate 1, plate 2 visualized by iodine vapor. Spots removed from plate 2 and analyzed by FTIR	Sample size: 2 µL	[39]

PP = polypropylene; PVC = polyvinyl chloride.

^aThis reference documents the chromatographic properties of over 100 rubber-related amine and phenolic antioxidants, antiozonants, guanidines, accelerators, and amine hydrochlorides.^bThis reference examined the chromatographic characteristics of the cited additives and, thus, did not characterize actual polymers.

Table 9 Examples of GC methods used to identify and/or quantify packaging system additives

Material	Additives	Sample preparation	Column	Oven program	Detection	Other	Ref.
PET	Diethylene glycol	High temperature and pressure extraction with water	Numerous ^a	Isothermal at 180°C	FID and thermal conductivity detector (TCD)	Injector $T = 260^{\circ}\text{C}$; detector $T = 270^{\circ}\text{C}$; He carrier at 50 mL/min	[40]
PET	BHET, EG, DEG, TA, MHET ^b	N/A; ^c samples TMS derivatized with BSFTA (80°C for 10 min)	3% OV101 on 80–100 mesh Chromosorb W, 6 ft, 0.125 in. o.d., 0.05 in. i.d.	80°C for 3 min, ramp at 15°C/min to 265°C	FID	Injector $T = 270^{\circ}\text{C}$; detector $T = 280^{\circ}\text{C}$; He carrier at 50 mL/min, 2 μL injection	[41]
Elastomers	Various antioxidants and additives	N/A ^c	3% SP2100 on 80–100 mesh Supelcoport	150°C for 2 min, ramp at 10°C/min to 250°C	MS	Injector $T = 270^{\circ}\text{C}$; He carrier at 35 mL/min	[42]
Polyolefins	BHT; Irganox 1010, 1076, 2246; Irgafos 168, Santowhite	Refluxed in acetone for 2–3 hr, evaporated to dryness and dissolved in chloroform	PS264, 15 m \times 0.32 mm i.d., 0.15- μm film	90°C to 280°C at 5°C/min	FID	Detector $T = 300^{\circ}\text{C}$; He carrier at inlet pressure of 0.5 kg/cm ²	[43]
PVC	Benzoflex 2860, ATBC, DEHA ^d	SFE	SPB-5 fused silica capillary, 30 m \times 0.25 mm i.d., 0.25- μm film	110°C to 260°C at 10°C/min	FID	Detector, injector $T = 300^{\circ}\text{C}$; He carrier at 50 cm/sec, 1 μL splitless	[44]

Polyolefins	Numerous ^e	Reflux with chloroform, evaporative concentration	HR-1701 (14% cyanopropylphenylmethylsiloxane) fused silica capillary, 15 m × 0.53 mm i.d., 1.0-μm film	100°C for 2 min, 20°C/min to 210°C, 1.5°C/min to 222°C, 8°C/min to 350°C, hold for 10 min	FID	Injector and detector <i>T</i> = 350°C; He carrier at 5 mL/min, 1 μL splitless injection	[45]
Petroleum resin	Numerous ^e	Dissolve in <i>n</i> -hexane, cleanup with silica column	DB-1701 (14% cyanopropylphenylmethylsiloxane) fused silica capillary, 15 m × 0.53 mm i.d., 1.0-μm film	150°C for 2 min, 20°C/min to 210°C, 1.5°C/min to 222°C, 8°C/min to 350°C, hold for 10 min	FID	Injector and detector <i>T</i> = 300°C; He carrier at 5 mL/min, 2 μL split injection (1:100 ratio)	[45]
PE	Numerous ^f	Dissolution	UA-1 HT (dimethylpolysiloxane) fused silica capillary, 30 m × 0.25 mm i.d., 0.1-μm film	Start at 50°C, ramp at 20°C/min to 300°C, hold for 10 min	MS, EI, 70 eV, 40–700 <i>m/z</i>	Injector <i>T</i> = 250°C; He carrier at 1 psi, 1 μL split injection (1/2 ratio)	[46]

PE = polyethylene; PET = polyethylene terephthalate; PVC = polyvinyl chloride.

^aColumns used included: Carbowax 20M, Chromosorb W-HMDS, Aeropak Number 30, 10 ft × 1/8 in. × 0.055 in. i.d.

^bBHET = bis(2-hydroxyethyl)terephthalate; EG = ethylene glycol; DEG = diethylene glycol; TA = terephthalic acid; MHET = mono-(2-hydroxyethyl)terephthalate.

^cThis reference examined the chromatographic characteristics of the cited additives and, thus, did not characterize actual polymers.

^dATBC = *o*-acetyl-*tri-n*-butyl citrate; DEHA = di(ethylhexyl) adipate.

^eAdditives chromatographed included antioxidants (BHT; Irganox 1076, 1330; Yoshinow BB, SR, 2246 R; Irgafos 168; Ultrinox 626; Topanol CA; DLTDP; DMTDP; DSTDP), light stabilizers (Sanol LS744, LS770; Tinuvin 120, 326, 327; UV 531), and slip agents (palmitic acid amide, oleic amide, stearic acid amide, erucic amide).

^fThis reference included the separation of 53 polymer additives including antioxidants, UV stabilizers, lubricants, and plasticizers. Performance details are provided.

Table 10 Examples of pyrolysis/GC methods used to identify and/or quantify packaging system additives

Material	Additives	Pyrolysis conditions	Column	Oven program	Detection	Other	Ref.
Polyolefin, PMMA	Hostanox O3; Hostavin N 20; Irganox 3052 FF; Irganox 3114; Tinuvin 320, 329, 350	100 µg sample at 550°C	RTX-5 fused silica capillary, 60 m × 0.32 mm i.d., 0.5-µm film	60° to 300°C at 7°C/min	MS (EI, 45 – 700 mass range)	Injector T = 260°C; detector T = 270°C; He carrier at 50 mL/min	[47]
PVC	DEHP	0.5 mg sample at 700°C	DB-5 fused silica	40°C for 4 min, ramp at 10°C/min to 320°C, hold for 18 min	MS (EI, 15 – 650 mass range)	Injector T = 300°C; detector T = 300°C; 30/1 injection split	[48] ^{a,b}
Cellulose Copolymer ^c	Diethyl adipate Dibutyl sebacate, tributyl acetyl/citrate TPP		capillary, 30 m × 0.25 mm i.d., 1.0-µm film				
PS/PC blend PU	Mixture of didecyl phthalate esters						
Epoxy resin ^d	Brominated bisphenol A						
Poly-(diallyl- phthalate) ABS	Decchlorane Plus	0.5 mg sample at 950°C	DB-5 fused silica capillary, 30 m × 0.25 mm i.d., 1.0-µm film	40°C for 4 min, ramp at 10°C/min to 320°C, hold for 18 min	MS (EI, 15 – 650 mass range)	Injector T = 300°C; detector T = 300°C; 30/1 injection split	[49] ^{a,e}
PC-ABS blend	Octabromodiphenyl oxide						
General	Brominated phenol, triphenyl phosphate Various waxes, stearic acid, butyl stearate, zinc stearate, butyl oleate, butyl palmitate, stearamide, AcraWax C	0.5 mg sample at 950°C	DB-5 fused silica capillary, 30 m × 0.25 mm i.d., 1.0-µm film	40°C for 4 min, ramp at 10°C/min to 320°C, hold for 18 min	MS (EI, 15 – 650 mass range)	Injector T = 300°C; detector T = 300°C; 30/1 injection split	[50] ^{a,f}
General	Irganox 565, 1010; MD1024, 1035, 1076, 1425, 3114; Irgafos 168	0.5 mg sample at 950°C	DB-5 fused silica capillary, 30 m × 0.25 mm i.d., 1.0-µm film	40°C for 4 min, ramp at 10°C/min to 320°C, hold for 18 min	MS (EI, 15 – 650 mass range)	Injector T = 300°C; detector T = 300°C; 30/1 injection split	[51] ^{a,g}

ABS = acrylonitrile–butadiene–styrene; PC = polycarbonate; PMMA = polymethylmethacrylate; PS = polystyrene; PU = polyurethane; PVC = polyvinyl chloride.

^aA more rapid oven program was also used to produce pyrograms via FID detection.

^bThis manuscript deals with plasticizers as a class of additives.

^cVinyl chloride–vinylidene chloride copolymer.

^dCross-linked epoxy resin (thermoset of bisphenol A diglycidyl ether).

^eThis manuscript deals with flame retardants as a class of additives.

^fThis manuscript deals with lubricants as a class of additives.

^gThis manuscript deals with antioxidants as a class of additives.

Table 11 Solubility of polymers

Polymer	Soluble in
Alkyd resin	Chlorinated hydrocarbons, lower alcohols, esters
Acrylonitrile-butadiene-styrene terpolymer	Methylene chloride
Polyacrylamide	Water
Polyamides	Phenols, <i>m</i> -cresol, concentrated mineral acids, formic acid
Polycarbonate	Ethanolamine, dioxane, chlorinated hydrocarbons, cyclohexanone
Polyethylene	Dichlorobenzene, pentachloroethylene, dichloroethylene, tetralin
Poly(ethylene terephthalate)	Cresol, concentrated sulfuric acid, chlorophenol, trichloroacetic acid
Polyformaldehyde	Dichlorobenzene, DMF, chlorophenol, benzyl alcohol
Polystyrene	Aromatic and chlorinated hydrocarbons, pyridine, ethyl acetate, dioxane, chloroform, acetone
Polytetrafluoroethylene	Fluorocarbon oil
Polyurethanes	Dioxane, THF, DMF, dimethylsulfoxide (DMSO), <i>m</i> -cresol, formic acid, 60% sulfuric acid
Poly(vinyl chloride)	Cyclohexanone, THF, dimethylformamide (DMF), ethylene dichloride
Poly(vinylidene chloride)	THF, ketones, DMF, chlorobenzene
Vinyl chloride-vinyl acetate copolymers	Methylene chloride, THF, cyclohexanone

remain capable of providing researchers with accurate, precise, and pertinent information. Thus this review attempts to maintain a historical perspective as well.

While it is not a chromatographic issue per se, preinjection sample preparation, nevertheless, is an important consideration in the successful application of a complete analytical process. This fact is borne out in the observation that recent technological advances in polymer characterization focus not only on the analytical characterization of a test sample but also on the method of generation of that sample. Innovation in sample preparation is driven both by scientific considerations [the difficulty, but necessity, of isolating the analytes of interest (additives) from the sample matrix (bulk polymer) in such a way that the additives are not impacted by the process (e.g., Ref. [52]) and by practical considerations associated with all analytical chemistry (e.g., time and cost efficiency). While it is beyond the scope of this manuscript to exhaustively discuss sample preparation strategies for polymer characterization, this general information is provided to facilitate an important step of the overall analytical process. In terms of specific sample preparation methods, Nerin et al.^[53] have recently provided a review of sample treatment techniques applicable to polymer extract analysis including headspace methods, supercritical fluid extraction, and solid-phase microextraction. In terms of general knowledge, Table 11 provides solubility information relevant to polymer dissolution.

REFERENCES

- Duval, M.; Giguere, Y. Simultaneous determination of the antioxidant, the crosslinking-agent and decomposition products in polyethylene by reversed-phase HPLC. *J. Liq. Chromatogr.* **1982**, *5*, 1847–1854.
- Sreenivasan, K. High-performance liquid chromatographic method for the simultaneous separation and determination of three additives in poly(vinyl chloride). *J. Chromatogr.* **1986**, *357*, 433–435.
- Francis, V.C.; Sharma, Y.N.; Bhardwaj, I.S. Quantitative determination of antioxidants and ultraviolet stabilizers in polymer by high performance liquid chromatography. *Angew. Makromol. Chem.* **1983**, *113*, 219–225.
- Nielson, R.C. Extraction and quantitation of polyolefin additives. *J. Liq. Chromatogr.* **1991**, *14*, 503–519.
- Jinno, K.; Yokoyama, Y. Retention prediction for polymer additives in reversed-phase liquid chromatography. *J. Chromatogr.* **1991**, *550*, 325–334.
- Lesellier, E.; Saint Martin, P.; Tchaplal, A. Separation of six polymer additives using mobile-phase optimization software. *LC GC Int.* **1992**, *5*, 38–43.
- Lesellier, E.; Tchaplal, A. Sequential optimization of the separation of a complex mixture of plastic additives by HPLC with a quaternary gradient and a dual detection system. *Chromatographia* **1993**, *36*, 135–143.
- Masoud, A.N.; Cha, Y.N. Simultaneous use of fluorescence, ultraviolet, and electrochemical detectors in high performance liquid chromatography-separation and identification of phenolic antioxidants and related compounds. *J. HRC & GC* **1982**, *5*, 299–305.
- Skelly, N.E.; Graham, J.D.; Iskandarani, Z.; Priddy, D. Reversed-phase liquid chromatographic separation of polymer additives combined with photodiode-array detection and spectral sort software. *Polym. Mater. Sci. Eng.* **1988**, *59*, 23–27.
- Bucherl, T.; Gruner, A.; Palibroda, N. Rapid analysis of polymer homologues and additives with SFE/SFC-MS coupling. *Packag. Technol. Sci.* **1994**, *7*, 139–154.
- Thilen, M.; Shishoo, R. Optimization of experimental parameters for the quantification of polymer additives

- using SFE/HPLC. *J. Appl. Polym. Sci.* **2000**, *76*, 938–946.
12. Marcato, M.; Vianello, M. Microwave-assisted extraction by fast sample preparation for the systematic analysis of additives in polyolefins by high-performance liquid chromatography. *J. Chromatogr., A* **2000**, *869*, 285–300.
13. Nasim, N.; Taylor, L.T. Polymer-additive extraction via pressurized fluids and organic solvents of variously cross-linked poly(methylmethacrylates). *J. Chromatogr. Sci.* **2002**, *40*, 181–186.
14. Patrick, D.W.; Strand, D.A.; Cortes, H.J. Automation and optimization of multidimensional microcolumn size exclusion chromatography-liquid chromatography for the analysis of photocrosslinkers in Cyclotene 400 series advanced electronic resins. *J. Sep. Sci.* **2002**, *25*, 519–526.
15. Sreenivasan, K. A combined chromatographic and IR spectroscopic method to identify antioxidant in biomedical polyurethane. *Chromatographia* **1991**, *32*, 285–286.
16. Somsen, G.W.; Rozendom, E.J.E.; Gooijer, C.; Velthorst, N.H.; Brinkman, U.A.Th. Polymer analysis by column liquid chromatography coupled semi-on-line with Fourier transform infrared spectrometry. *Analyst* **1996**, *121*, 1069–1074.
17. Sudo, E.; Esaki, Y.; Sugiura, M. Analysis of additives in a polymer by LC/IR using surface-enhanced infrared absorption spectroscopy. *Bunseki Kagaku* **2001**, *50*, 703–707.
18. Jordan, S.L.; Taylor, L.T. HPLC separation with solvent elimination FTIR detection of polymer additives. *J. Chromatogr. Sci.* **1997**, *35*, 7–13.
19. Vargo, J.D.; Olson, K.L. Identification of antioxidant and ultraviolet light stabilizing additives in plastics by liquid chromatography/mass spectrometry. *Anal. Chem.* **1985**, *57*, 672–675.
20. Baker, J.K. Characterization of phthalate plasticizers by HPLC/thermospray mass spectrometry. *J. Pharm. Biomed. Anal.* **1996**, *15*, 145–148.
21. Yu, K.; Block, E.; Balogh, M. LC-MS analysis of polymer additives by electron and atmospheric-pressure ionization: Identification and quantification. *LC GC* **2000**, *18*, 162–178.
22. Carrott, M.J.; Jones, D.C.; Davidson, G. Identification and analysis of polymer additives using packed-column supercritical fluid chromatography with APCI mass spectrometric detection. *Analyst* **1998**, *123*, 1827–1833.
23. Daimon, H.; Hirata, Y. Directly coupled supercritical-fluid extraction/capillary supercritical-fluid chromatography of polymer additives. *Chromatographia* **1991**, *32*, 549–554.
24. Arpino, P.J.; Dilettato, D.; Nguyen, K.; Bruchet, A. Investigation of antioxidants and UV stabilizers from plastics: Part I. Comparison of HPLC and SFC; Preliminary SFC/MS study. *J. High Resolut. Chromatogr.* **1990**, *13*, 5–12.
25. Arpino, P.J.; Dilettato, D.; Nguyen, K.; Bruchet, A. Investigation of antioxidants and UV stabilizers from plastics: Part II. Application to polyolefin soxhlet extracts. *J. High Resolut. Chromatogr.* **1991**, *14*, 335–342.
26. Raynor, M.W.; Bartle, K.D.; Davies, I.L.; Williams, A.; Clifford, A.A.; Chalmers, J.M.; Cook, B.W. Polymer additive characterization by capillary supercritical fluid chromatography/Fourier transform infrared microspectrometry. *Anal. Chem.* **1988**, *60*, 427–433.
27. Wieboldt, R.C.; Kempfert, K.D.; Dalrymple, D.L. Analysis of antioxidants in polyethylene using supercritical fluid extraction/supercritical fluid chromatography and infrared detection. *Appl. Spectrosc.* **1990**, *44*, 1028–1034.
28. Zhou, L.Y.; Asharf-Khorassani, M.; Taylor, L.T. Comparison of methods for quantitative analysis of additives in low density polyethylene using supercritical fluid and enhanced solvent extraction. *J. Chromatogr., A* **1999**, *858*, 209–218.
29. MacKay, G.A.; Smith, R.M. Supercritical fluid extraction-supercritical fluid chromatography-mass spectrometry for the analysis of additives in polyurethanes. *J. Chromatogr. Sci.* **1994**, *32*, 455–460.
30. Jordan, S.L.; Taylor, L.T.; Seemuth, P.D.; Miller, R.J. Analysis of additives and monomers in nylon and polystyrene. *Text. Chem. Color.* **1997**, *29*, 25–32.
31. Ryan, T.W.; Yocklovich, S.G.; Watkins, J.C.; Levy, E.J. Quantitative analysis of additives in polymers using coupled supercritical fluid extraction-supercritical fluid chromatography. *J. Chromatogr.* **1990**, *505*, 273–282.
32. Howard, J.M. Gel permeation chromatography and polymer additive systems. *J. Chromatogr.* **1971**, *55*, 15–24.
33. Shepherd, M.J.; Gilbert, J. Analysis of additives in plastics by high performance size exclusion chromatography. *J. Chromatogr.* **1981**, *218*, 703–713.
34. Nerfin, C.; Salafranca, J.; Cacho, J.; Rubio, C. Separation of polymer and on-line determination of several antioxidants and UV stabilizers by coupling size-exclusion and normal-phase high-performance liquid chromatography columns. *J. Chromatogr., A* **1995**, *690*, 230–236.
35. Cortes, H.J.; Bell, B.M.; Pfeiffer, C.D.; Graham, J.D. Multidimensional chromatography using on-line coupled microcolumn size exclusion chromatography-capillary gas chromatography-mass spectrometry for determination of polymer additives. *J. Microcolumn Sep.* **1989**, *1*, 278–288.
36. Kreiner, J.G.; Warner, W.C. The identification of rubber compounding ingredients using thin-layer chromatography. *J. Chromatogr.* **1969**, *44*, 315–330.
37. Sevini, F.; Marcato, B. Chromatographic determination of some hindered amine light stabilizers in polyolefins. *J. Chromatogr.* **1983**, *260*, 507–512.
38. Airaud, C.B.; Gayte-Sorbier, A.; Creusevau, R.; Dumont, R. Identification of phenolic antioxidants in elastomers for pharmaceutical and medical use. *Pharm. Res.* **1987**, *4*, 237–239.
39. He, W.; Shanks, R.; Amarasinghe, G. Analysis of additives in polymers by thin-layer chromatography coupled with Fourier transform-infrared microscopy. *Vibr. Spectrosc.* **2002**, *30*, 147–156.
40. Ponder, L.H. Gas chromatographic determination of diethylene glycol in poly(ethylene terephthalate). *Anal. Chem.* **1968**, *40*, 229–231.
41. Atkinson, E.R., Jr.; Calouche, S.L. Analysis of polyethyl-

- ene terephthalate prepolymer by trimethylsilylation and gas chromatography. *Anal. Chem.* **1971**, *43*, 460–462.
42. Kiang, P.H. The application of gas chromatography/mass spectrometry to the analysis of pharmaceutical packaging materials. *J. Parenter. Sci. Technol.* **1981**, *35*, 152–161.
 43. Pasquale, G.D.; Galli, M. Determination of additives in polyolefins by capillary gas chromatography. *J. High Resolut. Chromatogr. Chromatogr. Commun.* **1984**, *7*, 484–486.
 44. Guerra, R.M.; Marin, M.L.; Sanchez, A.; Jimenez, A. Analysis of citrates and benzoates used in poly(vinyl chloride) by supercritical fluid extraction and gas chromatography. *J. Chromatogr., A* **2002**, *950*, 31–39.
 45. Nagata, M.; Kishioka, Y. Determination of additives in polyolefins and petroleum resin by capillary GC. *J. High Resolut. Chromatogr.* **1991**, *14*, 639–642.
 46. Kawamura, Y.; Watanabe, Z.; Sayama, K.; Takeda, Y.; Yamada, T. Simultaneous determination of polymer additives in polyethylene by GC/MS. *Shokuhin Eiseigaku Zasshi* **1997**, *38*, 307–318.
 47. Meyer-Dulheuer, T.; Pasch, H.; Geissler, M. Direct analysis of additives in polymeric materials by pyrolysis-gas chromatography-mass spectrometry. *KSG Kautsch. Gummi Kunstst.* **2000**, *53*, 574–581.
 48. Wang, F.C. Polymer additive analysis by pyrolysis-gas chromatography. I. Plasticizers. *J. Chromatogr. A* **2000**, *883*, 199–210.
 49. Wang, F.C. Polymer additive analysis by pyrolysis-gas chromatography: II. Flame retardants. *J. Chromatogr., A* **2000**, *886*, 225–235.
 50. Wang, F.C.; Buzanowski, W.C. Polymer additive analysis by pyrolysis-gas chromatography: III. Lubricants. *J. Chromatogr., A* **2000**, *891*, 313–324.
 51. Wang, F.C. Polymer additive analysis by pyrolysis-gas chromatography: IV. Antioxidants. *J. Chromatogr., A* **2000**, *891*, 325–336.
 52. Gasslander, U.; Jaegfeldt, H. Stability and extraction features in the determination of Irganox-1330 in a poly-alkane copolymer. *Anal. Chim. Acta* **1984**, *166*, 243–251.
 53. Nerin, C.; Rubio, C.; Salafranca, J.; Batlle, R. The simplest sample treatment techniques to assess the quality and safety of food packaging materials. *Rev. Anal. Chem.* **2000**, *19*, 435–465.
 54. Hirata, Y.; Okamoto, Y. Supercritical fluid extraction combined with microcolumn liquid chromatography for the analysis of polymer additives. *J. Microcolumn Sep.* **1989**, *1*, 46–50.
 55. Loudon, D.; Handley, A.; Lenz, E.; Sinclair, I.; Taylor, S.; Wilson, I.D. Reversed-phase HPLC of polymer additives with multiple on-line spectroscopic analysis (UV, IR, ¹H NMR, and MS). *Anal. Bioanal. Chem.* **2002**, *373*, 508–515.

Classification of Organic Solvents in Capillary Electrophoresis

Ernst Kenndler

Institute for Analytical Chemistry, University of Vienna, Vienna, Austria

Introduction

In capillary electrophoresis (CE), several criteria can be applied to classify solvents [e.g., for practical purposes based on the solution ability for analytes, on ultraviolet (UV) absorbance (for suitability to the UV detector), toxicity, etc.]. Another parameter could be the viscosity of the solvent, a property that influences the mobilities of analytes and that of the electro-osmotic flow (EOF) and restricts handling of the background electrolyte (BGE). For more fundamental reasons, the dielectric constant (the relative permittivity) is a well-recognized parameter for classification. It was initially considered to interpret the change of ionization constants of acids and bases according to Born's approach. This approach has lost importance in this respect because it is based on too simple assumptions limited to electrostatic interactions. Indeed, a more appropriate concept reflects solvation effects, the ability for H-bonding, or the acido-base property of the solvent.

Classification of Solvents

A first classification, according to the dielectric constant ϵ (with a somewhat arbitrary value about 20 or 30 to distinguish the two main classes), is still useful, be-

cause the dielectric constant reflects the extent of ion association and ion-pairing. In solvents with a high dielectric constant, called polar solvents, ion-pairing is nearly negligible in dilute solutions. Acid strength can be assigned by a numerical value, independent of the base with which it undergoes reaction. Nonpolar solvents, on the other hand (i.e., those with low dielectric constant), support ion-pairing, and the acidity is dependent on the choice of the reference base. Further grouping of the solvents is based on their ability for H-bond formation. Note that this scheme disregards the solvents' own acidity or basicity (this criterion is taken for the latter scheme). This is shown in Table 1. A typical H-bonded solvent, termed protic solvents, is water or methanol. Aprotic solvents (although containing H atoms or being able to accept H bonds) lack the ability to donate hydrogen bonds. The lower alcohols (except methanol) are grouped in the class with low ϵ . They are protic as well (they are able to donate hydrogen bonds), in contrast to the fourth group, where, for example, dioxane and tetrahydrofuran are found.

The solvents can be grouped according to another classification scheme introduced by Brønsted. It has significance for the evaluation of acido-basic equilibria in the particular solvents, especially for the interpretation of the changes of the pK values of weakly acidic (or basic) analytes and their degree of protolysis. Obviously, it is also of main importance for the

Table 1 Classification of Solvents for Potential Use in CE, According to Their Dielectric Constant, ϵ , and Their Ability for H-Bond Formation

High ϵ		Low ϵ	
H-bonded	Non-H-bonded	H-bonded	Non-H-bonded
Water	Acetonitrile	Ethanol	Acetone
Methanol	<i>N,N</i> -Dimethylformamide	<i>n</i> -Propanol	Dioxane
Ethylene glycol	<i>N,N</i> -Dimethylacetamide	<i>i</i> -Propanol	Tetrahydrofuran
Formamide	Dimethyl sulfoxide	<i>n</i> -Butanol	
Acetamide		<i>tert</i> -Butanol	
<i>N</i> -Methylformamide			
<i>N</i> -Methylacetamide			



evaluation of the pH scales in the different solvents or solvent mixtures. It differentiates, mainly, three groups: amphiprotic, dipolar aprotic, and inert solvents. As the first scheme, it also relates to the "polarity" of the solvent (expressible by the dielectric constant, too). *Amphiprotic* solvents have acidic and basic properties as well. These solvents, HS, are able to form lyonium ions, H_2S^+ , with the proton, and stable lyate ions, S^- . Examples for *amphiprotic neutral* solvents (with high ϵ) are water and methanol. In the classification given in Table 1, they belong to the H-bonded solvents.

Amphiprotic protogenic solvents have higher acidic properties, but lower basic ones (always in comparison to water). Examples are formic and acetic acid. *Amphiprotic protophilic* solvents have lower acidity and higher basicity than water, with formamide or ethanolamine as examples. *Aprotic dipolar* solvents have low acidity and (occasionally) basicity as well, with *N,N*-dimethylformamide and dimethylsulfoxide as examples for protophilic dipolar solvents and acetonitrile for a protophobic dipolar solvent.

Solvents with low ϵ and without the ability to form H bonds are also classified as dipolar aprotic solvents in some cases. Examples are dioxane and tetrahydrofuran, which have ϵ values smaller than 7. They have reduced applicability in CE; however, their aqueous mixtures might be of some interest.

Inert solvents (according to the second classification scheme) have insignificant applicability for CE, as dissociation into free ions is reduced (and solubility of electrolytes is very low). Charged analytes form stable ion pairs there. Examples are the halogenated or aliphatic and aromatic hydrocarbons (e.g., octane, benzene).

Suggested Further Reading

- Bates, R. G., Medium effect and pH in nonaqueous and mixed solvents, in *Determination of pH, Theory and Practice*, John Wiley & Sons, New York, 1973, pp. 211–253.
- Covington, A. K. and T. Dickinson, Introduction and solvent properties, in *Physical Chemistry of Organic Solvents Systems* (A. K. Covington and T. Dickinson, eds.), Plenum Press, London, 1973, pp. 1–23.
- Kenndler, E., Organic solvents in capillary electrophoresis, in *Capillary Electrophoresis Technology* (N. A. Guzman, ed.), Basel, Hong Kong: Marcel Dekker, Inc., New York, 1993, pp. 161–186.
- King, E. J., Acid-base behaviour, in *Physical Chemistry of Organic Solvent Systems* (A. K. Covington and T. Dickinson, eds.), Plenum Press, London, 1973, pp. 331–403.
- Kolthoff, I. M. and M. K. Chantooni, General introduction to acid-base equilibria in nonaqueous organic solvents, in *Treatise on Analytical Chemistry, Part I, Theory and Practice* (I. M. Kolthoff and P. J. Elving, eds.), John Wiley & Sons, New York, 1979, pp. 239–301.



Coil Planet Centrifuges

Yoichiro Ito

National Institutes of Health, Bethesda, Maryland, U.S.A.

INTRODUCTION

We have defined “coil planet centrifuge (CPC)” as a term that designates all centrifuge devices in which the coiled separation column undergoes a planetary motion, i.e., the column rotates about its own axis while revolving around the central axis of the centrifuge. Except for the original CPC, all existing CPCs are equipped with a flow-through system so that the liquid can pass through the rotating coiled column. In most of these flow-through CPCs, the use of a conventional rotary seal device is eliminated. These sealless systems are classified into two categories according to their modes of planetary motion, i.e., synchronous and nonsynchronous (see instrumentation of countercurrent chromatography, Fig. 3). In the synchronous CPC, the coiled column rotates about its own axis during one revolution cycle, whereas in the nonsynchronous CPC, the rates of rotation and revolution of the coiled column are freely adjustable. Among several different types of CPCs, the following four instruments are described below in terms of their best applications: the original CPC, the type-J CPC, the cross-axis CPC, and the nonsynchronous CPC.

ORIGINAL CPC

This first CPC model was devised in an effort to improve the efficiency of lymphocyte separation which was conventionally performed in a short centrifuge tube. If a long tubing is wound into a coil and rotated in a centrifugal field, the particles present in the tube would travel through the tube from one end to the other at a rate depending on their size and density. This idea was implemented in the designs of the first device named the “CPC.”^[1]

Principle

Physical analysis of the motion of a particle in the rotating helical tube of a CPC has been carried out by means of a simple model is as follows.^[1]

(A) We consider a tube filled with a fluid of density ρ_0 coiled into a helix of radius R , with its axis horizontal. If a spherical particle of radius a , density ρ , is placed in the

tube, we can determine motion of the particle when the helix undergoes uniform rotation about its axis with angular velocity ω . As a first approximation, we neglect the lateral motion in the tube and assume that in a given turn of the coil, the particle moves on a vertical circle of radius R . The position of the particle can then be specified by the angle θ , as indicated in Fig. 1. With this approximation, the particle is acted on by only two forces, the Stokes drag

$$F_s = -6\pi a\eta R(d\theta/dt - \omega)$$

where η is the viscosity of the fluid, and the net gravitational force g tangent to the circular path

$$F_g = -(4\pi/3)a^3(\rho - \rho_0)g \sin \theta$$

The equation of motion is therefore

$$(4\pi/3)a^3\rho R(d^2\theta/dt^2) = F_s + F_g$$

and on introducing the total angle of rotation of the helix, $x = \omega t$, this can be written in the convenient form

$$d^2\theta/dx^2 + (1/\omega\tau)\{d\theta/dx - 1 + (\omega_c/\omega) \sin \theta\} = 0 \quad (1)$$

where τ is the relaxation time

$$\tau = 2\rho a^2/9\eta \quad (2)$$

and ω_c is the critical angular velocity

$$\omega_c = (2/9)\{(\rho - \rho_0)ga^2\}/\eta R = V_e/R \quad (3)$$

where V_e is the equilibrium Stokes velocity. We consider separately the motion for

$$\omega_c/\omega > 1 \text{ and } \omega_c/\omega < 1$$

(B) $\omega_c/\omega > 1$. In this case, Eq. 1 has a singular point at $\omega_c/\omega \sin \theta = 1$, i.e., at $\theta = \theta_2 = \sin^{-1}(\omega/\omega_c)$, $0 \leq \theta \leq \frac{\pi}{2}$, and at $\theta = \pi - \theta_c$. The terms θ_c and $\pi - \theta_c$ are the angles at which the drag of the liquid is just balanced by the gravitational force so that the particle is at equilibrium when at rest. It is readily seen from physical considerations that



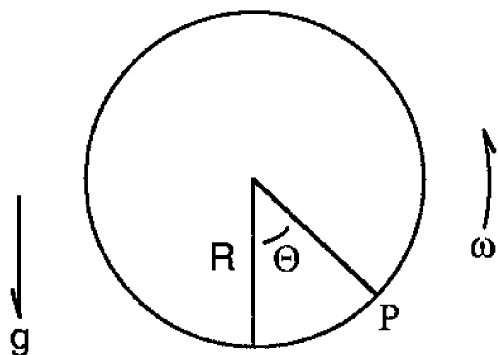


Fig. 1 The coil unit for mathematical analysis of the motion of a particle. (From Ref. [1].)

the equilibrium at θ_e is stable while that at $\pi - \theta_e$ is unstable. More precisely, an analysis in the neighborhood of the singular points shows that $\pi - \theta_e$ is an unstable saddle point, while θ_e is a stable node if $\omega\tau \leq 1/4 \tan \theta_e$ and a stable spiral point if $\omega\tau > 1/4 \tan \theta_e$. Consequently, after a time of the order of τ , the particle will remain fixed at θ_e . Its angular velocity relative to the tube will then be

$$\omega_{\text{rel}} = \omega \{d\theta/dx - 1\} = -\omega \quad (4)$$

That is, it will spiral down the helix at a rate independent of its size and density.

(C) $\omega_e/\omega < 1$, $\omega\tau < 1$. When $\omega_e/\omega < 1$, Eq. 1 has no singular points. The character of the motion, however, depends to some extent on the size of $\omega\tau$, and we shall consider in detail only the physically interesting case $\omega\tau \ll 1$. It can readily be shown that within this limit, after a time of the order of τ , angular velocity of the particle adjusts itself in such a way that the inertial term, $\omega\tau d^2\theta/dx^2$, becomes negligible, so that Eq. 1 reduces to

$$d\theta/dx = 1 - \omega_e/\omega \sin \theta \quad (5)$$

The particle then always rotates in the same direction as the tube, but more slowly than the tube when $0 < \theta < \pi$ and more rapidly when $\pi < \theta < 2\pi$. The two effects, however, do not quite cancel out, and the net effect is that, again, the particle spirals down the tube in a direction opposite to that of the tube rotation.

To determine the mean angular velocity of this spiraling motion, we first calculate the time required for the particle to traverse one turn of the coil. We have from Eq. 5

$$\begin{aligned} X(2\pi) - X(0) &= \int_0^{2\pi} d\theta / \{1 - (\omega_e/\omega) \sin \theta\} \\ &= 2\pi / \{1 - (\omega_e/\omega)^2\}^{1/2} \end{aligned}$$

The mean angular velocity of the particle relative to the tube is therefore

$$\begin{aligned} \omega_{\text{rel}} &= \omega \{2\pi / [X(2\pi) - X(0)] - 1\} \\ &= -\omega \{1 - [1 - (\omega_e/\omega)^2]^{1/2}\} \end{aligned} \quad (6)$$

which joins continuously on to the value at $\omega_e/\omega = 1$ of Eq. 4.

When ω is close to ω_e , ω_{rel} is rather insensitive to the size and density of the particle. When $\omega_e/\omega \ll 1$, however, Eq. 6 becomes

$$\omega_{\text{rel}} = -\omega_e^2/2\omega \quad (7)$$

so that the rate of motion down the tube is proportional to a^4 and $(\rho - \rho_0)$. Thus, when $\omega_e \ll \omega \ll 1/\tau$, the method should be quite effective in segregating particles of different size and density.

In order to apply (A)–(C) to the CPC, the value of g should be replaced by that of the centrifugal force acting on the axis of the rotating helical tube.

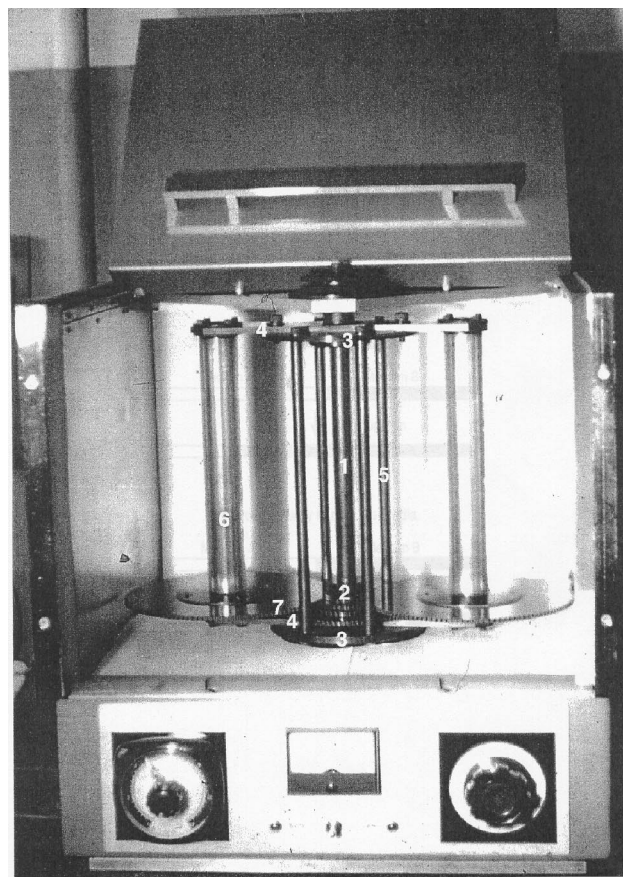


Fig. 2 The coil planet centrifuge fabricated by Sanki Engineering Ltd., Kyoto, Japan. (From Ref. [1].)

Design of the Original CPC

Fig. 2 shows the first commercial model of the CPC manufactured by Sanki Engineering, Ltd. (Kyoto, Japan).^[1,3] The main body of the apparatus consists of three parts, each capable to rotation as a unit: coil holder (6) and interchangeable gear (7) (part I); frame or a pair of arms (4) and discs (3) bridged with links (5) (part II); and central shaft (1) and gear 2 which interlocks to gear 7 of part I. Simultaneous rotation of parts II and III at different angular velocities results in revolution and rotation of part I as a planet. The rotation of part I is determined by the difference in angular velocity between parts II and III and by the gear ratio between 2 and 7.

The apparatus can produce $1000 \times g$ force where the ratio between the coil rotation and revolution can be adjustable to 1/100, 1/300, or 1/500 by interchanging the planetary gears (7) at the bottom of the column holder (6). Each coil holder is equipped with six straight grooves at its periphery to accommodate six coiled tubes that are covered by a transparent vinyl sheath protector tightly fitted to the outside of the holder. Each coil is made by winding either polyethylene or Teflon tubing (typically 0.3-mm ID) onto a glass core (15 cm long and 6-mm diameter). After the liquid and sample are introduced into the tube, both ends of the coil are closed before loading onto the holder.

Three Different Modes of Operation

Preliminary experiments with the CPC revealed some interesting features of the apparatus. The results are summarized in Fig. 3.^[1]

(I) Single medium: When the tube is filled with a single medium and a particle mixture is introduced at one end, centrifugation separates the particles according to the difference in size and relative density. The method was effectively demonstrated by a model experiment using polyacrylic resin particles.^[1]

(II) Two mutually miscible media (gradient method): When the tube is filled with two mutually miscible media, the heavier in one half and the lighter in the other half, centrifugation produces a density gradient. After centrifugation for some time, the gradient reaches a fairly stable state. In practice, such a stable gradient between water and isotonic saline solution can be introduced into the coil to measure osmotic fragility of erythrocytes. Erythrocytes introduced into the saline side of the coil are forced to travel through the gradient down to the point where hemolysis occurs, the distribution of hemoglobin thus formed, indicating the osmotic fragility of the sample.^[2]

(III) Two mutually immiscible media (countercurrent chromatography). When two mutually immiscible media

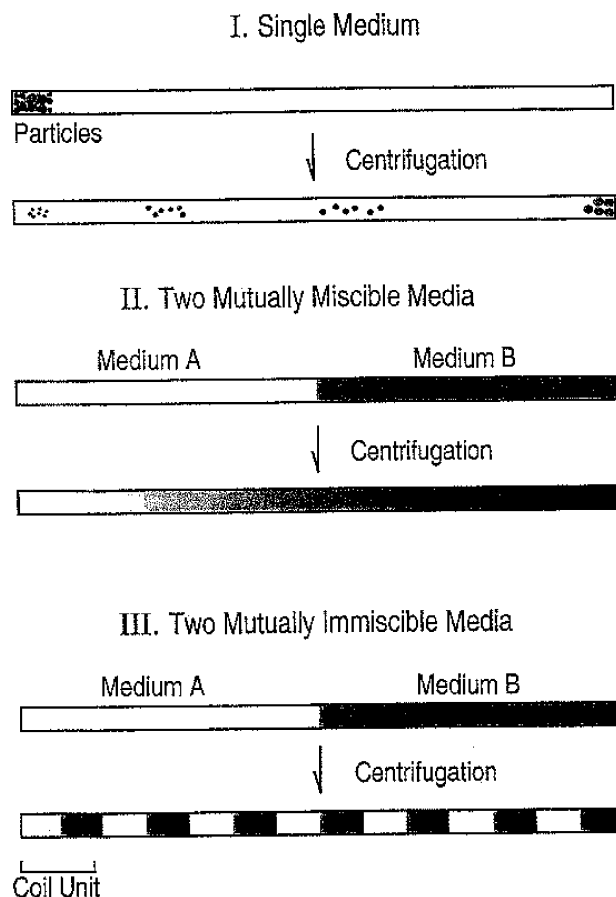


Fig. 3 The principle of three different applications of the coil planet centrifuge. All tubes are shown uncoiled before and after centrifugation. (From Ref. [1].)

are used similarly, centrifugation forces these two media to undergo countercurrent motion, and, in the final stage, each turn of the coil is occupied by the two media nearly half and half as illustrated in Fig. 3-III. Consequently, a small amount of a sample injected beforehand at the interface of the two media, i.e., the middle portion of the tube, is distributed along the tube according to its partition coefficient. This countercurrent chromatographic method is applicable to microgram amounts of chemicals with a high efficiency that may be equivalent to near 1000 units of a Craig countercurrent distribution apparatus.

Applications to Countercurrent Chromatography

Capability of the apparatus for performing microscale countercurrent chromatography has been demonstrated using three different samples, i.e., a mixture of dyes, agal proteins, and mammalian erythrocytes.^[3]

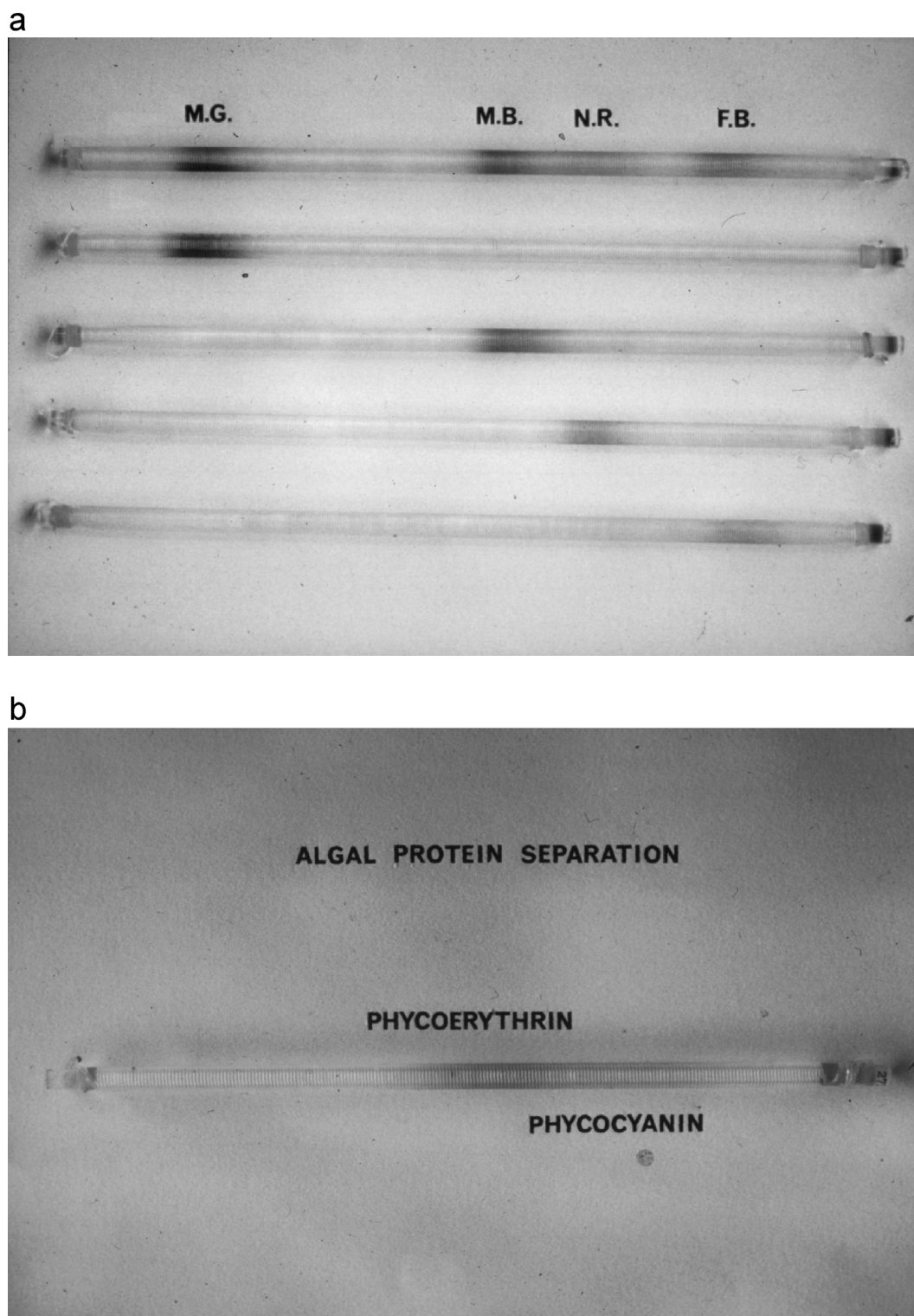


Fig. 4 Countercurrent separation of various samples by the coil planet centrifuge. (a) Separation of basic dyes with an organic/aqueous two-phase solvent system. M.G.: methyl green; M.B.: methylene blue; N.R.: neutral red; F.B.: basic fuchsin. (From Ref. [3].) Solvent system consisted of isoamyl alcohol/ethanol/acetic acid/water (4:2:1:5, v/v).

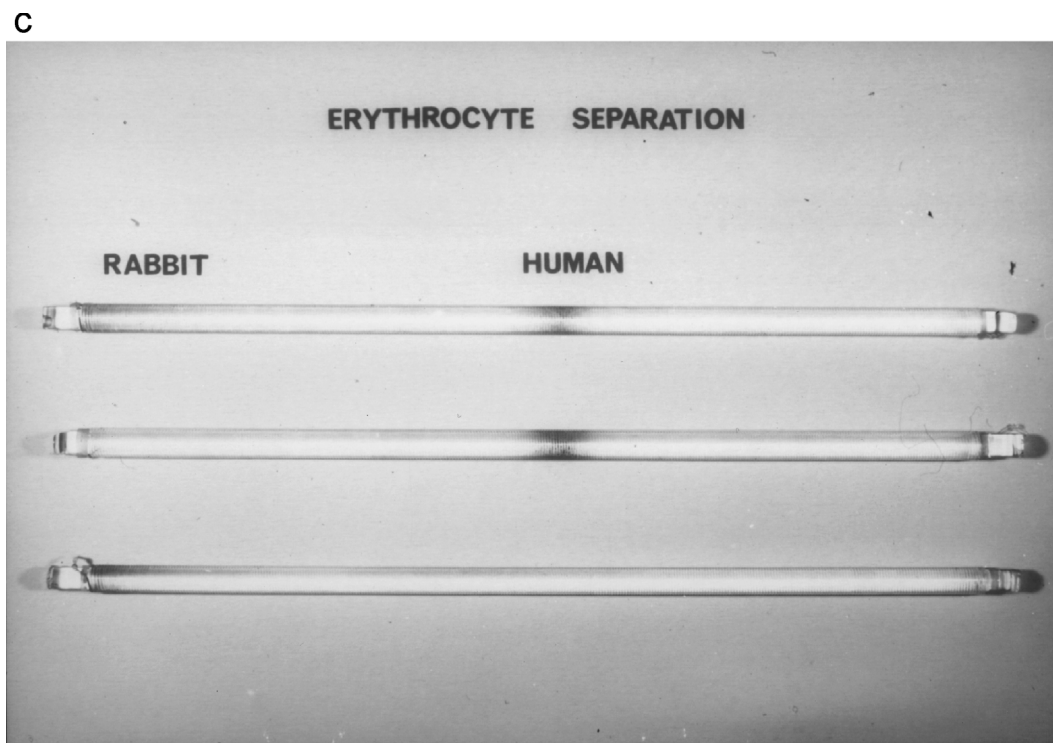


Fig. 4 (Continued).

Separation of dyes

Fig. 4a shows countercurrent chromatographic separation of four basic dyes, i.e., methyl green (MG), methylene blue (MB), neutral red (NR), and basic fuchsin using a two-phase solvent system composed of isoamyl alcohol-ethanol-acetic acid-distilled water (4:2:1:5, v/v). The first coil displays the separation of the mixture, and the other coils show distribution of individual dyes to demonstrate the reproducibility of the method. The separation was performed with 6 m of 0.35-mm-ID tubing (ca. 300 helical turns) at relative coil rotation of 0.25 rpm at $300 \times g$ for 10 hr.

Separation of algal proteins

Phycoerythrin and phycocyanin were extracted from dried Asakusa-nori (*Porphyra tenera*) and subjected to partition with an aqueous polymer phase system (Table 1) using the above standard countercurrent method. Fig. 4b shows the results of separation, where two components are well resolved.

Erythrocyte separation

The separation of human and rabbit erythrocytes was performed with a modified method using a gradient between a pair of polymer phase systems A and B (Table 2),

where the upper phase of A and the lower phase of B were used for separation. Before charging with sample, the coil was rotated at 1500 rpm at a relative rotation of 1/100 (15 rpm) for 30 min, which produced a gradient between the two phases along the coil. Then the sample cell mixture was loaded followed by centrifugation for 1 hr. Fig. 4c shows the partition of human and rabbit erythrocytes which were completely separated along the coil.

The results of the above studies using the original CPC led to the development of a series of new CPC devices equipped with a flow-through system that permits continuous elution through the column as in other chromatographic systems.

TYPE-J MULTILAYER CPC

Among all existing types of seal-free flow-through CPCs, the type-J CPC affords the most efficient and speedy separations or "high-speed CCC," and it has been extensively used for preparative separations of natural and synthetic products.

Mathematical Analysis of Planetary Motion

The type-J synchronous planetary motion of the coil holder is shown in Fig. 5a (see also instrumentation of



Table 1 Polymer phase system for separation of algal proteins

20%(w/w) Dextran 500	35.0 g
30%(w/w) PEG 8000 ^a	14.7 g
0.05 M KH ₂ PO ₄	10.0 ml
0.05 M K ₂ HPO ₄	10.0 ml
0.22 M KCl	10.0 ml
H ₂ O	20.3 ml

From Ref [3].

countercurrent chromatography, Fig. 3), where the holder rotates about its own axis and simultaneously revolves around the axis of the centrifuge at the same angular velocity but in the opposite direction. Simple mathematical analysis^[4] is performed using a coordinate system shown in Fig. 5b, where the center of the revolution coincides with the center of the coordinate system (point O). For convenience of analysis, the center of rotation and an arbitrary point are initially located on the *x*-axis. After the lapse of time *t*, the holder circles around point O by $\theta = \omega t$, while the arbitrary point circles around the axis of rotation by 2θ to reach *P*(*x*,*y*) where

$$x = R \cos \theta + r \cos 2\theta \quad (8)$$

$$y = R \sin \theta + r \sin 2\theta \quad (9)$$

The acceleration produced by the planetary motion is then obtained from the second derivatives of Eqs. 8 and 9,

$$d^2x/dt^2 = -R\omega^2(\cos \theta + 4\beta \cos 2\theta) \quad (10)$$

$$d^2y/dt^2 = -R\omega^2(\sin \theta + 4\beta \sin 2\theta) \quad (11)$$

where $\beta = r/R$.

From Eqs. 10 and 11, two centrifugal force components, i.e., *Fr* (radial component) and *Ft* (tangential component), are computed using the following formula:

$$Fr = R\omega^2(\cos \theta + 4\beta) \quad (12)$$

$$Ft = R\omega^2(\sin \theta) \quad (13)$$

Fig. 5c shows the distributions of force vectors computed from Eqs. 12 and 13 at various locations on the column holder. All vectors confined in a plane perpendicular to the holder axis. As the holder rotates, both the direction and the net strength of the force vector fluctuate in such a way that the vector becomes longest at the point remote from the centrifuge axis and shortest at the point close to the central axis of the centrifuge. In most locations, the vectors are directed outwardly from the circle except for $\beta < 0.25$, where its direction is reversed

at the vicinity of the center of revolution. This fluctuating centrifugal force field creates unique hydrodynamic effects on the two solvent phases in the coiled tube.

Stroboscopic Observation of Hydrodynamic Motion of Solvent Phases

Fig. 6 schematically illustrates motion of the two solvent phases in a spiral column, which is subjected to the type-J synchronous planetary motion. The upper diagram shows distribution of two solvent phases in the column observed under stroboscopic illumination. About one-fourth of the area near the center of revolution (point O) shows vigorous mixing of the two phases (mixing zone), whereas in the rest of the area, the two phases are separated by a strong centrifugal force in such a way that the lighter phase occupies the inner portion and the heavier phase occupies the outer portion of the tube. Four stretched tubes in the lower diagram illustrate the traveling pattern of the mixing zone through the spiral tube in one revolution cycle. In analogy to the motion of a wave advancing over water, the mixing zone travels one spiral turn for each revolution. This indicates that the solutes are subjected to an efficient partition process of repeating mixing and settling at a high rate of 13 times per second at 800 rpm of revolution. This accounts for the high partition efficiency of the present system, and we have called it ‘‘high-speed CCC.’’^[4]

Design of the Apparatus

Fig. 7 shows a photograph of the most advanced model of the multilayer CPC, which holds a set of three multilayer coil separation columns symmetrically around the rotary frame.^[5,6] All columns are connected in series with flow tubes which are supported by counterrotating pipes placed

Table 2 A pair of polymer phase systems for separation of erythrocytes

System A		System B	
20% (w/w)	25.0 g	20% (w/w)	25.0 g
Dextran 500		Dextran 500	
30% (w/w)	13.3 g	30% (w/w)	13.3 g
PEG 8000 ^a		PEG 8000 ^a	
0.55M NaH ₂ PO ₄	5.0 ml	0.55M NaH ₂ PO ₄	5.0 ml
0.55M Na ₂ HPO ₄	5.0 ml	0.55M Na ₂ HPO ₄	5.0 ml
25% HSA ^b	1.0 ml	25% HSA ^b	1.0 ml
H ₂ O	50.7 ml	1.5M NaCl	10.0 ml
		H ₂ O	40.7 ml

^aPEG 8000 was labeled as PEG 6000 in early applications.

^bHSA = human serum albumin.

From Ref [3].

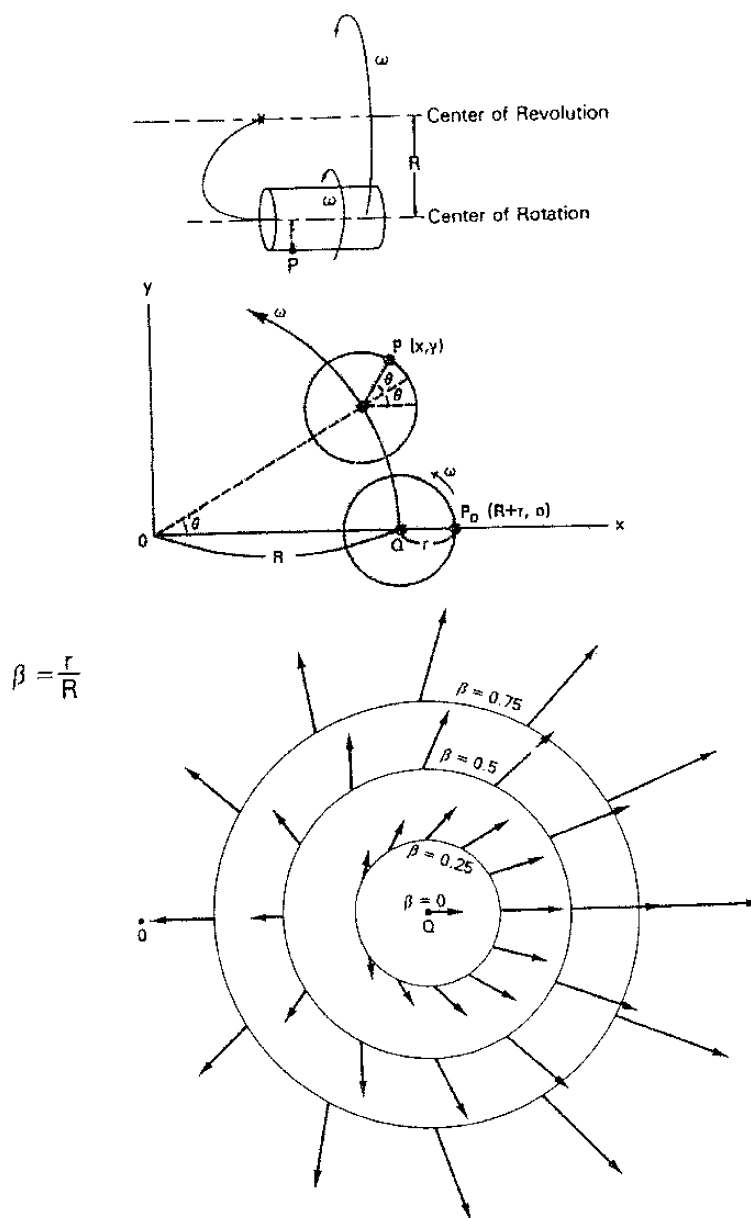


Fig. 5 Analysis of centrifugal force field for type-J planetary motion. (a) Planetary motion; (b) planetary motion in an x - y coordinate system for the analysis of centrifugal force; (c) distribution of the centrifugal vectors on the column holder. (From Ref. [12].)

between the column holders. The type-J synchronous planetary motion of the holder is provided by engaging a planetary gear on the column holder with an identical stationary sun gear mounted around the central stationary shaft of the centrifuge. The counterrotation of the tube holder is effected by interlocking a pair of identical gears, one mounted on the holder and the other on the tube holder. Flow tubes from each end of the column assembly are passed through the central rotary shaft to exit the centrifuge on each side, where they are tightly affixed with a pair of clamps.

The multilayer coil separation column is prepared by winding a single piece of Teflon or Tefzel tubing around a spool-shaped column holder making multiple coiled layers between a pair of flanges. Currently, three different sets of multilayer coils are commercially available: the large preparative scale (2.6-mm ID, ca. 1000 ml total capacity); the standard preparative column (1.6-mm ID, ca. 320 ml total capacity); and the analytical scale (0.85-mm ID, ca. 120 ml capacity). The optimal revolution speed of the apparatus ranges from 800 to 1200 rpm.



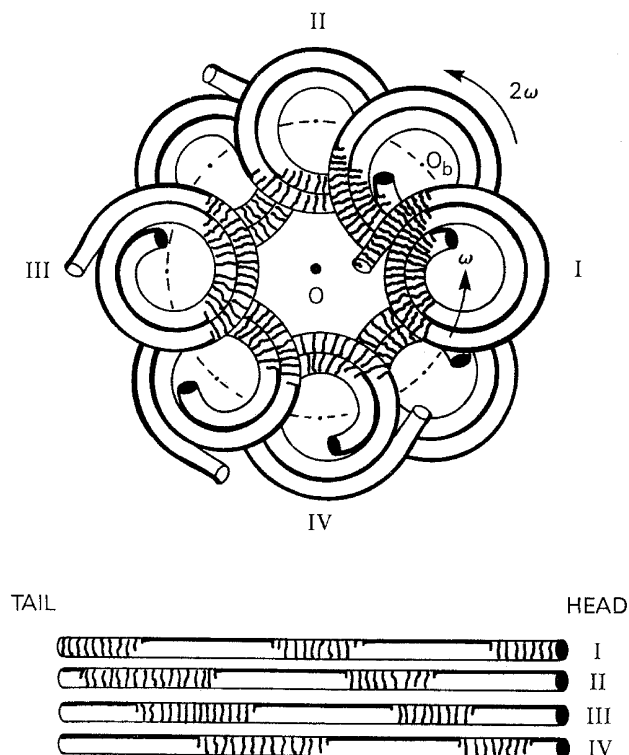


Fig. 6 Mixing and settling zones in the spiral column undergoing type-J planetary motion. (From Ref. [12].)

Applications

Because of its rapid and high separation efficiency, the multilayer coil CPC has been extensively used for separation and purification of variety of compounds using suitable organic/aqueous solvent systems. The application also covers special CCC techniques such as peak-focusing CCC and pH-zone-refining CCC^[7] (see pH-peak-focusing and pH-zone-refining countercurrent chromatography, pp. 606–611); chiral and affinity CCC (see chiral countercurrent chromatography, pp. 160–163); foam CCC^[8] (see foam countercurrent chromatography, pp. 342–345), liquid–liquid dual CCC;^[9] and CCC/MS (see countercurrent chromatography/mass spectrometry, pp. 208–211).

The method, however, fails to retain viscous, low interfacial tension polymer phase systems such as polyethylene glycol (PEG)–dextran systems^[10] due to its intensive mixing effect which tends to produce emulsification, resulting in carryover of the stationary phase. This problem is largely eliminated by the cross-axis CPC described below.

CROSS-AXIS CPC

The cross-axis CPC has a specific feature in that it permits the universal use of two-phase solvent systems

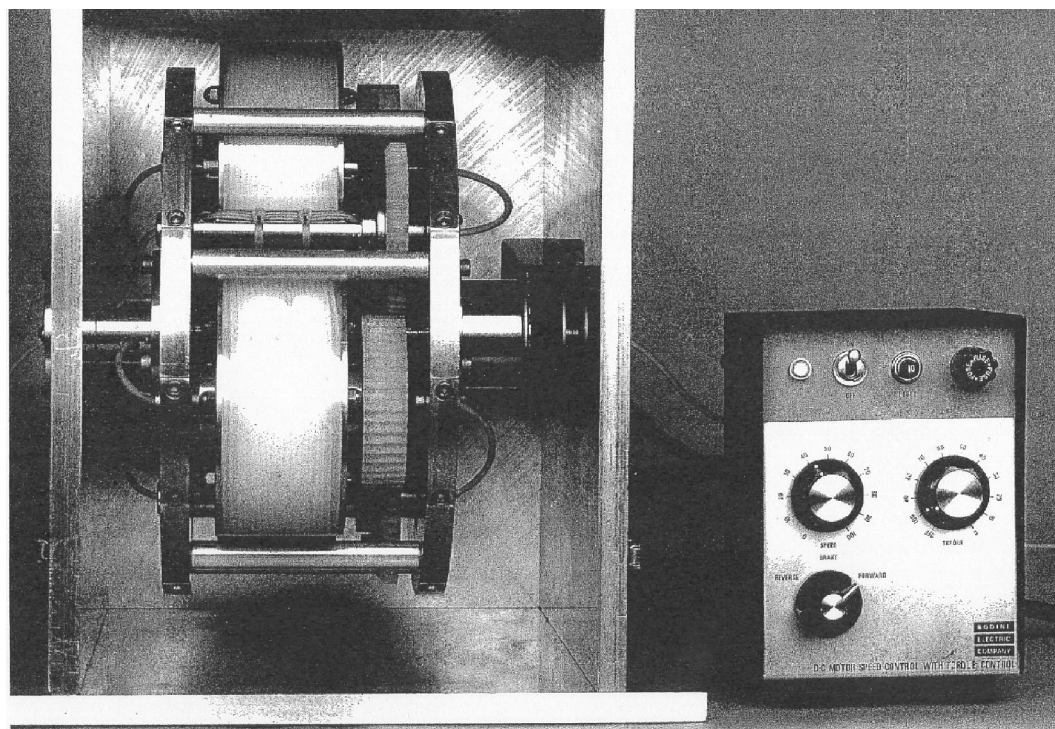


Fig. 7 Improved high-speed CCC centrifuge equipped with three column holders. (From Ref. [6].)

including aqueous–aqueous polymer phase systems which are useful for partitioning macromolecules and cell particles.^[10]

Acceleration Field

The design of the cross-axis CPC is based on the hybrid between type-L and type-X planetary motions, which results in an extremely complex centrifugal force field with a three-dimensional fluctuation of force vectors during each revolution cycle of the holder. The pattern of this centrifugal force field produced by the cross-axis CPC somewhat resembles that produced by the type-J planetary motion (Fig. 5c), but it is superimposed by a force component acting in parallel to the axis of the coil holder. This additional force component acts to improve the retention of the stationary phase. This beneficial effect is greatest in type-L planetary motion and becomes smallest in the type-X planetary motion. A detailed mathematical analysis on this planetary motion is described elsewhere.^[11]

Design of the Apparatus

Fig. 8 shows the general principle of various cross-axis CPCs. The geometrical parameter of the system is shown in Fig. 8a, where the orientation and planetary motion are indicated relative to the axis of the apparatus. The vertical axis of the apparatus and the horizontal axis of the coil are always kept perpendicular to each other at a fixed distance. The cylindrical column revolves at the central axis at the same rotational speed with which it rotates about its own axis. Three parameters displayed in Fig. 8a explain various versions of the cross-axis prototypes: r is the radius of the column holder, R is the distance between the two axis, and L is the measure of the lateral shift of the column holder along its axis. The name of a cross-axis device is based on the ratio L/R , when $R \neq 0$. Types X and L represent the limits for the column positions; type X involves no shifting of the column holder, while type L corresponds to an infinite shifting. Some examples of prototypes fabricated at the machine shop in the National Institutes of Health, Bethesda, MD, are shown in Fig. 8b.

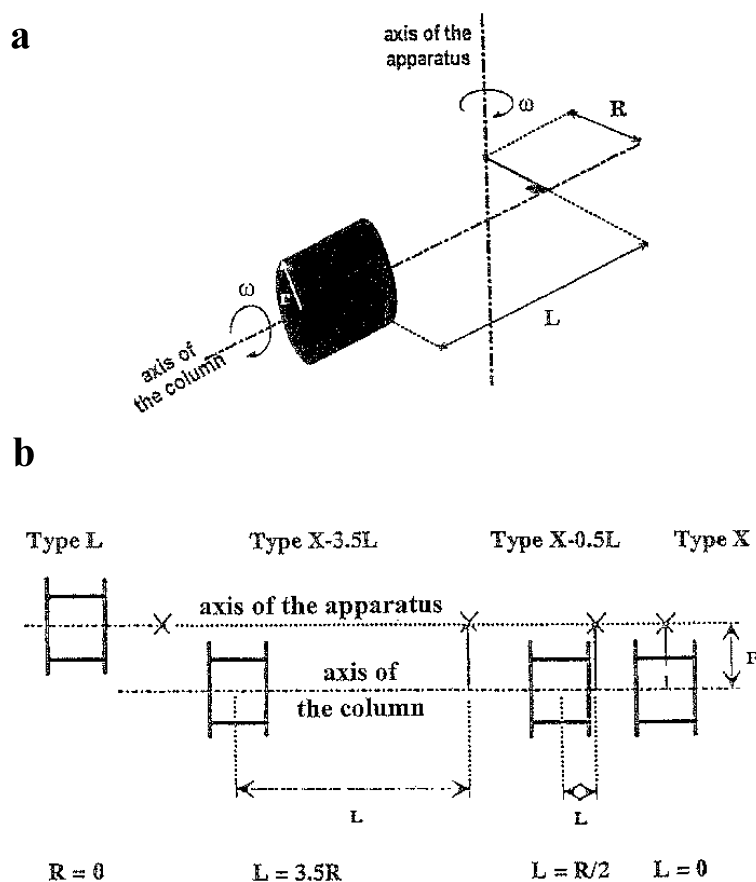


Fig. 8 General principle of various cross-axis CPCs. (a) Geometrical parameters; (b) some examples of prototypes built in NIH Machine Shop. X type in 1987; X-0.5L type in 1988; X-3.5L type in 1991; and L type in 1992. (From Ref. [12].)



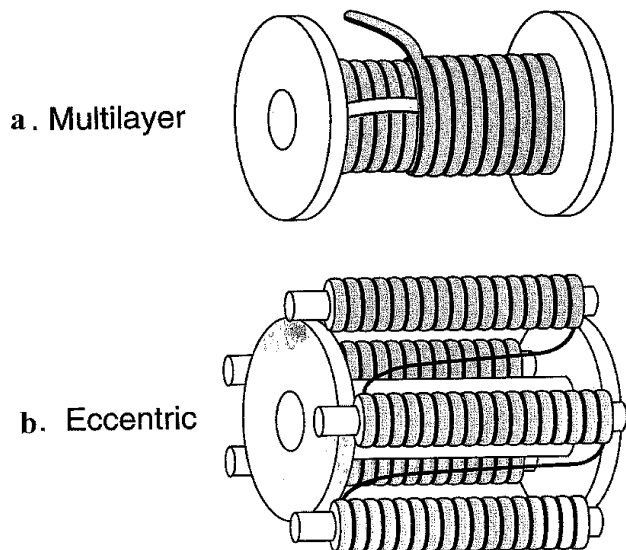


Fig. 9 Two different types of coiled columns for cross-axis CPC. Multilayer coil is for large-scale separations and eccentric coil assembly for small-scale separations.

The two different column designs are schematically shown in Fig. 9: The first column (multilayer coil) is used for preparative scale separations, while the second column (eccentric coil) is for analytical scale separations. The multilayer coil is prepared by winding a large Teflon

tubing (2.6-mm ID) directly onto the holder hub in such a way that after completing each coiled layer, the tubing is directly returned to the starting point to wind the second layer over this connecting tube segment, and so on. This results in multiple coiled layers of the same handedness that are connected in series with short-tube segments as shown in Fig. 9a. The eccentric coil is prepared by winding a piece of Teflon tubing (typically 0.85-mm ID) onto a set of multiple short cores (ca. 6-mm OD), which is arranged around the periphery of the holder hub as shown in Fig. 9b.

Fig. 10 shows a photograph of a recently designed cross-axis CPC equipped with a pair of multilayer coil separation columns.^[12] The column can be mounted on the rotary frame in two positions, X-1.5L (off-center position) and L (central position). The off-center position is used for both organic/aqueous and aqueous PEG—potassium phosphate systems, while the central position is used for viscous, low interfacial tension PEG—dextran systems.

Applications

Although cross-axis CPCs yield less efficient separations than the type-J multilayer CPC, they provide more stable retention of the stationary phase and are therefore useful for large-scale preparative separations with polar solvent systems. These are especially useful for the purification of

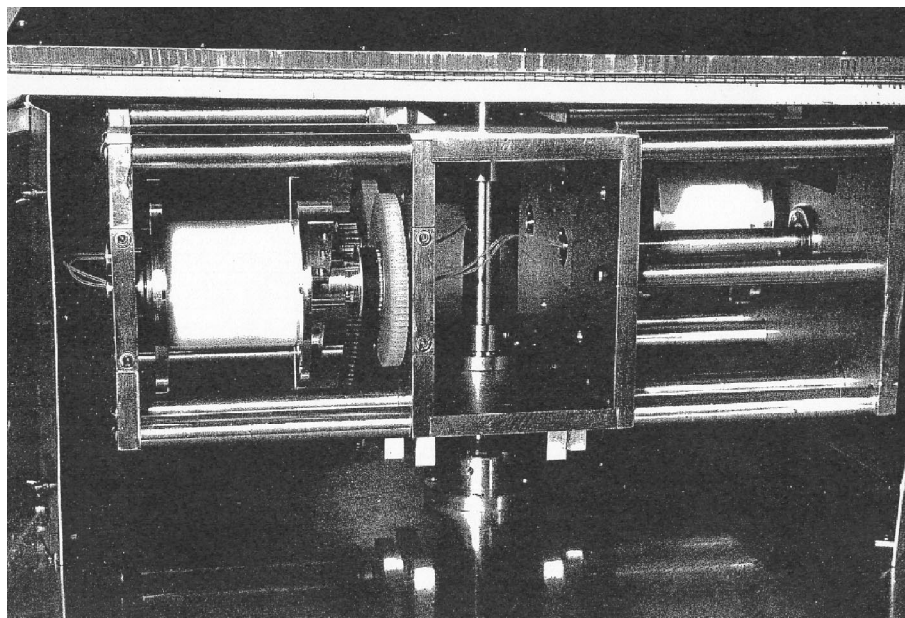


Fig. 10 Photograph of X-1.5L and L prototypes. The rotary frame of the apparatus is driven by a motor (back of the apparatus) by coupling a pair of toothed pulleys one on the motor shaft and the other on the central shaft with a belt. Two cylindrical holders are mounted in the X-1.5L or off-center position. The inlet and the outlet Teflon tubes go through the upper plate of the apparatus inside the hollow part of the central vertical axis. A circular metallic plate around the rotary frame decreases the torque by an average of 30%. (From Ref. [12].)

proteins with aqueous–aqueous polymer phase systems composed of PEG and potassium phosphate. The cross-axis CPC has been used for the purification of various enzymes including choline esterase, ketosteroid isomerase, purine nucleoside phosphorylase, lactic acid dehydrogenase, uridine phosphorylase (see cross-axis coil planet centrifuge for the separation of proteins, pp. 212–213).

NONSYNCHRONOUS CPC

The nonsynchronous flow-through CPC is a particular type of planetary centrifuge which allows adjustment of the rotational rate of the coiled separation column at a given revolution speed. The first prototype was equipped with a dual rotary seal for continuous elution.^[13] Later, an improved model^[14] was designed to eliminate the rotary seal which had become a source of complications such as leakage, contamination, and clogging.

Design Principle of the Seal-Free Nonsynchronous CPC

Fig. 11a shows a cross-sectional view through the central axis of the apparatus. The rotor consists of two major

rotary structures, i.e., frames I and II, which are coaxially bridged together with the center piece (dark shade).

Frame I consists of three plates rigidly linked together and directly driven by motor I. It holds three rotary elements, namely, the centerpiece (center), countershaft I (bottom), and countershaft II (top), all employing ball bearings. A pair of long arms extending symmetrically and perpendicularly from the middle plate forms the tube-supporting frame, which clears over frame II to reach the central shaft on the right side of frame II.

Frame II (light shade) consists of three pairs of arms linked together to rotate around the central shaft. It supports a pair of rotary shafts, one holding a coil holder assembly and the other the counterweight.

There are two motors, i.e., motors I and II, to drive the rotor. When motor I drives frame I, the stationary pulley 1 introduces counterrotation of pulley II through a toothed belt; therefore, countershaft I rotates at $-\omega_1$ with respect to rotating frame I. This motion is further conveyed to the centerpiece by 1:1 gearing between gears 1 and 2. Thus, the centerpiece rotates at $2\omega_1$ or at ω_1 with respect to the rotating frame I. The motion of frame I also depends upon the motion of motor II.

If motor II is at rest, pulley 5 becomes stationary same with pulley 1 so that countershaft II counterrotates at ω_1

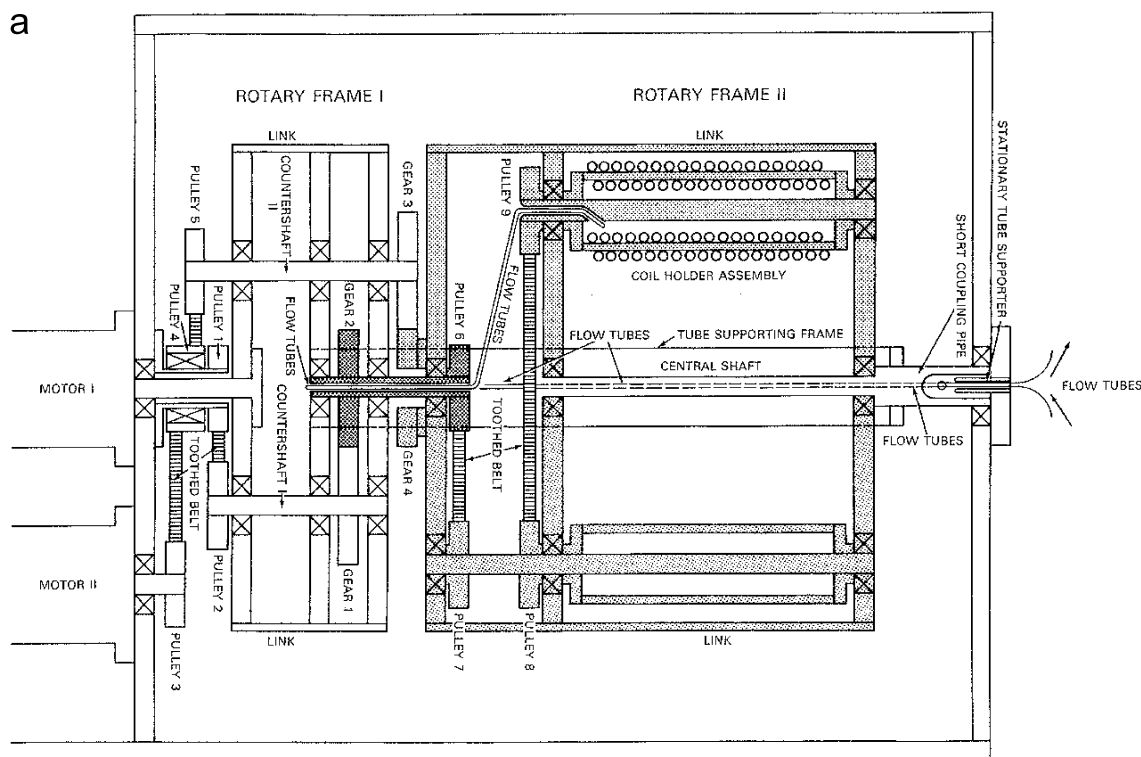


Fig. 11 Improved nonsynchronous flow-through coil planet centrifuge without rotary seals. (a) Cross-sectional view through the central axis of the apparatus; (b) photograph of the apparatus equipped with an eccentric coil assembly. (From Ref. [14].)



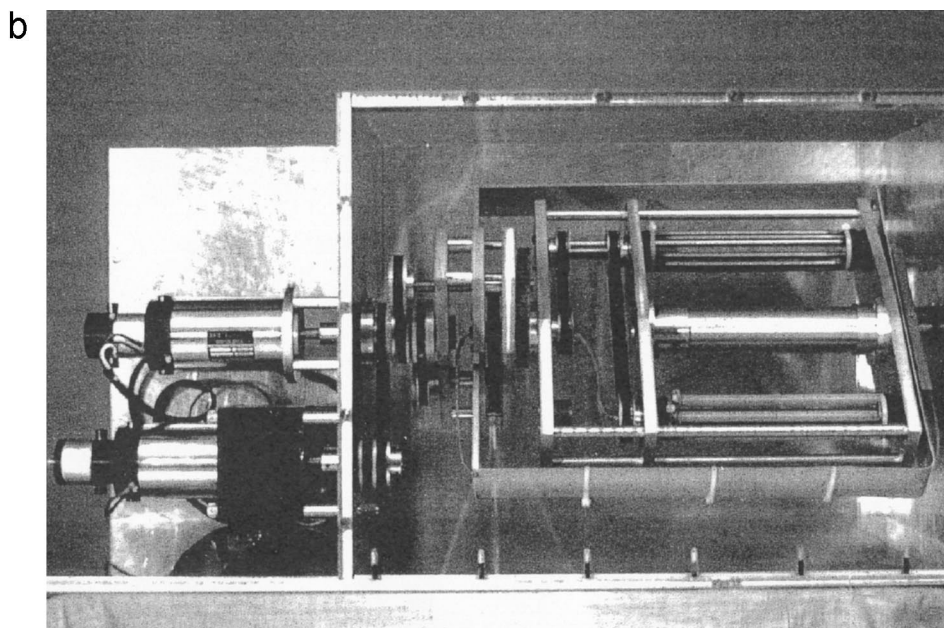


Fig. 11 (Continued).

as does countershaft I. This motion is similarly conveyed to the rotary arms of frame II by 1:1 gearing between gears 3 and 4, resulting in rotation of frame II at $2\omega_I$ or the same angular velocity as that of the centerpiece. Consequently, coupling of pulleys 6 to 7 and 8 to 9 with toothed belts produces no additional motion to the rotary shaft, which simply revolves with frame II at $2\omega_I$ around the central axis of the apparatus.

When motor II rotates at ω_{II} , idler pulley 4 coupled to pulley 3 on the motor shaft rotates at the same rate, which, in turn, modifies the rotational rate of pulley 5 on countershaft II. Thus, countershaft II now counter-rotates at $\omega_I - \omega_{II}$ on frame I. This motion further alters the rotational rate of frame II through 1:1 gear coupling between gears 3 and 4. Subsequently, frame II rotates at $2\omega_I - \omega_{II}$ with respect to the earth or at $-\omega_{II}$ relative to the centerpiece which always rotates at $2\omega_I$. The difference in rotational rate between frame II and the center piece is conveyed to the rotary shafts through coupling of pulleys 6 to 7 and 8 to 9. Consequently, both rotary shafts rotate at ω_{II} about their own axes while revolving around the central axis of the apparatus at $2\omega_I - \omega_{II}$. This gives the rotation/revolution ratio of the rotary shaft

$$r/R = \omega_{II}/(2\omega_I - \omega_{II}) \quad (14)$$

Therefore, any combination of revolutionary and rotational speeds of the coil holder assembly can be achieved by selecting the proper values of ω_I and ω_{II} .

Coiled Column and Flow Tubes

Two different column configurations are used: a multilayer coil and an eccentric coil assembly. The multilayer coil column is prepared by winding a piece of Teflon tubing, typically 1.6-mm ID, directly onto the holder hub (ca. 2.5-cm OD), making multiple coiled layers as those for the type-J high-speed CCC. The eccentric coil assembly was made by winding a piece of Teflon tubing, typically 1-mm ID, onto a set of six units of 0.68-cm-OD stainless steel pipe in series. These coil units are arranged around the holder with their axis in parallel to the holder axis (see eccentric coil assembly in Fig. 9, lower diagram). A pair of flow tubes from each end of the coiled column is first led through the hole of the rotary shaft and then pass through the opening of the centerpiece to exit at the middle portion of frame I. The flow tubes are then led along from the tube support to clear frame II and then reach the side hole of the central shaft near the right wall of the centrifuge where they are tightly held by the stationary tube supporter.

Fig. 11b shows the overall photograph of the apparatus equipped with an eccentric coil assembly. The revolution speed of the coil holder assembly is continuously adjustable up to 1000 rpm combined with any given rotational rate between 0 and 50 rpm in either direction.

Applications

The nonsynchronous CPC is a most versatile centrifuge which can be applied to a variety of samples including

cells, macromolecules, and small molecular weight compounds. Cell separations may be performed with a single phase such as physiological solution or culture medium^[14,15] and also with PEG–dextran polymer two-phase systems.^[16] DNA and RNA are partitioned with a PEG–dextran system by optimizing the pH.^[14]

CONCLUSIONS

The CPC, which was originally developed for separating blood lymphocytes, has evolved into several useful instruments for separations of cells, macromolecules, and small molecular weight compounds. Among those, the type-J multilayer CPC is most extensively utilized for high-speed CCC separations of natural and synthetic products. The utility of the type-J CPC may be extended to the polymer phase separation of macromolecules and cell particles with a spiral disk assembly currently being developed in our laboratory.

ACKNOWLEDGMENT

The author is indebted to Dr. Henry M. Fales of Laboratory of Biophysical Chemistry, National Heart, Lung, and Blood Institute, National Institutes of Health, Bethesda, MD, for editing the manuscript.

REFERENCES

1. Ito, Y.; Weinstein, M.A.; Aoki, I.; Harada, R.; Kimura, E.; Nunogaki, K. The coil planet centrifuge. *Nature* **1966**, *212*, 985–987.
2. Harada, R.; Ito, Y.; Kimura, E. A new method of osmotic fragility test of erythrocytes with coil planet centrifuge. *Jpn. J. Physiol.* **1969**, *19*, 306–314.
3. Ito, Y.; Aoki, I.; Kimura, E.; Nunogaki, K.; Nunogaki, Y. New micro liquid–liquid partition techniques with the coil planet centrifuge. *Anal. Chem.* **1969**, *41*, 1579–1584.
4. Ito, Y. High-speed countercurrent chromatography. *CRC Crit. Rev. Anal. Chem.* **1986**, *17* (1), 65–143.
5. Ito, Y.; Oka, H.; Slemp, J.L. Improved high-speed countercurrent chromatograph with three multilayer coils connected in series. I. Design of the apparatus and performance of semipreparative columns in DNP amino acid separation. *J. Chromatogr.* **1989**, *475*, 219–227.
6. Ito, Y.; Oka, H.; Lee, Y.-W. Improved high-speed countercurrent chromatograph with three multilayer coils connected in series. II. Separation of various biological samples with a semipreparative column. *J. Chromatogr.* **1990**, *498*, 169–178.
7. Ito, Y.; Ma, Y. pH-zone-refining countercurrent chromatography. *J. Chromatogr., A* **1996**, *753*, 1–36.
8. Ito, Y. Foam countercurrent chromatography based on dual countercurrent system. *J. Liq. Chromatogr.* **1985**, *8*, 2131–2152.
9. Lee, Y.-W.; Fang, Q.-C.; Cook, C.E.; Ito, Y. The application of true countercurrent chromatography in the isolation of bio-active natural products. *J. Nat. Prod.* **1989**, *52* (4), 706–710.
10. Albertsson, P. *Partition of Cell Particles and Macromolecules*; Wiley Interscience: New York, 1986.
11. Ito, Y.; Oka, H.; Slemp, J.L. Improved cross-axis synchronous flow-through coil planet centrifuge for performing countercurrent chromatography. I. Design of the apparatus and analysis of acceleration. *J. Chromatogr.* **1989**, *463*, 305–316.
12. Ito, Y.; Menet, J.-M. Coil Planet Centrifuges for High-Speed Countercurrent Chromatography. In *Countercurrent Chromatography*; Menet, J.-M., Thiebaut, D., Eds.; Marcel Dekker: New York, 1999; 87–119.
13. Ito, Y.; Carmeci, P.; Sutherland, I.A. Nonsynchronous flow-through coil planet centrifuge applied to cell separation with physiological solution. *Anal. Biochem.* **1979**, *94*, 249–252.
14. Ito, Y.; Bramblett, G.T.; Bhatnagar, R.; Huberman, M.; Leive, L.; Cullinane, L.M.; Groves, W. Improved nonsynchronous flow-through coil planet centrifuge without rotating seals. Principle and application. *Sep. Sci. Technol.* **1983**, *18* (1), 33–48.
15. Okada, T.; Metcalfe, D.D.; Ito, Y. Purification of mast cells with an improved nonsynchronous flow-through coil planet centrifuge. *Int. Arch. Allergy Immunol.* **1996**, *109*, 376–382.
16. Leive, L.; Cullinane, M.L.; Ito, Y.; Bramblett, G.T. Countercurrent chromatographic separation of bacteria with known difference in surface lipopolysaccharide. *J. Liq. Chromatogr.* **1984**, *7* (2), 403–418.

Cold-Wall Effects in Thermal FFF

Martin E. Schimpf

Boise State University, Boise, Idaho, U.S.A.

Introduction

In field-flow fractionation (FFF), like chromatography, retention and resolution are affected by temperature. For chromatographic systems, thermostatted ovens are used to precisely control the column temperature, but in thermal FFF, the issue of temperature control is more complex. Under a given set of conditions, the temperature in the channel varies between the hot and cold walls, but more importantly, the average temperature of an eluting component varies with the temperature of the cold wall. As a result, the retention of a given analyte in different channels will be identical only if the cold-wall temperatures (as well as the field strengths) are identical. The retention of polystyrene in ethylbenzene, for example, is reduced by 1% for each 2-degree increase in the cold-wall temperature (T_c), even when the temperature gradient is held constant [1].

Discussion

The effect of T_c on the retention of polystyrene in ethylbenzene is typical of most polymer-solvent systems. Therefore, fluctuations in T_c of only a couple degrees are generally not a problem. Larger fluctuations can be a significant problem, however, especially when retention is used to monitor small batch-to-batch variations in a quality control situation. The magnitude of T_c depends on several factors. Heat, which is transferred from the hot wall, is typically removed by heat exchange with water flowing beneath the cold wall. The cooling efficiency is affected by the temperature of the incoming water, which can vary by several degrees among different laboratories. The incoming water temperature may also vary by several degrees over time in a given laboratory. The effect of variations in the incoming water temperature can be attenuated with the use of a flow-control valve, because T_c also varies with the flow rate of the water. For example, a lower coolant flow rate can be used in the winter to offset the effect on T_c of the lower water temperature. An alternative to varying the flow rate is to maintain a con-

stant water temperature by running it through a thermostatted heater/chiller.

When T_c is not controlled to within a couple of degrees, the fluctuations ultimately affect the accuracy of molecular-weight determinations that rely on the calibration of thermal FFF retention to molecular weight. For a detailed discussion of the role of T_c in thermal FFF calibrations, see the entry Molecular Weight and Molecular-Weight Distributions by Thermal FFF. In summary, variations in retention with T_c can be handled when characterizing molecular-weight distributions by either matching the T_c between calibration and analysis or by incorporating the T_c into the calibration equation. Matching the T_c can be difficult when data are to be compared among channels in different laboratories. On the other hand, incorporating T_c into the calibration equation requires the systematic accumulation of large amounts of data.

In addition to molecular weight, thermal FFF is used to measure transport coefficients. For example, the measurement of thermodiffusion coefficients is important for obtaining compositional information on polymer blends and copolymers (see the entry Thermal FFF of Polymers and Particles). Thermal FFF is also used in fundamental studies of thermodiffusion because it is a relatively fast and accurate method for obtaining the Soret coefficient, which is used to quantify the concentration of material in a temperature gradient. However, the accuracy of Soret and thermodiffusion coefficients obtained from thermal FFF experiments depends on properly accounting for several factors that involve temperature. In order to understand the effect of temperature on transport coefficients, as well as the effect on thermal FFF calibration equations, a brief outline of retention theory is given next.

In all FFF subtechniques, retention depends on a balance of two opposing motions. The first motion is induced by the applied field and results in the concentration of material at the accumulation wall (typically, the cold wall in thermal FFF). The buildup in concentration induces the opposing motion of diffusion. Both motions are accounted for in the retention parameter λ , which is defined for all FFF subtechniques as

Encyclopedia of Chromatography

DOI: 10.1081/E-Echr 120004623

Copyright © 2002 by Marcel Dekker, Inc. All rights reserved.



$$\lambda = \frac{D}{Uw} \quad (1)$$

Here, D is the (mass) diffusion coefficient, U is the field-induced velocity of the sample, and w is the channel thickness. In thermal FFF, U is governed by the thermal diffusion coefficient (D_T) and the temperature gradient (dT/dx), which is applied in the same dimension (x) as the channel thickness (x varies in value from 0 at the cold wall to w at the hot wall). Using the dependence of U on D_T and dT/dx , the retention parameter in thermal FFF can be expressed as

$$\lambda = \frac{D}{D_T(dT/dx)w} \cong \frac{D}{D_T\Delta T} \quad (2)$$

where ΔT is the difference in temperature between the hot and cold walls. Because x and w are in the same dimension, dT/dx can be approximated by $\Delta T/w$; therefore, $w(dT/dx)$ is approximated by ΔT on the right-hand side of Eq. (2).

When the parameters in Eq. (1) are constant throughout the channel, the volume V_r of fluid required to flush a sample component through the channel is related to λ by the following equation:

$$V_r = \frac{V^\circ}{6\lambda} \left[\coth\left(\frac{1}{2\lambda} - 2\lambda\right) \right]^{-1} \quad (3)$$

Here, V° is the volume of fluid required to flush a sample that is not affected by the field ($U = 0$). In most FFF subtechniques, the parameters in Eq. (1) are, in fact, constant throughout the channel. In thermal FFF, however, these parameters vary across the channel because they depend on temperature, which varies between the hot and cold walls. As a result, Eq. (3) is only an approximation in thermal FFF. Fortunately, the approximations associated with Eq. (3) are inconsequential for the determination of molecular-weight distributions, so that the only concern is variations in T_c , as outlined earlier. For measuring transport coefficients, on the other hand, the approximations can lead to significant errors.

When calculating transport coefficients from measured values of V_r , the retention parameter λ is first calculated using Eq. (3). Next, the Soret coefficient D_T/D is calculated from λ using Eq. (2). From the Soret coefficient, the value of D_T can be calculated if an independent measure of D is available. The accuracy of the resulting value is compromised by the approxima-

tions involved in deriving Eq. (3). First, a parabolic velocity profile is assumed. In reality, the velocity profile is skewed toward the hot wall by a carrier-liquid viscosity (η) that varies across the channel as a result of the temperature gradient. Variations in thermal conductivity (κ) with temperature across the channel must also be considered. Finally, the accuracy of Eq. (3) is compromised by an assumption that the analyte forms an exponential concentration profile, whereas, in reality, the profile is more complicated due to the temperature dependence of the transport coefficients.

Conclusion

The consequences of the temperature dependence of η , κ , D , and D_T have been discussed in several articles [3–6]. Ko et al. [3] demonstrated that the temperature dependence of the Soret coefficient actually increases the resolution of different molecular-weight components. In a theoretical study by van Asten et al. [4], it was shown that the consequence of ignoring the temperature dependence of κ has a nearly negligible effect on the accuracy of D/D_T values calculated using Eqs. (2) and (3). Ignoring the temperature dependence of η and D/D_T , on the other hand, can lead to errors of up to 8% when D/D_T values are calculated from retention data. Several refinements to Eq. (3) have been made over the years [2,5,6]. When these refinements are used, they yield accurate values for the transport coefficients. Although the resulting equations are quite complex, they are not required for the routine analysis of polymers by thermal FFF.

References

1. S. L. Brimhall, M. N. Myers, K. D. Caldwell, and J. C. Giddings, *J. Polym. Sci. Polym. Phys. Ed.* 23:2443 (1985).
2. J. J. Gunderson, K. D. Caldwell, and J. C. Giddings, *Separ. Sci. Technol.* 19:667 (1984).
3. G.-H. Ko, R. Richards, and M. E. Schimpf, *Separ. Sci. Technol.* 31:1035 (1996).
4. A. C. van Asten, H. F. M. Boelens, W. Th. Kok, H. Poppe, P. S. Williams, and J. C. Giddings, *Separ. Sci. Technol.* 29:513 (1994).
5. M. Martin and J. C. Giddings, *J. Phys. Chem.* 85:727 (1981).
6. M. Martin, C. van Batten, and M. Hoyos, *Anal. Chem.* 69:1339 (1997).



Comprehensive Thermodynamic Approach to Ion Interaction Chromatography

Teresa Cecchi

Università degli Studi di Camerino, Camerino, Italy

INTRODUCTION

Reverse-phase (RP) chromatography is, by far, the most widely used separation mode in high-performance liquid chromatography (HPLC). A wide variety of mobile-phase additives that may also modify the surface of the packing material are used in optimization procedures. Ion interaction chromatography (IIC) is an RP technique that involves the use of ion interaction reagents (IIRs) that are large lipophilic ions; they are retained much more than their nonadsorbophilic counterions. An electrostatic potential difference between the stationary phase and the bulk mobile phase develops and influences ionic solute retention. When IIR is used, conventional RP columns are able to retain oppositely charged analytes with adequate retention. Improved resolution and selectivity broaden the scope of separation of organic and inorganic ions.

IIC analyses are challenging because of the high number of easily tunable but interdependent mobile-phase variables. Retention models are often sought because there is a need for a detailed understanding of the underlying phenomena that govern solute distribution between the two phases. The retention equations of a theoretical model can also be advantageously used during method development, involving the setup of custom modes in computer-supported software tools.

ION INTERACTION INTERPRETATION

To obtain a simple interpretation of the experimental findings in IIC, theoretical chromatographers first adopted a stoichiometric strategy that pioneered this separation mode. Unfortunately, the reaction schemes of stoichiometric models in both the mobile phase (ion pair model)^[1] and stationary phase (dynamic ion exchange model)^[2] lack a firm foundation in physical chemistry^[3] because they are not able to account for the stationary-phase modification that results from the addition of the IIR to the eluent, and they fail to properly describe experimental results, as pointed out by Bidlingmeyer et al.^[4] Key insights on these retention models were also provided by

Knox and Hartwick.^[5] The contrast between the simplicity and practicality of stoichiometric relationships, and the complexities of the thermodynamics solutes undergo is an important underlying theme of meditation for a model maker. Later, electrostatic theories^[3,6] tried to pattern chromatographic findings according to electrostatic interactions between charged IIRs and an analyte, thereby disregarding chemical equilibria in the IIC system, but some predictions of theirs are at variance with experimental evidence.^[7–9] Conversely, the recently developed extended thermodynamic approach to IIC^[7–18] considers that a major contribution to the distribution of charged solutes between phases is the electrostatic potential difference between them, but also capitalizes on the importance of complex formation at a thermodynamic level, and not a stoichiometric level, to take into account the stationary-phase electrostatic potential that results from IIR adsorption. In the following, we will discuss in detail how this retention model may help the chromatographer to make educated guesses and to simplify the complex task of a successful optimization in the parameter space of IIC separations.

THEORY

Influence of IIR Concentration on the Retention Behavior of Charged, Neutral, and Zwitterionic Analytes

Amphiphilic IIR ions (H) dynamically adsorb onto the stationary phase, forming a primary charged ion layer, and counterions in the diffuse outer region form an electrical double layer. The adsorption isotherm of an IIR can be described by the Freundlich equation:

$$[\text{LH}] = a[\text{H}]^b \quad (1)$$

where a and b are constants; $[\text{H}]$ and $[\text{LH}]$ are, respectively, the mobile-phase and the stationary-phase concentrations of the IIR. The use of the Freundlich adsorption isotherm is not empirical^[19] because it is related to the potential modified Langmuir adsorption

isotherm, which holds for the adsorption of ions that have a substantial hydrophobic moiety. Because IIR counterions have a negligible adsorbophilic aptitude, an electrical potential difference Ψ° develops between the surface and the bulk solution. This potential is given by the rigorous Gouy–Chapman theory equation: if the ionic strength is high enough and the Debye length is low, we are allowed to use a planar surface geometry;^[3] we have the following relationship:^[3,7]

$$\Psi^\circ = \frac{2RT}{F} \ln \left\{ \frac{[LH]|z_H|F}{\left(8\epsilon_0\epsilon_rRT \sum_i c_{0i}\right)^{\frac{1}{2}}} + \left[\frac{([LH]z_HF)^2}{8\epsilon_0\epsilon_rRT \sum_i c_{0i}} + 1 \right]^{\frac{1}{2}}} \right\} \quad (2)$$

where F is the Faraday constant, R is the gas constant, T is the absolute temperature, z_H is the charge of the IIR, ϵ_r is the dielectric constant of the medium, ϵ_0 is the vacuum permittivity, and $\sum c_{0i}$ is the mobile-phase concentration of singly charged electrolytes. For the sake of simplicity, we will indicate the following:

$$f = \frac{|z_H|F}{\left(8\epsilon_0\epsilon_rRT \sum_i c_{0i}\right)^{\frac{1}{2}}} \quad (3)$$

where f (m²/mol) is a constant, which can be evaluated from experimental conditions.

The complex equation (Eq. 2) can be advantageously approximated, for high surface potential, by the following very simple expression:^[10,12,14,19]

$$\Psi^\circ = \alpha + \beta \ln[LH] \quad (4)$$

where α and β are constants^[10] that depend on experimental conditions.

For surface potential below 25 mV, Eq. 2 can be linearized^[3,11,15] and approximated by the following:

$$\Psi^\circ = \frac{z_H[LH]F}{\kappa\epsilon_0\epsilon_r} \quad (5)$$

where κ is the inverse Debye length.

It has been demonstrated^[7] that the course of analyte retention on the mobile-phase and stationary-phase concentrations of the IIR can be described, respectively, by the following two expressions:

$$k = \phi[L]_T \times \frac{K_{LE} \frac{\gamma_L \gamma_E}{\gamma_{LE}} \exp(-z_E F \Psi^\circ / RT) + K_{EHL} \frac{\gamma_E \gamma_H \gamma_L}{\gamma_{EHL}} [H]}{\left(1 + K_{EH} \frac{\gamma_E \gamma_H}{\gamma_{EH}} [H]\right) \left(1 + K_{LH} \frac{\gamma_L \gamma_H}{\gamma_{LH}} \exp(-z_H F \Psi^\circ / RT) [H]\right)} \quad (6)$$

$$k = \phi \frac{K_{LE} \frac{\gamma_L \gamma_E}{\gamma_{LE}} \exp(-z_E F \Psi^\circ / RT) + \frac{K_{EHL}}{a^{1/b}} \frac{\gamma_E \gamma_H \gamma_L}{\gamma_{EHL}} [LH]^{1/b}}{\left(1 + \frac{K_{EH}}{a^{1/b}} \frac{\gamma_E \gamma_H}{\gamma_{EH}} [LH]^{1/b}\right)} \times ([L]_T - [LH]) \quad (7)$$

where ϕ is the phase ratio of the column; K_{EL} , K_{EHL} , K_{EH} , and K_{HL} , are the thermodynamic equilibrium constants for adsorption of the analyte E onto the stationary phase, ion pair formation in the stationary phase, ion pair formation in the eluent, and adsorption of the IIR onto the stationary phase, respectively; γ represents the activity coefficient for each species; z_E is the charge of the analyte; and $[L]_T$ estimates the total ligand surface concentration.

The first term in the numerator of Eqs. 6 and 7 describes the electrostatic interaction between the analyte and the charged stationary phase. This interaction will be attractive (repulsive) if the analyte is oppositely (similarly) charged to the IIR; hence, its retention increases (decreases) with increasing IIR concentration. The second term in the numerator of Eqs. 6 and 7 accounts for ion pair formation at the stationary phase that results in a retention increase. The left factor of the denominator of Eq. 6 and the denominator of Eq. 7 accounts for ion pair formation in the mobile phase that tends to reduce retention because the analyte is withdrawn from the stationary phase toward the eluent. Both terms concerning ion pair formation are missing if the analyte and IIR are similarly charged, or if the analyte is neutral. The right-hand factor of the denominator of Eq. 6 and the right-hand factor of Eq. 7 describe adsorption competition between the analyte and

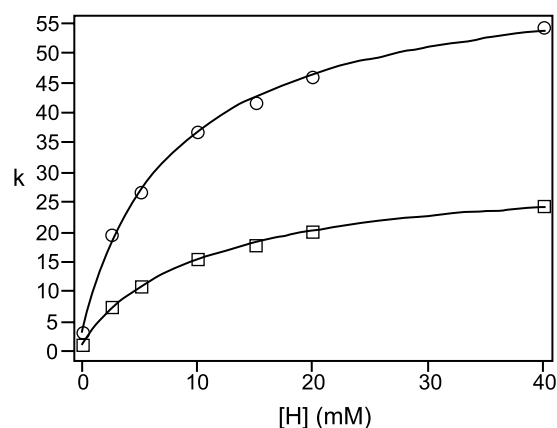


Fig. 1 Dependence of k on adrenaline (squares) and L-tyrosine hydrazide (circles), on mobile-phase concentration of 1-hexanesulfonate. Column: Synergi Hydro-RP (Phenomenex) 150 × 4.6 mm ID, particle size 4 μ m, and bonded phase coverage 4.05 μ mol/m². Eluent: phosphate buffer 37.10 mM KH₂PO₄ and 4.29 mM Na₂HPO₄ calculated to provide a pH of 6.0. After addition of the desired amount of sodium 1-hexanesulfonate, NaCl was added so that the total sodium concentration was 50 mM (constant ionic strength). Experimental data were fitted by Eq. 8.

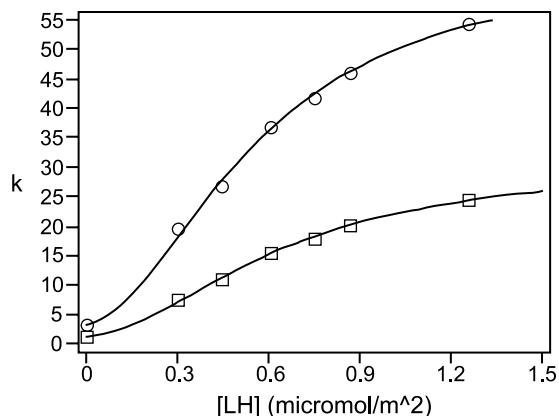


Fig. 2 Dependence of k on adrenaline (squares) and L-tyrosine hydrazide (circles), on stationary-phase concentration of 1-hexanesulfonate. Conditions as in Fig. 1. Experimental data were fitted by Eq. 9.

the IIR. From Eq. 6, it is clear that Ψ° always runs counter to further adsorption of the IIR because Ψ° is of the same sign as z_H . From Eq. 7, it is evident that adsorption competition, if it applies, shows only if $[LH]$ is high, compared to $[L]_T$.

Eluent pH is an important optimization parameter because it influences the analyte ionization, which, in turn, controls the magnitude of electrostatic interactions.

When Eqs. 1–3 are substituted into Eqs. 6 and 7, the following two expressions are obtained:

$$k = \frac{c_1 \left(a[H]^b f + \left((a[H]^b f)^2 + 1 \right)^{\frac{1}{2}} \right)^{(\pm 2|z_E|)} + c_2[H]}{(1 + c_3[H]) \left(1 + c_4[H] \left(a[H]^b f + \left((a[H]^b f)^2 + 1 \right)^{\frac{1}{2}} \right)^{(-2|z_H|)} \right)} \quad (8)$$

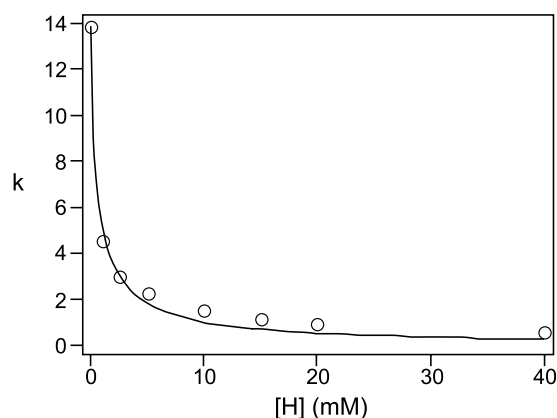


Fig. 3 Dependence of k on sodium *p*-toluenesulfonate, on mobile-phase concentration of 1-hexanesulfonate. Conditions as in Fig. 1. Experimental data were fitted by Eq. 8. (From Ref. [18]. Courtesy of Marcel Dekker, Inc.)

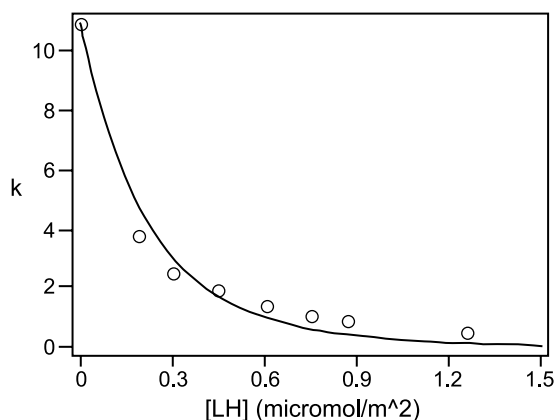


Fig. 4 Dependence of k sodium salicylate on the stationary-phase concentration of 1-hexanesulfonate. Conditions as in Fig. 1. Experimental data were fitted by Eq. 9. (From Ref. [18]. Courtesy of Marcel Dekker, Inc.)

$$k = \frac{d_1 \left([LH]f + \left(([LH]f)^2 + 1 \right)^{\frac{1}{2}} \right)^{\pm 2|z_E|} + d_2[LH]^{1/b}}{(1 + d_3[LH]^{1/b}) \times (d_4 - [LH])} \quad (9)$$

In the exponent of the first term of the numerator, the plus sign applies for oppositely charged analytes and IIRs, whereas the minus sign applies for similarly charged analytes and IIRs, as expected according to the electrostatic behavior; Eqs. 8 and 9 are also able to take into account, via the magnitude of z_E in the exponents, that the electrostatic interaction is stronger for multiply charged analytes.

When Eqs. 8 and 9 are fitted to experimental data, excellent results are obtained, as shown in Figs. 1 and 2

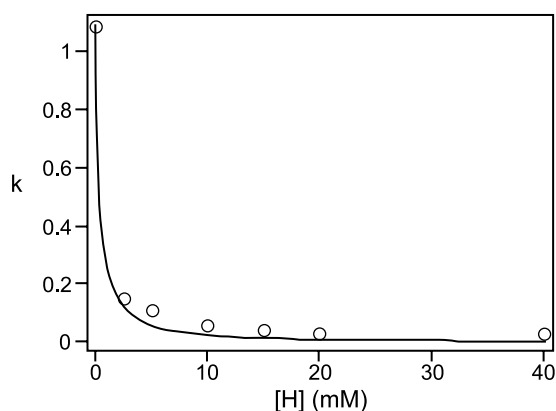


Fig. 5 Dependence of k on 2,6-naphthalenedisulfonate, on mobile-phase concentration of 1-hexanesulfonate. Conditions as in Fig. 1. Experimental data were fitted by Eq. 8. (From Ref. [18]. Courtesy of Marcel Dekker, Inc.)

Table 1 Summary of parameter estimates and their standard deviation, correlation coefficient (r), and sum of square errors (SSE) for the best fit of experimental retention data (some of them are shown in Figs. 1, 3, and 5) as a function of the mobile-phase concentration of the IIR by Eq. 8

Analyte	c_1	c_2 (mM ⁻¹)	c_3 (mM ⁻¹)	c_4 (mM ⁻¹)	r (Eq. 8)	SSE (Eq. 8)
L-Tyrosine hydrazide	—	4.627±0.295	0.111±0.006	—	0.999	2.531
Adrenaline	—	1.368±0.084	0.090±0.004	—	0.999	0.321
Octopamine	—	0.989±0.087	0.085±0.005	—	0.999	0.380
Sodium <i>p</i> -toluenesulfonate	—	—	—	0.629±0.144	0.995	1.337
Sodium salicylate	—	—	—	0.488±0.140	0.994	1.064
2,6-Naphthalenedisulfonate	1.097±0.035	—	—	—	0.996	0.007

Conditions as in Fig. 1.

Source: From Ref. [18]. (Courtesy of Marcel Dekker, Inc.)

for analytes charged oppositely to the IIRs; in Figs. 3 and 4 for analytes charged similarly to the IIRs; and in Fig. 5 for a doubly charged analyte, as detailed in the captions. Tables 1 and 2 detail parameter estimates and their standard deviations, correlation coefficients, and sum of square errors obtained from the best fit of these experimental data by Eqs. 8 and 9, respectively. Fitting parameters c_1 – c_4 and d_1 – d_4 are not simple adjustable constants, but have a clear physical meaning,^[7] and this allows the parameter estimates to be commented on. As expected, c_2 – c_3 and d_2 – d_3 , which are related to ion pair equilibrium constants, decrease with decreasing analyte lipophilicity; d_4 , which represents the total ligand concentration, compares well with the bonded phase coverage of the column (4.05 μmol/m²), as expected; from the estimated c_4 , which represents the equilibrium constant for the IIR adsorption, we obtain an averaged $\Delta G^\circ = -15.6$ kJ/mol, which is a very reasonable value for the standard free energy of adsorption of hexanesulfonate.^[19,20] In Table 1, c_1 is missing for all analytes except 2,6-naphthalenedisulphonate because it was not considered an optimization parameter, since it represents k_0 that is analyte retention without the IIR in the mobile phase and it can be obtained from experimental results. When c_1

was estimated by the model (as for the doubly charged 2,6-naphthalendisulphonate, for which other fitting parameters do not apply because electrostatic repulsion entirely models its retention behavior), the percent error is very low (0.6%).

When Eq. 4 is used to obtain the surface potential that has to be substituted into Eq. 6, we obtain^[10] the following expression (a parallel expression can also be obtained from Eq. 7 to model retention data as a function of the stationary-phase concentration of the IIR):

$$k = \frac{c_1[\text{H}]^{z_E/z_H(b-1)} + c_2[\text{H}]}{(1 + c_3[\text{H}]) (1 + c_4[\text{H}]^b)} \quad (10)$$

For a detailed description of c_1 – c_4 in Eq. 10, the reader is referred to Ref. [10]. Figure 6 details how this equation properly describes the retention of neutral analytes in IIC;^[12] in this case the above expression can be simplified because z_E , c_2 , and c_3 are all zero and only adsorption competitions model the retention decrease with increasing IIR concentration.

The surface potential is easily predicted to alter the retention behavior of zwitterions.^[13–15,21] The molecular electrical dipole is subjected to a torque moment that

Table 2 Summary of parameter estimates and their standard deviation, correlation coefficient (r), and sum of square errors (SSE) for the best fit of experimental retention data (some of them are shown in Figs. 2 and 4) as a function of the stationary-phase concentration of the IIR by Eq. 9

Analyte	d_1	d_2 (m ² /μmol) ^(1/b)	d_3 (m ² /μmol) ^(1/b)	d_4 (μmol/m ²)	r (Eq. 9)	SSE (Eq. 9)
L-Tyrosine hydrazide	—	101.829±10.444	3.011±0.229	—	0.999	4.587
Adrenaline	—	35.116±2.971	2.350±0.146	—	0.999	0.606
Octopamine	—	25.396±2.300	2.204±0.144	—	0.999	0.408
Sodium <i>p</i> -toluenesulfonate	—	—	—	1.311±0.393	0.987	3.380
Sodium salicylate	—	—	—	1.616±0.595	0.987	2.085
2,6-Naphthalenedisulfonate	1.097±0.036	—	—	—	0.996	0.008

Conditions as in Fig. 1.

Source: From Ref. [18]. (Courtesy of Marcel Dekker, Inc.)



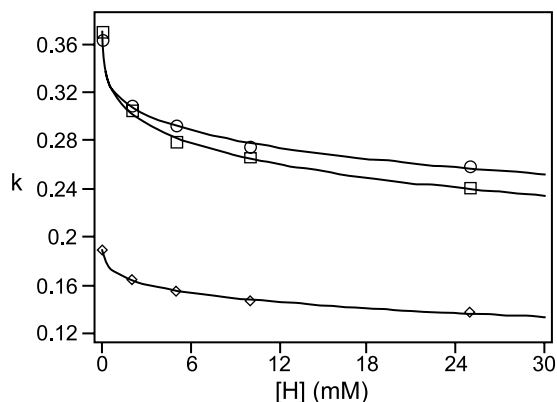


Fig. 6 Dependence of k on dimethylformamide (squares), dimethylacetone (circles), and dimethylsulfoxide (rhombuses), on mobile-phase concentration of tetrabutylammonium bromide. Column: Res Elut 5 C₁₈ (Varian), 25 cm × 4.6 mm ID, 5 μm. Eluent: 81.6 mM phosphate buffer, pH 7.2—methanol, 85:15, vol/vol containing tetrabutylammonium bromide. Experimental data were fitted by Eq. 10 with all z_E , c_2 , and c_3 equal to zero. (From Ref. [12]. Courtesy of Marcel Dekker, Inc.)

arranges it parallel to the lines of the nonhomogeneous electrical field, with the head oppositely charged to the electrostatic surface potential facing the stationary phase. Hence, the electrical force is always attractive and it pushes the dipole toward the interphase, where the field is stronger. This force was used to calculate the electrostatic contribution to the electrochemical potential of the analyte, and to the thermodynamic equilibrium constant for its adsorption. It was demonstrated that, from Eq. 6, the following relationship is quantitatively able to model zwitterions retention and can be advantageously used in life science chromatography:

$$k = \frac{c_1 \left(a[H]^b f + \left((a[H]^b f)^2 + 1 \right)^{\frac{1}{2}} \right)^{2c_2 K/F}}{1 + c_4 [H] \left(a[H]^b f + \left((a[H]^b f)^2 + 1 \right)^{\frac{1}{2}} \right)^{-2|z_H|}} \quad (11)$$

In Eq. 11, c_1 and c_4 are the already discussed parameters, whereas c_2 is related to the molecular dipole: the higher it is, the stronger is the retention increase on IIR addition. A parallel expression can also be obtained from Eq. 7 to model retention data as a function of the stationary-phase concentration of the IIR.^[13] A fractional charge approach to the IIC of zwitterions was also recently put forward.^[21]

Influence of Organic Modifier Concentration

A bivariate treatment of the simultaneous effects of IIR mobile-phase concentration and organic modifier percentage in the eluent on analyte retention gives the following relationship^[16] (see Eq. 12 below) where φ is the percentage (% vol/vol) of methanol in the mobile phase; c_{1_0} – c_{4_0} are the already discussed parameters c_1 – c_4 when the organic modifier is not present in the eluent; a_0 and b_0 are a and b when the organic modifier is not present in the eluent; and h is a parameter that accounts for the eluent ionic strength. If the latter is not constant and the dependence of h on total ionic concentration is explicitly introduced in Eq. 12, the above expression allows a multivariate approach to IIC; m_1 , m_2 , m_3 , m_4 , m_5 , and m_6 are parameters that depend on experimental conditions: m_1 depends on the analyte characteristic, m_2 , m_3 , and m_6 depend on the peculiarity of IIR, whereas m_4 and m_5 depend on the nature of both the analyte and the IIR. For analytes oppositely charged to the IIR, the active fitting parameters are m_1 , m_4 , m_5 , c_{2_0} , and c_{3_0} because m_2 , m_3 , a_0 , and b_0 are readily obtained from the fitting of the Freundlich constants as functions of the organic modifier concentration in the eluent. The bivariate nonlinear regression of the retention of a typical analyte oppositely charged to the IIR gives parameter estimates that were used to graphically present Eq. 12 in Fig. 7: it is rewarding to observe that retention decreases with increasing organic modifier concentration and increases with increasing IIR concentration. This increase is steeper at low organic modifier percentages because the organic modifier reduces analyte retention both directly (it decreases the analyte free energy of adsorption) and indirectly (it decreases the IIR

$$k = \frac{c_{1_0} e^{-m_1 \varphi} \left(\frac{a_0 e^{-m_2 \varphi} [H]^{(b_0 + m_3 \varphi)}}{(h(\varepsilon_{H_2O} - (\varepsilon_{H_2O} - \varepsilon_{MeOH})\varphi))^{\frac{1}{2}}} + \left(\left(\frac{a_0 e^{-m_2 \varphi} [H]^{(b_0 + m_3 \varphi)}}{(h(\varepsilon_{H_2O} - (\varepsilon_{H_2O} - \varepsilon_{MeOH})\varphi))^{\frac{1}{2}}} \right)^2 + 1 \right)^{\frac{1}{2}} \right)^{(\pm 2|z_E|)}}{1 + c_{3_0} e^{-m_5 \varphi} [H] \left(1 + c_{4_0} e^{-m_6 \varphi} [H] \left(\frac{a_0 e^{-m_2 \varphi} [H]^{(b_0 + m_3 \varphi)}}{(h(\varepsilon_{H_2O} - (\varepsilon_{H_2O} - \varepsilon_{MeOH})\varphi))^{\frac{1}{2}}} + \left(\left(\frac{a_0 e^{-m_2 \varphi} [H]^{(b_0 + m_3 \varphi)}}{(h(\varepsilon_{H_2O} - (\varepsilon_{H_2O} - \varepsilon_{MeOH})\varphi))^{\frac{1}{2}}} \right)^2 + 1 \right)^{\frac{1}{2}} \right)^{(-2|z_H|)}} \right)} + c_{2_0} e^{-m_4 \varphi} [H] \quad (12)$$

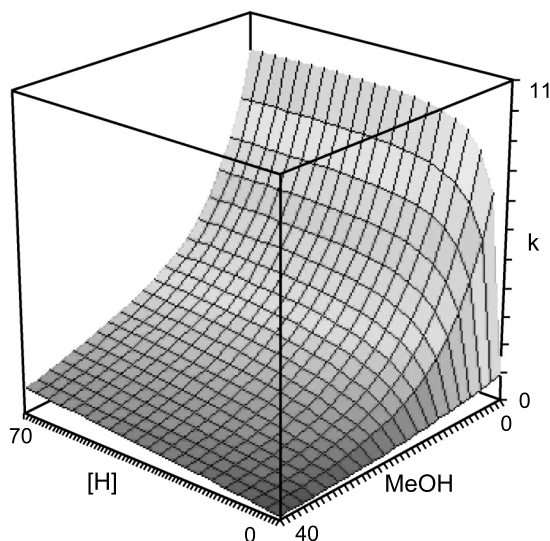


Fig. 7 Retention behavior of a typical analyte in IIC as a function of IIR mobile-phase concentration and organic modifier percentage in the eluent, according to Eq. 12.

free energy of adsorption: a lower surface concentration of the IIR results in a lower electrostatic attraction of the analyte and hence in a lower retention).

Noteworthy, in the absence of the IIR, Eq. 12 reduces to one which describes the influence of the organic modifier on RP-HPLC retention. A relationship similar to Eq. 12 can be obtained to describe the simultaneous effects of the IIR stationary-phase concentration and organic modifier percentage in the eluent on analyte retention.^[16]

Influence of Ionic Strength

In IIC method development, when a compensatory electrolyte is not added to the eluent, the ionic strength is not constant; hence, the dependence of f (Eq. 3) on the ionic concentration must be explicitly addressed.^[17] At a fixed IIR surface concentration, the electrostatic potential decreases with increasing electrolyte concentration because counterions in the diffuse layer shield the surface charge. However, with increasing ionic strength, there is an increased surface concentration of the IIR because counterions lower the self-repulsion forces between the similarly charged adsorbed IIR ions. Yet, this Donnan effect is not able to compensate the decreased surface potential due to a higher concentration of counterions in the diffuse layer. The strong interplay between these issues can be easily taken into account using the adsorption isotherm of the IIR obtained when its counterion concentration is not kept constant in the eluent.^[17] The retention of a solute oppositely (similarly) charged to the IIR is predicted to decrease (increase) with

increasing ionic strength because of the lower net electrostatic attraction (repulsion).

CONCLUSION

The distinguishing features that set this retention model apart are the following:^[7–18,21]

1. It is general. From two equations, quantitative predictions can be made for the retention behavior of charged, multiply charged, neutral, and zwitterionic solutes in IIC as a function of both the mobile-phase and the stationary-phase concentrations of the IIR. Retention equations can also quantitatively take into account the influence of the organic modifier concentration and the ionic strength; in the absence of IIR, they reduce to the well-known relationships of RP-HPLC.
2. It reduces to the relationships of stoichiometric or electrostatic approaches in IIC, respectively, if the surface potential or ion pairing equilibria are disregarded.
3. It is able to rationalize experimental behaviors that cannot be explained by other outstanding electrostatic retention models: 1) different theoretical curves when k is plotted as a function of the stationary-phase concentration of the IIR, for different IIRs; 2) dependence of the ratio of the retention of two different analytes on the IIR concentration; 3) dependence of the k/k_0 ratio on the analyte nature if the experimental conditions are the same; and 4) better agreement between electrostatic retention model predictions and experimental findings for analytes similarly charged as the IIR.
4. It is able to explain why the electrostatic approach is sometimes at variance with experimental evidence (this happens if experimental data underscore and involve complex formation).
5. Adjustable parameters have a clear physical meaning and their estimates are reliable because they compare well with literature estimates and with direct experimental measurements.
6. It is able to rationalize, in a quantitatively unprecedented way, with very low percent errors, experimental evidence qualitatively or semiquantitatively explained by other models.

As a concluding remark, it has to be emphasized that every acceptable retention theory must be consistent with fundamental physics, as well as describe experimental findings. The complex multiplicity of phenomena involved in an IIC system requires a complex description of the thermodynamics solutes have undergone: this description is epistemologically acceptable if the model is



well founded in physical chemistry and if it is able to describe experimental data better than previous models.

REFERENCES

- Horvath, C.; Melander, W.; Molnar, I.; Molnar, P. Enhancement of retention by ion-pair formation in liquid chromatography with nonpolar stationary phases. *Anal. Chem.* **1977**, *49* (14), 2295–2305.
- Kissinger, P.T. Comments on reverse-phase ion-pair partition chromatography. *Anal. Chem.* **1977**, *49* (6), 883.
- Bartha, A.; Stahlberg, J. Electrostatic retention model of reversed-phase ion-pair chromatography. *J. Chromatogr., A* **1994**, *668*, 255–284.
- Bidlingmeyer, B.A.; Deming, S.N.; Price, W.P., Jr.; Sachok, B.; Petrusek, M. Retention mechanism for reversed-phase ion-pair liquid chromatography. *J. Chromatogr.* **1979**, *186*, 419–434.
- Knox, J.H.; Hartwick, R.A. Mechanism of ion-pair liquid chromatography of amines, neutrals, zwitterions and acids using anionic heterons. *J. Chromatogr.* **1981**, *204*, 3–21.
- Cantwell, F.F. Retention model for ion-pair chromatography based on double-layer ionic adsorption and exchange. *J. Pharm. Biomed. Anal.* **1984**, *2* (2), 153–164.
- Cecchi, T.; Pucciarelli, F.; Passamonti, P. Extended thermodynamic approach to ion-interaction chromatography. *Anal. Chem.* **2001**, *73* (11), 2632–2639.
- Cecchi, T. Extended thermodynamic approach to ion-interaction chromatography: A thorough comparison with the electrostatic approach and further quantitative validation. *J. Chromatogr., A* **2002**, *958* (1–2), 51–58.
- Cecchi, T.; Pucciarelli, F.; Passamonti, P. Ion interaction chromatography of neutral molecules. *Chromatographia* **2001**, *53* (1–2), 27–34.
- Cecchi, T.; Pucciarelli, F.; Passamonti, P. An extended thermodynamic approach to ion-interaction chromatography for high surface potential: Use of a potential approximation to obtain a simplified retention equation. *Chromatographia* **2001**, *54* (9–10), 589–593.
- Cecchi, T.; Pucciarelli, F.; Passamonti, P. Extended thermodynamic approach to ion-interaction chromatography for low surface potential: Use of a linearized potential expression. *J. Liq. Chromatogr. Relat. Technol.* **2001**, *24* (17), 2551–2557.
- Cecchi, T.; Pucciarelli, F.; Passamonti, P. Ion interaction chromatography of neutral molecules: A potential approximation to obtain a simplified retention equation. *J. Liq. Chromatogr. Relat. Technol.* **2001**, *24* (3), 291–302.
- Cecchi, T.; Pucciarelli, F.; Passamonti, P.; Cecchi, P. The dipole approach to ion interaction chromatography of zwitterions. *Chromatographia* **2001**, *54* (1–2), 38–44.
- Cecchi, T.; Cecchi, P. The dipole approach to ion interaction chromatography of zwitterions: Use of a potential approximation to obtain a simplified retention equation. *Chromatographia* **2002**, *55* (5–6), 279–282.
- Cecchi, T.; Cecchi, P. The dipole approach to ion interaction chromatography of zwitterions: Use of the linearized potential expression for low surface potential. *J. Liq. Chromatogr. Relat. Technol.* **2002**, *25* (3), 415–420.
- Cecchi, T.; Pucciarelli, F.; Passamonti, P. Extended thermodynamic approach to ion-interaction chromatography. The influence of the organic modifier concentration. *Chromatographia* **2003**, *58* (7–8), 411–419.
- Cecchi, T.; Pucciarelli, F.; Passamonti, P. Extended thermodynamic approach to ion-interaction chromatography. A mono- and bivariate strategy to model the influence of ionic strength. *J. Sep. Sci.* **2004**, *27*, *in press*.
- Cecchi, T.; Pucciarelli, F.; Passamonti, P. Extended thermodynamic approach to ion-interaction chromatography: Effect of the electrical charge of the solute ion. *J. Liq. Chromatogr. Relat. Technol.* **2004**, *27* (1), 1–15.
- Davies, J.T.; Rideal, E.K. Adsorption at Liquid Interfaces. In *Interfacial Phenomena*; Academic Press: New York, 1961; 154–216.
- Rosen, M.J. Adsorption of Surface-Active Agents at Interfaces: The Electrical Double Layer. In *Surfactant and Interfacial Phenomena*, 2nd Ed.; Wiley: New York, 1978; 33–106.
- Cecchi, T.; Pucciarelli, F.; Passamonti, P. Ion-Interaction Chromatography of Zwitterions. The Fractional Charge Approach to Model the Influence of the Mobile Phase Concentration of the Ion-Interaction Reagent The Analyst. **2004**, *129*, 1037–1046. (article B404721D available: DOI 10.1039/b404721d <http://www.rsc.org/is/journals/current/analyst/anpub.htm>).



Concentration Effects on Polymer Separation and Characterization by ThFFF

Wenjie Cao

Mohan Gownder

Huntsman Polymers Corporation, Odessa, Texas, U.S.A.

Introduction

The understanding of the effects of sample concentration (sample mass) in field-flow fractionation (FFF) has been obtained gradually with the improvement of the sensitivity (detection limit) of high-performance liquid chromatography (HPLC) detectors. Overloading, which was used in earlier publications, emphasizes that there is an upper limit of sample amount (or concentration) below which sample retention will not be dependent on sample mass injected into the FFF channels [1]. Recent studies show that such limits may not exist for thermal FFF (may be true for all the FFF techniques in polymer separation), although some of the most sensitive detectors on the market were used [2].

Sample Concentration

Experimental results indicate that the effects of sample mass include, but not exclusively, the following aspects.

Increased Polymer Retention

Figure 1 shows the fractograms of thermal FFF (ThFFF) to show the concentration effects for poly(methyl methacrylate) (PMMA) in THF, where M_p is the peak average molecular weight, m is the sample mass in micrograms injected into the ThFFF channel, and t^0 is the retention time of a nonretained species such as toluene. When the molecular weight (MW) of a polymer is moderate or higher, say above 300×10^3 g/mol for PMMA in THF, a moderate increase in concentration will result in longer retention. As reported in Ref. 2, the detector limits for the study was $0.09 \mu\text{g}$ of sample mass for 1000×10^3 g/mol polystyrene using an ultraviolet (UV) detector and $1 \mu\text{g}$ for 570×10^3 g/mol PMMA with an evaporative light-scattering detector. The retention was measured for sample masses ranging

from these limits to more than $20 \mu\text{g}$ and was consistently found to increase with the increase in sample mass. The high limit, below which polymer retention is not dependent on concentration, was not found.

Broader Polymer Peaks

Increased concentration will increase band broadening in all chromatographic techniques, but it seems that the effect of concentration on band broadening is more serious in FFF, due to its concentration enhancement as shown by Fig. 1, and by Figure 5 of Ref. 1. More details will be discussed in the next section.

Distorted Peaks and Double-Topped Peaks (Ghost Peaks)

When the amount of sample mass injected into the ThFFF channel is moderate, say $1\text{--}10 \mu\text{g}$ for a typical channel, the peaks are pretty symmetrical and not much distortion may be observed for small polymers,

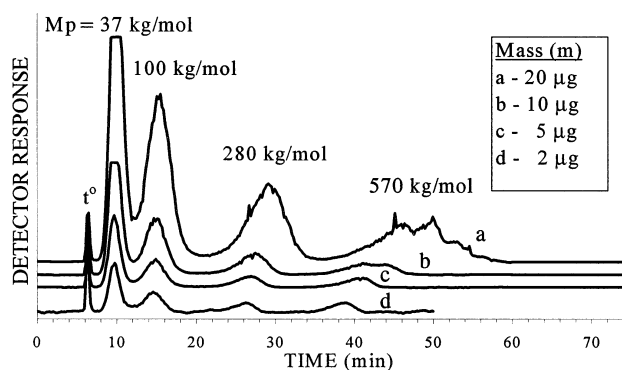


Fig. 1 Fractograms of PMMA in THF showing the effect of sample concentration on retention. Experimental conditions: cold-wall temperature, 25°C , T , 50°C ; flow rate, 0.1 mL/min .



as shown by Fig. 1. Increased retention may be observed for high-MW polymers [2]. When sample mass is further increased, say more than 20 μg , distorted peaks, even double-topped peaks or ghost peaks, may be observed for high-MW polymers as shown by Fig. 1, Fig. 6 of Ref. 1, and Fig. 3 of Ref. 2. The detailed report and discussion of double-topped peaks can be found in both Refs. 1 and 2.

Enhanced Viscosity Is Blamed for the Sample Concentration Effects

The viscosity of a polymer solution is highly dependent on concentration, temperature, and MW, as discussed below.

Concentration and Viscosity Enhancement in FFF

The amount of sample injected into the FFF channels can affect the retention time, primarily by influencing the viscosity of the solute-solvent mixture in the sample zone [1,2]. Unlike other chromatographic polymer separation methods [e.g., GPC-SEC (size-exclusion chromatography) and TREF, etc.], the viscosity of the fluid is not homogeneous at a given channel (column) cross section. In order for the samples to be retained by FFF, the concentration must be larger near the accumulation wall than that near the depletion wall [3,4]. In chromatography, sample concentration changes only along one dimension (i.e., the flow axis) whereas in FFF, sample concentration varies along two dimensions, one being the flow axis and the other one is across the channel thickness, which is perpendicular to the flow axis. The concentration across the channel thickness varies due to the migration of the molecules under the influence of the temperature gradient across the ThFFF channel [3]. The concentration distribution is approximately exponential as given by

$$c(x) = c_0 \exp\left(\frac{-x}{\lambda w}\right) \quad (1)$$

where $c(x)$ is the concentration at distance x across the channel thickness measured from the accumulation wall, c_0 is the concentration at the accumulation wall, w is the channel thickness, and λ is the retention parameter or reduced mean thickness of the sample zone. Shortly after injection, the sample zone is assumed to broaden into a Gaussian distribution along the z axis, corresponding to the direction of flow down

the channel. The two-dimensional concentration becomes [5]

$$c(x, z) = c_{00} \exp\left(\frac{-(z - Z)^2}{2\sigma^2}\right) \exp\left(\frac{-x}{\lambda w}\right) \quad (2)$$

where Z is the distance traveled by the center of the zone down the channel. The concentration at the accumulation wall at the center of the zone, c_{00} , is found from [6]

$$c_{00} \cong \frac{V_{\text{inj}} c_{\text{inj}} L}{(2\pi\sigma^2)^{1/2} V^0 \lambda} \quad (3)$$

where V_{inj} is the volume of sample injected, V^0 is the void volume (channel volume), c_{inj} is the concentration of the injected sample, L is the length of the channel, and σ is the sum of the variances contributing to the zone breadth.

A rough calculation using Eq. (3) indicates that the concentration of c_{00} can be as high as 20 times the concentration of the original polymer solution. The concentration of the sample zone, therefore, can be enhanced dramatically in FFF.

The relationship between viscosity and concentration of polymer solution is very complex. Several empirical equations are necessary to describe the viscosity behavior of a polymer solution's dependence upon concentration. As an example, the following equation can be used for dilute solutions [7]:

$$\eta = 0.54 + 1.3374C + 1.1593C^2 \quad (4)$$

where η is viscosity in centipoise and C is the concentration in grams per deciliter.

For the concentration where a microgel may be formed, the following equation is proposed [8]:

$$\eta = BM^3 C^{3.7} \quad (5)$$

where B is a constant and M is the polymer's molecular weight.

Although various empirical equations can be found in the literature, the common aspect is that the viscosity of a polymer solution is highly dependent on concentration and molecular weight.

Temperature Dependence of Viscosity

The effect of temperature on the viscosity of the carrier can be expressed as [5]

$$\frac{1}{\eta} = a_0 + a_1T + a_2T^2 + a_3T^3 \quad (6)$$

where a_0 , a_1 , a_2 , and a_3 , are empirically obtained coefficients.

As Eq. (6) shows, the viscosity of a polymer solution is highly dependent on temperature. The sample zone of a high-MW polymer is pressed much closer to the cold wall in ThFFF. Its viscosity is more enhanced than with a low-MW polymer. The concentration effect, therefore, is more serious for high-MW polymers in ThFFF.

Molecular-Weight Dependence of Viscosity

If the temperature and concentration are kept the same, the viscosity of higher-MW polymer solution is higher, as shown by Eq. (2); thus, more distortion of its peak is expected, as shown by Fig. 1.

Unlike most of the elution separation methods, such as HPLC, GPC/SEC, gas chromatography (GC), and so forth, where the concentration of the sample zone will never be higher than the stock solution before injection, FFF will concentrate the samples, that is to say that sample concentration will be enhanced near the accumulative wall of FFF and the cold wall in ThFFF. The higher the MW of the polymer, the more the concentration will be enhanced and the lower the temperature of the sample zone will be. All three factors, concentration, temperature, and MW, contribute simultaneously to enhance the viscosity of the sample zone of the polymers in ThFFF. The viscosity of the sample zone can reach such extension that there is a tendency for the carrier fluid to flow over the top of the zone, with increased velocity in the region above the sample zone. The moving fluid will go over the sample zone, thus resulting in a longer retention for the sample zone; this is like a sticky slump going slowly on the floor of a river. A longer retention will be observed even if the flow rate of the carrier is constant.

When the MW of the polymer is so large that its zone is compressed close to the cold wall, the temperature of the sample zone becomes, essentially, the temperature of the cold wall, 25°C in many experiments. The viscosity is enhanced so much that the flow velocity of the carrier fluid is further distorted, so that deformed or double-topped peaks will be produced.

For the double-topped peaks, pseudo-gel, formed near the cold wall, is also proposed due to the low tem-

perature and high concentration of the sample zone in ThFFF [2,9]. The behavior of a pseudo-gel solution is quite different from the polymer solution from which it is formed. The diffusion coefficient of a pseudo-gel is much smaller than that of the original polymer, and the viscosity of the pseudo-gel solution will be much larger than that of the original polymer solution. The pseudo-gel, in theory, will be compressed closer to the cold wall and will elute out of the channel later than the parent molecules. However, as the size of the pseudo-gel cluster increases, hydrodynamic effects will result in an earlier emergence from the channel [3]. If either of these scenarios occurs in the ThFFF channel, double peaks might be observed for a sample of a single peak without "overloading."

Conclusion

Any attempts to obtain the parameters of the chromatograms and the physicochemical constants which are measurable in theory, by FFF, will be affected by the sample mass injected into the FFF channel. All of the concentration effects on the chromatograms discussed in the previous sections will be transferred, in turn, to those measured parameters and the physicochemical constants, such as the mass selectivity (S_m), the common diffusion coefficient (D), the thermal diffusion coefficient (D_T), and so forth. The increased retention of large polymers will result in enhanced mass selectivity in ThFFF. For a long time, this enhanced selectivity, in turn, the enhanced ThFFF universal calibration constant n , has led to confusion concerning the accuracy and repeatability of FFF, because different research groups have reported different data for selectivity and physicochemical constants measured by FFF for a given polymer-solvent combination [2,11]. Recent studies show that the enhanced selectivity and the different values of the physicochemical constants reported by different laboratories, measured by ThFFF, may be caused by different concentrations (sample mass) used by different laboratories.

References

1. K. D. Caldwell, S. L. Brimhall, Y. Gao, and J. C. Giddings, *J. Appl. Polym. Sci.* 36:703 (1988).
2. W. J. Cao, M. N. Marcus, P. S. Williams, and J. C. Giddings, *Int. J. Polym. Anal. Charact.* 4:407 (1998).
3. J. C. Giddings, *Science* 260:1456 (1993).
4. J. C. Giddings, *Anal. Chem.* 66:2783 (1994).



5. J. C. Giddings, F. J. F. Yang, and M. N. Myers, *Anal. Chem.* 46:1917 (1974).
6. K. D. Caldwell, S. L. Brimhall, Y. Gao, and J. C. Giddings, *J. Appl. Polym. Sci.* 36:703 (1988).
7. C. Tanford, *Physical Chemistry of Macromolecules*, John Wiley & Sons, New York, 1961, Chap. 6.
8. P. G. DeGennes, *Macromolecules* 9:594 (1976).
9. H. Tan, A. Moet, A. Hiltner, and E. Baer, *Macromolecules* 16:28 (1983).
10. M. Hoyos and M. Martin, *Anal. Chem.* 66:1718 (1994).
11. R. M. Sisson and J. C. Giddings, *Anal. Chem.* 66:4043 (1994).



Concentration of Dilute Colloidal Samples by Field-Flow Fractionation

George Karaiskakis

University of Patras, Patras, Greece

Introduction

Many colloidal systems, such as those of natural water, are too dilute to be detected by the available detection systems. Thus, a simple and accurate method for the concentration and analysis of these dilute samples should be of great significance in analytical chemistry. In the present work, two methodologies of the field-flow fractionation (FFF) technique for the concentration and analysis of dilute colloidal samples are presented. Both the conventional and potential barrier methodologies of FFF are based on the “adhesion” of the samples at the beginning of the channel wall, followed by their total removal and analysis. In the conventional sedimentation FFF (SdFFF) concentration procedure, the apparent adhesion of a dilute sample is due to its strong retention, which can be achieved by applying high field strengths and low flow rates. In the potential barrier SdFFF (PBSdFFF) concentration procedure, the true adhesion of a dilute sample is due to its reverse adsorption at the beginning of the column, which can be achieved by the appropriate adjustment of various parameters influencing the interactions between the colloidal particles and the material of the channel wall. The total release of the adherent particles is accomplished either by reducing the field strength and increasing the solvent velocity (conventional SdFFF) or by varying the potential energy of interaction between the particles and the column material—for instance, by changing the ionic strength of the carrier solution (PBSdFFF).

Methodology

Field-flow fractionation is a one-phase chromatographic system in which an external field or gradient replaces the stationary phase. The applied field can be of any type that interacts with the sample components and causes them to move perpendicular to the flow direction in the open channel. The most highly developed of the various FFF subtechniques is sedimenta-

tion FFF (SdFFF), in which the separations of suspended particles are performed with a single, continuously flowing mobile phase in a very thin, open channel under the influence of an external centrifugal force field.

In the normal mode of the SdFFF operation, a balance is reached between the external centrifugal field, driving the particles toward the accumulation wall, and the molecular diffusion in the opposite direction. In that case, the retention volume increases with particle diameter until steric effects dominate, at which transition point there is a foldback in elution order.

Potential barrier SdFFF (PBSdFFF), which has been developed recently in our laboratory, is based either on particle size differences or on Hamaker constant, surface potential, and Debye–Hückel reciprocal distance differences.

The retention volume of a component under study, V_r , in the normal SdFFF and the PBSdFFF methodologies is a function of the following parameters:

1. SdFFF:

$$V_r = f(d, G, \Delta\rho) \quad (1)$$

2. PBSdFFF:

$$V_r = f(d, G, \Delta\rho, \psi_1, \psi_2, A, I) \quad (2)$$

where d is the particle diameter, G is the field strength expressed in acceleration, $\Delta\rho$ is the density difference between solute and solvent, ψ_1 and ψ_2 are the surface potentials of the particle and of the wall, respectively, A is the Hamaker constant, and I is the ionic strength of the carrier solution.

The conventional concentration procedure in SdFFF consists of two steps: the feeding (or concentration) and the separation (or elution) step. In the feeding step, the diluted samples are fed into the column with a small flow velocity while the channel is rotated at a high field strength to ensure the “apparent adhesion” of the total number of the colloidal particles at the beginning of the channel wall as a consequence



of the particles' strong retention. In the separation step, the field is reduced and the flow rate is increased to ensure the total release and the consequence elution of the adherent dilute particles.

In PBSdFFF, the concentration step consists of feeding the column with the diluted samples at such experimental conditions, so as to decrease the repulsive component and increase the attractive component of the total potential energy of the particles under study. Because the stability of a colloid varies (increases or decreases) with a number of parameters (surface potential, Hamaker constant and ionic strength of the suspending medium), the proper adjustment of one or more of these parameters can lead not only to the adhesion of the dilute colloidal samples, which leads to their "concentration," but also to the total release of the adherent particles during the elution step.

Applications

Conventional SdFFF

As model samples for the verification of the conventional SdFFF as a concentration methodology monodisperse polystyrene latex beads (Dow Chemical Co.) with nominal diameters of $0.357\ \mu\text{m}$ (PS1) and $0.481\ \mu\text{m}$ (PS2) were used. They were either used as dispersions containing 10% solids or diluted with the carrier solution (triple-distilled water + 0.1% (v/v) detergent FL-70 from Fisher Scientific Co. + 0.02% (w/w) NaN_3) to study sample dilution effects. Diluted samples in which the amount of the polystyrene was held constant ($1\ \mu\text{L}$ of the 10% solids) while the volume in which it was contained was varied over a 50,000-fold range (from 1 to 50 mL of carrier solution) were introduced into the SdFFF column. During the feeding step, the flow rate was 5.8 mL/h for the PS1 polystyrene, and 7.6 mL/h for the polystyrene PS2, and the channel was rotated at 1800 rpm for the PS1 sample and at 1400 rpm for the PS2 sample. In the separation (elution) step, the experimental conditions for the two samples were as follows:

- PS1: Field strength = 880 rpm,
flow rate = 12–53 mL/h
- PS2: Field strength = 500 rpm,
flow rate = 24–59 mL/h

Figure 1 provides a comparison of fractograms for the $0.357\text{-}\mu\text{m}$ polystyrene injected as a narrow pulse (Fig. 1a) and injected at 10 mL dilution (Fig. 1b) by the conventional SdFFF concentration procedure de-

scribed previously. Figure 1b shows that the eluted peak from the diluted sample emerges intact and without serious degradation, compared to the peak of Fig. 1a, despite the fact that the sample volume (10 mL) is over twice the channel volume (4.5 mL). The same concentration procedure was also successfully applied to the separation of the two polystyrene samples initially mixed together in a volume of 10 mL, as well as to the concentration of the colloidal particles contained in natural water samples collected from the Colorado, Green, and Price rivers in eastern Utah (U.S.A.).

As a general conclusion, the on-column concentration procedure of the conventional SdFFF method works quite successfully in dealing with highly diluted samples. Optimization, particularly higher field strengths during the concentration step, would allow higher flow rates and increased analysis speed. However, experimental confirmation would be necessary to give assurance that the particle–wall adhesion is not irreversible at higher spin rates.

Potential Barrier SdFFF

As model samples to test the validity of the PBSdFFF as a concentration procedure of diluted samples the monodisperse colloidal particles of $\alpha\text{-Fe}_2\text{O}_3$ with nominal diameters of $0.271\ \mu\text{m}$ were used. Diluted samples of $\alpha\text{-Fe}_2\text{O}_3$ containing $2\ \mu\text{L}$ of the 10% solid, in which the volume was varied over a 10,000-fold range (from 2 to 20 mL), were introduced into the column with a carrier solution containing 0.5% (v/v) detergent FL-70 + $3 \times 10^{-2}\text{M}$ KNO_3 to ensure the total adhesion of the $\alpha\text{-Fe}_2\text{O}_3$ particles at the beginning of the SdFFF Hastelloy-C channel wall. In the separation step, the carrier solution was changed to one containing only 0.5% (v/v) detergent FL-70 (without electrolyte) to ensure the total detachment of the adherent particles. In that case, a sample peak appeared (cf. Fig. 1c) as a consequence of the desorption of the $\alpha\text{-Fe}_2\text{O}_3$ particles. The mean diameter of the $\alpha\text{-Fe}_2\text{O}_3$ particles ($0.280\ \mu\text{m}$) obtained by the proposed PBSdFFF methodology for the on-channel concentration procedure of the sample diluted in 8 mL of the carrier solution is very close to that found ($0.271\ \mu\text{m}$) by the direct injection of the same particles into the channel, using a carrier in which no adsorption occurs.

As a general conclusion, one could say that the proposed PBSdFFF concentration procedure works quite successfully in dealing with highly dilute samples, separating them according to size, surface potential, and Hamaker constant. At the same time, as separa-



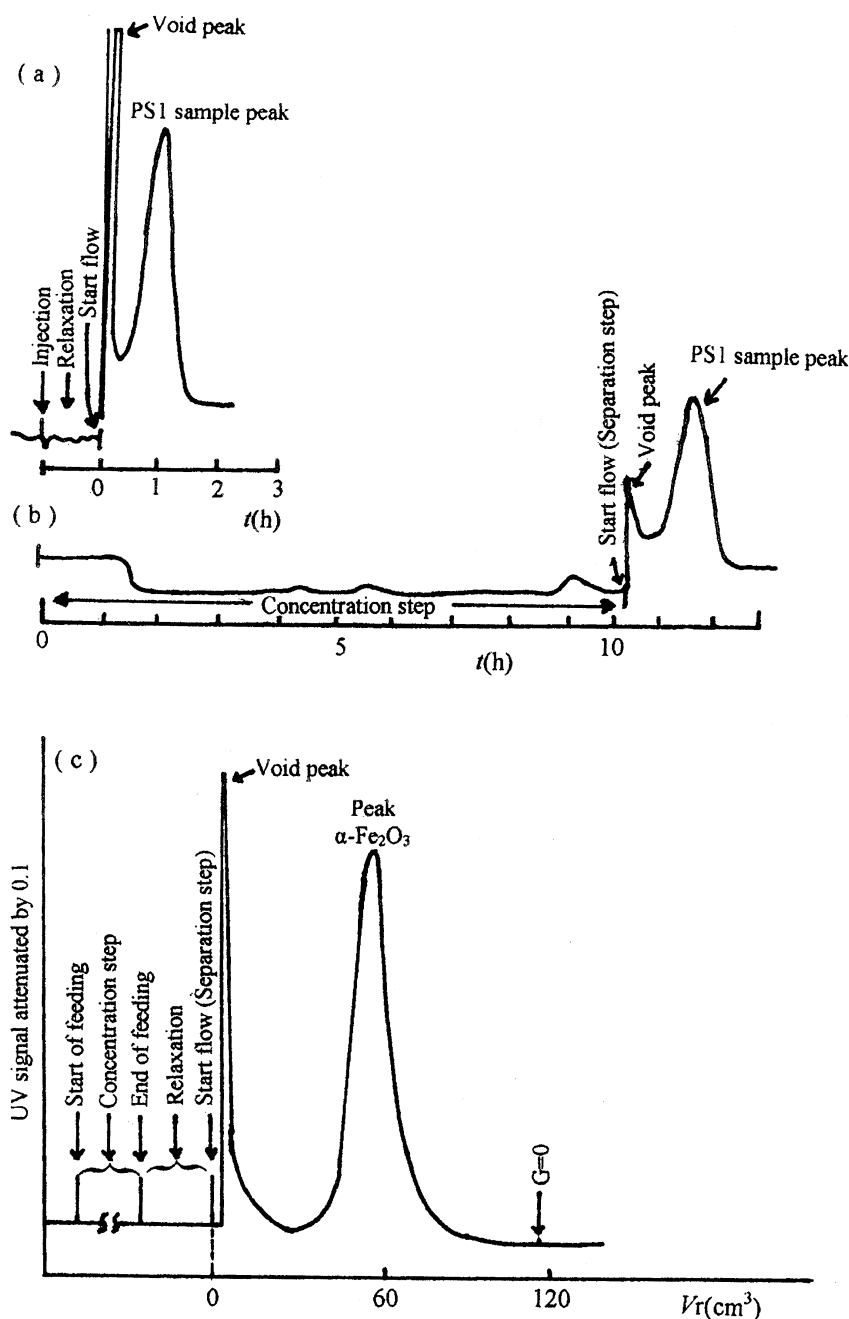


Fig. 1 Fractograms of the polystyrene latex beads of $0.357\ \mu\text{m}$ (PS1) obtained by the direct injection of $1\ \mu\text{L}$ of PS1 (a) and by the concentration procedure of the PS1 sample diluted in $10\ \text{mL}$ of the carrier solution (b) using the conventional SdFFF technique, as well as of the $\alpha\text{-Fe}_2\text{O}_3$ sample with nominal particle diameter of $0.271\ \mu\text{m}$ diluted in $6\ \text{mL}$ of the carrier solution obtained by the PBSdFFF concentration methodology (1c).

tion occurs, the particle sizes of the colloidal materials of the diluted mixture can be determined. The major advantage of the proposed concentration procedure is that the method can concentrate and analyze dilute mixtures of colloidal particles even of the same size but

with different surface potentials and/or Hamaker constants. The method has considerable promise for the separation and characterization, in terms of particle size, of dilute complex colloidal materials, where particles are present in low concentration.



Future Developments

Looking to the future, we believe that the efforts of the researchers will be focused on the extension of the FFF concentration methodologies to the ranges of more dilute and complex colloidal samples, without lengthening the analysis time.

Suggested Further Reading

A. Athanasopoulou, A. Koliadima, and G. Karaiskakis, *Instrum. Sci. Technol.* 24(2):79 (1996).

J. C. Giddings, G. Karaiskakis, and K. D. Caldwell, *Separ. Sci. Technol.* 16(6):725 (1981).

P. C. Hiemenz, *Principles of Colloid and Surface Chemistry*, Marcel Dekker, Inc., New York, 1977.

G. Karaiskakis and J. Cazes (eds.), *J. Liquid Chromatogr. Related Technol.* 20(16 & 17) (1997).

G. Karaiskakis, K. A. Graff, K. D. Caldwell, and J. C. Giddings, *Int. J. Environ. Anal. Chem.* 12:1 (1982).

A. Koliadima and G. Karaiskakis, *J. Liquid Chromatogr.* 11:2863 (1988).

A. Koliadima and G. Karaiskakis, *J. Chromatogr.* 517:345 (1990).

A. Koliadima and G. Karaiskakis, *Chromatographia* 39:74 (1994).



Conductivity Detection in Capillary Electrophoresis

Jetse C. Reijenga

Eindhoven University of Technology, Eindhoven, The Netherlands

Introduction

In contrast to component-specific detectors, such as ultraviolet (UV) absorbance and fluorescence, conductivity detection is a universal detection method. This means that a bulk property (conductivity) of the buffer solution is continuously measured. A migrating ionic component locally changes the conductivity and this change is monitored. As such, conductivity detection is universally sensitive because, in principle, all migrating ionic compounds show detector response, although not to the same extent.

Types of Conductivity Detection

Two kinds of conductivity detector are distinguished: contact detectors and contactless detectors. Both types were originally developed for isotachopheresis in 0.2–0.5-mm-inner diameter (i.d.) PTFE tubes. Contactless detectors are based on the measurement of high-frequency cell resistance and, as such, inversely proportional to the conductivity. The advantage is that electrodes do not make contact with the buffer solution and are, therefore, outside the electric field. As these types of detectors are difficult to miniaturize down to the usual 50–75- μm capillar inner diameter, their actual application in capillary electrophoresis (CE) is limited.

Contact detectors are somewhat easier to miniaturize. There are generally two subtypes: those with twin axially mounted electrodes and those with twin or quadruple radially mounted electrodes. The former can be operated in DC mode or AC mode. In the DC mode, the detector signal directly originates from the field strength between the electrodes and, given the current, is inversely proportional to the detector cell resistance. In the AC mode, both axially and radially mounted electrodes form part of a closed primary circuit of an isolation transformer, the output of which is also inversely proportional to the cell conductivity. Alternatively, the output can be linearized with respect to the conductivity.

Conductivity Detector Response

As mentioned, the detector continually measures the conductivity of the buffer solution in the capillary. If an ionic component enters the detector cell, the local conductivity will change. At first glance, one would expect the conductivity to increase, because of additional ionic material. This is a simplified and incorrect approach, however. Suppose, in a buffer consisting of 0.01M potassium and 0.02M acetate (pH 4.7), a 10^{-4}M sodium solution is analyzed. Electroneutrality requires that with an increase of the sodium concentration from zero to, in this case, initially 10^{-4}M , the potassium and/or charged acetate concentration cannot remain unchanged. This process is governed by the so-called Kohlrausch law. For strong ions, this equation reads

$$\Lambda = \sum_i \frac{c_i}{\mu_i}$$

in which Λ is the so-called Kohlrausch regulating function, c_i is the concentration of component i , and μ_i is the mobility of component i . Generally speaking, potassium will be partly displaced by sodium, whereas acetate will remain approximately (but not, by definition, exactly) constant. In the example given, the conductivity detector will give a negative response (see line A in Fig. 1), because potassium (with a high mobility and, hence, a higher contribution to conductivity) is, to some extent, replaced with sodium which has a $\sim 30\%$ lower mobility. From this example, it automatically follows that a potassium peak in a sodium acetate buffer, by contrast, will yield a positive amplitude. This makes interpretation of conductivity detector signals less straightforward.

Sensitivity of Conductivity Detection

A further example will illustrate aspects related to sensitivity. Suppose a 100 times more concentrated (10 mM) solution of ammonium is coseparated in the



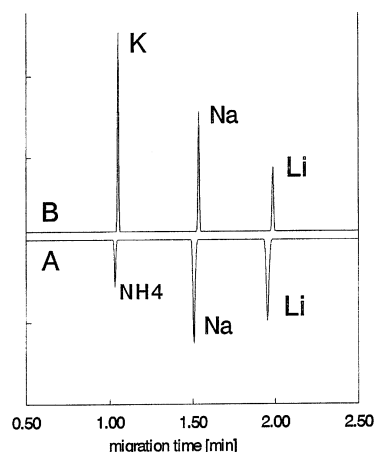


Fig. 1 Relative sensitivities in conductivity detection in CE. Trace A: sample of 10 mM NH_4 , 0.1 mM Na, and 0.005 mM Li in a 0.01M potassium–acetate buffer; trace B: sample of 0.1 mM each of K, Na, and Li in a 10 mM Tris–acetate buffer.

potassium–acetate system mentioned earlier. Naturally, ammonium will displace potassium, but as the mobilities of potassium and ammonium are almost equal, the resulting change in conductivity is minor. Sensitivity in this example is, consequently, very low (line A in Fig. 1). On the other hand, 0.005 mM lithium has a much lower conductivity than sodium and, consequently, shows a higher specific response (line A in Fig. 1).

Conductivity Detection in Capillary Electrophoresis

Generally, one cannot expect a high sensitivity anyhow, as the background signal (originating from the buffer) is generally much higher than the eventual change superimposed upon that background. One might argue that background conductivity can easily be decreased by diluting the buffer. Potential gain with this approach is very limited, because diluting the buffer below an ionic strength of 1 mM will lead to unacceptable loss in buffering capacity and, moreover, in severe sample overload. Another possibility to decrease the background conductivity is to use buffer components with lower mobility, such as GOOD buffers. This, however, will sooner lead to nonsymmetric peaks on sample overload (peak triangulation). Using low-mobility Tris as a buffer co-ion will lead to positive peaks for 0.1 mM potassium, sodium, and lithium alike (line B in Fig. 1).

Suggested Further Reading

- Beckers, J. L., *Isotachophoresis, some fundamental aspects, Thesis*, Eindhoven University of Technology, 1973.
- Everaerts, F. M., J. L. Beckers, and Th. P. E. M. Verheggen, *Isotachophoresis: Theory, Instrumentation and Applications*, Elsevier, Amsterdam, 1976.
- Hjertén, S., *Chromatogr. Rev.* 9:122 (1967).
- Kohlrausch, F., *Ann. Phys. (Leipzig)* 62:209 (1897).
- Li, S. F. Y., *Capillary Electrophoresis – Principles, Practice and Applications*, Elsevier, Amsterdam, 1992.
- Reijenga, J. C., Th. P. E. M. Verheggen, J. H. P. A. Martens, and F. M. Everaerts, *J. Chromatogr. A* 744:147 (1996).

Conductivity Detection in HPLC

Ioannis N. Papadoyannis

Victoria F. Samanidou

Aristotle University of Thessaloniki, Thessaloniki, Greece

Introduction

Conductivity detection is used to detect inorganic and organic ionic species in liquid chromatography. As all ionic species are electrically conducting, conductometric detection is a universal detection technique, considered as the mainstay in high-pressure ion chromatography, in the same way as is ultraviolet (UV) detection in high-performance liquid chromatography (HPLC).

Discussion

The principle of operation of a conductivity detector lies in differential measurement of mobile-phase conductivity prior to and during solute ion elution. The conductivity cell is either placed directly after an analytical column or after a suppression device required to reduce background conductivity, in order to increase the signal-to-noise ratio and, thus, sensitivity. In the first mode, known as *nonsuppressed* or *single-column ion chromatography*, aromatic acid eluents are used, with low-capacity fixed-site ion exchangers and dynamically or permanently coated reversed-phase columns. In the second mode, known as *eluent-suppressed ion chromatography*, the separated ions are detected by conductance after passing through a suppression column or a membrane, to convert the solute ions to higher conducting species (e.g., hydrochloric acid in the case of chloride ions and sodium hydroxide in the case of sodium ions). In the meantime, the eluent ions are converted to a low-residual-conductivity medium such as carbonic acid or water, thus reducing background noise.

Conductance G is the ability of electrolyte solutions in an electric field applied between two electrodes to transport current by ion migration. According to Ohm's law, ohmic resistance R is given by

$$R = \frac{U}{I} \quad (1)$$

where U is the voltage (V) and I is the current intensity (A). The reciprocal of ohmic resistance is the conductance G , where

$$G = \frac{1}{R} \quad (2)$$

expressed in Siemens in the International System of Units (SI), formerly reported in the literature as mho (Ω^{-1}). The measured conductance of a solution is related to the interelectrode distance d (cm) and the microscopic surface area (A) (geometric area \times roughness factor) of each electrode (A is assumed identical for the two electrodes) as well as the ionic concentration, given by

$$G = \frac{kA}{d} \quad (3)$$

where k is the specific conductance or conductivity. The ratio d/A is a constant for a particular cell, referred as the cell constant K_c (cm^{-1}) and is determined by calibration. The usual measured variable in conductometry is conductivity k (S/cm):

$$k = GK_c \quad (4)$$

The conductance G (in μS) of a solution is given by

$$G = \frac{(\lambda^+ + \lambda^-)CI}{10^{-3}K_c} \quad (5)$$

where λ^+ and λ^- are limiting molar conductivities of the cation and anion, respectively, and C is the molarity and I the fraction of eluent that is ionized. If the eluent and solute are fully ionized, the conductance change accompanying solute elution is

$$\Delta G = \frac{(\lambda_s - \lambda_e)C_s}{10^{-3}K_c} \quad (6)$$

The specific conductance/conductivity k (S/cm) of salts measured by a conductivity detector is given by



$$k = \frac{(\lambda_{s+} + \lambda_{s-})C_s + (\lambda_{e+} + \lambda_{e-})C_e}{1000} = \frac{\Lambda_s C_s + \Lambda_e C_e}{1000} \quad (7)$$

where C_s and C_e are the concentration (mol/L) of the solute and eluent ions, respectively, and Λ is the molar conductivity of the electrolyte.

The change in conductance when a sample solute band passes through the detector results from replacement of some of the eluent ions by solute ions, although the total ion concentration C_{tot} remains constant:

$$C_{\text{tot}} = C_s + C_e \quad (8)$$

The background ion conductivity when $C_s = 0$ is

$$k_1 = \frac{\Lambda_e C_{\text{tot}}}{1000} \quad (9)$$

When a solute band is eluted, the ion conductivity k_2 is given by

$$k_2 = \frac{\Lambda_e C_{\text{tot}}}{1000} + \frac{(\Lambda_s - \Lambda_e)C_s}{1000} \quad (10)$$

The difference in conductivity is obtained after subtraction of the first equation from the second:

$$\Delta k = k_2 - k_1 = \frac{(\Lambda_s - \Lambda_e)C_s}{1000} \quad (11)$$

From Eq. (11), it is obvious that when a sample band is eluted, the observed difference in conductivity is proportional to the concentration of the sample solute C_s .

However, the linear relation holds only for dilute solutions, as Λ is itself dependent on concentration, according to Kohlrausch's law:

$$\Lambda = \Lambda^\circ - A\sqrt{C} \quad (12)$$

where A is a constant and Λ° is the limiting molar conductivity in an infinitely dilute solution, given by the sum

$$\Lambda^\circ = \Lambda^{\circ+} + \Lambda^{\circ-} \quad (13)$$

or

$$\Lambda^\circ = \nu_+ \lambda_+^\circ + \nu_- \lambda_-^\circ \quad (14)$$

where ν_+ and ν_- represent stoichiometric coefficients for the cation and anion, respectively, in the electrolyte.

Eq. (11) shows that the signal observed during solute ion elution is also proportional to the difference in limiting molar ionic conductivities between the eluent and the solute ions.

Values of limiting molar ionic conductivities for a few common ions are shown in Table 1. The data tabulated are referred to 25°C temperature. The term *limiting molar ionic conductivity* is used according to IUPAC recommendation, rather than the formerly used *limiting ionic equivalent conductivity*. The molar and equivalent values are interconvertible through stoichiometric coefficient z .

Conductivity is measured by applying an alternating voltage to two electrodes of various geometric shapes

Table 1 Limiting Molar Ionic Conductivities of some Anions and Cations (S cm²/mol) at 25°C

Anions	λ^-	Cations	λ^+
OH ⁻	199.1	H ⁺	349.6
F ⁻	55.4	Li ⁺	38.7
Cl ⁻	76.4	Na ⁺	50.1
Br ⁻	78.1	K ⁺	73.5
I ⁻	76.8	NH ₄ ⁺	73.5
NO ₃ ⁻	71.46	Mg ²⁺	106
NO ₂ ⁻	71.8	Cu ²⁺	107.2
SO ₄ ²⁻	160.0	Ca ²⁺	120
Benzoate ⁻	32.4	Sr ²⁺	118.9
Phthalate ²⁻	76	Ba ²⁺	127.2
Citrate ³⁻	168	Ethylammonium	47.2
CO ₃ ²⁻	138.6	Diethylammonium	42.0
C ₂ O ₄ ²⁻	148.2	Triethylammonium	34.3
PO ₄ ³⁻	207	Tetraethylammonium	32.6
CH ₃ COO ⁻	40.9	Trimethylammonium	47.2
HCOO ⁻	54.6	Tetramethylammonium	44.9

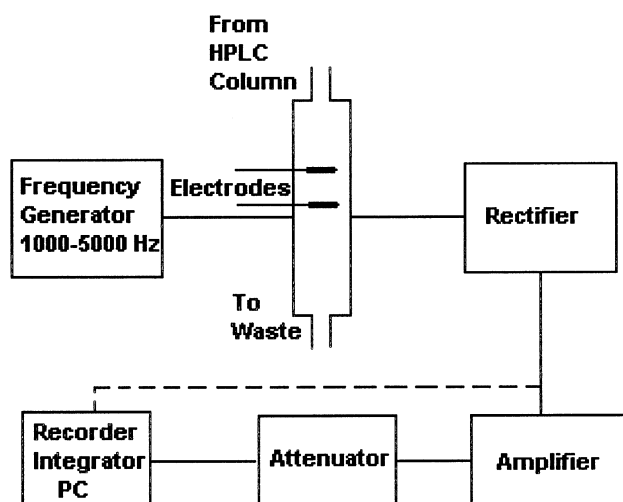


Fig. 1 Block diagram of electrical conductivity detector in HPLC.

in a flow-through cell, which results in anion migration, as negatively charged, toward the anode (positive electrode) and cation migration, as positively charged, toward the negative electrode (cathode). An AC potential (frequency 1000–5000 Hz) is required in order to avoid electrode polarization. The cell current is measured and the solution's resistance (or more strictly the impedance) is calculated by Ohm's law. Conductance is further corrected by the conductivity cell constant, thus giving conductivity.

The requirements for a typical conductivity detection cell are small volume (to eliminate dispersion effects), high sensitivity, wide linear range, rapid response, and acceptable stability. The cell generally consists of a small-volume chamber ($<5 \mu\text{L}$) fitted with two or more electrodes constructed of platinum, stainless steel, or gold.

Most conductivity detectors function according to the Wheatstone Bridge principle. What is actually measured is resistance of the solution. Electronically, the electrodes are arranged in that way to constitute one arm of a Wheatstone Bridge. Eluting ions from chromatographic column subsequently enter the detector cell, leading to a change of electrical resistance and the out-of-balance signal is rectified with a precision rectifier. The DC signal is either digitized and sent to a computer data acquisition system or is passed to a potentiometric recorder, by means of a linearizing amplifier, which modifies the signal so that the output is linearly related to ion concentration. Sometimes, a variable resistance is situated in one of the other arms of

the bridge and is used for zero adjustment to compensate for any signal from mobile-phase ions. As mentioned earlier, at constant voltage applied to the cell, the current will be proportional to the conductivity (Fig. 1).

The conductivity k is a characteristic property of the solution rather than a property of the cell used. It contains all the chemical information available from the measurement, such as concentration and mobilities of the ions present. Accordingly, the conductivity detector is a bulk property detector and, as such, it responds to all electrolytes present in the mobile phase as well as the solutes. Thus, the experimentally determined conductivity is the sum of the contributions from all ions pres-

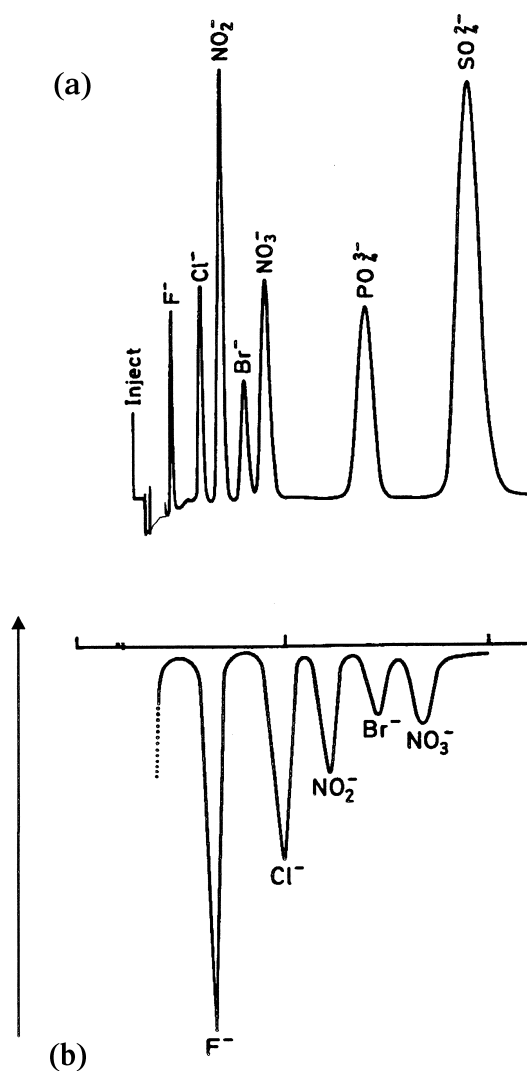


Fig. 2 Conductivity detection of anions in nonsuppressed (single column) ion chromatography using an eluent of (a) low background conductance (direct detection) and (b) high background conductance (indirect detection). The direction of the arrow indicates the increase of conductivity.



ent in the solution. The sensitivity of the conductivity detector depends on the difference between the limiting ionic conductivities of the solute and eluent ions.

The differential mode of detection is mostly effective, provided there is a significant difference in the values of the measured property between the eluent and solute ions. This difference may be either positive or negative. The former case refers to lower conductivity of the eluent ion, described as *direct detection method*, the latter to greater conductivity of the eluent ion, described as *indirect detection method* (Fig. 2).

The thermal stability of a conductivity detector is of great importance. Effective thermostating is highly required, as the temperature greatly affects the mobility of ions and, therefore, conductivity. A 0.5–3% increase of conductivity is usually expected per degree Celsius. Close temperature control is necessary to minimize background noise and maximize sensitivity; this is an especially important issue if nonsuppressed eluents are used.

Typical specifications for an electrical conductivity detector are as follows: sensitivity, 5×10^{-9} g/mL; linear dynamic range, 5×10^{-9} to 1×10^{-6} g/mL; response index, 0.97–1.03.

Conclusion

Conductivity detection in HPLC or, more precisely HPIC, can be applied to ionic species, including all an-

ions and cations of strong acids and bases (e.g., chloride, sulfate, sodium, potassium, etc.). Ions of weaker acids and bases are detected provided that the pH value of the eluent is chosen to maximize the analyte's ionization so as to increase sensitivity. The relatively simple design requirements, accuracy, and low cost contribute to its utility and popularity; thus, it is almost used in over 95% of analyses, where ion-exchange separation procedures are involved.

Suggested Further Reading

- Coury, L., *Curr. Separ.* 18(3):91 (1999).
- Papadoyannis, I., V. Samanidou, and A. Zotou, *J. Liquid Chromatogr.* 18(7):1383 (1995).
- Parriott, D., *A Practical Guide to HPLC Detection*, Academic Press, San Diego, CA, 1993.
- Schaefer, H., M. Laubli, and R. Doerig, *Ion Chromatography*, Metrohm Monograph 50143, Metrohm AG, Herisau, 1996.
- Scott, R., *Techniques and Practice of Chromatography*, Marcel Dekker, Inc., New York, 1995.
- Scott, R., *Chromatographic Detectors, Design, Function and Operation*, Marcel Dekker, Inc., New York, 1996.
- Tarter, J., *Ion Chromatography*, Chromatographic Science Series Vol. 37, Marcel Dekker, Inc., New York, 1987.



Congener-Specific PCB Analysis

George M. Frame II

Consultant, Halfmoon, New York, New York, U.S.A.

Introduction

Polychlorinated biphenyls (PCBs) are complex mixtures of 209 possible chlorinated biphenyl molecules, referred to as congeners. There are from 3 to 46 isomers at each of the 10 possible levels of chlorination. Isomers of a given chlorination level are referred to as homologs. About 150 of these congeners appear at significant levels in the commercial mixtures. These mixtures, trade named Aroclor (U.S.A.), Clophen (Germany), Kanechlor (Japan), and so forth, found use as electrical insulating fluids in transformers and capacitors and as binders for a wide variety of uncontained applications. Although their manufacture has been largely discontinued, their long-term stability, dispersion into the environment by prior uncontrolled releases, lipophilicity (resulting in biomagnification up food chains), and potential toxicity to humans and biota have sparked extensive research and the requirement for detailed analytical characterization of these mixtures.

Discussion

This article will not discuss the extensive literature on sample preparation, cleanup, and proper instrumental operation. Adsorption column chromatography and high-performance liquid chromatography (HPLC) procedures find application here, and the book by Erickson [1] provides exhaustive discussions of these and of the history of PCB use and analysis. Methods for measuring total PCB content or measuring and reporting the mixtures by their commercial designation will not be detailed. Congener-specific PCB analysis demands separation and quantitation of either short lists of priority PCB congeners or of the PCB content of all chromatographic PCB peaks that can be separated in particular system(s). This latter mode is referred to as Comprehensive, Quantitative, Congener-Specific Analysis (CQCS). The methods of choice for CQCS PCB analysis employ high-resolution gas chromatography (HRGC) on capillary columns with sensitive and selective detection by electron-capture detec-

tors (ECD), selected ion monitoring–mass spectrometry (MS–SIM), or full-scan, ion-trap MS (ITMS). The most complete discussion of target congeners for specific research applications is in Ref. 2. A descriptive overview of CQCS PCB analysis appears in an *Analytical Chemistry* A-page article [3], and extensive reviews [4–6] provide detailed discussions and large bibliographies.

Figure 1 summarizes PCB congener structure, nomenclature, the Ballschmiter and Zell (BZ) congener numbering system, and the relative abundances in the commercial Aroclor mixtures as a function of single-ring chlorine-substitution patterns. The BZ numbers in the matrix correspond to the chlorine-substitution positions in each ring of the biphenyl structure, which are listed along the top and right sides of the figure matrix. The abbreviated nomenclature (e.g., 234–245 = PCB #138) defines each congener by the substitution pattern in each ring, with the hyphen representing the bond between the two phenyl rings. Rotation about this bond is possible except in congeners with three or four chlorines in the ortho (2 or 6) positions.

In the United States, the commercial mixtures were manufactured until 1977 by Monsanto under the trade name Aroclor. In the four-digit Aroclor designations (e.g., Aroclor 1242), the 12 indicates a biphenyl nucleus and the 42 the weight percentage of chlorine in the mixture. Reference to the matrix in Fig. 1 reveals congeners in black cells which never exceed 0.1 wt% in the mixtures. These “non-Aroclor” congeners are absent due to unfavored or improbable formation in the electrophilic chlorination process employed in the manufacture of Aroclors [7]. Conversely, the ring chlorine-substitution patterns giving rise to the congeners in gray cells are especially favored.

Whereas three or more *ortho*-chlorines block rotation about the ring-connecting bond, congeners with none, or only one, *ortho*-chlorine can relatively easily achieve a planar configuration (colloquially referred to as “coplanars”) and may behave as isosteres (compounds with similar shape, functionality, and polarity) to 2,3,7,8–tetrachlorodibenzodioxin (TCDD). These bind significantly to the “dioxin receptor,” and meas-

Encyclopedia of Chromatography

DOI: 10.1081/E-Echr 120004628

Copyright © 2002 by Marcel Dekker, Inc. All rights reserved.



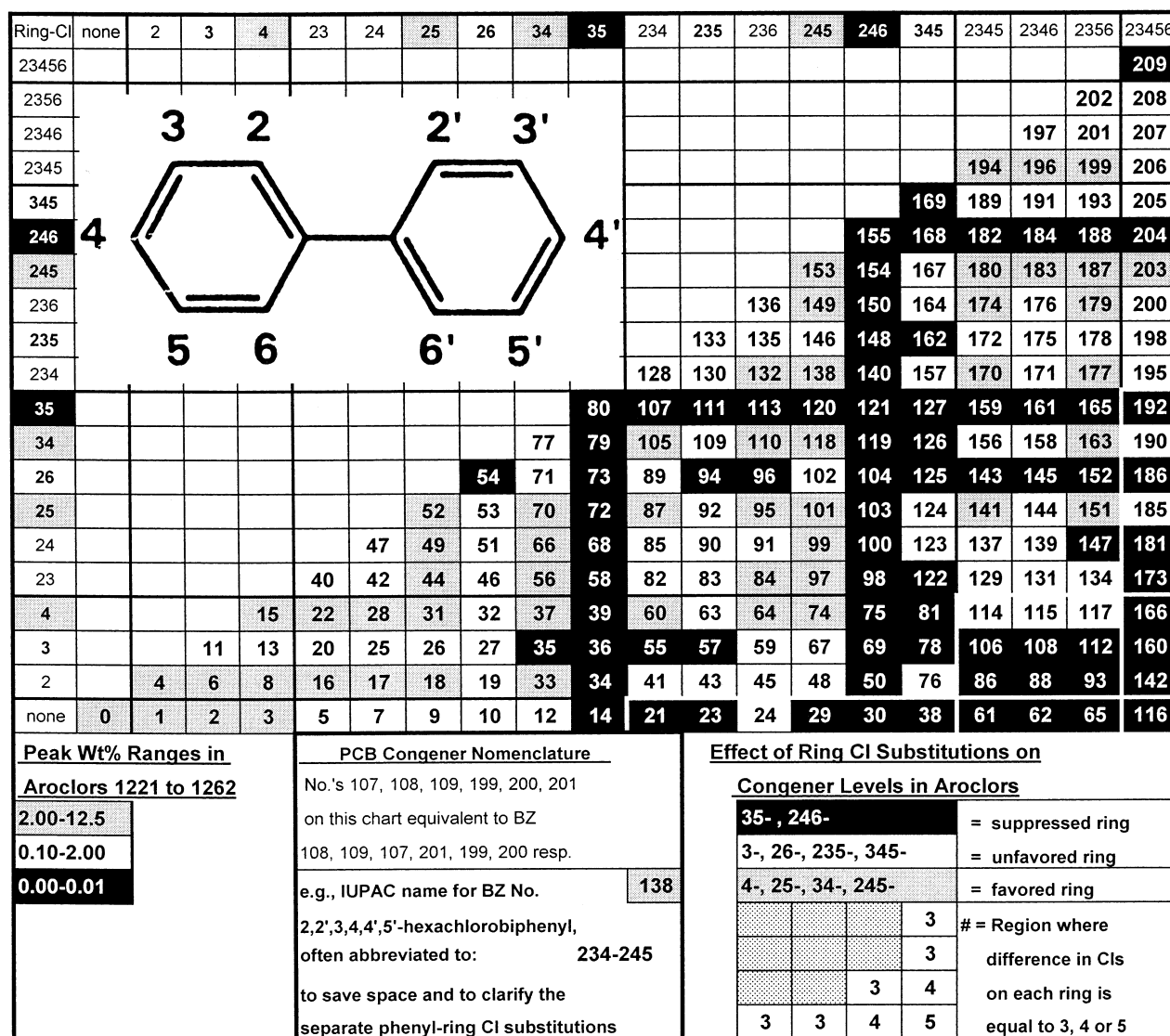


Fig. 1 PCB congener structure, nomenclature, BZ congener numbering system, and relative abundances in Aroclor mixtures.

urement of their concentrations can be combined with their “dioxin-like toxic equivalency factors (TEFs)” to give an estimate of a PCB mixture’s “dioxin-like toxic equivalency (TEQ)” [2]. Thus, one “short list” analysis specified by the World Health Organization (WHO) is for 12 such congeners found in commercial mixtures, namely PCBs 77, 81, 105, 114, 118, 123, 126, 156, 157, 167, 169, and 189. Although PCB 126 is generally a trace component, it has such a high TEF that it often dominates the TEQ calculation.

In the United States, the initial regulatory methods were the USEPA 8080 series. In 8080, packed column GC-ECD was recommended and calibration was

against Aroclor mixtures and results were reported as Aroclor equivalents. Method 8081 encouraged use of higher-resolution capillary GC columns and MS-SIM detection, and the current version 8082 extends this to suggest measuring some individual congeners against primary standards. An early version of CQCS analysis is EPA Method 680, which employs MS-SIM detection at the molecular ion cluster mass for each homolog level. It does not provide for actually identifying all congeners by determining their elution times and is, thus, not classified as congener-specific, but rather homolog-class-specific. It is quantitatively calibrated against an average response at each level, resulting in

less precise measurement of individual congeners, but it will detect and measure all PCB-containing peaks whether Aroclor derived or not. It is, thus, superior to the 8080 series when a PCB mixture arising from a non-Aroclor source or a substantially altered Aroclor congener distribution is encountered. In Europe, the Community Bureau of Reference (BCR) specifies measurement of a short list of major persistent "indicator congeners," namely PCBs 28, 52, 101, 118, 138, 153, and 180. A number of other congener short lists are detailed in Refs. 2 and 3. A powerful but expensive and difficult-to-implement congener-specific PCB analysis is USEPA Method 1668. The target list is the WHO list of coplanar PCBs with dioxinlike TEQs. The methodology is HRGC with $>10,000$ resolution HRMS detection and ^{13}C -isotope dilution internal standards for all the analytes. The procedures are modeled on the well-established HRGC–HRMS USEPA Method 1613 for PCDD/Fs. The newer USEPA Method 1668 Revision A (December 1999) describes procedures for extending the analyte list to all 209 congeners which can be resolved on either a SPB-Octyl capillary column or a DB-1 (100% methyl silicone) capillary. Primary standards for all 209 congeners are distributed among 5 calibration solutions, which avoid any isomer co-elutions on the SPB-Octyl column.

No single column, nor any pair of columns, can completely separate all 209 congeners, or even the 150 or so found in Aroclors. Analysts developing CQCS or even "short list" congener-specific PCB analyses must select GC stationary phases capable of resolving congeners in their target list. Many analysts have employed 5% phenyl-,95% methyl-substituted silicone polymers (e.g., DB-5) since a very similar phase was the first one for which the relative retention times for all 209 PCB congeners were published [3]. Methyl silicone phases with 50% *n*-octyl or *n*-octadecyl substituents have PCB retention characteristics similar to those of hydrocarbon columns such as Apeizon L or Apolane, but much greater stability and higher temperature limits than the latter. They permit resolution of many pairs of lower homologs which co-elute on the more polar phases. This feature is valuable for characterizing the products of dechlorination by anaerobic bacteria [7]. Phases with arylene or carborane units substituted in the silicone backbone to decrease column bleed (e.g., DB-5MS, DB-XLB, HT-8) have been found to have particularly useful congener-separation capabilities [3,7–9].

A database of relative retention times and co-elutions for all 209 congeners on 20 different stationary phases has been published [8]. For 12 of the most useful of these phases, the elution orders of 9 solutions of

all 209 congeners are available from a standard supplier which markets these solutions (AccuStandard, New Haven, CT, U.S.A.). By surveying the database, one can determine the most suitable column(s) for a particular application and can quickly establish a method component table by nine injections of the standard mixtures. This greatly facilitates the development of new CQCS PCB analyses. Tables of the weight percentages of all congeners in each of the numbered Aroclor mixtures, from which the information condensed in the figure matrix were derived, are available [7,8]. These help reduce the number of congeners which a CQCS method is required to separate when one anticipates analyzing only relatively unaltered Aroclor congener mixtures.

Prior to the availability of all 209 congeners in well-designed primary standard mixtures, much effort was expended to use structure–retention relationships on various phases to predict retention for congeners for which standards were not available [5]. In general, PCB retention times increase with chlorination level, and within chlorination levels, with less chlorine substitution in the ortho position (i.e., "coplanar PCBs" are more strongly retained). These relationships are of theoretical interest but are of less use now that accurate retention time assignments are possible with actual standards. The use of commercial mixtures such as Aroclors as quantitative secondary standards for CQCS PCB analysis is now to be discouraged [4], as detailed studies of congener distributions show significantly different proportions among different lots [7]. In the case of Aroclor 1254, there are actually two different mixtures of radically different composition produced by totally different synthetic processes [9].

The other major factor affecting the capability of CQCS PCB analyses is the selection of the GC detector. Initially, the ECD has been most useful for this application. It is selective for halogenated compounds, and its sensitivity is outstanding for the more chlorinated ($\text{Cl} \geq 4$) congeners. Its drawbacks are twofold: It has a limited linear range, necessitating multilevel calibration, and the relative response factors vary widely from instrument to instrument and among congeners even at the same chlorination level [3]. For mono- and dichloro-substituted congeners, it is less sensitive than the corresponding MS detectors. Other halogenated compounds such as organochlorine pesticides will produce ECD responsive peaks which may interfere by co-elution with certain PCB congeners. For these reasons, CQCS PCB analyses with ECD detection often employ a procedure of splitting the injected sample to two columns (each with ECD detector) of different polarity and PCB congener elution order [3,7]. To be re-



ported, a congener must be measured on at least one column without co-elution of PCB or another interfering compound. If separately measurable on each column, the quantities found must match within a preset limit to preclude the possibility of an unexpected co-eluting contaminant on one of the columns. Given the large number of congeners which may need to be measured, the data reduction algorithm for such a procedure is complex and not easily automated.

Another approach to providing a second dimension to CQCS PCB analysis is to employ much more selective mass spectrometric detection [3,6–8]. In EI–MS, the spectra consist of a molecular ion cluster of chlorine isotope MS peaks and similar fragment ion clusters resulting from the successive loss of chlorine atoms. Congeners differing by one chlorine substituent which co-elute on the GC column may often be separately quantitated by MS detection, if the more chlorinated one is not in great excess. This is because the $[M - 1Cl]^+$ fragment which interferes with the lower congener's signal is from a ^{13}C isotope peak and typically has 0.5–12% the signal level of its M^+ peak [9]. In contrast to the ECD, the sensitivity of MS–SIM or full-scan ITMS is greater for the less chlorinated congeners, as their electron affinity is lower and the positive charge of the ions is distributed over a smaller number of fragments. The linearity of the MS detectors is better than that of ECDs, and the ions monitored are more specific for PCBs and less prone to interference from non-PCB compounds. ECDs continue to hold the edge in absolute sensitivity (for the higher chlorinated congeners), and the dual-column/ECD detector systems are slightly less expensive than comparable bench-top, unit-mass-resolution, single-column GC–MS systems. Application to PCB analysis of more advanced (and expensive) MS detection systems, such as high-resolution mass spectrometry (HRMS), MS–MS, and negative-ion MS, is described in several reviews [4,6].

A final refinement of congener-specific PCB analysis arises from the fact that 19 of the congeners actually exist as stable enantiomeric pairs, either component of which can withstand racemization even at the elevated temperatures required to elute them from a capillary GC separation [6]. Some congeners containing either a 236- or 2346-chlorine-substituted ring and three or more chlorines in the ortho position exist in two mirror-image forms by virtue of their inability to rotate around the bond between the two rings. These so-called atropisomers do not contain asymmetric carbon

centers. They are PCB numbers 45, 84, 91, 95, 132, 135, 136, 149, 174, and 176 (containing the 236-ring), as well as PCB numbers 88, 131, 139, 144, 171, 175, 176, 183, 196, and 197 (containing the 2346-ring). They may be separated on chiral GC stationary phases, primarily those employing a family of modified cyclodextrins. A series of 7 such columns has been found, which among them can achieve resolution of all 19 stable PCB atropisomers as well as separation of 11 of them from other possible coeluting PCBs if MS detection is employed [10]. Observation of PCB enantiomeric ratios significantly different from 1 is a certain indication of the action of an enzyme-mediated biological process operating on these congeners.

References

1. M. D. Erickson, *Analytical Chemistry of PCBs*, 2nd ed., Lewis Publishers, New York, 1997.
2. L. G. Hansen, *The ortho Side of PCBs: Occurrence and Disposition*, Kluwer Academic, Boston, 1999.
3. G. M. Frame, Congener-specific PCB analysis, *Anal. Chem.* 69:468A (1997).
4. P. Hess, J. de Boer, W. P. Cofino, P. E. G. Leonards, and D. E. Wells, Critical review of the analysis of non- and mono-ortho-chlorobiphenyls, *J. Chromatogr. A* 703:417 (1995).
5. B. R. Larsen, HRGC separation of PCB congeners, *J. High Resolut. Chromatogr.*, 18:141 (1995).
6. J. W. Cochran and G. M. Frame, Recent developments in the high resolution gas chromatography of polychlorinated biphenyls, *J. Chromatogr. A* 843:323 (1999).
7. G. M. Frame, J. W. Cochran, and S. S. Bøwadt, Complete PCB congener distributions for 17 Aroclor mixtures determined by 3 HRGC systems optimized for comprehensive, quantitative, congener-specific analysis, *J. High Resolut. Chromatogr.* 19:657 (1996).
8. G. M. Frame, A collaborative study of 209 PCB congeners and 6 Aroclors on 20 different HRGC columns: 1. Retention and coelution database, 2. Semi-quantitative Aroclor distributions, *Fresenius J. Anal. Chem.* 357:701 (1997).
9. G. M. Frame, Improved procedure for single DB-XLB column GC–MS–SIM quantitation of PCB congener distributions and characterization of two different preparations sold as “Aroclor 1254”, *J. High Resolut. Chromatogr.* 22:533 (1999).
10. C. S. Wong and A. W. Garrison, Enantiomer separation of polychlorinated biphenyl atropisomers and polychlorinated biphenyl retention behavior on modified cyclodextrin capillary gas chromatography columns, *J. Chromatogr. A* 866:213 (2000).



Copolymer Analysis by LC Methods, Including Two-Dimensional Chromatography

Peter Kilz

Polymer Standards Service, Mainz, Germany

Introduction

Gel permeation chromatography (GPC) is the established method for the determination of molar mass averages and the molar mass distributions of polymers. GPC retention is based on the separation of macromolecules in solution by molecular sizes and, therefore, requires a molar mass calibration to transform elution time or elution volume into molar mass information. This kind of calibration is typically performed with narrow molecular mass distribution polymer standards, universal, or broad calibration methods or molar-mass-sensitive detectors like light-scattering or viscosity detectors.

Copolymer GPC Analysis by Multiple Detection

Conventional GPC data processing is unable to determine other important polymer properties such as copolymer composition or copolymer molar mass. The reason is that the GPC separation is based on hydrodynamic volume rather than the molar mass of the polymer and that molar mass calibration data are only valid for polymers of identical molecular structures. This means that polymer topology (e.g., linear, star-shaped, comb, ring, or branched polymers), copolymer composition, and chain conformation (isomerization, tacticity, etc.) determine the apparent molecular weight. The main problem of copolymer analysis is the calibration of the size-exclusion chromatography (SEC) instrument for copolymers with varying comonomer compositions. However, even if the bulk composition is constant, second-order chemical heterogeneity has to be taken into account (i.e., the composition will vary for a given chain length, in general).

Several attempts have been made to solve the calibration dilemma. Some are based on the universal calibration concept, which has been extended for copolymers. Another approach to copolymer calibration is multiple detection [1]. The advantage of multiple detection can be seen in its flexibility and its ability to

yield the composition distribution as well as molar masses for the copolymer under investigation. This method requires a molar mass calibration and an additional detector response calibration to determine chemical composition at each point of the elution profile. No other kind of information, parameters, or special equipment are necessary to do this kind of analysis [2] and to calculate compositional drift, bulk composition, and copolymer molar mass.

Determination of Comonomer Concentration

In order to characterize the composition of a copolymer of k comonomers, the same number of independent detector signals d are necessary in the GPC experiment; that is, in the case of a binary copolymer, two independent detectors (e.g., LUV and RI) are required to calculate the composition distribution $w_k(M)$ and the overall (bulk) composition \bar{w}_k . The detector output U_d of each detector d is the superposition of all individual responses from all comonomers present in the detector cell at a given elution volume V . Therefore,

$$U_d(V) = \sum_k f_{dk} c_k(V) \quad (1)$$

with f_{dk} the response factor of comonomer k in detector d , and c_k the true concentration of comonomer k in the detector cell at elution volume V . The detector response factors are determined in the usual way by injecting homopolymers for each comonomer of known concentration and correlating that with the area of the corresponding peak. If no homopolymers are available, model compounds have been used to estimate the detector response factors. In the case of a binary copolymer, the weight fraction, w_A , of comonomer A is then given by

$$w_A(V) = \left(1 + \frac{[U_1(V) - (f_{1B}/f_{2B})U_2(V)][f_{1A} - (f_{1B}/f_{2B})f_{2A}]}{[U_1(V) - (f_{1A}/f_{2A})U_2(V)][f_{1B} - (f_{1A}/f_{2A})f_{2B}]} \right)^{-1} \quad (2)$$

Encyclopedia of Chromatography

DOI: 10.1081/E-Echr 120004629

Copyright © 2002 by Marcel Dekker, Inc. All rights reserved.

Copyright © Marcel Dekker, Inc. All rights reserved.



Obviously, the sum of all comonomer weight fractions is unity. The accurate copolymer concentration and the distribution of the comonomers across the chromatogram can be calculated from the apparent chromatogram and the individual comonomer concentrations [3].

The accuracy of the compositional information is not affected by the polymer architecture. Deviations from the true comonomer ratios are only possible if the detected property is dependent on the local environment. This is the case if neighbor-group effects exist. The possibility of electronic interactions causing such deviations is very small, because there are too many chemical bonds between two different monomer units. Other types of interactions, especially those which proceed across space (e.g., charge-transfer interactions), may influence composition accuracy [4].

Determination of Copolymer Molar Mass Averages

The major difficulty in the determination of the copolymer molar mass distribution is the fact that the GPC separation is based on the molecular size of the copolymer chain. Its hydrodynamic radius, however, is dependent on the type of the comonomers incorporated into the macromolecule as well as their placement (sequence distribution).

Consequently, there can be a co-elution of species possessing different chain length *and* chemical composition. The influence of different comonomers copolymerized into the macromolecule on the chain size can be measured by the GPC elution of homopolymer standards of this comonomer. Unfortunately, the influence of the comonomer sequence distribution on the hydrodynamic radius cannot be described explicitly by any theory at present. However, there are limiting cases which can be discussed to evaluate the influence of the comonomer placement in a macromolecular chain.

From a GPC point of view, the most simple copolymer is an alternating copolymer (AB)_n, which can be treated exactly like a homopolymer with a repeating unit (AB). The next simple copolymer architecture is a AB block copolymer, where a sequence of comonomer A is followed by a block of B units. The only heterocontact in this chain is the A–B link, which can influence the size of the macromolecule. The A segment and the B segment of the AB block copolymer will hydrodynamically behave like a pure homopolymer of the same chain length. In the case of long A and B segments in the AB block copolymer, only the A–B link acts as a defect position and will not change the

overall hydrodynamic behavior of the AB block copolymer chain. Consequently, the molar mass of the copolymer chain can be approximated by the molar masses of the respective segments. Similar considerations are true for ABA, ABC, and other types of block structure and for comb-shaped copolymers with low side-chain densities.

In such cases, the copolymer molar mass *M* can be determined from the interpolation of homopolymer calibration curves *M_k(V)* and the weight fractions *w_k* of the comonomers *k* according to [1]

$$\log M_c(V) = \sum_k w_k(V) \log M_k(V) \quad (3)$$

The calculation of copolymer molar mass averages *M_{n,c}*, *M_{w,c}*, and so on, and copolymer polydispersity *D* is done as in conventional GPC calculations using the copolymer molar mass calculated from Eq. (3).

In cases where the number of heterocontacts can no longer be neglected, this simplified reasoning breaks down and copolymer molar masses cannot be measured accurately by GPC alone. This is the case with statistical copolymers, polymers with only short comonomer sequences and high side-chain densities [2]. In such cases, more powerful and universal methods have to be employed (e.g., 2D separations) (see below).

Copolymer Characterization by GPC

Block copolymers are an important class of polymers used in many applications from thermoplastic elastomers to polymer-blend stabilizers. Their synthesis is most often done by ionic polymerization, which is both costly and sometimes difficult to control. However, block copolymer properties strongly depend, for example, on the exact chemical composition, block molar mass, and block yield. These parameters can be evaluated in a single experiment using copolymer GPC with multiple detection.

Figure 1 shows the measured molar mass distribution of a styrene–MMA block copolymer using refractive index (RI) and ultraviolet (UV) detection. The RI responds to the styrene and MMA units, whereas the UV, tuned to 260 nm, predominantly picks up the presence of styrene in the copolymer. After detector calibration, the styrene and MMA content in each fraction can be measured. The MMA content distribution (black solid line) is superimposed on the MWD of the product in Fig. 1. It is obvious that the MMA content is not constant throughout the MWD, but continuously increases with the molar



mass. The trimodal MWD itself only shows the presence of three different species. The MMA content information clearly reveals that the copolymerization process was not producing block structures, but that the MMA was added to chains of different styrene molar masses.

Two-Dimensional Chromatography

Complex polymer topologies, polymer blends, and multicomponent formulations require a different approach to perform a proper molecular characterization. In two-dimensional (2D) chromatography, different separation techniques are used to avoid co-elution of species and to measure molar mass and chemical composition in a truly independent way [5].

It is obvious that n independent molecular properties require n -dimensional methods for accurate (independent) characterization of all parameters. Additionally, the separation efficiency of any single separation method is limited by the efficiency and selectivity of this separation mode (i.e., the plate count N of the column and the phase system selected). Adding more columns will not overcome the need to identify more components in a complex sample, due to the limitation of peak capacities, n . The corresponding peak capacity

in an n -dimensional separation is substantially higher due to the fact that each dimension contributes to the total peak capacity as a factor and not as an additive term for single-dimension methods:

$$n_{\text{total}} = \prod_{i=1}^n n_i \sin^{(i-1)} \theta_i \quad (4)$$

for example, for a 2D system, $n_{2D} = n_1 n_2 \sin \theta$, where n_{total} represents the total peak capacity, n_i is the peak capacity in dimension i , and θ_i is the “angle” between two dimensions; for orthogonal separations, this angle will be 90° and the peak capacity will be maximized. The angle between dimensions is determined by the independence of the methods; a 90° angle is obtained using two methods which are completely independent of each other and will, thus, separate two properties solely on a single parameter without influencing each other.

In 2D chromatography separations, an aliquot from a first column (method) is transferred into the next separation method in a sequential and repetitive manner using automated sample transfer valves which are equipped with one or more sample loops. Alternatively, as a simpler and not quite as useful transfer technique, “heart cuts” from peaks in the first separation

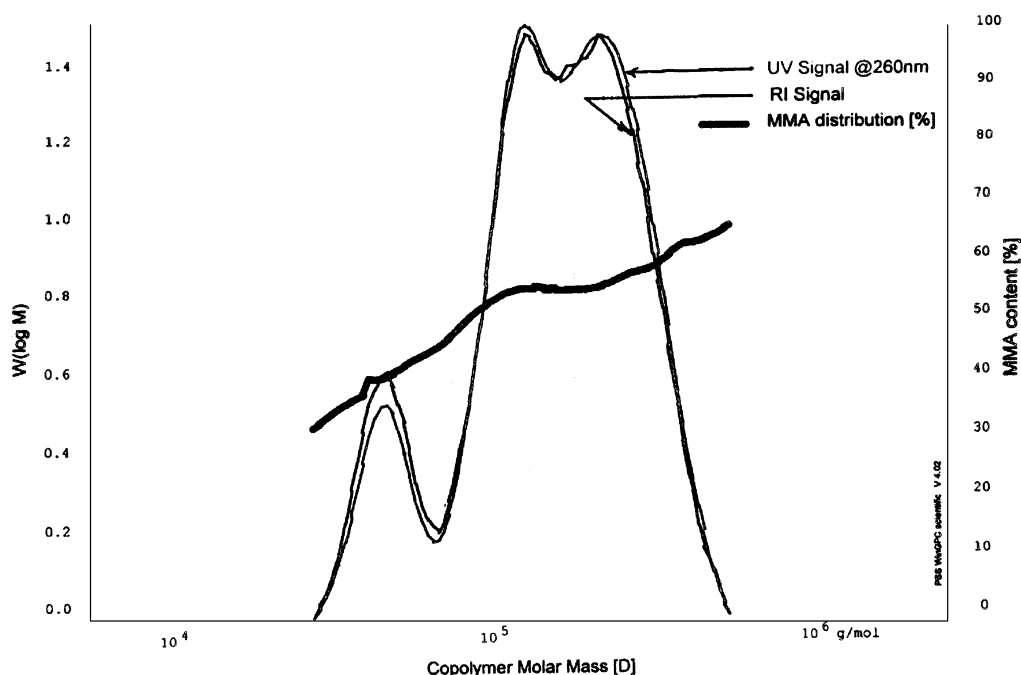


Fig. 1 Molar mass distribution with overlaid chemical composition distribution of a styrene–MMA block copolymer with poor block formation.

mode can be manually injected into the next separation column (second dimension).

The use of different modes of liquid chromatography facilitates the separation of complex samples, selectively, with respect to different properties like hydrodynamic volume, molar mass, chemical composition, or functionality. Using these techniques in combination, multidimensional information on different aspects of molecular heterogeneity can be obtained. If, for example, two different chromatographic techniques are combined in a "cross-fractionation" mode, information on chemical composition distribution and molar mass distribution can be obtained. Reviews on different techniques and applications involving the combination of GPC and various LC methods can be found in the literature [6–8].

Experimental Aspects of Two-Dimensional Separations

Setting up a 2D chromatographic separation system is actually not as difficult as one might first think. As long as well-known separation methods exist for each dimension [8], the experimental aspects can be handled quite easily in most cases. Off-line systems just require a fraction collection device and something or someone who reinjects the fractions into the next chromatographic dimension. In on-line 2D systems, the transfer of fractions is preferentially done by automated injection valves, as was proposed by Kilz et al. [9].

The sequence of the separation methods is important, in order to realize the best resolution and accurate determination of property distributions [10]. It is advisable to use the method with highest selectivity for the separation of one property as the first dimension. This ensures highest purity of eluting fractions being transferred into the subsequent separation. In many cases, interaction chromatography has proven to be the best and most easily adjustable method for the first dimension separation, because (a) more parameters (mobile phase, mobile-phase composition, mobile-phase modifiers, stationary phase, temperature, etc.) can be used to adjust the separation according to the chemical nature of the sample, (b) better fine-tuning in interaction chromatography allows for more homogeneous fractions, and (c) sample load on such columns can be much higher as compared to, for example, GPC columns.

Because of the consecutive dilution of fractions, detectability and sensitivity become important criteria in 2D experimental design [11]. If low-level components have to be detected, only the most sensitive and/or se-

lective detection methods can be used. ELSD detection, despite several drawbacks, has been used mostly due to its high sensitivity for compounds which will not evaporate or sublime under detection conditions. Fluorescence and diode-array UV/VIS are also sensitive detection methods, which can pick up samples at nanogram levels. Mass spectrometers have a high potential in this respect too; however, they are currently not developed to a state where they would be generally usable. Only in special cases, refractive index detection, otherwise very popular in GPC, has been used in multidimensional separations, because of its low sensitivity and strong dependence on mobile-phase composition.

Time consumption is another important aspect of 2D analyses. All early 2D chromatography work was done in either off-line mode or in a stop-flow mode, which are both time-consuming and have poor reproducibility. The first fully automated 2D chromatographic system was developed by Kilz et al. [11]. This system uses 2D chromatography software for data acquisition and processing, which also controls the 2D transfer valve. This setup relieves the operator from all the time-consuming tasks and does all 2D and 3D data processing and reporting.

The recent introduction of high-speed GPC columns reduces time consumption even further and allows a complete 2D analysis in about an hour.

2D Analysis of Complex Copolymer Blends

The potential of 2D separations can be explained best by a 16-component blend of a styrene–butadiene star block copolymer. The copolymer mixture consisted of four different molar masses (1*M*, 2*M*, 3*M*, and 4*M* reflecting the 1-, 2-, 3- and 4-arm star molecules) and four styrene compositions (20%, 40%, 60%, and 80%) for each arm. Molar mass and composition were very thoroughly controlled by a special anionic polymerization technique to ensure macromolecular architecture [7]. Gradient HPLC analysis only showed a broad elution profile, whereas high-resolution GPC just separated out the molar masses of the four arms. The GPC result gave no indication of additional peaks with identical molecular weight but different composition hiding behind the detected peaks. The online combination of both techniques, under otherwise identical conditions, allowed for the separation of all 16 species in the mixture. The separation was not completely orthogonal, because the gradient high-performance liquid chromatography (HPLC) separation was partially dependent on molar mass (cf. Fig. 2c).



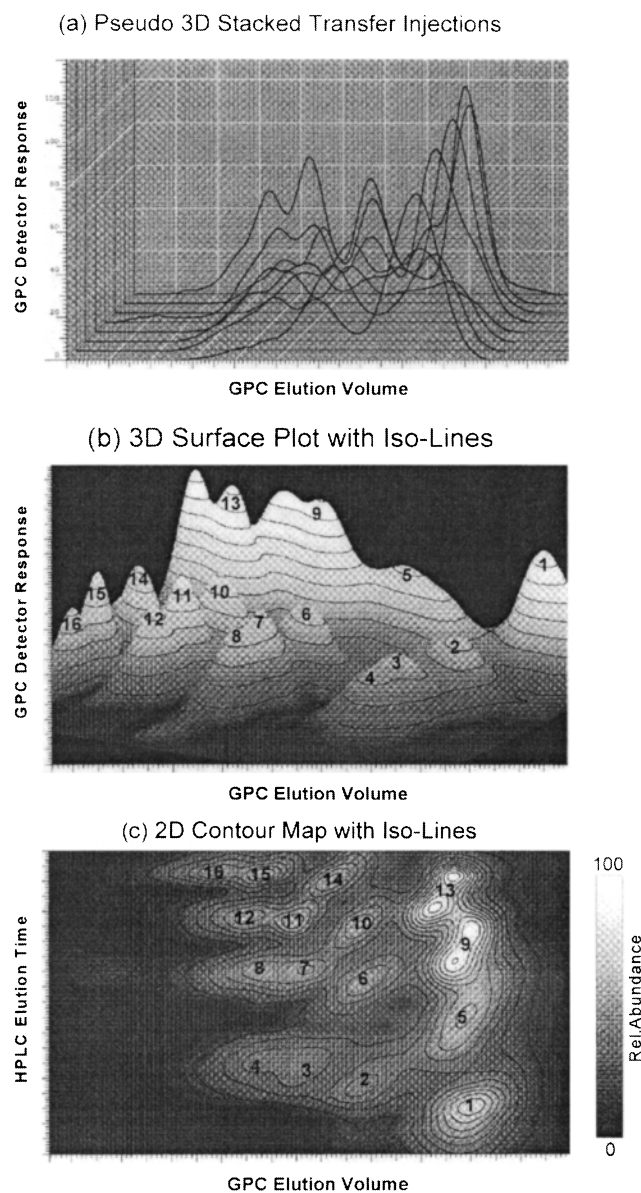


Fig. 2 Various data presentation views in 2D chromatography showing the 2D analysis of a 16-component star block copolymer (see text for details).

Further data analysis allows the determination of molar mass, chemical composition, and relative concentration for each component. The 2D chromatography data can be displayed in various forms (cf. Fig. 2): (a) stacked or waterfall presentation showing the individual traces transferred into the second dimension; (b) surface plot allowing to view the 3D surface from different angles; (c) 2D contour maps, which are most

useful for data analysis and interpretation. Other data views can be also calculated from the 3D data set: cuts in any direction of properties (e.g., composition or molar mass) and true projections (accumulation) of data to create virtual chromatograms for each separation dimension.

Conclusions

Multidimensional chromatography separations are currently one of the most promising and powerful methods for the fractionation and characterization of complex sample mixtures in different property coordinates. This technique combines extraordinary resolution and peak capacity with flexibility, and it overcomes the limitations of any given single chromatographic method. This is the ideal basis for the identification and quantification of major compounds and by-products, which might adversely affect product properties if not detected in time.

Copolymer GPC is a proven analytical tool to investigate molecular properties of block and other highly segmented copolymers and to correlate structure with bulk properties.

References

1. J. R. Runyon, D. E. Barnes, J. F. Rudel, and L. H. Tung, *J. Appl. Polym. Sci.* 13:2359 (1969).
2. F. Gores and P. Kilz, Copolymer characterization using conventional SEC and molar mass-sensitive detectors, in *Chromatography of Polymers* (T. Provder, ed.), ACS Symposium Series 521, American Chemical Society, Washington, DC, 1993, Chap. 10.
3. B. Trathnigg, S. Feichtenhofer, and M. Kollroser, *J. Chromatogr. A* 786:75 (1997).
4. C. Johann and P. Kilz, *Proc. Int. Conf. Molar Mass Charact.* 1989.
5. H. Pasch, *Adv. Polym. Sci.* 150:1 (2000).
6. G. Glöckner, *Gradient HPLC of Copolymers and Chromatographic Cross-Fractionation*, Springer-Verlag, Berlin, 1991.
7. P. Kilz, R.-P. Krüger, H. Much, and G. Schulz, in *Chromatographic Characterization of Polymers: Hyphenated and Multidimensional Techniques* (T. Provder, M. W. Urban, and H. G. Barth, eds.), Advances in Chemistry Vol. 247, American Chemical Society, Washington, DC, 1995.
8. H. Pasch and B. Trathnigg, *HPLC of Polymers*, Springer-Verlag, Berlin, 1997.
9. P. Kilz, R.-P. Krüger, H. Much, and G. Schulz, *Polym. Mater. Sci. Eng.* 69:114 (1993).
10. M. R. Schure, *Anal. Chem.* 71:1645 (1999).
11. P. Kilz, *Laborpraxis*, 6:628 (1992).



Copolymer Composition by GPC–SEC

Sadao Mori

PAC Research Institute, Mie University, Nagoya, Japan

Introduction

Determination of the average chemical composition and polymer composition by size-exclusion chromatography (SEC) has been reported in the literature. Two different types of concentration detector or two different absorption wavelengths of an ultraviolet or an infrared detectors are employed; the composition at each retention volume is calculated by measuring peak responses at the identical retention points of the two chromatograms.

Discussion

Synthetic copolymers have both molecular-weight and chemical composition distributions and copolymer molecules of the same molecular size, which are eluted at the same retention volume in SEC, may have different molecular weights in addition to different compositions. This is because separation in SEC is achieved according to the sizes of molecules in solution, not according to their molecular weights or chemical compositions.

Molecules that appear at the same retention volume may have different compositions, so that accurate information on chemical heterogeneity cannot be obtained by SEC alone. When the chemical heterogeneity of a copolymer, as a function of molecular weight, is observed, the copolymer is said to have a heterogeneous composition, but, even though it shows constant composition over the entire range of molecular weights, it cannot be concluded that it has a homogeneous composition [1]. Nevertheless, SEC is still extremely useful in copolymer analysis, due to its rapidity, simplicity, and wide applicability.

When one of the constituents, A or B of a copolymer A–B, has an ultraviolet (UV) absorption and the other does not, a UV detector–refractive index (RI) combined detector system can be used for the determination of chemical composition or heterogeneity of the copolymer. A point-to-point composition, with respect to retention volume, is calculated from two chromatograms and a variation of composition is plotted as a function of molecular weight. The response factors of

the two components in the two detectors must first be calibrated.

Let A be a constituent that has UV absorption. K_A and K_B are defined as the response factors of an RI detector for the A and B constituents, and K'_A as the response of the UV detector for A. These response factors are calculated by injecting known amounts of homopolymers A and B into the SEC dual-detector system, calculating the areas of the corresponding chromatograms, and dividing the areas by the weights of homopolymers injected as

$$F_A = K_A G_A, \quad F_B = K_B G_B, \quad F'_A = K'_A G_A$$

where F_A , F_B , and F'_A are areas of homopolymers A and B in the RI detector and of homopolymer A in the UV detector, and G_A and G_B are the weights of homopolymers A and B injected into the SEC system.

The weight fraction $W_{A,I}$ of constituent A, at each retention volume I of the chromatogram for the copolymer, is given by

$$W_{A,I} = \frac{K_B}{R_I K'_A - K_A + K_B}$$

where $R_I = F_{RI,I}/F_{UV,I}$ for the copolymer at retention volume I . Retention volume I for the RI detector is not equal to the retention volume I for the UV detector. Usually, the UV detector is connected to the column outlet and is followed by an RI detector, and the dead volume between these two detectors must be corrected. The dead volume can normally be measured by injecting a polymer sample having a narrow molecular-weight distribution and by measuring the retention difference between the two peak maxima.

Because the additivity of the RI increments of homopolymers is valid for copolymers, the additivity of the response factors is also valid:

$$K_C = W_A K_A + W_B K_B$$

where K_C is the response factor for the copolymer in the RI detector. If the response factors of one or two homopolymers that comprise a copolymer cannot be

Encyclopedia of Chromatography

DOI: 10.1081/E-Echr 120004630

Copyright © 2002 by Marcel Dekker, Inc. All rights reserved.



measured because of insolubility of the homopolymer(s), then this equation is employed.

Alternatively, the extrapolation of the plot of RI response factors of copolymers of known compositions can be used. An example is that the RI response for polystyrene was 2800 and that for polyacrylonitrile was 2250.

Although the values of these response factors are dependent on several parameters, the ratio of K_A to K_B is almost constant in the same mobile phase.

An infrared detector can be used, at an appropriate wavelength, for detecting one component in copolymers or terpolymers and, thus, expand its range of applicability to copolymers analysis. Information on composition can be obtained by repeating runs, using different wavelengths to monitor different functional groups. A single-detector system is more advantageous than a dual-detector system, such as a combination of UV and RI detectors.

Instead of measuring chromatograms two or three times at different wavelengths for different functional groups, operation in a stop-and-go fashion was introduced for rapid determination of copolymer composition as a function of molecular weight [2].

Pyrolysis gas chromatography has been widely used for copolymer analysis. This technique may offer many advantages over other detection techniques for copolymer analysis by SEC. One obvious advantage is the small sample size required. Another is the capability of application to copolymers which cannot utilize UV or IR detectors [3].

Combination with other liquid chromatographic techniques is also reported by several workers. Orthogonal coupling of an SEC system to another high-performance liquid chromatography (HPLC) system

to achieve a desired cross-fractionation was proposed [4]. It was an SEC-SEC mode, using the same polystyrene column, but the mobile phase in the first system was chosen to accomplish only a hydrodynamic volume separation, and the mobile phase in the second system was chosen so as to be a thermodynamically poorer solvent for one of the monomer types in the copolymer, in order to fractionate by composition under adsorption or partition modes as well as size exclusion.

A combination of liquid adsorption chromatography with SEC has recently been developed by several workers. Poly(styrene-methyl methacrylate) copolymers were fractionated according to chemical composition by liquid adsorption chromatography and the molecular weight averages of each fraction were measured by SEC [5,6].

References

1. S. Mori, *J. Chromatogr.* 411:355 (1987).
2. F. M. Mirabella, Jr., E. M. Barrall II, and J. F. Johnson, *J. Appl. Polym. Sci.* 19:2131 (1975).
3. S. Mori, *J. Chromatogr.* 194:163 (1980).
4. S. T. Balke and R. D. Patel, *J. Polym. Sci. Polym. Lett. Ed.* 18:453 (1980).
5. S. Mori, *Anal. Chem.* 60:1125 (1988).
6. S. Mori, *Trends Polym. Sci.* 2:208 (1994).
7. S. Mori and H. G. Barth, *Size Exclusion Chromatography*, Springer-Verlag, New York, 1999, Chap. 12.
8. S. Mori, Copolymer analysis, in *Size Exclusion Chromatography* (B. J. Hunt and S. R. Hodling, eds.), Blackie, Oxford, 1989.



Copolymer Molecular Weights by GPC–SEC

Sadao Mori

PAC Research Institute, Mie University, Nagoya, Japan

Introduction

It is well known that most copolymers have both molecular weight and composition distributions and that copolymer properties are affected by both distributions. Therefore, we must know average values of molecular weights and composition, and their distributions. These two distributions are inherently independent of each other. However, it is not easy to determine the molecular-weight distribution independently of the composition, even by modern techniques.

Discussion

Size-exclusion chromatography (SEC) is a rapid technique used to obtain the molecular-weight averages and the molecular-weight distributions of synthetic polymers. The objective of SEC for copolymer analysis must be not only the determination of molecular-weight averages and its distribution but also the measurement of average copolymer composition and its distribution. However, separation by SEC is achieved according to the sizes of molecules in the solution, not according to their molecular weights. Therefore, the retention volume of a copolymer molecule obtained by SEC reflects not the molecular weight, as in the case of a homopolymer, but simply the molecular size.

For example, the elution order of polystyrene (PS), poly(methyl methacrylate) (PMMA), and their copolymers [P(S–MMA)], both random and block, all having the same molecular weight are as follows: random copolymer of P(S–MMA), PS, block copolymer (MMA–S–MMA), and PMMA [1]. Copolymers having the same molecular weight but different composition are different in molecular size and elute at different retention volumes. Therefore, the accurate determination of the values of molecular-weight averages and the molecular-weight distribution for a copolymer by SEC might be limited to the case when the copolymer has the homogeneous composition across the whole range of molecular weights.

A calibration curve for a copolymer consisting of components A and B can be constructed from those for the two homopolymers A and B, if the relationships of the molecular weights and the molecular sizes of the two homopolymers are the same as their copolymer and if the size of the copolymer molecules in the solution is the sum of the sizes of the two homopolymers times the corresponding weight fractions. The molecular weight of the copolymer at retention volume I , $M_{C,I}$, is calculated using

$$\log M_{C,I} = W_{A,I} \log M_{A,I} + W_{B,I} \log M_{B,I}$$

where $M_{A,I}$ and $M_{B,I}$ are the molecular weights of homopolymers A and B, respectively, and $W_{A,I}$ and $W_{B,I}$ are the weight fractions of components A and B, respectively, in the copolymer at retention volume I . This equation was empirically postulated for block copolymers [2].

The use of the so-called “universal calibration” is a theoretically reliable procedure for calibration. For ethylene–propylene (EP) copolymers, Mark–Houwink parameters in *o*-dichlorobenzene at 135°C are calculated as [3]

$$a_{EP} = (a_{PE}a_{PP})^{1/2}$$

$$K_{EP} = W_E K_{PE} + W_P K_{PP} - 2(K_{PE}K_{PP})^{1/2}W_E W_P$$

where W_E and W_P are the weight fractions of the ethylene and propylene units of the copolymer, respectively.

Calculated Mark–Houwink parameters for P(S–MMA) block and statistical copolymers at several compositions in tetrahydrofuran at 25°C are listed in Table 1 [4]. The parameters for PS and PMMA used in the calculation are as follows:

$$\text{PS: } K = 0.682 \times 10^{-2} \text{ mL/g, } a = 0.766$$

$$\text{PMMA: } K = 1.28 \times 10^{-2} \text{ mL/g, } a = 0.69$$

If copolymer molecules and PS molecules are eluted at the same retention volume, then

$$[\mu]_C M_C = [\mu]_S M_S$$



Table 1 Calculated Mark-Houwink Parameters for P(S-MMA) Block and Statistical Copolymers at Several Compositions in Tetrahydrofuran at 25°C

Composition (styrene wt%)	Block copolymer		Statistical copolymer	
	$K \times 10^2$ (mL/g)	a	$K \times 10^2$ (mL/g)	a
20	1.124	0.705	1.044	0.718
30	1.054	0.714	0.953	0.731
40	0.989	0.721	0.879	0.742
50	0.929	0.729	0.821	0.750
60	0.872	0.736	0.779	0.756
70	0.820	0.744	0.747	0.760
80	0.771	0.751	0.722	0.763

where M_C and M_S are the molecular weights of the copolymer and PS, respectively, and $[\mu]_C$ and $[\mu]_S$ are the intrinsic viscosities of the copolymer and PS, respectively. A differential pressure viscometer can measure intrinsic viscosities for the fractions of the copolymer and PS continuously, followed by the determination of M_C of the copolymer fraction at retention volume i .

The application of a light-scattering detector in SEC does not require the construction of a calibration curve using narrow molecular-weight distribution polymers. However, this method is not generally applicable to copolymers because the intensity of light scattering is a function not only of molecular weight but

also of the specific refractive index (the refractive index increment) of the copolymer in the mobile phase. The refractive index increment is also a function of composition. In the case of a styrene-butyl acrylate (30:70) emulsion copolymer, the apparent molecular weight of the copolymer in tetrahydrofuran was only 7% lower than true one [5]. A recent study concluded that if refractive index increments of the corresponding homopolymers do not differ widely, SEC measurements combined with light scattering and concentration detectors yield good approximations to molecular weight and its distribution, even if the chemical composition distribution is very broad [6].

References

1. A. Dondos, P. Rempp, and H. Benoit, *Macromol. Chem.* 175:1659 (1984).
2. J. R. Runyon, D. E. Barnes, J. F. Rudd, and L. H. Tung, *J. Appl. Polym. Sci.* 13:2359 (1969).
3. T. Ogawa and T. Inaba, *J. Appl. Polym. Sci.* 21:2979 (1988).
4. J. M. Goldwasser and A. Rudin, *J. Liquid Chromatogr.* 6:2433 (1983).
5. F. B. Malihi, C. Y. Kuo, and T. Provder, *J. Appl. Polym. Sci.* 29:925 (1984).
6. P. Kratochvil, 8th International Symposium on Polymer Analysis and Characterization (ISPAC-8), 1995, Abstract L14.
7. S. Mori and H. G. Barth, *Size Exclusion Chromatography*, Springer-Verlag, New York, 1999, Chap. 12.
8. S. Mori, Copolymer analysis, in *Size Exclusion Chromatography* (B. J. Hunt and S. R. Holding, eds.), Blackie, Oxford, 1989.



Coriolis Force in Countercurrent Chromatography

Yoichiro Ito

National Heart, Lung, and Blood Institute, National Institutes of Health, Bethesda, Maryland, U.S.A.

Introduction

The Coriolis force acts on a moving object on a rotating body such as the Earth and centrifuge bowl. It was first analyzed by a French engineer and mathematician, Gaspard de Coriolis (1835) [1].

Discussion

The effect of the Coriolis force produced by the Earth's rotation is weak, whereas that on the rotating centrifuge is strong and easily detected. Figure 1 illustrates the effect of the Coriolis force on the moving droplets in a rotating centrifuge where the path of the sinking droplets shifts toward the opposite direction to the rotation (left) and this effect is reversed on the floating droplets (right) [2]. The moving droplets on a rotating centrifuge have been photographed under stroboscopic illumination [3,4].

The effects of the Coriolis force on countercurrent chromatography have been demonstrated on the toroidal coil centrifuge which uses a coiled tube mounted around the periphery of the centrifuge bowl [2]. When a protein mixture containing cytochrome-c,

myoglobin and lysozyme was separated on an aqueous-aqueous polymer-phase system composed of 12.5% (w/w) poly(ethylene glycol) 1000 and 12.5% (w/w) dibasic potassium phosphate, the direction of the elution through the toroidal coil produced substantial effects on peak resolution, as shown in Fig. 2 and Table 1 [2]. Because the toroidal coil separation column has a symmetrical orientation except for the handedness, the above effect is best explained on the basis of the Coriolis force as follows. If the Coriolis force acts parallel to the effective coil segments (parallel orientation), the two phases form multiple droplets which provide a broad interface area to enhance the mass-transfer process, hence improving the partition efficiency (Fig. 3a). When the Coriolis force acts across the effecting coil segments, the two phases form a streaming flow, minimizing the interfacial area for mass transfer and resulting in lower partition efficiency (Fig. 3b).

Conclusion

It is interesting to note that the above effects have not been observed on the separation of low-molecular-

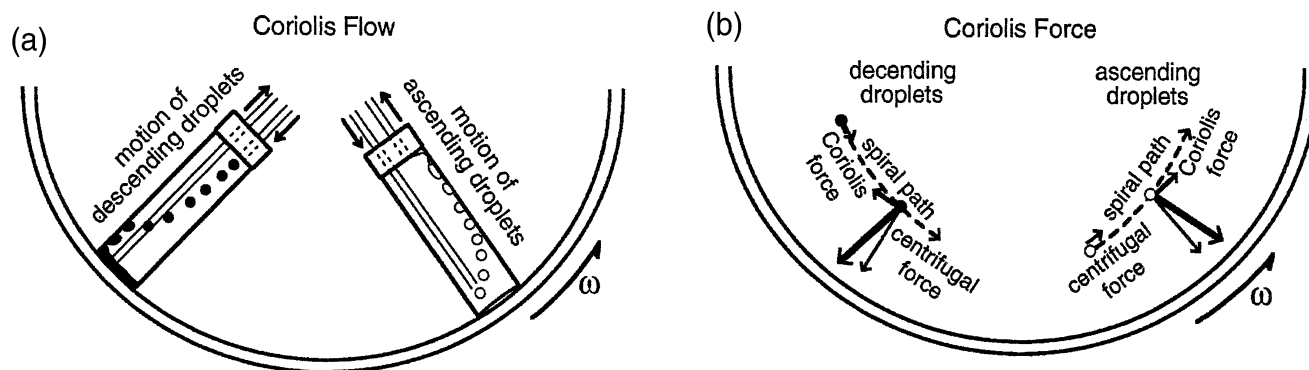


Fig. 1 Effects of Coriolis force on moving droplets in a rotating centrifuge. (a) Motion of the droplets in a flow through cell in a rotating centrifuge; (b) direction of the Coriolis force acting on droplets on the rotating centrifuge bowl.



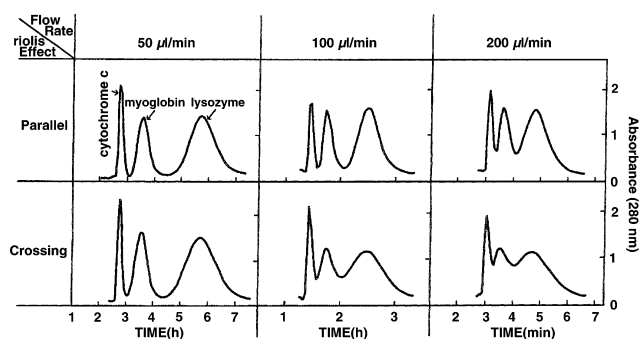


Fig. 2 Effects of Coriolis force on partition efficiency and retention of the stationary phase in protein separation by the toroidal coil centrifuge.

weight compounds such as dipeptides [2] and DNP (dinitrophenyl) amino acids [5] on the conventional organic–aqueous two-phase solvent systems, except that at a relatively low revolution speed, the Coriolis force acting across the effective coil segments slightly improves the partition efficiency, probably due to the substantially higher retention of the stationary phase.

Coriolis Force in Countercurrent Chromatography

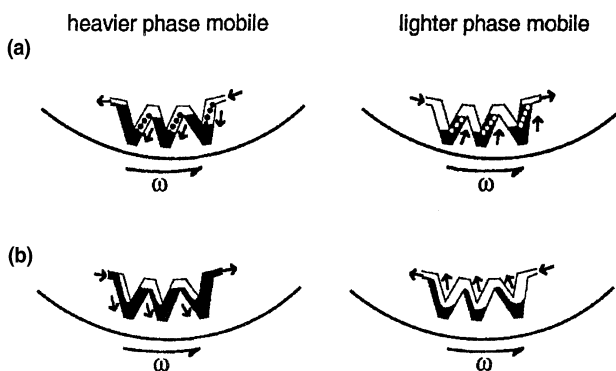


Fig. 3 Effects of Coriolis force on the two-phase flow in the separation coil of the toroidal coil centrifuge: (a) Coriolis force parallel; (b) Coriolis force crossing.

References

1. *New Encyclopedia Britannica*, 1995, Vol. 3, p. 632.
2. Y. Ito and Y. Ma, Effect of Coriolis force on countercurrent chromatography, *J. Liquid Chromatogr.* 21:1 (1998).
3. L. Marchal, A. Foucault, G. Patissier, J. M. Rosant, and J. Legrand, *J. Chromatogr. A* 869:339 (2000).
4. A. Morvan, A. Foucault, G. Patissier, J. M. Rosant and J. Legrand, *J. Hydrodyn.* (in press).
5. Y. Ito, K. Matsuda, Y. Ma, and L. Qi, *J. Chromatogr. A* 808:95 (1998).

Table 1 Effects of Coriolis Force on Partition Efficiencies of Three Stable Proteins in Toroidal Coil CCC

Flow rate ($\mu\text{L}/\text{min}$)	Analyte peak	TP (Para/Cross)	R_s (Para/Cross)	Retention (%) (Para/Cross)
50	Cytochrome-c	1860/1490	1.62/1.39	29.2/32.0
	Myoglobin	365/266		
	Lysozyme	156/104	1.66/1.40	
100	Cytochrome-c	1760/2821	1.27/0.86	30.0/30.3
	Myoglobin	433/172		
	Lysozyme	172/63	1.39/0.84	
200	Cytochrome-c	1296/—	0.84/—	22.8/21.3
	Myoglobin	330/—		
	Lysozyme	123/—	0.92/—	

Corrected Retention Time and Corrected Retention Volume

Raymond P. W. Scott

Scientific Detectors Ltd., Banbury, Oxfordshire, England

Introduction

The corrected retention time of a solute is the elapsed time between the dead point and the peak maximum of the solute. The different properties of the chromatogram are shown in Fig. 1. The volume of mobile phase that passes through the column between the dead point and the peak maximum is called the corrected retention volume. If the mobile phase is incompressible, as in liquid chromatography, the retention volume (as so far defined) will be the simple product of the exit flow-rate and the corrected retention time.

If the mobile phase is compressible, the simple product of the corrected retention time and flow rate will be incorrect, and the corrected retention volume must be taken as the product of the corrected retention time and the *mean* flow rate. The true corrected retention volume has been shown to be given by [1]

$$V'_r = V_r \frac{3}{2} \left(\frac{\gamma^2 - 1}{\gamma^3 - 1} \right) = Q_0 t'_r \frac{3}{2} \left(\frac{\gamma^2 - 1}{\gamma^3 - 1} \right)$$

where the symbols have the meaning defined in Fig. 1, and V'_r is the corrected retention volume measured at the column exit and γ is the inlet/outlet pressure ratio.

The corrected retention volume, V'_r , will be the difference between the retention volume and the dead volume V_0 , which, in turn, will include the actual dead volume V_m and the extra column volume V_E . Thus,

$$V'_r = V_r - (V_E + V_m)$$

The retention time can be taken as the product of the distance on the chart between the dead point and the peak maximum and the chart speed, using appropriate units. As in the case of the retention time, it can be more accurately measured with a stopwatch. Again, the most accurate method of measuring V'_r for a non-compressible mobile phase, although considered antiquated, is to attach an accurate burette to the detector exit and measure the retention volume in volume units. This is an absolute method of measurement and

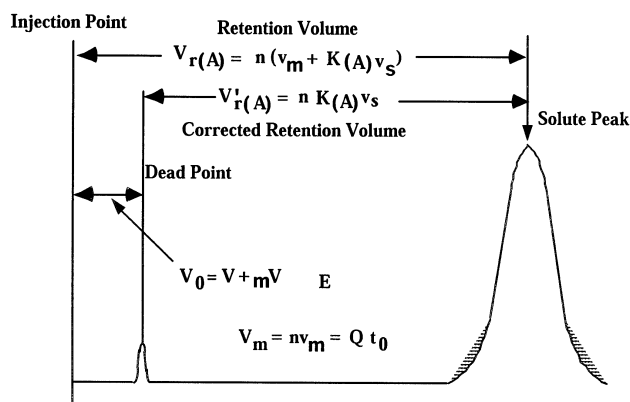


Fig. 1 Diagram depicting the retention volume, corrected retention volume, dead point, dead volume, and dead time of a chromatogram. V_0 : total volume passed through the column between the point of injection and the peak maximum of a completely unretained peak; V_m : total volume of mobile phase in the column; $V_{r(A)}$: retention volume of solute A; $V'_{r(A)}$: corrected retention volume of solute A; V_E : extra column volume of mobile phase; v_m : volume of mobile phase, per theoretical plate; v_s : volume of stationary phase per theoretical plate; $K_{(A)}$: distribution coefficient of the solute between the two phases; n : number of theoretical plates in the column; Q : column flow rate measured at the exit.

does not depend on the accurate calibration of the pump, chart speed, or computer acquisition level and processing.

Reference

1. R. P. W. Scott, *Introduction to Analytical Gas Chromatography*, Marcel Dekker, Inc., New York, 1998, p. 77.

Suggested Further Reading

- Scott, R. P. W., *Liquid Chromatography Column Theory*, John Wiley & Sons, Chichester, 1992, p. 19.
 Scott, R. P. W., *Techniques and Practice of Chromatography*, Marcel Dekker, Inc., New York, 1996.



Coumarins: Analysis by TLC

Kazimierz Głowniak

Medical University, Lublin, Poland

Introduction

Coumarins are natural compounds that contain characteristic benzo[a]pyrone (2H-benzopyran-2-one) moiety. They are especially abundant in Umbelliferae, Rutaceae, Leguminosae, and other plant families. Different coumarin derivatives have been isolated. Usually the substituents are at the positions C₅, C₆, C₇, and C₈ [e.g., umbelliferone (7-hydroxycoumarin), hieroniarin (7-methoxycoumarin), esculetin (6,7-dihydroxycoumarin), scopoletin (6-methoxy-7-hydroxycoumarin), osthonol (7-hydroxy-8-prenylcoumarin), osthonol (7-methoxy-8-prenylcoumarin), and others].

Discussion

In addition to simple coumarin derivatives, furano- and pyrano-coumarins are also commonly encountered in the Umbelliferae and Rutaceae families. The essential chemical moiety of linear furano-coumarins consists of 2H-furan[3.2-g]benzo[b]pyran-2-one ring called psoralen (its derivatives; e.g., bergapten, xanthotoxin, isopimpinelin, imperatorin, isoimperatorin, oxypeucedanin, and others). The second type of furano-coumarins (the angular type of angelicin) has a 2H-furan[2.3-h]-benzo[b]pyran-2-one structure (the angelicin derivatives; e.g., isobergapten, pimpinelin, sphondin). There are also both linear and angular types of pyrano-coumarins. In the linear type, which is named alloxanthiletin, the 2H,8H-pyran[3.2g]-benzo[b]pyran-2-one ring is characteristic, whereas in the angular type called seselin, the 2H,8H-pyran[2.3-h]benzo[b]pyran-2-one moiety is typical.

Thin-layer chromatography (TLC) is a very useful method for separation of natural coumarins, furano-coumarins and pyrano-coumarins. Natural coumarins exhibit fluorescence properties which they display in ultraviolet (UV) light (365 nm). Their spots can be easily detected on paper and thin-layer chromatograms without the use of any chromogenic reagents. It is often possible to recognize the structural class of coumarin from the color it displays under UV detection (Table 1). Purple fluorescence generally signifies 7-

alkoxycoumarins, whereas 7-hydroxycoumarins and 5,7-dioxygenated coumarins tend to fluoresce blue. In general, furano-coumarins possess a dull yellow or ochre fluorescence, except for psoralen, sphondin, and angelicin. Spot fluorescence is more intense or its color is changed after spraying the TLC chromatogram with ammonia (see Table 1) [1].

Thin-layer chromatograms can also be detected by several nonspecific chromatogenic reactions:

1. 1% aqueous solution of iron(III) chloride
2. 1% aqueous solution of potassium ferricyanide
3. Diazotized sulfonilic acid and diazotized p-nitroaniline

None of these reagents is very specific for hydroxycoumarins and its confirmation should be substantiated by other methods. Exposed groups present in many natural coumarins can be detected due to their susceptibility to cleavage by acids and applied over a phosphoric acid spot on a silica TLC plate.

The linear (psoralens) and angular (angelicins) furanocoumarins can be readily differentiated with the Emerson reagent. It is used, also, for detection of pyrano-coumarins (selinidin, pteryxin) on TLC chromatograms.

Thin-Layer Chromatography

Conventional TLC is a well-known technique, used for many years in systematic research on coumarin content of numerous plant species, as well as for chemotaxonomic relationships between those species. Great progress in optimization of the TLC-separation process was made by the design of modern, horizontal chambers for TLC. It is a universal design, offering the possibility of developing chromatograms in the space saturated or nonsaturated with mobile-phase vapors; moreover, it is possible to perform gradient elution, stepwise or continuous, or to accomplish micropreparative separation of chemical compound composites (e.g., plant extracts) [2].

Gradient elution in TLC can be obtained in several ways [1]:



Table 1 Chromatographic Methods of Coumarins
Identification: Fluorescence Colors of Coumarins
Under UV Irradiation (365 nm)

Fluores- cence color ^a	Fluorescence color with ammonia	Coumarin or coumarin type
Blue	L. Blue	7-Hydroxycoumarin
B. blue	V. blue	7-Hydroxycoumarins
Blue	B. blue	7-Hydroxy-6-alkoxycoumarins
Blue	Blue	5,7-Dialkoxycoumarins
B. blue	B. blue	6,7-Dialkoxycoumarins
Blue	Blue	6,7,8-Trialkoxycoumarins
W. blue	W. blue	5,6,7-Trialkoxycoumarins
W. blue	B. blue	7-Hydroxy-5,6-dialkoxycoumarins
Blue		Psoralen
Blue	B. blue	6-Methoxyangelicin
Blue	Green	7,8-Dihydroxycoumarin
Pink	Yellow	6-Hydroxy-7-glucosyloxycoumarin
Purple	Purple	8-Hydroxy-5-alkoxypsoralens
W. purple	Pink	6-Hydroxy-7-alkoxycoumarins
Purple	Green	Angelicin, coumestrol
Green		5-Methoxyangelicin
Green		8-Hydroxy-6,7-dimethoxycoumarin
Green	Yellow	7,8-Dihydroxy-6-methoxycoumarin
Yellow		7-Hydroxy-8-methoxycoumarin
Yellow		3,4,5-Trimethoxypsoralen
Yellow	Yellow	6-Hydroxy-5,7-dimethoxycoumarin
Yellow	Yellow	5-Hydroxy-6,7-dimethoxycoumarin
Yellow	Yellow	5-Hydroxypsoralen
Yellow	Yellow	5,6-Dimethoxyangelicin
Yellow	Yellow	8-Alkoxypsoralens
Yellow– green	Yellow– green	5-Alkoxypsoralens
B. yellow	B. yellow	5,8-Dialkoxypsoralens

^aB. = bright; V. = very bright; L. = light; W. = weak

Source: Ref. 1.

1. Multizonal development: the use of multicomponent eluents which are partially separated during development (frontal chromatography), forming an eluent strength gradient along the layer
2. Development with a strong solvent (e.g., acetone) of an adsorbent layer exposed to vapors of a less polar solvent
3. The use of mixed layers of varying surface area, activity (comparison silica and florisil)
4. Delivery of an eluent whose composition is varied in a continuous or stepwise manner by introducing small volumes of more polar eluent fractions (e.g., 0.2 mL).

The possibility of zonal sample dosage in equilibrium conditions (after the front of mobile-phase and continuous-chromatogram development, which is provided by a horizontal “sandwich” chamber) was utilized by Głowniak et al. [3] in preparative chromatography of simple coumarins and furano-coumarins found in *Archangelica* fruits, performed with a short-bed continuous development (SB–CD) technique.

The latter possibility was employed by Wawrzynowicz and Waksmundzka-Hajnos for micropreparative TLC isolation of furano-coumarins from *Archangelica*, *Pastinaca*, and *Heracleum* fruits on silica gel, silanized gel, and florisil.

Superior coumarin compounds separation with use of the described flat “sandwich” chambers was achieved with gradient chromatography on silica gel and stepwise variation of polar modifier concentration in mobile phase, as less polar solvents (hexane, cyclohexane, toluene, or dichloromethane) and polar modifiers (acetonitrile, diisopropyl ether, ethyl acetate) are used.

Complex pyrano-coumarin mixtures can be separated with the TLC technique by alternative use of two different polar adsorbents (silica gel, florisil) and various binary and ternary eluents with different mechanisms of adsorption centers effect on the molecules to be separated [4]. Improved separation can be achieved by high-performance thin-layer chromatography (HPTLC), which employs new highly effective adsorbents of narrow particle size distribution, or with a chemically modified surface. Because of its similarity, HPTLC is applied in designing optimal HPLC systems. Another gradient technique in coumarin compounds separation is programmed multiple development (PMD), also called “reverse gradient” technique, in which chromatograms are developed to increasing distances by a sequence of eluents with decreasing polarity, with eluent evaporation after each stage. Automated multiple development (AMD), providing automatic chromatogram developing and drying, is a novel form of the PMD technique.

Two-dimensional thin-layer chromatography (2D–TLC), is particularly effective in the case of complex extracts when one-dimensional developing yields partial separation. Moreover, it offers the possibility of modifying separation procedures when the development direction is changed.

Overpressured Layer Chromatography

The term “overpressured layer chromatography” (OPLC) was originally introduced by Tyihak et al. [5] in



the late seventies. The crucial factor is pressurized mobile-phase flow through the planar media. A short analysis time, low solvent consumption, high resolution, and availability of on-line and off-line modes are the main OPLC advantages in comparison with the classical TLC techniques. OPLC was proved effective in qualitative and quantitative analysis of furano-coumarins by densitometric on-line detection. OPLC can also be performed in two-dimensional mode (2D-OPLC).

Long-distance OPLC is a novel form of OPLC, in which chromatograms are developed over a long distance with optimal (empiric) mobile-phase flow. Used in combination with specialized equipment designs, it produces high performance (70,000 to 80,000 of theoretic plates) and excellent resolution. Botz et al. [6], who initiated long-distance OPLC, proved its efficiency in separation of eight furano-coumarin isomers and in isolation of furanocoumarin complex from *Peucedanum palustre* roots raw extract.

Rotation Planar Chromatography

Rotation planar chromatography (RPC), as with OPLC, is another thin-layer technique with forced

eluent flow, employing a centrifugal force of a revolving rotor to move the mobile phase and separate chemical compounds. The RPC equipment can vary in chamber size, operative mode (analytical or preparative), separation type (circular, anticircular, or linear), and detection mode (off-line or on-line). The described technique was applied in analytical and micro-preparative separation of coumarin compounds from plant extracts.

References

1. R. D. H. Murray, Nat. Prod. Rep. 591–624 (1989).
2. E. Soczewinski, *Chromatography*, 138:443 (1977).
3. K. Głowniak, E. Soczewinski, and T. Wawrzynowicz, *Chem. Anal. (Warsaw)* 32:797 (1987).
4. K. Głowniak, *J. Chromatogr.* 552:453 (1991).
5. E. Tyihák, E. Mincsovisc, and H. Kalász, *J. Chromatogr.* 174:75 (1979).
6. L. Botz, S. Nyiredy, and O. Sticher, *J. Planar Chromatogr.* 4:115 (1991).





Countercurrent Chromatographic Separation of Vitamins by Cross-Axis Coil Planet Centrifuge

Kazufusa Shinomiya

Nihon University, Chiba, Japan

Yoichiro Ito

National Institutes of Health, Bethesda, Maryland, U.S.A.

INTRODUCTION

Cross-axis coil planet centrifuges (cross-axis CPC), which have been widely used in the separation of natural and synthetic products, are some of the most useful models among various types of countercurrent chromatographic (CCC) apparatuses.^[1–3] It produces a unique mode of planetary motion such that the column holder rotates about its horizontal axis while revolving around the vertical axis of the centrifuge.^[4,5] The centrifugal force field produced by the planetary motion provides stable retention of the stationary phase for polar two-phase solvent systems such as aqueous–aqueous polymer phase systems with extremely low interfacial tension and high viscosity. Our previous studies demonstrated that cross-axis CPC, equipped with either a multilayer coil or eccentric coil assembly in the off-center position of the column holder, can be effectively applied for the separation of proteins^[6–8] and sugars.^[9]

This article illustrates the CCC separation of various vitamins by means of cross-axis CPC equipped with eccentric coil assemblies.^[10,11]

APPARATUS AND SEPARATION COLUMNS

All existing cross-axis CPCs are classified according to their relative column position on the rotary frame, e.g., X ,^[4,5] XL ,^[12] XLL ,^[13] and $XLLL$,^[14] where X is the distance from the column holder axis to the central axis of the centrifuge, and L is the distance between the holder and the middle point of the rotary shaft. Increasing the ratio L/X improves the retention of the stationary phase by moderating phase mixing. The separations of vitamins described below were performed using the $X - 1.5L$ cross-axis CPC, which holds the separation column at $X = 10$ cm and $L = 15$ cm.

The separation column was prepared by means of a pair of eccentric coil assemblies, which were made by winding a single piece of 1-mm-ID polytetrafluoro-

ethylene (PTFE) tubing onto 7.6-cm-long, 5-mm-OD nylon pipes forming 20 units of serially connected left-handed coils. Then, a set of these coil units was arranged around the holder with their axes parallel to the holder axis. A pair of identical coil assemblies was connected in series to obtain a total column capacity of 26.5 mL.

CCC SEPARATION OF WATER-SOLUBLE VITAMINS

In CCC, the partition coefficient (K) is an important parameter which is used for selecting the optimal solvent

Table 1 Partition coefficients of water-soluble vitamins in 1-butanol/aqueous 0.15 M monobasic potassium phosphate two-phase solvent systems

1-Butanol	1	4	8
Ethanol	0	1	3
0.15 M KH_2PO_4	1	4	8
Thiamine nitrate (M.W. 327.36)	0.03	0.05	0.11
Thiamine hydrochloride (M.W. 327.27)	0.14	0.05	0.17
Riboflavin (M.W. 376.37)	0.54	0.83	1.08
Riboflavin sodium phosphate (M.W. 478.33)	0.11	0.18	0.34
Pyridoxine hydrochloride (M.W. 205.64)	0.23	0.43	0.59
Cyanocobalamin (M.W. 1355.38)	0.04	0.12	0.24
L-Ascorbic acid (M.W. 176.12)	0.07	0.11	0.15
Nicotinamide (M.W. 122.13)	1.84	1.41	1.34

Partition coefficients were calculated from the absorbance of the upper phase divided by that of lower phase at 260 nm.

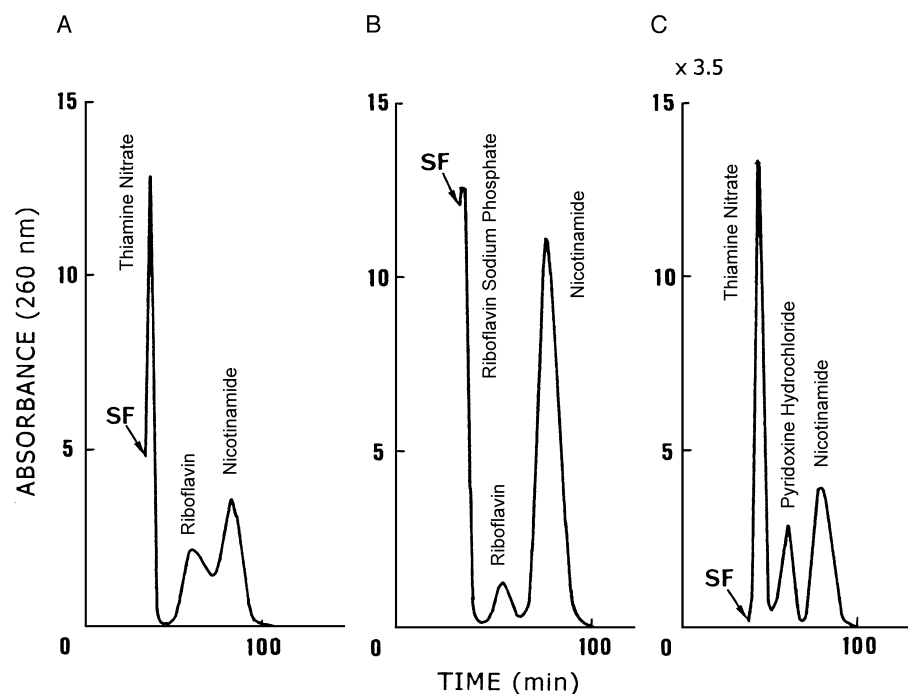


Fig. 1 CCC separation of water-soluble vitamins by cross-axis CPC. Experimental conditions: apparatus, cross-axis CPC equipped with a pair of eccentric coil assemblies, 1 mm ID and 26.5 mL capacity; sample. (A) thiamine nitrate (2.5 mg)+riboflavin (1.5 mg)+nicotinamide (2.5 mg) (B) riboflavin sodium phosphate (2.5 mg)+nicotinamide (2.5 mg) and (C) thiamine nitrate (2.8 mg)+pyridoxine hydrochloride (4.0 mg)+nicotinamide (3.0 mg); solvent system: (A) and (B) 1-butanol/aqueous 0.15 M monobasic potassium phosphate (1:1) and (C) 1-butanol/ethanol/aqueous 0.15 M monobasic potassium phosphate (8:3:8); mobile phase: lower phase; flow rate: 0.4 mL/min; revolution: 800 rpm. SF = solvent front.

system because it predicts the retention time of each component. Table 1 shows the K values of various water-soluble vitamins in the 1-butanol/aqueous 0.15 M monobasic potassium phosphate system. Most of the water-soluble vitamins were partitioned, almost unilaterally, into the aqueous phase in this solvent system, except that riboflavin and nicotinamide were distributed

significantly into the organic phase ($K=0.54-1.84$). Adding ethanol to the two-phase solvent system significantly increased the partition coefficients of riboflavin and pyridoxine hydrochloride.

Fig. 1A illustrates the CCC separation of thiamine nitrate, riboflavin, and nicotinamide by cross-axis CPC, with the 1-butanol/aqueous 0.15 M monobasic potassium

Table 2 Effect of ion-pair reagents on partition coefficients of water-soluble vitamins in 1-butanol/aqueous 0.15 M KH_2PO_4 solvent systems

Ion-pair reagent Concentration (%)	1-Butane sulfonic acid		1-Pentane sulfonic acid		1-Octane sulfonic acid
	1.5	2.5	1.5	2.5	1.5
Thiamine nitrate (M.W. 327.36)	0.18	0.29	0.76	1.01	2.45
Thiamine hydrochloride (M.W. 327.27)	0.17	0.25	0.73	0.97	2.42
Riboflavin (M.W. 376.37)	0.58	0.70	0.57	0.95	1.07
Riboflavin sodium phosphate (M.W. 478.33)	0.04	0.29	0.08	0.20	0.13
Pyridoxine hydrochloride (M.W. 205.64)	0.57	0.73	0.77	0.86	1.63
Cyanocobalamin (M.W. 1355.38)	0.08	0.44	0.37	0.35	0.47
L-Ascorbic acid (M.W. 176.12)	0.04	0.13	0.09	0.09	0.09
Nicotinamide (M.W. 122.13)	1.32	0.78	1.46	1.39	1.49

Partition coefficients were calculated from the absorbance of the upper phase divided by that of lower phase at 260 nm.

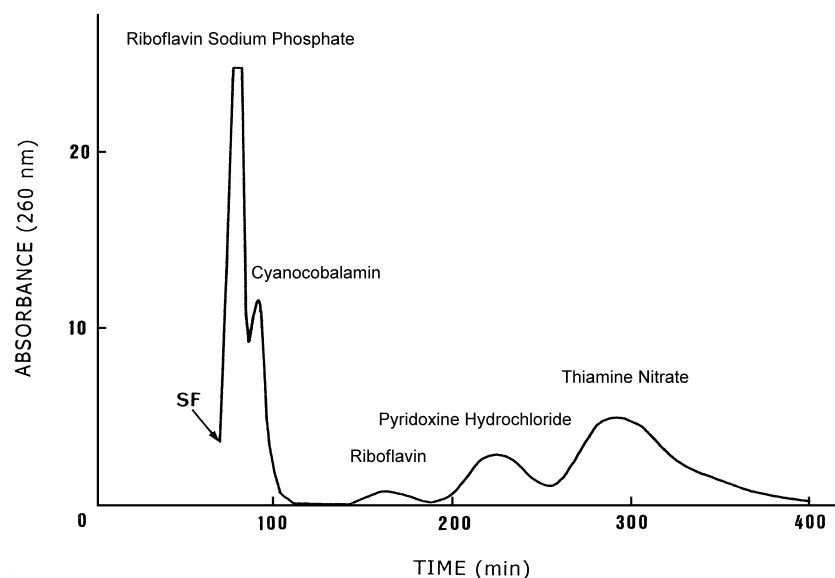


Fig. 2 CCC separation of water-soluble vitamins by cross-axis CPC. Experimental conditions: sample, riboflavin sodium phosphate (2.5 mg) + cyanocobalamin (2.5 mg) + pyridoxine hydrochloride (2.5 mg) + thiamine nitrate (2.5 mg); solvent system, 1-butanol and aqueous 0.15 M monobasic potassium phosphate containing 1.5% of 1-octanesulfonic acid sodium salt; mobile phase, lower phase; flow rate, 0.2 mL/min. For other experimental conditions, see Fig. 1 caption. SF = solvent front.

phosphate (1:1) system. Riboflavin sodium phosphate is also resolved from riboflavin with the same solvent system (Fig. 1B). When a more polar solvent system consisting of 1-butanol/ethanol/aqueous 0.15 M monobasic potassium phosphate (8:3:8) is used, thiamine nitrate, pyridoxine hydrochloride, and nicotinamide are well resolved from each other, as shown in Fig. 1C.

In order to improve the separation of each water-soluble vitamin by cross-axis CPC, three ion-pair reagents were added to the 1-butanol/aqueous 0.15 M monobasic potassium phosphate system. The K values of

the vitamins in this solvent system are summarized in Table 2. Most of the K values increased by increasing the concentration and carbon number of ion-pairing reagents added in the two-phase solvent system. Among these ion-pairing reagents, 1-octanesulfonic acid sodium salt was found to be most suitable and was selected for the separation of water-soluble vitamins by cross-axis CPC.

Fig. 2 illustrates the CCC chromatogram of water-soluble vitamins obtained with the above solvent system, which comprise 1-butanol and aqueous 0.15 M mono-

Table 3 Partition coefficients of fat-soluble vitamins in four different two-phase solvent systems

	<i>n</i> -Hexane/aqueous 90% acetonitrile (1:1)	<i>n</i> -Hexane/ acetonitrile (1:1)	2,2,4-Trimethyl pentane/methanol (1:1)	<i>n</i> -Hexane/ethyl acetate/methanol/ water (1:1:1:1)
Vitamin A acetate	5.34	1.69	1.34	130
Calciferol (M.W. 396.66)	8.14	3.29	0.83	71.2
(±)- α -Tocopherol acetate (M.W. 472.25)	48.5	10.1	3.11	62.6
Vitamin K ₁ (M.W. 450.71)	61.6	5.79	3.92	9.23
Vitamin K ₃ (M.W. 172.19)	0.31	0.22	0.35	2.40

Partition coefficients were calculated from the absorbance of the upper phase divided by that of lower phase at 280 nm.

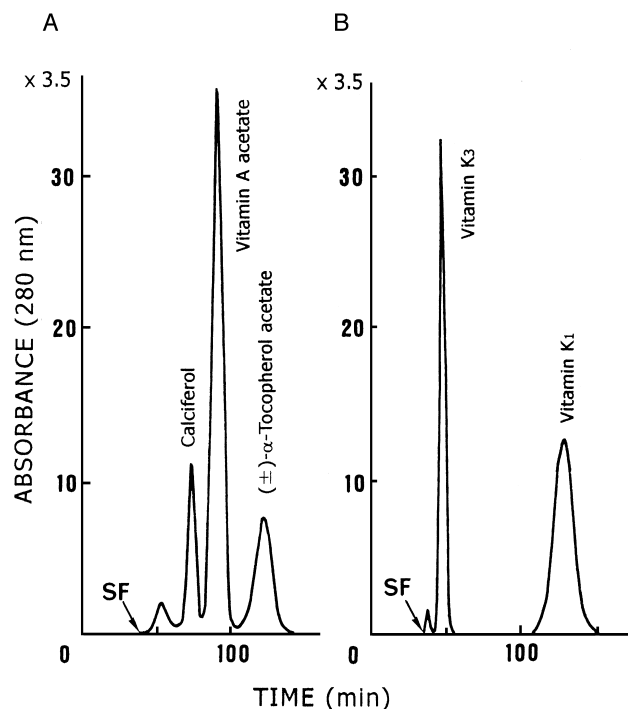


Fig. 3 CCC separation of fat-soluble vitamins by cross-axis CPC. Experimental conditions: sample, (A) calciferol (3 mg) + vitamin A acetate (30 mg) + (±)- α -tocopherol acetate (40 mg) and (B) vitamin K₃ (3 mg) + vitamin K₁ (10 mg); solvent system, 2,2,4-trimethyl pentane/methanol (1:1); mobile phase, lower phase. For other experimental conditions, see Fig. 1 caption. SF = solvent front.

basic potassium phosphate, including 1.5% of 1-octane-sulfonic acid sodium salt. Riboflavin sodium phosphate, cyanocobalamin, riboflavin, pyridoxine hydrochloride, and thiamine nitrate were separated using the lower phase as the mobile phase. Riboflavin was found as an impurity contained in the riboflavin sodium phosphate sample.

CCC SEPARATION OF FAT-SOLUBLE VITAMINS

The K values of fat-soluble vitamins obtained with four different kinds of solvent systems are summarized in Table 3. The most suitable solvent system was found to be the 2,2,4-trimethyl pentane (isooctane)/methanol binary system.

Fig. 3A illustrates the CCC separation of fat-soluble vitamins using the cross-axis CPC equipped with eccentric coil assemblies. Calciferol, vitamin A acetate, and (±)- α -tocopherol acetate were well resolved from each other and eluted within 2.5 h. Vitamin K₃ and Vitamin K₁ were also completely resolved with the same solvent system, as shown in Fig. 3B.

CONCLUSION

As described above, the cross-axis CPC, equipped with eccentric coil assemblies, can be used for the separation of both water-soluble and fat-soluble vitamins by selecting suitable two-phase solvent systems.

REFERENCES

1. *Countercurrent Chromatography: Theory and Practice*; Mandava, N.B., Ito, Y., Eds.; Marcel Dekker, Inc.: New York, 1988; 79.
2. Conway, W.D. *Countercurrent Chromatography: Apparatus, Theory and Applications*; VCH: New York, 1990; 37.
3. *High Speed Countercurrent Chromatography*; Ito, Y., Conway, W.D., Eds.; Wiley-Interscience: New York, 1996; 3.
4. Ito, Y. Cross-axis synchronous flow-through coil planet centrifuge free of rotary seals for preparative countercurrent chromatography. Part I: Apparatus and analysis of acceleration. *Sep. Sci. Technol.* **1987**, 22, 1971.
5. Ito, Y. Cross-axis synchronous flow-through coil planet centrifuge free of rotary seals for preparative countercurrent chromatography. Part II: Studies on phase distri-



- bution and partition efficiency in coaxial coils. *Sep. Sci. Technol.* **1987**, 22, 1989.
6. Shinomiya, K.; Menet, J.-M.; Fales, H.M.; Ito, Y. Studies on a new cross-axis coil planet centrifuge for performing counter-current chromatography. I. Design of the apparatus, retention of the stationary phase, and efficiency in the separation of proteins with polymer phase systems. *J. Chromatogr.* **1993**, 644, 215.
 7. Shinomiya, K.; Inokuchi, N.; Gnabre, J.N.; Muto, M.; Kabasawa, Y.; Fales, H.M.; Ito, Y. Countercurrent chromatographic analysis of ovalbumin obtained from various sources using the cross-axis coil planet centrifuge. *J. Chromatogr., A* **1996**, 724, 179.
 8. Shinomiya, K.; Muto, M.; Kabasawa, Y.; Fales, H.M.; Ito, Y. Protein separation by improved cross-axis coil planet centrifuge with eccentric coil assemblies. *J. Liq. Chromatogr. Relat. Technol.* **1996**, 19, 415.
 9. Shinomiya, K.; Kabasawa, Y.; Ito, Y. Countercurrent chromatographic separation of sugars and their p-nitrophenyl derivatives by cross-axis coil planet centrifuge. *J. Liq. Chromatogr. Relat. Technol.* **1999**, 22, 579.
 10. Shinomiya, K.; Komatsu, T.; Murata, T.; Kabasawa, Y.; Ito, Y. Countercurrent chromatographic separation of vitamins by cross-axis coil planet centrifuge with eccentric coil assemblies. *J. Liq. Chromatogr. Relat. Technol.* **2000**, 23, 1403.
 11. Shinomiya, K.; Yoshida, K.; Kabasawa, Y.; Ito, Y. Countercurrent chromatographic separation of water-soluble vitamins by cross-axis coil planet centrifuge using an ion-pair reagent with polar two-phase solvent system. *J. Liq. Chromatogr. Relat. Technol.* **2001**, 24, 2615.
 12. Ito, Y.; Oka, H.; Slempe, J. Improved cross-axis synchronous flow-through coil planet centrifuge for performing counter-current chromatography. I. Design of the apparatus and analysis of acceleration. *J. Chromatogr.* **1989**, 463, 305.
 13. Ito, Y.; Kitazume, E.; Bhatnagar, M.; Trimble, F. Cross-axis synchronous flow-through coil planet centrifuge (Type XLL). I. Design of the apparatus and studies on retention of stationary phase. *J. Chromatogr.* **1991**, 538, 59.
 14. Shibusawa, Y.; Ito, Y. Countercurrent chromatography of proteins with polyethylene glycol-dextran polymer phase systems using type-XLLL cross-axis coil planet centrifuge. *J. Liq. Chromatogr.* **1992**, 15, 2787.

Countercurrent Chromatography–Mass Spectrometry

Hisao Oka

Aichi Prefectural Institute of Public Health, Nagoya, Japan

Yoichiro Ito

National Heart, Lung, and Blood Institute, National Institutes of Health, Bethesda, Maryland, U.S.A.

Introduction

Countercurrent chromatography (CCC) is a unique liquid–liquid partition technique which does not require the use of a solid support [1–5], hence eliminating various complications associated with conventional liquid chromatography, such as tailing of solute peaks, adsorptive sample loss and deactivation, contamination, and so forth. Since 1970, the CCC technology has advanced in various directions, including preparative and trace analysis, dual CCC, foam CCC, and, more recently, partition of macromolecules with polymer-phase systems. However, most of these methods were only suitable for preparative applications due to relatively long separation times required. In order to fully explore the potential of CCC, efforts have been made to develop analytical high-speed CCC (HSCCC) by designing a miniature multilayer coil planet centrifuge; interfacing analytical HSCCC to a mass spectrometer (HSCCC–MS) began in the late 1980s.

Integration of the high-purity eluate of HSCCC with a low detection limit of MS has led to the identification of a number of natural products, as shown in Table 1 [6–10].

Various HSCCC–MS techniques and their applications are described herein.

Interfacing HSCCC to Thermospray Mass Spectrometry

HSCCC–thermospray (TSP) MS was initiated using an analytical HSCCC apparatus of a 5-cm revolution radius, equipped with a 0.85-mm-inner diameter (i.d.) polytetrafluoroethylene (PTFE) column at 2000 rpm [6–8]. Directly interfacing HSCCC to the MS produced, however, a problem in that the high back-pressure generated by the TSP vaporizer often damaged the HSCCC column. To overcome this problem, an additional high-performance liquid chromatography

(HPLC) pump was inserted at the interface junction between HSCCC and MS to protect the column against high back-pressures. The effluent from the HSCCC column (0.8 mL/min) was introduced into the HPLC pump through a zero-dead-volume tee fitted with a reservoir supplying extra solvent or venting excess solvent from the HSCCC system. The effluent from the HPLC pump, after being mixed with 0.3M ammonium acetate at a rate of 0.3 mL/min, was introduced into the TSP interface. This system has been successfully applied to the analyses of alkaloids [6], triterpenic acids, [7] and lignans [8] from plant natural products, thereby providing useful structural information. However, a large dead space in the pump at the interface junction adversely affected the resulting chromatogram, as evidenced by loss of a minor peak when HSCCC–UV and HSCCC–TSP–MS total ion current (TIC) chromatograms of plant alkaloids were compared.

In the subsequently developed techniques, the HSCCC effluent is directly introduced into the MS to preserve the peak resolution. Direct HSCCC–MS techniques have many advantages over the HSCCC–TSP method as follows:

1. High enrichment of sample in the ion source
2. High yield of sample reaching the MS
3. No peak broadening
4. High applicability to nonvolatile samples

Various types of HSCCC–MS have been developed using frit fast-atom bombardment (FAB) including continuous flow (CF) FAB, frit electron ionization (EI), frit chemical ionization (CI), TSP, atmospheric pressure chemical ionization (APCI), and electrospray ionization (ESI). Each interface has its specific features. Among those, frit MS and ESI are particularly suitable for directly interfacing to HSCCC, because they generate low back-pressures of approximately 2 kg/cm², which is only one-tenth of that produced by TSP.



Table 1 Summary of Previously Reported HSCCC–MS Conditions

Sample	Column	Column capacity (mL)	Revolu-tional speed (rpm)	Solvent system	Mobile phase	Flow rate (mL/min)	Retention of station-ary phase (%)	Ionization	Ref.
Alkaloids	0.85-mm PTFE tube	38	1500	<i>n</i> -Hexane–ethanol–water (6:5:5)	Lower phase	0.7	—	Thermospray	6
Triterpenoic acids	0.85-mm PTFE tube	38	1500	<i>n</i> -Hexane–ethanol–water (6:5:5)	Lower phase	0.7	—	Thermospray	7
Lignans	0.85-mm PTFE tube	38	1500	<i>n</i> -Hexane–ethanol–water (6:5:5)	Lower phase	0.7	—	Thermospray	8
Indole auxins	0.3-mm PTFE tube	7	4000	<i>n</i> -Hexane–ethyl acetate–methanol–water (1:1:1:1)	Lower phase	0.2	27.2	Frit–EI	9
Mycinamicins	0.3-mm PTFE tube	7	4000	<i>n</i> -Hexane–ethyl acetate–methanol–8% ammonia (1:1:1:1)	Lower phase	0.1	40.4	Frit–CI	9
Colistins	0.55-mm PTFE tube	6	4000	<i>n</i> -Butanol–0.04 <i>M</i> TFA (1:1)	Lower phase	0.16	34.3	Frit–FAB	9
Erythromycins	0.85-mm PTFE tube	17	1200	Ethyl acetate–methanol–water (4:7:4:3)	Lower phase	0.8	—	Electrospray	10
Didemnins	0.85-mm PTFE tube	17	1200	Ethyl acetate–methanol–water (1:4:1:4)	Lower phase	0.8	—	Electrospray	10

Interfacing of HSCCC to Frit EI, CI, and FAB–MS

In our laboratory, separations were conducted by newly developed HSCCC-4000 with a 2.5-cm revolution radius, equipped with a 0.3-mm or 0.55-mm-i.d. multilayer coil at a maximum revolution speed of 4000 rpm [9]. The system produced an excellent partition efficiency at a flow rate ranging between 0.1 and 0.2 mL/min, whereas the suitable flow rate for HSCCC–frit MS is between 1 and 5 μ L/min. Therefore, the effluent of the HSCCC column was introduced into the MS through a splitting tee which was adjusted to a split ratio of 1:40 to meet the above requirement. A 0.06-mm-i.d. fused-silica tube was led to the MS and a 0.5-mm-i.d. stainless-steel tube was connected to the HSCCC column. The other side of the fused-silica tube extended deeply into the stainless-steel tube to receive a small portion of the effluent from the HSCCC column, and the rest of the effluent was discarded through a 0.1-mm-i.d. PTFE tube. The split ratio of the effluent depended on the flow rate of the effluent and the length of the 0.1-mm-i.d. tube. For adjusting the split ratio at 40:1, a 2-cm length of the 0.1-

mm-i.d. tube was needed. Figure 1 shows the HSCCC–MS system, including an HPLC pump, sample injection port, HSCCC-4000, the split tee, and mass spectrometer [9].

In order to demonstrate the potential of HSCCC–frit MS, indole auxins, mycinamicins (macrolide antibiotics), and colistin complex (peptide antibiotics) were analyzed under HSCCC–frit, EI, CI, and FAB–MS conditions.

Three indole auxins, including indole-3-acetamide (IA, MW: 174), indole-3-acetic acid (IAA, MW: 175), and indole-3-butyric acid (IBA, MW: 203) were analyzed under frit EI–MS conditions. In comparison of a TIC with a UV chromatogram, both showed similar chromatographic resolution with excellent theoretical plate numbers ranging from 12,000 to 5500. The results indicate that MS interfacing does not adversely affect chromatographic resolution. In frit EI–MS, the mobile phase behaves like a reagent gas in CI–MS. Both molecular ions and protonated molecules appear in all mass spectra and these data are very useful for the estimation of the molecular weight. Common fragment ions originating from the indole nuclei are found at m/z 116 and 130.



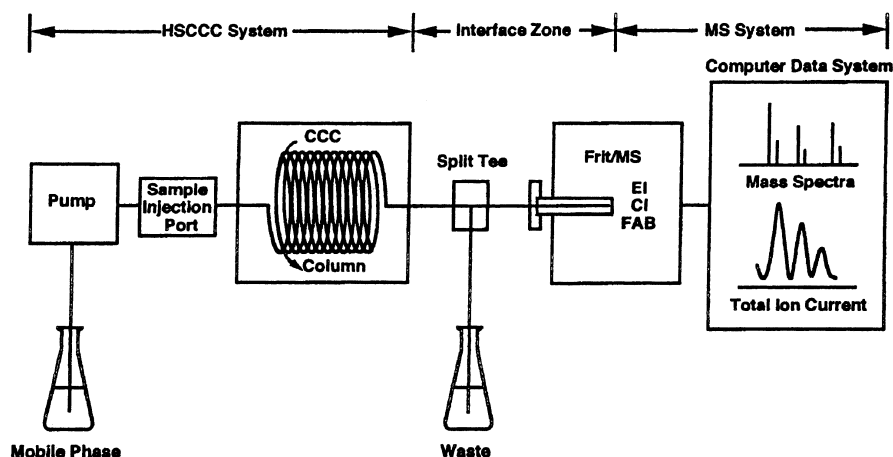


Fig. 1 HSCCC–frit MS system.

A mixture of mycinamicins was analyzed under HSCCC–frit CI–MS conditions. Mycinamicins consist of six components, mycinamicins I to VI, and isolated mycinamicins IV (MN-IV, MW: 695) and V (MN-V, MW: 711) were used. The structural difference is derived from the hydroxyl group at C-14. These antibiotics were detected under CI conditions, but a reagent gas such as methane, isobutane, or ammonia was not introduced, because the mobile phase behaves like a reagent gas, as described earlier. Both UV and TIC chromatograms showed similar efficiencies, indicating that the MS interfacing does not affect peak resolution, as demonstrated in the analysis of indole auxins. An applicability of this HSCCC–MS system to less volatile compounds was examined under frit FAB–MS conditions.

A peptide antibiotic colistin complex consisting of two major components of colistins A (CL-A, MW: 1168) and B (CL-B, MW: 1154) is difficult to ionize by CI and EI–MS. For HSCCC analysis of these polar compounds, a wider column of 0.55 mm i.d. (instead of 0.3 mm i.d.) was used to achieve satisfactory retention of the stationary phase for a polar *n*-butanol–trifluoroacetic acid (TFA) solvent system. In addition, for obtaining FAB mass spectra, it is necessary to introduce a sample with an appropriate matrix such as glycerol, thioglycerol, and *m*-nitrobenzyl alcohol into the FAB–MS ion source. In the present study, glycerol was added as a matrix to the mobile phase at a concentration of 1%. Although a two-phase solvent system containing glycerol was the first trial for a HSCCC study, similarly satisfactory results were obtained in both retention and separation efficiency. Because of

the use of a wider column with a viscous *n*-butanol–aqueous TFA solvent system, the separation was less efficient compared with those obtained from the above two experiments, but the peaks corresponding to CL-A and CL-B were clearly resolved. Mass chromatograms at individual protonated molecules showed symmetrical peaks without a significant loss of peak resolution due to MS interfacing. In all spectra, protonated molecules appeared well above the chemical noise to indicate the molecular weights. These experiments demonstrated that the present HSCCC–frit MS system including EI, CI, and FAB is very potent and is applicable to various analytes having a broad range of polarity. For a nonvolatile, thermally labile and/or polar compound, HSCCC–frit FAB is most suitable, whereas both HSCCC–frit EI and CI can be effectively used for a relatively nonpolar compound.

Interfacing HSCCC to ESI–MS

The experiment was carried out using a small analytical coiled column (17 mL) at 1200 rpm. The effluent from the CCC column at 800 μ L/min was split at a 1:7 ratio to introduce the smaller portion of the effluent into ESI–MS using a tee adaptor, as described earlier.

The performance of HSCCC–ESI–MS was evaluated by analyzing erythromycins and didemnins [10]. Because erythromycins (macrolide antibiotics) show weak UV absorbance and cannot be detected easily with a conventional UV detector, mass spectrometric detection is a very useful technique for analysis of these antibiotics. A mixture of erythromycin A (Er-A,



MW: 733), erythromycin estolate (Er-E, MW: 789), and erythromycin ethyl succinate (Er-S, MW: 789) was analyzed using HSCCC–ESI–MS with a two-phase solvent system composed of *n*-hexane–ethyl acetate–methanol–water (4:7:4:3). TIC showed, clearly, four peaks corresponding to Er-A, Er-E, Er-S, and an unknown substance. The mass spectra of Er-E and Er-S gave $[M + H]^+$ at m/z 862 and 789 and $[M + H - H_2O]^+$ at m/z 844 and 772, respectively. In the mass spectrum of Er-A, $[M + H - H_2O]^+$ was observed at m/z 761; however, no $[M + H]^+$ was given. The mass spectrum of the unknown peak indicated that it consists of two components with molecular weights of 843 and 772, which correspond to dehydrated Er-S and Er-E, respectively.

Didemnin A (Did-A, MW: 942) is one of the main components of didemnis (cyclic depsipeptides) and is a precursor for synthesis of other didemnins which exhibit antiviral, antitumor, and immunosuppressive activities. Therefore, its purification is very important in the field of pharmaceutical science. However, large-scale purification of Did-A using conventional liquid chromatography is difficult due to the presence of nordidemnin A (Nordid-A), which contaminates the target fraction. HSCCC–ESI–MS has been successfully applied to the separation and detection of didemnins. Three peaks were observed on TIC corresponding to didemnins A and B and nordidemnin A. Their mass spectra gave only protonated molecules without fragmentation. The first eluted peak was dideminin B, which gave $[M + H]^+$ and $[M + Na]^+$ at m/z 1112 and 1134, respectively. Did-A appeared as the second peak with $[M + H]^+$ at m/z 943 and $[M + Na]^+$ at m/z 965. The third peak was Nordid-A, showing $[M + H]^+$ at m/z 929 and $[M + Na]^+$ at m/z 951. The results indicated that Did-A can be isolated by HSCCC.

Future Prospects

HSCCC–MS has many desirable features for performing the separation and identification of natural and synthetic products, because it eliminates various complications arising from the use of solid support and offers a powerful identification capacity of MS with its low detection limit. We believe that the combination of these two methods, HSCCC–MS, has great a potential for screening, identification, and structural characterization of natural products and will contribute to a rapid advance in natural products chemistry.

References

1. N. B. Mandava and Y. Ito (eds.), *Countercurrent Chromatography: Theory and Practice*, Marcel Dekker, Inc., New York, 1988.
2. W. D. Conway, *Countercurrent Chromatography: Apparatus, Theory and Applications*, VCH, New York, 1990.
3. A. Foucault (ed.), *Centrifugal Partition Chromatography*, Marcel Dekker, Inc., New York, 1995.
4. Y. Ito, *CRC Crit. Rev. Anal. Chem.* 17:65 (1986).
5. Y. Ito and W. D. Conway (eds.), *High-Speed Countercurrent Chromatography*, Wiley–Interscience, New York, 1996.
6. Y.-W. Lee, R. D. Voyksner, Q.-C. Fang, C. E. Cook, and Y. Ito, *J. Liquid Chromatogr.* 11:153 (1988).
7. Y.-W. Lee, T. W. Pack, R. D. Voyksner, Q.-C. Fang, and Y. Ito, *J. Liquid Chromatogr.* 13:2389 (1990).
8. Y.-W. Lee, R. D. Voyksner, T. W. Pack, C. E. Cook, Q.-C. Fang, and Y. Ito, *Anal. Chem.* 62:244 (1990).
9. H. Oka, Y. Ikai, N. Kawamura, J. Hayakawa, K.-I. Harada, H. Murata, and M. Suzuki, *Anal. Chem.* 63:2861 (1991).
10. Z. Kong, K. L. Rinehart, R. M. Milberg, and W. D. Conway, *J. Liquid Chromatogr.* 21:65 (1998).



Creatinine and Purine Derivatives, Analysis by HPLC

M. J. Arin

M. T. Diez

P. Garcia-del Moral

J. A. Resines

Universidad de León, León, Spain

INTRODUCTION

Several compounds, such as creatinine and purine derivatives (allantoin, uric acid, hypoxanthine, and xanthine) present in biological samples, are important analytes for diagnoses of certain types of metabolic diseases and can serve as markers for these processes. Analyses for such substances are crucial for the diagnosis and monitoring of renal diseases, metabolic disorders, and various types of tumorigenic activity.

OVERVIEW

Creatinine results from the irreversible, nonenzymatic dehydration and loss of phosphate from phosphocreatine (Fig. 1). Creatinine is used as an indicator of skeletal muscle mass because it is a by-product of the creatine kinase reaction and it is one of the most widely used clinical markers to assess renal function. Urine levels of creatinine are good indicators of the glomerular filtration rate of the kidneys (i.e., the amount of fluid filtered per unit time).

Allantoin is the catabolic end product of purines in most mammals. It is formed by the action of the enzyme uricase on urate. Humans and other primates lack uricase and excrete urate as the final product of purine metabolism. However, small amounts of allantoin are present in human serum. Some authors demonstrated that free radical attack on urate generates allantoin. Therefore small amounts of allantoin detected in human serum may provide a marker of free radical activity *in vivo*.

Uric acid is the major product of catabolism of purine nucleosides adenosine and guanosine. Hypoxanthine and xanthine are intermediates along this pathway (Fig. 2). Under normal conditions, they reflect the balance between the synthesis and breakdown of nucleotides. Levels of these compounds change in various situations (e.g., they decrease in experimental tumors) when synthesis prevails over catabolism, and are enhanced during oxidative stress and hypoxia. Uric acid serves as a marker for tubular

reabsorption of nephrons, in addition to glomerular filtration rate. An imbalance in uric acid level can lead to gout—the formation of urate crystals in joints. Uric acid and xanthines are also markers for metabolic disorders such as Lesch–Nyhan syndrome and xanthinuria, to indicate a few.

However, creatinine and purine derivatives are very important in the field of animal nutrition because measurements of urinary excretion of these compounds have been proposed as an internal marker for microbial protein synthesis.

SAMPLE PREPARATION

Determination of these compounds is carried out frequently in biological fluids. Analysis in urine requires a previous filtration to remove cells and other particulate matter; then, the samples are diluted and directly injected onto the column. With cerebrospinal fluid, the samples are obtained by lumbar puncture; each aliquot is centrifuged and decanted before analysis. Often in plasma or serum, some form of protein removal is needed because the presence of these compounds in injected samples can cause modifications of the column and bias in chromatographic results. Protein removal can be performed by various methods such as protein precipitation, ultrafiltration, centrifugation, liquid-phase or solid-phase extraction, and column-switching techniques.

ANALYSIS OF CREATININE

For determination of creatinine, the nonspecific Jaffé method, although subject to perturbation by many interfering substances of endogenous and exogenous origin, is the most widely used. However, a batchwise kinetic procedure and flow injection analysis have shown the possibility to determine creatinine in human urine samples by this reaction, free from any systematic error.^[1] Enzymatic assays have higher specificities, but still suffer

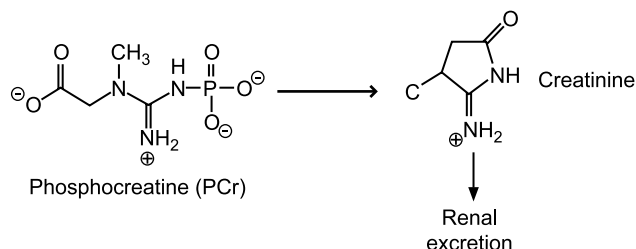


Fig. 1 Degradation of purine nucleotides and formation of purine derivatives.

from interferences. To avoid these problems, new analytical methods were developed: potentiometry, capillary electrophoresis (CE), and isotope dilution–gas chromatography–mass spectrometry (ID-GC-MS),^[2] with the latter being proposed as a reference method.

Chromatographic techniques have been very useful for clinical analysis, with advantages of simultaneous measurements of different components and elimination of interfering species. Previous reviews have been realized for the determination of creatinine.^[3] High-performance liquid chromatography (HPLC) methods include ion exchange chromatography, reversed-phase chromatography, ion pair chromatography, and micellar electrokinetic capillary chromatography (MEKC), and more complicated column-switching and tandem methods^[4] have been described as well.

Urinary creatinine can be analyzed by HPLC using a variety of columns. Detection methods include absorption, fluorescence after postcolumn derivatization, mass spectrometry, and some other methods. Review of recent

literature reveals that the method of choice for the measurement of creatinine has been RP-HPLC. C₈ and C₁₈ columns, and UV or electrochemical detection (ED) with isocratic elution or gradient elution were the most commonly used.^[5,6]

In most cases, reversed-phase ion pairing HPLC with UV photometric detection was used. The advantage of this technique is the broad range of parameters that may be conveniently adjusted to optimize the separation method; they include the concentration of organic modifier in the mobile phase, the type and concentration of buffer in the mobile phase, and the type and concentration of the counterion.^[7] In addition to ion exchange methods, some authors have developed a procedure for the determination of creatinine and a wide range of amino acids that provides for fixed-site ion exchangers and eliminates the addition of ion-pairing agent to the mobile phase.^[8] Creatinine has been analyzed in sera and tissues using HPLC and CE methods. Many of these determinations could also be applied to urinary creatinine analysis.

Various papers related to the simultaneous determination of creatinine and uric acid can be found in the literature. Several authors have developed capillary zone electrophoresis (CZE) methods for simultaneous analysis of these compounds in urine. The CE analysis of these renal markers offers some advantages when compared with chromatography, such as shortened separation time, reduced reagent consumption, and increased resolution. Capillary micellar electrokinetic chromatography has been applied to the simultaneous separation of creatinine and uric acid in human plasma and urine. However, chromatographic techniques are widely accepted for the determination of these compounds. Reversed-phase and ion

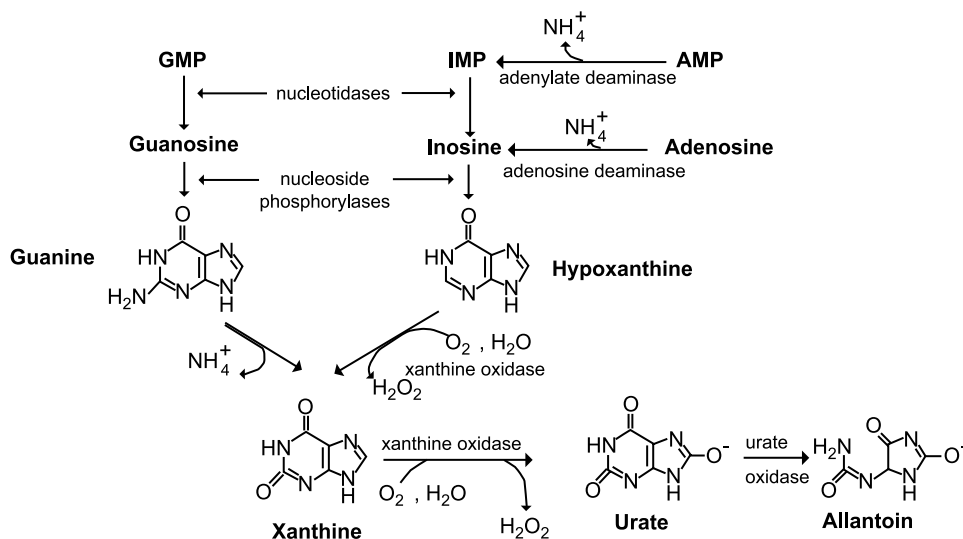


Fig. 2 Phosphocreatine metabolism.



pair HPLC methods have been applied for the simultaneous determination of these compounds in sera.^[9,10] These methods were consistent with the ID-GC-MS reference method.

PURINE DERIVATIVES: ALLANTOIN, URIC ACID, XANTHINE, AND HYPOXANTHINE

Traditionally, oxypurines allantoin, uric acid, and, in some cases, xanthines have been analyzed in biofluids by colorimetric methods.

The analysis of allantoin is based on the Rimini-Schrivver reaction, in which allantoin is converted to glyoxylic acid by sequential hydrolysis under alkaline and acidic conditions, and then derivatized with 2,4-dinitrophenylhydrazine to obtain the chromophore glyoxylate-2,4-dinitrophenylhydrazone.

The two predominant analyses of uric acid are the phosphotungstic acid (PTA) method and the uricase method. In the PTA method, urate reduces PTA to form a blue product. In the uricase analysis method, urate is oxidized by uricase oxidoreductase.

Xanthine and hypoxanthine have been often quantified colorimetrically or as uric acid following enzymatic conversion. Both approaches are problematic due to interference by compounds contained in biological fluids, whereas enzymatic conversion to uric acid has been often incomplete.

These photometric and enzymatic methods suffer from interferences by endogenous and exogenous compounds and can lead to inaccurate results. To avoid these problems, in recent years, CE, gas chromatography–mass spectrometry (GC-MS), and HPLC methods have been developed. Reversed-phase, normal phase, ion exchange, ion pair, column-switching, MEKC, and size exclusion chromatography were used for purine derivative determination.

Different methods, mostly colorimetric and chromatographic, for the determination of allantoin have been reviewed by Chen.^[11] The chromatographic procedures are mainly based on separation by HPLC using C₁₈ reversed-phase columns and monitoring at wavelengths around 200 nm. Many compounds present in plasma and urine also exhibit absorbance at these wavelengths; therefore, the detection of allantoin is not selective enough when the concentration is low (<60 μmol/L).^[11] To avoid this problem, allantoin can be converted, prior to elution, to a derivative, which can be monitored at a more specific detection wavelength. However, allantoin is an extremely polar compound that has poor retention on C₁₈ reversed-phase columns. To achieve a good separation from other polar compounds, the column length often needs to be extended (i.e., using long columns or two columns connected in series).^[12] Another way to overcome the

problem is the use of ion-pairing reagents to slow down the elution.^[11]

For uric acid, ID-GC-MS^[2] has been proposed as candidate reference method. Reversed-phase methods have been most widely employed. RP C₈ and C₁₈ columns, ranging from 150 to 250 mm in length and usually with an internal diameter of 3.9–4.6 mm, were used. Both isocratic elution and gradient elution were applied. Variable wavelength UV or diode array detectors are the most commonly used, in the range 210–292 nm. Electrochemical and online combination of UV with ED detection improves the selectivity and sensitivity of analysis and decreases the probability that interfering substances are present in analyte peaks. Some methods make use of ion exchange HPLC for the determination of uric acid and other organic compounds. In most cases, reversed-phase ion pairing HPLC methods were used to determine uric acid in biological samples. One of these^[13] has been proposed as a candidate reference method for the determination of uric acid. Data obtained by this method were compared with those from ID-GC-MS using [1,3-¹⁵N₂] uric acid as internal standard.

The main advantage of these methods is that they allow direct determination of urine samples, whereas plasma samples only need deproteinization; in addition, they offer the possibility to simultaneously determine other purine derivatives.

Various methods have been proposed for the simultaneous determination of uric acid and allantoin in different biological matrices. For urine samples, GC-MS was applied for the determination of both compounds.^[14] However, HPLC methods are still widely accepted.

Several HPLC methods have been reported for the determination of xanthine and hypoxanthine. Different RP-HPLC methods, using gradient elution and UV detection, have been described to determine these metabolites and other methylated purines.^[15] To improve xanthine determination in urine samples, analyses were carried out with two columns—reversed-phase column and anion exchange column—connected by a column switch.^[16] With this method, urinary hypoxanthine and xanthine can be measured without any sample preparation other than filtration.

Simultaneous determination of uric acid, hypoxanthine, and xanthine in different biological matrices such as urine, urinary calculi, cerebrospinal fluid, and plasma was carried out by RP-HPLC with isocratic elution and UV detection.^[17,18]

Various analytical methods for the simultaneous determination of allantoin, uric acid, and xanthine in biological samples, such as urine, blood plasma, and serum, have been described. These procedures are mainly based on separation by HPLC using reversed-phase C₁₈ columns, UV detection, and isocratic elution or gradient

elution. In some cases, allantoin was converted to a derivative with a chromophoric group, but other authors avoid the disadvantages of the allantoin derivatization process.^[19] The HPLC and CE methods have been compared for the determination of these compounds on plasma and atherosclerotic plaque. Comparison of results showed that CZE may have similar, or even superior, analytical performance to HPLC, especially for the determination of allantoin in biological samples.^[20]

SIMULTANEOUS DETERMINATION OF CREATININE AND PURINE DERIVATIVES

Several papers can be found in the literature concerning the simultaneous determination of creatinine and uric acid or various purine metabolites; however, only a few have reported the simultaneous determination of creatinine and purine derivatives.

Kochansky and Strein^[21] reviewed recent developments in chromatography and CE for the determination of creatinine, uric acid, and xanthine in biological fluids.

RP-HPLC procedures for the determination of creatinine and purine metabolites, such as allantoin, uric acid, xanthine, and hypoxanthine in ruminant urine, were described. Chromatography was achieved with a C₁₈ column under isocratic conditions, and detection at 218 nm without allantoin derivatization. The chromatographic conditions were a compromise between the sensitivity and specificity of the measurement of each analyte, analysis time, and resolution of all analyte peaks from interfering compounds.^[22,23] Uremic toxins creatine, creatinine, uric acid, and xanthine were simultaneously determined in human biofluids, simply after dilution, with UV detection at 200 nm. This method was compared, for creatinine and uric acid, with conventional routine methods and did not give significantly different results.^[24]

An ion pair HPLC method for the determination of creatinine and purine derivatives (allantoin, uric acid, and hypoxanthine in sheep urine) using allopurinol as internal standard is described.^[25] In this work, various variables were tested to optimize the simultaneous determination of these compounds, including alkyl chain length of the ion-pairing agent (C₆, C₈, and C₁₀), buffer concentration, pH, percentage of methanol of the mobile phase, and column temperature. The mobile phase composition was 10 mM phosphate buffer with 3 mM 1-octanesulfonic acid, sodium salt, pH 4, mixed with methanol:eluent A (5%) and eluent B (20%). The gradient program was 0–13 min, 0–100% B, flow rate 0.5 mL/min; 13–25 min, 100–0% B, flow rate 1.5 mL/min; reequilibration time at 0% B, 10 min. The injection volume was 20 μ L. The column temperature was set at 30°C. The chromatographic conditions adopted represented a compromise between

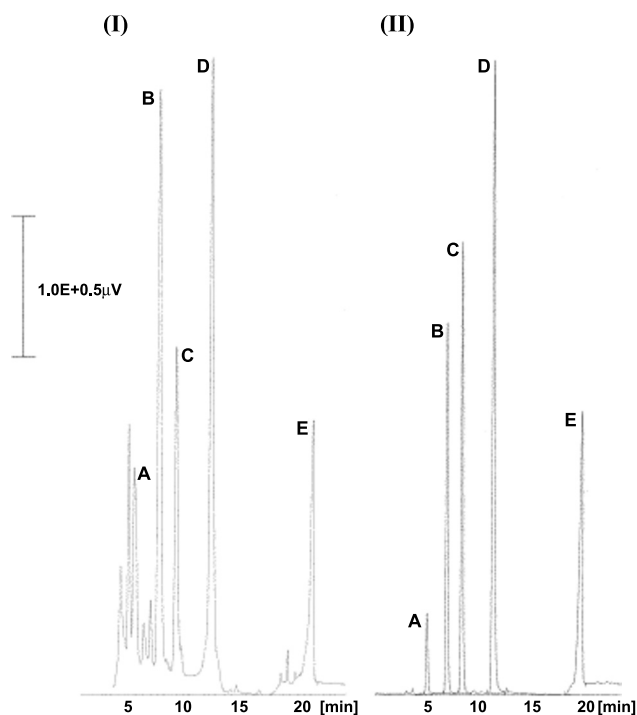


Fig. 3 (I) Chromatogram of 10-fold diluted sheep urine. (II) Chromatographic separation of standard solutions. Peaks: A=allantoin; B=uric acid; C=hypoxanthine; D=allopurinol (IS); and E=creatinine. (From Ref. [25].)

good separation and reasonable analysis time. Figure 3 shows the chromatograms resulting from the injection of pure standards and 10-fold diluted sheep urine sample under adopted chromatographic conditions. Under these conditions, there were no other endogenous urinary components that can interfere with the analyte peaks.

CONCLUSION

HPLC, when compared to other instrumental methods, presents significant advantages for the simultaneous analysis of creatinine and purine derivatives. The variety of instrumental and experimental conditions (columns, buffers, organic modifiers, detectors, etc.) of these methods reported in the literature offers versatility and flexibility. Chromatographic conditions for these analytes are not complicated when reversed-phase columns are employed. New stationary phases with high separation power provide short analysis times. The mobile phases used are also very simple ones (organic–water mixtures with controlled pH); both isocratic elution and gradient elution are recommended. Different sensitivity detectors (UV, electrochemical, fluorescence, and combined techniques such as HPLC-MS) are very valuable for the



identification of all analyzed compounds. In some cases, only CE shows some advantages over HPLC, such as short analysis time, reduced reagent consumption, and increased resolution. However, detection limits are often inferior when using UV absorbance detectors.

REFERENCES

- Campins, P.; Tortajada, L.A.; Meseger, S.; Blasco, F.; Sevillano, A.; Molins, C. Creatinine determination in urine samples by batchwise kinetic procedure and for injection analysis using the Jaffé reaction: Chemometric study. *Talanta* **2001**, *55*, 1079–1089.
- Thienpont, L.M.; Van Nieuwenhove, B.; Reinuer, H.; De Leenheer, A.P. Determination of reference method values by isotope dilution–gas chromatography–mass spectrometry: A five years' experience of two European reference laboratories. *Eur. J. Clin. Chem. Clin. Biochem.* **1996**, *34*, 853–860.
- Smith-Palmer, T. Separation methods applicable to urinary creatine and creatinine. *J. Chromatogr., B* **2002**, *781*, 93–106.
- Stokes, P.; O'Connor, G. Development of a liquid chromatography–mass spectrometry method for the high-accuracy determination of creatinine in serum. *J. Chromatogr., B* **2003**, *794*, 125–136.
- Hewavitharana, A.K.; Bruce, H.L. Simultaneous determination of creatinine and pseudouridine concentrations in bovine plasma by reversed-phase liquid chromatography with photodiode array detection. *J. Chromatogr., B* **2003**, *784*, 275–281.
- Mo, Y.; Dobberpuhl, D.; Dash, A.K. A simple HPLC method with pulsed EC detection for the analysis of creatine. *J. Pharm. Biomed. Anal.* **2003**, *32*, 125–132.
- Resines, J.A.; Arín, M.J.; Díez, M.T.; García del Moral, P. Ion-pair reversed-phase HPLC determination of creatinine in urine. *J. Liq. Chromatogr. Relat. Technol.* **1999**, *22* (16), 2503–2510.
- Yokoyama, Y.; Horikoshi, S.; Takahashi, T.; Sato, H. Low-capacity cation-exchange chromatography of ultraviolet-absorbing urinary basic metabolites using a reversed-phase column coated with hexadecylsulfonate. *J. Chromatogr., A* **2000**, *886*, 297–302.
- Werner, G.; Schneider, V.; Emmert, J. Simultaneous determination of creatine, uric acid and creatinine by high-performance liquid chromatography with direct serum injection and multi-wavelength detection. *J. Chromatogr.* **1990**, *525*, 265–275.
- Kock, R.; Seitz, S.; Delvoux, B.; Greiling, H. A method for the simultaneous determination of creatinine and uric acid in serum by high-performance-liquid-chromatography evaluated versus reference methods. *Eur. J. Clin. Chem. Clin. Biochem.* **1995**, *33*, 23–29.
- Chen, X.B. Determination of allantoin in biological, cosmetic and pharmaceutical samples. *J. AOAC Int.* **1996**, *79* (3), 628–635.
- Balcells, J.A.; Guada, J.M.; Peiro, J.A.; Parker, D.S. Simultaneous determination of allantoin and oxypurines in biological fluids by high-performance liquid chromatography. *J. Chromatogr.* **1992**, *575*, 153–157.
- Kock, R.; Delvoux, B.; Tillmanns, U.; Greiling, H. A candidate reference method for the determination of uric acid in serum based on high-performance liquid chromatography, compared with an isotope dilution–gas chromatography–mass spectrometer method. *J. Clin. Chem. Clin. Biochem.* **1989**, *27*, 157–162.
- Chen, X.B.; Calder, A.F.; Prasitkusol, P.; Kyle, D.L.; Jayasuriya, M.C.N. Determination of ¹⁵N isotopic enrichment and concentrations of allantoin and uric acid in urine by gas chromatography/mass spectrometry. *J. Mass Spectrom.* **1998**, *33*, 130–137.
- Di Pietro, M.C.; Vannoni, D.; Leoncini, R.; Liso, G.; Guerranti, R.; Marinello, E. Determination of urinary methylated purine pattern by high-performance liquid chromatography. *J. Chromatogr., B* **2001**, *751*, 87–92.
- Sumi, S.; Kidouchi, K.; Ohba, S.; Wada, Y. Automated determination of hypoxanthine and xanthine in urine by high-performance liquid chromatography with column switching. *J. Chromatogr., B* **1995**, *670*, 376–378.
- Safranow, K.; Zygmunt, M.; Ciechanowski, K. Analysis of purines in urinary calculi by high-performance liquid chromatography. *Anal. Biochem.* **2000**, *286*, 224–230.
- Kuracka, L.; Kalnovicova, T.; Liska, B.; Turcani, P. HPLC method for measurement of purine nucleotide degradation products in cerebrospinal fluid. *Clin. Chem.* **1996**, *42* (5), 756–760.
- Czauderna, M.; Kowalczyk, J. Quantification of allantoin, uric acid, xanthine and hypoxanthine in ovine urine by high-performance liquid chromatography and photodiode array detection. *J. Chromatogr., B* **2000**, *744*, 129–138.
- Terzuoli, L.; Porcelli, B.; Setacci, C.; Giubolini, M.; Cinci, G.; Carlucci, F.; Pagani, R.; Marinello, E. Comparative determination of purine compounds in carotid plaque by capillary zone electrophoresis and high-performance liquid chromatography. *J. Chromatogr., B* **1999**, *728*, 185–192.
- Kochansky, C.J.; Strein, T.G. Determination of uremic toxins in biofluids: Creatinine, creatine, uric acid and xanthines. *J. Chromatogr., B* **2000**, *747*, 217–227.
- Resines, J.A.; Arín, M.J.; Díez, M.T. Determination of creatinine and purine derivatives in ruminant's urine by reversed-phase high-performance liquid chromatography. *J. Chromatogr.* **1992**, *607*, 199–202.
- Shingfield, K.J.; Offer, N.W. Simultaneous determination of purine metabolites, creatinine and pseudouridine in ruminant urine by reversed-phase high-performance liquid chromatography. *J. Chromatogr., B* **1999**, *723*, 81–94.
- Samanidou, V.F.; Metaxa, A.S.; Papadoyannis, I.N. Direct simultaneous determination of uremic toxins: Creatine, creatinine, uric acid and xanthine in human biofluids by HPLC. *J. Liq. Chromatogr. Relat. Technol.* **2002**, *25* (1), 43–57.
- Del Moral, P.; Díez, M.T.; Resines, J.A.; Bravo, I.G.; Arín, M.J. Simultaneous measurements of creatinine and purine derivatives in ruminant's urine using ion-pair HPLC. *J. Liq. Chromatogr. Relat. Technol.* **2003**, *26* (17), 2961–2968.



Cross-Axis Coil Planet Centrifuge for the Separation of Proteins

Yoichi Shibusawa

School of Pharmacy, Tokyo University of Pharmacy and Life Science, Tokyo, Japan

Yoichiro Ito

National Heart, Lung, and Blood Institute, National Institutes of Health, Bethesda, Maryland, U.S.A.

Introduction

Countercurrent chromatography (CCC) is a form of support-free liquid-liquid partition chromatography in which the stationary phase is retained in the column with the aid of the Earth's gravity or a centrifugal force [1]. Partition of biological samples such as proteins, nucleic acids, and cells has been carried out using various aqueous polymer-phase systems [2]. Among many existing polymer-phase systems, PEG [poly(ethylene glycol)]-dextran and PEG-phosphate systems have been most commonly used for the partition of biological samples. Whereas these polymer-phase systems provide an ideal environment for biopolymers and live cells, high viscosity and low interfacial tension between the two phases tend to cause a detrimental loss of stationary phase from the column in the standard high-speed CCC centrifuge system (known as type J).

The cross-axis CPC (coil planet centrifuge), with column holders at the off-center position on the rotary shaft, enables retention of the stationary phase of aqueous-aqueous polymer-phase systems such as PEG 1000-potassium phosphate and PEG 8000-dextran T500 [3,4]. Since the last decade, various types of cross-axis CPC (types XL, XLL, XLLL, and L) have been developed for performing CCC with highly viscous aqueous polymer-phase systems. The separation and purification of protein samples, including lactic acid dehydrogenase [5], recombinant enzymes, profilin-actin complex, and so on, were achieved using these cross-axis CPCs [6].

Apparatus

The cross-axis CPCs which include types X and L and their hybrids are mainly used for protein separations. These modified versions of the high-speed CCC centrifuge have a unique feature among the CPC systems in that the system provides reliable retention of the sta-

tionary phase for viscous polymer-phase systems. Figure 1 presents a photograph of the type XLLL CPC unit and schematically illustrates the orientation and motion of the coil holder in the cross-axis CPC system, where R is a radius of revolution; there are five types of the cross-axis CPC in which the degree of the lateral shift of the coil holder is conventionally expressed by L/R . This parameter for type X, XL, XLL, XLLL, and L CPCs is 0, 1, 2, 3.5, and infinity, respectively. Our studies have shown that the stationary-phase retention is enhanced by laterally shifting the position of the coil holder along the rotary shaft, apparently due to the enhancement of a laterally acting force field across the diameter of the tubing.

The polymer-phase system composed of PEG and potassium phosphate has a relatively large difference in density between the two phases, so that it can be retained well in both XL and XLL column positions which provide efficient mixing of the two phases. On the other hand, the viscous PEG-dextran system, with an extremely low interfacial tension and a small density difference between the two phases, has a high tendency of emulsification under vigorous mixing. Therefore, the use of either the XLLL or L column position, which produces less violent mixing and an enhanced lateral force field, is required to achieve satisfactory phase retention of the PEG-dextran system.

The photograph of the XLLL cross-axis CPC ($L/R = 3.5$) equipped with a pair of multilayer coil separation columns is shown in fig. 1. The apparatus holds a pair of horizontal rotary shafts symmetrically, one on each side of the rotary frame, at a distance of 3.8 cm from the centrifuge axis. A spool-shaped column holder is mounted on each rotary shaft at an off-center position 13.5 cm away from the midpoint. Each multilayer coil separation column was prepared from a 2.6-mm-inner diameter (i.d.) PTFE (polytetrafluoroethylene) tubing by winding it onto the coil holder hub, forming multiple layers of left-handed coils.

Encyclopedia of Chromatography

DOI: 10.1081/E-Echr 120004636

Copyright © 2002 by Marcel Dekker, Inc. All rights reserved.



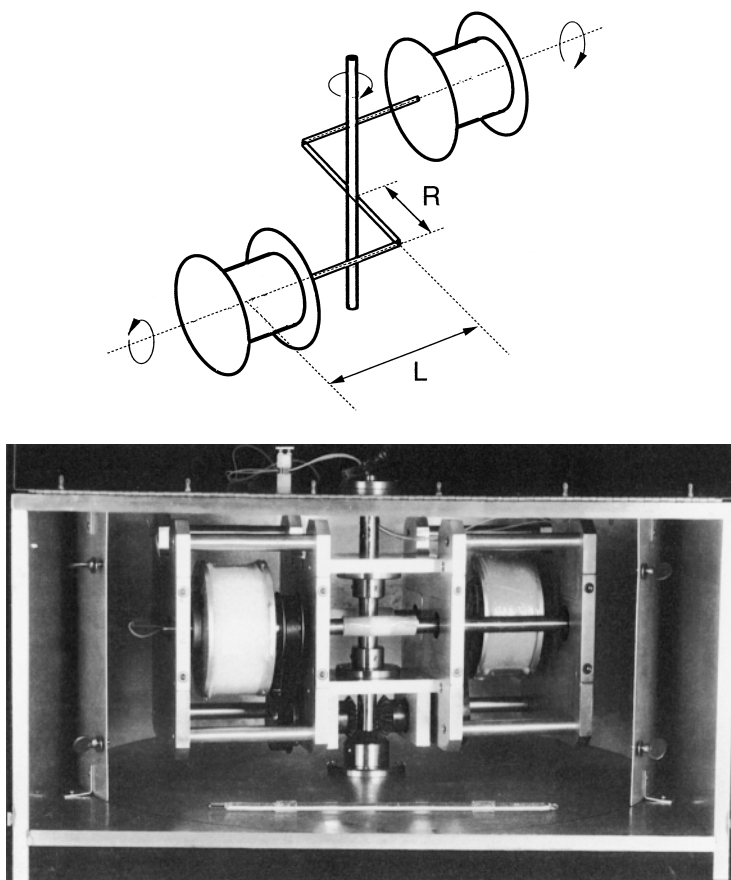


Fig. 1 Diagram of the cross-axis coil planet centrifuge and the photograph of the type XLCC CPC.

Polymer-Phase Systems for Protein Separation

Countercurrent chromatography utilizes a pair of immiscible solvent phases which have been preequilibrated in a separatory funnel: One phase is used as the stationary phase and the other as the mobile phase. A solvent system composed of 12.5% or 16.0% (w/w) PEG 1000 and 12.5% (w/w) potassium phosphate was usually used for the type XL and XLL cross-axis CPCs. These solutions form two layers; the upper layer is rich in PEG and the lower layer is rich in potassium phosphate. The ratio of monobasic to dibasic potassium phosphates determines the pH of the solvent system; this effect can be used for optimizing the partition coefficient of proteins.

A solvent system composed of 4.4% (w/w) PEG 8000, 7.0% (w/w) dextran T500, and 10 mM potassium phosphate is used with the type XLCC and L cross-axis

CPCs for separation of proteins which are not soluble in the PEG-phosphate system. This two-phase solvent system consists of the PEG-rich upper phase and dextran-rich lower phase. The cross-axis CPC may be operated in four different elution modes: P_IHO , $P_{II}TO$, P_ITI , and P_{IITHI} . The parameters P_I and P_{II} indicate the direction of the planetary motion where P_I indicates counterclockwise and P_{II} clockwise when observed from the top of the centrifuge. H and T indicate the head-tail elution mode, and O and I the inward-outward elution mode along the holder axis. In mode I (inward), the mobile phase is eluted against the laterally acting centrifugal force, and in mode O (outward), this flow direction is reversed. These three parameters yield a total of four combinations for the left-handed coils. Among these elution modes, the inward-outward elution mode plays the most important role in the stationary-phase retention for the polymer-phase sys-

tems. To obtain a satisfactory retention of the stationary phase, the lower phase should be eluted outwardly along the direction of the lateral force field (P_{IHO} and P_{ITO}) or the upper phase in the opposite direction (P_{ITI} or P_{IHI}).

Application of Cross-Axis CPC for Proteins

Type XL Cross-Axis CPC

The performance of the XL cross-axis CPC, equipped with a pair of columns with a 165-mL capacity, was evaluated for purification of lactic acid dehydrogenase (LDH) from a crude bovine heart filtrate. Successful separation of the LDH fraction was achieved with 16% (w/w) PEG 1000–12.5% (w/w) potassium phosphate at pH 7.3. The separation was performed at 500 rpm at a flow rate of 1.0 mL/min using the potassium phosphate-rich lower phase as a mobile phase. The sodium dodecyl sulfate–polyacrylamide gel electrophoresis (SDS–PAGE) analysis of the LDH fractions showed no detectable contamination by other proteins. The enzymatic activity was also preserved in these fractions.

Type XLL Cross-Axis CPC

The XLL cross-axis CPC, with a 250-mL capacity column, was used for the purification of recombinant enzymes such as purine nucleoside phosphorylase (PNP) and uridine phosphorylase (UrdPase) from a crude *Escherichia coli* lysate. The polymer-phase system used in these separations was 16% (w/w) PEG 1000–12.5% (w/w) potassium phosphate at pH 6.8. The separation was performed at 750 rpm at a flow rate of 0.5 mL/min using the upper phase as a mobile phase. About 1.0 mL of crude lysate, containing PNP in 10 mL of the above solvent system, was loaded into the multilayer coil. Purified PNP was harvested in 45-mL fractions. The SDS–PAGE analysis clearly demonstrated that PNP was highly purified in a one-step elution with the XLL cross-axis CPC.

The capability of the XLL cross-axis CPC was further examined in the purification of a recombinant UrdPase from a crude *E. coli* lysate under the same experimental conditions as described earlier. The majority of the protein mass was eluted immediately after the solvent front (between 105 mL and 165 mL elution volume), whereas the enzyme activity of UrdPase coincided with the fourth

protein peak (between 225 mL and 265 mL elution volume). The result indicated that the recombinant UrdPase can be highly purified from a crude *E. coli* lysate within 10 h using the XLL cross-axis CPC.

Type XLLL Cross-Axis CPC

Although PEG–phosphate systems yield a high-efficiency separation, some proteins show a low solubility due to a high salt concentration in the solvent system. In this case, the PEG–dextran polymer-phase system with a low salt concentration can be alternatively used for the separation of such proteins. Because the dextran–PEG system has a high viscosity and an extremely low interfacial tension, it tends to cause emulsification and loss of the stationary phase in the XLL or XL cross-axis CPCs. This problem is minimized using the XLLL cross-axis CPC, which provides a strong lateral centrifugal force to provide a more stable retention of the stationary phase.

Type L Cross-Axis CPC

This cross-axis CPC provides the universal application of protein samples with a dextran–PEG polymer-phase system. Using a prototype of the L cross-axis CPC with a 130-mL column capacity, profilin–actin complex was purified directly from a crude extract of *Acanthamoeba* with the same solvent system as used for the serum protein separation earlier. The sample solution was prepared by adding proper amounts of PEG 8000 and dextran T500 to 2.5 g of the *Acanthamoeba* crude extract to adjust the two-phase composition similar to that of the solvent system used for the separation. The experiment was performed by eluting the upper phase at 0.5 mL/min under a high revolution rate of 1000 rpm. The profilin–actin complex was eluted between 60 mL and 84 mL fractions and well separated from other compounds. The retention of the stationary phase was 69.0% of the total column capacity.

Conclusion

The overall results of our studies indicate that the retention of the stationary phase of polymer-phase systems in the cross-axis CPCs is increased by shifting the column holder laterally along the rotary shaft. Separation of proteins with high solubility in the PEG–phosphate system can be performed with the XL or XLL cross-axis CPC at a high partition efficiency. Proteins



with low solubility in PEG–phosphate systems may be separated with a dextran–PEG system using the XLLL or L cross-axis CPC, which provides more stable retention of the stationary phase.

References

1. W. D. Conway, *Countercurrent Chromatography: Apparatus and Applications*, VCH, New York, 1990.
2. P.-Å. Albertsson, *Partition of Cell Particles and Macromolecules*, 3rd ed., Wiley–Interscience, New York, 1986.
3. Y. Ito, E. Kitazume, and M. Bhatnagar, *J. Chromatogr.* 538:59 (1991).
4. Y. Ito, *J. Chromatogr.* 538:67 (1991).
5. Y. Shibusawa, Y. Eriguchi, and Y. Ito, *J. Chromatogr. B* 696:25 (1997).
6. Y. Shibusawa, in *High-Speed Countercurrent Chromatography* (Y. Ito and W. D. Conway, eds.), Chemical Analysis Series Vol. 132, Wiley–Interscience, 1996, p. 121.



CZE of Biopolymers

Feng Xu

Yoshinobu Baba

The University of Tokushima, CREST, JST, Tokushima, Japan

INTRODUCTION

Since Jorgenson and Lukacs^[1] separated peptides in 1981 using free zone electrophoresis in glass capillaries, capillary electrophoresis (CE) has become a highly efficient technique for the separation of biopolymers such as proteins, peptides, carbohydrates, and DNA. Free solution CE, or capillary zone electrophoresis (CZE), is an electrophoresis in free homogeneous solution.^[2,3] Charged solutes are simply separated on the basis of the solute charge-to-mass ratio, applied electric field, and the pH and ionic strength of the background electrolyte (BGE).

Separation of DNA is generally conducted by capillary gel electrophoresis (CGE), in which gel or polymer solutions act as sieving media, rather than by CZE, because each DNA has the same charge-to-mass ratio. The CZE separation of DNA can only be achieved by using some special modifications to break the charge-to-mass symmetry through either trapping analytes into sodium dodecyl sulfate (SDS) micelles or labeling analytes with large and weakly charged molecules at the DNA fragment ends (end-labeled free-solution electrophoresis).^[4] Separation of DNA is not covered here. Interested readers are referred to our previous articles,^[5,6] dealing with DNA size separation and sequencing, in the *Encyclopedia of Chromatography*. Here we concentrate on the CZE separations of three kinds of biopolymers (proteins, peptides, and carbohydrates), including the factors influencing the separations and the promising development of CZE in microchip and capillary array platforms.

PROTEINS AND PEPTIDES

Proteins are key participants in all biological activities. Peptides, generally shorter than proteins, have important biological functions, as hormones, neurotransmitters, etc. Owing to the similarity in structure, the general principles of the separations of proteins and peptides are alike. A semiempirical relation exists between mobility, charge, and size of a peptide or protein:

$$\mu = A \frac{q}{M^p} + B$$

where μ is mobility, q is charge, M is molecular mass, A and B denote empirical constants, and p varies from 1/3 to 2/3 as a function of the pH and ionic strength of BGE, and shape of peptides and proteins, etc. For a protein, the most difficult part is estimation of the charge.^[7]

Sample Preconcentration

The CZE of a low concentration protein or peptide requires preconcentration of the sample before analysis, either off-line or on-line. Preconcentration is commonly performed by using solid-phase packing material at the inlet end of the capillary and is based on chromatographic or electrophoretic principle. Solid-phase extraction (SPE) on C₁₈ or C₈ cartridges can be on-line connected to CZE and the concentrated nonspecific analytes are released by an organic solvent (e.g., acetonitrile).^[8] Alternatively, specific analytes can be concentrated by the use of antibody-containing cartridges and enzyme-immobilized microreactors. Desalting is important in protein processing. Microdialysis sampling can be used for the desalting of samples prior to introduction into electrospray ionization mass spectrometry (ESI-MS). Capillary isoelectric focusing (CIEF), with slow ramping of voltage, can achieve on-line desalting of proteins in cerebrospinal fluid. Head column stacking has a long history and is now a popular technique in which the injected sample is simply dissolved in water and is focused at the interface between the sample plug and separation buffer, as a result of different mobilities in the two solutions. Capillary isotachopheresis (CITP) can also be utilized to achieve on-column sample preconcentration. The sample is introduced as a plug between a leading electrolyte, which has a higher mobility than the sample, and a trailing electrolyte, which has a lower mobility than the sample. After applying the voltage, the sample components are focused as a concentrated band. Very large sample zones can be accommodated by isotachopheresis to enhance the limit of detection.^[9]

Detection

Peptide bonds enable proteins and peptides to be directly detected by ultraviolet (UV) radiation, at 200–220 nm, where the absorption is proportional to the number of



peptide bonds. Sometimes, detection is performed around 254 or 280 nm, where proteins have modest absorbance in the presence of aromatic residues. However, the sensitivity of UV detection is relatively poor (mM to μ M). Several commercially available Z-type cells and bubble-shaped cells can help, somewhat, in improving the sensitivity.

Laser-induced fluorescence (LIF) produces low limits of detection and a wide dynamic range. Native fluorescence of proteins is primarily associated with emission from tryptophan and tyrosine, between 300 and 400 nm. Proteins are easy to derivatize with a fluorescent reagent prior to electrophoresis. Postcolumn derivatization can be performed in sheath flow systems where the sheath flow cell acts as a postseparation labeling reactor. To avoid the formation of a mixture of multiply labeled products for originally single species, some special procedures utilizing Edman degradation chemistry or fluorescein isothiocyanate (FITC) labeling at lower than normal derivatization buffer pH have been developed. Noncovalent labeling is performed with dyes that interact with proteins, either by H bonding or through hydrophobic interactions. The sensitivity of LIF approaches the absolute limit of detection of a single molecule. A number of fluorescent dyes are widely used,^[10] such as fluorescamine, 1-anilinonaphthalene-8-sulfonic acid, 4,4'-dianilino-1,1'-binaphthyl-5,5'-disulfonic acid, 2-(*p*-toluidino)-naphthalene-6-sulfonic acid, 3-(2-furoyl)quinoline-2-carboxaldehyde, naphthalene-2,3-dicarboxaldehyde, 4-chloro-7-nitrobenzofurazan, 4-fluoro-7-nitrobenzofurazan, *o*-phthalaldehyde-2-mercaptoethanol, and 3-(4-carboxybenzoyl)-2-quinolinecarboxaldehyde, etc.

Mass spectrometric detection has come into frequent use, as it provides significant information relating to the solute structure. Protein analysis using CZE-MS has been applied to abundant proteins in a single cell after the single intact cell was introduced into a separation capillary and after being lyzed. On the other hand, ESI-MS is a soft ionization technique that can form molecular ions. On-line ESI detection requires an external interface and volatile buffers to avoid contamination of the ionization chamber. Proteins can also be off-line identified by matrix-assisted laser desorption ionization/time-of-flight mass spectrometry (MALDI-TOF-MS), in which the matrix utilizes a low-molecular-weight organic acid that absorbs laser light and dissipates the energy in such a way that protein is evaporated, usually in a single protonated form. Time of flight has an advantage of having no upper mass-to-charge limit.

Coatings and Additives

The interaction of proteins with the negative charges of the ionized silanol groups on the inner capillary wall

should be overcome prior to separation. The interaction results in peak tailing, poor resolution, unstable electroosmotic flow (EOF), and sample adsorption loss. A variety of approaches have been developed to overcome this problem, including the use of extreme buffer pH, coated capillaries, and additives in BGE.

The simplest way is to use extreme buffer pH, i.e., either a low pH at which the dissociation of silanol groups is suppressed so as to prevent their electrostatic interactions with positively charged polypeptides, or an alkaline pH that is at least two units above the isoelectric point of an analyzed polypeptide, which leads to electrostatic repulsion between the negatively charged polypeptide and the negatively charged silanol groups on the capillary wall. Unfortunately, even proteins that behave as anions still have a positively charged section on their surface that can interact with the capillary wall. In addition, more extreme pHs may denature proteins.

Static wall coatings are usually made by reacting the capillary wall with a small bifunctional reagent, which is then used to bind a polymer to the wall. The polymer is usually prepared in situ. γ -methacryloxypropyltrimethoxysilane is a classical bifunctional reagent, while polyacrylamide is a frequently used polymer for coatings. A variety of polymer coatings can be anchored onto capillaries, such as polystyrene, polybrene, polyvinyl alcohol, polyethyleneimine, polyethylene glycerol, polyvinylpyrrolidone, polyethylene oxide, and nonionic surfactant coatings. Hydrophilic coating, epoxy-poly(dimethylacrylamide), can separate proteins over the range of pH 4–10 with the recovery of both cationic and anionic proteins over 90%.

Dynamic wall coatings are replaceable. There are two kinds of dynamic coatings: One is performed by introducing a neutral polymer to the BGE, and the other is performed by adding ions to the BGE. The neutral polymers not only shield capillary wall from interactions with solutes, but also increase the viscosity in the electric double layer and reduce EOF. Various cellulose derivatives and other hydrophilic polymers, such as polyvinyl alcohol, polyethyleneoxide, hydroxyethyl cellulose, copolymer of hydroxypropylcellulose and hydroxyethylmethacrylate, and polysaccharide guaran, have been used for this purpose. Ionic (mainly cationic) additives titrate the negative charge of the capillary wall so that the EOF is decreased, neutralized, or even reversed. Polyionic species reduce the pH dependence of the EOF if, for example, the coating contains sulfonic acid groups that are fully ionized over a wide pH range. One can also add, to the BGE,^[11,12] oligoamines such as putrescine, spermine, and tetraethylene pentamine, cationic surfactants such as cetyltrimethylammonium bromide (CTAB) and didodecyltrimethylammonium bromide (DDAB), high concentration of anionic surfactants such as SDS,

zwitterionic phospholipids such as 1,2-dilauroyl-*sn*-phosphatidylcholine, high concentration of alkali salts and phytic acid, other compounds such as cyclodextrins, etc. A mixture of cationic and anionic fluorosurfactants pro-

duces efficient separations of acidic and basic proteins in a single run at neutral pH. Zwitterionic surfactants are typically superior to the nonionogenic ones. The protein interactions with the capillary wall are inversely proportional to the critical micellar concentration (CMC) of surfactants.

In addition to reducing the adsorption, the dynamic additives also play important roles in selectivity enhancement. pH is an important option for protein and peptide separation. An increase in the buffer ionic strength can increase the resolution. Any ion that displays a preferential affinity with the peptides has a potential modifying effect on the selectivity. The addition of organic modifiers, e.g., methanol, ethanol, and acetonitrile, in the BGE, can induce different solvation of the peptide chains and modify the migration order and selectivity of peptides. For separation of very hydrophobic proteins, e.g., lipoproteins, surfactants can act as buffer additives to improve solubilization.

Using amphoteric, isoelectric buffers at pH close to their isoelectric points (pI), at which the electrolytes have a net charge of zero, is an efficient way to decrease the BGE conductivity and apply extremely high field strength. Thus the separation time can be reduced to the order of a few minutes, and high resolution is achieved as a result of minimal diffusion-driven peak spreading. Several acidic isoelectric buffers, such as cysteic acid (pI 1.85), iminodiacetic acid (pI 2.23), aspartic acid (pI 2.77), and glutamic acid (pI 3.22), all at 50 mM concentration,^[13] have been used in CZE separation of proteins and peptides. Fig. 1 shows a decrease of total running time from 70 to 12 min when using an isoelectric solution.

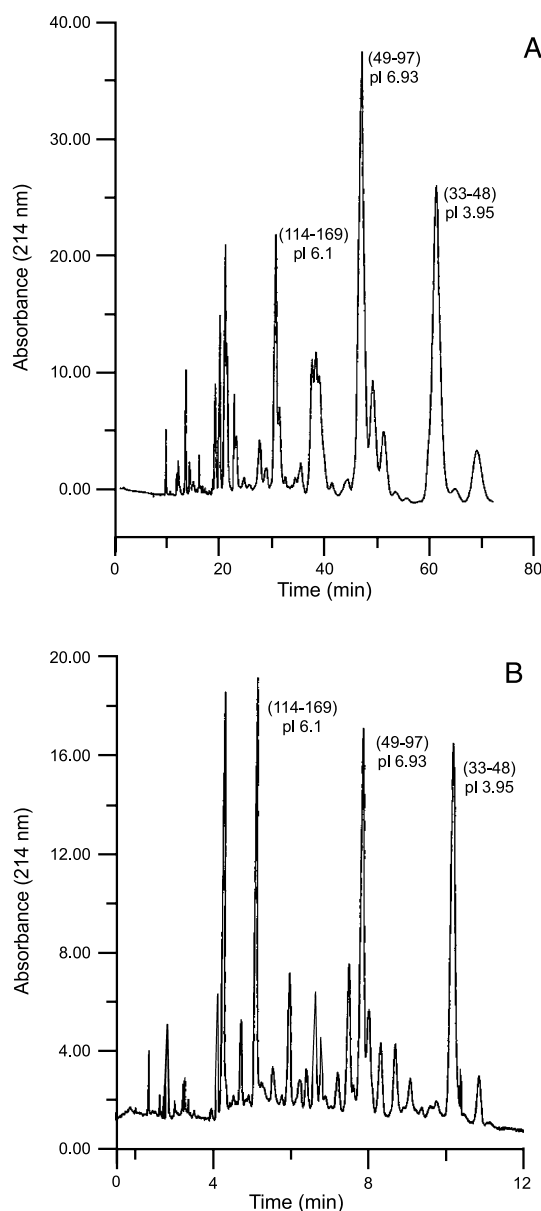


Fig. 1 Capillary zone electrophoresis of tryptic digests of β -casein in 100 mm i.d. \times 37-cm capillary. (A) BGE: 80 mM phosphate buffer, pH 2.0; injection: 0.5 p.s.i. for 3 sec; applied field strength: 110 V/cm. The three major peaks are: 1) pI 6.1, fragment β -CN (114–169); 2) pI 6.93, fragment β -CN (49–97); and 3) pI 3.95, fragment β -CN (33–48). Note that the total running time is 70 min. (B) BGE: 50 mM isoelectric aspartic acid (pH = pI = 2.77) added with 0.5% hydroxyethyl cellulose (HEC) (M_n 27,000 Da) and 5% trifluoroethanol; applied field strength: 600 V/cm. (From Ref. [13].)

CARBOHYDRATES

Carbohydrates are the third most important class of biopolymers, next to proteins and DNA. However, their analyses by CZE are still in infancy because of the complexity and diversity of their structures. In terms of ionization ability, carbohydrates may be divided into acidic and weakly ionizable classes. Acidic carbohydrates are negatively charged at neutral pH and can be conveniently separated. Weakly ionizable carbohydrates are neutral at mild pH, but deprotonate at extremely basic condition (e.g., pH > 12).

Underivatized Carbohydrates

The borate buffer is the most effective buffer for the CZE separation of native (and derivatized) carbohydrates. Borate complexes with adjacent hydroxyl groups on carbohydrates to form a negatively charged complex, which has a 2- to 20-fold increased UV absorbance at 195 nm.^[9]



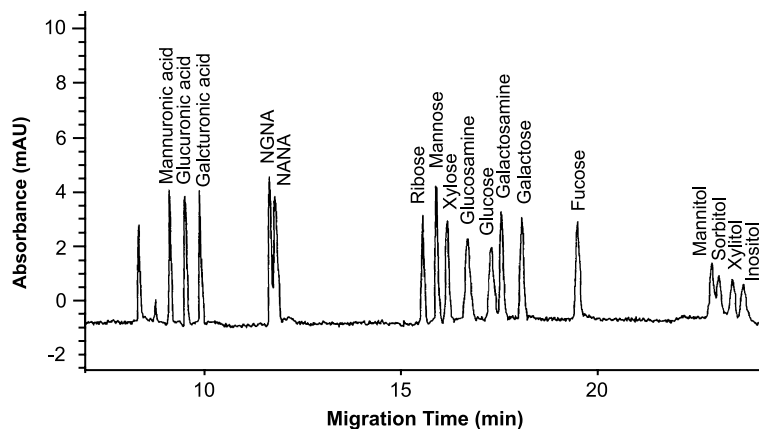


Fig. 2 Capillary zone electrophoresis of saccharides (1 mM each) standard mixture. Capillary: Fused silica, 50 μm i.d. \times 80.5 cm (72-cm effective length); BGE: 20 mM 2,6-pyridinedicarboxylic acid (PDC) and 0.5 mM CTAB, pH 12.1; voltage: -25 kV. The signal wavelength was set at 350 nm with a reference at 275 nm. (From Ref. [14].)

The stability of sugar–borate complexes increases with increasing pH and borate concentration, and depends on the number and configuration of the hydroxyl groups. The presence of a surfactant (e.g., tetrabutylammonium) in a borate buffer also enhances the solute selectivity by interacting with anionic borate–sugar complexes. Saccharides, e.g., sucrose, glucose, fructose, etc. can also be separated by chelating with Cu^{2+} present in the BGE. Elevated temperature up to 60°C facilitates the enhancement of resolution and efficiency.

Underivatized carbohydrates are mainly detected using low-wavelength UV (at 190–200 nm), indirect UV, or indirect LIF. The indirect method is based on the physical displacement of analytes with the added chromophoric or fluorophoric compounds in the BGE. Indirect UV detection, using sorbic acid as both carrier electrolyte and chromophore, and employing high pH to achieve ionization of saccharides, permits the analysis of underivatized saccharides in low concentration. Fig. 2 shows the separation of underivatized acidic, neutral, and amino sugars and sugar alcohols by CZE-indirect UV.^[14] Capillary electrophoresis-pulsed amperometric detection (CE-PAD) in the analysis of oligosaccharides derived from glycopeptides provides structural information through simply modulating the detection potentials. Refractive index detection is a universal detection and is also useful for oligosaccharide analysis. However, the detection limit is rather poor.

Derivatized Carbohydrates

Derivatization provides the advantage of incorporating chromophoric or fluorophoric functions into carbohydrates to achieve highly sensitive detection. Electromi-

gration can also be achieved by derivatization of neutral saccharides with reagents possessing ionizable functions. Derivatization of the reducing aldehyde and/or keto groups present in carbohydrates can be performed by reductive amination and condensation reaction.

The reaction of reductive amination is based on the reducing end of a saccharide reacting with the primary amino group of a chromophoric or fluorophoric reagent to form a Schiff base that is subsequently reduced to a stable secondary amine. For example, in the reductive amination of malto-oligosaccharides, 8-aminonaphthalene-1,3,6-trisulfonic acid (ANTS) introduces both electric charge and fluorescence to the saccharides.^[15] The products are ionized at a pH as low as 2.5, allowing CZE of carbohydrates under conditions where both EOF and adsorption to the internal capillary wall are negligible, even in the absence of any coating. Aminobenzoic acid and related compounds have the merit to react with both ketoses and aldoses of oligosaccharides in less than 15 min at 90°C . Such fast reactions could be compatible with the CE separation speed. Other conventional fluorophores for carbohydrate labeling include 8-aminopyrene-1,3,6-trisulfonate (APTS), 7-amino-4-methylcoumarin, 3-(4-carboxybenzoyl)-2-quinolinecarboxaldehyde, 2-aminobenzamide, 4-aminobenzoate, 4-aminobenzonitrile, etc.

The derivatization of aldehydes in reducing carbohydrates can also be performed by a condensation reaction between the active hydrogens of 1-phenyl-3-methyl-5-pyrazolone (PMP) and the aldehyde functionality under slightly basic condition. The formed bis-PMP derivatives can be separated by CZE and detected by UV absorbance.^[16] Oligosaccharides can also be separated as complexes with a variety of compounds, including acetate, molybdate, germanate, stannate, arsenite, wolframate, vanadate, and tellurate of various alkali and alkaline

earth metal ions. In a BGE containing calcium, barium, or strontium acetate, a mixture of PMP-derivatized reducing carbohydrates such as arabinose, ribose, galactose, glucose, and mannose was fully resolved.^[16]

Glycoprotein analysis requires both protein and glycan identification. Capillary electrophoresis/laser-induced fluorescence (CE-LIF) is widely used in the fingerprinting of fluorescently labeled glycans and in detection differences in maps of the oligosaccharides released from glycoproteins. The analysis of the complete composition of saccharides occurring in glycoproteins can be performed by separating the hydrolyzed sugars using CZE. Useful information about the glycoprotein structure can be obtained by combining CZE with MALDI-MS and ESI-MS. The techniques are well suited for the sensitive determination of the degree of heterogeneity, the site of glycosylation in a protein, and the composition and branching patterns of *N*- and *O*-linked glycans.

CONCLUSION

Capillary zone electrophoresis, with its automation, simplicity, and rapid method development, is an attractive choice for biopolymer separation. Future methodological advances include novel capillary wall coatings, specific buffer additives, effective sample preconcentration, and highly sensitive detection. At the same time, CZE development will move toward two promising directions: High-throughput and ultrafast separations (in seconds not minutes). Previously, CZE was a sequential technique, which allowed analysis of one sample per analysis. One remedy to this problem is the use of the capillary array electrophoresis (CAE) technique. Array instruments use 100 or more capillaries in parallel, with the laser excited fluorescence signals from each channel simultaneously recorded, e.g., by a charge-coupled device (CCD) array. Another remedy for fast analysis is the use of microchip-based CE devices. All operations, e.g., sample manipulation, separation, and detection, are performed on the microstructures of the chips. The short sample injecting plug, essentially zero dead volume intersections, and high field strength result in extremely rapid and high efficient separation.^[17] The advantage of microfabricated devices is also the potential of producing arrays of separation channels for high-throughput applications in a single run. After solving some technical problems, the microchip-based separations are expected to become a highly powerful tool in future separations of biopolymers.

REFERENCES

1. Jorgenson, J.W.; Lukacs, K.D. Zone electrophoresis in open-tubular glass capillaries. *Anal. Chem.* **1981**, 53 (8), 1298–1302.
2. *Capillary Electrophoresis in Analytical Biotechnology*; Righetti, P.G., Ed.; CRC Press: Boca Raton, FL, 1996.
3. *Capillary Electrophoresis—Theory and Practice. New Directions in Organic and Biological Chemistry Series*; Camilleri, P., Ed.; CRC Press: Boca Raton, FL, 1997.
4. Heller, C.; Slater, G.W.; Mayer, P.; Dovichi, N.; Pinto, D.; Viovy, J.-L.; Drouin, G. Free-solution electrophoresis of DNA. *J. Chromatogr., A* **1998**, 806 (1), 113–221.
5. Baba, Y. DNA Sequencing Studies by CE. In *Encyclopedia of Chromatography*; Cazes, J., Ed.; Marcel Dekker, Inc.: New York, 2001; 259–261.
6. Kiba, Y.; Baba, Y. Nucleic Acids, Oligonucleotides, and DNA: Capillary Electrophoresis. In *Encyclopedia of Chromatography*; Cazes, J., Ed.; Marcel Dekker, Inc.: New York, 2001; 556–560.
7. Kašička, V. Recent advances in capillary electrophoresis of peptides. *Electrophoresis* **2001**, 22 (19), 4139–4162.
8. Dolník, V.; Hutterer, K.M. Capillary electrophoresis of proteins 1999–2001. *Electrophoresis* **2001**, 22 (19), 4163–4178.
9. Krylov, S.N.; Dovichi, N.J. Capillary electrophoresis for the analysis of biopolymers. *Anal. Chem.* **2000**, 72 (12), 111R–128R.
10. Bardelmeijer, H.A.; Waterval, J.C.M.; Lingeman, H.; van't Hof, R.; Bult, A.; Underberg, W.J.M. Pre-, on-, and post-column derivatization in capillary electrophoresis. *Electrophoresis* **1997**, 18 (12–13), 2214–2227.
11. Tabuchi, M.; Baba, Y. A separation carrier in high-speed proteome analysis by capillary electrophoresis. *Electrophoresis* **2001**, 22 (16), 3449–3457.
12. Cunliffe, J.M.; Barylá, N.E.; Lucy, C.A. Phospholipid bilayer coatings for the separation of proteins in capillary electrophoresis. *Anal. Chem.* **2002**, 74 (4), 776–783.
13. Righetti, P.G.; Nembri, F. Capillary electrophoresis of peptides in isoelectric buffers. *J. Chromatogr., A* **1997**, 772 (1–2), 203–211.
14. Soga, T.; Heiger, D.N. Simultaneous determination of monosaccharides in glycoproteins by capillary electrophoresis. *Anal. Biochem.* **1998**, 261 (1), 73–78.
15. El Rassi, Z. Recent developments in capillary electrophoresis and capillary electrochromatography of carbohydrate species. *Electrophoresis* **1999**, 20 (15–16), 3134–3144.
16. Honda, S.; Yamamoto, K.; Suzuki, S.; Ueda, M.; Kakehi, K. High-performance capillary zone electrophoresis of carbohydrates in the presence of alkaline earth metal ions. *J. Chromatogr.* **1991**, 588 (1–2), 327–333.
17. Effenhauser, C.S.; Bruin, G.J.M.; Paulus, A. Integrated chip-based capillary electrophoresis. *Electrophoresis* **1997**, 18 (12–13), 2203–2213.

Dead Point (Volume or Time)

Raymond P.W. Scott

Scientific Detectors Ltd., Banbury, Oxfordshire, England

Introduction

The *injection point* on a chromatogram is that position where the sample is injected. The *dead point* on a chromatogram is the position of the peak maximum of a completely unretained solute. The different attributes of the chromatogram are shown in Fig. 1. The *dead time* is the elapsed time between the injection point and the dead point. The volume that passes through the column between the injection point and the dead point is called the *dead volume*.

Discussion

If the mobile phase is *incompressible*, as in liquid chromatography (LC), the *dead volume* (as so far defined) will be the simple product of the *exit* flow rate and the dead time. However, in LC, where the stationary phase is a porous matrix, the dead volume can be a very ambiguous column property and requires closer inspection and a tighter definition.

If the mobile phase is compressible, the simple product of dead time and flow rate will be incorrect, and the dead volume must be taken as the product of the dead time and the *mean* flow rate. The dead volume has been shown to be given by [1]

$$V_0 = V'_0 \frac{3}{2} \left(\frac{\gamma^2 - 1}{\gamma^3 - 1} \right) = Q_0 t_0 \frac{3}{2} \left(\frac{\gamma^2 - 1}{\gamma^3 - 1} \right)$$

where the symbols have the meaning defined in Fig. 1, and V'_0 is the dead volume measured at the column exit and γ is the inlet/outlet pressure ratio.

The dead volume will not simply be the total volume of mobile phase in the column system (V_m) but will include extra-column dead volumes (V_E) comprising volumes involved in the sample valve, connecting tubes, and detector. If these volumes are significant, then they must be taken into account when measuring the dead volume.

There are two types of dead volume (i.e., the *dynamic* dead volume and the *thermodynamic* dead volume [2]). The dynamic dead volume is the volume of

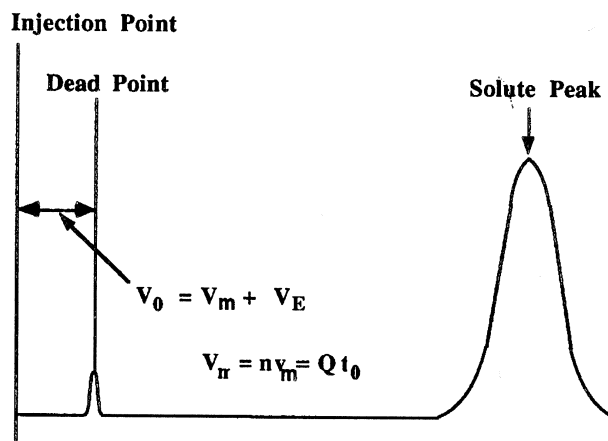


Fig. 1 Diagram depicting the dead point, dead volume, and dead time of a chromatogram. If the mobile phase is not compressible, then V_0 is the total volume passed through the column between the point of injection and the peak maximum of a completely unretained peak, V_m is the total volume of the mobile phase in the column, V_E is the extra column volume of the mobile phase, v_m is the volume of the mobile phase per theoretical plate, t_0 is the time elapsed between the time of injection and the retention time of a completely unretained peak, n is the number of theoretical plates in the column, and Q is the column flow rate measured at the exit.

the *moving phase* in the column and is used in kinetic studies to calculate mobile-phase velocities. In gas chromatography, both the dynamic dead volume and the thermodynamic dead volume can be taken as the difference between the dead volume and the extra-column volume. In LC, however, where a porous packing is involved, some of the mobile phase will be in pores (the *pore volume*) and some between the particles (the *interstitial volume*). In addition, some of the mobile phase in the interstitial volume which is close to the points of contact of the particles will also be stationary. The dynamic dead volume (i.e., the volume of the moving phase) is best taken as the retention volume of a relatively large inorganic salt such as potassium nitroprusside. This salt will be excluded from the pores of the packing by ionic exclusion and



will only explore the moving volumes of the mobile phase [2]. The thermodynamic dead volume will include all the mobile phase that is available to the solute that is under thermodynamic examination. It is best measured as the retention volume of a solvent sample of very similar type to that of the mobile phase and of small molecular weight. If a binary solvent mixture is used (which is the more common situation), then one component of the mobile phase, in pure form, can be used to measure the thermodynamic dead volume. Careful consideration must be given to the measurement of the column dead volume when determining thermodynamic data by LC using columns packed with porous materials.

References

1. R. P. W. Scott, *Introduction to Analytical Gas Chromatography*, Marcel Dekker, Inc., New York, 1998, p. 77.
2. A. Alhedai, D. E. Martire, and R. P. W. Scott, *Analyst* 114: 869 (1989).

Suggested Further Reading

Scott, R. P. W., *Liquid Chromatography Column Theory*, John Wiley & Sons, Chichester, 1992, p. 19.
Scott, R. P. W., *Techniques and Practice of Chromatography*, Marcel Dekker, Inc., New York, 1996.



Degassing of Solvents

Richard DeMuro

Shimadzu Scientific Instruments, Inc., Columbia, Maryland, U.S.A.

Introduction

Degassing, an important step in the preparation of high-performance liquid chromatography (HPLC) mobile phases, is used to remove dissolved atmospheric gases from mobile-phase solvents which may interfere with the normal operation of the HPLC pump and detector. Bubbles that form when these gases come out of solution may result in loss of pump prime and other irregularities, such as inaccurate and irreproducible flow, ultimately resulting in inconsistent retention times and noisy or drifting chromatographic baselines.

Discussion

A bubble in the detector's flow cell typically manifests itself as a "spike" which may hinder peak detection and integration. Dissolved oxygen poses special problems such as baseline shifts caused by the formation of ultraviolet (UV) absorbing O₂-solvent complexes and diminished fluorescence response (quenching).

Three methods are commonly used to degas HPLC solvents: applying a vacuum, helium sparging, or using an in-line membrane degassing device.

Vacuum Degassing

Applying a vacuum for several minutes (alone, or in combination with filtration) to a solvent reservoir is an inexpensive, effective method of degassing. It is typically performed with a side-arm filtration flask and a vacuum aspirator attached to a laboratory faucet. Alternatively, a vacuum pump may be used. Care must be taken when employing vacuum degassing. Because it is an off-line, noncontinuous process, its long-term effectiveness is limited, as air will begin to redissolve as soon as the vacuum is removed. Complete resaturation of the mobile phase will occur within several hours. It is most effective when used on premixed solvents for isocratic separations and is generally unacceptable when performing gradient separations with a low-pressure

solvent proportioning device. In addition, vigorous vacuum degassing may alter the composition of mixed solutions as the more volatile organic components (e.g., methanol, acetonitrile, etc.) are selectively evaporated. This may lead to variability in the retention times of separations performed with different batches of mobile phase.

Helium Degassing

Bubbling helium through a solvent, a technique known as sparging, is a highly effective means of degassing. The rationale behind such an approach is that the helium will displace all other gases present in the solvent, but because the solubility of helium is low in virtually all solvents, the helium-saturated solution is immune from the problems of air-saturated mobile phases. In practice, ultrapure helium is delivered from a gas cylinder and connected to a high-porosity frit via Teflon or similar polymeric tubing. The frit is placed at the bottom of the solvent reservoir and a relatively high flow rate of helium is allowed to bubble through the mobile phase for several minutes. Once the solvent is degassed, the helium flow rate is stopped or, more typically, reduced to a trickle to maintain a continuous deaerated state. Many helium degassing devices are available commercially, including those that allow the solvent reservoirs to be sealed. After the helium flow is reduced to a trickle, the reservoir is sealed, thus blanketing the mobile phase with helium, pressurizing the reservoir, and conserving the sparge gas.

Continuous helium degassing is extremely useful when performing low- or high-pressure solvent proportioning. However, like vacuum degassing, care must be exercised when sparging at high helium flow rates to avoid selective evaporation of the more volatile components of a mixture.

In-Line Membrane Degassing

The third common method of degassing performs its function continuously as mobile-phase solvents flow through it. An in-line membrane degasser consists of a



vacuum chamber housing coils of gas-permeable tubing, typically composed of thin-walled Teflon. As aerated solvent flows through the tubing, the vacuum removes the dissolved gasses. Typical commercial devices incorporate up to four separate solvent channels to accommodate up to four channels of mobile-phase flow. In-line membrane degassing is an efficient, cost-effective alternative to continuous helium sparging. Selective solvent evaporation is not a problem with these devices, but degassing efficiency does decrease as the mobile-phase flow rate increases.

Whereas degassing is important for all HPLC systems, it is especially important when blending mobile phases automatically with solvent-proportioning devices. The solubility of gases in pure solvents is different than in mixtures, as evidenced by the release of bubbles when two solvents such as methanol and water are mixed together. Because solvent-proportioning devices used to form HPLC gradients continuously blend two or more solvents, it is essential that each solvent be deaerated before meeting in the mixing device. This is particularly true of low-pressure proportioning HPLC systems in which the solvents meet at atmospheric pressure. These systems often require the use of a continuous degassing device such as helium sparging or in-line vacuum. In high-pressure proportioning HPLC systems, the solvents meet under conditions of elevated pressure. This pressure helps to keep the gas in

solution and a continuous form of degassing is not always needed.

Conclusion

Although degassing is widely accepted as a necessary step in the preparation of HPLC mobile phases, cases involving the appearance of anomalous peaks have been reported when there is a difference between the amount of dissolved gas in the mobile phase and that of the sample solvent. This is most commonly seen when continuous forms of degassing are used. Although a variety of remedies may be employed, suspension of continuous degassing may be recommended, provided low-pressure solvent proportioning is not being used.

Suggested Further Reading

- Bakalyar, S. R., M. P. T. Bradley, and R. Honganen, The role of dissolved gases in high performance liquid chromatography, *J. Chromatogr.* 158: 277 (1978).
- Egi, Y. and A. Ueyanagi, Ghost peaks and aerated sample solvent, *LC-GC* 16(2): 112 (1998).
- Snyder, L. R. and J. J. Kirkland, *Introduction to Modern Liquid Chromatography*, 2nd ed., John Wiley & Sons, New York, 1979.



Dendrimers and Hyperbranched Polymers: Analysis by GPC–SEC

Nikolay Vladimirov

Hercules, Inc., Wilmington, Delaware, U.S.A.

Introduction

Dendrimers and hyperbranched polymers are globular macromolecules having a highly branched structure, in which all bonds converge to a focal point or core, and a multiplicity of reactive chain ends. Because of the obvious similarity of their building blocks, many assume that the properties of these two families of dendritic macromolecules are almost identical and that the terms “dendrimer” and “hyperbranched polymer” can be used interchangeably. These assumptions are incorrect because only dendrimers have a precise end-group multiplicity and functionality. Furthermore, they exhibit properties totally unlike that of other families of macromolecules.

Historical Background

Highly branched and generally irregular dendritic structures have been known for some time, being found, for example, in polysaccharides, such as amylopectin, glycogen, and some other biopolymers. In the area of synthetic structures, Flory discussed, as early as 1952, the theoretical growth of highly branched polymers obtained by the polycondensation of AB_x structures in which x is at least equal to 2. Such highly branched structures are now known as “hyperbranched polymers.”

Today, regular dendrimers can only be prepared using rather tedious, multistep syntheses that require intermediate purifications. In contrast, hyperbranched polymers are easily obtained using a variety of one-pot procedures, some of which mimic, but do not truly achieve, regular dendritic growth [1]. The presence of such a large number of atoms within each dendritic or hyperbranched macromolecule permits an enormous variety of conformations with different shapes and sizes. The distribution of molecular weights focuses on the polydispersity index (M_w/M_n), and the requirements for gelation (or avoidance of gelation) when multimodal monomers are incorporated into the macromolecule. Each of these topics are discussed in Newcome's monograph [2]. Lists of reviews between 1986 and 1996 and *Advances* series are also given.

Buchard et al. [3] outlined some properties of hyperbranched chains. The dilute solution properties of branched macromolecules are governed by the higher segment density found with linear chains. The dimensions appear to be shrunk when compared with linear chains of the same molar mass and composition. It is shown that the apparent shrinking has an influence also on the intrinsic viscosity and the second virial coefficient. The broad molecular-weight distribution (MWD) has a strong influence on these shrinking factors, which can be defined and used for quantitative determination of the branching density (i.e., the number of branching points in a macromolecule). Here, the branching density can be determined only by size-exclusion chromatography (SEC) in on-line combination with light-scattering and viscosity detectors. The technique and possibilities are discussed in detail.

Discussion

A dendritic structure generally gives rise to better solubility than the corresponding linear analog. For example, aromatic polyamide dendrimers and hyperbranched polymers are soluble in amide-type solvents and even in tetrahydrofuran. Gel permeation chromatography (GPC) was performed on a Jasco HPLC 880PU fitted with polystyrene–divinylbenzene columns (two Shodex KD806M and KD802) and a Shodex RI-71 refractive index detector in DMF containing 0.01 mol/L of lithium bromide as an eluent. Absolute molecular weights (M_w) of 74,600, 47,800 and 36,800 were determined by light scattering using a MiniDawn apparatus (Wyatt Technology Co.) and a Shimadzu RID-6A refractive index detector. A specific refractive index increment (dn/dc) of the polymer in DMF at 690 nm was measured to be 0.216 mL/g [4].

Standards commonly employed [5] to calibrate SEC columns do not have a well-defined size. Carefully characterized spherical solutes in the appropriate size range are therefore of considerable interest. The chromatographic behavior of carboxylated starburst dendrimers — characterized by quasi-elastic light scatter-



ing and viscometry — on a Superose SEC column was explored. Carboxylated starburst dendrimers appear to behave as noninteracting spheres during chromatography in the presence of an appropriate mobile phase. The dependence of the retention time on the solute size seems to coincide with data collected on the same column for Ficoll. Chromatography of the dendrimers yields to a remarkable correlation of the chromatographic partition coefficient with the generation number; this result is, in part, a consequence of the exponential relationship between the generation number and the molecular volume of these dendrimers. All measurements were made in a 9:1 mixture of $\text{NaNO}_3:\text{Na}_2\text{HPO}_4$, $\text{pH} = 5.5$, $0.38M$, which has been previously known to minimize electrostatic interactions between a variety of proteins and this stationary phase [4].

The SEC partition coefficient [6] (K_{SEC}) was measured on a Superose 6 column for three sets of well-characterized symmetrical solutes: the compact, densely branched nonionic polysaccharide, Ficoll; the flexible chain nonionic polysaccharide, pullulan; and compact, anionic synthetic polymers, carboxylated starburst dendrimers. All three solutes display a congruent dependence of K_{SEC} on solute radius, R . In accord with a simple geometric model for SEC, all of these data conform to the same linear plot of $K_{\text{SEC}}^{1/2}$ versus R . This plot reveals the behavior of noninteracting spheres on this column. The mobile phase for the first two solutes was $0.2M$ NaH_2PO_4 – Na_2HPO_4 , $\text{pH} 7.0$. In order to ensure the suppression of electrostatic repulsive interactions between the dendrimer and the packing, the ionic strength was increased to $0.30M$ for that solute.

The MWD [7] is derived for polymers generated by self-condensing vinyl polymerization (SCVP) of a monomer having a vinyl and an initiator group (“inimer”) in the presence of multifunctional initiator. If the monomer is added slowly to the initiator solution (semibatch process), this leads to hyperbranched polymers with a multifunctional core. If monomer and initiator are mixed simultaneously (batch process), even at vinyl group conversions as high as 99%, the total MWD consists of polymers, which have grown via reactions between inimer molecules (i.e., the normal SCVP process) and those which have reacted with the initiator. Consequently, the weight distribution, $w(M)$, is bimodal. However, the z -distribution, $z(M)$, equivalent to the “GPC distribution,” $w(\log M)$ versus $\log M$, is unimodal. Their theoretical studies showed that the hyperbranched polymers generated from an SCVP pos-

sess a very wide MWD $M_w/M_n \cong P_n$, where P_n is the number-average degree of polymerization. The evolution of the weight-distribution and z -distribution curves of the total resultant polymer during the SCVP in the presence of the core moiety with $f = 10$ is given. The weight distributions become less bimodal with increasing conversion. In contrast, all z -distributions are unimodal.

Striegel et al. [8] employed SEC with universal calibration to determine the molecular-weight averages, distributions, intrinsic viscosities, and structural parameters of Starburst dendrimers, dextrans, and the starch-degradation polysaccharides (maltodextrins). A comparison has been made in the dilute solution behavior of dendrimers and polysaccharides with equivalent weight-average molecular weights. Intrinsic viscosities decreased in the order $[\eta_{\text{dextrans}}] > [\eta_{\text{dextrin}}] > [\eta_{\text{dendrimer}}]$. A comparison between the molecular radii obtained from SEC data and the radii from molecular dynamics studies show that Starburst dendrimers behave as θ -stars with functionality between 1 and 4. Additionally, electrospray ionization mass spectrometry was employed to determine M_w , M_n , and the PD of Astramol dendrimers.

Size-exclusion chromatography experiments were carried out on a Waters 150CV⁺ instrument (Waters Associates, Milford, MA) equipped with both differential refractive index single-capillary viscometer detectors. The solvent/mobile phase was $\text{H}_2\text{O}/0.02\%$ NaN_3 , at the flow rate of 1.0 mL/min. Pump, solvent, and detector compartments were maintained at 50°C . Separation occurred over a column bank consisting of three analytical columns preceded by a guard column: Shodex KB-G, KS-802, KS-803, and KB-804 (Phenomenex, Torrance, CA). Universal calibration was performed using a series of oligosaccharides (Sigma, St. Louis, MO), and Pullulan Standards (American Polymer Standards, Mentor, OH, and Polymer Laboratories, Amherst, MA).

The solution behavior of several generations of Starburst poly(amido amine) dendrimers, low-molecular-weight ($M_w < 60,000$) dextrans, and maltodextrins was also examined by SEC, using the universal calibration. For Starburst and Astramols, supplied M_w values are theoretical average molecular weights. Weight-average molecular weights for the dendrimers determined by SEC with universal calibration using oligosaccharide and polysaccharide narrow standards were slightly, albeit consistently lower than the theoretical averages. In general, the intrinsic viscosity of polymers tends to increase with increasing molecular weight (M),

which accompanies an increase in the size of the macromolecule. Exceptions to this are the hyperbranched polymers, in which the Mark–Houwink double logarithmic $[\eta]$ versus M curve passes through a minimum in the low-molecular-weight region before steadily increasing. For solutions of the dendrimers studied in their experiments, it is evident that as M increases, $[\eta]$ decreases. This corresponds to the molecules growing faster in density than in radial growth. Fréchet has pointed out the special situation of this class of polymers, in which their volume increases cubically and their mass increases exponentially [9]. The exponent a in the Mark–Houwink equation for the dendrimers is -0.2 for convergent growth for the generation studied (located in the inverted region of the Mark–Houwink plot). This value for the Starburst dendrimers is comparable to the a value of -0.2 for convergent-growth dendrimers, generations 3–6, studied by Mourey et al. [9]. When the results from SEC are combined with those from computer modeling by comparing the ratios of geometric to hydrodynamic radii for the trifunctional Starbursts to the ratios derived for the other molecular geometries, the dendrimers appear to resemble θ -stars.

Size-exclusion chromatography [9] with a coupled molecular-weight-sensitive detection is a simple convenient method for characterizing dendrimers for which limited sample quantities are available. The polyether dendrimers increase in hydrodynamic radius approximately linearly with generation and have a characteristic maximum in viscosity. These properties distinguish these dendrimers from completely collapsed, globular structures. The experimental data also indicate that these structures are extended to approximately two-thirds of the theoretical, fully extended length.

Puskas and Grasmüller characterized the synthesized star-branched and hyperbranched polyisobutylenes (PIBs) by SEC–light scattering in tetrahydrofuran (THF), with the dn/dc measured as 0.09 mL/g . The radius of gyration gave a slope of 0.3 , demonstrating the formation of a star-branched polymer [10].

Gitsov and Fréchet [11] reported the syntheses of novel linear-dendritic triblock copolymers achieved via anionic polymerization of styrene and final quenching with reactive dendrimers. For the characterization of the products in the reaction mixture, SEC with double detection was performed at 45°C on a chromatography line consisting of a 510 pump, a U6K universal injector, three Ultrastaygel columns with

pore sizes 100 \AA and 500 \AA and Linear, a DRI detector M410, and a photodiode array detector M991 (all Millipore Co., Waters Chromatography Division). THF was used as the eluent at a flow rate of 1 mL/min . SEC with coupled PDA detection proves to be particularly useful in the separation and identification of all compounds in the reaction mixture. A detailed discussion can be found in Ref. 11. SEC/VISC studies show that the ABA copolymers are not entangled and undergo a transition from an extended globular form to a statistical coil when the molecular weight of their linear central block exceeds $50,000$.

The solution properties of hybrid–linear dendritic polyether copolymers are investigated by SEC with coupled viscometric detection from the same authors [12]. The results obtained show that the block copolymers are able to form monomolecular and multimolecular micelles depending on the dendrimer generation and the concentration in methanol–water (good solvent for the linear blocks).

Large macromolecular assemblies and agglomerates play an important role in living matter and its artificial reproduction. AB and ABA block copolymers are convenient tools used for modeling of these processes. Usually in a specific solvent–nonsolvent system, ABA triblocks form micelles with a core consisting of insoluble B blocks and a surrounding shell of A blocks that extend into the solvent phase. Two Waters/Shodex PROTEIN KW 802.5 and 804 columns were used for the aqueous SEC measurements. The columns were calibrated with 14 PEO and PEG standards. The radius of gyration (R_g) was calculated from the intrinsic viscosity $[\eta]$ and Unical 4.04 software (Viscotek). The calculated values for the Mark–Houwink–Sakurada constant a are 0.583 for PEG ($K = 9.616 \times 10^{-4}$) and 0.776 for PEO ($K = 2.042 \times 10^{-4}$). They are in close agreement with the data reported for the same polymer in other aqueous mixtures (compositions).

The significant decrease in the $[\eta]$ of the copolymer solutions and the parallel decrease in R_g of the hybrid structures containing [G-4] blocks indicate that the block copolymers are undergoing intramolecular micellization. Unimolecular micelles consisting of a small, dense, dendritic core tightly surrounded by a PEO corona are formed. The influence of the size of the dendritic block was investigated with PEO7500. The solution behavior of ABA hybrid copolymers is documented. In general, materials containing more than 30 wt\% of dendritic blocks are not soluble in methanol–water. However, it should be emphasized that the solubility of copolymers is also strongly



influenced by the size of the dendritic block. Obviously, an optimal balance between the size of the dendrimer and the length of the linear block is required to enable the dissolution of the copolymer in the solvent composition.

Performing SEC with dual detection (DRI and viscometry) permitted application of the concept of universal calibration.

References

1. J. M. J. Fréchet, C. J. Hawker, I. Gitsov, and J. W. Leon, *J. M. S.-Pure Appl. Chem. A33*: 1399 (1996).
2. G. R. Newcome, C. N. Moorefield, and F. Vögtle, *Dendritic Molecules, Concepts, Syntheses, Perspectives*, VCH, Weinheim, 1996.
3. W. Buchard, *Adv. Polym. Sci. 143*: 113 (1999).
4. G. Yang, M. Jikey, and M. Kakimoto, *Macromolecules* 32: 2215 (1999).
5. P. L. Dubin, S. L. Edwards, I. Kaplan, M. S. Mehta, D. Tomalia, and J. Xia, *Anal. Chem.* 64: 2344 (1992).
6. P. L. Dubin, S. L. Edwards, M. S. Mehta, and D. Tomalia, *J. Chromatogr.* 635: 51 (1993).
7. D. Yan, Z. Zhou, and A. Müller, *Macromolecules* 32: 245 (1999).
8. A. M. Strigel, R. D. Plattner, and J. L. Willet, *Anal. Chem.* 71: 978 (1999).
9. T. H. Mourey, S. R. Turner, M. Rubinstein, J. M. J. Fréchet, C. J. Hawker, and K. L. Wooley, *Macromolecules* 25: 2401 (1992).
10. J. E. Puskas and M. Grasmüller, *Macromol. Symp.* 132: 117 (1998).
11. I. Gitsov and J. M. J. Fréchet, *Macromolecules* 27: 7309 (1994).
12. I. Gitsov and J. M. J. Fréchet, *Macromolecules* 26: 6536 (1993).



Derivatization of Acids for GC Analysis

Igor G. Zenkevich

Chemical Research Institute, St. Petersburg State University, St. Petersburg, Russia

Introduction

The class of “acids” includes various types of compounds with active hydrogen atoms. The most important group of organic acids is the compounds with the carboxyl fragment —COOH. Some other compounds can be classified not only as O acids [e.g., hydroxamic acids, —CONHOH \rightleftharpoons —C(OH)=NOH], but C—H acids [in the presence of structural fragments —CH(NO₂)₂, —CH(CN)₂, etc.]. The known substances of this class for gas chromatography (GC) analysis are fatty acids from triglycerides, numerous nonvolatile polyfunctional biogenic compounds (including phenolic carboxylic acids: gallic, vanillic, syringic, etc.), acidic herbicides (e.g., 2,4-D, 2,4,5-T, MCPB, MCPA, fenoprop, haloxyfop, etc.), and many other substances. Strong inorganic acids (e.g., volatile hydrogen halides HHal or nonvolatile H₂SO₄, H₃PO₄, etc.) can also be the objects of GC analysis.

Discussion

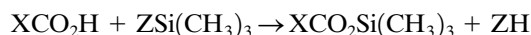
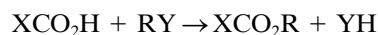
The simplest monofunctional carboxylic acids have boiling points at atmospheric pressure without decomposition and, hence, can be analyzed directly by GC. However, owing to the high polarities of carboxyl compounds, the typical problem of their GC analysis with standard nonpolar phases is a nonlinear sorption isotherm. As a result, these compounds yield broad, nonsymmetrical peaks that lead to poor detection limits and unsatisfactory reproducibility of their retention indices. The recommended stationary phases for direct analysis of free carboxylic acids are polar polyethylene glycols (Carbowax 20M, DB Wax, SP-1000, FFAP, etc.). However, these phases have less thermal stability compared with polydimethyl siloxanes (approximately 220–230°C versus 300–350°C). This means that the upper limit of GC columns with these polar phases in RI units is not more than 3000–3500 IU. High homologs, even of monocarboxylic acids, cannot be eluted within this RI window (keep in mind that the absence of RI data for palmitic acid C₁₅H₃₁COOH on the mentioned type of polar phases).

Compound	pK _a	T _b (°C)	RI _{nonpolar}	RI _{polar}
Acetic acid	4.75	118	638 ± 10 ^a	1428 ± 30
Palmitic acid	4.9	351.5	1966 ± 7	No data
Benzoic acid	4.2	250	1201 ± 24	2387 ± 5
Phenylacetic acid	4.2	266	1290 ± 44	No data

^aRI data with standard deviations are randomized interlaboratory data.

Some of dicarboxylic acids can also be distilled, without decomposition, under reduced pressures. This is at least a theoretical ground for the possibility of their direct GC analysis. Few successful attempts have been described, but these analytes require “on-column” injection of samples and extremely high inertness of chromatographic systems. Many types of polyfunctional carboxylic acids (hydroxy-, mercapto-, amino-, etc.) cannot be analyzed in free, underivatized form, owing to either nonvolatility and/or absence of thermal stability. These features are the principal reasons for the conversion of carboxylic acids, before their GC analysis, into less polar derivatives without active hydrogen atoms.

The general approach for carboxylic acids derivatization is their esterification with formation of alkyl (arylalkyl, halogenated alkyl) or silyl esters:



Some of the most widely used reagents for the synthesis of alkyl carboxylates are listed in Table 1. The general recommendations for the silylation of carboxylic acids (TMS and more stable *tert*-butyldimethylsilyl derivatives) are the same as those for other hydroxy-containing compounds (see the entry Derivatization of Hydroxy Compounds for GC Analysis).

The simplest esterification reagents are the corresponding alcohols ROH themselves. Different esters have been used as the analytical derivatives of carboxylic acids: Me, Et, Pr, iso-Pr, isomeric Bu (excluding *tert*-Bu esters, owing to their poorer synthetic yields), and so forth. This method requires the use of excess of dry alcohol and acid catalysis by BCl₃, BF₃, CH₃COCl, SOCl₂,

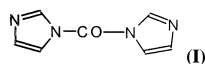
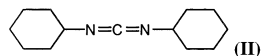


Table 1 Physicochemical and Gas Chromatographic Properties of Some Alkylating Derivatization Reagents

Reagent (abbreviation)	MW	$T_b(^{\circ}\text{C})$	RI _{nonpolar}	By-products (RI _{nonpolar})
Methanol (BCl ₃ , BF ₃ , HCl, DCC, etc.)	32	64.6	381 ± 15	—
Diazomethane (in ethyl ether solution)	42	−23	None (unstable)	—
Methyl iodide (DMFA, K ₂ CO ₃)	142	42.8	515 ± 7	CH ₃ OH (381 ± 15)
Dimethyl sulfate (<i>tert</i> -amines)	126	188.5	853 ± 22	CH ₃ OH (381 ± 15)
1-Iodopropane (DMFA, K ₂ CO ₃)	170	102	711 ± 11	C ₃ H ₇ OH (552 ± 13), (C ₃ H ₇) ₂ O (680 ± 6)
2-Bromopropane (LiH, DMSO)	122	59.4	571 ± 5	(CH ₃) ₂ CHOH (486 ± 9), (iso-Pr) ₂ O (598 ± 5)
Methyl chloroformate	94	71	582 ± 17	CH ₃ OH (381 ± 15)
Ethyl chloroformate	108	—	640 ± 12	C ₂ H ₅ OH (452 ± 18)
Butyl chloroformate	136	—	832 ± 10	C ₄ H ₉ OH (658 ± 12)
Pentafluorobenzyl bromide (PFB–Br)	260	174–175	991 ± 11 ^a	C ₆ F ₅ CH ₂ OH (934 ± 16) ^a
3,5-bis-(Trifluoromethyl)benzyl bromide (BTBDMA–Br)	306	—	1103 ± 9 ^a	(CF ₃) ₂ C ₆ H ₃ CH ₂ OH (1046 ± 15) ^a
Tetramethylammonium hydroxide (TMAH; in 25% aqueous solution)	74	—	Nonvolatile	(CH ₃) ₃ N (418 ± 9)
Trimethylanilinium hydroxide (TMPAH; in 0.2M MeOH solution)	136	—	Nonvolatile	C ₆ H ₅ N(CH ₃) ₂ (1065 ± 9)
3,5-bis-(Trifluoromethylbenzyl)-dimethylanilinium fluoride	258	—	Nonvolatile	3,5-(CF ₃) ₂ C ₆ H ₃ CH ₂ N(CH ₃) ₂ (no data), C ₆ H ₅ N(CH ₃) ₂ (1065 ± 9)
2-Bromoacetophenone (phenacyl bromide)	198	260	1321 ± 4	C ₆ H ₅ COCH ₂ OH (1118) ^b
Silylating reagents	See table in the entry Derivatization of Hydroxy Compounds for GC Analysis			

^aEstimated RI values.^bSingle experimental value.

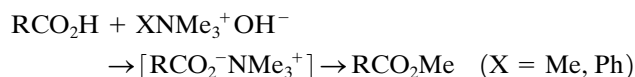
and so on. Otherwise, the alcohol being used can be saturated with gaseous HCl, which must then be removed by heating the reaction mixtures after completion of the reaction. The same procedure is used for the synthesis of 2-chloroethyl (RCO₂CH₂CH₂Cl), 2,2,2-trichloroethyl (RCO₂CH₂CCl₃), and hexafluoroisopropyl esters [RCO₂CH(CF₃)₂] for GC analysis with selective detection. Instead of acid catalysis of this reaction, some reagents for the coupling of water were recommended, namely 1,1'-carbonyldiimidazole (**I**) and 1,3-dicyclohexylcarbodiimide (DCC, **II**):

**(I)****(II)**

The application of any additional reagents usually leads to the appearance of additional peaks in the chromatograms (including the peaks of by-products; for example, imidazole, RI_{nonpolar} = 1072 ± 17), which must be reliably identified and excluded from data interpretation. The by-product from compound (**II**) — 1,3-dicyclohexylurea — is nonvolatile for GC analysis.

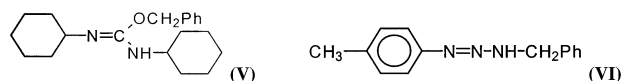
Other classes of esterification reagents are halogenated compounds (alkyl iodides, substituted benzyl and phenacyl bromides, etc.), which need basic media

for their reaction (K₂CO₃ or DMFA are used usually for the neutralization of HBr or HCl as acid by-products). For methylation of carboxylic acids, some tetra-substituted ammonium hydroxides can be used, namely tetramethylammonium hydroxide (in aqueous solutions) or trimethylanilinium hydroxide (in methanolic solutions). The intermediate ammonium carboxylates are thermally unstable and can produce methylalkanoates during subsequent heating of reaction mixtures or even during their introduction into the hot injector of the gas chromatograph (flash methylation):

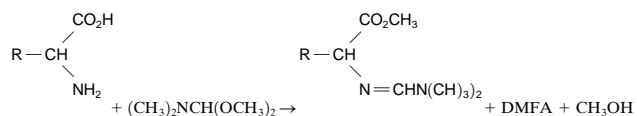


The possible by-products of these reactions are corresponding amines (Me₃N or PhNMe₂). If the appearance of any volatile by-products is undesirable, the methylation of carboxylic acids by diazomethane can be recommended. This reagent (*warning*: highly toxic) is synthesized by alkaline cleavage of *N*-methyl-*N*-nitrosourea (**III**) or *N*-methyl-*N*-nitrosotoluenesulfamide (**IV**) and, owing to its low boiling point (−23°C), can be used only in diethyl ether solutions. In the absence of acid catalysis, diazomethane reacts only with carboxylic acids (p*K*_a = 4–5), and phenols

($pK_a = 9-10$), but has no influence on aliphatic OH groups. Besides CH_2N_2 , some more complex diazo compounds (diazioethane, diazotoluene) have been recommended for the synthesis of other esters (ethyl and benzyl, correspondingly). For the synthesis of benzyl (or substituted benzyl) esters, some special reagents have also been proposed [e.g., *N,N'*-dicyclohexyl-*O*-benzylurea (**V**) and 1-(4-methylphenyl)-3-benzyltriazene (**VI**)]:

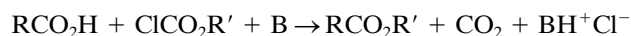


The esterification of carboxylic acids can be provided, also, by synthetic equivalents of alcohols: acetals $\text{RCH}(\text{OR}')_2$ (with acid catalysis), ortho-esters $\text{RC}(\text{OR}')_3$ (acid catalysis), and dialkylcarbonates $\text{CO}(\text{OR})_2$ (base catalysis). The series of bifunctional reagents of this type [dimethylformamide dialkylacetals $(\text{CH}_3)_2\text{N}-\text{CH}(\text{OR})_2$] is commercially available. Besides the esterification of carboxyl groups, these compounds react with primary amino groups and, thus, are used for GC analysis of amino acids (see the entry "Derivatization of Amines, Amino Acids, and Related Compounds for GC Analysis"):

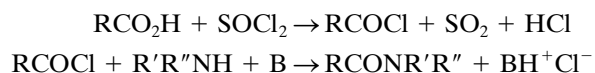


A "sandwich" technique (flash methylation) can also be used in this case. This implies the injection the combined sample and reagent in the same syringe into the gas chromatograph (e.g., successively placed 1 mL of derivatization reagent, 1 mL of pyridine with internal standard, and 1 mL of the solution of analytes in the same solvent).

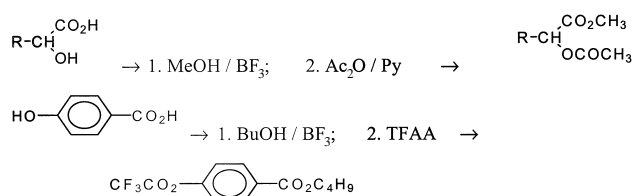
Alkyl chloroformates ClCO_2R ($\text{R} = \text{Me}, \text{Et}, \text{Bu}$) have been recently proposed as convenient alkylating reagents for carboxylic acids:



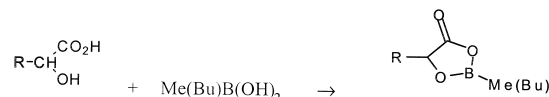
Two-stage single-pot derivatization of carboxylic acids (with intermediate formation of chloroanhydrides with thionyl chloride, followed by their conversion into amides) was recommended for high-performance liquid chromatography analysis, but the simplest dialkylamides are also volatile enough for GC analysis (the mixture of Ph_3P and CCl_4 can be used in this reaction instead of SOCl_2). Moreover, the same procedure is used for the synthesis of diastereomeric derivatives of enantiomeric carboxylic acids (see below):



The reactivities of carboxy and OH groups in the polyfunctional hydroxy and phenolic carboxylic acids are different. This indicates the possibility of an independent two-stage derivatization of these compounds, for example,



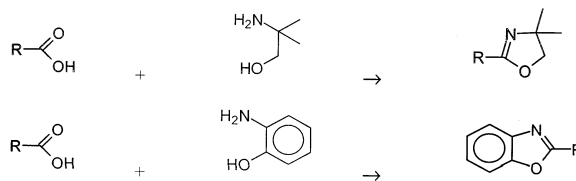
If these functional groups are located in vic- (aliphatic series) or ortho-positions (arenecarboxylic acids), methyl or butyl boronic acids are convenient reagents for their one-step derivatization, with the formation of cyclic methyl (butyl) boronates:



A similar method for simultaneous derivatization of two functional groups is the formation of cyclic silylene derivatives for the same types of compounds:



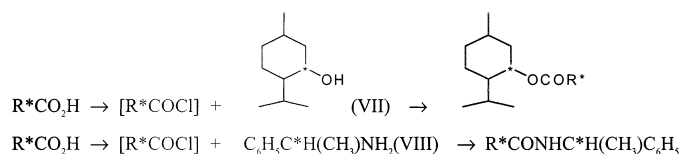
The special type of carbonyl-group derivatization is aimed for gas chromatography-mass spectrometry (GC-MS) determination of double-bond $\text{C}=\text{C}$ positions in the unsaturated long-chain acids. The analytical derivatives for the solution of this problem are nitrogen-containing heterocycles. These compounds can be synthesized by condensation of carboxylic acids with 2-amino-2-methyl-1-propanol (2-substituted 4,4-dimethyloxazolines), 2-aminophenol (2-substituted benzoxazoles), and so forth.



Gas chromatographic separation of enantiomeric carboxylic acids is based on the formation of their esters or amides with optically active alcohols [e.g., (-)-



menthol (**VII**) or amines [α -methylbenz-
emethaneamine (**VIII**)], usually through the intermedi-
ate chloroanhydrides. These diastereomeric products
are not as volatile as other acid derivatives, but, owing
to presence of two asymmetric carbon atoms (*) in the
molecule, they can be separated on nonchiral phases:



A problem closely related to the derivatization of
free carboxylic acids is the determination of their com-
position in the biogenic triglycerides, lipids, and so
forth. The sample preparation includes the reesterifica-
tion (preferably with formation of methyl es-
ters) of these compounds in acid (MeOH/BF₃,
MeOH/AcCl, etc.) or basic (MeONa, MeOH/KOH,
etc.) media. Methyl esters of fatty acids are compounds
that are well characterized by both standard mass spec-
tra and GC retention indices on standard phases. The
combination of these analytical parameters provides
their reliable identification.

The general method of organic sulfo- (RSO₂OH) and
various substituted phosphorus acids [ROP(O)(OH)₂,
RP(O)(OH)₂, etc.] is their silylation. Analogous recom-
mendations have been proposed for the determination
of inorganic anions. The values of retention indices on
standard nonpolar phases (SE-30) are known for TMS
derivatives of most important inorganic acids:

Derivatization of Acids for GC Analysis

Anion	Volatile derivative for GC analysis	RI _{nonpolar}	Anion	Volatile derivative for GC analysis	RI _{nonpolar}
Borate	B(OTMS) ₃	1010	Arsenite	As(OTMS) ₃	1149
Carbonate	CO(OTMS) ₂	1048	Phosphate	PO(OTMS) ₃	1273
Phosphite	P(OTMS) ₃	1115	Vanadate	VO(OTMS) ₃	1301
Sulfate	SO ₂ (OTMS) ₂	1148	Arsenate	AsO(OTMS) ₃	1353

Suggested Further Reading

- Blau, K. and J. M. Halket (eds.), *Handbook of Deriva-
tives for Chromatography*, 2nd ed., John Wiley &
Sons, New York, 1993.
- Brooks, C. J. W. and W. T. Cole, *J. Chromatogr.* 441: 13
(1988).
- Burke, D. J. and B. Halpern, *Anal. Chem.* 55: 822
(1983).
- Butz, S. and H.-J. Stan, *J. Chromatogr.* 643: 227 (1993).
- Drozd, J., *Chemical Derivatization in Gas Chromatog-
raphy*, Elsevier, Amsterdam, 1981.
- Gabelish, C. L., P. Crisp, and R. P. Schneider, *J. Chro-
matogr. A* 749: 165 (1996).
- Gonzalez, G., R. Ventura, A. K. Smith, R. de la Torre,
and J. Segura, *J. Chromatogr. A* 719: 251 (1996).
- Knapp, D. R., *Handbook of Analytical Derivatization
Reactions*, John Wiley & Sons, New York, 1979.
- Umeh, E. O., *J. Chromatogr.* 51: 139, 147 (1970).
- Zhang, J. T., Q. T. Yu, B. N. Lin, and Z. H. Huang, *Bio-
med. Environ. Mass Spectrom.* 15: 33 (1988).



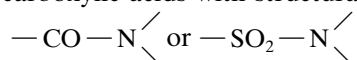
Derivatization of Amines, Amino Acids, Amides, and Imides for GC Analysis

Igor G. Zenkevich

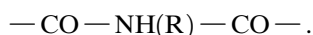
Chemical Research Institute, St. Petersburg State University, St. Petersburg, Russia

Introduction

The amines are the extensive class of organic compounds of general formulas RNH_2 (primary), $\text{RR}'\text{NH}$ (secondary), and $\text{RR}'\text{R}''\text{N}$ (tertiary). Their chemical and chromatographic properties are determined by the presence of a basic functional group and active hydrogen atoms in the molecule. Their basicity is strongly different for aliphatic amines ($\text{p}K_a = 10.5 \pm 0.8$) and substituted anilines ($\text{p}K_a = 4.9 \pm 0.3$) owing to $\text{p}-\pi$ conjugation $\text{N}-\text{Ar}$. Amides are the derivatives of carboxylic acids with structural fragments



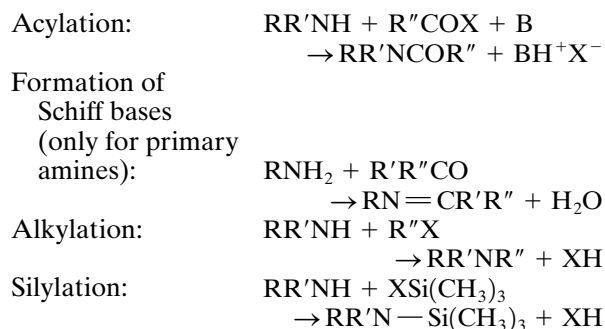
(including cyclic structures), whereas imides have the fragments



The simplest members of all amine classes usually are volatile enough for their direct gas chromatography (GC) analysis. When other polar functional groups with active hydrogen atoms are present in the molecule, the derivatization of one or all of them becomes necessary. A typical example of these compounds is amino acids, which exist in the form of inner-molecular salts $\text{RCH}(\text{NH}_3^+)\text{CO}_2^-$ in the solid state.

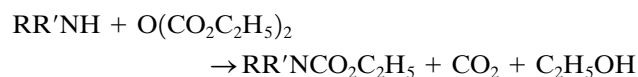
Discussion

The principal directions of amino compound derivatization for GC analysis include the following types of chemical reactions:



The first group of reactions (acylation) includes the greatest number of examples. Numerous recommended reagents are listed in the Table 1; they belong to two classes of reagents: anhydrides ($\text{X} = \text{OCOR}''$) and chloroanhydrides ($\text{X} = \text{Cl}$). Most widely used of them are acetic and trifluoroacetic anhydrides. The by-products of acylation, in all cases, are acids; these reactions need basic media (additives of pyridine or *tert*-amines) to prevent the formation of nonvolatile salts from the analytes. The technique of derivatization is extremely simple: Samples mixtures are allowed to stand with acylating reagents for some minutes prior to analysis.

The anhydrides and chloroanhydrides of chlorinated acetic acids and pentafluorobenzoyl chloride are used for the synthesis of chlorinated amides for GC analysis with selective detectors. Diethylpyrocarbonate converts primary and secondary amines (including NH_3) to *N*-substituted carbamates:



The next group of derivatization reactions is the formation of Schiff bases from the reaction of primary amines with carbonyl compounds. Some recommended reagents are listed in Table 2. Aromatic aldehydes are much more reactive in this condensation, compared with ketones and aliphatic compounds (from the latter, only low-boiling acetone and cyclohexanone have been used in GC practice). All carbonyl compounds can be taken into reaction with amines in the form of their various synthetic analogs, at first acetals or ketals. So, dimethylformamide dialkylacetals $(\text{CH}_3)_2\text{N}-\text{CH}(\text{OCH}_3)_2$ react with primary amines with formation of *N*-dimethylaminomethylene derivatives $\text{R}-\text{N}=\text{CH}-\text{N}(\text{CH}_3)_2$. So far, because these reagents at the same time provide the esterification of carboxyl groups, they have been recommended for single-stage derivatization of amino acids (discussed later).

Carbon disulfide, as the thio analog of carbonyl compounds, reacts with primary amines with resultant formation of alkyl isothiocyanates, which have lower

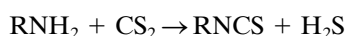


Table 1 Physicochemical and Gas-Chromatographic Properties of Some Acylation Reagents

Reagent (abbreviation)	MW	$T_b(^{\circ}\text{C})$ (P)	d_4^{20}	n_D^{20}	RI _{nonpolar}	By-products (RI _{nonpolar})
Acetic anhydride	102	139.6	1.08	1.390	706 ± 9	CH ₃ CO ₂ H (638 ± 10)
Trifluoroacetic anhydride (TFA)	210	39–40	1.511	1.268	515 ± 6	CF ₃ CO ₂ H (744 ± 6)
Pentafluoropropionic anhydride (PFPA)	310	70–72	1.588	—	606 ± 6 ^a	C ₂ F ₅ CO ₂ H (781 ± 12)
Heptafluorobutyric anhydride (HFBA)	410	109–111	1.674	—	745 ± 4 ^a	C ₃ F ₇ CO ₂ H (863 ± 16)
bis-Trifluoroacetyl methylamine (MBTFA)	223	120–122	1.547	1.346	773 ± 16 ^a	CF ₃ CONHCH (540)
<i>N</i> -Trifluoroacetyl imidazole (TFAI)	164	137–138	1.442	1.424	830 ± 21 ^a	Imidazole (1072 ± 17)
Chloroacetic anhydride	170	203	1.550	—	1116 ± 18 ^a	ClCH ₂ CO ₂ H (864 ± 3)
Dichloroacetic anhydride	238	214–216	—	—	1248 ± 14 ^a	Cl ₂ CHCO ₂ H (1048 ± 23)
Trichloroacetic anhydride	306	222–224	1.691	1.484	1471 ± 27 ^a	CCl ₃ CO ₂ H (1270 ^a)
Benzoyl chloride	140	197–198	1.211	1.553	1046 ± 9	C ₆ H ₅ CO ₂ H (1201 ± 24)
Pentafluorobenzoyl chloride	230	158–159	1.669	1.453	922 ± 14 ^a	C ₆ F ₅ CH ₂ OH (934 ± 16 ^a)
Chlorodifluoroacetic anhydride	242	92–93	—	1.348	679 ± 8 ^a	ClCF ₂ CO ₂ H (793 ^a)
Acetyl chloride	78	51.8	1.104	1.389	542 ± 7	CH ₃ CO ₂ H (638 ± 10)
Chloroacetyl chloride	112	106.1	1.419	1.454	622 ± 8	ClCH ₂ CO ₂ H (864 ± 3)
Dichloroacetyl chloride	146	107–108	1.532	1.460	726 ± 19 ^a	Cl ₂ CHCO ₂ H (1048 ± 23)
Trichloroacetyl chloride	180	118	1.629	1.470	778 ± 15	CCl ₃ CO ₂ H (1270 ^a)
Pivaloyl anhydride	186	192–193	0.918	1.409	1053 ± 31 ^a	(CH ₃) ₃ CCO ₂ H (804)
Diethylpyrocarbonate	162	93–94 (18)	1.101	1.398	—	C ₂ H ₅ OH (452 ± 18)

^aEstimated RI values.

retention indices than other derivatives of primary amines, including *N*-trimethylsilylated amines. The sole by-product of this reaction is gaseous hydrogen sulfide:



R in RNHSi(CH ₃) ₃	RI _{nonpolar}	R in R—NCS	RI _{nonpolar}
Me	689 ± 21 ^a	Me	689 ± 16
Et	756 ± 11	Et	736 ± 5

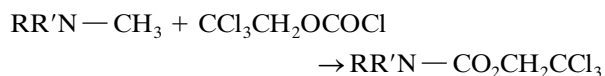
^aRI data with standard deviations are randomized interlaboratory data.

The alkylation of amines (including polyamines formed by reduction of polypeptides) was a highly popular method of derivatization in peptide chemistry before the appearance of contemporary mass-spectrometric techniques for analysis of nonvolatile compounds (FFAB, MALDI, etc.). Direct alkylation of amines by alkyl halides (Hoffman reaction) can lead to the final nonvolatile ammonium salts and, hence, other soft reagents must be used. For example, exhaustive methylation can be provided by the mixtures CH₂O/NaBH₄/H⁺ or CH₂O/formic acid.

Silylation of amines is a relatively rarely used method for their derivatization at present. The problem is the facile hydrolysis of *N*-TMS compounds. It leads to the formation in the reaction mixtures of both

mono-TMS (RNHTMS), and bis-TMS [RN(TMS)₂] derivatives. This multiplicity of products from the same precursor creates some difficulties in data interpretation. The recently introduced *N*-(*tert*-butyldimethylsilyl) (DMTBS) derivatives are more stable to the hydrolysis and their formation is more unambiguous (only monosubstituted compounds are formed) owing to steric reasons.

Tertiary amines have no active hydrogen atoms and their derivatization in the generally accepted sense is not required. Only in special cases (GC analysis with selective detectors), the cleavage of N—CH₃ bonds by chloroformates can be used:



Mixtures of amino acids are among of the most important substances for chromatographic analysis. Some dozens of methods for derivatization of these compounds for their GC determination have been proposed. The most widely used can be subdivided into two types:

1. Separate derivatization of functional groups —CO₂H and —NH₂ by different reagents.
2. Protection of both groups by only one reagent.

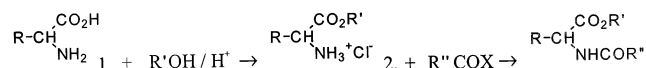
The typical derivatives of the first type are various esters (Me, Et, Pr, iso-Pr, Bu, iso-Bu, sec-Bu, Am, iso-Am, etc.) of *N*-acyl (acetyl, trifluoroacetyl,

Table 2 Physicochemical and GC Properties of Some Carbonyl Reagents and Their Analogs for Derivatization of Amino Compounds

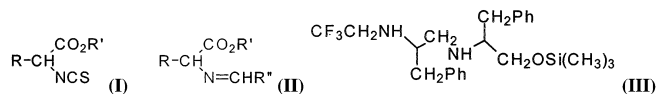
Reagent (abbreviation)	MW	$T_b(^{\circ}\text{C})$	d_4^{20}	n_D^{20}	RI _{nonpolar}
Acetone	58	56.2	0.791	1.359	472 \pm 12
Pentafluorobenzaldehyde	196	166–168	1.588	1.450	943 \pm 22 ^a
Thiophen-2-carboxaldehyde	112	198	1.200	1.590	966 \pm 9
Carbon disulfide	76	46.3	1.263	1.628	530 \pm 9
Methyl isothiocyanate ^b	73	118	1.069	1.525	689 \pm 16
Phenyl isothiocyanate ^b	135	219–221	1.130	1.652	1163 \pm 7
Dimethylformamide dimethyl acetal (DMFDMA) ^c	119	106	0.897	1.397	726 \pm 4
Dimethylformamide diethyl acetal (DMFDEA) ^c	147	134–136	0.859	1.400	826 \pm 5 ^a

^aEstimated RI values.^bOnly for derivatization of amino acids; with monofunctional amines nonvolatile products can be formed.^cBifunctional reagents; the by-products are MeOH (EtOH) and DMFA (749 \pm 16).

pentafluoropropionyl, heptafluorobutyl, etc.) amino acids. The butyl esters of *N*-TFA amino acids even have been given the special abbreviation: TAB derivatives. The two-stage process includes the esterification of amino acids by an excess of the corresponding alcohol in the presence of HCl and, after evaporation of volatile compounds, the treatment of the nonvolatile hydrochlorides of alkyl esters by acylating reagents:

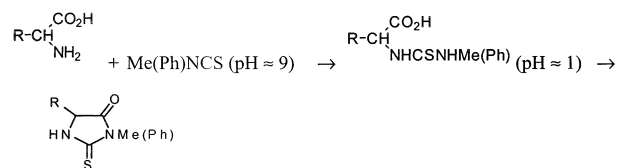


Some variations of this procedure are known. Instead of *N*-acylation, the treatment of intermediate esters by CS₂/Et₃N and CH₃OCOCl, with the formation of 2-alkoxycarbonylisothiocyanates (**I**), or by carbonyl compounds, which leads to the Schiff bases (**II**), have been proposed. However, the analytical advantages of these derivatives are not so obvious.



The same types of *N*-acyl-*O*-alkyl derivatives can also be used for GC analysis of the simplest oligopeptides (at least dipeptides and tripeptides). Other, obsolete, recommendations on the GC analysis of these compounds include various sequences for their reduction by LiAlH₄ into polyaminoalcohols, followed by *N*-acylation or permethylation and, finally, silylation of OH groups. For example, *N*-TFA dipeptide Phe-Phe after reduction and silylation gives the compound (**III**) with a retention index of 2390 on semistandard-phase Dexsil-300.

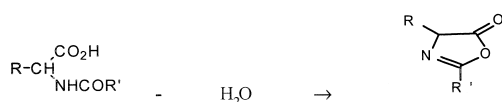
The typical example of one-stage derivatization of amino acids is their treatment by isopropyl bromide in presence LiH with the formation of *N*-isopropylated isopropyl esters. Unfortunately, this reaction can take place only in high-boiling aprotic bipolar solvents like dimethyl sulfoxide (DMSO, T_b = 189°C, RI_{nonpolar} = 790 \pm 18); this is a significant restriction for its application, in practice. A more important method is based on the reaction of amino acids with methyl or phenyl isothiocyanates with the formation of 3-methyl (phenyl) hydantoin:



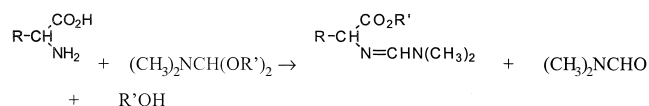
The stable nonvolatile intermediate phenylthiocarbamoyl derivatives are formed in basic media and can be analyzed directly by reverse-phase high-performance liquid chromatography (RP-HPLC). Their cyclization into hydantoin requires acid catalysis. This mode of derivatization is a very important supplement to the Edman's method of *N*-terminated sequencing of polypeptides. Before GC analysis, any hydantoin can be converted into *N*-trifluoroacetyl or enol-*O*-trimethylsilyl derivatives, which increases the selectivity of their determination in complex matrices.

N-Acylated amino acids, in the presence of water-coupling reagents (dicyclohexylcarbodiimide or the excess of TFAA), form other cyclic derivatives – azlactones (2,4-disubstituted oxazolin-5-ones):

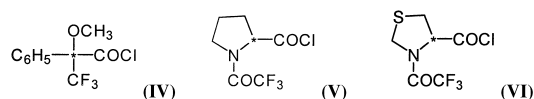




One of the most popular methods of single-stage amino acid derivatization at present is their conversion to *N,O(S) tert*-butyldimethylsilyl derivatives [the reagent *tert*-butyldimethylsilyl trifluoroacetamide (MTBSTFA) or its *N*-Me analog]. Another way, which was proposed at the beginning of the 1970s is based on amino acid interaction with dimethylformamide dialkylacetals $(\text{CH}_3)_2\text{NCH}(\text{OR}')_2$ ($\text{R} = \text{Me, Et, Pr, iso-Pr, Bu, Am}$) with formation of *N*-dimethylaminomethylene derivatives of amino acids esters:



The GC separation of enantiomeric D- and L-amino acids with nonchiral phases requires their conversion to diastereomeric derivatives. The second asymmetric center in the molecule (*) arises after esterification by optically active alcohols [2-BuOH, 2-AmOH, pinacolol, (–)-menthol, etc.] or NH_2 group acylation by chiral reagents {e.g., α -methoxy- α -trifluoromethylphenylacetyl chloride [MTPAC (**IV**)], *N*-trifluoroacetyl-L-prolyl chloride [N-TFA-L-Pro-Cl (**V**)], *N*-trifluoroacetyl-thiazolidine-4-carbonyl chloride (**VI**)}, etc.):



The selection of derivatization methods for amides and imides is not as great as for other classes of amino compounds. The active hydrogen atom in the structural fragments $-\text{CO}-\text{NH}-$ or $\text{SO}_2-\text{NH}-$ is highly acidic and, hence, sometimes recommended TMS, acetyl, or TFA derivatives of these compounds are unstable during hydrolysis. The best derivatization method is their exhaustive alkylation (preferably methylation), because permethylated amides and imides are volatile enough for their GC analysis. This general statement can be illustrated by retention data

for methylated derivatives of urea $\text{CO}(\text{NH}_2)_2$ as the simplest amide: Both the initial compound and its monomethyl and two dimethyl homologs cannot be analyzed by GC, owing to their nonvolatility. The retention index of trimethyl urea on the standard non-polar polysimethyl siloxanes is 976 ± 28 , whereas, for tetramethyl urea, it is 956 ± 5 (see the high interlaboratory reproducibility of this value compared with the previous one).

The exhaustive methylation of amides can be realized with rather high yields by their reactions with dimethyl sulfate/ $\text{EtN}(\text{iso-Pr})_2$, by CH_3I in acetone solution, with CH_3I in the presence of K_2CO_3 or LiH in DMSO, in heterophaseous “water–organic solvent” systems (together with the extraction of derivatives from matrices), and, directly, in the injector of gas chromatograph (so-called flash methylation) by $\text{PhNMe}_3^+\text{OH}^-$ (TMPAH). These modes of derivatization precede the GC determination of numerous diuretics (acetazolamide, ethacrinic acid, clopamide, etc.), some barbiturates and their metabolites, xanthines (theophylline), various urea and carbamate pesticides (monuron, fenuron, linuron and their metabolites), and so forth.

Suggested Further Reading

- Avery, M. J. and G. A. Junk, *Anal. Chem.* 57: 790 (1985).
 Biermann, C. J., C. M. Kinoshita, J. A. Marlett, and R. D. Steele, *J. Chromatogr.* 357: 330 (1986).
 Blau, K. and J. M. Halket (eds), *Handbook of Derivatives for Chromatography*, 2nd ed., John Wiley & Sons, New York, 1993.
 Carreras, D., C. Imas, R. Navajas, M. A. Garcia, C. Rodrigues, A. F. Rodrigues, and R. J. Cortes, *J. Chromatogr. A* 683: 195 (1994).
 Drozd, J., *Chemical Derivatization in Gas Chromatography*, Elsevier, Amsterdam, 1981.
 Horman, I. and F. J. Hesford, *Biomed. Mass Spectrom.* 1: 115 (1974); *Nestle Research News* 100 (1976/77).
 Knapp, D. R., *Handbook of Analytical Derivatization Reactions*, John Wiley & Sons, New York, 1979.
 Mawhinney, T. P., R. S. R. Robinett, A. Atalay, and M. A. Madson, *J. Chromatogr.* 358: 231 (1986).
 Nazareth, A., M. Joppich, A. Panthani, D. Fisher, and R. W. Giese, *J. Chromatogr.* 319: 382 (1985).
 Thenot, J. P. and E. C. Horning, *Anal. Lett.* 5: 519 (1972).

Derivatization of Analytes in Chromatography: General Aspects

Igor G. Zenkevich

Chemical Research Institute, St. Petersburg State University, St. Petersburg, Russia

Introduction

Any chromatographic analysis is preceded by a priori available information about analytes. Depending on the quantity of this available information, all determinations may be classified as (a) preferably confirmatory (determined components are known) and (b) prospective (any propositions concerning their chemical nature are very approximate). Numerous differences in the design of analytical procedures in these two cases are manifested in the features of all stages of analysis: sampling, sample preparation, the analysis itself, and interpretation of results. Only for procedures being classified as confirmatory, the stage of sample preparation can be supplemented by their chemical treatment by different reagents for the optimization of subsequent chromatographic analysis. The most widely used type of treatment is the synthesis of various chemical derivatives of target analytes, namely derivatization.

Discussion

Derivatization is a special subgroup of organic reactions used in chromatography for compounds with specific types of functional group. Not all known reactions can be applied as methods for derivatization, because these processes must be in accordance with some specific conditions:

1. The experimental operations must be as simple as possible. The mixing of sample with reagent(s) at ambient temperature, without additional treatment of mixtures, is preferable. In chromatographic practice, the time needed for the completion of the derivatization reaction may be up to 24 h (so-called "stay overnight"). Instead of this long time, the heating of reaction mixtures in ampoules is also permitted. Some processes (including silylation) can be realized by simple injection of reaction mixtures into the hot injector of the GC equipment.
2. The number of stages for every type of functional group must be minimal (one or 2, but no more!). For multistaged processes, the condi-

tion "single-pot synthesis" is necessary. Such operations as extraction or reextraction may be used only when the quantities of analytes are not very small or when it is necessary to isolate them from complex matrices. The large excess of derivatization reagent(s) and/or solvents must be easily removable or have no influence on the results of the analysis. The use of high-boiling solvents, typically, is not recommended. The possible by-products of reaction of must have no influence on the results as well.

3. The degree of transformation of initial compounds into products (yield, %) must be maximal and reproducible to provide valid quantitative determination of these compounds by analysis of their derivatives.
4. Mutually unambiguous correspondence between initial analytes and derivatives must be assured. The optimal case is $1 \rightarrow 1$, but some examples of type $1 \rightarrow 2$ are known (e.g., when the derivatives of enantiomers form a pair of diastereomers, *O*-alkyl ethers of oximes exist in syn and anti isomers, etc.). All processes that lead to further uncertainty (chemical multiplication of analytical signals) [e.g., $1 \rightarrow N$ ($N \geq 3$) must be excluded].

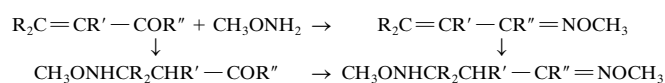
In accordance with the last criterion, for example, *N,O*-trimethylsilyl derivatives of amino acids seem not useful in analytical practice, owing to the nonspecific silylation of amino groups or postreaction hydrolysis of the resultant N—Si bonds. Even the simplest compounds of this class $H_2N-CHR-CO_2H$ form three possible products: $H_2N-CHR-CO_2TMS$, $TMSNH-CHR-CO_2TMS$, and $(TMS)_2N-CHR-CO_2TMS$ [TMS = $Si(CH_3)_3$] with different GC retention parameters. In the case of diamino monocarboxylic acids with nonequivalent amino groups [e.g., lysine $H_2N(CH_2)_4CH(NH_2)CO_2H$], the number of similar semisilylated derivatives is theoretically increased to nine.

The greatest principal difference between organic reactions in general and those which can be considered as chromatographic derivatization reactions is *de facto* commonly accepted absence of necessity of product



structure determinations in the last case. In "classical" organic chemistry, every synthesized compound must be isolated from its reaction mixture and characterized by physicochemical constants or spectral parameters for confirmation or estimation (for new objects) of its structure. However, for the processes that have been classified as derivatization reactions, these operations are not necessary and are really not used in analytical practice. *The reaction itself is considered as the confirmation of structures of derivatives.* Of course, any exceptions from this important rule are very dangerous and must be pronounced as the special warning for applications of every method of derivatization.

The examples of chemical uncertainty (some products of different structures are formed) are the reactions of barbiturates with diazomethane CH_2N_2 , which leads to different *N*- and/or *O*-methyl derivatives [1], or the interaction of dimethyl disulfide with conjugate dienes [2]. One of the frequently used derivatization methods for carbonyl compounds $\text{RR}'\text{CO}$ (including an important group of steroids) implies their one-step treatment by *O*-alkyl hydroxylamines $\text{R}''\text{ONH}_2$, with formation of alkyl ethers of oximes $\text{RR}'\text{C}=\text{NOR}''$. However, this reaction has an anomaly for compounds with double bonds $\text{C}=\text{C}$ conjugated with carbonyl groups, namely the parallel addition of reagent with active hydrogen atoms to the polarized $\text{C}=\text{C}$ bonds [3]:



This means that, instead of one expected product with molecular weight (MW) = $M_0 + 29$ (with *O*-methyl hydroxylamine as reagent), reaction mixtures may contain two additional compounds with $\text{MW} = M_0 + 47$ and $M_0 + 76$. This feature is negligible for analysis of individual compounds, but when samples are mixtures of components of interest, the analysis becomes impossible because of the complexity of the resultant interpretation.

Only if the organic reaction is in accordance with all above-mentioned criteria can it be considered as a method for derivatization. Finding new appropriate processes of this type is complex and often not obvious. Some reagents have been recommended only for synthesis of derivatives for chromatography.

One of the main purposes of derivatization is the transformation of nonvolatile compounds into volatile derivatives. However, it is not the sole purpose of this treatment of analytes. Each chromatographic method [gas chromatography (GC), GC-mass spectroscopy (MS), high-performance liquid chromatography (HPLC), capillary electrophoresis (CE), etc.] being

supplemented by derivatization permits us to solve some specific problems. Most principal of them are summarized briefly in Table 1, followed by more detailed comments.

Most monofunctional organic compounds (including alcohols ROH , carboxylic acids RCO_2H , amides RCONH_2 , etc.) are volatile enough for direct GC analysis. Exceptions are only those compounds with high melting points (sometimes with decomposition) because of strong intermolecular interactions in their condensed phases [e.g., semicarbazones $\text{RR}'\text{C}=\text{N}-\text{NHCSNH}_2$, guanidines $\text{RNH}-\text{C}(=\text{NH})-\text{NH}_2$, etc.]. Ionic compounds (e.g., quaternary ammonium salts $[\text{R}_4\text{N}]^+\text{X}^-$ are nonvolatile as well. If the compounds contain two or more functional groups with active hydrogen atoms [including the case of inner-molecular ionic structures, such as that seen in amino acids $\text{RCH}(\text{NH}_3^+)\text{CO}_2^-$], their volatility decreases significantly. The purpose of derivatization of all these objects is to substitute active hydrogen atoms by covalently bonded fragments that provide more volatile products. Direct GC analysis of highly reactive compounds (free halogens, hydrogen halides, sulfonic acids RSO_2OH , etc.) is accompanied by their interaction with stationary phases of chromatographic columns; they also require derivatization. If the initial compound A can be analyzed together with derivative B, the comparison of their GC retention indices is an important source of information about the nature of these compounds. The average value of the retention indices $\Delta\text{RI}_r = \text{RI}(\text{B}) - \text{RI}(\text{A})$ may be used for identification of both analytes. Some selected ΔRI_r values are presented in Table 2.

Gas chromatography-mass spectrometry analysis completely excludes the second item from the possible aims of derivatization, insofar as the mass spectrometer itself is both a universal and a selective GC detector. At the same time, two new important reasons for derivatization appear in this method. The intensities of molecular ion (M^+) signals are small if the compounds have no structural fragments to provide the effective delocalization of a charge and unpaired electron. These fragments are conjugated bonds-atoms systems and isolated heteroatoms with high polarizabilities (S, Se, I). In accordance with this regularity, *O*-TMS derivatives of alcohols indicate no M^+ peaks in mass spectra, whereas for the TMS ethers of carbonyl compounds' enols $\text{RCH}_2\text{COR}' \rightarrow \text{RCH}=\text{CR}'-\text{OSiMe}_3$ (π - p - d conjugation system), they are very intense.

The determination of double-bond $\text{C}=\text{C}$ positions in the carbon skeletons of molecules very often is impossible, owing to uncertain charge distribution in molecular ions. The solution of this problem implies the conversion of unsaturated compounds into products whose molecu-



Table 1 The Principal Applications of Derivatization in Different Chromatographic Techniques

Aims of derivatization	Typical examples
Gas Chromatography	
1. Transformation of nonvolatile, thermally unstable and/or highly reactive compounds into stable volatile derivatives	$\text{ROH} \rightarrow \text{ROSiMe}_3$ $\text{ArOH} \rightarrow \text{ArOCOCF}_3$ $\text{RR}'\text{CO} \rightarrow \text{RR}'\text{C}=\text{NOCH}_3$ $\text{ROH} \rightarrow \text{ROCOCCl}_3$ (ECD) $\text{RCO}_2\text{H} \rightarrow \text{RCO}_2\text{CH}_2\text{CCl}_3$ (ECD) $\text{HCO}_2\text{H} \rightarrow \text{HCO}_2\text{CH}_2\text{C}_6\text{H}_5$ (FID) $\text{RCHO} \rightarrow 2,4\text{-(NO}_2)_2\text{C}_6\text{H}_3\text{—NH—N=CHR}$
2. Synthesis of derivatives for element-specific GC detectors or conversion of nondetectable compounds into suitable products for the minimization of detection limit	
3. Combination with the stage of sampling (preferably in the environment analyses when derivatization are used as the method of chemosorption)	
4. Separation of enantiomeric compounds on non-chiral phases after their conversion into diastereomeric derivatives	$\text{RR}'\text{C}^*\text{HNNH}_2 + \text{C}_6\text{H}_5\text{C}^*\text{H(OMe)COCl} \rightarrow$ $\text{RR}'\text{C}^*\text{HNNH—COC}^*\text{H(OMe)C}_6\text{H}_5$ (C* = asymmetrical carbon atoms)
Gas chromatography–mass spectrometry	
5. Determination of molecular weights of compounds with $W_M \approx 0$ at the electron impact ionization (synthesis of derivatives with conjugated bonds–atoms systems)	$\text{RR}'\text{CO} \rightarrow \text{RR}'\text{C}=\text{NNH—C}_6\text{F}_5$ (π – p – π conjugation system) $\text{RNH}_2 \rightarrow \text{RN}=\text{CH—NMe}_2$ (p – π conjugation system)
6. The increasing of specificity of molecular ion fragmentation for estimation of structure of analytes (an example: the determination of double bonds C=C position in carbon skeleton of the molecules)	“On-site” derivatization: $\text{RCH}=\text{CHR}' \rightarrow \text{R—CH(SMe)—CH(SMe)—R}'$ “Remote-site” derivatization: $\text{RCH}=\text{CH(CH}_2)_n\text{CO}_2\text{H} + \text{H}_2\text{NCH}_2\text{CH}_2\text{OH} \rightarrow$ 2-Substituted oxazoline
High-performance liquid chromatography with UV detection	
7. Synthesis of chromogenic derivatives (with chromophores which provide the adsorption within typical range of UV detection 190–700 nm)	$\text{C}_6\text{H}_7\text{O(OH)}_5 \rightarrow \text{C}_6\text{H}_7\text{O(OCOC}_6\text{H}_5)_5$
8. The conversion of hydrophilic analytes into more hydrophobic derivatives	$\text{RCH(NH}_2\text{)CO}_2\text{H} \rightarrow$ $\text{RCH(NHCSNHC}_6\text{H}_5\text{)CO}_2\text{H}$
9. The determination of number of functional groups with active hydrogen atoms	$\text{X(OH)}_n + [(\text{R}_1\text{CO})_2\text{O} + (\text{R}_2\text{CO})_2\text{O}] \rightarrow$ miscellaneous acyl derivatives

lar ions have sufficiently fixed charge localization. There are two concepts to provide this localization: (a) by the addition of heteroatomic reagents to the C=C bond (so-called “on-site” derivatization with the formation of TMS ethers of corresponding diols, adducts with dimethyl disulfide, etc.) and (b) after introduction or formation of nitrogen-containing heterocycles rather far from an unchanged C=C bond (“remote-site” derivatization).

The formation of new chromophores for the optimization of ultraviolet (UV) detection of analytes in HPLC implies the synthesis of derivatives with conjugated systems in the molecule. Compared with GC, there are no restrictions on the volatilities of these derivatives for HPLC analysis. They may be synthesized before analysis (precolumn derivatization) or after chromatographic separation (postcolumn derivatization). The latter technique is rarely used and then only for a few classes of compounds, but it permits us to

combine the measurement of retention parameters of initial analytes with the detection of their derivatives.

The range of the most convenient hydrophobicities of organic compounds for reversed-phase HPLC separation may be estimated approximately as $-1 \leq \log P \leq +5$ ($\log P$ is the logarithm of the partition coefficient of the compound being characterized in the standard solvent system *n*-octanol–water). Highly hydrophilic substances with $\log P \leq -1$ need the special choice of analysis condition (e.g., use of ion-pair reagents). Another approach is their conversion to more hydrophobic derivatives by modification of functional groups with active hydrogen atoms.

The examples mentioned here for RP–HPLC analysis of monosaccharides in the form of perbenzoates and amino acids as *N*-phenylthiocarbamoyl derivatives (Table 1) satisfy both principal criteria: introducing the chromophores into molecules of the analytes



Table 2 Average Values of Retention Indices Differences ΔRI_r for Different Derivatization Reactions

$\Delta M = M_{\text{deriv}} - M_{\text{initial}}$	Scheme of reaction (for mono-functional compounds only)	$\Delta RI_r \pm s_{\Delta RI}$ (standard non-polar polydimethyl siloxanes)
14	$\text{RCO}_2\text{H} \rightarrow \text{RCO}_2\text{Me}$	-102 ± 28
14	$\text{ArOH} \rightarrow \text{ArOMe}$	-62 ± 16
28	$\text{RCO}_2\text{H} \rightarrow \text{RCO}_2\text{Et}$	-42 ± 7
28	$\text{RR}'\text{CO} \rightarrow \text{RR}'\text{C}=\text{NNHMe}$	229 ± 23
29	$\text{ROH} \rightarrow \text{RONO}$	-66 ± 27
42	$\text{ROH} \rightarrow \text{ROCOMe}$	142 ± 18
42	$\text{ArOH} \rightarrow \text{ArOCOMe}$	97 ± 20
42	$\text{RNH}_2 \rightarrow \text{RNHCOMe}$	437 ± 29
42	$\text{ArNH}_2 \rightarrow \text{ArNHCOMe}$	401 ± 7
42	$\text{RR}'\text{CO} \rightarrow \text{RR}'\text{C}=\text{NNMe}_2$	302 ± 20
72	$\text{ROH} \rightarrow \text{ROSiMe}_3$	119 ± 18
72	$\text{RCO}_2\text{H} \rightarrow \text{RCO}_2\text{SiMe}_3$	76 ± 16
90	$\text{RR}'\text{CO} \rightarrow \text{RR}'\text{C}=\text{NNHC}_6\text{H}_5$	858 ± 22
96	$\text{ROH} \rightarrow \text{ROCOCF}_3$	-85 ± 24
114	$\text{RCO}_2\text{H} \rightarrow \text{RCO}_2\text{SiMe}_2\text{-tert-Bu}$	288 ± 29
144	$\text{ROH} \rightarrow \text{ROCOCCl}_3$	494 ± 18

($\text{C}_6\text{H}_5\text{CO}-$ and $\text{C}_6\text{H}_5\text{NH}-\text{CS}-\text{NH}-$) and optimization of their retention parameters.

Sometimes, the generally prohibited multiplication of analytical signals of derivatives may be attained artificially for the solution of partial problems. For example, the treatment of polyhydroxy compounds (phenols, phenolcarboxylic acids, etc.) $\text{X}(\text{OH})_n$ by an equimolar mixture of acylation reagents $(\text{R}_1\text{CO})_2\text{O} + (\text{R}_2\text{CO})_2\text{O}$ leads to the formation of $n + 1$ miscellaneous acyl derivatives $\text{X}(\text{OCOR}_1)_n$, $\text{X}(\text{OCOR}_1)_{n-1}(\text{OCOR}_2)$, . . . , $\text{X}(\text{OCOR}_2)_n$. The relative abundances of their chromatographic peaks are similar to the binomial coefficients (i.e., 1:1 at $n = 1$, 1:2:1 at $n = 2$, 1:3:3:1 at $n = 3$, and so forth). The differences between retention indices of these derivatives at $\text{R}_1 = \text{CH}_3$ and $\text{R}_2 = \text{C}_3\text{H}_7$ are small and their average value for phenols is 160 ± 23 [4]. These two regularities permit us to determine the number of hydroxyl groups (n) in analytes.

References

1. D. J. Harvey, J. Nowlin, P. Hickert, C. Butler, O. Gansow, and M. G. Horning, *Biomed. Mass Spectrom.* 1: 340 (1974).

2. M. Vincentini, G. Guglielmetti, G. Gassani, and C. Tonini, *Anal. Chem.* 59: 694 (1987).
3. I. G. Zenkevich, Ju. P. Artsybasheva, and B. V. Ioffe, *Zh. Org. Khim. (Russ.)*, 25: 487 (1989).
4. I. G. Zenkevich, *Fresenius' J. Anal. Chem.* 365: 305–309 (1999).

Suggested Further Reading

- Blau, K. and G. S. King (eds.), *Handbook of Derivatives for Chromatography*, John Wiley & Sons, New York, 1978.
- Blau, K. and J. M. Halket (eds.), *Handbook of Derivatives for Chromatography*, 2nd ed., John Wiley & Sons, New York, 1993.
- Drozd, J., *Chemical Derivatization in Gas Chromatography*, Chromatography Library Vol. 19, Elsevier, Amsterdam, 1981.
- Heberle, J. and G. Simchen, *Silylating Agents*, 2nd ed., Fluka Chemie AG, 1995.
- Knapp, D. R., *Handbook of Analytical Derivatization Reactions*, John Wiley & Sons, New York, 1979.



Derivatization of Carbohydrates for GC Analysis

Raymond P.W. Scott

Scientific Detectors Ltd., Banbury, Oxfordshire, England

Introduction

As a result of the development of special bonded phases, carbohydrates or their derivatives are usually separated by liquid chromatography. However, certain carbohydrate samples are still analyzed by GC due to the inherent high efficiencies obtainable from the technique and to the associated short elution times. In addition, gas chromatography–mass spectrometry (GC–MS) is a particularly powerful analytical technique for carbohydrates, especially for their identification. As a consequence, appropriate derivatives must be formed to render them sufficiently volatile but still easily recognizable from their mass spectra.

Discussion

It is relatively easy to form the trimethylsilyl derivatives, employing standard silyl reagents such as trimethylchlorsilane or hexamethyltrisilazane, and the reactions normally can be made to proceed to completion. However, there is a major problem associated with the derivatization of natural sugars which arises from the formation of anomers and the pyranose–furanose interconversion. Reducing sugars in solution (e.g., glucose) exist as an equilibrium mixture of anomers. Consequently, each sugar produces five tautomeric forms—two pyranose, two furanose, and one open-chain form. In general, all the anomers can be separated by GC. This autoconversion can be minimized by mild and rapid derivatization. Equilibrium mixtures are to be expected from reducing sugars isolated from natural products.

Mixtures of hexamethyltrisilazane and trimethylchlorsilane are frequently used to derivatize sugars. Pure sugars (e.g., glucose, mannose, and xylose) can be readily derivatized using a mixture of hexamethyltrisilazane:trimethylchlorsilane:pyridine (2:1:10 v/v/v), giving single GC peaks; however, if the pro-

portion of trimethylchlorsilane is doubled, small amounts of the anomeric forins are observed. One disadvantage of this procedure is the formation of an ammonium chloride precipitate, which, if injected directly onto the column, can cause column contamination and eventually column blockage. The formation of ammonium chloride can be avoided by extracting the derivative into hexane or by the use of an alternative derivatizing agent.

N,O-Bis(trimethylsilyl)trifluoroacetamide, usually combined with trimethylchlorsilane (10:1, v/v) is also a popular derivatizing agent for carbohydrates and the reaction mixture can be injected directly onto the column without fear of column contamination. The formation of anomers can also be avoided by preparing the alditols by treating with sodium borohydride. The alditols can then be separated after derivatizing with trimethylchlorsilane, a procedure that is considered preferable to the preparation of their acetates. The rapid preparation of trimethylsilylalditols using trimethylsilylimidazole in pyridine mixtures at room temperature has the advantage over other methods, which require longer reaction times and higher temperatures. The use of silylaldolnitrile derivatives has been reported for the separation of aldoses. The sugars are reacted with hydroxylamine-*O*-sulfonic acid to form aldonitriles which are then silanated with *N,O*-bis(trimethylsilyl)trifluoroacetamide:pyridine (1:1 v/v). The silylaldonitrile derivatives are readily separated on open tubular columns.

Another silanization procedure for the derivatization of carbohydrates is the formation of trimethylsilyl oximes. The methyloxime is heated with hexamethyldisilazane:trifluoroacetic anhydride (9:1 v/v) for 1 h at 100°C. Anthrone *O*-glucoside is an important ingredient in skin care cosmetics and can be fully silylated by reaction with *N,O*-bis(trimethylsilyl)acetamide:acetonitrile mixture (1:1 v/v) for 1 h at 90°C, and subsequently separated by GC.



Conclusion

Acetylation and the use of trifluoroacetates, originally the more popular derivatives for the separation of carbohydrates by GC, are still used on occasion, but the various silanization methods are, today, the most common and considered the most effective for GC carbohydrate analysis.

Suggested Further Reading

- Blau, K. and J. Halket (eds.), *Handbook of Derivatives for Chromatography*, John Wiley & Sons, New York, 1993.
- D. W. Grant, *Capillary Gas Chromatography*, John Wiley & Sons, New York, 1996.
- R. P. W. Scott, *Techniques of Chromatography*, Marcel Dekker, Inc., New York, 1995.
- R. P. W. Scott, *Introduction to Analytical Gas Chromatography*, Marcel Dekker, Inc., New York, 1998.



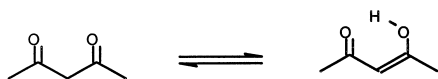
Derivatization of Carbonyls for GC Analysis

Igor G. Zenkevich

Chemical Research Institute, St. Petersburg State University, St. Petersburg, Russia

Introduction

The carbonyl group in aldehydes (RCHO) and ketones (RCOR') is one of the frequently encountered functionalities in the composition of organic compounds. This group has no active hydrogen atoms, excluding the cases of high content of enols for β -dicarbonyl compounds (β -diketones, esters of β -ketocarboxylic acids, etc.):



Discussion

The derivatization, at least of monofunctional carbonyl compounds, is not the obligatory stage of sample preparation before their gas chromatography (GC) analysis. Nevertheless, the objective reasons for their derivatization are the following

1. The simplest aldehydes and ketones are slightly polar, low-boiling substances with small retention indices (RI) both on standard nonpolar and polar stationary phases; for example:

Aldehyde	RI _{nonpolar}	RI _{polar}
Ethanal	369 \pm 7 ^a	701 \pm 14
Propanal	479 \pm 9	794 \pm 9

Ketone	RI _{nonpolar}	RI _{polar}
Acetone	472 \pm 12	820 \pm 11
2-Butanone	578 \pm 12	907 \pm 14

^aHere and later, RI values with standard deviations are randomized interlaboratory data.

In the numerous GC analytical procedures, the first part of chromatograms very often can be overloaded by intensive peaks of auxiliary compounds (solvents, by-products, etc.). The optimization of the determination of target carbonyl compounds usually needs the "replacement" of their analytical signals into less "populated" areas of chromatograms (the derivatives

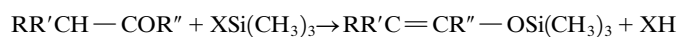
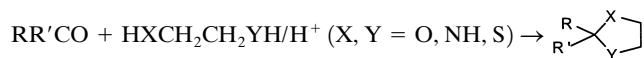
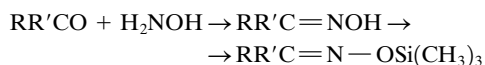
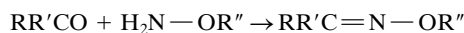
with retention parameters which exceed that for initial analytes).

2. The simplest monofunctional compounds with active hydrogens in the functional groups — OH, — CO₂H, NH₂, and so forth typically are volatile enough for their GC determinations. However, the presence in the molecules of any extra polar fragments (including C=O) makes the possibilities of GC analysis of these compounds worse; they usually need derivatization of one or (better) of both polar functional groups. Thus, in many cases, the necessity of derivatization of carbonyl fragment in polyfunctional compounds is a secondary procedure, which is caused by the presence of other functional groups.
3. Both aliphatic and aromatic aldehydes are easily oxidized compounds (even by atmospheric oxygen). Hence, one of the aims of their derivatization is to prevent the oxidation of analytes with resultant formation of carboxylic acids.

Some methods of carbonyl compound derivatization have been known in "classical" organic chemistry since the last century. Their predestination was simply the identification by comparison of melting points of purified solid derivatives with reference data. These derivatives are, for example, semicarbazones RR'C=NNHCONH₂, thiosemicarbazones RR'C=NNHCSNH₂, 2,4-dinitrophenylhydrazones RR'C=NNHC₆H₃(NO₂)₂, and so forth. However, most of these derivatives with structural fragments =N—NH—C(=X)—NH₂ are not volatile enough for their direct GC analysis, because of the presence of three active hydrogen atoms in these fragments. The convenient derivatives for GC determinations must include not more than one of these atoms (monosubstituted arylhydrazones) or they need to be free of them (*O*-alkyl and *O*-benzyl ethers of oximes). The oximes themselves can be synthesized by the reaction of carbonyl compounds with hydroxylamine, but they are usually used in GC practice in the form of *O*-TMS ethers.

Other types of carbonyl derivatives are acetals and/or ketals, preferably cyclic 1,3-dioxolanes, 1,3-oxathiolanes, or thiazolidines. Some carbonyl compounds (especially steroids) can be analyzed as their enol-TMS derivatives:





All of these processes (excluding the last one) can be classified as condensation reactions. Hence, in all cases, the target derivatives are theoretically the sole components and no other volatile by-products, excluding water, have been formed. However, some common features of these reactions must be considered:

1. Both *O*-alkyl hydroxylamines and, especially, arylhydrazines, are slightly oxidized compounds. The presence of any oxidizers in the reaction mixtures must be excluded. Nevertheless, in real practice, these mixtures very often contain some by-products (e.g., $ArNH_2$, $ArOH$, ArH , etc.). Usually, there are no problems to reveal their chromatographic peaks, because all of them have lower retention parameters than those for the initial reagents and, moreover, all target derivatives.
2. The condensation reaction of the considered type can be characterized by statistically processed differences of retention indices of products and initial substrates. This mode of additive scheme permits us to estimate these analytical parameters for any new derivatives on standard nonpolar polydimethyl siloxanes. For the simplest reaction scheme, $A + \dots \rightarrow B + \dots$, $\Delta MW = MW(B) - MW(A)$ and $\Delta RI_r = RI(B) - RI(A)$:

Scheme of reaction	ΔMW	$\langle \Delta RI_r \rangle$ (IU)
$RR'CO \rightarrow RR'C=NNHCH_3$	28	229 ± 23
$ArRCO \rightarrow ArR=NNHCH_3$	28	320 ± 30
$RR'CO \rightarrow RR'C=NN(CH_3)_2$	42	302 ± 20
$RR'CO \rightarrow RR'C=NNHC_2H_5$	42	345 ± 16
$RR'CO \rightarrow RR'C=NNHC_6H_5$	90	858 ± 22
$ArCHO \rightarrow ArCH=NNHC_6H_5$	90	996 ± 50
$RR'CO \rightarrow RR'C(OCH_3)_2$	46	189 ± 17
$ROH \rightarrow ROSi(CH_3)_3$	72	119 ± 18
(for the comparison)		

Derivatization of Carbonyls for GC Analysis

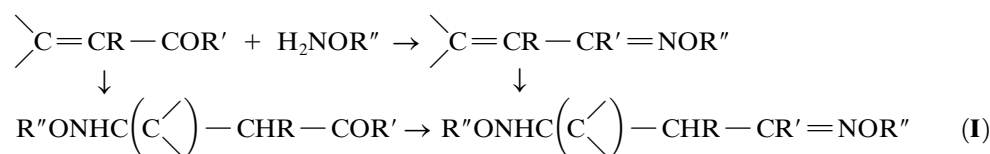
This set of ΔRI_r values illustrate that the simplest alkylhydrazones (methyl, ethyl, dimethyl, etc.) have appropriate GC retention parameters and, theoretically, can be recommended as the derivatives for carbonyl compounds. However, in real analytical practice, these hydrazones are not used because of their low yields, especially for the aliphatic ketones.

3. All considered condensation reactions have some anomalies for the α,β -unsaturated carbonyl compounds. Most reagents with active hydrogen atoms can react not only with carbonyl groups but also with polarized conjugated double bonds $C=C$. As a result of this regularity, three products, instead of the estimated one target derivative, are formed in the reactions of α,β -unsaturated carbonyl compounds with *O*-alkyl hydroxylamines:

The relative ratio of these products depends on the excess of derivatization reagent and the pH of the reaction mixtures. The chemical origin of products of the reaction of phenyl hydrazine with unsaturated carbonyl compounds depends on the same factors and, moreover, on the order of the components' mixing (it exerts the influence on the current pH of reaction media). The 2-pyrazolines have resulted, in some cases, as the sole reaction products instead of hydrazones:

The formation of hydrazinohydrazones [similar to compounds **(I)**] have been reported for the reaction of unsaturated carbonyl compounds with dialkyl hydrazines. Hence, the existence of different products means that the quantitative yield of each of them is not enough, as is necessary for GC analysis of derivatives. It is quite probable that the same anomalies can take place in the reactions of unsaturated carbonyls with other reagents. For example, unsaturated 2,4-DNPHs seem unstable at the high temperatures of injectors and GC columns. This fact explains the small number of published RI data for the derivatives of these compounds and the necessity to search the new types of derivatization reactions for them.

4. Both hydrazones and *O*-alkyl oximes of asymmetrical carbonyl compounds exist in two iso-

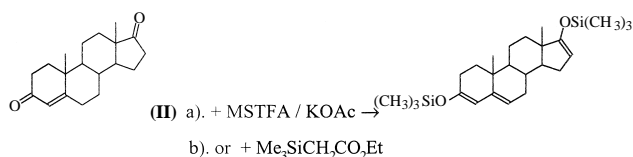


meric structures with slightly different GC retention parameters:

Hence, most of these derivatives give two analytical signals (antiisomers typically are more stable and their peaks prevail over the syn derivatives). If the assignment of these two peaks to the isomeric compounds is not obvious, they can be marked by symbols #1 and #2 in the accordance with the usual chromatographic practice. The same duplication of analytical signals takes place, for example, during reversed-phase high-performance liquid chromatography (RP-HPLC) analysis of 2,4-DNPHs.

For the polyfunctional organic compounds, the considered condensation reactions of carbonyls can be combined with different derivatizations of other functional groups. So, the "standard" method of hydroxyketosteroids derivatization for GC analysis is their two-stage treatment with *O*-methyl hydroxylamine ($\text{>C=O} \rightarrow \text{>C=NOCH}_3$) followed by silylation of OH groups.

The resulting MO-TMS derivatives of numerous important compounds of this class are characterized by standard mass spectra and GC retention indices on standard nonpolar phases for their identification. The use of most active silylating reagents permits us to exclude the stage of *O*-methyl oxime formation, so far as ketosteroids can form the enol-TMS ethers. For example, androstenedione (**II**) gives the bis-*O*-TMS derivative:

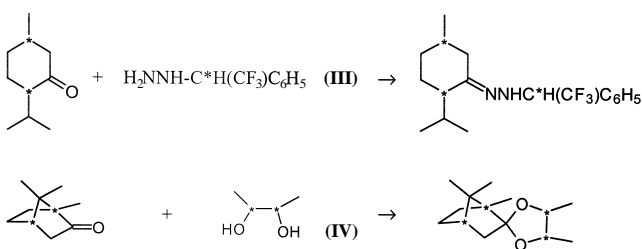


Because of the presence of p - π -(d) conjugated systems $\text{C}=\text{C}-\text{O}-(\text{Si})$, these derivatives indicate the intensive signals of the molecular ions in their mass spectra.

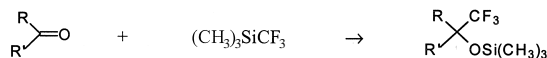
The formation of acetals from carbonyl compounds requires acid catalysis and (sometimes) the presence of water-coupling reagents (for instance, anhydrous CuSO_4). The conversion of aliphatic aldehydes into dimethyl acetals slightly increases the retention parameters of analytes ($\Delta\text{RI}_r = 189 \pm 17$). The cyclic ethylene derivatives (1,3-dioxolanes, $\Delta\text{RI}_r = 212 \pm 7$, this value is valid only for acyclic carbonyl compounds) are more stable to the hydrolysis and used in GC practice

preferably. Their important advantage for gas chromatography-mass spectrometry (GC-MS) analysis is the very specific fragmentation of molecular ions with the loss of substituents R and R' in the second position of the cycle and the formation of daughter ions $[\text{M}-\text{R}]^+$ and $[\text{M}-\text{R}']^+$, that give useful information for the determination of the initial carbonyl compound structure. The use of 2-aminoethanethiol in this reaction instead of ethylene glycol leads to the thiazolidines, which indicate the intense signals of molecular ions.

The GC separation of chiral carbonyl compounds (at first natural terpenoids, for example, camphor, menthone, carvone, etc.) on the nonchiral phases can be carried out in the accordance with the same principles as those for enantiomers of other classes. Their conversion into diastereomers by the reaction with chiral derivatization reagents is necessary. Examples of them are α -trifluoromethylbenzyl hydrazine (**III**) and optically active 2,3-butanediol (**IV**):



In connection with the problem of carbonyl compounds derivatization, it is expedient to touch upon a question of the application of new proposed reagents which are not yet widely used in GC analytical practice, but seem like promising ones in accordance with different criteria. One of them is low-boiling trimethyl-trifluoromethyl silane $(\text{CH}_3)_3\text{SiCF}_3$ which converts the carbonyl groups into α -trifluoromethyl *O*-TMS carbinol fragments:



Moreover, the carbonyl groups are represented in the numerous derivatives of carboxylic acids, namely amides, imides, and so forth. There are no derivatization methods for these compounds at present (excluding reduction), which are based on the reactions of the carbonyl group. Nevertheless, the amides react with $(\text{CH}_3)_3\text{SiCF}_3$ in a manner similar to other carbonyl compounds. The hydrolysis of intermediate *O*-TMS derivatives followed by dehydration leads to the low boiling α -trifluoromethyl enamines

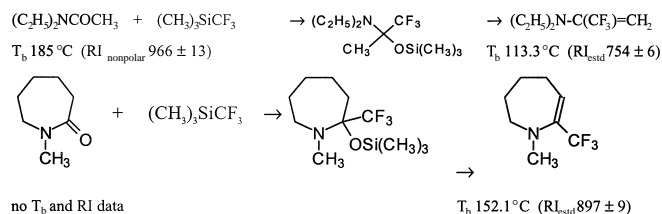


Table 1 Physicochemical and Gas Chromatographic Properties of Some Reagents for the Derivatization of Carbonyl Compounds

Reagent (abbreviation)	MW	T_b ($^{\circ}\text{C}$)(m.p., $^{\circ}\text{C}$)	RI _{nonpolar}
Phenyl hydrazine	108	244	1157 \pm 11
Pentafluorophenyl hydrazine (PFPH)	198	(74–75)	1164 \pm 16 ^a
2,4,6-Trichlorophenyl hydrazine (TCOH)	210	(141–143)	1654 ^b
2,4-Dinitrophenyl hydrazine	198	(200.5–201.5)	—
N-Aminopiperidine	100	146	859 \pm 14
O-Methyl hydroxylamine (HCl)	47	47 (148)	—
O-Ethyl hydroxylamine (HCl)	61	68 (130–133)	—
O-Pentafluorobenzyl hydroxylamine hydroxylamine (HCl) (PFBHA)	213	227 (subl)	1068 \pm 12 ^a
Hydroxylamine (HCl) (with following silylation of oximes)	33	(151)	—
Methanol/H ⁺	32	64.6	381 \pm 15
Ethylene glycol/H ⁺ , CuSO ₄	62	197.8	726 \pm 28
Trimethyltrifluoromethyl silane	142	45	532 \pm 3 ^a
Silylating reagents (for synthesis of enols' TMS ethers)	See table in the entry Derivatization of Hydroxy Compounds for GC Analysis		

^aEstimated RI values.^bSingle experimental data.

These structures are in the mutually unambiguous accordance with the structures of initial amides and, hence, can be considered as new types of derivatives.



The retention indices of any members of this new class of derivatives are unknown at present (only the boiling points have been determined). Nevertheless, this information is enough for the estimation of retention index (RI) values on the standard nonpolar phases with the following nonlinear equation:

$$\log \text{RI} = a \log T_b + b \text{MR}_D + c$$

where T_b is the boiling point and MR_D is the molar refraction (can be estimated by additive schemes); the coefficients of this equation are calculated by a least squares method with the data for compounds with known RI, T_b , and MR_D . Some results of calculations are presented in Table 1: They indicate that the RIs of α -trifluoromethyl enamines are less than the RIs of ini-

tial amides by approximately 200 IU; this is a very important fact for the choice of appropriate derivatization methods for the more complex nonvolatile compounds of this class.

Suggested Further Reading

- Biondi, P. A., F. Manca, A. Negri, C. Secchi, and M. Montana, *J. Chromatogr.* 411: 275 (1987).
- Blau, K. and J. M. Halket (eds.), *Handbook of Derivatives for Chromatography*, 2nd ed., John Wiley & Sons, New York, 1993.
- Droz, J., *Chemical Derivatization in Gas Chromatography*, Elsevier, Amsterdam, 1981.
- Gleispach, H., *J. Chromatogr.* 91: 407 (1974).
- Knapp, D. R., *Handbook of Analytical Derivatization Reactions*, John Wiley & Sons, New York, 1979.
- Lehmpuhl, D. W. and J. W. Birks, *J. Chromatogr. A* 740: 71 (1996).
- Levine, S. P., T. M. Harvey, T. J. Waeghe, and R. H. Shapiro, *Anal. Chem.* 53: 805 (1981).
- Nawrocki, J., I. Kalkowska, and A. Dabrowska, *J. Chromatogr. A* 749: 157 (1996).
- Zenkevich, I. G., *J. High Resolut. Chromatogr.* 21: 565 (1998).
- Zenkevich, I. G., Ju. P. Artsybasheva, and B. V. Ioffe. *Zh. Org. Khim. (Russ.)*. 25: 487 (1989).



Derivatization of Hydroxy Compounds for GC Analysis

Igor G. Zenkevich

Chemical Research Institute, St. Petersburg State University, St. Petersburg, Russia

Introduction

The hydroxyl group is one of the most propagated functional groups in organic compounds. Important biogenic substances (carbohydrates, flavones, phenolic acids, etc.) belong to the class of hydroxy compounds. One of the principal directions of the metabolism of different ecotoxicants and drugs in vivo is their hydroxylation followed by formation of conjugates with carbohydrates or amino acids. For example, the oxidation of widespread environmental pollutants—polychlorinated biphenyls (PCBs)—by cytochrome P450 leads to hydroxy-PCBs. The determination of OH compounds was one of the important problems of GC analysis during the almost half a century that this method has been in existence.

Discussion

The simple rule for the prediction of the possibility of GC analysis of organic compounds is based on the reference data of their boiling points. If any compound can be distilled without decomposition at the pressures from atmospheric to 0.01–0.1 torr, it can be subjected to GC analysis, at least on standard nonpolar polydimethylsiloxane stationary phases. In accordance with this rule, most of the monofunctional —OH compounds (alcohols, phenols) and their S analogs (thiols, thiophenols, etc.) may be analyzed directly. The confirmation of chromatographic properties of any analytes must be not only verbal (at the binary level “yes/no”) but also based on their GC Kovats retention indices as the most objective criteria; for example:

Compound	T_b (°C)	RI (nonpolar)
1-Tetradecanol	290.8	1664 ± 12 ^a
1-Decanethiol	239.2	1320 ± 7
2,6-Di- <i>tert</i> -butyl-4-methyl phenol	265	1491 ± 10
2-Methylbenzenethiol	194	1061 ± 11

^aRI's with standard deviations are randomized interlaboratory data.

Chemical properties of hydroxy compounds depend on the presence of active hydrogen atoms in the

molecule. The pK_a values for aliphatic alcohols are comparable to that of water (≈ 16), but phenols are weak acids ($pK_a \approx 9$ –10). An increase in the number of polar functional groups in the molecules leads to an increase of the strength of intermolecular interactions. This is manifested in the rising of melting and boiling points, which can increase the temperature limits of thermal stability of the compounds. For example, some aliphatic diols and triols have boiling points at atmospheric pressure and, hence, are volatile enough for GC analysis. Similar compounds with four or more hydroxyl groups have no boiling points at atmospheric pressure; this means the impossibility of their GC analysis. The same restrictions are valid within the series of polyfunctional phenols:

Compound	T_b (°C)	RI (nonpolar)
Glycerol (three OH groups)	290.5	1196 ± 28
Hydroquinone	287	1338 ± 14
<i>meso</i> -Erythritol (four OH groups)	329–331	1319
Pyrogallol	309	1548
Xylitol (five OH groups)	None	None
1,2,4-Benzenetriol	None	None

Even the simplest bifunctional compounds of these classes being analyzed on nonpolar phases indicate broad nonsymmetrical peaks on chromatograms. This leads to poor detection limits and reproducibility of retention indices (the position of peaks' maxima depends on the quantity of analytes) compared with nonpolar compounds. The general way to avoid these problems is based on the conversion of hydroxy compounds to thermally stable volatile derivatives. This task is a most important purpose of derivatization (see the entry Derivatization of Analytes in Chromatography, General Aspects). This chemical treatment may be used not only for nonvolatile compounds but also for volatile substances. The less polar products typically yield narrower chromatographic peaks that provide the better signal-to-noise ratio and, hence, lower detection limits. Nonpolar derivatives have much better interlaboratory reproducibility of retention indices compared with this parameter for initially polar compounds.



Table 1 Physicochemical and Gas Chromatographic Properties of Some Silylating Reagents

Reagent (abbreviation)	MW	T_b (°C)(P)	d_4^{20}	n_D^{20}	RI _{nonpolar}	By-products (RI _{nonpolar}) ^a
Most widely used reagents (in order of increasing silyl donor strength)						
Hexamethyldisilazane (HMDS)	161	126	0.774	1.408	817 ± 29	NH ₃ (ND) ^b
Trimethylchlorosilane (TMCS)	108	57.7	0.858	1.338	560 ± 8	HCl (ND)
<i>N</i> -Methyl- <i>N</i> -trimethylsilyl acetamide (MSA)	145	159–161	0.904	1.439	947 ± 14	CH ₃ CONHCH ₃ (816 ± 22)
<i>N</i> -Trimethylsilyl diethylamine (TMSDEA)	145	125–126	0.767	1.411	817 ± 11 ^c	(C ₂ H ₅) ₂ NH (548 ± 8)
<i>N</i> -Trimethylsilyl dimethylamine (TMSDMA)	117	84	0.732	1.397	660 ± 4 ^c	(CH ₃) ₂ NH (425 ± 16)
<i>N</i> -Methyl- <i>N</i> -trimethylsilyl trifluoroacetamide (MSTFA)	199	130–132	1.079	1.380	826 ± 3 ^c	CF ₃ CONHCH ₃ (540)
<i>N,O</i> -bis-Trimethylsilyl acetamide (BSA)	203	71–73 (35)	0.832	1.418	1008 ^c	CH ₃ CONH ₂ (711 ± 19)
<i>N,O</i> -bis-Trimethylsilyl trifluoroacetamide (BSTFA)	257	145–147	0.974	1.384	887 ^c	CF ₃ CONH ₂ (675 ± 11)
<i>N</i> -Trimethylsilyl imidazole (TMSI)	140	222–223	0.957	1.476	1176 ± 18 ^c	Imidazole (1072 ± 17)
New proposed and special reagents (in order of molecular weights increasing)						
2-(Trimethylsilyloxy)propene (IPOTMS)	130	—	0.780	1.395	675 ± 12	Acetone (472 ± 12)
Chloromethyldimethyl chlorosilane (CMDCS)	142	114	1.086	1.437	755 ± 8 ^c	HCl (ND)
<i>N</i> -Trimethylsilyl pyrrolidine (TMSP)	143	139 — 140	0.821	1.433	862 ± 5 ^c	Pyrrolidine (686 ± 10)
Dimethyl- <i>tert</i> -butyl chlorosilane (DMTBCS, TBDMS-Cl)	150	125	—	—	729 ± 11 ^c	HCl (ND)
Ethyl (trimethylsilyl)acetate (ETSA)	160	156–159	0.876	1.415	930 ± 5 ^c	CH ₃ CO ₂ C ₂ H ₅ (602 ± 9)
bis-Trimethylsilyl methylamine (BSMA)	175	144–147	0.799	1.421	903 ± 18 ^c	CH ₃ NH ₂ (348 ± 12)
Trimethylsilyl trifluoroacetate (TMSTFA)	186	88–90	1.076	1.336	674 ± 5 ^c	CF ₃ CO ₂ H (744 ± 6)
Bromomethyldimethyl chlorosilane (BMDCS)	186	—	—	—	842 ± 14 ^c	HCl (ND)
bis-Trimethylsilyl formamide (BSFA)	189	158	0.885	1.437	948 ± 14 ^c	HCONH ₂ (637 ± 6)
Bis-Trimethylsilyl urea (BSU)	204	—	—	—	1237 ± 11	CO(NH ₂) ₂ (ND)
<i>N,O</i> -bis-Trimethylsilyl carbamic acid	205	77–78 (mp)	—	—	—	H ₂ NCO ₂ H, NH ₃ , CO ₂ (ND)
Trimethylsilyl trifluoromethanesulfonate	222	77 (80)	1.228	1.360	—	CF ₃ SO ₂ OH
Dimethyl- <i>tert</i> -butylsilyl trifluoroacetamide (MTBSTFA)	241	168–170	1.023	1.402	996 ± 13 ^c	CF ₃ CONH ₂ (675 ± 11)
Dimethylpentafluorophenyl chlorosilane (in the mixture with dimethylpentafluoro-silyl amine, 1:1 v/v)	260	88–90 (10)	1.384	1.447	—	HCl (ND)
<i>N</i> -Methyl- <i>N</i> -trimethylsilyl heptafluoro-butanamide (MSHFBA)	299	148	1.254	1.353	906 ± 11 ^c	C ₃ F ₇ CONH ₂ (750 ± 18)

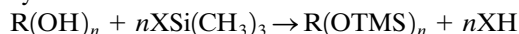
^aCommon hydrolysis by-products for all reagents are trimethylsilanol (CH₃)₃SiOH (RI = 584 ± 8) or dimethyl-*tert*-butyl silanol (RI = 753 ± 18, estimated value).

^bND: By-product is not detected after formation of nonvolatile salts with bases (HCl) or acids (NH₃).

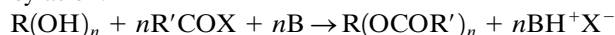
^cEstimated RI values may be defined more precisely afterward.

Principal methods of hydroxy compound derivatization may be classified in accordance with types of chemical reactions:

Silylation:



Acylation:



Alkylation: $R(OH)_n + nR'X \rightarrow R(OR')_n + nXH$

The large group of silylation reactions (trimethylsilyl derivatives are most widely used) implies the replace-

ment of active hydrogen atoms in molecules of analytes by a silyl group donated from different O-, N-, or C-silylating reagents. The relative order of —OH compounds reactivity is *n*-OH > *sec*-OH > *tert*-OH > Ar — OH > R — SH. The first part of Table 1 includes physicochemical and gas chromatographic constants of numerous reagents, listed in the order of increasing silyl-donor strength. The second part of this table presents compounds which have been recently introduced into analytical practice with still unestimated relative silylation activities and some non-TMS

reagents. Besides the individual chemicals, their different combinations have been considered as so-called silylating mixtures (e.g., HMDS + TMCS or HMDS + DMFA). The triple mixture BSA + TMSI + TMCS (1:1:1 v/v/v) seems to be the most active currently known silylating agent. It may be used for derivatization of all types of compounds with active hydrogen atoms, including carbonyl's enols and aci forms of aliphatic nitro compounds.

Every reagent in Table 1 is characterized, not only by its own retention index but also by retention index (RI) values of principal by-products of the reaction. This permits us to predict the possible overlapping of their chromatographic peaks with signals of derivatives of target compounds.

The list of recommended silylating compounds is constantly changing. Some older ones have been excluded and replaced by more effective reagents. For example, in one textbook (Knapp, 1979), *N*-trimethylsilyl-*N*-phenyl acetamide $C_6H_5N(COCH_3)SiMe_3$ (Phanalog of MSA) was presented as the silylating reagent. However, no new examples of its application have been recently published. The most principal reason for its being excluded from analytical practice is the inconvenient RIs, both for this reagent itself (1493 ± 28 , estimated value) and for the by-product of the reaction (*N*-phenylacetamide, 1362 ± 11). This window of GC retention indices may include peaks of target derivatives and, hence, it must be free from overlap with the initial reagents and by-products.

Standard mass spectra of TMS derivatives of aliphatic hydroxy compounds indicate no peaks of molecular ions M^{++} but, in all cases, ions $[M - CH_3]^+$ are reliably registered. The same derivatives of phenols and carbonyl compound's enols with $p-\pi$ conjugated systems $C=C-O$ in the molecules indicate the signals of M^{++} of high intensities. Some typical base peaks in mass spectra of *O*-TMS derivatives are $[Si(CH_3)_3]^+$ (m/z 73) and $[Si(CH_3)_2OH]^+$ (m/z 75).

The principal disadvantage of TMS derivatives is the ease of postreaction hydrolysis in the presence of water. Most of these compounds cannot exist in aqueous media. Other types of derivatives, namely dimethyl-*tert*-butyl silyl ethers, have approximately 10^3 times lower hydrolysis constants, owing to steric hindrance of Si—O bonds by *tert*-butyl groups. Unfortunately, their mass spectra are not so informative for elucidation of the structures of unknown analytes, because the base peaks for all of them belong to noncharacteristic ions $[C_4H_9]^+$ with m/z 57 and $[M - C_4Hg]^+$.

Some halogenated silylating reagents are used in the synthesis of derivatives for GC analysis with

selective (element-specific) detectors; for example, $ClCH_2SiMe_2Cl$, $BrCH_2SiMe_2Cl$, and $C_6F_5SiMe_2Cl$.

The second group of hydroxy compound derivatization reactions includes acylation of OH groups with the formation of esters. The most important are listed below (for the table of physicochemical and gas chromatographic constants of acylation reagents refer to the entry Derivatization of Amines, Amino Acids, Amides, and Imides for GC Analysis).

Reagent (abbreviation)	Derivative	ΔMW
Acetic anhydride/(H ⁺)	$R(Ar)OCOCH_3$	42
Trifluoroacetic anhydride (TFAA), bis-trifluoroacetyl methylamine (MBTFA), or trifluoroacetylimidazole (TFAI)	$R(Ar)OCOCF_3$	42
Pentafluoropropionic anhydride (PFPA)	$R(Ar)OCOC_2F_5$	146
Heptafluorobutyric anhydride (HFBA)	$R(Ar)OCOC_3F_7$	196
Pentafluorobenzoyl chloride	$R(Ar)OCOC_6F_5$	194
Chloroacetic anhydride	$R(Ar)OCOCH_2Cl$	76
Dichloroacetic anhydride	$R(Ar)OCOCHCl_2$	110
Trichloroacetic anhydride or trichloroacetyl chloride	$R(Ar)OCOCCL_3$	144
<i>N</i> -Trifluoroacetyl-L-prolyl chloride (<i>N</i> -TFA-L- Pro-Cl) ^a	<i>N</i> -TFA L-prolyl esters	193
Diethyl chlorophosphate	$R(Ar)OP(O)(OC_2H_5)_2$	136
2-Chloro-1,3,2-dioxaphospholane	2-Alkoxy-1,3,2-dioxaphospholanes	90
$NaNO_2/(H^+)$ (special derivatization of simplest C_1-C_5 aliphatic alcohols into volatile alkyl nitrites for headspace analysis)	RONO	29

^aUsed for synthesis of diastereomeric derivatives of enantiomeric alcohols.

It is recommended that these reactions be conducted in the presence of bases without active hydrogen atoms (pyridine, triethylamine, etc.). Exceptions are indicated by the symbol "reagent/(H⁺).". These basic media are necessary for the connection of acidic by-products into nonvolatile salts to protect the acid-sensitive analytes from decomposition and avoid the appearance of extra peaks of by-products on the chromatograms. Phenols can be converted into Na salts before acylation.

The third group of derivatization reactions of hydroxy compounds for GC analysis includes formation of their alkyl or substituted benzyl ethers



(see also the entry Derivatization of Acids for GC Analysis):

Reagent (abbreviation)	Derivative	ΔMW
Diazomethane (in diethyl ether solutions in presence of HBF_4)	R(Ar)OCH_3	14
Methyl iodide/DMFA (dimethylformamide), K_2CO_3	R(Ar)OCH_3	14
Pentafluorobenzyl bromide (PFB-Br)	$\text{R(Ar)OCH}_2\text{C}_6\text{F}_5$	180
3,5-bis-(Trifluoromethylbenzyl)dimethylanilinium fluoride (BTBDMA-F) (only for phenols during GC injection)	$\text{ArOCH}_2\text{C}_6\text{H}_3\text{-(CF}_3)_2$	226

Methylation by diazomethane is a simple method for derivatization of relatively acidic compounds [e.g., phenols ($\text{p}K_a = 9\text{--}10$) or carboxylic acids ($\text{p}K_a = 4.4 \pm 0.2$)]. The application of this reagent for methylation of aliphatic alcohols requires additional acid catalysis. Methyl iodide is the most convenient reagent for synthesis of permethylated derivatives of polyols (including carbohydrates) and phenols. Dimethyl sulfate [$(\text{CH}_3\text{O})_2\text{SO}_2$] can be used in basic aqueous media for methylation of phenols, but the yields of methyl ethers, in this case, are not enough for quantitative determinations of initial compounds by GC.

Some special derivatization methods, which lead to the formation of cyclic products, have been recommended for glycols (triols, tetrols, etc., including carbohydrates) and amino alcohols. An appropriate orientation of two functional groups $(\text{OH})_2$ or $(\text{OH}) + (\text{NH}_2)$ in 1,2- (*vic*) or (sometimes) in 1,3- and more remote positions, is necessary for their realization:

Initial compound	Reagent (s)	Product	ΔMW
1,2-Diols	Acetone/ (H^+)	2,2-Dimethyl-1,3-dioxolanes	40
	Methane- or butaneboronic acid $\text{CH}_3\text{B(OH)}_2$ or $\text{C}_4\text{H}_9\text{B(OH)}_2$	2-Methyl or 2-butyl 1,3,2-dioxaborolanes (Me or Bu boronates)	24 (Me) 66 (Bu)
2-Amino alcohols	Methane- or butaneboronic acid	2-Methyl or 2-butyl 1,3,2-oxazaborolanes	24 (Me) 66 (Bu)

The number of proposed methods for alcoholic and phenolic S-analog derivatization for GC analysis is significantly less than those for alcohols. The most objective reason for this is the lower frequency of their determinations in real analytical practice. In accordance with general recommendations, thiols and thio-phenols may be converted into TFA (PFP, HFB) esters or PFB ethers (S-TMS derivatives seems not as stable as O-TMS ethers). In addition to the optimization of chromatographic parameters, the derivatization of these compounds is necessary to prevent their oxidation by atmospheric oxygen.

The experimental details of numerous derivatization reactions are presented in specialized textbooks (see below).

Suggested Further Reading

- Amijee, M., J. Cheung, and R. J. Wells, *J. Chromatogr. A.* 738: 57–72 (1996).
- Blau, K. and G. S. King (eds.), *Handbook of Derivatives for Chromatography*, John Wiley & Sons, New York, 1978.
- Blau, K. and J. M. Halket (eds.), *Handbook of Derivatives for Chromatography*, 2nd ed., John Wiley & Sons, New York, 1993.
- Drozd, J., *Chemical Derivatization in Gas Chromatography*, Elsevier, Amsterdam, 1981.
- Heberle, J. and G. Simchen, *Silylating Agents*, 2nd ed., Fluka Chemie AG, 1995.
- Knapp, D. R., *Handbook of Analytical Derivatization Reactions*, John Wiley & Sons, New York, 1979.
- Little, J. L., *J. Chromatogr. A.* 844: 1–22 (1999).



Derivatization of Steroids for GC Analysis

Raymond P.W. Scott

Scientific Detectors Ltd., Banbury, Oxfordshire, England

Introduction

Steroids, bile acids, and similar compounds pose certain problems when they require to be derivatized for separation by GC. The hydroxyl groups in the respective structures differ greatly in their reaction rate, which will depend on their nature (whether they are primary, secondary, or tertiary) and also, to a certain extent, on their steric environment.

Discussion

After considerable research, which examined a wide variety of different derivatives, trimethylsilylation has emerged as the procedure of popular choice for steroid and steroidlike compounds. Pure compounds or biological extracts containing 3β -hydroxyl groups can be readily silylated by treatment with *N,O*-bistrimethylsilyltrifluoroacetamide containing 1% trimethylchlorosilane at 60°C for 30 min, with or without added pyridine. *N,O*-Bistri-methylsilyltrifluoroacetamide, under some circumstances, can also be used alone or with a mixture of hexamethyl-disilazane and trimethylchlorosilane (10:10:5 v/v/v) at 60°C for 30–60 min. The trimethylsilyl derivatives separate well on capillary columns carrying apolar stationary phases. The derivatives also provide excellent electron-impact mass spectra.

In addition, *N,O*-bistrimethylsilyltrifluoroacetamide has been used very effectively for the silylation of estradiol and catechol estrogens. Employing *N,O*-bistrimethylsilyltrifluoroacetamide:pyridine:trimethylchlorosilane (5:5:1 v/v/v) at 40°C for 8–10 h, tetrahydroaldosterone (11 β ,18-epoxy-3 α ,16,21-trihydroxy-5 β -pregnene-20-one) and aldosterone (11 β ,21-dihydroxy-3,20-dio-exopregn-4-en-18-al) have been derivatized. Employing stable isotope dilution, cortisol has been determined in human plasma by gas chromatography–mass spectrometry (GC–MS) after reacting the dimethoxime cortisol derivative with 50 μ L of *N,O*-bistrimethylsilyltrifluoroacetamide at 100°C for 2 h.

More sterically hindered steroids and, in particular, the polyhydroxylated compounds were more

efficiently derivatized with trimethylsilylimidazole. The ease of silylation of the ecdysteroids (polyhydroxylated arthropod moulting hormones) tracked the following order: 2, 3, 22, 25 > 20 \gg 14. Those substances containing a 14 α -hydroxyl group require very strong reaction conditions. For example, 20-hydroxyecdysone could only be silylated using neat trimethylsilylimidazole at 100°C over a reaction period of 15 h. It has also been established that the addition of 1% trimethylchlorosilane to the trimethylsilylimidazole catalyzed the reaction of the reagent with the 14 α -hydroxyl group, reducing the reaction time to 4 h at 100°C. The use of larger quantities of trimethylchlorosilane caused confusing side reactions to occur and should be avoided. However, the addition of potassium acetate also appeared to increase the reaction rate, allowing the reaction time to be reduced to 2–3 h.

The conversion of the enol form of keto steroids to a silyl derivative is somewhat fraught with difficulties, as mixtures of silylated substances can be easily formed. Nevertheless, the quantitative conversion of keto steroids to their trimethylsilyl-enol ethers has been optimized. Silylation of dexamethasone (9 α -fluor-11 β , 17 α ,21-trihydroxy-16 α -methyl-pregna-1,4-diene-3,20-dione) using *N,O*-bistrimethylsilyltrifluoroacetamide in the presence of sodium acetate yielded the pure tetra-trimethylsilyl derivative. In this case, the trimethylsilyl-enol ether of the 20-one moiety was produced, leaving the 3-one group unreacted. An unusual reaction associated with the enolization of keto steroids is the aromatization of the (A) ring of norethynodrel (a 3-keto-5,10-ene-nor-19-methyl steroid) during trimethylsilylation. It has been suggested that, under routine silylation conditions, aromatic derivatives are very likely to form from 3-keto-4,5-epoxides of nor-19-methyl steroids. The yield of aromatic silylated products were greater when the more basic reagents were employed and at higher temperatures.

Formyl derivatives are also popular in situations where several groups have to be blocked, as in steroid analysis, because the formyl group adds little to the molecular weight. To prevent the formation of artifacts, the strength of the formic acid should be kept at 95% and reaction allowed to take place for 30 min at



40°C. Alternatively, sodium formate can be used, an example of which is in the preparation of the enol *tert*-butyldimethylsilyl derivatives of steroids and bile acids. Sodium formate solution (1 mg in 100 μ L) is dried under a stream of nitrogen in a 1-mL reaction tube fitted with a Teflon-lined screw cap. The tube is then heated to 270°C for 30 min, cooled, and 10 μ g of the steroid in 100 μ L of methanol added. The solvent is evaporated under a stream of nitrogen and 20 μ L of *t*-butyldimethylsilylimidazole added. The tube is then filled with nitrogen, sealed, and heated at 100°C for 4 h. Twenty microliters of 2-propanol are then added to remove excess reagent, the tube sealed, and then heated again to 100°C for 10 min. One-half milliliter of water is then added to the reaction mixture and then extracted three times with 0.5 mL of hexane. The hexane solution is concentrated under a stream of nitrogen and the concentrated solution is used for analysis.

The literature indicates that *t*-butyldimethylsilylimidazole is probably the most popular reagent for derivatizing steroids, and it is often used in conjunction with *t*-butyldimethylchlorosilane. These reagents form derivatives under relatively mild conditions (room temperature, reaction time, 1 h), reaction goes close to completion, and relatively few side products are generated.

Suggested Further Reading

- Blau, K. and J. Halket (eds.), *Handbook of Derivatives for Chromatography*, John Wiley & Sons, New York, 1993.
- Grant, D. W., *Capillary Gas Chromatography*, John Wiley & Sons, New York, 1996.
- Scott, R. P. W., *Techniques of Chromatography*, Marcel Dekker, Inc., New York, 1995.
- Scott, R. P. W., *Introduction to Analytical Gas Chromatography*, Marcel Dekker, Inc., New York, 1998.



Detection (Visualization) of TLC Zones

Joseph Sherma

Lafayette College, Easton, Pennsylvania, U.S.A.

Introduction

After development with the mobile phase, the plate is dried in a fume hood and heated to completely evaporate the mobile phase. Separated compounds are detected on the layer by viewing their natural color (e.g., plant pigments, food colors, dyestuffs), natural fluorescence (aflatoxins, polycyclic aromatic hydrocarbons, riboflavin, quinine), or quenching of fluorescence. Substances that cannot be seen in visible or ultraviolet (UV) light must be visualized with suitable detection reagents to form colored, fluorescent, or UV-absorbing compounds by means of derivatization reactions (postchromatographic derivatization). Although dependent on the particular analyte and the detection method chosen, sensitivity values are generally in the nanogram range for absorbance and picogram range for fluorescence. Detection may be obtained by prechromatographic derivatization, either in solution prior to sample application or directly on the plate at the origin. As an example, dansyl derivatives of amino acids are detected directly by their fluorescence. Prechromatographic derivatization may enhance compound stability or chromatographic selectivity as well as serving for detection.

Direct Detection

Compounds that are naturally colored are viewed directly on the layer in daylight, whereas compounds with native fluorescence are viewed as bright zones on a dark background under UV light. Viewing cabinets or boxes incorporating short-wave (254 nm) and long-wave (366 nm) UV-emitting mercury lamps are available for inspecting chromatograms in an undarkened room.

Fluorescence Quenching

Compounds that absorb around 254 nm, including most compounds with aromatic rings and conjugated double bonds and some unsaturated compounds, can be detected on an "F layer" containing a phosphor or

fluorescent indicator (often zinc silicate). When excited with 254-nm UV light, absorbing compounds diminish (quench) the uniform layer fluorescence and are detected as dark violet spots on a bright green background. Detection by natural fluorescence or fluorescence quenching does not modify or destroy the compounds, and the methods are therefore suitable for preparative layer chromatography. Derivatization reactions modify or destroy the structure of the compounds detected, but they are often more sensitive than detection with UV radiation.

Universal Detection Reagents

Universal reactions such as iodine absorption or spraying with sulfuric acid and heat treatment are quite unspecific and are valuable for completely characterizing an unknown sample. Absorption of iodine vapor from crystals in a closed chamber produces brown spots on a yellow background with almost all organic compounds except for some saturated alkanes. Iodine staining is nondestructive and reversible upon evaporation, whereas sulfuric acid charring is destructive. Besides sulfuric acid, 3% copper acetate in 8% phosphoric acid is a widely used charring reagent. The plate, which must contain a sorbent and binder that do not char, is typically heated at 120–130°C for 20–30 min to transform zones containing organic compounds into black to brown zones of carbon on a white background. Some charring reagents initially produce fluorescent zones at a lower temperature before the charring occurs at a higher temperature.

Selective Detection Reagents

Selective reagents form colored or fluorescent compounds on a group- or substance-specific basis and aid in compound identification. They also allow the use of a thin-layer chromatography (TLC) system with less resolution because interfering zones will not be detected. Examples include the formation of red to purple zones by reaction of α -amino acids with ninhydrin, detection of acidic and/or basic analytes with the



indicator bromocresol green, and location of aldehydes as orange zones after reaction with 2,4-dinitrophenylhydrazine hydrochloride.

Certain specialized reagents are used to visualize compounds based on their biological activity. Cholinesterase-inhibiting pesticides (e.g., organophosphates, carbamates) are detected sensitively by treating the layer with the enzyme and a suitable substrate, which react to produce a colored product over the entire layer except where colorless pesticide zones are located due to their inhibition of the enzyme–substrate reaction.

Application of Detection Reagents

Chromogenic and fluorogenic liquid detection reagents are applied by spraying or dipping the layer. Various types of aerosol sprayers that connect to air or nitrogen lines are available commercially for manual operation. For safety purposes, spraying is carried out inside a laboratory fume hood or commercial TLC spray cabinet with a blower (fan) and exhaust hose, and protective eyewear and laboratory gloves are worn. The developed, dried plate is placed on a sheet of paper or supported upright inside a cardboard spray box. The spray is applied from a distance of about 15 cm with a uniform up-and-down and side-to-side motion until the layer is completely covered. It is usually better to spray a layer two or three times lightly and evenly with intermediate drying rather than a single, saturating application that might cause zones to become diffuse. Studies are required with each reagent to determine the optimum total amount of reagent that should be sprayed, but, generally, the layer is sprayed until it begins to become translucent. After visualization, zones should be marked with a soft lead pencil because zones formed with some reagents may fade or change color with time.

Dipping is usually the best method for uniform reagent application and will produce the most reproducible results in quantitative densitometric analysis. The simplest method is to manually dip for a short time (5–10 s) in a glass or metal dip tank. A more uniform dip application of reagents can be achieved by the use of a battery-operated automatic, mechanical chromatogram immersion instrument (Fig. 1), which provides selectable, consistent vertical immersion and withdrawal speeds between 30 and 50 mm/s and immersion times between 1 and 8 s for plates with 10- or 20-cm heights. The immersion device can also be used for impregnation of layers with detection reagents prior to initial zone application and development and

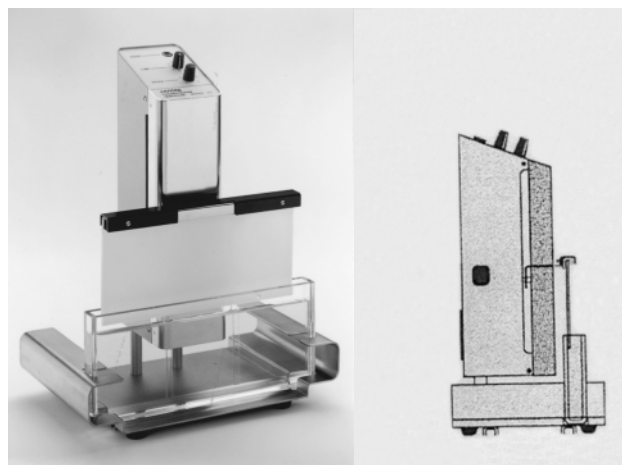


Fig. 1 Camag chromatogram immersion device set for a 10-cm dipping depth with high-performance TLC plates. Vertical dipping and removal rates and the residence time in the reagent can be preselected. [Photograph (left) supplied by D. Jaenchen, Camag, Muttenz, Switzerland; schematic diagram (right) reprinted from *Handbook of Thin Layer Chromatography* (J. Sherma and B. Freid, eds.), p. 146, with permission of Marcel Dekker, Inc.]

for postdevelopment impregnation of chromatograms containing fluorescent zones with a fluorescence enhancement and stabilization reagent such as paraffin. Dip application to the layer cannot be used when two or more aqueous reagents must be used in sequence without intermediate drying, such as the detection of primary aromatic amines as pink to violet zones by diazotization and coupling with the Bratton–Marshall reagent composed of sodium nitrite and *N*-(1-naphthyl)ethylenediamine dihydrochloride aqueous spray solutions. Dip reagents must be prepared in a solvent that does not cause the layer to be removed from the plate or the zones to be dissolved from the layer or to become diffuse.

Heating the Layer

Layers often require heating after applying the reagent in order to complete the reaction upon which detection is based and ensure optimum color development. Typical conditions are 10–15 min at 105–110°C. If a laboratory oven is used, the plate should be supported on a solid metal tray to help ensure uniform heat distribution. A plate heater (Fig. 2), which contains a 20 × 20-cm flat, evenly heated surface, a grid to facilitate proper positioning of TLC and high-performance TLC plates, programmable temperature between 25°C and

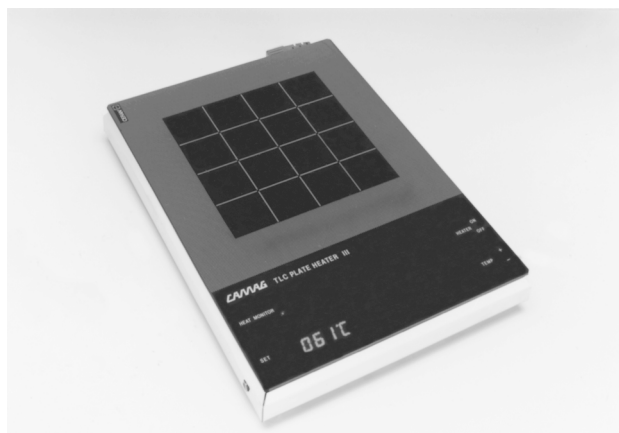


Fig. 2 Camag TLC plate heater. (Photograph supplied by D. Jaenchen, Camag, Muttenz, Switzerland.)

200°C, and digital display of the programmed and actual temperatures, will usually provide more consistent heating conditions than an oven. Prolonged heating time or excessive temperature can cause decomposition of the analytes and darkening of the layer background and should be avoided.

Some reagents can be impregnated into the layer before spotting of samples if the selectivity of the separation is not affected. Detection takes place only upon heating after development. This method has been used for the detection of lipids as blue spots on a yellow background on silica gel layers preimpregnated with phosphomolybdic acid. A few detection reagents (HCl, sulfuryl chloride, iodine) can be transferred uniformly to the layer as vapors in a closed chamber rather than as solutions.

Zone Identification and Confirmation

The identity of the detected TLC zones is obtained initially by comparison of characteristic R_f values between samples and reference standards chromatographed on the same plate; R_f equals the migration distance of the center of the zone from the start (origin) divided by the migration distance of the mobile phase front from the start. Identity is more certain if a selective chromogenic detection reagent yields the same characteristic color for sample and standard zones. Because the chromatogram is stored on the layer, multiple compatible, specific detection reagents

can be applied in sequence to confirm the identity of unknown zones. As an example, almost all lipids are detected as light green fluorescent zones by use of 2,7-dichlorofluorescein reagent, and absorption of iodine vapor differentiates between saturated and unsaturated lipids or lipids containing nitrogen. The identity of zones is confirmed further by recording UV or visible absorption spectra directly on the layer using a densitometer (*in situ* spectra) or by direct or indirect (after scraping and elution) measurement of Fourier transform infrared, Raman, or mass spectra.

Suggested Further Reading

Details of procedures, results, and applications for many hundreds of reagents for detection of all classes of compounds and ions are available in the following literature references:

- Bauer, K., L. Gros, and W. Sauer, *Thin Layer Chromatography: An Introduction*, EM Science, Darmstadt, 1991.
- Fried, B. and J. Sherma, *Thin Layer Chromatography: Techniques and Applications*, 4th ed., Marcel Dekker, Inc., New York, 1999, pp. 145–175.
- Jork, H., W. Funk, W. Fischer, and H. Wimmer, *Thin Layer Chromatography, Volume 1a, Physical and Chemical Detection Methods*, VCH, Weinheim, 1990.
- Jork, H., W. Funk, W. Fischer, and H. Wimmer, *Thin Layer Chromatography, Volume 1b, Reagents and Detection Methods*, VCH, Weinheim, 1994.
- Kovar, K.-A. and G. E. Morlock, Detection, identification, and documentation, in *Handbook of Thin Layer Chromatography* 2nd ed., (J. Sherma and B. Fried, eds.), Marcel Dekker, Inc., New York, 1996, pp. 205–239.
- Macherey-Nagel GmbH & Co. KG, *TLC Applications*, Dueren, pp. 75–78.
- Merck, KGaA, *Dyeing Reagents for Thin Layer Chromatography and Paper Chromatography*, Darmstadt.
- Stahl, E., *Thin Layer Chromatography: A Laboratory Handbook*, Academic Press, San Diego, CA, 1965, pp. 485–502.
- Touchstone, J. C., *Practice of Thin Layer Chromatography*, 3rd ed., Wiley-Interscience, New York, 1992, pp. 139–183.
- Zweig, G., and J. Sherma, *Handbook of Chromatography, Volume II*, CRC Press, Boca Raton, FL, 1972, pp. 103–189.



Detection in Countercurrent Chromatography

M.-C. Rolet-Menet

Laboratoire de Chimie Analytique, UFR des Sciences Pharmacochimie et Biologie, Paris, France

Introduction

Detection of solutes is an essential link in the separation chain. It has to reveal the solutes separation by detecting them in the column effluent and, in some cases, it could permit their characterization. Toward these objectives, it is based on the various physical properties of substances.

Countercurrent chromatography (CCC) is a chromatographic method which separates solutes more or less retained in the column by a stationary phase (liquid in this case) and are eluted at the outlet of column by a mobile phase. Two treatments of column effluent have been used until now in CCC. Either the column outlet is directly connected to a detector commonly used in high-performance liquid chromatography (HPLC) (on-line detection) or fractions of the mobile phase are collected and analyzed by spectrophotometric, electrophoretic, or chromatographic methods (off-line detection).

The first one is more practical and easier to perform. It is commonly used in analytical applications of CCC and also in preparative CCC to analyze effluent continuously and to follow the steps of the separation.

The second one is often tedious, because each fraction must be analyzed individually. However, it is really interesting in preparative applications of CCC, especially to measure the purities of fractions and the biological activities of separated compounds and also to recover a product from one or some selected fractions to resolve its chemical structure.

On-Line Detection

This type of detection can be used as much in preparative CCC to monitor separations, before the fraction collector if any, as in analytical CCC (for instance, during the determination of $\log P_{\text{octanol/water}}$).

Several detectors used in HPLC and in supercritical fluid chromatography (SFC) can be connected to a CCC column [1] to detect solutes and, thus, follow separation. They can be, for instance, fluorimetry (very

sensitive and used without modifications in CCC), ultraviolet (UV)-visible spectroscopy [1], evaporative light-scattering detection [1], and atomic emission spectroscopy [2]. Some detectors give more information than the detection of the solute, such as structural information of separated components (e.g., infrared spectroscopy [3], mass spectrometry [4], or nuclear magnetic resonance [5]). These detectors are used either on-line with a fraction collector or in parallel if they are destructive detectors.

UV Detection

The UV-visible detector is the universal detector used in analytical and preparative CCC. It does not destroy solutes. It is used to detect organic molecules with a chromophoric moiety or mineral species after formation of a UV-absorbing complex (the rare earth elements with Arsenazo III [6], for instance). Several problems can occur in direct UV detection, as has already been described by Oka and Ito [7]: (a) carryover of the stationary phase due to improper choice of operating conditions with appearance of stationary phase droplets in the effluent of the column, or (b) overloading of the sample, vibrations, or fluctuations of the revolution speed, (c) turbidity of the mobile phase due to the difference in temperature between the column and the detection cell, or (d) gas bubbling after reduction of the effluent pressure. Some of these problems can be solved by optimization of the operating conditions, better control of the temperature of mobile phase, or addition of some length of capillary tubing or a narrow-bore tube at the outlet of the column, before the detector, to stabilize the effluent flow and to prevent bubble formation. The problem of the stationary-phase carryover (especially encountered with hydrodynamic mode CCC devices) can be solved by the addition, between the column outlet and UV detector, of a solvent which is miscible with both stationary and mobile phases and which allows to obtain a monophasic liquid in the cell of detector [1] (a common example is isopropanol).



Evaporative Light-Scattering Detection

Evaporative light-scattering detection (ELSD) involves atomization of the column effluent into a gas stream via a Venturi nebulizer, evaporation of solvents by passing it through a heated tube to yield an aerosol of nonvolatile solutes, and, finally, measurement of the intensity of light scattered by the aerosol. After a suitable evaporation step, in the worst case of segmented or emulsified mobile phase, the column effluent should always be an aerosol of the solutes before reaching the detection cell. It can be used without modifications. For molecules without chromophore or fluorophore groups, or with mobile phases with a high UV cutoff (acetone, ethyl acetate, etc.), ELSD is useful [1]. However, it cannot detect fragile or easy sublimable solutes because nebulizer is heated. Moreover, this detection method does not preserve the solutes. To collect column effluent, a split must be installed at the outlet of the column to allow ELSD in a parallel direction to fraction collection, with a consequent loss of solutes.

Atomic Emission Spectrometry

This detection mode can be used during ion separation. Kitazume et al. [2] used a direct plasma-atomic emission spectrometer (DCP, Spectra-Metrics Model SpectraSpan IIIB system with fixed-wavelength channels) for observation of the elution profile during the separation of nickel, cobalt, magnesium, and copper by CCC. For profile measurement of a single element, an analog recorder signal from the DCP was converted into a digital signal. The digital data was stored in a work station and the elution profile was plotted. For simultaneous multielement measurement, the emission signal for each channel was integrated for 10 s at intervals of 20 s, and the integrated data were printed out.

Infrared Spectrometry

Romanach and de Haseth [3] have used, in CCC, a flow cell for LC-FTIR (liquid chromatography-Fourier transform infrared) spectrometry. The main difficulty is the absorbance of the liquid mobile phase. This problem is exacerbated in LC by low solute-to-solvent ratios in the eluates. On the contrary, CCC leads to a high solute-to-solvent ratio so that it can be used with a very simple interface with a CCC column, without any complex solvent removal procedures. High sample loadings are possible by using the variable path length of the IR detector (from 0.025 to 1.0 mm).

Mass Spectrometry [5]

Several interfaces have been used for CCC-MS (mass spectrometry). The first employed is thermospray (TSP). When a column is directly coupled with TSP MS, the CCC column often breaks due to the high back-pressure generated by the thermospray vaporizer. By contrast, other interfaces, such as fast atom bombardment (FAB), electron ionization (EI), and chemical ionization (CI), have been directly connected to a CCC column without generating high back-pressure. Such interfaces can be applied to analytes with a broad range of polarities. As it is suitable to introduce effluent from the column CCC into MS at a flow rate of only between 1 and 5 $\mu\text{L}/\text{min}$, the effluent is usually introduced into the MS through a splitting tee, which is adjusted to an appropriate ratio.

Nuclear Magnetic Resonance

Nuclear magnetic resonance (NMR) gives maximum structural information and allows the measurement of the relative concentrations of eluted compounds. Spraul et al. [5] experimented with the coupling of pH zone-refining centrifugal partition chromatography (CPC) with NMR by using a biphasic system based on D_2O and an organic solvent. In pH zone refining, solutes are not eluted as separated peaks but as contiguous blocks of constant concentrations, so that it is highly difficult to monitor the separation by means of a UV detector. On-line pH monitoring is generally used, allowing the observation of transitions between solutes, because each zone has its own characteristic pH determined by the pK_a and the solute concentration it contains. The experiment was carried out in stop-flow mode.

Off-Line Detection

The analysis of the mobile-phase fractions collected at the outlet of column is the oldest method used in CCC (droplet countercurrent chromatography and rotation locular countercurrent chromatography) to elucidate the quality of separation and to characterize solutes. With modern CCC, such as CPC, CCC type J, and crossaxis, numerous applications have been described for preconcentration and preparative chromatography.

Table 1 gathers some applications described in the literature [4,8]. The type of detection used with each fraction depends on the isolated solute. They include thin-layer chromatography (TLC) and HPLC, which also enables an estimation of each fraction's purity, for



Table 1 Off-Line Detection

Molecules [Ref.]	Fractions analysis
Schisanhenol acetate 5 and 6 of <i>Schisandra rubriflora</i> [4]	TLC
Bacitracine complex [4]	Purity control by HPLC
	Absorbance measure at 234 nm
	Purity control by HPLC
Dye species [4]	Mass spectrometry
Thyroid hormone derivatives [4]	UV on line at 280 nm; gamma radioactivity measure of fractions
	Purity control by TLC, HPLC, and UV spectra
Cerium chloride and erbium chloride [4]	Inductively coupled plasma–atomic emission spectroscopy
Recombinant uridine phosphorylase [8]	SDS-PAGE
	Enzymatic activity by Magni method

organic solutes, the inductively coupled plasma–atomic emission spectroscopy (ICP–AES) for mineral species, and polyacrylamide gel electrophoresis (PAGE) for biological molecules. If the purity of the compound is satisfactory, a study by direct injection–mass spectrometry and nuclear magnetic resonance allows one to determine its chemical structure. Biochemical tests are also available to verify the biological activity of biomolecules which are often separated and collected in aqueous two-phase CCC solvent systems.

References

1. S. Drogue, M.-C. Rolet, D. Thiébaud, and R. Rosset. *J. Chromatogr.* 538: 91–97 (1991).
2. E. Kitazume, N. Sato, and Y. Ito, *Anal. Chem.* 65: 2225–2228 (1993).
3. R. J. Romanach and J. A. de Haseth. *J. Liquid Chromatogr.* 11(1): 133–152 (1988).
4. H. Oka, High-speed counter current chromatography/mass spectrometry, In *High-Speed Counter Current Chromatography* (Y. Ito and W. D. Conway, eds.), John Wiley and Sons, New York, 1995, pp. 73–91.
5. M. Spraul, U. Braumann, J.-H. Renault, P. Thépinier, and J.-M. Nuzillard, *J. Chromatogr.* 766: 255–260 (1997).
6. E. Kitazume, M. Bhatnagar, and Y. Ito, *J. Chromatogr.* 538: 133–140 (1991).
7. H. Oka and Y. Ito, *J. Chromatogr.* 475: 229–235 (1989).
8. Y. W. Lee, Cross-axis counter current chromatography: A versatile technique for biotech purification, in *Counter Current Chromatography* (J.-M. Menet and D. Thiébaud, eds.), Marcel Dekker, Inc., New York, 1999, pp. 149–169.



Detection Methods in Field-Flow Fractionation

Martin Hassellöv

Göteborg University, Gothenburg, Sweden

Introduction

An analytical separation technique requires a detection method responding to some or all of the components eluting from the separation system. The choice of detector is determined by the demands of the sample and analysis. For Field-Flow Fractionation (FFF) techniques many of the detection systems have evolved from those used in liquid chromatography (LC) techniques.

Detection can be carried out either with an on-line detector coupled to the eluent flow or by the collection and subsequent analysis of discrete fractions. For collected fractions, a range of analytical methods can be used, both quantitative (e.g., radiotracer and metal analysis) and more qualitative (e.g., microscopic techniques). On-line detectors suitable for coupling to the FFF channels include both nondestructive flow through cell systems and destructive analysis systems. It is often desirable to use on-line detection if possible because the total analysis time is much less than for discrete fraction analysis. Regardless of detector type, the dead volumes and flows in the system between the FFF channel and detector or fraction collector must be accurately determined and corrected for.

If the signal from a detector consists of a factor of two properties, it is possible to use another detector on-line to resolve the different properties [e.g., multi-angle light scattering (MALS) in combination with the differential refractive index (DRI) or continuous viscometry + DRI]. Alternatively, the two detectors may respond to two different properties of interest; in either case, it is almost as simple to acquire multiple detector signals as a single one. Multiple detectors can be arranged either in series or in parallel. A parallel detector arrangement avoids the band-broadening problem encountered in the serial arrangement, where the first detector may cause significant band-broadening for the second, due to the dead volume in the flow cell. For a serial detector connection, it is best to have the one with the smallest dead volume first, as long as it is not a destructive detector. For parallel coupling, the outflow from the FFF channel needs to be split into two or more detectors, and it is then essential to have

control of the individual flows because changes can induce drift in sensitivity and shifts in the dead times between the channel and detector during a run.

When choosing detector and experimental conditions, one needs to consider analyte concentration, detector sensitivity, background level, and detection limits. The maximum amount of analytes that can be injected is usually limited by sample overloading in the FFF channel, which can cause interparticle interactions which disturb the separation. It is necessary to have an analyte detection limit well below the overloading sample concentration to be able to quantify the peaks without a too noisy background. When using multiple detectors on-line, their sensitivity may be quite different either overall or as a function of size range. An example of this is the use of a MALS detector, which has much higher sensitivity for larger particles, together with a DRI detector, which has the opposite sensitivity properties, making the small and large particle ranges difficult to cover.

Optical Detection Systems

Ultraviolet (UV) detectors are the most commonly used detectors for FFF applications because of their availability, simplicity and low cost. The majority of FFF work to date has focused on separation method development, in which the use of a UV detector showing the quality of the separations is sufficient. However, the quantification of the separated particles or macromolecules is not always straightforward because the UV signal is actually a turbidimetric measure, which is a combination of light scattering and absorbance. The absorbance contribution is only dependent on concentration, but there is a more complicated relationship involved in the scattering signal. Large particles scatter light much more effectively than smaller particles, and particles with varying composition and refractive indices give rise to further complications. The correction of the detector signal according to Mie scattering theory is complicated but can often be simplified with appropriate assumptions [1]. For particles larger than 1 μm , efforts have been put



into development of an absolute or standard free-quantification method using UV Detection for Gravitational FFF [2].

The DRI detector is very common in LC and records any change in refractive index of the sample stream relative to a reference stream. DRI is a general detector with the advantage of responding to almost all solutes and it is concentration selective. The sensitivity of a DRI detector is not always the best, but new detector models offer different lengths of the optical path, so that the sensitivity can be adjusted to match sample concentration. The DRI detector is not sensitive to changes in flow rate but they are highly sensitive to temperature changes. It is probably the most frequently used detector for FFF applications after UV detectors.

Flow-through fluorescence detectors are very common in liquid chromatography, due to the high selectivity and good signal-to-noise ratio. Only a few articles on FFF with fluorescence detectors are published, but when the analytes have suitable fluorescence properties, this is an excellent choice.

Photon correlation spectroscopy (PCS), also called dynamic light scattering or quasi-elastic light scattering, correlates the frequency of the light-scattering signal to the diffusion coefficients of the sample particles. PCS is a valuable tool in the validation of FFF separations, but it is too slow to be of practical use as an on-line detector. PCS has, for example, been used for verification of the average sizes obtained from FFF theory for discrete fractions of emulsion separated using sedimentation FFF [3]. Improvements in light-scattering theory and instrumentation has been going on for decades, but the development of the MALS instrument from the earlier Low Angle Light Scattering (LALS) technology, presents a breakthrough in particle sizing. Compared to LALS instruments multian-gle detection (up to 18 detectors measuring the scattered light at individual angles) allows more physical properties of the particles to be derived from the results. Also, the MALS instrument has a higher sensitivity and is less affected by dust particles in the sample. Light-scattering techniques give average values of the properties of the particle population in the sample and do not describe the property distribution of the sample, but when coupled to a particle sizing technique, such as FFF, distribution of the different properties are derived from each size fraction.

The MALS theory has been thoroughly described in several articles by Wyatt [4] and will only be mentioned briefly here. For each size fraction or batch measurement, the following applies if the assumptions

Detection Methods in Field-Flow Fractionation

that all diffraction of the light is due to scattering of the particles (i.e., similar refractive index of sample and solvent; no change of light wave front when passing through the sample):

$$\frac{Kc}{R_\theta} = \frac{1}{M_w P(\theta)} + 2A_2c + \dots \quad (1)$$

$$P(\theta) = 1 - a_1[2k \sin(\theta/2)]^2 + a_2[2k \sin(\theta/2)]^4 - \dots \quad (2)$$

where K is the light-scattering constant including the refractive index increment and the wavelength of the scattering light and A_2 is the second viral coefficient. If a sample is very diluted, the second term of Eq. (1) can be neglected and the excess Rayleigh ratio, R_θ (net light-scattering contribution from each component at angle θ), becomes directly proportional to $M_w P(\theta)$. On plotting R_θ/Kc against $\sin^2(\theta/2)$, the intercept yields the molecular weight (M_w) at the concentration c , and from the slope the root mean square radius can be derived. One great advantage with the MALS detector is that it does not demand calibration of the channel with reference materials, but the absolute concentration of the analyte is necessary because the signal includes a factor of the concentration. To acquire the sample concentration at each time slice, a concentration-calibrated DRI detector is commonly used on-line with the MALS detector. The FFF-MALS-DRI is receiving much interest and attention and many applications have been developed in recent years, especially in polymer characterization. Thielking and co-workers have published articles on the coupling of FFF-MALS-DRI for analysis of both polystyrene particles and smaller polystyrene sulfonates (PSS) [5]. Figure 1

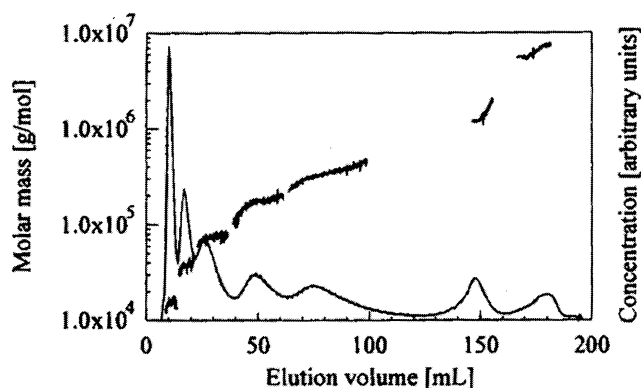


Fig. 1 Results from FIFFF-MALS-DRI analysis of seven PSS standards. The molecular weight is derived from MALS data and the concentration is given by the DRI detector. (From Ref. 5.)

shows their results of DRI-derived concentration and molecular weight given from MALS data as a function of elution volume for seven PSS standards. However, for small molecules (<10 kDa), the sensitivity of the MALS detector is rather poor.

In an evaporative light-scattering detector (ELSD), the sample is nebulized and when the solvent in the resulting droplets is evaporated, their mass content is proportional to the particle's mass in the sample stream. The particles are detected with a laser-light-scattering detector and the signal is related to their size. ELSD has not been extensively used in FFF. Openheimer and Mourey [6] showed that it can be a good complement to turbidimetric detection in sedimentation FFF for particles smaller than 0.2 μm . This detector is free from the problems associated with UV detectors when applied to a broad size range or samples with differing extinction coefficients over the size range. Further, it can be used for samples lacking absorbance characteristics. Compton et al. [7] presented a single-particle detector for steric FFF (1–70 μm) based on light scattering of single particles flowing through the laser-light path. Today, there are several other commercial flow-stream particle counters available.

A continuous-viscosity detector has been shown to be a good detection tool for thermal FFF analysis of polymer solutions [8]. Due to the high sample dilution in FFF, the viscosity detector response above the solvent baseline, ΔS , is only dependent on the intrinsic viscosity of every sample point, $[\eta]$, multiplied by the concentration, c , at the corresponding points:

$$\Delta S = [\eta]c \quad (3)$$

If a concentration-selective detector, such as a DRI, is connected on-line with the viscosity detector, the ratio of the two signals yields the intrinsic viscosity distribution of the polymer sample. In polymer characterization, the intrinsic viscosity can be a property just as important as the molecular-weight distribution. Furthermore, polymer intrinsic viscosity follows the Mark–Houwink relation to the molecular weight, M , where K and a are Mark–Houwink viscosity constants:

$$[\eta] = KM^a \quad (4)$$

Mass Spectrometric Detection Systems

The mass spectrometry (MS) detection methods covered here are mainly a selection of commonly used

LC–MS methods, some of which have been optimized for FFF techniques or could potentially be good detection tools for FFF separations. The issue in the coupling of a liquid-based separation method to a mass spectrometer is the ion source conversion of dissolved analytes to ions in the high vacuum mass analyzer, which, for instance, can be magnetic sectors, quadrupoles, ion traps, or time-of-flight analyzers. Different ion sources give different information depending on the ionization mechanisms and will be discussed for each method.

In most FFF separations, a moderate concentration of dispersion agent, electrolyte, or surfactant is used to improve the separations. A common feature for most MS instruments is that salt in the liquid entering the ion source is deteriorating the performance of the MS by lowering the signal-to-noise ratio and by condensing on surfaces inside the MS, thus continuously increasing the background level.

Today, the most frequently used LC–MS ion source is electrospray ionization (ESI) in which the sample stream ends in a narrow capillary, put on a high voltage (positive or negative). This potential, sometimes together with a sheath gas flow, gives rise to a spray of small charged droplets ($\sim 1 \mu\text{m}$). When the solvent is evaporated from these droplets, electrostatic repulsion forces smaller droplets ($\sim 10 \text{ nm}$) to leave. Before entering the semivacuum region, free analytes with one or more net charges, usually due to proton transfer or ion adducts (e.g., Li^+ , Na^+ , or NH_4^+), dominate.

Electrospray ionization is a mild ionization source (i.e., almost no fragmentation of the ions occur). It is applicable to all organic compounds applicable to proton exchange or binding to ions in the gas phase, which includes almost all biomolecules and polymers. In ESI–MS, multiple charges occur with a charge distribution for all components. This charge envelope has usually maximum intensity at m/z about 1000 and rarely ranging beyond 2000 in m/z . This has the advantage that large molecules, such as peptides, DNA molecules, or polymers, can be analyzed by all common MS analyzers, but the drawback is that the resulting spectra can be complicated to interpret. For single-mass molecules such as peptides, there are numerical models to deconvolute the single-charge molecular weight from the ESI–MS m/z spectra, but for not completely separated polymer components the overlapping charge distributions for the individual polymer components makes the interpretation complicated. ESI–MS sensitivity is dramatically reduced due to cluster formation in the presence of more than a few mmol/L salt, and surfactants can have a devastating effect on the ESI–MS spectra.



Therefore, a volatile buffer should be used if possible (e.g., ammonium acetate, ammonium nitrate). ESI-MS has been used as a detector for FFF analysis of low-molecular-weight ethylene glycol polymers [9], where the effect of different carriers on cluster formation was investigated. ESI-MS has been coupled to size-exclusion chromatography (SEC) in several applications for polymer analysis and other applications where FFF techniques can be successfully used, including proteins, neuropeptides, and DNA molecule segments. Modern ESI-MS has a broad range of flow rates from nanoliters per minute up to milliliters per minute.

Atmospheric pressure chemical ionization (APCI) is a method not yet applied to FFF but could potentially be a good alternative to ESI for semivolatile analytes lacking a natural site for a charge. The analytes are evaporated and exposed to gas-phase molecules ionized by a high-voltage corona discharge electrode. The analytes are subsequently ionized by a charge transfer from the gas molecules. APCI has been shown to be less sensitive to buffer salts than ESI and no fragmentation occurs in the ion source. Primarily, singly charged ions are formed, making APCI less applicable to large molecules, depending on the upper range of the MS analyzer. APCI has a good flow-rate compatibility (0.3–1.5 mL/min) with FFF.

Matrix-assisted laser desorption/ionization (MALDI) is a frequently used ionization technique, but it is rarely used as an on-line detector. The sample stream is applied to a target plate, and it is allowed to cocrystallize with the matrix, which is subsequently desorbed, ionized with a laser, and analyzed in the MS. There has been attempts of combining FFF and MALDI, and for biomolecules, MALDI is a good ion source, due to the soft ionization with high efficiency and simple mass spectra, even for heavier molecules because the majority carry only single charge.

Inductively coupled plasma-ionization mass spectrometry (ICP-MS) is an ion source for elemental analysis where the analyte stream is introduced into a high-energy plasma with efficient atomization and ionization, producing almost entirely singly-charged elemental ions. ICP-MS has multielement capability with excellent sensitivity and has good flow-rate compatibility (0.3–1.5 mL/min) with FFF techniques. ICP-MS has previously been applied to Sedimentation FFF for determination of major element composition in different size fractions of suspended riverine particles and soil particles in the size range 50–800 nm [10] and recently Flow FFF coupled on-line to ICP-MS has been used to determine elemental size distributions for over 30 elements in freshwater colloidal material (1–50 nm) [11]. Figure 2 shows a selection of elements and the sig-

nal from the UV detector, coupled on-line before the ICP-MS, from a river water sample. An interface between the FFF channel and the ICP-MS was used to supply acid, to improve the performance of the nebulizer-spray chamber system, and the internal standard. The interface also serves to dilute and split away some half of the salt content. The salt is necessary for the FFF separation, but harmful to the ICPMS.

Density-Based Detection

A continuous-density detector is working on the principles of a liquid flowing through a oscillating U-shaped glass tube where the oscillating frequency is found re-

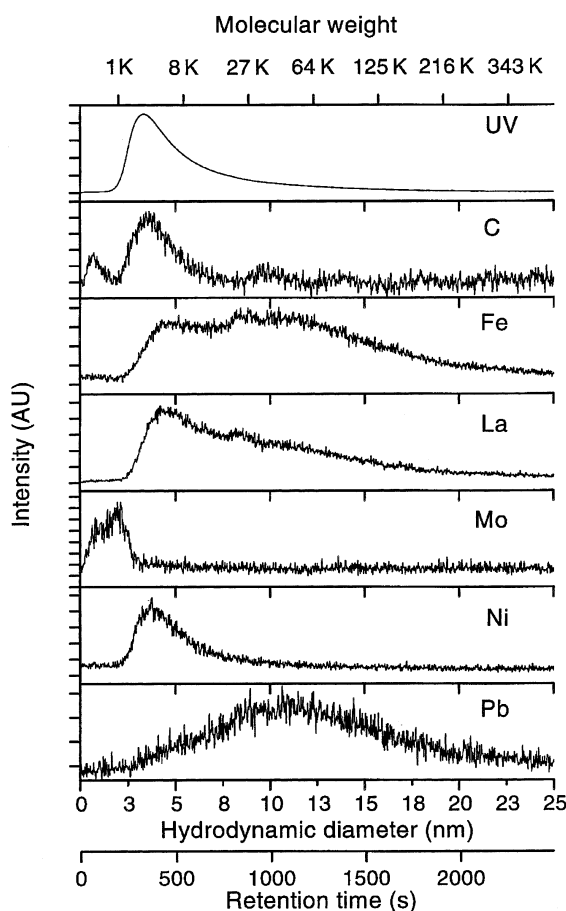


Fig. 2 Elemental size distributions of the colloidal material in a freshwater sample as given from a FIFFF coupled to ICPMS. A UV detector is placed on-line prior to the ICPMS and the UV size distribution is included. The signals are plotted as a function of retention time, hydrodynamic diameter (from FFF theory) and molecular weight (from standardization with PSS standards). (From Ref. 11.)

lating the oscillations to the density of the flowing liquid. A densimetric detector has been evaluated for sedimentation FFF [12], and the conclusions were that it is a universal concentration-selective detector without the need for signal correction or transformation. However, the sensitivity is a limiting factor because the sensitivity is dependent on the density difference between the sample and the carrier liquid. A density difference of 0.2 g/mL is sometimes sufficient, but to achieve higher sensitivity, a difference up to 1.0 is desirable, making the densimetric detection suitable for inorganic particles, but less appropriate for lighter organic analytes. The densimeter detector is sensitive to temperature changes, but insensitive to flow changes, making it most suitable for flow programming applications.

References

1. F.-S. Yang, K. D. Caldwell, and J. C. Giddings, *J. Colloid Interf. Sci.* 92: 81–91 (1983).
2. P. Reschiglian, D. Melucci, A. Zattoni, and T. Giancarlo, *J. Microcol. Separ.* 9: 545–556 (1997).
3. K. D. Caldwell and J. Li, *J. Colloid Interf. Sci.* 132: 256–268 (1989).
4. P. J. Wyatt, *J. Colloid Interf. Sci.* 197: 9–20 (1998).
5. H. Thielking and W.-M. Kulicke, *Anal. Chem.* 68: 1169–1173 (1996).
6. L. E. Oppenheimer and T. H. Mourey, *J. Chromatogr.* 298: 217–224 (1984).
7. B. J. Compton, M. N. Myers, and J. C. Giddings, *Chem. Biomed. Environ. Instrum.* 12: 299–317 (1983).
8. J. J. Kirkland, S. W. Rementer, and W. W. Yau, *J. Appl. Polym. Sci.* 38: 1383–1395 (1989).
9. M. Hassellöv, G. Hulthe, B. Lyvén, and G. Stenhagen, *J. Liquid Chromatogr. Related Technol.* 20: 2843–2856 (1997).
10. H. E. Taylor, J. R. Garbarino, D. M. Hotchin, and R. Beckett, *Anal. Chem.* 64: 2036 (1992).
11. M. Hassellöv, B. Lyvén, C. Haraldsson, and W. Sirinawin, *Anal. Chem.* 71: 3497–3502 (1999).
12. J. J. Kirkland and W. W. Yau, *J. Chromatogr.* 550:





Detection Principles

Kiyokatsu Jinno

Toyohashi University of Technology, Toyohashi, Japan

INTRODUCTION

Various methods of detection are employed in chromatography. Each approach for the detection of solutes is based on their physical or chemical properties. Some of the more commonly used detectors are discussed here for liquid chromatography (LC), gas chromatography (GC), and supercritical fluid chromatography (SFC).

LIQUID CHROMATOGRAPHY

The most commonly used detectors in LC are concentration-sensitive. The detector output signal is a function of the concentrations of the analytes passing through the detector cell. In order to use the information for quantitation, the detector must respond linearly to changes in concentration over a wide concentration range, which is called the linear dynamic range of the detector. Criteria for the evaluation of the quality or the suitability of the detector are as follows: the magnitude of the linear dynamic range, the noise level, the sensitivity, and the selectivity. The sensitivity is determined by the specific characteristics of the analytes and by the extent to which these differ from the characteristics of the sample matrix. The most important parameters are noise, drift, detection limit (sensitivity), selectivity, stability, and compatibility with various elution modes.

Noise is the high-frequency variation of the detector signal, which becomes visible when the baseline is recorded at the higher-sensitivity settings. To determine the noise level, parallel lines are drawn around the noise envelope and the distance between these lines; the actual noise level is expressed in detector signal units (for instance, AU, mV, or μ A). This parameter is dependent upon the lamp, the amplifier, and the cell geometry, and is specified differently by many manufacturers. Static measurements usually provide better values for the noise level than those obtained under flow conditions. Noise levels are calculated using the mean of the baseline envelope. A measure for the sensitivity of a detector is the minimum detectable amount of a given compound (detection limit). Most LC detectors measure optical or spectroscopic characteristics of the analytes. Other detectors use electrical (conductivity) or electrochemical cha-

acteristics, such as oxidation or reduction (electrochemical detector, EcD) of the analytes. A detector is said to be more selective when it measures a more unique characteristic of an analyte.

Ultraviolet (UV) Detector

UV detection is the most popular, i.e., most commonly utilized, in the LC detection mode. Depending on instrumental design, three types of UV detectors are used today: single wavelength detectors, where a fixed wavelength is used for the absorbance monitoring of the analytes; variable wavelength detectors, with which one can choose the most appropriate wavelength for the analyte detection; and UV detectors which provide spectral information, such as fast-scanning UV detectors and diode array detectors.

UV detectors make use of the spectral absorption properties of the analytes in the UV and visible (Vis) wavelength range. The absorption measured at a given wavelength generally follows Beer's law and is transformed to a concentration-dependent signal. The change in absorption is proportional to the concentration when all parameters are kept constant. The detector cell volumes range from 5 and 10 μ L; the light path typically ranges from 6 to 10 mm.

The fixed wavelength detector is the most widely used in LC. It is simple in design and, consequently, the least expensive although it is still the most sensitive. Its widespread use is historic in origin and is due to the fact that the strong emission line of the mercury lamp at 254 nm is well suited for absorption measurements of many organic compounds, provided that they possess an aromatic system. Some advantages of the fixed wavelength detector are as follows:

1. The simple design; the detector is relatively inexpensive.
2. The mercury spectral line is very strong and narrow.
3. The intensity of the light beam entering the system allows for a wide linear response range and high sensitivity.

Variable wavelength detectors use a continuous light source in combination with monochromators to select the

desired detection wavelength. The monochromator, in general, is a rotating diffraction grating which is positioned in the light path of the detector cell. Some instruments possess an additional variable bandwidth. In microprocessor-driven instruments, the desired wavelength and slit width can be selected and read on a display. Almost all instruments contain “classical” optics with spectral dispersion of the light occurring prior to passage through the flow cell. “Reversed optics” UV detectors have recently become popular. A holographic grating is placed between the flow cell and the photodiodes; it disperses the light beam through the detector cell. This design makes it possible to obtain spectral information at any point in time, which can then be further processed depending on the requirements of the analysis. Spectral information can be obtained from the diode array within 40–200 msec. Even for very narrow peaks, it is possible to scan spectra without stopping the flow. The diode array detector contains no moving parts; consequently, the spectra are of high quality in terms of resolution and reproducibility. Data can be acquired and evaluated, and relevant spectra can be stored and compared with spectral libraries via a computer. Of course, this type detector can be useful as a variable wavelength detector and, also, this provides information on peak identity and peak purity; it is routinely used in method development for separation of UV-active compounds.

Refractive Index (RI) Detectors

RI detection is the oldest in various LC detection modes and is commonly used in carbohydrate and polymer analysis. The RI (n) is a bulk property of the eluate. The RI detector is therefore a universal and rather nonspecific detector but offers relatively low sensitivity. In RI detection, the specific physical parameter is the RI increment, dn/dc , which detects the differential change in the RI (n) that is a dimensionless parameter, and dn/dc is therefore expressed in mL/g. For most compounds in common solvents, dn/dc lies between 0.8–0.15 mL/g. The actual parameter used in RI detection is the RI itself, whose minute changes are transformed into a detector signal. Three types of RI detectors are commercially available: Fresnel (reflection), deflection, and interference. Fresnel RI detectors measure the difference between the RI of a glass prism with reference to the eluate. At the glass/liquid phase boundary, part of the incident beam is completely reflected. The intensity of the transmitted light is then measured at a given angle. When the RI changes, the angle and the intensity of the beam hitting the photodiode changes accordingly.

In the deflection-type RI detector, the optical system is designed differently. The light beam actually passes

through the detector cell twice. After passage through the detector and the reference cell, the light beam is reflected back through the detector cell. The beam is balanced by an optical zero control, divided into two beams of equal intensity by a prism, and focuses onto two photodiodes. One half of the detector cell is filled with pure mobile phase (reference cell), while the column eluate flows through the other half. The RI (n) is the same in each cell when only mobile phase passes through the cell. When an analyte passes through the flow cell, the RI (n) in the flow cell will change with respect to the reference cell. The light beam is deflected during forward and return passage through the cells. The resulting difference in light intensity is sensed by the photodiodes and the differential signal of the diodes is amplified and passed on to signal output devices.

In the interference-type RI detector, a monochromatic coherent light beam is split and the resulting two beams are directed through a reference and a sample cell, respectively. After passage through the cells, the difference in RI between the cells causes interference of two beams, which is measured by a photodiode.

Fluorescence (FL) Detector

Absorption of UV light by certain compounds triggers the emission of light with a longer wavelength. The spectral range of the emitted light depends on the excitation wavelength. Fluorescence emission can only be triggered at wavelengths at which the analytes absorb in the UV. Not all UV-absorbing compounds are also fluorescence emitters although some compounds possess native fluorescence. Nonfluorescent compounds can be converted into fluorescent compounds by derivatization with a suitable fluorophore before (so-called pre-column derivatization) or after (post-column derivatization) LC separation. The most selective and most flexible design contains two diffraction gratings with variable wavelength monochromators at the excitation side and at the emission side of the system. These types of detectors contain an additional cut-off filter to control stray light/light scattering and noise. In the stopped-flow mode, excitation, as well as emission spectra, of labile compounds can be scanned, and the optimum wavelengths for routine measurements can be determined. Of course, photodiode array detection is also available for this detector type.

Electrochemical Detectors

EcDs are used for quantitation of compounds which can be easily oxidized or reduced by an applied potential. The standard reduction potential at the electrode is measured

Detection Principles

3

and transformed into a detector signal. The number of compounds which can be electrochemically detected is, however, considerably smaller than the number of optically detectable compounds by UV, RI, and FL. To become oxidized or reduced, a compound must possess electrochemically active groups. EcDs are mainly used in clinical, food, and environmental analysis.

GC

In contrast to LC detectors, GC detectors often require a specific gas, either as a reactant gas or as fuel (such as hydrogen gas as fuel for flame ionization). Most GC detectors work best when the total gas flow rate through the detector is 20–40 mL/min. Because packed columns deliver 20–40 mL/min of carrier gas, this requirement is easily met. Capillary columns deliver 0.5–10 mL/min; thus, the total flow rate of gas is too low for optimum detector performance. In order to overcome the problem when using capillary columns, an appropriate makeup gas should be supplied at the detector. Some detectors use the reactant gas as the makeup gas, thus eliminating the need for two gases. The type and flow rate of the detector gases are dependent on the detector and can be different even for the same type of detector from different manufacturers. It is often necessary to refer the specific instrument manuals for details to obtain the information on the proper selection of gases and flow rates. All detectors are heated, primarily to keep the

analytes from condensing on the detector surfaces. Some detectors require high temperatures to function properly; some detectors are very sensitive to changes in temperature although others are only affected by very large changes in temperature. Some detectors are flow-sensitive; thus, their response changes or the baseline shifts according to the total gas flow rate through the detector.

Flame Ionization Detector (FID)

The FID is the most powerful and popular detector in GC, for which a basic structure is demonstrated in Fig. 1. Hydrogen and air are used to maintain a flame at the tip of the jet and into the flame where the organic components are burned. Ions are created in this combustion process; they are attracted to the charged collector electrode. This induced ion flow generates a current that can be measured and transformed to an output voltage by an electrometer. The amount of current generated should be dependent on the concentrations of the compounds introduced into the flame. The FID responds best to compounds containing a carbon–hydrogen bond. The lack of a carbon–hydrogen bond does not completely eliminate any response; however, the response is significantly depressed. Some notable compounds such as water, carbon monoxide, and carbon dioxide are nonresponding. Typical sensitivities for most organic compounds are 0.1–1 ng. The linear range is 5–6 orders magnitudes. Helium and nitrogen are typical as the makeup gases for capillary columns. Nitrogen is less costly and provides slightly

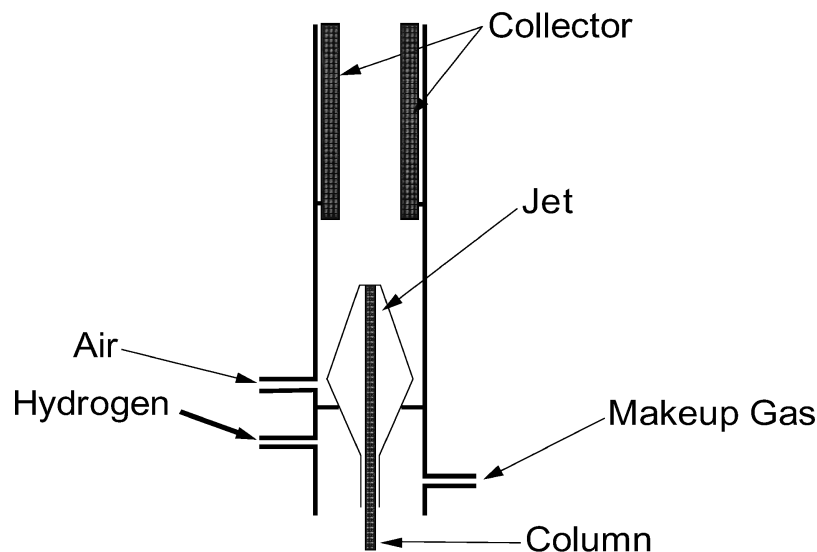


Fig. 1 Basic structure of FID for capillary GC.

better sensitivity. Near universal response, ease of use, wide linear range, and good sensitivity make the FID suitable for a wide variety of samples. Since FID is a simple detector, there is little routine maintenance required. The response of an FID is dependent on the hydrogen and gas flow rates; therefore, periodic measurement of these gas flow rates is necessary to maintain a stable performance. FIDs are not very temperature-sensitive and temperature changes of 50°C or greater are needed before any performance alterations are observed. FIDs are not sensitive to changes in the carrier gas flow rates; thus, baseline shifts or drifting is rarely found by changing the experimental conditions.

Nitrogen–Phosphorus Detector (NPD)

An alkali metal bead, usually rubidium sulfate, is positioned above the jet in NPD, as seen in Fig. 2, and the current is applied to this bead, which causes it to achieve temperatures up to 800°C. The addition of hydrogen and air generates plasma around the bead, and carrier gas containing the solutes is delivered to the tip of the jet and the plasma. Specific ions are produced in the plasma from nitrogen- or phosphorus-containing compounds. These ions move to the charged collector. This movement of ions generates a current that is measured

and transformed to an output voltage by an electrometer. The amount of the current is dependent on the amount of the compound introduced into the plasma. The NPD exhibits excellent selectivity and sensitivity for nitrogen- and phosphorus-containing compounds. The sensitivity is approximately 10,000 times greater for nitrogen and phosphorus compounds than for hydrocarbons. Typical NPD sensitivities are in the range of 0.5–1 pg with a linear range of 5–6 orders. Helium is the preferred make-up gas. Many compounds in the sample may not contain nitrogen or phosphorus, so a response is not observed for these compounds and, therefore, specific detection for nitrogen and phosphorus can be attained. Peak separation, identification, and measurement are made much easier because there are fewer peaks in the chromatogram. Also, less preparation of the sample prior to final determination is required because fewer of the potential interferences yield a response in the detector signal. Pesticides and pharmaceuticals analysis are generally the fields of application of the NPD.

Flame Photometric Detector (FPD)

Hydrogen and air are used to maintain a flame at the tip of the jet in the FPD. The carrier gas containing the analytes is delivered to the tip of the jet and into the flame. Some

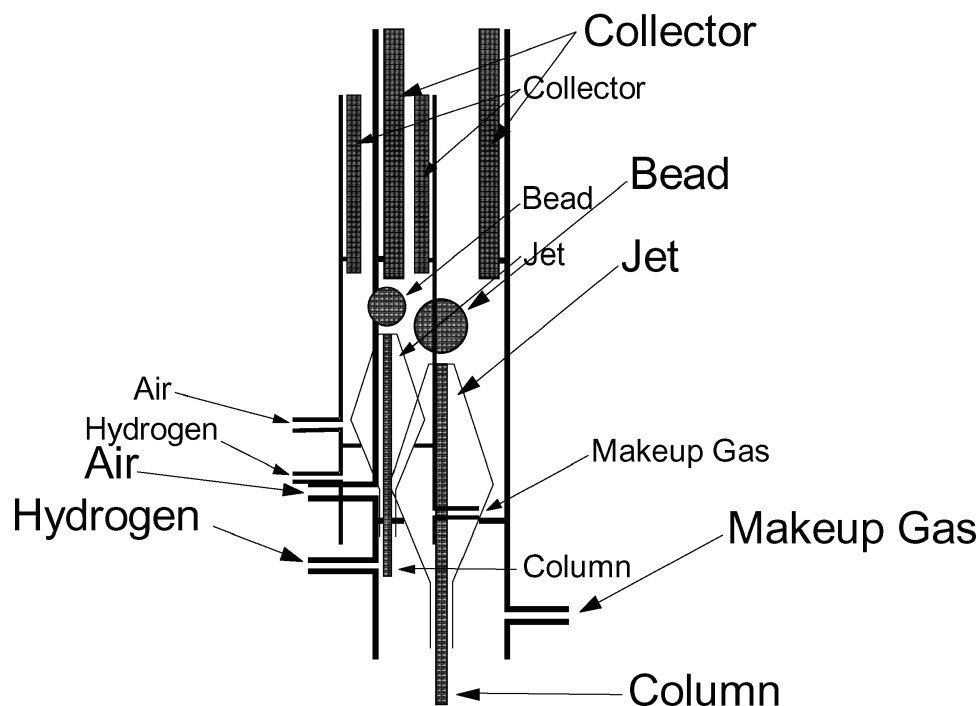


Fig. 2 Basic structure of NPD for capillary GC.



Detection Principles

5

FPDs use a dual jet or burner design, but the overall process is not significantly different. The solutes are burned in the flame, forming S₂ and HPO. Due to excitation in the flame, light at 392 nm for S₂ and at 526 nm for HPO are emitted. A photomultiplier tube is used to measure the light intensity after the optical filter. A current is generated, which can be measured and transformed to an output voltage by an electrometer. The amount of light created at each wavelength is dependent on the amount of compound introduced into the flame. The selectivity of the FPD for sulfur and phosphorus compounds is 3–4 orders of magnitude. Typical sensitivities are 10–100 pg for sulfur and 1–10 pg for phosphorus compounds. FPD responses are usually nonlinear for sulfur compounds. Nitrogen is the best makeup gas because its use results in the best sensitivity especially in the sulfur detection mode. FPDs are temperature- and flow-sensitive and, therefore, sensitivity changes are common when the temperature or carrier gas flow rates are changed. Increasing the detector temperature results in a decrease in sensitivity. FPD sensitivity for phosphorus compounds is comparable to NPD sensitivity. Due to some of the difficulties with NPDs, FPDs are frequently preferred for phosphorus-specific detection purposes. The increase of 500–1000 times in sensitivity of the FPD over the thermal conductivity detector (TCD) and FID often makes its nonlinear response behavior tolerable.

Electron-Capture Detector (ECD)

Carrier gas containing the solutes is delivered into the heated cell in the ECD. A ⁶³Ni source lining the cell acts as a source of electrons, and a moderating or auxiliary gas of nitrogen or argon/methane (95/5) is introduced into the cell to create thermal electrons which are attracted to the anode, creating a current. When an electronegative compound enters the cell, it captures thermal electrons and reduces the cell current. The amount of current reduction is measured and transformed to an output voltage by an electrometer. The size of the current loss is dependent on the amount of the compound entering the cell. The ECD primarily responds to compounds that contain a halogen, carbonyl, or nitrate group. Halogens have 100–100,000 times, nitrates have 100–1000 times, and carbonyls have 20–100 times better response than hydrocarbons. Polyhalogenated compounds, or compounds containing multiple nitrate or carbonyl groups, yield significantly increased detector responses. Also, the response for different halogens and types of carbonyls are varied, depending upon the structures of the analytes. Sensitivities approaching 1 pg for halogens, 10 pg for nitrates, and 50 pg for carbonyls are typical. The linear range is 2–3 orders and

poor; therefore, multiple-point calibration curves are required for accurate quantitation. The auxiliary gas is often used as the makeup gas in situations where makeup gas is necessary. Nitrogen is less costly and provides slightly better sensitivity than others. Argon/methane provides a slightly better linear dynamic range than nitrogen. The primary application of ECDs is for the detection of halogenated compounds. The flow rates of the carrier gas and auxiliary gas have a pronounced effect on the sensitivity and linear range of an ECD. The ECD temperature also affects the sensitivity.

Thermal Conductivity Detector (TCD)

The TCD consists of two heated cells, one of which is a sample cell and the other is a reference cell. The carrier gas containing the separated compounds enters the sample cell, while the reference cell is supplied with the same type and flow rate of carrier gas that flows into the sample cell. There is a TCD design that utilizes a single cell and a switching valve to accomplish the same task. Current is applied to the filaments, which causes them to reach an elevated equilibrium temperature when the current and gas flows are constant. When a compound that has a thermal conductivity different from that of the carrier gas is eluted from the column, it induces a change in the filament temperature. Because the reference cell filament remains at a constant temperature, the temperature difference between the two filaments is compared. The difference is measured via a Wheatstone bridge, which produces an output voltage. It is dependent on the amount of compound entering the sample cell. The best TCD sensitivity is established when the difference in thermal conductivities between the carrier gas and the component is maximized. Helium or hydrogen is usually the carrier gas of choice because these gases have thermal conductivities 10–15 times greater than that of most organic molecules, whereas nitrogen is only seven times higher than most organic molecules. This means that the TCD is a universal detector in GC although the sensitivity is relatively low, 5–50 ng per component or 10–100 times less than that of the FID. The linear range is five orders magnitude. TCDs are flow- and temperature-dependent.

Other detectors

There are a number of other GC detectors commercially available. Photoionization detectors (PID) are primarily used for the selective, low-level detection of the compounds which have double or triple bonds or an aromatic moiety in their structures. Electrolytic conductivity



detectors (ELCD) are used for the selective detection of chlorine-, nitrogen-, or sulfur-containing compounds at low levels. Chemiluminescence detectors are usually employed for the detection of sulfur compounds. The atomic emission detectors (AED) can be set up to respond only to selected atoms, or group of atoms, and they are very useful for element-specific detection and element-speciation work.

SFC

All detectors in GC and LC can be easily made useful for SFC. Basically, however, we can say that GC detectors are useful for capillary SFC, and LC detectors are useful for packed-column SFC. The most important and convenient features of SFC are that any detection sys-

tems available in chromatography can be useful and all work well.

FURTHER READING

Chromatography Fundamentals, Applications, and Troubleshooting; Walker, J.Q., Ed.; Preston Publications: Niles, IL, 1996.

Diode Array Detection in HPLC; Huber, L., George, S.A., Eds.; Marcel Dekker, Inc.: New York, 1993.

Detectors for Liquid Chromatography; Yeung, E.S., Ed.; Wiley-Interscience: New York, 1986.

Gilbert, M.T. *High Performance Liquid Chromatography*; Wright Co.: Bristol, 1987.

Hyphenated Techniques in Supercritical Fluid Chromatography and Extraction; Jinno, K., Ed.; Elsevier: Amsterdam, 1992.

Smith, R.M. *Gas and Liquid Chromatography in Analytical Chemistry*; John Wiley & Sons: Chichester, 1988.

Detector Linear Dynamic Range

Raymond P.W. Scott

Scientific Detectors Ltd., Banbury, Oxfordshire, England

Introduction

The linearity of most detectors deteriorates at high concentrations and, thus, the *linear dynamic range* of a detector will always be less than its dynamic range.

Discussion

The symbol for the linear dynamic range is usually taken as (D_{LR}). As an example, the linear dynamic range of a flame ionization detector might be specified as

$$D_{LR} = 2 \times 10^5 \quad \text{for } 0.98 < r < 1.02$$

where r is the response index of the detector.

Alternatively, according to the ASTM E19 committee report on detector linearity, the linear range may also be defined as that concentration range over which the response of the detector is constant to within 5%, as determined from a linearity plot. This definition is significantly looser than that using the response index.

The lowest concentration in the linear dynamic range is usually taken as equal to the *minimum detectable concentration* or the *sensitivity* of the detector. The largest concentration in the linear dynamic range would be that where the response factor (r) falls outside the range specified, or the deviation from linearity exceeds 5% depending on how the linearity is defined. Unfortunately, many manufacturers do not differentiate between the dynamic range of the detector (D_R) and the linear dynamic range (D_{LR}) and do not quote a range for the response index (r). Some manufacturers do mark the least sensitive setting on a detector as N/L (nonlinear), which, in effect, accepts that there is a difference between the linear dynamic range and the dynamic range.

Suggested Further Reading

Fowles, I. A. and R. P. W. Scott, *J. Chromatogr.*, **11**: 1 (1963).

Scott, R. P. W., *Chromatographic Detectors*, Marcel Dekker, Inc., New York, 1996.



Detector Linearity and Response Index

Raymond P.W. Scott

Scientific Detectors Ltd., Banbury, Oxfordshire, England

Introduction

It is essential that any detector that is to be used directly for quantitative analysis has a linear response. A detector is said to be truly linear if the detector output (V) can be described by the simple linear function

$$V = Ac$$

where A is a constant and c is the concentration of the solute in the mobile phase (carrier gas) passing through it.

Discussion

As a result of the imperfections inherent in all electro-mechanical and electrical devices, true linearity is a hypothetical concept, and practical detectors can only approach this ideal response. Consequently, it is essential for the analyst to have some measure of detector linearity that can be given in numerical terms. Such a specification would allow quantitative comparison between detectors and indicate how close the response of the detector was to true linearity. Fowles and Scott [1] proposed a simple method for measuring detector linearity. They assumed that for an approximately linear detector, the response can be described by the power function

$$V = Ac^r$$

where r is defined as the response index of the detector.

For a truly linear detector, $r = 1$, and the proximity of r to unity will indicate the extent to which the response of the detector deviates from true linearity. The response of some detectors having different values for r are shown as curves relating the detector output (V) to solute concentration (c) in Fig. 1. It is seen that the individual curves appear as straight lines but the errors that occur in assuming true linearity can be quite large. The errors actually involved are shown in the following, which is an analysis of a binary mixture employing detectors with different response indices:

Solute	$r = 0.94$	$r = 0.97$	$r = 1.00$	$r = 1.03$	$r = 1.05$
1	11.25%	10.60%	10.00%	9.42%	9.05%
2	88.75%	89.40%	90.00%	90.58%	90.95%

It is clear that the magnitude of the error for the lower-level components can be as great as 12.5% (1.25% absolute) for $r = 0.94$ and 9.5% (0.95% absolute) for $r = 1.05$. In general analytical work, if reasonable linearity is assumed, then $0.98 < r < 1.03$. The basic advantage of defining linearity in this way is that if the detector is not perfectly linear, but the value for r is known, then a correction can be applied to accommodate the nonlinearity.

There are alternative methods for defining linearity which, in the author's opinion, are somewhat less precise and less useful. The recommendations of the ASTM E19 committee on linearity measurement are as follows:

The linear range of a detector is that concentration range of the test substance over which the response of the detector is constant to within 5%

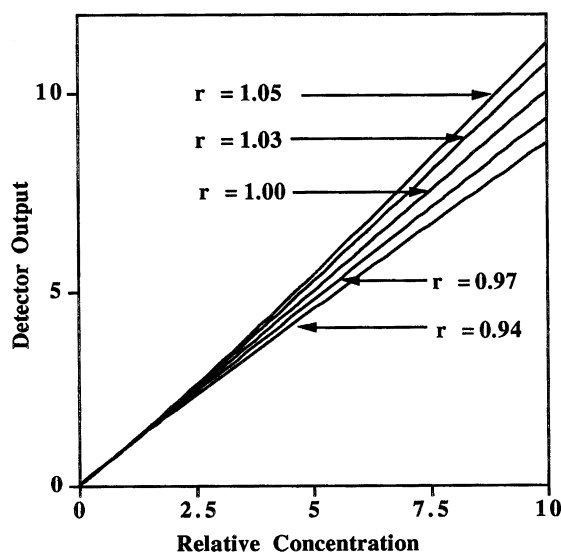


Fig. 1 Graph of detector output against solute concentration for detectors having different response indices.



as determined from a linearity plot,— the linear range should be expressed as the ratio of the highest concentration on the linearity scale to the minimum detectable concentration.

This method for defining detector linearity is satisfactory up to a point and ensures a minimum linearity from the detector and, consequently, an acceptable quantitative accuracy. However, the specification is significantly “looser” than that given above, and it is not possible to correct for any nonlinearity that may exist, as there is no correction factor provided that is equivalent to the response index. It is strongly advised that the response index should be determined for any detector that is to be used for quantitative analysis. In most cases, r need only be measured once, unless the detector undergoes some catastrophic event that is liable to distort its response, in which case, r may need to be checked again.

There are two methods that can be used to measure the response index of a detector: the *incremental method* of measurement and the *logarithmic dilution method* of measurement [2]. The former requires no special apparatus, but the latter requires a log-dilution vessel, which, fortunately, is relatively easy to fabricate. The incremental method of measurement is the one recommended for general use.

The apparatus necessary is the detector itself with its associated electronics and recorder or computer system, a mobile-phase supply, pump, sample valve, and virtually any kind of column. In practice, the chromatograph to be used for the subsequent analyses is normally employed. The solute is chosen as typical of the type of substances that will be analyzed and a mobile phase is chosen that will elute the solute from the column in a reasonable time. Initial sample concentrations are chosen to be appropriate for the detector under examination.

Duplicate samples are placed on the column, the sample solution is diluted by a factor of 3 and duplicate samples are again placed on the column. This procedure is repeated, increasing the detector sensitivity setting where necessary until the height of the eluted peak is commensurate with the noise level. If the de-

tector has no data acquisition and processing facilities, then the peaks from the chart recorder can be used. The width of each peak at 0.607 of the peak height is measured and the peak volume can be calculated from the chart speed and the mobile-phase flow rate. Now, the concentration at the peak maximum will be twice the average peak concentration, which can be calculated from

$$c_p = \frac{ms}{wQ}$$

where c_p is the concentration of solute in the mobile phase at the peak height (g/mL), m is the mass of solute injected, w is the peak width at 0.6067 of the peak height, s is the chart speed of the recorder or printer, and Q is the flow rate (mL/min).

The logarithm of the peak height y (where y is the peak height in millivolts) is then plotted against the log of the solute concentration at the peak maximum (c_p). Now,

$$\log(V) = \log(A) + (r) \log(c_p)$$

Thus, the slope of the $\log(V)/\log(c_p)$ curve will give the value of the response index (r). If the detector is truly linear, $r = 1$ (i.e., the slope of the curve will be $\tan \pi/4 = 1$). Alternatively, if suitable software is available, the data can be curved fitted to a power function and the value of r extracted directly from the curve-fitting analysis. The same data can be employed to determine the linear range as defined by the ASTM E19 committee. In this case, however, a linear plot of detector output against solute concentration at the peak maximum should be used and the point where the line deviates from 45° by 5% determines the limit of the linear dynamic range.

References

1. I. A. Fowles and R. P. W. Scott, *J. Chromatogr.*, 11: 1 (1963).
2. R. P. W. Scott, *Chromatographic Detectors*, Marcel Dekker, Inc., New York, 1996.

Detector Noise

Raymond P.W. Scott

Scientific Detectors Ltd., Banbury, Oxfordshire, England

Introduction

Detector noise is the term given to any perturbation on the detector output that is not related to the presence of an eluted solute. As the minimum detectable concentration, or detector sensitivity, is defined as that concentration of solute that provides a signal equivalent to twice the noise, the detector noise determines the ultimate performance of the detector. Detector noise has been arbitrarily divided into three types, *short-term noise*, *long-term noise*, and *drift*, all three of which are depicted in Fig. 1.

Short-Term Noise

Short-term noise consists of baseline perturbations that have a frequency that is significantly higher than that of the eluted peak. Short-term detector noise is usually not a serious problem in practice, as it can be easily removed by appropriate electronic noise filters that do not significantly affect the profiles of the peaks. The source of this noise is usually electronic, originating from either the detector sensor system or the amplifier electronics.

Long-Term Noise

Baseline perturbations that have a frequency that is similar to that of the eluted peak are termed long-term noise.

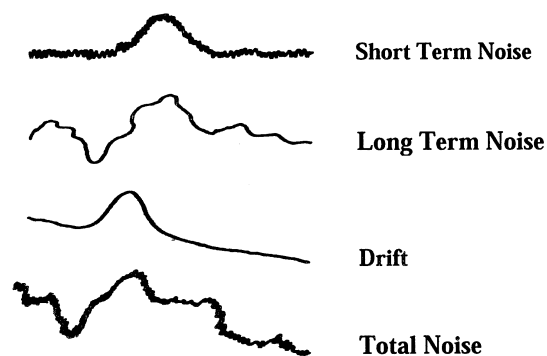


Fig. 1 Different types of detector noise.

This type of detector noise is the most significant and damaging, as it is often indiscernible from very small peaks in the chromatogram. Long-term noise cannot be removed by electronic filtering without affecting the profiles of the eluted peaks and, thus, destroying the integrity of the chromatogram. It is clear in Fig. 1 that the peak profile can easily be discerned above the high-frequency noise, but it is lost in the long-term noise. Long-term noise usually arises from temperature, pressure, or flow-rate changes in the sensing cell. Long-term noise can be controlled by careful detector cell design, the rigorous stabilization of operating variables such as sensor temperature, flow rate, and sensor pressure. Long-term noise is the primary factor that ultimately limits the detector *sensitivity* or the *minimum detectable concentration*.

Drift

Baseline perturbations that have a frequency significantly larger than that of the eluted peak are called drift. In gas chromatography (GC), drift is almost always due to either changes in detector temperature, changes in carrier gas flow rate, or column bleed. As a consequence, with certain detectors, baseline drift can become very significant at high column temperatures. Drift is easily constrained by choosing operating parameters that are within detector and column specifications.

A combination of all three sources of noise is shown by the trace at the bottom of Fig. 1. In general, the sensitivity of the detector (i.e., in most cases, the amplifier setting) should never be set above the level where the combined noise exceeds 2% of the FSD (full scale deflection) of the recorder (if one is used), or appears as more than 2% FSD of the computer simulation of the chromatogram.

Measurement of Detector Noise

The detector noise is defined as the maximum amplitude of the combined short- and long-term noise measured over a period of 10 min (the ASTM E19 committee recommends a period of 15 min). The detector must be connected to a column and carrier gas passed through it during measurement. The detector noise is obtained by



constructing parallel lines embracing the maximum excursions of the recorder trace over the defined time period. The distance between the parallel lines, measured in millivolts, is taken as the measured noise (v_n), and the noise level (N_D) is calculated in the following manner:

$$N_D = v_n A = \frac{v_n}{B}$$

where v_n is the noise measured in volts from the recorder trace, A is the attenuation factor, and B is the alternative amplification factor.

Note: Attenuation is the reciprocal of amplification; manufacturers may use either function as a control of detector sensitivity.

The noise levels of detectors that are particularly susceptible to variations in column pressure or flow rate (e.g., the katharometer) are sometimes measured under static conditions (i.e., no flow of carrier gas). Such specifications are not really useful, as the analyst can never use the detector without a column flow. It could be argued that the manufacturer of the detector should not be held respon-

sible for the precise control of the mobile phase, whether it may be a gas flow controller or pressure controller. However, all carrier supply systems show some variation in flow rates (and, consequently, pressure) and it is the responsibility of the detector manufacturer to design devices that are as insensitive to pressure and flow changes as possible.

At the high-sensitivity-range settings of some detectors, electronic filter circuits are automatically introduced to reduce the noise. Under such circumstances, the noise level should be determined at the lowest attenuation (or highest amplification) that does not include noise-filtering devices (or, at best, the lowest attenuation with the fastest response time) and then corrected to an attenuation of unity.

Suggested Further Reading

Scott, R. P. W., *Chromatographic Detectors*, Marcel Dekker, Inc., New York, 1996.

Scott, R. P. W., *Introduction to Gas Chromatography*, Marcel Dekker, Inc., New York, 1998.



Displacement Chromatography

John C. Ford

Indiana University of Pennsylvania, Indiana, Pennsylvania, U.S.A.

Introduction

Displacement chromatography is one of the three basic modes of chromatographic operation, the other two being frontal analysis and elution chromatography. Displacement chromatography is rarely, if ever, used for analytical separations, but it is useful for preparative separations. It has also been used for trace enrichment. Many retentive chromatographic methods have been performed in the displacement mode, including normal-phase, reversed-phase, ion-exchange, and metal affinity chromatographies. Much of the recent work has focused on the use of ion-exchange displacement chromatography for the preparative purification of the products of biotechnological products. Solutes purified by displacement chromatography have included metal cations, small organic molecules, antibiotics, sugars, peptides, proteins, and nucleic acids.

Discussion

Tswett recognized the difference between elution and displacement development, although Tiselius was the first to clearly define these differences. Although displacement was popular in the 1940s, that popularity waned in the 1950s. In the 1980s, there was a resurgence of interest in displacement operation due to the efficient utilization of the stationary phase possible in that mode. Frenz and Horvath have published a comprehensive review of the history and applications of displacement chromatography.

Displacement chromatography is characterized by the introduction of a discrete volume of sample into the chromatographic column that has been previously equilibrated with a weak mobile phase, termed the carrier. This carrier is chosen so that the individual components of the sample (the solutes) are significantly retained by the stationary phase. The displacement is accomplished by following the sample with a new mobile phase containing some concentration of the displacer, a molecule with a higher affinity for the stationary phase than that of any of the solutes. The solutes are displaced from the stationary phase by the higher-

affinity displacer and move further down the column, readsorbing. That solute with the highest affinity for the stationary phase moves the least before readsorbing and that solute with the lowest affinity for the stationary phase moves the most. This process is repeated as the displacer solution moves further down the column until a series of separated, but adjacent, bands is formed, termed the isotachic train. Each component of the train moves at the same velocity as the velocity of the displacer front.

Following elution of the isotachic train and the displacer solution from the column, the column must be regenerated and reequilibrated with the carrier before any subsequent displacement separation. This reequilibration step can be lengthy and is frequently considered a major limitation to efficient displacement operation. Displacement chromatography requires the competitive isotherms of the solutes and the displacer to be convex upward and to not intersect each other. (See the entry Distribution Coefficient for related information.)

The isotherm of the displacer must have a higher saturation capacity than any of the solutes. This is shown in Fig. 1a. The operating line is the line that connects the origin with the concentration of the displacer used: 9 g/L in the figure. The points of intersection between the operating line and the isotherms of each of the solutes determine the concentrations of each solute in the isotachic train, roughly 3.4, 4.5, and 6.8 g/L as shown in Fig. 1b. The width, not the height, of the solute band within the train varies as the amount of solute in the sample varies. The concentration of the eluted solutes can be greater than their concentrations in the sample in displacement chromatography, unlike isocratic elution chromatography, wherein dilution necessarily occurs. Note that an actual displacement chromatogram would not have the appearance of that shown in the figure unless all solutes and the displacer had equal response factors for the detector employed.

The choice of the displacer concentration, which determines the operating line for a given displacement system, is critical for successful displacement. If the displacer concentration is increased (i.e., the



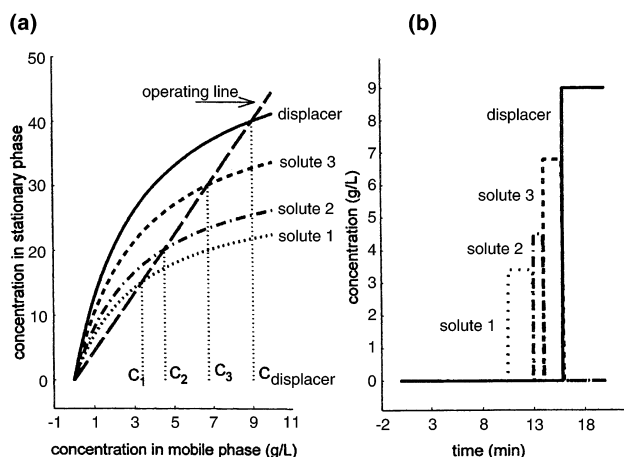


Fig. 1 Relationship between solute and displacer adsorption isotherms and the resultant isotachic train. (a) Nested set of upward isotherms showing the operating line at a displacer concentration of 9 g/L. (b) Resultant isotachic train showing that each solute elutes at the concentration determined by the intersection of the operating line with that solute's isotherm.

slope of the operating line is decreased), then the solute concentrations in the isotachic train also increase. If the displacer concentration is decreased to the point that the operating line does not intersect the isotherms of the solutes, then displacement does not occur and the solutes elute as overloaded peaks in the elution mode. Rhee and Amundson have shown that there is a critical displacer concentration below which displacement cannot occur. This concentration depends primarily on the saturation capacities of the solutes and displacer.

When the solute isotherms cross one another, the situation becomes more complex. It then becomes possible to experience selectivity reversal; that is, at one displacer concentration, the solutes elute in the order A first, then B, whereas at another displacer concentration, the order is B first, then A. In a study of this problem, Antia and Horvath showed the existence of the separation gap. This is a region in the isotherm plane, the position of which depends on the ratio of the saturation capacities of the solutes in question. If the operating line is outside the separation gap, displacement occurs in the normal fashion. The elution order of the solutes then depends on the position of the operating line relative to the separation gap. However, if the operating line is within the separation gap, displacement operation does not separate the displaced solutes, but results in the elution of a mixture of the solutes.

In addition to appropriate isotherm behavior and displacer concentration, other factors are important in determining the effectiveness of a displacement chromatographic method. Highly efficient columns and fast-mass-transfer kinetics are necessary to achieve sharp boundaries between the adjacent solute bands in the isotachic train. Diffuse boundaries mean significant regions of overlap between adjacent solute bands, and thus a low recovery of purified material.

Successful displacement requires the establishment of the isotachic train before elution of the solutes from the column. As might be expected, the column length is an important parameter in displacement chromatography. The column should be sufficiently long (or sufficiently efficient) to allow complete formation of the isotachic train while lengths beyond that minimum do not improve the separation and increase the separation time. An inadequate length results in the elution of an incompletely formed isotachic train with inadequately resolved solute bands, again reducing the recovery yield.

Similarly, the sample size, column length, and displacer concentration jointly influence the establishment of the isotachic train and, thus, the effectiveness of the displacement separation. For a given displacer concentration and column length, increasing amounts of sample result in increasingly diffuse boundaries, and in sufficiently large samples, significant deterioration of the isotachic train. Likewise, for a given sample size and column length, increasingly high concentrations of displacer cause increasingly diffuse boundaries—termed overdisplacement.

Conclusion

Displacement chromatography has the attractive benefit of concentrating the solute. If the conditions are selected appropriately, large injection volumes of low-concentration samples can result in isotachic trains having high solute concentrations, essentially identical to those obtained for narrow pulses of high-concentration samples. This is one of the features that has caused the increased interest in displacement as a preparative mode. However, detailed comparisons of the production rates of displacement versus overloaded elution operation are limited. The limited experimental studies suggest that displacement operation is superior, although regeneration time was not included in the production rate calculation. Alternately, extensive theoretical studies indicate that for solutes having Langmuirian behavior, optimized overloaded elution chromatography is superior. Resolution of this issue currently awaits further studies.

Suggested Further Reading

- Anita, F. D. and Cs. Horvath, Displacement chromatography of peptides and proteins, in *HPLC of Peptides and Proteins: Separation, Analysis, and Conformation* (C. Mant and R. Hodges, eds.), CRC Press, Boca Raton, FL, 1990, pp. 809–821.
- Antia, F. and Cs. Horvath, *J. Chromatogr.* 556: 119–143 (1991).
- Cramer, S. M. and G. Subramanian, *Separ. Purif. Methods* 19(1): 31–91 (1990).
- Freitag, R., Displacement chromatography: application to downstream processing in biotechnology, in *Bioseparation Bioprocess* (G. Subramanian, ed.), Wiley-VCH, Weinheim, 1998, Vol. 1, pp. 89–112.
- Frenz, J. and Cs. Horvath, High-performance displacement chromatography, in *High-Performance Liquid Chromatography: Advances and Perspectives* (Cs. Horvath, ed.), Academic Press, San Diego, CA, 1988, Vol. 5, pp. 211–314.
- Guiochon, G. and S. G. Shirazi, and A. M. Katti, *Fundamentals of Preparative and Nonlinear Chromatography*, Academic Press, Boston, 1994.
- Rhee, H.-K. and N. R. Amundson, *AIChE J.* 28: 423–433 (1982).



Displacement Thin-Layer Chromatography

Mária Báthori

University of Szeged, Szeged, Hungary

INTRODUCTION

Displacement takes place in a broad scale when a stronger species replaces a weaker one. Displacement of ligands on the receptor is a typical phenomenon in pharmacology which explains drug–drug interactions.

Displacement equilibrium is also known in chromatography, by which ligands compete for binding sites. This competition can be preferentially utilized for either analytical or preparative scale separations.

DISPLACEMENT CHROMATOGRAPHY WITH COLUMN HIGH-PERFORMANCE LIQUID CHROMATOGRAPHY

Chromatography may be performed as elution, frontal, or displacement. When the mode of development is not specified, a chromatographic separation is considered to be an elution.

The displacement phenomenon in chromatography was recognized from the beginning of separation processes in the present-day sense.^[1] Classical displacement chromatography was used to separate biologically active compounds, such as amino acids, peptides, and fatty acids.^[2] High-performance displacement chromatography (HPDC) was developed in Horváth's laboratory at Yale University. They realized displacement type of development on a microparticulate stationary phase; various applications were accomplished to demonstrate the power of HPDC in preparative scale separation of compounds of biological and medical interest.^[3–6]

Experimental work of Kalász et al.^[6] resulted in the statement of the characteristics and basic rules of displacement chromatography. They conceived properties of the fully developed displacement train, factors affecting displacement development, efficacy of separation, analysis of displaced fractions, determination of displacement diagrams from Langmuirian isotherms, as well as selection of the column, carrier, and displacer for displacement chromatography. Concentration of the sample is a particular feature of displacement chromatography. However, the displacer in the carrier is also definitely concentrated through the development of the displacement train.

Furthermore, certain prerequisites of HPDC were stated, such as the limit of the mobile phase flow velocity, slight overlapping of peaks during fractionation, etc.

Displacement thin-layer chromatography (D-TLC) also stemmed from the activity of Horváth's group at Yale University. Experimental work with D-TLC has proven the validity of the rules of displacement chromatography, found by using high-performance liquid chromatography (HPLC).^[5,6] Kalász et al.^[6–8] continued the research on D-TLC, mainly with the separation of steroids.

There are basic unique characteristics solely for displacement chromatography (DC). Displacement chromatography works with a mobile phase containing both the carrier and the displacer. A special front moves forward during the development; it is the front of the displacer. Of course, certain compounds are moving forward ahead of the displacer front; that is, the displacer (front) displaces the components from the binding sites of the stationary phase. This complex of the components is terminated by the displacer and the components, and also the displacer is moving forward in the form of clearly defined zone(s) instead of as the Gaussian peaks seen with elution chromatography. The concentration (zone height or peak height) of individual displaced zones is determined by the crossing point of the Langmuirian isotherm and the operating line, instead of the amount of sample components (Table 1).

DISPLACEMENT THIN-LAYER CHROMATOGRAPHY

Displacement thin-layer chromatography started with the experiments of Kalász and Horváth,^[5–7] who stated the basic rules of D-TLC. A direct connection was found between the volumetric load of HPLC and the size (length) of sample in TLC. The size of displaced zones depends on the weight size of the load, but never on the volume of the injected sample with D-HPLC. Similarly, the dimensions of the displaced band are independent from that of the spotted sample. A surprisingly short distance of advancement totally developed the displacement train, e.g., a 20-mm development. It is even more surprising that 75 µg of the sample load could become part

Table 1 Comparison of elution and displacement modes of development

Elution development	Displacement development
<p>Linear and nonlinear (overloaded) elution. The components are diluted (relative to their concentrations in the sample). There is one mobile phase, consisting of the elements of the eluent. Gradient elution can also be performed by the use of several mobile phases. Either stepwise gradient or continuous gradient elution is possible. The components travel with different migration speeds.</p> <p>Gaussian (or quasi-Gaussian) peaks. The peak area is proportional to the amount of the component. In some approximations, the peak height is considered instead of peak area.</p> <p>Separation means physical removal of the peaks from each other, the maximum of peaks have to be far away from each other, the distance should be at least one peak width measured at the baseline.</p>	<p>The components are concentrated (relative to their concentrations in the sample). There are two consecutively supplied mobile phases, the carrier and the displacer. This latter consists of an adequate amount of displacer in the carrier. Isotachic migration of the component zones in the fully developed displacement train. Adjacent square-wave-shaped zones. The zone height is determined by the crossing of the Langmuirian isotherm of the component with the operating line. The zone width is proportional to the amount of the component. The adjacent zones of a totally developed displacement train touch each other, even in the optimal separation.</p>

of a displacement train after having utilized about 250 mg of stationary phase.^[6,7]

Displacement thin-layer chromatography has several analogs to column displacement HPLC, such as:

- A displacer is supplied after the samples have been loaded onto the stationary phase.
- A displacer front is generated in situ on the stationary phase.
- The sample components start to move because of the effect of displacer, and the displacer front forms a displacement train of adjacent spots.
- After having reached the state of a fully developed displacement train, all bands move with the same velocity, which is the velocity of the displacer front.

There are two conditions required for any component in the displacement train:

- The component has to show very moderate movement on the stationary phase from the effect of carrier.
- The displacer has to have stronger absorption to the displacement train than the component to be displaced.

There are four different migration types of any solute in the displacing system; for example,

1. The solute is displaced in the front of the displacer.
2. The solute migrates faster than the displacer front.
3. The solute migrates slower than the displacer front.
4. The solute remains at the start.

Cases 1–3 are given in Fig. 1. Case no. 1 generally represents the real displacement (bona fide displacement).^[9] Further proof of the bona fide displacing process can be given by the use of spacers, varying the front distance (and, thereby, the displacement front distance), and control of the load vs. spot length principle. This latter rule means that the higher the load, the longer will be the spot length. Bona fide displacement and quasi-displacement can also be differentiated on the basis of the chromatogram. Bona fide displacement gives a homogeneous peak, which consists of both the displacer front and the displaced component. In the case of quasi-displacement, the two peaks are partially separated, and the peak of the displaced component is a little bit wider. A change of carrier generally solves this problem. Participation in the displacement train is the principal assignment.

Kalász et al.^[10] showed that even a very short distance (e.g., 2 cm in the case of 5% displacer) may be sufficient for the formation of a fully developed displacement train. High-performance displacement chromatography (HPDC) is devoted to preparative scale separation.^[3] Fractions result in HPDC; the fractions are collected and analyzed “off-line.” The appropriate fractions can be combined to yield the pure compounds. Displacement thin-layer chromatography was grown into an approach for scouting the optimum conditions for HPDC. Its goals are to find the proper carrier, the proper displacer, and the appropriate displacer concentration in the carrier. A series of experiments proved that the results of D-TLC can be transferred to HPDC.^[5] Even the zone-concentrating effect of the increase of displacer concentration was directly proven using off-line quantitative determination



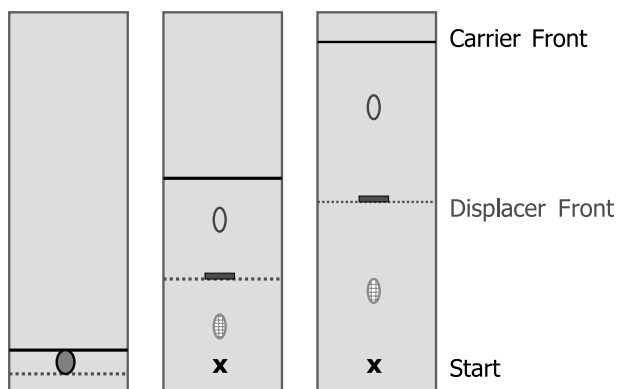


Fig. 1 Development of displacement chromatogram can take place on a plane. The faster-running front represents the carrier, and the slower running front is the displacer in the carrier. Certain components can be eluted by the carrier (blue open circle), and another one is eluted with the displacer (green circle, shaded). If there is any component displaced, it is located just before the displacer front (red square, filled). (View this art in color at www.dekker.com.)

of the fractions obtained by HPDC.^[5] However, the major field of application of D-TLC remains qualitative analysis, such as identification of compounds such as metabolites. Displacement thin-layer chromatography is mainly performed for such analytical purposes. On plain silica stationary phase, the 20:1:4:2 mixture of *n*-butanol–hydrochloric acid–water–methanol properly displaced several morphine derivatives, including morphine, azido-dihydroisomorphine, 14-hydroxy-dihydromorphine, dihydromorphine, 14-hydroxy-azido-dihydroisocodeine, 14-hydroxy-azido-dihydroisomorphine, codeine, azido-dihydroisocodeine, and 14-hydroxy-dihydrocodeine. Nonetheless, the adequate choice of the displacement system can alter the order of components and even the participation of the components in the displacement train. Using the same stationary phase (plain silica), the chlorinated hydrocarbon carriers (chloroform, dichloromethane, and dichloroethane) make less migration possible, as compared with the *n*-butanol–methanol–water–hydrochloric acid system. When triethanolamine displacer in chloroform carrier was used, certain otherwise eluted components became part of the displacement train. The ECAM (*O*-ethyl-*N*-cyclopropyl-norazido-dihydroisomorphine), CAM (*N*-cyclopropyl-norazido-dihydroisomorphine), norazido-dihydroisomorphine, normorphine, and nalorphine changed their situation from eluted positions to displaced ones. The most surprising change happened in the case of 6-amino-dihydromorphine, which was eluted with the carrier well before the displacer front, but it was left behind the displacer front in chlorinated hydrocarbon carrier and triethanolamine displacer. This phenomenon

can be explained by the reaction of amino group to the change of acidic to basic conditions caused by substituting triethylamine for the hydrochloric acid. The change of the stationary phase from silica to alumina also altered the components, in the displacement train, and the lengths of the displaced zones were changed as well. Remarkably, certain components show faster mobility on alumina when chloroform carrier is used. In addition, the displacement zones are also generally longer.^[11] The change of the stationary phase from plain silica to reversed-phase silica (TLC plate RP-18 F₂₅₄S, precoated, layer thickness 0.25 mm) turned the order of components upside-down (Fig. 2). Some of the components, however, remained in the displacement train, e.g., azido-dihydroisomorphine, ethyl-morphine, and norazido-dihydroisomorphine. Preparative work can also be performed by scraping the spots from the plate. Displacement thin-layer chromatography separation of morphine analogs was performed using volatile mobile phases including the carrier and the displacer. The mixture of *n*-butanol–hydrochloric acid–water–methanol (20:1:4:2) can be preferentially used for preparative separation of semisynthetic morphine derivatives. The separation includes the removal of the intermediates of the synthesis as well as the purification of the member of metabolic pathway. Another important factor to be considered was the concentration of displacer in the carrier. The higher the displacer concentration, the larger will be the R_F of its front (i.e., R_D). The displacer front could reach the migration position of certain eluted components, which may be part of the displacement train.^[9]

Displacement chromatography of substituted phenyl-isopropylamines can be easily accomplished. Both normal phase and octadecyl-substituted silica (reversed-phase) plates were used with the chloroform/triethanolamine and water–acetonitrile/tetrabutylammonium chloride carrier/displacer pairs, respectively. Only a few exceptionally

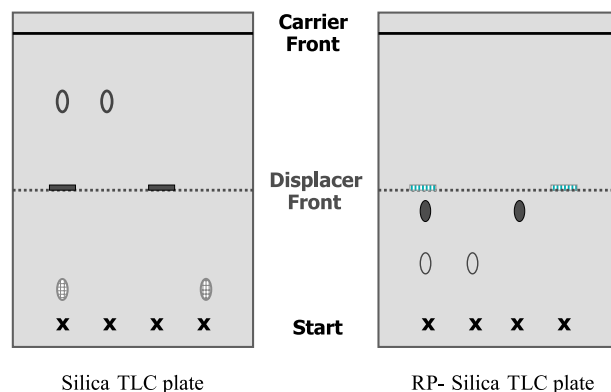


Fig. 2 The order of the spots is generally reversed when the stationary phase is changed from plain silica to reversed-phase silica. (View this art in color at www.dekker.com.)

behaving compounds moved faster or slower than the displacer front in the normal-phase and reversed-phase systems, respectively. The displacement chromatogram of HPDC can be characterized as series of sequentially increasing steps of the weight distribution or that of ultraviolet absorbance. This is the reason why off-line detection is used to characterize HPDC. Displacement thin-layer chromatography would have a similar profile, but specific detection may improve differentiation of the individual components. Further possibility is given by the application of spacers.

Kalász et al.^[12] used spacer to improve separation of radiolabeled metabolites, and the method was called spacer displacement thin-layer chromatography. They also constructed specific parameters of displacement chromatography, especially for calculation of the resolution (R_D), yield (Y), loss (L), and efficiency (E). Displacement of radiolabeled compounds was readily visualized using X-ray film with contact autoradiography.^[6,12,13] Two-dimensional chromatography can be simply arranged when a planar stationary phase is used. The stationary phase must be rotated 90° after the 1st dimensional development; then, the system is ready for the 2nd dimensional run. Elution type of development followed by displacement is an easy and useful means of two-dimensional thin-layer chromatography (2D-TLC). The 2D-TLC method has several increments to the elution-elution developments, such as the discrimination factors are different in the 1st and in the 2nd dimensional separations. The spots are concentrated through the 2nd dimensional development. Use of a spacer may further increase the separation of the spots that are located close to each other. Extensive work was devoted to the D-TLC using forced flow of the mobile phase (FFMP)^[6,14] and to the comparison of the effect of forced flow of the mobile phase to that of the classical (capillary flow) TLC.^[8]

The decrease of the mobile phase flow rate from 0.6 to 0.5 and then to 0.3 caused the appearance of the doubled fronts, such as alpha and beta fronts of the carrier and also α and β fronts of the displacer. This phenomenon can be explained by a particular characteristic of planar chromatography, as the mobile phase runs on a dry stationary phase. In addition to the chromatographic occurrences, there is an additional process; it is the wetting of the stationary phase with the components of the mobile phase. If the mobile phase supply is not adequate (this is the case of slow-traveling mobile phase), the wetting of the dry stationary phase is the rate-limiting step. Such cases are unknown in either HPDC or HPLC, when the stationary phase is presaturated and extensively washed by the mobile phase prior to loading a sample. Therefore development of HPDC is restrained by the high flow velocity of the mobile phase, and that of D-TLC is limited by using a slow velocity. Two-dimensional thin-layer

chromatography is the proper choice for separation of a single compound from a multicomponent mixture. When the 2nd dimensional run is carried out using D-TLC, one or several components can be well separated from all others. In addition, the displaced components are extensively concentrated.^[14]

When varying the conditions of D-TLC, various components can be a part of the displacement train. An interesting application of displacement chromatography is given by the identification of metabolically generated radiolabeled formaldehyde from the radiolabeled (–)-deprenyl [(–)-C¹⁴-*N*-methyl-*N*-propynyl-phenyl-isopropylamine]. The analysis was carried out after reacting the metabolites in a urine sample with 2,4-dinitrophenylhydrazine. The essence of the identification included the use of a standard (2,4-dinitrophenylhydrazone of formaldehyde) and comparing the urine samples with, and without, reaction of 2,4-dinitrophenylhydrazine.^[15,16] This method has been called reaction-displacement thin-layer chromatography.^[16] Kalász et al.^[9,17] reported front deformation when the stationary phase per load mass ratio was under 10, e.g., when 0.5 or 1 mg of solute was loaded onto 2.5 mg of the stationary phase.

The list of substances subjected to planar displacement chromatography includes a broad range of organic compounds. For instance, Kalász and Horváth^[5] separated three corticosteroids, Reichstein's Q, Reichstein's S, and Reichstein's H compounds. Kalász^[13] also separated phenylalkylamines, e.g., deprenyl, deprenyl metabolites, and related compounds. Báthori et al.^[18–21] separated ecdysteroids; Kamano et al.^[22] separated toad-poison bufadienolides, such as resibufogenin, cinobufagin, bufalin, bufotalin, cinobufotalin, telocinobufagin, and gamabufotalin. Kalász et al.^[10] separated morphine and semisynthetic morphine derivatives from each other. Kalász et al.^[15,16] also identified formaldehyde as an efferent metabolite of *N*-demethylation.

CONCLUSION

There are advantages which are offered by D-TLC. The planar stationary phase offers numerous advantages which cannot easily be realized using column (or capillary) arrangements. The entire displacement process can be readily visually followed. The separation can be directly evaluated. Sensitivity of the UV/visible scanners is well suited for the concentrations of substances in the displacement train. Radioactive spots on the planar stationary phase may be easily monitored by the use of X-ray film or digital autoradiography (DAR). Spacers can be inserted between the displaced bands. The plates are disposable; therefore the regeneration process is generally ignored. Two-dimensional developments (elution displacement)



can be easily performed. The actual concentration of displacer in the carrier can be calculated on the basis of its retardation. A detailed general summary of D-TLC is also given in a recently published book on TLC.^[23]

ACKNOWLEDGMENTS

This project was sponsored by the grant of OTKA T032185. The advice of Ms. Bogi Kalász is appreciated.

REFERENCES

1. Ettre, L.S. Evolution of Liquid Chromatography. In *High-Performance Liquid Chromatography. Advances and Perspectives*; Horváth, Cs., Ed.; Academic Press: New York, 1980; Vol. 1, 25.
2. Tiselius, A. Displacement development in adsorption analysis. *Ark. Kemi, Mineral. Geol.* **1943**, *16A*, 1–18.
3. Horváth, Cs.; Nahum, A.; Frenz, J. High-performance displacement chromatography. *J. Chromatogr.* **1981**, *218*, 365–393.
4. Kalász, H.; Horváth, Cs. Preparative scale separation of polymyxin B's by high performance displacement chromatography. *J. Chromatogr.* **1981**, *215*, 295–302.
5. Kalász, H.; Horváth, Cs. High-performance displacement chromatography of corticosteroids. Scouting for displacer and analysis of the effluent by thin-layer chromatography. *J. Chromatogr.* **1982**, *239*, 423–438.
6. Kalász, H.; Kerecsen, L.; Knoll, J.; Báthori, M. Displacement Chromatography of Steroids: Steroid Analysis. Proceedings of the Symposium on the Analysis of Steroids, Sopron, Hungary, 1987; Görög, S., Ed.; Akadémiai Kiadó: Budapest, 1988; 405–410.
7. Kalász, H.; Horváth, Cs. Effects of Operating Conditions in Displacement Thin-Layer Chromatography. In *New Approaches in Liquid Chromatography*; Kalász, H., Ed.; Elsevier: Amsterdam, 1984; 57–67.
8. Kalász, H.; Báthori, M.; Kerecsen, L.; Tóth, L. Displacement thin-layer chromatography of some plant ecdysteroids. *J. Planar Chromatogr.* **1993**, *6*, 38–42.
9. Bariska, J.; Csermely, T.; Fürst, S.; Kalász, H.; Báthori, M. Displacement thin-layer chromatography. *J. Liq. Chromatogr. Relat. Technol.* **2000**, *23*, 531–549.
10. Kalász, H.; Kerecsen, L.; Csermely, T.; Götz, H.; Friedmann, T.; Hosztafi, S. Displacement thin-layer chromatographic investigation of morphine and its semi-synthetic derivatives. *J. Liq. Chromatogr.* **1996**, *19*, 23–35.
11. Kalász, H.; Báthori, M.; Csermely, T. Planar versus microcolumn chromatography. *Am. Lab.* **2000**, *32* (9), 28–32.
12. Kalász, H.; Báthori, M.; Matkovics, B. Spacer and carrier spacer-displacement thin-layer chromatography. *J. Chromatogr.* **1990**, *520*, 287–293.
13. Kalász, H. Carrier displacement chromatography for identification of deprenyl and its metabolites. *J. High Resol. Chromatogr. Chromatogr. Commun.* **1983**, *6*, 49–50.
14. Kalász, H.; Báthori, M.; Ettre, L.S.; Polyák, B. Displacement thin-layer chromatography of some plant ecdysteroids with forced-flow development. *J. Planar Chromatogr.* **1993**, *6*, 481–486.
15. Kalász, H.; Szarvas, T.; Szarkáné-Bohóvszky, A.; Lengyel, J. TLC analysis of formaldehyde produced by metabolic *N*-demethylation. *J. Liq. Chromatogr. Relat. Technol.* **2002**, *25*, 1589–1598.
16. Kalász, H.; Lengyel, J.; Szarvas, T.; Morovjan, Gy.; Klebovich, I. *J. Planar Chromatogr.* submitted.
17. Kalász, H.; Báthori, M. Spacer displacement chromatography of steroids. Experiments, considerations and calculations. *Invertebr. Reprod. Dev.* **1990**, *18*, 119–120.
18. Kalász, H.; Kerecsen, L.; Nagy, J. Conditions dominating displacement thin-layer chromatography. *J. Chromatogr.* **1984**, *316*, 95–104.
19. Csermely, T.; Kalász, H.; Rischák, K.; Báthori, M.; Tarjányi, Zs.; Fürst, S. Planar chromatography of (–)-deprenyl and some structurally related compounds. *J. Planar Chromatogr.* **1998**, *11*, 247–253.
20. Lengyel, J.; Magyar, K.; Hollósi, I.; Bartók, T.; Báthori, M.; Kalász, H.; Fürst, S. Urinary excretion of deprenyl metabolites. *J. Chromatogr.* **1997**, *762*, 321–326.
21. Kalász, H.; Kerecsen, L.; Csermely, T.; Götz, H.; Friedmann, T.; Hosztafi, S. Thin-layer chromatographic investigation of some morphine derivatives. *J. Planar Chromatogr.* **1995**, *8*, 17–22.
22. Kamano, Y.; Kotake, A.; Nogawa, T.; Tozawa, M.; Pettit, G. Application of displacement thin-layer chromatography to toad-poison bufadienolides. *J. Planar Chromatogr.* **1999**, *12*, 120–123.
23. Kalász, H.; Báthori, M. Displacement Chromatography and Its Application Using a Planar Stationary Phase. In *Planar Chromatography, a Retrospective View for the Third Millennium*; Nyiredy, Sz., Ed.; Springer: Budapest, 2001; 220–233.



Distribution Coefficient

M. Caude

A. Jardy

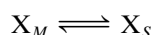
ESPCI, Paris, France

Introduction

In high-performance liquid chromatography (HPLC), as in many chromatographic techniques, separations result from the great number of repetitions of the analyte distribution between the mobile and stationary phases that are linked.

Discussion

At each elementary step, the distribution is governed by the distribution equilibrium



where X stands for the solute and the subscripts *M* and *S* for the mobile phase and the stationary phase, respectively. Conventionally, this equilibrium is characterized by the distribution coefficient

$$K = \frac{C_S}{C_M} \quad (1)$$

where C_S and C_M are the molar concentrations of the solute X in the two phases. The distribution coefficient is also sometimes defined in terms of mole fractions of the solute in both phases. In elution analytical chromatography, concentrations are low enough to be comparable to the activities as an approximation. Although *K* should be dimensionless, as any thermodynamic constant, some authors use different units for the concentrations in both phases. For example, in LSC chromatography, concentrations are given in moles per square meter for the adsorbent. In such a case, *K* should be considered as an “apparent” constant, the dimension of which is *m*. However, in practice, the product KV_S in Eq. (2) must have the dimension of a volume.

K is interrelated with the retention factor *k'* by

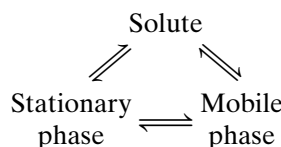
$$k' = Kq$$

where *q* is the phase ratio, defined as the ratio of stationary phase volume V_S to the mobile phase volume V_M . Under linear conditions, *K* is linked to the solute

retention volume (first-order moment of the elution peak) through

$$V_R = V_M + KV_S \quad (2)$$

The distribution coefficient is the reflection of the ternary interactions schematically represented by



These interactions are as follows:

Solute \leftrightarrow stationary phase for the retention

Solute \leftrightarrow mobile phase for the solubilization

Mobile phase \leftrightarrow stationary phase because of the competition between at least one constituent of the mobile phase (the strongest, also called the modifier) and the solute toward the active sites.

For an isobaric and isothermal process, the equilibrium constant *K* is given by

$$\ln K = -\frac{\Delta G^\circ}{RT} \quad (3)$$

where ΔG° is the difference in standard Gibbs free energy linked with the solute transfer from the mobile phase to the stationary phase:

$$\Delta G^\circ = \Delta H^\circ - T\Delta S^\circ \quad (4)$$

where ΔH° and ΔS° are the enthalpy and entropy, respectively.

In many cases, the value of ΔH° is independent of temperature so that linear Van't Hoff plots ($\ln K$ versus $1/T$) are observed. However, irregular retention behaviors are often observed, in practice, due to the dependence of ΔH° on the temperature.

Relationship (3) shows, clearly, the obtaining of reproducible results needed to thermoregulate the chromatographic apparatus, especially the column and mobile phase. Similarly, Eq. (3) explains why temperature changes implemented in order to



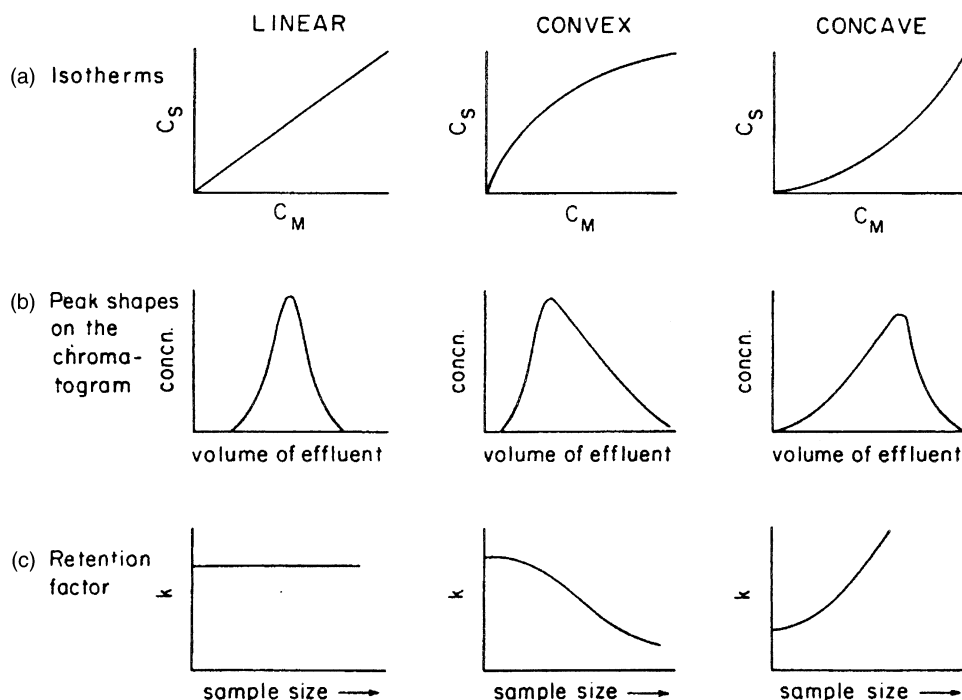


Fig. 1 Effect of isotherm shape on certain chromatographic properties. (a) Three different shapes of sorption isotherms encountered in chromatography; (b) peak shapes resulting from these isotherms; (c) dependence of the retention factor on the amount of solute injected. (From Karger, B. L., L. R. Snyder, and C. Horvath, *An Introduction to Separation Science*, John Wiley & Sons, New York, 1973.)

increase efficiency can affect, drastically, the selectivity.

From Eq. (1), K can be related to the sorption isotherm, as it corresponds to the chord slope at each point. Therefore, Eq. (2) is valid only if K is constant; that is, the sorption isotherm is linear or, at least, is in a region where it becomes linear (i.e., if the dilution is great enough). The effect of the isotherm shape is shown in Fig. 1.

For the low concentrations used in liquid chromatography, the elution peak is Gaussian in shape and its retention factor is independent of the sample size. When isotherms are nonlinear (convex or concave, as illustrated in Fig. 1), an asymmetric elution peak is obtained and the retention factor measured at the peak apex is dependant on the sample size.

This peak asymmetry is due to the dependence of the solute migration velocity versus the slope of the isotherm, which varies the solution concentration in the mobile phase.

Suggested Further Reading

- Katz, E., R. Eksteen, P. Schoenmakers, and N. Miller, *Handbook of HPLC*, Marcel Dekker, Inc., New York, 1998, Chap. 1.
- Karger, B. L., L. R. Snyder, and C. Horvath, *An Introduction to Separation Science*, John Wiley & Sons, New York, 1973, pp. 12–33.
- Rosset, R., M. Caude, and A. Jardy, *Chromatographies en phases liquide et supercritique*, Masson, Paris, 1991, pp. 729–730.

DNA Sequencing Studies by CE

Yoshinobu Baba

University of Tokushima, Tokushima, Japan

Introduction

Development and commercialization of capillary array electrophoresis has a great impact on the Human Genome Project. The commercial 96-capillary array instrument has been achieved high-throughput DNA sequencing in the Human Genome Project and a 384-capillary array version has been developing to obtain a fourfold increase in throughput. Accordingly, the original key deadline for sequencing the 3 billion bases of the human genome by the end of 2005 has been brought forward significantly by use of capillary array electrophoresis. June 26, 2000, President Clinton announced that scientists in the international sequencing effort completed a working draft, which covers at least 90% of the human genome.

Human Genome Sequencing

Because the read length for each capillary of the commercial instrument is limited to less than 500–600 bases with >99% accuracy, long read sequencing more than 1000 bases for each capillary with >99% accuracy is required to achieve much higher throughput for DNA sequencing. Unfortunately, sequence read length degrades as the electric field and sequencing speed increases. Several investigations to improve the read length for DNA sequencing have been reported and elevated capillary temperature, development of new separation matrices, use of lower electric fields, use of a gradient of electric field strength, and a change in denaturing agent proved to be effective in achieving long reading for DNA sequencing. The longest sequencing read lengths have been obtained at modest electric fields, high temperature, and with low-concentration, non-cross-linked polymers. In parallel, the second track of DNA sequencing development is the design of large-scale capillary instruments, wherein hundreds of DNA samples can be sequenced in parallel.

Four-color LIF Detector

To develop a four-color detectable laser-induced fluorescence (LIF) detection system for capillary elec-

trophoresis is the first challenge toward accurate DNA sequencing, because the sequencing DNA fragment is fluorescently labeled with four different dyes on every base. The first high-speed, four-color capillary electrophoresis system for DNA sequencing was reported in 1990. The DNA sequencing fragments, which are fluorescently labeled with four different dyes on every base, were separated in a single capillary. A multiline argon ion laser was used to illuminate the narrow capillary simultaneously with light at 488 and 514 nm. Fluorescence was collected at right angles from the capillary. A set of beam splitters was used to direct the fluorescence to a set of four photomultiplier tubes, each equipped with a bandpass spectral filter, and fluorescence was recorded simultaneously in the four spectral channels. At an electric field of 300 V/cm, 80 min were required to separate fragments up to 360 bases in length. Some other detection schemes for DNA sequencing using a single capillary have been developed, including time-multiplexed fluorescence detection, two-spectral channel direct reading fluorescence spectrometer, and four-level peak-height encoded sequencing technique.

Capillary Array

Capillary electrophoresis (CE) provides rapid separation of long DNA sequencing fragments. However, the use of capillary arrays, instead of a single capillary, allows capillary DNA sequencing instrumentation to function as a high-throughput system. Array instruments typically use about 100 capillaries. A number of capillary array instruments have been reported. The systems fall into two classes: systems built around a scanning optical detector and systems that employ a detector array. Capillary array instruments put special requirements on the detection system. The first instrument used a confocal fluorescence scanner. In another approach, a multiple-capillary DNA sequencer was reported, in which a ribbon of capillaries was illuminated with a line-focused laser beam. Fluorescence was collected at right angles and imaged onto a CCD camera. The use of the CCD camera ensured that all capillaries



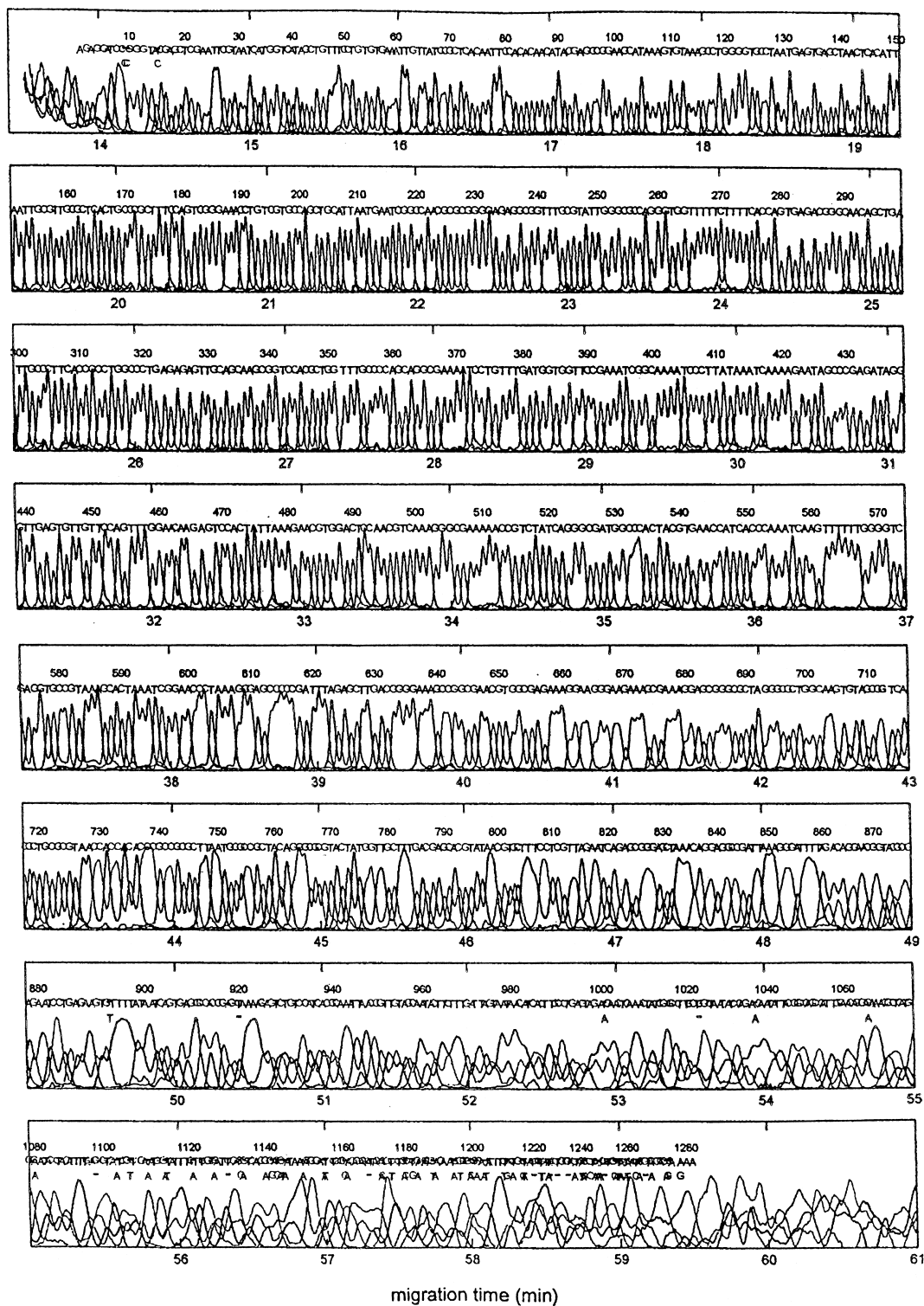


Fig. 1 Rapid 1000-base DNA sequencing by capillary electrophoresis.

were monitored simultaneously. To eliminate light scattering, a sheath-flow cuvette for multiple capillaries was developed (a multiple-sheath flow method). Fluorescence was collected at right angles and imaged onto a CCD camera. Optical waveguides have been proposed to collect fluorescence in the detection cell. A postelectrophoresis capillary scanning method has been developed to detect DNA sequencing fragments. The confocal fluorescence-scanning method is used in the first commercial system for DNA sequencing by capillary array electrophoresis, the MegaBACE 1000 by Molecular Dynamics, and the multiple-sheath flow detection method produces the second commercially system, PE-Biosystems PRISM 3700.

Microfabricated Chip

Substantial effort is being directed toward microfabrication of a device on a chip for DNA sequencing by capillary electrophoresis. Several laser-confocal scanners have been developed to be applicable to the detection of DNA sequencing fragments migrating in the microchannel array on a glass chip. An efficient microfabricated 96-microchannel (capillary) array chip was developed for DNA sequencing and achieved 570 bases sequencing within only 20 min. Capillary array electrophoresis on a chip brings new potentials into DNA sequencing and, after solving some technical problems, it may become a starting point for an instrument of future.

Separation Matrix

A key characteristic of an electrophoresis system is the sequencing read length. The number of primers required for directed sequencing strategy and the number of templates generated and sequenced in shotgun sequencing are inversely proportional to the read length. A long read length minimizes sample preparation. More subtly, long reads minimize the computational effort required to assemble shotgun-generated data into finished sequence. Finally, a long read length allows sequencing of difficult templates that contain long stretches of repeated sequence.

Among several factors affecting the read length for DNA sequencing, the separation matrix is the most important factor to gain long sequencing read length, even 1000 bases sequencing. The first experiments with DNA sequencing by capillary electrophoresis used cross-linked polyacrylamide gels. However, the cross-linked polyacrylamide capillary had a rather limited

lifetime. The use of cross-linked polymers in capillary electrophoresis leads to a serious limitation: The entire capillary must be replaced when the separation medium has degraded. The replacement can be quite tedious because of alignment constraints of the optical system with the narrow-diameter capillaries. Instead, it is attractive to use low-viscosity polymers for DNA sequencing by capillary electrophoresis. Low-viscosity polymers may be pumped from the capillary and replaced with a fresh matrix without replacement of the capillary or realignment of the optical system. Replaceable sieving matrices of linear polymers were introduced with the use of a linear polyacrylamide. With some exceptions, replaceable sieving matrices are now used in DNA sequencing, exclusively.

Several polymers have been used successfully in DNA sequencing: linear polyacrylamide (PAA), poly(ethylene oxide) (PEO), hydroxyethyl cellulose (HEC), polydimethylacrylamide (PDMA), polyvinylpyrrolidone (PVP), poly(ethylene glycol) (PEG) with a fluorocarbon tail, polyacryloylaminopropanol, and a copolymer of acrylamide and allylglucopyranose. It is not well understood why some polymers are better sieving matrices than others. It has been observed that a larger molecular mass of the polymer means a longer read length but results in poorer separation of short fragments. Linear polymers are much more suitable for separation of long DNA sequencing fragments than are branched polymers.

Linear polyacrylamide represents the best replaceable sieving polymer today in terms of read length and speed, although formation of a dynamic wall coating by PDMA and PEO, which allows DNA sequencing in bare fused-silica capillaries, sometimes makes these latter polymers the preferred choice. DNA sequencing performance, expressed as the read length generated per unit time, is the more important criterion. The read length itself depends on a number of factors, namely temperature, voltage, and the molecular mass of the polymer. It is not clear why polyacrylamide currently provides the best DNA sequencing data. It may be because of inherently superior properties of linear polyacrylamide or it may simply be because acrylamide is available in much higher purity than other monomers. Karger and his colleagues showed that linear polyacrylamide can generate DNA-sequencing read lengths beyond 1000 bases with an accuracy of almost 99% in 53 min (Fig. 1). This accuracy is good enough, because the value generally accepted for routine DNA sequencing is 98.5%. With linear polyacrylamide, the run-to-run base calling accuracy was 99.2% for the first 800 bases and 98.1% for the first



900 bases. Poly(ethylene oxide) is another extensively studied sieving polymer. A mixture of low-molecular-mass populations of PEO was possible to separate DNA sequencing fragments over 1000 bases, but the separation time exceeded 7 h.

Suggested Further Reading

- Dolnik, V., *J. Biochem. Biophys. Methods* 41: 103–119 (1999).
- Dovich, N. J., *Electrophoresis* 18: 2393–2399 (1997).
- Kambara, H. and S. Takahashi, *Nature* 361: 565–566 (1993).
- Karger, B. L., *Nature* 339: 641–642 (1989).
- Mathies, R. A., *Anal. Chem.* 71: 31A–37A (1999).
- Mathies, R. A. and X. C. Hunag, *Nature* 359: 167–169 (1992).
- Salas-Solano, E. Carrilho, L. Kotler, A. W. Miller, W. Goettinger, Z. Sasic, and B. L. Karger, *Anal. Chem.* 70: 3996–4003 (1998).
- Simpson, P. C., D. Roach, A. R. Woolley, T. Thorsen, R. Johanston, G. F. Sensbauch, and R. A. Mathies, *Proc. Natl. Acad. Sci. USA* 95: 2256–2261 (1998).
- Ueno, K. and E. S. Yeung, *Anal. Chem.* 66: 1424–1431 (1994).
- Zhang, J., Y. Fang, J. Y. Hou, H. J. Ren, R. Jiang, P. Roos, and N. J. Dovich, *Anal. Chem.* 67: 4589–4593 (1995).



Drug Residues in Food, Detection/Confirmation by LC-MS

Nikolaos A. Botsoglou

Aristotle University, Thessaloniki, Greece

INTRODUCTION

Numerous detection systems based on almost all kinds of known analytical techniques have been developed for screening, identifying, and quantifying drug residues in food. Each detection system has its own advantages and drawbacks which must be carefully considered in the selection of the most convenient system for a particular analyte in a particular matrix. The problem of analyzing for drug residues in food is complicated by the fact that it is not known whether residues exist and, if they exist, the type and quantity are not known.

Microbiological or immunochemical detection systems offer the advantage to screen, rapidly and at low cost, a large number of food samples for potential residues, but cannot provide definitive information on the identity of violative residues found in suspected samples. For samples found positive by the screening assays, residues can be tentatively identified and quantified by means of the combined force of an efficient liquid chromatographic (LC) separation and a selective physicochemical detection system such as UV, fluorescence, or electrochemical detection. The potential of pre- or postcolumn derivatization can further enhance the selectivity and sensitivity of the analysis. Nevertheless, unequivocal identification by these methods is not possible unless a more efficient detection system is applied.

The possibility for unambiguous identification of the analytes is offered by liquid chromatography–mass spectrometry (LC-MS). Mass spectrometry detection systems use the difference in mass-to-charge ratio (m/z) of ionized atoms or molecules to separate them from each other. Molecules have distinctive fragmentation patterns that provide structural information to identify structural components. The on-line coupling of LC with MS for the determination of drug residues in food has been under investigation for almost two decades.

LC-MS COUPLING

When LC is coupled with MS, three major problems generally arise. The first concerns the ionization of nonvolatile and/or thermolabile analytes. As MS operation is based on magnetic and electric fields that exert

forces on charged ions in a vacuum, a compound must be charged or ionized in the source to be introduced in the gas phase into the vacuum system of the MS. This is easily attainable for thermally volatile samples, but thermally labile analytes may decompose upon heating. The second is due to mobile-phase incompatibility as a result of the frequent use of nonvolatile mobile-phase buffers and additives in LC. This is why routine or long-term use of nonvolatile mobile-phase constituents, such as phosphate buffers and ion-pairing agents, is prohibited by all current LC-MS methods. As far as the third problem is concerned, this is related to the apparent flow rate incompatibility as expressed in the need to introduce a mobile phase eluting from the column at a flow rate of around 1 mL/min into the high vacuum of the MS.

To eliminate these problems, several different interfaces that provide broad analytical coverage have been developed. The main limitation of LC-MS interfaces is the lack of fragmentation data provided for structure determination because most interfaces operate basically in a chemical ionization (CI) mode, providing mild ionization and making identification of unknowns difficult or impossible. Hence the choice of a suitable interface for a particular application always has to be related to the analytes considered, especially their polarity and molecular mass, and the specific analytical problem as well.^[1]

Among the currently available interfaces for drug residue analysis, the most powerful and promising appear to be the particle-beam (PB) interface, the thermospray (TSP) interface that works well with substances of medium polarity, and the atmospheric pressure ionization (API) interfaces that have opened up important application areas of LC to LC-MS for ionizable compounds. Among the API interfaces, electrospray (ESP) and ionspray (ISP) appear to be the most versatile as they are suitable for substances ranging from polar to ionic and from low to high molecular mass. Ionspray, in particular, is compatible with the flow rates used with conventional LC columns. In addition, both ESP and ISP appear to be valuable in terms of analyte detectability.

Complementary to ESP and ISP interfaces, with respect to the analyte polarity, is the atmospheric pressure chemical ionization (APCI) interface equipped with a heated nebulizer. This is a powerful interface for both structural confirmation and quantitative analysis.

Particle-Beam Interface

The PB interface is an analyte-enrichment interface in which the column effluent is pneumatically nebulized into a near atmospheric-pressure desolvation chamber connected to a momentum separator, where the high-mass analytes are preferentially directed to the MS ion source while the low-mass solvent molecules are efficiently pumped away. With this interface, mobile-phase flow rates within the range 0.1–1.0 mL/min can be applied. Particle-beam–mass spectrometry appears to have high potential as an identification method for residues of some antibiotics in foods as it generates library-searchable EI spectra and CI solvent-independent spectra. Limitations of the PB-MS interface, as compared with other LC-MS interfaces, include lower sensitivity, difficulty in quantification, and lower response with highly aqueous mobile phases. The low sensitivity can be attributed, in part, to chromatographic band broadening during the transmission of the sample through the interface and, in part, to nonlinearity effects that appear at low analyte concentrations.^[2]

Liquid chromatography–particle beam–mass spectrometry has been investigated as a potential confirmatory method for the determination of malachite green in incurred catfish tissue,^[3] and cephalixin, furosemide, and methylene blue in milk, kidney, and muscle tissue, respectively.^[4] Liquid chromatography–particle beam–mass spectrometry has also been investigated for the analysis of ivermectin residues in bovine liver and milk.^[5] The specificity required for regulatory confirmation was obtained by monitoring the molecular ion and characteristic fragment ions of the drug under negative-ion chemical ionization (NCI)–selective ion monitoring (SIM) conditions. Quantification and confirmation of tetracycline, oxytetracycline, and chlortetracycline residues in milk,^[6] as well as chloramphenicol residues in calf muscle,^[7] have also been carried out using LC-PB-NCI-MS.

Thermospray Interface

The thermospray (TSP) interface is widely used for the determination of drug residues in foods.^[1] Thermospray is typically used with reversed-phase columns and volatile buffers. Aqueous mobile phases containing an electrolyte, such as ammonium acetate, are passed through a heated capillary prior to entering a heated ion source. As the end of the capillary lies opposite a vacuum line, nebulization takes place and a jet of vapor containing a mist of electrically charged droplets is formed. As the droplets move through the hot source area, they continue to vaporize, and ions present in the eluent are ejected from the droplet and

sampled through a conical exit aperture in the mass analyzer. The ionization of the analytes takes place by means of direct ion evaporation of the sample ion or by solvent-mediated CI reactions. With ionic analytes, the mechanism of ion evaporation is supposed to be primarily operative as ions are produced spontaneously from the mobile phase. Drawbacks of LC-TSP-MS are the requirements for volatile modifiers and the control of temperature, particularly for thermolabile compounds.^[8] Also, ion evaporation often yields mass spectra with little structural information. Lack of structural information from LC-TSP-MS applications can be overcome by the use of LC-TSP-MS-MS. Use of this tandem MS approach provides enhanced selectivity, generally at the cost of loss of sensitivity as a consequence of decreased ion transmission.

Liquid chromatography–thermospray–mass spectrometry has been successfully applied for the detection/confirmation of nicarbazin residues in chicken tissues using negative-ion detection in SIM mode.^[9] Liquid chromatography–thermospray–mass spectrometry in SIM mode has also been used for the quantification of residues of moxidectin in cattle tissues and fat,^[10] and nitroxylin, raxofenamide, and levamisole in muscle.^[11] Confirmatory methods based on LC-TSP-MS have been further reported for the determination of penicillin G,^[12] cephalixin,^[13] and various penicillin derivatives^[14] in milk. Comparative evaluation of the confirmatory efficiency of LC-TSP-MS and LC-TSP-MS-MS in the assay of maduramycin in chicken fat showed the former approach to be marginally appropriate, whereas the latter is highly efficient.^[15] Tandem LC-MS-MS has also been successfully applied in the analysis of residues of chloramphenicol in milk and fish.^[16]

Electrospray Interface

The ESP interface, which is a widely applicable soft ionization technique, operates at the low microliter per minute flow rate, necessitating the use of either capillary columns or postcolumn splitting of the mobile phase. For ESP ionization, the analytes must be ionic or have an ionizable functional group, or be able to form an ionic adduct in solution; the analytes are commonly detected as deprotonated species or as cation adducts of a proton or an alkali metal ion. When using positive ion ESP ionization, the use of ammonium acetate as a mobile-phase modifier is generally unsuitable. Instead, organic modifiers, such as heptafluorobutyric or trifluoroacetic acid, usually at a concentration of 0.1%, are strongly recommended. For negative ion applications, the choice of the modifier is even more limited, triethylamine currently being the only suitable compound.



Liquid chromatography–electrospray–mass spectrometry has been successfully used for the multiresidue assay of penicillin G, ampicillin, amoxicillin, cloxacillin, and cephalixin in milk ultrafiltrate at the 100-ppb level after postcolumn splitting of the eluent and recording under SIM conditions in the positive-ion mode.^[17] Significantly lower detection limits were reported by other workers who described an LC-ESP-MS confirmatory procedure for the simultaneous determination of five penicillins in milk and meat under SIM conditions in the negative-ion mode.^[18] Electrospray has been further shown to be useful in the analysis of several classes of veterinary drugs, including sulfonamides and tetracyclines, which exhibit spectra with four common ions; however, this was not possible for the group of β -agonists because of their more diverse chemical structures.^[19] Negative-ion ESP-MS has also been used for the detection/identification of a number of nonsteroidal anti-inflammatory drugs, including phenylbutazone, flunixin, oxyphenbutazone, and diclofenac, after their reversed-phase separation.^[20] Liquid chromatography–electrospray–mass spectrometry has also been found suitable for the determination of four coccidiostats in poultry products.^[21]

Ionspray Interface

The ISP interface is closely related to the ESP. However, unlike the ESP interface, ISP allows higher flow rates by virtue of pneumatically assisted vaporization. As both ESP and ISP produce quasi-molecular ions, more sophisticated techniques, such as LC-MS-MS, are required to obtain diagnostic fragment ions and thus analyte structure elucidation. Identification can often be achieved by using daughter ion MS-MS scans and collisionally induced dissociation (CID), most commonly on a triple quadrupole MS; in this way, dissociation of the quasi-molecular ion occurs and diagnostic structural information can be obtained.

Liquid chromatography–ionspray–mass spectrometry has been shown to be an attractive approach for the determination of semduramicin in chicken liver.^[22] Tandem MS using the CID of the molecular ions further enhanced the specificity providing structure elucidation and selective detection down to 30 ppb. Liquid chromatography–ionspray–mass spectrometry has also been successfully applied for the assay of 21 sulfonamides in salmon flesh.^[23] Coupling of LC with either ISP-MS or ISP-MS-MS has also been investigated as an attractive alternative for the determination of erythromycin A and its metabolites in salmon tissue.^[24] The combination of these methods permitted the identification of a number of degradation products and metabolites of erythromycin at the 10–50 ppb level. Tandem MS with CID has also been

applied for the specific monitoring of danofloxacin and its metabolites in chicken and cattle tissues at levels down to 50 ppb.^[25] Both ISP-MS in SIM mode and pulsed amperometric detection were found to be suitable for the determination of aminoglycoside antibiotics in bovine tissues.^[26]

Atmospheric Pressure Chemical Ionization Interface

Complementary to ESP and ISP interfaces is the APCI interface equipped with a heated nebulizer. The nebulized liquid effluent is swept through the heated tube by an additional gas flow, which circumvents the nebulizer. The heated mixture of solvent and vapor is then introduced into the ionization source where a corona discharge electrode initiates APCI. The spectra and chromatograms from APCI are somewhat similar to those from TSP, but the technique is more robust, especially with gradient LC, and it is often more sensitive. Atmospheric pressure chemical ionization is particularly useful for heat labile compounds and for low-mass, as well as high-mass, compounds. In contrast to the TSP interface, no extensive temperature optimization is needed with APCI.

The applicability of the APCI interface is restricted to the analysis of compounds with lower polarity and lower molecular mass, compared with ESP and ISP. Applications include the LC-APCI-MS multiresidue determination of quinolone antibiotics,^[27] the determination of tetracyclines in muscle at the 100-ppb level,^[28] and the determination of fenbendazole, oxfendazole, and the sulfone metabolite in muscle at the 10-ppb level.^[29]

CONCLUSION

The need to use drugs in animal husbandry will continue well into the future, and therefore monitoring of edible animal products for violative residues will remain an area of increasing concern and importance because of the potential impact on human health. The successful hyphenation of LC with MS has led to the development of highly flexible, computer-aided analytical methods that offer the required possibility for unambiguous identification of drug residues in food. Liquid chromatography–mass spectrometry is now in a mature state, but it still cannot be considered routine in the field of drug residue analysis. Possible reasons are the high initial cost, which is two to four times higher than that of gas chromatography–MS (GC-MS), and the poor detection limits, which are approximately 100 times higher than in GC-MS.

Coupling of LC with tandem MS may be a solution for improving detection limits by reducing the background noise, but this combination is two or three times more expensive than its LC-MS analogue. Mass spectrometry has become a standard tool in every modern laboratory, but there will be a growing need for even more sophisticated couplings.

REFERENCES

1. Botsoglou, N.A.; Fletouris, D.J. *Drug Residues in Food. Pharmacology, Food Safety, and Analysis*; Marcel Dekker, Inc.: New York, 2001.
2. Tinke, A.P.; Van der Hoeven, R.A.M.; Niessen, W.M.A.; Tjaden, U.R.; Van der Greef, J. Some aspects of peak broadening in particle-beam liquid-chromatography mass-spectrometry. *J. Chromatogr.* **1991**, *554*, 119–124.
3. Turnipseed, S.B.; Roybal, J.E.; Rupp, H.S.; Hurlbut, J.A.; Long, A.R. Particle-beam liquid-chromatography mass-spectrometry of triphenylmethane dyes—Application to confirmation of malachite green in incurred catfish tissue. *J. Chromatogr.* **1995**, *670*, 55–62.
4. Voyksner, R.D.; Smith, C.S.; Knox, P.C. Optimization and application of particle beam high-performance liquid-chromatography mass-spectrometry to compounds of pharmaceutical interest. *Biomed. Environ. Mass Spectrom.* **1990**, *19*, 523–534.
5. Heller, D.N.; Schenck, F.J. Particle beam liquid-chromatography mass-spectrometry with negative-ion chemical ionization for the confirmation of ivermectin residues in bovine milk and liver. *Biol. Mass Spectrom.* **1993**, *22*, 184–193.
6. Kijak, P.J.; Leadbetter, M.G.; Thomas, M.H.; Thompson, E.A. Confirmation of oxytetracycline, tetracycline and chlortetracycline residues in milk by particle beam liquid-chromatography mass-spectrometry. *Biol. Mass Spectrom.* **1991**, *20*, 789–795.
7. Delepine, B.; Sanders, P. Determination of chloramphenicol in muscle using a particle beam interface for combining liquid-chromatography with negative-ion chemical ionization mass-spectrometry. *J. Chromatogr.* **1992**, *582*, 113–121.
8. Niessen, W.M.A.; Van der Greef, J. *Liquid Chromatography–Mass Spectrometry, Principles and Application*; Marcel Dekker, Inc.: New York, 1992.
9. Lewis, J.L.; Macy, T.D.; Garteiz, D.A. Determination of nicarbazin in chicken tissues by liquid-chromatography and confirmation of identity by thermospray liquid-chromatography mass-spectrometry. *J. Assoc. Off. Anal. Chem.* **1989**, *72*, 577–581.
10. Khunachak, A.; Dakunha, A.R.; Stout, S.J. Liquid-chromatographic determination of moxidectin residues in cattle tissues and confirmation in cattle fat by liquid-chromatography mass-spectrometry. *J. AOAC Int.* **1993**, *76*, 1230–1235.
11. Cannavan, A.; Blanchflower, W.J.; Kennedy, D.G. Determination of levamisole in animal tissues using liquid-chromatography thermospray mass-spectrometry. *Analyst* **1997**, *120*, 331–333.
12. Boison, J.O.K.; Keng, L.J.-Y.; MacNeil, J.D. Analysis of penicillin-G in milk by liquid-chromatography. *J. AOAC Int.* **1994**, *77*, 565–570.
13. Tyczkowska, K.L.; Voyksner, R.D.; Aronson, A.L. Development of an analytical method for cephalixin and its metabolite in bovine milk and serum by liquid-chromatography with UV–Vis detection and confirmation by thermospray mass-spectrometry. *J. Vet. Pharmacol. Ther.* **1991**, *14*, 51–60.
14. Voyksner, R.D.; Tyczkowska, K.L.; Aronson, A.L. Development of analytical methods for some penicillins in bovine milk by ion-paired chromatography and confirmation by thermospray mass-spectrometry. *J. Chromatogr.* **1991**, *567*, 389–404.
15. Stout, S.J.; Wilson, L.A.; Kleiner, A.I.; Dacunha, A.R.; Franc, T.J. Mass-spectrometric approaches to the confirmation of maduramicin-alpha in chicken fat. *Biomed. Environ. Mass Spectrom.* **1989**, *18*, 57–63.
16. Ramsey, E.D.; Games, D.E.; Startin, J.R.; Crews, C.; Gilbert, J. Detection of residues of chloramphenicol in crude extracts of fish and milk by tandem mass-spectrometry. *Biomed. Environ. Mass Spectrom.* **1989**, *18*, 5–11.
17. Straub, R.F.; Voyksner, R.D. Determination of penicillin-G, ampicillin, amoxicillin, cloxacillin and cephalixin by high-performance liquid-chromatography electrospray mass-spectrometry. *J. Chromatogr.* **1993**, *647*, 167–181.
18. Tyczkowska, K.L.; Voyksner, R.D.; Straub, R.F.; Aronson, A.L. Simultaneous multiresidue analysis of beta-lactam antibiotics in bovine milk by liquid-chromatography with ultraviolet detection and confirmation by electrospray mass-spectrometry. *J. AOAC Int.* **1994**, *77*, 1122–1131.
19. Harris, J.; Wilkins, J. The Application of HPLC–Cone Voltage Assisted Fragmentation Electrospray Mass Spectrometry to the Determination of Veterinary Drug Residues. In *Residues of Veterinary Drugs in Food*, Proceedings of the Euroresidue III Conference, Veldhoven, May 6–8, 1996; Haagsma, N., Ruiter, A., Eds.; Fac. Vet. Med., Univ. Utrecht: The Netherlands, 1996.
20. Gowik, P.; Julicher, B. Behaviour of Some Selected NSAID's Under Electrospray LC-MS Conditions. In *Residues of Veterinary Drugs in Food*, Proceedings of the Euroresidue III Conference, Veldhoven, May 6–8, 1996; Haagsma, N., Ruiter, A., Eds.; Fac. Vet. Med., Univ. Utrecht: The Netherlands, 1996.
21. Blanchflower, W.J.; Kennedy, D.G. Determination of lasalocid in eggs using liquid chromatography-electrospray mass-spectrometry. *Analyst* **1995**, *120*, 1129–1132.
22. Schneider, R.P.; Lynch, M.J.; Ericson, J.F.; Fouda, H.G. Electrospray ionization mass-spectrometry of semduramicin and other polyether ionophores. *Anal. Chem.* **1991**, *63*, 1789–1794.
23. Pleasance, S.; Blay, P.; Quilliam, M.A.; O'Hara, G.



- Determination of sulphonamides by liquid-chromatography, ultraviolet diode-array detection and ion-spray tandem mass-spectrometry with application to cultured salmon flesh. *J. Chromatogr.* **1991**, 558, 155–173.
24. Pleasance, S.; Kelly, J.; Leblanc, M.D.; Quilliam, M.A.; Boyd, R.K.; Kitts, D.D.; McErlane, K.; Bailey, M.R.; North, D.H. Determination of erythromycin-A in salmon tissue by liquid-chromatography with ionspray mass-spectrometry. *Biol. Mass Spectrom.* **1992**, 21, 675–687.
 25. McLaughlin, L.G.; Henion, J.D. Determination of aminoglycoside antibiotics by reversed-phase ion-pair high-performance liquid-chromatography coupled with pulsed amperometry and ion spray mass-spectrometry. *J. Chromatogr.* **1992**, 591, 195–206.
 26. Schneider, R.P.; Ericson, J.F.; Lynch, M.J.; Fouda, H.G. Confirmation of danofloxacin residues in chicken and cattle liver by microbore high-performance liquid-chromatography electrospray-ionization tandem mass-spectrometry. *Biol. Mass Spectrom.* **1993**, 22, 595–599.
 27. Doerge, D.R.; Bajic, S. Multiresidue determination of quinolone antibiotics using liquid-chromatography coupled to atmospheric-pressure chemical-ionization mass-spectrometry and tandem mass-spectrometry. *Rapid Commun. Mass Spectrom.* **1993**, 9, 1012–1016.
 28. McCracken, R.J.; Blanchflower, W.J.; Haggan, S.A.; Kennedy, D.G. Simultaneous determination of oxytetracycline, tetracycline and chlortetracycline in animal tissues using liquid-chromatography, postcolumn derivatization with aluminum, and fluorescence detection. *Analyst* **1995**, 120, 1761–1766.
 29. Blanchflower, W.J.; Cannavan, A.; Kennedy, D.J. Determination of fenbendazole and oxfendazole in liver and muscle using liquid-chromatography mass-spectrometry. *Analyst* **1994**, 119, 1325–1328.



Dry-Column Chromatography

Mark Moskovitz

Scientific Adsorbents, Inc., Atlanta, Georgia, U.S.A.

Introduction

Dry-column chromatography (DCC) is a modern chromatographic technique that allows easy and rapid transfer of the operating parameters of analytical thin-layer chromatography (TLC) to preparative column chromatography (CC). The dry-column technique bridges the gap between preparative column chromatography and analytical thin-layer chromatography.

Discussion

Thin-layer chromatography has become an important technique in laboratory work, because it permits the rapid determination of the composition of complex mixtures. TLC allows the isolation of substances in micro amounts. If, however, milligrams or even grams of substance are required, column chromatography (CC) has to be applied, as TLC would involve a high cost and excessive time. In many cases, even the so-called thick layer or prep layer is but a poor choice because of time, cost, and sometimes inadequate transferability of the parameters of the analytical technique. In addition, the transfer from TLC to column chromatography, however, often proves to be difficult because the column chromatographic adsorbent is not usually analogous to the TLC adsorbent.

It is imperative that when transferring conditions of TLC separations to preparative columns, the conditions responsible for the TLC separation be meticulously transferred. Both CC and TLC use the same principle of separation. For normal operating conditions, a TLC layer has a chromatographic activity of II–III of the Brockmann and Schodder scale. Therefore, the sorbent used for DCC has to be brought to the same grade of activity. TLC layers often contain a fluorescent indicator in which case the DCC sorbent has to contain the same phosphor.

In TLC, the silica or alumina layer is “dry” before it is used and contacts the solvent only after it has been placed into the developing chamber. This is why, in DCC, the dry column is charged with the sample. Contrary to the normal CC, DCC is a nonelution tech-

nique. Therefore, only a limited amount of eluent is used in DCC to merely fill the interstitial volume between the adsorbent particles.

Scientific Adsorbents, Inc. DCC adsorbents, which are commercially available from Scientific Adsorbents, Inc. (Atlanta, GA, U.S.A.) are adjusted to meet the physical–chemical properties of TLC as closely as possible. These adjustments are made during the manufacturing cycle, and the material is packaged ready to use. With similar physical–chemical properties, the R_f values obtained for the substances under investigation from TLC are practically identical to those obtained with dry-column chromatography.

Using these especially adjusted adsorbents for DCC, one can use the same sorbent and the same solvent for the column work and can transfer the TLC results to a preparative scale column operation rapidly, saving time and money. DCC materials are available corresponding with the most common thin layers: silica DCC and alumina DCC.

These DCC sorbents have found wide use when it is necessary to scale up TLC separations in order to prepare sufficient quantities of compounds for further chemical reactions and/or analytical processes. DCC can be practically used for every separation achievable by TLC (Fig. 1).

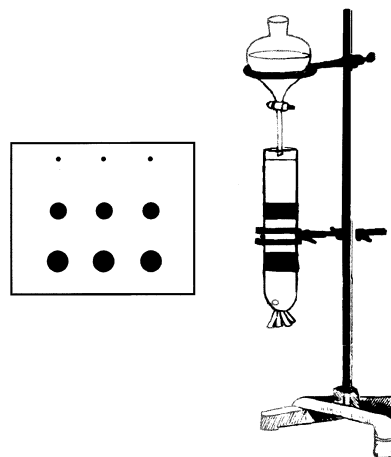


Fig. 1



Simplified Procedure

Preparation

1. Use the same solvent system that was developed on a TLC plate.
2. Cut a Nylon tube to the desired length. To isolate 1 g of material, use approximately 300 g of sorbent in a 1-m \times 740-mm tube (Fig. 2).

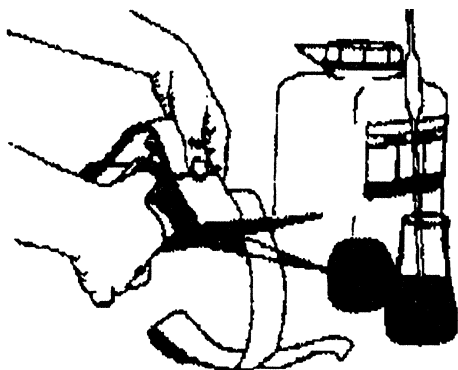


Fig. 2

3. Close the tube by rolling one end and securing it by a seal or a clip/staple.
4. Insert a small pad or wad of glass wool at the bottom of the column; pierce holes at the bottom with a needle.
5. Dry fill the column to three-fourths of its length (Fig. 3).

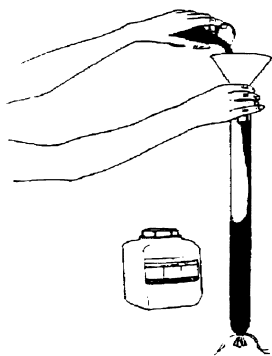


Fig. 3

6. The sample to be separated should be combined with at least 10 times its weight of the same sorbent in a conical test tube.
7. Add an additional centimeter of sorbent on top of the sample, followed by a small pad of glass wool (Fig. 4).

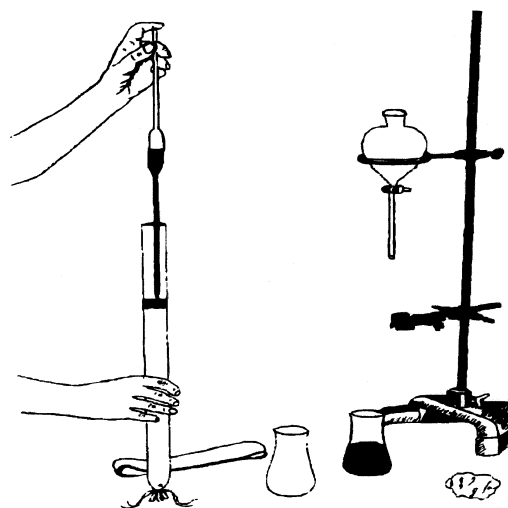


Fig. 4

8. Fasten the tube to a clamp on a stand.
9. Open the stopcock of the solvent reservoir and add solvent until it reaches the bottom of the column. Stop. Elapsed time: approximately 30 min. (Fig. 5).

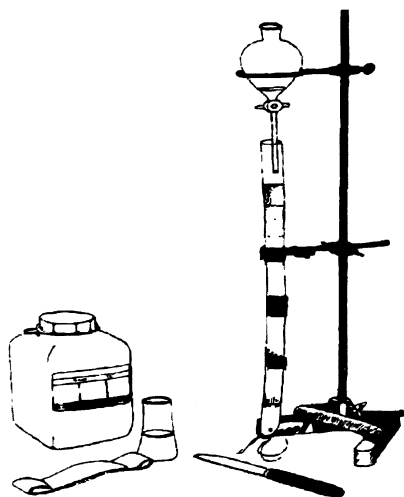


Fig. 5

10. Find the locations of the separated bands by visible, ultraviolet (UV), or UV quenching. Alternatively, cut a 1/16-in. vertical slice off the tube. Spray the exposed area with an appropriate visualization reagent and align with the untreated column to identify (mark) the separated bands.
11. Mark the location of the bands on the Nylon tube.

12. Remove the column from the clamp.
13. Slice the column into the desired sections (Fig. 6).
14. Elute the pure compounds from the sliced sections with polar solvents.

Suggested Further Reading

Love, B. and M. M. Goodman, *Chem. Ind. (London)* 2026 (1967).
Love, B. and K. M. Snyder, *Chem. Ind. (London)* 15 (1965).

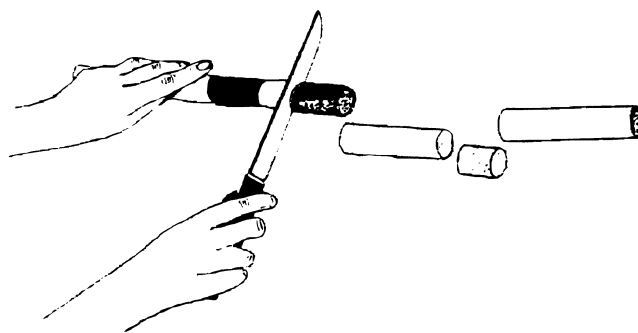


Fig. 6



Dual Countercurrent Chromatography

David Y.W. Lee

McLean Hospital, Harvard Medical School, Belmont, Massachusetts, U.S.A.

Introduction

Dual countercurrent chromatography (DuCCC) is a powerful separation method, which allows the performance of classic countercurrent distribution in a highly efficient manner. The system consists of a multilayer coiled column integrated with two inlet and two outlet flow tubes for a nonmiscible two-phase solvent system and a sample feed line, which is connected to the middle of the coiled column. Subjecting the system to a particular combination of centrifugal and planetary motions produces a unique hydrodynamic effect, which allows two immiscible liquids to flow countercurrently through the coiled column. The sample solution is fed at the middle portion of the column and eluted simultaneously through the column in opposite directions by the two solvents. This distinct feature of maintaining constant fresh two mobile phases within the coiled column permits a rich domain of applications. The principles of DuCCC and its applications in the purification of natural products and synthetic peptides are reviewed.

Discussion

The development, in the 1980s, of modern high-speed countercurrent chromatography (HSCCC) based on the fundamental principles of liquid–liquid partition has caused a resurgence of interest in the separation sciences. The advantages of applying continuous liquid–liquid extraction, a process for separating of a multicomponent mixture according to the differential solubility of each component in two immiscible solvents, have long been recognized. For instance, the countercurrent distribution method, which prevailed in the 1950s and 1960s, was applied successfully to fractionate commercial insulin into two subfractions, which differed only by one amide group in a molecular weight of 6000 [1]. In recent years, significant improvements have been made to enhance the performance and efficiency of liquid–liquid partitioning [2–8]. The high-speed centrifugal partition chromatographic (CPC) technique utilizes a particular combination of coil orientation and planetary motion to produce a unique hydrodynamic, unilateral phase distribution of two

immiscible solvents in a coiled column. The hydrodynamic properties can effectively be applied to perform a variety of liquid–liquid partition chromatographies including HSCCC [2], foam countercurrent chromatography [8,9] and DuCCC [10,11]. In most cases, for the two-phase solvent system selected for HSCCC, one liquid phase serves as a stationary phase and the second phase is used as a mobile phase. An efficient separation can be achieved by continuous partitioning of a mixture between the stationary phase and the mobile phase.

By definition, this mode of separation should be called high-speed liquid–liquid partition chromatography or centrifugal partition chromatography, because only one solvent phase is mobile. In the case of DuCCC, for the two-phase solvents countercrossing each other inside the coiled column from opposite directions, both phases are mobile and there is no stationary phase involved.

The name “dual” countercurrent chromatography is redundant; however, it is useful to distinguish it from ordinary HSCCC. DuCCC shares several common advantages with other types of liquid–liquid partition chromatography. For instance, there are an unlimited number of two-phase solvent systems which can be employed, and there are no sample losses from irreversible adsorption or decomposition on the solid support. In addition, DuCCC is extremely powerful in separating crude natural products, which usually consist of multicomponents with an extremely wide range of polarities. In a standard operation, the crude sample is fed through the middle portion of the column. The extreme polar and nonpolar components are readily eluted from the opposite ends of the column followed by components with decreasing orders of polarity in one phase and increasing order of polarity in the other phase. A component with a partition coefficient equal to 1.0 will remain inside the coiled column. Essentially, the DuCCC resembles a highly efficient performance of classic countercurrent distribution. They differ in that CCC is a dynamic process, whereas CCD is an equilibrium process. The principles, instrumentation of DuCCC, and its capabilities in natural products isolation are illustrated in the remainder of the article.



Principles and Mechanism

The fundamental principle of separation for modern DuCCC is identical to classic countercurrent distribution. It is based on the differential partitions of a multicomponent mixture between two countercrossing and immiscible solvents. The separation of a particular component within a complex mixture is based on the selection of a two-phase solvent system, which provides an optimized partition coefficient difference between the desired component and the impurities. In other words, DuCCC and HSCCC cannot be expected to resolve all the components with one particular two-phase solvent system. Nevertheless, it is always possible to select a two-phase solvent system, which will separate the desired component. In general, the crude sample is applied to the middle of the coiled column through the sample inlet, and the extreme polar and nonpolar components are readily eluted by two immiscible solvents to opposite outlets of the column.

Contrary to the classic countercurrent distribution method, modern DuCCC allows the entire operation to be carried out in a continuous and highly efficient manner. DuCCC is based on the ingenious design of Ito [8]. A cylindrical coil holder is equipped with a planetary gear, which is coupled to an identical stationary sun gear (shaded) placed around the central axis of the centrifuge. This gear arrangement produces an epicyclic motion; the holder rotates about its own axis relative to the rotating frame and simultaneously revolves around the central axis of the centrifuge at the same angular velocity as indicated by the pair of arrows. The epicyclic rotation of the holder is necessary to unwind the twist of the five flow tubes caused by the revolution, eliminating the use of rotary seals to connect each flow tube.

As shown in Fig. 1, this unique design enables the performance of DuCCC using five flow channels con-

nected directly to the column without using a rotational seal. When a column with a particular coil orientation is subjected to an epicyclic rotation, it produces a unique hydrodynamic phenomenon in the coiled column in which one phase entirely occupies the head side and the other phase occupies the tail side of the coil column. This unilateral phase distribution enables the performance of DuCCC in an efficient manner. A theoretical calculation of the hydrodynamic forces resulting from such an epicyclic rotation is very complicated and has not been elucidated.

Methods and Apparatus

The DuCCC experiments are performed with a tabletop (type J) high-speed plant centrifuge equipped with a multilayer coiled column connected to five flow channels. The multilayer coiled column is prepared from 2.6-mm-inner diameter PTFE tubing by winding it coaxially onto the holder to a total volume capacity of 400 mL. The multilayer coiled column is subjected to an epicyclic rotation at 500–800 rpm. The fractions are collected simultaneously from both ends of the column and analyzed by thin-layer chromatography (TLC) or high-performance liquid chromatography (HPLC) [8,12].

Applications

In the past decade, the rapid development of sophisticated spectroscopic techniques, including various two-dimensional nuclear magnetic resonance (2D NMR) methods, automated instrumentation and routine availability of x-ray crystallography has greatly simplified structural elucidation in natural product investigations. Consequently, the challenge to today's chemists has shifted to one's capability of isolating the bioactive components from crude extracts of either plants or animals. The extract of crude natural products usually is comprised of hundreds of components over a wide range of polarities. In isolating these natural products, it is essential to preserve the biological activity while performing chromatographic purifications. DuCCC represents one of the most efficient methods for isolation of the desired compound from a complex mixture.

Dual CCC has several advantages over HSCCC or CPC [13] in dealing with crude natural products. One distinct feature of DuCCC is the capability of performing normal-phase and reversed-phase elutions simultaneously. This provides a highly efficient and unique method for separation of crude natural products. In

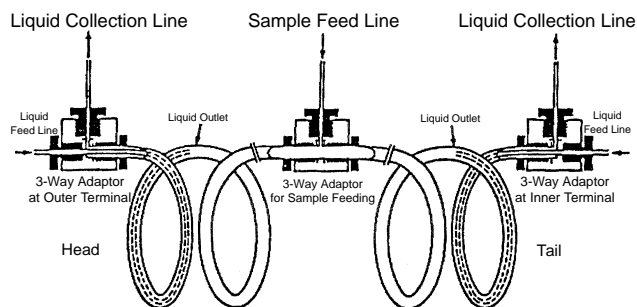


Fig. 1 Column design for DuCCC.

many instances, fractions eluted from DuCCC are pure enough for recrystallization or structural study. For example, an HPLC trace of the crude ethanol extract of *Schisandra rubriflora* shows that the major bioactive lignan, schisanhenol, is closely eluted with its acetate, it has been a major problem to isolate the pure schisanhenol. The fractions collected from DuCCC after injection of a crude ethanol extract of *Schisandra rubriflora* (125 mg) were analyzed by TLC and reversed-phase HPLC. The solvent system employed for DuCCC was hexane:ethyl acetate:methanol:water (10:5:5:1).

The upper phase, being less polar than the lower phase, results in a sequence of elution similar to normal-phase chromatography, whereas the lower phase provides a sequence of elution resembling reversed-phase chromatography. The bioactive components, schisanhenol acetate and schisanhenol, were eluted in the lower phase. Reversed-phase HPLC analyses of fractions 36–40 accounted for 32 mg of almost pure schisanhenol [6]. A total of 4 mg of schisanhenol ac-

etate was also obtained from fractions 50–57. As evidenced by this experiment, DuCCC offers an excellent method for semipreparative isolation of bioactive components from very crude natural products [11]. The isolation of the topoisomerase inhibitor boswellic acid acetate from its triterpenoic acid mixture has also been accomplished by DuCCC [12]. As shown in Fig. 2, when an isomeric mixture of triterpenoic acids (400 mg) was subjected to DuCCC, using a hexane: ethanol:water (6:5:1) as the solvent system, 215 mg of the boswellic acid acetates and 135 mg of the corresponding boswellic acid were obtained. Some highly polar impurities were eluted immediately in the solvent front, from fraction 1 to 4. The isomeric boswellic acid was eluted in the lower-phase solvent and the less polar acetates were eluted simultaneously in the upper-phase solvent. Although the isomers were only partially resolved by DuCCC, this experiment demonstrates that DuCCC is a highly efficient system for preparative purification.

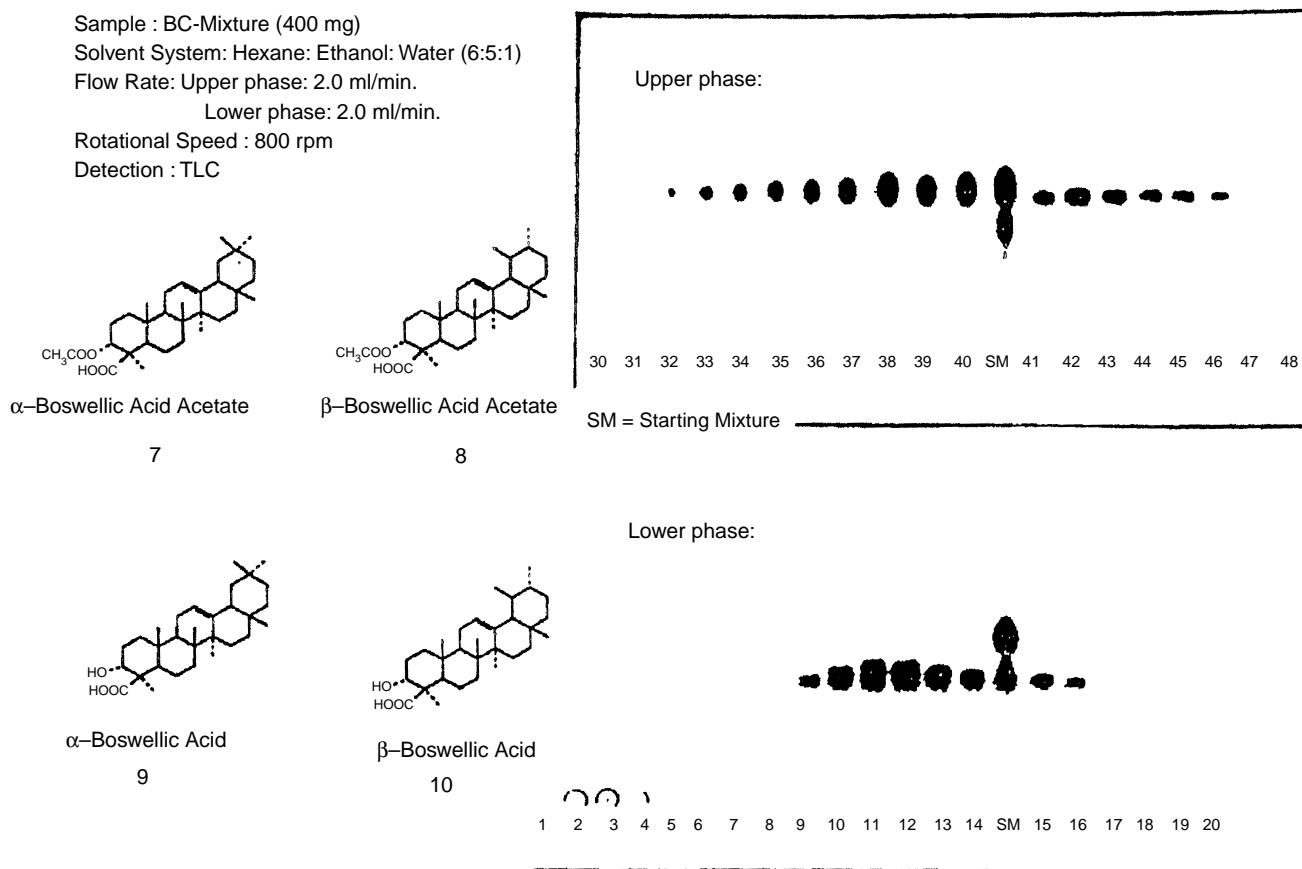


Fig. 2 DuCCC of triterpenoic acids.



The conformationally restricted cyclic, disulfide-containing, enkephalin analog (D-Pen, D-Pen) enkephalin (DPDPE) was synthesized by solid-phase methods. Its purification was accomplished previously by partition on Sephadex G-25 block polymerizate using the solvent system (1-butanol:acetic acid:water: 4:1:5), followed by gel filtration on Sephadex G-15 with 30% acetic acid as the eluent [14]. DuCCC demonstrated a highly efficient and one step method for the purification of DPDPE. The crude DPDPE (500 mg), which contained impurities and salts, was purified by DuCCC with a two-phase solvent system consisting of 1-butanol containing 0.1% TFA and water also containing 0.1% TFA in a 1:1 (v/v) ratio. The desired DPDPE was eluted from the upper phase in fractions 15–19. The purity of each fraction collected was monitored by HPLC. A total of 24 mg pure DPDPE was obtained within 2 h. As evidenced, DuCCC can be a highly cost-effective procedure for the purification of polypeptides.

Conclusion

The capability and efficiency of DuCCC in performing classic countercurrent distribution has been demonstrated in the isolation of bioactive lignans and triterpenoic acids from crude natural products and in the purification of synthetic polypeptides. DuCCC provides excellent resolution and sample loading capacity. It offers a unique feature of elution of the nonpolar components in the upper-phase solvent (assuming the upper phase is less polar than the lower phase) and concomitant elution of the polar components in the lower phase. This capability results in an efficient and convenient preparative method for purification of the crude complex mixture. The capability of DuCCC has not yet been fully explored. For instance, a particular solvent system can be selected to give the desired bioactive component a partition coefficient of 1. This

will allow the “stripping” of the crude extract with DuCCC to remove the impurities or inactive components. Consequently, the bioactive component will be concentrated inside the column for subsequent collection. This strategy can also be applied to extract and concentrate certain metabolites in biological fluids such as urine or plasma. Because there is no saturation of the stationary phase, a large amount of sample can also be processed by DuCCC. In addition, the system can be easily automated with computer-assisted sample injection and fractionation.

References

1. L. C. Craig, W. Hausmann, P. Ahrens, and E. J. Harfenist, *Anal. Chem.* 23: 1326 (1951).
2. Y. Ito, *CRC Crit. Rev. Anal. Chem.* 17: 65–143 (1986).
3. Y. W. Lee, Y. Ito, Q. C. Fang, and C. E. Cook, *J. Liquid Chromatogr.* 11(1): 75–89 (1988).
4. T. Y. Zhang, X. Hua, R. Xiao, and S. Kong, *J. Liquid Chromatogr.* 11(1): 233–244 (1988).
5. Y. W. Lee, C. E. Cook, Q. C. Fang, and Y. Ito, *J. Chromatogr.* 477: 434–438 (1989).
6. G. M. Brill, J. B. McAlpine, and E. J. Hochlowski, *J. Liquid Chromatogr.* 8: 2259 (1985).
7. D. G. Martin, R. E. Peltonen, and J. W. Nielsen, *J. Antibiot.* 39: 721 (1986).
8. Y. Ito, *J. Liquid Chromatogr.* 8(12): 2131 (1985).
9. H. Oka, K.-L. Harada, M. Suzuki, H. Nakazawa, and Y. Ito, *J. Chromatogr.* 482: 197 (1989).
10. Y. W. Lee, C. E. Cook, and Y. Ito, *J. Liquid Chromatogr.* 11(1): 37–53 (1988).
11. Y. W. Lee, Q. C. Fang, Y. Ito, and C. E. Cook, *J. Nat. Products* 52(1): 706–710 (1989).
12. W. Lee, unpublished data.
13. W. Murayama, Y. Kosuge, N. Nakaya, Y. Nunogaki, N. Nunogaki, J. Cazes, and H. Nunogaki, *J. Liquid Chromatogr.* 11(1): 283–300 (1988).
14. H. J. Mosberg, R. Hurst, V. J. Hruby, K. Gee, H. I. Yamamura, J. J. Galligan, and T. F. Burks, *Proc. Natl. Acad. Sci. USA* 80: 5871–5874 (1983).



Dyes: Separation by Countercurrent Chromatography

Adrian Weisz

Center for Food Safety and Applied Nutrition, USFDA, Washington, D.C., U.S.A.

Introduction

Countercurrent chromatography (CCC) is a liquid–liquid partition technique that does not involve use of a solid support. In high-speed countercurrent chromatography (HSCCC), one of the liquid phases (the stationary phase) is retained in an Ito multilayered coil column by centrifugal force while the other liquid phase (the mobile phase) is pumped through the column. A variation of HSCCC was recently developed and is known as pH-zone-refining CCC. Both conventional HSCCC and pH-zone-refining CCC have been applied to the separation of dyes. The principles of these techniques, the instrumentation involved, the basis for selecting the two-phase solvent systems, and the separation procedure itself have all been discussed by Ito in the countercurrent chromatography entries of the present volume.

Conventional HSCCC

Conventional HSCCC has been used for dye separations since the mid-1980s. At that time, Fales et al. [1] separated various methylated homologs and contaminants from a 6-mg portion of the triphenylmethane dye Methyl Violet 2B (CI 42535), and Freeman and Willard [2] purified up to 520 mg of azo textile and ink dyes. Later documented applications have been for the colors Sulforhodamine B (CI 45100) [3] and Gardenia Yellow [4].

There are two notable advantages of this technique for the separation of dyes. One is its applicability for the separation of both the ionic and nonionic components of a dye mixture. Second, it has been shown to be one of the best methods for successfully separating small quantities (20 mg or less) of dye mixtures. On the other hand, several hundred milligrams of dye mixtures represent the upper limit beyond which conventional HSCCC cannot be applied as the method of separation when the common 1.6-mm-inner diameter, 325-mL-volume column is used.

pH-Zone-Refining CCC

pH-Zone-refining CCC is a relatively new preparative method of separation [5,6] that allows separation of or-

ganic acids and bases according to their pK_a values and hydrophobicities. In contrast to conventional HSCCC, it permits the separation or purification of multigram quantities of dye mixtures, as long as those mixtures contain ionic or ionizable components. It has been applied to the separation of dyes containing various functional groups, such as $-\text{COOH}$, $-\text{OH}$, $-\text{NH}_2$, and $-\text{SO}_3\text{H}$. Details on its application to dye separation were recently described [7]. Briefly, pH-zone-refining CCC of dyes can be divided into two categories:

1. Standard separations, for carboxylic acid- or amine-containing dyes
2. Affinity-ligand separations, for sulfonated dyes

Standard pH-Zone-Refining CCC

For separation by standard pH-zone-refining CCC, the sample components should be stable over a pH range of 1–10 during the separation period and the minimum quantity of each targeted component should be no less than 0.1 mmol and preferably over 1 mmol. The requirements for the selection of a solvent system are different from those needed to select a solvent system for conventional HSCCC separations. Carboxylic acid-containing dyes (e.g., xanthene dyes or their lactone analogs, fluoran dyes) may be separated by using an organic acid (e.g., trifluoroacetic acid) as a retainer in the organic stationary phase and a base (e.g., ammonia) as an eluter in the aqueous mobile phase. Dyes containing amino groups may be separated by using an organic base as a retainer (e.g., triethylamine) and an inorganic acid (e.g., HCl) as an eluter. The recommended steps in selecting an appropriate solvent system for the separation of dyes and the separation procedure have been described in detail elsewhere [7].

Standard pH-zone-refining CCC was applied to the separation of pure components, sometimes multigram quantities, from various halogenated fluorescein (F) dyes such as 4,5,6,7-tetrachloroF, D&C Orange No. 5 (mainly 4',5'-dibromoF), D&C Red No. 22 (Eosin Y, mainly the disodium salt of 2',4',5',7'-tetrabromoF), D&C Orange No. 10 (mainly 4',5'-diiodoF), FD&C Red No. 3 (Erythrosine, mainly the



disodium salt of 2',4',5',7'-tetraiodoF), D&C Red No. 28 (Phloxine B, mainly the disodium salt of 2',4',5',7'-tetrabromo-4,5,6,7-tetrachloroF), and Rose Bengal (mainly the disodium salt of 2',4',5',7'-tetraiodo-4,5,6,7-tetrachloroF). These dyes are used as biological stains and, except for Rose Bengal, for coloring food (FD&C Red No. 3), drugs, and cosmetics in the United States. Standard pH-zone-refining CCC was also applied to the separation of contaminants from these colors and their intermediates. The

purified contaminants were further used as reference materials for the development of analytical methods [high-performance liquid chromatography (HPLC), thin-layer chromatography (TLC), etc.]. Furthermore, the capability of this method to purify multi-gram quantities of dyes used as biological stains may facilitate standardization of the biological stains themselves, a well-documented goal. A detailed review [8] describes the separation of the above-mentioned dyes by standard pH-zone-refining CCC.

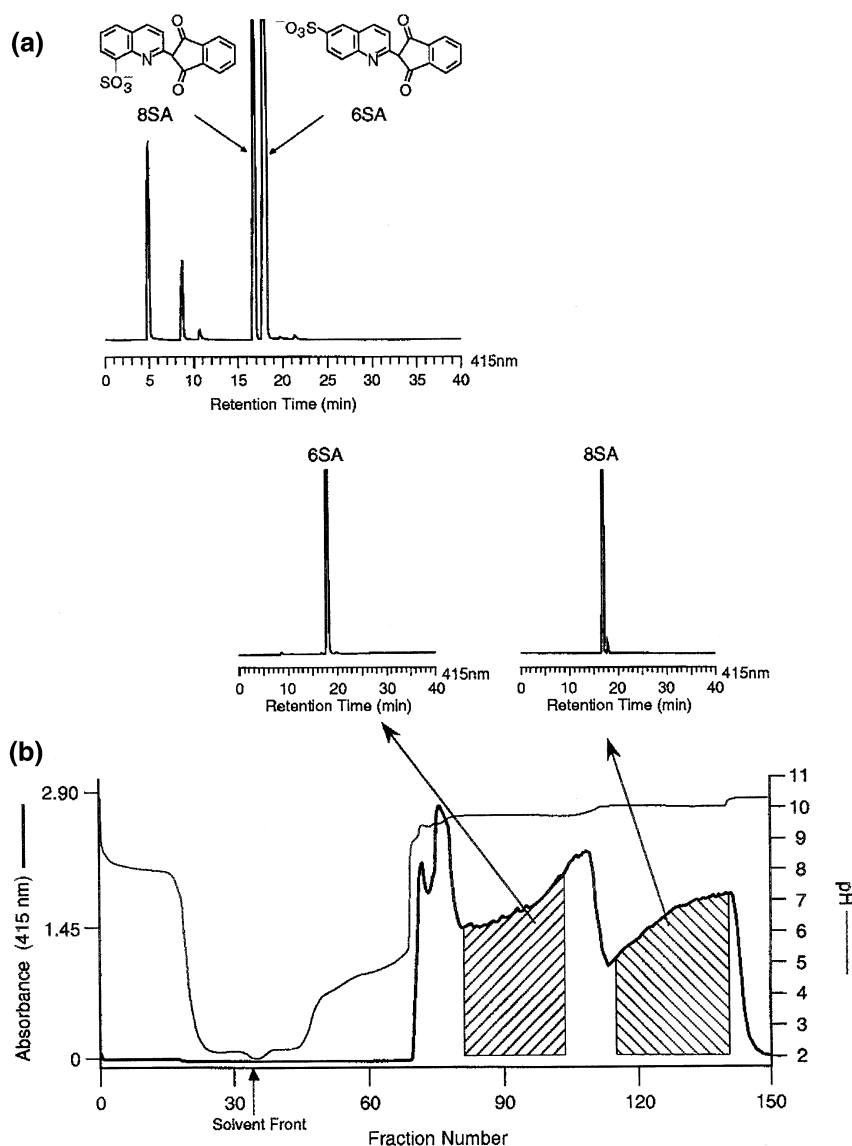


Fig. 1 Separation by affinity-ligand pH-zone-refining CCC in the ion-exchange mode of the main components from a sample of D&C Yellow No. 10 (Quinoline Yellow, CI 47005). (a) HPLC analysis of the original mixture; (b) pH-zone-refining CCC elution profile and HPLC analyses of the combined fractions 81–103 and 114–138, respectively. For experimental conditions, see text and Ref. 9.

Affinity-Ligand pH-Zone-Refining CCC

Sulfonated dyes have not been amenable to separation by standard pH-zone-refining CCC because of their very low pK_a values, which prevent their partitioning into the organic phase of a conventional two-phase solvent system. The addition of a ligand, an ion-exchange reagent (e.g., dodecylamine) or an ion-pairing reagent (tetrabutylammonium hydroxide), and a retainer acid (e.g., HCl, H_2SO_4) will enhance the partitioning of the sulfonated dye components into the organic stationary phase, thus enabling their separation by pH-zone-refining CCC. The more stringent conditions require that the components of a sulfonated dye mixture be stable over a pH range of 0.5–13.5 during the time of the experiment. The details and conditions required for the separation of sulfonated dyes by affinity-ligand pH-zone-refining CCC in the ion-exchange mode and in the ion-pairing mode can be found elsewhere [7]. An example [9] of such a separation is described below. Figure 1 shows the separation by affinity-ligand pH-zone-refining CCC in the ion-exchange mode of the main components from a 1.8-g portion of U.S. certified color additive D&C Yellow No. 10 (Quinoline Yellow, CI 47005). The two-phase solvent system used consisted of iso-amyl alcohol:methyl *tert*-butyl ether:acetonitrile:water (3:1:1:5). The ligand (dodecylamine) at a concentration of 5%, and sulfuric acid were added to the organic stationary phase as the retainer. The separation obtained for the two monosulfonated positional isomers 6SA (0.6 g) and 8SA (0.18 g) is shown by the associated HPLC chromatograms in Fig. 1.

Using a modified procedure, the applications of this technique have been extended to the separation of the highly polar disulfonated and trisulfonated components of D&C Yellow No. 10 and Yellow No. 203 (the Japanese Quinoline Yellow, CI 47005) (7) and of other sulfonated dyes such as FD&C Yellow No. 6 (Sunset Yellow, CI 15985), D&C Green No. 8 (Pyranine, CI 59040), and FD&C Red No. 40 (Allura Red, CI 16035).

References

1. H. M. Fales, L. K. Pannell, E. A. Sokoloski, and P. Carmeci, Separation of methyl violet 2B by high-speed countercurrent chromatography and identification by Californium-252 plasma desorption mass spectrometry, *Anal. Chem.* 57: 376–378 (1985).
2. H. S. Freeman and C. S. Williard, Purification procedures for synthetic dyes: 2. Countercurrent chromatography, *Dyes Pigments* 7: 407–417 (1986).
3. H. Oka, Y. Ikai, N. Kawamura, J. Hayakawa, M. Yamada, K.-I. Harada, H. Murata, M. Suzuki, H. Nakazawa, S. Suzuki, T. Sakita, M. Fujita, Y. Maeda, and Y. Ito, Purification of food color Red No. 106 (Acid Red) using high-speed countercurrent chromatography, *J. Chromatogr.* 538: 149–156 (1991).
4. H. Oka, Y. Ikai, S. Yamada, J. Hayakawa, K.-I. Harada, M. Suzuki, H. Nakazawa, and Y. Ito, Separation of Gardenia Yellow components by high-speed countercurrent chromatography, in *Modern Countercurrent Chromatography* (W. D. Conway and R. J. Petroski, eds.), American Chemical Society, Washington, DC, ACS Symposium Series, Vol. 593 1995, pp. 92–106.
5. A. Weisz, A. L. Scher, K. Shinomiya, H. M. Fales, and Y. Ito, A new preparative-scale purification technique: pH-Zone-refining countercurrent chromatography, *J. Am Chem Soc* 116: 704–708 (1994).
6. Y. Ito and Y. Ma, Review: pH-Zone-refining countercurrent chromatography, *J. Chromatogr. A*, 753: 1–36 (1996).
7. A. Weisz and Y. Ito, High-Speed countercurrent chromatography. Dyes, in *Encyclopedia of Separation Science*, Academic Press, London 2000 vol. 6 pp. 2588–2602.
8. A. Weisz, Separation and purification of dyes by conventional high-speed countercurrent chromatography and pH-zone-refining countercurrent chromatography, in *High-Speed Countercurrent Chromatography* (Y. Ito and W. D. Conway, eds.), John Wiley & Sons, New York, 1996, pp. 337–384.
9. A. Weisz, E. P. Mazzola, J. E. Matusik, and Y. Ito, Preparative separation of isomeric 2- (2-quinolinyl)-1H-indene-1, 3 (2H)-dione monosulfonic acids of the color additive D&C Yellow No. 10 (Quinoline Yellow) by pH-zone-refining countercurrent chromatography, *J. Chromatogr. A* 923:87–96 (2001).



Eddy Diffusion in Liquid Chromatography

J.E. Haky

Florida Atlantic University, Boca Raton, Florida, U.S.A.

Introduction

Among the causes of widening of peaks corresponding to components of a mixture undergoing separation by liquid chromatography (LC) is the phenomenon known as eddy diffusion. This results from molecules of a solute traversing a packed bed of a column through different pathways, in and around the stationary phase. Some molecules travel more rapidly through the column through more open, shorter pathways, whereas others will encounter longer, restricted areas and lag behind. The result is a solute band that passes through the column with a Gaussian distribution around its center [1].

Discussion

The degree of band broadening of any chromatographic peak may be described in terms of the height equivalent to a theoretical plate, H , given by

$$H = \frac{L}{N} \quad (1)$$

where L is the length of the column (usually measured in cm) and N is the number of theoretical plates, which can be calculated from Eq. (2), where t_R and W are the retention time and width of the peak of interest, respectively:

$$N = 16 \left(\frac{t_R}{W} \right)^2 \quad (2)$$

Because higher values of N correspond to lower degrees of band broadening and narrower peaks, the opposite is true for H . Therefore, the goal of any chromatographic separation is to obtain the lowest possible values for H .

The contribution of eddy diffusion and other factors to band broadening in liquid chromatography can be quantitatively described by the following equation, which relates the column plate height H to the linear velocity of the solute, μ :

$$H = A\mu^{0.33} + \frac{B}{\mu} + C\mu + D\mu \quad (3)$$

where A , B , C , and D are constants for a given column [2]. The linear velocity μ is related to the mobile-phase flow rate and is determined by

$$\mu = \frac{L}{t_0} \quad (4)$$

where t_0 (the so-called “dead time”) is determined from the retention time of a solute which is known not to interact with the stationary phase of the column. The first term in Eq. (4), $A\mu^{0.33}$, includes the contribution of eddy diffusion to chromatographic band broadening. This term, which is dependent on the cube root of the linear velocity, is less dependent on mobile-phase flow rate than the other terms in the equation, which are either directly or inversely proportional to linear velocity.

Minimizing eddy diffusion in an LC column results in a lower $A\mu^{0.33}$ term in Eq. (3), which minimizes band spreading and gives narrower chromatographic peaks. The most common methods used for this purpose, in LC, are the following: (a) using a column of the smallest practical diameter; this obviously reduces the number of alternate pathways which a solute can take through the column; (b) using a stationary phase of smallest practical particle size; Giddings [3] and others have shown that the effects of eddy diffusion are directly proportional to the average diameter of stationary-phase particles; thus, smaller stationary phase particles give narrower peaks; (c) making sure the column is uniformly packed; again, this limits open space in the column, thus minimizing the number of pathways.

Those who prepare and/or manufacture LC columns must use the above methods to limit the effects of eddy diffusion on the chromatographic separations. However, there are practical limitations. Column and stationary-phase particle diameters can only be reduced to points that are compatible with the pressure limitations of the pumps used in chromatographic instruments and the required sample capacities of the columns. The degree of training and experience of those who pack the columns may also limit the quality of the procedure used in packing the column. Nevertheless, most commercial manufactur-



ers of LC columns have adopted column designs and packing procedures which generally reduce the effects of eddy diffusion on modern LC separations to an inconsequential level. Still, these effects may increase as a column ages, and practicing chromatographers should be on the watch for them.

References

1. C. F. Poole and S. K. Poole, *Chromatography Today*, Elsevier, New York, 1991, Chap. 1.
2. L. R. Snyder and J. J. Kirkland, *Introduction to Modern Liquid Chromatography*, 2nd ed., John Wiley & Sons, New York, 1979, pp. 15–37.
3. J. C. Giddings, *Dynamics of Chromatography*, Marcel Dekker, Inc., New York, 1965, pp. 35–36.



Effect of Organic Solvents on Ion Mobility

Ernst Kenndler

Institute for Analytical Chemistry, University of Vienna, Vienna, Austria

Introduction

The ionic mobility, μ_i , of a species, i , is the velocity, v , of a particle that moves under the influence of an electric field, E , of unit strength:

$$\mu_i = \frac{v_i}{E} \quad (1)$$

The dimension of the mobility is square meter per volt per second. The values of the mobilities range from more than 300 units for the proton in water to about 5 units for large organic ions in solvents with high viscosities. The mobility depends on the size and shape of the solvated ion, on its charge, and on the viscosity and temperature of the solution. Thus, it is clear that the mobility is a function of the solvent.

Three kinds of mobility can be distinguished: the absolute mobility, μ_i^0 , in an infinitely diluted solution, the actual mobility of the fully charged ion at the ionic strength, I , of the solution, and the effective mobility, μ_i^{eff} , which depends on the degree of ionization, α .

Ionic Mobilities of Weak Electrolytes

For higher ionic strengths, no quantitative theoretical description of the dependence of the mobility on the ionic strength exists. Even for lower ionic strengths, theory is directed, rather, to spherical ions of 1:1 electrolytes with low charge (Debye–Hückel–Onsager theory, see below) than to multiple charged ions with irregular geometry. An expression derived empirically relates the logarithm of the correction factor for the mobility on the square root of the ionic strength and the charge number of the analyte.

The degree of dissociation, on the other hand, depends, in a well-defined manner, on the pK of the analyte and the pH of the solution, according to the Henderson–Hasselbalch equation. α , is a function of pK_a and pH: for example, for monobasic neutral acids

$$\alpha = \frac{1}{1 + 10^{\text{pK}_a - \text{pH}}} \quad (2)$$

For this type of acid, the total mobility can be expressed as

$$\mu_i^{\text{tot}} = \mu_i^{\text{eff}} + \mu_{\text{EOF}} = \frac{\mu_i^0 f}{1 + 10^{\text{pK}_{a,i} - \text{pH}}} + \mu_{\text{EOF}} \quad (3)$$

Here, μ_i^0 is the absolute mobility, that of the ion at infinite dilution, f is the correction factor that takes into account the deviation from ideal behavior. It can be seen that an additional parameter occurs in this equation: the mobility of the electro-osmotic flow, μ_{EOF} , which occurs in many cases in the separation systems and leads to an additional velocity vector of the solutes.

Influence of Organic Solvents

Equation (3) is the key expression that enables understanding of the influence of the solvent on the mobility. From this expression, it follows that solvents may affect the following:

- the absolute mobility
- the correction factor, f
- the ionization constants, K_a , of the analytes and the buffering electrolytes
- the mobility of the EOF

Absolute Mobility

A first approach to take into account the solvent's effect on the absolute mobility of an ion was made by Walden. It is based on the Stokes' law of frictional resistance. Walden's rule states that the product of absolute mobility and solvent viscosity is constant. It is clear that the serious limitation of this model is that it does not consider specific solvation effects, because it is based on the *sphere-in-continuum* model. However, it delivers an appropriate explanation for the fact that, within a given solvent, the mobility depends on temperature to the same extent as the viscosity (in water, for example, the mobility increases by about 2.5% per degree Kelvin). The mobilities do not deviate too



much from Walden's rule in some binary mixtures of water with organic solvents. This model is, on the other hand, not appropriate for forecasting or explaining the effect of the solvent on the mobility in a more general manner (see Table 1).

Taking specific solvation effects into account makes it clear that the hydrodynamic radius, r_h , of an ion depends on the solvent, due to the different solvation shell established:

$$r_{h,i} = \frac{z_i e_0}{6\pi\eta\mu_i} \quad (4)$$

where e_0 is the electron charge and z_i is the charge number. This expression is valid for a spherical ion. It is obvious that by a simple geometrical argument, this radius changes for an ion with crystal radius, r_{cryst} , according to solvation by n_h molecules of solvent, S , with radius, r_s , in the solvation shell:

$$r_h^3 = r_{\text{cryst}}^3 + n_h r_s^3 \quad (5)$$

Because n_h and r_s may change, the hydrodynamic radius and, therefore, the absolute mobility change as well.

Correction Factor

The correction factor, f , relates the actual mobility of a fully charged particle at the ionic strength under the experimental conditions to the absolute mobility. It takes ionic interactions into account and is derived for not-too-concentrated solutions by the theory of Debye–Hückel–Onsager using the model of an ionic cloud around a given central ion. It depends, in a com-

plex way on the mean ionic activity coefficient. The resulting equation contains the solvent viscosity and dielectric constant in the denominator. In all cases, the factor is <1 . The actual mobility is always smaller than the absolute mobility.

Ionization Constant

Organic solvents influence the ionization constants of weak acids or bases in several ways (note that they influence the analytes and the buffer as well). Concerning ionization equilibria, an important solvent property is the basicity (in comparison to water), which reflects the interaction with the proton. From the most common solvents, the lower alcohols and acetonitrile are less basic than water. Dimethyl sulfoxide is clearly more basic. However, stabilization of all particles involved in the acido-basic equilibrium is decisive for the pK_a shift as well. For neutral acids of type HA, the particles are the free, molecular acid, and the anion, A^- . In the equilibrium of bases, B, stabilization of B and its conjugated acid, HB^+ , takes place. As most solvents have a lower stabilization ability toward anions (compared to water), they shift the pK_a values of acids of type HA to higher values in general. No such clear direction of the change is found for the pK_a values of bases; however, they undergo less pronounced shifts.

Mobility of the EOF

According to the Smoluchowsky equation, the mobility of the EOF is

$$\mu_{\text{EOF}} = -\frac{\varepsilon\varepsilon_0\zeta}{\eta} \quad (6)$$

where ε and ε_0 are the permittivity of the medium and the vacuum, respectively, η is the solvent viscosity, and ζ is the zeta potential of the electric double layer. Roughly, the mobility of the EOF should depend on the ratio of relative permittivity to viscosity of the solvent and on the conditions of the electric double layer of the surface of the capillary in capillary electrophoresis (CE). As in most cases, fused-silica capillaries are used in CE, and its ζ potential is a function of the buffer pH, because the silanol groups at the surface are weak acids, with pK values around 5–6. It follows that the solvent affects the pK of the silanol as well, in a manner similar to that for the ionization constants of the analytes and the buffers. Nearly all solvents shift the pK values of the silanol groups toward a higher, pure acetonitrile and to even to very high values.

Table 1 Absolute Mobilities and Walden Products of Some Anions in Pure Solvents

Ion	Water		Methanol		Acetonitrile	
	μ_{abs}	$\eta\lambda^0$	μ_{abs}	$\eta\lambda^0$	μ_{abs}	$\eta\lambda^0$
Li^+	40.0	0.34	41.0	0.22	71.8	0.24
K^+	76.2	0.65	54.5	0.29	86.6	0.29
$(\text{CH}_3)_4\text{N}^+$	46.5	0.40	71.2	0.33	98.0	0.33
$(\text{C}_4\text{H}_9)_4\text{N}^+$	20.2	0.17	40.4	0.21	63.6	0.21
Cl^-	79.2	0.68	54.3	0.28	92.2	0.31
J^-	79.6	0.68	65.1	0.34	105.7	0.35
CH_3COO^-	42.4	0.36	40.8	0.21	110.9	0.37

Note: μ_{abs} is measured in $10^{-5} \text{ cm}^2/\text{Vs}$; $\eta\lambda^0$ is measured in $\text{Pcm}^2/\Omega\text{mol}$ where λ^0 is the single ion conductance at infinite dilution.

Suggested Further Reading

Conway, B. E., *Ion Hydration in Chemistry and Biophysics*. Elsevier, Amsterdam, 1981.

Fernandez-Prini, R. and M. Spiro, Conductance and transference numbers, in *Physical Chemistry of Organic Solvent Systems* (A. K. Covington and T. Dickinson, eds.), Plenum, London, 1973, pp. 525–679.

Kenndler, E., Organic solvents in capillary electrophoresis, in *Capillary Electrophoresis Technology* (N. A. Guzman, ed.), Marcel Dekker, Inc., New York, 1993, pp. 161–86.

Schwer, C. and E. Kenndler, Electrophoresis in fused-silica capillaries: The influence of organic solvent on the electroosmotic velocity and the zeta potential, *Anal. Chem.* 63: 1801–1807 (1991).



Effect of Temperature and Mobile Phase Composition on RP-HPLC Separation of β -Lactam Antibiotics

J. Martín-Villacorta

R. Méndez

N. Montes

J. C. García-Glez

University of León, León, Spain

INTRODUCTION

In previous papers,^[1,2] we reported the effect of column temperature on resolution in RP-HPLC to separate various β -lactams (penicillins and cephalosporins) from a single sample. In this work we describe the effect of column temperature and volume fraction of an organic solvent on resolution in the isocratic elution conditions of some β -lactam antibiotics.

Mobile phase composition and column temperature are two important experimental parameters that can be altered when a mixture of several compounds is to be separated.^[3–5]

The relationships between capacity factor, k' , and organic modifier concentration in the mobile phase, and the effect of the column temperature on k' for the antibiotics studied have been used to define k' as a function of T and V (volume fraction) on the basis of a small number of experimental measurements for a given combination of column, organic solvent, and type of antibiotic. From calculated values of k' , resolution values, R_S , may be estimated for adjacent band-pairs under all conditions. The method developed enables the optimization of RP-HPLC separations of the β -lactam antibiotics in the absence of difficult theoretical calculations, using a small number of experimental data, including the influence of the organic solvent in the mobile phase (isopropanol) and the column temperature.

INSTRUMENTS

The HPLC system consisted of a Model 600E multi-solvent delivery system equipped with a heated column compartment, a Model 484 variable-wavelength detector, and a Model 745B computing integrator, all from Waters Assoc., Inc., Milford, MA. The chromatograph was equipped with a Spherisorb ODS column (10 μ m particle size, 25 cm \times 4.6 mm I.D.).

CHROMATOGRAPHIC PROCEDURE

The mobile phases used to separate the compounds were acetate buffer (pH 5.00, 0.1 M)/isopropanol, 96.5/3.5, 95/5, 93/7, and 90/10 (v/v). A precolumn (3 cm \times 4.6 mm I.D.), packed with the same packing materials, was used to guard the main column. The detector was set at 254 nm. The flow rate of the mobile phase was 1.0 mL/min. The column dead time, t_0 , was measured by injecting methanol.

RESULTS AND DISCUSSION

The mixture of β -lactams was chromatographed at each of five column temperatures from 20°C to 60°C, and at four different volume fractions of isopropanol in mobile phase, from 0.035 to 0.1. Figure 1A shows chromatograms with the volume fraction of isopropanol ranging from 0.035 to 0.1 at a constant column temperature (30°C). Figure 1B shows the chromatograms obtained for each column temperature at 0.05 volume fraction of isopropanol. As one can see, a marked effect is produced for both parameters on the chromatographic behavior of each antibiotic.

Capacity Factor as a Function of Volume Fraction of Isopropanol in the Mobile Phase

The volume fraction (V) of organic solvent in the mobile phase is one of the most important parameters controlling capacity factor in RP-HPLC. Many reported studies^[6–10] show that, for a given solute and separation temperature, T , the relationship between capacity factor (k') and the volume fraction (V), or the eluent concentration, can be expressed as follows:

$$k' = aV^{-b} \quad (1)$$

where a and b are constants.

For all antibiotics, the plots of $\log k'$ vs. $\log V$ gave straight lines for all temperatures, with a correlation of

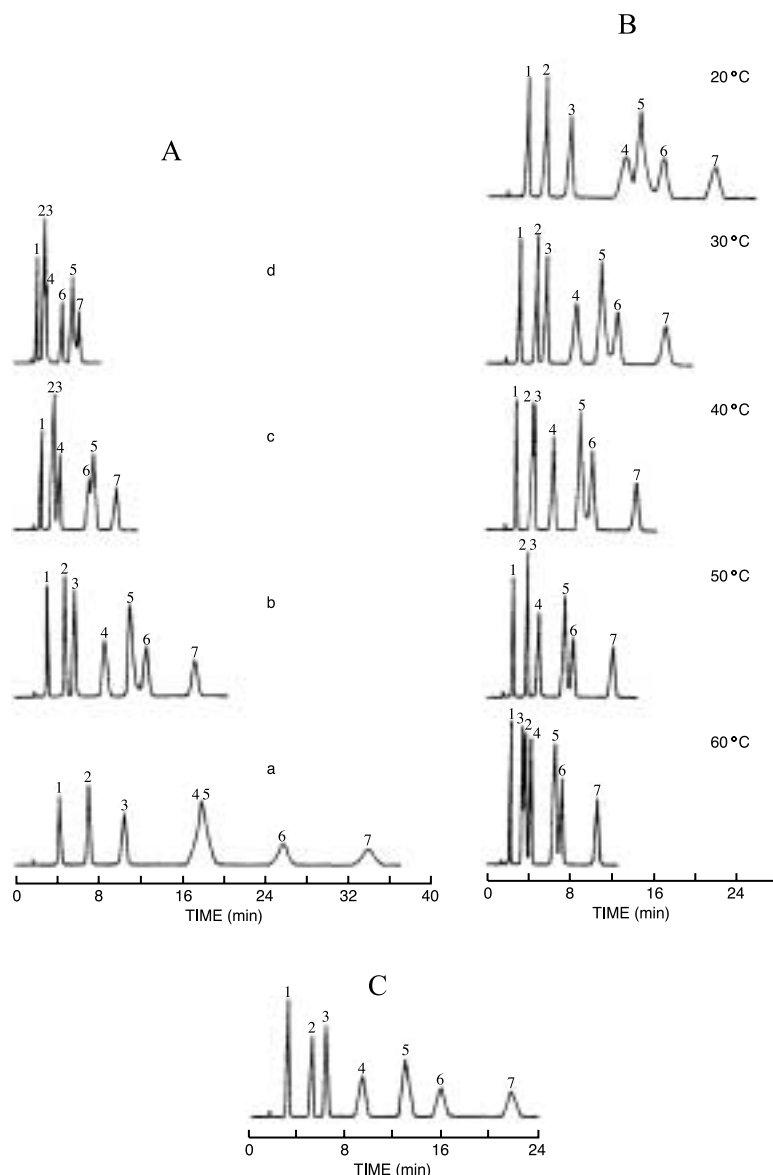


Fig. 1 (A) Effect of changing isopropanol volume fraction in the mobile phase on the elution profiles of cefonicid (1), cefaclor (2), cephalozin (3), cefodizime (4), cephaloridine (5), cephamandole (6), and cephalotin (7), using a mobile phase of 0.1 M acetate buffer (pH 5.00)/isopropanol (v/v) $a=(96.5/3.5)$, $b=(95/5)$, $c=(93/7)$, and $d=(90/10)$ at a column temperature of 30°C. (B) Effect of column temperature on the elution profiles of cephalosporins studied [numbering as in (A)], using a mobile phase of 0.1 M acetate buffer (pH 5.00)/isopropanol (95/5) (v/v). (C) Isocratic elution profile under optimal conditions. Mobile phase 0.1 M acetate buffer (pH 5.00)/isopropanol (95.4/4.6) (v/v), column temperature, 32°C, numbering as in (A).

0.9992 or greater (Fig. 2A). As one can see, there are different slopes, which may probably be ascribed to different separation mechanisms.

Table 1 lists constants a and b , calculated from the intercepts and the slopes, respectively, by means of a least-squares method. The slopes for 1, 2, and 7 were found to be slightly affected by the column temperature, especially the slope for 1 (Cefonicid).

Capacity Factor as a Function of Column Temperature

Figure 1B shows five chromatograms for the mixture of β -lactams, obtained at different temperatures. As one can see, the retention time of each antibiotic increased strongly as the column temperature was increased from 20°C to 60°C.



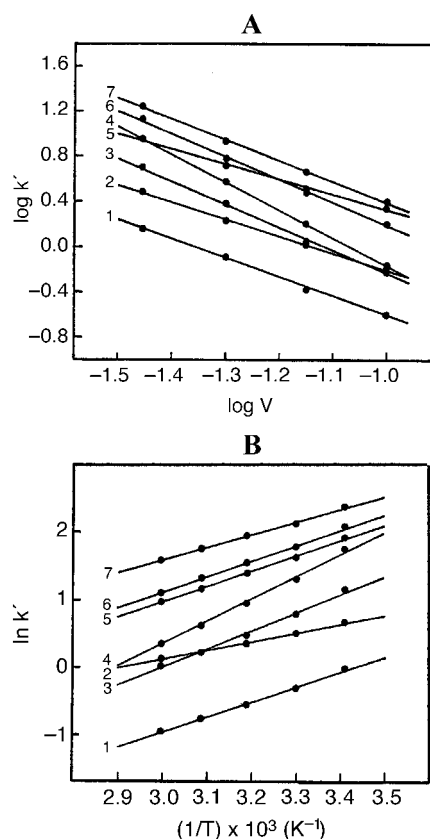


Fig. 2 (A) Effect of isopropanol volume fraction (V) in mobile phase on the capacity factor (k') at 30°C. Mobile phases as in Fig. 1B and numbering as in Fig. 1A. (B) Effect of column temperature on the capacity factor (k'). Mobile phase as in Fig. 1B and numbering as in Fig. 1A.

The dependence of the capacity factor on temperature is given by the Van't Hoff equation:

$$\ln k' = -\Delta H^\circ/RT + \Delta S^\circ/R + \Phi \quad (2)$$

where R is the gas constant, ΔH° and ΔS° are the enthalpy and entropy changes, respectively, associated with the solute retention process. The parameter Φ is the phase ratio and T is the absolute temperature.

Figure 2B shows a Van't Hoff plot for each antibiotic. It can be seen that the lines generated from the $\ln k'$ of each compound at different temperatures are linear with a correlation coefficient of 0.995 or greater. The linearity of the plots supports the assumption that single sorption mechanisms are operative for each antibiotic. As for β -lactams and other compounds,^[2,11,12] the slopes of these lines were not all the same, as one might expect if the effect of temperature was generalized.

For all antibiotics, the values of enthalpy change are negative, which indicates that the transfer of antibiotic from the mobile phase to sorption sites is favored.

Determination of Capacity Factor for Any Value of Volume Fraction of Isopropanol and Column Temperature

Following the methodology developed by Gant et al.,^[3] it is possible to obtain the values for the capacity factor ($k'_{T,V}$) for any value of volume fraction of isopropanol and any column temperature. In this methodology, a standard state is defined by a temperature (T_S) and mobile phase composition (V_S). In the present study, $T_S=20^\circ\text{C}$ (293.3 K) and $V_S=0.035$. The standard state value of k' for the solute in question is k'_{T_S,V_S} .

From Eq. 1, we can write:

$$\log k'_{T_S,V} = \log k'_{T_S,V_S} - b(\log V - \log V_S) \quad (3)$$

where $k'_{T_S,V}$ is the capacity factor for a value of V and the temperature T_S .

Table 1 Values of constants a and b in Eq. 1 at different column temperatures

Cephalosporin	Column temperature ($^\circ\text{C}$)									
	20		30		40		50		60	
	b	$a \times 10^3$	b	$a \times 10^3$	b	$a \times 10^3$	b	$a \times 10^3$	b	$a \times 10^3$
1	1.43	13.9	1.67	5.07	1.82	2.48	2.18	0.665	2.24	0.472
2	1.41	29.5	1.49	20.0	1.55	14.1	1.52	13.4	1.65	7.86
3	2.01	7.86	2.03	5.23	1.99	4.23	2.20	1.71	2.14	1.60
4	2.50	3.22	2.46	2.29	2.48	1.54	2.71	0.559	2.70	0.410
5	1.24	163.7	1.35	92.6	1.36	68.7	1.33	60.3	1.42	37.6
6	1.96	22.8	2.03	14.1	2.03	10.4	2.04	8.25	2.20	4.30
7	1.74	59.5	1.86	33.0	1.87	25.9	2.02	13.7	1.99	12.6



Table 2 Experimental vs. calculated capacity factor (k') values for cephalosporins studied at different temperatures

Cephalosporin	Temperature (°C)											
	20				30				40			
	Experimental	Calculated	Experimental	Calculated	Experimental	Calculated	Experimental	Calculated	Experimental	Calculated	Experimental	Calculated
1	1.01	1.01	0.75	0.79	0.58	0.62	0.47	0.49	0.39	0.38	0.39	0.38
2	2.03	2.03	1.69	1.75	1.46	1.51	1.26	1.30	1.14	1.12	1.14	1.12
3	3.36	3.33	2.23	2.46	1.63	1.82	1.26	1.34	1.01	0.99	1.01	0.99
4	6.31	5.52	3.75	3.85	2.60	2.69	1.87	1.88	1.42	1.31	1.42	1.31
5	7.03	6.78	5.21	5.33	4.00	4.18	3.23	3.29	2.69	2.58	2.69	2.58
6	8.34	8.05	6.03	6.33	4.66	4.98	3.73	3.92	3.08	3.08	3.08	3.08
7	11.1	10.9	8.58	8.94	7.00	7.30	5.85	5.96	4.98	4.86	4.98	4.86

Volume fraction of isopropanol $V = 0.05$. Numbering as in Table 1.

From Eq. 2, we can write at any value of T and V :

$$\log k'_{T,V} = \log k'_{T_s,V} - c(1/T_s - 1/T) \quad (4)$$

where $k'_{T,V}$ is the capacity factor for any value of T and V , and the parameter c varies with the β -lactam and with mobile phase composition.

According to Eqs. 3 and 4, the temperature coefficient c must be of the form:

$$c = d - e \log V \quad (5)$$

where d and e are constant for a given β -lactam and system.

Using Eqs. 3, 4, and 5, it is possible to calculate the capacity factor $k'_{T,V}$ for any value of T and V , after determining the values of b and c from these equations and the experimental data. The parameter c used for each volume fraction of isopropanol is determined from Eq. 5, using the constants d and e previously determined by plotting experimental c values vs. $\log V$. Table 2 compares the experimental and calculated values of the capacity factor, k' , for the antibiotic studied, experimental k' values being predicted generally with good agreement.

EFFECT OF ELUTION CONDITIONS ON RESOLUTION

The conventional equation to evaluate the effect of elution conditions on resolution (R_s) is:

$$R_s = 1/4\sqrt{N}(k'_1/1 + k')(\alpha - 1/\alpha) \quad (6)$$

Here, N is the plate number, α is the selectivity factor (defined as k'_2/k'_1), where k'_1 and k'_2 are the capacity factors for bands 1 and 2, and k' is the average capacity factor of k'_1 and k'_2 . The three factors, α , N , and k' , control the resolution. It is assumed that the three terms of Eq. 6 are approximately independent, which allows their separate optimization. The resolution equation (Eq. 6) must be applied to each of the adjacent band-pairs considered.

As one can see in Fig. 1B, the band broadening of any peak appearing at a fixed retention time decreases as the temperature increases; accordingly, the N value increases with increasing temperature. A linear relationship was obtained for the plot of N vs. T : $N=24.7 T-6560$ (T has the dimension of absolute temperature) with a correlation coefficient of 0.991. The N value is practically independent of the volume fraction of isopropanol for the β -lactam studied.

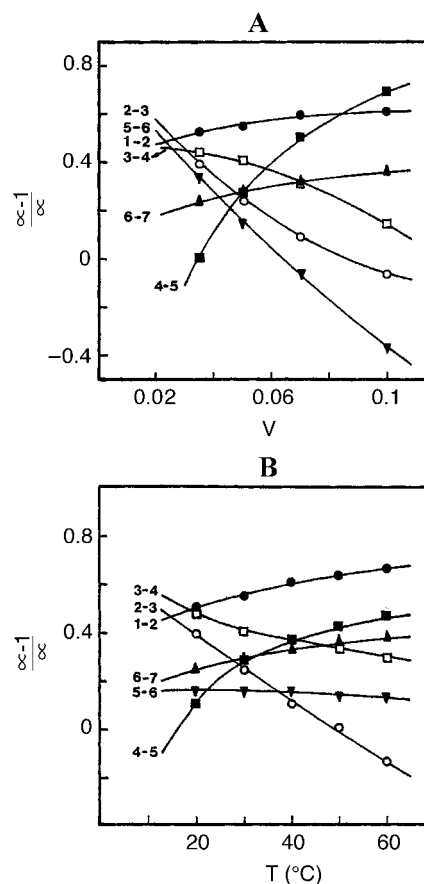


Fig. 3 (A) Effect of column temperature on the selectivity factor ($\alpha - 1/\alpha$) of the six pairs of sequentially resolved peaks. Mobile phase as in Fig. 1B and numbering as in Fig. 1A. (B) Effect of isopropanol volume fraction (V) in mobile phase on the selectivity factor ($\alpha - 1/\alpha$) of the six pairs of sequentially resolved peaks at 30°C. Mobile phases and numbering as in Fig. 1B and numbering as in Fig. 1A.

In general, the contribution of $k'_1/1+k'$ terms to R_s is approximately constant as long as k' is not small. As the selectivity factor (α) is of greater concern in Eq. 6, the separate optimization of the influence of the temperature and mobile phase composition in values is in many cases a good criterion for establishing the elution conditions of the separation.

Figure 3 shows the influence of temperature and isopropanol volume fraction in the term: ($\alpha - 1/\alpha$). There are examples of different situations: for pairs 5-6 and 4-5, the ($\alpha - 1/\alpha$) term is markedly influenced by the isopropanol volume fraction; the column temperature also exerts an important influence on this term for pairs 2-3 and 4-5. It is interesting to note that both parameters (T and V) have important and similar effects on pairs 4-5 and 2-3 in this resolution term. For these

cases, both parameters can be used to obtain a better resolution. Figure 1C shows an elution profile under optimal elution conditions.

CONCLUSION

The present work demonstrates that there is linear relationship between the $\log k'$ and both the $\log V$ (volume fraction of organic solvent in the mobile phase) and the reciprocal of the absolute temperature. Therefore, it is possible with a small number of initial experimental data of the capacity factor (k') to predict k' for each cephalosporin as a function of T and V , which reveals the optimal elution conditions for the isocratic separation of a mixture of cephalosporins.

REFERENCES

1. Martín-Villacorta, J.; Méndez, R.; Negro, A. Effect of temperature on HPLC separation of penicillins. *J. Liq. Chromatogr.* **1988**, *11* (8), 1707.
2. Martín-Villacorta, J.; Méndez, R. Effect of temperature and mobile phase composition on RP-HPLC separation of cephalosporins. *J. Liq. Chromatogr.* **1990**, *13* (16), 3269.
3. Gant, J.R.; Dolan, J.W.; Snyder, L.R. Systematic approach to optimizing resolution in reversed-phase liquid chromatography, with emphasis on the role of temperature. *J. Chromatogr.* **1979**, *185*, 153.
4. Baba, Y.; Yoza, N.; Ohashi, S. Effect of column temperature on high-performance liquid chromatographic behaviour of inorganic polyphosphates: I. Isocratic ion-exchange chromatography. *J. Chromatogr.* **1985**, *348*, 27.
5. Atamna, I.; Gruska, E. Optimization by isochronal analysis: II. Changes in mobile phase velocity and temperature, and in mobile phase composition and temperature. *J. Chromatogr.* **1986**, *355*, 41.
6. Rothbart, H.L.; Weymouth, J.W.; Rieman, W., III. Separation of the oligophosphates. *Talanta* **1964**, *11*, 33.
7. Ohashi, S. Chromatography of phosphorous oxoacids. *Pure Appl. Chem.* **1975**, *44*, 415.
8. Ohashi, S.; Tsuji, N.; Ueno, Y.; Takeshita, M.; Muto, M. Elution peak positions of linear phosphates in gradient elution chromatography with an anion-exchange resin. *J. Chromatogr.* **1970**, *50*, 349.
9. Nakamura, T.; Kimura, M.; Waki, H.; Ohashi, S. The pH dependence of anion exchange chromatographic separation of tri- and tetraphosphate anions. *Bull. Chem. Soc. Jpn.* **1971**, *44*, 1302.
10. Schoenmakers, P.J.; Billiet, H.A.H.; Tijssen, R.; de Galan, L. Gradient selection in reversed-phase liquid chromatography. *J. Chromatogr.* **1978**, *149*, 519.
11. Chemielowiec, J.; Sawatzky, H. Entropy dominated high performance liquid chromatographic separations of polynuclear aromatic hydrocarbons. Temperature as a separation parameter. *J. Chromatogr. Sci.* **1979**, *17*, 245.
12. Diasio, R.B.; Wilburn, M.E. Effect of subambient column temperature on resolution of fluorouracyl metabolites in reversed-phase high performance liquid chromatography. *J. Chromatogr. Sci.* **1979**, *17*, 565.



Efficiency in Chromatography

Nelu Grinberg

Merck Research Laboratories, Rahway, New Jersey, U.S.A.

Rosario LoBrutto*

Seton Hall University, South Orange, New Jersey, U.S.A.

Introduction

One of the most important characteristics of a chromatographic system is the efficiency or the number of theoretical plates, N .

Discussion

The number of theoretical plates can be defined from a chromatogram of a single band as

$$N = \left(\frac{t_R}{\sigma_t} \right)^2 = \frac{L^2}{\sigma_t^2} \quad (1)$$

where, for a Gaussian shaped peak, t_R is the time for elution of the band center, σ_t is the band variance in time units, and L is the column length [1]. N is a dimensionless quantity; it can also be expressed as a function of the band elution volume and variance in volume units:

$$N = \left(\frac{V_R}{\sigma_V} \right)^2 = 5.56 \left(\frac{t_R}{W_{1/2}} \right)^2 \quad (2)$$

In a chromatographic system, it is desirable to have a high column plate number. The column plate number increases with several factors [2]:

- Well-packed column
- Longer columns
- Smaller column packing particles
- Lower mobile-phase viscosity and higher temperature
- Smaller sample molecules
- Minimum extracolumn effects

In an open-bed system, N can be measured from the distance passed by a zone along the bed:

$$N = \left(\frac{d_R}{\sigma_d} \right)^2 \quad (3)$$

where d_R is the distance from the point of sample application to the point of the band center and σ_d is the variance of the band in distance units [1].

*Current affiliation: Merck Research Laboratories, Rahway, New Jersey, U.S.A.

In fact, the plate theory describes the movement of a particular zone through the chromatographic bed. As the zone is washed through the first several plates, a highly discontinuous concentration profile is obtained, with the solute being distributed in plates following the Poisson distribution [3]. At an intermediate stage (approximately 30–50 plates), much of the abrupt discontinuity disappears due to a similar concentration of the analyte in the neighboring plates. As the process continues (after 100 plates), the concentration profile is smooth and, even though the distribution is still Poisson, it can be approximated by a Gaussian curve. The standard deviation, σ , of the Gaussian curve, which is a direct measure of the zone spreading, is found to be

$$\sigma = \sqrt{HL} \quad (4)$$

where H is the plate height and L is the distance migrated by the center of the zone. In practice, the plate height is used to describe the zone spreading, including both nonequilibrium and longitudinal effects. In a uniform column, free from concentration and velocity gradients, the plate height is defined as

$$H = \frac{\sigma^2}{L} \quad (5)$$

In a nonuniform column, the zone spreading varies from point to point and its local value is

$$H = \frac{d\sigma^2}{dL} \quad (6)$$

which represents the increment of plate height in the variance σ^2 per unit length of migration. In practice, the smaller the value of H , the smaller the magnitude of band spreading per unit length of the column. The determination of H does not require the measurement of σ^2 , as long as N is known. Thus, combining Eqs. (1) and (6) yields [4]

$$H = L \left(\frac{\sigma}{L} \right)^2 = \frac{L}{N} \quad (7)$$

In practice, because the separation in a particular chromatographic column is linked to the time spent by



the analyte in the stationary phase and the time spent by the analyte in the mobile phase is irrelevant for the separation, a new parameter is defined (i.e., *effective plate number*, N_{eff}). The effective plate number is related to the separation factor k' and N by

$$N_{\text{eff}} = N \left(\frac{k'}{1 + k'} \right)^2 \quad (8)$$

Similarly, an expression for H_{eff} can be written

$$H_{\text{eff}} = H \left(\frac{1 + k'}{k'} \right)^2 \quad (9)$$

The effective parameters are more meaningful when comparing different columns [4].

There are several major contributions that will influence the band broadening and, consequently, H [5]: eddy diffusion, mobile-phase mass transfer, longitudinal diffusion, stagnant mobile-phase mass transfer, and stationary-phase mass transfer. The effect of each process on the band broadening and, consequently, on the plate height is related to all the experimental variables: mobile-phase velocity, u ; particle diameter, d_p ; sample diffusion coefficient in the mobile phase, D_m ; the thickness of the stationary-phase layer, d_s ; and the sample diffusion coefficient in the stationary phase, D_s . In general, H will vary with the velocity of the mobile phase, u , as it travels through the column. In a gas chromatography (GC) system, a plot of u versus H will lead to a curve which has a hyperbolic shape [6], characterized by the equation

$$H = A + \frac{B}{u} + Cu \quad (10)$$

Equation (10) is known as the van Deemter equation, and no correction was made for gas compressibility. Using the reduced parameters $h = H/d_p$ and $v = ud_p/D_m$, Eq. (10) becomes

$$h = a + \frac{b}{v} + cv \quad (11)$$

where A , B , C , a , b , and c are constants for a particular sample compound and set of experimental conditions as the flow rate varies. The B term in Eq. (10) relates to band broadening occurring by diffusion in the gas phase in the longitudinal direction of the column. According to Einstein's equation for diffusion,

$$\sigma^2 = 2D_m t_0 = \frac{2D_m L}{u} \quad (12)$$

Because $H = \sigma^2/L$, the B term becomes

$$B = 2 \frac{D_m}{u} \quad (13)$$

The inverse velocity term in Eq. (13) becomes important at low velocities. Because the D_m in liquids is 10^5 times smaller than in gases, the longitudinal term plays no practical role in band broadening in liquid chromatography.

The A term in Eq. (10) describes the nonhomogeneous flow, also called eddy diffusion. In this case,

$$\frac{\sigma^2}{L} = 2\lambda d_p = A \quad (14)$$

where λ is a packing correction factor of ~ 0.5 . In classical GC, the A term is a constant, representing a lower limit on column efficiency, equivalent to $H = d_p$ or $h = 1$.

At velocities above H_{min} , the C term controls H and relates to nonequilibrium resulting from resistance to mass transfer in the stationary and mobile phases [6].

In high-performance liquid chromatography (HPLC), the van Deemter equation still holds. However, Giddings [7] argued that the equation is too simplistic because it ignores the coupling that exists between the flow velocity and the radial diffusion in the void space of the packing around the particles. He suggested replacing the term A by a term $a/(1 + bu^{-1})$ to account for the flow velocity, because both the eddy diffusion and the radial diffusion are responsible for the transfer of the molecules between the different flow paths of unequal velocity. To include the coupling between the laminar flow and the molecular diffusion in porous media, Horvath and Lin [8] introduced a new parameter, δ , which is the thickness of the stagnant film surrounding each stationary-phase particle. However, at high velocities required in HPLC, Horvath and Lin's model reduces to the Knox equation, which is a variation of the van Deemter equation [9]:

$$h = av^{0.33} + \frac{b}{v} + cv \quad (15)$$

where a , b , and c are empirical parameters related to the analyte and the experimental flow rate conditions.

References

1. B. L. Karger, L. R. Snyder, and Cs. Horvath, *An Introduction to Separation Science*, John Wiley & Sons, New York, 1973, p. 136.
2. L. R. Snyder, J. J. Kirkland, and J. L. Glajch, *Practical HPLC Method Development*, John Wiley & Sons, New York, 1997, p. 42.
3. J. C. Giddings, *Dynamic of Chromatography, Part I, Principles and Theory*, Marcel Dekker, Inc., New York, 1965, p. 23.

4. Cs. Horvath and W. R. Melander, in *Chromatography, Fundamentals and Applications of Chromatographic and Electrophoretic Methods, Part A: Fundamentals and Techniques* (E. Heftmann, ed.), Elsevier Scientific, Amsterdam, 1983, p. A45.
5. L. R. Snyder and J. J. Kirkland, *Introduction to Modern Liquid Chromatography*, 2nd ed., John Wiley & Sons, New York, p. 168.
6. B. L. Karger, *Modern Practice of Liquid Chromatography* (J. J. Kirkland, ed.), Wiley-Interscience, New York, 1971, p. 23.
7. J. C. Giddings, *Dynamics of Chromatography, Part I, Principles and Theory*, Marcel Dekker, Inc., New York, 1965, p. 61.
8. Cs. Horvath and H. J. Lin, *J. Chromatogr.*, 149:43 (1978).
9. G. Guiochon, S. G. Shirazi, and A. M. Katti, *Fundamentals of Preparative and Nonlinear Chromatography*, Academic Press, Boston, 1994, p. 201.



Efficiency of a Thin-Layer Chromatography Plate

Wojciech Markowski

Medical University, Lublin, Poland

INTRODUCTION

Chromatography, by definition, is a separation methodology for a multicomponent sample mixture, which is based on differentiating movement zones of the sample. An essential feature of chromatographic separation is that the components of the sample are transported through the separation medium—in the case of thin layer chromatography (TLC), through an open bed. Differences in interaction with the medium lead to a selective redistribution of the component zones, from overlapping zones at the start following injection, toward largely individual regions inside the separation medium. The appearance of individual component zones, after the development process, can be recorded with the aid of scanning densitometry, to convert the plate chromatogram into realistic two-dimensional representation of the chromatographic process in a form suitable for evaluation of kinetic parameters. The underlying fundamental processes responsible for chromatographic separations can be explained by thermodynamic and kinetic considerations. Thermodynamic relationships are responsible for retention and selectivity, and kinetic properties are responsible for band broadening. Thus, the position and separation of peaks in a chromatogram are thermodynamic properties, whereas the axial dimensions of the peaks are governed by kinetic considerations, and both phenomena must be considered to optimize resolution. As Giddings^[1] emphasizes in his book, “separation is the art and science of maximizing separative transport relative to the dispersive transport.”

RESOLUTION

The most useful criterion for the estimation of the quality of a separation is the resolution. The resolution is given by:^[2]

$$R_s = \frac{(z_f - z_o)(R_{f(2)} - R_{f(1)})}{0.5(w_1 + w_2)} \quad (1)$$

where $R_{f(1)}$ and $R_{f(2)}$ are the R_f values of chromatographic spots 1 and 2, respectively; and w_1 and w_2 are widths of spots at the base. Eq. 1 clearly shows the two competing aspects of a chromatographic separation: the separation distance achieved by the primary separation process

(numerator) is opposed by the “blurring” action of the zone broadening (denominator). Eq. 1 allows for direct calculation of R_s based on the parameters measured on the chromatogram. Eq. 1 can be transformed to the form:^[3]

$$R_s = (1 - R_{f(1)}) \left[1 - \frac{R_{f(1)}}{R_{f(2)}} \right] N^{0.5} \quad (2)$$

Eq. 2 demonstrates that the plate resolution, as in other forms of chromatography, depends on the number of theoretical plates N , the selectivity, and the retention coefficient of the solute for the particular layer concerned.

CONCEPT OF THEORETICAL PLATES AND THEIR MEASUREMENT

The measurement of plate efficiency is depicted in Fig. 1a and b.^[4] The number of “theoretical plates” is a measure of the quality or “efficiency” of a chromatographic layer. By analogy with the theoretical plates of a distillation column, the chromatographic separations distance and the layer are divided into theoretical separation plates. For a given problem, sorbent, and solvent, a specific minimum number of theoretical plates is necessary to achieve the desired separation. For a capillary flow-controlled system, the mobile-phase velocity is not constant throughout the chromatogram and, at any position within the chromatogram, its value depends on the system variables. The mobile-phase velocity is not under external control and its range cannot be varied independently to study the relationship between the layer plate height and the mobile-phase velocity. Because all zones do not migrate the same distance in TLC, individual zones experience only those theoretical plates through which they travel and the plate height is directly dependent on the migration distance. A further complicating factor is that the size of the starting zone applied to the layer is always a finite value with respect to the size of a developed zone. Therefore, it is not adequate to use the measured zone width as the starting point from which to determine the extent of zone broadening for the layer. The plate number N can be experimentally determined via the “ H value” (i.e., “height equivalent to a theoretical plate,” or HETP).^[5] The measured H value is an average over the



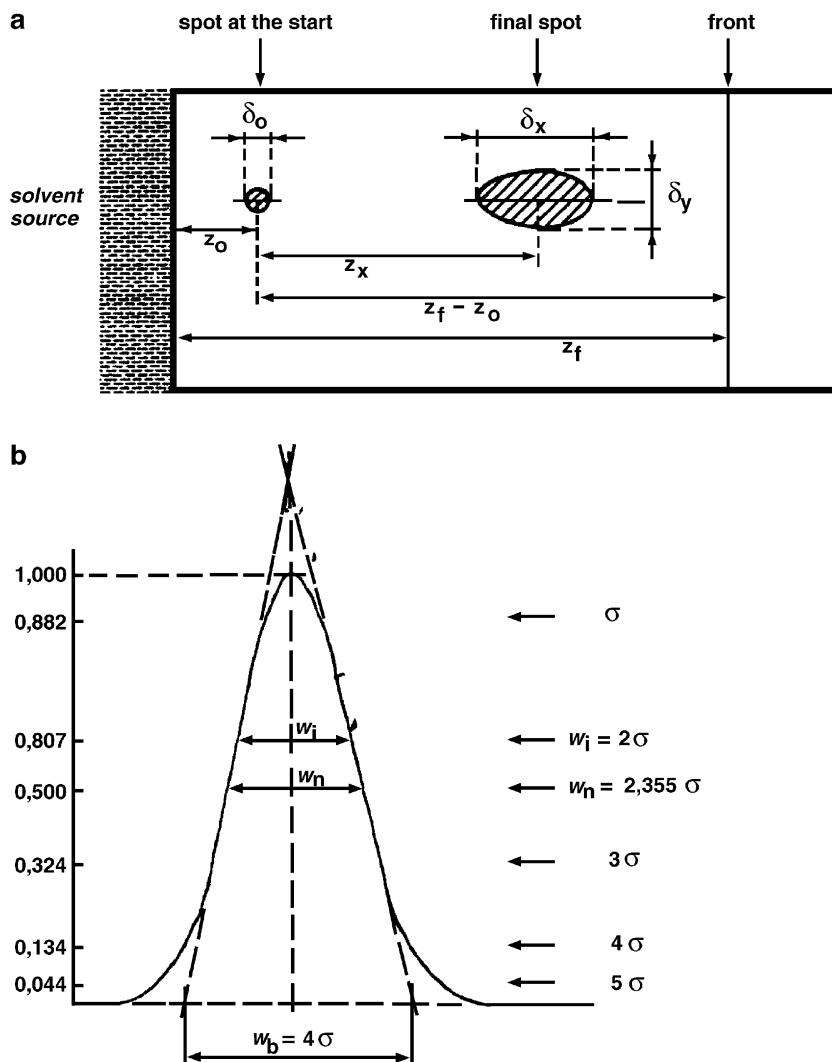


Fig. 1 (a) Basic symbols for TLC spot migration. z_x is the migration length of the spot, $z_f - z_0$ is the separation length, and z_f is the front migration length. (b) Width of a Gaussian band at different percentages of maximum height.

separation length and the symbol H_{obs} or \bar{H} is given and is obtained from the integration of the expression for the local plate height H_{loc} (quantity introduced by Giddings^[1]):^[1,4]

$$N = \frac{z_f - z_0}{H} \quad (3)$$

$$H_{\text{loc}} = \frac{d\sigma_x^2}{dz} \quad (4)$$

and, in practical terms,

$$\bar{H} = H_{\text{obs}} = \frac{\int_{z_0}^{z_x} H_{\text{loc}} dz}{\int_{z_0}^{z_x} dz} = \frac{\sigma_x^2}{z_x} = \frac{b_{0,5}^2}{5.54 z_x} \quad (5)$$

The average plate number N of the whole separation length is:

$$N \approx \bar{N} = \frac{z_f - z_0}{H_{\text{obs}}} = \frac{z_x}{H_{\text{obs}} R_f} \quad (6)$$

Hence, the average theoretical plate number can be calculated from the experimental data for $b_{0,5}$ and the lengths z_f and z_x in the chromatogram. To obtain reliable H values, it is recommended that the experiment comply with the following rules:^[4]

- 1) The band maximum should be at least 10 times greater than the detection limit.
- 2) Asymmetrical or poorly resolved spots should not be used for determining H .
- 3) Only σ_{chrom}^2 should be used.

Failure to do this results in excessively high H values. The measured zone variance σ_x^2 in the direction of flow is composed of:

$$\sigma_x^2 = \sigma_{\text{spotting}}^2 + \sigma_{\text{chrom}}^2 + \sigma_{\text{inst}}^2 + \sigma_{\text{other}}^2 \quad (7)$$

The contribution of the length of the starting zone to the length of the separated zone could be removed by considering their variances, such that:

$$\sigma_{\text{chrom}}^2 = \sigma_x^2 - \sigma_{\text{spotting}}^2 \quad (8)$$

where σ_x^2 is the variance of the developed zone, σ_{chrom}^2 is the variance due to the zone expansion during the migration through the layer, and $\sigma_{\text{spotting}}^2$ is the variance associated with sample application; here, we are assuming that the contributions to zone broadening associated with the properties of the detection and recording devices σ_{inst}^2 are negligible. The form of the starting zone is immaterial—only its dimension and sample distribution along its axis parallel to the direction of development (first-order approximation) are significant. It is obvious that the characteristic dimension of the starting zone in the direction of migration is never infinitely small compared with the same characteristic dimension of the zone after normal development. The determination of peak variance is straightforward for developed zones, but presents some difficulty for the undeveloped starting zone. The starting zone is applied to the dry layer. At the start of the migration process, it is contacted by the advancing mobile phase, which is moving at its highest velocity and is probably not fully saturated at its leading edge. Several processes take place quickly, which can lead to changes in the dimensions of the starting zone at the moment the chromatogram begins. The solvent front contacts the bottom portion of the starting zone first, pushing it forward with a characteristic migration velocity (which depends on the solute R_f value) into the upper portion of the starting zone, which is fixed in position until it is contacted by the advancing mobile phase. This causes a reconcentration of the starting zone and a reduction of its characteristic dimension in the direction of development. In addition, because the flow of mobile phase is unsaturated, all the pores holding sample will not be filled simultaneously; adsorbed samples may not be displaced from the sorbent surface instantaneously, and localized solvent saturation may limit the rate of solute dissolution in the mobile phase. The dimensions of the starting zone in the direction of migration are too large to ignore.

It can be assumed that the variance of the starting zone is equivalent to the properties of the sample zone, after it has been transported a few millimeters from its point of application by the mobile phase. In this way, some account is taken of the capacity of the mobile phase to

reshape the deposited sample zone at the beginning of the chromatogram.^[6]

CAPILLARY FLOW

As normally practiced in TLC, capillary forces control the migration of the mobile phase through the layer. Under these conditions, the velocity at which the solvent front moves is a function of the distance of the front from the solvent entry position and declines as this distance increases.^[4] There are two consequences of this effect:

- 1) The mobile-phase velocity is not constant throughout the chromatogram.
- 2) The mobile-phase velocity is set by the system variables and cannot be independently optimized unless forced flow development conditions are used.

If the migration distance is not excessively long, then the solvent front position as a function of time is adequately described by:

$$z_f^2 = \chi t \quad (9)$$

where z_f is the distance of the solvent front position above the solvent entry position, χ is the mobile-phase velocity constant, and t is the elapsed time since the solvent commenced migration through the layer. At any position on the layer, the solvent front will be moving with a velocity given by:

$$u_f = \frac{\chi}{2z_f} \quad (10)$$

There are two features of importance when using Eqs. 9 and 10. The velocity constant χ depends on the identity of the solvent; layer characteristics such as average particle size, layer permeability, layer thickness, etc.; and the state of equilibrium between solvent vapors in contact with the layer and the bulk solvent moving through the layer. As the solvent permeates the layer, the channels of narrower diameter are filled first, leading to more rapid advancement of the mobile phase. Large pores below the solvent front fill more slowly, resulting in an increase in the thickness of the layer of mobile phase. The bulk mobile-phase velocity, representing saturated flow through the region occupied by the sample zones, is moving at a lower velocity than the solvent u_f front velocity. As a reasonable approximation, the bulk solvent velocity is usually taken to be $0.8u_f$.^[6] The velocity constant χ is related to the experimental condition by Eq. 11:

$$\chi = 2k_0 d_p \frac{\gamma}{\eta} \cos \theta \quad (11)$$



where κ_o is the layer permeability constant, d_p is the average particle diameter, γ is the surface tension, η is the viscosity of the mobile phase, and θ is the contact angle. The layer permeability constant is dimensionless and takes into account the effect of porosity on the permeability of the layer and the difference between the bulk liquid velocity and the solvent front velocity. A typical value of permeability is $1-2 \times 10^{-3}$,^[6] virtually identical with typical column values. Assuming a narrow particle size distribution, Eq. 11 indicates that the velocity constant should increase linearly with average particle size. The solvent front velocity should be larger for coarse particle layers than for fine particle layers, in good agreement with experimental observations. In addition, from Eq. 11, we see that the velocity constant depends linearly on the ratio of the surface tension of the solvent to its viscosity, and the solvents that maximize this ratio are most useful for TLC. The contact angle for most mobile phases on polar adsorbent layers is generally close to zero and there does not exist the problem of wetting. In the case of reversed-phase layers containing bonded, long-chain, alkyl groups, it is not possible to apply the mobile phase with a content of water below 40%. The optimum mobile-phase velocity for a separation can be established by forced flow development^[6] and it is considerably higher than the mobile-phase velocity obtained by the use of capillary flow under different experimental conditions. This is illustrated in Fig. 2a and b.

BAND-BROADENING INTERPRETATION

The kinetic contributions to zone broadening are evaluated by fitting data for the column plate height, as a function of the mobile-phase velocity, to a mathematical model describing the relationship between the two parameters. Several models have been used in the above experiment, but those by de Ligny and Remijnsee^[7] and Knox and Pryde,^[11] and developed by Guiochon and Siouffi^[9], are most widely used and, at least for a first approximation, allow for comparison and determination of the differences between TLC and column chromatography.^[7-11]

$$\bar{H} = \frac{3A_k d^{5/3} \theta^{1/3}}{2(2D_m)^{1/3} z_f^{1/3}} \frac{(z_f^{2/3} - z_0^{2/3})}{z_f - z_0} + \frac{B_k D_m}{\theta d_p} (z_f - z_0) + \frac{C_k \theta d_p^3}{2D_m(z_f - z_0)} \lg \frac{z_f}{z_0} \quad (12)$$

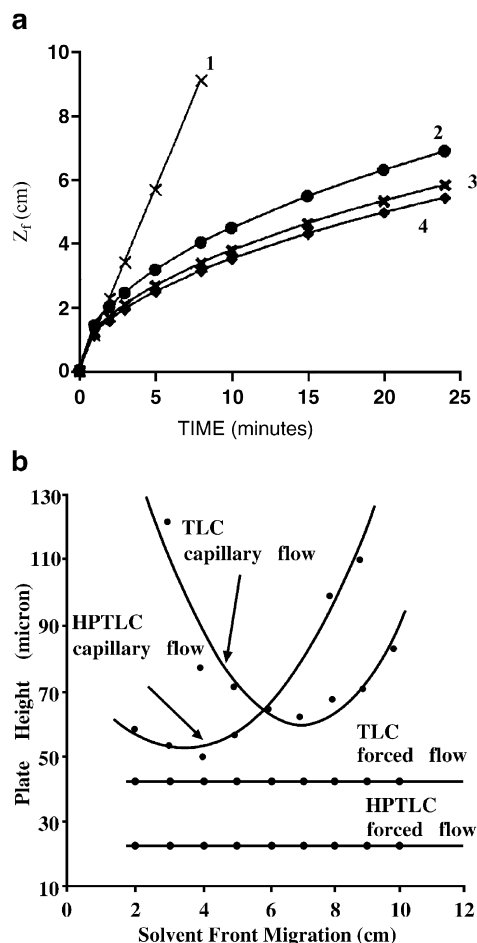


Fig. 2 (a) Plot of solvent front migration distance z_f for dichloromethane on a high-performance silica gel layer as a function of time under different experimental conditions. Identification: 1 = forced flow development at u_{opt} ; 2 = capillary flow in a saturated developing chamber; 3 = capillary flow in a sandwich chamber; and 4 = capillary flow in an unsaturated developing chamber. (b) Variation of the observed plate height as a function of the solvent front migration distance for conventional (TLC) and high-performance (HPTLC) silica layers under capillary flow and forced flow (u_{opt}) conditions.

where d_p is the average particle size, χ is the mobile-phase velocity constant, and D_m is the solute diffusion coefficient in the mobile phase. A_k , B_k , and C_k are dimensionless coefficients characterizing the packing quality (A_k), the diffusion in the mobile phase (B_k), and the resistance to mass transfer (C_k). Eq. 12 can be helpful in the interpretation of the influence of layer structure on plate height. Results of simulations of the relationship between plate height and different parameters are presented in Fig. 3 and parameters used in simulation are presented in Table 1.

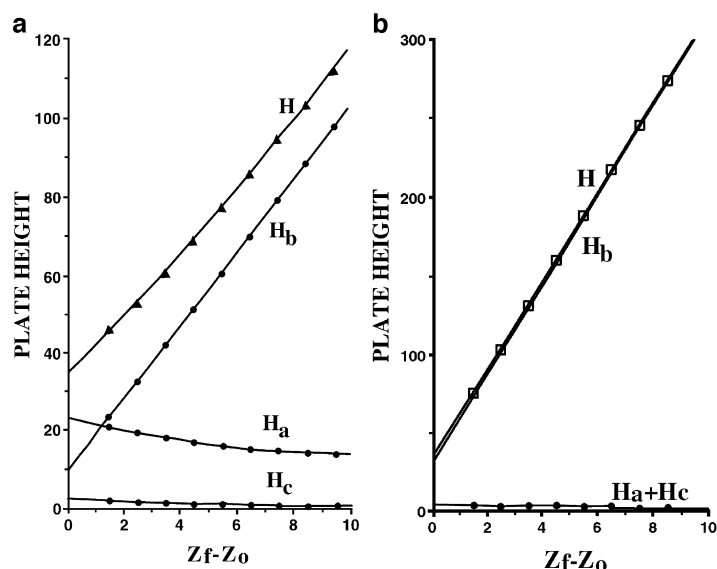


Fig. 3 (a) Simulation of the average plate height for a TLC layer by use (Eq. 12) and properties listed in Table 1. The contribution from flow anisotropy is represented by H_a , that from longitudinal diffusion by H_b , and that from resistance to mass transfer by H_c . (b) Simulation of the average plate height for an HPTLC layer by use (Eq. 12) and properties listed in Table 1. The contribution from flow anisotropy is represented by H_a , that from longitudinal diffusion by H_b , and that from resistance to mass transfer by H_c .

UNIDIMENSIONAL MULTIPLE DEVELOPMENT

Unidimensional multiple development provides a complementary approach to forced flow for minimizing zone broadening.^[13] All unidimensional multiple development techniques employ successive repeated development of

the layer in the same direction, with removal of the mobile phase between developments. Approaches differ in the changes made (e.g., mobile-phase composition and solvent front migration distance) between consecutive development steps; the total number of successive development steps employed can also be varied. Capillary forces are responsible for migration of the mobile phase,

Table 1 Characteristic properties of precoated layers and HPLC columns

Property	HPTLC	TLC	HPLC
Porosity total	0.65–0.70	0.65–0.75	0.8–0.9
Interparticle	0.35–0.45	0.35–0.45	0.4–0.5
Intraparticle	0.28	0.28	0.4–0.5
Flow resistance parameter	875–1500	600–1200	500–1000
Apparent particle size (μm)	5–7	8–10	d_p
Minimum plate height (μm)	22–25	35–45	$2-3d_p$
Optimum velocity (cm sec^{-1})	0.03–0.05	0.02–0.05	0.2
Minimum reduced plate height	3.5–4.5	3.5–4.5	1.5–3
Optimum reduced velocity	0.7–1.0	0.6–1.2	3–5
Separation impedance 9,000–70,000	10,500–19,800	11,100–60,200	2,000–9,000
Mean pore diameter (Si 60) (nm)	5.9–7.0	6.1–7.0	
<i>Knox coefficients</i>			
A_k	0.75	2.83	0.5–1
B_k	1.56	1.18	1–4
C_k	1.42	0.84	0.05

(From Refs. [6], [12])



but a zone-focusing mechanism is used to counteract the normal zone broadening that occurs in each successive development. Each time the solvent front traverses the stationary sample zone, the zone is compressed in the direction of development. The compression occurs because the mobile phase contacts the bottom edge of the zone first; here, the sample molecules start to move forward before those molecules are still ahead of the solvent front. When the solvent front has moved beyond the zone, the focused zone migrates and is subject to the normal zone-broadening mechanisms. Experiment indicates that, beyond a minimum number of development steps, zone widths converge to a constant value that is roughly independent of migration distance.

SOLVENT GRADIENTS

A similar phenomenon, compression of chromatographic zones, occurs in gradient TLC when the concentration of mobile phase delivered to the layer is varied in a stepwise manner. In the case where the concentration front traverses the sample zone, the zone is compressed in the direction of development. The compression takes place on the length equal to the diameter of the spot. Application of multicomponent eluent for the development of the layer, when the components differ in polarity, causes the creation of a natural gradient in the mobile phase. The gradient appears as multiconcentration fronts.^[14] As in step gradients, the compression takes place and the widths of the spots are much smaller. This should improve resolution.

Table 2 Zone capacity calculated or predicted for different separation conditions in TLC^[6]

Method	Dimensions	Zone capacity
<i>(A) Predictions from theory</i>		
Capillary flow	1	< 25
Forced flow	1	< 80 (up to 150, depending on pressure limit)
Capillary flow	2	< 400
Forced flow	2	Several thousands
<i>(B) Based on experimental observations</i>		
Capillary flow	1	12–14
Forced flow	1	30–40
Capillary flow (AMD)	1	30–40
Capillary flow	2	ca. 100
<i>(C) Predictions based on results in (B)</i>		
Forced flow	2	ca. 1500
Capillary flow (AMD)	2	ca. 1500

MOVING PLATE

Changing the solvent entry position for each, or some, of the development steps enables the separation in each segment to be achieved in the shortest possible time under favorable capillary flow conditions. With as few as 10 developments, it is relatively easy to achieve 15,000–25,000 apparent theoretical plates for a zone migration distance of 6–11 cm.^[6,15,16]

ZONE CAPACITY

The potential of a chromatographic system to achieve a particular separation can be estimated from its zone capacity, also referred to as the separation number (SN). It provides a method of comparison of different TLC systems and an indication of the possibility of separating a given mixture:^[8]

$$SN = \frac{z_f}{b_0 + b_1} - 1 \quad (13)$$

where b_0 is the extrapolated width of the starting spot at half-height of the concentration curve, and b_1 is the extrapolated width of the spot with $R_f = 1$. Some typical results for the zone capacity, either predicted from theory or by experiment, are summarized in Table 2.^[6] Experimental observations are indicated for zone capacity of approximately 12–14 for a single development in a capillary flow, increasing to 30–40 if forced flow is used. Use of capillary flow and the zone-focusing mechanism of multiple development leads to a zone capacity similar to that for forced flow.

CONCLUSION

In capillary flow conditions, there is an inadequate range of mobile-phase velocities, which does not allow working at u_{opt} values; the role of the binder remains not completely clear. The zone-focusing mechanism causes an increase of separation performance of the system in the most simple way. Forced flow offers a modest increase in performance with a reduction in separation time.

REFERENCES

- Giddings, J.C. *Unified Separation Science*; John Wiley & Sons, Inc.: New York, 1991; 10.
- Kowalska, T. Theory and Mechanism of Thin-Layer Chromatography. In *Handbook of Thin Layer Chroma-*

- topography, 2nd Ed.; Sherma, J., Fried, B., Eds.; Marcel Dekker, Inc.: New York, 1996; Vol. 71, 49–80.
3. Cazes, J.; Scott, R.P.W. Thin Layer Chromatography. In *Chromatography Theory*; Marcel Dekker, Inc.: New York, 2002; 443–454.
 4. Geiss, F. *Fundamentals of Thin Layer Chromatography*; Hüthig: Heidelberg, 1987; 9–82.
 5. Van Deemter, J.J.; Zuiderweg, F.; Klinkenberg, A. Longitudinal diffusion and resistance to mass transfer as causes of nonideality in chromatography. *Chem. Eng. Sci.* **1956**, 5, 271.
 6. Poole, C.F. Kinetic Theory of Planar Chromatography. In *Planar Chromatography. A Retrospective View for the Third Millennium*; Nyiredy, Sz., Ed.; Springer: Budapest, 2001; 13–32.
 7. de Ligny, C.L.; Remijnse, A.G. *J. Chromatogr.* **1968**, 33, 242–254, 257–268.
 8. Zlatkis, A.; Kaiser, R.E. *HPTLC High Performance Thin Layer Chromatography*; Elsevier: Amsterdam, 1977; 15–38.
 9. Guiochon, G.; Siouffi, A. Band broadening and plate height equation. III. Flow velocity. *J. Chromatogr. Sci.* **1978**, 16, 470–481, 598–609.
 - 10a. Belenkii, B.B.; Nesterov, V.V.; Smirnov, V.V. Differential equation for thin-layer chromatography and its solution. *Russ. J. Phys. Chem.* **1968**, 42, 773–775.
 - 10b. Belenkii, B.B.; Nesterov, V.V.; Smirnov, V.V. Comparison of theory with experimental results. *Russ. J. Phys. Chem.* **1968**, 42, 1527–1530.
 11. Knox, J.H.; Pryde, A. Performance and selected applications of a new range of chemically bonded packing materials in high-performance liquid chromatography. *J. Chromatogr.* **1975**, 112, 171–188.
 12. Poole, C.K.; Poole, S.K. Instrumental thin-layer chromatography. *Anal. Chem.* **1994**, 66, 27A–37A.
 13. Poole, C.K.; Poole, S.K. *Chromatography Today*; Elsevier: Amsterdam, 1991.
 14. Niederwieser, A.; Honegger, C.C. Gradient Techniques in Thin-Layer Chromatography. In *Advances in Chromatography*; Giddings, J.J., Keller, R.A., Eds.; Marcel Dekker, Inc.: New York, 1966; Vol. 2, 123.
 15. Fernando, W.P.N.; Poole, C.F. Determination of kinetic parameters for precoated silica gel thin layer chromatography plates by forced flow development. *J. Planar Chromatogr.* **1991**, 4, 278–287.
 16. Fernando, W.P.N.; Poole, C.F. Comparison of the kinetic properties of commercially available precoated silica gel plates. *J. Planar Chromatogr.* **1993**, 6, 357–361.

SUGGESTED ADDITIONAL READING

- Grinberg, N.; LoBrutto, R. Efficiency in Chromatography. In *Encyclopedia of Chromatography*; Cazes, J., Ed.; Marcel Dekker, Inc.: New York, 2001; 274.
- Modern Thin-Layer Chromatography*; Grinberg, N., Ed.; Marcel Dekker, Inc.: New York, 1990.
- Tijssen, R. The Mechanisms and Importance of Zone-Spreading. In *Handbook of HPLC*; Katz, E., Eksteen, R., Schoenmakers, P., Miller, N., Eds.; Marcel Dekker, Inc.: New York, 1998; 55–142.

Electro-osmotic Flow

Danilo Corradini

Institute of Chromatography, Rome, Italy

Introduction

Electro-osmosis refers to the movement of the liquid adjacent to a charged surface, in contact with a polar liquid, under the influence of an electric field applied parallel to the solid–liquid interface. The bulk fluid of liquid originated by this electrokinetic process is termed electro-osmotic flow (EOF). It may be produced both in open and in packed capillary tubes, as well as in planar electrophoretic systems employing a variety of supports, such as paper or hydrophilic polymers.

Discussion

The formation of an electric double layer at the interfacial region between the charged surface and the surrounding liquid is of key importance in the generation of the electro-osmotic flow [1–3]. Most solid surfaces acquire a superficial charge when are brought into contact with a polar liquid. The acquired charge may result from dissociation of ionizable groups on the surface, adsorption of ions from solution, or by virtue of unequal dissolution of oppositely charged ions of which the surface is composed. This superficial charge causes a variation in the distribution of ions near the solid–liquid interface. Ions of opposite charge (counterions) are attracted toward the surface, whereas ions of the same charge (co-ions) are repulsed away from the surface. This, in combination with the mixing tendency of thermal motion, leads to the generation of an electric double layer formed by the charged surface and a neutralizing excess of counterion over co-ions distributed in a diffuse manner in the polar liquid. Part of the counterions are firmly held in the region of the double layer closer to the surface (the compact or Stern layer) and are believed to be less hydrated than those in the diffuse region of the double layer where ions are distributed according to the influence of electrical forces and random thermal motion. A plane (the Stern plane) located at about one ion radius from the surface separates these two regions of the electric double layer.

Certain counterions may be held in the compact region of the double layer by forces additional to those of

purely electrostatic origin, resulting in their adsorption in the Stern layer. Specifically, adsorbed ions are attracted to the surface by electrostatic and/or van der Waals forces strongly enough to overcome the thermal agitation. Usually, the specific adsorption of counterions predominates over co-ion adsorption.

The variation of the electric potential in the electric double layer with the distance from the charged surface is depicted in Fig. 1. The potential at the surface (ψ_0) linearly decreases in the Stern layer with respect to the value of the zeta potential (ζ). This is the electric potential at the plane of shear between the Stern layer (plus that part of the double layer occupied by the molecules of solvent associated with the adsorbed ions) and the diffuse part of the double layer. The zeta potential decays exponentially from ζ to zero with the distance from the plane of shear between the Stern layer and the diffuse part of the double layer. The location of the plane of shear, a small distance further out from the surface than the Stern plane, renders the zeta potential marginally smaller in magnitude than the potential at the Stern plane (ψ_δ). However, in order to simplify the mathematical models describing the electric double layer, it is customary to assume identity of ψ_δ and ζ , and the bulk experimental evidence indicates that errors introduced through this approximation are usually small.

According to the Gouy–Chapman–Stern–Grahame (GCSG) model of the electric double layer [4], the surface density of the charge in the Stern layer is related to the adsorption of the counterions, which is described by a Langmuir-type adsorption model, modified by the incorporation of a Boltzman factor. Considering only the adsorption of counterions, the surface charge density σ_s of the Stern layer is related to the ion concentration C in the bulk solution by the following equation:

$$\sigma_s = ze n_0 \frac{C}{V_m} \exp\left(\frac{ze\xi + \Phi}{kT}\right) \times \left[1 + \frac{C}{V_m} \exp\left(\frac{ze\xi + \Phi}{kT}\right)\right]^{-1} \quad (1)$$

where e is the elementary charge, z is the valence of the ion, k is the Boltzman constant, T is the temperature,



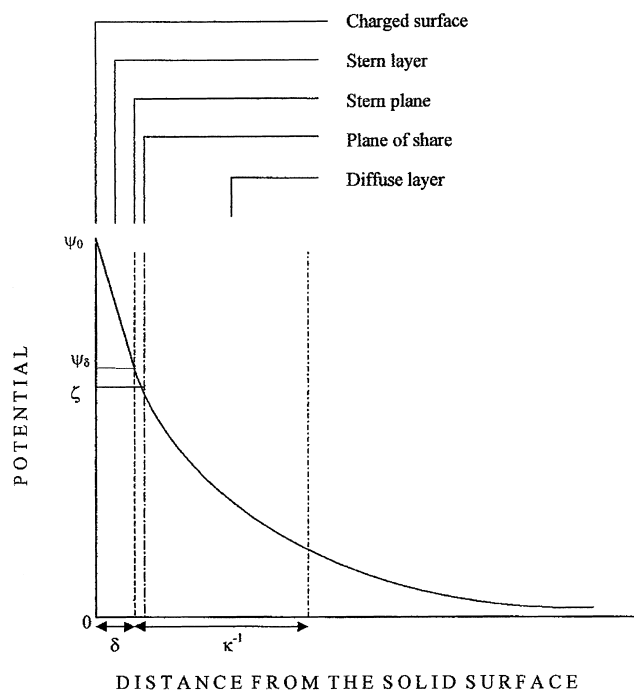


Fig. 1 Schematic representation of the electric double layer at a solid-liquid interface and variation of potential with the distance from the solid surface: ψ_0 , surface potential; ψ_δ , potential at the Stern plane; ζ , potential at the plane of share (zeta potential); δ , distance of the Stern plane from the surface (thickness of the Stern layer); κ^{-1} , thickness of the diffuse region of the double layer.

n_0 is the number of accessible sites, V_m is the molar volume of the solvent, and Φ is the specific adsorption potential of counterions.

The surface charge density of the diffuse part of the double layer is given by the Gouy-Chapman equation

$$\sigma_G = (8\epsilon k T c_0) \sinh\left(\frac{ze\xi}{2kT}\right) \quad (2)$$

where ϵ is the permittivity of the electrolyte solution and c_0 is the bulk concentration of each ionic species in the electrolyte solution.

At low potentials, Eq. (2) reduces to

$$\sigma_G = \frac{\epsilon \xi}{\kappa^{-1}} \quad (3)$$

where κ^{-1} is the reciprocal Debye-Hückel parameter, which is defined as the “thickness” of the electric double layer. This quantity has the dimension of length and is given by

$$\kappa^{-1} = \left(\frac{\epsilon k T}{2e^2 I}\right)^{1/2} \quad (4)$$

in which I is the ionic strength of the electrolyte solution.

Equation (3) is identical to the equation that relates the charge density, voltage difference, and distance of separation of a parallel-plate capacitor. This result indicates that a diffuse double layer at low potentials behaves like a parallel capacitor, in which the separation distance between the plates is given by κ^{-1} . This explains why κ^{-1} is called the double-layer thickness.

Equation (2) can be written in the form

$$\xi = \frac{\sigma_G \kappa^{-1}}{\epsilon} \quad (5)$$

which indicates that the zeta potential can change due to variations in the density of the electric charge, in the permittivity of the electrolyte solution, and in the thickness of the electric double layer, which depends, throughout the ionic strength [see Eq. (4)], on the concentration and valence of the ions in solution.

The dependence of the velocity of the electro-osmotic flow (v_{eo}) on the zeta potential is expressed by the Helmholtz-von Smoluchowski equation

$$v_{eo} = -\frac{\epsilon_0 \epsilon \xi}{\eta} E \quad (6)$$

where E is the applied electric field, ϵ_0 is the permittivity of vacuum, and ϵ and η are the dielectric constant and the viscosity of the electrolyte solution, respectively. This expression assumes that the dielectric constant and viscosity of the electrolyte solution are the same in the electric double layer as in the bulk solution.

The Helmholtz-von Smoluchowski equation indicates that under constant composition of the electrolyte solution, the electro-osmotic flow depends on the magnitude of the zeta potential, which is determined by the different factors influencing the formation of the electric double layer, as discussed earlier. Each of these factors depends on several variables, such as pH, specific adsorption of ionic species in the compact region of the double layer, ionic strength, and temperature.

The specific adsorption of counterions at the interface between the surface and the electrolyte solution results in a drastic variation of the charge density in the Stern layer, which reduces the zeta potential and, hence, the electro-osmotic flow. If the charge density of the adsorbed counterions exceeds the charge density on the surface, the zeta potential changes sign and the direction of the electro-osmotic flow is reversed.

The ratio of the velocity of the electro-osmotic flow to the applied electric field, which expresses the velocity per unit field, is defined as electro-osmotic

coefficient or, more properly, electro-osmotic mobility (μ_{eo}).

$$\frac{v_{eo}}{E} = \mu_{eo} = \frac{\varepsilon_0 \varepsilon \zeta}{\eta} \quad (7)$$

Using SI units, the velocity of the electro-osmotic flow is expressed in meters per second (m/s) and the electric field in volts per meter (V/m). Consequently, in analogy to the electrophoretic mobility, the electro-osmotic mobility has the dimension square meters per volt per second. Because electro-osmotic and electrophoretic mobilities are converse manifestations of the same underlying phenomenon, the Helmholtz–von Smoluchowski equation applies to electro-osmosis as well as to electrophoresis. In fact, when an electric field is applied to an ion, this moves relative to the electrolyte solution, whereas in the case of electro-osmosis, it is the mobile diffuse layer that moves under an applied electric field, carrying the electrolyte solution with it.

According to Eq. (6), the velocity of the electro-osmotic flow is directly proportional to the intensity of the applied electric field. However, in practice, the nonlinear dependence of the electro-osmotic flow on the applied electric field is obtained as a result of Joule heat production, which causes an increase of the electrolyte temperature with a consequent decrease of viscosity and variation of all other temperature-dependent parameters (protonic equilibrium, ion distribution in the double layer, etc.). The electro-osmotic flow can also be altered during a run by variations of the protonic and hydroxylic concentration in the anodic and cathodic electrolyte solutions as a result of electrolysis. This effect can be minimized by using electrolyte solutions with a high buffering capacity and electrolyte reservoirs of relatively large volume and by frequent replacement of the electrolyte in the electrode compartments with fresh solution.

The magnitude and direction of the electro-osmotic flow depend also on the composition, pH, and ionic strength of the electrolyte solution [5–7]. Both the pH and ionic strength influence the protonic equilibrium of fixed-charged groups on the surface and of ionogenic substances in the electrolyte solution which affect the charge density in the electric double layer and, consequently, the zeta potential. In addition, the ionic strength influences the thickness of the double layer (κ^{-1}). According to Eq. (4), increasing the ionic strength causes a decrease in κ^{-1} , which is currently referred to as the compression of the double layer that results in lowering the zeta potential. Consequently, increasing the ionic strength results in decreasing the electro-osmotic flow.

The charge density in the electric double layer and, hence, the electro-osmotic flow are also influenced by the adsorption of potential-determining ions in the Stern region of the electric double layer. A variety of additives can be incorporated into the electrolyte solution with the purpose of controlling the electro-osmotic flow by modifying the solid surface dynamically. These include simple and complex ionic compounds, ionic and zwitterionic surfactants, and neutral and charged polymers. The incorporation of these additives into the electrolyte solution may result either in increasing or in reducing the electro-osmotic flow, or even in reversing its direction. The impact of these additives on the electro-osmotic flow is generally concentration dependent. Such behavior is in accordance to the Langmuir-like adsorption model describing the variation of the charge density in the Stern layer on the concentration of adsorbing ions in the electrolyte solution [see Eq. (1)].

The proper control of the electro-osmotic flow can be also obtained by adding organic solvents to the electrolyte solution. The influence of organic solvents on the electro-osmotic flow may result from a multiplicity of mechanisms. Organic solvents are expected to influence both the dielectric constant and viscosity of the bulk electrolyte solution. Generally, this leads to the variation of the ratio of the dielectric constant to the viscosity of the electrolyte solution, to which the electro-osmotic flow depends according to Eq. (6). In addition, the local viscosity within the electric double layer [8] can be varied by the adsorption of the organic–solvent molecules in the Stern layer, which may also influence the adsorption of counterions, depending on the different solvation properties of the organic solvent. Organic solvents may also influence the zeta potential by affecting the ionization of potential-determining ions on the surface.

Different methods can be employed to measure the magnitude of the electro-osmotic flow [9]. One possibility involves measuring the velocity of the electro-osmotic flow by measuring the change in weight or in volume in one of the electrolyte solution reservoirs. The addition of an electrically neutral dye to one electrode reservoir and its detection in the other where the electro-osmotic flow is directed is another possible method. Other methods based on monitoring electric current while an electrolyte solution of different conductivity is drawn into the system by electro-osmosis or determining the zeta potential from streaming potential measurements are less popular and accurate. More com-



mon is the method of calculating the electro-osmotic velocity from the migration time of an electrically neutral marker substance incorporated into the sample solution. The selected compound must be soluble in the electrolyte solution, neutral in a wide pH range, and easily detectable. In addition, it should neither become partially charged by complexation with the components of the electrolyte solution nor interact with the capillary tube, the chromatographic stationary phase, or the slab gel employed in capillary electrophoresis, capillary electrochromatography, and planar electrophoresis, respectively. This method has the advantage of simplicity and can be used to monitor the electro-osmotic flow during analysis in any of the above techniques, provided that the analytes and the electro-osmotic flow are directed toward the same electrode.

References

1. P. C. Hiemenz, *Principles of Colloid and Surface Chemistry*, 2nd ed., Marcel Dekker, Inc., New York, 1986, pp. 677–735.
2. A. W. Adamson, *Physical Chemistry of Surfaces*, 5th ed., John Wiley & Sons, New York, 1990, pp. 203–257.
3. D. J. Shaw, *Introduction to Colloid and Surface Chemistry*, 3th ed., Butterworths, London, 1980, pp. 148–182.
4. D. C. Grahame, *Chem. Rev.* 41: 441–501 (1947).
5. K. D. Lukacs and J. W. Jorgenson, *J. High Resolut. Chromatogr. Chromatogr. Commun.* 8: 407–411 (1985).
6. K. D. Altria and C. F. Simpson, *Chromatographia* 24: 527–532 (1987).
7. M. G. Cikalo, K. D. Bartle, and P. Myers, *J. Chromatogr. A* 836: 35–51 (1999).
8. S. Hjerten, *Chromatogr. Rev.* 9: 122–219 (1967).
9. A. A. A. M. Van de Goor, B. J. Wanders, and F. M. Everaerts, *J. Chromatogr.* 470: 95–104 (1989).



Electro-osmotic Flow in Capillary Tubes

Danilo Corradini

Institute of Chromatography, Rome, Italy

Introduction

The electro-osmotic flow in open capillary tubes is generated by the effect of the applied electric field across the tube on the uneven distribution of ions in the electric double layer at the interface between the capillary wall and the electrolyte solution. In bare fused-silica capillaries, ionizable silanol groups are present at the surface of the capillary wall, which is exposed to the electrolyte solution. In this case, the electric double layer is the result of the excess of cations in the solution in contact with the capillary tube to balance the negative charges on the wall arising from the ionization of the silanol groups. Part of the excess cations are firmly held in the region of the double layer closer to the capillary wall (the compact or Stern layer) and are believed to be less hydrated than those in the diffuse region of the double layer [1]. When an electric field is applied across the capillary, the remaining excess cations in the diffuse part of the electric double layer move toward the cathode, dragging their hydration spheres with them. Because the molecules of water associated with the cations are in direct contact with the bulk solvent, all the electrolyte solution moves toward the cathode, producing a pluglike flow having a flat velocity distribution across the capillary diameter [2].

Discussion

The flow of liquid caused by electro-osmosis displays a pluglike profile because the driving force is uniformly distributed along the capillary tube. Consequently, a uniform flow velocity vector occurs across the capillary. The flow velocity approaches zero only in the region of the double layer very close to the capillary surface. Therefore, no peak broadening is caused by sample transport carried out by the electro-osmotic flow. This is in contrast to the laminar or parabolic flow profile generated in a pressure-driven system, where there is a strong pressure drop across the capillary caused by frictional forces at the liquid–solid boundary. A schematic representation of the flow profile due

to electro-osmosis in comparison to that obtained in the same capillary column in a pressure-driven system, such as a capillary high-performance liquid chromatography (HPLC), is displayed in Fig. 1.

The dependence of the velocity of the electro-osmotic flow (v_{eo}) on the applied electric field (E) is expressed by the Helmholtz–von Smoluchowski equation

$$v_{eo} = -\frac{\epsilon_0 \epsilon_r \zeta}{\eta} E \quad (1)$$

where ζ is the zeta potential, ϵ_0 is the permittivity of vacuum, ϵ_r is the dielectric constant, and η is the viscosity of the electrolyte solution. This expression assumes that the dielectric constant and viscosity of the electrolyte solution are the same in the electric double layer as in the bulk solution. The term $-\epsilon_0 \epsilon_r \zeta / \eta$ is the defined electro-osmotic coefficient or, more properly,

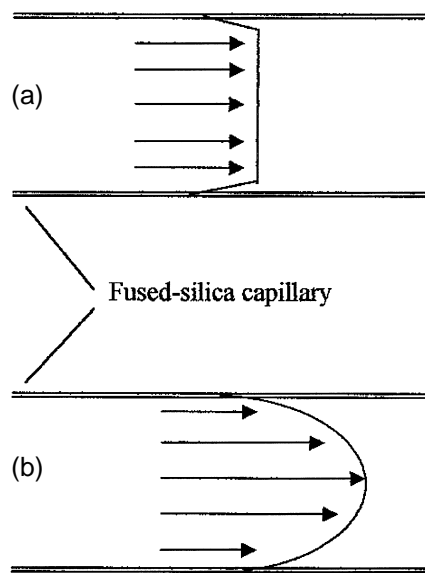


Fig. 1 Schematic representation of the flow profiles obtained with the same capillary column connected to an electric-driven system (a) and to a pressure-driven system (b). Arrows indicate flow velocity vectors.



electro-osmotic mobility (μ_{eo}) and expresses the velocity of the electro-osmotic flow per unit field. Accordingly, the Helmholtz–von Smoluchowski equation can be written

$$\mu_{eo} = \frac{v_{eo}}{E} \quad (2)$$

In a capillary tube, the applied electric field E is expressed by the ratio V/L_T , where V is the potential difference in volts across the capillary tube of length L_T (in meters). The velocity of the electro-osmotic flow, v_{eo} (in meters per second), can be evaluated from the migration time t_{eof} (in seconds) of an electrically neutral marker substance and the distance L_D (in meters) from the end of the capillary where the samples are introduced to the detection windows (effective length of the capillary). This indicates that, experimentally, the electro-osmotic mobility can be easily calculated using the Helmholtz–von Smoluchowski equation in the following form:

$$\mu_{eo} = \frac{L_T L_D}{V t_{eof}} \quad (\text{m}^2/\text{V/s}) \quad (3)$$

which demonstrates that, by analogy to the electrophoretic mobility, the electro-osmotic mobility has the dimension of square meters per volt per second.

The electrically neutral marker substance employed to measure the velocity of the electro-osmotic flow has to fulfill the following requirements. The compound must be soluble in the electrolyte solution and neutral in a wide pH range and no interaction with the capillary wall must occur. In addition, the electrically neutral marker substance should be easily detectable in order to allow a small amount to be injected. If the electrically neutral marker interacts with the capillary wall or becomes partially charged by complexation with the components of the electrolyte solution, the measured electro-osmotic velocity may appear slower or faster than the real flow. Some compounds that adequately serve as electrically neutral markers include benzyl alcohol, riboflavin, acetone, dimethyl-formamide, dimethyl sulfoxide, and mesityl oxide.

Alternatively, the velocity of the electro-osmotic flow can be measured by weighing the volume of the electrolyte solution displayed by electro-osmosis from the anodic to the cathodic reservoir. When detection is performed by ultraviolet (UV) absorbance, a “solvent dip” equal to the electro-osmotic flow appears in the electropherogram after any sample injection. In most cases, the sample solvent has a lower UV absorbance than the electrolyte

solution, resulting in a negative UV signal. On the other hand, if the UV absorbance of the sample solvent is higher than that of the electrolyte solution, a positive system peak can be observed at the time corresponding to the velocity of the electro-osmotic flow. The time at which the “solvent dip” appears in the electropherogram can be used to measure the velocity of the electro-osmotic flow in a very simple but less accurate way than those using an electrically neutral marker substance or the weight of the displaced liquid.

The Helmholtz–von Smoluchowski equation indicates that under constant composition of the electrolyte solution, the electro-osmotic flow depends on the magnitude of the zeta potential which is determined by many different factors, the most important being the dissociation of the silanol groups on the capillary wall, the charge density in the Stern layer, and the thickness of the diffuse layer. Each of these factors depends on several variables, such as pH, specific adsorption of ionic species in the compact region of the electric double layer, ionic strength, viscosity, and temperature.

Secondary equilibrium in solution, generation of Joule heat, and variation of protonic and hydroxylic concentration due to electrolysis may alter the hydrogen ion concentration in the capillary tube when electrolyte solutions having low buffering capacities are employed. A change in the protonic equilibrium directly influences the zeta potential through the variation of the charge density on the capillary wall resulting from the deprotonation of the surface silanol groups, which increases with increasing pH. The shape of a curve describing the dependence of the zeta potential on the electrolyte pH resembles a titration curve, the inflection point of which may be interpreted as the pK value of the surface silanol groups. At acidic pH, the ionization of the surface silanol groups is suppressed and the zeta potential approaches zero, determining the virtual annihilation of the electro-osmotic flow. Under alkaline conditions, the silanol groups are fully charged and the zeta potential reaches its maximum value, which corresponds to a plateau value of the electro-osmotic flow. Between these extreme conditions, the zeta potential rapidly increases with increasing pH up to the complete dissociation of the silanol groups, determining the well-known sigmoidal pH dependence of the electro-osmotic flow. The concentration and ionic strength of the electrolyte solution also have a strong impact on the electro-osmotic flow. The ionic strength influences the thickness of the diffuse part of

the electric double layer to which the zeta potential is directly proportional. Because the thickness of the diffuse part of the electric double layer is inversely proportional to the square root of the ionic strength, the electro-osmotic flow decreases with the concentration of the electrolyte solution according to the following relationship [3]:

$$\mu_{eo} \approx \frac{e}{3 \times 10^7 |z| \eta \sqrt{C}} \quad (4)$$

where, e , z , η , and C are the total charge per unit surface area, the electron valence of the electrolyte, the viscosity, and the concentration of the electrolyte in the bulk solution, respectively.

Another model that accounts for the decrease of the electro-osmotic flow with increasing the electrolyte concentration relates the electro-osmotic mobility to the concentration of a monovalent counterion, introduced with the buffer, according to the following relationship [4]:

$$\mu_{eo} = \frac{Q_0}{\eta(1 + K_{wall}[M^+])} \left(d_0 + \frac{1}{K' \sqrt{[M^+]}} \right) \quad (5)$$

where η is the viscosity of the electrolyte solution and K' is a constant that, for a dilute aqueous solution at 25°C, is equal to $3 \times 10^9 / \text{m}(\text{mol/L})^{-1/2}$. The first term on the right side of Eq. (5) is related to the dependence of the surface charge on the concentration of the monovalent cation in the electrolyte solution. The model postulates that the initial charge per unit area at the surface of the silica capillary wall (Q_0) is reduced by the factor $1/(1 + K_{wall}[M^+])$ upon incorporating a monovalent buffer of concentration $[M^+]$ into the electrolyte solution. This is a result of the neutralization of the free silanol groups on the capillary surface caused by the adsorption of the monovalent cations. The constant K_{wall} is defined as the equilibrium constant between the cations in the buffer solution and adsorption sites on the capillary wall. The second term describes the influence of the concentration of the monovalent cation on the thickness of the mobile region of the electric double layer. This is postulated to be composed of a fixed thickness (d_0) and the Debye–Hückel thickness $\delta = 1/K'[M^+]^{1/2}$, which is inversely proportional to the square root of the concentration of the monovalent ion. According to this model, increasing the concentration of the monovalent buffer cation in the bulk solution influences the electro-osmotic mobility by reducing the Debye–Hückel thickness of the diffuse double layer and by neutralizing the negative charges

on the capillary wall resulting from the ionization of the silanol groups.

Certain counterions, such as polycationic species, cationic surfactants, and several amino compounds can be firmly held in the compact region of the electric double layer by forces additional to those of simple Coulombic origin. The specific adsorption of counterions at the interface between the capillary wall and the electrolyte solution results in a drastic variation of the positive charge density in the Stern layer, which reduces the zeta potential and, hence, the electro-osmotic flow. If the positive charge density of the adsorbed counterions exceeds the negative charge density on the capillary wall resulting from the ionization of silanol groups, the zeta potential becomes positive and the concomitant electro-osmotic flow is reversed from cathodic to anodic.

The dependence of the electro-osmotic flow on the specific adsorption of counterions in the electric double layer can be described by a model which correlates the electro-osmotic mobility to the charge density in the Stern part of the electric double layer (arising from the adsorption of counterions) and the charge density at the capillary wall (resulting from the ionization of silanol groups) [5]. According to this model, the dependence of the electro-osmotic mobility on the concentration of the adsorbing ions (C) in the electrolyte solution is expressed as

$$\mu_{eo} = \frac{\kappa^{-1}}{\eta} \left\{ zen_0 \frac{C}{V_m} \exp\left(\frac{ze\psi_d + \Phi}{kT}\right) \times \left[1 + \frac{C}{V_m} \exp\left(\frac{ze\psi_\delta + \Phi}{kT}\right) \right]^{-1} - \left(\frac{\gamma}{1 + [H^+]/K_a} \right) \right\} \quad (6)$$

where κ^{-1} is the Debye–Hückel thickness of the diffuse double layer, η is the viscosity of the electrolyte solution, e is the elementary charge, z is the valence of the adsorbing ion, k is the Boltzmann constant, T is the absolute temperature, n_0 is the number of accessible sites in the Stern layer, V_m is the molar volume of the solvent, Φ is the specific adsorption potential of counterions, γ is the sum of the ionized and protonated surface silanol groups, $[H^+]$ is the bulk electrolyte hydrogen ion concentration, and K_a is the silanol dissociation constant. According to this equation, at constant ionic strength, viscosity, and pH, the electro-osmotic mobility depends mainly on the surface density of the adsorbed counterions in the Stern region of the electric double layer, which follow a Langmuir-type adsorption model.



The reversal of the direction of the electro-osmotic flow by the adsorption onto the capillary wall of alkylammonium surfactants and polymeric ion-pair agents incorporated into the electrolyte solution is widely employed in capillary zone electrophoresis (CZE) of organic acids, amino acids, and metal ions. The dependence of the electro-osmotic mobility on the concentration of these additives has been interpreted on the basis of the model proposed by Fuerstenau [6] to explain the adsorption of alkylammonium salts on quartz. According to this model, the adsorption in the Stern layer as individual ions of surfactant molecules in dilute solution results from the electrostatic attraction between the head groups of the surfactant and the ionized silanol groups at the surface of the capillary wall. As the concentration of the surfactant in the solution is increased, the concentration of the adsorbed alkylammonium ions increases too and reaches a critical concentration at which the van der Waals attraction forces between the hydrocarbon chains of adsorbed and free-surfactant molecules in solution cause their association into hemimicelles (i.e., pairs of surfactant molecules with one cationic group directed toward the capillary wall and the other directed out into the solution).

Lowering the velocity or reversing the direction of the electro-osmotic flow may have a beneficial effect of on the resolution of two adjacent peaks, as evidenced by the following expression for resolution in electrophoresis elaborated by Giddings [7]:

$$R_s = \frac{\sqrt{N}}{4} \left(\frac{\Delta\mu}{\mu_{av} + \mu_{eo}} \right) \quad (7)$$

where N is the number of theoretical plates, $\Delta\mu$ and μ_{av} are the difference and the average value of the electrophoretic mobilities of two adjacent peaks, respectively, and μ_{eo} is the electro-osmotic mobility. According to this equation, the highest resolution is obtained when the electro-osmotic mobility has the same value but opposite direction of the average electrophoretic mobility of the two adjacent peaks.

Neutral polymeric molecules, such as polysaccharides and synthetic polymers, may also adsorb onto the Stern layer, causing a variation of viscosity in the double layer with distance from the capillary wall, which affects the electro-osmotic mobility according to the following relationship [2]:

$$\mu_{eo} = \frac{\varepsilon_r}{4\pi} \int_0^{\xi} \frac{1}{\eta} d\psi \quad (8)$$

where ε_r is the dielectric constant, ξ is the zeta potential, η is the viscosity, and ψ is the electric potential. The value of the integral in this expression will approach zero when the viscosity in the double layer approaches infinity. Accordingly, the electro-osmotic flow is drastically reduced when the local viscosity of the double layer is increased as a result of the adsorption of a neutral polymer onto the Stern layer. It is worth noting that at constant value of the viscosity in the electric double layer, Eq. (8) is equivalent to the Helmholtz–von Smoluchowski expression for the electro-osmotic flow.

The incorporation of an organic solvent into the aqueous electrolyte solution also leads to a variation of the electro-osmotic flow [8]. The general trend is that the electro-osmotic flow decreases steadily with increasing concentration of the organic solvent in the hydro-organic electrolyte solution. This effect can be attributed, to some extent, to the increasing viscosity and decreasing dielectric constant of most hydro-organic electrolyte solutions with increasing concentration of organic solvent. However, in most cases, the decrease of the electro-osmotic flow is also observed at organic solvent concentrations greater than 50–60% (v/v), at which the ratio of the dielectric constant and the viscosity, ε_r/η , is generally increasing. This indicates that the variation of the electro-osmotic flow caused by the incorporation of an organic solvent into the electrolyte solution cannot be solely related to the changes of the ratio ε_r/η .

Similar to the neutral polymers, organic solvents can adsorb at the interface between the capillary wall and the electrolyte solution, through hydrogen-bonding or dipole interaction, thus increasing the local viscosity within the electric double layer. Organic solvents may also influence the zeta potential by affecting the ionization of the silanol groups at the capillary surface, whose pK_a has been found to be shifted toward higher values with increasing the content of organic solvents in the electrolyte solution. The dependence of the zeta potential on the fraction of an organic solvent incorporated into the electrolyte solution may be also related to the variation of both the dielectric constant and the adsorption of counterions in the Stern layer. In practice, introducing a neutral polymer or an organic solvent into the electrolyte solution results in multiple changes, generally involving the viscosity and the dielectric constant of the bulk solution, the ionization of the silanol groups on the capillary wall, and the charge density in the Stern layer, as well as the local viscosity and the dielectric constant of the electric double layer.

References

1. P. C. Hiemenz, *Principles of Colloid and Surface Chemistry*, 2nd ed., Marcel Dekker, Inc., New York, 1986, pp. 677–735.
2. S. Hjertén, *Chromatogr. Rev.* 9: 122–219 (1967).
3. T. Tsuda, K. Nomura, and G. Nakagawa, *J. Chromatogr.* 248: 241–247 (1982).
4. K. Salomon, D. S. Burgi, and J. C. Helmer, *J. Chromatogr.* 559: 69–80 (1991).
5. D. Corradini, A. Rhomberg, and C. Corradini, *J. Chromatogr. A* 661: 305–313 (1994).
6. D. W. Fuerstenau, *J. Phys. Chem.* 60: 981–985 (1956).
7. J. C. Giddings, *Separ. Sci.* 4: 181–189 (1969).
8. C. Schwer and E. Kenndler, *Anal. Chem.* 63: 1801–1807 (1991).



Electro-osmotic Flow Nonuniformity: Influence on Efficiency of Capillary Electrophoresis

Victor P. Andreev

Institute for Analytical Instrumentation, Russian Academy of Sciences, St. Petersburg, Russia

Introduction

There are two types of nonuniformities of electro-osmotic flow (EOF) that can contribute significantly to the solute peak broadening and are important for capillary electrophoresis (CE). The first is the transversal nonuniformity of the usual EOF in the capillary with the zeta potential of the walls and longitudinal electric field strength constant and independent of coordinates. The second one is the nonuniformity of EOF caused by the dependence of the zeta potential of the walls or electric field strength on coordinates.

Discussion

The first type of EOF nonuniformity was described in the classical article by Rice and Whitehead [1] written much earlier than the first works on CE. The equation for the EOF velocity profile in the infinitely long tube with radius a was given by

$$V(r) = \frac{\zeta \varepsilon \varepsilon_0 E}{\eta} \left(1 - \frac{I_0(\kappa r)}{I_0(\kappa a)} \right) \quad (1)$$

where ζ is the zeta potential of the wall, ε and η are the dielectric constant and viscosity of the buffer, respectively, ε_0 is the permittivity of the free space, $\kappa^{-1} = (\varepsilon \varepsilon_0 k_B T / 2 n e^2)^{1/2}$ is the Debye layer thickness, k_B is the Boltzmann constant, T is the temperature, n is the number of ions per unit volume (proportional to the concentration of buffer C_0), e is the proton charge, and $I_0(x)$ is the modified Bessel function. It is evident from Eq. (1) that the nonuniformity of the EOF profile can be substantial only if the capillary radius and Debye length are commensurate. In fact, for the case of $\kappa a \approx 1$, the profile of EOF according to Eq. (1) is very close to parabolic. Luckily, it is not the case of usual capillaries for CE with $a \geq 25 \mu\text{m}$ because, even for distilled water, $\kappa^{-1} \approx 0.1 \mu\text{m}$. Another important result of Ref. 1 is the prediction of the EOF profile in the long capillary with closed ends. In such a capillary, liquid moves in one direction in the vicinity of the walls and in the opposite direction near the axis of the capillary, thus making the total flow through the cross section equal to zero. With

this result, it is quite evident that CE must be realized in a capillary with open ends; otherwise, nonuniformity of EOF would ruin the separation.

Results of Ref. 1 were produced by employing a linear approximation of the exponential terms in the Poisson–Boltzmann equation for electrical potential and charge distribution. Strictly speaking, this linearization is valid only for $|\zeta| \ll kT/e \approx 0.03 \text{ V}$, whereas the range of the values of the zeta potential is $|\zeta| \leq 0.1 \text{ V}$. In Ref. 2, the Poisson–Boltzmann equation and the Navier–Stokes equations for EOF velocity profile were solved numerically without linearization. The dependence of buffer viscosity on temperature and the existence of temperature gradients due to Joule heating were also taken into consideration. Calculated EOF profiles were compared with and predicted by Eq. (1), showing that the difference in flow profiles for $|\zeta| = 0.1 \text{ V}$ could be significant, especially for thin capillaries and low buffer concentrations ($\kappa a \approx 10$). Calculated flow profiles were used to predict the stationary value of HETP by using the results of generalized dispersion theory. It was shown that for low buffer concentrations ($C_0 \leq 10^{-4} \text{ M}$), the contribution of electro-osmotic flow nonuniformity to the HETP value could be larger than the contribution of the thermal effects and molecular diffusion.

A similar approach was used in Ref. 3, where the contributions of EOF nonuniformity (H_{eo}) and molecular diffusion (H_{diff}) to HETP were compared for different values of solute diffusion coefficients. It was shown [3] that for the typical CE velocities of EOF (1–2 mm/s) and rather high buffer concentration ($C_0 = 10^{-2} \text{ M}$), $H_{\text{eo}}/H_{\text{diff}} \geq 1$ for $D \leq 2 \times 10^{-12} \text{ m}^2/\text{s}$. For lower buffer concentrations, the influence of EOF nonuniformity is substantial for smaller molecules also ($H_{\text{eo}} = 1.3 \times 10^{-8} \text{ m}$, $H_{\text{diff}} = 1.6 \times 10^{-8} \text{ m}$ for $D = 2.4 \times 10^{-11} \text{ m}^2/\text{s}$, corresponding to α_2 -macroglobulin).

The joint effect of EOF nonuniformity and particle–wall electrostatic interactions was studied in Ref. 4. Two types of solute particles were examined: one with the charge of the same sign as the zeta potential of the wall, and the other of the opposite sign. The particles of the first type are moving electrophoretically in the direction opposite to the direction of EOF and are elec-



trostatically subtracted by the wall, whereas the particles of the second type are attracted by the wall and are moving electrophoretically in the same direction as EOF. Particles of the second type spend a large portion of time in the vicinity of the capillary wall and, so, EOF nonuniformity contributes significantly to peak broadening, whereas for the particles subtracted by the wall, the influence of EOF nonuniformity is negligible because their residence time in the vicinity of the wall is close to zero. For example, for the particles with $D = 5 \times 10^{-11} \text{ m}^2/\text{s}$, in the capillary with $a = 10 \text{ }\mu\text{m}$, $\zeta = -0.1 \text{ V}$, and $E = 40 \text{ kV/m}$, filled with diluted buffer ($C_0 = 10^{-5} \text{ M}$), one has $\text{HETP} \approx 10 \text{ }\mu\text{m}$ for particles attracted by the wall, whereas for particles subtracted by the wall, $\text{HETP} \approx 0.1 \text{ }\mu\text{m}$. For neutral particles not interacting with the walls, $\text{HETP} \approx 0.2 \text{ }\mu\text{m}$ was predicted. The difference was much less dramatic for the case of the higher buffer concentrations and the lower zeta potential. For example, for $\zeta = -0.02 \text{ V}$, $C_0 = 10^{-3} \text{ M}$, and the rest of parameters being the same as described earlier, HETP is determined mainly by molecular diffusion and is close to $0.1 \text{ }\mu\text{m}$.

The influence of EOF nonuniformity on efficiency of CE in the capillary with the zeta potential of the wall being the function $\zeta(x)$ of the longitudinal coordinate x was studied in Ref. 5. To calculate the EOF velocity profile, an important approximation was justified by the fact that usually $\kappa a \gg 1$ in CE. Thus, the double-layer region was neglected and the following boundary condition was formulated:

$$V_x(x, a, t) = \frac{\varepsilon \varepsilon_0 E}{\eta} \zeta(x) \quad (2)$$

With this boundary condition, the Navier–Stokes equations for longitudinal V_x and radial V_r components of EOF velocity were solved numerically, and the calculated EOF profiles were used to simulate the solute peak shapes. The situation where the part of the capillary length was modified to the zero value of the zeta potential and the part of capillary was not modified ($\zeta \neq 0$) was studied. It was shown that the radial component of the velocity is nonzero only in the rather short transition region between the uncovered and covered parts of the capillary. At a distance of a few capillary diameters from the transient region, the radial flows are negligible and the axial component of the velocity in the covered section of the capillary has an almost parabolic profile. Peak shapes and peak variances were studied, and the general conclusion of Ref. 5 was that the main contribution to the peak width was from the parabolic velocity profiles, the contribution of the radial flow in the transient regions being less significant. Based on this result, the mathematical model of CE in the capillary made of

several sections with various nonequal values of the zeta potentials and radii was developed [6]. For each of the sections, the total flow was considered to be the sum of EOF caused by electrical potential differences along the section and the Poiseuille flow, caused by the pressure drop along the section. The values of the pressure drops and potentials differences were determined by the solution of the set of $2N$ algebraic equations, where N is the number of sections in the capillary. These equations reflect the fact that the total flow of liquid and total current are constant along the capillary, and the sums of pressure drops and potential differences at the sections are equal to the total pressure drop and total potential difference at the whole capillary, respectively. The lengths of the sections were considered to be much larger than the capillary radius, so the results of the model are valid everywhere except the immediate vicinity of the points where the radius of capillary or the zeta potential of the wall change their values. When calculating the values of HETP in such a capillary, particle–wall electrostatic interactions were taken into consideration, and it was shown that HETP values are considerably larger for particles attracted by the wall. It was also shown that differences in the values of the zeta potential contributes to HETP much more significantly than the differences in radii values. The situation that might happen in the case of a bubble-cell detector was modeled and considerable growth of HETP was predicted.

In Ref. 7, the case was studied in which the zeta potential of the wall was the linear function of the longitudinal coordinate. This situation may happen when the value of the zeta potential is controlled by the external electrical potential applied to the wall. Electrical potential value inside the capillary is naturally a linear function of the longitudinal coordinate x ; therefore, if the electrical potential applied to the outer boundary of the capillary wall is constant, then the potential difference across the wall is a linear function of x . The theoretical approach used in Ref. 7 is similar to the one in Ref. 5. Secondary parabolic flow was shown to be generated, leading to the increase of HETP. It was predicted theoretically, and verified experimentally, that a pressure profile superimposed on the capillary can, in some cases, compensate for the disturbed profile and reduce the HETP value.

In Ref. 8, the mathematical model of capillary electrophoresis in rectangular channels with nonequal values of the zeta potentials of the walls was developed. This model may be of interest for the case of CE on a microchip, where the microgrooves are produced by wet chemical etching and, so, the walls of the groove can have different values of zeta potential than the cover

plate that is not etched. Flow profiles for the channels with different aspect ratios and different combinations of the zeta potential values were examined. It was shown, for example, that a 10% difference in the values of the zeta potentials of upper and lower walls can cause a sixfold growth of the HETP value.

The above-mentioned examples show that EOF nonuniformities may occur in different situations and must be given considerable attention, as they can reduce the CE efficiency dramatically.

References

1. C. L. Rice and R. Whitehead, Electrokinetic flow in a narrow cylindrical capillary, *J. Phys. Chem.* 69: 4017 (1965).
2. V. P. Andreev and E. E. Lisin, Investigation of the electroosmotic flow effect on the efficiency of capillary electrophoresis, *Electrophoresis* 13: 832 (1992).
3. B. Gas, M. Stedry, and E. Kenndler, Contribution of the electroosmotic flow to peak broadening in capillary zone electrophoresis with uniform zeta potential, *J. Chromatogr. A* 709: 63 (1995).
4. V. P. Andreev and E. E. Lisin, On the mathematical model of capillary electrophoresis, *Chromatographia* 37: 202 (1993).
5. B. Potocek, B. Gas, E. Kenndler, and M. Stedry, Electroosmosis in capillary zone electrophoresis with non-uniform zeta potential, *J. Chromatogr. A* 709: 51 (1995).
6. V. P. Andreev and N. V. Shirokih, Electroosmotic flow profile in the capillary made of several sections, 20th Int. Symp. on Capillary Chromatography, Proceedings on CD, 1998, paper H 11.
7. C. A. Keely, T. A. A. M. van de Goor, and D. McManigill, Modeling flow profiles and dispersion in capillary electrophoresis with nonuniform zeta potential, *Anal. Chem.* 66: 4236 (1994).
8. V. P. Andreev, S. G. Dubrovsky, and Y. V. Stepanov, Mathematical modeling of capillary electrophoresis in rectangular channels, *J. Microcol. Separ.* 9: 443 (1997).



Electrochemical Detection

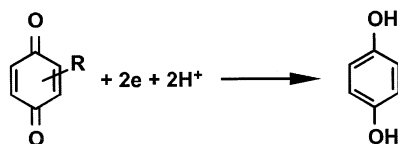
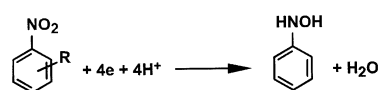
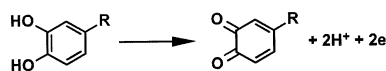
Peter T. Kissinger

Bioanalytical Systems, Inc., and Purdue University, West Lafayette, Indiana, U.S.A.

Introduction

With respect to chromatography, “electrochemical detection” means amperometric detection. Amperometry is the measurement of electrolysis current versus time at a controlled electrode potential. It has a relationship to voltammetry similar to the relationship of an ultraviolet (UV) detector to spectroscopy. Whereas conductometric detection is used in ion chromatography, potentiometric detection is never used in routine practice. Electrochemical detection has even been used in gas chromatography in a few unusual circumstances. It has even been attempted with thin-layer chromatography (TLC). Its practical success has only been with liquid chromatography (LC) and that will be the focus here.

Most chemists remember electrochemistry as a difficult subject they heard about in physical chemistry courses and they regard it as having something to do with batteries. Both of these impressions are true! What is important here is to understand that (a) redox reactions can be made to occur at surfaces (electrodes) and (b) amazingly enough, such reactions are not just the fate of metals ($\text{Fe}^{3+} \rightarrow \text{Fe}^{2+}$) but actually occur quite widely among organic compounds of interest such as drugs, pesticides, explosives, food additives, neurotransmitters, DNA, and so forth. There are good references for the novice wishing to understand the analytical electrochemistry of organic substances [1]. A few common examples are presented for both oxidations (electrons are lost, the process is anodic) and reductions (electrons are gained by the analyte, the process is cathodic):



Although we all remember (or try not to) the confusing math associated with electrochemistry and thermodynamics, all we need here is an appreciation of the fact that the current, i , is proportional to the moles, N , of analyte reacted per unit time. The latter is proportional to concentration at a constant flow rate through a detector cell. The key equation is

$$i = \frac{dQ}{dt} = nF \frac{dN}{dt}$$

where Q is the amount of electricity (charge in coulombs), n is the number of electrons, and F is the Faraday constant. As one can see from the above examples, most organic analytes are involved in reactions where $n = 1, 2$, or 4 . To use an electrochemical detector, it is very important to know that i is proportional to the concentration and the amount injected, just as UV absorbance is proportional to the concentration or the amount injected.

Liquid chromatography–electrochemistry (LC–EC) is now over 30 years old [1]. In recent years, an emphasis has been placed on miniaturizing the technology to accommodate the study of smaller biological samples, often with a total available volume of only a few microliters. Both liquid chromatography and electrochemistry are largely controlled by surface science. Considering this fact, both technologies benefit from reducing the distance from the bulk of the solution phase to the surface. In LC, this is accomplished by using smaller-diameter stationary-phase particles. In electrochemistry, it is accomplished by using packed-bed or porous electrodes and/or thin-layer cells with greatly restricted diffusion pathways.

For analytical purposes, there is no loss in the concentration detection limit by reducing the total surface area available in both methodologies. In LC, this reduction is accomplished by using smaller-di-



ameter columns, and in EC, by using smaller electrodes. With LC column diameters of 0.1–1.0 mm and radial flow thin-layer cells with dead volumes of a few tens of nanoliters, it is possible to build analytical instruments capable of routine use by neuroscientists, drug metabolism groups, and pharmacokinetics experts. LC–EC has been used for foods, industrial chemicals, and environmental work. Nevertheless, biomedical applications have dominated. It shows no potential for preparative chromatography and is generally used when nanograms or picograms hold some appeal.

Detector Cells

A wide variety of detector cells has been used for LC–EC [1]. The choice can be baffling to a nonexpert. These all “work” to some degree. The key issues are as follows:

1. An electrode (the “working electrode”) exposed to the mobile phase in a dead volume (small) appropriate to the column diameter chosen
2. A place to locate at least one other electrode (a “counter electrode”) or preferentially two (an auxiliary electrode and a reference electrode)
3. The possibility for a choice of different working electrode materials (see the following section)
4. The possibility of multiple channels in series or parallel

Figure 1 is representative of one choice that meets these criteria. Such a cell is normally described as a “thin-layer sandwich configuration.” The working electrode(s) is in the form of an interchangeable block. Electrodes of different sizes, shapes, or materials can be accommodated with a flow pattern established by a gasket shape and thickness. Such cells can easily be adapted for LC flow rates of from 5 to 5000 $\mu\text{L}/\text{min}$. Different designs are used for capillary separation tools such as capillary electrophoresis (CE).

Electrode Materials

The most common electrode material used in LC–EC is carbon, either as solid “glassy carbon” disks in thin-layer cells, or as a high-surface-area porous matrix through which the mobile phase can flow. Gold electrodes are useful to support a mercury film and these are primarily used to determine thiols and disulfides, and also for carbohydrates using pulsed electrochemical detection

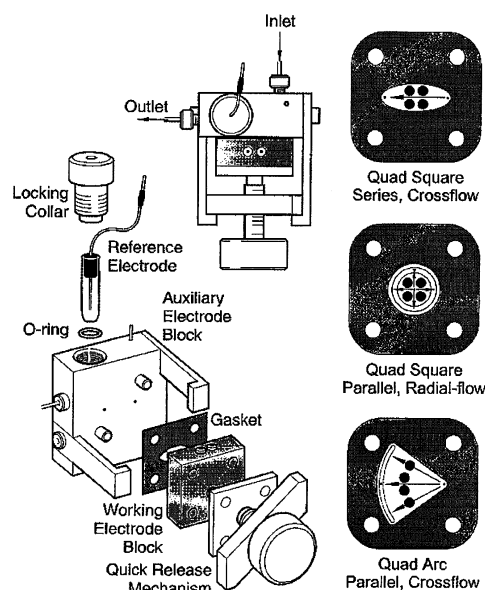


Fig. 1 One example of a sandwich-type thin-layer LC–EC detector with adjustable dead volume, flow pattern, and up to four channels. [Reprinted with permission from *Current Separations* 18: 114 (2000).]

(PED) with high-pH mobile phases. Platinum electrodes are occasionally useful for specific analytes, but they are most frequently employed to determine hydrogen peroxide following an oxidase immobilized enzyme reactor (IMER). More recently, copper electrodes have begun to attract serious interest for the determination of carbohydrates in basic mobile phases. Glassy carbon is the overwhelming favorite choice because of its wide range of applicable potentials and its rugged convenience. Bulk glassy carbon is difficult to use in geometries other than disks and plates. There are a number of other geometries that have practical interest for multiple-electrode detectors. One of the more valuable recent contributions to LC–EC derives from the ability to deposit conducting vitreous carbon films on silicon or quartz substrates using lithography techniques. The lithography technology makes it possible to lay down a variety of electrode geometries, which could not possibly be manufactured in small sizes by traditional machining. Although such electrodes are still at the research stage, they show considerable promise. Detector cells with 2, 4, or even 16 electrodes are commercially available. There are obvious parallels with diode-array detection (DAD). When two electrodes are used in series, there are similarities to fluorescence or mass spectrometry–mass spectrometry (MS–MS) in the way that selectivity is often enhanced.

Pulsed Electrochemical Detection

There are many substances which would appear to be good candidates for LC–EC from a thermodynamic point of view but which do not behave well due to kinetic limitations. Johnson and co-workers at Iowa State University used some fundamental ideas about electrocatalysis to revolutionize the determination of carbohydrates, nearly intractable substances which do not readily lend themselves to ultraviolet absorption (LC–UV), fluorescence (LC–F), or traditional DC amperometry (LC–EC) [2]. At the time that this work began, the LC of carbohydrates was more or less relegated to refractive index detection (LC–RI) of microgram amounts. The importance of polysaccharides and glycoproteins, as well as traditional sugars, has focused a lot of attention on pulsed electrochemical detection (PED) methodology. The detection limits are not competitive with DC amperometry of more easily oxidized substances such as phenols and aromatic amines; however, they are far superior to optical detection approaches.

Postcolumn Reactions

Electrochemical detection is inherently a “chemical” rather than a “physical” technique (such as ultraviolet, infrared, fluorescence, or refractive index). It is, therefore, not surprising to find that many imaginative post-column reactions have been coupled to LC–EC. These include photochemical reactions, enzymatic reactions, halogenation reactions, and Biuret reactions. In each case, the purpose is to enhance selectivity and therefore improve limits of detection. While simplicity is sacrificed with such schemes, there are many published methods that have been quite successful.

Capillary Electrophoresis and Capillary Electrochromatography

Because there is LC–EC, it is only logical that there should be CE–EC and capillary electrochromatography (CEC)–EC. This area was pioneered by Andrew Ewing at the Pennsylvania State University. Richard Zare (Stanford University) and Susan Lunte (Kansas University) have explored this idea in a number of unique ways. The basic technology has been recently reviewed [3]. There are several fundamental problems that do not occur with LC–EC. First, the capillaries must be of small diameter to properly dissipate resistive heating. Thus, the electrodes used in CE–EC are normally carbon fibers or metallic wires placed in or at the capillary end.

Second, the electrical current through the capillary which establishes the electro-osmotic pumping is much larger than the electrolysis current measured in determining analytes of interest. The ionic and electrolytic currents need to be “decoupled” in some way. A third concern is that the flow rate in CE or CEC is not independent of the choice of “mobile phase” or even the sample, whereas in LC, it is easily predetermined and maintained by a volume displacement pump. In spite of these concerns, CE is very attractive because of its high resolution per unit time and the small sample volumes required. In the case of CEEC, the concentration detection limits are frequently superior to optical detectors for suitable analytes. This is because electrochemical detection is a surface (not volume)-dependent technique. In the grand scheme of things, at this writing, CE and CEC are very rarely used instead of LC and, therefore, CE–EC and CEC–EC must be considered academic curiosities until this situation changes.

Conclusions

Electrochemical detection has matured considerably in recent years and is routinely used by many laboratories, often for a very specific biomedical application. The most popular applications include acetylcholine, serotonin, catecholamines, thiols and disulfides, phenols, aromatic amines, macrocyclic antibiotics, ascorbic acid, nitro compounds, hydroxylamines, and carbohydrates. As the last century concluded, it is fair to say that many applications for which LC–EC would be an obvious choice are now pursued with LC–MS–MS. This only became practical in the 1990s and is clearly a more general method applicable to a wider variety of substances. In a similar fashion, LC–MS–MS has also largely supplanted LC–F for new bioanalytical methods. Nevertheless, there remain a number of key applications for these more traditional detectors known for their selectivity (and therefore excellent detection limits).

References

1. P. T. Kissinger and W. R. Heineman (eds.), *Laboratory Techniques in Electroanalytical Chemistry*, 2nd ed., Marcel Dekker, Inc., New York, 1996.
2. W. R. LaCourse, *Pulsed Electrochemical Detection in High-Performance Liquid Chromatography*, John Wiley & Sons, New York, 1997.
3. L. A. Holland and S. M. Lunte, Capillary electrophoresis coupled to electrochemical detection: A review of recent advances, *Anal. Commun.* 35: 1H–4H (1998).



Electrochemical Detection in CE

Oliver Klett

Institute of Chemistry, Uppsala University, Uppsala, Sweden

Introduction

Capillary electrophoresis (CE) is a powerful separation tool which has its primary strength in the high separation efficiency and short analysis times.

Discussion

By decreasing the internal diameter (i.d.) of the capillaries used, the situation can be further improved due to the possibility of using higher separation voltages. Such a miniaturization, however, often involves a challenge regarding how the detection is to be made in the narrow capillaries for sample volumes in the nanoliter to sub-picoliter range. Electrochemical (EC) methods, usually based on the use of microelectrodes, are relatively inexpensive and are readily miniaturized and adapted to such low volumes and capillary sizes without loss of performance. Electrochemical detection is based on the monitoring of changes in an electrical signal due to a chemical system at an electrode surface, usually as a result of an imposed potential or current. The principles, advantages, and drawbacks of currently used EC methods will be discussed briefly below.

In a solution, the equilibrium concentrations of the reduced and oxidized forms of a redox couple are linked to the potential (E) via the Nernst equation

$$E = E^0 + \frac{RT}{nF} \ln \left(\frac{c(\text{ox})}{c(\text{red})} \right) \quad (1)$$

with E^0 the standard potential and $c(\text{ox})$ and $c(\text{red})$ the concentration of the oxidized and reduced forms, respectively; the other symbols have their usual meaning.

In electrochemical detection, the potential of a working electrode can be measured versus a reference electrode, usually while no net current is flowing between the electrodes. This type of detection is referred to as “potentiometry.” Alternatively, a potential is applied to the working electrode with respect to the reference electrode while the generated oxidation or reduction current is measured. This technique is referred to as “amperometry.” When applying a negative po-

tential to the working electrode, the energy of the electrons in the electrode is increased and, eventually, an electron can be transferred to the lowest unoccupied level of a species in the nearby solution. This species is thus reduced; vice versa, species can be oxidized by applying a sufficiently high positive potential. In both cases, the generated current (i) can be expressed by

$$i = -aFDnc\delta_N^{-1} \quad (2)$$

with a being the electrode area, D the diffusion coefficient, δ_N the thickness of diffusion layer; the other symbols have their usual meaning. For each redox couple, there exists a potential, the standard potential E^0 , for which the reduced and oxidized forms are present in equal concentrations. By applying a potential more positive than E^0 , the concentration of the reduced form is forced to decrease at the electrode surface while the concentration of the oxidized form increases. This process is the cause of the current measured in amperometric techniques. By choosing the applied potential, it is also possible to discriminate between different analytes. The range of potentials that can be applied in amperometric detection is, however, generally limited by redox processes involving the solvent [e.g., the oxidative and reductive evolution of oxygen ($2\text{H}_2\text{O} \rightarrow \text{O}_2 + 4\text{H}^+ + 4e^-$) and hydrogen ($\text{H}_2\text{O} + e^- \rightarrow 0.5\text{H}_2 + \text{OH}^-$), respectively, in water]. A wide range of physiologically and pharmacologically important substances, as well as many heavy metals, transition metals, and their complexes, exhibit standard potentials within this accessible potential range. In fact, many metabolic pathways involve redox processes taking place in aqueous systems. Neurotransmitters of the catechol type (*o*-dihydroxy benzene derivatives) were consequently among the first reported analytes for electrochemical detection in CE (CE–EC). Detection limits down to 10^{-9} mol/L can be achieved in this way.

The choice of working electrode material is an important factor in amperometric detection. For catechols and similar substances, such as phenolic acids, electrodes made of glassy carbon have shown good performances. Other good detectable and biological important substances include thiols and disulfides (e.g., cysteine, glutathione, and their disulfides which



are best detected on an Au/Hg amalgam electrode); amino acids and peptides, which can be detected using Cu electrodes, and carbohydrates, glycopeptides, and nucleotides, detected on Au, Cu, or Ni electrodes.

Commonly in amperometric detection, a fiber or disk microelectrode is used where the electrode is positioned in or close to the outlet of the capillary (see Fig. 1). A complication when working with EC in CE is the need for careful alignment of the electrode(s) and capillary outlet. This alignment, which mostly is carried out with micromanipulators under a microscope, is essential to ensure both a good sensitivity and reproducibility and, hence, constitutes the main challenge while adapting EC for routine CE. Another complication in CEEC involves the interference of the high-voltage (HV) separation field on the EC detection. In the first combination of EC and CE, it was assumed that the HV field had to be totally removed from the detection area. This was done by various kinds of decouplers, which unfortunately also introduced additional band broadening and decreased sensitivities. Furthermore, the manufacturing of the decouplers requires considerable labor-intensive experience and skill.

A later approach is based on the utilization of small-inner-diameter (<25 μm) capillaries to reduce the influence of the HV field.

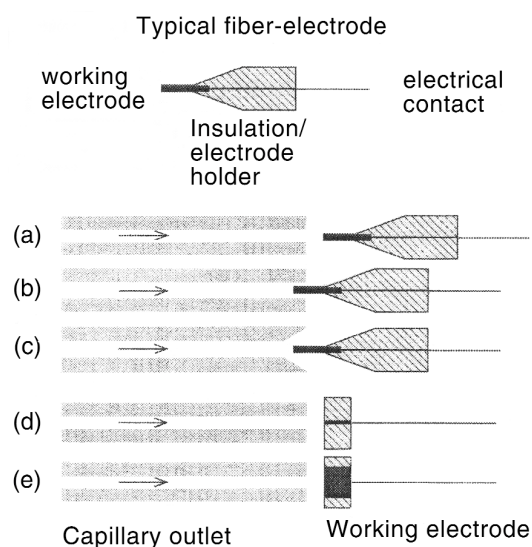


Fig. 1 Electrode setups for CE–EC with fiber microelectrodes: (a) end column, (b) on-column, (c) improved on-column, (d) wall tube, and (e) wall-jet detection.

In potentiometry, all ions present in the solution principally contribute to the potential of the working electrode. As the ratio between the analyte concentration and that of other species in the solution generally is rather low, the analyte contribution to the detector signal is often low, which results in relatively poor detection limits. To circumvent this problem, ion-selective membranes (ISM), which permit only some ions to pass through the membranes, are commonly employed. In this way, detection limits down to 10^{-7} mol/L can be achieved. The ISM also reduces the influence from matrix components, which allows measurements in complex matrices such as blood or serum without interferences. The long-term stability of these electrode may, however, be a problem, as the electrodes might have to be replaced after a few hours or days. Common analytes are inorganic anions and cations, especially alkali and alkaline earth metals ions. A further application is the indirect detection of amino acids, where the complexing of amino acids with Cu^+ ions selectively alters the potential of a copper electrode.

In conductometry, two working electrodes placed either in or at the end of the capillary, along the capillary axis, are commonly employed. A high-frequency AC potential is applied between the working electrodes and the conductance (L) of the solution is continually monitored. In this way, the passing of any zone deviating in its ion composition from the background is detected. As the ion mobilities contribute to the magnitude of the signal as seen in Eq. (3), slowly moving large molecules and low charged biomolecules are less straightforwardly detected, whereas detection limits down to some hundred parts per thousand have been reported for small inorganic and organic ions:

$$L = \frac{FA \sum i |z_i| u_i c_i}{l} \quad (3)$$

with A as the cross-sectional area perpendicular to the AC field, l the electrode distance, and u the mobility. Applications have been described for ions up to a size of sulfate or Cd^+ and MES or benzylamine, respectively.

Suggested Further Reading

The field of electrochemical detection in CE have been extensively reviewed in Refs. 1–3. Instructive applications can be found for amperometry in Ref. 4, for potentiometry in Ref. 5, and for conductometry in Ref. 6.

An example of miniaturized on-chip EC–CE is given in Ref. 7. The theoretical aspects of electrochemical detection have been discussed in detail in Ref. 8.

References

1. P. D. Voegel and R. P. Baldwin, *Electrophoresis*, 18(12–13): 2267–2278 (1997).
2. S. M. Lunte, et al., *Pharmaceut. Res.*, 14(4): 372–387 (1997).
3. T. Kappes and P. C. Hauser, *J. Chromatogr. A* 834(1–2): 89–101 (1999).
4. L. A. Holland and S. M. Lunte, *Anal. Chem.* 71(2): 407 (1999).
5. T. Kappes and P. C. Hauser, *Anal. Chim. Acta* 354: 129–134 (1997).
6. C. Haber, et al., *J. Capillary Electrophoresis* 3(1): 1–11 (1996).
7. A. T. Woolley, K. Lao, A. N. Glazer, and R. A. Mathies, *Anal. Chem.* 70(4): 684 (1998).
8. C. M. A. Brett and A. M. Oliveira Brett, *Electrochemistry*, Oxford University Press, Oxford, 1993.



Electrokinetic Chromatography Including Micellar Electrokinetic Chromatography

Hassan Y. Aboul-Enein

Vince Serignese

Pharmaceutical Analysis Laboratory, King Faisal Specialist Hospital and Research Centre, Riyadh, Saudi Arabia

Introduction

Separation science technology has provided the analyst with numerous methods for quantitative determinations, the more established being high-performance liquid chromatography (HPLC) and gas chromatography (GC). With huge advancements in computer technology, extremely sensitive methods have been made available to the user such as tandem mass spectrometry (MS–MS), liquid chromatography–mass spectrometry (LC–MS), and gas chromatography–mass spectrometry (GC–MS). However, an electrophoretic technique which has been developed through joint efforts from a number of scientific disciplines is rapidly generating interest for its wide applicability and highly sensitive assays. The field of capillary electrophoresis (CE) borrows principles from conventional electrophoresis, liquid chromatography, and gas chromatography. High-performance capillary electrophoresis (HPCE) refers to all techniques that have been developed on the subject. In this article, the electrokinetic chromatographic (EKC) analysis method will be discussed, with emphasis on micellar electrokinetic chromatography (MEKC). Before doing so, some fundamental principles of capillary electrophoresis will be discussed.

Electrophoretic and Electro-osmotic Migration

Capillary zone electrophoresis (CZE) [1] is a basic mode of HPCE and serves as a good starting point for laying the background information on EKC and MEKC. Only ionic or charged compounds are separated, based on their differential electrophoretic mobilities. Figure 1 illustrates the setup for a CE system. In summary, electrolyte buffer solutions and electrodes are present at both ends of the open-tube fused-silica capillary. A positive high-voltage power supply is the source of current. A sample is injected hydrostatically or electrokinetically at the positive end of the capillary (capillary head) and, in the presence of an applied voltage potential, moves toward the negative electrode, where it is detected by an ultraviolet (UV) absorbance

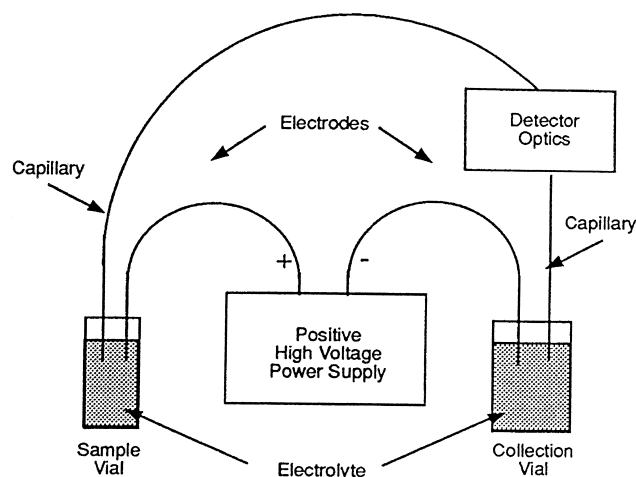


Fig. 1 Diagram of a CE system. [Reprinted from Waters Quanta 4000E Capillary Electrophoresis System Operator's Manual, Waters Corp., 1993.]

instrument. The signal produced is recorded as a chromatogram where sample components are identified as chromatographic peaks according to their retention times, and peak areas or heights are calculated for quantitative purposes.

During analyte migration, electrophoresis and electro-osmosis are taking place. The velocity (v_s , cm/s) and mobility (μ_s , cm²/V s) of the solute are defined by the following equations:

$$v_s = v_{eo} + v_{ep} \quad (1)$$

$$\mu_s = \mu_{eo} + \mu_{ep} \quad (2)$$

where v_{eo} and μ_{eo} are electro-osmotic velocity and mobility, respectively, and v_{ep} and μ_{ep} are electrophoretic velocity and mobility, respectively. The relationship between velocity and mobility is given by

$$v = \mu E \quad (3)$$

where E (V/cm) is the electric field strength. Because E is constant for all solutes in a separation analysis, the solute velocities are differentiated by their mobilities.

Electrophoresis is an electrokinetic phenomenon whereby charged compounds in an electric field move through a continuous medium and separate by prefer-



entially obtaining different electrophoretic mobilities according to their charges and sizes. Cations move toward the negative electrode (cathode) and anions move toward the positive electrode (anode).

Electro-osmosis is created by the electric double-layer effect [2]. A fused-silica capillary at neutral pH attains fixed negative charges at the inner wall surface as its silanol groups undergo ionization. A layer of hydrated cations will form adjacent to the inner wall to counter the fixed negative charges. An applied voltage potential will cause the positively charged layer to migrate toward the cathode with a flat velocity profile, simultaneously dragging the bulk solution inside the capillary and transporting charged compounds at the electro-osmotic flow velocity. It is assumed that v_{eo} is faster than v_{ep} and determines the direction of solute migration. Hence, a cation will have its sum total [Eq. (1)] greater than the individual component velocities ($v_s > v_{eo}$) and the anion will migrate slower than the electro-osmotic flow ($v_s < v_{eo}$).

Electro-osmosis need not be present in open-tube CE. Coatings exist that can be applied to the capillary surface to eliminate the electrical double layer. However, electro-osmotic flow can be used to reduce solute retention times, which can be advantageous for certain analyses.

As previously mentioned, electrophoretic separations using open-tube capillaries are based on solute differential mobility, which is a function of charge and molecular size. A different approach is required for separating neutral or uncharged compounds. Because charge is absent, electrophoretic mobility is zero. Electro-osmotic flow would allow them to migrate, but their velocities would be equal. Separation would not be possible with the above method.

Electrokinetic Chromatography

Terabe [3] developed a method that separates neutral or uncharged compounds; he named it electrokinetic chromatography. The experimental design is that of capillary zone electrophoresis (Fig. 1). The difference lies in the separation principle. In liquid chromatography, a solute freely distributes itself between two phases [i.e., a mobile phase usually made of a mixture of aqueous and organic solvents and a stationary phase (a solid material packed in a steel housing known as a chromatographic column)]. Under high pressure, the mobile phase is delivered by a liquid chromatographic pump and continuously solvates the stationary phase, thereby transporting nonvolatile compounds of interest that are introduced into the sys-

tem via chromatographic injection. Separation is based on their phase-distribution profiles. EKC follows the above principle but uses electro-osmosis and electrophoresis to displace analytes and "chromatographic phases" in capillaries.

The electrolyte buffer solution is analogous to the mobile phase. A charged substance, referred to as the carrier, is dissolved in the electrolyte buffer. The neutral solute present in the separation medium will partition itself between the carrier (incorporated form) and the surrounding solution (free form). The carrier ("chromatographic phase") corresponds to the stationary phase in conventional chromatography with modifications, in that it is not a fixed support and exists homogeneously in solution. For this reason, the carrier is called the "pseudo-stationary phase." As discussed in the previous section, the charged carrier will transport the incorporated solute electrophoretically (here, v_{ep} is the carrier velocity) at a slower velocity than the free solute migrating with the electro-osmotic flow velocity (v_{eo}) in the opposite direction. The point to keep in mind is that the carrier migrates with a different velocity than the bulk solution. The variation of the ratio of the amount of incorporated solute to the amount of total solute between separands in a sample mixture will lead to sample component separation.

Micelles in Electrokinetic Chromatography

Different types of EKC have been developed. Cyclodextrins (CDEKC) have been used to form inclusion complexes with solutes to effect their separation. Other examples of EKC include microemulsion electrokinetic chromatography (MEEKC). The MEKC technique (for a detailed treatise, the reader is referred to Ref. 4) utilizes the presence of micelles in the electrolyte buffer solution to influence the migration time of solutes. In this case, the separation carrier is the micelle [5].

Surfactants produce micelles. Their amphiphilic nature classifies them as detergents, surface-active agents that are composed of a hydrophilic group and a hydrophobic hydrocarbon chain. In addition to what is known as the critical micelle concentration (CMC), individual surfactant molecules (monomers) interact with each other to form aggregates or micelles, establishing a state of equilibrium between a constant monomer concentration and a rapidly increasing micelle concentration.

As shown in Fig. 2a, micelles are depicted as "roundlike" structures with their polar moieties exte-

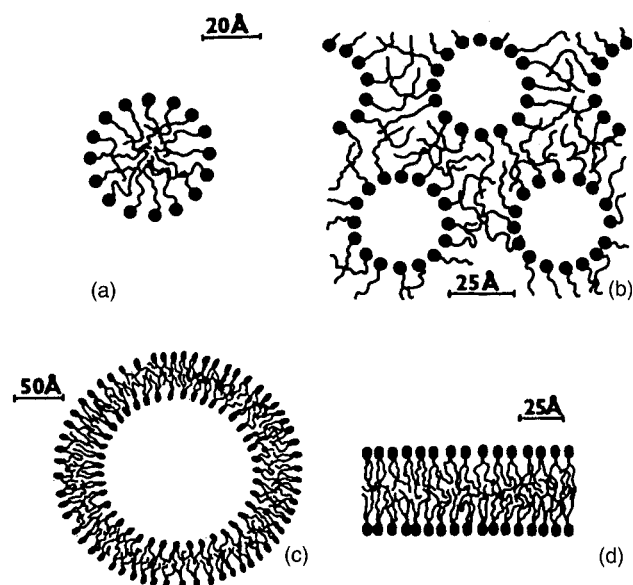


Fig. 2 Examples of aggregate structures of surfactants in solution: (a) micelle; (b) inverted micelles; (c) bilayer vesicle; (d) bilayer. (From Ref. 7.)

riorly located in the vicinity of the aqueous medium and their hydrophobic tails oriented inward forming a cavity. The sizes and shapes of the structures formed when monomer units aggregate is affected by electrolyte concentration, pH, temperature, and hydrocarbon chain length. During aggregation, interactions occur not only between the aggregates but also among the monomer units within the aggregate structure. Monomer unit distribution (the number of surfactant molecules in an aggregate) is characteristic of the surfactant used. Figure 2 displays several forms of aggregates that exist in solution and Table 1 gives examples of surfactants.

Basically, MEKC is an EKC application with the micelle as the designated carrier. A surfactant at a concentration above the CMC is added to the running buffer and initiates micelle formation. Because the separation principle has already been dealt with and the flow scheme in Fig. 3 is an illustrative summary notated for MEKC, it is clear that a neutral analyte residing in the hydrophobic interior of a micelle (depicted as a sphere in Fig. 3) will be transported with the micelle's velocity (v_{mc}). The free analyte will migrate with the electro-osmotic flow velocity (v_{eo}).

The chromatographic aspect (solute partitioning) of the separation [6] can be explained in terms of a commonly used parameter in chromatography, the retention or capacity factor (k'). We begin with the following equation:

$$k' = \frac{n_{mc}}{n_{aq}} \quad (4)$$

where n_{mc} and n_{aq} are the mole amounts of the analyte in the micellar and aqueous phases, respectively. The corresponding mole fractions are given by

$$\frac{n_{mc}}{n_{mc} + n_{aq}} \quad \text{and} \quad \frac{n_{aq}}{n_{mc} + n_{aq}}$$

where $n_{mc} + n_{aq}$ is the total amount of analyte present in the electrolyte buffer. The relationship in Eq. (4) and appropriate substitutions transform the above ratios into $k'/(1 + k')$ for the micelle analyte mole fraction and $1/(1 + k')$ for the aqueous analyte mole fraction. The total analyte velocity (v_s) takes the form

$$v_s = \frac{1}{1 + k'} v_{eo} + \frac{k'}{1 + k'} v_{mc} \quad (5)$$

where $[1/(1 + k')]v_{eo}$ represents the velocity of the analyte mole fraction in the aqueous phase and

Table 1 Some Common Surface-Active Agents

Anionic	
Sodium stearate	$\text{CH}_3(\text{CH}_2)_{16}\text{COO}^-\text{Na}^+$
Sodium oleate	$\text{CH}_3(\text{CH}_2)_7\text{CH}=\text{CH}(\text{CH}_2)_7\text{COO}^-\text{Na}^+$
Sodium dodecyl sulfate	$\text{CH}_3(\text{CH}_2)_{11}\text{SO}_4^-\text{Na}^+$
Sodium dodecyl benzene sulfonate	$\text{CH}_3(\text{CH}_2)_{11} \cdot \text{C}_6\text{H}_4 \cdot \text{SO}_3^-\text{Na}^+$
Cationic	
Laurylamine hydrochloride	$\text{CH}_3(\text{CH}_2)_{11}\text{NH}_3^+\text{Cl}^-$
Cetyltrimethylammonium bromide	$\text{CH}_3(\text{CH}_2)_{15}\text{N}(\text{CH}_3)_3^+\text{Br}^-$
Nonionic	
Polyethylene oxides	$\text{CH}_3(\text{CH}_2)_7 \cdot \text{C}_6\text{H}_4 \cdot (\text{O} \cdot \text{CH}_2 \cdot \text{CH}_2)_8\text{OH}$

Source: Ref. 9.



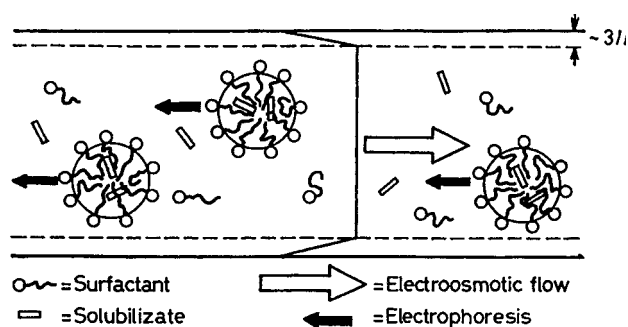


Fig. 3 Schematics of the separation principle of MEKC. (From Ref. 6.)

$[k'/(1 + k')]v_{mc}$ is the velocity of the analyte mole fraction in the micellar phase.

Because velocity is a function of length (the capillary length from the point of injection to the detector cell) over time ($v = l/t$), we can substitute and rearrange the terms in Eq. (5) to obtain a relationship between the migration time (t_R) of the analyte and k' :

$$t_R = \frac{1 + k'}{1 + (t_0/t_{mc})k'} t_0 \quad (6)$$

$$k' = \frac{t_R - t_0}{(1 - t_R/t_{mc})t_0} \left[\left(\frac{1 - t_R}{t_{mc}} \right) t_0 \right]^{-1} \quad (7)$$

Figure 4a is a snapshot of the capillary tube following a sample injection at its positive end (inj.). The micelle, neutral solute, and aqueous solution (water) migrate toward the negative electrode (det.), establishing zones depicted by vertical bands, as they separate inside the capillary. The corresponding chromatogram in Fig. 4b shows the migration order where the t_R value for a neutral analyte is range bound between the migration times of the

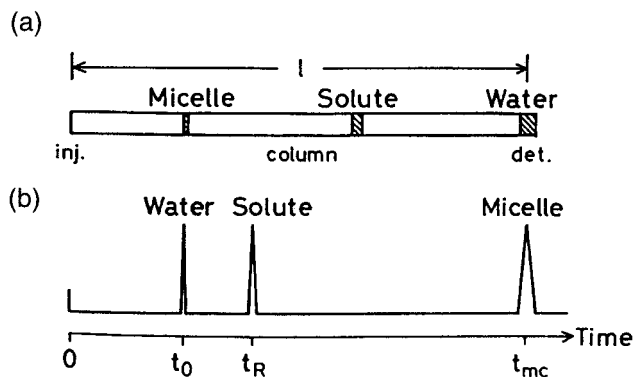


Fig. 4 (a) Representation of zone migration inside the capillary tube and (b) the corresponding chromatogram. (From Ref. 8.)

micelle (t_{mc}) and water (t_0). This limitation is reflected in the denominator of Eq. (6). When t_{mc} approaches infinity, the micelle is assumed to be stationary. The ratio t_0/t_{mc} will become zero and Eq. (6) turns into

$$t_R = 1 + k' \quad (8)$$

In this case, a neutral solute completely solubilized within the micelle will have a t_R value approaching infinity as its k' value does the same. Solute elution is assumed not to occur. Similarly, the free neutral analyte is unretained and its k' is equal to zero. Therefore, the t_R value will be equal to t_0 [Eq. (8)]. This explains why the neutral solute can migrate no slower than the micelle (t_{mc}) and no faster than the aqueous solution (t_0).

Although the above discussion focuses on neutral analyte separation, MEKC can be applied to ionic species which have their own electrophoretic mobilities and a broader migration time range.

Conclusion

The purpose of this article was to provide the reader with a basic understanding of capillary electrophoresis and to describe how a technique such as MEKC uses basic principles of chromatography to perform separations which are not possible electrophoretically. As the applications for electrokinetic chromatography rapidly expand, the future direction will develop on two fronts:

1. The development of novel separation carriers that will broaden the species range of separable analytes. EKC is suitable for separating small molecules, considering the size of the cavities of the established carriers.
2. The scope for further partition mechanisms, as new separation carriers are discovered, is promising. The separation principle is basic chromatography and with research efforts introducing new carriers in the pipeline, modified versions of the separation mechanism are possible.

Its rapid analysis time, low sample and solvent volume requirements, high resolution, and selectivity will continue to attract researchers who are involved in separation analysis.

References

1. B. J. Radola (ed.), *Capillary Zone Electrophoresis*, VCH, Weinheim, 1993.
2. B. L. Karger and F. Foret, Capillary electrophoresis: Introduction and assessment, in *Capillary Electrophoresis*

- Technology* (N. A. Guzman, ed.), Marcel Dekker, Inc., New York, 1993, pp. 3–64.
3. S. Terabe, *Trends Anal. Chem.* 8: 129 (1989).
 4. P. Muijselaar, Micellar electrokinetic chromatography: Fundamentals and applications, Ph.D. thesis, Eindhoven University of Technology, Eindhoven, The Netherlands, 1996.
 5. F. Foret, L. Kivánková, and P. Boek, Principles of capillary electrophoretic techniques: Micellar electrokinetic chromatography, in *Capillary Zone Electrophoresis* (B. J. Radola, ed.), VCH, Weinheim, 1993, pp. 67–74.
 6. S. Terabe, Micellar electrokinetic chromatography, in *Capillary Electrophoresis Technology* (N. A. Guzman, ed.), Marcel Dekker, Inc., New York, 1993, pp. 65–87.
 7. J. N. Israelchvili, in *Physics of Amphiphiles: Micelles, Vesicles and Microemulsions* (V. Degiorgio and M. Corti, eds.), Proceedings of the International School of Physics “Enrico Fermi,” CourseXC, North-Holland, Amsterdam, 1985, pp. 24–37.
 8. S. Terabe, K. Otsuka, and T. Ando, *Anal. Chem.* 57: 834 (1985).
 9. D. J. Shaw, *Introduction to Colloid and Surface Chemistry*, Butterworths, London, 1966, pp. 57–72.



Electron-Capture Detector

Raymond P.W. Scott

Scientific Detectors Ltd., Banbury, Oxfordshire, England

Introduction

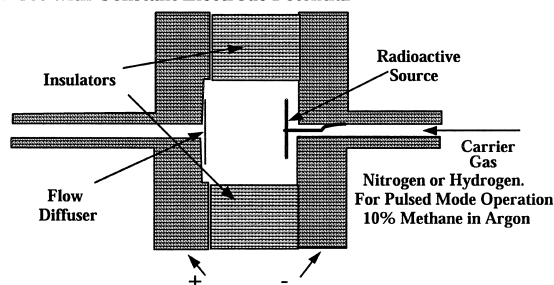
The electron-capture detector (ECD) is probably the most sensitive GC detector presently available. However, like most high-sensitivity detectors, it is also very specific and will only sense those substances that are electron capturing (e.g., *halogenated* substances, particularly fluorinated materials).

Discussion

The ECD detector was invented by Lovelock [1] and functions on an entirely different principle from that of the argon detector. A low-energy β -ray source is used in the sensor to produce electrons and ions. The first source to be used was tritium absorbed onto a silver foil, but, due to its relative instability at high temperatures, this was replaced by the far more thermally stable ^{63}Ni source. The detector can be made to function in two ways: either a constant potential is applied across the sensor electrodes (the DC mode) or a pulsed potential is used (the pulsed mode).

A diagram of the ECD is shown in Fig. 1. In the DC mode, a constant electrode potential (a few volts) is employed that is just sufficient to collect all the electrons that are produced and provide a small standing current. If an electron-capturing molecule (e.g., a molecule containing a halogen atom which has only seven electrons in its outer shell) enters the sensor, the electrons are captured by the molecules and the molecules become charged. The mobility of the captured electrons are much reduced compared with the free electrons and, furthermore, are more likely to be neutralized by collision with any positive ions that are also generated. As a consequence, the electrode current falls dramatically. In the pulsed mode of operation, which is usually the preferred mode, a mixture of methane in argon is usually em-

ECD for Use with Constant Electrode Potential



ECD for Use with Pulsed Electrode Potential

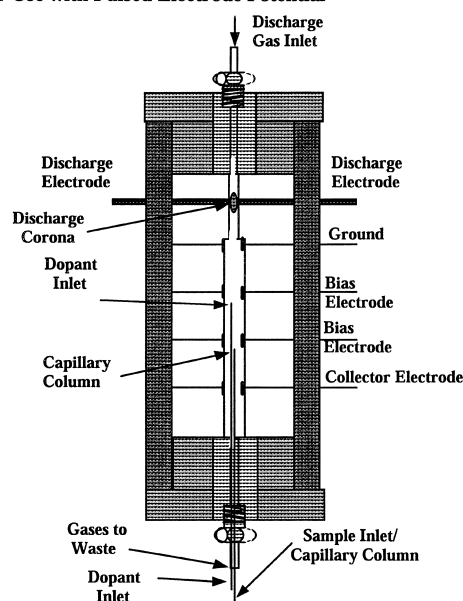


Fig. 1 The two types of electron capture detector. (Courtesy of Valco Instruments Company, Inc.)

ployed as the carrier gas. Pure argon cannot be used very effectively as the carrier gas, as the diffusion rate of electrons in argon is 10 times less than that in a 10% methane–90% argon mixture. The period of



the pulsed potential is adjusted such that relatively few of the slow negatively charged molecules reach the anode, but the faster moving electrons are all collected. During the “off-period,” the electrons reestablish equilibrium with the gas. In general use, the pulse width is set at about $1\ \mu\text{s}$ and the frequency of the pulses at about 1 kHz. This allows about 1 ms for the sensor to reestablish equilibrium in the cell before the next electron collection occurs. The peak potential of each pulse is usually about 30 V but will depend on the geometry of the sensor and the strength of the radioactive source. The average current resulting from the electrons collected at each pulse is about $1 \times 10^{-8}\ \text{A}$ and usually has an associated noise level of about $5 \times 10^{-12}\ \text{A}$. Both the standing current and the noise will also vary with the strength of the radioactive source that is used.

The sensor consists of a small chamber, 1 or 2 mL in volume, with metal ends separated by a suitable insulator. The metal ends act both as electrodes and as fluid conduits for the carrier gas to enter and leave the cell. The cell contains the radioactive source, electrically connected to the conduit through which the carrier gas enters and to the negative side of the power supply. A gauze “diffuser” is connected to the exit of the cell and to the positive side of the power supply. In the pulsed mode, the sensor operates with oxygen-free nitrogen or argon–methane mixtures. The active source is ^{63}Ni , which is stable up to 450°C . The sensor is thermostatted in a separate oven which can be operated at temperatures ranging from 100°C to 350°C . The column is connected to the sensor at the base and makeup gas can be introduced into the base of the detector. If open tubular columns are employed, the columns are operated with hydrogen or helium as the carrier gas. The electron-capture detector is extremely sensitive (i.e., minimum detectable concentration $\sim 1 \times 10^{-13}\ \text{g/mL}$) and is widely used in trace analysis of halogenated compounds—in particular, pesticides.

In the DC mode, the linear dynamic range is relatively small, perhaps two orders of magnitude, with the response index lying between 0.97 and 1.03. The pulsed mode has a much wider linear dynamic range and values up to five orders of magnitude have been reported. The linear dynamic range will also depend on the strength of the radioactive source and the detector geometry. The values reported will also rest on how the linearity is measured and defined. If a response index lying between 0.98 and 1.02 is assumed, then a linear dynamic range of at least three orders of magnitude should be obtainable from most pulsed-mode electron-capture detectors.

Pulsed-Discharge Electron-Capture Detector

The pulsed-discharge electron-capture detector is a variant of the pulsed ECD detector, a diagram of which is shown in the lower part of Fig. 1. The detector functions in exactly the same way as that of the traditional electron-capture detector but differs in the method of electron production. The sensor consists of two sections: the upper section, where the discharge takes place, has a small diameter and the lower section where the column eluent is sensed and the electron capturing occurs, has a wider diameter. The potential across the discharge electrodes is pulsed at about 3 kHz with a discharge pulse width of about $45\ \mu\text{s}$ for optimum performance. The discharge produces electrons and high-energy photons (which can also produce electrons) and some metastable helium atoms. The helium doped with propane enters just below the second electrode, metastable atoms are removed, and electrons are generated both by the decay of the metastable atoms and by the photons. The electrons are collected by appropriate potentials applied to each electrode in the section between the third and fourth electrode and, finally, collected at the fourth electrode. The collector electrode potential (the potential between the third and fourth electrodes) is pulsed at about 3 kHz with a pulse width of about $23\ \mu\text{s}$ and a pulse height of 30 V.

The device functions in the same way as the conventional electron-capture detector with a radioactive source. The column eluent enters just below the third electrode, any electron-capturing substance present removes some of the free electrons, and the current collected by the fourth electrode falls. The sensitivity claimed for the detector is 0.2–1.0 ng, but this is not very informative as its significance depends on the characteristics of the column used and on the k' of the solute peak on which the measurements were made. The sensitivity should be given as that solute *concentration* that produces a signal equivalent to twice the noise. Such data allow a rational comparison between detectors. The sensitivity or minimum detectable concentration of this detector is probably similar to the conventional pulsed ECD (viz. $1 \times 10^{-13}\ \text{g/mL}$). The linear dynamic range appears to be at least three orders of magnitude for a response index of r , where $0.97 < r < 1.03$, but this is



an estimate from the published data. The modified form of the electron-capture detector, devoid of a radioactive source, is obviously an attractive alternative to the conventional device and appears to have similar, if not better, performance characteristics.

The high sensitivity of the electron-capture detector makes it very popular for use in forensic and environmental chemistry. It is very simple to use and is one of the less expensive, high-sensitivity selective detectors available.

Reference

1. J. E. Lovelock and S. R. Lipsky, *J. Am. Chem. Soc.* 82: 431 (1960).

Suggested Further Reading

- R. P. W. Scott, *Chromatographic Detectors*, Marcel Dekker, Inc., New York, 1996.
R. P. W. Scott, *Introduction to Gas Chromatography*, Marcel Dekker, Inc., New York, 1998.



Electrospray Ionization Interface for CE-MS

Joanne Severs

Bayer Pharmaceuticals, Berkeley, California, U.S.A.

Introduction

The development of the electrospray ionization (ESI) source for mass spectrometry provided an ideal means of detection for capillary electrophoretic (CE) separations. The ESI source is currently the preferred interface for CE-MS, due to the fact that it can produce ions directly from liquids at atmospheric pressure and with high sensitivity and selectivity for a wide range of analytes.

Discussion

Electrospray ionization is initiated by generating a high potential difference between the spray capillary tip and a counterelectrode [1]. This electric field leads to the production of micron-sized droplets with an uneven charge distribution, generally accepted to be due to an electrophoretic mechanism acting on electrolytes in the solvent [2]. This mechanism, combined with a shrinkage of the droplets due to solvent evaporation (aided by heat and an applied gas flow into the source), leads to electrostatic repulsion overcoming surface tension in the droplet. The “Rayleigh” limit is reached, a “Taylor cone” is formed, and smaller highly charged droplets are emitted, eventually leading to the production of gas-phase ions [1–3]. These ions are accelerated through a skimmer into successive vacuum stages of the mass analyzer. The ESI source has been demonstrated to act as an electrolytic cell, generating electrochemical oxidation and reduction [2]. The exact ionization mechanism will vary with experimental conditions and is still an area of continuing in-depth research and discussion [3].

Electrospray ionization is classified as a “soft” ionization technique. It produces molecular-weight information and very little, if any, fragmentation of the analyte ion, unless induced in the vacuum region of the mass analyzer. The number of charges accumulated by an analyte ion is proportional to its number of basic or acidic sites. The spray polarity and conditions, solution pH and nature, as well as solute concentration will all effect the charge state distribution observed in the mass spectrum. Multiple charging of an analyte ion en-

courages the release of very high-molecular-weight ions. It is mainly due to this fact that ESI has gained such enormous interest, especially among biochemists. Employing only small, relatively inexpensive mass analyzers, spectrometrists are able to obtain high-sensitivity information on analytes with molecular weights of up to 200 kDa. The multiple-charging phenomenon means that the mass-to-charge (m/z) range of the analyzer does not generally need to exceed 3000. A deconvolution algorithm [4], generally built nowadays into the instrument software, can be applied to the series of multiply-charged, molecular-ion peaks, and a single peak, representing the molecular weight, is then displayed on a “true mass” scale. The m/z scale is calibrated with standards of known exact mass. Whereas ESI-MS (mass spectrometry) has made the largest impact on large biomolecule analysis, CE-ESI-MS has also been applied with great success to the analysis of many small-molecule applications.

The development of the first CE-MS was prompted by the early reports on electrospray ionization (ESI-MS) by Fenn and co-workers in the mid-1980s [1], when it was recognized that CE would provide an optimal flow rate of polar and ionic species to the ESI source. In this initial CE-MS report, a metal coating on the tip of the CE capillary made contact with a metal sheath capillary to which the ESI voltage was applied [5]. In this way, the sheath capillary acted as both the CE cathode, closing the CE electrical circuit, and the ESI source (emitter). Ideally, the interface between CE and MS should maintain separation efficiency and resolution, be sensitive, precise, linear in response, maintain electrical continuity across the separation capillary so as to define the CE field gradient, be able to cope with all eluents presented by the CE separation step, and be able to provide efficient ionization from low flow rates for mass analysis.

Several research groups have presented work on the development of CE-ESI-MS interfaces. The interfaces developed can be categorized into three main groups: coaxial sheath flow, liquid junction, and sheathless interfaces. A schematic of the sheath-flow interface first developed for CE-ESI-MS by Smith et al. [6] is illustrated in Fig. 1a. A sheath liquid, with



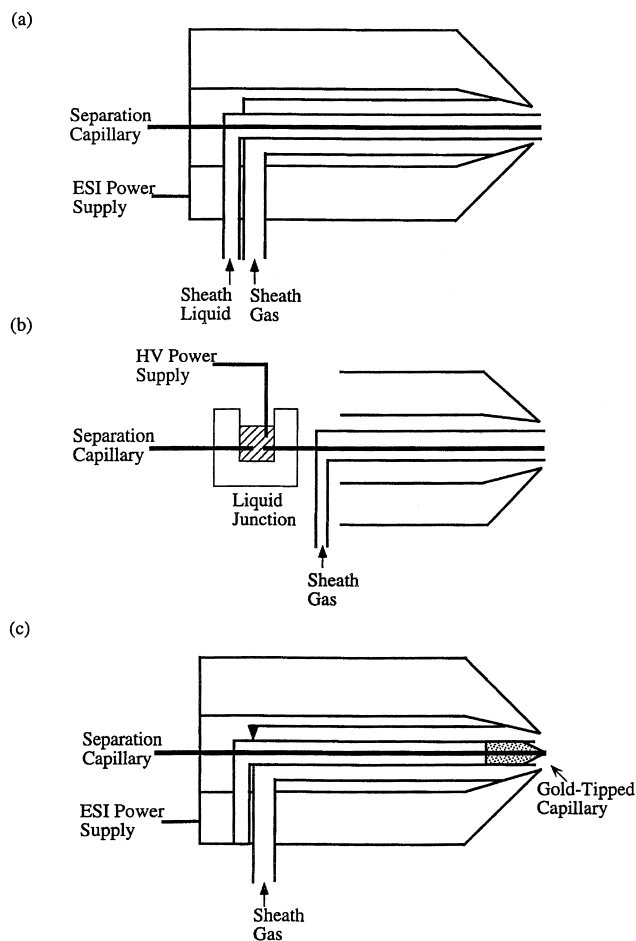


Fig. 1 Schematic illustration of CE-MS interfaces to an ESI source: (a) a coaxial sheath-flow interface; (b) a liquid-junction interface; (c) a sheathless interface.

an electrolytic content, is infused into the ESI source at a constant rate, through the coaxial sheath capillary which surrounds the end of the separation capillary and terminates near the end of the separation capillary. This sheath liquid mixes with the separation buffer as it elutes from the tip of the CE capillary, thus providing the necessary electrical contact between the ESI needle and the CE buffer, and closing the CE circuit. Because the CE terminus and ESI source are at the same voltage, if the ESI source requires a high voltage (2–5 kV) (rather than ground potential), then the ESI voltage chosen also directly affects the potential difference across the separation capillary. To date, the sheath-liquid interface has been the most widely used and accepted system, being the simplest to construct, with numerous results published employing sheath liquids typically containing 60–80% organic solvent, modified with 1–3% acid in water and typically intro-

duced at flow rates of 1–4 $\mu\text{L}/\text{min}$. The composition of the sheath liquid should be optimized for the specific systems under investigation. Recent reports have confirmed that the relative dimensions and positioning of the separation and sheath capillaries also influence sensitivity and stability.

Although the additional flow of an organic-containing electrolyte into the ESI source moderately extends the range of CE buffer systems that can be used, the CE buffer composition still has a dramatic effect on the ESI signal, minimizing the buffer choice for best sensitivity to volatile solutions. Reports have also highlighted the need for a considered selection of sheath-liquid composition due to the possibility of formation of moving ionic boundaries inside the capillary [7]. The possibility of these effects occurring should be considered and minimized when transferring a CE method from an alternative detection system to MS. It should be noted, however, that these effects are minimized or eliminated when there is a sufficiently strong flow toward the CE terminus.

A “liquid-junction interface” has also been suggested and applied for CE-ESI-MS [8]. Electrical contact with this interface is established through the liquid reservoir which surrounds the junction of the separation capillary and a transfer capillary, as shown in Fig. 1b. The gap between the two capillaries is approximately 10–20 μm , allowing sufficient makeup liquid from the reservoir to be drawn into the transfer capillary while avoiding analyte loss. The flow of makeup liquid into the transfer capillary is induced by a combination of gravity and the Venturi effect of the nebulizing gas at the capillary tip [8].

In comparisons of coaxial sheath-flow and liquid-junction interfaces, it has been noted that although both provide efficient coupling, the former is generally easier to operate. One of the major disadvantages in employing the liquid-junction interface is in establishing a reproducible connection inside the tee piece. Also, the use of a transfer capillary, which has no potential difference applied across it, can lead to peak broadening. Advantages of this interface, however, include the possibility of combining different outer-diameter capillaries through the junction and the extra mixing time provided for the makeup liquid and CE eluant.

The problem with both interfaces described so far is that they depend on the addition of excess electrolyte to the ESI source to maintain the circuit, generally leading to a decrease in analyte sensitivity. As previously mentioned, the first CE-MS interface reported made electrical connection between the separation buffer and the ESI needle via a metal coating on the tip

of the CE capillary [5], as represented in Fig. 1c. Although femtomole detection limits and separation efficiencies of up to half a million theoretical plates were achieved, problems included a high dependence on the buffer system used and the need to regularly replace the metal coating on the capillary tip.

The further development of interfaces which do not rely on an additional liquid flow are currently underway. Generally, they have employed metal deposition on the CE terminus that is tapered (by chemical etching or mechanical pulling) to provide an increased electric field at the capillary tip. These so-called "microspray" and "nanospray" approaches, with more effective ionization mechanisms, have been adopted recently by several groups for interfacing infusion systems, LC and CE to ESI-MS, and in all cases, significant gains in sensitivity and sample usage have been observed [9]. Attomole level detection limits from nanoliter sample volumes can now be attained, and the ability to form an electrospray from a purely aqueous solution is now possible. Alternative sheathless interfaces have also been briefly investigated [10]. Stability problems still need consideration in most cases. An interface which does not use an additional makeup flow can, as well as aiding sensitivity, also avoid such problems as charge state distribution shifts in the mass spectrum. In addition, the ability to electrospray purely aqueous systems is often advantageous for looking at fragile biological and noncovalently bound analytes. In some cases, however, a makeup liquid may be found necessary. For example, for certain separations, the EOF may need to be minimized or eliminated in the CE capillary, and thus flow rates into the source will not be sufficiently high as to maintain a stable electrospray. If a capillary needs to be coated to avoid analyte interaction with the capillary wall, then a cationic coating, which reverses the EOF rather than eliminating it, should preferably be chosen if a sheathless system is to be employed. Also, it may be found that a makeup liquid is necessary to increase the volatility of a specific CE electrolyte system.

Another disadvantage at present in using the sheathless interface is the time dispensed in preparing the tapered, coated tips. Although the coatings now employed are more stable than those initially used, the tips do not regularly survive more than a day or two of use. This can, however, be due to the tip "plugging" rather than the metal coating deteriorating. Filtering of electrolyte and analytes and rinsing of the capillary can, therefore, often prolong the capillary lifetime.

An instrumental attribute which aids the development and interfacing of CE to ESI-MS is the ability to pressurize the CE capillary, at low pressure for sample

injection and higher pressures for capillary content elution. Balancing of the heights of the capillary termini is also an important consideration in order to avoid syphoning effects. In all cases of CE-ESI-MS application, safety, with respect to the electrical circuits, should be considered. It should be verified that all circuits have a common ground, and the addition of a resistor in the ESI power supply line when interfaced to CE is a wise precaution.

An incompatibility that does need to be considered in CE-MS method development is the use of certain CE buffer systems and additives which are detrimental to the ESI process. For example, although sample concentration can be increased by the use of more conductive buffers, this approach is not advantageous for ESI-MS detection. These characteristics result in a significant demand upon ESI interface efficiency [11]. Ideally, the chosen CE buffer should be volatile, such as ammonium acetate or formate. The use of pure acids or bases rather than a true buffer has also been shown to be advantageous for certain molecules. Nonaqueous buffer systems are also being employed more widely.

Capillary electrokinetic chromatography (CEKC) with ESI-MS requires either the use of additives that do not significantly impact the ESI process or a method for their removal prior to the electrospray. Although this problem has not yet been completely solved, recent reports have suggested that considered choices of surfactant type and reduction of electroosmotic flow (EOF) and surfactant in the capillary can decrease problems. Because most analytes that benefit from the CEKC mode of operation can be effectively addressed by the interface of other separations methods with MS, more emphasis has until now been placed upon interfacing with other CE modes. For "small-molecule" CE analysis, in which micellar and inclusion complex systems are commonly used, atmospheric pressure chemical ionization (APCI) may provide a useful alternative to ESI, as it is not as greatly affected by involatile salts and additives.

The efficiency of the ESI detection process for CE-MS can be considered in terms of the simple model of Kebarle and Tang [3] and has been discussed in great detail by Smith and co-workers [11]. These considerations indicate that analyte sensitivity in CE-ESI-MS may be increased by reducing the mass flow rate of the background components. This decrease in background flow rates can be experimentally accomplished by decreasing the electric field or employing smaller-diameter capillaries, and this predicted increase in analyte sensitivity is now well supported by experimental studies [11].



To reduce the elution speed of the analyte ions into the source, the electrophoretic voltage can be decreased just prior to elution of the first analyte of interest, minimizing the experimental analysis time while allowing more scans to be recorded without a significant loss in ion intensity [11]. Alternatively, the use of smaller-diameter capillaries than conventionally used for CE also increases sensitivity [11]. A capillary diameter should, ideally, be commercially available, amenable to alternative detection methods, provide the necessary detector sensitivity, and be free from clogging. Capillary internal diameters of between 20 and 40 μm have been shown to be optimal and are compatible with "microspray" techniques.

The further development of microscale preconcentration and cleanup techniques and the resulting improvements in CE-MS concentration detection limits are likely to expand the use of this analytical technique. The more common use of small-diameter capillaries and even tiny etched microplate devices [10], along with the improvements in ESI spray techniques are pushing research along. Further investigations into improving interface design, durability, reproducibility and sensitivity are still necessary. The availability of improved, less expensive, and smaller mass spectrometers will almost certainly lead to increased use of CE-MS. However, the sensitivity and selectivity already demonstrated by CE-MS systems, in combina-

tion with the minute analyte volumes sampled, already make this a highly powerful technique.

References

1. C. M. Whitehouse, R. N. Dreyer, M. Yamashita, and J. B. Fenn, *Anal. Chem.* 57: 675-679 (1985).
2. P. Kebarle and L. Tang, *Anal. Chem.* 65: 972A (1993).
3. M. G. Ikonomou, A. T. Blades, and P. Kebarle, *Anal. Chem.* 63: 1989-1998 (1991).
4. M. Mann, C. K. Meng, and J. B. Fenn, *Anal. Chem.* 61: 1702-1708 (1989).
5. J. A. Olivares, N. T. Nguyen, C. R. Yonker, and R. D. Smith, *Anal. Chem.* 59: 1230-1232 (1987).
6. R. D. Smith, J. A. Olivares, N. T. Nguyen, and H. R. Udseth, *Anal. Chem.* 60: 436-441 (1988).
7. F. Foret, T. J. Thompson, P. Vouros, B. L. Karger, P. Gebauer, and P. Bocek, *Anal. Chem.* 66: 4450-4458 (1994).
8. E. D. Lee, W. Mück, J. D. Henion, and T. R. Covey, *Bio-med. Environ. Mass Spectrom.* 18: 844-850 (1989).
9. S. K. Chowdhury and B. T. Chait, *Anal. Chem.* 63: 1660-1664 (1991); M. Wilm and M. Mann, *Anal. Chem.* 68: 1-8 (1996).
10. D. Figeys and R. Aebersold, *Electrophoresis* 19: 885-892 (1998) and references therein.
11. J. H. Wahl, D. R. Goodlett, H. R. Udseth, and R. D. Smith, *Electrophoresis* 14: 448-457 (1993); J. P. Landers, Capillary electrophoresis-mass spectrometry, in *Handbook of Capillary Electrophoresis*, CRC Press, Boca Raton, FL, 1997, and references therein.



Eluotropic Series of Solvents for Thin-Layer Chromatography

Simion Gocan

"Babeş-Bolyai" University, Cluj-Napoca, Romania

INTRODUCTION

The easiest way to vary the relative adsorption of the sample (and its R_f value, migration rate, respectively) is to change the solvent: strong (polar) eluents decrease adsorption, and weak (no polar) eluents increase it. When benzene, for instance, is used as solvent on silica gels or alumina layers, the ethers and esters are found on top of the chromatogram (with high R_f values), ketones and aldehydes are approximately in the center (medium R_f values), and the alcohols are below them (low R_f values), whereas the acids remain at the starting point ($R_f=0$). Thus the separation sequence follows the polarities of the compounds.

The dielectric constant may be taken as an indication of solvent polarity, but the interfacial tension between solvents and polar adsorbents, approximated by the interfacial tension between the solvent and water, has been suggested as a fundamental basis for correlating solvent strength.

The physical factors that determine solvent strength in a given adsorption system have long been understood in general terms. Solvent strength can be interpreted in terms of the following basic contributions: 1) interactions between solvent molecules and a sample molecule in solution; 2) interactions between solvent molecules and a sample molecule in the adsorbed phase; and 3) interactions between an adsorbed solvent molecule and the adsorbent.

ELUOTROPIC SERIES

Normal-Phase Thin-Layer Chromatography (NPTLC)

A series of authors has defined the solvent relative strength for polar adsorbents in the form of eluotropic series, grouping them in order of their chromatographic elution strength, with both pure solvents and mixtures of solvents included. The most familiar of these is, of course, the one set up by Trappe,^[1] and variations of this have been published from time to time. Trappe gave the

following series (listed in order of increasing elution power): light petroleum, cyclohexane, carbon tetrachloride, trichloroethylene, toluene, benzene, dichloromethane, chloroform, ether, ethyl acetate, acetone, *n*-propanol, ethanol, and methanol.

The eluotropic series of pure solvents is generally referred to a particular adsorbent. The magnitude of ϵ° , the solvent strength parameter, can be defined as the adsorption energy of the solvent per unit of the standard activity surface. All these ϵ° values are relative to the solvent pentane, for which ϵ° is defined equal to zero. This parameter is defined as a measure of the degree of the adsorption interaction of the solvent with the stationary phase. As a function of this magnitude, the eluotropic series for various polar adsorbents is presented in Table 1.

It is well recognized that the eluotropic series of solvents, according to Snyder, is suited for monoactive site-type adsorbents, but in the case of multiactive site-type adsorbents (e.g., alumina), their imperfection becomes acute. Thus for multiactive-site-type adsorbents, the eluotropic series sequence and eluent strength values are highly dependent on the class of test solutes employed.^[7]

A practical eluotropic series of solvents, based on the expended solubility parameter concept, was reported.^[8] This series was defined based on partial specific solubility parameter (δ_s) that is equal to the sum of Keeson (δ_o) and acid-base ($2\delta_a\delta_b$), which represents the contribution to interaction forces introduced to characterize the solute, the mobile, and the stationary phase in liquid-solid chromatography. Exactly the same two interaction forces define ϵ° and, consequently, there should exist a direct relation between ϵ° and $\delta_s^2 = \delta_o^2 + 2\delta_a\delta_b$. Unfortunately, the general correlation for all the solvents on alumina is poor ($r^2=0.75$).

Snyder^[2] has shown that there is a correlation between the ϵ° values for a certain polar adsorbent (i.e., silica gel, Florisil, magnesia, and alumina). These values can be estimated from values for alumina using the following equations:

$$\epsilon_{\text{silica gel}}^\circ = 0.77\epsilon_{\text{alumina}}^\circ$$

$$\epsilon_{\text{Florisil}}^\circ = 0.52\epsilon_{\text{alumina}}^\circ$$

Table 1 Relative strengths of different solvents on various adsorbents: eluotropic series

Solvent	ϵ^0				P'_i [3,4]	S_i [5]
	Al_2O_3 [2]	Silica gel [2]	Florisil [2]	MgO [2]		
<i>n</i> -Pentane	0.00	0.00	0.00	0.00	0.1 (–) ^a	
<i>n</i> -Hexane	0.01				–0.14	
Cyclohexane	0.04				0.2 (VIa)	
Carbon tetrachloride	0.18	0.11	0.04	0.10	1.6 (–) ^a	
					1.56	
<i>m,p</i> -Xylene	0.25				2.7 (VII)	
Amyl chloride	0.26					
<i>o</i> -Xylene	0.27					
Isopropyl ether	0.28				2.4 (I)	
Isopropyl chloride	0.29					
Toluene	0.29				2.4 (VII)	
Benzene	0.32	0.25	0.17	0.22	2.7 (VII)	
					3.19	
Ethyl ether	0.38	0.38	0.30	0.21	2.8 (I)	
					3.15	
Chloroform	0.40	0.26	0.19	0.26	4.1 (VIII) ^b	
					4.31	
Methylene chloride	0.42	0.32	0.23	0.26	3.1 (V)	
Methyl isobutyl ketone	0.43					
1,2-Dichloroethane	0.43				3.1 (V)	
					4.29	
Acetone	0.56	0.47			5.1 (VIa)	3.4
					5.10	
Ethyl acetate	0.58	0.38			4.4 (VIa)	
					4.24	
Methyl acetate	0.60			0.28		
Amyl alcohol	0.61					
Dioxane	0.63	0.49			4.8 (VIa)	3.5
					5.27	
Pyridine	0.71				5.3 (III)	
Butyl-cellosolve ($\text{C}_4\text{H}_9\text{-O-C}_2\text{H}_4\text{OH}$)	0.74					
Acetonitrile	0.79	0.50			5.8 (VIb)	3.4
					5.64	
Tetrahydrofuran					4.0 (III)	4.4
					4.28	
Isopropanol	0.82				3.9 (II)	4.2
					3.92	
Methanol	0.95				5.1 (II)	2.9
					5.10	
Ethanol					4.3 (II)	3.6
Acetic acid					6.0 (IV)	
					6.13	
Water					10.2 (VIII)	0.0
					10.2	

I–VIII represent groups from Snyder's classification.

^aSelectivity group irrelevant because of low P' values.

^bClose to group and VIII.



and

$$\varepsilon_{\text{magnesia}}^{\circ} = 0.58\varepsilon_{\text{alumina}}^{\circ}$$

The values calculated by means of these equations show the standard deviation of ε° values ± 0.004 units with respect to the experimental values.

The relationships between eluent strength and composition for binary (one to two) and ternary (one to three) solvents have been derived:^[2]

$$\varepsilon_1 - \varepsilon_2 = \varepsilon_1 + \frac{\log[X_2 10^{\alpha n_2 (\varepsilon_2 - \varepsilon_1)} + 1 - X_2]}{\alpha n_2} \quad (1)$$

$$\varepsilon_1 \rightarrow \varepsilon_3 = \varepsilon_2 - \frac{\log[X_3 10^{\alpha n_3 (\varepsilon_3 - \varepsilon_2)} + X_2]}{\alpha n_3} \quad (2)$$

Eluent strength is assumed to increase in the order $\varepsilon_1 < \varepsilon_2 < \varepsilon_3$ for solvents A, B, and C; n_2 and n_3 are the effective molecular areas of adsorbed solvent molecules B and C, respectively (with the exception of certain very strong solvents); X_2 and X_3 are the mole fractions of B and C in the solvent mixtures; and α represents the adsorbent's surface activity. To use Eqs. 1 and 2, we must know the activity degree of the adsorbent. Consequently, the α (adsorbent surface activity function) values for a few adsorbents with respect to water content are presented in Table 2. Based on the data in Tables 1 and 2, and by using Eq. 1, an infinite number of such series can be established.

The principle of the variation of solvent composition while holding solvent strength constant was first developed by Neher^[9] for separation of steroids. Figure 1 is a representation of the eluotropic series of Neher for application in this fashion. Six solvents, which will act as solvent S_1 (100% concentration, on the left), are arranged vertically, whereas the same solvents, acting as solvent S_2 (100% concentration, on the right of the

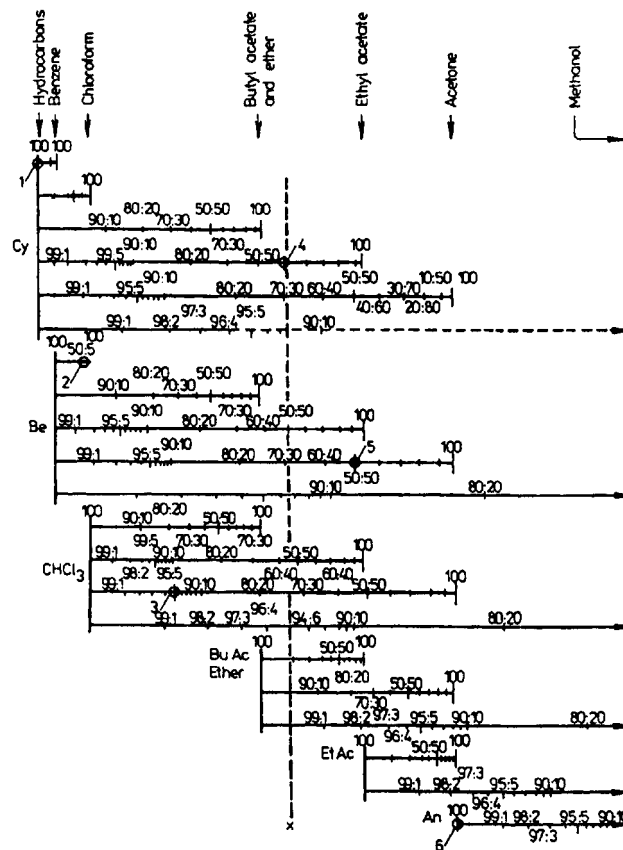


Fig. 1 Eluotropic series of Neher. Cy=cyclohexane; Be=benzene; BuAc=butyl acetate; EtAc=ethyl acetate; An=acetone.

horizontal lines) in a binary solvent eluotropic series, are arranged horizontally. We can obtain a very large number of binary systems, of the same or different strength, by means of this nomogram. The dashed line X determines 12 compositions of binary systems of the same average eluotropic properties. These systems are called equieluotropic systems. The nomogram in Fig. 1 corresponds to adsorption on silica gel.

Saunders^[10] obtained another nomogram by using six very common solvents. With the help of the nomogram presented in Fig. 2, we can achieve binary solvent mixtures of certain strength in the interval 0.0–0.75. In this graph, ε° is plotted across the top and in various binary solvent compositions in each of the horizontal lines below it. Each line corresponds to the range 0–100% by volume of binary solvent composition. Its manner of use is similar to that described for Neher's nomogram.

For NPTLC, the solvent strength weighting factor S_i is the same as the polarity index P' given in Table 1. The polarity index P' is given by the sum of the logarithms of the polar distribution constants for ethanol, dioxane, and nitromethane, and the selectivity parameters x_i is given as the ratio of polar distribution constant for solute I to the

Table 2 α values for some common chromatographic adsorbents

H_2O^a (%)	Silica gel (wide pore)			
	Alumina	TLC	Florasil	Magnesia
0	1.00	0.83	1.61	1.00
0.5	0.90	0.79	1.18	1.00
1.0	0.84	0.75	1.00	1.00
2.0	0.75	0.71	0.90	0.98
4.0	0.63	0.70	0.81	0.93
7.0	0.59	0.69	0.79	0.86
10.0	0.59	0.69		
15.0	0.59			

Source: Ref. [6].

^aWater added to activated adsorbent.



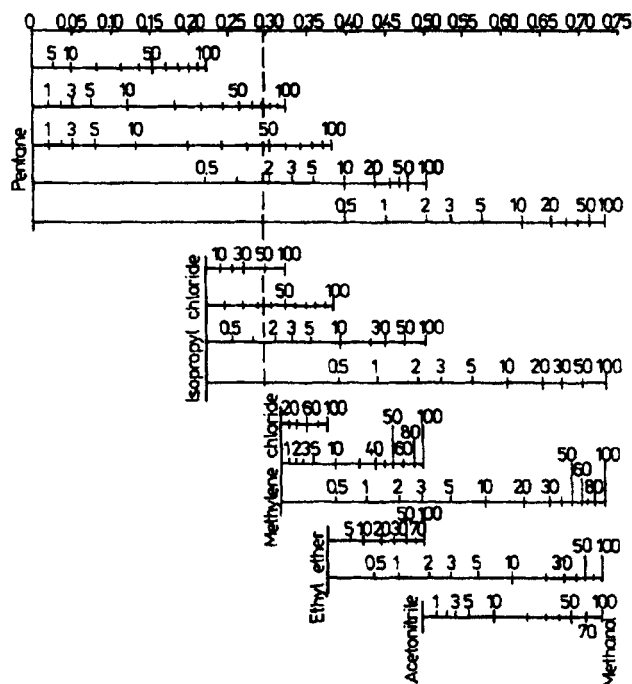


Fig. 2 Mixed solvent strengths on silica gel after Saunders. (From Ref. [10].)

total solvent polarity (P'). The sum of the three values for x_i will be normalized up to 1.0. Snyder was able to show that the many solvents available could be grouped into eight classes with distinctly different selectivities. Solvents within the same selectivity group exhibit similar separation properties (Table 1).^[3] The polarity index P' of a mixed mobile phase is the arithmetic average of the solvent polarity index weighting factor adjusted according to the volume fraction of each solvent as is given by:^[11]

$$P' = \sum_i P'_i \phi_i \quad (3)$$

where P'_i is the polarity index weighting factor of solvent i (Table 1) and ϕ_i is the volume fraction of solvent i . For a binary solvent mixture containing 95% dichloromethane and 5% methanol, the polarity index of the mixed solvent is calculated as follows:

$$P' = (4.29)(0.95) + (5.10)(0.05) = 4.33$$

Reversed-Phase Thin-Layer Chromatography (RPTLC)

A general characteristic of RTLPC systems is that the stationary phase is nonpolar vs. the mobile phase that is polar. Thus a decrease in polarity of the mobile phase leads to a decrease in retention. This situation is the reverse of the general trends observed in NPTLC. A

decrease in polarity of the mobile phase can be realized by increasing the volume fraction of organic solvent in an aqueous organic mobile phase. The most common method for varying the chromatographic selectivity for neutral molecules is to change the type of organic modifier in the mobile phase. Eq. 4 can often be used as an acceptable approximation for the variation of the retention with the volume fraction of organic solvent in the mobile phase:^[11]

$$\log k = \log k_w - S\phi \quad (4)$$

where k is the solute capacity factor, k_w is the solute capacity factor with pure water as the mobile phase, ϕ is the volume fraction of organic solvent, and S is a solute-dependent factor related to the solvent strength of the organic solvent.

The literature data suggest that RPTLC solvent strength varies as water (weakest) < methanol < acetonitrile < ethanol < tetrahydrofuran < propanol < (methylene chloride) (strongest). Thus solvent strength increases as solvent polarity decreases.

The eluotropic scale is a relative one; it is necessary to choose a reference. To obtain a positive value for solvent eluotropic strength, the reference solvent has to be water. The S values determined from the slope of Eq. 4 can be used as descriptor, in a semiquantitative way, of the solvent strength (S_i) of the organic solvent.^[11] Some typical S_i values for common solvents are presented in Table 1. The solvent strength of a mixed mobile phase (S_T) is the arithmetic average of the solvent strength weighting factors adjusted according to the volume fraction ϕ of each solvent (Eq. 5):

$$S_T = \sum_i S_i \phi_i \quad (5)$$

where S_i is the solvent strength weighting factor of solvent i and ϕ_i is the volume fraction of solvent i . If we want to change solvent selectivity to adjust resolution, then the volume fraction of the new solvent required to obtain an isoeluotropic mixture could be calculated from Eq. 5. For example, for methanol–water (60:40), $S_T = 1.56$; using acetonitrile as an example and the same value of $S_T = 1.56$, we obtain $1.56 = 3.2\phi_a + 0\phi_w = 0.49$. Thus a mixture of acetonitrile–water (49:51) is similar in solvent strength to a mixture of methanol–water (60:40). In a similar manner, it is possible to calculate several eluotropic eluents.

TLC APPLICATIONS

In adsorption TLC, there exists a competition between the sample and eluent molecules for a place on the adsorbent surface. If we assume that one molecule of sample (X) replaces m solvent molecules (S) on adsorption, we may represent the adsorption process as:





In this case, Snyder^[12] found an important relationship for adsorption chromatography:

$$\log K^o = \log V_a + \alpha(S^o - A_s \varepsilon^o) \quad (7)$$

where the sample adsorption distribution coefficient K^o [mL/g] is defined as being equal to the ratio of sample concentrations in adsorbent and unadsorbed phases; V_a is adsorbent surface volume [mL]; S^o is dimensionless free energy of adsorption of a sample compound on adsorbent of standard activity ($\alpha=0$) from pentane as solvent; and A_s is molecular area of adsorbed sample. For adsorbents of the same type, Eq. 7 expresses K^o as a function of some fundamental properties of the sample (S^o , A_s), adsorbent (V_a , α), and solvent (ε^o). The parameter ε^o defines the effect of the solvent on the adsorption of a given sample; therefore it may be equated with solvent strength. The larger is the solvent strength parameter ε^o , the smaller is the value of K^o for a given sample and adsorbent. Eq. 7 predicts that sample separation order can vary with solvent for sample components of different sizes (A_s). Let K^o and ε^o for solvent 1 be K_1 and ε_1 , and K_2 and ε_2 for solvent 2. Thus from Eq. 4, the ratio of K values for a sample component adsorbent from two solvents is given as:

$$\log(K_1/K_2) = \alpha A_s(\varepsilon_2 - \varepsilon_1) \quad (8)$$

According to Eq. 8, the change in K on changing the solvent is predicted to be proportional to the difference in eluent strengths ($\varepsilon_2 - \varepsilon_1$) and to the sample molecule size A_s .

For the TLC or other bed, there were analogous relationships derived:^[12]

$$R'_M = \log(V_a W/V^o) + \alpha(S^o - A_s \varepsilon^o) \quad (9)$$

where $R'_M = \log [(1/\xi R_f) - 1]$, W is total weight of adsorbent in the bed, V^o is bed void volume equal to the volume of solvent in a solvent wet bed, and $(R_f)_{true} = \xi(R_f)_{exp}$. Eq. 9 can be written for a given sample and adsorbent, for solvents 1 and 2, respectively. Then, subtracting the second equation from the first gives:

$$(R'_M)_1 - (R'_M)_2 = \alpha A_s(\varepsilon_2 - \varepsilon_1) \quad (10)$$

Eq. 10 can be useful in estimating the effect on sample R_f values of a change in solvent strength.

Eqs. 7 and 9 are a generally reliable relationship for adsorption systems with weak or moderately strong solvents. But, in their derivation, two major approximations were made:^[12] 1) interactions between solvent and sample molecules are assumed unimportant; and 2) interactions between the adsorbent and various adsorbed molecules are assumed to be fundamentally similar

in type. Both of these assumptions can be defended in the case of weak solvent systems, but they are poor approximations for strong solvents. These equations are concerned only with the primary effect of the solvent on sample adsorption. However, in the case of the majority of adsorption systems based on weak or moderately strong solvents, these approximate relationships are adequate for most purposes. For the strongest solvent systems (e.g., alcohols, acids, water, and their solutions), these equations can be corrected for secondary solvent effect by addition of a correction term Δ_{eas} :

$$R'_M = \log(V_a W/V^o) + \alpha(S^o - A_s \varepsilon^o) + \Delta_{eas} \quad (11)$$

where Δ_{eas} represents the secondary adsorption effect and is a complex function of solvent elution strength, adsorbent activity, solute structure, and various possible interactions between the solute adsorbent, and solvent and adsorbent. These aspects are largely discussed in Ref. [2]. If $(\Delta_{eas})_1$ and $(\Delta_{eas})_2$ refer to the secondary solvent effects for a particular sample and solvents 1 and 2, respectively, then we can write:

$$(R'_M)_1 - (R'_M)_2 = \alpha A_s(\varepsilon_2 - \varepsilon_1) + (\Delta_{eas})_1 - (\Delta_{eas})_2 \quad (12)$$

Eq. 12 gives the difference in $\Delta R'_M$ values for a particular sample (A_s) in two solvents 1 and 2, with ε_1 and ε_2 , respectively, as a function of adsorbent activity α , and the secondary solvent terms for the particular solvent contribution. The largest Δ_{eas} values were found for samples with free hydroxyl groups, and between these samples, two free hydroxyl groups in the sample molecule give a larger value of Δ_{eas} than does a single free hydroxyl. Sample molecules with intramolecularly bonded hydroxyl groups give much smaller values of Δ_{eas} , but limited hydrogen bonding of these groups with basic solvents is still possible. For the same sample molecule, the Δ_{eas} value will be a function of the eluent composition.

Now let us write Eq. 11 for a particular eluent and sample molecules 1 and 2, respectively:

$$(R'_M)_1 - (R'_M)_2 = \alpha(S_1^o - S_2^o) + \alpha\varepsilon(A_{s2} - A_{s1}) + (\Delta_{eas})_1 - (\Delta_{eas})_2 \quad (13)$$

In this equation, we find the different source and the selectivity between the two solutes, which can differ by the difference in energy of adsorption ($S_1^o - S_2^o$), molecular size ($A_{s2} - A_{s1}$), and secondary adsorption effect ($(\Delta_{eas})_1 - (\Delta_{eas})_2$). These considerations are valuable for a large number of compounds, but in the case of some isomers, the second terms of Eq. 13 can be considered practically equal to zero and only difference sources for selectivity remain in the difference in energy of adsorption

and the secondary adsorption effect. The secondary adsorption effect plays a major role in the separation of the isomers. For instance, in adsorption on silica gel with benzene–pyridine (90:10, vol/vol) as eluent, the following Δ_{eas} values: -0.90 ± 0.17 and $+0.05 \pm 0.11$ for *m*-hydroxybenzaldehyde and *o*-hydroxybenzaldehyde, respectively, were obtained. These sample molecules can be very easily separated.

Adsorption TLC selection of the mobile phase is conditioned by sample and stationary-phase polarities. The following polarity scale is valid for various compound classes in NPTLC in decreasing order of *K* values: carboxylic acids>amides>amines>alcohols>aldehydes>ketones>esters>nitro compounds>ethers>halogenated compounds>aromatics>olefins>saturated hydrocarbons>fluorocarbons. For example, retention on silica gel is controlled by the number and functional groups present in the sample and their spatial locations. Proton donor/acceptor functional groups show the greatest retention, followed by dipolar molecules, and, finally, nonpolar groups.

The activity degree is another important characteristic for adsorbents. As is well known, the adsorbent is in contact with large amounts of water in the thin-layer preparation process water that has to be removed by drying at 100–120°C for approximately 30–60 min. This process is known as activation. The activity of the layer is directly correlated with the water content of the adsorbent. The silanol groups show a great affinity for water, which is bound by hydrogen bonds. Thus the activity degree can be controlled by the content of physisorbed water onto the adsorbent. Lower *R_f* values will be obtained on the adsorbent with a high degree of activity.

Generally speaking, the first problem with which the analyst is confronted concerns gathering information regarding the mixture to be separated, in terms of mixture polarity and the range of molecular masses. For example, if the mixtures that have to be separated are nonpolar, then we can select an active stationary phase and nonpolar mobile phase from the following scheme:

Sample to be separated:	nonpolar → medium polar → polar
Stationary phase:	active → medium active → inactive
Mobile phase:	nonpolar → medium polar → polar

Several mobile-phase optimization strategies in TLC are based on the use of isoeluotropic solvents (i.e., solvent mixtures of identical strengths but different selectivities). Selecting mobile phase will be achieved based on the eluotropic series (Figs. 1 and 2). These considerations are

very general. The selection and optimization of one system of eluent is a more complex problem and must be discussed for each particular system. For example, the separation of 13 phenylurea and *s*-triazine herbicides was performed by overpressured layer chromatography (OPLC) with a binary mobile phase.^[12] The optimization of the mobile-phase composition for the separation of these herbicides on silica gel was achieved by means of the “ELUO” method in which solvents are selected from an eluotropic series based on solvent power. The method is complementary to the “PRISMA” method for optimizing the compositions of binary, ternary, and quaternary mobile phase for OPLC and TLC.^[13] The phenylurea herbicides could be separated with hexane–ethyl acetate (1:1, vol/vol), ethyl ether–benzene (9:1, vol/vol), or chloroform–ethyl acetate, and triazine herbicides could be separated with hexane–ethyl acetate (13: 7, vol/vol), ethyl ether–benzene (9:1, vol/vol), or chloroform–ethyl acetate (3: 1, vol/vol). The simultaneous separation of the herbicide classes could not be achieved and compounds that were chemically closely related were not well separated.

To maximize the differences in selectivity, solvents must be selected from different selectivity groups that are situated close to the Snyder’s triangle apexes. For example, for NPTLC, a suitable selection could be solvents from several groups of Snyder’s classifications (I, VII, and VIII), mixed with hexane to control solvent strength.^[3]

REFERENCES

1. Trappe, W. *Biochem. Z.* **1940**, 305, 150.
2. Snyder, L.R. *Principles of Adsorption Chromatography*; Marcel Dekker: New York, 1968.
3. Snyder, L.R. *J. Chromatogr. Sci.* **1978**, 16, 223–234.
4. Poole, C.V.; Poole, S.K. *Chromatography Today*; Elsevier: Amsterdam, 1991.
5. Snyder, L.R.; Dolan, J.W.; Gant, J.R. *J. Chromatogr.* **1979**, 165, 3–9.
6. Gocan, S. The Mobile Phase in Thin-Layer Chromatography. In *Modern Thin-Layer Chromatography*; Grinberg, N., Ed.; Marcel Dekker: New York, 1990; 139. Chap. 3.
7. Kovalsca, T.; Klama, B. *JPC, J. Planar Chromatogr.* **1997**, 10, 353–357.
8. Buchmann, M.L.; Kesselring, U.K. *Pharm. Acta Helv.* **1981**, 56, 166–273.
9. Neher, R. *Thin Layer Chromatography*; Marini-Bettolo, G.B., Ed.; Elsevier: Amsterdam, 1964; 75–86.
10. Saunders, D.L. *Anal. Chem.* **1974**, 46, 470–473.
11. Poole, C.F.; Poole, S.K. *Chromatography Today*; Elsevier: Amsterdam, 1991.
12. Tekei, J. *JPC, J. Planar Chromatogr.* **1990**, 3, 326–330.
13. Nyiredy, S.Z.; Meier, B.; Erdelmeier, C.A.J.; Sticher, O. *HRC CC* **1985**, 8, 186–188.



Elution Chromatography

John C. Ford

Indiana University of Pennsylvania, Indiana, Pennsylvania, U.S.A.

Introduction

Elution chromatography is the one of the three basic modes of chromatographic operation, the other two being frontal analysis and displacement chromatography. All three modes were known to Tswett in the early 1900s, although a systematic definition was not made until 1943. Elution chromatography is, by far, the most common chromatographic mode and is virtually the only mode used for analytical separations. Most theoretical work has been directed at the elution mode, although, frequently, the results are applicable to other modes as well.

Discussion

Elution chromatography is characterized by the introduction of a discrete volume of sample into the chromatographic column that has been previously equilibrated with the mobile phase. Typically, the volume of the sample is small compared to the volume of the column. The individual components of the sample (the solutes) move through the column at different average velocities, each less than the velocity of the mobile phase. The differences in velocities are caused by differences in the interactions of the solutes with the stationary and mobile phases. Assuming essentially equivalent interactions with the mobile phase, solutes which interact strongly with the stationary phase spend less time on the average in the mobile phase and, consequently, have a lower average velocity than components which interact weakly with the stationary phase. If the difference in the average velocities of two solutes is sufficiently large, the dispersive transport within the column is sufficiently small, and the column is sufficiently long, the solute bands will be resolved from one another by the time they exit the column.

Elution chromatography can be performed with a constant mobile-phase composition (isocratic elution) or with a mobile-phase composition that changes during the elution process (gradient elution). The following discussion focuses on isocratic operation (see the entry Gradient Elution, Overview for further information on gradient operation).

Further, each of the mechanistic categories of chromatography can be performed in the elution mode and additional information on elution chromatography can be obtained by reference to the appropriate entries of this encyclopedia.

Elution chromatography is categorized as being linear or nonlinear, depending on the distribution isotherm, and as being ideal or nonideal, with ideal behavior requiring both infinite mass-transfer kinetics and negligible axial dispersion. Although truly linear distribution isotherms are rare, at low solute concentrations or over small ranges of solute concentration, sufficient linearity may exist to approximate linear elution. Linear, ideal elution would result in band profiles that are identical to the injection profiles — an unrealistic situation. Under linear, nonideal elution conditions, thermodynamic factors control band retention and kinetic factors such as mass-transfer resistances control the band shape.

Figure 1 shows the effect of isotherm nonlinearity on band shape. Figure 1a corresponds to linear elution; the band shape is independent of the solute concentration because the isotherm is linear. In Fig. 1b, increasing amounts of solute result in a diffuse rear edge and a sharp leading edge (i.e., tailing). The peak maximum moves forward with increasing sample load. If the isotherm were curved in the other direction, the leading edge would be diffuse and the rear edge sharp (fronting) and the peak maximum would move back with increasing sample load. However, isotherm nonlinearity is not the only cause of asymmetric peak shape.

The retention of a solute in elution chromatography is usually expressed as the retention factor, k (capacity factor or k'), given by $k = (t_R - t_M)/t_M$, where t_R is the retention time of the solute and t_M is the holdup time (void time or t_0). The holdup time is the time required to elute a component that is not retained at all by the stationary phase. [See the entry Dead Point (Volume or Time).] One can relate k to the distribution coefficient, K , by $k = K\beta$, where β is the phase ratio, the ratio of the stationary-phase volume to the mobile-phase volume. Rearranging the definition of retention factor, we find that $t_R = t_M(1 + k) = t_M(1 + K\beta)$. Be-



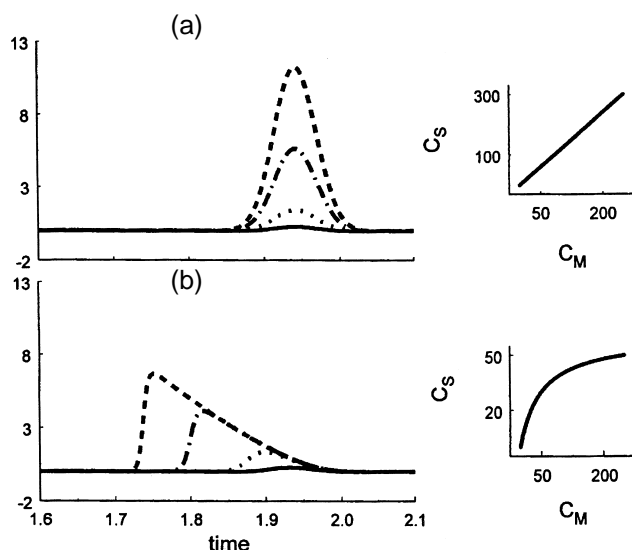


Fig. 1 Effect of distribution isotherm curvature on peak shape in elution chromatography. (a) A linear isotherm resulting in linear elution; the band shape is independent of the solute concentration; (b) a nonlinear isotherm results in asymmetric peaks when increasing amounts of solute are injected. In the example shown, the isotherm results in a diffuse rear edge and a sharp leading edge (i.e., tailing). If the isotherm were curved in the other direction, the leading edge would be diffuse and the rear edge sharp (fronting).

cause it is usually reasonable to assume that t_M and β are the same for different solutes, the retention time differences are due to distribution coefficient differences. Under the appropriate conditions, the distribution coefficient can be related to the thermodynamic distribution constant, and the elution chromatographic measurements can be used for physicochemical determinations of thermodynamic parameters.

Differences in solute retention are usually expressed as the separation factor (selectivity coefficient or α), given by $\alpha = k_b/k_a$, where k_a and k_b are the retention factors of the two solutes in question. By convention, k_b is the more retained solute and $\alpha > 1$, although this is not always followed. Again, because it is reasonable to assume that β is the same for different solutes, $\alpha = K_b/K_a$, where K_a and K_b are the distribution coefficients of the two solutes, and, again, retention time differences are due to distribution coefficient differences. If two solutes have the same distribution coefficient (i.e., $\alpha = 1$) in a particular combination of mobile and stationary phases, they cannot be separated by elution chromatography in that system. However, $\alpha \neq 1$ is a necessary, but not sufficient, condition for a successful separation.

As a solute moves through the column, it undergoes dispersive transport as well as separative transport. Under typical elution chromatographic conditions, the dispersive transport is caused by axial diffusion and mass-transfer considerations, such as slow adsorption–desorption kinetics. This dispersive transport results in band spreading (see the entry Band Spreading, Mechanism), which can prevent adequate separation of different solutes. The plate number (plate count, number of theoretical plates, theoretical plate number, or N), defined as $N = t_R^2/\sigma_t^2$, where σ_t^2 is the variance of the band in time units, is a measure of the column efficiency (i.e., the ratio of separative to dispersive transport). Several alternate forms of this equation are commonly used, usually based on the assumption of a Gaussian peak shape. The effective plate number, N_{eff} , is a combination of the plate number and the capacity factor [i.e., $N_{\text{eff}} = N[k/(1 + k)]^2$] and is generally more useful than N for comparing the resolving power of different columns. Another common measure of column efficiency is the plate height (HETP, height equivalent to a theoretical plate, or H), defined by $H = L/N$, where L is the length of the column, usually in centimeters. This is frequently presented as the reduced plate height h , the ratio of the plate height to the diameter of the packing material. A “good” column has a high plate count (a low plate height, $2 < h < 5$). Further discussion can be found in the Further Readings section.

Efficiency in High-Performance Liquid Chromatography

The overall quality of the separation of two solutes is measured by their resolution (R_S), a combination of the thermodynamic factors causing separative transport and the kinetic factors causing dispersive transport and is an index of the effectiveness of the separation. Defined by $R_S = (t_{r,b} - t_{r,a})/(\frac{1}{2}(w_{t,b} + w_{t,a}))$, where a and b refer to the two solutes, $t_{r,x}$ is the retention time of solute x , and $w_{t,x}$ is the peak width at the base of solute x in units of time, it is frequently estimated by use of the fundamental resolution equation,

$$R_S = \left(\frac{\sqrt{N}}{4} \right) \left(\frac{\alpha - 1}{\alpha} \right) \left(\frac{k_b}{1 + k_b} \right)$$

where k_b is the retention factor of the more retained solute, α is the separation factor of the solute pair under consideration, and N is the plate count. This equation assumes that the peak shapes are Gaussian and that the peak widths are equivalent.

Easy recognition of the two peaks over a wide range of relative concentrations is possible for $R_s = 1$ and this is essentially the practical minimum resolution desirable. It is usually stated that $R_s = 1$ corresponds to a peak purity of about 98%; however, this is correct only for equal concentrations of the two solutes. As the ratio of relative concentrations of the two solutes deviates from 1, the recovery of the lower concentration solute at a given level of purity becomes poorer.

Examination of the fundamental resolution equation shows that improvements in resolution can be obtained by the following:

Increasing the column efficiency. The dependence of R_s on \sqrt{N} , rather than N , means that this method is most effective when the column efficiency is initially low. In other words, when using efficient columns to develop a separation, major improvements in R_s are not generally obtained by increasing N .

Increasing α . If α is close to 1.0, the greatest increase in R_s can be obtained by changing those parameters which influence α (i.e., the mobile-phase composition, the choice of stationary phase, the temperature, or, less frequently, the pressure). Increasing α from 1.1 to 1.2 increases R_s by more than 80%. However, as α increases, the amount of increase in R_s decreases, so that increasing α from 2.1 to 2.2 increases R_s by only about 4%.

Increasing k . If k_b (and thus k_a) < 1 , R_s can be significantly increased by changing the mobile-phase composition to increase k_b . As for α , the amount of increase decreases as k_b increases, so that changing k_b from 0.5 to 1.5 improves R_s by about 80%, increasing k_b from 1.5 to 2.5 increases R_s by about 20%. Moreover, increasing k_b increases the analysis time; thus, this approach is also of limited practicality.

To summarize, the most successful approach to obtaining an adequate R_s is usually to increase α by varying the mobile-phase composition [e.g., choice of solvent(s), pH, or temperature] or by varying the stationary phase. Increasing R_s by increasing N or k_b works in selected instances, but it is not as generally applicable.

Developing an elution separation method to be used for the analysis of numerous samples requires more than obtaining the minimal resolution of the solutes of interest. A successful method should not only achieve the desired separation but should also do so in a cost-effective and robust manner. High-performance liquid chromatography (HPLC) method development has its own, extensive literature, reflecting the importance of HPLC as an analytical technique.

Snyder *et al.* state the goals of the HPLC method development as follows: (a) precise and rugged quantitative analysis requires that R_s be greater than 1.5; (b) a separation time of < 5 –10 min; (c) $\leq 2\%$ RSD for quantitation in assays ($\leq 5\%$ for less demanding analyses and $\leq 15\%$ for trace analysis); (d) a pressure drop of < 150 bar; (e) narrow peaks to give large signal-to-noise ratios; and (f) minimal mobile-phase consumption per run. Additionally, thorough testing of the robustness of proposed methods is recommended.

Suggested Further Reading

- Bidlingmeyer, B. A., *Practical HPLC Methodology and Applications*, John Wiley & Sons, New York, 1992.
- Giddings, J. C., *Unified Separation Science*, John Wiley & Sons, New York, 1991.
- Guiochon, G., S. G. Shirazi, and A. M. Katti, *Fundamentals of Preparative and Nonlinear Chromatography*, Academic Press, Boston, 1994.
- Karger, B. L., L. R. Snyder, and Cs. Horvath, *An Introduction to Separation Science*, John Wiley & Sons, New York, 1973, pp. 11–167.
- Meyer, V. R., *Practical High-Performance Liquid Chromatography*, 3rd ed., John Wiley & Sons, New York, 1998.
- Rizzi, A., Retention and selectivity, in *Handbook of HPLC* (E. Katz, R. Eksteen, P. Schoenmakers, and N. Miller, eds.), Marcel Dekker, Inc., New York, 1998, pp. 1–54.
- Snyder, L. R. and J. J. Kirkland, *Introduction to Modern Liquid Chromatography*, 2nd ed., John Wiley & Sons, New York, 1979.
- Snyder, L. R., J. J. Kirkland, and J. L. Glajch, *Practical HPLC Method Development*, 2nd ed., John Wiley & Sons, New York, 1997.



Elution Modes in Field-Flow Fractionation

Josef Chmelík

Institute of Analytical Chemistry, Academy of Sciences of the Czech Republic, Brno, Czech Republic

Introduction

Field-flow fractionation is, in principle, based on the coupled action of a nonuniform flow velocity profile of a carrier liquid with a nonuniform transverse concentration profile of the analyte caused by an external field applied perpendicularly to the direction of the flow. Based on the magnitude of the acting field, on the properties of the analyte, and, in some cases, on the flow rate of the carrier liquid, different elution modes are observed. They basically differ in the type of the concentration profiles of the analyte. Three types of the concentration profile can be derived by the same procedure from the general transport equation. The differences among them arise from the course and magnitude of the resulting force acting on the analyte (in comparison to the effect of diffusion of the analyte). Based on these concentration profiles, three elution modes are described.

Background Information

Field-flow fractionation (FFF) represents a family of versatile elution techniques suited for the separation and characterization of macromolecules and particles. Separation results from the combination of a nonuniform flow velocity profile of a carrier liquid and a nonuniform transverse concentration profile of an analyte caused by the action of a force field. The field, oriented perpendicularly to the direction of the flow, forms a specific concentration distribution of the analyte inside the channel. Because of the flow velocity profile, different analytes are displaced along the channel with different mean velocities, and, thus, their separation is achieved.

According to the original concept [1], the field drives the analytes to the accumulation wall of the channel. This concentrating effect is opposed by diffusion, driven by Brownian motion of the analytes, which causes a steady state when the convective flux is exactly balanced by the diffusive flux. The concentration profile is exponential and the corresponding elution

mode is referred to as the normal mode. Recently, it has been called the Brownian elution mode [2].

During last two decades, new elution modes were described [3–5] that were not suggested in the original concept [1]. Basically, they differ in the type of the analyte concentration profile.

In 1978, Giddings and Myers described another elution mode for large particles under conditions when diffusion effects can be neglected [3]. The particles form a layer on the channel wall and, under the influence of the carrier liquid flow, they roll on the channel bottom to the channel outlet. This elution mode is referred to as the steric mode [3].

The above-mentioned elution modes apply to the situation when the resulting force acting on the analytes does not change its orientation inside the channel. However, there exist conditions when the resulting force acting on analytes may change its orientation inside the channel [e.g., two counteracting forces, a gradient of a property (pH, density) of the carrier liquid, influence of hydrodynamic lift forces]. Under such conditions, the analytes form narrow zones at the positions where the resulting forces acting on them equal zero. The resulting force is changing its sign below and above this position in such a way that the analyte is focused into this equilibrium position. The concept of formation of narrow zones of analytes inside the FFF channel was first described in 1977 by Giddings [6]. In 1982, a technique utilizing sedimentation–flotation equilibrium and centrifugal field was suggested [7]. However, this technique has not been yet verified experimentally. Later, the general features of this elution mode were described and several techniques were implemented; for a review, see Ref. 8. The mode was called either the hyperlayer [4] or focusing [5] elution mode.

Some other elution modes have been described. They are induced by various factors—cyclical field, secondary chemical equilibria, adhesion chromatography, asymmetrical electro-osmotic flow; for a review, see Ref. 2. However, the number of their implementations is rather limited, and for this reason, these modes are not discussed here.



Theory

Field-flow fractionation experiments are mainly performed in a thin ribbonlike channel with tapered inlet and outlet ends (see Fig. 1). This simple geometry is advantageous for the exact and simple calculation of separation characteristics in FFF. Theories of infinite parallel plates are often used to describe the behavior of analytes because the cross-sectional aspect ratio of the channel is usually large and, thus, the end effects can be neglected. This means that the flow velocity and concentration profiles are not dependent on the coordinate y . It has been shown that, under suitable conditions, the analytes move along the channel as steady-state zones. Then, equilibrium concentration profiles of analytes can be easily calculated.

Generally, the concentration profile of analytes in FFF can be obtained from the solution of the general transport equation. For the sake of simplicity, the concentration profile of the steady-state zone of the analyte along the axis of the applied field is calculated from the one-dimensional transport equation:

$$J_x = W_x c(x) - D \frac{\partial c}{\partial x} \quad (1)$$

where J_x and W_x are the components of the flux density of the analyte and of the transport velocity of the analyte along the axis of the applied field, $c(x)$ is the analyte concentration distribution along the direction of the applied field, and D is the total effective diffusion coefficient. The term $W_x c(x)$ corresponds to the x component of the convective flux of the analyte and the term $D(\partial c/\partial x)$ corresponds to the x component of the diffusive flux of the analyte. W_x equals the sum of the x

components of the transport velocity of the analyte induced by the external field applied U_x and the transport velocity of the analyte induced by the carrier liquid flow v_x ($W_x = U_x + v_x$). Because of the direction of the carrier liquid flow inside the FFF channel, the component v_x equals zero (the x axis is perpendicular to the direction of the flow) and, thus, W_x equals U_x .

Following the treatment given by Giddings [9], imposing for the condition of the steady-state zone of the analyte, which is characterized by the null flux density, and applying the equation of continuity, the general solution of the analyte concentration profile can be expressed in the form

$$c(x) = c_0 \exp \left[\int_0^x \left(\frac{U_x}{D} \right) dx \right] \quad (2)$$

The integration limit $x = 0$ corresponds to the accumulation wall boundary. The particular solutions for the concentration profile are dependent on the course of the force field inducing the transport of the analyte, and the ratio of U_x and D .

The equation of the field-induced transport velocity was derived by Giddings [10]:

$$U_x = -ax^n \quad (3)$$

where a is constant and n equals 0 or 1. If $n = 0$, then U_x is constant; if $n = 1$, then U_x is dependent on the position inside the channel.

Discussion

Brownian Elution Mode

The field-induced velocity of the analyte in the separation channel is constant and comparable with its diffusive motion ($U_x = \text{constant}$, $U_x t \approx \sqrt{2Dt}$, where t is time). The resulting concentration profile of the analyte is given by the exponential relationship [9]

$$c(x) = c_0 \exp \left(-\frac{|U_x|}{D} x \right) \quad (4)$$

where c_0 is the maximum concentration at the accumulation channel wall. The elution mode with the exponential concentration profile is called Brownian [2].

It is known that there are two main factors influencing the behavior of analytes in this elution mode: the properties of the analytes (characterized by the so-called analyte-field interaction parameter [11] and the diffusion coefficient) and the strength of the field applied.

In Brownian elution mode, the retention ratio R is indirectly dependent on both the applied force F and

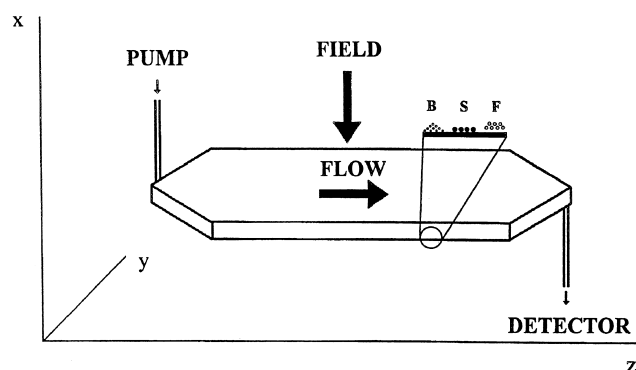


Fig. 1 The orientation of the field and flow in the given coordinate system. The zoomed inset shows the schematic representation of the zone shapes in particular elution modes (B for Brownian, S for steric, and F for focusing).

the thickness of the channel w , and independent on the flow rate [9]. It can be expressed in an approximate form:

$$R = \frac{6kT}{Fw} \quad (5)$$

where k is the Boltzmann constant and T is the absolute temperature.

Steric Elution Mode

The velocity of transport induced by the force field in the separation channel is constant and much higher than the velocity caused by the diffusive motion of the analyte ($U_x = \text{constant}$, $U_x t \gg \sqrt{2Dt}$). In this case, the analyte forms a layer on the accumulation channel wall and its concentration in any other position inside the channel equals zero. The particle radius r_p describes the distance of the particle center from the accumulation wall:

$$c(r_p) = c_0 \quad \text{and} \quad c(x \neq r_p) = 0 \quad (6)$$

The elution mode is called steric [3]. The retention ratio can be expressed in the form

$$R = \frac{6r_p}{w} \quad (7)$$

This shows that R is independent of both the field applied and the flow rate, and it is dependent only on the particle radius and the channel thickness. In fact, the retention ratio values corresponding to the pure steric elution mode have been seldom observed experimentally [12]. The observed values often correspond to the focusing elution mode as a result of the action of some additional forces influencing retention behavior of analytes.

Focusing Elution Mode

In this elution mode, the velocity of analyte transport induced by a force field in the separation channel is dependent on the position across the channel ($U_x \neq \text{constant}$). Based on Eq. (3), the nonconstant transport velocity can be, in the simplest case, described as

$$U_x = -a(x - s) \quad (8)$$

where s is the distance of the center of the focused zone from the channel wall (i.e., the position where the resulting force acting on the analyte equals zero). Com-

binning this equation with Eq. (2), we obtain a relation for the resulting concentration profile of the analyte:

$$c(x) = c_0 \exp\left(-\frac{a}{2D}(x - s)^2\right) \quad (9)$$

where c_0 is the maximum concentration at the center of the focused zone at the position s . The concentration profile of the analyte across the channel thickness, in this simplest case, is Gaussian. In other cases, where other secondary effects act on the retention in the focusing elution mode, the observed concentration profile is more complex. However, even in these cases, the main feature remains the same; that is, the maximum concentration of the analyte is at the equilibrium position, where the resulting force acting on the analyte is zero, and not on the channel wall as in the case of the Brownian and steric elution modes. The elution mode is called focusing [5] or hyperlayer [4]. In the focusing elution mode, the retention ratio can be expressed in a form formally similar to the expression given for the steric elution mode [see Eq. (7)]:

$$R = \frac{6s}{w} \quad (10)$$

At least two counteracting forces are necessary for the formation of the focused zone of the analyte. The center of the zone is located at the position s where the resulting force is zero. Changing of both forces can control the resulting position of the particle zone.

Conclusions

In the majority of FFF techniques, the retention ratio is dependent on the analyte size. This dependence for Brownian and steric mode is described by Eq. (11), derived by Giddings [13]:

$$R = 6(\alpha - \alpha^2) + 6\lambda(1 - 2\alpha)\left[\coth\left(\frac{1 - 2\alpha}{2\lambda}\right) - \frac{2\lambda}{1 - 2\alpha}\right] \quad (11)$$

where $\alpha = d/2w$, $\lambda = kT/Fw$, and d is the analyte diameter. The curve describing this dependence is shown in Fig. 2. The values of R for the focusing mode lie above the curve. This complex situation shows that determination of the elution mode is very important for evaluation of the measured retention data because different elution modes can act on particular analytes in the same experiment.



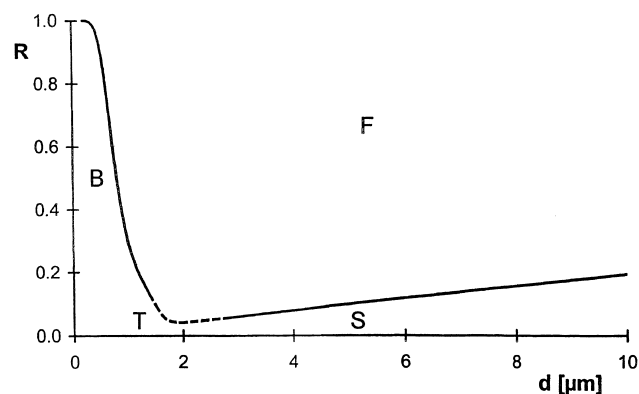


Fig. 2 Schematic representation of the dependence of the retention ratio R on the analyte size. Curve B corresponds to Brownian mode and the line S to the steric mode. The dashed part T denotes the transition between these two modes. The area F shows the range of applicability of the focusing mode.

Acknowledgment

This work was supported by a grant No. A4031805 from the Grant Agency of Academy of Sciences of the Czech Republic.

References

1. J. C. Giddings, *Separ. Sci.* 1: 123 (1966).
2. M. Martin, in *Advances in Chromatography*, Vol. 39 (P. R. Brown and E. Grushka, eds.), Marcel Dekker, Inc., New York, 1998, pp. 1–138.
3. J. C. Giddings and M. N. Myers, *Separ. Sci. Technol.* 13: 637 (1978).
4. J. C. Giddings, *Separ. Sci. Technol.* 18: 765 (1983).
5. J. Janča and J. Chmelík, *Anal. Chem.* 56: 2481 (1984).
6. J. C. Giddings, *Am. Lab.* 24: 20D (1992).
7. J. Janča, *Makromol. Chem. Rapid Commun.* 3: 887 (1982).
8. J. Janča, J. Chmelík, V. Jahnová, N. Nováková, and E. Urbánková, *Chem. Anal.* 36: 657 (1991).
9. J. C. Giddings, *Unified Separation Science*, John Wiley & Sons, New York, 1991.
10. J. C. Giddings, *J. Chem. Phys.* 49: 81 (1968).
11. J. C. Giddings and K. D. Caldwell, in *Physical Methods of Chemistry*, Vol. 3B (B. W. Rossiter and J. F. Hamilton, eds.), John Wiley & Sons, New York, 1989, p. 867.
12. J. Pazourek, K.-G. Wahlund, and J. Chmelík, *J. Microcol. Separ.* 8: 331 (1996).
13. J. C. Giddings, *Separ. Sci. Technol.* 13: 241 (1978); 14: 869 (1979).

Enantiomer Separations by TLC

Luciano Lepri

Alessandra Cincinelli

Università degli Studi di Firenze, Firenze, Italy

Introduction

Enantiomers are compounds which have the same chemical structure but different conformations, whose molecular structures are not superimposable on their mirror images, and, because of their molecular asymmetry, these compounds are optically active. The most common cause of optical activity is the presence of one or more chiral centers which, in organic chemistry, are usually related to tetrahedral structures formed by four different groups around carbon, silicon, tin, nitrogen, phosphorus, or sulfur.

Many molecules are chiral, even in the absence of stereogenic centers; that is, molecules containing adjacent π -systems, which cannot adopt a coplanar conformation because of rotational restrictions due to steric hindrance, can exist in two mirror forms (atropisomers). This is the case for some dienes or olefins, for some nonplanar amides, and for the biphenyl or binaphthyl types of compounds.

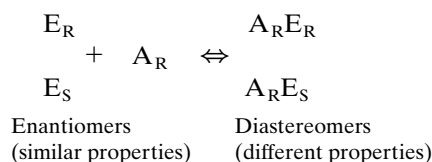
Designation of optical isomers can be by the symbols D and L, which are used to indicate the relationship between configurations based on D (+)-glyceraldehyde as an arbitrary standard. If such relationship is unknown, the symbols (+) and (–) are used to indicate the sign of rotation of plane polarized light (i.e., dextrorotatory and levorotatory). In 1956, Cahn et al. [1] presented a new system, the (R) and (S) absolute configurations of compounds.

Many enantiomers show different physiological behaviors and it is, therefore, desirable to have reliable methods for the resolution of racemates and the determination of the enantiomeric purity. To this end, thin-layer chromatography (TLC) is a simple, sensitive, economic, and fast method which allows easy control of a synthetic process and can be used for preparative separations.

TLC Separation of Enantiomers by Use of Diastereomeric Derivatives

Because the stationary phases originally used in liquid chromatography were achiral, much research was de-

voted to the separation of enantiomers as diastereomeric derivatives produced by reaction of the enantiomers with an optically pure reagent (A_R). The resultant diastereomers could, because of their different physicochemical properties, then be separated on conventional stationary phases:



In addition, a significant increase in the sensitivity of detection and the location on the layers of some compounds not otherwise identifiable can be achieved by this method. There are, however, some disadvantages: (a) It is very important to use derivatization reagents with 100% optical purity; (b) quantitation is founded on the assumption that the reaction is complete and not associated with racemization; (c) the distance between the two chiral centers should be as close as possible to each other in order to maximize the difference in chromatographic properties.

Many chiral derivatization reactions were used and the compounds examined are mostly amphetamines, β -blocking agents, amino acids, and anti-inflammatory drugs. Silica gel and, to a lesser extent, silanized silica were used as stationary phases. The ΔR_f values obtained for the diastereomeric pairs were not usually very high (0.04–0.07), with the exception of amino alcohol and amino acid diastereomers obtained with Marphey's reagent, a derivative of L-alanine amide (0.06–0.22).

TLC Separations of Enantiomers by Chiral Chromatography

In chiral chromatography, the two diastereomeric adducts $A_R E_R$ and $A_R E_S$ are formed during elution, rather than synthetically, prior to chromatography. The adducts differ in their stability using chiral stationary phases (CSP) or chiral coated phases (CCP) and/or in their interphase distribution ratio adding a chiral selec-



tor to the mobile phase (CMP). The difference between the interactions of the chiral environment with the two enantiomers is called enantioselectivity.

According to Dalgliesh [2], three active positions on the selector must interact simultaneously with the active positions of the enantiomer to reveal differences between optical antipodes. This is a sufficient condition for resolution to occur, but it is not necessary. Chiral discrimination may happen as a result of hydrogen-bonding and steric interactions, making only one attractive force necessary in this type of chromatography. Moreover, the creation of specific chiral cavities in a polymer network (as in "molecular imprinting" techniques) could make it possible to base enantiomeric separations entirely on steric fit.

The most important technique for enantiomeric separation in TLC is chiral ligand-exchange chromatography (LEC). LEC is based on the copper(II) complex formation of a chiral selector and the respective optical antipodes. Differences in the retention of the enantiomers are caused by dissimilar stabilities of their diastereomeric metal complexes. The requirement of sufficient stability of the ternary complex involves five-membered ring formation, and compounds such as α -amino and α -hydroxyacids are the most suitable.

Chiral Stationary Phases and Chiral Coated Phases

Few chiral phases are used in TLC; one of the main reasons for this is that stationary phases with a very high ultraviolet (UV) background can be used only with fluorescent or colored solutes. For example, amino-modified ready-to-use layers bonded or coated with Pirkle-type selectors [3], such as *N*-(3,5-dinitrobenzoyl)-L-leucine or *R*(-)- α -phenylglycine, are pale yellow and strongly adsorb UV radiation.

Another reason is the high price of most CSPs. In spite of this, Pirkle-type CSPs, based on a combination of aromatic π - π bonding interactions (charge-transfer complexation), hydrogen-bonding and dipole interactions, allows the resolution of racemic mixtures of 2,2,2-trifluoro-1-(9-anthryl)ethanol, 1,1'-bi-2-naphthol, benzodiazepines, hexobarbital, and β -blocking agents derivatized with achiral 1-isocyanatonaphthalene. However, the most widely used CSPs or CCPs are polysaccharides and their derivatives (cellulose, cellulose triacetate, and triphenylcarbamate) and silanized silica gel impregnated with an optically active copper(II) complex of (2*S*,4*R*, 2'*RS*)-*N*-(2'-hydroxydodecyl)-4-hydroxyproline (ChiralPlate,

Macherey-Nagel, and HPTLC-Chir, Merck, Germany) for ligand-exchange chromatography. The chiral layer on the latter plates is combined with a so-called "concentrating zone."

The resolution of optical antipodes on polysaccharides is mainly governed by the shape and size of solutes (inclusion phenomena) and only to a minor extent by other interactions involving the functional groups of the molecules. In the case of microcrystalline cellulose triacetate (MCTA), the type and composition of the aqueous-organic eluent affect the separation because these result in different swelling of MCTA.

The use of silica gel impregnated with chiral polar selector, such as D-galacturonic acid, (+)-tartaric acid, (-)-brucine, L-aspartic acid, or a complex of copper(II) with L-proline, should also be mentioned.

In CSPs, owing to the nature of the polymeric structure, the simultaneous participation of several chiral sites or several polymeric chains is conceivable. In CCPs, the chiral sites are distributed at the surface or in the network of the achiral matrix relatively far away from each other and only a bimolecular interaction is generally possible with the optical antipodes.

A survey of optically active substance classes separated with ChiralPlate and HPTLC Chir layers and with MCTA plates is shown in Fig. 1.

Chiral Mobile Phases

Chiral mobile phases enable the use of conventional stationary phases and show minor detection problems compared to CSPs or CCPs. However, high cost chiral selectors (i.e., γ -cyclodextrin) are certainly not advisable for TLC. Enantiomer separations can be achieved using chiral mobile phases in both normal- and reversed-phase chromatography. The first technique uses silica gel and, mostly, diol F₂₅₄ HPTLC plates (Merck) and, as chiral selectors, D-galacturonic acid for ephedrine, *N*-carbobenzoxy (CBZ)-L-amino acids or peptides and 1*R*(-)-ammonium-10-camphorsulfonate for several drugs and 2-*O*-[(*R*)-2-hydroxypropyl]- β -cyclodextrin for underivatized amino acids. Extremely high ΔR_f values (0.05–0.25) were observed for the various pairs of enantiomers, proving the strong enantioselectivity of this system.

Most separations have been obtained by reversed-phase chromatography on hydrophobic silica gel (RP-18W/UV₂₅₄ and Sil C₁₈-50/UV₂₅₄ from Macherey-Nagel, Germany; KC2F, KC18F and chemically bonded diphenyl-F from Whatman, USA, and RP-18W/F₂₅₄ from Merck, Germany) as stationary phase



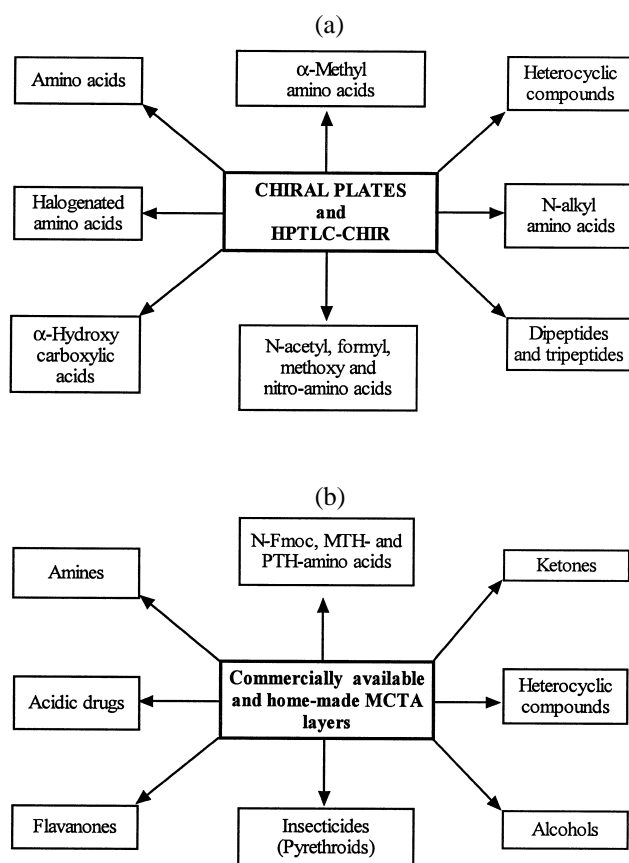


Fig. 1 Classes of chiral organic compounds resolved (a) by ligand-exchange chromatography on Chiral and HPTLC Chir plates and (b) on MCTA layers.

and β -cyclodextrin and its derivatives, bovine serum albumin (BSA), and the macrocyclic antibiotic vancomycin as chiral agents. Enantiomers which interact selectively with β -cyclodextrin cavities are generally N-derivatized amino acids, whereas the use of BSA as chiral selector is able to resolve many N-derivatized amino acids, tryptophan and its derivatives, derivatized lactic acid, and unusual optical antipodes such as binaphthols.

Quantitative Analysis of TLC-Separated Enantiomers

Although TLC-MS (mass spectrometry) has been shown to be technically feasible and applicable to a variety of problems, thin-layer chromatography is generally coupled with spectrophotometric methods for quantitative analysis of enantiomers. Optical quantitation can be achieved by *in situ* densitometry by measurement of UV-vis absorption, fluorescence or fluorescence quenching, or after extraction of solutes from the scraped layer. The evaluation of detection limits for separated enantiomers is essential because precise determinations of trace levels of a D- or L-enantiomer in an excess of the other become more and more important. Detection limits as low as 0.1% of an enantiomer in the other have been obtained.

References

1. R. S. Cahn, C. K. Ingold, and V. Prelog, Specification of asymmetric configuration in organic chemistry, *Experientia* 12: 81–94 (1956).
2. C. E. Dalgliesh, The optical resolution of aromatic amino acids on paper chromatograms, *J. Chem. Soc.* 3: 3940–3943 (1952).
3. W. H. Pirkle and J. M. Finn, Chiral high-pressure liquid chromatographic stationary phases. General resolution of arylalkylcarbinols, *J. Org. Chem.* 46: 2935–2938 (1981).

Suggested Further Reading

- Gunther, R. and K. Möller, Enantiomer separations, in *Handbook of Thin Layer Chromatography* (J. Sherma and B. Fried, eds.), Marcel Dekker, Inc., New York, 1996, pp. 621–682.
- Lepri, L., Enantiomer separation by TLC, *J. Planar Chromatogr. Mod. TLC* 10: 320–331 (1997).
- Prosek, M. and M. Puki, Basic principles of optical quantitation in TLC, in *Handbook of Thin Layer Chromatography* (J. Sherma and B. Fried, eds.), Marcel Dekker, Inc., New York, 1996, pp. 273–306.



Enantioseparation by Capillary Electrochromatography

Yulin Deng

University of Saskatchewan, Saskatoon, Saskatchewan, Canada

Introduction

Capillary electrochromatography (CEC) is considered to be a hybrid technique that combines the features of both capillary high-performance liquid chromatography (HPLC) and capillary electrophoresis (CE). In CEC, a mobile phase is driven through a packed or an open tubular coating capillary column by electro-osmotic flow [1,2] and/or pressurized flow [3]. The first electrochromatographic experiments were done in early 1974 by Pretorius et al. [4], who applied an electric field across a packed column. This allows the analyte to partition between the mobile and stationary phases. As a high voltage is applied, electrophoretic mobility should also contribute to the chromatographic separation for charged analyses. The ability of CEC to combine electrophoretic mobility with partitioning mechanisms is one of its strongest advantages. For electroosmotically driven capillary electrochromatography (ED-CEC), the resulting flow profile is almost pluglike; thus, a high column efficiency, comparable to that in CE, can be obtained. For pressure-driven capillary electrochromatography (PD-CEC), although dispersion caused by flow velocity differences causes zone broadening, plate numbers are higher than in capillary HPLC due to the contribution of the electric field to total flow rate. Unlike ED-CEC, the use of an HPLC pump provides stable flow conditions and, thus, offers improvements in retention reproducibility, in sample introduction (e.g., split injection), in suppression of bubble formation, and in gradient elution. More importantly, because the solvent can be mainly driven by pressurized flow, the change of the direction of electric field is no longer limited, and the separation of mixtures of cationic, anionic and neutral compounds becomes possible in a single run. Additionally, neutral molecules can be separated without micelles or other organic additives; this makes CEC more amenable to coupling with mass spectrometry.

Chiral separation in capillary electrophoresis is usually achieved by the addition of chiral complexing agents to form *in situ* diastereometric complexes between the enantiomers and the chiral complexing

agent. Many of the chiral selectors successfully used in HPLC [5] can also be applied in CE, and thus the experience from both HPLC and CE can be transferred to CEC. During the last few years, interest in CEC has increased due to the improvement in the preparation of capillary columns [6,7] and in the stability and efficiency of separations [6–9]. A limited but dramatically increasing number of chiral separations in CEC have been reported so far. This review will be mainly devoted to recent developments and applications. We are also interested in exploring the potential advantages offered by capillary electrochromatography and, in particular, its practical utility for enantioseparation.

Enantioselectivity in CEC

Capillary electrochromatography is a more complicated system than CE and HPLC due to the combination of both electrophoretic and chromatographic transport mechanisms. It is difficult to define an effective selectivity (separation factor) as in the case of general chromatography or general electrophoresis. To better illustrate the interactions that control selectivity, we defined a relative selectivity ($\alpha_r = \Delta t_e/t_{e2}$), and postulated a model that illustrates the effect of separation parameters on the enantioselectivity [10].

For enantioseparation chiral stationary phases (CSPs), an expression of the relative selectivity is obtained:

$$\alpha_r = \frac{\phi(K_{f2} - K_{f1})}{1 + \phi K_2 + \phi K_{f2}} \quad (1)$$

Interestingly, this equation indicates that the electrophoresis mechanism does not influence the enantioselectivity and the electric field only plays a role in driving the mobile phase.

For enantioseparation with chiral additives in CEC, we derived another expression:

$$\alpha_r = \frac{(K_{f1} - K_{f2})[\phi K v_c + (\mu_c - \mu_f)E][C]_m}{(1 + \phi K + K_{f2}[C]_m)(v_f + v_c K_{f1}[C]_m)} \quad (2)$$



where v_f and v_c are the apparent flow velocity of the free analyte and the complexed analyte, respectively. Both Eqs. (1) and (2) show that the enantioselectivity is not only dependent on the difference in formation constants (K_f) between a pair of enantiomers with the chiral agents but also is influenced by some experimental factors. Substantially, chiral recognition of enantiomers is the direct result of the transient formation of diastereomeric complex between enantiomeric analytes and the chiral complexing agent (i.e., the difference in formation constants). However, the importance of experimental factors lies in the fact that they can convert the intrinsic difference into the apparent difference in migration velocity along the column. Therefore, the overall selectivity in chiral separation can be considered to be made up of two contributing factors: the intrinsic difference (intrinsic selectivity) in formation constants of a pair of enantiomers, and the conversion efficiency (exogenous selectivity) of the intrinsic difference into the apparent difference in the migration velocity. According to Eq. (2), these experimental factors may include the equilibrium concentration of a chiral selector, the electric field strength, and the properties of the stationary phase.

In CEC with chiral additives, Eq. (2) shows that there exists a maximum selectivity at the optimal concentration of chiral selector. The optimal concentration is not only dependent on the formation constants (K_{f1} , K_{f2}) but also on properties of the column (ϕ and K) [i.e., $[C]_{\text{opt}} = \sqrt{(1 + \phi K)/K_{f1}K_{f2}}$].

Unlike in the case of a chiral column, the selectivity in CEC with chiral additives is determined by both partition and electrophoresis, and the electric field either increases or decreases the selectivity. Table 1 summarizes the relationship between the direction of field

strength and the electrophoretic mobility of the free and complexed analytes. For PD-CEC, the solvent is mainly driven by pressurized flow; thus, there is no limitation to change the direction of electric field.

For enantioseparation on CSPs in CEC, nonstereospecific interactions, expressed as ϕK , contribute only to the denominator as shown in Eq. (1), indicating that any nonstereospecific interaction with the stationary phase is detrimental to the chiral separation. This conclusion is identical to that obtained from most theoretical models in HPLC. However, for separation with a chiral mobile phase, ϕK appears in both the numerator and denominator [Eq. (2)]. A suitable ϕK is advantageous to the improvement of enantioselectivity in this separation mode. It is interesting to compare the enantioselectivity in conventional capillary electrophoresis with that in CEC. For the chiral separation of salsolinols using β -CyD as a chiral selector in conventional capillary electrophoresis, a plate number of 178,464 is required for a resolution of 1.5. With CEC (i.e., $\phi K = 10$), the required plate number is only 5976 for the same resolution [10]. For PD-CEC, the column plate number is sacrificed due to the introduction of hydrodynamic flow, but the increased selectivity markedly reduces the requirement for the column efficiency.

Chiral Separation in CEC

There are different ways of performing chiral separation by CEC. Mayer and Schurig immobilized the chiral selectors by coating or chemically binding them to the wall of the capillary [11,12]. Permethylated β - or γ -CyD was attached via an octamethylene spacer to dimethylpolysiloxane (Chirasil-Dex) as the stationary phase. A high efficiency ($\sim 250,000/M$) was obtained for the separation of 1,1'-dinaphthyl-2,2'-diyl hydrogenphosphate. An alternative coating approach was developed by Sezeman and Ganzler. Linear acrylamide was coated on the capillary wall, and after polymerization, CyD derivatives were bound to the polymer [13].

Chiral separation can also be performed with packed capillaries. β -CyD-bonded CSPs that are most frequently used in HPLC and CE were successfully applied in CEC. The separation of a variety of chiral compounds, such as some amino acid derivatives benzoin and hexobarbital was achieved by using CSPs bonded with different CyD derivatives [14,15]. Proteins are not ideal for use as buffer additives in CE because of their large detector response; however, CEC may be a good way to use this type of chi-

Table 1 Relationship Between the Field Strength and the Electrophoretic Mobility for Getting High Enantioselectivity in CEC

Direction of μ_{ep}		Size relationship (absolute value)	Direction of E
μ_f	μ_c		
+	+	$\mu_f < \mu_c$	+
+	+	$\mu_f > \mu_c$	—
+	—	^a	—
—	—	$\mu_f < \mu_c$	—
—	—	$\mu_f > \mu_c$	+
—	+	^a	+

^aThe selection of direction of electric field is not influenced by size relationship in absolute values between the electrophoretic mobility of the free and complexed analytes.

ral selectors. Lloyd et al. have performed CEC enantioseparation by using commercially available protein CSPs, such as AGP and HAS [16,17]. The resolution obtained on protein CSPs was good; the efficiency, however, was rather poor. Another HPLC–CSP based on cellulose derivatives has been also reported for enantioseparation by CEC [18]. CSPs modified by covalent attachment of poly-*N*-acryloyl-L-phenylalanineethyl ester or by coating with cellulose tris(3,5-dimethylphenylcarbamate) can be performed in the reversed-phase mode. Acetonitrile as organic modifier was found to be advantageous for this type of CSP. An anion-exchange-type CSP was recently developed for the separation of *N*-derivatized amino acids [19]. The new chiral sorbent was modified with a basic *tert*-butyl carbamoyl quinine. Enantioselectivity obtained in CEC was as high as in HPLC and efficiency was typically a factor of 2–3 higher than in HPLC. A recent innovative approach is the use of imprinted polymers as CSPs in CEC [20,21]. Imprinted polymers possess a permanent memory for the imprinted species, and, thus, their enantioselectivity is predetermined by the enantiomeric form of the templating ligand. The use of imprint-based CSPs in HPLC is hampered by their poor chromatographic performance. CEC, however, was found to greatly improve the efficiency of the imprint-based separation. The most successful approach is the use of capillary columns filled with a monolithic, superporous imprinted polymer obtained by an *in situ* photo-initiated polymerization process. This technique enables imprint-based column to be operational within 3 h from the start of preparation. Generally, the imprint-based CSPs show high enantioselectivity but somewhat low efficiency and are limited to the separation of very closely related compounds.

Enantioseparation can be achieved on a conventional achiral stationary phase by the inclusion of an appropriate chiral additive into the mobile phase. It is theoretically predicted that the enantioselectivity in CEC with a chiral additive may be higher than that using a chiral column with the same chiral selector [10]. Lelievre et al. compared an HP- β -CyD column and HP- β -CyD as an additive in the mobile phase with an achiral phase (ODS) to resolve chlortalidone by CEC [22]. It was demonstrated that resolution on ODS with the chiral additive was superior on the CSP; however, efficiency was low. With an increasing amount of acetonitrile, the peak shape was improved and the migration time was decreased. We achieved the separation of salsolinol by the use of CEC with β -CyD as a chiral

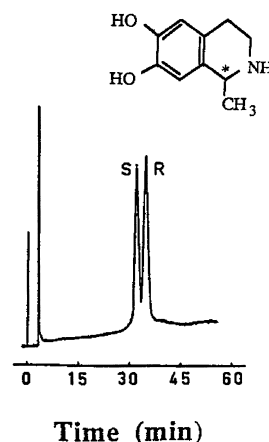


Fig. 1 Electrochromatogram of salsolinol enantiomers on a packed capillary column. Column: ODS-C18, 29 cm (23 cm effective length) \times 75 μ m ID; applied electric field strength: \sim 250 V/cm; mobile phase: 20 mM sodium phosphate buffer (pH 3.0) containing 12 mM β -cyclodextrin and 5 mM sodium 1-heptanesulfonate. The pump was set at the constant pressure of 100 kg/cm².

additive in the mobile phase containing sodium 1-heptanesulfonate, as shown in Fig. 1. Salsolinol is a hydrophilic amine and is difficult to enantioseparate due to the small k' values on the reversed stationary phases. Sodium 1-heptanesulfonate was used as a counterion to improve the retention.

In conclusion, CEC has great potential in separation technology. Our theoretical model as well as many published practices in CEC show clearly that the benefit of combining electrophoresis and partitioning mechanisms in CEC is the increase in selectivity for the separation. The intrinsic difference in formation constants is critical, but the experimental factors, such as electric field or the stationary and mobile phases, can also contribute to the improvement of the overall enantioselectivity via increasing the conversion efficiency. However, only when both electrophoretic and partitioning mechanisms act in the positive effects, can high overall enantioselectivity in CEC be obtained.

References

1. T. Tsuda, K. Nomura, and G. Nagakawa, *J. Chromatogr.* 248: 241 (1982).
2. J. W. Jorgenson and K. D. Lukacs, *J. Chromatogr.* 218: 209 (1981).



3. T. Tsuda, *LC-GC Int.* 5:26 (1992).
4. V. Pretorius, B. J. Hopkins, and J. D. Schieke, *J. Chromatogr.* 99: 23 (1974).
5. Y. Deng, W. Maruyama, M. Kawai, P. Dostert, and M. Naoi, *Progress in HPLC and HPCE*, VSP, Utrecht, 1997, Vol. 6, pp. 301.
6. R. J. Boughtflower, T. Underwood, and C. J. Paterson, *Chromatographia* 40: 329 (1995).
7. C. Yan, U.S. Patent 5453163 (1995).
8. M. R. Taloy, P. Teale, S. A. Westwood, and D. Perrett, *Anal. Chem.* 69: 2554 (1997).
9. J. Eimer, K. K. Unger, and T. Tsuda, *Fresenius J. Anal. Chem.* 352: 649 (1995).
10. Y. Deng, J. Zhang, T. Tsuda, P. H. Yu, A. A. Boulton, and R. M. Cassidy, *Anal. Chem.* 70: 4586 (1998).
11. S. Mayer and V. Schurig, *J. High Resolut. Chromatogr.* 15: 129 (1992).
12. S. Mayer and V. Schurig, *J. Liquid Chromatogr.* 16: 915 (1993).
13. J. Sezemam and K. Ganzler, *J. Chromatogr. A* 668: 509 (1994).
14. S. Li and D. K. Lloyd, *J. Chromatogr. A* 666: 321 (1994).
15. D. Wistuba, H. Czesla, M. Roeder, and V. Schurig, *J. Chromatogr. A* 815: 183 (1998).
16. S. Li and D. K. Lloyd, *Anal. Chem.* 65: 3684 (1993).
17. D. K. Lloyd, S. Li, and P. Ryan, *J. Chromatogr. A* 694: 285 (1995).
18. K. Krause, M. Girod, B. Chankvetadze, and G. Blasehk, *J. Chromatogr. A* 837: 51 (1999).
19. M. Lammerhofer and W. Lindner, *J. Chromatogr. A* 829: 115 (1998).
20. L. Schweitz, L. I. Andersson, and S. Nilsson, *Anal. Chem.* 69: 1179 (1997).
21. L. Schweitz, L. I. Andersson, and S. Nilsson, *J. Chromatogr. A* 817: 5 (1998).
22. F. Lelievre, C. Yan, R. N. Zare, and P. Gareil, *J. Chromatogr. A* 723: 145 (1996).



End Capping

Kiyokatsu Jinno

School of Materials Science, Toyohashi University of Technology, Toyohashi, Japan

Introduction

A typical stationary phase for chromatography, especially liquid chromatography (LC), is a chemically alkyl (C_{18})-bonded phase on silica gel particles. For the preparation of this type of bonded phase, alkylsilane is used to react with the silica gel surface by a silane-coupling reaction. In order to perform this synthesis, the silica gel to be bonded is treated to remove heavy metals and to prepare the surface for better bonding. Generally, only one of the functional groups bonds to form a Si—O—Si bond. Less often, two of the functional groups react to form adjacent Si—O—Si bonds. The remaining functional groups on each reagent molecule hydrolyze to form Si—O—H groups during workup, following the initial reaction. These groups, however, which form with the di- and tri- functional reagents, can cross-link with one another near the surface of the silica gel support. Thus, bonded phases made with any di- or tri-functional reagents are termed “polymeric” phases. A monofunctional silane reagent can only bond to the silanols and any excess is washed free as the ether resulting from hydrolysis of the reagent. Any packing made with a monofunctional silane reagent is referred to as a “monomeric” bonded phase. These schemes are summarized in Fig. 1a(i) and (ii). Other chemically bonded phases, such as cyano-, amino-, and shorter or longer alkyl phases are synthesized by similar bonding chemistries.

Discussion

The products made by the above synthetic processes still have large numbers of residual silanols, which lead to poor peak shapes or irreversible adsorption, because chemically bonded groups on the silica gel surface have large, bulky molecular sizes and, after the bonding, the functionalized silane cannot react with the silanols around the bonded ligands. Because such alkyl-bonded phases are used for reversed-phase separations, especially for chromatography of polar molecules, any silanol groups that remain accessible to sol-

utes after the bonding are likely to make an important contribution to the chromatography of such solutes; this is generally detrimental to the typical reversed-phase LC separations. It is a common fact that the residual silanols produce peak tailing for highly polar compounds which will interact with these silanol groups with deleterious effects. Therefore, the attempt to reduce the number of residual silanols on the silica gel is a common procedure in the preparation of chemically bonded stationary phases, where the surface of a reversed-phase material is ensured to be uniformly hydrophobic, for example, by blocking residual silanol groups with some functional groups. This process is the so-called “end capping.” The end-capping process is possible with a smaller molecule than alkylchlorosilanes, such as a trimethyl-substituted silane (from trimethylchlorosilane or hexamethyldisilazane) as seen in Fig. 1a(iii). Because the molecular weights of these reagents are small, they do not add much to the total percent carbon, compared with the initial bonded phase. It must be known that all chemically bonded phases on silica gel cannot be end-capped by this process, because the above reagents can react with diol and amino phases, and not only with silanol groups on the surface. To block, end cap, and then unblock these phases would be very time-consuming and too expensive to be practical. If the final bonded phase is, in fact, a diol, this silane-bonding reagent is made from glycerol and has the structure Si—O—CHOH—CH₂OH. The cyano or amino phases are most often attached with a propyl group between the silicon atom and the CN or NH₂ group.

Often, when various bonded phases are studied for suitability for a particular separation, the question arises as to which is bonded most completely. This is a common question, because all phases, no matter how they are bonded, will have some residual silanols, even after an end-capping process. It is impossible for the bulkier bonding reagents to reach any but the most sterically accessible silanols. It is much easier for the smaller solutes to reach the silanols, however, and be affected by them. The final surface of the silica gel has three different structures, as demonstrated in Fig. 1b(i), (ii), and (iii), for a



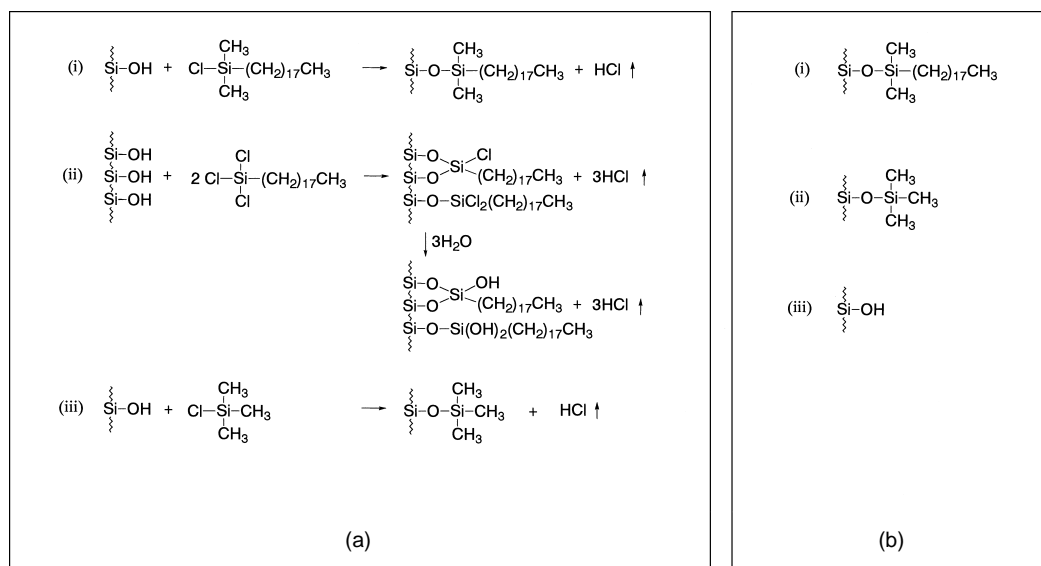


Fig. 1 (a) Scheme of bonding chemistry for chemically bonded C_{18} silica phase: (i) synthesis of monomeric C_{18} ; (ii) synthesis of polymeric C_{18} ; (iii) end-capping process. (b) Surface structure of a monomeric C_{18} phase: (i) monomeric C_{18} ligand; (ii) end-capped trimethyl ligand; (iii) residual silanol.

monomeric C_{18} , end capped by trimethylchlorosilane and residual silanols, respectively.

The presence of residual silanol groups can be detected most readily by using Methyl Red indicator [1], which turns red in the presence of acidic silanol groups, but a more sensitive test is to chromatograph a polar solute on the reversed-phase material.

To test, chromatographically, any phase for residual silanols, the column has to be conditioned with heptane or hexane (which has been dried overnight with spherical 4A molecular sieves). The series of solvents to use if the column has been used with water or a water-organic mobile phase, such as water \rightarrow ethanol \rightarrow acetone \rightarrow ethyl acetate \rightarrow chloroform \rightarrow heptane. Once activated, a sample of nitrobenzene or nitrotoluene is injected, eluted with heptane or hexane, and detected at 254 nm. The degree of retention is then a sensitive guide to the presence or absence of residual silanols; if the solute is essentially unretained, the absence of silanols may be assumed. The better the bonding, the faster the polar compound will be eluted from the column. A well-bonded and end-capped phase will have a retention factor of between 0 and 1. Less well-covered silicas can have retention factors greater than 10. This is a comparative test, but it can also be useful for examining a phase to see if the end-capping reagent or primary phase has been cleaved by the mobile phase used over

a period of time. Other methods to measure the silanol content of silica and bonded silica have been discussed by Unger [2]. Solid-state nuclear magnetic resonance spectrometry is the most powerful method to identify the species of residual silanol groups on the silica gel surface [3].

In order to avoid the contribution of the residual silanols to solute retention, many packing materials that should not have silanols have been developed [4]. They are polymer-based materials and also polymer-coated silica phases. These polymer-based or polymer-coated phases can be recommended as very useful and stable stationary phases in LC separations of polar compounds; they also offer much better stability for use at higher pH alkaline conditions.

References

1. K. Karch, I. Sebastian, and I. Halasz, *J. Chromatogr.* 122: 3 (1976).
2. K. K. Unger (ed.), *Packings and Stationary Phases in Chromatographic Techniques*, Marcel Dekker, Inc., New York, 1990.
3. M. Pursch, L. C. Sander, and K. Albert, *Anal. Chem.* 71: 733A (1999).
4. K. K. Unger and E. Weber, *A Guide to Practical HPLC*, GIT Verlag, Darmstadt, 1999.



Enoxacin: Analysis by Capillary Electrophoresis and HPLC

Hassan Y. Aboul-Enein

Imran Ali

King Faisal Specialist Hospital and Research Centre, Riyadh, Saudi Arabia

INTRODUCTION

Enoxacin, 1-ethyl-6-fluoro-1,4-dihydro-4-oxo-7-(1-piperazinyl)-1,8-naphthyridine-3-carboxylic acid (ENX; Fig. 1), is a new broad spectrum fluorinated 4-quinolone antibacterial agent.^[1] It has a broad spectrum of antibacterial activity and is particularly potent against Gram-negative organisms and staphylococci.^[2] The 4-quinolone antibiotics have been used in the treatment of many soft tissue infections including bacterial prostatitis.^[3] ENX is excreted, mainly, in urine as the unchanged drug. It is metabolized by oxidation (to oxo-enoxacin), by conjugation with formic and acetic acid (ring opening), and by deamination of the piperazinyl ring. Its major metabolite, oxo-enoxacin, accounts for 10–15% of the administered dose and each of the other metabolites constitutes less than 1% of the dose.^[2] It has also been reported that ENX has potent competitive inhibitory effects on theophylline metabolism, causing elevated plasma theophylline concentration and potential toxicity.^[4] Because of these properties of ENX, it is very important to develop suitable analytical methods for this substance. High-performance liquid chromatography (HPLC) is the most commonly employed method for the determination of ENX and its metabolites in plasma, urine, and tissues.^[5–12] Capillary electrophoresis (CE) is becoming a reliable, preferable, and alternative method, especially for the analysis of drugs in biological matrices.^[13,14] CE offers some advantages such as rapidity, short analysis time, and low cost.^[15–17] Only one report on the analysis of ENX by CE is presented by Tuncel et al.^[18] Further, the authors have also carried out the analysis of ENX by HPLC and compared this method with the CE method in pharmaceutical dosage forms and in biological fluids.

DETERMINATION OF ENX BY CE

Instruments

The experiments were conducted using a Spectrophoresis 100 system equipped with a modular injector and high-voltage power supply, and a model Spectra FOCUS

scanning CE detector (Thermo Separation Products, California, U.S.A.) connected to a Model Etacomp 486 DX 4-100 computer which processed the data using PC 1000 (Version 2.6) running under the OS/2 Warp program (Version 3.0). The analysis was performed in a fused silica capillary which has a total length of 88 cm, an effective length of 58 cm, and an I.D. of 75 μm (Phenomenex, California, U.S.A.). The pHs of the solutions were measured with a Multiline P4 pH meter with SenTix glass electrode (WTW, Weilheim, Germany). All the solutions were filtered using a Phenex microfilter (25 mm, 0.45 μm) (Phenomenex) and were degassed using a model B-220 ultrasonic bath (Branson, Connecticut, U.S.A.).

Chemicals

Acetonitrile, methanol (HPLC grade), ethanol, propanol, hydrochloric acid, sodium hydroxide, borax, acetylpipemidic acid (internal standard (IS) for CE), and 3,4-dihydroxybenzylamine HBr (IS for HPLC) were from Merck (Darmstadt, Germany). Enoxacin was generously provided by Eczacibasi Ilac Sanayi ve Ticaret A.S. (Istanbul, Turkey). Blood samples were withdrawn from healthy volunteers after obtaining their consent. The serum samples were separated by centrifuging for 10 min at 5000 \times g. Double-distilled water was used to prepare all the solutions. A stock solution of ENX (10 mg/25 mL of methanol) was prepared. Dilutions were made in the range of 2.5×10^{-5} to 1.2×10^{-4} M, each containing 0.25 μmol IS (acetylpipemidic acid) for CE and 0.11 μmol IS (3,4-dihydroxybenzylamine HBr) for HPLC. All the dilutions for CE were prepared in a background electrolyte. The background electrolyte was a 20 mM borate buffer at pH 8.6 for the CE experiments. The dilutions were analyzed by applying a +30-kV potential, injecting the sample 1s and detecting at 265 nm where ENX and acetylpipemidic acid (IS) absorb the monochromatic light equivalently.

Procedure for CE Analysis

The fused silica capillary tubing was filled with the background electrolyte (pH 8.6; 20 mM borate). Both

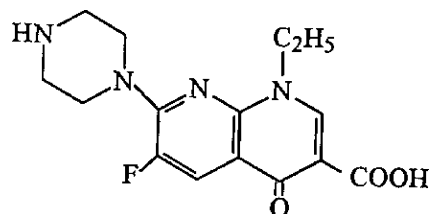


Fig. 1 The chemical structure of ENX.

ends of the tube were dipped into a reservoir (8 mL) and a vial (1.1 mL) filled with the background buffer. The end part where the sample (side of vial) was introduced was connected with a platinum electrode to the positive high-voltage side of the power supply. The reservoir side at the detector end was connected with a platinum electrode to the ground. Samples at a concentration of 7.7×10^{-5} M for the optimization of CE parameters were introduced by 1 s of vacuum injection corresponding to almost 65 nL. Before each run, the capillary was purged for 2 min with 0.1 M sodium hydroxide solution, then for another 2 min with double-distilled water. It was then equilibrated by passing the background electrolyte for 5 min prior to operation.

A background electrolyte consisting of borax was preferred for conducting the initial CE experiments because ENX has a carboxylic group on its structure. Several pH values were tested in the range from 8.45 to 9.95 using the concentration of 20 mM borax buffer. It was observed that the ENX (1.26×10^{-4} M) peak appeared in all the studied pH values, but the migration time of ENX, as expected, increased with increasing pH. Phosphate and citrate buffers of the same pH and concentration (8.6, 20 mM) were used to compare the effect of the nature of the buffer components. The migration time (t_M) of ENX was not affected by the buffer components, but the repeatability of the peak areas decreased with the use of citrate and phosphate buffers. It is concluded that some optimization studies are required if these buffer systems are to be used.

The influence of borax buffer concentration was investigated in the range from 10 to 100 mM. The sharpest peaks were obtained in the use of 10–30 mM concentrations and the t_M of ENX was almost constant, and an increase was observed in the use of borax concentration above 30 mM, but peak deformation also occurred due to the heat production by the Joule effect. In order to achieve optimization of the proposed analytical

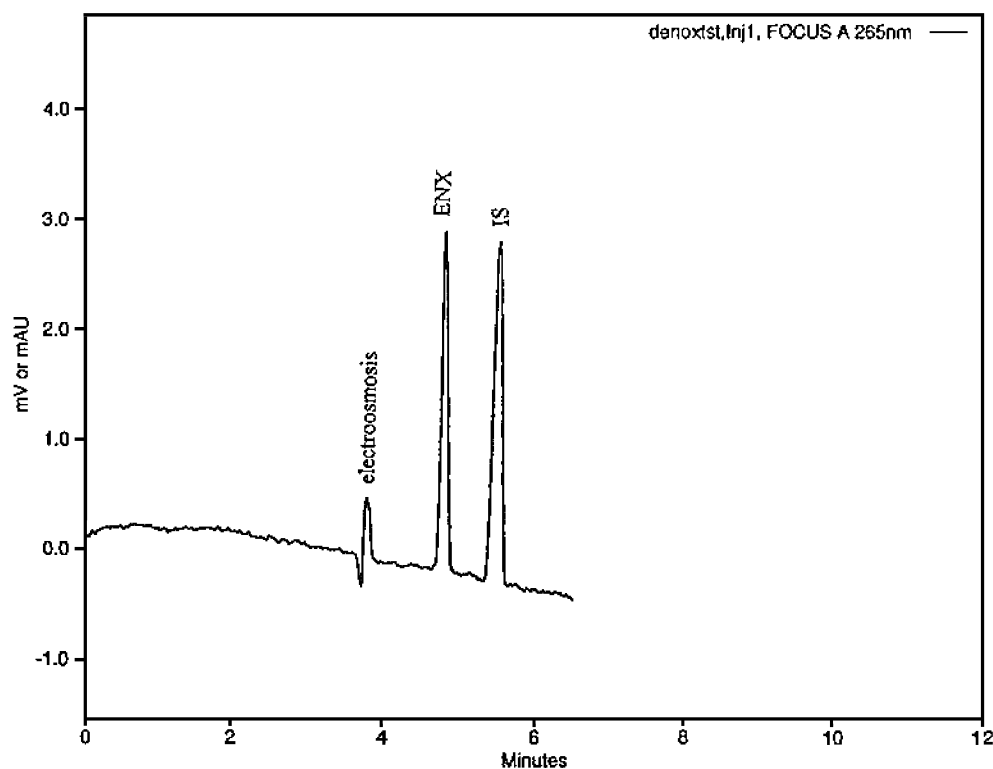


Fig. 2 Typical electropherogram of standard ENX (7.7×10^{-5} M) and IS (acetylpipecimic acid, 5.18×10^{-5} M). Conditions: 20 mM borax pH 8.6; injection, hydrodynamically 1 s; applied voltage, +30 kV; capillary, uncoated fused silica, 75 μ m I.D., 88 cm total, and 58 cm effective length; detection at 265 nm.

Table 1 Precision of peak areas (days = 3; $n = 6$)

Precision of peak areas (RSD%)	PN no IS	IS no PN	IS and PN
Repeatability	2.80	0.99	0.99
Intermediate precision	3.24	2.86	1.36

procedure, low buffer concentration was considered to decrease the electrophoretic mobility that corresponds to short analysis time. Based on the above results, the most convenient buffer system was 20 mM borate buffer at pH 8.6. Since the separation depends on the conditioning of the capillary inner surface in the CE analysis, the t_M and peak integration values might be very similar to the HPLC techniques.

The electropherogram of ENX and acetylpipemidic acid (IS) in the background electrolyte is shown in Fig. 2. The signal of electroosmosis and the migration time of the peaks of ENX and IS appeared at 3.8, 4.8, and 5.5 min, respectively. From the integration data, the net mobility toward the cathode (electroosmosis) and the ENX and IS toward the anode (electrophoretic) were 7.56×10^{-4} , 5.96×10^{-4} , and $4.6 \times 10^{-4} \text{ cm}^2 \text{ V}^{-1} \text{ s}^{-1}$, respectively. The capacity factors were 3.82 (ENX) and 4.53 (IS).

Certain evaluation methods were examined based on the quantification processes. These can be divided into three groups, employing only the values of peak normalization (PN). The effect of the use of IS and certain evaluation methods, such as correction of peak area (normalization), was calculated by dividing the related peak area into t_M on which the precision was examined. These can be divided into three groups: a) employing only the area values of PN (PN no IS), b) computing the ratio values (IS no PN), and c) using the area values of peak normalized IS and ENX (IS and PN). The precision of the peak areas was calculated as shown in Table 1.

The success of the CE experiments from an analytical point of view depends on the conditioning of the capillary surface. Therefore, cleaning and conditioning processes, as explained in the experimental part, must be repeated

after each injection to provide optimum resolution and reproducibility. The precision of the peak area was also assessed by considering certain evaluations, such as the effects of correction of peak area (normalization), which were found by the division of the related peaks into the corresponding migration times; the use of an internal standard was studied.

As seen from Table 1, the lowest RSD% values were obtained from those of IS and PN. Thus, such evaluation was considered throughout the rest of the study. A series of standard ENX solutions in the concentration range of 2.5×10^{-5} through $1.2 \times 10^{-4} \text{ M}$, with each solution containing 0.25 μmol at a fix concentration of IS, were prepared and injected ($n = 3$). Linear regression lines were obtained by plotting the ratios of normalized peak areas to those of the internal standard vs. the analyte concentration. The calibration equation was computed using a regression analysis program, considering the ratio values vs. the related concentrations. The results are presented in Table 2.

Method Validation and Accuracy

From the electropherogram in Fig. 2, no interference from the formulation excipients could be observed at the migration times of ENX and IS. The limit of the detection (LOD) was $3.85 \times 10^{-7} \text{ M}$, while the limit of quantification (LOQ) was $1.16 \times 10^{-6} \text{ M}$. The results indicate good precision. Method accuracy was determined by analyzing a placebo (mixture of excipients) spiked with ENX at three concentration levels ($n = 6$) covering the same range as that used for linearity. Mean recoveries with 95% confidence intervals are given in Table 3.

Determination of ENX by HPLC

HPLC experiments were carried out using a Model 510 Liquid Chromatograph equipped with a Model 481 UV detector (Waters Associates, Milford, Massachusetts, U.S.A.). The chromatograms were processed by means of a chromatographic workstation (Baseline 810). Separation was performed on a reversed-phase Supel-

Table 2 Linearity and accuracy of the method (spiked placebos)

Regression parameters			
Linearity	$r^2 = 0.9998$	intercept (mean \pm SD) $= -0.02342 \pm 7.32 \times 10^{-3}$	slope (mean \pm SD) $= 9813.18 \pm 102.31$
Accuracy	50%	100%	150%
Mean recovery \pm CI%	101.4 ± 2.12	101.1 ± 2.63	100.4 ± 2.25

Table 3 Precision of the method (spiked placebos)

Concentration levels (%)	50	100	150
Repeatability (days = 3; $n = 6$, RSD%)	2.0	2.5	2.1
Intermediate precision (days = 3; $n = 6$, RSD%)	3.3	3.0	3.1

cosil LC-18 column (250×4.6 mm I.D., 5 μ m particle size) (Supelco, St. Louis, Missouri, U.S.A.). The samples were injected into a 50- μ L loop using a Rheodyne 7125 valve (Rheodyne, Cotati, California, U.S.A.).

Procedure for HPLC Analysis

The HPLC conditions were optimized by using different mobile and stationary phases. During HPLC experiments, a 10 mM phosphate buffer (pH 4.0)/acetonitrile (85:15, v/v) was used as a mobile phase. 3,4-Dihydroxybenzylamine-HBr (IS) was found to be a suitable internal standard for the HPLC experiments. The flow rate was 1.5 mL min^{-1} and detection was carried out at 260 nm. The ENX in tablet and the serum were identified by comparing the retention times of the pure ENX under the identical chromatographic conditions.

RESULTS AND DISCUSSION

Under the described chromatographic conditions, ENX has a retention time of 10.03 min, whereas IS eluted at 2 min. Peak area ratios were linearly proportional to ENX concentrations in the range 3.12×10^{-6} through 3.12×10^{-4} M, with a detection limit of 1.56×10^{-6} M. The calibration equation was found to be $[R = -0.51 + 2.1 \times 10^5 C \text{ (M)}; r = 0.9992]$, where $C \text{ (M)}$ is the molar concentration of ENX. The results of the HPLC experiments were compared with those obtained by the CE experiments. As described earlier, various reports on enoxacin analysis by HPLC are available. The different stationary phases used are μ -Bondapak C_{18} , Spherisorb S5 ODS2, Nucleosil C_{18} , Hypersil ODS, etc. The mobile phases used for the analysis of ENX are different ratios of water–acetonitrile, buffers–acetonitrile, acetonitrile–salt solutions, methanol–salt solutions, etc.^[5–12]

Analysis of ENX in Tablets by CE and HPLC Methods

Enoxacin tablets (containing 400 mg active material) were obtained from the local market. Ten ENX tablets were accurately weighed. The average weight of one tablet was calculated, and then the tablets were finely

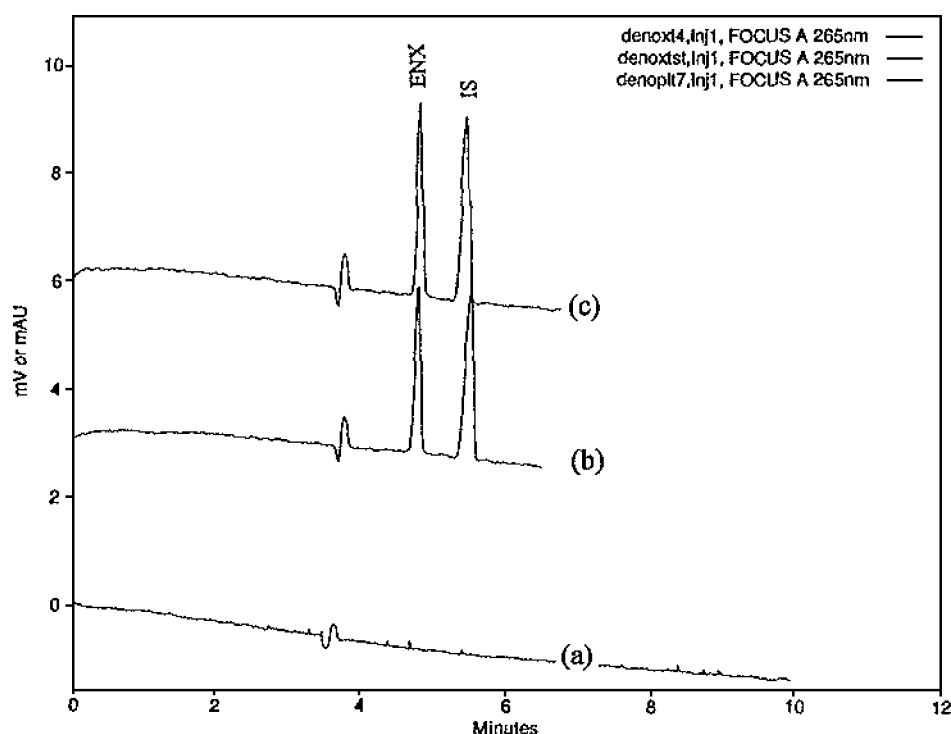


Fig. 3 Electropherograms of (a) inactive ingredients of a tablet solution of ENX; (b) standard ENX (7.7×10^{-5} M) and IS (acetylpipecimic acid, 5.18×10^{-5} M); and (c) enoxacin tablet solution containing IS. Conditions are the same as in Fig. 2.

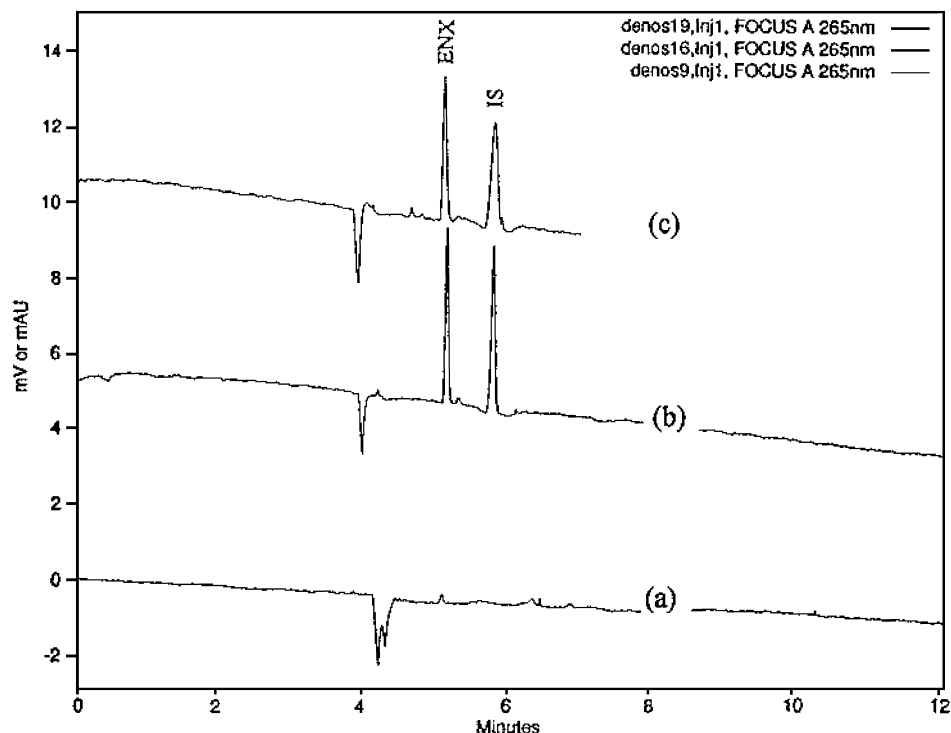


Fig. 4 Electropherogram of (a) blank serum deproteinized with ethanol; (b) serum spiked with the standard ENX solution (0.25 μmol) and IS (0.15 μmol); and (c) water spiked with the standard ENX solution (0.25 μmol). Conditions are the same as in Fig. 2.

powdered in a mortar. A sufficient amount of tablet powder, equivalent to 10 mg of ENX, was accurately weighed, then transferred to a 25-mL volumetric flask, and methanol was added to dissolve the active material. It was magnetically stirred for 10 min and made up to the final volume with the related solvent. The solution was then centrifuged at $5000 \times g$ for 10 min. The supernatant and a fixed amount of IS solution were diluted with a background electrolyte or mobile phase to carry out either the CE or the HPLC assay. The electropherograms of ENX in tablets with IS are shown in Fig. 3.

Analysis of ENX in Serum by CE and HPLC Methods

For the CE analysis, 0.25 μmol of ENX (in 1 mL) was added to 1 mL of serum and was vigorously shaken. Then 3 mL of ethanol was added and mixed well using a shaker. The precipitated proteins were separated by centrifuging for 10 min at $5000 \times g$. A specific amount of clear supernatant was transferred to a tube, IS solution was added, and the final solution was directly injected to the CE instrument under the same conditions. It was reported that some determinations have been carried out by directly injecting the supernatant of the homogenates

and urine into the CE.^[16] This kind of application shortens the total analysis time. For HPLC, the precipitation of proteins of 1 mL serum was achieved according to the methods described by Nangia et al.,^[17] i.e., by adding 50 μL HClO_4 (60% w/v), centrifuging for 10 min at $5000 \times g$, and directly injecting the supernatant into the column of the HPLC system under the conditions mentioned above. The electropherograms of ENX with IS in the serum are given in Fig. 4.

Table 4 Comparative studies for the determination of ENX tablet

No. of experiment	Amount found (mg) using CE	Amount found (mg) using HPLC
1	419.7	410.1
2	428.5	417.4
3	422.3	414.9
4	417.1	419.9
5	419.4	417.4
Mean	421.4	415.9
RSD%	1.04	0.89
$t_{\text{calculated}}$	2.13	
t_{table}		2.78 ($p = 0.05$)

(Declared amount, 400 mg per tablet).

CONCLUSION

A typical electropherogram is shown in Fig. 2, which indicates no interferences from the tablet excipients. In order to examine the applicability and validity of the CE method, ENX pharmaceutical tablets were analyzed by CE and HPLC methods. Results of the comparative studies are shown in Table 4. The results indicate that both methods, i.e., by CE and HPLC, show insignificant differences at the 95% probability level and the ENX tablet formulations satisfy the official requirements.^[19] Certain experiments were conducted to elucidate the recovery of ENX and to validate the CE studies. Three sets of experiments with definite amounts of ENX were added to the serum and to the double-distilled water, and were analyzed. The same experiment was also performed without any ENX. The recovery was found to be 89.7 ± 0.63 (RSD%). The recovery experiments were also tested by HPLC and were found to be 78.8 ± 4.94 (RSD%). The difference between the methods could be due to the different precipitation procedures applied.

These results show that the proposed CE method is simple, rapid, and low cost, as compared to HPLC, especially for the quality-control analysis of ENX. It has also been observed that the amount of ENX found (Table 4) was always greater with CE than with HPLC. The presented CE method can be used for the analysis of ENX at trace levels in unknown matrices and also for routine quality control of ENX.

REFERENCES

1. Wolfson, J.S.; Hooper, C. *Quinolone Antimicrobial Agents*; American Society for Microbiology: Washington, DC, 1989.
2. Henwood, J.M.; Monk, J.P. Enoxacin: A review of its antibacterial activity, pharmacokinetic properties and therapeutic use. *Drugs* **1988**, *36*, 32–66.
3. Guimaraes, M.A.; Noone, P. The comparative in-vitro activity of norfloxacin, ciprofloxacin, enoxacin and nalidixic acid against 423 strains of Gram-negative rods and staphylococci isolated from infected hospitalised patients. *J. Antimicrob. Chemother.* **1986**, *17*, 63–68.
4. Wijnands, W.J.; Vree, T.B.; Van Herwaarden, C.L. The influence of quinolone derivatives on theophylline clearance. *Br. J. Clin. Pharmacol.* **1986**, *22*, 677–683.
5. Vree, T.B.; Baars, A.M.; Wijnands, W.J.A. High performance liquid chromatography and preliminary pharmacokinetics of enoxacin and its 4-oxo metabolite in human plasma, urine and saliva. *J. Chromatogr., Biomed. Appl.* **1985**, *343*, 449–454.
6. Griggs, D.J.; Wise, R. A simple isocratic high pressure liquid chromatographic assay of quinolones in serum. *J. Antimicrob. Chemother.* **1989**, *24*, 437–445.
7. Nangia, A.; Lam, F.; Hung, C.T. Reversed phase ion-pair high performance liquid chromatographic determination of fluoroquinolones in human plasma. *J. Pharm. Sci.* **1990**, *79*, 988–991.
8. Goebel, K.J.; Stolz, H.; Ehret, I.; Nussbaum, W. A validated ion-pairing high performance liquid chromatographic method for the determination of enoxacin and its metabolite oxo-enoxacin in plasma and urine. *J. Liq. Chromatogr.* **1991**, *14*, 733–751.
9. Zhai, S.; Korrapati, M.R.; Wei, X.; Muppalla, S.; Vestal, R.E. Simultaneous determination of theophylline, enoxacin and ciprofloxacin in human plasma and saliva by high performance liquid chromatography. *J. Chromatogr., Biomed. Appl.* **1995**, *669*, 372–376.
10. Davis, J.D.; Aarons, L.; Houston, J.B. Simultaneous assay of fluoroquinolones and theophylline in plasma by high performance liquid chromatography. *J. Chromatogr., Biomed. Appl.* **1993**, *621*, 105–109.
11. Hamel, B.; Audran, M.; Costa, P.; Bressolle, F. Reversed phase high performance liquid chromatographic determination of enoxacin and 4-oxo-enoxacin in human plasma and prostatic tissue: Application to a pharmacokinetic study. *J. Chromatogr., A* **1998**, *812*, 369–379.
12. Barbosa, J.; Berges, R.; Sanz-Nebot, V. Retention behaviour of quinolone derivatives in high performance liquid chromatography: Effect of pH and evaluation of ionization constants. *J. Chromatogr., A* **1998**, *823*, 411–422.
13. Boone, C.M.; Douma, J.W.; Franke, J.P.; de Zeeuw, R.A.; Ensing, K. Screening for the presence of drugs in serum and urine using different separation modes of capillary electrophoresis. *Forensic Sci. Int.* **2001**, *121*, 89–96.
14. Lemos, N.P.; Bortolotti, F.; Manetto, G.; Anderson, R.A.; Cittadini, F.; Tagliaro, F. Capillary electrophoresis: A new tool in forensic medicine and science. *Sci. Justice* **2001**, *41*, 203–210.
15. Baker, D.R. *Capillary Electrophoresis*; J. Wiley & Sons, Inc.: New York, 1995.
16. Xu, Y. Capillary electrophoresis. *Anal. Chem.* **1995**, *67*, 463R–473R.
17. Altria, K.D. Overview of capillary electrophoresis and capillary electrochromatography. *J. Chromatogr.* **1999**, *856*, 443–463.
18. Tuncel, M.; Dogrukol-Ak, D.; Senturk, Z.; Ozkan, S.A.; Aboul-Enein, H.Y. Capillary electrophoretic behaviour and determination of enoxacin in pharmaceutical preparations and human serum. *J. Liq. Chromatogr. Relat. Technol.* **2001**, *24*, 2455–2467.
19. *United States Pharmacopoeia (USP) 22, NF-17*; U.S. Pharmacopeial Convention: Rockville, Maryland, 1990.

Environmental Applications of SFC

Yu Yang

East Carolina University, Greenville, North Carolina, U.S.A.

Introduction

Because supercritical fluids have liquidlike solvating power and gaslike mass-transfer properties, supercritical fluid chromatography (SFC) is considered to be the bridge between gas chromatography (GC) and liquid chromatography (LC) and possesses several advantages over GC and LC, as summarized in Table 1. For example, SFC can separate nonvolatile, thermally labile, and high-molecular-weight compounds in short analysis times. Another advantage of SFC is its compatibility with both GC and high-performance liquid chromatographic (HPLC) detectors. Because of these advantages of SFC, there is a large number of SFC applications in environmental analysis. However, only selected recent works are reviewed here. Although sample preparation is often required before SFC analysis to remove the analytes from environmental matrices and to enrich them, sample preparation is not intensively discussed in this review. To facilitate the discussion, the environmental pollutants are classified and reviewed separately in this article.

Pesticides and Herbicides

The analysis of pesticides and herbicides has mainly been done either by GC with selective detectors or by HPLC with ultraviolet (UV) detection. As summarized

in Table 1, GC is limited to thermally stable volatile compounds, whereas the HPLC with UV can only detect compounds with chromophores. These limitations of GC and HPLC led to the use of SFC in the analysis of pesticides and herbicides. Among the SFC works in environmental analysis, one-third of the works concerns the analysis of pesticides and herbicides.

Many detectors have been used to detect pesticides and herbicides in SFC. Among these detectors, the flame ionization detector (FID) is most commonly used for detection of a wide range of pesticides and herbicides, with a detection limit ranging from 1 ppm (for carbonfuran) to 80 ppm (for Karmex, Harmony, Glean, and Oust herbicides). The UV detector has frequently been used for the detection of compounds with chromophores. The detection limit was as low as 10 ppt when solid-phase extraction (SPE) was on-line coupled to SFC. The mass spectrometric detector (MSD) has also been used in many applications as a universal detector. The MSD detection limit reached 10 ppb with on-line SFE (supercritical fluid extraction)–SFC. Selective detection of chlorinated pesticides and herbicides has been achieved by an electron-capture detector (ECD). The limit of detection for triazole fungicide metabolite was reported to be 35 ppb. Other detectors used for detection of pesticides and herbicides include thermoionic, infrared, photometric, and atomic emission detectors.

Table 1 Comparison of Characteristics of GC, SFC, and LC

	GC ^a	SFC	LC ^b
Suitability for polar and thermolabile compounds	Low	High	High
Size of analyte molecule	Small–Medium	Small–Large	Small–Large
Sample capacity	Low	High (packed column)	High
Possibility of introducing selectivity in the mobile phase	Low	High	Medium
Toxicity and disposal cost of the mobile phase	No	No (with pure CO ₂) Low (with modifier)	High
Efficiency	High	Medium–High	Low
Use of gas-phase detectors	Yes	Yes	No
Analysis time	Medium	Medium	Long

^aOnly capillary GC is used for these evaluations. Fast GC and packed column GC are not included here.

^bCapillary HPLC is not included.



A variety of both packed and open tubular columns have been used for separation of pesticides and herbicides. The columns were either used separately or coupled in series to achieve better separations. Although environmental water samples were mostly analyzed by SFC, analyses of pesticides and herbicides from soil, foods, and other samples were also reported.

Polychlorinated Biphenyls

Since 1929, polychlorinated biphenyls (PCBs) have been produced and used as heat-transfer, hydraulic, and dielectric fluids. Because of their chemical and physical stability, PCBs have been found in many environmental samples. Generally, PCBs have been analyzed by GC with electron-capture detection. There are many reports on subcritical and supercritical fluid extraction of PCBs, but only a few on supercritical fluid separation of PCBs.

Among the works of supercritical fluid separations of PCBs, UV has been the most popular detector. A Microbore C₁₈ column was used to separate individual PCB congeners in Aroclor mixtures. Density and temperature programming was also utilized for separation of PCBs. Both packed (with phenyl and C₁₈) and capillary (Sphery-5 cyanopropyl) columns were used in this work. Carbon dioxide, nitrous oxide, and sulfur hexafluoride were tested as mobile phases for the separation of PCBs.

A flame ionization detector and MSD were also used for detection of PCBs in SFC. Capillary columns packed with aminosilane-bonded silica and open tubular columns coated with polysiloxane were employed for PCB separation in these works.

Polycyclic Aromatic Hydrocarbons

Polycyclic aromatic hydrocarbons (PAHs) have routinely been analyzed by GC and LC. However, both techniques have limitations in terms of analyte molecular weight and analysis time. The greater molecular-weight range of SFC with respect to GC makes it better suited for determining a wide range of PAHs. SFC also has advantages over HPLC for the analysis of PAHs when the same kind of columns is used. Supercritical fluid has similar solvating power as a liquid does, and the solute diffusion coefficients are much greater than those found in liquids. Therefore, comparable efficiencies to HPLC can be obtained by SFC in shorter analysis time. Because of these characteristics of SFC, the separation of PAHs by SFC with different

kinds of packed and capillary columns is a well-investigated and established method.

The most popular detector for PAHs is the UV detector. The detection limit was 0.2–2.5 ppb for 16 PAHs. A diode-array detector was also used for PAHs in SFC, and the detection limit was reported to be as low as 0.4 ppb. Other detections used for PAHs include mass spectrometric, thermoionic, infrared, photoionization, sulfur chemiluminescence, and fluorescence detectors.

Although CO₂ has mainly been used as the mobile phase in SFC, modifiers have often been added to CO₂ to increase the solvating power of the mobile phase. Although the most frequently used modifier has been methanol, many other modifiers were also tested. The modifier effect on retention is discussed separately in this encyclopedia. Because organic modifiers are incompatible with FID, flame ionization detection was rarely used for PAHs in SFC.

Fast separations of 16 PAHs were achieved within 6–7 min using packed columns. A comparison study of the PAH molecular shape recognition properties of liquid-crystal-bonded phases in packed-column SFC and HPLC found that the selectivity was enhanced in SFC. The result of an interlaboratory round-robin evaluation of SFC for the determination of PAHs also shows that SFC possesses distinct advantages over GC–mass spectrometry (MS) and nuclear magnetic resonance (NMR) including speed, cost, and applicability.

Polar Pollutants

Because carbon dioxide is nonpolar, the separation of polar compounds by supercritical carbon dioxide is difficult. Thus, polar modifiers are often used for the separation of phenols and amines. Derivatization has also been employed to obtain nonpolar analytes in some applications. The UV detector has mainly been used for the detection of polar compounds. Oxidative and reductive amperometric detection was also utilized with a detection limit of 250 pg for oxidative detection of 2,6-dimethylphenol. The detection of amines has generally been achieved by FID. Other detectors used for the detection of polar analytes include Fourier transform infrared (FTIR), photodiode array, and flame photometry.

It should be pointed out that separation of more than one class of organic compounds can be achieved by SFC. For example, Fig. 1 shows the chromatogram of 35 PAHs, herbicides, and phenols from a contaminated water sample. Solid-phase extraction was used



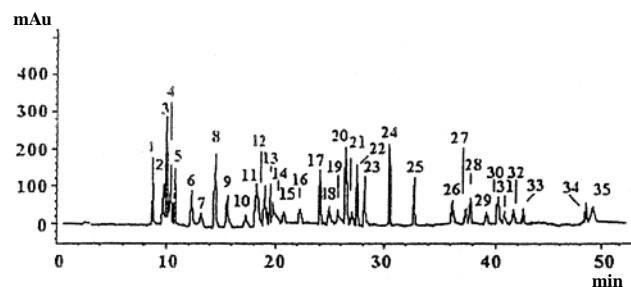


Fig. 1 Chromatogram of PAHs, herbicides, and phenols obtained by supercritical carbon dioxide modified with methanol. [Reprinted from L. Toribio, M. J. del Nozal, J. L. Bernal, J. J. Jimenez, and M. L. Serna, Packed-column supercritical fluid chromatography coupled with solid-phase extraction for the determination of organic microcontaminants in water, *J. Chromatogr. A* 823: 164 (1998). Copyright 1998, with permission from Elsevier Science.]

for sample preparation. Five Hypersil silica columns were coupled in series for separation of these contaminants. The percentage of methanol (as modifier) was varied from 2% (5 min) to 10% (29 min) at 0.5%/min. A pressure program was also applied. A diode-array detector was used in this work.

Organotin, Mercury, and Other Inorganic Pollutants

Organotin compounds are used extensively as biocides and in marine antifouling paints. These compounds accumulate in sediments, marine organisms, and water, as they are continuously released into the marine environment. Many of these organotin compounds are toxic to aquatic life. Most organotin separation techniques have been based on the GC resolution of volatile derivatives and coupled to elemental detection techniques that are often not sensitive enough to detect trace organotin compounds. However, the separation of organotin compounds was achieved by capillary columns (SB-Biphenyl-30 or SE-52) with pure CO_2 as the mobile phase. Inductively coupled plasma-mass spectrometry (ICP-MS) was used in most of the applications to improve the sensitivity for detecting trace organotin species. The reported detection limits range from 0.2 to 0.8 pg for tetrabutyltin chloride, tributyltin chloride, triphenyltin chloride, and tetraphenyltin. However, the detection limits obtained by FID are 15- to 45-fold higher than those obtained by ICP-MS for the above-mentioned organotin compounds. Flame photometric detector

was also used to detect organotin species with a detection limit of 40 pg for tributyltin chloride.

The separation of organomercury was conducted by using a SB-methyl-100 capillary column and pure CO_2 as the mobile phase. FID and atomic fluorescence were used for detection. The same column was also used for separation of mercury, arsenic, and antimony species using carbon dioxide as the mobile phase. A chelating reagent, bis(trifluoroethyl)dithiocarbamate, was used in this case to convert the metal ions to organometallic compounds before the separation. The detection limit of FID was 7 and 11 pg for arsenic and antimony, respectively.

Figure 2 shows an example of separating organomercury using supercritical CO_2 . A 10-m \times 50- μm -inner diameter SB-Methyl 100 column was used for the separation. Due to their poor solubility in supercritical carbon dioxide, monoorganomercury compounds were derivatized by diethyldithiocarbamate. An interface for a system consisting of SFC and atomic fluorescence spectrometry was developed for the detection of organomercurials.

In closing, supercritical fluid chromatography is a promising technique for the analysis of environmental pollutants. The analytes range from inorganic species to polar and nonpolar organic compounds. The sample matrices cover water, soil, sediments, sludge,

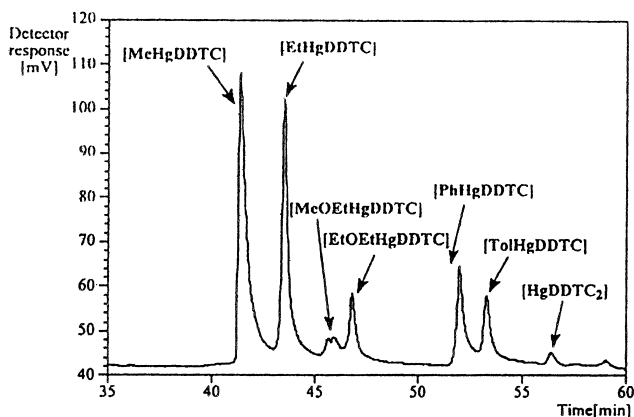


Fig. 2 Chromatogram of a standard mixture after complexation with sodium diethyldithiocarbamate. Composition of the standard: mercury dichloride, methylmercury chloride, ethylmercury chloride, methoxyethylmercury chloride, ethoxyethylmercury chloride, phenylmercury chloride, and tolylmercury chloride. [Reprinted from A. Knochel and H. Potteger, Interfacing supercritical fluid chromatography with atomic fluorescence spectrometry for the determination of organomercury compounds, *J. Chromatogr. A* 786: 192 (1997). Copyright 1997, with permission from Elsevier Science.]



and air particulate matters. The sample preparation has been done by solid-phase extraction, supercritical fluid extraction, or traditional solvent extraction. Modifiers are often used to enhance the solubility of analytes and to yield a better separation for polar and high-molecular-weight analytes. Packed columns are preferred for trace analysis because of their high sample capacity. Both gas-phase and liquid-phase detectors have been used in SFC to detect a wide range of environmental pollutants.

Suggested Further Reading

- J. M. Bayona and Y. Cai, *Trends Anal. Chem.* 13: 327–332 (1994).
- T. A. Berger, *J. Chromatogr. A* 785: 3–33 (1997).
- T. L. Chester, J. D. Pinkston, and D. E. Raynie, *Anal. Chem.* 70: 301R–319R (1998).
- S. F. Dressman, A. M. Simeone, and A. C. Michael, *Anal. Chem.* 68: 3121–3127 (1996).
- Z. Juvancz, K. M. Payne, K. E. Markides, and M. L. Lee, *Anal. Chem.* 62: 1384–1388 (1990).
- A. Knochel and H. Potgeter, *J. Chromatogr. A* 786: 188–193 (1997).
- K. E. Laintz, G. M. Shieh, and C. M. Wai, *J. Chromatogr. Sci.* 30: 120–123 (1992).
- D. R. Luffer and M. Novotny, *J. Chromatogr.* 517: 477–489 (1990).
- A. Medvedovici, A. Kot, F. David, and P. Sandra, The use of supercritical fluids in environmental analysis, in *Supercritical Fluid Chromatography with Packed Columns* (K. Anton and C. Berger, eds.), Marcel Dekker, Inc., New York, 1998, pp. 369–401.
- A. Medvedovici, F. David, G. Desmet, and P. Sandra, *J. Microcol. Separ.* 10: 89–97 (1998).
- E. Moyano, M. McCullagh, M. T. Galceran, and D. E. Games, *J. Chromatogr. A* 777: 167–176 (1997).
- L. J. Mulcahey, C. L. Rankin, and M. E. P. McNally, Environmental applications of supercritical fluid chromatography, in *Advances in Chromatography Vol. 34*, 1994, pp. 251–308.
- S. Shan, M. Ashraf-Khorassani, and L. T. Taylor, *J. Chromatogr.* 505: 293–298 (1990).
- R. M. Smith and D. A. Briggs, *J. Chromatogr. A* 688: 261–271 (1994).
- L. Toribio, M. J. del Nozal, J. L. Bernal, J. J. Jimenez, and M. L. Serna, *J. Chromatogr. A* 823: 163–170 (1998).



Environmental Pollutants Analysis by Capillary Electrophoresis

Imran Ali

Hassan Y. Aboul-Enein

King Faisal Specialist Hospital and Research Center, Riyadh, Saudi Arabia

INTRODUCTION

The quality of the environment is degrading continuously, due to the accumulation of various undesirable constituents. Water resources, the most important and useful components of the environment, are most affected by pollution. The ground and surface water at many places in the world are not suitable for drinking purposes, due to the presence of aesthetic and toxic pollutants. Therefore, the importance of water quality preservation and improvement is essential and continuously increasing.^[1,2] The most important toxic pollutants are inorganic and organic chemicals. Therefore, determination of these water pollutants at trace levels is essential in environmental hydrology.

The analysis of these pollutants has been widely carried out using gas chromatography (GC)^[3,4] and high performance liquid chromatography (HPLC).^[3,4] The high polarity, low vapor pressure, and required derivatization of some of the organic pollutants are the factors that complicate GC analysis. On the other hand, due to the inherently limited resolving power of conventional HPLC techniques, optimization of pollutant analysis often involves complex procedures or numerous experiments leading to the consumption of large amounts of solvents and sample volumes. Presently, capillary electrophoresis (CE), a versatile technique of high speed, high sensitivity, lower limit of detection, and reproducible results, is a major trend in analytical science and the number of publications on water pollutants analysis have increased exponentially in recent years.^[3,5–11] Therefore, attempts have been made, here, to summarize the various CE methods for the analysis of different water pollutants. Critical comments are also presented to improve the application of CE in water pollutant analysis.

PRINCIPLE OF CAPILLARY ELECTROPHORESIS

The schematic representation of a CE apparatus is shown in Fig. 1. The mechanism of separation of water pollutants in CE is based on the electroosmotic flow (EOF) and

electrophoretic mobilities of the pollutants. The EOF propels all pollutants (cationic, neutral, and anionic) toward the detector and, ultimately, separation occurs due to the differences in the electrophoretic migration of the individual pollutants. Under the CE conditions, the migration of the pollutant is controlled by the sum of the intrinsic electrophoretic mobility (μ_{ep}) and the electroosmotic mobility (μ_{eo}), due to the action of EOF. The observed mobility (μ_{obs}) of the pollutants is related to μ_{eo} and μ_{ep} by the following equation:

$$\mu_{obs} = \mu_{eo} + \mu_{ep} \quad (1)$$

The electrophoretic mobilities of cations (μ_{obs}) can be related to the limiting ionic equivalent conductivity, λ_{ekv} , by the following equation:

$$\mu_{obs} = \lambda_{ekv}/F = q_i/6\pi\eta r_i \quad (2)$$

where, F is the Faraday constant ($F = 9.6487 \times 10^4$ A sec mol⁻¹), λ_{ekv} (cm² mol⁻¹ ohm⁻¹) is related, by the Stokes law, to the charge of the hydrated cation q_i , to the dynamic viscosity of the electrolyte, η (g cm² sec⁻¹), and to the radius of the hydrated cation r_i (cm). The μ_{ep} values can be calculated from the experimental data, the mobility of the cation (μ_{obs}), and the mobility of the EOF μ_{eo} , according to the following equation:

$$\mu_{ep} = \mu_{obs} - \mu_{eo} = [1/t_{m(ion)} - 1/t_{m(eo)}][l_T \cdot L_d/V] \quad (3)$$

where, $t_{m(ion)}$, $t_{m(eo)}$, l_T and L_d are the migration time of the cation (sec), migration time of the EOF (sec), the overall capillary length, and the length of the capillary to the detector (cm), respectively. Thus, EOF plays an important role in the determination of metal ions by CE. The determination of water pollutants can be carried out by several modes of CE. The various modes of CE include capillary zone electrophoresis (CZE), micellar electrokinetic capillary chromatography (MECC), capillary isotachopheresis (CIEF), capillary gel electrophoresis (CGE), ion-exchange electrokinetic chromatography (IEEC), capillary isoelectric focusing (CIEF), affinity capillary electrophoresis (ACE), capillary electrochromatography (CEC), separation on microchips (MC), and nonaqueous

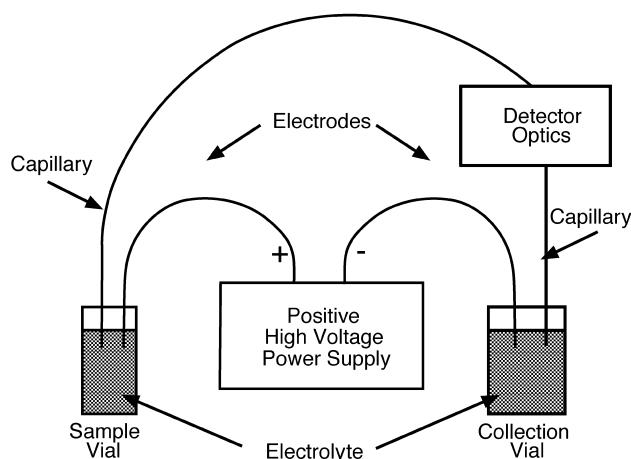


Fig. 1 Diagram of the CE system. (Reprinted from Waters Quanta 4000E Capillary Electrophoresis System Operator's Manual, Waters Corp., Milford, Massachusetts, U.S.A., 1993.)

capillary electrophoresis (NACE).^[8] However, most of the water pollutant analyses have been carried out in the CZE mode.

SAMPLE PRETREATMENT

The treatment of the samples from environmental matrices is an important issue in CE. Little attention has been given for the water sample treatment in CE analysis of environmental pollutants. Soil samples have been extracted by the usual methods. Besides, the sediment samples were digested using strong acids. The samples containing a highly ionic matrix may cause problems in CE. Electroosmotic flow in the capillary can be altered by the influence of the sample matrix, resulting in poor resolution. Additionally, the detector baseline is usually perturbed when the pH of the sample differs greatly from the pH of the background electrolyte (BGE). The samples containing UV absorbing materials are also problematic in the detection of the environmental pollutants. Due to all of these factors, some authors have suggested sample cleanup processes, solid/liquid phase extractions, and sample preparations prior to loading onto CE.^[10–13] Real samples often require the application of simple procedures, such as filtration, extraction, dilution, etc. Electromigration of sample cleanup suffers severely from matrix dependence effects; even then, it has been used for pre-concentration in inorganic analysis. The sample treatment methods have been discussed in several reviews.^[7–9,12] The use of ion-exchange and chelating resins to pre-concentrate the metal ion samples prior to CE application has been reported.^[9,12] An on-line dialysis sample cleanup method for CE analysis has also been presented. Besides, several reports have been published on dialy-

Environmental Pollutants Analysis by Capillary Electrophoresis

sis and electro dialysis for sample cleanup prior to CE injection.^[7–9,12]

DETECTION

Generally, UV detection is used for the determination of most environmental pollutants. However, the use of UV detectors in CE for metal ion and anion analysis is not suitable due to the poor absorbance of UV radiation by metal ions and anions. The most common method to solve this problem is indirect UV detection. The main advantage of the indirect UV detection method is its universal applicability. The complexation of metal ions with ligands also increases the sensitivity of their detection. The complexing agent is either added to the electrolyte (in situ, on-line complexation) or to the sample before the introduction into the capillary column (off-line complexation). The most commonly used ligands are azo dyes, quinoline dyes, porphyrin, dithiocarbamate, aminopolycarboxylic acids, 4-(2-pyridylazo) resorcinol, 8-hydroxyquinoline-5-sulfonic acid, ethylenediaminetetraacetic acid, cyanides, various hydroxy carboxylic acids, crown ethers, and other organic chelating agents. Besides, UV visualizing agents (probe) have also been used to increase the sensitivity of detection in the UV mode. The important probes include, e.g., Cu(II) salts, chromate, aromatic amines, and cyclic compounds, e.g., benzylamine, 4-methylbenzylamine, dimethylbenzylamine, imidazole, *p*-toluidine, pyridine, creatinine, ephedrine, and anionic chromophores (benzoate and anisates).^[7–9,12,14] Care must be taken to avoid the interaction of the cations and visualizing agent with the capillary wall. Besides, the visualizing agents should exhibit a mobility close to that of the cations, its UV absorbance should be as high as possible, and the detector noise as low as possible. Furthermore, sensitivity of the UV detection has been increased by using a double beam laser as the light source.

To overcome the problem of detection in CE, many workers have used inductively coupled plasma-mass spectrometry (ICP-MS) as the method of detection.^[7–9,12–14] Electrochemical detection in CE includes conductivity, amperometry, and potentiometry detection. The detection limit of amperometric detectors has been reported to be up to 10^{-7} M. A special design of the conductivity cell has been described by many workers. The pulsed-amperometric and cyclic voltammetry waveforms, as well as multi step waveforms, have been used as detection systems for various pollutants. Potentiometric detection in CE was first introduced in 1991 and was further developed by various workers.^[7–9,12,14] 8-Hydroxyquinoline-5-sulfonic acid and lumogallion exhibit fluorescent properties and, hence, have been used for metal ion detection in CE by fluorescence detectors.^[7–9,12,14] Over-

all, fluorescence detectors have not yet received wide acceptance in CE for metal ions analysis, although their gains in sensitivity and selectivity over photometric detectors are significant. Moreover, these detectors are also commercially available. Some other devices, such as chemiluminescence, atomic emission spectrometry (AES), refractive index, radioactivity, and X-ray diffraction, have also been used as detectors in CE for metal ions analysis,^[14] but their use is still limited.

SEPARATION EFFICIENCY IN CAPILLARY ELECTROPHORESIS

From the literature available and discussed herein, it may be assumed that the selectivity of various environmental pollutants by CE is quite good. However, the detection sensitivity for metal ions and anions is poor. Therefore, many attempts have been made to solve this problem. Organic solvents have been added to the BGE to improve the selectivities of many of the pollutants. It has also been reported that the organic solvents ameliorate the solubility of hydrophobic complexes, reduce the adsorption onto the capillary wall, regulate the distribution of complexes between aqueous phase and micellar phase, adjust the viscosity of the separation medium and, accordingly, accomplish an improvement in detection. The pH of the electrolyte solution is very important from the selectivity point of view. The pH controls the behavior of EOF, acid/base dissociation equilibria of complexes, and the state of existing complexes. Therefore, the selectivity can be improved by adjusting the pH of the BGE. Besides, ion pairing can be used to improve the separation in CE. Six types of ion pairing agents have been developed and used. Ion pairing has also been used in MECC for the improvement of the separation of hydrophobic or weakly hydrophobic metal complexes. In addition, the selectivity of the separation of environmental pollutants has also been increased by varying the partition and ion-association (micellar interactions) mechanisms.

APPLICATIONS

During the last decade, CE has been increasingly used for the determination of environmental pollutants. Some of the methods of pre-treatment of waste environmental samples have been carried out prior to the injection into the CE system, as discussed above. CE has been applied for the determination of inorganic and organic pollutants. The major inorganic pollutants include metal ions and anions. On the other hand, the most common toxic organic environmental pollutants analysed by CE are phenols, pesticides, polynuclear aromatic hydrocarbons,

amines, carbonyl compounds, surfactants, dyes, and others. Recently, chiral separation of pollutants and xenobiotics has emerged as the most important issue for the environmental chemist. Therefore, CE has also been used for the analysis of the chiral pollutants. The application of CE for the determination of environmental pollutants is summarized in Table 1, which contains the type of pollutants, their sources, BGE used, detection method, and detection limit. As a specimen sample, a typical electropherogram of separated metal ions in a water sample by CE is shown in Fig. 2.^[7]

Validation of Methods

There are only a few studies dealing with method validation of the determination of environmental pollutants by CE. However, some authors have demonstrated the application of their developed separation methods. The accuracy determination for Na, K, Ca, and Mg metal ions has been presented.^[7-9] Similarly, the precision of migration times and peak areas for seven alkali and alkaline earth metals has been measured; RSD values were less than 0.4% for migration times and from 0.8% to 1.8% for peak areas.^[7-9] In one of the experiments, the reported %RSD varied from 2.79 to 3.38 for Zn, Cu, and Fe metal ions.^[15] Several other studies have shown reliable results with recoveries close to 100%, or good agreement with the results obtained by other methods.^[15] In spite of this, the precision of linearity, sensitivity, and reproducibility of CE methods for metal ions and anions analysis are not better than ion chromatography.

CONCLUSION

The determination of environmental pollutants at trace level is currently a very important and challenging issue. Gas chromatography and high performance liquid chromatography have been used for the analysis of environmental pollutants but, in recent years, capillary electrophoresis has also been used for the determination of environmental pollutants. A search of the literature indicates several reports of the analysis of environmental pollutants by CE, but CE could not have yet achieved a place in the routine analysis of these pollutants. The reason for this is the poor detection of metal ions and anions and the poor reproducibility of CE methods. Therefore, many workers have suggested various modifications and alternatives to make CE a method of choice. To obtain good sensitivity and reproducibility, the selection of the capillary wall chemistry, pH and ionic strength of the BGE, complexing and visualizing agents, detectors, and optimization of BGE have been described and suggested.^[7-9,14-17]

**Table 1** The applications of capillary electrophoresis for the determination of environmental pollutants

Pollutants	Sample matrix	Electrolytes	Detection	Detection limit
<i>Metal Ions in Water, Sediment, and Soil</i> ^[7-9]				
Arsenic and selenium	Drinking water	20 mM KHP, 20 mM Boric acid (pH 9.03) hydrodynamically modified EOF	Hydride generation ICP-MS	6–58 ng/L
		75 mM Dihydrogen phosphate, 25 mM tetraborate (pH 7.65)	Direct UV 195	12 µg/L
		Chromate, 0.5 mM TTAOH (pH 10.5)	Indirect UV 254 nm	10 µg/L
Mg, Ca, Na, and K	Well water	5 mM Imidazole, 6.5 mM HIBA	Indirect UV 214 nm	–
		2 mM 18-crown-6 (pH 4.1)		
Alkali and alkaline Earth metals	Tap and mineral waters	10 mM Imidazole (pH 4.5)	Indirect UV 214 nm	0.05 mg/L
Uranyl cation (UO ₂ ²⁺)	River water	10 mM Perchloric acid, 1 mM phosphate, 0.6 mM borate, 0.01–0.1 mM arsenazo III 650 nm, 50–150 mM NaCl, 10% MeOH	Direct UV-VIS	10 µg/L
Zn and other transition metals	Tap water	10 mM Borate buffer, 0.1 mM HQS (pH 9.2)	Direct UV 254 nm	3–225 µg/L
Al	River, reservoir, and spring waters	40 mM AcOH, 10 mM NH ₄ Ac (pH 4.0)	Fluorescence 419 and 576 nm	19 µg/L
Ca, Mg, Ba, Na, K, and Li	Mineral water	3–5 mM Imidazole, pH 4.5	Indirect 214 nm	0.05 ppb
Cu, Ni, Co, Hg, Mn, Fe, Pb, Pd, Zn, Cd, Mg, Sr, Ca, and Ba	River water	2 mM Na ₂ B ₄ O ₇ , 2 mM EDTA pH 4.4	Direct UV 200 and 214 nm	10 µM
Ca, Sr, Ba, Li, Na, K, Rb, Sc, and Mg	Tap, rain, and mineral waters	5 mM Benzimidazole, tartarate, pH 5.2, +0.1% HEC or methy-HEC, +40 mM 18C6	Indirect UV 254 nm	–
Chromate	Waste water	0.02 mM Phosphate buffer, (pH 7)	Direct UV	–
Fe, Ni, Pd, Pt, and Cu(I) cyano complexes	Leaching solutions of automobile catalytic converters	20 mM Phosphate buffer, 100 Mm NaCl, 1.2 mM TBABr, 40 µM TTABr (pH 11)	Direct UV 208 nm	20 µg/L
<i>Speciation of Metal Ions</i> ^[7-9]				
Arsenic species	Drinking water	0.025 mM Phosphate buffer, pH 6.8	Direct UV 190 nm	<2 mg/L
	Water	50 mM CHES, 20 mM LiOH	Conductivity	0.4 mg/L
	Tin mining	15 mM Phosphate buffer, 1 mM	Conductivity	0.4 mg/L
As(III), As(V), and dimethyl arsenic acid	Process water	CTAB 50 mM CHES, 0.03% Triton X-100	ICP-MS	1 ppb
	–	20 mM LiOH, pH 9.4		
		60 mM Calcium chloride (pH 6.7)		
		cetyltrimethyl ammonium bromide, pH 10.0		

Table 1 The applications of capillary electrophoresis for the determination of environmental pollutants (*Continued*)

Pollutants	Sample matrix	Electrolytes	Detection	Detection limit
Arsenic and selenium species	Drinking water	20 mM KHP, 20 mM Boric acid (pH 9.03) hydrodynamically modified EOF	Hydride generation ICP-MS	6 ng/L
	Tap and drinking waters	75 mM Dihydrogen phosphate 25 mM, tetraborate (pH 7.65)	Direct UV 12 µg/L 195 nm	–
	–	20 mM Na ₂ HPO ₄ , 5 mM DTPA, pH 8.0 or 8.5	Indirect UV 214 nm	10 ^{–6} M
Cr(IV) and Cr(VI)	Rinse water from chromium platings	1 mM CDTA, 10 mM Formate buffer (pH 3.8)	Direct UV 214 and 254 nm	10 µg/L
	Chromium plating water	10 mM Formate buffer, 1 mM CDTA (pH 3.0)	Direct UV 214 nm	10 ppb
	Electroplating water	10 mM Formate buffer, (pH 3.0)	Indirect UV 214 nm	50 ppb
	Waste water	20 mM Na ₂ HPO ₄ , 0.05 mM TTAOH	Direct UV 214 and 254 nm	–
Fe(II) and Fe(III)	Electroplating waters	20 mM Phosphate buffer (pH 7.0)	Direct UV 214 nm	10 ^{–5} M
Hg(II), CH ₃ Hg ⁺ , and CH ₃ CH ₂ Hg ⁺	–	25 mM Na ₂ B ₄ O ₇ ·10 H ₂ O, pH 9.3	ICP-MS	81–275 ppb
Ir(II) and Ir(III)	–	4 mM H ⁺ , 23 mM Cl [–] , pH 2.4	Indirect UV 214 nm	–
Pb(II), triethyl lead (IV), trimethyl lead (IV), and diphenyl lead (IV)	–	Na ₂ HPO ₄ –Na ₂ B ₄ O ₇ , 2.5 mM TTHA, 2.0 mM SDS, pH 7.5	Indirect UV 220 nm	ppb level
Pt(II) and Pt(IV)	–	4 mM H ⁺ , 23 mM Cl [–] , pH 2.4	Indirect UV 214 nm	–
V(IV) and V(V)	Electroplating bath	20 mM Na ₂ HPO ₄ , 5 mM DTPA, pH 8.0 or 8.5	Indirect UV 214 nm	10 ^{–6} M
<i>Anions Analysis</i> ^[9,12]				
F [–]	Rain water	1.13 mM PMA, 0.8 mM TEA, 2.13 mM HMOH, pH 7.7	Indirect UV 254 nm	0.6 µM
F [–] , Cl [–] , Br [–] , SO ₄ ^{–2} , NO ₃ [–] , NO ₂ [–] , PO ₄ ^{–3} , and thiosulphate	Tap water	2.25 mM PMA, 6.5 mM NaOH, 0.75 mM HMOH, 1.6 mM TEA, pH 7.7	Indirect UV 250 nm	1–3 mg/L
HClO ₄ [–] , Br [–] , F [–] , NO ₃ [–] , and NO ₂ [–]	Tap water	20 mM Sodium sulphate, pH 2.5	Ionselective microelectrode	5 µg/L
Br [–] , BrO ₄ [–] , I [–] , IO ₄ [–] , NO ₃ [–] , NO ₂ [–] , and selenite	River water	Phosphate buffer, pH 2.9	Direct UV 200 nm	–
organic and inorganic anions	Water from dumping area	9 mM PDCA, 0.05 mM TTABr, pH 7.8	Indirect UV 254 nm	–

(Continued)

**Table 1** The applications of capillary electrophoresis for the determination of environmental pollutants (*Continued*)

Pollutants	Sample matrix	Electrolytes	Detection	Detection limit
Br^- , NO_2^- , $\text{S}_2\text{O}_3^{2-}$, NO_3^- , N_3^- , $\text{Fe}(\text{CN})_6^{4-}$, MoO_4^{2-} , WO_4^{2-} , CrO_x^{3-} , and ReO_4^-	—	10 mM Borate, 220 mM NaCl, pH adjusted to 8.5 by sodium hydroxide	UV 214 nm	—
<i>Phenols and its Derivatives</i> ^[3,10]				
Alkyl phenols		1.25 mM $\text{Na}_2\text{B}_4\text{O}_7$, 15 mM NaH_2PO_4 pH 11.0 with 0.001% HDB	UV 254 nm	—
Chlorophenols		50 mM Na_2HPO_4 / NaH_2PO_4 , pH 6.9	UV 214 nm	0.06 mg/L
Miscellaneous derivatives of phenols		10 mM $\text{Na}_2\text{B}_4\text{O}_7$ / Na_3PO_4 , pH 9.8	UV 210 nm	0.3 mg/L
		20 mM CHES, pH 10.1	Amperometric	0.03 mg/L
		15 mM Na_3BO_3 , pH 9.9	Indirect fluorimetry	0.01 mg/L
Pentachlorophenols	Drinking water	40 mM Sodium borate, pH 10	—	ng level
Chloro- and nitro-phenols	Tap water	20 mM Sodium borate	—	µg level
<i>Pesticides</i> ^[11]				
Hexazinone and its metabolite	Ground water	50 mM SDS, 12 mM Sodium phosphate, 0 mM sodium borate, and 15% MeOH, pH 9.0	UV 220–247 nm	—
Primisulfuron and triasulfuron	Water and soil	25 mM NaH_2PO_4 + 50 mM LiDS buffer	UV at 214 nm	—
Triazines and chlorotriazines	Tap and river Water	30 mM Sodium borate, 30 mM SDS, pH 9.3	UV at 210 nm	—
Chlorinated acid herbicides and related compounds	Water	5 mM Ammonium acetate in isopropanol-water (40:60, v/v), pH 10	MS	—
Chlorpyrifos	Air and soil	—	—	—
Triazine pesticides		50 mM Ammonium acetate, 0.7 mM CTAB, pH 4.5	MS and UV (230 nm)	—
<i>Polyaromatic Hydrocarbons</i> ^[5]				
PAHs	Standard	8 mM $\text{Na}_2\text{B}_4\text{O}_7$, pH 9.0, 50 mM DOSS, 40% acetonitrile	UV 254 nm	—
	Standard	5 mM Resorcarene, pH 13.25, 6 M Urea, 50% acetonitrile	UV 260 nm	—
<i>Amines</i> ^[5]				
Methyl, dimethyl trimethyl, and ethyl amines	Atmospheric aerosols	5 mM DHBP, 6 mM glycine, 2 mM 18-crown-6 ether, pH 6.5	Indirect UV 280 nm	—
Substituted anilines	Tap and ground water, soil, and sediment	50 mM NaH_2PO_4 , pH 2.35, 7 mM 1,3-diaminopropane	UV 280 nm	0.06 mg/L
Heterocyclic aromatic amines	Rain water	50 mM NaH_2PO_4 –20 mM citric acid, 30 mM NaCl, 26% methanol	UV 190, 240, and 263 nm	0.05 mg/L

**Table 1** The applications of capillary electrophoresis for the determination of environmental pollutants (*Continued*)

Pollutants	Sample matrix	Electrolytes	Detection	Detection limit
<i>Carbonyls</i> ^[5]				
Acetaldehyde, benzaldehyde, formaldehyde, and glyoxal	Rain water	5 mM Na ₃ PO ₄ –10 mM Na ₂ B ₄ O ₇ , pH 8.0, 20% acetonitrile	Laser-induced fluorescence 325 and 442 nm	–
<i>Dyes</i> ^[5,10]				
Synthetic cationic dyes	Standard	10 mM Citric acid, pH 3.0, 0.1% PVP	UV 214 nm	–
Anionic synthetic azo dyes	Standard	10 mM BTP-HCl, pH 6.5, 0.5% PEG, 0.05% PVP	UV 214 nm	–
Photoactive dyes	Coffee and beans	50 mM Boric acid/10 mM sodium borate, pH 8.5	–	0.08 µg L ^{–1}
<i>Chiral Separations</i> ^[11,18]				
Fenoprop, mecoprop, and dichlorprop	–	20 mM Tributyl-β-CD in 50 mM, ammonium acetate, pH 4.6	MS	–
2-Phenoxypropionic acid, dichlorprop, fenoprop, fluaziprop, haloxyfop, and diclofop enantiomers	–	10–4 M 75 mM Britton-Robinson buffer with 6 mM Vancomycin	–	–
Imazaquin isomer	–	50 mM Sodium acetate, 10 mM dimethyl-β-CD, pH 4.6	–	–
Phenoxy acid herbicides	–	200 mM Sodium phosphate, pH 6.5 with various concentrations of OG and NG	–	–
Diclofop	–	50 mM Sodium acetate, 10 mM trimethyl-β-CD, pH 3.6	–	–
Imazamethabenz isomers	–	50 mM Sodium acetate, 10 mM dimethyl-β-CD, pH 4.6	–	–
2-(2-methyl-4-chlorophenoxy) propionic acid,	–	0.05 M Lithium acetate containing α-cyclodextrins	UV 200 nm	–
2-(2-methyl-4, 6-dichlorophenoxy) propionic acid	–	0.05 M Lithium acetate containing β-cyclodextrin	UV 200 nm	–
2-(2,4-dichlorophenoxy) propionic acid	–	0.05 M Lithium acetate containing heptakis-(2,6-di- <i>O</i> -methyl)-β-cyclodextrin	UV 200 nm	–
propionic acid, and 2-(2-methyl-4-chlorophenoxy) propionic acid	–	0.03 M Lithium acetate containing heptakis-(2,6-di- <i>O</i> -methyl)-β-cyclodextrin	UV 200 nm	–
1,1'-Binaphthyl-2-2'-dicarboxylic acid, 1,1'-binaphthyl-2, 2'-dihydrogen phosphate, and 2,2'-dihydroxy-1-1'-binaphthyl-3, 3'-dicarboxylic acid	–	0.04 M Carbonate, pH 9.0, with noncyclo-oligosaccharides	UV 215–235 nm	–

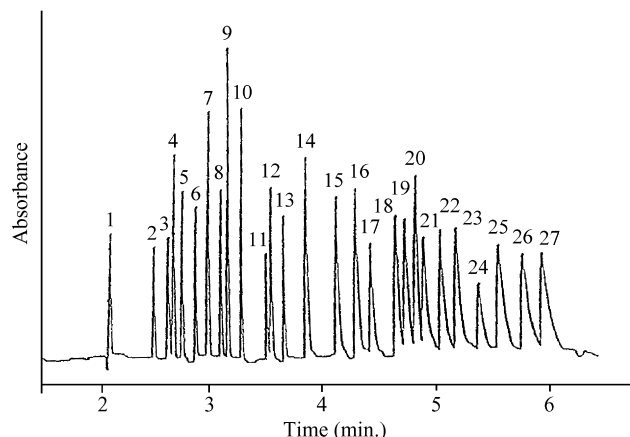


Fig. 2 The electropherogram of the separation of alkali, alkaline earth, transition metals, and lanthanoids on a fused silica capillary (60 cm \times 75 μ m) using 15 nM lactic acid, 8 mM 4-methylbenzylamine and 5% MeOH, pH 4.25, as running electrolyte with 30 kV as the separation voltage, 20°C temperature, and UV detection (214 nm).^[7] Peaks: 1=K; 2=Ba; 3=Sr; 4=Na; 5=Ca; 6=Mg; 7=Mn; 8=Cd; 9=Li; 10=Co; 11=Pb; 12=Ni; 13=Zn; 14=La; 15=Ce; 16=Pr; 17=Nd; 18=Sm; 19=Gd; 20=Cu; 21=Tb; 22=Dy; 23=Ho; 24=Er; 25=Tm; 26=Yb; and 27=Lu.

Apart from the points discussed for improvement of CE applications for the determination of environmental pollutants, some other aspects should also be addressed so that CE can be used as the routine method of choice in this field. The important points relating to this include the development and wide use of fluorescent and radioactive complexing agents, since detection by fluorescent and radioactive detectors is more sensitive and reproducible with low limits of detection. To make CE application more reproducible, the BGE should be developed in such a way to ensure its physical and chemical properties remain unchanged during the experimental run. The nonreproducibility of the methods may be due to the heating of BGE during a long analysis. Therefore, to keep the temperature constant throughout the experiments, a cooling device should be included in the instrument. Besides, especially for the determination of anions, the CE instrument should be designed with the facility to reverse the electrodes. There are only a few reports dealing with method validation. To make the developed method more applicable, the validation of the methodology should be performed. All the capabilities and possibilities of CE have not yet been explored but they are underway. However, eventually CE will be realized as a widely recognized method of choice for the determination of environmental pollutants.

In summary, there is much to be developed for the advancement of CE for the analysis of environmental pollutants. Definitely, CE will prove itself as the best

technique for the determination of environmental pollutants within the next few years; it will achieve the status of the technique of routine analysis in most of the environmental laboratories.

LIST OF ABBREVIATIONS

AcOH:	Acetic acid
BTP:	Bis-trispropane
CD:	Cyclodextrin
CDTA:	Cyclohexane-1,2-diaminetetraacetic acid
CHES:	2-(<i>N</i> -Cyclohexylamino)-ethanesulphonic acid
CTAB:	Cetyltrimethylammonium bromide
DHBP:	1,1'-Di- <i>n</i> -heptyl-4,4'-bipyridinium hydroxide
DOSS:	Sodium dioctyl sulfosuccinate
DTPA:	Diethylenetriaminepenta acetic acid
EDTA:	Ethylenediaminetetraacetic acid
EOF:	Electroosmotic flow
HDB:	Hexadimethrine bromide
HEC:	Hydroxyethyl cellulose
HIBA:	α -Hydroxyisobutyric acid
HMOH:	Hexamethonium hydroxide
HQS:	8-Hydroxyquinoline-5-sulfonic acid
ICP-MS:	Inductively coupled plasma-mass spectrometer
KHP:	Potassium hydrogenphthalate
LiOH:	Lithium hydroxide
MeOH:	Methanol
MES:	Morpholinoethanesulfonic acid
NaAc:	Sodium acetate
NaCl:	Sodium chloride
NH ₄ Ac:	Ammonium acetate
NaOH:	Sodium hydroxide
NG:	Nonyl- β -d-glucopyranoside
OG:	Octyl- β -d-glucopyranoside
PAHs:	Polyaromatic hydrocarbons
PDCA:	Pyridine-2,6-dicarboxylic acid
PEG:	Polyethylene glycol
PMA:	Pyromellitic acid
PVP:	Polyvinylpyrrolidone
RSD:	Lower standard deviation
SDS:	Sodium dodecyl sulfate
TBABr:	Tetrabutylammonium bromide
TEA:	Triethanolamine
TTABr:	Tetradecyl-trimethylammonium bromide
TTAOH:	Tetradecyl-trimethylammonium hydroxide
TTHA:	Triethylenetetraminehexa acetic acid
UV:	Ultraviolet

REFERENCES

1. Franklin, L.B. *Wastewater Engineering: Treatment, Disposal and Reuse*; McGraw-Hill, Inc.: New York, 1991.



2. Droste, R.L. *Theory and Practice of Water and Wastewater Treatment*; John Wiley & Sons, Inc.: New York, 1997.
3. Crego, A.L.; Marina, M.L. Capillary zone electrophoresis versus micellar electrokinetic chromatography in the separation of phenols of environmental interest. *J. Liq. Chromatogr. Relat. Technol.* **1997**, *20*, 1–20.
4. Kallenborn, R.; Huhnerfuss, H. *Chiral Environmental Pollutants: Trace Analysis and Ecotoxicology*; Springer-Verlag: Berlin, 2000.
5. Dabek-Zlotorzynska, E. Capillary electrophoresis in the determination of pollutants. *Electrophoresis* **1997**, *18*, 2453–2464.
6. Sovocool, G.W.; Brumley, W.C.; Donnelly, J.R. Capillary electrophoresis and capillary electro-chromatography of organic pollutants. *Electrophoresis* **1999**, *20*, 3297–3310.
7. Pacakova, V.; Coufal, P.; Stulik, K. Capillary electrophoresis of inorganic cations. *J. Chromatogr. A* **1999**, *834*, 257–275.
8. Liu, B.F.; Liu, B.L.; Cheng, J.K. Analysis of inorganic cations as their complexes by capillary electrophoresis. *J. Chromatogr. A* **1999**, *834*, 277–308.
9. Valsecchi, S.M.; Polesello, S. Analysis of inorganic species in the environmental samples by capillary electrophoresis. *J. Chromatogr. A* **1999**, *834*, 363–385.
10. Martinez, D.; Cugat, M.J.; Borrull, F.; Calull, M. Solid phase extraction coupling to capillary electrophoresis with emphasis on environmental analysis. *J. Chromatogr. A* **2000**, *902*, 65–89.
11. Malik, A.K.; Faubel, W. A review of analysis of pesticides using capillary electrophoresis. *Crit. Rev. Anal. Chem.* **2001**, *31*, 223–279.
12. Haddad, P.R.; Doble, P.; Macka, M. Development in sample preparation and separation techniques for the determination of inorganic ions by ion chromatography and capillary electrophoresis. *J. Chromatogr. A* **1999**, *856*, 145–177.
13. Dabek-Zlotorzynska, E.; Aranda-Rodriguez, R.; Keppel-Jones, K. Recent advances in capillary electrophoresis and capillary electro-chromatography of pollutants. *Electrophoresis* **2001**, *22*, 4262–4280.
14. Timerbaev, A.R.; Buchberger, W. Prospects for the detection and sensitivity enhancement of inorganic ions in capillary electrophoresis. *J. Chromatogr. A* **1999**, *834*, 117–132.
15. Macka, M.; Haddad, P.R. Determination of metal ions by capillary electrophoresis. *Electrophoresis* **1997**, *18*, 2482–2501.
16. Horvath, J.; Dolnik, V. Polymer wall coating for capillary electrophoresis. *Electrophoresis* **2001**, *22*, 644–655.
17. Mayer, B.X. How to increase precision in capillary electrophoresis. *J. Chromatogr. A* **2001**, *907*, 21–37.
18. Marina, M.L.; Crego, A.L. Capillary electrophoresis: A good alternative for the separation of chiral compounds of environmental interest. *J. Liq. Chromatogr. Relat. Technol.* **1997**, *20*, 1337–1365.

Essential Oils Analysis by Gas Chromatography

M. Soledad Prats

Alfonso Jiménez

University of Alicante, Alicante, Spain

INTRODUCTION

Essential oils are highly concentrated substances extracted from flowers, leaves, stems, roots, seeds, barks, resins, or fruit rinds. The levels of essential oils found in plants can be anywhere from 0.01% to 10% of the total. This is why tons of plant materials are required for just a few hundred pounds of oil. These oils are often used for their flavor and their therapeutic or odoriferous properties, in a wide selection of products such as foods, medicines, and cosmetics.

Pure essential oils are mixtures of more than 200 components, normally mixtures of terpenes or phenylpropanic derivatives, in which the chemical and structural differences between compounds are minimal. They can be essentially classified into two groups: A volatile fraction, constituting 90–95% of the oil in weight, containing the monoterpene and sesquiterpene hydrocarbons, as well as their oxygenated derivatives along with aliphatic aldehydes, alcohols, and esters; and a nonvolatile residue that comprises 1–10% of the oil, containing hydrocarbons, fatty acids, sterols, carotenoids, waxes, and flavonoids.

OVERVIEW

Because of the enormous amount of raw products used to obtain a small amount of essential oil, many products on the market have been polluted with lower-quality commercial oils to reduce their cost, a fact not usually indicated on the label. This is why it is important to study the chemical composition of the volatile fraction once the essential oil is extracted. This fraction is characterized by the complexity in the separation of its components, which belong to various classes of compounds and which are present in a wide range of concentrations. Therefore it is complicated to establish a composition profile of essential oils.

The gas chromatographic method (GC) is almost exclusively used for the qualitative analysis of volatiles. The analysis of essential oils was developed in parallel with the technological developments in GC, such as

stationary phases, detection devices, etc. However, advances in instrumentation were not the only important factor in the development of analytical methods for essential oils in plants. Sample extraction and concentration were also improved. The most outstanding improvements in the determination of the composition of essential oils came from the introduction of tandem techniques involving prior/further chromatography or spectroscopy. The great amount of information on the application of GC and hyphenated techniques to essential oils has led to much research in this field, and to the publication of recent reviews.^[1–3]

EXTRACTION METHODS

Extraction of essential oils is one of the most time- and effort-consuming processes in the analysis of the constituents of plants. Various extraction methods were traditionally employed, depending on the material or the available devices. The most commonly used methods are steam distillation and distillation-solvent extraction. The introduction of innovative extraction methods, such as microwave-assisted extraction (MAE) and supercritical fluid extraction (SFE), has led to significant improvement, not only in the analytical performance, but also in the accuracy and reproducibility of methods.

Steam distillation has been traditionally used for isolation of essential oils, but some problems were recently reported; for example, degradation of certain monoterpenes can occur because of acid-catalyzed hydration.^[4] An alternative method, useful for much smaller sample sizes, involves extraction with organic solvents, such as dichloromethane, followed by evaporation of solvent from the extract.^[5] However, this approach is not very popular when the obtained extracts are to be used in the cosmetic or food industry, because of the possible toxic organic solvent residue.

Supercritical fluid extraction and microwave-assisted extraction have been recently applied to the extraction of essential oils. Both techniques are based on the application of high pressures and temperatures for the total extraction of analytes. Supercritical fluid extraction has



shown much potential for the isolation of organic compounds from various samples by minimizing sample handling, providing relatively clean extracts, expediting sample preparation, and reducing the use and disposal of environmentally aggressive solvents. Additionally, in many cases, SFE provides recoveries even better than those of conventional solvent extraction techniques.

One of the most important subjects of research in this field is the modeling of the essential oil extractions. Several kinds of models have been presented in recent literature.^[6-8] Most of these models consider the natural matrix as a porous sphere and the extractable material as a single chemical species. The application to multicomponent systems permits the extension of the extraction model to simulate SFE in essential oils and the selective extraction of the mixed constituents.^[7] Therefore the most important extraction parameters can be controlled for an optimized process with these complicated samples.

The use of SFE and MAE has been generalized to many essential oils and different samples. These techniques have improved recoveries in the determination of most organic additives, as well as permitted considerable reductions in solvent volume and extraction time. However, the comparison of extraction methods was usually reduced to relative recoveries of target analytes, ignoring important analytical parameters of the method. Selectivity is one of these, as the coextraction of other organics from the matrix usually requires a postextraction cleanup step before chromatographic analysis. There is still much effort to be carried out in this field in order to optimize the extraction of essential oils from different natural matrices. The selection of the best extraction method depends on the components to be extracted, and this is something to be carefully considered in each particular case.

CONCENTRATION OF ANALYTES

Another important aspect to take into account for a reproducible and accurate separation and determination of essential oils is the concentration of each component. In many cases, a preconcentration of the sample, prior to any other step in the analytical process, is necessary to assure a concentration range for an accurate determination. This is the way small amounts of each constituent in plants or complex matrices, such as pharmaceuticals, can be collected and concentrated using the headspace technique (HS-GC), which involves volatilization of the terpenoids and other substances in a closely confined space, followed with analysis of constituents in the gaseous phase. This process can be carried out as an equilibrium process (static headspace) or as a continuous process (dynamic headspace). Some essential oil

applications of HS-GC were described using different enrichment and cryogenic techniques. Solid phase microextraction (SPME) is one of the most promising ones.^[9] A headspace-SPME system, coupled with gas chromatography/mass spectrometry (GC/MS), has recently been reported as a powerful separation tool for essential oil analysis. Results were compared with those from steam-distilled samples and, in general, most of the monoterpene compounds were detected at higher levels by using HS-SPME with 30-sec extraction time. In addition, detailed information about terpenic compounds was obtained by using HS-SPME.^[10]

GAS CHROMATOGRAPHIC ANALYSIS

The separation of essential oil components is usually carried out by GC with fused-silica capillary columns. The properties and conditions of columns used are variable, depending on the polarity of the components to be separated. The most used columns include stationary phases such as DB-1, Carbowax, OV-1, OV-101, PEG 20M, BP5, and DB-5, which cover a wide range of polarities. Column lengths normally range from 25 to 100 m, and stationary phase film thickness ranges from 0.2 to 0.7 μm . Elution of components is usually performed with a temperature gradient ranging from 50°C to 280°C.

New developments in stationary phases for use with essential oils have been recently reported.^[12] These developments have led to the production of thermally and chemically stable phases, with greater selectivity and efficiency. It is advantageous to use a more selective phase for a given separation as the overlapping of peaks in the final chromatogram is often a significant drawback of chromatographic techniques in natural samples. The discovery of chiral phases (mostly based on cyclodextrin derivatives) allows the resolution of enantiomers of volatile components. These phases can give different elution sequences for a polarity range and provide a distinct advantage in identification because of large changes in solute relative retention times.

The information obtained from high-resolution GC analysis of the volatile fraction of essential oils must be sufficient to determine whether the product is genuine or not. If the product is adulterated, the kind and level of adulteration must be detected. Therefore a selective and accurate separation is absolutely necessary in the case of industrial analysis. On the other hand, GC sometimes permits the separation and further identification of some components of the nonvolatile residue as well.

An important drawback in the separation of essential oils is the time required for complete GC resolution of the

components of interest, which sometimes can take hours. In fact, the analysis of essential oil samples is usually carried out with slow temperature programs, which take long times for the development of the whole chromatogram. There are several ways to reduce analysis time in GC. The most common approach is to use shorter capillary columns with reduced internal diameter and reduced film thickness. When using these columns, the optimum carrier gas velocity is higher, and it is possible to work with higher average linear velocity without the loss of efficiency. However, this increase in linear velocity must be linked with some specific conditions of measurement, such as fast oven heating, fast acquisition rate, high inlet pressures, and higher split ratios. Some work has been carried out in this area, using 10-m-long columns with 0.1-mm internal diameter and conventional instrumentation for the analysis of citrus essential oils by fast gas chromatography/flame ionization detection (GC/FID) and fast GC/MS.^[11]

DETECTION AND CHARACTERIZATION OF CONSTITUENTS

The flame ionization detector (FID) is still widely applied for the detection and quantitation of some of the essential oil components, such as terpenoids. As usual in GC/FID, the primary criterion for the identification of peaks is the comparison of the standard retention times with the retention times of peaks in the sample's chromatogram. However, this procedure is sometimes not useful as the identification is quite difficult and overlapping of peaks makes determination not possible.

The easiest and most frequently used way to identify essential oil components when using GC/FID is comparison with Kovats retention indices (RI). The use of this type of retention data, derived from two GC columns of different polarities, allows highly reliable identification of large numbers of components in a particular sample.

By far, mass spectrometry (MS) is the most popular detection technique for performing chromatographic studies of essential oils. The use of retention indices, in conjunction with GC/MS studies, is well established. Many laboratories use such procedures in their routine analyses to confirm the identities of unknown components. The identification of components is usually performed by comparing the mass spectra with an MS library. However, a feature of MS for essential oils is that mass spectra are not particularly unique in many cases because of the large numbers of isomers of the same molecular formula, but with different structures, that could exist. Therefore their mass spectra are similar and

their identification is sometimes not so easy. The most common approach to solve this problem, as well as the presence of unknowns on whom very little other structural information is available, is the use of algorithms and powerful MS databases, as has been recently proposed.^[12] Two different MS databases are commonly used as references: National Institute of Standards and Technology (NIST)/Environment Protection Agency (EPA)/National Institutes of Health (NIH) and the Registry of Mass Spectral Data. The first one contains more than 62,000 mass spectra of different chemicals. The largest database is the Registry of Mass Spectral Data, called the Wiley database, containing more than 300,000 different spectra, resulting from the work of many researchers in the field of MS. One of the most used algorithms was proposed by Oprean et al.,^[11] which considers two parameters as identification criteria for an unknown peak, i.e., the match index of the unknown mass spectrum with spectral libraries, and the relative retention indices computed from the retention times of the unknowns relative to a mixture of *n*-alkanes.

One of the most recently proposed methods to improve the analysis of complex mixtures, especially for deconvolution of overlapping mass spectra, is time-of-flight mass spectrometry (TOFMS). This technique allows assignment of a spectrum to each individual solute in significantly overlapping elution profiles. This is an important advantage that can be exploited when fast GC methods are applied for complex samples because each overlapping peak may be deconvoluted and the individual spectrum of each overlapping solute may be obtained. Although great efforts have been recently carried out in this field, it remains to be determined if TOFMS can be used on a routine basis.

The identification of compounds comprising more than 1% in the oils can be also carried out by ¹³C-NMR and computer-aided analysis.^[13] The chemical shift of each carbon in the experimental spectrum can be compared with those of the spectra of pure compounds. These spectra are listed in the laboratory spectral data bank, which contains approximately 350 spectra of mono-, sesqui- and diterpenes, as well as with literature data. Each compound can be unambiguously identified, taking into account the number of identified carbons, the number of overlapped signals, as well as the difference between the chemical shift of each resonance in the mixture and in the reference.

The combination of GC with olfactometry is another possibility for detection that has been used in essential oil analysis. Olfactometry adapters are commercially available and should include humidity of the GC effluent at the nose adapter and provide auxiliary gas flow. The correlation among eluted peaks with specific odors allows accurate retention indices or retention times to be

established for the essential oil components. Some of them can be detected in such way after applying chemometric techniques, such as cluster analysis and principal component analysis, to the data from the sensors.

HYPHENATED OR MULTIDIMENSIONAL ANALYSIS OF ESSENTIAL OILS

Hyphenated or multidimensional techniques have been recently introduced for the analysis of essential oils. Various approaches were recently proposed to obtain better results in the identification and quantification of essential oil components. Thus it is possible to use systems that incorporate separations prior to GC, multicolumn separations, and specific identification methods.

With respect to separations preceding GC analysis, some hyphenated techniques have been successfully used when there is a lack of resolution of the single capillary GC method. One of these is the combination of high-performance liquid chromatography (HPLC) with GC. The prior HPLC step achieves the isolation of components of similar chemical composition, primarily based on polarity. Hence, this will separate saturated hydrocarbons from unsaturated or aromatic hydrocarbons, for example.^[14] These systems are fully automated, but there is a problem with off-line sampling of HPLC fractions. The selection of the HPLC injection port will determine the particular method of separation. Therefore in this instrumental arrangement, each transferred fraction must be separately analyzed before the introduction of a subsequent fraction into the GC system. In general, the prior separation will be introduced to simplify the subsequent GC analysis, leading to improved resolution.

Multidimensional Gas Chromatography

The application of multidimensional gas chromatography (MDGC) to essential oil analysis is a great development in the determination of such complex samples. This is an appropriate approach when there are zones on the chromatogram where the peaks are not well resolved, which is a common situation in natural samples. The fractions corresponding to the zones with unresolved peaks are transferred to a second column containing a different stationary phase, where they are separated and completely resolved. Therefore MDGC permits the separation of poorly resolved peaks and increases resolution, with the final result of an improvement in both identification and quantification of components of essential oils.

However, this evidently improved approach in instrumentation is only available to relatively few regions of chromatographic analysis, as overlapping of peaks in the same area can be too complex for a complete resolution

of each component, even by applying multiple-column couplings. The use of conventional MDGC technology is not possible for the entire analysis because this would involve transferring all the components to the second column, with the inherent technical problems of loss of selectivity and sensitivity. This is why the MDGC analysis of essential oils is not focused on the increase of resolution for the whole sample, but only for specific components of interest in the quality control of the natural product. The use of chiral columns in one or both separation processes should be an additional improvement in the resolution of chromatograms, but this is an area requiring further attention.

A possible solution to the above problems would be the triple-dimensional analysis by using GC \times GC coupled to TOFMS.^[15] Mass spectrometric techniques improve component identification and sensitivity, especially for the limited spectral fragmentation produced by soft ionization methods, such as chemical ionization (CI) and field ionization (FI). The use of MS to provide a unique identity for overlapping components in the chromatogram makes identification much easier. Thus MS is the most recognized spectroscopic tool for identification of GC \times GC-separated components. However, quadrupole conventional mass spectrometers are unable to reach the resolution levels required for such separations. Only TOFMS possess the necessary speed of spectral acquisition to give more than 50 spectra/sec. This area of recent development is one of the most important and promising methods to improve the analysis of essential oil components.

CONCLUSION

The identification and determination of essential oils in many natural samples have improved greatly with the use of more powerful analytical techniques, such as fast extraction methods, better chromatographic detectors, and hyphenation. This improvement in analytical parameters open a great future for the development of analytical methods for essential oil determinations, even at low limits of detection.

REFERENCES

1. Oprean, R.; Tamas, M.; Sandulescu, R.; Roman, L. Essential oil analysis. I. Evaluation of essential oil composition using both GC and MS fingerprints. *J. Pharm. Biomed. Anal.* **1998**, *18*, 651–657.
2. Marriot, P.J.; Shellie, R.; Cornwell, C. Gas chromatographic techniques for the analysis of essential oils. *J. Chromatogr., A* **2001**, *936*, 1–22.

3. Lockwood, G.B. Techniques for gas chromatography of volatile terpenoids from a range of matrices. *J. Chromatogr., A* **2001**, *936*, 23–31.
4. Griffiths, D.W.; Robertson, G.W.; Birch, A.N.E.; Brennan, R.M. Evaluation of thermal desorption and solvent elution combined with polymer entrainment for the analysis of volatiles released by leaves from midge (*Dasineura tetensi*) resistant and susceptible blackcurrant (*Ribesnigrum* L.) cultivars. *Phytochem. Anal.* **1999**, *10*, 328–334.
5. Zhu, W.; Lockwood, G.B. Enhanced biotransformation of terpenes in plant cell suspensions using controlled release polymer. *Biotechnol. Lett.* **2000**, *22*, 659–662.
6. Spricigo, C.B.; Pinto, L.T.; Bolzan, A.; Novais, A.F. Extraction of essential oil and lipids from nutmeg by liquid carbon dioxide. *J. Supercrit. Fluids* **1999**, *15*, 253–259.
7. Tezel, A.; Hortaçsu, A.; Hortaçsu, O. Multi-component models for seed and essential oil extraction. *J. Supercrit. Fluids* **2000**, *19*, 3–17.
8. Benyoussef, E.H.; Hasni, S.; Belabbès, R.; Bessière, J.M. Modélisation du transfert de matière lors de l'extraction de l'huile essentielle des fruits de coriandre. *Chem. Eng. J.* **2002**, *85*, 1–5.
9. Pawliszyn, J. *Applications of Solid Phase Microextraction*; Royal Society of Chemistry: Cambridge, 1999.
10. Rohloff, J. Essential oil composition of sachalinmint from Norway detected by solid phase microextraction and gas chromatography-mass spectrometry analysis. *J. Agric. Food Chem.* **2002**, *50*, 1543–1547.
11. Mondello, L.; Zappia, G.; Bonaccorsi, I.; Dugo, G.; McNair, H.M. Fast GC for the analysis of natural matrices. Preliminary note: The determination of fatty acid methyl esters in natural fats. *J. Microcolumn September* **2000**, *12*, 41–47.
12. Oprean, R.; Oprean, L.; Tamas, M.; Sandulescu, R.; Roman, L. Essential oils analysis. II. Mass spectra identification of terpene and phenylpropane derivatives. *J. Pharm. Biomed. Anal.* **2001**, *24*, 1163–1168.
13. Mundina, M.; Vila, R.; Tomi, F.; Gupta, M.P.; Adzet, T.; Casanova, J.; Cañigüeral, S. Leaf essential oils of three Panamanian piper species. *Phytochemistry* **1998**, *47*, 1277–1282.
14. Mondello, L.; Dugo, G.; Bartle, K.D. On-line microbore high performance liquid chromatography capillary gas chromatography for food and water analyses. A review. *J. Microcolumn September* **1996**, *8*, 275–310.
15. Shellie, R.; Marriot, P.; Morrison, P. Concepts and preliminary observations on the triple-dimensional analysis of complex volatile samples by using GC × GC-TOFMS. *Anal. Chem.* **2001**, *73*, 1336–1344.



Evaporative Light Scattering Detection for Liquid Chromatography

Sarah Chen

Merck Research Laboratories, Rahway, New Jersey, U.S.A.

INTRODUCTION

Evaporative light scattering detection (ELSD) is a powerful technique that can be applied in liquid chromatography to all solutes having lower volatility than the mobile phase. It consists of a nebulizer that transforms the eluent from the HPLC into an aerosol, a drift tube to vaporize the solvent, and a light scattering cell (Fig. 1). When using ELSD in conjunction with liquid chromatography, the eluent is nebulized immediately into a stream of warm gas. The solvent then vaporizes leaving a cloud of solute particles. The particles are subjected to a light source and scattering occurs in the scattering chamber. The amount of light scattered by the particles is proportional to the analyte concentration. These principles make ELSD a universal detector that can be used for analytes with low UV chromophores. Evaporative light scattering detection has been used for the detection of polymers in size exclusion chromatography.^[1] It has also been used in the detection of small molecules in reversed phase and normal phase liquid chromatography.^[2–4]

THEORY AND INSTRUMENTATION

Light scattering detection cannot be used if the analyte particles or solvent vapors absorb at the wavelength range of the light source. When particles are hit with a beam of light, the light may be absorbed, refracted, reflected, or scattered. Reflection and refraction always occur together and they prevail when the wavelength of light approaches the particle's size.^[5] The sum of the reflection and refraction intensities equals the intensity of the incident light when there is no absorbance. Scattering occurs when the particle diameter is close to one-tenth of the wavelength. There are two types of scattering: Mie scattering and Rayleigh scattering. Mie scattering occurs when the ratio of particle diameter to the wavelength of light is greater than 0.1.^[6] Rayleigh scattering occurs when the ratio is less than 0.1.^[7] These numbers are approximate and a transition region does exist. The property of scattering has been used in the

evaporative light scattering detector (ELSD) for liquid chromatography. In ELSD, the eluent for liquid chromatography is nebulized, and the amount of light scattered by the nebulized eluent particles is proportional to the analyte concentration.

Evaporative light scattering detection involves three successive and interrelated processes: nebulization of the chromatographic eluent, evaporation of the volatile solvent (mobile phase), and scattering of light by residual analyte particles. The three major parts of the system are the nebulizer, drift tube, and light-scattering cell.

Nebulizer

The nebulizer is normally interfaced directly to the LC column. It combines the eluent with a stream of gas to produce an aerosol. Much of the theoretical and practical basis of nebulization comes from atomic spectroscopy. The average droplet diameter and uniformity of the aerosol are the most important factors for ELSD sensitivity and reproducibility. As larger solute particles scatter light more intensely, an aerosol with large droplets and a narrow droplet size distribution leads to the most precise and sensitive detection. A good nebulizer should produce a uniform aerosol of large droplets with narrow droplet size distribution. The droplets cannot be too large, however; otherwise, the solvent in a droplet will not be completely vaporized and errors in detection will occur. The nebulizer properties that can be adjusted to obtain the desired droplet properties are, primarily, the gas flow rate and the LC mobile phase flow rate.^[8]

Drift Tube

Volatile components of the aerosol produced by the nebulizer are evaporated in the drift tube to produce nonvolatile particles in a dispersed mixture of carrier gas and solvent vapors. Ideally, the temperature in the drift tube should be high enough to ensure the complete evaporation of solvents, yet not so high as to be able to volatilize the analytes. If solvent removal is incomplete, detector noise will increase. When extremely large

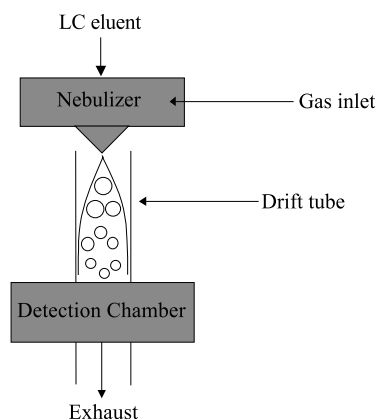


Fig. 1 Schematic diagram of evaporative light scattering detector. (View this art in color at www.dekker.com.)

droplets reach the light scattering cell, they will be seen as spikes. If the drift tube temperature is too high, solute may be vaporized or partially vaporized, resulting in decreased sensitivity and accuracy. Droplet aggregation is another phenomenon that can occur in the drift tube. It can cause incomplete solvent removal and detector signal spiking. Overall, the drift tube should be wide enough, long enough, and hot enough to ensure complete and rapid solvent removal. Its outlet into the light-scattering cell should be shaped to send all of the particles past the detector window. There has been an increased need for a low temperature ELSD to address the detection of thermally labile compounds and volatile compounds. A low-temperature ELSD that can evaporate solvent at near-ambient temperature, 26–40°C, is now available from several vendors. These instruments are designed in a way that extremely large droplets are expelled to waste. Only droplets of optimum size can survive and the surface area of these droplets will allow maximum vaporization of solvents at moderate drift tube temperatures.

Light Scattering Cell

The particle cloud leaves the drift tube and enters into a light scattering cell. Laser light is passed into the cell through a window, scattered by the analyte, and detected at an angle to the incident light. Single wavelength light at 632, 650, or 670 nm has been generally used in various instrument designs. Other instruments use a polychromatic light source. It is believed that a polychromatic light source emits a distribution of wavelengths where specific absorbance effects are minimized and mass sensitivity predominates over structural sensitivity. The

Evaporative Light Scattering Detection for Liquid Chromatography

response increases monotonically with analyte mass because of the averaging effects that occur when polychromatic scattered light is collected. Thus a polychromatic light source can be found more often than a single wavelength source in instruments. The detector is usually constructed in a way that material in the particle cloud will not stick to the window and fumes are properly vented. In addition, light traps are used to dissipate nonscattered light.

EXPERIMENTAL CONSIDERATIONS

The response factor of an ELSD largely depends on the size of analyte particles entering the detection chamber. After exiting from the HPLC column, the eluent stream is nebulized, and a scavenger gas stream carries the effluent cloud through a hot drift tube where the solvent vaporizes. The droplet shrinks to the volume of the nonvolatile material contained in the eluent. The average particle size in the cloud at a given time and the particle size distribution can be derived from the elution profile of the analyte and the droplet size distribution given by the nebulizer. The average diameter, D_o , of the particles formed in a concentric nebulizer is given by the Atkinson equation:^[9]

$$D_o = \frac{A\sigma_1^{1/2}}{u\rho_1^{1/2}} + B\left(\frac{\eta_1}{(\sigma_1\rho_1)^{1/2}}\right)^{0.45}\left(\frac{1000Q_1}{Q_g}\right)^{1.5} \quad (1)$$

where A and B are constants, σ_1 is the surface tension of the mobile phase, ρ_1 is the density of the mobile phase, η_1 is the viscosity of the mobile phase, u is the relative velocity of the gas and liquid streams in the nebulizer (i.e., the cross-section average velocity of the gas stream between the gas and the liquid nozzles, minus the cross-sectional average velocity of the solvent in the liquid tube), Q_1 is the volume flow rate of the mobile phase, and Q_g is the volume flow rate of the scavenger gas.

Eq. 1 predicts that the average droplet size depends on the gas and solvent flow rate. It also predicts that the average droplet size will depend on the nature of the solvent, because of the dependency on the density, surface tension, and viscosity of the nebulized liquid. The initial droplet size formed in the nebulizer has little to do with the property of the analyte as it predominantly contains mobile phase. The final droplet size in the scattering chamber is dependent on the analyte concentration. When optimizing detector conditions, the experimental parameters that can be adjusted are nebulizer gas flow rate, mobile phase flow rate, and drift tube temperature.



Effect of Scavenger Gas Flow Rate

While keeping mobile phase constant, a plot of the response for a constant sample amount vs. the scavenger gas flow rate exhibits a maximum at an intermediate flow rate, and so does the plot of the signal-to-noise ratio vs. flow rate. At large flow rates, the decrease in response is due to the fact that the average particle size of the solute cloud decreases with increasing gas flow rate according to Eq. 1. The response decreases accordingly with the particle size. At low flow rate, the response factor decreases rapidly with decreasing flow rate, while the noise increases and spikes appear. This is related to the fact that the flow velocity of the scavenger gas in the concentric nebulizer should be in the sonic range in order for the nebulizer to function properly. A low gas flow rate results in very large droplets that vaporize too slowly; hence a spike appears. Precipitation or aggregation can occur if the nebulizer gas pressure is too low. Precipitation in the drift tube can also cause a decrease in sensitivity.

Effect of Mobile Phase Flow Rate

An increase in eluent flow rate will result in increased droplet size and high response factor. However, a flow rate that is too high will result in the incomplete vaporization of the mobile phase and high background noise. When ELSD is used in conjunction with liquid chromatography, the effect of flow rate on the separation should also be considered.

Effect of Drift Tube Temperature

The solvent contained in the droplets formed in the nebulizer must be completely vaporized during the migration of these droplets down through the drift tube. Thus a compromise between the scavenger gas pressure, the mobile phase flow velocity, and drift tube temperature has to be chosen. The residence time of the droplets of solution in the drift tube should be large enough and the drift tube temperature should be high enough to ensure the complete vaporization of solvents. Meanwhile, the temperature must be low enough so that the analytes are not vaporized, as this would result either in a systematic error (small extent of analyte vaporization) or in a total loss of signal (total vaporization of analyte). Low temperatures avoid evaporation of semivolatile analytes and destruction of thermally labile compounds. Vaporization of the solvent is facile with organic mobile phases such as acetonitrile, hexane, or chloroform, but relatively difficult with aqueous mobile phases.

Other Considerations

The response of the evaporative light scattering detector is not linear. This is because the droplets scatter light with an intensity that increases much faster than the third power of their diameter.^[10] The response of the detector is not linear but is given by

$$A = aC^b \quad (2)$$

where A is the response of the detector, a and b are numerical coefficients, C is the concentration of solute. The data can be plotted as $\log A$ vs. $\log C$ to obtain a graph that has a large linear region with a slope b and an ordinate a . This region can be used for quantitation. Slope b tends to be similar for similar compounds and falls between 1 and 2. A slope of 2 is the limiting value for Rayleigh scattering.^[11]

One advantage of ELSD is that a wide range of solvents can be used, including acetone and chloroform which are not useful with UV detection. One drawback is that the solvent must be significantly more volatile than the analytes; thus the use of nonvolatile buffers should be strictly avoided. Only high-quality HPLC solvents with minimum particulates should be used.

If the solvents remain clean and totally volatilized, baseline drift should not be observed during gradient elution. However, sensitivity may change in solvent gradients, mainly due to the change in droplet size as a result of the change in eluent properties such as surface tension, viscosity, and density. In general, shallow gradients are preferable.

Outlet waste gas stream from the ELSD may contain organic solvent vapors. For safety reasons, it is essential to ensure that the outlet of ELSD is properly directed to a safe vented outlet (e.g., a fume hood). Waste ventilation should occur at atmospheric pressure. A vacuum or restriction may result in pressure changes within the optical detection chamber and cause detector baseline instability.

CONCLUSION

Evaporative light scattering detection can be used as a universal detector for liquid chromatography. Its operation includes the nebulization of the eluent in the nebulizer, solvent evaporation in the drift tube, and scattered light detection at the light scattering chamber. Experimental conditions which can be adjusted in most ELSD systems to optimize the detector sensitivity are the nebulizer gas flow rate, mobile phase flow rate, and drift tube temperature. The detector response is nonlinear, but



can be used in quantitative work if a calibration curve is obtained.

REFERENCES

1. Nagy, D.J. *J. Appl. Polym. Sci.* **1996**, 62 (5), 845.
2. Toussaint, B.; Duchateau, A.L.L.; van der Wal, S.J.; Albert, A.; Hubert, Ph.; Crommen, J. *J. Chromatogr., A* **2000**, 890, 239–249.
3. Risley, D.S.; Strege, M.A. *Anal. Chem.* **2000**, 72, 1736–1739.
4. Chen, S.; Yuan, H.; Grinberg, N.; Dovletoglou, A.; Bicker, G. *J. Liq. Chromatogr. Relat. Technol.* **2003**, 26 (3), 425–442.
5. Charlesworth, J. *Anal. Chem.* **1978**, 50 (11), 1402–1414.
6. Righezza, M.; Guiochon, G. *J. Liq. Chromatogr.* **1988**, 11 (9,10), 1967–2004.
7. Mourey, T.; Oppenheimer, L. *Anal. Chem.* **1984**, 56, 2427–2434.
8. Stolyhwo, A.; Colin, H.; Martin, M.; Guiochon, G. *J. Chromatogr.* **1984**, 288, 253–275.
9. Nukiyama, S.; Tanasawa, Y. *Trans. Soc. Mech. Eng., Tokyo* **1938**, 4, 86.
10. Guiochon, G.; Moysan, A.; Holley, C. *J. Liq. Chromatogr.* **1988**, 11 (12), 2547–2570.
11. Oppenheimer, L.; Mourey, T. *J. Chromatogr.* **1985**, 323, 297–304.



Exclusion Limit in GPC–SEC

Iwao Teraoka

Polytechnic University, Brooklyn, New York, U.S.A.

Introduction

A given gel permeation chromatography–size-exclusion chromatography (GPC–SEC) column can analyze the molecular weight (MW) of a polymer only over a limited range of MWs. Figure 1 illustrates a typical calibration curve for the column. The logarithm of the MW is plotted as a function of the retention time t_R . At low and high ends of MW, t_R barely depends on MW, effectively limiting the range of analysis to $M_1 < MW < M_2$. The exclusion limit refers to M_2 .

Discussion

The sharp slope of the calibration curve at the high-MW end of the calibration curve is caused by a drastic decline of the partition coefficient as the chain dimen-

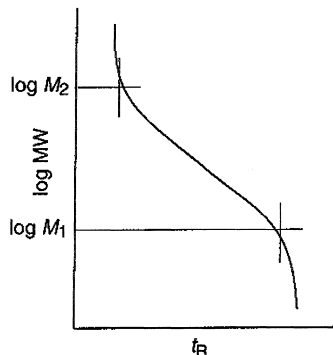


Fig. 1 Calibration curve of GPC–SEC column. Logarithm of the molecular weight, M , is plotted as a function of the retention time (volume) t_R (V_R).

sion increases beyond the accessible pore size of the column packing material. Polymer chains of $MW > M_2$ have a molecular size dimension which is much greater than the pore size. It is virtually impossible for these chains to enter the stationary-phase pores. Thus, at almost every plate in the column, they are partitioned to the mobile phase, thus eluting with little separation at around the dead time (volume) of the column. By contrast, polymer chains smaller or comparable to the available pore sizes can penetrate the pores to be partitioned to the stationary phase with a partition coefficient which depends on their chain dimensions. The dependence of the partition coefficient on the chain dimension allows polymer chains of different MWs to be separated and elute at different times. Columns packed with porous materials of a larger pore size have greater M_1 and M_2 .

For the high-MW chains that are excluded by the pores, there is a small dependence of t_R (V_R) on MW. The latter is mostly caused by the velocity gradient of the mobile phase and the population gradient of the polymer near the stationary-phase particles' surface. The mobile phase flows more slowly near the particles' surface because of the no-slip boundary condition of the fluid at the particles' surface. Among sufficiently long polymer chains to be excluded by the pore, those with a smaller dimension can more easily approach the particles' surface, compared with those of a greater dimension. Therefore, shorter chains flow more slowly. Longer chains stay away from the particles and flow along the fastest-flowing mobile phase, eluting earlier than other components. This mode of separation is called "hydrodynamic chromatography."



Extra-Column Dispersion

Raymond P. W. Scott

Scientific Detectors Ltd., Banbury, Oxfordshire, England

Introduction

In addition to the dispersion that takes place during the normal function of the column, dispersion can also occur in connecting tubes, injection system, and detector sensing volume, and as a result of injecting a finite sample mass and sample volume onto the column.

Discussion

The major sources of extra column dispersion are as follows:

1. Dispersion due to the sample volume (σ_s^2)
2. Dispersion occurring in valve-column and column-detector connecting tubes (σ_T^2)
3. Dispersion in the sensor volume from Newtonian flow (σ_{CF}^2)
4. Dispersion in the sensor volume from peak merging (σ_{CM}^2)
5. Dispersion from the sensor and electronics time constant (σ_i^2)

The sum of the variances will give the overall variance for the extra-column dispersion (σ_E^2). Thus,

$$\sigma_E^2 = \sigma_s^2 + \sigma_T^2 + \sigma_{CF}^2 + \sigma_{CM}^2 + \sigma_i^2 \quad (1)$$

Equation (1) shows how the various contributions to extra-column dispersion can be combined. According to Klinkenberg [1], the total extra-column dispersion must not exceed 10% of the column variance if the resolution of the column is not to be seriously denigrated; that is,

$$\sigma_E^2 = \sigma_s^2 + \sigma_T^2 + \sigma_{CF}^2 + \sigma_{CM}^2 + \sigma_i^2 = 0.1\sigma_c^2$$

In practice, σ_T^2 , σ_{CF}^2 , σ_{CM}^2 , and σ_i^2 are all kept to a minimum to allow the largest contribution to extra-column dispersion to come from σ_s^2 . This will allow the largest possible sample to be placed on the column, if so desired, to aid in trace analysis. Each extra-column dispersion process can be examined theoretically and two examples will be the evaluation of σ_s^2 and σ_T^2 .

Maximum Sample Volume

Consider the injection of a sample volume (V_i) that forms a rectangular distribution of solute at the front of the column. The variance of the final peak will be the sum of the variance of the sample volume plus the normal variance from a peak for a small sample. Now, the variance of a rectangular distribution of sample volume (V_i) is $V_i^2/12$, and assuming the peak width is increased by 5% due to the dispersing effect of the sample volume (a 5% increase in standard deviation is approximately equivalent to a 10% increase in peak variance), then by summing the variances,

$$\frac{V_i^2}{12} + [\sqrt{n}(v_m + Kv_s)]^2 = [1.05\sqrt{n}(v_m + Kv_s)]^2$$

where the dispersion due to the column alone is $[\sqrt{n}(v_m + Kv_s)]^2$ (see the entry Plate Theory). Simplifying and rearranging,

$$V_i^2 = n(v_m + Kv_s)^2(1.22)$$

Bearing in mind that

$$V_r = n(v_m + Kv_s)$$

then

$$V_i = \frac{1.1V_r}{\sqrt{n}}$$

Thus, the maximum sample volume that can be tolerated can be calculated from the retention volume of the solute concerned and the efficiency of the column. A knowledge of the maximum sample volume can be important when the column efficiency available is only just adequate, and the compounds of interest are minor components that are only partly resolved.

Dispersion in Connecting Tubes

The column variance is given by V_r^2/n , and for a peak eluted at the dead volume, the variance will be V_0^2/n (see the entry Plate Theory). Thus, for a connecting



tube of radius r_t and length l_t , the dead volume (V_0) (i.e., the volume of the tube) is

$$V_0 = \pi r_t^2 l_t$$

Thus,

$$\sigma_E^2 = \frac{0.1(\pi r_t^2 l_t)^2}{n}$$

Now, for the dead volume peak from an open tube, $n = 1/0.6r_t$ (see the entry Golay Dispersion Equation for Open-Tubular Columns). Thus,

$$\sigma_E^2 = 0.06\pi^2 r_t^5 l_t$$

However, when assessing the length of tube that can be tolerated, it must be remembered that the 10% increase in variance that can be tolerated before resolution is seriously denigrated involves *all* sources of extra-column dispersion, not just for a connecting tube. In practice, the connecting tube should be made as short as possible and the radius as small as

Extra-Column Dispersion

possible commensurate with reasonable pressures and the possibility that if the radius is too small, the tube may become blocked. The different sources of extra-column dispersion have been examined in Refs. 2 and 3.

References

1. A. Klinkenberg, *Gas Chromatography 1960* (R. P. W. Scott, ed.), Butterworths, London, 1960, p. 194.
2. R. P. W. Scott, *Liquid Chromatography Column Theory*, John Wiley & Sons, New York, 1992, p. 19.
3. R. P. W. Scott, *Introduction to Gas Chromatography*, Marcel Dekker, Inc., New York, 1998.

Suggested Further Reading

Scott, R. P. W., *Chromatographic Detectors*, Marcel Dekker, Inc., New York, 1998.



Extra-Column Volume

Kiyokatsu Jinno

Toyohashi University of Technology, Toyohashi, Japan

INTRODUCTION

Three mechanisms produce dispersion of a band of solute in a chromatographic system as it passes through the separation column: 1) eddy diffusion; 2) longitudinal diffusion; and 3) mass transfer effects. These effects are discussed, in some detail, in this article.

EXTRA-COLUMN BAND BROADENING

Three mechanisms produce dispersion of a band of solute in a chromatographic system as it passes through the separation column.

- Eddy diffusion and flow dispersion, which is the term for the dispersion produced because of the existence of different flow paths through which solutes can progress through the column. These differences of traveling distance arise because the stationary phase particles have different sizes and shapes, and because the packing of the column is imperfect, causing gaps or voids in the column bed. To reduce dispersion due to the multiple path effect, we need to pack the column with small particles, with as narrow a size distribution as possible.
- Longitudinal diffusion, which also arises because of diffusion of solute in the longitudinal (axial) direction in the column. This is an important source of dispersion in GC, but less so in LC, because rates of diffusion are very much slower in liquids than they are in gases. This effect becomes more serious the longer the solute species spend in the column; so, unlike flow dispersion, using a rapid flow rate of mobile phase reduces this effect.
- Mass transfer effects, which arise because the rate of the distribution process (sorption and desorption) of the solute species between mobile and stationary phases may be slow, compared to the rate at which the solute is moving in the mobile phase.

Except for the above general dispersions produced in the separation mechanisms, an unexpected, but important, dispersion can be produced outside the separation column by dead volumes in other parts of the chromatographic

system, such as in the injector, the detector, the connecting tubing, and connectors. The combined effect of all of these parts is called “extra-column volume” and the dispersion produced by this volume is called “extra-column dispersion.”^[1–4] Fig. 1 demonstrates an example of this extra-column dispersion, in which different dead volumes are inserted between the column and the detector. One can see, from this figure, that the effect of extra-column volume can cause a serious loss in separation performance of the chromatographic system.

The variance (the square of the standard deviation) of the observed peak (σ^2) can be expressed as the sum of the peak variances caused only by the contribution of the column (σ_p^2) and all the contributions to the peak broadening due to the extra-column volume (σ_{ex}^2). This is expressed as

$$\sigma^2 = \sigma_p^2 + \sigma_{ex}^2 \quad (1)$$

Since the peak volume is four times the standard deviation (σ_s), Eq. 1 can be rewritten as

$$V_t^2 = V_p^2 + V_{ex}^2 \quad (2)$$

where V_p is the peak volume obtained only from column contribution and V_{ex} is the extra-column peak volume corresponding to the contributions of the injector,

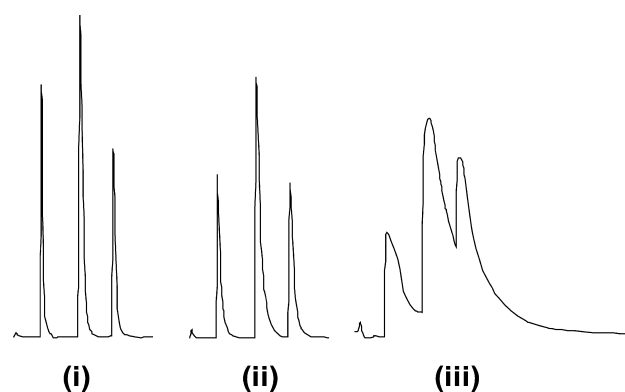


Fig. 1 Extra-column effects on the chromatogram. i) Normal chromatogram for a test separation; ii) chromatogram obtained by inserting 75 μ L of extra volume between the column and the detector inlet tube; iii) chromatogram obtained by inserting 2 mL of extra volume between the column and the detector inlet tube.

**Table 1** Maximum extra-column peak volumes for peaks eluted by various columns^a

	Column type (length, mm; ID, mm)		
	Conventional (250; 4.6)	Semi-microcolumn (250; 1.5)	Microcolumn (250; 0.5)
Maximum extra column			
Peak volume (V_{ex} , μL)	53	5.5	0.6
Peak volume (V_p , μL)	116	12	1.4

^aThe above numbers have been estimated by assuming as follows: Column porosity = 0.7; retention factor = 0; and theoretical plate number = 10,000.

detector cell, and connecting tubing. Dividing Eq. 2 by V_p^2 produces

$$(V_t/V_p)^2 = 1 + (V_{ex}/V_p)^2 \quad (3)$$

Therefore, if the observed peak is allowed to have a volume 10% greater than the column peak volume, the extra-column peak volume should be one-half (ca. 46%) of the column peak volume. Table 1 lists column peak volumes and maximum extra-column peak volumes for various types of columns for LC; because the largest contribution from this extra-column volume should be considered in liquid phase separations, the diffusion coefficients in liquids are very small.

From Table 1, it is very clear that, as the absolute volume of a microcolumn is relatively small, the extra-column volume will contribute significantly to disturb the separation performance of the chromatography system. Because the small extra-column volume is still a large portion of the total system volume which, in turn, is much smaller than the conventional column system, and it is hard to eliminate such small extra-column volume, even if attempts to reduce are applied, a serious problem would be produced. Most typical discussions on the applicability

of microcolumn separations in LC are concerned with how to reduce the extra-column volume; this makes microcolumn LC techniques still unpopular, although many advantages are proven and acknowledged. In conclusion, the minimum column volume one can use will depend on the amount of extra-column dispersion and on what we consider to be an acceptable increase in peak width that is produced by the extra-column effects. In practice, this acceptable increase is assumed to be 10%, based on an unretained solute and, if we take 50 μL as a typical value for extra-column dispersion, then the minimum column diameter in LC works out to about 4.6 mm for a column 25 cm long, which is the most popular conventional LC separation column configuration that is commercially available.

REFERENCES

1. Knox, J.H. *J. Chromatogr. Sci.* **1977**, *15*, 352.
2. Golay, M.J.E.; Atwood, J.G. *J. Chromatogr.* **1979**, *186*, 353.
3. Katz, E.D.; Scott, R.P.W. *J. Chromatogr.* **1983**, *268*, 169.
4. Hupe, K.P.; Jonker, R.J.; Rozing, G. *J. Chromatogr.* **1984**, *285*, 253.

Fast Gas Chromatography

Richard C. Striebich

University of Dayton Research Institute, Dayton, Ohio, U.S.A.

INTRODUCTION

The examination of ways to conduct fast gas chromatography (GC) has been a popular research topic since the 1960s, and even more so in the past 10 years. The need to analyze complex mixtures by GC is often a balance between the ability to separate adjacent peaks in a chromatogram (resolution) and analysis time. Especially with complex mixtures, analysts can use longer columns and much slower programming rates to increase resolution; however, there is a penalty to be paid in analysis time. Because petroleum samples are arguably the most complex samples known, a good deal of work has been performed to provide the greatest possible resolution without regard for the consideration of time. Some GC petroleum analyses have been reported, which take 2–4 hr and longer.^[1] However, there is a definite application for faster analyses with less resolution.

The history, methods, and applications for conducting fast analyses by GC are delineated in several excellent reviews.^[2–6] In these works, the authors discuss several ways to shorten analysis time, such as the following:

1. decrease the column length
2. increase the carrier gas flow rate
3. use multichannel columns^[6]
4. provide rapid heating of the column with heating rates up to 1200°C/min and sometimes higher^[2]

Fast GC in these instances is best described as conducting analyses as fast as is possible to provide just enough separation of the compounds of interest. Often-times, in the search for maximum resolution, compounds can be overseparated, which usually lengthens the time of analysis.

OVERVIEW

In petroleum analyses, and specifically for aviation fuels, there are a good many separations where complete resolution is not needed. GC fingerprinting of different types of fuels (diesel, gasoline, aviation fuels, kerosene, etc.) can be performed quickly to characterize the mixtures in useful ways. Simulated distillation^[1] is one good example of

a chromatographic analysis that has low resolution, but can be conducted very quickly, (i.e., $\ll 5$ min). Fortunately, excellent resolution is not usually necessary to obtain the critical information about distillation range,^[7] and so this application is a good example of fast GC where limited resolution is acceptable. In this article, we introduce simple fast GC concepts that can speed up the low-resolution analysis of petroleum products.

EXPERIMENTAL

Short (3–7 m) microbore gas chromatographic columns (0.10 mm internal diameter, 0.17 μ m film thickness) can be used to provide much faster analyses with acceptable resolution for at least two different types of useful analyses: *fuel GC fingerprinting* and *simulated distillation analysis*. The detector for the instrument used for these analyses is a hydrogen flame ionization detector (FID) capable of very fast sampling rates (adjustable up to 200 Hz), which is necessary because of the narrow peaks that are generated. Carrier gas is one of the parameters investigated; both helium and hydrogen carrier gases were used, with high-pressure hydrogen routinely providing the best and fastest separations (in agreement with previous work and theory). In this work, the programming rates were limited to that which was available using an Agilent 6890 instrument with a fast heating option (i.e., input rates to 120°C/min with trackable rates to approximately 75°C/min). No attempts were made to increase programming rate by resistively heating the column.

RESULTS AND DISCUSSION

Analysis of aviation fuels by capillary GC can be performed using a variable level of resolution (peak separation) by changing the conditions of the GC. For the purposes of this work, the approximate resolution required was that obtained with conventional methods. That is, an experiment that is completed in 20–30 min is typical because it is fast enough to be productive with regard to research and testing, and provides enough resolution to obtain the needed useful information. In addition to this level of resolution, we briefly examined

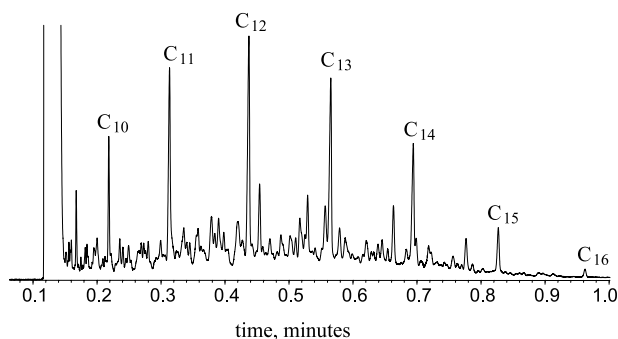


Fig. 1 Fast GC analysis of aviation turbine engine fuel using a typical laboratory GC instrument. Conditions: hydrogen carrier gas; temperature programming rate, 70–170°C at 120°C/min (actual 75°C/min); microbore column: 3 m × 0.10 mm ID.

the output of a GC analysis conducted using a column of 50 μm internal diameter, half the diameter of typical fast GC columns. These conditions represent our laboratory's (present-day) limit of speed and resolving power (Fig. 1).

Effect of Column Dimensions

Table 1 shows a comparison of the general relationship that exists between GC efficiency as measured by the number of theoretical plates per meter and a particular column dimension. Because microbore columns (0.10 mm internal diameter) have more resolving power per meter, the length of these columns can be typically one third the length of standard bore columns (0.25 mm internal diameter) and still provide approximately the same resolution. Thus fast GC is really faster because of the use of shorter columns, which are more efficient because of their smaller inner diameter. Figure 2a shows a typical high-resolution analysis using a conventional 30-m column (0.25 mm internal diameter) and a fast chromatogram with similar resolution, but with greatly reduced time.

Table 1 Chromatographic column diameter vs. efficiency

Column internal diameter (ID) [mm]	Theoretical plates per meter
0.10	12,500
0.18	6,600
0.20	5,940
0.25 ^a	4,750
0.32	3,710
0.45	2,640
0.53	2,240

^aMost typically used in our laboratory.

Source: Ref. [8].

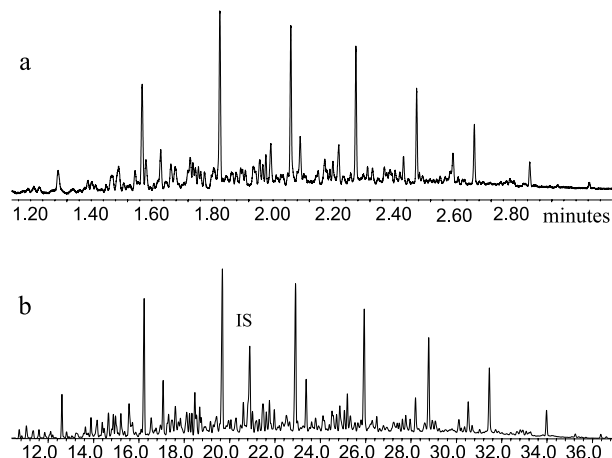


Fig. 2 Comparison of conventional 3 m × 0.25 mm ID (standard bore) column (b) with a 10 m × 0.10 mm ID column (a) with similar resolution.

Changing column diameter and length is one of the easiest ways to decrease analysis times, but it is not without a price. Usually, this cost is in decreased column capacity (mass of solute chromatographed without overloading), or in the need to increase carrier head pressure.^[4,6]

Effect of Carrier Gas

The widely accepted carrier gas for fast GC analyses is hydrogen, whereas in the United States, helium is the usual choice for conventional analyses. The use of hydrogen is typically better because faster optimal linear velocities are possible at the same generated resolution. Column efficiency is usually expressed in terms of H (i.e., the height equivalent of a theoretical plate, which, when minimized, expresses an optimal efficiency of separation between two components). By plotting the average velocity of the carrier gas vs. the H value, a van Deemter plot is generated. The optimal velocity of the carrier gas for the most efficient separation is higher for hydrogen carrier gas. Thus hydrogen can operate at higher carrier gas velocities without loss of resolution. Although helium carrier gas can be used above its optimal velocity, significant resolution decreases will occur at high flow rates. Because the van Deemter plot for hydrogen is flatter for higher velocities than it is for helium, less resolution is lost with higher velocities of hydrogen, compared to helium.

Effect of Temperature Programming

The ability to quickly ramp column temperature is an excellent way to increase analysis speed, given appropriate carrier gas flow rates and fast detector sampling rates. Along with column dimensions and operation above



optimal velocities of hydrogen carrier gas, analyses can be performed extremely fast and with high resolution. Temperature programming for all of the experiments shown was at 70°C/min, which was approximately the fastest rate that the GC oven could reasonably track. Temperature programming rates of up to 120°C/min are possible to input into the GC, but the heaters cannot reliably heat the large oven at this rate. Clearly, faster temperature programs, using resistively heated columns and sheaths,^[2] would lead to faster analyses. However, resolution is sacrificed if the column is heated so fast that large portions of the column act as a transfer line for GC solutes, whose boiling points have been exceeded too quickly. It is difficult to balance speed and accuracy with mixtures with wide boiling range.

APPLICATIONS

Fuel samples were examined using conditions similar to those used in this study, with 100- μ m capillary columns and conventional GC instrumentation (Agilent 6890). Jet fuels are more of an analytical challenge because of their multicomponent nature; indeed, any analysis of jet fuel probably contains many unresolved solute zones. Enough chromatographic separation must be generated to conduct the particular task of the analysis, but must also be balanced with acceptable speed. The following applications show separations of various mixtures conducted with speed as the primary consideration.

Fuel GC Fingerprinting

Figure 3 shows four examples of fuel “fingerprinting”; the normal alkane distribution helps to indicate the fuel type. Because of the high resolution in this example, it is possible to obtain useful information from the chromatogram and to be able to compare this output tracing to those

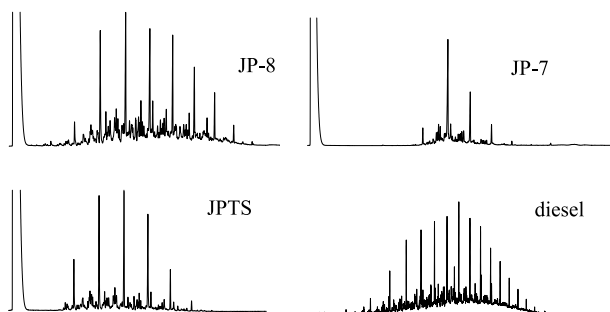


Fig. 3 Fast GC analysis of four fuels including (a) JP-8; (b) JP-7; (c) JP-TS; and (d) diesel fuel.

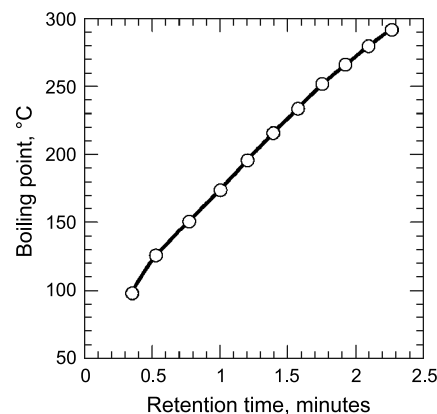


Fig. 4 Calibration curve for simulated distillation of JP-8, JP-TS, and JP-7. (View this art in color at www.dekker.com.)

generated by other fuels. In many cases of fuel contamination, mixing of fuels, mislabeling of containers, and other commonly encountered problems, it is necessary to perform a “general pattern recognition” to identify or characterize the fuel.

Simulated Distillation

By conducting a calibration curve based on the boiling points of *n*-alkanes, it is possible to estimate the distillation temperatures according to the ASTM D2887 method.^[9] Figures 4 and 5 show the calibration and the

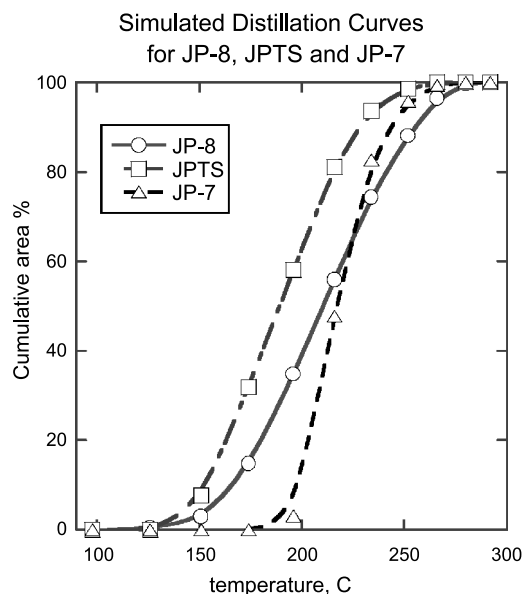


Fig. 5 Simulated distillation analysis of JP-8, JP-TS, and JP-7. (View this art in color at www.dekker.com.)

simulated distillation curves, respectively, for JP-8, JP-TS, and JP-7, which were obtained from the fast GC analyses. These analyses are directly comparable to fuel specification tests for distillation range. Even analyses faster than these are possible because simulated distillation is a technique where very low resolution is required and generated. Relatively high resolution was maintained for these runs because the chromatographic data were correlated to other specification properties, such as freeze point and flash point.^[7]

CONCLUSIONS

Fast GC has great potential as a highly productive investigative tool in today's analytical laboratory. It is becoming more widely used as more advanced GC systems are introduced. We have shown applications of GC analyses with acceptable resolution for aviation fuels, analyzed in fewer than 5 min. The speed of analysis may eventually improve to the point where the GC could produce jet fuel analyses in much less than 1 min.

ACKNOWLEDGMENTS

This work was partially supported by the Fuels Branch of the Air Force Research Laboratory, Propulsion Sciences and Advanced Concepts Division, AFRL/PRSF under the program entitled "Advanced Integrated Fuel/Combustion

System" (contract no. F33615-97-C-2719). Mr. Robert Morris was the technical monitor.

REFERENCES

1. *Chromatography in Petroleum Analysis*; Altgelt, K.H., Gouw, T.H., Eds.; Marcel Dekker, Inc.: New York, NY, 1979; 75–89.
2. McNair, H.M.; Reed, G.L. Fast gas chromatography: The effect of fast temperature programming. *J. Microcolumn Sep.* **2000**, *12* (6), 351–355.
3. Cramers, C.A.; Janssen, H.-G.; van Deursen, M.M.; Leclercq, P.A. High-speed gas chromatography: An overview of various concepts. *J. Chromatogr., A* **1999**, *856*, 315–329.
4. Cramers, C.A.; Leclercq, P.A. Strategies for speed optimization in gas chromatography: An overview. *J. Chromatogr., A* **1999**, *842*, 3–13.
5. David, F.; Gere, D.R.; Scanlan, F.; Sandra, P. Instrumentation and applications of fast high-resolution capillary gas chromatography. *J. Chromatogr., A* **1999**, *842*, 309–319.
6. van Lieshout, M.; van Deursen, M.; Derks, R.; Janssen, H.-G.; Cramers, C. A practical comparison of two recent strategies for fast gas chromatography: Packed capillary columns and multicapillary columns. *J. Microcolumn Sep.* **1999**, *11* (2), 155–162.
7. Striebich, R.C. Fast gas chromatography for middle-distillate aviation turbine fuels. *Assoc. Can. Stud. Pet. Chem. Prepr.* **2002**, *47* (3), 219–222.
8. J&W Inc. *GC Reference Guide*; Folsom, CA, 1998; 13 pp.
9. ASTM D2887-93. Boiling Range Distribution of Petroleum Fractions by Gas Chromatography. In *Section 5 Annual Book of ASTM Standards*; 1996; 192–201. Conshohocken, PA.



Field-Flow Fractionation Data Treatment

Josef Janča

Université de La Rochelle, La Rochelle, France

Introduction

Field-flow fractionation (FFF) methods are classified into two main categories [1–3]: *polarization* FFF and *focusing* FFF. Their basic characterization is given in the entry Field-Flow Fractionation Fundamentals. Whereas the polarization FFF methods allow to fractionate the samples on the basis of the differences in the extensive properties (such as the molar mass or particle size, etc.) of the individual species, the focusing FFF methods discriminate among the species, according to their intensive property differences (such as the charge or density, etc.). This article deals with the data treatment of the experimental results from polarization FFF, thus with the quantitative characterization of the extensive properties. However, a principally identical approach can be applied to the intensive properties data treatment of the results obtained from the focusing FFF experiments.

Discussion

In general, the methodology of the data treatment, concerning the separations of the macromolecular or particulate samples, does not depend on the particular separation method or technique. The basics of this methodology were elaborated in parallel with the development of size-exclusion chromatography (SEC) [4] and of the techniques of particle size analysis [5], but they originate at the very beginning [6,7] of liquid chromatography of macromolecules and remain substantially unchanged until today.

Macromolecular or particulate samples fractionated by the FFF are usually not uniform but exhibit a distribution of the concerned extensive or intensive parameter [8] or, in other words, a polydispersity. Molar mass distribution (MMD), sometimes called molecular weight distribution (MWD), or particle size distribution (PSD) describes the relative proportion of each molar mass (molecular weight), M , or particle size (diameter), d_p , species composing the sample. This proportion can be expressed as a number of the macromolecules or particles of a given molar mass or diameter, respectively, relative to the number of all macromolecules or particles in the sample:

$$N(M) = \frac{n_i(M)}{\sum_{i=1}^{\infty} n_i} \quad (1)$$

$$N(d_p) = \frac{n_i(d_p)}{\sum_{i=1}^{\infty} n_i}$$

or as a mass (weight) of the macromolecules or particles of a given molar mass or diameter relative to the total mass of the sample:

$$W(M) = \frac{m_i(M)}{\sum_{i=1}^{\infty} m_i} \quad (2)$$

$$W(d_p) = \frac{m_i(d_p)}{\sum_{i=1}^{\infty} m_i}$$

Accordingly, the MMD (MWD) and PSD are called number or mass (weight) MMD or PSD, respectively. FFF provides a fractogram which has to be treated to obtain the required MMD or PSD. These distributions can be used to calculate various average molar masses or particle sizes and polydispersity indices.

Average Molar Masses, Particle Sizes, and Polydispersities

As mentioned, in addition to the MMD and PSD, various average molar masses, particle sizes, and polydispersity indexes can be calculated from the FFF fractograms. If the detector response, h , is proportional to the mass of the macromolecules or particles, the mass-average molar mass or mass average particle diameter can be calculated from

$$\begin{aligned} \overline{M}_m = \overline{M}_w &= \frac{\sum_{i=1}^{\infty} M_i h_i}{\sum_{i=1}^{\infty} h_i} \\ \overline{d}_m = \overline{d}_w &= \frac{\sum_{i=1}^{\infty} d_i h_i}{\sum_{i=1}^{\infty} h_i} \end{aligned} \quad (3)$$

and the corresponding number average values are calculated from

$$\overline{M}_n = \frac{\sum_{i=1}^{\infty} M_i n_i}{\sum_{i=1}^{\infty} n_i} = \frac{\sum_{i=1}^{\infty} h_i}{\sum_{i=1}^{\infty} (h_i/M_i)} \quad (4)$$



$$\overline{d}_n = \frac{\sum_{i=1}^{\infty} d_i n_i}{\sum_{i=1}^{\infty} n_i} = \frac{\sum_{i=1}^{\infty} h_i}{\sum_{i=1}^{\infty} (h_i/d_i)}$$

The width of the MMD or PSD (polydispersity) can be characterized by the index of polydispersity:

$$I_{\text{MMD}} = \frac{\overline{M}_m}{\overline{M}_n} \quad (5)$$

$$I_{\text{PSD}} = \frac{\overline{d}_m}{\overline{d}_n}$$

Practical Data Treatment

Provided that the correction for the zone broadening should not be applied, the first step in the data treatment is to convert the retention volumes (or the retention ratios R) into the corresponding molecular or particulate parameter, characterizing the fractionated species. Whenever the zone broadening correction procedure has to be applied, the data treatment protocol is modified, as described in the entry Zone Dispersion in Field-Flow Fractionation.

The dependences of the retention ratio R on the size of the fractionated species (molar mass for the macromolecules or particle diameter for the particulate matter) are presented for various polarization FFF methods in the entry Field-Flow Fractionation Fundamentals. The raw, digitized fractogram, which is a record of the detector response as a function of the retention volume, is represented by a differential distribution function $h(V)$. It can be processed to obtain a series of the height values h_i corresponding to the retention volumes V_i , as shown in Fig. 1. Subsequently, the retention volumes V_i , are converted into the retention ratios R_i :

$$R_i = \frac{V_0}{V_i} \quad (6)$$

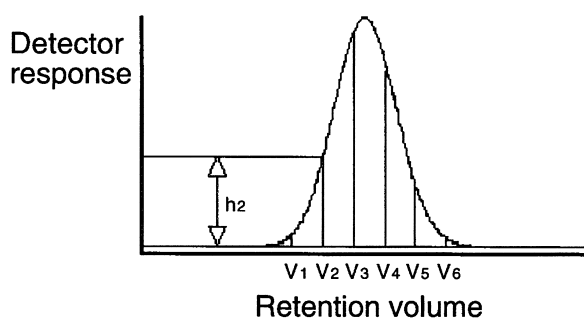


Fig. 1 Treatment of an experimental FFF fractogram of a polydisperse sample.

The retention ratio R in polarization FFF is related to the retention parameter λ (see the entry Field-Flow Fractionation Fundamentals) by

$$R = 6\lambda \left[\coth\left(\frac{1}{2\lambda}\right) - 2\lambda \right] \quad (7)$$

or by an approximate relationship

$$(\lim R)_{\lambda \rightarrow 0} = 6\lambda \quad (8)$$

and the parameter λ is directly related to the molecular or particulate parameters by the general relationships

$$\lambda = f(M^{-n}) \quad \text{or} \quad \lambda = f(d_p^{-n}) \quad (9)$$

where the exponent $n = 1, 2$, or 3 . As concerns the focusing FFF methods, similar relationships exist between the retention ratio R and the intensive properties of the fractionated species.

Having the V_i values converted into the R_i values by using Eq. (6), the corresponding molar mass M_i or the particle diameter d_i values are calculated by applying Eqs. (7)–(9). The difficulty is that Eq. (7) is a transcendental function $R = f(\lambda)$ for which the inversion function $\lambda = f'(R)$ does not exist. As a result, Eq. (8) can be used as a first approximation to estimate the λ_i values from the experimental R_i data, and by applying a rapidly converging iteration procedure, the accurate λ_i values can be calculated. The subsequent attribution of the corresponding M_i or d_i values to the calculated λ_i values, by using the appropriate relationship, Eq. (9), is not mathematically complicated.

In order to obtain an accurate result, the regular segmentation ΔV_i of the raw fractogram must be converted into the ΔR_i and, thereafter, into the appropriate increment of the molar mass ΔM_i or of the particle diameter Δd_i . The corresponding conversions of the raw experimental fractograms into the MMD or PSD can be carried out according to the following protocol. Equations (3) and (4) can be rewritten in integral form:

$$\overline{M}_m = \frac{\int_0^{\infty} W(M) M dM}{\int_0^{\infty} W(M) dM} \quad (10)$$

$$\overline{d}_m = \frac{\int_0^{\infty} d_p W(d_p) dd_p}{\int_0^{\infty} W(d_p) dd_p}$$

and

$$\overline{M}_n = \frac{\int_0^{\infty} N(M) M dM}{\int_0^{\infty} N(M) dM} \quad (11)$$

$$\overline{dn} = \frac{\int_0^\infty d_p N(d_p) dd_p}{\int_0^\infty N(d_p) dd_p}$$

where it holds for the normalized MMD or PSD:

$$\begin{aligned} \int_0^\infty W(M) dM &= \int_0^\infty W(d_p) dd_p \\ &= \int_0^\infty N(M) dM = \int_0^\infty N(d_p) dd_p = 1 \end{aligned} \quad (12)$$

By considering all of the above-mentioned transformations, Eqs. (10)–(12) give

$$\begin{aligned} \overline{M_m} &= \int_0^\infty W(M) M \left(\frac{\partial M}{\partial \lambda} \right) \left(\frac{\partial \lambda}{\partial R} \right) \left(\frac{\partial R}{\partial V} \right) dV \left(\int_0^\infty W(M) dV \right)^{-1} \\ \overline{d_m} &= \int_0^\infty W(d_p) d_p \left(\frac{\partial d_p}{\partial \lambda} \right) \left(\frac{\partial \lambda}{\partial R} \right) \left(\frac{\partial R}{\partial V} \right) dV \left(\int_0^\infty W(d_p) dV \right)^{-1} \\ \overline{M_n} &= \int_0^\infty N(M) M \left(\frac{\partial M}{\partial \lambda} \right) \left(\frac{\partial \lambda}{\partial R} \right) \left(\frac{\partial R}{\partial V} \right) dV \left(\int_0^\infty N(M) dV \right)^{-1} \\ \overline{d_n} &= \int_0^\infty N(d_p) d_p \left(\frac{\partial d_p}{\partial \lambda} \right) \left(\frac{\partial \lambda}{\partial R} \right) \left(\frac{\partial R}{\partial V} \right) dV \left(\int_0^\infty N(d_p) dV \right)^{-1} \end{aligned} \quad (13)$$

Any of Eqs. (13) can further be rewritten in a numerical form of Eqs. (3) and (4), which are convenient for the data treatment and calculations using the discrete M_i or d_i and h_i values. The acquisition of the experimental data and the treatment of the fractogram is easily performed by a computer connected on-line to the separation system.

References

1. J. Janča, *Field-Flow Fractionation: Analysis of Macromolecules and Particles*, Marcel Dekker, Inc., New York, 1988.
2. J. Janča, *J. Liquid Chromatogr. Related Technol.* 20: 2555 (1997).
3. H. Cölfen and M. Antonietti, *Adv. Polym. Sci.* 150: 67 (2000).
4. C. Quivoron, in *Steric Exclusion Chromatography of Polymers* (J. Janča, ed.), Marcel Dekker, Inc., New York, 1984.
5. H. G. Barth (ed.), *Modern Methods of Particle Size Analysis*, John Wiley & Sons, New York, 1984.
6. J. Cazes, *J. Chem. Educ.* 43: A567 (1966).
7. J. Cazes, *J. Chem. Educ.* 43: A625 (1966).
8. J. V. Dawkins, in *Comprehensive Polymer Science, Vol. 1* (C. Booth and C. Price, eds.), Pergamon Press, Oxford, 1989.



Field-Flow Fractionation Fundamentals

Josef Janča

Université de La Rochelle, La Rochelle, France

Introduction

Field-flow fractionation (FFF) is a separation methodology suitable for the analysis and characterization of the macromolecules and particles. The separation is based on the interaction of the effective physical or chemical forces (e.g., temperature gradient; electric, magnetic, gravitational, or centrifugal forces; chemical potential gradient; etc.) with the separated species. The field acting across a separation channel concentrates them at a given position inside the channel. The formed concentration gradient induces an opposite diffusion flux. This leads to a steady-state distribution of the sample components across the channel. The velocity of the longitudinal flow of the carrier liquid also varies across the channel. A flow velocity profile is established inside the channel. As a result, the components of the separated sample are transported in the longitudinal direction at different velocities depending on their transversal positions within the flow of the carrier liquid. This general principle of the FFF is demonstrated in Fig. 1.

Discussion

Two mechanisms, *polarization* [1] and *focusing* [2], lead to the formation of different concentration distributions across the fractionation channel. The components of the fractionated sample are either compressed to the accumulation wall of the channel or focused at different positions, as shown in Fig. 1. Steady state inside the channel is reached in a short time due to a small channel thickness. The strength of the field can be controlled within a wide range in order to manipulate the retention conveniently. Many operational variables in FFF can be manipulated during the experiment by a suitable programming.

The *polarization FFF* methods are classified according to the nature of the applied field, whereas the *focusing FFF* methods are classified by considering the combination of various gradients and fields emphasizing the focusing processes. Polarization

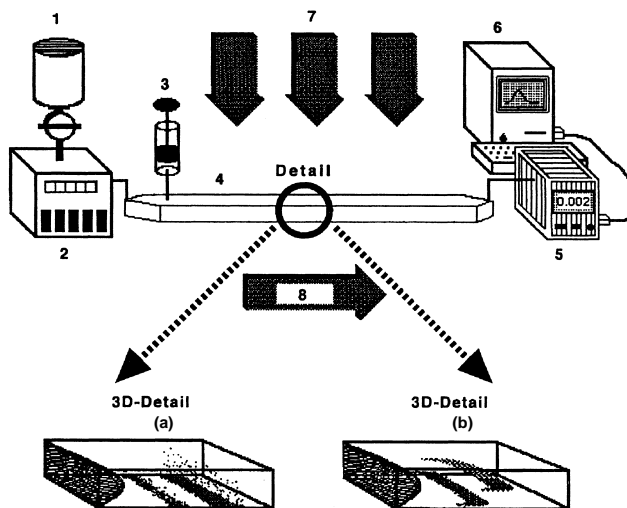


Fig. 1 Principle of field-flow fractionation: (1) solvent reservoir, (2) carrier liquid pump, (3) injection of the sample, (4) separation channel, (5) detector, (6) computer for data acquisition, (7) transversal effective field forces, (8) longitudinal flow of the carrier liquid. (a) Section of the channel demonstrating the principle of polarization FFF with two distinct zones compressed differently at the accumulation wall and the parabolic flow velocity profile. (b) Section of the channel demonstrating the principle of focusing FFF with two distinct zones focused at different positions and the parabolic flow velocity profile.

FFF methods make use of the formation of an exponential concentration distribution of each sample component across the channel with the maximum concentration at the accumulation wall, which is a consequence of constant and position-independent velocity of transversal migration of the affected species due to the field forces. This concentration distribution is combined with the velocity profile formed in the flowing liquid. Focusing FFF methods make use of transversal migration of each sample component under the effect of driving forces that vary across the channel. As a result, the sample components are focused at the positions where the



intensity of the effective forces is zero and are transported longitudinally with different velocities according to the established flow velocity profile. The concentration distribution within a zone of a focused sample component can be described by Gaussian or similar distribution function.

Principle and Theory

The carrier liquid flows in the direction of the channel longitudinal axis, whereas the field forces act perpendicularly across the channel. The driving forces can be generated by a single field or by the coupled action of two or more different fields. Polarizing and focusing forces can operate simultaneously, resulting in a complex mechanism of separation. The field force F and, consequently, the velocity U are independent of the position in the direction of the x axis in polarization FFF:

$$F \neq 0 \quad \text{and} \quad U \neq 0 \quad \text{for } 0 < x < w \quad (1)$$

where w is the distance between the main channel walls in the direction of the x axis with $x = 0$ at the accumulation wall. On the other hand, it holds for the x -axis-dependent direction of the field force in focusing FFF:

$$F = F(x) \quad \text{and} \quad U = U(x) \quad \text{within } 0 < x < w \quad (2)$$

$$F(x) = 0 \quad \text{and} \quad U(x) = 0 \quad \text{for } x = x_{\max} \quad (3)$$

with $0 < x_{\max} < w$

$$F(x) > 0 \quad \text{and} \quad U(x) > 0 \quad \text{for } x < x_{\max} \quad (4)$$

$$F(x) < 0 \quad \text{and} \quad U(x) < 0 \quad \text{for } x > x_{\max} \quad (5)$$

where the coordinate x_{\max} corresponds to the position at which the concentration distribution of a sample component across the channel attains its maximal value.

Polarization FFF

The equilibrium concentration distribution in the direction of the x axis across the channel of a given component of the sample can be calculated from the continuity equation

$$-D \frac{\partial c}{\partial x} - Uc = 0 \quad (6)$$

where D is the diffusion coefficient and c is the concentration. The solution of Eq. (6) gives the exponential concentration distribution of the sample component across the channel [3]:

$$c(x) = c(0) \exp\left(-\frac{xU}{D}\right) \quad (7)$$

By defining the mean layer thickness, $l = D/U$, Eq. (7) can be rewritten

$$c(x) = c(0) \exp\left(-\frac{x}{l}\right) \quad (8)$$

The mean layer thickness is practically equal to the center of gravity of the concentration distribution.

Focusing FFF

It holds for a focused species at equilibrium that

$$D \frac{\partial c}{\partial x} - U(x)c = 0 \quad (9)$$

The force $F(x)$, acting on one particle undergoing the focusing, can be written as

$$F(x) = U(x)f \quad (10)$$

with the friction coefficient defined by

$$f = \frac{kT}{D} \quad (11)$$

where k is the Boltzmann constant and T is the absolute temperature. Then, it holds that

$$\frac{dc}{dx} = \frac{F(x)c}{kT} \quad (12)$$

The focusing force can be approximated by [4]

$$F(x) = -\left|\left(\frac{dF(x)}{dx}\right)_{x \approx x_{\max}}\right|(x - x_{\max}) \quad (13)$$

where $(dF(x)/dx)_{x=x_{\max}}$ is the gradient of the driving force. The solution is

$$c(x) = c_{\max} \exp\left[-\frac{1}{2kT}\left|\left(\frac{dF(x)}{dx}\right)_{x \approx x_{\max}}\right|(x - x_{\max})^2\right] \quad (14)$$

which is a Gaussian concentration profile of a single focused component. A more accurate approach [4] is based on the real gradient of the focusing forces and results in a concentration distribution of the focused species, which is not Gaussian.

Flow Velocity Profiles

The separation is usually carried out in a belt-shaped narrow channel of constant thickness. The cross section of the channel is rectangular. Velocity distribution in such a channel (provided that the flow is isoviscous) is parabolic:

$$v(x) = \frac{\Delta P x(w - x)}{2L\mu} \quad (15)$$

where $v(x)$ is the longitudinal velocity at the x coordinate, ΔP is the pressure drop along the channel of the length L , and μ is the viscosity of the carrier liquid. The average velocity is

$$\langle v(x) \rangle = \frac{\Delta P w^2}{12L\mu} \quad (16)$$

Other shapes of the flow velocity profiles can be formed in channels whose cross section is not rectangular but, for example, trapezoidal. The use of such nonparabolic flow velocity profiles can be advantageous, especially in focusing FFF.

Separation

The separation is due to the coupled action of the concentration and flow velocity distributions. The concentration distribution across the channel of each sample component is established and the sample components are eluted along the channel with different velocities, depending on the distance of their centers of gravity from the accumulation wall. The average velocity of the zone of a retained sample component is

$$\langle v \rangle = \frac{\langle c(x)v(x) \rangle}{\langle c(x) \rangle} \quad (17)$$

The retention ratio R is defined as the average velocity of a retained sample component to the average velocity of the carrier liquid:

$$R = \frac{\int_0^w c(x)v(x) dx \int_0^w dx}{\int_0^w c(x) dx \int_0^w v(x) dx} \quad (18)$$

where $v(x)$ and $c(x)$ are the local velocity and concentration, respectively, of the retained species. From the practical point of view, the retention ratio R can be expressed as the ratio of the experimental retention time t_0 or the retention volume V_0 of an unretained sample component to the retention time t_r or the retention volume V_r of the retained sample component.

Provided that the relationship between the position of the center of gravity of the zone and the molecular parameters of the sample component exists, these parameters can be calculated from the retention data without a calibration.

The retention ratio in polarization FFF is thus given by [5]

$$R = 6\lambda \left[\coth\left(\frac{1}{2\lambda}\right) - 2\lambda \right] \quad (19)$$

where $\lambda = l/w$. If λ is small, the following approximations hold:

$$(\lim R)_{\lambda \rightarrow 0} = 6(\lambda - 2\lambda^2) \quad \text{or} \quad (\lim R)_{\lambda \rightarrow 0} = 6\lambda \quad (20)$$

The retention parameter λ is the ratio of thermal energy to the effective of the field on the retained species:

$$\lambda = \frac{kT}{Fw} \quad (21)$$

When the size of the separated species is commensurable with the thickness of the channel, the limit retention ratio in this mode of steric FFF is [6]

$$\lim_{\alpha \rightarrow 0} R = 6\alpha \quad (22)$$

where $\alpha = r/w$ and r is the particle radius.

The retention ratio in focusing FFF carried out in rectangular cross-section channel is given by the approximate relationship [7]

$$R = 6(\Gamma_{\max} - \Gamma_{\max}^2) \quad (23)$$

where $\Gamma_{\max} = x_{\max}/w$ is the dimensionless coordinate of the maximal concentration of the focused zone.

Methods and Applications

The retention is related to the size, charge, diffusion coefficient, thermal diffusion factor, and so forth of the separated species in polarization FFF. As concerns the focusing FFF, the retention is usually related with the intensive properties of the fractionated species. Consequently, the FFF can be used to characterize the properties related to the retention. Because the entry Focusing FFF of Particles and Macromolecules is fully devoted to the focusing FFF, only the polarization FFF methods will be described here.

The particular methods of polarization FFF are denominated by the nature of the applied field. The most important of them are described in the following subsections.



Sedimentation FFF

The sedimentation FFF is shown schematically in Fig. 2a. The separation channel is situated inside a centrifuge rotor and the centrifugal forces are applied radially [8]. The method can be used for the analysis and characterization of various latexes, inorganic particles, emulsions, biological cells, and so forth. The retention parameter λ depends on the effective mass of the particles:

$$\lambda = \frac{6kT}{\pi d^3 g w \Delta \rho} \quad (24)$$

where g is the gravitational or centrifugal acceleration and $\Delta \rho$ is the density difference between the particles and the carrier liquid. The calculation of the particle size distribution is possible directly from the retention data.

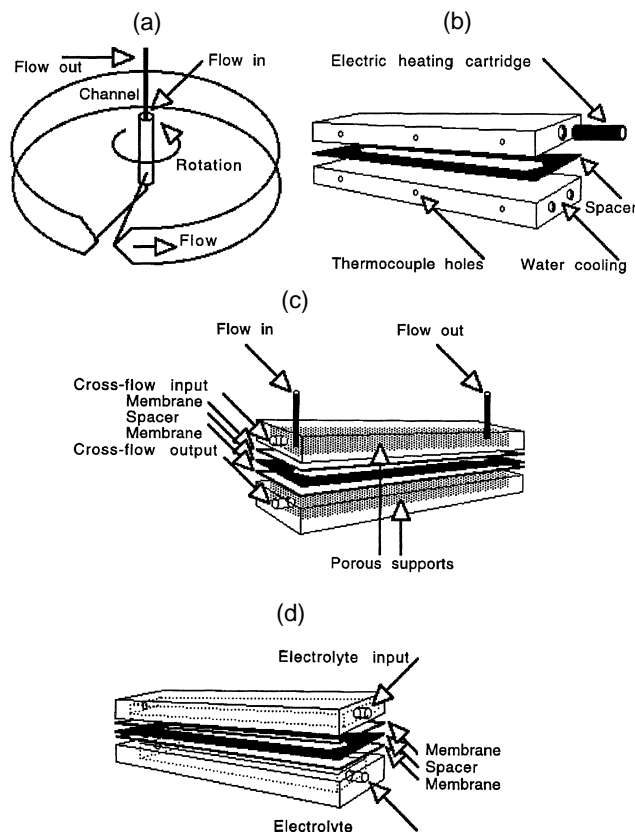


Fig. 2 Methods of polarization field-flow fractionation: (a) sedimentation FFF; (b) thermal FFF; (c) flow FFF; (d) electric FFF.

Thermal FFF

Thermal FFF was the first experimentally implemented method [9]. It is used mostly for the fractionation of macromolecules. The temperature difference between two metallic bars, forming the channel walls with highly polished surfaces and separated by a spacer in which the channel proper is cut, produces the flux of the sample components, usually toward the cold wall. The channel for thermal FFF is shown in Fig. 2b. The relation between λ and the operational variables is given by

$$\lambda = \frac{D}{w D_T (dT/dx)} \quad (25)$$

where D_T is the coefficient of the thermal diffusion which depends on the chemical composition and structure of the fractionated species but not on their size. On the other hand, the diffusion coefficient D depends on the size. As a result, the differences in thermal diffusion coefficients allow the fractionation according to differences in chemical composition and structure, whereas different diffusion coefficients allow the fractionation based on the size differences. The performances favor thermal FFF over the competitive methods.

Flow FFF

Flow FFF is the most universal method because the cross-flow field acts on all fractionated species in the same manner and the separation is due to the differences in diffusion coefficients [10]. The channel, schematically demonstrated in Fig. 2c, is formed between two parallel semipermeable membranes. The carrier liquid can permeate through the membranes but not the separated species. The retention parameter λ is related to the diameter d_p of the separated species by

$$\lambda = \frac{kTV_0}{3\pi\mu V_c w^2 d_p} \quad (26)$$

where V_0 is the void volume of the channel, μ is the viscosity of the carrier liquid, and V_c is the volumetric velocity of the cross-flow. The separations of various kinds of particles such as proteins, biological cells, colloidal silica, polymer latexes, and so forth, were described as well as of the soluble macromolecules.

Electric FFF

Electric FFF uses the electric potential across the channel to generate the transversal flux of the charged

species [11]. The walls of the channel can be formed by semipermeable membranes that allow the passage of small ions but not of the separated species. The channel is shown in Fig. 2d. The dependence of the retention parameter λ on the electrophoretic mobility μ_e , and the diffusion coefficient of the charged particles is given by

$$\lambda = \frac{D}{\mu_e E w} \quad (27)$$

where E is the electric field strength. As a result, the ratio of the diffusion coefficient to the electrophoretic mobility determines the retention. The species exhibiting only small differences in electrophoretic mobilities but important differences in diffusion coefficients can be separated. Electric FFF is especially suited for the separations of the biological cells as well as for charged polymer latexes and other colloidal particles and charged macromolecules.

Other Polarization FFF Methods

Other polarization FFF methods have recently been proposed theoretically and some of them implemented experimentally. Their use in current laboratory practice needs further development in methodology and instrumentation. One of the most recent review articles brings an excellent review of the state of the art of the polarization FFF methods [12].

References

1. J. C. Giddings, *Separ. Sci. Technol.* 18: 765 (1983).
2. J. Janča, *Makromol. Chem. Rapid Commun.* 3: 887 (1982).
3. J. Janča, *Field-Flow Fractionation: Analysis of Macromolecules and Particles*, Marcel Dekker, Inc., New York, 1988.
4. J. Janča, in *Chromatographic Characterization of Polymers, Hyphenated and Multidimensional Techniques* (T. Provder, H. G. Barth, and M. W. Urban, eds.), *Advances in Chemistry Series Vol. 247*, American Chemical Society, Washington, DC, 1995.
5. M. E. Hovingh, G. H. Thompson, and J. C. Giddings, *Anal. Chem.* 42: 195 (1970).
6. J. C. Giddings and M. N. Myers, *Separ. Sci. Technol.* 13: 637 (1978).
7. J. Janča and J. Chmelík, *Anal. Chem.* 56: 2481 (1984).
8. J. C. Giddings, M. N. Myers, M. H. Moon, and B. N. Barman, in *Particle Size Distribution* (T. Provder, ed.), ACS Symposium Series Vol. 472, American Chemical Society, Washington, DC, 1991.
9. S. J. Jeon and M. E. Schimpf, in *Particle Size Distribution III: Assessment and Characterization* (T. Provder, ed.), American Chemical Society, Washington, DC, 1998.
10. S. K. Ratanathanawongs and J. C. Giddings, in *Chromatography of Polymers: Characterization by SEC and FFF* (T. Provder, ed.), ACS Symposium Series Vol. 521, American Chemical Society, Washington, DC, 1993.
11. M. E. Schimpf and K. D. Caldwell, *Am. Lab.* 27: 64 (1995).
12. H. Cölfen and M. Antonietti, *Adv. Polym. Sci.* 150: 67 (2000).



Field-Flow Fractionation with Electro-osmotic Flow

Victor P. Andreev

Institute for Analytical Instrumentation, Russian Academy of Sciences, St. Petersburg, Russia

Introduction

It is well known that the essence of field-flow fractionation (FFF) is in the interaction between the distribution of the sample particles in the transversal field and the nonuniformity of the longitudinal flow profile. The classical FFF is realized in the channel with the flow driven by the pressure drop. The flow, in this case, is called Poiseuille flow and its profile is parabolic.

Discussion

Electro-osmotic flow (EOF) is widely used for the propulsion of liquid in modern chromatographic methods, so it was natural to study the possibility of FFF with EOF, generated by applying an electric field, E , along a channel or a tube with charged (having the nonzero zeta-potentials) walls. The usual EOF is very close to uniform. For the cylindrical tube of radius a , the EOF velocity profile is described by

$$V(r) = \frac{\zeta \varepsilon \varepsilon_0 E}{\eta} \left(1 - \frac{I_0(\kappa r)}{I_0(\kappa a)} \right) \quad (1)$$

where ζ is the zeta-potential of the wall, ε and η are the dielectric constant and viscosity of the buffer, respectively, ε_0 is the permittivity of the free space, $\kappa^{-1} = (\varepsilon \varepsilon_0 k_B T / 2 n e^2)^{1/2}$ is the Debye layer thickness [k_B is the Boltzman constant, T is the temperature, n is the number of ions per unit volume (proportional to the concentration of buffer C_0), e is the proton charge], and $I_0(x)$ is the modified Bessel function. As can be seen from Eq. (1), the velocity profile of the EOF in the tube is very close to uniform everywhere except the Debye layer vicinity of the wall. Thus, it is hard to exploit such a profile for FFF unless the concentration of buffer is very low.

That is why it was proposed [1,2] to realize the asymmetrical FFF in the flat channel by making its walls of different materials or chemically modifying them. If the channel walls have nonequal values of the zeta-potentials, then the shape of the EOF profile can be quite different from uniform. The flow profiles that can be generated in the FFF channel with the applied

electric field E and pressure drop Δp are presented in Fig. 1. These profiles can be described by

$$V(r) = \frac{\zeta_2 \varepsilon \varepsilon_0 E}{\eta} \cdot \left[(\zeta_R - 1) \frac{\sinh kY}{\sinh k} + (\zeta_R + 1) \frac{\cosh kY}{\cosh k} + (1 - \zeta_R)Y - (1 + \zeta_R) \right] + V_0(1 - Y^2) \quad (2)$$

where $\zeta_R = \zeta_1/\zeta_2$ is the ratio of the zeta-potential of the accumulation wall to the zeta-potential of the depletion wall, $k = \kappa w/2$, w is the channel depth, $Y = 1 - 2y/w$, and $V_0 = \Delta p/2\eta L$.

For large values of k , the first two terms in the square brackets are substantially nonzero only in the Debye layer vicinity of the walls, whereas everywhere else the EOF profile is dominated by the last two linear terms in the square brackets. Therefore, the asymmetric EOF profile can be close to trapezoidal or close to triangular depending on the exact values of the zeta-potentials of the walls. If the signs of the zeta-potentials of the walls are different, then the liquid moves in one direction near one wall and in the opposite direction near another wall (this case can be interesting for the pre separation of the particles having different densities). The last term in Eq. (2) corresponds to the pressure-driven Poiseuille flow.

Having Eq. (2) for flow profile enables one to calculate the retention ratio R and χ coefficient describing the Taylor dispersion part of the theoretical plate height H for arbitrary flow profile, according to [3]

$$H = \frac{2D}{R(V)} + \chi \frac{w^2(V)}{D} \quad (3)$$

where $\langle V \rangle$ is the average velocity of the flow and D is the diffusion coefficient of sample molecules. Usually, in FFF, the second term of Eq. (3) is much larger than the first one.



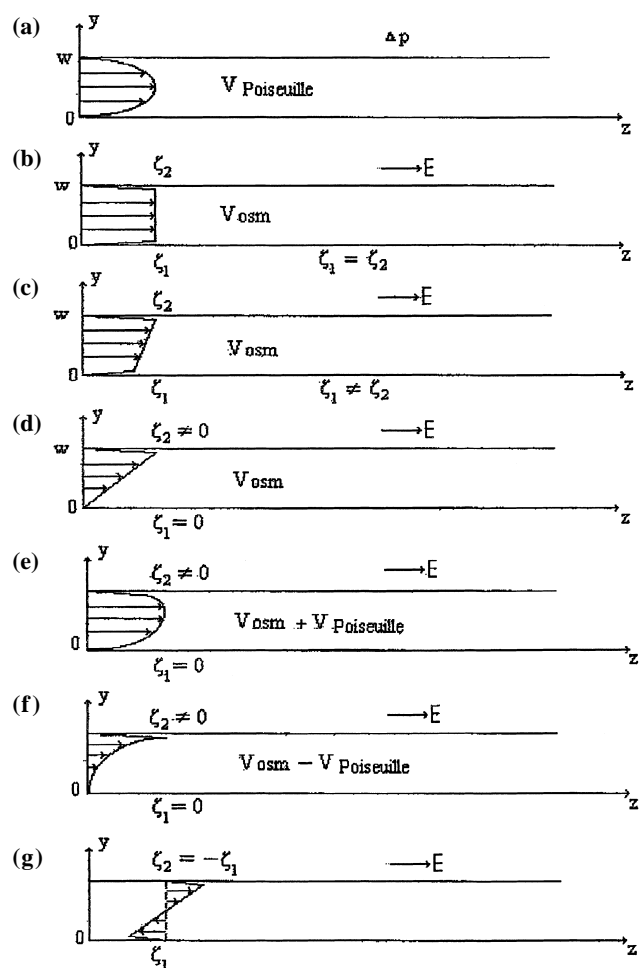


Fig. 1 Outline of the flow profiles in the FFF channels: (a) Poiseuille flow; (b) EOF (the equal zeta-potentials of the walls); (c) trapezoidal EOF (the nonequal zeta-potentials of the walls); (d) triangular EOF (the zero zeta-potential of the accumulating wall); (e) codirected triangular EOF and Poiseuille flow; (f) counterdirected triangular EOF and Poiseuille flow; (g) antisymmetric EOF (different signs of the zeta-potentials of the walls).

Comparison of R and χ values for the flow profiles presented in Fig. 1 for the case of the FFF parameter $\lambda \ll 1$ gives $R = 6\lambda$ and $\chi = 24\lambda^3$ for classical FFF with Poiseuille flow and $R = 2\lambda$ and $\chi = 8\lambda^3$ for FFF with a triangular EOF ($\zeta_1 = 0$). The most interesting result corresponds to the case of FFF with a combined triangular EOF and counterdirected Poiseuille flow (with $V_0 = \zeta_2 \varepsilon \varepsilon_0 E / 4\eta$ leading to $dV/dY = 0$ for $Y = 0$). In this case, $R = 6\lambda^2$ and $\chi = 24\lambda^4$. Thus, the selectivity $S = d \ln R / d \ln \lambda = 2$ and is twice as large as in the case of classical FFF and FFF with a triangular EOF. The χ

coefficient is very small for $\lambda \ll 1$, so that the Taylor dispersion is very low and efficiency is high. The function $F = S/\sqrt{\chi}$ (fractionating power), characterizing the resolution for the given value of $\langle V \rangle$, is proportional to λ^{-2} in this case; in the rest of the cases, it is proportional to $\lambda^{-3/2}$. The situation with this kind of combined flow is very similar to the one described in Ref. 4 for the case of Poiseuille flow combined with the natural convection flow in the thermogravitational FFF channel.

High selectivity, efficiency, and fractionating power makes FFF with combined EOF and Poiseuille flows very interesting, as it can, at least theoretically, lead to finer separations for given values of λ . Experimental realization of FFF with asymmetrical EOF have not yet been reported due to some technical problems. However, considerable progress in this field is accomplished by a Finnish group (Riekkola, Vastamaki, and Jussila) working on the experimental realization of thermal FFF with asymmetrical EOF [5] and a Russian group (Andreev, Stepanov, and Tihomolov) working on gravitational FFF with asymmetrical EOF [6].

The situation is more complicated, even theoretically, when the sample particles are charged. In this case, they are not only moving with the longitudinal flow (here, asymmetrical EOF) but are also forced by the longitudinal electric field to move along the channel electrophoretically. If the electrophoretic mobilities of the particles are different, then there are two types of separations combined: The FFF type due to the difference in λ values and the capillary zone electrophoresis (CZE) type due to the difference in electrophoretic mobilities. A great variety of variants of FFF and CZE combinations in the FFF channel with asymmetrical EOF could be imagined, depending on various factors such as the ratio of the zeta-potentials of the channel walls, the sign and the value of the ratio of electrophoretic and electro-osmotic velocities, and the type of the transversal field. Some of these combinations are examined in Ref. 6. They could lead both to the new possibilities of the method and to some new complications in the interpretation of the experimental results.

Another possibility for realizing FFF with EOF is to reduce the concentration of the buffer, thus making the Debye length commensurate, if not with the depth of the channel, then with the thickness $l = \lambda w$ of the layer of sample particles compressed to the accumulating wall of FFF channel (for $C_0 = 10^{-5} M$ Debye length, $\kappa^{-1} = 0.1 \mu m$). In this case, EOF will be nonuniform enough to realize FFF in a channel with equal zeta-potentials of the walls.

In Ref. 7 the mathematical model of CZE, taking into consideration EOF nonuniformity and particle–

wall electrostatic interactions, was developed. It was shown that for the particles electrostatically attracted by the wall of the capillary, two mechanisms of separation exist. The first is the usual CZE mechanism and it dominates for the case of high buffer concentrations; the second is the FFF accompanying the CZE mechanism and it dominates for low buffer concentrations. As is usual in CZE, the total velocity of the particle is the sum of its electrophoretic velocity and electro-osmotic velocity of the flow. The larger the electrical charge of sample particles, the stronger they are attracted to the wall and the higher is their concentration in the Debye layer vicinity of the wall, where the EOF is substantially nonuniform. Thus, for the particles with a higher charge, the mean velocity of movement with EOF will be lower than for the particles with the lower charge. Especially interesting with this type of FFF is for the particles with equal electrophoretic mobilities but different charges. Such types of particles (e.g., DNA fragments) cannot be fractionated by usual CZE, but can be fractionated by FFF accompanying CZE, where the separation is due to the difference of electrical charges, not the difference of mobilities. Note that for this type of FFF, there is no need for any external transversal field, because the particles are attracted to the walls by the field of the electrical double layer. As is usual in FFF, there is the transition point from normal diffusional FFF to steric FFF mode, taking place when the size of the particle is commensurable with λw . In Ref. 8, it was theoretically predicted that steric FFF accompanying the CZE mode can be realized for the separation of DNA fragments in the range of 20–3000 bases with high resolution and speed. To realize this type of separation, one needs to develop a modified capillary

with the positive value of the zeta-potential of the wall and without the irreversible sorption of DNA fragments on the walls. Such an attempt seems to be worthy because, unlike DNA separation by CZE in gel or polymer solution, in the case of FFF–CZE there is the possibility of on-line coupling with a mass spectrometer without the risk of gel particles going inside the spectrometer.

References

1. V. P. Andreev, M. E. Miller, and J. C. Giddings, Field-flow fractionation with asymmetrical electroosmotic flow, *5th Int. Symp on FFF*, 1995.
2. V. P. Andreev, Y. V. Stepanov, and J. C. Giddings. Field-flow fractionation with asymmetrical electroosmotic flow. I. Uncharged particles, *J. Microcol. Separ.* 9: 163 (1997).
3. M. Martin and J. C. Giddings, Retention and nonequilibrium peak broadening for generalized flow profile in FFF, *J. Phys. Chem.* 85: 727 (1981).
4. J. C. Giddings, M. Martin, and M. N. Myers, Thermogravitational FFF: An elution thermogravitational column, *Separ. Sci. Technol.* 14: 611 (1979).
5. P. Vastamaki, M. Jussila, and M.-L. Riekkola, The effect of electrically nonconductive wall coating on retention in ThFFF, *7th Int. Symp. on FFF*, 1998.
6. V. P. Andreev and Y. V. Stepanov, Field-flow fractionation with asymmetrical electroosmotic flow. II. Charged particles, *J. Liquid Chromatogr. Related Technol.* 20: 2873 (1997).
7. V. P. Andreev and E. E. Lisin, On the mathematical model of capillary electrophoresis, *Chromatographia* 37: 202 (1993).
8. V. P. Andreev and Y. V. Stepanov, Steric FFF accompanying capillary electrophoresis, *5th Int. Symp on FFF*, 1995.



Flame Ionization Detector for GC



Raymond P. W. Scott

Scientific Detectors Ltd., Banbury, Oxfordshire, England

Introduction

The flame ionization detector (FID) is, by far, the most commonly used detector in gas chromatography (GC) and is probably the most important. It is a little uncertain as to who was the first to invent the FID; some gave the credit to Harley and Pretorius [1], others to McWilliams and Dewar [2]. In any event, it would appear that both contenders developed the device at about the same time, and independently of one another; the controversy had more patent significance than historical interest. The FID is an extension of the flame thermocouple detector and is physically very similar, the fundamentally important difference being that the ions produced in the flame are measured, as opposed to the heat generated.

Discussion

The principle of detection is as follows. Hydrogen is mixed with the column eluent and burned at a small jet. Surrounding the flame is a cylindrical electrode and a relatively high voltage is applied between the jet and the electrode to collect the ions that are formed in the flame. The resulting current is amplified by a high-impedance amplifier and the output fed to a data acquisition system or a potentiometric recorder.

A detailed diagram of the FID sensor is shown in Fig. 1. The body and the cylindrical electrode is usually made of stainless steel and stainless-steel fittings connect the detector to the appropriate gas supplies. The jet and the electrodes are insulated from the main body of the sensor with appropriate high-temperature insulators. Some care must be taken in selecting appropriate insulators as many glasses (with the exception of fused quartz) and some ceramic materials become conducting at high temperatures (200–300°C) [3].

As a result of the relatively high voltages used in conjunction with the very small ionic currents being measured, all connections to the jet or electrode must be well insulated and electrically screened. In

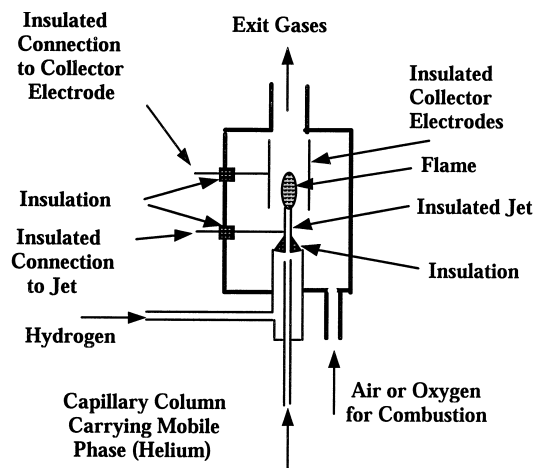


Fig. 1 The FID sensor.

addition, the screening and insulating materials must be stable at the elevated temperature of the detector oven. In order to accommodate the high temperatures that exist at the jet tip, the jet is usually constructed of a metal that is not easily oxidized, such as stainless steel, platinum, or platinum-rhodium. The detector electronics consist of a high-voltage power supply and a high-impedance amplifier. The jet and electrode can be connected to the power supply and amplifier in basically two configurations. The floating jet configuration is the most commonly used and in this arrangement, +250 to +400 V is applied to the cylindrical electrodes and the jet is connected to a ground by a very high resistance. The signal developed across the resistance is amplified, modified, and passed to a recorder of the data acquisition system. In the second alternative, the jet is grounded and the high-voltage power supply is electrically floated. Then, +250 to +400 V is applied to the cylindrical electrodes and the negative terminal of the power supply is connected to a ground by a very high resistance. The signal that is developed across the resistance is again amplified, modified, and passed to a recorder of the data acquisition system.



Response Mechanism of the FID

The flame ionization detector has a very wide dynamic range, has a high sensitivity, and, with the exception of about half a dozen low-molecular-weight compounds, will detect all substances that contain carbon. The response mechanism of the FID has been carefully investigated by a number of workers. It was originally thought that the ionization mechanism in the FID flame is similar to the ionization process in a hydrocarbon flame, but it quickly became apparent that ionization in the hydrogen flame is many times higher than could be accounted for by thermal ionization alone. It would appear that the ionization potentials of organic materials become much lower when they enter the flame.

The generally accepted explanation of this effect is that the ions are not formed by thermal ionization but by thermal emission from small carbon particles that are formed during the combustion process. Consequently, the dominating factor in the ionization of organic material is not their ionization potential but the work function of the carbon that is transiently formed during their combustion. The flame plasma contains both positive ions and electrons which are collected on either the jet or the plate, depending on the polarity of the applied voltage. Initially, the current increases with applied voltage, the magnitude of which depends on the electrode spacing. The current continues to increase with the applied voltage and eventually reaches a plateau at which the current remains sensibly constant. The voltage at which this plateau is reached also depends on the electrode distances.

As soon as the electron-ion pair is produced, recombination starts to take place. The longer the ions take to reach the electrode and be collected, the more the recombination takes place. Thus, the greater the distance between the electrodes and the lower the voltage, the greater the recombination. As a result, initially the current increases with the applied voltage and then eventually flattens out, and at this point, it would appear that all the ion-electron pairs were being collected. In practice, the applied voltage would be adjusted to suit the electrode geometry and ensure that the detector operates under conditions where all electrons and ions are collected.

It was also shown that the airflow should be at least six times that of the hydrogen flow for stable conditions and complete combustion. The base current from the hydrogen flow depends strongly on the purity of the hydrogen. Traces of hydrocarbons significantly increase the base current, as would be expected. Consequently, very pure hydrogen should be employed with the FID if maximum sensitivity is required. Employing purified hydrogen,

Desty et al. reported a base current of 1.45×10^{-12} A for a hydrogen flow of 20 mL/min. This was equivalent to 1×10^{-7} C/mol. The sensitivity reported for *n*-heptane, assuming a noise level equivalent to the base current from hydrogen of $\sim 2 \times 10^{-14}$ A (a fairly generous assumption), was 5×10^{-12} g/mL at a flow rate of 20 mL/min. It follows that although the sensitivity is amazingly high, the ionization efficiency is still very small ($\sim 0.0015\%$). The general response of the FID to substances of different type varies very significantly from one to another. For a given homologous series, the response appears to increase linearly with carbon number, but there is a large difference in response between different homologous series (e.g., hydrocarbons and alcohols).

The linear dynamic range of the FID covers at least four to five orders of magnitude for $0.98 < r < 1.02$. This is a remarkably wide range that also helps explain the popularity of the detector. Examination of the different commercially available detectors shows considerable difference in electrode geometry and operating electrode voltages, yet they all have very similar performance specifications.

Operation of the FID

The FID is one of the simplest and most reliable detectors to operate. Generally, the appropriate flow rates for the different gases are given in the detector manual. The hydrogen flow usually ranges between 20 and 30 mL/min and the airflow is about six times that of the hydrogen flow (e.g., 120–200 mL/min. The column flow that can be tolerated is usually about 20–25 mL/min, depending on the chosen hydrogen flow. However, if a capillary column is used, the flow rate may be less than 1 mL/min for very small-diameter columns. The mobile phase can be any inert gas — helium, nitrogen, argon, and so forth. To some extent, the detector is self-cleaning and rarely becomes fouled. However, this depends a little on the substances being analyzed. If silane derivatives are continuously injected on the column, then silica is deposited both on the jet and on the electrodes and may need to be regularly cleaned. In a similar way, the regular analysis of phosphate-containing compounds may eventually contaminate the electrode system. Electrode cleaning is best carried out by the qualified instrument service engineer.

Apparently, the sole disadvantage of the FID as a general detector is that it normally requires three separate gas supplies, together with their precision flow regulators. The need for three gas supplies is a decided inconvenience but is readily tolerated in order to take advantage of the many other attributes of the FID. The detector is normally thermostatted in a separate oven;



this is not because the response of the FID is particularly temperature sensitive but to ensure that no solutes condense in the connecting tubes.

The FID has an extremely wide field of application and is used in the analysis of hydrocarbons, solvents, essential oils, flavors, drugs, and their metabolites — in fact, any mixture of volatile substances that contain carbon.

References

1. J. Harley, W. Nel, and V. Pretorius, *Nature (London)*, **181**: 177 (1958).
2. I. G. McWilliams and R. A. Dewar, *Gas Chromatography 1958* (D. H. Desty, ed.), Butterworths, London, 1957, p. 142.
3. S. A. Beres, C. D. Halfmann, E. D. Katz, and R. P. W. Scott, *Analyst* **112**: 91 (1987).

Suggested Further Reading

Scott, R. P. W., *Chromatographic Detectors*, Marcel Dekker, Inc., New York, 1996.

Scott, R. P. W., *Introduction to Analytical Gas Chromatography*, Marcel Dekker, Inc., New York, 1998.



Flavonoids, Analysis by Supercritical Fluid Chromatography

Xia Yang

Huwei Liu

Peking University, Beijing, P.R. China

INTRODUCTION

Several kinds of flavonoids are efficiently separated and analyzed using packed or capillary column supercritical fluid chromatography. The composition of mobile phase, stationary phase, temperature, and pressure all affect the resolution. This article mainly focuses on the separation of polymethoxylated flavones, polyhydroxyl flavonoids, and flavonol isomers.

FLAVONOIDS

As a result of the development of chromatography technology, supercritical fluid chromatography (SFC) has been used to separate more and more compounds, owing to the low viscosity and high diffusivity of its mobile phase compared to the liquid mobile phase in high-performance liquid chromatography (HPLC). Supercritical carbon dioxide is the most popular SFC mobile phase because it is nontoxic, nonflammable, and easy to obtain, and it has a near-ambient critical temperature (approximately 31°C at 74 bar). However, CO₂ has weak solvating power for polar compounds. Supercritical fluids that are substantially more polar than carbon dioxide generally tend to have extreme critical temperatures and pressures (e.g., water with a critical temperature near 400°C), which makes them difficult or dangerous to work with and raises questions about the effect of such conditions on labile solutes themselves.^[1] So CO₂ is the best choice, but it is often modified by such polar organic solvents as methanol, ethanol, etc. However, this binary mobile phase cannot elute very polar compounds efficiently. To widen the applicability of SFC, a small amount (<1%) of additive is added to a modifier to form a ternary mixture with CO₂. Organic acids, such as trifluoroacetic acid and citric acid, were used as additives to cause polar solutes (e.g., hydroxybenzoic and polycarboxylic acids) to be eluted rapidly and efficiently from packed SFC columns.^[2–4]

Flavonoids are a group of naturally occurring substances derived from flavone (phenyl- γ -benzopyrone) that

are widely distributed in the plant kingdom and used in herbal medicines throughout the world. They are 15-carbon compounds consisting of two aromatic rings and, based on the oxidation level of another ring, are classified into several groups, i.e., chalcones, flavanones, flavones, isoflavones, and flavonols, which are collectively known as the “yellow pigments,” and the colored “anthocyanin pigments.” Flavonoid compounds may undergo further enzymatic hydroxylation, methylation, glycosylation, sulfonation, acylation, and/or prenylation reactions, resulting in the immense diversity of flavonoid structures. There are more than 5000 identified flavonoid compounds found in nature.

Traditionally, flavonoids have been separated and analyzed by HPLC^[5,6] and gas chromatography (GC).^[7] However, recent developments of SFC may permit a more accurate and complete analysis of plant phenolic compounds. Supercritical fluid chromatography brings together the advantages of both HPLC and GC techniques because it may be readily employed in the analysis of nonvolatile and thermolabile compounds and provides facile coupling to detector technologies such as mass spectrometry and Fourier transform infrared (FT-IR) spectroscopy. In recent years, SFC has been used to separate flavonoid compounds, most of which are polymethoxylated flavones and polyhydroxylflavonoids.

SEPARATION OF FLAVONOIDS

Separation of Polyhydroxylflavonoids by Packed-Column SFC

Liu et al.^[8] separated polyhydroxylflavonoids, quercetin, and risetin by packed-column SFC with a ternary mobile phase. They designed an SFC apparatus with two syringe pumps and a variable-wavelength UV detector. A manual back-pressure regulator was also used to control the flow rate. This experiment showed that there are several factors affecting the result.

Mobile Phase

Neither pure supercritical CO₂ nor ethanol-modified CO₂ eluted all the flavonoids tested in this experiment. But when phosphoric acid and ethanol modifiers were added to the mobile phase together, the separation on a silica-based column was significantly improved, and quercetin and risetin were eluted rapidly and efficiently. With an increase of phosphoric acid concentration, the peak shapes were also improved. Because the phosphoric acid molecules could be adsorbed onto the active sites of the stationary phase, which could prevent solute molecules from being strongly adsorbed, the interaction between solutes and stationary phase was eliminated, making the solutes easily elute from the chromatographic system.

Stationary Phase

The polarity of the column packing is in the following order: cyanopropyl>phenyl>ODS C₁₈. It is understandable that the ODS column is not suitable for the separation because of its low polarity. Both the cyanopropyl and phenyl columns could separate these solutes efficiently, but the latter exhibited shorter separation times.

Pressure and Temperature

The capacity factor for the separation of flavonoids is decreased with the increase of operating pressure, in addition to the effect of the decrease in modifier concentration, thus indicating that the pressure effect is a very important one.

The retention times of solutes slightly increased with increasing temperature in the range of 40.0–65.0°C. As the volatilities of the solutes were increased with an increase in the temperature (which is favorable to shorten the retention time), the density of the mobile phase decreases with the temperature, which is not favorable for eluting the solute. In the range of temperatures mentioned above, the second factor is dominant; thus a lower temperature is desirable for the separation of quercetin and risetin.

Separation of Polymethoxylated Flavones by Packed-Column SFC

Morin et al.^[9] successfully separated polymethoxylated flavones (PMFs) by packed-column SFC, illustrating that the SFC procedure is considerably faster than HPLC, with good resolution and adequate accuracy for the quantitative analysis of the PMFs. The chromatographic system

Table 1 Structures of polymethoxylated flavones

PMF	Systematic name
Heptamethoxyflavone	3,5,6,7,8,3',4'-Heptamethoxyflavone
Hexamethoxyflaxone	3,5,6,7,3',4'-Hexamethoxyflavone
Nobiletin	5,6,7,8,3',4'-Hexamethoxyflavone
Sinensetin	5,6,7,3',4'-Pentamethoxyflavone
Tangeretin	5,6,7,8,4'-Pentamethoxyflaxone
Isosinensetin	5,7,8,3',4'-Pentamethoxyflavone
Tetramethylisoscuteallarein	5,8,7,4'-Tetramethoxyflavone
Tetramethylscuteallarein	5,6,7,4'-Tetramethoxyflavone

consisted of a bare silica column (250 × 4.6 mm I.D.) with a carbon dioxide–methanol mobile phase and UV detection (313 nm). The pressure was controlled by a manual back-pressure regulator connected in series after the detector and maintained at 40°C with a water bath. Six compounds, including tangeretin, heptamethoxyflavone, nobiletin, sinensetin, tetramethylisoscuteallarein, and isosinensetin (Table 1), were separated in less than 12 min as shown in Fig. 1. The resolution between nobiletin and heptamethoxyflavone is greater than 1.5, whereas reversed-phase HPLC required the use of water–tetrahydrofuran solvent to resolve these two compounds satisfactorily. If the carbon dioxide and methanol flow rates are increased from 3 and 0.3 mL/min to 9 and 0.9 mL/min, respectively, the polymethoxylated flavones (tangeretin, nobiletin, sinensetin, and tetramethylisoscuteallarein) are separated in 2 min without any significant loss of efficiency and resolution. Thus packed-column SFC appears to be useful for rapid analyses of the main polymethoxylated flavonones.

Separation of Flavonol Isomers by Packed-Column SFC

Flavonol isomers, which differ only in the position of hydroxyl group on their chemical structures, showed different chromatographic behaviors. Liu et al.^[10] separated three flavonol isomers (3-hydroxyflavone, 6-hydroxyflavone, and 7-hydroxyflavone) by a lab-constructed packed column SFC system with carbon dioxide modified with ethanol containing 0.5% (V/V) phosphoric acid as the mobile phase. The effects of temperature, pressure, composition of mobile phase, and packed-column type on



the separation were studied. It was indicated that the addition of phosphoric acid to the mobile phase enabled flavonol isomers to be eluted from the column. It was also shown that a phenyl-bonded silica column was better and the ODS column was not as effective for the isomer separation. Increasing pressure shortened the retention time of each compound, with good resolution, and higher temperature led to longer retention times, and even the loss of the bioactivities of these components. Under

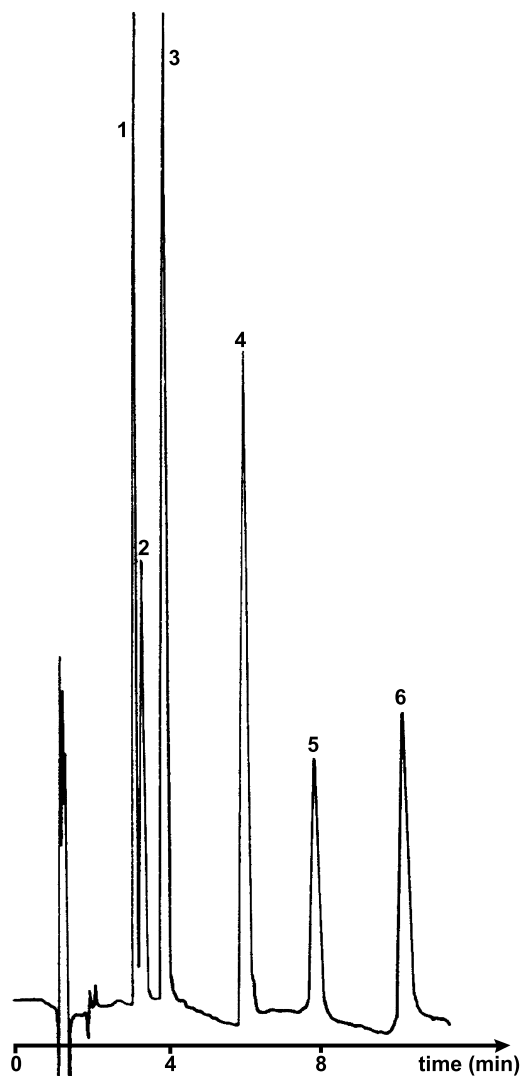


Fig. 1 SFC separation of synthetic mixture of polymethoxylated flavones. Column, 250 mm \times 4.6 mm I.D.; stationary phase, Zorbax (5 μ m) silica; mobile phase, carbon dioxide modified with 10% methanol; inlet pressure, 220 atm; outlet pressure, 200 atm; column temperature, 40°C; carbon dioxide flow-rate, 3 mL/min; methanol flow-rate, 0.3 mL/min; UV detection at 313 nm. Peaks: 1=tangeretin; 2=heptamethoxyflavone; 3=nobiletin; 4=sinensetin; 5=tetramethylisoscutellarin; 6=isosinensetin.

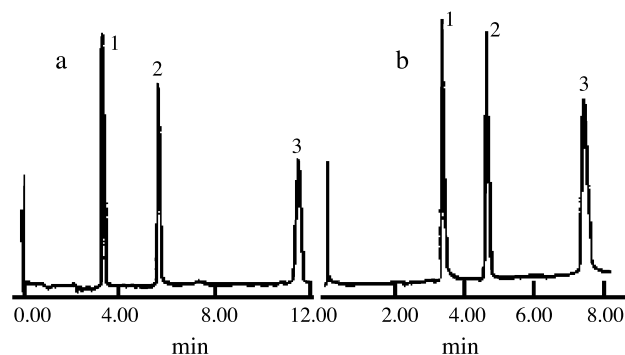


Fig. 2 Effect of stationary phase Pressure: 25 MPa, temperature: 50°C, mobile phase: carbon dioxide-ethanol with 0.5% phosphoric acid: 90:10, flowrate: 1.05 mL/min, stationary phase: a) cyano column, b) phenyl column.

selected conditions, the separation of these isomers was very satisfactory, as illustrated in Fig. 2.

Separation of Polymethoxylated and Polyhydroxylated Flavones by Open-Tubular Capillary SFC

Solvent modifiers and additives can be used to adjust the retention and selectivity of separation in packed-column SFC. Similar effects have been reported with open-tubular capillary SFC.^[11] The advantage of capillary column over packed column arises from the differences in permeability. Pressure ramps are much easier to use in capillary columns to modify the solvent strength (via density modification) as compared to packed columns. Therefore it should be entirely feasible, with capillary SFC, to combine the benefit of solvent density (pressure) programming with simultaneous modification of the solvent strength.^[12,13]

Hadj-Mahammed et al.^[11] analyzed a mixture of flavone, 5-methoxyflavone, and tangeretin by supercritical CO₂ SFC on capillary columns with two types of detectors: flame ionization (FID) and FT-IR. Peak identification was achieved with the help of the FT-IR fingerprint of each compound. However, the separation was satisfactory only by the use of supercritical CO₂ density programs, without the use of a phase modifier. The separations were accomplished using a Carlo Erba SFC system equipped with a Model SFC 300 pump and a Model SFC 3000 oven. The fused silica capillary columns were BP1 (12 m \times 0.1 mm I.D.; 0.1- μ m film of dimethylpolysiloxane) and DB5 (15 m \times 0.1 mm I.D.; 0.4- μ m film of 94% dimethyl-, 5% diphenyl-, and 1% vinylpolysiloxane). The two supercritical CO₂ density programs used in this work were P1 [from 0.127 g/mL

Table 2 Comparison of retention times and capacity factors of flavones analyzed using capillary columns DB5 and BP1 with supercritical CO₂ density program P2

Flavones	DB5		BP1	
	<i>t_R</i> (min)	<i>k'</i>	<i>t_R</i> (min)	<i>k'</i>
Flavone	17.93	2.40	9.52	1.36
5-Methoxyflavone	20.83	2.93	11.82	1.93
Tangeretin	25.84	3.90	16.53	3.10

(at a pressure of 73.3 bars) to 0.689 g/mL (324.2 bars) isothermally at 100°C] and P2 [from 0.111 g/mL (at a pressure of 79.0 bars) to 0.511 g/mL (318.5 bars) isothermally at 150°C].

On the DB5 capillary column, satisfactory separation of hydroxyl- and methoxyflavones could be obtained using either of the two gradient systems, but the retention times of the analytes for P2 were shorter than those for P1. This is due to the variation in the solubilities of flavones in the supercritical mobile phase when the density gradient was employed. The polarity effect of the stationary phase (BP1 phase is less polar than the DB5) is illustrated in Table 2. It can be seen that, on BP1, the flavones are less retained and the analysis time is decreased by nearly half, while conserving a satisfactory separation.

In summary, the use of a polar capillary column and an appropriate gradient of supercritical CO₂ density at a temperature of about 150°C permits the flavonoids to be separated rapidly and effectively.

CONCLUSION

Both packed-column and open-tubular capillary SFC can be used to separate flavonoids, and, in most cases, the separation is improved by changing the composition of mobile phase, stationary phase, temperature, and pressure.

Although HPLC has been used more often than SFC for the separation of flavonoids until now, SFC still has its particular merits and can be listed as the promising approach.

ACKNOWLEDGMENTS

This study is financially supported by the National Nature Science Foundation of China (NSFC), Grant Nos. 20275001 and 90209056.

REFERENCES

- Berger, T.A.; Deye, J.F. Separation of benzene polycarboxylic acids by packed column supercritical fluid chromatography using methanol-carbon dioxide mixtures with very polar additives. *J. Chromatogr. Sci.* **1991**, *29*, 141.
- Berger, T.A.; Deye, J.F. Separation of phenols by packed column supercritical fluid chromatography. *J. Chromatogr. Sci.* **1991**, *29*, 54–59.
- Berger, T.A.; Deye, J.F. Separation of hydroxybenzoic acids by packed column supercritical fluid chromatography using modified fluids with very polar additives. *J. Chromatogr. Sci.* **1991**, *29*, 26–30.
- Berger, T.A.; Deye, J.F. Separation of benzene polycarboxylic acids by packed column supercritical fluid chromatography using methane-carbon dioxide mixtures with very polar additives. *J. Chromatogr. Sci.* **1991**, *29*, 141–146.
- Sendra, J.M.; Swift, J.L.; Izquierdo, L. C₁₈ solid-phase isolation and high-performance liquid chromatography/ultraviolet diode array determination of fully methoxylated flavones in citrus juices. *J. Chromatogr. Sci.* **1988**, *26*, 443.
- Hernburger, B.; Galensa, R.; Herrmann, K. High-performance liquid chromatography determination of polymethoxylated flavones in orange juice after solid-phase extraction. *J. Chromatogr.* **1988**, *439*, 481.
- Drawert, F.; Leupold, G.; Pivernetz, H. Quantitative gaschromatographische bestimmung von Rutin, Hesperidin und Naringin in Orangensaft. *Chem. Mikrobiol. Technol. Lebensm.* **1980**, *20*, 111–114.
- Liu, Z.; Zhao, S.; Wang, R.; Yang, G. Separation of polyhydroxylflavonoids by packed-column supercritical fluid chromatography. *J. Chromatogr. Sci.* **1999**, *37*, 155–158.
- Morin, P.; Gallois, A.; Richard, H.; Gaydou, E. Fast separation of polymethoxylated flavones by carbon dioxide supercritical fluid chromatography. *J. Chromatogr.* **1991**, *586*, 171–176.
- Liu, Z.; Zhao, S.; Wang, R.; Yang, G. Separation of flavonol isomers by packed column supercritical fluids chromatography. *Chin. J. Chromatogr.* **1997**, *15* (4), 288–291.
- Hadj-Mahammed, M.; Badjah-Hadj-Ahmed, Y.; Meklati, B.Y. Behaviour of polymethoxylated and polyhydroxylated flavones by carbon dioxide supercritical fluid chromatography with flame ionization and Fourier transform infrared detectors. *Phytochem. Anal.* **1993**, *4*, 275–278.
- Schmitz, F.P.; Hilger, H.; Lorenschat, B.; Klesper, E. Separation of oligomers with UV-absorbing side groups by supercritical fluid chromatography using eluent gradients. *J. Chromatogr.* **1985**, *346*, 69.
- Blilie, A.L.; Greibrokk, T. Gradient programming and combined gradient-pressure programming in supercritical fluid chromatography. *J. Chromatogr.* **1985**, *349*, 317–322.



Flow Field-Flow Fractionation: Introduction

Myeong Hee Moon

Pusan National University, Pusan, Korea

Introduction

Flow field-flow fractionation (flow FFF or FIFFF) is one of the FFF subtechniques in which particles and macromolecules are separated in a thin channel by aqueous flow under a field force generated by a secondary flow. As with other FFF techniques, separation in FIFFF is based on the applied force directed across the axis of separation flow. In FIFFF, this force is generated by cross-flow of liquid delivered across the channel walls. In order to maintain the uniformity of cross-flow moving in a typical rectangular channel, two ceramic permeable frits are used as channel walls and the flow stream enters and exits through these walls. The force applied in FIFFF is a Stokes force that depends only on the sizes of sample components.

Principles

In FIFFF, particles or macromolecules entering the channel are driven toward an accumulation wall by the cross-flow. Normally, a sheet of semipermeable membrane is placed at the accumulation wall in order to keep sample materials from being lost by the wall. While sample components are being transported close to the accumulation wall, they are projected against the wall by Brownian diffusion. The diffusive transport against the wall leads the sample components to be differentially distributed against the wall, according to their sizes: The larger particles, having a small diffusion coefficient, are placed at an equilibrium position closer to the vicinity of accumulation wall than the smaller ones. Thus, small particles, which are located further from the wall, will be exposed to the fast streamline of a parabolic flow profile, and they will be eluted earlier than the larger ones. This is the typical elution profile that can be observed in the normal operating mode of FFF (denoted as FI/NI FFF). Retention time in FI/NI FFF is inversely proportional to the diffusion coefficient of the sample; it is represented as

$$t_r = \frac{w^2}{6D} \frac{\dot{V}_c}{\dot{V}} \quad \left(\text{where } D = \frac{kT}{3\pi\eta d_s} \right) \quad (1)$$

where w is the channel thickness, D is the diffusion coefficient, \dot{V}_c is the cross-flow rate, and \dot{V} is the channel flow rate. Because the diffusion coefficient D is inversely proportional to the viscosity of carrier solution η and hydrodynamic radius d_s , the retention time can be simply predicted provided the particle diameter or the diffusion coefficient is known. Conversely, the particle diameter of an unknown sample can be calculated from experimental retention time by rearranging Eq. 1.

As the particle size becomes large at or above $1 \mu\text{m}$, the diffusional process of particles becomes less dominant in FFF. In this regime, a particle's retention is largely governed by the particle size itself, in which the center of large particles is located at a higher position than small ones. Thus, large particles meet the faster streamlines and they elute earlier than the small ones; the elution order is reversed. However, it is known, from experimental results, that particles migrate at certain positions elevated from the wall due to the existence of hydrodynamic lift forces that act in the opposite direction to the field. This is described as the steric/hyperlayer operating mode of separation in flow FFF and is denoted by FI/Hy FFF. Whereas the theoretical expectation of particle retention in FI/NI FFF is clearly understood, retention in FI/Hy FFF is not predictable because the hydrodynamic lift forces are not yet completely understood. Therefore, the particle size calculation in FI/Hy FFF relies on the calibration process in which a set of standard latex particles of known diameter is run beforehand as

$$\log t_r = -S_d \log d_s + \log t_{r1} \quad (2)$$

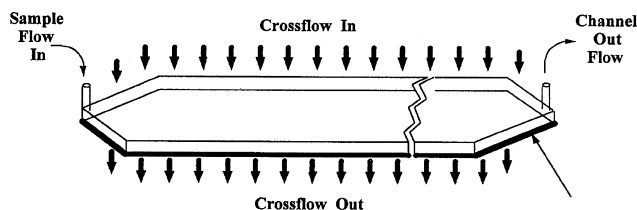
where S_d is the diameter-based selectivity and t_{r1} is the interpolated intercept representing the retention time of a unit diameter. The S_d values found experimentally are about 1.5 in FI/Hy FFF. By using Eq. (2), the particle diameters of unknown samples can be calculated once the calibration parameters S_d and t_{r1} are provided.

Types of Channel in FIFFF

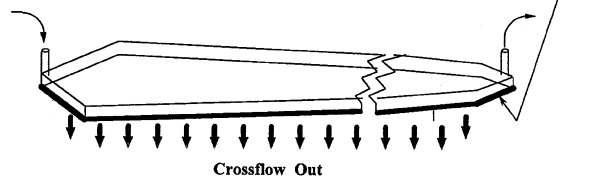
There are two main categories of flow FFF channel systems, depending on the use of frit wall. The above-



(a) symmetrical, rectangular



(b) asymmetrical, trapezoidal



(c) hollow fiber

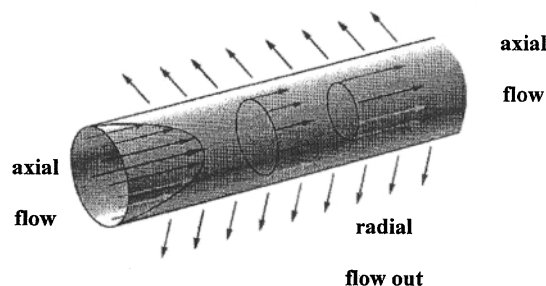


Fig. 1 Types of channel in FFF.

described flow FFF system has a frit on both walls; this is classified as a symmetrical channel, as shown in Fig. 1a. An asymmetrical channel system is being widely studied in which only one permeable frit wall is used, at the accumulation wall, and the depletion wall is replaced with a glass plate (Fig. 1b). In an asymmetrical channel, part of the flow entering the channel is lost by the accumulation wall and this acts as a field force to retain the sample components in the channel, as does the cross-flow in a symmetrical channel.

The separation efficiency of an asymmetrical flow FFF system has been known to be higher than that of a conventional symmetrical channel. Because an asymmetrical channel utilizes only one frit, nonuniformity of flow that could arise from the imperfection of frits can be reduced. In addition, the initial sample band can be kept narrower in an asymmetrical channel, due to the focusing-relaxation procedure, which is an essential process in an asymmetrical channel. The relaxation processes, which provide an equilibrium status for sample components, are necessary in both symmetrical

and asymmetrical channels for a period of time prior to the separation. For a symmetrical channel, this is normally achieved by stopping channel flow immediately after sample injection, while the cross-flow is applied.

During the relaxation process, sample components seek their equilibrium positions where the drag of the cross-flow is counterbalanced with diffusive transports (or lift forces) against the walls. After relaxation, flow is resumed and separation begins. However, in an asymmetrical channel, the relaxation process is achieved by two convergent focusing flow streams originating at the channel inlet and outlet (focusing-relaxation). Thus, injected sample can be focused at a certain position near the inlet end and the broadening of the initial sample band can be better minimized. This will lead to a decrease in band broadening of an eluted peak in an asymmetrical channel.

In asymmetrical flow FFF, two channel designs are utilized: rectangular and trapezoidal. Because flow velocity decreases along the axis of migration, a trapezoidal channel in which the channel breadth decreases toward the outlet is known to be more efficient in eluting low-retaining materials such as high-molecular-weight proteins. Retention in an asymmetrical flow FFF system follows the basic FFF principle and the retention time is calculated as

$$t_r = \frac{w^2}{6D} \ln \left(1 + \frac{\dot{V}_c}{\dot{V}_{out}} \right) \quad (3)$$

where \dot{V}_c is the cross-flow rate and \dot{V}_{out} is the outlet flow rate.

In addition to the rectangular channels in FIFFF described thus far, a cylindrical channel system has been developed with the use of hollow fibers in which the fiber wall is made of a porous membrane, as shown in Fig. 1c. It also requires a focusing-relaxation process, as does an asymmetrical channel. Retention in hollow-fiber flow FFF (HF-FIFFF) is controlled by the radial flow, which effectively acts as the cross-flow of a conventional flow FFF system, and the retention in a hollow fiber resembles that of an asymmetrical channel system.

However, the retention ratio in HF-FIFFF is approximately 4λ for a sufficiently retained component, which is somewhat different from that of a conventional channel system ($R \cong 6\lambda$). The retention time in a hollow fiber is calculated as

$$t_r = \frac{r_f^2}{8D} \ln \left(1 + \frac{\dot{V}_{rad}}{\dot{V}_{out}} \right) \quad (4)$$

where r_f^2 is the radius of the fiber and \dot{V}_{rad} is the radial flow rate. Although a number of experiments have indicated a great potential of hollow fibers as an alterna-

tive for a flow FFF channel, a great deal of study related to their performance and optimization is needed.

Suggested Further Readings

- Giddings, J. C., *Science* 260: 1456 (1993).
Giddings, J. C., F. J. Yang, and M. N. Myers, *Anal. Chem.* 48: 1126 (1976).
Jönsson, J. A., and A. Carlshaf, *Anal. Chem.* 61: 11 (1989).
Litzén, A. and K.-G. Wahlund, *J. Chromatogr.* 476: 413 (1989).
Litzén, A. and K.-G. Wahlund, *Anal. Chem.* 63: 1001 (1991).
Moon, M. H., Y. H. Kim, and I. Park, *J. Chromatogr.* 813: 91 (1998).
Ratanathanawongs, S. K. and J. C. Giddings, in *Chromatography of Polymers: Characterization by SEC and FFF* (T. Provder, ed.), ACS Symposium Series Vol. 521, American Chemical Society, Washington, DC, 1993, pp. 13–29.



Fluorescence Detection in Capillary Electrophoresis

Robert Weinberger

CE Technologies, Inc., Chappaqua, New York, U.S.A.

Introduction

One cannot overestimate the importance of fluorescence detection in high-performance capillary electrophoresis (HPCE) [1]. The success of the human genome project along with the forthcoming revolutions in forensic testing and genetic analysis might not have occurred without the sensitivity and selectivity of laser-induced fluorescence (LIF) detection.

Basic Concepts

The stunning sensitivity of fluorescence detection arises from two areas: (a) detection is performed against a very dark background and (b) the use of the laser as an excitation source provides a high photon flux. The combination of the two can yield single-molecule detection in exceptional circumstances, although picomolar ($10^{-12}M$) is typically obtained. Under conditions that are easy to replicate, LIF detection is often 10^6 times more sensitive compared to ultraviolet (UV) absorption detection.

Most molecules absorb light in the ultraviolet or visible portion of the spectrum, but only few produce significant fluorescence. This provides for the extreme selectivity of the technique. Molecular fluorescence is usually quenched through vibronic or collisional events resulting in a radiationless decay of excited singlet-state energy to the ground state. In aromatic structurally rigid molecules, quenching is less significant and the quantum yield increases.

The selectivity of fluorescence is to itself a problem because the technique is applicable to fewer separations. Sophisticated derivatization schemes have been developed for these applications to take advantage of the attributes contributed by fluorescence detection. Because there are two instrumental parameters to adjust, the excitation and emission wavelengths, the inherent selectivity of the method is further enhanced.

The fundamental equation governing fluorescence is

$$I_f = \Phi_f I_0 abc E_x E_c E_m E_{\text{pmt}}$$

where I_f is the measured fluorescence intensity, Φ_f is the quantum yield (photons emitted/photons absorbed), I_0 is the excitation power of the light source, a , b , and c are the Beer's Law terms, and the E terms are the efficiencies of the excitation monochromator or filter, the optical portion of the capillary, the emission monochromator or filter, and the detector (photomultiplier or charge-coupled device), respectively. It is no wonder why optimization of fluorescence detection is difficult for the uninitiated.

Excitation Sources

The optimal excitation wavelength is usually a combination of the power of the light source and the molar absorptivity of the solute at the selected wavelength. The argon-ion laser is used for most DNA applications since the primers, intercalators, and dye terminators have been optimized for 488-nm excitation. For other applications, particularly for small molecules, where native fluorescence is measured, a tunable light source is desirable. The deuterium lamp is useful for low-UV excitation and the xenon arc is superior in the near-UV to visible region. With a 75-W xenon arc, the limit of detection (LOD) is 2 ng/mL ($6 \times 10^{-9}M$) for fluorescein using fiber-optic collection of the fluorescence emission [2]. This is a 100-fold improvement compared to absorption detection. By using a microscope objective to focus the light along with a sheath-flow cuvette (to reduce scattering, see below) and lens to collect the light, the LOD is reduced to $8 \times 10^{-11}M$ [3]. Nevertheless, the LOD using conventional tunable sources will never be superior to that found with the laser.

It is possible to select lasers other than the argon-ion laser for LIF detection. A 625-nm diode laser is available on a commercial unit (Beckman P/ACE and MDQ). Tunable dye lasers would be desirable but cost and reliability has precluded widespread use. The KrF laser is particularly useful because it emits in the UV at 248 nm. If fiber optics are employed to direct the laser light, then a UV transparent fiber optic must be used. A table of lasers and their wavelengths of emission is given in Table 1.



Table 1 Laser Light Sources for LIF Detection

Laser	Available wavelengths (nm)
Ar ion (air-cooled)	457, 472, 476, 488, 496, 501, 514
Ar ion (full frame)	275, 300, 305, 333, 351, 364, 385, 457, 472, 476, 488, 496, 501, 514
Ar ion (full frame, frequency doubled)	229, 238, 244, 248, 257
ArKr	350–360, 457, 472, 476, 488, 496, 501, 514, 521, 514, 521, 531, 568, 647, 752
HeNe	543, 594, 604, 612, 633
Excimer	
XeCl (pulsed)	308
KrF (pulsed)	248
Nitrogen (pulsed)	337
Nitrogen-pumped dye (tunable)	360–950
Solid state	
YAG (frequency doubled)	532
YAG (frequency quadrupled)	266
Diode lasers	
Frequency doubled (LiNbO ₃)	415
Frequency doubled (KTP)	424
Frequency tripled (Nd-doped YLiF)	349

Source: Data from Ref. 13.

Low-power lasers are often used in HPCE. Because scattered light is the factor that often limits detectability, raising the power level is ineffective. At high laser power, photobleaching becomes more likely to occur as well.

Methods for Collecting Fluorescent Emission

The goal here is to minimize the collection of scattered radiation and optimize the collection of emitted fluorescence. Scattered radiation comes from two sources: Rayleigh scattering and Raman scattering. Rayleigh scattering occurs at the wavelength of excitation. To optimize the LOD, virtually all of this radiation must be excluded from detection. Raman scattering is observed at longer wavelengths than Rayleigh scattering and it is 10^6 times less intense. Despite the weakness of Raman scattering, this effect can significantly elevate the background if left unchecked. Bandpass and/or cutoff filters are often used to reduce the impact of scattering. It is important to ascertain that the selected filter does not fluoresce as well.

Fluorescence Detection in Capillary Electrophoresis

Fiber optics held at right angles to the capillary can be employed to route emitted light toward the photomultiplier tube (PMT) [2]. The Beckman LIF detector employs a collecting mirror to increase the amount of collected emission. One problem with both of these approaches is the failure to prevent small amounts of scattered light from reaching the PMT. Cutoff and/or bandpass filters are not 100% efficient in this regard. This is particularly important when lasers are used because of the intense scattering of light.

The sheath-flow design is an important advance in reducing scattering because detection occurs after the solutes have exited the capillary [4]. Scattering occurs whenever a refractive index (RI) change occurs in the optical path. These RI changes include the air–capillary interface and the buffer–capillary interface. Eliminating the capillary from the optical path effectively removes four scattering surfaces. This becomes most important in multiple-capillary systems such as the DNA sequencer because many surfaces are now involved. The sheath-flow device patented in 1998 [5] is illustrated in Fig. 1 for a five-capillary system. In actual

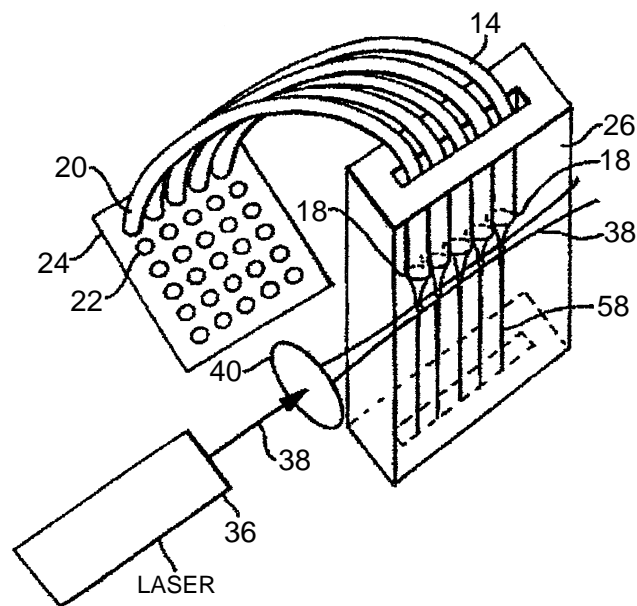


Fig. 1 Multiple-capillary instrument employing the sheath-flow technique. Key: 14, capillary; 18, capillary outlet; 20, capillary inlet; 22, buffer well; 24, microtiter plate; 26, quartz chamber; 36, laser; 38, laser beam; 40, lens; 58, fluidic stream. The electrodes are not shown nor is the device for delivering the sheath fluid. (Reprinted in part from U.S. Patent No. 5,741,412, Figure 1.)

practice, 96 capillaries are employed. The laser beam is sufficiently strong that attenuation is not significant or at least can be compensated for in the software. Fluorescence from each capillary is then imaged onto a charge-coupled device (CCD) camera.

For single-capillary systems, a conventional PMT is used for detection. Light is routed to that PMT either with fiber optics, a collecting mirror, epi-illumination microscopy, or a microscope objective. For multiple-capillary systems, the system must be scanned [6] or the light imaged onto a CCD camera.

Derivatization

Derivatization is important in capillary electrophoresis to enhance the detectability of solutes that are nonfluorescent [7]. The chemistry can occur precapillary, on capillary, postcapillary. Typically, the solutes are amino acids, catecholamines, peptides, or proteins, all of which contain primary or secondary amine groups.

Reagents such as *ortho*-phthaldehyde (OPA), naphthalenedialdehyde (NDA), 3-(4-carboxy-benzoyl)-2-quinoline carboxaldehyde (CBQCA), fluorescein, and fluorenylmethyl chloroformate (Fmoc) are all useful for precapillary derivatization, the most common of the three techniques. For carbohydrates, reagents such as aminopyrene naphthalene sulfonate (APTS) are used for precapillary derivatization. For chiral recognition, prederivatization with optically pure fluorenyl ethyl chloroformate (FLEC) provides for both enantioseparation by micellar electrokinetic capillary chromatography (MECC or MEKC) and a tag that absorbs at 260 nm and emits above 305 nm. Reagents for derivatizing carbonyl, hydroxyl, and other functional groups are also available.

For on-capillary and postcapillary derivatization, the reagent must not fluoresce until reacted with the solute. For these purposes, NDA and OPA are the best choices. With on-capillary derivatization, it is possible to use a reagent that fluoresces, but its removal prior to solute detection can be difficult.

The advantage of precapillary and on-capillary derivatization is the lack of the need for additional instrumentation beyond the basic HPCE instrumentation. The disadvantage of precapillary derivatization is the need for extra sample-handling steps. For postcapillary derivatization, the need for additional miniaturized instrumentation is the principle disadvantage. This problem may be overcome when dedicated microfabricated systems become available.

Important non-DNA application areas for precapillary derivatization with LIF detection include the determination of amino acids and amines in cerebrospinal fluid to distinguish disease states such as Alzheimer's disease and leukemia from the normal population. In vivo monitoring of microdialysates from the brain of living animals has been employed for the determination of neuropeptides, amphetamine, neurotransmitters, and amino acids. The contents of single neurons and red blood cells have been studied as well.

A variant of postcapillary derivatization is chemiluminescence (CL) detection [8]. In this case, the chemical reaction replaces the light source for excitation. The detector is a PMT run at high voltage. Solute can be tagged with CL reagents such as luminol or directly excited via the peroxyoxalate reaction. The latter works best for aminoaromatic hydrocarbons such as dansylated amines. The LODs using CL detection approach laser levels because of the low background. However, the need for specialized apparatus has limited the applicability of CL detection.

Fluorescence Detection for Microfabricated Systems

The so-called micro-total analytical systems (μ TAS) can integrate sample handling, separation, and detection on a single chip [9]. Postcapillary reaction detectors can be incorporated as well [10]. Fluorescence detection is the most common method employed for these chip-based systems. A commercial instrument (Agilent 2100 Bioanalyzer) is available for DNA and RNA separations on disposable chips using a diode laser for LIF detection. In research laboratories, polymerase chain reaction (PCR) has been integrated into a chip that provides size separation and LIF detection [11].

Indirect Fluorescence Detection

When detecting solutes that neither absorb nor fluoresce, indirect detection can be employed. With this technique, a reagent is added to the background electrolyte that absorbs or fluoresces and is of the same charge for the solute being separated. This reagent elevates the baseline. When solute ions are present, they displace the additive as required by the principle of electroneutrality. As the separated ions migrate past the detector window, they are measured as negative peaks relative to the high baseline. The advantage of indirect fluorescence compared to indirect absorption is an improved LOD.



The sensitivity of indirect detection is given by the following equation [12]:

$$C_{\text{LOD}} = \frac{C_R}{(\text{DR})(\text{TR})}$$

where the CLOD is the concentration limit of detection, C_R is the concentration of the reagent, DR is the dynamic reserve, and TR is the transfer ratio. Thus, the lowest CLOD occurs when the reagent concentration is minimized.

With 100 μM fluorescein, a mass limit of detection of 20 μM was measured for lactate and pyruvate in single red blood cells. Fluorescein is a good reagent because it absorbs at 488 nm and thus matches the argon-ion laser emission wavelength. In indirect absorption detection, the additive concentration is usually 5–10 mM. Band broadening due to electrodispersion is less unimportant in indirect fluorescence detection because the solute concentration is so low. At higher solute concentrations, the system will be less useful because of electrodispersion. The concentration of the indirect reagent could be increased, but then indirect absorption detection becomes applicable.

With the advent of microfabricated systems that employ LIF detection, it is expected that indirect

Fluorescence Detection in Capillary Electrophoresis

fluorescence will gain importance as a general-purpose detection scheme.

References

1. C. E. MacTaylor and A. G. Ewing, *Electrophoresis* 18: 2279 (1997).
2. M. Albin, R. Weinberger, E. Sapp, and S. Moring, *Anal. Chem.* 63: 417 (1991).
3. E. Arriaga, D. Y. Chen, X. L. Cheng, and N. J. Dovichi, *J. Chromatogr.* 652: 347 (1993).
4. Y. F. Cheng and N. J. Dovichi, *SPIE* 910: 111 (1988).
5. N. J. Dovichi and J. Z. Zhang, U.S. Patent 5,741,412 (April 21, 1998).
6. X. C. Huang, M. A. Quesada, and R. A. Mathies, *Anal. Chem.* 64: 967 (1992).
7. H. A. Bardelmeijer, et al., *Electrophoresis* 18: 2214 (1997).
8. T. D. Staller and M. J. Sepaniak, *Electrophoresis* 18: 2291 (1997).
9. A. Manz, et al., *Analysis* 22: M25 (1994).
10. S. C. Jacobson, L. B. Koutny, R. Hergenroeder, and A. W. Moore, Jr., *Anal. Chem.* 66: 4372 (1994).
11. L. C. Waters, et al., *Anal. Chem.* 70: 158 (1998).
12. E. S. Yeung and W. G. Kuhr, *Anal. Chem.* 63: 275 (1991).
13. H. E. Schwartz, K. J. Ulfelder, F.-T. A. Chen, and J. Pen-tony, *J. Capillary Electrophoresis* 1: 36 (1994).



Fluorescence Detection in HPLC

Ioannis N. Papadoyannis

Anastasia Zotou

Aristotle University of Thessaloniki, Thessaloniki, Greece

Introduction

Detection based on analyte fluorescence can be extremely sensitive and selective, making it ideal for trace analysis and complex matrices. Fluorescence has allowed liquid chromatography to expand into a high-performance technique. High-performance liquid chromatography (HPLC) procedures with fluorescence detection are used in routine analysis for assays in the low nanogram per milliliter range and concentrations as low as picogram per milliliter often can be measured. The linearity range for these detectors is similar to that of ultraviolet (UV) detectors (i.e., 10^3 – 10^4).

Discussion

One major advantage of fluorescence detection is the possibility of obtaining three orders of magnitude increased sensitivity over absorbance detection and its ability to discriminate analyte from interference or background peaks. Contrary to absorbance, fluorescence is a “low-background” technique. In an absorbance detector, the signal measured is related to the difference in light intensity in the presence of the sample versus the signal in the absence of the sample. For traces of analyte, this difference becomes extremely small and the noise level of the detector increases significantly. In a fluorescence detector, however, the light emitted from the analyte is measured against a very low-light (dark) background and, thus, against a very low noise level. The result is a much lower detection limit, which is limited by the electronic noise of the instrument and the dark current of the photomultiplier tube.

Another major advantage of fluorescence detection is selectivity. The increased selectivity of fluorescence versus absorbance is mainly due to the following reasons: (a) Most organic molecules will absorb UV/visible light but not all will fluoresce. (b) Fluorescence makes use of two different wavelengths (excitation and emission) as opposed to one in absorbance, thus decreasing the chance of detecting interfering chromatographic peaks.

Quantitative analysis can be performed with fluorescence detection even when poor column resolution occurs, provided there is enough detection selectivity to resolve the peaks.

One of the weak points of fluorescence is that relatively few compounds fluoresce in a practical range of wavelengths. However, chemical derivatization allows many nonfluorescent molecules containing derivatizable functional groups to be detected, thus expanding the number of applications. Fluorescence derivatization can be accomplished either via precolumn or post-column methods.

Theoretical Background of Fluorescence Detection

Fluorescence is a specific type of luminescence. When a molecule is excited by absorbing electromagnetic radiation (a photon) supplied by an external source (i.e., an incandescent lamp or a laser), an excited electronic singlet state is created. Eventually, the molecule will attempt to lower its energy state, either by reemitting energy (heat or light) by internal rearrangement or by transferring the energy to another molecule through a molecular collision. This process distinguishes fluorescence from chemiluminescence, in which the excited state is created by a chemical reaction. If the release of electromagnetic energy is immediate or stops upon the removal of the excitation source, the substance is said to be fluorescent.

In fluorescence, the excited state exists for a finite time (1–10 ns). If, however, the release of energy is delayed or persists after the removal of the exciting radiation, then the substance is said to be phosphorescent.

Once a photon of energy $h\nu_{\text{exc}}$ excites an electron to a higher singlet (absorbance) state (1 fs), emission of the photon $h\nu_{\text{em}}$ occurs at longer wavelengths. This is due to the competing nonradiative processes (such as heat or bond breakage) occurring during energy deactivation. The difference in energy or wavelength represented by $h\nu_{\text{em}} - h\nu_{\text{exc}}$ is called the *Stokes shift*.



The fluorescence signal, I_f , is given by

$$I_f = \phi I_0 (1 - e^{-kcl})$$

where ϕ is the quantum yield (the ratio of the number of photons emitted to the number of photons absorbed), I_0 is the intensity of the incident light, c is the concentration of the analyte, k is the molar absorbance, and l is the path length of the cell.

With few exceptions, the *fluorescence excitation spectrum* of a single fluorophore in dilute solution is *identical to its absorption spectrum*. Under the same conditions, the *fluorescence emission spectrum is independent of the excitation wavelength*, due to the partial dissipation of the excitation energy during the excited lifetime. The emission intensity is proportional to the amplitude of the fluorescence excitation spectrum at the excitation wavelength.

Deactivation Pathways in Fluorescence

The excited state exists for a finite time (1–10 ns) during which the fluorophore undergoes conformational changes and is also subject to several interactions with its molecular environment. The processes which deactivate the excited state may be radiational or nonradiational (see Fig. 1) and are the following.

Internal Conversion

A transition from a higher (S_3 , S_2) to the first singlet excited state (S_1) occurs through an internal conversion (in 1 ps). Internal conversion is increased with increasing solvent polarity.

External Conversion (Quenching)

This is a chemical or matrix effect and can be defined as a bimolecular process that reduce the fluorescence quantum yield without changing the emission spectrum. Fluorescence radiation is transferred to foreign molecules after collisions.

Vibrational Relaxation

The energy of the first excited singlet state is partially dissipated through vibrations, yielding a relaxed singlet excited state. *Increased vibrations lower the fluorescence intensity*, due to the fact that they occur much faster (1 ps) than the fluorescence event. The molecular structure itself will determine the amount of vibrations. Rigid and planar molecules usually do not favor vibrations and they are prone to fluoresce.

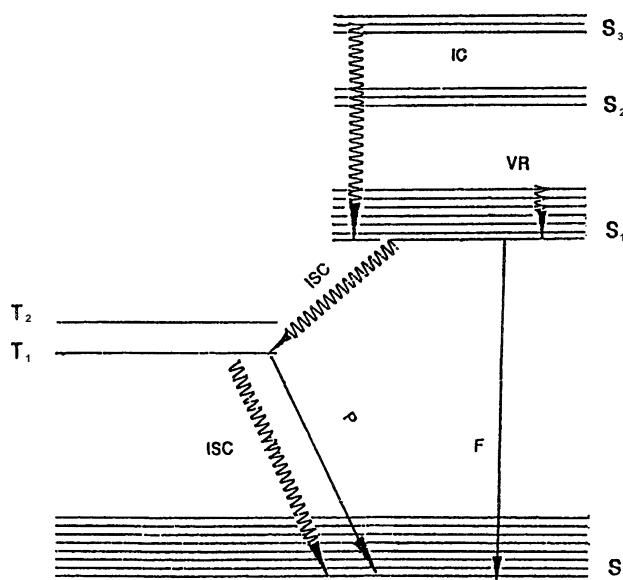


Fig. 1 Deactivation pathways in fluorescence; S_1 , S_2 , and S_3 are singlet excited states; S_0 is the ground state; T_1 and T_2 are triplet excited states; VR is vibrational relaxation, IC is internal conversion, ISC is intersystem crossing, P is phosphorescence, and F is fluorescence.

Intersystem Crossing (Photobleaching)

This is a nonradiational process under high-intensity illumination conditions and in the same timescale as fluorescence (1–10 ns). It is defined as a transition from the first excited singlet (S_1) to the excited triplet (T_1) state. This is a “forbidden” transfer and necessitates the change of electron spin. *The quantum yield of fluorescence is reduced and phosphorescence also occurs.*

Phosphorescence

This event occurs due to a radiational relaxation to the ground singlet (S_1) state and in the 0.1 ms to 10 s time frame. Therefore, the emission is at even longer wavelengths than in fluorescence. Energy addition to the molecule in the form of heat or collisions of two triplet-state molecules can cause delayed fluorescence.

Factors Affecting Fluorescence

Molecular structure and environmental factors such as acidity, solvent polarity, and temperature variations exert significant influence on fluorescence intensity. Also, variations in mobile-phase composition will

cause excitation and emission-wavelength changes in the fluorophore.

Molecular Structure

Common fluorophores possess aromaticity and electron-donating substituents on the ring. Only compounds with a high degree of conjugation will fluoresce. The possible molecular transitions resulting in fluorescence are $\sigma \rightarrow \sigma^*$, occurring only on alkanes in the vacuum UV region, and $\pi \rightarrow \pi^*$ with very high extinction coefficients, occurring in alkenes, carbonyls, alkynes, and azo compounds. The majority of strong fluorophores undergo this transition and the excited state is more polar than the ground state.

Solvent Polarity

Polar solvents affect the excited state differently in $\pi \rightarrow \pi^*$ and $n \rightarrow \pi^*$ transitions. The excited state in $\pi \rightarrow \pi^*$ transition is stabilized. A reduction in the energy gap will occur and the emission will be shifted to a longer wavelength (red shift). Therefore, the difference between excitation and emission wavelengths will be greater in polar solvents.

Temperature

A rise in temperature increases the rate of vibrations and collisions, resulting in increased intersystem crossing, internal and external conversion. Consequently, the fluorescence intensity is inversely proportional to the temperature increase. Additionally, an increased temperature causes a red shift of the emission wavelength.

Acidity

Acidity can drastically affect the fluorescence intensity. The pK_a of concern is the pK_a of the excited state. Because protonation is faster than fluorescence, the pK_a can be quite different than it is for the molecule in the ground state. Therefore, a pH optimization versus fluorescence intensity is needed for molecules that are particularly prone to pH changes.

Fluorescence Detector Instrumentation

Fluorescence detectors for HPLC use come in many designs from the manufacturer. Differences in detector

design can lead to markedly different results during interlaboratory comparisons.

Fluorescence detectors are based either on the straight-path design (similar to UV photometers) or on the more often encountered right-angle design. The common excitation source lamps used are continuous deuterium, xenon, xenon–mercury, and pulsed xenon. Recently, the use of high-power light sources for excitation, such as laser sources, allows the development of much smaller volume flow cells with less scatter (noise), resulting in improved efficiency. Photomultiplier tubes are commonly used as the photodetectors (photocells) versus photodiodes in UV detectors. They convert a light signal to an electronic signal.

Detector flow cells are the link between the chromatographic system and the detector system. The cell cuvettes are made of quartz, with either cylindrical or square shapes and volumes between 5 and 20 μL . The sensitivity is directly proportional to the volume. However, resolution decreases with increasing volume. Fluorescence is normally measured at an angle perpendicular to the incident light. An angle of 90° has the lowest scatter of incident light. However, fluorescence from the flow cell is isotropic and can be collected from the entire 360° .

With the straight-path design, a standard UV cell can be used, but the filters must be selected so as to prevent stray light from reaching the photodetector. The right-angle design often uses a cylindrical cell. This design is less efficient than the straight-path cell because light-scattering problems result in a lower light intensity reaching the photodetector. However, this design is less susceptible to interference from stray light from the lamp, because the photodetector is not in line with the lamp.

With respect to monochromator type, three general detector designs are available: filter–filter, grating–filter, and grating–grating, where either a filter or monochromator grating is used to select the correct excitation and emission wavelengths. Gratings allow a choice of any desired wavelength, whereas filters are limited to a single wavelength.

Fluorescence detectors that use *filters* to select excitation and emission wavelengths are called *filter fluorimeters*. This type of detector is the most sensitive, yet the simplest and least expensive. A diagram of this simple form of fluorescence detector is shown in Fig. 2. Usually, in order to enhance the fluorescence collected from the flow cell, lenses are employed along with filters. The lenses are positioned before the excitation filter and after the flow cell to focus and collect the light.



The ultimate in fluorescence detection is a detector that uses a diffraction grating to select the excitation wavelength and a second grating to select the wavelength of the fluorescent light. These dual monochromatic *grating-grating* fluorescence detectors are called *spectrofluorometers*. If the gratings are used in the scanning mode, the detector is a *scanning spectrofluorometer*. A fluorescence or excitation spectrum can be provided by arresting the flow (stop-flow technique) of the mobile phase when the solute resides in the detecting cell or by scanning the excitation or fluorescent light, respectively. In this way, it is possible to obtain excitation spectra at any chosen fluorescent wavelength or fluorescence spectra at any chosen excitation wavelength.

The *grating-filter* detector is a hybrid between the filter-filter and the grating-grating types. Both high sensitivity and intermediate selectivity are achieved. The use of a filter in combination with gratings is ideal for lowering the background.

Grating-grating fluorometers are convenient for method development, because they permit selection of any excitation or emission wavelength. Filter-filter instruments, on the other hand, are simpler, easier in use, less expensive, more sensitive, and better suited for transferring an HPLC method between laboratories.

With the vast development of technology, fluorescence detectors have become programmable. Optimization of wavelength-pair maxima for each analyte can be time programmed during the chromatographic run.

The proper use of fluorescence detectors necessitates knowledge and understanding of noise sources. Dual monochromatic detectors have stray light leakage. When the wavelength pair is close, the background noise can significantly limit the detection limit. The *stray light*, along with *reflection* and *scattering*, increases the blank signal, resulting in reduced signal-to-noise ratio. Reflection occurs at interfaces that have a difference in the refractive index. Scattering can be of *Rayleigh* or *Raman* type.

In Rayleigh scatter, the wavelength of the absorbed and emitted photons are the same. Ultraviolet wavelengths scatter more than visible. Rayleigh scatter can be a significant problem when the wavelength pair overlaps (less than 50 nm) and instruments do not have filter accommodations and adjustable slits.

Raman scatter can also be troublesome. Depending on the wavelength pair of the sample, Raman scatter from the mobile phase can overlap the fluorescence

signal and, thus, can be misdiagnosed as the fluorescence signal itself. This problem arises during increasing instrument sensitivity. However, satisfactory separation can be achieved by changing the excitation wavelength because emission is independent of the excitation wavelength.

To summarize, in terms of instrumental operation, the following practices should be followed: proper zeroing of the blank and nontampering with the gain during serial dilutions. Increased sensitivity should be accomplished by varying the full-scale range.

The basic sequence in instrumental adjustments is to select the minimum gain necessary to allow a full-scale deflection, at the least sensitive scale. When linear curves are prepared, the gain need not be adjusted. Amplification should always be done using the range control. Any small changes in the gain during calibration will cause nonlinearity. Once the gain has been set, the zero can be set. To ensure reproducibility, zeroing the detector from time to time during the day is recommended, because the dark current can change during the day.

Suggested Further Reading

- Dolan, J. W. and L. R. Snyder, *Troubleshooting LC Systems*, Humana Press, Clifton, NJ, 1989, pp. 337–339.
- Gilbert, M. T., *High Performance Liquid Chromatography*, IOP Publishing, Bristol, U.K., 1987, pp. 34–35.
- Hancock, W. S. and J. T. Sparrow, *HPLC Analysis of Biological Compounds, A Laboratory Guide*, Marcel Dekker, Inc., New York, 1984, pp. 166–169.
- Haugland, R. P., *Handbook of Fluorescent Probes and Research Chemicals*, 6th ed., Molecular Probes, Inc., Eugene, OR, 1996, pp. 1–4.
- O'Flaherty, B., *Fluorescence Detection*, in *A Practical Guide to HPLC Detection* (D. Parriott, ed.), Academic Press, San Diego, CA, 1993, pp. 111–139.
- Papadoyannis, I. N., *HPLC in Clinical Chemistry*, Marcel Dekker, Inc., New York, 1990, pp. 74–75.
- Scott, R. P. W., *Techniques and Practice of Chromatography*, Marcel Dekker, Inc., New York, 1995, pp. 288–292.
- Scott, R. P. W., *Chromatographic Detectors, Design, Function and Operation*, Marcel Dekker, Inc., New York, 1996, pp. 199–211.
- Snyder, L. R. and J. J. Kirkland, *Introduction to Modern Liquid Chromatography*, 2nd ed., John Wiley & Sons, New York, 1979, pp. 145–147.
- Snyder, R. L., J. J. Kirkland, and J. L. Glajch, *Practical HPLC Method Development*, John Wiley & Sons, New York, 1997, pp. 81–84.



Foam Countercurrent Chromatography

Hisao Oka

Aichi Prefectural Institute of Public Health, Nagoya, Japan

Yoichiro Ito

National Heart, Lung, and Blood Institute, National Institutes of Health, Bethesda, Maryland, U.S.A.

Introduction

When a foam moves through a liquid, it carries particles caught at its interface, resulting in the accumulation of these particles at the surface. For many years, this phenomenon has been utilized for the separation of minerals and metal ions. Because the method only employs an inert gas and an aqueous solution, it should have a great potential for the separation of biological samples. This idea has been realized using the high-speed countercurrent chromatographic (CCC) system. In this foam CCC method, foam and liquid undergo rapid countercurrent movement through a long, fine Teflon tubing [2.6 mm inner diameter (i.d.) \times 10 m] under a centrifugal force field. This foam CCC technology has been applied to the separation of variety of samples.

Apparatus for Foam CCC

Figure 1a illustrates a cross-sectional view of the foam CCC apparatus. The rotary frame holds a coiled separation column and a counterweight symmetrically at a distance of 20 cm from the central axis of the centrifuge. When the motor drives the rotary frame, a set of gears and pulleys produces synchronous planetary motion of the coiled column in such a manner that the column revolves around the central axis of the centrifuge while it rotates about its own axis at the same angular velocity, in the same direction. The rotating force field resulting from this planetary motion induces a countercurrent movement between foam and its mother liquid through a long, narrow coiled tube. Introduction of a sample mixture into the coil results in the separation of sample components. Foam active components are quickly carried with the foaming stream and are collected from one end of the coil while the rest moves with the liquid stream in the opposite direction and is collected from the other end of the coil.

Figure 1b illustrates the column design for foam CCC. The coiled column consists of a 10-m-long, 2.6-mm-i.d. Teflon tube with a 50-mL capacity. The column is equipped with five flow channels. The liquid is fed from the liquid feed line at the tail and collected from the liq-

uid collection line at the head. Nitrogen gas is fed from the gas feed line at the head and discharged through the foam collection line at the tail while the sample solution is introduced through the sample feed line at the middle portion of the coil. The head–tail relationship of the rotating coil is conventionally defined by an Archimedean screw force, where all objects in different density are driven toward the head. The liquid feed rate and sample injection rate are each separately regulated with a needle valve and the foam collection line is left open.

Application

Foam CCC can be applied to two types of samples: with (a) the affinity to the foam-producing carrier and (b) the direct affinity to the gas–liquid interface.

Foam Separation Using Surfactants

This technique was demonstrated by the separation of methylene blue and DNP-leucine, having affinity to the foam-producing carrier. Sodium dodecyl sulfate (SDS) and cetyl pyridinium chloride (CPC) were used as carriers to study their effects of electric charges on the foam affinities of various compounds. When the sample mixture was introduced with the anionic SDS surfactant, the positively charged Methylene Blue was adsorbed onto the foam and quickly eluted through the foam collection line; the negatively charged DNP-leucine was carried with the liquid stream in the opposite direction and eluted through the liquid collection line. Similarly, when the same sample mixture was introduced with the cationic CPC surfactant, the negatively charged DNP-leucine was totally eluted through the foam collection line, and positively charged Methylene Blue through the liquid collection line.

Foam Separation Without a Surfactant

Many natural products have foaming capacity, so foam CCC may be performed without a surfactant.



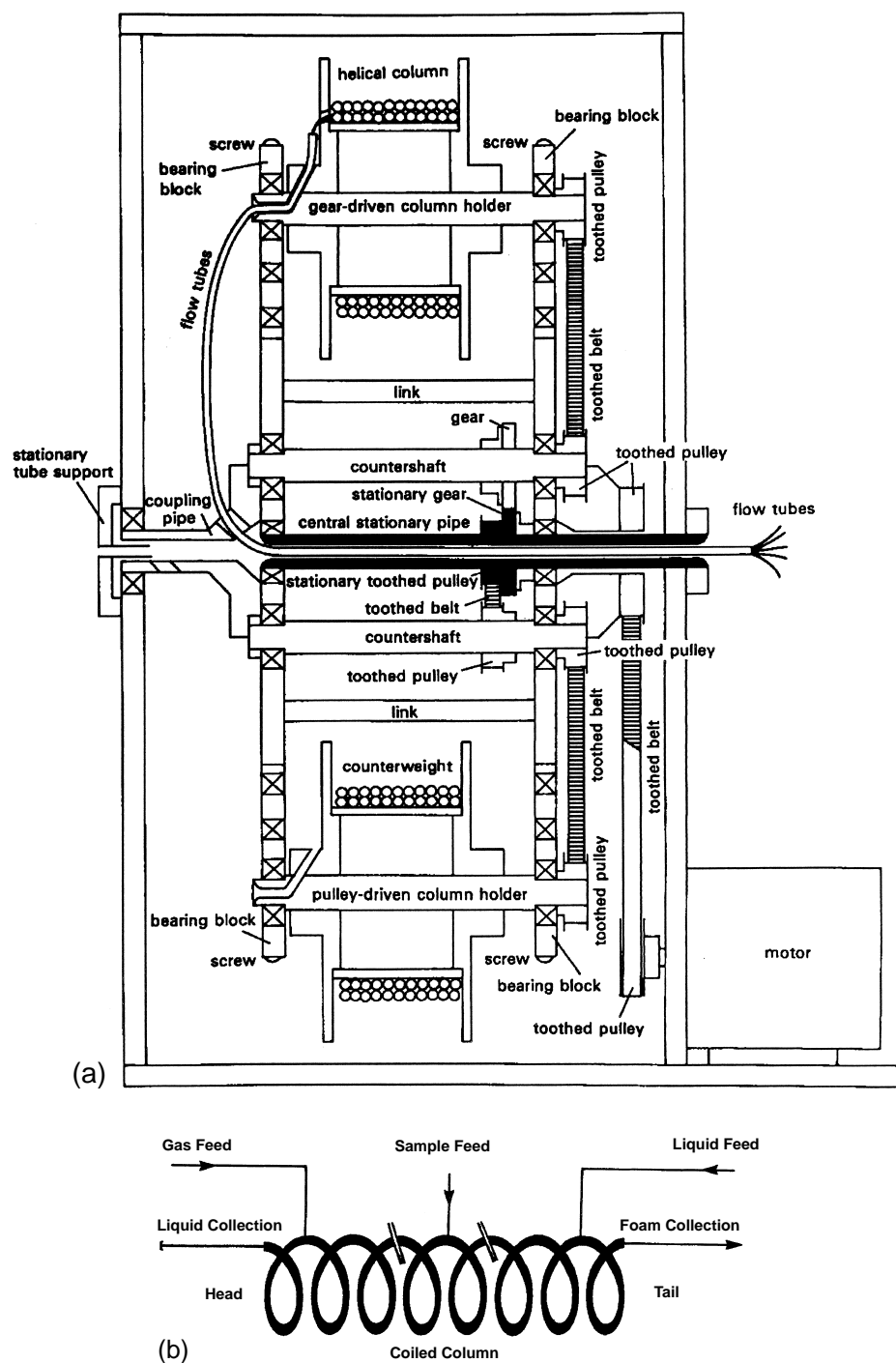


Fig. 1 (a) Foam CCC apparatus; (b) column design for foam CCC.

This technique was demonstrated using the bacitracin complex (BC) as a test sample because of its strong foaming capacity. The foam CCC experiment for sep-

aration and enrichment of BC components was conducted using nitrogen gas and distilled water, which was entirely free of surfactant or other additives.

Batch Sample Loading

Bacitracin is a basic cyclic peptide antibiotic consisting of more than 20 components, but, except for the major components BC-A and BC-F, the chemical structures of other components are still unknown.

Foam CCC of BC components was initiated by simultaneously introducing distilled water from the liquid feed line at the tail and nitrogen gas from the gas feed line at the head into the rotating column while the needle valve at the liquid collection line was fully open. After a steady-state hydrodynamic equilibrium was reached, the pump was stopped and the sample solution was injected through the sample feed line at the middle of the column. After a lapse of the predetermined standing time, the needle valve opening was adjusted to the desired level and pumping was resumed. Effluents were collected at 15-s intervals. The bacitracin components were separated in the order of hydrophobicities of the molecules in the foam fractions, with the most hydrophobic compounds being eluted first. This method can also be applied to continuous sample feeding, as described in the next section.

Continuous Sample Feeding

The experiment was initiated by introducing nitrogen gas from the gas feed line at the head of the rotating column. Then, a 2.5-L volume of the BC solution was continuously introduced into the coil from the sample feed

line at 1.5 mL/min. The hydrophobic components produced a thick foam which was carried with the gas stream and collected from the foam collection line at the tail; other components stayed in the liquid stream and eluted from the liquid collection line at the head. High-performance liquid chromatographic analysis of the foam fraction revealed that the degree of enrichment increased with the hydrophobicity of the components. These results clearly indicate that the present method will be quite effective for the detection and isolation of small amounts of natural products present in a large volume of aqueous solution.

Foaming Parameters

For application of foam CCC to various natural products, it is desirable to establish a set of physicochemical parameters which reliably indicate their applicability to foam CCC. Two parameters were selected for this purpose (i.e., "foaming power" and "foam stability")

which can be simultaneously determined by the following simple procedure. In each test, the sample solution (20 mL) is delivered into a 100-mL graduated cylinder with a ground-glass stopper, and the cylinder vigorously shaken for 10 s. The foaming power is expressed by the volume ratio of the resultant foam to the remaining solution; the foam stability is expressed by the duration of the foam.

In order to correlate the foaming parameters to the foam productivity in foam CCC, the following five samples were selected because of their strong foaming capacities: bacitracin, gardenia yellow, rose bengal, phloxine B, and senega methanol extract. The results of our studies indicated that a sample having the foaming power greater than 1.0 and a foam stability for over 250 min could be effectively enriched by foam CCC. These minimum requirements of foaming parameters, derived from the bacitracin experiment, were found to be applicable to other four samples.

Conclusions

Foam CCC can be applied successfully to a variety of samples having foam affinity, with or without surfactants. The method offers important advantages over the conventional foam separation methods by allowing the efficient chromatographic separation of sample in both batch loading and continuous feeding. The foam CCC technique has a great potential in enrichment, stripping, and isolation of foam active components from various natural and synthetic products in both research laboratories and industrial plants.

Suggested Further Reading

- Bhatnagar, M. and Ito, Y., Foam countercurrent chromatography on various test samples and the effects of additives on foam affinity, *J. Liquid Chromatogr.* 11: 21 (1988).
- Ito, Y., Foam countercurrent chromatography: New foam separation technique with flow-through coil planet centrifuge, *Separ. Sci.* 11: 201 (1976).
- Ito, Y., Foam countercurrent chromatography based on dual countercurrent system, *J. Liquid Chromatogr.* 8: 2131 (1985).
- Ito, Y., Foam countercurrent chromatography with the cross-axis synchronous flow-through coil planet centrifuge, *J. Chromatogr.* 403: 77 (1987).
- Oka, H., Foam countercurrent chromatography of bacitracin complex, in *High-Speed Countercurrent Chromatography* (Y. Ito and W. D. Conway, eds.), John Wiley & Sons, New York, 1996, pp. 107–120.



Oka, H., Harada, K.-I., Suzuki, M., Nakazawa, H., and Ito, Y., Foam countercurrent chromatography of bacitracin with nitrogen and additive-free water, *Anal. Chem.* 61: 1998 (1989).

Oka, H., Harada, K.-I., Suzuki, M., Nakazawa, H., and Ito, Y., Foam countercurrent chromatography of bacitracin I. Batch separation with nitrogen and water free of additives, *J. Chromatogr.* 482: 197 (1989).

Oka, H., Harada, K.-I., Suzuki, M., Nakazawa, H., and

Ito, Y., Foam countercurrent chromatography of bacitracin II. Continuous removal and concentration of hydrophobic components with nitrogen gas and distilled water free of surfactants or other additives, *J. Chromatogr.* 538: 213 (1991).

Oka, H., Iwaya, M., Harada, K.-I., Muarata, H., Suzuki, M., Ikai, Y., Hayakawa, J., and Ito, Y., Effect of foaming power and foam stability on continuous concentration with foam countercurrent chromatography, *J. Chromatogr. A* 791: 53 (1997).



Focusing Field-Flow Fractionation of Particles and Macromolecules

Josef Janča

Université de La Rochelle, La Rochelle, France

Introduction

The original idea of the focusing field-flow fractionation (focusing FFF) [1] appeared in 1982. Giddings [2] proposed an identical principle in 1983 under the name hyperlayer FFF. More detailed methodology of focusing FFF was developed, subsequently, by exploiting various separation mechanisms [3]. Recently, emerging isoperichoric focusing FFF represents the generalization of the original concept [4].

The principle of the focusing FFF is different compared with that of polarization FFF. The crucial difference between the focusing and polarization mechanisms is that the intensity and direction of the driving field force must be dependent on the position across the channel and converging in focusing FFF, whereas it is position independent in polarization FFF. The sample components are focused at different altitudes across the channel and, consequently, eluted at different velocities corresponding to their positions within the flow velocity profile in focusing FFF, as shown in Fig. 1a. Although focusing FFF is still in a stage of fundamental investigation, some applications concerning the fractionation of the macromolecular and particulate species were published.

Methods and Techniques

The focusing can appear only if a gradient of the effective forces exists, and the magnitude of these converging forces is position dependent and is zero at the focusing point. Various combinations of the fields and gradients determining the focusing FFF methods and techniques can be exploited, as demonstrated in the following subsections.

Effective Property Gradient of the Carrier Liquid, Combined with a Field Action

The gradient of an effective property of the carrier liquid, combined with the action of a field, can lead to the focusing of the macromolecules or particles; for example, a density gradient combined with the gravita-

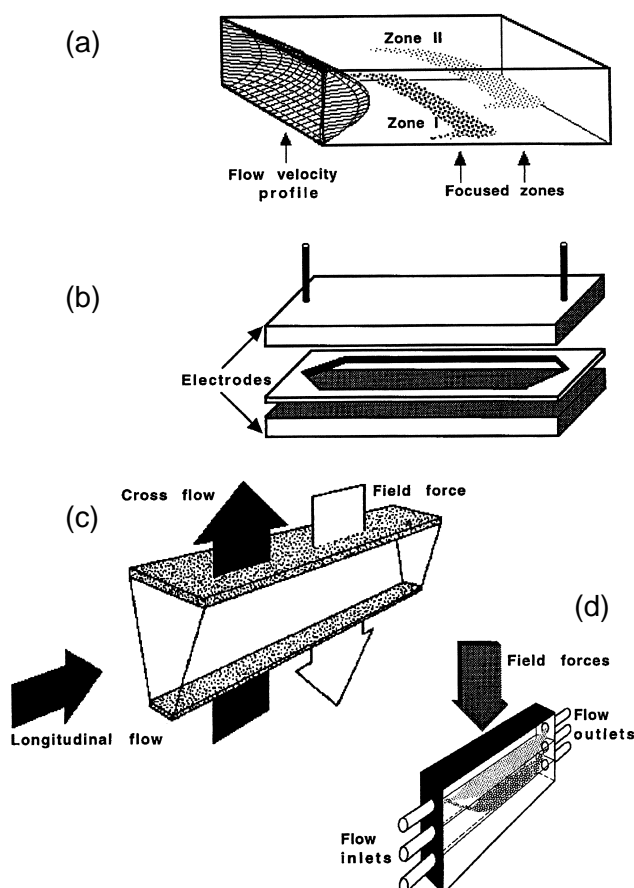


Fig. 1 Principle of focusing field-flow fractionation. (a) Section of the channel demonstrating the principle of focusing FFF with two distinct zones focused at different positions and the parabolic flow velocity profile. (b) Design of the channel for dynamic focusing FFF in coupled electrical and gravitational fields. (c) Schematic representation of the trapezoidal cross-section channel for elutriation focusing FFF. (d) Separation channel for continuous preparative focusing FFF operating in natural gravitational field with three inlet capillaries allowing one to preform the step density gradient by pumping three liquids of different densities and with three outlet capillaries to collect the separated fractions.

tional or centrifugal field generates the focusing of the species at their isopycnic positions, the amphoteric species focus in the pH gradient combined with the



electrical field at their isoelectric points, and so forth. All of these phenomena are called by the general term *isoperichoric focusing*, introduced by Kolin [5].

Usually, the same primary field forces which produce the effective property gradient are used to generate the focusing. However, the use of the secondary field forces of a different nature to generate the focusing phenomenon within the corresponding gradient established by the primary field is possible; for example, the isopycnic focusing of the large-sized uncharged particles due to the weak gravitational field force was found effective under dynamic focusing FFF conditions, whereas the density gradient was generated by the electrical field acting on small charged colloidal particles suspended in the carrier liquid. The construction of the fractionation channel was extremely simple, as shown in Fig. 1b. This principle, applied under static or dynamic FFF conditions, is promising for high-performance analytical and micro-preparative separations.

Although the focusing under the static conditions, without the action of perpendicularly (with respect to the focusing axis) applied bulk flow, can lead to a good separation of the focused species, the theoretical calculations, as well as the experimental tests, have shown the increase of the resolution under the dynamic conditions of focusing FFF.

Cross-Flow Velocity Gradient Combined with a Field Action

The velocity gradient of the carrier liquid across the fractionation channel, generated by the transversal flow through the semipermeable walls, which opposes the action of an external field, can produce the focusing phenomenon. The longitudinal flow is applied simultaneously. This method is called elutriation focusing FFF and was used to separate model mixtures of polystyrene latex particles and silica particles in a trapezoidal cross-section channel. The principle of such a fractionation channel is demonstrated in Fig. 1c. A similar focusing FFF principle can be exploited in a rectangular cross-section channel with two opposite semipermeable walls if the flow rates through the walls are different.

Lift Forces Combined with a Field Action

The hydrodynamic lift forces appearing at high flow rates of the carrier liquid, combined with the field forces, are able to concentrate the suspended particles into the focused layers. While the field forces in polarization FFF concentrate the retained species at the ac-

cumulation wall, the lift forces, becoming operational at high flow rates, pull the particles away from this wall. As a result, the transition from polarization to focusing FFF appears first, followed by the proper focusing effect. For example, Wahlund and Litzen [6] observed the interference of the lift forces in polarization flow FFF carried out in an asymmetrical channel with one semipermeable wall.

Moreover, the retention of the particles can vary with the nature of the field forces. Consequently, the fractionation data interpretation concerning the species eluting within the transition range must be performed with care.

Shear Stress Combined with a Field Action

A high-shear gradient can lead to the deformation of the macromolecular coils. The entropy gradient thus generated produces the driving forces that displace the macromolecules into a low-shear zone. The reversed elution order of high-molecular-weight polystyrenes in thermal FFF at high flow rates could be attributed to this phenomenon [7], but another possibility to explain the reversed elution order cannot be neglected [8].

Gradient of a Nonhomogeneous Field Action

The use of a high-gradient magnetic field was proposed to separate the paramagnetic and diamagnetic species by a mechanism of focusing FFF [9]. Various aspects of focusing FFF carried out under these conditions were discussed, but no experimental results appeared until now.

Preparative Fractionation

No principal difference distinguishes the analytical and preparative uses of focusing FFF. Both types of fractionations can be carried out under conditions of continuous operation [10], which represents the high-performance experimental arrangement for preparative FFF. The fractionation channel, equipped with several outlet capillaries at various positions (and occasionally with several inlets to preform a stepwise gradient in the direction of the focusing), allows one to fractionate the sample which is introduced continuously into the channel and to collect the focused layers eluting by the individual outlets. A schematic representation of such a fractionation channel is shown in Fig. 1d.

The experimental demonstration of this technique was given by the fractionations of various samples of

silica particles, by applying natural gravitation and a counteracting cross-flow gradient. The silica particles were separated according to size. The isopycnic or isoelectric focusing FFF already performed on an analytical scale can easily be transformed into such continuous large-scale separations.

Applications

Focusing FFF represents an important contribution to the science and technology of separation and analysis of the macromolecules of synthetic or natural origin. The range of molar masses and of the sizes of the particles in submicron and micron ranges, of the supramolecular structures, and of the organized biological species, such as the cells, microorganisms, and so forth, which can be fractionated by focusing FFF, is very large.

The molecules which do not interact sufficiently with the imposed fields, such as low-molar-mass species, and which, consequently, do not exhibit the focusing effect can still be separated. The condition is that an equilibrium between them and the effectively focused species is established. As a result, the species which originally do not undergo the separation processes can be transported and thus fractionated with the "carrier" focused species.

The most important field of potential applications of focusing FFF is in the research and technologies related to the life sciences and to macromolecular chemistry. The problems related to trace analysis, which have an enormous importance in the protection of the environment and many other scientific and technological activities, have already stimulated the development of new analytical separation methods. Focusing FFF is one of them, representing an alternative of choice whenever macromolecular or particulate species are concerned.

The newest achievements in focusing FFF clearly indicate that most of the experimental implementations have been obtained with model systems. Practical applications for daily laboratory use, elaborated to the minutest details, were not yet described. However, the

most significant advantages of these methods, mentioned earlier, are evident. Some of these advantages are inherently related to the separation principle of the focusing FFF, such as the absence of a large surface area within the separation channel, which is of crucial importance for sensitive biological materials that can be denatured in contact with the active surfaces.

The operational variables, such as the strength of the field, the flow rate, and so forth, can be continuously manipulated within a very wide range. Another advantage is that although the specific FFF apparatuses are already produced, the commercially available instrumentation for liquid chromatography can be adapted easily for use with focusing FFF methodology. All particular components of the complete focusing FFF apparatus are identical to those for liquid chromatography, except the separation channel, which, in most cases, is not difficult to build in the laboratory. Certainly, focusing FFF represents a large field of challenges, soliciting the creativity and invention in the theory, methodology, and practical applications.

References

1. J. Janča, *Makromol. Chem. Rapid Commun.* 3: 887 (1982).
2. J. C. Giddings, *Separ. Sci. Technol.* 18: 765 (1983).
3. J. Janča, *Field-Flow Fractionation: Analysis of Macromolecules and Particles*, Marcel Dekker, Inc., New York, 1988.
4. J. Janča, *J. Liquid Chromatogr. Related Technol.* 20: 2555 (1997).
5. A. Kolin, in *Electrofocusing and Isotachopheresis* (B. J. Radola and D. Graesslin, eds.), de Gruyter, Berlin, 1977.
6. K. G. Wahlund and A. Litzen, *J. Chromatogr.* 461: 73 (1989).
7. J. C. Giddings, S. Li, P. S. Williams, and M. E. Schimpf, *Makromol. Chem. Rapid Commun.* 9: 817 (1988).
8. J. Janča and M. Martin, *Chromatographia* 34: 125 (1992).
9. S. N. Semyonov, A. A. Kuznetsov, and P. P. Zolotaryov, *J. Chromatogr.* 364: 389 (1986).
10. J. Janča and J. Chmelik, *Anal. Chem.* 56: 2481 (1984).



Forensic Applications of Capillary Electrophoresis

Ivan Mikšík

Institute of Physiology, Academy of Sciences of the Czech Republic, Prague, Czech Republic

Introduction

During the last decade, capillary electrophoresis (CE) has developed into a widely applied method for the analysis of pharmaceuticals (both for the evaluation of pharmaceutical formulations and metabolites). These applications established the basis for introducing CE into the forensic field also. Today, capillary electrophoresis can be applied to a number of analytical problems in forensic science, including the analysis of gunshot residues, explosives, inks, dusts, soils, and, of course, illicit drugs, diverse toxicants, DNA fingerprinting, protein analysis, and so forth (for reviews, see Refs. 1 and 2).

Several features of capillary electrophoresis are particularly interesting for forensic scientists, namely high separation efficiency, sensitivity, and small amount of samples (nanoliters) and solvents (a few milliliters per day). Regarding different operational modes, all of them are applied, although to a different extent, depending on the type of compounds to be assayed.

Forensic Toxicology

Capillary electrophoresis has a particularly wide potential for the analysis of illicit drugs [3]. For this category of applications, mainly capillary zone electrophoresis (CZE) and micellar electrokinetic chromatography (MEKC) are used; however, other modifications of this approach, such as separation in buffers containing a high proportion (up to 20%) of an organic modifier in the background electrolyte, can be used also. More recently, some hints appeared indicating the possibility of applying electrochromatographic techniques for this purpose as well, although, admittedly, this latter approach has not reached the stage of maturity of other techniques. It is to be foreseen that particularly electrokinetic separations exploiting the properties of reversed-phase packings, will be used for these purposes in the near future.

Regarding tissues and body fluids to be analyzed, blood and urine serve most frequently as source material, although the interest of forensic analytical chemists can be easily extended to other specimens (e.g., saliva, bile, or vitreous humor). A tissue that has attracted a lot of inter-

est in the course of recent years is hair [4]; at the root end, the tissue is penetrated by a number of drugs during hair matrix formation. Because the hair stalk is basically devoid of metabolic processes, the drugs, once sorbed, remain in the tissue (depository effects). If one considers the average hair growth of about 1 cm/month the analysis of hair sections may yield information about past exposure of the individual to the toxicants; it has to be kept in mind, however, that external contamination may contribute also to the amount of the toxicant recovered.

As the analytes to be assayed are nearly always present in minute amounts, preconcentration steps are almost always necessary. The techniques used for this purpose have been mostly adopted from analytical procedures using gas or liquid chromatography as the separation step [5]. This fact is emphasized here because the appropriate adjustment of the sample preparation is necessary because the original procedures do not respect the fact that the sample volume injected into a CE system represents a few nanoliters only and requires a relatively high concentration of analytes assayed. However, in selected types of analysis, direct sample application is also possible (for a review, see Ref. 3).

There are three points emphasized in the quoted review which limit the use of direct injection: (a) protein-bound drugs display a different mobility in CZE in comparison to unbound species, (b) high conductivity of the untreated biological samples may cause undesirable peak broadening, and (c) selectivity of the analysis may be negatively influenced by using a nonselective wavelength for detection (usually 200 nm), which is needed to reveal low concentrations of the analytes of interest. Consequently, desalting and deproteinization (at last partial) is frequently done by adding different proportions of organic solvents to the sample ($\sim 1:1 \rightarrow 1:4$). If MEKC is to be used, it is recommended to remove the organic solvent prior to analysis (for the first application of MEKC for forensic purposes, see Ref. 6; for additional information, see Ref. 7). Standard preconcentration conditions, such as solid-phase and liquid–solid extractions, are widely used.

Some idea about actual conditions applicable for the separation of drugs of forensic interest can be obtained from Table 1. Extensive information about the MEKC of drugs is offered in a review of Nishi and Terabe [8].



Table 1 Examples of the Capillary Electrophoretic Separations of Misused Drugs, Their Enantiomers, and Metabolites

Analytes (remarks)	Detection	Separation
17 Basic drugs (amphetamine, lidocaine, codeine, diazepam, methaqualone, etc.; extracted by chloroform–2-propanol, 9:1 v/v)	UV at 214 nm	CZE, 50 mM phosphate buffer pH 2.35
Abused drugs (includes heroin, heroin impurities, <i>cis</i> - and <i>trans</i> -cinnamoyl cocaine)	UV at 210 nm	MEKC, 85 mM SDS, 8.5 mM borate, pH 8.5; containing 15% acetonitrile
Abused drugs and metabolites (includes benzoyl-ecgonine, morphine, heroin, methamphetamine, codeine, amphetamine, cocaine, methadone, benzodiazepines)	Fast scanning UV	MEKC, borate–phosphate buffer pH 9.1, 75 mM SDS
Amphetamines (enantiomers; LLE ^a or SPE ^b)	UV at 200 nm	CZE, 20 mM (2-hydroxy)-propyl- β -cyclodextrin in 200 mM phosphate pH 2.5
Amphetamines and ephedrine (enantiomers; LLE)	UV at 200 nm	CZE, 20 mM β -cyclodextrin in 150 mM phosphate pH 2.5
Barbiturates (after LLE)	UV at 214 nm	MEKC, 100 mM SDS in 10 mM borate, 10 mM phosphate, pH 8.5, 15% acetonitrile added (by volume)
Barbiturates (phenobarbital can be assayed without sample pretreatment)	Multiwavelength detection (195 and 320 nm)	MEKC, 50 mM SDS, phosphate–borate buffer, pH 7.8
Caffeine metabolites (direct injection, LLE)	UV at 254 nm	MEKC, 70 mM SDS, phosphate–borate, pH 8.43
Caffeine metabolites (LLE)	Scanning UV 195–320 nm	MEKC, 70 mM SDS, 16.2 mM phosphate, pH 8.6
Cannabis constituents (alkaline hydrolysis of urine followed by SPE ^b)	Fast scanning UV	MEKC, 75 mM SDS in phosphate–borate buffer pH 9.1)
Dextromethorphan and dextrophan (direct injection)	UV at 200 nm	CZE, 175 mM borate pH 9.3
Dihydrocodeine metabolites and O-demethylation (hydrolysis, direct injection, SPE)	UV at 213 nm, scanning UV 195–320 nm	MEKC, 75 mM SDS, 6 mM borate, 10 mM phosphate, pH 9.2
Flurazepam metabolites, sulfonamides (hydrolysis, LLE)	UV at 254 nm; MS	CZE, 15 or 0.2 mM ammonium acetate pH 2.5 or 1.3 adjusted with TFA, 15% methanol
Haloperidol metabolites (SPE)	UV at 214 nm, scanning UV 195–320 nm, MS	CZE, 50 mM ammonium acetate, 10% methanol, 1% acetic acid, pH 4
Mephentoin and dextromethorphan metabolites (hydrolysis)	Scanning UV 195–320 nm	MEKC, 75 mM SDS, 6 mM borate, 10 mM phosphate pH 9.2–9.3 or CZE, 140 mM borate pH 9.4
Morphine and cocaine in hair (hydrolysis by 0.25 M HCl at 45°C followed by LLE)	UV at 200 nm (230 nm for cocaine, 214 nm for morphine)	CZE, 50 mM borate pH 9.2
Nitrazepam and metabolites (SPE)	UV at 220 nm	MEKC, 60 mM SDS in 6 mM phosphate–borate buffer pH 8.5, 15% methanol (by volume)
Opiates (heroin, morphine, and metabolites; SPE)	Spectral UV analysis	CZE, 12 mM borate, 20 mM phosphate, pH 9.8 or MEKC, 75 mM SDS in phosphate borate buffer, pH 9.2
Opiates (morphine, heroin, codeine, etc., SPE)	UV at 200 nm	CZE, 100 mM phosphate pH 6
Opiates (morphine, heroin, codeine, amphetamine, caffeine)	UV at 200 nm	MEKC, 50 mM SDS, 50 mM glycine, pH 10.5
Purines, substituted (direct injection, LLE, SPE)	Scanning UV 195–320 nm	MEKC, 75 mM SDS, 6 mM borate, 10 mM phosphate pH 9
Racemethorphan, racemorphan (optical isomers)	UV at 200 nm	MEKC, 60 mM β -cyclodextrin in 50 mM borate pH 9.05, 50 mM SDS, 20% 1-propanol
Theophylline metabolites (SPE)	Scanning UV 195–320 nm	MEKC, 200 mM SDS in 100 mM borate, 100 mM phosphate, pH 8.5 (ratio 12:7, final pH 6.5)

Note: For detailed specifications of individual procedures, see Ref. 2.

^aLiquid–liquid extraction.

^bSolid-phase extraction.



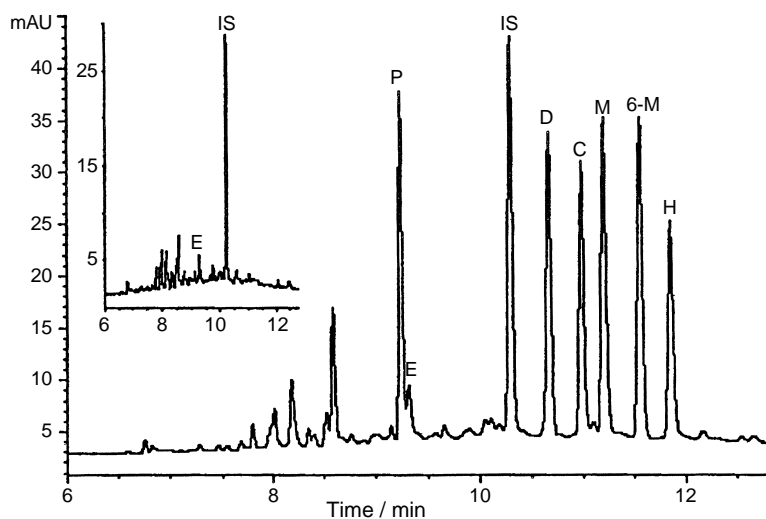


Fig. 1 Capillary electrophoretic separation of opiates. Running conditions: 100 mM phosphate buffer pH 6.0. Electrokinetic injection with field-amplified sample stacking after solid-phase extraction of spiked urine using “double mechanism” cartridges. Precision of migration times 1.2% R.S.D. (relative standard deviation), resolution >2 with all peaks shown. Within the day and day-to-day repeatability 1–4% R.S.D., respectively; detection by UV at 200 nm. Peak identification: pholcodine (P), MAM (6-M), heroin (H), codeine (C), morphine (M), dihydrocodeine (D), and levallorphan (I.S.); E represents an unidentified endogenous compound present in urine (see inset). (From Ref. 9 with permission.)

As indicated in Table 1, ultraviolet (UV) light at short wavelengths (190–220 nm) is routinely used for detection. In these cases, laser-induced fluorescence appears to be the method of choice. Unfortunately, the commercially available laser units emit at wavelengths not suitable for direct drug analysis, which limits the practical applicability of this approach. Nevertheless, where applicable, laser-induced fluorescence can easily improve the detection limit by a factor of 1000, in comparison with UV detection; Ar-ion lasers (emitting at 488 nm wavelength) or He–Cd lasers (emitting at 325 nm wavelength) are commonly used for this purpose. Typically, with enzymatically hydrolyzed urine, the detection limit can be about 2 ng/mL of the assayed compound (zolpidem).

If the investigated drug does not possess a suitable fluorophore, derivatization may be required [fluorescein isothiocyanate for compounds possessing a free amino group (e.g., amphetamines) may serve as a typical example; an Ar-ion laser emitting at 488 nm was used for this purpose]. Generally, detection limits achieved with laser-induced fluorescence after derivatization can be around 3 mM in concentration terms (or 3 μ mol in terms of absolute mass detection). This is about three orders of magnitude less

than what can be achieved with gas chromatography–mass spectrometry.

Another possibility is to use xenon-arc lamp irradiation for the same purpose, which extends the possibilities of excitation wavelengths to the 272–382-nm range. Exploiting competitive binding of trace amounts of (misused) drugs with fluorescence-labeled immunotracers can be spotted in the literature; however, this is not a widely used approach at the moment.

Amperometric detection, which generally offers quite high sensitivity, has not been used so far for forensic (toxicological) applications. The reason probably reflects some problems with commercially available coupling of the high-performance amperometric cell with the capillary electrophoresis device.

Surprisingly, not very many methods using the capillary electrophoresis–mass spectrometry (CE–MS) combination (mainly electrospray ionization) are in use in the area of forensic drug analysis. The first application of CE–MS for forensic purposes was described by Johansson et al. in 1991 [10] for the analysis of sulfonamides and benzodiazepines in urine. The main problem faced in this case is the need of improving the concentration sensitivity of the CE–MS combination. In order to improve the concentration of ana-



lytes, a special method of in-capillary coupling of isotachopheresis with CZE-MS has been proposed. CE-MS instrumentation and its application was reviewed by Cai and Henion [11].

Forensic Biology

One of the major areas of forensic science is DNA fingerprinting, which is used for personal identification and paternity testing. Most of these analyses are based on the polymerase chain reaction (PCR) of individual loci, followed by analysis of differences in length or sequence. Capillary electrophoresis, with laser-induced fluorescence detection, is becoming an alternative method to polyacrylamide gel electrophoresis (PAGE) and agarose slab gel electrophoresis. Fully automated CE-based instruments are now available for DNA sizing, quantitation, screening, and sequencing. Detailed information about the separation of nucleic acids is a matter of a specialized entry; for detailed information, specialized reviews are available (see, e.g., Refs. 12 and 13).

Using the separation of DNA fragments in media with cross-linked polyacrylamide or agarose gels makes it possible to achieve high efficiency (tens of millions of theoretical plates); however, from the practical point of view, replaceable, entangled polymers (e.g., derivatives of cellulose, linear polyacrylamide) are preferred. The main advantage of replaceable media is the ease of renewing the gel media in the capillary with every single run.

Ultraviolet light is routinely used for detection; however, laser-induced fluorescence of labeled DNA offers better results. For example, a PCR-amplified DNA fragment comprised of 120–400 base pairs can be separated with a resolution up to four base pairs using 1% hydroxyethylcellulose and DB-17 capillary (60 cm effective length \times 0.1 mm inner diameter with 0.1 μ m phase thickness). Laser-induced fluorescence detection can yield a sensitivity of about 500 pg/mL of DNA (after staining with fluorescent intercalating dye YO-PRO-1) [14].

Capillary electrophoresis can be also applied for DNA sequencing. For this purpose, multicapillary (array) instruments with laser-induced fluorescence detection are being developed. Detailed descriptions of these methods is beyond the scope of this entry.

Proteins and enzymes are also of interest in forensic science. In this context, it is possible to mention acetaldehyde-protein adducts, which can be used as potential markers of alcoholism. Another application is

Forensic Applications of Capillary Electrophoresis

the determination of globins, saliva, and semen proteins. Capillary electrophoresis of proteins is a broad and complex area of analytical chemistry which, like the separation of nucleic acids, is beyond the scope of this entry (for a review, see, e.g., Ref. 15 and many others). In principle, it is possible to use different operational modes such as CZE in acid or alkaline media, capillary isotachopheresis, capillary isoelectric focusing, capillary gel electrophoresis, and, recently, MEKC. A considerable problem in protein-enzyme separations in untreated capillaries is sticking of these analytes to the inner capillary wall, which can be eliminated (at least in part) by running the separation at very high or very low pH values, by adding some modifiers (as salts, etc.) to the buffer, or by appropriate modification of the capillary surface.

Conclusion

In conclusion, CE is a valuable analytical tool that offers a number of possibilities for the analysis of a wide spectrum of forensically interesting compounds. Practically all compounds which have been traditionally analyzed by GC, high-performance liquid chromatography, thin-layer chromatography, or slab-gel electrophoresis, can be assayed by capillary electrophoretic procedures. All methods of capillary electrophoresis can be validated and can meet the demands of good laboratory practice.

References

1. F. Tagliaro, F. P. Smith, L. Tadeschi, F. Castagna, M. Dobosz, I. Boschi, and V. Pascali, Toxicological and forensic applications, in *Advanced Chromatographic and Electromigration Methods in BioSciences* (Z. Deyl, I. Mikšík, F. Tagliaro, E. Tesarová, eds.), Journal of Chromatography Library Vol. 60, Elsevier, Amsterdam, 1998, pp. 917–961.
2. F. Tagliaro, Z. Deyl, and I. Mikšík, Applications of HPLC/HPCE in forensic, in *HPLC in Enzymatic Analysis* (E. F. Rossomando, ed.), Methods in Biochemical Analysis Vol. 38, John Wiley & Sons, New York, 1998, pp. 164–206.
3. F. Tagliaro, S. Turrina, P. Pisi, F. P. Smith, and M. Marigo, *J. Chromatogr. B* 713: 27 (1998) (and reviews therein).
4. F. Tagliaro, W. P. Smyth, S. Turrina, Z. Deyl, and M. Marigo, *Forensic Sci. Int.* 70: 93 (1995).
5. D. K. Lloyd, *J. Chromatogr. A* 735: 29 (1996).
6. R. Weinberger and I. S. Lurie, *Anal. Chem.* 63: 823 (1991).



7. P. Wernly and W. Thormann, *Anal. Chem.* 63: 2878 (1991).
8. H. Nishi and S. Terabe, *J. Chromatogr. A* 735: 3 (1996).
9. R. B. Taylor, A. S. Low, and R. G. Reid, *J. Chromatogr. B* 675: 213 (1996).
10. I. M. Johansson, R. Pavelka, and J. D. Henion, *J. Chromatogr.* 559: 515 (1991).
11. J. Cai and J. Henion, *J. Anal. Toxicol.* 20: 27 (1996).
12. A. Guttman and K. J. Ulfelder, *Adv. Chromatogr.* 38: 301 (1998).
13. P. G. Righetti and C. Gelfi, *Forensic Sci. Int.* 92: 239 (1998).
14. B. R. McCord, D. L. McClure, and J. M. Jung, *J. Chromatogr. A* 652: 75 (1993).
15. J. F. Banks, Protein analysis, in *Advanced Chromatographic and Electromigration Methods in BioSciences* (Z. Deyl, I. Mikšík, F. Tagliaro, E. Tesarová, eds.), Journal of Chromatography Library Vol. 60, Elsevier, Amsterdam, 1998, pp. 525–573.



Forskolin Purification Using an Immunoaffinity Column Combined with an Anti-Forskolin Monoclonal Antibody

Hiroyuki Tanaka

Yukihiro Shoyama

Kyushu University, Fukuoka, Japan

Introduction

Forskolin, a labdane diterpenoid, was isolated from the tuberous roots of *Coleus forskohlii* Briq. (Lamiaceae) [1]. *C. forskohlii* has been used as an important folk medicine in India. Forskolin was found to be an activator of adenylate cyclase [2], leading to an increase of c-AMP, and now a medicine in India, Germany, and Japan. The production of forskolin is completely dependent on the commercial collection of wild and cultivated plants in India. We have already set up the production of monoclonal antibodies (MAbs) against forskolin [3]. The practical application of enzyme-linked immunosorbent assay (ELISA) for the distribution of forskolin contained in clonally propagated plant organs and the quantitative fluctuation of forskolin depend on the age of *C. forskohlii* [4,5]. As an extension of this approach, we present the production of the immunoaffinity column using anti-forskolin MAb and its application [6].

Materials and Methods

Chemicals

Bovine serum albumin (BSA) was provided by Pierce (Rockford, U.S.A.). Forskolin and 7-deacetyl forskolin were isolated from the tuberous root of *C. forskohlii*, as previously reported [1]. 1-Deoxyforskolin, 1,9-dideoxyforskolin, and 6-acetyl-7-deacetylforskolin were purchased from Sigma Chemical Company (St. Louis, MO, U.S.A.). The mixture (approximately 20 μ g) of forskolin and 7-deacetyl forskolin, purified by the immunoaffinity column, was acetylated with pyridine and acetic anhydride mixture (each 100 ml) at 4°C for 2 h to give pure forskolin.

Preparation of Immunoaffinity Column Using Anti-Forskolin Monoclonal Antibody [6]

Purified IgG (10 mg) in PBS was added to a slurry of CNBr-activated Sepharose 4B (600 mg; Pharmacia Biotech) in coupling buffer (0.1M NaHCO₃ containing 0.5M NaCl). The slurry was stirred for 2 h at room temperature and then treated with 0.2M glycine at pH 8.0 for blocking of activated groups. The affinity gel was washed four times with 0.1M NaHCO₃ containing 0.5M NaCl and 0.1M acetate buffer (pH 4.0). Finally, the affinity gel was centrifuged and the supernatant was removed. The immunoaffinity gel was washed with phosphate buffer solution (PBS) and packed into a plastic minicolumn in volumes of 2.5 mL. Columns were washed until the absorption at 280 nm was equal to the background absorption. The columns were stored at 4°C in PBS containing 0.01% sodium azide.

Direct Isolation of Forskolin from Crude Extractives of Tuberous Roots and Callus Culture of C. forskohlii by Immunoaffinity Column

The dried powder (10 mg dry weight) of tuberous root was extracted five times with diethyl ether (5 mL). After evaporation of the solvent, the residue was redissolved in MeOH and diluted with PBS (1:16), and then filtered by Millex-HV filter (0.45- μ m filter unit; Millipore Products, Bedford, MA, U.S.A.) to remove insoluble portions. The filtrate was loaded onto the immunoaffinity column and allowed to stand for 90 min at 4°C. The column was washed with the washing buffer solution (10 mL). After forskolin disappeared, the column was eluted with PBSM (45%) at a flow rate of 0.1 mL/min. The fraction containing forskolin was lyophilized and extracted with diethyl ether. Forskolin



was determined by thin-layer chromatography (TLC) developed with C_6H_6 -EtOAc (85:15) [Rf; forskolin (0.21), 7-deacetyl forskolin (0.16)] and ELISA.

Results and Discussion

We established a simple and reproducible purification method for forskolin using an immunoaffinity column chromatography method. Because forskolin is almost insoluble in water, various buffer solutions were tested for the solubilization of forskolin. It became evident that 6% MeOH in PBS was necessary for the solubilization of forskolin [3,5]. Next, the elution system for the immunoaffinity column was investigated by using

various elution buffers based on PBS. Only 9% of bound forskolin can be recovered by the PBS supplemented with 10% of MeOH. The forskolin concentrations eluted increased rapidly from 20% of MeOH, and reached the optimum at 45% of MeOH.

To assess the capacity and the recovery of forskolin from the affinity column, 30 μ g of forskolin was added and passed through the column (2.5 mL of gel), and the forskolin content was analyzed by ELISA. After washing with 5 column volumes of PBST, 22.5 μ g of forskolin remained bound and was then completely eluted with the PBS containing 45% of MeOH. Therefore, the capacity of affinity column chromatography was determined to be 9.4 μ g/mL.

The crude diethyl ether extracts of the tuberous root of *C. forskohlii* were loaded onto the immunoaffinity column chromatography system, washed five times with PBS containing 6% of MeOH, and eluted with the PBS containing 45% of MeOH. Figure 1 shows a chromatogram detected by ELISA. Fractions 2–8 contained 45 μ g of forskolin that were over the column capacity, together with the related compounds 1-deoxyforskolin, 1,9-dideoxyforskolin, 7-deacetylforskolin and 6-acetyl-7-deacetylforskolin, and other unknown compounds which were detected by TLC, as indicated in Fig. 2. The peak of fractions 26–30 shows the elution of forskolin (21 μ g) eluted with the PBS containing 45% of MeOH. Forskolin eluted by washing solution (fractions 2–8) was repeatedly loaded and finally isolated. However, forskolin purified by the immunoaffinity column chromatography was still contaminated with a small amount of 7-deacetyl forskolin (Fig. 2) because this compound has a 5.5% cross-reactivity against Mab, as previously indicated [3]. Therefore, the mixture was treated with pyridine and acetic anhydride at 4°C for 2 h to give pure forskolin. In our case, the stability of antibody against PBS containing 45% MeOH is also quite high, because the immunoaffinity column has been used over 10 times, under the same conditions, without any substantial loss of capacity. Therefore, we concluded that the PBS supplemented with 45% MeOH can be routinely used as an elution buffer solution.

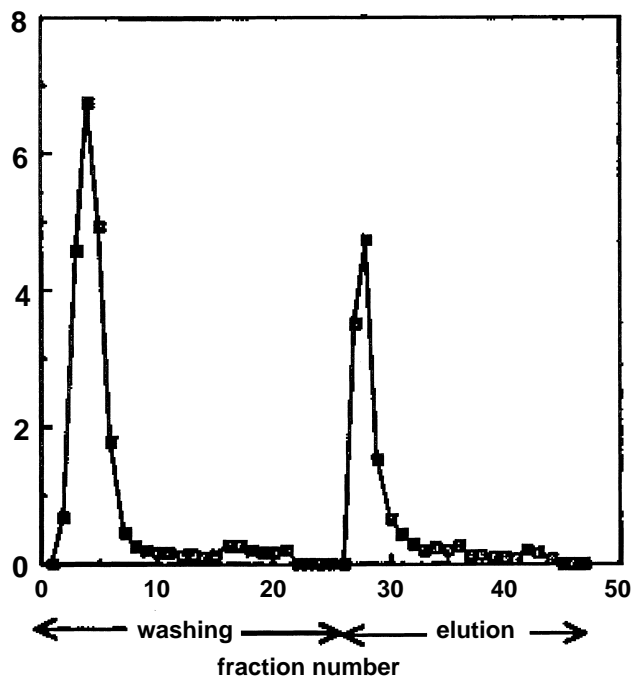


Fig. 1 Elution profile of forskolin in the tuberous root of *C. forskohlii* by purification on immunoaffinity column chromatography. The column was washed with PBSM, then eluted by PBS containing 45% of methanol after the forskolin disappeared. Individual fractions were assayed by ELISA.

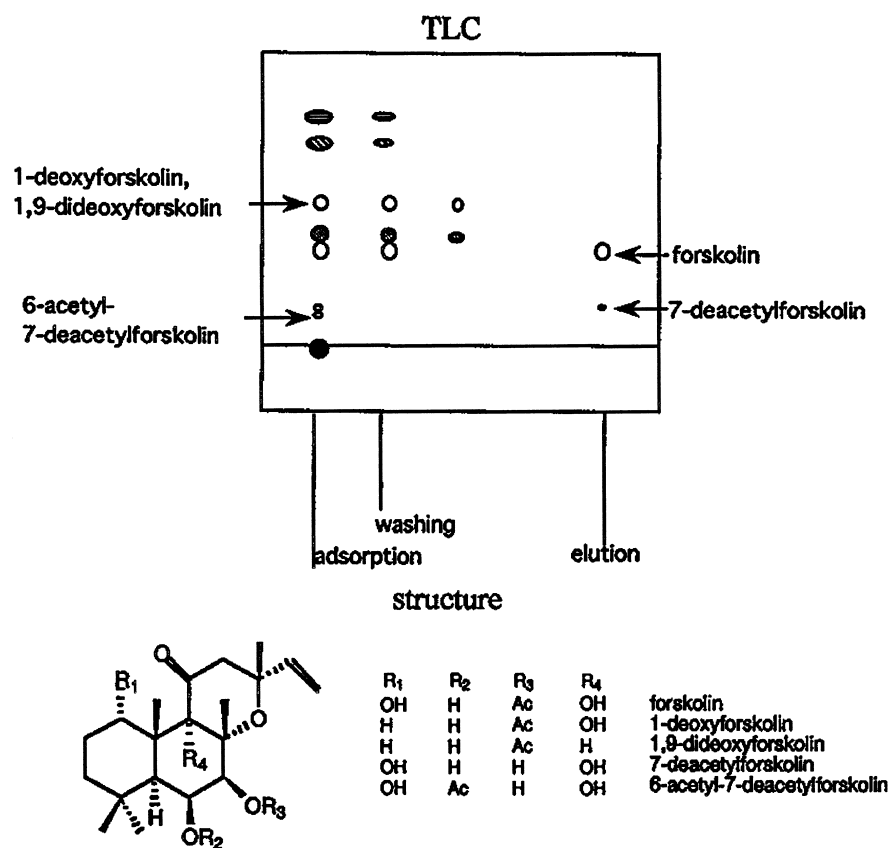


Fig. 2 TLC of adsorption, washing, and elution solutions, and structures of forskolin and the related compounds.

References

1. S. V. Bhat, B. S. Bajwa, H. Dornauer, N. J. de Sousa, and H. W. Fehlhaber, *Tetrahedron Lett.* 1669–1672 (1977).
2. H. Metzger and E. Lindner, *Drug Res.* 31: 1248–1250 (1981).
3. R. Sakata, Y. Shoyama, and H. Murakami, *Cytotechnology* 16: 101–108 (1994).
4. H. Yanagihara, R. Sakata, Y. Shoyama, and H. Murakami, *Biotronics* 24: 1–6 (1995).
5. H. Yanagihara, R. Sakata, Y. Shoyama, and H. Murakami, *Planta Med.* 62: 169–172 (1996).
6. H. Yanagihara, H. Minami, H. Tanaka, Y. Shoyama, and H. Murakami, *Anal. Chim. Acta* 335: 63–70 (1996).



Fraction Collection Devices

Gordon S. Hunter

Gilson, Inc., Middleton, Wisconsin, U.S.A.

Introduction

The growth of high-performance liquid chromatography (HPLC) has prompted significant interest in preparative liquid chromatography as a tool for purifying organic compounds in complex liquid mixtures. On any scale, preparative LC implies separation of target compounds and subsequent collection of the column eluent, containing the compounds, in appropriate vessels for their isolation. This frequently occurs in complex mixtures containing both major and minor peaks. Characterization of the isolated compound is then usually performed by complementary techniques such as mass spectroscopy (MS), nuclear magnetic resonance (NMR), or infrared (IR) spectroscopy.

Purposes and Uses

Fraction collectors are especially useful in applications involving unattended, overnight, and automated chromatographic purification schemes. If only several fractions are to be collected from the liquid chromatograph and only a few samples are to be purified, then the eluent from the column can sometimes be collected manually. However, a fraction collection device is recommended if the analyst has many samples to process and/or if there are many fractions to collect.

The goals of preparative HPLC are different compared to analytical and trace analyses. In analytical applications, the goal is to obtain quantitative and qualitative information about the sample. With preparative HPLC, however, the goal is to isolate and purify compounds from complex mixtures. Preparative liquid chromatography traditionally meant large flow rates, large-inner-diameter (i.d.) columns and relatively large column particles to isolate and purify milligram to gram quantities of compounds of interest. In recent years, however, preparative liquid chromatography has been "scaled down" to analytical (4.6 mm i.d.) and narrow-bore (≤ 2 mm i.d.) column proportions as biopharmaceutical and biomedical research focuses on trace analytes at the picogram level or lower.

Preparative liquid chromatography and fraction collectors are widely used to purify target compounds for applications found in many disciplines:

Pharmaceuticals. Determination of drug candidate/metabolite structure in discovery and development studies; end product and intermediate purification

Organic chemistry. Preparation of standards; purification of starting materials; identification of impurities in end products; determination of intermediate structures during organic synthesis

Biotechnology/biomedical. Identification of molecular structures in genetic engineering applications; end product and intermediate purification; isolation and purification of enzymes, proteins, nucleic acids, carbohydrates, lipids, and other biomolecules; polymerase chain reaction (PCR) product and monoclonal antibody purifications

Food/beverage. Additive purification; determination of intermediate structures during fermentation processes

Operational Considerations of Fraction Collectors in Liquid Chromatography

The functional requirements of fraction collectors have changed as liquid chromatography evolved from low-pressure (low-resolution) to high-pressure (high-resolution) techniques. This evolution was led by developments in column technologies and packing materials, and followed by adaptations to pumps, detectors, injectors, and fraction collectors. The following subsections briefly describe some of the key operational considerations of fraction collection devices.

Low-Pressure (Low-Resolution) Techniques

Classical low-pressure LC is a relatively simple technique developed in the 1950s, but still commonly used today by organic chemists and biochemists. It is very effective as a crude purification step, especially before preparative HPLC, to remove contaminants and inter-



ferences, even though it is slow and offers low resolution. For many laboratory studies using classical low-pressure LC, requirements are generally for simple time and drop mode fraction collectors. The entire chromatographic eluent is automatically collected by selecting equal fractions based on time per tube or drops per tube, as shown in Fig. 1.

If the elution time(s) of peaks of interest are known and reproducible, the user can program most microprocessor-based fraction collectors to automatically collect only the peaks of interest and discard the between-peak eluent or peaks of noninterest. This is a variable time window programming mode, also known as Time Program plus Time (or Drop) mode, and involves a sequence of time-based collection and drain steps, as shown in Fig. 2. Each collection step is commonly referred to as a collection time window. It conveniently allows the user to define time intervals during which the column eluent is either collected into fractions or discarded into waste. Each selected peak will be subfractionated by equal slices based on time counting or drop counting. Column void volumes, equilibration volumes, and peaks of no interest are discarded.

High-Pressure (High-Resolution) Techniques

Advances in column technology and small-particle packing materials ($\leq 15 \mu\text{m}$) have enabled small-scale

preparative chromatography using “analytical scale” HPLC columns, pumps, injectors, and detectors. However, the resultant high-resolution chromatograms are frequently very complex and require fraction collectors capable of “cutting” pure peaks of less than 20 s duration.

This has created a need for a new generation of flexible fraction collectors capable of sophisticated collection based on the detector output signal that corresponds to the target compound(s). This is sometimes known as peak detection and enables isolation of the purest part of each peak into a single vessel. When very high-purity levels are required, peaks of interest containing target compounds should not be contaminated by neighboring peaks or diluted with mobile phase, which would be the case if the collector were to collect equal fractions throughout the run based simply on time or drop counts (see Fig. 1). These high-purity requirements are usually found in small-scale laboratory studies where optimum purity of fractions (sometimes $\geq 99.9\%$) is critical.

Detection of chromatographic peaks by the fraction collector is determined by either calculation of a minimum baseline slope or by a user-specified millivolt threshold level of the detector's output. In the former case, sophisticated algorithms are used to calculate the baseline slope based on user input of peak width and peak sensitivity. An example of fraction collection based on the detector signal is shown

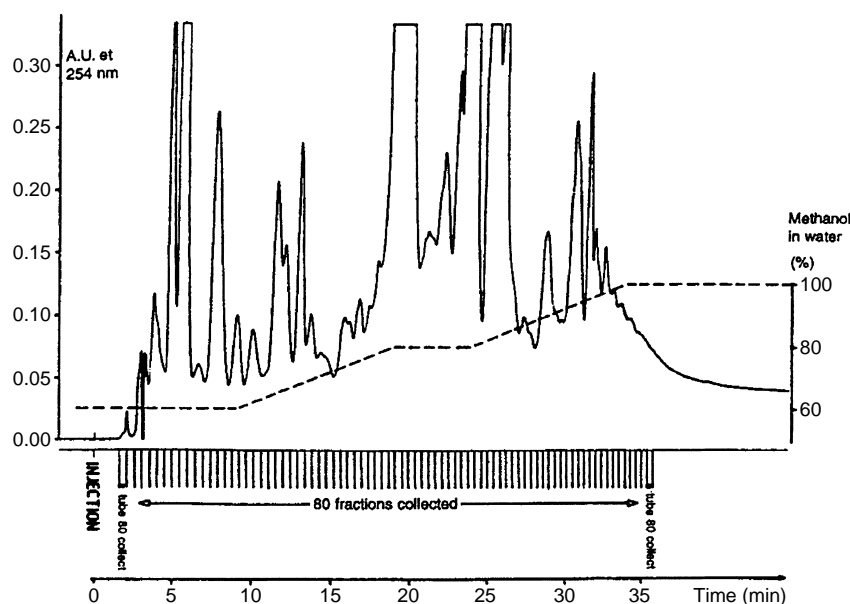


Fig. 1 Collection in Drop mode. The entire run is collected by selecting equal fractions based on drops per tube.

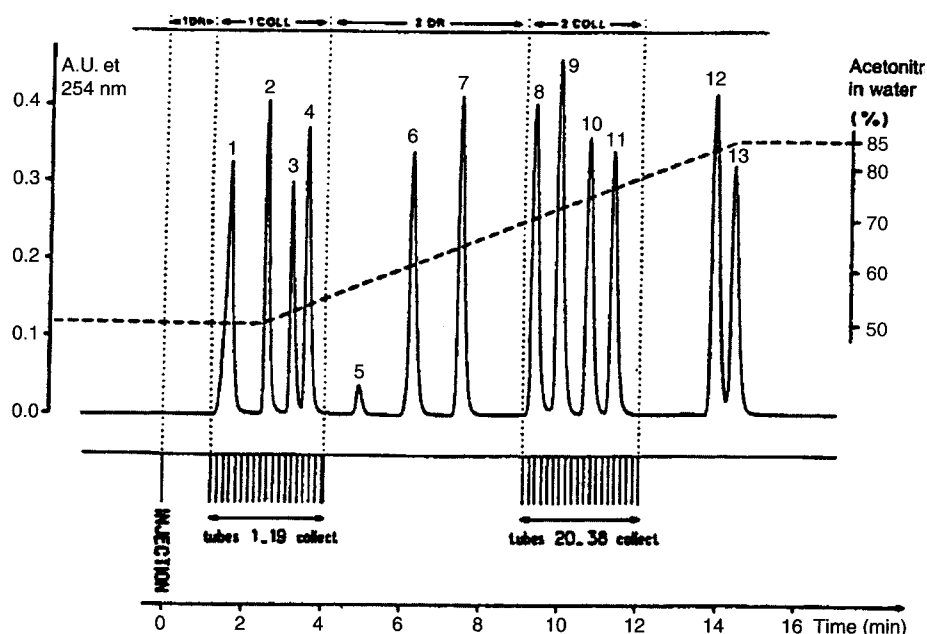


Fig. 2 Collection in Time Program plus Time mode. Two collection time windows are subfractionated into equivalent fractions based on time per tube.

in Fig. 3. Each fraction corresponds to a peak detected by the collector. Unwanted peaks, between-peak eluent, column void volumes, and equilibration volumes are discarded to waste. Because the chro-

matographer is not collecting the entire column effluent from beginning to end, there is no need to stop the system and change tubes or racks, thereby enabling automated, unattended operation.

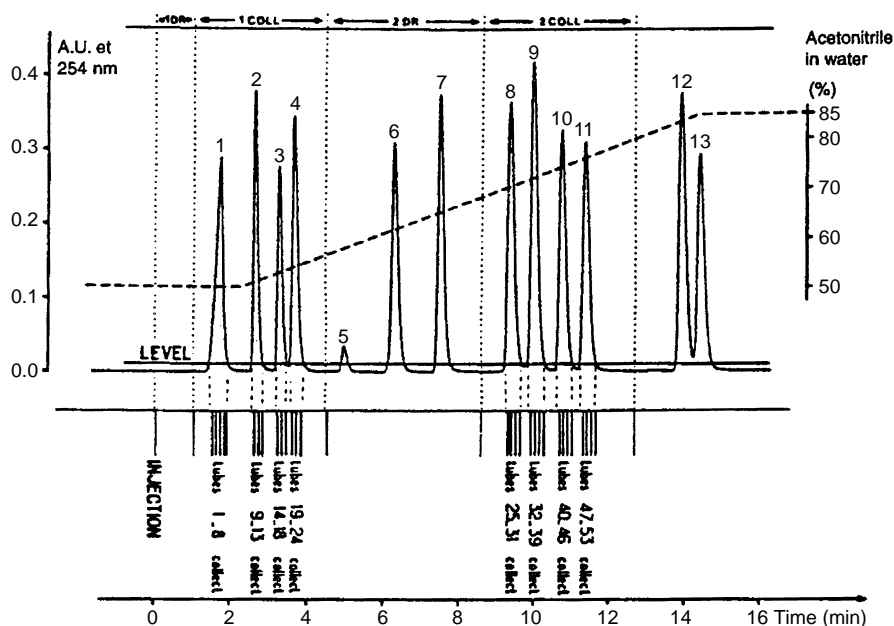


Fig. 3 Collection in Time Program plus Peak plus Time mode. This multimode protocol involves two collection time windows, peak detection (based on slope) within those time windows, and subfractionation of the peaks by time per tube.



Applications

In preparative HPLC, fraction collection is likely to be employed for two extreme applications: (a) the purification of one or a few major components or (b) the isolation of trace components or impurities in the presence of main components. The first problem is generally solved by the millivolt level (threshold) collection mode with time or drop “subfractionation” of each peak. A

slope-detecting peak collection mode with equal time slices is often the best solution to the second problem.

Suggested Further Reading

Katz, A., Eksteen, R., Schoenmakers, P., and Miller, N., Collection devices, in *Handbook of HPLC*, Marcel Dekker, Inc., New York, 1998, Chap. 19.



Frit-Inlet Asymmetrical Flow Field-Flow Fractionation

Myeong Hee Moon

Pusan National University, Pusan Korea

Introduction

Frit-inlet asymmetrical flow field-flow fractionation (FIA-FIFFF) [1–3] utilizes the frit-inlet injection technique, with an asymmetrical flow FFF channel which has one porous wall at the bottom and an upper wall that is replaced by a glass plate. In an asymmetrical flow FFF channel, channel flow is divided into two parts: axial flow for driving sample components toward a detector, and the cross-flow, which penetrates through the bottom of the channel wall [4,5]. Thus, the field (driving force of separation) is created by the movement of cross-flow, which is constantly lost through the porous wall of the channel bottom. FIA-FIFFF has been developed to utilize the stopless sample injection technique with the conventional asymmetrical channel by implementing an inlet frit nearby the channel inlet end and to reduce possible flow imperfections caused by the porous walls.

Discussion

The asymmetrical channel design in flow FFF has been shown to offer high-speed and more efficient separation for proteins and macromolecules than the conventional symmetrical channel. However, an asymmetrical channel requires a focusing–relaxation procedure for sample components to reach their equilibrium states before the separation begins. The focusing–relaxation procedure is achieved by two counterdirecting flow streams from both the channel inlet and outlet to a certain point slightly apart from the channel inlet end for a period of time. This is a necessary step equivalent to the stop-flow procedure as is normally used in a conventional symmetrical channel system. Although the stop-flow and the focusing–relaxation procedures are essential in each technique (symmetrical and asymmetrical channels, respectively), they are basically cumbersome in system operation due to the stoppage of flow with valve operations. In addition, they often cause baseline shifts during the conversion of flow. For these reasons, the frit-inlet injection technique, which can be an alternative to bypass those flow-halting pro-

cesses, is adapted to an asymmetrical flow FFF channel in order to take advantage of hydrodynamic relaxation of sample components.

The frit-inlet injection device was originally applied to the conventional symmetrical channel in order to bypass the stop-flow procedure [6]. However, the lowest axial flow rate that can be manipulated in a frit-inlet symmetrical system is limited, because the total axial flow rate becomes the sum of the injection flow rate and frit flow rate, and the incoming cross-flow penetrates through the bottom wall at the same rate. The relatively high axial flow rate in a symmetrical system needs a very high cross-flow rate in order to separate relatively low-retaining materials, such as proteins or low-molecular-weight components.

Compared to the limited choice in the selection of flow rate conditions, application of the frit-inlet injection technique to an asymmetrical flow FFF channel can be more flexible in allowing the selection of a low axial flow rate condition which is suitable for low-retaining materials without the need of using a very high cross-flow rates and for the reduction of injection amount resulting from the concentration effect.

In FIA-FIFFF, sample materials entering the channel are quickly driven toward the accumulation wall and are transported to their equilibrium positions by the compressing action of a rapidly flowing frit flow entering through the inlet frit. The schematic view of an FIA-FIFFF channel is shown in Fig. 1. In the relaxation segment of a FIA-FIFFF channel, the frit flow stream and the sample stream of relatively low speed will merge smoothly. During this process, sample materials are expected to be pushed below the inlet splitting plane formed by the compressing effect of frit flow, as illustrated in Fig. 1b. Thus, sample relaxation is achieved hydrodynamically in the relaxation segment (under the inlet frit region), and the sample components are continuously carried to the separation segment where the separation of sample components takes place. System operation requires only a simple one-step injection procedure, with no need for valve switching or interruption of flow. This is far simpler and more convenient than the operation of the con-



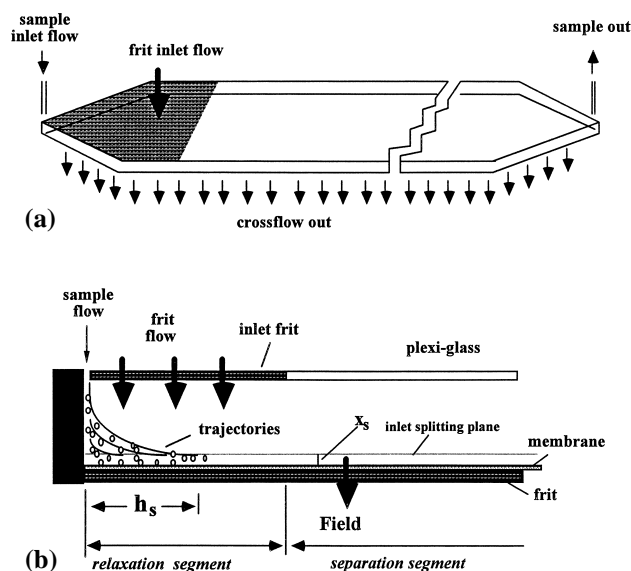


Fig. 1 Schematic view of an FIA-FIFFF channel.

ventional relaxation techniques, such as stop-flow and focusing-relaxation procedures.

In the first experimental work on FIA-FIFF [1], the system efficiency was studied by examining the effect of the ratio of injection flow rate to frit flow rate on hydrodynamic relaxation; the initial tests showed a possibility of using hydrodynamic relaxation in asymmetrical flow FFF with a number of polystyrene latex standards, in both normal and steric/hyperlayer modes of FFF. Normally, relaxational band broadening under hydrodynamic relaxation arises from a broadened starting band. The length of an initial sample band during hydrodynamic relaxation is dependent on flow rates as

$$h_s = \frac{\dot{V}_s}{\dot{V}_f} \frac{\dot{V}}{\dot{V}_c} L \quad (1)$$

where L is the channel length; \dot{V}_s , \dot{V}_f , \dot{V} , and \dot{V}_c represent the flow rates of the sample stream, frit stream, effective channel flow, and cross-flow, respectively. Equation (1) suggests that a small ratio of sample flow rate to frit flow rate, with a combined high cross-flow rate, is preferable in reducing h_s , leading to minimized relaxational band broadening.

Experimentally, the optimum ratio of \dot{V}_s/\dot{V}_f has been found to be about 0.03–0.05 for the separation of latex beads and for proteins.

Retention in the separation segment of the FIA-FIFFF channel is expected to be equivalent to that ob-

Frit-Inlet Asymmetrical Flow Field-Flow Fractionation

served in a conventional asymmetrical channel system, if complete hydrodynamic relaxation can be obtained. It will follow basic principles, as shown by the retention ratio, R , given by

$$R = \frac{t^0}{t_r} = 6\lambda \left[\coth \left(\frac{1}{2\lambda} - 2\lambda \right) \right] \quad \left(\text{where } \lambda = \frac{D}{w^2} \frac{V^0}{\dot{V}_c} \right) \quad (2)$$

where t^0 is the void time, t_r is the retention time, λ is the retention parameter, D is the diffusion coefficient, w is the channel thickness, and V^0 is the channel void volume. The void time in an FIA-FIFFF channel system is complicated to calculate, because sample flow and frit flow enter the channel simultaneously, and part of the merged flow exits through the accumulation wall. For this reason, channel flow velocity varies along the axial direction of channel. By considering these, the determination of void time can be represented as

$$t^0 = \frac{V^0 A_f / A_c}{\dot{V}_f - \dot{V}_c A_f / A_c} \ln \left(\frac{\dot{V}_s + \dot{V}_f - \dot{V}_c A_f / A_c}{\dot{V}_s} \right) + \frac{V^0}{\dot{V}_c} \ln \left(\frac{\dot{V}_s + \dot{V}_f - \dot{V}_c A_f / A_c}{\dot{V}_{out}} \right) \quad (3)$$

where \dot{V}_{out} is the channel outflow rate and A_f and A_c are the area of the inlet frit and the accumulation wall, respectively. Equation (3) represents the void time calculation in terms of volumetric flow rate and channel dimensions only; it is valid for any channel geometry, such as rectangular, trapezoidal, and even exponential design. Retention in FIA-FIFFF has been shown to follow the general principles of FFF with the confirmation of experimental work. It has also been found that the trapezoidal channel design provides a better resolving power for the separation of protein mixtures than a rectangular channel in FIA-FIFFF.

References

1. M. H. Moon, H. S. Kwon, and I. Park, *Anal. Chem.* 69: 1436 (1997).
2. M. H. Moon, H. S. Kwon, and I. Park, *J. Liquid Chromatogr. Related Technol.* 20: 2803 (1997).
3. M. H. Moon, P. Stephen Williams, and H. S. Kwon, *Anal. Chem.* 71: 2657 (1999).
4. A. Litzén and K.-G. Wahlund, *Anal. Chem.* 63: 1001 (1991).
5. A. Litzén, *Anal. Chem.* 65: 461 (1993).
6. J. C. Giddings, *Anal. Chem.* 57: 945 (1985).

Frontal Chromatography

Peter Sajonz

Merck Research Laboratories, Rahway, New Jersey, U.S.A.

Introduction

Frontal chromatography is a mode of chromatography in which the sample is introduced continuously into the column. The sample components migrate through the column at different velocities and eventually break through as a series of fronts. Only the least retained component exits the column in pure form and can, therefore, be isolated; all other sample components exit the column as mixed zones. The resulting chromatogram of a frontal chromatography experiment is generally referred to as a breakthrough curve, although the expression *frontal-gram* has also been used in the literature [1].

The exact shape of a breakthrough curve is mainly determined by the functional form of the underlying equilibrium isotherms of the sample components, but secondary factors such as diffusion and mass-transfer kinetics also have influence. The capacity of the column is an important parameter in frontal chromatography, because it determines when the column is saturated with the sample components and, therefore, is no longer able to adsorb more sample. The mixture then flows through the column with its original composition.

The Use of Frontal Chromatography

Frontal chromatography can also be called *adsorptive filtration* because it can be used for the purpose of filtration. The purification of gases and solvents are two classical applications of frontal chromatography. Another important use is the purification of proteins, where a frontal chromatography step is used in the initial purification procedure [2,3].

One of the most important applications of frontal chromatography is the determination of equilibrium adsorption isotherms. It was introduced for this purpose by Shay and Szekely and by James and Phillips [4,5]. The simplicity as well as the accuracy and precision of this method are reasons why the method is so popular today and why it is often preferred over other chromatographic methods [e.g., elution by characteristic points (ECP) or frontal analysis by characteristic points (FACP) [6,7]]. Frontal chromatography as a tool

for the determination of single-component adsorption isotherms will be discussed in the following section.

Frontal Chromatography for the Determination of Isotherms

Theory

First, the column is filled only with sample at concentration C_n ; then, a step injection is performed (i.e., sample with the concentration C_{n+1} is introduced into the column). This results in a breakthrough curve, as shown in Fig. 1. The amount adsorbed at the stationary phase Q_{n+1} can be calculated by

$$Q_{n+1} = q_{n+1}V_s = (C_{n+1} - C_n)(V_{R,n+1} - V_0) + q_nV_s$$

where q_n and q_{n+1} are the initial and final sample concentrations, respectively, in the stationary phase and C_n and C_{n+1} are the initial and final sample concentrations in the mobile phase, respectively. V_s is the volume of adsorbent in the column, V_0 is the holdup volume, and $V_{R,n+1}$ is the retention volume of the breakthrough curve. The retention volume is calculated from the area over the breakthrough curve:

$$V_R = \int_0^\infty \frac{(C_{n+1} - C) dV}{C_{n+1} - C_n}$$

The retention volume defined by the area method always gives the theoretically correct result for the amount adsorbed. In practice, it is, however, often easier and better to use the retention volume from half-height [i.e., at the concentration $(C_{n+1} + C_n)/2$] or the retention volume derived from the inflection point of the breakthrough curve. The reason for this is that the calculation of the area incorporates signal noise and it is very dependent on the integration limits. This is often a problem, especially when the mass transfer is slow, because, in this case, the plateau concentration C_{n+1} is only reached slowly and, therefore, systematic errors in the calculated area occur. It has been shown that the use of the retention volumes derived from the inflection point or the half-height gives satisfactory results. The half-height method is, however, easier to use and slightly more accurate than the inflection-point method [5].



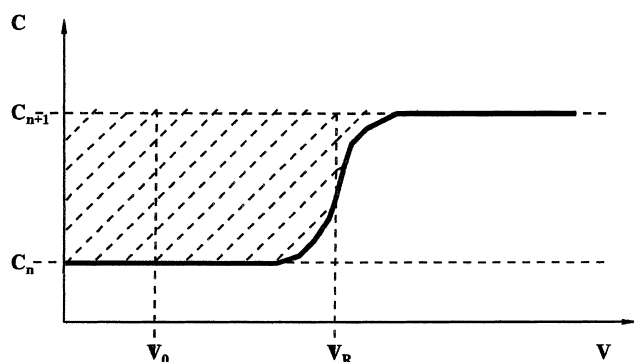


Fig. 1 Example of a frontal chromatography experiment; breakthrough curve of a single component.

It has to be noted that the half-height and inflection-point methods do not give reliable results if the isotherm is concave upward and ascending concentration steps are performed. The same is true for a convex upward isotherm and descending concentration steps. The reason for this is that, in these cases, a diffuse breakthrough profile is obtained and, consequently, errors are made in the accurate determination of the retention volumes when they are derived from the half-height or the inflection point. The diffuse profile can, however, be used for the determination of isotherms by the frontal analysis by characteristic points method (FACP).

Modes of Frontal Analysis

There are two possibilities for performing a frontal chromatography experiment for the purpose of the determination of equilibrium isotherms. The step-series method uses a series of steps starting from $C_n = 0$ to C_{n+1} . After each experiment, the column has to be reequilibrated and a new step injection with a different end concentration C_{n+1} can be performed. In the staircase method, a series of steps is performed in a single run with concentration steps from 0 to C_1 , C_1 to C_2 , ..., C_n to C_{n+1} . The column does not have to be reequilibrated after each step and, therefore, the staircase method is faster than the step-series method. Both modes of frontal analysis give very accurate isotherm results.

Determination of Multicomponent Isotherms by Frontal Analysis

It is possible to extend the frontal chromatography method for the measurement of binary and multicomponent isotherms. In this case, the profiles are characterized by successive elution of several steep fronts.

The use of these profiles for the determination of competitive isotherms in the binary case has been developed by Jacobsen et al. [8].

Combination of Frontal Analysis with Chromatographic Models

Frontal chromatography can be used in combination with chromatographic models to study mass-transfer and dispersion processes (e.g., the equilibrium dispersive or the transport model of chromatography [7]).

Constant Pattern, Self-Sharpening Effect, Shock-Layer Theory

Frontal chromatography generally requires the adsorption isotherm to be convex upward if the step injection is performed with ascending concentration (i.e., $C_{n+1} > C_n$) because, in this case, the profile of a breakthrough curve tends asymptotically toward a limit. After this constant profile has been reached, the profile migrates along the column without changing its shape. This state is called *constant pattern* [9]. This phenomenon arises because the self-sharpening effect associated with a convex isotherm is balanced by the dispersive effect of axial dispersion and a finite rate of mass-transfer kinetics. If the equilibrium adsorption isotherm is linear or concave upward, no constant pattern behavior is observed and the breakthrough curve spreads constantly during its migration through the column. This case is unfavorable. If the adsorption isotherm is concave upward, then a descending concentration step (i.e., $C_{n+1} < C_n$) leads to the formation of a constant pattern.

A very detailed study of the combined effects of axial dispersion and mass-transfer resistance under a constant pattern behavior has been conducted by Rhee and Amundson [10]. They used the *shock-layer* theory. The shock layer is defined as a zone of a breakthrough curve where a specific concentration change occurs (i.e., a concentration change from 10% to 90%). The study of the shock-layer thickness is a new approach to the study of column performance in non-linear chromatography. The optimum velocity for minimum shock-layer thickness (SLT) can be quite different from the optimum velocity for the height equivalent to a theoretical plate (HETP) [9].

Instrumentation

There are many possibilities for performing frontal chromatography experiments. In general, standard

chromatographic equipment can be used. The preparation of a series of solutions of known concentration can be easily accomplished by using a chromatograph with a gradient delivery system applied as a mobile-phase mixer. If this system is not available, then the solutions have to be prepared manually. Two pumps can be used to perform the step injections or a single pump with a gradient delivery system. An injector having a sufficient large loop can also be used. Even a single pump without gradient delivery system can be used. In this case, the step injection has to be made by manually switching the solvent inlet line to the prepared sample reservoir. The choice of the system is dependent on the application. For fast and accurate measurements of adsorption isotherms, a multisolvent gradient system with two pumps and a high-pressure mixer is a very good choice.

References

1. J. Parcher, *Adv. Chromatogr.* 16: 151 (1978).
2. F. Antia and Cs. Horváth, *Ber. Bunsenges. Phys. Chem.* 93: 968 (1989).
3. A. Lee, Aliao, and Cs. Horváth, *J. Chromatogr.* 443: 31 (1988).
4. D. James and C. Phillips, *J. Chem. Soc.*, 1066 (1954).
5. G. Shay and G. Szekely, *Acta Chim. Hung.* 5: 167 (1954).
6. H. Guan, B. Stanley, and G. Guiochon, *J. Chromatogr. A* 659: 27 (1994).
7. P. Sajonz, Ph.D. thesis, University Saarbrücken, Germany, 1996.
8. J. Jacobsen, J. Frenz, and Cs. Horváth, *Ind. Eng. Chem. Res.* 26: 43 (1987).
9. G. Guiochon, S. Golshan-Shirazi, and A. Katti, *Fundamentals of Preparative and Nonlinear Chromatography*, Academic Press, Boston, 1994.
10. H. Rhee and N. Amundson, *Chem. Engng. Sci.* 27: 199 (1972).



Fronting of Chromatographic Peaks: Causes

Ioannis N. Papadoyannis

Anastasia Zotou

Aristotle University of Thessaloniki, Thessaloniki, Greece

Introduction

Peaks with strange shapes represent one of the most vexing problems that can arise in a chromatographic laboratory. Fronting of peaks is a condition in which the front of a peak is less steep than the rear relative to the baseline. This condition results from nonideal equilibria in the chromatographic process.

Discussion

Fronting peaks, as well as tailing or other misshaped peaks, can be hard to quantitate. Some data systems have difficulty in measuring peak size accurately. As a result, the precision and/or reliability of assay methods involving fronting or other misshaped peaks is often poor when compared to good chromatography. There are a number of different causes of peak fronting, and discovering why peaks are thus misshaped and then fixing the problem can be a difficult undertaking. Fortunately, there is a systematic approach based on logical analysis plus practical fixes that have now been documented in numerous laboratories.

Fronting peaks are less commonly encountered in liquid chromatography (LC), but they are readily distinguished from other peak-shape problems. Fronting peaks are the opposite of tailing peaks. Whereas tailing peaks suggest that sample retention decreases with increasing sample size or concentration, fronting peaks suggest the opposite: retention increases with larger samples. In both cases, a decrease in sample size may eliminate peak distortion. However, this is often not practical, because some minimum sample size is required for good detectability. In the case of tailing peaks, it is believed that peak distortion often arises because large samples use up some part of the stationary phase. However, the cause of fronting peaks is seldom fully understood.

Ion-pair chromatography (IPC) is more susceptible to peak fronting than other modes in LC. *Column temperature* problems can cause fronting peaks in IPC. Figure 1 shows the separation of an antibiotic amine at ambient temperature. Repeating the

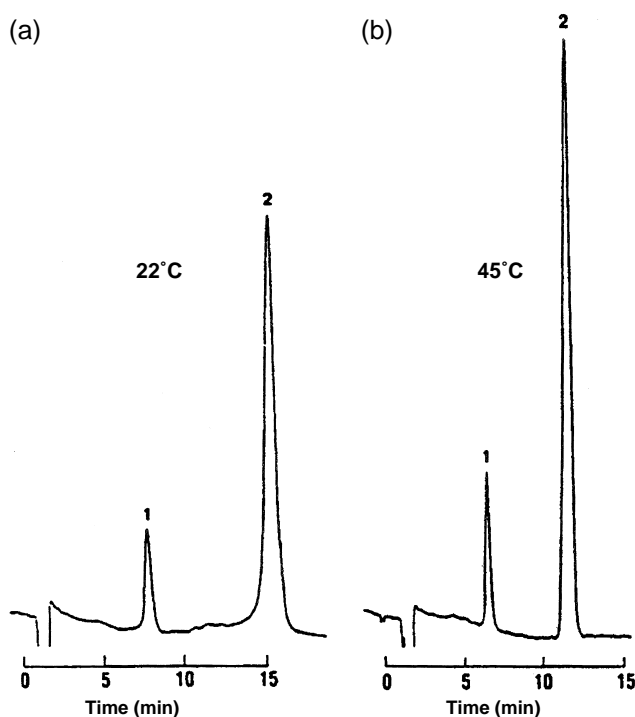


Fig. 1 Peak fronting in IPC as a function of separation temperature. Column: Zorbax C₈; mobile phase: 10 mM sodium dodecyl sulfate and 150 mM ammonium phosphate in 33% acetonitrile; pH: 6.0; flow rate: 2.0 mL/min; temperature: (a) = 22°C and (b) = 45°C. Peaks: 1 = lincomycin B; 2 = lincomycin A. (Reprinted from Ref. 1 with permission from Elsevier Science.)

separation at 45°C eliminated the fronting problem. Some studies have shown peak fronting in IPC that can be corrected by operating at a higher column temperature, whereas some other separations are best carried out at lower temperatures. The reason for this peculiar peak-shape behavior is unclear, but it may be related to the presence of reagent micelles in the mobile phase for some experimental IPC conditions. Generally, it is good practice to run ion-pair separations under thermostatted conditions, because relative retention tends to vary with temperature in IPC. Usually, narrower bands and better sep-



aration results when temperatures of 40–50°C are used for IPC.

The use of a *sample solvent other than the mobile phase* is another cause of fronting peaks in IPC. In this case, the sample should only be injected as a solution in the mobile phase. No more than 25–50 μl of sample should be injected, if possible.

Silanol effects can adversely alter peak shape in IPC, just as in reversed-phase separations. Therefore, when separating basic (cationic) compounds, the column and mobile phase should be chosen bearing this in mind. When ion-pair reagents are used, however, silanol effects are often less important. The reason is that an anionic (acidic) reagent confers an additional negative charge on the column packing and this reduces the relative importance of sample retention by ion exchange with silanol groups. Similarly, cationic (basic) reagents are quite effective at blocking silanols because of the strong interaction between reagent and ionized silanol groups.

Still another cause of peak fronting is for the case of *anionic (acidic) sample molecules separated with higher-pH mobile phases*. For silica-based packings, the packing has an increasingly negative charge as the

pH increases, and this results in the repulsion of anionic sample molecules from the pores of the packing. With larger sample sizes, however, this effect is overcome by the corresponding increase in ionic strength, caused by the sample. A remedy for this problem is to increase the ionic strength of the mobile phase, by increasing the mobile-phase buffer concentration to the range of 25–100 mM. It should be mentioned here that ionic or ionizable samples should never be separated with unbuffered mobile phases.

Finally, *column voids* and *blocked frits* can also cause peak fronting.

Suggested Further Reading

- Asmus, P. A., J. B. Landis, and C. L. Vila, *J. Chromatogr.* 264(2): 241 (1983).
- Bidlingmeyer, B. A., *Practical HPLC Methodology and Applications*, John Wiley & Sons, New York, 1992, p. 20.
- Dolan, J. W. and L. R. Snyder. *Troubleshooting LC Systems*, Humana Press, Totowa, NJ, 1989, pp. 400–401.
- Sadek, P. C., P. W. Carr, and L. D. Bowers, *LC, Liq. Chromatogr. HPLC Mag.* 3: 590 (1985).



Gas Chromatography System Instrumentation

Mochammad Yuwono

Gunawan Indrayanto

Airlangga University, Surabaya, Indonesia

INTRODUCTION

Gas chromatography (GC) was first described by Martin and James in 1952. It has become one of the most frequently used separation techniques for the analysis of gases and volatile liquids and solids. An important breakthrough in GC was the introduction of the open tubular column by Golay in 1958 and the adoption of fused silica capillary columns by Dandeneau and Zerenner in 1979.

Today, using of the capillary columns can solve many kinds of analytical problems, such as isomer separation and analysis of complex mixtures of natural products and biologicals.

The gas chromatograph involves volatilization of the sample in a heated inlet port (injector), separation of the component mixtures in a column, and detection of each component by a detector.

GAS CHROMATOGRAPHY SYSTEM INSTRUMENTATION

Gas chromatography, first described by James and Martin^[1] in 1952, has become one of the most frequently used separation technique for the analysis of gases, volatile liquids, and solids. The major breakthrough of GC was the introduction of the open tubular column by Golay and Desty^[2] in 1958 and the adoption of fused silica capillary columns by Dandeneau and Zerenner^[3] in 1979. Today, using of the capillary columns can solve many analytical problems, such as isomeric separation and analysis of complex mixtures of natural products and biological samples.

The basic principle of a gas chromatograph involves volatilization of the sample in a heated inlet port (injector), separation of the component mixtures in a column, and detection of each component by a detector. Although the basic components remain the same, some improvements in gas chromatograph appeared in the commercial marketplace. Gas chromatography with electronic integrators and computer-based data processing systems became common in 1970s, whereas in the 1980s, a computer was introduced to control all GC parameters

automatically, such as column temperature, flow rates, inlet pressure, and sample injection, and to evaluate the data obtained. The automated equipment can be operated unattended overnight.^[4,5]

Combinations of highly efficient separation columns, with specific or selective detectors, such as electron capture detector (ECD), GC-mass spectrometer (MS), and GC-Fourier transform infrared (FTIR) detector, make GC a more favorable technique. Multidimensional GC systems, which contain at least two columns operated in series, have also proved to be a powerful tool in the analytical chemistry of complex mixtures.

The dramatic advance in GC instrumentation is the introduction of portable gas chromatographs, which have been developed during 1990s to provide a field-based analysis. Recently, the micro high-speed GC portable has also appeared to carry out the analysis up to 10 times faster than conventional laboratory GCs.^[6–8]

The GC system (Fig. 1) consists of a carrier gas supply system, an inlet to deliver sample to a column, the column where the separations occur, an oven as a thermostat for the column, a detector to register the presence of a chemical in the column effluent, and a data system to record, display, and evaluate the chromatogram.

CARRIER GAS

The carrier gas that is used as the mobile phase transfers the sample from the injector, through the column, and into the detector. For a laboratory gas chromatograph, the carrier gas is usually obtained from a commercial pressurized gas cylinder equipped with a two-stage regulator for coarse and fine flow control. In most instruments, provision is made for secondary fine-tuning of pressure and gas flow. In 1990, electronic pressure control was developed, which allows operation at constant pressure, constant flow, and pressure-programming modes. The gas flow can be read electronically on the instrument panel or measured using a soap-bubble flow meter at the outlet of the column. The carrier gas flow is directed through a sieve trap, or a series of traps to remove the moisture, organic matter, and oxygen, and then through frits to filter off any particulate matter.^[9] It is also

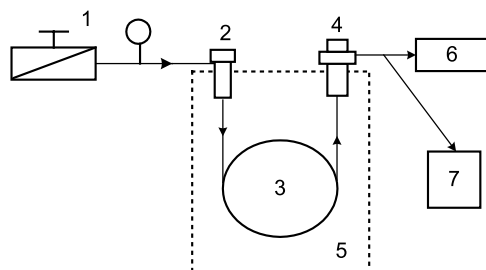


Fig. 1 Gas chromatography system schematic.

suggested to use copper tubing for the connection of the gas cylinder to the gas chromatographs. Polymer tubing should be avoided because the oxygen from the atmosphere can often permeate the tubing walls. The oxygen in the gas stream may cause degradation of some column stationary phases at elevated operating temperatures, thereby producing unstable baselines with the electron-capture detector and shortening filament lifetime for the thermal conductivity detector. To minimize contamination, high purity carrier gases are used, combined with additional chemical and/or catalytic gas purifying devices. The gas chromatograph may have thermostatically controlled pneumatics to prevent drift, in which pressure regulators, flow controllers, and additional gas purifying traps and filters are housed. The carrier gas must be inert so that it reacts neither with the sample nor with the stationary phase at the operating temperature.^[9] The choice of carrier gas requires consideration of the detector used, the separation problem to be solved, and the purity of the gases available. A further consideration in the selection of carrier gas is its availability and its cost. In practice, the choice of carrier gas will determine the efficiency of the GC system because the height equivalent to a theoretical plate depends on solute diffusivity in the carrier. The influence of the mobile-phase velocity on column efficiency and practical consequences of the carrier gas selection in capillary GC have been described in previous publications.^[9,10] Normally, a compromise between inertness, efficiency, and operating cost make nitrogen or helium the most common GC carrier gases. The carrier gas flow can be determined by either linear velocity, expressed in cm sec^{-1} , or volumetric flow rate, expressed in mL min^{-1} . The linear velocity is independent of the column diameter, whereas the flow rate is dependent on the column diameter. For capillary columns, makeup gas is added at the column exit to obtain a total gas flow of $30\text{--}40 \text{ mL min}^{-1}$ into the detector; it can be the same gas as the carrier gas or a different gas, depending on the type of detector being used.

SAMPLE INLET SYSTEMS

Sample introduction into the gas chromatograph is the first stage in the chromatographic process. It is of primary importance, especially in capillary GC, because its efficiency is reflected in the overall efficiency of the separation procedure and the quantitative results. The basic prerequisite of the sample injection system is that the sample should be introduced into the column as a narrow band, ideally with maintenance of constant pressure and flow. The specially designed inlet should be hot enough to flash-evaporate the sample and large enough in volume to allow the sample vapor to expand without blowing back through the septum. Care must be taken not to overheat the injector because the injection cell or the sample may decompose. The sample must be gaseous or an easily vaporized liquid or solid. Most organic compounds may be introduced onto the column in the form of a liquid sample, either as the neat compound or, in the case of a solid, as a solution. When the dilution of the solid sample would be undesirable, the solid may be encapsulated in glass capillaries and mechanically pushed into the heated injection block and crushed.^[10,11]

For injecting gases and vapors, gas-tight syringes with Teflon-tipped plungers and syringe barrels are available. Many analysts favor using gas syringes for gas samples; however, the introduction of accurately measured volumes of gases remains a problem. In the alternative method, gas samples can be introduced onto a column using rotary gas switching valves, which generally consist of a rotating polymeric core, encased in a stainless-steel body. For repetitive or periodic injection of a large number of the same or different samples, auto samplers may be used.^[10,12] The sample volume for analytical work depends on the dimensions of the column and on the sensitivity of the detector. For a packed column, sample size ranges from tenths of $1 \mu\text{L}$ up to $20 \mu\text{L}$. Capillary columns need much less sample ($0.01\text{--}1 \mu\text{L}$). The most commonly used silicone-rubber septa may contain impurities that may bleed into the column above a certain temperature, resulting in unsteady baseline and ghost peaks. Recently, various kinds of septa have become available which can be used at very high temperatures.^[13]

Packed and Open Tubular Column Inlet

Because of the variety of columns and samples that can be analyzed by GC, several injection techniques have been developed. The packed inlet system is designed mainly for packed and wide-bore columns. However, an adapter can



be used to enable capillary columns to be used. When injection is carried out in the on-column mode, glass wool can be used for packing the injector. For capillary GC, split technique is most common, which is used for high concentration samples. This technique allows injection of samples virtually independent of the selection of solvent, at any column temperature, with little risk of band broadening or disturbing solvent effects. The splitless technique, on the other hand, is used for trace level analysis. The so-called cold injection techniques (on-column, temperature programmed vaporization, cooled needle split) have also been recently developed.^[4,14,15]

Pyrolysis Gas Chromatography

Pyrolysis involves the thermal decomposition, degradation, or cracking of a large molecule into smaller fragments. Pyrolysis GC is an excellent technique for identifying certain types of compounds which cannot be analyzed by derivatization, e.g., polymers. The pyrolysis temperature is typically between 400°C and 1000°C. A number of analytical pyrolyzers have been introduced and are commercially available. The devices consist of platinum resistively heated and Curie point pyrolyzers. The carrier gas is directed through the system, and the platinum wire is heated to a certain temperature. The material decomposes, and the fragmentation products are analyzed.^[16,17]

Headspace Analysis

Headspace analysis is an excellent technique for gas chromatography to analyze volatile samples in which the matrix is of no interest. It is readily applied to many analytical problems, such as monitoring of volatiles in soil and water, determination of monomers in polymers, aromas in food and beverages, etc. A variety of headspace auto samplers are commercially available, based on the principle of static or dynamic headspace. In static headspace, the sample is transferred to a headspace vial that is sealed and placed in a thermostat to drive the desirable component into the headspace sampling. An aliquot of the vapor phase is introduced into the GC system via a gas-tight syringe or a sample loop of a gas-sampling valve. Static headspace implies that the sample is taken from a single-phase equilibrium. To increase the detectability, dynamic headspace analysis has been developed. Driving the headspace out of the vial via an inert gas continuously displaces the phase equilibrium. A detailed discussion of headspace GC is reported in the previous work.^[18]

Solid-Phase Microextraction

Solid-phase microextraction, first reported by Belardi and Pawliszyn in 1989, is an alternative sampling technique. The method has the advantages of convenience and simplicity, and it does not release environmentally polluting organic solvents into the atmosphere. The method is based on the extraction of analytes directly from liquid samples or from headspace of the samples onto a polymer- or adsorbent-coated fused silica fiber. After equilibration, the fiber is then removed and injected onto the gas chromatograph.^[19-22]

Purge-and-Trap Methods

Purge and trap samplers have been developed for analysis of nonpolar and medium-polarity pollutants in water samples. The commercially available systems are all based on the same principle. Helium is purged through the sample that is contained in a sealed system, and the volatiles are swept continuously through an adsorbent trap where they are concentrated. After a selected time, purging is stopped, the carrier gas is directed through the trap via a six-way valve, and the trap is heated rapidly to desorb the solutes.^[4,9]

OVEN

The column is ordinarily housed in a thermostatically controlled oven, which is equipped with fans to ensure a uniform temperature. The column temperature should not be affected by changes in the detector, injector, and ambient temperatures. Temperature fluctuations in column ovens can decrease the accuracy of the measured retention times and may also cause the peak splitting effect. For conventional ovens, the oven wall is well insulated using a wire coil of high thermal capacity, which is able to radiate heat into the inner volume of the oven. The characteristics of a more efficient method can accurately control the temperature of a column and allow the operator to change the temperature conveniently and rapidly for temperature programming. It is designed by suspending the column in an insulated air oven through which the air circulated at high velocity by means of fans or pumps. Most commercial instruments employ this design and allow for the adjustment and control of temperature between 50°C and 450°C. Subambient temperature operation would normally require a cryogenic cooling system using liquid nitrogen or carbon dioxide.^[4,9,10]



DETECTOR

The detector in a gas chromatograph senses the differences in the composition of the effluent gases from the column and converts the column's separation process into an electrical signal, which is recorded. There are many detectors that can be used in gas chromatography, and each detector gives a different type of selectivity. An excellent discussion and review on developments of GC detectors has been published.^[23]

Detectors may be classified on the basis of selectivity. A universal detector responds to all compounds in the mobile phase except carrier gas. A selective detector responds only to a related group of substances, and a specific detector responds to a single chemical compound. Most common GC detectors fall into the selective designation. Examples include flame ionization detector (FID), ECD, flame photometric detector (FPD), and thermoionic ionization detector. The common GC detector that has a truly universal response is the thermal conductivity detector (TCD). Mass spectrometer is another commercial detector with either universal or quasi-universal response capabilities.

Detectors can also be grouped into concentration-dependent detectors and mass-flow-dependent detectors. Detectors whose responses are related to the concentration of solute in the detector cell, and do not destroy the sample, are called concentration-dependent detectors, whereas detectors whose response is related to the rate at which solute molecules enter the detector are called mass-flow-dependent detectors. Typical concentration-dependent detectors are TCD and GC-FTIR. Important mass-flow-dependent detectors are the FID, thermoionic detector for N and P (N-, P-FID), flame photometric detector for S and P (FPD), ECD, and selected ion monitoring MS detector.

The FID is one of the most widely used GC detectors. The detection principle is based on the change in the electric conductivity of a hydrogen flame in an electric field when fed by organic compound(s). The resulting current is then directed into a high impedance operational amplifier for measurement. The FID is sensitive to all compounds which contain C-C or C-H linkages and considerably less sensitive up to insensitive to certain functional groups of organic compounds, such as alcohol, amine, carbonyl, and halogen. In addition, the detector is also insensitive toward noncombustible gases such as H₂O, CO₂, SO₂, and NO. A TCD, which was one of the earliest detectors for GC, is based on changes in the thermal conductivity of the gas stream caused by the presence of analyte molecules. This device is sometimes called a katharometer. Because the TCD reacts nonspecifically, it can be used universally for the detection of either organic or inorganic substances. In the ECD, the

column effluent passes over a beta-emitter, such as nickel-63 or tritium. The electrons from emitter bombard the carrier gas (nitrogen), giving rise to ions and a burst of electrons. In the absence of an analyte, the ionization process yields a constant standing current. However, this background current decreases in the presence of organic compounds that can capture electrons. The applications of the ECD illustrate the advantages of a highly sensitive special detector toward molecules that contain electro-negative functional groups such as halogens, peroxide, quinines, or nitro groups.^[22-24]

GAS CHROMATOGRAPHY DATA SYSTEM

The GC data system performs the tasks of recording, handling, evaluation, and documentation of the chromatogram. In a modern gas chromatographic system, these can be performed by means of a computer with specialized software. Nowadays, software for calculating the quantitative results and for the method validation is available.^[4]

CONCLUSION

Since the introduction of GC, the basic parts of a gas chromatograph have been unchanged in function and purpose, even though the improvement has been occurring in design and materials. One area of dramatic advance in GC instrumentation was the introduction of the open tubular columns. Consequently, most GC analyses in practice are performed in capillary columns that show the separation with high efficiencies and high resolution. The developments of GC instrumentation are occurring with sample handling techniques and refinements of detectors. The dramatic advance in GC instrumentation is the development of a small, high-speed, and portable gas chromatograph to provide a field-based analysis.

REFERENCES

1. James, A.T.; Martin, A.J.P. Gas-liquid partition chromatography: The separation and micro-estimation of volatile fatty acids from formic acid to dodecanoic acid. *Biochem. J.* **1952**, *50*, 679.
2. Golay, M.J.E.; Desty, D. *Gas Chromatography*; Butterworths: London, 1958.
3. Dandeneau, R.D.; Zerenner, E.H. *J. High Res. Chromatogr.* **1979**, *2*, 351.
4. Schomburg, G. *Gas Chromatography, A Practical Course*; VCH Verlagsgesellschaft: Weinheim, 1990.
5. Poole, C.F.; Poole, S.K. *Chromatography Today*; Elsevier: Amsterdam, 1991.
6. Eiceman, G.A.; Gardea-Torresdey, J.; Overton, E.; Carney,



- K.; Dorman, F. Gas chromatography. *Anal. Chem.* **2002**, 74, 2771–2780.
7. See <http://www.agilent.com/about/newsroom/pesrel/2002/30sep2002b.html>.
8. See <http://www.hnu.com/fpi/gc311.htm>.
9. Sandra, J.F. Gas Chromatography. In *Ullmann's Encyclopedia of Industrial Chemistry*; Wiley-VCH Verlag GmbH: Weinheim, 2002.
10. Ravindranath, B. *Principles and Practice of Chromatography*; Ellis Horwood Limited: Chichester, UK, 1989.
11. Sandra, P. *Sample Introduction in Capillary Gas Chromatography*; Hüthig Verlag: Heidelberg, 1985.
12. Grob, K.; Neukom, H.P., Jr. The influence of syringe needle on the precision and accuracy of vaporizing GC injections. *J. High Res. Chrom. Comm.* **1979**, 2, 15–21.
13. Olsavicky, V.M. A comparison of high temperature septa for gas chromatography. *J. Chromatogr. Sci.* **1978**, 16, 197–200.
14. Grob, K. *Classical Split and Splitless Injection in Capillary GC*; Hüthig Verlag: Heidelberg, 1986.
15. Grob, K. *On Column Injection in Capillary GC*; Hüthig Verlag: Heidelberg, 1987.
16. Wang, F.C.Y.; Bursleson, A.D. Development of pyrolysis fast gas chromatography for analysis of synthetic polymers. *J. Chromatogr. A* **1999**, 833 (1), 111–119.
17. Haken, J.K. Pyrolysis gas chromatography of synthetic polymers: A bibliography. *J. Chromatogr. A* **1998**, 825 (2), 171–187.
18. Joffe, B.V.; Vitenberg, A.G. *Headspace Analysis and Related Methods in Gas Chromatography*; John Wiley: New York, 1984.
19. See http://gc.discussing.info/gs/r_hs-gs/microextraction.html (accessed 12/2/2002).
20. Scarlata, C.J.; Ebeler, S.E. Headspace solid-phase microextraction for the analysis of dimethyl sulfide in beer. *J. Agric. Food Chem.* **1999**, 47 (7), 2505–2508.
21. Mills, G.A.; Walker, V.; Mughal, H. Quantitative determination of trimethylamine in urine by solid-phase microextraction and gas chromatography mass spectrometry. *J. Chromatogr. B* **1999**, 723 (1–2), 281–285.
22. Pinho, O.; Ferreira, I.M.P.L.V.O.; Ferreira, M.A. Solid-phase microextraction in combination with GC/MS for quantification of the major volatile free fatty acids in ewe cheese. *Anal. Chem.* **2002**, 74, 5199–5204.
23. Buffington, R.; Wilson, M.K. *Detectors for Gas Chromatography—A Practical Primer*; Hewlett-Packard Corporation, 1987. Part No. 5958-9433.
24. *Detectors for Capillary Chromatography*; Hill, H.H., McMinn, D.G., Eds.; J. Wiley & Sons: New York, 1992.



Gas Chromatography–Mass Spectrometry Systems

Raymond P.W. Scott

Scientific Detectors Ltd., Banbury, Oxfordshire, England

Introduction

Despite the speed and accuracy of contemporary analytical techniques, the use of more than one, separately and in sequence, is still very time-consuming. To reduce the analysis time, many techniques are operated concurrently, so that two or more analytical procedures can be carried out simultaneously. The tandem use of two different instruments can increase the analytical efficiency, but due to unpredictable interactions between one technique and the other, the combination can be quite difficult in practice. These difficulties become exacerbated if optimum performance is required from both instruments. The mass spectrometer was a natural choice for the early tandem systems to be developed with the gas chromatograph, as it could easily accept samples present as a vapor in a permanent gas.

Background Information

The first gas chromatography–mass spectrometry (GC–MS) system was reported by Holmes and Morrell in 1957, only 4 years after the first description of GC by James and Martin in 1953. The column eluent was split and passed directly to the mass spectrometer. Initially, only packed GC columns were available and thus the major problem encountered was the disposal of the relatively high flow of carrier gas from the chromatograph (~ 25 mL/min or more). These high flow rates were in direct conflict with the relatively low pumping rate of the MS vacuum system. This problem was solved either by the use of an eluent split system or by employing a vapor concentrator. A number of concentrating devices were developed (e.g., the jet concentrator invented by Ryhage and the helium diffuser developed by Biemann).

The jet concentrator consisted of a succession of jets that were aligned in series but separated from each other by carefully adjusted gaps. The helium diffused away in the gap between the jets and was removed by appropriate vacuum pumps. In contrast, the solute vapor, having greater momentum, continued into the next jet and, finally, into the mass spectrometer. The

concentration factor was about an order of magnitude and the sample recovery could be in excess of 25%.

The Biemann concentrator consisted of a heated glass jacket surrounding a sintered glass tube. The eluent from the chromatograph passed directly through the sintered glass tube and the helium diffused radially through the porous walls and was continuously pumped away. The helium stream enriched with solute vapor passed into the mass spectrometer. Solute concentration and sample recovery were similar to the Ryhage device, but the apparatus was bulkier although somewhat easier to operate. An alternative system employed a length of porous polytetrafluoroethylene (PTFE) tube, as opposed to one of sintered glass, but otherwise functioned in the same manner.

The introduction of the open-tubular columns eliminated the need for concentrating devices as the mass spectrometer pumping system could cope with the entire column eluent. Consequently, the column eluent could be passed directly into the mass spectrometer and the total sample can enter the ionization source. The first mass spectrometer used in a GC–MS tandem system was a rapid-scanning magnetic sector instrument that easily provided a resolution of one mass unit. Contemporary mass spectrometers have vastly improved resolution and the most advanced system (involving the triple quadrupole mass spectrometer) gives high in-line sensitivity, selectivity, and resolution.

Ionization Techniques for GC–MS

There are a number of ionization processes that are used, probably the most important being electron-impact ionization. Electron-impact ionization is a harsh method of ionization and produces a range of molecular fragments that can help to elucidate the structure of the molecule. Nevertheless, although molecular ions are usually produced that are important for structure elucidation, sometimes only small fragments of the molecule are observed, with no molecular ion invoking the use of alternative ionizing procedures. A diagram showing the configuration of an electron-impact ion source is shown in Fig. 1. Electrons, generated by a



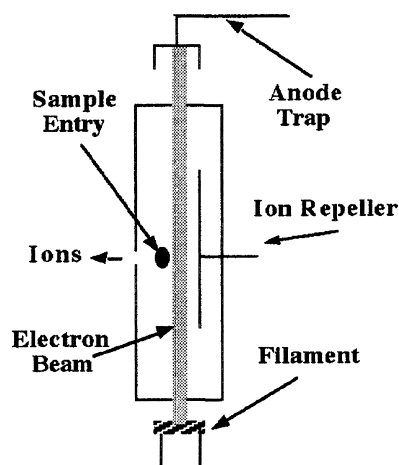
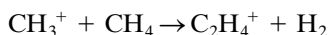
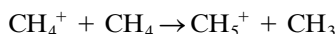
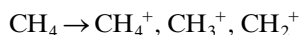


Fig. 1 An electron-impact ionization source: (a) Reagent gas methane; (b) reagent gas isobutane.

heated filament, pass across the ion source to an anode trap. The sample vapor is introduced in the center of the source and the solute molecules drift, by diffusion, into the path of the electron beam. Collision with the electrons produce molecular ions and ionized molecular fragments, the size of which is determined by the energy of the electrons. The electrons are generated by thermal emission from a heated tungsten or rhenium filament and accelerated by an appropriate potential to the anode trap. The magnitude of the collection potential may range from 5 to 100 V, depending on the electrode geometry and the ionization potential of the substances being ionized. The ions that are produced are driven by a potential applied to the ion-repeller electrode into the accelerating region of the mass spectrometer.

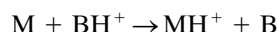
Unfortunately, with electron-impact ionization, there is a frequent absence of a molecular ion in the mass spectrum, which makes identification uncertain and complicates structure elucidation. One solution is to employ chemical ionization. If an excess of an appropriate reagent gas is fed into an electron-impact source, an entirely different type of ionization takes place. As the reagent gas is in excess, the reagent molecules are preferentially ionized and the reagent ions then collide with the sample molecules and produce sample + reagent ions or, in some cases, protonated ions. In this type of ionization, very little fragmentation takes place and parent ions + a proton or + a molecule of the reagent gas are produced. Little modification to the normal electron impact source is required and an additional conduit to supply the reagent gas is all that is necessary.

Chemical ionization was first observed by Munson and Field, who introduced it as an ionization procedure in 1966. A common reagent gas is methane and the partial pressure of the reagent gas is arranged to be about two orders of magnitude greater than that of the sample. The process is gentle and the energy of the most reactive reagent ions never exceeds 5 eV. Consequently, there is little fragmentation, and the most abundant ion usually has a m/z value close to that of the singly-charged molecular ion. The spectrum produced depends strongly on the nature of the reagent ion; thus, different structural information can be obtained by choosing different reagent gases. This adds another degree of freedom in the operation of the mass spectrometer. Using methane as the reagent ion, the following reagent ions can be produced:

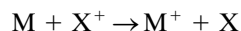


Other reactions can occur that are not useful for ionization but, in general, these are in the minority. The interaction of positively charged ions with the uncharged sample molecules can also occur in a number of ways, and the four most common are as follows:

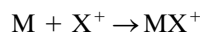
1. Proton transfer between the sample molecule and the reagent ion



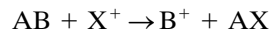
2. Exchange of charge between the sample molecule and the reagent ion



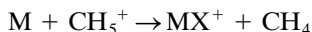
3. Simple addition of the sample molecule to the reagent ion



4. anion extraction



As an example, CH_5^+ ions, which are formed when methane is used as the reagent gas, will react with a sample molecule largely by proton transfer; that is,



Some reagent gases produce more reactive ions than others and will produce more fragmentation. For

example, methane produces more aggressive reagent ions than isobutane. Consequently, whereas methane ions produce a number of fragments by protonation, isobutane, by a similar protonation process, will produce almost exclusively the protonated molecular ion. This is shown in the mass spectra of methyl stearate in Fig. 2. Spectrum (a) was produced using methane as the reagent gas and exhibits fragments other than the protonated parent ion. In contrast, spectrum b obtained with butane as the reagent gas, exhibits the protonated molecular ion only. Continuous use of a chemical ionization source causes significant source contamination, which impairs the performance of the spectrometer and thus the source requires cleaning by baking-out fairly frequently. Retention data on two-phase systems coupled with matching electron-impact mass spectra or confirmation of the molecular weight from chemical ionization spectra are usually sufficient to establish the identity of a solute.

The inductively coupled plasma (ICP) source is used largely for specific element identification and evolved from the ICP atomic emission spectrometer; it is probably more commonly employed in liquid chromatography (LC–MS) than GC–MS. In GC–MS, the ICP ion source is used in the assay of organometallic materials and in metal speciation analyses. The ICP ion source is very similar to the volatilizing unit of the ICP atomic emission spectrometer, and a diagram of the device is shown in Fig. 3. The argon plasma is an electrodeless discharge, often initiated by a Tesla coil spark, and maintained by radio-frequency (rf) energy, inductively coupled to the inside of the torch by an external coil, wrapped around the torch stem. The

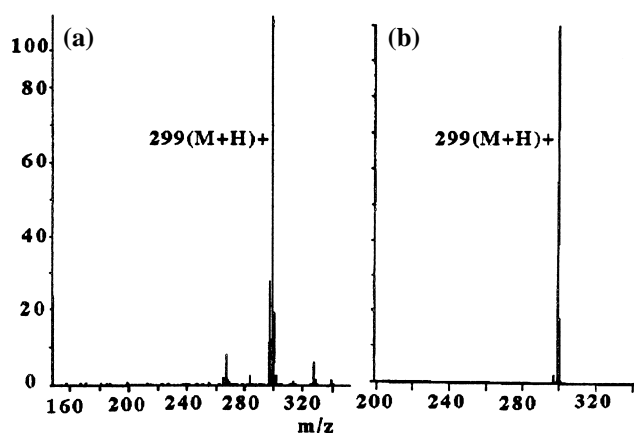


Fig. 2 Mass spectrum of methyl stearate produced by chemical ionization.

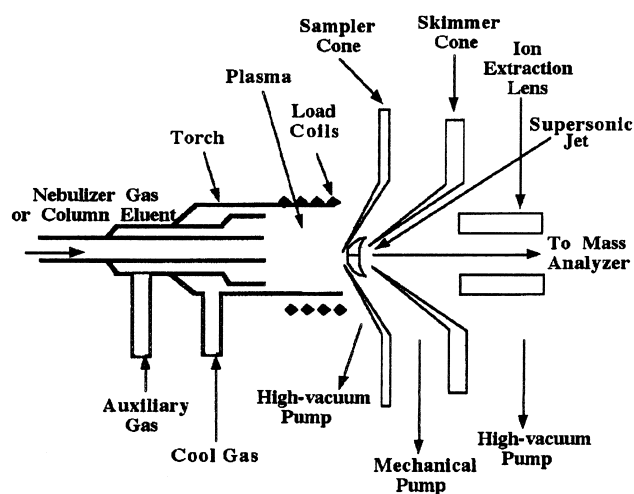


Fig. 3 ICP mass spectrometer ion source.

plasma is maintained at atmospheric pressure and at an average temperature of about 8000 K. The ICP torch consists of three concentric tubes made from fused silica. The center tube carries the nebulizing gas, or the column eluent, from the gas chromatograph. Argon is used as the carrier gas, and the next tube carries an auxiliary supply of argon to help maintain the plasma and also to prevent the hot plasma from reaching the tip of the sample inlet tube. The outer tube also carries another supply of argon at a very high flow rate that cools the two inner tubes and prevents them from melting at the plasma temperature. The coupling coil consists of two to four turns of water cooled copper tubing, situated a few millimeters behind the mouth of the torch. The rf generator produces about 1300 W of rf at 27 or 40 MHz, which induces a fluctuating magnetic field along the axis of the torch. Temperature in the induction region of the torch can reach 10,000 K, but in the ionizing region, close to the mouth of the sample tube, the temperature is 7000–9000 K.

The sample atoms account for less than 10^{-6} of the total number of atoms present in the plasma region; thus, there is little or no self-quenching. At the plasma temperature, over 50% of most elements are ionized. The ions, once formed, pass through the apertures in the apex of two cones. The first has an aperture about 1 mm inner diameter (i.d.) and ions pass through it to the second skimmer cone. The space in front of the first cone is evacuated by a high-vacuum pump. The region between the first cone and the second skimmer cone is evacuated by a mechanical pump to about 2 mbar and, as the sample expands into this region, a supersonic jet is formed. This jet of gas and ions flows through a



slightly smaller orifice into the apex of the second cone. The emerging ions are extracted by negatively charged electrodes (-100 to -600 V) into the focusing region of the spectrometer, and then into the mass analyzer.

The ICP ion source has the advantages that the sample is introduced at atmospheric pressure, the degree of ionization is relatively uniform for all elements, and singly-charged ions are the principal ion product. Furthermore, sample dissociation is extremely efficient and few, if any, molecular fragments of the original sample remain to pass into the mass spectrometer. High ion populations of trace components in the sample are produced, making the system extremely sensitive. Nevertheless, there are some disadvantages: the high gas temperature and pressure evoke an interface design that is not very efficient and only about 1% of the ions that pass the sample orifice pass through the skimmer orifice. Furthermore, some molecular ion formation does occur in the plasma, the most troublesome being molecular ions formed with oxygen. These can only be reduced by adjusting the position of the cones, so that only those portions of the plasma where the oxygen population is low are sampled.

Although the detection limit of an ICP–MS is about 1 part in a trillion, as already stated, the device is rather inefficient in the transport of the ions from the plasma to the analyzer. Only about 1% pass through the sample and skimming cones and only about 10^{-6} ions will eventually reach the detector. One reason for ion loss is the diverging nature of the beam, but a second is due to space-charge effects, which, in simple terms, is the mutual repulsion of the positive ions away from each other. Mutual ion repulsion could also be responsible for some nonspectroscopic interelement interference (i.e., matrix effects). The heavier ions having greater momentum suffer less dispersion than the lighter elements, thus causing a preferential loss of the lighter elements.

Mass Spectrometers for MS–GC Tandem Operation

The most common mass spectrometer used in GC–MS systems is the quadrupole mass spectrometer, either as a single quadrupole or as a triple quadrupole, which can also provide MS–MS spectra. A diagram of a quadrupole mass spectrometer is shown in Fig. 4. The operation of the quadrupole mass spectrometer is quite different from that of the sector instrument. The instrument consists of four rods which must be precisely straight and parallel and so arranged that the beam of ions is directed axially between them. Theoretically, the rods should have a hyperbolic cross section, but in practice, less ex-

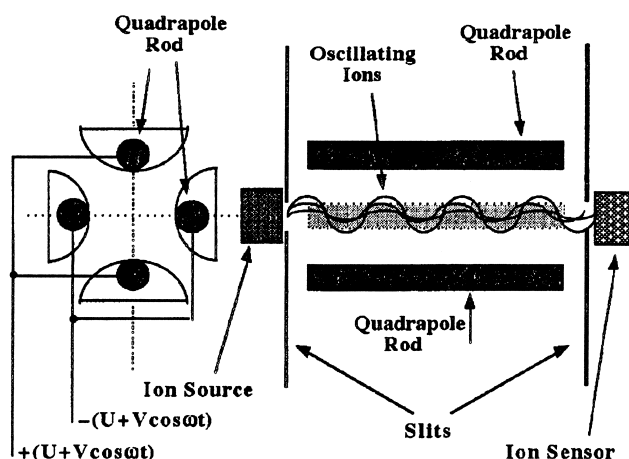


Fig. 4 Quadrupole mass spectrometer.

pensive cylindrical rods are nearly as satisfactory. A voltage comprising a DC component (U) and a rf component ($V_0 \cos \omega t$) is applied between adjacent rods, opposite rods being electrically connected. Ions are accelerated into the center, between the rods, by a potential ranging from 10 to 20 V. Once inside the quadrupole, the ions oscillate in the x and y dimensions induced by the high-frequency electric field. The mass range is scanned by changing U and V_0 while keeping the ratio U/V_0 constant. The quadrupole mass spectrometer is compact, rugged, and easy to operate, but its mass range does not extend to very high values. However, under certain circumstances, multiply-charged ions can be generated and identified by the mass spectrometer. This, in effect, increases the mass range of the device proportionally to the number of charges on the ion.

The quadrupole mass spectrometer can also be constructed to provide MS–MS spectra by combining three quadrupole units in series. A diagram of a triple quadrupole mass spectrometer is shown in Fig. 5. The sample enters the ion source and is usually fragmented by either an electron-impact or chemical ionization process. In the first analyzer, the various charged fragments are separated in the usual way, which then pass into the second quadrupole section, sometimes called the collision cell. The first quadrupole behaves as a straightforward mass spectrometer. Instead of the ions passing to a sensor, the ions pass into a second mass spectrometer and a specific ion can be selected for further study. In the center quadrupole section, the selected ion is further fragmented by collision ionization and the new fragments pass into the third quadrupole, which functions as a second analyzer. The second analyzer resolves the new fragments into their individual masses producing the

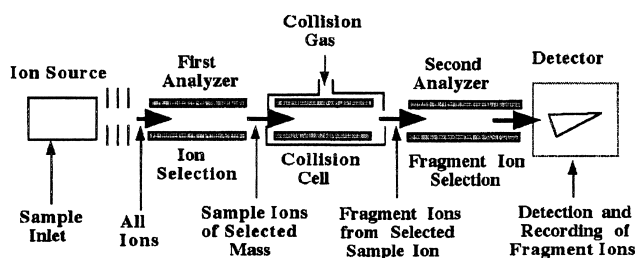


Fig. 5 Triple quadrupole mass spectrometer.

mass spectrum. Thus, the exclusive mass spectrum of a particular molecular or fragment ion can be obtained from the myriad of ions that may be produced from the sample in the first analyzer. This is an extremely powerful analytical system that can handle exceedingly complex mixtures and very involved molecular structures.

Another form of the quadrupole mass spectrometer is the ion trap detector, which has been designed more specifically as a chromatography detector than for use as a tandem instrument. The electrode orientation of the quadrupole ion trap mass spectrometer is shown in Fig. 6. The ion trap mass spectrometer has an electrode arrangement that consists of three cylindrically symmetrical electrodes comprised of two end caps and a ring. The device is small, the opposite internal electrode faces being only 2 cm apart. Each electrode has accurately machined hyperbolic internal faces. An rf voltage together with an additional DC voltage is applied to the ring, and the end caps are grounded. The rf voltage causes rapid reversals of field direction, so any ions are alternately accelerated and decelerated in the axial direction and vice versa in the radial direction. At a given voltage, ions of a specific mass range are held oscillating in the trap. Initially, the electron beam is used to produce ions, and after a given time, the beam is turned off.

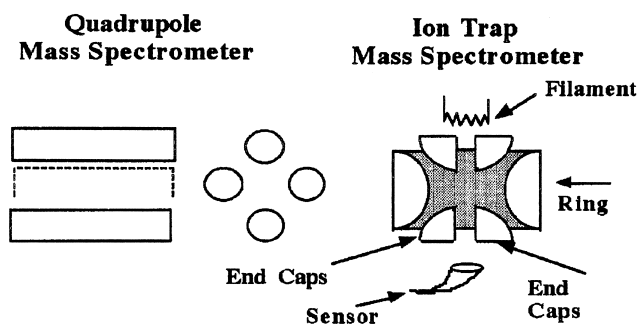


Fig. 6 Pole arrangement for the quadrupole and ion trap mass spectrometers.

All the ions, except those selected by the magnitude of the applied rf voltage, are lost to the walls of the trap, and the remainder continue oscillating in the trap. The potential of the applied rf voltage is then increased, and the ions sequentially assume unstable trajectories and leave the trap via the aperture to the sensor. The ions exit the trap in order of their increasing m/z values. The first ion trap mass spectrometers were not very efficient, but it was found that the introduction of traces of helium to the ion trap significantly improved the quality of the spectra. The improvement appeared to result from ion–helium collisions that reduced the energy of the ions and allow them to concentrate in the center of the trap. The spectra produced are quite satisfactory for solute identification by comparison with reference spectra. However, the spectrum produced for a given substance will probably differ considerably from that produced by the normal quadrupole mass spectrometer.

The time-of-flight mass spectrometer was invented many years ago, but the performance of the modern version is greatly improved. A diagram of the time-of-flight mass spectrometer is shown in Fig. 7. In a time-of-flight mass spectrometer, the following relationship holds:

$$t = \left(\frac{m}{2zeV} \right)^{1/2} L$$

where t is the time taken for the ion to travel a distance L , V is the accelerating voltage applied to the ion, and L is the distance traveled by the ion to the ion sensor.

The mass of the ion is directly proportional to the square of the transit time to the sensor. The sample is

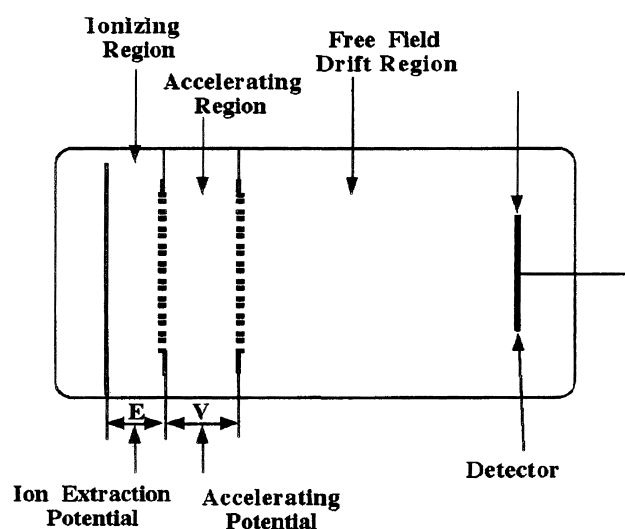


Fig. 7 The time-of-flight mass spectrometer. (Courtesy of VG Organic Inc.)



volatilized into the space between the first and second electrodes and a microsecond burst of electrons is allowed to produce ions. An extraction voltage is then applied for another short time period, which, as those further from the second electrode will experience a greater force than those closer to the second electrode, will focus the ions. After focusing, the accelerating potential (V) is applied for about 100 ns so that all the ions in the source are accelerated almost simultaneously. The ions then pass through the third electrode into the drift zone and are then collected by the sensor electrode. The particular advantage of the time-of-flight mass spectrometer is that it is directly compatible with surface desorption procedures. Consequently, it can be employed with laser-desorption and plasma-desorption techniques. An excellent discussion on general organic mass spectrometry is given in *Practical Organic Mass Spectrometry* edited by Chapman [1].

The combination of the gas chromatograph with the single quadrupole mass spectrometer or with the triple quadrupole mass spectrometer are the most commonly used tandem systems. They are used extensively in forensic chemistry, in pollution monitoring and control, and in metabolism studies. The quadrupole mass spectrometers provide both high sensitivity and good mass spectrometric resolution. They can be readily used with open-tubular columns, and an example of the use of the single quadrupole monitoring a separation from an open-tubular column is shown in Fig. 8. The column was 30 m long with a 0.25-mm i.d. and carried a 0.5-mm film of stationary phase. A 1-mL sample was used and the column was programmed from 50°C to 300°C at 10°C/min.

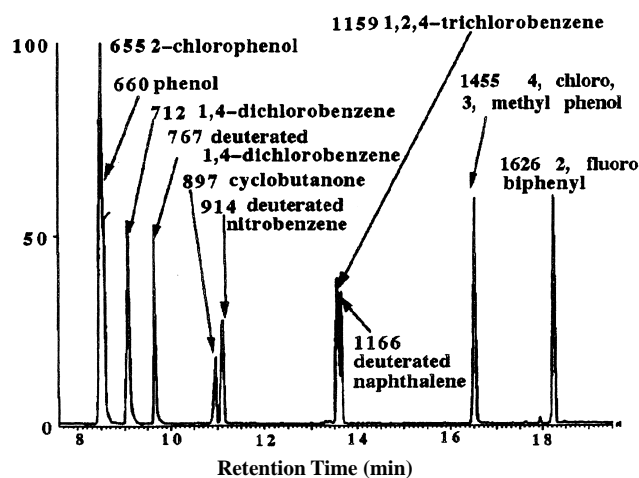


Fig. 8 A separation from an open-tubular column monitored by a single quadrupole mass spectrometer.

Gas Chromatography–Mass Spectrometry Systems

An elegant example of the use of GC–MS in the analysis of pesticides in river water is given by Vreuls et al. [2]. A 1-mL sample was collected in an LC sample loop and the internal standard added. The sample was then displaced through a short column 1 cm long with a 2-mm i.d. packed with 10- μ m particles of a proprietary PLRP-S adsorbent (styrene–divinylbenzene copolymer) by a stream of pure water. The extraction column was then dried with nitrogen and the adsorbed materials displaced into a gas chromatograph with 180 mL of ethyl acetate. The sample was passed through a short retention gap column and then to a retaining column. The GC oven was maintained at 70°C so that the ethyl acetate passed through the retaining column and was vented to waste. The solutes of interest were held in the retaining column at this temperature during the removal of the ethyl acetate. The temperature was then increased and the residual material separated on an an-

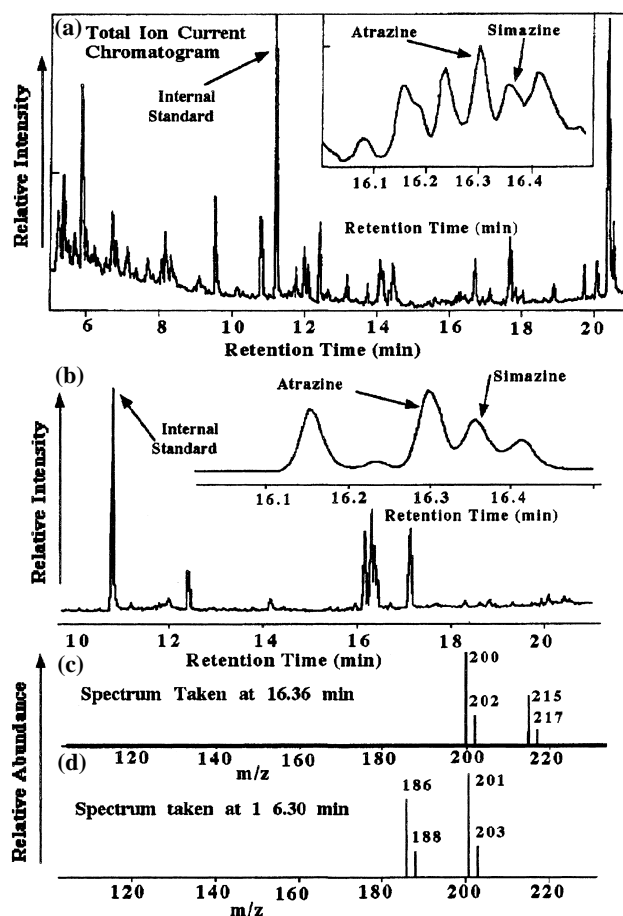


Fig. 9 Chromatogram and spectra from a sample of river water containing 200 ppt of atrazine and simazine. (From Ref. 2.)

alytical column using an appropriate temperature program. The eluents from the analytical column passed to a quadrupole mass spectrometer. An example of the chromatograms and spectra obtained are shown in Fig. 9. Figure 9a shows the total ion current chromatogram from a sample of Rhine River water containing 200 ppt of the herbicides atrazine and simazine. The pertinent peaks are shown enlarged in the inset. Figure 9b shows a section of the same chromatogram presented in the selected ion mode. It is seen that the herbicide peaks are clearly and unambiguously revealed. In Figs. 9c and 9d, the individual mass spectra of atrazine (eluted at 16.30 min) and simazine (eluted at 16.36 min) are shown. The spectra are clear and more than adequate to confirm the identity of the two herbicides.

References

1. J. R. Chapman (ed.), *Practical Organic Mass Spectrometry*, John Wiley & Sons, New York, 1994.
2. J. J. Vreuls, A.-J. Bulterman, R. T. Ghijsen, and U. Th. Brinkman, *Analyst* 117: 1701 (1992).

Suggested Further Reading

Message, G. M., *Practical Aspects of GC/MS*, John Wiley & Sons, New York, 1984.
Scott, R. P. W., *Tandem Techniques*, John Wiley & Sons, New York, 1984.



Golay Dispersion Equation for Open-Tubular Columns

Raymond P.W. Scott

Scientific Detectors Ltd., Banbury, Oxfordshire, England

Introduction

The open-tubular column or capillary column is the one most commonly used in gas chromatography (GC) today. The equation that describes dispersion in open tubes was developed by Golay [1], who employed a modified form of the rate theory, and is similar in form to that for packed columns. However, as there is no packing, there can be no multipath term and, thus, the equation only describes two types of dispersion. One function describes the longitudinal diffusion effect and two others describe the combined resistance to mass-transfer terms for the mobile and stationary phases.

Discussion

The Golay equation takes the following form:

$$H = \frac{2D_m}{u} + \frac{f_1(k')r^2}{D_m}u + \frac{f_2(k')r^2}{K^2D_s}u \quad (1)$$

where H is the height of a theoretical plate or the variance/unit length, D_m is the diffusivity of the solute in the mobile phase, D_s is the diffusivity of the solute in the stationary phase, r is the column radius, k' is the capacity ratio of the solute, K is the distribution coefficient of the solute, and u is the mobile-phase linear velocity.

Open-tubular columns behave in exactly the same way as packed columns with respect to pressure. The same mathematical arguments can be deduced which results in the modified form of the equation shown in Eq. (2). As the column is geometrically simple, the respective functions of k' can also be explicitly developed.

$$H = \frac{2D_m}{u_0} + \frac{(1 + 6k' + 11k'^2)r^2}{24(1 + k')^2D_{m(0)}}u_0 + \frac{2k' df^2}{3(1 + k')^2D_s(\gamma + 1)}u_0 \quad (2)$$

where u_0 is the exit velocity of the mobile phase and $D_{m(0)}$ is the diffusivity of the solute measured at the exit pressure. As the film is thin, $r \gg df$; then,

$$\frac{(1 + 6k' + 11k'^2)r^2}{24(1 + k')^2D_{m(0)}} \gg \frac{2k' df^2}{3(1 + k')^2D_s(\gamma + 1)}$$

and, thus,

$$H = \frac{2D_{m(0)}}{u} + \frac{(1 + 6k' + 11k'^2)r^2}{24(1 + k')^2D_{m(0)}}u_0 \quad (3)$$

By differentiating Eq. (3) and equating it to zero, expressions can be obtained for u_{opt} and H_{min} in a manner similar to the method used for a packed column:

$$u_{0(\text{opt})} = 2 \frac{D_{m(0)}}{r} \left(\frac{12(1 + k')^2}{1 + 6k' + 11k'^2} \right)^{1/2} \quad (4)$$

$$H_{\text{min}} = \frac{r}{2} \left(\frac{1 + 6k' + 11k'^2}{3(1 + k')^2} \right)^{1/2} \quad (5)$$

The approximate efficiency of a capillary column operated at its optimum velocity (assuming the inlet/outlet pressure ratio is small) can be simply calculated. If only the dead volume is considered (i.e., $k' = 0$), Eq. (3) reduces to



$$H = \frac{2D_m}{u} + \frac{1}{24} \frac{r^2}{D_m} u \quad (6)$$

Differentiating and equating to zero,

$$\frac{dH}{du} = -\frac{2D_m}{u^2} + \frac{1}{24} \frac{r^2}{D_m} = 0 \quad \text{or} \quad u = \frac{\sqrt{48}D_m}{r}$$

Substituting for u in Eq. (6) and simplifying,

$$\begin{aligned} H &= \frac{2D_m r}{\sqrt{48}D_m} + \frac{1}{24} \frac{r^2}{D_m} \frac{\sqrt{48}D_m}{r} \\ &= 0.289r + 0.289r = 0.577r \end{aligned}$$

Thus, the efficiency of a capillary column of length (l) can be assessed as

$$n = \frac{l}{0.6r} \quad (7)$$

Golay Dispersion Equation for Open-Tubular Columns

The column efficiency will be inversely proportional to the column radius and the analysis time will directly proportional to the column radius and inversely proportional to the diffusivity of the solute in the mobile phase.

Reference

1. M. J. E. Golay, *Gas Chromatography*. 1958 (D. H. Desty, ed.), Butterworths, London, 1958, p. 36.

Suggested Further Reading

- Scott, R. P. W., *Techniques and Practice of Chromatography*, Marcel Dekker, Inc., New York, 1996.
 Scott, R. P. W., *Introduction to Analytical Gas Chromatography*, Marcel Dekker, Inc., New York, 1998.



GPC–SEC Analysis of Nonionic Surfactants

Ivan Gitsov

College of Environmental Science and Forestry, State University of New York, Syracuse, New York, U.S.A.

Introduction

Nonionic surfactants are one of the most important and largest surfactant groups. They are amphiphilic molecules composed, in most cases, of poly(oxyethylene) blocks (PEO) as the water-soluble fragment and fatty alcohols, fatty acids, alkylated phenol derivatives, or various synthetic polymers as the hydrophobic part [1]. This class of surfactants is widely used as surface wetting agents, emulsifiers, detergents, phase-transfer agents, and solubilizers for diverse industrial and biomedical applications [2]. Several of them have been used for many years under different trade names: Brij (ethoxylated fatty alcohols), Synperonic (PEO copolymers) and Tween (ethoxylated sorbitan esters) by ICI Surfactants; Igepal (PEO copolymers) by Rhone-Poulenc, Rhodia; Pluronic [poly(oxyethylene)-*block*-poly(oxypropylene) copolymers] by BASF; Triton DF (ethoxylated fatty alcohols) and Triton X (ethoxylated octylphenols) by Union Carbide; and others. The exploitation characteristics of nonionic surfactants depend on the oligomer distribution, the molecular-weight characteristics of the constituent blocks, and the hydrophilic/hydrophobic ratio of their chemical composition. Therefore, the quantitative determination of these factors is of primary importance for their performance evaluation.

Discussion

Several high-performance liquid chromatography (HPLC) separation techniques have been used in combination with different detection methods to characterize poly(ethylene glycol)s and their amphiphilic derivatives [3]. Size-exclusion chromatography (SEC) is a particularly attractive analytical tool for the investigation of nonionic surfactants because it can provide information for their composition, molecular weight, and molecular-weight distribution along with their micellization in selective solvents. This entry will survey briefly both applications with major emphasis on the choice of the most appropriate eluent and stationary phase.

Molecular-weight determinations are performed in good solvents for both blocks of the PEO copolymers. The most widely used analysis conditions are as follows: eluents—tetrahydrofuran (THF) and chloroform (CHL); flow rate—1.0 mL/min; detection—differential refractive index (dRI) detector. The temperature interval is between 20°C and 40°C. The stationary phase is typically a polystyrene–divinylbenzene cross-linked matrix supplied by different vendors: Phenogel (Phenomenex, USA); PL Gel (Polymer Laboratories, UK), PSS Gel (Polymer Standards Service, Germany), TSKgel (TosoHaas, U.S.A.); UltraStyrigel (Waters Corporation, U.S.A.); and others. The pore size range of the column set should be adjusted to the molecular-weight range of the investigated materials. The SEC analysis in THF requires low-dRI response correction factors (1.66 for $M_n = 106$ and 1.00 for $M_n = 20,000$ [4]), whereas the low-molecular-weight PEO derivatives are almost invisible in CHL. On the other side, the solubility of PEO in THF decreases with the molecular weight, as evidenced by steeper calibration curves and broadening of the peaks in the eluograms (Fig. 1). This complicates the precise molecular weight calculations of PEO copolymers and the choice of calibration standards becomes crucial [5]. The increasing content of PEO in the copolymer results in lower hydrodynamic volumes in THF and, consequently, yields lower apparent molecular weights, regardless of the macromolecular architecture of the analytes [6]. The problems with calibration mismatch can be avoided to some extent by using the universal calibration approach with on-line differential viscometry. This method provides accurate molecular-weight information for most linear and comb-graft PEO copolymers but has been proved less precise for copolymers with complex linear-dendritic or hyperbranched architecture. On-line laser-light-scattering detection eliminates the need for a calibration curve and yields correct M_w values for macromolecules with molecular weights higher than 500 g/mol. The precision of the method depends largely on accurate dn/dc values that need to be measured for each copolymer investigated.



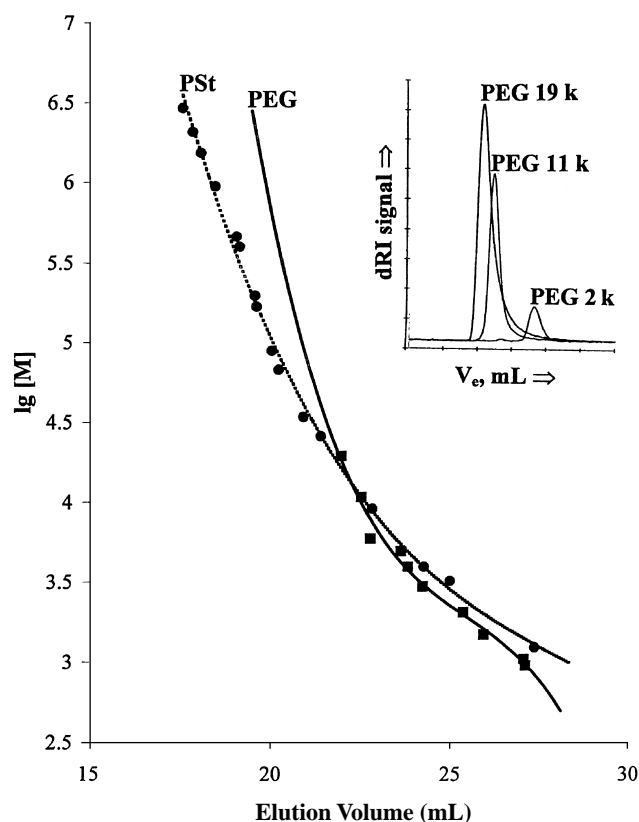


Fig. 1 Polystyrene, PSt, and poly(ethylene glycol), PEG, calibration curves obtained on PL Gel column set (Mixed C, 10^3 Å, 5×10^2 Å, and 10^2 Å). Eluent: THF; flow rate: 1 mL/min; temperature: 40°C. Inset: SEC elution profiles of poly(ethylene glycol)s (PEGs) at the same analysis conditions.

The self-assembly process of nonionic surfactants in aqueous media differs in several aspects from the micellization of amphiphilic copolymers:

1. Micelles constructed of low-molecular-weight surfactants have much lower molecular weights than that of polymeric ones.
2. The critical micelle concentration (CMC) is much lower for polymer surfactants.
3. The vast majority of polymer micelles have spherical shape in dilute or semidilute solutions, whereas low-molecular-weight surfactants form structures that are strongly concentration dependent: lamellae, sheets, rods, and spheres.
4. The kinetics of micelle formation and the dynamics of the micelle-unimer equilibrium are considerably slower for polymeric surfactants.

The last factor is particularly important for the successful utilization of aqueous SEC in the investigation of the micellization process. In order to provide a realistic picture for the micellization equilibrium, the chromatographic system needs to meet several strict requirements: The packing material and the eluent should be appropriately chosen to prevent the occurrence of non-size-exclusion phenomena and adsorption of micelles in the stationary phase. In all cases, mass balance of the material injected and recovered from the columns must be performed in order to verify the absence copolymer entrapment. Cross-linked copolymers containing either poly(vinyl alcohol) or poly(glycidyl methacrylate) as the hydrophilic component are the most widely used column packing materials for aqueous SEC. Both Shodex Protein KW (Showa Denko, Japan) and Micropak TSK-gel PW (Toyo Soda, Japan) columns have been reported to afford good information on the micellization behavior of PEO copolymers without interference of side effects [7]. The mobile phase is methanol–water (1:1, v/v) or pure water eluting at 1.0 mL/min. The analysis temperature is between 22°C and 40°C. Historically, the major concern for the use of SEC in the investigation of micellar systems has always been the lack of suitable calibration and, consequently, the inability of the method to furnish accurate information for the size (hydrodynamic volume) of the micelles and their molecular weight. The incorporation of light-scattering and viscosity detectors for on-line measurement seems to eliminate this problem. With no solute–column interaction present and slow unimer–micelle equilibrium, a multiangle light-scattering detector (DAWN-DSP, Wyatt Technology, U.S.A.) provides accurate information for the molecular weight and radius of gyration of the micelle using Zimm's formalism:

$$\frac{R_\theta}{K^*c} = M_w P(\theta) - 2A_2 c M_w^2 P^2(\theta)$$

where R_θ is the excess Rayleigh ratio, K^* is an optical constant that includes the differential refractive index increment (dn/dc) of the solvent–solute mixture, c is the concentration of the solute molecules in the analyzed solution, M_w is the weight-average molecular weight, $P(\theta)$ is a form factor, and A_2 is the second virial coefficient. If the dn/dc value for the copolymer above CMC is known, the extrapolation to zero concentration and zero angle will yield the Z -average of the radius of gyration and A_2 , respectively. The double extrapolation to zero angle and zero concentration will afford M_w . The hydrodynamic radii can be calculated

using an on-line viscometric detector (Viskotec, U.S.A., and Waters) and the following relationship:

$$R_{\eta}^3 = \frac{3[\eta]M}{10\pi N_A}$$

where the value of $[\eta]M$ could be extracted directly from the universal calibration and N_A is Avogadro's number (6.022×10^{23}). It should be pointed out, however, that this formula is strictly valid only for spherical structures. The hydrodynamic radius can also be measured by a combination of SEC and dynamic light scattering (Precision Detectors, U.S.A.) or NMR spectroscopy [8]. However, the same assumption for a spherical shape of the investigated macromolecules has to be made.

In conclusion, modern SEC is a versatile technique for the investigation of nonionic surfactants in aqueous and organic media. In combination with different spectroscopic and viscometric detectors it will provide useful information for the molecular weight characteristics, chemical composition and solution behavior of this important class of materials.

References

1. B. Jönsson, B. Lindman, K. Holmberg, and B. Kronberg, *Surfactants and Polymers in Aqueous Solution*, John Wiley & Sons, New York, 1998.
2. J. E. Glass (ed.), *Hydrophilic Polymers: Performance with Environmental Acceptability*, Advances in Chemistry Series Vol. 248, American Chemical Society, Washington, DC, 1996.
3. K. Rissler, *J. Chromatogr. A* 742: 1 (1996).
4. S. Mori, *Anal. Chem.* 50: 1639 (1978).
5. B. Trathnigg, S. Feichtenhofer, and M. Kollroser, *J. Chromatogr. A* 786: 75 (1997), and references therein.
6. D. Taton, E. Cloutet, and Y. Gnanou, *Macromol. Chem. Phys.* 199: 2501 (1998); I. V. Berlinova, I. V. Dimitrov, and I. Gitsov, *J. Polym. Sci., Part A: Polym. Chem.* 35: 673 (1997); I. V. Berlinova, A. Amzil, and N. G. Vladimirov, *J. Polym. Sci., Part A: Polym. Chem.* 33: 1751 (1995).
7. I. V. Berlinova, N. G. Vladimirov, and I. M. Panayotov, *Makromol. Chem. Rapid Commun.* 10: 163 (1989); R. Xu, Y. Hu, M. A. Winnik, G. Riess, and M. D. Crocher, *J. Chromatogr.* 547: 434 (1991).
8. G. R. Newkome, J. K. Young, G. R. Baker, R. L. Potter, L. Audoly, D. Cooper, C. D. Weis, K. Morris, and C. S. Johnson, Jr., *Macromolecules* 26: 2394 (1993).



GPC–SEC Viscometry from Multiangle Light Scattering

Philip J. Wyatt

Ron Myers

Wyatt Technology Corporation, Santa Barbara, California, U.S.A.

Introduction

Viscometric techniques have long been used in combination with GPC–SEC separations since the early discovery [1] that the elution of many classes of divers polymers follows a so-called “universal calibration” curve. A plot of the logarithm of the hydrodynamic volume, $M[\eta]$, where M is the molar mass and $[\eta]$ the intrinsic (or “limiting”) viscosity, against the elution volume V yields a common curve (differing for each mobile phase, operating temperature, and column set) along which polymers of greatly differing conformation appear to lie. Neglecting the fact that the errors of such fits can be quite large (the results are usually presented on a logarithmic scale), the concept of universal calibration (UC) allows one to estimate (from the UC curve) the molar mass of an eluting fraction by measuring only the intrinsic viscosity, $[\eta]$, and the corresponding elution volume (time). Key to the measurement of $[\eta]$ is the determination of the specific, η_{sp} , or relative, η_{rel} , viscosity and the concentration c , both in the limit as $c \rightarrow 0$. These viscosities are defined by

$$\eta_{\text{sp}} = \frac{\eta - \eta_0}{c} \quad (1)$$

and

$$\eta_{\text{rel}} = \frac{\eta}{\eta_0} \quad (2)$$

where η is the solution viscosity and η_0 is the viscosity of the pure solvent. Because $\eta_{\text{rel}} = \eta_{\text{sp}} + 1$, it is easily shown for η_{sp} small compared to unity that

$$\lim_{c \rightarrow 0} \frac{\ln(\eta_{\text{rel}})}{c} = \lim_{c \rightarrow 0} \frac{\eta_{\text{sp}}}{c} = [\eta] \quad (3)$$

For the case of GPC–SEC elutions, the concentration c following separation is generally so small that Eq. (3) is assumed to be valid.

The Mark–Houwink–Sakurada Equation

Even without the use of a UC curve (one must be generated for each series of measurements), measurement of $[\eta_0]$ is believed by some to yield an intrinsic viscosity-weighted molar mass [2]. Most importantly, there is a historic interest in the relation of $[\eta]$ to molar mass and/or size. Indeed, the study and explanation of UC has occupied the theorists for some time and, accordingly, there are various formulations describing such relationships [2]. For linear polymers, the most popular empirical relationship between $[\eta]$ and molar mass is the Mark–Houwink–Sakurada (MHS) equation

$$[\eta] = KM^a \quad (4)$$

where K and a are the MHS coefficients. For many polymer–solvent combinations, a plot of $\log([\eta])$ versus $\log(M)$ is linear over a wide range of molar masses. In other words, both K and a are constant throughout the range. Thus, the equation may be used for such polymer–solvent combinations to determine molar mass by measuring $[\eta]$.

Unfortunately, for some solvent–polymer combinations, even for nearly ideal random coils such as polystyrene, the coefficients are not constant but vary with molar mass.

The Flory–Fox Equation

In the various theoretical attempts to explain the relation between $[\eta]$ and the molar mass M , a relation derived by Flory and Fox for random coil molecules is often applied to interpret viscometric measurements for even more general polymer structures. Although applicable to a broader range of polymers than the MHS equation, the Flory–Fox relation has its own shortcomings. Nevertheless, its frequent use and good correlation with experimental data over a



wide range of polymer types confirms its potential for combination with light-scattering measurements to eliminate the need for separate viscometric determinations. In its most general form, the Flory-Fox equation is given by

$$M[\eta] = \Phi(\sqrt{6}r_g)^3 \quad (5)$$

where r_g is the root mean square radius (or “radius of gyration”). The excluded volume effect is taken into account by representing the Flory-Fox coefficient as $\Phi = \Phi_0(1 \pm 2.63\varepsilon + 2.86\varepsilon^2)$. The constant $\Phi_0 = 2.87 \times 10^{23}$ and ε is related to the MHS coefficient a by the relation $2a = 1 + 3\varepsilon$. Thus, ε ranges from 0 at the theta point to 0.2 for a good solvent. Equation (5) is of particular interest because multiangle light-scattering (MALS) measurements [3] determine M and r_g directly. Thus, if a polymer-solvent combination is well characterized by Eq. (5), then this equation may be used directly to calculate the intrinsic viscosity without need for a viscometer.

Viscometry Without a Viscometer

As we have seen earlier, $[\eta]$ may be calculated directly from the (absolute) MALS measurements of M and r_g using Eq. (5). For linear polymers spanning a relatively broad molecular range (an order of magnitude or more), the measurement of M and r_g permits the determination of the molecular conformation defined by

$$r_g = kM^\alpha \quad (6)$$

where k and α are constants generally calculated from the intercept and slope of the least-squares fitted plot of $\log(M)$ against $\log(r_g)$. Combining Eqs. (4) and (5), we obtain

$$KM^{\alpha-1} = (\Phi\sqrt{6}r_g)^3 \quad (7)$$

Solving for r_g and substituting into Eq. (6) yields

$$\frac{K^{1/3}M^{(a-1)/3}}{\Phi\sqrt{6}} = kM^\alpha \quad (8)$$

Therefore, we have the following relations between the coefficients:

$$a = 3\alpha - 1 \quad \text{and} \quad K = \Phi(\sqrt{6}k)^3 \quad (9)$$

Equations (9) show that we can obtain the MHS coefficients a and K directly from a MALS measurement and a determination from such measurements of the molecular conformation parameters α and k . Note that when long-chain branching becomes significant and the molecular conformation becomes more compact such that $\alpha \rightarrow \frac{1}{3}$, the MHS equation, Eq. (4), shows that the intrinsic viscosity no longer varies with molar mass, but becomes constant. This condition also represents a failure of the Flory-Fox equation and the concepts associated with the use of intrinsic viscosity as a means (through UC, for example) to determine molar mass. For linear polymers for which MALS measurements yield values for r_g and M at each eluting slice, all of the important viscometric parameters may be derived directly from the Flory-Fox relation and the MHS equation, as has been shown. For more complex molecular structures or solvent-solute interactions, the MHS coefficients are no longer constants and the empirical theory itself begins to fail.

It is well known [3], however, that the MALS measurements begin to fail in the determination of r_g once r_g falls below about 8–10 nm, even though the M values generated still remain precise. This lack of precision is due to the limitations of the laser “ruler” to resolve a size much below about one-twentieth of the incident wavelength. The trouble with empirical relations, such as the relation between intrinsic viscosity and molar mass, is that they too are often limited to regions where such concepts are applicable. For very small molar

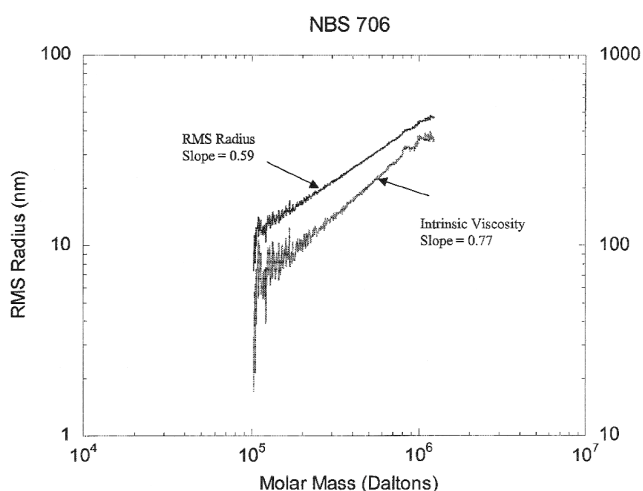


Fig. 1 Conformation plot for $\log(r_g)$ versus $\log(M)$.

masses, the conformation of a polymer molecule may be poorly described by the same theory applied for the larger constituents of a sample. Although MALS conformation measurements may be extrapolated in r_g for the case of linear polymers, such extrapolations must be used with great caution. Similar remarks apply, of course, to the use of viscometric measurements for characterizing complex molecules whose conformations (and, therefore, MHS coefficients) are changing with M .

Figure 1 presents the conformation plot for $\log(r_g)$ versus $\log(M)$ as obtained from a MALS measurement for the polystyrene broad linear standard NIST706 in toluene. Superimposed thereon is a plot of the calculated $\log[\eta]$ as a function of $\log(M)$ for the same sample. From the latter plot, the MHS coefficients may be deduced by inspection of the slope and intercept to yield $a = 0.77$ and $K \approx 0.008$.

References

1. H. Benoit, Z. Grubisic, and R. Rempp, *J. Polym. Sci. B5*, 753: (1967).
2. K. Kamide and M. Saito, in *Determination of Molecular Weight* (A. R. Cooper, ed.), John Wiley & Sons, New York, 1989.
3. P. J. Wyatt, *Anal. Chim. Acta* 272: 1 (1993).

Suggested Further Reading

Billingham, N. C., *Molar Mass Measurements in Polymer Science*, John Wiley & Sons, New York, 1977.
Zimm, B. H., *J. Chem. Phys.* 16: 1093 (1948); 16: 1099 (1948).



GPC–SEC–HPLC Without Calibration: Multiangle Light Scattering Techniques

Philip J. Wyatt

Wyatt Technology Corporation, Santa Barbara, California, U.S.A.

Introduction

Traditional size-exclusion chromatography [SEC or gel permeation chromatography (GPC)] as used to obtain molar masses and their distributions has been described elsewhere in this volume. The method suffers from three shortcomings:

1. The calibration standards generally differ from the unknown sample;
2. The results are sensitive to fluctuations in chromatography conditions (*e.g.* temperature, pump speed fluctuations, *etc.*); and
3. Calibration must be repeated frequently.

Discussion

By adding a multiangle light-scattering [1] detector directly into the separation line, as shown schematically in Fig. 1, the eluting molar masses are determined *ab-*

solutely, thus obviating the need for calibration and elimination of all of the three shortcomings listed. Figure 1 illustrates also two most important elements associated with making quality light-scattering measurements: an in-line degasser and an in-line filter. The in-line degasser is essential to minimize dissolved gases and, thereby, prevent the production of bubbles during the measurement process. Scattering from such bubbles can overwhelm the signals from the solute molecules or particles. Perhaps even more importantly, the system requires that the mobile phase be dust-free. The filter illustrated is placed between the pump and the injector. Usually, this filter station is comprised of two holders, holding, respectively, a 0.20- μm filter followed by a 0.02- or 0.01- μm filter. Although providing for such pristine operating conditions may seem bothersome, it has been shown that so-called “dirty” solvents, although rarely affecting the refractive index detector (RID) signal, do actually contribute significantly to the degradation of high-performance liquid chromatography (HPLC) and SEC columns as well as resulting in the more frequent need to rebuild pumps. The additional solvent cleanup effort is well worth it!

An “absolute” light-scattering (LS) measurement is one that is independent of calibration standards which have “known” molar masses to which the unknown is compared. A LS measurement requires the chromatographer to determine the fundamental properties of the solution (refractive index, dn/dc value) and the detector response (field of view, sensitivity, solid angle subtended at the scattering volume). In addition, other factors must be determined, such as the light wavelength and polarization, geometry of the scattering cell, refractive index of all regions through which the scattered and incident light will pass, and the ratio of the scattered light to the incident light. Generally, these determinations are made in conjunction with appropriate multiangle light-scattering (MALS) software. The importance of light scattering’s independence of a set of reference molar masses to determine the molar mass of an unknown cannot be over-emphasized.

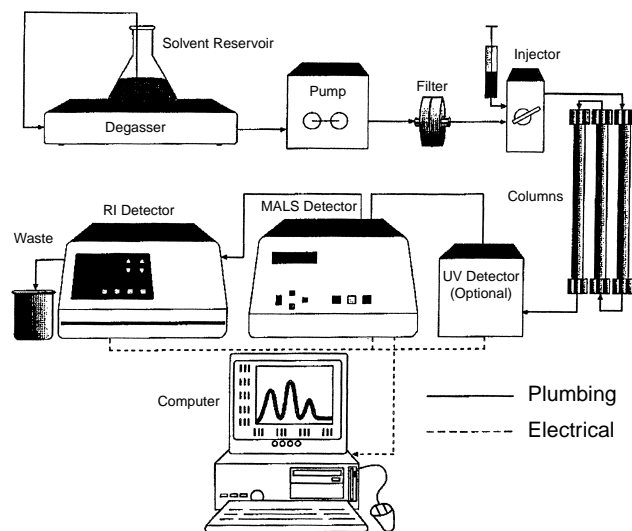


Fig. 1 Schematic diagram showing elements of traditional chromatograph with added MALS detector and dust- and bubble-reducing elements.



Theory

As described in detail in Refs. 1–3, the fundamental equation relating the quantities measured during a MALS detection and the quantities derived is, in the limit of “. . . vanishingly low concentrations. . .” [2], given by

$$\frac{K^*c}{R(\theta)} \approx \frac{1}{MP(\theta)} + 2A_2c \quad (1)$$

where $K^* = 4\pi^2(dn/dc)^2n_0^2(N_A\lambda_0^4)^{-1}$, M is the weight-average molar mass, N_A is Avogadro's number, dn/dc is the refractive index increment, λ_0 is the vacuum wavelength, θ is the angle between the incident beam and the scattered light, and n_0 is the refractive index of the solvent. The refractive index increment, dn/dc , is measured off-line (or looked up in the literature) by means of a differential refractive index (DRI) operating at the same wavelength as the one used for the MALS measurements. It represents the incremental refractive index change dn of the solution (solvent plus solute) for an incremental change dc of the concentration in the limit of vanishingly small concentration. Most importantly, the excess Rayleigh ratio, $R(\theta)$, and form factor $P(\theta)$ are defined respectively by

$$R(\theta) = \frac{f(\theta)_{\text{geom}}[I(\theta) - I_s(\theta)]}{I_0} \quad (2)$$

$$P(\theta) = 1 - \alpha_1 \sin^2(\theta/2) + \alpha_2 \sin^4(\theta/2) - \dots \quad (3)$$

where

$$\alpha_1 = \frac{1}{3} \left(\frac{4\pi n_0}{\lambda_0} \right) \langle r_g^2 \rangle \quad (4)$$

I_0 is the incident light intensity (ergs/cm² s), $f(\theta)_{\text{geom}}$ is a geometrical calibration constant that is a function of the solvent and scattering cell's refractive index and geometry, and $I(\theta)$ and $I_s(\theta)$ are the normalized intensities respectively of light scattered by the solution and by the solvent per solid angle. The mean square radius is given by Eq. (5), where the distances r_i are measured from the molecule's center of mass to the mass element m_i :

$$\langle r_g^2 \rangle = \frac{\sum_i r_i^2 m_i}{\sum_i m_i} = \frac{1}{M} \int r^2 dm \quad (5)$$

For MALS measurement following GPC separation, the sample concentration at the LS detector is usually diluted sufficiently that the term $2A_2c$ often may be safely dropped from Eq. (1). In some applica-

tions involving very high molar masses, it is often worthwhile to perform an off-line determination of the second virial coefficient from a Zimm plot [1,2] to confirm its negligible effect on the derived molar mass of Eq. (1).

Basic Principles

In the limit of vanishingly small concentrations, and the extrapolation of Eq. (3) to very small angles, the two basic principles of light scattering are evident:

1. The amount of light scattered (in excess of that scattered by the mobile phase) at $\theta \approx 0$ is directly proportional to the product of the weight-average molar mass and the concentration (*ergo*, measure the concentration and derive the mass!).
2. The angular variation of the scattered light at $\theta \approx 0$ is directly proportional to the molecule's mean square radius (i.e., size).

The successful application of absolute MALS measurements requires a sufficient number of resolved scattering angles to permit an accurate extrapolation to $\theta \approx 0$. Again, all required calculations are performed by the software. Whenever the mobile phase is changed, its corresponding refractive index must be entered into the software program, which should correct automatically for the resultant change of scattering geometry. Figure 2 shows the normalized light-scattering signals at each scattering angle (detector) as a function of elution volume for a relatively broad sample. Also indicated is the corresponding concentration detector signal.

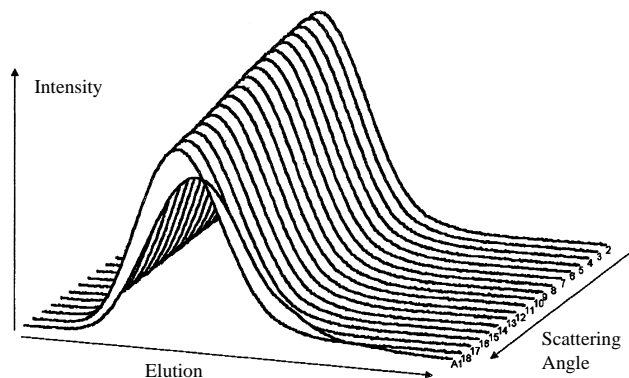


Fig. 2 Light-scattering and DRI signals from MALS setup shown in Fig. 1.

In conventional SEC measurements, it is necessary to calibrate the mass detector [DRI or ultraviolet (UV)] so that its response yields concentration directly. For example, a DRI detector, following calibration, should produce a response proportional to the refractive index change (Δn) detected. This is related to the concentration change Δc by the simple result $\Delta c = \Delta n / (dn/dc)$. Implicit in the use of a DRI detector, therefore, is that measurement of the concentration of the unknown requires that its differential refractive index, dn/dc , be measured, or otherwise determined.

Combining SEC with MALS to produce absolute molar mass data without molecular calibration standards also requires prior calibration of the concentration detector as well as calibration of the MALS detector itself. The latter calibration involves the determination of all geometrical contributions such that the MALS detector measures the Rayleigh excess ratio at each scattering angle. This is most easily achieved by using a turbidity standard such as toluene. Details are found in Ref. 2. Once the refractive index of the mobile phase is entered, the software [4] performs the required calibration.

Derived Mass, Size, and Conformation

The MALS detector produces the absolute molar mass and mean square radius $\langle r_g^2 \rangle$ at each eluting slice. The *root mean square (rms) radius* $r_g = \langle r_g^2 \rangle^{1/2}$ is often referred to by the misnomer “radius of gyration.” There is a lower limit to its determination, which is generally about 8–10 nm. Below this value, MALS cannot generally produce a reliable value. Nevertheless, whenever both r_g and molar mass M are determined by MALS over a range of fractions present in an unknown sample, the sample’s so-called conformation may be determined by plotting the logarithm of the rms radius versus the logarithm of the corresponding molar mass. A resultant slope of unity indicates a rodlike structure, a slope of 0.5–0.6 corresponds to a random coil, and a slope of $\frac{1}{3}$ would indicate a sphere. Values below $\frac{1}{3}$ generally suggest a highly branched molecular conformation.

Figure 3 shows the MALS-derived molar mass and rms radius as a function of elution volume for a broad polystyrene sample. Measurements were made in toluene at 690 nm. The value of dn/dc chosen was 0.11. From Fig. 3, it should be noted that the radius data be-

gins to deteriorate around 10 nm, whereas the mass data extends to its detection limits. From the mass and radius data of Fig. 3, a conformation plot is easily generated with a slope of about 0.57 (i.e., corresponding to a random coil). These same data can also be used immediately to calculate the mass and size moments of the sample as well as its polydispersity as shown in the next section.

Mass and Size Moments

If we assume that the molecules in each slice, i , following separation by SEC, are monodisperse, the mass moments of each sample peak selected are calculated from the conventional definitions [3,5] by

$$M_n = \frac{\sum_i n_i M_i}{\sum_i n_i} = \frac{\sum_i c_i}{\sum_i c_i / M_i} \quad (6)$$

for the *number-average* molar mass, where n_i is the number of molecules of mass M_i in slice i and the summations are over all the slices present in the peak; the concentration c_i of the i th species, therefore, is proportional to $M_i n_i$;

$$M_w = \frac{\sum_i c_i M_i}{\sum_i c_i} = \frac{\sum_i n_i M_i^2}{\sum_i n_i M_i} \quad (7)$$

for the *weight-average* molar mass; and

$$M_z = \frac{\sum_i n_i M_i^3}{\sum_i n_i M_i^2} = \frac{\sum_i c_i M_i^2}{\sum_i c_i M_i} \quad (8)$$

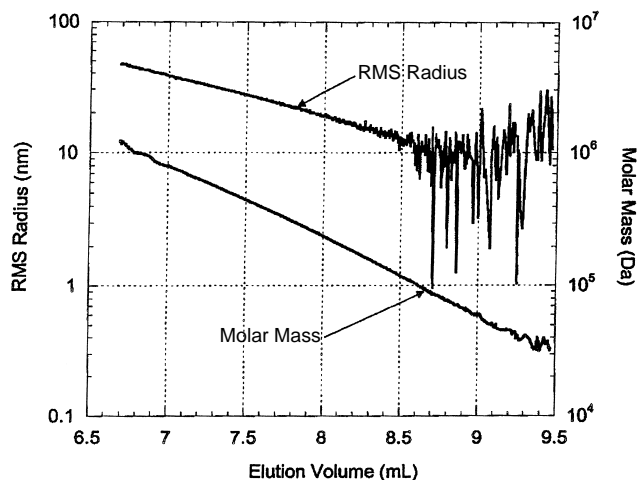


Fig. 3 Molar mass and rms radius generated from data of Fig. 2 as a function of elution volume.



for the z -average (“centrifuge”) molar mass. Note how these “moments” are defined. In particular, the z -average moment corresponds to “the next higher weighting” of both numerator and denominator by the factor M_i . Equations (6) and (7), of course, have a simple physical interpretation in terms of molecular numbers and concentration. From Eq. (8), it is a simple matter to write down expressions for the $z + 1$, $z + 2$, . . . moments.

A similar set of expressions may be written down for the so-called size number and weight moments by replacing the mass terms M_i by the mean square radius values at each slice $\langle r_{g,i}^2 \rangle$ in Eqs. (6) and (7). A z -average term, on the other hand, takes on a more convoluted form [5]. For a random coil conformation under so-called theta conditions, the molar mass is directly proportional to $\langle r_g^2 \rangle$, and an expression that looks identical to Eq. (8) with one of the M_i of the numerator sum replaced by $\langle r_{g,i}^2 \rangle$ is obtained. However, in general, this “equivalence” is not the case and the “light-scattering” value LS is a better description, namely

$$\langle r_g^2 \rangle_{\text{LS}} = \frac{\sum_i c_i M_i \langle r_{g,i}^2 \rangle}{\sum_i M_i c_i} \quad (9)$$

Despite the non-random-coil-at-theta conditions, Eq. (9) is commonly referred to as the z -average mean square radius. The cross-term $M_i \langle r_{g,i}^2 \rangle c_i$ of Eq. (9) is a quantity measured directly by light scattering, at small $\sin^2(\theta/2)$, as clearly may be seen by expanding the term $1/P(\theta)$ in Eq. (1) using the expansion of $P(\theta)$ of Eq. (3).

Polydispersity

Within the peak selected, the sample polydispersity is simply the ratio of the weight to number average (viz. M_w/M_n) obtained from Eqs. (7) and (6), respectively.

Differential Mass Weight Fraction Distribution

The MALS measurements illustrated by Fig. 2 also may be used directly to calculate the differential mass weight fraction distribution, $x(M) = dW(M)/d(\log_{10}M)$ by using the measured $\log_{10}M$ as a function of the elution volume V . Thus, if the concentration detector’s baseline subtracted response is $h(V)$, then $dW/dV = \pm h(V)/\int h(V) dV$, the integral representing the sum over all contributing concentrations to the peak. It is then easily shown [6] that

$$x(M) = -\frac{h(V)/\int h(V) dV}{d(\log_{10}M)/dV} \quad (10)$$

Note that for so-called “linear” column separations, the denominator $d(\log_{10}M)/dV$ is just a constant and, therefore, the differential weight fraction distribution will appear as a reflection (small mass first, from left to right) of the DRI signal. In general, column separations are not linear, so the DRI signal is not a good representation of the mass-elution distribution.

Branching

The MALS measurements which eliminate the need for column calibration and all of its subsequent aberrations also permit the direct evaluation of branching phenomena in macromolecules because the basic quantitation of branching may only be achieved from such measurements as shown in the article by Zimm and Stockmayer [7]. Empirical approaches to quantitate branching, using such techniques as viscometry, have been shown to yield consistently erroneous results especially when long-chain branching becomes dominant.

Reversed-Phase and Other Separation Techniques

Because MALS determinations are independent of the separation mechanism, they may be applied to many types of HPLC. Reversed-phase separations are of particular significance because they cannot be calibrated, as sequential elutions do not occur in a monotonic or otherwise predictable manner. Again, as with all MALS chromatography measurements, all that is required is that the concentration and MALS’s signals be available at each elution volume (slice).

Another separation technique of particular application for proteins, high-molar-mass molecules, and particles is the general class known as field-flow fractionation (FFF) in its various forms (cross-flow, sedimentation, thermal, and electrical). Once again, MALS detection permits mass and size determinations in an absolute sense without calibration. For homogeneous particles of relatively simple structure, a concentration detector is not required to calculate size and differential size and mass fraction distributions. Capillary hydrodynamic fractionation (CHDF) is another particle separation technique that may be used successfully with MALS detection.

References

1. P. J. Wyatt, *Anal. Chim. Acta* 272: 1 (1993).
2. B. H. Zimm, *J. Chem. Phys.* 16: 1093 (1948); 16, 1099 (1948).
3. N. C. Billingham, *Molar Mass Measurements in Polymer Science*, John Wiley & Sons, New York, 1977.
4. ASTRA® software, Wyatt Technology, Santa Barbara, CA, 1999.
5. P. J. Wyatt, in *Analytical and Preparative Separation Methods of Biomacromolecules* (H. Y. Aboul-Enein, ed.), Marcel Dekker, Inc., New York, 1999.
6. D. W. Shortt, *J. Liquid Chrom.*, 16, 3371 \pm 3391 (1993).
7. B. H. Zimm and W. H. Stockmayer, *J. Chem Phys.* 17: 1301 (1949).

Suggested Further Reading

Huglin, M. B. (ed.) *Light scattering from Polymer Solutions*, Academic, London, 1972.



GPC–SEC: Effect of Experimental Conditions

Sadao Mori

PAC Research Institute, Mie University, Nagoya, Japan

Introduction

In order to calculate the molecular-weight averages of a polymer from the SEC chromatogram, the relationship between the molecular weight and the retention volume (called the “calibration curve”) needs to be known, unless a molecular-weight-sensitive detector is used. The retention volume of a polymer changes with changing experimental conditions; therefore, when molecular-weight averages of the polymer are calculated using the calibration curve, care must be taken with the effect of experimental conditions [1].

Discussion

Sample concentration is one of the most important operating variables in SEC, because the retention volumes of polymers increase with increased concentration of the sample solution. The concentration dependence of the retention volume is a well-known phenomenon and the magnitude of the peak shift to higher retention volume is more pronounced for polymers with a higher molecular weights than for those with lower molecular weights. This phenomenon is almost improbable for polymers with a molecular weight lower than 10^4 and is observed ever at a low concentration, such as 0.01%, although the peak shift is smaller than that at a higher concentration.

In this sense, this concentration dependence of the retention volume should be called the “concentration effect,” not “overload effect” or “viscosity effect.” If a large volume of a sample solution is injected, an appreciable shift in retention volume is observed, even for low-molecular-weight polymers; this is called the “overload effect.”

The retention volume increases with increasing concentration of the sample solution and the magnitude of the increase is related to the increasing molecular weight of the sample polymers [2]. The reason for the increase in retention volume with increasing polymer concentration is considered to result from the decrease in the hydrodynamic volume of the polymer molecules in the solution

Molecular-weight averages calculated with calibration curves of varying concentrations may differ in value. As the influence of the sample concentration on the retention volume is based on the essential nature of the hydrodynamic volume of the polymer in solution, it is necessary to select experimental conditions that will reduce the errors produced by the concentration effect.

By rule of thumb, the preferred sample concentrations, if two SEC columns of 8 mm inner diameter (i.d.) \times 25 cm in length are used, are as follows. The sample concentrations should be as low as possible and no more than 0.2%. For high-molecular-weight polymers, concentrations less than 0.1% are often required, and for low-molecular-weight polymers, concentrations of more than 0.2% are possible. The concentrations of polystyrene standards for calibration should be one-half of the unknown sample concentration. For polystyrene standards with a molecular weight over 10^6 , it is preferable that they are one-eighth to one-tenth and for those with a molecular weights between 5×10^5 and 10^6 , a quarter to one-fifth of the sample concentration.

The retention volume of a polymer sample increases as the injection volume increases [3]. In some cases, the increase in the retention volume from an injection volume increase from 0.1 to 0.25 mL was 0.65 mL, whereas that from 0.25 to 0.5 mL was only 0.05 mL, suggesting that a precise or constant injection is required even if the injection volume is as small as 0.1 or 0.05 mL. In view of the significant effect of the injection volume on the retention volume, it is important to use the same injection volume for the sample under examination as that used when constructing the calibration curve. The use of a loop injector is essential, and the same injection volume must be employed for all sample solutions including calibration standards, regardless of their molecular-weight values. The increase in the injection volume results in a decrease in the number of theoretical plates, due to band broadening, which means that the calculated values of the molecular-weight averages and distribution deviate from the true values (Fig. 1).



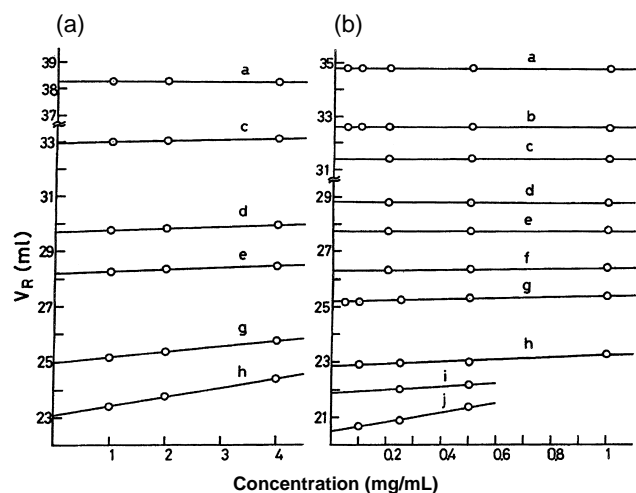


Fig. 1 Concentration dependence of retention volume for polystyrene in good solvents on polystyrene gel columns: (a) in toluene on microstyragel columns ($\frac{3}{8}$ in. \times 1 ft \times 4) (10^6 , 10^5 , 10^4 , and 10^3 nominal porosity) at a flow rate 2 mL/min and injected volume 0.25 mL; (b) in Tetrahydrofuran on Shodex A 80M columns (8 mm \times 50 cm \times 2) (mixed polystyrene gels of several nominal porosities) at a flow rate 1.5 mL/min and injected volume 0.25 mL. Molecular weight of polystyrene standards: (a) 2100; (b) 10,000; (c) 20,400; (d) 97,200; (e) 180,000; (f) 411,000; (g) 670,000; (h) 1,800,000; (i) 3,800,000; (j) 8,500,000.

The retention volume in SEC increases with increasing flow rate [3]. This is attributed to nonequilibrium effects, because polymer diffusion between the intrapores and extrapores of gels is sufficiently slow that equilibrium cannot be attained at each point in the column. With a decreasing flow rate, the efficiency and the resolution are increased. Bimodal distribution of a PS standard (NBS706) with a narrow molecular weight distribution was clearly observed at the lower flow rate.

Separation of molecules in SEC is governed, mainly, by the entropy change of the molecules between the mobile phase and the stationary phase, and the temperature independence of peak retention can be predicted. However, an increase in retention volume with increasing column temperature is often observed. A temperature difference of 10°C results in a 1% increase in the retention volume, which corresponds to a 10–15% change in molecular weight [4].

Two main factors that cause retention-volume variations with column temperature are assumed: an expansion or a contraction of the mobile phase in the column and the secondary effects of the solute to the stationary phase. When the column temperature is

10°C higher than room temperature, the mobile phase (temperature of the mobile phase is supposed to be the same as room temperature in this case) will expand about 1% from when it entered the columns, resulting in an increase in the real flow rate in the column due to the expansion of the mobile phase and the decrease in the retention volume. The magnitude of the retention-volume dependence on the solvent expansion is evaluated to be about one-half of the total change in the retention volume. The residual contribution to the change in retention volume is assumed to be that due to gel-solute interactions such as adsorption.

In order to obtain accurate and precise molecular-weight averages, the column temperature, as well as the difference of both temperatures, the solvent reservoir and the column oven, must be maintained.

Other factors affecting retention volume are the viscosity of the mobile phase, the sizes of gel pores, and the effective size of the solute molecules. Of these, the former two can be ignored, because they exhibit either no effect or only a small effect. The effective size of a solute molecule may also change with changing column temperature. The dependence of intrinsic viscosity on column temperature for PS in chloroform, tetrahydrofuran, and cyclohexane were tested [5]. The temperature dependence of intrinsic viscosity of PS solutions was observed over a range of temperatures. The intrinsic viscosity of PS in tetrahydrofuran is almost unchanged from 20°C up to 55°C, whereas the intrinsic viscosity in chloroform decreased from 30°C to 40°C. Cyclohexane is a theta solvent for PS at around 35°C and intrinsic viscosity in cyclohexane increased with increasing column temperature.

Because the hydrodynamic volume is proportional to the molecular size, the intrinsic viscosity can be used as a measure of the molecular size and optimum column temperatures and solvents must be those where no changes in intrinsic viscosity are observed.

References

1. S. Mori and H. G. Barth, *Size Exclusion Chromatography*, Springer-Verlag, New York, 1999, Chap 5.
2. S. Mori, Effect of experimental conditions, in *Steric Exclusion Liquid Chromatography of Polymers* (J. Janča, ed.), Marcel Dekker, Inc., New York, 1984.
3. S. Mori, *J. Appl. Polym. Sci.* 21: 1921 (1977).
4. S. Mori and T. Suzuki, *Anal. Chem.* 52: 1625 (1980).
5. S. Mori and M. Suzuki, *J. Liquid Chromatogr.* 7: 1841 (1984).

GPC–SEC: Introduction and Principles

Vaishali Soneji Lafita

Abbott Laboratories, Inc., Abbott Park, Illinois, U.S.A.

Introduction

The basic principle of chromatography involves the introduction of the sample into a stream of mobile phase that flows through a bed of a stationary phase. The sample molecules will distribute so that each spends some time in each phase. *Size-exclusion chromatography* (SEC) is a liquid column chromatographic technique which separates molecules on the basis of their sizes or hydrodynamic volumes with respect to the average pore size of the packing. The stationary phase consists of small polymeric or silica-based particles that are porous and semirigid to rigid. Sample molecules that are smaller than the pore size can enter the stationary-phase particles and, therefore, have a longer path and longer retention time than larger molecules that cannot enter the pore structure. Very small molecules can enter virtually every pore they encounter and, therefore, elute last. The sizes, and sometimes the shapes, of the mid-size molecules regulate the extent to which they can enter the pores. Larger molecules are excluded and, therefore, are rapidly carried through the system. The porosity of the packing material can be adjusted to exclude all molecules above a certain size. SEC is generally used to separate biological macromolecules and to determine molecular-weight distributions of polymers.

History

It is not obvious who was the first to use SEC. However, the first effective separation of polymers based on *gel filtration chromatography* (GFC) appears to be that reported by Porath and Flodin [1]. Porath and Flodin employed insoluble cross-linked polydextran gels, swollen in aqueous medium, to separate various water-soluble macromolecules. GFC generally employs aqueous solvents and hydrophilic column packings, which swell heavily in water. Moreover, at high flow rates and pressures, these lightly cross-linked soft gels have low mechanical stability and collapse. Therefore, GFC stationary phases are generally used with low flow rates to minimize high-back pressures. GFC is

mainly used for biomolecule separations at low pressure [2].

Moore described an improved separation technique relative to GFC and introduced the term *gel permeation chromatography* (GPC) in 1964 [3]. GPC performs the same separation as GFC, but it utilizes organic solvents and hydrophobic packings. Moore developed rigid polystyrene gels, cross-linked with divinylbenzene, for separating synthetic polymers soluble in organic media. These extensively cross-linked gels are mechanically stable enough to withstand high pressures and flow rates. The more rugged GPC quickly flourished in industrial laboratories where polymer characterization and quality control are of primary concern. Since its introduction in the 1960s, the understanding and utility of GPC has substantially evolved. GPC has been widely used for the determination of molecular weight (MW) and molecular-weight distribution (MWD) for numerous synthetic polymers [4].

Other names such as gel chromatography, exclusion chromatography, molecular sieve chromatography, gel exclusion chromatography, size separation chromatography, steric exclusion chromatography, and restricted diffusion chromatography have been utilized to reflect the principal mechanism for the separation. The fundamental mechanism of this chromatographic method is complex and certainly will not be readily incorporated into one term. Strong arguments have been made for many of the above-listed titles [5]. In an attempt to minimize the dispute over the proper name, the term SEC will be used in this entry, as it appears to be the most widely used.

Mechanism

Size-exclusion chromatography is a liquid chromatography technique in which a polymer sample, dissolved in a solvent, is injected into a packed column (or a series of packed columns) and flows through the column(s) and its concentration as a function of time is determined by a suitable detector. The column packing material differentiates SEC from other liquid chro-



matography techniques where sample components primarily separate by differential adsorption and desorption. The SEC packing consists of a polymer, generally polystyrene, which is chemically cross-linked so that varying size pores are created. Several models are discussed by Barth et al. [6] to illustrate SEC separation theory. A rather simplified separation mechanism is described here. A polymer sample dissolved in the SEC mobile phase is injected in the chromatographic system. The column eluent is monitored by a mass-sensitive detector, which responds to the weight concentration of polymer in the mobile phase. The most common detector for SEC is a differential refractometer. The raw data in SEC consists of a trace of detector response proportional to the amount of polymer in solution and the corresponding retention volume. A typical SEC sample chromatogram is depicted in Fig. 1. An SEC chromatogram generally is a broad peak representing the entire range of molecular weights in the sample. For synthetic polymers, this can extend from a

few hundred mass units up to a million or more. The average molecular weight can be calculated in a number of ways. Both natural and synthetic polymers are molecules containing a distribution of molecular weights. The most commonly calculated molecular-weight averages using SEC are the weight-average molecular weight (M_w) and number-average molecular weight (M_n). These terms have been well defined by Cazes [7].

The weight-average molecular weight is defined as

$$\overline{M}_w = \frac{\sum_{i=1}^{\infty} W_i M_i}{\sum_{i=1}^{\infty} W_i} \quad (1)$$

and the number-average molecular weight is defined as

$$\overline{M}_n = \frac{W}{\sum_{i=1}^{\infty} N_i} = \frac{\sum_{i=1}^{\infty} M_i N_i}{\sum_{i=1}^{\infty} N_i} \quad (2)$$

where W is the total weight of the polymer, W_i is the weight fraction of a given molecule i , N_i is the number of moles of each species i , and M_i is the molecular weight of each species i .

M_w is generally greater than or equal to M_n . The samples in which all of the molecules have a single molecular weight ($M_w = M_n$) are called monodisperse polymers. The degree of polydispersity (i.e., the ratio of M_w to M_n) describes the spread of the molecular-weight-distribution curve. The broader the SEC curve, the larger the polydispersity.

The detector response on the SEC chromatogram is proportional to the weight fraction of total polymer, and suitable calibration permits the translation of the retention volume axis into a logarithmic molecular-weight scale. Calibration of SEC is perhaps the most difficult aspect of the technique because polymer molecules are separated by size rather than by molecular weight. Size, in turn, is most directly proportional to the lengths of the polymer molecules in solution. A length, however, is proportional to molecular weight only within a single polymer type. An absolute SEC calibration would require the use of narrow molecular-weight range standards of the same polymer that is being analyzed. This is not always practical because a wide range of polymer types needs to be evaluated. SEC calibration is often achieved using the "universal calibration" technique, which assumes hydrodynamic volume is the sole determinate of retention time or volume [8]. A series of commercially available monodisperse molecular-weight polystyrenes are the most commonly used SEC calibration standards. If polystyrene standards are used to calibrate the analyses of any other type of polymer, the molecular weights ob-

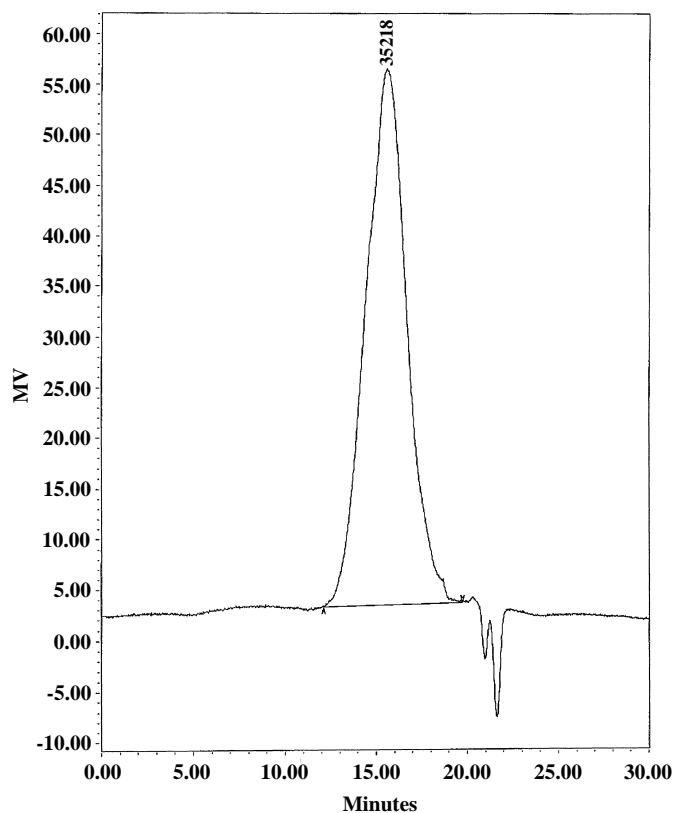


Fig. 1 Typical size-exclusion chromatogram of a polymer sample. SampleName: 6B Vial: 15 Inj: 1 Ch: 410 Type: Broad Unknown.

tained for a polymer sample are actually “polystyrene-equivalent” molecular weights. Numeric conversion factors are available for correlating “molecular weight per polystyrene length” to that of other polymers, but this approach only produces marginally better estimates of the absolute molecular weights. In addition, approaches such as these are usually invalid because the calibration curve for the polymer being analyzed does not often have the same shape as the curve generated with the polystyrene standards.

Size-exclusion chromatograms of narrow-distribution polystyrene standards along with a typical polystyrene calibration curve are shown in Fig. 2. The peak retention volume and corresponding molecular weights produce a calibration curve. With a calibration curve, it is possible to determine M_w and M_n for a poly-

mer. The SEC curve of a polymer sample is divided into vertical segments of equal retention volume. The height or area of each segment and the corresponding average molecular weight, calculated from the calibration curve, are then used for M_w and M_n calculations. There are several commercially available software packages that simplify the calculation process for molecular-weight determinations.

Application

Until the mid-1960s, molecular-weight averages were determined only by techniques such as dilute solution viscosity, osmometry, and light scattering. Most of these techniques work best for polymers with a narrow

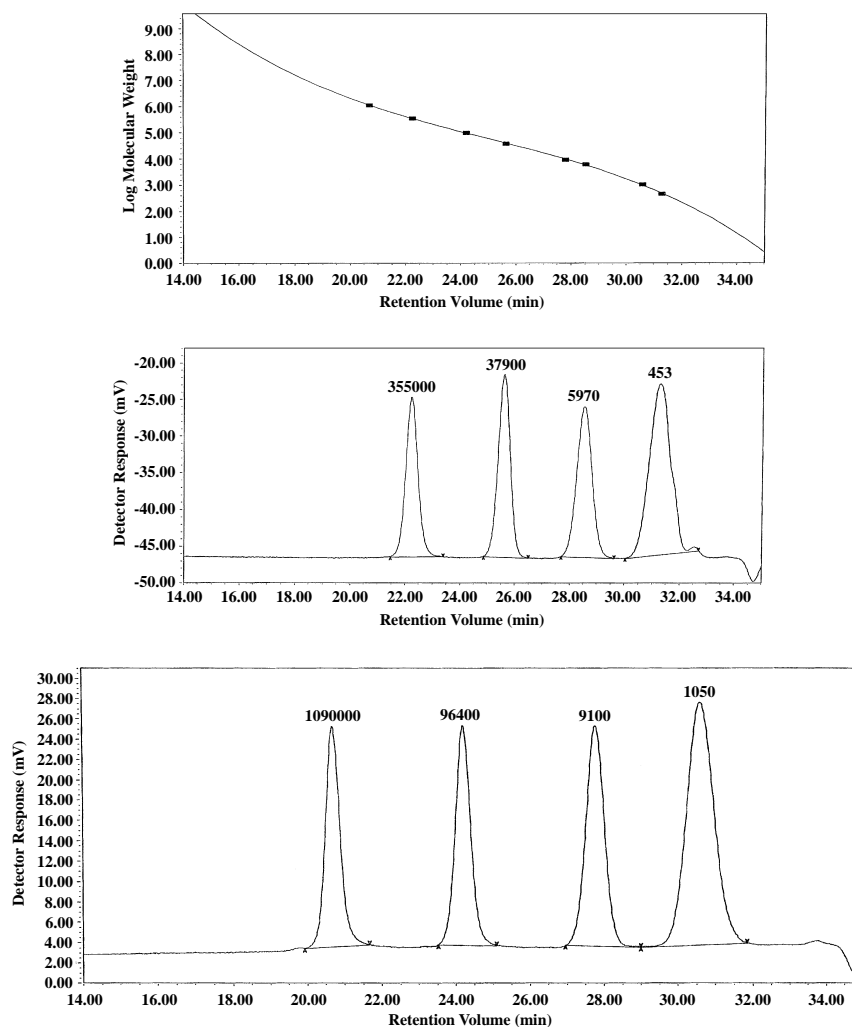


Fig. 2 Typical polystyrene narrow molecular-weight range standard chromatograms and calibration curve.



MWD. None of these techniques, either alone or in combination, could readily identify the range of molecular weights in a given sample. SEC was introduced in the mid-1960s to determine MWDs and other properties of polymers. During the first two decades of SEC acceptance, the emphasis was on improving the fundamental aspects of chromatography, such as column technology, optimizing solvents, and the precision of analysis. Over the past 10 years, there has been an increasing demand for deriving more information from SEC, driven by the need to characterize, more fully, an increasingly complex array of new polymers. Significant developments in SEC detection systems include light scattering, viscometry, and matrix-assisted laser desorption ionization time-of-flight (MALDI-TOF) mass spectrometry and, most recently, nuclear magnetic resonance (NMR) detection in conjunction with SEC for determining MW and chemical composition of polymers. The use of SEC for measuring physiological properties of polymers, especially biopolymers, has become an important area of research.

Finally, SEC is merely a separation technique based on differences in hydrodynamic volumes of molecules. No direct measurement of molecular weight is made. SEC itself does not render absolute information on molecular weights and their distribution or on the structure of the polymers studied without the use of more specialized detectors (e.g., viscometry and light scattering). With these detectors, a "self-calibration" may be achieved for each polymer sample while it is

being analyzed by SEC. However, it is possible to calibrate the elution time in relation to molecular weight of known standards. With proper column calibration, or by the use of molecular-weight-sensitive detectors such as light scattering, viscometry, or mass spectrometry, MWD and average molecular weights can be obtained readily [6]. The combined use of concentration sensitive and molecular-weight-sensitive detectors has greatly improved the accuracy and precision of SEC measurements. Thus, SEC has become an essential technique that provides valuable molecular-weight information, which can be related to polymer physical properties, chemical resistance, and processability.

References

1. J. Porath and P. Flodin, *Nature* 183: 1657 (1959).
2. A. V. Danilov, I. V. Vagenina, L. G. Mustaeva, S. A. Moshnikov, E. Y. Gorbunova, V. V. Cherskii, and M. B. Baru, *J. Chromatogr. A* 773: 103 (1997).
3. J. C. Moore, *J. Polym. Sci., Part A* 2: 835 (1964).
4. V. S. Lafita, Y. Tian, D. Stephens, J. Deng, M. Meisters, L. Li, B. Mattern, and P. Reiter, *Proc. Int. GPC Symp. 1998*, Waters Corp.; Milford, MA, 1998, pp. 474–490.
5. J. Johnson, R. Porter, and M. Cantow, *J. Macromol. Chem., Part C* 1: 393 (1966).
6. H. G. Barth, B. E. Boyes, and C. Jackson, *Anal. Chem.* 70: 251R (1998).
7. J. Cazes, *J. Chem. Educ.*, 43: A567 (1966).
8. R. H. Boyd, R. R. Chance, and G. Ver Strate, *Macromolecules* 29: 1182 (1996).



Gradient Development in Thin-Layer Chromatography

Wojciech Markowski

Medical University, Lublin, Poland

Introduction

The main tasks of analytical thin-layer chromatography (TLC) are the separation of sample components and the measurement of peak heights or areas for quantitative analysis. In the final effect, the peaks should be narrow and symmetrical. Two problems are related to analysis: choice of suitable conditions of elution and full separation. In practice, two modes of development are applied (i.e., isocratic and gradient elution). In isocratic elution, the band migrates under constant conditions; in gradient elution, the changes in migration conditions are consciously programmed. Both in column and in thin-layer chromatography, the isocratic mode is preferred unless the “general elution problem” is encountered. Its solution may consist in gradient elution (stepwise or continuous), gradient of stationary phase, development with a mixed eluent composed of solvents of different polarity (polyzonal TLC), or temperature programming [1].

Discussion

The gradient of the mobile phase is both simple and practical in application. In gradient and isocratic development, we consider the properties and composition of the eluent delivered to the adsorbent bed; if these are constant, we have isocratic analysis, if varied — usually stepwise — it is the gradient of the mobile phase. In a simple gradient, the eluent strength is increased from the beginning to the end of development process. One of advantages of gradient TLC is the feasibility of application of both simple and reversed gradients (decreasing modifier concentration) and a complex gradient — combination of both types of gradient. The reversed gradient can be applied in the case of multiple development.

The gradient is defined by the variation of composition of the mobile phase: by the percent contents of the weaker component A and the stronger component B, called the modifier. The gradient is also characterized by its steepness and shape. The steepness is defined by the concentration of the modifier of the first and last

fractions of the eluent delivered to the adsorbent layer. When the differences of modifier concentrations among all steps are constant, the gradient is called linear. When these differences are large in the beginning and then decrease in the consecutive steps, it is known as a convex gradient program, and in the opposite case, a concave gradient.

To illustrate the “general elution problem” and its solution, let us consider the following situation. Consider a 20-component mixture with capacity factors k of the components forming a geometrical progression and exponentially dependent on the modifier concentration (molar or volume fraction c), in accordance with the Snyder–Soczewinski model of adsorption [2]. The $\log k$ versus $\log c$ plots of the 20 solutes are given in Fig. 1, which has a parallel R_f axis subordinated to the right-hand-side $\log k$ axis. It can be seen that no isocratic eluent can separate all the components. A pure modifier [$c = 1.0$ (100%)] separates well solutes 1–7, and the less polar solutes are accumulated near the solvent front; for $c = 0.1$ (10%), solutes 8–14 are

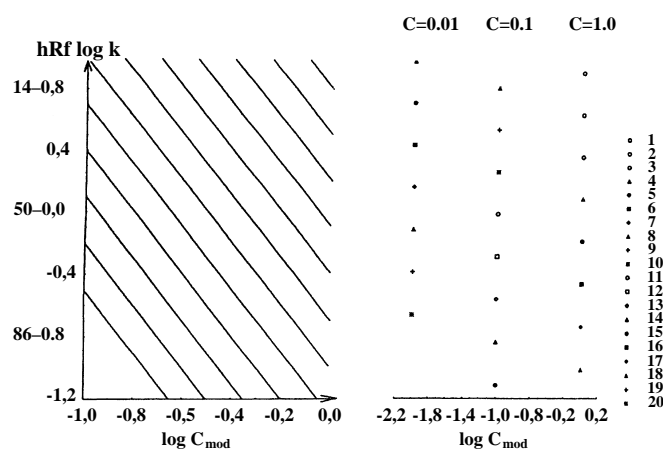


Fig. 1 Family of $\log k$ versus $\log C_{\text{mod}}$ plots for hypothetical solutes 1–20 with capacity factors forming a geometrical progression according to Snyder–Soczewinski equation. For isocratic elution at $C_{\text{mod}} = 1.0, 0.1$, and 0.01 . Only seven to eight solutes give R_f values in the range 0.09 – 0.9 (left-hand ordinate).



well separated, the remaining ones being accumulated either near the start line or the front line; for $c = 0.01$ (1%), solutes 1–14 are accumulated on the start line. Thus, only less than half of the components can be satisfactorily separated by isocratic elution.

Mobile-Phase Gradients

The use of a stepwise gradient of the mobile phase is well described by theoretical models [1,3,4]. The migration of zones is shown in Fig. 2a. In the ideal situation, the spots of solutes overtaken by the consecutive fronts of increased modifier concentrations accelerate their migration so that the strongly retained solutes also start to migrate. Depending on the polarities of the solutes, they migrate all the time in the first concentration zones or are overtaken by the consecutive

Gradient Development in Thin-Layer Chromatography

zones of higher concentration. It can be seen that both weakly polar (A–E) and strongly polar (F–K) compounds are well separated in the final chromatogram. The migration of the components is given by the following equation [3]:

$$R_f = \sum_{i=1}^{h-1} \frac{V(i)R_{f(j,i)}}{1 - R_{f(j,i)}} + R_{f(j,h)} \left(1 - \sum_{i=1}^{h-1} \frac{V(i)}{1 - R_{f(j,i)}} \right) \quad (1)$$

(For detailed derivation and discussion, see Ref. 3.)

This equation could be applied to formulate computer programs that calculate the final R_f values for a given gradient program and retention–eluent composition relationships. In the equation, it is assumed that the stagnant mobile phase in the pores of adsorbent is rapidly displaced. In reality, demixing takes place (especially in the first fractions of slow concentrations of B) and the exchange of the stagnant solvent in the pores with the mobile phase is low; therefore, the boundaries of the concentration zones are not sharp but somewhat diffuse and the solutes migrate in zones of intermediate properties. Planning the gradient program, it is necessary to choose conditions under which the weakly retained components do not migrate with the front of the mobile phase and the strongly retained ones do not remain on the start line. The following series of solvents can be applied to TLC on silica: heptane, trichloroethylene, dichloromethane, diisopropyl ether, ethyl acetate, and isopropanol. The application of the stepwise mobile-phase gradient greatly improves the separation of complex mixtures (e.g., plant extracts); in many cases, twice as many spots were obtained in comparison to isocratic elution. Densitograms of lanatosides obtained by isocratic and gradient elution, for example, indicated that the polar lanatosides were separated on silica using a rapid non-aqueous eluent, avoiding the frequently used cellulose powder and viscous aqueous eluents [5].

Gradient Multiple Development

In all techniques of multiple development, the plate is repeatedly developed in the same direction, with intermittent evaporation of the mobile phase between the consecutive developments (Fig. 2b). If the layer is developed many times to the same distance with the same eluent, the technique is called unidimensional multiple chromatography. A variation of this technique, called incremental multiple development, consists in the stepwise change of the development distance that is the shortest in the first step and is then increased, usually by a constant increment (equal dis-

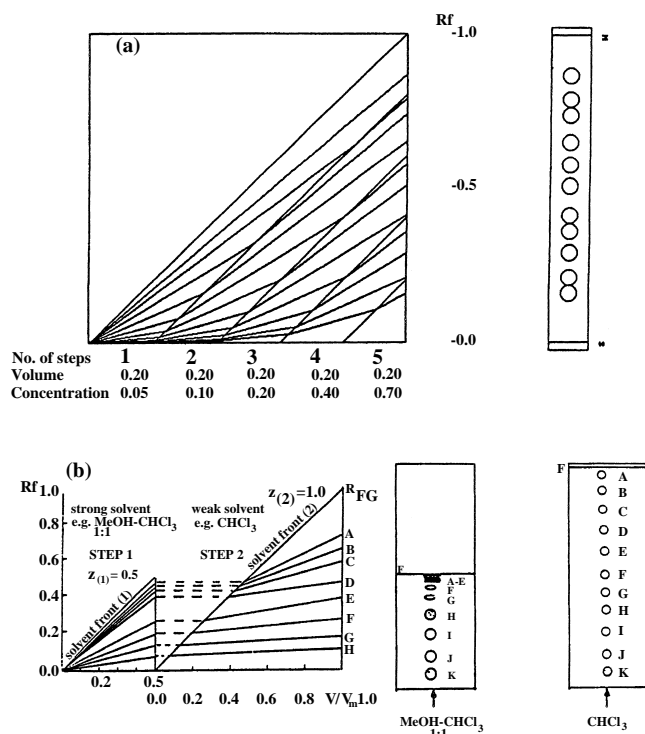


Fig. 2 Separation of hypothetical solutes A–K with a wide range of polarity: (a) five-step simple gradient of mobile phase (concentration of modifier C_{mod} in the range 0.05–0.7), volume of solvent expressed in void volume units (dimensionless); (b) two-step development (solid lines). In the first step, polar solutes E–H are separated; the less polar solutes A–D, poorly separated during the first step, are separated during the second step.

tance or time); the last development step corresponds to the maximum development distance. If, in the process of multiple development, the solvent strength of the mobile phase is varied, the technique is then called gradient multiple development in either the unidimensional or the incremental version. The change in the mobile phase may concern several or all steps.

Depending on the properties of the components of the mixture to be analyzed, an increasing or decreasing gradient of solvent strength can be applied. The process of multiple development with any variation of the mobile-phase composition can be described by a model and equations reported, modified to take into account the intermittent evaporations of solvents:

$$R_{f(n)} = S_{(n-1)} + (Z_{(n)} - S_{(n-1)})R_{(n)} \quad (2)$$

where $S_{(n-1)}$ is the position of the zone in the $n - 1$ development step and $Z_{(n)}$ is the final development distance [1,6]. In the simplest case of a decreasing stepwise gradient, the layer is developed to half the distance with a polar eluent that separates the most polar components in the lower part of the chromatogram; the less polar components are accumulated in the front area. Their separation occurs in the second stage when the layer is developed to the full distance with a less polar eluent (Fig. 2b). The incremental, multistep version of this technique, with programmed, automated development and evaporation steps, is called automated multiple development (AMD) [7] and the method is considered to be the most effective and versatile TLC technique [8].

Mechanism of Compression of Chromatographic Zones

One of the advantages of gradient elution is the compression of zones. Each passage of the front of the increased concentration of the mobile phase through the spot leads to compression of the spot in the direction of development. This is due to the fact that the front of the increased eluent concentration first reaches the lower edge of the spot so that the solute molecules in this fragment start to move (multiple development) or accelerate their migration (gradient) earlier than the molecules in the farther part of the spot. When the front of the mobile phase or of the concentration zone overtakes the whole spot, the compressed spot continues to migrate and gradually becomes more diffuse as in isocratic elution. If the two mechanisms, compression and diffusion, become

counterbalanced, the spot may migrate through considerable distances without any marked broadening (Fig. 3). Incremental multiple development provides a superior separation compared to multiple chromatography, in this case, by minimizing zone broadening and enhancing the zone center separation by migrations of the sample components over a longer distance while maintaining a mobile-phase flow rate range closer to the best value for the separation. This variant can also be achieved by the change of the point of delivery of the eluent to the layer.

Not all compounds are suitable for separation by multiple development. Compounds with significant vapor pressure may be lost during the repeated solvent evaporation steps. Certain solvents of low volatility and/or high polarity, such as acetic acid, triethylamine, dimethyl sulfoxide, and so forth, are unsuitable selections for mobile phases because of the difficulty of removing them from the layer by vacuum evaporation between development steps. Water can be used, but the drying steps will then be lengthy. Solvent residues remaining after the drying step can modify the selectivity of mobile phases used in later steps, resulting in irreproducible separations. Although precautions can be taken to minimize the production of artifact peaks in multiple development, the separation of light and/or air-sensitive compounds is probably better handled by other techniques such as simple gradient development.

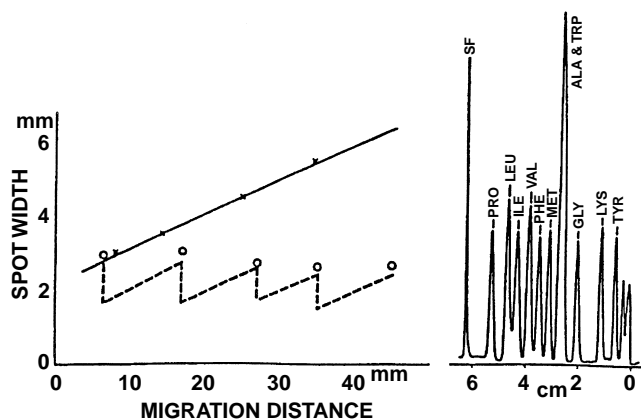


Fig. 3 An illustration of the zone refocusing mechanism (left) and its application to the separation of a mixture of phenylthiohydantoin-amino acids (right). The broken line on the left-hand side represents the change in spot size due to the expansion and contraction stages in multiple development and the solid line depicts the expected zone width for a zone migrating the same distance in a single development.



Polyzonal TLC

Polyzonal TLC is the simplest method for formation of gradients in TLC. The main effect utilized is solvent demixing, which occurs in the case of the application of binary and polycomponent solvents, especially those of differentiated polarity. For an n -component mixed eluent, $n - 1$ solvent fronts are formed, ordered in the sequence of polarity of the components. A gradient of eluent strength is thus formed along the layer; the solutes migrate in various zones, and the passage of fronts leads to compression of TLC spots.

Equipment for Gradient TLC

Depending on the type of the gradient, various apparatuses are applied for its generation. Numerous gradient generators have been described [1]. The gradient of the mobile phase can be formed in some types of horizontal chamber (e.g., Camag, Muttenz, Switzerland; Chromdes, Lublin, Poland). The generation of stepwise gradients is simple for sandwich chambers with distributors, which allow for complete absorption of the eluent fractions from the reservoir. For both chambers, the eluent fractions of increasing eluent strength (increasing concentrations of the polar modifier) are introduced under the distributor. After absorption of the preceding eluent fraction by the adsorbent layer, the next fraction of eluent of changed strength is delivered; the total volume of the eluent fractions corresponds to the development distance. Any gradient program, including continuous or multiple-component gradients, can be generated in this way. The process of multiple development can be fully automated (AMD chamber, Camag Scientific [7]). An apparatus comprises an N -type chamber with connections for adding and removing solvents and gas phases. AMD involves the use of a stepwise gradient of different mobile phases with decreasing strength in 10–30 successive developments increasing in length about 1–5 mm. The initial solvent, which is the strongest, focuses the zones during the first short run, and the solvent is changed for each, or most, of the following cycles. The mobile phase is removed from the chamber, the plate dried and activated by vacuum evaporation, and the layer conditioned with a controlled atmosphere of vapors prior to the next develop-

ment. High resolution and improved detection limits are achieved because zones are reconcentrated during each development stage. Widths of the separated zones are approximately constant at 2–3 mm, and separation capacity for baseline-resolved peaks is 25–40. Zones migrate different distances according to their polarity. The reproducibility of R_f values is 1–2% (CV) for multiple spots on the same plate or different plates from the same batch. A typical universal gradient for a silica gel layer involves 25 steps, with methanol, dichloromethane, or *tert*-butyl ether, and hexane as the solvents.

Discontinuous gradient of the stationary phase can be obtained easily using an ordinary spreader. The trough is divided into separate chambers filled with suspensions of mixtures of adsorbents. The carrier plates are covered in the usual way [1]. Another method of formation of gradients of stationary-phase activity is the use of a Vario-KS chamber, which permits adsorption of various vapors on the adsorbent surface or to control the activity of adsorbent.

To sum up, gradient elution may be applied to the separation of samples composed of solutes of differentiated chromatographic behavior, for increasing throughput in preparative TLC, for removal of ballast (nonpolar) matrix from the analytes in the first gradient step, for decreasing the detection limit by the compression of spots, for the preliminary estimation of the polarity of sample components, and for acceleration of the choice of optimal conditions of chromatographic analysis.

References

1. W. Golkiewicz, Gradient development in thin-layer chromatography, in *Handbook of Thin-layer Chromatography* (J. Sherma and B. Fried, eds.), Marcel Dekker, Inc., New York, 1997, pp. 135–154.
2. E. Soczewinski, *Anal. Chem.* 41: 179 (1969).
3. E. Soczewinski and W. Markowski, *J. Chromatogr.* 370: 63 (1986).
4. E. Soczewinski, *J. Chromatogr.* 369: 11 (1986).
5. G. Matysik and E. Soczewinski, *J. Planar Chromatogr.* 9: 404 (1996).
6. W. Markowski, *J. Chromatogr.* 485: 517 (1989).
7. C. F. Poole and S. K. Poole, *J. Chromatogr.* 703: 573 (1995).
8. C. F. Poole and M. T. Belay, *J. Planar Chromatogr.* 4: 345 (1991).



Gradient Elution

J.E. Haky

Florida Atlantic University, Boca Raton, Florida, U.S.A.

Introduction

The term *gradient elution* refers to a systematic, programmed increase in the elution strength of the mobile phase during the chromatographic run. Of all the techniques used to provide quality separations among complex mixtures, gradient elution offers the greatest potential [1]. Basically, the composition of the mobile phase is varied throughout the separation so as to provide a continual increase in solvent strength and, thereby, a more convenient elution time and sharper peaks for all sample components [2]. What makes this method so useful is the ability to choose from a variety of different eluents. Although most instruments permit gradients to be automatically prepared from various concentrations of only a two-eluent mixture, sample mixtures of a wide range of polarities can be separated efficiently.

Discussion

The process of mixing eluents is a sensitive one. When two solvents with a large difference in their elution strengths are used, even a small increase in the polar component produces a sharp rise in elution strength. Such an effect is undesirable because the components are almost always eluted at the beginning of the analysis and displacement effects may result from demixing of eluent mixtures [1]. According to Poole et al. [3], the most frequently used gradients are binary solvent systems with a linear, convex, or concave increase in the percent volume fraction of the stronger solvent, as depicted in the following equations:

Linear gradient

$$\theta_B = \frac{t}{t_G} \quad (1)$$

Convex gradient

$$\theta_B = 1 - \left(1 - \frac{t}{t_G}\right)^n \quad (2)$$

Concave gradient

$$\theta_B = \left(\frac{t}{t_B}\right)^n \quad (3)$$

In these equations, θ_B is the volume fraction of the stronger eluting solvent, t is the time after the gradient begins, t_G is the total gradient time, and n is an integer controlling gradient steepness.

Complex gradients can be constructed by combining several gradient segments (i.e., rates of increase of strong solvent composition) to form the complete gradient program [3]. Linear gradients are most commonly used, with convex and concave gradients employed only when necessary to optimize more complex separations. In a linear-solvent-strength gradient, the logarithm of the capacity factor for each sample component, k' , decreases linearly with time, according to Eq. (4):

$$\log k = \log k_0 - b \frac{[t]}{[t_m]} \quad (4)$$

In this equation, k_0 is the value of k determined isocratically in the starting solvent, b is the gradient steepness parameter, t is the time after the start of gradient and sample injection, and t_m is the column dead time. Ideally, this equation shows that a linear-solvent-strength gradient should result in equal resolution and bandwidths of all components. Unfortunately, this is not always possible. There are certain cases where linear-solvent-strength gradient is not the ideal method. In some cases, for example, b actually increases regularly with solute retention, which reduces the separation of late-eluting components. Such an effect is observed in the separation of polycyclic aromatic hydrocarbons [3].

There are three things to consider when finding a suitable gradient for a separation: (a) the initial and final mobile-phase compositions, (b) the gradient shape, and (c) the gradient steepness [3]. A convex gradient leads to the elution of bands with a lower average capacity factor and a shorter total analysis time. In other words, the later-eluting bands appear wider and better resolved than the early eluting bands. A concave gradient resolves the early bands to a greater degree than the later bands.

Solvent selection is one of the most important facets of gradient elution. The choice of the first solvent



influences the separation of the initial bands, whereas the strength of the final solvent influences the selectivity of the separation and the retention times and peak shapes of later-eluting bands. If solvent B is too weak, the analysis time may become very long and the later-eluting bands might broaden excessively; thus, a stronger solvent B may be required [3].

Abbott et al. [4] devised a method designed to predict the retention times in gradient elution under the assumption that the retention factor as determined under isocratic conditions is a log-linear function of solvent composition according to Eq. (5), where k_w is the retention factor obtained in water, φ_0 refers to the volume fraction of the organic component, and S refers to the solvent strength for which the values can be obtained as the negative slope of plots of $\log k$ versus volume fraction:

$$\log k = \log k_w - S\varphi_0 \quad (5)$$

Engelhardt and Elgass [5] found that if the gradient volume is held constant and the initial and final compositions of the eluent are fixed, each component of a sample is eluted at a given solvent composition. Snyder et al. [6] derived a simple relationship between the elution time of a solute and the rate of change of solvent composition in gradient elution. Utilizing Eq. (6), they found that the elution time t_e is related to column dead time, t_0 , and an experimental parameter b whereby k_0 is the retention factor that would be obtained in isocratic elution with mobile-phase composition used at the beginning of the gradient. [1]:

$$t_e = \left(\frac{t_0}{b} \right) \log(2.31 k_0 b + 1) + t_0 \quad (6)$$

The parameter b is defined as

$$b = \frac{\Phi S t_0}{100} \quad (7)$$

where Φ is the rate of increase in the concentration of the solvent component having eluent strength S and given as volume percent of organic solvent component per minute [1].

Many technical problems can occur with gradient elution, some of which can be avoided through various methods. To begin, gradient elution relies upon the purity of the solvents used. The high-performance liquid chromatography (HPLC) column can collect impurities,

in the mobile phase, which may or may not elute as sharp peaks at a certain eluent composition. These can be mistaken for sample components. Such peaks are called "ghost peaks" and can result in inaccurate data. Water presents its own set of problems. Contaminated water can also result in ghost peaks. Even deionization of water by ion exchangers can leach out organics from the resin [1]. For this reason, it is advisable to run a gradient first without injecting the sample and use commercially available, purified solvents, including the water, to determine if they result in the elution of ghost peaks.

Another thing to consider with gradient elution is changes in the eluent viscosity. When gradient elution with a hydro-organic mobile phase is used (e.g., methanol-water), systematic variations in the flow rate are expected under conditions of constant-pressure operation, and systematic variations in the operating pressure will be found when a constant flow rate is used [1]. The compressibility of the solvent is species-specific.

In summary, gradient elution is a powerful method for the separation and analysis of complex mixtures containing components with a wide variety of polarities and hydrophobicities. It can also be used to help establish an isocratic mobile phase for the analysis of simpler mixtures. In either case, utmost care must be taken in the selection and use of solvents of high purity and selectivity.

Acknowledgments

The author wishes to thank D.A. Teifer for technical assistance.

References

1. C. Horvath, *High Performance Liquid Chromatography: Advances and Perspectives*, Vol. 2, Academic Press, New York, 1980.
2. J. J. Kirkland and J. L. Glajch, *J. Chromatogr.* 255: 27 (1983).
3. C. F. Poole and S. A. Schuette, *Contemporary Practice of Chromatography*, Elsevier, Amsterdam, 1984.
4. S. R. Abbott, J. R. Berg, P. Achener, and R. L. Stevenson, *J. Chromatogr.* 126: 421 (1976).
5. H. Engelhardt, and H. Elgass, *J. Chromatogr.* 158: 249 (1978).
6. L. R. Snyder, J. W. Dolan, and J. R. Gant, *J. Chromatogr.* 165: 3 (1979).



Gradient Elution in Capillary Electrophoresis

Haleem J. Issaq

NCI-Frederick Cancer Research and Development Center, Frederick, Maryland, U.S.A.

Introduction

Gradient elution is routinely used in high-performance liquid chromatography (HPLC) to achieve the complete resolution of a mixture which could not be resolved using isocratic elution. Unlike isocratic elution, where the mobile-phase composition remains constant throughout the experiment, in gradient elution the mobile-phase composition changes with time. The change could be continuous or stepwise, known as the *step-gradient*. In the continuous gradient, the analyst can pick one of three general shapes: linear, concave, or convex.

Discussion

Gradient elution in HPLC is achieved using two pumps, two different solvent reservoirs, and a solvent mixer. In capillary electrophoresis (CE), electro-osmotic flow controls the flow of the mobile phase, which is, in most cases, an aqueous buffer and is used in place of a mechanical pump.

A manual step-gradient was used by Balchunas and Sepaniak [1] to separate a mixture of amines by micellar electrokinetic chromatography (MEKC). Stepwise gradients were produced by pipetting aliquots of a gradient solvent to the inlet reservoir which was filled with 2.5 mL of running buffer. A small magnetic stirring bar was used to ensure thorough mixing of the added gradient solvent with the starting mobile phase. The gradient elution solvent was manually added, in four 0.5 mL increments, spaced 5 min apart, 5 min after start of the experiment.

Bocek and his group [2] developed a method for controlling the composition of the operational electrolyte directly in the separation capillary in isotachopheresis (ITP) and capillary zone electrophoresis (CZE). The method is based on feeding the capillary with two different ionic species from two separate electrode chambers by simultaneous electromigration. The composition and pH of the electrolyte in the separation capillary is thus controlled by setting the ratio of two electric currents. This procedure can be used, in

addition to generating the mobile-phase gradient, for generating pH gradients [3,4]. Sepaniak et al. [5–7] produced continuous gradients of different shapes (linear, concave, or convex) by using a negative-polarity configuration in which the inlet reservoir is at ground potential and the outlet reservoir at a very high negative potential. This configuration allows two syringe pumps to pump solutions into and out of the inlet reservoir. Tsuda [8] used a solvent-program delivery system, similar to that used in HPLC, to generate pH gradients in CZE. A pH gradient derived from temperature changes has also been reported [9]. Chang and Yeung [10] used two different techniques (i.e., the dynamic pH gradient and electro-osmotic flow gradient) to control selectivity in CZE. A dynamic pH gradient from pH 3.0 to 5.2 was generated by a HPLC gradient pump. An electro-osmotic flow gradient was produced by changing the reservoirs containing different concentrations of cetylammmonium bromide for injection and running.

Capillary electrochromatography (CEC) is a separation technique which combines the advantages of micro-HPLC and CE. In CEC, the HPLC pump is replaced by electro-osmotic flow. Behnke and Bayer [11] developed a micro-bore system for gradient elution using 50- and 100- μm fused-silica capillaries, packed with 5 μm octadecyl reversed phase silica gel and voltage gradients, up to 30,000 V, across the length of the capillary. A modular CE system was combined with a gradient HPLC system to generate gradient CEC. Enhanced column efficiency and resolution were realized. Zare and his co-workers [12] used two high-voltage power supplies and a packed fused-silica capillary to generate an electro-osmotically driven gradient flow in an automated manner. The separation of 16 polycyclic aromatic hydrocarbons was resolved in the gradient mode; these compounds were not separated when the isocratic mode was employed. Others [13–16] used gradient elution in combination with CEC to resolve various mixtures.

Multiple, intersecting narrow channels can be formed on a glass chip to form a manifold of flow channels in which CE can be used to resolve a mixture of solutes in seconds. Harrison and co-workers



[17] showed that judicious application of voltages to multiple channels within a manifold can be used to control the mixing of solutions and to direct the flow at the intersection of channels. The authors concluded that such a system, in which the applied voltages can be used to control the flow, can be used for sample dilution, pH adjustment, derivatization, complexation, or masking of interferences. Ramsey and co-workers [18] used a microchip device with electrokinetically controlled solvent mixing for isocratic and gradient elution in MEKC. Isocratic and gradient conditions are controlled by proper setting of voltages applied to the buffer reservoirs of the microchip. The precision of such control was successfully tested for gradients of various shapes (linear, concave, or convex) by mixing pure buffer and buffer doped with a fluorescent dye. By making use of the electro-osmotic flow and employing computer control, very precise manipulation of the solvent was possible and allowed fast and efficient optimization of separation problems.

Acknowledgment

This project has been funded in whole or in part with federal funds from the National Cancer Institute, National Institutes of Health, under Contract No. NO1-CO-56000.

By acceptance of this article, the publisher or recipient acknowledges the right of the U.S. government to retain nonexclusive, royalty-free license to any copyright covering the article.

The content of this publication does not necessarily reflect the views of the Department of Health and Human Services, nor does the mention of trade names,

commercial products, or organizations imply endorsement by the U.S. government.

References

1. A. T. Balachunas and M. J. Sepaniak, *Anal. Chem.* 60: 617 (1988).
2. J. Popsichal, M. Deml, P. Gebauer, and P. Bocek, *J. Chromatogr.* 470: 43 (1989).
3. P. Bocek, M. Deml, J. Popsichal, and J. Sudor, *J. Chromatogr.* 470: 309 (1989).
4. V. Sustacek, F. Foret, and P. Bocek, *J. Chromatogr.* 480: 271 (1989).
5. M. J. Sepaniak, D. F. Swaile, and A. C. Powell, *J. Chromatogr.* 480: 185 (1989).
6. A. C. Powell and M. J. Sepaniak, *J. Microcol. Separ.* 2: 278 (1990).
7. A. C. Powell and M. J. Sepaniak, *Anal. Instrum.* 21: 25 (1993).
8. T. Tsuda, *Anal. Chem.* 64: 386 (1992).
9. C. W. Wang and E. S. Yeung, *Anal. Chem.* 64: 502 (1992).
10. H-T. Chang and E. S. Yeung, *J. Chromatogr.* 608: 65 (1992).
11. B. Behnke and E. Bayer, *J. Chromatogr.* 680: 93 (1994).
12. C. Yan, R. Dadoo, R. N. Zare, D. J. Rakestraw, and D. S. Anex, *Anal. Chem.* 68: 2726 (1996).
13. K. Schmeer, B. Behnke, and E. Bayer, *Anal. Chem.* 67: 3656 (1995).
14. M. R. Taylor, P. Teale, S. A. Westwood, and D. Perrett, *Anal. Chem.* 69: 2554, (1997).
15. M. R. Taylor and P. Teale, *J. Chromatogr. A* 768: 89 (1997).
16. P. Gfrorer, J. Schewitz, K. Psecker, L-H. Tseng., K. Albert, and E. Bayer, *Electrophoresis* 20: 3 (1999).
17. K. Seller, Z. H. Fan, K. Fluri and J. Harrison, *Anal. Chem.* 66: 3485 (1994).
18. J. P. Kutter, S. J. Jacobson, and J. M. Ramsey, *Anal. Chem.* 69: 5165 (1997).



Gradient Elution: Overview

Ioannis N. Papadoyannis

Kalliopi A. Georga

Aristotle University of Thessaloniki, Thessaloniki, Greece

Introduction

Gradient elution is the elution method in which the mobile-phase composition changes during time. It may be considered as an analogy to the temperature programming in gas chromatography.

Discussion

The main purpose of gradient elution is to move strongly retained components of a mixture faster, while having the least retained components well resolved. At the beginning of the analysis, the solvent used is appropriate to elute some of the components, but is “weak” in terms of its ability to remove other compounds from the column and separate them from one another.

Gradient elution operates on the principle that, under the initial mobile-phase conditions, many of the components have a k' (capacity factor) value of essentially infinity, in that these components are stopped in a narrow band near the head of the column. As the solvent composition is changed and its solvent strength is increased, sample components dissolve at a characteristic solvent strength and then migrate down the column, leaving the remaining components behind. Changes in the mobile-phase composition may be “continuous” with a predetermined set of conditions or may be done in “steps” of substantial solvent composition changes.

The typical gradients used in reversed-phase chromatography are linear or binary (i.e., involving two mobile phases). Convex and concave gradients are used occasionally for analytical purposes, particularly when dealing with multicomponent samples requiring extra resolution either at the beginning or at the end of the gradient (Fig. 1).

The concentration of the organic solvent is lower in the initial mobile phase (mobile phase A) than it is in the final mobile phase (mobile phase B). The gradient then, regardless of the absolute change in percent organic modifier, always proceeds from a condition of

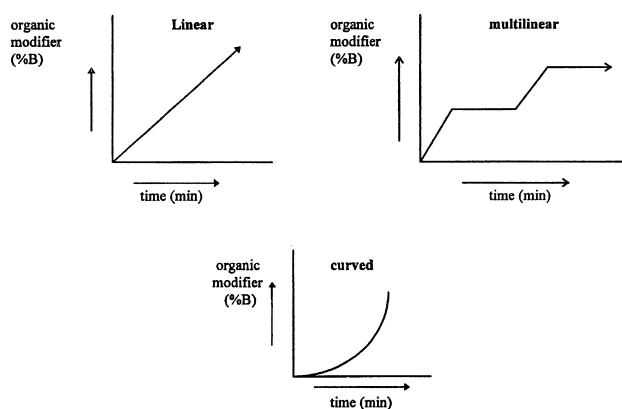


Fig. 1 Various gradient shapes.

high polarity (high aqueous content, low concentration of organic modifier) to low polarity (higher concentration of organic modifier, lower aqueous content). Reversed-phase separations can be achieved using either a stepwise or a continuous gradient to elute sample components. Step gradients (i.e., a series of isocratic elutions at different percentages of B) are useful for applications such as desalting, but for separations requiring high resolution, a linear continuous gradient is required.

Step gradients are also ideal when performing process scale applications providing the desired resolution can be obtained; less complex instrumentation is required to generate step gradients. Additionally, step gradients can be generated more reproducibly than linear gradients.

Gradient shape (combination of linear gradient and isocratic conditions), gradient slope, and gradient volume are all important considerations in reversed-phase chromatography. Typically, when first performing a reversed-phase separation of a complex sample, a broad gradient is used for initial screening in order to determine the optimum gradient shape.

The ideal gradient shape and volume are empirically determined for a particular separation. Generally, the sample is chromatographed using a broad-



range linear gradient to determine where the molecules of interest will elute. The initial conditions usually consist of mobile phase A containing 10% or less organic modifier and mobile phase B containing 90% or more organic modifier. The initial gradient runs from 0% B to 100% B over 10–30 column volumes. A blank gradient is usually run prior to injecting the sample, in order to detect any baseline disturbances resulting from the column or impurities originating in the mobile phase.

After the initial screening is completed, the gradient shape may be adjusted to optimize the separation of the desired components. This is usually accomplished by decreasing the gradient slope, where the desired components elute, and increasing it before and after. The choice of gradient slope will depend on how closely the contaminants elute to the target molecule. Generally, decreasing the gradient slope increases the resolution. However, the peak volume and retention time increase with decreasing gradient slope. Shallow gradients with short columns are generally optimal for high-molecular-weight biomolecules.

Gradient slopes are generally reported as change in percent B per unit time (% B/min) or per unit volume (% B/mL). When programming a chromatography system in the time mode, it is important to remember that changes in flow rate will affect gradient slope and, therefore, resolution.

Resolution is also affected by the total gradient volume (gradient volume \times flow rate). Although the optimum value must be determined empirically, a good rule of thumb is to begin with a gradient volume that is approximately 10–20 times the column volume. The slope can then be increased or decreased in order to optimize the resolution.

Except for optimizing gradient elution methods, which is a very important parameter in chromatographic analysis, another parameter of great significance is the mixing of the mobile-phase components.

There are two primary methods of mixing the mobile-phase components, known as “low-pressure mixing” and “high-pressure mixing.” The first method employs electrically actuated solenoid valves located ahead of a single-solvent delivery system (pump). The precision of the gradient depends on the ability of the solenoid to reproducibly dispense solvents in segments of variable size (volume), depending on the composition desired. If reproducible retention times and stable detector baselines are to be obtained, these “segments

of solvent plugs” must be well mixed into a homogeneous mobile-phase stream before entering the chromatographic column.

The second method uses a separate solvent delivery device for each solvent, with each being capable of delivering smooth, precise flow rates of as low as a few microliters per minute. Gradients are formed by varying the delivery speeds and simply blending the concurrent solvent streams on the high-pressure side of the pumps.

Each method of gradient formation has advantages and disadvantages. The low-pressure gradient formation is preferred most of the time, because it uses only one pump, whereas the high-pressure method uses two pumps which might go wrong during use. Because low-pressure gradient systems have only one pump, they are, of course, less expensive. These systems require extensive degassing and have a large lag time (delay volume) in starting the gradient, whereas, in high-pressure systems, degassing is desired but not essential.

Moreover, low-pressure systems often use three or four solvents. This multiple-solvent blending might also be useful for the optimization of both isocratic and gradient elution methods. This is an advantage that the high-pressure system also has; when not using a gradient system, the operator has two independent isocratic pumps.

Gradient elution is ideal for separating certain kinds of sample which cannot be easily handled by isocratic methods, because of their wide k' range. Nevertheless, there is a strong bias against the use of gradient elution in many laboratories.

Some of the reasons for not preferring gradient elution are as follows: Gradient equipment is not available in some laboratories, because of its higher cost, and gradient elution is more complicated and makes both method development and routine analysis more difficult; the most important issue is that it is not compatible with some high-performance liquid chromatographic (HPLC) detectors (e.g., refractive index detectors). Furthermore, gradient runs take longer, because of the need of column equilibration after each run. Baseline problems are more common with gradient elution and the solvent must be of high purity.

Although the disadvantages of gradient elution must be taken into serious consideration, many separations are only possible using gradient elution. The use of gradient elution for routine applications is suggested for the following kinds of sample:



1. Samples with a wide range of k'
2. Samples composed of large molecules > 1000 in molecular weight
3. Samples containing late eluting interferences that can either foul the column or overlap subsequent chromatograms

Using gradient elution to develop HPLC methods has many advantages compared with using isocratic experiments. First, errors in solvent strength can be adjusted when changing from one solvent to another. Second, the ability to increase resolution during early exploratory runs is a distinct advantage when doing solvent mapping. Early bands often are severely overlapped in isocratic separations, so that it may not be clear how resolution is changing as separation condi-

tions are varied. Gradient elution opens up the front of the chromatogram, allowing a better view of what is happening as conditions are varied (Fig. 2).

Third, using gradient elution runs during the initial stages of method development makes it easier to locate compounds that elute either very early or very late in the chromatogram. With isocratic separation, early-eluting compounds are often lost in the solvent front, whereas late-eluting compounds disappear into the baseline or overlap the next sample. Finally, gradient elution method development works for either gradient or isocratic elution.

In conclusion, gradient elution is not preferred as a quantitative technique because it is more complex than isocratic elution and, hence, more things can potentially go wrong. However, with proper control

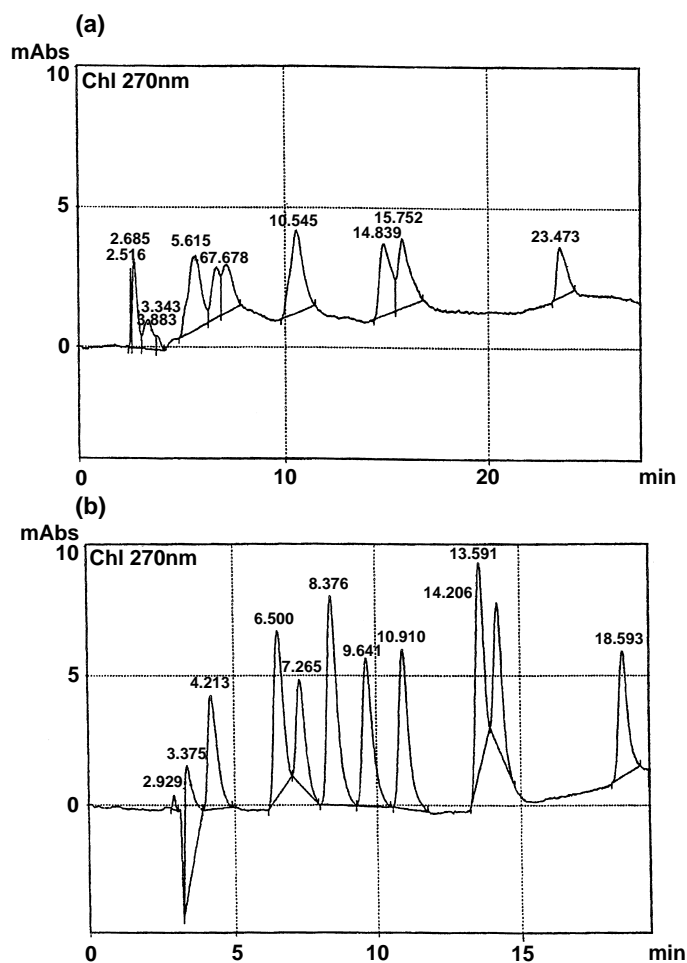


Fig. 2 HPLC analysis of eight methylxanthines: (a) with isocratic elution; (b) with gradient elution.



of operating parameters and good instrumentation, it is possible to obtain a separation with excellent quantitative results. This requires that the operator understand the hardware and determine that it is working correctly before attempting a separation. The ideal gradient system should be easy to operate, reproducible to provide consistent retention times, versatile to provide capability of generating various concave, convex, and linear gradient shapes, and convenient to provide a rapid turnaround time to initial eluent conditions (equilibration) for fast throughput from analysis to analysis.

Suggested Further Reading

1. Bidlingmeyer, B. A., *Practical HPLC Methodology and Applications*, John Wiley and Sons, Inc., New York, 1992.
2. Papadoyannis, I., V. Samanidou, and K. Georga, *J. Liq. Chromatogr.* 19(16): 2559 (1996).
3. Pharmacia Biotech, *Reversed Phase Chromatography*, Pharmacia Biotech, Uppsala, Sweden, 1996.
4. Snyder, L. R., J. L. Glajch, and J. J. Kirkland, *Practical HPLC Method Development*, John Wiley and Sons, Inc., New York, 1988.
5. Snyder, L. R., J. J. Kirkland and J. L. Glajch, *Practical HPLC Method Development*, 2nd ed., New York, 1997.



Gradient Generation Devices and Methods

Miroslav Petro

Symyx Technologies, Santa Clara, California, U.S.A.

Introduction

Chromatography represents a large number of principles, methods, and approaches and can be divided into many different groups. One of the classifications is based on the “continuity” of conditions during the separation. Using such a classification, we can recognize two types of chromatographic elution or separation (i.e., isocratic and gradient).

Discussion

Isocratic elution is the term used when the sample is introduced into the separation unit and eluted from it under a constant set of conditions. Isocratic separation is suitable for those applications in which the sample components have similar retention behavior and are eluted rapidly, one after the other.

Gradient elution involves a change in chromatographic conditions during a chromatographic run in order to achieve separation of sample components of widely varying affinities for the stationary phase or of different solubilities in the mobile phase.

There is a good correlation between the retention behavior of solutes under isocratic conditions and the retention observed under conditions of gradient elution [1]. Migration of the solute bands through a chromatographic column under both isocratic and gradient conditions is described in Fig. 1. It demonstrates that the gradient elution cannot improve the resolution, but it is a convenient tool for controlling the speed of the solute migration through the column and, as a result of this, the position of the solute peaks on a chromatogram.

From the practical point of view, it is not important which mechanism controls the chromatographic process during a gradient elution, but how the changes in experimental conditions affect the resulting retention times of separated compounds. Typically, conditions that support a strong retention are applied at the start of the run, and conditions enhancing an elution are applied more and more over the course of the separation. This allows for sufficient resolution of the early eluted,

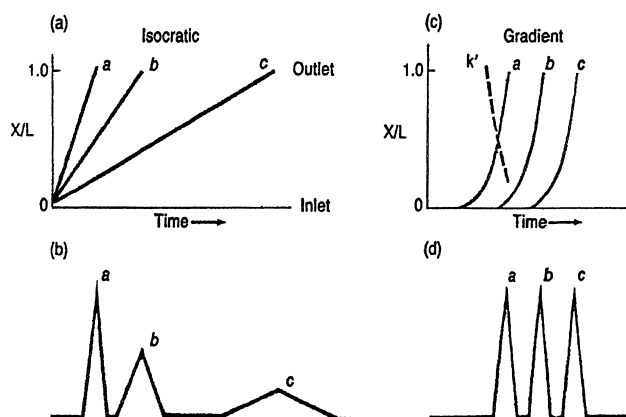


Fig. 1 Fractional migration (X/L) of solute bands along the column and resulting chromatograms for isocratic versus gradient elution. (Reprinted with permission from L. R. Snyder, M. A. Stadalius, and M. A. Quarry, *Analytical Chemistry*, Vol. 55, No. 14, 1983, pp. 1413A–1430A. Copyright 1983 American Chemical Society.)

weakly retained solutes, while ensuring that the elution time of the later peaks is not excessively long. Changes in experimental conditions that affect elution can be either continuous or happening in discrete steps. The continuous gradient can be of any shape. The most popular is a linear gradient, but convex, concave, or a combination of several profiles are also used. Step-elution involves a sudden change in the composition of the mobile phase, followed by a period where the mobile phase is held constant. This process may be repeated several times during an analysis. Optimization of the gradient profile may lead to a successful separation of a large variety of the solutes in a single run.

Theoretical principles, approaches, applications, and advantages of gradient elution are described in detail in a large variety of books and review articles. We recommend reading some of those issued in the last 2 years and the papers referenced therein (see Ref. 2 for some examples). In this entry, we will briefly discuss various types of gradient elution and compare different ways of gradient generation.



Materials and Methods

The devices and methods for gradient generation can be sorted out, for example, according to parameters that are being intentionally changed during the chromatographic run. From those parameters, composition of the mobile phase, flow rate, and temperature are the most important factors influencing the separation in a desirable way.

Mobile-Phase Composition Gradient

The mobile-phase composition gradient involves a change in solvent ratio or concentration of an additive. The properties that affect the separation conditions are, for example, solvent strength, polarity, ionic strength, and pH. Some gradients can be simply generated by an injection of a liquid having an elution strength different from that of the original mobile phase [3]. In a vast majority of cases, the gradient is created by a controlled blending of several eluents together before entering the injection port. A binary gradient refers to a gradient employing two different eluents, a ternary gradient refers to a system in which three different eluents are used, and a quaternary gradient where four different eluents are used.

Gradient Pumps

Gradient pumping (solvent delivery) systems are those that can accurately mix and deliver more than one solvent during an analysis. There is a large variety of gradient pumps for liquid chromatography on the market [4] and many different ways of using them [5]. The major parameters for judging the quality of an isocratic pump are the flow rate precision and accuracy, robustness, and back-pressure capability. In addition to this, accuracy and smoothness of the mobile-phase mixing are the main parameters describing the quality of a gradient pump. The blending of the solvents can occur in one of two ways (i.e., high-pressure mixing or low-pressure mixing).

High-Pressure Mixing

High-pressure mixing means that the eluents are blended on the “high-pressure” side of the pump. Two or more isocratic pumps are required, one for each solvent used to generate the gradient. The output fluid lines of the pumps are joined with a mixing device. Then, the mobile-phase composition during the gradi-

ent is easily controlled by controlling the ratio of the flow rates of the pumps. The schematic of such a setup is shown in Fig. 2a. More than two solvents can also be mixed in this way, by using pumps connected to the mixing device.

For some “high-speed” or “low-volume” applications, it is very important to minimize the time interval needed for the mobile phase to travel from the mixing point to the injection port. High-pressure mixing has an advantage of very low delay volumes, which makes it attractive for rapid analyses, micro high performance liquid chromatography (HPLC), mass spectrometry (MS), and many other applications. The gradient solvent delivery systems can be configured with delay volumes of only a few microliters. The disadvantage of the high-pressure mixing is that piston pumps have limited precision at the extremes of the flow rate ranges, which becomes worse with increasing volume of the piston and decreasing volume of the mixing device. In addition, blending of solvents, compressibility, or combining volumes which are nonadditive may result in unwanted fluctuations of the flow rate at the injector and through the column.

Typically, a constant flow rate (i.e., the sum of the flow rates of all of the isocratic pumps) is desired at any

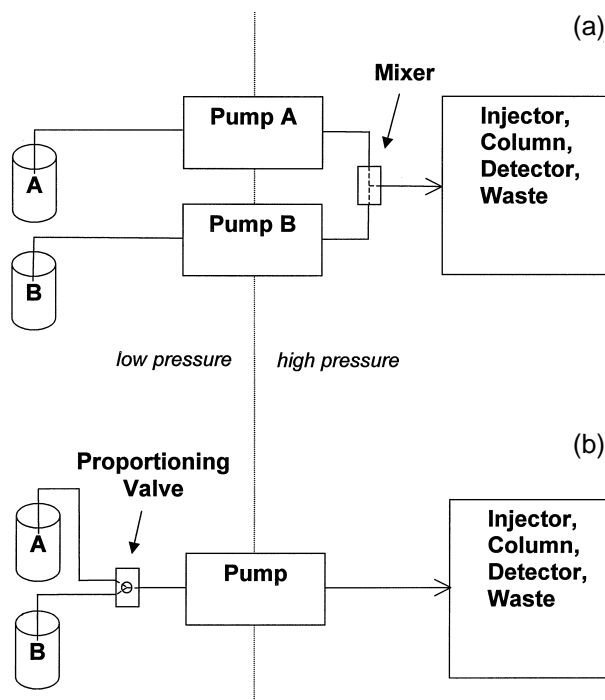


Fig. 2 Schematic of the mobile-phase gradient generation device based on high-pressure (a) and low-pressure (b) mixing of two liquids.

point of the run. However, in certain cases, a combination of the mobile-phase composition and flow rate gradients might be useful.

Low-Pressure Mixing

In contrast to the high-pressure mixing that had prevailed in the early years of gradient liquid chromatography, low-pressure mixing became a common configuration for most of the modern HPLC systems. In the low-pressure mixing arrangement, the solvents are blended at atmospheric pressure, ahead of the pump, and a single high-pressure pump is used to deliver the mixture to injector and column. Figure 2b shows the schematic of such a configuration. It is easier to control mixing of several solvents at the low-pressure side of the pump, as compared to a high-pressure mixing. Therefore, the precision of the blending is good, even at extremes of mobile-phase compositions. Typically, the low-pressure gradient pumps are equipped with a valve that can mix up to four solvents. After the mixing, the blend of the solvents travels through the pump head, pressure transducer, and pulse damper before entering the injection port. This results in a slightly higher delay volume than that offered by a high-pressure gradient system. The delay volume was reduced below 1 mL only for the most advanced low-pressure gradient systems, recommended for separations requiring short and narrow columns or for connection to a low flow rate requiring detection systems such as mass spectrometer.

Electro-osmotic Mixing

The mobile phase can be driven through the chromatographic column not only by a mechanical pressure but also by applying voltage on both ends of the column that generates an electro-osmotic flow. The technique, which uses electro-osmotic flow for driving a mobile phase through a column to achieve a chromatographic separation, is called electrochromatography. Various approaches for gradient elution in electrochromatography have been explored. Simple combination of pressure-driven mixing with electro-osmotic delivery of the resulting blend has been used [6]; however, a more perspective approach seems to be the one that includes merging of two or more electro-osmotic flows, regulated by computer-controlled voltages [7]. An example of such a system is shown in Fig. 3. The mobile-phase composition can be easily changed in time via changes of the applied voltages. One of the main advantages of this approach is that the

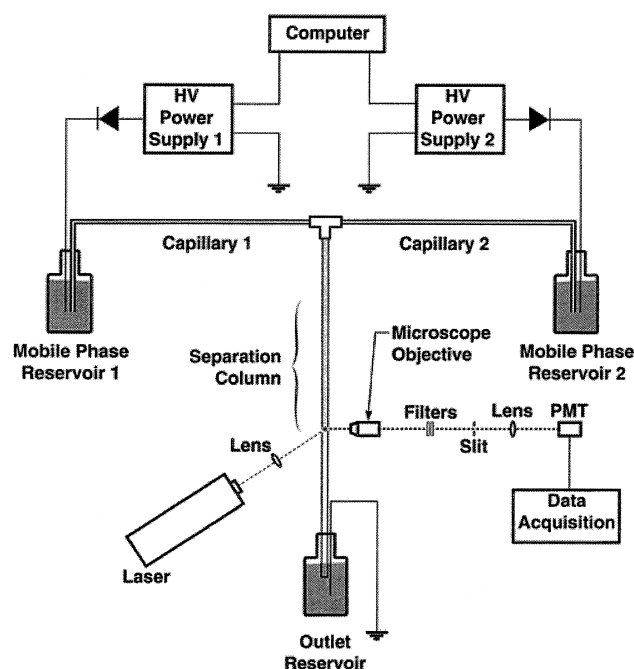


Fig. 3 Schematic of the mobile-phase gradient generation device based on electro-osmotic mixing of two liquids. (Reprinted with permission from C. Yan, R. Dadoo, R. N. Zare, D. J. Rakestraw, and D. S. Anex, *Analytical Chemistry*, Vol. 68, No. 17, 1996, pp. 2726–2730. Copyright 1996 American Chemical Society.)

electro-osmotically driven gradient devices can be miniaturized to the extreme level and micromachined to a high precision to be a part of the new “lab-on-a-chip” technology [8].

On-Line Gradient Generation

Various gradient generation devices have been used for transforming deionized water into solutions of varying pH or ionic strength. The on-line generator allows one to apply mobile-phase gradients without the necessity of blending several starting eluents [9]. In addition, those systems offer very short gradient delays and prevent the corrosive acidic, basic, or salt solutions from contacting sensitive parts of the pump.

Flow Rate Gradient

The main purpose of gradient elution is to achieve separation of sample components which differ widely in retention properties, in a single run. This means that, after eluting all of the fast-moving components of the sample,



we want to speed up the elution of the more retained ones. It is obvious that an increase in the flow rate during the run would serve well for this purpose. Any isocratic pump that allows one to program flow rate versus time can be used for the flow rate gradient elution. In contrast to the mobile-phase composition changes, the speed of the sample band migration through a column increases only linearly with a linear change in the flow rate. Also, the back-pressure increases proportionally with the flow rate increase. These factors severely limit applicability of the flow rate gradients.

Temperature Gradient

Because viscosity of the mobile-phase decreases and the speed of diffusion of the separated molecules increases with an increase in temperature, the temperature gradient represents another way of speeding up elution during a chromatographic run. In addition to these effects, the stationary-phase surface or some of the separated molecules may go through phase-transition changes during the temperature gradient, leading to a strong effect on the separation. Unfortunately, temperature changes, especially during the cooling period, often require significant time for equilibration; this limits the applicability of the temperature-gradient elution in liquid chromatography.

On the other hand, optimization of the column temperature may significantly improve the overall performance of the chromatographic system. Several studies describe a combination of temperature control with the mobile-phase composition changes and the effect of the combined parameters on reversed-phase separations [10].

References

1. L. R. Snyder, M. A. Stadalius, and M. A. Quarry, *Anal. Chem.* 55: 1413A (1983).
2. L. R. Snyder and J. W. Dolan, *Adv. Chromatogr. (NY)* 38: 115 (1998); J. B. Li, J. Morawski, *LC-GC* 16: 468 (1998); P. Schoenmakers, Programmed analysis, in *Handbook of HPLC* (E. Katz, R. Eksteen, P. Schoenmakers, and N. Miller, eds.), Chromatography Science Series Vol. 78, Marcel Dekker, Inc., New York, 1998, pp. 193–231; A. Weston and P. Brown, *HPLC and CE: Principles and Practice*, Academic Press, San Diego, CA, 1997, pp. 1–130.
3. B. Streel, A. Ceccato, P. Chiap, Ph. Hubert, and J. Crommen, *Biomed. Chromatogr.* 9: 254 (1995); V. Berry, *J. Liq. Chromatogr.* 13: 1529 (1990).
4. See for example, <http://www.lcgmag.com/lcgc/bg/prod42.htm>
5. R. L. Stevenson, Mobile-phase delivery systems for HPLC, in *Handbook of HPLC* (E. Katz, R. Eksteen, P. Schoenmakers, and N. Miller, eds.), Chromatography Science Series Vol. 78, Marcel Dekker, Inc., New York, 1998.
6. C. G. Huber, G. Choudhary, and C. Horvath, *Anal. Chem.* 69: 4429 (1997).
7. C. Yan, R. Dadoo, R. N. Zare, D. J. Rakestraw, and D. S. Anex, *Anal. Chem.* 68: 2726 (1996).
8. D. Figeys and R. Aebersold, *Anal. Chem.* 70: 3721 (1998); J. P. Kutter, S. C. Jacobson, and J. M. Ramsey, *Anal. Chem.* 69: 5165 (1997).
9. Y. Liu, N. Avdalovic, C. Pohl, R. Matt, H. Dhillon, and R. Kiser, *Am. Lab.* 30 (22): 48 (1998).
10. J. W. Dolan, L. R. Snyder, N. M. Djordjevic, D. W. Hill, D. L. Saunders, L. Van Heukelem, and T. J. Waeghe, *J. Chromatogr. A* 803: 1 (1998); M. H. Chen and C. Horvath, *J. Chromatogr. A* 788: 51 (1997).



Headspace Sampling

Raymond P.W. Scott

Scientific Detectors Ltd., Banbury, Oxfordshire, England

Introduction

Headspace sampling is usually employed to identify the volatile constituents of a complex matrix without actually taking a sample of the material itself. There are three variations of the technique: (a) static headspace sampling, (b) dynamic headspace sampling, and (c) purge and trapping.

Discussion

The first technique, commonly used to monitor the condition of foodstuffs, particularly for detecting food deterioration (food deterioration is often accompanied by the characteristic generation of volatile products such as low-molecular-weight organic acids, alcohols, and ketones, etc.), involves first placing the sample in a flask or some other appropriate container and warming to about 40°C. Raising the temperature increases the distribution of the volatile substances of interest in the gas phase. A defined volume of the air above the material is withdrawn through an adsorption tube by means of a gas syringe. Graphitized carbon is often used as the adsorbing material, although other substances such as porous polymers can also be employed. Carbon adsorbents having relatively large surface areas ($\sim 100 \text{ m}^2/\text{g}$) are used for adsorbing low-molecular-weight materials, whereas for large molecules, adsorbents of lower surface areas are used ($\sim 5 \text{ m}^2/\text{g}$). After sampling, the adsorption trap is placed in an oven and connected to the chromatograph. The column is maintained at a low temperature (50°C or less) to allow the desorbed solutes to concentrate at the beginning of the column. The trap is then heated rapidly to about 300°C and a stream of carrier gas sweeps the desorbed solutes onto the column. When desorption is complete, the temperature of the column is programmed up to an appropriate temperature and the components of the headspace sample are separated and quantitatively assayed. The proportions of each component in the gas phase will not be the same as that in the sample, as they are modified by the distribution coefficient. Thus, analyses will be comparative or relative, but not absolute.

The second analytical procedure is somewhat similar, but a continuous stream of gas is passed over the sample and through the trap. This produces a much larger sample of the volatile substances of interest and, thus, can often detect trace materials. The adsorbed components are desorbed by heat in the same manner and passed directly onto a gas chromatography (GC) column. The results are still determined by the distribution coefficient of each solute between the sample matrix and the air and, thus, the quantitative results remain comparative or relative, but not absolute.

The third method (purge and trap) is used for liquids and, in particular, for testing for water pollution by volatile solvents. In this method, air or nitrogen is bubbled through the water sample and then through the adsorbent tube. In this way, the substances of interest can be completely leached from the water; the results will give the total quantity of each solute in the original water sample. Thus, with this method, the results can be actual and not relative or comparative. The solutes are desorbed by heat in exactly the same way as the previous two methods, but provision is usually made to remove the water that is also collected before developing the separation.

A good example of the use of headspace analysis is in the quality control of tobacco. Despite the health concern in the United States, tobacco is an extremely valuable export and its quality needs to be carefully monitored. Tobacco can be flue cured, air cured, fire cured, or sun cured, but the quality of the product can often be monitored by analyzing the vapors in the headspace above the tobacco.

The headspace over tobacco can be sampled and analyzed using a solid-phase micro-extraction (SPME) technique. The apparatus used for SPME is shown in Fig. 1. The basic extraction device consists of a length of fused-silica fiber, coated with a suitable polymeric adsorbent, which is attached to the steel plunger contained in a protective holder. The steps that are taken to sample a vapor are depicted in Fig. 1. The sample is first placed in a small headspace vial and allowed to come to equilibrium with the air in the vial (1). The needle of the syringe containing the fiber is then made to pierce the cap, and the plunger pressed to expose the fiber to



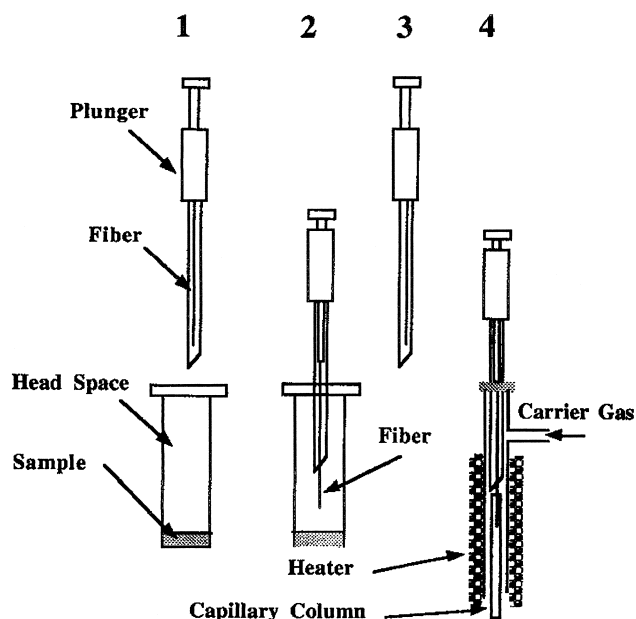


Fig. 1 The SPME apparatus.

the headspace vapor. The fiber is left in contact with air above the sample for periods that can range from 3 to 60 min, depending on the nature of the sample (2).

The fiber is then removed from the vial (3) and then passed through the septum of the injection system of the gas chromatograph into the region surrounded by a heater (4). The plunger is again depressed and the fiber, now protruding into the heater, is rapidly heated to desorb the sample onto the GC column. In most cases, the column is kept cool so the components concentrate on the front of the column. When desorption is complete (a few seconds), the column can then be appropriately temperature programmed to separate the components of the sample. A chromatogram of the headspace sample, taken over tobacco, is shown in Fig. 2. The actual experimental details were as follows. One gram of tobacco (12% moisture) is placed in a 20-mL headspace vial and 3.0 mL of 3M potassium chloride solution is added. The fiber is coated with polydimethyl siloxane (a highly dispersive adsorbent) as a 100- μ m film. The vial is heated to 95°C and the fiber is left in contact with the headspace for 30 min. The sample is then desorbed from the fiber for 1 min at 259°C. The separation can be carried out on a column 30 cm long with a 250- μ m inner diameter, carrying a 0.25- μ m-thick film of 5% phenylmethylsiloxane. The

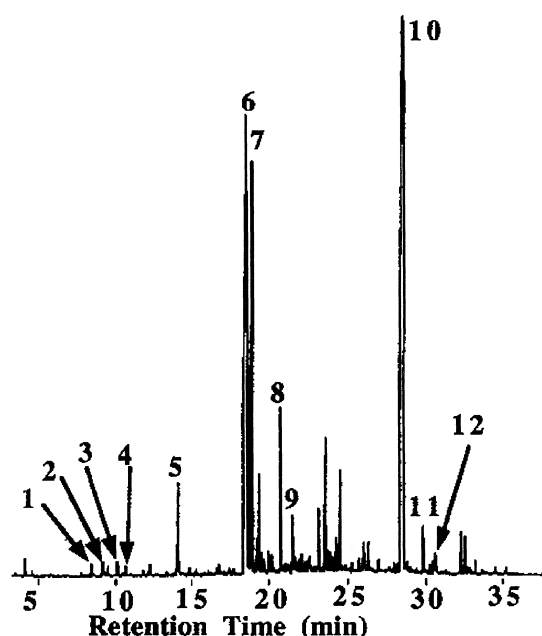


Fig. 2 A chromatogram of tobacco headspace. 1: Benzaldehyde; 2: 6-methyl-5-heptene-2-one; 3: phenylacetaldehyde; 4: ninanal; 5: menthol; 6: nicotine; 7: solanone; 8: geranyl acetone; 9: β -nicotyrine; 10: neophytadiene; 11: famesylacetone; 12: cembrene.

stationary phase is predominantly dispersive, with a slight capability of polar interactions with strong polarizing solute groups by the polarized aromatic nuclei of the phenyl groups. Helium can be used as the carrier gas, at 30 cm/s. The column is held isothermally at 40°C for 1 min, then programmed to 250°C at 6°C/min and held at 250°C for 2 min. It is seen that a clean separation of the components of the tobacco headspace is obtained and the resolution is quite adequate to compare tobaccos from different sources, tobaccos with different histories, and tobaccos of different quality.

References

1. D. W. Grant, *Capillary Gas Chromatography* (R. P. W. Scott, C. F. Simpson, and E. D. Katz, eds.), John Wiley & Sons, Chichester, 1996.
2. R. P. W. Scott, *Introduction to Analytical Gas Chromatography*, Marcel Dekker, Inc., New York, 1998.
3. R. P. W. Scott, *Techniques of Chromatography*, Marcel Dekker, Inc., New York, 1995.

Helium Detector

Raymond P.W. Scott

Scientific Detectors Ltd., Banbury, Oxfordshire, England

Introduction

The outer group of electrons in the noble gases is complete, and as a consequence, collisions between noble gas atoms and electrons are perfectly elastic. It follows that if a high potential is set up between two electrodes in a noble gas and ionization is initiated by a suitable radioactive source, electrons will be accelerated toward the anode and will not be impeded by energy absorbed from collisions with the noble gas atoms. However, if the potential of the anode is high enough, the electrons will develop sufficient kinetic energy that, on collision with a the noble gas atom, energy can be absorbed and a *metastable* atom can be produced. A metastable atom carries *no* charge, but adsorbs energy from collision with a high-energy electron by displacing an orbiting electron to an outer orbit.

Discussion

Metastable helium atoms have an energy of 19.8 and 20.6 eV and thus can ionize and, consequently, detect all permanent gas molecules and, in fact, the molecules of all other volatile substances. A collision between a metastable atom and an organic molecule will result in the outer electron of the metastable atom collapsing back to its original orbit, followed by the expulsion of an electron from the organic molecule. The electrons produced by this process are collected at the anode and produce a large increase in anode current. However, when an ion is produced by collision between a metastable atom and an organic molecule, the electron, simultaneously produced, is also immediately accelerated toward the anode. This results in a further increase in metastable atoms and a consequent increase in the ionization of other organic molecules.

This cascade effect, unless controlled, results in an exponential increase in ion current. It is clear that the helium must be extremely pure or the production of metastable helium atoms would be quenched by traces of any other permanent gases that may be present.

Originally, a very complicated helium-purifying chain was necessary to ensure the helium detector's op-

timum operation. However, with high-purity helium becoming generally available, the helium detector is now a more practical system.

The metastable atoms that must be produced in the argon and helium detectors need not necessarily be generated from electrons induced by radioactive decay. Electrons can be generated by electric discharge or photometrically, which can then be accelerated in an inert gas atmosphere under an appropriate electrical potential to produce metastable atoms. This procedure is the basis of a highly sensitive helium detector that is depicted on the left-hand side of Fig. 1. The detector does not depend solely on metastable helium atoms for ionization and, for this reason, is called the helium discharge ionization detector (HDID).

The sensor consists of two cavities, one carrying a pair of electrodes across which a potential of about 550 V is applied. In the presence of helium, this poten-

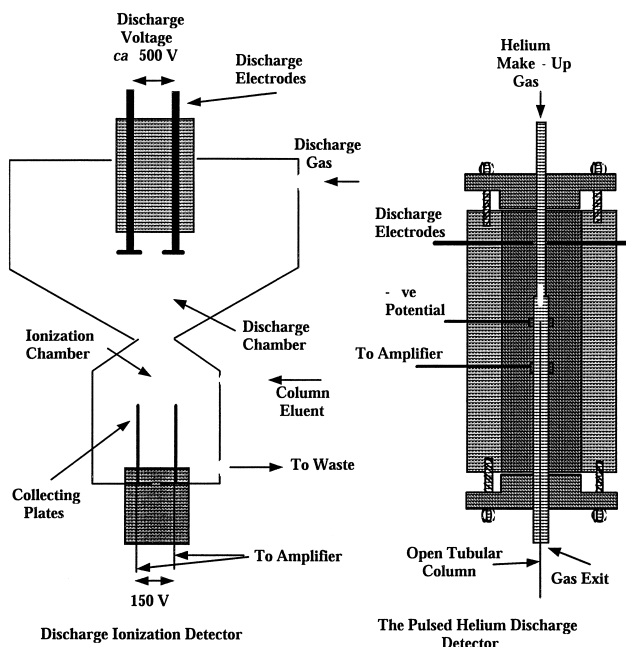


Fig. 1 The discharge ionization detector (courtesy of GOW-MAC Instruments) and the pulsed helium discharge detector (courtesy of Valco Instruments).



tial initiates a gas discharge across the electrodes. The discharge gas passes into a second chamber that acts as the ionization chamber and any ions formed are collected by two plate electrodes having a potential difference of about 160 V. The column eluent enters the top of the ionization chamber and mixes with the helium from the discharge chamber and exits at the base of the ionization chamber.

In this particular detector, ionization probably occurs as a result of a number of processes. The electric discharge produces both electrons and photons. The electrons can be accelerated to produce metastable helium atoms which, in turn, can ionize the components in the column eluent. However, the photons generated in the discharge have, themselves, sufficient energy to ionize many eluent components and so ions will probably be produced by both mechanisms. It is possible that other ionization processes may also be involved, but the two mentioned are likely to account for the majority of the ions produced. The response of the detector is largely controlled by the collecting voltage and is very sensitive to traces of inert gases in the carrier gas. Peak reversal is often experienced at high collecting voltages, which may also indicate that some form of electron capturing may take place between the collecting electrodes. This peak reversal appears to be significantly reduced by the introduction of traces of neon in the helium carrier gas.

The helium discharge ionization detector has a high sensitivity toward the permanent gases and has been used very successfully for the analysis of trace components in ultrapure gases. It would appear that the detector response is linear over at least two, and possibly three, orders of magnitude, with a response index probably lying between 0.97 and 1.03. In any event, any slight nonlinearity of the sensor can be corrected by an appropriate signal-modifying amplifier. The potential sensitivity of the detector to organic vapors appears to be about 1×10^{-13} g/mL.

The Pulsed Helium Discharge Detector

The pulsed helium discharge detector [1,2] is an extension of the helium detector, a diagram of which is shown on the right-hand side of Fig. 1. The detector has two

sections: the upper section consisting of a tube 1.6 mm i.d. (where the discharge takes place) and the lower section, 3 mm i.d. (where reaction with metastable helium atoms and photons takes place). Helium makeup gas enters the top of the sensor and passes into the discharge section. The potential (about 20 V) applied across the discharge electrodes and for optimum performance is pulsed at about 3 kHz with a discharge pulse width of about 45 μ s. The discharge produces electrons and high-energy photons (that can also produce electrons), and probably some metastable helium atoms. The photons and metastable helium atoms enter the reaction zone where they meet the eluent from the capillary column. The solute molecules are ionized and the electrons produced are collected at the lower electrode and measured by an appropriate high-impedance amplifier. The distance between the collecting electrodes is about 1.5 mm. The helium must be 99.9995 pure, otherwise permanent gas impurities quench the production of metastable atoms. The base current ranges from 1×10^{-9} to 5×10^{-9} A, the noise level is about 1.2×10^{-13} A, and the ionization efficiency is about 0.07%. It is claimed to be about 10 times more sensitive than the flame ionization detector and to have a linear dynamic range of 10^5 . The pulsed helium discharge detector appears to be an attractive alternative to the flame ionization detector and would eliminate the need for three different gas supplies. It does, however, require equipment to provide specially purified helium, which diminishes the advantage of using a single gas.

References

1. W. E. Wentworth, S. V. Vasin, S. D. Stearns, and C. J. Meyer, *Chromatographia* 34: 219 (1992).
2. W. E. Wentworth, H. Cai, and S. D. Stearns, *J. Chromatogr.* 688: 135 (1994).

Suggested Further Reading

Scott, R. P. W., *Chromatographic Detectors*, Marcel Dekker, Inc., New York, 1996.
 Scott, R. P. W., *Introduction to Analytical Gas Chromatography*, Marcel Dekker, Inc., New York, 1998.



High-Speed SEC Methods

Peter Kilz

Polymer Standards Service GmbH, Mainz, Germany

INTRODUCTION

Size-exclusion chromatography (SEC) is the established method to determine macromolecular properties in solution. It is the only technique that allows efficient measurement of property distributions for a wide range of applications. Recent trends in industrial laboratories and research institutes have been focused on increasing the analytical throughput in order to increase productivity. Quality control and combinatorial chemistry demand the optimization of high-throughput methods. Increased analytical throughput can also save time and resources (e.g., instrumentation) in production-related fields. In combinatorial research, high-throughput analytical techniques are a bare necessity, because of the huge numbers of samples being synthesized.^[1,2; and references therein] In either situation, the slowest step in the process will determine the overall turnaround time. The importance of high-speed analytical techniques becomes obvious when research companies synthesize over 500 targets per day, but only about 100 samples can be analyzed. The potential of new synthetic methods and in-line production control cannot be fully utilized until the typical SEC run times of 40 min are substantially reduced.

METHODS FOR FAST SEC ANALYSES

There have been several approaches to overcome the traditionally slow SEC separations, which are caused by the diffusion processes in SEC columns. Most of them are column-related (see “High-Speed SEC Columns,” “Small Particle Technology,” and “Smaller SEC Column Dimensions”); one utilizes the column void volume (cf. “Overlaid Injections”), while another replaces separation with simplified sample preparation (see “Flow Injection Analysis”). Cloning existing methods and instrumentation is also reviewed with respect to the potential time gain (see “Cloning of SEC Systems”). Benefits and limitations of each method are summarized in Table 1.

High-Speed SEC Columns

The pore volume of the column packing has been shown to be one of the major factors influencing peak resolution in SEC. True high-speed separations, with good resolu-

tion, requires special high-speed columns, which allow fast flow rates, possess high separation volumes, and allow solutes to easily access the pores.^[3] PSS GmbH is currently the only vendor of high-speed columns for SEC. Their high-speed columns replace conventional columns one to one, which allows for a trouble-free method transfer from an existing conventional application to a high-speed application. High-speed SEC can be performed in about 1 min, cutting down analysis time by about 10%, with similar resolution on existing instrumentation.^[4] Fig. 1 shows a comparison of an SEC separation of polystyrene standards in THF on a conventional column and on a high-speed column, analyzed on the same instrument.

Precision and accuracy of high-speed separations have been investigated for various applications. Both the accuracy of molar mass results and the reproducibility have been comparable to results from conventional columns.^[3]

Fig. 2 shows the overlay of 10 out of 60 repeats of a commercial polycarbonate sample analyzed in tetrahydrofuran (THF). They overlap almost perfectly. Each run took about 2.5 min, and the total run time for 60 repeats was about 2 hr.

The overall time savings can even be larger when taking the complete analytical process into account. The total run time of an instrument consists of the preparation and equilibration time, the time needed for running the calibration standards, and the run times for the unknown samples. If 10 individual standards are used for calibration and 10 samples are run, the total run time on a conventional system will be about 2 days. The same work carried out on a high-speed system will only require about 3 hr, and can be easily performed in a single day.^[4]

The cost-saving aspects of high-throughput SEC techniques can be substantial and have been evaluated for different scenarios.^[5]

Polyolefins, other synthetic polymers, and water-soluble macromolecules have been investigated in high-speed SEC systems. High-speed SEC can be a major time saver in two-dimensional chromatography applications, which require about 10 hr analysis time for cross-fractionation.^[6] This can be reduced by a factor of 10, to about 1 hr, which makes it much more interesting for many laboratories. Details on these and additional high-speed applications can be found in Ref. [4].

**Table 1** Synopsis of methods for increased SEC throughput

Approach	Advantages	Disadvantages	Beneficial for...
Instrument cloning	No method change Easy to implement No additional training	High investment cost High maintenance Higher operating cost More people More space Limited throughput gain No eluent savings	Sample increase of up to 3 ×
High-speed column	No method change Uses existing equipment 1:1 application transfer No additional training Minimizes investment (column only) SEC separations in 1 min Time gain ca. 10 × No additional shear High efficiency Runs with conventional software	No separation Limited time gain Not applicable for copolymers/blends Requires molar mass sensitive detectors Only primary information (conc., Mw, IV) Needs method change Needs special software Needs overlaid injection-ready software	QC/QA Increased throughput (10 ×) Use with exiting methods
FIA	Uses existing equipment Saves eluent	Only primary information (conc., Mw, IV) Needs method change Needs special software Needs overlaid injection-ready software	Samples difficult to separate Utilize existing instruments
Overlaid injections	No method change Uses existing equipment No additional training Low cost	Limited time savings Needs method adaption Optimization of: injection volumes detection systems Shear degradation Low efficiency Needs training Limited throughput increase	QC/QA known samples
Small columns	Uses existing equipment Minimizes investment Saves eluent Runs with current software	Limited time savings Needs method adaption Optimization of: injection volumes detection systems Shear degradation Low efficiency Needs training Limited throughput increase	Low-resolution applications Low time-saving requirements Single detector applications

Small Particle Technology

Reducing particle size of the SEC column packings reduces the time requirements in SEC because of the increased mass transfer and resultant separation efficiency. Hence, columns can become smaller in dimensions while maintaining resolution. This approach has been used for many years. Column bank lengths dropped from several meters to now typically 60 cm with current SEC column particle sizes of 5 μm as compared with about 100 μm in the early 1960s. During the same period, time requirements dropped from about 6 hr to less than 1 hr.

Unfortunately, this approach is very limited now because of the high shear rates in columns packed with small particles (less than 5 μm), which can cause polymer degradation.

Smaller SEC Column Dimensions

The reduction of column dimensions can, in theory, substantially reduce the time requirements of the separation. However, several limitations predicted by chromatographic theory have to be considered.^[7,8] A study of

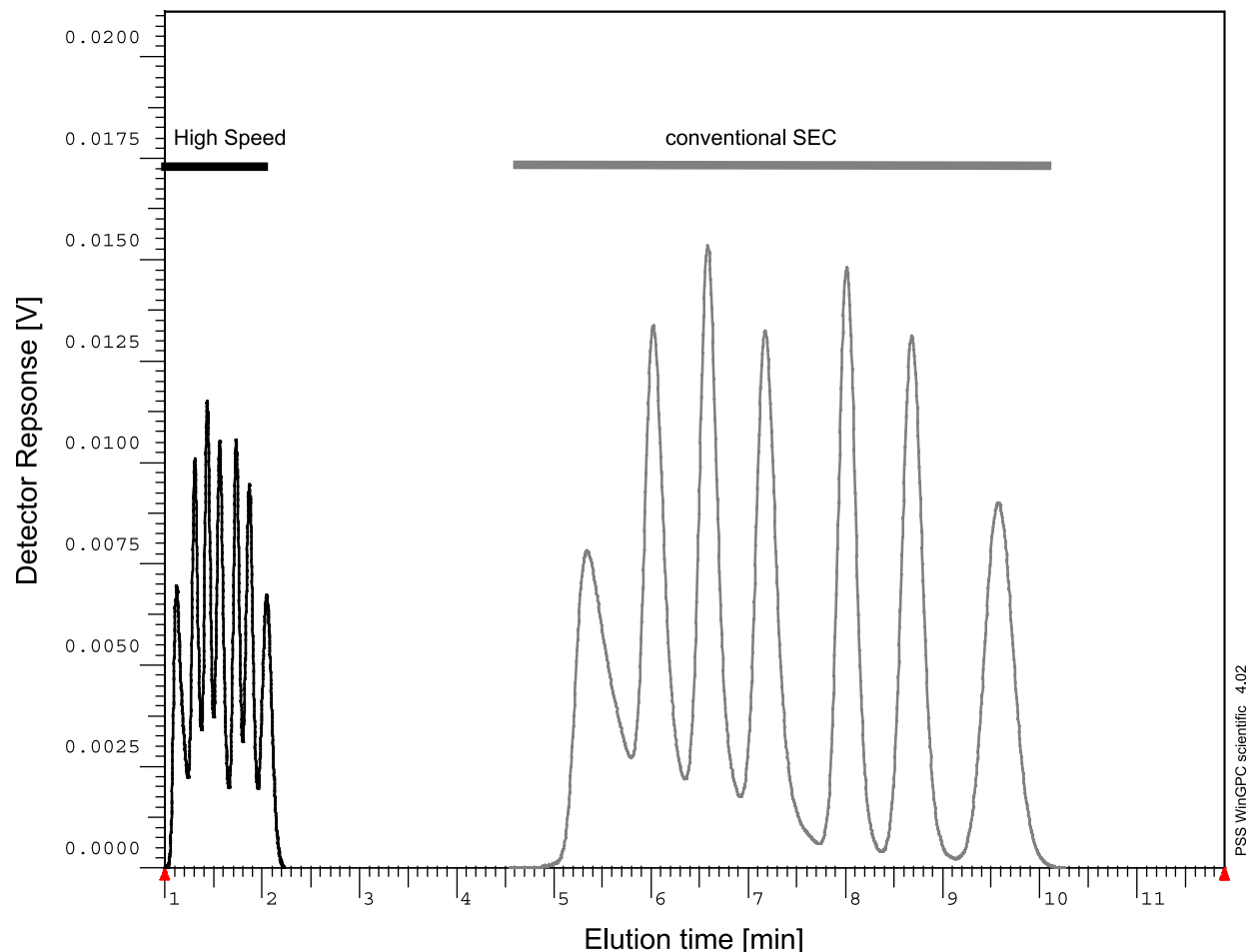


Fig. 1 Chromatogram of conventional SEC column (right part) compared to HighSpeed SEC column (left part); tested on identical instrument with polystyrene standards, in THF.

the influence of column dimensions on fast SEC separations has been published in Ref. [4]. It has been found difficult to optimize and transfer existing methods and, in many cases, new equipment had to be purchased.

Overlaid Injections

This approach has also been used when SEC separations required hours; it can cut down analysis time by a factor of 2. It utilizes the fact that about 50% of the SEC elution time is needed to transport the solutes through the interstitial volume of the columns. This allows us to inject another sample before the current one is already totally eluted. The optimum injection interval, Δt_{\min} , can be calculated from the separation properties of the instrument:

$$\Delta t_{\min} = (V_t - V_0)/F$$

where V_t is the total penetration volume of column(s), V_0 is the total exclusion volume of column(s), and F is the volumetric flow rate.

The required parameters are easily determined from a molar mass calibration curve.

Today, this method can be combined with appropriate software to automate data acquisition and data processing. It is easy to use, requires no additional investment, and no method modifications are necessary.

Flow Injection Analysis (FIA)

Another approach to cut down on analysis time is to avoid separation and inject samples directly into detector cells. FIA has received some attention recently and is, therefore, mentioned in this review. Because it does not rely on any separation, advantages and limitations will be summarized only.

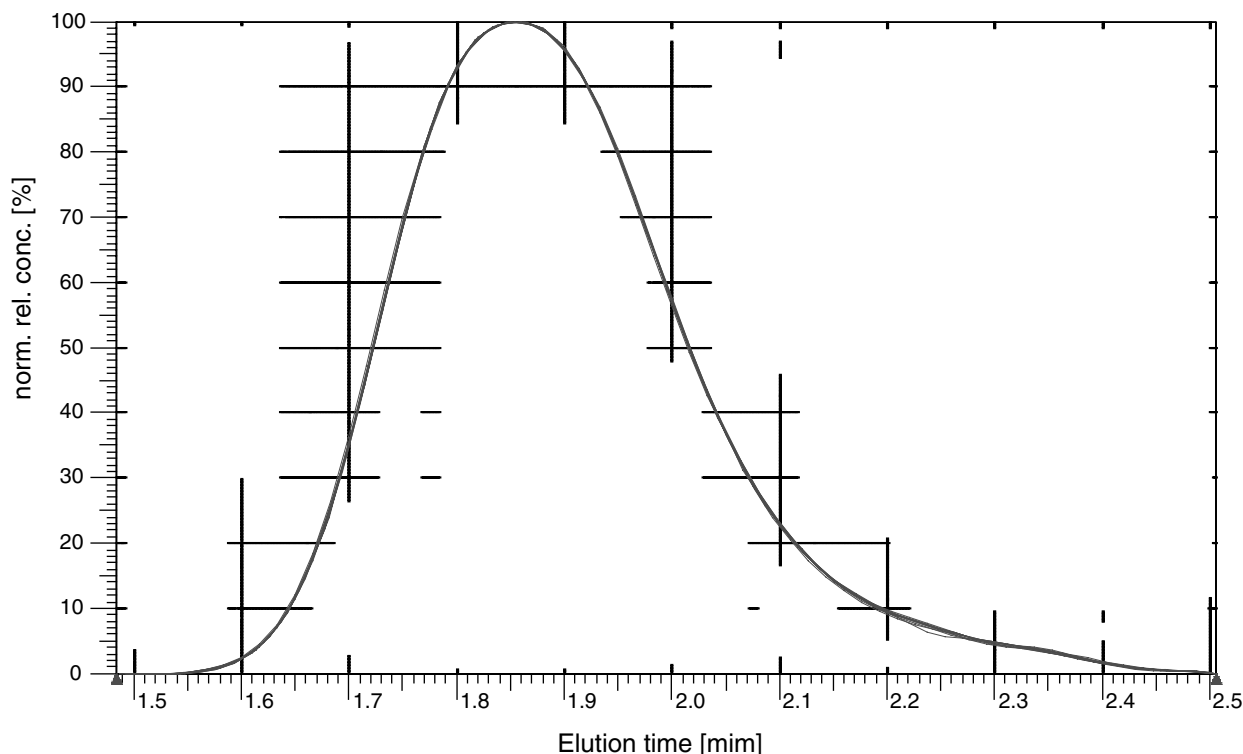


Fig. 2 Overlay of 10 out of 60 repeats of a commercial polycarbonate analysis, in THF, on PSS SDV 5 μm HighSpeed 10^3 , 10^5 Å column; measured $M_w = (29,610 \pm 150)$ g/mol (nominal sample molar mass by producer: 30,000 g/mol).

This method uses the high-performance liquid chromatography (HPLC) equipment for sample handling and requires molar mass sensitive detectors (such as light scattering and/or viscometry) to obtain a mean property values from each detector (M_w and/or IV, respectively). The FIA result from a concentration detector yields polymer content in a sample, which can also be determined with other well-established methods. The FIA approach requires expensive and well-maintained equipment, and will not save much time or solvent; furthermore, no distribution information is available.

Cloning of SEC Systems

The number of processed samples can be increased proportionally by increasing the number identical systems. The time and analytical requirements for each sample are not changed, but the number of samples per hour can be increased. Because no change in analytical methods is necessary, cloning SEC instruments and methods is straightforward and can be carried out in most environments.

This approach, however, is clearly limited by the availability of important resources such as laboratory

space, operators, instrumentation, and software licenses. Cloning systems can become very costly; time and effort for instrument maintenance and operation increases proportionally.

True parallelization of analytical processes has, so far, not been very successful. In such set-ups, only the separation module (in general the column) is set up in parallel, while solvent delivery, injection, detection, and data processing are multiplexed. These systems will no longer be as simple in operation and maintenance as the cloned systems.

CONCLUSION

Time requirements of SEC experiments can be reduced substantially by using high-speed SEC columns. The availability of high-speed columns allows an increase in SEC separations by a factor of 10 and run times of 1 min are possible. Precision and accuracy of results are comparable with existing methods. Existing methods and instrumentation can still be used with high-speed columns.



The time gain of high-speed columns can open up SEC methodology for

- a) monitoring and controlling processes on-line;
- b) using SEC methods routinely in QC labs;
- c) allowing high-throughput screening for new materials design;
- d) being a useful tool in combinatorial chemistry; and
- e) studying monitoring time-critical processes.

REFERENCES

1. Nielson, R.B.; Safir, A.L.; Petro, M.; Lee, T.S.; Huefner, P. *Polym. Mater. Sci. Eng.* **1999**, 80, 92.
2. Brocchini, S.; James, K.; Tangpasuthadol, V.; Kohn, J. J. *Am. Chem. Soc.* **1997**, 119, 4553.
3. Kilz, P.; Reinhold, G.; Dauwe, C. *Proceedings of the International GPC Symposium 2000; Las Vegas, NV*; Waters Corp.: Milford, MA, 2001; (CD-ROM).
4. Kilz, P. Methods and Columns for High Speed SEC Separations. In *Handbook for Size Exclusion Chromatography and Related Techniques*; Wu, C.-S., Ed.; Marcel Dekker: New York, 2002, *in press*.
5. Reinhold, G.; Hofe, T. *GIT Fachz. Lab.* **2000**, 44, 556.
6. Kilz, P.; Pasch, H. Coupled LC Techniques in Molecular Characterization. In *Encyclopedia of Analytical Chemistry*; Meyers, R.A., Ed.; Wiley: New York, 2000; Vol. 9, 7495–7543.
7. Giddings, J.C.; Kucera, E.; Russell, C.P.; Myers, M.N. *J. Phys. Chem.* **1968**, 72, 4397.
8. Glockner, G. *Liquid Chromatography of Polymers*; Hüthig: Heidelberg, 1982.

High-Temperature High-Resolution Gas Chromatography

Fernando M. Lanças

J.J.S. Moreira

Laboratório de Cromatografia, Instituto de Química de São Carlos, Universidade de São Paulo, São Carlos/SP, Brazil

Introduction

Gas chromatography (GC), in its early days, used packed columns with chemically inert solid supports coated with stationary phases. These columns presented low efficiency due to the wide range of particle sizes used, causing inhomogeneity in the packed bed and, consequently, high instability due to a poor deactivation and thermal instability at high-temperature operations [1]. This characteristic limited the use of the GC to only volatile and low-mass molecular compounds. The later development of columns with a stationary phase coated on the inner wall of the capillary provided a more inert environment. In this form, columns with higher thermal stability and more efficiency (higher N) were produced, allowing the analysis of semivolatile and medium molecular mass compounds. This technique was named high-resolution gas chromatography (HRGC) [1]. The possibility of using thermally stable, highly efficient columns, stimulated scientists to search for new stationary phases and chemical manufacturing processes to produce capillary columns with high thermal stabilities, capable of operating at higher temperatures [2] (to 360°C).

Lipsky and McMurray [3] suggested, in their pioneering work on high-temperature high-resolution gas chromatography (HT-HRGC), the use of column temperatures equal to, or higher than, 360°C. However, other column temperature values have also been reported for this technique [4].

The thermal stability of the high-temperature capillary columns allowed the analysis of higher molecular masses (more than 600 Da) and nonvolatile compounds never before directly analyzed by gas chromatography [2].

Instrumentation for HT-HRGC

The instrumentation used for HT-HRGC is the same as used for conventional GC, with only minor modifications.

Columns

The columns utilized in HT-HRGC are short (usually equal to, or shorter than, 10 m) coated with thin films

($\sim 0.1 \mu\text{m}$ or less) and having an inner diameter (i.d.) around 0.2 mm [5].

A smaller inner diameter (e.g., 0.1 mm) can also be used, but with the inconvenience of limiting the work to more diluted samples in order to avoid column overload. On the other hand, this type of column permits carrier gas speeds higher than with columns of inner diameters in the range 0.2–0.3 mm. Columns with inner diameters equal to 0.1 mm exhibit fewer plates with the increment of the carrier gas speed, in contrast to the columns with equivalent characteristics, but of 0.3 mm i.d. [5]. The increase of the carrier gas speed in smaller-i.d. columns performs an analysis in a shorter time, without undermining the efficiency of separation [6].

Capillary columns, to be suitable to HT-HRGC, must be extremely robust and must be coated with a thin film of the stationary phase with the purpose of reducing the retention of the less volatile compounds and preventing stationary-phase bleed at high temperatures [7].

Using such proper columns, elution of substances with carbon numbers in excess of $n\text{-C}_{130}$ has been reported, at column temperatures of up to 430°C [8].

Tubing Material for HT-HRGC Columns

There are four major types of materials being utilized to prepare columns for high-temperature capillary columns [2]:

1. Glass (borosilicate)
2. Polyimide-clad fused silica
3. Aluminum-clad fused silica
4. Metal-clad fused silica

Columns of aluminum-clad fused silica [2,4] and metal-clad fused silica support temperatures up to 500°C, representing an advantage in comparison with borosilicate glass columns, with a temperature limit to 450°C, and columns of polyimide-clad fused silica for high temperature [2,9], limited temperature to 400–420°C. On the other hand, aluminum-clad fused silica columns present leakage, principally in the connec-



tions, after a short time of use [2,9]. Polyimide-clad fused-silica capillaries, after prolonged exposure to temperatures above 380°C, tend to break spontaneously at many points, thus losing the polyimide coating [9]. Borosilicate columns are inexpensive, being an alternative to fused silica for high-temperature applications. However, these columns have been reported to leak when coupled with retention gap and to mass spectrometry detectors [2]. An important alternative for HT-HRGC are HT metal-clad fused-silica columns which resist temperatures above 500°C for long-term exposure [9].

Stationary Phases

The first results on HT-HRGC [3,10] were published in 1983, dealing with stationary-phase immobilization (polysiloxane — OH terminated). Due to the column instability, when submitted to high temperature, stationary-phase loss was common at that time. These works can be considered to be the precursor of high-temperature gas chromatography, because the phase immobilization process developed resulted in a series of OH-terminated polysiloxane phases compatible with the inner surfaces of borosilicate glass and fused-silica tubing. These phases are thermally stable and capable of withstanding elevated temperatures [11] used in HT-HRGC. After this report, many other articles dealing with the ideal stationary phase for high-temperature gas chromatography appeared. Nonpolar stationary phases of the carborane-siloxane-type bonded phase (temperature range >480°C) and siloxane-silarylene copolymers suitable for HTGC were developed [7] around 1988.

A medium-polarity stationary phase based on fluoralkyl-phenyl substitution, which is thermally stable up to 400°C, was reported [12], and a CH₃O-terminated polydimethyl siloxane, diphenyl-substituted stationary phase made possible the analysis of complex high-molecular-mass mixtures such as free-base porphyrins and triglycerides using narrow-bore capillary columns [5]. Since these developments, a variety of stationary phases for analysis of specific analytes by HT-HRGC were found [2].

Sample Introduction

The sampling and elution of such high-molecular-weight materials requires careful attention in order to avoid quantitative sample losses during the sample introduction step. In general, “cold” injection techniques are required for accurate nondiscriminative

sample transfer into the column. Cold on-column and programmed temperature (PT) split/splitless injection have been used with success for a large number of HT-HRGC analyses. In certain cases, however, significant losses of compounds above *n*-C₆₀ have been observed with PT splitless injection [13]. This effect was identified as a time-based discrimination process caused by purging the PT inlet too soon after injection, resulting in incomplete sample vaporization [14].

Actually, same articles show the possibility of use split injection [8] in HT-HRGC analyses of substances up to C₇₈. However, volatile materials from the septum accumulate at the head of the column during the cool-down portion of the temperature program. When the columns are reheated to analyze the next sample, these accumulated volatiles are eluted, producing peaks, a baseline rise, or both. This difficulty can be solved using commercial septa already available for HT-HRGC, which exhibit very low bleed levels.

Detectors

High-temperature high-resolution GC is a technique similar to conventional GC; however, it presents high column bleeding due to the high temperature to which the column is submitted. Selective detectors, when used in HT-HRGC, require special attention. As an example, the electron-capture detector (ECD) is a very sensitive detector and should not be used in HT-HRGC because of its ability to detect column bleeding. This fact limits the detectors used to a few, such as the flame ionization detector (FID), alkali-flame ionization detector (AFID), and mass spectrometry detector (MS). In HT-HRGC, these detectors usually need small adjustments; for example, the MS detector requires a special interface when used for HT-HRGC [2].

HT-HRGC Application

High-temperature high-resolution GC has opened to many scientists the opportunity to analyze compounds of high molecular mass (600 Da or more) with similar efficiency to conventional high-resolution gas chromatography (HRGC). Actually, HT-HRGC has been applied to the analyses of compounds from several different areas [15–18]. As a general rule, this will avoid the time-consuming and usually expensive step of derivatization. In natural products, underivatized triterpenic compounds found in medicinal plants can be analyzed by this technique. The HT-HRGC analysis of



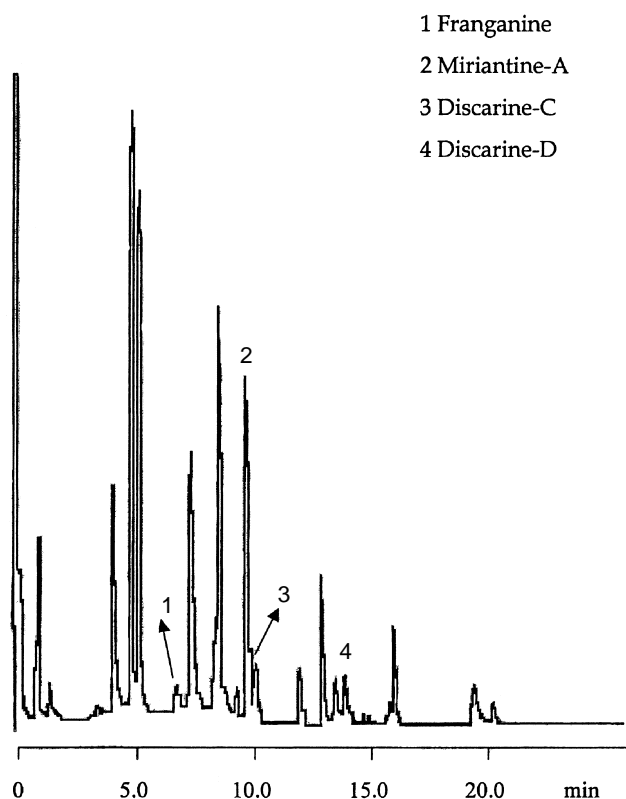


Fig. 1 Analysis of underivatized cyclopeptidic alkaloids in chloroform extract using HT-HRGC. Condition: fused-silica capillary column (6 m \times 0.25 mm \times 0.08 μ m) coated with a LM-5 (5% phenyl, 95% polymethylsiloxane immobilized bonded phase) stationary phase. Temperature condition: column at 200°C (1 min), increased by 4°C/min, then 300°C (5 min); inlet: 250°C; FID detector: 310°C.

triterpenes in aqueous alcoholic extracts of *Maytenus ilicifolia* and *M. aquifolium* leaves clearly allows the detection of the presence of friedelan-3-ol and friedelin and, therefore, allows distinguishing between the two varieties [15]; this differentiation is very important in pharmacological studies, because they present different biological activities.

Cyclopeptidic alkaloids (molecular mass \sim 600 Da), a class of important alkaloids which present biological activity, were analyzed by HT-HRGC without derivatization [16]. Figure 1 illustrates the separation of cyclopeptidic alkaloids in the chloroform fraction. The following selected compounds were identified: (1) Franganine, (2) Miriantine-A, (3) Discarine-C, and (4) Discarine-D.

Triacylglycerides from animal and vegetable sources have been separated and identified by HT-HRGC and high-temperature gas chromatography

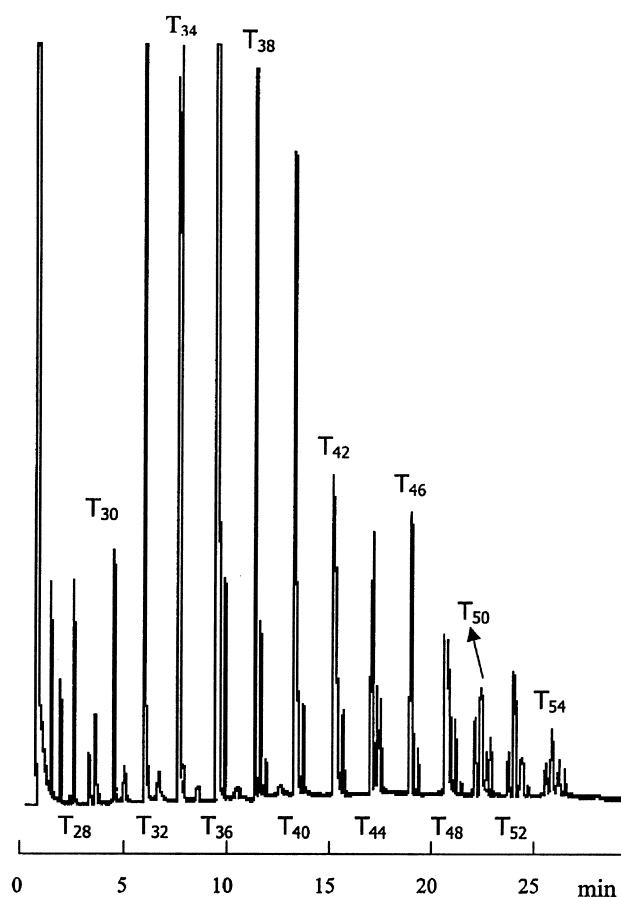


Fig. 2 Chromatogram of underivatized Palmist Oil (*Elaeis guineensis* L.) triacylglyceridic fraction using HT-HRGC. Condition: fused-silica capillary column (25 m \times 0.25 mm \times 0.1 μ m) with the stationary phase OV-17-OH (50% phenyl, 50% methylpolysiloxane immobilized phase). Temperature condition: column at 350°C isothermic; injector: 360°C; FID detector: 380°C. T is the number of the underivatized triacylglyceride (e.g., T₅₀ means a triacylglyceride having 50 carbon atoms).

coupled to mass spectrometry (HT-HRGC/MS). Figure 2 shows the chromatographic profile of palm oil (*Elaeis guineensis* L.) by HT-HRGC, and the triacylglyceride compounds identification [17].

The HT-HRGC/MS technique was also used as an important tool to identify and quantify cholesterol present in the total lipid extracts of archeological bones and teeth, constituents of a new source of paleodietary information [19].

The detection of vanadium, nickel, and porphyrins in crude oils were analyzed by high-temperature gas chromatography–atomic emission spectroscopy (HT-GC–AES), presenting characteristic metal distribu-



tions of oils from different sources [18]. Other related applications of HT-HRGC, including the analysis of α , β , and γ cyclodextrins, antioxidants, and oligosaccharides [2].

Considering that HT-HRGC is still a young separation technique and that it presents several attractive features, including the analysis of higher-molecular-weight compounds within short analysis times, without the necessity of sample derivatization, we can envisage a bright future for this technique, with many new applications being developed in the near future.

References

1. I. A. Fowles, *Gas Chromatography*, 2nd ed., John Wiley & Sons, New York, 1994, pp. 1–11.
2. W. Blum and R. Aichholtz, *Hochtemperatur Gas-Chromatographie*, Hüthig, Germany, 1991, pp. 26–114.
3. S. R. Lipsky and W. J. McMurray, *J. Chromatogr.* 279: 59 (1983).
4. F. M. Lanças and M. S. Galhiane, *J. High Resolut. Chromatogr. Chromatogr. Commun.* 13: 654 (1990).
5. L. M. P. Damasceno, J. N. Cardoso, and R. B. Coelho, *J. High Resolut. Chromatogr. Chromatogr. Commun.* 15: 256 (1992).
6. K. Grob and R. Tschuor, *J. High Resolut. Chromatogr. Chromatogr. Commun.* 13: 193 (1990).
7. J. Hubball, *LC-GC* 8: 12 (1990).
8. J. V. Hinshaw and L. S. Ettre, *J. High Resolut. Chromatogr. Chromatogr. Commun.* 12: 251 (1989).
9. W. Blum and L. Damasceno, *J. High Resolut. Chromatogr. Chromatogr. Commun.* 10: 472 (1987).
10. M. Verzele, F. David, M. van Roelenbosch, G. Diricks, and P. Sandra, *J. Chromatogr.* 270: 99 (1983).
11. S. R. Lipsky and M. L. Duffy, *J. High Resolut. Chromatogr. Chromatogr. Commun.* 9: 376 (1986).
12. R. Aichholz and E. Lorbeer, *J. Microcol. Separ.* 8: 553 (1996).
13. S. Trestianu, G. Zilioli, A. Sironi, C. Saravelle, F. Munari, M. Galli, G. Gaspar, J. Colin, and J. L. Jovelín, *J. High Resolut. Chromatogr. Chromatogr. Commun.* 8: 771 (1985).
14. J. V. Hinshaw, *J. Chromatogr. Sci.* 25: 49 (1987).
15. F. M. Lanças, J. H. Y. Vilegas, and N. R. Antoniosi Filho, *Chromatographia* 40: 341 (1995).
16. F. M. Lanças and J. J. S. Moreira, High temperature gas chromatography (HT-GC) analysis of underivatized cyclopeptidic alkaloids, Proc. of the 23rd Int. Symp. Capill. Chromatogr., 2000.
17. N. R. Antoniosi Filho, Analysis of the vegetable oils and fats using high resolution gas chromatography and computational methods, Ph.D. thesis, University of São Paulo, Institute of Chemistry at São Carlos, Brazil, 1995, pp. 140–152.
18. Y. Zeng and P. C. Uden, *J. High Resolut. Chromatogr. Chromatogr. Commun.* 17: 223 (1994).
19. A. W. Stott and R. P. Evershed, *Anal. Chem.* 68: 4402 (1996).



Histidine in Body Fluids, Specific Determination by HPLC

Toshiaki Miura

Hokkaido University, Sapporo, Japan

Naohiro Tateda

Kiichi Matsuhisa

Asahikawa National College of Technology, Asahikawa, Japan

INTRODUCTION

Amino acids in biological samples have been principally determined by high-performance liquid chromatography (HPLC) with pre- or postcolumn chemical derivatization selective for a primary amino group. Although HPLC methods are applicable to the assay of all commonly encountered amino acids in biological samples, they are time-consuming and inadequate for the assay of a large number of samples when a specific amino acid is required to be assayed. In such cases, a rapid assay can be achieved by the use of a chemical derivatization that is selective for the individual amino acid, which renders the HPLC separation conditions to be very simple. As an example of such a case, this paper describes a rapid HPLC method for the determination of histidine in body fluids. The method is based on the separation by a reversed-phase, ion-pair chromatography followed by the selective postcolumn detection of histidine with fluorescence derivatization using *ortho*-phthalaldehyde (OPA).

SELECTIVE FLUORESCENCE DETECTION OF HISTIDINE WITH OPA

OPA has been known to give a fluorescent adduct with most primary amines in the presence of a thiol compound, but only with several biogenic amines such as histidine, histamine, and glutathione in the absence of a thiol compound in a neutral or alkaline medium. In the case of histidine, it gradually reacts with OPA alone in an alkaline medium, to give a relatively stable fluorescent adduct showing excitation and emission maxima at 360 and 440 nm, respectively.^[1] Håkanson et al. optimized these reaction conditions and showed that the fluorescence intensity due to histidine reached a maximum 10 min after initiation of the reaction at pH 11.2–11.5, at 40°C. This fluorescence reaction is relatively selective for histidine and has been used in a batch method for the assay of histidine.^[1]

On the other hand, we revealed the mechanistic pathway of the OPA-induced fluorescence reaction of

histidine, as shown in Fig. 1.^[2] In addition, we found that the fluorescent adduct of histidine rapidly forms in a neutral medium, although its stability is low.^[3] These findings led us to optimize this fluorescence reaction for a postcolumn detection of histidine in its HPLC determination. Under the optimized conditions (for 30 sec at pH 7 and at 40°C), no significant fluorescence was observed with other biological substances, except for histamine and glutathione. The relative fluorescence intensities of histamine and glutathione were 14.4% and 11.8% of that given by histidine on a molar base, respectively.^[3] Such high selectivity of this fluorescence reaction was reasonably explained by the fact that both the primary amino group and imidazole ring of histidine participate in the formation of the fluorescent adduct (Fig. 1).

Because the reaction temperature markedly influences the rates of formation and degradation of the fluorescent adduct, its precise control is an essential factor for the reproducibility of the postcolumn fluorescence detection. Therefore preheating of both the eluent and OPA reagent to a constant temperature of 40°C is required before their mixing, and these was achieved by insertion of preheater tubes for both the eluent and OPA reagent into the line. As described in the section ‘‘HPLC System and Conditions,’’ the preheater tubes, as well as columns, resistor tube, and the reactor tube were placed in a column oven maintained at 40°C.

HPLC CONDITIONS FOR SEPARATION OF HISTIDINE

As described above, histamine and glutathione also show significant fluorescence in the postcolumn detection with OPA. The levels of glutathione are comparable or higher than those of histidine in many biological samples, such as liver, kidney, and blood (mainly in the erythrocytes). On the other hand, most biological samples normally contain histamine at markedly lower levels than histidine; in particular, the level of histamine in human serum or plasma is 10,000-fold lower than that of histidine. These facts indicate that the interfering biological substance is

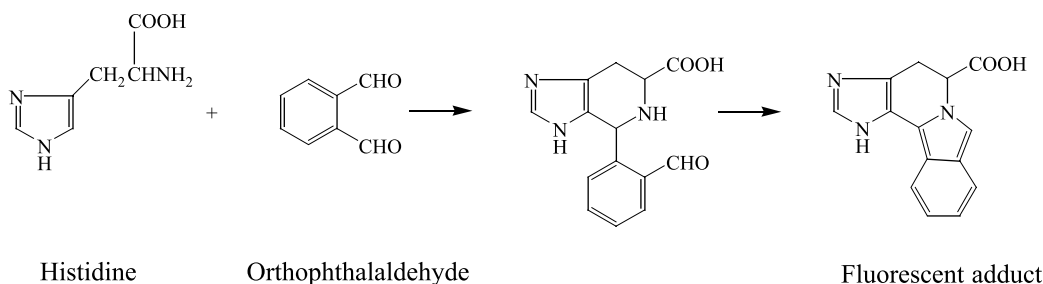


Fig. 1 Mechanistic pathway for the formation of fluorescent adduct in the reaction of histidine with *ortho*-phthalaldehyde.

limited to glutathione in the HPLC method in the post-column fluorescence detection using OPA. Thus HPLC separation conditions had only to separate histidine from glutathione, which was easily achieved by a reversed-phase ion-pair chromatography on an ODS short column with a 5:95 (v/v) mixture of methanol and sodium phosphate buffer (35 mM, pH 6.2) containing 5.3 mM sodium octanesulfonate, at a flow rate of 0.5 mL/min and at 40°C. Under these conditions, histidine and glutathione were eluted at 2.7 and 1.4 min, respectively (Fig. 2A).

DETERMINATION OF HISTIDINE IN BODY FLUIDS

HPLC System and Conditions

The HPLC system comprised an L-6000 pump (Hitachi, Tokyo, Japan) and an LC-9A pump (Shimadzu, Kyoto, Japan) for deliveries of an eluent and the OPA reagent, a DGU-12A degasser (Shimadzu), a Rheodyne Model 7725i sample injector (Rheodyne, Cotati, CA, USA), a CTO-10A column oven (Shimadzu), an F-1050 fluorescence detector equipped with a 12-μL square flow cell, and a D-2500 data processor (Hitachi). Separation was performed at 40°C with a Develosil ODS UG-3 column (30 × 4.6 mm i.d., 3 μm; Nomura Chemical, Seto, Japan) as an analytical column, which was protected by a guard-pak cartridge column (Develosil ODS UG-5, 10 × 4.0 mm i.d., 5 μm), and with a 1:19 (v/v) mixture of methanol and sodium phosphate buffer (35 mM, pH 6.2) containing 5.3 mM sodium octanesulfonate as an eluent. The OPA reagent was a 15:1 (v/v) mixture of 50 mM sodium phosphate buffer (pH 8.0) and 50 mM OPA in methanol. Both the eluent and OPA reagent were filtered through a 0.45 μm membrane filter (Millipore, Bedford, MA, USA) before use. The eluent was delivered to the column at a flow rate of 0.5 mL/min through a preheater tube (stainless-steel tube, 10 m × 0.8 mm i.d.). Ten microliters of the sample solution was introduced to the column. The eluate from the column was added with OPA

reagent delivered at a flow rate of 0.5 mL/min to a mixing T-joint attached to the column through a pre-heater tube (stainless-steel tube, 10 m × 0.8 mm i.d.) and a resistor polytetrafluoroethylene (PTFE) tube (20 m × 0.25 mm i.d.). The mixture was passed through a reactor tube (coiled PTFE tube, 2.5 m × 0.5 mm i.d., coil diameter of 20 mm) and the generated fluorescence was detected at 435 nm with an excitation wavelength of 365 nm. All columns, preheater, resistor, and reactor tube were placed in the column oven which was maintained at 40°C.

Sample Preparation

Because of high selectivity of the postcolumn fluorescence detection with OPA, no sample pretreatment other than deproteinization was required for the assay of his-

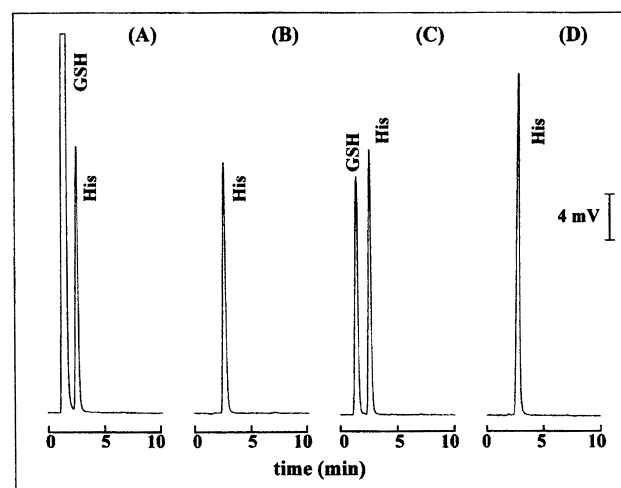


Fig. 2 Typical HPLC chromatograms of histidine. (A) Standard histidine and glutathione. Injected amounts: histidine (His), 5 pmol; glutathione (GSH), 500 pmol. (B) Human serum. (C) Human blood. (D) Human urine. See the section "HPLC system and Conditions" for chromatographic conditions.

tidine in body fluids such as human serum, blood, and urine as follows:

Human serum was mixed with an equal volume of 6% (w/v) perchloric acid and was vortexed several times. The mixture was centrifuged at $10,000 \times g$ for 10 min at 4°C , then the supernatant was diluted 10-fold with water and was filtered through the $0.45\text{-}\mu\text{m}$ membrane filter. A portion of the filtrate was further diluted 10-fold with 0.01 M HCl for HPLC analysis.

Heparinized human blood (1.0 mL) was mixed with water (0.9 mL) and 60% (w/v) perchloric acid (0.1 mL), vortexed, and then centrifuged at 4°C and $10,000 \times g$ for 10 min. The supernatant ($400\text{ }\mu\text{L}$) was transferred to an Ultrafree-MC centrifugal filter unit (Durapore type, $0.22\text{ }\mu\text{m}$) (Millipore) and centrifuged at 4°C and $10,000 \times g$ for 1 min. A portion of the filtrate was diluted 200-fold with 0.01 M HCl and injected onto the HPLC column.

Human urine was mixed with an equal volume of 6% (w/v) perchloric acid and was then filtered through the membrane filter. The filtrate was diluted 1000-fold with 0.01 M HCl and injected onto the HPLC column.

Evaluation of the Present HPLC Method

Fig. 2A shows the chromatogram of a 1:100 mixture of standard histidine and glutathione. The peak due to histidine was observed at 2.7 min with no interference from 100-fold excess of glutathione. The HPLC method gave a linear calibration curve ($r = 1.000$) over the range of 0.25–1000 pmol per injection ($10\text{ }\mu\text{L}$) with the coefficient of variation of 0.9% at 2 pmol ($n = 10$) and with the detection limit ($S/N = 8$) of 25 fmol.

Fig. 2B and D shows the typical chromatograms of deproteinized human serum and urine, respectively, which contain less glutathione than histidine. The high selectivity of the postcolumn detection made the chromatograms quite simple, where the peak due to histidine appeared as a sole peak. On the other hand, both glutathione and histidine were detected in human blood, which contains glutathione at a higher level than histidine (Fig. 2C).

Recoveries of the present HPLC method were tested by using a pooled human serum, blood, or urine, to which were added various amounts of histidine prior to the sample preparation. The mean recovery values were in the range of 101–104%. The values of histidine in human sera, blood, and urine, determined by the HPLC method, were $85.6 \pm 15.0\text{ }\mu\text{M}$ ($n = 47$, mean \pm SD), $95.3\text{ }\mu\text{M}$ ($n = 2$,

96.8 and $93.8\text{ }\mu\text{M}$), and $1.13 \pm 0.48\text{ mmol/mg}$ of creatinine ($n = 10$, mean \pm S.D.), respectively, which were in good agreement with their reported values. The coefficients of the day-to-day variation obtained with a pooled human serum, blood, or urine were below 1.0%.

CONCLUSION

Because of the high selectivity and sensitivity of the postcolumn fluorescence detection of histidine with OPA, the present HPLC method is applicable to a specific and rapid assay of histidine in human serum, blood, and urine after simple pretreatment. A recent paper demonstrated that the postcolumn detection with OPA was applicable to the simultaneous assays of histidine and its major metabolites (*cis*- and *trans*-urocanic acids) in human stratum corneum.^[4] The postcolumn detection system was also applicable to the flow injection analysis (FIA) method for the assay of histidine in serum and urine. The FIA method enabled us to determine histidine in blood after pretreatment of the sample with *N*-ethylmaleimide (masking reagent of glutathione).^[5] These methods are useful in the diagnosis of histidinemia, one of hereditary metabolic disorders characterized by a virtual deficiency of histidine ammonia-lyase.

REFERENCES

1. Håkanson, R.; Rönnberg, A.L.; Sjölund, K. Improved fluorometric assay of histidine and peptides having NH_2 -terminal histidine using *o*-phthalaldehyde. *Anal. Biochem.* **1974**, *59*, 98–109.
2. Yoshimura, T.; Kamataki, T.; Miura, T. Difference between histidine and histamine in the mechanistic pathway of the fluorescence reaction with *ortho*-phthalaldehyde. *Anal. Biochem.* **1990**, *188*, 132–135.
3. Tateda, N.; Matsuhisa, K.; Hasebe, K.; Kitajima, N.; Miura, T. High-performance liquid chromatographic method for rapid and highly sensitive determination of histidine using postcolumn fluorescence detection with *o*-phthalaldehyde. *J. Chromatogr., B* **1998**, *718*, 235–241.
4. Tateda, N.; Matsuhisa, K.; Hasebe, K.; Miura, T. Simultaneous determination of urocanic acid isomers and histidine in human stratum corneum by high-performance liquid chromatography. *Anal. Sci.* **2001**, *17*, 775–778.
5. Tateda, N.; Matsuhisa, K.; Hasebe, K.; Miura, T. Sensitive and specific determination of histidine in human serum, urine and stratum corneum by a flow injection method based on fluorescence derivatization with *o*-phthalaldehyde. *J. Liq. Chromatogr. Relat. Technol.* **2001**, *24*, 3181–3196.



HPLC Analysis of Amino Acids

Ioannis N. Papadoyannis
Georgios A. Theodoridis

Laboratory of Analytical Chemistry, Chemistry Department, Aristotle University of Thessaloniki, Thessaloniki, Greece

Introduction

Amino acids are small organic molecules that possess both an amino and a carboxyl group. Amino acids occur in nature in a multitude of biological forms, either free or conjugated to various types of compounds, or as the building blocks of proteins. The amino acids that occur in proteins are named α -amino acids and have the empirical formula $\text{RCH}(\text{NH}_2)\text{COOH}$. Only 20 amino acids are used in nature for the biosynthesis of the proteins, because only 20 amino acids are coded by the nucleic acids.

Discussion

Amino acids show acid–base properties, which are strongly dependent on the varying R groups present in each molecule. The varying R groups of individual amino acids are responsible for specific properties: polarity, hydrophilicity–hydrophobicity [1,2]. Hence, the 20 α -amino acids could be categorized in the 4 distinct groups listed in Table 1.

Their dipolar (zwitterionic) behavior is a fundamental factor in any separation approach. At low pH, amino acids exist in their cationic form with both amino and carboxyl groups protonated. The ampholyte form appears at a pH of 6–7, whereas at higher values, amino acids are in their anionic form (carboxyl group dissociated). Another important parameter is that all α -amino acids (with the exception of Gly) are asymmetrical molecules exhibiting optical isomerization (L being the isomer found in nature). As can be seen in Table 1, amino acids are actually small [molecular weight (MW) ranging from 75 to 204] molecules, exhibiting pronounced differences in polarity and a few chromophoric moieties.

The determination of amino acids in various samples is a usual task in many research, industrial, quality control, and service laboratories. Hence, there is a substantial interest in the high-performance liquid chromatography (HPLC) analysis of amino acids from many diverse areas like biochemistry, biotechnology, food quality control, diagnostic services, neuro-chemis-

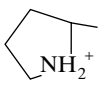
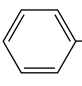
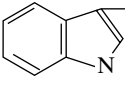
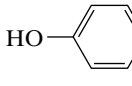
try/biology, and so forth. As a result, the separation of amino acids is probably the most extensively studied and best developed chromatographic separation in biological sciences. The most known system is the separation on a cation-exchange column and postcolumn derivatization with ninhydrin, which was described in 1951 by Moore and Stein. With this approach, a sulfonated polystyrene column achieved a separation of the 20 naturally occurring amino acids within approximately 6 h; modifications of the original protocol enhanced color stabilization of the derivatives and enabled the application of the method in various real samples. Since then, immense developments in instrumentation, column technologies, and automation established HPLC as the dominant separation technique in chemical analysis. Numerous published reports described the HPLC analysis of amino acids in a great variety of samples. To no surprise, a two-volume handbook is entirely devoted to HPLC for the separation of amino acids, peptides and proteins [3]. Many of the initial reports employed soft resins or ion exchangers such as polystyrene or cellulose as stationary phases. These materials show some disadvantages (e.g., compaction under pressure, reduced porosity, and wide particle size distribution). The last decades' developments in manufacturing silica-based materials resulted in the domination of reversed-phase (RP) silica-based packing in liquid chromatography. As a result, RP-HPLC is, at present, widely used for the separation of amino acids, because it offers high resolution, short analysis time, ease in handling combined with low cost, and environmental impact per analysis circle.

In ligand-exchange chromatography (LEC), the separation of analytes is due to the exchange of ligands from the mobile phase with other ligands coordinated to metal ions immobilized on a stationary phase. LEC has been used successfully for the resolution of free amino acids, amino acid derivatives, and for enantiomeric resolution of racemic mixtures [3].

Apart from ninhydrin, many other derivatization reagents have been used; both precolumn and postcolumn derivatization modes have been extensively employed [3–5]. Derivatization procedures offer significant advantages in both separation and detection aspects and, thus,



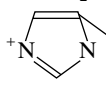
Table 1 Amino Acids Found in Proteins

Amino acid		Structure at pH 6-7	MW	pKa
Hydrophobic Aminoacids (Nonpolar R)	Alanine Ala	$\text{CH}_3\text{—CH—COO}^-$ NH_3^+	89	2.35, 9.69
	Leucine Leu	$\text{CH(Me)}_2\text{CH}_2\text{—CH—COO}^-$ NH_3^+	131	2.36, 9.60
	Isoleucine Ile	$\text{C}_2\text{H}_5\text{CH(CH}_3\text{)—CH—COO}^-$ NH_3^+	131	2.36, 9.68
	Valine Val	$\text{CH(Me)}_2\text{—CH—COO}^-$ NH_3^+	117	2.36, 9.68
	Proline Pro		115	1.99, 10.60
	Methionine Met	$\text{CH}_3\text{SC}_2\text{H}_5\text{—CH—COO}^-$ NH_3^+	149	2.28, 9.21
	Phenylalanine Phe		165	1.83, 9.13
Hydrophilic Aminoacids (Not Charged R)	Tryptophan Trp		204	2.38, 9.39
	Glycine Gly	H—CH—COO^- NH_3^+	75	2.34, 9.6
	Serine Ser	$\text{CH}_2\text{OH—CH—COO}^-$ NH_3^+	105	2.21, 9.15
	Threonine Thr	$\text{CH}_3\text{CHOH—CH—COO}^-$ NH_3^+	119	2.63, 10.43
	Cysteine Cys	$\text{HSCH}_2\text{—CH—COO}^-$ NH_3^+	121	1.71, 10.78
	Tyrosine Tyr		181	2.20, 9.11
	Glutamine Gln	$\text{NH}_2\text{COC}_2\text{H}_5\text{—CH—COO}^-$ NH_3^+	146	2.17, 9.13
Acidic Aminoacids	Asparagine Asn	$\text{NH}_2\text{COCH}_2\text{—CH—COO}^-$ NH_3^+	132	2.02, 8.8
	Aspartic Acid Asp	$^- \text{OOCCH}_2\text{—CH—COO}^-$ NH_3^+	133	2.09, 3.86, 9.86
	Glutamic Acid Glu	$^- \text{OOC}_2\text{H}_5\text{—CH—COO}^-$ NH_3^+	147	2.19, 4.25, 9.67

(continued)



Table 1 Continued

Amino acid		Structure at pH 6-7	MW	pKa
Basic Aminoacids	Lysine Lys	${}^+\text{H}_3\text{NC}_4\text{H}_8\text{—CH—COO}^-$ NH_3^+	133	2.18, 8.95, 10.53
	Arginine Arg	$\text{H}_2\text{NCHNHC}_3\text{H}_6\text{—CH—COO}^-$ ${}^+\text{NH}_2$ NH_3^+	133	2.17, 9.04, 12.48
	Histidine His	 $\text{CH}_2\text{—CH—COO}^-$ NH_3^+	155	1.82, 8.95, 10.53

will be discussed in further detail. The rest of the entry will be divided into two sections: separation of underivatized amino acids, where the determination of free amino acids and postcolumn derivatization procedures are described; and separation of derivatized amino acids, where precolumn derivatization approaches are discussed.

Separation of Underivatized Amino Acids

The differing solubilities, polarities, and acid–base properties of free amino acids have been exploited in their separation by partition chromatography, ion-exchange chromatography, and electrophoresis. For example, the elution order obtained from a polystyrene ion-exchange resin with an acidic mobile phase corresponds to the amino acid classification depicted in Table 1: Acidic amino acids are eluted early, neutral between, and basic amino acids later. In this case, ionic interactions between the sample and the stationary phase are the driving force for the separation of the groups. However, hydrophobic van der Waals and π – π aromatic interactions are responsible for the separation of amino acids within the groups [3].

The dominant stationary phase in HPLC is modified silica and, to be more specific, octadecyl silica (ODS). It should be pointed out that there could be great differences between various types of ODS materials or even between different batches of the same material. Carbon load, free silanol content, endcapping, type of silica, and coupling chemistry to the C_{18} moiety, not to mention the several physical characteristics of the packing material all involve the behavior of an ODS column. However, a rather safe generalization is that, in such material, hydrophobic interactions are a dominant mechanism of separation [3–7].

In typical ODS materials, polar amino acids are very weakly retained on column; thus, they are insufficiently resolved. In contrast, nonpolar amino acids

are stronger retained and adequately separated. To overcome the poor resolution of polar amino acids, two strategies are the most promising:

1. Derivatization (as discussed in the next section)
2. Modification of the mobile phase with the addition of ion-pairing reagents

Alkyl sulfates/sulfonates added to the mobile phase form a micellar layer interacting with both the stationary phase and the amino acids (which under these conditions are protonated). A mixed mechanism (ion-pairing and dynamic ion exchange) is observed. Furthermore, the ion-pairing reagent masks underivatized silanols of the ODS material, reducing nonspecific unwanted interactions. Sodium dodecyl sulfate (SDS) is the most often used ion-pairing reagent. Gradient elution is often required to achieve reasonable analysis time for nonpolar amino acids. Despite the above-mentioned advantages, ion-pairing shows some disadvantages, such as irreproducibility (especially in gradient runs), long equilibration times, and difficulties in ultraviolet (UV) detection.

Another possibility is the use of alternative stationary phases. A strong trend of the last decade is the employment of specialty phases in challenging and complex separations. Thus, newer C_8 , NH_2 , CN, mixed-mode phases (materials incorporating both ion exchange and reversed-phase moieties), new polymeric phases, and zirconia-based materials offer attractive stationary-phase selectivities.

Postcolumn Derivatization

The nonderivatized amino acids, following their chromatographic separation, can either be directly detected as free amino acids, on-line derivatized, or by postcolumn derivatization. Derivatization with ninhydrin, the classical amino acid analysis, was the first re-



ported postcolumn derivatization method. Modern postcolumn derivatization protocols employ sophisticated instrumentation and achieve high resolution and sensitivity. In such configurations, derivatization occurs in a reaction coil placed between the analytical column and the detector. Additional pumps and valves are required; thus, such systems typically run fully automated and controlled by a computer. The major disadvantages of postcolumn derivatization are the need for sophisticated and complex instrumentation and the band broadening occurring in the reactor. *Ortho*-phthalaldehyde (OPT) is the most common reagent in postcolumn derivatization. OPT reacts with primary amino acids under basic conditions, forming a fluorescent derivative (OPA derivative) that allows detection at femtomole levels. Disadvantages of OPA derivatization are the instability of the resultant derivatives and the fact that secondary amino acids are not detected.

If no derivatization takes place, detection is preferably accomplished by UV at a low wavelength (200–210 nm) in order to enhance detection sensitivity. However, detection selectivity is sacrificed at such low wavelengths. Electrochemical detection, when applied to the analysis of free amino acids, offers higher selectivity but suffers from a small linearity range. Furthermore, most amino acids (with the exception of tryptophan, tyrosine, and cysteine) are not intrinsically electrochemically active within the current useful potential range [5]. Lately, the development of the evaporative light-scattering detector (ELSD) offers an attractive alternative for the determination of nonderivatized amino acids (see Fig. 1).

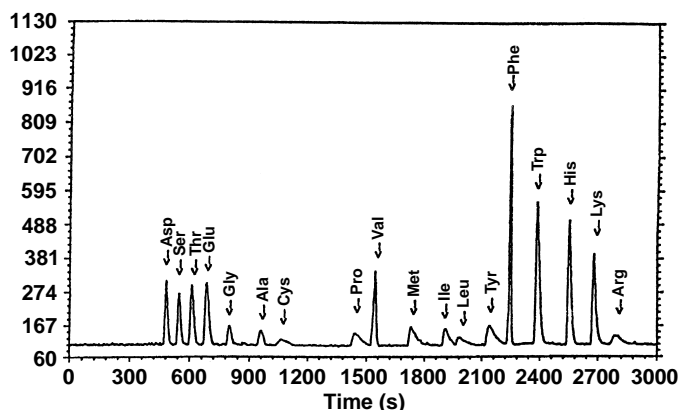


Fig. 1 HPLC analysis of 18 common amino acids. Conditions: stationary phase: CS-10 cation exchange; mobile phase: gradient of aqueous 0.01% TFA and ammonium acetate; detection at the ELSD. (From Ref. 11.)

Separation of Derivatized Amino Acids

Precolumn derivatization is the generally accepted approach for the determination of amino acids, because it offers significant advantages: increased detection sensitivity, enhanced selectivity, enhanced resolution, and limited needs for sophisticated instrumentation (in contrast with postcolumn derivatization techniques).

In modern instrument configurations, derivatization can take place in a conventional autosampler; the resultant derivatives are separated on the analytical column. Detection limits at the femtomole level are achieved, and the resolution of polar amino acids is greatly enhanced.

The most common derivatization reagents are as follows:

- Dimethylamino azobenzene isothiocyanate (DABITC)
- 4-(Dimethylamino)azobenzene-4-sulfonyl chloride (dabsyl chloride or DABS-Cl) [dabsyl derivatives]
- 1-*N,N*-Dimethylaminonaphthalene-5-sulfonyl chloride [dansyl derivatives]
- Fluorodinitrobenzene (DNP derivatives)
- Fluorescamine
- 9-Fluorenylmethyl chloroformate (FMOC-Cl)
- 4-Chloro-7-nitro-2,1,3-benzoxadiazole (NBD-Cl)
- Phenylisothiocyanate (PITC) [phenylthiohydantoin (PTH) derivatives]
- Methylisothiocyanate (MITC) [methylthiohydantoin (MTH) derivatives]

Figure 2 illustrates the structure of the product resulting from the derivatization of an amino acid with the above-mentioned reagents. Mixtures of derivatives with the most commonly used reagents (dansyl, DNP, PTH) are readily provided in kits, to be directly used as reference standards in HPLC analysis.

Phenylthiohydantoin derivatization offers a special value because it is actually performed during Edman degradation, the sequencing technique mostly used for the determination of the primary structure of proteins and peptides. PTH derivatives are separated in many different stationary phases, in either normal- or reversed-phase mode and are mostly detected at 254 nm [8,9]. Using radiolabeled proteins, sequencing of proteins down to the 1–100-pmol range can be achieved. The formed derivatives are basic and thus interact strongly with base silica materials. RP separations are mostly carried out in acidic conditions with the addition of appropriate buffers (sodium acetate mostly, but

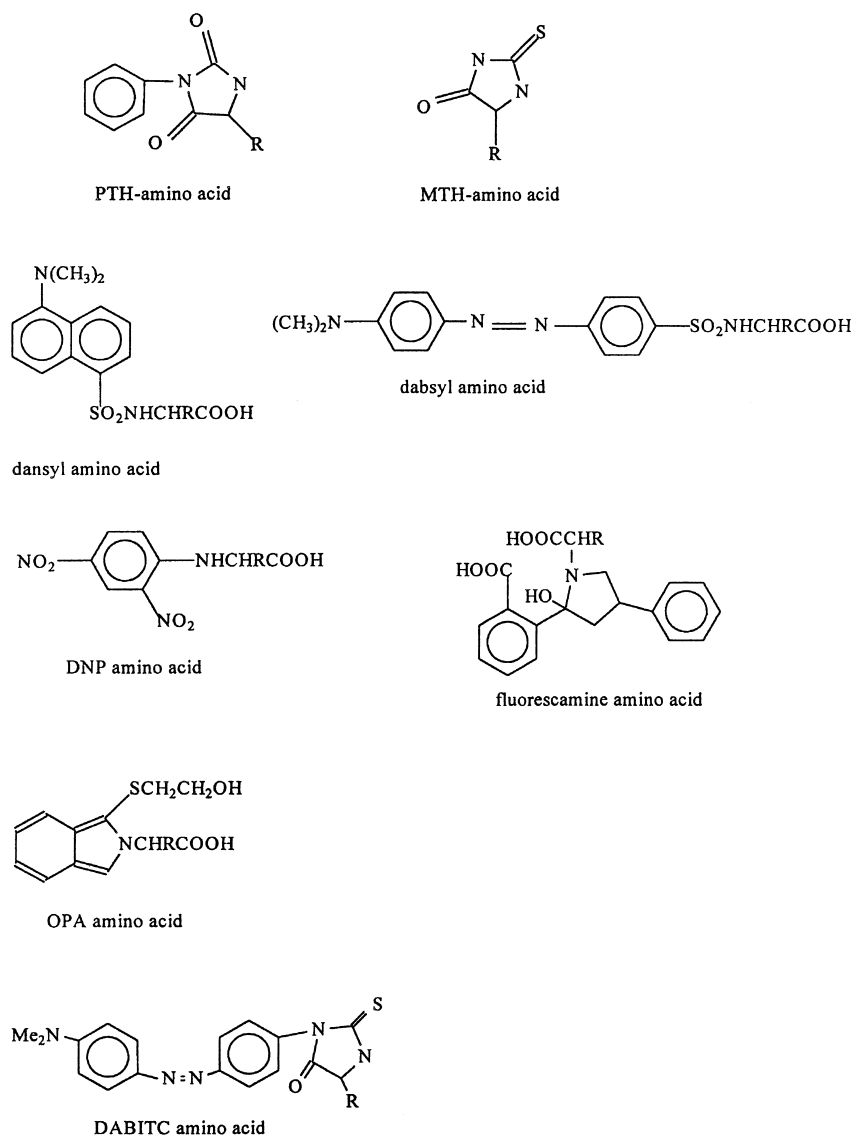


Fig. 2 Structures of the most common amino acid derivatives.

also phosphate, perchlorate, etc). Failings of PTH derivatization are the lengthy procedure and the higher detection limits obtained (compared to fluorescent derivatives). Potent advantages of the method are its robustness and reproducibility, and the extensive research literature that covers any possible requirement. An alternative to PTH is MTH derivatization, a method well suited for solid-phase sequencing [3].

Dimethylamino azobenzene isothiocyanate microsequencing results in red–orange derivatives, which exhibit their absorbance maximum at 420 nm with $\epsilon = 47,000$, in other words offering threefold higher sensitivity compared to PTH derivatives. DABITC deriva-

tives are separated in C_8 or C_{18} columns in acidic environment, within 20 min.

Dabsyl chloride is an alternative to DABITC as a derivatization reagent to be used for manual sequencing. Dabsyl chloride reacts with primary and secondary amino acids forming red–orange derivatives that are stable for months. The method offers excellent sensitivity, ease, and speed of preparation and high-resolution capabilities. However, it suffers from interferences with ammonia present in biological samples. Furthermore, it results in a relatively reduced column lifetime due to the utilization of excess of Dabsyl chloride [9].



The dansyl derivatization has been extensively studied to label α - or ϵ -amino groups. DNS derivatives are formed within 2 min and are detected by either UV or fluorescence. A typical example of a separation of dansyl amino acids is illustrated in Fig. 3.

The FMOc derivatization offers high fluorescent detection sensitivity, but it requires an extraction step to remove unreacted FMOc and by-products. This step is a potential cause of analyte losses. Furthermore, it is not suitable for Trp and Cys, because the corresponding derivatives exhibit a lower response due to intramolecular quenching of fluorescence.

The DNP derivatives are analyzed either in normal or reversed phase. Disadvantages of this method are the lower detection sensitivity (60 times less sensitive compared to dansyl detection) and the lower separation resolution. However, this approach has proven useful for the determination of lysine in food materials.

Finally, the incorporation of an electroactive functionality into a chromatographic label is an attractive alternative for the HPLC of amino acids. Reagents like π -N and N-dimethylaminosothiocyanate have been used to facilitate amperometric detection of the derivatives.

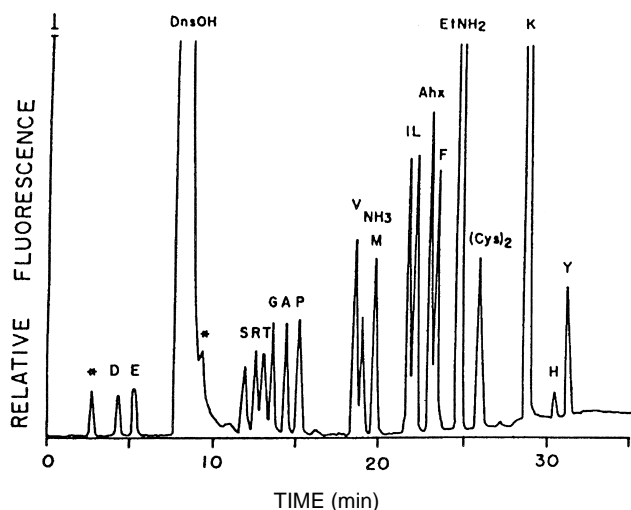


Fig. 3 RP-HPLC analysis of a mixture of dansyl amino acids. Conditions: stationary phase: 4 μ m Nova Pak C₁₈; mobile phase: gradient of methanol and tetrahydrofuran versus aqueous phosphate buffer; detection in a fluorescent detector; excitation 338 nm, emission 455 nm. Amino acids are abbreviated by the one-letter system. (From Ref. 12.)

Chiral Separation of Amino Acids

The importance of chirality has rapidly evolved the last decade. Both analytical and preparative separations are needed for biochemical, pharmaceutical, and alimentary purposes. Amino acids are asymmetrical molecules. L is the form appearing in proteins; however the D form is also present in nature. Enantiomeric separation of amino acids has been achieved in various stationary phases, such as polystyrene and polyacrylamide to which chiral ligands were covalently bound. Metal ions, in conjunction with chiral ligands, have also been utilized in the mobile phase in the reversed-phase and ligand-exchange mode. Novel stationary chiral phases developed for enantiomeric analysis incorporate chiral ligands (e.g., cyclodextrins or even amino acids) immobilized on silica. Generally, L-amino acid-bonded phases retain L-amino acids stronger than the D species [3,5,10].

Recently, a strong trend in molecular recognition is the development of molecular imprinting polymers (MIP). MIPs have been used as synthetic antibodies in immunoassays and biosensors, but also as catalysts and separation media (employed both in analysis and extraction). One of the first applications of MIPs in separations was the enantiomeric separation of amino acids derivatives.

Conclusions

High-performance liquid chromatography, when compared to other instrumental methods [thin-layer chromatography (TLC), GC, automated amino acid analyzer], offers significant advantages in the analysis of amino acids: high resolution, high sensitivity, low cost, time saving (one-third of the analysis time of an amino acid analyzer), and a multivariate optimization scheme offering versatility and flexibility. Furthermore, optimization of HPLC determination enables the practitioner to overcome typical problems of other methods (e.g., the well-known interferences of ammonia in amino acid analyzer). An additional advantage of HPLC is its direct compatibility with mass spectrometry. The widespread use of LC-MS in proteomic analysis, which at present utilizes state of the art mass spectrometers (e.g., matrix-assisted laser desorption ionization-time-of-flight-mass spectrometry), is seen as a potent future trend.

The variety of instrumentation and experimental conditions (columns, buffers, organic modifiers, derivatization procedures, etc.) reported in the vast literature

may hinder the novice from pinpointing the best method to use. The choice of the appropriate method depends on the specific needs of each analytical problem and the nature of the sample to be analyzed. Aspects such as specificity and speed of the derivatization reaction should always be considered. Furthermore, in such multivariate dynamic systems, precision, accuracy, and linearity of the chosen method is a very important factor. The practitioner should carefully follow the developed protocol; the use of automated systems, especially in derivatization procedures, could greatly enhance the reproducibility of the method.

References

1. L. M. Silverman and R. H. Christenson, Amino Acids and Proteins, in *Fundamentals of Clinical Chemistry*, 4th ed. (C. A. Burtis and E. R. Ashwood, eds.), Saunders, Philadelphia, 1996.
2. C. K. Matthews and K. E. van Holde, Biochemistry, 2nd ed., Benjamin-Cummings, Menlo Park, CA, 1995, pp. 129–214.
3. W. S. Hancock (ed.), *CRC Handbook of HPLC for the Separation of Amino Acids, Peptides and Proteins*, CRC Press, Boca Raton, FL, 1984.
4. W. S. Hancock and J. T. Sparrow, *HPLC of Biological Compounds*, Marcel Dekker, Inc., New York, 1984, pp. 187–207.
5. I. N. Papadoyannis, HPLC in the analysis of amino acids, in *HPLC in Clinical Chemistry*, Marcel Dekker, Inc., New York, 1990, pp. 97–154.
6. R. M. Kamp, High sensitivity Amino acid analysis, in *Protein Structure Analysis* (R. M. Kamp, T. Choli-Papadopolou, and B. Wittman-Liebold, eds.), Springer-Verlag, Berlin, 1997.
7. F. Lottspeich and A. Herschen, Amino acids, peptides, proteins, in *HPLC in Biochemistry* (A. Herschen, K. P. Hupe, F. Lottspeich, and W. Voelter, eds.), VCH Weinheim, 1985.
8. M. D. Waterfield, G. Scrace, and N. Totty, Analysis of phenylthiohydantoin amino acids, in *Practical Protein Chemistry—A Handbook* (A. Darbre, ed.), John Wiley & Sons, Chichester, 1986.
9. T. Bergman, M. Carlquist, H. Jornvall, Amino acid analysis by high performance liquid chromatography of phenylthiocarbamyl derivatives, and amino acid analysis using DABS-Cl precolumn derivatization method, R. Knecht and J. Y. Chang, in *Advanced Methods in Protein Microsequence Analysis* (B. Wittmann-Liebold, J. Salnikow, and V. A. Erdmann, eds.), Springer-Verlag, Berlin, 1986.
10. D. Vollenbroich and K. Krause, Quantitative Analysis of D- and L-amino acids by HPLC, in *Protein Structure Analysis* (R. M. Kamp, T. Choli-Papadopolou, and B. Wittman-Liebold, eds.), Springer-Verlag, Berlin, 1997.
11. J. Petterson, L. J. Lorenz, D. S. Risley, and B. J. Sanmann, *J. Liquid Chromatogr. Related Technol.* 22: 1009 (1999).
12. A. R. Martins and A. F. Padovan, *J. Liquid Chromatogr. Related Technol.* 19: 467 (1999).



HPLC Analysis of Flavonoids

Marina Stefova

Trajče Stafilov

Svetlana Kulevanova

Sts. Cyril and Methodius University, Skopje, Republic of Macedonia

INTRODUCTION

Flavonoids are widely spread plant secondary metabolites called $C_6-C_3-C_6$ phenolics, which are classified in three groups, depending on the nature of the C_3 fragment and the type of the heterocyclic ring, as follows: 1) chromone derivatives (flavones, flavonols, flavanones, and flavanols); 2) chromane derivatives (catechines and antocyanidines); and 3) flavonoids with open propane chain (chalcones) and with a furane ring (aurones). From all of these, flavones, flavonols, and flavanones are the most abundant in the plant kingdom and their skeleton is given in Fig. 1. Substitution in the positions 3, 5, 6, 7, 8, 2', 3', 4', 5', and 6' gives all the compounds from these groups, with hydroxylation, methoxylation, and glycosylation being the most common substitution. Thousands of various flavonoids with various substitution patterns are recognized today as *free* flavones, flavonols, and flavanones, i.e., *aglycones*, and as *flavonoid glycosides*, which consist of flavonoid, nonsugar component *aglycone*, connected to the *sugar moiety* (mostly monosaccharides and disaccharides). Bonding to sugars makes flavonoids soluble in water and enables their easy transport within plants.

Flavonoids are a well-defined group of compounds with established physical and chemical characteristics. This especially counts for their absorption of ultraviolet (UV) radiation, which makes their UV spectra very characteristic and UV spectroscopy a method of choice for their characterization.^[1] Two main absorption bands are observed: 1) band I (300–380 nm) due to absorption of ring B; and 2) band II (240–280 nm) due to absorption of ring A. The position of these bands gives information about the kind of the flavonoid and its substitution pattern; thus UV spectroscopy is used as a main method for the identification and the quantification of flavonoids for decades.

There are several published information regarding the isolation and the identification of flavonoids in plant material using different methods, mainly chromatographic and spectroscopic. Today, high-performance liquid chromatography (HPLC) is established as the most convenient method which enables separation and identification of

flavonoids using various detection systems.^[2–4] As for the quantitative analysis, much data have been published in the last few years confirming the suitability of this technique for simultaneous determination of flavonoid compounds in various samples, which gives an insight into the distribution of flavonoids in the studied material. High-performance liquid chromatography methods are developed for qualitative and quantitative analyses of flavonoids in fruits and beverages, wine, honey, propolis, and, especially, in various plant materials^[5–14] using different detection systems, from which UV diode array detectors are settled as the most suitable for these compounds and the most accessible as well.

EXPERIMENTAL

Stationary Phases

High-performance liquid chromatography is the method of choice for the separation of complex mixtures containing nonvolatile compounds such as various flavonoids in extracts prepared from different samples. A survey of literatures revealed that most researchers have used C_{18} -reversed stationary phases, which proved to be superior to the normal phase technique. The reversed phases are suitable for separating flavonoids in a wide range of polarities, as Vande Castele et al.^[15] have demonstrated the separation of 141 flavonoids from polar triglycosides to relatively nonpolar polymethoxylated aglycones belonging to the classes of flavones, flavonols, flavanones, dihydroflavonols, chalcones, and dihydrochalcones.

The use of normal phase silica columns was also described but after acetylation of the flavonoids and then isocratic elution on silica gel.^[16] Polystyrene divinylbenzene as a stationary phase was also found to give satisfactory separation and good peak shapes without using acidic mobile phases,^[17] which are not so favorable for use with reversed phases.

The choice of a column involves matching the class of flavonoids to be separated to the characteristics of the stationary phase capable of providing satisfactory



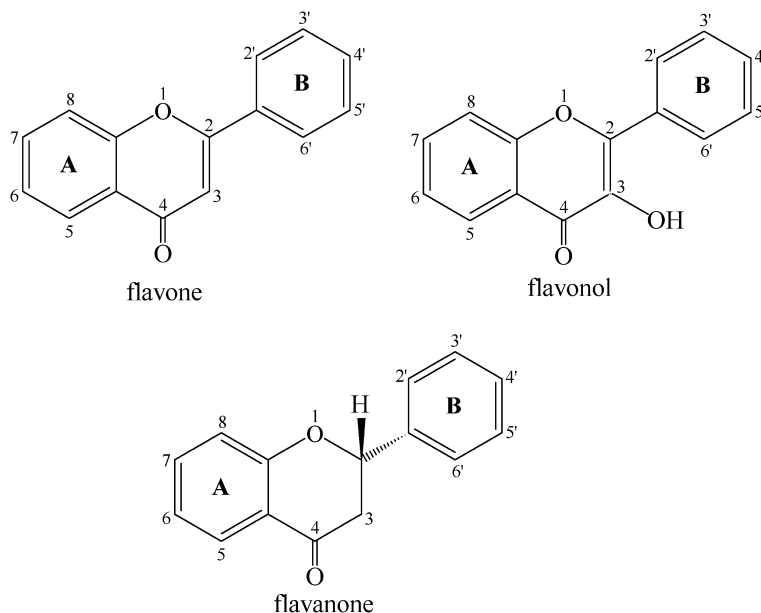


Fig. 1 Structure of flavone, flavonol, and flavanone.

retention, selectivity, and peak shapes. As for the dimensions, the most popular are 150 and 250 mm long, with 5 μm particle size, although phases with 3 μm particles are becoming more popular because of better efficiency and less solvent consumption. The use of guard columns is recommended in order to extend their lifetime by protecting the analytical column from impurities in the samples prepared from various natural products.

Mobile Phases

The preferred solvent system used for the separation of flavonoids on reversed-phase stationary phases is methanol–water, followed closely by acetonitrile–water. Usually, acetic or formic acid is added (sometimes phosphoric acid, potassium dihydrogen phosphate, ammonium dihydrogen phosphate, and perchloric acid), which enables improved separation and prevention of peak tailing with respect to the phenolic character of the flavonoids. Ion pairing has also been used for improving the separation of neutral glycosides from flavonol sulfates.^[4]

Often, gradient elution with a linear gradient, combined with isocratic steps, usually gives the best separation of flavonoids, differing in the degree of saturation, hydroxylation, methylation, and/or glycosylation. Optimization of the elution program is usually performed by changing the elution program until a satisfactory resolution and analysis time is achieved, depending on the analysis purpose, i.e., qualitative or quantitative analysis.

Detection Systems

Identification of flavonoids separated by HPLC is commonly performed by comparing the obtained retention times with the ones of authentic samples as well as by analysis of their characteristics collected by the detector.

Detection of flavonoids separated by HPLC can be performed using several detection systems. Photodiode array detectors (DADs) are the most convenient for use because of their availability and easy maintenance, and mainly because of the valuable information for the identification of flavonoids contained in their UV [or ultraviolet–visible (UV–VIS)] spectra. The sophisticated software packages enable storage of all the spectra obtained during the elution process, which can later be analyzed and compared to the spectra from a library previously prepared from authentic samples of flavonoids. An experienced analyst working on flavonoids can recognize the peaks from flavonoids in the chromatogram from the spectra, which are, as previously mentioned, very characteristic, although they are not enough for identification. As for the quantitative analysis, scanning over a wide wavelength range enables measuring all the components at wavelengths of their absorption maxima, which provides maximum sensitivity.

Fluorescence detectors have also been employed for flavonoid determination, offering higher sensitivity and selectivity, as suggested by the results in the analysis of 3',4',5'-trimethoxyflavone, which has been determined by excitation at 330 nm and by detection at 440 nm.^[18]

Overcoming the difficulty in introducing the liquid sample into the mass spectrometer in the last decade enabled their use for HPLC detection, even in routine practical applications. The atmospheric pressure chemical ionization, thermospray, and electrospray ionization systems have proved to be most convenient for flavonoid analysis by HPLC–MS.^[18,19] Mass spectrometry is a more specific and extremely selective detection technique, although it is not enough for structure elucidation (it reveals the structural fragments that are present, but not the exact substitution pattern). It offers the molecular weight of the molecular ion, which helps the tentative identification of the flavonoid. The use of HPLC–MS–MS gives additional information about the characteristic fragmentation pattern—“fingerprint” of the substance, which is very useful for qualitative and quantitative analyses in complex matrices. An excellent illustration of the use of HPLC–MS for the identification of flavonoids is presented in the work of Huck et al.,^[19] who have isolated and characterized polymethoxylated flavones from *Primulae veris flos* using HPLC–ESI–MS. The six detected flavonoid compounds were found to be mono-, di-, tri-, and pentamethoxyflavones, but their exact substitution pattern could not be revealed, except for 3',4',5'-trimethoxyflavone, for which ¹³C NMR spectral data were available.

As regards the sensitivity of the MS detection in HPLC analysis of flavonoids, this technique has proved to be the most sensitive as compared to UV and fluorescence detection. A very comprehensive comparison of the four detection systems—UV, fluorescence, and two MS systems [atmospheric pressure chemical ionization (APCI) and electrospray ionization (ESI)]—for the determination of the previously identified 3',4',5'-trimethoxyflavone^[18] is presented in Table 1. Fluorescence detection is 10 times more sensitive than UV detection, whereas MS detection is 50 times more sensitive than UV detection and 5 times more sensitive than fluorescence detection.

Similar assay of the detection systems is performed by Stecher et al.,^[9] who analyzed flavonols and stilbenes in wine and biological products and found that ESI–MS detection gave two, three, and nine times lower limit of detection (LOD) for myricetin, quercetin, and kaempferol,

respectively, as compared to UV absorbance detection at 377 nm (absorption maximum of flavonols).

A significant amount of literature regarding the antioxidant properties of flavonoids and other plant polyphenols is available. As the essence of redox chemistry involves electron transfer, it seems natural that electrochemical detection rivals spectrophotometric detection techniques for the compounds that are supposed to be antioxidants. With the improvements in electrochemical detector geometries and electronics over the last decade, coupled with a requirement for increased sensitivity, the use of electrochemical detectors offers significant additional advantages when combined with the traditional UV–VIS detection in the analysis of flavonoids and other plant polyphenols.^[20]

APPLICATIONS

Several information regarding HPLC analysis of flavonoids, often together with other phenolic constituents, in various samples, such as fruits, vegetables, juices, wines, honey, propolis, and, especially, plant material, are published. The enormous interest in studying these compounds is a result of their potential importance to health and antioxidant defense mechanisms, which has imposed the need for developing methods for their identification and quantification in various natural products. Reversed-phase HPLC (RP HPLC) with combined isocratic and gradient elution with acidic mobile phases and UV diode array or mass spectrometer detector is the most often used system for flavonoid analysis. Depending on the nature of the sample, a variety of sample preparation techniques has been developed in order to achieve good recovery of the analyzed compounds in a simple sample preparation procedure. The procedure includes extraction of the flavonoids in a polar solvent; this extract is then used either for injection onto the column (after filtration) or for further fractionation and purification of the flavonoids to obtain a relatively “clean” sample for injection. The latter step can be carried out in several ways: by liquid–liquid extraction in suitable solvents; by chromatographic techniques (thin layer or column chromatography) on various

Table 1 Regression equations for the calibration curves (logarithmic), regression coefficients, and detection limits for the determination of 3',4',5'-trimethoxyflavone

Detection method	Regression equation	Regression coefficient (R^2)	Detection limit
UV at 213 nm	$y = 0.990x + 13.158$	0.9986	0.244 ng
Fluorescence at 330/440 nm	$y = 0.879x + 12.926$	0.9946	24.4 pg
ESI–MS	$y = 0.692x + 17.349$	0.9956	5.00 pg
APCI–MS	$y = 0.899x + 15.798$	0.9997	5.00 pg

(From Ref. [18].)

stationary phases (silica, reversed phases, Amberlite, and Sephadex); or by solid-phase extraction techniques using different adsorbents, which in the last decade has been found very convenient for the isolation of flavonoids from complex matrices.

Flavonoids in Fruits, Juices, and Wine

During the past decades, extensive analytical research has been performed on the separation of phenolic constituents in various fresh fruits and fruit products. A very thorough examination was performed by Barberán et al.^[11] on samples of several types of fresh nectarines, peaches, and plums using RP HPLC–DAD–ESI–MS and combined isocratic and gradient elution with a mobile phase of water–methanol with 5% formic acid. The samples were prepared by extraction of a homogenized frozen fruit material with water–methanol (2:8), by centrifugation, by filtration, and by injection into the column. This procedure recovers 85–92% of all phenolic compounds including hydroxycinnamates, procyanidins, flavonols, and anthocyanins. In the chromatograms obtained for nectarin and peach samples, three peaks from flavonols (quercetin 3-glucoside, quercetin 3-rutinoside, and, probably, quercetin 3-galactoside), several peaks from flavan-3-ols (catechin, epicatechin, and dimer procyanindines), and two anthocyanin pigments (cyanidine 3-glucoside and cyanidine 3-rutinoside) have been identified by comparing the retention data, the UV, and the mass spectra of the detected flavonoids with the ones obtained for authentic markers. Quantification was done using external standards: quercetin 3-rutinoside for flavonols at 340 nm, cyanidine 3-rutinoside for anthocyanins at 510 nm, and catechin for flavan-3-ols at 280 nm.

An HPLC–DAD method was developed for the separation and the determination of flavonoid and phenolic antioxidants in commercial and freshly prepared cranberry juice.^[6] Two sample preparation procedures were used: with and without hydrolysis of the glycoside forms of flavonoids carried out by the addition of HCl in the step prior to solid-phase extraction (SPE). The flavonoid and phenolic compounds were then fractionated into neutral and acidic groups via a solid-phase extraction method (Sep-Pak C₁₈), followed by a RP HPLC separation with gradient elution with water–methanol–acetic acid and a detection at 280 and 360 nm. A comparison of the chromatograms obtained for extracts prepared with and without hydrolysis showed that flavonoids and phenolic acids exist predominantly in combined forms such as glycosides and esters. In a freshly squeezed cranberry juice, for instance, 400 mg of total flavonoids and phenolics per liter of sample was found, 56% of which were flavonoids. Quercetin was the main flavonoid in the hydrolyzed products, where it accounted for about 75% of the total flavonoids, while it was absent in the unhydrolyzed products.

The flavonoid constituents of *Citrus* have attracted attention in the last decade because of their biological activities (anticarcinogenic, anti-inflammatory effects, etc.) together with the chemotaxonomic importance of the specific flavanone glycosides found in this species. The presence of 12 flavonoids (9 flavanone glycosides, 2 flavanone aglycones, and 1 flavone glycoside) was detected in samples from leaves and fruits of *Citrus aurantium*.^[7] The use of different extraction solvents was studied (methanol, dioxane–methanol 1:1, 0.1% NaOH aq., 0.01% KOH methanolic, pyridin, dimethylformamide, and dimethylsulfoxide), with dimethylsulfoxide

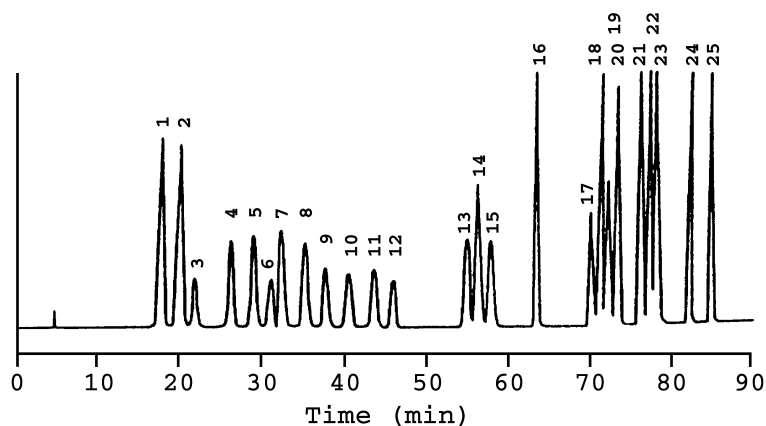


Fig. 2 Separation of 25 flavonoid standards (1—eriocitrin; 2—neeroiocitrin; 3—robinetin; 4—narirutin; 5—naringin; 6—rutin; 7—hesperidin; 8—neohesperidin; 9—isorhoifolin; 10—rhoifolin; 11—diosmin; 12—neodiosmin; 13—neoponcirin; 14—quercetin; 15—poncirin; 16—luteolin; 17—kaempferol; 18—apigenin; 19—isorhamnetin; 20—diosmetin; 21—rhamnetin; 22—isosakuranetin; 23—sinensetin; 24—acacetin; 25—tangeretin) using C₁₈ Lichrospher 100, 250 × 4.0 mm, 5 μm, Merck; gradient elution with 0.01 M phosphoric acid–methanol with flow rate of 0.6 mL/min at 40°C and detection at 285 nm. (From Ref. [8].)

representing the best results. Also, an exhaustive description of the optimization process by studying the quantitative chromatographic parameters— k' , w , α , N , height equivalent to a theoretical plate (HETP), and R —is given with the discussion of the effects of the variation of the methanol (acetonitrile) content in the mobile phase, the degree of mobile phase acidity, together with the influence of the structural characteristics of the studied flavonoids on their behavior in the reversed-phase chromatographic system.

Another thorough procedure for flavonoid analysis in *Citrus* samples is presented in the work of Nogata et al.^[8] They developed a method for separation of 9 flavanones, 10 flavones, and 6 flavonols using a RP HPLC system with gradient elution with 0.01 M phosphoric acid–methanol and for detection at 285 nm, which is presented in Fig. 2. Identification was carried out by comparing the retention data and the spectra of the sample components with the ones of the standards. For quantitative analysis, all flavonoids exhibited good linearity ($r = 0.988$ – 1.00) between concentration and peak area in the investigated concentration range (10–200 ppm) with detection limits from 0.5 to 2.5 ppm.

To investigate the probable health benefits of flavonoids and stilbenes in red wine, a RP HPLC method with enhanced separation efficiency, selectivity, sensitivity, and speed has been established for the determination of the flavonols quercetin, myricetin, and kaempferol and the stilbenes *cis*- and *trans*-resveratrol in a single run.^[9] The sample preparation step for wines and grape juices included only filtration prior to injection. Identification was carried out by the comparison of the retention data, the UV, and the mass spectra of the flavonoids and the stilbenes with the ones obtained for standards. Quantitative analysis using external standards showed good linearity ($R^2 > 0.999$ for UV and $R^2 > 0.9878$ for MS detection), recoveries between 95% and 105%, and limits of detection in the nanogram range, with MS being more sensitive.

An interesting improvement in the sample preparation step has been suggested^[10] using only filtering of the sample prior to injection into the system composed of two columns: clean-up column (50×2.1 mm packed with C_{18} stationary phase, 5 μ m) and analytical column (250×2.1 mm, C_{18} , 5 μ m). A column-switching procedure enables the sample introduced in the first column to be cleaned from the disturbing matrix compounds for 2 min (elution phosphate buffer, pH = 7, with 10% acetonitrile), and then by a gradient of the mobile phase (phosphate buffer, pH = 2.5, with acetonitrile); the retained analytes—flavonoids—are eluted to the analytical column, where they are separated and detected at 365 nm. The method was used for the determination of flavonoid profiles of berry wines containing the flavonols quercetin, myricetin, kaempferol, rutin, and isoquercitrin.

Flavonoids of Honey and Propolis

A very interesting application of flavonoid analysis by HPLC has been carried out by Barberán et al.^[11] on honey samples. They used RP HPLC–DAD for the analysis of 20 flavonoid aglycones, which could be considered as markers for the floral origin of honey. Different solvent systems were applied to the analysis of flavonoids from citrus and rosemary honeys. The sample preparation included dilution with water and HCl (pH = 2–3) for hydrolysis of glycosides, followed by purification using chromatography on Amberlite XAD-2 and Sephadex LH-20. The flavonoid markers of the botanical origin, hesperetin and apigenin, were detected using methanol–water and acetonitrile–water mixtures with formic acid. Quercetin and kaempferol were separated using Prizma-optimized conditions, whereas tectochrysin was eluted with methanol–water and acetonitrile–water mixtures by increasing the content of the organic solvent at the end of the elution programs. The use of diode array detection was found essential in studies of the floral origin of honey by flavonoid analysis.

Flavonoid analysis has also been carried out in propolis, another beehive product rich in flavonoids, which are partly responsible for its pharmacological activity.^[12] Qualitative and quantitative analyses were performed by using a reversed-phase column and isocratic elution with water–methanol–acetic acid (60:75:5) and by monitoring at 275 and 320 nm. The propolis sample was cut into small pieces, extracted with boiling methanol, and the methanolic extract was then diluted with water and, subsequently, extracted with light petroleum and diethyl ether. The last extract contained the propolis flavonoids pinocembrin (21.4%), galangin (5%), chrysin (4.8%), quercetin (2.2%), and tectochrysin (1.1%).

Plant Material

Flavonoids play important roles in plant biochemistry and physiology; they are responsible for the biological effects of plants and their extracts as well as preparations on humans. High-performance liquid chromatography is found very suitable for the detection and the determination of flavonoids present in various plants and plant products; the so-called HPLC fingerprint analysis is suggested for quality control and standardization because of the ability of good separation and resolution of complex mixtures as well as peak purity control. One of the limitations of the assays of flavonoids in plant material is the fact that many compounds, especially glycosides, are not commercially available. One of the possible solutions to this problem is the hydrolysis of flavonoid glycosides during the extraction procedure, which aids the identification on flavonoid aglycones. Such a procedure (the

extraction in acetone with the addition of HCl for hydrolysis of glycosides) is proposed for the screening of flavonols and the determination of quercetin in medicinal plants using RP HPLC with gradient elution with water–acetonitrile–acetic acid and UV diode array detection.^[13] Quercetin was found to be the most abundant, especially in *Hyperici herba* and *Pruni spinosae flos*, kaempferol in *Robiniae pseudoacaciae flos* and *P. spinosae flos*, whereas myricetin was detected only in *Betulae folium*, as can be seen in the chromatograms presented in Fig. 3. The content of quercetin ranged from 0.026% in *Bursae pastoris herba* to 0.552% in *Hyperici herba*.

Another quantitative RP HPLC method, based on the reduction of the complex flavonoid glycoside pattern by acid hydrolysis to one major aglycone (quercetin) and one C-glycoside (vitexin), was developed and employed for the characterization of *Crataegus* leaves and flowers.^[14] A qualitative fingerprint method was also developed for the separation and the identification of all characteristic flavonoids (glycosides and aglycones). Samples for fingerprint analysis were prepared by extraction with 80% methanol and then filtered through Bond Elut C₁₈ cartridge prior to injection. Elution was performed by a mobile phase composed of tetrahydrofuran–acetonitrile–methanol and 0.5% orthophosphoric acid and was monitored at 370, 336, and 260 nm. For quantitative analysis, extraction was carried out with methanol in a Soxhlet apparatus, HCl was added to the methanolic extracts for the hydrolysis of glycosides, and, finally, they were filtered through Bond Elut C₁₈ before injection. Separation and quantification of vitexin and quercetin were

performed for characterization and standardization of the plant material as well as its extracts and preparations.

Structure–RP HPLC Retention Relationships of Flavonoids

The ability to predict the chromatographic mobility of a compound under given conditions, based on its structure, offers many advantages in analysis. The elution sequence of individual flavonoids can be interpreted by assuming that the compounds are first adsorbed on the reversed stationary phase by “hydrophobic interaction,” and then subsequently eluted with the mobile phase according to the extent of hydrogen bond formation. Therefore the hydrogen bond donating and/or accepting ability of a given substituent as well as its contribution to the hydrophobic interaction have to be considered. The retention data of 141 flavonoids^[15] imply the balance between these two effects, resulting in almost identical retention of tricetin pentamethylether (pentamethoxy flavone) and unsubstituted flavone.

Hydroxylation in positions other than 3 and 5 decreases retention owing to increasing polarity (hydrogen bond formation ability). The presence of an OH group in positions 3 and 5 is specific because of the formation of an intramolecular hydrogen bond with the carbonyl group on C-4, which is the strongest hydrogen bond acceptor in flavones and isoflavones. This is the reason for the increase in retention, especially when OH is substituted in position 5, whereas another OH group in position C-3 only slightly lowers the retention. This produces poor separation of the so-called critical pairs flavone–flavonol differing only in the OH group in position 3.

Methylation of the OH groups more or less prevents their effect, which means that flavonoids and their partial methyl ethers are easily separated. On the other hand, the introduction of additional methoxy groups has little or no effect on retention—introducing another type of critical pair differing only in one methoxy group.

Glycosylation of an OH group means introducing a hydrophilic moiety together with shielding (by hydrogen bonding or just by steric hindrance) some hydrophilic substituents already present in the vicinity. The shielding effect plays a role when an OH group located *ortho* to another OH group is glycosylated (e.g., glycosylation of 7- or 4'-OH without an adjacent *ortho*-OH decreases the t_R values by 4.26–3.83 min, whereas, in the presence of an *ortho*-OH, the decrease is only 2.28–1.55 min^[15]). The fact that the t_R value of luteolin-5- β -d-glucopyranoside is only 0.37 min smaller than that of the corresponding 7- β -d-glucopyranoside can also be explained by the shielding effect of sugar on the carbonyl group. The contributions of various types of sugars to the hydrophilic interaction decrease from hexoses through pentoses to methylpentoses.

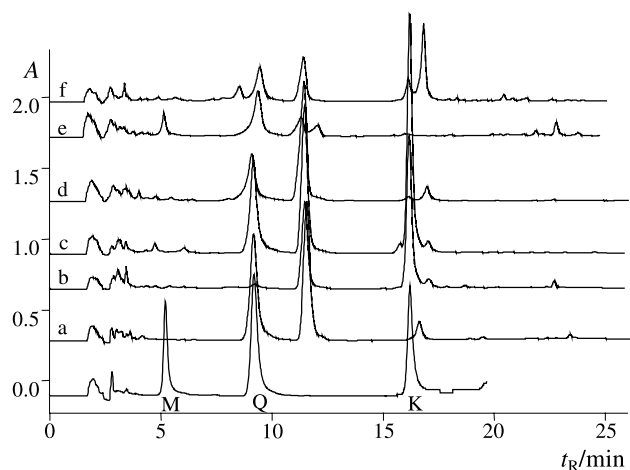


Fig. 3 Chromatograms obtained for extracts of the following: a) *H. herba*; b) *R. pseudoacaciae flos*; c) *P. spinosae flos*; d) *Sambuci flos*; e) *B. folium*; and f) *Primula flos*, and for mixture of authentic samples of myricetin (M), quercetin (Q), and kaempferol (K) using: C₁₈ (250 × 4.6 mm, 5 μ m, Varian); gradient elution with 5% acetic acid–acetonitrile with flow rate of 1.0 mL/min at 30°C and detection at 367 nm. (From Ref. [13].)

Saturation of the C₃ ring, which means transformation of flavones to flavanones and of flavonols to dihydroflavonols, affects the retention in a very complex way. The saturation itself has a small effect; however, in the presence of OH groups, the retention is always decreased. This is explained by the interruption of the conjugation in the system, affecting the acidity and therefore the hydrogen bond accepting and donating abilities of the OH groups, especially the 3-OH groups which are phenolic in flavones and alcoholic in flavanones.

CONCLUSION

Reversed-phase high-performance liquid chromatography has proved to be the method of choice for the separation of a variety of flavonoids in different samples. The phenolic nature of these compounds requires the use of acidic mobile phases for satisfactory separation and peak shapes, whereas the detection is usually carried out with photodiode array detectors which are also very helpful for their identification of the characteristic absorption spectra of the flavonoids. In the last decade, mass spectrometers connected to HPLC systems introduced a greater selectivity and sensitivity in flavonoid analysis. Improving the characteristics of the stationary phases and developing more sophisticated instruments as well as devices for more efficient and faster sample preparation are the challenges for all modern analysts. Discovering the beneficial health effects of flavonoids and the “going-back-to-nature” trend motivates the development of more efficient and fast procedures for their identification and quantification, with HPLC remaining the most powerful technique for their separation from the complex mixtures.

REFERENCES

- Mabry, T.J.; Markham, K.R.; Thomas, M.B. *The Systematic Identification of Flavonoids*; Springer-Verlag: New York, 1970.
- Harborne, J.B. *Phytochemical Methods (A Guide to Modern Techniques of Plant Analysis)*; Chapman and Hall: London, 1984.
- Wollenweber, E.; Jay, M. Flavones and Flavonols. In *The Flavonoids*; Harborn, J.B., Ed.; Chapman and Hall: London, 1988.
- Daigle, D.J.; Conkerton, E.J. Analysis of flavonoids by HPLC: An update. *J. Liq. Chromatogr.* **1988**, *11* (2), 309–325.
- Barberán, F.A.T.; Gil, M.I.; Cremin, P.; Waterhouse, A.L.; Hess-Pierce, B.; Kader, A.A. HPLC–DAD–ESIMS analysis of phenolic compounds in nectarines, peaches, and plums. *J. Agric. Food Chem.* **2001**, *49*, 4748–4760.
- Chen, H.; Zuo, Y.; Deng, Y. Separation and determination of flavonoids and other phenolic compounds in cranberry juice by high-performance liquid chromatography. *J. Chromatogr. A* **2001**, *913*, 387–395.
- Castillo, J.; Benavente-García, O.; Del Rio, J.A. Study and optimization of *Citrus* flavanone and flavones elucidation by reverse phase HPLC with several mobile phases: Influence of the structural characteristics. *J. Liq. Chromatogr.* **1994**, *17* (7), 1497–1523.
- Nogata, Y.; Ohta, H.; Yoza, K.I.; Berhow, M.; Hasegawa, S. High-performance liquid chromatographic determination of naturally occurring flavonoids in *Citrus* with a photodiode-array detector. *J. Chromatogr. A* **1994**, *667*, 59–66.
- Stecher, G.; Huch, C.W.; Popp, M.; Bonn, G.K. Determination of flavonoids and stilbenes in red wine and related biological product by HPLC and HPLC–ESI–MS–MS. *Fresenius' J. Anal. Chem.* **2001**, *371*, 73–80.
- Ollanketo, M.; Riekkola, M.L. Column-switching technique for selective determination of flavonoids in Finnish berry wines by high-performance liquid chromatography with diode array detection. *J. Liq. Chromatogr. Relat. Technol.* **2000**, *23* (9), 1339–1351.
- Barberán, F.A.T.; Ferreres, F.; Blázquez, M.A.; García-Viguera, C.; Tomás-Lorente, F. High-performance liquid chromatography of honey flavonoids. *J. Chromatogr.* **1993**, *634*, 41–46.
- Bankova, V.S.; Popov, S.S.; Marekov, N.L. High-performance liquid chromatographic analysis of flavonoids from propolis. *J. Chromatogr.* **1982**, *242*, 135–143.
- Stefova, M.; Kulevanova, S.; Stafilov, T. Assay of flavonols and quantification of quercetin in medicinal plants by HPLC with UV-diode array detection. *J. Liq. Chromatogr. Relat. Technol.* **2001**, *24* (15), 2283–2292.
- Rehwald, A.; Meier, B.; Sticher, O. Qualitative and quantitative reversed-phase high-performance liquid chromatography of *Crataegus* leaves and flowers. *J. Chromatogr. A* **1994**, *677*, 25–33.
- Vande Castele, K.; Geiger, H.; Van Sumere, C.F. Separation of flavonoids by reversed-phase high-performance liquid chromatography. *J. Chromatogr.* **1982**, *240*, 81–94.
- Galensa, R.; Herrmann, K. Analysis of flavonoids by high-performance liquid chromatography. *J. Chromatogr.* **1980**, *189*, 217–224.
- Jagota, N.K.; Cheathan, S.F. HPLC separation of flavonoids and flavonoid glycosides using a polystyrene/divinylbenzene column. *J. Liq. Chromatogr.* **1992**, *15* (4), 603–615.
- Huck, C.W.; Bonn, G.K. Evaluation of detection methods for the reversed-phase HPLC determination of 3',4',5'-trimethoxyflavone in different phytopharmaceutical products and in human serum. *Phytochem. Anal.* **2001**, *12*, 104–109.
- Huck, C.W.; Huber, C.G.; Ongania, K.H.; Bonn, G.K. Isolation and characterization of methoxylated flavones in the flowers of *Primula veris* by liquid chromatography and mass spectrometry. *J. Chromatogr. A* **2000**, *870*, 453–462.
- Milbury, P.E. Analysis of complex mixtures of flavonoids and polyphenols by high-performance liquid chromatography electrochemical detection methods. *Methods Enzymol.* **2001**, *335*, 15–26.

HPLC Column Maintenance

Sarah Chen

Merck Research Laboratories, Rahway, New Jersey, U.S.A.

INTRODUCTION

The column is arguably the most important component in HPLC separations. The availability of a stable, high-performance column is essential for developing a rugged, reproducible analytical method. Performance of columns from different vendors can vary widely. Separation selectivity, resolution, and efficiency depend on the type and quality of the column. Proper column maintenance is the key to ensure optimum column performance as well as an extended column lifetime. It ensures stability of column plate number, band symmetry, retention, and resolution. The major issues related to column performance and maintenance are discussed here.

COLUMN CONFIGURATION

The HPLC column usually consists of a length of stainless steel tubing packed with porous particles for separation. These particles are sealed in the tubing by an HPLC column end fitting at each end, containing porous frits to retain the packing particles. Typically, 2- and 0.5- μm pore size stainless steel frits are used for 5- and 3- μm particles, respectively.^[1] Many problems arising from stainless steel columns can be traced to the inlet stainless steel frit, which has a higher surface area than the column walls, leading to possible sample adsorption. High backpressure, poor peak shapes, and low sample yields are indications of possible frit problems.

COLUMN PACKING MATERIALS

Silica-based packings are the most popular HPLC column packing materials because of their favorable physical and chemical properties.^[2,3] The silica particles have high mechanical strength, as well as narrow pore size and particle size distribution. The surface of silica can be chemically modified with a large variety of bonding molecules having different functionalities. Silica-based packings are compatible with water and all organic solvents, and exhibit no swelling with change in solvents; this is in contrast to most polymer-based stationary phases.

Columns packed with porous, polymeric particles such as divinylbenzene cross-linked polystyrene, substituted methacrylates, and polyvinyl alcohols can also be used for HPLC method development^[4] as can modified alumina and zirconia stationary phases.^[5,6]

COLUMN MAINTENANCE

Proper column maintenance is very important to ensure optimal performance and extended column lifetimes. There are common procedures that apply to all columns, e.g., avoiding mechanical or thermal shock. There are procedures that are column specific, such as avoiding chloride-containing mobile phases to prevent “halide cracking” if the column tubing and frits are made of stainless steel (especially at low pH). Nonetheless, columns made with stainless steel tubing and packed with silica-based stationary phases are the most commonly used in HPLC. Thus problems associated with these columns and how to prevent such problems by proper column maintenance will be discussed here.

How to Ensure Retention and Resolution Reproducibility of HPLC Columns

Reproducible retention and resolution are very important when developing routine methods. Changes in resolution and retention can be a function of the column quality, its operation, instrumental effects, or variations in separation conditions. The first important step in maintaining retention reproducibility is through selection of a good-quality column with a less acidic and highly purified support. Choosing a favorable mobile-phase condition (pH, buffer type and concentration, additives, etc.) that can eliminate surface silanol interactions when separating basic compounds is also very important for column retention reproducibility. There should be minimal variation in laboratory temperature or column temperature for retention and resolution reproducibility. Proper laboratory instrumentation and column storage conditions cannot be neglected either.

Poor retention reproducibility and tailing peaks often occur in poorly buffered mobile phases, because of an inappropriately selected buffer, too low a buffer

concentration, or a pH out of the effective range of a buffer. Increasing buffer concentration can minimize some of the problems. However, the buffer concentration must not be too high; otherwise, the buffer may not be miscible with the organic portion of the mobile phase. Other factors such as tailing peaks, high backpressure, or loss of stationary phase will also result in poor retention reproducibility and will be discussed later.

How to Avoid Band Tailing

Band tailing causes inferior resolution and reduced precision. Thus conditions resulting in tailing or asymmetric peaks should be avoided. Peak asymmetry or band tailing can arise from several sources: partially plugged column frits, void(s) in the column, buildup of sample components and impurities on the column inlet following multiple sample injections, sample overload, solvent mismatch with reference to the sample, chemical or nonspecific interactions (e.g., silanol effects), contamination by heavy metals, and excess void volume in the HPLC system.

Tailing peaks are common with heavily used columns. During use, columns can develop severe band tailing or even a split peak for a single component. Such effects usually arise from the presence of a void in the inlet of the column and/or a dirty or partially plugged inlet frit. The cause of the void can be either a poorly packed column in which the packing settles during use or dissolution of silica packing at excessively high pH. Excessive system backpressure or pressure surges, caused by poorly operating pumps or sample injection valves, can also cause column voiding. The void can be eliminated by the addition of a new packing material at the inlet end of the column to fill the void. This can be done by carefully removing the end fittings from the column inlet. Packing material is added in a slurry form to the void column volume. For best results, packing material of the same type as the column packing should be used. Old frits should be replaced with new ones of the same type. However, sometimes it is difficult to achieve the initial column efficiency after such procedures.

The presence of strongly retained materials in real-world samples can result in peaks that are eluted long after the normal run time is over. These peaks can cause three kinds of problems in later runs. If the peaks are large, they can sometimes show up in a subsequent run as very broad peaks. If the peaks are very small, they can be hidden under a peak of interest and cause peak distortion. It is also possible that peaks eluting late in a run can be small enough or so strongly retained that they appear only as a minor baseline hump. The development of broader tailing peaks during column use may also indicate the buildup of strongly retained sample components (garbage) on the column. Purging the column with

a strong solvent can eliminate this buildup. For reversed-phase columns, a 20-column volume purge (about 50 mL for a 250 × 4.6-mm i.d. column) with 100% acetonitrile is often adequate. In case a stronger solvent is needed, a mixture of 96% dichloromethane and 4% methanol with 0.1% ammonium hydroxide is often effective. Because dichloromethane is not miscible with aqueous mobile phases, it is necessary to flush the reversed-phase column with acetonitrile prior to and after the use of dichloromethane. Methanol is used for normal phase columns. Sometimes it may be sufficient to flush the column once a day. If strongly retained materials are known to exist in the sample, it is a good idea to flush the column with a strong solvent at the end of each run sequence so that any strongly retained materials are flushed out before the next analysis.

How to Avoid High Backpressure

High backpressure is one of the most commonly encountered problems when performing HPLC analysis. Normal column backpressure is observed after a new column has been installed and equilibrated with the mobile phase. Unfortunately, this pressure often will increase with time of use because of particles collecting on the column inlet or outlet frit. These particles can be sample impurities, mobile phase contaminants, or materials from the injector or autosampler rotary seal. Unfavorable buffer conditions, such as high pH, can dissolve silica particles. Following the breakdown of particles, resultant small particles can clog the frit at the outlet of the column. The presence of small particles in the system can result in increased backpressure, split peaks, tailing, and, eventually, overpressure shutdown of the HPLC system. Most often, plugged frits can be eliminated by back flushing the column with a strong solvent. If this does not alleviate the problem, the plugged inlet frit can be replaced with a new frit without disturbing the packing. When replacing the inlet frit, addition of packing material is often needed if a void is noticed at the column inlet. To reduce backpressure problems, samples should be cleaned up before injection. The sample treatment may include filtering the samples through a submicron membrane filter to remove particulates or using solid-phase extraction techniques to remove highly retained sample components or matrix components. Only HPLC-grade or superior-grade solvents should be used to prepare the mobile phase, and buffer solutions should be filtered; alternatively, prefilters may be installed at the buffer reservoir. Rotary valve seals should be changed during routine maintenance procedures. Along with these preventive measures, it is advisable to use column prefilters, e.g., a guard column protection system. Particles then build up on the inexpensive, replaceable frit in the prefilter instead of in the permanent frit at the head of the analytical column.



is best to choose a guard column containing the same type of stationary phase as is contained in the analytical column. The length of a guard cartridge is usually 1 or 2 cm, with typical diameters ranging from 2.0 to 4.6 mm.

How to Prevent Loss of Stationary Phases

Column lifetime can be reduced significantly by the loss of the stationary phase during the separations. Stationary/mobile-phase combinations that lead to a rapid loss of bonded phase should be avoided. Column manufacturers' recommendations should be followed when using an HPLC column for separations. Commonly, reversed-phase columns with short-chain silane groups are the least stable, as the silane groups can be easily hydrolyzed with aggressive mobile phases (e.g., pH < 2.0). Reversed-phase columns with longer alkyl groups, such as C₈ or C₁₈ (Fig. 1), are usually considered relatively stable because of the inaccessibility of the surface Si-O-R group. Polymeric C₈ or C₁₈ is considered to be more stable than its monomeric counterparts. However, over long periods at very low or very high pH values, these columns can also lose bonded molecules. Use of sterically protected silane stationary phases will provide additional stability in aggressive low-pH environments.

The stability of the bonded organic ligand on a reversed-phase column also depends on the type and acidity of the silica used as the support. Packings made with fully hydroxylated silicas with a homogeneous distribution of silanol groups show superior stability. Higher bonded-phase stability apparently can occur for columns made with highly purified silica supports having a lower surface acidity.

Loss of stationary phase from silica-based columns is accelerated at higher temperatures. Temperatures above

~40°C should be used with caution when operating at intermediate or high pH values with phosphate buffers. Operation at pH < 3 and elevated temperature can degrade the bonded stationary phase more rapidly and cause retention reproducibility instabilities. However, there are specially end-capped columns available commercially that can withstand higher temperatures with significantly less hydrolysis.

One Hundred Percent Aqueous Mobile Phase with Reversed-Phase Column

Unless specified by the manufacturer, 100% aqueous mobile phase should be avoided with a reversed-phase column, such as C₁₈ or C₈. Most reversed-phase columns exhibit decreased and poorly reproducible retention under more than 98% aqueous conditions. This problem has been attributed to the ligand collapse or incomplete wetting of the stationary phase. It has been reported that when a C₁₈ column is washed with water, the bonded phase collapses or is incompletely wetted.^[7] Subsequent flushing with mobile phase removes the wash solvent, but the stationary phase remained in the collapsed configuration; this has caused a change in retention and selectivity. It has been suggested that washing a reversed-phase column with water should be avoided. Furthermore, if the organic content of a mobile phase is too low, the stationary phase will tend to collapse onto itself in a low energy conformation. This collapse/incomplete wetting could lead to abnormal chromatographic behavior and generally undesirable results. To avoid this phenomenon, workers have sometimes used embedded polar phases, including amide or carbamate groups^[8-11] which presumably do not undergo phase collapse in 100% water and can withstand mobile phases with high aqueous content. If

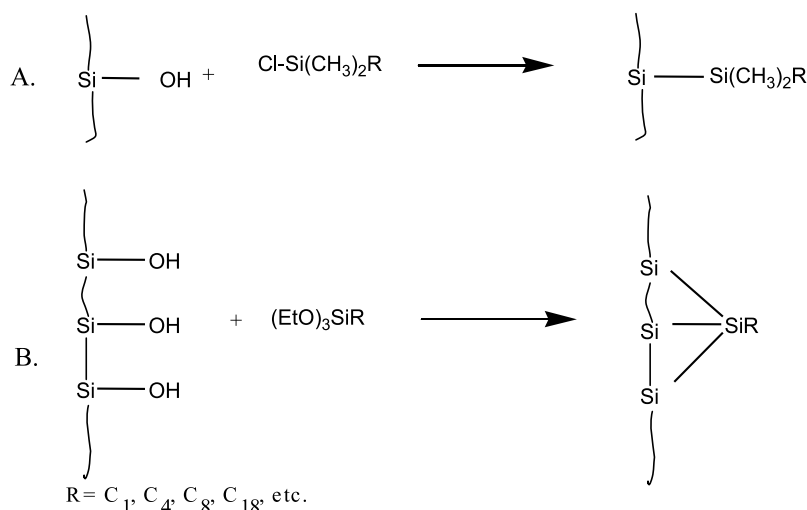


Fig. 1 Schematic diagram of monomeric (A) and polymeric (B) stationary phases for reversed phase HPLC.



100% aqueous mobile phase is needed for a reversed-phase separation, columns with embedded polar groups should be used.

Other Factors in Column Maintenance

Storing a column filled with 100% organic solvent, such as acetonitrile, preserves the performance and lifetime of bonded-phase columns. Storage with buffered solutions (particularly those containing high concentrations of water and alcohols) should be avoided. When buffers are used, columns should be flushed with 15 to 20 column volumes of the same aqueous/organic mobile phase without buffer before converting to 100% organic for storage. Columns should be capped tightly during storage to prevent the packed bed from completely drying. Bacterial growth often occurs in buffers and aqueous mobile phases contained in columns that are prepared and stored at ambient temperature for more than a day. Particulates from this source can plug the column inlet and reduce column life significantly. As a result, mobile phases that are free of organic solvents should be discarded at the end of each day. Alternatively, 20% of organic modifier in the mobile phase retards bacterial growth. The organic modifier also assists in the mobile-phase degassing process.

CONCLUSION

In general, mechanical and thermal shock should be avoided to prevent disturbing the column packing bed. Pressure surges in the system should also be avoided. Choosing a suitable buffer system is very critical to

maintaining retention and resolution reproducibility and preventing the loss of stationary phase. Samples containing particulates should be filtered before injection. The use of guard columns can reduce the "garbage" build up at the column inlet and reduce the risk of high back-pressure. It is a good practice to flush the column frequently with a strong solvent after heavy use and to store it in an appropriate solvent.

REFERENCES

1. Snyder, L.R.; Kirkland, J.J.; Glajch, J.L. *Practical HPLC Method Development*, 2nd Ed.; John Wiley & Sons, Inc.: New York, 1997.
2. Iler, R.K. *The Chemistry of Silica*; Wiley: New York, 1979.
3. Unger, K.K. Porous silica. *J. Chromatogr. Libr.* **1979**, *16*, Elsevier, Amsterdam.
4. Tanaka, N.; Araki, M. *Adv. Chromatogr.* **1989**, *30*, 81.
5. Pesek, J.J.; Sandoval, J.E.; Su, M. *J. Chromatogr.* **1990**, *630*, 91.
6. Sun, L.; Annen, M.J.; Lorenzano-Porras, F.; Carr, P.W.; McCormick, A.V. *J. Colloid Interface Sci.* **1993**, *163* (2), 91.
7. Wolcott, R.G.; Dolan, J.W. *LC-GC* **1999**, *17* (4), 316.
8. O'Gara, J.E.; Alden, B.A.; Walter, T.H.; Petersen, J.S.; Niederlander, C.L.; Neue, U.D. *Anal. Chem.* **1995**, *67*, 3809.
9. Cqajkwaka, T.; Hrabovsky, I.; Buszewski, B.; Gilpin, R.K.; Jaroniec, M. *J. Chromatogr., A* **1995**, *691*, 217.
10. Ascah, T.L.; Kallury, K.M.R.; Szafranski, C.A.; Corman, S.K.; Liu, F. *J. Liq. Chromatogr. Relat. Technol.* **1996**, *19*, 3409.
11. Czajkowaka, T.; Jaroniec, M. *J. Chromatogr., A* **1997**, *762*, 147.





Hybrid Micellar Mobile Phases

M.C. García-Alvarez-Coque

J.R. Torres-Lapasio

Universidad de Valencia, Valencia, Spain

INTRODUCTION

The first report on the analytical use of an aqueous solution of a surfactant, above its critical micellar concentration (CMC), as mobile phase in reversed-phase liquid chromatography (RPLC) was published in 1980.^[1] The technique, named micellar liquid chromatography (MLC), is an interesting example of the modification of the chromatographic behavior taking advantage of secondary equilibria to vary both retention and selectivity.

Most MLC procedures use micelles of the anionic surfactant sodium dodecyl sulfate (SDS). Other useful surfactants include the cationic cetyltrimethylammonium bromide or chloride (CTAB or CTAC) and the nonionic Brij-35.^[2] The separations are usually carried out in C₁₈ or C₈ columns.

Inside the column, solutes are affected by the presence of micelles in the mobile phase and by the nature of the alkyl-bonded stationary phase, which is coated with monomers of surfactant (Fig. 1). As a consequence, at least two partition equilibria can affect the retention behavior. In the mobile phase, solutes can remain in the bulk water, be associated to the free surfactant monomers or micelle surface, be inserted into the micelle palisade layer, or penetrate into the micelle core. The surface of the surfactant-modified stationary phase is micelle-like and can give rise to similar interactions with the solutes, which are mainly hydrophobic in nature. With ionic surfactants, the charged heads of the surfactant in micelles and monomers adsorbed on the stationary phase are in contact with the polar solution, producing additional electrostatic interactions with charged solutes. Finally, the association of solutes with the nonmodified bonded stationary phase and free silanol groups still exists.

The most serious limitations of pure micellar solutions are their weak elution strength and poor efficiencies. As early as 1983,^[3] the addition of a small percentage of 1-propanol was found to enhance the efficiencies and decrease the asymmetries of chromatographic peaks. Later, the term “hybrid micellar mobile phases” was given to the ternary eluents of water/organic solvent/micelles. Although 1-propanol is still the most frequently used additive, other alcohols (methanol, ethanol, 1-butanol, and 1-pentanol) and organic solvents common

in conventional RPLC (acetonitrile and tetrahydrofuran) have also been used. It should be noted that micellar solutions increase the solubility of butanol and pentanol in water to reach concentration levels considered useful in chromatography.

The concentration of organic solvent should be low enough to make the existence of micelles possible. Such maximal amount depends on the type of surfactant and organic solvent, and is usually unknown. For SDS, the maximal volume fractions of acetonitrile, propanol, butanol, and pentanol that seem to guarantee the presence of micelles are 20%, 15%, 10%, and 7% (v/v), respectively. However, analytical reports where authors claim the use of hybrid micellar mobile phases and these maximal values are exceeded—micelles do not exist—are not unusual. In such conditions, the system bears closer resemblance to an aqueous–organic system, although the surfactant monomers still affect the retention and efficiencies.

NATURE OF THE MOBILE AND STATIONARY PHASES

The presence of a small amount of an organic solvent in the micellar mobile phase produces changes in the micellization process which depend on the nature of the additive. A progressive increase in the CMC of SDS (8.2×10^{-3} M in water at 25°C) is observed by adding methanol and acetonitrile; the reverse is observed when ethanol, propanol, butanol, and pentanol are added. As an example, the CMC of SDS in the presence of 4% (v/v) organic solvent is 8.7×10^{-3} M (methanol), 9.2×10^{-3} M (acetonitrile), 7.4×10^{-3} M (ethanol), 5.9×10^{-3} M (propanol), 2.7×10^{-3} M (butanol), and 2.0×10^{-3} M (pentanol).^[4]

Methanol, which has the shortest carbon chain, is more polar and soluble than other alcohols. SDS monomers are more easily solvated in an aqueous–methanol medium. This inhibits them from interacting and forming micelles. A similar behavior is expected for acetonitrile. Ethanol and propanol, which are also miscible with water, remain outside the micelles, dissolved in the bulk liquid, but interact with the micelle surface. Repulsion among the



Fig. 1 Solute–micelle and solute–stationary phase interactions in hybrid micellar mobile phases (see text for meaning of equilibrium constants).

ionic heads of surfactant monomers is reduced in the presence of these two alcohols, thus aiding the formation of micelles.

As the length of the alcohol alkyl chain increases, its affinity for the SDS micelle is enhanced. Butanol and pentanol are inserted in the intermonomer spaces of the micelle palisade (aligned with the surfactant molecules), the polar hydroxyl group orientated toward the Stern layer and the alkyl chains located in the nonpolar micelle core. A swollen mixed micelle is thus formed. Such micelles are geometrically hindered to allocate additional surfactant monomers, which is translated into a CMC reduction. However, above 4% butanol and 1.5% pentanol, the decay rate in the CMC values changes. An explanation for this behavior is that above a given concentration, the amount of alcohol entering the palisade is not significant, and the excess is solubilized in the core of the swollen micelle. Further additions of alcohol lead to a dramatic change in the mobile phase microstructure, yielding a microemulsion.

Organic solvents also induce changes in the properties of surfactant-coated stationary phases, such as polarity, surface area, or pore volume. Several studies have demonstrated that *n*-alcohols interpenetrate the C₁₈-bonded alkyl chains to form a single monolayer, structurally similar to an opened micelle (i.e., the hydroxyl group orientated toward the aqueous phase). The competition between organic solvent and surfactant molecules for the active sites on the column explains the reduction of adsorbed surfactant at increasing concentration of organic solvent in the mobile phase. For ionic surfactants, this

reduction is linear with slopes that depend on the strength of the solvent (methanol < ethanol < propanol < butanol < pentanol). Substitution of alcohol by some surfactant molecules on the stationary phase increases its effective polarity and decreases the retention time. With hybrid micellar mobile phases, the stationary phase resembles a solvated phase in aqueous–organic systems more, rather than in pure micellar systems.^[5]

Solute retention varies with the concentration of propanol, butanol, and pentanol in the mobile phase in the same way as CMC does. This means that the collateral effects which change the CMC in an organic–micellar system are, at least partially, those that induce shorter retention with hybrid mobile phases: the modification of bulk water and micelle. As noted, another important factor that affects retention is the modification of the structure of the stationary phase. The analogous effects on both microenvironments (micelle and stationary phase) are evident in the parallel variation of solute–micelle and solute–stationary phase partition coefficients, as the concentration of organic solvent changes.^[6]

In the hybrid system, solute partition equilibria are significantly displaced away from the micelle and the stationary phase toward the bulk aqueous–organic phase, which is more nonpolar (Fig. 1). However, as long as the integrity of micelles is maintained, the addition of organic solvent to micellar mobile phases will not create an aqueous–organic system. The chromatographic behavior of alkyl homologous series has been used to demonstrate that the separation mechanism in hybrid MLC is more similar to pure MLC than to conventional RPLC. In aqueous–organic systems, the retention of homologue compounds is described as follows:

$$\log k = \log \alpha(\text{CH}_2)n_C + \log \beta \quad (1)$$

where n_C is the number of carbon atoms in the homologue, $\alpha(\text{CH}_2)$ is the nonspecific selectivity of a methylene group, and β is the contribution of the series functional group to the retention. In contrast to this behavior, a linear relationship between k and n_C is observed with either pure or hybrid micellar mobile phases.

RETENTION BEHAVIOR

In pure micellar mobile phases, retention is described by a hyperbolic relationship.^[7]

$$k = \frac{\phi P_{AS}}{1 + v(P_{AM} - 1)[M]} = \frac{K_{AS}}{1 + K_{AM}[M]} \quad (2)$$

where k is the retention factor, ϕ is the phase ratio, P_{AS} and P_{AM} are the solute–stationary phase and solute–

micelle partition coefficients, v is the specific volume of surfactant monomers, and $[M]$ is the concentration of surfactant forming micelles (total surfactant concentration minus the CMC). The expression with K_{AS} and K_{AM} is often used for simplicity.

The same model is valid for hybrid micellar mobile phases at fixed concentration of organic solvent, although both constants, K_{AS} and K_{AM} , decrease when the modifier concentration increases, especially for non-polar solutes. An extended model, including the effect of changes in organic solvent concentration, has also been proposed.^[17,8]

$$k = \frac{K_{AS} \frac{1 + K_{SD}\varphi}{1 + K_{AD}\varphi}}{1 + K_{AM} \frac{1 + K_{MD}\varphi}{1 + K_{AD}\varphi}} [M] \quad (3)$$

where φ is the volume fraction of organic solvent; K_{AS} and K_{AM} are the partition constants in pure micellar eluents; and K_{AD} , K_{MD} , and K_{SD} measure the relative variations in solute concentration in bulk water, micelle, and stationary phase, respectively, in the presence of organic solvent, taking the pure micellar solution as reference. These constants increase with the organic solvent strength. For polar and moderately polar solutes eluted with propanol, K_{SD} can be disregarded and Eq. 3 is simplified as follows:

$$\frac{1}{k} = c_0 + c_1[M] + c_2\varphi + c_{12}[M]\varphi \quad (4)$$

Chromatographic optimizations are usually performed at a preselected pH. However, a simultaneous consideration of the three factors (i.e., surfactant, organic solvent, and pH) expands the separation capability for some problems. The retention can be predicted from: (see below) where K_{AS} , K_{AM} , K_{AD} , K_{MD} , and K_{SD} are the equilibrium constants associated to the basic species; and K_{HAS} , K_{HAM} , K_{HAD} , K_{HMD} , and K_{HSD} correspond to the acidic species. K_H is the protonation constant in the aqueous-organic bulk solvent, and $[H]$ is the proton concentration.

Eqs. 2–5 give accurate predictions of the retention with several types of surfactant (anionic, cationic, and nonionic) and organic solvent (alcohols and acetonitrile), and solutes of different polarity and charge, with errors usually below 3–5%.

ELUTION STRENGTH

One of the most serious problems of pure micellar eluents is their weak elution strengths. Shorter retention times are obtained by increasing the surfactant concentration, but the chromatographic efficiency usually deteriorates. The use of ultrawide pore or shorter chain-length-bonded stationary phases constitutes other alternatives, but the most practical solution seems to be the addition of a small amount of an organic solvent to the mobile phase. This strategy may result in adequate elution strengths, together with improved chromatographic efficiencies and selectivities, which will produce a favorable effect on both the resolution and the length of analysis time. However, the addition of an organic solvent is unsuitable for low retained solutes because the retention level may fall below the optimal retention range. In other instances, adequate retention times are achieved, but the efficiencies remain low.

The elution strength of the organic solvent in MLC has been described according to Eq. 3.^[9] However, a simple logarithmic relationship (similar to that used in conventional RPLC) is customary:^[10]

$$\log k = \log k_0 - S\varphi \quad (5)$$

where S is the sensitivity of solute retention to changes in the volume fraction of organic solvent, and $\log k_0$ is the retention in a pure aqueous micellar solution. A similar equation has been used for the surfactant:

$$\log k = \log k'_0 - S'[M] \quad (6)$$

If Eq. 2 is rewritten in the logarithmic form:

$$\log k = \log K_{AS} - \log (1 + K_{AM}[M]) \quad (7)$$

and linear relationships are assumed between $\log K_{AS}$ and $\log (1 + K_{AM}[M])$ with φ , the following results:

$$S = S_s - S_m \quad (8)$$

S_s and S_m represent the sensitivity of variations in solute partitioning from bulk solvent into the stationary phase and micelles, respectively, with changes in φ . The negative sign in Eq. 9 reflects the competing nature of the two partitioning equilibria. In the absence of micelles, $S_m=0$ and $S=S_s$, which represents the solvent strength parameter in conventional aqueous-organic RPLC. Eq. 9 also shows that the elution strength in hybrid micellar

$$k = \frac{K_{AS} \frac{1 + K_{SD}\varphi}{1 + K_{AD}\varphi} + K_{HAS} \frac{1 + K_{HSD}\varphi}{1 + K_{HAD}\varphi} K_H[H]}{\left(1 + K_{AM} \frac{1 + K_{MD}\varphi}{1 + K_{AD}\varphi} [M]\right) + \left(1 + K_{HAM} \frac{1 + K_{HMD}\varphi}{1 + K_{HAD}\varphi} [M] K_H[H]\right)} \quad (9)$$

systems will be generally smaller. The magnitude of the reduction depends on the interaction degree of solutes and organic solvents with micelles. Also, the range of elution strength values for solutes of diverse polarity is narrower than in conventional RPLC.

Longer-length alcohols, which are more hydrophobic, are able to shorten the retention in a larger extent. Retention times are smaller for micellar solutions containing greater amounts of additive, but even relatively low amounts can produce dramatic effects. These are attenuated as the surfactant concentration is increased. Finally, decrease in retention times is more intense for more hydrophobic solutes. Elution strength is usually greater in alcohols than in surfactants. However, changes in the retention of positively charged solutes—such as catecholamines and β -blockers, eluted with SDS micellar mobile phases—are larger when the concentration of surfactant is varied due to the high affinity of these compounds for the negatively charged micelles.

The elution strength of hybrid micellar mobile phases was measured for a number of organic additives (alcohols, alkane diols, alkanes, alkylnitriles, and dipolar aprotic solvents, such as dimethyl sulfoxide and dioxane) added to micellar SDS, CTAC, and Brij-35.^[11] Benzene and 2-ethylantraquinone were used as probe compounds. The presence of alcohols, alkane diols, alkylnitriles, and dipolar aprotic solvents produced a diminution of the retention times, reaching remarkable levels for the most hydrophobic compound (2-ethylantraquinone). The observed elution strength order roughly paralleled the octanol–water partition coefficients of the additives, $P_{o/w}^a$ (Fig. 2), or their ability to bind to micelles, K_{AM}^a . In contrast, alkanes (pentane, hexane, and cyclohexane) had relatively little effect on the retention.

Selection of the most suitable organic solvent should consider the polarity of analytes and their association with the surfactant. Solute $\log P_{o/w}$ values can be used, in most cases, as a guide to make this decision.^[12] Thus, with SDS as surfactant, a low concentration of propanol ($\sim 1\%$ v/v) is useful to separate compounds with $\log P_{o/w} < 1$ as amino acids. A greater concentration of this solvent ($\sim 5\%$ to 7%) is needed for compounds in the range $1 < \log P_{o/w} < 2$ as diuretics and sulfonamides. Pentanol ($\sim 2\%$ to 6%) is more convenient for low polar compounds with $\log P_{o/w} > 3$ as steroids. For basic compounds, such as phenethylamines with $0 < \log P_{o/w} < 2$ and β -blockers with $1 < \log P_{o/w} < 3$, propanol is too weak due to the strong electrostatic interaction between the positively charged solutes and the anionic surfactant adsorbed on the stationary phase. In this case, a high concentration of propanol ($\sim 15\%$), or preferably, a moderate concentration of butanol ($< 10\%$) should be used.

When complex mixtures of compounds in a wide range of polarities are eluted with hybrid micellar mobile

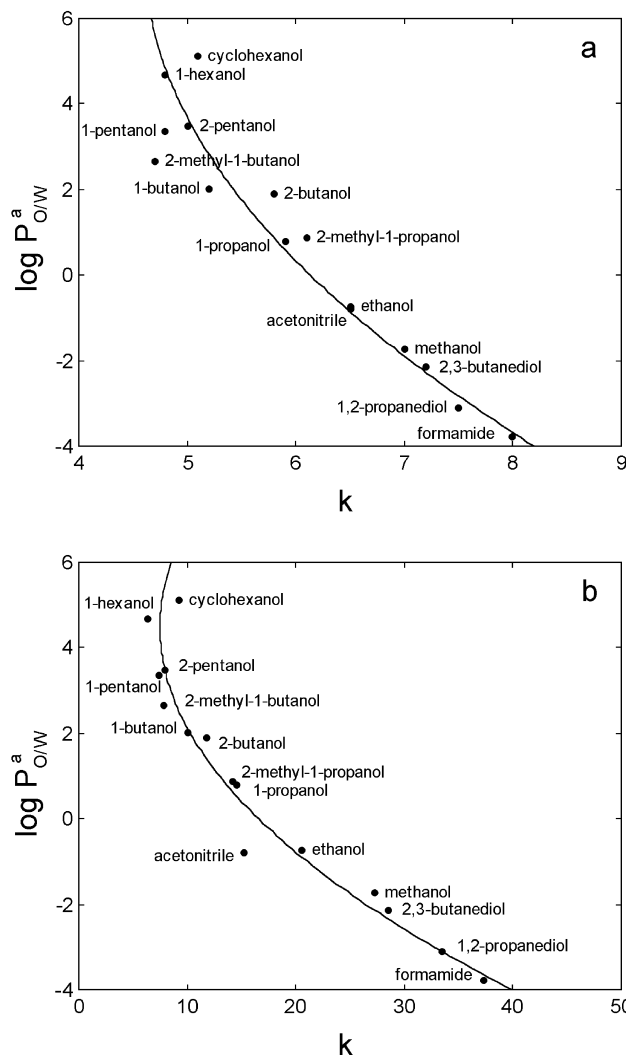


Fig. 2 Correlation between octanol–water partition coefficients of the organic solvents ($\log P_{o/w}^a$), and the retention factors of: (a) benzene and (b) 2-ethylantraquinone in hybrid SDS micellar mobile phases. The concentration of surfactant and organic solvent was 0.285 M and 5% (v/v), respectively. (From Ref. [11].)

phases at increasing volume fraction of organic solvent, the retention times of late-eluting compounds are reduced in a larger extent than earlier peaks. The effect is similar to that obtained with gradient elution in conventional RPLC but using isocratic elution and low amounts of organic solvent.

EFFICIENCY

Low efficiencies, observed especially for highly hydrophobic solutes eluted with pure micellar mobile phases,

Hybrid Micellar Mobile Phases

5

hindered the initial development of MLC. The addition of a small amount of organic solvent at least partially remedied this situation. Efficiency enhancements—dramatic in some cases—have been reported for solutes eluted with SDS mobile phases in the presence of alcohols, alkane diols, alkylnitriles, and dipolar aprotic solvents. Concomitant with the enhanced efficiencies, improvements in peak asymmetry are observed. The reason for these effects is an increased solute mass transfer between micelles/stationary phase and aqueous phase due to the greater solute–micelle exchange rate constants, lower stationary phase viscosity, and smaller amount of adsorbed surfactant.^[5,11]

Plots of $P_{o/w}^a$ or K_{AM}^a vs. plate counts for benzene and 2-ethylantraquinone eluted with micellar SDS, in the presence of several alkanols and alkane diols, show an initial steep increase in efficiency, after which an approximately constant value is reached (Fig. 3). Among the alcohols, maximal efficiency for benzene and 2-ethylantraquinone is obtained with the butanols and the pentanols, with enhancement factors of ~ 2.5 and ~ 25 (compared to pure SDS), respectively. However, final efficiencies for the latter compound are much lower compared to that for benzene. Dipolar aprotic modifiers (acetonitrile or dimethylsulfoxide) appear to be somewhat more effective in enhancing efficiencies than alcohols with comparable $P_{o/w}^a$. Some recent work has shown the advantage of using acetonitrile as additive in MLC for the analysis of sulfonamides, tetracyclines, and the most polar steroids.

Chromatographic efficiency seems to be linked to the additive-to-surfactant concentration ratio in the micellar mobile phase. The plate numbers increase with this ratio but reach a maximum level (e.g., at pentanol/SDS = 6 and acetonitrile/CTAC = 12).^[5] The organic solvent/surfactant ratio affects the exchange rates of the solute between micelle/stationary and aqueous phases. It also controls the extent of the surfactant coverage and the fluidity of the organic layer on the stationary phase.

Satisfactory results are obtained with compounds of different nature. Of particular interest is the case of basic compounds, such as phenethylamines and β -blockers, which experience large efficiency enhancements in SDS systems.^[12] This makes the use of special columns less necessary. The surfactant layer adsorbed on the column prevents the interaction of basic compounds with free silanol groups, which accounts for the low efficiencies observed with conventional columns in aqueous–organic RPLC. For acidic compounds such as sulfonamides, the efficiencies are comparable with both MLC and conventional RPLC, but for low polar compounds such as steroids, efficiencies are comparably poorer in MLC. However, in this technique, low polar steroids are eluted at sufficiently short retention times via a small amount of

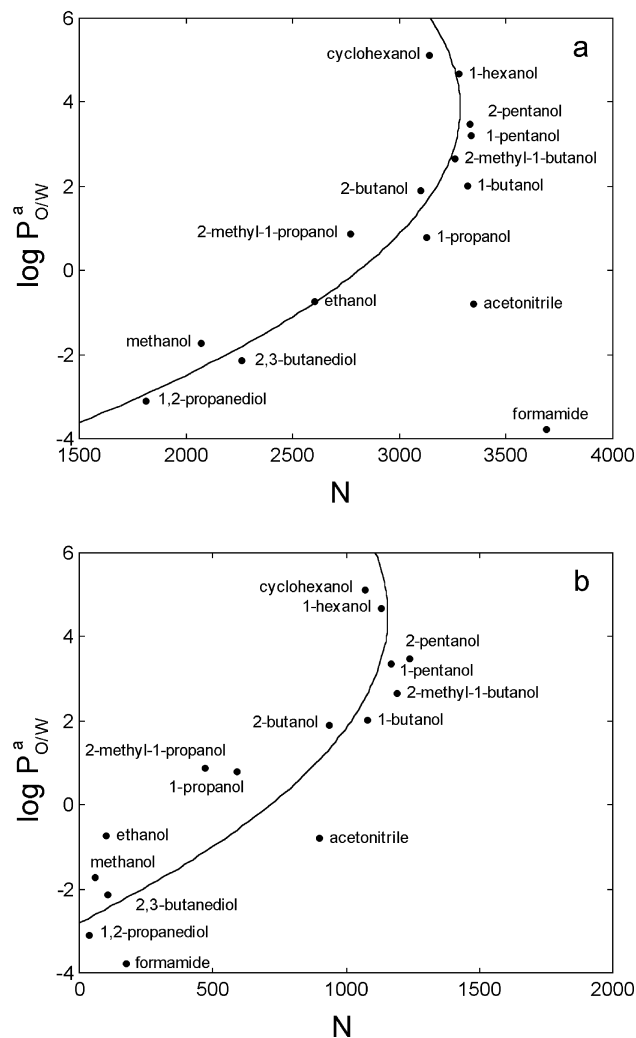


Fig. 3 Correlation between octanol–water partition coefficients of the organic solvents and the efficiencies (plate counts) of: (a) benzene and (b) 2-ethylantraquinone in hybrid SDS micellar mobile phases. See details in Fig. 2.

a strong organic solvent. Meanwhile, in conventional RPLC, a high amount of organic solvent is needed to decrease the retention time to practical values.

SELECTIVITY

The rate of change in retention at varying surfactant and organic solvent concentration depends on the solute charge and polarity, as well as on the nature of both modifiers. The existence of different intermolecular forces governing the retention, the magnitude of which is altered by each modifier, explains this behavior. The more hydrophobic the solute, the more intense is the

effect of the organic solvent on the elution strength (i.e., for a given increment in the concentration of an organic solvent, the partition coefficients for more hydrophobic solutes decrease more than for hydrophilic solutes). Hence, the selectivity changes. Several examples have been published where a hybrid mobile phase was able to achieve an acceptable separation—impossible with pure micellar eluents—within much shorter analysis time.

The presence of micelles has a great influence on the chromatographic selectivity of organic solvents. As a result, the solvent classification established by Snyder in conventional RPLC, based on selectivity, does not seem to be valid in MLC with hybrid mobile phases.^[10] Thus, for example, according to Snyder, 1-propanol and 1-butanol belong to the same selectivity group and, consequently, although the elution strength is greater when using butanol, both alcohols yield similar chromatographic selectivities in aqueous–organic mobile phases. Because in MLC organic solvents not only associate with micelles but also compete with them to interact with the solutes, the selectivities for 1-propanol and 1-butanol vary. The different impact of micelles of different surfactants on the selectivity is another factor that should be considered.

In conventional RPLC, a systematic decrease in selectivity usually occurs when the volume fraction of organic solvent is increased.^[10] In contrast, in the presence of micelles, the selectivity may increase, decrease, or remain unchanged with the addition of both surfactant and organic solvent. Although the elution strength increases with the concentration of both micelle and organic solvent, their effect on the selectivity can be quite different, even opposite.

The behavior of solutes depends on the relative change of their apparent solute–micelle association constants and partitioning constants into the stationary phase. These usually decrease with an increase in volume fraction of modifier. The magnitude of the diminution is, however, not equal for various solutes. Improving the resolution and simultaneously reducing the separation time are the two more important goals in most optimization strategies. Simultaneous enhancements in selectivity and elution strength can lead to better separations in shorter analysis times.

Method development in MLC requires first the selection of a surfactant/organic solvent system. The second step concerns the optimization of the selectivity. The separation can be improved by varying only one factor, or modifying one after optimizing the other (i.e., proton, surfactant, and organic solvent concentration). However, in operations like this, the best separation conditions can be easily missed. Reliable optimal conditions can be obtained only when all factors are simultaneously taken into account. This requires the use

of an interpretive optimization strategy (i.e., based on the description of the retention behavior and peak shape of solutes). In this task, the product of free peak areas or purities has proved to be the best optimization criterion.^[13] An interactive computer program is available to obtain the best separation conditions.^[14]

The experimental domain that should be examined to obtain the best separation should cover a region of concentrations of surfactant and organic solvent as wide as possible, with some restrictions. The lower concentration of surfactant should be well above the CMC (e.g., 0.05 M for SDS and 0.04 M for CTAB). Surfactant concentrations exceeding 0.20 M are not convenient due to the high viscosity of the mobile phase and degradation of the efficiencies. Polarity of the solutes should be considered for the choice of the right organic solvent (nature and concentration range). This concentration must be low enough to guarantee the existence of micelles. Typically, resolution diagrams are complex, with several local maxima.

The optimization methodologies currently developed allow the separation of complex mixtures and the comparison of chromatographic performance in different situations (i.e., different organic solvents or columns). Analyses are often possible via a single organic solvent, but a mixture of solutes showing a wide range of polarities, such as steroids with $\log P_{o/w} = 3-8$, may require two mobile phases, each with a particular organic solvent. In this example, acetonitrile permits the appropriate elution of the least retained steroids with higher efficiencies, whereas pentanol is used to elute highly non-polar steroids with lower retention times.

CONCLUSIONS

Pure micellar mobile phases are certainly attractive, considering the increasing restriction in the use of organic solvents in laboratories. For this reason, hybrid micellar mobile phases were first belittled because some of MLC's appeal was considered to be lost. However, most reported analytical procedures in MLC utilize these eluents. The main reason is that in most cases, retention of solutes with pure micellar mobile phases is too high, which necessitates the addition of an organic solvent to achieve adequate retention times. Peak shape and symmetry are also improved. Procedures that use the hybrid eluents still have the advantage of requiring significantly smaller amounts of organic solvent with respect to conventional RPLC. In MLC, the organic solvent is also highly retained in micellar solution, which reduces the risk of evaporation. The mobile phases can therefore be kept stable for a long time. The toxicity, flammability, environmental impact, and cost of RPLC are consequently reduced.



Finally, sample preparation is expedited due to the solubilization capability of micellar media, avoiding laborious steps to separate the matrix, previously performed to sample injection. All these features have allowed the development of multiple applications that are highly competitive against conventional RPLC.

ACKNOWLEDGMENTS

This work was supported by Project BQU2001-3047 (Ministerio de Ciencia y Tecnología, MCYT, Spain and FEDER funds). JRTL thanks the MCYT for a Ramón y Cajal position.

REFERENCES

1. Armstrong, D.W.; Henry, S.J. Use of an aqueous mobile phase for separation of phenols and PAHs via HPLC. *J. Liq. Chromatogr.* **1980**, *3*, 657–662.
2. Berthod, A.; García-Alvarez-Coque, C. *Micellar Liquid Chromatography*; Cazes, J., Ed.; Marcel Dekker, Inc.: New York, 2000.
3. Dorsey, J.G.; DeEchegaray, M.T.; Landy, J.S. Efficiency enhancement in micellar liquid chromatography. *Anal. Chem.* **1983**, *55*, 924–928.
4. Lopez-Grio, S.; Baeza-Baeza, J.J.; García-Alvarez-Coque, M.C. Influence of the addition of modifiers on solute–micelle interaction in hybrid micellar liquid chromatography. *Chromatographia* **1998**, *48*, 655–663.
5. Berthod, A. Causes and remediation of reduced efficiency in micellar liquid chromatography. *J. Chromatogr., A* **1997**, *780*, 191–206.
6. Marina, M.L.; García, M.A. Evaluation of distribution coefficients in micellar liquid chromatography. *J. Chromatogr., A* **1997**, *780*, 103–116.
7. García-Alvarez-Coque, M.C.; Torres-Lapasio, J.R.; Baeza-Baeza, J.J. Modelling of retention behaviour of solutes in micellar liquid chromatography. A review. *J. Chromatogr., A* **1997**, *780*, 129–148.
8. Lopez-Grio, S.; Baeza-Baeza, J.J.; García-Alvarez-Coque, M.C. Modelling of the elution behaviour in hybrid micellar eluents with different organic modifiers. *Anal. Chim. Acta* **1999**, *381*, 275–285.
9. Lopez-Grio, S.; Baeza-Baeza, J.J.; García-Alvarez-Coque, M.C. Evaluation of the elution strength of organic modifier, and surfactant in micellar mobile phases. *J. Liq. Chromatogr. Relat. Technol.* **2001**, *24*, 2765–2783.
10. Kord, A.S.; Khaledi, M.G. Controlling solvent strength and selectivity in MLC: Role of organic modifiers and micelles. *Anal. Chem.* **1992**, *64*, 1894–1900.
11. Lopez-Grio, S.; García-Alvarez-Coque, M.C.; Hinze, W.L.; Quina, F.H.; Berthod, A. Effect of a variety of organic additives on retention, and efficiency in micellar liquid chromatography. *Anal. Chem.* **2000**, *72*, 4826–4835.
12. Caballero, R.D.; Ruiz-Angel, M.J.; Simo-Alfonso, E.; García-Alvarez-Coque, M.C. Micellar liquid chromatography: A suitable technique for screening analysis. *J. Chromatogr., A* **2002**, *947*, 31–45.
13. Carda-Broch, S.; Torres-Lapasio, J.R.; García-Alvarez-Coque, M.C. Evaluation of several global resolution functions for liquid chromatography. *Anal. Chim. Acta* **1999**, *396*, 61–74.
14. Torres-Lapasio, J.R. *Michrom Software*; Cazes, J., Ed.; Marcel Dekker, Inc.: New York, 2000.

Hydrodynamic Equilibrium in CCC

Petr S. Fedotov

Boris Ya. Spivakov

Vernadsky Institute of Geochemistry and Analytical Chemistry, Russian Academy of Sciences, Moscow, Russia

Introduction

In all cases, countercurrent chromatography (CCC) utilizes a hydrodynamic behavior of two immiscible liquid phases through a tubular column space which is free of a solid support matrix. The most versatile form of CCC, called the hydrodynamic equilibrium system, applies a rotating coil in an acceleration field (either in the unit gravity or in the centrifuge force field). Two immiscible liquid phases confined in such a coil distribute themselves along the length of the coil to form various patterns of hydrodynamic equilibrium [1].

Discussion

According to the hypothesis proposed by Ito [2], the multitude of hydrodynamic phenomena observed in the rotating coils can be attributed to the following types of liquid distribution.

1. The basic hydrodynamic equilibrium (the two liquid phases are evenly distributed from one end of the coil, called the head, and any excess of either phase is accumulated at the other end, called the tail). Here, the tail-head relationship of the rotating coil is defined by the direction of the Archimedean screw force which drives all objects toward the head of the coil.
2. The unilateral hydrodynamic equilibrium [the two solvent phases are unilaterally distributed along the length of the coil, one phase (head phase) entirely occupying the head side and the other phase (tail phase) the tail side of the coil]. The head phase can be the lighter or the heavier phase and also can be the aqueous or the non-aqueous phase, depending on the physical properties of the liquid system and the applied experimental conditions. This type of equilibrium may also be called bilateral, indicating the distribution of the one phase on the head side and the other phase on the tail side [3].

To illustrate the process of establishing the hydrodynamic equilibrium, it is worthwhile to begin with the dis-

tribution of two immiscible solvent phases in the “closed” coil, simply rotated around the horizontal axis in the unit gravitational field. The coil is filled with equal volumes of the lighter and heavier phase and then sealed at both ends. At a slow rotation of 10–20 revolutions per minute (rpm), two liquid phases are evenly distributed in the coil (basic hydrodynamic equilibrium) due to the Archimedean screw force. As the rotational speed increases, the heavier phase quickly occupies more space on the head side of the coil and, at the critical speed range of 60–100 rpm, the two phases are completely separated along the length of the coil, with the heavier phase on the head side and the lighter phase on the tail side (unilateral hydrodynamic equilibrium).

After this critical speed range, the amount of the heavier phase on the head side decreases sharply, reaching substantially below the 50% level at about 160 rpm. Further increase of the rotational speed again distributes the two phases fairly evenly throughout the coil, apparently due to the strong radial centrifugal force field produced by the rotation of the coil. The phase distribution described can be observed in many solvent systems [chloroform–acetic acid–water (2/2/1), hexane–methanol, *n*-butanol–water, etc.], glass coils [10–20 mm inner diameter (i.d.)] with different helical diameters (5–20 cm) being applied.

As a first approximation, the complex hydrodynamic phenomenon taking place in the rotating coil may be explained by the interplay between two force components acting on the fluid. The tangential force component (F_t) generates the Archimedean screw effect to move two phases toward the head of the coil, and the radial force component (F_r) which acts against the Archimedean force. The critical speed range is the most interesting. An increase of the rotational speed up to 60–100 rpm alters the balance of the hydrodynamic equilibrium by an enhanced radial centrifugal force field that increases the net force field acting at the bottom of the coil and decreases that acting at the top. Under this asymmetrical force distribution, the movement of the heavier phase toward the head is accelerated, whereas the movement of the lighter phase toward the head is retarded. This results in a unilateral hydrodynamic phase distribution in the rotating coil.



The hydrodynamic equilibrium condition may be used for performing CCC as follows. First, the coil is completely filled with the stationary phase, either the lighter or the heavier phase, and the other phase is introduced from the head end of the coil while the coil is rotated around its axis. Then, the two liquid phases establish equilibrium in each turn of the coil and the mobile phase finally emerges from the tail end of the coil, leaving some amount of the stationary phase permanently in the coil. Solutes locally introduced at the head of the coil are subjected to a partition process between two phases and eluted in order of their partition coefficients. In general, higher retention of the stationary phase significantly improves the peak resolution. Consequently, the unilateral hydrodynamic equilibrium condition provides a great advantage in performing CCC, because the system permits retention of a large amount of stationary phase in the coil if the lighter phase is eluted in a normal mode (head-to-tail direction) or the heavier phase in a reversed mode (tail-to-head direction).

In general, the retention of the stationary phase in the coil rotated in the unit gravity field entirely relies on relatively weak Archimedean screw force. In this situation, application of a high flow rate of the mobile phase would cause a depletion of the stationary phase from the column. This problem can be solved by the utilization of synchronous planetary centrifuges, free of rotary seals, which enable one to increase the rotational speed and, consequently, enhance the Archimedean screw force. The seal-free principle can be applied to various types of synchronous planetary motion. In all cases, the holder revolves around the centrifuge axis and simultaneously rotates about its own axis at the same angular velocity ω .

When the coil is mounted coaxially around the holder, which revolves around the central axis of the device and counterrotates about its own axis, two axes being parallel (Type I), two solvent phases are distributed along the length of the coil according to the basic hydrodynamic equilibrium. It does not favor the stationary-phase retention. Another, similar planetary motion, except that the holder revolves around the central axis of the centrifuge and rotates about its own axis in the same direction (Type J), produces, regardless of the rotational speed, a totally different phase-distribution pattern which is typical for the unilateral hydrodynamic equilibrium. The unilateral distribution can also be attained in the coaxially mounted coils in cross-axis planetary centrifuges [4]. It is important to note that all the planetary motions providing the unilateral distribution form an asymmetrical centrifuge

force field that closely resembles that observed in the coil rotating at the critical speed in the unit gravity.

The unilateral hydrodynamic equilibrium conditions provide the basis for high-speed CCC (HSCCC, $\omega = 800$ rpm or more) which has mainly gained acceptance for CCC separations. The stroboscopic observation on two-phase flow through the running spiral column of a Type J system reveals the following pattern. When the lower phase (chloroform) is eluted through the stationary lighter phase (water) from the head toward the tail of the spiral column, a large volume of the stationary phase is retained in the column and the spiral column is divided into two distinct zones: the mixing zone in about one-fourth of the area near the center of the centrifuge and the settling zone showing a linear interface between the two phases in the rest of the area. The mixing zone is always fixed at the vicinity of the central axis of the centrifuge while the spiral column undergoes the planetary motion. In other words, the mixing zone in each loop is traveling through the spiral column toward the head at a rate equal to the column rotation. Consequently, at any portion of the column, the two liquid phases are subjected to a typical partition process of repetitive mixing and settling at a high frequency, over 13 times per second at 800 rpm of column revolution, while the mobile phase is being continuously pumped through the stationary phase [3].

At a first approximation, the hydrodynamic phenomenon observed also may be explained by the interplay between two force components acting on the fluid. At the distal portion of the coil, both the strong radial force field and the reduced relative flow of the two phases establish a clear and stable interface between the two liquid phases. At the proximal portion of the spiral column, where the strength of the radial-force component is minimized, the effect of the Archimedean screw force becomes visualized as agitation at the interface caused by the relative movement of two liquid layers [2].

It should be noted that the centrifuge force field acts on the fluid in the rotated coil in parallel with other forces of different nature [5]:

- F_A , buoyancy force due to the difference between the stationary and mobile phases
- F_i , inertial force caused by coil motion, comprises components of centrifugal force field
- F_η , viscosity force due to the overflow of the stationary phase along the coil tube walls
- F_γ , interfacial tension force
- F_w , adhesion force
- F_h , hydraulic resistance force caused by moving of two immiscible phases relative to each other



The following balance of these forces of a different nature is considered:

$$F_i = F_A + F_\eta + F_\gamma + F_W + F_h$$

From this, the basic equation of the stationary-phase retention process can be derived, a number of assumptions and complex theoretical treatments being required. Taking as example the planetary centrifuge of Type J, the average cross-sectional area of a stationary-phase layer has been estimated for hydrophobic liquid systems, which are characterized by high values of interfacial tension γ , low values of viscosity η , and low hydrodynamic equilibrium settling times:

$$\left(\sqrt{\frac{S_c}{S}} - 1\right)(S_c - S) \approx \frac{v_m^{1/2} r^{1/2} \eta_s}{\rho_m \Delta \rho R \omega^{3/2}}$$

where S and S_c are the cross-sectional areas of the stationary-phase layer and the spiral column, respectively, v_m is the linear speed of the mobile phase flow, η_s is the viscosity of the stationary phase, and r and R are rotation and revolution radii, respectively; ρ_m is the density of the mobile phase and $\Delta \rho$ is the density difference between two phases. After a few assumptions, it can be rewritten as

$$\frac{S}{S_c} \approx 1 - k_1 \frac{\beta^{1/4}}{\omega^{3/4} R^{1/4}} \approx 1 - k_2 \frac{1}{\omega^{3/4}}$$

where $\beta = r/R$, k_1 is a proportional coefficient characterizing peculiarities of the liquid system (it is dependent on the interfacial tension, viscosity of the stationary phase, and density difference between two phases); $k_2 = k_1(r^{1/4}/R^{1/2})$.

The ratio of the cross-sectional area of the stationary-phase layer to that of the coil tube (S/S_c) governs the volume of the stationary phase retained in the column. The theoretical dependence of S/S_c on the rotation speed ω and the experimental dependencies of the S_f value (ratio of the volume of the stationary phase retained in the column to the total column volume) on ω for *n*-decane–water and chloroform–water liquid systems are in good agreement (Fig. 1).

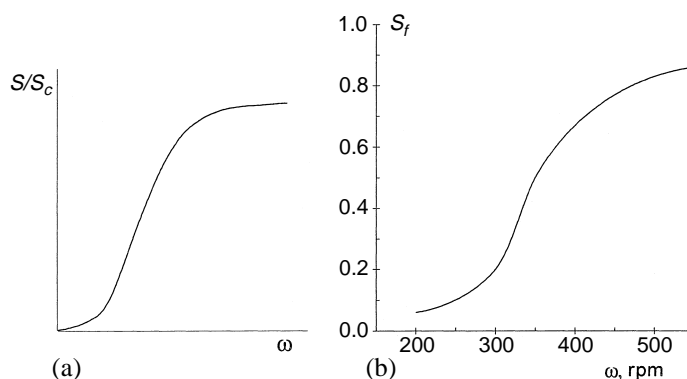


Fig. 1 (a) Theoretical ω -dependence of S/S_c ; (b) Experimental ω dependence of S_f for the *n*-decane–water system. Planetary centrifuge of Type J; $\beta = 0.37$; flow rate = 1 mL/min.

Hence, an approach based on considering the balance of forces of a different nature acting on the fluid in the rotating coil may give some correlation among the peculiarities of the liquid system, operation conditions, design parameters of the planetary centrifuge, and the stationary-phase retention. However, any rigorous mathematical model describing the complex hydrodynamic equilibrium of two liquid phases in the rotating coiled column has not been yet elaborated. This issue remains open.

References

1. W. D. Conway, *Countercurrent Chromatography. Apparatus, Theory and Application*, VCH, New York, 1990.
2. Y. Ito, *J. Liquid Chromatogr.* 15: 2639 (1992).
3. Y. Ito, Principle, apparatus, and methodology of high-speed countercurrent chromatography, in *High-Speed Countercurrent Chromatography* (Y. Ito and W. D. Conway, eds.), John Wiley & Sons, New York, 1996, pp. 3–44.
4. J.-M. Menet, K. Shimomiya, and Y. Ito, *J. Chromatogr.* 644: 239 (1993).
5. P. S. Fedotov, V. A. Kronrod, T. A. Maryutina, and B. Ya. Spivakov, *J. Liquid Chromatogr. Related Technol.* 19: 3237 (1996).



Hydrophilic Vitamins, Analysis by TLC

Fumio Watanabe

Emi Miyamoto

Kochi Women's University, Kochi, Japan

INTRODUCTION

The benefit of using thin-layer chromatography (TLC) for the identification of unknown vitamins and related compounds by comparing R_f values of the unknown compounds with authentic vitamins is beyond doubt. The quantification of the separated vitamins can be performed by the use of modern densitometry. TLC [or high-performance thin-layer chromatography (HPTLC)], as a powerful separation and analytic tool, is used particularly with pharmaceutical preparations and food products. Because amounts of most hydrophilic vitamins are low, or very low, in tissues or body fluids, bioautography or derivatization is used before densitometry.

In this section, we summarize the recent advance of TLC analysis for hydrophilic vitamins.

THIAMINE (VITAMIN B₁)

To investigate thiamine metabolism in mammals, thiamine (R_f values: 0.16, 0.04, and 0.03), urinary excretion of thiamine metabolites [thiochrome (R_f values: 0.31, 0.28, and 0.33), thiazole (R_f values: 0.85, 0.79, and 0.81), and 2-methyl-4-amino-pyrimidinecarboxylic acid (R_f values: 0.42, 0.21, and 0.26)], and related compounds [pyrimidinesulfonic acid (R_f values: 0.48, 0.39, and 0.46), α -hydroxyethylthiamine (R_f values: 0.23, 0.09, and 0.06), N' -methylnicotinamide (R_f values: 0.31, 0.06, and 0.05)] were analyzed and identified by TLC on silica gel with acetonitrile–water (40:10 vol/vol) adjusted to a pH of 2.54, 4.03, and 7.85 with formic acid as solvents, respectively.^[1] Although N' -methylnicotinamide and thiochrome could not be separated in single-phase chromatography at pH 2.54, a second phase at right angle, with a pH 4.03 solvent, separated these quite clearly without affecting the resolution of the other compounds.^[1]

The quantitative analysis of thiamine hydrochloride (vitamin B₁), using HPTLC on silica gel plates with two different mobile phases, was elaborated.^[2] After TLC separation, vitamin B₁ was derivatized by the use of *tert*-butyl hypochlorite or potassium hexacyanoferrate (III)–sodium hydroxide as reagents. The *tert*-butyl

hypochlorite reagent formed yellow-fluorescing derivatives with a limit of detection of less than 3 ng per chromatogram zone. The potassium hexacyanoferrate(III)–sodium hydroxide reagent led to a bluish-fluorescing derivative with a limit of detection of 500 ng per chromatogram zone.

RIBOFLAVIN (VITAMIN B₂)

TLC on silica gel 60 plates was used in various TLC solvent systems for both determination and identification of flavin derivatives in baker's yeast^[3] and foods (plain yogurt and bioyogurt, raw egg white, and egg powder).^[4,5] The R_f values of two unknown compounds found in plain yogurt were identical to those of 7 α -hydroxyriboflavin (R_f values: 0.32 and 0.21) and riboflavin- β -galactoside (R_f values: 0.14 and 0.10), but not to those of other flavin compounds [flavin adenine dinucleotide or FAD (R_f values: 0 and 0), flavine mononucleotide or FMN (R_f values: 0 and 0.05), 10-hydroxyethylflavin (R_f values: 0.71 and 0.40), riboflavin (R_f values: 0.55 and 0.32), and 10-formylmethylflavin (R_f values: 0.86 and 0.76)] by TLC on silica gel with chloroform–methanol–ethyl acetate (5:5:2) and 1-butanol–benzyl alcohol–glacial acetic acid (8:4:3) as solvents, respectively.^[4]

7 α -Hydroxyriboflavin was identified in blood plasma from humans, following oral administration of riboflavin supplements, by fluorescence after TLC [benzene–1-butanol–methanol–water (1:2:1:1 vol/vol)] and by its spectrum.^[6]

PYRIDOXINE (VITAMIN B₆)

TLC of vitamin B₆ compounds, on various layers in different solvents, was studied.^[7] The R_f values of pyridoxine, pyridoxal, pyridoxamine, pyridoxal ethyl acetate, 4-pyridoxic acid, 4-pyridoxic acid lactone, pyridoxine phosphate, pyridoxal phosphate, and pyridoxamine phosphate were 0.62, 0.68, 0.12, 0.54, 0.91, 0.91, 0.95, 0.95, and 0.86, respectively, by TLC on silica gel HF₂₅₄ with

0.2% NH_4OH in water as solvent. When adsorbents containing fluorescent indicators are used, all forms and derivatives of vitamin B_6 can be detected through fluorescence, or through quenching of indicator fluorescence in ultraviolet (UV) light (254 nm).

When radioactive pyridoxine hydrochloride was orally supplemented to evaluate vitamin B_6 metabolism in adult domestic cats, two unknown radioactive compounds (compounds X and Y) were excreted in the urine.^[8] The R_f values of compound X (R_f values: 0.95, 0.83, 0.2, 0.5, and 0.62) and compound Y (R_f values: 0.35, 0.20, 0.22, 0.32, and 0.25) were identical to those of pyridoxine-3-sulfate and *N*-methylpyridoxine, respectively, but not to those of pyridoxine (R_f values: 0.73, 0.83, 0.78, 0.52, and 0.62) in various solvent systems [0.5% ammonium hydroxide, 95% ethanol, chloroform-methanol (3:1 vol/vol), isoamyl alcohol-acetone-triethylamine-water (24:18:8:6 vol/vol), and 2-butanol-1.5N ammonium hydroxide (3:1 vol/vol), respectively] by TLC on silica gel plates.

COBALAMIN (VITAMIN B_{12})

Usual dietary sources of vitamin B_{12} are animal food products (meat, milk, eggs, and shellfish), but not plant food products. To evaluate whether foods contain true vitamin B_{12} or inactive corrinoids, vitamin B_{12} compounds were purified and characterized using TLC on silica gel.^[9] The R_f values of the unknown vitamin B_{12} compound, purified from an algal health food (*Spirulina* tablets) were identical to those of pseudovitamin B_{12} (R_f values: 0.14 and 0.42), but not to those of vitamin B_{12} (or 5,6-dimethylbenzimidazolyl cyanocobamide) (R_f values: 0.23 and 0.56), benzimidazolyl cyanocobamide (R_f values: 0.18 and 0.52), 5-dihydroxybenzimidazolyl cyanocobamide (R_f values: 0.20 and 0.47), and *p*-cresolyl cyanocobamide (R_f values: 0.38 and 0.62) by TLC on silica gel 60 with 1-butanol-2-propanol-water (10:7:10 vol/vol) and 2-propanol- NH_4OH (28%)-water (7:1:2 vol/vol) as solvents, respectively. The results indicate that an inactive vitamin B_{12} compound (pseudovitamin B_{12}) is predominant in *Spirulina* tablets.^[10]

Because amounts of vitamin B_{12} are very low in foods, tissues, and body fluids, bioautography is used before densitometry. A selected strain of *Escherichia coli* is used as a microorganism for the bioautography. Growth spots are enhanced by the addition of 2,3,5-triphenyltetrazolium chloride, which is converted to the red-colored formazan by *E. coli* growth. Determination of vitamin B_{12} in human plasma and erythrocytes was accomplished by one-dimensional bioautography.^[11] A

sensitive two-dimensional bioautography was also developed to investigate B_{12} metabolism in health and a wide range of diseases.^[12]

NICOTINIC ACID AND NICOTINAMIDE

Nicotinic acid and nicotinamide and their derivatives were analyzed by TLC on MN 300G cellulose plates in various solvent systems (K. Shibata, personal communications, October 16, 2001). The R_f values of nicotinamide adenine dinucleotide phosphate or NADP^+ (R_f values: 0.03, 0.50, and 0.70), nicotinamide adenine dinucleotide or NAD^+ (R_f values: 0.13, 0.61, and 0.58), nicotinic acid adenine dinucleotide (R_f values: 0.15, 0.52, and 0.57), nicotinamide mononucleotide (R_f values: 0.11, 0.63, and 0.73), nicotinic acid mononucleotide (R_f values: 0.13, 0.47, and 0.75), nicotinamide (R_f values: 0.87, 0.88, and 0.45), and nicotinic acid (R_f values: 0.77, 0.82, and 0.55) are shown in various solvent systems [1 M ammonium acetate-95% ethanol (3:7), pH 5.0; 2-butyric acid-ammonia-water (66:1.7:33), and 600 g of ammonium sulfate in 0.1 M sodium phosphate-2% 1-propanol (pH 6.8), respectively]. The detection is performed by illumination under short-wavelength (257.3 nm) UV light. Urinary metabolites of the vitamin could be analyzed by TLC.^[13]

PANTOTHENIC ACID

A rapid, simple, and specific TLC method has been developed for the estimation of panthenol and pantothenic acid in pharmaceutical preparations containing other vitamins, amino acids, syrups, enzymes, etc.^[14] The vitamin was extracted with ethanol (from tablets and capsules) or benzyl alcohol (from liquid oral preparations) and isolated from other ingredients by TLC on silica gel 60 plates with 2-propanol-water (85:15 vol/vol) as a solvent. β -Alanine (panthothenate) or β -alanol (panthenol) was liberated by heating for 20 min at 160°C. The liberated amines were visualized with the ninhydrin reaction and estimated by spectrodensitometry at 490 nm. Recoveries for panthenol and pantothenic acid were $99.8 \pm 2.25\%$ and $100.2 \pm 1.7\%$, respectively.

BIOTIN

Unidentified biotin metabolites were analyzed and identified in urine from healthy adults by TLC.^[15,16] Three unknown biotin metabolites were identified as



biotin sulfone (R_f values: 0.49 and 0.17), bisnorbiotin methyl ketone (R_f values: 0.78 and 0.29), and tetranorbiotin-*l*-sulfoxide (R_f values: 0.22 and 0.01) by derivatization with *p*-demethylaminocinnamaldehyde after TLC on microcellulose with 1-butanol–acetic acid–water (4:1:1) and 1-butanol as solvents, respectively.^[15]

FOLIC ACID

Folates [pteroylmonoglutamates (PteGlu)] and related compounds were separated by TLC on cellulose powder (MN300 UV₂₅₄) with 3.0% (wt/vol) NH₄Cl and 0.5% (vol/vol) 2-mercaptoethanol as solvents.^[17] The R_f values of PteGlu (R_f value: 0.24), H₂-PteGlu (R_f value: 0.1), 5,10-CH=H₄-PteGlu (R_f value: 0.32), H₄-PteGlu (R_f value: 0.56), 5-CHO-H₂-PteGlu (R_f value: 0.72), 5-HCNH-H₄-PteGlu (R_f value: 0.72), 5,10-CH₂-H₄-PteGlu (R_f value: 0.75), 5-CH₃-H₄-PteGlu (R_f value: 0.8), 10-CHO-H₄-PteGlu (R_f value: 0.82), 5-CH₃-H₂-PteGlu (R_f value: 0.87), 10-CHO-PteGlu (R_f value: 0.7), and 10-CHO-H₂-PteGlu (R_f value: 0.73) were shown in this TLC system, which is applied to evaluate the transport and metabolism of reduced folates in blood.

A TLC densitometric method could be applied to evaluate the purity of folic acid preparations for the final purpose of determination of the *N*-(4-aminobenzol)-L-glutamic acid content as an impurity.^[18] The separation was performed in 1-propanol–NH₄OH (25%)–ethanol (2:2:1) and toluene–methanol–glacial acetic acid–acetone (14:4:1:1) as solvents. The silica gel plates developed were scanned at 278 nm.

ASCORBIC ACID (VITAMIN C)

TLC has been widely used to determine ascorbic acid concentrations in foods,^[19–21] pharmaceutical preparations,^[21–23] and biological materials.^[21,24,25] Isomers of ascorbic acid and their oxidation product, dehydroascorbic acid, were separated by TLC on sodium borate-impregnated silica gel and cellulose plates.^[21] This TLC method has been adapted to separate and identify ascorbic acid and dehydroascorbic acid in fresh orange and lime juices, pharmaceutical preparations (ascorbic acid), and guinea pig tissues (liver, kidney, and eye lens) and fluids (plasma and urine).

The components of an analgesic mixture (paracetamol, ascorbic acid, caffeine, and phenylephrine hydrochloride) were separated by HPTLC on silica gel plates with methylene chloride–ethylacetate–ethanol–formic acid (3.5:2:4:0.5 vol/vol) as the mobile phase.^[22] The plates

were scanned at 264 nm for ascorbic acid (R_f value: 0.53), 254 nm for paracetamol (R_f value: 0.87), and 274 nm for phenylephrine hydrochloride (R_f value: 0.22) and caffeine (R_f value: 0.69).

Ascorbic acid and dipyrone (metamizole) are sometimes combined in pharmaceutical dosage forms to relieve pain and fever. Simultaneous determination of ascorbic acid and dipyrone was done by TLC on silica gel using water–methanol (95:5 vol/vol) as the solvent.^[23] The developed plates were directly scanned at 260 nm. The R_f values for ascorbic acid and dipyrone were 0.92 and 0.65, respectively.

MULTIVITAMIN COMPLEX

Vitamin B₁, vitamin B₂, and nicotinic acid, all of which frequently occur together in foods, were separated by TLC and fluorimetrically determined by using a commercially available fiber optic-based instrument.^[26] A fluorescent tracer (fluoresceinamine, isomer II) was used to label the nicotinic acid. Vitamin B₁ was converted to fluorescent thiochrome by oxidizing with potassium ferricyanide solution in aqueous sodium hydroxide. These vitamins were separated by HPTLC on silica gel using methanol–water (70:30 vol/vol) as mobile phase. Under these conditions, the R_f values of the vitamin B₁, vitamin B₂, and nicotinic acid derivatives were 0.73, 0.86, and 0.91, respectively.

A vitamin B complex (vitamin B₁, vitamin B₂, vitamin B₆, vitamin B₁₂, and folic acid) was also separated into its components using TLC plates impregnated with different transition metal ions.^[27] CuSO₄ at 0.4% impregnation in all the employed solvent systems resulted in the simultaneous resolution of constituents of the vitamin B complex with appreciable differences in R_f values.

Water-soluble vitamins (vitamin B₁, vitamin B₆, vitamin B₁₂, and vitamin C) in “Kombucha” drink (a curative liquor) were separated by TLC on silica gel plates with water as the solvent.^[28] The plates were visually examined under UV light at 254- and 366-nm wavelengths. The four vitamins were identified and determined by comparing the R_f values with the reference values (vitamin B₁, 0.21; vitamin B₆, 0.73; vitamin B₁₂, 0.34; and vitamin C, 0.96).

An overpressured layer chromatographic procedure with photodensitometric detection for the simultaneous determination of water-soluble vitamins in multivitamin pharmaceutical preparations, was developed and evaluated.^[29] HPTLC on silica gel plates with 1-butanol–pyridine–water (50:35:15 vol/vol) as mobile phase was used. The quantitation was carried out without



derivatization [vitamin B₂ (R_f value: 0.30), vitamin B₆ (R_f value: 0.64), folic acid (R_f value: 0.37), nicotinamide (R_f value: 0.80), and vitamin C (R_f value: 1.02)] or after spraying ninhydrin reagent [calcium pantothenate (R_f value: 0.72)] or 4-demethylaminocinnamaldehyde [vitamin B₁₂ (R_f value: 1.84) and biotin (R_f value: 0)].

CONCLUSION

TLC is used as a powerful separation tool particularly for the analysis of pharmaceutical preparations and food products. The separated vitamins can be quantified by the use of densitometry. In biological materials (tissues and body fluids), which contain only trace amounts of vitamins, bioautography or derivatization is used before densitometry.

TLC offers great advantages (simplicity, flexibility, speed, and relative low expense) for the separation and analysis of hydrophilic vitamins.

REFERENCES

1. Ziporin, Z.Z.; Waring, P.P. Thin-layer chromatography for the separation of thiamine, *N*'-methylnicotinamide, and related compounds. *Methods Enzymol.* **1970**, *18A*, 86–87.
2. Funk, W.; Derr, P. Characterization and quantitative HPTLC determination of vitamin B₁ (thiamine hydrochloride) in a pharmaceutical product. *J. Planar Chromatogr.* **1990**, *3*, 149–152.
3. Gliszczynska, A.; Koziolowa, A. Chromatographic determination of flavin derivatives in baker's yeast. *J. Chromatogr., A* **1998**, *822*, 59–66.
4. Gliszczynska-Swiglo, A.; Koziolowa, A. Chromatographic determination of riboflavin and its derivatives in food. *J. Chromatogr., A* **2000**, *881*, 285–297.
5. Gliszczynska, A.; Koziolowa, A. Chromatographic identification of a new flavin derivative in plain yogurt. *J. Agric. Food Chem.* **1999**, *47*, 3197–3201.
6. Zemleni, J.; Galloway, J.R.; McCormick, D.B. The identification and kinetics of 7 α -hydroxyriboflavin (7-hydroxymethylriboflavin) in blood plasma from humans following oral administration of riboflavin supplements. *Int. J. Vitam. Nutr. Res.* **1996**, *66*, 151–157.
7. Ahrens, H.; Korytnyk, W. Pyridoxine chemistry: XXI. Thin-layer chromatography and thin-layer electrophoresis of compounds in the vitamin B₆ group. *Anal. Biochem.* **1969**, *30*, 413–420.
8. Coburn, S.P.; Mahuren, J.D. Identification of pyridoxine 3-sulfate, pyridoxal 3-sulfate, and *N*-methylpyridoxine as major urinary metabolites of vitamin B₆ in domestic cats. *J. Biol. Chem.* **1987**, *262*, 2642–2644.
9. Watanabe, F.; Miyamoto, E. TLC separation and analysis of vitamin B₁₂ and related compounds in food. *J. Liq. Chromatogr. Relat. Technol.* **2002**, *25*, 1561–1577.
10. Watanabe, F.; Katsura, H.; Takenaka, S.; Fujita, T.; Abe, K.; Tamura, Y.; Nakatsuka, T.; Nakano, Y. Pseudovitamin B₁₂ is the predominant cobamide of an algal health food, *Spirulina* tablets. *J. Agric. Food Chem.* **1999**, *47*, 4736–4741.
11. Gimsing, P.; Nexø, E.; Hippe, E. Determination of cobalamins in biological material: II. The cobalamins in human plasma and erythrocytes after desalting on nonpolar adsorbent material, and separation by one-dimensional thin-layer chromatography. *Anal. Biochem.* **1983**, *129*, 296–304.
12. Linnell, J.C.; Hoffbrand, A.V.; Peters, T.J.; Matthews, D.M. Chromatographic and bioautographic estimation of plasma cobalamins in various disturbances of vitamin B₁₂ metabolism. *Clin. Sci.* **1971**, *40*, 1–16.
13. Shibata, K.; Taguchi, H. Nicotinic Acid and Nicotinamide. In *Modern Chromatographic Analysis of Vitamins*, 3rd Ed.; De Leenheer, A.P., Lambert, W.E., Van Bocxlaer, J.F., Eds.; Marcel Dekker, Inc.: New York, 2000; 325–364.
14. Nag, S.S.; Das, S. Identification and quantitation of pantothenic acid in pharmaceutical preparations by thin-layer chromatography and densitometry. *J. AOAC Int.* **1992**, *75*, 898–901.
15. Zemleni, J.; McCormick, B.; Mock, D.M. Identification of biotin sulfone, bisnorbiotin methyl ketone, and tetra-norbiotin-*l*-sulfoxide in human urine. *Am. J. Clin. Nutr.* **1997**, *65*, 508–511.
16. Zemleni, J.; Mock, D.M. Advanced analysis of biotin metabolites in body fluids allows a more accurate measurement of biotin bioavailability and metabolism in humans. *J. Nutr.* **1999**, *129*, 494S–497S.
17. Brown, J.P.; Davidson, G.E.; Scott, J.M. Thin-layer chromatography of pteroglutamates and related compounds. Application to transport and metabolism of reduced folates in blood. *J. Chromatogr.* **1973**, *79*, 195–207.
18. Krzek, J.; Kwiecien, A. Densitometric determination of impurities in drugs: Part IV. Determination of *N*-(4-aminobenzoyl)-*L*-glutamic acid in preparations of folic acid. *J. Pharm. Biomed. Anal.* **1999**, *21*, 451–457.
19. Beljaars, P.R.; Horrocks, W.V.S.; Rondags, T.M.M. Assay of L(+)-ascorbic acid in buttermilk by densitometric transmittance measurement of the dehydroascorbic acid. *J. Assoc. Off. Anal. Chem.* **1974**, *57*, 65–69.
20. Okamura, M. Distribution of ascorbic acid analogs and associated glycosides in mushrooms. *J. Nutr. Sci. Vitaminol.* **1994**, *40*, 81–94.
21. Roomi, M.W.; Tsao, C.S. Thin-layer chromatographic separation of isomers of ascorbic acid and dehydroascorbic acid as sodium borate complexes on silica gel and cellulose plates. *J. Agric. Food Chem.* **1998**, *46*, 1406–1409.
22. El-Sadek, M.; El-Shanawany, A.; Aboul Khier, A.



- Determination of the components of analgesic mixture using high-performance thin-layer chromatography. *Analyst* **1990**, *115*, 1181–1184.
23. Aburjai, T.; Amro, B.I.; Aiedeh, K.; Abuirjeie, M.; Al-Khalil, S. Second derivative ultraviolet spectrophotometry and HPTLC for the simultaneous determination of vitamin C and dipyrone. *Pharmazie* **2000**, *55*, 751–754.
 24. DiMattio, J. A comparative study of ascorbic acid entry into aqueous and vitreous tumors of the rat and guinea pig. *Invest. Ophthalmol. Vis. Sci.* **1989**, *30*, 2320–2331.
 25. Chatterjee, I.B.; Banerjee, A. Estimation of dehydroascorbic acid in blood of diabetic patients. *Anal. Biochem.* **1979**, *98*, 368–374.
 26. Diaz, A.N.; Paniaqua, A.G.; Sanchez, F.G. Thin-layer chromatography and fibre-optic fluorimetric quantitation of thiamine, riboflavin and niacin. *J. Chromatogr., A* **1993**, *655*, 39–43.
 27. Bhushan, R.; Parshad, V. Improved separation of vitamin B complex and folic acid using some new solvent systems and impregnated TLC. *J. Liq. Chromatogr. Relat. Technol.* **1999**, *22*, 1607–1623.
 28. Bauer-Petrovska, B.; Petrushevska-Tozi, L. Mineral and water soluble vitamin content in the Kombucha drink. *Int. J. Food Sci. Technol.* **2000**, *35*, 201–205.
 29. Postaire, E.; Cisse, M.; Le Hoang, M.D.; Pradeau, D. Simultaneous determination of water-soluble vitamins by over-pressure layer chromatography and photodensitometric detection. *J. Pharm. Sci.* **1991**, *80*, 368–370.



Hydrophobic Interaction Chromatography

Karen M. Gooding

Eli Lilly and Company, Indianapolis, Indiana, U.S.A.

Introduction

Hydrophobic interaction chromatography (HIC) is a mode of separation in which molecules in a high-salt environment interact hydrophobically with a nonpolar bonded phase. HIC has been predominantly used to analyze proteins, nucleic acids, and other biological macromolecules by a hydrophobic mechanism when maintenance of the three-dimensional structure is a primary concern [1–4]. The main applications of HIC have been in the area of protein purification because the recovery is frequently quantitative in terms of both mass and biological activity.

In HIC, a high-salt environment causes the association of hydrophobic patches on the surface of an analyte with the nonpolar ligands of the bonded phase. Elution is generally effected by an “inverse” gradient to lower salt concentration. This is considered “inverse” because it is the opposite of gradients used for ion-exchange chromatography. Effective salts for HIC are those which are “antichaotropic”; that is, they promote the ordering of water molecules at interfaces. Because interaction is only with the surface of a macromolecule such as a protein, the number of amino acids involved in the chromatography is relatively small, and changes in surface structure can cause differential binding and, hence, separation.

Reversed-phase chromatography (RPC) and HIC are both based on interactions between hydrophobic moieties, but the operational aspects of the techniques render selectivities totally different. The physical properties and selectivities of the two methods are contrasted in Fig. 1. The bonded phase of HIC supports consists of a hydrophilic matrix into which hydrophobic chains are inserted, generally in low density. This can be contrasted with the higher-density organosilane chemistry used in RPC. The chromatograms illustrate that both the selectivity and the number of peaks obtained for a protein mixture vary between the two modes. Cytochrome c is not retained at all by HIC and myoglobin is split into two peaks by RPC. A primary reason for the vast difference is the mobile-phase environment for each method. The organic solvents and generally acidic conditions used in RPC cause dena-

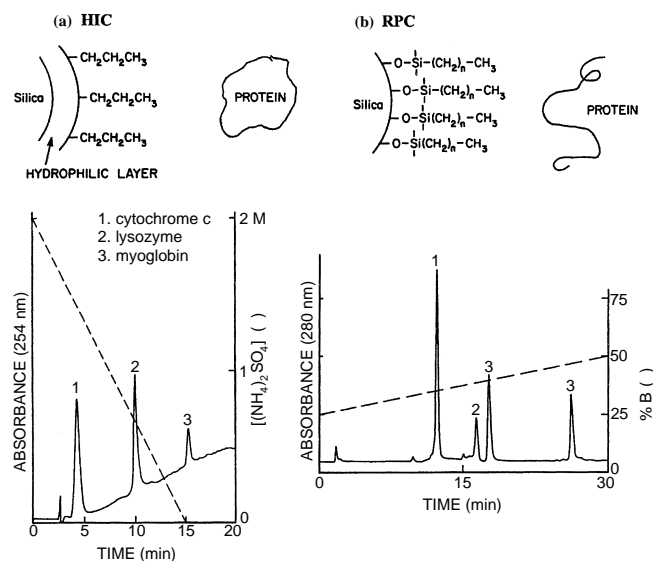


Fig. 1 (a) SynChropak Propyl; 15 min gradient from 2M–0M (NH₄)₂SO₄ in 0.1M potassium phosphate, pH 6.8. (b) SynChropak RPP (C₁₈); 30-min gradient from 25% to 50% ACN with 0.1% TFA. (Used with permission of Eichrom.)

turation of most proteins and even splitting into subunits, whereas the high-salt concentrations at neutral pH used in HIC result in stabilization of globular or three-dimensional structures for biological macromolecules. The hydrophobic amino acid residues of globular proteins are generally folded inside the structure or located in a few patches on the surface. As a protein is denatured, the buried amino acids are exposed, yielding more sites for hydrophobic binding. The hydrophobic interaction system thus encounters primarily surface amino acids—far fewer hydrophobic residues than the reversed phase.

Supports

Bonded phases for HIC consist of a hydrophilic polymeric layer into which hydrophobic ligands are inserted. The hydrophilic layer totally covers the silica or



polymer matrix, providing a wettable and noninteractive surface which is neutral to the protein. In HIC, even short ligands cause substantial binding and there is a definite relationship between ligand chain length and retention, contrary to the minimal effect of chain length observed in the RPC of proteins and peptides. The ligand chains are postulated either to interact with hydrophobic surface patches on the proteins or to be inserted into their hydrophobic pockets; it is the latter interaction which is strengthened by and related to chain length. The strength of the binding causes some proteins to bind irreversibly if the ligand is too long; therefore, most ligands are either aromatic or 1–3 carbon alkyl chains.

Because HIC supports are designed for macromolecules, they either possess pore diameters of at least 300 Å to allow inclusion or are nonporous. Both silica and polymer matrices are used because the hydrophilic polymeric coating minimizes or eliminates most matrix-based effects. The absolute retention and selectivity of an HIC support may be affected by the specific composition of the bonded phase, as well as the ligand. For example, protein mixtures have shown distinct selectivity on different HIC columns which have propyl functional groups [5].

Operation

Mobile Phase

In HIC, the concept of weak and strong solvents is different than in other modes because the weak solvent, or the one which promotes binding, is that containing high-salt concentration. The strong solvent, or one which causes elution, is that with low-salt concentration.

Salt

The most important variable in HIC retention, other than the ligand chain, is the composition of the salt used to promote binding. The effectiveness is based on the molal surface tension increment, which is parallel to the Hofmeister salting-out series for precipitation of proteins. The strength of HIC binding for some commonly used salts is $K_3\text{citrate} > \text{Na}_2\text{SO}_4 > (\text{NH}_4)_2\text{SO}_4 > \text{Na}_2\text{HPO}_4 > \text{NaCl}$.

Although potassium citrate and sodium sulfate cause stronger retention, ammonium sulfate is probably the most popular choice for HIC. Besides being effective for retention, it is highly soluble, stabilizing for enzymes, and resistant to microbial growth. Ammonium sulfate is available in high purity because of

its use for salt fractionation. Sodium sulfate is less soluble and may precipitate under conditions of high concentration. The initial concentration of salt must be at a level high enough to cause binding of all the proteins to the bonded phase to avoid variable retention of early eluting peaks, which may also be broad [6]. Most proteins will bind when 2M ammonium sulfate is used. In HIC, the concentration of anticholotropic salt is proportional to $\log k$, as has been shown for conalbumin in four different salts [7]. The exact relationship varies for each salt, as well as for the specific protein.

pH

In HIC, the mobile phase should be buffered to provide control of ionization because amino acids which are not ionized are more hydrophobic than those which are charged. The effect of pH on hydrophobicity produces some variation of retention with pH; however, it is not directly related to the *pI* of the analyte because only surface amino acids interact with the ligands. In a study of the effect of pH on retention by HIC for a series of lysozymes from different bird species, those containing histidine residues in the hydrophobic contact region exhibited deviation for pH values of 6–8, which is near the *pK* of histidine (*pK* = 6) [7].

Additives

Because HIC is based on surface-tension phenomena, changing those characteristics by the addition of surfactants affects retention. In a study of the effects of surfactants on retention of proteins by HIC, the addition of CHAPS {3-[(3-cholamidopropyl) dimethylammonio]-1-propane sulfonate} to the mobile phase resulted in shortened retention, improvement of peak shape, and a change in peak order for enolase and bovine pancreatic trypsin inhibitor [8]. The effects were dependent on the concentration of the surfactant. Surfactants can usually be washed easily from hydrophobic interaction columns because the bonded phases are neither highly hydrophobic nor ionic.

The hydrophobic basis of HIC means that alcohols may reduce interaction with supports; however, disruption of protein conformation may also occur. Because of the high salt concentrations used in HIC, organic solvents should only be added after compatibility with the mobile phase has been tested to ensure that precipitation will not take place. Generally, no more

than 10% organic is added. Other additives that increase the stability of a given protein can often be included in the mobile phase for HIC without adversely changing the separation.

Flow Rate and Gradient

Almost all HIC separations are performed in the gradient mode because proteins bind with multipoint interactions. The flow rate and gradient have an effect on retention in HIC because HIC follows the linear solvent strength model [9]. The time of the gradient is another determinant in improving resolution in that longer gradients provide increased resolution. Generally, a 20–60-min gradient from 2M–0M ammonium sulfate in 0.02M buffer at neutral pH, with a moderate flow rate (1 mL/min for a 4.6-mm inner diameter), will provide a satisfactory starting point for an HIC analysis [1].

Temperature

Hydrophobic interaction chromatography is different than other modes of chromatography in that it is an entropy-driven process, characterized by increased retention with increased temperature. This is a major benefit when subambient temperatures must be used to preserve the structure and biological activity of labile proteins. Retention is usually decreased rather than increased as temperatures are lowered. In one study, the retention of lysozyme was relatively unchanged throughout a temperature range 0–45°C, whereas bovine serum albumin exhibited two peaks which changed in proportion with temperature, as well as increased in retention [10]. Some of the increase in retention with elevated temperatures, in this or other studies, can be attributed to protein unfolding and the increased exposure of internal hydrophobic residues, especially when peak broadening also occurs.

Loading

Loading capacities for proteins on HIC columns are quite high because proteins retain their globular forms during the procedure [1,4]. High loading is generally accompanied by high recoveries of biological activity. Dynamic and absolute loading capacities of HIC supports are in the range of 10 mg/mL and 30 mg/mL, respectively. Loading is also related to the relative sizes of the pore diameter and the solute, with 300 Å giving maximum capacity for many proteins.

Applications

The primary application for HIC has been in protein analysis and purification due to the good selectivity and preservation of biological activity [1–4]. Because of the major differences in selectivity, HIC can be used as an orthogonal technique to RPC, as well as to ion-exchange and size-exclusion chromatography.

Although the best HPLC method for peptide analysis is RPC, HIC offers a different selectivity for those peptides possessing three-dimensional conformations under high-salt conditions. When the separations of peptide mixtures by HIC and RPC have been compared, peaks were generally narrower on RPC due to the organic mobile phase. In a study of calcitonin variants, it was seen that peptides with certain amino acid substitutions could not be resolved by RPC, but were separated by HIC [11]. The main utility of HIC for peptide separations seems to lie in applications for extremely hydrophilic or hydrophobic peptides, or those with three-dimensional structures stable in high salt.

The separation of nucleic acids, particularly t-RNA, has been another useful application of HIC for biological macromolecules. The tertiary structure of t-RNA has made analysis under the gentle conditions of HIC very feasible [12]. Figure 2 shows an example of the purification of t-RNA molecules specific for different amino acids on a 100-nm polyol HIC column. Separation of t-RNA molecules has also been accomplished successfully by using HIC conditions on supports with alkylamino ligands, which are functionally similar to those traditionally used to separate nucleic acids [1].

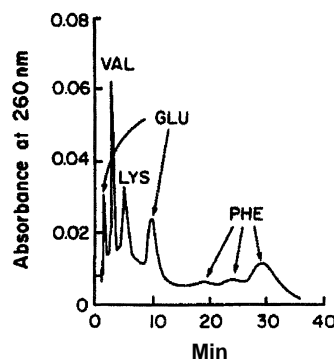


Fig. 2 Column: Polyol HIC, 100 nm; mobile phase: 0.7M disodium hydrogen phosphate, pH 6.3. [Reprinted from El Rassi and Horvath, *J. Chromatogr.* 326 (1985) p. 79 with kind permission of Elsevier Science NL, Sara Burgerhartstraat 25, 1055 Amsterdam, The Netherlands.]



Conclusions

Hydrophobic interaction chromatography is a mode of chromatography particularly effective for the analysis of proteins and other macromolecules. The hydrophobic interactions are primarily with nonpolar groups on the surface of the analytes due to maintenance of the tertiary structure. High loading and recovery of both mass and biological activity are achieved.

References

1. R. L. Cunico, K. M. Gooding, and T. Wehr, Hydrophobic interaction chromatography, in *Basic HPLC and CE of Biomolecules*, Bay Bioanalytical Laboratories, Richmond, CA, 1998.
2. R. E. Shansky, S.-L. Wu, A. Figueroa, and B. L. Karger, Hydrophobic interaction chromatography of proteins, in *HPLC of Biological Macromolecules* (K. M. Gooding and F. E. Regnier, eds.), Marcel Dekker, Inc., New York, 1990, p. 95.
3. M. I. Aguilar and M. T. W. Hearn, Reversed-phase and hydrophobic-interaction chromatography of proteins, in *HPLC of Proteins, Peptides and Polynucleotides* (M. T. W. Hearn, ed.), VCH, New York, 1991, p. 247.
4. R. H. Ingraham, Hydrophobic interaction chromatography of proteins, in *High-Performance Liquid Chromatography of Peptides and Proteins* (C. T. Mant and R. S. Hodges, eds.), CRC Press, Boca Raton, FL, 1991, p. 425.
5. A. J. Alpert, *J. Chromatogr.* 359: 85 (1986).
6. Y. Kato, T. Kitamura, S. Nakatani, and T. Hashimoto, *J. Chromatogr.* 483: 401 (1989).
7. J. L. Fausnaugh and F. E. Regnier, *J. Chromatogr.* 359: 131 (1986).
8. D. B. Wetlaufer and M. R. Koenigbauer, *J. Chromatogr.* 359: 55 (1986).
9. L. R. Snyder, Gradient elution separation of large biomolecules, in *HPLC of Biological Macromolecules* (K. M. Gooding and F. E. Regnier, eds.), Marcel Dekker, Inc., New York, 1990, p. 95.
10. S. C. Goheen and S. C. Engelhorn, *J. Chromatogr.* 317: 55 (1984).
11. M. L. Heinritz, E. Flanigin, R. C. Orlowski, and F. E. Regnier, *J. Chromatogr.* 443: 229 (1988).
12. Z. El Rassi and Cs. Horvath, *J. Chromatogr.* 326: 79 (1985).



Immobilized Metal Affinity Chromatography

Roy A. Musil

Althea Technologies, Inc., San Diego, California, U.S.A.

Introduction

The foundations for immobilized metal affinity chromatography (IMAC) were first laid in 1961 when Helferich introduced “ligand-exchange chromatography” [1]. The modern-day usage of this technique and its practical applications as a purification tool did not emerge, however, until 1975 and the seminal work by Porath et al. [2].

Among the many new protein purification approaches introduced in recent years, IMAC stands out for its ease of use and widespread applicability. This highly versatile and efficient technique is based on the interaction between biological molecules and covalently bound chelating ligands immobilized on a chromatographic support. Indeed, because the popularization of the Qiagen Qiaexpress® bacterial expression and one-step purification system [3], the use of IMAC has become nearly ubiquitous as tool for molecular biologists.

Discussion

The principle behind IMAC lies in the fact that many transition metal ions [i.e., Ni(II) and Cu(II)] can coordinate to the amino acids histidine, cysteine, and tryptophan via electron-donor groups on the amino acid side chains.

An IMAC column may be loaded with a given metal-ion by perfusing the column with a metal-ion solution until equilibrium is reached between the metal chelated to the stationary phase and the metal ion in solution. The solid support (typically agarose, cross-linked dextran, or silica) is covalently linked to a metal-chelating ligand. The two most common ligands are iminodiacetic acid (IDA) and nitrilotriacetic acid (NTA) [4]. All major chromatography suppliers now offer their own brands of IMAC supports, with IDA typically the ligand of choice. The IDA residue is very suitable as an immobilized chelating agent because a bidentate chelating moiety remains free after immobilization, to which a metal ion can be coordinated. The NTA ligand contains an additional chelating site for

metal ions, which can minimize metal leakage on the column. Free coordination sites of the metal ion are then used to bind different proteins and peptides.

Pearson systematized metal ions into three categories according to their reactivity toward nucleophiles: hard, intermediate, and soft [5]. Hard metal ions, such as Fe(III), prefer oxygen, whereas soft metal ions prefer sulfur. Intermediate types of ions such as Cu(II), Zn(II), Ni(II), and Co(II) coordinate nitrogen but also oxygen and sulfur. All the metals mentioned have been successfully employed for use in IMAC [6]. The immobilized metal-ion adsorbents may be prepared by charging the chelating gels with a slightly acid solution of the metal salt (pH 3–5). Charging the gel under acidic conditions is essential in the case of Fe(III) to avoid the formation of ferric hydroxide particles in solution. The use of colored Ni(II) or Cu(II) ions facilitates checking of leakage and the possible presence of metal ions bound to the protein eluate.

In his pioneering contribution, Porath postulated that the histidine, cysteine, and tryptophan residues of a protein were most likely to form stable coordination bonds with chelated metal ions at near neutral pH [2]. To date, an analysis of several protein models [7] lend full to his original theory. Having said that, histidine, by far and away, plays the most prominent role in IMAC binding. In a very real sense, IMAC has subtly become synonymous as a histidine affinity technique. The absence of a histidine residue on a protein surface correlates with the lack of retention of that protein on any IDA–metal column. The presence of even a single histidine on a protein surface, available for coordination, results in retention of that protein on an IDA–Cu(II) column. Also, a protein needs to display at least two histidine residues on its surface to be retained on an IDA–Ni(II) column. Thus, beyond its role as a purification technique, IMAC has been used as a tool to probe the surface topography of proteins [6].

The Qiaexpress® system is based on the selectivity of Ni–NTA for proteins with an affinity tag of six consecutive histidine residues: the 6x His tag. The 6x His tag is much smaller than such affinity tags as glutathione *S*-transferase, protein A, and maltose-binding protein and is uncharged at physiological pH. It has



been shown to rarely contribute to a protein's immunogenicity, interfere with protein structure, function, or affect secretion from its expression system [3].

As in any chromatography technique, one can break down the separation process to its two most fundamental aspects: adsorption and elution. On a more practical level, the execution of an IMAC experiment involves five discrete steps which can be readily automated: column equilibration (charging of the gel), sample loading, removal of unbound material (washing), elution, and regeneration.

Adsorption of a protein to an IMAC column has to be performed at a pH at which an electron-donor group(s) on the protein's surface is at least partially unprotonated. Because the pK_a value of histidine groups (which supply the strongest metal interactions) lies in the neutral range, the binding of protein samples to the column should normally occur at a pH value of approximately 7. However, the actual pK_a value of an individual amino acid varies strongly depending on the neighboring amino acid value. Various experiments show that depending on the protein structure, the pK_a value of an amino acid can deviate from the theoretical value up to one pH unit [4]. Therefore, an application buffer of pH 8 often achieves improved binding. In order to eliminate any nonspecific electrostatic interactions, it is common to include salt in the equilibrating buffer. Typically, sodium chloride is used in concentrations between 0.1M and 1.0M [8].

The buffer itself should not effectively compete with a protein for coordination to the metal ligand. Sodium phosphate or sodium acetate are recommended buffers (depending on the pH choice) and the presence of EDTA or sodium citrate should be avoided. The presence of detergents (Triton X-100, Tween-20, urea, etc.) in the buffer does not normally affect the adsorption of proteins [4].

Elution of proteins can be achieved by one of three methods: protonation, ligand exchange, or column stripping. Protonation is the most common method and probably the simplest. The pH is reduced by either a linear gradient or step-gradient in the range of pH 8 to 3 or 4, reflecting the titration of the histidyl residues. Most proteins elute between pH 6 and 4. Again, sodium phosphate or sodium acetate are the buffers of choice. Competitive elution with ammonium chloride (0M–2.0M), imidazole (0M–0.5M) or its analogs histidine (0M–0.05M) and histamine yield similar selectivity [8]. Competitive elution with a linear gradient or step-gradient is best run at a constant nearly neutral pH. The final method of elution is to use chelating agents such as EDTA or EGTA (0.05M solutions)

which will strip the metal ions from the gel and cause the proteins to elute. Unless the protein of interest is the only one still bound on the column, this method will result only in recovery and not in purification or resolution [3]. Another undesirable feature of this protocol is that the eluate will contain a high concentration of free metal ion.

Most resin manufacturers recommend that to maintain reproducibility and consistency, IMAC columns should be stripped of their metal ligands after each use and subsequently recharged with metal before the next run [6].

Recently, Fe(III)–IMAC has found specific application in the separation of phosphorylated macromolecules and other biological substances [9]. Unlike Cu(II)–IDA complexes which have no formal charge, the metal–ligand complex Fe(III)–IDA has a net positive charge. In terms of use, the highest protein capacity is reached at low pH (< 6) rather than at or above neutrality and at low ionic strength rather than at high salt concentrations. Electrostatic interactions for Fe(III) complexes play an important in protein binding [2]. However, Fe(III)–IMAC systems do not interact with phosphoproteins in the same way as ordinary ion-exchange resins. Fe(III)–IMAC can be employed to resolve proteins with a wide range of isoelectric points (pI 4–11) something that is not generally possible in a simple, single ion-exchange chromatographic step.

Immobilized metal affinity chromatography has been shown to be effective for isolating proteins from crude mixtures, as well as for selective separations of closely related proteins [2]. With respect to separation efficiency, IMAC compares well with biospecific affinity chromatography and the immobilized metal-ion complexes are much more robust than antibodies or enzymes. These factors make IMAC particularly well suited for scale-up to process scale chromatography. The main scale-up points to be aware of are the degree to which the column is metal saturated, the chelating agent content of the sample, and the potential of leached metal (or its interactions) within the product eluate.

Leakage of metals from the column during elution can be the most significant problem due to their toxicity, but there are several ways to avoid this pitfall. Some references suggest the precaution of underloading IMAC columns (by as much as 20%) with the metal ion to begin with [8]. Another precaution is to add EDTA with imidazole, histidine, or histamine to the column fractions. EDTA competitively blocks formation of coordination complexes between protein

carboxyl clusters and divalent metal cations, whereas the imidazolium groups block histidyl-metal complexation. For best reproducibility and general ease of use, a two-column format is preferred for process scale. A second scavenging column with 5% of the volume of the metal saturated purification column is simply placed in line.

Besides accommodating raw feedstreams, the relative independence of protein binding from salt concentration offers a great deal of flexibility for process sequencing. IMAC can follow virtually any other technique without the requirement for buffer exchange. The main exception is hydrophilic interaction chromatography (HIC) with ammonium sulfate. IMAC can also be used as the initial capture step enabling purification up to a 1000-fold [4] and subsequent preequilibration for downstream low-ionic-strength methods. Although high salt loading improves IMAC-binding specificity [5], its concentration can be reduced after the major contaminants are

washed through the column. Even with sodium chloride concentrations of up to 0.1M, just a minor dilution can allow for the following charge-based chromatography method. This flexibility reveals IMAC as a valuable tool for streamlining the overall process design.

References

1. F. Helfferich, *Nature* 189: 1001 (1961).
2. J. Porath, J. Carlsson, I. Olsson, and G. Belfrage, *Nature* 258: 598 (1975).
3. *The Qiaexpressionist*, 2nd ed., Qiagen Inc., Chatsworth, CA, 1992.
4. J. Porath, *Protein Express. Purif.* 3: 263 (1992).
5. E. Sulkowski, *Trends Biotechnol.* 3: 170 (1985).
6. E. Sulkowski, *BioEssays* 10: 170 (1989).
7. R. D. Johnson and F. H. Arnold, *Biotechnol. Bioeng.* 48: 437 (1995).
8. J. Porath and B. Olin, *Biochemistry* 22: 1621 (1983).
9. L. D. Holmes and M. R. Schiller, *J. Liquid Chromatography Related Technol.* 20: 123 (1997).



Immunoaffinity Chromatography

David S. Hage
John Austin

University of Nebraska, Lincoln, Nebraska, U.S.A.

Introduction

Immunoaffinity chromatography (IAC) refers to any chromatographic method in which the stationary phase consists of antibodies or antibody-related binding agents. *Antibodies*, or *immunoglobulins*, are a diverse class of glycoproteins that are produced by the body in response to a foreign agent, or *antigen*. The high selectivity of antibodies in their interactions with other molecules and the ability to produce antibodies against a wide range of substances has made IAC a popular purification tool for the isolation of hormones, peptides, enzymes, proteins, receptors, viruses, and subcellular components. The high selectivity of IAC has also made it appealing as a means for developing a variety of specific analytical methods.

Antibody Structure

The key component of any IAC method is the antibody preparation that is used as the stationary phase. The basic structure of a typical antibody (i.e., immunoglobulin G or an IgG-class antibody) consists of four polypeptides that are linked by disulfide bonds to form a Y- or T-shaped structure. The two upper arms of this structure are called the *Fab fragments* and contain two identical antigen-binding regions. The lower stem region is known as the *Fc fragment* and has a structure which is highly conserved between antibodies that belong to the same class. Other classes of antibodies (e.g., IgA, IgM, IgD, and IgE) have the same basic structure as IgG but may contain multiple units that are cross-linked through the presence of additional peptide chains. The amino acid composition within the Fab fragments is highly variable from one type of antibody to the next. It is this variability that allows the body to produce antibodies that have a large variety of affinities and binding specificities for foreign agents.

Typical antigens in nature include bacteria, viruses, and foreign proteins from animals or plants. All of these agents are fairly large compared to the binding sites on an antibody. As a result, these antigens usually

have many different locations on their surfaces to which an antibody can bind; each of these locations is called an *epitope*. Smaller antigens (i.e., those with molecular masses below several thousand Daltons) are too small to produce an immune response by themselves. However, these can be made to give rise to antibody production if they are first coupled to a larger species, such as a *carrier protein*. The agent that is coupled to the carrier protein is then called a *hapten*.

Antibody Production

One way to produce antibodies to a given compound is to inject the corresponding antigen or hapten-carrier protein conjugate into a suitable laboratory animal, such as a mouse or rabbit. Samples of the animal's blood are then taken at specified intervals to collect any antibodies that have been produced to the foreign agent. This method results in a heterogeneous mixture of antibodies that bind with a variety of strengths and to various epitopes on the antigen or hapten-carrier protein conjugate. These antibodies are called *polyclonal antibodies*, because they are produced by several different immune system cell lines within the body. Techniques have also been developed that allow for the isolation of single antibody-producing cells and the subsequent hybridization of these with cancer cells to produce new cell lines that are stable and relatively easy to grow over long periods of time. These combined immune system/cancer cells are known as *hybridomas*, and their product is a single type of well-defined antibody called a *monoclonal antibody*. Both polyclonal and monoclonal antibodies are commonly used in IAC methods.

Immunoaffinity Supports

The support material is another important item to consider in the development of a successful IAC method. In the past, most IAC applications have been based on low-performance supports (i.e., nonrigid media that can be operated under gravity or in the presence of



peristaltic flow or a small applied vacuum). The supports used in this situation have typically been carbohydrate-related materials, like agarose and cellulose, or synthetic organic supports, like acrylamide-based polymers. However, IAC can also be used in high-performance liquid chromatography (HPLC) if more rigid, pressure-resistant, and higher efficiency materials are employed. Some examples of HPLC supports that have been used for IAC include derivatized glass, silica, polystyrene-based perfusion media, and azalac-tone beads. When these types of supports are used in IAC, the resulting method is often referred to as *high-performance immunoaffinity chromatography (HPIAC)*. Of these two approaches, low-performance IAC is the method most often used for the purification of solutes or in sample pretreatment prior to analysis by other techniques. HPIAC can also be used for sample pretreatment or compound isolation, but it is more commonly employed as an analytical tool for the measurement of specific chemicals in complex mixtures.

Antibody Immobilization

One common approach to antibody immobilization involves direct, covalent attachment between the support and free amine groups on the antibodies. Examples include reductive amination (i.e., the Schiff base method) or the reaction of antibodies with supports that have been activated with reagents such as carbonyldiimidazole or *N*-hydroxysuccinimide. Antibodies or antibody fragments can also be covalently immobilized through more site-selective methods. For instance, free sulfhydryl groups that are generated during the production of Fab fragments can be used to couple these fragments to thiol-activated supports. Another example involves the mild oxidation of the carbohydrate residues which occur in the Fc region of antibodies, followed by the reaction of these oxidized residues with amine- or hydrazide-activated materials. The main advantage of site-selective immobilization is that it produces immobilized antibodies or antibody fragments that have fairly well-defined points of attachment and greater accessibility of their binding regions to analytes, thus giving rise to higher binding activities than are obtained by more general coupling methods.

Noncovalent immobilization can also be used for the site-selective coupling of antibodies to supports. One common approach for this involves absorbing the antibody to a secondary ligand such as protein A or protein G, which both bind to the Fc region of many

antibody classes. This binding is quite strong under physiological conditions but can be easily disrupted by decreasing the pH of the surrounding solution. This method is useful when high antibody activity is needed or when it is desirable to have frequent replacement of antibodies in the IAC column.

Application and Elution Conditions

The mobile phases that are used in IAC are another group of factors that need to be considered when using this method. The *application buffer* that is used during sample injection should facilitate quick and efficient binding of the analyte to immobilized antibodies. This mobile phase is usually selected so that it mimics the natural surroundings of the antibody (i.e., physiological pH and ionic strength). The association equilibrium constants for antibody–antigen interactions under such conditions are often in the range of $10^6 M^{-1}$ – $10^{12} M^{-1}$. This results in extremely strong binding between the analytes and the immunoaffinity column during sample application.

Although it is possible to use isocratic elution for IAC columns that contain low-affinity antibodies (i.e., those with association constants below $10^6 M^{-1}$), this is not practical for higher-affinity antibodies. The only way that solutes can be quickly eluted from these antibodies is to change the column conditions to lower the effective strength of the antibody–analyte interaction. This is done by applying an *elution buffer* to the column. Usually, an acidic buffer (pH 1–3) or one that contains a chaotropic agent such as sodium thiocyanate is used for analyte elution, but, occasionally, a competing agent, an organic modifier, a temperature change, or a denaturing agent is employed. The elution buffer is typically applied in a step-gradient; however, more gradual linear or nonlinear gradients can also be used.

Traditional IAC

There a variety of formats in which IAC can be performed. Some examples of these are shown in Fig. 1. The simplest format is the *on–off mode* or *direct-detection mode* of IAC. In this technique, the sample is first injected onto the IAC column in the presence of the application buffer. As the analyte is being retained, other solutes present in the sample pass through nonretained and are washed from the column. After these nonretained solutes have been removed, the elution buffer is applied. The analyte is then collected or detected as it elutes from the column. Afterward, the initial application buffer is



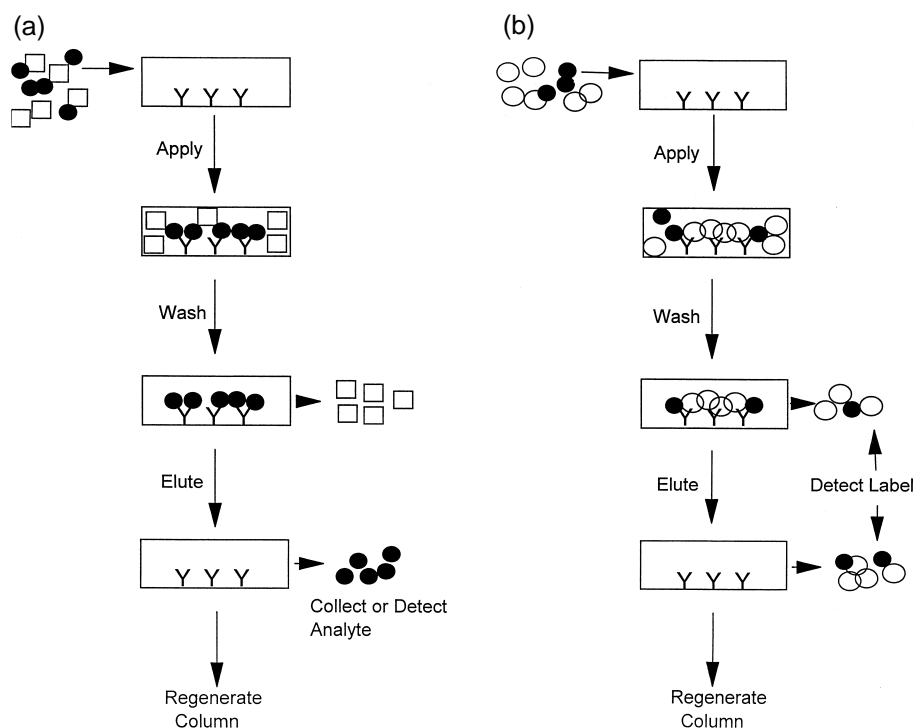


Fig. 1 Typical schemes for (a) the on-off mode of immunoaffinity chromatography and (b) a chromatography-based competitive binding immunoassay. The solid circles represent the analyte, the open circles represent a labeled analog of the analyte, and the open squares represent nonretained sample components.

reapplied and the antibodies are allowed to regenerate before the next sample is injected. This particular format is the one most commonly used in IAC for the purification of compounds. The on-off mode is also used in analytical applications that involve analytes which are labeled or occur at sufficiently high levels to allow direct detection as they elute from the IAC column.

Immunoextraction Methods

Another set of IAC methods are those that involve *immunoextraction*. This refers to the use of IAC for the removal of a specific solute or group of solutes from a sample prior to determination by a second analytical method. *Off-line immunoextraction* is generally the easiest way for combining IAC with other techniques. For this method, antibodies are typically immobilized onto a low-performance support that is packed into a small disposable syringe or solid-phase extraction cartridge. After sample application and the washing away of undesired sample components, an elution buffer is applied and the analyte is collected. In most situations, the collected fraction is dried down and reconstituted

in a solvent that is more suited for a subsequent analysis (e.g., a volatile solvent for compound quantitation by gas chromatography). This approach has been used to analyze substances in a variety of samples, ranging from plasma and urine to food, water, and soil extracts.

The relative ease with which IAC can be directly coupled to an HPLC system makes *on-line immunoextraction* appealing as a means for automating and reducing the time required for sample pretreatment in HPLC. Although IAC has been directly coupled with both size-exclusion and ion-exchange chromatography, the vast majority of on-line immunoextraction has involved coupling IAC with reversed-phase liquid chromatography. Part of the reason for this is the popularity of reversed-phase HPLC in routine chemical separations. Another reason is the fact that the elution buffer for an IAC column is an aqueous solvent with little or no organic modifier, making this act as a weak mobile phase for reversed-phase columns. On-line immunoextraction coupled with reversed-phase HPLC has been used to quantitate compounds in such samples as food extracts, bodily fluids, enzyme digests, cell extracts, and environmental samples.



Chromatographic Immunoassays

Another important technique in IAC is the use of immobilized antibody columns to perform *chromatographic* (or *flow-injection*) *immunoassays*. One way this can be done is in a competitive binding format. The simplest approach to a competitive binding scheme is to mix the sample and a labeled analyte analog (the label) and apply these simultaneously to the IAC column; this is a method known as a *simultaneous injection competitive binding immunoassay*. If the sample is applied to the IAC column and followed later by a separate injection of the label, then the technique is called a *sequential injection competitive binding immunoassay*. In both formats, an indirect measure of the sample analyte is obtained by examining the amount of label that elutes in either the nonretained or retained IAC fractions.

An alternative format is the *displacement competitive binding immunoassay*. Here, the IAC column is first saturated with the labeled analog, followed by application of sample to the column. As the sample travels through the column, it is able to bind to any antibody-binding regions that are momentarily unoccupied by the label as this undergoes local dissociation and reassociation with the immobilized antibodies. This results in displacement of the label from the column, with the degree of this displacement being directly proportional to the amount of applied analyte.

A *sandwich immunoassay* in IAC involves the use of two different types of antibody that each bind to the analyte of interest. The first type is attached to a solid-phase support and is used for extraction of the analyte from samples. The second contains an easily measured label and is added in solution to the analyte either before or after extraction. This label allows a substance to be quantitated by providing a signal that is directly proportional to the amount of analyte that is present in the IAC column.

In a *one-site immunometric assay*, the sample is first incubated with a known excess of labeled antibodies (or Fab fragments) that are specific for the analyte of interest. After this binding has occurred, the mixture is applied to a column that contains an immobilized analog

of the analyte; this is done to extract any antibodies that are not bound to the analyte. Those antibodies that are bound to the analyte will pass through the column in the nonretained peak. Detection is performed by either looking at the nonretained labeled antibodies or by monitoring the amount of excess antibodies that later dissociate from the column during the elution step.

Postcolumn Immunodetection

The technique of *postcolumn immunodetection* involves the use of an IAC column that is attached to the exit of an analytical HPLC system. The IAC column in this approach serves to collect and retain a specific analyte from the HPLC column eluent for later detection. Both the on-off mode and immunoassay formats of IAC have been used as strategies for postcolumn immunodetection. The most common of these approaches is the one-site immunometric assay. One reason for this is that the immobilized analog columns in one-site immunometric assays often have a much more flexible selection of elution conditions than immobilized antibody columns. Another reason is that one-site immunometric columns can usually be used for many sample injections before they are eluted and regenerated, which helps to decrease the overall analysis time associated with their use in postcolumn detection.

Suggested Further Reading

- Calton, G., *Methods Enzymol.* 104: 381 (1984).
- de Frutos, M. and F. E. Regnier, *Anal. Chem.* 65: 17A (1993).
- Hage, D. S., *J. Clin. Ligand Assay* 20: 293 (1997).
- Hage, D. S., D. H. Thomas, and M. S. Beck, *Anal. Chem.* 65: 1622 (1993).
- Irth, H., A. J. Oosterkamp, U. R. Tjaden, and J. van der Greef, *Trends Anal. Chem.* 14: 355 (1995).
- Oosterkamp, A. J., H. Irth, U. R. Tjaden, and J. van der Greef, *Anal. Chem.* 66: 4295 (1994).
- Wilchek, M., T. Miron, and J. Kohn, *Methods Enzymol.* 104: 3 (1984).



Immunodetection

E.S.M. Lutz

AstraZeneca R&D Mölndal, Mölndal, Sweden

Introduction

Monitoring a liquid chromatographic effluent by means of an immunoassay provides sensitive and selective detection in combination with the separation of cross-reactive compounds [1,2]. When implementing the immunoassay as a postcolumn reaction detection system after liquid chromatography, it is frequently referred to as immunodetection [3,4]. Automation and assay speed are the main advantages of immunodetection over off-line coupling of immunoassays to liquid chromatography by means of fraction collection [5,6].

The typical setup of immunodetection is illustrated in Fig. 1 [5,6]. The column effluent is mixed with labeled antibodies which will bind selectively to the analytes while passing through a reaction coil. This binding is based on the affinity between analyte and antibody and is characterized by the association and dissociation rate constants of the affinity reaction. Whereas the association rate constant (k_{+1}) is diffusion controlled, the dissociation rate constant (k_{-1}) depends on the interactions between the antibody and its antigen. Generally, k_{+1} lies in the range of 10^7 – 10^8 L/ml s, whereas k_{-1} is comparably slow (10^3 – 10^{-5} s $^{-1}$). The volume of the reaction coil and the flow rates used determine the reaction time during which the labeled antibodies can bind to analyte molecules. Typical reaction times lie in the range of a few minutes and thus allow the fast association reaction to take place, whereas the dissociation reaction can practically be neglected. Quantification of the analyte concentration is

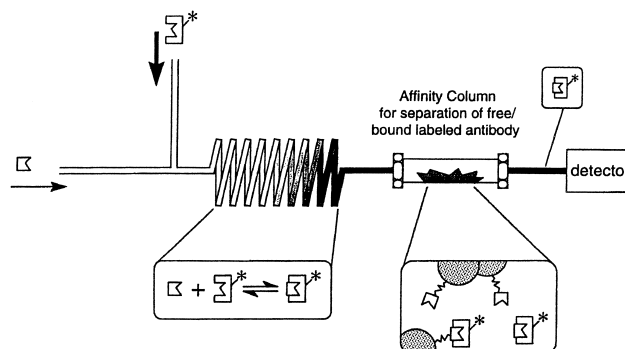


Fig. 1 Scheme of the immunodetection system employing labeled antibodies (\square^*) and an affinity column for separating labelled antibodies which have reacted with an analyte (\square) from free-labeled antibodies.

then possible by distinguishing labeled antibody which has bound to analyte from free antibody. For that purpose, the free and the bound antibody needs to be separated (e.g., by means of an affinity column which traps free antibody), whereas the analyte–antibody complex passes the affinity column unretained for detection in a conventional flow through the detector. Using this setup, both analyte recognition and quantification occurs through the labeled antibody.

Alternatively, it is possible to use untreated antibodies in combination with a labeled antigen; see Fig. 2 [5,6]. Under these circumstances, a two-step reaction

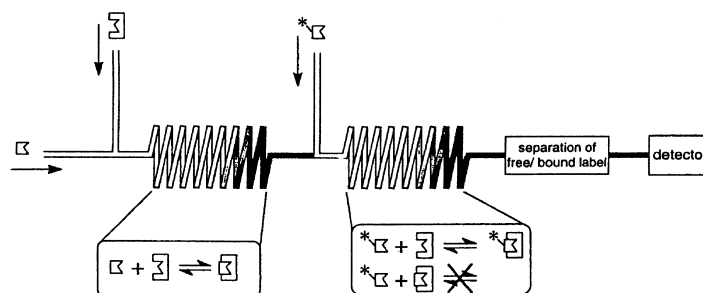


Fig. 2 Scheme of the immunodetection system employing untreated antibodies (\square) and a labeled antigen (\square^*).



is performed after the analytical separation. First, the column effluent is mixed with antibodies to allow the recognition of analyte(s). In the second step, the labeled antigen is added to saturate the fraction of free antibodies and allow quantification. When binding of labeled antigen to the antibody causes a change in detection properties, the reaction mixture can be monitored directly for quantification (homogeneous assay). However, generally the labeled antigen which has reacted with the antibody needs to be separated from the free labeled antigen to allow quantification. Again, affinity columns can be used for this purpose. Other forms of separating free and bound labeled antigens comprise restricted access columns, free-flow electrophoresis, and cross-flow filtration.

Reagents

So far, primarily antibodies and their Fab fragments have been implemented in immunodetection for analyte recognition. Antibodies can be raised against virtually any compound of interest; accordingly, their implementation into detection for liquid chromatography provides a general approach. Antibody affinity and selectivity can be modulated by appropriate design of the hapten, by adequate screening of the antibodies, and by site-directed mutagenesis. Because the chemical structure and properties of antibodies against different antigens is comparatively homogenous, immobilization, stabilization, calibration, and storage procedures can be standardized.

The approach of implementing a biological assay as a postcolumn reaction detection system after liquid chromatography can not only be applied to antibody-based assays (immunoassays) but also to assays employing other affinity interactions with high association and low dissociation rate constants, such as receptors. Information obtained from such a detection system not only provides quantitative results but also indicates the biological activity of the detected compound.

Requirements with respect to the label used to mark one of the immunoreagents are comparable to those in other postcolumn reaction detection systems [4]. The label should preferably allow sensitive and rapid detection and be nontoxic, stable, and commercially available. So far, mainly fluorescence labels have been employed (e.g., fluorescein), although, in principle, also liposomes, time-resolved fluorescence, and electrochemical or enzymatic labels are feasible. On the other hand, labels providing a slow response, including radioactive isotopes and glow-type chemiluminescence, are less suitable for immunodetection.

When attaching the label to the immunoreagent, care has to be taken not to affect the affinity reaction between the antibody and its antigens and thus deteriorate assay performance.

A concern in recent research involving immunodetection has been availability, quality, and cost of reagents, especially of antibody and receptor preparations. In the future, this concern may be overcome with novel cloning techniques providing possibilities to drastically reduce the cost of producing proteins as well as to develop proteins for specific applications.

Interfacing Liquid Chromatography–Immunodetection

The attractiveness of immunodetection consists in its on-line coupling to a separation step, such as liquid chromatography. Parameters to consider are band broadening caused by the postcolumn reaction and interference of the liquid chromatographic mobile phase with the immunoreaction [4,7].

In conventional immunoassays with long incubation times, the environment in which the affinity reaction is taking place needs to be strictly controlled with respect to, for example, pH, salt, and organic modifier content. In contrast, immunodetection takes place within a few minutes, entailing less stringent requirements with respect to reaction conditions. Nevertheless, the mobile phase needs to be consistent with the affinity reaction; that is, the mobile phase should not denature the immunoreagents or compete with the analyte for the available binding sites. Mobile-phase compatibility has mainly been evaluated with reversed-phase liquid chromatography, as it is a frequently used analytical separation technique and constitutes the greatest challenges in interfacing to biological assays. The crucial consideration is the organic-modifier content in the reversed-phase liquid-chromatography mobile phase. Investigations have shown that up to 15–25% (v/v) of organic modifier can be used in immunodetection without affecting the antibody–antigen interaction [5]. These results are in concurrence with immunodetection systems which have been coupled to reversed-phase liquid chromatography. At higher concentrations of organic modifier, the affinity reaction can be hampered seriously, which typically is overcome by dilution of the column effluent [8,9].

However, many interesting analytes (e.g., peptides and proteins) are commonly separated by means of a gradient. The challenge of coupling immunodetection to gradient liquid chromatography is twofold: On the one hand, the affinity interaction will be affected; on



the other hand, the detection properties of the label will vary. For example, using a gradient of organic modifier affects the conformation of the antibody and, thus, its affinity characteristics, as well as the detection properties of a fluorescence label. When acceptance of an increasing baseline [10,11] is out of the question, additional interfacing between the separation step and the immunodetection is required. One approach is to introduce a buffer-exchange step after the separation (e.g., with on-line dialysis [12] or an ion-exchange column [7]). However, this will introduce extra band broadening as well as affect robustness with yet another part in the system.

Applications

Feasibility of liquid chromatography-immunodetection has been shown for quantitative analysis and for screening for biological activity, as summarized in Table 1. For analytical purposes, immunodetection in combination with liquid chromatography is most promising in those cases when conventional immunoassays or conventional liquid chromatographic methods by themselves do not suffice for accurate analytical determinations. Being an approach offering high selectivity and sensitivity, applications are directed toward measurement of trace levels of compounds which lack appropriate detection properties in complex matrices. This is illustrated, for example, by measuring endogenous levels of the protein granulo-

cyte colony-stimulating factor (GCSF) in biological matrices [10]. Affinity chromatography for sample preparation introduces high selectivity into the system but does not provide a means to improve detection properties of the protein. By combining the affinity chromatography for sample preparation with an analytical separation by means of reversed-phase liquid chromatography and immunodetection, levels of GCSF were determined in plasma.

In other bioanalytical applications, the emphasis lies more on overcoming cross-reactivity. For example, the heart glycoside digoxin is cross-reactive with several of its metabolites as well as with plasma constituents, thus hampering approaches solely based on immunoassays. By treating plasma samples with solid-phase extraction on a C_{18} -restricted access column, coupled on-line to reversed-phase liquid chromatography-immunodetection, digoxin and two of its cross-reactive metabolites were analyzed in patients treated with the heart glycoside [8].

A key to successful drug development is the identification of new lead compounds. Lead compounds can be identified through receptor assays, where the receptor-ligand interaction reflects the biomolecular mechanism associated with a disorder. By implementing the receptor interactions into postcolumn reaction detection systems, biologically active compounds can be separated and detected with high sensitivity and selectivity. This concept has been described for the analysis of estrogens using a recombinant steroid-binding domain of the human estrogen receptor for analyte recognition

Table 1 Review of Immunodetection Applications

Application area	Compound	Matrix	Immunodetection type	Detection limit	Ref.
Protein bioanalysis	Granulocyte colony-stimulating factor (GCSF)	Plasma	Fluorescence-labeled antibodies, affinity chromatography	0.6 nmol/L	10
	Growth-hormone-releasing factor (GHRF)	Plasma	Fluorescence- and enzyme-labeled antibodies, affinity chromatography, interface for dilution between liquid chromatography and immunodetection for compatibility	0.2 ng/mL	9
	Urokinase	Plasma	Fluorescence-labeled receptor, affinity column	40 nmol/L	11
	Interleukine 4	?	fluorescence-labeled antibodies, affinity chromatography	2 fmol	16
Drug bioanalysis	Diogoxin	Plasma	Fluorescence-labeled antibodies, affinity chromatography	0.2 nmol/L	8
Biomarker analysis	Sulfodipeptide Leukotrienes	Urine, human cell culture extract	Untreated antibodies and fluorescence-labeled ligand, reversed-phase restricted-access chromatography	0.4 nmol/L	15



and coumestrol, a fluorescent estrogen, as reporter molecule [13]. Prior to detection, samples were treated on-line and automated by reversed-phase solid-phase extraction and reversed-phase liquid chromatography. Selectivity of this system is demonstrated for analysis in urine samples, which shows the feasibility of using this method in the determination of the abuse of steroid hormones in performance doping or cattle breeding. When performing both liquid chromatography–immunodetection and mass spectrometry, information on biological activity is combined with structure elucidation [11].

Recently, also direct recognition of active ligands attached to bead surfaces has been achieved with immunodetection [14]. This provides a rapid and automated screening tool which is compatible with solid-phase bound compounds originating from solid-phase chemistry in combinatorial chemistry. However, this approach has so far only been published for a model system.

Conclusions

Immunodetection coupled on-line to liquid chromatography as a tool for quantitative analysis has been developed for model compounds as well as been applied in relevant applications. The approach is particularly appealing for trace analysis in complicated matrices and for identifying ligands for certain receptors in drug discovery. However, each application still requires a fair amount of method development and optimization, and obtaining the desired, pure immunoreagents still is a concern, although advances in recombinant protein production are providing us with an increased choice and availability of affinity reagents at reduced cost.

In parallel with miniaturization of liquid chromatography, immunodetection will be downscaled, thus lowering reagent consumption and, consequently, cost. However, increased challenges with respect to band broadening in a postcolumn reaction detection system and nonspecific binding to capillary walls will need to be addressed. The trend toward miniaturization will simultaneously give the opportunity to couple immunodetection to other analytical separation methods, such as capillary electrophoresis. Combination of im-

munodetection with mass spectrometry enables the combination of information of biological activity with structure elucidation. Other developments in immunodetection concern the separation of free and bound labels, enabling the implementation of suspended materials in detection liquid chromatography, including, for example, suspended membrane receptors, whole cells, and molecularly imprinted polymers serving as artificial receptors. Consequently, immunodetection potentially conquer new application areas, such as the evaluation of absorption profiles of drugs and the investigation of drug metabolism on a cellular level.

References

1. B. Mattiasson, M. Nilsson, P. Berdén, and H. Håkansson, *Tr. A. C.* 9: 317 (1990).
2. M. De Frutos and F. E. Regnier, *Anal. Chem.* 65: 17 (1992).
3. D. S. Hage, *J. Chromatogr. B* 715: 3 (1998).
4. I. S. Krull, B.-Y. Cho, R. Strong, and M. Vanderlaan, *LC–GC Int.* 278 (May 1997).
5. H. Irth and A. J. Oosterkamp, *Tr. A. C.* 14: 355 (1995).
6. E. S. M. Lutz, A. J. Oosterkamp, and H. Irth, *Chim. Oggi* 15: 11 (1997).
7. K. Shahdeo, C. March, and H. T. Karnes, *Anal. Chem.* 69: 4278 (1997).
8. A. J. Oosterkamp, H. Irth, M. Beth, K. K. Unger, U. R. Tjaden, and J. van der Greef, *J. Chromatogr. B* 653: 55 (1994).
9. B.-Y. Cho, H. Zou, R. Strong, D. H. Fisher, J. Nappier, and I. S. Krull, *J. Chromatogr. A* 743: 181 (1996).
10. K. J. Miller and A. C. Herman, *Anal. Chem.* 68: 3077 (1996).
11. A. J. Oosterkamp, R. van der Hoeven, W. Glässgen, B. König, U. R. Tjaden, J. van der Greef, and H. Irth, *J. Chromatogr. B* 715: 331 (1998).
12. M. Kaufmann, T. Schwarz, and P. Batholmes, *J. Chromatogr. A* 639: 33 (1993).
13. A. J. Oosterkamp, M. T. Villaverde Herraiz, H. Irth, U. R. Tjaden, and J. van der Greef, *Anal. Chem.* 68: 1201 (1996).
14. E. S. M. Lutz, H. Irth, U. R. Tjaden, and J. van der Greef, *Anal. Chem.* 69: 4878 (1997).
15. A. J. Oosterkamp, H. Irth, L. Heintz, G. Marko-Varga, U. R. Tjaden, and J. van der Greef, *Anal. Chem.* 68: 4101 (1996).
16. T. Schenk, H. Irth, L. Heintz, G. Marko-Varga, U. R. Tjaden, and J. van der Greef, submitted.



Industrial Applications of CCC

Alain Berthod

Laboratoire des Sciences Analytiques, CNRS, Université de Lyon I, Villeurbanne, France

Serge Alex

Centre d'Etudes des Procédés Chimiques du Québec, Montreal, Canada

Sylvain Caravieilles

Laboratoire des Sciences Analytiques, CNRS, Université de Lyon I, Villeurbanne, France

Claude De Bellefon

Laboratoire de Génie des Procédés Catalytiques, CNRS, CPE Lyon I, Villeurbanne, France

Introduction

In human activity, industry has to produce material products and goods. The chemical industry produces millions of metric tons of basic chemicals such as soda, ethylene, sulfuric acid, or urea, and a few kilograms or less of fine and/or complicated chemicals such as chiral drugs, catalysts, antibiotics, or delicate perfumes. Countercurrent chromatography (CCC) is useful in the production of the latter class of chemicals. This entry explains the role that CCC can play in industrial processes, revealing concepts and ideas rather than detailing examples that can be found elsewhere. At the moment, only a handful of chemical companies are using CCC in commercial processes. Often, they are, apparently, very successful with the technique, because they purchase more CCC systems and CCC becomes part of the production process. The problem is the companies do not make nor want their chemical competitors to know that CCC works.

The Liquid Stationary Phase

It is the liquid nature of the stationary phase in CCC that renders it useful, for three reasons:

1. The solutes can access the whole volume of the stationary phase, not only the surface of a solid stationary phase as in most other chromatographic techniques. Large amounts of substance can be processed in a single run. CCC is truly a preparative technique.
2. The retention mechanism is very simple. The only physicochemical parameter responsible for solute retention is the liquid–liquid partition coefficient, P . The retention volume, V_R , is simply

$$V_R = V_M + PV_S = V_C + (P - 1)V_S \quad (1)$$

where V_M and V_S are the volumes of the mobile and stationary phases, respectively, inside the CCC system. The sum of these two volumes is the CCC system volume, V_C .

3. It is possible to switch the roles of the phases during a run. The mobile phase becomes the stationary phase and vice versa (see the entry Measurement of $P_{O/W}$ by CCC). The combination of these three points produces the following advantages.

A study and optimization of a separation of a complex mixture can be accomplished with a low-volume CCC system, V_C , injecting small quantities of the sample. The biphasic liquid system composition is *optimized rapidly* because the V_R volumes are reduced.

If the retention volumes of some constituents of the sample are too large, the dual mode is used. The retained constituents are eluted in the reversed mode. It is absolutely certain that *no part of the sample can be trapped* inside the CCC apparatus.

Once the separation is optimized, the partition coefficient of each constituent is then calculated [Eq. (1)]. The very same liquid system is used in a large-volume CCC system. So, the *retention volumes can be predicted* because the partition coefficients, which depend entirely upon the liquid–liquid system, are the same as for the small-volume system. The scaling-up is straightforward [1].

Large-Scale Separation or Purification

Classical Use of the Technique

In a recent work, the fractionation of a tannin sample was studied. The separation was optimized with a 150-mL CCC apparatus. The butanol–ethyl acetate–water



(pH 2.8) system (3.5:46.5:50% v/v) was found to be efficient for the separation. The partition coefficients of the 12 peaks were calculated. Then, it was possible to fractionate 26 g of the tannin sample in one run with the same liquid system and a 2-L CCC system [1]. The dual-mode approach was used for this separation.

The high loading capability of large-volume CCC systems is commonly used in industry. Large amounts (gram to kilogram scale) of natural products with high added values are separated by CCC. Alkaloids, antibiotics, enzymes, macrolides, peptides, rare fatty acids, saponins, tannins, taxoids and/or precursors of Taxol®, and other fine chemicals have been isolated, separated, and/or purified by preparative CCC [1].

What makes CCC preferred to classical prep liquid chromatography (LC) are as follows:

- An original or unique selectivity obtained with a subtle polarity difference between the two liquid phases
- The possibility of injecting heavily concentrated or even polyphasic samples (e.g., fermentation broths)
- The gentle interactions during the separation process that preserve delicate molecules (e.g., proteins) from denaturation.

Displacement Chromatography

In displacement chromatography, the sample to be purified is injected in a large volume, or even continuously, into the CCC machine. The sample components have different affinities for the stationary phase in an exclusive way: The component with a higher affinity for the stationary phase displaces another one with a lower affinity. Bands of pure components form. This method of using CCC offers the maximum throughput capability [1].

pH Zone Refining

pH Zone refining sorts compounds by their ionization constants, K_a , using a stationary phase with a different pH from the mobile phase [2]. For example, the stationary phase will be an acidic organic phase [e.g., methyl *tert*-butyl ether (MTBE) with 1% acetic acid] and the mobile phase is an aqueous basic buffer (e.g., 0.015M NH_3 solution, pH = 10). Up to 60% of the CCC system volume of a mixture of organic acids can be injected into the apparatus (in the ammonium salt form at pH = 10) [2]. The injected organic salts are protonated by the acidic stationary MTBE. The protonated

molecular forms stay in the organic phase, and the ionized basic forms prefer the aqueous phase. The weaker acid is protonated first, so it is the most retained. Bands of pure organic acids form in the order of decreasing $\text{p}K_a$ values.

Complexation

Complexation can be used to separate metallic ions on an industrial scale. Figure 1 illustrates the process in the case of the separation of nickel and cobalt ions [3]. A complexing agent (e.g., diethyl hexyl phosphoric acid) is added to a heptane stationary phase. A large volume (up to 20 times the CCC machine volume V_C)

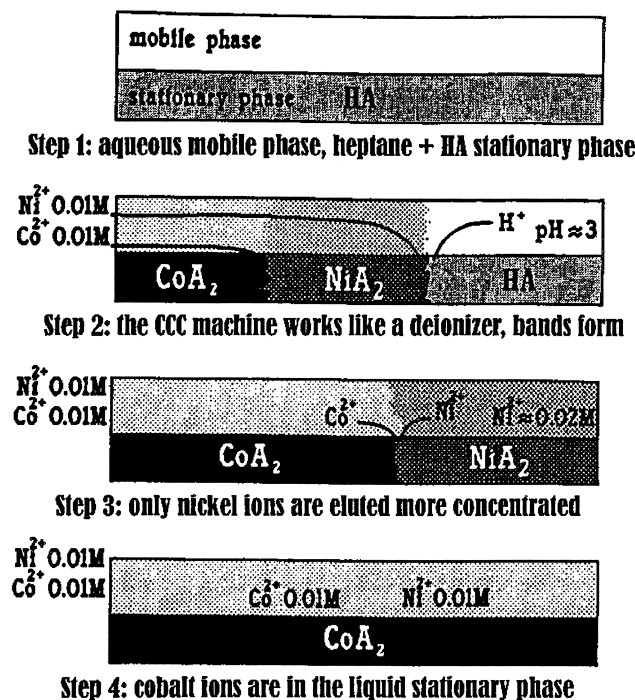


Fig. 1 Removal and separation of cobalt and nickel ions by CCC. Stationary phase: heptane + diethyl hexyl phosphoric acid (HA 0.5M); mobile phase: aqueous solution of cobalt and nickel acetate (0.01M each). Step 1: The CCC machine is equilibrated with water. Step 2: The ionic solution is introduced in the machine, the ions are extracted into the stationary phase, and the cobalt complex displaces the nickel one less stable. Step 3: The stationary phase is saturated in nickel ions. The greenish effluent leaving the machine contains only nickel ions two times more concentrated than the entering solution. Cobalt ions are still extracted, displacing nickel ions. Step 4: End of the process — the stationary phase is saturated in cobalt ions. The machine is stopped, the dark blue stationary phase is collected, and cobalt ions are recovered by an acid wash. (From Ref. 3.)

of the ionic solution is injected. The nickel ions are displaced in the aqueous phase. The cobalt ions can be collected in the stationary phase. More than two ions can be separated in bands of increasing complexation constants order [3]. Because no ions can stay trapped inside the CCC machine, it could be a very potent tool in the separation of radionuclides in the processing of nuclear wastes.

Extraction

Countercurrent chromatography can be used to extract and to concentrate, in a low volume of stationary phase, a component present in large volumes of mobile phase. It was shown that a 60-mL CCC instrument was able to extract 285 mg of a nonionic surfactant contained in 20 L of water (at 16.5 ppm or mg/L) and to concentrate it into 30 mL of ethyl acetate (at 9500 ppm or 9.5 g/L) [4].

A Continuous Plug-Flow Reactor

Recently, the use of a CCC system as an original and powerful plug-flow liquid–liquid reactor for a biphasic catalytic reaction was demonstrated [5]. Benzaldehyde (BZA) can be reduced to benzyl alcohol (BZO) by sodium formate in the aqueous phase, at room temperature, when a ruthenium phosphine complex is used. BZA is located in the cyclohexane mobile phase. Sodium formate, the complex, and BZO are located in the aqueous stationary phase. A 79% conversion of BZA to BZO was obtained at 30°C [5]. Even more interesting, injecting a 200- μ L plug of BZA into the CCC apparatus with the aqueous phase containing the catalyst and sodium formate (5M), the result shown in Figure 2 was obtained. The elution band profile of the BZO formed should allow one to model the kinetic behavior of the catalyst complex used. This study would need numerous batch experiments with different experimental conditions using, each time, some amount of an expensive and rare new catalyst. This can be done in one run, for one temperature, with the CCC reactor, saving time and catalyst.

At the moment, CCC is scarcely used in industry. The reasons are that the technique is not well known and few small-instrument companies market good

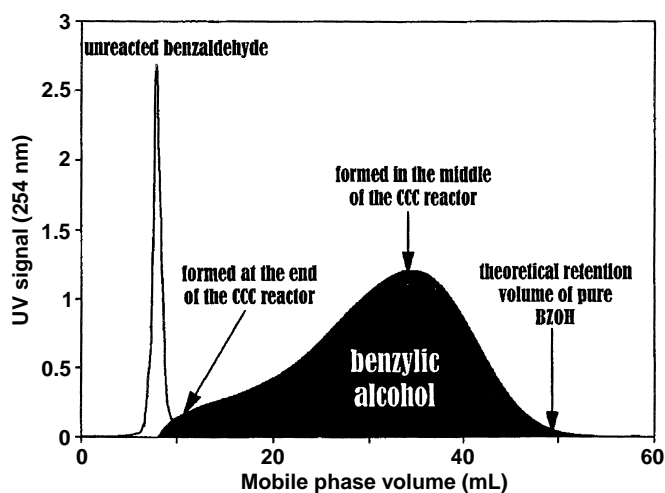


Fig. 2 Fast evaluation of a new catalyst capability: reduction of benzaldehyde (BZA) in benzylic alcohol (BZO) by sodium formate catalyzed by a ruthenium–triphenylphosphine trisulfonated sodium complex. Twenty Tmoles BZA were injected. Seventeen Tmoles BZO were formed (85% conversion). A 59-mL CCC machine, $V_S = 52$ mL of 5M sodium formate aqueous solution, $V_M = 7$ mL cyclohexane at 1.5 mL/min in the ascending tail to head direction, 750 rpm. (From Ref. 5.)

CCC systems. The capabilities of the technique could be of great help in many industrial processes such as classical: extraction, purification, and separation of fragile compounds, as well as novel: use of a CCC system as a powerful liquid–liquid reactor.

References

1. A. Berthod and B. Billardello, *Adv. Chromatogr.* 40: 503–538 (1999).
2. Y. Ito, K. Shinomiya, H. M. Fales, and A. Weisz, in *Modern Countercurrent Chromatography* (W. D. Conway and R. J. Petroski, eds.), ACS Symposium Series No. 368, American Chemical Society, Washington, DC, (1995), pp. 156–183.
3. A. Berthod, J. Xiang, S. Alex, and C. Collet-Gonnet, *Can. J. Chem.* 74: 277–286 (1996).
4. A. Berthod, C. D. Chang, and D. W. Armstrong, in *Centrifugal Partition Chromatography* (A. P. Foucault, ed.), Chromatography Science Series No. 68, 1995, pp. 1–23.
5. A. Berthod, K. Talabardon, S. Caravieilhies, and C. De Bellefon, *J. Chromatogr.* 828: 523–530 (1998).



Influence of Organic Solvents on pK_a

Ernst Kenndler

Institute for Analytical Chemistry, University of Vienna, Vienna, Austria

Introduction

The influence of solvents on the ionization equilibrium is related to their electrostatic and their solvation properties. The value of the ionization constant of an analyte is closely determined, in practice, by the pH scale in the particular solvent. It is clear that it is most desirable to have a universal scale which is able to describe acidity (and basicity) in a way that is generally valid for all solvents. It is, in principle, not the definition of an acidity scale in theory which complicates the problem; it is the difficulty of approximating the measured values in practice to the specifications of the definition. The pH scale, as is common in water, is applicable only to some organic solvents (i.e., mainly those for which the solvated proton activity is compatible with the Brønsted theory of acidity). The applicability of an analog to the pH scale in water decreases with decreasing relative permittivity of the solvents and with their increasing aprotic character.

A scale that would enable us to compare the acidity in all solvents could be based on the transfer activity coefficient on the proton (see the entry Capillary Electrophoresis in Nonaqueous Media). The effect of the solvent of any species can be expressed in the same way as for the proton by this concept and applied to all particles involved in the thermodynamic equilibrium.

Medium Effect and Ionization Constants of Weak Acids and Bases

The ionization of a weak neutral acid, HA, is described according to



For the weak base, B, for formal reasons, it is favourably expressed for its conjugated cation acid:



The corresponding changes of the ionization constants of these weak acids can be expressed by the particular transfer activity coefficients, ${}_m\gamma_i$, on the single species, i , according to

$$\Delta pK_{a,\text{HA}} = {}_s pK_{a,\text{HA}} - {}_w pK_{a,\text{HA}} = \log \left(\frac{{}_m\gamma_{\text{H}^+} {}_m\gamma_{\text{A}^-}}{{}_m\gamma_{\text{HA}}} \right) \quad (1)$$

$$\Delta pK_{a,\text{HB}^+} = {}_s pK_{a,\text{HB}^+} - {}_w pK_{a,\text{HB}^+} = \log \left(\frac{{}_m\gamma_{\text{H}^+} {}_m\gamma_{\text{B}}}{{}_m\gamma_{\text{HB}^+}} \right) \quad (2)$$

S and W indicate organic solvent and water, respectively. The transfer activity coefficients, ${}_m\gamma_i$, is the ratio of the activity coefficients in the particular solvents: ${}_m\gamma_i = {}_w\gamma_i / {}_s\gamma_i$.

Equations (1) and (2) enable the interpretation of the changes in pK_a values in the different organic solvents, compared to water. One must take into account not only the stabilization of the proton (this is given by the mutual basicity of the solvents) but also the different ability to stabilize the other individual particles. Besides the neutral particles HA and B, oppositely charged ions H^+ and A^- take part in the equilibrium in case of the neutral acids, and equally charged HB^+ and B^+ ions in case of the cation acid. This occurrence leads to a different change of the pK_a values for these two different types of weak electrolytes, depending on the ability of the solvent to stabilize anions or cations.

Nearly all organic solvents stabilize anions worse than water. For this reason, the pK_a values of neutral acids are larger in organic solvents (it is obvious that strongly basic solvents like amines may level out this effect). In lower alcohols, for example, the pK_a values increase by several units. In acetonitrile, which has generally even less cation stabilization ability in addition, the pK_a values may increase by 16 units. The effect of many solvents on weak bases (expressed by the pK_a of the corresponding cation acid) is much lower. pK_a values change only by few units. An exception is acetonitrile, due to the reason mentioned earlier.

It should be noted that traces of water have a great influence on the shift of pK_a values in all solvents, because there is a steep change of the pK_a with increasing



Table 1 Ionization Constants of Neutral and Cation Acids of type HA and HB^+ , respectively, in Water, Amphiprotic, and Dipolar Aprotic Solvents

Acid	pK_a						
	W	MeOH	EtOH	<i>t</i> -BuOH	ACN	DMSO	DMF
Acetic	4.73	9.7	10.3	14.2	22.3		13.3
Chloro acetic	2.81	7.8	8.3	12.2	18.8		10.1
Benzoic	4.21	9.4	10.1	15.1	20.7	11.0	12.3
3,4-Dimethyl benzoic	4.4	9.7		15.4	21.2	11.4	13.0
3-Bromo benzoic	3.81	8.8	9.4	13.5	20.3	9.7	11.3
4-Nitro benzoic	3.45	8.3	8.9	12.0	18.7	9.0	10.6
2,4,6-Trinitro phenol	0.3	3.7	4.1	4.8	11.0		
Ammonium	9.2				16.5	10.5	
Ethylammonium	10.6				18.4	11.0	
Triethylammonium	10.7	10.9			18.5	9.0	
Anilinium	4.6		5.7		10.6	3.6	
Pyridinium	5.2	5.2			12.3	3.4	

water content of the organic solvent. It should be also pointed out that the pK_a of the silanol groups at the surface of the commonly used fused-silica material is affected by the choice of the solvent, too. It is also shifted to higher values (in water the pK_a is around 5–6).

Suggested Further Reading

Bates, R. G., Medium effect and pH in nonaqueous and mixed solvents, in *Determination of pH, Theory and Practice*. John Wiley & Sons, New York, 1973, pp. 211–253.

Kenndler, E., Organic solvents in capillary electrophoresis, in *Capillary Electrophoresis Technology* (N. A. Guzman, ed.), Marcel Dekker, Inc., New York, 1993, pp. 161–186.

Kolthoff, I. M. and M. K. Chantooni, General introduction to acid–base equilibria in nonaqueous organic solvents, in *Treatise on Analytical Chemistry* (I. M. Kolthoff and P. J. Elving, eds.), John Wiley & Sons, New York, 1979, pp. 239–301.

Sarmini, K. and E. Kenndler, Ionization constants of weak acids and bases in organic solvents, *J. Biophys. Biochem. Methods* 38: 123–137 (1999).



Injection Techniques for Capillary Electrophoresis

Robert Weinberger

CE Technologies Inc., Chappaqua, New York, U.S.A.

Introduction

In liquid chromatography, a loop containing a defined volume is used to introduce the sample into the flowing mobile phase. Injection in high-performance capillary electrophoresis (HPCE) differs in two ways: (a) the injection volume is not as well defined and (b) injection is performed with the electric field turned off. Both of these features can contribute to quantitative errors of analysis. In addition, the length of the injection plug must be kept quite small to maintain the efficiency of the electrophoretic process [1]. The use of stacking electrolytes permits large injections to be made [2]. This is necessary to achieve acceptable limits of detection.

There are two modes of injection in capillary electrophoresis: hydrodynamic injection and electrokinetic injection. In hydrodynamic injection, pressure or vacuum are placed on the inlet sample vial or the outlet waste vial, respectively. For electrokinetic injection, the voltage is activated for a short time with the capillary and electrode immersed in the sample.

The general process of performing an injection and run is as follows:

1. The capillary is rinsed with 0.1*N* sodium hydroxide or 0.1*N* phosphoric acid for 1–2 min.
2. A second rinse with background electrolyte (BGE) is performed for 2–3 min.
3. The inlet side of the capillary is immersed in the sample.
4. Injection is performed for 1–30 s.
5. The voltage is ramped up (15 s) to the designated value and the separation is performed.
6. The process repeats for the next sample.

Volumetric Constraints on Injection Size

Because the entire internal volume of a 50-cm × 50-μm-inner diameter (i.d.) capillary is only 981 nL, the injection volume must be kept quite small. The contribution to band broadening (variance) from a plug injection is given by

$$\sigma_{\text{inj}}^2 = \frac{l_{\text{inj}}^2}{12} \quad (1)$$

where l is the length of the injection plug. To calculate the band broadening from the injection process, the diffusion-limiting case can be considered using the Einstein equation:

$$\sigma_{\text{diff}}^2 = 2D_m t \quad (2)$$

Because the squares of the variances are additive, the contributions to band broadening from injection and diffusion can be inserted into the theoretical plate equation:

$$N = \left(\frac{L_d}{\sigma_{\text{tot}}} \right)^2 \quad (3)$$

For a 50-cm capillary and a solute migration time of 600 s, the impact of the injection size for a small molecule ($D_m = 10^{-5} \text{ cm}^2/\text{s}$) and large molecule ($D_m = 10^{-6} \text{ cm}^2/\text{s}$) is shown in Fig. 1.

As illustrated in Fig. 1, injection of 1% (0.5 cm) of the capillary volume with sample produces a 92% loss of efficiency for a large molecule and an 8% loss of efficiency for a small molecule. Because diffusion is a limiting cause of efficiency, the large molecule provides a higher number of theoretical plates. The more

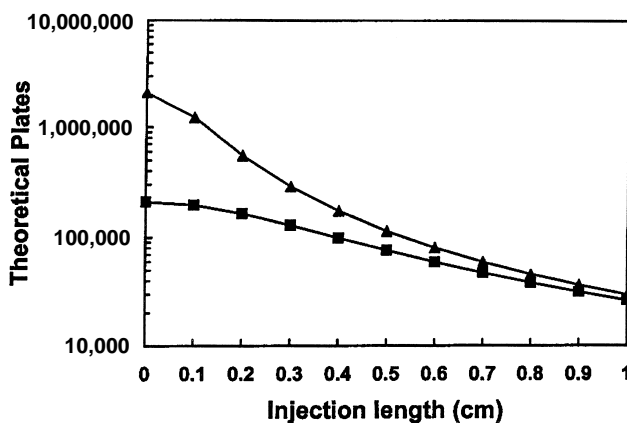


Fig. 1 Effect of the injection zone length on the number of theoretical plates for a small molecule (■, $D_m = 10^{-5} \text{ cm}^2/\text{s}$) and large molecule (▲, $D_m = 10^{-6} \text{ cm}^2/\text{s}$) as solved by Eq. (3). Conditions: capillary length = 50 cm to detector; migration time = 600 s.



efficient the separation process, the more difficult it is to maintain that inherent efficiency.

This model assumes that the sample is dissolved in BGE. Through the use of a low-ionic-strength solution as the sample diluent, sample stacking permits large-volume injections to be made.

In a well-controlled separation, injection can be the greatest source of band broadening [1]. This is one of the reasons that micromachined systems may become important for high-resolution DNA separations. In this case, it is possible to inject minute amounts of sample and use shortened separation channels [3]. Sensitivity does not suffer because laser-induced detection is employed.

Hydrodynamic Injection

The volume of material injected per unit time (V_i , nL/s) is determined by the Poiseuille equation.

$$V_i = \frac{\Delta P D^4 \pi}{128 \eta L} \quad (4)$$

where ΔP equals the pressure drop, D is the capillary internal diameter, η is the viscosity, and L is the length of the capillary. On some instruments, the pressure is generated by raising the capillary inlet side (siphoning).

The problems generated using an open-ended injection system as shown by the Poiseuille equation dictate that changes in the experimental conditions will result in variations of the amount of material injected. Internal standards are best used to compensate for some of the experimental variables.

Pressure-driven systems are preferred compared to vacuum-driven systems for two reasons: (a) Generation of pressures over 1 atm is important when viscous polymer networks are used for size separations and (b) interface to the mass spectrometer is simpler.

Electrokinetic Injection

The quantity (Q) of a solute injected is given by

$$Q = (\mu_{ep} + \mu_{eo}) \pi r^2 E C t \quad (5)$$

where μ_{ep} and μ_{eo} are the electrophoretic and electroosmotic mobilities, respectively, r is the capillary radius, E is the field strength, t is the time of injection, and C is the concentration of each solute.

As illustrated in Fig. 2, solutes with high mobility are preferably injected compared to those with low mobility [4]. Note the smaller peak heights for lithium and arginine compared to rubidium when electrokinetic injection is employed. Solute that have identical mobility in free solution show no such bias (e.g.,

Injection Techniques for Capillary Electrophoresis

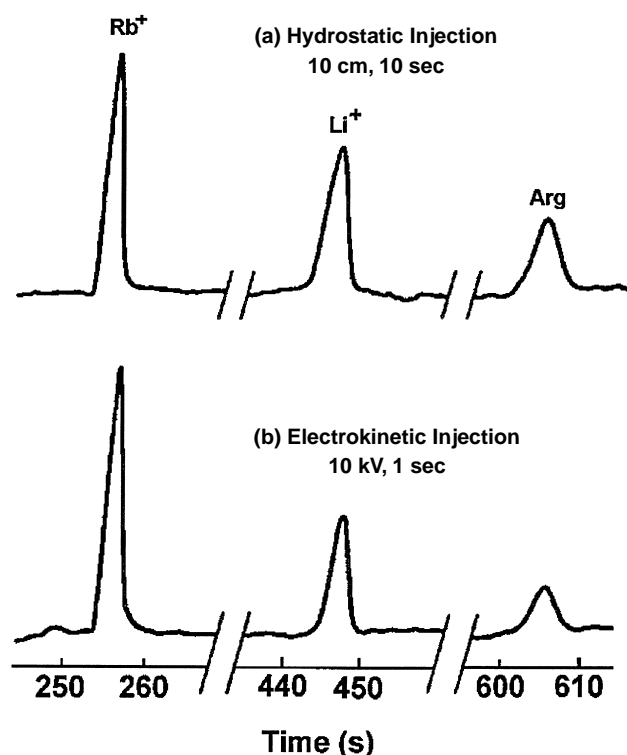


Fig. 2 Hydrostatic versus electrokinetic injection. Buffer: 20 mM MES adjusted with histidine to pH 6.0; solutes: Rb^+ , Li^+ , and arginine, $5 \times 10^{-5} \text{ M}$; injection: (top) hydrostatic, $\Delta h = 10 \text{ cm}$, $t = 10 \text{ s}$; (bottom) electrokinetic, 1 s at 10 kV; detection: conductivity. [Reprinted with permission from *Anal. Chem.* 60: 375 (1988), copyright © 1988 American Chemical Society.]

oligonucleotides and DNA fragments). This is fortunate because it is often necessary to use electrokinetic injection with gel-filled capillaries or when high-viscosity polymer networks are employed.

The problem with electrokinetic injection is that the field strength at the point of injection is inversely proportional to the sample conductivity. Calibration curves for ionic solutes show negative deviations from linearity because of this. Internal standards are necessary unless it is certain that the sample conductivities are identical. Low-conductivity samples are preferable because they stack.

The advantage of electrokinetic injection is that extreme trace enrichment is possible [5]. If the electroosmotic flow approaches zero, it is possible to inject only solute ions, omitting the sample diluent.

"Short-End" Injection

The section of capillary between the outlet vial and the detector can be used for high-speed separations if

sufficient selectivity is designed into the separation [6]. The process is as follows. (1) Equilibrate the capillary in BGE as usual. (2) Place the sample at the capillary outlet. (3) Inject by pressuring the outlet vial or with electrokinetic injection using negative polarity (inlet-side negative). (4) Set the power supply to negative polarity and perform the usual voltage ramp. Because the capillary length is short, the injection should also be kept small and stacking buffers should be used. Be sure to set the detector time constant to 10–20% of the peak width to minimize that form of band broadening. Depending on the instrument, the short-end of the capillary usually ranges from 6 to 10 cm.

Injection Artifacts, Problems, and Solutions

No Injection

A plugged capillary is the usual culprit. Cut a few millimeters of the inlet or pressurize the outlet with a syringe to unplug it. When plugged, the observed current is usually zero. No injection can also occur if an empty or incorrect sample vial is used, if an incorrect vial is called for in the method, if the vial cap is missing or badly leaking, or if the external pressure source (if required) is not activated. It is possible that the capillary is broken. Breaks usually occur at the detection window. Check that the voltage polarity is correctly set.

Peak Tailing

Peak tailing can result from a poorly cut capillary inlet. If the capillary is not cut squarely, a concentration gradient can occur upon injection [7].

Peak Splitting

Artifactual-injection-related peak splitting can occur under certain conditions. When the sample diluent

contains organic solvents and micellar electrokinetic capillary electrophoresis or cyclodextrin containing electrolytes are employed, splitting can occur due to the distribution of the solute between two phases moving at different speeds at the point of injection [8]. The problem is solved by dissolving the solute in aqueous media. If the sample is insoluble in totally aqueous solvents, 6M urea can be added both to the BGE and the sample diluent.

A fracture near the capillary inlet can also cause peak splitting. The break can occur if the capillary hits a vial wall or seal. The polyimide coating keeps the cracked portion intact. During injection, the sample moves into the capillary from both the open end of the tube and through the crack. The split peak is usually smaller than the main component and always has a migration time that is a little shorter. This is confirmed by examining the capillary inlet. If fractured, a small piece often detaches and the peak splitting is resolved.

References

1. X. Huang, W. F. Coleman, and R. N. Zare, *J. Chromatogr.* 480: 95 (1989).
2. D. Burgi and R.-L. Chien, *Anal. Chem.* 63: 2042 (1991).
3. S. C. Jacobson, R. Hergenroder, L. B. Koutny, R. J. Warmack, and M. J. Ramsey, *Anal. Chem.* 66: 1107 (1994).
4. X. Huang, M. J. Gordon, and R. N. Zare, *Anal. Chem.* 60: 375 (1988).
5. C.-X. Zhang and W. Thormann, *Anal. Chem.* 70: 540 (1998).
6. M. R. Euerby, C. M. Johnson, M. Cikalo, and K. D. Bartle, *Chromatographia* 47: 135 (1998).
7. A. Guttman and H. E. Schwartz, *Anal. Chem.* 67: 2279 (1995).
8. R. Weinberger, *Am. Lab.* 29: 24 (1997).



Inorganic Analysis by CCC

E. Kitazume

Iwate University, Morioka, Japan

INTRODUCTION

Countercurrent chromatography (CCC) has been applied to preconcentration and separation of inorganic elements since the end of the 1980s. Since the early 1990s, certain inorganic elements, including rare earths, have been separated by high-speed countercurrent chromatography (HSCCC). In addition, preconcentration and separation of inorganics from geological samples have been studied. Many of the features of HSCCC have convinced us that this method can be successfully used in separation of inorganic elements and inorganic analytical chemistry. However, the liquid systems for inorganics are somewhat complicated as compared with those for the separation of organics because they usually contain significant amounts of an extracting reagent which influences kinetic properties and viscosities of the two-phase system.

To achieve high sensitivity for analyzing trace inorganic elements in a sample solution using an atomic absorption spectrometry (AAS) or ICP atomic emission spectrometry (ICP-AES), conventional preconcentration methods such as evaporation, ion exchange, solvent extraction techniques, etc. have been used. However, there are several problems in their methodologies for the determination of ultratrace elements; for example, peak broadening for the ion exchange technique, low enrichment factor for solvent extraction techniques, etc. are encountered. It is difficult to directly work with under 0.5-mL concentrated sample solution by conventional methods. If there were effective methods for concentrating traces into 0.1 mL or less volume solution, absolute detection limits for trace analysis using techniques such as AAS, ICP-AES, and ICP-mass spectrometry (ICP-MS) would be greatly decreased, as well as eliminating their matrix effects.

pH PEAK FOCUSING

pH-peak-focusing countercurrent chromatography (pH-PFCCC) is a unique technique which is based on neutralization between mobile and stationary phases.^[1,2] It has been applied to the separation and enrichment of organic compounds such as indole auxins, bromoacetyl thyroxine and its analogs, dinitrophenyl amino acids,

transretinoic acid, and diazepam. Neutralization is initiated at the mobile phase front, but advances through the column at a slower pace, forming a sharp border between basic and acidic zones. Trace impurities in the sample solution are concentrated at this narrow pH boundary in the column. This has great potential for on-line enrichment and subsequent analysis of trace inorganic elements by interfacing HSCCC with analytical instruments such as nonflame atomic absorption spectrometry (NFAAS), ICP-AES, and ICP-MS.

Recently, the feasibility of a HSCCC centrifuge in enriching several metallic elements was demonstrated using pH-PFCCC. Under optimum conditions, an excellent enrichment factor of over 100 is achieved with good recovery of Ca, Cd, Mg, Mn, Pb, and Zn at a concentration of several parts per billion by on-line detection using a direct-current plasma atomic emission spectrometer (DCP-AES) as the detector.^[3] In addition, many metal ions were efficiently enriched into an eluent of 100 μ L or less by HSCCC, resulting in a greater than 100-fold increase in peak intensities for a 10-mL sample solution. Preconcentrating the sample solution, substantially improving detection limits, facilitates conventional trace determination of inorganic elements by instrumental analysis; however, usually, metals could not be separated from each other. If the pH border can be sufficiently broad, and the order of the elements in the column is maintained until the final stage of the elution, each concentrated metal ion may be separated mutually, as in displacement chromatography.

Under appropriate experimental conditions with pH-PFCCC, major matrix elements such as Ca and Mg in enriched tap water were found to be separated from trace elements.^[4] Trace Cd, which will appear between chromatographic bands of Mg and Ca when using di(2-ethylhexyl) phosphoric acid (DEHPA) as an extracting reagent, was well determined without interference by alkali metals.

EXTRACTION REAGENT FOR SEPARATION OF INORGANIC ELEMENTS

The existence of extracting reagent in the mobile phase is an essential factor in separation and enrichment of

Table 1 Typical extracting reagent for separation and enrichment of inorganic elements using HSCCC

Extracting reagent	Two-phase system	Inorganic element
Di(2-ethylhexyl) phosphoric acid (DEHPA)	HCl, organic acid–heptane	Rare earth, heavy metals
2-Ethylhexylphosphonic acid mono-2-ethylhexyl ester (EHPA)	Carboxylic acid–toluene	Rare earth
Dinonyltin dichloride	HCl, HNO ₃ –Methylisobutylketone (MIBK)	Orthophosphate and pyrophosphate
Cobalt dicarbide	HNO ₃ –nitrobenzen	Cs and Sr
Tetraoctylethylenediamine (TOEDA)	HCl, HNO ₃ , organic acid–chloroform	Alkali, alkaline-earth, rare earth, heavy metals, Hf, Zr, Nb, Ta

inorganic elements. It complicates the determination of several important factors, e.g., distribution coefficients, peak resolution, and separation efficiency. Some basic researches revealed that kinetic properties of specific systems used in HSCCC affect the separation efficiency. Moreover, mass-transfer rates into organic stationary phases are significantly responsible for separating mode, i.e., stepwise or isocratic elution. In addition, the values of the distribution coefficients, determined by the batch extraction measurements in the systems, are sometimes considerably different from those of the dynamic distribution coefficients calculated from elution curves plotted from experimental data. Further theoretical and basic investigations are necessarily concerned with extraction kinetics, as well as hydrodynamic behavior of the two phases in the HSCCC column.

In Table 1, typical extracting reagents used for separation and enrichment of inorganic elements are summarized. Organophosphorus extractants are often used because of their solubility properties. Di(2-ethylhexyl) phosphoric acid is commonly applied to industrial separations because of its high extractability and high separation factors between many inorganic elements, especially for rare earth elements. Other metal ions are extracted as well as the trivalent metal ions.

ENRICHMENT ANALYSIS IN THE EFFLUENT

Large-Scale Enrichment Followed by Conventional Elution

Enrichment of the desired trace elements prior to their determination cannot simply overcome such problems as interference, toxic or radioactive samples, etc., but can also provide highly sensitive determination of trace elements.

The parts-per-billion level of metal ions in 500 mL of the mobile phase was continuously concentrated into small volumes of the stationary phase retained in the column. Concentrated metal ions were simultaneously

eluted with nitric acid and determined by the emission intensity with a direct current plasma atomic emission spectrometer. The recoveries of Ca, Cd, Mg, Mn, Pb, and Zn ranged over 88% at the concentration, of each, of 10 ppb in 500 mL of the sample solution. Versatility of this method was further demonstrated in determination of trace metals in tap water and deionized water.

Rare earth elements have been enriched into a stationary phase composed of toluene including 2-ethylhexylphosphonic acid mono-2-ethylhexyl ester (EHPA) from 1 L of aqueous solution and eluted with a stepwise pH gradient. As many elements remained in the column head because of their high partition coefficients to the stationary phase, they can be eluted with mobile phase and also separated mutually.

A large-scale enrichment technique is very useful for determining extremely low level concentrations of metals in solution when a large amount of sample such as natural water is available.

Enrichment Using pH-Zone Refining Technique as Preconcentration Method of Inorganic Analysis for Subsequent Determination

Even if sufficient sample size, in volume, may not be available, enrichment techniques that concentrate trace metals in microliter samples are sometimes quite useful because modern instrumental detection systems such as AAS, ICP-AES, ICP-MS, etc. do not need a large sample size. Moreover, if trace metals that have been separated from their major substances can be concentrated in an extremely small area of the polytetrafluoroethylene (PTFE) tube in HSCCC, this would be an ideal flow-injection analysis system for determination of inorganics. From this point of view, the recently developed pH-zone refining technique has great potential for enrichment, especially for instrumental inorganic trace analysis.

In the pH-zone refining technique, a basic organic solution containing a complex-forming reagent, such as



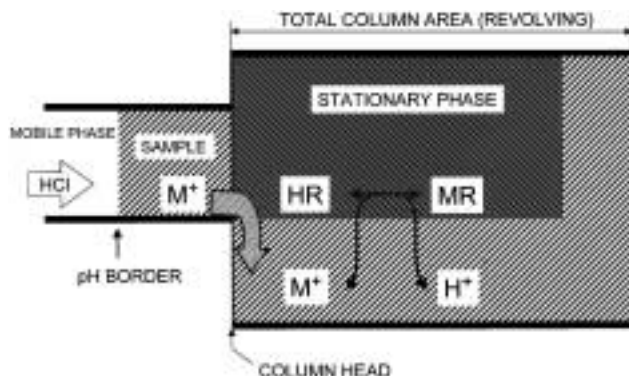


Fig. 1 Metal extraction into stationary phase.

DEHPA, as a stationary phase is used. After sample solution is introduced into the column, metal ions stay close to the sharp pH border region in the small-bore PTFE tube. Then, the trace inorganic ions in the sample are moved by the acid effluent (diluted hydrochloric or nitric acid, etc.) to the tail of the column while concentrating in the sharp-moving pH "interface," and finally eluted as small fractions containing concentrated inorganic ions. This enrichment method for trace organic impurities has been called "pH-peak-focusing counter-current chromatography (pH-PFCCC)."

The concentration procedure is modeled in Figs. 1–3. In Fig. 1, sample ion is concentrated into the column head just after the concentration procedure is started. After the stationary phase has been introduced into the system, the HSCCC is started at an appropriate rotational rate, followed by the sample and the mobile-phase pumps. For example, monovalent metal or inorganic ions (M^+) are concentrated into the stationary phase as MR in Fig. 1. The dark-shaded zone shows an organic stationary phase, which includes organophosphorus extractants (HR) and an alkali such as ammonia. The bright-shaded zone shows a sample phase with the pH adjusted by ammonia. When the

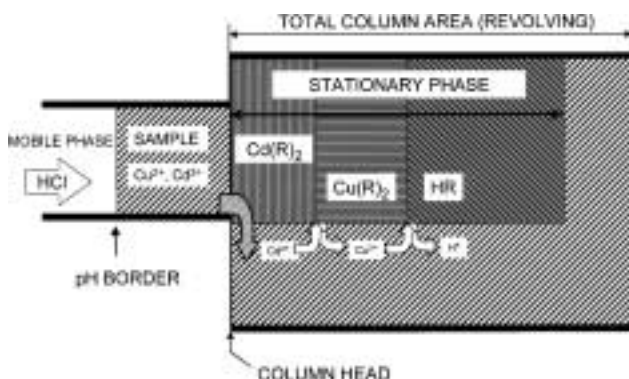


Fig. 2 Metal displacement process in stationary phase.

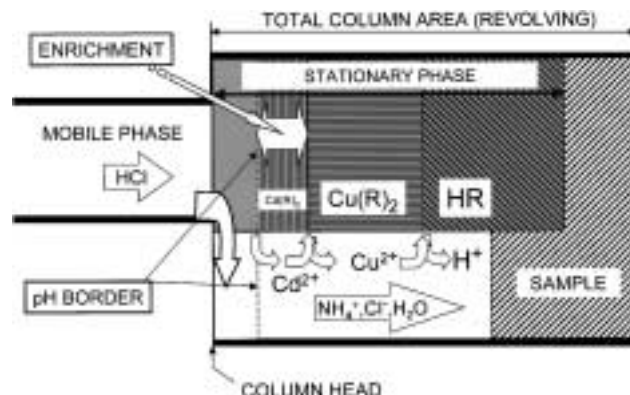


Fig. 3 Metal enrichment process after sample injection.

column rotation is started, as the organic stationary phase is lighter than the mobile phase (diluted acid solution, HCl in Fig. 1), it moves to the head of the column by an Archimedean screw effect (ASE). The driving force, based on ASE, increases with the rotational speed of the column. Therefore the stationary phase can be retained in the column by selecting an appropriate rotational rate and pump rate, even if the mobile phase is introduced from the head direction (left side in Fig. 1) into the column. The retention ratio of the stationary phase to the whole column varies from 20% to 70%, but is stable when all conditions including pump and rotational speed are constant. So the position of the mobile phase is stable in a column while in operation. Inorganic ions (M^+) form complexes with ligand ions (R^-) and are mainly concentrated on the column head, shown as MR in Fig. 1. A proton is transferred into the mobile phase when the inorganic ion extracted into the stationary phase.

Figure 2 shows a displacement procedure as well as the concentration procedure in the HSCCC column after most ions in the sample are extracted on the top of the stationary phase. If sample contains two kinds of divalent metal ions (Cu and Cd) in a large amount of solution, each metal might be arranged by difference of its affinity or partition rate to the stationary phase. As Cd ion is usually more extractable than Cu ion, Cd can displace Cu at the end (left) of the Cu band in the stationary phase. However, the bandwidth of Cd is increasing until the entire sample was introduced into the column.

Metal-focusing process after the sample injection is shown in Fig. 3. After all ions in the sample are extracted in the stationary phase, mobile phase is introduced in the column. Ammonia in the stationary phase begins to be neutralized with hydrochloric acid in the mobile phase. The neutralization area, where reaction between the acid and the base has just finished, is shown as pH border in Fig. 3. The pH border proceeds from left to right (the same direction as the mobile phase); however, its flow rate is

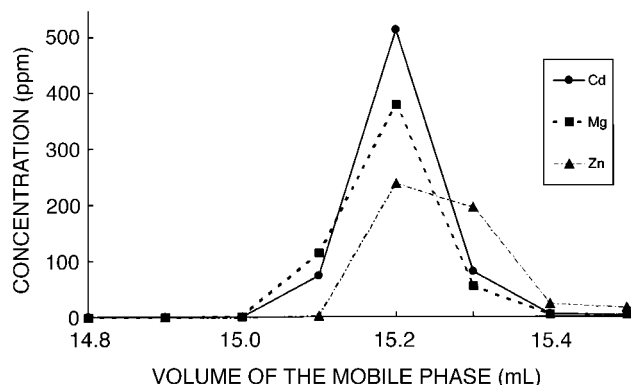


Fig. 4 Typical concentration results for 10-ppm solution of cadmium, manganese, and zinc. Apparatus: HSCCC centrifuge with 10.0-cm revolution radius; column: one multilayer coil; sample: 5 mL of each 10-ppm solution (pH 9.25) in 0.1 M tartaric acid; mobile phase: 0.1 M HCl saturated with ether; stationary phase: 6 mL of 0.2 M DEHPA and 0.18 M ammonia in ether; column: 0.5 mm i.d. \times 32 m; flow rate: 0.05 mL/min; rotational speed: 950 rpm.

lower than that of the mobile phase because of the delay based on the neutralization between the acid in the mobile phase and the base in the stationary phase. Therefore the flow rate of the pH border may be controlled by adjusting the concentration of base and acid in each phase.

As a result, Cd zone will be enriched despite increasing its retention time of chromatogram. On the other hand, as the border between Cd and Cu also moves by proceeding elution of Cd, Cu zone also moves to tail with enrichment.

If the concentration of hydrochloric acid just after the sample is very low or in case of using gradient elution

mode, pH border shown as dotted line in Fig. 3 will move more slowly.

If the speed of pH border would be relatively so high compared with the movement of Cu zone, pH border will catch up the border between Cu zone and reagent zone shown as HR in Fig. 3. Then, both peaks could not be separated well in such quick movement of pH border.

In both concentration mechanisms described above, there is little diffusion process observed as in usual elution procedures with ion exchange or other chromatographic separation method, such as conventional HSCCC and HPLC. If there is no basic compound such as ammonia in the stationary phase, ions move to the tail with a different flow rate as a function of distribution ratio between the stationary phase and the mobile phase. Many ions can be separated from each other in that case, but because there is no pH border in the column, concentration is not effected, but only separation with diffusion.

Figure 4 shows the typical concentration results for a 10-ppm solution of cadmium, magnesium, and zinc. The injected sample solution contained 50 μ g of each in 5 mL of 0.1 M tartaric acid solution, adjusted to pH to 9.25. The mobile phase was pumped at a flow rate of 0.05 mL/min. Rotational speed was 950 rpm. The eluent was collected every 2 min (0.1-mL fractions). The fractions were diluted 1:10 with water, and the emission intensity for each element was measured by plasma atomic emission spectrometer. The emission intensities for each element were increased 20-fold compared with the original sample solution. The results of this study demonstrated the high-performance capabilities of the pH-zone refining technique. Trace elements in the sample solution could be successfully concentrated into a small volume, almost under 0.1 mL with an enormous level of enrichment.

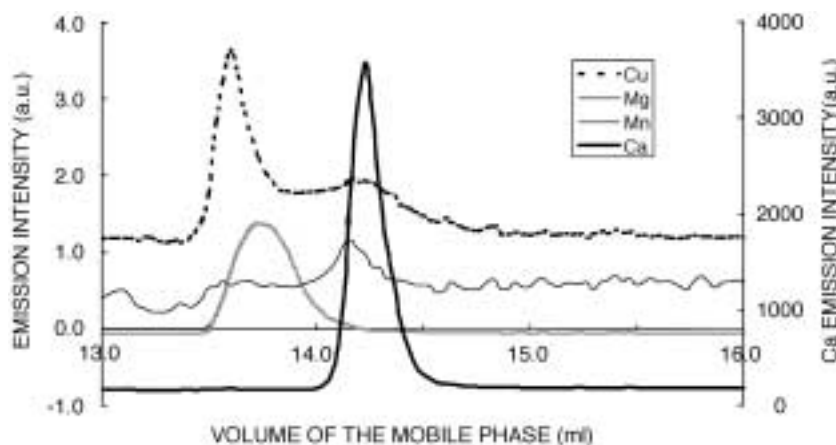


Fig. 5 Enrichment profiles of Mg, Cu, Mn, and Ca in 10-mL tap water. Experimental conditions: column, one monolayer coil, 0.5 mm i.d. \times 10 m (2 mL); sample, 10 mL of tap water (pH 8.0) in 0.1 M tartaric acid; mobile phase, 0.1 M HCl including 0.1 M tartaric acid; stationary phase, 0.22 M DEHPA and 0.20 M ammonia in heptane; flow rate, 0.1 mL/min at enrichment stage and 1.0 mL/min at detection stage; rotational speed, 1200 rpm; Sf, 7.5%.

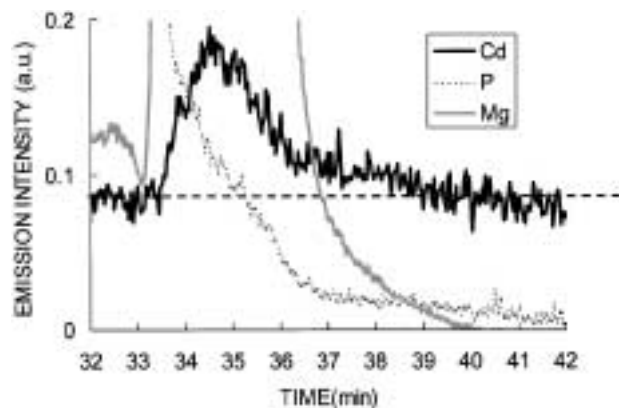


Fig. 6 Enrichment profiles of Cd and Mg in 30-mL tap water. Experimental conditions: column, one monolayer coil, 1.6 mm i.d. \times 0.86 m (2 mL); sample, 30 mL of tap water (pH 7.1) in 0.1 M tartaric acid; mobile phase, 0.1 M HCl including 0.1 M tartaric acid; stationary phase, 2 mL of 0.22 M DEHPA and 0.20 M ammonia in heptane; flow rate, 1.0 mL/min; rotational speed, 800 rpm; Sf, 20%.

On the other hand, if the speed of pH border would be relatively slow as in Fig. 3, so that the pH border cannot catch up the border between the Cu zone and the reagent zone until the border passes through the stationary phase, both peaks would be separated because the Cu zone will be eluted before coming close to the enriched Cd zone. So the order of the elements will be maintained until the final stage of elution in the tail of the column. Whereas the use of large-bore column may accelerate the peak appearance because of the longitudinally short distance of the stationary phase, each metal may be separated well compared with the case of using a small-bore column. As well as enrichment, chromatographic separation would be essential for exact measurement. The speed of the pH border can be controlled by choosing appropriate experimental conditions, such as bore size of a column and molar ratio between acid and base.

When a small-bore column, such as 0.5 mm i.d., was used, all peaks appeared simultaneously if the volume of the retained stationary phase was over 15%.^[3] However, if the retention volume of the stationary phase was less than 10% in a small-bore column, peak separation was observed as shown in Fig. 5.^[4] Each peak was detected by plasma atomic emission spectrometry. This peak profile shows enrichment profiles with separation of Mg, Cu, Mn, and Ca in tap water. The intensity of Ca is shown in the right axis, 3 orders higher than that of the other elements, while the intensity of Mn is amplified 10 times. The spectral interference of Ca to the signal of Cu is observed. This separation phenomenon is considered to be quite useful for exact determination of trace metals.

On the other hand, in the case of using a large bore column, such as 1.6 mm i.d., with the same volume of

stationary phase, peak separation was observed even if there was sufficient retention volume of more than 15%. This phenomenon may be explained by shorter longitude of the stationary phase in a large bore column, compared with a small-bore column. Figure 6 shows the signals of Mg, phosphorus, and Cd for 30 mL of tap water. The large peak of the Cd emission line may be the result of spectral interference caused by the scaled-out peak of Mg. On the shoulder of the Cd peak, a small peak was observed. This may be the real emission signal of Cd. If using a large peak on the determination of Cd, the result was 3 ppb. On the other hand, the result determined by the small peak was about 1 ppb. Using the pH-PFCCC system, precision results for the determination of Cd or other elements which are influenced by matrices elements could be obtained.

CONCLUSION

In contrast to HPLC, the unique feature of CCC is that there is no solid support in the column. As the distribution, abilities, including the capacity of the stationary phase, are easy to control, CCC can be applied to the separation, enrichment, and purification of inorganics over a wide range of concentration. In particular, enrichment of trace elements using pH-peak-focusing countercurrent chromatography will be an ideal preconcentration method for subsequent inorganic determination of modern instrumental analytical methods. Countercurrent chromatography can be combined directly with the flow injection technique, and it shows great potential for preconcentration of selected desired trace inorganic elements prior to their final detection and quantitation. On-line enrichment and subsequent analysis, based on a simple and high-performance enrichment system for inorganics, may take the place of conventional sample preparation using a beaker and separatory funnel in future investigations in this field.

REFERENCES

1. *High-Speed Countercurrent Chromatography*; Ito, Y., Conway, W.D., Eds.; John Wiley & Sons: New York, 1996.
2. Ito, Y.; Shibusawa, Y.; Fales, H.M.; Cahnmann, H.J. Studies on an abnormally sharpened elution peak observed in countercurrent chromatography. *J. Chromatogr., A* **1992**, 625, 177.
3. Kitazume, E.; Higashiyama, T.; Sato, N.; Kanetomo, M.; Tajima, T.; Kobayashi, S. On-line microextraction of metal traces for subsequent determination by plasma atomic emission spectrometry using pH peak focusing countercurrent chromatography. *Anal. Chem.* **1999**, 71, 5515.
4. Kitazume, E.; Takatsuka, T.; Sato, N.; Ito, Y. Mutual metal separation system with enrichment using pH-peak focusing countercurrent chromatography. *J. Liq. Chromatogr. Relat. Technol.* **2003**, 27, 427.

Instrumentation of Countercurrent Chromatography

Yoichiro Ito

National Heart, Lung, and Blood Institute, National Institutes of Health, Bethesda, Maryland, U.S.A.

Introduction

Countercurrent chromatography (CCC) is a support-free liquid–liquid partition system in which solutes are partitioned between the mobile and stationary phases in an open-column space. The instrumentation, therefore, requires a unique approach for achieving both retention of the stationary phase and high partition efficiency in the absence of a solid support. A variety of existing CCC systems may be divided into two classes [1] (i.e., hydrostatic and hydrodynamic equilibrium systems). The principle of each system may be illustrated by a simple coil as shown in Fig. 1.

Two Basic CCC Systems

The basic hydrostatic equilibrium system (Fig. 1, left) utilizes a stationary coil. The mobile phase is introduced into the inlet of the coil which has been filled with the stationary phase. The mobile phase then displaces the stationary phase completely on one side of the coil (dead space), but only partially displaces it on the other side of the coil due to the effect of gravity. This process continues until the mobile phase elutes from the coil. Once this hydrostatic equilibrium state is established

throughout the column, the mobile phase only displaces the same phase, leaving the stationary phase permanently in the coil. Consequently, the solutes locally introduced at the inlet of the coil is subjected to a continuous partition process between two phases in each helical turn and separated according to their partition coefficient in the absence of a solid support.

The basic hydrodynamic equilibrium system (Fig. 1, right) uses a rotating coil which generates an Archimedian screw effect where all objects in different density present in the coil are driven toward one end, conventionally called the “head.” The mobile phase introduced through the head of the coil is mixed with the stationary phase to establish a hydrodynamic equilibrium, where a portion of the stationary phase is retained in each turn of the coil. This process continues until the mobile phase elutes from the tail of the coil. After the hydrodynamic equilibrium is established throughout the coil, the mobile phase displaces only the same phase, leaving the other phase stationary in the coil. Consequently, solutes introduced locally at the head of the coil is subjected to an efficient partition process between the two phases and separated according their partition coefficients.

Each basic system has its specific advantages as well as disadvantages. The hydrostatic system provides stable retention of the stationary phase while it yields relatively low partition efficiency due to a limited degree of mixing. The hydrodynamic system, on the other hand, produces a high partition efficiency in a short elution time while the retention of the stationary phase tends to become unstable due to violent mixing, often resulting in emulsification and extensive carryover of the stationary phase.

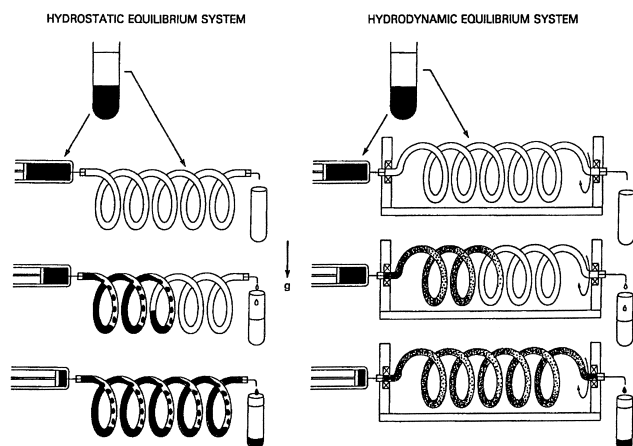


Fig. 1 Two basic CCC systems.

Development of Hydrostatic CCC Systems

In the early 1970s, the hydrostatic system was quickly developed into several efficient CCC schemes, as shown in Fig. 2 [2]. The development has been made by utilizing the unit gravity (Fig. 2, top) or the centrifugal force (Fig. 2, bottom).

In droplet CCC, which utilizes unit gravity, one side of the coil (Fig. 1, left) entirely occupied by the mobile phase is reduced to a fine-flow tube and the other side



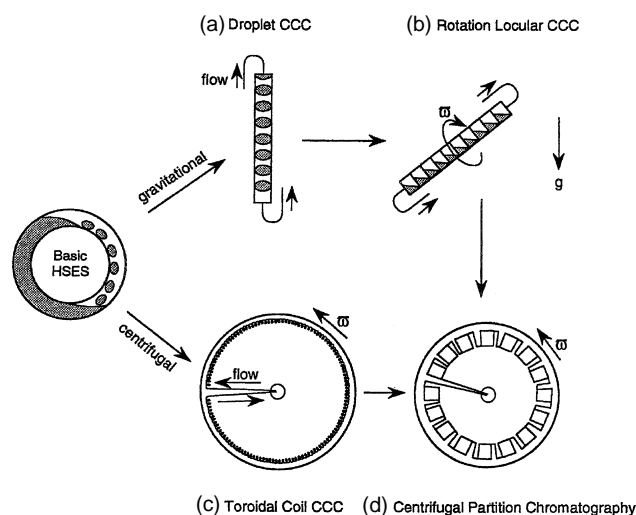


Fig. 2 Development of hydrostatic CCC systems.

of the coil is replaced by a straight tubular column. The column is first filled with the stationary phase, and the mobile phase is introduced into the column in a proper direction so that it forms a parade of droplets in the stationary phase by the effect of gravity. The system necessitates the formation of droplets, which limits the choice of the solvent system. In order to allow a more universal application of solvent systems, a locular column was devised by inserting centrally perforated disks into the tube at regular intervals to form a number of compartments called locules. The locular column is held in an angle and rotated along its axis to mix the two phases in each locule. As in droplet CCC, the lower phase is eluted from the upper end of the locular column, and the upper phase is eluted from the lower end for better retention of the stationary phase.

In the toroidal coil CCC (helix CCC) system operated under a centrifugal force, the dimensions of the coil is reduced (Fig. 2c). The coil is mounted around the periphery of the centrifuge bowl so that the stable radially acting centrifugal force field retains the stationary phase, either upper or lower phase, in one side of the coil as in the basic hydrostatic system (Fig. 1, left). The effective column capacity and retention of the stationary phase can be increased by replacing the coil with a locular column arrangement (centrifugal partition chromatography).

Development of Hydrodynamic CCC Systems

The performance of the hydrodynamic CCC system is remarkably improved by rotating the coil in the centrifugal force field, but this requires a planetary mo-

Instrumentation of Countercurrent Chromatography

tion of the coil. During the 1970s, a series of flow-through centrifuge schemes has been developed for performing CCC. In these centrifuge systems, the use of the conventional rotary seal device is eliminated because it would produce various complications such as leakage, clogging, and cross-contamination. These sealless flow-through centrifuge schemes are divided into three classes: synchronous, nonplanetary, and nonsynchronous according to their mode of planetary motion (Fig. 3).

In type I synchronous planetary motion (Fig. 3, upper left), a vertical holder revolves around the center of the centrifuge while it counterrotates around its own axis at the same angular velocity. This counterrotation of the holder unwinds the twist of the tube bundle caused by revolution, thus eliminating the need for the rotary seal. This principle works well for the rest of the synchronous schemes with tilted (types I-L and I-X), horizontal (types L and X), inversely tilted (types J-L and J-X), and even inverted orientation (type J) of the holder. When the holder of type I is moved to the center of the centrifuge, the counterrotation of the holder cancels out the revolution effect, resulting in no rotation (Fig. 3, upper center). On the contrary, when this shift is applied to the type J planetary motion, the rotation of the holder is added to the revolution, resulting in the rotation of the holder at a

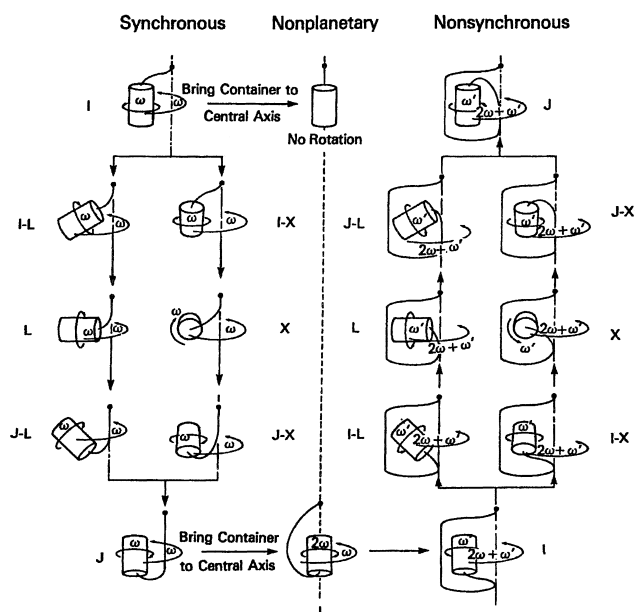


Fig. 3 A series of sealless flow-through centrifuge systems for performing CCC.

doubled speed while the tube bundle revolves around the holder to unwind the twisting (Fig. 3, bottom center). This nonplanetary scheme is a transitional form to the nonsynchronous planetary motions. On the base of the non-planetary scheme, the holder is again shifted toward the periphery to undergo a synchronous planetary motion. Because the net revolution speed of the coil is the sum of the nonplanetary and the synchronous planetary motions, the ratio of the rotation and revolution becomes freely adjustable.

Several useful CCC systems have been developed from these centrifuge schemes. The nonplanetary scheme has been used for toroidal coil CCC [3,4], centrifugal precipitation chromatography [5], and on-line apheresis in the blood bank [6,7]. The nonsynchronous scheme has been applied to partition of cells with polymer phase systems and also to cell elutriation with physiological solutions [8,9]. The type J synchronous scheme is further developed into a highly efficient CCC system called high-speed CCC (HSCCC) [10].

Development of HSCCC

The development of HSCCC was initiated by the discovery that when the type J planetary motion is applied to an end-closed coil coaxially mounted on the holder, the two solvent phases are completely separated in such a way that one phase occupies the head side and the other phase the tail side of the coil. This bilateral hydrodynamic distribution can be utilized for performing CCC, as illustrated in Fig. 4, where all coils are each schematically shown as a straight tube to indicate the overall distribution of the two phases.

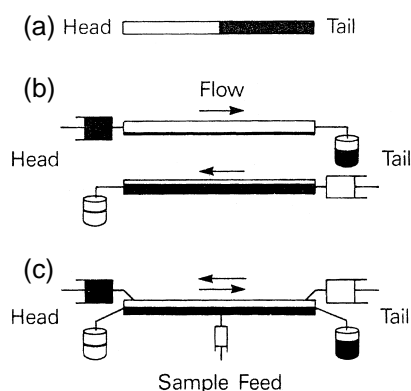


Fig. 4 Mechanism of high-speed CCC: (a) bilateral phase distribution in an end-closed coil; (b) two elution procedures for high-speed CCC; (c) dual CCC system.

Figure 4a shows the bilateral distribution of the two phases as mentioned earlier, where the white phase occupies the head side and the black phase the tail side. This hydrodynamic distribution of the two phases can be utilized for performing CCC.

In Fig. 4b, the upper coil is filled with the white phase and the black phase is introduced from the head end. The mobile black phase then travels rapidly through the coil, leaving a large volume of the white phase stationary in the coil. Similarly, the lower coil is filled with the black phase and the white phase is introduced from the tail end. The mobile white phase then travels through the coil, leaving a large volume of the black phase stationary in the coil. In either case, solutes locally injected at the inlet of the coil are efficiently partitioned between the two phases and quickly eluted from the coil in the order of their partition coefficient, thus yielding a high partition efficiency in a short elution time.

The present system also permits simultaneous introduction of the two phases through the respective terminals, as illustrated in Fig. 4c. This dual countercurrent operation requires an additional flow tube at each terminal to collect the effluent, and if desired, a sample injection port is made in the middle portion of the coil. This system has been effectively applied to foam CCC [11,12] and dual CCC [13].

References

1. Y. Ito, Minireview: Countercurrent chromatography, *J. Biophys. Biochem. Methods* 3: 77–87 (1980).
2. Y. Ito, Review: Recent advances in countercurrent chromatography, *J. Chromatogr.* 538: 3–25 (1991).
3. Y. Ito and R. L. Bowman, Countercurrent chromatography with flow-through centrifuge without rotating seals, *Anal. Biochem.* 85: 614–617 (1978).
4. K. Matsuda, S. Matsuda, and Y. Ito, Toroidal coil countercurrent chromatography. Achievement of high resolution by optimizing flow-rate, rotation speed, sample volume and tube length, *J. Chromatogr. A* 808: 95–104 (1998).
5. Y. Ito, Centrifugal precipitation chromatography applied to fractionation of proteins with ammonium sulfate, *J. Biophys. Biochem. Methods*, submitted.
6. Y. Ito, J. Suaudeau, and R. L. Bowman, New flow-through centrifuge without rotating seals applied to plasmapheresis, *Science* 189: 999–1000 (1975).
7. Y. Ito, Sealless continuous flow centrifuge, in *Apheresis: Principles and Practice* (B. McLeod, T. H. Price, and M. J. Drew, eds.), AABB Press, Bethesda, MD, 1997, pp. 9–13.
8. Y. Ito, G. T. Blamblett, R. Bhatnagar, M. Huberman, L. Leive, L. M. Cullinane, and W. Groves, Improved



non-synchronous flow-through coil planet centrifuge without rotating seals. Principle and application, *Separ. Sci. Technol.* 18: 33–48 (1983).

9. T. Okada, D. D. Metcalf, and Y. Ito, Purification of mast cells with an improved nonsynchronous flow-through coil planet centrifuge, *Int. Arch. Allergy Immunol.* 109: 376–382 (1996).
10. Y. Ito and W. D. Conway (eds.), *High-speed Countercurrent Chromatography*, Wiley–Interscience, New York, 1996.
11. Y. Ito, Foam countercurrent chromatography based on dual countercurrent system, *J. Liquid Chromatogr.* 8: 2131–2152 (1985).
12. H. Oka, Foam countercurrent chromatography, in *High-Speed Countercurrent Chromatography* (Y. Ito and W. D. Conway, eds.), Wiley–Interscience, New York, 1996, pp. 107–120.
13. Y. W. Lee, Dual countercurrent chromatography, in *High-Speed Countercurrent Chromatography* (Y. Ito and W. D. Conway, eds.), Wiley–Interscience, New York, 1996, pp. 93–104.

Instrumentation of Countercurrent Chromatography



Intrinsic Viscosity of Polymers: Determination by GPC

Yefim Brun

Waters Corporation, Milford, Massachusetts, U.S.A.

Introduction

The intrinsic viscosity is a widely used measure of molecular weight, M , and size (dimensions) of macromolecules in dilute solution. Important information about macromolecular architecture and conformations can be obtained from the molecular-weight dependence of intrinsic viscosity for a homologous series of polymers. Size-exclusion chromatography (SEC) provides a unique opportunity to measure this dependence in a single chromatographic run. Another striking coincidence is that the dimensions of a macromolecule associated with its frictional properties in dilute solution (i.e., with the intrinsic viscosity) determine the elution time (volume) in size-exclusion separation. This allows one to use the intrinsic viscosity measurement as a crucial intermediate step in the determination of molecular weights and molecular-weight distributions of polymers. From the above, it might be assumed that on-line intrinsic viscosity measurements represent an important aspect of contemporary gel permeation chromatography (GPC).

Solution Viscosity

There are several dilute solution viscosity quantities used in the determination of the intrinsic viscosity. The size of macromolecules in solution is associated with an increase in viscosity of the solvent brought about by the presence of these molecules. Relative viscosity is a dimensionless quantity representing a solution/solvent viscosity ratio, $\eta_r = \eta/\eta_0$, where η and η_0 are the solution and solvent viscosities, respectively. The specific viscosity $\eta_{sp} = \eta_r - 1$ is the fractional increase in viscosity between the solution and solvent. The effect of the concentration can be normalized by division of η_{sp} by the concentration C , expressed in grams per deciliter (g/dL). This concentration-normalized viscosity is termed the reduced specific viscosity or η_{sp}/C (the IUPAC preferred term is viscosity number). Another related term, the inherent viscosity, is expressed as $\eta_{inh} = (\ln \eta_r)/C$ (the IUPAC preferred term is logarithmic viscosity number).

In order to relate viscosity to molecular weight, the value of reduced (or inherent) viscosity is extrapolated to zero concentration. This parameter is called the intrinsic viscosity, $[\eta]$, and is usually expressed in deciliters per gram (dL/g) (the IUPAC preferred term is limiting viscosity number, mL/g):

$$[\eta] = \lim(\eta_{sp}/C) = \lim \eta_{inh} \quad (C \rightarrow 0) \quad (1)$$

Practically, the limit in Eq. (1) is achieved when the concentration is so low that the frictional interactions between an individual macromolecule and a solvent are not affected by the presence of other macromolecules in the same solution. Under these conditions, which are typical for the GPC-SEC experiments, the difference between the reduced and intrinsic viscosities is negligible.

Calculation of Intrinsic Viscosity in GPC

The opportunity to measure the dilute polymer solution viscosity in GPC came with the continuous capillary-type viscometers (single capillary or differential multicapillary detectors) coupled to the traditional chromatographic system before or after a concentration detector in series (see the entry Viscometric Detection in GPC-SEC). Because liquid continuously flows through the capillary tube, the detected pressure drop across the capillary provides the measure for the fluid viscosity according to the Poiseuille's equation for laminar flow of incompressible liquids [1]. Most commercial on-line viscometers provide either relative or specific viscosities measured continuously across the entire polymer peak. These measurements produce a viscometry elution profile (chromatogram). Combined with a concentration-detector chromatogram (the concentration versus retention volume elution curve), this profile allows one to calculate the instantaneous intrinsic viscosity $[\eta]_i$ of a polymer solution at each data point i (time slice) of a polymer distribution. Thus, if the differential refractometer is used as a concentration detector, then for each sample slice i ,

$$[\eta]_i \approx \frac{\eta_{sp,i}}{C_i} = \frac{\nu \eta_{sp,i}}{\Delta n_i} \quad (2)$$



where Δn is the refractive index change due to the polymer in solution, detected by the refractometer and $\nu = dn/dc$ is the refractive index increment of the polymer. The quantity calculated from Eq. (2) is often designated as “observed” intrinsic viscosity, $[\eta]_{\text{obs}}$.

As can be seen from Eq. (2), the observed intrinsic viscosity for each slice is proportional to the ratio of two detectors’ responses. It follows that detector noise, which is an irreducible component of the measurement process, introduces noise in the intrinsic viscosity that depends on this ratio. However, two detectors have different sensitivities at the tails of polymer distribution: the concentration detector is less sensitive to the high-molecular-weight end and the viscometer is less sensitive to the opposite end. Thus, the noise increases dramatically on both tails of the distribution, where the ratio (2) does not produce physically meaningful values. For example, the logarithm of intrinsic viscosity computed from the slice ratios (2) sometimes does not increase monotonically with molecular weight (i.e., with decreasing elution volume V) even for the flexible coil-like polymers (curves 2 in Fig. 1).

Fitting a smooth, multivariate model to a time series of noisy data is an effective way to produce a more precise estimate of the measured quantity at each sample time. Typically, the logarithm of intrinsic viscosity is

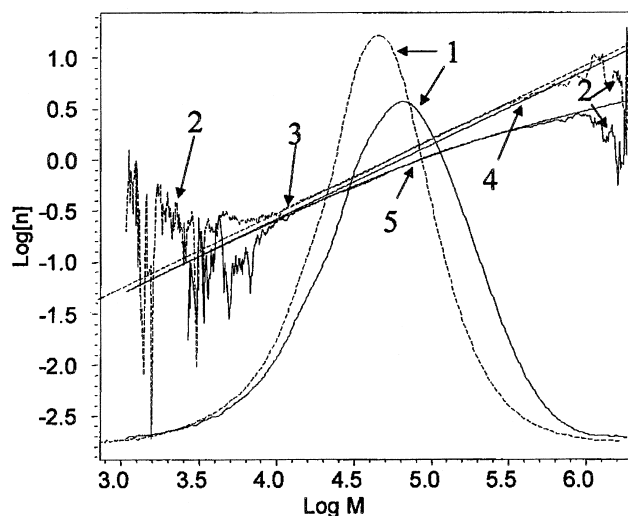


Fig. 1 Molecular-weight-distribution (MWD) and viscosity-law plots for NIST PE1475 high-density polyethylene (dashed lines) and NIST PE1476 low-density polyethylene (solid lines). The curves are (1) MWD, (2) observed viscosity, (3) fitted viscosity for linear polyethylene, (4) extrapolated fitted viscosity for polyethylene with short-chain branches only, and (5) fitted viscosity for branched polyethylene.

Intrinsic Viscosity of Polymers: Determination by GPC

modeled as a low-order polynomial in elution volume V using a least-squares fitting to the experimental data [2–4]. The intrinsic viscosity calibration curve ($\log[\eta]_{\text{fit}}$ versus V) obtained this way depends on properties of the polymer as well as that of the chromatographic system (e.g., columns). It can be used for diagnostic information concerning the GPC–viscometry system [5] and also to refine such system parameters as interdetector volume (see the entry Interdetector Delay Volume) and band broadening (see the entry Axial Dispersion Correction in GPC–SEC).

Application of Intrinsic Viscosity in GPC to Polymer Characterization

Molecular Weight and Molecular-Weight Distribution Determination

The most important feature that has been added to conventional GPC by the viscometer detector through the intrinsic viscosity calculation is the ability to determine the “absolute” MWD without any additional assumptions about the polymer chemical structure. This goal is accomplished by applying the universal calibration concept, which establishes the hydrodynamic volume $H = [\eta]M$ as a universal parameter governing the size-exclusion separation. The MWD can be determined in three steps. First, the set of narrow polydispersity polymers with known molecular weights (narrow standards) covering the entire region of column size-exclusion separation is selected to construct the universal (or hydrodynamic volume) calibration curve, $\log H$ versus elution volume V (see the entry Calibration of GPC–SEC with Universal Calibration Techniques). This curve is then used to calculate the molecular-weight calibration curve via the relationship $\log M = \log H - \log[\eta]_{\text{fit}}$, where these quantities are obtained from the (smooth) hydrodynamic and intrinsic viscosity calibration curves. Finally, the MWD is constructed by plotting the concentration C as a function of $\log M$ across the polymer distribution (curves 1 in Fig. 1). Different statistical moments of this distribution (i.e., average molecular weights, including viscosity-average molecular weight M_v) can be calculated by appropriate summation over the slice data and compared with the values obtained by bulk measurements [6].

Intrinsic Viscosity Distribution

The intrinsic viscosity is a fundamental property of the polymer sample in solution, and thus the intrinsic viscosity distribution (IVD) (C versus $\log[\eta]$) with associ-

ated statistical moments may be used to characterize polymers without converting this distribution into a MWD [7]. The IVD can be determined in GPC-viscometry directly, without resorting to universal calibration. This distribution depends not only on the polymer sample itself but also on the solvent and the temperature, and hence does not possess the versatility of the MWD. Nevertheless, the IVD measurement in GPC-viscometry is much less sensitive to experimental conditions than any calibration curve and, hence, can be successfully used in industry (e.g., for quality control of polymers in production).

Size and Molecular Structure of Polymers

The GPC-viscometry with universal calibration provides the unique opportunity to measure the intrinsic viscosity as a function of molecular weight (viscosity law, $\log[\eta]_{\text{fit}}$ versus $\log M$) across the polymer distribution (curves 3 and 4 in Fig. 1). This dependence is an important source of information about the macromolecule architecture and conformations in a dilute solution. Thus, the Mark-Houwink equation usually describes this law for linear polymers: $\log[\eta] = \log K + \alpha \log M$ (see the entry Mark-Houwink Relationship). The value of the exponent α is affected by the macromolecule conformations: Flexible coils have the values between 0.5 and 0.8, the higher values are typical for stiff anisotropic ("rod"-like) molecules, and much lower (even negative) values are associated with dense spherical conformations.

The determination of the viscosity law in GPC-viscometry is even more important for branched polymers. Branches reduce the sizes of a macromolecule, including its hydrodynamic volume H . This size reduction is reflected by the changes in the shape and position of the viscosity law plot for a branched polymer. Short-chain branches usually do not change the linearity and slope of the Mark-Houwink plot and just decrease the value of parameter K , whereas the long-chain branches cause bending of the corresponding plot.

These features of the viscosity-law plots for branched polymers are demonstrated in Fig. 1 with two NIST (National Institute of Standards and Technology, U.S.A.) polyethylene standards as examples:

high-density linear polyethylene PE1475 and low-density branched polyethylene PE1476. This last one contains both short- and long-chain branches. Dashed straight line 3 represents the Mark-Houwink plot for linear polyethylene, parallel solid line 4 takes into account the short-chain branches, and polyethylene with both types of branches (PE1476) is described by solid curve 5 (see the entry Long-Chain Polymer Branching, Determination by GPC-SEC for further discussion).

For further information on the intrinsic viscosity determination in GPC, including the use of the light-scattering detector, see Ref. 8 and the entry GPC-SEC Viscometry from Multiangle Light Scattering.

References

1. J. W. Mays and N. Hadjichristidis, Polymer characterization using dilute solution viscometry, in *Modern Methods of Polymer Characterization* (H. G. Barth and J. W. Mays, eds.), John Wiley & Sons, New York, 1991, pp. 227-269.
2. C.-Y. Kuo, T. Provder, M. E. Koehler, and A. F. Kah, Use of a viscometric detector for size exclusion chromatography, in *Detection and Data Analysis in Size Exclusion Chromatography* (T. Provder, ed.), American Chemical Society, Washington, DC, 1987, pp. 130-154.
3. R. Lew, P. Cheung, S. T. Balke, and T. H. Mourey, *J. Appl. Polym. Sci.* 47: 1685-1700 (1993).
4. Y. Brun, R. Nielson, M. Gorenstein, and N. Hay, New results in polymer characterization using multidetector GPC, in *Proceedings, International GPC Symposium*, 1998, pp. 48-67.
5. S. T. Balke, P. Cheung, R. Lew, and T. H. Mourey, *J. Liquid Chromatogr.* 13: 2929-2955 (1990).
6. J. Lesec, Problems encountered in the determination of average molecular weights by GPC viscometry, in *Liquid Chromatography of Polymers and Related Materials II* (J. Cazes and X. Delamare, eds.), Chromatographic Science Series, Vol. 13, Marcel Dekker, Inc., New York, 1980, pp. 1-17.
7. W. W. Yau and S. W. Rementer, *J. Liquid Chromatogr.* 13: 627-675 (1990).
8. C. Jackson and H. G. Barth, Molecular weight-sensitive detectors for size exclusion chromatography, in *Handbook of Size Exclusion Chromatography* (C. Wu, ed.), Chromatographic Science Series, Vol. 69, Marcel Dekker, Inc., New York, 1995, pp. 103-145.



Ion Chromatography Principles, Suppressed and Nonsuppressed

Ioannis N. Papadoyannis

Victoria F. Samanidou

Aristotle University of Thessaloniki, Thessaloniki, Greece

Introduction

Ion chromatography (IC) is a mode of high-performance liquid chromatography (HPLC) in which ionic analyte species are separated on cationic or anionic sites of the stationary phase. The separation mechanisms can be broadly compared to ion exchange, using fixed-site exchange resins of various composition and ion-interaction methods, using a variety of columns as substrates to support dynamically exchanged or permanently bonded ionic groups. Alternative approaches of minor significance also exist. The mobile phase is an aqueous buffer solution. The rate of migration of the ion (inorganic ions and organic acids and bases) through the column is directly dependent on the type and concentration of eluent ions. Retention is based on the affinity of different ions for the ion-exchange sites and on the competition between eluent buffer ions and analyte ions, which is dependent on the ionic strength of the buffer and can be adjusted by altering the pH of the mobile phase or the concentration of any organic modifier in it.

Discussion

Ion chromatography operates at pressures ranging from several hundred to several thousand pounds per square inch. In most cases, the same chromatographic components (pumps, injectors, etc.) can be employed in both HPLC and IC. Most of the chromatographic principles developed in HPLC stand for IC also, with possible minor modifications. Injection volumes in ion chromatography are generally somewhat larger than those normally in HPLC, typically in the range 50–100 μL , in contrast to HPLC, where 5–20 μL are injected.

It was in 1975 when Small and his co-workers introduced the high-pressure operation mode of ion chromatography. In their original paper, they described a novel system for the chromatographic determination of inorganic ions, in which a resin was used for the sep-

aration and a second ion-exchange column was combined to chemically suppress the background conductance of the eluent, thus improving detection limits for eluted ions. Since 1975, IC has grown rapidly and ion chromatographic methods for ions are currently among the best available and have been applied to a wide range of inorganic species. This can be attributed to concurrent advances in separation technology and detection methods.

Detection techniques can be subdivided into three broad categories:

1. Electrochemical detection (using conductivity, amperometry, or potentiometry).
2. Spectroscopic detection (using ultraviolet/visible (UV/vis) absorbance, refractive index, fluorescence, atomic absorption or atomic emission).
3. Techniques based on postcolumn reactions.

Conductivity detectors provide the advantage of universal detection, as all ions are electrochemically conducting. Thus, the majority of ion chromatography detectors rely upon conductivity measurements.

The principle of conductivity-detector operation is the differential measurement of conductance of the eluent, prior to and during elution of the analyte ion. The detector response depends on analyte concentration, the degree of ionization of both eluent and analyte (governed by the eluent pH), and limiting equivalent conductances of the eluent cation and of the eluent and analyte anions (where an anion-exchange system is considered). If the eluent and analyte are fully ionized, the signal is proportional to the analyte concentration and to the difference (positive or negative) in limiting equivalent conductances which determines sensitivity.

Conductivity detection provides a sensitive measure of ion concentrations in solution, but its measurement is hampered by high conductivity of the eluent, as ion exchange requires a competing electrolyte to displace the analytes from the column. In order to eliminate



background conductivity and thus to improve the analyte signal, *H. Smith et al.* proposed the use of a second ion-exchange column. In this way, two different ion chromatography techniques are distinguished: eluent suppressed and nonsuppressed (also called single-column ion chromatography) using different packing materials and different eluents, leading to specific advantages and disadvantages for each technique.

Eluent Suppressed Ion Chromatography

Various schemes have been devised to improve the signal-to-noise ratio (S/N) by decreasing the background signal of the eluent/displacer or increasing the conductance of the analyte, or both.

The principle of conductivity suppression is the reduction of background conductivity by converting the eluent to a less conductive medium (H_2O) through acid-base neutralization while the analyte ions' conductivity is increased, by converting them to a more conductive medium: Anions are converted to their acid forms and cations to their hydroxide forms. These reactions lead to higher S/N ratios, thus significantly improving baseline stability and detection limits.

Suppressor devices include packed column suppressors, hollow-fiber membrane suppressors, micromembrane suppressors, suspension postcolumn reaction suppressors, autoregenerated electrochemical suppressors, and so forth.

The packed column suppressor, originally introduced by *Small et al.*, suffers from a number of drawbacks, such as time shifts due to Donnan exclusion effects, band broadening (due to a large dead volume and high dispersion), and oxidation of nitrite, which is easily oxidized to nitrate, due to the formation of nitrous acid in the suppressor. Because of these limitations, they were only practical for isocratic elution. However, the main disadvantage of the method is the necessity for periodical regeneration of the suppressor (also called stripper) to restore its ion-exchange capacity.

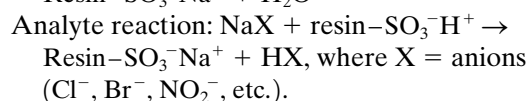
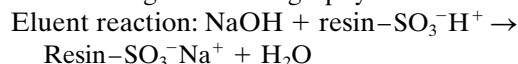
For anion analysis, the regenerant must supply a source of hydrogen ions to convert the eluent anions to a less conductive form. The most common regenerant is dilute sulfuric acid, whereas for cation analysis, the most common regenerant is hydroxide (sodium, potassium, or tetramethylammonium hydroxide).

The preferred eluents for anions are dilute carbonate-bicarbonate mixture, sodium hydroxide and, for common alkali metals and simple amines, dilute mineral acids (HCl , HNO_3 , BaCl_2 , AgNO_3 , amino acids, alkyl and aryl sulfonic acids). The most common

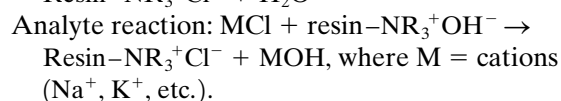
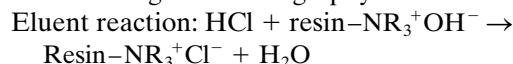
choice is HCl , but in the case of divalent ions, an eluent of much higher affinity for the ion-exchange resin, such as AgNO_3 , must be used.

Typical neutralization reactions for chemical suppressors are as follows:

Anion-exchange chromatography:



Cation-exchange chromatography:



The reaction, in the case of bicarbonate, yields the largely undissociated carbonic acid that does not contribute significantly to the conductivity.

Without chemical suppression, the contribution to the total measured conductivity from the eluent is many orders of magnitude higher than that from the analyte, leading to low sensitivity (*Fig. 1*).

Some of the drawbacks that packed column suppressors have were eliminated when hollow-fiber membrane suppressors were introduced in 1981. These were found to be even more convenient and efficient, with low dead volume and high capacity, and they are dynamically regenerated. Eluent passes through the

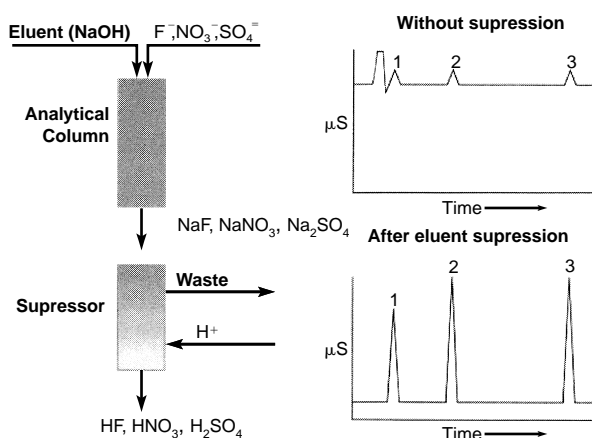
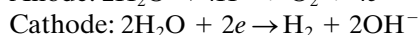
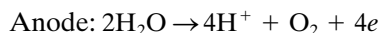


Fig. 1 The effect of the background conductivity suppression on the monitored signal of the analyte anions, after separation by means of ion chromatography. Peaks: 1 = fluoride, 2 = nitrate, 3 = sulfate.

core of the fiber and regenerant washes the outside. However, they have also limited suppression capacity and are restricted only to isocratic operation.

Micromembrane suppressors introduced in 1985 use thin, flat ion-exchange membranes to enhance ion transport while maintaining a very low dead volume, providing a high suppression capacity, with low dispersion.

Later, electrochemically regenerated suppression modules were introduced, where an electrochemical process is used to regenerate a solid-phase chemical suppressor for continuous reagent-free operation. Self-regenerating suppressors are similar to micromembrane suppressors, except that regenerant hydronium and hydroxide ions are produced, *in situ*, by electrolysis of water supplied by recycle or an external source. This is achieved by incorporating electrodes inside the regenerant chambers; thus, external acid or base supply are unnecessary. The two electrolysis reactions taking place are



Another technique of improving the S/N ratio is the one that uses postcolumn addition of a solid-phase reagent (SPR), which is a colloidal suspension of ultrafine ion-exchange particles. The SPR reacts with the analyte to increase its conductivity. Additionally, the SPR has a low electrophoretic mobility and, hence, conductance. This technique avoids the dead time due to suppressor column and also eliminates the regeneration cycle.

Nonsuppressed Single-Column Ion Chromatography

Another approach of ion chromatography is the nonsuppressed single column, in which no suppressor device is used. In this case, the only method for improving the sensitivity is to maximize the difference between mobile-phase conductivity and analyte conductivity.

Nonsuppressed single-column ion chromatography (SCIC) was introduced in 1979 by Gierde and co-workers, based on a two-principal innovation:

1. The use of a special anion-exchange resin of very low capacity (0.007–0.007 mEq/g).
2. The adoption of an eluent having a very low conductivity, which can be passed directly through the conductometric detector. Typical eluents used are benzoate, phthalate, or other aromatic acid salts, with low limiting equivalent conductances (leading to direct detection) or potassium hydroxide eluent, with high conduc-

tivity for anions or dilute nitric acid for cations, leading to indirect detection mode (decrease of conductivity as the analyte is eluting).

The major limitation of nonsuppressed conductivity detection is that gradient systems cannot be used; thus, the background conductivity remains constant.

Virtually every type of high-performance liquid chromatography (HPLC) detector can be combined with SCIC: refractive index, UV absorbance (direct and indirect), electrochemical, and so forth.

A typical nonsuppressed SCIC separation obtained with a low-capacity resin-based strong anion exchanger (PRP-X100 Hamilton) used as the analytical column is illustrated in Fig. 2 for the simultaneous determination

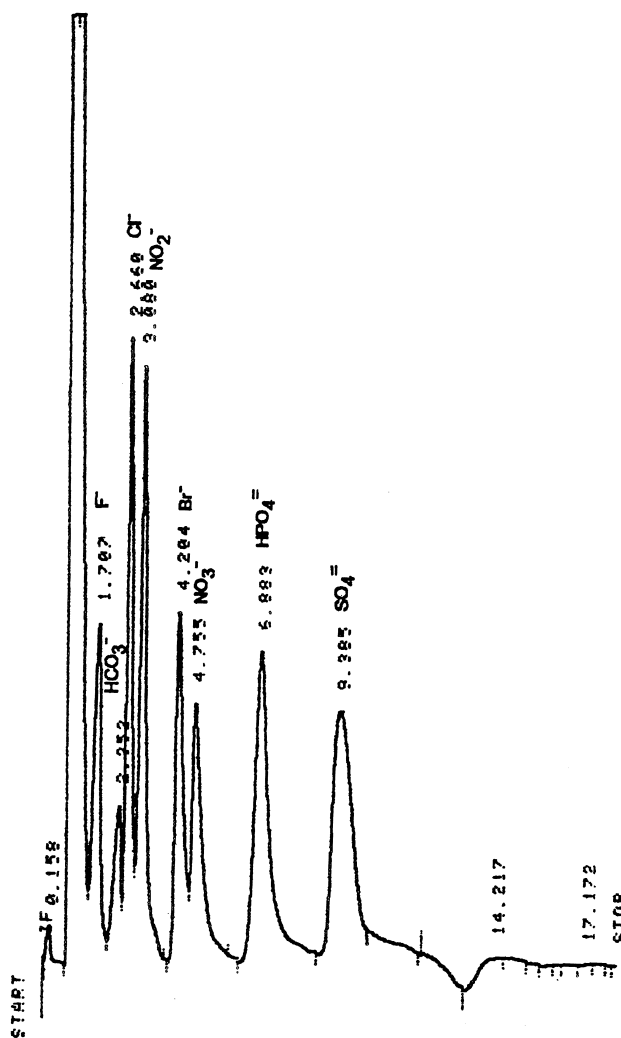


Fig. 2 Nonsuppressed SCIC determination of eight inorganic anions.



of eight inorganic anions (F^- , Br^- , NO_2^- , Cl^- , NO_3^- , PO_4^{3-} , SO_4^{2-} , CO_3^{2-}), with conductometric detection, using a mixture of 2.0 mM sodium benzoate and 2.5 mM *p*-hydroxybenzoic acid (pH 9.0 adjusted with 1N NaOH) as eluent, with the organic modifier methanol 8% v/v, at a flow rate of 0.7 mL/min. The detection limits ($S/N = 3$) were 100 $\mu\text{g/L}$ for carbonate and 50 $\mu\text{g/L}$ for the rest of the cited anions, when 50 μL of the samples were injected onto the analytical column.

Columns

Two types of packing materials are commonly used for ion chromatography: silica-based and polymer-based ion exchangers. The polymer-based ion exchangers typically contain a PSDVB (polystyrenedivinylbenzene) backbone, lightly sulfonated (cation exchanger) or lightly aminated (anion exchanger), whereas the silica-based ion exchangers use a porous silica bead, chemically prepared to form the anion or cation exchanger. The resins have the advantage that they can be used over the entire pH range, whereas silica based materials can be used in a narrow working pH range (2–6.5).

Detection limits for ions vary with the sensitivity of the detector, with the volume of sample injected, and with the identity, concentration, and pH of the eluent, as well as with chromatographic factors, such as column efficiency and so forth.

Comparison of ESIC and SCIC

The main advantages of eluent suppressed ion chromatography (ESIC) are that a wide range of eluents and columns can be used, the wide dynamic range, and the higher sensitivity; the main disadvantage is the periodical necessity for suppressor-column regeneration.

On the other hand, SCIC is rapid, sensitive, with easy sample preparation, and simple instrumentation; however, it requires a significant difference in conductance between eluent and analyte ions and the temperature stability is crucial. The answer to the question of which IC technique is most efficient is dependent on several considerations, such as the nature of sample analytes, the concentration of the solute ions, the sensitivity required, the equipment available, and so forth.

Applications

Ion chromatography, suppressed and nonsuppressed, can be applied both to anion and cation analysis. The

current situation is that the methods for anion determination have far outnumbered those for cation analysis, for the reason that there are available methods for the latter, which are rapid and sensitive (e.g., AAS, ICP, ASV). It is difficult to mention all the ionic species detectable by this analytical technique. Practically, any compound that can be converted to an ionic form is amenable to analysis by IC. Among the inorganic ions determined are (F^- , Br^- , NO_2^- , Cl^- , NO_3^- , PO_4^{3-} , SO_4^{2-} , CO_3^{2-} , CrO_4^{2-} , I^- , IO_3^- , $C_2O_4^{2-}$, BrO_3^- , SCN^- , Na^+ , K^+ , Mg^{2+} , Ca^{2+} , NH_4^+ , at the ppm or ppb levels, in drinking water, food samples, food additives, beverages, environmental samples (soil extracts, rain water, surface water or groundwater), cosmetics, pharmaceuticals, biomedical, plating bath analysis, biological fluids, industrial process products, wastewater, and so forth. IC is also capable of speciation analysis of polyvalent anions or transition metal ions with multiple oxidation states, at levels lower than those possible with ICP or AAS. Organic species of biological and biochemical interest can also be determined.

Suggested Further Reading

- Dasgupta, P., *Anal. Chem.* 64(15): 775A–783A (1992).
 Gierde, D., J. Fritz, and G. Schmuckler, *J. Chromatogr.* 186: 509–519 (1979).
 Gierde, D., G. Schmuckler, and J. Fritz, *J. Chromatogr.* 187: 35–45 (1980).
 Haddad, P., and A. Heckenberg, *J. Chromatogr.* 300: 357–394 (1984).
 Henderson, I., R. Saari-Nordhaus, and J. Anderson, Jr., *J. Chromatogr.* 546: 61–71 (1991).
 Henshall, A., S. Rabin, J. Statler, and J. Stilian, *Int. Chromatogr. Lab.* 12: 7–14 (1993).
 Papadoyannis, I., V. Samanidou, and K. Moutsis, *J. Liquid Chromatogr.* 21(3): 361–379 (1998).
 Papadoyannis, I., V. Samanidou, and A. Zotou, *J. Liquid Chromatogr.* 18(7): 1383–1403 (1995).
 Pietrzyk, D., Z. Iskandarani, and G. Schmitt, *J. Liquid Chromatogr.* 9(12): 2633–2659 (1986).
 Saari-Nordhaus, R. and J. Anderson, Jr., *Int. Chromatogr. Lab.* 18: 4–10 (1994).
 Schmuckler, G., *J. Chromatogr.* 313: 47–57 (1984).
 Small, H., T. Stevens, and W. Bauman, *Anal. Chem.* 47(11): 1801–1809 (1975).
 Tarter, J., *Ion Chromatography*, Chromatographic Science Series Vol. 37. Marcel Dekker Inc., New York, 1987.
 Walker, T., N. Akbari, and T. Ho, *J. Liquid Chromatogr.* 14(4): 619–641 (1991).



Ion Exchange: Mechanism and Factors Affecting Separation

Karen M. Gooding

Eli Lilly and Company, Indianapolis, Indiana, U.S.A.

Introduction

Ion-exchange chromatography (IEC) is a technique in which ionic solutes bind to charged functional groups on the bonded phase. The power and versatility of IEC as an analytical and preparative technique is due in large part to the ability to drastically change the selectivity through manipulation of the mobile phase. Although it is obvious that the pH determines the charge on the support and the analytes, the nature of the salt is an equally important parameter. The constituent ions of the salt associate with the support functional groups and/or those of the solute, yielding distinct ionic interactions. Mobile-phase additives, temperature, and gradient conditions also contribute to the separation in IEC.

Mobile Phase

pH

Adjustment of the pH is a critical factor in IEC because the pH dictates the charge of both the solutes and the ion exchanger, thus controlling their affinity for one another or their ability to release from a bound state. The essential nature of pH in the process necessitates its exact control; therefore, any mobile phase used for IEC should contain an effective buffer (0.02M–0.1M) within its optimum pH range. Some common buffers which cover much of the range of pH used in IEC are phosphate, citrate, acetate, and tris(hydroxymethyl)aminomethane (Tris) [1,2]. The pH should be selected to yield ionization of the functional groups on the support as well as those on the analytes. For molecules with a single charge, the pH should be at least two units from the pK in the direction of ionization. The guideline for zwitterions is that the pH be at least two units from the isoelectric point (pI). A pH near neutrality is often effective for complex mixtures of diverse substances. Even carbohydrates, whose hydroxyl groups do not ionize until the pH is greater than 12, can be separated by IEC when the pH is adjusted to a high enough value with low concentrations of base as the mobile phase [3].

The choice of pH for IEC of proteins or other macromolecules is not as simplistic as it is for small molecules. Although using the pI as a guide frequently yields an adequate separation, the pI encompasses all the charged groups in the molecule, whereas, because of their defined tertiary structures, only the surface amino acids of proteins are actually involved in the binding. Under denaturing conditions, more amino acids are likely to be exposed to the bonded phase.

Salt Concentration

Ion-exchange chromatography is a very predictable technique because the mechanism is well defined. The capacity factor (k) for the binding of an ionic solute to an ion-exchange functional group in IEC is directly related to the concentration (c) of salt in the mobile phase:

$$\log k = \log K_0 + Z_c \log \left(\frac{1}{c} \right)$$

where K_0 is the distribution coefficient and Z_c is an experimentally determined parameter that reflects the apparent number of ionic charges associated with the process of a specific solute with a specific surface [4]. For isocratic separations of simple molecules with up to several charges, the analysis time can be optimized along with resolution by adjustment of the salt concentration. For more complex analytes or mixtures, salt gradients are often necessary to achieve acceptable separations. Generally, a gradient from 0M to 1M salt in a buffer at a suitable pH will yield a preliminary separation.

An opposite mechanism to ion exchange occurs when the ionic strength is too low. Ion exclusion is a phenomenon in which a charged analyte is repelled by the like charges within a pore. This is very likely to occur if water is used alone as the mobile phase with ion-exchange supports or with other modes of silica-based columns. Adding buffer and salt usually eliminates the problem.

Salt Composition

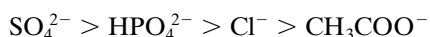
Elution with increased concentrations of salt is the most common and readily controlled method of achiev-



ing displacement of molecules which are strongly bound by an ion exchanger. The salt counterions competitively displace solute ions from the charged sites on the stationary phase. Smaller, more highly charged ions are most effective at this displacement. Specifically, the strength of displacement for cations is



and for anions, it is



The strength of the ions for displacement is not necessarily related to optimum selectivity or resolution. Selectivity is dictated by the effect of the salt on both the solute and the bonded phase. Besides displacing the solute from the support, either of the ions of the salt can complex with the ion-exchange functional group or the solute, alter the tertiary structure of the solute, or enhance hydrophobic properties. It is this combination of effects which results in selectivity. For example, when a mixture of proteins was run on a polyethyleneimine (PEI) weak anion-exchange column with gradients formed with 1.0*N* salt, substitution of sodium acetate for sodium phosphate produced not only longer retention but also much better resolution of the proteins [5]. Sodium phosphate produced narrower peaks with less tailing, but the peaks had only slight differences in retention. In this case, the short retention was proven to be due to a special affinity of phosphate for PEI, which did not occur with anion-exchange supports having quaternary (*Q*) or diethylaminoethanol (DEAE) functional groups. The salt effects on selectivity encompass anions and cations in both anion-exchange and cation-exchange chromatography, as illustrated in Fig. 1, implying that the selectivity occurs because of ionic interactions with the functional groups of both the support and the solute. In the case of adenosine 5'-diphosphate (ADP), divalent ions like calcium can bridge between the oxygens in the phosphate and thus reduce the ionic properties. Phosphate salts reduce the retention of ADP on PEI supports due to the phosphate-PEI affinity discussed earlier. Another example of ion-based selectivity is the excellent resolution obtained for sugars when a calcium salt is used with a cation-exchange resin. This ability to change selectivity so dramatically by varying the salt significantly broadens the utility of IEC.

The only restrictions on the choice of salt are those involving analyte solubility or stability. Volatile salts such as ammonium acetate even allow IEC to be interfaced with mass spectrometry or evaporative light-scattering detection. It is very important that a given salt be totally stripped from a support before changing

to other ions to avoid mixed ion effects. An acid such as trifluoroacetic acid is often effective as a bridge/washing solvent for this purpose.

Surfactants and Organic Solvents

Secondary separation which may be present in IEC is generally size exclusion or hydrophobicity. Size exclusion will occur if macromolecules are larger than the pores in a support. Hydrophobic interactions are most often observed under conditions of high salt for solutes with significant nonpolar characteristics, such as certain peptides. The hydrophobicity of an ion-exchange support is due to either the matrix or the cross-linking agents which were employed in the synthesis of the bonded phase. Any hydrophobic interactions are fundamentally undesirable and can be minimized by the addition of 1–10% of an organic solvent, such as methanol, ethanol, or acetonitrile, to the running buffer. The solubility of the salt in the organic mobile phase should always be verified to avoid precipitation.

Nonionic detergents may also reduce hydrophobic interactions with a column. These detergents, such as CHAPS or urea, can also be added to ion-exchange mobile phases to aid in the solubilization of membrane or other insoluble proteins. Such detergents are easy to equilibrate and remove from ion-exchange columns; however, ionic detergents should be avoided because of their very strong binding to the column or the solutes.

Flow Rate and Gradient

Small molecules can often be effectively separated isocratically by IEC; however, due to multipoint interactions, isocratic IEC of proteins and most biological macromolecules is not usually feasible, yielding no resolution and extreme tailing. Such complex molecules are generally separated by gradient elution.

As a salt gradient proceeds to higher levels in IEC, molecules elute at a specific salt concentration, generally without binding from secondary effects. The relationship of gradient conditions to elution (k^*) can be described by

$$k^* = 0.87 t_G \frac{F}{V_M} \left(\log \frac{C_2}{C_1} \right) Z$$

where C_1 and C_2 are the total salt concentrations (salt plus buffer) at the beginning and the end of the gradient, respectively, Z is the effective charge on the solute molecule, F is the flow rate; V_M is the total mo-

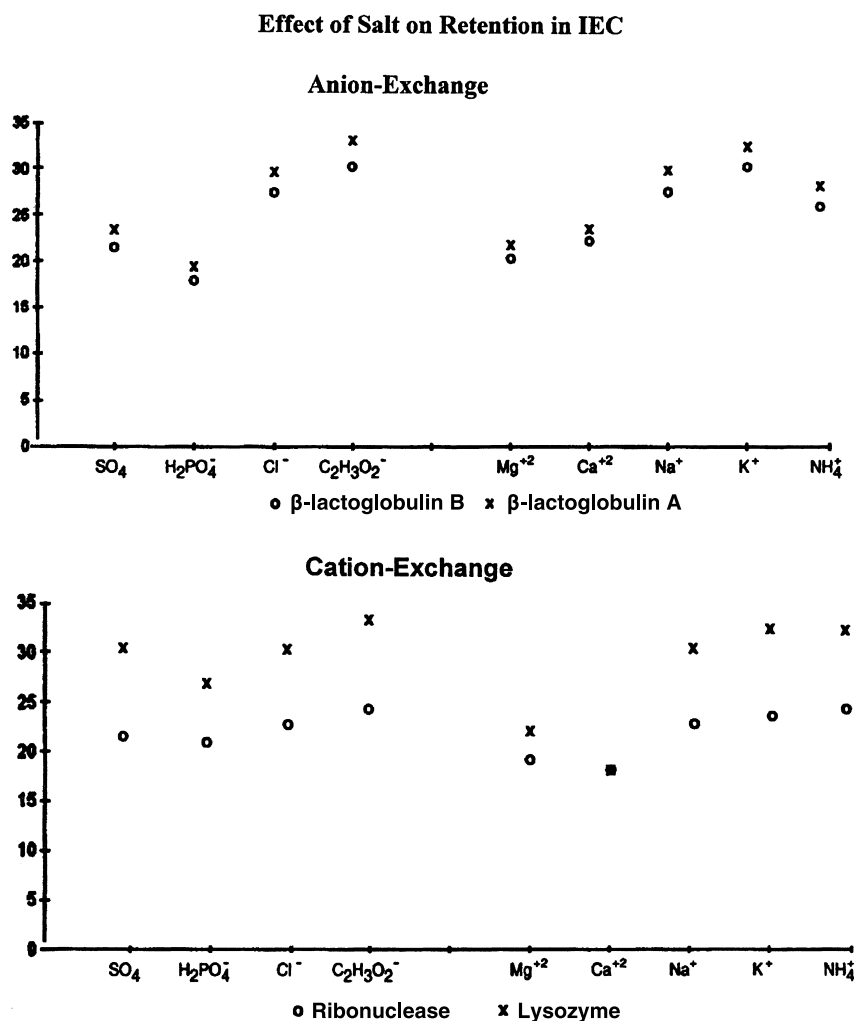


Fig. 1 Anion-exchange chromatography (AEX): SynChropak AX300 (polyethyleneimine, 300 Å, 6 μm); cation-exchange chromatography (CEX): SynChropak CM300 (carboxymethyl, 300 Å, 6 μm); 30-min gradient (0–1*N*) of sodium or chloride salts in 0.02*M* Tris, pH 7. (Reprinted with permission of MICRA Scientific.)

bile-phase volume, and t_G is the gradient time [6]. The Z number will vary with solute and pH. An initial ion-exchange protocol of a 20–30-min linear gradient from 0*M*–1*M* salt in a buffer at a suitable pH will usually yield a separation which can be later optimized, if necessary. For shortest analysis times, a gradient should begin at the highest salt concentration where the analytes are bound and it should end at the lowest ionic strength that causes elution. The pH gradients may also be used to elicit elution during IEC, although this has been a less popular strategy than salt gradients. Ion-exchange columns can be effectively washed with a mobile phase of higher ionic strength than the upper gradient limit or with low pH. For gradients, intermediate flow rates of

1mL/min for a 4.6-mm-inner diameter column are usually satisfactory.

Temperature

The use of elevated temperature in IEC reduces the mobile-phase diffusion coefficient and concomitantly decreases band spreading. Most mobile phases in IEC are composed of water with salts and thus produce efficiencies which are less than those obtained in modes using organic solvents. Because increased temperatures decrease retention, they may permit the use of lower salt concentrations. Elevated temperatures have been especially effective in amino



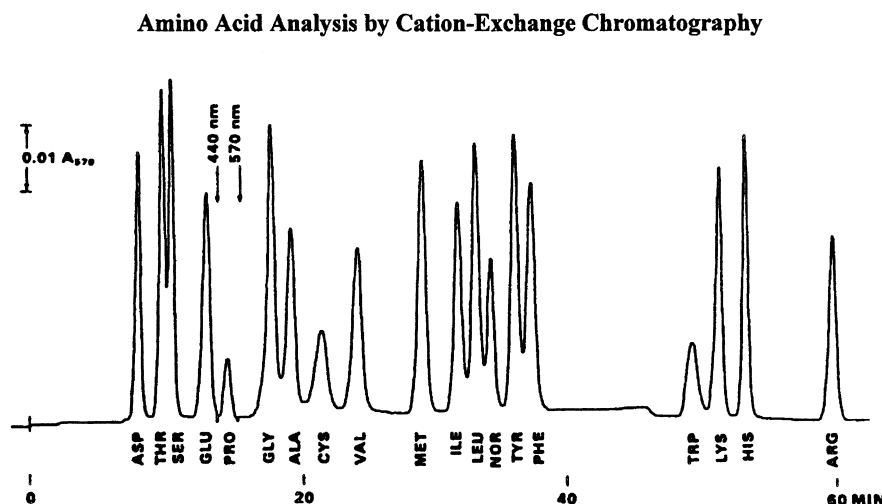


Fig. 2 Column: Micropak AA (sulfonated polystyrene); solvent A: 0.2M sodium citrate, pH 3.25; solvent B: 1M sodium citrate, pH 7.40. Gradient: 5 min 100% A; 100–75% A in 20 min; 75–70% A in 5 min; 70–35% A in 5 min; 10 min 35%; 35–0% A in 1 min. $T = 50^{\circ}\text{C}$ for 25 min, then 90°C . Detection after ninhydrin postcolumn reaction. (Reprinted from Amino acid analysis with ninhydrin postcolumn derivatization, *LC at Work*, Varian Associates with permission.)

acid analyses by cation-exchange chromatography, as illustrated in Fig. 2.

Conclusions

The effectiveness of ion-exchange chromatography as a method for separating charged species is enhanced by the ability of many operational factors to change the selectivity and resolution. Salt concentration, salt composition, and pH are the most important operational parameters which strengthen the versatility of the technique.

References

1. R. L. Cunico, K. M. Gooding, and T. Wehr, Ion-exchange chromatography, in *Basic HPLC and CE of Biomolecules*, Bay Bioanalytical Laboratories, Richmond, VA, 1998.
2. *Ion-Exchange Chromatography, Principles and Methods*, Pharmacia Biotech, Sweden.
3. R. R. Townsend, High-pH anion exchange chromatography of recombinant glycoprotein glycans, in *High Performance Liquid Chromatography: Principles and Methods in Biotechnology* (E. D. Katz, ed.), John Wiley & Sons, New York, 1996.
4. M. I. Aguilar, A. N. Hodder, and M. T. W. Hearn, HPIEC of proteins, in *HPLC of Proteins, Peptides and Polynucleotides* (M. T. W. Hearn, ed.), VCH, New York, 1991, p. 199.
5. M. P. Nowlan and K. M. Gooding, HPIEC of proteins, in *High-Performance Liquid Chromatography of Peptides and Proteins* (C. T. Mant and R. S. Hodges, eds.), CRC Press, Boca Raton, FL, 1991.
6. L. R. Snyder, Gradient elution separation of large biomolecules, in *HPLC of Biological Macromolecules: Methods and Applications* (K. M. Gooding and F. E. Regnier, eds.), Marcel Dekker, Inc., New York, 1990.

Ion-Exchange Buffers

J.E. Haky

Florida Atlantic University, Boca Raton, Florida, U.S.A.

Introduction

Ion-exchange chromatography is a separation method based on the exchanging of ions in a solution with ions of the same charge present in a porous insoluble solid. The method is used for the deionization of water [1,2]. It is often employed for the separation and identification of the rare earth and transuranium elements [2]. Additionally, ion-exchange chromatography is also used in clinical laboratories for the automated separation and analysis of amino acids and other physiologically important amines used for pharmaceutical purposes [3].

Discussion

In ion-exchange chromatography, ions are separated on the basis of their differences in relative affinity for ionic functional groups on the stationary phase. Anionic and cationic functional groups are covalently attached to the stationary phase, usually resins, which are amorphous particles of organic material [1–3]. Sulfonated styrene-based polymers are the most widely used cation-exchange resin, and similar polymers containing quaternary ammonium groups are the most widely used anion exchangers [4]. Oppositely charged solute ions are attracted to ionic functional groups on the stationary phase by electrostatic forces. Retention is based on the attraction between solute ions and charged sites bound to the stationary phase [4,5].

Due to the desirable solvent and ionizing properties of water, most ion-exchange chromatographic separations are carried out in aqueous media. Once the selection of the column type has been made, the resolution of components in the sample can be optimized by adjusting ionic strength, temperature, flow rate, and, most importantly, the pH and concentration of buffer or organic modifier in the mobile phase.

Solvent strength, which is defined as the ability of the solvent to elute a given solute from the stationary phase, increases with increased ionic strength of the mobile phase. Selectivity is generally not affected by changes in ionic strength, except for samples containing solutes with different valence charges. With in-

creased temperature, the rate of solute exchange between the stationary phases and mobile phases increases, and the viscosity of the mobile phase decreases, resulting in increased solvent strength. Solvent strength also increases with the volume percent of organic modifier for hydrophobic solutes. However, most ion-exchange chromatography is performed in totally aqueous mobile phases, due to the hydrophilic nature of most ionic solutes. Flow rates of the mobile phase can change resolution in ion-exchange chromatography, but the effects are often minimal [5].

Increases in mobile-phase pH cause decreases in solute retention in cation-exchange chromatography and increases in retention in anion-exchange chromatography. Separation selectivity can also be greatly influenced by small changes in pH. In ion-exchange chromatography with aqueous mobile phases, buffers are used to maintain the pH in the mobile phase. A buffered solution can resist the changes in pH when an acid or base is added or when dilution is occurring. The pH of a buffer is given by the Henderson–Hasselbalch equation:

$$\text{pH} = \text{p}K_a + 109 \frac{[\text{A}^-]}{[\text{HA}]} \quad (1)$$

where $\text{p}K_a$ refers to the acid dissociation constant of the species in the denominator, HA, and A refers to the conjugate base of the acid HA. Buffer capacity, the measure of how well a solution resists changes in pH when a strong acid or base is added, increases as the concentration of the buffer increases. However, the pH of a buffer solution is virtually independent of dilution. When the $\text{pH} = \text{p}K_a$, the maximum buffer capacity is met and a good working range of the buffer is approximately when the $\text{pH} = \text{p}K_a = 1 \pm 1$ [1]. A buffer is very easy to make. For example, to prepare 1.00 L of buffer containing 0.100M tris(hydroxymethyl)aminomethane hydrochloride at pH of 7.4, simply weigh out 0.100 mol of its hydrochloride salt and dissolve it in a beaker containing about 900 mL of water. Then, add a base (e.g., NaOH), until the pH is exactly 7.4. Then, quantitatively transfer the solution to a volumetric flask. Finally, dilute to the volumetric mark and mix [1].

By increasing the buffer concentration, the concentration of the counterions are increased in the mo-



bile phase and stronger competition is provided between the sample components and the counterions for the exchangeable ionic centers, resulting in reduced solute retention [5]. As stated earlier, selectivity and retention can also be adjusted by changing the pH of the mobile phase. This occurs because such a change in pH modifies the character of both the ion-exchange medium and the acid-base equilibrium as well as the degree of ionization of the sample [3]. A pH gradient in which the pH of the mobile phase is changed during the chromatographic analysis can also be used to control the solvent strength and retention of ionic solutes. Such gradients can also be used to control selectivity [6].

The working pH range for a separation can be estimated from the pK_a values of the sample components. If such pK_a values are not available, they can often be estimated by considering the number and types of functional groups present and the molecular structures of the components in the sample [1]. In order to ensure that solutes are ionized and retained by the ion exchanger, the optimum buffer pH of the mobile phase should be 1 or 2 pH units above the pK_a of acids and 1 or 2 pH units below the pK_a of bases [3].

Two criteria should be met when choosing the components of the buffer. First, the buffer must be able to maintain the operating pH for the separation to be performed. Second, the exchangeable buffer counterion must yield the desired eluent strength [3]. Some common buffer salts used in ion-exchange chromatography and their usable pH ranges are summarized in Table 1. Examples of their use includes the chromatography of amino acids, polymeric, cation exchanger using various combinations of citrate and borate buffer [3]. Additionally, carbohydrates can be separated by anion-exchange chromatography using an aqueous solution of sodium hydroxide-sodium acetate as the eluent [3]. Being weak acids, the ion-exchange behavior of such compounds is significantly affected by the pH of the mobile phase. Similar separations of ionizable compounds through the use of ion-exchange chroma-

Table 1 Typical Buffers for Ion-Exchange Chromatography

Buffer salt	pH Range
Ammonia	8.2–10.2
Ammonium acetate	8.6–9.8
Ammonium phosphate	2.2–6.5
Citric acid	2.0–6.0
Disodium hydrogen citrate	2.6–6.5
Potassium dihydrogen phosphate	2.0–8.0 / 9.0–13
Potassium hydrogen phthalate	2.2–6.5
Sodium acetate	4.2–5.4
Sodium borate	8.0–9.8
Sodium dihydrogen phosphate	2.0–6.0 / 8.0–12
Sodium formate	3.0–4.4
Sodium perchlorate	8.0–9.8
Sodium nitrate	8.0–10.0
Triethanolamine	6.7–8.7

tography with these and other buffers have been reported [1–7].

Acknowledgment

The author wishes to thank H. Seegulum for technical assistance.

References

1. D. C. Harris, *Quantitative Chemical Analysis*, 5th ed., W. H. Freeman, New York, 1998, pp. 755–766.
2. H. F. Walton, *Ion-Exchange Chromatography*, Hutchinson and Ross, Dowden, U.K., 1976.
3. C. F. Poole and S. K. Poole, *Chromatography Today*, Elsevier, New York, 1991, pp. 422–439.
4. H. Small, *Ion Chromatography*, Plenum, New York.
5. D. T. Gjerde and J. S. Fritz, *Ion Chromatography*, 2nd ed., Huthig, New York, 1987.
6. L. R. Snyder and J. J. Kirkland, *Introduction to Modern Liquid Chromatography*, 2nd ed., John Wiley & Sons, New York, 1979, pp. 410–452.
7. W. Rieman and H. F. Walton, *Ion Exchange in Analytical Chemistry*, Pergamon Press, New York, 1976.



Ion-Exchange Stationary Phases

Karen M. Gooding

Eli Lilly and Company, Indianapolis, Indiana, U.S.A.

Introduction

In ion-exchange chromatography (IEC), molecules bind by the reversible attraction of electrostatic charges located on the outer surface of a solute molecule with dense clusters of groups with an opposite charge on an ion-exchange support. To maintain electrical neutrality, the charges on both the analytes and the matrix are associated with ions of opposite charge, termed counterions, which are either provided by preequilibration with the mobile phase or during manufacturing. Because a solute must displace the counterions on the matrix during attachment, the technique is termed "ion exchange." If the support possesses a positive charge, it is used for anion-exchange chromatography, whereas if it carries a negative charge, it is for cation exchange. Generally, the molecule of interest will have a charge that is opposite (positive or negative) to that on the support and the same as the competitively displaced counterions.

There are several major variables which distinguish ion-exchange packings and determine their utility for specific classes of solutes and for analytical or preparative applications. Those variables are as follows:

1. Structure of the bonded phase, including the chemistry of the functional group, its pK , and the properties of the spacer arm and/or bonded phase layer
2. Charge density and related nominal capacity
3. Properties of the support matrix, including composition and pore diameter

Bonded Phase

Functional Groups

The functional groups of an ion-exchange bonded phase are ionizable under specific pH conditions. The extent of their charge dependence on pH is the basis for distinguishing two types of ion exchangers — strong and weak. These designations do not refer to the strength of binding or to the capacity of the gel, but simply to the pK of the ionizable ligand group, similar

to the designations for acids and bases. The structures and approximate pK and pH ranges of some typical strong and weak ion-exchange groups are shown in Table 1 [1–5].

Generally, strong ion-exchange groups retain their charge over a wide range of pH, with binding capacity dropping off at the extremes. For example, quaternary ammonium (Q) resins are strong anion-exchange groups which are effective throughout the pH range of about 2–12. Similarly, sulfonyl groups are strong cation-exchange groups that remain negatively charged until acidic pH levels are used. Strong ion-exchange groups can be considered to possess a permanent positive or negative charge.

The diminished ionization of weak ion-exchange groups near neutral pH result in less predictable separations if operation in this range is necessary for analyte stability, as in the case of many proteins. In these cases, the use of a strong ion exchanger allows the pH of the mobile phase to be manipulated to protonate or deprotonate the analytes without changing the ionic properties of the packing. For example, certain amino acids are most highly charged at pH less than 4, where a weak cation-exchange support would not be fully charged, but a strong cation-exchange group would.

Because weak ion-exchange groups are not fully charged in certain pH ranges, column equilibration may require more mobile phase or time under those conditions. Conversely, highly bound molecules may release more easily from supports which are not totally ionized. Clearly, careful consideration of the titration curves for an ion-exchange support is an essential aspect of designing appropriate conditions for a separation. A complete description of the charged group of an ion exchanger is necessary to understand its pH characteristics because they are dependent on the exact chemical composition of the bonded phase and the matrix. Convenient descriptions such as "strong," "S," "stable weak ion-exchange," and so forth do not sufficiently describe the ionic characteristics of the packing. The exact pK and functional pH range are also affected by the chemistry of the remainder of the bonded phase and of the matrix. For example, a silica matrix may ion-pair with cationic functional groups or a polymeric layer with amines may



Table 1 Properties of Ion-Exchange Groups

	Functional group	Type	pK	pH Range (approximate)
Anion exchange				
DEAE (diethylaminoethyl)	$-\text{O}-\text{CH}_2-\text{CH}_2-\text{N}^+\text{H}(\text{CH}_2\text{CH}_3)_2$	Weak	5–9	2–9
PEI (polyethyleneimine)	$(-\text{NHCH}_2\text{CH}_2)_n-\text{N}(\text{CH}_2\text{CH}_2-)_m\text{CH}_2\text{CH}_2\text{NH}_2$	Weak	5–9	2–9
Q (quaternary ammonium)	$-\text{CHOH}-\text{CH}_2-\text{N}^+(\text{CH}_3)_3$	Strong	>13	2–12
Cation exchange				
CM (carboxymethyl)	$-\text{O}-\text{CH}_2-\text{COO}^-$	Weak	4–6	6–10
SP (sulfopropyl)	$-\text{CH}_2-\text{CH}_2-\text{CH}_2\text{SO}_3^-$	Strong	<1	4–13
S (sulfonate)	$-\text{R}-\text{CH}_2\text{SO}_3^-$ (R may be methyl with hydroxyl or amide groups)	Strong	<1	3–11

ion-pair with anionic functional groups. The actual titration curves, pK, and/or pH range for a given support should always be consulted.

Hydrophobic Spacer Arms

Ion-exchange functional groups are chemically bonded to the support, often through a polymeric layer which totally covers the matrix. The chemical nature of this coupling chemistry and its spatial characteristics can affect the chromatographic properties. Hydrophobic linkages may impart a nonpolar aspect to the separations. Spacer arms make the functional groups more accessible by distancing them from the support surface. Tentacle IEC bonded phases are a spacer design incorporating a hydrophilic ligand arm [6].

Charge Density

The number of charges, as measured by titration, defines the nominal capacity of a support. The charge density of an ion-exchange support is determined by the number of ionic groups divided by the surface area or the volume. Typical values range from 3 to 370 $\mu\text{Eq/mL}$ of support. The lower values are generally found in non-porous supports. High loading capacities are associated with IEC, especially for porous supports. Weak ion-exchange groups only have maximum capacity in the pH range where they maintain charge — pH less than 9 for DEAE supports and pH greater than 6 for CM.

Counterions

In certain cases, ion-exchange columns are preequilibrated with distinct counterions by the manufacturer.

These ions, such as calcium for amino acids, impart a specific selectivity (see the entry Ion-Exchange, Mechanism and Factors Affecting Separation). Alternatively, a layer of counterions is applied by the user by conditioning a column with the salt of interest. An intermediate step of washing with a weak acid may accelerate the equilibration process.

Matrix

Composition

Ion-exchange supports based on derivatized cellulose and agarose have been popular since the 1960s, particularly for protein analysis. For high-performance liquid chromatography (HPLC), less compressible supports, such as silica and cross-linked polymers, are most commonly used.

Carbohydrate Matrix

Carbohydrate supports such as dextran or agarose are very hydrophilic and easily derivatized with ionic functional groups. They have been very popular for analysis and purification of biological molecules like proteins. One major drawback to these supports is that their volume changes with mobile-phase composition. This has been alleviated in part by higher cross-linking.

Silica Matrix

In silica-based ion exchangers, the silica is bonded through a polymeric layer to a charged ligand group. Operating pH is generally limited to pH 2–8 due to the silica backbone. Although some small-pore silica-based ion exchangers have been synthesized with



silane bonding, large-pore supports (≥ 300 Å) designed for protein analysis have polymeric layers containing ionic functional groups which are very stable and even protect the silica matrix from erosion. Silica columns have several advantages:

1. High mechanical stability
2. Minimal shrinkage or swelling with changes in counterions
3. Stability to organic modifiers (with the restriction of salt solubility)
4. High capacity
5. Good mass transfer
6. Large variety of particle and pore sizes

Polymeric Matrix

Polymeric matrices are also widely available for IEC. Polystyrene cross-linked with divinylbenzene (PS-DVB) is one such polymer, typically available with pore diameters of at least 1000 Å. The repetitive structure of polystyrene permits reproducible coupling of both strong and weak ion-exchange groups; cross-linking adds the rigidity required for high-pressure applications. These polymeric supports have most of the same advantages as silica for IEC. Methacrylate copolymers, which are also used as matrices in IEC, are more hydrophilic than PSDVB.

Pellicular Matrix

A third group of ion-exchange supports are pellicular, consisting of a solid inert core made of PSDVB agglomerated with 350 nm functionalized latex. The quaternary amine groups are closely and uniformly bound on the microbeads, improving flow and reducing non-specific retention. These pellicular supports are primarily used for carbohydrate analysis [7].

Pore Diameter

Pore diameter is a major determinant in ion-exchange capacity because as the pore diameter decreases, there is a tremendous increase in surface area. Nominal loading capacity is directly related to the surface area

and the ligand density; consequently, matrices with the smallest pores exhibit the highest ion-exchange capacities for small, totally included solutes.

The ion-exchange capacities of picric acid correlate with surface area. For example, that of a 100-Å pore was seen to be 1415 $\mu\text{mol/g}$, whereas that of a 300-Å pore was only 656 $\mu\text{mol/g}$ [8]. The capacities for macromolecules such as proteins do not relate directly to surface area because they are excluded by size from portions of small pores and are effectively prevented from reaching all the reactive exchange sites [5,8]. Consequently, larger pores exhibit maximum capacity for macromolecules. For example, a 300-Å pore exhibited maximum capacities of 98 and 130 mg/g for ovalbumin (45,000 MW) and bovine serum albumin (65,000 MW) respectively, because they were able to permeate and bind to the optimum available surface area [5,8].

References

1. R. L. Cunico, K. M. Gooding, and T. Wehr, Ion-exchange chromatography, in *Basic HPLC and CE of Biomolecules*, Bay Bioanalytical Laboratories, Richmond, VA, 1998.
2. *Ion-Exchange Chromatography, Principles and Methods*, Pharmacia Biotech, Sweden.
3. E. D. Katz (ed.), *High Performance Liquid Chromatography: Principles and Methods in Biotechnology*, John Wiley & Sons, New York, 1996.
4. M. I. Aguilar, A. N. Hodder, and M. T. W. Hearn, HPIEC of Proteins, in *HPLC of Proteins, Peptides and Polynucleotides* (M. T. W. Hearn, ed.), VCH, New York, 1991, p. 199.
5. C. T. Mant and R. S. Hodges (eds.), *High-Performance Liquid Chromatography of Peptides and Proteins*, CRC Press, Boca Raton, FL, 1991.
6. W. Muller, *J. Chromatogr.* 510: 133 (1990).
7. Analysis of Carbohydrates by HPAE-PAD, Technical Note 20, Dionex, 1993.
8. G. Vanecek and F. E. Regnier, *Anal. Biochem.* 109: 345 (1980).
9. M. P. Nowlan and K. M. Gooding, HPIEC of proteins, in *High-Performance Liquid Chromatography of Peptides and Proteins* (C. T. Mant and R. S. Hodges, eds.), CRC Press, Boca Raton, FL, 1991, p. 203.



Ion-Exclusion Chromatography

Ioannis N. Papadoyannis

Victoria F. Samanidou

Aristotle University of Thessaloniki, Thessaloniki, Greece

Introduction

Ion exclusion is the term that describes the mechanism by which ion-exchange resins are used for the fractionation of neutral and ionic species. Ionic compounds are rejected by the resin, due to Donnan exclusion, and they are eluted in the void volume of the column. Non-ionic or weakly ionic substances penetrate into the pores of the packing, they are retained and, thus, separation is achieved, as they partition between the liquid inside and outside the resin particles.

Ion-exclusion chromatography is a mode of high-performance liquid chromatography (HPLC) and, thus, the same equipment can be used, with the proper eluent, column, and detection technique. The technique is mostly used for the analysis of organic acids, sugars, alcohols, phenols, and organic bases. It provides a convenient way to separate molecular acids from highly ionized substances. Ionized acids pass rapidly through the column while molecular acids are held up to varying degrees. A conductivity detector is commonly used. Carboxylic acids can be separated by using water, a dilute mineral acid, or a dilute benzoic or succinic acid as eluent.

Discussion

As neutral species, rather than ions, are being separated, ion-exclusion chromatography cannot be considered as a form of ion chromatography; although ion-exchange polymers are used, ion-exchange mechanisms are not involved.

Anions, most commonly simple carboxylic acids (e.g., tartaric, malic, citric, lactic, acetic, succinic, formic, propionic, butyric, etc.), are separated on cation-exchange resins in acidic form. Salts of weak acids can also be analyzed, as they are converted to the corresponding acid by the hydrogen ions in the exchanger. Cations (weak bases and their salts) are separated on anion-exchange resins in the hydroxide form.

In order to understand the mechanism of ion-exclusion chromatography, the behavior of the resin, in an

aquatic medium, must be taken into account. In this case, three parts can be distinguished:

1. The resin network
2. The liquid inside the resin particles
3. The liquid between the resin particles

The first acts as a semipermeable membrane between the stationary liquid phase within the resin and the mobile liquid phase between the resin beads.

Ionic groups are fixed on the resin and movement of ions across the membrane takes place as predicted by Donnan theory. The ion-exclusion mechanism involves interaction between partially ionized species and fully ionized polymer matrix. Electrostatic repulsive forces, between strong electrolytes (e.g., chloride, in the case of using HCl as eluent) and the ionic groups fixed on the resin (e.g., sulfonate), prevent them from entering into the resin, due to high ionic concentration inside the resin. Because ionized analytes are not retained, they are excluded from the polymer, migrate rapidly through the column, and are eluted at the column void volume. Partially ionized and neutral species (e.g., the undissociated forms of the analyte acids), as they penetrate into the pores of the resin, are distributed between the mobile phase in the column and the immobilized liquid in the pores of the packing. Separation is accomplished by differences in acid strength, size, and hydrophobicity.

The degree of retardation increases with the decrease of the ionization degree and, additionally, depends on polar attractions between analyte and fixed functional groups and on different van der Waals forces between an analyte and the hydrocarbon part of the resin. Elution order is related to pK_a values for ionic species and to the molecular size for neutral compounds.

Members of a homologous series, such as formic, acetic, and propionic acids, elute in the order of increasing pK_a (decreasing acid strength). Dibasic acids elute sooner than monobasic acids of the same carbon number. Isoacids elute earlier than normal acids. Double bonds retard elution, whereas keto groups increase elution rate.



Microporous polystyrene divinylbenzene resins are used, operating at pressures sometimes exceeding 3000 psi; unlike silica-based packings, they are stable from pH 0 to 14. For ion-exclusion separation of organic acids and weakly acidic compounds, strongly acidic, high-capacity, sulfonated styrene divinylbenzene in the hydrogen form are used. For organic bases, separation columns are packed with strongly basic copolymer with a quaternary ammonium functional group. The degree of cross-linking (the percentage of divinylbenzene in the copolymer) affects the retention of weakly ionized species; the lower the degree of cross-linking, the longer the retention time of acid, either strong or weak. This is due to the fact that as cross-linking decreases, ions more readily penetrate the resin, where they are held up.

As aforementioned, a large number of organic and weak inorganic acids can be eluted from the hydrogen form of cation-exchange resin using water as the eluent. However, the addition of mineral acid to the water eluent suppresses the ionization of strong and moderately strong organic acids, allowing them to partition into the resin phase and, thus, improve selectivity, as retention times on the resin are increased. The addition of inorganic salts, such as $(\text{NH}_4)_2\text{SO}_4$ or organic modifiers (acetonitrile, isopropanol, ethanol, methanol), to the eluent may improve separation. Acetonitrile, for example, decreases the retention time of relatively nonpolar compounds.

Ion-exclusion chromatography can couple to ion chromatography to improve the chromatographic resolution of inorganic anions and organic acids in complex matrices. The dual system can be either in the order IEC/IC or IC/IEC.

Various detection systems can be used in ion-exclusion chromatography, among them ultraviolet (UV)/vis spectrophotometry, conductivity, electrochemistry, fluorometry, refractive index (RI) measurement, are the most common techniques. Additionally, combined detection systems (e.g., UV/amperometry, UV/RI) may be used, leading to enhanced selectivity.

Ultraviolet detection is useful, especially when water or sulfuric acid, which do not absorb in the UV region, are used. Detection for most nonaromatic carboxylic acids is accomplished at 210 nm.

Conductivity detection is preferred when water is used as eluent; then ionizable analytes are readily detected. However, in the case where HCl is used as the eluent, the analytical column is followed by a suppressor column, packed with a cation-exchange resin

in the silver form. The hydrogen ions of the eluent are exchanged for silver ions, which then precipitate chloride ions, thus removing the ions contributed by the eluent and enhancing the analyte's signal.

Electrochemical detectors (coulometric and amperometric) are used when the analytes are electrochemically active or capable of being coupled to an electrochemical reaction.

Refractive index monitors are used in food analysis, for detecting carbohydrates, alcohols, and other substances with weak or no UV absorption.

With the combination of RI and UV, simultaneous detection of organic acids, carbohydrates, and alcohols with one sample injection can be achieved. Postcolumn reactions can be used for fluorometric detection of amino acids, with excellent sensitivity and selectivity.

Ion-exclusion chromatography finds numerous applications for identification and determination of acidic species in complex matrix materials, such as dairy products, coffee, wine, beer, fruit juice, and other commercial products which can be quickly analyzed with minimal sample preparation before injection (usually only filtration, dilution, or centrifugation). Organic acid determination is also of great importance in biomedical research (e.g., physiological samples, in which most of the Krebs cycle acids (tricarboxylic acid cycle) are present).

Organic acids can be detected in the parts per billion range. With preconcentration, this limit can be further decreased. A typical ion-exclusion chromatogram of organic acids separation is presented in Fig. 1.

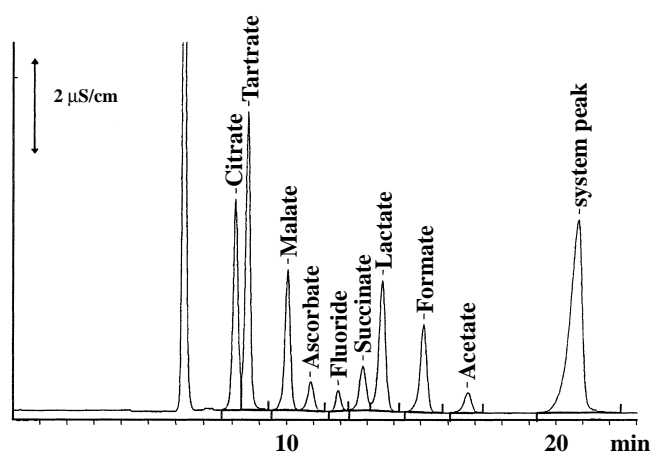


Fig. 1 Determination of organic acids and fluoride using ion-exclusion chromatography with direct conductivity detection, using mmol/L H_2SO_4 , and 10% acetone as eluent. (From Metrohm Ltd., with permission.)

Suggested Further Reading

- Gierde, D. and J. Fritz, *Ion Chromatography*, 2nd ed., Alfred Huethig Verlag, New York, 1987.
- Gierde, D. and H. Mehra, *Advances in Ion Chromatography Volume 1* (P. Jandik and R. Cassidy, eds.), Century International, Franklin, MA, 1989.
- Haddad, P. and P. Jackson, *Ion Chromatography, Principles and Application*, Elsevier, Amsterdam, 1990.
- Kaine, L., J. Crowe, and K. Wolnic, *J. Chromatogr.* 602: 141–247 (1992).
- Metrohm IC Application Note No. O-5, Application Notes, Metrohm, Herisau (1996).
- Small, H., *Ion Chromatography*, Plenum Press, New York, 1989.
- Tanaka, K. and J. Fritz, *Anal. Chem.* 59: 708–712 (1987).
- Tarter, J., *Ion Chromatography*, Chromatographic Science Series Vol. 37, Marcel Dekker, Inc., New York, 1987.
- Togami, D., L. Treat-Clemons, and D. Hometchko, *Int. Lab.* 2: 29–33 (1990).



Ion-Interaction Chromatography

Teresa Cecchi

Università degli Studi di Camerino, Camerino, Italy

Introduction

Under reversed-phase high-performance liquid chromatography (HPLC) conditions, ionic compounds are weakly retained. On the contrary, when an ion-interaction reagent (IIR), which is a large lipophilic ion, is added to the mobile phase, ionized species of opposite charge are separated on reversed-phase columns with adequate retention. This is the chromatographic approach of reversed-phase ion-interaction chromatography (IIC). It has become a widely used separation mode in analytical HPLC because it provides a useful and flexible alternative to ion-exchange chromatography. Better selectivity, enhanced resolution, and retention are usually gained by this separation strategy.

According to the qualitative retention model of Bidlingmeyer, the lipophilic IIR, flowing under isocratic conditions, dynamically adsorbs onto the alkyl-bonded apolar surface of the stationary phase, forming a primary charged ion layer. The corresponding counterions are found in the diffuse outer region to form an electrical double layer. This charged stationary phase can then more strongly retain analyte ions of the opposite charge.

Unlike conventional ion exchange, IIC can be used to separate nonionic and ionic or ionizable compounds in the same sample, because retention of an analyte involves its transfer through the electrical double layer and depends on both electrostatic interactions and adsorptive (reversed-phase) effects.

In recent years, many examples of applications of IIC have been reported. They essentially concern the separation of organic and inorganic ions in the environmental, pharmaceutical, food, and clinical fields.

Retention Mechanism

The larger number of names (e.g., ion-pair chromatography, dynamic ion-exchange chromatography, heteric chromatography, soap chromatography) which have been given to the IIC mode sheds light on the uncertainty concerning the retention mechanism. A majority of the proposed models are stoichiometric. They

suggest that the oppositely charged analyte and IIR form a complex, according to a clear reaction scheme, either in the mobile-phase (ion-pair model) or at the stationary-phase surface (dynamic ion-exchange model). According to the first theory, the uncharged ion pair between oppositely charged analyte and IIR, which is formed in the mobile phase, is then more strongly retained by the stationary phase. The second theory presumes that solute ions undergo an ion-exchange process, at exchange sites dynamically generated by the adsorption of the IIR at the stationary phase. Knox and Hartwick demonstrated that both models lead to identical retention equation.

These models, although of practical and intuitive value, are not well founded in physical chemistry. The pioneering, even if qualitative, work of Bidlingmeyer demonstrated that IIRs adsorb onto the stationary phase. It follows that stoichiometric equilibrium constants, which depend on the change in free energy of adsorption of the analyte, cannot be considered constant if the IIR concentration in the mobile phase increases, because the stationary phase surface properties (including its charge density) are modified. The multibody interactions and long-term forces involved in IIC can better be described by a thermodynamic approach.

A quantitative nonstoichiometric model was developed by Ståhlberg and coworkers. The model applies the Gouy–Chapman electrostatic theory to describe the interactions between charged species and it does not assume the formation of any chemical complexes: The adsorption of the IIR onto the stationary phase establishes a certain electrostatic surface potential, because its counterion has a lower adsorption tendency. An electrical double layer develops and a difference in electrostatic potential is created between the electroneutral bulk of the mobile phase and the net charged surface. The intuitive view of the effect of the IIR on retention is an electrostatic repulsion or attraction of the analyte to the charged stationary-phase surface, according to the analyte and IIR charge status. However, the adsorptive (reversed phase) effects are also considered, to evaluate the total free energy of adsorption of the solute: The latter is partitioned into a



“chemical” and an electrostatic free energy. This is a first approximation: The “chemical” part depends on the concentration of the IIR, as it determines a dynamic modification of the stationary-phase properties. This electrostatic theory of IIC has been implemented by taking into account the competition between IIR and analyte for a limited surface area, and the different surface area requirements of analyte and IIR (multi-site occupancy model). However, the main drawback of this powerful electrostatic theory is the complex algebraic form of the resulting equations; hence, a series of approximations has to be made to obtain a relationship between the analyte capacity factor and mobile-phase concentration of IIR, which is of interest for practical work.

Cantwell and co-workers proposed a surface adsorption, diffuse-layer ion-exchange double-layer model in which they underlined the role of the diffuse part of the double layer by assigning a stoichiometric constant for the exchange of ions.

Stranahan and Deming proposed a thermodynamic model for IIC in which the distribution a sample between the mobile and the stationary phase is discussed in terms of chemical potentials in both phases.

Additional peaks relative to the number of components injected are often obtained in IIC. These so-called “system peaks” confirm the proposed mechanism of dynamic functionalization of the stationary phase. They can be explained by taking into account that IIR ions are locally adsorbed onto (desorbed from) the stationary phase by injection of adsorbophilic solute ion of the opposite charge (of same charge). This change in the eluent composition, created by the sample injection, migrates along the column and give a signal if at least one of the eluent components can be detected. The same rationale provides the explanation for the indirect ultraviolet (UV) visualization (or amplification) of otherwise non-UV-absorbing samples, when a UV-absorbing lipophilic ion is added to the eluent.

Influence of Experimental Parameters on Retention

The optimization of separations performed with IIC and the rationalization of analytes retention behavior are not easy tasks because they are influenced by many interdependent factors. This allows a fine modulation of their effects to achieve tailor-made separations.

Experimental design can be very helpful, and a number of chemometric optimization methods are

present in the literature. Neural network models provided a good prediction power and a great versatility, without the need to develop any equations.

The following presents the effect of varying some individual factors on analyte retention.

Ion-Interaction Reagent

Type

The hydrophobic character of the IIR increases with increasing its chain length. More lipophilic reagents have higher adsorption constants, hence the effect of increasing chain length is qualitatively similar to the effect of increasing IIR concentration (see below) with regard to the degree of stationary-phase coverage. The use of multiply-charged IIRs allows the chromatographer to obtain larger changes of analyte retention. If chiral compounds are used as the IIR, the separation of the enantiomeric forms of the analyte may be achieved. The most popular IIRs are listed in Table 1.

Concentration

If the eluent concentration of the IIR increases, the amount of the adsorbed IIR also increases, according to its adsorption isotherm. This induces a higher surface potential on the stationary phase but also adsorption competes between analyte and IIR for the available stationary phase sites. Therefore, the following hold:

1. If the charge status of analyte and the IIR is the same, a decrease in retention is observed because of electrostatic repulsion between solute and charged stationary phase, and because of adsorption competition.
2. If the charge status of analyte and the IIR is the opposite, an increase in retention is expected because of electrostatic attraction between solute and charged stationary phase. A parabola-like dependence of analyte capacity factors on

Table 1 Commonly Used Ion-Interaction Reagents

Cationic IIRs	Anionic IIRs
Tetramethylammonium	Butanesulfonate
Tetraethylammonium	Pentanesulfonate
Tetrabutylammonium	Hexanesulfonate
Cetyltrimethylammonium	Octanesulfonate
Octylammonium (from octylamine)	Dodecanesulfonate

IIR concentration is observed if the investigated concentration range is broad. For narrower ranges, a linear increase may hold. Some authors have emphasized that analyte retention passes through a maximum because if the ionic strength is not kept constant when increasing the IIR concentration, there is a competition between analyte ion and IIR counterion; this competition counteracts the retention increase. However, a foldover of the plot may still occur even if the ionic strength is kept constant, because there is a critical value of the IIR concentration at which the positive effect of the electrostatic attraction is balanced by the negative effect of adsorption competition for the available stationary-phase surface area.

3. If the analyte is uncharged, a very weak decrease in retention is usually observed, primarily because of adsorption competition for the stationary phase.

Increasing the IIR above its critical micelle concentration leads into the field of micellar chromatography in which analyte may partition between the mobile phase and both the stationary phase and the micelle.

Mobile-Phase Composition

Organic-Modifier Concentration

In IIC, the logarithm of the analyte capacity factor is described as a linear function of the organic-modifier concentration in the mobile phase. When the sample ion is in the same charge status as the IIR, the slope of the linear relationship, if compared to the original reversed-phase slope, becomes steeper (the contrary is observed for oppositely charged combinations). This can be explained by taking into account that the organic modifier, through desorption effects, decreases the retention of ionic solutes via the simultaneous decrease of the free energy of adsorption of both the analyte and IIR.

Ionic Strength

An increase in salt concentration in the bulk mobile phase provides those counterions which are able to reduce, according to the Gouy–Chapman electrostatic theory, the electrostatic stationary-phase surface potential. Hence, the adsorption of the IIR may increase, even if its concentration in the eluent is the same, because of lower electrostatic “self”-repulsion. However,

the net effect is a reduced surface potential: The ion interactions decrease, and analyte retention may be modulated.

From an intuitive point of view, the inorganic ions are eluting agents because they limit the interaction of oppositely charged analyte and IIR, via a competing equilibrium for adsorbed lipophilic ions. This view gives the rationale for the use of mobile-phase additives, such as sodium carbonate, to avoid the unnecessarily high resolution which may be obtained between analytes of different charge.

It has to be emphasized that the nature of the electrolyte ions influences the surface potential value because the effective surface charge concentration is reduced if slight hydrophobic, adsorbophilic electrolytic counterions are included in the eluent.

The influence of moderate increase of ionic strength on the “chemical” part of the free energy relative to the analyte transfer from the mobile to the stationary phase has been usually neglected.

Mobile-Phase pH

The eluent pH value affects the degree of ionization of the species involved in ion interaction. Hence, the greatest retention is obtained for completely dissociated species. This is the opposite of what is observed in reverse-phase chromatography.

Unexpected pH dependencies were explained by (a) competition between negative analyte ions and OH^- ions for interaction with the electrical double layer and (b) a mixed retention mechanism in which reverse-phase partition or interaction with unreacted silanols from the stationary-phase base may play a significant role.

Reversed-Phase Stationary Phase

A number of different packings were used in IIC, including the newly developed graphitized carbon column, which has excellent chemical and physical resistance. The use of polymeric material has the drawback of poor physical resistance. However, a wider pH range is investigable and the affinity for certain IIR is higher, by comparison with the silica-based reversed-phase columns. However, discordant results are present in literature reports with regard to the chromatographic efficiency.

With regard to the silica-based reversed-phase stationary phase, unreacted residual silanol groups may play a significant role in IIC because it was shown that



they are ion-exchange sites not only for analyte cations but also for alkylammonium IIR. The higher retentions that were noticed for the silica-based stationary phase if compared to end-capped or polymer-based packings supports this.

The reproducibility of results obtained with silica-based reversed phases, of the same declared characteristics but from different manufacturers, was sometimes poor, probably because of the properties of the silica used and the different reaction conditions in the alkylation of the support.

Stationary phases with higher hydrophobicities and adsorption capacities show increased retention of both solute and IIR. Hence, an increased capacity factor value should be expected, even if anomalies can be due to direct competition of solute and IIR for the available stationary phase.

Temperature

Temperature control is very important for obtaining reproducible separations. Indeed, the adsorption of the IIR onto the stationary phase follows an adsorption isotherm; hence, an increase of the column temperature leads to a decreased amount of the adsorbed IIR, even if its concentration in the mobile phase is constant. This, in turn, determines a decreased absolute surface potential and a modification of the solutes' capacity

factors. Usually, a temperature increase results in an improved resolution and faster separation, even if a reversal of the elution sequence of the components of a mixture may sometimes be observed, because of the interplay of electrostatic and reversed-phase interaction which are characterized by different enthalpies.

Suggested Further Reading

- Bartha, A. and J. Ståhlberg, *J. Chromatogr. A* 668: 255–284 (1994).
 Bidlingmeyer, B. A., *J. Chromatogr. Sci.* 18: 525–539 (1980).
 Chen, J. C., S. G. Weber, L. L. Glavina, and F. F. Cantwell, *J. Chromatogr.* 656: 549–576 (1993).
 Gennaro, M. C., *Adv. Chromatogr.* 35: 343–381 (1995).
 Knox, J. H. and R. A. Hartwick, *J. Chromatogr.* 204: 3–21 (1981).
 Okamoto, T., A. Isozaki, and H. Nagashima, *J. Chromatogr. A* 800: 239–245 (1998).
 Pietrzy, D. J., *Chromatogr. Sci.* 78: 413–462 (1998).
 Saccherio, G., M. C. Bruzzoniti, C. Sarzanini, E. Menastasi, H. J. Metting, and P. M. J. Coenegracht, *J. Chromatogr. A* 799: 35–45 (1998).
 Stranahan, J. J. and S. N. Deming, *Anal. Chem.* 54: 2251–2256 (1982).
 Weiss, J., *Ion Chromatography*, 2nd ed. VCH, Weinheim, 1995, pp. 239–289.



Ion-Pairing Techniques

Ioannis N. Papadoyannis

Anastasia Zotou

Aristotle University of Thessaloniki, Thessaloniki, Greece

Introduction

Ion-pair chromatography (IPC) is of relatively recent origin, being first applied in the mid-1970s. Much of the development work in both theory and practice was performed by Schill and co-workers. At various times, IPC has also been called extraction chromatography, chromatography with a liquid ion exchanger, soap chromatography, paired-ion chromatography and ion-pair partition chromatography.

Background Information

When solute ions (A^-) are added to a chromatographic system containing pairing ions (B^+) and associated counter ions (C^-), the degree of retention of (A^-) depends on the following equilibrium:



with an extraction constant

$$E_{AB} = \frac{[AB_{org}]}{[A_{aq}^-][B_{aq}^+]} \quad (2)$$

In the simplest case of IPC, it can be assumed that the sample and counterions are soluble only in the aqueous mobile phase and the ion pair formed is soluble only in the organic stationary phase.

Assuming that the concentration of the pairing ion in the aqueous phase is high compared to that of the solute ion, the *distribution coefficient* of A^- , D_A^- , is given by

$$D_A^- = \frac{[AB_{org}]}{[A_{aq}^-]} = E_{AB}[B_{aq}^+] \quad (3)$$

The *capacity factor* k' is related to E_{AB} as follows (in the reversed-phase mode):

$$k' = \frac{V_S}{V_m} \left(\frac{[AB_{org}]}{[A_{aq}^-]} \right) \quad (4)$$

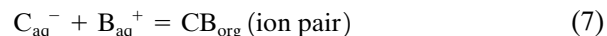
$$= \frac{V_S}{V_m} (E_{AB}[B_{aq}^+]) \quad (5)$$

or

$$k' = D_A^- \frac{V_S}{V_m} \quad (6)$$

Because the capacity factor k' is proportional to $1/D$ in normal-phase chromatography and to D in reversed-phase chromatography, it follows that k' in IPC is inversely proportional to the pairing ion concentration in the normal-phase situation but directly proportional in the reversed-phase case.

When the pairing ion is very hydrophobic, B^+ will be extracted into the organic phase with its normal counterion C^- , according to



Subtracting it from Eq. (1) gives



This is very similar to ion-exchange chromatography with an equilibrium constant:

$$K_{IE} = \frac{[AB_{org}][C_{aq}^-]}{[CB_{org}][A_{aq}^-]} \quad (9)$$

This gives

$$D_A^- = \frac{[AB_{org}]}{[A_{aq}^-]} = K_{IE} \frac{[CB_{org}]}{[C_{aq}^-]} \quad (10)$$

from which it follows that k' is inversely proportional to the concentration of the counterion in the aqueous phase.

The latter situation is usual in the reversed-phase mode, where the hydrophobic ion is adsorbed onto the bonded hydrocarbon of the packing material. Thus, we can distinguish three different techniques:

1. Normal-phase IPC, where the support is coated with an aqueous stationary phase containing the pairing ion and the ion pairs are partitioned between the stationary phase and an organic mobile phase
2. Reversed-phase IPC, where the liquid stationary phase is organic and the pairing ion is introduced in the aqueous mobile phase
3. Reversed-phase IPC, using a chemically bonded stationary phase and a hydrophobic pairing ion in the aqueous mobile phase



The use of bonded-phase partition systems is generally preferred over mechanically held stationary phases; this gives advantage to technique 3.

Normal-Phase Ion-Pair Chromatography

The support is loaded with the aqueous stationary phase containing the pairing ion by one of the following three methods:

1. The stationary phase or a concentrated solution of the stationary phase in acetone is pumped through the packed column bed. The excess is then removed by passing eluent or hexane, followed by eluent saturated with stationary phase, until equilibrium is reached. Equilibrium is normally achieved when stable k' values are obtained for a series of representative solutes. This usually requires passage of several hundred milliliters of eluent.
2. The stationary phase can be loaded onto the column in several large plugs (0.1–1.0 mL) using a stopped-flow technique and equilibrium is achieved in the same way as previously.
3. The eluent, which has been preequilibrated with the stationary phase, is pumped through the column until stable k' values are obtained. The stationary phase is adsorbed onto the support surface, but at equilibrium, the pores of the support are not as completely filled as they are in the columns obtained by the first two methods. The equilibration can be a very time-consuming procedure, but the columns thus obtained are stable and reproducible.

Because the columns are in an equilibrium situation, it is obvious that gradient elution is not possible. In the normal-phase situation, the k' value of a solute is inversely proportional to the pairing ion concentration. Because the pairing ion is in the stationary phase, this concentration is not readily changed, and for this reason, retention is normally controlled by modification of the eluent. Hydrocarbon or chlorinated hydrocarbon solvents are usually employed with a small percentage of alcohol as a modifier. Varying the concentration or nature of the alcohol can produce the required changes in retention or selectivity.

Very high efficiencies have not usually been achieved with normal-phase IPC; the advantage of the reversed-phase mode, where the pairing ion concentration can be easily altered, has led to almost total takeover in the ion-pair field. The normal phase has two advantages compared to the reversed-phase mode:

1. The use of ultraviolet (UV) absorbing or fluorescent ions to enhance or enable the detection of nonabsorbing solutes
2. The possibility of varying selectivity by varying the organic-phase composition.

Reversed-Phase Ion-Pair Chromatography

Most often, pentanol or butyronitrile is used as the stationary phase loaded onto a hydrophobic support such as silanized silica.

The equilibration time depends on the hydrophobicity of the support (the coating of pentanol on a hydrocarbon-bonded silica takes no longer than 2 h at a flow rate of approximately 1 mL/min).

The retention of analytes can be regulated by varying the following factors:

1. The capacity factor increases with the hydrophobicity of the pairing ion. For hydrophilic solutes, hydrophobic pairing ions are chosen, and vice versa.
2. The capacity factor increases linearly with pairing ion concentration. Alternatively, gradient elution can be performed by decreasing the pairing ion concentration.
3. The choice of the organic phase affects the selectivity of the system.

Reversed-Phase Ion-Pair Chromatography Using a Chemically Bonded Stationary Phase

This is, by far, the most commonly used form of reversed-phase IPC. This technique has been also called *soap chromatography* although, in soap chromatography, the use of detergents as counterions is introduced.

Here, the columns (with C_8 or C_{18} packings) are prepared by equilibrating the stationary bonded phase with the mobile phase containing the pairing ion. The ion-pair reagent is attracted to the stationary phase because of its hydrophobic alkyl group and the charge carried by the reagent thereby attaches to the stationary phase.

The surface of a C_8 or C_{18} column packing is shown in Fig. 1 as a rectangle covered by sorbed molecules of a negative ion-pair reagent (e.g., hexane sulfonate, $C_6\text{-SO}_3^-$). The negative charge on the stationary phase is balanced by the positive ions (Na^+) from the reagent and/or buffer. A positively charged sample ion (protonated base BH^+) can exchange with a Na^+ ion as shown (arrows), resulting in the retention of the sample ion by an ion-exchange process.



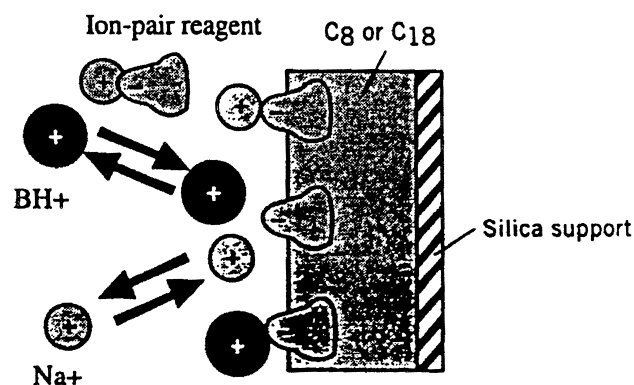


Fig. 1 Pictorial representation of IPC retention of a protonated base (BH⁺); Na⁺ is the mobile-phase cation; the IPC reagent is hexane sulfonate. (Reprinted from L. R. Snyder, J. J. Kirkland, and J. L. Glajch, *Practical HPLC Method Development*, 2nd ed., 1997, by permission of John Wiley & Sons, Inc.)

For each ion-pair reagent, the column uptake increases for a higher reagent concentration in the mobile phase, but then levels off as the column becomes saturated with the reagent. The more hydrophobic reagents are retained more strongly and saturate the column at a lower mobile-phase reagent concentration (10⁻⁵M), but equilibration may take several hours. Less hydrophobic ion-pair reagents are added at a slightly higher concentration (10⁻⁴M–10⁻³M) and equilibrium is reached much faster (1–2 h at a flow rate of 1 mL/min). This is shown in Fig. 2a, where the concentration of reagent in the stationary phase (P⁻)_s is plotted versus the concentration of reagent in the mobile phase (P⁻)_m for two reagents of different hydrophobicity.

The change in sample retention, as the ion-pair reagent concentration increases, is shown in Fig. 2b for a hydrophilic sample compound BH⁺. Once the column becomes saturated with the reagent, the sample retention levels off. Because IPC retention involves an ion-exchange process, further increases in reagent concentration lead to an increase in the counterion concentration (Na⁺), which competes with the retention of the sample ion on the column.

In practice, when very hydrophobic pairing ions are used, the columns are irreversibly altered, because the ions can never be completely removed. Once equilibrium is reached, the columns are stable and can be used for several months. The columns should be stored in the mobile phase because of the lengthy equilibration times. Only if the column is not used for an extended period of time should one consider storing the column in an organic solvent.

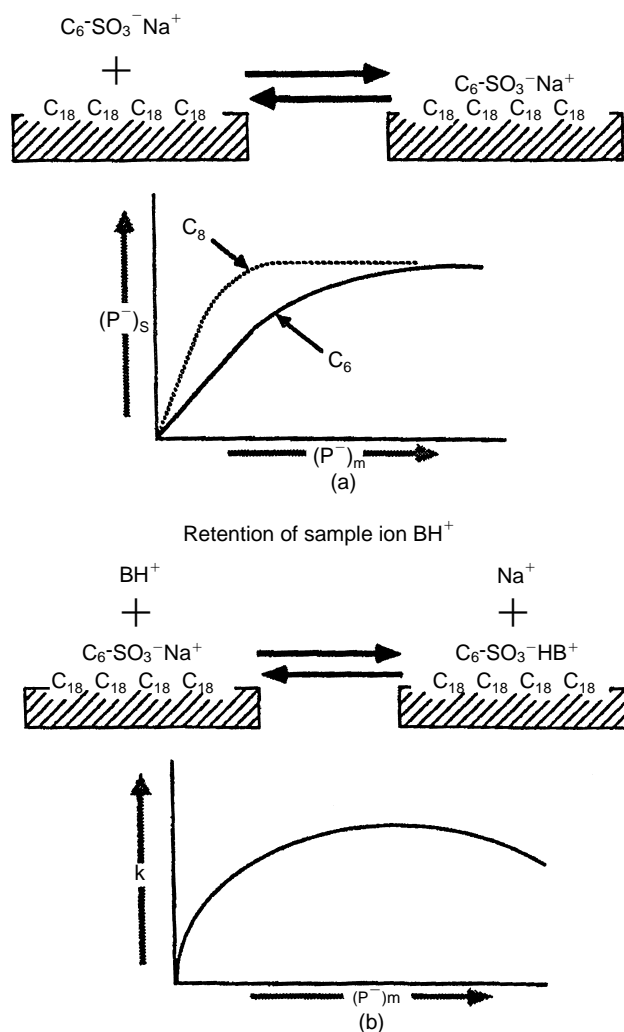


Fig. 2 Effect of ion-pair reagent concentration on separation. (a) Sorption of the ion-pair reagent as a function of concentration for reagents of different hydrophobicity (C₆- and C₈-sulfonates); (b) retention as a function of reagent concentration. (Reprinted from L. R. Snyder, J. J. Kirkland, and J. L. Glajch, *Practical HPLC Method Development*, 2nd ed., 1997, by permission of John Wiley & Sons.)

Design of an Ion-Pair Separation

Unless there is a specific reason to choose a normal-phase system, IPC should be carried on in the reversed-phase mode, using chemically bonded stationary phases.

The best counterion and pH depend on the kind of sample to be separated. Most ion-pair reagents used today are either alkyl sulfonates or tetraalkyl ammonium salts, either of which allow UV detection above 210 nm. The IPC aqueous phase must be adequately



buffered with respect to both pH and concentration of the counterion.

Inadequate buffering of the aqueous phase is a source of band tailing in IPC. Conventional buffers, such as citrate and phosphate, have been used and, in some cases, the counterion itself is an adequate buffer. For separations at low pH, 0.1M–0.2M solutions of a strong acid provide adequate buffering. Inadequate buffering of the aqueous phase is a source of band tailing in IPC.

In reversed-phase IPC, maximum k' values are obtained at intermediate values of pH, where the sample compounds are completely ionized and ion-pair formation is at a maximum. As the pH of the mobile phase is lowered, sample anions A^- begin to form the un-ionized acids HA, leading to a smaller number of sample ion pairs in the stationary phase. Acids are usually separated at a pH of 7–9, whereas bases are separated at a pH of 1–6.

In reversed-phase systems, the solvent strength is readily varied by changing the counterion or its concentration. When all sample ions are fully ionized, a change in solvent strength via a change in counterion concentration leads to minimal changes in separation selectivity. The concentration of the counterion is usually 0.005M–0.05M, except for perchlorate (0.5M–1M) or the detergents used in soap chromatography (e.g., 1 wt% of counterion). Buffer concentrations are similar to those used in ion-exchange chromatography (0.001M–0.5M).

An increase in the alkyl chain length of the counter-ion increases retention in reversed-phase

IPC by up to 2.5 times per added $-\text{CH}_2-$ group in the counterion.

Apart from an increase in the counterion concentration, an increase in ionic strength of the aqueous phase generally reduces the formation of ion pairs, as a result of the competition of secondary ions in forming ion pairs with the counterion. One study showed a twofold to threefold change in k' for each doubling of ionic strength.

For reproducible separations by IPC, it is important to thermostat the column. Temperature effects in IPC are more important than in some other liquid chromatography methods.

Suggested Further Reading

- Bidlingmeyer, B. A., *Practical HPLC Methodology and Applications*, John Wiley & Sons, New York, 1992, pp. 157–165.
- Gilbert, M. T., *High Performance Liquid Chromatography*. IOP Publishing, Wright, Bristol, U.K., 1987, pp. 227–253.
- Snyder, L. R. and J. J. Kirkland, *Introduction to Modern Liquid Chromatography*, 2nd ed. John Wiley & Sons, New York, 1979, pp. 454–482.
- Snyder, L. R., J. J. Kirkland, and J. L. Glajch, *Practical HPLC Method Development*, 2nd ed. John Wiley & Sons, New York, 1997, pp. 317–341.
- Su, S. C., A. V. Hartkopf, and B. L. Karger, *J. Chromatogr.* 199: 523 (1976).



Katharometer Detector for Gas Chromatography

Raymond P.W. Scott

Scientific Detectors Ltd., Banbury, Oxfordshire, England

Introduction

The katharometer detector [sometimes spelled “catharometer” and often referred to as the *thermal conductivity detector* (TCD) or the *hot-wire detector* (HWD)] is the oldest commercially available gas chromatographic (GC) detector still in common use. Compared with other GC detectors, it is a relatively insensitive detector and has survived largely as a result of its almost universal response. In particular, it is sensitive to the permanent gases to which few other detectors have a significant response. Despite its relatively low sensitivity, the frequent need for permanent gas analysis in many industries probably accounts for it still being the fourth most commonly used GC detector. It is simple in design and requires minimal electronic support and, as a consequence, is also relatively inexpensive compared with other detectors.

Discussion

In the late 1940s and early 1950s, the katharometer was developed for measuring the amount of carbon dioxide in flue gases. However, with the advent of GC, its use as a detector was investigated by Ray [1]. It was soon established as a very effective GC detector and was found to be simpler to fabricate than the gas density bridge, but had about the same sensitivity and linearity. For a while, it was the only detector that was commercially available. At the time, its mode of action was the subject of some controversy, as it was not clear whether it responded to changes in the *thermal conductivity* or the *specific heat* of the column eluent. The response of the detector was examined in detail by Mellor [2] and Harvey and Morgan [3] in 1956 and it would appear that no such detailed studies have been carried out since that time. It was concluded that the katharometer responded to both changes in thermal conductivity *and* to changes in the specific heat of its surroundings. In any particular system, depending on the operating conditions employed, one or the other property may dominate in controlling the response of the detector. The relationship, however, is

not simple and it was not found possible to accurately predict the response of the detector from a knowledge of the specific heat and thermal conductivity of the gases or vapors involved.

The basic design of a katharometer is as follows. A filament carrying a current is situated in the column eluent. Under equilibrium conditions, the heat generated in the filament will equal the heat lost by conduction, convection, and radiation and the filament will assume a constant temperature. The filament is constructed from a metal, such as platinum, that has a high temperature coefficient of resistance, and at the equilibrium temperature, the resistance of the filament and, thus, the potential across it will be constant. The heat lost from the filament will depend on the thermal conductivity of the gas, its specific heat, and the thermal emissivity of the filament surface. Both the thermal conductivity and the specific heat of the gas will change in the presence of a different gas or solute vapor. As a result, the temperature of the filament will change, causing a change in potential across the filament. This potential change is amplified and either fed to a suitable recorder or regularly sampled by an appropriate data acquisition system.

As the device responds to the heat lost from the filament, the katharometer detector is extremely *flow* and *pressure* sensitive. Consequently, all katharometer detectors must be carefully thermostatted and must be fitted with reference cells to help compensate for changes in pressure or flow rate. There are two basic katharometer designs: the “in-line” cell, where the column eluent actually passes directly over the filament, and the “off-line” cell, where the filaments are situated away from the main carrier gas stream and the gases or vapors only reach the sensing element by diffusion. Due to the high diffusivity of vapors in gases, the diffusion process can be considered as almost instantaneous. Diagrams of the two katharometer designs are shown in Fig. 1.

The sensitivity of the katharometer is only about 10^{-6} g/mL (probably the least sensitive of all GC detectors) and has a linear dynamic range of about 500 (the response index lying between 0.98 and 1.02). It is, however, a general detector and will sense all permanent



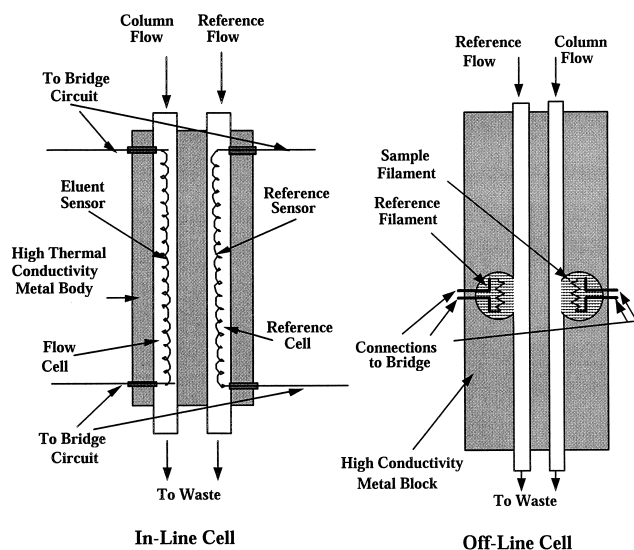


Fig. 1 Katharometer cells.

gases and vapors other than the gas that is used as the carrier gas. Its universal response is one reason for its survival as a GC detector, despite its very limited sensitivity. Although the least glamorous, this detector can be used in most GC analyses that utilize packed columns and where there is no limitation to sample availability. Although small-volume katharometers have been designed for use with capillary columns, the

katharometer is rarely used with such columns, again due to its relatively low sensitivity. The device is simple, reliable, rugged, and, as already stated, comparatively inexpensive. As a consequence, it has found use in less than ideal environments where GC is employed for process monitoring and process control. If constructed of platinum and Teflon, the katharometer is one of the few detectors that can be used for detecting very corrosive materials such as the halogens, uranium hexafluoride, volatile inorganic acids, and so forth.

References

1. N. H. Ray, *J. Appl. Chem.* 4: 21 (1954).
2. N. Mellor, in *Vapor Phase Chromatography* (D. H. Desty and C. L. A. Harbourn, eds.), Butterworths, London, 1957, p. 63.
3. D. Harvey and G. O. Morgan, in *Vapor Phase Chromatography* (D. H. Desty and C. L. A. Harbourn, eds.), Butterworths, London, 1957, p. 74.

Suggested Further Reading

Scott, R. P. W., *Chromatographic Detectors*, Marcel Dekker, Inc., New York, 1996.
 Scott, R. P. W., *Introduction to Gas Chromatography*, Marcel Dekker, Inc., New York, 1998.

Kovats Retention Index System

Igor G. Zenkevich

Chemical Research Institute, St. Petersburg State University, St. Petersburg, Russia

Introduction

In “classical” chromatographic methods (excluding hyphenated techniques), analytical signals are two dimensional. Every chromatographic peak may be characterized by two parameters: area, which is proportional to the quantity of substance being eluted from column, and position on the chromatogram (retention time, t_R), which reflects the interaction between the sorbate (analyte) and sorbent (stationary phase). This interaction is the sole source of information about the chemical nature and structure of the analytes. However, the “raw” retention times by themselves are not useful for any chemical interpretation, owing to their dependence on numerical conditions of analysis. In gas chromatography, for example, these conditions include oven temperature, type of stationary phase, its content on the support of packed columns or film thickness in the capillary columns, length of the column, carrier gas flow, and the pressure gradient between the inlet and outlet of the chromatographic system. The characterization of analytes in chromatography by net retention times may be compared to the measurement of temperature by thermometers with different arbitrary scales, or even without any scales at all. Thus, the standardization of chromatographic retention parameters is a problem of extremely high importance.

Discussion

One possible solution is based on the complete interlaboratory standardization of all of the above-mentioned experimental conditions. The realization of the so-called RTL concept (retention time locking) became possible only during the middle of the 1990s. The second most widely used solution requires the recalculation of the data being measured at different conditions into the interlaboratory comparable scale. The mathematical method suitable for this recalculation — linear interpolation — has been known long before the appearance of chromatography. Given pairs of function (y) and argument (x)

values $[y_1(x_1), y_2(x_2), \dots, y_n(x_n)]$ that are connected by a known or unknown functional dependence $y = f(x)$, we can estimate the unknown values y_i , which are located between the known values $y_k < y_i < y_{k+1}$ from the value x_i ($x_k < x_i < x_{k+1}$) by the following relationship:

$$y_i = y_k + \frac{(y_{k+1} - y_k)(x_i - x_k)}{x_{k+1} - x_k} \quad (1)$$

In the case of a nonlinear or unknown dependence $y = f(x)$, the application of simple linear interpolation leads to some uncertainty in the results. However, if the equation for nonlinear dependence is known, a transformation of Eq. (1) into Eq. (2) can be applied to remove the nonlinearity. This approach gives the results of the same precision as that of direct calculation with the equation $y = f(x)$:

$$y_i = y_k + (y_{k+1} - y_k) \left(\frac{f(x_i) - f(x_k)}{f(x_{k+1}) - f(x_k)} \right) \quad (2)$$

The application of this concept in chromatography requires the introduction of some extra components with previously known (postulated) retention indices $[RI = f(t_R)]$ into the samples being analyzed. Their peaks form a “mobile” coordinate system for the recalculation of t_R data of the target analytes. Hence, the establishment of any retention index system needs the following:

1. The choice of set of reference compounds (most often they are members of the same homologous series which differ by a homologous difference CH_2)
2. The attribution of standard (conventional) RI values for these compounds
3. The choice of a formula for the calculation of RI values for all other analytes

The first RI system was proposed by Kovats in 1958 [1] for isothermal conditions of gas chromatographic (GC) analysis. The easily accepted n -alkanes $n\text{-C}_n\text{H}_{2n+2}$ with postulated RI values of $100n_C$ [e.g., methane (CH_4)—100; n -nonane (C_9H_{20})—900, n -hentriacontane ($\text{C}_{31}\text{H}_{64}$)—3100, etc.] was recommended as reference compounds. Insofar as, at the



isothermal conditions of GC analysis, the linear dependence of logarithms of corrected retention times $t'_R = t_R - t_0$ (t_0 is the dead time of chromatographic system) versus the number of carbon atoms in the molecule of the homolog is observed, $\log t'_R = an_C + b$, and (by definition) $100n_C = \text{RI}$; this means the existence of following linear dependence:

$$\text{RI} = a \log t'_R + b \quad (3)$$

If we consider the last relationship as the function $y = f(x)$ in Eq. (2), we come to the final equation of the Kovats Retention Index System:

$$\text{RI}_x = \text{RI}_k + (\text{RI}_{k+1} - \text{RI}_k) \left(\frac{\log(t'_{R,x}) - \log(t'_{R,k})}{\log(t'_{R,k+1}) - \log(t'_{R,k})} \right) \quad (4)$$

where $t'_{R,x} < t'_{R,k} < t'_{R,k+1}$ are the corrected retention times of reference n -alkanes with number of carbon atoms k and $k + 1$ being eluted immediately before ($t'_{R,k}$) and after ($t'_{R,k+1}$) the target compound ($t'_{R,x}$).

As far as the basis of formula (4) is linear dependence [Eq. (3)], it is possible to use retention times of reference n -alkanes which differ by not one but by a greater number of carbon atoms [i.e., RI_{k+m} and RI_k with $t_{R,k+m}$ and $t_{R,k}$ (in the original publication of Kovats [1] just the difference $m = 2$ was used)]. When $m = 1$, Eq. (3) may be simplified to the various visually different but the same relationship formulas; for example,

$$\text{RI}_x = 100 \left(k + \frac{\log(t'_{R,x}/t'_{R,k})}{\log(t'_{R,k+1}/t'_{R,k})} \right) \quad (5)$$

where k is the number of carbon atoms in the n -alkane that elutes before the compound undergoes characterization.

The proposed form of data presentation became highly popular and opportune in gas chromatography. Up to the present, some thousand references to the Kovats' work [1] have been known. The RI values are proportional to the free energies of sorption; this is their thermodynamic interpretation. Further development of the RI concept was aimed at its application to nonisothermal conditions of gas chromatographic (GC) analysis. For linear temperature programming regimes (which are characterized by two variables: initial temperature, T_0 , and rate of its increase, r , $\text{deg} \times \text{min}^{-1}$), the linear relationship (3) does not hold. In some partial cases, other linear dependence seems more precise for the retention time approximation:

$$\text{RI} \approx at_R + b \quad (6)$$

This is a reason to change the formula for the RI calculation (the set of reference compounds and their attributed RI values remain the same). This version of RIs developed especially for a linear temperature programming regime (linear retention indices) have been proposed by Van den Dool and Kratz in 1963 [2]:

$$\text{RI}_x = \text{RI}_k + (\text{RI}_{k+1} - \text{RI}_k) \frac{t_{R,x} - t_{R,k}}{t_{R,k+1} - t_{R,k}} \quad (7)$$

or, after the same simplifications as those which were used for Eq. (4),

$$\text{RI}_x = 100 \left(k + \frac{t_{R,x} - t_{R,k}}{t_{R,k+1} - t_{R,k}} \right) \quad (8)$$

Owing to the approximate character of dependence (6), Eqs. (7) and (8) give less comparable results for the same compounds in different temperature programming regimes. As a consequence, the replacement of the $k, k + 1$ pair of reference n -alkanes on the $k, k + m$ ($m > 1$) also increases the errors to an unpredictable extent and is usually not recommended.

Complex dependencies $\text{RI} = f(t_R)$ in nonisothermal conditions of GC analysis may be described by polynomials of different degrees (up to 13 have been tested) or splines (cubic splines seem most convenient). However, the calculation of coefficients of an N -degree polynomial needs t_R data for at least $N + 1$ reference compounds instead of only two t_R values as in "classical" RI systems. In connection with this fact, it is interesting to mention the combined lin-log RI system, which was proposed in 1984 (3,4). If both the dependencies (3) and (6) are nonlinear at temperature programming, every local window of retention times for reference compounds may be precisely approximated by linear and logarithmic addends in variable proportion:

$$\text{RI} = a(t_R + q \log t'_R) + c \quad (9)$$

and

$$\text{RI}_x = \text{RI}_k + (\text{RI}_{k+m} - \text{RI}_k) \left(\frac{f(t'_{R,x}) - f(t'_{R,k})}{f(t'_{R,k+m}) - f(t'_{R,k})} \right) \quad (10)$$

where $f(t'_R) = t_R + q \log t'_R$. The variable parameter q may be calculated in different manners, but in the simplest case, it needs t_R data only for three successive reference compounds with retention times $t_{R,k-1}$, t_R , and $t_{R,k+1}$:

$$q = \frac{2t_{R,k} - t_{R,k-1} - t_{R,k+1}}{\log t'_{R,k-1} + \log t'_{R,k+1} - 2 \log t'_{R,k}} \quad (11)$$

The most convenient advantage of a lin-log RI system is the possibility of its application in any temperature regime of GC analysis without special choice of formulas for calculations. Under isothermal conditions, the logarithmic contribution to the total dependence $RI = f(t_R)$ exceeds the linear one by many times, which automatically reflects on the value of q ($|q| \rightarrow \infty$). Only the lin-log RI system provides the most comparable results for different temperature conditions of analysis.

The maximal influence on RI values is the nature of stationary phase in the chromatographic column. Use of these parameters as the constants of chemical compounds (similar to other known physicochemical constants like boiling points, T_b , refractive index, n_D^{20} , density, d_4^{20} , etc.) requires the choice of standard phases for their determination. In accordance with the criteria of the most often used application in practice, two types of phases may be classified as standards:

Nonpolar polydimethyl siloxanes:

$[-Si(CH_3)_2-O-]_n$; maximal temperature of application $\approx 300^\circ C$

Polar polyethylene glycols: $[-CH_2CH_2-O-]_n$; maximal temperature of application $\approx 225^\circ C$

Each of these groups of phases includes the numerous items of various trade names, different average molecular weights, viscosity, thermal stability, and so forth, but all of them are very close to each other by polarity. Up to the middle of the 1970s, the preferred nonpolar phase was squalane (isoprenoid alkane $C_{30}H_{62}$). This phase is no longer used because of its low thermal stability (only about $110^\circ C$). However, this obsolete phase maintains its importance as a nonpolar standard in gas chromatography. Other phases may be characterized by differences of RI values of specially selected test compounds between the phase under consideration and squalane, for example:

The comparison of RI values of the same compounds measured with the same stationary phase but at different conditions of analysis indicates some deviations. From some objective reasons for these deviations, the temperature dependence of retention indices seems like the most important contribution (coefficients β are the measure of this dependence, typically $\beta > 0$):

$$\beta = \frac{dRI}{dT} \approx \frac{RI(T_2) - RI(T_1)}{T_2 - T_1} \quad (12)$$

Among the multitude of organic compounds, there are objects with $\beta \approx 0$ (all types of noncyclic compounds most topologically relevant to n -alkanes). The increase in the number of cycles in the molecules leads to the increase of β up to 0.3–0.5 (cycloalkanes, arenes, etc.), 0.5–0.8 (naphthalenes, biphenyl, etc.), and 1.0 and more retention index units per degree (i.u. $\times \text{deg}^{-1}$) for tricyclic and polycyclic structures. Hence, it is not surprising that RI data for isoalkanes, ethers, esters, and so forth being measured at different conditions are in good agreement with each other (standard deviations of randomized interlaboratory values are not more than 1–3 i.u.). The same statistical characteristic for substituted benzenes is about 8 i.u., and for naphthalenes it may exceed 10–15 i.u.

The choice of n -alkanes as a reference set of compounds for the determination of RI values is accepted up to the present. Meanwhile, numerous other homologous series have been recommended for different specific applications. For example, GC analysis with electron-capture detectors (selective to halogenated compounds) requires other reference compounds of similar chemical origin. These series are alkyl trichloroacetates $CCl_3CO_2C_nH_{2n+1}$, alkyl methyl phosphonofluoridates $CH_3P(O)(F)OC_nH_{2n+1}$ (so-called P series), O -alkyl bis(trifluoromethyl)phosphinothionates $(CF_3)_2P(S)OC_nH_{2n+1}$ (A series), alkyl bis(trifluoromethyl)thiophosphines $(CF_3)_2P(S)C_nH_{2n+1}$ (M series), and others. The last two series seem most universal for different types of GC detectors, owing to the simultaneous presence of various

	Test compounds				
	Benzene	1-Butanol	2-Pentanone	Nitro propane	Pyridine
$\Delta RI = RI_{\text{polydimethyl siloxanes}} - RI_{\text{squalane}}$	16 ± 1	53 ± 2	44 ± 1	65 ± 2	42 ± 1



elements in the molecule (Hal, P, S, CH). A special set of reference objects have been proposed by Lee [5] for the analysis of polycyclic aromatic compounds to eliminate the strong temperature dependence of their RIs in the n -alkane scale. This system is based on benzene (postulated RI value $100 = 100 \times \text{number of cycles}$), naphthalene (200), phenanthrene (300), chrysene (400), picene (500), benzo[*b*]picene (600), and dinaphtho[2,1-*a*:2,1-*h*]anthracene (700) (i.e., condensed aromatic hydrocarbons). Of course, RI values being measured with different reference series are not directly comparable to each other but, if necessary, may be recalculated.

Since the 1980s, some applications of the RI system have been reported for reversed-phase high-performance liquid chromatography (RP-HPLC). The principal requirement for the reference compounds in this method, with UV detection, is the presence of chromophores in the molecules. The most widely accepted RI system in HPLC is based on homologous alkyl phenyl ketones $\text{PhCOC}_n\text{H}_{2n+1}$ (so-called Smith's system of retention indices; by analogy with GC, the RI values, attributed for reference compounds, are $100n_C$). Other RI scales imply the use of homologous monoalkylbenzenes $\text{PhC}_n\text{H}_{2n+1}$, 1-nitroalkanes $\text{C}_n\text{H}_{2n+1}\text{NO}_2$, glycerol 1-(4-acylphenyl) ethers $4\text{-C}_n\text{H}_{2n+1}\text{CO-C}_6\text{H}_4\text{-OCH}_2\text{-CH(OH)-CH}_2\text{OH}$, and so forth. The last set of substances is convenient for the determination of RIs of most hydrophilic organic compounds; this set is eluted before simplest reference components of other series. In the isocratic regimes of HPLC separation, which are analogous to isothermal conditions in GC, linear dependence (3) is correct and RIs must be calculated with formulas (4) and (5). With gradient elution, by analogy with temperature programming, formulas (7) and (8), which are based on dependence (6), are preferable. Of course, lin-log RI system may be used in any regimes of RP-HPLC, as well as in gas chromatography.

It is interesting to note that by analogy with chromatographic retention parameters, the values of some other properties of organic compounds may be presented in the linear interpolated form relative to the set of reference compounds. These equivalent to indices forms are known for boiling points [6], molecular weights [7], and molar refractions, $\text{MR}_D = (\text{MW}/d)(n^2 - 1)/(n^2 + 2)$, where MW is the molecular weight, n_D^{20} is the refractive index, and d_4^{20} is the density [8]. For example,

$$I(T_b) = 100 \left(k + \frac{\log(T_{b,x}/T_{b,k})}{\log(T_{b,k+1}/T_{b,k})} \right) \quad (13)$$

where $T_{b,k} < T_{b,x} < T_{b,k+1}$ are the boiling points of n -alkanes with k and $k + 1$ carbon atoms in the molecule

and the target compound. For nonpolar compounds, the values of $I(T_b)$ are close to the experimental RI data being measured with nonpolar stationary phases.

The most significant feature of retention indices, as the constants of organic compounds, seems to be the possibility of their precalculation both from other physicochemical parameters and by different additive schemes [9]; this is impossible for values of net retention times themselves. The methods of RI precalculation unite as complex algorithms, as very simple but useful rules. For instance, it is interesting to note that even in the first publication of Kovats [1], the rule for precalculation of RIs for compounds of general type A-B by arithmetical averaging of data for compounds A-A and B-B were recommended [i.e., $\text{RI(A-B)} = [\text{RI(A-A)} + \text{RI(B-B)}]/2$]. It is very surprising that any attempts to use the same rule in mathematically transformed form, namely $\text{RI(B-B)} = 2\text{RI(A-B)} - \text{RI(A-A)}$ were unknown during the past 40 years. Nevertheless, if B is a more complex structural fragment of molecule than A, this is simplest way to precalculate RIs of high-molecular-weight compounds from data for more simple precursors. This general statement may be illustrated by the following example: The estimation of unknown RI value of 1,1,1,3,3,3-hexachloropropane $\text{CCl}_3\text{-CH}_2\text{-CCl}_3$ needs the data for 1,1,1-trichloroethane and propane, so far as $2 \times \text{CCl}_3\text{-CH}_2\text{-CH}_3 - \text{C}_3\text{H}_8 = \text{CCl}_3\text{-CH}_2\text{-CCl}_3$, namely $2(736 \pm 3) - 300 = 1172 \pm 4$.

One of the most practical contemporary problems of GC RI application seems to be the formation of available and representative databases by analogy with well-organized databases in mass spectrometry.

References

1. E. Kovats, *Helv. Chim. Acta* 41: 1915 (1958).
2. H. Van den Dool and P. Kratz, *J. Chromatogr.* 11: 463 (1963).
3. I. G. Zenkevich, *Zh. Anal. Khim. (Russ.)* 42: 1297 (1984).
4. I. G. Zenkevich and B. V. Ioffe, *J. Chromatogr.* 439: 185 (1988).
5. M. L. Lee, M. V. Novotny, and K. D. Bartle, *Analytical Chemistry of Polynuclear Aromatic Hydrocarbons*, Academic Press, New York, 1981.
6. P. G. Pobinson and A. L. Odell, *J. Chromatogr.* 57: 1 (1971).
7. M. B. Evans, J. K. Haken, and T. Toth, *J. Chromatogr.* 351: 155 (1986).
8. I. G. Zenkevich and L. M. Kuznetsova, *Collect. Czech Chem. Commun.* 56: 2042 (1991).
9. R. Kaliszan, *Quantitative Structure—Chromatographic Retention Relationships*, John Wiley & Sons, New York, 1987.



Large-Volume Injection for Gas Chromatography

Yong Cai

Florida International University, Miami, Florida, U.S.A.

Introduction

Trace or ultratrace analyses for environmental and biological samples require sensitive methods, including sample preparation and detection techniques, to be used. The enhancement of the detectability of analytical procedure is often brought about by some form of pre-concentration, such as Soxhlet extraction, liquid-liquid extraction, and solid-phase extraction. Capillary gas chromatography (GC) coupled with different detectors is one of the most frequently employed techniques for trace analysis of micropollutants. However, because of the limited sample capacity of the capillary column, only a small portion (1–5 μL) of the final sample extract is introduced into the gas chromatographic system. This means that after careful workup, which often comprises analyte isolation by extraction and changing to a GC-compatible solvent, a maximum few percent could be injected and reach the detector [1]. The concentration detection limit of the method can be improved by increasing the concentration factor of the extraction and cleanup procedure. This is generally achieved by using a larger amount of sample or/and by reducing the volume of final extract through evaporation. Both methods have limitations for practical application. Extraction of a large amount of sample is very time consuming and requires a large volume of toxic organic solvents. Sampling a large amount of sample is sometimes difficult or even impossible. Although solvent evaporation is frequently used, it is a rather critical step in which the more volatile compounds may be lost from the sample because of the coevaporation with the solvent [1,2]. Recently, there has been increased interest in the introduction of large sample volumes in capillary GC [1–6]. Several hundred microliters of sample can be introduced by using these techniques. Among the several techniques for the introduction of a large volume of sample, on-column injection and programmed-temperature vaporization (PTV) injection are best developed.

On-Column Injection

The on-column injection techniques, in which the solvent is generally vaporized in a few meters of uncoated

deactivated capillary (retention gap) and vented via an early vapor exit valve, are of good accuracy and reproducibility [3–5]. A schematic diagram for on-column injection is shown in Fig. 1. The on-column large-volume injection system generally consists of a regular gas chromatograph equipped with an on-column injector, a retention gap, a retaining precolumn, an analytical column, and a heated early solvent vapor exit.

The introduction of a large volume of sample can be performed using a technique called partially concurrent solvent evaporation (PCSE). With PCSE, some 90% of the solvent injected is evaporated during the injection through the early solvent vapor exit [1]. The injection rate of the sample is controlled based on the length of the retention gap and the boiling points of the analytes. If the sample volume exceeds the capacity of the uncoated retention gap to retain liquid (it is true for most large-volume injection applications), the injection speed should be adjusted to result in a sufficiently large proportion of concurrent evaporation to prevent liquid solvent from spreading into the analytical column [2]. Most of the vapor escapes through the open solvent vapor exit. After large-volume on-column injection, the analytes are spread out over several meters of the uncoated retention gap. Solvent evaporation continues, removing solvent from the rear

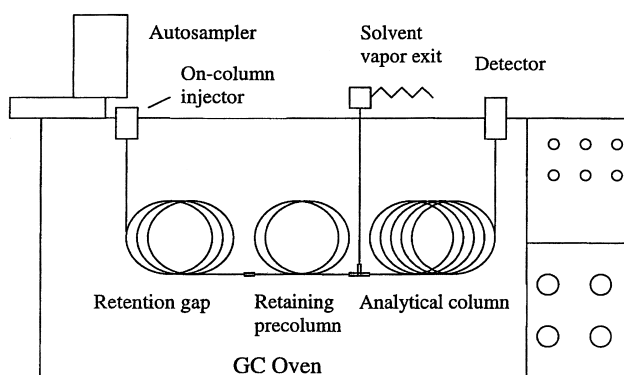


Fig. 1 Schematic diagram of GC with on-column large-volume injection.



to the front of the sample film. Relatively volatile analytes evaporate and are re-concentrated by the liquid ahead. This process is described as the solvent-trapping effect. Less volatile components do not evaporate with the solvent and remain on the dry retention gap surface. The vapor exit valve is closed shortly before the end of solvent evaporation when the residual liquid still remains the volatile components. The rest of the solvent is discharged through the analytical column. Re-concentrations of the less volatile compounds are carried out by phase-ratio focusing; that is, the difference in migration speed in the retention gap and in the coated column causes the rear end of the zone to catch up with the front end at an appropriately increased oven temperature [1,2]. As soon as the front end of the zone reaches the stationary phase, its migration speed reduces dramatically, while the remaining part, which is still in the retention gap, continues to migrate at a higher speed.

With on-column large-volume injection, the selection of appropriate experimental conditions is complicated [2]. Generally, the following parameters need to be carefully optimized.

1. The sample must be introduced at a rate slightly exceeding the evaporation rate. Slower injection causes the loss of solvent trapping because all solvent evaporate concurrently, whereas a too high introduction rate results in flooding of the solvent into the retaining precolumn and, eventually, the analytical column and the vapor exit.
2. The temperature of the column oven during injection should be set slightly below the pressure-corrected boiling point of the solvent used. At too high temperatures, the solvent starts to boil and causes the backflush of solvent into the injector.
3. The vapor exit valve must be closed at a right time. Early closing of the valve may cause the remaining solvent in the retention gap to exceed the capacity of the analytical column. However, delayed closure will result in the loss of volatile components.

On-column large-volume injection has wide applications in terms of volatility and thermostability of the analytes [4]. If the solvent exit valve is operated carefully, compounds with boiling points only slightly above that of the solvent can be recovered quantitatively. However, the technique is generally not very suitable for dirty samples. Frequent analysis of samples with high contents of matrix com-

Large-Volume Injection for Gas Chromatography

pounds can rapidly decrease the column performance [3–6].

Programmed-Temperature Vaporization

Vogt and co-workers in 1979 described an injector that allowed the injection of up to 250 μL into a cold glass insert filled with glass wool [7,8]. This technique has been modified and refined in the recent years [3–6,9,10]. In fact, the large-volume sampling technique using PTV injectors is modified from a conventional split/splitless injector [1]. The main differences between the conventional split/splitless and the PTV injectors are the temperature control of the injector and the solvent venting capacity of the split/splitless valve. In PTV injectors, the injection port should be heated or cooled rapidly, and the split/splitless valve should be large enough to be able to vent the solvent vapor produced during injection. Before a large volume of sample is introduced, the temperature of the injection port is reduced to below the boiling point of the solvent. The sample is injected into the liner of the injector at a controlled rate. Upon introduction, the solvent is selectively eliminated and solvent vapor is vented via the split/splitless valve. The less volatile components are retained in the cold liner. When solvent elimination is finished, the components retained in the liner are transferred to the analytical column by rapid temperature-programmed heating of the injector.

In order to obtain a quantitative analysis for the analytes with a wide range of volatility using the PTV injection technique, the following parameters are of great importance: injection speed, liner packing material, solvent venting temperature, and solvent venting time. The speed of sample introduction should roughly equal the rate of solvent elimination [1]. If the sample is injected at a rate exceeding the evaporation rate, the sample will accumulate in the liner, which eventually will result in overloading of the liner. This will cause flooding of the analytical column and severe losses of both volatile and non-volatile components via the split exit. On the other hand, a too slow sample introduction rate will cause losses of volatile sample components. The use of liners packed with an absorbent is an efficient means to retain the liquid sample and minimize losses of volatile compounds [1,10]. A number of packing materials, such as glass wool, quartz wool, cup liner, Tenax TA, PTFE wool, have been investigated in terms of their interaction with different types of analytes [10]. An unsuitable choice of the packing material

can cause degradation of the analyte in the liner. The solvent venting temperature and solvent venting time must be carefully optimized. The liner temperature is held below the boiling point of the solvent during the solvent venting time. The split/splitless valve must be closed at the right time. Early closing will cause accumulation of the solvent, which may exceed the capacity of the column, whereas delayed closure can result in losses of the volatile sample components.

It has been shown that the PTV injector is a very useful technique for large-volume injection, especially for the analysis of a dirty sample. Because the vaporization of the solvent is carried out at a low temperature, nonvolatile matrix constituents remaining in the liner will not contaminate the GC column. However, the PTV injection technique is less suited when analyzing volatile compounds because only components with volatility significantly below that of the solvent are trapped in the cold liner, unless liners packed with a selective adsorbent is used [4].

References

1. H. G. J. Mol, H. G. M. Janssen, C. A. Cramers, J. J. Vreuls, and U. A. Th. Brinkman, *J. Chromatogr. A* 703: 277 (1995).
2. K. Grab, *J. Chromatogr. A* 703: 265 (1995).
3. H. G. J. Mol, M. Althuisen, H. G. Janssen, C. A. Cramers, and U. A. Th. Brinkman, *J. High Resolut. Chromatogr.* 19: 69 (1996).
4. J. C. Bosboom, H. G. Janssen, H. G. J. Mol, and C. A. Cramers, *J. Chromatogr. A* 724: 384 (1996).
5. H. J. Stan and M. Linkerhagner, *J. Chromatogr. A* 727: 275 (1996).
6. F. Munari, P. A. Colombo, P. Magni, G. Zilioli, S. Trestianu, and K. Grab, *J. Microcol. Separ.* 7: 403 (1995).
7. W. Vogt, K. Jacob, and H. W. Obwexer, *J. Chromatogr.* 174: 437 (1979).
8. W. Vogt, K. Jacob, A. B. Ohnesorge, and H. W. Obwexer, *J. Chromatogr.* 186: 197 (1979).
9. S. Ramalho, T. Hankemeier, M. de Jong, U. A. Th. Brinkman, and R. J. J. Vreuls, *J. Microcol. Separ.* 7: 383 (1995).
10. H. G. J. Mol, P. J. M. Hendriks, H. G. Janssen, C. A. Cramers, and U. A. Th. Brinkman, *J. High Resol. Chromatogr.* 18: 124 (1995).



Large-Volume Sample Injection in FFF

Martin Hassellöv

Göteborg University, Gothenburg, Sweden

Introduction

Field-flow fractionation (FFF) techniques are used for a range of sample types, including polymers, macromolecules, glass beads, silica, and other inorganic particles due to their good separation characteristics (e.g., high-molecular-weight separation selectivity and a large dynamic operating range). These analytes are dissolved or suspended in an appropriate liquid and small aliquots of the suspensions (typically 2–20 μL) are injected into the FFF channel. For these applications, it has usually been possible to adjust the analyte concentration to ensure an acceptable signal-to-noise ratio given detector sensitivity and the dilution in the FFF system. However, there are a number of applications where the solutes are very dilute and any preconcentration may cause perturbation of the size distribution or other changes of sample characteristics. Such applications could include most of the groups of sample types mentioned, and especially in environmental particles and colloids, which are often present in low concentrations and are easily disturbed.

Discussion

Schure has recently evaluated dilution factors and detection limits for FFF in comparison with liquid chromatography and capillary electrophoresis [1]. It is obvious that samples are subject to much higher dilution in FFF channels (~200–1000 times) compared with most liquid chromatography techniques (~3–25) due to the rather low efficiency and large elution volumes. A narrower and thinner channel than one with more conventional dimensions would improve the dilution factors, but there are practical problems involved in the production and maintenance of such a channel. There is the option of using any of the outlet flow splitting devices which have been developed. These are different approaches having in common removal of some of the overlying liquid at the end of the channel and thus reducing the dilution. The principles build on horizontal flow splitters, capillaries exiting both above and below the channel, or a second porous frit section

in the overlying channel wall letting out liquid. There have been difficulties in accurate production, maintenance, and precision of some of these technical solutions, but there is now one system commercially available using the frit-outlet system in flow FFF (FIFFF) for removal of excess liquid [2], with which at least a 10-fold reduction in dilution is achieved.

The injection volume of the conventional stop-flow sample injection technique is limited typically to 2–20 μL . This procedure is carried out using a sample loop and injecting the sample plug just onto the channel carried with the channel flow before stopping that flow and letting the sample attain its equilibrium distribution relative to the accumulation wall (relaxation). Sedimentation FFF (SdFFF) is the only technique where the field is not applied during the complete stop-flow procedure, but the centrifuge is started as soon as the sample is injected and the channel flow switched away for practical reasons.

Kirkland et al. [3] introduced an injection technique for SdFFF, where the sample is slowly injected with the centrifuge spinning at a high field and thereby retaining the analytes in a narrow band at the entrance of the channel. When the sample is injected, the flow is stopped, the centrifuge speed is decreased to the initial elution speed, and an appropriate relaxation time is allowed. This technique has been further refined and developed by Giddings and co-workers into an on-channel preconcentration step for concentrating dilute particulate samples in SdFFF [4].

Another injection technique, which involves a sample injection port a small distance downstream of the channel inlet, where the sample was injected and relaxed between two focusing flows with a reversed flow from the channel outlet, was first employed for asymmetrical FIFFF [5]. The theoretical basis of the horizontal transport was derived and fundamental practical aspects were discussed. This procedure is now standard for asymmetrical FIFFF, partly due to the difficulties of adapting the stop-flow injection mode and was further optimized by Wahlund and Litzén [6] to include injection of up to 5 mL of sample in a 0.8-mL channel.



This approach has subsequently been used in symmetrical FIFFF [7,8], where the sample is injected in either the forward or backward focusing flow streams (Fig. 1). Lyvén et al. [7] showed a virtually quantitative recovery for preconcentration of 1.7 to over 100 mL of low-molecular-weight polymers and natural water colloids (Fig. 2) with a molecular weight of the same order as the membrane cutoff by optimizing injection flows, membrane, and carrier. Injection in both the forward and backward focusing flow stream was evaluated. An experimental approach was used to determine the minimum time for sample loading and focusing. In or-

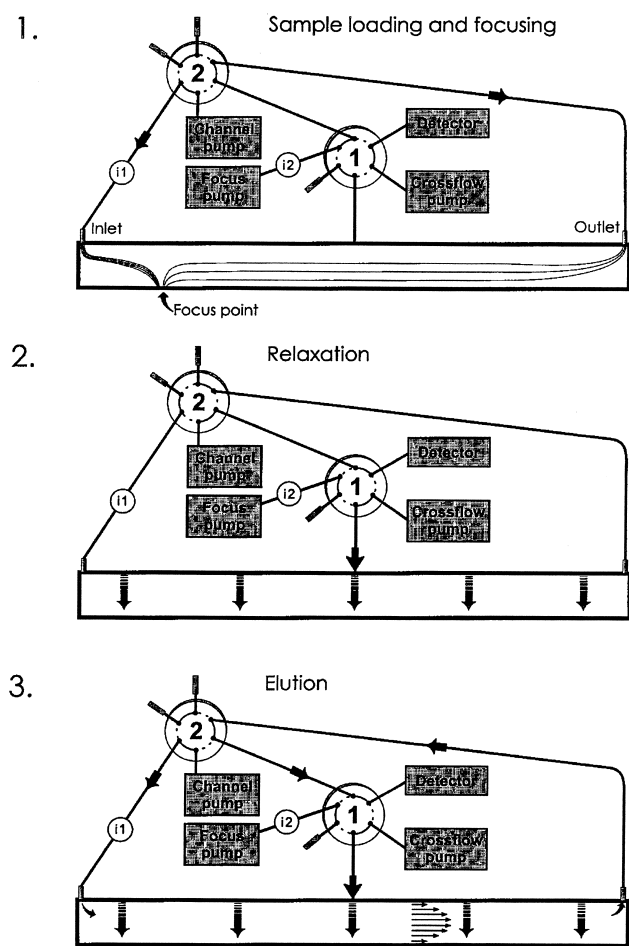


Fig. 1 Instrumental schematics of FIFFF with on-channel preconcentration showing the three different procedure steps. The first involves emptying of the sample loop into either the forward or backward flows and subsequent focusing of the sample material at the focusing point. During the next step (2), the sample is allowed relaxation to the equilibrium position by applying cross-flow only, and then the channel flow is switched on and elution is commenced.

Large-Volume Sample Injection in FFF

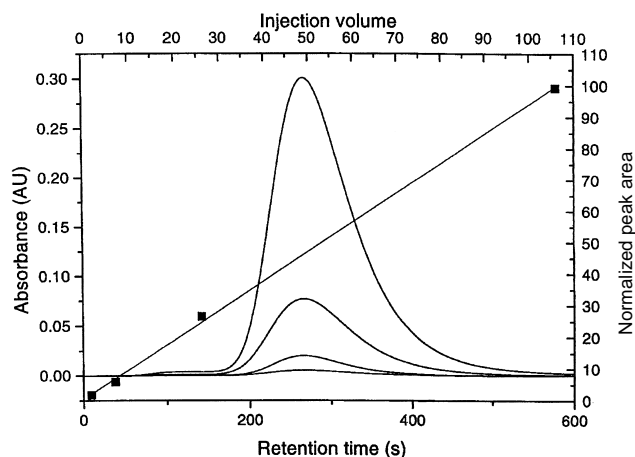


Fig. 2 Results showing preconcentration of 1.7–106 mL of a natural freshwater sample using the procedure in Fig. 1. The solid lines show the ultraviolet detector response, and the squares with the regression line (slope 0.94 and $R^2 = 0.9993$) represent peak area versus injection volume. The sample was first diluted in order not to exceed the overloading point. (From Ref. 7.)

der to ensure sufficient focusing time for all colloids, the focusing time was increased until a stable retention time was attained for the largest reference standard. This on-channel preconcentration method has later been used in a FIFFF coupling with inductively coupled plasma-mass spectrometry for trace element size distributions for natural water colloids [9]. The colloids and the associated metals would have been impossible to study without the preconcentration procedure due to the very low concentrations of both colloids and trace metals often found in natural waters. Lee et al. [8] presented a method for preconcentrating 10-mL samples of dilute polystyrene latex beads, river sediment particles, and proteins, which are injected in the channel inlet stream with an opposed focusing flow from the channel outlet. Results of recoveries are shown for different membrane materials. On-channel preconcentration for FIFFF and SdFFF are rather simple to incorporate in a conventional instrument, just with the addition of a second switching valve and a liquid pump. The sample is exposed to the same media as in the separation step and the preconcentration step is carried out just prior to analysis, which is not always the case for external preconcentration techniques such as ultrafiltration or centrifugation.

Precautions must be taken in all FFF analysis when injecting a large amount of material with any injection technique. During the sample relaxation, local concen-

trations of analytes can become quite high and, at some point, the sample components start affecting each other. Then, conformational changes or intermolecular repulsion can occur, preventing the analytes from attaining a true equilibrium distribution in the channel. This phenomenon is often referred to as overloading and is usually indicated by a later eluting peak with a fronting peak shape.

Overloading in polymer analysis using flow and thermal FFF is thoroughly described by Caldwell et al. [10], where different overloading mechanisms during relaxation and elution are theoretically and experimentally evaluated. Usually, for FFF separations, the detector sensitivity is sufficiently high to detect the separated components at sample concentrations well below the overloading concentration. For further characterization of the particulate material by other detection systems (e.g. mass spectrometry) or subsequent analysis of a collected fractions, it is often necessary to inject large amounts of sample material to exceed the detection limits and then it is essential to be observant of overloading effects. The best way of investigating the elution behavior in order to rule out overloading is to inject various amounts of sample and follow the retention time as well as the shape of the peak. The applied field in stop-flow relaxation or focusing flows in on-channel preconcentration could also have an affect on nonideal behavior; that is, the sample

components are compressed during high fields, causing both higher local concentrations and potential interaction with the accumulation wall. When working with sample amounts near the overloading point, varying the field strength acting on the analytes can be used to find conditions where overloading starts and thereby avoid it.

References

1. M. R. Schure, *Anal. Chem.* 71: 1645–1657 (1999).
2. P. Li, M. Hansen, and J. C. Giddings, *J. Microcol. Separ.* 10 (1998).
3. J. J. Kirkland, W. W. Yau, and W. A. Doerner, *Anal. Chem.* 52: 1944–1954 (1980).
4. J. C. Giddings, G. Karaiskakis, and K. D. Caldwell, *Separ. Sci. Technol.* 16: 725–744 (1981).
5. K.-G. Wahlund and J. C. Giddings, *Anal. Chem.* 59: 1332–1339 (1987).
6. K.-G. Wahlund and A. Litzén, *J. Chromatogr.* 461: 73–87 (1989).
7. B. Lyvén, M. Hassellöv, C. Haraldsson, and D. R. Turner, *Anal. Chim. Acta* 357: 187–196 (1997).
8. H. Lee, S. K. Ratanathanawongs Williams, and J. C. Giddings, *Anal. Chem.* 70: 2495–2503 (1998).
9. M. Hassellöv, B. Lyvén, C. Haraldsson, and W. Sirinawin, *Anal. Chem.* (in press).
10. K. C. Caldwell, L. B. Steven, Y. Gao, and J. C. Giddings,



Laser-Induced Fluorescence Detection for Capillary Electrophoresis

Huan-Tsung Chang
Tai-Chia Chiu
Chih-Ching Huang

National Taiwan University, Taipei, Taiwan

INTRODUCTION

Separations of small solutes and macromolecules by capillary electrophoresis (CE) have been widely accepted by the scientific community, mainly due to its inherent advantages such as high resolution, compatibility with smaller samples, consumption of less buffer, rapidity, and ease of automation. Some of these advantages stem from the use of capillaries with inner diameters of 1–100 μm . With such small diameters, injection volumes are typically 0.1–10 nL, leading to a difficulty of detection. For detecting an analyte present at 1 nM concentration, with a 0.1-nL injection volume, extremely sensitive detection systems, providing a detection limit below 100 zmol for the analyte, are needed. Over the past 20 years, a number of nanoscale detectors, based on mass spectrometry, amperometry, chemiluminescence, radiochemistry, and fluorescence, have been developed to meet the extraordinary sensitivity challenges posed by CE. Of these, laser-induced fluorescence (LIF) has been the most successful and has been applied to single-cell analysis, DNA sequencing and separations, protein analysis, single-molecule detection, etc. One good example is that LIF, in conjunction with capillary array electrophoresis (CAE), has been successfully used for DNA sequencing, which has considerably assisted in the rapid progress of the Human Genome Project.

FLUORESCENCE

Fluorescence is the process of emission of light after absorption; its intensity is generally small, which depends on the extinction coefficient and quantum efficiency of the analyte, optical length, power of the light source, and light collection efficiency. In fluorescence measurements, one molecule can be reexcited thousands of times during the measurement to generate sufficient numbers of photons for detection. Thus it is essential to minimize the stray light from the optics and Rayleigh and Raman scattering of the solvent molecules. Once stray light and

background signals are under control, a laser can be used to increase the excitation intensity, leading to larger signals and improved limit of detection (LOD) in fluorescence. To prevent photobleaching of analytes and damages of capillaries, lasers with 1–10-mW power are commonly used in CE; some are listed in Table 1.

Instrumentation

Since the first successful use of LIF for CE by Gassmann et al.,^[1] several designs have been tested, including cross-beam excitation, epi-illumination, axial-beam excitation, and sheath-flow cuvette. Of these, the design of cross-beam excitation has been most commonly adopted in CE. Because laser light is well collimated, it can be focused to a beam diameter smaller than any practical capillaries used in CE. Thus the maximum photon flux can be delivered to the interior of a capillary to allow efficient excitation of analytes and to reduce the scattering from the capillary wall. With the capillary tilted at an angle to the laser beam, and the emitted fluorescence collected in a direction perpendicular to the plane of the capillary and excitation beam, the background from refracted light is minimized after appropriate spatial and spectral filtering. One basic instrumental setup of CE-LIF is shown in Fig. 1. With such a simple system, Tseng et al. were able to detect 11.1 nM human serum albumin labeled with albumin blue 580, using a low-cost He–Ne laser.^[2]

A novel LIF detector, which uses a sheath flow cuvette developed by Wu and Dovichi, provides better sensitivity than the design of cross-beam excitation.^[3] For example, LOD values as low as 1.7 zmol for fluorescein derivatives of amino acids have been achieved when injecting a 1.3-nL sample. Briefly, a sheath flow cuvette uses a flowing jacket of refractive index-matching buffer to hydrodynamically focus solutes as they exit from the capillary, leading to a thin stream in the center of the flow chamber. Thus it is easy to excite fluorophores migrating in such a thin stream by a focused laser beam, with a minimum Rayleigh scattering from the capillary wall and Raman scattering from water.



Table 1 Lasers commonly used in CE-LIF

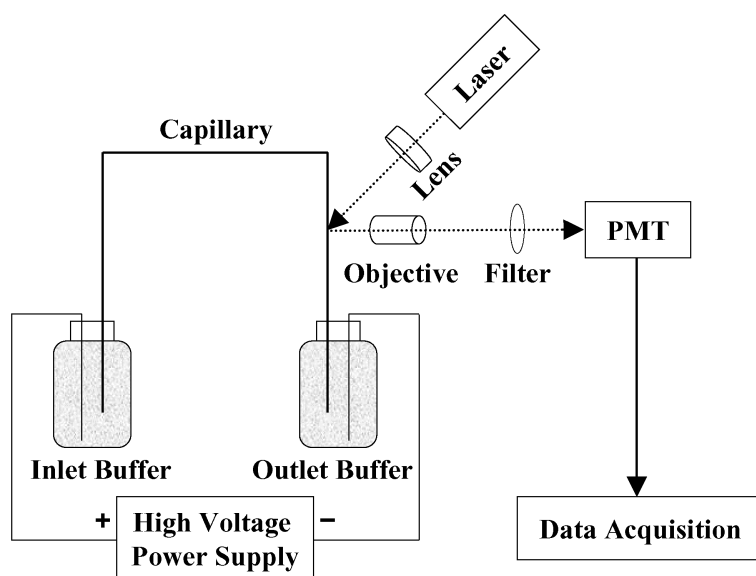
Wavelength (nm)	Type	Representative applications	Derivatizing agent	Comments
248	KrF	Proteins and DNA	none	pulsed, KrF gas used
266	Nd:YAG	Proteins, PAHs, and catecholamines	none	pulsed
275	Ar ⁺	Proteins, PAHs, and catecholamines	none	continuous
305	Ar ⁺	PAHs and catecholamines	none	continuous
325	He–Cd	Proteins	NBD	short lifetime
334	Ar ⁺	Proteins	DNS, OPA	continuous
355	Nd:YAG	Enzyme assay	NAD ⁺ + substrate → NADH + product	pulsed
363	Ar ⁺	Enzyme assay	NAD ⁺ + substrate → NADH + product	continuous
442	He–Cd	Proteins	NBD	short lifetime
488	Ar ⁺	Proteins and amino acids	FITC	continuous
543.6	He–Ne	DNA	YOYO-1	cheap, stable, low power

PAHs: polycyclic aromatic hydrocarbons. FITC: fluorescein isothiocyanate. DNS: dansyl halide. OPA: *o*-phthaldialdehyde. NBD: 4-chloro-7-nitro-2-oxa-1,3-diazole. YOYO-1: benzoxazolium-4-quinolinium dimer. NAD⁺: nicotinamide adenine dinucleotide.

Fluorescence Signal

Compared to absorption, fluorescence is highly selective and sensitive. However, only very few solutes of interest have excellent photophysical properties, including high molar absorptivity, quantum yield, and photostability.

Some solutes that can be detected by laser-induced native fluorescence (LINF) in CE, using mid- to deep-UV lasers, include proteins, nucleic acids, polycyclic aromatic hydrocarbons, and catecholamines. Most commonly used UV lasers include a continuous frequency-doubled Ar⁺ laser as well as pulsed excimer lasers and quadruplet

**Fig. 1** Instrumental setup of CE-LIF.

Nd:YAG laser. Although the analyses of proteins within single human erythrocytes and enzyme activity in cancer cells have been demonstrated by using a continuous UV laser,^[4] high costs and maintenance of the laser are problematic.

For those without native fluorescence, two common approaches have been employed, namely, derivatization and indirect fluorescence. Derivatizing agents should be pure, low fluorescent, and stable, as well as react quickly and uniquely with the analytes and, thus, formed compounds should be strongly fluorescent and stable. These include dansyl chloride, fluorescamine, 4-chloro-7-nitro-benz-2-oxa-1,3-diazole (NBD), *o*-phthalaldehyde (OPA), fluorescein isothiocyanate (FITC), and naphthalene-2,3-dicarboxaldehyde (NDA), which have been used for the analyses of amino acids, peptides, proteins, thiols, and sugars with LOD in 1–100 nM range. Compared to LINF, approaches based on derivatization provide the advantages of relatively low cost and versatility in instrumentation, but they may suffer from contamination and loss of temporal information.

Indirect LIF (ILIF), in conjunction with CE, has been widely used for the analysis of ionic solutes, including organic acids, inorganic anions, carbohydrates, amino acids, and metal ions.^[5] To optimize sensitivity, the use of an ionic dye with a greater fluorescent quantum yield and a very stable laser is essential, according to Eq. 1:

$$C_{\text{LOD}} = C_m / (\text{DR} \times \text{TR}) \quad (1)$$

where C_{LOD} is the concentration limit of detection; C_m is the concentration of relevant mobile-phase components; DR is the ability to measure a small change on top of a large signal and is equal to a signal-to-noise ratio (S/N) of the background signal; and TR refers to transfer ratio, which is the degree of displacement of the probe (co-ion) by the analyte. A system providing a high TR is also required for optimum sensitivity, as shown in Eq. 1, which can be realized by the use of fluorophores with a high charge density and a comparable mobility with analytes. By carefully controlling these factors, an LOD down to submicromolar for an analyte is easily achieved. As a result, the analysis of metal ions in single human erythrocytes by ILIF-CE has been demonstrated,^[6] but its use for macromolecules such as proteins and DNA has been limited. Owing to the use of low ionic-strength buffers for achieving a high TR, matrix interference is a common problem.

APPLICATIONS

With high resolution, rapidity, and sensitivity, CE-LIF has become one of the most important separation tools in

many fields. Most exciting research goals target at DNA sequencing, analysis of polymerase chain reaction products, single-cell analysis, single-molecule analysis, monitoring trace peptides and proteins in clinical analysis, determination of toxic chemicals, enantiospecific analyses in the fields of pharmaceutical drug research and production, etc. Herein we show some examples focusing on the analyses of DNA, proteins, and single cells.

DNA Sequencing and Separation

Although CE-LINF, using a UV Ar^+ laser, has been applied to the analysis of DNA, the majority has been performed by using visible lasers such as Ar^+ at 488 nm and He–Ne laser at 543.6 nm. These visible lasers are employed to excite DNA labeled covalently with fluorophores, such as modified fluorescein and rhodamine or intercalated DNA complexes. Some intercalating dyes, such as ethidium bromide (EtBr), benzothiazolium-4-quinolinium dimer (TOTO-1), benzoxazolium-4-quinolinium dimer (YOYO-1), and quinolinium-4-[(3-methyl-2(3*H*)-benzothiazolylidene)methyl]-1-[3-(trimethylammonio)propyl]-diodide (TOPRO-1), have been developed that fluoresce weakly unless they insert inside a DNA strand, resulting in a low background and strong fluorescence. Detection limits in the level of zeptomole for these intercalated complexes have been demonstrated. Owing to high quantum yields, greater stability of these intercalated complexes, and multiple labeled capability, single-molecule detection for large DNA molecules has been achieved.^[7] Moreover, some novel single-molecule-detection techniques have been developed and used to monitor the changes in DNA conformation (U-J-I) when migrating through gel matrices at applied electric fields.

Although DNA separation in CE relies on a sieving mechanism, like that in slab gel electrophoresis, polymer solutions prepared from linear polymers, such as linear polyacrylamide, poly(ethylene oxide), and cellulose derivatives, are commonly used, simply because they are of relatively low viscosity and are replaceable between runs. Polymer solutions can be filled into capillaries either under the influence of pressure prior to analysis in the absence of electroosmotic flow (EOF), or by electrokinetic means during analysis in the presence of EOF. By taking advantage of EOF, Huang et al. have demonstrated gradient CE techniques for optimizing resolution, sensitivity, and speed in the analysis of DNA,^[8] and on-line concentration techniques for DNA analysis with more than 400-fold improvement in the sensitivity, as shown in Fig. 2.^[9] One should note that the migration order is the reverse of that observed in conventional CE methods (in the absence of EOF), because of DNA migrating against EOF.



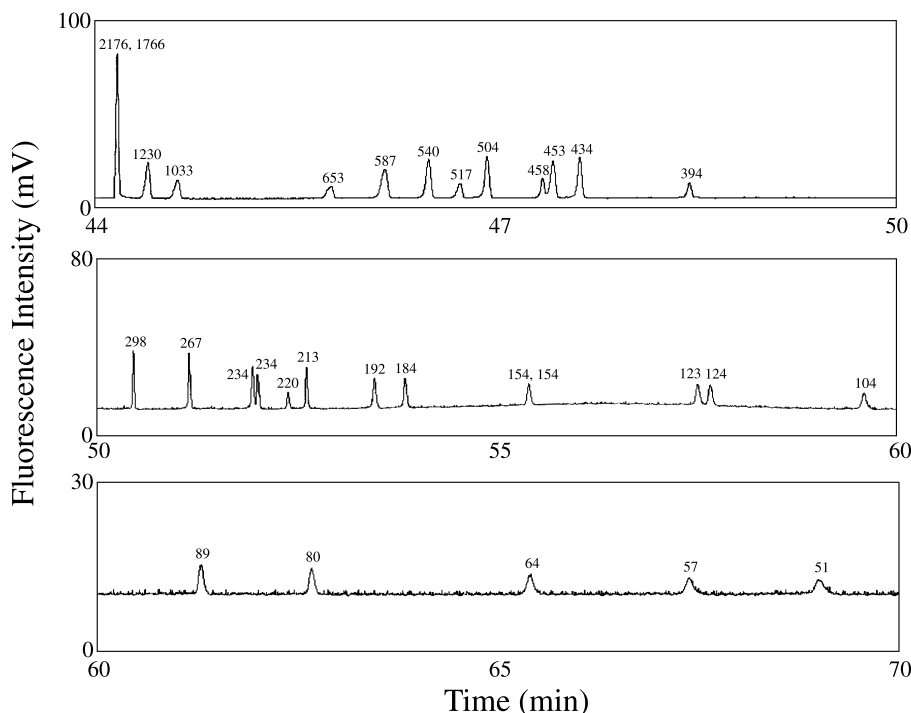


Fig. 2 Separation of 5 μ L 0.1 μ g/mL DNA markers V and VI prepared in 10 mM Tris-Borate (TB), pH 10.0, containing 2.5 mM NaCl at 444 V/cm for 30 min and, subsequently, at 222 V/cm for the rest using 2.5% PEO prepared in 200 mM TB, pH 9.0. Capillary: 45 cm in total length, 35 cm in effective length, 150 μ m ID, filled with 400 mM TB, pH 10.0. (From Ref. [9].)

The speed of CE is excellent compared to slab gel electrophoresis, but it is not throughput comparable to DNA sequencing. To overcome this disadvantage, the concept of high-throughput DNA analyzers, using an array of capillaries, has been realized and tested for DNA sequencing. One representative example is shown in Fig. 3.^[10] Parallel separations result in significant challenges, such as reproducibility among capillaries, detecting DNA migrating through as many as 1000 capillaries at one time, cross talk between capillaries, and signal procession. So far, some novel CAE systems utilizing multiple sheath flow, line focus illumination, confocal fluorescence scanner, rotary confocal fluorescence scanner, fiber optic array illumination, together with CCD detection, have been developed and tested for DNA sequencing, forensic short tandem repeats, and genotyping.

Single-Cell Analysis

Generally, capillaries with inner diameters of 5–25 μ m are used to inject and analyze single cells in CE. With such small capillaries, several features can be achieved, including low risk of injection of more than one cell at a time, low dilution factors after cell lysis, high resolving power, and rapidity at high electric field strengths. It is important to keep a very small dilution factor, as the

amounts of important markers in single cells are extremely low, mostly in the range of atomole–yoctomole. Besides, high resolving power is needed in order to separate a number of markers from a complicated cell environment. Although CE, in conjunction with mass spectrometry or amperometry, has been tested for single-cell analysis, most successful examples were conducted by CE-LIF. After injection of a cell into a capillary by pressure or electrokinetic means, lysis by osmosis, detergents, high voltage, or light takes place. When CE-LINF, using an Ar^+ laser at 275 nm is applied to detect proteins in erythrocytes, insulin contents in single islet cells, or catecholamines in adrenal medullary cells, the lysis components are directly subject to separation and detection. The success of these methods relies on the high sensitivity of LINF, with LOD values for proteins and catecholamines lower than nanomolar. For example, the determination of epinephrine and norepinephrine in individual bovine adrenal medullary cells, under acidic conditions, has been demonstrated.^[11] Using a 285 groove/mm holographic grating and a CCD camera for detection, identification of ~ 30 compounds within single-neuron cells has been demonstrated using a frequency-doubled Ar^+ laser at 257 nm. When derivatization is required, background electrolytes containing suitable derivatizing agents are commonly used to perform on-column reaction. Compared to

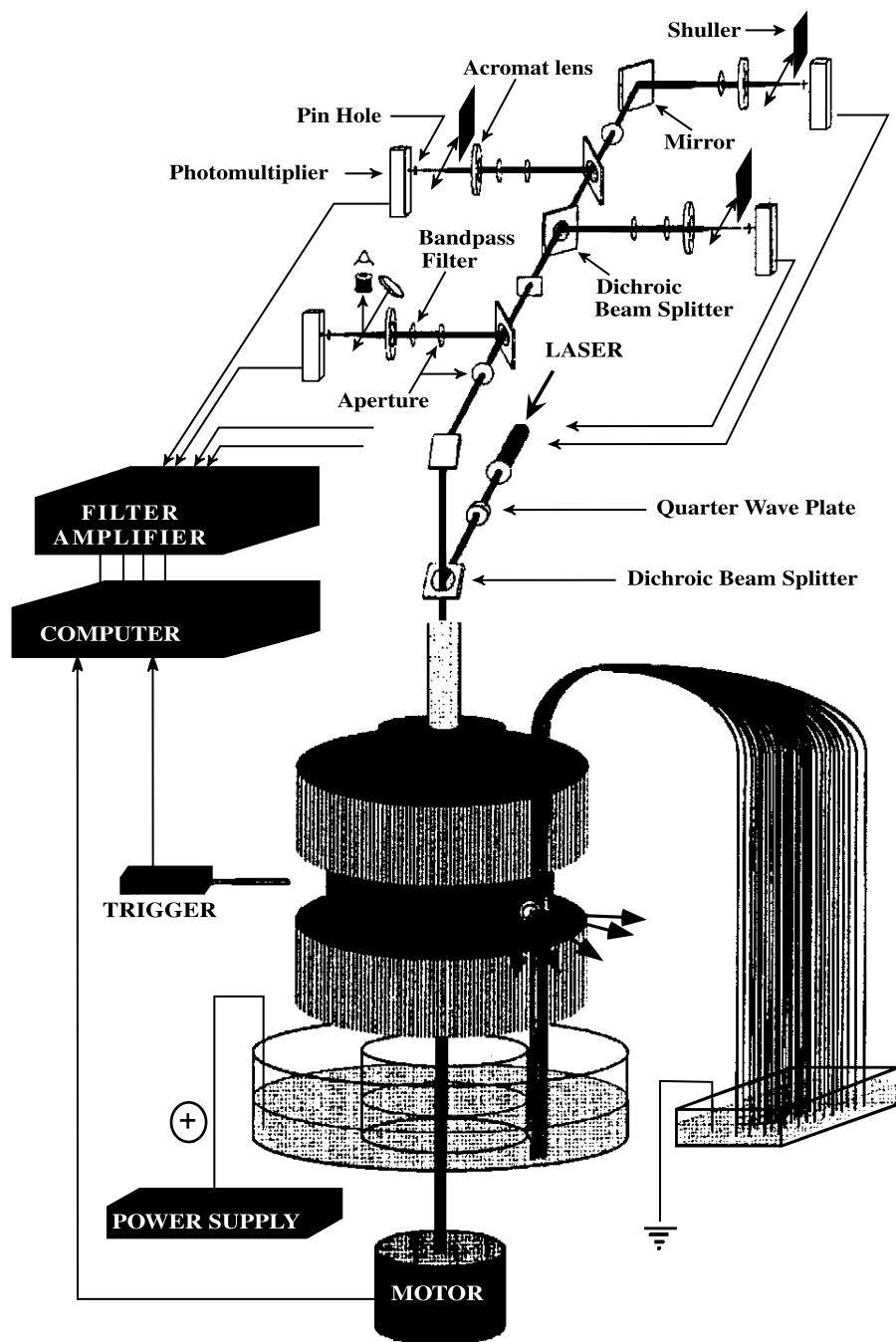


Fig. 3 Schematic representation of a 1000-capillary rotary scanner and a four-color confocal fluorescence detection system. (From Ref. [10].)

off-column derivatization, on-column reaction provides the advantages of low risk of contamination, low dilution factors, simplicity, and rapidity. One example is the use of naphthalene-2,3-dicarboxaldehyde and CN^- for the determination of dopamine and five amino acids in individual rat pheochromocytoma cells.^[12] To increase the sensitivity and specificity, capillary affinity electrophor-

esis, in conjunction with immunoassay using antibody-fluorescein, has been developed for the determination of insulin in single islet cells.^[13] In addition, the application of on-line enzyme assay, using an Ar^+ laser at 366 nm, has been demonstrated in the comparison of the activity of lactate dehydrogenase (LDH) in lymphoblastic cells and leukemia cells. With a high turnover number and



low LOD for NADH, the same strategy has also been applied to the determination of the activity of single LDH molecules.

Protein Analysis

Proteomics is becoming increasingly important following the human genome era because proteins are the main catalysts, structural elements, signaling messengers, and molecular machines of biological tissues. A proteome represents the protein pattern of an organism, a cell, an organelle, or even a body fluid determined quantitatively at a certain time under precisely defined conditions. With high sensitivity and resolution, CE-LIF has shown high potential for quantification of proteins and exploration of their localization, modification, interaction, activity, and, ultimately, their function. In addition to separations based on a sieving mechanism, capillary zone electrophoresis using fused-silica capillary at low pH, high pH, or in high-conductivity background electrolytes, or using coated capillaries under mild conditions has been applied to the analysis of proteins. Besides, isotachopheresis and iso-electric focusing in capillaries have shown to be useful for separation of proteins. Although an Ar⁺ laser at 275 nm and Kr⁺ laser at 280 nm have been commonly used for protein analysis in CE-LINF, relatively inexpensive Nd:YAG pulsed laser at 266 nm and KrF excimer laser at 248 nm have also been employed. Generally speaking, pulsed lasers provide about 10 times higher LOD than continuous laser sources (former case). In spite of this, the LOD values down to picomolar for proteins have been achieved using a Nd:YAG laser when applying an on-line concentration technique.^[14] When performing CE-LINF for protein analysis, a great effort must be made to minimize interferences, photobleaching, and quenching that may occur at low pH, high pH, high salt concentrations, and the existence of detergents. On the other hand, these problems can be minimized or prevented by careful selection of visible lasers, such as He-Ne lasers and dyes such as 3-(2-furoyl)quinoline-2-carboxaldehyde (FQ), NDA, Sypro Red, and Nile Red. Lee et al. have demonstrated protein analysis by on-column reaction using FQ, with a LOD of picomolar when excited with Ar⁺ laser at 488 nm.^[15] One drawback of performing derivatization is that multiple derivatization and byproducts might occur, leading to difficulty of separation.

CONCLUSION

With high sensitivity, rapidity, and high efficiency, CE-LIF has proved to be a powerful tool in the analysis of

DNA, proteins, amino acids, glycoproteins, and single cells. To prevent photobleaching, as well as to reduce autofluorescence background and the cost of lasers, the use of diode lasers in the near-infrared region, together with suitable dyes, as well as sensitive detectors such as avalanche photodiode, has attracted much interest, which has been demonstrated in DNA sequencing and single-molecule detection. As the analyses of a single DNA molecule and single enzyme activity by CE-LIF have been demonstrated, its role in disease diagnosis and fundamental research, such as the interactions between DNA and proteins, will soon be recognized in many realms, such as in the life sciences. Recently, micrototal-analysis systems with LIF have become increasingly important in modern science and have been applied to the analysis of PCR products or enzyme activity in a chip. Thus it is our belief that, despite LIF, some other laser techniques such as thermal lens absorption and Raman scattering spectroscopy will continue to play a strong role in the life sciences.

ACKNOWLEDGMENT

This work was supported by the National Science Council of the Republic of China under contract number NSC 90-2113-M002-058.

REFERENCES

1. Gassmann, E.; Kuo, J.E.; Zare, R.N. Electrokinetic separation of chiral compounds. *Science* **1985**, *230* (4727), 813–814.
2. Tseng, W.-L.; Chiu, T.-C.; Weng, J.-M.; Chang, H.-T. Analysis of albumins using albumin blue 580, by capillary electrophoresis and laser-induced fluorescence. *J. Liq. Chromatogr. Relat. Technol.* **2001**, *24* (19), 2971–2982.
3. Wu, S.; Dovichi, N.J. High-sensitivity fluorescence detector for fluorescein isothiocyanate derivatives of amino acids separated by capillary zone electrophoresis. *J. Chromatogr.* **1989**, *480* (1), 141–155.
4. Yeung, E.S. Study of single cells by using capillary electrophoresis and native fluorescence detection. *J. Chromatogr., A* **1999**, *830* (2), 243–262.
5. Chiu, T.-C.; Huang, M.-F.; Huang, C.-C.; Hsieh, M.-M.; Chang, H.-T. Indirect fluorescence of aliphatic carboxylic acids in non-aqueous capillary electrophoresis using merocyanine 540. *Electrophoresis* **2002**, *23* (2), 449–455.
6. Hogan, B.L.; Yeung, E.S. Determination of intracellular species at the level of a single erythrocyte via capillary electrophoresis with direct and indirect fluorescence detection. *Anal. Chem.* **1992**, *64* (22), 2841–2845.

7. Ma, Y.; Shortreed, M.R.; Yeung, E.S. High-throughput single-molecule spectroscopy in free solution. *Anal. Chem.* **2000**, *72* (19), 4640–4645.
8. Huang, M.-F.; Hsu, C.-E.; Tseng, W.-L.; Lin, Y.-C.; Chang, H.-T. Separation of dsDNA in the presence of electroosmotic flow under discontinuous conditions. *Electrophoresis* **2001**, *1* (11), 2281–2290.
9. Huang, C.-C.; Hsieh, M.-M.; Chiu, T.-C.; Lin, Y.-C.; Chang, H.-T. Maximization of injection volumes for DNA analysis in capillary electrophoresis. *Electrophoresis* **2001**, *22* (20), 4328–4332.
10. Scherer, J.R.; Kheterpal, I.; Radhakrishnan, A.; Ja, W.W.; Mathies, R.A. Ultra-high throughput rotary capillary array electrophoresis scanner for fluorescent DNA sequencing and analysis. *Electrophoresis* **1999**, *20* (7), 1508–1517.
11. Chang, H.-T.; Yeung, E.S. Determination of catecholamines in single adrenal medullary cells by capillary electrophoresis and laser-induced native fluorescence. *Anal. Chem.* **1995**, *67* (6), 1079–1083.
12. Gilman, S.D.; Ewing, A.G. Analysis of single cells by capillary electrophoresis with on-column derivatization and laser-induced fluorescence detection. *Anal. Chem.* **1995**, *67* (1), 58–64.
13. Tao, L.; Kennedy, R.T. On-line competitive immunoassay for insulin based on capillary electrophoresis with laser-induced fluorescence detection. *Anal. Chem.* **1996**, *68* (22), 3899–3906.
14. Tseng, W.-L.; Chang, H.-T. On-line concentration and separation of proteins by capillary electrophoresis using polymer solutions. *Anal. Chem.* **2000**, *72* (20), 4805–4811.
15. Lee, I.H.; Pinto, D.; Arriaga, E.A.; Zhang, Z.; Dovichi, N.J. Picomolar analysis of proteins using electrophoretically mediated microanalysis and capillary electrophoresis with laser-induced fluorescence detection. *Anal. Chem.* **1998**, *70* (21), 4546–4548.



LC-NMR and LC-MS-NMR: Recent Technological Advancements

Maria Victoria Silva Elipe

Merck Research Laboratories, Rahway, New Jersey, U.S.A.

INTRODUCTION

During the last decade, hyphenated analytical techniques have grown rapidly to solve complex analytical problems. The combination of separation technologies with spectroscopic techniques is extremely powerful in carrying out qualitative and quantitative analysis of unknown compounds in complex matrices. High-performance liquid chromatography (HPLC) is the most widely used analytical separation technique for the qualitative and quantitative determination of compounds in solution. Mass spectrometry (MS) and nuclear magnetic resonance (NMR) are the primary analytical techniques that provide structural information for the analytes. The physical connection of HPLC and MS (liquid chromatography-mass spectrometry, LC-MS) or NMR (LC-NMR) increases the capability of analysts to solve structural problems of mixtures of unknown compounds. LC-MS has been the more extensively applied hyphenated technique because MS has higher sensitivity than NMR.^[1-3] Recent advances in NMR, LC-NMR, and even LC-MS-NMR have enabled these techniques to become routine analytical tools in many laboratories. This article provides an overview of the LC-NMR and LC-MS-NMR techniques with a description of their limitations, together with an example of LC-MS-NMR to illustrate the data generated by these hyphenated techniques. This article is not meant to imply that LC-MS-NMR will replace LC-MS, LC-NMR, or NMR techniques for structural elucidation of compounds. LC-MS-NMR, together with LC-MS, LC-NMR, and NMR, are techniques that should be available and applied to appropriate cases based on their advantages and limitations.

PRACTICAL ISSUES OF LC-NMR

NMR is one of the most powerful techniques for elucidating the structures of organic compounds. Before undertaking the NMR analysis of a complex mixture, separation of the individual components by chromatography is required. LC-MS is routinely used to analyze mixtures without prior isolation of their components. In many cases, however, NMR is needed for the identifica-

tion of ambiguous structures. Although hyphenated LC-NMR has been known since the late 1970s,^[4-6] it has not been widely implemented until the last decade.^[7,8] The major technical considerations of LC-NMR are NMR sensitivity, NMR and chromatographically compatible solvents, solvent suppression, NMR flow-probe design, and compatibility of the sensitivity vs. the volume for the chromatographic peak with the volume of the NMR flow cell.

NMR is a less sensitive technique compared to MS and, hence, requires much larger samples for analysis. MS analysis is routinely carried out in the picogram range. Modern high field NMR spectrometers (400 MHz and higher) can detect proton signals from pure demonstration samples well into the nanogram range (MW 300 Da). For real world samples, however, purity problems become more intrusive with diminishing sample size and can be overwhelming in the submicrogram domain. This places a practical lower limit for most structural elucidation by NMR, which is estimated by the author to be close to 500 ng (MW 300 Da).

Although several other important nuclides can be detected by NMR, proton (¹H) NMR remains the most widely used because of its high sensitivity, high isotopic natural abundance (99.985%), and its ubiquitous presence in organic compounds. Of comparable importance is carbon (¹³C), with 1.108% abundance which, because of substantial improvements in instrument sensitivity, is now utilized as routinely as proton. Fluorine (¹⁹F), with 100% abundance, is used less often because it is present in only about 10% of pharmaceutical compounds. Another consequence of the intrinsic low sensitivity of NMR is that virtually all samples require signal averaging to reach an acceptable signal-to-noise level. Depending on the sample size, signal averaging may range anywhere from several minutes to several days. For metabolites in the 1–10 µg range, for example, overnight experiments are generally necessary.

Liquid NMR requires the use of deuterated solvents. Conventionally, the sample is analyzed as a solution using a 5- or 3-mm NMR tube, depending on the NMR probe, which requires ca. 500 or 150 µL, respectively, of deuterated solvents. The increased solvent requirement for LC-NMR makes this technique highly expensive.



Deuterium oxide (D_2O) is the most readily available, reasonably priced solvent (over \$300/L). The cost of deuterated acetonitrile (CD_3CN) is dropping and varies, depending on the percentage of included D_2O , but still exceeds \$1000/L. Deuterated methanol (CD_3OD) is even more expensive. Deuterated solvents for normal-phase columns are not readily available, but those that are available have even more prohibitive price tags. This necessitates the use of reverse-phase columns. Another factor that raises concern is the compatibility of the HPLC gradient-solvent system with the NMR operations. An HPLC gradient-solvent system greater than 2–3%/min causes problems in optimizing the magnetic field homogeneity (shimming) because of solvent mixing in the flow cell.

During the LC-NMR run, the solvent signal in the chromatographic peak is much larger than those of the sample and needs to be suppressed. Even with deuterated solvents, the residual proton solvent signals need to be suppressed. In the case of acetonitrile, the two ^{13}C satellite peaks of either the protonated or residual protonated methyl group for CH_3CN or CD_3CN need to be suppressed because they are typically much larger than signals from the sample. In 1995, Smallcombe and coworkers^[9] optimized the WET (water suppression enhanced through T1 effects) solvent suppression technique, which greatly improves the quality of spectra generated during LC-NMR. One disadvantage of suppressing the solvent lines is that any nearby analyte signal will also be suppressed, resulting in loss of structural information.

Conventional NMR flow cells have an active volume of 60 μL (i.e., corresponds to the length of the receiver coil), and a total volume of 120 μL . This means that NMR will only “see” 60 μL of the chromatographic peak. If the flow rate in the HPLC system is 1 mL/min, when 4.6 mm columns are used, only 3.6 sec of the chromatographic peak will be “seen” by NMR. Chromatographic peaks are generally much wider than 4 sec, indicating that less than half of the chromatographic peak will be detected. This is one of the disadvantages of LC-NMR, compared with conventional 3-mm NMR probes where the amount of sample “seen” by NMR receiver coil is independent of the width of the chromatographic peak.

Because NMR is a low-sensitivity technique that requires samples in the order of several micrograms, analytical HPLC columns have to be saturated when injecting samples in that range. This will affect the chromatographic resolution and separation because resolution is often degraded when sample injection is scaled-up to that level. Another factor that can affect chromatographic performance is the use of deuterated solvents. In many cases, analytes show different retention times from nondeuterated solvents, resulting in occasional peak broadening.

When this occurs, more study is required in order to obtain reasonable resolution.

There are many examples in the literature of applications of LC-NMR in natural products,^[10–13] food analysis,^[14] metabolites^[15–17] degradation products,^[18] drug impurities,^[19] and drug discovery.^[20]

Other chromatographic techniques have been coupled on-line to NMR for additional applications—such as size-exclusion chromatography (SEC), as SEC-NMR;^[21] solid-phase extraction (SPE), as SPE-NMR;^[22] capillary electrophoresis (CE), as CE-NMR;^[23] and capillary electrochromatography (CEC), as CEC-NMR^[24]—as examples. CE-NMR and CEC-NMR are techniques that work with very small-volume NMR probes, with capillary separations. Recently, more developments have been carried out to hyphenate capillary-based HPLC (capLC) with NMR (capLC-NMR) and the use of commercial microcoil NMR probes.^[25,26] With microcoil NMR probes, the range of sample used in capLC-NMR could reach the nanogram level (low nanogram level only for detection limit, but not for structural analysis).^[25,26] With this technique, the volume of the chromatographic peak is comparable with the volume of the microcoil NMR flow cell.

OPERATIONAL MODES OF LC-NMR

The HPLC is connected by red PEEK tubing to the NMR flow cell, which is inside the magnet. With shielded cryomagnets, the HPLC can be as close as 30–50 cm to the magnet vs. 1.5–2 m for conventional magnets. Normally, an ultraviolet (UV) detector is used in the HPLC system to monitor the chromatographic run. Radioactivity or fluorescent detectors can also be used to trigger the chromatographic peak of interest.

There are four general modes of operation for LC-NMR: on-flow, stop-flow, time-sliced, and loop collection.

On-flow or continuous-flow experiments require more sample to analyze “on the fly” because the resident time in the NMR flow cell is very short (3.6 sec at 1 mL/min) during the chromatographic run.

Stop-flow requires the calibration of the delay time, which is the time required for the sample to travel from the UV detector to the NMR flow cell, which depends, in turn, on the flow rate and the length of the tubing connecting HPLC with NMR. Because the chromatographic run is automatically stopped when the chromatographic peak of interest is in the flow cell, the amount of sample required for the analysis can be reduced and 2-D NMR experiments, such as correlation spectroscopy (COSY), total correlation spectroscopy (TOCSY), and others, can be obtained because the sample can remain inside the flow cell for days. It is possible to obtain NMR

data on a number of chromatographic peaks in a series of stops during the chromatographic run without on-column diffusion that causes loss of resolution, but only if the NMR data for each chromatographic peak can be acquired in a short time (30 min or less).

“Time-sliced” operation involves a series of stops during the elution of a chromatographic peak of interest. Time-sliced is used when two analytes elute together or with close retention times, or when the separation is poor.

Loop collection can be used when there is more than one chromatographic peak of interest. Chromatographic peaks are stored in loops for later off-line NMR study. In this case, the analytes must be stable inside the loops during the extended period of the analysis. Capillary tubing should be used to avoid peak broadening with concomitant loss of analyte “seen” by the NMR spectrometer.

PRACTICAL ISSUES OF LC-MS-NMR

NMR and MS data for the same analyte is crucial for structural elucidation. When different isolates are analyzed by NMR and MS, one cannot always be certain that the NMR and the MS data apply to the same analyte. To avoid this ambiguity, LC-MS and LC-NMR are combined. MS data should be obtained initially because with NMR, data collection in the stop-flow mode can take hours or

days, depending on the complexity of the structure and the amount of sample. This is why it is preferable to designate this operation as LC-MS-NMR rather than LC-NMR-MS.

Because MS is considerably more sensitive than NMR, a splitter is incorporated after the HPLC to direct the sample to the MS and NMR units separately. In our laboratories, the MS used in these studies is a Classic LCQ instrument (ThermoFinnigan, CA). A custom-made splitter was used with a splitting ratio of 1:100 (Acurate™, LC Packings, CA). It was designed to deliver 1% of the sample initially to the MS and the balance 20 sec later to the NMR. With a flow rate of 1 mL/min, the final flow rate going to the NMR will be 0.990 mL/min and to the MS will be 0.010 mL/min. Electrospray is the only source of ionization that will work with such a low flow rate (10 μ L/min) in LCQ. Fig. 1 depicts the scheme of our LC-MS-NMR system.

Another consideration for the LC-MS-NMR is the use of deuterated solvents needed for NMR. Analytes with exchangeable or “active” hydrogens can exchange (i.e., equilibrate) with deuterium (^2H) at different rates. The analyst should be alerted to this possibility because it could result in the appearance of several closely spaced molecular ions.

There are examples in the literature for the application of LC-MS-NMR in natural products^[27] and drug metabolism.^[28–33]

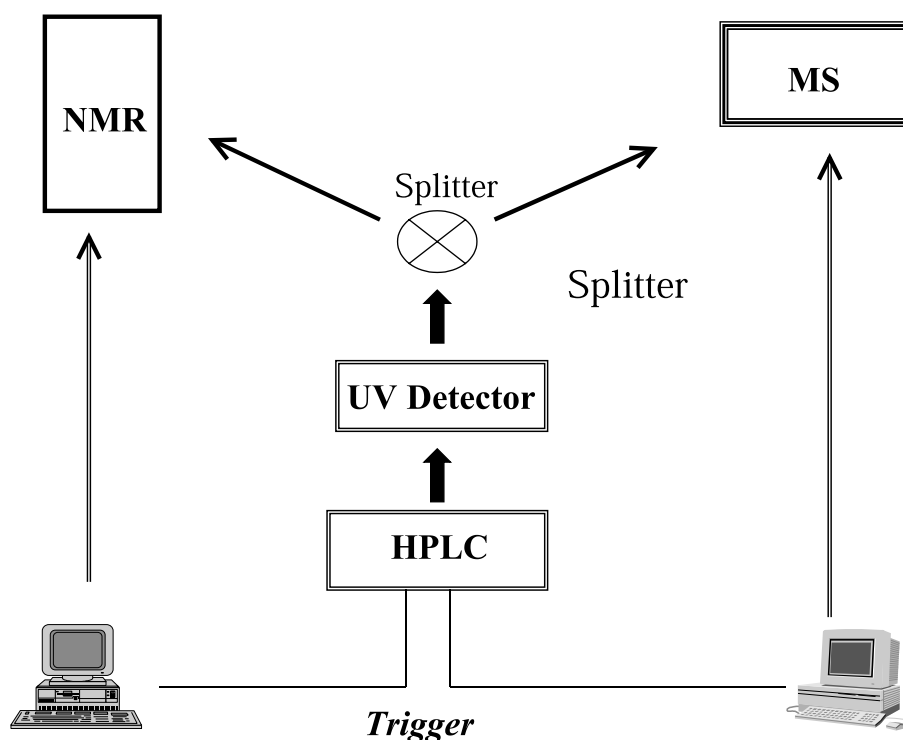


Fig. 1 Schematic set-up for the LC-MS-NMR system.



OPERATIONAL MODES OF LC-MS-NMR

As mentioned in the section "Operational Modes of LC-NMR," with the use of shielded cryomagnets the location of the MS instrument will follow the same rule as that for the HPLC. The most common modes of operation for LC-MS-NMR are on-flow and stop-flow. With stop-flow, the MS instrument can also be used to stop the flow on the chromatographic peak of interest that is to be analyzed by NMR.

In the last three years, there have been relatively few examples in the literature that deal with the application of LC-MS-NMR. We have been interested in evaluating this technology in our laboratory to determine the pros and cons, and to decide which cases are suitable for this application. To illustrate these modes of operation, a group of flavonoids was chosen. These compounds have simple structures with primarily aromatic protons; some have low field aliphatic protons, which would not be

hidden under the NMR solvent peaks. Phenolic protons exchange fast enough with D₂O so that each compound will only show one molecular ion. Flavonoids are natural products with important biological functions, acting as antioxidants, free radical scavengers, and metal chelators, and are related to the food industry. Fig. 2 shows the group of eight flavonoids chosen for these studies.

The chromatographic conditions used for these studies were as follows: 35–50% B 0–10 min, 50–80% B 10–15 min, A: D₂O, B: ACN, 1 mL/min, 287 nm, Discovery C18 column 15 × 4.6 cm, 5 μm. Stock solutions of each compound were prepared at 1 μg/μL in ACN/MeOH (1:1).

A Varian Unity Inova 600 MHz NMR instrument (Palo Alto, CA), equipped with a ¹H{¹³C/¹⁵N} pulse field gradient triple resonance microflow NMR probe (flow cell 60 μL; 3 mm O.D.), was used. Reverse-phase HPLC of the samples was carried out with a Varian modular HPLC system (a 9012 pump and a 9065 photodiode array UV detector). The Varian HPLC software was also

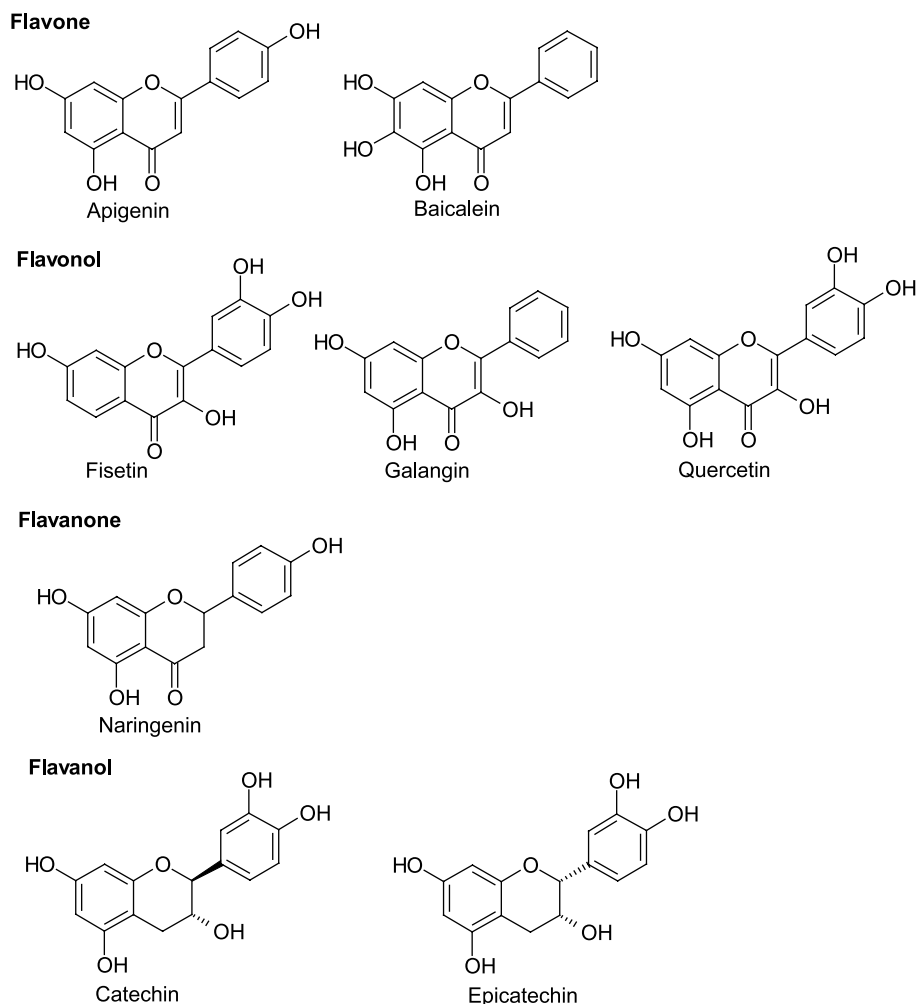


Fig. 2 Structures of eight flavonoids used for the LC-MS-NMR technology development studies.

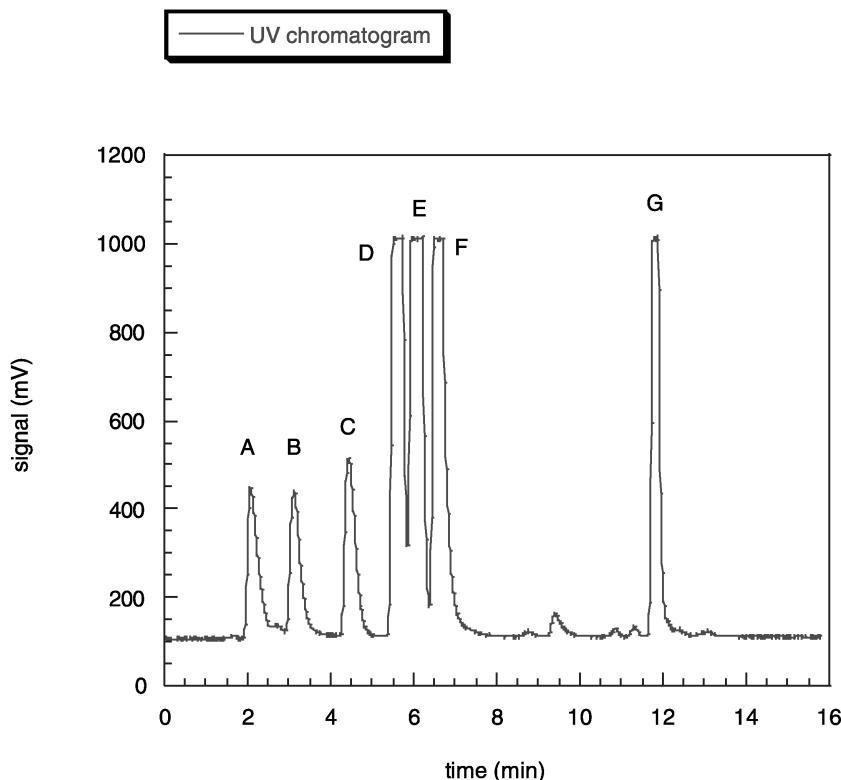


Fig. 3 UV chromatogram of the on-flow experiment injecting a mixture of eight flavonoids (A: Catechin + Epicatechin; B: Fisetin; C: Quercetin; D: Apigenin; E: Naringenin; F: Baicalein; G: Galangin).

equipped with the capability for programmable stop-flow experiments based on UV peak detection. An LCQ classic MS instrument, mentioned in the previous section, was connected, on-line, to the HPLC–UV system of the LC-NMR by contact closure. The ^2H resonance of the D_2O was used for field-frequency lock and the spectra were centered on the ACN methyl resonance. Suppression of resonances from HOD, the residual protonated signal of D_2O , and the methyl of ACN and its two ^{13}C satellites was accomplished by means of a train of four selective WET pulses, each followed by a B_0 gradient pulse and a composite 90° read pulse.^[9]

The on-flow experiment was carried out on a mixture of eight flavonoids (Fig. 2) (20 μg each). MS and NMR data were obtained during this on-flow experiment. The UV chromatogram is depicted in Fig. 3. Table 1 and Fig. 4 show the pseudo-molecular ion information $[\text{M}-^2\text{H}]^-$, where M is the molecular weight with all the hydroxyl protons deuterated, in negative mode, for the eight flavonoids obtained in this on-flow experiment. Fig. 5 is the 2-D data set (time vs. chemical shift) where each ^1H NMR spectrum was acquired for 16 scans and decreasing the delays (total time per spectrum of 20 s). Fig. 6 depicts the ^1H NMR traces of each flavonoid extracted from the 2-D data set. It is notable that catechin

and epicatechin co-elute under these conditions (peak A of the UV chromatogram of Fig. 3). Distinguishing these diastereomers by MS alone is not feasible. Differences in the NMR spectra would be expected, and are in fact, observed. The ability of LC-MS-NMR to distinguish signals from individual diastereomers is illustrated in Figs. 5 and 6a.

Two stop-flow experiments were carried out on apigenin (10 μg) (Fig. 2) by using, independently, the UV peak maximum or the molecular ion chromatographic

Table 1 MS data of flavonoids in negative mode from the on-flow run in the LC-MS–NMR

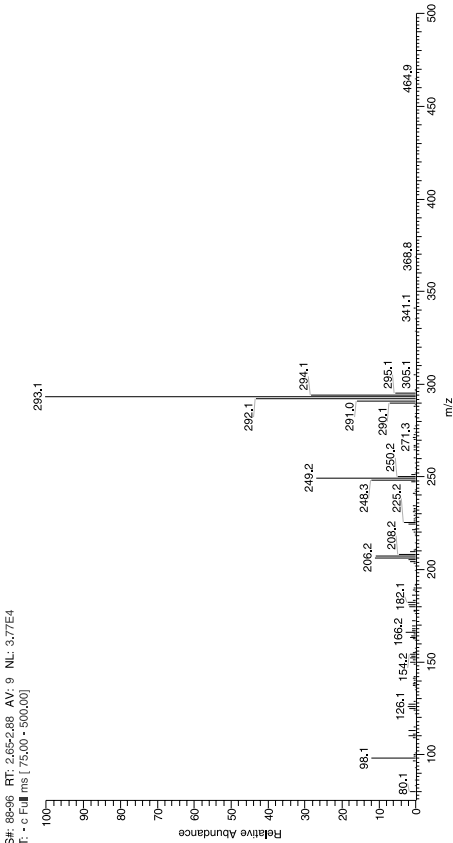
Peak	Compound	MW ^a	MW ^b	<i>m/z</i>
A	Catechin + Epicatechin	290	295	293
B	Fisetin	286	290	288
C	Quercetin	302	307	305
D	Apigenin	270	273	271
E	Naringenin	272	275	273
F	Baicalein	270	273	271
G	Galangin	270	273	271

^aMolecular weight.

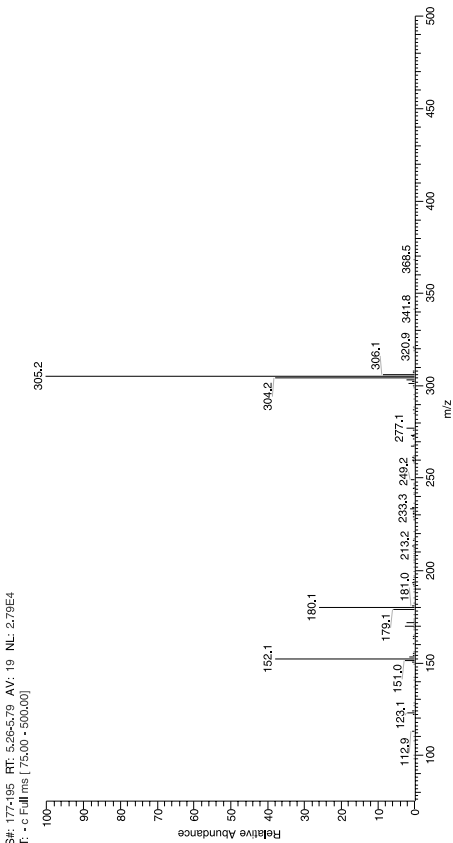
^bMolecular weight with all the hydroxyl protons deuterated.



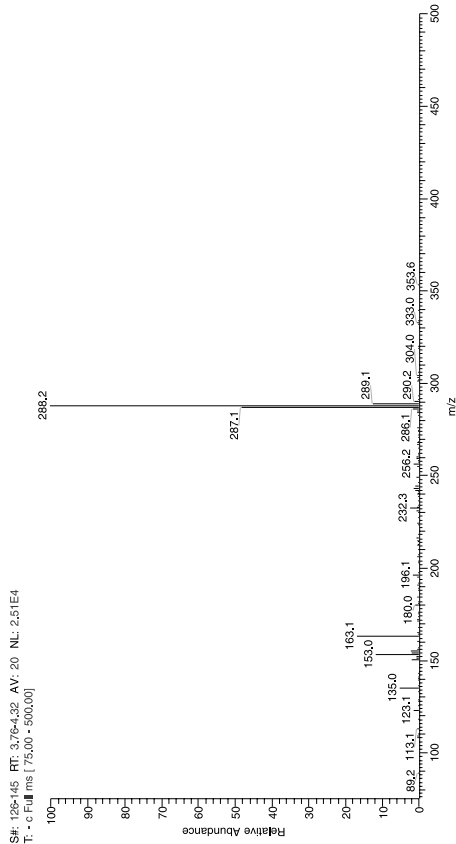
A: Catechin + Epicatechin



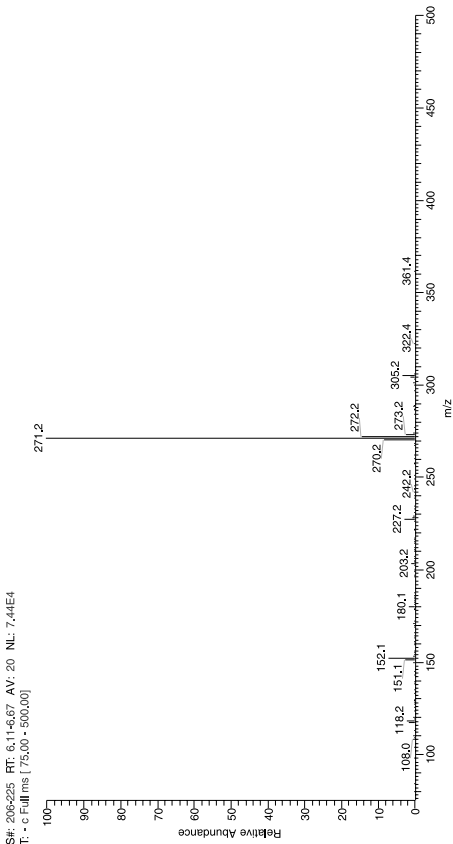
C: Quercetin



B: Fisetin



D: Apigenin



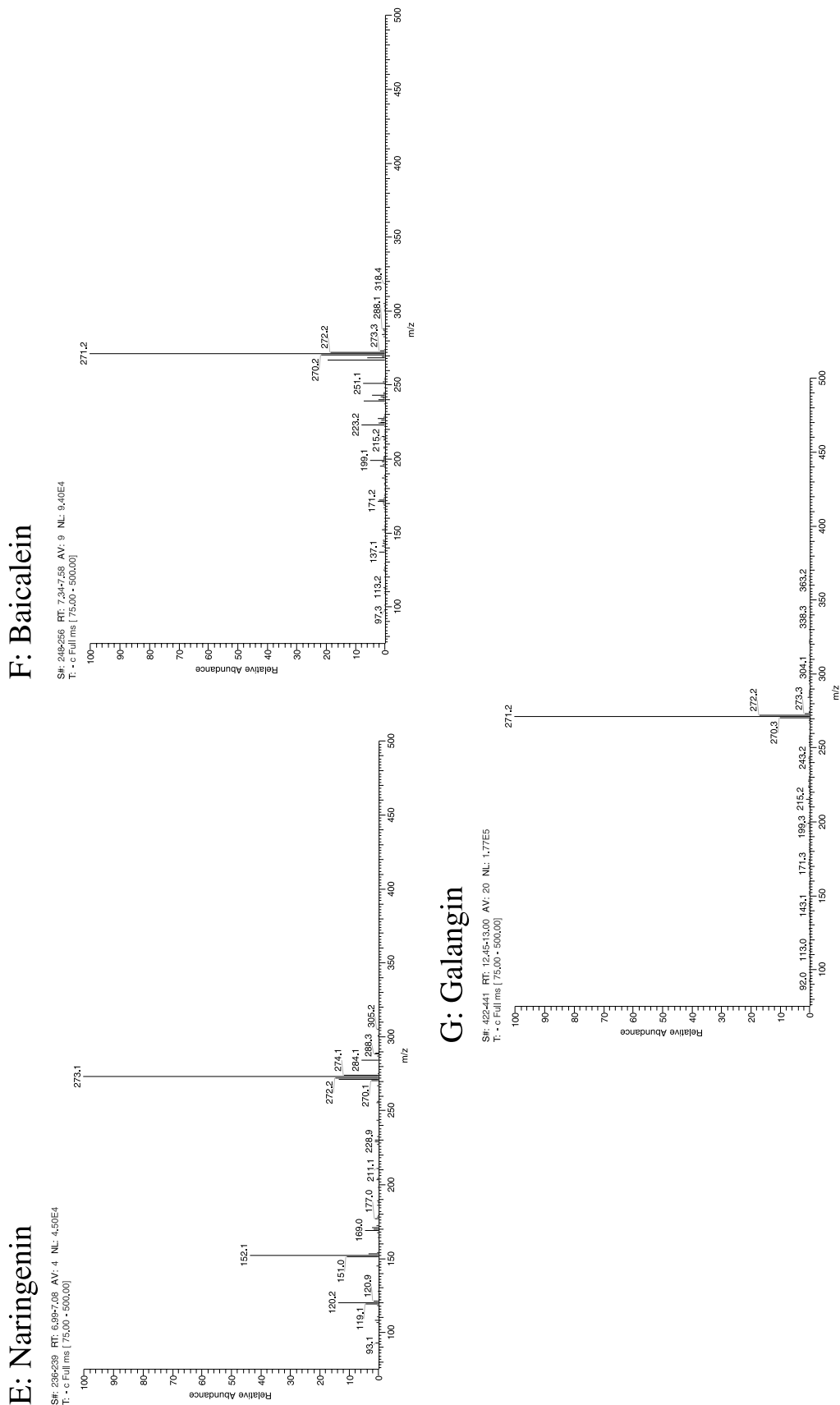


Fig. 4 MS data on the on-flow experiment of the eight flavonoids (A: Catechin + Epicatechin; B: Fisetin; C: Quercetin; D: Apigenin; E: Naringenin; F: Baicalein; G: Galangin).



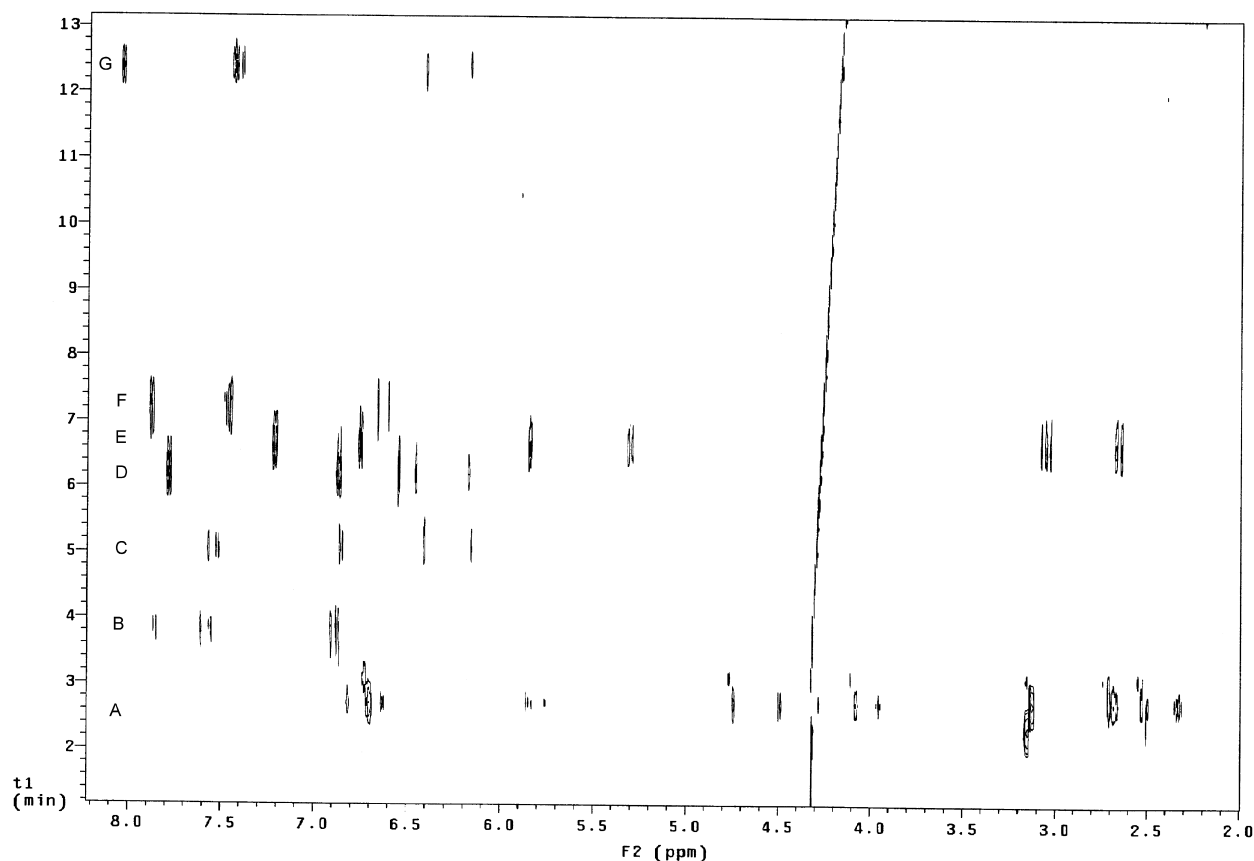


Fig. 5 2-D data set (time/min vs. chemical shift/ppm) for the on-flow experiment injecting a mixture of eight flavonoids (A: Catechin+Epicatechin; B: Fisetin; C: Quercetin; D: Apigenin; E: Naringenin; F: Baicalein; G: Galangin).

peak seen in the MS instrument to trigger the stop-flow. The Varian software triggers the stop-flow automatically with the UV peak, so this mode was used as a reference point. When the MS was used to trigger the stop-flow, it was carried out manually with a chronometer while the molecular ion of apigenin was being monitored in negative mode (m/z 275). After peak detection in the UV or MS and a time delay of about 52 or 20 sec, respectively, the HPLC pump was stopped, trapping the peak of interest in the LC-NMR microprobe. ^1H NMR stop-flow spectra were acquired using an acquisition time of 1.5 sec, a delay between the successive pulses of 0.5 sec, a spectral width of 9000 Hz, and 32 K time-domain data points. The methyl resonance of ACN was referenced to 1.94 ppm. These two experiments were carried out by injecting 10 μg of apigenin and acquiring ^1H NMR spectra for ca. 4.5 min (128 scans), giving rise to the same quality of ^1H NMR spectra of apigenin (Fig. 7).

These experiments indicate that for sample mixtures, the on-flow mode of LC-MS-NMR is useful in obtaining structural information for the major components. If more detailed analysis is required, or the amount of sample is

small and the compound(s) cannot be isolated because of instability, stop-flow is the mode of choice. LC-MS and LC-NMR chromatographic conditions must be compatible; in addition, prior evaluation of the LC conditions on the LC-MS-NMR system needs to be carried out to assure consistency with the chromatographic resolution needed in the LC-NMR part of the system. The sample must ionize well by electrospray to obtain MS data. To use MS to trigger halting the flow in the stop-flow mode, prior MS information of the chromatographic peak(s) of interest in deuterated solvent(s) is needed to evaluate the suitability of the system in providing structural information.

CONCLUSIONS

Hyphenated analytical and spectroscopic techniques have enhanced the ability of analysts to solve structural problems. Until the advent of recent developments in NMR, LC-MS had been the only hyphenated technique for qualitative analysis of structures on mixtures. NMR could

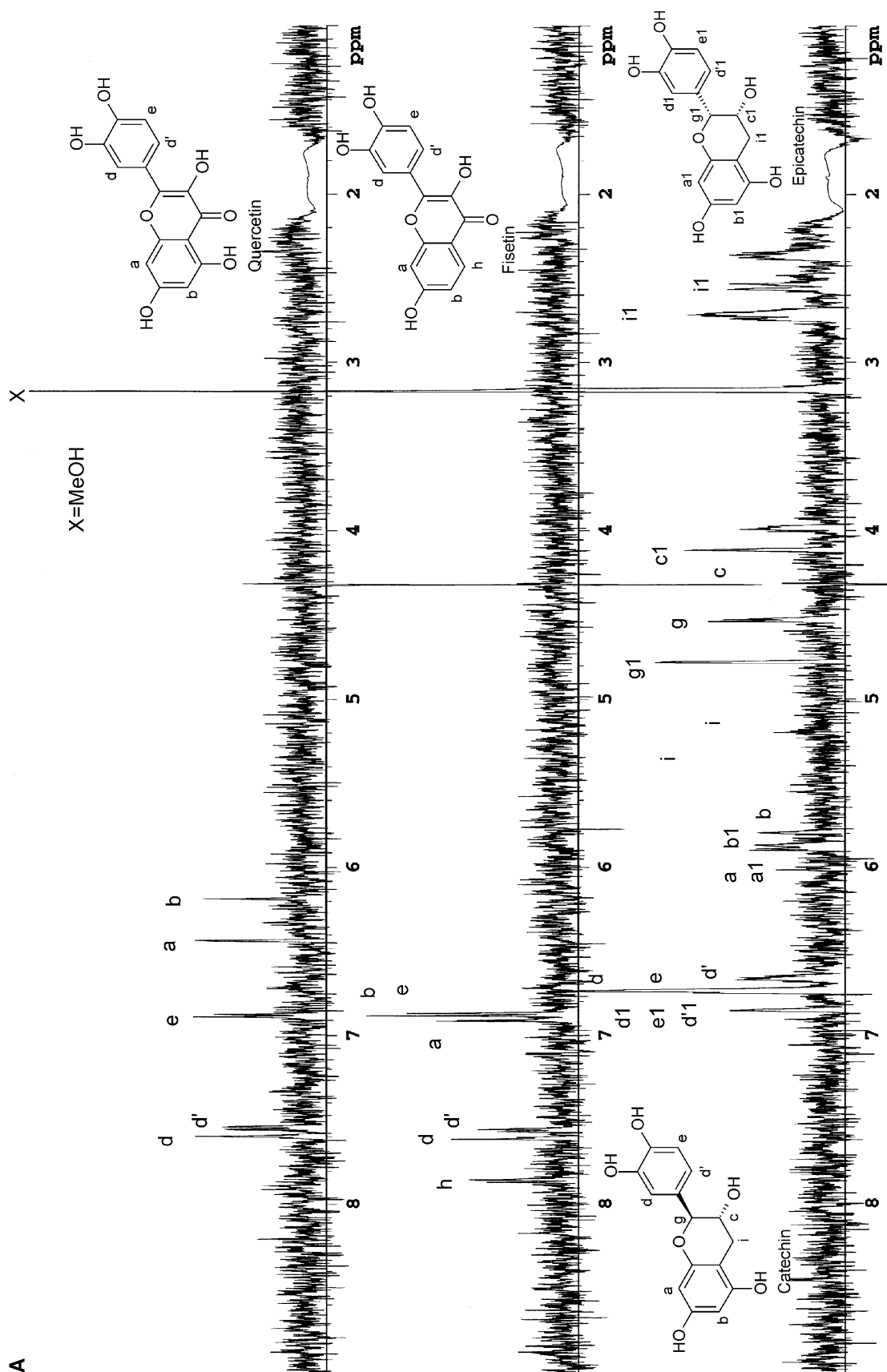


Fig. 6 (A) ^1H NMR trace spectra from the 2-D data set of the on-flow experiment of Catechin and Epicatechin (bottom), Fisetin (middle) and Quercetin (top). (B) ^1H NMR trace spectra from the 2-D data set of the on-flow experiment of Apigenin (bottom), Naringenin (middle down), Baicalein (middle up), and Galangin (top).

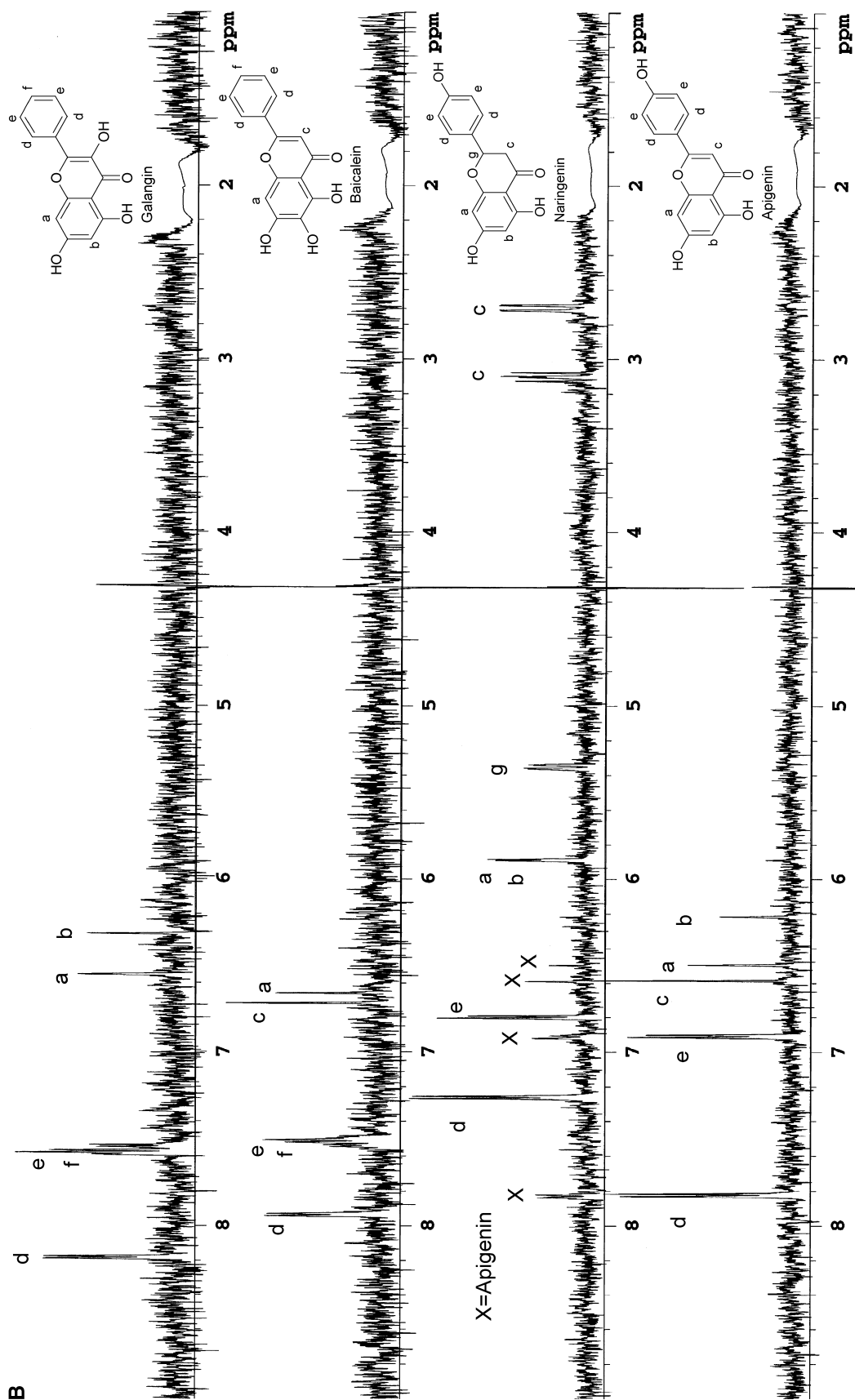


Fig. 6 (Continued).

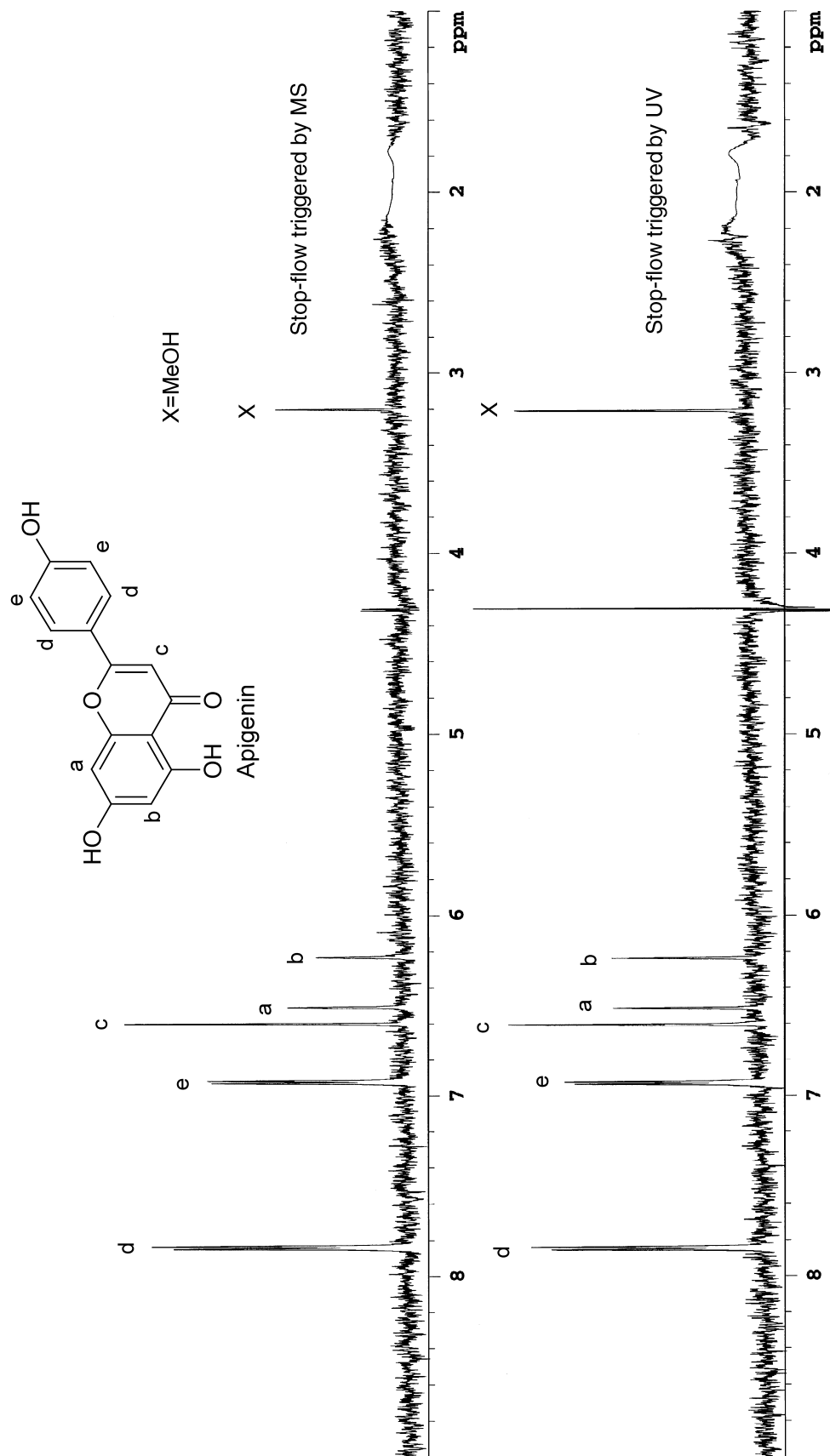


Fig. 7 ^1H NMR spectra of Apigenin triggering the stop-flow by UV (bottom) and by MS (top).

only be applied to reasonably pure compounds until the last decade. LC-NMR has expanded the capability of solving structural problems in complex mixtures. LC-NMR, however, is not comparable to LC-MS because of its lower sensitivity, the need of expensive deuterated solvents, the need of solvent suppression of the residual protonated solvents, and the compatibility of the volume of the chromatographic peak with the volume of the NMR flow cell. To overcome some of these problems, more development has led to the hyphenation of capillary HPLC (capLC) and NMR, where the amount of solvent used is minimal and the volume of the chromatographic peak is comparable to the volume of the NMR flow cell, but the suppression of the residual protonated solvents must still be carried out.

Within the last decade, hyphenation of LC-MS, LC-NMR, and LC-MS-NMR have become available. Because MS is destructive (in contrast to NMR) and requires far less sample than NMR, a splitter is incorporated, on-line, to direct the bulk of the sample to the less sensitive technique. In addition to the advantage of having MS and NMR information for the same chromatographic peak, the combination of these two techniques with different sensitivities must deal with other issues, such as the effect of deuterated solvents on the MS, the limitation of source of ionization on the MS compatible with low flow rates, and the timing which depends on the slower NMR technique. There is still room for improvement for LC-MS-NMR and the next decade will define the areas where this hyphenated technique is best suited.

LC-MS-NMR cannot replace LC-MS, LC-NMR or even NMR techniques for the structural elucidation of compounds. There will always be cases where purification of the analyte(s) is required when the structural problem is too complex or the separation of the chromatographic peak is not suitable. LC-MS-NMR, LC-MS, LC-NMR, and NMR have to be available so the analyst can choose the appropriate technique for each structural problem. The success rate of problem solution will depend on choosing the right technique, depending on the difficulty and nature of the problem. Each technique has its own advantages and limitations.

ACKNOWLEDGMENTS

The author is thankful to Dr. Ray Bakhtiar (Drug Metabolism of MRL at Rahway) for the preparation of Fig. 1, his support, encouragement in writing this manuscript, to Dr. Byron H. Arison (Drug Metabolism of MRL at Rahway) for his interest, support, encouragement, and constructive discussions during the course of this work, and David Knapp and Uresh Parikh (Medicinal Chemistry of MRL at Rahway) for technical help connecting the MS detector on-line to the LC-NMR system.

REFERENCES

1. Lee, M.S.; Kerns, E.H. LC/MS applications in drug development. *Mass Spectrom. Rev.* **1999**, *18*, 187–279.
2. Wu, Y. The use of liquid chromatography-mass spectrometry for the identification of drug degradation products in pharmaceutical formulations. *Biomed. Chromatogr.* **2000**, *14*, 384–396.
3. Clarke, N.J.; Rindgen, D.; Korfmacher, W.A.; Cox, K.A. Systematic LC/MS metabolite identification in drug discovery. *Anal. Chem.* **2001**, *73* (15), 430A–439A.
4. Watanabe, N.; Niki, E. Direct-coupling of FT-NMR to high performance liquid chromatography. *Proc. Jpn. Acad., Ser. B Phys. Biol. Sci.* **1978**, *54*, 194–199.
5. Bayer, E.; Albert, K.; Nieder, M.; Grom, E.; Keller, T. On-line coupling of high-performance liquid chromatography and nuclear magnetic resonance. *J. Chromatogr.* **1979**, *186*, 497–507.
6. Haw, J.F.; Glass, T.E.; Hausler, D.W.; Motell, E.; Dorn, H.C. Direct coupling of a liquid chromatograph to a continuous flow hydrogen nuclear magnetic resonance detector for analysis of petroleum and synthetic fuels. *Anal. Chem.* **1980**, *52*, 1135–1140.
7. Albert, K. Liquid chromatography-nuclear magnetic resonance spectroscopy. *J. Chromatogr., A* **1999**, *856*, 199–211.
8. Lindon, J.C.; Nicholson, J.K.; Wilson, I.D. Directly coupled HPLC-NMR and HPLC-NMR-MS in pharmaceutical research and development. *J. Chromatogr., B, Biomed. Sci. Appl.* **2000**, *748*, 233–258.
9. Smallcombe, S.H.; Patt, S.L.; Keifer, P.A. WET solvent suppression and its applications to LC NMR and high-resolution NMR spectroscopy. *J. Magn. Reson. Ser. A* **1995**, *117*, 295–303.
10. Bobzin, S.C.; Yang, S.; Kasten, T.P. Application of liquid chromatography-nuclear magnetic resonance spectroscopy to the identification of natural products. *J. Chromatogr., B, Biomed. Sci. Appl.* **2000**, *748*, 259–267.
11. Bobzin, S.C.; Yang, S.; Kasten, T.P. LC-NMR: A new tool to expedite the dereplication and identification of natural products. *J. Ind. Microbiol. Biotech.* **2000**, *25*, 342–345.
12. Bringmann, G.; Wohlfarth, M.; Rischer, H.; Heubes, M.; Saeb, W.; Diem, S.; Herderich, M.; Schlauer, J. A photometric screening method for dimeric naphthylisoquinoline alkaloids and complete on-line structural elucidation of a dimer in crude plant extracts, by the LC-MS/LC-NMR/LC-CD triad. *Anal. Chem.* **2001**, *73*, 2571–2577.
13. Wolfender, J.-L.; Ndjoko, K.; Hostettmann, K. The potential of LC-NMR in phytochemical analysis. *Phytochem. Anal.* **2001**, *12*, 2–22.
14. Careri, M.; Mangia, A. Multidimensional detection methods for separations and their application in food analysis. *Trends Anal. Chem.* **1996**, *15* (10), 538–550.
15. Mutlib, A.E.; Strupczewski, J.T.; Chesson, S.M. Application of hyphenated LC/NMR and LC/MS techniques in rapid identification of in vitro and in vivo metabolites of iloperidone. *Drug Metab. Dispos.* **1995**, *23* (9), 951–964.
16. Lindon, J.C.; Nicholson, J.K.; Sidelmann, U.G.; Wilson,

- I.D. Directly coupled HPLC-NMR and its application to drug metabolism. *Drug Metab. Rev.* **1997**, 29 (3), 705–746.
17. Zhang, K.E.; Hee, B.; Lee, C.A.; Liang, B.; Potts, B.C.M. Liquid chromatography-mass spectrometry and liquid chromatography-NMR characterization of in vitro metabolites of a potent and irreversible peptidomimetic inhibitor of rhinovirus 3C protease. *Drug Metab. Dispos.* **2001**, 29 (5), 729–734.
18. Peng, S.X.; Borah, B.; Dobson, R.L.M.; Liu, Y.D.; Pikul, S. Application of LC-NMR and LC-MS to the identification of degradation products of a protease inhibitor in dosage formulations. *J. Pharm. Biomed. Anal.* **1999**, 20, 75–89.
19. Potts, B.C.M.; Albizati, K.F.; O'Neil Johnson, M.; James, J.P. Application of LC-NMR to the identification of bulk drug impurities in GART inhibitor AG2034. *Magn. Reson. Chem.* **1999**, 37, 393–400.
20. Peng, S.E. Hyphenated HPLC-NMR and its applications in drug discovery. *Biomed. Chromatogr.* **2000**, 14, 430–441.
21. Ludlow, M.; Loudon, D.; Handley, A.; Taylor, S.; Wright, B.; Wilson, I.D. Size-exclusion chromatography with on-line ultraviolet, proton nuclear magnetic resonance and mass spectrometric detection and on-line collection for off-line Fourier transform infrared spectroscopy. *J. Chromatogr., A* **1999**, 857, 89–96.
22. De Koning, J.A.; Hogenboom, A.C.; Lacker, T.; Strhosein, S.; Albert, K.; Brinkman, U.A.Th. On-line trace enrichment in hyphenated liquid chromatography-nuclear magnetic resonance spectroscopy. *J. Chromatogr., A* **1998**, 813, 55–61.
23. Wu, N.; Peck, T.L.; Webb, A.G.; Magin, R.L.; Sweedler, J.V. Nanoliter volume sample cells for ^1H NMR. Application to on-line detection in capillary electrophoresis. *J. Am. Chem. Soc.* **1994**, 116 (17), 7929–7930.
24. Pusecker, K.; Schewitz, J.; Gfrörer, P.; Tseng, L.-H.; Albert, K.; Bayer, E.; Wilson, I.D.; Bailey, N.J.; Scarfe, G.B.; Nicholson, J.K.; Lindon, J.C. On-flow identification of metabolites of paracetamol from human urine using directly coupled CZE-NMR and CEC-NMR spectroscopy. *Anal. Commun.* **1998**, 35, 213–215.
25. Lacey, M.E.; Subramanian, R.; Olson, D.L.; Webb, A.G.; Sweedler, J.V. High-resolution NMR spectroscopy of sample volumes from 1 nL to 1 μL . *Chem. Rev.* **1999**, 99, 3133–3152.
26. Lacey, M.E.; Tan, Z.J.; Webb, A.G.; Sweedler, J.V. Union of capillary high-performance liquid chromatography and microcoil nuclear magnetic resonance spectroscopy applied to the separation and identification of terpenoids. *J. Chromatogr., A* **2001**, 922, 139–149.
27. Sandvoss, M.; Weltring, A.; Preiss, A.; Levsen, K.; Wuensch, G. Combination of matrix solid-phase dispersion extraction and direct on-line chromatography-nuclear magnetic resonance spectroscopy-tandem mass spectrometry as a new efficient approach for the rapid screening of natural products: Application to the total asterosaponin fraction of the starfish *Asterias rubens*. *J. Chromatogr., A* **2001**, 917, 75–86.
28. Burton, K.I.; Everett, J.R.; Newman, M.J.; Pullen, F.S.; Richards, D.S.; Swanson, A.G. On-line liquid chromatography coupled with high field NMR and mass spectrometry (LC-NMR-MS): A new technique for drug metabolite structure elucidation. *J. Pharm. Biomed. Anal.* **1997**, 15, 1903–1912.
29. Dear, G.J.; Ayrton, J.; Plumb, R.; Sweatman, B.C.; Ismail, I.M.; Fraser, I.J.; Mutch, P.J. A rapid and efficient approach to metabolite identification using nuclear magnetic resonance spectroscopy, liquid chromatography/mass spectrometry and liquid chromatography/nuclear magnetic resonance spectroscopy/sequential mass spectrometry. *Rapid Commun. Mass Spectrom.* **1998**, 12, 2023–2030.
30. Scarfe, G.B.; Wilson, I.D.; Spraul, M.; Hofmann, M.; Braumann, U.; Lindon, J.C.; Nicholson, J.K. Application of directly coupled high-performance liquid chromatography-nuclear magnetic resonance-mass spectrometry to the detection and characterization of metabolites of 2-bromo-4-trifluoromethylaniline in rat urine. *Anal. Commun.* **1997**, 34, 37–39.
31. Scarfe, G.B.; Wright, B.; Clayton, E.; Taylor, S.; Wilson, I.D.; Lindon, J.C.; Nicholson, J.K. ^{19}F -NMR and directly coupled HPLC-NMR-MS investigations into the metabolism of 2-bromo-4-trifluoromethylaniline in rat: A urinary excretion balance study without the use of radiolabelling. *Xenobiotica* **1998**, 28 (4), 373–388.
32. Scarfe, G.B.; Wright, B.; Clayton, E.; Taylor, S.; Wilson, I.D.; Lindon, J.C.; Nicholson, J.K. Quantitative studies on the urinary metabolic fate of 2-chloro-4-trifluoromethylaniline in the rat using ^{19}F -NMR spectroscopy and directly coupled HPLC-NMR-MS. *Xenobiotica* **1999**, 29 (1), 77–91.
33. Shockcor, J.P.; Unger, S.E.; Savina, P.; Nicholson, J.K.; Lindon, J.C. Application of directly coupled LC-NMR-MS to the structural elucidation of metabolites of the HIV-1 reverse-transcriptase inhibitor BW935U83. *J. Chromatogr., B, Biomed. Sci. Appl.* **2000**, 748, 269–279.





Lewis Base–Modified Zirconia as Stationary Phases for HPLC

Y.-L. Hu

Y.-Q. Feng

S.-L. Da

Wuhan University, Wuhan, P.R. China

INTRODUCTION

The developments of the Lewis base–modified zirconia and mixed-oxide containing zirconia as stationary phases for high-performance liquid chromatography (HPLC) are reviewed. In this context, the preparation methods of porous spherical zirconia, and zirconia supports for HPLC based on modification with fluoride, phosphate, phosphonate, carboxylic acid, phenols, and protein, as well as cyclodextrin derivative, are covered. The application of modified-zirconia in capillary electrochromatography (CEC) is also discussed.

ALTERNATIVES TO SILICA AS HPLC SUPPORTS

Over the past few years, there has been considerable interest expressed in materials that can serve as alternatives to silica as the basis of supports in different mode of HPLC. Zirconia is chemically and mechanically stable relative to silica and polymeric phases. It is resistant to chemical degradation from pH 1 to pH 14. The material's thermal stability is excellent over any liquid chromatographically accessible temperature, leading to increased flexibility when designing separation.^[1]

However, the surface of zirconia is much more complex than silica. A number of distinct classes of sites exist which can significantly contribute to the retention of a given solute. These sites include Brönsted acid sites, Brönsted base sites, and Lewis acid sites. Among these, the most chromatographically troublesome sites on the zirconia surface are the Lewis acid sites. These sites arise from the surface discontinuity in bonding between metal and oxygen atoms. They can form coordinate complexes with a number of Lewis bases and are responsible for the irreversible adsorption for proteins and other solutes. However, these sites can be blocked by adsorption with competing Lewis bases. This can be compared to adding amines to the mobile phase when silica-based stationary phases are used to decrease peak tailing due to silano-

philic interaction. The effective candidates for modification of the zirconia surface are those species that interact strongly with these hard surface Lewis acid sites, such as fluoride, inorganic phosphate, organic phosphonate, and carboxylic acid. When the surface of zirconia was modified by these species, they exhibited quicker kinetics in the chromatographic process, as well as different selectivity and separation mechanism. This review will cover some aspects of Lewis base–modified zirconia as stationary phases for HPLC.

Preparation of Porous Zirconia Spheres for HPLC

The preparation of porous zirconia with narrow particle size distribution is the foundation for further Lewis base modification. There are several methods reported for the preparation of spherical zirconia. Among these, an oil emulsion method is most widely used in several laboratories for its simplicity and good reproducibility.^[2–4] The method involves mechanically dispersing micrometer-scale droplets of an aqueous zirconia sol in an oil phase, in the presence of surfactants. Simultaneous gelation of the colloids within the droplets and extraction of water from the droplets yields zirconia aggregates that are further strengthened by sintering. The oil emulsion method has also been successfully applied for the synthesis of zirconia-containing mixed oxides in our laboratory.^[5–7] Sun et al.^[8] and Reeder et al.^[9] developed another promising method referred as the polymerization-induced colloid aggregation (PICA) for the preparation of spherical, porous zirconia. In this method, an aqueous zirconia sol is mixed with urea and formaldehyde, which are polymerized by the acidic sol. The oligomer so formed adsorbs on the surface of colloids, causing the colloids to aggregate. Zirconia prepared by the PICA method usually has a relatively narrow particle size distribution. Techniques based on a spray-drying process have also been used for the preparation of porous zirconia.^[2,10] In this process, a zirconia sol, which may contain a reactive binder, is forced through a nozzle. Droplets of

zirconia solution are dried to yield rigid particles. Zirconia spheres prepared by this method usually have a broad size distribution; so size classification is necessary to make them useful for HPLC.

Fluoride-Modified Zirconia as a Biocompatible Stationary Phase

Because fluoride ion forms some of its strongest coordination compounds with zirconium ion in solution, it should be a very powerful displacing agent toward any Lewis base on a zirconium oxide surface. Blackwell and Carr^[11] have studied the fluoride adsorption characteristics of porous zirconium oxide. They found that the composition of fluoride coordinated to the surface of zirconia is pH and ionic strength dependent. At low pH, the fluoride was more easily adsorbed onto the surface, due to less effective competition from hydroxide ion. Washing the zirconia particles with 0.1 M sodium hydroxide quantitatively desorbs bound fluoride. To maintain chromatographic reproducibility, a small amount of fluoride is added to the mobile phase for separation of proteins.^[12] The fluoride-modified zirconia is very biocompatible. The unique overall retention properties of this material are operationally analogous to those of calcium hydroxyapatite. However, the system does not have the chemical and physical weaknesses that limit the use of hydroxyapatite. Fig. 1 shows that very efficient separation can be implemented in any of a number of elution schemes.^[12] In addition, the substantial base stability allows sterilization of the packing material and strip-

ping of irreversibly bound proteins with sodium hydroxide solution.

Inorganic Phosphate and Organic Phosphonate as Modifiers

The Lewis acid of zirconia can be blocked by other than fluoride. The effectiveness of the blocking of the Lewis acid sites should be related to the strength of the interaction between the Lewis base used and the zirconium ion coordination site. Blackwell and Carr^[13] have developed the relative eluotropic strength of a number of Lewis bases in terms of their ability to elute a wide variety of benzoic acid derivatives. Phosphate ranks at the top of the elution series. It brought about elution of the benzoic acid derivatives in the column dead volume. This proves that phosphate binds strongly to the surface of zirconia. The strong affinity of zirconia for phosphate suggested that a phosphate modification of the surface should be a reasonable approach. Schafer et al.^[14] used several spectroscopic techniques to characterize the surface species on phosphate-modified zirconia particles. Their results show that phosphate merely adsorbs on the surface of zirconia under the "mildest" phosphate concentration, i.e., neutral pH, room temperature, and short contact times. However, at acidic pH and higher temperatures, esterification of the phosphate with surface hydroxyls takes place as the kinetic barriers are overcome. The solid ³¹P NMR studies clearly show the presence of covalently bound phosphate. This phosphate modification effectively blocks the sites responsible for the strong interaction of certain Lewis

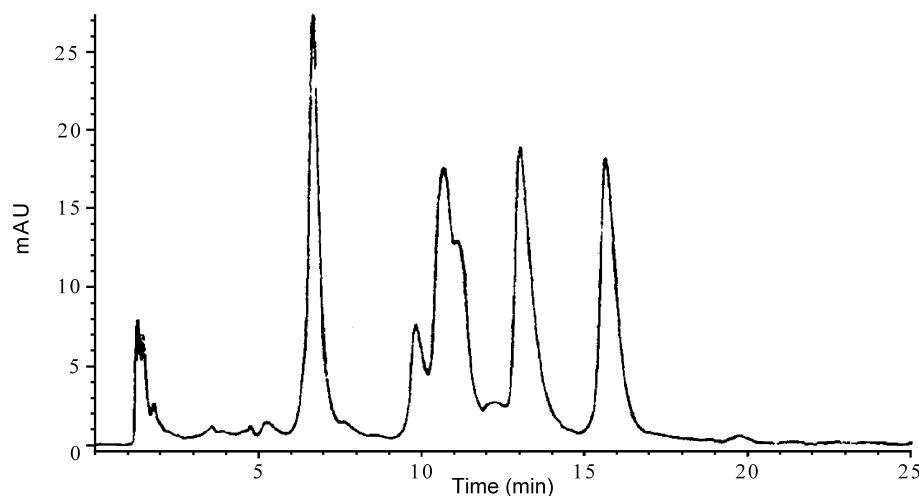


Fig. 1 Protein separation on fluoride modified zirconium oxide. A linear gradient of 0–0.75 M Na₂SO₄ in 100 mM NaF and 20 mM MES at pH 5.5 was used. Flow-rate was 0.5 mL/min at 35. Protein loadings were 4.4 µg lysozyme, 15.4 µg α-chymotrypsin, 13.6 µg myoglobin and 15.4 µg cytochrome c. (From Ref. [12].)

bases with the zirconia surface, resulting in a more bio-compatible stationary phase.^[15] Unlike fluoride-modified zirconia, phosphate-modified zirconia behaves as a classic cation exchanger and not as a mixed-mode medium analogous to hydroxyapatite, despite spectroscopic evidence of zirconium phosphate formation on the surface. This limits the applicability of the supports, as most proteins and enzymes are anionic at neutral pH. Nevertheless, its ability to separate proteins with high *pI* values still deserves much attention. The preparative-scale separation of murine IgGs from a fermentation broth demonstrates the utility of the supports for solutes that are retained.

Porous zirconia particles were also treated with polyphosphates of chain lengths between 3 and 100 for affinity chromatography of nucleic acids and proteins.^[16] The affinity matrix was stable in the pH range of 3 to 11 during a 120-h incubation period. It is demonstrated that polyphosphate-modified zirconia not only is a useful support for the separation of cationic proteins as is phosphate-modified zirconia, but also can be used for the binding of neutral proteins (e.g., DNase I) and anionic proteins (e.g., alkaline phosphatase). Applying both high-performance liquid chromatography and batch procedures can perform protein separation on this packing. The polyphosphate-modified zirconia can also be used in the effective purification of nucleic acids. It was found that 1) double-stranded DNA does not bind to the zirconia either in the absence or presence of Mg^{2+} ions, and 2) single-stranded DNA and RNA, in the absence of Mg^{2+} ions, also does not bind to the matrix; however, after addition of Mg^{2+} or other divalent cations, they bind strongly to the matrix. Elution of DNA and RNA can be performed with ethylenediaminetetraacetic acid (EDTA).

Based on the successful utility of phosphate-modified zirconia for protein separation, Clausen and Carr^[17] have extended their investigation to include the study of ethylenediamine-*N,N'*-tetramethylphosphonic acid (EDTPA), a phosphonate analog of EDTA, as a surface modifier for zirconia. They compared EDTPA-modified zirconia (PEZ) with inorganic phosphate-modified zirconia ($ZrPO_4$). Similar to $ZrPO_4$, cation-exchange is the dominant mechanism of protein retention on zirconia. However, PEZ showed increased efficiency, as well as unique selectivity for chromatography of proteins on the chelator-modified surface. Fig. 2^[17] shows the chromatogram of the protein mixture on the PEZ and the $ZrPO_4$ phases using the same elution conditions. It can be seen that PEZ is less retentive for all proteins but lysozyme relative to the $ZrPO_4$ phase, but PEZ is able to better resolve proteins especially for α -chymotrypsin and ribonuclease A. This can be accounted for by a mix of lower surface coverage of EDTPA and a change in the chemical nature of the modifier ligand. The presence of

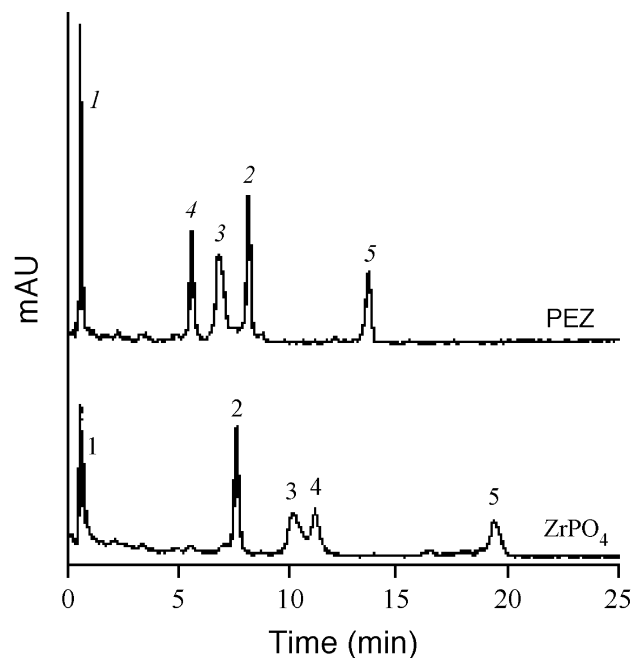


Fig. 2 Chromatographic comparison of protein elution profiles from PEZ and $ZrPO_4$ phases. Particles (4.5 μm) were packed in 50 mm \times 4.6 mm i.d. columns. Mobile phase: 30 min linear gradient from 50 to 500 mM potassium phosphate dibasic, pH 7.0; 0.5 mL/min; ambient temperature; detection at 280 nm. Peaks: 1—myoglobin, 2—lysozyme, 3— α -chymotrypsin, 4—ribonuclease A, 5—cytochrome *c*. (From Ref. [17].)

ionizable nitrogens in EDTPA should render the zirconia surface less negatively charged than orthophosphate-modified zirconia, resulting in the decrease in retention for all proteins other than lysozyme, as well as to serve, in part, to change the selectivity. It is important, as with $ZrPO_4$, to maintain a small concentration of EDTPA in the mobile phase to keep the stability. Subramanian et al.^[18] have used the spray-dried zirconia microsphere (20–30 μm) modified with EDTPA for the isolation of monoclonal antibodies (MAb) from cell culture supernatant. The selectivity between MAb and bovine serum albumin (BSA), which are the main constituents in the sample matrix, is very high. Analysis by enzyme-linked immunosorbent assay (ELISA) and gel electrophoresis demonstrates that MAbs can be recovered from a cell culture supernatant at high yield (92–98%) and high purity (95%) in a single chromatographic step.

As reversed-phase high-performance liquid chromatography is the most common mode of HPLC, many efforts have been made by chromatographers to introduce hydrophobic moieties on the zirconia surface. Polybutadiene-coated zirconia (PBD- ZrO_2) was proven to be an excellent reversed-phase packing material.^[19] PBD- ZrO_2 has excellent pH and thermal stability and is efficient for

the separation of some small molecules. However, the separation of peptides and proteins on PBD-ZrO₂ has not been successful, due to irreversible adsorption. The addition of phosphate to the mobile phase can alleviate interaction between the Lewis acid sites on zirconia and carboxyl groups on proteins.^[20] The phosphate-modified PBD-ZrO₂ phase has both reversed-phase and cation-exchange characteristics under acidic mobile-phase conditions. The PBD coating provides hydrophobic moieties, and the phosphate ions adsorbed on zirconia's surface provide cation-exchange sites. The phosphate-modified PBD-ZrO₂ performs satisfactorily for both hydrophobic peptides and positively charged peptides. The limitation of the phase is the reduced efficiency due to secondary equilibrium in the mixed-mode retention mechanism. As an alternative to adding Lewis bases to the eluent, Trammell et al.^[21] also studied the effect of permanently modifying PBD-ZrO₂ by covalently attaching vinylphosphonic acid (VPA) to PBD which was predeposited in the pores of zirconia. The resultant stationary phase allows catechol and carboxylates to elute with 100% recovery, without the use of mobile-phase additives. Although this is a tremendous improvement over previous PBD-ZrO₂ phases, a mobile-phase Lewis base additive is still required to provide acceptable peak shapes and plate counts. Evaluation of the cation exchange characteristic of VPA-PBD-ZrO₂ shows that it is significantly more negatively charged than is PBD-ZrO₂ in the presence of phosphate or phosphonate eluent additive. A tremendous improvement in the separation of peptides is achieved when ultralow-pH eluents are used.

Particle pore characteristics are crucial factors for chromatographic performance. Recently, other metal oxides, such as magnesia and ceria, were introduced into zirconia for improvement of its physicochemical properties in our laboratory.^[5–7] The mixed-oxides demonstrate higher specific surface area, large specific pore volume, and better pore connectivity than pure zirconia. Increased surface basicity was also observed on magnesia–zirconia and ceria–zirconia, but especially on magnesia–zirconia, which led to stronger affinity toward Lewis base solutes. In the consequent study, alkylphosphonate with 15 carbons, which was synthesized in our laboratory, was adopted to modify magnesia–zirconia^[22] and ceria–zirconia.^[23] The new materials illustrated satisfactory pH stability, even in the absence of alkylphosphonic acid in the mobile phase. Alkylphosphonic acid–modified magnesia–zirconia is very stable against extreme pH conditions, e.g., from pH 2 to pH 11.^[22] This might be ascribed to be the existence of magnesia on the surface of magnesia–zirconia. The chromatographic performance of the new materials was studied by using polycyclic aromatic hydrocarbons (PAHs) and basic compounds as probes. PAHs were retained on alkylphos-

Lewis Base–Modified Zirconia as Stationary Phases for HPLC

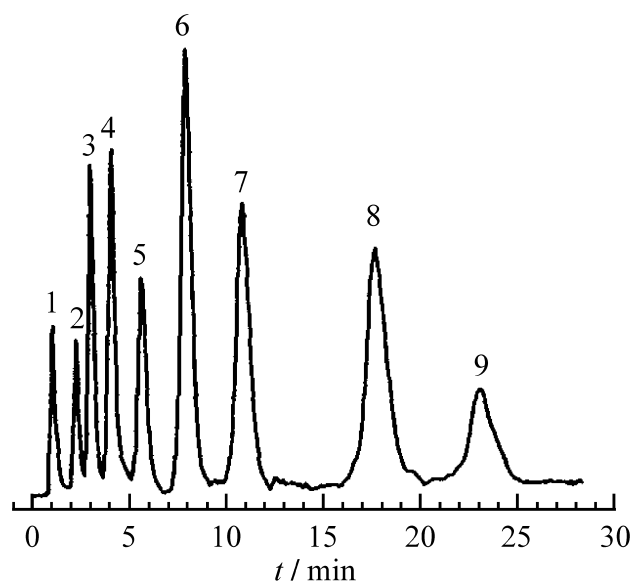


Fig. 3 PAHs separation on alkylphosphonate modified magnesia–zirconia composite (4–6 μm , 150 mm \times 4.6 mm i.d. column). Mobile phase: methanol–water (75:25, v/v). 1—Solvent; 2—Benzene; 3—Toluene; 4—Naphthalene; 5—Biphenyl; 6—Fluorene; 7—*O*-terphenyl; 8—*M*-terphenyl; 9—*P*-terphenyl. (From Ref. [26].)

phonic acid–modified mixed oxides by typical reversed-phase mechanism in the entire pH range studied. Basic solutes were retarded on stationary phases, mainly by hydrophobic interaction at higher pH, whereas they also showed cation-exchange interaction with the stationary phase at relatively lower pH conditions.^[24] It is found that the alkylphosphonic acid–modified magnesia–zirconia and ceria–zirconia are more viable supports for reversed-phase chromatography of basic solutes, relative to silica-based hydrophobic stationary phases, for less peak tailing of these solutes.^[22–25] The separations of PAHs and basic solutes on alkylphosphonic acid–modified magnesia–zirconia are illustrated in Fig. 3^[26] and Fig. 4,^[25] respectively. Application of this material to the separation of nucleosides and nucleobases was also confirmed successful.^[27] However, acidic compounds still exhibit strong interaction with alkylphosphonic acid–modified magnesia–zirconia and ceria–zirconia using a typical reversed-phase mobile phase.

Stearic Acid Modified Zirconia and Ceria–Zirconia for RP-HPLC

Octadecyl-silica stationary phases (ODS) are among the most widely used packing materials in all modalities of HPLC, owing to their applicability to the separation of

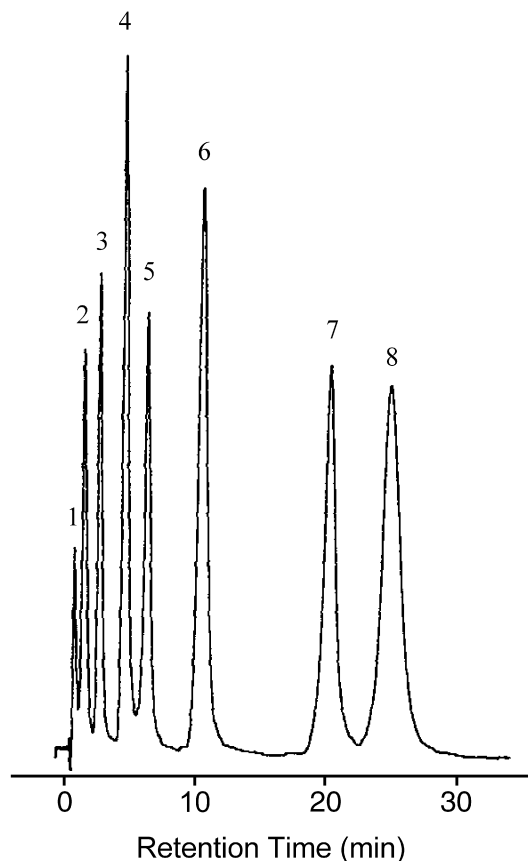


Fig. 4 Separation of basic compounds on the alkylphosphonate-modified magnesia-zirconia composite column with 35:65 (v/v) methanol-TRIS buffer (5.0 mM TRIS and 50 mM NaCl, pH 10.0) as mobile phase at a flow rate of 1.0 mL/min. 1—Solvent; 2—Caffeine; 3—Aniline; 4—*O*-toluidine; 5—*N*-methylaniline; 6—*O*-nitroaniline; 7—*N,N'*-dimethylaniline; 8— β -aminonaphthalene. (From Ref. [25].)

solutes of very different polarity, molecular weight, and chemical functionality. Yu and Rassi^[28] have investigated the expansion of chemical bonding octadecylsilane on the zirconia's surface. The resulting octadecyl-zirconia was quite useful in the separation of PAHs, alkylbenzenes, alkylalcohol homologous series, oligosaccharides, and peptides. However, this method has its limitation for lower stability of Zr-O-Si-R relative to Si-O-Si-R bonds. As zirconia and zirconia-containing mixed-oxides have strong affinity toward carboxyl acid derivatives, we^[7,29] developed a simple method to dynamically modify zirconia and ceria-zirconia with stearic acid, a fatty acid with 18 carbons, and comparable to octadecylsilane. Stearic acid-modified ceria-zirconia illustrates better chromatographic properties than stearic acid-modified zirconia, owing to its improved column efficiency and hydrophobicity. PAHs and basic compounds are well

resolved on the material. Better selectivity of basic compounds was obtained on stearic acid-modified ceria-zirconia than on an ODS column. However, the stability of the stationary phases is worse than for alkylphosphonic acid-modified mixed-oxides in higher pH eluents. This is predictable, since phosphates are stronger Lewis bases than carboxyl acids.

Zirconia-Containing Mixed-Oxides Modified with Phenol Derivatives for Separation of Fullerene Compounds

Chromatographic separation of fullerene compounds has been of great interest during the past few years. Silica-based stationary phases were the most widely used materials for fullerene purification. As synthesis of new silica bonded stationary phase is always time-consuming, we have recently attempted to prepare a useful stationary phase for fullerene separation by a simple method. As mentioned previously, Lewis bases, including some phenol derivatives, strongly adsorb onto the surface of zirconia-containing mixed-oxides. Although these phenol derivatives can be gradually stripped from the matrix in polar solvents, they exhibit high stability while exposed to nonpolar solvents which are commonly used as the mobile phase for fullerene separation. Therefore, zirconia-containing mixed-oxides were modified with various phenolic compounds to test their ability for separation of fullerene compounds.^[30] A consequence of the retention behavior of fullerene compounds on these station-

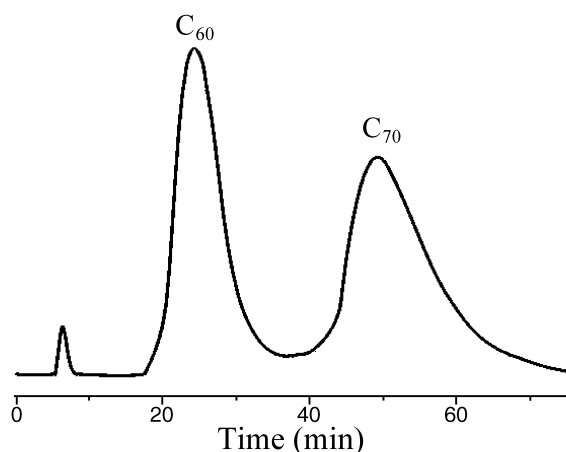


Fig. 5 Separation of C_{60} and C_{70} on 2,4,6-trinitrophenol-modified zirconia-ceria stationary phase (4–6 μ m, 150 mm \times 4.6 mm i.d. column). Mobile phase: toluene-cyclohexane (30:70, v/v). Sample: 11.4 mg/mL of C_{60} , C_{70} mixture in toluene. Injection volume: 0.8 mL. Flow rate: 0.25 mL/min. UV detection at 380 nm.

ary phases was that charge-transfer interaction was the main retention mechanism. Based on the results of a column loading capacity test, 2,4,6-trinitrophenol-modified ceria–zirconia and alumina–zirconia are considered as a potential material for the separation of C₆₀ and C₇₀ in large amounts. Fig. 5 illustrated their separation under the overloaded condition on an analytical column.

Other Lewis Bases as Modifier

The results of Blackwell and Carr's study show that the chromatographic properties of the zirconia surface in aqueous media are highly dependent upon the chemical composition of the eluent.^[31] They investigated the retention of various small solutes in the presence of glycolic acid, malic acid, succinic acid, citrate, or borate, and concluded that these Lewis base eluent components act to control retention in two ways. They modify the net ligand exchange contribution to retention, and they serve as sites for secondary interactions, such as hydrogen bonding and hydrophobic interaction between solutes and the dynamic stationary phase.

Whitman et al.^[32] also evaluated the effect of pre-treatments of zirconia with a number of Lewis bases on normal phase selectivity. Chemometric methodology was used to characterize the similarities and differences between the "acid"- and "base"-washed supports. Hydrogen bonding interactions are quite pronounced for the Lewis base-modified zirconia, the extent of which differs greatly among the various Lewis bases used to modify the zirconia.

The irreversible binding of many proteins to bare zirconia can be modulated by addition of some weaker Lewis bases other than phosphate and fluoride.^[33] Phosphate and fluoride are able to bring about elution of nearly all proteins, as they are the strongest Lewis bases. On the other hand, there is not much leeway for modulating the strength of the competitive ligand exchange interaction through adjustments of their concentrations for the ease of saturation of their adsorption isotherm. In contrast, weaker Lewis bases such as borate, sulfate, and bromide are able to elute only those proteins retained primarily by ionic interaction. Proteins that contain a large number of accessible Lewis base sites cannot be eluted from zirconia in weak eluents.

Blackwell and Carr investigated the ligand exchange chromatography of free amino acids on copper-loaded zirconia.^[34,35] It was shown that the use of Lewis base buffers in this system improved the operating efficiency. Acetate, sulfate, fluoride, and phosphate are the effective competing ions.

Lewis Base–Modified Zirconia as Stationary Phases for HPLC

Park et al.^[36] reported a method to modify zirconia by adsorption with BSA and, subsequently, crosslinked by glutaraldehyde. The BSA–zirconia showed good enantioselectivity for some enantiomers and could be used for RPLC separation in mobile phases of alkaline pH. They also developed a carboxymethyl- β -cyclodextrin-coated zirconia stationary phase for the separation of racemic 2,4-dinitrophenyl amino acids.^[37]

Lewis Base–Modified Zirconia–Magnesia in Capillary Electrochromatography (CEC)

Capillary electrochromatography (CEC) is a relatively new technique for chemical analysis. It brings together the advantages of the capillary electrophoresis (CE) and high-performance liquid chromatography (HPLC). Capillary electrochromatography can be performed in open tubes or packed structures. To date, the most commonly used packing materials for CEC are the silica-based stationary phases. Recently, zirconia and zirconia–magnesia were successfully utilized as packing or coating material for CEC in our laboratory.^[38–40] As mentioned above, alkylphosphonic acid–modified zirconia–magnesia has exhibited excellent chromatographic properties in HPLC. In the subsequent study, Xia et al.^[38] demonstrated its usefulness as packing material in CEC. The alkylphosphonic acid–modified zirconia–magnesia shows distinct electroosmotic flow (EOF), compared with the unmodified zirconia–magnesia for its negative surface at lower pH. Successful separation of polycyclic aromatic hydrocarbons can be obtained within a shorter time in the CEC mode than in the HPLC mode, due to the higher column efficiency in CEC. A zirconia–magnesia coating was also fabricated inside fused-silica capillaries for open tubular capillary electrochromatography (OTCE).^[39] The capillaries coated with zirconia–magnesia exhibited switchable EOF at pH 5.2. Then, its surface was further modified with SO₄^{2–} and alkylphosphonic acid, respectively, and the isoelectric point of the capillary shifted accordingly. The capillary coated by SO₄^{2–} modified zirconia–magnesia shows better chromatography toward basic compounds than unmodified zirconia–magnesia, with less peak tailing; the alkylphosphonate modified magnesnia–zirconia coated capillary can separate six PAHs within 13 min.

REFERENCES

1. Nawrocki, J.; Rigney, M.P.; McCormick, A.; Carr, P.W. Chemistry of zirconia and its use in chromatography. *J. Chromatogr.* **1993**, 657, 229–282.



2. Carr, P.W.; Funkenbusch, E.F.; Rigney, M.P.; Coleman, P.L.; Hanggi, D.L.; Schafer, W.A. U.S. Patent 5015373, 1991.
3. Trudinger, U.; Muller, G.; Unger, K.K. Porous zirconia and titania as packing materials for high-performance liquid-chromatography. *J. Chromatogr.* **1990**, *535*, 111–125.
4. Yu, J.; El-Rassi, Z. Reversed-phase liquid-chromatography with microspherical octadecyl-zirconia bonded stationary phases. *J. Chromatogr.* **1993**, *631*, 91–106.
5. Zhang, Q.H.; Feng, Y.Q.; Da, S.L. Characterization and evaluation of magnesia-zirconia supports for normal-phase liquid chromatography. *Chromatographia* **1999**, *50*, 654–660.
6. Zhang, Q.H.; Feng, Y.Q.; Da, S.L. Preparation and characterization of silica-zirconia supports for normal-phase liquid chromatography. *J. Liq. Chromatogr. Relat. Technol.* **2000**, *23*, 1461–1470.
7. Hu, Y.L.; Feng, Y.Q.; Wan, J.D.; Da, S.L.; Hu, L. Native and stearic acid modified ceria-zirconia supports in normal and reversed-phase HPLC. *Talanta* **2001**, *54*, 79–88.
8. Sun, L.; Annen, J.; Lorenzano-Porras, C.F.; Carr, P.W.; McCormick, A.V. Synthesis of porous zirconia spheres for HPLC by polymerization-induced colloid aggregation (pica). *J. Colloid Interf. Sci.* **1994**, *163*, 464–473.
9. Reeder, D.H.; Clausen, M.J.; Annen, M.J.; Carr, P.W.; Flickinger, M.C.; McCormick, A.V. An approach to hierarchically structured porous zirconia aggregates. *J. Colloid Interf. Sci.* **1996**, *184*, 328–330.
10. Wax, M.J.; Grasselli, R.K. EP Patent 0 490 226 A1, 1991.
11. Blackwell, J.A.; Carr, P.W. Study of the fluoride adsorption characteristics of porous microparticulate zirconium-oxide. *J. Chromatogr.* **1991**, *549*, 43–57.
12. Blackwell, J.A.; Carr, P.W. Fluoride-modified zirconium-oxide as a biocompatible stationary phase for high-performance liquid-chromatography. *J. Chromatogr.* **1991**, *549*, 59–75.
13. Blackwell, J.A.; Carr, P.W. Development of an eluotropic series for the chromatography of Lewis-bases on zirconium-oxide. *Anal. Chem.* **1992**, *64*, 863–873.
14. Schafer, W.A.; Carr, P.W.; Funkenbusch, E.F.; Parson, K.A. Physical and chemical characterization of a porous phosphate-modified zirconia substrate. *J. Chromatogr.* **1991**, *587*, 137–147.
15. Schafer, W.A.; Carr, P.W. Chromatographic characterization of a phosphate-modified zirconia support for biochromatographic applications. *J. Chromatogr.* **1991**, *587*, 149–160.
16. Lorenz, B.; Marmé, S.; Muller, W.E.G.; Unger, K.; Schroeder, H.C. Preparation and use of polyphosphate-modified zirconia for purification of nucleic-acids and proteins. *Anal. Biochem.* **1994**, *216*, 118–126.
17. Clausen, A.M.; Carr, P.W. Chromatographic characterization of phosphonate analog EDTA-modified zirconia support for biochromatographic applications. *Anal. Chem.* **1998**, *70*, 378–385.
18. Subramanian, A.; Carr, P.W.; McNeff, C.V. Use of spray-dried zirconia microspheres in the separation of immunoglobulins from cell culture supernatant. *J. Chromatogr. A* **2000**, *890*, 15–23.
19. Rigney, M.P.; Weber, T.P.; Carr, P.W. Preparation and evaluation of a polymer-coated zirconia reversed-phase chromatographic support. *J. Chromatogr.* **1989**, *484*, 273–291.
20. Sun, L.F.; Carr, P.W. Mixed-mode retention of peptides on phosphate-modified polybutadiene-coated zirconia. *Anal. Chem.* **1995**, *67*, 2517–2523.
21. Trammell, B.C.; Hillmyer, M.A.; Carr, P.W. A study of the Lewis acid-base interactions of vinylphosphonic acid-modified polybutadiene-coated zirconia. *Anal. Chem.* **2001**, *73*, 3323–3331.
22. Feng, Y.Q.; Zhang, Q.H.; Da, S.L.; Zhang, Y. Preparation and characterization of alkylphosphonate-modified magnesia-zirconia composite for reversed-phase liquid chromatography. *Anal. Sci.* **2000**, *16*, 579–583.
23. Hu, Y.L.; Feng, Y.Q.; Da, S.L. Chromatographic evaluation of alkylphosphonic acid-modified ceria-zirconia in reversed-phase HPLC. *J. Liq. Chromatogr. Relat. Technol.* **2001**, *24*, 957–971.
24. Hu, Y.L.; Feng, Y.Q.; Da, S.L. Comparison of chromatographic properties of Lewis base-modified mixed oxides as stationary phases for HPLC. *J. Liq. Chromatogr. Relat. Technol.* **2002**, *25*, 83–99.
25. Feng, Y.Q.; Fu, H.J.; Zhang, Q.H.; Da, S.L.; Zhang, Y.J. Retention behavior of basic compounds on alkylphosphonate-modified magnesia-zirconia composite stationary phase in RPHPLC. *Chromatographia* **2000**, *52*, 165–168.
26. Fu, H.J.; Feng, Y.Q.; Zhang, Q.H.; Da, S.L.; Zhang, Y.J. Retention behavior of some polycyclic aromatic hydrocarbons on alkylphosphonate-modified magnesia-zirconia composite stationary phase for reversed-phase liquid chromatography. *Chin. J. Chromatogr.* **2000**, *18*, 194–197.
27. Fu, H.J.; Feng, Y.Q.; Zhang, Q.H.; Da, S.L.; Zhang, Y.J. High-performance liquid chromatography of some bases and nucleosides on alkylphosphonate-modified magnesia-zirconia column. *Anal. Lett.* **1999**, *32*, 2761.
28. Yu, J.; Rassi, Z.E. Reversed-phase liquid-chromatography with microspherical octadecyl-zirconia bonded stationary phases. *J. Chromatogr.* **1993**, *631*, 91–106.
29. Zhang, Q.H.; Feng, Y.Q.; Yan, L.; Da, S.L.; Wang, Z.H. Retention behavior of solutes on liquid chromatographic column packed with dynamically modified zirconia. *Chin. J. Chromatogr.* **1999**, *17*, 229–231.
30. Hu, Y.L.; Feng, Y.Q.; Wan, J.D.; Da, S.L. Phenol-modified ceria-zirconia and calcia-zirconia as chromatographic packings for separation of C₆₀ and C₇₀. *Anal. Sci.*, **2001**, *17*, Supplement a321–a324. Wan, J.D.; Feng, Y.Q.; Hu, Y.L.; Da, S.L.; Wang, Z.H. Preparation and evaluation of 2,4,6-trinitrophenol-modified zirconia-alumina for high performance liquid chromatography and its application in the separation of fullerenes. *Chem. J. Chin. Univ.* **2002**, *23*, 1259–1263.
31. Blackwell, J.A.; Carr, P.W. A chromatographic study of



- the Lewis acid-base chemistry of zirconia surfaces. *J. Liq. Chromatogr.* **1991**, *14*, 2875–2889.
32. Whitman, D.A.; Weber, T.P.; Blackwell, J.A. Chemo-metric characterization of Lewis base-modified zirconia for normal-phase chromatography. *J. Chromatogr. A* **1995**, *691*, 205–212.
 33. Blackwell, J.A.; Carr, P.W. Ion-exchange and ligand-exchange chromatography of proteins using porous zirconium-oxide supports in organic and inorganic Lewis base eluents. *J. Chromatogr.* **1992**, *596*, 27–41.
 34. Blackwell, J.A.; Carr, P.W. Ligand-exchange chromatography of free amino-acids and proteins on porous micro-particulate zirconium-oxide. *J. Liq. Chromatogr.* **1992**, *15*, 1487–1506.
 35. Blackwell, J.A.; Carr, P.W. Ligand-exchange chromatography of free amino-acids on phosphated zirconium-oxide supports. *J. Liq. Chromatogr.* **1992**, *15*, 727–751.
 36. Park, J.H.; Ryu, J.K.; Park, J.K.; McNeff, C.V.; Carr, P.W. Separation of enantiomers on bovine serum albumin coated zirconia in reversed-phase liquid chromatography. *Chromatographia* **2001**, *53*, 405–408.
 37. Park, S.Y.; Park, J.K.; Park, J.H.; McNeff, C.V.; Carr, P.W. Separation of racemic 2,4-dinitrophenyl amino acids on carboxymethyl-beta-cyclodextrin coated zirconia in RPLC. *Microchem. J.* **2001**, *70*, 179–185.
 38. Xia, D.; Feng, Y.Q.; Da, S.L. Capillary electrochromatography with alkylphosphonate-modified magnesia-zirconia as the chromatographic support material. *J. Liq. Chromatogr. Relat. Technol.* **2001**, *24*, 1881–1894.
 39. Xie, M.J.; Feng, Y.Q.; Da, S.L.; Meng, D.Y.; Ren, L.W. Capillary electrophoresis and open tubular capillary electrochromatography using a magnesia-zirconia coated capillary. *Anal. Chim. Acta* **2001**, *428*, 255–263.
 40. Xie, M.J.; Feng, Y.Q.; Da, S.L. Capillary electrophoresis using zirconia-coated fused silica capillaries. *J. Sep. Sci.* **2001**, *24*, 62–66.

Lipid Analysis by HPLC

Jahangir Emrani

Novartis Crop Protection, Inc., Greensboro, North Carolina, U.S.A.

Introduction

Lipids are mixtures of fatty molecules that contain polar and nonpolar groups. Polar lipids include phospholipids and glycolipids, whereas nonpolar lipids include fatty acids and their esters, cholesterol and its esters, essential oils, wax esters, and squalene. Lipids are important ingredients in the production of modern food and play key roles in physiological systems. The role of lipids in certain cardiovascular and dermatological conditions has been established. Understanding the roles of lipids in cellular and physiological systems have been the driving force behind recent developments in lipid analysis. Historically, thin-layer chromatography (TLC) and gas chromatography (GC) have been used for the analysis of lipids. Due to the limitations of these techniques and the advances in high-performance liquid chromatography (HPLC) detection technology, HPLC is gaining popularity for lipid analysis. The high temperatures used in the GC causes degradation of some molecules, whereas many fat molecules are not volatile enough to go through the GC. On the other hand, detection of fats on TLC is somewhat cumbersome.

Today, HPLC is the dominant analytical technique used for the analysis of most classes of compounds. The analyses can be carried out at room temperature and the collection of fractions for reanalysis or further manipulation is straightforward. The main reason for the slow acceptance of the HPLC technique for lipid analysis has been the detection system. Traditionally, HPLC used ultraviolet/visible (UV/vis) detection, which requires the presence of a chromophore in the analyte. Most lipid molecules do not contain chromophores and therefore would not be detected by UV/vis. Modern HPLC detection techniques, such as the use of a mass spectrometer as the detector, derivatization techniques to introduce chromophores, and the availability of pure solvents to reduce interference, have allowed HPLC to compete with and/or complement GC and other traditional methods of lipid analysis. In addition to analytical HPLC, preparative HPLC has been used extensively to collect pure samples of the lipids for the derivatization or synthesis of new compounds.

Modes of Separation of Lipids by HPLC

The mode of separation in the HPLC depends on the selection of the stationary and mobile phases. In HPLC of lipids, normal- and reversed-phase modes are primarily used, with the reverse phase being more common than the normal phase. Separation in the reversed-phase mode is mainly by partition chromatography, whereas separation in the normal phase mode is primarily by adsorption chromatography. Normal-phase HPLC is used for the separation of the lipids into classes of lipids [1,F]. Reversed-phase HPLC (RP-HPLC), on the other hand, is mainly used to separate each lipid class into individual species [2,B1]. For example, several triglycerides were separated from each other via nonaqueous reversed-phase HPLC, involving an octadecyl (ODS) column and a nonpolar (non-aqueous) mobile phase. RP-HPLC alone can be used to separate the fat molecules into classes and species [2,B1].

In reversed-phase chromatography of lipids [B2], the lipophilic interaction between the octadecyl chains of the column and the fatty molecules of the analyte determines the retention. For this reason, the retention times of the lipid molecules depend on the stationary-phase chain length and number of double bonds in each lipid structure. In general, the retention time increases as the number of double bonds decrease. Glycerides with the shortest acyl chain length and highest number of double bonds elute first. This general rule applies if the column contains a C₈ or C₁₈ stationary phase. Using such a general correlation and knowing the relative retention time of a reference compound such as a phospholipid on ODS columns, the retention time of other phospholipids can be calculated [B1].

In addition to normal- and reversed-phase chromatography, silver ion HPLC, RP ion-pair HPLC, chiral separation, and supercritical fluid chromatography have been used for analysis of lipids [3]. In silver-ion HPLC, the counterion of an ion-exchange column such as sulfonate is exchanged with silver ions. Only the degree of unsaturation in the lipid molecule determines retention. In RP ion-pair HPLC, different ion-pairing agents, such



as alkylammonium phosphates, are added to the ODS column for molecular species separation. In supercritical fluid chromatography (SFC), which is used in combination with flame ionization detection (FID), solubility of lipids in carbon dioxide allows the separation to be performed. This mode of analysis is not widely used.

Selection of the Stationary Phase

The type of packing in the HPLC column is the most important factor affecting the HPLC separation. Silica is the most common packing material for normal-phase chromatography because it is stable under pressure and has a neutral pH. Silica-bonded C_{18} and C_8 , on the other hand, are the most common packing materials for RP chromatography because they are stable to pressure and low pH. Diol-bonded phases are also used as polar column packing [4]. In cases where gradient elution is necessary, diol-bonded stationary phases are more suitable than silica. For lipid classes found in plants, chemically bonded phases have produced better resolution than silica gel [5]. Cyano-propyl, amino, and other stationary phases have all been used. Aminopropyl phases are suitable for acidic and nonpolar lipids. These columns are compatible with commonly used solvents and modifiers. Florisil is another stationary phase used for the separation of lipids; however, irreversible retention may occur.

The method of stationary-phase preparation has a major effect on the resolution, column stability, retention time, reproducibility, and peak shape. When preparing C_{18} or C_8 , for example, it is important that the residual silanol groups are capped to prevent peak tailing. The extent of capping must be consistently maintained between different batches of the stationary phase for reproducible results.

In terms of particle size and column dimensions, stationary phases with particle sizes of 5–10 μm in 250 \times 4.6-mm analytical columns are most common. HPLC columns with smaller particle sizes (2–3 μm) have also been prepared and used. Such columns have the advantages of higher efficiency, better resolution, and shorter analysis times. For example, the triglycerides of cocoa butter were baseline separated with columns that contained 2–3- μm particles. Research and development of columns with smaller particles is very active.

Selection of the Mobile Phase

The mobile phase consists of one or more solvents that are pumped through the chromatographic system, re-

sulting in the separation of analytes. Mobile phases may also contain modifiers. Examples of frequently used solvents include hexane, methanol, 2-propanol, acetonitrile (ACN), and water. Examples of modifiers include trifluoroacetic acid, acetic acid, or formic acid. In general, the composition of the mobile phase should be kept simple. Factors that influence the choice of mobile phase include the solubility of the sample in the mobile phase, the polarity of the mobile phase, ultraviolet (UV) absorption wavelength, refractive index, and viscosity of the solvents. The purity of the solvents in the mobile phase is also important because the region of UV that is used for the detection of lipids (200–215 nm) must be free of interferences. For phospholipids, the most popular solvent systems are transparent to UV in the range of 200–215 nm; they include hexane–2-propanol–water and acetonitrile–methanol–water. Variations include hexane–methanol–isopropanol or water–methanol. The ratios of these solvents in the mobile phase depends on the nature of the lipid substances being separated. Several examples of mobile phases commonly used in the analysis of lipids are listed in the general references.

In order to separate the molecular species of lipids that have very close characteristics, small differences such as the number of double bonds in each molecule can occasionally be used as a guide to devise a solvent system to separate the molecules. This method is not always successful and may have to be further optimized for a good separation.

Detection

No single HPLC detector has all the characteristics of a good detector, which include sensitivity, specificity, detectability, linearity, repeatability, and dependability. Detection by UV/vis is widely used for the analysis of lipids; it is simple, concentration sensitive, and nondestructive. However, the analyte to be monitored by UV/vis absorption must contain a chromophore, and because many fat molecules do not contain a chromophore, this detection system cannot be used in many cases. Fortunately, in cases where no chromophore is present in the molecule, a chromophore can be introduced through derivatization. If the derivatization is done before the analyte enters the column, it is called precolumn derivatization, whereas if it is done after the elution of analyte, it is called postcolumn derivatization.

For the detection of phospholipids, UV/vis at 205 nm is often used. In cases where the molecules contain several lipid groups, UV detection in the

range of 205–215 nm has been used. Vitamin E, α -, β -, δ -, and γ -tocopherols have been analyzed by RP-HPLC using UV at 215 [B1] and 280 nm. In other cases, UV diode-array detection at 190–350 nm or 200–400 nm has been used. Tocopherols and triglycerides from vegetable oils and human lipoproteins were analyzed by RP-HPLC using a UV/vis diode-array detector. With diode-array detection, UV spectra of the peaks can be collected during the analysis. In many analyses, the UV absorption of the lipid analyte is due to the carbonyl group C=O in the acyl group of the molecules.

More recently, a less sensitive detection technique, refractive index (RI) detection, has been used. The disadvantage of RI is that one is limited to isocratic elution, because RI detection is affected by changes in the pressure and temperature of the mobile phase. On the other hand, infrared (IR) detection can be used when the solvents in the mobile phase do not absorb infrared light, which can create interference. Because of these limitations, RI and IR have not been used as widely as UV detection.

In contrast, newer techniques such as FID and evaporative light-scattering detection (ELSD, “Universal Detector”) are more sensitive and have been used for the analysis of many lipids, including the polar and neutral lipid classes [6]. For preparative scale separations, if the UV absorbance is more than what the detector can handle, an evaporative light-scattering detector is used [B2].

Fluorescence (FL) detection is another selective and sensitive technique. Vitamin E, α -, β -, δ -, and γ -tocopherols have been analyzed by RP-HPLC using FL as well as UV detection. In addition, a newer technique, electrochemical detection, has been reported in the analysis of phenolic compounds of olive oil [7].

Finally, the detection by liquid chromatograph-mass spectrometer (LC-MS), which has been largely dependent on the price, mode of ionization, and ease of operation of the mass spectrometer, is becoming popular [8]. It is predicted that LC-MS will become the method of choice for lipid analysis in coming years.

Derivatization

Samples of lipids may be derivatized either before they are injected into the HPLC or after they emerge from the HPLC column. The purpose of derivatization is either to make the lipid molecules detectable or to improve peak shape during the analysis. The addition of functional groups, such as phenyl, 2,4-dinitrophenyl, or

anisyl to the molecule enhances the detectability by changing the absorption wavelength of a lipid molecule. On the other hand, making derivatives such as acetates or methyl esters help to improve the peak shape. To make the lipid molecules fluorescent, groups such as anthroyl, 7-methoxycoumaryl, naproxen, and naphthyl [B1] are added to the lipid molecules. The reactions are carried out postcolumn and the derivatized molecules can be detected by both excitation and emission. For the detection of fatty acids, they are derivatized by reacting with either *p*-bromophenacylbromide, 9-anthryldiazomethane, or bromomethyl-methoxy-cumarin. These derivatizations also make the molecules UV absorbers. Fatty acids have also been analyzed directly without derivatization using conductivity for detection (Fig. 1). Many examples of derivatization techniques have been tabulated in Ref. B1. Phosphatidic acids, which result from the enzymatic reaction of phospholipase D with phospholipids, are derivatized to the methyl ester by treatment with diazomethane. In the reaction, the phosphate salt is converted to a neutral organophosphate, thereby changing its chromatographic behavior without affecting UV absorption of the lipid. Several commercially available phosphatidylethanolamines (PEs) have been derivatized for HPLC analysis as dansyl, pyrene-sulphonyl, and fluoresceinthiocarbomoyl derivatives.

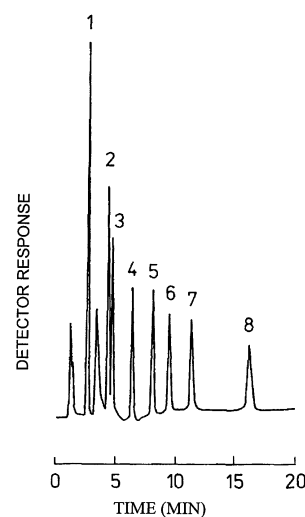


Fig. 1 Separation of free fatty acids by HPLC with conductivity detection. Mobile phase is methanol–5 mM tetrabutylammonium salt (75:25, v/v; pH 7.5) at a flow rate of 0.8 mL/min. Peaks: 1, lauric (12:0); 2, myristic (14:0); 3, linolenic (18:3); 4, linoleic (18:2); 5, palmitic (16:0); 6, oleic (18:1); 7, margaric (17:0); 8, stearic acids (18:0). (Reproduced by kind permission of the authors and of *Journal of Chromatography*).



Diacylglycerol acetates, from bovine brain ethanol-amineglycerophospholipid (EGP), were separated into molecular species using an ODS column. The chromatograms of derivatized phospholipids showed better resolution when compared with the chromatograms of underivatized phospholipids.

Sample Cleanup

Before analysis, lipids are extracted from biological matrices with either a single organic solvent or a mixture of several organic solvents, such as chloroform-methanol or 2-propanol-hexane. Some lipids that contain several double bonds are easily oxidized by air during extraction. To prevent oxidation of such lipids, it is best to perform the extraction in an atmosphere of nitrogen and/or at low temperature. Prior to extraction, an antioxidant, such as BHT, may be added to inhibit oxidation. After the extraction, the extracts are cleaned up by solid-phase extraction (e.g., aminopropyl), column chromatography, or TLC [9]. Then, one-dimensional or two-dimensional TLC is used to separate the lipids. The separated lipids are eluted from the silica gel by scraping the zones of interest from the plate and extracting the lipids with a solvent.

In many cases, HPLC can replace TLC in this step. HPLC has the advantage that, during the analysis, oxygen-sensitive lipids are not exposed to air and autoxidation is limited. After the cleanup steps, samples are analyzed by GC or HPLC. Analysis of triglycerides often involves saponification before the HPLC analysis. Because samples of lipids may originate from a variety of different sources, the specific cleanup steps prior to analysis depend largely on the sample and the original sample matrix. For analysis of cholesterol in blood plasma, a sample of plasma was mixed with isopropanol and centrifuged. After centrifugation, the supernatant was directly analyzed by HPLC [9]. For analysis of monoglycerides in emulsifiers, the sample was dissolved in hexane-2-propanol (90:10), diluted, and injected into the HPLC. For analysis of vegetable oils, a dilute solution of oil in hexane-2-propanol is prepared and analyzed.

For quantitation of cholesterol and its derivatives in muscle and liver tissues, the extracts of the tissue homogenates are evaporated, dissolved in a mobile phase such as hexane-isopropanol, and injected onto a normal-phase column. For analysis of soybean oil by reversed-phase HPLC, after extraction with chloroform-methanol (9:1), the neutral lipids,

chlorophylls, and the phospholipids are separated by TLC. The lipids recovered from the TLC are analyzed by HPLC.

Examples of Lipid Analysis by HPLC

For examples of separation of lipids see general references. For tabulated examples, see Ref. B1 for separation of molecular species of phospholipids by HPLC, Ref. I for separation of lipids in food by HPLC, Ref. H for HPLC of phosphatidic acid, and Ref. B2 for preparative HPLC of lipids.

For separation of intact polar lipids by HPLC and detection by mass spectrometer, see Ref. 8. For triglycerides and fatty acids, see Ref. B4. For separation of neutral lipids into classes and species, see Ref. 2.

Acknowledgments

The author wishes to thank Sue Hammer for preparation of the manuscript, Andrea Wong for reviewing the manuscript, and Peter Austin for library searches.

References

General References

For important references in lipid analysis see Appendices in *Advances in Lipid Methodology, Volumes 1-4* (W. W. Christie, ed.), The Oily Press, Dundee (1990, 1992, 1994, 1997).

For more detailed description of the subjects consult the following:

The following chapters in *Advances in Lipid Methodology, Volume 4*: (B1) Chapter 2, Separation of molecular species of phospholipids by high-performance liquid chromatography, M. V. Bell; (B2) Chapter 3, Preparative high-performance liquid chromatography of lipids, P. Van der Meeren and J. Vanderdeelen; (B3) Chapter 4: Structural analysis of fatty acids, W. W. Christie; (B4) Chapter 6: Reverse-phase high-performance liquid chromatography: General principles and application to the analysis of fatty acids and triglycerols, B. Nikolova-Damyanova.

The following chapters in *Advances in Lipid Methodology, Volume 3*: (C1) Chapter 3, Separation of phospholipid classes by high-performance liquid chromatography. W. W. Christie; (C2) Chapter 6, Plant glycolipids: Structure, isolation and analysis, E. Heinz.

The following chapters in *Advances in Lipid Methodology, Volume 2*: (D1) Chapter 2, Preparation of ester

derivatives of fatty acids for chromatographic analysis, W. W. Christie; (D2) Chapter 3, Size exclusion chromatography in the analysis of lipids, M. C. Dobarganes and G. Marquez-Ruiz; (D3) Chapter 5, Capillary isotachopheresis in the analysis of lipoproteins, G. Schmitz, G. Nowicka, and C. Mollers; (D4) Chapter 6, Preparation of lipid extracts from tissues, W. W. Christie.

The following chapters in *Advances in Lipid Methodology, Volume 1*: (E1) Chapter 1, Solid-phase extraction columns in the analysis of lipids, W. W. Christie; (E2) Chapter 3, Supercritical fluid chromatography of lipids, P. Laakso; (E3) Chapter 4, The chromatographic resolution of chiral lipids, W. W. Christie; (E4) Chapter 6, Silver ion chromatography and lipids, B. Nikolova-Damyanova; (E5) Chapter 7, Detectors for high-performance liquid chromatography of lipids with special reference to evaporative light-scattering detection, W. W. Christie.

Also, consult the following:

Christie, W. W., Lipid class separations using high-performance liquid chromatography, in *New Trends in Lipid and Lipoprotein Analyses* (J. L. Sebedio and E. G. Perkins, eds.), AOCS Press, Champaign, IL, 1995, p. 1934.

Shulka, High performance liquid chromatography, normal phase, reverse phase detection methodology, in *New Trends in Lipid and Lipoprotein Analyses* (J. L. Sebedio and E. G. Perkins, eds.), AOCS Press, Champaign, IL, 1995, p. 38.

Abidi, S. L. and T. L. Mounts, High-performance liquid chromatography of phosphatidic acid, *J. Chromatogr. B* 671: 281–297 (1995).

Berg, K. A. and C. E. Canessa, HPLC applications in food and nutritional analysis, in *Chromatographic Science, Volume 78* (L. M. L. Nollet, ed.), Marcel Dekker, Inc., New York, 1998, pp. 753–787.

Additional References

1. J. G. Hamilton and K. Comai, Separation of neutral lipid, free fatty acid and phospholipid classes by normal phase HPLC, *Lipids* 23: 1150–1158 (1988).
2. Antonopoulou, N. K. Andrikopolos, and C. A. Demopoulos, Separation of the main neutral lipids into classes and species by RP-HPLC and UV detection, *J. Liquid Chromatogr.* 17(3): 633–648 (1994).
3. W. W. Christie, Some recent advances in the chromatographic analysis of lipids, *ANALYSIS Mag.* 26(3): M34–M40 (1998).
4. I. Elfman-Borjesson and M. Harrod, Analysis of non-polar lipids by HPLC on a diol column, *J. High Resolut. Chromatogr.* 20: 516 (1997).
5. W. W. Christie and R. Anne Urwin, Separation of lipid classes from plant tissues by HPLC on chemically bonded stationary phases, *J. High Resolut. Chromatogr.* 18: 97 (1995).
6. Liu, T. Lee, E. Bobik, Jr., M. Guzman-Harty, and C. Hastilow, Quantitative determination of monoglycerides and diglycerides by HPLC and evaporative light-scattering detection, *J. Am. Oil Chem. Soc.* 70: 343 (1993).
7. K. Seta, H. Nakamura, and T. Okuyama, Determination of α -tocopherol, free cholesterol, esterified cholesterol and triacylglycerols in human lipoproteins by HPLC, *J. Chromatogr.* 515: 585–595 (1990).
8. A. A. Karlsson, Analysis of intact polar lipids by HPLC-mass spectrometry/tandem mass spectrometry with use of thermospray or atmospheric pressure ionization, in *Lipid Anal. Oils Fats* (R. J. Hamilton, ed.), Blackie, London, 1998, pp. 290–316.
9. H. P. Nissen and H. W. Kreysel, The use of HPLC for determination of lipids in biological samples, *Chromatographia* 30(11/12): 686 (1990).
10. Y. Tsuyama, T. Uchida, and T. Goto, Analysis of underivatized C12–C18 fatty acids by reverse phase ion-pair high-performance liquid chromatography with conductivity detection, *J. Chromatogr.* 596: 181–184 (1992).



Lipid Classes: Purification by Solid-Phase Extraction

Jacques Bodennec
Jacques Portoukalian

Laboratory of Tumor Glycobiology, Université Claude Bernard Lyon I, Oullins, France

Introduction

In recent years, solid-phase extraction (SPE) has emerged as an important tool for the purification of compounds in various fields of chemistry and biochemistry. This technique is taking place with others such as thin-layer chromatography (TLC) and high-performance liquid chromatography (HPLC) in the wide range of preparative tools available to the analyst. Solid-phase extraction technology is relatively new, as the first applications were published during the past two decades, and its real development occurred only in the nineties. The advantages of SPE, as compared to other methods, makes it an attractive method of choice for purification of molecules. Among these advantages are less time and lower solvent consumption when compared to classical liquid-liquid extraction, low cost, and excellent reproducibility of SPE products. Moreover, SPE is easily automated, so that numerous samples can be processed at the same time. SPE is frequently used in lipid chemistry and biochemistry for the isolation of particular compounds or groups of molecules for analytical or preparative purposes [1–3]. Here, we will focus on the applications of SPE in the field of lipid biochemistry, and, primarily, on the use of the aminopropyl-bonded silica gel matrix for lipid fractionation.

General Principles and Methodology of SPE

Solid-phase extraction is a technique which is used for concentration and purification of analytes from solution by adsorption onto a disposable solid-phase-containing cartridge, disk, or syringe barrel, followed by elution of analytes with an appropriate solvent. From a general point of view, the principles of SPE are the same as conventional liquid chromatography and HPLC, so that the retention and elution depend on interactions of the analyte with the stationary solid and mobile liquid phases. Retention mechanisms include normal and reversed phases and ion exchange. The SPE procedure begins by sorbent conditioning to remove cartridge impurities and to wet the functional

groups at the surface of the matrix. Then, the sample is loaded onto the SPE matrix and the sorbent is rinsed to remove the components which are not desired. In a final step, the analytes are eluted from the SPE matrix and recovered in an appropriate solvent for further analysis. A wide variety of solid phases are available. Most applications are performed on the silica gel solid phase, which can be bonded with the same substituents used for HPLC or conventional liquid chromatography columns. SPE principles are described in detail in ad hoc reviews or books [1,4]. This method (as with all chromatographic methods) requires an accurate determination of the conditions of column preparation, sample loading, and stepwise elution. Hence, incomplete elution or analyte breakthrough can occur if optimal conditioning or elution parameters are not well defined. A good choice of solid sorbent must be made according to the nature of the analytes that are to be recovered. The choice of solvents and their volumes, as well as flow rates, must also be carefully determined to ensure optimal recovery of analytes. An understanding of the interactions between sorbent and analytes is needed to develop and optimize SPE procedures [4].

Its advantages and ease of use have made SPE an appropriate method for concentration and fractionation of lipid classes [2,3]. Many different solid-phase types have been used in lipid fractionation on silica, alumina, porous carbon, and ion-exchange resins. Various bonded phases have been used, particularly with the silica gel matrix.

Separation of Lipid Classes by Reversed-Phase SPE

The reversed-phase procedure has been applied in some cases for the isolation of lipid classes on SPE columns. This procedure is mainly suitable for the isolation of lipids dissolved in polar solvents, such as aqueous samples. The mechanism involves partitioning of organic solutes from the polar mobile phase to a non-polar sorbent phase, which can be C₂, C₄, C₈, and C₁₈ aliphatic chains, or cyclohexyl and phenyl groups. Elution of analytes is accomplished by choosing a solvent



that will disrupt the van der Waals forces retaining the molecules on the matrix. Methanol, ethyl acetate, and acetonitrile are often used for this purpose, as they can overcome van der Waals forces and they succeed in bonding to free silanol groups of the column and dissolve residual water coming from the aqueous matrix sample. Reversed-phase separations are not as common as normal-phase separation of lipids by SPE. C₁₈ SPE tubes have been often used in the isolation of phosphatidylcholine, cerebroside, sulfatides, and gangliosides from water-soluble compounds (Figlewicz et al., 1985., quoted in Ref. 2). C₁₈ has been shown to be an efficient tool for the purification of these lipids and is easier to use than other liquid-liquid methods. Reversed-phase SPE columns have also been used for the isolation of short- and long-chain fatty acids from distilled water and seawater (Pempkowiak, J. 1983, quoted in Ref. 2). For more information on the use of SPE in the reverse phase, references cited at the end of this entry should be consulted.

Separation of Lipid Classes by Normal-Phase SPE

Most of applications deal with silica gel sorbent and with aminopropyl-bonded silica sorbents. Silica is a sorbent of choice for lipid fractionation, because these analytes are first recovered in nonpolar solvents as chloroform. The polar silanol groups present at the surface of the silica sorbent will more strongly adsorb polar compounds such as phospholipids, rather than neutral lipids such as sterols and triglycerides. The retention of analytes and their elution will depend on solvent polarity. The mildly acidic nature of silica can also interfere with the separation mechanism by ion-exchange effects. Silica matrix solid-phase extraction has been used to purify some individual lipid classes, such as phosphatidylcholine (PC) or phosphatidylethanolamine (PE) from total lipids. More complex separations are also possible with silica SPE columns. Hence, a procedure for isolating cholesterol esters, triglycerides, free fatty acids (FFAs), cholesterol, acidic phospholipids such as phosphatidylinositol (PI) and phosphatidylethanolamine (PE) from a neutral phospholipid fraction containing PC, lyso-PC, and sphingomyelin (SPH) has been described [5]. This procedure was modified and adapted for further isolation of specific classes of molecules such as the choline phospholipid platelet-activating factor (PAF).

Numerous chemically bonded stationary phases can be formed by reacting the silanol groups of silica with various organic reagents. These can be successfully

Lipid Classes: Purification by Solid-Phase Extraction

used for the isolation of specific lipid classes, because the bonded phases will have greater bonding potential for some specific molecules according to their functional groups. This is the case for aminopropyl-bonded phases whose primary amine group can develop a strong interaction by hydrogen-bonding with molecules having functional groups such as hydroxyl. The amino group can also be used to separate molecules on the basis of an ion-exchange mechanism, because it can also have weak anion-exchange properties [2].

As with silica gel sorbent, neutral lipids will be poorly retained as compared to polar lipids such as phospholipids or glycosphingolipids. Aminopropyl-bonded silica gel SPE sorbent can be used according to its chemical properties, compared to an unbonded silica matrix. Surprisingly, relatively few procedures have been described for lipid fractionation and purification using aminopropyl-bonded silica SPE columns. Kaluzny et al. [6] first described a detailed procedure which allows the fractionation of neutral lipids into different classes. In this procedure, all neutral lipids were eluted from the column with a mixture of chloroform-methanol (2:1, v/v) and transferred for further fractionation onto a second column to obtain cholesterol esters, triacylglycerols, cholesterol, diacylglycerols, and monoacylglycerols to separate fractions, with good yields. With such elution, FFAs and phospholipids still bind to the column. They are then eluted in a stepwise manner by washing this column with 2% acetic acid in diethyl ether (FFA) followed by methanol to elute neutral phospholipids such as PC and SPH. Aminopropyl columns show, here, some advantage compared to un-bonded silica matrix to isolate FFA, since these molecules are firmly bound to the amino group of the column and with relative selectivity compared to other neutral lipids. In the case of an unbonded silica matrix, FFAs would have been eluted before monoacylglycerols, with the other neutral lipids.

Elution of FFAs from the aminopropyl-bonded column requires a change in pH of the elution solvent to weaken the interaction between the FFA carboxyl and the column's amino groups. This is achieved by washing the column with diethyl ether containing 2% acetic acid. This example shows the advantage which can be realized by adapting the nature of the solid phase to the kind of molecule to be recovered. This is particularly useful with molecules which tend to elute together on an unbonded silica sorbent. This is often the case with free ceramides and FFAs, which will tend to migrate close to each other on a silica gel matrix; thus, it can sometimes be difficult to individually purify these compounds, particularly when high levels of

FFAs are present in the sample. By choosing aminopropyl SPE tubes, this problem can be avoided, as FFA will be firmly retained, allowing further efficient elution and purification of these compounds.

However, Hamilton and Comai described a procedure which allows good recovery and separation of the neutral lipids from FFA on a silica SPE matrix [5]. Separation of the different phospholipids can be also achieved on an aminopropyl column. These polar compounds are tightly bound to the matrix, so they are retained while eluting neutral lipids and FFAs. Then, the different phospholipids can be washed from the column by changing the pH and the ionic strength of the solvent. Stepwise elution of phospholipids was obtained (PC, PE, PS, and PI) by increasing, progressively, the polarity of the solvent and its pH [7].

Suzuki et al. also separated phospholipids by using a combination of aminopropyl-bonded silica and an unbonded silica SPE to recover PC, PE, cardiolipin, phosphatidylglycerol, and phosphatidylserine. Phospholipids were recovered with good purity and high yields [8]. The present procedure allows the optimized use of the advantages of each kind of column. Such a combination of two SPE tubes with different matrices was already successfully used by Prietto et al. (1992, in Ref. 2). Steryl esters, TGs, FFAs, diglycerides, monoglycerides, monogalactosylmonoglycerides, and monogalactosyldiglycerides and their digalactosyl derivatives were separated from PC and lysoPC onto a silica gel SPE tube by different solvents of increasing polarity. Then, phosphatidylethanolamine and its lyso derivatives, which were co-eluting from the silica tube, were separated on an aminopropyl-bonded SPE.

Recovery of phospholipids, as well as the various neutral lipids, is obtained with good yields on aminopropyl tubes. Hence, Kaluzny's procedure was shown to recover up to 100% of all the lipid classes studied, giving better results than the TLC procedure [6]. This latter procedure has been extensively used by many workers to separate lipid mixtures from different origins. It has been slightly modified and adapted for particular use with poorer fractionation of lipid samples

[2]. This SPE procedure has been used to achieve partial fractionation of phospholipids by various researchers [2] and, particularly, to recover acidic phospholipids, which can only be eluted from an aminopropyl matrix by changing the ionic strength of the solvent.

Surprisingly, the development of SPE procedures for fractionation of lipid samples has attracted relatively little attention as compared to conventional methods, such as TLC. However, because of its qualities and advantages, it promises to be applied much more in the future. The development of such separation methods is still in progress, as new sorbents and enhanced quality of packing will become available in the near future, from the more than 50 manufacturers currently making SPE products [9].

References

1. W. W. Christie, Solid-phase extraction columns in the analysis of lipids, in *Advances in Lipid Methodology, Volume 1* (W. W. Christie, ed.), The Oily Press, Arly, Scotland, 1992, pp. 1–17.
2. S. E. Ebeler and T. Shibamoto, Overview and recent developments in solid-phase extraction for separation of lipid classes, in *Lipid Chromatographic Analysis* (T. Shibamoto, ed.), Marcel Dekker, Inc., New York, 1994, pp. 1–49.
3. S. E. Ebeler and J. D. Ebeler, *INFORM* 7: 1094–1103 (1996).
4. E. M. Thurman and M. S. Mills, in *Solid-Phase Extraction. Principles and Practice* (J. D. Winefordner, ed.), John Wiley & Sons, New York, 1998.
5. J. G. Hamilton and K. Comai, *Lipids* 23: 1146–1149 (1988).
6. M. A. Kaluzny, L. A. Duncan, M. V. Merritt, and D. E. Epps, *J. Lipid Res.* 26: 135–140 (1985).
7. A. Pietsch and R. L. Lorenz, *Lipids* 28: 945–947 (1993).
8. E. Suzuki, A. Sano, T. Kuriki, and T. Miki, *Biol. Pharm. Bull.* 20: 299–304 (1997).
9. R. E. Majors, Current trends and developments in sample preparation, *LC–GC Int.* 11(Suppl.): 8–16



Lipid Separation by Countercurrent Chromatography

Kazuhiro Matsuda

National Cancer Center Research Institute, Tokyo, Japan

Sachie Matsuda

Horikiri Central Hospital, Tokyo, Japan

Yoichiro Ito

National Institutes of Health, Bethesda, Maryland, U.S.A.

INTRODUCTION

We demonstrate the separation of human brain lipids by using toroidal-coil countercurrent chromatography (TC-CCC). It becomes possible to select the suitable two-phase solvent systems because retention of a stationary phase is much more stable in TC-CCC than in high-speed countercurrent chromatography (HS-CCC). Optimizing the solvent systems, we succeeded in separating major brain lipids. The two-phase solvent, consisting of chloroform/methanol/water (5:4:3), was suitable for the separation of acidic phospholipids (phosphatidic acid [PA], phosphatidylserine [PS], phosphatidylinositol [PI], lysophosphatidylinositol [lysoPI], and lysophosphatidylserine [lysoPS]). By using hexane/ethylacetate/ethanol/0.1% aqueous ammonia (5:5:5:4), neutral phospholipids (phosphatidylcholine [PC], sphingomyelin [SPM], and lysophosphatidylcholine [lysoPC]) were separated. Nonpolar lipids (cholesterol, alkali-labile glycolipids, and cerebroside [CS]) were separated by using the solvent of hexane/ethanol/water (10:15:4). Sphingomyelin (SPM), cerebroside, and phosphatidylcholine are each reported to have more than 100 molecular species, which are derived from variations of the hydrophobic tail group in mammalian tissues. For this reason, SPM was further separated into two groups (SPM-I and SPM-II). Cerebrosides were separated into several groups by using hexane/ethanol/water (5:4:3). It was clearly shown that synthesized PC (distearoyl phosphatidylglycerol and dipalmitoyl phosphatidylglycerol) was completely separated. Because the partition behavior of molecules in the two-phase solvent system can be measured, TC-CCC could be useful not only for the separation, but also for the biological analysis of mammalian cell-membrane lipids.

COUNTERCURRENT CHROMATOGRAPHY

Phospholipids, glycolipids, and cholesterol are the major components of mammalian cell-membrane lipids. They

play important roles in cell-signaling transduction and cell-to-cell recognition or modification of enzyme functions. All of these lipids have amphipathic properties, and contain hydrophobic and hydrophilic regions. In the cell membrane, the hydrophobic and hydrophilic residues and their behavior play an important role in cell functions. The amphipathic property disturbs the separation of these compounds via a countercurrent distribution method because the vigorous mixing of the two solvent phases causes the formation of an emulsion.

Countercurrent chromatography (CCC) is a liquid partition chromatographic technique which eliminates the use of a solid support.^[1,2] CCC utilizes two immiscible solvent phases. The partition process takes place in an open column in which one phase (the stationary phase) is retained while the other phase (the mobile phase) is continuously equilibrating with the stationary phase. To retain the stationary phase in the column, the system uses various combinations of column configuration and force fields (gravitational and centrifugal). Countercurrent liquid partition chromatography is a system without a solid phase. Therefore it may become a useful method for analyzing the hydrophobicity and the behavior of lipids, avoiding the influence of a solid phase or spacers.

Previously, we showed that HS-CCC could separate alkali-labile glycolipids (ALGLs), which were isolated from the human brain, into several groups.^[3] In that experiment, HS-CCC could finely separate the molecular species in the final step of purification. Nevertheless, the retention of a stationary phase is poor in HS-CCC. Therefore the available two-phase solvent systems have their limitations. Moreover, it was actually difficult to separate them from crude materials because of severe emulsification and the subsequent loss of the stationary phase from the column. To overcome this problem, we developed an analytical-scale TC-CCC, which has the advantage of using centrifugal force to retain the stationary phase.^[4] In this system, a stable two-phase separation can be obtained by increasing the rotational speed (centrifugal force) and/or decreasing the flow rate to avoid



emulsification. We can use most of the two-phase solvent systems for this TC-CCC.

In this study, the TC-CCC system was applied to solve the problem of emulsification, and satisfactory stationary phase retention was obtained. Human brain lipids could then be separated. We established the solvent systems that are used for the separation of most of the phospholipids, glycolipids, and less-polar lipids of the human brain. Furthermore, we demonstrated that molecular species, which are derived from variations of the hydrophobic tail group, were separated by optimizing the composition of the solvents. TC-CCC is available for analyzing the hydrophobicities of various lipid molecules in biomembranes.^[15]

EXPERIMENTAL APPROACH

Apparatus

The present studies employ a commercial model of the toroidal coil centrifuge (TC-CCC 1000) purchased from Pharma-Tech Research (Baltimore, MD, USA). The apparatus is a compact tabletop unit measuring 30 × 630 × 640 cm. It is equipped with a flow-through device without the use of rotary seals, according to a previously described principle.^[16] In this implement, rotation speed is continuously adjustable up to 3000 rpm, having a speed regulator equipped with a digital display. The toroidal coil separation column was prepared by winding a 0.4-mm ID, 15–100 m polytetrafluoroethylene (PTFE) tubing (Zeus Industrial Products, Raritan, NJ, USA) onto a nylon pipe of 1.5-mm OD, thus making a right-handed coil. Next, the coiled tube was affixed to the inner wall of the cylindrical centrifuge bowl (diameter: 12 cm and height: 5 cm), thus forming a doughnut-shaped configuration (toroidal coil) consisting of two to three coiled layers. The toroidal coil is about 6 m in length (made from 60-m-long PTFE tubing) and consists of 12,000 helical turns with a total capacity of about 8 mL. The inlet and outlet flow lines were made of thick-wall PTFE tubes (0.35 mm ID) to withstand constant flexing movements. A chromatographic metering pump (model 515 HPLC pump, Waters, USA) was used for pumping in the mobile phase, and a fraction collector (Ultrac, LKB Instruments, Stockholm, Sweden) was used to collect the eluate into test tubes.

Reagents

Phospholipid standards (Phospholipid kit) were purchased from Funakoshi (Tokyo, Japan). Cerebroside (bovine), D- α -phosphatidylcholine dipalmitoyl, and D- α -phosphatidylcholine distearoyl were purchased from

Sigma (St. Louis, MO, USA). Chloroform and methanol, both of glass-distilled chromatographic grades were purchased from Burdick and Jackson Labs. (Muskegon, MI, USA), and a reagent-grade glacial acetic acid, water, hexane, and ethyl acetate from Fisher Scientific (Fair Lawn, NJ, USA). Ethanol was purchased from Pharmacoproduits (Brookfield, CT, USA). Trifluoroacetic acid (TFA) was from Pierce Chemical (Rockford, IL, USA). Ammonium hydroxide was from J.T. Baker (Philipsburg, NJ, USA).

Lipid Extraction and Purification

Human brain tissue (200 g, wet weight) was homogenized, and the total lipids were successively extracted with 3 L each of mixtures composed of chloroform/methanol, 2:1, 1:1, and 1:2 (v/v). The lipid extracts were combined and evaporated to dryness in a rotary evaporator, then suspended and dialyzed against distilled water, and, finally, lyophilized. Unbound (neutral) lipids and bound (acidic) lipid fractions were separated with a column packed with DEAE Sephadex A-25 (Pharmacia LKB Biotechnology, Uppsala, Sweden) (bed volume, 200 mL).

Preparation of Two-Phase Solvent System and Sample Solution

Each solvent system was thoroughly equilibrated in a funnel at room temperature. The sample solution was prepared by dissolving 1–5 mg of lipids in 0.05 mL each of the upper and lower phases.

CCC Procedure

In each separation, the toroidal coil was first entirely filled with a stationary phase (either the upper or the lower phase), and a sample solution was injected into the coil. Next, the mobile phase (organic phase) was pumped into the column while the column was rotated at the desired rate. The effluent from the outlet of the column was collected in test tubes at a rate of 0.2 mL/tube, and at a flow rate of 0.1 mL/min. After the desired peaks eluted, the centrifuge run was terminated and the column contents were fractionated into test tubes at 0.5 mL/tube by eluting the column with the solvent initially used as the stationary phase, at a flow rate of 0.25 mL/min.

High-Performance Thin-Layer Chromatography

The lipids were separated on a high-performance thin-layer chromatography (HPTLC) plate. The developing

solvent was a mixture of chloroform, methanol, and 0.2% aqueous CaCl_2 . Orcinol reagent^[7] and Dittmer's reagent^[8] were used to detect glycolipids and phospholipids.

RESULTS

Fig. 1A shows the procedure for acidic and neutral lipid preparation. Human brain tissue was homogenized and extracted by using a mixture of chloroform and methanol. Next, the lipid extract was dialyzed and applied to the anion exchange column. Then, the binding fraction

(acidic fraction) and the nonbinding fraction (neutral fraction) were separated. Cholesterol, phospholipids, and glycolipids were the main components of these fractions. The general structures of these lipids are summarized in Fig. 1B. There are two types of glycolipids and phospholipids. One is a sphingo type and the other is a glycerol type. In humans, sphingomyelin is only one sphingo type of phospholipid. In glycosphingolipids, X represents various carbohydrates. The carbohydrate containing sialic acid is called a ganglioside, which is eluted as a binding fraction by using anion-exchange column chromatography. We tried various solvent systems and various compositions for each solvent system. We then determined

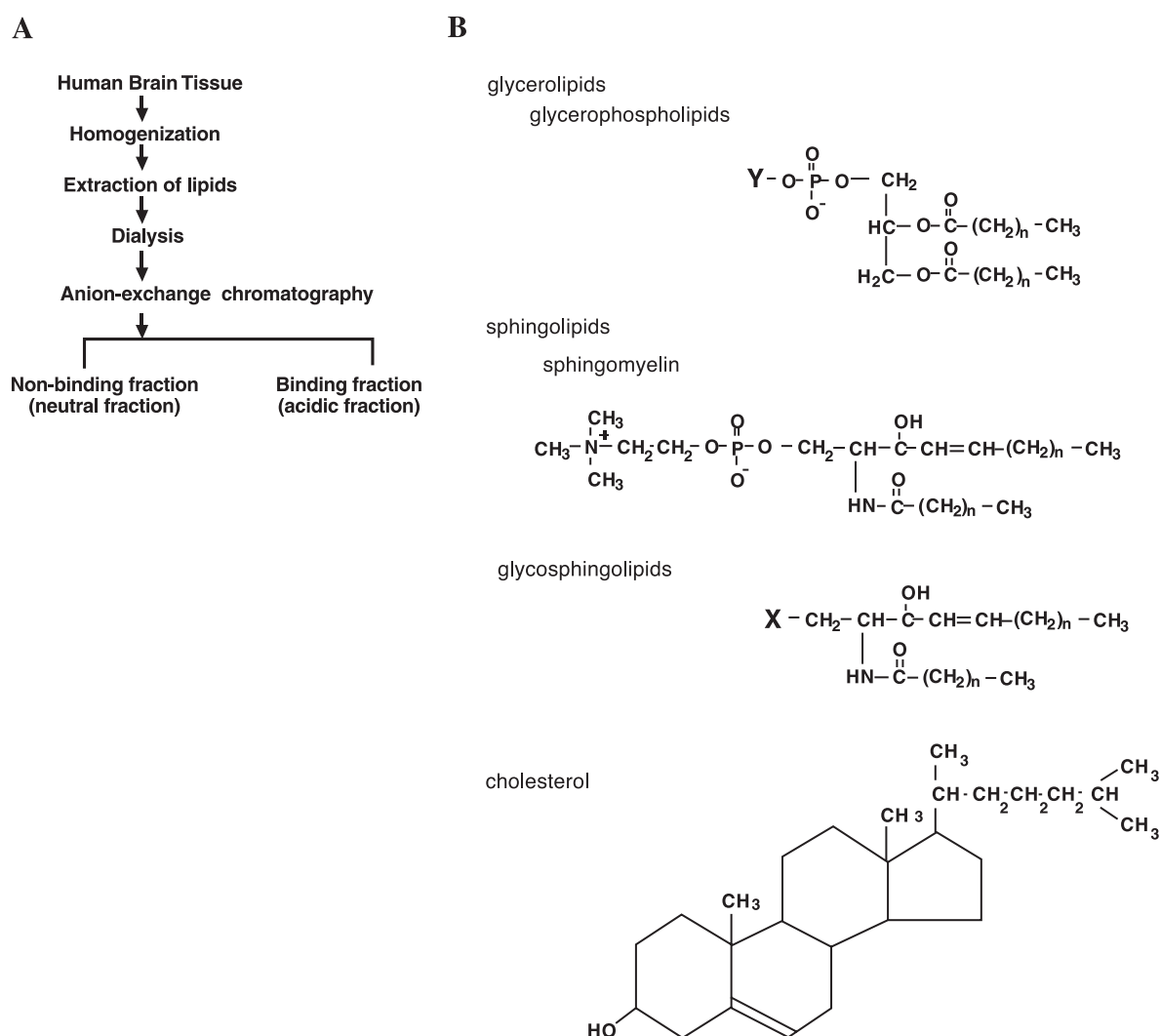


Fig. 1 (A) Procedure to obtain acidic and neutral fractions. (B) General structures of lipids analyzed in this study. Glycosphingolipid is composed of a ceramide (a hydrophobic-tail group) and a carbohydrate (X). X represents various sugar chains. If the X contains sialic acid, it is called a ganglioside. The gangliosides are eluted as acidic fraction in anion-exchange column chromatography. A glycerophospholipid is composed of diacylglycerol (a hydrophobic-tail group) and Y. Y is a hydrophilic head group. Phospholipid classes show differences in Y residue as follows: $-\text{H}$, PA; $-\text{CH}_2\text{CH}_2\text{NH}_3^+$, PE; $-\text{CH}_2\text{CHN}(\text{CH}_3)_3$, PC; $-\text{CH}_2\text{CHNH}_3^+ + \text{COO}^-$, PS; myo-inositol, PI.

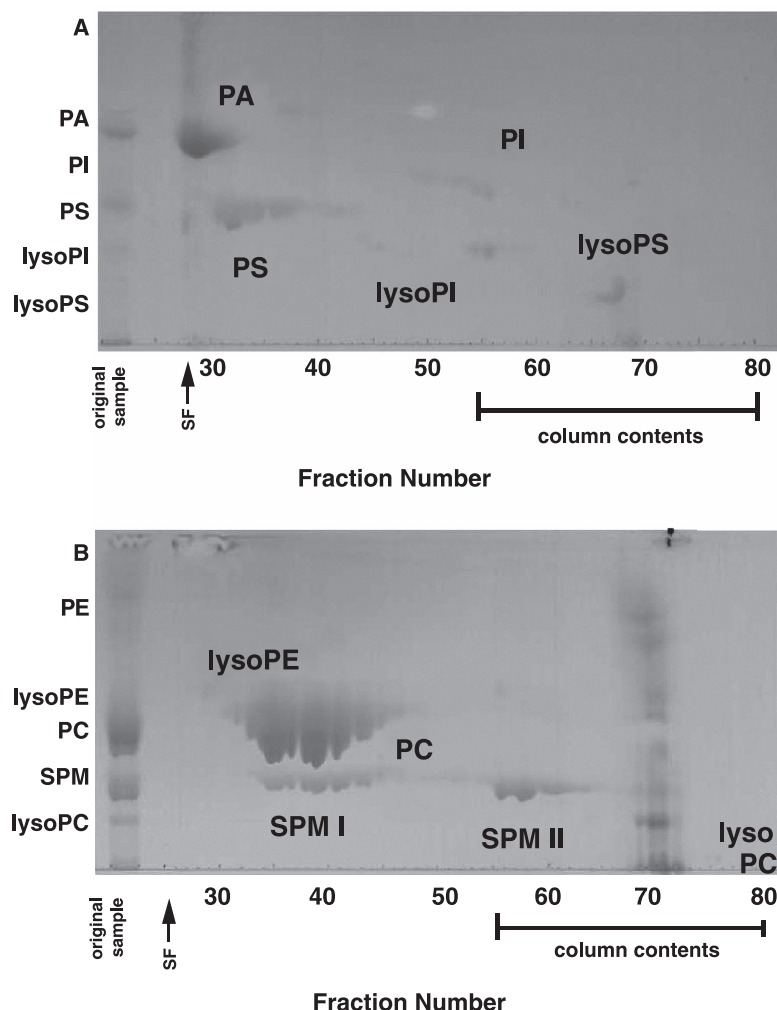


Fig. 2 Separation of acidic phospholipids in the human brain. (A) The solvent system used for TC-CCC was chloroform/methanol/water (5:4:3). The lower phase (organic phase) was mobile. The revolution speed was maintained at 1500–700 rpm. The highest column pressure was 350 psi. A 2-mg portion of the acidic fraction of human brain lipids was loaded. Each fraction was spotted and developed on the HPTLC using chloroform/methanol/0.2% CaCl_2 (60:32:4). Phospholipids were stained with Dittmer's reagent. PA, phosphatidic acid; PS, phosphatidylserine; PI, phosphatidylinositol; lysoPI, lysophosphatidylinositol; lysoPS, lysophosphatidylserine. SF, solvent front. (B) Separation of neutral phospholipids in the human brain. The solvent system used for the TC-CCC was hexane/ethyl acetate/ethanol/0.1% aqueous ammonia (5:5:5:4). The upper phase (organic phase) was mobile. The revolution speed was controlled to run from 1500 to 700 rpm. The highest column pressure was 350 psi. A total of 5 mg of a neutral fraction of human brain lipids was loaded. Each fraction was spotted and developed on the HPTLC using chloroform/methanol/0.2% CaCl_2 (60:32:4). Phospholipids were stained with Dittmer's reagent. PC, phosphatidylcholine; SPM, sphingomyelin; PE, phosphatidylethanolamine; lysoPE, lysophosphatidylethanolamine; lysoPC, lysophosphatidylcholine. SF, solvent front.

that the following conditions are the most appropriate for the separation of the lipids.

Separation of Acidic Fraction

A chloroform/methanol/water system is appropriate for the separation of an acidic fraction. If the solvent compositions are not optimized, the phospholipids and glycolipids are eluted at the solvent front or in the column contents. When we chose a suitable solvent, acidic phospholipids (phosphatidic acid, phosphatidylserine, phosphatidylinositol,

lysophosphatidyl-inositol, and lysophosphatidylserine) were satisfactorily separated between the solvent front and the column contents (Fig. 2A). Samples (2 mg each) of the acidic fraction of human brain lipids was applied to TC-CCC by using the chloroform/methanol/water (5:4:3) solvent system. Aliquots of each fraction were spotted and developed by HPTLC.

Phospholipids were visualized as blue-colored bands by using Dittmer's reagent, which specifically stains phospholipids. Phosphatidylinositol is completely separated from phosphatidic acid (PA) and phosphatidylserine

(PS). The PA, which is the most hydrophobic phospholipid in this solvent system, eluted first, followed by PS, PI, lysoPI, and lysoPS. These phospholipids were identified by using phospholipid standards. The minor phospholipid components (frs. 65–68) may either be phosphatidylinositol phosphate (PIP) or phosphatidylinositol bisphosphate (PIP₂). Each phospholipid (e.g., PS or PI) was further separated into some groups, because each phospholipid has various molecular species, which are derived from variations of hydrophobic tails (ceramide or diacylglycerol). Glycolipids were visualized as pink- or purple-colored bands by using orcinol reagent (data not shown). Sulfatides (fractions [frs.] 40–64) and gangliosides (GM1, GD1a, and GD1b) (frs. 68–70) were eluted. The abbreviations for gangliosides (GM1, GD1a, and GD1b) are according to Svennerholm's nomenclature.^[15] The sulfatides and phospholipids were eluted in the same fraction by TC-CCC.

Separation of the Neutral Fraction

Most of the lipids of the neutral fraction were eluted at the solvent front when the chloroform/methanol/water solvent system, which is suitable for the separation of the acidic fraction, was used. We then tried solvent systems which can separate more hydrophobic lipids. Using the hexane/ethyl acetate/ethanol/0.1% aqueous ammonia solvent system, we could separate phospholipids (Fig. 2B) and glycolipids (data not shown). A 5-mg amount of a neutral fraction from human brain lipids was applied to TC-CCC by using hexane/ethyl acetate/ethanol/0.1% aqueous ammonia (5:5:5:4). Phosphatidylcholine (PC), sphingomyelin (SPM), and lysophosphatidylcholine (lysoPC) were successively eluted. Phosphatidylethanolamine (PE) and lysophosphatidylethanolamine (lysoPE) and other minor phospholipid components were retained as the column contents with this solvent system. Cerebroside (fr. 28/36) and some

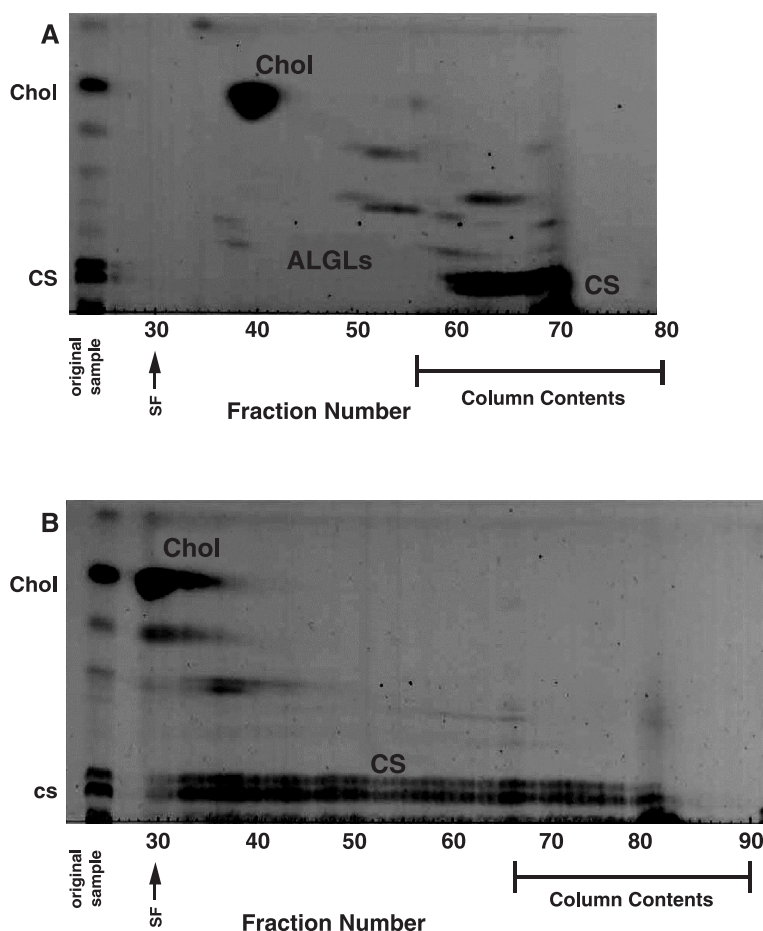


Fig. 3 Separation of highly nonpolar neutral glycolipids in the human brain. The solvent system used for the TC-CCC was hexane/ethanol/water (10:15:4) (A) and (5:4:3) (B). The upper phase (organic phase) was mobile. The revolution speed was controlled to run from 1500 to 700 rpm. The highest column pressure was 350 psi. A total of 5 mg of a neutral fraction of human brain lipids was loaded. Each fraction was spotted and developed on the HPTLC using chloroform/methanol/0.2% CaCl_2 (90:12:1). Chol, cholesterol; CS, cerebroside. SF, solvent front.



other neutral glycolipids (frs. 35–43 and 55–63) were visualized on HPTLC when we used orcinol staining (data not shown). Cholesterol (Chol) is eluted at the solvent front (frs. 28–32) and nonspecifically stained (a brown color). It should be noted that SPM, which is usually difficult to separate into two groups with a silica bead column, is completely separated into two groups (SPM I and SPM II) (Fig. 2).

Separation of Less-Polar Neutral Lipids

Cholesterol and cerebrosides were difficult to separate via the hexane/ethyl acetate/ethanol/0.1% aqueous ammonia system. Therefore we used another solvent system to separate less hydrophobic lipids. A 5-mg amount of a

neutral fraction from human brain lipids was applied to TC-CCC by using hexane/ethanol/water at a volume ratio of 10:15:4 (Fig. 3). In Fig. 3, the orcinol staining shows the specific purple color for cerebroside (CS) and ALGLs,^[3] and a nonspecific brown color for other lipids (not identified). Most of the phospholipids and glycolipids were retained in the column contents. Cholesterol was isolated from other lipids (frs. 38–43) (Fig. 3A). Cerebroside is eluted at frs. 60–72.

We changed the composition of the solvent system to determine whether TC-CCC could separate molecular species of CS. Fig. 3B shows the result when we used hexane/ethanol/water at a volume ratio of 5:4:3. It has been reported that CS is composed of more than 100 molecular species. The difference in intensity in the two

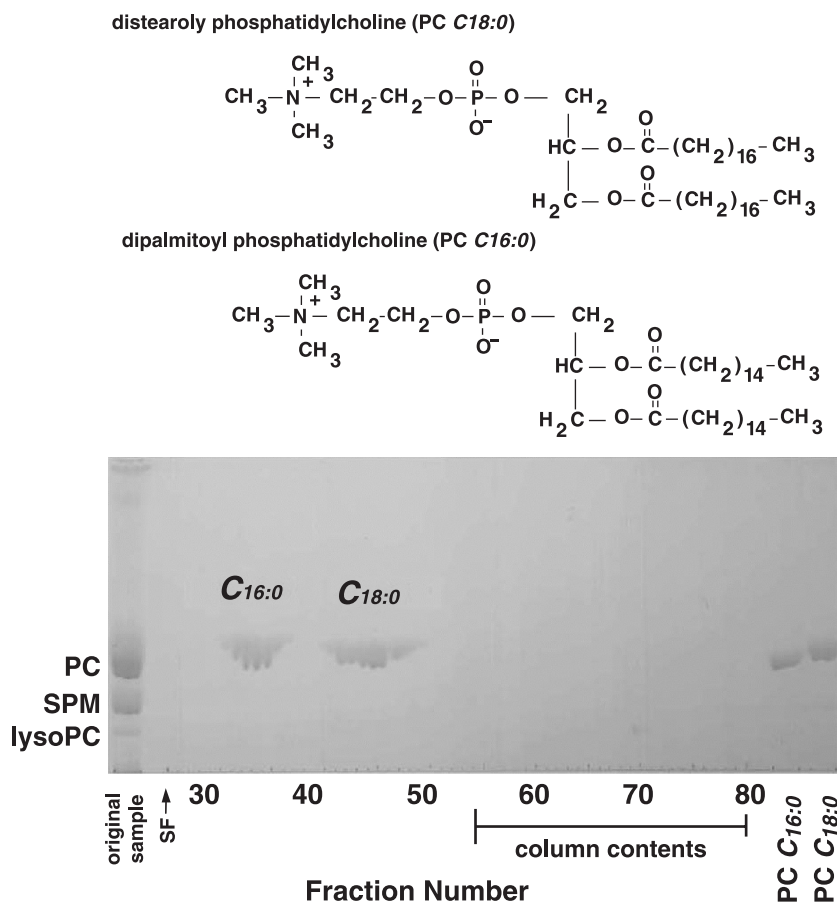


Fig. 4 Separation of dipalmitoyl phosphatidylcholine and distearoyl phosphatidylcholine. The solvent system used for the TC-CCC was hexane/ethyl acetate/ethanol/1% trifluoroacetic acid (5:5:5:4). The upper phase (organic phase) was mobile. The rotational speed was maintained at 1500–700 rpm. The highest column pressure was 360 psi. Amounts (100 µg each) of phosphatidylcholine dipalmitoyl and phosphatidylcholine distearoyl were loaded. Each fraction was spotted and developed on the HPTLC using chloroform/methanol/0.2% CaCl₂ (60:32:4). Distearoyl phosphatidylcholine contains 2 mol of esterified stearic acids and dipalmitoyl phosphatidylcholine contains 2 mol of esterified palmitic acids. PC C16:0, dipalmitoyl phosphatidylcholine; PC C18:0, distearoyl phosphatidylcholine. SF, solvent front.

bands represents the different molecular species. To show more clearly that TC-CCC can separate molecular species, the following studies were carried out.

Separation of Molecular Species

To assess the ability of the TC-CCC molecular species, two molecular species of phosphatidylcholine, which were synthesized, were subjected to TC-CCC. Dipalmitoyl phosphatidylcholine (PC C16:0) and distearoyl phosphatidylcholine (PC C18:0), two of the major molecular species of phosphatidylcholine, were completely separated as shown in Fig. 4. Distearoyl phosphatidylcholine contains 2 mol of esterified stearic acids and dipalmitoyl phosphatidylcholine contains 2 mol of esterified palmitic acid. The structures of these compounds are shown in Fig. 4. These two compounds were completely separated. This result indicates that the TC-CCC system can separate molecular species in both phospholipids and glycolipids categories.

DISCUSSION

Advantages of TC-CCC

Applications of countercurrent distribution to lipid purification were already reported in the 1950s. These included the isolation of PC, SPM, or cerebrosides from brain tissue^[9,10] or the placenta.^[11] It was then mentioned that lipids easily emulsify, and this adversely affects the ability to separate them. Therefore these methods were only used for crude separation. The method also requires a long time for phase separation before each phase transfer, and this procedure needs to be repeated 500–3000 times. Otsuka and Yamakawa^[12] reported the application of droplet countercurrent chromatography to the purification of phospholipids and glycolipids. Because the stationary phase retention is much more stable in TC-CCC than with high-speed countercurrent chromatography (HS-CCC), it has become possible to select appropriate two-phase solvent systems. In this study, we showed the successful separation of human brain lipids by using TC-CCC. Additionally, if an isolated band can be observed on HPTLC, the lipid can be purified by using silica column chromatography after TC-CCC crude separation.

Reverse-phase column chromatography using HPLC can be used to separate these compounds according to their hydrophobicities. However, the reported solvent systems contain salt. The TC-CCC system has an advantage in that lipids can be separated without the use of salted buffer. We plan to monitor the eluted lipids from

TC-CCC by using a mass spectrometer, and this can be achieved employing salted, buffer-free solvent systems.

Separation of Molecular Species

In this paper, we have shown that this system can separate molecular species. One example is shown for cerebrosides (Fig. 3B). Human phospholipids and glycolipids have many forms (molecular species) because of the variation in fatty acids or ceramides. Phosphatidylcholine, sphingomyelin, and cerebroside are each reported to consist of more than 100 molecular species.^[13] As shown in Fig. 4, it is possible to obtain better resolution by changing the flow rate and the volumes of the fractions. Furthermore, better conditions can be optimized by changing the composition of the solvents to target one lipid, as shown.

It should be emphasized that the SPM was completely separated into at least two groups (SPM I and SPM II). It was reported that there are two forms of dihydro-sphingomyelin (DHS) and sphingomyelin (SPM) in commercially available bovine brain SPM;^[14] SPM I and SPM II may correspond to these. TC-CCC is still in the prototype stage because there are many factors that still need to be improved, e.g., the flow volume, the flow rate, and the tube length, as previously described. In addition, the injection system and the detection system could be improved. If these elements can be enhanced, resolution may dramatically improve.

Applications for Biological Analysis

There is a possibility that TC-CCC can be useful not only for the separation of lipids, but also as an instrument for showing the hydrophobic behavior of lipids in cell membranes. Both phospholipids and glycolipids are important components of cell membranes, in which molecular interactions between hydrophilic or hydrophobic molecules play an important role in a cell's physiology. Avoiding the effects of hydrophobicity in a solid phase system, we are able to study molecular interactions between lipids and hydrophobic molecules. The advantage of the present system is that the net partition behavior of molecules in the two-phase solvent system can be measured by monitoring the retention volumes of eluted molecules. As a result, we can obtain the partition coefficient (*K*) of molecules in the two-phase solvent system. This may provide a method for measuring the lipid–protein interaction in a cell membrane. This method may be useful for purifying and analyzing of caveolae, lipoprotein, or such hydrophobic microdomains in biomembranes.

Next, we determined appropriate solvent systems, and showed the hydrophobicity of lipids. In other words, most of the major human brain lipids were mapped with



HPTLC using TC-CCC. Calcium plays an important role in a biomembrane. It is interesting to note that calcium improves the separation of lipids by the HPTLC.^[15] In this system, it is possible to see the effect of either calcium or pH on the elution profiles of lipids.

CONCLUSION

Phospholipids, glycolipids, and cholesterol are the major components of mammalian cell-membrane lipids. They play important roles in cell-signaling transduction and cell-to-cell recognition or modification of enzyme functions. In this study, the toroidal-coil countercurrent chromatography (TC-CCC) system was applied to solve the problem of emulsification, and satisfactory stationary phase retention was obtained. Human brain lipids could then be separated. We established the solvent systems that are used for the separation of most of the phospholipids, glycolipids, and less-polar lipids of the human brain. Furthermore, we demonstrated that molecular species, which are derived from variations of the hydrophobic tail group, were separated by optimizing the composition of the solvents. TC-CCC is available for analyzing the hydrophobicities of various lipid molecules in biomembranes.

ACKNOWLEDGMENT

The authors thank Dr. Henry M. Fales of the National Institutes of Health for editing the manuscript with valuable suggestions.

REFERENCES

1. Ito, Y.; Bowman, R.L. Countercurrent chromatography: Liquid-liquid partition chromatography without solid support. *Science* **1970**, *167*, 281–283.
2. Ito, Y.; Bowman, R.L. *Countercurrent Chromatography*; Mandava, N.B., Ito, Y., Eds.; Marcel Dekker, Inc: New York, 1988; 79.
3. Matsuda, K.; Ma, Y.; Baughout, V.; Ito, Y.; Chatterjee, S. Isolation of less polar alkali-labile glycolipids of human brain by high-speed countercurrent chromatography. *J. Liq. Chromatogr. Relat. Technol.* **1998**, *21*, 103–110.
4. Matsuda, K.; Matsuda, S.; Ito, Y. Toroidal coil countercurrent chromatography: Achievement of high resolution by optimizing flow-rate, rotation speed, sample volume and tube length. *J. Chromatogr. A* **1998**, *808*, 95–104.
5. Matsuda, K.; Matsuda, S.; Saito, M.; Ito, Y. Separation of phospholipids and glycolipids using analytical toroidal-coil countercurrent chromatography. I. Separation of human brain lipids. *J. Liq. Chromatogr. Relat. Technol.* **2002**, *25*, 1255–1269.
6. Ito, Y.; Suaudeau, J.; Bowman, R.L. New flow-through centrifuge without rotating seals applied to plasmapheresis. *Science* **1975**, *189*, 999–1000.
7. Svennerholm, L. The quantitative estimation of cerebroside in nervous tissue. *J. Neurochem.* **1956**, *1*, 42–53.
8. Dittmer, J.C.; Lester, R.L. A simple, specific spray for the detection of phospholipids on thin-layer chromatograms. *J. Lipid Res* **1964**, *5*, 126–127.
9. Nielsen, K. A preliminary note on the composition of the non-hydratable soyabean phosphatide. *Acta Chem. Scand.* **1955**, *9*, 173.
10. Cole, P.; Lathe, G.; Ruthven, C. The application of countercurrent methods to the fractionation of lipid material from brain. *Biochem. J. (London)* **1953**, *54*, 449–458.
11. Lovern, J. The application of counter-current distribution to the separation of phospholipids. *Biochem. J. (London)* **1952**, *51*, 464–470.
12. Otsuka, K.; Yamakawa, T. The application of droplet counter-current chromatography (DCC) for the separation of acidic glycolipids. *J. Biochem. (Tokyo)* **1981**, *90*, 247–254.
13. Kim, Y.; Wang, T.C.; Ma, Y.C. Liquid chromatography/mass spectrometry of phospholipids using electrospray ionization. *Anal. Chem.* **1994**, *66*, 3977.
14. Byrdwell, Y.C. Dual parallel mass spectrometers for analysis of sphingolipid, glycerophospholipid and plasmalogen molecular species. *Rapid Commun. Mass Spectrom.* **1998**, *12*, 256–272.
15. Svennerholm, L. Chromatographic separation of human brain gangliosides. *J. Neurochem.* **1963**, *10*, 613–623.



Lipids Analysis by Thin-Layer Chromatography

Boryana Nikolova-Damyanova

Institute of Organic Chemistry, Bulgarian Academy of Sciences, Sofia, Bulgaria

Introduction

The term *lipids* in this entry is restricted to esters and amides of the long-chain aliphatic monocarboxylic acids, the fatty acids, and to their biosynthetically or functionally related compounds. The most abundant lipids are the esters of fatty acids with glycerol (1,2,3-trihydroxypropane), denoted as glycerolipids. Lipids are classified according to the number of hydrolytic products per mole. *Simple* (or *neutral*) lipids release two types of products (e.g., fatty acids and glycerol). The most abundant simple lipids are the triacylglycerols. *Complex* (or *polar*) lipids give three or more products, such as fatty acids, glycerol, phosphoric acid, and an organic base. Typical complex lipids are the glycerophospholipids (phospholipids), glycolipids (galactolipids), and the sphingolipids. A natural lipid mixture comprises different types (denoted as lipid classes) of simple and complex lipids.

Lipids are important constituents of all living organisms. Thus, for example, the triacylglycerols serve as an energy reserve, whereas complex lipids are structural components of the cell membranes with a substantial role in cell functions. Lipids are also important components of the human and animal diet. Disturbances in the lipid metabolism of the organism lead to various disorders and malfunctions. In humans, these are unambiguously related to the development of cardiovascular disease.

The complexity of natural lipids requires relevant methods for examination. Adequate approaches for separation and isolation of lipid components are mandatory, and among these, the chromatography techniques are of primary importance. Among the different chromatographic methods, thin-layer chromatography (TLC) has its special place, being one of the first separation methods applied in lipid analysis. Most of the present basic knowledge on the structure and biological role of lipids has been achieved by using various TLC techniques.

The first description of TLC goes back to 1938, but Kirchner (1951) and Stahl (1965) were those who converted the idea into a full-scale analytical technique. In the early 1960s, Kaufmann and co-workers in Ger-

many and the group of Privet in the United States introduced TLC in the lipid analysis.

Thin-layer chromatography is a powerful tool in the analysis of lipids. It is easy to perform, versatile, and relatively cheap, and it allows for direct quantitative measurements of the separated compounds by means of scanning densitometry. An important feature is that the analyst gets a full picture of the examined sample.

The General TLC Technique for Lipids

Thin-layer chromatography is a separation technique in which the components of a lipid mixture are differently distributed between a solid stationary phase, spread as a thin layer on a plate made of inert material, and a solvent mobile phase. Depending on their type, the components are retained with different strengths on the layer to give distinctive spots or bands. The migration of a band is presented quantitatively by the corresponding R_f value. The stronger the retention, the lower is the R_f value.

Three modifications of TLC are in use in lipid analysis: (a) separation on unmodified silica gel layer, silica gel TLC; (b) separation on a layer impregnated with silver ions, silver-ion TLC (Ag TLC), and (c) separation on a layer modified with silanes or long-chain hydrocarbons to give a nonpolar stationary phase, reverse-phase TLC (RP-TLC).

The universal TLC facilities are utilized: plates, adsorbents, microcapillars or micropipettes for sample application, development tanks, detection spray reagents and devices for spraying, and densitometers for quantification. Plates are either commercially precoated or handmade. Silica gel G (G, for gypsum as a binding substance), silica gel H (no binding substance), and, rarely, alumina and kieselguhr form the thin-layer stationary phases. Complete sets of devices necessary for the preparation of handmade plates are commercially available. After the silica gel slurry is spread on the plates, they are left to dry in the air for at least 24 h and briefly in an oven at 110°C. The plates are then ready for either direct use or for modification of the layer. From the great variety of precoated plates which



are commercially available and preferred nowadays, silica gel plates and plates with layers modified with carbon chains from C₂ to C₁₈ are of interest in lipid analysis. Understandably, precoated plates for Ag TLC are not commercially available. Preparative TLC is performed mostly on 20-cm × 20-cm plates with a layer thickness of 1 mm. Analytical separations are usually performed on 5-cm × 20-cm plates with a layer thickness of 0.2 mm.

The preparation of a lipid sample includes extraction of the lipid material from the examined object (seeds, tissues, food, etc.), choosing among the several widely accepted procedures. The extraction with chloroform–methanol (2:1) (the Folch extraction) is the most popular. A solution of known concentration in hexane or dichloroethane is prepared and a suitable aliquot is applied on the plate as a small spot or, better, as a narrow band. Two, three, or more solvents, mixed in different proportions, give the mobile phase. Development is performed in common tanks (Desaga type, for example), in the ascending mode. For fine separations, cylindrical or sandwich-type tanks provide better results.

In preparative TLC, detection is performed by spraying the plate with 2,7-dichlorofluorescein and viewing the plate under ultraviolet (UV) light. The spraying reagent does not affect the lipid and can be easily removed during the isolation process, if necessary. Nonspecific destructive reagents are used in analytical TLC. Those most widely used are the alcoholic solutions of sulfuric (up to 50%) or phosphomolybdic (5%) acid, applied as spraying reagents. They are equally suitable for nonmodified as well as for modified layers. Reliable results are also obtained by saturating the layer with vapors of sulfurylchloride (for silica gel TLC and Ag TLC only). To visualize the separated components, the plate is heated at 180–220°C. The substances carbonize to give intensively stained spots, contrasting well with the background. The concentration of the lipid substance in the spots can be measured directly on the plate by using scanning densitometry.

Separation by Silica Gel TLC

Silica gel TLC is used for the identification of lipid classes in the sample (analytical TLC) and for isolation of a given lipid class for further examination (preparative TLC). Silica gel TLC is a good aid in checking both the identity and purity of individual components and different derivatives.

The separation is based on the interaction (hydrogen-bonding, van der Waals' forces, and ionic bonding)

between the lipid molecule and the silica gel. Lipid classes with free hydroxyl, keto, and carboxyl groups are held stronger than those which contain only fatty acid residues.

Mobile phases of hexane or light petroleum ether as main components and acetone or diethyl ether as polar modifiers are used for the separation of simple lipids. Acetic or formic acid is often added to keep the free fatty acids in the fully protonated form. The retention of simple lipids increases in the order waxes, sterol esters, methyl esters, triacylglycerols, free fatty acid, sterols, diacylglycerols, and monoacylglycerols (see Fig. 1a). If no acid is present in the mobile phase, the free fatty acids migrate between diacylglycerols and monoacylglycerols. The

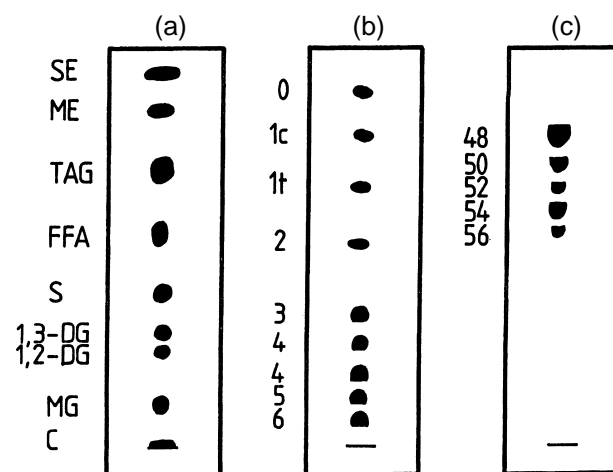


Fig. 1 Schematic presentation of lipid separation by TLC: (a) Reference mixture of simple lipid classes, silica gel TLC; mobile phase: hexane–ethyl ether–acetic acid, 80:20:2 (v/v/v); SE = sterol esters, ME = fatty acid methyl esters, TG = triacylglycerols, FFA = free fatty acids, S = sterols, 1,3-DG = 1,3-diacylglycerols, 1,2-DG = 1,2-diacylglycerols, MG = monoacylglycerols, C = complex lipids; detection by spraying with 5% ethanolic phosphomolibdic acid and heating for several minutes at 180°C; (b) reference mixture of fatty acid methyl esters, Ag TLC on silica gel layer impregnated with 0.5% methanolic solution of silver nitrate; mobile phase: 5 mL of light petroleum ether–acetone–formic acid, 92:2:1 (v/v/v), development in open cylindrical tank; detection by treatment for 30 min with sulfurylchloride vapors and heating for 5 min at 180°C; the numbers denote the number of double bonds, *t*, for a trans double bond, *c* for a cis double bond; (c) triacylglycerols of the 001 class (0 for zero and 1 for one double bond in the molecule), reversed-phase TLC on kieselguhr layer silanized by treatment with dimethyldichlorosilane vapors; mobile phase: acetone–acetonitrile–water, 70:30:12 (v/v/v), detection by spraying with 50% ethanolic sulfuric acid and heating at 220°C for 10 min; the numbers denote the partition number.

complex lipids remain on the start. The retention of phospholipids depends on the nature of the polar “head” and increases in the order cardiolipin, phosphatidylethanolamin, phosphatidylserine, phosphatidylinositol, phosphatidylcholine, [silica gel H, mobile-phase chloroform–methanol–acetic acid–water, 25:15:4:2 (v/v/v/v)]. Galactolipids can be separated with the same solvent system after changing the solvent proportions to increase the polarity. Predictably, monogalactosyl diacylglycerols migrate ahead digalactosyl diacylglycerols.

Identification of the lipid components is performed easily by applying a standard lipid mixture on the same plate prior to the development.

Separation by Ag TLC

Silver-ion TLC is the modification with the most important impact on the development of lipid chemistry and has been of immense importance for the understanding of lipid structure. It is used to resolve the molecular species of a single lipid class. The separation is based on the ability of unsaturated fatty acid moieties in lipid molecules to form weak reversible charge-transfer complexes with silver ions. The complexation includes the formation of a σ -type bond between the occupied $2p$ orbitals of the olefinic double bond in the fatty acid (FA) moiety and the free $5s$ and $5p$ orbitals of the silver ion, and a (probably weaker) π -acceptor backbond between the occupied $4d$ orbitals of the silver ion and the free antibonding $2p\pi^*$ orbitals of the olefinic bond. Thus, Ag TLC separates lipid classes into molecular types depending on the number, configuration, and, occasionally, the position of the double bond in the fatty acid moieties.

The impregnation of the layer is performed by immersing the plate in a solution of the silver salt in methanol, acetone or acetonitrile or by spraying the plate with one of these solutions. Preparative plates are usually treated with 1–20% silver nitrate solutions. For analytical Ag TLC, the concentration of silver nitrate varies in the range 0.5–10%. The impregnation procedures must be standardized to provide reproducible separation. Plates are left in the air for the solvent to evaporate and are usually activated prior to use (between 5 min and 1 h depending on the purpose) by heating at 110°C.

The separation is affected by the dimensions of the tank, the volume of the mobile phase, the development mode (covered or “open” tanks, with or without saturation of the atmosphere, respectively),

the atmospheric humidity, and the temperature. The Ag TLC plates are normally developed at ambient temperature.

Hexane or light petroleum ether, chloroform, benzene, and toluene are most often the major components of the mobile phase, whereas smaller proportions of diethyl ether, acetone, methanol, ethanol, or acetic acid are added as modifiers. Chloroform–methanol and hexane–acetone mobile phases reportedly provide very good separations. Often more than one development is required for reliable resolution. The separation starts with the most polar phase and proceeds, after drying between runs, with mobile phases of gradually decreasing polarity. Highly unsaturated components are resolved first and do not move further with subsequent developments when the more saturated components are separated.

In general, the migration order of any lipid class is determined by the overall number of double bonds in the molecule. Thus, the retention of common fatty acids (chain lengths of 16–22 carbon atoms, methylene-interrupted double bonds) increases with increasing number of double bonds from zero to six (Fig. 1b). For the triacylglycerols which contain the above type of acyl moieties, the order of increasing retention is 000, 001, 011, 002, 111, 012, 112, 003, 112, 013, 113, 222, 023, 123, 223, 133, 233, and 333 (the numbers indicate the number of double bonds in the fatty acid residue but not the position in the glycerol backbone). The same order of retention is valid for complex lipids, but because of different technical difficulties, Ag TLC is only rarely applied in the analysis of these lipids. Species with *cis* double bonds are held stronger than those with *trans* double bonds and this differentiation is of great practical importance. Ag TLC is capable, under specific conditions, to differentiate fatty acids and triacylglycerols according to the position of the double bond in the carbon chain.

Both handmade and precoated plates provide reliable separation of fatty acids. Successful separation of triacylglycerols has been achieved on handmade plates only.

Silver ion TLC offers an effective means of fractionation of lipid mixtures into distinct fractions differing in the number of double bonds. It is often used to simplify the further examination with gas chromatography, GC–mass spectrometry, Fourier transform infrared, and so forth. Ag TLC serves also as an enrichment procedure for minor components and allows for more accurate estimation of their content and identity. Quantitative procedures have been developed for the determination of fatty acids and triacylglycerols by using Ag TLC and densitometry.



Separation by RP-TLC

Reversed-phase (RP) TLC is less popular and has been applied so far only for the resolution of fatty acids and triacylglycerols. It is based on the distribution of lipid molecules between a nonpolar stationary phase and a relatively polar mobile phase. Lipids are, therefore, separated according to their overall polarity, expressed by the partition number (PN). PN relates the migration of a component to the total number of carbon atoms, CN (in the acyl residues only), and the total number of double bonds, n , so that $PN = CN - 2n$. The higher the PN, the stronger is the component retained in the nonpolar layer (the lower the R_f value).

Reversed-phase TLC also uses the common supporting facilities. In the laboratory, the nonpolar stationary phase can be produced by impregnating the layer (kieselguhr G or silica gel G) with long-chain hydrocarbons or liquid paraffin or by treatment with dimethyldichlorosilane (DMCS). Although commercial RP-TLC plates are available, so far it has been experimented with C₁₈ plates only.

Mobile phases which provide good separation for triacylglycerols are (a) acetone–acetonitrile–water, 70:30:X (v/v/v, the water proportion, X, increases with the increasing unsaturation of the lipid class) which is suitable for handmade kieselguhr layers, treated with DMCS and (b) acetonitrile–2-butanone–chloroform, 50:35:15 (by volume) which is suitable for precoated C₁₈ plates.

At present, RP-TLC finds application only as a quantitative technique complementary to the analytical and preparative Ag TLC of triacylglycerols. The triacylglycerol mixture is first fractionated into classes according to the unsaturation and then each class is subjected to RP-TLC to give a series of species with different PNs. An example is shown on Fig. 1c.

Suggested Further Reading

- Ackman, R. G., Application of thin-layer chromatography to lipid separation, in *Analysis of Fats, Oils and Lipoproteins* (G. E. Perkins, ed.), American Oil Chemical Society, Champaign, IL, 1991, pp. 60–82.
- Christie, W. W., *Lipid Analysis*, 2nd ed., Pergamon Press, Oxford, 1982.
- Fried, B. and J. Sherma, *Thin-Layer Chromatography, Techniques and Applications*, Marcel Dekker, Inc., New York, 1994.
- Hamilton, R. J., Thin-layer chromatography and high-performance liquid chromatography, in *Analysis of Oils and Fats* (R. J. Hamilton and J. B. Rossel, eds.), Elsevier, London, 1986, pp. 243–311.
- Kuksis, A., Lipids, in *Chromatography, Part B. Application*, 5th ed. (E. Heftman, ed.), Elsevier, Amsterdam, 1992, pp. B171–B227.
- Nikolova-Damyanova, B., Silver ion chromatography of lipids, in *Advances of Lipid Methodology, Volume 1* (W. W. Christie, ed.), The Oily Press Ltd., Ayr, U.K., 1992, pp. 181–237.



Lipids Analysis by TLC

Boryana Nikolova-Damyanova

Bulgarian Academy of Sciences, Sofia, Bulgaria

INTRODUCTION

The term lipids in this article is restricted (according to Christie) to esters and amides of the long-chain aliphatic monocarboxylic acids, the fatty acids, and to their bio-synthetically or functionally related compounds. The most abundant lipids are the esters of fatty acids with glycerol (1,2,3-trihydroxypropane), which are denoted as glycerolipids. Lipids are classified according to the number of hydrolytic products per mol.

Simple (or *neutral*) lipids release two types of products, e.g., fatty acids and glycerol. The most abundant simple lipids are the triacylglycerols.

Complex (or *polar*) lipids give three or more products, such as fatty acids, glycerol, phosphoric acid, and an organic base. Typical complex lipids include the glycerophospholipids (phospholipids), glycoglycerolipids (galactolipids), and the sphingolipids. A natural lipid mixture comprises different types (denoted as lipid classes) of simple and complex lipids.

LIPIDS

Lipids are important constituents of all living organisms. Thus, for example, triacylglycerols serve as an energy reserve while complex lipids are structural components of the cell membranes with substantial role in cell functions. Lipids are also important components of the human and animal diet. Disturbances in the lipid metabolism of the organism leads to various disorders and malfunctions. In humans, these are unambiguously related to the development of cardiovascular disease.

The complexity of natural lipids requires relevant methods for examination. Adequate approaches for separation and isolation of lipid components are mandatory and, among these, the chromatographic techniques are of primary importance. Among the different chromatographic methods, thin-layer chromatography (TLC) occupies a special place, being one of the first separation methods applied to lipid analysis. Most of the present basic knowledge on the structure and biological role of lipids has been achieved by using various TLC techniques.

The first description of TLC goes back to 1938, but Kirchner (in the fifties) and later Stahl (1965) were those

who converted the idea into a full-scale analytical technique. In the early 1960s, Kaufmann and coworkers in Germany and the group of Privet in the United States introduced TLC to lipid analysis.

TLC is a powerful tool in the analysis of lipids.^[1–7] It is easy to perform, versatile, and relatively cheap, and it allows for direct quantitative measurements of the separated compounds via scanning densitometry. An important feature is that the analyst obtains a full picture of the examined sample.

The General TLC Technique for Lipids

TLC is a separation technique in which the components of a lipid mixture are differentially distributed between a solid stationary phase, spread as a thin layer on a plate made of inert material, and a solvent mobile phase. Depending on their type, the components are retained with different strengths on the layer to give distinctive spots or bands. The migration of a band is presented quantitatively by the corresponding R_f value. The stronger the retention, the lower the R_f value becomes.

Three modifications of TLC are in use for lipid analysis: 1) separation on unmodified silica gel layer, silica gel TLC; 2) separation on a layer impregnated with silver ions, silver ion-TLC (Ag-TLC); and 3) separation on a layer modified with silanes or long-chain hydrocarbons to give a nonpolar stationary phase, reverse-phase TLC (RP-TLC).

The universal TLC facilities are utilized: plates, adsorbents, microcapillaries, or micropipettes for sample application, development tanks, detection spray reagents, devices for spraying, and densitometers for quantification. Plates are either commercially precoated or handmade. Silica gel G (G, for gypsum as a binding substance), silica gel H (no binding substance) and, rarely, alumina and kieselguhr, form the thin-layer stationary phases. Complete sets of devices necessary for the preparation of handmade plates are commercially available. After the silica gel slurry is spread on the plates, they are left to dry in the air for at least 24 hr and shortly in an oven at 110°C. The plates are then ready for either direct use or for modification of the layer. From the great variety of precoated plates, which are commercially available and preferred nowadays, silica gel plates and plates with layers

modified with carbon chains from C₂ to C₁₈ are of interest in lipid analysis. Understandably, precoated plates for Ag-TLC are not commercially available. Preparative TLC is performed mostly on 20 × 20 cm plates with layer thickness of 1 mm. Analytical separations are usually performed on 5 × 20 cm plates with layer thickness of 0.2 mm.

The preparation of a lipid sample includes extraction of the lipid material from the examined object (seeds, tissues, food, etc.) and choosing which among the several widely accepted procedures should be used. Extraction with chloroform-methanol, 2:1 (the Folch extraction) is the most popular. A solution of known concentration in hexane or dichloroethane is prepared and a suitable aliquot is applied onto the plate as a small spot or, better yet, as a narrow band. Two, three, or more solvents, mixed in different proportions, comprise the mobile phase. Development is performed in common tanks (Desaga-type, for example), in the ascending mode. For fine separations, cylindrical or sandwich-type tanks provide better results.

In preparative TLC, detection is performed by spraying the plate with 2,7-dichlorofluorescein and viewing the plate under UV light. The spraying reagent does not affect the lipid and it can be easily removed during the isolation process, if necessary. Nonspecific destructive reagents are used in analytical TLC. The most widely used of these are the alcoholic solutions of sulfuric (up to 50%) or phosphomolybdic (5%) acid, applied as spraying reagents. They are equally suitable for nonmodified, as well as for modified layers. Reliable results are also obtained by saturating the layer with vapors of suluryl chloride (for silica gel TLC and Ag-TLC only). To visualize the separated components, the plate is heated at 180–220°C. The substances carbonize to give intensively stained spots, contrasting well with the background. The concentration of the lipid substance in the spots can be directly measured on the plate by using scanning densitometry.

Separation by Silica Gel TLC

Silica gel TLC is used for the identification of lipid classes in the sample (analytical TLC) and for isolation of a given lipid class for further examination (preparative TLC). Silica gel TLC is a good aid in checking both the identity and purity of individual components and different derivatives.

Separation is based on the interaction (hydrogen bonding, van der Waals forces, and ionic bonding) between the lipid molecules and the silica gel. Lipid classes with free hydroxyl-, keto-, and carboxyl groups are held stronger than those containing only fatty acid residues.

Mobile phases of hexane or light petroleum ether as main components and acetone or diethyl ether as polar

modifiers are used for the separation of simple lipids. Acetic or formic acid is often added to keep the free fatty acids in the fully protonated form. The retention of simple lipids increases in the order: waxes, sterol esters, methyl esters, triacylglycerols, free fatty acids, sterols, diacylglycerols, monoacylglycerols (Fig. 1A). If no acid is present in the mobile phase, the free fatty acids migrate between diacylglycerols and monoacylglycerols. Complex lipids remain at the starting point. Retention of phospholipids depends on the nature of the polar "head" and increases in the order: cardiolipin, phosphatidylethanolamine, phosphatidylserine, phosphatidylinositol, phosphatidylcholine [silica gel H, mobile phase chloroform-methanol-acetic acid-water, 25:15:4:2 (v/v/v/v)]. Galactolipids can be separated with the same solvent

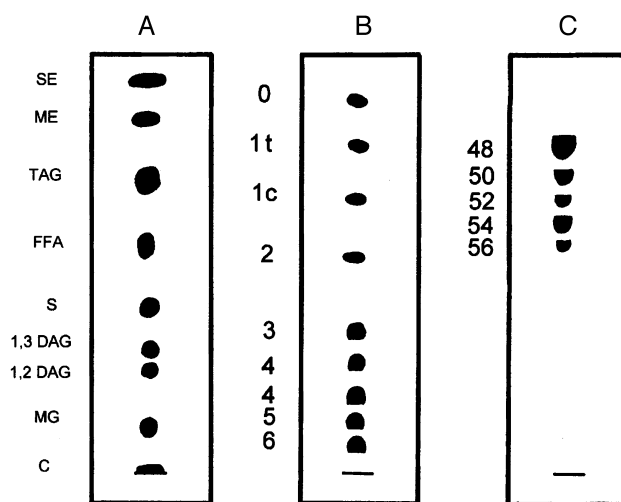


Fig. 1 Schematic presentation of lipid separation by TLC. A) Reference mixture of simple lipid classes, silica gel TLC, mobile phase: hexane-ethyl ether-acetic acid, 80:20:2 (v/v/v); SE, sterol esters; ME, fatty acid methyl esters; TG, triacylglycerols; FFA, free fatty acids; S, sterols; 1,3-DG, 1,3-diacylglycerols; 1,2-DG, 1,2-diacylglycerols; MG, monoacylglycerols; C, complex lipids; detection by spraying with 5% ethanolic phosphomolibdic acid and heating for several minutes at 180°C. B) Reference mixture of fatty acid methyl esters, Ag-TLC on silica gel layer impregnated with 0.5% methanolic solution of silver nitrate, mobile phase 5 mL of light petroleum ether-acetone-formic acid, 92:2:1 (v/v/v), development in open cylindrical tank; detection by treatment for 30 min with sulurylchloride vapors and heating for 5 min at 180°C; the figures denote the number of double bonds, t, for a *trans* double bond, c, for a *cis* double bond. C) triacylglycerols of the 001 class (0 for zero and 1 for one double bond in the molecule), RP-TLC on kieselguhr layer silanized by treatment with dimethyldichlorosilane vapors, mobile phase acetone-acetonitrile-water, 70:30:12 (v/v/v), detection by spraying with 50% ethanolic sulfuric acid and heating at 220°C for 10 min; the figures denote the partition number of the triacylglycerol species.

system after the solvent proportions are changed to increase the polarity. Predictably, monogalactosyl diacylglycerols migrate ahead of digalactosyl diacylglycerols.

Identification of the lipid components is easily performed by applying a standard lipid mixture on the same plate prior to the development.

Separation by Ag-TLC

Ag-TLC is the modification with the most important impact on the development of lipid chemistry and has been of immense importance for the understanding of lipid structure. The separation is based on the ability of unsaturated fatty acid residues in lipid molecules to form weak, reversible charge-transfer complexes with silver ions. Thus Ag-TLC separates lipid classes into molecular types depending on the number, configuration, and occasionally, on the position of the double bonds in the fatty acid residues.

The impregnation of the layer is performed by immersing the plate in a solution of the silver salt in methanol, acetone, or acetonitrile, or by spraying the plate with one of these solutions. Preparative plates are usually treated with 1–20% silver nitrate solutions. For analytical Ag-TLC, the concentration of silver nitrate varies in the range 0.5–10%. The impregnation procedures must be standardized to provide reproducible separation. Plates are left in the air for the solvent to evaporate and are usually activated prior to use (between 5 min and 1 hr depending on the purpose) by heating at 110°C.

The separation is affected by the dimensions of the tank, the volume of the mobile phase, the development mode (covered or “open” tanks, with or without saturation of the atmosphere, respectively), the atmospheric humidity, and the temperature. Ag-TLC plates are normally developed at ambient temperature.

Hexane or light petroleum ether, chloroform, benzene, and toluene are most often the major components of the mobile phase, while smaller proportions of diethyl ether, acetone, methanol, ethanol, or acetic acid are added as modifiers. Chloroform–methanol and hexane–acetone mobile phases reportedly provide very good separations. Often, more than one development is required for reliable resolution. The separation starts with the most polar phase and proceeds, after drying between runs, with mobile phases of gradually decreasing polarity. Highly unsaturated components are resolved first and do not move further with subsequent developments when the more saturated components are separated.

In general, the migration order of any lipid class is determined by the overall number of double bonds in the molecule. Thus the retention of common fatty acids (chain lengths of 16–22 carbon atoms, methylene interrupted double bonds) increases with increasing number of double

bonds from 0 to 6 (Fig. 1B). For the triacylglycerols, which contain the above type of acyl residues, the order of increasing retention is: 000, 001, 011, 002, 111, 012, 112, 003, 112, 013, 113, 222, 023, 123, 223, 133, 233, 333 (the figures indicate the number of double bonds in the fatty acid residue but not the position in the glycerol backbone). The same order of retention is valid for complex lipids but, because of different technical difficulties, Ag-TLC is only rarely applied in the analysis of these lipids. Species with *cis*-double bonds are held stronger than those with *trans* double bonds, and this differentiation is of great practical importance. Ag-TLC is capable, under specific conditions, of differentiating fatty acids and triacylglycerols according to the position of the double bond in the carbon chain.

Both handmade and precoated plates provide reliable separation of fatty acids. Successful separation of triacylglycerols has been achieved on handmade plates only.

Ag-TLC offers an effective means of fractionation of lipid mixtures into distinct fractions differing in the number of double bonds, thus ensuring unambiguous results by further chromatographic and spectral characterization. Ag-TLC serves also as an enrichment procedure for minor components and allows for a more accurate identification and quantification. Quantitative procedures have been developed for the determination of fatty acids and triacylglycerols by using Ag-TLC and densitometry.

Separation by RP-TLC

RP-TLC is less popular and has been applied, so far, only for the resolution of fatty acids and triacylglycerols. It is based on the distribution of lipid molecules between a nonpolar stationary phase and a relatively polar mobile phase. Lipids are, therefore, separated according to their overall polarity, expressed by the Partition Number (PN). PN relates the migration of a component to the total number of carbon atoms, CN (in the acyl residues only) and the total number of double bonds, n , so that $PN = CN - n$; the higher is the PN, the stronger the component is retained in the nonpolar layer (the lower the R_f value becomes).

RP-TLC also uses the common supporting facilities. In the laboratory, the nonpolar stationary phase can be produced by impregnating the layer (kieselguhr G or silica gel G) with long-chain hydrocarbons or liquid paraffin or by treatment with dimethyldichlorosilane (DMCS). Although commercial RP-TLC plates are available, so far, experiments have only employed C_{18} plates.

Mobile phases that provide good separation for triacylglycerols include: 1) acetone–acetonitrile water, 70:30:X (v/v/v, the water proportion, X, increases with the increasing unsaturation of the lipid class) which is suitable

for handmade kieselguhr layers, treated with DMCS; and 2) acetonitrile-2-butanone-chloroform, 50:35:15 (by volume), which is suitable for precoated C_{18} plates.

At present, RP-TLC finds application only as a quantitative technique, complementary to the analytical and preparative Ag-TLC of triacylglycerols. The triacylglycerol mixture is first fractionated into classes according to the unsaturation, and then each class is subjected to RP-TLC to give a series of species with different PN. An example is shown in Fig. 1C.

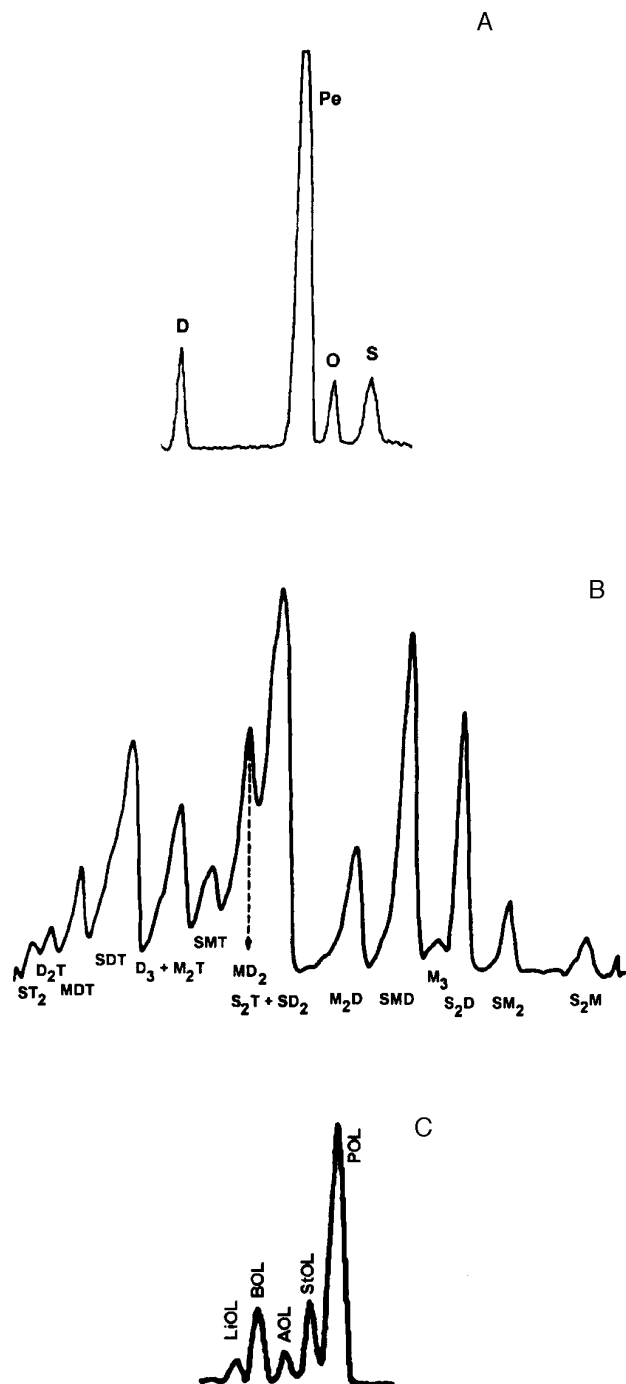
Quantification

The most widely applied procedure is indirect quantification by extracting the fractions from the adsorbent layer in the presence of an internal standard, transmethylation, and subjecting the methyl esters of the fatty acids to gas chromatography (GC) analysis. Information is simultaneously obtained on the composition of the fractions and their absolute amounts. In practice, the sample is resolved on a preparative plate, each distinct zone is carefully scraped off, a standard solution of the internal standard (usually an odd-chain fatty acid methyl ester) is added, and the material is extracted with a suitable polar solvent such as diethyl ether or a chloroform-methanol mixture. More complicated extraction procedures are sometimes needed for polar complex lipids. Fatty acid methyl esters

are directly subjected to GC while triacylglycerols and other lipids are usually transmethyated with the internal standard before analysis by GC. Indirect quantification is the method of choice in the determination of lipid classes.

Direct, in situ, quantification by scanning photodensitometry (a technique developed especially for TLC) is more advantageous. Densitometric measurements are based on the difference in optical response between the

Fig. 2 Densitograms for quantitative determination of fatty acid and triacylglycerol in lipid samples produced on Shimadzu CS-930 scanner in zigzag reflection mode at 450 nm, beam slit varies depending on the sample. A) Determination of fatty acids, as phenacyl esters, in *Petroselinum sativum* seed oil by Ag-TLC, 4×19 cm glass plate covered with 0.2mm thick silica gel layer; layer was impregnated by dipping with 1.0% methanolic silver nitrate and the plate was developed twice in closed cylindrical tank with 3 mL of chloroform-acetone, 100:0.25 (v/v); visualization by successive treatment with bromine (30 min) and sulfuryl chloride (30 min) vapors and heating on a hot plate at 180–200°C; scanning with beam slit 0.4×0.4 mm; S, saturated, O, oleic, Pe, petroselinic, D, dienoic fatty acid. B) Determination of lemon seed oil triacylglycerols by Ag-TLC, TLC plate as in panel A, impregnated by dipping with 0.5% methanolic silver nitrate and developed with 8 mL petroleum ether-acetone, 100:6 (v/v) in open cylindrical tank; visualization by successive treatment with bromine (30 min) and sulfuryl chloride (30 min) vapors and heating on a hot plate at 180–200°C; scanning with beam slit 1.2×1.2 mm; S, saturated, M, monenoic, D, dienoic, T, trienoic acyl residues. C) Determination of triacylglycerols by RP-TLC on kieselguhr layer silanized by treatment with dimethyldichlorosilane vapours, mobile phase acetone-acetonitrile-water, 70:30:18 (v/v/v), visualization by spraying with 50% ethanolic sulfuric acid and heating at 220°C for 10 min; P, palmitic, St, stearic, A, arachidic, B, behenic, Li, lignoceric, O, oleic, L, linoleic acyl residues.



blank part of the plate and regions where the analytes are present. Nowadays, excellent instrumentation is available and the problems that arise are rarely a function of the densitometer and depend mainly on the properties of the chromatogram. A uniform layer, a clean background, well-resolved, distinct, and evenly stained zones, and good contrast between spots and background are required. Zigzag (or flying spot) scanning is greatly superior to linear scanning and should be preferred. Modern instruments are fully computerized and quantify the peaks in the most accurate, reproducible, and convenient manner.

The problem in applying scanning photodensitometry is that lipids do not possess any chromogenic groups and are usually visualized for direct quantification by charring and carbonization. Although charring is a sensitive detection procedure, all steps, including treatment of the plate with the charring reagent, and the temperature and duration of heating must be standardized as far as possible to obtain reproducible results. In most instances, the charring procedure is therefore the critical step. However, efforts to replace charring by another visualization procedure have not led to satisfactory results. An important requirement is that the charring reagent should react in an equal manner with all components, and in particular, staining should not be influenced by the different degree of unsaturation of the separated species. Spraying of the layer with charring reagents (50–70% aqueous, methanolic, or ethanolic solutions of sulfuric acid) or treatment with vapors of such charring reagents such as sulfuryl chloride have been tested, and which one to choose depends on the specific application of TLC.

The recommended procedure for densitometric quantification of fatty acid esters and triacylglycerol separated by Ag-TLC is the successive treatment of the plate with bromine and sulfuryl chloride vapors, followed by heating at 180–200°C (Fig. 2A,B). Correction factors are not required because the quantitative results do not depend on the unsaturation. Spraying with a 50% ethanolic solution of sulfuric acid is suitable for densitometric quantification of triacylglycerols separated by RP-TLC (Fig. 2C).

Lipid analysts have often been skeptical about the possibilities for quantification offered by densitometry,

their opinions generally being formed by earlier experience when the instrumentation was quite primitive. Today, however, the situation is greatly changed and laboratories whose staff are well trained in silver ion TLC methods can successfully apply densitometry. It can be claimed that the overall procedure is cheaper and more suitable for routine analysis of large numbers of samples compared to any alternative technique, while providing results of the same range of accuracy and reproducibility.

ACKNOWLEDGMENTS

Partial financial support of the Bulgarian National Scientific Fund, Contract No X-1009, is gratefully acknowledged.

REFERENCES

1. Ackman, R.G. Application of Thin-Layer Chromatography to Lipid Separation. In *Analysis of Fats, Oils and Lipoproteins*; Perkins, G.E., Ed.; Amer. Oil Chem. Soc.: Champaign, IL, 1991; 60–82.
2. Christie, W.W. *Lipid Analysis*, 2nd Ed.; Pergamon Press: Oxford, 1982.
3. Fried, B.; Sherma, J. *Thin-Layer Chromatography, Techniques and Applications*; Marcel Dekker, Inc.: New York, 1994.
4. Hamilton, R.J. Thin-Layer Chromatography and High-Performance Liquid Chromatography. In *Analysis of Oils and Fats*; Hamilton, R.J., Rossel, J.B., Eds.; Elsevier: London, 1986; 243–311.
5. Kuksis, A. Lipids. In *Chromatography. Part B—Application*, 5th Ed.; Heftman, E., Ed.; Elsevier: Amsterdam, 1992; B171–B227.
6. Nikolova-Damyanova, B. Silver Ion Chromatography of Lipids. In *Advances of Lipid Methodology—One*; Christie, W.W., Ed.; The Oily Press Ltd.: Ayr, 1992; 181–237.
7. Nikolova-Damyanova, B. Quantitative thin-layer chromatography of triacylglycerols: Principles and application. *J. Liq. Chromatogr. Relat. Technol.* **1999**, 22, 1513–1537.



Lipophilic Vitamins by Thin-Layer Chromatography

Alina Pyka

Silesian Academy of Medicine, Sosnowiec, Poland

Introduction

Vitamins are defined as biologically active, organic compounds, controlling agents which are essential for an organism's normal health and growth, not synthesized within the organism, available in the diet in small amounts, and carried in the circulatory system in low concentrations to act on target organs or tissues. Vitamins are classified according to their solubility in water and in fats. Lipophilic vitamins are the vitamins of the groups A, D, E, and K. In chromatography of vitamins, the following problems must be solved: identification and the determination of vitamins in pharmaceutical preparations, identification and determination of vitamins and related substances in natural materials and foodstuffs, and chemical and biochemical determination of vitamins and their metabolites in fats and tissues. The isolation of the vitamins, their metabolites, and related substances from natural material is the most difficult task [1–4].

Vitamin A

There are different physiological forms known as vitamins A, namely retinol (vitamin A₁) and esters, 3-dehydroretinol (vitamin A₂) and esters, retinal (retinene, vitamin A aldehyde), 3-dehydroretinal (retine-2), retinoic acid, neovitamin A, and neo-b-vitamin A₁. There are active analogs and related compounds known as vitamins A, namely α -, β -, and γ -carotene, neo- β -carotene B, cryptoxanthine, myxoxanthine, torularhodin, aphanicin, and echinenone [3]. Vitamin A is susceptible to oxidation and degradation. Therefore, the control of the vitamin A level is recommended.

On silica gel thin-layer chromatography (TLC) plates eluted with a mixture of cyclohexane–ethanol (97:3, by volume), vitamin A₁ alcohol and *retro*-vitamin A₁ alcohol (R_F values 0.10 and 0.09, respectively) are separated from the pair vitamin A₁ acetate/*retro*-vitamin A₁ acetate (R_F values 0.48 and 0.45, respectively) and vitamin A₁ palmitate (R_F value 0.78) and anhydrovitamin A₁ (R_F value 0.87) [5]. Geometric isomers of retinol are separated on silica gel plates using

hexane–ether (50:50, by volume) mixture as a mobile phase. Syn and anti forms of retinal oximes are separated from each other using cyclohexane–toluene–ethyl acetate (50:30:20, by volume) as a mobile phase [1,2]. On magnesium hydroxide, plates eluted with a benzene retinol (R_F value 0.29) is separated from retinal (R_F value 0.61) and retinyl acetate (R_F value 0.75). On magnesium oxide layers, and eluted with petrol ether (boiling point 90–110°C)–benzene (50:50, by volume) as the solvent, the carotenes are separated: ϵ -carotene, α -carotene, β -carotene, δ -carotene, and γ -carotene (R_F values 0.70, 0.66, 0.49, 0.20, and 0.11, respectively) [4]. In partition TLC on kieselguhr G, plates impregnated with paraffin oil (8% paraffin oil in petrol ether), and eluted with acetone–methanol–water (50:47:3, by volume), cryptoxanthin, echinenone, torularhodin methyl ester, and β -carotene (R_F values 0.91, 0.69, 0.57, and 0.22, respectively) are separated [4].

Very small amounts of the intensely colored pigments can be detected in ultraviolet (UV) light and also in visible light; the limit of detection is 0.01 μg of the carotenoids; 0.02–0.03 μg retinal can be detected after spraying of the rhodanine (orange-red color of the spot of retinal). Many vitamin A compounds fluoresce yellow–green in light of 365 nm wavelength (limit of detection 0.05 μg). Vitamin A compounds can be detected with antimony(III) and antimony(V)-chlorides (blue color of spot), with concentrated sulfuric acid (blue color of spot), with molybdophosphoric acid (green–blue color of spot), and with potassium dichromate in sulfuric acid (limits of detection 0.1–0.3 μg) [1,2,4].

Vitamin D

There are various physiological forms known as vitamins D, namely vitamin D₂ (calciferol, ergocalciferol), vitamin D₃ (cholecalciferol), phosphate esters of D₂, D₃, 25-hydroxycholecalciferol, 1,25-dihydroxycholecalciferol, and 5,25-dihydroxycholecalciferol. There are active analogs and related compounds known as vitamins D, namely 22-dihydroergosterol (vitamin D₄), 2-dehydrostigmaterol (vitamin D₆), and 7-dehydro-sitosterol (vitamin D₅) [3].



On silica gel plates, using a mixture of cyclohexane–dichloroethane–diethyl ether (5:3:2, by volume) as a mobile phase, provitamin D₃, tachysterol, lumisterol, and previtamin D₃ (R_F values 0.18, 0.23, 0.27, and 0.31, respectively) are separated [1,2]. The vitamins D₂ and D₃ (R_F values 0.50 and 0.41, respectively) are separated on kieselguhr F₂₅₄ plates impregnated with a 10% solution of paraffin oil in benzene and eluted with binary mixtures of acetonitrile–water (9.5:0.5, by volume) [6]. Previtamins D₂ and D₃ (R_F value 0.50) are separated from vitamins D₂ and D₃ (R_F value 0.40) on silica gel GF₂₅₄ plates using a mixture of cyclohexane–ether (50:50, by volume) as solvent. Vitamins D₂ and D₃ (R_F values 0.79 and 0.57, respectively) are separated from cholesterol, ergosterol, and 7-dehydrocholesterol (R_F values 0.41, 0.30, and 0.13, respectively) on silica gel G impregnated with silver nitrate and eluted with acetic acid–acetonitrile (25:75, by volume) as solvent [4]. On silica gel high-performance thin-layer chromatography (HP–TLC) plates, eluted with a mixture of hexane–isopropanol (85:15, by volume), vitamin D₃ (R_F value 0.66) is separated from hydroxylated metabolites of vitamin D₃: 1,24,25(OH)₃D₃, 1,25(OH)₂D₃, 25,26(OH)₂D₃, 24,25(OH)₂D₃, 23,25(OH)₂D₃, and 25(OH)D₃ (R_F values 0.14, 0.26, 0.35, 0.46, 0.51, and 0.59, respectively) [1,2].

Spots of vitamin D derivatives can be inspected in short-wavelength ultraviolet (UV) light (limit of detection 0.025–0.5 μ g). Vitamins D₂ and D₃ can be detected with antimony(III) and antimony(V) chlorides (gray–blue and orange–red color of spots, respectively; limit of detection 0.025–0.3 μ g), with concentrated sulfuric acid (brown and green color of spots respectively of vitamins D₂ and D₃; limit of detection 30 μ g), with tungstophosphoric acid (gray–brown color of spots; limit of detection 0.2 μ g), with molybdophosphoric acid (gray–blue color of spots; limit of detection 0.3 μ g), and with trichloroacetic and trifluoroacetic acids (limit of detection 0.1–0.2 μ g) [4].

Vitamin E

There are different physiological forms known as vitamins E, namely *d*- α -tocopherol, tocopheronolactone, and their phosphate esters. There are active analogs and related compounds known as vitamins E, namely *dl*- α -tocopherol, *l*- α -tocopherol, esters (succinate, acetate, phosphate), and β -, ζ_1 -, ζ_2 -tocopherols [3].

α -, β -, γ -, and δ -Tocopherols are separated (R_F values 0.26, 0.48, 0.50, and 0.65, respectively) on kieselguhr G plates impregnated with a 10% solution paraffin oil in hexane and using a mixture of methanol–water (9.5:0.5, by volume) as solvent [7]. Tocotrienols

Lipophilic Vitamins by Thin-Layer Chromatography

are separated on silica gel G plates using a mixture of methanol–benzene (1:99, by volume); the R_F values for ζ_1 -, ϵ -, and η -tocopherol and δ -T-3 are 0.55, 0.41, 0.39, and 0.29, respectively [4].

Vitamin E compounds can be detected (about 20 μ g) as dark spots in UV light. They appear violet and detection is appreciably more sensitive (0.02 μ g) on layers that contain 0.02% Na-fluorescein. Moreover, these are visible in daylight as reddish spots (limit of detection 2 μ g). The same effect is produced by spraying with fluorescein or dichlorofluorescein reagent. Nonspecific visualization procedures for tocopherols and tocotrienols are based on spraying with sulfuric acid, molybdophosphoric acid, antimony(V) chloride, dipyridyl-iron reagent, nitric acid, and copper(II) sulfate–phosphoric acid [1–4].

Vitamin K

There are different physiological forms known as vitamins K, namely vitamin K₁ (phyloquinone, phytonadione) and vitamin K₂ (farnokinone). There are active analogs and related compounds known as vitamins K, namely menadiol diphosphate, menadione (vitamin K₃), menadione bisulfite, phthiocol, synkayvite, menadiol (vitamin K₄), menaquinone-*n* (MK-*n*), ubiquinone (Q-*n*), and plastoquinone (PQ-*n*) [3].

Selected K vitamins and related quinones are separated on silica gel G impregnated with silver nitrate using a diisopropyl ether as a solvent; the R_F values for vitamin K (trans K-4), MK-3, MK-4, MK-5, MK-6, MK-7, and menadione are 0.72, 0.58, 0.49, 0.41, 0.29, 0.21, and 0.45, respectively [4].

All lipoquinones in amounts of 0.5 μ g and more are visible as dark spots on layers containing inorganic fluorescent material when illuminated with UV light, by adding Na-fluorescein or rhodamine B or 6G to the adsorbent or by spraying the chromatographed layer with fluorescein or dichlorofluorescein reagents. These compounds can be detected in daylight and, with high sensitivity, in UV light. Vitamin K compounds can be detected with iodine vapor (brown color of spots), with concentrated sulfuric acid followed by heating (violet color of spots, limit of detection 3 μ g), with molybdophosphoric acid (gray–blue color of spots, limit of detection 0.5 μ g) [1–4].

Lipophilic vitamins A, D₂, and E (α -tocopherol) (R_F values 0.34, 0.44, and 0.62, respectively) are separated on silica gel plates and a mixture of benzene–chloroform–acetone (88.5:8.8:2.7, by volume) applied [8]. Table 1 gives information about detection and the hR_F values of lipophilic vitamins in mixtures, using the various layers and solvents.

Table 1 hR_F Values of Lipophilic Vitamins Using Various Separation Systems and Detection of Lipophilic Vitamins

Layer ^a (~0.25 mm): Solvent ^b :	S ₁ F ₁	S ₁ F ₂	S ₁ F ₃	S ₂ F ₂	Detection in		
					UV (254 nm)	UV (365 nm)	Daylight
β -Carotene ^a	84	100	100	78	Dark ^d	Dark ^d	Orange
Vitamin A–alcohol ^c	10	8	22	8	Dark ^d	Yellow–green ^e	—
Vitamin A–acetate ^c	45	41	69	62	Dark ^d	—	—
Vitamin A–palmitate ^c	72	75	94	74	Dark ^d	—	—
Vitamin D ₂ or D ₃	15	9	14	17	Dark ^d	—	—
α -Tocopherol	32	35	56	37	Dark ^d	—	—
α -Tocopherol–acetate	40	40	76	60	Dark ^d	—	—
Vitamin K ₁ ^c	61	67	81	73	Dark ^d	Dark ^d	Yellow
Vitamin K ₃ ^c	38	29	49	63	—	—	—

^aS₁ = silica gel G; S₂ = alumina G.^bF₁ = cyclohexane–ether (80:20, by volume); F₂ = benzene; F₃ = chloroform.^cAll-trans compounds.^dAbsorption.^eFluorescence.

The assay of vitamins A, D, E, and K in food, feed-stuffs, pharmaceutical preparations, organs, blood, and vegetable matter is described in Refs. 1–4. The application of TLC techniques, together with a densitometric scanning apparatus, now permit precise and sensitive quantification of vitamins A, D, E, and K compounds on TLC plates.

References

1. A. P. de Leenheer, W. E. Lambert, and H. J. Nelis, Lipophilic vitamins, in *Handbook of Thin-Layer Chromatography* (J. Sherma and B. Fried, eds.), Chromatographic Science Series Vol. 55, Marcel Dekker, Inc., New York, 1991, pp. 993–1019.
2. A. P. de Leenheer and W. E. Lambert, Lipophilic vitamins, in *Handbook of Thin-Layer Chromatography* (J. Sherma and B. Fried, eds.), Chromatographic Science Series Vol. 71, Marcel Dekker, Inc., New York, 1996, pp. 1055–1077.
3. R. Strohecker and H. M. Henning, *Vitamin Assay, Tested Methods*, Verlag Chemie, Weinheim, 1966.
4. E. Stahl (ed.), *Thin-Layer Chromatography, A Laboratory Handbook*, Springer-Verlag, Berlin, 1969.
5. J. Kahan, *J. Chromatogr.* 30: 506–513 (1967).
6. B. Kocjan and J. •liwiok, *J. Planar Chromatogr. Mod. TLC* 7: 327–328 (1994).
7. J. •liwiok and B. Kocjan, *Fat. Sci. Technol.* 94: 157–159 (1992).
8. M. Ranný, *Thin-Layer Chromatography with Flame Ionization Detection*, Prague, 1987.



Lipophilicity Determination of Organic Substances by Reversed-Phase Thin-Layer Chromatography

Gabriela Cimpan

"Babes-Bolyai" University, Cluj-Napoca, Romania

Introduction

Lipophilicity seems to be an important physicochemical parameter for organic substances, influencing their biological activity. Usually, lipophilicity is defined by the partition coefficient, P , of an organic compound between an organic phase and water:

$$P = \frac{C_o}{C_a} \quad (1)$$

where C_o and C_a are the compound concentrations in the organic and the aqueous phases, respectively, when equilibrium is established. The organic phase can be a hydrocarbon, oil, or, most frequently, n -octanol. From a qualitative point of view, the partition coefficient measures the preference of the compound for the non-polar phase, and from the thermodynamic perspective, it gives information about the intermolecular forces affecting a compound in solution.

Discussion

The partition coefficient between n -octanol and water, $P_{o/w}$, can be measured experimentally using the "shake-flask" method or can be calculated from structural fragments. The direct measurement of $\log P_{o/w}$ values by equilibration between n -octanol and water faces some difficulties, such as the necessary high purity of the substance that must be available in an adequate quantity, and the method is time-consuming too. In addition, it is not applicable to very lipophilic or very hydrophilic compounds.

Reversed-phase liquid chromatography (RP-LC) has been proposed as an alternative method for $\log P_{o/w}$ determination, simulating the partition of a specific compound between the lipid layer and the biological membrane of a cell. This is the process which rules the biological activity of substances, such as the absorption of drugs and their metabolites, the bioaccumulation of organic compounds, and so forth.

Reversed-phase thin-layer chromatography (RP-TLC) is one of the liquid chromatographic techniques showing distinct advantages compared to conventional methods for $\log P_{o/w}$ determination. It is a rapid and reliable method, having a good reproducibility, and it needs only a small amount of sample that does not have to be of high purity. In a RP-TLC experiment, several samples can be run simultaneously. In TLC, the retention parameter, R_F , is defined as the ratio between the migration distances of the compound and of the mobile phase [Eq. (2)]; The term R_M was introduced for a linear relationship between the $\log P$ and R_M values [Eq. (3)]:

$$R_F = \frac{z_x}{z_f} \quad (2)$$

where z_x and z_f are the migration distances of the component and of the mobile phase between the start and the front line, and

$$R_M = \log \left(\frac{1}{R_F} - 1 \right) \quad (3)$$

The stationary phase in RP-TLC can be silica-C₈ or silica-C₁₈; however, better correlations between the R_M values and $\log P$ have been obtained for silica-C₁₈, probably due to the strong interactions which appear between the polar groups of organic compounds and the more accessible free silanol groups on silica-C₈. Impregnated silica with paraffin oil or silicone oil was also used in order to improve the detectability of different organic compounds by spraying with derivatisation reagents. The measurements of R_M values on silica layers impregnated with oils have a lower reproducibility than the measurements on silica C₈- or C₁₈-bonded phases.

The mobile phase used in the lipophilicity measurements by RP-TLC is usually a binary mixture between an organic solvent and water. The organic solvent can be methanol, acetonitrile, or acetone. The first two can also be used in reversed-phase high-performance liquid chromatography (RP-HPLC) measurements, but



acetone is restricted by its absorption in ultraviolet (UV) light.

When a compound contains one or more dissociable polar substituents, the pH and the ionic strength of the mobile phase influence the apparent lipophilicity of the compound. Usually, the mobile phase is buffered at a pH which ensures the neutral form of the studied compound.

The lipophilicity determination of organic substances by RP-TLC is based on the linear relationship established between the R_M values and the concentration of organic modifier in the mobile phase [Eq. (4)]:

$$R_M = a_0 + a_1\varphi \quad (4)$$

where φ is the concentration of the organic modifier in the mobile phase, a_0 and a_1 are the intercept and the slope of the linear relationship (4). The significance of a_0 is the R_{M_w} value obtained for pure water as the mobile phase. Experimentally, the R_{M_w} value can be measured only for very hydrophilic compounds. Practically, the R_{M_w} value is extrapolated from the linear relationship (4) to 0% organic modifier in the mobile phase. The extrapolation method was confirmed by the good correlations obtained between the experimental and the extrapolated R_{M_w} values. From a theoretical point of view, the nature of the organic modifier in the aqueous mobile phase should lead to the same R_{M_w} value. Practically, these values are slightly different, but they do not affect the lipophilicity measurements. Sometimes, a positive or negative deviation of R_M values from the linear relationship (4) was observed, especially at a low concentration of organic modifier in the mobile phase (Fig. 1).

The use of the R_{M_w} value as a measure of a compound lipophilicity is based on the linear relationship with $\log P_{o/w}$ values [Eq. (5)]:

$$R_M = b_0 + b_1 \log P_{o/w} \quad (5)$$

where b_0 and b_1 are the coefficients, the intercept, and the slope, respectively. Equation (5) is similar to the linear relationships obtained in RP-HPLC between $\log k$ and $\log P$ values.

The extreme values for R_F are 0 and 1. As a consequence, the obtained R_M values can be situated between $-\infty$ and $+\infty$. Practically, the R_F values can be measured in the range 0.03–0.97, which means that $-1.5 \leq R_M \leq +1.5$. A particular case corresponds to very hydrophilic compounds, which migrates in the mobile-phase front even at a low concentration of the organic modifier.

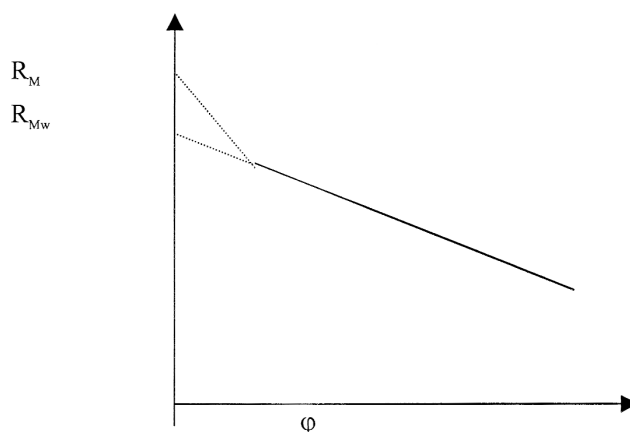


Fig. 1 The relationship between the R_M values and the organic-modifier concentration (φ) in the mobile phase for RP-TLC lipophilicity measurements.

For hydrophilic compounds, the R_{M_w} values can be obtained experimentally, or by extrapolation. The relationship obtained between the direct experimental and the extrapolated R_{M_w} is linear, having an intercept value $m \approx 0$ and the slope n of approximately 1 [Eq. (6)]:

$$R_{M_w, \text{experimental}} = m + nR_{M_w, \text{extrapolated}} \quad (6)$$

Equation (6) proves the validity of the extrapolation method for obtaining the R_{M_w} values in cases when the direct measurement is not possible, due to the lipophilic character of the substance.

The R_{M_w} values obtained in different solvent systems are similar for acetone or methanol aqueous mobile phases, but for *N,N*-dimethylformamide, they are significantly lower. This observation can be explained by the structure of *N,N*-dimethylformamide, which is very different from water.

Irrespective of the organic modifier used in the aqueous mobile phase, a linear relationship can be obtained between the intercept and the slope of Eq. (4). This means that the intercept value, $a_0 = R_{M_w}$, is correlated with the slope a_1 [Eq. (7)]:

$$R_{M_w} = a + ba_1 \quad (7)$$

The linear correlation shown in Eq. (7) is not influenced by the value of the slope a_1 . For a methanol–water mobile phase, an increase of methanol concentration will produce a more rapid decrease of R_M values for the lipophilic compounds than for the hydrophilic ones. In other words, the lipophilic sub-

stances are more sensitive to variations in the mobile-phase composition.

The linear relationship between a_0 and a_1 values [Eq. (4)] is an important characteristic of lipophilicity measurements. The intercept, $a_0 = R_{M_w}$, can be considered a measure for the partition of a compound between a polar mobile phase and a nonpolar stationary phase. The physicochemical significance of the slope, a_1 , is not completely established. It was demonstrated experimentally that the slope shows the rate of increasing the compound solubility in the mobile phase. The solubility increases as a consequence of the decreasing of the mobile-phase polarity. The slope, a_1 , depends on the nonpolar surface of the organic compound (i.e., the part of the compound which interacts with the nonpolar stationary phase).

The correct measurement of the R_F values is very important because it affects the calculation of the R_{M_w} values and the further correlations. The manual measurement of the R_F values will include a error of ± 1 mm, comparing with the precision of a densitometer, which is ± 0.01 mm. The start and the front lines should be also exactly established, in order to reduce the measurement error. The "front line" in TLC is approximately equivalent

with the "dead time" in HPLC. The marker substance used in HPLC (such as inorganic salts) can be applied to estimate the exact front line in TLC. The measurement error for the front line is about 0.03 mm for a migration distance of 80 mm, for any concentration of the organic modifier in the aqueous mobile phase.

Suggested Further Reading

- G. L. Biagi, A. M. Barbaro, and M. Recanatini, *J. Chromatogr. A* 678: 127–137 (1994).
G. L. Biagi, A. M. Barbaro, A. Sapone, and M. Recanatini, *J. Chromatogr. A* 669: 246–253 (1994).
G. L. Biagi, A. M. Barbaro, A. Sapone, and M. Recanatini, *J. Chromatogr. A* 662: 341–361 (1994).
G. Cimpan, C. Bota, M. Coman, N. Grinberg, and S. Gocan, *J. Liquid Chromatogr. Related Technol.* 22: 29–40 (1999).
R. Kaliszan, *Quantitative Structure–Chromatographic Retention Relationships*, John Wiley & Sons, New York, 1987.
Lambert, W. J., *J. Chromatogr. A* 656: 469–484 (1993).
Leo, A. and C. Hansch, *Chem. Rev.* 71: 525–616 (1971).
Tomlinson, E., *J. Chromatogr.* 113: 1–45 (1975).



Lipoprotein Separation by Combined Use of Countercurrent Chromatography and Liquid Chromatography

Yoichi Shibusawa

Tokyo University of Pharmacy and Life Science, Tokyo, Japan

Yoichiro Ito

National Institutes of Health, Bethesda, Maryland, U.S.A.

INTRODUCTION

Polymer phase systems were first introduced by Albertsson^[1] in the 1950s for partitioning macromolecules and cell particles. One of these two-phase solvent systems consists of one polymeric component, such as polyethylene glycol (PEG), and a high concentration of a salt such as potassium phosphate in water. Being free from the organic solvent, the system can preserve a natural structure of proteins if the pH of the system is kept within their physiological range. In the past, polymer phase systems composed of PEG and potassium phosphate were most successfully used for protein separations. In these polymer phase systems, proteins are distributed according to their partition coefficients; these provide the basis for their purification. For example, relatively hydrophobic proteins distribute more into the PEG-rich upper phase and hydrophilic proteins into the phosphate-rich lower phase.

Chromatographic partitioning of the proteins with polymer phase systems can be performed by countercurrent chromatography (CCC)^[2] using a centrifugal device: the cross-axis coil-planet centrifuge (cross-axis CPC) is mainly used for preparative-scale separations. Because of the protective effects of high polymer-salt concentrations, proteins can maintain their integrity at room temperature for a relatively long period of time, and, usually, the purification can be performed without cooling the column or collecting fractions. Combined with liquid chromatography, this method has been successfully applied to separation of lipoproteins directly from human serum as described below.^[3]

APPARATUS

A photograph of the cross-axis CPC is shown in Fig. 1. The apparatus holds a pair of horizontal rotary shafts,

symmetrically mounted, one on each side of the rotary frame, at a distance of 10 cm from the centrifuge axis. A spool-shaped column holder is mounted on each rotary shaft at an off-center position 10 cm from its midpoint. The large multilayer coil separation column was prepared from 2.6mm I.D. polytetrafluoroethylene (PTFE) tubing by winding it on a 15.2-cm diameter holder hub, forming a single layer of left-handed coils between a pair of flanges spaced 5 cm apart. A pair of columns mounted on the rotary frame is connected in series with a flow tube to give a total capacity of 60 mL. Both inflow and outflow tubes exit together at the center of the top plate of the centrifuge case where they are tightly supported with a pair of clamps equipped with silicone rubber pads. The speed of the apparatus is regulated at 500 rpm with a speed control unit.

PARTITION COEFFICIENTS OF LIPOPROTEINS AND SERUM PROTEINS

Countercurrent chromatography is a two-phase procedure where the separation is based on the difference in partition coefficients of solutes within the phases. To achieve efficient separation of lipoproteins from human serum, it is essential to optimize the partition coefficient of each component by selecting an appropriate pH for the polymer phase system.

Fig. 2 shows the partition coefficients of three lipoproteins and three serum proteins plotted on a logarithmic scale against pH of 16% PEG 1000–12.5% potassium phosphate buffer. The partition coefficients of serum proteins and VLDL show an increase with increased pH from 6.8 to 9.2, while those of HDL and LDL display quite different trends, i.e., they become less than 1.0 at pH 9.2, indicating that these lipoproteins are mainly distributed to the potassium phosphate-rich lower phase at high pH.

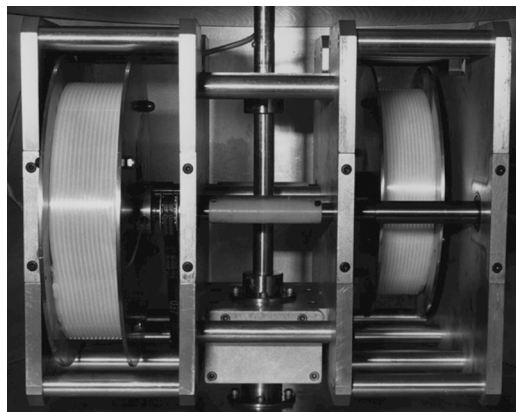


Fig. 1 Photograph of the type XL cross-axis coil-planet centrifuge.

Countercurrent Chromatography of Human Serum

Two lipoprotein fractions (HDL-LDL and VLDL-serum proteins) from human serum were obtained using the *X*-axis CPC equipped with a small-capacity column (60 mL). Fig. 3 shows a chromatogram of human serum (4 mL) obtained with the *X*-axis CPC using 16% PEG 1000–12.5% potassium phosphate buffer (pH 9.2). The separation was performed at 500 rpm and at a flow rate of 0.5 mL/min using the lower phase as the mobile phase where HDLs and LDLs were eluted together near the solvent front (SF), while other proteins were retained in the column for a much longer period of time. After collecting the HDL-LDL fraction, VLDL was eluted together with serum proteins (VLDL-serum proteins fraction) by pumping the upper phase in the reverse direction (marked

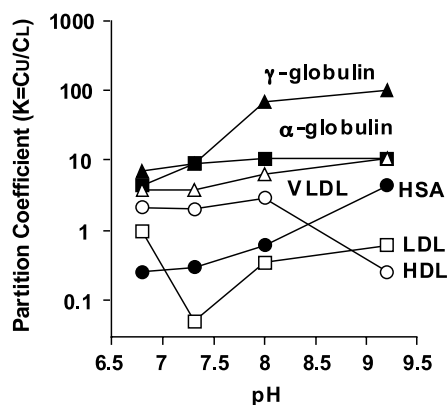


Fig. 2 Partition coefficients (K) of HDLs, LDLs, VLDLs, and serum proteins in polymer phase systems composed of 16% PEG 1000 and 12.5% potassium phosphate buffers.

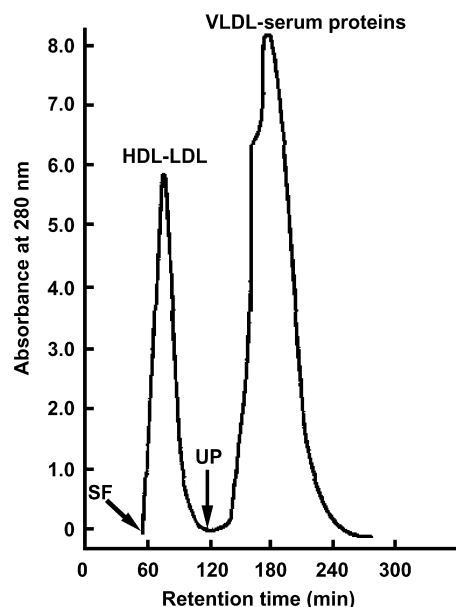


Fig. 3 Countercurrent chromatographic separation of HDL-LDL and VLDL-serum protein fractions from human serum with an aqueous polymer phase system. Column: 2.6mm I.D. PTFE single-layer coil ($\times 2$) with 60-mL capacity; sample: 4 mL of human serum; solvent system: 16% PEG 1000–12.5% dibasic potassium phosphate at pH 9.2; mobile phase: lower phase; flow rate: 0.5 mL/min; revolution speed: 500 rpm. SF = solvent front, UP = starting point of the reversed elution mode with the upper phase.

“UP” in Fig. 3). The separation was completed within 4.5 hr. The lipoprotein in each peak fraction was confirmed by agarose gel electrophoresis with Oil Red 7B staining, and the serum proteins were also detected by SDS-PAGE with Coomassie Brilliant Blue protein staining. The first peak contained HDLs and LDLs but no serum proteins, and the second peak contained VLDLs mixed with serum proteins.

Hydroxyapatite Chromatography of Countercurrent Chromatography Fractions

The CCC fractions, HDL-LDL and VLDL-serum proteins, were each separately dialyzed against distilled water until the concentration of the potassium phosphate was decreased to that in the starting buffer used for the hydroxyapatite chromatography. These two fractions were concentrated separately by ultrafiltration. The concentrates of both fractions were chromatographed on the hydroxyapatite column. Fig. 4 shows the elution profile on hydroxyapatite obtained from the HDL-LDL fraction. A 1.4-mL volume of the concentrate was loaded onto a Bio-Gel HTP DNA-grade column (5.0 \times 2.5 cm I.D.)



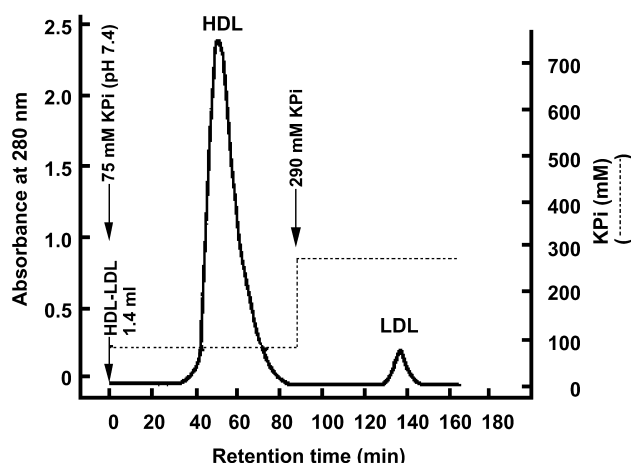


Fig. 4 Stepwise elution profile of HDLs and LDLs by hydroxyapatite chromatography. Column: Bio-Gel HTP DNA-grade hydroxyapatite (5.0×2.5 cm I.D.); eluents: 75 and 290 mM potassium phosphate buffers at pH 7.4; flow rate: 1.0 mL/min; sample: 1.4 mL concentrated HDL-LDL CCC fraction.

and eluted at 1.0 mL/min with 75 and 290 mM potassium phosphate buffer at pH 7.4. Two lipoprotein peaks were eluted; the first peak contained HDLs and the second peak contained LDLs.

The concentrate (1.5 mL) of the VLDL-serum protein fraction was similarly chromatographed (Fig. 5). The separation was performed with a two-step elution with 290 and 650 mM potassium phosphate buffer at pH 7.4. Most of the serum proteins, including albumin and globulins, were eluted with 290 mM potassium phosphate buffer at pH 7.4. The VLDLs, on the other hand, were retained in the column for a much longer period of time and were eluted with 650 mM potassium phosphate buffer. Lipoproteins in the hydroxyapatite chromatographic fractions were confirmed by agarose gel electrophoresis.

CONCLUSION

Countercurrent chromatography is a very useful technique for the separation and fractionation of human serum lipoproteins. The HDL-LDL and VLDL-serum protein fractions were directly obtained from human serum using

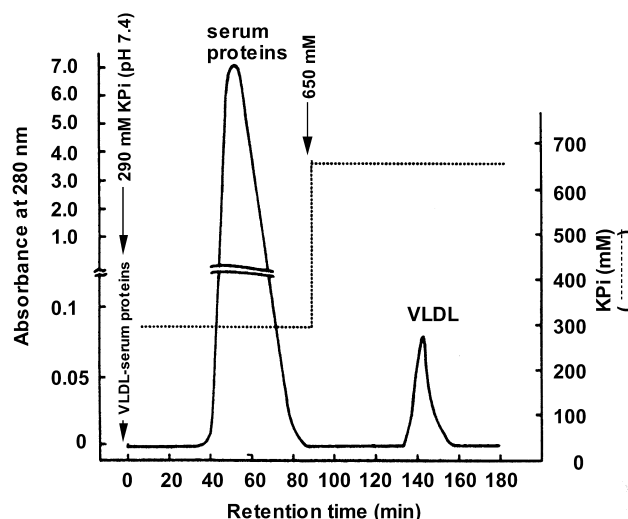


Fig. 5 Stepwise elution profile of serum proteins and VLDLs by hydroxyapatite chromatography. Column: Bio-Gel HTP DNA-grade hydroxyapatite (5.0×2.5 cm I.D.); eluents: 290 and 650 mM potassium phosphate buffers at pH 7.4; flow rate: 1.0 mL/min; sample: 1.5 mL concentrated VLDL-serum protein CCC fraction.

the solvent system composed of 16% PEG 1000–12.5% potassium phosphate at pH 9.2. The separated HDL-LDL and VLDL-serum protein fractions were loaded onto hydroxyapatite columns and separated into HDLs, LDLs, VLDLs, and serum proteins, respectively. The combined use of countercurrent chromatography and hydroxyapatite chromatography is a useful method for the separation of three main classes of lipoproteins from human serum, without prior ultracentrifugation.

REFERENCES

1. Albertsson, P.A. *Partition of Cell Particles and Macromolecules*, 3rd Ed.; Wiley-Interscience: New York, 1986.
2. Ito, Y. Principle and Instrumentation of Countercurrent Chromatography. In *Countercurrent Chromatography: Theory and Practice*; Ito, Y., Mandava, N.B., Eds.; Marcel Dekker: New York, 1988; 79–442.
3. Shibusawa, Y.; Mugiyama, M.; Matsumoto, U.; Ito, Y. J. Chromatogr. B **1997**, *664*, 295–301.



Liquid Chromatography–Mass Spectrometry

Ioannis N. Papadoyannis

Georgios A. Theodoridis

Aristotle University of Thessaloniki, Thessaloniki, Greece

Introduction

The coupling of liquid chromatography and mass spectrometry (LC–MS) was initially considered impossible and actually is still characterized as a hyphenated technique. This can be seen, at first glance, to be due to the incompatibilities of the two methods. In order to introduce a conventional LC flow (0.5–1.5 mL/min) into the mass spectrometer, one should evaporate it, producing a vapor of a volume that is far beyond the capacity of the pump systems of a mass spectrometer. This means that an interface is required to couple the instruments, thus increasing price, complexity, and prestige of any such system. Until recently, most LC–MS systems were state-of-the-art, room-filling machines, reachable only by specialists. The last years' evolution in technology and electronics, together with stronger cooperation of LC with MS manufacturers, brought to the market bench-top, low-price, dedicated systems that require less handling and can even be used for routine analysis.

Discussion

The advantages of an on-line LC–MS approach are many. Both techniques show high separation power and their combination on-line is a powerful tool for identification purposes as well as quantitative studies. Many detectors are available for high-performance liquid chromatography (HPLC): ultraviolet (UV), conductivity, electrochemical, fluorescence, refractometer, and so forth. Unfortunately, most of them lack specificity, selectivity, and sensitivity. Hence, identification of unknown compounds is actually impossible.

An ideal detector for HPLC should combine optimum sensitivity with maximum identification capability. It should also respond to all solutes and increase its signal linearly with the amount of the solute but, at the same time, be unaffected by changes in the mobile phase. Finally, it should also not contribute to extra-column peak broadening and should be reliable and robust. Of the detectors used with HPLC, the mass spectrometer is the closest to the above requirements.

A mass spectrometer offers many attractive features as a chromatographic detector. Low detection limits down to the picogram range can be accomplished in optimized configurations. Mass spectrometry offers high specificity and mass distinction according to nominal mass (low-resolution MS). The specificity is even further increased in high-resolution MS, where mass distinction is made according to accurate mass. This enables the resolution of compounds with the same nominal mass but with different elemental composition (e.g., isomers). Mass spectrometry provides compound-specific information by fragmentation obtained either by hard ionization or by tandem mass spectrometry. Fragmentation patterns greatly increase identification power in the analysis of unknown compounds in complex matrices. Finally, a mass spectrometer is potentially a universal detector.

A diagram of a typical mass spectrometer scheme is depicted in Fig. 1. The simplest form of an MS system should perform the following fundamental tasks:

1. Vaporize compounds of varying volatility. This is accomplished in the inlet system. Introduction of the sample is done by direct insertion probe, reservoir inlet, or following a chromatographic separation (GC, HPLC, and CE). As mentioned earlier, to introduce the LC flow to the mass spectrometer on-line, we need an appropriate interface. Development of appropriate interfaces was the utmost for evolution of the LC–MS coupling.
2. Produce ions from neutral molecules in the vapor phase. This takes place in the ion source. As can be seen in Fig. 1, there are several modes of ion sources. Of those, the most used in LC–MS are electron spray ionization (ESI), chemical ionization (CI), thermospray ionization (TSP), fast-atom bombardment (FAB), and electron impact (EI).
3. Separate the formed ions according to their mass-to-charge ratio (m/z ratio). This takes place in the mass analyzer. By far, the most used analyzer is the quadrupole, either as single or as triple quadrupole, combined with a soft ioniza-



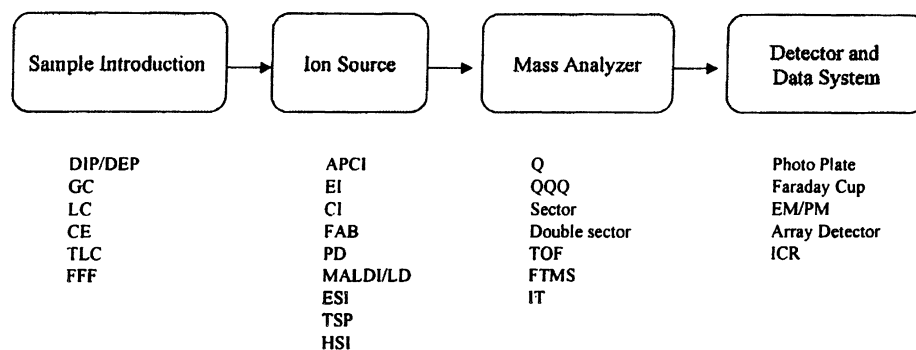


Fig. 1 Schematic representation of a mass spectrometer depicting its main components and the different modes used. Abbreviations: DIP: direct insertion probe; DEP: direct exposure probe; GC: gas chromatography; LC: liquid chromatography; CE: capillary chromatography; TLC: thin-layer chromatography; FFF: field-flow fractionation; APCI: atmospheric pressure ionization; EI: electron impact; CI: chemical ionization; FAB: fast-atom bombardment; PD: plasma desorption; MALDI: matrix-assisted laser desorption ionization; LD: laser desorption; TSP: thermospray; ESI: electron spray ionization; HSI: hyperthermal surface ionization; Q: quadrupole; QQQ: triple quadrupole; TOF: time-of-flight; FTMS: Fourier transform mass spectrometer; IT: ion trap; EM: electrom multiplier; PM: photo-multiplier; ICR: ion cyclotron resonance.

tion technique. In the latter configuration, tandem mass spectrometry can be accomplished. The magnetic sector is also coupled to LC when there is a need for higher-resolution power or higher sensitivity.

4. Detect and record the separated ions. Multipliers are the most common detectors used in LC–MS instruments. Proper fully computerized data manipulation systems are required to handle the massive information flux from the detector.

Interfacing LC and MS benefits both techniques. An obvious question could be: Why do you need such a seemingly unorthodox coupling when other robust and well-behaving techniques (GC–MS) are already available? The great potential of the LC–MS approach is its applicability in the analysis of thermolabile or nonvolatile compounds; this is of great interest in bioanalysis. Despite its high-resolving power, GC is actually suitable only for the analysis of volatile compounds of low molecular mass. LC–MS analysis gives a real boost to bioanalysis, enabling the positive identification and low-level detection of peptides, proteins, carbohydrates, polar analytes, and many other types of synthetic or naturally occurring compounds.

Interfaces

Numerous types of LC–MS interface have been developed. Early attempts were focused on methods of overcoming the incompatibility of the liquid flow rate

and maintenance of the MS high vacuum. Recent approaches pay more respect to the practical use of ionization techniques that do not require sample volatilization. The main approaches to overcome incompatibilities are as follows:

1. Splitting of the flow. A high proportion of the sample is wasted this way.
2. Increasing the source housing pump speed, usually with the addition of a cryopump.
3. Miniaturizing the LC step.
4. Removal of the solvent prior to the introduction in the MS. This approach is used in transport interfaces (MB) and PB.
5. Attaching additional pump to the ion source, which can then accept higher flow rates. This approach is used in TSP.
6. Atmospheric pressure ionization (ESI, ISP).

The main features of LC–MS interfaces are illustrated in Table 1.

The first commercially available LC–MS system (Finnigan, 1976) used a moving-belt interface. This was a straightforward approach based on the 1960s instruments design of moving wires and cords. An endless continuous moving belt transports the analytes from the LC system to the MS. The LC flow is deposited on a polyimide belt and the mobile phase is removed by heating and subsequent evaporation in two consecutive vacuum chambers. Next, the analyte is desorbed from the belt and introduced into the ion source. On the return path, the belt passes over a cleaner heater to remove residual solvent and

Table 1 General Features and Applicability of Various LC–MS Interfaces

Type	Solvent	Flow rate ($\mu\text{L}/\text{min}$)	Ionization	Analyte type
MB	NP	<2000	EI, CI, FAB	Non/slightly polar
	RP (<50% H_2O)	<500	EI, CI, FAB	RV
DLI	RP (<50% H_2O)	<50	Solvent-CI	Non/medium polar, MV
PB	RP, NP	100–500	EI, CI, FAB	Non/medium polar, MV
TSP	RP, NP	500–2000	TSP, solvent-CI	Nonpolar to polar V to RIV
ESI	RP, NP	1–1000	IE, API	Polar, IV
ISP	RP, NP	10–1000	IE, API	Polar, IV
HNI	RP, NP	1–2000	APCI	Non/medium polar, RV
cfFAB	RP, NP	<20	FAB	Polar, IV

Note: MB: moving belt; DLI: direct liquid introduction; ISP: ion spray; HNI: heated nebuliser interface; cfFAB: continuous-flow FAB; RP: reversed phase; NP: normal phase; IE: ion evaporation; API: atmospheric pressure ionization; RV: relatively volatile; RIV: relatively involatile; IV: involatile. The rest of the abbreviations as in Fig. 1.

sample and, finally, through a water bath to remove any nonvolatile material.

More robust, sensitive, and user-friendly devices soon replaced the first types of interfaces (MB and DLI). During the 1980s, much effort was put on the development of TSP and PB. In the 1990s, ESI is by far the most used interface for LC–MS.

In ESI, the column effluent is passed through a small jet maintained at a high voltage (kilovolt range). Due to electronic charging, the liquid is dispersed into very small droplets. Desolvation of the droplets increases the electric field strength at the surface and leads to the ejection of charged compounds by ion evaporation. ESI demonstrates three major advantages: It is a gentle technique and leads to less thermal degradation compared to other techniques; because it is an atmospheric pressure ionization technique, up to 100% ionization can be achieved, thus enhancing method sensitivity; and multiple ions (sometimes up to 70–100 charges) are often formed, thus lowering the m/z ratio and permitting the analysis of high-molecular-weight compounds.

However, despite the great advantages it offers, LC–MS coupling has some limitations, apart from the interfacing need: Incompatibility with some of the nonvolatile buffers and other mobile phase additives. Hence, phosphates, ion-pairing agents, and amine modifiers are replaced by ammonium acetate, ammonium formate, and so forth.

Care has to be taken that any connection will not introduce peak broadening; Interfaces are not compatible with all the ionization modes, thus although the MS is a universal detector, the fact remains that not all compounds can be analyzed with any instrumental configuration. The price still remains much higher compared to GC–MS.

The application area of LC–MS is rapidly growing. LC–MS is now regularly used for the analysis of many different types of compound: drugs and metabolites, herbicides–pesticides and metabolites, surfactants, dyes, saccharides, lipids–phospholipids, steroids, and many others. In our opinion, the area that profits more from the development of LC–MS is bioanalysis: natural products, proteins, peptides, nucleosides, and metabolic studies. Despite the current trends toward immunoassays–biospecific assays and capillary electrophoresis, LC–MS is an extremely powerful analytical technique that is considered complementary to the above mentioned, rather than competitive.

Finally, an aspect that should not be left out of consideration is the off-line combination of LC with MS. A great advantage of on-line techniques is the integration of the evaluation systems used. In on-line LC–MS systems, identification of incompletely resolved peaks is easily and unambiguously accomplished, taking advantage of the mass spectrometer separation power. In contrast, with off-line LC–MS, complete resolution of the peaks is essential. Moreover, fraction collection,

Table 2 Characteristics of Various LC Modes

LC mode	Inner diameter	Injection volume	Flow rate
Conventional	3–6 mm	10–50 μL	0.5–2 mL/min
Microbore	0.5–2 mm	0.5–2 μL	10–300 $\mu\text{L}/\text{min}$
Packed micro-capillary	0.2–0.5 mm	0.1 μL	1–10 $\mu\text{L}/\text{min}$
Drawn packed capillary	50–200 μm	10 nL	<0.1 $\mu\text{L}/\text{min}$
Open tubular	5–25 μm	1 nL	<0.1 $\mu\text{L}/\text{min}$



evaporation, and sample introduction may result in sample loss or contamination. However, off-line LC–MS can still be of great value, for preparative purposes or in cases where a special mass spectrometry technique is required. For example, characterization of biopolymers or proteins by MALDI–TOF cannot be performed on-line with a chromatographic separation method, due to the absence of an appropriate interface. In this case, off-line LC–MS is the method of choice, enabling separation and analysis of very high molecular compounds (more than 1,000,000 Da).

Suggested Further Reading

- P. J. Arpino, Combined liquid chromatography/mass spectrometry. A review, in *Mass Spectrometry in Biological Sciences: A Tutorial* (M. L. Gross, ed.), Kluwer, Dordrecht, 1992.
- J. R. Chapman, Mass spectrometry as an LC detection technique, in *A Practical Guide to HPLC Detection* (D. Parriott, ed.), Academic Press, San Diego, CA, 1993.
- C. Heeremans, Thermospray liquid chromatography tandem mass spectrometry, Ph.D. thesis, Leiden University, 1990.
- P. S. Kokkonen, Continuous-flow fast atom bombardment liquid chromatography mass spectrometry in bioanalysis, Ph.D. thesis, Oulou University, 1991.
- W. M. A. Niessen and J. Van der Greef, *Liquid Chromatography–Mass Spectrometry*, Marcel Dekker, Inc., New York, 1991.
- A. P. Tinke, Surface ionization. A new approach in liquid chromatography–mass spectrometry, Ph.D. thesis, Leiden University, 1996.
- K. B. Tomer, HPLC detection by mass spectrometry, in *HPLC Detection, Newer Methods* (G. Patonay, ed.), VCH, New York, 1992.
- E. R. Verheij, Strategies for compatibility enhancement in liquid chromatography–mass spectrometry, Ph.D. thesis, Leiden University, 1993.
- A. L. Yergey, C. G. Edmonds, I. A. S. Lewis, and M. L. Vestal, *Liquid Chromatography–Mass Spectrometry Techniques and Applications*, Plenum Press, New York, 1990.



Liquid–Liquid Partition Chromatography

Anant Vailaya

Merck Research Laboratories, Rahway, New Jersey, U.S.A.

Introduction

Liquid–liquid partition chromatography (LLPC), employing an organic–aqueous two-phase solvent system and a silica support to separate amino acids, was pioneered by Martin and Synge [1], for which they received the Nobel Prize. Its invention presented a significant advancement over conventional adsorption-based chromatographic processes that were rather unfavorable, due to the energetic heterogeneity of the adsorbent surface. By replacing the solid surface with a layer of an immiscible liquid to retain the solutes, much higher separation efficiencies could be obtained with LLPC. Its scope was later expanded to resolve water-insoluble sample mixtures as well as to isolate biopolymers by introducing organic–organic and aqueous–aqueous two-phase systems, respectively, and by extending the range of supports to include cellulose, dextran, and polymer-based supports.

The rapid development of hydrocarbonaceous bonded phases (nonpolar stationary phases with hydrocarbon chains covalently attached to the silica support) in the 1970s and 1980s for the popular reversed-phase chromatographic (RPC) technique has, however, eclipsed this technique somewhat, lately. Nevertheless, LLPC has become one of the most powerful separation techniques for the isolation of natural products and biopolymers.

Fundamental Principles and Theoretical Background

Martin and Synge provided the first theoretical treatment of LLPC by adapting the concept of theoretical plates which had been developed, mainly, for distillation and countercurrent extraction. According to the theory, a chromatographic column is considered to consist of a number of theoretical plates, within each of which perfect equilibrium occurs between the mobile and the stationary phases. Unlike in RPC employing hydrocarbonaceous bonded stationary phases where the retention mechanism is still the subject of contro-

versy [2], three distribution processes contributing to the total retention of the solute may be clearly identified in LLPC systems. They are (a) partitioning between the two bulk liquid phases, (b) adsorption at the surface of the support, and (c) adsorption at the liquid–liquid interface. Assuming an inert support with large pores that minimize solute adsorption at the support surface and weak adsorption at the liquid–liquid interface, solute retention associated with undesirable adsorption effects may be neglected. Thus, separation in LLPC may be visualized as a multistep partition process, similar to countercurrent distribution, in which the differential migrations of various sample constituents are governed by their partition coefficients and by the volume ratio of the two phases. Then, the magnitude of solute retention in LLPC, measured under isocratic condition by the retention factor, k' , is given by

$$k' = \frac{KV_s}{V_m} \quad (1)$$

where K is the partition coefficient of the solute in the two-phase system employed, V_m is the volume of the mobile phase, measured by an inert tracer and V_s is the volume of the stationary phase. The retention factor is evaluated directly from the chromatogram as

$$k' = \frac{V_r - V_m}{V_m} \quad (2)$$

where V_r is the retention volume of the solute.

Shake-flask measurements are often employed to design a suitable LLPC system for a given sample mixture by assisting in the selection of the two phases in which the compound of interest shows a partition coefficient sufficiently different from those of the impurities. One of the two phases is then immobilized on a suitable support that is packed into the column, and the second phase is used as the mobile phase. In general, partition coefficients of solutes obtained from static experiments compare favorably with those obtained from chromatographic experiments [3]. A comprehensive thermodynamic treatment of LLPC can be found in Ref. 4, and the prediction and control of zone migration is discussed extensively in Ref. 5.



Supports for Stationary Phases

Liquid-liquid partition chromatography systems have been used with or without stationary-phase support. Support-free LLPC has been classified as countercurrent chromatography (CCC). High-speed CCC techniques, based on planetary motion and coaxial orientation of the coiled column, have been developed that achieve both high partition efficiency and excellent retention of the stationary phase, thus circumventing the need for stationary-phase supports [6].

Liquid-liquid partition chromatography systems employing stationary-phase supports have been applied in both paper and column chromatographic modes. Paper strips impregnated with the liquid stationary phase are employed as supports for paper chromatography [5]. Column supports for LLPC bind the liquid stationary phase selectively enough to immobilize it and thus prevent its bleeding by the mobile phase. The support surface is homogeneously coated with the stationary phase and is sufficiently large to generate an interface for solute partitioning. Given these considerations, macroporous supports of average pore diameter greater than 50 nm are most suitable as column packings. Supports with smaller pores might contribute to retention by adsorption of solutes. In principle, both organic- and inorganic-based column packings can be employed in LLPC. Soft packings, such as cellulose, dextran, polymers, and diatomaceous earth, which do not withstand high pressures, are preferably used as larger particles at low pressures. On the other hand, microparticulate and bonded silicas are the supports of choice in the high-performance mode.

In the separation of large biopolymers, such as proteins and nucleic acids, specific supports characterized by large pores and bonded structure have been developed for LLPC employing poly(ethylene glycol) (PEG)-dextran two-phase aqueous-aqueous system. Bonded silica [e.g., LiChrospher® Diol (typically 1000 Å pore size and 10 µm particle size)] or a hydrophilic methacrylate polymer (e.g., Fractogel®) are chemically modified to form polyacrylamide chains of defined lengths that facilitate the selective binding of a dextran-rich aqueous phase. Polymer-based materials serve frequently as phase supports insensitive to high-pH systems.

Columns for LLPC are prepared by using solvent evaporation, direct coating, precipitation, or a dynamic coating technique [3]. In the solvent-evaporation technique, the nonvolatile liquid stationary phase is dissolved in a volatile solvent and mixed with the dry sup-

port. Then, the solvent is slowly removed by rotating the suspension in a rotary evaporator until the coated support remains as a dry, free-flowing powder. In the direct coating technique, the liquid stationary phase is pumped through the column, and then the excess is displaced by elution with a mobile phase saturated with the stationary phase. In the precipitation technique, the liquid stationary phase precipitates in the support pores when a solvent, which is not miscible with the liquid stationary phase, is pumped through the column. Finally, the liquid mobile phase saturated with a liquid stationary phase is pumped through the prepacked column in the dynamic coating technique. The liquid stationary phase is adsorbed at the surface of the support until it builds a multilayer and completely fills the pore volume.

Liquid-Liquid Systems

Binary and sometimes ternary systems employing phases of different polarity, which is characterized by Hildebrand's solubility parameter [7] or Snyder's polarity index [8], are used for LLPC separations. Applying the solubility parameter concept, various organic-organic, organic-aqueous, and aqueous-aqueous LLPC systems have been utilized to modulate solute retention. Based on polarity differences, LLPC can be operated in both normal phase (polar stationary phase, nonpolar mobile phase) and reversed-phase (polar mobile phase and nonpolar stationary phase) modes. Mobile phases typically used in the normal-phase mode are aliphatic hydrocarbons such as hexane, heptane and isooctane, alcohols, tetrahydrofuran (THF), methylene chloride, dioxane, and aromatic solvents. Stationary phases in the normal-phase mode include water, formamide, glycerol, and glycols. In the reversed-phase mode, hydro-organic mixtures such as acetonitrile-water and methanol-water are employed as mobile phases, whereas nonpolar solvents such as squalane, octanol, and aliphatic hydrocarbons are used as stationary phases. For the separation of large biopolymers based on aqueous-aqueous LLPC systems, a PEG-rich aqueous phase forms the mobile phase, and the dextran-rich aqueous phase is immobilized on the polyacrylamide support to form the stationary phase.

Applications

A number of advantages of current LLPC systems make them attractive for widespread application in the separation and isolation of low-molecular-weight com-

pounds as well as macromolecules. Among them are simple preparation of bulk liquid phases, high reproducibility of retention and selectivity under isothermal conditions and lesser contamination, higher efficiency, and longer lifetime compared to adsorbent columns. Some of the most common applications of LLPC are now described.

Small Molecules

Liquid-liquid partition chromatography employing organic-organic, organic-aqueous, and aqueous-organic binary systems with column support have been used to separate small molecules of wide polarity [3]. A majority of applications involve the use of LLPC systems in the normal-phase mode (e.g., the separation of polyaromatic hydrocarbons, alcohols, esters, alkylated and chlorinated aromatic derivatives, pesticides, herbicides, and steroids). Several nitrogen-containing compounds, radionuclides, derivatives of aromatic carboxylic acids, benzodiazepines, aromatic compounds, and naphthalenesulfonic acids have successfully been separated in the reversed-phase mode. Many ternary LLPC systems in both the normal-phase and reversed-phase modes have also been employed in the separation of polyaromatic hydrocarbons, benzodiazepines, steroids, metal chelates, glycosides, metabolites, dansyl amino acids, herbicides, aliphatic carboxylic and dicarboxylic acids, sulfonic acids, nucleosides, barbiturates, chlorinated phenols, and alkylbenzenes. Support-free high-speed CCC has been employed in the separation of dyes, rare earth and certain inorganic elements, as well as in the preparative and analytical applications of medicinal herbs and other natural products, such as alkaloids, tannins, flavonoids, marine compounds, and anthraquinones [6].

Biopolymers

Classical LLPC using aqueous-aqueous polymer systems based on Albertsson's [9] PEG-dextran system has provided a versatile tool for the separation of proteins and nucleic acids, thus increasing the arsenal of biopolymer purification methods currently dominated by gel filtration, ion-exchange chromatography, and affinity chromatography RPC. The technique operates

on the basis of the biopolymers partitioning between the top PEG-rich aqueous mobile phase and the bottom dextran-rich aqueous stationary [10]. Factors that depend on the nature of the protein, such as size, surface area, and hydrophobicity, determine their partition in the PEG-dextran systems. Other factors associated with the nature of the two-phase system that strongly influence protein retention in LLPC are the size of the phase-forming polymers, the pH of the system, and the presence of salts, zwitterions, detergents and organic solvents.

Liquid-liquid partition chromatography techniques based on aqueous-aqueous systems have successfully been employed in the fractionation of crude human serum, purification of steroid hormone-binding proteins from human serum, isolation of basic proteins from crude bacterial extracts, purification of immunoglobulins and monoclonal antibodies, DNA fractionations by size, topology and base sequence, as well as the isolation of soluble and ribosomal RNAs in preparative amounts from bulky mixtures [10]. High-speed CCC using PEG-dextran system has also been employed in the separation of proteins [6].

References

1. A. J. P. Martin and R. L. M. Synge, *Biochem. J.* 35: 1358-1368 (1941).
2. A. Vailaya and Cs. Horváth, *J. Chromatogr. A.* 829: 1-27 (1998).
3. J. C. Kraak and J. P. Crombeen, in *Practice of High Performance Liquid Chromatography* (H. Engelhardt, ed.), Springer-Verlag, Berlin, 1986, pp. 182-194.
4. D. C. Locke, *Adv. Chromatogr.* 8: 47-89 (1969).
5. E. Soczewinski, *Adv. Chromatogr.* 5: 3-78 (1968).
6. Y. Ito and W. D. Conway, *High Speed Countercurrent Chromatography*, Wiley-Interscience, New York, 1996.
7. Cs. Horváth, L. R. Snyder, and B. L. Karger, *Introduction to Separation Science*, Wiley-Interscience, New York, 1974, pp. 49-55, 268-276.
8. L. R. Snyder, *J. Chromatogr. Sci.* 16: 223-234 (1978).
9. P. Å. Albertsson, *Partition of Cell Particles and Macromolecules*, 2nd ed., Wiley-Interscience, New York, 1971.
10. W. Müller, *Bioseparation I*: 265-282 (1990).



Long-Chain Polymer Branching: Determination by GPC–SEC

André M. Striegel

Solutia, Inc., Springfield, Massachusetts, U.S.A.

Introduction

Polymer branching has long been recognized as a main influencer of macromolecular properties, both chemical and physical. The increase in the number (and, possibly, variety) of end groups of a branched polymer, with respect to its linear counterpart, along with the concomitant increase in the number of branch points, has the potential to greatly alter the chemical reactivity of the polymer, the polymer's ability to crystallize, and so forth. The effects of branching, however, tend to manifest themselves most greatly in changes in the physical or space-filling properties of the molecule, both in the melt and in solution. Properties such as the viscosity and elasticity of melts, as well as the intrinsic viscosity, angular distribution of scattered radiation, and sedimentation behavior of dilute solutions are all affected by branching. As a branched molecule will possess a more compact structure in solution than a linear molecule composed of the same type and number of repeat units, its elution behavior as determined via size-exclusion chromatography [SEC, also known as gel permeation chromatography (GPC)] will be likewise altered, the branched molecule taking a longer time to elute from the column under identical chromatographic conditions. At this point, two factors should be mentioned. First, for the sake of the present discussion, it is assumed that only homopolymers are being analyzed. Nonetheless, when confronted by two SEC peaks with different retention volumes, the possibility presents itself that these peaks could either be different with respect to molecular weight, to chain branching, or to both. The synergistic nature of combining various SEC detectors, which are sensitive to dissimilar polymer properties, has now become a favored way to address this concern. These combinations of detectors have also proven to be fundamental in determining and quantifying polymer branching by SEC. Second, this entry deals exclusively with long-chain branching (LCB) in polymers, not with short-chain branching (SCB). Although a clear difference between these two types of branching is yet to be established, LCB is usually thought of as when the length of the side chains is comparable to that of the main chain or, in the absence of the latter, when random dendritic branching occurs.

Polymer Branching by SEC

Virtually every method of quantifying branching of dilute polymer solutions harkens back to a single publication by Zimm and Stockmayer from 1949 [1]. Here, the authors derived the root-mean-square radius of a polymer ($\langle R_g^2 \rangle^{1/2}$) and showed how the ratio of the mean-square radius of a branched polymer ($\langle R_g^2 \rangle_B$) to that of a linear polymer ($\langle R_g^2 \rangle_L$) may be used as the basis for branching calculations. This ratio, termed the ratio of the mean-square radii, has been given the symbol g and is defined by

$$g = \left[\frac{\langle R_g^2 \rangle_B}{\langle R_g^2 \rangle_L} \right]_M \quad (1)$$

with the subscript M referring to values obtained for the same molecular weight. (It should be noted that the term “radius of gyration” is often used in the literature both indiscriminately and mistakenly to describe, variously, the root-mean-square radius, the viscosity radius, the Stokes radius, and the hydrodynamic radius of a molecule. Caution is recommended when encountering this term undefined.) The assumptions inherent in the branching calculations were well recognized at the time: Only materials of equal chemistry and molecular weight should be compared, and the type (functionality, f) of the branch points should remain uniform throughout the molecule. The calculations were shown to be invariant to changes in the length of the branches throughout the molecular-weight distribution (MWD) of the polymer. In the case of trifunctional ($f = 3$) branching, the number- and weight-average number of branches per molecule (B_{3n} and B_{3w} , respectively) are given by Eqs. (2) and (3),

$$g = [(1 + B_{3n}/7)^{0.5} + 4B_{3n}/9\pi]^{-0.5} \quad (2)$$

$$g = \frac{6}{B_{3w}} \left[0.5 \left(\frac{2 + B_{3w}}{B_{3w}} \right)^{-0.5} \cdot \ln \left(\frac{(2 + B_{3w})^{0.5} + B_{3w}^{0.5}}{(2 + B_{3w})^{0.5} - B_{3w}^{0.5}} \right) - 1 \right] \quad (3)$$



whereas for tetrafunctional branching ($f = 4$), these same parameters are defined via Eqs. (4) and (5):

$$g = \left[\left(1 + \frac{B_{4n}}{6} \right)^{0.5} + \frac{4B_{4n}}{3\pi} \right]^{-0.5} \quad (4)$$

$$g = \frac{\ln(1 + B_{4w})}{B_{4w}} \quad (5)$$

(Many of the symbols used here are those which have found favor in the literature over the years and which are presently being used. As such, they may differ from the symbols used in the original publications.) From the number of branches, the branching frequency (λ) of the molecule may be calculated by Eq. (6),

$$\lambda = \frac{RB}{M} \quad (6)$$

where B is defined by Eqs. (2)–(5), R is the molecular weight of the repeat unit and M is the molecular weight of the branched material for the SEC slice under consideration. For f -functional stars, Stockmayer and Fixman [2] computed the number of arms (f) from g using

$$g = \frac{3f - 2}{f^2} \quad (7)$$

$\langle R_g^2 \rangle^{1/2}$ averages and the $\langle R_g^2 \rangle^{1/2}$ distribution with respect to the molecular weight of the polymer are best calculated by SEC using either a variable-angle or, more commonly and conveniently, a multiangle laser light-scattering (MALLS) detector, in conjunction with a concentration-sensitive detector (e.g., a differential refractometer). Various MALLS detectors are available commercially, and their data acquisition and manipulation software has the ability to perform the desired branching calculations. For a truly quantitative measure of the branching number and branching frequency of a polymer, it should be compared to a linear standard with identical chemical composition. Moreover, the MWD of the linear standard should span that of the unknown, so that at each molecular weight slice, the $\langle R_g^2 \rangle$ of the latter may be compared to that of the former. Also, the functionality of the polymer should be known, so that the proper branching equations (either those for B_3 or those for B_4) may be used.

If a viscometer is used instead of a MALLS detector in SEC (again in conjunction with a concentration-sensitive detector), either by applying universal calibration or the newly emerging technique of SEC³, the ratio (g') of the intrinsic viscosities of the branched molecule and the linear standard at the same molecu-

lar weight may be used for the branching calculations (Eq. (8) [1]):

$$g' = \left(\frac{[\eta]_B}{[\eta]_L} \right)_M \quad (8)$$

(the same requirements for a linear standard as mentioned earlier continue to apply). The relationship between g and g' is given by

$$g' = g^\epsilon \quad (9)$$

where ϵ is known as the viscosity shielding ratio. This ratio was defined by Debye and Bueche [3] as the distance within the hydrodynamic sphere occupied by the molecule in solution over which the flow of solvent decreases by a factor $1/e$ of that in the free solution, divided by the radius of said hydrodynamic sphere. (It should be noted that even though this definition applied strictly to the Debye–Bueche linear-density pearl-string model of a polymer in solution, the authors demonstrated its suitability to the more accurate Kirkwood–Riseman Gaussian-density polymer model.) The value of ϵ is dependent on a number of factors, including solvent, temperature, and branching, and may be considered indicative of how “draining” a polymer coil is in dilute solution. ϵ has been found to fall in the range 0.5–1.5, with the smaller value determined by Zimm and Kilb [4] to correspond to non-free-draining, high-molecular-weight, regular stars, and the larger value determined by Berry [5] for comb-shaped polystyrenes in good solvents. It has been noted that the majority of values for ϵ fall in the range 0.7–0.8 [6], although it is recommended that an exact value be either sought in the literature for the appropriate polymer under the given solvent/temperature conditions of the experiment or determined by a comparison of MALLS and viscometry data or by other experimental techniques (for a table of ϵ values, see Ref. 6).

An alternative method, also using viscometry, for determining g' without recourse to a linear standard is that implemented in the Waters Millennium software for SEC. In this method, the lower-molecular-weight portion of the MWD is assumed to be nonbranched, as branching normally does not express itself markedly at low molecular weights. The linear double-logarithmic intrinsic viscosity–molecular weight relationship (also known as the Mark–Houwink plot) is extrapolated from this portion, and deviations from this relationship at high molecular weights are used to calculate g' . Although this method has proven effective in corroborating the linearity of natural polymers and should be useful for calculating g' in certain types of LCB, doubts exist as to its applicability to extremely highly branched molecules such as hyperbranched polymers

and dendrimers that have no linear portion in their MWDs from which to perform the requisite extrapolation [7]. One may alternatively calculate g by what is known as the “mass method” [8], by comparing the molecular weights of the unknown (M_B) and of the linear standard (M_L) at the same elution volume (V), via

$$g = \left(\frac{M_L}{M_B} \right)_V^{(a+1)/\varepsilon} \quad (10)$$

with a being the exponent of the Mark–Houwink relationship ($[\eta] = KM^a$) and ε the viscosity shielding ratio.

In 1953, Stockmayer and Fixman [2] observed that the ratio of hydrodynamic (Stokes) radii (R_H), given by the symbol h , could also be used as a measure of branching. Although they presented their relationship as a ratio of intrinsic viscosities [see Eq. (11)], the relatively recent introduction of on-line dynamic light scattering (DLS) detectors

$$h^3 = \frac{[\eta]_B}{[\eta]_L} \quad (11)$$

permits direct determination of h by

$$h = \frac{(R_H)_B}{(R_H)_L} \quad (12)$$

In certain cases, such as with lightly branched polymers, the h^3 rule appears more suitable than either the $g^{0.5}$ or $g^{1.5}$ rule. Future research on polymer branching using SEC with on-line DLS detection may shed new light on this area of polymer characterization.

Applications

For a detailed list of applications of SEC to determining LCB in polymers through the mid-1970s, see Ref. 9. For comprehensive, up-to-date reviews of the solu-

tion and conformational properties of branched molecules, see Ref. 10.

Conclusions

Long-chain polymer branching, which can have a great effect on the physical and chemical properties of macromolecules, may be determined using multidetector SEC by a variety of means; calculations will likely be aided by the rapid advances in computer modeling of polymer conformations and properties [7]. Whether one employs static or dynamic light scattering, viscometry, or a combination of viscometry, refractometry, and light scattering, stringent requirements on the nature of the linear standard must be met in order to assure accurate, quantitative results.

References

1. B. H. Zimm and W. H. Stockmayer, *J. Chem. Phys.* 17: 1301–1314 (1949).
2. W. H. Stockmayer and M. Fixman, *Ann. NY Acad. Sci.* 57: 334–352 (1953).
3. P. Debye and A. M. Bueche, *J. Chem. Phys.* 16: 573–579 (1948).
4. B. H. Zimm and R. W. Kilb, *J. Polym. Sci.* 37: 19–42 (1959).
5. G. C. Berry, *J. Polym. Sci. A-2* 9: 687–715 (1971).
6. J. Roovers, *Encyclopedia of Polymer Science and Engineering*, Volume 2, John Wiley & Sons, New York, 1985, pp. 478–499.
7. A. M. Striegel, R. D. Plattner, and J. L. Willett, *Anal. Chem.* 71: 978–986 (1999).
8. L.-P. Yu and J. E. Rollings, *J. Appl. Polym. Sci.* 33: 1909–1921 (1987).
9. E. E. Drott, *Liquid Chromatography of Polymers and Related Materials* (J. Cazes, ed.), Marcel Dekker, Inc., New York, 1977, pp. 161–167.
10. J. Roovers (ed.), *Advances in Polymer Science*, Volume 143, Springer-Verlag, Berlin, 1999.



Longitudinal Diffusion in Liquid Chromatography

J.E. Haky

Florida Atlantic University, Boca Raton, Florida, U.S.A.

Introduction

Longitudinal diffusion refers to the natural spreading of a solute band from regions of high concentration to those of lower concentration as it passes through a chromatographic system [1]. It is a simple process which is dependent on the time that the solute spends on the chromatographic system, which, in turn, is related to the flow rate of the mobile phase.

Discussion

As an extreme illustration of the longitudinal diffusion process, consider a situation in which a solute is put onto a liquid chromatographic column and the flow of the mobile phase is shut off prior to any of the solute eluting from the column. The column is then sealed. Under these conditions, the solute molecules in the column would begin to diffuse from a concentrated band outward to regions of lower concentrations in the column. Given enough time, this diffusion would continue until the solute concentration throughout the mobile phase in the sealed column is constant. Although this is an extreme example of band broadening caused by this phenomenon, such longitudinal diffusion occurs to a lesser extent even when the mobile phase is flowing.

The degree of band broadening of any chromatographic peak may be described in terms of the height equivalent to a theoretical plate, H , given by

$$H = \frac{L}{N} \quad (1)$$

where L is the length of the column (usually in cm) and N is the number of theoretical plates, which can be calculated from Eq. (2),

$$N = 16 \left(\frac{t_R}{W} \right)^2 \quad (2)$$

where t_R and W are the retention time and width of the peak of interest, respectively. Because higher values of N correspond to lower degrees of band broadening

and narrower peaks, the opposite is true for H . Therefore, the goal of any chromatographic separation is to obtain the lowest possible values for H .

The contribution of longitudinal diffusion and other factors to band broadening in liquid chromatography can be quantitatively described by the following equation, which relates the column plate height H to the linear velocity of the solute, μ :

$$H = A\mu^{0.33} + \frac{B}{\mu} + C\mu + D\mu \quad (3)$$

In this equation, A , B , C , and D are constants for a given column [2]. The linear velocity μ is related to the mobile-phase flow rate and is determined by

$$\mu = \frac{L}{t_0} \quad (4)$$

where t_0 (the so-called "dead time") is determined from the retention time of a solute which is known not to interact with the stationary phase of the column.

The second term in Eq. (3), B/μ , describes the contribution of longitudinal diffusion to band broadening of the solute as it passes through the chromatographic system. This is the only term in the equation inversely proportional to the linear velocity of the mobile phase; the other terms increase in value as the linear velocity increases. Giddings and others have also shown that this term is also directly proportional to the diffusion coefficient D_m of the solute in the mobile phase according to the following equation, where C_d is a constant [3]:

$$\frac{B}{\mu} = \frac{C_d D_m}{\mu}$$

Fortunately, the mobile-phase flow rates used in most modern liquid chromatographic separations are sufficiently high enough to minimize the effects of longitudinal diffusion on chromatographic band broadening under usual conditions. Other factors, such as solute mass transfer, are usually more important contributors to band broadening in LC. However, longitudinal diffusion can be an important



factor in situations where the flow rate of the mobile phase is either stopped or significantly reduced during a chromatographic separation. Additionally, because it occurs throughout the path of a solute passing through a chromatographic system, efforts should be made to minimize longitudinal diffusion effects by minimizing open space (“extracolumn volume”) in the chromatographic system before and after the column.

Longitudinal Diffusion in Liquid Chromatography

References

1. D. C. Harris, *Quantitative Chemical Analysis*, W. H. Freeman, New York, 1999, p. 662.
2. L. R. Snyder and J. J. Kirkland, *Introduction to Modern Liquid Chromatography*, 2nd ed., John Wiley & Sons, New York, 1979, pp. 168–173.
3. J. C. Giddings, *Dynamics of Chromatography*, Marcel Dekker, Inc., New York, 1965, pp. 47–61.



Magnetic FFF and Magnetic SPLITT

Maciej Zborowski

The Cleveland Clinic Foundation, Cleveland, Ohio, U.S.A.

Jeffrey J. Chalmers

The Ohio State University, Columbus, Ohio, U.S.A.

P. Stephen Williams

The Cleveland Clinic Foundation, Cleveland, Ohio, U.S.A.

Introduction

Magnetic field-flow fractionation (FFF) employs static or quasi-static magnetic fields and excludes electromagnetic fields. Electromagnetic fields having frequencies in the kilohertz to megahertz range are used in dielectrophoretic FFF. Static electric fields are used in electrical FFF (see the entry Field-Flow Fractionation Fundamentals).

Magnetophoretic Mobility and Magnetic Field Energy Density Gradient

The magnetic field is described by two vectors: magnetic field strength, H , and magnetic flux density (also called magnetic induction or, simply, magnetic field), B , described by Maxwell's equations. The magnetic field is solenoidal; that is, its sources are electric currents or magnetic dipoles (but not "magnetic charges"). The magnetic property of matter is described by its magnetic permeability, μ , which for an isotropic medium is a scalar. The difference between the external, applied field H and the induced field B is the magnetization of the matter, which is a vector quantity M . An external magnetic field always induces magnetization in matter and, in this sense, all matter is magnetic. (The microscopic basis of magnetization is provided by quantum physics and is beyond the scope of this entry.) For a large class of materials, magnetization is a linear function of the applied, external magnetic field strength, and it always consists of a diamagnetic contribution and, less often, a paramagnetic contribution. In the International System of Units, we have

$$B = \mu\mu_0 H, \quad M = \frac{1}{\mu_0} B - H, \quad \chi = \frac{|M|}{|H|} = \frac{M}{H}$$

where B is measured in tesla (T), H is measured in A/m, $\mu_0 = 4\pi \times 10^{-7}$ T m/A is a constant called the magnetic permeability of a vacuum, χ is the volumet-

ric susceptibility of the material (dimensionless), and the symbol $|\cdot|$ denotes the magnitude of the vector. Note that $\mu = 1 + \chi$. Diamagnetic magnetization is antiparallel to the field strength ($\chi < 0$), and paramagnetic magnetization is parallel to the field strength ($\chi > 0$). Diamagnetic effects are very weak (with the notable exceptions of bismuth and graphite) and are dominated by much stronger paramagnetic effects.

Typical fluid media encountered in magnetic separation are diamagnetic (for water, $\chi = 9.05 \times 10^{-6}$). For certain metals, their alloys, and oxides, the coordinated behavior of the neighboring atoms or molecules (the totality of which is referred to as a magnetic domain) gives rise to very strong magnetic effects known as ferromagnetism and ferrimagnetism. For such material, magnetization increases very rapidly with the external field strength H , and the value of the magnetization depends on the history of the material (hysteresis effect). In particular, the magnetization does not disappear with the removal of the external field (residual magnetization) and requires application of an opposite field to be brought down to zero (coercive force). For convenience, diamagnetics and paramagnetics are characterized by their magnetic susceptibility, χ (typically, $\chi = 10^{-2}$ to 10^{-5}), whereas ferromagnetics are characterized by their magnetic permeability, μ (typically, $\mu = 10^5$). For particles having a size not larger than that of the magnetic domain, the hysteresis curve reduces to a straight line, and such particles are referred to as superparamagnetic particles. Paramagnetic and superparamagnetic particles and colloids are used to tag (or label) weakly magnetic particles and biological cells for their selective separation.

The fluid dynamic properties of continuous magnetic media, including liquid ferromagnetic media (ferrofluids), are described by the Navier–Stokes equations with the addition of terms describing the interaction with the magnetic field and are the subject of a considerable number of studies (for a review, see Ref. 1). The motion of discrete magnetic particles in a very

Encyclopedia of Chromatography

DOI: 10.1081/E-Echr 120005221

Copyright © 2002 by Marcel Dekker, Inc. All rights reserved.



weakly magnetic (“nonmagnetic”) medium can be described by a combination of long-range, magnetic body forces and local shear stresses due to the resulting motion through the viscous medium. In the case of colloidal particles for which inertial effects are much lower than the viscous effects (low-particle Reynolds number), and for laminar flows (low-channel Reynolds number), the equation of motion reduces to

$$0 = 6\pi\eta R\nu - \Delta\chi V \nabla \left(\frac{B^2}{2\mu_0} \right)$$

from which

$$|\nu| = \nu = \frac{\Delta\chi V}{6\pi\eta R} \left| \nabla \left(\frac{B^2}{2\mu_0} \right) \right|$$

where η is the viscosity of the medium, R is the particle radius, V is the particle volume, ν is the particle linear velocity vector relative to the medium, and $\Delta\chi$ is the difference between the particle magnetic susceptibility and that of the medium. The operand acted on by the nabla operator, ∇ (resulting in a gradient of scalar quantity), is the external magnetic field energy density, $B^2/2\mu_0$, in a nonmagnetic medium. The expression for the field-induced velocity can be conveniently presented as a product of the particle magnetophoretic mobility, m , and the magnetic field energy density gradient, S_m ,

$$\nu = mS_m$$

where

$$m = \frac{\Delta\chi V}{6\pi\eta R} \quad \text{and} \quad S_m = \left| \nabla \left(\frac{B^2}{2\mu_0} \right) \right|$$

For paramagnetic (and diamagnetic) particles in diamagnetic media, $\Delta\chi$ is independent of S_m and the magnetophoretic mobility depends entirely on the intrinsic properties of the particle and those of the medium. For a ferromagnetic particle, $\Delta\chi$ is, in general, a function of H , and therefore the magnetophoretic mobility depends on the properties of the particle, the medium, and the field strength. Particle magnetophoretic mobility provides the basis of magnetic separation, and its role is analogous to the electric and sedimentation mobilities encountered in the electrical and sedimentation split-flow thin-channel (SPLITT) separations, respectively.

The order-of-magnitude analysis of the magnetophoretic mobility of weakly paramagnetic particles, 10 μm in diameter, acted on by the body forces available for the magnetic separation, returns the following

numerical values: $\Delta\chi = 10^{-3}$, $V = 524 \mu\text{m}^3$, $\eta = 10^{-3} \text{ kg/m s}$, $R = 5 \mu\text{m}$, $B = 1 \text{ T}$, gradient of $B = 200 \text{ T/m}$, $m = 5.6 \times 10^{-15} (\text{m/s})/(\text{N/m}^3)$, and $S_m = 1.6 \times 10^8 \text{ N/m}^3$. It follows, that the particle velocity induced by the magnetic field, $\nu = 9 \times 10^{-7} \text{ m/s}$, or about 1 $\mu\text{m/s}$.

Advantages of the magnetostatic or quasi-static field as compared to the oscillating electromagnetic fields in application to separation include the following: no interaction with the solvent, which typically is diamagnetic or very weakly paramagnetic, and therefore no Joule heating, no convective effects, and no need for a cooling system; no electro-osmotic effects; long range of the magnetic interactions (as compared to dielectrophoresis); the possibility of using permanent magnets for the magnetic field and thus no requirement for power supply; high specificity in targeting the separands by using magnetic labels as ligands to specific receptors; and no demonstrated biological effects in the practical range of magnetic fields and gradients. The limitations of the magnetic separation include a requirement for magnetic labels for nonmagnetic separands and, generally, a complex geometry of the magnetic force field, which tends to make it difficult to control the separation process.

Magnetic FFF

There is a limited number of publications concerning magnetic field-flow fractionation (magnetic FFF or MgFFF), which, characteristically, describe different technical approaches to achieve a uniformly high magnetic field and gradient over the entire channel volume. In this sense, magnetic FFF has not achieved the level of maturity of other FFF techniques for which the field and flow geometries are well established. Interestingly, there is a large volume of work on “magnetic chromatography,” or “magnetic affinity chromatography,” or “magnetic columns,” which does not make reference to FFF and does not use its analytical methods, although it is based on differential retention of separands in the magnetic field [2]. The most successful of those devices is the “high-gradient magnetic separation” (HGMS) column, which is used for separation of small particulate matter (such as cells using magnetic ligands as labels) in biological and clinical laboratories [3].

The earliest, explicit reference to magnetic FFF was made by Vickrey and Garcia-Ramirez [4], although their methods and conclusions were questioned by Semenov and Kuznetsov [5]. Those early efforts pointed to the difficulties of achieving a high, uniform magnetic

field energy gradient over a substantial part of a thin flow channel. (Vickrey and Garcia-Ramirez proposed an electromagnet with an iron core, and Semenov and Kuznetsov a ferromagnetic fiber exposed to an external magnetic field, as a source for S_m). There were no experimental data in the Semenov and Kuznetsov study however. In a more rigorous work by Schunk et al. [6], an electromagnet with an iron core and a variable current was used to generate a well-characterized magnetic field. Due to the low field gradient, and thus low S_m , these investigations were limited to particulate materials of high magnetic permeability (iron oxide, Fe_2O_3 , 0.8- μm particles used in recording media). They showed that their magnetic FFF method was able to characterize flocculation of those particles in suspension in acetonitrile (singlets from dimers). In a more recent work, Ohara discussed theoretically the separation of small radioactive waste particles (1–50 nm in diameter) from nuclear fuel (not specified) using magnetic FFF consisting of a very thin flow channel (50 μm) lined with a regular grid of 20- μm ferromagnetic wires in the field of a superconducting magnet (2.0–28.0 T) and concluded that magnetic FFF would be superior to HGMS for such separations (no experimental data to support this conclusion were given) [7].

Magnetic SPLITT

The requirement of a highly regular field and flow geometries is even more stringent in split-flow thin channel (SPLITT) separation than it is in FFF separation and this may be the reason for a relatively late appearance of the magnetic SPLITT technique. The solenoidal character of the magnetic field requires a radical departure from the usual rectangular geometry of the SPLITT channel. This has led to the design of an annular channel around an axisymmetric magnetic quadrupole field (similar to that used in quadrupole mass spectroscopy) [8]. Quadrupole magnetic SPLITT offers the advantages of a highly regular S_m , which is a linear function of the distance from the axis of symmetry and directed along the radial position vector, and of an edgeless flow channel. The theory of the quadrupole magnetic SPLITT separation has been developed and its experimental verification in biological applications is ongoing [9]. It appears that it has advantages over a more traditional approach utilizing a rectangular channel.

A SPLITT system based on a quadrupole magnetic field combined with annular channel geometry possesses an axial symmetry that not only lends itself to the separation but also to the tractability of the mathemat-

ical description of the separation process. Given the magnetophoretic mobility of a paramagnetic particle, m , the magnetic field energy gradient in the annular channel, the system dimensions, and flow rates, it is possible to predict particle trajectory through the system as a function of starting position. It follows that it is possible to calculate the flow rate conditions required to obtain any desired cutoff in mobility. All particles having mobilities higher than a specified critical value will be collected at the outer channel outlet, and those having mobilities lower than another critical mobility will be collected at the inner channel outlet; see Fig. 1. The resolution of the fractionation is related to how close these two critical values are and the volumetric throughput is inversely related to this resolution.

The availability of immunomagnetic colloidal labels opens up the possibility of purifying or isolating certain specific biological cell types using magnetic SPLITT. These procedures are useful for cancer treatment and various cell therapies. Unlabeled biological cells tend to be only very weakly influenced by magnetic fields. Flow conditions may be selected so that when a mixture of labeled and unlabeled cells is passed through the magnetic SPLITT system, the labeled cells are selectively drawn toward the outer channel wall and are collected at the outer channel outlet. An example of this type of separation is shown in Fig. 1.

In general, the magnetophoretic mobility of a weakly magnetic particle, or a cell, labeled with a magnetic ligand, is directly proportional to the number of ligand molecules, or moieties, attached to the target particle or cell. An important question in magnetic SPLITT is this: Given the upper and lower limit of the number of magnetic receptors per particle (or cell), and an upper and lower limit of the particle diameter, into how many different fractions may one separate the sample? If one assumes a Normal distribution in size for the particle (or cell), the theoretical number of subpopulations that a magnetically labeled particle (or cell) population can be divided into is given by

$$n = \ln\left(\frac{\alpha_n}{\alpha_0}\right) \left[\ln\left(\frac{1 + z\sigma}{1 - z\sigma}\right) \right]^{-1}, \quad 0 < |z\sigma| < 1$$

where α_n and α_0 are the high and low values, respectively, of the magnetic receptor density and σ is the relative standard deviation in cell diameter. The number z is chosen according to the desired level of certainty of including cells of a given receptor density in a sorted fraction. For example, for $z = 2$, the percentage of cells of a given receptor density in the sorted fraction is 95.5%. A more complete discussion of this relationship can be found in Ref. 10.



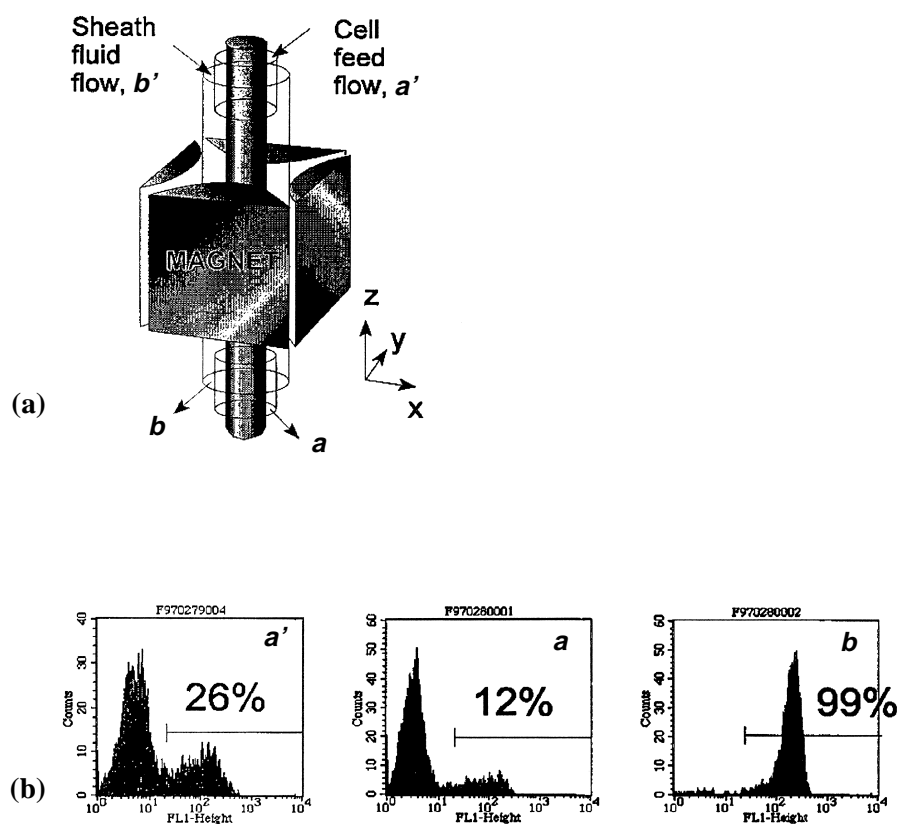


Fig. 1 (a) Schematic view of magnetic SPLITT based on quadrupole magnetic field and annular flow channel. Note the positions of short cylindrical flow splitters, concentric with the solid cylindrical core. Note direction of the feed flow, a' sheath fluid flow, b' , and sorted fraction flows (a and b) as indicated by arrows. (b) Composition of human peripheral lymphocytes labeled with anti-CD8 antibody and magnetic colloid, as analyzed by flow cytometry, before and after magnetic SPLITT sorting: a' = original sample, a = non-magnetic fraction, b = magnetic fraction. The percentages indicate fractional composition of the magnetically labeled cells in the sample. Note enrichment of the positive cells in b fraction as compared to the original cell sample, a' .

References

1. R. E. Rosensweig, *Ferrohydrodynamics*, Cambridge University Press, New York, 1985.
2. C. H. Evans, A. P. Russell, and V. C. Westcott, Demonstration of the principle of paramagnetic chromatography for resolving mixtures of particles, *J. Chromatogr.* 351: 409–415 (1986).
3. A. Radbruch, B. Mechtold, A. Thiel, S. Miltenyi, and E. Pflueger, High-gradient magnetic sorting, *Methods Cell Biol.* 42: 387–403 (1994).
4. T. M. Vickrey and J. A. Garcia-Ramirez, Magnetic field-flow fractionation: Theoretical basis, *Separ. Sci. Technol.* 15: 1297–1304 (1980).
5. S. N. Semenov and A. A. Kuznetsov, Flow fractionation in a transverse high-gradient magnetic field, *Russ. J. Phys. Chem.* 60: 424–428 (1986) (translated from *Zh. Fiz. Khim.*).
6. T. C. Schunk, J. Gorse, and M. F. Burke, Parameters affecting magnetic field-flow fractionation of metal oxide particles, *Separ. Sci. Technol.* 19: 653–666 (1984).
7. T. Ohara, Feasibility of using magnetic chromatography for ultra-fine particle separation, in *High Magnetic Fields: Applications, Generation, Materials* (H. J. Schneider-Muntau, ed.), World Scientific, Singapore, 1997.
8. M. Zborowski, P. S. Williams, L. Sun, L. R. Moore, and J. J. Chalmers, Cylindrical SPLITT and quadrupole magnetic field in application to continuous-flow magnetic cell sorting, *J. Liquid Chromatogr. Related Technol.* 20: 2887–2905 (1997).
9. P. S. Williams, M. Zborowski, and J. J. Chalmers, Flow rate optimization for the quadrupole magnetic cell sorter, *Anal. Chem.* (1999).
10. J. J. Chalmers, M. Zborowski, L. R. Moore, S. Mandal, B. Fang, and L. Sun, Theoretical analysis of cell separation based on cell surface marker density, *Biotechnol. Bioeng.* 59: 10–20 (1998).

Mark–Houwink Relationship

Oscar Chiantore

Università degli Studi di Torino, Torino, Italy

Introduction

The molecular weight of polymer molecules can be determined by the measurement of the viscosity of dilute polymer solutions [1]. The relationship used is the so-called Mark–Houwink (MH) empirical equation:

$$[\eta] = KM^a \quad (1)$$

where the intrinsic viscosity $[\eta]$, also called the limiting viscosity number, is proportional to the polymer molecular weight, M , through the constants K and a , valid for each polymer–solvent system at a given temperature.

Applications

The constants of Eq. (1) are obtained by measuring the intrinsic viscosities, in the solvent and at the temperature of choice, of a series of polymer samples having different and known molecular weights.

For flexible macromolecules, the exponent a takes values between 0.5 and 0.8, whereas, for rigid chains, it can reach values higher than 1, up to 2.

The intrinsic viscosity of a polymer is obtained from the viscosities η and η_0 of solution and solvent, respectively, through the following transformations. The relative viscosity is the ratio $\eta_{\text{rel}} = \eta/\eta_0$. By assuming that the viscosity η of a dilute solution is given by the sum of viscosities from solvent and solute molecules, the specific viscosity, η_{sp} , represents the polymer contribution to viscosity:

$$\eta_{\text{sp}} = \frac{\eta - \eta_0}{\eta_0} = \eta_{\text{rel}} - 1 \quad (2)$$

and dividing by the concentration, c , the reduced viscosity η_{sp}/c is obtained. The intrinsic viscosity is the value of reduced viscosity at infinite dilution:

$$[\eta] = \lim_{c \rightarrow 0} \frac{\eta_{\text{sp}}}{c} \quad (3)$$

Experimentally, the viscosity of dilute polymer solutions is, in most cases, determined with glass capillary viscometers, making application of the Hagen–

Poiseuille's law for laminar flow of liquids. The time required for a specific volume of a liquid to flow through a capillary of defined length and radius is proportional to the ratio of the viscosity by the density of the liquid itself. As the density of a dilute solution may be considered practically equal to that of the pure solvent, the ratio of efflux time of the solution, t , to that of solvent t_0 , gives the relative viscosity:

$$\eta_{\text{rel}} = \frac{t}{t_0} = \frac{\eta}{\eta_0} \quad (4)$$

The relative viscosities of polymer solutions are measured at different concentrations and a plot of the reduced viscosity versus concentration is made, in order to extrapolate to zero concentration. The concentration dependence of the viscosity of polymer solutions, in the dilute regime, may be expressed by several linear equations. For practical extrapolation to zero concentration, the most commonly employed are the Huggins equation:

$$\frac{\eta_{\text{sp}}}{c} = [\eta] + k_H[\eta]^2c \quad (5)$$

and the Kraemer equation, where a new quantity, the inherent viscosity η_{inh} , is defined:

$$\eta_{\text{inh}} = \ln\left(\frac{\eta_{\text{rel}}}{c}\right) = [\eta] + k_K[\eta]^2c \quad (6)$$

The constants of the two equations are connected by the relationships $k_K = k_H - 0.5$. Given that, for flexible polymers, the k_H values vary between 0.3 and 0.5, the slope of Kraemer equation is generally negative, with absolute values lower than the Huggins slope. This helps in the extrapolation procedure which is conveniently made, in order to reduce experimental uncertainties, by plotting in the same graph the viscosity data according to Eqs. (5) and (6), as shown in the example of Fig. 1.

The combination of Eqs. (5) and (6) with the assumption that $k_H + k_K = 0.5$ leads to the Solomon–Ciuta equation:

$$[\eta] = \frac{[2(\eta_{\text{sp}} - \ln \eta_{\text{rel}})]^{0.5}}{c} \quad (7)$$



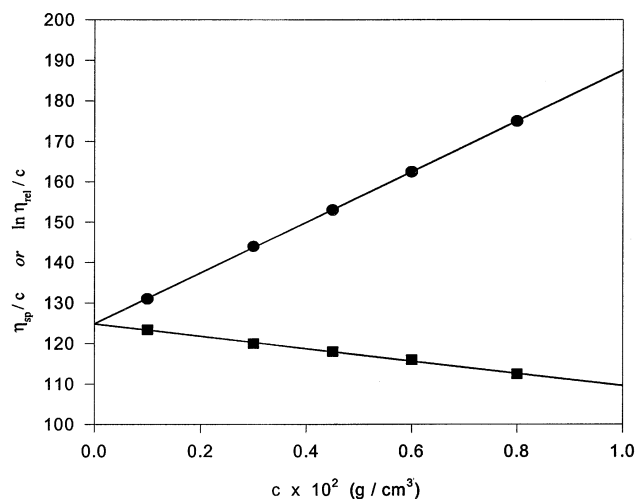


Fig. 1 Double extrapolation of viscometric data according to the Huggins and Kraemer equations: ●: reduced viscosity; ■: inherent viscosity.

which may be used to obtain intrinsic viscosity by a single measurement performed at reasonably low concentration. Equation (7) finds application also in the evaluation of data from viscometer absolute detectors in gel permeation–size-exclusion permeation (GPC–SEC) [2].

In the case of polymers with different chain lengths, the molecular weight obtained from the Mark–Houwink equation is a viscosity-average molecular weight, M_v , whereas the intrinsic viscosity is the weight average. In fact, at infinite dilution, one may write

$$[\eta] = \sum \left(\frac{\eta_{sp,i}}{c_i} \right) = \sum \left(\frac{c_i [\eta]_i}{c_i} \right) = \sum w_i [\eta]_i = [\eta]_w \quad (8)$$

where $w_i = c_i / \sum c_i$ is the weight fraction of the i th component.

The expression for M_v is immediately derived by combining Eq. (8) with the Mark–Houwink relationship:

$$[\eta]_w = \sum w_i [\eta]_i = K \sum w_i M_i^a = K M_v^a \quad (9)$$

$$M_v = (\sum w_i M_i^a)^{1/a} \quad (10)$$

The viscosity-average molecular weight is located between the number- and weight-average values but is, in any case, closer to the weight average. From Eq. (10), it may be seen that viscosity and weight averages coincide for $a = 1$. It is also worth noting that the M_v of a polymer is not a unique definite value because, depending on the exponent a , it varies with the solvent, where the polymer is dissolved.

Mark–Houwink relationships are also important for the application of the universal calibration procedure in GPC–SEC of polymer molecules, where the

calibration curve is expressed in terms of the size of fractionated molecules against retention volumes. The intrinsic viscosity of a polymer (expressed in cm^3/g) is, in practice, a measure of the volume occupied by a unit weight of the macromolecules in the solution. From the Flory–Fox equation for viscosity of flexible chain molecules and from the Einstein relationship for viscosity of a dispersion of spheres [3], it turns out that the product $[\eta]M$ can be used to represent the dimension of polymer molecules in the solution:

$$[\eta]M = \Phi' \alpha^3 \langle s_0^2 \rangle^{3/2} = 2.5 N_A V_h \quad (11)$$

Φ' is the so-called Flory's constant, α is the expansion factor of the polymer molecule, which depends from the thermodynamic quality of the solvent ($\alpha = 1$ in ideal solvent), $\langle s_0^2 \rangle$ is the mean-square radius of gyration, N_A is Avogadro's number, and V_h is the volume of the equivalent hydrodynamic sphere.

In GPC–SEC with universal calibration, at each retention volume i of the chromatogram, a value of $[\eta]_i M_i$ is read, and for molecular-weight and molecular-weight-distribution calculations the values of $[\eta]_i$ are needed. These are obtained, whenever the equation is known, from the Mark–Houwink constants of the polymer in the solvent and at the temperature of chromatographic elution.

A selection of literature values for Mark–Houwink constants K and a in tetrahydrofuran, which is the eluent most commonly used in size-exclusion chromatography, is collected in Table 1 for the principal polymer structures. An accurate, more extensive compilation of the same constants for homopolymers and copolymers may be found in Ref. 22.

References

1. N. C. Billingham, *Molar Mass Measurements in Polymer Science*, John Wiley & Sons, New York, 1977.
2. W. W. Yau, S. D. Abbot, G. A. Smith, and M. Y. Keating, *ACS Symp. Ser.* 352: 80 (1987).
3. P. J. Flory, *Principles of Polymer Chemistry*, Cornell University Press, Ithaca, NY, 1953.
4. M. Kolinsky and J. Janca, *J. Polym. Sci. A-1* 12: 1181 (1974).
5. U. K. O. Schroder and K. H. Ebert, *Makromol. Chem.* 188: 1415 (1987).
6. D. Goedhar and A. Opshoor, *J. Polym. Sci. A-2* 8: 1227 (1970).
7. Z. Grubisic, P. Rempp, and H. Benoit, *J. Polym. Sci. B* 5: 753 (1967).
8. Y.-J. Chen, J. Li, N. Hadjichristidis, and J. W. Mays, *Polym. Bull.* 30: 575 (1993).
9. G. Samay, M. Kubin, and J. Podesva, *Angew. Makromol. Chem.* 72: 185 (1978).

Table 1 Literature Values for Mark–Houwink Constants K and a in Tetrahydrofuran

Polymer	Temp. (°C)	$K \times 10^2$ (cm ³ /g)	a	Ref.
Polystyrene	23	1.11	0.723	4
Poly(methyl styrene)	25	4.2	0.608	5
Poly(vinyl chloride)	25	1.50	0.77	4
Poly(vinyl acetate)	25	3.50	0.63	6
Poly(methyl methacrylate)	23	0.93	0.69	7
	25	1.08	0.702	8
Poly(ethyl methacrylate)	25	1.549	0.679	9
Poly(butyl methacrylate)	25	0.503	0.758	9
Poly(methyl acrylate)	25	0.388	0.82	10
Polyisobutylene)	40	5.79	0.593	11
Polycarbonate	25	3.99	0.77	12
Polybutadiene	30	2.56	0.74	13
Polyisoprene	25	1.77	0.753	14
Butyl rubber	25	0.85	0.75	12
Poly(vinyl butyral)	25	1.4	0.80	15
Poly(2-vinyl pyridine)	25	2.23	0.66	16
Poly(dimethyl siloxane)	25	0.65	0.77	17
Cellulose nitrate	25	25.0	1.00	18
Poly(DL-lactic acid)	31.15	5.49	0.639	19
Poly(ethylene-co-vinyl acetate) (27–29% VA)	20	9.7	0.62	20
Poly(ethylene-co-propylene-co-ethylidene norbornene) (EPDM: 27% PP, 11.5%: ENB)	35	27.4	0.54	21

10. M. Szesztay and F. Tuedoes, *Polym. Bull.* 5: 429 (1981).
11. J. Xie, *Polymer* 35: 2385 (1994).
12. J. M. Evans, *Polym. Eng. Sci.* 13: 401 (1973).
13. X. Zhongde, S. Minghsi, N. Hadjichristidis, and L. J. Fetters, *Macromolecules* 14: 1591 (1981).
14. C. Kraus and C. J. Stacy, *J. Polym. Sci. A-2* 10: 657 (1972).
15. L. Mrkvickova, J. Danhelka, and S. Pokorny, *J. Appl. Polym. Sci.* 29: 803 (1984).
16. C. Hugelin and A. Dondos, *Makromol. Chem.* 126: 207 (1969).
17. L. Mrkvickova and N. Radhakrisnan, *Eur. Polym. J.* 33: 1403 (1997).
18. A. Rudin and H. W. Hoegy, *J. Polym. Sci. A-1* 10: 217 (1972).
19. J. A. P. P. van Dijk, J. A. M. Smit, F. E. Kohn, and J. Feijten, *J. Polym. Sci., Polym. Chem. Ed.* 21: 197 (1983).
20. J. Echarri, J. J. Iruin, G. M. Guzman, and J. Amsorena, *Makromol. Chem.* 180: 2749 (1979).
21. O. Chiantore, P. Cinquina, and M. Guaita, *Eur. Polym. J.* 30: 1043 (1994).
22. S. Mori and H. Barth, *Size Exclusion Chromatography*, Springer-Verlag, Berlin, 1999.



Mass Transfer Between Phases

J.E. Haky

Florida Atlantic University, Boca Raton, Florida, U.S.A.

Introduction

Chromatography is a separation method which involves two phases — one stationary and one mobile. A mixture is introduced into the mobile phase and is carried through the system by it. At some point, the mobile phase passes over and through the stationary phase. The components of the mixture partition between the two phases, resulting in different migration rates through the system [1]. At any given point, an analyte molecule will either be moving along the mobile phase or be held immobile in the stationary phase. A separation results as the molecules emerge from the bed at different times, which are called retention times.

Background Information

The retention time of a solute is partially controlled by how effectively it interacts with the stationary phase as it passes through the column. As a solute molecule moves through a chromatographic system, it is carried through the mobile phase to a new solution site in the stationary phase. Simultaneously, other solute molecules are moving from the stationary phase and are being conducted through the column by the mobile phase. In any separation of components of a mixture by liquid chromatography, the rate at which this repeated transfer of solutes between the stationary phase and the mobile phase is an important factor affecting retention, peak shape, and resolution.

Mass transfer in both the stationary and mobile phases are not instantaneous and, consequently, complete equilibrium is not established under normal separation conditions [2]. The result is that the solute concentration profile in the stationary phase is always displaced slightly behind the equilibrium position and the mobile-phase profile is slightly in advance of the equilibrium position [2]. A high degree of displacement will lead to wider peaks and reduced resolution. In fact, the largest problem associated with mass transport in the packed column revolves around moving the solute from the stationary phase to the mobile phase.

The degree of band broadening of any chromatographic peak may be described in terms of the height equivalent to a theoretical plate, H , given by

$$H = \frac{L}{N} \quad (1)$$

where L is the length of the column (usually in cm) and N is the number of theoretical plates, which can be calculated from

$$N = 16 \left(\frac{t_R}{W} \right)^2 \quad (2)$$

where t_R and W are the retention time and width of the peak of interest, respectively.

Because higher values of N correspond to lower degrees of band broadening and narrower peaks, the opposite is true for H . Therefore, the goal of any chromatographic separation is to obtain the lowest possible values for H .

The contribution of mass transfer and other factors to band broadening in liquid chromatography can be quantitatively described by the following equation, which relates the column plate height H to the linear velocity of the solute, μ :

$$H = A\mu^{0.33} + \frac{B}{\mu} + C\mu + D\mu \quad (3)$$

In this equation, A , B , C , and D are constants for a given column [3]. The linear velocity μ is related to the mobile-phase flow rate and is determined by

$$\mu = \frac{L}{t_0} \quad (4)$$

where t_0 (the so-called “dead time”) is determined from the retention time of a solute, which is known not to interact with the stationary phase of the column.

The first term in Eq. (3), $A\mu^{0.33}$, includes the contribution of eddy diffusion to band broadening as well as that of mass transfer of the solute through the mobile phase. This contribution of this mobile-phase mass transfer to this term, H_i , increases with the square of the stationary-phase particle diameter d_p . It is also in-



versely proportional to the diffusion coefficient of the solute in the mobile phase, D_m , according to

$$H_i = \frac{C_m d_p^2 \mu}{D_m} \quad (5)$$

where C_m is a constant.

The third and fourth terms of Eq. (3) also relate to mass transfer. The third term, C_μ , describes the contribution of mass transfer of solutes to and from areas in the column where the mobile phase is stagnant (e.g., within the pores of the packing). The size of this term is related to stationary-phase particle diameter and solute diffusion coefficient according to

$$C_\mu = \frac{C_{sm} d_p^2 \mu}{D_m} \quad (6)$$

where C_{sm} is a constant.

Finally, the fourth term in Eq. (3), D_μ , describes the contribution of mass transfer of solutes to and from the stationary phases. This term is related to the thickness d_f of the phase that coats the stationary phase and the diffusion coefficient D_s of the solute in the stationary phase according to

$$D_\mu = \frac{C_s d_s^2 \mu}{D_s} \quad (6)$$

where C_s is a constant.

To minimize band broadening in liquid chromatography, conditions must be established to minimize each of the terms described by Eqs. (5)–(7). Because each of these terms is directly proportional to mobile-phase linear velocity, employing the lowest possible mobile-phase flow rates would seem to serve this purpose. However, use of extremely low flow rates [<0.5 mL/min for a standard high-performance liquid chromatography (HPLC) column] can increase solute retention times to impractical levels and may actually increase band broadening due to increased longitudinal diffusion [described by the second term in Eq. (3)]. For this reason, other factors are usually adjusted to minimize these mass transfer terms. Such adjustments include (a) using monomerically bonded stationary phases with small particle diameters [this reduces the size of d_f and d_p terms in Eqs. (5)–(7), which, in turn, has an exponential effect on reducing the size of the mass transfer terms]; (b) employing mobile phases of low viscosity at high temperatures (this increases the sizes of the diffusion coefficients D_s and D_m

in the equations, resulting in fast mass transfer and narrow chromatographic bands [4].)

Column manufacturers and researchers have optimized the above parameters to produce LC columns of remarkably high selectivities and efficiencies. However, there are practical limitations to adjustments of these parameters. For example, stationary phases with particle diameters below $3 \mu\text{m}$ generally cannot be routinely used, owing to excessively high back-pressures and short column lifetimes. Additionally, for obvious reasons, operating temperatures must be kept below the boiling points of the components of the mobile phase. Use of nonporous pellicular column packings has also been attempted in an effort to eliminate any areas of stagnant mobile phase in the chromatographic system, thus reducing the size of the third term in Eq. (3) to zero. However, such pellicular stationary phases have very low sample capacities, and diffusion coefficients of many solutes on their polymeric coatings are often low, which, of course, results in increased band broadening [3].

At commonly used mobile-phase flow rates, mass transfer of solutes through and between the stationary phase and the mobile phase is generally the most important factor controlling the widths of chromatographic bands in liquid chromatography. Although manufacturers have designed packings and columns to minimize their effects, consideration of solute mass-transfer effects are extremely important in the development of any chromatographic method.

Acknowledgments

The author wishes to thank D.A. Teifer for technical assistance.

References

1. J. M. Miller, *Chromatography: Concepts and Contrasts*, John Wiley & Sons, New York, 1988, Chap. 2.
2. J. C. Giddings, *Dynamics of Chromatography*, Marcel Dekker, Inc., New York, 1965, pp. 95–118.
3. L. R. Snyder and J. J. Kirkland, *Introduction to Modern Liquid Chromatography*, 2nd ed., John Wiley & Sons, New York, 1979, Chap. 5.
4. L. R. Snyder, J. J. Kirkland, and J. L. Glajch, *Practical HPLC Method Development*, 2nd ed., John Wiley & Sons, New York, 1997, Chap. 2.



Metal-Ion Enrichment by Countercurrent Chromatography

Eiichi Kitazume

Laboratory of Chemistry, Iwate University, Morioka, Japan

Introduction

Countercurrent chromatography (CCC) is a useful method for separating metal ions as well as organic compounds. In addition, highly efficient chromatographic separation has been achieved using a multi-layer coil system and strong force field by over several hundreds of revolutions per minute. However, there have been no applications to the enrichment of inorganic elements until quite recently.

The latest study has revealed that CCC has a great potential in the ultratrace determination of metals, because it can concentrate minute amounts of metal prior to the instrumental multielement analysis, such as atomic absorption spectrometry (AAS), inductively coupled plasma–atomic emission spectrometry (ICP–AES), and inductively coupled plasma–mass spectrometry (ICP–MS).

Enrichment of the desired trace elements would not only allow highly sensitive determination of the trace elements but also alleviate various problems including interferences, high risk of exposure to toxic chemicals and radiation from radioactive samples, and so forth.

Extraction of Metal Ions in the Stationary Phase

The existence of the extracting reagent in the stationary phase is one of the essential factors in the enrichment of inorganic elements as well as in the separation itself. However, the values of the distribution ratios, determined by batch extraction measurements in the two-phase system, is sometimes considerably different from that of the dynamic distribution ratios calculated from the elution curve. Further theoretical and basic investigations are necessarily concerned with extraction kinetics, as well as hydrodynamics behavior of two phases in the high-speed CCC (HSCCC) column [1].

Organophosphorus extractants such as di(2-ethylhexyl) phosphoric acid (DEHPA), 2-ethylhexylphosphonic acid mono-2-ethylhexyl ester (EHPA), *N*-benzoyl-*N*-phenylhydroxylamine (BPHA), and tetraoctylethylenediamine (TOEDA) are often used due to their solubility properties in the stationary organic phase [1–3].

Enrichment in the Effluent by Conventional Elution

After metal ions are enriched in the organic stationary phase including the extracting reagent in the CCC column, they can be eluted simultaneously or chromatographically into the eluent stream by a conventional elution mode.

It was demonstrated that systems with DEHPA can extract and preconcentrate Zr(IV), Hf(IV), and Nb(V) into the organic stationary phase and can separate them from the majority of other elements [1]. The preconcentration of Zr(IV) and Hf(IV) and subsequent back-extraction, as well as the selective extraction of Zr(IV), Hf(IV), Nb(V), and Ta(V) into a 4-mL volume of the organic phase can be performed with a mixture of DEHPA and BPHA.

A 1000-mL sample solution containing $5 \times 10^{-7}M$ of each rare earth element were effectively enriched onto the CCC column head using carboxylic acid–toluene including the EHPA system [2]. Then, each element concentrated on the column head was eluted chromatographically by the mobile phase with a step-wise pH gradient.

On the other hand, the capability of sample preconcentration for instruments such as AAS, ICP–AES, ICP–MS, and so forth was studied [3]. After metal ions were enriched, they were eluted almost simultaneously by inorganic acid at low pH, because of their diffusion in the column is at a disadvantage for improvement of the detection limits. It has been demonstrated that metal ions such as Ca, Cd, Mg, Mn, Pb, and Zn were enriched with a good recovery at a concentration of 10 ppb each in 500 mL of the sample solution. However, the final enriched sample volume eluted from the CCC column was as large as several milliliters, due to longitudinal diffusion of the sample band in the retained stationary phase [1,3]. Additional band spreading occurred in the flow tube when the concentrated solution was eluted with an acid solution for subsequent analysis.

Also, the mechanism of the separation, based on displacement chromatography followed by the enrichment in the CCC column, was studied and a 10-fold en-



richment of the transition metal ions was observed in the stationary phase [4]. However, the diffusion of the sample is an inherent process in chromatographic elution, and spreading of the sample bands in the column is unavoidable in CCC as it is in conventional liquid chromatography.

Therefore, it may be difficult to obtain highly concentrated metal ions in an extremely small volume of effluent such as under-mL-order, even if a small-bore column was used with higher concentration efficiency.

Enrichment in the Effluent by pH-Peak Focusing Technique

Recently, pH-zone-refining countercurrent chromatography (pH-ZRCCC), which is a quite unique technique based on neutralization reaction between mobile and stationary phases, has been developed for preparative-scale separation and enrichment of various organic compounds [5]. The pH-ZRCCC can realize chemical reaction in a quite limited thin area (i.e., the interface between organic and aqueous phase, where there is spreading over wide direction in a small-bore tube). If the pH between two phases in the column is reversed, the stationary phase will be continuously neutralized with the mobile phase. Therefore, the pH border, where neutralization has just finished, moves to the tail (outlet) from the head (inlet) of the column. The moving rate of the pH border in the column can be controlled by adjusting the pH in each phase. This means that "another flow rate" concerned with pH, different from the "real flow rate of the eluent," can be realized in the column. Impurities in the sample solution can be quantitatively trapped and enriched in the pH border at a specific condition of the moving rate. This enrichment method for trace organic impurities has been called pH-peak-focusing countercurrent chromatography (pH-PFCCC).

It has been shown that the pH-PFCCC could be successfully applied to enrichment of inorganic trace elements in solution [6–8]. It has great potential for on-line enrichment and subsequent analysis, when CCC is combined with another analytical instrument for solution. The peak intensities for a 10-mL standard sample in the effluent stream was increased over 100-fold, compared with the conventional plasma atomic emission spectrometry. In this method, Ca, Cd, Cu, Mg, Mn, and Zn are chromatographically extracted, in a basic organic stationary phase containing a complex-forming reagent such as DEHPA, by introducing the sample solution into the column rotating at 1200 rpm. When the column is eluted with the acidified mobile

phase, metal ions are trapped and concentrated around the sharp pH border formed between the acidic and the basic zones, moving toward the outlet of the column. Enriched metal ions are finally eluted with the sharp pH border as a highly concentrated peak into less than a 100- μ L volume.

The conditions of distribution ratio (K) between the two-phase solvent for pH-PFCCC are shown in Fig. 1. In a relatively basic environment at the first stage of the sample injection, the metal ion present in an aqueous phase forms a complex with the ligand and it partitions into the organic phase with a distribution ratio of K_b , whereas in an acidic environment, the metal ion is mainly distributed into the aqueous phase with distribution ratio of K_a .

As the elution proceeds, acid (e.g., HCl) present in the mobile phase steadily neutralizes the base (e.g., NH_3) in the stationary phase, forming a narrow pH border between the basic front zone and the acidic rear zone. The traveling rate of this sharp pH border through the column is determined mainly by the molar ratio between the base in the stationary phase and acid in the mobile phase, but it is substantially lower than the flow rate of the mobile phase. The metal ion present in the acidic zone quickly moves with the mobile phase passing through the pH border into the basic zone, where it forms a metal–ligand complex and is transferred into the stationary phase. As the pH bor-

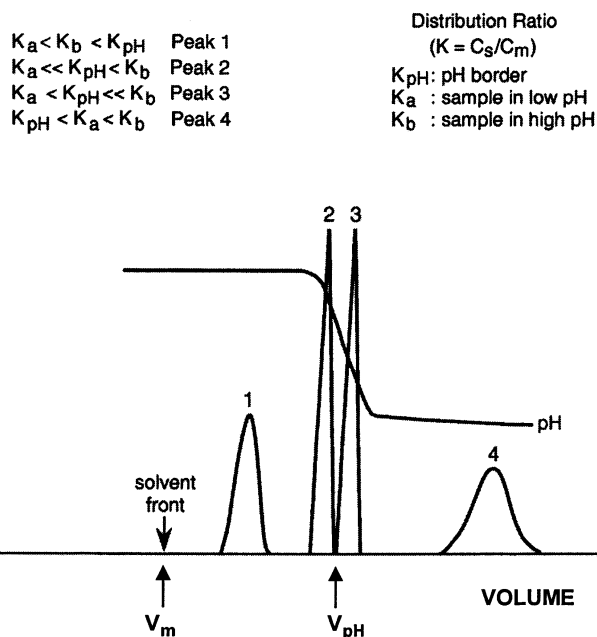


Fig. 1 Conditions of distribution ratio between two-phase solvent for pH-peak focusing.

der moves forward, the complex is exposed to a lower pH where the metal is displaced by a proton (H^+) and released into the aqueous phase as its ionic form (M^+) to repeat the above cycle. Consequently, the metal element is always confined to a narrow region around the sharp pH border and, finally, eluted as a highly concentrated sharp peaks (peaks 2 and 3) in the pH slope, as shown in Fig. 1. Thus, the system eliminates longitudinal spreading of the sample band due to the separation process, which is inherent in other liquid chromatographic methods.

In above method, trapping the metal element by the sharp pH border is essential, and this requires a certain relationship between the distribution ratios of the metal element and the traveling rate of the pH border through the column, as illustrated in Fig. 1. The distribution ratio is shown as K_a and K_b in the acidic and the basic zones, respectively. V_{pH} shows the volume of the eluent when the pH border comes out on the chromatogram. K_{pH} is assumed as a temporary distribution ratio when solute peak was appeared at the retention volume of V_{pH} . K_{pH} is adjustable by changing the molarity between the basic phase and the acidic phase. If K_{pH} is greater than K_a and K_b , the metal ion will elute earlier than the sharp pH border (peak 1), and if K_{pH} is smaller than K_a and K_b , the metal ion will elute after the sharp pH border (peak 4). The peak trapping takes place only when K_{pH} falls between K_a and K_b (peaks 2 and 3). The two metal peaks (peaks 2 and 3) may be resolved within a narrow range if they have a substantial difference in their K_a and K_b values, as shown in Fig. 1.

Conclusion

In contrast to HPLC, CCC has the unique feature that there is no solid support in the column. Because the distribution abilities, including the capacity of the stationary phase, are easy to control, CCC can be applied to the various inorganic treatment, such as enrichment as well as separation and purification, over a wide range in concentration. Moreover, the reproducibility for the enrichment operation has a substan-

tial advantage over other enrichment systems, such as ion exchange, because the absorber system in CCC is always "fresh" in each operation. In particular, enrichment of trace elements using pH-PFCCC will be an ideal preconcentration method for subsequent inorganic determination of modern instrumental analytical methods. It can be combined directly with the flow injection technique, so there would be great potentials for a new enrichment (preconcentration) system of a desired trace element prior to the determination. On-line enrichment and subsequent analysis may take the place of conventional sample preparation using a beaker and separatory funnel, in the future investigation in this field.

References

1. P. S. Fedotov, T. A. Maryutina, O. N. Grebneva, N. M. Kuz'min, and B. Ya. Spivakov, *J. Anal. Chem.* 52: 1034 (1997).
2. S. Nakamura, H. Hashimoto, and K. Akiba, *J. Liquid Chromatogr. A* 789: 381 (1997).
3. E. Kitazume, N. Sato, and Y. Ito, *J. Liquid Chromatogr. Related Technol.* 21: 251 (1998).
4. K. Talabardon, M. Gagean, J. M. Marmet, and A. Berthod, *J. Liquid Chromatogr. Related Technol.* 21: 231 (1998).
5. Y. Ito and Y. Ma, *J. Chromatogr. A* 753: 1 (1996).
6. E. Kitazume, N. Sato, and Y. Ito, A new preconcentration-detection method for trace metals by pH-zone-refining countercurrent chromatography, 1995 Pittsburgh Conference and Exposition on Analytical Chemistry and Applied Spectroscopy, 1995.
7. E. Kitazume, N. Sato, and Y. Ito, Effective concentration method for trace metals in solution by pH-zone-refining countercurrent chromatography, 1997 Pittsburgh Conference and Exposition on Analytical Chemistry and Applied Spectroscopy, 1997.
8. E. Kitazume, T. Higashiyama, N. Sato, M. Kanetomo, T. Tajima, S. Kobayashi, and Y. Ito, A novel on-line micro extraction system of metal traces for their subsequent determination by plasma atomic emission spectrometry using pH-zone refining high speed countercurrent chromatography, 1999 Pittsburgh Conference and Exposition on Analytical Chemistry and Applied Spectroscopy, 1999.



Metal-Ion Separation by Micellar High Performance Liquid Chromatography

S. Muralidharan

Western Michigan University, Kalamazoo, Michigan, U.S.A.

Introduction

The separation of target metal ions from a complex mixture is an extremely important area of research for the purpose of recovery of metal values from wastes and for environmental remediation and restoration. Conventional approaches to metal-ion separation and recovery fall into two broad classes, namely (a) solid-liquid and (b) liquid-liquid separations.

Solid-liquid methods include ion-exchange resins, which involve electrostatic interaction between the positively charged metal ions in solution and a negatively charged functional group on a polymer backbone such as SO_3^- , chelating polymers containing complexing ligands such as iminodiacetic acid, and membrane-mediated separations using solid membranes.

Liquid-liquid methods include solvent extraction with immiscible liquid-liquid systems in which a suitable ligand is dissolved in an organic phase and contacted with a metal ion containing an aqueous phase and liquid membranes. Separations can also be achieved with pseudo-phase systems such as micelles, microemulsions, and vesicles. Such separations can be solid-liquid or liquid-liquid and include separations with normal- and reversed-phase silica, and polymeric supports where the mobile phase contains the organized molecular assembly (OMA) of micelles, microemulsions, or vesicles. Separation of metal ions using the pseudo-phase systems is still in its infancy and a brief account will be provided here.

OMAs

Organized molecular assemblies (OMAs) are inherently capable of providing greater selectivities in separations of both organic compounds and metal ions mainly due to the ability of the organized microenvironments to discriminate among analytes with similar properties. Selectivities in metal-ion separation are best achieved through complexation rather than through ion-pair formation, and, in general, chelating

ligands provide higher selectivities than monodentate ligands. The selectivities of the chelating ligands are limited in the conventional approaches using chelating resins and solvent extraction because the ligands are present in random macroenvironments. The incorporation of these ligands into organized microstructures such as micelles can provide dramatic improvements in their metal-ion selectivities. The factors that influence metal-ion selectivities are the stability constants of their complexes, the geometry and coordination number of the complexes, and the equilibrium and kinetics of metal complex formation and dissociation reactions, especially in the interfacial region. It is evident that these factors can be better exploited to achieve metal-ion selectivities in an organized microenvironment compared to a random macroenvironment. High metal-ion selectivities are needed for the separation of target metal ions from complex matrices such as spent catalysts and electrochemical baths, geothermal brines, and nuclear wastes. Organized microenvironments will be key to achieving the selectivities demanded by such complex and difficult matrices.

Micelles

Separations of metal ions mediated by the OMA micelles will be the focus of this entry. Micelles are formed from surfactants in aqueous solutions above a certain concentration of the surfactants called the critical micelle concentration (CMC) [1]. These surfactants can be neutral, such as Triton X-100 and Brij 35, which have the general structure $\text{R}(\text{OCH}_2\text{CH}_2)_n\text{OH}$, where R is a long-chain alkyl group (C_{12} and above) and n the number of oxyethylene groups ($n = 9$ for Triton X-100 and 23 for Brij 35), or anionic such as sodium dodecyl sulfate (SDS; $\text{C}_{12}\text{H}_{25}\text{SO}_4^-\text{Na}^+$), or cationic such as cetyltrimethylammonium bromide [CTAB; $\text{C}_{16}\text{H}_{33}\text{N}(\text{CH}_3)_3^+\text{Br}^-$]. The CMC values of Triton X-100, SDS, and CTAB at an ionic strength of 0.1 are $2 \times 10^{-4}\text{M}$, $2 \times 10^{-3}\text{M}$, and $1.8 \times 10^{-4}\text{M}$, respectively, and their aggregation numbers are 100, 40, and 60, respectively. The neutral micelles in addition to the



CMC are also characterized by the cloud point, which is the temperature at which a solution of the neutral micelle separates into two phases, namely the surfactant-rich phase and the water-rich phase. This property has been exploited to achieve cloud point separations analogous to separations employing two immiscible liquid phases. When the micelles are formed in the aqueous phase, the polar head groups of the surfactants, namely OH, SO_4^- , and $\text{C}_{16}\text{H}_{33}\text{N}(\text{CH}_3)_3^+$, are present on the surface of the micelles, and the interior of the micelle is hydrophobic like an organic phase in the case of the anionic and cationic micelles. In the case of the neutral micelles, the interior is composed of the oxyethylene groups terminating in an alkyl chain which form the hydrophobic interior called the corona. Neutral surfactants form reverse micelles in nonpolar solvents where the OH group is in the interior and the R group is on the surface. The presence of polar groups on the surface of the normal micelles in the aqueous phase results in an electrical double layer and an interfacial potential, which have significant influence on metal-ion selectivities. This potential is close to zero for neutral micelles, negative for anionic micelles, and positive for cationic micelles.

Adsorption of Surfactants on Silica and Reversed-Phase Silica

The neutral, anionic, and cationic surfactants will adsorb on silica and reversed-phase silica such as octadecylsilanized silica (ODS) from an aqueous solution to form a monolayer of the surfactant on the surface. The adsorption of surfactants on silica surface is more complex than their adsorption on ODS surface. The SiO_2 surface is polar due to the presence of surface silanol groups, and, as a result, the surfactants will adsorb with the polar group on the surface, namely the OH , SO_4^- , and $\text{C}_{16}\text{H}_{33}\text{N}(\text{CH}_3)_3^+$, with the alkyl groups pointed away from the surface. The adsorption of the surfactants on SiO_2 is pH dependent as the surface charge changes with pH. This adsorption is also dependent on the concentration of the surfactant with monolayers being formed at

low surfactant concentrations and bilayers being formed at high surfactant concentrations. The bilayers are formed when a second layer of the surfactant adsorbs on the initial monolayer through its alkyl chains and the bilayer has the polar head groups pointing toward the bulk aqueous phase. Due to the complex adsorption phenomenon associated with adsorption of surfactants on SiO₂ surface, it is not a useful stationary phase for performing micellar chromatography.

The adsorption of surfactants onto ODS is more straightforward and well understood. Here, the formation of the monolayer of the surfactant on the ODS surface proceeds through the adsorption of the surfactant through its alkyl chain with the polar head group pointing into the bulk aqueous phase. Such an adsorption only results in a monolayer coverage, and the chromatographic behavior of these adsorbed monolayers can be discerned with established principles. The adsorbed monolayers of surfactants on reversed-phase silica have been characterized by several spectroscopic methods [2] and will not be discussed here.

Micellar Chromatographic Separations of Metal Ions

The adsorbed monolayers of surfactants on reversed-phase silica can be utilized as stationary phases and an aqueous solution of the same surfactant above its CMC as the mobile phase to separate both organic and inorganic analyte mixtures [3]. In the case of organic analytes, the selectivity between analyte components can be improved dramatically by employing micellar chromatography. The mechanism of separation, as in reversed-phase chromatography, is the distribution of the analyte between the micellar pseudo-phase and the stationary phase containing the adsorbed monolayer of the surfactant. Because the partitioning of the analyte now occurs between the organized microstructure of the micellar pseudo-phase and the adsorbed monolayer, the selectivity between closely related analytes is significantly improved. The separation of metal ions requires the addition of a complexing ligand in order

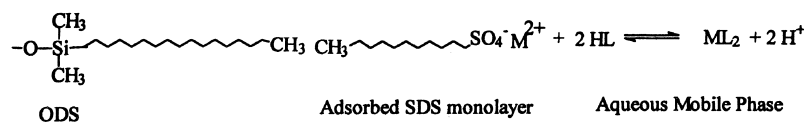


Fig. 1 Mechanism of separation of metal ions by micellar chromatography employing sodium dodecyl sulfate micelles in the mobile phase and octadecylsilanized silica as the stationary phase.

to discriminate among the various metal ions. The SDS adsorbed on ODS as shown in Fig. 1 can function as an ion-exchange column but will not possess any selectivity between metal ions with similar charges analogous to a cation-exchange resin. Metal-ion separations can be achieved, in principle, on neutral, anionic, and cationic surfactants adsorbed on ODS columns, but only the separation with anionic surfactants adsorbed on ODS columns has been studied so far because of its complementary nature to conventional cation-exchange resins. The separations with neutral and cationic surfactants adsorbed are more complex and their behavior needs to be understood before they will be useful for the separation of metal ions.

Metal-Ion Separations on the ODS–SDS Column

The separation on the ODS–SDS column is achieved by the addition of a suitable complexing ligand to the mobile phase to discriminate between the various metal ions. The selectivity between two metal ions is achieved through two competing equilibria, namely the complexation equilibrium of the free metal ion in the micellar pseudo-phase and the complexation equilibrium of the metal ion adsorbed on the SDS monolayer and this is shown in Fig. 1. It is evident from this equilibrium that the distribution ratio (capacity factor) of the metal ion M^{2+} is given by Eq. (1), where the subscripts a and s represent the concentration of the free metal ion in the bulk aqueous phase and the adsorbed monolayer, respectively:

$$D = \frac{[M^{2+}]_s}{[M^{2+}]_a} \quad (1)$$

The associated equilibrium constant is defined in Eq. (2), where HL represents the ligand, and the relationship between $\log D$ and $\log[HL]$ and pH is given in Eq. (3):

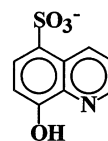
$$K_{eq} = \frac{D[HL]^2}{[H^+]^2} \quad (2)$$

$$\log D = \log K_{eq} - 2 \log[HL] - 2pH \quad (3)$$

As is evident from Eq. (3), a plot of $\log D$ as a function of $\log[HL]$ at constant pH and as a function of pH at constant $[HL]$ will yield the stoichiometry of the equilibrium involved in the separation of the metal ion and the associated equilibrium constants.

The above-mentioned separation principle can be understood by the separation of Co(II), Ni(II), Cu(II), and Zn(II) by micellar chromatography employing SDS above its CMC in the mobile phase, ODS as the

stationary phase, and 8-quinolinol-5-sulfonic acid ($pK_1 = 3.84$; $pK_2 = 8.35$) as the ligand [4]:



The logarithm of the stability constant for the 1:2 metal: ligand complex of this ligand with Co(II), Ni(II), Cu(II), and Zn(II) are 16.1, 16.77, 21.9, and 14.3, respectively. This separation employing a pH gradient is shown in Fig. 2, from which it is evident that the metal ions are eluted in the reverse order of their stability constants with 8-quinolinol-5-sulfonic acid. This elution order is readily understood from the equilibrium in Fig. 2, which indicates that the metal ion with the larger stability constant will be stripped from the adsorbed SDS monolayer more easily compared to the metal ion with a smaller stability constant. It may also be noted that the chromatographic bandwidths are much larger than those encountered with organic analytes and this is a direct consequence of slow metal complex formation and dissociation kinetics. Information on such kinetics can be obtained by studying the dependence of HETP on the concentrations of ligand and pH. This indicates that in the case of Co(II), Cu(II), and Zn(II), the dissociation of the metal complex is mainly responsible for the band broadening, whereas in the case of Ni(II), both metal complex formation and dissociation affect the efficiency.

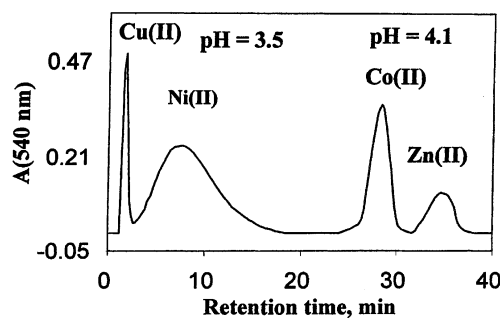


Fig. 2 Separation of Co^{2+} , Ni^{2+} , Cu^{2+} , and Zn^{2+} by micellar chromatography employing a pH gradient. Experimental conditions: mobile phase: $[SDS] = 0.004M$, $[8\text{-quinolinol-5-sulfonic acid}] = 0.002M$, ionic strength = 0.1; ODS stationary phase. $10\ \mu L$ of the metal-ion mixture containing $0.002M$ of each ion was injected at a mobile-phase flow rate of $1\ mL/min$. Cu^{2+} and Ni^{2+} elute at $pH = 3.5$ and Co^{2+} and Zn^{2+} elute at $pH = 4.1$.



Several simple water-soluble chelating ligands such as iminodiacetic acid have been employed for the separation of a variety of metal ions. Okada demonstrated the separation of several divalent metal ions (Mn^{2+} , Co^{2+} , Ni^{2+} , Cu^{2+} , Zn^{2+} , Cd^{2+}) on ODS column with SDS micelles in the mobile phase and tartaric acid as the ligand [5]. The selectivity between the various divalent metal ions is much smaller than that observed with 8-quinolinol-5-sulfonic acid, which forms complexes with much larger stability constants than does tartaric acid. The stability constants of the metal complexes with a given ligand as mentioned earlier is one of the factors that affect selectivity. Karcher and Krull have published a review of the use of simple water-soluble ligands such as acetic acid, oxalic acid, hydroxyisobutyric acid, citric acid, tartaric acid, oxalic acid, and EDTA in micellar chromatography and with simple ion-exchange columns [6]. The selectivities obtained with these simple ligands is not as large as with ligands of the 8-quinolinol, acylpyrazolone, and aromatic oxime families, which are yet to be extensively investigated. Inorganic anions such as nitrate, nitrite, and phosphate can be separated by micellar chromatography using cationic micelles in the mobile phase and ODS as the stationary phase, as shown by Cassidy and Elchuk [7].

Chelating Micelles

The studies that have been conducted so far have involved the addition of a suitable ligand to the micellar pseudo-phase in order to separate the mixture of metal ions. The location of the ligand in this pseudo-phase is a function of the hydrophilic and hydrophobic nature of the ligand. If the ligand is hydrophilic simple ones such as tartaric acid, then they will be present predominantly in the bulk aqueous phase, and if the ligand is hydrophobic such as 8-quinolinols, then they will distribute into the micellar pseudo-phase. The location of the ligands in the micellar pseudo-phase is a function of the hydrophobicity of the ligand. Thus, the distribution of the ligand between the bulk aqueous phase and the micellar pseudo-phase introduces uncertainty in the location of the ligand and does not fully exploit the organized microenvironment. The aqueous-micelle interfacial region has a very high interfacial area and possesses an electrical double layer with an interfacial potential. These can be effectively exploited to achieve even higher selectivities in metal-ion separations if the ligand can be specifically located at the interfacial region. We have recently achieved this by chemically derivatizing neutral surfactants such as Brij 35 such that a chelating ligand like 8-quinolinol or acylpyrazolone

is the head group instead of OH. Such chelating surfactants form chelating micelles at CMC values much lower than Brij 35. The charge of the micelle is pH and ligand dependent and can be neutral, anionic, or cationic. In these chelating micelles, the ligand is exclusively present on the surface of the micelle and its chelating properties and metal-ion selectivities are strongly influenced by the interfacial region. We have synthesized chelating surfactants containing 2-methyl-8-quinolinol and 1-phenyl-3-methyl-4-benzoyl-5-pyrazolone as the head groups [8]. We have been able to obtain very large selectivities in the separation of divalent transition metal ions and trivalent lanthanide ions using these chelating micelles. The selectivities that we have achieved in the separation of the trivalent lanthanide metal ions are unprecedented and clearly indicate the tremendous gains in selectivities that can be achieved by the incorporation of ligands into organized microstructures. We have also shown that the mixed system of chelating surfactants with the 8-quinolinol and acylpyrazolone head groups form vesicles which also exhibit unique selectivities in the separation of transition and lanthanide metal ions on an ODS stationary phase. The chelating micelles are also interesting candidates for the separation of metal ions by electrokinetic chromatography, where the interfacial properties of the chelating micelles can be further exploited to achieve very high metal-ion selectivities.

References

1. M. J. Rosen, *Surfactants and Interfacial Phenomena*, John Wiley & Sons, New York, 1989.
2. D. A. Piasecki and M. A. Wirth, Spectroscopic probing of the interfacial roughness of sodium dodecyl sulfate adsorbed to a hydrocarbon surface, *Langmuir* 10: 1913 (1994).
3. W. L. Hinze and D. W. Armstrong, eds., *Ordered Media in Chemical Separations* American Chemical Society, Washington, DC, 1987.
4. S. Muralidharan, unpublished results.
5. T. Okada, Interpretation of retention behavior of transition-metal cations in micellar chromatography using an ion-exchange model, *Anal. Chem.* 64: 589 (1992).
6. B. D. Karcher and I. S. Krull, The use of complexing eluents for the high performance liquid chromatographic determination of metal species, in *Trace Metal Analysis and Speciation* (I. S. Krull, ed.), Journal of Chromatography Library Series Vol. 47, Elsevier, Amsterdam, 1991, pp. 123–166.
7. R. M. Cassidy and S. Elchuk, Dynamically coated columns for the separation of metal ions and anions by ion chromatography, *Anal. Chem.* 54: 1558 (1982).
8. S. Muralidharan, unpublished results.



Metals and Organometallics: Gas Chromatography for Speciation and Analysis

Yong Cai

Weihoa Zhang

Florida International University, Miami, Florida, U.S.A.

Introduction

Speciation analysis is usually defined as the determination of the concentrations of the individual physico-chemical forms of the element in a sample that together constitute its total concentration. Recently, there has been increasing interest in speciation information of elements present in environmental and biological samples because the toxicological and biological importance of many metals and metalloids greatly depends on their chemical forms [1–3]. The determination of the total amount of an element is important, but it is not sufficient to assess its toxicity. Information about concentrations of the individual species of an element, including its organic derivatives, is particularly crucial. Frequently, the lack of the speciation information is the major limitation to our understanding of the biogeochemical cycling of the element.

The identification of the chemical forms of an element has become an important and challenging research area in environmental and biomedical studies. Two complementary techniques are necessary for trace element speciation. One provides an efficient and reliable separation procedure, and the other provides adequate detection and quantitation [4]. In its various analytical manifestations, chromatography is a powerful tool for the separation of a vast variety of chemical species. Some popular chromatographic detectors, such as flame ionization (FID) and thermal conductivity (TCD) detectors are bulk-property detectors, responding to changes produced by eluates in a characteristic mobile-phase physical property [5]. These detectors are effectively “universal,” but they provide little specific information about the nature of the separated chemical species. Atomic spectroscopy offers the possibility of selectively detecting a wide range of metals and nonmetals. The use of detectors responsive only to selected elements in a multicomponent mixture drastically reduces the constraints placed on the separation step, as only those components in the mixture which contain the element of interest will be detected

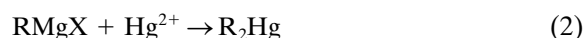
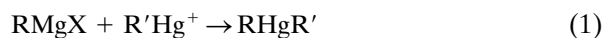
[6]. It is not surprising that the coupling of chromatographic techniques [gas chromatography (GC) and high-performance liquid chromatography (HPLC)] with a highly sensitive and selective atomic spectrometry detector has been widely exploited and accepted for the speciation of metals and organometals. GC has enjoyed particular attention because of its high sensitivity and simplicity of coupling. Details about GC coupled to atomic absorption spectrometry (AAS), MIP–AES, and inductively coupled plasma–mass spectrometry (ICP–MS) are discussed here.

Sample Preparation

The native species of most metals and metalloids, such as mercury, lead, tin, arsenic, and selenium, are generally present as ionic forms in sample matrices. For GC-based coupling techniques, these compounds need to be extracted from the sample matrix and to be converted to volatile and thermally stable derivatives. Frequently, the derivatives are then concentrated by cryotrapping or extracting into an organic solvent prior to injection onto a GC column [1].

Grignard Reaction

The Grignard reaction is one of the most widely used derivatization techniques for the speciation of a number of elements [7,8]. The main advantage of this reaction is that different alkyl groups can be chosen to make fully alkylated species. Reactions for mercury analysis can be described as follows:



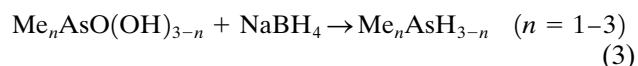
where R = propyl, butyl, and pentyl groups and R' = methyl and ethyl groups. However, Grignard reagents are very sensitive to water. As a consequence, metal and organometallic compounds have to be extracted prior to derivatization into organic solvent with assis-



tance of complexing reagents, such as dithiocarbamates and tropolone. The whole sample preparation can be tedious and time-consuming.

Hydride Generation

Several elements (Hg, Ge, Sn, Pb, Se, As, Te, Sb, Bi, and Cd) can be transformed into volatile hydrides, providing the basis of their analysis [1,3]. Sodium borohydride (NaBH_4) is commonly used as a derivatization reagent. The reaction for methylarsenicals is



The usefulness of this procedure for speciation analysis, however, is restricted by either the thermodynamic inability of hydride formation for some species or considerable kinetic limitation to hydride formation. Nevertheless, the technique is still essential for some classes of compounds [1].

Aqueous Derivatization with Tetraalkyl(aryl)borates

The restricted versatility can, to a certain degree, be overcome by replacing NaBH_4 by alkyl or arylborates [1]. The most common derivatization procedure relies on ethylation with sodium tetraethylborate, which was initiated for determining methyllead ionic compounds [9]:



NaBEt_4 acts as an aqueous-phase ethylation reagent, quantitatively transferring Et^- ions to ionic metals and organometals. Direct aqueous-phase ethylation with NaBEt_4 has been used for the speciation of a variety of metals, such as lead, mercury, and tin in different environmental and biological samples. This reaction has significant advantages because the derivatization reaction is performed in the aqueous phase, subsequently reducing the analysis time and eliminating the need for organic solvent extraction. However, this method cannot be used for the speciation of the natively occurring ethylated species, such as ethyllead and ethylmercury [8].

Several efforts have been carried out to develop a new aqueous derivatization reagent. Phenylation with sodium tetraphenylborate is a promising procedure for the speciation of several metals. Its application for organomercury analysis has been comprehensively studied [10]. Sodium tetrapropylborate is another reagent that has been investigated for determining organolead, tin, and mercury compounds [1]. However, its application is limited because it is not commercially available.

Coupling GC with Atomic Spectrometric Detection

GC-AAS

Gas chromatography coupled with AAS has been the most popular hyphenated technique for the speciation of metals and organometals. Among different atomizer designs employed in coupling GC with AAS, electrothermal atomization, especially the electrothermally heated quartz tube, is preferred because of its high sensitivity, simple operation, and low cost [6]. The quartz tube ($\sim 100 \times 10$ mm inner diameter) is usually constructed in house and wrapped with Nichrome resistance wire and ceramic isolation material. A thermocouple is attached to the surface of the quartz burner for temperature control (Fig. 1). If necessary, hydrogen and air can be supplied from side arms of the burner. The furnace can be heated to more than 1000°C by means of a variable transformer.

Two types of sample introduction-interface coupling GC and quartz furnace have been generally used. Figure 1 shows a schematic representation of the first design, usually called purge and trap. The instrumental setup consists of a reaction vessel where the sample is brought in contact with a reagent, such as NaBH_4 and NaBEt_4 , and a U-tube filled with a GC sorbent. During the reaction, the U-tube is maintained in liquid nitrogen and the produced derivatives are purged with helium, then trapped on the sorbent. Once the reaction is finished, the liquid nitrogen is removed and the U-tube is heated electrically. The trapped compounds are then separated according to their volatility and measured by AAS. The principal advantages of this setup are its very

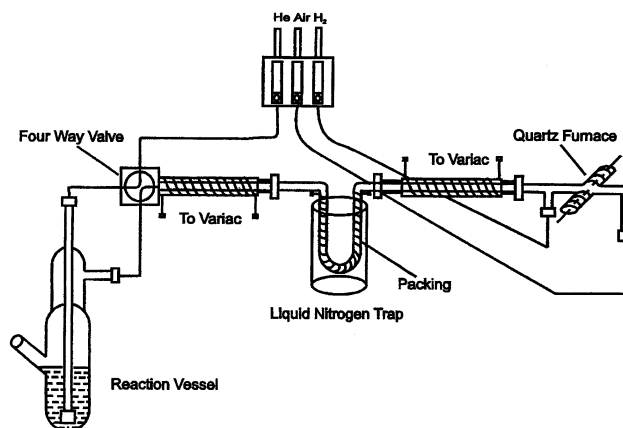


Fig. 1 Schematic diagram of a purge-and-trap GC-AAS system.

high sensitivity and on-line aqueous derivatization. However, it suffers from a water-condensation problem in the U-trap, which limits the length of the purge time. A water trap is often installed upstream from the sorbent tube to avoid its blocking with ice crystals [1].

The second design is actually modified from a regular GC device equipped with either a packed or a capillary column. The outlet of the GC is directly connected to the entrance of the quartz furnace through a piece of stainless-steel tubing, which is electrically heated to avoid condensation of the compounds of interest. To be able to use this technique, the target compounds have to be extracted from the sample matrix, derivatized with the appropriate reagent, and back-extracted into organic solvent before injection. Absolute detection limits obtained with this system are similar to those using purge and trap because they use same detection technique. However, the concentration detection limits can be different as large as several orders of magnitude. With the purge-and-trap system, all target compounds in the sample are on-line preconcentrated and analyzed at once, whereas with regular GC, only a small portion of the sample extract is injected for analysis. However, the regular GC method offers a high versatility because of the possibility of using different Grignard reagents.

GC/MIP-AES

MIP-AES has two basic characteristics that can be utilized when coupling to a GC instrument [6]. The low gas temperature of the MIP allows small amounts of sample, compatible with those of GC solutes, to be introduced without extinguishing the plasma. In addition, sample introduction is easily facilitated because the carrier and plasma gases are the same (helium). These advantages have made the coupled GC/MIP-AES a popular technique and many applications have been reported [5,6,10]. A commercial instrument is currently available.

Helium plasma is maintained within a "cavity" which serves to focus power from a microwave source (usually operated at 2.45 GHz) into a discharge cell (usually a quartz capillary tube). The cavity, which has been most used for GC detection, has been the atmospheric-pressure TM_{010} cylindrical resonance cavity developed by Beenakker [11]. The effluent from a GC is connected directly to the discharge tube via a heated transfer line to prevent analyte condensation. The GC/MIP-AES requires a consistent supply of high-purity gases for optimal performance. Hydrogen and oxygen are often used as plasma reagent gases for metal and metalloid analysis. In addition, the AED spectrometer requires a continuous nitrogen purge.

Advantages of MIP-AES are low cost, simple operation, and high sensitivity. Its sensitivity for mercury analysis is compatible with that using GC coupled with atomic fluorescence detection [10], which is currently recognized as the most sensitive method for determining mercury. The main drawback is the low tolerance for organic solvents. A venting system has to be used to prevent solvent from getting into plasma tube.

GC/ICP-MS

Over the last decade, ICP-MS has proven to be a highly sensitive and selective technique for the determination of trace and ultratrace amounts of metals in various samples. It allows multielement detection in a single run and offers isotopic information of the elements of interest [12–14]. Solvent venting to prevent plasma instability is unnecessary, unlike in GC/MIP-AES, and no carbon accumulates, as it does on the MIP discharge tube. These features make the hyphenation GC/ICP-MS unique.

Coupling GC to ICP-MS is easily accomplished by connecting the column to the inner tube of torch using a transfer line between the GC oven and the plasma torch (Fig. 2). The transfer line usually consists of an electrically heated stainless-steel tube through which a piece of deactivated fused silica is passed. The transfer line capillary ends at the tip of the ICP injector. Generally, the stainless-steel tubing is maintained at a temperature that prevents the condensation of the GC effluent in the transfer line. Fluctuation in the transfer line temperature can affect GC peak shape and resolution.

The ICP-MS instrument requires a carrier gas flow rate of approximately 1 L/min, whereas the capillary GC effluent is less than 5 mL/min. It is, therefore, necessary to introduce argon as a makeup gas. The makeup gas produces a central channel in the plasma

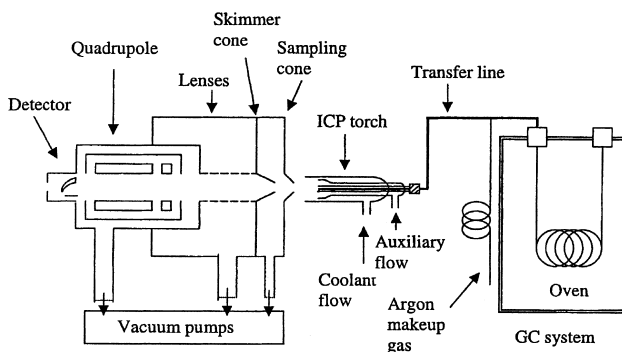


Fig. 2 Schematic diagram of a GC/ICP-MS system.



and helps to carry analytes from the GC column to the plasma. The makeup gas must be heated to avoid condensation of the column effluent and this has been done by passing the argon gas through a heated stainless-steel tubing and added it at the beginning of the transfer line [12]. However, a high flow rate of argon makeup gas results in an undesirable dilution effect.

This hyphenated technique has been successfully applied to the speciation of a number of metals, including lead, mercury, and tin. The advantages of determining multielements simultaneously and the wide dynamic liner range are obvious [13].

References

1. R. Lobinski and F. C. Adams, *Spectrochim. Acta B* 52: 1865 (1997).
2. K. Sutton, R. M. C. Sutton, and J. A. Caruso, *J. Chromatogr. A* 789: 85 (1997).
3. Y. Cai, *Trend Anal. Chem.* (2000).
4. N. P. Vela, L. K. Olson, and J. A. Caruso, *Anal. Chem.* 65: 585A (1993).
5. P. Uden, in *Element-Specific Chromatographic Detection by Atomic Emission Spectroscopy* (P. Uden, ed.), ACS Symposium Series Vol. 479, American Chemical Society, Washington, DC, 1990.
6. L. Ebdon, S. Hill, and R. W. Ward, *Analyst* 111: 1113 (1986).
7. Y. K. Chau, P. T. S. Wong, G. A. Bengert, and J. L. Dunn, *Anal. Chem.* 56: 271 (1984).
8. Y. Cai, R. Jaffe, and R. D. Jones, *Environ. Sci. Technol.* 31: 302 (1997).
9. S. Rapsomanikis, O. F. X. Donard, and J. H. Weber, *Anal. Chem.* 58: 38 (1986).
10. S. Monsalud, M.S. thesis, Florida International University, 1999.
11. C. I. M. Beenakker, *Spectrochim. Acta* 32B: 173 (1977).
12. T. De Smaele, L. Moens, R. Dams, and P. Sandra, *LC-GC* 14: 876 (1996).
13. T. De Smaele, J. Vercauteren, L. Moens, R. Dams, and P. Sandra, *Hewlett-Packard Peak*, N. 2, 10 (1999).
14. F. A. Byrdy and J. A. Caruso, *Environ. Sci. Technol.* 28: 529A (1994).



Metformin and Glibenclamide, Simultaneous Determination by HPLC

B. L. Kolte

B. B. Raut

Dr. Babasaheb Ambedkar Marathwada University, Aurangabad, Maharashtra State, India

A. A. Deo

M. A. Bagool

Wockhardt Research Centre, Aurangabad, Maharashtra State, India

D. B. Shinde

Dr. Babasaheb Ambedkar Marathwada University, Aurangabad, Maharashtra State, India

INTRODUCTION

A high-performance liquid chromatography (HPLC) method was developed for the simultaneous determination of metformin and glibenclamide in a combined dosage form using a Zorbax XDB C₁₈, 15-cm column. The mobile phase was composed of the buffer and acetonitrile in the ratio 68:32, vol/vol; pH was adjusted to 7.5 with orthophosphoric acid. The buffer used in the mobile phase contains 10 mM disodium hydrogen phosphate and 10 mM sodium dodecyl sulphate (SDS) in double-distilled water. The mobile phase flow rate was 1 mL/min, column oven temperature was maintained at 40°C, and analytes were detected at a wavelength of 226 nm. The developed method was validated and shown to be linear. The correlation coefficients for metformin and glibenclamide were 1.0 and 0.9999, respectively. The relative standard deviations for six replicate measurements in two sets of each drug in the tablets were always less than 2%.

OVERVIEW

Metformin HCl is 1,1-dimethyl biguanide hydrochloride and glibenclamide is 5-chloro-*N*-[2-[4-[[[(cyclohexylamino)carboxyl]amino]sulfonyl]phenyl]ethyl]-2-methoxybenzamide. A combination of 500 mg of metformin HCl and 5 mg of glibenclamide is available commercially as tablets.^[1] It has been concluded, from the comparative study, that combined treatment with metformin and sulphonylurea is more effective than these drugs alone for improving glycemic control in type II diabetes, while also allowing a reduction of the dosage of each drug.^[2]

A literature survey revealed that few methods are reported for the individual estimation of metformin and glibenclamide. Both of these drugs are official in the IP^[3] and BP,^[4] glibenclamide is also reported in the United

States Pharmacopeia (USP).^[5] The methods for metformin^[6–11] and glibenclamide^[12–15] are reported for the estimation of these drugs in tablets and plasma. One method is reported for the estimation of metformin and glibenclamide in a combined dosage form.^[16] In the reported method,^[16] glibenclamide was estimated at 300 nm and metformin was estimated at 232 nm. The estimation of the analytes was performed by preparing two different sample preparations.

In the present article, attempts have been made to develop a simple and rapid method for the simultaneous determination of metformin and glibenclamide. Adequate separation was achieved by using a mobile phase containing 10 mM SDS and 10 mM disodium hydrogen phosphate in double-distilled water and acetonitrile in the ratio of 68:32, vol/vol, with pH adjusted to 7.5 with orthophosphoric acid. In the present developed method, the analytes of the combined dosage form were analyzed using the same sample preparation and were detected at a wavelength of 226 nm. In the reported method,^[16] the recovery values for metformin HCl and glibenclamide were 99.37% and 101.57%, respectively. In the present method, the recovery values for metformin HCl and glibenclamide were 99.2% and 100.0%, respectively. The method is validated and shown to be linear, accurate, and precise. The method has been applied for the analysis of the ingredients of the combined dosage forms available in the commercial market.

EXPERIMENTAL TECHNIQUES

Materials and Reagents

Metformin HCl and glibenclamide were obtained from Wockhardt Research Centre (Aurangabad, Maharashtra State, India). SDS and disodium hydrogen phosphate were

obtained from E. Merck (India) Ltd. (Worli, Mumbai, India). Orthophosphoric acid and acetonitrile (HPLC grade) were obtained from Qualigens Fine Chemicals (Dr. Annie Besant Road, Mumbai, India). The 0.45- μ m nylon filter was obtained from Advanced Microdevices Pvt. Ltd. (Ambala Cantt, India) and Whatman filter paper 41 was obtained from Whatman International Ltd. (Maidstone, England, UK). The tablets containing a combination of metformin and glibenclamide were purchased from the Indian market. Double-distilled water was used throughout the experiments. Other chemicals were of analytical or HPLC grade.

Chromatographic Conditions

A Thermoseparation Products Co. HPLC was utilized, consisting of the following components: Constametric 3500 pump, AS 3000 autosampler, and UV 1000 detector. A Zorbax XDB C₁₈ (5 μ m, 4.6 \times 150 mm; Agilent Technologies) column was used. The mobile phase flow rate was 1 mL/min and the column oven temperature was maintained at 40°C; the analytes were detected at a wavelength of 226 nm. The injection volume was 25 μ L. Data acquisition was performed with the software, PC 1000. Peak purity was checked with a photodiode array detector (UV6000 LP; Thermoseparation Products Co.).

Preparation of Solutions

Mobile phase

The mobile phase was composed of a buffer and acetonitrile in the ratio of 68:32, vol/vol. The pH of the mobile phase was adjusted to 7.5 with orthophosphoric acid. The buffer used in the mobile phase consisted of 10 mM disodium hydrogen phosphate and 10 mM SDS in double-distilled water. The mobile phase was premixed and filtered through a 0.45- μ m nylon filter and degassed.

Standard stock solutions

Standard solutions were prepared by dissolving the drugs in the diluents and diluting them to the desired concentration. The buffer and diluents used for the standard preparation and sample preparation were prepared as follows:

Buffer: contained 10 mM disodium hydrogen phosphate in double-distilled water; pH was adjusted to 4.0 with orthophosphoric acid.

Diluent: contained the buffer and acetonitrile in the ratio 60:40, vol/vol.

Metformin HCl

A 125-mg portion of metformin HCl standard was accurately weighed and transferred to a 50-mL volumetric flask; it was dissolved and diluted to 50 mL with the diluent.

Glibenclamide

A 25-mg portion of glibenclamide standard was accurately weighed and transferred to a 50-mL volumetric flask; 30 mL of acetonitrile was then added and sonication was applied for 5 min. After sonication, 10 mL of the buffer was then added and the volume was made up to 50 mL with the diluent. From this solution, 2.5 mL was transferred into a 50-mL volumetric flask and diluted to the mark with the diluent.

Mixed standard preparation

For mixed standard solution, 2 mL of a metformin standard solution and 2 mL of glibenclamide standard solution were transferred to a 50-mL volumetric flask and diluted to the mark with the diluent. This solution contains 100 μ g/mL metformin HCl and 1.0 μ g/mL glibenclamide.

Assay preparation

Ten tablets were weighed and finely powdered. A quantity of powder equivalent to one tablet, containing 500 mg of metformin HCl and 5 mg of glibenclamide, was transferred to a 100-mL volumetric flask; 50 mL of acetonitrile was then added and sonication was applied for 5 min. After sonication, 20 mL of buffer was added and further sonication was applied for 20 min with swirling. The solution was cooled to ambient temperature and diluted to the desired volume with the diluent and mixed well. The solution was filtered through Whatman filter paper 41. The first 5-mL portion of the filtrate was rejected and then 1 mL of the filtered solution was transferred into a 50-mL volumetric flask and diluted with the diluent.

RESULTS AND DISCUSSION

Chromatography

A reverse-phase HPLC procedure was proposed as a suitable method for the simultaneous determination of metformin and glibenclamide in a combined dosage form. The chromatographic conditions were adjusted to provide adequate retention and resolution of metformin and glibenclamide. A mixture of buffer and acetonitrile, in



the ratio of 68:32, vol/vol, with pH adjusted to 7.5 with orthophosphoric acid at a flow rate of 1 mL/min, was found to be an appropriate mobile phase, allowing adequate separation of active substances of the combined

dosage form. Typical chromatograms obtained by using the aforementioned mobile phase, from 25 μ L of the mixed standard preparation and assay preparation, are illustrated in Fig. 1a and b, respectively. The retention

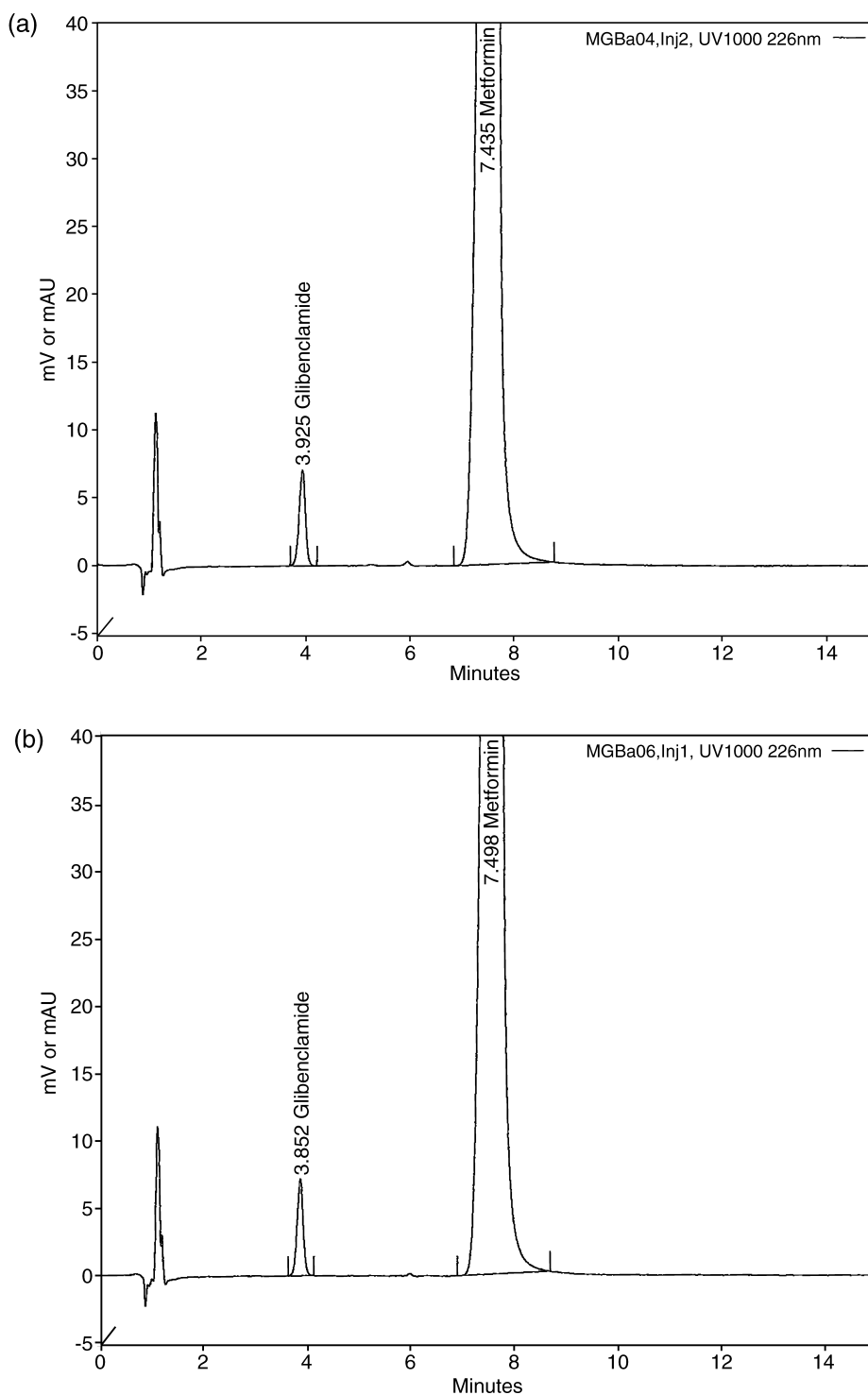


Fig. 1 (a) A typical chromatogram of a mixed standard preparation. (b) A typical chromatogram of an assay preparation.

Table 1 Results of the recovery tests for the drugs

Level of addition (%)	Ingredient	Amount added (mg)	Amount recovered (%) (\pm SD)	Overall recovery (%) ($n=9$)
80	Metformin HCl	400.0	99.8 (\pm 0.08)	99.2 (\pm 0.5)
	Glibenclamide	4.0	100.7 (\pm 0.36)	100.0 (\pm 0.6)
100	Metformin HCl	500.0	99.1 (\pm 0.05)	
	Glibenclamide	5.0	99.6 (\pm 0.08)	
120	Metformin HCl	600.0	98.7 (\pm 0.17)	
	Glibenclamide	6.0	99.8 (\pm 0.34)	

times of glibenclamide and metformin were 3.9 and 7.4 min, respectively.

150.79, and the correlation coefficients for the regression lines were 1.0 and 0.9999, respectively.

Specificity

The specificity of the method was checked with a peak purity test of the assay preparation performed with a photodiode array detector. The peak purity values for metformin and glibenclamide were observed to be 995 and 999, respectively. The results of the peak purity analysis show that the peaks of the analytes were pure and that the formulation excipients did not interfere with the analyte peaks.

Linearity

Linearity of the method was tested from 25% to 150% of the targeted level of the assay concentration (100 μ g/mL metformin HCl and 1.0 μ g/mL glibenclamide) for the two analytes. The mixed standard solutions containing 25–150 μ g/mL metformin HCl and 0.25–1.50 μ g/mL glibenclamide were prepared from the standard stock solutions of metformin and glibenclamide. Linearity test solutions were injected and analyzed in triplicate. The calibration graphs were plotted by using peak areas of the analytes against the concentration of the drug (in micrograms per milliliter). In the simultaneous determination, the calibration graphs were found to be linear for both the analytes in the mentioned concentration ranges. The regression equations for metformin and glibenclamide were found to be $y=74,383x+22,660$ and $y=60,424x-$

Accuracy

The accuracy of the method was studied by recovery experiments. The recovery experiments were performed by adding known amounts of the drugs into a placebo. The recovery was performed at three levels (80%, 100%, and 120%) of the label claim per tablet (500 mg of metformin HCl and 5 mg of glibenclamide). Three samples were prepared for each recovery level. The recovery values for metformin HCl and glibenclamide ranged from 98.5% to 99.9% and from 99.3% to 101.2%, respectively (Table 1). The average recovery of three levels (nine determinations) for metformin HCl and glibenclamide were 99.2% and 100.0%, respectively.

Precision

The precision (repeatability and intermediate precision) of the method was determined from one lot of the combined dosage form.

Repeatability

For repeatability of the method, six determinations of the concentrations of each ingredient in the tablets were performed. The results are shown in Table 2.

Table 2 Assay results of active ingredients in tablets

Set	Ingredient	Label claim (mg)	Found (mg) ($n=6$)	% Label claim (\pm SD)
Repeatability	Metformin HCl	500	498.0	99.6 (\pm 1.6)
	Glibenclamide	5	5.12	102.3 (\pm 1.6)
Intermediate	Metformin HCl	500	496.0	99.2 (\pm 1.3)
Precision	Glibenclamide	5	5.07	101.3 (\pm 1.5)



Table 3 System suitability

Analyte	RSD (%)	Tailing factor	Theoretical plates	Resolution
Metformin	0.61	1.04	9193	13.6
Glibenclamide	0.62	1.03	6395	

Intermediate Precision

Intermediate precision of the method was assessed by analyzing the samples six times on different days, by different chemists, by using different analytical columns of the same manufacture and different HPLC systems. The percentage assay was calculated using the area of the mixed standard preparation. The assay results are shown in Table 2.

Determination of the Limit of Detection and Limit of Quantitation

To determine the limit of detection (LOD) and the limit of quantitation (LOQ), the method based on the residual standard deviation of a regression line and slope was adopted. To determine the LOD and LOQ, a specific calibration curve was studied by using samples containing the analytes in the range of the detection limit and the quantitation limit. The limits of detection for metformin and glibenclamide were 0.013 and 0.007 $\mu\text{g/mL}$, respectively, and the limits of quantitation were 0.040 and 0.021 $\mu\text{g/mL}$, respectively.

Stability of Analytical Solutions

The stability of the analytical solutions was determined in terms of the assay of the drugs in the standard preparation and the assay preparation at room temperature. These solutions were analyzed at 0, 24, 48, and 72 hr against a freshly prepared standard at each time interval. The relative standard deviations for the assay values, determined up to 72 hr for metformin and glibenclamide in assay preparation and standard preparation, were 0.75% and 0.62%, respectively. The assay values were within $\pm 2\%$ after 72 hr. The results indicate that the solutions were stable for 72 hr at room temperature.

System Suitability

For system suitability studies, five replicate injections of mixed standard solutions were injected and parameters such as relative standard deviation of peak area, column efficiency, resolution, and tailing factors of the peaks were calculated. Results are shown in Table 3.

CONCLUSION

The described isocratic HPLC method is validated and shown to be precise and accurate. This method can be used in quality control departments for the simultaneous determination of metformin and glibenclamide in the combined dosage form.

ACKNOWLEDGMENTS

The authors are grateful to the Wockhardt Research Centre and to the Head of the Department of Chemical Technology, Dr. Babasaheb Ambedkar Marathwada University, Aurangabad, Maharashtra State, India, for providing the facilities for this research work.

REFERENCES

1. *Indian Drugs Review (IDR)*; Sanjiv, M., Ed.; Mediworld Publications Pvt. Ltd.: New Delhi, 2003; Vol. 9 (4), 514.
2. Tosi, F.; Muggeo, M.; Brun, E.; Spiazzi, G.; Perobelli, L.; Zanolin, E.; Gori, M.; Coppini, A.; Moghetti, P. Combination treatment with metformin and glibenclamide versus single-drug therapies in type 2-diabetes mellitus: A randomized, double blind, comparative study. *Metabolism* **2003**, 52 (7), 862–867.
3. *Indian Pharmacopoeia*; The Controller of Publications: New Delhi, 1996.
4. *British Pharmacopoeia*; The Stationery Office: London, 1998.
5. *The United States Pharmacopeia*; U.S. Pharmacopeial Convention: Rockville, MD, 2002.
6. Vasudevan, M.; Ravi, J.; Ravisankar, S.; Suresh, B. Ion-pair liquid chromatography technique for the estimation of metformin in its multicomponent dosage forms. *J. Pharm. Biomed. Anal.* **2001**, 25, 77–84.
7. Zarghi, A.; Foroutan, S.M.; Shafaati, A.; Khoddam, A. Rapid determination of metformin in human plasma using ion-pair HPLC. *J. Pharm. Biomed. Anal.* **2003**, 31 (1), 197–200.
8. Zhang, M.; Moore, G.A.; Lever, M.; Gardiner, S.J.; Kirkpatrick, C.M.; Begg, E.J. Rapid and simple high performance liquid chromatographic assay for the determination of metformin in human plasma and breast milk. *J. Chromatogr., B, Anal. Technol. Biomed. Life Sci.* **2002**, 766 (1), 175–179.

9. Cheng, C.L.; Chou, C.H. Determination of metformin in human plasma by high performance liquid chromatography with spectrophotometric detection. *J. Chromatogr., B, Biomed. Sci. Appl.* **2001**, *762* (1), 51–58.
10. Bonfigli, A.R.; Manfrini, S.; Gregorio, F.; Testa, R.; De Sio, G.; Coppa, G. Determination of plasma metformin by a new cation exchange HPLC technique. *Ther. Drug Monit.* **1999**, *21* (3), 330–334.
11. Veterqvist, O.; Nabbie, F.; Swanson, B. Determination of metformin in plasma by high performance liquid chromatography after ultrafiltration. *J. Chromatogr., B, Biomed. Sci. Appl.* **1998**, *716* (1–2), 299–304.
12. Han, F.M.; Cheng, Z.Y.; Chen, Y. Separation and determination of glibenclamide in xiaotangling tablets by micellar electrokinetic capillary chromatography. *Se Puede* **2000**, *18* (5), 456–458.
13. Niopas, I.; Daftsios, A.C. A validated high-performance liquid chromatographic method for the determination of glibenclamide in human plasma and its application to pharmacokinetic studies. *J. Pharm. Biomed. Anal.* **2002**, *28* (3–4), 653–657.
14. Khatri, J.; Qassim, S.; Abed, O.; Abraham, B.; Al-Lami, A.; Masood, S. A novel extractionless HPLC fluorescence method for the determination of glyburide in the human plasma: Application to a bioequivalence study. *J. Pharm. Pharm. Sci.* **2001**, *4* (2), 201–206.
15. Valdes Santurio, J.R.; Gonzalez Porto, E. Determination of glibenclamide in human plasma by solid-phase extraction and high-performance liquid chromatography. *J. Chromatogr., B, Biomed. Appl.* **1996**, *682* (2), 364–370.
16. Khanolkar, D.H.; Shinde, V.M. RP-HPLC method for the estimation of glibenclamide and metformin HCl from combined dosage form. *Indian Drugs* **1999**, *36* (12), 739–742.



Microcystin, Isolation by Supercritical Fluid Extraction

Bing Yu
Huwei Liu

Peking University, Beijing, P.R. China

INTRODUCTION

Microcystins are an increasingly important group of bioactive compounds, produced mainly by planktonic cyanobacteria. They are a family of cyclic heptapeptides that cause both acute and chronic toxicity. Purified microcystins are utilized in a range of research applications. This review summarizes the isolation of microcystins from the cyanobacteria by supercritical fluid extraction (SFE). The microcystins can be successfully extracted when a modifier is used in supercritical carbon dioxide fluid. The advantage of the method is that the sample handling steps are minimized, thus reducing possible losses of microcystin and saving extraction and purification time.

MICROCYSTINS

Microcystins are a family of more than 50 structurally similar hepatotoxins produced by species of freshwater cyanobacteria (blue-green algae), primarily *Microcystis aeruginosa*.^[1] Microcystins are potent toxins that inhibit the regulatory enzymes protein phosphatase 1 and 2A (PP1 and PP2A).^[2–4] It is reported that liver is the target organ that shows the greatest degree of histopathological change when animals are poisoned by these cyclic peptides. Therefore their presence in water bodies has caused the death of wild and domestic animals worldwide,^[5] and, more recently, they have been implicated in human fatalities.^[6,7]

Microcystins are cyclic heptapeptides that share a general structure, as shown in Fig. 1 and Table 1, containing g-linked D-glutamic acid (D-Glu), D-alanine (D-Ala), β -linked D-erythro- β -methylaspartic acid (D-MeAsp), N-methyldehydroalanine (Mdha), and a unique C20 β -amino acid, (2S,3S,8S,9S)-3-amino-9-methoxy-2,6,8-trimethyl-10-phenyldeca-4(E), 6(E)-dienoic acid (Adda). The other two L-amino acids are variable (denoted X and Z) and are found in positions 2 and 4 of the cyclic structure. The single-letter abbreviation of the variable amino acids is used to distinguish different microcystins; for example, the most commonly occurring microcystin

contains leucine and arginine in these positions and is therefore called microcystin LR.^[8] Variation in these two amino acids accounts for many of the microcystin variants that have been characterized; however, other minor modifications, such as demethylation, increase the number of microcystin variants to at least 60.^[5] The need for extensive research into their detection, toxicology, and the investigation of water-treatment strategies requires the availability of purified microcystins. Therefore the isolation of microcystins is very important and urgent.

ISOLATION AND PURIFICATION MODES

Microcystins were first purified by Botes et al.^[9] in 1982, and, since then, many different approaches^[10–14] have been adopted for the isolation of microcystins from cyanobacterial cells. The most widely used procedures^[13,15–17] are as follows: The lyophilized cyanobacterial cells which contain microcystins are extracted with organic solvents several times, and then the extracts are applied to multistep column chromatography and thin-layer chromatography.^[15] For example, Harada et al.^[13] established an effective analysis method for microcystins RR and LR. They used 5% aqueous acetic acid solution as an extracting solvent and isolated microcystins by using preparative or semipreparative liquid chromatography with ODS, silica gel, or gel permeation columns.

In this review, we provide an in-depth survey of a rapid method for isolation of microcystin LR from cyanobacterial cells. The unique feature of the method is that it uses a one-step SFE and a one-step chromatography, instead of multiple extractions with organic solvents and multistep column chromatography.

PRINCIPLE AND INSTRUMENTATION FOR SFE

SFE is a well-recognized alternative to conventional solvent-based extraction techniques, which has the main advantages of being environmentally benign and available as fully automated instruments. Because SFE can

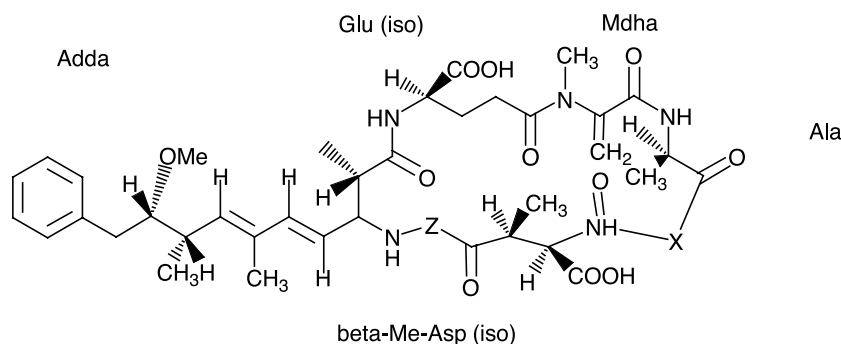


Fig. 1 General structure of microcystin where X and Z represent variable amino acids as presented in Table 1.

Table 1 Microcystins characterized to date indicating the molecular mass of each variant

Z compound	Variable amino acid X										
	Ala (A)	Arg (R)	Glu (E)	E (OMe)	Homo IsoL	Leu (L)	Methionine -S-oxide	Phe (F)	Try (W)	Tyr (Y)	Val (V)
Alanine						909				959	
Aminoisobutyric acid						923					
Arginine	952	1037			1008	994	1028	1028	1067	1044, 1048 ^t , 1058 ^{hY} , 1030 ^{hY}	
D-Asp ³ , Dha ⁷		1099				966				1030 ^{hY}	
D-Asp ³		1023				980		1014, 1028 ^{hF}		1030, 1044 ^{hY}	
Dha ⁷		1023				980				1030, 1044 ^{hY}	
L-Ser ⁷		1041				998				1062 ^{hY}	
DMAdda ⁵						980					
D-Asp ³ , D-Glu(OCH ₃) ⁶						994					
(6Z)-Adda ⁵		1037				994					
D-Asp ³ , ADMAdda ⁵						1008, 1022 ^{hR}					
D-Glu(OCH) ⁶						1008					
D-Asp ³ , ADMAdda ⁵ , Dhb ⁷		1052				1009				1073 ^{hY}	
L-MeSer ⁷						1012					
D-Asp ³ , L-MeSer ⁷		1041									
ADMAdda ⁵						1022, 1036 ^{hR}					
D-Ser ¹ , ADMAdda ⁵						1038					
D-Glu-OC ₂ H ₃ (CH ₃)OH ⁶						1052					
ADMAdda ⁵ , MeSer ⁷						1040					
N-Methylanthionine						1115					
E (OMe)											
D-Asp ³ , Dha ⁷			969	983							
Dha ⁷			983	997							
L-Ser ⁷			1001	1015							
D-Asp ³ , Ser ⁷				1001							
Leucine						951					
Methionine-S-oxide									1035		
Phenylalanine						985					971
Tryptophan						1024					
Tyrosine						1001					

Abbreviations and superscripts: ^hHomo variant of the amino acid indicated by single letter; ^tTetrahydrotyrosine; ADMAdda, 6 *O*-Acetyl-*O*-demethylAdda; DMAdda, *O*-demethylAdda; (6Z)-Adda, stereoisomer of Adda at the Δ⁶ double bond; Dha, dehydroalanine; Dhb, dehydrobutyrine; MeSer, *N*-methylserine; E(OMe), glutamic acid methyl ester.



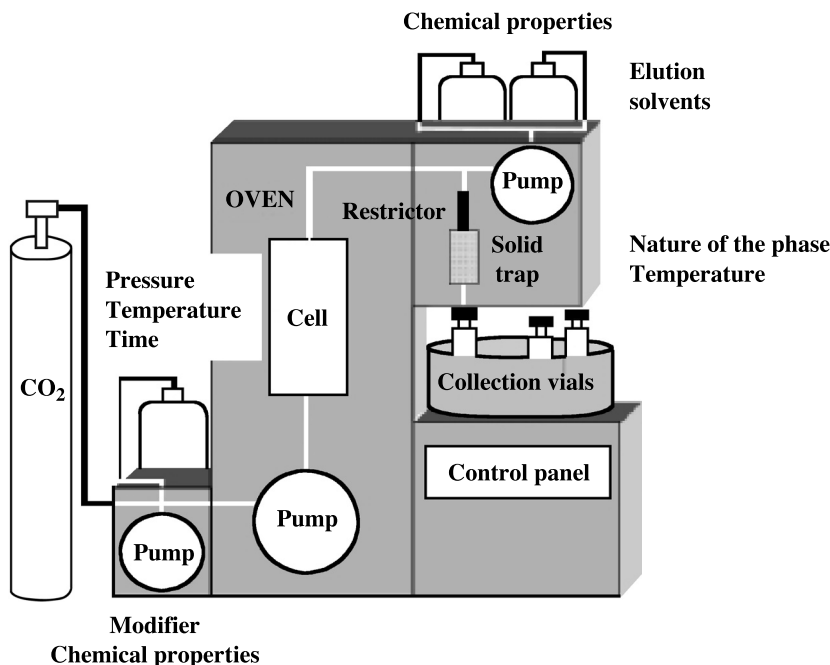


Fig. 2 Principle of an SFE system and influencing parameters. (From Ref. [24].)

minimize organic solvent consumption and increase sample throughput,^[18] extraction with supercritical fluids has received wide attention in recent years.

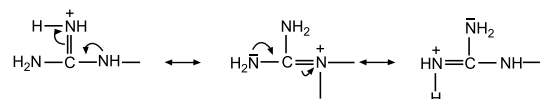
From the chromatographic point of view, the physico-chemical properties of a supercritical fluid are intermediate between those of the gases and liquids, and they are dependent upon the fluid composition, pressure, and temperature. Obviously, SFE possesses the following properties: low viscosity of gases, higher diffusion coefficients, higher compressibility, and solubilization power of liquids. Therefore SFE possesses a number of advantages including more rapid extraction rates, more efficient extractions, higher selectivity, and easy coupling on-line to other analytical technologies. In particular, the solvating strength of a supercritical fluid is related to its density, which may be adjusted by varying both the pressure and the temperature.^[19] Consequently, the pressure and the temperature of the supercritical fluid are the two most important parameters to be optimized for most SFE experiments.

A typical SFE system comprises three integrated parts (Fig. 2): fluid delivery system, extraction cell of the analytes from the sample matrix, and subsequent collection (trapping) of the analytes.^[18,20]

MICROCYSTINS ISOLATED BY SFE

From Fig. 1, both microcystins RR and LR contain a strongly basic functional group (NHCNH-NH₂), i.e., a

guanidine moiety. (Microcystin LR contains one guanidine moiety and microcystin RR contains two guanidine moieties.) These microcystins would be present mainly in the following cationic form:^[20]



The poor extraction result obtained with neat CO₂ is probably caused by the fact that microcystins consist of fairly polar functional groups. The use of cosolvents can have a profound effect on increasing the solubility levels of polar solutes in supercritical fluids. In addition, water plays an important role in the SFE of microcystins. Dongjin Pyo^[21] used aqueous acetic acid modified CO₂ for the extraction of microcystins from cyanobacteria. One of the difficulties with using aqueous acetic acid as a cosolvent was the high fluctuation of the pressure gauge which results from the clogging of the extraction line. Subsequently, Dongjin Pyo used aqueous methanol as a cosolvent, which could avoid the clogging and maintain the pressure of the extracting fluid fairly constant during SFE. Therefore the most suitable medium for the SFE of microcystins is a ternary mixed fluid (90% CO₂, 9.0% methanol, and 1.0% water). When 90% aqueous methanol was used as a cosolvent at 40°C and 250 atm. and the flow rate of the cosolvent and supercritical CO₂ fluid were 0.2 and 2.0 mL/min, respectively, 95% of microcystin RR and 94% of microcystin LR were extracted.^[21-23]

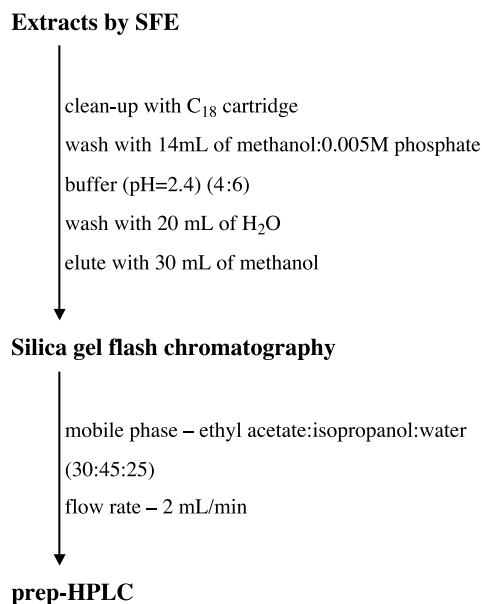


Fig. 3 Purification procedure for microcystin LR. (From Ref. [23].)

PURIFICATION PROCEDURE FOR MICROCYSTIN BY HPLC SYSTEM

The extracts collected from SFE were treated according to the isolation procedures shown in Fig. 3.

Purification of Microcystin LR

Dongjin Pyo also reported some other procedures: The extraction by SFE was performed with a Beckman 116 pump (System Gold programmable solvent module 126), a 15 cm × 10 mm I.D. ODS column and Agilent HPLC 1100 series diode-array detector. Methanol/0.05 M phosphate buffer (52:48), pH 3, was used as a mobile phase at a flow rate of 2 mL/min. The analytical results obtained from real lake samples indicate the viability of the method for the determination of microcystins in real samples.^[20]

CONCLUSION

SFE is very suitable for extracting thermolabile compounds, as it allows the possibility to perform fast extractions at moderate temperatures (around 40°C).^[24] Therefore numerous applications of the technique have been reported. A large field has been covered: environmental matrices, plants, foods and fats, and polymers. As legislation will tend to restrict, or even ban, the use of many common solvents, recent extraction techniques will,

in the future, undoubtedly supercede the traditional methods, as SFE considerably reduces the solvent volumes required, along with a reduction in the time devoted to the extraction step. SFE appears, undoubtedly, to be the most potentially selective extraction technique.

The isolation of microcystins by SFE is effective and successful. However, the main drawbacks of SFE are the difficulties in a tedious optimization of SFE methods, as several parameters need to be considered with this technique. In addition, because of the high investment cost of the technique, economic considerations will, in practice, also influence the choice of the extraction technique. Yet future trends will depend on the availability of commercial apparatus.

REFERENCES

1. Dawson, R.M. The toxicology of microcystins. *Toxicon* **1998**, 36 (7), 953–962.
2. Carmichael, W.W. *Toxins of Freshwater Algae: Handbook of Natural Toxins*; Marcel Dekker: New York, 1988; Vol. 3, 121–127.
3. Namikoshi, M.; Rinehart, K.L.; Sakai, R.; Sivonen, K.; Carmichael, W.W. Structures of three new cyclic hepatotoxins produced by the cyanobacterium (blue-green algae) *Nostoc* sp. strain 152. *J. Org. Chem.* **1990**, 55, 6135–6141.
4. Sivonen, K.; Carmichael, W.W.; Namikoshi, M.; Rinehart, M.L.; Dahlem, A.M.; Niemela, S.I. Isolation and characterization of hepatotoxic microcystin homologues from the filamentous freshwater cyanobacterium *Nostoc* sp. strain 152. *Appl. Environ. Microbiol.* **1991**, 56, 2650–2657.
5. Sivonen, K.; Jones, G. *Toxic Cyanobacteria in Water*; Chorus, I., Bartram, J., Eds.; E&FN Spon: London, 1999; 41.
6. Bell, S.G.; Codd, G.A. Cyanobacterial toxins and human health. *Rev. Med. Microbiol.* **1994**, 5, 256–264.
7. An, J.; Carmichael, W.W. Use of a colorimetric protein phosphatase inhibition assay and enzyme linked immunosorbent assay for the study of microcystins and nodularins. *Toxicon* **1994**, 32, 1495–1507.
8. Lawton, L.A.; Edwards, C. Purification of microcystins. *J. Chromatogr., A* **2001**, 912, 191–209.
9. Botes, D.P.; Kruger, H.; Viljoen, C.C. Isolation and characterization of four toxins from the blue green alga *Microcystis aeruginosa*. *Toxicon* **1982**, 20, 945–954.
10. Brooks, W.P.; Codd, G.A. Extraction and purification of toxic peptides from natural blooms and laboratory isolate of the cyanobacterium *Microcystis aeruginosa*. *Lett. Appl. Microbiol.* **1986**, 2, 1–7.
11. Krishnamarty, T.; Carmichael, W.W.; Sarver, E.W. Investigations of freshwater cyanobacteria (blue-green algae) toxic peptides: I. Isolation, purification and characterization of peptides from *Microcystis aeruginosa* and *Anabaena flos-aquae*. *Toxicon* **1986**, 24, 865–872.
12. Berg, K.; Carmichael, W.W.; Skulberg, O.M.; Benestad,

- C.; Underdal, B. Investigation of a toxic water-bloom of *Microcystis aeruginosa* (Cyanophyceae) in Lake Akersvatn, Norway. *Hydrobiologia* **1987**, *144*, 97–103.
13. Harada, K.I.; Matsuura, K.; Suzuki, M.; Oka, H.; Watanabe, M.F.; Oishi, S.; Dahlem, A.M.; Beasley, V.R.; Carmichael, W.W. Analysis and purification of toxic peptides from cyanobacteria by reversed-phased high-performance liquid chromatography. *J. Chromatogr.* **1988**, *448*, 275–281.
14. Poon, G.K.; Priestley, I.M.; Hunt, S.M.; Fawell, J.K.; Cood, G.A. Purification procedure for peptide toxins from the cyanobacterium *Microcystis aeruginosa* involving high-performance thin-layer chromatography. *J. Chromatogr.* **1987**, *387*, 551–558.
15. Pravda, M.; Kreuzer, M.P.; Guilbault, G.G. Analysis of important freshwater and marine toxins. *Anal. Lett.* **2002**, *35*, 1–15.
16. Namikoshi, M.; Sivonen, K.; Evans, W.R.; Carmichael, W.W.; Sun, F.; Rouhiainen, L.; Luukkainen, R.; Rinehart, K.L. Two new L-serine variants of microcystins-LR and -RD from *Anabaena* sp. strains. *Toxicon* **1992**, *30*, 1457–1462.
17. Meriluoto, J. Chromatography of microcystin. *Anal. Chim. Acta* **1997**, *352*, 277–298.
18. Turner, C.; Eskilsson, C.S.; Bjorklund, E. Collection in analytical-scale supercritical fluid extraction. *J. Chromatogr., A* **2002**, *947*, 1–22.
19. McHugh, M.A.; Krukonis, V.J. *Supercritical Fluid Extraction: Principles and Practice*; Butterworth: Boston, MA, 1986.
20. Dongjin, P.; Shin, H. Supercritical fluid extraction of microcystins from cyanobacteria. *Anal. Chem.* **1999**, *71*, 4772–4775.
21. Pyo, D.; Park, K.; Shin, H.; Moon, M. Extraction of microcystin from the cyanobacteria by acetic-acid modified supercritical CO₂. *Chromatographia* **1999**, *49* (9/10), 539–542.
22. Dongjin, P.; Yonsook, K. Rapid and efficient method for extraction and isolation of microcystin RR from the cyanobacterium. *J. Liq. Chromatogr. Relat. Technol.* **2001**, *24* (17), 2685–2696.
23. Dongjin, P.; Soyoung, L. Rapid purification of microcystin-LR using supercritical fluid extraction and flash chromatography. *Anal. Lett.* **2002**, *35* (9), 1591–1602.
24. Camel, V. Recent extraction techniques for solid matrices—Supercritical fluid extraction, pressurized fluid extraction and microwave-assisted extraction: Their potential and pitfalls. *Analyst* **2001**, *126*, 1182–1193.



Migration Behavior: Reproducibility in Capillary Electrophoresis

Jetse C. Reijenga

Eindhoven University of Technology, Eindhoven, The Netherlands

Introduction

Identification of sample components based solely on migration time in capillary electrophoresis (CE) requires reproducibilities not normally obtained. These are caused, mainly, by two effects: temperature effects and electro-osmotic effects. Migration times in CE are determined by the electro-osmotic velocity v_{EOF} and effective electrophoretic migration velocity v_{EFF} ; the net migration velocity v_i is the vector sum of both velocities:

$$v_i = v_{\text{EFF}} + v_{\text{EOF}}$$

In terms of mobilities, this relationship becomes

$$v_i = \left(-\frac{\zeta \varepsilon}{\eta} + \mu_i \right) \cdot E$$

in which ζ is the zeta-potential of the capillary, ε is the dielectric constant of the liquid, η is the viscosity of the liquid, μ_{eff} is the effective mobility of the sample component, and E is the electric field strength. From this relationship, it is obvious that migration time reproducibility depends on the reproducibility of a number of parameters. In addition to the ones mentioned, sample matrix effects can also play a significant role.

Electrophoretic Effects

The reproducibility of the effective mobility is governed by temperature and pH effects. An acceptable run-to-run pH reproducibility can usually be assured, at least in equipment where the effects of possible electrode reactions can be avoided. Again, temperature plays a leading role: The effective mobility has a temperature coefficient of 2–3% per degree. Most buffer solutions, incidentally, have a temperature-dependent pH value, so that changing the temperature in the capillary will, for weak ions, even lead to changing degrees of dissociation and, hence, effective mobility. These effects are, by definition, different for different buffers and different sample components.

Sample Matrix and Injection Effects

When injecting very dilute sample solutions, a relatively large proportion of the total voltage drop across the capillary will take place over this sample plug, resulting in a proportionally lower field strength in the remainder of the separation capillary. This will lead to systematically longer migration times. In this case, also, identification on the basis of effective mobilities is better than on migration times alone.

Another effect takes place when injecting different sample volumes in the capillary: This may systematically change the migration length and, thus, migration times. A constant injection volume is, therefore, advised in cases of required high migration time reproducibility.

Electro-osmotic Effects

In coated capillaries, the $\zeta \varepsilon E / \eta$ term is small, possibly close to zero, compared to the $\mu_{\text{EFF}} \cdot E$ term. If, however, one works with unsuppressed electro-osmosis, the reproducibility of the $\zeta \varepsilon E / \eta$ term plays an important role. Both ζ and η depend on temperature, and in some equipment, thermostating is not perfect, at least not in all parts of the capillary. The viscosity alone accounts for an $\sim 2\%$ per degree dependence. Another effect that might take place is the gradual change in ζ -potential due to adsorption of sample matrix components on the inner capillary surface. The good news is that run-to-run change in electro-osmotic velocity is directly obvious from the EOF marker peak in the detection signal, so that changes in EOF can be accounted for in cases where they cannot be avoided. However, this also means that measures have to be taken to assure a clear EOF marker peak [e.g., by addition to the sample of a neutral ultraviolet (UV)-absorbing component, such as mesityloxide]. In complicated samples, such an EOF marker peak may not be possible. For reasons of EOF reproducibility, identification is preferentially



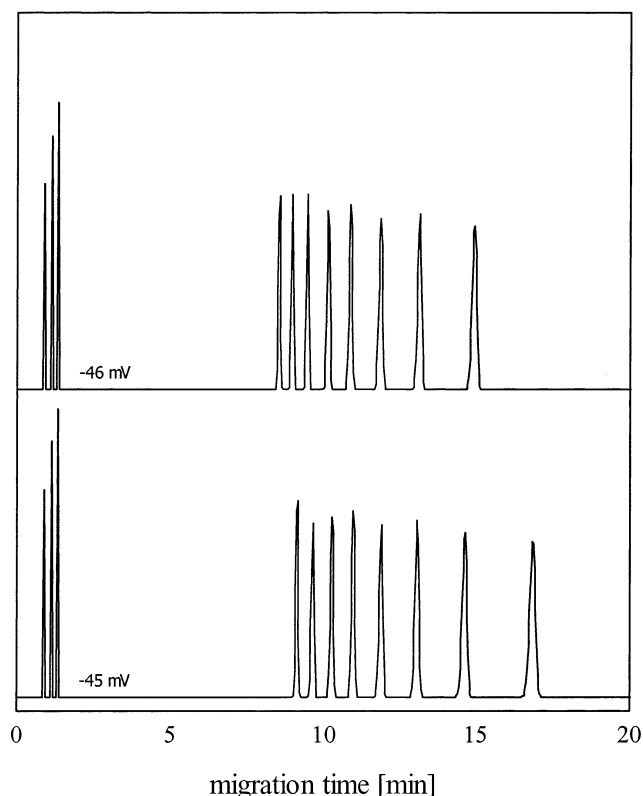


Fig. 1 Effect of capillary ζ -potential on the analysis of a mixture of anions in an uncoated fused-silica capillary in a 10 mM Tris/acetate buffer of pH 8. Normal ζ -potentials are around 50 mV at this pH.

based not on migration time but on effective mobility calculation by means of

$$\mu_{\text{EFF}} = \frac{L_d}{t_i E} - \mu_{\text{EOF}}$$

in which L_d is the capillary length to the detector and t_i is the migration time of the component i .

For quantitation under conditions of changing migration velocity, peak areas are usually divided by corresponding migration times to make them more independent of run-to-run differences in EOF. Migration times are especially susceptible to small EOF variations in the case of opposite signs for EOF and sample mobility (i.e., usually for anions). This is illustrated in Fig. 1, a separation of three cations before and eight anions after the EOF marker (not indicated in the figure). The traces given are for a ζ -potential of -46 and -45 mV, respectively. This 2% EOF change corresponds to the equivalent of only 1 degree temperature effect.

References

1. J. W. Jorgenson and K. D. Lucaks, *Science* 222: 266 (1983).
2. S. F. Y. Li, *Capillary Electrophoresis — Principles, Practice and Applications*, Elsevier, Amsterdam, 1992.
3. E. Kenndler, *J. Capillary Electrophor.* 3(4): 191–198 (1996).

Minimum Detectable Concentration (Sensitivity)

Raymond P.W. Scott

Scientific Detectors Ltd., Banbury, Oxfordshire, England

Introduction

Detector sensitivity or the minimum detectable concentration (MDC) is defined as the minimum concentration of solute passing through the detector that can be unambiguously distinguished from the noise. The size of the signal that will be distinct from the noise (the signal-to-noise ratio) will be an arbitrary choice. In electronic measuring systems, it is generally accepted that a signal can be differentiated from the noise when the signal-to-noise ratio is 2. This criterion has been generally adopted for physical-chemical measurements and is used to define detector sensitivity in chromatography.

Discussion

For a concentration-sensitive detector, the detector sensitivity (X_D) or MDC is given by

$$X_D = \frac{2N_D}{R_c} \left(\frac{\text{g}}{\text{mL}} \right)$$

where R_c is the response of the detector (i.e., the voltage output for unit change in concentration (V/g/mL) and N_D is the detector noise level (V).

The sensitivity or MDC of a detector is *not* the same as the minimum mass that can be detected. This would be the *system mass sensitivity*, which will depend on the characteristics of the column and the chromatographic properties of the solute, as well as the detector specifications. In all chromatographic systems, the peak becomes broader as the retention increases. Con-

sequently, a given mass may be detected if eluted as a narrow peak early in the chromatogram, but if eluted later, its peak height may be reduced to such an extent that it is impossible to discern it from the noise. Thus, detector sensitivity quoted as the “minimum mass detectable” must be carefully examined and related to the chromatographic system and, particularly, the column with which it is to be used. If the data to do this are not available, then the sensitivity must be calculated from the detector response and the noise level in the manner described earlier.

Some manufacturers have taken the minimum detectable concentration and multiplied it by the sensor volume and defined the product as the minimum detectable mass. This gives values that are very misleading. For example, a detector having a true sensitivity of 10^{-6} g/mL and a sensor volume of $10 \mu\text{L}$ would be attributed to a mass sensitivity of 10^{-8} g. This is grossly incorrect, as it is the *peak volume* that controls the mass sensitivity, not the *sensor volume*. Conversely, if the peak volume does approach that of the sensor, then a very serious peak distortion occurs with loss of resolution; thus, this way of specifying sensitivity remains meaningless.

Suggested Further Reading

Scott, R. P. W., *Chromatographic Detectors*, Marcel Dekker, Inc., New York, 1996.

Scott, R. P. W., *Introduction to Gas Chromatography*, Marcel Dekker, Inc., New York, 1998.



Mixed Stationary Phases in GC

Raymond P.W. Scott

Scientific Detectors Ltd., Banbury, Oxfordshire, England

Introduction

The desired interactive character of a GC stationary phase is usually obtained by choosing a thermally stable substance that contains the appropriate polar and dispersive groups that can provide the necessary molecular interactions for sample resolution.

Background Information

Purnell and co-workers [1] pioneered an alternative approach to stationary-phase polarity control for GC. These workers demonstrated that for a wide range of stationary phases made up of binary mixtures, the corrected retention volume of a solute was linearly related to the volume fraction of either one of the two phases. At the time of discovery, this was quite an unexpected relationship, as it was generally accepted that the expression for the retention volume would take the form of the exponent of the stationary-phase composition. The results of Purnell and his co-workers can be summarized by

$$V'_{r(A)} = K_A \alpha V_S + K_B (1 - \alpha) V_S$$

where $V'_{r(AB)}$ is the retention volume of the solute on a mixture of stationary phases A and B, K_A is the distribution coefficient of the solute with respect to the pure stationary phase A, K_B is the distribution coefficient of the solute with respect to the pure stationary phase B, V_S is the total volume of the stationary phase in the column, and α is the volume fraction of phase A in the stationary-phase mixture; that is,

$$V'_{r(AB)} = \alpha V'_A + (1 - \alpha) V'_B \quad (1)$$

where V'_A is the retention volume of the solute on the same volume of pure phase A and V'_B is the retention volume of the solute on the same volume of pure phase B.

Rearranging Eq. (1),

$$V'_{AB} = \alpha(V'_A - V'_B) + V'_B \quad (2)$$

This remarkably simple relationship is depicted in Fig. 1.

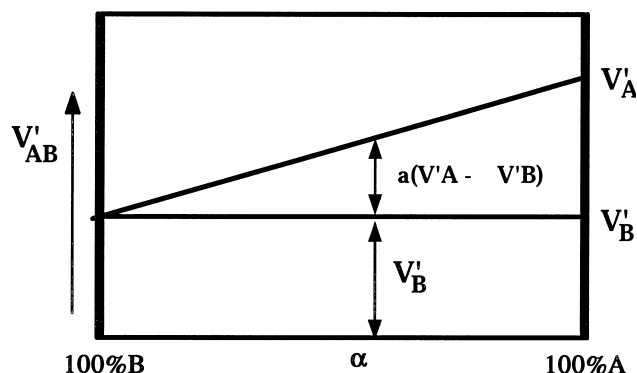


Fig. 1 Graph of corrected retention volume versus volume fraction of the stationary phase.

Purnell carried out three experiments to examine the effect of the composition of binary mixtures of stationary phases on solute retention. In the first experiment, the two fractions were mixed, coated on some support, and packed into the column. In the second experiment, each of the two fractions was coated on separate aliquots of support and the coated supports mixed and packed in a column. In the third experiment, each fraction was coated on a support and each support packed into separate columns and the columns joined in series. Purnell demonstrated that all three columns gave exactly the same corrected retention volume for a given solute.

It was found, however, that where strong association occurred between the two phases, there were exceptions to this relationship. If a strong association took place, the blend would no longer be a simple binary mixture but would contain the associate of the two phases as a third component. It is clear that for a ternary mixture, the simple linear relationship obtained for a binary mixture would not hold. The simple linear relationship for the binary mixture is not surprising. The distribution coefficient of the solute with either pure component is a constant. It follows that the volume fraction of each phase will determine the probability that a solute molecule will interact with a molecule of that phase. This is analogous to the partial pres-



sure of solute determining the probability that a solute molecule will collide with a gas molecule.

Doubling the volume fraction of one phase doubles the probability of solute interaction and, consequently, doubles its contribution to retention. There is another interesting outcome from the results of Purnell and his co-workers. Where a linear relationship existed between the retention volume and the volume fraction of the stationary phase, the linear functions of the distribution coefficients could be summed directly, but their logarithms could *not*. In many classical thermodynamic descriptions of the effect of the stationary-phase composition on solute retention, the stationary-phase composition is often taken into account by including an extra term in the expression for the standard free energy of distribution. The results of Purnell indicate that this is not acceptable, as the solute retention or distribution coefficient is *linearly* not exponentially related to the stationary-phase composition. The stationary phases of intermediate polarities can easily be constructed from

binary mixtures of a strongly dispersive stationary phase and one that is strongly polar. This procedure is not commonly used for commercial columns, although it is a simple and economic method for constructing columns having intermediate polarities. Mixed phases are always worth considering as a flexible alternative to the use of a specific proprietary material.

References

1. M. McCann, J. H. Purnell, and C. A. Wellington, Proceedings of the Faraday Symposium, Chemical Society, 1980, p. 83.

Suggested Further Reading

Scott, R. P. W., *Techniques of Chromatography*, Marcel Dekker, Inc., New York, 1995.
Scott, R. P. W., *Introduction to Gas Chromatography*, Marcel Dekker, Inc., New York, 1998.



Mobile Phase Modifiers for SFC: Influence on Retention

Yu Yang

East Carolina University, Greenville, North Carolina, U.S.A.

Introduction

Carbon dioxide has been the most common mobile phase in supercritical fluid chromatography (SFC) due to its low critical point, nontoxicity, and wide availability in pure form. However, the polarity and solvating power of carbon dioxide are fairly low, which prevents polar and high-molecular-weight compounds to elute by using pure CO₂ as the mobile phase. Therefore, a small amount of organic or inorganic solvents are often added to CO₂ to enhance the solvating power of the mobile phase, so that polar and high-molecular-weight solutes can be eluted. Both polar and nonpolar modifiers have been added to carbon dioxide to alter the chromatographic retention and selectivity. The modifiers and CO₂ can be either premixed in a compressed cylinder, mixed using a saturator column (device), or mixed by using two delivery pumps. Among many modifiers tested in SFC, methanol has been the most popular additive for carbon dioxide. Although binary systems have been used in many applications, ternary systems have also been investigated and found to be very successful in separating organic acids and bases. The modifier influence on chromatographic retention and the mechanism of modifier effect in SFC are also discussed in this entry.

Preparation of the Modified Mobile Phase

There are a number of ways to mix modifiers with CO₂. A mixture of modifier and CO₂ can be purchased as premixed cylinders. Because the modifier is premixed with CO₂ in a cylinder, a modifier gradient cannot be carried out by this approach. Another drawback of this premixing method is that the concentration of the modifier may be increased as the cylinder is evacuated. Modifiers can also be directly introduced into an empty syringe pump that is then filled with CO₂. Again, similar limitations exist in this method. Another way to mix the modifier with CO₂ is to use a saturator column, usually a silica column saturated with polar modifiers. However, because the modifier-hold-

ing capacity of the silica column is limited, the amount of modifier dissolved in the mobile phase varies as the mobile phase passes through the saturator column. An improved mixing device in which highly porous stainless-steel filters were used to generate a modified CO₂ mobile phase has been developed to substitute for the saturator column. Although this mixing device can maintain the amount of modifiers dissolved in supercritical CO₂ for a long time, the performance of the modifier gradient remains impossible with this system. The best and most effective (also the most expensive) way of delivering a modifier in SFC is by using two supply pumps. One pump is used for CO₂ delivery and the other for modifier delivery. The modifier and CO₂ meet inside a mixing chamber that mixes the modifier with CO₂ and equilibrates the mixture in a thermostated zone, and then the mixed fluid is delivered to the SFC injection port and column.

Methanol as the Modifier

Among the published articles regarding modifiers in SFC, methanol has been involved in at least two-thirds of the works. Therefore, methanol has been the most popular modifier for CO₂ in SFC. The mole fraction of methanol in the mobile phase is generally low, ranging from 1% to 10%. However, methanol concentrations up to 45% have also been tested. Due to the high cost of dual-pump systems, a constant concentration of methanol has normally been used to modify carbon dioxide. Once a dual-pump system is available, a programmed concentration of the modifier is preferred, as better separations can be achieved by using the modifier gradient technique. The methanol-modified mobile phase has been used to successfully separate phenols and their derivatives, amines and their derivatives, carboxylic acids, carbohydrates and their derivatives, herbicides and pesticides, alkylbenzenes, chlorobenzenes, chlorophenyls, higher-molecular-weight *n*-alkanes, polycyclic aromatic hydrocarbons (PAHs) and their derivatives, polychlorinated biphenyls (PCBs), pharmaceutical compounds, active ingredients in natural products, explosives, and other solutes.



Ternary Systems

Because methanol is not very polar, the elution of strong organic acids and bases requires a mobile phase with even greater polarity. This has normally been done by adding a very low concentration of acids or bases into methanol, and then the modified methanol is mixed with CO₂ for separation. Citric, acetic, and chlorinated acetic acids have been used as acidic secondary modifiers, whereas isopropylamine, triethylamine, and tetrabutylammonium hydroxide have been served as basic secondary modifiers. A good example with ternary systems is the separation of benzylamines, as shown in Fig. 1. None of the three tested amines were effectively eluted by pure CO₂ (Fig. 1a); however, some of these amines were eluted with very poor peak shapes when methanol was added to the CO₂ (Fig. 1b). However, the addition of isopropylamine to the methanol-modified mobile phase effectively eluted all of the three benzylamines and dramatically improved the peak shapes, as shown in Fig. 1c.

Other Modifiers

Besides methanol, many other polar and nonpolar modifiers have also been used to successfully improve the separation in SFC. These modifiers include acetone, acetonitrile, acetic acid, butane, butanol, *n*-butyl chloride, carbon tetrachloride, dioxane, ethanol, formic acid, heptane, hexane, *n*-hexylamine, methylene chloride, nitromethane, propanol, propionitrile, tetrahydrofuran, toluene, triethanolamine, trifluoroacetic acid, trifluoroethanol, trimethyl phosphate, and water.

FID-Compatible Modifiers

One of the major advantages of SFC over HPLC (high-performance liquid chromatography) is its compatibility with the flame ionization detector (FID), a universal and sensitive detector for carbon compounds. Unfortunately, most modifiers used in SFC are incompatible with FID. Therefore, a search for polar modifiers that have less response to FID led to the use of water, formic acid, and formamide. These modifiers produce acceptably low background noise and enable the use of FID. Because both water and formic acid have poor solubilities in carbon dioxide, they have been used as modifiers at very low concentrations. However, the modifier effect is significant even at this low level. For example, when water or formic acid was used as modifiers, the resolution of free fatty acids was significantly improved.

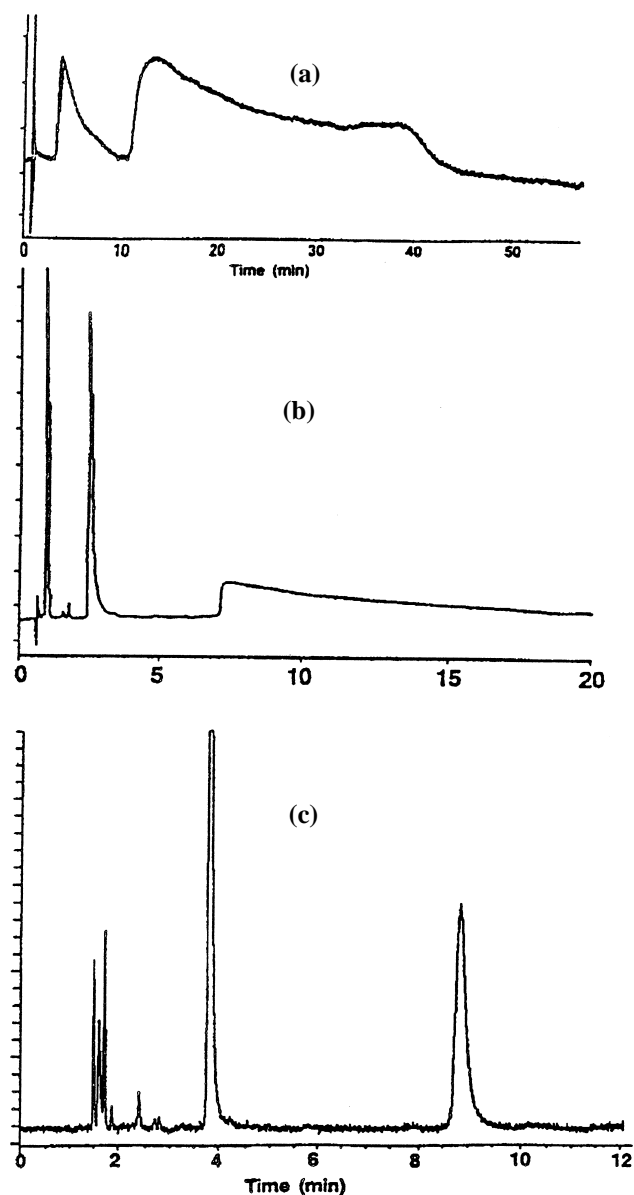


Fig. 1 Separation of benzylamines: (a) On a Deltabond Octyl column (100 × 2 mm, 5 μm) using pure carbon dioxide (0.5 mL/min) at 40°C and 180 bar; (b) on a Diol column (100 × 2 mm, 7 μm) using 5% methanol in carbon dioxide (0.5 mL/min) at 40°C and 182 bar; (c) on a Diol column (250 × 4.6 mm, 5 μm) using 10% methanol (containing 0.6% isopropylamine) in carbon dioxide (2 mL/min) at 40°C and 200 bar. Reprinted from *J. Chromatogr. A* Vol. 785, T. A. Berger, Separation of polar solutes by packed column supercritical fluid chromatography, p. 9. Copyright ©1997, with permission from Elsevier Science.)

Very recently, the separation of polar analytes has also been performed by using pure water under subcritical conditions. Subcritical water has several unique characteristics. For example, the dielectric constant, surface tension, and viscosity of water are dramatically decreased by raising the water temperature while a moderate pressure is applied to keep water in the liquid state. At 200–250°C, the values of these physical properties are similar to those of pure methanol or acetonitrile at ambient conditions. Therefore, subcritical water may be a potential mobile phase for polar analytes. SFC mobile phases other than CO₂ are reviewed separately in this encyclopedia.

Modifier Effect on Retention

It is very clear that chromatographic retention is changed by adding modifiers into carbon dioxide. However, modifiers used in SFC can be classified in three groups, depending on the retention behavior of the solutes. Figure 2 shows a good example of the modifier effect on the retention of α -carotene. For separations using heptane-, tetrahydrofuran-, and methylene chloride-modified CO₂ (group 1), the retention of α -carotene was decreased rapidly and almost inversely proportional to the modifier concentration, as shown in Fig. 2. The second group of modifiers include ethanol, propionitrile, acetone, and 1-propanol. A more grad-

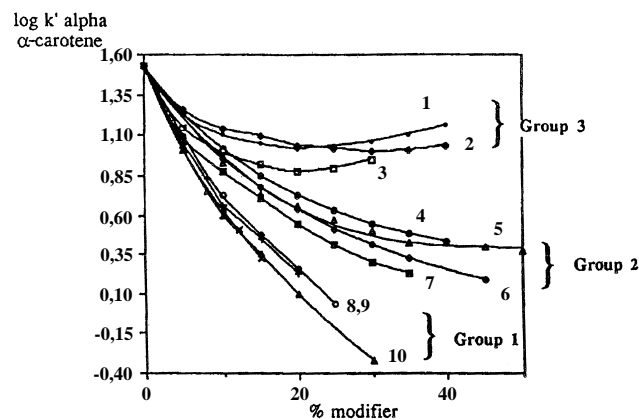


Fig. 2 Variation of the log k' for α -carotene versus the percentage of modifier in carbon dioxide. Temperature: 25°C (subcritical); outlet pressure: 150 bar; flow rate: 3 mL/min; UV at 450 nm; column: UB 225 (250 \times 4.6 nm; 5 μ m). 1. Acetonitrile; 2. methanol; 3. nitromethane; 4. ethanol; 5. propionitrile; 6. acetone; 7. 1-propanol; 8. heptane; 9. tetrahydrofuran; 10. methylene chloride. [Reprinted from *Chromatographia*, 36: 275 (1993), E. Lesellier, A. M. Krstulovic, and A. Tchaplá, with permission from Friedr Vieweg und Sohn Verlagsgesellschaft mbH.]

ual decrease in the retention of α -carotene was obtained by using modifiers in this group. Methanol, acetonitrile, and nitromethane are in the third group. Even though the retention decreased significantly with increasing modifier percentage up to $\sim 10\%$ for all three modifiers in this group, the retention reached a minimum with acetonitrile- and nitromethane-modified carbon dioxide. For separation using the methanol-modified CO₂, the retention remained almost unchanged at higher methanol concentrations. A similar behavior was observed for separations of many other solutes with methanol as the modifier.

Mechanism of the Modifier Effect

Although the exact mechanism is not very clear, the following factors may contribute to the modifier effect on chromatographic retention. Polar modifiers may cover the active sites of the stationary phase (deactivation) so that solute retention is reduced. This can be explained by the differences in retention change between packed and open-tubular columns when small amounts of modifiers were used. Open-tubular columns normally do not show the drastic changes in retention or efficiency upon the addition of small amounts ($<2\%$) of modifier as most packed columns do. These less drastic differences were caused by the differences in the degree of deactivation of the packed column stationary phase as compared with the open-tubular-column stationary phase. An open-tubular column has fewer active sites present and, thus, fewer active sites are present for the modifier to deactivate.

Modifiers may also swell the stationary phase, causing retention change of solutes. The density of the mobile phase can be increased by most polar and nonpolar modifiers so that the solvating power of the mobile phase is enhanced. The polarity of the mobile phase is definitely increased by adding polar modifiers; thus, the retention of polar analytes is reduced. Specific intermolecular interactions between the solute and the modifier in the mobile phase may be additional factors for the modifier effect.

In conclusion, both polar and nonpolar modifiers can be added to the SFC mobile phase to increase the solvent strength. Unlike pure carbon dioxide, the modified CO₂ can elute polar and high-molecular-weight solutes due to its enhanced solvating power. The retention factors are reduced and peak shapes greatly improved by using binary or ternary mobile phases. Although ultraviolet detection can be applied for separations with many modifiers, only water, formic acid, and formamide are compatible with FID.



Suggested Further Reading

- Berger, T. A. and Deye, J. F., *Chromatographia* 31: 529–534 (1991).
- Berger, T. A., *J. Chromatogr. A* 785: 3–33 (1997).
- Cantrell, G. O., Stringham, R. W., Blackwell, J. A., Weckwerth, J. D., and Carr, P. W., *Anal. Chem.* 68: 3645–3650 (1996).
- Francis, E. S., Lee, M. L., and Richter, B. E., *J. Microcol. Separ.* 6: 449–457 (1994).
- Janssen, H.-G., Schoenmakers, P. J., and Cramers, C. A., *J. Chromatogr.* 552: 527–537 (1991).
- Kuepper, S., Grosse-Ophoff, M., and Klesper, E., *J. Chromatogr.* 629: 345–359 (1993).
- Lesellier, E., Krstulovic, A. M., and Tchaplal, A., *Chromatographia* 36: 275 (1993).
- Lesellier, E. and Tchaplal, A., Supercritical fluid chromatography with organic modifiers on octadecyl packed columns: Recent developments for the analysis of high molecular organic compounds, in *Supercritical Fluid Chromatography with Packed Columns*, (K. Anton and C. Berger, eds.), Marcel Dekker, Inc., New York, 1998, pp. 195–221.
- Morrissey, M. A., Giorgetti, A., Polasek, M., Pericles, N., and Widmer, H. M., *J. Chromatogr. Sci.* 29: 237–242 (1991).
- Pyo, D. and Ju, D., *Anal. Sci.* 10: 171–174 (1994).
- Pyo, D., Li, W., Lee, M. L., Weckwerth, J. D., and Carr, P. W., *J. Chromatogr. A* 753: 291–298 (1996).
- Roth, M., *J. Phys. Chem.* 100: 2372–2375 (1996).
- Smith, R. M. and Briggs, D. A., *J. Chromatogr. A* 688: 261–271 (1994).
- Taylor, L. T., *J. Chromatogr. Sci.* 35: 374–381 (1997).
- Upmoor, D. and Brunner, G., *Chromatographia* 33: 261–266 (1992).



Molecular Interactions in GC

Raymond P.W. Scott

Scientific Detectors Ltd., Banbury, Oxfordshire, England

Introduction

The retention of a solute is directly proportional to the magnitude of its distribution coefficient (K) between the mobile phase (gas) and the stationary phase. The magnitude of K depends on the relative affinity of the solute for the two phases; thus, the stronger the forces between the solute molecule and the molecules of the stationary phase, the larger the distribution coefficient and the more the solute is retained. It follows that the stationary phase must interact strongly with the solutes to be retained and to achieve a separation. Molecular interaction results from *intermolecular forces*, of which there are only two types effective in gas chromatography (GC).

In total, there are three different basic types of molecular force, all of which are electrical in nature. These forces are called *dispersion forces*, *polar forces*, and *ionic forces*. Despite there being many different terms used to describe molecular interactions (e.g., hydrophobic forces, π - π interactions, hydrogen-bonding, etc.), all interactions between molecules are the result of composites of these three different types of molecular force.

Dispersion Forces

Dispersion forces [1] arise from charge fluctuations throughout a molecule, resulting from electron/nuclei vibrations. Glasstone [2] described them in the following way:

Although the physical significance probably cannot be clearly defined, it may be imagined that an instantaneous picture of a molecule would show various arrangements of nuclei and electrons having dipole moments. These rapidly varying dipoles, when averaged over a large number of configurations, would give a resultant of zero. However, at any instant, they would offer electrical interactions with another molecule, resulting in interactive forces.

Dispersion forces are those that occur between hydrocarbons and other substances that have either no permanent dipoles or can have no dipoles induced in them. In biotechnology and biochemistry, dispersive interactions are often referred to as “hydrophobic” or “lyophobic” interactions, apparently because dispersive substance such as the aliphatic hydrocarbons do not dissolve readily in water. To a first approximation, the interaction energy (U_D) involved with dispersive forces has been deduced to be

$$U_D = \frac{3h\nu_0\alpha^2}{4r^6}$$

where α is the polarizability of the molecule, ν_0 is a characteristic frequency of the molecule, h is Planck's constant, and r is the distance between the molecules. The dominant factor that controls dispersive force is the polarizability (α) of the molecule, which for substances that have no dipoles is given by

$$\frac{D-1}{D+2} = \frac{4}{3}\pi n\alpha$$

where D is the dielectric constant of the material and n is the number of molecules per unit volume.

If ρ is the density of the medium and M is the molecular weight, then the number of molecules per unit volume is N_ρ/M , where N is Avogadro's number. Thus,

$$\frac{4}{3}\pi N\alpha = \frac{D-1}{D+2} \frac{M}{\rho} = P$$

where P is called the molar polarizability. It is seen that the molar polarizability is proportional to M/ρ , the molar volume.

Polar Forces

Polar interactions arise from electrical forces between localized charges such as permanent or induced dipoles. Polar forces are always accompanied by dispersive interactions and may also be combined with ionic interactions.



tions. Polar interactions can be very strong and produce molecular associations that approach, in energy, that of a weak chemical bond (e.g., "hydrogen-bonding").

Dipole–Dipole Interactions

The interaction energy (U_P) between two dipoles molecules is given, to a first approximation, by

$$U_P = \frac{2\alpha\mu^2}{r^6}$$

where α is the polarizability of the molecule, μ is the dipole moment of the molecule, and r is the distance between the molecules. The energy depends on the square of the dipole moment, which can vary widely in strength. The numerical value of the dipole moment does not always give an indication of the strength of any polar interactions, as there is often internal electric field compensation when more than one dipole is present in the molecule. Although, the *polarizability* of a substance containing no dipoles may give an indication of the *strength of the dispersive* interactions, due to possible self-association or internal compensation, the *dipole moment* of a substance will *not* always give an indication of the *strength of any polar interaction* that might take place with another molecule.

Dipole–Induced-Dipole Interactions

Compounds, such as those containing the aromatic nucleus and thus π electrons, are polarizable. When such molecules are in close proximity to a molecule with a permanent dipole, the electric field from the dipole induces a counterdipole in the polarizable molecule. This induced dipole acts in the same manner as a permanent dipole and, thus, polar interactions occur between the molecules. Induced-dipole interactions are, as with polar interactions, always accompanied by dispersive interactions. Aromatic hydrocarbons can be

retained and separated in GC purely by dispersive interactions when using a hydrocarbon stationary phase or they can be retained and separated by combined induced-polar and dispersive interactions using a poly(ethylene glycol) stationary phase. Molecules can possess different types of polarity, phenyl ethanol, for example, will possess both a permanent dipole as a result of the hydroxyl group and also be polarizable due to the aromatic ring. More complex molecules can have many different interactive groups.

Ionic Forces

Ionic interactions arise from permanent negative or positive charges on the molecule and, thus, usually occur between ions. Ionic interactions are exploited in ion-exchange chromatography, where the counterions to the ions being separated are situated in the stationary phase; ionic interactions are rarely active in GC separations.

To achieve the necessary retention and selectivity between the solutes for complete resolution, it is necessary to select a stationary phase that will provide the optimum balance of dispersive, polar, and induced-polar interactions between the solute molecules and those of the mobile phase.

References

1. F. London, *Phys. Z* 60: 245 (1930).
2. S. Glasstone, *Textbook of Physical Chemistry*, D. Van Nostrand, New York, 1946, pp. 298 and 534.

Suggested Further Reading

- Scott, R. P. W., *Techniques of Chromatography*, Marcel Dekker, Inc., New York, 1995.
- Scott, R. P. W., *Introduction to Analytical Gas Chromatography*, Marcel Dekker, Inc., New York, 1998.



Molecular Weight and Molecular-Weight Distributions by Thermal FFF

Martin E. Schimpf

Boise State University, Boise, Idaho, U.S.A.

Introduction

In field-flow fractionation (FFF), retention can be related through a well-defined equation to the applied field and governing physicochemical parameters of the analyte. Therefore, in principle, FFF is a primary measurement technique that does not require calibration, but only if the governing physicochemical parameters are either the analyte parameters of interest or their relationship to the parameter of interest (such a molecular weight) is well defined.

In thermal FFF, the applied field is a temperature drop (ΔT) across the channel, and the physicochemical parameter that governs retention is the Soret coefficient, which is the ratio of the thermodiffusion coefficient (D_T) to the ordinary (mass) diffusion coefficient (D). Because ΔT is set by the user, retention in a thermal FFF channel can be used to calculate the Soret coefficient of a polymer-solvent system.

Discussion

In order to calculate the molecular weight (M) or molecular-weight distribution (MWD) of the polymer, the dependence of the Soret coefficient on M must be known. Because D_T is virtually independent of M , at least for random coil polymers, the dependence of retention on M reduces to the dependence of D on M . The separation of molecular-weight components by D (or hydrodynamic volume, which scales directly with D) is a feature that thermal FFF shares with size-exclusion chromatography (SEC). In the latter technique, the dependence of retention on D forms the basis for universal calibration, as D scales directly with the product $[\eta]M$, where $[\eta]$ is the intrinsic viscosity. Thus, a single calibration plot prepared in terms of $\log([\eta]M)$ versus retention volume (V_r) can be used to measure M for different polymer compositions, provided an independent measure of $[\eta]$ is available. In thermal FFF, a single calibration plot can only be used for multiple polymers when the values of D_T for each polymer-solvent system of interest are known. However, a single calibration plot can be used with multiple channels. In

summary, calibration plots in SEC are specific to each column but can be made universal with respect to their application to a variety of different polymer compositions. Calibration plots in thermal FFF are specific to each polymer-solvent system but universal with respect to different thermal FFF channels. The following discussion outlines the various forms that can be used to calibrate a thermal FFF channel and how they are used to obtain average values of M and MWDs.

The simplest calibration plot takes the following form:

$$\log V_r = a + S_m \log M \quad (1)$$

where a and S_m are calibration constants. The parameter S_m is referred to as the mass-based selectivity in the FFF literature and is very close but not identical in value to the exponent (b) which defines the dependence of D on M :

$$D = AM^b \quad (2)$$

The difference between S_m and b can be explained by the fact that components of different M experience different temperatures as they separate in the thermal FFF channel [1].

An alternate form of Eq. (1) allows for the use of low levels of retention (associated with components of low molecular weight) without losing linearity in the calibration plot [2]:

$$\log(V_r - V^\circ) = a + S_m \log M \quad (3)$$

Here, V° is the geometric (void) volume of the FFF channel.

Because ΔT can be varied to optimize the separation of different samples, it is convenient to incorporate the dependence of retention on ΔT into the calibration plot:

$$\log(\lambda \Delta T) = \phi + n \log M \quad (4)$$

Here, n and ϕ are calibration constants and λ is the FFF retention parameter, which is calculated from V_r using

$$V_r = \frac{V^\circ}{6\lambda[\coth(2\lambda)^{-1} - 2\lambda]} \quad (5)$$



When ΔT is incorporated into the calibration plot, retention parameter λ is used in place of $V_r - V^\circ$ in order to maintain linearity in the plot over a wide range of applied fields and retention levels.

Once the calibration constants ϕ and n have been determined for a given polymer-solvent system, Eq. (4) can be used for all thermal FFF channels, provided the temperature of the cold wall (T_c) is held constant. The cold-wall temperature affects the calibration plot because the Soret coefficient (D_T/D) and, therefore, ϕ varies with T_c . For a detailed discussion of temperature effects; see the entry Cold-Wall Effects in Thermal FFF. In a thorough study of temperature effects, Myers and co-workers [3] demonstrated that the dependence of the Soret coefficient on T_c can be accurately modeled by

$$\frac{D}{D_T} = \lambda \Delta T = a' T_c^m \quad (6)$$

The validity of this model is illustrated in Fig. 1 by the linearity in plots of $\log(\lambda \Delta T)$ versus $\log(T_c/298)$. Based on Eq. (6), the following universal calibration equation has been proposed:

$$\log(\lambda \Delta T) = \phi + m \log(T_c/298) - n \log\left(\frac{M}{10^6}\right) \quad (7)$$

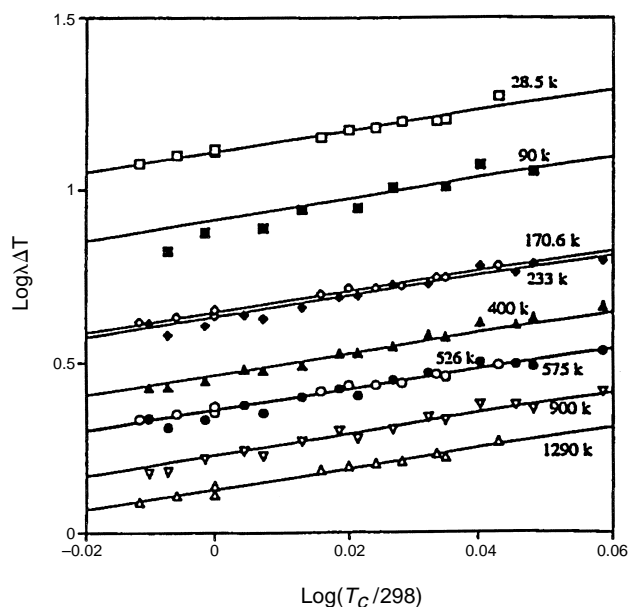


Fig. 1 Plots of $\log(\lambda \Delta T)$ versus $\log(T_c/298)$ for polystyrene in tetrahydrofuran. The data were gathered using a variety of different thermal FFF channels. Values of ΔT ranged from 30 to 70 K.

In order to utilize Eq. (7), a set of linear plots of $\log(\lambda \Delta T)$ versus $\log(M/10^6)$ is established for a given polymer-solvent system, with one plot being generated for each of several cold-wall temperatures. Such plots run parallel to one another with a slope equal to n and with intercepts that equal $\phi + m \log(T_c/298)$. To obtain the values of ϕ and m , linear regression is performed on the intercept values as a function of $T_c/298$. In Eq. (7), T_c and M are divided by 298 and 10^6 , respectively, to avoid large extrapolations in obtaining the various intercept values by regression.

When a mass-sensitive detector such as a refractometer or photometer is used, the weight-average molecular weight (M_w) of a polymer sample is calculated from the calibration equation using the value of V_r that corresponds to the center of gravity of the elution profile. The center of gravity is defined by placing a vertical line through the elution profile such that the line bisects the profile into two halves of equal area. The intersection of this line with the elution-volume axis defines the weight-average V_r , which is converted to M_w through the calibration equation. If the elution profile has a Gaussian or other symmetrical shape, then the weight-average V_r is the value of V_r that corresponds to the peak of the elution profile.

In thermal FFF, the shape of the elution profile is not significantly affected by band broadening for polydisperse ($\mu > 1.2$) polymers, provided that low flow rates (< 0.2 mL/min) are used. In that case, accurate information on the MWD can be obtained directly from the elution profile. For example, if a mass-sensitive detector is used, the signal (s) is linearly related to the mass of polymer in the eluting stream, and the number-average molecular weight (M_n) of the sample is calculated as [2,4]

$$M_n = \frac{\sum s_i}{\sum s_i/M_i} \quad (8)$$

Here, the summation extends over small equal elements of elution volume from the beginning to the end of the elution profile. Thus, s_i is the detector signal of the i th digitized increment and M_i is calculated from the associated value of V_r using the calibration equation. The weight-average molecular weight (M_w) is calculated as

$$M_w = \frac{\sum s_i M_i}{\sum s_i} \quad (9)$$

The polydispersity, μ , defined as the ratio M_w/M_n , thus becomes

$$\mu = \frac{(\sum s_i M_i)(\sum s_i / M_i)}{(\sum s_i)^2} \quad (10)$$

Thermal FFF elution profiles can also be converted into a detailed MWD. With a mass-sensitive detector, the elution profile is essentially a plot of the polymer concentration c (with units of mass/volume) in the eluting stream versus V_r . In order to obtain the mass-based MWD, $m(M)$, we need to transform this profile using

$$m(M) = c(V_r) \frac{dV_r}{dM} \quad (11)$$

The normalized and digitized form of this equation is

$$m_i = \frac{s_i}{\sum s_i} \frac{\Delta V_r}{\Delta M_i} \quad (12)$$

where ΔV_r is the fixed elution volume element corresponding to one digitized interval. In the case of linear calibrations, as defined by Eqs. (1) and (3), $d(\log V_r)/d(\log M)$ is a constant equal to S_m and Eq. (12) is more conveniently expressed as

$$m_i = \frac{s_i}{\sum s_i} \frac{M_i}{V_{r,i}} S_m \quad (13)$$

If needed, the differential number MWD can be obtained by dividing $m(M)$ by M :

$$n(M) = \frac{m(M)}{M} \quad (14)$$

For polymers with a low polydispersity ($\mu < 1.2$), a detailed MWD is not generally needed, and simply calculating M_n and M_w from Eqs. (8) and (9) is generally adequate. However, the elution profile of such a narrow MWD is affected significantly by band broadening, which must be accounted for in order to obtain the most accurate possible values of M_n and μ [5]. Even the elution profile of more polydisperse samples ($\mu > 1.2$) can be affected by band broadening if high flow rates (> 0.2 mL/min) are used. Fortunately, band broadening is well defined in thermal FFF and can be removed by one of two methods. For samples of low polydispersity, μ is well approximated by [5]

$$\mu = 1 + \frac{H_p}{LS_m^2} \quad (15)$$

where L is the channel length and H_p is the polydispersity contribution to plate height. H_p is obtained by plotting the experimental plate height as a function of flow rate.

With the proper technique [5], such plots are linear and the y intercept is equivalent to H_p . Alternatively, H_p can be obtained by subtracting the nonequilibrium band-broadening contribution to plate height (H_N) from the experimentally measured value. Methods for calculating

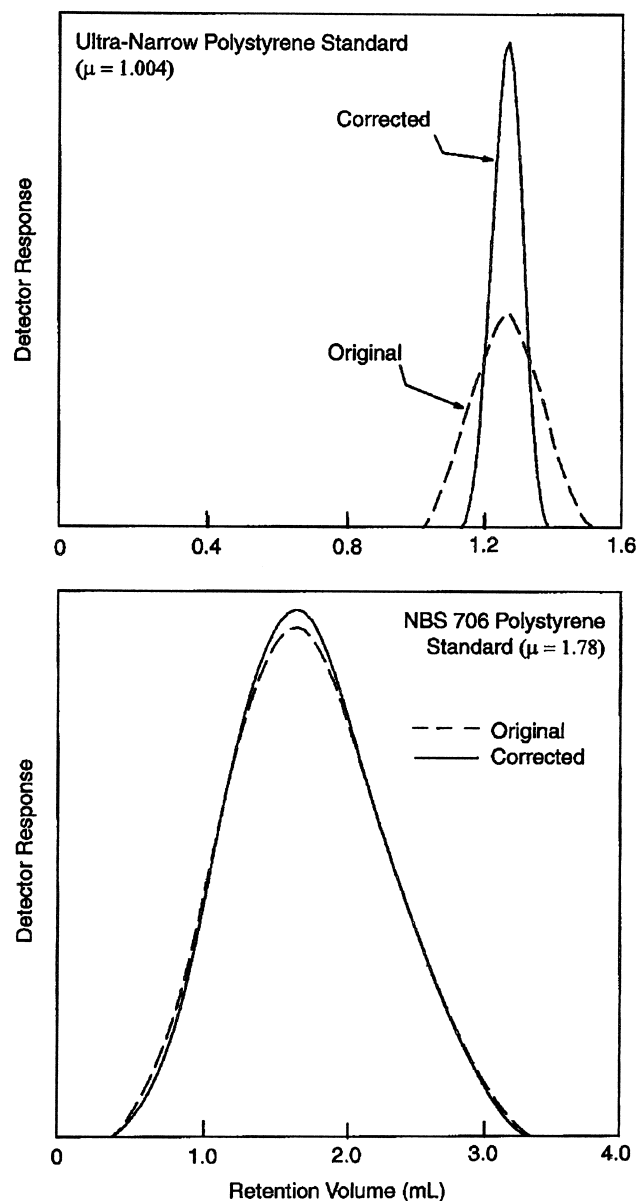


Fig. 2 Thermal FFF elution profiles before (original) and after (corrected) removing the effects of band broadening. With the polydisperse sample (NBS 706), which was analyzed at a flow rate of 0.4 mL/min, the effect of band broadening on the elution profile is minimal. The polydispersity values listed were determined using thermal FFF.



H_N from well-established models of band broadening in thermal FFF can be found in the literature [2]. Because the elution profile of samples with low polydispersity are generally symmetrical, M_w is calculated using the peak value of V_r in the calibration equation, Eq. (15) is used to calculate μ . Finally, M_n is calculated from $\mu = M_w/M_n$.

Samples with higher polydispersity do not generally yield symmetrical elution profiles. Moreover, a detailed MWD [either $m(M)$ or $n(M)$] is often desired. As mentioned earlier, band broadening does not significantly affect the elution profile when low flow rates are used. Therefore, the elution profile can be directly converted into a MWD by the procedures outlined. If, on the other hand, fast flow rates are used to shorten the analysis time, the observed elution profile must be adjusted to account for the effects of band broadening. A deconvolution algorithm that filters out the band-broadening contribution to the elution

profile is described in the literature [2]. Figure 2 illustrates the elution profiles before and after the effects of band broadening are removed for samples of both low and high polydispersity.

References

1. G. H. Ko, R. Richards, and M. E. Schimpf, *Separ. Sci. Technol.* 31: 1035 (1996).
2. M. E. Schimpf, P. S. Williams, and J. C. Giddings, *J. Appl. Polym. Sci.* 37: 2059 (1989).
3. M. N. Myers, W. Cao, C.-I. Chen, V. Kumar, and J. C. Giddings, *J. Liquid Chromatography Related Technol.* 20(16 & 17): 2757 (1997).
4. L. H. Tung, in *Polymer Fractionation* (M. J. R. Cantow, ed.), Academic, New York, 1967.
5. M. E. Schimpf, M. N. Myers, and J. C. Giddings, *J. Appl. Polym. Sci.* 33: 117 (1987).





Molecularly Imprinted Polymers for Affinity Chromatography

Georgios A. Theodoridis

Aristotle University of Thessaloniki, Thessaloniki, Greece

INTRODUCTION

In the last decade, molecular imprinting has evolved into an elegant technique for the generation of synthetic media with a predetermined selectivity. Selectivity is a major parameter in separation science. Optimization of a chromatographic separation is often based on the enhancement of the selectivity of the separation system for a given analyte. This optimization procedure can aim at: 1) the mobile-phase composition, 2) the stationary-phase choice, and 3) the simultaneous optimization of both mobile and stationary phases. The first approach was, for years (and still remains, but to a lesser extent), the subject of extensive research and development. The last few years, however, have seen tremendous increase in the drive toward the optimization of the selectivity of the chromatographic stationary phase. Affinity chromatography, utilizing immobilized antibodies, receptors, or other proteinaceous recognition elements, is an important development in contemporary separation science.

Molecular imprinting is now established as a powerful technique for producing artificial receptors. The dominant application area of molecularly imprinted polymers (MIPs) is analytical chemistry; thus, it is not surprising that in 2001, at least two leading research journals have dedicated an entire issue in the upcoming technology of molecular imprinting (*Analyst*, vol. 126 and *Anal. Chim. Acta*, vol. 435). The imprinting process is based on the production of a polymeric network in the presence of a template molecule. The latter is subsequently removed from the polymer, thus leaving an active site, a “cavity” exhibiting molecular recognition toward the template molecule. Such cavities are complementary to the template molecule in terms of stereochemistry, shape, and chemical interactions. Fig. 1 depicts a simplified scheme of the imprinting process. When, at a later stage, a sample containing the template is administered to the polymer, selective binding of the template molecule will occur. Such polymers are called MIPs and have been used in separations, binding assays, sensors, and catalysis.

MOLECULAR IMPRINTING, KEY ISSUES

The synthesis of MIPs is performed by copolymerization of appropriate monomers in the presence of a template ligand. The monomers interact with the template by non-covalent interactions, reversible covalent interactions, or metal ion-mediated interactions. The types of interactions that are usually exploited in molecular imprinting are as follows:

- i) Covalent bonds.
- ii) π - π Interactions.
- iii) Hydrogen bonds.
- iv) Hydrophobic, van der Waals interactions.
- v) Crown-ether/cyclodextrin-type interactions.
- vi) Metal-ligand bonds.
- vii) Ionic forces.

The imprinting effect is maximized when the template interacts to more than one binding site, and when the interactions involved have directional or spatial determination.

Noncovalent Approach

The noncovalent, or “self-assembly” approach, was pioneered by Klaus Mosbach and is now the most widely applied mode in molecular imprinting. The template is mixed with monomers and cross-linkers in an appropriate solvent. In this prepolymerization mixture, complexes of template with monomers are formed as a result of polar interactions such as hydrogen bonds, ionic interactions, van der Waals forces, etc. The strength of these interactions and the resulting complexes is of vital importance for the templating effect in the final polymer. Hence, “selective” interactions, such as the spatially determined hydrogen bonds, are preferred in contrast to more generic forces (hydrophobic interactions, van der Waals forces). Aprotic solvents allow polar interactions (hydrogen bonds) and are usually chosen, provided that they can dissolve the template molecule and the monomers. In contrast, polar protic solvents suppress the formation

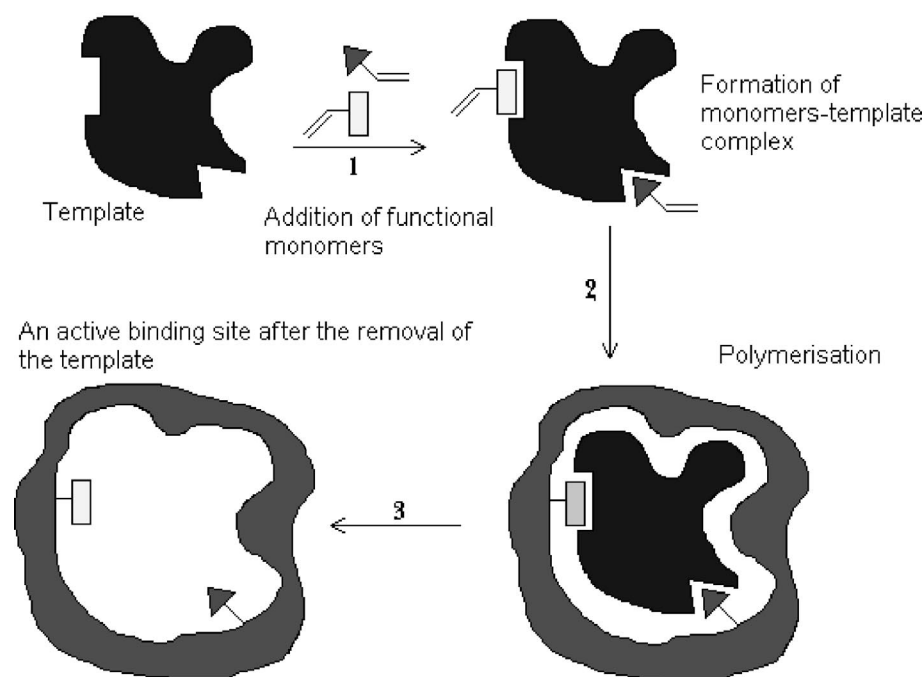


Fig. 1 Schematic representation of the imprinting process.

of hydrogen bonds but promote hydrophobic and ionic interactions between the template and the monomers. Typical polymerization solvents are chloroform, acetonitrile, and dimethylsulfoxide. Protic solvents like methanol have found limited use in specific cases. The role of the solvent is not only to provide the environment for the polymerization reaction but also to produce a porous structure in the resulting polymer. A meso-macroporous structure is necessary to ensure reasonable operating flow and pressure in liquid chromatographic applications and, most of all, good accessibility to the imprinted binding sites. Hence, the choice of polymerization solvent also presides over the rigidity and the pore size of the MIP.

Covalent and Semicovalent Approach

Covalent imprinting was first described in 1972 by G. Wulff as a method of manufacturing enzyme analogue-built polymers. This work is considered by many researchers as a major breakthrough, the actual initiation of molecular imprinting. In covalent imprinting, the template molecule is modified in order to incorporate a polymerization functionality in it. Typically, the template is bound to an appropriate monomer by labile covalent bonds. The monomers frequently used are 4-vinylphenylboronic acid and 4-vinylbenzylamine. During polymerization, the template is fixed in spatial arrangement within the

polymer network. To recover the polymer, the labile bonds are cleaved, thereby releasing the active binding sites.

The advantage of this technique is the known stoichiometry between the template and the functional monomer. As a result, covalent imprinting results in a high density of well-defined sites. One disadvantage of this approach is the synthetic effort that is required to obtain specific bonds that will tolerate polymerization conditions and, additionally, will then easily break in order to recover the template and free the active sites. Rebinding occurs by the formation of either covalent bonds or by formation of other types of interactions, as in the noncovalent approach. In the first case, an additional drawback is the slow kinetics of bond formation. The latter method of imprinting with covalent bond and using the polymer as a noncovalent entity has been called semicovalent imprinting and is an ingenious hybrid technique that combines the attractive features of the two methods. The template molecule is bound to the functional monomer via a sacrificing spacer (e.g., a carbonate ester). Following polymerization, the ester is cleaved with the loss of CO_2 , leaving the monomer capable of forming a noncovalent recognition site.

Monomers used for noncovalent molecular imprinting include methacrylic acid (MAA), 2- and 4-vinylpyridine (2- and 4-VP), trifluoromethacrylic acid (TFMA) acrylamide, and hydroxymethacrylate (HEMA). Ethyleneglycol dimethyl acrylate (EGDMA) is the most common cross-

linker, whereas divinylbenzene (DVB) and trimethylolpropane trimethacrylate (TRIM) have been used to a lesser extent. The cross-linker is added in excessive concentrations (up to 80–90% of the molar ratio in the polymerization mixture), in order to obtain a rigid, highly dense polymeric network. This enables the imprinted sites to retain their shape and size, and tolerate different environments, “resisting” shrinkage and swelling. Most researchers base their work on the abovementioned monomers or their combinations (cocktail of monomers). In this approach, the formation of the template–monomer complex is expected to occur via selected functionalities of the corresponding molecules. Recently, the development of novel monomers specific for a given template has opened new ways in molecular imprinting. To achieve this, existing monomers are modified, or totally new entities are prepared, aiming at a multipoint association with the template molecule. It is expected that such complexes will be stronger and more specific for the template molecule; thus, the resulting MIP will exhibit higher affinity/avidity toward the template.

After the template–monomer complexes have been formed, an azo initiator (usually azo-*N,N*-bis-isobutyronitrile, AIBN) is added to the polymerization mixture. Free-radical polymerization is initiated by heating at 40–60°C or by photochemical homolysis by ultraviolet (UV) radiation (0–15°C). MIPs prepared at lower temperatures (0°C) by photopolymerization have been found to exhibit better molecular recognition. It is theorized that the template–monomer complexes are more stable at lower temperatures; thus, the imprints are more homogeneous and better defined in the resulting MIPs.

Polymerization is allowed to take place for 10–24 hr. Next, the polymer is further processed to back extract the template molecule. This step is of great importance for the successful future use of the MIP. Typical extraction solvents are mixtures of protic solvents with acids (e.g., methanol, with 10% acetic acid). Such mixtures suppress binding interactions and extract the template, almost quantitatively, from the polymer core. Soxhlet extraction, extensive washing, or alternative acid–base washing are the main experimental protocols used. Quantitative removal of the template is essential for two reasons: 1) the more template is removed, the higher the number of active sites revealed in the MIP, and 2) it has been repeatedly reported that leakage or the so-called “bleeding” of the remaining template from the MIP may occur. In such a case, even a minimal amount of template (added as an artifact in a sample) may, to a great extent, influence the results of the analysis. An elegant solution to this problem is the utilization of an analyte analogue, i.e., a “dummy template,” during polymerization. In this approach, even if leakage of the “dummy template” occurs, it will not interfere with the analysis, provided that a

separation step capable of separating the two analogue molecules is used.

Bulk polymerization is the dominant method in molecular imprinting. Polymerization occurs in sealed tubes, resulting in a rigid, highly cross-linked, polymeric network exhibiting macroporous and mesoporous structure. Following template removal, the polymer is processed by grinding and sieving in order to reduce the size of polymer particles. Grinding is performed manually by mortar and pestle or in a mechanical mill; this leads to irregularly shaped particles, including a large quantity of fine particles. Fine grains should be removed if the MIP is to be used for separation; otherwise, these particles may block the frits or tubing and, thus, build high pressure. Fine particles, however, may be used successfully for binding assays. Typically, a selected size range is collected (e.g., 20–50 μm in diameter) and is subsequently used as a chromatographic material in solid-phase extraction (SPE) cartridges or high-performance liquid chromatography (HPLC) columns. It is estimated that about 50% of the produced MIPs are recovered for use as chromatographic material.

Alternative polymerization methods, such as suspension polymerization, dispersion polymerization, and microbead production, have been shown to produce spherical particles of a determined size; however, their use is limited. Finally, the production of monolithic polymeric imprinted materials is a straightforward method of producing MIP rods inside a stainless steel or a PEEK column; however, this method still needs to provide further evidence of enhanced selectivity and molecular recognition.

MIPS AS CHROMATOGRAPHIC MEDIA

The use of MIPs as chromatographic stationary phases is the most studied application of MIPs. This method is, in fact, the best way to quickly and efficiently validate the performance of a developed MIP. To achieve this, the MIP is packed into an HPLC column and the retention characteristics of the template and/or analogue molecules are collected in various selected mobile phases. From the collected data, useful parameters, such as capacity factor, imprinting factor, and peak asymmetry, are calculated and used to evaluate polymer affinity, cross reactivity, and other features of the MIP.

Another attractive feature of using MIPs is the attainment of chiral stationary phases (CSPs). Molecular imprinting offers a very efficient way of producing receptors against an enantiomer within a stationary phase. A major advantage of using MIPs is predetermined selectivity. Hence, by preparing an MIP against an optically pure *R*-template, chiral separations of remarkable

selectivity are easily achieved. The *R*-enantiomer will preferentially bind to the MIP and, thus, elute late; whereas the *S*-enantiomer will elute much earlier. Pharmaceuticals accounted for most of the studied template molecules, given that the pharmaceutical industry needs for chiral separation are still considerable. MIP-based chiral separations of various types of drugs, peptides, protected aminoacids, alkaloids, and other chiral compounds exhibited enantioselectivities higher than conventional CSPs. "Enantiopolishing" is a useful application in that direction. In this approach, a synthetic product is assayed in an MIP CSP manufactured against an enantiomer. Optical impurities elute fast, leading to a purification of the desired enantiomer.

Despite these attractive features, MIP-based CSPs exhibit limitations, the dominant being the heterogeneity of the active binding sites. During the polymerization process, active sites of higher and lesser affinities are both produced. High-affinity sites are produced where best-defined interactions occur; sites of one-point interaction or other sites in the polymer network that exhibit non-selective interaction are responsible for lower affinity. This heterogeneity may result in peak asymmetry and tailing and to a great decrease in separation efficiency. As a result, nonlinear adsorption isotherms are typically observed for the template molecule. Another limitation of MIPs is its capacity, which is, in general, lower than other CSPs. Finally, the achievement of molecular recognition in aqueous environment remains a challenge for MIP technologies. This challenge, however, is to be exploited not only in chiral separations but also in sensing, catalysis, and other application areas.

Apart from HPLC, MIPs have also been used as media for capillary electrochromatography (CEC) and thin-layer chromatography (TLC). CEC is a hybrid separation technique that utilizes a stationary phase as in liquid chromatography and an electroosmotic flow as in capillary electrophoresis (CE). MIPs have been successfully employed as stationary phases of predetermined selectivity for CEC. In fact, the high efficiency of CEC may potentially overcome the efficiency problems encountered with MIP chromatographic media. Mass transfer and kinetic limitations in MIP-based liquid chromatography could be addressed by the enhanced flow dynamics of CEC. A problem that needs to be addressed is the introduction and immobilization of polymer particles in packed capillaries. The usual technique used is the employment of a plug of polyacrylamide as a retaining frit. Alternatively, *in situ* polymerization is used to produce monolithic MIP rods inside the column. Another alternative is the coating of the inner walls of the capillary with thin imprinted polymeric films. Additional obstacles include the known problems of capillary techniques: the need for increased sensitivity and column/polymer's capacity.

Molecularly Imprinted Polymers for Affinity Chromatography

In general, the use of MIPs as stationary phases in either electrochromatography or conventional liquid chromatography has to surmount important problems, such as the production of particles of reproducible size and shape, the tedious grinding-sieving process, and the need for a large amount of template molecule.

USE OF MIPS IN EXTRACTION AND SAMPLE PRETREATMENT

The use of MIPs as media for selective SPE is the application area closer to viable completion and product commercialization. This combination is abbreviated either as MI-SPE or MIP-SPE and is the most successful application of MIPs so far. SPE is now an established technique for sample preparation, due to its advantages vs. other extraction methods: ease and simplicity, automation capability, reduced consumption of organic solvents, choice between several stationary phases (C_8 , C_{18} , CN, NH_2 , Ph, ion exchange, mixed mode, etc.). These generic phases are the first choice for a number of protocols because they offer high capacity, interaction with a wide range of analytes, and good reproducibility. The mechanism involved in extraction is the same one that governs chromatographic analysis; thus, it is rather easily conceived, controlled, and optimized. This conventional mechanism may also be considered to be a drawback; therefore, in many cases, the need for alternative separation mechanisms of higher selectivity is evident.

Extraction mechanisms that take advantage of molecular recognition interactions (immuno-extraction and MI-SPE) are increasingly developed to cover this need. Advantages of MIPs vs. immunoaffinity sorbents are their low cost and ease of preparation, the elimination of the biological receptor (and, thus, the long and tedious immunization experiments), the robustness and long life of the MIP, and the compatibility with elevated temperatures, organic solvents, and environments of increased ionic strength.

MI-SPE has been applied in either on-line or off-line mode for several analytes. In the first case, MIP is packed as an HPLC precolumn. Column switching and pulsed elution modes are employed in on-line MI-SPE. One advantage of this design is the automation capability and the direct coupling to HPLC or other separation modes. Despite these advantages, the off-line mode, which has been successfully applied to bio and environmental and food analysis, is the most commonly practiced method.

There are some critical issues to be taken into consideration for the successful application of MI-SPE. Sample loading may occur under conditions of molecular recognition. In this case, the entrapment of the analytes is selective and the following elution will provide an enriched sample to be further analyzed. Usually, this

selective adsorption/entrapment occurs in the polymerization solvent. It is theorized that by mimicking the conditions of polymerization, the assembly of the template–monomers complex will recur between the MIP and the template. Therefore, it is expected, and has also been found experimentally, that molecular recognition and selective retention of the template is enhanced in the polymerization solvent.

A second strategy is the entrapment of the analytes by nonselective sorption on the MIP. Usually this is achieved by loading in aqueous environment and trapping by hydrophobic interactions. Next, a selective washing step removes unwanted matrix compounds from the SPE cartridge; whereas it facilitates selective binding of the analyte on the MIP. Finally, a selective desorption/elution solvent step obstructs hydrogen bonds or other such specific interactions and recovers the analyte. This mode employs additional extraction steps but offers the advantage of straightforward application of aqueous samples (biofluids or environmental samples). The two above-mentioned modes of analyte trapping could be easily understood by chromatographers as binding in the two chromatographic modes: normal phase for selective binding and reversed phase for nonselective binding-selective desorption. Fig. 2 depicts the operational principles of off-line MIP-SPE in either normal or reversed phase.

USE OF MIPS IN SENSORS AND BINDING ASSAYS

MIPs are ideal media to be used in sensing devices. Typically, sensors include a substrate-selective element

(a receptor or an enzyme) immobilized on an appropriate surface (a membrane or an electrode). Binding of a ligand causes a signal which is translated by an appropriate transducer to a quantitative response. MIPs provide inherent molecular recognition properties with no need for tedious chemical modifications. Therefore, it is not surprising that various sensors have been developed utilizing MIPs as the recognition element: quartz crystal microbalance, acoustic, piezoelectric odor, luminescent, fiber optics, electrochemical, conductometric. Surface plasmon resonance sensors have been used in the analysis of a diversified range of analytes: polyaromatic hydrocarbons, propranolol, nitrate, pesticides, nerve agents, caffeine, nucleotides, fluorescent-labeled aminoacids, chloramphenicol, cholesterol, etc. The methods have been applied to the analysis of various samples and matrices (biological, environmental, etc.). Molecular imprinting may prove to be a smooth way toward the effective and straightforward production of sensors. Virtually any low molecular mass compound can be imprinted. Recently, larger entities, such as proteins, bacteria, and living cells, were targeted by MIP base sensors, dramatically increasing the applicability and prospects of MIP technologies.

Alternatively, MIPs have also been used in biological receptors for competitive binding assays. The assay principle is similar to that in other known biological assays such as radioimmunoassay (RIA) or enzyme-linked immunosorbent assay (ELISA) except that instead of antibodies, MIPs are utilized. This method is often called molecularly imprinted assay (MIA). Typically, in MIA methods, a marker molecule (a labeled analyte analogue) is incubated together with the sample and the MIPs. Analyte and marker molecules compete for the binding

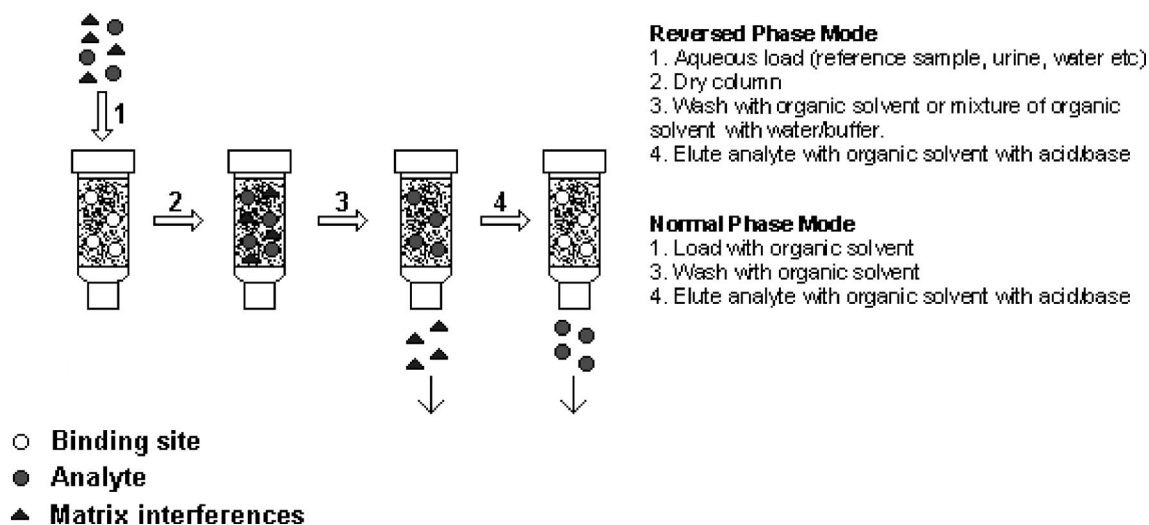


Fig. 2 Off-line application of MIP-SPE. Representation of the two modes of operation: normal phase (selective binding) and reversed phase (nonselective binding-selective desorption).

sites of the polymer. Provided that the number of the polymer's binding sites is limited and within an optimum range of the assay, the amount of marker bound on the polymer will depend on the amount of analyte in the sample. Hence, in samples rich in analyte molecule, the marker will not bind to the polymer. In contrast, in samples with zero or minimal quantities of analyte, the lot of the marker molecule will bind onto the MIP. MIA protocols have been developed, so far, only in the heterogeneous format, meaning that a separation step follows in order to separate the MIP particles from the sample. Marker molecules are often radiolabeled, but lately, fluorescence tagging tends to substitute for radioassays.

The advantages of using MIPs instead of antibodies in binding assays are the same attractive features that drive the utilization of MIPs as affinity chromatographic media: ease of preparation, lower cost, tolerance to extreme chemical and thermal conditions, long shelf life, and no need for animal immunization. For example, MIA protocols employ organic solvents, offering an attractive alternative to conventional immunoassays. Additionally, MIPs have been found to provide affinity/avidity, and cross reactivity comparable to antibodies.

CONCLUDING REMARKS

Molecular imprinting technologies have found a niche in separation science. MIPs offer a good alternative to proteinaceous receptors and have been successfully used in affinity-based separations. Furthermore, the polymeric nature of the MIPs bears attractive features for applications that could not be achieved by antibodies or enzymes: gas chromatography, solid-phase microextraction, etc. As further fundamental research and application efforts are invested in MIP technologies, it is expected that MIPs will soon be commercialized. MIP-SPE is expected to the first commercial application area.

The number of research groups working in the field is expanding; thus, significant advances are made and new targets are addressed. Imprinting in aqueous environment, imprinting of large biomolecules, and implementation of existing recognition elements (e.g., cyclodextrins) are some of the areas where remarkable developments are expected. Parallel to these developments, antibody/receptor technologies spread out and become more robust. Techniques like solid-phase peptide synthesis, recombinant protein technologies, and antibody engineering expand continuously. Taking into account the rapid growth in biotechnology and immunology, a central role of molecular recognition technologies is seen in many scientific disciplines: analytical chemistry, medicinal chemistry,

Molecularly Imprinted Polymers for Affinity Chromatography

drug and gene delivery, synthetic catalysis, proteome research. In that direction, MIPs could serve as a powerful tool that could prove to be complementary and/or alternative to biological receptors.

SUGGESTED ADDITIONAL READING

- Andersson, L.I. Molecular imprinting: Developments, and applications in the analytical chemistry field. *J. Chromatogr., B, Biomed. Sci. Appl.* **2000**, 745 (1), 3–13.
- Andersson, L.I. Molecular imprinting for drug bioanalysis—A review on the application of imprinted polymers to solid-phase extraction, and binding assay. *J. Chromatogr., B, Biomed. Sci. Appl.* **2000**, 739 (1), 163–173.
- Ansell, R.J.; Ramstrom, O.; Mosbach, K. Towards artificial antibodies prepared by molecular imprinting. *Clin. Chem.* **1996**, 42 (9), 1506–1512.
- Asanuma, H.; Hishiya, T.; Komiyama, M. Tailor-made receptors by molecular imprinting. *Adv. Mater.* **2000**, 12 (14), 1019–1030.
- Bartsch, R.A.; Maeda, M. *Molecular, and Ionic Recognition With Imprinted Polymers*; ACS Symp. Ser., American Chemical Society: Washington, 1998; Vol. 703.
- Dickert, F.L.; Hayden, O. Molecular imprinting in chemical sensing. *TrAC, Trends Anal. Chem.* **1999**, 18 (3), 192–199.
- Haupt, K.; Mosbach, K. Plastic antibodies: Developments, and applications. *Trends Biotechnol.* **1998**, 16 (11), 468–475.
- Lanza, F.; Sellergren, B. The application of molecular imprinting technology to solid phase extraction. *Chromatographia* **2001**, 53 (11–12), 599–611.
- Owens, P.K.; Karlsson, L.; Lutz, E.S.M.; Andersson, L.I. Molecular imprinting for bio-, and pharmaceutical analysis. *TrAC, Trends Anal. Chem.* **1999**, 18 (3), 146–154.
- Sellergren, B.; Andersson, L.I. Application of imprinted synthetic polymers in binding assay development. *Methods: Companion Meth. Enzymol.* **2000**, 22 (1), 92–106.
- Sellergren, B. *Molecularly Imprinted Polymers*; Elsevier: Amsterdam, 2000.
- Stevenson, D. Molecular imprinted polymers for solid-phase extraction. *TrAC, Trends Anal. Chem.* **1999**, 18 (3), 154–158.
- Valano, P.T.; Remcho, K. Highly selective separations by capillary electrochromatography: Molecular imprint polymer sorbents. *J. Chromatogr., A* **2000**, 887, 125–135.
- Whitcombe, M.J.; Rodriguez, M.E.; Villar, P.; Vulfson, E.N. A new method for the introduction of recognition site functionality into polymers prepared by molecular imprinting: Synthesis, and characterization of polymeric receptors for cholesterol. *J. Am. Chem. Soc.* **1995**, 117 (27), 7105–7111.
- Wulff, G. Molecular imprinting in crosslinked materials with the aid of molecular templates—A way towards artificial antibodies. *Angew. Chem.* **1995**, 34, 1812–1832.
- Wulff, G. Molecular imprinting in crosslinked polymers—The role of the binding sites. *Mol. Cryst. Liq. Cryst. Sci. Technol., Sect. A* **1996**, 276, 1–6.

Monolithic Disk Supports for HPLC

A. Podgornik

M. Barut

A. Strancar

BIA Separations d.o.o., Ljubljana, Slovenia

INTRODUCTION

Chromatographic columns are typically several centimeters in length, resulting in a high number of column plates, and, consequently, such columns have high efficiency. These properties allow even very similar molecules to be separated. This is especially true for smaller molecules, where the separation is based on selective migration. For large molecules, a different separation mechanism is usually required. Large molecules normally interact with the matrix at several binding sites. Consequently, their adsorption isotherms are very steep, almost rectangular. For such molecules, there exists only a very narrow mobile phase range within which they interact with the active moieties on the stationary phase, but are not irreversibly retained. To elute them from the matrix, a change of the mobile phase composition is required. Therefore the separation is based upon the selective elution and requires the use of gradient chromatographic methods. For this type of separation, the column length is less important and the efficient separations can be achieved even with extremely short columns.

Because it is possible to use short columns, high flow rates can be used because of the low-pressure drop on the column. When this is accompanied with a steep gradient, extremely fast separations of large molecules can be achieved. However, to obtain efficient, fast separation, the mass transfer between the mobile and the stationary phase should also be fast. This might be a problem for large molecules having a very low mobility. Therefore suitable stationary phases should be used. In order to decrease the diffusion limitations, which are especially pronounced for large molecules, convection must be a significant part of the materials' mass transfer characteristics. To overcome a diffusion bottleneck, several types of stationary phases have been proposed, e.g., nonporous and perfusion particles. Despite significantly improved mass transfer in comparison to porous particles, preparation of short columns, as a result of the problems connected with column packing, can be problematic.

An alternative approach is represented by membranes. They are, by definition, very thin and seem ideally suited for the preparation of short columns. In fact, several

successful large molecule separations were reported.^[1] Membranes possess excellent mass transfer characteristics, enabling the fast exchange of molecules between the mobile and stationary phases. Because of their extreme thinness, several membranes are normally stacked to achieve acceptable binding capacity. This inherently introduces voids between the membranes that decrease the continuous nature of the matrix.

A decade ago, a new type of stationary phase was developed. It is commonly referred to as a monolith to emphasize that the matrix consists of a single piece of a highly porous material. Similar to the membranes, the monoliths have open pores that form a highly interconnected network of channels which are uniformly distributed in all directions. In contrast to the membranes, however, they can be prepared in various shapes and dimensions. The porous structure enables very good hydrodynamic characteristics. The mobile phase flows through the channels, and convection is the predominant transport mechanism. In this way, the mass transfer of large molecules is increased by at least an order of magnitude and, consequently, the analysis times can be significantly shortened without loss of resolution. In addition, chromatographic characteristics such as column efficiency and dynamic binding capacity are practically flow-independent. Similar to other chromatographic supports, monoliths can be prepared with different active groups. It is beyond the scope of this article to describe in detail the characteristics of monoliths, but those interested in the subject are referred to a recent book entitled "Monolithic Separation Media."^[2] Because the monoliths combine the advantageous hydrodynamic characteristics of the membranes with a flexible geometry, they are an ideal matrix for short chromatographic columns.

EFFECT OF THE COLUMN LENGTH ON THE RESOLUTION UNDER THE CONDITIONS OF A LINEAR GRADIENT ELUTION

Several decades ago, the theory of gradient elution was proposed by Snyder and Stadalius.^[3] In this work, it



was shown that the column length does not influence the resolution. This is especially true for steep gradients, where the separation is entirely based on selective elution. In contrast to isocratic separations, where a longer column normally results in better separations, the elution time for gradient elutions depends upon the composition of the mobile phase. As a consequence, only a small part of the column is used for the separation. This conclusion is based upon the assumption of instantaneous equilibrium between the sample and the mobile phase. For large molecules, however, this assumption is hardly justified because of the significantly different mobilities of large and small molecules. Indeed, a detailed work by Dubinina, Kurenbin, and Tennikova^[4] demonstrated that the gradient should be adjusted to the column length. Furthermore, they demonstrated that longer columns might even decrease the resolution because of pronounced band spreading. They introduced a term of gradient length, which depends on mobile phase velocity, concentration at which the molecule is eluted, steepness of the gradient, and the *Z* factor. The theoretical analysis showed that there is an increase in band spreading in the area where the gradient length is shorter than the column length. The spreading, together with the resolution, increases while the column length approaches the calculated gradient length. When the gradient and the column length are comparable, the bandwidth remains constant. Further increases in the column length result in a pronounced band spreading without improving the separation. The reason for this behavior lies in the equilibrium between the sample and the mobile phase. Once the molecules are released from the active groups, they start to move through the column with the mobile phase. Because of the lower mobility, however, their velocity is lower than the velocity of the eluting mobile phase. Therefore they become surrounded by the mobile phase with higher ionic strength, which, consequently, accelerates them. This results in a so-called sharpening effect resulting in lower bandwidth. When the gradient approaches the physical length of the column, the equilibrium between the sample molecules and the mobile phase composition is achieved at the end of the column. Therefore the mobile phase composition determines the band spreading and, in this way, preserves the resolution efficiency. A longer column does not contribute to a better separation, but only to additional band spreading because of axial dispersion, resulting in decreased resolution. Therefore for molecules that require a steep gradient for an efficient separation, short columns are not only a method of choice, but can even be superior to longer columns.

DEVELOPMENT AND CHARACTERISTICS OF DISK MONOLITHIC COLUMNS

The concept of monolithic columns in the shape of disks was first introduced at the beginning of the 1990s by Tennikova, Belenkii, and Svec.^[5] They prepared hydrophobic methacrylate-based monolithic disks with a diameter of 20 mm and a thickness of 1 mm which demonstrated a very efficient separation of a protein mixture. After this initial research, monolithic disks of different diameters and thicknesses were prepared and used for various chromatographic separations. The smallest monolith had a diameter of only 1.8 mm, while the largest had a diameter of 50 mm. The thickness was between 0.3 and 7 mm.^[6] In this way, the monolith volume differed by several orders of magnitude. The monolithic disks contained different chemical moieties which were used for separations in ion exchange, hydrophobic, and affinity interactions, as well as reversed phase modes.

Along with the development of the monolithic disks, a suitable housing had to be designed. The housing needed to facilitate the usage of the monolithic disks and enable the connection of the disk monolithic columns to an HPLC/LC or flow injection analysis (FIA) system. In addition, it needed to provide a uniform sample distribution over the entire monolith surface, ensure the mechanical stability of the monolithic disk when a high flow rate is applied, and prevent any bypass of the mobile phase. Furthermore, the peak spreading and the dead volume of such a unit should be as low as possible. Historically, this represented a major challenge. Several attempts to fulfill these requirements have been reported over the last several years.^[7] In the initial experiments, the monolith was simply installed at the bottom of a filtration device. Despite the simplicity of such an approach, the large dead volume limited its wide applicability. To overcome this problem, a special housing with optimized sample distribution was constructed. This device enabled excellent separation of proteins within several minutes. The monolithic disk was placed between

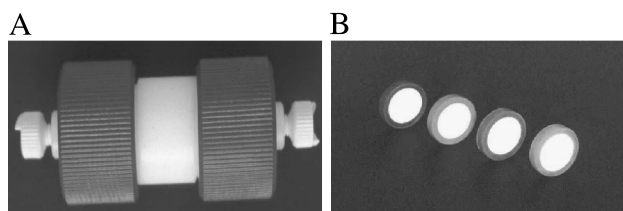


Fig. 1 The outlook of (A) the CIM[®] Disk Monolithic Column and (B) the CIM[®] Disks from BIA Separations, Ljubljana, Slovenia.

two sample distributors, and o-rings created a seal around the monolith. Because of the way the monoliths were fixed in the housing, the replacement often damaged the monolith. In 1998, a commercial product under the trademark CIM Convective Interaction Media[®] was launched.^[8] The housing enables highly efficient separations and easy exchange of the monolithic disks. Along with the construction of the housing, the dimensions of the monolithic disks were standardized to have a diameter of 12 mm and a thickness of 3 mm. To provide additional mechanical stability to the monolith, a self-sealing nonporous ring was fixed around the monolith. These commercially available units are shown in Fig. 1.

CHROMATOGRAPHIC CHARACTERISTICS OF MONOLITHIC DISKS

Despite the existing theory claiming that, under the conditions of a gradient elution, resolution does not improve with increased column length, very short chromatographic columns were not routinely used for separations in a gradient mode at the time the monolithic disks were introduced. To evaluate the chromatographic characteristics of the monolithic disks, a detailed analysis of their properties under gradient elution was published in 1993 by Tennikova and Svec.^[9] They prepared monolithic disks with different chemistries, enabling ion-exchange (IEX), HIC, and RP separation modes. They investigated the effect of the gradient volume on the separation efficiency and concluded that the monolithic disks obey the same chromatographic rules as conventional particulate chromatographic columns. On the other hand, because of the enhanced transport mechanism, the separation characteristics were almost independent of the applied flow rate. Furthermore, the resolution increased even with the increases in linear velocity, which was explained by the narrowing of the peaks. They estimated that the apparent diffusivity of the proteins, as a result of the convective flow through the pores of the monolithic disk, was four magnitudes higher than the free diffusivity of proteins in solution.

In 1999, a similar analysis was performed for an isocratic separation.^[10] The investigators examined the effect of the mobile phase composition and the monolithic disk thickness on band spreading. Again, it was found that, despite an extremely short column length and the monolithic structure, all conclusions for the conventional HPLC columns were applicable to these columns. Separation of oligonucleotides gave a height equivalent of theoretical plate (HETP) value of 18 μm , which is comparable to the chromatographic columns filled with 5–7 μm particles. Investigation of the effects of flow rate

demonstrated a slightly improved separation at a higher flow rate. This surprising conclusion was explained by the increased flow through the small pores, which are not “permeable” at lower flow rates.^[10] Both works demonstrated that the monolithic disks should be considered as “real” chromatographic columns.

All monolithic disks reported so far were methacrylate- or styrene-based. Because of that, they have a rigid structure, which minimizes compression when high flow rates are applied. This is confirmed by a linear correlation between the pressure drop and the linear velocity. For the commercially available CIM[®] disks of 12-mm diameter and 3-mm thickness, it was found that there is a pressure drop of about 0.5 bar per each mL/min. A low-pressure drop is very important for working at high flow rates. Because the mass exchange is not a limiting factor, the gradient can be adjusted in a way to optimally match the thickness of the monolithic disk. In this way, efficient separations in a very short time can be obtained. The extremely short separation times were investigated by Strancar et al.^[11] (Fig. 2). The authors were able to separate a mixture of proteins within a few seconds at room temperature. For even faster separations, current HPLC equipment becomes a bottleneck.

Another consequence of the very fast mass exchange between the mobile and the stationary phase are the flow-independent characteristics of these units. In Fig. 3a, the comparison of a protein separation performed at flow rates from 2 up to 8 mL/min is shown. As can be seen, the chromatograms overlap, indicating no loss of separation efficiency. Similar results were achieved for the dynamic

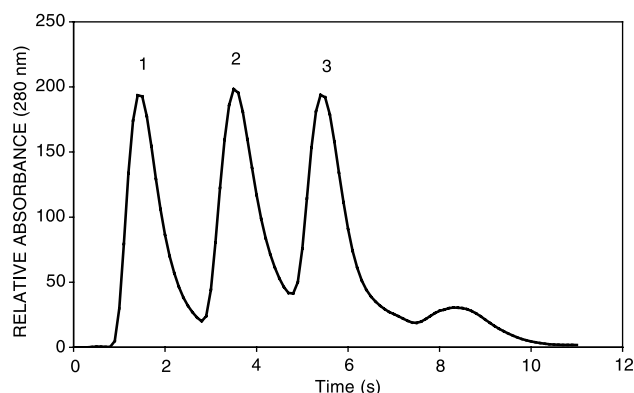


Fig. 2 Separation of test proteins in seconds on a CIM[®] QA disk monolithic column. Conditions—buffer A: 20 mM Tris–HCl buffer, pH 7.4; buffer B: 1 M NaCl in buffer A, pH 7.4; flow rate: 10 mL/min; detection: UV at 280 nm; gradient: step gradient at 0%, 20%, and 50% buffer B for 2 sec each; sample: (1) myoglobin (0.5 mg/mL), (2) conalbumin (1.5 mg/mL), (3) soybean trypsin inhibitor (2 mg/mL); injection volume: 20 μL . (From Ref. [11].)



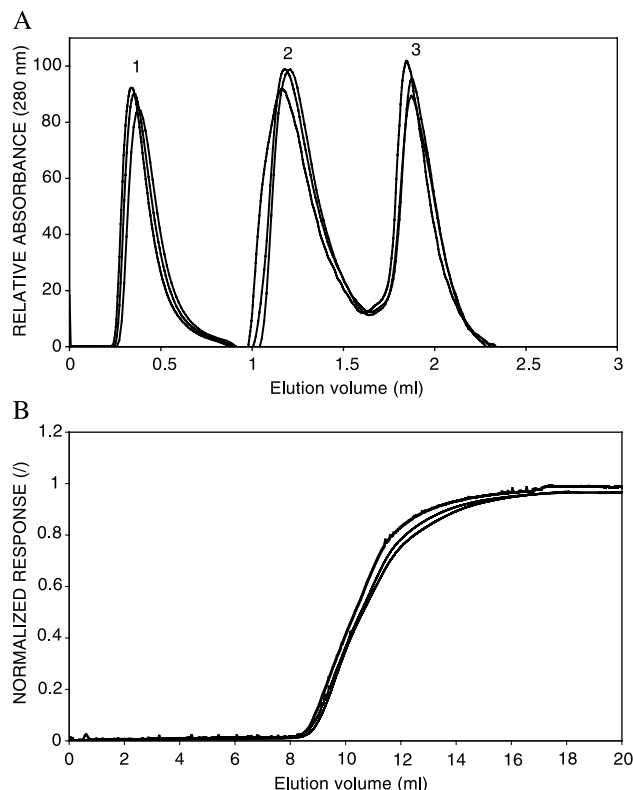


Fig. 3 Flow characteristics of the monolithic disks: (A) flow-independent resolution and (B) flow-independent dynamic binding capacity. (A) Conditions—buffer A: 20 mM Tris–HCl buffer, pH 7.4; buffer B: 1 M NaCl in buffer A, pH 7.4; flow rate: 10 mL/min; detection: UV at 280 nm; gradient: 0–70% buffer B in 30 sec; sample: (1) myoglobin (0.5 mg/mL), (2) conalbumin (1.5 mg/mL), (3) soybean trypsin inhibitor (2 mg/mL); injection volume: 20 μ L. (B) Conditions—binding buffer: 20 mM Tris–HCl buffer, pH 7.4; flow rate: 2, 4, and 8 mL/min; detection: UV at 280 nm; sample: human serum albumin dissolved in buffer A (1 mg/mL).

binding capacity. In Fig. 3b, breakthrough curves are presented. Again, they match closely, indicating a constant binding capacity.

Because of their small thickness, one might speculate that the monolithic disks can only separate a few substances during a chromatographic run. However, by precise gradient adjustments, more than 10 substances can be separated in a few minutes. In Fig. 4, a separation of 14 oligonucleotides was performed in 3 min at room temperature^[12]—a feat hardly achievable with a conventional particulate column.

Monolithic structures enable two additional interesting features. Because of their defined dimension, several monolithic disks can be stacked together forming a single chromatographic column. Such a column has much better performance in comparison to a group of several columns

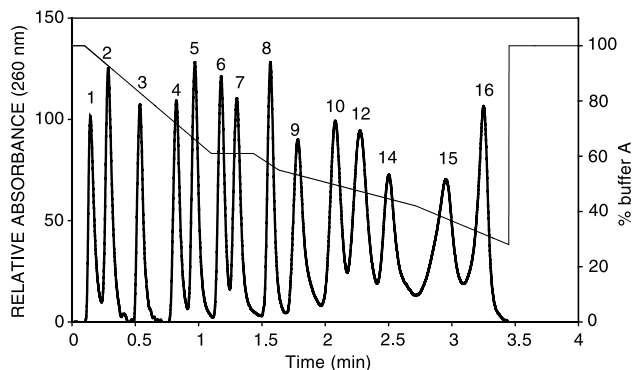


Fig. 4 Separation of oligomers using optimized gradient conditions. Conditions: mobile phase—buffer A: 20 mM Tris–HCl buffer, pH 8.5; buffer B: 1 M NaCl in 20 mM Tris–HCl buffer, pH 8.5; flow rate: 4 mL/min; stationary phase—CIM disk monolithic column comprising of a single disk; sample: oligonucleotides of different lengths (see “Chromatographic Characteristics of Monolithic Disks”). Number near the peak represents the oligonucleotide length. Gradient: as shown in the figure; injection volume: 20 μ L; detection: UV at 260 nm. (From Ref. [12].)

in series comprising a single monolithic disk.^[13] In this way, the capacity of the column increases linearly. It is important to note that this can be performed by the user without any additional equipment. Several disks also increase the column length, resulting in an increased number of theoretical plates and, consequently, better efficiency in isocratic separation. In Fig. 5, a separation of organic acids with a monolithic column consisting of four monolithic disks is presented.

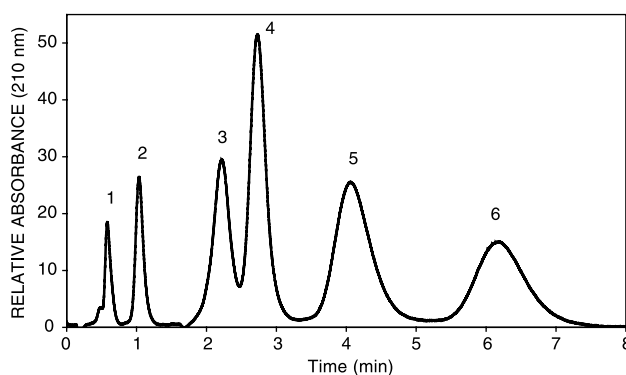


Fig. 5 Separation of the organic acid on CIM disk monolithic column. Conditions—mobile phase: 130 mM NaCl in 20 mM phosphate buffer, pH 8.0; separation unit: CIM[®] disk monolithic column comprising of four CIM[®] QA disks; flow rate: 5 mL/min; sample: (1) 0.03 g/L pyruvic acid, (2) 0.5 g/L malic acid, (3) 0.2 g/L α -ketoglutaric acid, (4) 0.007 g/L fumaric acid, (5) 2 g/L citric acid, and (6) 2 g/L isocitric acid; injection volume: 20 μ L; detection: UV at 210 nm. (From Ref. [17].)

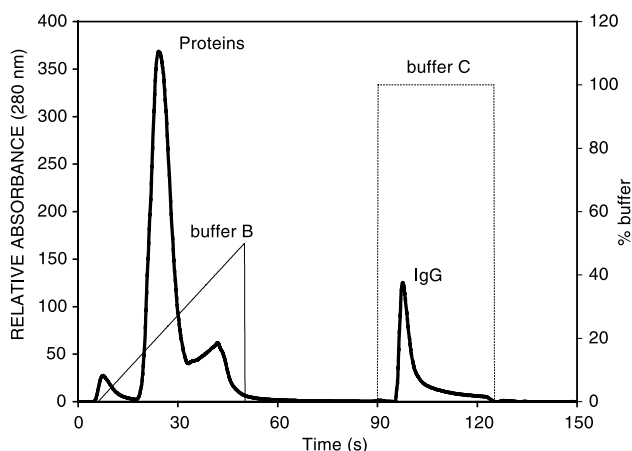


Fig. 6 Conjoint liquid chromatography (CLC): separation of proteins from mouse ascites and isolation of monoclonal antibody IgG in one step obtained by a combination of CIM[®] QA and CIM[®] Protein A Disks. Conditions—separation mode: CLC (first disk: CIM[®] QA; second disk: CIM[®] Protein A, inserted in one-disk monolithic column housing); instrumentation: gradient HPLC system with extra low dead volume mixing chamber; sample: mouse ascites; injection volume: 20 μ L; mobile phase: buffer A—20 mM Tris-HCl, pH 7.4; buffer B—buffer A + 1 M NaCl; buffer C—0.1 M acetic acid; conditions: gradient—0–50% B in 50 sec, 100% A for 40 sec, and 100% C for 30 sec; flow rate—4 mL/min; detection—UV at 280 nm. (From Ref. [13].)

A similar approach using monolithic disks of different chemistries enables multidimensional separations. This approach, using monolithic disks, was called conjoint liquid chromatography (CLC).^[13] The main advantage is that these columns can be reconstructed by placing the disks in a different order or exchanging some of the disks. This is possible because the stationary phases bearing different chemistries do not mix. An example of such a separation is shown in Fig. 6, applying affinity and ion-exchange disks in a single column.

The features clearly indicate that the monolithic disks enable efficient separations and purification of different types of molecules. This is demonstrated in a number of examples where these columns were used in the separation of complex biological mixtures.

APPLICATION OF MONOLITHIC DISKS

Monolithic disks have been successfully used in the separation of different types of molecules. Most of the applications, however, deal with the separation of proteins. Initially, the studies were conducted with test solutions to prove the power of the separation media, but many applications with real samples have also been

reported. All of these separations were performed in a short period of time, typically a few minutes or even less. Some of the representative ones are described.

Ion-Exchange, Hydrophobic, and Reverse Phase High-Performance Liquid Chromatography Disk Monolithic Columns

Separation of proteins

There are several reports about the application of the disk monolithic columns for the separation and purification of plasma proteins.^[14,15] Purification and monitoring of clotting Factor IX (FIX) from human plasma were performed using the ion-exchange monolithic disks. In addition, separation of vitronectin from FIX was possible. A similar system was used for the separation of a complex between clotting Factor VIII and von Willebrand factor (FVIII-vWF). Another application was the monitoring of α_1 -antitrypsin production. Separation of impurities such as human serum albumin and transferrin was achieved in a few minutes.

Another well-studied system was the monitoring and purification of extracellular ligninolytic enzymes from the fermentation broth of fungus *Phanerochaete chrysosporium*. Again, the ion-exchange disk monolithic columns were used. The different enzyme isoforms present in a fermentation broth have similar molecular weights. An efficient separation was achieved in a few minutes, thus reducing the required separation time by an order of magnitude, as compared with a conventional column. The purities of the isoforms were comparable using monolithic vs. conventional columns. The method was also used for monitoring the isoenzyme profiles during the fermentation process.^[16]

Separation of polynucleotides

Monolithic disks seem to be very efficient columns for the separation of polynucleotides. They enabled not only the separation of pDNA from RNA, but also the separation of pDNA isoforms: supercoiled, open circular, and linear forms.^[14] Besides a separation time of only a few minutes, the most outstanding characteristic of the monolithic disks is their high dynamic binding capacity for pDNA, which is in the range of 10 mg/mL of support.^[6] In addition, the monolithic disks seem to be very attractive for the purification of even larger molecules, e.g., viruses.^[6]

Small molecules

While most of the papers deal with the separation of large molecules, a few successful separations of small

molecules were recently reported.^[14] By stacking several disks of the same chemistry into a single monolithic column, it was possible to apply it for monitoring the organic acid formation during the fermentation of yeast *Yarrowia lipolytica*.^[17] A similar column was used for the determination of Mn^{3+} tartrate complex in a fermentation medium of *P. chrysosporium*. Very recently, the separation of Zn complexes of citrate, oxalate, and EDTA, as well as hydrated Zn^{2+} species, was compared on an ion-exchange disk monolithic column and Mono Q. The former was found to be more efficient.^[18]

More information about the applications of the monolithic disk columns can be found in several reviews.^[14,15,17,19]

Affinity Monolithic Columns

Methacrylate-based monolithic disks are very suitable for the immobilization of various ligands because they contain epoxy groups which form very stable covalent bonds with the amino or sulfhydryl groups of the ligand. Recently, an extensive description of different immobilization procedures was published.^[20]

Low molecular mass ligands

The first report about the immobilization of a small affinity ligand on monolithic disks was published in 1991.^[21] Immobilized *p*-(amino methyl) benzol sulfonamide, a carbonic anhydrase inhibitor, was used for the purification of carbonic anhydrase. The immobilization of various peptides, including the hormone bradykinin, on a CIM[®] disk monolithic column, was performed to investigate the possibility of purifying monospecific polyclonal antibodies in serum. Several disks, each with a different immobilized peptide, were placed in a single housing. This CLC approach demonstrated that the simultaneous loading of immunoglobulins can be performed in a few minutes. The specific immunoglobulins were then released from each monolithic disk separately.^[21]

An important issue related to the small affinity ligands is their utilization (capacity per unit of ligand) on the matrix. Because of their size, they are more sensitive toward matrix composition and immobilization chemistry in comparison to large affinity ligands. A detailed study of the characteristics of a model peptide with affinity to chicken egg lysozyme immobilized to different supports such as agarose, cellulose, and methacrylate-based supports and via different immobilization chemistries revealed that the highest utilization of the ligand was achieved with the methacrylate-based monolithic disks.^[15] This means that the ligand is optimally presented on the matrix surface, which additionally facilitates mass transfer between the mobile and stationary phases.

High molecular mass ligands

Different high molecular mass affinity ligands were successfully immobilized to monolithic disks.^[14,20,21] Monolithic disks with immobilized heparin and collagen were used for the purification of membrane proteins and annexins. The heparin unit was also used in the quality control of the preparation of the plasma proteins Antithrombin III and clotting Factor IX. Purification of IgG was successfully performed by immobilizing Protein A, Protein G, and Protein L.^[14,20] Because the elution is carried out under harsh conditions, which might cause denaturation, the fast separation enabled by the monolithic disks decreased such a risk. Indeed, the separation on a monolithic disk was performed within a few seconds.

Affinity monolithic disks were not only used in combination with an HPLC system, but also for the monitoring of specific compounds as part of an FIA system. The use of the monolithic disks is beneficial because it is compatible with high flow rates at low to medium pressure, has little to no dependency on the flow rate, is compatible with typical bioprocess samples, has long-term stability, and performs stable immobilization of highly active biologicals such as antibodies and enzymes.^[20] The monitoring of recombinant protein G concentrations from a cell lysate of *E. coli* was performed using monolithic disks with immobilized IgG. A similar approach, this time with the enzyme glucose oxidase immobilized, was used for the monitoring of the glucose concentration in a fermentation broth.

Monolithic Disks as Bioreactors

Enzymes immobilized to monolithic disks were not applied only as biosensors, but also as bioreactors.^[20,21] The first report, in 1991, describes the immobilization of carbonic anhydrase. Interestingly, an increase in enzyme activity with the increase of flow rate through the bioreactor was observed. Recently, the immobilization of trypsin was reported. Contrary to the previous work, increased flow rate diminished the extent of protein degradation. In contrast to the previously mentioned experiments, where the immobilized enzyme was used for substrate degradation, the synthesis of polyriboadenylate from ADP was studied by polynucleotide phosphorylase immobilized on a monolithic disk.

SCALE-UP OF MONOLITHIC DISK

An obvious approach for scaling-up the monolithic disks is by increasing their diameter. Because of the mechanical properties, however, this approach seems not to be the most appropriate one. The problem of increasing the

volume while preserving the short column length was solved with the introduction of the tubular monolithic columns. Furthermore, with the introduction of the tube-in-tube approach, the CLC approach can also be scaled. Detailed information about the preparation and characteristics of the tube monolithic columns can be found elsewhere.^[6,22]

CONCLUSION

Monoliths represent a novel stationary phase with advantageous chromatographic characteristics. Monolithic disks have proven to be very efficient separation media despite their short column length. Their main advantage is an extremely short separation time. This makes them a promising tool for the in-process monitoring of, for example, preparative chromatographic purification or bioprocesses, where fast analyses of complex mixtures are required to perform real-time actions. In addition, they are well suited for the very fast purification of small quantities of labile compounds, as well as in the fast development of chromatographic methods adapted to a preparative purification on larger monolithic columns.

REFERENCES

1. Tennikova, T.B.; Freitag, R. High-Performance Membrane Chromatography of Proteins. In *Analytical and Preparative Separation Methods of Biomacromolecules*; Aboul-Enein, H.Y., Ed.; Marcel Dekker, Inc.: New York-Basel, 1999; 255–300.
2. *Monolithic Separation Media*; Svec, F., Deyl, Z., Tennikova, T.B., Eds.; Elsevier: Amsterdam, 2003, *in press*.
3. Snyder, L.R.; Stadalius, M.A. High-Performance Liquid Chromatography Separations of Large Molecules: A General Model. In *High-Performance Liquid Chromatography, Advances and Perspectives*; Horvath, Cs., Ed.; Academic Press: Orlando, 1986; Vol. 4, 195.
4. Dubinina, N.I.; Kurenbin, O.I.; Tennikova, T.B. Peculiarities of gradient ion-exchange high-performance liquid chromatography of proteins. *J. Chromatogr.* **1996**, *753*, 217–225.
5. Tennikova, T.B.; Belenkii, B.G.; Svec, F. High-performance membrane chromatography. A novel method of protein separation. *J. Liq. Chromatogr.* **1990**, *13* (1), 63–70.
6. Štrancar, A.; Podgornik, A.; Barut, M.; Necina, R. Short Monolithic Columns as Stationary Phases for Biochromatography. In *Advances in Biochemical Engineering/Biotechnology; Modern Advances Chromatography*; Freitag, R., Ed.; Springer-Verlag: Heidelberg, 2002; 49–85.
7. Josić, Dj.; Strancar, A. Application of membranes and compact, porous units for separation of biopolymers. *Ind. Eng. Chem. Res.* **1999**, *38* (2), 333–342.
8. <http://www.biaseparations.com> (accessed March 2002).
9. Tennikova, T.B.; Svec, F. High-performance membrane chromatography: Highly efficient separation method for proteins in ion-exchange, hydrophobic interaction and reversed-phase modes. *J. Chromatogr.* **1993**, *646*, 279–288.
10. Podgornik, A.; Barut, M.; Jancar, J.; Strancar, A. Isocratic separations on thin glycidyl methacrylate-ethylenedimethacrylate monoliths. *J. Chromatogr., A* **1999**, *848*, 51–60.
11. Strancar, A.; Koselj, P.; Schwinn, H.; Josic, Dj. Application of compact porous disks for fast separations of biopolymers and in-process control in biotechnology. *Anal. Chem.* **1996**, *68* (19), 3483–3488.
12. Podgornik, A.; Barut, M.; Jaksa, S.; Jancar, J.; Strancar, A. Application of very short monolithic columns for separation of low and high molecular mass substances. *J. Liq. Chromatogr. Relat. Technol.* **2002**, *25*, 3099–3116.
13. Strancar, A.; Barut, M.; Podgornik, A.; Koselj, P.; Josic, Dj.; Buchacher, A. Convective interaction media: Polymer-based supports for fast separation of biomolecules. *LC GC* **1998**, *11*, 660–669.
14. Tennikova, T.B.; Freitag, R. An introduction to monolithic disks as stationary phases for high performance biochromatography (review). *J. High Resol. Chromatogr.* **2000**, *23*, 27–38.
15. Josic, Dj.; Buchacher, A. Monoliths as stationary phases for separation of proteins and polynucleotides and enzymatic conversion. (Review). *J. Chromatogr., B, Biomed. Sci. Appl.* **2001**, *752* (2), 191–205.
16. Podgornik, H.; Podgornik, A.; Perdih, A. A method of fast separation of lignin peroxidases using convective interaction media disks. *Anal. Biochem.* **1999**, *272*, 43–47.
17. Vodopivec, M.; Podgornik, A.; Berovic, M.; Strancar, A. Application of Convective Interaction Media (CIM®) disk monolithic columns for fast separation and monitoring of organic acids. *JCS* **2000**, *38* (11), 489–495.
18. Svete, P.; Milacic, R.; Mitrovic, B.; Pihlar, B. Potential for the speciation of Zn using fast protein liquid chromatography (FPLC) and convective interaction media (CIM®) fast monolithic chromatography with FAAS and electrospray (ES)–MS–MS detection. *Analyst* **2001**, *126*, 1346–1354.
19. Barut, M.; Podgornik, A.; Merhar, M.; Strancar, A. Rigid Discs. In *Monolithic Separation Media*; Svec, F., Deyl, Z., Tennikova, T.B., Eds.; Elsevier: Amsterdam, 2003, *in press*.
20. Berruex, L.G.; Freitag, R. Affinity-based Interactions on Disks for Fast Analysis, Isolation and Conversion of Biomolecules. In *Methods for Affinity-Based Separations of Enzymes and Proteins*; Gupta, M.N., Ed.; Birkhauser: Basel, 2002; Chapter 7.
21. Josic, Dj.; Buchacher, A. Application of monoliths as supports for affinity chromatography and fast enzymatic conversion. *J. Biochem. Biophys. Methods* **2001**, *49*, 153–174.
22. Podgornik, A.; Barut, M.; Mihelic, I.; Strancar, A. Tubes. In *Monolithic Separation Media*; Svec, F., Deyl, Z., Tennikova, T.B., Eds.; Elsevier: Amsterdam, 2003, *in press*.

Multidimensional TLC

Simion Gocan

"Babes-Bolyai" University, Cluj-Napoca, Romania

Introduction

Since the introduction of thin-layer chromatography (TLC), there has been great interest regarding the increase of separation capacity (spot capacity). This interest was motivated by the separation of complex mixtures that contain a great number of compounds. Some of them are difficult to separate because they have similar properties.

Two-Dimensional Development

Two-dimensional thin-layer chromatography (2D TLC) involves the application of a single sample to one corner of a TLC plate, which is subjected to two development processes. The TLC plate is developed with the first mobile phase, dried, and redeveloped in an orthogonal (the plate rotated through 90°) direction with a second mobile phase having different selectivity characteristics. Thus, the components migrate from the point of application into a two-dimensional thin layer, ensuring more space for resolution compared to one-dimensional separation.

Two-dimensional TLC is an analytical separation technique recommended for the separation of sample of compounds that are difficult to separate in a single dimension. This technique has been mostly used for qualitative clinical and biochemical analysis, where high selectivity separation is required.

In 2D TLC, any spot can be defined by a pair of x and y coordinates; the quality of a separation can be established by comparing the distance between all pairs of spots in the chromatogram. High resolution will be obtained when the selectivity between the two directions will be significantly different. In practice, several methods have been used to achieve this purpose. The potential methods for obtaining two different separation mechanisms in orthogonal directions are the following:

1. Two eluent systems of different selectivities for the sample components are used and a single sorbent thin layer for two dimensions is developed.

2. Two sorbent layers (e.g., silica gel and reversed phase) as adjacent zones with different selectivities can be used. The sorbent layer for the first development is a narrow strip (reversed phase), and for the second development, it is a large surface (normal phase). A suitable eluent system has to be used for each sorbent layer.

There are others possibilities, but all of them have the same principle (i.e., the selectivities to be different in the two orthogonal developments). If the selectivities are close to each other, the 2D separation effect will be a diagonal arrangement of the spots. A separation will be considered better when the spots will be uniformly spread along the entire surface of the plate.

Two-dimensional TLC is used for a great number of compounds. When spot capacity in the first direction is n_1 and is n_2 in the orthogonal direction, then the total spot capacity will be equal to $n_1 n_2$. References 1 and 2 should also be consulted for routine procedures.

Multiple Unidimensional Development

Multiple unidimensional development (MUD) is the simplest approach for enhancement of the separation capacity in TLC [2]. In this approach, the TLC plate is developed for a selected distance, then the plate is withdrawn from the developing chamber and the adsorbed solvent is evaporated before repeating the development process. MUD is a very versatile strategy for the separation of complex mixtures. The main feature of MUD is that it leads to an increase in the spot reconcentration mechanism. There is an optimum number of developments that provide maximum separation.

Programmed Multiple Development

The term *programmed multiple development* (PMD) was introduced by Perry et al. [3] for a TLC developing technique and defined as follows: A TLC plate is repeatedly developed in the same direction with the



same solvent. Each development run is longer than the previous development step. Following each run, the layer is dried by radiant heat, optionally assisted by a flow of inert gas. The lower edge of the layer remains, at all times, in the contact with the solvent in the reservoir, which is shielded from the radiant heat. The solvent migration distance is controlled, programmed via the lengths of intervals between the heating cycles.

Automated Multiple Development

Automated multiple development (AMD) combines the advantages of MUD and mobile-phase gradient elution. This multiple development approach was improved by Burger [4], who maintained the basic idea of development. The chromatogram is developed in the same direction, stepwise, over an increasing solvent migration distance, but changes all other characteristics. The characteristics of the AMD system, according to Burger, are as follows: An HPTLC plate is developed several times in the same direction with eluents differing in elution power. In general, the polarity of the eluent is decreased step by step over the solvent migration distance. Between each run, the plate is completely dried by vacuum.

Gradient elution in AMD starts with the most polar eluent and is varied toward decreasing polarity. Figure 1a shows a typical universal elution gradient, made up of the three solvents: methanol, dichloromethane, and hexane. Figure 1b illustrates the increasing duration of the development cycles. Time increments are chosen to obtain uniform increases of the running distance of ~ 3 mm/step.

Automated multiple development causes sample fractions to become concentrated into narrow bands. The eluent flows over the lower part of a sample before reaching the upper part, concentrating the sample in the top to bottom direction. This is due to the fact that molecules in the lower part of the sample zone start their upward movement earlier than those in the upper part of that sample zone each time the eluent front passes through that area. A strong solvent used at the beginning of AMD causes concentration effects similar to a plate with a concentration zone. The separation power is increased by factor of 3, as compared with regular high-pressure TLC (HP-TLC). The combination of the focusing effect and gradient elution results in extremely narrow bands. Their typical peak width is about 1 mm. This means that with the available separation distance of 80 mm, up to 40 components can be completely resolved (i.e., with a resolution greater than 1).

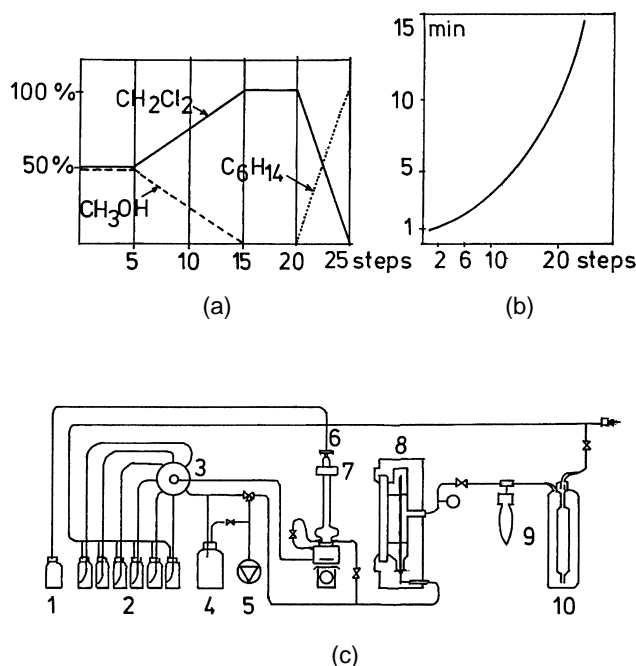


Fig. 1 (a) Typical universal elution gradient; (b) time of development versus number of steps; (c) AMD system flow diagram.

Design and Operation of an AMD System [5]

The Camag AMD system consists of two main components: the AMD developing unit (Fig. 1c) and the microprocessor-based controller. This system provides an AMD under reproducible conditions. For the AMD microprocessor-based controller, the following parameters may be chosen: the eluent composition, by selecting the number of solvent reservoir; the number of developing steps; the developing time for each step; the number of preconditions; the option of emptying the mixer after a selected step.

Functional Principle of the AMD Device

During the development process, the system is controlled by computer. The main component is an enclosed developing chamber (8), which is connected for introducing and withdrawing the developing solvent and for pumping the gas phase in and out. The six reservoir bottles (2) contain the individual solvent components. The gradient mixer (6) is connected, via motor valve (3), to reservoir bottles (2). The gas phase is made up externally by passing nitrogen through the wash bottle (10) into the gas-phase reservoir (9). At the same time, the mixer is filled with solvent from the solvent

reservoir bottle (1). Then, the chamber is equilibrated for 15 s with gas from the reservoir (9). The first step of development can start after filling the chamber (8) with the contents (8 mL) of the upper part of the gradient mixer (6), which is controlled by a light barrier (7).

Migration of the solvent in the layer starts immediately. At the end of the programmed time (determining the migration distance), the liquid solvent is removed by vacuum from the chamber (8) into the waste-collecting container (4). Then, after all liquid solvent has been removed, vacuum is applied by pump (5), thus drying the layer. The drying period is time programmed. Before the next developing cycle is started, the chromatographic thin layer is reconditioned by feeding the gas phase from the blender (9) into the chamber. After reconditioning the chamber, the next development step can start. While the drying phase is carried out, the solvent for the next step is made up in the gradient mixer (6).

Application

When the sample components differ widely in their polarities, they can be separated by using a universal elution gradient. With AMD, it is possible to simultaneously analyze 12 samples. AMD-HP-TLC has been applied for screening of pesticides from groundwater or drinking water and soil. A universal gradient based on dichloromethane was used to detect the presence of pesticides from different classes such as organochlorine, organophosphorus, carbamate, phenylureas, triazines, phenoxy-carboxylic acids, and others. In this way, 283 pesticides were analyzed using this universal gradient [6,7].

Plant extracts have a widespread application in the drug and cosmetic industries. For the separation of plant extracts, the AMD-HP-TLC method is the most suitable because it has a higher separating power. Isocratic and AMD development are shown in Fig. 2 [8].

On-Line Coupling of HPLC-AMD-TLC

Combining different separation methods, governed by different separation mechanisms, to multidimensional methods is suitable for multiplying the potential of the individual techniques. Reversed-phase chromatography high-performance columns (RP-HPLC) can be coupled with normal phase TLC [9,10].

Principle

The system for mass transfer HPLC-TLC consists of a column filled with RP-C₁₈ sorbent and a modified

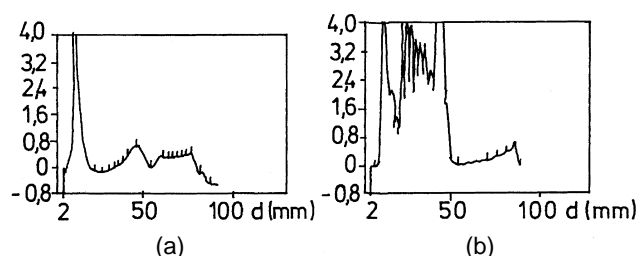


Fig. 2 Densitograms: (a) isocratic development TLC; (b) AMD-TLC.

Linomat (Camag) sample spray unit for TLC. The effluent is transferred, via a capillary tubing, to a TLC applicator unit. While the effluent of the HPLC column is sprayed onto the thin layer with nitrogen, the plate is moved. The separation of 56 pesticide residues in drinking water in a single sample using RP-HPLC coupled with TLC and AMD has been demonstrated. For example, by AMD, a chromatogram of RP-HPLC cut no. 13 was separated and over 10 pesticides were detected through multiwavelength scanning by absorbance between 200 and 300 nm, [11].

References

1. N. Grinberg (ed.), *Modern Thin-layer Chromatography*, Marcel Dekker, Inc., New York, 1990.
2. C. F. Poole and S. K. Poole, *Chromatography Today*, Elsevier, Amsterdam, 1991.
3. J. A. Perry, K. W. Haag, and L. J. Glunz, *J. Chromatogr. Sci.* 11: 447 (1973).
4. K. Burger, *Z. Anal. Chem.* 318: 228 (1984).
5. D. E. Jaenchen, in *Proceedings 3rd International Symposium on Instrumental HPTLC* (R. E. Kaiser (ed.), Institute for Chromatography, Bad Duerkheim, Germany, 1985, p. 71.
6. S. Butz and H. J. Stan, *Anal. Chem.* 67: 620 (1995).
7. R. Koeber and R. Niessner, *Fresenius J. Anal. Chem.* 354 (1996).
8. S. Gocan, G. Cimpan, and L. Muresan, *J. Pharm. Biomed. Anal.* 14: 1221 (1986).
9. D. E. Jaenchen, in *Proceedings 4th International Symposium on Instrumental High Performance Thin-Layer Chromatography*, H. Trautler, A. Studer, and Kaiser (eds.), Institute for Chromatography, Bad Duerkheim, Germany, 1987, p. 185.
10. J. W. Hofstra, M. Engelsman, R. J. Van De Nesse, C. Gooijer, N. H. Velthorst, and U. A. Th. Brinkman, *Anal. Chim. Acta* 186: 247 (1986).
11. B. Protze, Diploma thesis, Fachhochschule Niederrhein Krefeld, Germany, 1986.



Natural Products Analysis by CE

Noh-Hong Myoung

Institute of Health and Environment, Seoul, Korea

Introduction

Natural products chemistry is a science that investigates the identification, metabolism, biosynthesis, distribution, and biological activity of various organic compounds derived from living things. It concerns, essentially, the separation, purification, and structural determination of each compound. It was not until the late 1700s that, in plants or animals, the separation of natural products was carried out; for example, tartaric acid was extracted from grapes, citric acid from lemons, and malic acid from the apple by Scheele, a pharmacist in Sweden. In the nineteenth century, most of the compounds, alkaloid, terpenoid, and glycoside, were first isolated in pure form and elucidated structurally, since morphine was extracted from opium by Serturner. In the twentieth century, natural products chemistry achieved a great promotion through development of micro element analysis and column chromatography, which allowed physiological activity materials in crude form to be isolated with ease. Natural products are the organic and inorganic compounds found in nature: in plants (leaves, roots, barks, rhizoma, flowers, and seeds), in marine organisms (plants, animals, and microbes), in the fungi found in highly diverse and sometimes extreme environments, and in soil [1].

Discussion

There are two major classes of natural products: primary and secondary metabolites. Primary metabolites are compounds that exist in all organisms and are involved in basal and vital metabolism (e.g., glucose, fatty acids, amino acids, etc.). Secondary metabolites, alkaloids, terpenoids, and flavonoids, are unique to a particular species and vary in their basic structures. Secondary metabolites are usually accumulated, as most of their end metabolites are in plants, but are excreted in animals and microorganisms and some of these are proven to have pharmacological and ecological significance.

The pharmaceutical industry, in its drug discovery efforts, has relied heavily on natural products. Not all

natural products are bioactive; in fact, most have little or no measurable activity at all. Simple sugars, lipids, amino acids, flavonoids, and so forth are nature's essential building blocks, and measurements of their quantities are needed for the study of metabolism, disease processes, and aging. In today's public marketplace, there is a growing interest in the so-called crude drugs, where an increasing number of herbal products claimed as health aids, bodybuilding supplements, nutrients, vitamin supplements, cosmetics, and so forth are being sold.

In Asia, plants have been applied in various diseases and studied with their components for many years. For research of their components, at first, fresh plants are dried at low temperature, for short times, in well-ventilated places so as to minimize chemical change of components, and then they are extracted. They are generally finely ground and extracted first with an organic solvent, then by water, to remove the widest possible range of compounds, from the hydrophilic to the most hydrophobic. The solvent is then removed and the crude extracts are tested for biological activity. If they are found to be active, fractionation by a variety of chromatographic techniques is initiated. At each step, the fractions are reevaluated, and only those fractions in which bioactivity is increasing are fractionated further. Finally, a pure chemical and structural identity of the molecule is determined by a combination of nuclear magnetic resonance (NMR), infrared (IR), ultraviolet (UV), mass spectrometry (MS), x-ray crystallography, and other analytical tools. Once the structure and chemical properties of an active compound are known, quantitative and qualitative analytical methods are employed to detect and quantify it. Recently, the pharmacological significance of the crude drugs is highlighted in terms of the suitability of their medicinal value and low number of side effects. Most crude drugs are comprised of more than one component and their number is determined through the analysis of major components.

Although high-performance liquid chromatography (HPLC) and gas chromatography (GC) have been mainly applied in quantitative method of analysis, they



have difficulty with simultaneous quantitative analysis of crude drugs and have problems concerning the instability of experimental conditions, poor reproducibility because of pretreatment of crude drugs, efficacy of columns, and delay of separation time. GC has a limitation that components must be volatile. HPLC requires longer times for simultaneous analysis of samples, although gradient could be used advantageously for shortening analysis times.

With capillary electrophoresis (CE), it is possible to carry out simultaneous quantitative analysis with small sample volumes (1–10 nL); the amount of solvent waste generated is in the order of 1–2 mL/day and requires much less analysis time, with outstanding resolution. CE may be able to resolve a component of interest more quickly and with less effort invested in sample preparation than alternative techniques, because it can resolve neutral as well as ionic compounds using the same column in the same analytical run. Although CE is an excellent micro-analytical technique, its use in a preparative format is limited at the present time. CE in its capillary zone electrophoresis (CZE) and micellar electrokinetic chromatography (MEKC) formats allows the analyst to resolve both ionic and neutral compounds on the same column using simple buffers, with or without an organic modifier, a micelle, a cyclodextrin, or a mixture of all of these. The reproducibility of migration time is the factor requiring improvement with CE, as the longer the migration time is, the more the peak area increases.

The velocity of a solute in the capillary is determined by its electrophoretic mobility and electro-osmotic flow (EOF), which are affected by temperature, and which is influenced by the diameter and length of the capillary, its contents, concentration, and pH of running buffer, applied voltage, current, viscosity, and zeta-potential. The subtle variation of EOF is also a main factor in maintaining high reproducibility if CE is automated by the constant temperature of the capillary and running buffer with proper buffering capacity. However, it is difficult to keep the temperature constant, as EOF depends on the condition of the fused silica.

The zeta-potential present on the silica surface is changed by the cleaning, preconditioning, storage method, and use time. Therefore, it is important to keep the surface condition reproducible. Usually, herb drugs are made of several crude drugs, as extracts, powders, or pills. The components of herb drugs are so varied that their quality control is applied to just one or two of their index components. CE has been applied to the analyti-

cal study of various components ever since it was applied to individual components in glycyrrhizin of an herb drug by Iwagami in 1991 [2]. Presently, new analysis methods that are combinations of MEKC have been developed for the distribution of samples in an interfacially active agent by Terabe. CZE is able to analyze components with and/or without electric charge [3].

Micellar electrokinetic chromatography was originally developed for the separation of electrically neutral substances by capillary electrophoresis and has proven to be a highly efficient separation method for various kinds of analyte. Although various ionic substances can be separated by CE alone, the separation of many components in complex mixtures is not always successful. For example, a number of drugs are ionic, but some of them are not easily separated by CE. MEKC has been shown to be a powerful technique for the separation of complex drug mixtures. Although most of these drugs can be separated by HPLC, MEKC usually gives a better resolution in shorter analysis times.

Compared to HPLC, CE is simpler, faster, more convenient, and has a higher resolution power, which is a necessity when analyzing complex multicomponent mixtures.

A literature search reveals that CE has been used for the analysis of widely different natural compounds from extracts of leaves and needles, bark, roots, marine organisms, moss, soils, and so forth. To illustrate the problems associated with analyzing natural product extracts, especially from plant materials, by chromatography and to demonstrate how CE can overcome some of these problems as a consequence of its high resolving power, we compared the separation of an extract from the radix of the *Scutellaria baicalensis* Georgi by HPLC and CE. *Scutellaria radix* is the root of *Scutellaria baicalensis* Georgi. It is well known and is frequently used in oriental pharmaceutical preparations as a remedy for inflammation, suppurative dermatitis, allergic diseases, hyperlipidemia, and arteriosclerosis [4].

Flavonoids are major components of *Scutellaria radix*, and about 40 kinds of flavonoids have been identified in it so far [5]. These flavonoids are known to have a broad range of physiological activities. The activities of baicalin, which is the main component, baicalein, and wogonin, in particular, have been investigated. From the results, it has been concluded that the most potent antiallergic material is baicalein, and the other flavonoids have low activities. Therefore, the quantitative analysis of individual flavonoids is important for evaluating the quality of *Scutellaria radix*. Figures 1 and 2 show the HPLC



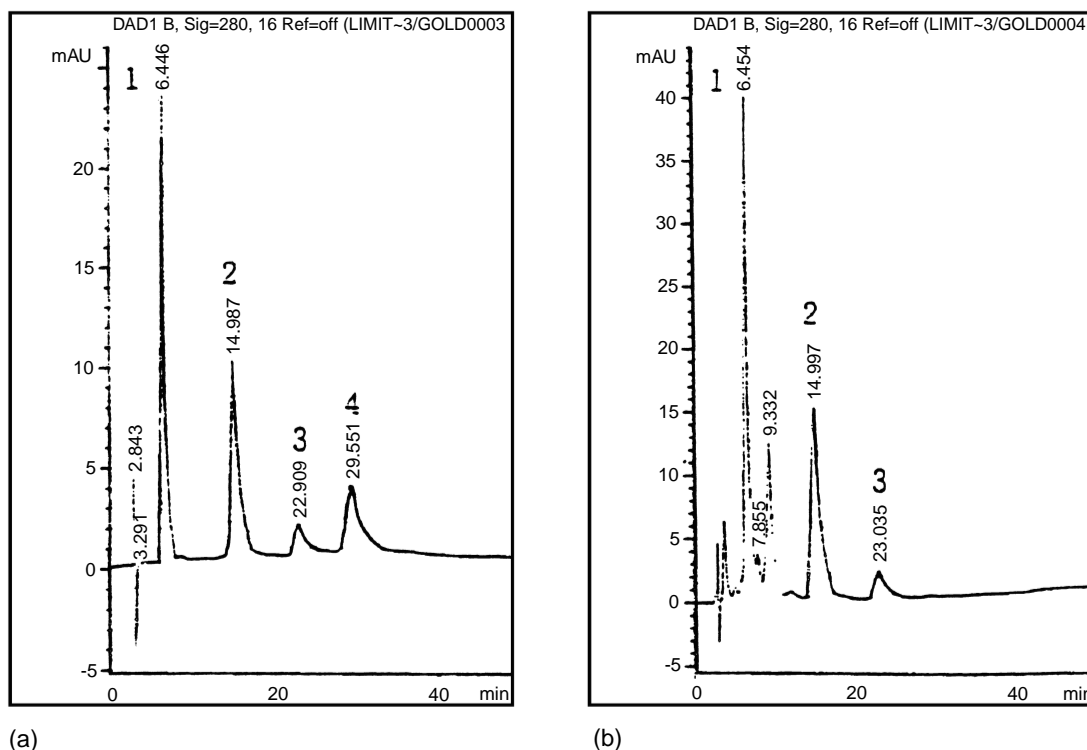


Fig. 1 HPLC chromatogram of standard mixtures (a) and a *Scutellaria radix* extract (b). Key: 1: baicalin; 2: baicalein; 3: wogonin; 4: chrysin.

chromatogram and CE electropherogram of a crude drug radix extract (*Scutellaria baicalensis* Georgi). These samples were obtained by first extracting with 50% ethanol. In the ethanol extract, many compounds are left. It is clear from Fig. 1 that HPLC is not the method of choice in this case. Important characteristics of an analytical procedure are sufficiently high precision and accuracy and also the time of analysis. Therefore, often it is not relevant in method development to simply maximize the resolution of the sample components without fulfilling the demands on analysis time. Decreasing the pH of the buffer leads to an increase in the degree of dissociation of baicalin, baicalein, wogonin, and chrysin. However, crude drugs have many components. As *Scutellariae radix* has about 40 kinds of flavonoid, it is very difficult to simultaneously separate baicalin, baicalein, wogonin, chrysin, and other flavonoids in a short time. Based on the dependence of the migration times and resolution on pH and phosphate buffer concentration (Fig. 2), it can be concluded that the most favorable electrolyte system is that with pH 7.0, 35 mM phosphate buffer. This system was applied for the determination of baicalin,

baicalein, wogonin, and chrysin in the extracts of *Scutellariae radix*. A typical HPLC chromatogram obtained from the extract of *Scutellariae radix* with a KFDA regulation is shown in Fig. 1. Baicalin is not clearly distinguished from other components and the analysis time is greater than 35 min.

By comparing the records of Figs. 1 and 2 for the results of HPLC and CE analysis, it is seen that (a) CE provides higher sensitivity than HPLC and (b) the CE analysis time is shorter than HPLC.

Conclusions

The proposed method is well suited for the rapid and simultaneous determination of baicalin, baicalein, wogonin, and chrysin. The data presented in this report indicates that CE has application for crude drugs. The separation by CE is completed within 15 min and is much faster than HPLC. A comparison of the analysis time for both techniques is made. Resolution, recovery, and reproducibility for four flavonoids in *Scutellariae radix*, separated by CE, are greatly improved in crude drug analysis.



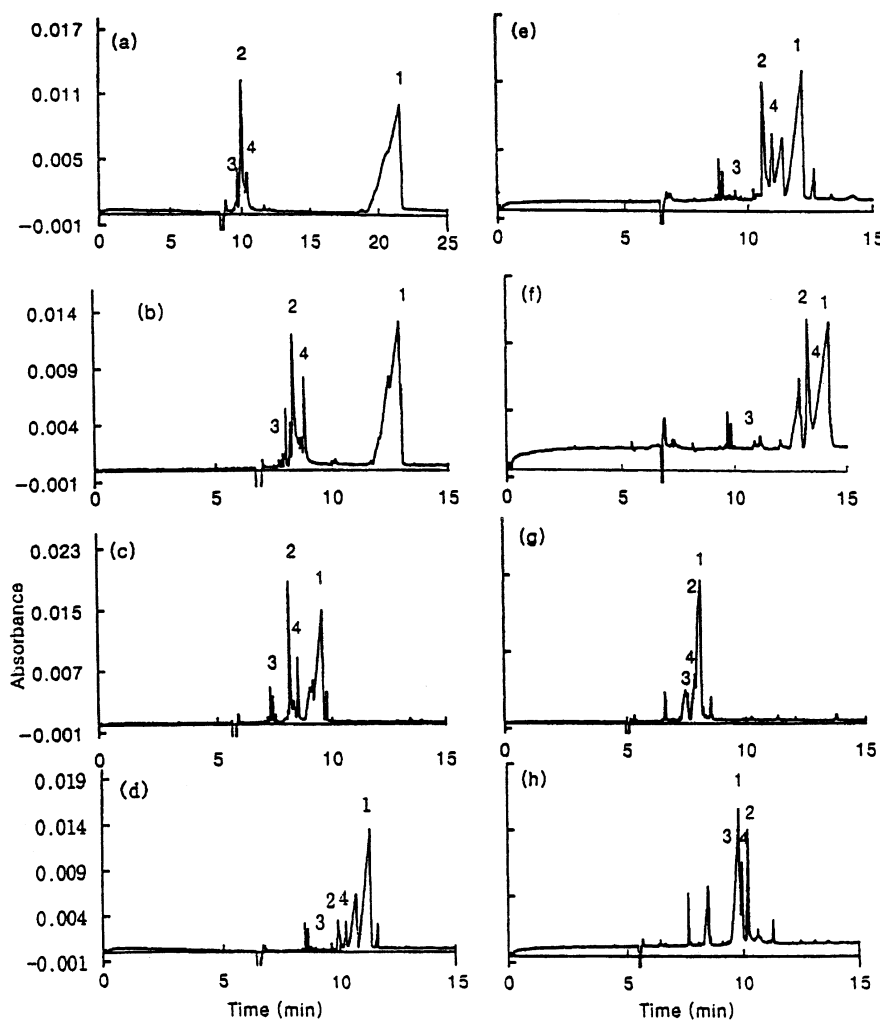


Fig. 2 Effect of running buffer pH and phosphate concentration on the separation of four components in the *Scutellaria radix* CE (1: baicalin; 2: bicalcin; 3: chrysin; 4: wogonin). (a) pH 6.0 sodium citrate buffer (20 mM), (b) pH 6.5 sodium phosphate buffer (20 mM), (c) pH 7.0 sodium phosphate buffer (20 mM), (d) pH 7.0 sodium phosphate buffer (35 mM), (e) pH 7.0 sodium phosphate buffer (50 mM), (f) pH 7.0 sodium phosphate buffer (100 mM), (g) pH 7.5 sodium phosphate buffer (50 mM), (h) pH 8.0 sodium phosphate buffer (35 mM).

References

1. H. J. Issaq, Capillary electrophoresis of natural products, *Electrophoresis* 18: 2438 (1997).
2. S. Iwagami, Y. Sawaba, and T. Nakagawa, Micellar electrokinetic chromatography for the analysis of crude drugs. Determination of glycyrrhizin in oriental pharmaceutical preparations, *Shoykugaku Zasshi* 45(3): 233 (1991).
3. S. Terabe, K. Otsuka, K. Ichikawa, A. Tsuchiya, and T. Ando, Electrokinetic separations with micellar solutions and open-tubular capillaries, *Anal. Chem* 56: 111 (1984).
4. S. I. Lee and D. G. An, Natural herb products sciences, Young Lim Co., Seoul, p. 178 (1992).
5. H. S. Yoon, Flavonoid components in plants of the Genus *Scutellaria*. *Korean J. Pharmacogen.* 23: 201 (1992).

Natural Rubber: GPC–SEC Analysis

Frederic Bonfils

CIRAD-CP, Programme Hevea, Montpellier, France

Introduction

Natural rubber, produced from *Hevea brasiliensis*, a very high-molar-mass polymer, differs from most of its synthetic counterparts through its more complex microstructure, due to the interactions of nonrubber compounds with the polyisoprene chains. This “associative” microstructure is gradually destroyed and, part when the polyisoprene is dissolved in a conventional solvent. However, in very many cases, a proportion of the natural rubber remains insoluble in such solvents; this fraction is commonly called the gel or macrogel phase [1,2] and is usually eliminated and quantified by centrifugation. The soluble fraction contains the polyisoprene macromolecules and a variable quantity of microaggregates, between 1 and 15 μm in diameter [3], forming the microgel.

Numerous *Hevea* varieties, referred to as “clones” in the professional jargon, can be found in estates. Subramaniam [4] was the first to study natural rubber from various clones by size-exclusion chromatography (SEC), to study the native molar mass distribution.

This article describes the different stages of natural rubber analysis by SEC, concentrating on the points that distinguish natural rubber from other more conventional polymers.

Dissolving and Eluant

In most cases, tetrahydrofuran (THF) has been used as the mobile phase, except by Bartels et al. [5], who used cyclohexane. However, using THF to analyze natural rubber by SEC can raise certain problems [6].

As a general rule in our laboratory, the samples of natural rubber are dissolved in cyclohexane (HPLC grade) stabilized with 2,6-di-*tert*-butyl-4-methylphenol (internal standard) at a rate of 120 mg for 30 mL of solvent. The solutions, stored at 30°C, are gently stirred for 1 h, periodically, for 14 days.

Equipment

The equipment used consists of a conventional SEC system [gas extractor, a pumping system, an injector, col-

umn(s), and detector(s)]. It is important to use a column oven. At room temperature, injecting natural rubber solutions into an SEC system can block the columns. The oven temperature used depends on the solvent used as the mobile phase. With cyclohexane, the oven temperature must be 65°C to overcome adsorption phenomena due to the very low polarity of this solvent. When using THF, the oven is heated to 50°C.

Using columns with a porosity of 20 μm is also recommended, in order to minimize shearing the long chains of the polyisoprene. As molar mass distribution (MMD) in natural rubber is quite broad ($12 < I < 3$), the columns need to offer a considerable separation range.

Because cyclohexane does not require an added stabilizer in the mobile phase, this means that ultraviolet (UV) detection at 220 nm can be used. This is important, as this type of detector is more sensitive than a refractometer. In fact, as natural rubber is a polymer with a very high molecular weight, it is recommended that low-concentration solutions at around 0.2 mg/mL are injected, so as to overcome viscosity effects and avoid excessive shearing of the macromolecules [7]. Of course, a light-scattering detector, or viscometer, can be added to the system to access the branching rate [8,9], which is an important parameter for natural rubber.

Calibration

Cyclohexane as the mobile phase requires the use of polyisoprene standards, as polystyrene standards are not soluble in this solvent. It should be noted that calibration by polystyrenes results in an overestimation of molar masses by a factor of around 2, compared to the use of polyisoprene standards [10]. It is, therefore, necessary to carry out universal calibration or to convert molar masses using the Mark–Houwink coefficients relative to synthetic or natural polyisoprenes [4,5,8,11,12].

Determining the Quantity of Macrogel

Once solubilization is complete, the solution is centrifuged (35,000g for 1 h at 17°C). The quantity of



macrogel is determined by weighing the centrifugation residue, after drying.

Filtering the Solutions Prior to Injection

The solution obtained after centrifugation is diluted to 0.2 mg/mL. It is allowed to stand for 24 h and is filtered through a disposable filter (glass fiber) with a porosity of 1 μm to eliminate the microgel. The filter porosity is very important, as the MMD observed after filtration through 0.45 μm or 1 μm are very different (Fig. 1). By filtering through 0.45 μm , shearing is considerable in the case of natural rubber.

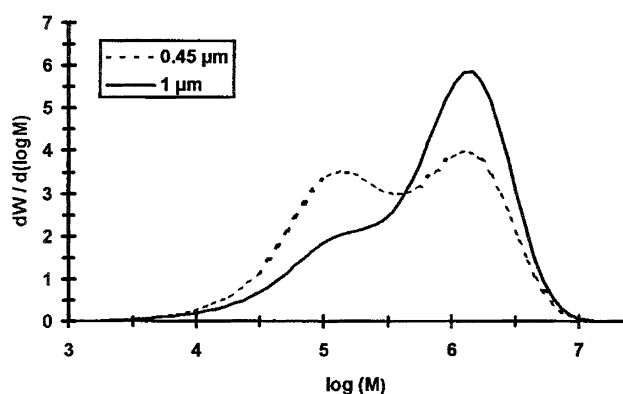


Fig. 1 Influence of the filter porosity on the molar mass distribution.

References

1. P. W. Allen and G. M. Bristow, *J. Appl. Polym. Sci.* 7: 603 (1963).
2. Y. Tanaka, J. Tangpakdee, and S. Kawahara, *Kautsch. Gummi Kunstst.* 50: 6 (1997).
3. A. P. Voznyakovskii, I. P. Dmitrieva, V. V. Klyubin, and S. A. Tumanova, *Polym. Sci. Series A* 38(10): 1153 (1996).
4. A. Subramaniam, *Rubber Chem. Technol.* 45: 346 (1972).
5. H. Bartels, M. L. Hallensleben, G. Pampus, and G. Schulz, *Angew. Makromol. Chem.* 180: 73 (1990).
6. F. Bonfils, A. K. Achi, J. Sainte Beuve, S. Sylla, A. Allet Don, and J. C. Laigneau, *J. Nat. Rubber Res.* 10(3): 143 (1995).
7. A. D. Edwards, in *Natural Rubber Science and Technology* (A. D. Roberts, ed.), Oxford University Press, Oxford, 1988, pp. 995–997.
8. J. L. Angulo-Sanchez and P. Caballero-Mata, *Rubber Chem. Technol.* 54: 34 (1981).
9. J. Tangpakdee and Y. Tanaka, *J. Nat. Rubber Res.* 1(1): 14 (1998).
10. C. L. Swanson, M. E. Carr, and H. C. Nielsen, *J. Polym. Mater.* 3: 211 (1986).
11. A. K. Bhowmick, J. Cho, A. MacArthur, and D. MacIntyre, *Polymer* 27: 1889 (1986).
12. K. N. G. Fuller and W. S. Fulton, *Polymer* 31: 609 (1990).

Neuropeptides and Neuroproteins by Capillary Electrophoresis

E.S.M. Lutz

AstraZeneca R&D Mölndal, Mölndal, Sweden

Introduction

Neuropeptides comprise peptide neurotransmitters and neuromodulators occurring primarily in the central nervous system (CNS), but may also be found in peripheral tissues. In order to study their physiological effects and their role in a variety of physiological functions (e.g., sensory information, food intake control, regulation of hormone secretion, and control of the sleep–waking cycle), methods for accurate determination of neuropeptides in biological tissues and fluids are required. Typically, immunoassays are used for this purpose, but cross-reactivity, especially with unknown fragments and matrix components, compromises quantitative analysis. In addition, immunoassays are generally designed for a single analyte, whereas neuropeptide research regularly aims to separately determine several neuropeptides in the same sample. One approach to inducing selectivity and allowing multiple neuropeptide analysis is to employ high-performance separations such as capillary electrophoresis (CE) in combination with appropriate sample handling and sensitive detection.

Capillary Electrophoresis of Neuropeptides and Neuroproteins

Because peptides and proteins are zwitterionic substances whose charge can be controlled through the pH, CE is well suited to provide high-speed separations with high efficiency, good mass sensitivity, low sample consumption, and high resolution. Differences relative to CE of low-molecular-mass compounds are due to the larger size of peptides and proteins, their secondary and tertiary structures, and their tendency to interact with the wall of bare fused-silica capillaries. This is valid for peptides and proteins occurring primarily in the CNS and for other peptide and protein analytes. For further reading, see the entry on Capillary Isoelectric Focusing of Peptides, Proteins, and Antibodies as well as to more extensive reviews (e.g., CE on opioid peptides by Lee et al. [1]).

Briefly, CE of peptides and proteins is often performed in uncoated fused-silica capillaries. In order to reduce interactions with the wall and to ensure that all peptides and proteins are charged, a buffer with a low pH (e.g., 50 mmol/L phosphate pH 2.5) is commonly used. Consistent rinsing protocols are required between runs, such as 0.1 mol/L NaOH followed by rinsing with the running buffer in order to remove adsorbed contaminants. When such rinsing procedures are not in compliance with the total analytical system or when adsorption of the analyte and/or matrix components hampers analysis, coating of the capillaries may prove useful. Adsorption phenomena can also be influenced by pH adjustment, temperature control, or by adding ionic and nonionic surfactants, organic solvents, or ion-pairing reagents to the running buffer. Both capillary coating and use of buffer additives affect the electro-osmotic flow leading to a reduction or a reversal of the flow, which, in turn, will affect the time required for separation.

Concentration sensitivities achieved in CE typically lie in the micromoles per liter or nanograms per liter range and are limited by sample loadability and detector path length (often 20–100 μm). Whether such concentration sensitivity is sufficient for a certain biochemical or pharmacological investigation depends primarily on the application. Complexity of the sample, concentration range of the analyte, and sample volume are all factors determining whether CE can be applied to analyze neuropeptides and neuroproteins in real-life samples. Plasma concentrations often are in the picomoles per liter range and can, accordingly, only be analyzed by CE after rigorous sample concentration. For instance, average concentrations of β -endorphin, methionin and leucine–enkephalin in 20 human plasma samples were determined to be 20 ng/ml, 2 ng/ml, and 2 ng/ml, respectively [2]. On the other hand, sampling of discrete areas in the brain can provide small samples with considerably higher concentrations of neuropeptides, and clear differences in concentrations may exist in the healthy and diseased states. For example, base levels of vasoactive intestinal peptide, substance P, and neuropeptide Y in nasal tissue of normal individuals are 28, 16, and 12 pg/ μg pro-

Encyclopedia of Chromatography

DOI: 10.1081/E-Echr 120005236

Copyright © 2002 by Marcel Dekker, Inc. All rights reserved.



tein, whereas patients suffering from allergy may have concentrations of 63, 165, and 98 pg/ μ g protein in perivascular lesion areas in the nasal tissue [3].

Even though free-solution CE is most commonly used for neuropeptides and neuroproteins, other forms of CE have also been employed. For instance, as an alternative to conventional slab-gel electrophoresis, a method using sodium dodecyl sulfate (SDS) capillary gel electrophoresis was developed. It was applied to low-molecular-mass proteins (β -trace protein, β_2 -microglobulin, ϕ -trace protein, and myelin basic protein) in cerebrospinal fluid [4]. Advantageous features of capillary gel electrophoresis over slab-gel electrophoresis are compatibility with small sample volumes, shorter analysis times, and more accurate quantification of the analytes.

Generally, integration of sample collection, preparation, and introduction with the analytical separation and detection is decisive for successful application of CE to neuropeptide analysis; why both sample handling and detection will be discussed in this context.

Sample Handling

Sample collection and preparation are crucial issues for any bioanalytical application in order to address the complexity of samples originating from biological tissues and fluids. It is necessary to cope with the lack in concentration sensitivity typical for capillary separation techniques, to avoid interference from matrix components as well as to ensure analyte stability. In peptide analysis, a strong focus exists on handling small-volume samples and on selective concentration of the analyte in order to overcome limitations with respect to loadability. In addition, loss of analyte frequently occurs due to degradation by proteases and due to adsorption to surfaces, which accordingly needs to be minimized.

In brain research, microdialysis sampling employing a miniaturized dialysis unit (probe) containing a dialysis membrane of a few millimeters length has become popular. The probe is implanted into the tissue or organ of the test animal and is infused with an isotonic solution (typically at 0.5–25 μ L/min). A steady-state osmotic flux across the membrane removes molecules with a mass below the cutoff of the membrane from the extracellular matrix. Microdialysis yields relatively clean samples of volumes in the range 20–100 μ L. However, the recovery of neuropeptides can be as low as 0.5–15%, leading to a low neuropeptide concentration in the samples [5,6].

Problems with recovery are avoided when sampling the extracellular brain tissue by means of a push–pull cannula. A push–pull cannula consists of two coaxial assembled hollow needles (cannulae) which are implanted into the brain. Artificial cerebrospinal fluid is infused through the inner cannula and withdrawn through the outer cannula [5–8].

In addition, a whole-tissue sample can be taken by means of routine pathological biopsy. Tissue samples are typically homogenized under denaturing conditions (0.1 mol/L HCl), centrifuged, and the supernatant is then used for further analysis [5]. When of interest, even morphologically defined areas can be investigated after being isolated by means of microdissection prior to further sample treatment. For example, nasal tissue biopsies were taken and perivascular lesion tissue or normal tissue 5 mm from the lesion were isolated by means of microdissection preceding further analysis [3].

As discussed in-depth elsewhere in this encyclopedia, sample composition is important with respect to peak efficiencies achieved in CE. When the sample has a lower conductivity than the running buffer, focusing occurs, which often is referred to as sample stacking. This is a convenient way of increasing concentration sensitivity 5–10-fold. However, when the sample has a higher conductivity than the running buffer, uneven migration of the analyte(s) and zone spreading will occur, resulting in lower concentration sensitivities. Biological samples therefore need to be desalted prior to submitting them to capillary electrophoretic separation.

Desalting of biological samples can be achieved with traditional sample preparation methods, including ultrafiltration, liquid–liquid extraction, and solid-phase extraction (SPE). Sample preparation, especially of plasma samples, involves, most often, protein precipitation by means of an acid or an organic solvent (e.g., acetonitrile), followed by SPE. After evaporation of the eluate and reconstitution in the running buffer used for CE, [D-Pen^{2,5}]enkephalin was analyzed in rat serum in this way [9]. These traditional sample preparation methods usually include deproteination, which reduces the protease content of the sample and improves analyte stability. Another option to reduce peptide degradation during sample handling is to add a protease inhibitor (e.g., 1 mmol/L leupeptin) [3].

Even under ideal circumstances, samples that are ready for CE analysis are in the microliter range, whereas typical injection volumes in CE are a few nanoliters. In order to take full advantage of the sample, increased injection volumes without column over-



load are desirable and can be achieved by coupling (transient) isotachopheresis (ITP) to CE. During ITP, the concentration of the sample introduced into the capillary is adapted to the concentration of the leading buffer, thus focusing the sample in a discrete zone. A discontinuous buffer is used during ITP, and after a change in conditions, separation by capillary zone electrophoresis continues. On-column ITP enables focusing of 10–100 times higher injection volumes (100–1000 nL), but it is limited to the total volume of the analytical system.

Another approach to increase the loadability is to enrich the analyte at the capillary inlet by means of an adsorptive phase, as reviewed in detail in Ref. 10. Reversed-phase materials such as octadecyl-bonded silica have regularly been used in the form of membranes or column materials, thus, in principle, performing miniaturized SPE (μ SPE) in-line with CE, allowing injections of 10–15 μ L. More selective sample concentration is obtained when using antibodies or Fab fragments for coating the inner wall of the capillary inlet [3,5].

Often a combination of techniques is used to achieve a sufficient concentration of the sample in combination with selective cleanup—for instance, a combination of microdialysis and immunoaffinity CE [11], microdissection and SPE [7], or microdialysis and μ SPE [12].

Detection

Detection of neuropeptides in CE is usually performed by ultraviolet (UV) absorbance, fluorescence and mass spectrometry (MS). UV absorbance is widely used for detection in CE, often at 214 nm, because it is inexpensive, robust, and widely available on commercial instruments. Typically, concentration sensitivities lie in the micromoles per liter range, as shown in an application starting from 2.5-mL lumbar cerebrospinal fluid, where detection limits of neuroproteins with UV absorbance detection at 214 nm between 5 and 10 μ g/mL, corresponding to 0.1–1 μ mol/L, were reported [4]. In order to address the lack of sensitivity achieved with UV absorbance detection, path lengths in the detection window have been increased threefold by means of the bubble cell and 10-fold by applying the so-called z -cell.

Tryptophan and tyrosine are intrinsic fluorophores that are present in many peptides, which then can be identified with fluorescence detection. However, most peptides have no native fluorescence, thus making de-

derivatization a prerequisite for fluorescence detection. Derivatization has been described with naphthalene-2,3-dicarboxaldehyde- β -mercaptoethanol for determination of substance P and its metabolites [6], fluorescamine [5], and 5-carboxyfluorescein succinimidyl ester [8] for luteinizing hormone-releasing hormone (LHRH), neuropeptide Y, and β -endorphin. Kostel and Lunte [6] compared various postcolumn reactor designs, whereas Advis et al. [5,8] employed pre-column derivatization, among others. In order to improve sensitivity, laser light is frequently employed for exciting the fluorescent molecules referred to as laser-induced fluorescence (LIF) and provides a 500–1000 times improved sensitivity compared to UV detection.

Mass spectrometry is another detection technique widely used in neuropeptide analysis. Concentration sensitivities in CE–MS do not reach those obtained by CE–LIF; nevertheless, tedious derivatization procedures are avoided. In addition, CE–MS has proven to be a powerful tool for structure elucidation as illustrated by the investigation of the *in vivo* metabolic fate of peptide E by Caprioli's group [12]. After microdialysis and in-line SPE, neuropeptides migrating out of the electrophoresis capillary were deposited directly onto a precoated cellulose target used in matrix-assisted laser desorption–time of flight (MALDI–TOF) MS subsequently. Structural information is then obtained along with the mass of the peptide(s).

More extensive structural information is obtained when using MS–MS, where information on the peptide sequence can be extracted from the fragmentation pattern. So far, CE–MS–MS has predominantly been performed with electrospray ionization (ESI)–triple quadrupole and ESI–ion trap instruments, as reviewed in Ref. 13. The advent of ESI–TOF and ESI–quadrupole–TOF instruments is believed to have a strong impact on CE–MS. TOF instruments require an extremely short time to produce a full mass spectrum and are especially attractive as a detection device for a separation technique producing sharp peaks, as illustrated by the separation of three enkephalins in a time window of 6 s with detection by means of ESI–TOF [14].

Conclusions

In this entry, an overview is given over the implementation of CE in neuropeptide and neuroprotein analysis. So far, relatively few applications in biological matrices, including cerebrospinal fluid, plasma, and neural tissue, have been published; nevertheless, the potential of this approach has been demonstrated over the past years and the number of publications is growing steadily. Ac-



cordingly, it is expected that more research groups will be enticed to use CE for neuropeptide and neuroprotein analysis.

References

1. H. G. Lee and D. M. Desiderio, *Anal. Chim. Acta* 383: 79 (1999).
2. E. Ban, D. Kim, E. A. Yoo, and Y. S. Yoo, *Anal. Sci.* 13: 489 (1997).
3. T. M. Phillips, *Anal. Chim. Acta* 372: 209 (1998).
4. A. Hiraoka, T. Arato, I. Tominaga, N. Eguchi, H. Oda, and Y. Urade, *J. Chromatogr. B* 697: 141 (1997).
5. J. P. Advis, K. Iqbal, A. W. Malick, and N. A. Guzman, *Handbook of Endocrine Research Techniques*, Academic Press, San Diego, CA, 1993, p. 127.
6. K. L. Kostel and S. M. Lunte, *J. Chromatogr. B* 695: 27 (1997).
7. J. P. Advis, L. Hernandez, and N. A. Guzman, *Peptide Res.* 2: 389 (1989).
8. S. P. SungAe, W.-L. Hung, D. E. Schaufelberger, N. A. Guzman, and J. P. Advis, *Methods in Molecular Biology, Neuropeptide Protocols* (G. B. Irvine and C. H. Williams, eds.), Humana Press, Totowa, NJ, 1997, Vol. 73, p. 101.
9. C. Chen, D. Jeffery, J. W. Jorgenson, M. A. Moseley, and G. M. Pollack, *J. Chromatogr. B* 697: 149 (1997).
10. A. J. Tomlinson, L. M. Bensson, N. A. Guzman, and S. Naylor, *J. Chromatogr. A* 744: 3 (1996).
11. T. M. Phillips, L. M. Kennedy, and E. C. De Fabo, *J. Chromatogr. B* 697: 101 (1997).
12. H. Zhang, M. Stoeckli, P. E. Andren, and R. M. Caprioli, *J. Mass Spectrom.* 34: 377 (1999).
13. D. Figeys and R. Aebersold, *Electrophoresis* 19: 885 (1998).
14. I. M. Lazar, E. D. Lee, A. L. Rockwood, and M. L. Lee, *J. Chromatogr. A* 829: 1 (1998).



Neurotransmitter and Hormone Receptors: Purification by Affinity

Terry M. Phillips

Ultramicro Analytical Immunochemistry Resource, DBEPS, ORS, OD, NIH, Rockville, Maryland, U.S.A.

Introduction

The isolation of membrane receptors has great application in a number of fields ranging from structural biochemistry to pharmacology and the medicinal sciences. Although many biochemical approaches to receptor purification are available, the application of affinity techniques holds great promise. The use of selective receptor ligands promises isolation not only of a specific receptor but also possibly in a bioactive form. The use of immobilized receptor ligands often ensures that the integrity of the receptor structure is maintained during the isolation process due to protection of the receptor-binding domains by the ligand itself. Additionally, receptors can be isolated either via a chromatographic system or by batch technology. The application of ligand-coated magnetic beads offers a quick and relatively simple approach to receptor isolation, although its use is only just becoming evident.

Discussion

The application of biotinylated receptor substrates is another approach, incubating the labeled substrate with the receptors prior to isolation on an avidin-coated support. In such cases, biotinylation with a cleavable biotinylation reagent such as Sulfo-NHS-SS-biotin or NHS-Iminobiotin would be essential for recovery of the isolated receptor. Alternatively, the receptor could be recovered by substrate competition. Perhaps one of the major drawbacks to the application of affinity techniques is the relative low molecular weight or small size of the receptor substrates, making them difficult ligands to immobilize. However, affinity procedures have been applied to the purification of a number of different receptors although relatively little work has been reported on those involved in the processing of neurotransmitters, neuropeptides, and hormones [1,2].

Ligands used to isolate neurotransmitter and hormone receptors have ranged from immobilized receptor substrates to immobilized antireceptor antibodies, the latter being used extensively in recent years. This marks the increased availability of specific monoclonal

antibodies to specific receptors and/or receptor domains and the increasing popularity of using solid-phase extraction techniques over more physicochemical ones. The use of antibodies also circumvents problems arising from the immobilization chemistry required not only to maintain the integrity of the ligand but also its correct orientation. The rise of molecular biological techniques has opened a new approach to studying receptor structure and function. Cloning and expression of recombinant receptors in bacterial, yeast, or insect cells allows the investigator to engineer the receptor structure as well as the quantity of materials available for study. This situation has also increased the use of antibodies for the isolation of these recombinant receptors from culture medium.

Cosgrove et al. [3] described studies that isolated a recombinant ectodomain of the human insulin receptor using immobilized insulin as an affinity ligand. The ligand was immobilized to a chromatographic support and the receptor domain was isolated by affinity chromatography. The efficiency of the system was shown by the similarities between the isolated receptor domain and the native form isolated by physicochemical techniques. The process also allowed for the receptor to be isolated in a bioactive form as shown by its ability to bind insulin with a K_d of approximately 2×10^{-9} M. Feng et al. [4] approached the isolation of a recombinant human estrogen α -receptor in a different manner. They used a sequential heparin and 17- β -estradiol-17-hemisuccinate-bovine serum albumin affinity chromatography system to first remove the majority of the contaminating materials in the culture medium, followed by selective binding of the receptor to its substrate. This approach easily isolated the receptor yielding a 100-fold purification of a bioactive receptor. Ohtaki et al. [5] employed a biotinylated substrate to isolate a recombinant human pituitary adenylate cyclase-activating polypeptide (PACAP) receptor expressed in both insect cells and Chinese hamster ovary cells. The biotinylated ligand was immobilized on an avidin-coated support, allowing the receptor to be isolated by affinity chromatography.

The use of immobilized antibodies is perhaps the most popular approach to isolating these receptors.



Andersen and Stevens [6] employed a combination of immobilized metal affinity and immunoaffinity chromatography to isolate a functional recombinant human D1A dopamine receptor expressed in *Saccharomyces cerevisiae*. This was achieved by engineering both a FLAG and a His6 tag to the C-terminus of the receptor. The histamine tag was used to perform a primary selection via metal affinity chromatography followed by a second purification step involving immobilized antibodies directed against the FLAG tag. In this way, a bioactive recombinant receptor could be isolated in a relatively pure form. Recombinant human β -1 thyroid hormone receptors can be isolated using a one-step immunoaffinity chromatography procedure [7]. Antibodies directed against the receptor are immobilized to a suitable chromatographic support, enabling the recovery of a bioactive receptor capable of binding 3,3',5-triiodo-L-thyronine with a $K_d = 2 \times 10^{-9}$ M.

Eckard et al. [8] isolated a series of rhodopsin-like, G-protein-coupled neuropeptide Y receptors (Y1, Y2, Y4, and Y5) using immunoaffinity chromatography. Antibodies were raised against synthetic fragments of the second (E2) and third (E3) extracellular loops of the Y receptors and used to recover the receptors of interest. In a similar manner, murine glucocorticoid receptors have been isolated from a lymphoma cell line by immunoaffinity chromatography using an immobilized monoclonal antibody [9]. The antibody called BUGR-2 was coupled to protein A-coated Sepharose 4B beads and used in a chromatography system. Recovery of the bound receptors was achieved by epitope competition. This procedure released not only multiple receptors but also the heat-shock proteins 70 and 90, suggesting that the murine receptor interacts with these proteins, which may act as chaperones under physiological conditions. Immunoaffinity chromatography was also used by Repa et al. [10] for the isolation of members of the steroid/thyroid hormone receptor

superfamily. Isolation of recombinant retinoic acid receptors expressed in an insect cell line was achieved by immunoaffinity chromatography using a monoclonal antibody to the human γ -retinoic acid receptor. The immunoaffinity-purified receptor was found to be biochemically greater than 90% pure as revealed by silver-stained electrophoretic gels. The isolated receptor was also shown to be functional, binding its ligand with a K_d of approximately 2 nM.

References

1. A. Azzi, U. Brodbeck, and P. Zahler, *Membrane Proteins. A Laboratory Manual*, Springer-Verlag, New York, 1981.
2. J. C. Venter, *Receptor Biochem. Methodol.* 4: 117–139 (1984).
3. L. Cosgrove, G. O. Lovrecz, A. Verkuylen, L. Cavaleri, L. A. Black, J. D. Bentley, G. J. Howlett, P. P. Gray, C. W. Ward, and N. M. McKern, *Protein Express. Purif.* 6:789–798 (1995).
4. W. Feng, K. Graumann, R. Hahn, and A. Jungbauer, *J. Chromatogr. A* 852: 161–173 (1999).
5. T. Ohtaki, K. Ogi, Y. Masuda, K. Mitsuoka, Y. Fujiyoshi, C. Kitada, H. Sawada, H. Onda, and M. Fujino, *J. Biol. Chem.* 273: 15,464–15,473 (1998).
6. B. Andersen and R. C. Stevens, *Protein Express. Purif.* 13: 111–119 (1998).
7. J. B. Park, K. Ashizawa, C. Parkison, and S. Y. Cheng, *J. Biochem. Biophys. Methods* 27: 95–103 (1993).
8. C. P. Eckard, A. G. Beck-Sickinger, and H. A. Wieland, *J. Recept. Signal Transduct. Res.* 19: 379–394 (1999).
9. C. E. Powell, C. S. Watson, and B. Gametchu, *Endocrine* 10: 271–280 (1999).
10. J. J. Repa, J. A. Berg, M. E. Kaiser, K. K. Hanson, S. A. Strugnell, and M. Clagett-Dame, *Protein Express. Purif.* 9: 319–330 (1997).



Nitrogen/Phosphorus Detector

Raymond P.W. Scott

Scientific Detectors Ltd., Banbury, Oxfordshire, England

Introduction

The nitrogen/phosphorus detector (NPD) is extremely sensitive [more so than the flame ionization detector (FID)] but is also highly selective. As its name suggests, it responds strongly to substances containing nitrogen and/or phosphorus. Physically, the design appears very similar to that of the FID but, in fact, operates on an entirely different principle. A diagram of an NPD detector is shown in Fig. 1.

Discussion

The essential change that differentiates the NPD sensor from that of the FID is a rubidium or cesium bead contained inside a heater coil and situated close to the hydrogen flame. The bead, heated by a current through the coil, is situated above a jet, through which passes the helium carrier gas from the column mixed with hydrogen from a separate supply. If the detector is to respond to both nitrogen and phosphorus, then

the hydrogen flow is arranged to be minimal so that the gas does not ignite at the jet. If the detector is to respond to phosphorus only, a large flow of hydrogen can be used and the mixture burned at the jet.

The detector functions in the following manner. The heated alkali bead emits electrons by thermionic emission, which are collected at the anode, providing a base current across the electrode system. When a solute that contains nitrogen or phosphorus is eluted, the partially combusted nitrogen and phosphorus materials are adsorbed on the surface of the bead. This adsorbed material *reduces* the work function of the surface and, as a consequence, the emission of electrons is increased, which *increases* the current collected at the anode. The sensitivity of the NPD is very high and only about an order of magnitude less than that of the electron capture detector ($\sim 10^{-12}$ g/mL for phosphorus and 10^{-11} g/mL for nitrogen).

A significant disadvantage of this type of detector is that its performance deteriorates gradually with time and eventually does not function at all. Reese [1] examined the performance of the NPD in great detail. The alkali salt employed as the bead is usually a silicate and Reese demonstrated that the loss in response was due to water vapor from the burning hydrogen converting the alkali silicate to the hydroxide and free silica.

Unfortunately, at the normal operating temperature of the bead, the alkali hydroxide has a significant vapor pressure and, consequently, the rubidium or cesium is continually lost during the operation of the detector. Eventually, all the alkali is evaporated, leaving a bead of inactive silica. This is an inherent problem with all NPDs and, as a result, the bead needs to be replaced regularly if the detector is in continuous use. The detector can be made "linear" over three orders of magnitude, although no values for the response index appear to have been reported. Like the FID, it is relatively insensitive to pressure, flow rate, and temperature changes but is usually thermostatted at 260°C or above.

The specific nature of the NPD response to nitrogen and phosphorus, coupled with its relatively high sensitivity, makes it especially useful for the analysis

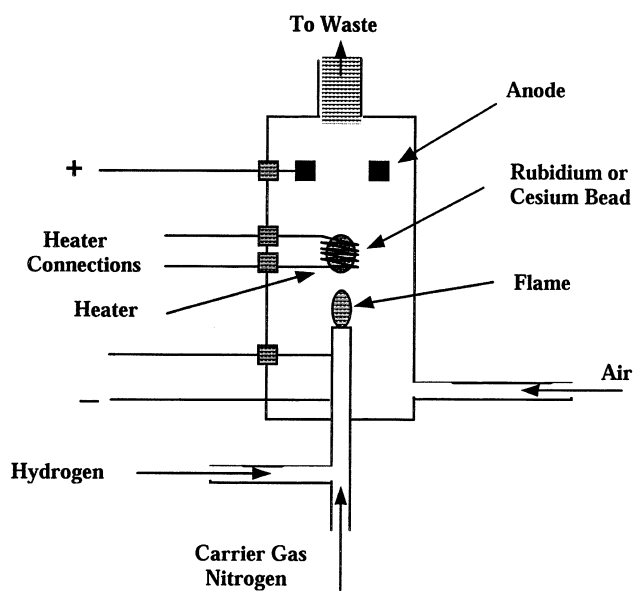


Fig. 1 The nitrogen/phosphorus detector.



of many pharmaceuticals and, in particular, in environmental analyses of samples containing herbicides. Employing appropriate column systems, traces of herbicides at the 500-pg level can easily be determined. Virtually all the basic drugs presently employed in medicine contain nitrogen. Consequently, the specific detection of the NPD allows these drugs to be selectively monitored and quantitatively assayed, even when they are eluted among a large number of other unresolved compounds not containing nitrogen.

Reference

1. C. H. Reese, Ph.D. thesis, University of London (Birkbeck College), 1992.

Suggested Further Reading

Scott, R. P. W., *Chromatographic Detectors*, Marcel Dekker, Inc., New York, 1996.

Scott, R. P. W., *Introduction to Analytical Gas Chromatography*, Marcel Dekker, Inc., New York, 1998.



Nonionic Surfactants: GPC–SEC Analysis

Ivan Gitsov

College of Environmental Science and Forestry, State University of New York, Syracuse, New York, U.S.A.

Introduction

Nonionic surfactants are one of the most important and largest surfactant groups. They are amphiphilic molecules composed, in most cases, of poly(ethylene oxide) (PEO) blocks as the water-soluble fragment and fatty alcohols, fatty acids, alkylated phenol derivatives, or various synthetic polymers as the hydrophobic part [1]. This class of surfactants is widely used as surface wetting agents, emulsifiers, detergents, phase-transfer agents, and solubilizers for diverse industrial and biomedical applications [2].

Discussion

Several nonionic surfactants have been used for many years under different trade names: Brij (ethoxylated fatty alcohols), Synperonic (PEO copolymers) and Tween (ethoxylated sorbitan esters) by ICI Surfactants; Igepal (PEO copolymers) by Rhone-Poulenc, Rhodia; Pluronic [poly(oxyethylene)-*block*-poly(oxypropylene) copolymers] by BASF; Triton DF (ethoxylated fatty alcohols), and Triton X (ethoxylated octylphenols) by Union Carbide; and others. The exploitation characteristics of nonionic surfactants depend on the oligomer distribution, the molecular-weight characteristics of the constituent blocks, and the hydrophilic/hydrophobic ratio of their chemical composition. Therefore, the quantitative determination of these factors is of primary importance for their performance evaluation. Several high-performance liquid chromatography (HPLC) separation techniques have been used in combination with different detection methods to characterize poly(ethylene glycol)s and their amphiphilic derivatives [3]. Size-exclusion chromatography (SEC) is a particularly attractive analytical tool for the investigation of nonionic surfactants because it can provide information for their composition, molecular weight and molecular-weight distribution, and their micellization in selective solvents. This entry will survey briefly both applications, with

major emphasis on the choice of the most appropriate eluent and stationary phase.

Molecular-weight determinations are performed in good solvents for both blocks of the PEO copolymers. The most widely used analysis conditions are eluents [tetrahydrofuran (THF) and chloroform (CHL)], flow rate (1.0 mL/min), and detection [differential refractive index (dRI) detector]. The temperature interval is between 20°C and 40°C. The stationary phase is typically a polystyrene/divinylbenzene cross-linked matrix supplied by different vendors: Phenogel (Phenomenex, U.S.A.); PL Gel (Polymer Laboratories, U.K.), PSS Gel (Polymer Standards Service, Germany), TSKgel (TosoHaas, U.S.A.), UltraStyrigel (Waters Corporation, U.S.A.), and others. The pore size range of the column set should be adjusted to the molecular-weight range of the investigated materials. The SEC analysis in THF requires low dRI response correction factors, between 1.66 for $M_n = 106$ and 1.00 for $M_n = 20,000$ [4], whereas the low-molecular-weight PEO derivatives are almost invisible in CHL. On the other hand, the solubility of PEO in THF decreases with the molecular weight, as evidenced by steeper calibration curves and broadening of the peaks in the eluograms; see Fig. 1. This complicates the precise molecular-weight calculations of PEO copolymers and the choice of calibration standards becomes crucial [5]. Increasing the content of PEO in the copolymer results in lower hydrodynamic volumes in THF and, consequently, yields lower apparent molecular weights, regardless of the macromolecular architecture of the analytes [6]. The problems with calibration mismatch can be avoided to some extent by using the universal calibration approach with on-line differential viscometry. This method provides accurate molecular-weight information for most linear and comb-graft PEO copolymers, but has been proved less precise for copolymers with complex linear-dendritic or hyperbranched architecture. On-line laser-light-scattering detection eliminates the need for a calibration curve and yields correct M_w values for macromolecules with molecular weights higher than 500 g/mol.



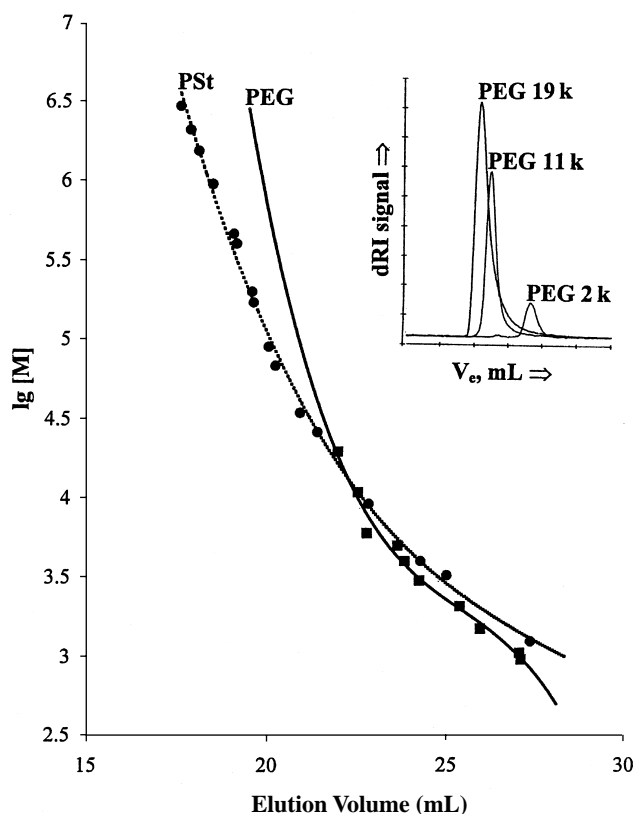


Fig. 1 Poly(styrene) (PSt) and poly(ethylene glycol) (PEG) calibration curves obtained on PL Gel column set (Mixed C, 10^3 Å, 5×10^2 Å, and 10^2 Å). Eluent: THF; flow rate: 1 mL/min; temperature: 40°C. Inset: SEC elution profiles of PEGs at the same analysis conditions.

The precision of the method depends largely on accurate dn/dc values that need to be measured for each copolymer investigated.

The self-assembly process of nonionic surfactants in aqueous media differs in several aspects from the micellization of amphiphilic copolymers:

1. Micelles constructed of low-molecular-weight surfactants have much lower molecular weights than that of polymeric ones.
2. The critical micelle concentration (CMC) is much lower for polymer surfactants.
3. The vast majority of polymer micelles have spherical shape in dilute or semidilute solutions, whereas low-molecular-weight surfactants form structures that are strongly concentration dependent—lamellae, sheets, rods, and spheres.
4. The kinetics of micelle formation and the dynamics of the micelle–unimer equilibrium are considerably slower for polymeric surfactants.

The last factor is particularly important for the successful utilization of aqueous SEC in the investigation of the micellization process. In order to provide a realistic picture for the micellization equilibrium, the chromatographic system needs to meet several strict requirements: The packing material and the eluent should be appropriately chosen to prevent the occurrence of non-size-exclusion phenomena and adsorption of micelles in the stationary phase. In all cases, mass balance of the material injected and recovered from the columns must be performed in order to verify the absence of copolymer entrapment. Cross-linked copolymers containing either poly(vinyl alcohol) or poly(glycidyl methacrylate) as the hydrophilic component are the most widely used column packing materials for aqueous SEC. Both Shodex Protein KW (Showa Denko, Japan) and Micropak TSK-gel PW (Toyo Soda, Japan) columns have been reported to afford good information on the micellization behavior of PEO copolymers without the interference of side effects [7]. The mobile phase is methanol–water (1:1, v/v) or pure water eluting at 1.0 mL/min. The analysis temperature is between 22°C and 40°C.

Historically, the major concern for the use of SEC in the investigation of micellar systems has always been the lack of suitable calibration and, consequently, the inability of the method to furnish accurate information for the size (hydrodynamic volume) of the micelles and their molecular weight. The incorporation of light-scattering and viscosity detectors for on-line measurement seems to eliminate this problem. With no solute–column interaction present and slow unimer–micelle equilibrium, a multiangle light-scattering detector (DAWN-DSP, Wyatt Technology, U.S.A.) provides accurate information for the molecular weight and radius of gyration of the micelle using Zimm's formalism:

$$\frac{R_\theta}{K^*c} = M_w P(\theta) - 2A_2 c M_w^2 P^2(\theta)$$

where R_θ is the excess Rayleigh ratio, K^* is an optical constant that includes the differential refractive index increment (dn/dc) of the solvent–solute mixture, c is the concentration of the solute molecules in the analyzed solution, M_w is the weight-average molecular weight, $P(\theta)$ is a form factor, and A_2 is the second virial coefficient. If the dn/dc value for the copolymer above the CMC is known, the extrapolation to zero concentration and zero angle will yield the Z-average of the radius of gyration and A_2 , respectively. The double extrapolation to zero angle

and zero concentration will afford M_w . The hydrodynamic radii can be calculated using on-line viscometric detector (Viskotec, U.S.A., and Waters) and the following relationship:

$$R_\eta^3 = \frac{3[\eta]M}{10\pi N_A}$$

where the value of $[\eta]M$ could be extracted directly from the universal calibration and N_A is Avogadro's number (6.022×10^{22}). It should be pointed out, however, that this formula is strictly valid only for spherical structures. The hydrodynamic radius can also be measured by a combination of SEC and dynamic light scattering (Precision Detectors, U.S.A.) or nuclear magnetic resonance spectroscopy [8]. However, the same assumption for a spherical shape of the investigated macromolecules has to be made.

In conclusion, modern SEC is a versatile technique for the investigation of nonionic surfactants in aqueous and organic media. In combination with different spectroscopic and viscometric detectors, it will provide useful information for the molecular-weight characteristics, chemical composition, and solution behavior of this important class of materials.

References

1. B. Jönsson, B. Lindman, K. Holmberg, and B. Kronberg, *Surfactants and Polymers in Aqueous Solution*, John Wiley & Sons, New York, 1998.
2. J. E. Glass (ed.), *Hydrophilic Polymers: Performance with Environmental Acceptability*, Advances in Chemistry Series Vol. 248, American Chemical Society, Washington, DC, 1996.
3. K. Rissler, *J. Chromatogr. A* 742: 1–54 (1996).
4. S. Mori, *Anal. Chem.* 50: 1639–1643 (1978).
5. B. Trathnigg, S. Feichtenhofer, and M. Kollroser, *J. Chromatogr. A* 786: 75–84 (1997), and references therein.
6. D. Taton, E. Cloutet, and Y. Gnanou, *Macromol. Chem. Phys.* 199: 2501–2510 (1998); I. V. Berlinova, I. V. Dimitrov, and I. Gitsov, *J. Polym. Sci., Part A: Polym. Chem.* 35: 673–679 (1997); I. V. Berlinova, A. Amzil, and N. G. Vladimirov, *J. Polym. Sci., Part A: Polym. Chem.* 33: 1751–1758 (1995).
7. I. V. Berlinova, N. G. Vladimirov, and I. M. Panayotov, *Makromol. Chem., Rapid Commun.* 10: 163–166 (1989); R. Xu, Y. Hu, M. A. Winnik, G. Riess, and M. D. Crocher, *J. Chromatogr.* 547: 434–438 (1991).
8. G. R. Newkome, J. K. Young, G. R. Baker, R. L. Potter, L. Audoly, D. Cooper, C. D. Weis, K. Morris, and C. S. Johnson, Jr., *Macromolecules* 26: 2394–2396 (1993).



Normal-Phase Chromatography

Fred M. Rabel

EM Science, Gibbstown, New Jersey, U.S.A.

Introduction

There are a number of modes or mechanisms into which chromatography is divided. These include adsorption, normal-phase partition, reversed-phase partition, and ion exchange. Often, the term “partition” is deleted from the discussions of the differences and similarities of these modes. The word “partition” initially arose when supports had to be coated with a liquid phase (and the mobile phases saturated with them) to accomplish separations with these two modes. Today, bonded-phase versions of these liquid phases are available, making them easier to use with greater reproducibility. Perhaps it has been the use of these bonded supports that have enabled the name of the mode to be simplified.

The reasons for distinguishing between these modes are as follows:

1. To better understand the operating parameters of each mode
2. To understand what type of separations (isomers, equal polarity, different polarity) each is able to do better than another mode

Often the modes can be complementary, allowing various types of selectivity. This is advantageous when doing separations of unknown substances, as different mechanisms will allow unique selectivities, thereby guaranteeing more complete separation. Applying different modes of chromatography to a single-separation problem is often called “multidimensional” chromatography.

Before bonded phases became available, all normal-phase partition — and reversed-phase partition — separations were done on silica and other supports which were only “coated” with different polar and nonpolar phases or oils. Obviously, their use presented many problems, because it was absolutely necessary to keep both the mobile phase and the stationary phases saturated with these phases. The laboratory work of the analytical chemist was made infinitely simpler with the introduction of bonded phases, which this topic addresses.

Normal-phase chromatography is a close parallel to adsorption chromatography. Briefly, adsorption chromatography most often uses polar silica gel as the stationary phase and a mobile phase that is predominantly nonpolar, possibly with some polar modifier. An example of such a mobile phase would be hexane with 2% ethanol. When increasing the percentage of the polar modifier, the elution times decrease.

Normal-phase (NP) chromatography generally uses the same types of mobile phase as for the adsorption mode. The difference, however, is the nature of the stationary phase. In NP chromatography, the packing is silica gel that has been bonded with a polar phase. The usual polar phases widely available from many manufacturers include cyano, amino, nitro, and diol phases. These are illustrated in Fig. 1. The first three often have a propyl group between the Si—O— and the X groups. The diol phase is derived from glycerol bonded to the silane reagent. Of course, each manufacturer uses a different silica, different reagents, different reaction conditions, and a different final workup; thus, any given polar bonded phase from the various suppliers can differ in relative selectivity and/or observed retention times.

There are two major differences between using silica gel (for adsorption) and a polar bonded phase (for normal phase) for a separation. First, the polar bonded phase adds a different surface to the silica gel, which can impart unique selectivities (i.e., separation characteristics) to an analysis. This is because the stationary-

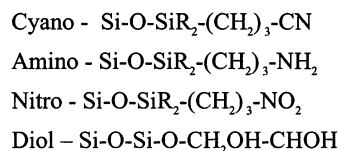


Fig. 1 The usual structures of polar bonded phases. The R groups may be —OCH₃, —OCH₂CH₃, —H, —CH₃, —CH₂CH₃, or others. Combinations of reagents or active groups are also possible. One manufacturer, for instance, offers a PAC (polar aminocyano) bonded phase.



phase surface is no longer as polar as it was before bonding. Many of the silanols are replaced with the organo-polar groups. As with any bonded phase, perhaps only 50% of the available silanols are actually bonded, because of their incomplete accessibility to any reagent. It is possible to also endcap (a second-step bonding reaction, with a trimethylsilyl reagent) more of the remaining silanols. This is not generally done; so, there is often some definite silanol interaction and, also, with amino and diol phases, they would, themselves, react with the reagent, silanizing them. This would defeat the purpose of trying to produce a different selectivity packing.

The second difference comes from the fact that if there are fewer silanols available on the surface of the packing, it will be less sensitive to any moisture that gets into the mobile phase. One of the biggest problems observed by users of silica gel separations in the adsorption mode is the control of the separation's reproducibility. Unless one is very careful to use dry solvents, or "controlled water content" mobile phases, the retention times of their compounds can change dramatically from analysis to analysis. If more water gets onto the silanols, they are deactivated, and sample components elute more rapidly. Removing water with an exhaustively dried solvent combination, for instance, removes moisture from the silanol groups and components are then retained longer. As a result, with less silanols available for deactivation by water, the polar bonded phases are more reproducible and often preferred by chromatographers.

If variable retention times become a problem in the adsorption mode, a switch to a polar bonded-phase column is often the simplest solution. When using the same solvent mixture as was used on the bare, unbonded silica gel column, it is often found that the elution order is often the same or very similar. Of course, a switch in mode would necessitate identifying the sample components, to guarantee that their elution order is, indeed, changed or not. With fewer silanols, however, the components of the mixture will elute faster, so readjusting the mobile phase is required to ensure adequate resolution. As mentioned earlier, the polar bonded-phase separation will be much less sensitive to small moisture variations in the mobile phase. Moisture in the mobile phase should, nevertheless, be controlled, but will present few, if any, problems over the time the samples in a study are being run.

As with adsorption chromatography, the normal-phase mode separates molecules on the basis of solubility in the mobile phase (so it dissolves relatively nonpolar compounds) and the differences in the polarities

of the components in the mixture and their attraction to the solvated polar bonded phase. Relatively nonpolar components elute first; more polar components elute later. These relative polarities and elution orders are summarized in Table 1.

At the nonpolar end of the elution scheme, the elution of alkanes to ethers with perhaps only hexane or heptane would be expected. For elution of moderate to polar compounds, a polar modifier has to be added to the major nonpolar component of the mobile phase. Much of the guesswork as to which solvent combinations to use has been simplified by the work of Kirkland and Snyder [1]. Their work has grouped solvents of similar selectivities [e.g., alcohols give identical (or similar) elution sequences; only the elution times change from one alcohol to another]. As a result of their studies, the recommended solvents to be mixed with hexane or heptane to effect the greatest possible selectivity differences are diethyl ether, chloroform, and methylene dichloride.

It is possible to separate more polar components by introducing a gradient from a low concentration (0–10%) of a polar modifier to a higher concentration of the same polar solvent (to 90%, for example). The important consideration is the solubility limit of the polar component. Thus, methanol is only soluble in hexane to about 5%, but ethanol can be brought up to 20% before reaching maximum solubility. If more polar samples are to be separated, then hexane can be replaced by ethyl acetate or chloroform.

Using such an approach does not limit the chromatographer to the use of only relatively nonpolar mobile phases. Much work with these bonded phases is also done with polar solvent mixtures, such as methanol–water or acetonitrile–water. They might appear to be reversed-phase separations, but this may not be the case. Often, when a CN (cyanopropyl) phase is used, it is used as a slightly more polar bonded phase than would be a C4 bonded phase. Then, the polar organic–

Table 1 Relative Group Polarity and Elution Order in Normal-Phase Partition Chromatography

RH < RX < RNO ₂ < ROR < RCOOR < RCONHR < RNH ₂ < ROH	
RCRO	R ₂ NH
RCHO	R ₃ N

Increasing polarity of organic structures/groups → →
 Increasing retention of compounds containing these structures/groups → →

Notes: (a) The more functional groups in the compound, the greater its polarity; (b) for polyfunctional cpds, the *most polar* group determines the retention of the compound.



water combinations used almost always are invoking the reversed-phase mode.

One widely used application using NP chromatography in which the mobile-phase composition is deceptive in the actual mode being used is the separation of sugars (carbohydrates) and oligosaccharides. The packing used is an NH_2 (aminopropyl, most often) bonded phase and the mobile phase is acetonitrile–water in the ratio of 20–35% water. This mobile phase might lead one to suspect a reversed-phase mechanism at work, but, in fact, adding more water (the polar component) to the mobile phase decreases the retention times of the sugars, proving it is, indeed, a normal-phase partition mode being used (if it were a reversed phase, the addition of more water would increase the retention of the compounds). *Note:* If this column is supplied by the manufacturer in heptane or hexane, an intermediate solvent such as ethyl acetate should be used, on going to the acetonitrile–water mobile phase, to prevent immisibility of one solvent in another.

It is also possible to also use an NH_2 bonded phase as an ion exchanger, because it will form the quaternary ion, NH_3^+ in buffers between pH's of 2 to 6 (i.e., a weak cationic exchanger). This can also be a problem when attempting the sugar separation described earlier, if acidic components in the mixture inadvertently transform the NH_2 to the NH_3^+ form. The separation will not work as well, if at all. This, fortunately, is reversible by taking the column to pure water, then pass-

ing through 10 column volumes ($V_M \times 10$) of 0.01M NH_4OH , then pure water, to regenerate the free base.

Other possible problems with this reactive bonded phase is that it can form Schiff bases with aldehydes and ketones, so samples containing these should be avoided. The NH_2 group also can be easily oxidized, so peroxides in any easily oxidizable solvents (e.g., diethyl ether, dioxane and tetrahydrofuran) should be avoided [2].

The types of compounds that can be separated in the normal-phase mode is as vast as for the adsorption mode. Likewise, because the range of solvents which can be used in this mode is virtually unlimited, it will lend itself to even more sample types. Unfortunately, not as many references exist for normal-phase separations as do for reversed-phase separations. As a guide to the types of solvents to use in the normal-phase mode, refer to the many references on silica gel. As mentioned, usually only minor changes, if any, need be made to the mobile phase when adapting to the normal bonded-phase column.

References

1. L. R. Snyder and J. J. Kirkland, *Introduction to Modern Liquid Chromatography*, 2nd ed., John Wiley & Sons, New York 1979, pp. 247–264.
2. V. R. Meyer, *Practical High Performance Liquid Chromatography*, 2nd ed., John Wiley & Sons, New York, 1994, p. 166.



Normal-Phase Stationary Packings

Rosario LoBrutto

Seton Hall University, South Orange, New Jersey, U.S.A.

Introduction

Normal-phase chromatography is a mode of liquid chromatography employing polar stationary phases and nonpolar eluents. Retention is predominately governed by hydrogen-bonding, electrostatic interactions, and, more specifically, dipole–dipole interactions. The stationary phases most typically used for the normal phase are silica, alumina, and chemically bonded phases such as aminoisopropyl, cyanopropyl, nitrophenyl, and diol. Other phases designed for particular types of analytes have also proved to be successful. These include modified alumina, titania, and zirconia, modified silica gels, impregnated silica gels, and nitrophases.

Silica

Silica is the most widely used commercially available normal-phase packing in various forms, having standard particle sizes ranging from 3 to 10 μm and surface areas from 200 to 800 m^2/g [1]. It is classified as an acidic adsorbent because its surface consists of acidic hydroxyl groups that are covalently bound to the Si atoms (i.e., silanol groups). Silica contains weak Brønsted acidic sites and does not contain any Lewis-acid sites.

The silica gel surface is heterogeneous and consists of siloxane and silanol groups. The active silanol groups on the surface are electron acceptors and hydrogen-bond with polar or unsaturated molecules. They exist in several forms: single (isolated or free), geminal, bound, and reactive surface hydroxyls (vicinal). Free silanols contain an Si atom that has three bonds in the bulk structure and the fourth bond is attached to a single OH group. Geminal silanols contain two hydroxyl groups attached to one silicon atom that are unable to hydrogen-bond. A bound hydroxyl is denoted as a hydrogen-bound surface hydroxyl. The reactive surface hydroxyls have two hydroxyl groups attached to different silicon atoms that are able to hydrogen-bond with each other. The reactive surface hydroxyls are believed to have the greatest relative

strength as adsorption sites, among all hydroxyls formed. At higher temperatures (200–400°C), surface siloxane groups are formed from the condensation of reactive and geminal silanols and decomposition of free silanols.

The geometric properties of silica also play a role on the retention of analytes, because they vary the surface activity. Because the silica surface is heterogeneous, different silica gels have varied surface hydroxyls and, therefore, their concentrations can be different in pores of different dimensions. The smaller the pore diameter, the higher the surface area of the corresponding silica. It also has been shown that higher concentrations of reactive and bound hydroxyls are present in smaller-pore silicas, typically with a pore diameter less than 100 Å, whereas free hydroxyls predominate on large-pore silicas having pore diameters greater than 150 Å [1].

Silica may have different amounts of adsorbed water on the surface which decrease the activity of the silica, because the water blocks the underlying surface. If the silica is heated between 150°C and 250°C, the water may then be removed without the loss of surface hydroxyls and, therefore, the silica retains maximum activity [2]. Water is selectively adsorbed onto reactive hydroxyls, and because the concentration of the reactive hydroxyls is greater in small-pore silicas, there is a large deactivation effect, consequently leaving a surface of bound hydroxyls. Deactivation of the large-pore silicas generally leaves, mostly, free hydroxyls. Therefore, heavily deactivated large-pore silicas, when compared to small-pore silicas, have a higher surface activity due to the presence of the free hydroxyls versus bound hydroxyls.

The silica may also be contaminated by metallic impurities such as aluminum, nickel, and iron, depending on the synthesis of the silica or the manufacturing process. These metals may be present either in the form of oxides and hydrous oxides or through oxygen bonds attached to an Si atom [3]. The metal impurities may also have an effect on the chromatography, causing peak tailing due to complexation with the trace metal impurities. The acidity of the surface silanols is increased with the presence of these metal impurities.



Depending on the pH of the silica, metal ions can exist in either nonhydrated or hydrated forms.

The surface of the silica can be modified with the use of a buffer and this may be an effective alternative method for the separation of polar analytes. This may lead to the enhancement and change in selectivity of ionic samples while exhibiting no effect on the behavior of nonionic samples. The pH of the buffer, concentration, and the type of buffer used have a significant effect on the retention and peak shape of the analytes [4–6]. However, the most influential parameter is the pH of the buffer, where the pH of the buffer solution should be lower than the pK_a of the acidic analytes and be higher than the pK_a of the basic analytes.

The surface of the silica may be coated with heavy metals and the selectivities observed can be attributed to the complexes formed between the metal ions and analyte species. The use of silver-impregnated silica has been used for the analysis of saturated and unsaturated fatty acid methyl esters (FAME) and triacylglycerols (TAG) [7]. The retention of the unsaturated FAME and TAG can be attributed to the stability of the complex that is formed between the π electrons of the carbon–carbon double bonds and the silver ions. The predominant interaction for saturated analytes is with the polar silanol groups. The secondary interactions are those of the silver ions with the unpaired electrons of the carbonyl oxygens of the analytes. The amount of silver adsorbed onto the silica and the pH have been determined to have an effect on the retention and resolution of certain acidic and basic compounds and fatty acids [8].

Alumina

Alumina is an inorganic oxide just as silica, but it is less widely used. Alumina may exist in many forms containing several hydroxides and oxide–hydroxides which are stable only at low temperatures. γ -Alumina, a low-temperature crystalline form, is the type that is most commercially available, having surface areas of 50–200 m²/g, specific pore volumes ranging up to 0.6 mL/g, pore structures consisting of cylindrical micropores, and larger-diameter irregularly shaped pores [3]. The characteristics of low-temperature aluminas include different surface hydration and imperfect crystal structure, in which different crystal planes may be formed. The alumina surface contains weak Brønsted-acid sites and, upon calcination treatment, these sites are transformed into aprotic Lewis-acid sites (Al^{3+} atoms) that lie in one plane and Lewis-base sites (oxide ions, O^{2-}),

which form the surface layer [1]. The pretreatment of the alumina determines the acidity, basicity, or neutrality of the packing; the basic alumina has cation-exchange properties and the acidic alumina behaves as an anion exchanger.

The surface of alumina is covered by five distinct types of surface hydroxyls in their coordination to the aluminum. The total hydroxyl groups of the γ -alumina is about 3 $\mu\text{mol}/\text{m}^2$. Upon heating to temperatures above 200°C, there is a consequent loss of these surface hydroxyls. Even though there is a loss of surface hydroxyls that may participate as weak Brønsted sites, the activity of the alumina increases with increase of hydroxyl loss, because they are converted into Lewis acidic and basic sites which may act as stronger adsorption sites. The activity of the five types of hydroxyl sites on the alumina is dependent on the amount of water present on the surface. Furthermore, the highest surface activity would be obtained with lesser amounts of physically sorbed water. The presence of Na_2O , a common impurity of the γ -alumina, is known to affect the pH of the γ -alumina to a more basic alumina [3].

γ -Alumina is generally more polar and, therefore, more retentive than silica. It is typically used for the analysis of organic compounds that have carbon–carbon double bonds, such as olefinic hydrocarbons, weak acids, and electron-rich aromatic compounds such as polynuclear aromatic hydrocarbons. The aromatic π electrons can interact with the Lewis acid.

Some drawbacks of this packing include a strong interaction with polar analytes such as organic acids, leading to peak tailing or maybe even irreversible adsorption, and decomposition of the analyte due to chemisorption. On the other hand, if acid-treated aluminas are employed for the analysis of strongly acidic samples, then some of the aforementioned deleterious effects may be avoided. The analysis of basic compounds may also be used on acid-treated and neutral aluminas.

Zirconia and Titania

Zirconia and titania both contain Lewis-acid and Lewis-base sites, with the latter having stronger adsorption properties. The titania phase also has strong Brønsted acidic sites. Basic compounds are less retained on zirconia and titania phases, due to their basic nature. Neutral compounds such as polyaromatic hydrocarbons (PAH), due to their π -electron system, behave as Lewis bases and the interactions with Lewis acid sites on the zirconia and titania packing materials become dominant for retention.

Chemically Bonded Phases

Polar bonded phases for normal-phase separations have recently gained popularity. These include the dihydroxypropyl propyl ether (diol), aminopropyl, cyanopropyl, and nitrophenyl bonded silicas. These phases are advantageous to silica because they are less active and, yet, produce similar interactions, require shorter equilibration times, and are influenced less by the water content of the mobile phase. The retention of most analytes upon the diol and amino phases is similar to that of the parent silica and alumina, whereas the cyanopropyl and nitrophenyl phases generally show less retention.

Amino Propyl Silica

The aminopropyl phase is generally prepared from trimethoxy or triethoxy aminopropylsilanes. The amino phase acts as a strong proton donor. It generally retains acids longer than bases. For example, phenol elutes after aniline in various mobile-phase solvents of different solvent strengths such as chloroform and methyl-tert-butyl ether (MTBE) [9]. The amino phase generally shows more retention for samples of acidic nature than do silica, diol, and cyanopropyl phases. Alcohols and phenols were shown to be preferentially retained on amino, compared to diol and cyano, in pentane–diethyl ether mobile phases [10]. It also has been shown that steroids with phenolic groups generally show a higher retentivity on the amino phase [11,12]. The separation of a mixture of saturated hydrocarbons, olefinic hydrocarbons, and aromatic compounds have been shown to be separated on the amino and alumina phases, but not on the silica [13].

Basic solutes such as amines, ethers, esters, and ketones are preferentially retained on amino and diol columns when compared to cyano columns [14,15]. The amino phase is a good alternative to the cyano column for a change in selectivity. When analyzing ketones and aldehydes, the aminopropyl phase should be carefully used due to the possible reactivity of the amino group with these substances. This may lead to the formation of imines and the bonded phase may be easily oxidized [13].

Cyano

The cyano column may be used in the normal- or reversed-phase mode and can be regarded as the first column of choice for method development when both modes are under consideration. Typically, it is prepared from mono-, di-, or trifunctional silane. A more

reproducible packing is obtained when monofunctional silanes are used for synthesis.

Dipolar compounds such as those with chloro, nitro, and nitrile substituents are more strongly retained on cyano columns, compared to amino or diol [14]. Also, cyanopropyl silica can exhibit acidic or basic character, depending on the mobile phase used. It was shown that a complete reversal of elution order was obtained for phenol and aniline when MTBE and chloroform were used as the mobile phases, because phenol eluted first in the MTBE solvent and second in the chloroform solvent [9].

The cyano phase may physically collapse in solvents of intermediate polarity and it is recommended to be used solely with nonpolar or polar solvents. If solvents of intermediate polarity are to be used, the flow should not be changed or stopped, because the back-pressure holds the bonded phase in place and this helps prevent the collapse of the packed bed [13].

Diol Phases

The diol phases are usually prepared from trimethoxyglycidoxypyl or triethoxyglycidoxypyl silane, followed by hydrolysis of the epoxy group to form the diol functionality. The most widely used diol phase is the 1,2-dihydroxypropyl propyl ether phase.

Esters and ethers are preferentially retained on diol silica when compared to amino or cyano in systems when employing a pentane–diethyl ether mobile phase. The diol groups can form hydrogen bonds with esters and may interact strongly with sp^3 -hybridized oxygen of ether bridges, thus leading to an increased adsorption [10]. For a change in selectivity, the diol phase is a good alternative to the cyano column, but it is less stable [14]. The interaction of basic and acidic samples is equivalent, because the diol phase is neutral and possesses no ionizable groups.

Nitrophenyl Phases

The phase that is most commercially available contains a weak π -electron acceptor mononitrophenyl bonded to the silica and usually contains a propyl spacer arm. This packing interacts with analytes through π -donor interactions. Other nitrophenyl phases exist and, as the number of nitro groups increases on these acceptor-type phases, an increased retention of aromatic donor compounds occurs. The phases of 3-(2,4-dinitroanilino)-propyl and (2,4,6-trinitroanilino)-propyl have shown preferential adsorption of PAHs, alkyl aromatic hydrocarbons, and polyarylalkanes, in comparison to aminopropyl silica [3].



Retention and Adsorption in Normal Phase

Retention in normal-phase chromatography increases as the polarity of the mobile phase decreases. The selectivity of the analytes may arise from the differences in solvent strengths (ϵ_0), acidity, basicity, and dipolar nature of the mobile phase. Furthermore, solvent localization of the mobile phase plays a major role in the retention of the analytes [15,16]. These solvent strengths have been shown to be different when used with varied stationary-phase packings such as alumina, diol, and silica [3,17].

The retention mechanism in the normal phase is often referred to as adsorption chromatography. It is described as the competition between analyte molecules and mobile-phase molecules on the surface of the stationary phase. It is assumed that the adsorbing analyte displaces an approximate equivalent amount of the adsorbed solvent molecules from the monolayer on the surface of the packing throughout the retention process [18]. The solvent molecules that cover the surface of the adsorbent may or may not interact with the adsorption sites, depending on the properties of the solvent. This retention model, proposed by Snyder, was originally used to describe retention with silica and alumina adsorbents, but several other studies have shown that this model may also be used for polar bonded phases, such as diol, cyano, and amino bonded silica [10,19].

References

1. L. L. Snyder, *Principles of Adsorption Chromatography*, Marcel Dekker, Inc., New York, 1968.
2. E. Heftmann, *Chromatography*, 2nd ed., Reinhold Publishing, New York, 1961.
3. K. K. Unger, *Packings and Stationary Phases in Chromatographic Techniques*, Marcel Dekker, Inc., New York, 1990.
4. R. Schwarzenbach, *J. Liquid Chromatogr.* 2(2): 205–216 (1979).
5. R. Schwarzenbach, *J. Liquid Chromatogr.* 334: 35 (1985).
6. S. H. Hansen, P. Helboe, and M. Thomsen, *J. Chromatogr.* 368: 39 (1986).
7. O. R. Adlof, *J. Chromatogr. A* 764: 337–340 (1997).
8. M. Okamoto, H. Kakamu, K. Nobuhara, and D. Ishii, *J. Chromatogr. A* 722: 81–85 (1996).
9. P. L. Smith and W. T. Cooper, *J. Chromatogr.* 410: 249 (1987).
10. M. Lubke, J. L. le Quere, and D. Barron, *J. Chromatogr. A* 690: 41 (1995).
11. S. Hara and S. Ohnishi, *J. Liquid Chromatogr.* 7(1): 59–68 (1984).
12. S. Hara and S. Ohnishi, *J. Liquid Chromatogr.* 7(1): 69–82 (1984).
13. U. D. Neue, *HPLC Columns*, Wiley-VCH, New York, 1997.
14. L. R. Snyder, J. J. Kirkland, and J. L. Glach, *Practical HPLC Method Development*, 2nd ed., Wiley-Interscience, New York, 1997.
15. L. R. Snyder, J. L. Glajch, and J. J. Kirkland, *J. Chromatogr.* 218: 299 (1981).
16. J. J. Kirkland, J. L. Glajch, and L. R. Snyder, *J. Chromatogr.* 238: 269 (1982).
17. L. R. Snyder, *High-Performance Liquid Chromatography Advances and Perspectives*, C. Horvath, ed., Academic Press, San Diego, CA, 1983, Vol. 3, p. 157.
18. L. R. Snyder and H. Poppe, *J. Chromatogr.* 184: 363–413 (1980).
19. T. C. Schunk and M. F. Burke, *Int. J. Environ. Anal. Chem.* 25: 81 (1986).

Nucleic Acids, Oligonucleotides, and DNA: Capillary Electrophoresis

Yuriko Kiba

Yoshinobu Baba

University of Tokushima, Tokushima, Japan

Introduction

Rapid progress in the Human Genome Project has stimulated investigations for gene therapy and DNA diagnosis of human diseases through mutation or polymorphism analysis of disease-causing genes. The recent development of capillary electrophoresis (CE) technologies has facilitated the application of CE to the analysis of polymorphism and mutations on human genome toward DNA diagnosis and gene therapy for human diseases.

A CE system is a very simple analytical separation instrumentation consisting of only a high-voltage power supply, detector, and capillary. Separations are performed in fused-silica capillaries which are supplied with a thin outer coating of polyimide to make them strong and flexible. Coated capillaries with an internal diameter of 50–100 μm were usually filled with gel or polymer solution for DNA separation.

The advantage of electrophoresis using a capillary is to be able to apply a high voltage, compared with gel electrophoresis, that has enabled us to analyze DNA with high resolution and with high speed. This is because a small-diameter capillary leads to efficient heat dissipation, because the fused-silica wall acts as a heat sink, absorbing heat generated inside the capillary by Joule heating and dissipates it from the relatively large surface area of the outer wall of the capillary. In addition, DNA separation by CE is performed in a buffer including a polymer such as non-cross-linked polyacrylamide, cellulose derivatives, or poly(ethylene glycol), not only in gel. The polymer solution is set automatically into the capillary, which is much easier than with gel electrophoresis. DNA is detected with PDA (photodiode array) or LIF (laser-induced fluorescence).

Theory for DNA Analysis by CE

In a polymer solution such as methylcellulose, polymer molecules start to overlap to form dynamic pores. The

pores do not have a definite size, but the average mesh size depends on the polymer concentration. DNA separation is achieved by a molecular sieving effect during electrophoresis in polymer solution, as well as in gel. DNA is separated depending on its size while migrating in the entanglement polymer solution. Polymer solution can be separated into three different concentration regimes; dilute, semidilute, and entangled. When the polymer concentration is low enough, polymer chains are hydrodynamically isolated from one another in solution. As the concentration of polymer is increased, the polymer chains begin to overlap. With higher concentration of polymer, each polymer molecule strongly interacts with other polymer molecules in the solution, forming physical networks. The transition between dilute and entangled solution is called a semidilute regime, which occurs at concentrations near their entanglement threshold. Thus, we need the information of such an entanglement threshold for testing polymer solutions to use the molecular sieving effect. The entanglement threshold for the polymer, c^* , is

$$c^* = \left(\frac{1.5}{K} \right) M_w^{-a} = I M_w^{-a} \quad (1)$$

where M_w is the molecular mass of the polymer, and K , I , and a are all molecular parameters which are different for each polymer. For example, the molecular mass of methylcellulose is about 400,000, so the value of c^* , in this case, is estimated at 0.4%.

An entangled solution can be characterized as a network with an average mesh size, ξ , similar to the pore size of the gel. Mesh sizes for various polymers are expressed as a function of the polymer concentration:

$$\xi = 1.43 \left[\frac{1.5^{1+1/a}}{2.5 N_A} \right]^{1/3} K^{-1/3a} c^{-(a+1)/3a} = J c^{-\beta} \quad (2)$$

where N_A is Avogadro number, and J and b are parameters which differ for each polymer. Each mesh size for various concentrations of methylcellulose was estimated as $\xi = 48 \text{ nm}$ (0.4%), $\xi = 39 \text{ nm}$ (0.5%), $\xi =$



33 nm (0.6%), $\xi = 28$ nm (0.7%), $\xi = 25$ nm (0.8%), $\xi = 22$ nm (0.9%), and $\xi = 20$ nm (1.0%).

To explain electrophoretic behavior of DNA, the Ogston model and theory are well used, in general. On the basis of the Ogston model, a separation medium, such as gel or polymer, is treated as a random network of fibers with limited lengths. A sample DNA molecule is assumed to migrate through the network as a sphere with radius R . The sample molecule migrates as a whole toward the direction of the electric field, diffusing laterally until it encounters a pore large enough to allow its passage. The network of the polymer matrix is assumed to be a round post with radius r ; the probability that a sample does not go through those regions is equal to the probability that a sample passes through polymer matrices. In the Ogston model, the mobility, μ , or the migration time, t , of DNA is expressed as follows:

$$\log\left(\frac{\mu}{\mu_0}\right) = -\log\left(\frac{t}{t_0}\right) = -\pi l'(r + R)^2 T \times 10^{-16} \quad (3)$$

where l' (cm) is the total fiber length produced by 1 g of dry polymer, T is the concentration of polymer (or gel), μ and t are the mobility and the migration time of DNA in the polymer solution, respectively, and μ_0 and t_0 are those in free solution, respectively.

DNA molecules, however, are not actually spheres; rather, they are considered random coil polymers with some degree of flexibility. Thus, DNA molecules with total length L (nm) as a random coil polymer can be assumed to adopt a spherical shape with radius of gyration, R_g , given by

$$R_g^2 = \frac{1}{3}pL \left[1 - \frac{p}{L} + \left(\frac{p}{L}\right) \exp\left(\frac{-L}{p}\right) \right] \quad (4)$$

In this equation, p (nm) is the persistence length, a measure of the flexibility of the DNA chain. Because single-stranded DNA is extremely flexible, the p/L terms are assumed to be negligible for smaller DNA molecules, which allows us to express R_g^2 with a simpler formula:

$$R_g^2 = \frac{1}{3}pL = \lambda N \quad (5)$$

where N is the length of the chain, expressed in nucleotide units, and λ is a constant.

Using the radius of gyration, R_g , instead of R in Eq. (3), R_g is much larger than the polymer strand radius, we obtain the relationship $(r + R)^2 = R_g^2$. Further, using Eq. (3) allows us to obtain Eq. (6) as follows:

$$\ln(\mu) = \ln(\mu_0) - CTN \quad (6)$$

where $C (= \pi/\lambda \times 10^{-16})$ is a constant. This formula predicts the linear relationship between the logarithm of mobility and the DNA size, N , or polymer concentration, T , with the Ogston model. Although Eq. (6) is successfully used in the analysis of DNA mobilities in both gel and polymer solution, the migrating molecule is treated as a spherical coil in this theory, and it is generally applied only for the molecules that can be treated as small spherical coils, typically with a radius of gyration R_g much smaller than the average pore size ξ .

The Ogston model has been successful in fitting experimental data for small DNA fragments with the limitation of low electric fields. However, DNA with radii of gyration much larger than the average gel pore size will still migrate rapidly through the gel during electrophoresis, implying that the assumptions inherent in the Ogston model are invalid for larger DNA.

Because a DNA molecule is a flexible polymer, the assumption in the Ogston model that DNA migrates as an undeformable particle loses validity with increasing size of DNA. The Ogston model predicts that the mobility of DNA with R_g larger than the pore size of the gel will approach 0. However, it actually was observed experimentally that DNA with its R_g larger than the gel pore size keeps migrating.

The reptation theory has been established to explain the movement of polyelectrolyte during the electrophoresis in neutral polymer network, and the reptation theory was applied to biomolecules. In the reptation theory, a polymer chain moves through a network, not as an undeformable particle, but rather snakelike through "tubes" in the polymer network. DNA chains move through the "tube" and the friction coefficient, ζ , is proportional to chain length, $\zeta = \zeta_0 L$, where ζ_0 is the friction coefficient per unit length.

According to the reptation theory, the polyelectrolyte (it can be DNA in this case) is assumed to be something which consists of N units (length = a , the number of bases in case of DNA). The total length of DNA is equal to Na . In the reptation theory, only the force along the DNA chain (longitudinal force) is taken into account in the electric field. The mobility of DNA, μ , therefore, is then expressed by

$$\mu = \frac{Q(hx^2)}{\zeta_0 a L^2} \quad (7)$$

where Q is the total charge of DNA and hx is the end-to-end distance of the molecule in the direction of the electric field.

When the electric field is low enough, the DNA molecule can be considered as a random coil polymer

with some degree of flexibility. When the DNA size is very large, electrophoretic behavior is expressed as

$$\mu \propto L^{-1} \propto N^{-1} \quad (8)$$

On the other hand, when the electric field is strong, DNA is no longer considered to move as a random coil polymer, but moves with extended rodlike conformation. If DNA is completely extended and moves straight to the field direction, $\langle hx^2 \rangle = L^2$, showing that the mobility in Eq. (7) is independent of DNA size:

$$\mu \propto L^0 \propto N^0 \quad (9)$$

This can be well applied to the electrophoretic behavior for extremely large sizes of DNA as well as the case of strong electric field.

The regime for Eq. (8) obtained from reptation theory is termed reptation-without-stretching regime; the one for Eq. (9) is termed reptation with stretching regime. The mobility decreases exponentially in accordance with DNA size when it is small enough (Ogston regime); then, as the size becomes larger, the mobility is proportional to the size (reptation-without-stretching regime).

Separation Matrix and Capillary Detection

Separation matrices mainly used for the separation of DNA by capillary electrophoresis are gel or polymer solutions as listed in Table 1. The separation of single-strand oligonucleotide is achieved by using cross-linked polyacrylamide gel, in which the concentration varies from 3% to 8% *T* and the degree of cross-linking varies from 3% to 5% *C*. High-concentration linear polyacrylamide (8–10%) has been successfully applied

to the separation of oligonucleotides, too. Because linear polyacrylamide is replaceable from the capillary, gels are now increasingly being replaced by polymer solution. Electric fields between 200 and 500 V/cm have been used.

For the separation of double-stranded DNA fragments, several polymer networks are used primarily, as well as cross-linked polyacrylamide gel. The matrices currently used are methyl cellulose (MC), hydroxyethyl cellulose (HEC), hydroxypropyl cellulose, hydroxypropylmethyl cellulose (HPMC), poly(ethylene glycol) (PEG), poly(ethylene oxide) (PEO), poly(vinyl alcohol) (PVA), and agarose. For the separation of polymerase chain reaction (PCR) products and restricted DNA fragments, less concentrated solutions of polymers can be used. Typical polymer concentrations are about 0.1–1.0%, as listed in Table 1, and most commercially available capillary electrophoresis instruments are now able to fill and empty the capillaries with such solutions automatically. For the separation of DNA fragments ranging from 300 to 5000 bp, 0.5% cellulose derivative solution would be selected. Concentrations of cellulose derivative solution should be higher (0.7–1.0%) for the separation of shorter DNA fragments less than 300 bp. The application of dilute polymer solution (less than 0.3%) will be appropriate for the separation of larger DNA fragments ranging from 5000 to 50,000 bp. When low-concentration polymer solutions are applied, inner-wall-coated capillaries are usually used for eliminating electro-osmotic flow. Such capillaries are prepared by the chemical attachment of linear polyacrylamide to the capillary inner wall or some commercially available coated capillaries are used (e.g., J&W DB-17). The electric fields between 50 and 800 V/cm have been used for the separation of double-stranded DNA. For the optimization of the separation of double-stranded DNA fragments, some systematic studies on the separation conditions have been published. We can easily reach the optimum conditions for our own separations by choosing appropriate length, diameter, and coating for the capillary, electric field, temperature, pH of the buffer, type of polymer network, and its concentration.

DNA fragments separated by polymer networks are detected by ultraviolet (UV) detector or laser-induced fluorescence (LIF) detection. UV detection of DNA fragments is based on the UV absorption of the DNA bases; that is, the wavelength and the molar absorption coefficient for the UV absorption maxima of DNA bases are 260 nm for *A*, 254 nm for *G*, 267 nm for *T*, and 271 nm for *C*, respectively.

Table 1 Proposed Concentration Range of the Polymer-Type Separation Matrices for the Separation of DNA Fragments

Effective DNA size range of separation (bp)	Concentration range of polymer (% w/v)		
	PAA	HEC, MC	PEG, PEO
1–100	8.0–12	1.0–3.0	6.0–8.0
100–300	7.0–8.0	0.7–1.0	3.0–6.0
300–1,000	5.0–7.0	0.5–0.7	2.0–3.0
1,000–10,000	3.0–5.0	0.3–0.5	0.5–2.0
10,000–30,000	2.0–3.0	0.01–0.3	

Note: PAA = polyacrylamide; MC = methylcellulose; HEC = hydroxyethylcellulose; PEG = poly(ethylene glycol); PEO = poly(ethylene oxide).



The LIF detection of DNA fragments requires some fluorescent dye (e.g., intercalating dyes and chemically labeling dyes). The intercalating dyes are currently used for the LIF detection of DNA fragments. Ethidium bromide has been the most widely used as an intercalating dye for capillary electrophoresis, but it has some disadvantages (e.g., high background and low sensitivity). More recently, some new, efficient intercalating dyes have been developed. Some monomeric dye including thiazole orange (TO), TO-PRO-1, and oxazole yellow (YO), YO-PRO-1, and dimeric dyes including TOTO-1, YOYO-1, and YOYO-3 are applied to the highly sensitive detection of double-stranded DNA fragments. These dyes have several advantages, including low background and high sensitivity. Monomeric dyes, TO, TO6, and YO-PRO-1 are especially better in detection sensitivity than dimeric dyes. Recently, another monomeric dye, SYBR Green I, has been developed as a fluorescent dye well suited for efficient separation and quantitative, sensitive, and precise determination of double-stranded DNA using capillary electrophoresis. Most monomeric dyes, including ethidium bromide, acridine orange, TO, YO-PRO-1, TO PRO-1, and SYBR Green I, are optimally excited by the argon ion laser (488 nm and/or 514 nm). Some dimeric dyes, YOYO-1 and TOTO-1, are suitable for the excitation by argon ion laser too, and others, YOYO-3 and POPO-3, are excited by the He-Ne laser (543 nm and/or 633 nm). YOYO-1 is a benzoxazolium-4-quinolinium dimer that has one carbon atom bridging the aromatic rings of the unsymmetrical cyanines. YOYO-3, which differs from YOYO-1 only in the number of bridging carbon atoms (three), has longer wavelength spectral properties. The addition of intercalating dye also improves the resolution of DNA fragments.

Another LIF detection scheme for DNA involves direct labeling of the analyte with a suitable fluorophore. Fluorescently labeled probes and primers are used in many molecular biology applications involving hybridization, PCR, DNA sequencing, and multicolor detection for accurate SSCP analysis. Mostly used fluorescent labeling agents are so-called ABI dyes, including FAM, JOE, TAMRA, and ROX. Recently, new types of labeling agents called energy-transfer (ET) primers have been developed. DNA primers and probes are usually synthesized with a fluorescent label attached to the 5' end of the molecule.

Suggested Further Reading

- Baba, Y., *Mol. Biotech.* 6: 143–153 (1996).
 Baba, Y., *J. Chromatogr. B* 687: 271–302 (1996).
 Dolnik, V., *J. Biochem. Biophys. Methods* 41: 103–119 (1999).
 Heller, C. (ed.), *Analysis of Nucleic Acids by Capillary Electrophoresis*, Vieweg, Weinbaden, 1997.
 Heller, M. and A. Guttman (eds.), *Integrated Microfabricated Device Technology: Advances in Genomic, Drug Discovery, and Clinical Diagnosis*, Marcel Dekker, Inc., New York, 2001.
 Mitchelson, K. and J. Cheng (eds.), *Capillary Electrophoresis of Nucleic Acids*, Humana Press, Totowa, NJ, 2001.
 Mitnik, L., L. Salome, J. L. Viovy, and C. Heller, *J. Chromatogr. A* 710: 309–321 (1995).
 Righetti, P. G. (ed.), *Capillary Electrophoresis in Analytical Biotechnology*, CRC Press, Boca Raton, FL, 1996.
 Righetti, P. G. and C. Gelfi, *J. Chromatogr. A* 806: 97–112 (1998).
 Sunada, W. M. and H. W. Blanch, *Electrophoresis* 18: 2243–2254 (1997).



Octanol–Water Partition Coefficients by CCC

Alain Berthod

Laboratoire des Sciences Analytiques, CNRS, Université de Lyon I, Villeurbanne, France

Introduction

Hydrophobicity, from the greek *hydro* water and *phobia* aversion, is a term referring to the way a molecule “likes” or “does not like” water. A compound with a high hydrophobicity will not be water soluble. It is apolar. Conversely, a compound with a low hydrophobicity is said to be hydrophilic or polar. It is likely to be water soluble. In between the two extremes, the hydrophobicity varies. A scale is needed. The problem is that the hydrophobicity, or the polarity of a compound, depends on several parameters such as the dipole moment, the dielectric constant, the polarizability, the proton donor or acceptor character, or even the boiling point to molecular mass ratio. Since the end of the nineteenth century, the *octanol–water partition coefficient*, $P_{o/w}$, was used with success as a measure of hydrophobicity. The $\log P_{o/w}$ is the convenient scale. Compounds with a positive $\log P_{o/w}$ value are more and more hydrophobic or apolar as the value increases. Compounds with a negative $\log P_{o/w}$ value are hydrophilic or polar [1].

It is of paramount importance to be able to measure, accurately, the $P_{o/w}$ and $\log P_{o/w}$ value of a compound, because it is the accepted parameter used by the Food and Drug Administration (FDA) and the Environmental Protection Agency (EPA) and many other international drug and environmental agencies to estimate the tendency of an organic chemical to bioconcentrate into living cells. A new drug cannot be accepted by the FDA and EPA without the $P_{o/w}$ parameter.

The most extensive and useful sets of $P_{o/w}$ data were obtained by simply shaking a solute with the two immiscible octanol and water phases and then analyzing the solute concentration in one or both phases. For many solutes, repeated inversion (say ~ 100) of a 25-mL tube with $\sim 0.01M$ solute and the two phases establishes equilibrium in ~ 15 min. Very vigorous shaking can produce troublesome emulsions. The solute can be analyzed in only one phase and the concentration in the other can be obtained by the difference. The phase analysis is most often done by gas chromatography, liquid chromatogra-

phy, or ultraviolet (UV)-visible spectroscopy. The shake flask method gives reliable results over the wide 10^{-4} – 10^4 $P_{o/w}$ range. However, it requires highly pure solutes and is very sensitive to the smallest contamination.

Reversed-phase liquid chromatography (RPLC), capillary electrophoresis (CE), micellar liquid chromatography (MLC), and electrochromatography (EC) can be used to estimate values of $\log P_{o/w}$ from the corresponding $\log k$ values; k is the retention factor, directly related to the retention parameter of the solute of interest. Good correlations are generally found between $\log k$ and $\log P_{o/w}$ for structural congeners. Unfortunately, the correlations are much poorer with dissimilar compounds. Trace amounts of octanol were added in the mobile phase to enhance $\log k$ – $\log P_{o/w}$ correlations with a wide variety of solutes. The $P_{o/w}$ range is 1 – $10^{5.5}$. The advantages of the RPLC method are its relative simplicity and the fact that it does not need highly pure solutes. At the moment, the correlation remains the main drawback.

Direct $P_{o/w}$ Measurement by CCC

The decisive advantage of countercurrent chromatography (CCC) in $P_{o/w}$ measurement is that there is no correlation at all. Water, saturated with octanol, is the mobile phase. Octanol saturated with water is the stationary phase. The octanol–water partition coefficient of a given solute is the only physicochemical parameter responsible for the solute retention. If the solute is not highly pure, it is likely that the impurities will have differing $P_{o/w}$ values. This means that if the impurities have differing retention volumes, they are separated during the measurement from the solute of interest. The $P_{o/w}$ value is easily derived from the CCC retention equation:

$$V_R = V_M + PV_S \quad (1)$$

using

$$P_{o/w} = \frac{V_R - V_M}{V_S} = 1 + \frac{V_R - V_C}{V_S} \quad (2)$$



If octanol is the stationary phase and water the mobile phase, $P_{o/w}$ is the octanol–water partition coefficient without any assumption. Correlations of the $P_{o/w}$ or $\log P_{o/w}$ values obtained with the same liquid system by the shake flask method and by CCC produce straight lines with a slope unity and a negligible intercept. The validity and solidity of the method was assessed by Gluck and Martin for $P_{o/w}$ coefficients [2]. The $P_{o/w}$ range that can be obtained directly by CCC is 0.05–200 [1]. It is limited on the high side by the experiment duration. A $P_{o/w}$ value of 200 corresponds to a V_R retention volume of 6 L with a V_S value of only 30 mL [Eq. (1)]. This is 1200 min or 20 h with a 5-mL/min flow rate. The lower-side limitation is due to experimental precision. The difference between the retention volume V_R and the dead volume V_M is equal to PV_S [Eq. (1)]. With a 30-mL V_S volume, the $P_{o/w}$ value of 0.05 corresponds to a $V_R - V_M$ value of only 1.5 mL. Such a low value may be difficult to evaluate with an acceptable accuracy. To increase the measurable $P_{o/w}$ range, the fact that the CCC stationary phase is a liquid can be used. This led to the dual-mode use of CCC and the cocurrent operation.

Dual-Mode CCC

The idea is simple: Solutes with very high $P_{o/w}$ values move very slowly in the octanol phase; they need too long a time to emerge from the apparatus. To force them out of the CCC apparatus, the role of the aqueous and octanol phases and their flow directions are reversed after some reasonable flowing time in the normal direction. The dual-mode operation is illustrated in Fig. 1. It was demonstrated that the $P_{o/w}$ value can be simply expressed by

$$P_{o/w} = V_{aq}/V_{oct} \quad (3)$$

in which V_{aq} is the aqueous-phase volume passed in the normal way (descending or head to tail, Steps 1 and 2) and V_{oct} is the octanol-phase volume passed in the reversed way (ascending or tail to head, Step 3). The highest $P_{o/w}$ value that can be measured is again limited by the lowest V_{oct} volume that can be accurately determined. Due to band broadening, the practical minimum V_{oct} value is about 3 mL [1]. Then, with a 6000-mL V_{aq} volume, the corresponding $P_{o/w}$ value is 2000. Table 1 shows the experimental conditions corresponding to the dual-mode measurement of some $P_{o/w}$ values in the 40–3000 range. It was shown that the error on the $P_{o/w}$ determination was minimized when the octanol flow rate in the reversed mode was very low.

Octanol–Water Partition Coefficients by CCC

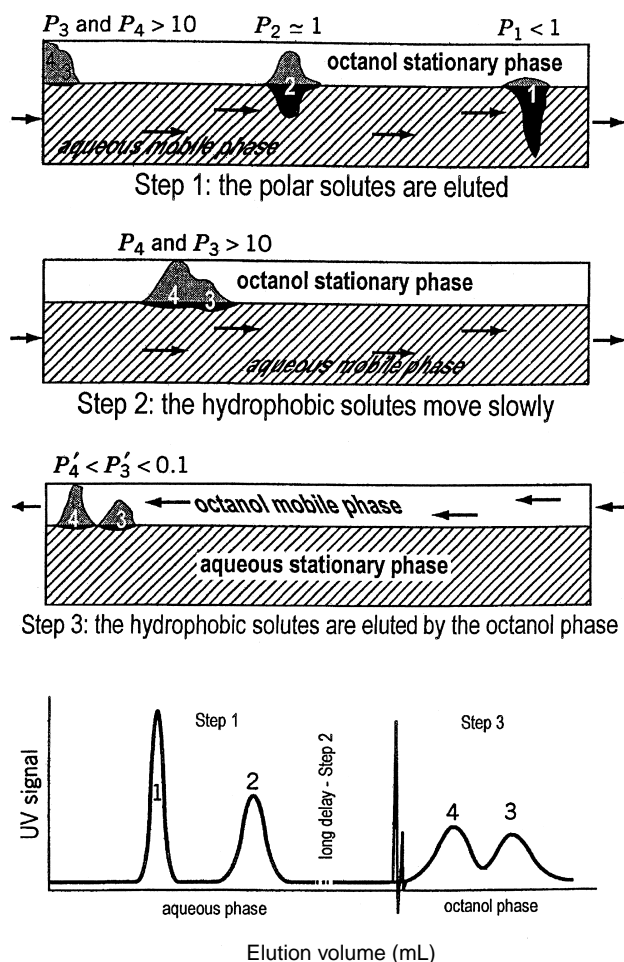


Fig. 1 Dual-mode CCC.

Cocurrent CCC

The cocurrent CCC operation takes advantage of the liquid nature of the stationary phase. If a lipophilic solute stays too long inside the CCC apparatus, why not push it out, pushing the liquid stationary phase, slowly, in the same direction as the mobile phase? The theoretical treatment [3] and the practical promise of the method were established [4]. Three pumps are needed. Pump 1 allows the adjustment of the aqueous-phase flow rate in the few milliliter per minute range. Pump 2 governs the octanol phase flow rate in the microliter per minute range. Pump 3 is used to add a clarifying agent to the phase mixture leaving the CCC apparatus. The clarifying agent can be 2-propanol; it solubilizes the trace amounts of octanol present in the aqueous phase. The interest of the method is that there is no

Table 1 Some Practical Examples of $P_{o/w}$ Measurements by CCC

Solute					$\log P_{o/w}$	$\log P_{o/w}$
Direct measurement	V_R (mL)	t_R (h)	$P_{o/w}$	CCC	Literature	
Benzamide	240	0.8	4.4	0.643	0.64	
Acetophenone	1,020	3.4	40	1.60	1.6	
2-Chlorobenzoic acid	2,280	7.6	97	1.99	2.0	
2-Chlorophenol	3,270	10.9	145	2.16	2.15	
Dual-Mode CCC	V_{aq} (mL)	V_{oct} (mL)	t_R (h)	$P_{o/w}$	$\log P_{o/w}$	$\log P_{o/w}$ (lit.)
Benzoic acid	178	2.36	0.8	75.4	1.88	1.87
2-Chlorophenol	487	2.71	2.2	180	2.25	2.15
Toluene	2,630	5.5	9.0	480	2.68	2.71
Biphenyl	19,600	1.0	65	19,600	4.29	3.80
Cocurrent CCC	V_{oct} (mL)	V_R (mL)	t_R (h)	$P_{o/w}$	$\log P_{o/w}$	$\log P_{o/w}$ (lit.)
Benzene	29.7	2,530	10.5	107	2.03	2.14
Toluene	20.2	6,520	12	500	2.70	2.71
Naphthalene	20.2	15,500	28.6	5,100	3.7	3.2
Phenanthrene	22.2	9,790	18.1	20,000	4.3	4.4

Source: Data from Refs. 1–4.

abrupt change; that is, it is continuous. The octanol volume retained in the CCC system is very stable, more stable than with other methods because there is a constant input of octanol. The octanol volume changes, due to dissolution that was noted in the direct method or due to phase reversal as noted in the back-flushing method, do not exist with the cocurrent CCC method. The V_{oct} volume was determined using a test solute (2-chlorophenol, $P_{o/w} = 147$ in Ref. 4). Another very important effect that was experimentally observed is the increased peak efficiency due to the octanol flow rate. The measurable $P_{o/w}$ range was extended up to 20,000 ($\log P_{o/w} = 4.3$). Table 1 lists the actual conditions of some $P_{o/w}$ measurements by the cocurrent CCC method. The CCC methods presented here were extensively used to measure the $P_{o/w}$ value of molecular compounds.

They were recently adapted to measure the $P_{o/w}$ values of ionizable compounds using buffered octanol-saturated aqueous phases [5].

References

1. A. Berthod, Liquid–liquid partition coefficients, in *Centrifugal Partition Chromatography* (A. P. Foucault, ed.), Chromatographic Science Series Vol. 68, Marcel Dekker Inc., New York, 1995, pp. 167–198.
2. S. J. Gluck and E. J. Martin, *J. Liquid Chromatogr.* **13**: 2529–2551 (1990).
3. A. Berthod, *Analisis* **18**: 352–358 (1990).
4. A. Berthod, R. A. Menges, and D. W. Armstrong, *J. Liquid Chromatogr.* **15**: 2769–2785 (1992).
5. A. Berthod, S. Carda-Broch, and M. C. G. Alvarez-Coque, *Anal. Chem.* **71**: 879–888 (1999).



On-Column Injection for GC

Mochammad Yuwono

Gunawan Indrayanto

Airlangga University, Surabaya, Indonesia

INTRODUCTION

The injection system in a GC analysis provides a means of introducing the sample onto the column. This is normally a simple injector design when packed columns are used. Capillary or open tubular columns require, however, more sophisticated design than do packed columns, because of their very low capacities and small internal diameters. A number of different injector designs have been recently developed. Unfortunately, no universal injector has so far been commercially available to handle all sample types. This article will discuss various approaches to sample injection.

SELECTION OF INJECTION MODE

The selection of the most suitable injection system becomes important, especially when samples containing widely different boiling point components and different concentrations are to be analyzed.^[1,2] Today, the most commonly used injectors for capillary GC fall into one of four techniques, i.e., split, splitless, on-column injection, and programmed-temperature vaporizers (PTV). The split injection mode was the first sample introduction system developed for capillary GC which, as the name signifies, splits the vaporized sample into two unequal portions, allowing only the smaller portion of it into the column and venting the larger from the system. The injector involves a heated chamber including a glass liner, into which the sample is introduced through an injection septum. For many applications, it is the most convenient sampling method, as it is very easy to operate, producing perfect peak shapes and good resolution after injecting concentrated samples in the same manner as for packed column systems.^[3] A major drawback of the split injection technique is the so-called sample discrimination due to the uneven flash vaporization of the sample. The discrimination means that not all components of the vaporized samples are brought quantitatively into the column. When a sample containing compounds with widely different boiling points is analyzed with the split

sampling technique, the less volatile components are discriminated. Consequently, the resultant chromatogram does not truly describe the real composition of the sample components; so the quantitative analysis becomes unreliable.^[3,4] To minimize or prevent this, the use of other injection techniques is suggested, such as cooled needle injection, very fast injection, cold on-column or programmable vaporization.^[5] Using an internal standard or an autosampler can also greatly enhance the accuracy of the results. With split techniques, problems arise also in analyzing thermally labile compounds which may decompose at the injection operating temperature. Introducing the samples using cold on-column injection technique is the best solution to solve this problem.^[5,6] Because the split technique is beneficial for analysis of samples containing compounds at high concentration, the splitless injection mode was then developed for analyzing trace-level compounds. In this splitless technique, the entire vaporized sample volume is directed into the column by closing the split vent (purge off mode). In this way, the sample is transferred completely and slowly into the column; this ensures quantitative and representative sample introduction. Most split injectors today can operate in the splitless mode. These injectors are normally called split/splitless injectors, which can be operated first in a splitless mode (usually less than 1 min), allowing to gradually force the majority of the vaporized sample to the column inlet. The mode is then operated in split mode to purge the excess solvent. The method does not need fast vaporization, so that it is advantageous for the analysis of thermally unstable compounds. However, the solvent focusing techniques and other parameters must be gently optimized; otherwise, the results obtained are not reproducible and are low in accuracy.^[5,7] The splitless injection technique is still used for the routine determination of trace-level compounds, such as for pesticide residues, drug impurities, etc. Direct and on-column flash vaporization injection has also been applied recently, which offers some advantages over the splitless technique for trace samples.^[8] For the same purpose, cold on-column injection is also increasing in popularity as a technique for the analysis of the trace compounds, because of its higher precision and accuracy.

DIRECT AND ON-COLUMN INJECTION

Direct injection is often confused with on-column injection. Direct injection allows the injection of liquid samples into a heated injection port. After injection, the sample is subsequently vaporized and then completely directed onto the column.^[5,9] The evaporation of sample occurs in the inlet, which is heated independently from the column oven. The most commonly used inlet is a glass liner, and no sample splitting or venting occurs during or after injection. Direct injection is limited to widebore or megabore columns.^[5] In on-column injection, the sample enters the column directly from the syringe and does not contact other surfaces. On-column injection generally indicates cold on-column injection for capillary columns.^[5] The terms “hot on-column injection” and “on-column flash vaporization” are elsewhere introduced.^[9] The hot on-column mode is different from the direct injection in the inlet that is used and in the termination point of the syringe needle during injection.^[8] The technique is called direct injection when a glass inlet sleeve is used, and the evaporation of the injected sample occurs outside the column. With an on-column injection, a specially designed liner or a part of the column is used as inlet which allows the injection of the liquid sample inside the column and the evaporation of the sample also occurs on the column wall surface.^[5,9] This simple technique is usually used for packed column GC. However, it has recently become popular because it can also be used with capillary columns (0.32 and 0.53 mm ID).

Specially designed injection port inlet sleeves have been available on the market for direct and hot on-column injection.^[7,8] In the direct injection mode, 2–4-mm-ID inlet sleeves are commonly used, which permit a sufficient space for sample evaporation; however, the on-column mode is usually performed by inserting a 26-gauge needle inside a 0.53-mm-ID column. Direct injection is more favorable because it is less problematic than the hot on-column mode.^[9] Because the liner can trap nonvolatile residues before entering the column, this technique is suitable for dirty samples. Compared to the splitless mode, the direct injection is advantageous, involving less adsorption of the solutes and better sensitivity. However, with this technique, the adsorption of the sample may occur on the inlet sleeve during the evaporation process.^[9] In this case, the hot on-column mode offers more benefits.

COLD ON-COLUMN INJECTION TECHNIQUE

As the name indicates, the cold on-column injector allows the injection of the sample directly as a liquid onto the column, of which the inlet and/or outlet section is

maintained at a lower temperature than the oven. After the solutes are focused in the inlet section of column, the sample is then vaporized as the oven temperature is increased. In this way, all of the sample components are transferred into the column, so that the sample discrimination attributed to the syringe needle heating during injection is eliminated; it is also convenient for the analysis of thermally labile compounds.^[1,10] The possibility of peak broadening is due only to band broadening in space.^[5,11] This technique yields excellent quantitative precision and accuracy for samples that contain less volatile and highly volatile compounds.^[12–14] Unlike the on-column flash vaporization injection, cold on-column is the true on-column technique, because both the injection of the sample and the evaporation occur inside the column.

An injector device for on-column work was first introduced by Schomburg in 1977.^[15] In 1978, Grob and Grob^[16] developed an excellent injector design which requires, principally, a syringe guide and a stop valve. A standard syringe with stainless steel needle of 0.23 mm ID (32-gauge) and 8 cm in length was used for the commonly used 0.32-mm-ID glass capillary column. The needle is introduced through a conical aperture into the 0.3-mm inlet channel, close to the stop valve. By pushing down the syringe and guiding the needle into the capillary column, the sample is injected onto the column. After injection, the syringe is moved back, the valve is closed, and the syringe is finally withdrawn. The bottom of the body is cooled by a fan-driven air circulator to maintain the low temperature of the column inlet. This is called primary cooling. Complete construction of the design was described by Grob and Grob.^[16] Further development of the cold on-column injection device included the use of secondary cooling, which is done by circulating air directed from a jacket surrounding the capillary inlet toward the injection area of the column.^[17] The secondary cooling system is to cool the area of the column where the sample is actually injected. The use of secondary cooling can totally eliminate syringe discrimination and ensures that the temperature of the needle channel can be controlled to avoid solvent evaporation. The secondary cooling is advantageous, especially when the injector is combined with temperature programming.^[1,18] Figure 1 shows a typical on-column injector with provision for secondary cooling of the column inlet. The evolution of the cold on-column injection technique occurred because syringes with fused silica needles had been introduced to replace commonly employed metal needles; the injection onto a capillary column of 0.22 mm ID then became reality. The fused silica needles are inert and perfectly straight.^[5,7] This innovative work makes the on-column injection technique gain more acceptance. The programmed-temperature on-column injector was then developed, in



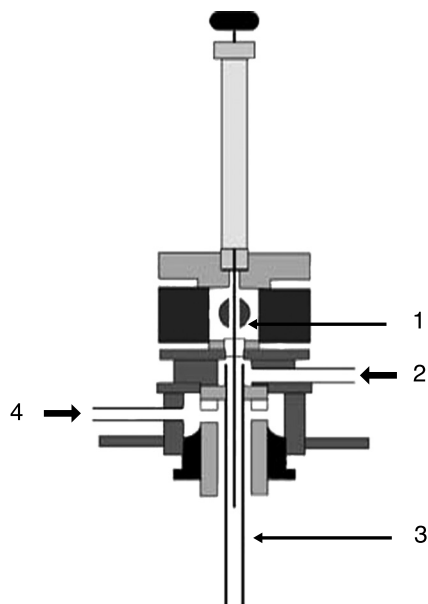


Fig. 1 Schematic diagram of a typical cold on-column injector with provision for secondary cooling of the column inlet. 1: Rotating valve, 2: carrier gas, 3: capillary column, 4: secondary cooling.

which the column inlet is housed in a separate injection oven, so that the column inlet temperature can be programmed from subambient to about 350°C and thermostated independently of the column oven.^[1] For thermally labile compounds, it is suggested that the temperature is programmed at a low heating rate, whereas a rapid rise is favored for vaporization of samples containing highly different boiling point components.^[6,7] A version of an on-column injector design that offers a low thermal mass, which facilitates cooling, has been developed. In this injector, a duck-bill valve constructed from a soft elastomer, such as in a flexible septum, is applied to form a gas-tight seal compressed by the column inlet pressure. When the needle guide is depressed, the isolation valve is parted and the metal guide is forced through the duck-bill valve.^[5] This permits the syringe needle to pass the valve and enter the column. When the plunger is released, gas flow through the column is restored. The system can be performed for manual and automated injections. The duck-bill valve is modified with a disk septum when automated cool on-column injection is applied (Fig. 2). A movable on-column injector has also been introduced to facilitate the up-and-down movement of the column oven wall.^[13] The cold on-column injection technique can now be operated in the constant-pressure, constant-flow, or pressure-programmed modes, allowing the reduction of analysis times. Moreover, electronic

pressure programming offers the advantages that column pressure can be controlled accurately and precisely, resulting in very low relative standard deviations of retention time reproducibility.^[5] The most suitably used carrier gas is hydrogen.^[5,6]

The attractive features of cold on-column injection are that they allow analysis at a low temperature; thus it is the most convenient method for analysis for thermally unstable compounds. Compared with the flash vaporizing injection technique, it is also the method of choice for analysis of the samples with widely different boiling point components, because the cold on-column injection technique enables quantitative transfer of a sample and thereby provides a more accurate result. However, there are also difficulties with this method, such as peak splitting and peak spreading due to band broadening in space. These effects frequently result when large volume injections are performed. Because the sample enters the column inlet as a liquid plug, the injection of larger sample volumes forms several meters of a layer distributed on the column wall and they remain there until the column temperature increased. This is called a

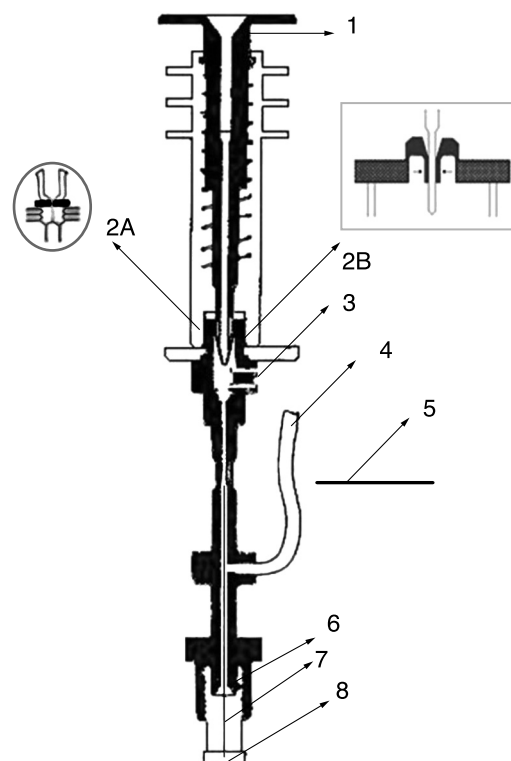


Fig. 2 Schematic diagram of a cross section of a cold on-column injector with a duck-bill valve. 1: Cool tower needle guide, 2A: disk septum for automated injections, 2B: isolation valve for manual injections, 3: frit, 4: carrier gas, 5: oven wall, 6: ferrule, 7: capillary column, 8: column nut. (Modified from Ref. [5].)

flooded zone situation, which is responsible for peak broadening and double peaks. The length of the flooded zone is related to the volume sample injected, the polarity difference between the solvent and the stationary phase, and the column temperature used. Injecting a small sample volume ($<1 \mu\text{L}$) can minimize the peak distortion and yield good results in terms of the peak shape and analytical precision. The speed of injecting the sample into the column also has an effect on sample loss during on-column injection. It is suggested to inject the samples rapidly at the temperature of the column oven, but not higher than the boiling point of the solvent. Depressing the plunger at a slow rate causes a part of the sample to adhere to the needle, and the sample component is discriminated. As the detection level is restricted by the small injection volume, a large volume sampling method is frequently required to enhance the detectability, especially for trace analysis.^[19] Using a technique called "retention gap," which allows the injection of a large volume of sample ($>2 \mu\text{L}$), can minimize the peak distortion. The retention gap is a length of fused silica tubing connected to the front of the analytical column by means of a suitable connector. It is actually a precolumn that does not contain any stationary phase, and the surface is deactivated to reduce solute interaction. Unlike the usual fused silica column, the retention gap has, consequently, a low or negligible retention character. To obtain a uniform sample film on the column wall, the solvent used should be selected in such a way that it wets the surface of the retention gap. Injection of the sample into the retention gap is followed by the evaporation of the solvent, leading to focusing of the sample components. When the solvent has completely evaporated, the solutes are sharply focused on the stationary phase. This approach has shown great success to improve peak shapes for many types of samples. As a general rule, typically used retention gaps are 25 to 50 cm in length, or about 25–30 cm for each microliter of solvent injected. A retention gap of $7 \text{ m} \times 0.32 \mu\text{m ID}$ enables injection of volumes up to about $50 \mu\text{L}$; whereas $250 \mu\text{L}$ can be injected using a $10\text{-m} \times 0.53\text{-}\mu\text{m-ID}$ uncoated precolumn. The use of a retention gap offers some advantages; it allows the operation of an automated injection with regular syringe needles.^[20,21] Moreover, the retention gap can act as guard column which reduces contamination when "dirty samples" are analyzed.^[4,6] On-column injection with a retention gap technique performs better than PTV solvent splitting for the analysis of volatile, labile, and high-boiling components, but it is sensitive to contamination of the precolumns with non-evaporating sample by-products. Large-volume, cold on-column injections are increasing in popularity as methods for analysis of trace-level components and, especially, for environmental analysis.^[22–25]

CONCLUSION

Cold on-column injection is an injection technique for GC which offers some advantages: elimination of sample discrimination, elimination of sample alteration, and high analytical precision and accuracy. Peak splitting or peak distortion, which may occur as a result of polarity mismatches of solvent, stationary phase, and solutes, can be reduced by means of a retention gap. Today, the cold on-column technique using a retention gap is one of the most commonly employed techniques for large-volume injections.

ACKNOWLEDGMENTS

The authors thank DAAD (Deutscher Akademischer Austauschdienst), Bonn, Germany, for the financial support during our short visit at TU Braunschweig and at the University of Duesseldorf in 2002. We are also grateful to Miss Ivy Widjaja and Mr. Dedy Triono for their technical assistance.

REFERENCES

- Schomburg, G. *Gas Chromatography, A Practical Course*; VCH Verlagsgesellschaft: Weinheim, 1990.
- Sandra, P. *Sample Introduction in Capillary Gas Chromatography*; Hüthig: Heidelberg, 1985.
- Grob, K. *Split and Splitless Injection in Capillary GC*; Hüthig: Heidelberg, 1998.
- Poole, C.F.; Poole, S.K. *Chromatography Today*; Elsevier: Amsterdam, 1991.
- Sandra, P. Sample Introduction. In *High Resolution Gas Chromatography*; Hyver, K.J., Ed.; Hewlett-Packard Co., 1989.
- Ravindranath, B. *Principles and Practice of Chromatography*; Ellis Horwood Limited: Chichester, 1989.
- Fowles, I.A. *Gas Chromatography: Analytical Chemistry by Open Learning*; John Wiley & Sons: New York, 1995.
- <http://www.chromtech.net.au/pdf/rtxflash.pdf>. (accessed in January 2004).
- Sandra, J.F. Gas Chromatography. In *Ullmann's Encyclopedia of Industrial Chemistry*; Wiley-VCH Verlag GmbH: Weinheim, 2002.
- Grob, R.L. *Modern Practice of Gas Chromatography*; Wiley Interscience: New York, 1997.
- Adamovics, J.A.; Eschbach, J.C. *Gas chromatography in Chromatographic Analysis of Pharmaceutical*; Marcel Dekker Inc: New York, 1997.
- Badings, H.T.; De Jong, C. Glass capillary gas chromatography of fatty acid methyl esters. A study of conditions for the quantitative analysis of short- and long-chain fatty acids in lipids. *J. Chromatogr.* **1983**, 279, 493–506.



13. Geeraert, E.; Sandra, P.; De Schepper, D. On-column injection in the capillary gas chromatography analysis of fats and oils. *J. Chromatogr.* **1983**, 279, 287–295.
14. Bonilla, M.; Enriquez, L.G.; McNair, H.M. Use of cold on-column injection for the analysis of putrescine and cadaverine by gas chromatography. *J. Chromatogr. Sci.* **1997**, 35 (2), 53–56.
15. Schomburg, G. Sampling technique in capillary gas chromatography. *J. Chromatogr.* **1977**, 142, 87–102.
16. Grob, K.; Grob, K., Jr. On-column injection on to glass capillary columns. *J. Chromatogr.* **1978**, 151, 311–320.
17. Galli, M.; Trestianu, S. Benefits of a special cooling system to improve precision and accuracy in non-vaporizing on-column injection procedures. *J. Chromatogr.* **1981**, 203, 193–205.
18. <http://www.gaschromatographs.com/sample.asp>. (accessed in January 2004).
19. Hinshaw, J. Capillary inlet systems for gas chromatographic trace analysis. *J. Chromatogr. Sci.* **1988**, 26, 49–55.
20. Grob, K. On-column injection of large volumes using the retention gap technique in capillary gas chromatography. *J. Chromatogr.* **1985**, 334, 129–155.
21. David, F.; Sandra, P.; Stafford, S.S. Application of Retention Gaps for Optimized Capillary GC. In *Application Note 228–245, Publ. No 43*; Hewlett-Packard Co., March 1994; 5962E–7904E.
22. <http://www.textronica.com/aplicate/struktur/an9142.pdf>. (accessed in January 2004) → LVIOCI.
23. <http://www.jtbaker.com/techlib/documents/quest2.htm>. (accessed in January 2004).
24. <http://www.chem.agilent.com/cpdocs/5890%20Series%20II%20Cool%20On%20Column%20Operating%20Manual.pdf>. (accessed in January 2004).
25. Wilson, B.; Nixon, D.; Klee, M. Large-Volume Injection for Gas Chromatography Using COC-SVE. In *Application Note 228–377, Publication No. 23*; Agilent Technology, March 1997; 5965E–7923E.

SUGGESTED FURTHER READING

Grob, K. *On Column Injection in Capillary Gas Chromatography*; Hüthig: Heidelberg, 1998.



Open-Tubular (Capillary) Columns

Raymond P.W. Scott

Scientific Detectors Ltd., Banbury, Oxfordshire, England

Introduction

Open-tubular columns were discovered by Golay [1] in the late 1950s and the first commercial columns were introduced in the early 1960s. The first capillary columns were fabricated from copper tubing 0.01 in. inner diameter but, due to their somewhat variable geometry, were quickly replaced with the more rigid cupronickel tubing and, subsequently, by stainless-steel tubing.

Discussion

Metal capillary columns need to be cleaned to remove traces of extrusion lubricants by washing them with methylene dichloride, methanol, and then water. They should also be washed with dilute acid to remove any metal oxides or corrosion products that remain adhering to the walls. The acid is removed with water and the tubing is again washed with methanol and methylene dichloride and dried in a stream of hot nitrogen.

Metal columns provide the expected high efficiencies and were used successfully for the analysis of low-polarity materials such as petroleum and fuel oils and, today, they are still extensively used for the analysis of hydrocarbons. Metal columns, however, although easily coated with dispersive stationary phases (e.g., squalane, Apiezon grease, etc.), do not coat well with the more polar stationary phases such as Carbowax®. In addition, the hot metal surface can cause decomposition and molecular rearrangement of many thermally labile materials that are being separated (e.g., the terpenes in essential oils). Metal can also react directly with some solutes by chelation and, as a result of surface adsorption, produce asymmetric and tailing peaks. Nevertheless, metal columns are rugged, easy to handle, and easy to remove and replace in the chromatograph, so their use has persisted in many applications despite the introduction of fused-silica columns.

In an attempt to eliminate surface activity, Desty et al. [2] introduced the first silica-based columns and invented an extremely clever device for drawing soft glass capillary columns. Desty produced both rigid soft glass and rigid Pyrex capillary columns, although their

permanent circular shape rendered them a little difficult to connect to the injector and detector. It was found that, with special surface treatment, the rigid glass tubes could be coated with polar stationary phases. The demand for special surface processing evoked a large number of proprietary methods for column treatment. Fortunately, the frenetic interest in the surface deactivation of soft glass capillary tubes was curtailed by the introduction of the flexible fused-silica capillary columns by Dandenau and Zenner [3].

The quartz fiber drawing technique used in the manufacture of data transmission lines was used to produce flexible *fused-silica* tubing. Basically, the solid quartz rod used in quartz fiber drawing was replaced by a quartz tube. In a similar manner to that used in the quartz fiber production, the quartz tubes were coated with polyimide to prevent moisture from attacking the surface and producing stress corrosion. Soft glass capillaries can be produced by the same technique at much lower temperatures [4], but the tubes are not as mechanically strong or as inert as quartz capillaries. Flexibility was the main advantage to quartz capillaries, as it greatly facilitated the installation of the columns in the chromatograph. However, surface treatment is still necessary with a fused-quartz column to reduce adsorption and catalytic activity and render the surface wettable for efficient coating. The treatment may involve washing with acid, silanization, and other types of chemical treatment, including the use of surfactants.

Deactivation procedures used for commercial columns also tend to be highly proprietary. A deactivation program for silica and soft glass columns that is suitable for most applications would first entail an acid wash. The column is filled with 10% (w/w) hydrochloric acid, the ends sealed, and the column then heated to 100°C for 1 h. The column is then washed free of acid with distilled water and dried. This procedure is believed to remove traces of heavy metal ions that can cause adsorption and peak tailing. The column is then filled with a solution of hexamethyldisilazane, sealed, and heated to the boiling point of the solvent for 1 h. This procedure blocks any hydroxyl groups on the surface that were generated during the acid wash. A polar



or semipolar silane reagent might be preferable to facilitate coating if a polar stationary phase is to be used. The column is then washed with the pure solvent, dried at an elevated temperature in a stream of pure nitrogen, and is ready for coating.

Open-tubular columns can be coated internally with a liquid stationary phase or with polymeric materials that are subsequently polymerized to form a relatively rigid polymer coating. The two methods of coating are the *dynamic method of coating* and the *static method of coating*. In the dynamic coating procedure, a plug of solvent containing the stationary phase is placed at the beginning of the column. The strength of the solution, among other factors, determines the thickness of the stationary-phase film. In general, the film thickness of an open-tubular column ranges from 0.25 μm to about 1.5 μm . As an estimate, a 5% (w/w) solution of stationary phase will provide a stationary film thickness of about 0.5 μm . After the plug has been run into the front of the column (sufficient solution should be added to fill about 10% of the column length), a gas pressure is used to force the plug through the column at about 2–4 mm/s. When the plug has passed through the column, the gas flow is continued for about 1 h. The gas flow should not be increased too soon, as ripples of stationary phase solution will form on the walls of the tube, which produces a very uneven film. After 1 h, the flow rate is increased and the column stripped of solvent. The last traces of the solvent are removed by heating the column above the boiling point of the solvent at an increased gas flow rate.

In static coating, the entire column is filled with a solution of the stationary phase and one end connected to a vacuum. As the solvent evaporates, it retreats back down the tube, leaving a coating on the walls. The optimum concentration will depend on the stationary phase, the solvent, the temperature, and the condition of the wall surface. This process is very time-consuming but can proceed without attention and is often carried out overnight. This procedure is more repeatable than the dynamic method of coating, but, in general, it produces columns having a similar performance to those dynamically coated.

However well the column may be coated, the stability of the column depends on the stability of the stationary phase film, and thus on the constant nature of the surface tension forces holding it to the column wall. These surface tension forces can change with temperature or be effected by the samples used for analysis. As a consequence, the surface tension can be suddenly reduced and the film break up. It follows that the stationary phase should be bonded in some way to the

column walls or polymerized *in situ*. Such coatings are called immobilized stationary phases and cannot be removed by solvent washing.

Some stationary phases that are polymeric in nature can sometimes be formed by coating the monomers or dimers on the walls and then initiating polymerization either by heat or a suitable catalyst. This locks the stationary phase to the column wall and is thus completely immobilized. Polymer coatings can be formed in the same way using dynamic coating. Techniques used for immobilizing the stationary phases are highly proprietary and little is known of the methods used. In any event, most chromatographers do not want to go to the trouble of coating their own columns and are usually content to purchase proprietary columns.

Porous-Layer Open-Tubular Columns

There are two basic disadvantages to the coated capillary column. First, the limited solute retention that results from the small quantity of stationary phase in the column. Second, if a thick film is coated on the column to compensate for this low retention, the film becomes unstable resulting in rapid column deterioration. Initially, attempts were made to increase the stationary-phase loading by increasing the internal surface area of the column. Attempts were first made to etch the internal column surface, which produced very little increase in surface area and very scant improvement. Attempts were then made to coat the internal surface with diatomaceous earth, to form a hybrid between a packed column and coated capillary. None of the techniques were particularly successful and the work was suddenly eclipsed by the production of immobilize films firmly attached to the tube walls. This solved both the problem of loading, because thick films could be immobilized on the tube surface, and that of phase stability. As a consequence, porous-layer open-tubular (PLOT) columns are not extensively used. The PLOT column, however, has been found to be an attractive alternative to the packed column for gas–solid chromatography (GSC) and effective methods for depositing adsorbents on the tube surface have been developed.

The open-tubular column is, by far, the most popular type of GC column in use today. As a result of its small internal cross section, however, extracolumn dispersion can become a serious problem. This means that open-tubular columns must be used with special types of injector and reduced volume connectors, and certain detectors must have specially designed sensor cells to avoid impairing column performance.



References

1. M. J. E. Golay, *Gas Chromatography. 1958* (D. H. Desty, ed.), Butterworths, London, 1958, p. 36.
2. D. H. Desty, A. Goldup, and B. F. Wyman, *J. Inst. Petrol.* 45: 287 (1959).
3. R. D. Dandenau and E. M. Zenner, *J. High Resolut. Chromatogr.* 2: 351 (1979).
4. K. L. Ogan, C. Reese, and R. P. W. Scott, *J. Chromatogr. Sci.* 20: 425 (1982).

Suggested Further Reading

Scott, R. P. W., *Techniques and Practice of Chromatography*, Marcel Dekker, Inc., New York, 1996.
Scott, R. P. W., *Introduction to Analytical Gas Chromatography*, Marcel Dekker, Inc., New York, 1998.



Open-Tubular and Micropacked Columns for Supercritical Fluid Chromatography

Brian Jones

Selerity Technologies, Inc., Salt Lake City, Utah, U.S.A.

Introduction

Supercritical fluid chromatography (SFC) with open-tubular columns was first demonstrated in 1981 by Novotny and co-workers [1]. This technique, known as capillary SFC, was made available to the analytical community through the introduction of several commercial instruments in 1986. Initially difficult to use, improvements in instrumentation and hardware, coupled with a wider array of columns and restrictor options designed specifically for the technique, becoming available, have led to a general acceptance of the method in many laboratories. Not only useful as a research tool, capillary SFC is firmly established as an essential analytical method for production support and quality control in many industries. Some of these include chemical and petroleum manufacturing, pharmaceuticals, polymers, and environmental monitoring.

Packed columns have also been used in SFC for many years, predating capillaries by nearly 20 years. Many columns originally developed for liquid chromatography have found utility in SFC and have varied in internal diameter from smaller than 50 μm to very large-preparative-scale sizes. Definitions vary, but for purposes here, micropacked columns are considered to have internal diameters less than 2 mm. These smaller-diameter columns are also in wide use and offer significant benefits with regard to mobile-phase consumption and detector compatibility than their large-bore counterparts. The selectivity and performance of micropacked columns are complimentary to those of capillaries, and instrumentation is available that is compatible with both separation techniques, allowing for the separation of a wide range of analytes and rapid switchover between methods. Several reviews have been published [2–4].

Pressure Drop Effects

Elution of a particular compound in SFC is a function of its extent of interaction with the column stationary phase and the solvating strength of the mobile phase, with the latter being a direct function of density. The

density is affected by temperature and pressure and, in the case of separations with capillary columns that are inherently open and exhibit little pressure drop across their length, it is essentially constant throughout. By contrast, packed columns exhibit much more resistance to mobile-phase flow and can experience a considerable density drop during SFC analysis, producing a potentially significant loss in separation efficiency. Commercial packed columns, tested only by high-performance liquid chromatography (HPLC), may not show these deficiencies in their test reports. The only reliable gauge of suitability of a column for SFC is a performance test in the SFC mode. Columns tested under SFC conditions and tested for suitability for a specific SFC method have been commercially available for some time.

The pressure drop effect limits the usable length of packed columns to approximately 25 cm, although micropacked columns prepared specifically for SFC can be used to longer lengths [5]. The particle size also plays a role, with packing materials smaller than 5 μm producing the highest pressure drops. Whereas short columns dominate in packed column SFC, typical parameters for capillary columns are 3–10 m in length, 50 μm in inner diameter, and a stationary-phase film thickness of 0.25 μm , which give the best compromise in loadability, analysis speed, and efficiency.

Calculated practical efficiencies for a compound with a capacity factor of 2 and a CO_2 mobile phase are shown for each type of column in Table 1. It is clear that capillary columns are capable of delivering high efficiency separations in SFC, but at the expense of analysis time when compared to packed columns.

Activity

Silica surfaces are the chief source of activity in columns for SFC and, even though many of the columns are well deactivated, the residual silanol sites can lead to tailing or adsorption of analytes. The low surface area of capillary columns is responsible for much higher levels of inertness than their packed counterparts based on silica particles. Capillary columns have been used successfully in the analysis of active com-



Table 1 Calculated Practical Efficiencies for Compound with a Capacity Factor of 2 and CO₂ Mobile Phase

Column type	Particle diameter, internal diameter (μm)	Length (m)	Plates at low density (100 atm, 100°C)	Plates at high density (400 atm, 100°C)	Linear velocity (cm/s) at low density	Linear velocity (cm/s) at high density
Packed	5	0.1	5,200	9,100	0.6	2.1
Capillary	50	10	102,000	19,000	2.5	5.8

Source: Data from Ref. 2.

pounds, including isocyanates, acid halides, organic acids, amines, peroxides, azo compounds, and many others. The low temperatures required for elution make analysis of active and labile compounds viable.

Silica particles have high surface areas and usually contain a large number of exposed residual silanol groups after derivatization. These groups impart a significant degree of polarity to packed columns and can be used to advantage, for example, in the determination of aromatics in fuels [6]. For more active solutes, modifiers are used to reduce tailing and improve quantitation.

Modifiers

The addition of cosolvents to the mobile phase can be effective in adjusting selectivity and improving sample solubility. As the most dramatic effect with polar modifiers is seen in the interaction with the surface silanol groups, even small amounts of cosolvents change the elution characteristics of packed columns. With capillary columns, the effect is related more to solvent strength of the mobile phase than surface modification, and higher modifier levels are required to produce significant changes in retention.

One of the drawbacks of using modifiers is their response in some of the detectors. The flame ionization detector (FID) is very popular with capillary and micropacked columns in SFC because of its near-universal response and high sensitivity and the lack of response of CO₂ as the most popular mobile phase. The low mass flow rate of the mobile phase in small columns allows for a direct interfacing of the column to the FID and other detectors without flow splitting or back-pressure regulation.

Sample Introduction

The small internal volume and low mobile-phase mass flow rates in capillary and micropacked column SFC place significant demands on the injection system and

connections. The injector must deliver a small, narrow band of material onto the head of the column and must not contain any void volume or unswept area in the flow path. Several methods of injection are in common use, including the following:

1. Split, where the column is placed in the injector such that it intercepts a portion of the sample stream with the excess carried past and out of the system through a flow restrictor. This method gives the highest efficiencies, but it can produce some sample discrimination.
2. Timed-split, where the sample loop is placed in the flow stream for short periods, and the time in the inject position determines the amount on column. This is the most popular injection method and gives good efficiency and reproducibility. It requires fast actuation and an internal sample loop.
3. Split-splitless, which is performed with a split assembly and a split vent shutoff valve. This method enables larger volumes to be admitted onto the columns and the split activates to reduce tailing by sweeping residual amounts of material out of the system.

The use of a retention gap can allow for higher efficiencies and larger injection volumes on capillary columns [7]. The retention gap is a section of uncoated tubing placed between the column and the injector, which allows the analytes to refocus into a narrow band at the head of the column. This uncoated section can be built right into the capillary column such that no additional connections are required.

Restrictors

Restrictors are required at the ends of SFC columns to maintain supercritical conditions throughout the column and to limit overall flow. Several options exist, with frit restrictors being the most popular, followed by integral and linear formats. The frit restrictor is

made by casting a porous ceramic material inside fused-silica tubing with the flow rate dependent on length and pore size. These restrictors are robust and are easily tuned to the desired flow rate by trimming small sections off of the frit end. The multiple flow paths are also resistant to plugging. Frit restrictors are supplied in varied porosities in the end of deactivated 50- μm -inner diameter tubing and are attached to the end of the column using low dead-volume connectors. Integral restrictors are made by heating fused-silica tubing to its melting point and allowing it to collapse to a single orifice of very small diameter. The end can be ground to form a larger opening, but this process requires considerable patience. This type of restrictor can be fabricated in the end of the column such that no connectors are required, but the single orifice is more susceptible to plugging with stray particles than are other types. Linear restrictors are made from short lengths of fused-silica tubing with narrow internal diameters. These are interfaced to the column with low-dead-volume connectors, but the long pressure drop across the tubing length can cause some analytes to precipitate prematurely and produce detector spiking.

Stationary Phases

A wide variety of stationary phases and bonded-phase particles for SFC are available. Capillary columns are coated with substituted and cross-linked polysiloxanes, which exhibit good inertness, efficiency, and stability. There are three main classes of capillary column stationary phases for SFC: apolar, polarizable, and polar.

Apolar

Methyl silicone, 5% phenyl-substituted silicone, and 50% octyl-substituted silicone separate generally on the basis of solute volatility. The most significant interactions are inherently weak van der Waal's. These phases have the highest diffusion properties and give the highest efficiencies. Highly polar materials overload easily on these columns and produce wedge-shaped peaks.

Polarizable

The 50% phenyl-substituted silicone and 30% biphenyl-substituted silicone stationary phases are moderately polar and contain polarizable aromatic rings that exhibit induced dipoles in the presence of dipolar solutes such as alcohols, phenols, amines, nitriles, ketones, and so forth. They give selectivity with-

out extended retention of polar solutes because the dipole-induced-dipole interaction is relatively weak. Temperature affects the extent of this polarization and can be used as a variable in optimizing separations.

Polar

The 25% and 50% cyanopropyl phases exhibit permanent dipoles that interact strongly with polar solutes. Because this translates into longer retention times for polar solutes, only lower-molecular-weight materials of this type can be eluted. Polarizable (aromatic and unsaturated hydrocarbons) and weakly dipolar solutes are good candidates for analysis with these phases. Aliphatic hydrocarbons overload easily but elute rapidly.

Micropacked columns are available with most of the bonded-phase packings used in high-performance liquid chromatography. Porous and nonporous silica particles are optionally functionalized with covalently bound silanes or other strongly adsorbed materials. Alkyl-bonded silicas produce separations, generally based on solute volatility, but with the potential for selectivity differences based on interaction with silanol groups. Underivatized silica is popular for petroleum separations of aliphatic and aromatic hydrocarbons. Silver-ion-containing silica columns are selective for olefin separations. Fluoroalkyl-bonded silicas produce unique selectivities and show good sample capacities for fluorocarbons. Polybutadiene-derivatized zirconia particles have also been used in SFC as have particles based on cross-linked organic polymers. These latter types show different selectivities because of the absence of surface silanol groups. Chiral-bonded phases capable of resolving enantiomers are seeing wide use, particularly in the pharmaceutical market.

Recent Advances

Recent developments in capillary and micropacked column SFC have centered on making the technique easier and more reliable to use. Columns are available that are fitted with restrictors, performance tested by SFC, and are ready to install. Dead-volume issues have been resolved with low-mass couplers and auto-depth-adjusting fingertight fittings suitable for high-pressure use. Packed columns have been developed and optimized for SFC use that have low pressure drops and high stabilities. The future should see a continuation of this trend, with more column options and formats becoming available and additional methods utilizing them seeing wide acceptance.



References

1. M. Novotny, S. R. Springston, P. A. Peaden, J. C. Fjeldstead, and M. L. Lee, *Anal. Chem.* 53: 407A (1981).
2. M. L. Lee and K. E. Markides (eds.), *Analytical Supercritical Fluid Chromatography and Extraction*, Chromatography Conferences, Provo, UT, 1990.
3. M. Caude and D. Thiebaut (eds.), *Practical Supercritical Fluid Chromatography and Extraction*, Harwood, Amsterdam, 1999.
4. L. G. Blomberg, M. Demirbueker, I. Haeggglund, and P. E. Andersson, *Trends Anal. Chem.* 13(3): 126–137 (1994).
5. W. Li, A. Malik, and M. L. Lee, *J. Microcol. Separ.* 6: 557–563 (1994).
6. W. Li, A. Malik, M. L. Lee, B. A. Jones, N. L. Porter, and B. E. Richter, *Anal. Chem.* 67(3): 647–654 (1995).
7. T. L. Chester and D. P. Innis, *Anal. Chem.* 67(17): 3057–3063 (1995).



Optical Activity Detectors

Hassan Y. Aboul-Enein

Ibrahim A. Al-Duraibi

Pharmaceutical Analysis Laboratory, King Faisal Specialist Hospital and Research Centre, Riyadh, Saudi Arabia

Introduction

Optical activity detectors are capable of specifically detecting chiral compounds, taking advantage of their unique interactions with polarized light. Much of the work on the development of prisms and other devices for the production of polarized light was done in the early part of the nineteenth century. However, the measurement of optical activity is often used for enantiomeric purity determination of chiral compounds, which by definition have either a center or plane of asymmetry. Enantiomers rotate the plane of polarized light in opposite directions, although in equal amounts. The isomer that rotates the plane to the left (counter-clockwise) is called the levo isomer and is designated (–), whereas the one that rotates the plane to the right (clockwise) is called the dextro isomer and is designated (+). Questions of optical activity are of extreme importance in the field of asymmetric chemical synthesis and in the pharmaceutical industry.

Detection Principle

Figure 1 shows the basic optimal system of the optical rotation detector, which is based on the nonmodulated polarized beam-splitting method. The light radiated from the light source is straightened by the plane polarizer, then to the lens for beam formation and concentration, and then to the flow cell.

The plane-polarized light which goes through the flow cell is rotated by optically active substances (chiral compounds) according to their specific optical rotations and concentrations. The light then enters the polarized beam splitter and is divided into two beams according to the polarized beam directions. These beams are detected by two photodiodes as shown.

The angle of the plane polarizer is adjusted so that the two photodiodes may receive the same beam intensity when no optically active substance is present in the flow cell. When optically active substances are present in the flow cell, the difference between the beam intensities received by the two photodiodes is not zero. Therefore, the difference has a linear relation

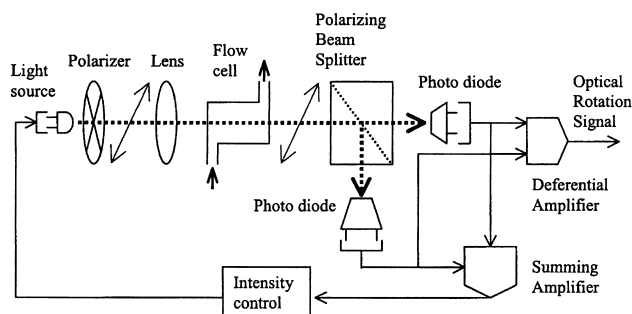


Fig. 1 Optical rotation detector.

with specific optical rotation and concentration of the optically active substance and can be expressed by

$$V_0 = K[\alpha]C$$

where V_0 is the difference of beam intensities received by the two photodiodes (i.e., output of signal level), K is a constant determined by cell structure and light intensity of the light source, $[\alpha]$ is the specific optical rotation of the chiral compound, and C is the concentration of the chiral compound.

Polarimetry Theory

Most forms of optical spectroscopy are usually concerned with the measurement of the absorption or emission of electromagnetic radiation. Ordinary, natural, unreflected light behaves as though it consists of a large number of electromagnetic waves vibrating in all possible orientations around the direction of propagation. If, by some means, we sort out from the natural conglomeration only those rays vibrating in one particular plane, we say that we have plane-polarized light. Of course, because a light wave consists of an electric and a magnetic component vibrating at right angles to each other, the term “plane” may not be quite descriptive, but the ray can be considered planar if we restrict ourselves to noting the direction of the electrical component. Circu-



lar polarized light represents a wave in which the electrical component (and, therefore, the magnetic component also) spirals around the direction of propagation of the ray, either clockwise ("right-handed" or dextrorotatory) or counterclockwise ("left-handed" or levorotatory). If, following the passage of the plane-polarized ray through some material, one of the circularly polarized components, say the left circularly polarized ray, has been slowed down, then the resultant would be a plane-polarized ray rotated somewhat to the right from its original position. In addition, lasers have been incorporated into two optical rotation methods to date: polarimetry and circular dichroism.

Optical Rotation and Optical Rotatory Dispersion

A polarimeter measures the direction of rotation of plane-polarized light caused by an optically active substance. The specific optical activity of an asymmetrical molecule varies with the wavelength of the light used for its determination. This variation is called optical rotatory dispersion (ORD). In ORD, rotations are measured over a range of wavelengths rather than at a single wavelength, usually covering the ultraviolet (UV) as well as the visible region.

Circular Dichroism

In this technique, the molecular extinction coefficients of a compound are measured with both left and right circularly polarized light, and the difference between these values is plotted against the wavelength of the light used. The phase angle between the projections of the two circularly polarized components is altered by passage through the chiral medium, but their amplitudes will be modified by the degree of absorption experienced by each component. This differential absorption of left- and right-circularly polarized light is termed circular dichroism (CD). So, circular dichroism measurements provide both absorbance and optical rotation information simultaneously.

Circularly Polarized Luminescence Spectroscopy

Circularly polarized luminescence spectroscopy (CPLS) is a measure of the chirality of a luminescent excited state. The excitation source can be either a laser or an arc lamp, but it is important that the source of excitation be unpolarized to avoid possible photoselection artifacts. The CPLS experiment produces two

measurable quantities, which are obtained in arbitrary units and related to the circular polarization condition of the luminescence. It is appropriate to consider CPLS spectroscopy as a technique that combines the selectivity of CD with the sensitivity of luminescence. The major limitation associated with CPLS spectroscopy is that it is confined to emissive molecules only.

Vibrational Optical Activity

The optical activity of vibrational transitions has been conducted. The infrared (IR) bands of a small molecule can easily be assigned with the performance of a normal coordinate analysis, and these can usually be well resolved. One of the problems associated with vibrational optical activity is the weakness of the effect. Instrumental limitations of infrared sources and detectors create additional experimental constraints on the signal-to-noise ratios.

Two methods suitable for the study of vibrational optical activity have been developed:

Vibrational Circular Dichroism: Vibrational circular dichroism (VCD) could be measured at good signal-to-noise levels. Vibrational optical activity is observed in the classic method of Grosjean and Legrand.

Raman Optical Activity: The Raman optical activity (ROA) effect is the differential scattering of left- or right-circularly polarized light by a chiral substrate where chirality is studied through Raman spectroscopy.

Fluorescence-Detected Circular Dichroism

Fluorescence-detected circular dichroism (FDCD) is a chiroptical technique in which the spectrum is obtained by measuring the difference in total luminescence obtained after the sample is excited by left- and right-circularly polarized light. For the FDCD spectrum of a given molecular species to match its CD spectrum, the luminescence excitation spectrum must be identical to the absorption spectrum.

Factors Affecting the Measurement of Optical Rotation

The rotation exhibited by an optically active substance depends on the thickness of the layer traversed by the light, the wavelength of the light used for the measurement, and the temperature of the system. In addition, if the substance being measured is a solution, then the

concentration of the optically active material is also involved and the nature of the solvent may also be important. There are certain substances that change their rotation with time. Some are substances that change from one structure to another with a different rotatory power and are said to show mutarotation. Mutarotation is common among the sugars. Other substances, owing to enolization within the molecules, may rotate so as to become symmetrical and, thus, lose their rotatory power. These substances are said to show racemization. Mutarotation and racemization are influenced not only by time, but also by pH, temperature, and other factors. Of course, rotations that determined for the same compound under the same conditions are identical. Therefore, in expressing the results of any polarimetric measurement, it is, therefore, very important to include all experimental conditions.

Temperature

Temperature changes have several effects on the rotation of a solution or liquid. An increase in temperature increases the length of the tube; it also decreases the density, thus reducing the number of molecules involved in the measurement. It causes changes in the rotatory power of the molecules themselves, due to association or dissociation and increased mobility of the atoms, and affects other properties. In addition, temperature changes cause expansion and contraction of the liquid and a consequent change in the number of active molecules in the path of the light.

The unique ability of the optical rotation detector to respond to the sign of rotation allows precise enantiomeric purity determination even if the enantiomers are only partially resolved. The sign of rotation is also useful in establishing enantiomer elution order.

Because the optical rotation detectors only respond to optically active compounds, enantiomeric purity determination to precisions of better than 0.5% can be achieved and is possible in even the complex mixtures. The detection can also be used as part of a flow injection analysis system to determine amount and enantiomeric purity of a drug in dosage form.

The applications using optical rotation detectors include the following:

1. Qualitative analysis of chiral compounds, including drugs, pesticides, carbohydrates, amino acids, liquid crystals, and other biochemicals
2. Determination of enantiomeric purity of chiral compounds
3. Monitoring an enzymatic reaction
4. Qualitative analysis of proteins
5. Use as a conventional polarimeter

However, the disadvantages of optical rotation detectors may be limited by shot or flicker noise, which are dependent on the optical and mechanical properties of the system or by noise in the detector electronics. Generally, the usefulness of this technique has been limited by the lack of sensitivity of commercially available instruments.

Suggested Further Reading

- Allenmark, S., Techniques used for studies of optically active compounds, in *Chromatographic Enantioseparation: Methods and Application*, 2nd ed., Ellis Horwood Ltd., London, 1991.
- Beesley, T. E. and R. P. W. Scott, An introduction to chiral chromatography, in *Chiral Chromatography*, John Wiley & Sons, Inc., New York, 1998, pp. 1–11.
- Dodziuk, H., Physical methods as a source of information on the spatial structure of organic molecules, in *Modern Conformational Analysis, Elucidating Novel Exciting Molecular Structures*, VCH, New York, 1995, pp. 48–54.
- Edkins, T. J. and D. C. Shelly, Measurement concepts and laser-based detection in high-performance micro separation, in *HPLC Detection: Newer Methods* (G. Patonay, ed.), VCH, New York, 1992, pp. 1–15.
- Goodall, D. M. and D. K. Lloyd, A note on an optical rotation detector for high-performance liquid chromatography, in *Chiral Separations* (D. Stevenson and D. Wilson, eds.), Plenum Press, New York, 1988, pp. 131–133.
- Sheldon, R. A., Introduction to optical isomerism, in *Chirotechnology: Industrial Synthesis of Optically Active Compounds*, Marcel Dekker, Inc., New York, 1993, pp. 25–27.
- Weston, A. and P. R. Brown, *HPLC and CE Principles and Practice*, Academic Press, San Diego, CA, 1997.
- Yeung, E. S., Polarimetric detectors, in *Detectors for Liquid Chromatography* (E. S. Yeung, ed.), John Wiley & Sons, New York, 1986, pp. 204–228.



Optical Quantification (Densitometry) in TLC

Joseph Sherma

Lafayette College, Easton, Pennsylvania, U.S.A.

Introduction

Quantitative evaluation of thin-layer chromatograms can be performed by direct, *in situ* visual, and indirect elution techniques. Visual evaluation involves comparison of the sizes and intensities of color or fluorescence between sample and standard zones spotted, developed, and detected on the same layer. The series of standards is chosen to have concentrations or weights that bracket those of the sample zones. After matching a sample with its closest standard, accuracy and precision are improved by respotting a more restricted series of bracketing standards with a separate sample spot between each of two standard zones. Accuracy no greater than 5–10% is possible for trained personnel using visual evaluation. The determination of mycotoxins in food samples is an example of a practical application of visual comparison of fluorescent zones.

The elution method involves scraping off the separated zones of samples and standards and elution of the substances from the layer material with a strong, volatile solvent. The eluates are concentrated and analyzed by use of a sensitive spectrometric method, gas or liquid column chromatography, or electroanalysis. Scraping and elution must be performed manually because the only commercial automatic micropreparative elution instrument has been discontinued by its manufacturer. The elution method is tedious and time-consuming and prone to errors caused by the incorrect choice of the sizes of the areas to scrape, incomplete collection of sorbent, and incomplete or inconsistent elution recovery of the analyte from the sorbent. However, the elution method is being rather widely used (e.g., some assay methods for pharmaceuticals and drugs in the USP Pharmacopoeia).

Introduction to Densitometry

In order to achieve the optimum accuracy, precision, and sensitivity, most quantitative analyses are performed by using high-performance thin-layer chromatography (TLC) plates and direct quantification by means of a modern optical densitometric scanner with

a fixed sample light beam in the form of a rectangular slit that is variable in height (e.g., 0.4–10 mm) and width (20 μm to 2 mm). Densitometers measure the difference in absorbance or fluorescence signal between a TLC zone and the empty plate background and relate the measured signals from a series of standards to those of unknown samples through a calibration curve. Modern computer-controlled densitometers can produce linear or polynomial calibration curves relating absorbance or fluorescence versus weight or concentration of the standards and determine bracketed unknowns by automatic interpolation from the curve. Samples and standards are best applied using an automated instrument such as the one shown in Fig. 1. Use of manual spotting and less efficient TLC plates results in greater errors and poorer reproducibility in quantitative results.

Instrumental Design and Scanning Modes

A commercial densitometer and a schematic diagram of the light-path arrangement used in scanning are shown in Fig. 2. The plate is mounted on a moveable stage controlled by a stepping motor drive that allows each chromatogram track to be scanned in or against the direction of development. A tungsten or halogen lamp is used as the source for scanning colored zones in the 400–800-nm range (visible absorption) and a deuterium lamp for scanning ultraviolet (UV)-absorbing zones directly or as quenched zones on phosphor-containing layers (F-layers) in the 190–450-nm range. The monochromator used with these continuous-wavelength sources can be a quartz prism or, more often, a grating. The detector is a photomultiplier or photodiode placed above the layer to measure reflected radiation. [Some scanners (e.g., Fig. 2) make use of a reference photomultiplier in addition to the measuring photomultiplier in the single-beam mode; the reference photomultiplier puts out a constant signal that is compared to the signal from the measuring photomultiplier to produce a difference signal that is more accurate than a direct signal from a single measuring photomultiplier would be.]



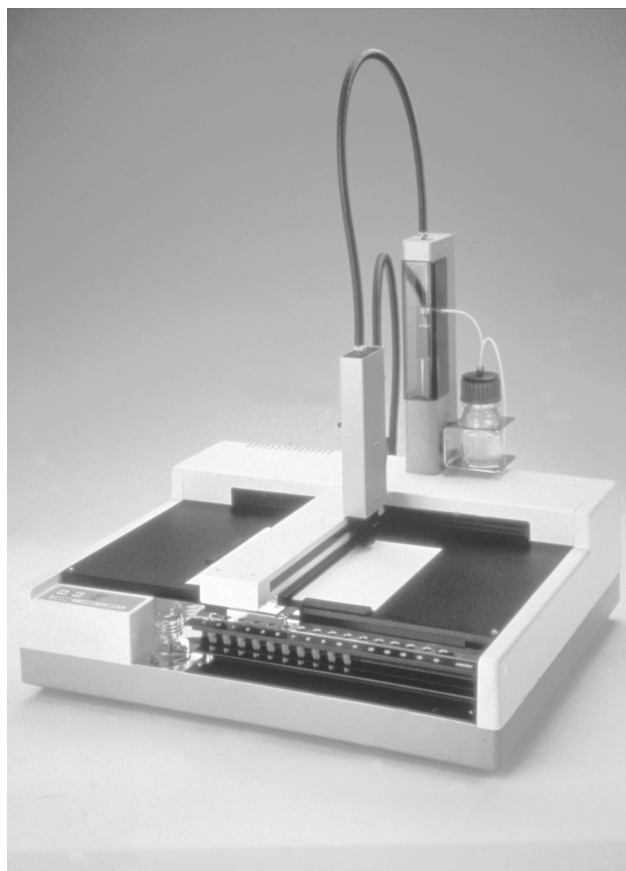


Fig. 1 Automatic TLC sampler (ATS 3) used for computer-controlled application of precisely controlled volumes of samples and standards between 10 nL and 50 μ L from a rack of vials as spots or bands to preselected origins on a plate. (Courtesy of Camag Scientific Inc., Wilmington, NC.)

For normal fluorescence scanning, a high-intensity xenon continuum source or a mercury vapor line source is used, and a cutoff filter is placed between the plate and detector to block the exciting UV radiation and transmit the visible emitted fluorescence. For fluorescence measurement in the reversed-beam mode, a monochromatic filter is placed between the source and plate and the monochromator between the plate and detector. In this mode, the monochromator selects the emission wavelength, rather than the excitation wavelength as in the normal mode.

Simultaneous measurement of reflection and transmission, or transmission alone, can be carried out by means of a detector positioned on the opposite side of the plate (Fig. 2). Ratio-recording double-beam densitometers, which can correct for background disturbances and drift caused by fluctuations in the source and detec-

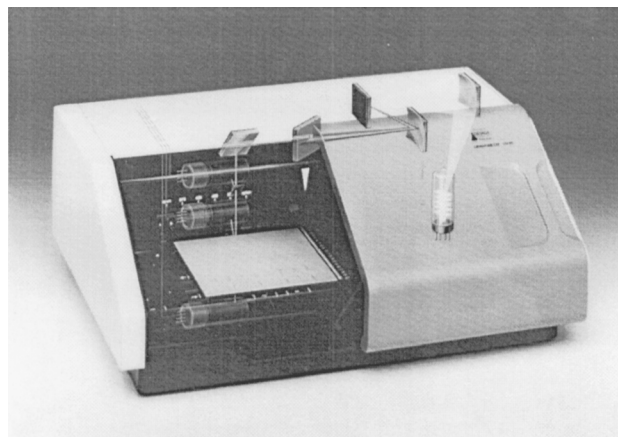


Fig. 2 Photograph of the DESAGA Densitometer CD 60 with a superimposed schematic diagram of the light path including (right to left) the source lamp, two mirrors, grating monochromator, mirror, beam splitter, plate with chromatograms to be scanned, reference and measuring detectors (reflection) above the plate and detector (transmission) below the plate. (Courtesy of DESAGA GmbH, Weisloch, Germany.)

tor, were designed earlier with two photomultiplier detectors simultaneously recording the two beams (double beam in space), but, today, such densitometers are equipped with a chopper and one detector (double beam in time). For dual-wavelength, single-beam scanning, which will correct for scattering of the absorbed light by subtracting out the (presumably equal) scattering at a nonabsorbed wavelength, a light beam is selected by a mirror and passes through two separate monochromators to isolate the two different wavelengths. The two beams are alternated by a chopper and recombined into a single beam representing a difference signal at the detector. Zigzag or meandering scanning with a small point or spot of light is possible with densitometers having two independent stepping motors to move the plate in the X and Y axes. Computer algorithms integrate the maximum absorbance measurements from each swing to produce a distribution profile of zones having any shape. The potential advantages of scanning with a moving light spot are offset by problems with lower spatial resolution and errors in data processing, and the method is not as widely used as conventional scanning of chromatographic tracks with a fixed slit. Some densitometers have the ability to rotate the plate while scanning for measurement of circular and anticircular chromatograms.

Single-wavelength, single-beam, fixed-slit scanning is most often used and can produce excellent results

when high-quality plates and analytical techniques are employed.

Spectral Measurement

Many modern scanners have a computer-controlled motor-driven monochromator that allows automatic recording of *in situ* absorption and fluorescence excitation spectra. These spectra can aid compound identification by comparison with stored standard spectra, test for identity by superimposition of spectra from different zones on a plate, and check zone purity by superimposition of spectra from different areas of a single zone. The spectral maximum determined from the *in situ* spectrum is usually the optimal wavelength for scanning standard and sample areas for quantitative analysis.

Data Handling

The densitometer is connected to a recorder, integrator, or computer. A personal computer with software designed specifically for TLC is most common for data handling and automation of the scanning process in modern instruments. With a fully automated system, the computer can carry out the following functions: data acquisition by scanning a complete plate following a preselected geometric pattern with control of all scanning parameters; automated peak searching and optimization of scanning for each fraction located; multiple-wavelength scanning to find, if possible, a common wavelength for all substances to be quantified, to optically resolve fractions incompletely separated by TLC, and to identify fractions by comparison of spectra with standards cochromatographed on the same plate or stored in a spectrum library through pattern recognition techniques; baseline location and correction; computation of peak areas and/or heights of samples and codeveloped standards and processing of the analog raw data to quantitative digital results, including calculation of calibration curves by linear or polynomial regression, interpolation of sample concentrations, statistical analysis of reproducibility, and presentation of a complete analysis report; and storage of raw data on disk for later reintegration, calibration, and evaluation with different parameters.

Calibration Curves

Densitometric calibration curves relating absorption signal and concentration or weight of standards on the layer are usually nonlinear, especially for higher

amounts of standards, and do not pass through the origin. Fluorescence calibration curves are generally linear and pass through the origin, and analyses based on fluorescence are more specific and 10–1000 times more sensitive. The advantages of fluorescence measurement may be realized for nonfluorescent compounds by prechromatographic or postchromatographic derivatization reactions with suitable fluorogenic reagents.

Because the incident monochromatic light is absorbed, reflected, and scattered by the opaque layer material, the theoretical relationship between amount of absorption and amount of substance does not follow the simple Beer–Lambert law that is valid for solutions. The Kubelka–Munk equation is the most accepted theoretical relationship for TLC, but its use is not necessary because of the ability of densitometer software to handle empirical nonlinear regression functions.

Image Analysis (Videodensitometry)

Video camera systems are available from several manufacturers for documentation and densitometric quantification of TLC plates. As an example, the Camag VideoScan instrument consists of a lighting module with short- and long-wave UV and visible sources upon which the layer is placed, a charge-coupled device (CCD) camera with zoom and long-time integration capability, and a PC under MS-Windows control with frame grabber, monitor, and printer. The available software for quantitative evaluation allows the display of the tracks of the chromatogram image acquired with the video camera as analog curves and calculation of their peak properties (R_f , height, area, height percent, and area percent). For quantification, the computer creates a standard curve from the areas or heights of the standards and interpolates unknown values from the curve.

Video scanners have potential advantages, including rapid data collection, simple design with virtually no moving parts, and ability to quantify two-dimensional chromatograms, but they have not yet been shown to have the required capabilities, such as sufficient spectral discrimination or the ability to illuminate the plate uniformly with monochromatic light of selected wavelength, to replace slit-scanning densitometers. Current video scanners can measure spots in the visible range in transmittance, reflectance, or fluorescence modes, but they cannot perform spectral analysis.



Applications and Practical Aspects of Densitometry

Densitometric quantification has been applied to virtually every type of analyte and sample. For example, the greatest number of applications is for the analysis of drug and pharmaceutical compounds, most of which have structures including chromophores that cause strong UV absorption. These compounds are readily quantified in the fluorescence quenching mode on F-layers or in the direct UV absorption mode on unimpregnated layers. Lipids are compounds that are not easily analyzed by gas chromatography (GC) or high-performance liquid chromatography (HPLC) because they lack volatility and the presence of a chromophore leading to UV absorption. The most successful way to quantify lipids is by densitometry after separation and detection on the layer with a chromogenic reagent, most notably phosphomolybdic acid. The quantification of amino acids after detection with ninhydrin is another example of densitometry in the visible absorption mode. Fluorescence densitometry has been applied to the determination of naturally fluorescent compounds (e.g., quinine in tonic water) or compounds derivatized with a fluorogenic reagent pre-TLC or post-TLC (e.g., amino acids reacted with fluorescamine, or carbamate pesticides with dansyl chloride after hydrolysis).

The steps in a typical densitometric quantitative analysis, regardless of analyte type, are the following:

1. Prepare a standard reference solution.
2. Prepare a sample solution in which the analyte is completely dissolved and impurities have been reduced to a level at which they do not interfere with scanning of the analyte.
3. Choose a layer and mobile-phase combination that will separate the analyte as a compact zone with an R_f value in the range 0.2–0.8.
4. Apply the standard and sample aliquots to the layer using an instrument (Fig. 1) or manually with a micropipette, onto preadsorbent, laned plates. Generally, three or four standard zones are applied in constant volumes from a series of standard solutions with increasing concentrations, or in a series of increasing volumes from a single standard solution. The sample volume applied must provide an amount of analyte zone with a weight or concentration that is bracketed by the standard amounts.
5. Develop the plate in an appropriate chamber and dry the mobile phase under in a fume hood or oven.

Optical Quantification (Densitometry) in TLC

6. Apply a detection reagent, if necessary, by spraying or dipping. The reagent should produce a stable colored, UV-absorbing, or fluorescent zone having high contrast with the layer background.
7. Scan the natural or induced absorption or fluorescence of the standard and sample zones on the plate using a densitometer with optimized parameters.
8. Generate a calibration curve by linear or polynomial regression of the scan areas and weights of the standards and interpolate the weights in the sample zones from the curve.
9. Calculate the concentration of analyte in the sample from the original weight of the sample, the original total volume of the sample test solution, the aliquot volume of the test solution that is spotted, the interpolated analyte weight in that spotted volume from the calibration curve, and any numerical factor required because of dilution or concentration steps needed for the test solution to produce a bracketed scan area for the analyte zone in the sample chromatogram.
10. Validate the precision of the TLC analysis by replicated determination of the sample and accuracy by comparison of the results to those obtained from analysis of the same sample by an established independent method or calculation of recovery from analysis of a spiked pre-analyzed sample or spiked blank sample.

The following are some advantages of TLC densitometry compared to HPLC:

1. The simultaneous analysis of multiple samples on a single plate leads to higher sample throughput (lower analysis time) and less cost per sample. Up to 36 tracks are available for samples and standards on a 10-cm × 20-cm high-performance TLC plate.
2. The ability to generate a unique calibration curve using standards developed under the same conditions as samples on each plate (in-system calibration) leads to statistical improvement in data handling and better analytical precision and accuracy and eliminates the need for an internal standard for most analyses.
3. Detection is versatile and flexible because the mobile phase is removed prior to detection. Because the detection process is static (the zones are stored on the layer), multiple, complementary detection methods can be used.



4. Storage of the chromatogram also allows scanning to be repeated with various parameters without time constraints and assures that the entire sample is available for detection and scanning.
5. Less sample cleanup is often required because plates are not reused. Every sample is analyzed on a fresh layer without sample carryover or cross-contamination.
6. Solvent use is very low for TLC, both on an absolute and per-sample basis, leading to reduced purchase and disposal costs and safety concerns.

Suggested Further Reading

- Fried, B. and J. Sherma, *Thin Layer Chromatography — Techniques and Applications*, 4th ed., Marcel Dekker, Inc., New York, 1999, pp. 197–222.
- Jaenchen, D. E., Instrumental thin layer chromatography, in *Handbook of Thin Layer Chromatography*, 2nd ed. (J. Sherma and B. Fried, eds.), Marcel Dekker, Inc., New York, 1996, pp. 129–148.
- Petrovic, M., M. Kastelan-Macan, K. Lazaric, and S. Babic, Validation of thin layer chromatography quantitation with CCD camera and slit-scanning densitometer, *J. AOAC Int.* 82: 25–39 (1999).
- Pollak, V. A., Theoretical foundations of optical quantitation, in *Handbook of Thin Layer Chromatography* (J. Sherma and B. Fried, eds.), Marcel Dekker, Inc., New York, 1991, pp. 249–281.
- Poole, C. F. and S. K. Poole, *Chromatography Today*, Elsevier, New York, 1991, pp. 649–734.
- Prosek, M. and M. Pukl, Basic principles of optical quantitation in TLC, in *Handbook of Thin Layer Chromatography*, 2nd ed. (J. Sherma and B. Fried, eds.), Marcel Dekker, Inc., New York, 1996, pp. 273–306.
- Robards, K., P. R. Haddad, and P. E. Jackson, *Principles and Practice of Modern Chromatographic Methods*, Academic Press, San Diego, CA, 1994, pp. 180–226.



Optimization of Thin-Layer Chromatography

Wojciech Prus

Technical University of Łódź, Bielsko-Biała, Poland

Teresa Kowalska

Institute of Chemistry, Silesian University, Katowice, Poland

Introduction

The principal task of chromatography is the separation of mixtures of substances. By “optimization” of the chromatographic process, we mean enhancement of the quality of the separation by changing one or more parameters of the chromatographic system. An ability to foresee, correctly, the direction and scope of these changes is the most important goal of each optimization procedure.

Use of chemometrics to devise procedures suitable for the most crucial stage of optimization, optimization of selectivity, is generally performed in three steps:

1. Selection of the experimental method which best suits the analytical problem considered. At this stage, a chromatographic technique is chosen that ensures that the best possible range of retention parameters is obtained for each individual component of the separated mixture.
2. Establishing the experimental conditions that enable quantification of the influence of the optimized parameters of a chromatographic system on solute retention.
3. Fixing the experimental conditions at values that provide the optimum separation selectivity.

Chemometric optimization of the chromatographic system consists, in fact, in predicting local maxima in multiparametric space and, then, in further deciding which of these parameters is global with regard to the overall efficiency of a given chromatographic system.

Quality of Chromatographic Separations

Elementary Criteria

The simplest way of quantifying the separation of two chromatographic bands, 1 and 2, is to calculate the dif-

ference between their respective retention parameters; that is, the difference between their R_F values,

$$\Delta R_F = R_{F_2} - R_{F_1} \quad (1)$$

or between their R_M values,

$$\Delta R_M = R_{M_1} - R_{M_2} = \log \frac{k_1}{k_2} = \log \alpha \quad (2)$$

where k_1 and k_2 are the capacity (retention) factors of the chromatographic bands and α is the separation factor.

The terms most frequently used to characterize the separation of two chromatographic bands are the separation factor, α ,

$$\alpha = \frac{k_1}{k_2} \quad (3)$$

where $k_1 > k_2$, and the resolution, R_S [1],

$$R_S = \frac{2(z_2 - z_1)}{w_1 + w_2} = \frac{2l\Delta R_F}{w_1 + w_2} \quad (4)$$

where z_1 and z_2 are the distances of the geometric centers of two chromatographic bands, 1 and 2, from the origin, l is the distance from the origin to the mobile phase front, and w_1 and w_2 are the diameters of the two chromatographic bands, measured in the direction of eluent flow.

Other elementary criteria include the separation factor, S [2],

$$S = \frac{k_2 - k_1}{k_1 + k_2 + 2} \quad (5)$$

the peak-to-valley ratio of the bands, P [3],

$$P = \frac{f}{g} \quad (6)$$

(where f and g are, respectively, the average peak height and valley depth, characteristic of a given pair of neighboring solutes on a chromatogram), the fractional peak overlap, FO [4],

$$\text{FO} = \frac{A_n - A_{n,n-1} - A_{n,n+1}}{A_n} \quad (7)$$



(where A_n is the surface area of the part of the band originating from the pure single compound, $A_{n,n-1}$ is the surface area of the fractional overlap of the n th and $(n-1)$ th bands, and $A_{n,n+1}$ is the surface area of the fractional overlap of the n th and $(n+1)$ th bands), and the selectivity parameter, R_R [5],

$$R_R = \frac{R_{F_1}}{R_{F_2}} \quad (8)$$

where $R_{F_1} > R_{F_2}$.

Criteria for the Quality of Chromatograms

One method which can be used to establish the optimum conditions for the separation of a complex mixture (i.e., not only a pair) of compounds consists in searching for the maximum of a function denoted the chromatogram quality criterion. The evaluation of separation selectivity can be conducted with the aid of different criteria of chromatogram quality such as the sum of resolution, ΣR_S [6], the sum of separation factors, ΣS [2], and other sums and products of elementary criteria, selected examples of which are the resolution product, ΠR_S [7],

$$\Pi R_S = \exp\left(\sum \ln R_S\right), \quad (9)$$

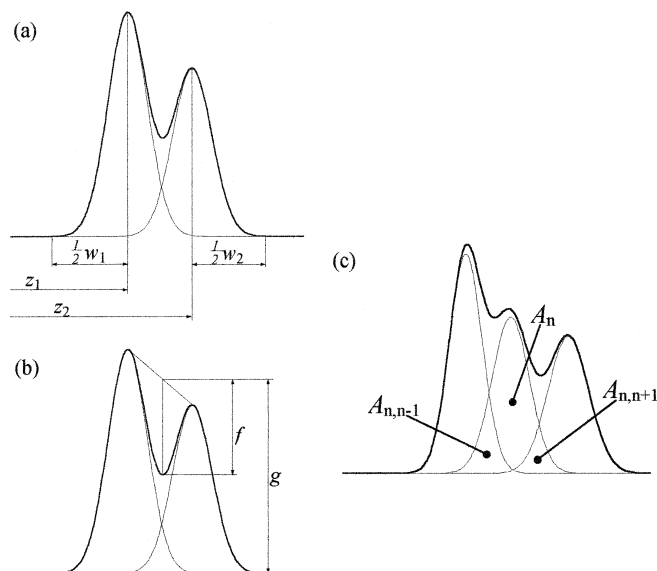


Fig. 1 Graphical interpretation of the selected elementary criteria: (a) resolution, R_S ; (b) the peak-to-valley ratio, P ; (c) the fractional peak overlap, FO.

the product of the separation factors, ΠS [8], the product of the fractional peak overlap, ΠFO [9], and the product of the peak-to-valley ratio of the bands, ΠP [10].

There are also other, more complex criteria, including the normalized resolution product, r [11],

$$r = \prod_{i=1}^{n-1} \frac{R_{S_{i,i+1}}}{R_S} = \prod_{i=1}^{n-1} \frac{S_{i,i+1}}{S} \quad (10)$$

where n is the number of the chromatographic bands,

$$\bar{R}_S = \frac{1}{n-1} \sum_{i=1}^{n-1} R_{S_{i,i+1}}$$

and

$$\bar{S} = \frac{1}{n-1} \sum_{i=1}^{n-1} S_{i,i+1}$$

and the minimum R_S [8],

$$R_{S,\min} \geq x \quad \text{or} \quad \max R_{S,\min} \quad (11)$$

The minimum of α is used as a criterion of the quality of chromatograms in liquid chromatography [12].

Other criteria are the total peak overlap, φ [13],

$$\varphi = \sum \exp(-2R_S), \quad (12)$$

the informing power, P_{inf} [14],

$$P_{\text{inf}} = \sum_{i=1}^n \log_2 S_i \quad (13)$$

and the chromatographic response function, CRF [10],

$$\text{CRF} = \sum_{i=1}^n \ln P_i \quad (14)$$

(where P_i is the peak-to-valley ratio for the i th pair of chromatographic bands).

Performance of the Chromatographic System

One measure of the performance of a given chromatographic system is the number of the theoretical plates per chromatographic band (N). In its simplest form, this can be defined as

$$N = \frac{l}{H} \quad (15)$$

where l is the distance from the origin to the eluent front and H is the height equivalent to one theoretical plate (H is sometimes also denoted HETP).

The average height equivalent to one theoretical plate (\bar{H}) can be calculated from the relationship [15]

$$\bar{H} = \frac{(\sigma_i)^2}{(z_r - z_0)R_F} = \frac{(w_i)^2}{16z_x} \quad (16)$$

where σ_i is the standard deviation, which characterizes the width of the chromatographic spot, or the band width on the densitogram, w_i is the spot width (or the width of the peak base on the densitogram), $z_r - z_0$ is the distance from the origin to the eluent front, and z_x is the distance from the origin to the geometric center of the chromatographic spot.

The relationship between the height equivalent to one theoretical plate (H) and the velocity of the mobile-phase flow is given by the simplified van Deemter equation [16]

$$H = A + \frac{B}{u} + Cu \quad (17)$$

where u is the linear velocity of the mobile phase, A is a constant characterizing eddy diffusion, B is a constant characterizing molecular diffusion, and C is a constant characterizing resistance to interphase mass transfer. This particular issue is of considerable significance in planar chromatographic separations, during the course of which the velocity of the mobile phase changes.

The concept of separation number (SN) in planar chromatography is a practical approach to the task of quantification of chromatographic system performance. According to this concept, such performance can simply be evaluated by calculating how many components of the separated mixture can be comfortably accommodated (i.e., without any overlap of adjacent components) along the direction of migration of the eluent. A convenient relationship proposed in Ref. 17 enables easy calculation of the numerical value of SN:

$$SN = \left(\log \frac{b_0}{b_1} \right) \left(\log \frac{1 - b_1 + b_0}{1 + b_1 - b_0} \right)^{-1},$$

or, simplified,

$$SN \approx \frac{1}{b_0 + b_1} \quad (18)$$

where b_0 is the width at half-height of a spot at the origin and b_1 is the width at half-height of a spot at $R_F = 1$ (extrapolated) (b_0 and b_1 are in R_F units).

Semiempirical Optimization Strategies

Strategies used for optimization of selectivity can basically be divided into three separate groups: (a) the simultaneous strategy, (b) the sequential strategy, and (c) the interpretative strategy.

Simultaneous Strategy

In this strategy, one must accomplish all the experiments according to a plan devised earlier. All the results obtained must then be carefully evaluated, the optimum experimental conditions being chosen on this basis.

Sequential Strategy

In this strategy, the optimum experimental conditions are approached in a series of consecutive steps. The choice of any step results strictly from the outcome of all those accomplished previously. One example of a relevant algorithm is the simplex method [18]; the PRISMA [19] geometrical method is a suitable example of the overall optimization approach.

Interpretative Strategy

This method enables prediction of the quality of a separation on the basis of a relatively limited number of the experimental data, collected in previous experiments. According to this approach, the chromatographic results are interpreted in terms of the retention functions, valid for each individual solute separately. Some good examples of the interpretative strategy are the so-called "window diagrams" approach [20] and the search for the extremum of the multiparameter response function with the aid of the genetical algorithm [21].

References

1. T. Kowalska, Theory and mechanism of thin-layer chromatography, in *Handbook of Thin-Layer Chromatography* (J. Sherma and B. Fried, eds.), Chromatographic Science Series. Vol. 55, Marcel Dekker, Inc., New York, 1991, p. 50.
2. P. Jones and C. A. Wellington, *J. Chromatogr.* 213: 357–361 (1981).
3. R. Kaiser, *Gas-Chromatographie*, Geest und Portig, Leipzig, 1960.
4. P. J. Schoenmakers, *Optimization of Chromatographic Selectivity. A Guide to Method Development*, Journal of Chromatography Library, Vol. 35, Elsevier, Amsterdam, 1986, pp. 123–125.
5. W. Prus and T. Kowalska, *J. Planar Chromatogr.* 8: 205–215 (1995).
6. J. C. Berridge, *J. Chromatogr.* 244: 1–14 (1982).
7. J. L. Glajch, J. J. Kirkland, K. M. Squire, and J. M. Minor, *J. Chromatogr.* 199: 57–79 (1980).
8. P. J. Schoenmakers, A. C. J. H. Drouen, H. A. H. Billiet, and L. de Galan, *Chromatographia* 15: 688–696 (1982).



9. R. Smits, C. Vanroelen, and D. L. Massart, *Fresenius Zeitschr. Anal. Chem.* 273: 1–5 (1975).
10. S. L. Morgan and S. N. Deming, *J. Chromatogr.* 112: 267–285 (1975).
11. A. C. J. H. Drouen, P. J. Schoenmakers, H. A. H. Billiet, and L. de Galan, *Chromatographia* 16: 48–52 (1982).
12. S. N. Deming and M. L. H. Turoff, *Anal. Chem.* 50: 546–548 (1978).
13. J. C. Giddings, *Anal. Chem.* 32: 1707–1711 (1960).
14. D. L. Massart and R. Smits, *Anal. Chem.* 46: 283–286 (1974).
15. G. Guiochon and A. M. Siouffi, *J. Chromatogr.* 245: 1–20 (1982).
16. J. J. Van Deemter, F. J. Zuiderweg, and A. Klinkenberg, *Chem. Eng. Sci.* 5: 271 (1965).
17. F. Geiss, *Fundamentals of TLC (Planar Chromatography)*, Hüthig, Heidelberg, 1987.
18. W. Spendley, G. R. Hext, and F. R. Hinsworth, *Technometrics* 4: 441 (1962).
19. Sz. Nyiredy, B. Meier, C. A. J. Erdelmeier, and O. Stichler, *J. High Resolut. Chromatogr. Chromatogr. Commun.* 8: 186–188 (1985).
20. R. J. Laub and J. H. Purnell, *J. Chromatogr.* 112: 71–79 (1975).
21. J. H. Holland, *Adaptation in Natural and Artificial Systems*, University of Michigan Press, Ann Arbor, 1975.



Organic Acids, Analysis by Thin Layer Chromatography

Nataša Brajenović

Ruđer Bošković Institute, Zagreb, Croatia

INTRODUCTION

A very large number of papers report new research works on analyses of organic acids by thin layer chromatography, paper chromatography, high-performance liquid chromatography, and other analytical techniques. One of the most popular and widely used separation techniques for qualitative and quantitative analyses in the laboratory is thin layer chromatography.

The reason for using thin layer chromatography is its wide applicability to a great number of different types of samples, high sensitivity, and speed of separation with relatively low cost. This technique is very fast, and many separations can be accomplished in less than an hour.

The development of different methods of analysis in thin layer chromatography is a very important area of organic chemistry and biochemistry. Analysis of organic acids by thin layer chromatography is widely applied in different fields of environmental, pharmaceutical, industry, industrial foods, organic chemistry, cosmetics, clinical, and biochemical assays.

OVERVIEW

Here, we present scientific activity in the analysis of organic acids by thin layer chromatography in a period from 1993 to 2004. The review is based on a search of *Current Contents and Science Citation Index*, using different combinations of key words relevant for thin layer chromatography, organic acids, and different kinds of organic acids, such as amino acids, carboxylic acids, humic acids, aromatic carboxylic acids, and fatty acids. In addition, the journals publishing papers covering specific topics related to the analysis of organic acids by thin layer chromatography were searched directly: *Analytica Chimica Acta*, *Analytical Chemistry*, *Journal of Microbiological Methods*, *Journal of Liquid Chromatography and Related Technologies*, *Journal of Chromatography (Parts A and B)*, *Chromatographia*, and *Journal of Pharmaceutical and Biochemical Analysis*.

GENERAL CONSIDERATIONS

Stationary Phase

Typical thin layer separations are performed on flat glass or plastic plates that are coated with a thin and adherent layer of particles, which constitute the stationary phase.^[1] Commercial plates come in two categories: conventional [thick layers (200–250 μm) of particles having sizes of 20 μm or greater] and high-performance plates (film thickness of 100 μm and particles whose diameters are 5 μm or less).

Silica gel is the most extensively used adsorbent in thin layer chromatography because it leads to excellent, uncomplicated separations. It can be successfully employed for both qualitative and quantitative thin layer chromatographic analyses. It is usually used as a stationary phase in separations and analysis of alkaloids, various organic acids (especially amino acids and their derivatives), steroids, lipids, vitamins, plant pigments, pesticides, drugs, carbohydrates, phenolic substances, etc.

Besides silica gel, cellulose, and aluminum oxide, various other impregnated plates are also frequently used as stationary phases.^[1]

Mobile Phase

Many different solvents and mixtures of solvents are used as mobile phases for the analysis of organic acids by thin layer chromatography, such as chloroform, ethyl acetate, methanol, benzene, etc.

Identification

For identification in qualitative thin layer chromatography, a great number of visualization reagents are used.^[1] If compounds are not colored, a UV lamp may be used to visualize the plates. The quantitative determination of sample components is performed according to the following:

1. Extracting the stained spot with solvent and analyzing it spectrophotometrically; or
2. Scanning the plate densitometrically.^[1]

APPLICATIONS

Pharmaceutical Industry, Medicine, Biochemistry, and Biology

Thin layer chromatography is used for the analysis of free amino acids from sanguine plasma in different progression states in maladies: diabetes, renal syndrome, and hepatic cirrhosis.^[2] Elution was performed on cellulose plates and the densitometry was achieved with a photo-densitometer (Shimadzu CS-9000) at 575 nm. In the case of hepatic cirrhosis, a better resolution was obtained. A mixture of *n*-butanol–acetone–acetic acid–water (35:35:7:23 vol/vol/vol/vol) was used as the mobile phase.

A simple and fast method for identification of bifidobacteria using thin layer chromatographic analysis of short chain fatty acids in a culture broth is proposed (Table 1).^[3] This approach has many advantages: the total time required to analyze organic acids is approximately 50 min; and the identification protocol is simpler, quicker, and more economical than conventional identification methods.

Mycolic acids analysis by thin layer chromatography has been employed by several laboratories worldwide as a method for fast identification of *Mycobacterium*.^[4] *Mycobacterium tuberculosis* strains identified by classical methods were confirmed by their mycolic acid content.

Using aminopropyl-modified silica gel plates in a normal phase system, the retention behavior of 12 acidic drugs and biologically active aromatic acids was investigated by high-performance thin layer chromatography.^[5]

The metabolism of aromatic amino acids (phenylalanine and tyrosine) can be studied following the excretion of their characteristic phenolic acid metabolites in urine using chromatographic methods. These apply acids to the investigations of amino acids themselves in diagnostics.

Table 1 Retention time (R_f) and detection color of standard organic acids

Organic acids	R_f value	Methyl red + bromophenol blue
Lactic acid	0.53 (Upper spot)	Red
	0.37 (Lower spot)	Red
Acetic acid	0.44	Blue
Propionic acid	0.54	Blue
Butyric acid	0.61	Blue
Succinic acid	0.12	Yellow
Citric acid	0.03	Dark yellow
	0.52	Red

Source: Ref. [3].

Table 2 R_f values ($\times 100$) of urinary phenolic acids

Compound	BzAc ^a		IprBuAm ^b		BuE ^c
	Cel ^d	SG ^e	Cel ^d	SG ^e	SG ^e
Phenyllactic acid	88	68	65	62	—
Phenylpyruvic acid	86	68	80	80	87
<i>p</i> -OH cinnamic acid	83	60	36	52	88
Hippuric acid	74	30	59	57	35
<i>p</i> -OH mandelic acid	11	6	28	40	34
<i>p</i> -OH phenylacetic acid	63	61	39	43	81
Vanillic acid	96	77	19	36	84

^aBzAc = benzene–acetic acid (glacial)–water (70:29:1).

^bIprBuAm = isopropanol–*n*-butanol–*t*-butanol–ammonia–water (40:20:20:10:20).

^cBuE = *n*-butanol–ethanol–water (100:5:10).

^dCellulose.

^eSilica gel.

Source: Ref. [6].

Thin layers of cellulose or silica gel on aluminum foil were used as stationary phases.^[6] The retention factor (R_f) of clinically important compounds in the three solvent systems is presented in Table 2.

Thin layer chromatography is also used for direct enantiomeric resolution of D,L-arginine, D,L-histidine, D,L-lysine, D,L-valine, and D,L-leucine on silica gel plates impregnated with optically pure (1*R*, 3*R*, 5*R*)-2-azabicyclo[3,3,0]octan-3-carboxylic acid, which serves as a chiral selector in the pharmaceutical industry.^[7] To successfully resolve D,L-amino acids, various combinations of acetonitrile–methanol–water were proposed. The spot was detected by ninhydrin (0.2% in acetone).

Thin layer chromatography is often applied as an industrial control procedure in the synthesis of 2-hydroxy-3-naphthalenecarboxylic acids, on silica gel plates with chloroform–methanol–acetic acid (50:20:1) as developer.^[8] 2-Hydroxy-3-naphthalenecarboxylic acid is an important intermediate in the synthesis of dyestuffs and drugs.

Separation of amino acids and their identification in different mixtures are frequent tasks encountered in biochemistry. Thin layer chromatography is a fast, simple, and inexpensive approach to attain this goal. Because some of the components are UV-inactive, other methods, such as vibrational spectroscopy, should be applied for detection and identification. Comparative study based on Raman spectroscopy of thin layer chromatography spots of some weak Raman scatterers (essential amino acids) was carried out using four different visible and near-infrared laser radiation wavelengths: 532, 633, 785, and 1064 nm.^[9] The best results were obtained with simple silica gel plates.



Table 3 Thin layer chromatographic procedures for separation of organic acids

Standards/simple	Stationary phase	Mobile phase
Mixture, organic acids	Merck silica gel	<i>n</i> -Butylformate/90% formic acids/H ₂ O (7:2:1, vol/vol)
	Cellulose powder or silica gel	1-Propanol concentrated in ammonium hydroxide (7:3 or 3:2)
2-Hydroxybenzoic acid (salicylic acid)	Silica gel or Fe(III)-impregnated silica gel or aluminum oxide	Tap water
4-Hydroxybenzoic acid	Silica gel or Fe(III)-impregnated silica gel or aluminum oxide	Tap water
3,4,5-Trimethoxybenzoic acid	Silica gel or Fe(III)-impregnated silica gel or aluminum oxide	Tap water
3,4,5-Trihydroxybenzoic acid (gallic acid)	Silica gel or Fe(III)-impregnated silica gel or aluminum oxide	Tap water
4-Hydroxy-3,5-dimethoxybenzoic acid	Silica gel or Fe(III)-impregnated silica gel or aluminum oxide	Tap water
1,2-Benzenedicarboxylic acid	Silica gel or Fe(III)-impregnated silica gel or aluminum oxide	Tap water

Source: Refs. [11], [14], and [15].

Environmental, Water, Plant, and Soil Applications

The occurrence of chlorinated organic compounds in fish from polluted waters is rather frequent.^[10] Chlorinated carboxylic acids of fatty acid character have also been shown to account for up to 90% of the extractable organically bound chloride (EOCl) in fish. Purification by thin layer chromatography of methyl esters of dichlorotetradecanoic, dichlorohexadecanoic, and dichlorooctadecanoic acids was used. They were detected at 1200 ppm of EOCl in fish.

Organic acid complexes with metal ions significantly affect the mobility of metal ions in plants and soils. Toxic

metals also react with organic acids and have a harmful influence on the environment.

Many plants contain a variety of free acids such as acetic acid, citric acid, fumaric acid, malic acid, succinic acid, oxalic acid, glycolic acid, etc.^[11-13] They are components of citric cycle, whereas the others are intermediates in the pathway from carbohydrates to aromatic compounds.^[11] Following extraction, organic acids can be separated and detected with a variety of techniques. Thin layer chromatographic methods have been also employed to separate certain organic acids,^[11,14,15] as presented in Table 3.

Thin layer chromatography of some plant phenolics, which play an important role in plant metabolism, was

Table 4 Chromatographic behavior of some plant phenolic acids

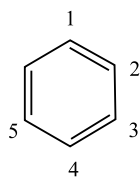
Compound	<i>R_f</i>				Detection		
	A	B	C	D	UV	DSA	DNA
<i>o</i> -Coumaric acid	0.34	0.39	0.29	0.51	F	Orange	Violet
<i>m</i> -Coumaric acid	0.43	0.26	0.33	0.52	F	Orange	Violet
<i>p</i> -Coumaric acid	0.34	0.33	0.28	0.47	Q	Red	Blue
<i>o</i> -Hydroxybenzoic acid (salicylic acid)	0.70	0.57	0.44	0.62	F	Yellow	Red
<i>m</i> -Hydroxybenzoic acid	0.37	0.63	0.58	0.70	F	Yellow	Rose
<i>p</i> -Hydroxybenzoic acid	0.27	0.59	0.52	0.70	Q	Yellow	Red
Gallic acid	0.09	0.33	0.31	0.46	F	Green-brown	Tan

F=fluorescence; Q=quenching; DSA=diazotized sulfanilic acid; DNA=diazotized *p*-nitroaniline.

Developers: A=2% formic acid; B=20% potassium chloride; C=isopropyl alcohol-ammonium hydroxide-water (8:1:1); D=10% acetic acid.

Source: Ref. [12].





	1	2	3	4	5
Benzoic acid	-COOH	-H	-H	-H	-H
Salicylic acid	-COOH	-OH	-H	-H	-H
Gallic acid	-COOH	-H	-OH	-OH	-OH
Pyrogallol	-H	-H	-OH	-OH	-OH
Hydroquinone	-OH	-H	-H	-OH	-H
Resorcinol	-H	-H	-OH	-H	-OH
Cinnamic acid	-CH=CH-COOH	-H	-H	-H	-H
Ferulic acid	-CH=CH-COOH	-H	-O-CH ₃	-OH	-H
p-Coumaric acid	-CH=CH-COOH	-H	-H	-OH	-H

Fig. 1 Chemical structure of simple phenolics and some components of lignin. (From Refs. [13] and [14].)

carried out on cellulose.^[12] The solvents were: 2% formic acid, 20% potassium chloride, isopropyl alcohol–ammonium hydroxide–water (8:1:1), and 10% acetic acid. The plates were examined under UV light after development. The results of the chromatographic analysis of some phenolic acids are shown in Table 4.

The composition of lignin (an important component of plant cell walls) is very complex.^[13] *p*-Coumaric acid, cinnamic acid, ferulic acid, and others are among the products of lignin biodegradation (Fig. 1). Thin layer chromatography is a very rapid method for their separation and is usually completed in a very short time. Six different solvents were used as developer (Table 5), with silica gel being used as a stationary phase.

Humic acids are also products of lignin biodegradation. The characterization of humic acids by thin layer chromatography on Fe(III)-impregnated silica gel with tap water as developer has been presented.^[14] During the chromatographic process, complexes between Fe(III) from the support group and the active functional group from humic acid are formed, causing successive attaching and detaching of Fe(III) from the support of Fe(III) hydroxy/oxide. These results could partially answer how the process of metal migration in soils and sediments progresses.

Some carboxy and benzene derivatives related to humic materials were also examined by thin layer

chromatography.^[15] Aluminum oxide, silica gel, and Fe(III)-impregnated silica gel plates were used as supports, whereas the mobile phase was water. The results are presented in Table 3. It was concluded that the hydroxy/oxide layer of iron and aluminum can affect the mobility of simple organic molecules in soil. On the other side, organic molecules having carboxy and hydroxy groups can improve the dissolution of hydroxy/oxides of iron or aluminum in soils and sediments.

Table 5 Different solvent systems were used as developers for thin layer chromatographic separation for simple phenolic and related compounds as cinnamic acid, *p*-coumaric acid, ferulic acid, and tannic acid

Solvent systems were used as developers for simple phenolic compounds and some acids, which are products of lignin biodegradation

- 1) Chloroform–methanol–acetic acid (90:10:1)
- 2) Petroleum ether (60–80°C)–ethyl acetate–formic acid (40:60:1)
- 3) Benzene–dioxane–acetic acid (85:15:1)
- 4) Chloroform–ethyl acetate–acetic acid (50:50:1)
- 5) Toluene–acetonitrile–formic acid (70:30:1)
- 6) Petroleum ether (60–80°C)–methanol–acetic acid (90:10:1)

Source: Ref. [13].



Food Analysis, Agriculture, and Industry

There are several acids that are widely used in industries. For example, synthetic carboxylic acid esters are used in the perfume industry. Benzoic acids are used as sodium salts in the food industry as inhibitors of microorganism growth.^[16]

Benzoic acid derivatives often contain amino, hydroxy, carboxy, and nitro groups. Analysis of substituted benzoic acids by thin layer chromatography was performed on silica gel, polyamide, and cellulose containing UF₂₅₄ fluorescent indicator.^[17] For the mobile phase, different mixtures were used: hexane–acetic acid; hexane–ethyl acetate–formic acid; chloroform–methanol–phosphoric acid; cyclohexane–acetic acid; benzene–ethanol; etc. Because benzoic acid derivatives have similar retention parameters, their separation requires a thorough optimization of conditions (the nature of the stationary phase, the composition of the mobile phase, and the pH of the solutions).

For the separation of benzoic acids, planar electrochromatography was used.^[18] In this approach, an electroosmotic flow is used to drive the mobile phase in thin layer chromatography. Planar electrochromatography has several advantages over classical thin layer chromatography, especially substantially faster separation. For example, separation by planar electrochromatography can be 10 times faster than that using ordinary thin layer chromatography.

Thin layer chromatographic analysis of agricultural products, foods, beverages, and plant constituents is described by Sherma^[19] in a review paper. In laboratories throughout the world, thin layer chromatography is widely used for food analysis and qualitative control. Numerous applications of thin layer chromatography have been reported in the area of food composition, involving determinations of compounds such as lipids, sugars, amines, vitamins, and organic acids such as amino acids and fatty acids.

VARIOUS ORGANIC COMPOUNDS

Thin layer chromatographic analysis is also highly applicable to the determination of aromatic organic acids.^[20] In human organisms, aromatic acids are synthesized as metabolites in intoxication by toluene, xylene, and ethyl benzene.^[16] These compounds are easily absorbed through the skin or respiratory system, and are oxidized to aromatic acids. The separation, identification, and quantitative analyses of aromatic acids are also necessary because they appear as semiproducts of the biosynthesis of aromatic amino acids in plants (phenolic acids), and metabolites of numerous toxic substances, drugs, and catecholamines. Polar adsorbents and polar-

bonded stationary phases are also widely used in carboxylic separation by thin layer chromatography, often coupled with densitometry.

Dansyl chloride (DNS-Cl; 5-dimethylaminonaphthalene-1-sulfonyl chloride) is used in analytical chemistry to fluorescently label substances. This process of dansylation creates fluorescent derivatives, which can be detected with great sensitivity. The method for the dansylation of hydroxyl (–OH) and carboxylic acid (–COOH) functional groups has been described.^[21] Fluorescent labeling by dansyl chloride has applications in liquid chromatography, high-performance liquid chromatography, thin layer chromatography, and mass spectrometry. Fast thin layer chromatography was accomplished using acetone as the resolving solvent, and resulted in good differentiation of analytes.

Many thin layer chromatography systems for the separation of amino acids have been described.^[22–24]

Copper sulphate and polyamide were tried as impregnants for improving the separation of 20 amino acids on silica gel layers. MeOH–BuOAc–AcOH–pyridine (20:20:10:5) was used as the solvent system.^[22]

D-enantiomers of amino acids have been frequently reported in various tissues of diverse organisms. A simple and rapid method of separating optical isomers of amino acids on a reverse-phase thin layer chromatography plate is described.^[23] Amino acids, derivatized with 1-fluoro-2,4-dinitrophenyl-5-L-alanine amide, were spotted onto a reverse-phase thin layer chromatography plate. Acetonitrile in triethylamine–phosphate buffer was used as the developer.

For the evaluation of protein structure, identification of amino acids is extremely important. Thin layer chromatography is an appropriate method in this field. A variety of spray reagents are used, among which ninhydrin is the most popular one due to its high sensitivity.^[24] Ninhydrin produces a purple/violet color with most amino acids. A typical experimental setup includes chromatographic plates prepared from silica gel; *n*-propanol–water (70:30) mixture was used as a mobile phase. For complex mixtures of substances, two-dimensional chromatography is preferred, using *n*-propanol–water (70:30) mixture and methanol–chloroform (3:1) mixture as the two developers.

CONCLUSION

Thin layer chromatography is a very widely used chromatographic technique in research activities of analytical chemists in many laboratories in the world. Many articles dealing with the development of new analytical methods for the analysis and separation of different organic acids in



various fields have been published. There is a constant need for qualitative and quantitative analyses of organic acids in the pharmaceutical, cosmetic, and food industries; in medicine, biology, organic chemistry, and biochemical analysis; and in environmental studies. The important reasons for frequent applications of thin layer chromatography in qualitative and quantitative analyses of organic acids are its high sensitivity, fast separation of components, and relatively low cost.

REFERENCES

1. Skoog, D.A.; Holler, J.F.; Nieman, T.A. High-Performance Liquid Chromatography. In *Principles of Instrumental Analysis*, 5th Ed.; Vondeling, J., Sherman, M., Bortel, J., Messina, F., Peculis, V., Eds.; M. Brooks/Cole, Thomson Learning, Inc.: London, 1998; 725–766.
2. Gocan, S.; Ghizdavu, L.; Ghizdavu, L. TLC of some free amino acids from sanguine plasma. *J. Pharm. Biomed. Anal.* **2001**, *26*, 681–685.
3. Ki-Yong, L.; Jae-Seong, S.; Tae-Ryeon, H. Thin layer chromatographic determination of organic acids for rapid identification of bifidobacteria at genus level. *J. Microbiol. Methods* **2001**, *45*, 1–6.
4. Leite, C.Q.F.; Desouza, C.W.O.; Leite, S.R.D. Identification of mycobacteria by thin layer chromatographic analysis of mycolic acids and conventional biochemical method—Four years of experience. *Mem. Inst. Oswaldo Cruz* **1998**, *93* (6), 801–805.
5. Bieganovska, M.L. Retention behaviour of some acids drugs and biologically active compounds on silica and aminopropyl silica layers. *Chem. Anal.* **1995**, *40* (6), 859–867.
6. Ersser, R.S.; Oakley, S.E.; Seakins, J.W.T. Urinary phenolic acids by thin-layer chromatography. *Clin. Chim. Acta* **1970**, *30*, 243–249.
7. Bhushan, R.; Martens, J.; Thuku Thiongo, G. Direct thin layer chromatography enantioresolution of some basic DL-amino acids using a pharmaceutical industry waste as chiral impregnating reagent. *J. Pharm. Biomed. Anal.* **2000**, *21*, 1143–1147.
8. Revilla, A.L.; Havel, J.; Borovcová, J.; Vrchlabsky, M. Capillary zone electrophoresis of hydroxynaphthalenecarboxylic acids. Purity monitoring of β -hydroxynaphthoic acid in industry. *J. Chromatogr., A* **1997**, *772*, 397–402.
9. István, K.; Keresztury, G.; Szép, A. Normal Raman and surface enhanced Raman spectroscopic experiments with thin layer chromatography spots of essential amino acids using different laser excitation sources. *Spectrochim. Acta, Part A: Mol. Biomol. Spectrosc.* **2003**, *59*, 1709–1723.
10. Mu, H.; Wesén, C.; Novák, T.; Sundin, P.; Skramstad, J.; Odham, G. Enrichment of chlorinated fatty acids in fish lipids prior to analysis by capillary gas chromatography with electrolytic conductivity detection and mass spectrometry. *J. Chromatogr., A* **1996**, *731*, 225–236.
11. Dashek, W.V.; Micales, J.A. Isolation, Separation, and Characterization of Organic Acids. In *Methods in Plant Biochemistry and Molecular Biology*; Dashek, W.V., Ed.; CRC Press: Boca Raton, FL, 1997; 107–113.
12. Jangaard, N.O. Thin-layer chromatography of some plant phenolics. *J. Chromatogr.* **1970**, *50*, 146–148.
13. Sharma, O.P.; Bhat, T.K.; Singh, B. Thin-layer chromatography of gallic acid, methyl gallate, pyrogallol, phloroglucinol, catechol, resorcinol, hydroquinone, catechin, epicatechin, cinnamic acid, *p*-coumaric acid, ferulic acid and tannic acid. *J. Chromatogr., A* **1998**, *822*, 167–171.
14. Iskrčić, S.; Hadžija, O.; Kveder, S. Behaviour of humic acids on Fe(III)-impregnated silica gel compared with model substances. *J. Liq. Chromatogr.* **1994**, *17* (7), 1653–1657.
15. Kveder, S.; Iskrčić, S.; Zambeli, N.; Hadžija, O. The behaviour of some benzene derivatives on thin layers of aluminum oxide—Comparison with plain and Fe(III) impregnated silica gel. *J. Liq. Chromatogr.* **1991**, *14* (18), 3277–3282.
16. Waksmundzka-Hajnos, M. Chromatographic separation of aromatic carboxylic acids. *J. Chromatogr., B* **1998**, *717*, 93–118.
17. Sumina, E.G.; Shtykov, S.N.; Dorofeeva, S.V. Ion-pair reversed-phase thin-layer chromatography and high-performance liquid chromatography of benzoic acids. *J. Anal. Chem.* **2002**, *57* (3), 210–214.
18. Nurk, D.; Koers, J.M.; Carmichael, A. Role of buffer concentration and applied voltage in obtaining a good separation in planar electrochromatography. *J. Chromatogr., A* **2003**, *983*, 247–253.
19. Sherma, J. Thin-layer chromatography in food and agricultural analysis. *J. Chromatogr., A* **2000**, *880*, 129–147.
20. Sherma, J. Planar chromatography. *Anal. Chem.* **1992**, *64*, 134R–147R.
21. Bartzatt, R. Dansylation of hydroxyl and carboxylic acid functional groups. *J. Biochem. Biophys. Methods* **2001**, *47*, 189–195.
22. Srivastava, S.P.; Bhushan, R.; Chauhan, R.S. TLC separations of amino acids on silica gel impregnated layers. *J. Liq. Chromatogr.* **1984**, *7* (7), 1359–1365.
23. Nagata, Y.; Iida, T.; Sakai, M. Enantiomeric resolution of amino acids by thin-layer chromatography. *J. Mol. Catal., B Enzym.* **2001**, *12*, 105–108.
24. Laskar, S.; Sinhababu, A.; Hazra, K.M. A modified spray reagent for the detection of amino acids on thin layer chromatography plates. *Amino Acids* **2001**, *21*, 201–204.



Organic Extractables from Packaging Materials: Chromatographic Methods Used for Identification and Quantification

Dennis Jenke

Baxter Healthcare Corporation, Round Lake, Illinois, U.S.A.

INTRODUCTION

Plastic materials are widely used in medical items, such as solution containers, transfusion sets, transfer tubing, devices, and packaging systems. The physiochemical nature of these materials provides medical products with their necessary, desirable performance characteristics. While an important performance characteristic of plastics used in medical application is chemical inertness, interactions between a plastic material and a contacted pharmaceutical product are well documented. Such interactions may include sorption, the uptake of product components by the plastic material, or leaching, i.e., the release of plastic material components into the product. In the case of leaching, both the identities of the leached substances and their accumulation levels may impact the ultimate utility of the product.

A review, related to the chromatographic methods used to assess the accumulation of leachable substances from packaging materials used for pharmaceutical products, is provided. This considers methods used to identify and/or quantify such leachables in actual products or product-simulating solvent systems.

DISCUSSION

The assessment of the impact of the accumulation of leached substances in pharmaceutical products contacted by a plastic material during their manufacture, storage, and/or use is a multifaceted undertaking involving disciplines within the applied physical, chemical, and biological sciences. While numerous strategies can be envisioned, and have been utilized to perform such an assessment, considerations include the identification of the leached substances and the measurement of the actual or probable accumulation levels of the identified substances. The identification process is an extensive investigation that utilizes sensitive and information-rich scouting of analytical methods for the dual purposes of

first revealing the leachables and then providing relevant information (e.g., formula and structure) that leads to their identification. In the worst-case scenario, such an analytical investigation is conducted blind; that is, the analytical team is faced with the unenviable challenge of finding an unknown number of unknown compounds, many of which accumulate in the product at levels much lower than its other constituents. These constituents may include both additives and nonmaterial-related contaminants such as ingredient impurities and degradation products. This search for material-derived leachables in pharmaceutical products is greatly facilitated if it is conducted with information-rich analytical methodologies that exhibit a comprehensive ability to respond to a large population of analytes in both a universal, but very specific, manner. The dual performance requirements of universality and specificity are the primary reasons why chromatographic methods are almost exclusively used in investigations specifically associated with organic leachables.

Given the variety of packaging materials used in pharmaceutical applications, the population of potential primary and secondary organic leachables is large and compositionally diverse. While an analytical chemist has a multitude of chromatographic tools with which to perform a leachables assessment, some guidance in terms of successfully applied strategies and methods can greatly facilitate the assessment. Thus this article contains a general compilation of published chromatographic methods and strategies that have been successfully applied to the identification and quantification of packaging material leachables. Examples are provided for each major separation strategy [e.g., high-performance liquid chromatography (HPLC), gas chromatography (GC), thin-layer chromatography (TLC), and supercritical fluid chromatography (SFC)] and for most commonly employed detection methods [e.g., ultraviolet (UV), mass spectrometry (MS), and flame ionization detection (FID)]. While the compilation in Tables 1–4 is by no means exhaustive, it is sufficiently broad in scope to provide the investigator with a general overview of the ways in which chromato-



Table 1 Examples of HPLC methods used to identify and/or quantify packaging system extractables

Material	Sample matrix	Sample preparation	Column	Mobile phase	λ (nm)	Other	Extractables	Ref.
PVC	Saline extracts	Extraction into hexane	Shandon ODS C ₁₈ , 200 \times 4.6 mm, 200 \times 2.1 mm	ACN/MeOH (9:1)	270	20 μ L, 0.8 or 0.17 mL/min	Di-ethylhexyl-phthalate	1 ^a
PVC, PE, PS	Organic solvents	Direct injection	Spherisorb C ₁₈ ODS-2, 250 \times 4.6 mm, 5 μ m	MEOH/phosphate buffer, pH 5.5 (1:1)	225	20 μ L, 1 mL/min	Monomers, caprolactam, aminocaproic acid	2
PVC, PE, PS	Organic solvents	Direct injection	Spherisorb C ₁₈ ODS-2, 250 \times 4.6 mm, 5 μ m	ACN/tetrahydrofuran (THF) (95:5)	280	20 μ L, 1 mL/min	Antioxidants [Butylated hydroxy toluene (BHT), Irganox 1010, Irganox 1076]	2
PET	Oils	Solvent partitioning (ACN/hexane) with evaporative concentration	Microsorb C8, 250 \times 4.6 mm, 5 μ m	A = water/ACN (85:15), B = ACN/water (85:15) ^b	254	20 μ L, 1.5 mL/min	PET oligomers (trimer-octamer), plasticizers (diethylene glycol dibenzoate)	3
PET	Oils	Solvent partitioning (ACN/hexane) with evaporative concentration	Microsorb C8, 250 \times 4.6 mm, 5 μ m	A = water/MEOH/AA (85:15:0.25), B = ACN/water (85:15) ^c	254	20 μ L, 1.5 mL/min	PET oligomers, terephthalic acid, dimethylterephthalate, bis(2-hydroxyethyl) terephthalate	4 ^a
PP	Solvent extracts (hexane, ethyl acetate, diethyl ether)	Solvent evaporation, reconstituted in chloroform/MEOH	Spherisorb ODS-1, 50 \times 4.6 mm, 5 μ m	15–40% ethyl acetate gradient in 75:25 MEOH/water	271	35°C, 2 mL/min	Antioxidants (BHT, Irganox 1010, Irganox 1076, Irganox 168)	5 ^a
HDPE	Dissolution with mobile phase	Direct injection	Spherisorb C ₁₈ ODS-2, 150 \times 4.6 mm, 3 μ m	MEOH/water/AA (66.5:32.5:1)	280	20 μ L, 1 mL/min	Phenolic antioxidants ^d , propyl <i>p</i> -hydroxybenzoate	6 ^a
Laminated polyolefin	Drug product	SPE concentration, residue reconstituted in ethanol	LiChrosorb C18 ODS-2, 250 \times 4.6 mm, 5 μ m	MEOH/water (70:30)	280	20 μ L	Caprolactam, butylhydroxytoluene, phthalic acid derivative	7

Filter cartridges	Water or ethanol extracts	Direct injection or after evaporative concentration	Nucleosil 100-5, RP18, 250 cm	MEOH/water (90:10), ACN/water (60:40)	220	20 μ L, 1 mL/min	Phthalates, fatty acids, phenols, siloxanes, acrylates, aliphatics, amides ^e	8 ^f
PC	Methylene chloride extract	Direct injection after polymer ppt with methanol	Shandon Hypercarb S, 150 \times 4.6 mm, 7 μ m ^g	MEOH/water/ACN (25.0:26.2:48.8)	^h	20 μ L, 0.5 mL/min	Bisphenol A	9
PET, PVC	Solvent extraction	Solvent evaporation reconstituted in IPA	Spherisorb ODS-2 ^g	Various binary mixtures	254	Various flow rates	Erucamide, PET oligomers	10
Polyolefin	Pharmaceutical products	Extract with chloroform, reconstituted in 2-propanol	Spherisorb LC-SI, 250 \times 4.6 mm, 5 μ m	<i>n</i> -hexane/2-propanol (9:1)	210	25 μ L, 1.5 mL/min	Caprolactam	11
PVC	Pharmaceutical products	Direct injection	Nucleosil ODS, 200 \times 4.6 mm, 5 μ m	ACN/water (pH 2.7) ^j	^j	1 mL	Phthalic acid, phenol Cyclohexanone Phthalide, benzoic acid Benzaldehyde, bisphenol A Butyl hydroxyanisol Mono-(2-ethylhexyl) phthalate Dibutyl phthalate Di(2-ethylhexyl) phthalate	12
PVC	Leaching of administration sets	Direct injection	Econosphere C18, 150 \times 4.6 mm, 5 μ m	A = 1% acetic acid B = ACN 50% B for 3.5 min, change to 65% B	254	1 mL/min, 50 μ L, 35°C	Phthalide Monobutyl phthalate Mono-(ethylhexyl) phthalate	13 ^a
Adhesives	Extraction with water, 50°C, 3 days	Direct injection	NovaPak C18, 150 \times 2.1 mm	40-min gradient from 5–85% ACN in 0.1% acetic acid	220 ^k	0.25 mL/min	1,3-Benzenedicarboxylic acid, mono(7,12-dioxo-3,6,13,16-tetraoxaoctadec-17-en-1-yl) ester Hexanedioic acid, 2-[2-[(5-carboxy-1-oxopentyl)oxy] ethoxy] ethyl 2-(ethenyl)oxy ethyl ester 1,3-Benzenedicarboxylic acid, 2-[2-[(carboxy benzoyl)oxy]ethoxy] ethyl 2-(ethyl)oxyethyl ester	14

(Continued)



Table 1 Examples of HPLC methods used to identify and/or quantify packaging system extractables (*Continued*)

Material	Sample matrix	Sample preparation	Column	Mobile phase	λ (nm)	Other	Extractables	Ref.
PP	Extraction with acetonitrile	Direct injection after filtration	Waters Symmetry C8, 150 \times 3.9 mm	Start at 30:70 ACN/water, to 100% ACN at 10 min, to 30% ACN at 30 min, hold at 30% ACN for 10 min	MS EI Atmospheric pressure chemical ionization (APCI) UV	0.4 mL/min, 10 μ L	Naugard XL, Irganox 1076 1-Octadecanol, NC-4 3-(3,5-Di- <i>tert</i> -butyl-4-hydroxyphenyl) propanoic acid 7,9-Di- <i>tert</i> -butyl-1-oxaspiro-[4,5]deca-6,9-diene-2,8-dione	15

Solvent abbreviations include MeOH = methanol; ACN = acetonitrile; AA = acetic acid.

Material abbreviations include PP = polypropylene; PVC = poly(vinyl chloride); HDPE = high-density polyethylene; PC = polycarbonate; PS = polystyrene; PET = polyethylene terephthalate.

^aMethod performance data provided in this reference.

^bGradient was as follows: 0.0 min, 70% A; 18.0 min, 0% A; 22.0 min, 0% A; 23.0 min, 70% A.

^cGradient was as follows: 0.0 min, 95% A; 8.0 min, 40% A; 16.0 min, 30% A; 17.0 min, 0% A; 21.0 min, 0% A; 22.0 min, 95% A.

^dSpecific compounds detected included propyl-3,4,5 trihydroxy benzoate, 2-*tert*-butyl-4-methoxy phenol, 2-*tert*-butylphenol, 2-*tert*-butyl-4-methylphenol, and octyl-3,4,5-trihydroxybenzoate.

^eThis cited reference documents numerous compounds in these and other general compound classes.

^fFourier transform-infrared spectroscopy analysis of collected peaks used to confirm analyte identification.

^gVarious column sizes used.

^hFluorescence detection.

ⁱGradient was as follows: 5% ACN for 2 min; 5–50% ACN in 28 min; 50–98% ACN in 15 min.

^jMultiple wavelengths are used.

^kCompound identification performed via MS and MS/MS using both APCI and electrospray ionization (ESI) in the positive ion mode.

Table 2 Examples of GC methods used to identify and/or quantify packaging system extractables

Material	Sample matrix	Sample preparation	Column	Oven program	Detection	Other	Extractables	Ref.
Rubber	Water extract, 121°C, 2 hr	Evaporative concentration	Cross-linked methyl silicone 25 m × 0.3 mm id	30°C for 1 min, ramp at 8°C/min to 250°C	FID 325°C ^a	Splitless injection, <i>T</i> = 250°C	2-Butoxyethanol Cyclohexanone Diphenylamine 9,10-Dihydro-9,9-dimethyl-acridine Dibutylformamide 1,1,2,2-Tetrachloroethane Acetophenone 2-Phenyl-2-propanol Benzothiazole 2,2,5,5-Tetramethyl-tetrahydrofuran Isophthalic acid Terephthalic acid PET oligomers Cyclohexanone	16
PET	Solvent extracts, 40°C, 10 days	Evaporative concentration	DB-Wax-30N, 0.25 mm id	34°C for 1 min, ramp at 6°C/min to 200°C				17
PVC	Water extract	Evaporative concentration	HP1, 50 × 0.25 mm	200–280°C at 8°C/min	FID 280°C	Split injection <i>T</i> = 250°C		18
PVC	Products	Acidification, solvent extraction, evaporative concentration	J&W DB-5, 15 m × 0.53 mm, 15 µm film	32°C, 1.5 min; to 75 °C at 6°C/min; to 250°C at 30°C/min, hold for 2 min	FID 350°	3 µL (splitless), <i>T</i> = 210°C		19 ^b
Filter cartridges	Water or ethanol extracts	Solid phase extraction (SPE) with evaporative concentration	J&W DB-5, 30 m × 0.32 mm, 0.25-µm film	30°C for 0.5 min, to 225°C at 6°C/min	FID 350°C	Cold on-column injection	Di(ethylhexyl) phthalate Dibutyl phthalate cyclohexanone, phthalide 2-Ethyl-1-hexanol 2,6-Di- <i>tert</i> -butyl- <i>p</i> -cresol Phthalates, fatty acids, phenols, siloxanes, acrylates, aliphatics, amides ^c	8
PC	Methylene chloride extract	Direct injection after polymer ppt with methanol	J&W DB-5, 60 m	60°C for 2 min, to 280°C at 10°C/min, hold	MS	1 mL, split, <i>T</i> = 250°C	Bisphenol A	9
PVC	Pharmaceutical products	Solvent extraction, evaporative concentration	Restek RTx-5 FSOT, 30 m × 0.25 mm, 1.0-µm film 3% QF-1 or 3% SE-30 on Supelcoport	100°C, to 280°C at 10°C/min, hold for 3 min 120°C for 1 min, to 225°C at 4°C/min	MS <i>m/z</i> 213, <i>T</i> = 290°C MS EI+, <i>T</i> = 230°C	2 µL, split, <i>T</i> = 280°C <i>T</i> = 230°C	9,10-Epoxysearate ester	20

(Continued)

Table 2 Examples of GC methods used to identify and/or quantify packaging system extractables (*Continued*)

Material	Sample matrix	Sample preparation	Column	Oven program	Detection	Other	Extractables	Ref.
Rubber stoppers	Methylene chloride extracts	Direct injection	J&W DB-5MS, 30 m × 0.25 mm, 0.25-μm film	50°C for 5 min, to 275°C at 10°C/min, hold for 20 min	MS EI +, T = 200°C, 50–650 amu	1 μL, splitless, 200°C	Tributoxyethylphosphate BHT, diphenylamine 4-(2,2,3,3-Tetramethylbutyl)phenol 2,2'-Methylenebis[6,(1,1 dimethylethyl)-4-ethyl]phenol Penta- to octa-decane Phthalic acid esters Mono- to hepta-cosane 13-dicosenoic acid Alkyl esters of nonanoic acid	21
Laminated polyolefin ^d	Soxhlet and <i>n</i> -heptane extracts	Evaporative concentration with and without silylation	J&W DB-5, 30 m × 0.32 mm, 0.25-μL film	From 100°C to 280°C at 10°C/min	MS ^e	T = 220°C	Ethylene glycol, BHT Phthalic acid esters Plamitic, stearic, oleic acid Terephthalic acid Alkyl terephthalic acid esters 2,6-bis-(1,1-methylethyl)-4-ethylphenol Pyrogallol	22,23 ^f
PET	Soxhlet extraction	Evaporative concentration, with and without silylation	J&W DB-1, 15 m × 0.53 mm, 1-μm film	50°C, hold for 10 min, to 280°C at 10°C/min	MS SIM mode, also FID	T = 280°C		24 ^f

Polyolefin	Solvent extraction	Evaporative concentration	TRB-5, 60 m × 0.25 mm, 0.5-μm film	40°C for 1 min, to 300°C at 20°C/min, hold for 26 min	MS EI +	1 μL, splitless, T = 300°C	Aliphatic hydrocarbons, straight-chained, branched and cyclic ^{fg}	25 ^h
PE ⁱ	Solvent extraction	Direct injection	DB-1, 30 m × 0.25 mm, 0.32-μm film	50°C for 2 min, to 340°C at 5°C/min, hold for 10 min	MS EI +, 40–700 Da, T = 270°C	Splitless, T = 250°C	1,3-Di- <i>tert</i> -butyl benzene Oligomers 2,4-Di- <i>tert</i> -butylphenol Oxidized antioxidants Butanoic acid vinylester Benzothiazole derivatives ^l	26 ^{f,j}
Rubber ^k	Water extraction	Evaporative concentration	3% OV17 on Cas-Chrom Q, 1.5 m × 2 mm	140–200°C at 10°C/min	MS EI +, T = 250°C	2 μL, T = 250°C		27

See legend of Table 1 for a list of material abbreviations.

^aMass spectrometry was used in compound identification.

^bMethod performance data are provided in this reference.

^cThis reference documents numerous extracted compounds in these general categories.

^dLaminated film consisting of glycol-modified polyethylene terephthalate (PETG), polyvinylidene chloride (PVDG), and polyethylene (PE) with a polyurethane adhesive.

^eGas chromatography/infrared spectroscopy analysis was also used under differing operating parameters to aid in compound identification.

^fThese cited references document numerous compounds in these and other general compound classes.

^gStraight chained = C₁₂–C₂₅; branched = C₁₉–C₃₀; cyclic = C₂₄–C₃₅.

^hSimilar methods were used to identify compounds from polystyrene (styrene, styrene derivatives, glycolic esters of C16–C25 fatty acids, *trans*-1,2-diphenylcyclobutane).

ⁱMaterial was gamma-irradiated prior to analysis.

^jA similar method was used to identify compounds from PP, PVC, PS, PET, and polyamide.

^kComponents of disposable syringes.

^lIdentified compounds include 2-hydroxybenzothiazole, 2-mercaptobenzothiazole, 2-(methylmercapto)benzothiazole, 2-(2-hydroxyethoxy)benzothiazole, and 2-(2-hydroxyethylmercapto)benzothiazole.

Table 3 Examples of GC methods used to identify and/or quantify volatile packaging system extractables

Material	Sample matrix	Sample preparation	Column	Oven program	Detection	Other	Extractables	Ref.
Paper and board	Extracts in water, ethanol, or chloroform	2.5 g sample per vial; 70°C for 30–60 min	Chrompack CP-Sil 8 CB, 50 m × 0.32 mm, 1.2-μm film	70°C for 2 min, ramp at 5°C/min to 110°C	MS	Also used diffusion trapping	Butanal, pentanal, hexanal Heptanal, 2-heptanal Ethyl acetate, chloroform Methyl acetate, nonanal <i>o</i> - and <i>p</i> -xylene, benzene, benzaldehyde, others Ethanol, pentane Acetic and formic acids Cyclohexanal, xylene Cyclohexanone, pentanal Heptanal, nonanal Phthalates, BHT Tetradecanoic acid Hexadecanoic acid	28
PVC bags	Portions of bags from actual products	1–5 mg sample per vial, 120°C for 5–20 min	SE-54, 20m × 0.2 mm	30°C for 2 min, ramp at 10°C/min to 280°C	MS	Evolved gas trapped in a container cooled with liquid nitrogen		12

Polyolefin packaging material	7-cm ² portion of the material	Investigated effect of temperature from 30°C to 125°C with a 3-min desorption	2% OV-7 on Aue 2 m × 2 mm	Start at 0°C, ramp at 10°C/min to 150°C	FID and MS	Also used purge and trap	Methanol, 1-propanol <i>t</i> -Butanol, toluene 2-Methyl-2-propanol 1-Ethoxy-2-propanol Methyl ethyl ketone 2-(2-Hydroxypropoxy)-1 propanol 2-Ethyl-1-hexanol Di-2-ethylhexyl phthalate	29 30
Drinking water in plastic bottles	Water solution	1 L of water stripped with N ₂ at 600/mL/min for 8 hr, trapped on activated carbon	HP Ultra 2, 30 m × 0.53 mm, 1.5-μm film	40°C for 2 min, ramp at 10°C/min to 120°C, hold for 3 min.	MS	Analyte desorbed with CS ₂ from activated carbon		
Irradiated poly-ethylene film	Pieces of film	Gas evolved at 80°C, transferred through trap with 3 L of N ₂ at 50 mL/min Trapped volatiles desorbed at 200°C into N ₂	Porapak Q, 3.1 m × 3.2 mm ^a or Ucon Oil HB2000 LB550X, 80 m × 0.2 mm ^b	60°C for 8 min, ramp to 230°C at 4°C/min ^a or 60°C for 16 min, ramp to 140°C at 4°C/min ^b	FID and MS	Tenax-GC 18 cm × 5 mm (60/80 mesh) rap used	Acetic acid, butyric acid Ethanol, isopropanol <i>n</i> -Propanol, <i>n</i> -butane 2-Pentanaone, 2-hexanone 3-Hexanaone, 3-heptanaone Toluene, butanal Acetaldehyde, propane Propionic acid	31

^aUsed for low-boiling compounds.^bUsed for high-boiling compounds.

Table 4 Examples of miscellaneous chromatographic methods used to identify or quantify material extractables

Material	Test sample	Method description	Extractables	Ref.
Polypropylene	Aqueous food-simulating solvents	Capillary SFC. Column: 10 m \times 50 μ m i.d. SB-Biphenyl-30, 0.25- μ m film. Mobile phase = CO ₂ , linear flow rate \approx 3 cm/sec. Pressure program, 100–400 bar; temperature program, 55–100°C. 1- μ L injection using solvent venting with gas purging. Retention gap was 1.8 m \times 100 μ m deactivated fused silica. Detection by FID and MS.	Pentaerythrityl-tetrakis(3-(3,5-di- <i>tert</i> -butyl-4-hydroxy-phenyl) propionate) (<i>N,N'</i> -bis(2-hydroxyethyl)-C12.C14-amine) Tris-2,4-di- <i>tert</i> -butylphenylphosphite	32
Polyolefins, polypropylene, polyethylene	Soxhlet extracts	Capillary SFC. Column: 10 m \times 50 μ m i.d. fused silica capillary coated with cross-linked 5% phenyl-methylpolysiloxane (0.4- μ m film). Mobile phase = CO ₂ . Various temperature and pressure gradients used. Detection = FID at 300°C	Stearic acid, Irganox 1010 Irganox PS802, Atmos 150 Mono- and di-glycerides Alkenes, cycloalkanes	33
Polypropylene	Soxhlet extracts	Capillary SFC. Column: 10 m \times 50 μ m i.d. fused silica capillary coated with cross-linked methylpolysiloxane (SB-Methyl-100) or 50% octyl-substituted methylpolysiloxane (SB-Octyl-50), 0.25- μ m film. Mobile phase = CO ₂ . Pressure program, 129–350 atm at 3 atm/min; temperature = 110°C. Detection = FID.	Additives including Topanol, Irgafos 168, Irganox 1076, Irganox 1330, Irganox 1010, ethylbenzoate, ethyl stearate	34
Polyolefin laminate	Drug product stored in plastic bags, SPE preparation	HPTLC. Plate = 10 \times 20 cm silica gel. Mobile phase: acetone–chloroform–concentrated sodium hydroxide (20:80:0.2). Photodensitometric detection, at 200 and 234 nm before derivitization, 388 nm after derivitization with ninhydrin and 580 nm after derivitization with Bratton/Marshall reagent.	ϵ -Caprolactam Irganox 1010 Butylhydroxytoluene 4,4'-methylene dianiline	7
Polyethylene	Organic and water extracts	HPTLC. Plate = 10 \times 10 cm Fertigplatten Kieselgel 40. Mobile phase: chloroform/cyclohexane (12:1). Densitometric detection.	Irganox 1076 3,5-di- <i>tert</i> -butyl-4-hydroxy-phenyl propionic acid	35

graphy has been applied to meet the objectives of a leachables investigation.

Tables 1–4 provide general method details, such as column type, elution and detection conditions, and other operating conditions. The materials investigated, as well as the specific leachables examined, are also indicated. General comments are provided in terms of sample preparation. Given the number of methods cited, it is not possible here to provide detailed chromatographic profiles, which are readily available in the cited references.

Preinjection sample preparation is not a chromatographic issue per se. Nevertheless, it is an important consideration in the successful application of a complete analytical process. Nerin et al.^[36] reviewed sample treatment techniques applicable to polymer extract analysis, including headspace methods, supercritical fluid extraction, and solid phase microextraction.

REFERENCES

1. Aignasse, M.F.; Prognon, P.; Stachowicz, M.; Gheyouché, R.; Pradeau, D. A simple and rapid HPLC method for determination of DEHP in PVC packaging and releasing studies. *Int. J. Pharm.* **1995**, *113*, 241–246.
2. Yagoubi, N.; Baillet, A.; Pellerin, F.; Ferrier, D. Physicochemical behavior of β -irradiated plastic materials currently used as packages and medical products. *Nucl. Instrum. Methods Phys. Res.* **1995**, *105*, 340–344.
3. Begley, T.H.; Hollifield, H.C. Migration of dibenzoate plasticizers and polyethylene terephthalate cyclic oligomers from microwave susceptor packaging into food-simulating liquids and foods. *J. Food Prot.* **1990**, *53*, 1062–1066.
4. Begley, T.H.; Hollifield, H.C. Liquid chromatographic determination of residual reactants and reaction by-products in polyethylene terephthalate. *J.A.O.A.C.* **1989**, *72*, 468–470.
5. Rybak, K.E.; Sarzynski, W.; Dawidowicz, A.L. Migration of antioxidant additives from polypropylene investigated by means of reversed phase high performance liquid chromatography. *Chem. Anal.* **1992**, *37*, 149–159.
6. Yagoubi, N.; Baillet, A.; Mur, C.; Baylocq-Ferrier, D. Determination of phenolic antioxidants in pharmaceutical formulations by liquid chromatography and migration study on HDPE packagings. *Chromatographia* **1993**, *35*, 455–458.
7. Sarbach, C.; Yagoubi, N.; Sauzies, J.; Renaux, C.; Ferrier, D.; Postaire, E. Migration of impurities from a multi-layer plastics container into a parenteral infusion solution. *Int. J. Pharm.* **1996**, *140*, 169–174.
8. Reif, O.W.; Solkner, P.; Rupp, J. Analysis and evaluation of filter cartridge extractables for validation in pharmaceutical downstream processing. *PDA J. Pharm. Sci. Technol.* **1996**, *50*, 399–410.
9. Biles, J.E.; McNeal, T.P.; Begley, T.H.; Hollifield, H.C. Determination of Bisphenol-A in reusable polycarbonate food-contact plastics and migration into food-simulating liquids. *J. Agric. Food Chem.* **1997**, *45*, 3541–3544.
10. Buiarelli, F.; Carboni, G.; Coccioli, F. HPLC and GC-MS determination of compounds released to mineral waters stored in plastic bottles of PET and PVC. *Annal. Chim.* **1993**, *83*, 93–104.
11. Ulsaker, G.A.; Teien, G. Identification of caprolactam as a potential contaminant in parenteral solutions stored in overwrapped PVC bags. *J. Pharm. Biomed. Anal.* **1992**, *10*, 77–80.
12. Arbin, A.; Jacobsson, S.; Hanninen, K.; Hagman, A.; Ostelius, J. Studies on contamination of intravenous solutions from PVC-bags with dynamic headspace GC-MS and LC-diode array techniques. *Int. J. Pharm.* **1986**, *28*, 211–221.
13. Snell, R.P. Solid-phase extraction and liquid chromatographic determination of monophthalates and phthalide extracted from solution administration sets. *J.A.O.A.C.* **1993**, *76*, 531–534.
14. Tiller, P.R.; El Fallah, Z.; Wilson, V.; Huysman, J.; Patel, D. Qualitative assessment of leachables using data-dependent liquid chromatography/mass spectrometry and liquid chromatography/tandem mass spectrometry. *Rapid Commun. Mass Spectrom.* **1997**, *11*, 1570–1574.
15. Yu, K.; Block, E.; Balogh, M. LC-MS analysis of polymer additives by electron and atmospheric-pressure ionization: Identification and quantification. *LC GC* **2000**, *18*, pp. 162, 164, 166, 168, 170, 172, 174, 176, 178.
16. Danielson, J.W. Toxicity potential of compounds found in parenteral solutions with rubber stoppers. *J. Parenter. Sci. Technol.* **1992**, *46*, 43–47.
17. Dobias, J.; Voldrich, M.; Proks, M. Migration of polyethylene terephthalate oligomers from packaging into food simulant liquids. *Potav. Vedy* **1996**, *14*, 25–32.
18. Snell, R.P. Gas chromatographic determination of cyclohexanone leached from hemodialysis tubing. *J.A.O.A.C.* **1993**, *76*, 1127–1132.
19. Snell, R.P. Capillary GC analysis of compounds leached into parenteral solutions packaged in plastic bag. *J. Chromatogr. Sci.* **1989**, *27*, 524–528.
20. Ulsaker, G.A.; Teien, G. Determination of 9,10-epoxystearate ester in intravenous solutions stored in poly(vinyl chloride) bags, using gas chromatography–single-ion monitoring mass spectrometry. *Analyst* **1984**, *109*, 967–971.
21. Milano, C.J.; Bailey, L.C. Evaluation of current compendial physicochemical test procedures for pharmaceutical elastomeric closures and development of an improved HPLC procedure. *PDA J. Pharm. Sci. Technol.* **1999**, *53*, 202–210.
22. Kim-Kang, H.; Gilbert, S.G. Permeation characteristics of and extractables from gamma-irradiated and non-irradiated plastic laminates for a unit dosage injection device. *Packag. Technol. Sci.* **1991**, *4*, 35–48.
23. Kim-Kang, H.; Gilbert, S.G. Isolation and identification of potential migrants in gamma-irradiated plastic laminates by using GC/MS and GC/IR. *Appl. Spectrosc.* **1991**, *45*, 572–580.

24. Kim, H.; Gilbert, S.G.; Johnson, J.B. Determination of potential migrants from commercial amber polyethylene terephthalate bottle wall. *Pharm. Res.* **1990**, *7*, 176–179.
25. Veiga-Rial, M.; Sarria-Vidal, M.; de la Montana-Miguel, J.; Simal-Gandura, J. Identification of residual constituents in plastic packaging for dairy products. *Rec. Res. Devel. Agric. Food Chem.* **1999**, *3*, 305–311.
26. Demertzis, P.G.; Franz, R.; Welle, F. The effects of γ -irradiation on compositional changes in plastic packaging films. *Packag. Technol. Sci.* **1999**, *12*, 119–130.
27. Salmons, G.; Assaf, A.; Gayte-Sorbier, A.; Airaud, C.B. Mass spectral identification of benzothiazole derivatives leached into injections by disposable syringes. *Biomed. Mass Spectrom.* **1984**, *11*, 450–454.
28. Castle, L.; Offen, C.P.; Baxter, M.J.; Gilbert, J. Migration studies from paper and board food packaging materials. I. Compositional analysis. *Food Addit. Contam.* **1997**, *14*, 35–44.
29. Eiceman, G.A.; Karasek, F.W. Identification of residual organic compounds in food packages. *J. Chromatogr.* **1981**, *210*, 93–103.
30. Vitali, M.; Leoni, V.; Chiavarni, S.; Cremisini, C. Determination of 2-ethyl-1-hexanol as contaminant in drinking water. *J.A.O.A.C.* **1993**, *76*, 1133–1137.
31. Azuma, K.; Hirata, T.; Tsunoda, H.; Ishitani, T.; Tanaka, Y. Identification of volatiles from low density polyethylene film irradiated with an electron beam. *Agric. Biol. Chem.* **1983**, *47*, 855–860.
32. Berg, B.E.; Hegna, D.R.; Orlin, N.; Greibrokk, T. Determination of low levels of polymer additives migrating from polypropylene to food simulated liquids by capillary SFC and solvent venting injection. *Chromatographia* **1993**, *37*, 271–276.
33. Dilettato, D.; Arpino, P.J.; Nguyen, K.; Bruchet, A. Investigation of low mass oligomers and polymer additives from plastics. Part II: Application to polyolefin soxhlet extracts. *J. High Res. Chromatogr.* **1991**, *14*, 335–342.
34. Moulder, R.; Kithinji, J.P.; Raynor, M.W.; Bartle, K.D.; Clifford, A.A. Analysis of chemical additives in polypropylene films using capillary supercritical fluid chromatography. *J. High Res. Chromatogr.* **1989**, *12*, 688–691.
35. Corti, P.; Murratzu, C.; Franchi, G.; Lencioni, E.; Pancini, R. Evaluation of chemical residues in food and drugs: Evaluation of an antioxidant given from high density polyethylene food containers. *Acta Toxicol. Ther.* **1988**, *9*, 205–221.
36. Nerin, C.; Rubio, C.; Salafranca, J.; Batlle, R. The simplest sample treatment techniques to assess the quality and safety of food packaging materials. *Rev. Anal. Chem.* **2000**, *19*, 435–465.

Overpressured Layer Chromatography

Jan K. Różyło

Marie Curie-Skłodowska University, Lublin, Poland

Introduction

Conventional thin-layer chromatography (TLC) in our experience, known under the name planar chromatography, uses horizontal or vertical glass or Teflon chambers for the development of chromatograms. As stationary phases, commonly known adsorbents or supports based on silica gel, aluminium oxide, magnesium silica, cellulose, and so forth are used; particle sizes are about 20 μm . The migration of the mobile phase is based on the phenomenon of capillary forces. This chromatographic method is described, in detail, in other sections of this volume.

This method is characterized by many limitations which either can cause unsatisfactory separation of a mixture of substances or lead to long development times (even up to several hours) or, sometimes, makes use of solvents of high viscosity impossible. The efficiencies of such chromatographic systems are also rather low.

Discussion

In conventional TLC, the velocity of chromatogram development depends on the dimension of stationary-phase particles, viscosity of the mobile phase, distance from the start line of the mobile phase, and other parameters. Therefore, there is no possibility of regulation of resolution by change of migration velocity of mobile-phase flow; the distance between the solvent reservoir and the solvent front (z_f) varies with time (t) according to

$$z_f^2 = kt$$

where k is a constant that depends on the chromatographic system (mobile phase and adsorbent) and the size of sorbent particles constituting the layer and presents a parabolic relationship.

As the most popular planar liquid chromatographic technique, TLC uses a vapor phase of solvent above the sorbent layer, which has an important influence on the resolving power.

Many of the inconveniences of TLC are avoided in overpressured layer chromatography (OPLC), which

is a logical extension of the theory and practice developed in high-pressure liquid chromatography (HPLC) which can now be used in the field of planar liquid chromatography. This extension offers some exceptional advantages to a chromatographer. OPLC is, in practical terms, a planar HPLC technique. OPLC integrates many of the benefits of TLC, high-performance TLC, and HPLC. This technique corresponds to an HPLC column having a relatively thin, wide cross section and using a pressurized ultramicrochamber with standard chromatoplates. Eluent is forced into the sorbent layer by the means of a pump which enables development of chromatograms with forced flow of the mobile phase (more precise penetration into micropores). The eluent migrates against the sorbent resistance imposed by external pressure on the sorbent surface, and the vapor phase is excluded. In the case of OPLC, there is a linear relationship between the distance (z_f) of the solvent front from the starting point and the migration time (t):

$$z_f = kt$$

where k is a constant that depends on the rate of solvent flow, on the externally applied pressure, and on the size of the particles constituting the layer. In principle, k is constant throughout the development and independent of the rate of solvent migration. In OPLC, the parameter R_F is also used to describe the position of the separated analyte and, in this case, the R_F values do not depend on the starting distance.

The parameters characterizing chromatographic systems in TLC, such as average plate height (H), reduced plate height (h), and theoretical plate number (N), are calculated in a similar way in OPLC, but, practically, they do not depend on either average particle diameter (d_p) or the start distance (s_0). In OPLC, the start distance has no influence on the efficiency of separation, and the average plate height is nearly constant on a layer of exceptionally fine particles, even over a longer development distance. Thus, the major advantage of OPLC over other planar techniques lies in this fact. We can say that OPLC permits relatively large plate numbers to be obtained and can be applied more favorably in the case of smaller particles.



Basic Instrumentation for OPLC

As far as OPLC is concerned, the method, in principle, differs from conventional TLC in the design of the equipment that is used. The first attempts at construction of chromatographic pressure chambers were made in the beginnings of the 1960s. However, only at the end of the 1970s, Tyihák, Mincsovcics, and Kalász were successful in construction of a well-operating OPLC chromatograph called Chrompress 10 (maximum pressure permitted in this chamber was 1.0 MPa) and, later, in the 1980s, Chrompress 25 (2.5 MPa) (Labor MIM, Hungary) and the most modern Personal OPLC BS-50 (OPLC-NIT, Budapest, Hungary) (5.0 MPa). In Poland, during 1980–1990, a pressure thin-layer chromatograph was constructed (Cobrabid, Warsaw); however, due to its narrow range of operating pressures (0.8 MPa), it was not widely used.

We will describe only the most up-to-date OPLC system. This fully automatic OPLC system allows separation of mixtures on an analytical and on a semipreparative scale. The fundamental separation process occurs on a chromatographic plate (constructed of glass or aluminum foil) with sorbent (Fig. 1) covered and compressed by a special polyethylene or Teflon foil, pressured by water. In this way, a flat, thin chromatographic column is created. This technique also requires a special chromatoplate which is sealed at the edges, which pre-

vents the eluent from flowing off the chromatoplate in an unwanted direction. According to the technique of chromatogram development used (unidirectional, bidirectional, circular, on-line, off-line, parallel coupled multilayer, serial coupled multilayer), all four margins of a plate, three margins, two opposite margins can be impregnated, or they can be left uncoated.

In linear development of a chromatogram, unidirectional or bidirectional developments of the chromatogram are possible. Similarly, as in liquid column chromatography, there are possible, in this case, either on-line or off-line techniques of sample application, separation, and detection, as well as various modifications (e.g., partly off-line method). Bidirectional development can also be vertical. Using vertical bidimensional development, applying different eluents, components of complex, difficult mixtures can be separated. The separation of such mixtures is also possible by means of this technique using multiple automatic development of chromatogram.

In OPLC, the changes in composition of the eluent give good possibilities for special separation techniques such as isocratic and gradient separation. The choice of mobile phase can be effectively and quickly determined using the optimization model Prisma according to Nyiredy. This is a three-dimensional model that correlates the solvent strength and the proportion of eluent constituent, which determines the selectivity of the mobile phases according to Snyder's solvent classification.

The newest apparatus for overpressured layer chromatography, "Personal OPLC BS-50" manufactured in Hungary, is shown in Fig. 2. Generally speaking, it consists of the separation chamber and a liquid delivery system. The separation chamber contains the following units: (a) holding unit, (b) hydraulic unit, (c) tray layer cassette, and (d) drain valve. The apparatus also has a pumping system for eluent delivery and for the hydraulic liquid delivery. The entire apparatus and the total chromatogram development process are controlled by a computer system. The apparatus and the method of chromatogram development is characterized by high reproducibility of results and chromatographic parameters. External pressure (5 MPa), eluent flow rate and its volume, and development time can be automatically programmed. The OPLC-BS-50 chamber works in off-line and on-line systems. Using this equipment, it is possible to separate 70–100 or even more samples at the same time, depending, of course, on the chosen technique of the OPLC process.

This OPLC method is characterized by high precision for determination of retention parameters and reproducibility of results.

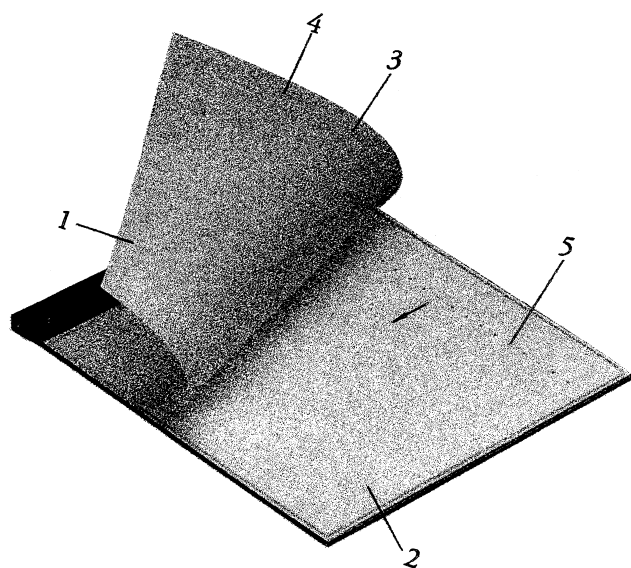


Fig. 1 Cassette of foil-backed layer for linear development: 1 = cover sheet, 2 = sorbent layer, 3 = eluent puncture, 4 = eluent trough, 5 = sample application site.

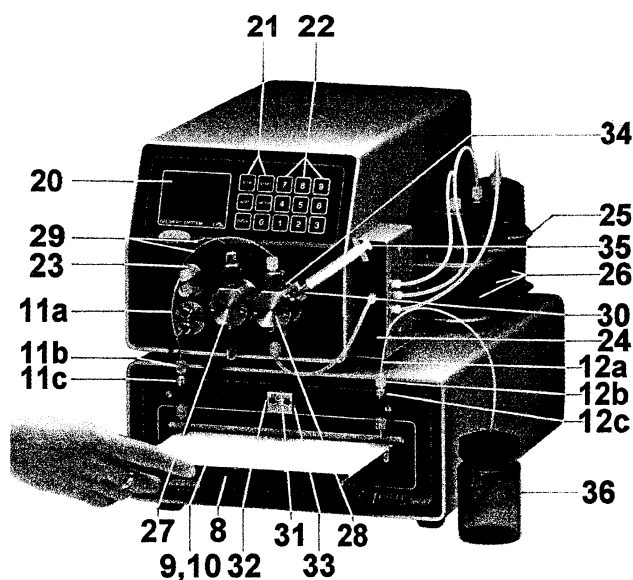


Fig. 2 Personal OPLC BS-50 apparatus: 9,10 = Teflon cover sheet of cassette, upper and lower, respectively; 11a = tube driving eluent from pressure gauge to chamber inlet connector; 11b = end connector for tube 11a; 11c = chamber-eluent-inlet connector; 12a = tube for eluent outlet of the chamber; 12b = end connector for tube 12a; 12c = chamber-eluent-outlet connector; 20 = display; 21 = function keys; 22 = numeric keys; 23 = pressure gauge for eluent; 24 = eluent switching valve; 25 = tank holder; 26 = eluent tanks A, B, and C; 27 = pump head for hydraulic liquid delivery; 28 = pump head for eluent delivery; 29 = hydraulic liquid and eluent connecting tubes; 30 = connecting stub for syringe to fill up eluent pump; 31 = middle hole of T distributor for fitting tubes in case of two-directional development; 32 = left hole of T distributor for fitting tubes in case of two-directional development; 33 = right hole of T distributor for fitting tubes in case of two-directional development; 34 = hole for piston rinsing against deposition; 35 = syringe.

Advantages

- Separation of components which the former TLC techniques failed to achieve
- Smaller attainable plate height over longer migration distances
- Rapid separation and high resolution for industrial control

- Optimization of resolution as a function of solvent velocity, development distance, and temperature
- Possibility of using high-viscosity eluents and poorly wettable stationary phases
- Possibility of both quantitative evaluation and preparative applications
- Efficient separation of multicomponent samples
- Different development modes: unidirectional, bi-dimensional, continuous on-line, and off-line
- Long migration distances on fine-particle layers with short development times
- No air interactions
- Minute consumption of developing solvent
- Programmable operating system.

Some applications include analytical and preparative analyses in all types of biological, biochemical, pharmaceutical, clinical, forensic, food, and environmental laboratories.

Suggested Further Reading

- Kaiser, R. E., *Einführung in die HPLC*, Huethig, Heidelberg, 1987.
- Kaiser, R. E. and R. I. Rieder, in *Planar Chromatography, Vol. 1* (R. E. Kaiser, ed.), Huethig, Heidelberg, 1986, p. 165.
- Mincsovcics, E., K. Ferenczi-Fodor, and E. Tyihák, in *Handbook Thin-Layer Chromatography* (J. Sherma and B. Fried, eds.), Marcel Dekker, Inc., New York, 1996, p. 173.
- Nyiredy, Sz., C. A. J. Erdelmeier, and O. Stichler, in *Proc. Int. Symp. TLC with Special Emphasis on Overpressured Layer Chromatography (OPLC)* (E. Tyihak, ed.), LABOR MIM, Budapest, 1986, p. 222.
- Nyiredy, Sz., S. Y. Meszaros, K. Dallenbach-Toelke, K. Nyiredy-Mikita, and O. Stichler, *J. High Resolut. Chromatogr. Chromatogr. Commun.* 10: 352 (1987).
- Rózyło, T. K., R. Siembida, and E. Tyihak, *Biomed. Chromatogr.* 13: 1 (1999).
- Ruoff, A. D. and J. C. Giddings, *J. Chromatogr.* 3: 438 (1960).
- Tyihák, E., E. Mincsovcics, and H. Kalász, *J. Chromatogr.* 174: 75 (1979).
- Tyihák, E., E. Mincsovcics, H. Kalász, and J. Nagy, *J. Chromatogr.* 211: 45 (1981).
- Tyihák, E., E. Mincsovcics, P. Tetenyi, I. Zambo, and H. Kalász, *Acta Horticult.* 96: 113 (1980).



Packed Capillary Liquid Chromatography

Fernando M. Lanças

Instituto de Química de São Carlos, Universidade de São Paulo, São Carlos/SP, Brazil

Introduction

Liquid chromatography (LC) was the first chromatographic mode to be developed in the beginning of the twentieth century. For almost 70 years, it was employed without major modifications until the end of the 1960s when an instrumental version of liquid chromatography was finally produced. Before this milestone, LC was performed mainly in large-bore glass tubing packed with large-diameter solid particles. To differentiate the instrumental version developed in the late 1960s from the noninstrumental, usually referred as the “classical” version, the former was named high-pressure liquid chromatography and, later, high-performance liquid chromatography (HPLC). Because HPLC used smaller particles as the stationary phase, the columns had to be packed at higher pressures in order to obtain a more stable bed required by the higher pressures used in these techniques. Altogether, HPLC offered a much higher efficiency (number of plates) than “conventional LC” and, as a consequence, higher resolution (separation power) as well. The standard HPLC columns used in the 1970s consisted of particles of 5–10 μm packed in stainless-steel tubing of 4.0–4.6 mm inner diameter (i.d.) and 15–25 cm long. Typical flow rates under these conditions are $\sim 1\text{--}2$ mL/min. In a typical quality control laboratory (8 h a day; 5 days a week, 20 days a month; 12 months a year), more than 100 L of chromatographic solvent are generated in a 1-year period. Most of these solvents are highly toxic to man and the environment, requiring special waste storage, transportation, and final disposal. As a consequence, a miniaturization of the HPLC techniques using less solvent became important immediately after its development.

A major step in the miniaturization of HPLC columns was done early in 1967 by Horváth and co-workers [1,2], when investigating the parameters that influence the separation of nucleotides in a 1-mm-i.d. column. These columns were then named microbore columns. A further step in the miniaturization process was done in 1973, by Ishii and co-workers, by separating polynuclear aromatic hydrocarbons (PAHs) in a

0.5-mm-i.d. PTFE column. The term micro-LC was then introduced to differentiate this technique from HPLC, which uses larger-bore columns [3–5]. Shortly after, Scott and Kucera published several articles dealing with microbore (1-mm-i.d. columns) LC [6,7].

In spite of the fast development in its early days (late 1960s and early 1970s), the miniaturization of HPLC followed a slow progress until recently, with the development of LC–mass spectrometry (MS) using electrospray-type interfaces.

Capillary Liquid Chromatography

Capillary liquid chromatography (CLC) is a mode of HPLC that deals with columns having internal diameters equal to, or smaller than, 0.5 mm. This number is limited by the internal diameter of the fused-silica tubing commercially available, which is the most popular tubing used in this area. The CLC columns are usually 15–60 cm long, having internal diameters < 0.5 mm and being either coated or packed with the stationary phase. Due to the small inner diameter of the CLC columns, this technique is more demanding in instrumentation than HPLC, particularly with respect to the solvent delivery, sample introduction, and detection systems.

Sample Introduction

Because the column inner diameter is small, the amount of stationary phase is also very small and, as a consequence, the amount of sample that can be introduced into the column without overloading is very small (typically a few nanoliters). In most cases, the preferred sample introduction system consists of an injection valve containing an internal loop smaller than 0.1 μL .

Pumping System

Because the eluent flow rate is relatively small (typically a few microliters per minute), the pump used to deliver it to the column is critical. There are two ma-



for approaches being used: pumps capable of delivering flow rates in the range of few microliters per minute (usually syringe-type pumps) or reciprocating pumps using a flow splitter. In both cases, reproducible flow rates are hard to obtain using commercially available pumps.

Detectors

Almost all detectors currently used in HPLC have been evaluated to be used in CLC. The major modification required, in most cases, is a decrease in the detector cell volume in order to accommodate the small sample volume without considerable peak broadening. Ultraviolet-visible (UV-vis), fluorescence, electrochemical, mass spectrometric, and several other detectors have been successfully used with CLC.

Columns

Capillary LC columns can be generally made in two different ways: wall-coated open tubular (WCOT) or packed columns. Coating the internal wall of the tubing (usually fused silica) with a thin film of a solvent-resistant polymer makes WCOT columns and is the same technology as used for capillary GC columns. Usually, cross-linked or immobilized phases are preferred in order to avoid stationary-phase removal by the eluent. The major drawback of these columns is that they have to be made with an internal diameter smaller than 20 μm in order to be highly efficient for complex separations, thus justifying their use instead of the packed capillary columns [8]. This places great demands on the instrumentation, the eluent quality, the sample preparation step, and so forth, thus making it impractical at this moment. As an alternative, the packed capillary columns using the technology already available to prepare HPLC columns is less instrument demanding and have been gaining more acceptance, every day becoming the preferred form of CLC.

Advantages of Capillary Liquid Chromatography

The advantages of CLC are consequences of its miniaturization [9]. Due to its miniaturized size, it requires much less stationary phase than does ordinary HPLC and, as a consequence, more expensive phases can be used to prepare the columns. This includes chiral phases, experimental new materials, expensive biocompounds, and so forth. In the same way, the amount of mobile phase is very small, thus leading to a savings in buying, storing, and discarding the solvent, allowing

the use of expensive eluents such as deuterated solvents and chiral modifiers such as cyclodextrins, transition metals, and so forth. In many cases, the total amount of mobile phase in one separation is just 10 μL (1 $\mu\text{L}/\text{min}$; 10-min run); this explains why this technique is sometimes referred to as "one-drop chromatography." The amount of sample injected is also very small, so it becomes an important technique when the sample size is critical, such as in biomedical studies (brain, spine liquid, newborn tests, etc.), forensic chemistry (fire debris, explosives, blood residues), environmental analysis, and several other application fields.

Other advantages of CLC, when compared to HPLC, includes its higher permeability [10], chemical inertia, easier coupling to other separation and identification systems such as mass spectrometry, gas chromatography, and nuclear magnetic resonance, and the possibility of making longer columns, thus achieving more plates (efficiency) and resolution.

Figure 1 shows a chromatogram of a separation of PAHs using a packed capillary column. As can be verified, a good separation is obtained with minute amounts of stationary phase, mobile phase, and sample.

Limitations of Capillary Liquid Chromatography

In spite of the several advantages over HPLC, CLC has not yet achieved its maturity as a separation technique to be used worldwide, particularly as a routine technique for quality control laboratories. Among the limitations still hindering the further development of CLC, one of the most critical ones is the very limited availability of commercial equipment dedicated to this

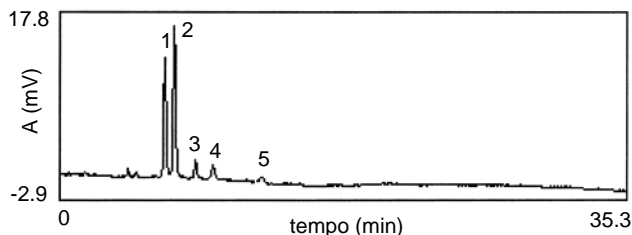


Fig. 1 Capillary LC chromatogram of a river water solid-phase extract containing PAHs. Column: fused silica (20 cm \times 0.25 mm) H_2O home-packed with RP-18 (5 μm). Mobile phase: ACN/ H_2O (75:25), flow rate 4 $\mu\text{L}/\text{min}$, UV detection at 254 nm. Compound identity: 1 = fenanthrene, 2 = anthracene, 3 = fluoranthene, 4 = pyrene, 5 = crysene.

technique. Even so, most systems are simple adaptations of parts already used for HPLC, by just decreasing their sizes and volumes without specifically having CLC in consideration. Therefore, in order to become a routine technique as its counterpart in gas chromatography, capillary liquid chromatography still has to have a broader interest for the instrument manufacturing companies in the technique before it will spread out beyond the academic environment. Those who have worked with packed columns in gas chromatography in the 1960s have already seen this same history.

Acknowledgments

Professor F. Lanças wishes to thank FAPESP (Fundação de Apoio à Pesquisa do Estado de São Paulo) and CNPq (Conselho Nacional de Desenvolvimento Científico e Tecnológico) for financial support to his laboratory.

References

1. C. G. Horváth, B. A. Preiss, and S. R. Lipsky, *Anal. Chem.* 39: 1422 (1967).
2. C. G. Horváth and S. R. Lipsky, *Anal. Chem.* 41: 1227 (1969).
3. D. Ishii and K. Sakurai, in *Tokyo Conference of Applied Spectrometry*, 1973, Abstract 1B05, p. 73.
4. D. Ishii, K. Asai, K. Hibi, T. Jonokuchi, and M. Nagaya, *J. Chromatogr.* 144: 157 (1977).
5. D. Ishii, K. Asai, and T. Jonokuchi, *J. Chromatogr.* 151: 147 (1978).
6. R. P. W. Scott and P. Kucera, *J. Chromatogr.* 125: 251 (1976).
7. R. P. W. Scott and P. Kucera, *J. Chromatogr.* 169: 51 (1979).
8. H. Menet, P. Gareil, and R. Rosset, *Anal. Chem.* 56: 2990 (1984).
9. M. Verzele and C. Dewaele, *J. High Resolut. Chromatogr.* 10: 280 (1987).
10. D. Shelly, J. Gluckman, and M. Novotny, *Anal. Chem.* 56: 2990 (1984).



Particle Size Determination by Gravitational FFF

Pierluigi Reschiglian

University of Bologna, Bologna, Italy

Introduction

Particle Size Distribution: A Key Property of Particulate Samples

Particle size distribution analysis was considered, in one of the latest Pittsburgh Conferences, as one of the most outstanding trends in analytical science. This is not an overstatement, as most of the real samples of analytical interest occur either in dispersed form or in dispersed matrices. Just for argument's sake, in industrial applications the characterization of the size of sample particles is routine and is an essential part of the overall quality control procedures. In the medical field, for particles used to carrier drugs, the size is a critical performance factor (e.g., liposomes). In the food industry, the alcoholic yield from fermentation of starch, and even the taste of chocolate, depends on the size of particles of which these samples are composed.

Before discussing our method for determining particle size, it is necessary to briefly review the definition of size distribution. If all particles of a given system were spherical in shape, the only size parameter would be the diameter. In most real cases of irregular particles, however, the size is usually expressed in terms of a sphere *equivalent* to the particle with regard to some property. Particles of a dispersed system are never of either perfectly identical size or shape: A spread around the mean (*distribution*) is found. Such a spread is often described in terms of standard deviation. However, a frequency function, or its integrated (cumulative) distribution function, more properly defines not only the spread but also the shape of such a spread around the mean value. This is commonly referred to as the *particle size distribution* (PSD) profile of the dispersed sample.

An examination of technical literature and trade publications indicates that a wide variety of instruments are commercially available for PSD analysis [1]. The classical methods are based on either electrical properties (e.g., the Coulter Counter® principle) or optical properties (e.g., laser scattering) of the analyte. However, none of these techniques are separation methods. Because particulate dispersions are often

highly complex in terms of the polydispersity index, multimodal size distribution, and density, it is hardly possible, without the use of separative methods, to obtain an accurate determination of their size distribution. Among separative chromatography-like methods, one can consider hydrodynamic chromatography and field-flow fractionation (FFF). The application to PSD of a subset of the latter family of methods is the topic of this article.

PSD by FFF

Field-flow fractionation is a broad family of liquid chromatographic-like techniques which have been shown, over more than 20 years, to be able to fractionate and characterize high-molecular-weight species in a size range spanning five orders of magnitude, from macromolecules to micron-size particles [2]. FFF has been demonstrated to be a rapid method for the determination of the mean diameters and polydispersities of particulate samples. When compared to standard methods for PSD analysis, the main advantage of FFF lies in the fact that FFF is a separation method which has some common features with liquid chromatography. The output from an FFF experiment is a function of the detector signal versus the retention time of the analyte. Whereas, in liquid chromatography, such an analytical response is referred to as the *chromatogram*, in FFF it is commonly defined as the *fractogram*. However, when it is compared to classical liquid chromatography, the existence of a direct relationship between retention and some physical properties of the analyte, such as the size, is a fundamental feature of most FFF techniques. The theory of FFF retention has been fully explained elsewhere, [2, and references therein] as well as in other entries of this encyclopedia. What is important to focus on here is that, in FFF, particle size determination of the analyte can be obtained by means of a direct numerical conversion of the retention scale, whereas the relative amount of separated analyte is, as in the case of chromatograms, in some way proportional to the signal intensity. The basic procedures for the two conversions is the topic of this entry.

Encyclopedia of Chromatography

DOI: 10.1081/E-Echr 120005251

Copyright © 2002 by Marcel Dekker, Inc. All rights reserved.



*Gravitational FFF: An Economical Device
for PSD Analysis of Micron-Size Dispersions*

Here, we treat the case of PSD analysis of particulate systems of micron-size range (i.e., with a size distribution extending above 1 μm). Since 1994, in our laboratories, this topic has been dealt with by means of a low-cost subset of sedimentation FFF (SdFFF), the gravitational field-flow fractionation (GrFFF) technique [3]. GrFFF had already been applied to the fractionation of a variety of micron-size dispersion, either inorganic as commercial chromatographic supports [4] or biological, as cells and parasites [5]. In no cases, however, had PSD been performed through GrFFF. As an SdFFF subset, GrFFF requires the application of a sedimentation field that, in this case, is simply Earth's gravity applied perpendicularly to a very thin, empty channel with a rectangular cross section. The big advantage of GrFFF, compared to other techniques for the characterization of particulate matter, lies in its very low cost ($\sim \$50$ for a homemade channel) and easy implementation in a standard high-pressure liquid chromatography (HPLC) system (the channel can simply replace the standard HPLC column). The GrFFF channel employed here can be easily built as described elsewhere [3–9]. It is basically a ribbon-like capillary channel which consists of two mirror-polished plates, of either glass or plastic material (e.g., polycarbonate) which are clamped together over a thin sheet of either Teflon or Mylar from which the channel volume has been removed. Simplicity and economy of use make it possible for laboratories that are not specialized in PSD analysis to perform dimensional characterization of supermicron particles dispersions with limited effort and cost.

We shall show here that GrFFF is capable of performing reliable, quantitative PSD analysis of particulate matter. Some basics of the overall procedure will be overviewed and the relevant questions presented. In fact, in order to obtain a PSD by means of GrFFF, the conversion of the retention time axis into the analyte size axis is necessary. For the same reason, the detector signal axis must be converted into mass (or concentration) of the fractionated analyte.

Procedure and Discussion

From a GrFFF Fractogram to a PSD

The diameter scale can be obtained from retention coordinates (i.e., the retention time axis) by applying to

Particle Size Determination by Gravitational FFF

the fractogram the well-known, approximate expression that is valid for highly retained samples in GrFFF [3]:

$$d_i = \frac{wV_0}{3\gamma} \frac{1}{V_{r,i}} \quad (1)$$

where d_i (cm) is the diameter value corresponding to the i th data point of the fractogram, the retention volume of which is $V_{r,i}$ (cm^3). V_0 (cm^3) is the void volume of the GrFFF channel, w (cm) is the channel thickness and γ is the so-called hydrodynamic correction factor, the knowledge of which is, therefore, required for PSD analysis.

In practice, PSD curves can be obtained directly from the experimental, digitized peak (fractogram), $y_i(V_{r,i})$ once it is converted to a function of particle diameter d_i with the use of Eq. (1). The frequency function of particle size f_m is expressed as [3]

$$f_{m,i} = \frac{\delta m_i}{\delta d_i} = \frac{\delta m_i}{\delta V_{r,i}} \frac{\delta V_{r,i}}{\delta d_i} \quad (2)$$

where $\delta m_i/\delta V_{r,i}$ (g/cm^3) is the mass concentration of the analyte at the i th digitized point and $\delta V_{r,i}$ and δd_i are the differences in retention volume and particle diameter between the i th and the $(i-1)$ th digitized points, respectively. The incremental quantity δd_i can be calculated for any given $\delta V_{r,i}$ by Eq. (1).

As far as the conversion of the analytical response y_i is concerned, the most used detectors in GrFFF have been, until now, conventional ultraviolet (UV) detectors commonly used for HPLC. With this type of detector, the amount of particles with diameter d_i is proportional to the detector response at the i th point. With particulate samples, in fact, because of UV detector optics, the response is a *turbidity* signal read within an angle between the incident light and the photosensor (i.e., usually smaller than $\sim 10^\circ$) rather than the *absorbance*. This turbidity signal can be assumed to be directly proportional to the sum of all cross-sectional areas of the particulate sample components at any time. The validity of the above assumption, in the case of particles which are about 10-fold larger than the incident wavelength, is discussed elsewhere [6]. The mass frequency function can thus be expressed as [7]

$$f_{m,i} \propto (\text{UV signal})_i(d_i) \frac{\delta V_{r,i}}{\delta d_i} \quad (3)$$

For the reader's convenience, a scheme of the required conversion is represented in Fig. 1. It is evident that it is rather straightforward to derive a PSD from a GrFFF experiment [3]. An example of GrFFF-PSD

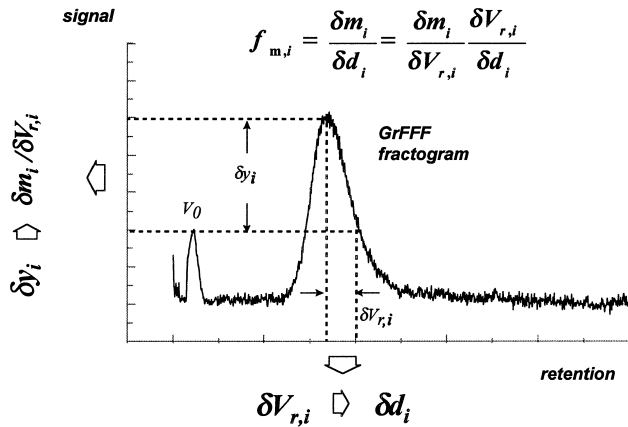


Fig. 1 Scheme for the conversion from a fractogram to a frequency function of particle size.

analysis for a sample of silica particles commonly used as the stationary phase in HPLC (5 μm LiChrospher, Merck) is reported in Fig. 2a. For the sake of comparison, the PSD of the same sample obtained by laser diffraction is reported in Fig. 2b. We can observe that PSD resolution is higher in GrFFF than in laser diffraction, where just a histogram is obtained. On the other hand, accuracy is comparable when the experimental distribution moments (i.e., the percentiles indicated as d_{10} , d_{50} , d_{90}) are compared to the nominal values given by the manufacturer. We must point out that differences in distribution moment values as high as 10% are commonly reported when different, uncorrelated techniques for PSD studies are compared [1].

Quantitative Particle Size and Sample Amount Distribution in GrFFF

We have derived an original method by which quantitative particle size and sample amount distribution (PSAD) in GrFFF can be obtained by applying to Eq. (2) a derivation of the Lambert–Beer law in flow-through systems [7]. If compared to standard PSD, a PSAD thus represents a distribution of the *real* mass of the analyte as a function of size, rather than a functional expression only *proportional* to mass.

For particle dispersions in the micron-size interval, which is the typical application range of GrFFF, it has been demonstrated that the sample amount exiting the detector cell, $N_0(g)$, can be expressed as

$$\frac{\bar{A}F}{Kb} = N_0 \quad (4)$$

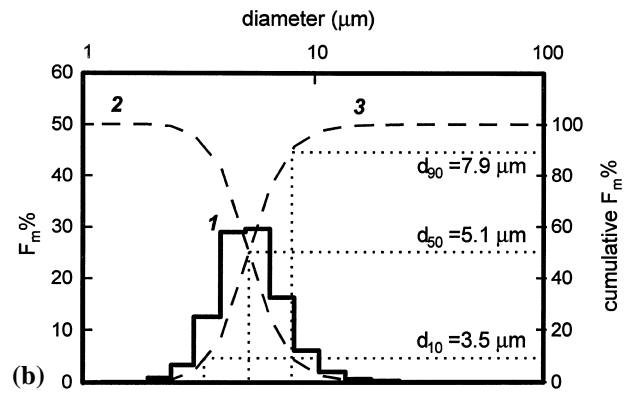
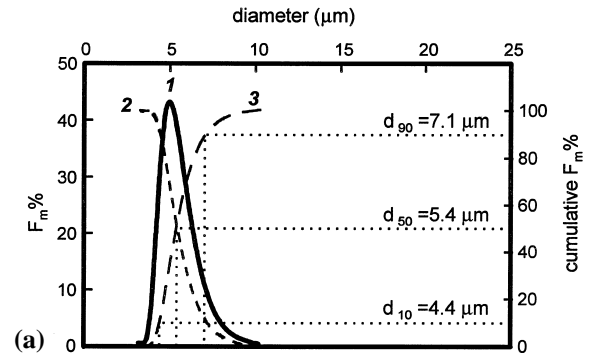


Fig. 2 Comparison between normalized, frequency functions of size (F_m %) of silica particles for HPLC packing (5 μm ; LiChrospher, Merck, Darmstadt); nominal distribution percentiles: $d_{10} = 3.7$ μm , $d_{50} = 5.0$ μm , $d_{90} = 6.8$ μm ; curve 1 (full line): F_m %; curve 2 (dashed line): F_{cum} %; curve 3 (dashed line): $100 - F_{\text{cum}}$ %. (a) GrFFF/PSD: Sample load: 100 μg ; channel: $90 \times 2 \times 0.020$ cm; mobile phase: Milli-Q water/Triton X-100, 0.1% (v/v)/ NaN_3 0.02% (w/v); flow rate: 1.010 ± 0.004 cm^3/min ; UV detection: 330 nm; experimental $\gamma = 0.70$. (b) Laser diffraction PSD (Malvern MASTERSIZER[®], Malvern Instruments Ltd., UK).

Where \bar{A} (min) is the peak area, F (cm^3/min) is the flow rate, b (cm) is the cell thickness, and K (cm^2/g) is the total extinction coefficient of the particulate sample. If the extinction coefficient can be assumed to be approximately constant, as in the case of particles whose size is at least 10 times higher than the incident wavelength [6], the detector reading, expressed as “absorbance” at the i th point (A_i), is related to the real turbidity signal from the detector (τ_i) by the equation [7]

$$A_i = Kc_i b = \frac{\tau_i}{2.303} b \quad (5)$$



where c_i (g/cm³) is the analyte concentration at the i th point of the fractogram; that is,

$$c_i = \frac{\delta m_i}{\delta V_{r,i}}$$

Therefore, the turbidity signal can be expressed as

$$\tau_i = 2.303K \frac{\delta m_i}{\delta V_{r,i}} \quad (6)$$

and the PSD expression for the frequency function, which is, in Eq. (3), just proportional to particle mass, can be transformed into a real function in mass directly from Eq. (6), thus giving [7]

$$f_{m,i} = \frac{\delta m_i}{\delta d_i} = \frac{\tau_i}{2.303K} \frac{\delta V_{r,i}}{\delta d_i} \quad (7)$$

Integration of Eq. (7) yields the cumulative distribution which gives, plotted as percent distribution, the size distribution percentiles (d_{10} , d_{50} , d_{90}). Moreover, once it is related to the injected sample amount, it gives the cumulative distribution of analyte mass as a function of size, with its asymptotic value giving the total sample recovery. Some examples of GrFFF/PSAD of silica samples used as HPLC column packing are reported in Ref. 7.

Direct Conversion of Retention to Size; Secondary Effects

As shown earlier, the direct conversion from retention time to particle diameter values [Eq. (1)] requires that the correction factor γ is predicted or experimentally estimated. It is known that, in GrFFF, γ can be influenced by either hydrodynamic or other effects as those due to the mobile phase [8] and the channel walls' nature [9]. All of these effects can influence particle size determination by GrFFF.

We have been developing an approach to the evaluation of the second-order effects, which act on GrFFF retention, and to the prediction of the correction factor γ . Among these effects, prominent are those due to hydrodynamic forces which lift the analyte particles away from the accumulation wall during their elution. GrFFF really shows a significant dependence of retention (and, thus, of the parameter γ) on the flow rate: The higher the flow rate, the higher the lift and, therefore, the lower the retention. In order to evaluate particle lift and, thus, particle retention, the semiempirical model given by Williams et al. has been applied [10–12]. This model is known to predict particle elevation from the accumulation wall in sedimentation field-flow fractionation (SdFFF), of which GrFFF it is

Particle Size Determination by Gravitational FFF

just a subset, as noted earlier. A description of the hydrodynamic and other secondary effects on GrFFF retention is far above the introductory nature of this entry. However, just to introduce the reader to the possibility of obtaining a direct conversion of retention to size by predicting γ , the above-mentioned model can be used for relating retention volume to particle mean elevation during elution as follows [10]:

$$V_{r,i} = V_0 \left[6f\left(\frac{2\delta}{d_i}\right) \frac{x_i}{w} \left(1 - \frac{x_i}{w}\right) \right]^{-1} \quad (8)$$

where x_i (cm) is the distance of the center of the particles from the accumulation wall ($x_i = \delta + d_i/2$) and $f(2\delta/d_i)$ is an empirical function. It was shown that under optimized experimental conditions, in a properly designed GrFFF system, a balance between secondary effects of forces other than hydrodynamic forces can give negligible effects [9]. In this way, particle elevation is predictable. In this case, also, the value of γ can be estimated, thus allowing for the direct conversion of retention time to analyte size without previous calibrations (*standardless*). This possibility of calculating γ is a task still in progress and it will open more promising uses of GrFFF for dimensional analysis of suspended particulate matter, because PSD can be obtained in the “single-run” mode (i.e., without previous calibration). This could be a significant enhancement in the future evolution of GrFFF/PSD. In fact, in the GrFFF/PSD example in Fig. 2a, the conversion from retention to size was performed only by means of an experimental evaluation of the parameter γ , with a calibration plot formerly obtained with standards [3].

Acknowledgments

Giancarlo Torsi, Dora Melucci, Andrea Zattoni, and Gabriele Berardi of the Department of Chemistry “G. Ciamician,” Bologna, Italy, are duly acknowledged.

References

1. H. G. Barth (ed.), *Modern Methods of Particle Size Analysis*, John Wiley & Sons, New York, 1984.
2. J. C. Giddings, *Science* 260: 1456 (1993).
3. P. Reschiglian and G. Torsi, *Chromatographia* 40: 467 (1995).
4. J. Pazourek and J. Chmelík, *J. Microcol. Separ.* 9: 611 (1997).
5. A. Bernard, B. Paulet, V. Colin, and Ph. J. P. Cardot, *Trends Anal. Chem.* 14: 266 (1995).
6. P. Reschiglian, D. Melucci, and G. Torsi, *Chromatographia* 44: 172 (1997).



7. P. Reschiglian, D. Melucci, A. Zattoni, and G. Torsi, *J. Microcol. Separ.* 9: 545 (1997).
8. P. Reschiglian, D. Melucci, and G. Torsi, *J. Chromatogr. A* 740: 245 (1996).
9. D. Melucci, G. Gianni, A. Torsi, A. Zattoni, and P. Reschiglian, *J. Liquid Chromatogr. Related Technol.* 20: 2615 (1997).
10. P. S. Williams, T. Koch, and J. C. Giddings, *Chem. Eng. Commun.* 111: 121 (1992).
11. P. S. Williams, S. Lee, and J. C. Giddings, *Chem. Eng. Commun.* 130: 143 (1994).
12. P. S. Williams, M. H. Moon, Y. Xu, and J. C. Giddings, *Chem. Eng. Sci.* 51: 4477 (1996).



Peak Identification with a Diode Array Detector

Ioannis N. Papadoyannis

H. G. Gika

Aristotle University of Thessaloniki, Thessaloniki, Greece

INTRODUCTION

The diode array detector (DAD), which arose from the analyst's needs to reduce data observations times in chromatography, has become a powerful tool in a research environment and in the quality assurance laboratory. Diode array adds a new dimension of analytical capability to liquid chromatography because it allows qualitative information to be obtained beyond simple identification by retention time.

Among the three advantages that diode array detector provides to the high-performance liquid chromatography (HPLC) analyst, peak identification is the one that allows the identification of unknown constituents in a sample whose matrix is complex.

PEAK IDENTIFICATION

The method-development laboratory is often set with a task of identifying unknown constituents in a complex sample. The identity or quantity of analytes is not well defined at this stage. Complicated sample-preparation steps and multiple HPLC analyses may be required to ascertain the nature of a sample. The diode array detector simplifies this process. In the case that more than 15 different peaks have been separated in a analysis of a multicomponent sample of known origin; more than a full day's work might be required just to establish the retention times of the unknowns with the use of a standard absorbance detector. A number of long-run HPLC analyses would have to be made with pure standards so that retention time correlations could be determined. This necessity is accomplished by the DAD's advantage of acquiring data in both the time and spectral domain.

The DAD has brought compound identification to HPLC. Previously, mass spectrometry was the sole domain in peak identification for gas or liquid chromatography (GC-MS or LC-MS). This can now be achieved as part of the HPLC analysis, and at a lower cost, because there is the ability to use an HPLC-DAD system as a scouting technique to check the possible identity of an unknown sample.

HPLC techniques often use absolute or relative retention times to identify compounds. Under well-defined

conditions, UV/visible spectra are useful data for the confirmation of peak identity. Thus, it is possible to qualify the compounds present through the use of spectra. This mode of identification by spectral similarity is also useful when retention times shift because of changing chromatography for similar sample runs.

However, spectral identity is a necessary but not a sufficient condition for compound identification. If the instrument parameters that determine how spectra are acquired are matched suitably, the spectral match of an unknown to a known spectrum can be used as strong indication of compound similarity or confirmation of identity. In a chromatogram, the retention time of a given peak offers an obvious means of preselection of candidate spectra through the application of a retention time window. All spectra from the set of possible candidates that fall in the window are compared to the unknown spectrum. The candidate with the best match factor above a certain threshold level is then used to identify the compound for the peak. Another possibility is to weigh both the match factor and the similarity in retention times and use the combined information for identification.

Peak identification is done by comparing a spectrum from an unknown peak to a spectrum from a user-created library. The best match of spectra is the closest to the correct identification. The comparison between the reference spectrum and the unknown spectrum is realized by the appropriate software.

With the DAD, spectra can be acquired automatically for each peak during the analysis. The spectra can be compared with those stored in a library, either interactively on the computer display or mathematically with the help of microprocessors. In Fig. 1, the spectral library matching is illustrated. The standard sample is analyzed and the spectrum of the target compound is registered in the library. The spectrum of the unknown sample is compared to standard spectra in the library.

SPECTRAL LIBRARIES

The UV spectra employed in HPLC can change for the same compound, depending on the mobile-phase environment at the time of elution. To have any success in



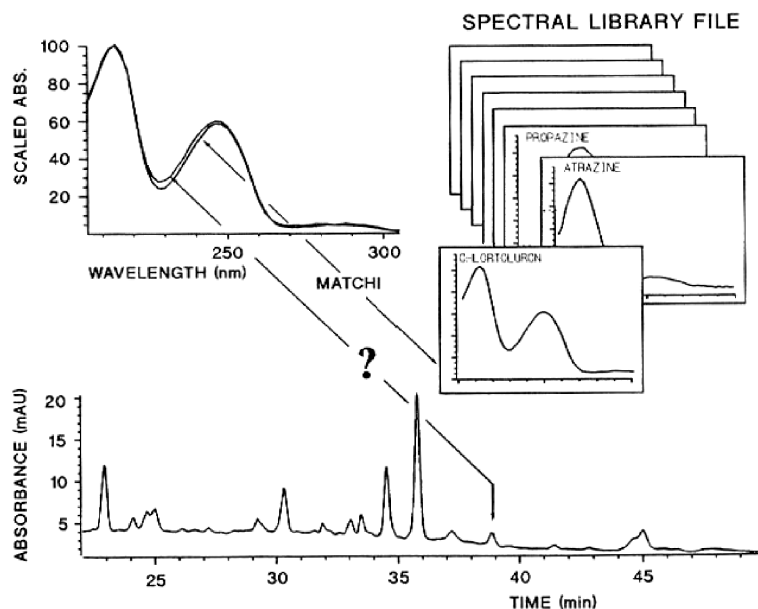


Fig. 1 Peak identification by spectral matching.

applying similar approaches to compound identification, the separation system used to acquire spectra for standards and unknown analytes needs to be the same and well defined. Several examples taken from the recent literature make a strong case for the necessity of clearly defining the column and the mobile phase used.

Two primary approaches to the use of spectral libraries in HPLC can be described:

1. In the forward library search, an attempt is made to identify each compound in an unknown sample from a large library of standard compounds, previously recorded under defined chromatographic conditions. Each compound spectrum from the sample, analyzed under the same conditions, is searched against the library for identification. In case this is not possible, it may be classified by comparison with similar compounds from the library. Because the unknown sample may contain compounds that are not present in the library, it is desirable to obtain, at least, a list of likely matches for each unknown. In some instances, preselection of spectra is employed, based on the retention time indexing or on rough comparison of spectral features such as number and position of the primary absorbance maxima. This is done primarily to reduce the time needed to search the full compound library. In HPLC, it is found mainly in toxicological screening and drug-testing applications.
2. For reverse library searching, a limited library of standard compounds, all of which are expected to be

present in the sample, is searched against the unknown spectrum in the current analysis. This search mode is an expansion of normal calibration procedures used currently in HPLC. Each peak of interest in a sample should be characterized through analysis of a standard. The spectral library, consequently, contains spectra for a limited number of compounds. In this case, we try to find the best match for each standard spectrum in the library by searching against all compound spectra identified in the current analysis. The question is to find all or some of the standard compounds in the unknown sample in a one-to-one assignment.

SPECTRAL MATCHING

Spectral matching can be defined as the process of comparing two spectra with the intention of determining their similarity. Once spectra could be digitized and the digital information manipulated mathematically, it became possible to base the comparison on a numeric evaluation of the digital data. Thus, in the modern definition, spectral matching is a procedure whereby the digital information available for a pair of spectra, each typically consisting of numerous discrete data points, is reduced to a single number indicative of the similarity between the two spectra. Ideally, this reduction in the number of data points does not involve any reduction in

the information contained in the relationship of two spectra to each other. More specifically, most matching procedures presently employed are based on a point-by-point comparison of the two spectra in question to establish the presence or absence of significant differences.

Generally, there are three ways of performing spectral comparison: 1) overlay of spectra and visual determination, which is a subjective test; 2) evaluation of spectral differences between the reference spectrum and the unknown spectrum using the appropriate software. Larger differences suggest that the unknown is a different compound than the reference or that it is a mixture; 3) use of sophisticated software to calculate a numerical value that mathematically defines the closeness of the match.

Following are descriptions of the most common mathematical approaches used through spectral matching software.

Vectorial Approach to Spectral Matching

One approach that facilitates the definition and comparison of various matching procedures and eliminates the confusion associated with normalization is to view each spectrum as a vector in N -dimensional space. A spectrum data is considered as the group of the absorbance at each wavelength and it is represented with the vector.

$$(a(\lambda_1), (a(\lambda_2), a(\lambda_3), \dots, a(\lambda_n))$$

where $a(\lambda_i)$ is the absorbance at the wavelength λ_i .

One spectrum corresponds to one vector:

$$\vec{S} = (a(\lambda_1), (a(\lambda_2), a(\lambda_3), \dots, a(\lambda_n))$$

If there are two spectra, spectrum S_1 corresponds to \vec{S}_1 and spectrum S_2 corresponds to \vec{S}_2 .

$$\vec{S}_1 = (a_1(\lambda_1), (a_1(\lambda_2), a_1(\lambda_3), \dots, a_1(\lambda_n))$$

$$\vec{S}_2 = (a_2(\lambda_1), (a_2(\lambda_2), a_2(\lambda_3), \dots, a_2(\lambda_n))$$

These vectors are simplified to a two-dimensional vector as shown in Fig. 2. The matching procedure can then be based either on determining the angle between the two vectors or on finding the distance between their tops. The first approach would seem to be independent of the relative magnitude of \vec{S}_1 and \vec{S}_2 ; the later definition implies normalization of \vec{S}_1 and \vec{S}_2 prior to the calculation of the distance.

If these spectra come from the same compound, the ratio between corresponding elements in S_1 and S_2 is constant and these vectors have the same direction. In that case, the angle θ in Fig. 2 becomes zero. As general rule,

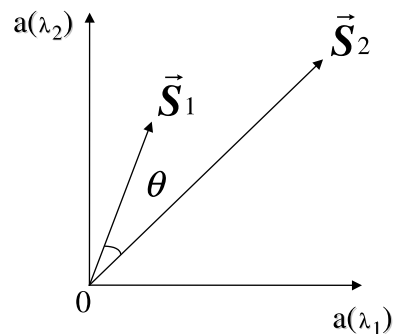


Fig. 2 Vectorial definitions of spectral matching.

the more the angle approaches zero, the greater the similarity between the two spectra. The following equation describes the degree to which the two spectra correspond [similarity index (SI)] based on the cosine of the angle of their component vectors formed at each point of measurement:

$$SI = \frac{\vec{S}_1 \cdot \vec{S}_2}{|\vec{S}_1| \cdot |\vec{S}_2|} = \cos \theta \quad (1)$$

or

$$SI = \frac{\sum_{\lambda_i} a_1(\lambda_i) \cdot a_2(\lambda_i)}{\sqrt{\sum_{\lambda_i} a_1(\lambda_i)^2} \cdot \sqrt{\sum_{\lambda_i} a_2(\lambda_i)^2}} \quad (2)$$

As the SI approaches zero, the pattern matching becomes poor (the angle θ between the vectors approaches 90°) and, conversely, as SI approaches unity, the pattern approaches a perfect match.

For easier manipulation, especially in the case of very similar spectra where differences may exist only in the third or fourth decimal place, the spectral match factor is often multiplied by 1000.

Another common measure of spectral similarity is the correlation coefficient r that is defined as:

$$r = \frac{\sum[(S_{1i} - \bar{S}_1)(S_{2i} - \bar{S}_2)]}{\sqrt{\sum(S_{1i} - \bar{S}_1)^2} \sqrt{\sum(S_{2i} - \bar{S}_2)^2}} \quad (3)$$

It expresses the correlation between paired absorbance values for the two spectra at each discrete wavelength interval. If we shift out two spectra S_1 and S_2 along the absorbance axis in a way that the mean absorbance for both spectra is zero, a process that is referred to as "mean centering," then \bar{S}_1 and \bar{S}_2 will both be zero.

Mean centering eliminates any spectral difference because of a fixed baseline offset that might be present in an individual spectrum. Eq. 3 further shows that the

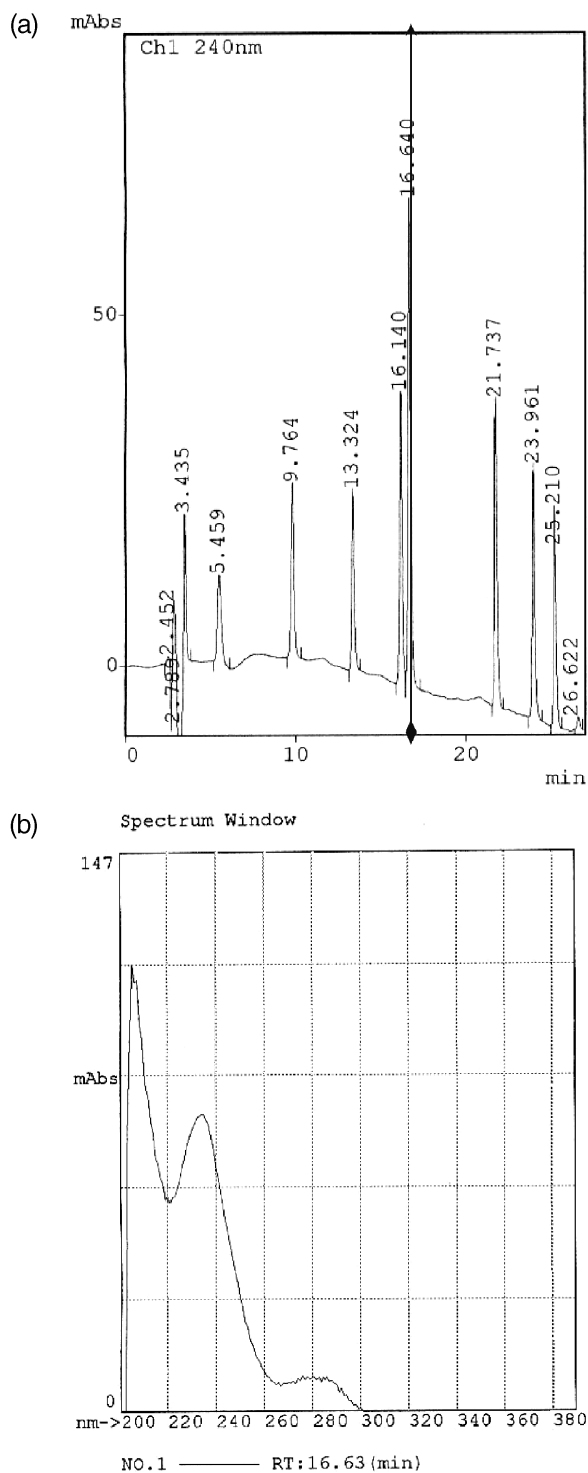
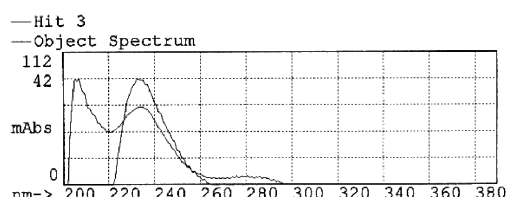
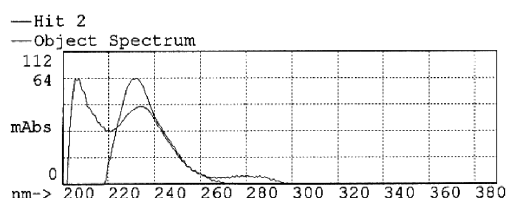
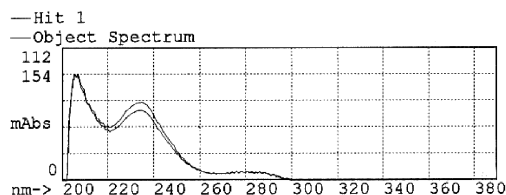


Fig. 3 (a) HPLC chromatogram of standard solution containing tyrosine, thyronine, and some of their iodo derivatives. Detection was performed with a Shimadzu SPD-M6A photodiode array detector at 240 nm. The spectrum (b) of the selected peak (thyronine) is acquired automatically and stored in the UV spectral library for comparison in further identification procedures. (c) Normalized spectral comparison and report results of chromatogram's thyronine peak with the best matching library spectrum. The similarity index indicates the closest match.

(c) Library Search Results



Library Name : HORMON.SLB
Object Spectrum : RT:16.61(min)
Max(nm) : 205, 207, 235, 220, 276

* Hit 1
Name : Thyr
Similarity : 0.9875
Threshold : 1.0000
Max(nm) : 205, 235, 220, 278, 276

* Hit 2
Name : T2
Similarity : 0.6800
Threshold : 1.0000
Max(nm) : 233, 258, 262, 266, 268

* Hit 3
Name : T3
Similarity : 0.4958
Threshold : 1.0000
Max(nm) : 233, 235, 237, 253, 255

Fig. 3 (Continued)

normalization of the spectral vectors to unit length is equivalent, in statistical terms, to the scaling of each spectrum by its standard deviation.

Measures of Dissimilarity

Reliant on the ultimate relationship of geometry:

$$\cos^2 + \sin^2 = 1, \quad (4)$$

we can define a factor of dissimilarity of spectra. Thus, the sine squared multiplied by 1000 could serve as an indicator of spectral dissimilarity.

Another possible measure of spectral dissimilarity, the Euclidean distance e between the tips of the two vectors, as shown in Fig. 2, can also be related to sine and cosine:

$$\begin{aligned} e &= S_1 - S_2 \\ &= \sqrt{\sin^2(S_1 - S_2) + [1 - \cos(S_1, S_2)]^2} \end{aligned} \quad (5)$$

$$e = \sqrt{\sin^2(S_1 - S_2) + 1 - 2\cos(S_1 - S_2) + \cos^2(S_1 - S_2)} \quad (6)$$

and upon the Eq. 4

$$e = \sqrt{2 - 2 \cos(S_1, S_2)} \quad (7)$$

$$e = \sqrt{1 - |\cos(S_1, S_2)|} \quad (8)$$

All the mathematical approaches mentioned above differ in the degree of change observed for spectral differences, most noticeably for angles below 15° . Between 0° and 10° , \sin^2 , \cos^2 , and cosine do not change very much, making it more difficult to differentiate among spectra with strong similarities. The rate of change varies, complicating the task of assessing the variability of the match score for different degrees of dissimilarity.

Normalization of Spectra

There are numerous procedures for the normalization of spectra, other than the one based on unit vector length. They all lead to the same result, if S_1 and S_2 differ only in concentration but there are essential differences in the case where S_1 and S_2 differ significantly.

The general normalization procedure for a given spectrum S follows the rule: $\langle S \rangle = NS$, where $\langle S \rangle$ corresponds



to the normalized spectrum S and N is the appropriate normalization factor. Some of the more commonly used normalization procedures are presented below.

For vector normalization, N is defined as $N = 1/\sqrt{\sum S_i^2}$. Further, normalization to unit area can be achieved as $N = 1/\sum |S_i|$.

Vector normalization and area normalization are fairly resistant to noise because all data points are included and small random fluctuations, due to noise, tend to cancel each other.

There are also two normalization procedures that are based on the forcing of the absorbance at a specific wavelength to a specific value V . The wavelength used can be either the same for both spectra, $N = S_\lambda/V$ or the wavelength of maximum absorbance can be found over a specific wavelength range for each spectrum, $N = S_{\max}/V$. In both cases, normalization is much more dependent on noise because a single absorbance value controls the normalization factor N .

FACTORS AFFECTING SPECTRAL COMPARISON

How to set a threshold level for the match factor to positively identify a compound spectrum is strongly dependent on a variety of factors. Below are mentioned those that play a major role in the success of the spectral matching procedure and are important tools in optimizing spectral comparison and threshold setting.

Wavelength Accuracy and Precision

Depending on the shape of the spectrum, small errors on the wavelength axis could translate into substantial errors on the absorbance axis and thus lead to false scores.

Detector Response Function

Initially, the optical resolution achieved by the spectrometer is governed by the size and shape of the entrance slit and determines the overall preservation of spectral fine structure. Secondly, the diode resolution obtained from the diode array is based on the geometry of the individual diodes, their spacing, and any grouping of diodes applied during processing of spectral data. Finally, stray light in the detector can cause deviations from Beer's law such that at low light throughput absorbance no longer changes linearly with concentration. Thus, depending on the analyte's concentration, spectra will be distorted at higher absorbance values, resulting in an

overall different shape when compared to a spectrum at lower concentrations.

Instrument Noise

The dissimilarity score for two identical spectra will never reach zero because of the presence of noise in the detector that cannot be compensated. There will always be some residual dissimilarity, which imposes a practical limit on the definition of a match threshold. The noise level of a given spectrum at a specific analyte concentration depends on the spectrometer, the characteristics of the diode array, and the scan speed of the detector, the lamp, and detector electronics.

Interference from Spectral Background

In most LC analyses, the spectra recorded contain some background absorption caused by either a change in the elution solvent, if a gradient system is employed, or by instabilities inherent in the instrumentation, or both. Therefore, some kind of background correction is typically indicated whenever spectra are compared, either for the purpose of determining whether a chromatographic peak contains an impurity or for the process of compound identification.

Selection of Wavelength Range Employed for Matching

The selection of the appropriate wavelength determines the selectivity of spectral comparisons because instrument noise, which is the sum of all electronic and optical imperfections, will certainly favor some wavelength regions over others.

Processing of Spectral Data Prior to Matching

Prior to calculation of a dissimilarity score, spectra can be treated mathematically, either to improve their noise characteristics or to enhance differences for very similar spectra. One mode of pretreatment, from classical spectroscopy, involves the use of derivatives, especially of the second and higher derivatives, to enhance the fine structure of absorbance bands. Smoothing of spectral data to reduce noise is another pretreatment mode that could potentially improve the selectivity of spectral matching.

Impurities

The spectrum of the unknown compound to be identified should not contain any spectral impurities as caused by

coeluting components. If a spectrum is known to contain a spectral impurity, it should be corrected for this impurity before the comparison with the standard spectra. Corrections for coeluting impurities are very difficult. If the impurity does not coelute completely, identification may still be possible, depending on the concentration and elution time of the impurity, relative to the main peak.

EXAMPLE OF APPLICATION

The identification of an unknown peak in a chromatographic analysis, performed by the Shimadzu SPD-M6A UV/Vis photodiode array detector, combined with data acquisition software Class M10A, is presented in Fig. 3a–c. The spectrum file of the selected peak is compared against reference spectra in a user-built library. Data processing through the mathematical approach mentioned above defines the best match. The numerical value of the SI indicates the spectrum of thyronine as the better match because, in this case, it is close to unity. The comparison is also made by visual evaluation through the overlaid spectra. The created spectral sublibrary consists of several iodothyronine and iodotyrosine spectra, which are those of interest in this application. Thus, the chromatographic peak, assuming it belongs to thyronine, can be identified among other related compounds by its UV spectrum, allowing qualitative analyses that are more accurate.

CONCLUSION

The mode of peak identification that the diode array detector provides allows identification of unknown peaks, not only by retention time but also by their UV spectra. The UV spectrum is very reproducible and its full shape is much more compound-specific than is generally assumed. It is a powerful tool that, beyond other applications, it can also be used as a scouting technique to find out the possible identity of an unknown sample. However, spectral identity is a necessary but not a sufficient precondition for compound identification. The information that is acquired by the comparison of an unknown and a known spectrum can be used as strong indication of compound similarity or confirmation of identity. Combinatorial estimation of retention time and spectral comparison results will give us a more definite idea.

RECOMMENDED READING

- http://hplc.chem.shu.edu/new/HPLC_book/detectors/det_uvda.htm.
- <http://www.chem.agilent.com/cag/peak/peak3-99/article01.html>.
- http://www.Waters.com/waters_website/pittcon98/p996.htm.
- Huber, L.; George, S.A. *Diode Array Detection in HPLC*; Chromatographic Science Series, Marcel Dekker, Inc.: New York; 1993; Vol. 62.
- LC GC Int. **1994**, 7 (11), 652–660. Nov.
- SPDM6A Photodiode Array Detector, Instruction Manual*; Shimadzu: Columbia, MD, 1989.



Peak Purity Determination with a Diode Array Detector

I. N. Papadoyannis

H. G. Gika

Aristotle University of Thessaloniki, Thessaloniki, Greece

INTRODUCTION

Peak purity analysis is an evaluation technique for detecting the presence of coeluting impurities in high-performance liquid chromatography (HPLC) data. Running a peak purity check prior to analytical quantitation helps to ensure accuracy. In the development of analytical methods, peak purity analysis can reveal the presence of contamination during standardization and, by doing so, can prevent the subsequent generation of false analytical data.

Peak purity analysis is also a useful addition to routine quality control procedures, especially in the analysis of pharmaceuticals and food products, for which contamination and quality of results are critical.

PEAK PURITY ANALYSIS WITH DIODE ARRAY DETECTOR

Peak purity analysis is designed to detect the presence of an impurity that is coeluting with the analyte peak. For impurity detection with a single-wavelength UV/Vis detector, one must see a shoulder, valley, or excessive tailing to suspect the presence of an impurity. The absence of these features on the chromatographic peak is not a foolproof assurance of peak purity. The impurity may not be seen simply because the chromatographic resolution is low (Fig. 1). A photodiode array detector can provide additional information by using the acquisition of UV/Vis spectra to determine peak purity.

A proper peak purity determination requires access to a significant portion of the eluting compound's spectrum without interrupting the separation. For this reason, peak purity analysis is performed using a multisignal UV/Vis diode array spectrophotometer as the HPLC detector. Unlike the diode array detector (DAD), the traditional variable-wavelength detector examines only a single wavelength of the sample spectrum, providing insufficient information for peak purity determination. The diode array spectrometer illuminates the sample with the entire spectrum of wavelengths emitted by the light source. Light transmitted by the sample is then broken into its

component wavelengths by a diffraction grating and directed to a bank of photodiodes, each of which is dedicated to measure a narrow band of the spectrum. As no mechanical scanning is required, spectral acquisition can be accomplished in as little as 12 msec, well within the precision limits for HPLC peak elution. The rapid spectral acquisition makes it possible to perform peak purity determinations using selected multiple spectra as inputs. Therefore, the absence of any mechanical action in the acquisition of spectra enhances the reproducibility and the accuracy of the peak purity analysis. For coeluting peaks, a DAD makes it possible to differentiate both compounds, even when their spectral absorption overlaps the entire range of captured wavelength data.^[1,2]

DIFFICULTIES OF PEAK PURITY CONFIRMATION

Before the quantitative information contained in a chromatographic peak can be used, the purity of the peak should be confirmed. Only after we are sure that no coeluting impurity was present, which could have contributed to the peak response, can we convert the peak's area or height into quantitative information based on the equivalent response of a pure standard. This peak purity analysis can be based on the comparison of the various spectra recorded during the elution of the peak. If the peak is pure, then, apart from concentration differences, the spectra taken at several points during a peak's elution should all be identical and the match scores obtained should be very close to the perfect match scores. If significant deviations are encountered, this can be seen as an indication of impurity.

Unfortunately, the inverse is not necessarily true. If the spectra are identical, based on the algorithm used for comparison, the peak can still be impure for one or several of three possible reasons:

- 1) The impurity is present at a much lower concentration than the main compound and is not detectable.
- 2) The impurity has the same or a very similar spectrum, compared to the main compound.



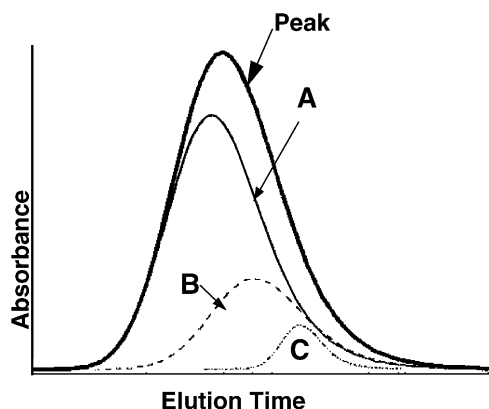


Fig. 1 Coelution of three compounds A, B, and C in the chromatographic peak. No shoulders, valleys, or excessive tailing are seen.

- 3) The impurity exhibits the same peak profile as does the main compound; that is, it completely coelutes with the main peak, across the entire peak.

One of the most important aspects of peak purity analysis that is often overlooked is the fact that any peak purity algorithm can only confirm the presence of impurities, but can never unambiguously prove that a peak is pure.

HPLC SIGNAL OVERLAY FOR PURITY ANALYSIS

One way of uncovering contributions because of impurities in an HPLC peak is to overlay peak profiles acquired at several wavelengths. As two different com-

pounds are unlikely to exhibit identical absorption over multiple wavelengths, the presence of an impurity is revealed by the deviation of the profiles. To compensate for the differences in spectral intensity at different wavelengths, the signals to be compared are first normalized to the maximum absorbance value or to equal areas. Peaks free of impurities exhibit good overlap, but the presence of an impurity is indicated by a shift in the retention time maximum at different wavelengths (Fig. 2).

The signal overlay method is not considered to be very sensitive, and is highly dependent on the resolution of analyte and impurity peaks. If care is taken to correct for solvent background and if the signals are normalized to the highest absorbance value in the time range plotted, the resulting ratiogram can provide conclusive information. It is usually recommended as an additional qualifier in conjunction with other peak purity analysis methods.

In addition to signal overlap, the ratios of signals acquired at different wavelengths can be calculated and plotted. The resulting ratiograms are good *indicators* of peak purity. Any significant distortion of the ratiogram's ideally rectangular form is an indication of differential absorption and the presence of an impurity (Fig. 3). Peak purity analysis based on signals is generally limited to instances for which the spectra of both analytes and impurities are well known, a requirement for selecting the wavelengths best suited for comparison. Typical applications for this information would be routine evaluations such as quality control checks.

PEAK PURITY USING SPECTRAL DATA

Comparison of spectra is the most popular method of peak purity determination. The primary advantage of this

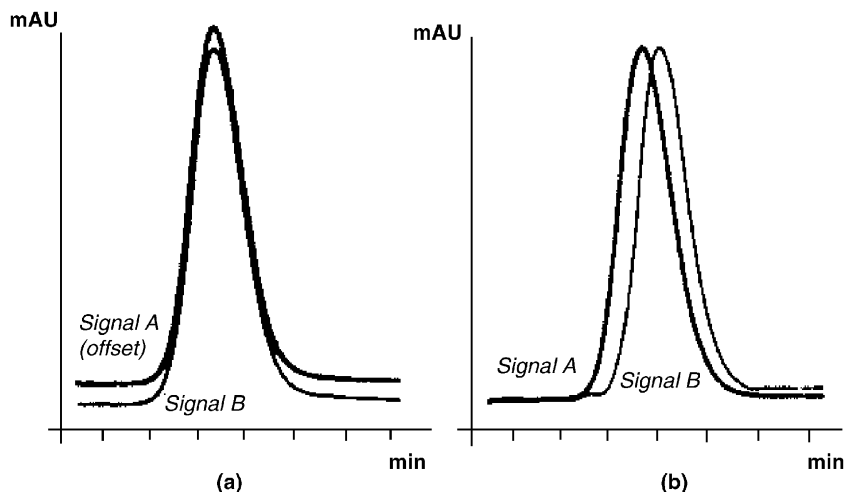


Fig. 2 Normalized signals for (a) pure and (b) impure peaks.

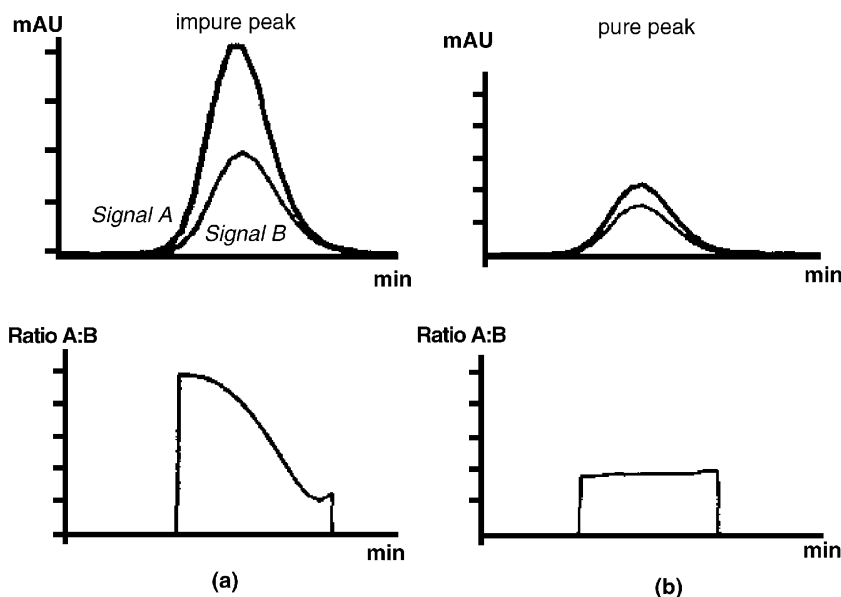


Fig. 3 Ratiograms taken from (a) an impure and (b) a pure peak.

approach is that prior knowledge of component spectra is not required. However, information derived using these techniques is not sufficient for determining the kind, number, and level of impurities present.

A number of selection criteria and data manipulation techniques can be applied prior to analysis to improve the quality of the analytical result. These include setting different spectrum acquisition modes, background corrections, normalization, and threshold settings.

Selection of Spectra for Comparison

Peak purity analysis software allows users to sample spectra at equidistant points across an HPLC peak. In general, the poorer the resolution between potentially coeluting peaks is, the more desirable it is to use greater numbers of data points to detect the impurity. Traditionally, spectra have been sampled upslope, at the apex, and downslope of the eluted peak. This selection pattern may overlook the presence of impurities near the peak extremities. However, acquisition of many spectra may increase calculation and display time without adding significant information.

Background Correction

A peak should not be labeled as impure because of spectral background, or because of tailing interference from a neighboring peak. Both effects can be corrected for by suitable background correction, with the under-

standing that spectral subtraction increases the noise of a spectrum and, thereby, lowers the ideal match factor.

Whether background correction needs to be applied depends on the separation system employed. If the instrument is balanced properly, then, for isocratic separations, the solvent background will be eliminated by the built-in automatic subtraction of the solvent spectrum, as present at the beginning of the analysis, from all recorded spectra. For gradient separations, background corrections will have to be applied after the analysis.

Different methods for correction are possible; the choice of method depends on the availability of spectra resulting from specific modes of spectral storage for different instruments. Ideally, all spectra are retained for an analysis, but because of processing and storage constraints, many instruments offer a mode of acquisition where spectra are stored only during the elution of a peak. Peak spectra can be limited to just the apex spectrum, or to a number of additional spectra across the peak, most commonly acquired at the baseline and the inflection points. If only apex spectra are available, no background correction is possible. For all other cases, the quality of background correction will depend on the availability of suitable baseline spectra.

In the simplest case, a single baseline spectrum is subtracted from all analyte spectra. This will work only for the elimination of constant spectral impurities. If several baseline spectra are available, linear combinations of those spectra can be used to generate a synthetic background spectrum at any point in the chromatogram. Ideally, the two spectra should be close to the beginning and the end of the peak being analyzed. If this is not



possible because of incomplete separation of the peak from its neighbors, baseline spectra could be taken from the beginning and the end of a peak group.

If only slope and apex spectra are available, background correction is still possible, in a limited fashion, by subtracting the apex spectrum from the two slope spectra. For isocratic separations or gradient with slow changes in solvent background, this approach will produce two baseline-corrected slope spectra with a loss in signal that is equal to the difference in amplitude between slope and apex spectrum.

Spectrum Normalization

Spectra used for comparison during peak purity determination should be normalized to compensate for differences in concentration. Normalization can be based on setting equal absorbance maxima or maximum wavelength ranges, on setting equal area of spectra or spectral region of interest, or on using a matching algorithm that minimizes area differences by shifting and scaling spectra.

Absorbance Threshold

Setting an absorbance threshold improves the accuracy of spectral comparison by screening out spectra near the signal baseline. These spectra tend to have a relatively high degree of noise, which adversely affects the accuracy of both normalization and subsequent spectrum matching.

Spectrum Overlay

After spectra are acquired and processed, they are overlaid for visual evaluation (Fig. 4). Although significant deviations between the profiles can indicate the presence of

an impurity, the converse is not necessarily true, and spectral profiles that match quite well may still mask the presence of an impurity. Factors that may contribute to nondetection of impurity include large concentration differences between analyte and impurity and either highly similar spectral profiles or identical chromatographic peak profiles and retention times for both analyte and impurity. As a rule of thumb, impurity concentrations in the 0.1–1% range may be detected when the spectra are dissimilar. However, if the spectra of the different components are highly similar and the HPLC peaks are not well resolved, the impurity detection limit is on the order of 5%.

ADVANCED TECHNIQUES

Simple peak purity analysis is relatively accurate when the impurity is present at significant concentration levels but, as the level of impurity diminishes, its impact on the target analyte spectrum becomes subtler and may require more sophisticated techniques. For this, statistical software routines are available for automated spectral comparisons. In these cases, peak purity determination and analysis of spectral differences are achieved using vector analysis algorithms. The more similar the spectra are, the closer the value is to 0.0°; the more spectrally different they are, the larger the value. All the spectral data points across the peak are analyzed; the data are converted into vectors, compared, and graphically plotted so that the results can be visualized. These software routines provide both numerical results and graphical representations such as similarity and threshold curves.

Similarity curves are plots of retention times versus similarity factors computed by comparing spectra across an eluted peak with one or more selected spectra.

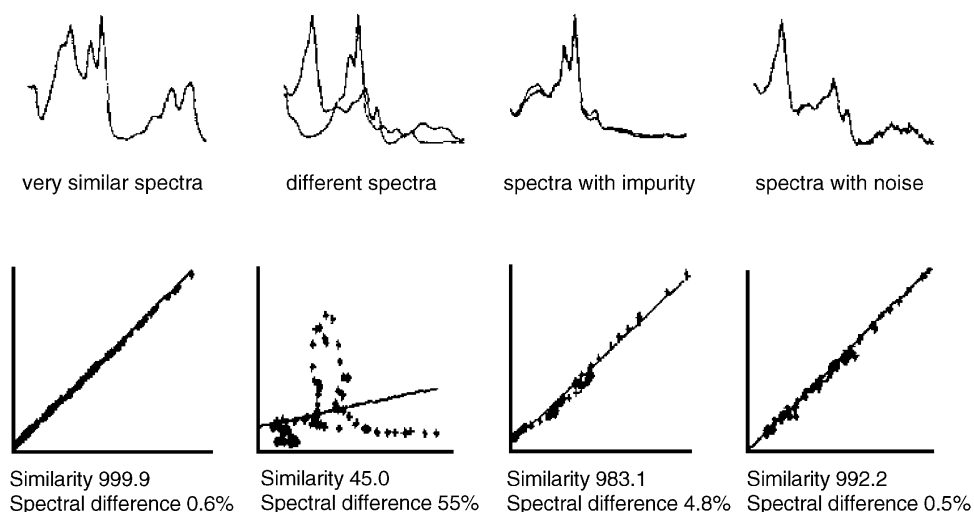


Fig. 4 Graphical display of similarity factors for different pairs of normalized spectra.

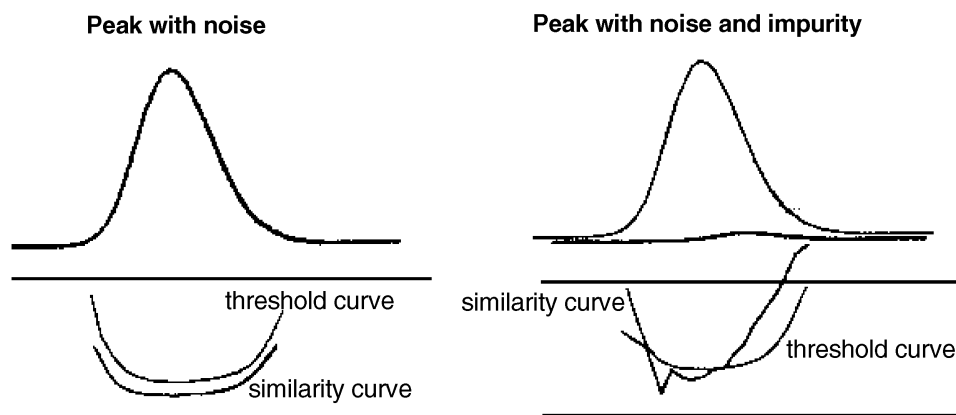


Fig. 5 Effect of impurity and noise on similarity and threshold curves of (a) a peak without impurity but with noise, and (b) a peak with impurity and noise.

Similarity curves improve the sensitivity of detecting impurities because they extract and highlight subtle impurity-generated anomalies in an analyte spectrum that might otherwise go unnoticed.

The threshold curve is a plot of retention time versus a similarity factor threshold, below which the presence of an impurity cannot be distinguished from spectral noise. The threshold trace may be computed automatically from the standard deviation of a number of user-selected pure noise spectra. Alternatively, the threshold may be set at a fixed value. Similarity and threshold curves tend to rise at the extremities of the eluted peak, even when no impurity is present. As signal strength decreases, a larger proportion of the spectral response is caused by noise. If an impurity is present at a detectable concentration, the similarity curve will intersect the threshold (Fig. 5).

Peak purity software incorporating routines for data acquisition and reduction, extraction and comparison of spectra, and display of analytical results can be utilized in either an interactive or automated fashion. A desired sequence of operations can be recorded in a peak purity analysis method file and can run unattended after input parameters are selected. As the quality of the determination is highly dependent on the preanalysis data treatment, results should be inspected visually to verify that peaks are properly baseline-separated and correctly integrated.

The evaluation of a peak purity analysis is assisted by a well-organized visual display of the output of various peak purity analysis techniques.^[3-5]

CONCLUSION

Peak purity analysis is designed to detect the presence of an impurity that is coeluting with the analyte peak. A DAD, using the almost instantaneous acquisition of a considerable portion of the UV/Vis spectrum of eluted peak components, can give accurate information to determine peak purity. The spectral uniqueness of each compound is used to indicate when there are two or more components present in the peak, to identify peaks, and to assess purity.

Peak purity analysis is very useful in chromatographic method development, to confirm that all components have been chromatographically separated, and in quality control, to warn the analyst that an unexpected coeluting impurity has appeared.

REFERENCES

1. Huber, L.; George, S.A. *Diode Array Detection in HPLC*; Marcel Dekker, Inc.: New York, 1993.
2. Kohn, A. The application of peak purity analysis in liquid chromatography and capillary electrophoresis. *LC-GC* **November 1994**, 7 (11).
3. Shimadzu SPDM6A Photodiode Array Detector, Instruction Manual.
4. <http://www.gcmsservice.com/879.htm>.
5. http://www.forumsci.co.il/HPLC/PEAK_PUR_web.pdf.

Peak Skimming for Overlapping Peaks

Wes Schafer

Merck Research Laboratories, Rahway, New Jersey, U.S.A.

Introduction

Any discussion of quantitating overlapped peaks should be prefaced by stating that baseline resolution of peaks is the only means of absolutely assuring the accuracy of their integration. All deconvolution methods involve assumptions that can affect accuracy. These methods are particularly inaccurate in cases of small peaks eluting on the tails of much larger peaks where percent errors are measured by two to three orders of magnitude [1,2]. In any case, the accuracy of all baseline methods generally increases with increasing resolution between the overlapping pair of peaks.

Discussion

This discussion is confined to single-channel chromatographic analyses such as high-performance liquid chromatography (HPLC) with single-wavelength ultraviolet (UV) detection or gas chromatography with flame ionization or thermal conductivity detection. Three-dimensional (multichannel) techniques such as photodiode-array, multiwavelength detection may allow deconvolution based on component characteristics such as absorptivity at multiple wavelengths rather than peak shape. These techniques and/or the required information about the components are not always available, however, and many routine analyses are still conducted with single-channel detection because of their lower cost and relative simplicity.

In the overlap region between two unresolved chromatographic peaks, the detector response is a function of the response due the first peak and the response due to the second peak. For a single-channel detector, this is mathematically equivalent to a single equation with two unknowns, which is impossible to solve. Detection and integration schemes, in such cases, must make assumptions regarding the shapes of the chromatographic peaks in order to attribute the response in the overlap region to one peak or the other. In some cases, the assumption is based on the ease of determining the baseline and, in other cases, on theoretical models of

chromatographic peaks such as Gaussian or exponentially modified Gaussian distributions.

Chromatographic data analysis systems generally employ three methods for determining baselines in overlapping peaks: *perpendicular drop*, *linear tangential skim*, and *exponential skim* (see Fig. 1). In order to choose the most appropriate method, the analyst must understand the assumptions and weaknesses of the three methods.

The perpendicular drop method produces accurate peak areas for symmetrical overlapped peaks of similar height and width. In this case, the portion of the second peak attributed to the first peak is offset by the portion of the first peak attributed to the second peak and vice versa. For overlapped peaks of significantly different size, the perpendicular drop method always overestimates the peak area of the smaller peak as the smaller peak gains more area from the larger peak than it “loses” to the larger peak. Quantitation errors are further exacerbated in the case of a smaller peak imposed on the tail of a much larger tailing peak. This method tends to show little injection-to-injection variability because of its simplicity.

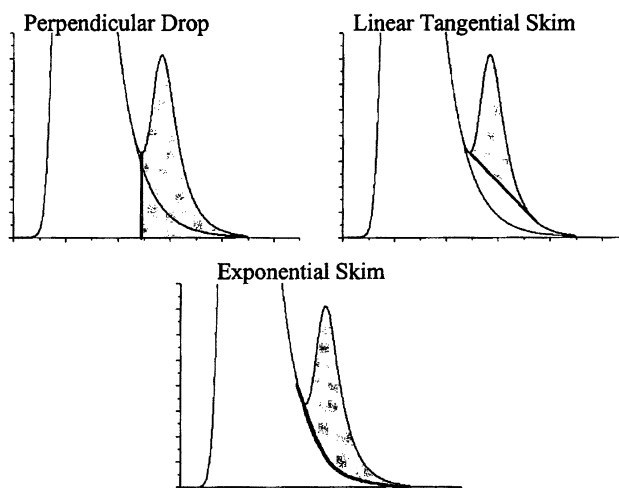


Fig. 1 Common methods for determining the baselines of overlapping peaks.



Linear tangential skimming, on the other hand, consistently underestimates the area of the smaller peak by neglecting that portion of the peak area under the tangential baseline. As seen in Fig. 1, it is easy to visually underestimate the size of a peak that is unresolved from a significantly larger one, giving the appearance that the linear tangential skim method is much more accurate than it is. The relative simplicity of this method makes it rugged as well.

Many commercial software packages offer a nonlinear exponential skimming method as well. As it has been estimated that 90% of all chromatographic peaks can be modeled by an exponentially modified Gaussian function (EMG) [3], this method should be the most accurate for tailing overlapped peaks. The algorithms for calculating such baselines are considerably more complicated, however, and the reproducibility of the technique may be problematic for some separations. The calculation of necessary parameters may limit its usefulness in extreme cases of tailing and peak width. In addition, the ability of exponential skimming to mimic symmetrical (Gaussian) peaks may also be an issue in some software. Examination of the constructed baselines is crucial in determining the proper use of this technique.

The peak area errors for the two most studied deconvolution methods (i.e., perpendicular drop and linear tangential skim) are dependent on a complex combination of resolution, relative peak width, relative peak height, and asymmetry ratio [1]. Exponential skimming assumes that the tailing of the first peak can be described by an exponential decay and that the peaks are sufficiently resolved to determine the decay parameters. Nonetheless, some broad generalizations can be made:

1. For symmetrical overlapped peaks of equal size and width, the perpendicular drop method provides accurate peak areas. Peak heights may still be overestimated.
2. In general, exponential skimming should be used when the first peak tails significantly or when the peak widths are significantly different. Care should be given that the area calculated by this method does not exceed the area by the perpendicular drop method, which already overestimates peak area.
3. For cases when exponential skimming is not possible or appropriate, due to extremely poor resolution or tailing, the tangential skim method should be used when the peak widths of the unresolved peaks vary significantly ($>2:1$) [2].
4. Quantitation by peak height should also be considered. It has been shown that peak height is more accurate in cases where the sizes of the overlapping peaks vary widely ($>100:1$). Quantitation is also generally more accurate for peak pairs of disparate size if the smaller peak elutes first [1].

Although only doublets have been considered here, the arguments can be extended to multiplets by considering the effects on the front and tail of surrounded peaks.

References

1. V. R. Meyer, *Chromatographia* 40(1): 15–22 (1995).
2. J. P. Foley, *Anal. Chem.* 59: 1984–1987 (1987).
3. A. N. Papas and T. P. Tougas, *Anal. Chem.* 62: 234–239 (1990).



Pellicular Supports for HPLC

Danilo Corradini

Institute of Chromatography, Rome, Italy

Introduction

In current practice, high-performance liquid chromatography (HPLC) supports consist of siliceous or polymer-based materials having pore sizes in the range of 80–120 Å for chromatography of small molecules and of 300–1000 Å for large biological molecules. Diffusional resistances in the stagnant mobile phase in the retentive material can have a significant influence on the efficiency of separation, particularly for large molecules of biological origin. Furthermore, pore size distribution of many mesoporous particles is rather wide and poor mass recovery is frequently encountered due to entrapment of macromolecules in the porous interior.

Discussion

One approach to minimize mass-transfer resistance in a stagnant mobile phase employs specially designed particles with a bimodal network of pores. The larger pores (≥ 1000 Å) facilitate convective transport of the mobile phase inside the particles, whereas the small pores (≤ 500 Å) are explored by the sample components by diffusion only and provide the necessary surface area for adequate sorption capacity.

Another approach consists in eliminating the pore structure, using pellicular column packing materials. These HPLC supports are mechanically stable, fluid-impervious microspheres with a thin retentive layer on the surface [1,2]. Such a stationary-phase configuration facilitates the interactions of the analytes with the active moieties of the stationary phase, which are completely exposed to the mobile-phase stream in the interstitial space of the column packing material. Because the diffusional path length in the retentive surface layer of the pellicular stationary phase is very short, the plate height contribution to the C term in the van Deemter equation is relatively small. It should be recalled that the C term in the van Deemter equation estimates the contribution to the plate height of the resistance to mass transfer. As a result, the absence of intraparticle diffusional resistance and the fast mass transfer between the stationary and the mobile phases

due to the small particle size allows high column efficiency, even at relatively high flow rates. In addition, the lack of internal pore structure eliminates the undesirable steric effects encountered in HPLC of large biological molecules with mesoporous stationary phases, resulting in good sample recovery.

With porous materials, the largest contribution to the total surface area is due to the area contained within particles; it is related to the pore volume, surface area, and pore diameter. As a result, there is little variation in the total surface area of packing materials with different diameters, but identical pore size. On the other hand, with pellicular particles, the total surface area within a column is a function of particle size. Consequently, stationary phases having the pellicular configuration have an adsorption capacity lower than the conventional mesoporous particles. This appears to be particularly so with micropellicular materials in HPLC of small molecules. With large molecules such as proteins, the loading capacity of columns packed with traditional mesoporous particles may be only three or four times higher than that of columns packed with the micropellicular stationary phases [3]. However, this somewhat low loading capacity is still adequate in the analytical mode and is more than compensated for by the high analytical speed and efficiency obtained with pellicular stationary phases.

Conventionally, the phase ratio is the volume of the active moieties of the stationary phase divided by the volume of the mobile phase in the column. From the particular configuration of pellicular stationary phases described earlier, it follows that they have a relatively low phase ratio with respect to that of the conventional packing materials employed in HPLC.

A variety of micropellicular packing materials has been developed for the analysis of both small and large molecules by various HPLC modes, including ion exchange (IEC), metal interaction (MIC), reversed phase (RPC) [4], and affinity chromatography (AC) [5]. Besides analytical applications, other possible utilization of micropellicular stationary phases includes fundamental kinetic and thermodynamic studies of the retention mechanisms on a well-defined surface. Nevertheless, a relatively limited variety of micropellicular



columns are commercially available. They are mainly restricted to ion-exchange and reversed-phase stationary phases. This may reflect certain practical disadvantages of micropellicular sorbents.

Columns packed with pellicular stationary phases of small particle size have low permeability and, therefore, cannot be operated at relatively high flow rates due to the pressure limitation of commercial HPLC instruments. However, due to the nonporous structure, micropellicular particles are generally more stable at higher temperature than conventional porous materials. Consequently, in the absence of limitation due to the thermal stability of either the sample or the bonded stationary phase, a column packed with nonporous materials can be operated at elevated temperatures with practical advantages from column permeability and sorption kinetics. This appears to be particularly so with several micropellicular materials employed in reversed-phase HPLC. By increasing the column temperature, the viscosity of the mobile phase decreases with concomitant increases in column permeability, which allows operating the column at high flow rates. In addition, with increasing temperature, sample diffusivity also increases and, in many cases, the sorption kinetic improves.

The elevated mechanical and thermal stabilities of pellicular stationary phases having a solid, fluid-imperious core have favored the development of nonporous particles tailored for the rapid HPLC analysis of peptides, proteins, and other biopolymers. Most of these applications are in RPC.

Although governed by the same separation mechanism, RPC of proteins differs significantly from that of small molecules because of high molecular weight and complex tertiary structure of these macromolecules. A large molecular size is associated with low diffusivity and molecular complexity is associated with multi-point interactions of proteins with the hydrophobic stationary phase, which complicate the dynamics of the separation process. In addition, the elution of certain proteins may be further complicated by conformational changes associated with the retention mechanism. Hence, RPC of proteins and other complex macromolecules is generally performed under the gradient elution mode, which reduces analysis time and improves the performance of separation. In the reversed-phase gradient elution mode, proteins are believed to be retained at the column inlet until, at some point in the gradient, corresponding to the proper mobile-phase composition, they are desorbed completely. Proteins then move through the column without apparent further interaction with the hydrophobic stationary phase.

In most cases, RPC of peptides and proteins are performed under denaturing conditions using hydro-organic mobile phases containing acidic additives such as trifluoroacetic or phosphoric acid. Because the elution strength of the mobile phase increases by decreasing its polarity, the appropriate gradient is produced by increasing the concentration of the organic solvent in the hydro-organic mobile phase during the chromatographic run. The variation of the eluent composition as a function of time gives the gradient shape, which is steep in the case of fast analysis performed with micropellicular reversed phase (i.e., high rate of change of mobile-phase composition during gradient elution).

Steep gradients require high flow rates in order to maintain satisfactory differences in retention of the analytes. According to Snyder and Standalus [6], the influence of the gradient parameters on retention is given by

$$k = \frac{t_g F}{1.15 \Delta \phi V_m S} \quad (1)$$

where k is the effective capacity factor for gradient elution, which is the value of the corresponding capacity factor under isocratic conditions (k') for the peak when it reaches the column midpoint, t_g is the gradient time (time from the beginning to the end of the gradient), F is the flow rate, $\Delta \phi$ is the variation of the fraction of organic solvent in the mobile phase during gradient, V_m is the column void volume, and S is the slope of the plot of the logarithmic retention factor (k') against mobile-phase composition under isocratic conditions. The value of the parameter S is related to the magnitude of the hydrophobic contact area and the number of the interaction sites established between the solutes and the stationary phase during the separation process. In comparison to small molecules, biopolymers have a larger contact area with the stationary-phase surface and, as a result, the retention is very sensitive to the content of the organic solvent in the hydro-organic mobile phase (i.e., the value of the parameter S is relatively large).

Equation (1) clearly shows that in order to maintain K constant while decreasing t_g , the flow rate must be proportionally increased. Because of the favorable mass-transfer properties of pellicular stationary phases, columns packed with such material can be employed at a high flow rate without loss in resolution. Moreover, pellicular column packings have a negligible intraparticulate void volume and, after the gradient, can be rapidly reequilibrated to the starting conditions. Finally, the thermal stability generally exhibited by these stationary phases allows running



the gradient at relatively elevated temperature with the beneficial effect of reducing the viscosity of the mobile phase, which reflects on reducing the column inlet pressure. In addition, temperature influences the retention behavior of the analytes. Generally, the chromatographic retention decreases with increasing temperature, with concomitant improvement in column efficiency due to increased solute diffusivity and faster mass transfer. However, with proteins, the retention may increase and efficiency decrease when temperature promotes further unfolding of the protein.

Pellicular packings may also consist of a fully functionalized layer encapsulating solid particles, where there is no physical attachment of the active layer to the core particles [7] or as colloidal particles bearing charged moieties (latex) electrostatically bound to a solid core functionalized with groups of opposite charge [8] (Fig. 1). Most of the anion-exchange columns in use today for either carbohydrate or ion chro-

matography are packed with electrostatically latex-coated pellicular ion exchangers. These sorbents consist of three parts: (a) a highly cross-linked polymeric nonporous core, (b) a sulfonated layer at the outer surface of the solid core, and (c) a monolayer coating of anion-exchange latex particles functionalized with quaternary ammonium compounds. The solid support and the latex particles are manufactured separately and brought together after independent quality control performed to remove particle agglomerates. This allows easy control of phase thickness, which results from the monodisperse latex particles, attached to the solid core by electrostatic forces. As a result, loading capacity increases with increasing the diameter of the latex particles, which generally ranges from 50 to 500 μm . For a 250-mm \times 4-mm-inner diameter column, the corresponding loading capacity ranges from 5 to 150 $\mu\text{Eq}/\text{column}$.

The highly cross-linked polymeric nonporous core may consist of either a polystyrene-divinylbenzene or an ethylvinylbenzene-divinylbenzene substrate. The latex coatings are generally made from vinylbenzylchloride polymer cross linked with divinylbenzene and fully functionalized with an appropriate quaternary amine for introducing anion-exchange properties.

Pellicular anion-exchange sorbents may also consist of quaternized latex hydrophobically coated onto the surface of an unsulfonated polystyrene solid core. However, using hydro-organic mobile phases can easily wash off the latex particles held onto the particle surface by hydrophobic interactions.

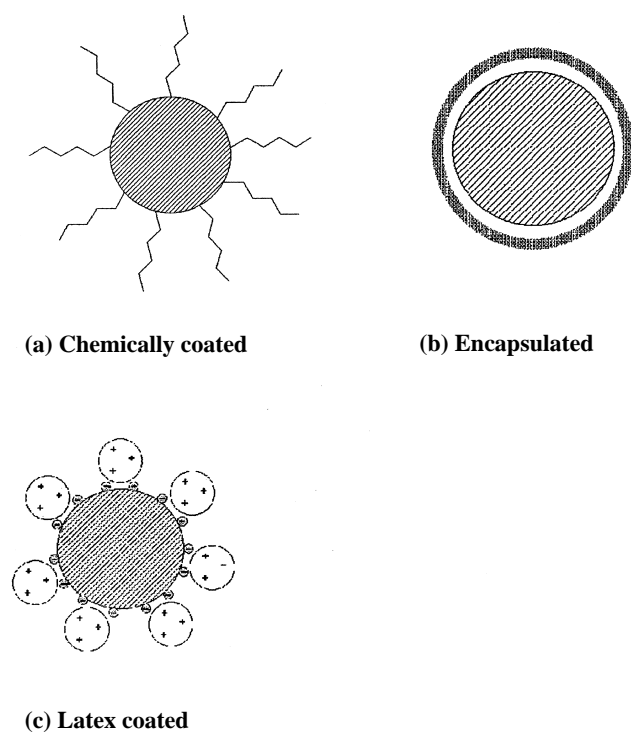


Fig. 1 Schematic representation of pellicular stationary phases consisting of covalently bonded functional groups at the surface (a), functionalized layer-encapsulating solid particles (b), and functionalized latex particles electrostatically bound to a solid core bearing groups of opposite charge (c).

References

1. Cs. Horváth, B. A. Preiss, and S. R. Lipsky, *Anal. Chem.* 39: 1422–1428 (1967).
2. K. K., Unger, G. Jilge, J. K. Kinkel, and M. T. W. Hearn, *J. Chromatogr.* 359: 61–72 (1986).
3. L. Varady, K. Kalghatgi, and Cs. Horváth, *J. Chromatogr.* 458, 207–215 (1988).
4. K. Kalghatgi, *J. Chromatogr.* 499: 267–278 (1990).
5. Q. M. Mao, A. Johnston, I. G. Prince, and M. T. W. Hearn, *J. Chromatogr.* 548: 147–163 (1991).
6. L. R. Snyder and M. A. Standalius, in *High-Performance Liquid Chromatography: Advances and Perspectives* (Cs. Horváth, ed.), Academic Press, New York, 1984, p. 195–309.
7. H. Giddings, U.S. Patent 3,488,922 (1970).
8. H. Small, T. S. Stevens, and W. C. Bauman, *Anal. Chem.* 47: 1801–1809 (1975).



Penicillin Antibiotics in Food: Liquid Chromatographic Analysis

Yuko Ito

Tomomi Goto

Hisao Oka

Aichi Prefectural Institute of Public Health, Nagoya, Japan

INTRODUCTION

Penicillin antibiotics are part of a wide variety of antimicrobial agents that are used as veterinary drugs to prevent and treat infectious diseases. Such use may lead to problems with residues in the livestock products. To provide safe products for consumers, the quantification of these residues in foods is required.

As most of the penicillins dissolve easily in water, high-performance liquid chromatography (HPLC) appears to be the best-suited approach for the analysis of residual penicillins in food. However, many HPLC methods require derivatization or special instrumentation because penicillins do not have any specific, strong ultraviolet (UV) absorption. Above all, the derivatization technique using mercury (II) chloride and 1,2,4-triazole or imidazole was applied to many analyses of penicillins. On the other hand, because it is not desirable to use toxic reagents such as mercury (II) chloride, there is a great need for a simpler, safer analytical method. To analyze the penicillins in food using a UV detector, a device is needed for sample preparation and chromatographic separation to remove interfering compounds which originate from the sample matrix. Because animal tissues (primarily muscle, kidney, and liver) include large amounts of sample matrix in comparison with milk, this causes difficulties for the development of simultaneous analysis of penicillins in these tissues. However, using an ion-exchange cartridge, in combination with ion-pair HPLC, has been reported to be very effective for simultaneous determination of the penicillins in the tissues. On the other hand, liquid chromatography/mass spectrometry (LC/MS) methods have also been published for the analysis of residual penicillins in food because mass spectrometric techniques can confirm and determine them, with high sensitivity and selectivity.

In this article, we deal with the simultaneous determination of penicillins in animal muscle, liver, and kidney using UV-HPLC and LC/MS.

UV-HPLC METHOD

Benzylpenicillin (PCG), phenoxymethylpenicillin (PCV), oxacillin (MPIPC), cloxacillin (MCIPC), nafcillin (NFPC), and dicloxacillin (MDIPC), all of which are representative weakly acidic penicillins, are widely used as veterinary drugs for livestock. We have reported, in our previous studies,^[1,2] the applicability of sample cleanup with an ion-exchange cartridge, in combination with ion-pair HPLC, for the analysis of ionizable compounds. We therefore applied the same technique to develop an analytical method for the quantitative determination of these residual penicillins in bovine muscle, kidney, and liver.^[3,4]

HPLC Conditions

After examination of several ion-pair reagents for acidic compounds, 12 mM of cetyltrimethylammonium chloride was chosen because it gave the best result in the separation of penicillins. When the pH of the mobile phase was adjusted to 6.2, the six penicillins exhibited good separations from each other, with adequate capacity factors.

Thus a satisfactory separation of the penicillins was obtained using TSKgel ODS-80Ts (5 μ m, 150 \times 4.6 mm, I.D.) column and acetonitrile-0.02 M phosphate buffer, pH 6.2, (4.3:5.7, v/v) containing 12 mM of cetyltrimethylammonium chloride, as the mobile phase (Fig. 1a).

Sample Extraction

Although the repeated (three times) extraction of the penicillins with 2% NaCl aqueous solution (60, 40, 40 mL) from bovine muscle was very simple and gave satisfactory extraction efficiency, the same extraction procedure could not be applied to bovine kidney and liver. Because the resultant extracts were foamy and viscous, it caused the serious problems in the sample cleanup procedure. To avoid these problems, the addition of aqueous solutions of sodium tungstate and sulfuric acid to the extraction



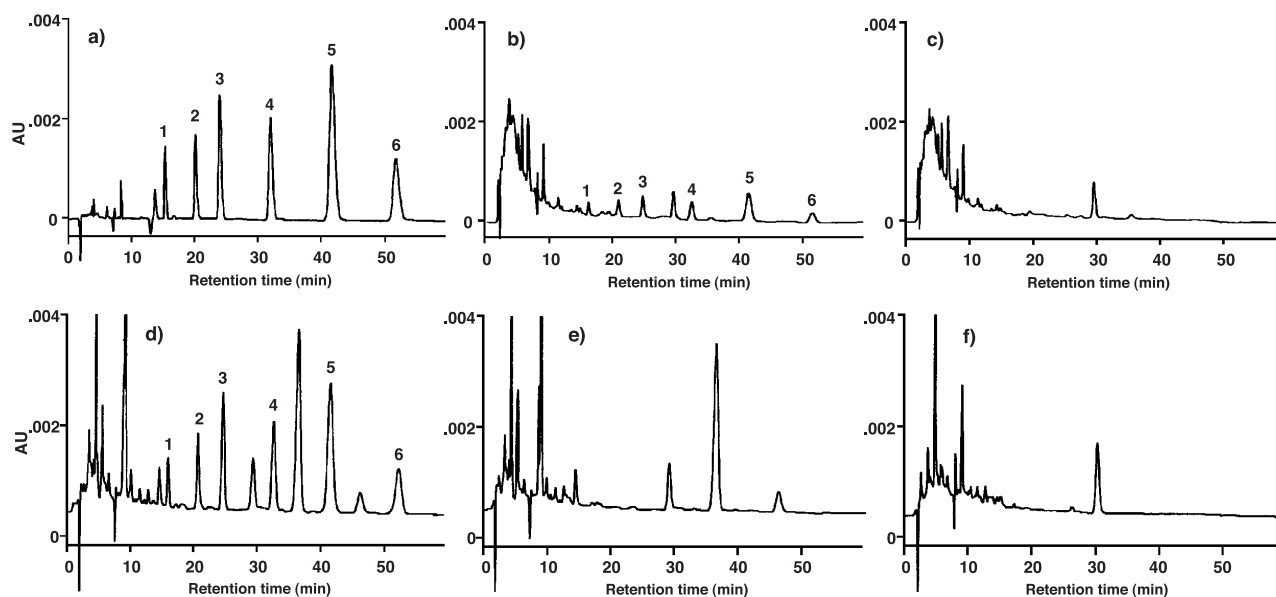


Fig. 1 Typical HPLC chromatograms of bovine tissue samples. a) Standard of six penicillins; b) muscle sample fortified at a concentration of 0.1 mg/kg each of penicillins; c) muscle sample; d) liver sample fortified at a concentration of 0.5 mg/kg each of penicillins; e) liver sample; f) kidney sample. 1) Benzylpenicillin; 2) phenoxymethylpenicillin; 3) oxacillin; 4) cloxacillin; 5) nafcillin; 6) dicloxacillin. Operating conditions—column: TSKgel ODS-80Ts (150 × 4.6 mm I.D.); mobile phase: acetonitrile-0.02 M phosphate buffer, pH 6.2, (4.3:5.7, v/v) containing 12 mM cetyltrimethylammonium chloride.; flow-rate: 0.8 ml/min; detector: UV 220 nm; column temp.: 30°C.

solution (2% NaCl), as deproteinization reagents, yielded satisfactory results. After a series of preliminary experiments, we decided to use 55 or 50 mL of 2% NaCl aqueous solution and 5 or 10 mL of the deproteinization reagent (5% sodium tungstate aqueous solution-0.17 M sulfuric acid solution, 1:1) as the first extraction solution for bovine kidney and liver. For the remaining two extractions, for each, 40 mL of 2% NaCl aqueous solution was used in the same manner as was used for muscle samples.

Purification of Crude Extracts

Pre-cleanup method

Because the tissue extract contains many substances which interfere with the ion-exchange capacity of the cartridge, it was necessary to develop a pre-cleanup method to retain the residual penicillins present in the tissue samples on the ion-exchange cartridge. It had been reported that washing a crude extract-loaded C18 cartridge with an aqueous methanolic solution containing NaCl was effective as a pre-cleanup of samples for the determination of PCG.^[5] After several experiments, the following pre-cleanup method was developed: the crude extract-loaded Bond Elut C18 cartridge was washed with 15% methanol containing 2% NaCl, followed by water; finally, the elution was carried out with 5 mL of 55% methanol.

Ion-exchange cartridge cleanup method

It is desirable to use the same solution for HPLC mobile phase and for the elution solvent from the cleanup cartridges to assure good reproducibility of the HPLC determination of the penicillins. After the investigation of the selected ion-exchange cartridges using 2 mL of the above-described mobile phase as the elution solvent, Sep-Pak Accell Plus QMA (QMA) produced the best results with all of the penicillins being completely eluted.

Even after the QMA cartridge cleanup procedure with the C18 cartridge pre-cleanup described above, there were nevertheless small amounts of the interfering substances overlapping the peaks of the penicillins. We therefore tried to wash the QMA cartridge to improve the cleanup. Judging from the results of several experiments, on the basis of the chemical properties of the QMA cartridge, we decided to use 3 mL each of 55% methanol and water for muscle samples and to use 3 mL each of 55% methanol, 10 mM acetic acid methanolic solution, and water for the kidney and liver samples.

Recoveries

Bovine tissue samples were fortified with the six penicillins (0.5 or 0.1, or 0.05 mg/kg of each) and performed the analyses according to the procedure described above.

Table 1 Recoveries of penicillins from bovine tissues

Penicillins	Muscle			Liver			Kidney		
	Fortified (mg/kg)	Recovery ^a (%)	C.V. (%)	Fortified (mg/kg)	Recovery ^a (%)	C.V. (%)	Fortified (mg/kg)	Recovery ^a (%)	C.V. (%)
Benzylpenicillin	0.5	92	2.9	0.5	82	4.2	0.5	83	4.7
	0.1	83	7.0	0.1	86	7.4	0.1	82	5.8
	0.05	77	6.4						
Phenoxymethylpenicillin	0.5	90	2.4	0.5	88	1.4	0.5	82	1.8
	0.1	82	4.8	0.1	83	4.1	0.1	86	7.8
	0.05	84	5.4						
Oxacillin	0.5	86	1.9	0.5	91	1.4	0.5	92	3.2
	0.1	74	3.5	0.1	96	3.4	0.1	92	4.2
	0.05	80	3.9						
Cloxacillin	0.5	85	1.8	0.5	91	2.9	0.5	89	2.9
	0.1	86	3.1	0.1	92	8.7	0.1	90	2.7
	0.05	82	4.0						
Nafcillin	0.5	89	1.7	0.5	84	1.7	0.5	80	3.5
	0.1	85	2.6	0.1	84	3.8	0.1	89	3.8
	0.05	90	5.2						
Dicloxacillin	0.5	83	4.4	0.5	73	3.1	0.5	79	5.9
	0.1	71	2.6	0.1	89	6.4	0.1	89	4.3
	0.05	79	6.4						

C.V.: coefficient of variation.

^aAverage of five trials.

As shown in Table 1, satisfactory recoveries (over 71%) and corresponding coefficients of variation (C.V., less than 8.7%) were obtained for these low concentrations of the penicillins. The detection limit was 0.02 mg/kg for each penicillin in the meat, and those were 0.02 mg/kg for MPIPC, MCIPC, and NFPC, 0.03 mg/kg for PCV, 0.04 mg/kg for PCG, and 0.05 mg/kg for MDIPC in the bovine kidney and liver (S/N ratio=3). Fig. 1 shows typical chromatograms of standard solution (a), fortified bovine muscle and liver samples (b and d), their corresponding controls (c and e), and bovine kidney sample (f), respectively. As shown by these chromatograms, satisfactory separation of PCs and cleanup effects were achieved

by using the ion-exchange cartridge cleanup in combination with the ion-pair HPLC described above.

LC/MS METHOD

Because mass spectrometric techniques can confirm and determine substances, with high sensitivity and selectivity, LC/MS methods have been published for the analysis of residual penicillins in food. However, only a few methods have been reported for the simultaneous analysis of penicillins in animal tissues; moreover, these methods are less sensitive than the UV-HPLC methods. It seemed

Table 2 Diagnostic ions of penicillins

Penicillins	Product ions ^a			Precursor ion ^a
	[M-H] ⁻	[M-H-CO ₂] ⁻	[M-H-141] ⁻	[M-H] ⁻
Benzylpenicillin	333	289	192	333
Phenoxymethylpenicillin	349	305	208	349
Oxacillin	400	356	259	400
Cloxacillin	434	390	293	434
Nafcillin	413	369	272	413
Dicloxacillin	468	424	327	468

^am/z.

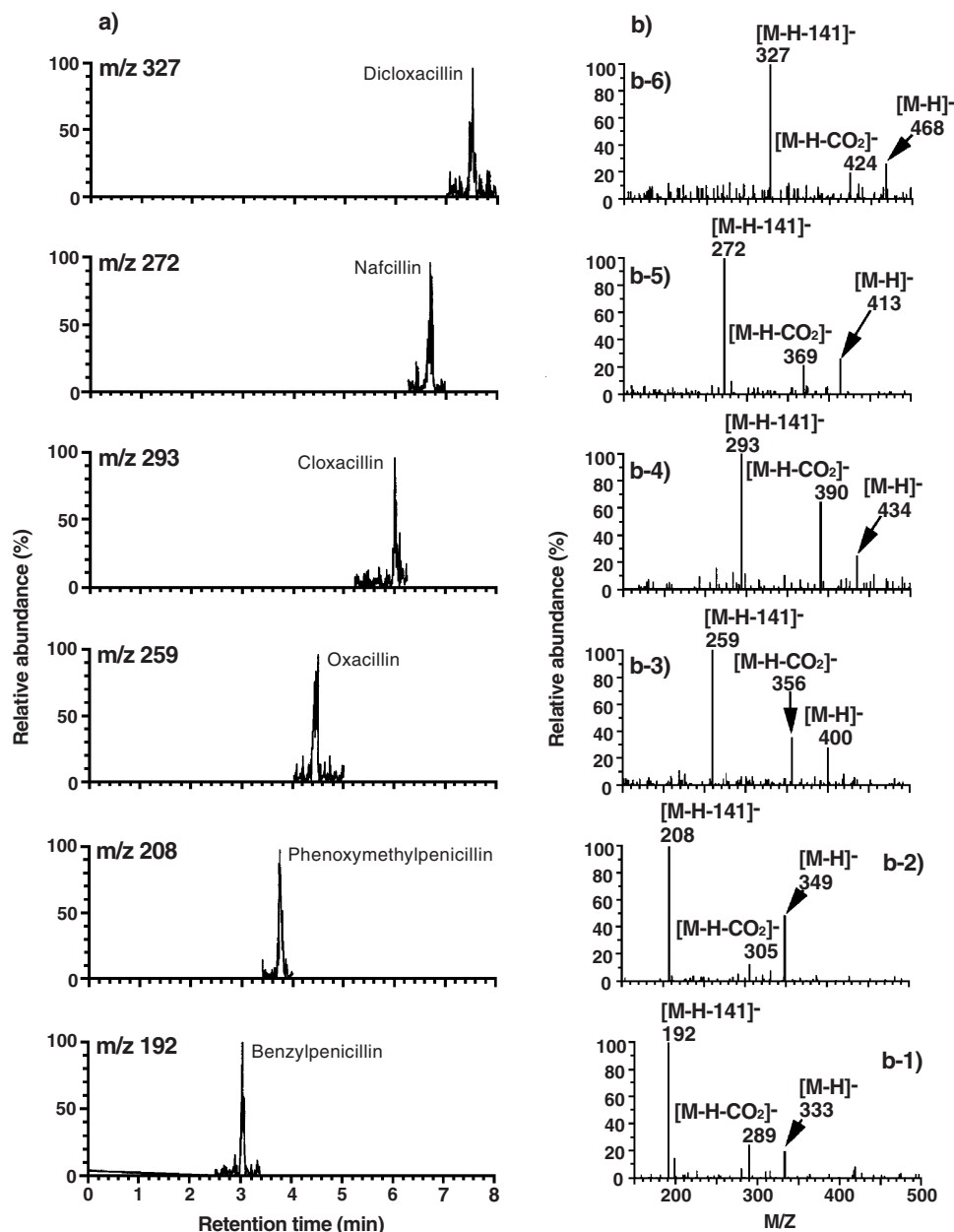


Fig. 2 ESI LC/MS/MS analysis of penicillins fortified at a concentration of 0.05 mg/kg in bovine liver. (a) Mass chromatograms monitored at $[M-H-141]^-$; (b) tandem mass spectra of penicillins recorded at the top of each peak on the mass chromatograms (a). (b-1) Benzylpenicillin; (b-2) phenoxymethylpenicillin; (b-3) oxacillin; (b-4) cloxacillin; (b-5) nafcillin; (b-6) dicloxacillin.

that their insufficient sample cleanup and separation under their LC conditions led to the lack of sensitivity. Accordingly, based on our determination method using the UV-HPLC approach described above, we decided to develop an accurate and highly sensitive confirmation method for penicillins in bovine tissues using ESI LC/MS/MS with a product ion scan mode.^[6] First, we reconstructed the LC conditions for ESI LC/MS analysis; hence 30% acetonitrile aqueous solution containing 2 mM of di-*n*-butylamine acetate (DBAA), which was a volatile

ion-pair reagent, was selected as the mobile phase. Gradient elution was used to increase the sensitivity. Then, we investigated whether or not the mobile phase described above can be used as the elution solvent for the cartridges used for cleanup. Because the mobile phase for ESI LC/MS analysis did not show satisfactory results, we decided to use the 30% acetonitrile aqueous solution containing 50 mM DBAA as the elution solvent.

Next, the optimal MS/MS conditions were investigated. Electrospray ionization mass spectra recorded for the six

penicillins gave $[M-H]^-$, $[M-H-CO_2]^-$, and $[M-H-141]^-$. When $[M-H]^-$ serves as a precursor ion for MS/MS, $[M-H-CO_2]^-$ and $[M-H-141]^-$ were generated as product ions (listed in Table 2), and they are very useful for the confirmation of penicillins. After a series of detailed examinations, the other MS/MS conditions including the compound-specific parameters were selected. To provide the applicability of the present method, the fortified bovine tissues, at a concentration of 0.05 mg/kg of each six penicillins, were analyzed. As shown in Fig. 2 left, all six penicillins from the liver sample appeared as separate peaks on the mass chromatograms monitored at $[M-H-141]^-$ under ESI LC/MS/MS conditions. Fig. 2 right shows the tandem mass spectra of the penicillins recorded at the top of each peak on the mass chromatograms shown in Fig. 2 left. All of these mass chromatograms and tandem mass spectra of fortified samples were almost the same as for the respective standards. Based on the results of the analyses of the fortified samples at 0.02 mg/kg, the lower limit of confirmation of the present method for muscle sample was estimated to be 0.02 mg/kg for all six penicillins, and those for kidney and liver were between 0.02 and 0.03 mg/kg.

As described above, we can hardly find the applicable LC/MS determination method of residual penicillins in animal tissue sample; however, those of penicillins in milk sample can be found. Recently, Riediker and Stadler^[7] reported the quantitative method for residual amoxicillin, ampicillin, MCIPC, MDIPC, and PCG in milk using ESI LC/MS/MS with a multiple ion monitoring mode and a stable isotope-labeled internal standard. A stable isotopically labeled compound is reasonable and useful for an internal standard of determination method using mass spectrometric techniques. The mixture of acetonitrile and water, including formic acid, as the LC mobile phase and gradient elution were selected. The milk sample with added internal standard (deuterated PCG) was washed with *n*-hexane and condensed before applying C18 cartridge for cleanup. The provided sample solution was filtered through a cutoff filter device (nominal molecular weight limit 10,000). For quantitation, matrix-matched calibration curves were established using a blank milk sample fortified at different concentrations of each target analyte. The mean recoveries of all target penicillins ranged from 76% to 94% at a single analyte concentration of 0.004 mg/kg. The LOQs were in the range of 0.0004–0.0008 mg/kg (mean of blank intensity + 10 SD).

CONCLUSION

We introduced the LC analysis for residual penicillin antibiotics in food, especially in bovine tissues. To avoid

the use of special instruments and toxic reagents, the combination of ion-exchange cartridge cleanup and ion-pair HPLC was very effective and was able to provide sufficient sensitivity and quantitation for the measurement of penicillins. Moreover, it was also able to be used for the development of the confirmation method using ESI LC/MS. The detection limits of all of these methods are able to satisfy the MRLs established by the WHO, FDA, EU, and Japan; so we strongly recommend these methods for the analysis of residual penicillins in tissues to provide safe products for consumers.

REFERENCES

1. Oka, H.; Ikai, Y.; Kawamura, N.; Uno, K.; Yamada, M.; Harada, K.; Uchiyama, M.; Asukabe, H.; Mori, Y.; Suzuki, M. Improvement of chemical analysis of antibiotics. IX. A simple method for residual tetracyclines analysis in honey using a tandem cartridge clean-up system. *J. Chromatogr.* **1987**, 389, 417–426.
2. Ito, Y.; Ikai, Y.; Oka, H.; Hayakawa, J.; Kagami, T. Application of ion-exchange cartridge clean-up in food analysis. I. Simultaneous determination of thiabendazole and imazalil in citrus fruit and banana using high-performance liquid chromatography with ultraviolet detection. *J. Chromatogr., A* **1998**, 810, 81–87.
3. Ito, Y.; Ikai, Y.; Oka, H.; Kagami, T.; Takeba, K. Application of ion-exchange cartridge clean-up in food analysis. II. Determination of benzylpenicillin, phenoxymethylpenicillin, oxacillin, cloxacillin, nafcillin and dicloxacillin in meat using liquid chromatography with ultraviolet detection. *J. Chromatogr., A* **1999**, 855, 247–253.
4. Ito, Y.; Ikai, Y.; Oka, H.; Matsumoto, H.; Kagami, T.; Takeba, K. Application of ion-exchange cartridge clean-up in food analysis. III. Determination of benzylpenicillin, phenoxymethylpenicillin, oxacillin, cloxacillin, nafcillin, and dicloxacillin in bovine liver and kidney by liquid chromatography with ultraviolet detection. *J. Chromatogr., A* **2000**, 880, 85–91.
5. Terada, H.; Asanoma, M.; Sakabe, Y. Studies on residual antibacterials in foods. III. High-performance liquid-chromatographic determination of penicillin G in animal tissues using an on-line pre-column concentration and purification system. *J. Chromatogr.* **1985**, 318, 299–306.
6. Ito, Y.; Ikai, Y.; Oka, H.; Matsumoto, H.; Miyazaki, Y.; Takeba, K.; Nagase, H. Application of ion-exchange cartridge clean-up in food analysis. IV. Confirmatory assay of benzylpenicillin, phenoxymethylpenicillin, oxacillin, cloxacillin, nafcillin and dicloxacillin in bovine tissues by liquid chromatography–electrospray ionization tandem mass spectrometry. *J. Chromatogr., A* **2001**, 911, 217–223.
7. Riediker, S.; Stadler, R.H. Simultaneous determination of five β -lactam antibiotics in bovine milk using liquid chromatography coupled with electrospray ionization tandem mass spectrometry. *Anal. Chem.* **2001**, 73, 1614–1621.

Peptide Analysis by HPLC

Karen M. Gooding

Eli Lilly and Company, Indianapolis, Indiana, U.S.A.

Introduction

The rapid advancement in peptide research over the past 25 years must be attributed, in part, to the effectiveness of high-performance liquid chromatography (HPLC), particularly reversed-phase chromatography, in the separation and analysis of peptides. The resolution and selectivity of this technique allows peptides to be effectively isolated and purified from closely related substances. It also separates most or all of the components of complex biological mixtures such as tryptic digests of proteins.

Modes of HPLC

Peptides, which are composed of amino acids linked by amide bonds, are often found in random coil to semi-defined conformations, depending on their lengths and structures. As such, most of the composite amino acids are available to interact with the bonded phase of an HPLC support. Although the variety of amino acid characteristics, such as charge, polarity, and hydrophobicity, would suggest that multiple modes of HPLC would be effective for separation, reversed-phase chromatography has shown the ultimate success in selectivity and resolution of peptides. Hydrophilic interaction chromatography is a good alternative for hydrophilic peptides or other mixtures that are not separated well by reversed-phase chromatography, whereas cation-exchange chromatography can be effective for highly cationic species. Size-exclusion chromatography is a difficult technique for analysis of peptides, due to their varying solubilities and high degrees of hydrophobicity and charge; however, it is invaluable for resolution from dimers and aggregates.

Reversed-Phase Chromatography

Reversed-phase chromatography (RPC) is a method in which molecules are bound hydrophobically to non-polar ligands in the presence of a polar solvent. Solutes are generally bound in an acidic mobile phase with elution occurring during a gradient to an organic solvent.

Molecules will tend to be unfolded due to the combination of acidic and organic mobile phases and the hydrophobic bonded phase. Consequently, binding involves most of the amino acids, depending on the conformation. RPC can differentiate peptides which vary in the positions of their amino acids, as well as in their identities, thus making it a powerful analysis tool. Very high selectivity is attained even for complex biological mixtures, such as the tryptic digest of human growth hormone shown in Fig. 1.

There are many ligands used for RPC, but the most popular for peptide analysis are octadecyl (C_{18}) and octyl (C_8) chains. Little difference in selectivity for peptides is observed with ligand chain-length variation; however, mass recovery of very hydrophobic species may be enhanced on the shorter chains. Many

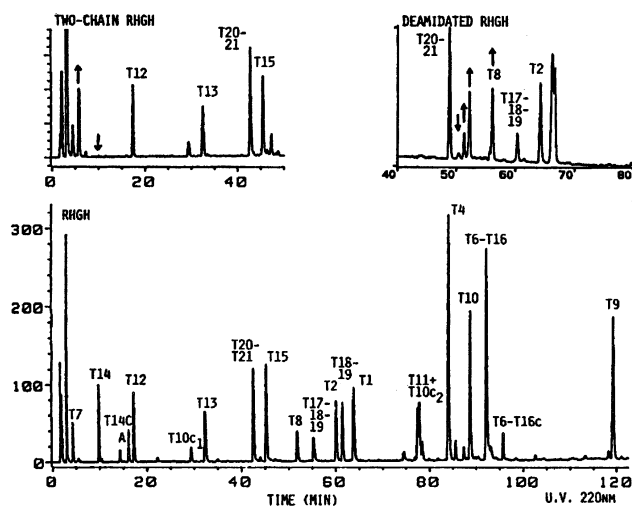


Fig. 1 Tryptic maps of the intact and (insets) degraded forms of recombinant human growth hormone (RHGH). The separation was achieved on a Nucleosil C-18 column (150 × 3.9 mm inner diameter) with a 120-min mobile-phase gradient from 10 mM potassium phosphate (pH 2.85) to 60% acetonitrile in the starting buffer. The flow rate was 1 mL/min and detection was at 214 nm. [Reprinted from J. Frenz, W.S. Hancock, W. J. Henzel and Cs. Horvath, in *HPLC of Biological Macromolecules: Methods and Applications* (K. M. Gooding and F. E. Regnier, eds.), Marcel Dekker, Inc., New York, 1990, p. 145.]



RPC bonded phases are synthesized by silane bonding, with or without endcapping, which results in a hydrophobic layer on a silanol surface. Recently, more hydrophilic–hydrophobic phases have been developed whereby amide linkages are embedded in the nonpolar layer to provide a wettable area which may be more compatible with some biological molecules. Due to their higher efficiencies, silica-based supports are generally used for peptide analysis; however, polymeric supports are effective for operation at high pH. The silica matrix is sometimes a factor in retention because silanols on reversed-phase supports are rarely totally eliminated. Most peptide analyses use supports with pore diameters of at least 300 Å to allow access to the bonded phase; nonporous supports offer a high-resolution option with significantly lower capacities. Dynamic loading capacities of peptides on porous analytical reversed-phase columns (250 × 4.6 mm inner diameter) are usually 100–500 µg.

Due to the multiple functional groups found in peptides, selectivity can be vastly changed by operational factors. Variable mobile-phase parameters include organic modifiers, pH, ion-pair agents, and gradient rates. Acetonitrile is the most popular organic solvent for RPC of peptides due to its transparency at low wavelengths (<210 nm) and its tendency to yield narrow peak widths. The strength of the organic solvent which causes elution increases from methanol to acetonitrile to isopropanol. Acidic pH is generally utilized to minimize silanol interactions; however, distinct pH conditions yield different selectivities. Ion-pairing agents, such as trifluoroacetic acid, are often added to the mobile phase to change the ionic or hydrophobic properties of either or both of the solute and the bonded phase. Amounts of 0.1% added to both the aqueous and the organic mobile phases are usually adequate, but optimal concentrations can be determined experimentally. Trifluoroacetic acid (TFA) is the most popular ion-pairing agent for peptides, imparting some additional hydrophobicity to amine groups and neutralizing cationic charges.

Most RPC peptide separations utilize gradient rather than isocratic conditions. Small peptides may be resolved well isocratically; however, due to multipoint interactions, larger ones yield broad peaks and tailing unless gradients are used. Shallow gradients generally improve resolution in an analytical mode or purity in preparative applications. For complex mixtures, 0.5–1% organic/min is usually a satisfactory rate. Increased temperatures can be implemented to reduce both retention times and the pressure generated by small-particle-diameter supports.

Hydrophilic Interaction Chromatography

Hydrophilic interaction chromatography (HILIC) is a variation of normal-phase chromatography in which solutes are retained on a polar bonded phase under high concentrations (80–90%) of organic solvent and released during a gradient to a more aqueous solvent. If the polar bonded phase contains a charge, a salt gradient can also be implemented, yielding separation by both charge and polarity. HILIC is most effective for polar peptides which are often poorly retained by RPC. Figure 2 compares the differences in selectivity and resolution of a cation-exchange (CEX) procedure on a HILIC column with that of RPC for a peptide mixture.

The HILIC bonded phases are hydrophilic, consisting of amide and/or polyhydroxy functionalities. Pore diameters are at least 300 Å to allow penetration of peptides. Supports can be based on either silica or polymer because the matrix is not exposed to the solutes.

Mobile-phase manipulation causes variations in selectivity in HILIC. Although a buffer is used for pH control, it may also serve to change the hydrophobicity of the solutes by ion-pairing. More hydrophobic ions such as acetate will decrease retention. The pH is a less important factor than the identity of the salt in HILIC selectivity. The organic modifier and its initial concentration directly affect retention and resolution. At least 80–90% organic is usually required to achieve adequate retention of hydrophilic peptides. For HILIC/cation exchange (HILIC/CEX), a salt gradient is implemented to separate the hydrophilic peptides by charge, as can be seen in Fig. 2.

Ion-Exchange Chromatography

Ion-exchange chromatography (IEC) separates peptides by ionic attraction of their composite amino acids to charges on the stationary phase. Selectivity is dependent on the number and the identity of the amino acids, as well as their spatial arrangement. A peptide with charges grouped together will bind differently than one whose charges are dispersed. IEC has been most successful for cationic peptides that cannot always be analyzed effectively by RPC.

Supports for IEC possess either anion- or cation-exchange functionalities which are positively or negatively charged, respectively. They are also classified as weak or strong to correspond to their titration curves, similar to acid and base designations. Generally, strong cation-exchange supports are used for peptide analy-



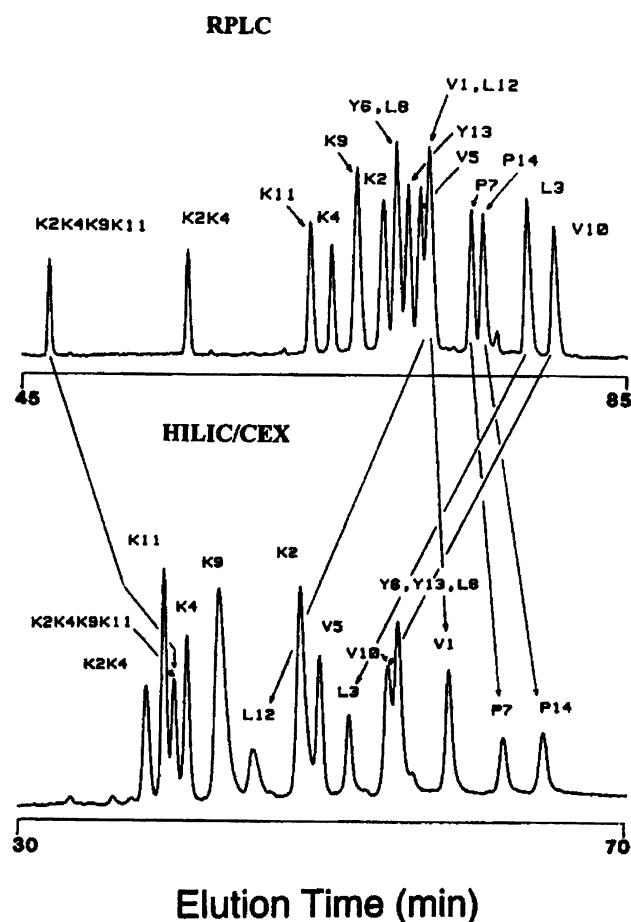


Fig. 2 Comparison of RPLC and HILIC/CEX elution profiles of cyclic peptides. RPLC: Zorbax 300XDB-C₈ column; linear gradient (0.5% acetonitrile/min) from 0.05% aqueous trifluoroacetic acid (TFA) to 0.05% TFA in acetonitrile at 1 mL/min; at 70°C and detection at 210 nm. HILIC/CEX: Polysulfoethyl A column; 5 min isocratic elution with buffer A (20 mM aqueous triethylammonium phosphate with 90% acetonitrile), followed by linear gradient (2.5 mM sodium perchlorate/min) from buffer A to buffer B (buffer A containing 400 mM sodium perchlorate with 80% acetonitrile); at 30°C and detection at 210 nm. [Reprinted from C. T. Mant, L. H. Kondejewski, and R. S. Hodges, *J. Chromatogr.* 816 (1998), p. 79, with permission of Elsevier Science.]

sis. The pore diameter is important in that it must be large enough to allow access of the peptides so that they are effectively retained and have optimum loading capacities.

In IEC, solutes are bound in a low-ionic-strength buffer (0.02M–0.05M) at an appropriate pH (often 1–2 pH units from the pI). Elution occurs when the ionic strength is increased during a concentration gradient of a salt in the same buffer. Isocratic elution may success-

fully separate small peptides with one or two charged groups, but larger peptides with more charged groups will require gradients for good peak shapes, resolution, and reproducibility. The nature of the salt in IEC has a major effect on selectivity due to interaction of the composite ions with either the stationary phase or the solutes. The hydrophobicity of many peptides may necessitate the addition of 5–10% organic solvent to improve peak shape. This can usually be included in the mobile phase without deleterious effects on the separation.

Size-Exclusion Chromatography

Size-exclusion chromatography (SEC) is a method in which molecules are separated by size due to differential permeation into a porous support. It requires complete solubility of the analytes in the mobile phase and elimination of all interactions with the bonded phase. In these respects, SEC is not as useful for the separation of peptides as it is for proteins because peptides vary drastically in solubility, charge, and hydrophobicity. Peak capacity in SEC is fairly low compared to other HPLC methods because all separations must occur in the internal volume (V_i) of the support, which is generally less than half the volume of mobile phase in the column. Despite these deficiencies, SEC can be very effective for separating peptides from dimers, aggregates, small molecules, proteins, and other molecules which differ by size.

Supports for SEC of proteins are designed to be neutral and very hydrophilic to avoid interaction of the solutes with the support by ionic or hydrophobic mechanisms. The base matrix can be either silica or polymer; efforts are made to totally mask its properties with a carbohydrate-like stationary phase. The pore structure is critical to successful SEC. Not only must the total pore volume (V_i) be adequate for separation, the pore diameter must be consistent and nearly homogeneous for attainment of maximum resolution between molecules with relatively small differences in molecular size (radius of gyration or molecular weight). A twofold difference in size is usually required for separation by SEC. Retention in SEC is directly related to the logarithm of the radius of gyration or the molecular weight. Because peptides do not all have the same shapes, their molecular volumes may not correspond uniformly to their molecular weights unless they are in the presence of sodium dodecyl sulfate (SDS) or another denaturing agent.

The mobile phase is a critical factor in SEC because it must eliminate all solute–support interactions. This may require adjustment to low pH or to an ionic strength which eliminates ionic interactions



(0.05M–0.2M) and/or the addition of 5–10% organic solvent to remove hydrophobic binding. Due to their variations in physical properties, it is sometimes difficult to eliminate all the ionic and hydrophobic interactions of a mixture of peptides using a single mobile phase.

Detection

The detectability of peptides varies greatly, depending on their amino acid composition. The aromatic amino acids (tyrosine, tryptophan, and phenylalanine) offer selective detection by ultraviolet (UV) light at 280 or 254 nm or by fluorescence detection. In the absence of these amino acids, low wavelengths (<220 nm), which also detect many other substances, including components of the mobile phase, must be used. TFA and acetonitrile are compatible with low wavelengths, making this system a popular one for peptide analysis by RPC. Alternatively, the amine functionalities of peptides can be derivatized using precolumn or postcolumn techniques with compounds such as fluorescamine. In this way, selective and sensitive detection methods like fluorescence can be implemented. Mass spectrometry also provides a viable, albeit, expensive means of detection of peptides.

Conclusions

High-performance liquid chromatography provides a rapid and effective means for the analysis and

purification of peptides. RPC is the primary and most universally successful mode, with HILIC and IEC offering alternative methods for hydrophilic peptides or others where RPC is ineffective. HILIC and IEC are also orthogonal modes to RPC for preparative or identification purposes. The ability to change selectivity using the mobile phase in HPLC methods makes them versatile techniques which can be rapidly optimized and implemented.

Suggested Further Reading

- Cunico, R. L., K. M. Gooding, and T. Wehr, *Basic HPLC and CE of Biomolecules*, Bay Bioanalytical Laboratories, Richmond, CA, 1998.
- Gooding, K. M., and F. E. Regnier (eds.), *HPLC of Biological Macromolecules: Methods and Applications*, Marcel Dekker, Inc., New York, 1990.
- Hancock, W. S. (ed.), *High Performance Liquid Chromatography in Biotechnology*, John Wiley & Sons, New York, 1990.
- Hearn, M. T. W. (ed.), *HPLC of Proteins, Peptides and Polynucleotides*, VCH, New York, 1991.
- Katz, E. D. (ed.), *High Performance Liquid Chromatography: Principles and Methods in Biotechnology*, John Wiley & Sons, New York, 1996.
- Mant, C. T. and R. S. Hodges (eds.), *High-Performance Liquid Chromatography of Peptides and Proteins*, CRC Press, Boca Raton, FL, 1991.
- Mant, C. T., L. H. Kondejewski, and R. S. Hodges, *J. Chromatogr. 816*: 79 (1998).



Peptide Separation by Countercurrent Chromatography

Ying Ma

Yoichiro Ito

National Heart, Lung, and Blood Institute–National Institutes of Health (NHLBI–NIH),
Bethesda, Maryland, U.S.A.

INTRODUCTION

Countercurrent chromatography (CCC),^[1–4] because it uses no solid support in the separation column, is particularly suitable for the separation and purification of peptides which often present a problem of irreversible adsorption onto solid supports. Since the 1970s, the horizontal flow-through coil planet centrifuge (CPC) has been used for the separation of a variety of natural and synthetic peptides.^[5] High-speed CCC,^[6,7] which was developed in the 1980s, has improved partition efficiency in terms of resolution and separation times, yielding up to a few thousand theoretical plates in a few hours. During the last decade, a preparative scheme called pH zone-refining CCC was developed. This method yields multi-gram quantities of pure fractions at an extremely high concentration.^[8,9] More recently, a new column, called spiral disk assembly, was designed for high-speed CCC to separate peptides and proteins using polar two-phase solvent systems.^[10]

The performance of these CCC instruments has been examined using butanol-based solvent systems and a set of dipeptide samples containing a tyrosine and/or a tryptophan moiety, which allows monitoring of the effluent at 280 nm.

HORIZONTAL FLOW-THROUGH CPC

Figure 1A shows the original prototype of the horizontal flow-through CPC (HCPC), which can be operated without rotary seals.^[5] A set of coiled tubes is arranged around the rotary shaft, which undergoes a specific planetary motion (type-J): The column assembly rotates about its own axis and revolves around the centrifuge axis at the same angular velocity, in the same direction. This planetary motion allows each helical turn of the column to retain the stationary phase of either the organic or the aqueous phase while vigorously mixing the two phases at each rotation cycle.

The system provides a stable retention for polar solvent systems up to 40% of the total column capacity. A typical separation of a set of dipeptides is illustrated in Fig. 1B. Using a two-phase solvent system composed of 1-butanol/

acetic acid/water (4:1:5, vol/vol/vol), seven components were well resolved in 70 hr.

Before the advent of high-speed CCC, the method was utilized for the purification of various samples such as synthetic peptides, cholecystokinin analogs, and their fragments (HCPC; Table 1).

HIGH-SPEED CCC USING TYPE-J PLANETARY MOTION

High-speed CCC is considered to be the most advanced form of CCC in terms of partition efficiency and separation times. The design of the apparatus is similar to that of the HCPC, except that the coiled column is mounted coaxially onto the column holder. Since the early 1980s, the method has been widely used for the separation and purification of a variety of natural and synthetic products, including peptides and their derivatives.^[6,7] Except for hydrophobic ring peptides such as gramicidin and bacitracin, most of the peptides are separated using polar butanol solvent systems, including 1-butanol/acetic acid/water (4:1:5), 1-butanol/aqueous trifluoroacetic acid (TFA; 1:1), and so on—typical examples of which are shown in Fig. 2A and B. Occasionally, one encounters a problem of carryover loss of the stationary phase from the multilayer coil separation column of the high-speed CCC centrifuge. To alleviate this problem, a new column, called spiral disk assembly, has recently been designed.^[10] When mounted on the type-J high-speed CCC rotor, it enhances the retention of the stationary phase because of its radially acting centrifugal force gradient through the spiral channel. Thus the method enables the use of highly polar solvent systems with low interfacial tension, such as aqueous–aqueous polymer phase systems used for protein separation.

HIGH-SPEED CCC USING CROSS-AXIS CPC

This CCC scheme produces a unique pattern of planetary motion: The axes of the rotation and the revolution are perpendicular to each other. This planetary motion

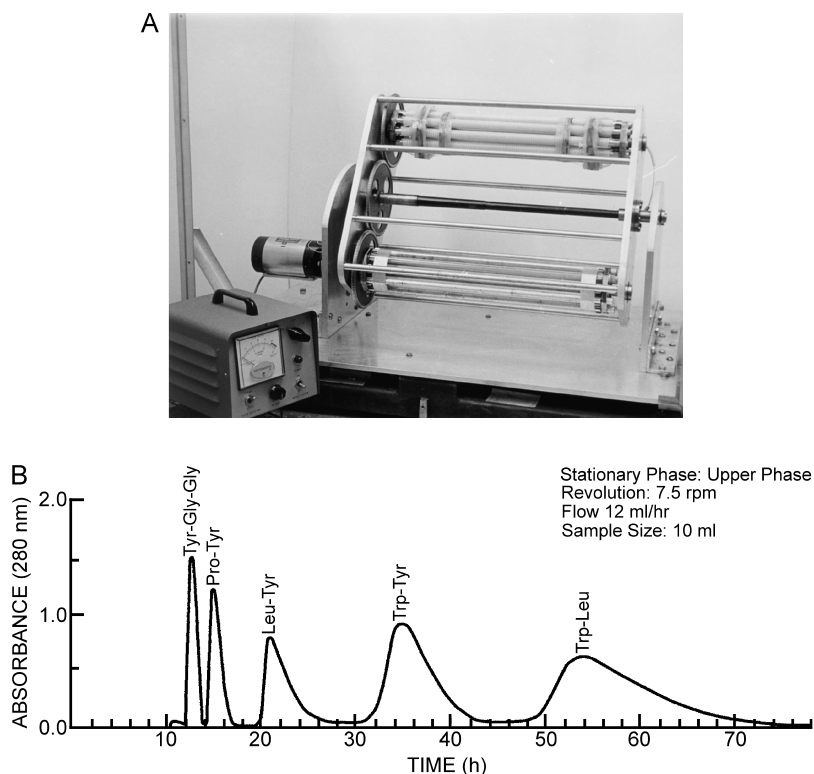


Fig. 1 Photograph of the horizontal flow-through coil planet centrifuge (A) and the chromatogram of dipeptide separation (B).

Table 1 Peptide samples and two-phase solvent systems for standard CCC techniques

Peptide sample	Solvent system ^a	CCC instrument ^b
Dipeptides	1-BuOH/AcOH/H ₂ O (4:1:5)	TCC, HCPC, MLCPC ICPC, SDA
Dipeptides	1-BuOH/DCA/NH ₄ OAc (100:1 → 2:100)	ICPC, ACPC
Synthetic peptide	1-BuOH/AcOH/H ₂ O (4:1:5)	HCPC (6, 5, 9, and 15 mers)
Des-enkephalin γ -endorphin (12 mers)	1-BuOH/0.1% TFA (1:1)	HCPC
Cholecystokinin fragments (four to eight mers)	1-BuOH/AcOH/H ₂ O (4:1:5)	HCPC
	1-BuOH/0.2–0.5M NH ₄ OAc (1:1)	HCPC
	1-BuOH/0.1% TFA (1:1)	HCPC
Cholecystokinin fragments sulfonated	1-BuOH/0.2–0.5M NH ₄ OAc (1:1)	HCPC
	1-BuOH/EtOH/Hex/AcOH/H ₂ O (3:1:2:1:5)	HCPC
	1-BuOH/AcOH/H ₂ O (4:1:5)	HCPC
Cholecystokinin analog	CHCl ₃ /AcOH/H ₂ O (2:2:1)	MLCPC
Bacitracins	CHCl ₃ /95% EtOH/H ₂ O (4:3:2)	HCPC, MLCPC, XCPC
Gramicidins	CHCl ₃ /C ₆ H ₆ /MeOH/H ₂ O (15/15/23/7)	HCPC, MLCPC, XCPC
WAP-8294A	1-BuOH/EtOH/0.005 TFA (pH 2.5) (1:3:4)	DCCC MLCPC
Tyrocidines	CHCl ₃ /MeOH/0.1 M HCl (19:19:12)	DCCC
Colistins A and B	1-BuOH/0.04 M TFA (1:1)	MLCPC
Kangdisu/colistin E	1-BuOH/2% DCA+5% NaCl (1:1)	MLCPC
Bombesin	1-BuOH/1% DCA (1:1) at 50°C	MLCPC
Bovine insulin	2-BuOH/3% DCA (1:1)	ICPC, ACPC
	1-BuOH/0.5% DCA (1:1) at 50°C	MLCPC

^aACN=acetonitrile; AcOH=acetic acid; BuOH=butanol; DCA=dichloroacetic acid; EtOH=ethanol; NH₄OAc=ammonium acetate; Hex=hexane; MeOH=methanol; TFA=trifluoroacetic acid.

^bCPC=coil planet centrifuge; ACPC=type-I L-angle rotor CPC; DCCC=droplet CCC; HCPC=horizontal flow-through CPC; MLCPC=type-J multilayer CPC; SDA=spiral disk assembly; TCC=toroidal coil centrifuge; ICPC=type-I CPC; XCPC=cross-axis CPC.

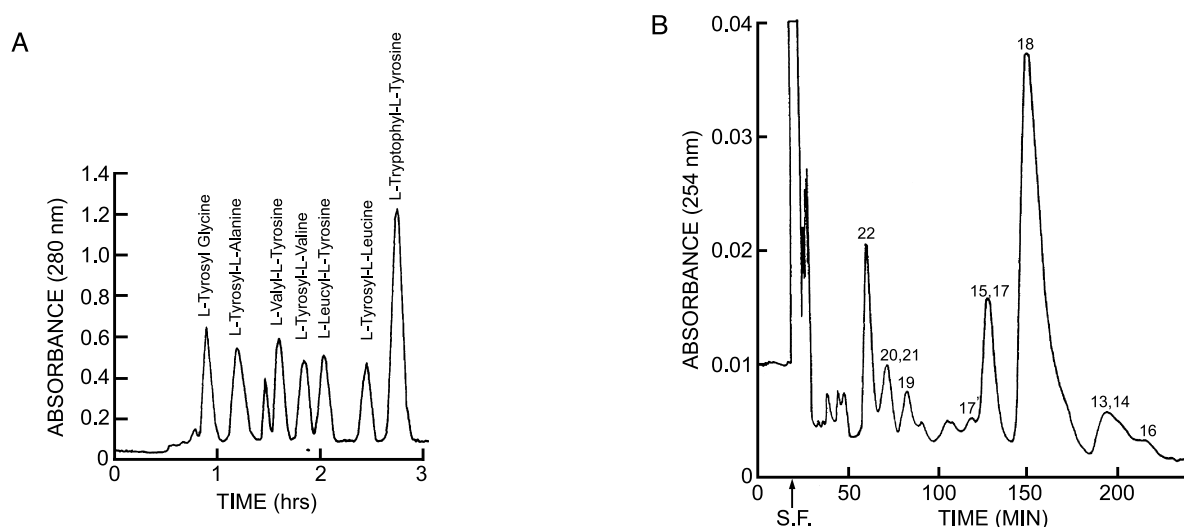


Fig. 2 Chromatograms obtained by high-speed CCC. (A) Separation of a set of dipeptides by gradient elution. Experimental conditions are as follows: apparatus: type-J multilayer CPC prototype with a 10-cm revolution radius; column: multilayer coil, 1.6-mm ID, 130 m length, 285 mL total capacity; sample: dipeptide mixture 70 mg; solvent system: linear gradient between the starting medium of 1-butanol/dichloroacetic acid/0.1 M ammonium formate (1:0.01:1) and the ending medium of 1-butanol/0.1 M ammonium formate (1:1); mobile phase for 4 hr: lower aqueous phase; flow rate—214 mL/hr; revolution: 800 rpm; detection: 280 nm; retention of stationary phase: 55% of the total column capacity. (B) Separation of bacitracins by high-speed CCC. Bacitracins A and F are separated in peaks 18 and 22, respectively. Separation conditions are as follows: apparatus: Shimadzu type-J multilayer CPC (model HSCCC-1A; Shimadzu Corporation, Kyoto, Japan) with a 10-cm revolution radius; column: multilayer coil, 1.6-mm ID, 325 mL capacity; sample: 50 mg; solvent system: chloroform/ethanol/methanol/water (5:3:3:4); mobile phase: lower organic phase; flow rate: 3 mL/min; detection: 254 nm.

produces a centrifugal force vector acting across the diameter of the multilayer coil to enhance the retention of the stationary phase, whereas the system yields less efficient resolution than the type-J high-speed CCC. Although the system was successfully utilized for the

separation of bacitracin and gramicidin having a potential for a large-scale preparative separation of more polar peptides, the method is currently used almost exclusively for the separation of proteins with aqueous–aqueous polymer phase system.^[11]

Table 2 Peptide samples and solvent systems for pH zone-refining CCC

Peptide ^a (weight; g)	Solvent system ^b	Key reagents ^c		
		Retainer	Eluter	Ligand
CBZ dipeptides (0.8 g)	MBE/ACN/H ₂ O (2:2:3)	TFA (16 mM/SP)	NH ₃ (5.5 mM/MP)	—
CBZ dipeptides (3 g)	MBE/ACN/H ₂ O (2:2:3)	TFA (16 mM/SP)	NH ₃ (5.5 mM/MP)	—
CBZ tripeptides (0.8 g)	1-BuOH/MBE/ACN/H ₂ O (2:2:1:5)	TFA (16 mM/SP)	NH ₃ (2.7 mM/MP)	—
Dipeptide βNA (0.3g)	MBE/ACN/H ₂ O (2:2:3)	TEA (5 mM/SP)	HCl (5 mM/MP)	—
Dipeptides (1 g)	MBE/ACN/50 mM HCl (4:1:5) (SP)	TEA (20 mM/SP)		DEHPA (30%/SP)
	MBE/1-BuOH/ACN/H ₂ O (2:2:5:1) (MP)		HCl (20 mM/MP)	
Bacitracins (5 g)	MBE/50 mM HCl (SP)	TEA (40 mM/SP)		DEHPA (10% SP)
	MBE/H ₂ O (MP)		HCl (20 mM/MP)	

^aCBZ = carbobenzoyle; βNA = naphthyl amide.

^bACN = acetonitrile; BuOH = butanol; MBE = methyl *tert*-butyl ether; MP = mobile phase; SP = stationary phase.

^cDEHPA = di-[2-ethylhexyl]phosphoric acid; TFA = trifluoroacetic acid; MP = mobile phase; SP = stationary phase.

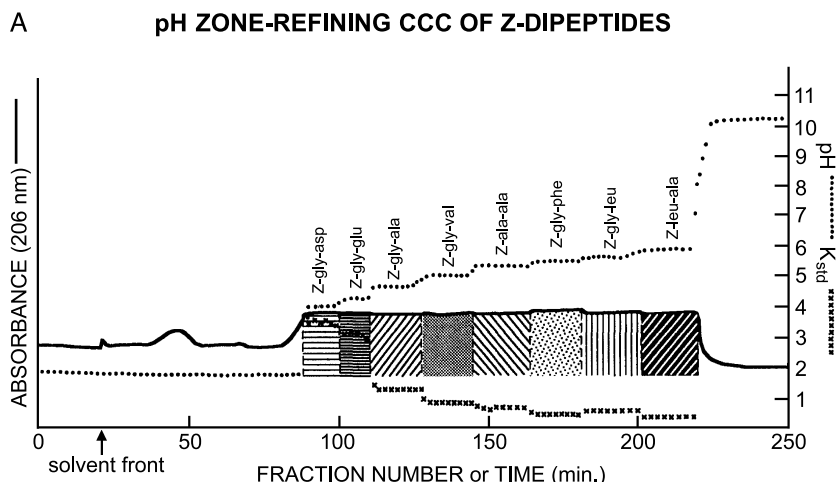


Fig. 3 Chromatograms obtained by pH zone-refining CCC. (A) Separation of CBZ(Z) dipeptides. Experimental conditions are as follows: apparatus: type-J multilayer CPC (PC Inc., Potomac, MD, USA) with a 10-cm revolution radius; column: multilayer coil, 1.6-mm ID, 325 mL capacity; solvent system: methyl *tert*-butyl ether/acetonitrile/water (2:2:3), 16 mM TFA in organic phase (pH 1.83), and 5.5 mM NH_3 in aqueous phase (pH 10.62); sample: eight CBZ(carbobenzoyloxy) dipeptides as indicated in the chromatogram, each 100 mg in 50 mL of solvent (25 mL in each phase); flow rate: 3.3 mL/hr in head-to-tail elution mode; detection: 206 nm; revolution: 800 rpm; retention of stationary phase: 65.1%. (B) Separation of bacitracin complex. High-performance liquid chromatography (HPLC) analysis indicated that two major components, bacitracins A and B, were isolated in peaks 3 and 5, respectively. Experimental conditions are as follows: apparatus and column: same as above; solvent system: methyl *tert*-butyl ether/acetonitrile/water (4:1:5), 40 mM triethylamine, 10% DEHPA in the organic stationary phase, and 20 mM HCl in aqueous mobile phase; flow rate: 3 mL/min; sample: 5 g of bacitracin dissolved in 40 mL of solvent (20 mL in each phase); revolution: 800 rpm; detection: 280 nm.

pH ZONE-REFINING CCC

In addition to the standard high-speed CCC technique described above, peptides can be purified by using a large-scale preparative method, called pH zone-refining CCC, in which analytes form a train of highly concentrated rectangular peaks with minimum overlapping.^[8,9] The solvent system and the separation procedure of this technique are quite different from the standard high-speed CCC. The method requires a pair of special agents called “retainer” and “eluter.” As suggested by their names, the retainer serves to retain the analyte in the stationary phase and the eluter serves to elute the analyte with the mobile phase. The separation of free peptides requires another agent, called an affinity ligand, such as di-[2-ethylhexyl]phosphoric acid (DEHPA), which is introduced into the stationary phase to enhance the retention of the analyte in the column. The typical retainers, eluters, and affinity ligands, together with the two-phase solvent systems, are listed in Table 2. Usually, the separation is performed with a two-phase solvent system containing *tert*-butyl methyl ether (MBE) as a major organic solvent (Table 2), which, because of its less viscous nature, gives higher stationary phase retention and partition efficiency than the butanol solvent systems.

Figure 3A and B illustrates typical chromatograms obtained by pH zone-refining CCC (Table 2).

CONCLUSION

The CCC technique is well suited for the separation of peptides and related compounds because it eliminates sample loss and denaturation caused by the solid support used in conventional liquid chromatography. The method separates multigram quantities of peptide samples using pH zone-refining CCC.

REFERENCES

1. Ito, Y.; Bowman, R.L. Countercurrent chromatography: Liquid-liquid partition chromatography without solid support. *Science* **1970**, *167*, 281–283.
2. Ito, Y. Principle and Instrumentation of Countercurrent Chromatography. In *Countercurrent Chromatography: Theory and Practice*; Mandava, N.B., Ito, Y., Eds.; Marcel Dekker Inc.: New York, 1988; 79–442. Chapter 3.
3. Conway, W.D. *Countercurrent Chromatography: Apparatus, Theory and Applications*; VCH: New York, 1990.

B pH ZONE-REFINING CCC OF BACITRACIN COMPLEX

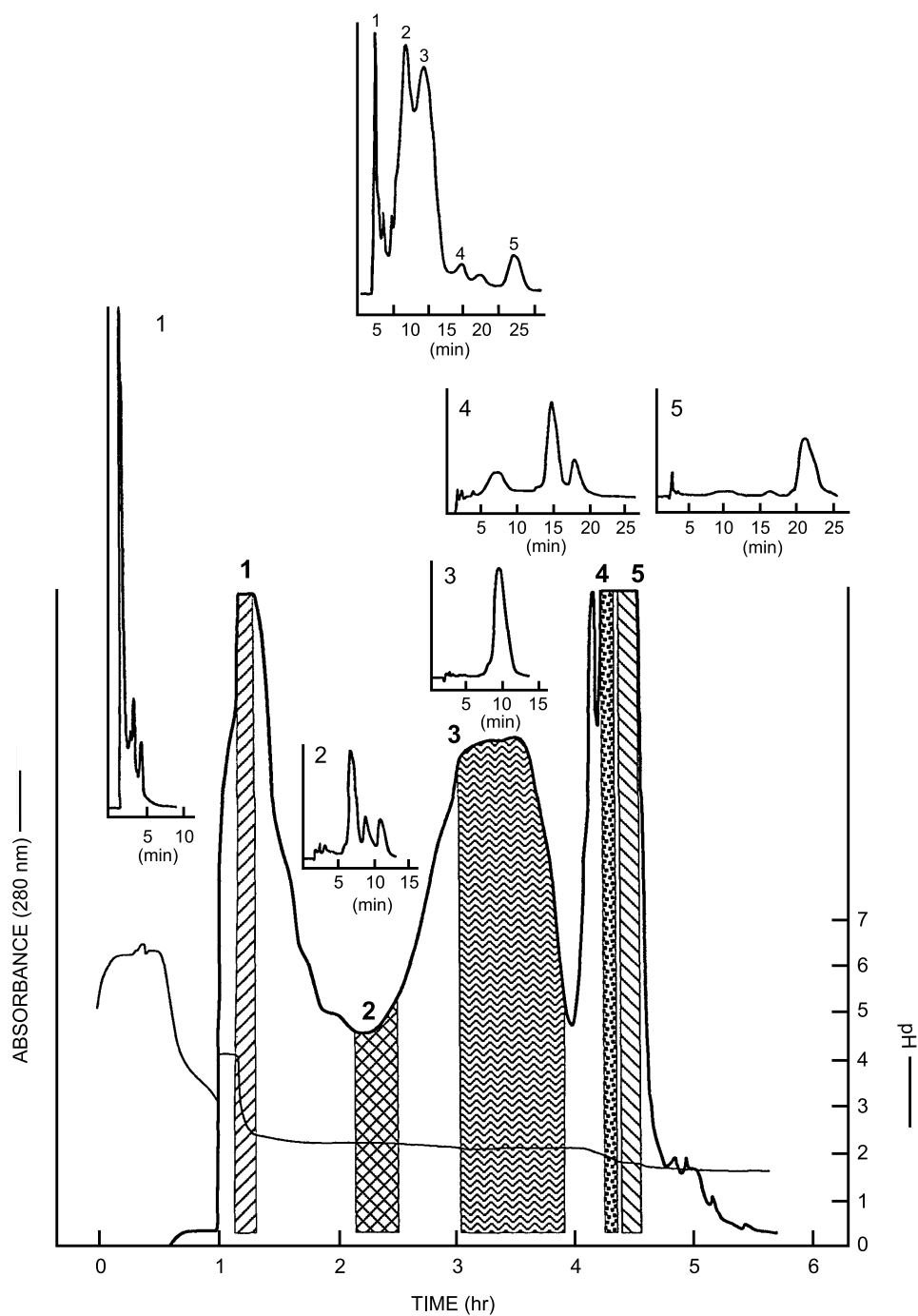


Fig. 3 (Continued).



4. Ito, Y. Countercurrent chromatography (minireview). *J. Biochem. Biophys. Methods* **1981**, 5 (2), 105–129.
5. Ito, Y. Countercurrent Chromatography. In *Methods in Enzymology*; Hirs, C.H.W., Timasheff, S.N., Eds.; Enzyme Structure, Part I; Academic Press: New York, 1983; Vol. 91, 335–351.
6. Ito, Y. Apparatus and Methodology of High-speed Countercurrent Chromatography. In *High-Speed Countercurrent Chromatography*; Yoichiro, I., Conway, W.D., Eds.; Chemical Analysis Series, Wiley Interscience: New York, 1996; Vol. 132, 3–43.
7. Ito, Y. High-speed countercurrent chromatography. *CRC Crit. Rev. Anal. Chem.* **1986**, 17 (1), 65–143.
8. Ito, Y.; Ma, Y. pH-Zone-refining countercurrent chromatography. *J. Chromatogr., A* **1996**, 753, 1–36.
9. Ma, Y.; Ito, Y. Peptide separation by pH-zone-refining countercurrent chromatography. *J. Chromatogr., A* **1997**, 771, 81–88.
10. Ito, Y.; Yang, F.-Q.; Fitze, P.E.; Sullivan, J.V. Spiral disk assembly for high-speed countercurrent chromatography. *J. Liq. Chromatogr. Relat. Technol.* **2003**, 26 (9&10), 1355–1372.
11. Ito, Y.; Menet, J.-M. Coil Planet Centrifuges for High-speed Countercurrent Chromatography. In *Countercurrent Chromatography*; Jean-Michel, M., Thiébaud, D., Eds.; Marcel Dekker: New York, 1999; 87–119. Chapter 3.



Pesticide Analysis by Gas Chromatography

Fernando M. Lanças

M.A. Barbirato

Instituto de Química de São Carlos, Universidade de São Paulo, São Carlos/SP, Brazil

Introduction

In spite of the worldwide controversy which has surrounded the use of pesticides for many years, there can be little doubt that they provide one of the most effective contributions to increasing crop production and they have helped the farmer to improve the quality and variety of our foodstuffs. However, even when used correctly, these compounds can cause ecological consequences, public health problems, and the occurrence of toxic residues in foodstuffs. These problems make necessary the development of analytical methodologies that allow the appropriate monitoring of pesticides residues.

One of the most important analytical techniques used today is high-resolution gas chromatography (HRGC). The pesticide residues can be analyzed by specific or multiresidue methods. When crops are treated with several pesticides, the use of a multiresidue method is preferable due the reduced cost and time of analysis. The methods of pesticides residue analysis usually present an initial step of extraction with a solvent which is not miscible with water, followed by a cleanup step and the analyte determination by gas chromatography.

Extraction Methods

Sample preparation represents a formidable challenge in the chemical analysis of the “real-world” samples. Not only is the majority of total analysis time spent in sample preparation, but also it is the most error-prone, least glamorous, and the most labor-intensive task in the laboratory. The components to be separated from the matrix are usually taken up with an auxiliary substance such as a carrier gas, an organic solvent, or an adsorbent. These separation processes can be regarded as extraction procedures (i.e., liquid–liquid extraction, liquid–solid extraction, Soxhlet extraction, solid-phase extraction, supercritical fluid extraction, solid-phase microextraction, etc.).

Soxhlet extraction (SE) has been the standard extraction method of the analyst for nearly 90 years. The

complete extraction produces a high-volume diluted solution that usually needs to be concentrated prior to analysis. The choice of solvent determines the solvating power as well as the temperature of the extraction. Perhaps the greatest disadvantage of using the Soxhlet method is the utilization of expensive, high-purity organic solvents such as acetone and methylene chloride.

Liquid–liquid extraction (LLE) uses two immiscible liquids as the two phases. The sample is dissolved in one of the liquids (refinate) which comes in contact with the other liquid (extractant) into a separatory funnel, under agitation, to increase the contact area among the phases. Some mixing time is usually necessary for efficient phase exchange. Multiple extractions are also mandatory if quantitative extraction is desired. Sample transfer can become a problem, especially if phase emulsions are produced.

Solid–liquid extraction (SLE), normally performed at room temperature, is a simpler version of Soxhlet extraction (see Fig. 1). The extraction of sample components is performed by blending the sample with a solvent. The choice of the extraction solvent can be determined by the analyst's experience, the equipment available in the laboratory, the type of sample to be analyzed, and the range of target analytes. Ethyl acetate is usually more powerful than acetone for extraction of more polar compounds. As regards selectivity, acetone is preferable because the amount of polar coextracted matrix interference will be less.

Solid-phase extraction (SPE) is based on low-pressure liquid chromatography, where a short column is filled with an adsorbent. The separation mechanisms are based on the intermolecular interactions among analyte molecules and functional groups of sorbent. The choice of eluent is made by the relationship between the electropic value (Σ°) and the analyte polarity. SPE is fast, selective, and economical if compared with the extraction methods described previously. It can be applicable to both nonpolar and polar analytes, but both matrix and analyte must be in the liquid state.

Supercritical fluid extraction (SFE) provides, for the first time, a viable alternative to other traditional sample preparation techniques which are slow, composed of several steps, and make use of organic sol-



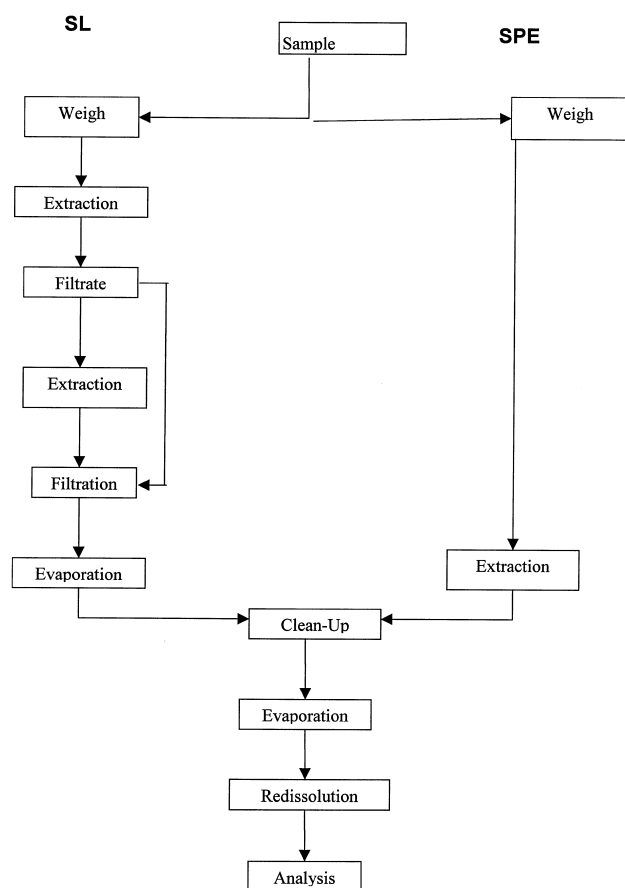


Fig. 1 Schematic diagram of the main steps of the solid-liquid extraction (SLE) and supercritical fluid extraction (SFE) methodologies for pesticide residue analysis.

vents. A supercritical fluid can be defined as any substance that is above its critical temperature and critical pressure. A supercritical fluid exhibits physicochemical properties intermediate between those of liquids and gases. Specifically, its relatively high (liquidlike) density gives good solvating power, whereas its relatively low viscosity and high diffusivity (gaslike) values provide appreciable penetrating power into the matrix. These latter two properties have been shown to give rise to higher rates of solute mass transfer into a supercritical fluid than into a liquid.

Supercritical CO₂ is the fluid with more applications at the present time, due to its readily amenable critical conditions ($T_c = 31.3^\circ\text{C}$; $P_c = 72.9\text{ atm}$) and high volatility and diffusivity, and it also is inert, inexpensive, nonflammable, nontoxic, and miscible with most solvents. It has been used to extract compounds ranging from low polarity to moderate polarity. The extraction

of polar compounds can be performed by supercritical CO₂ modified by the addition of a small volume of a polar liquid solvent.

The major parameters that influence the supercritical fluid extraction are temperature, pressure/density, fluid composition, particle size, matrix type, and extract collection system.

Solid-phase microextraction (SPME) is based on the adsorption of an analyte in a fused-silica fiber externally coated with a stationary phase and following a thermal desorption in the injector of a gas chromatograph. The fiber is introduced into the aqueous sample. In SPME, usually equilibrium among the aqueous samples and the stationary organic phase occurs instead of an exhaustive extraction. The pH, ionic strength, temperature, time, and agitation of the sample can exert an influence on the quality of the extract. The SPME process can integrate sampling, extraction, concentration, and sample introduction in just one step.

Cleanup Procedures

No single cleanup method is able to cover the entire matrix range. The need for a cleanup procedure prior to gas chromatography analysis is largely dependent on the complexity of the matrix and the range of analytes to be analyzed.

The most important cleanup procedures are liquid-liquid partition, liquid chromatography in a column of silica, florisil, and/or alumina, gel permeation chromatography, and solid-phase extraction.

Gel permeation chromatography (GPC) is the most universally applicable cleanup method for the removal of high-molecular-weight compounds. It is most favorable towards the multimatrix aspect and includes most pesticides. GPC has its limitations in the analyses of samples with a high load of coextractives and does not offer selectivity with respect to interference with low molecular weights. A selectivity gain can be obtained by the application of an additional cleanup using a small-scale chromatographic separation on silica, florisil, or alumina.

Gas Chromatographic Analysis

For the set up a GC-based multiresidue method for a specific pesticide-matrix combination, information is needed on GC retention and detectability of the analytes; also, the need for a cleanup procedure must be evaluated.

In general, the nature of the analyte determines the choice of stationary phase. For example, for the separation of organochlorine and pyrethroid pesticides, a nonpolar stationary phase such as DB-1 (or OV-1) is recommended. For the separation of somewhat more polar compounds, such as organophosphorus compounds, OV-17 (or DB-1701) can be applied. In addition, for confirmation purposes, the use of two columns with distinct stationary-phase polarities (e.g., DB-1 and DB-1701) is certainly required. A polar stationary phase (e.g., DB-wax) is suitable for the more polar compounds such as methamidofos, but its application to some detection modes is limited due to stationary-phase bleeding.

Due its robustness, particularly toward uncleaned samples, on-column, splitless injection is the most widely applied technique for sample introduction.

The conventional sensitive and specific GC detection such as electron-capture detector (ECD) (see Fig. 2), flame thermionic detector (FTD), and flame photometric detector (FPD) are still widely used in pesticide residue analysis. In recent years, mass spectrometric detection is becoming more and more important. Although other types of mass analyzers are commercially available, the equipment used in modern residue laboratories is based on two major types: the classical quadrupole mass analyzers and those based on the ion trap (also called tridimensional quadrupole).

For most compounds, the information on the m/z fragments were obtained with a quadrupole instru-

ment. It should be mentioned, however, that the sensitivity of quadrupole detectors must be enhanced by means of limited mass range scanning or by selected ion monitoring, whereas ion-trap-based instruments offer a fair sensitivity with simultaneous monitoring of the complete m/z range.

Acknowledgments

Professor Lanças wishes to express his appreciation to the Brazilian Agencies FAPESP (Fundação de Amparo à Pesquisa do Estado de São Paulo) and CNPq (Conselho Nacional de Desenvolvimento Científico e Tecnológico) for their financial support for our research programs.

Suggested Further Reading

- Font, G., J. Mañes, J. C. Moltó, and Y. Picó, Solid-phase extraction in multi-residue pesticides analysis of water, *J. Chromatogr.* 642: 135–161 (1993).
- General Inspectorate for Health Protection, Ministry of Public Health, Welfare and Sport, *Analytical Methods for Pesticides Residues in Foodstuffs*, 6th ed., The Netherlands, 1996.
- Hedrick, J. L., L. J. Mulcahey, and L. T. Taylor, Supercritical fluid extraction, *Microchim. Acta* 108: 115–132 (1992).
- Hennion, M. C., C. Call Dit-Coumes, and V. Pichon, Traces analysis of polar organic pollutants in aqueous samples: tools for the rapid prediction and optimisation of the SPE parameters, *J. Chromatogr. A* 823: 147–161 (1998).
- Ling, Y. C., H. C. Teng, and C. Castwright, Supercritical fluid extraction and cleanup of organochlorine pesticides in chinese herbal medicine, *J. Chromatogr. A* 835 (1-2), 145–157 (1999).
- Mol, H. G. J., H. G. M. Janssen, C. A. Cramers, J. J. Vreuls, and U. A. T. Brinkman, Trace level analysis of micropollutants in aqueous samples using gas chromatography with on-line sample enrichment and large volume injection, *J. Chromatogr. A* 703: 277–307 (1995).
- Peñalver, A., F. Pocurull, and R. M. Marcé, Trends in solid-phase microextraction for the determining organic pollutants in environmental samples, *Trends Anal. Chem.* 18(8): 557–568 (1999).
- van der Hoff, G. R. and P. van Zoonen, Traces analysis of pesticides by gas chromatography, *J. Chromatogr. A* 843: 301–322 (1999).

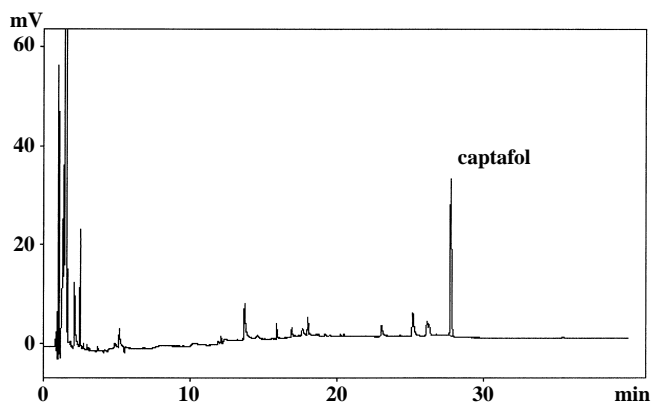


Fig. 2 Gas chromatogram (ECD) resultant from the analysis of captafol residues in tomato, after supercritical fluid extraction with neat CO₂ without further cleanup.



Pesticide Analysis by Thin-Layer Chromatography

Joseph Sherma

Lafayette College, Easton, Pennsylvania, U.S.A.

Introduction

Thin-layer chromatography (TLC) is complementary to gas chromatography (GC), high-performance liquid chromatography (HPLC), capillary electrophoresis, and immunochemical methods for the determination of single residues and multiresidues of many classes of pesticides in a variety of food, feed, biological, and environmental samples of importance in maintaining human health. The off-line, development arrangement of TLC allows significant advantages in many pesticide analyses, including high sample throughput, because many samples can be chromatographed simultaneously on a single plate.

Materials and Techniques

Sample Preparation

Trace pesticide analysis involves extraction and cleanup steps prior to TLC. Extraction is carried out with a solvent of appropriate polarity by Soxhlet, ultrasonication, homogenization, or shaking, followed by liquid-liquid partitioning and/or column adsorption or gel permeation chromatography (GPC) cleanup. Because each plate is used only once, another advantage of TLC is the possibility of analyzing cruder samples than could be injected into a GC or HPLC column without ruining the analysis, thereby reducing the number of sample preparation steps. These conventional procedures, which are slow and consume large volumes of solvents, have been superseded by solid-phase extraction (SPE) using small, disposable cartridges, columns, or disks for isolation and cleanup of pesticides from water and other samples prior to TLC analysis, especially using octadecyl (C_{18}) bonded silica gel phases. Microwave-assisted extraction is a time- and solvent-saving method for removing residues from samples such as soils. Supercritical fluid extraction (SFE) has been used for sample preparation in the screening of pesticide-contaminated soil by automated multiple development.

Stationary and Mobile Phases

Most pesticide analyses have been performed by normal- or straight-phase (NP) TLC using commercial plates precoated with silica gel and a less polar mobile phase containing combinations of two or more solvents such as acetone, methanol, chloroform, hexane, and toluene. Lipophilic bonded-phase silica gel, mainly C_{18} , and a more polar mobile phase, such as methanol or acetonitrile mixed with water, have been used for reversed-phase (RP) TLC. Other precoated layers used less often for pesticide analysis include aluminum oxide, magnesium silicate (Florisol), polyamide, cellulose, acetylated cellulose (reversed phase), and polar-modified silica gel layers containing bonded amino, cyano, diol, and thiol groups. Mixtures of sorbents or layers impregnated with various reagents have been used to prepare layers with special selectivity properties. High-performance TLC (HPTLC) plates with smaller particles of sorbent provide improved resolution, shorter analysis time, higher detection sensitivity, and more precise and accurate *in situ* quantification compared to conventional TLC plates. Plates with a preadsorbent or concentrating zone may provide cleanup by retaining some interfering substances from impure samples, and they allow the application of larger sample amounts for quantification of very low pesticide concentrations without loss of zone resolution.

The mobile phase for a particular separation is usually selected empirically using prior personal experience and literature reports of similar separations as a guide or by use of a systematic mobile-phase optimization scheme, usually the PRISMA model. Typical mobile phases that have been used for separations of many classes of pesticides on silica gel have been mixtures of hexane-acetone, toluene-acetone, chloroform-diethyl ether, and toluene-methanol, whereas mobile phases for RPTLC analyses on C_{18} layers are usually methanol-water and acetonitrile-water mixtures.

Application of Samples and Standards

Initial zones in the form of round spots are applied manually to the origins of the layer using a glass mi-



cropipette such as a 10- or 25- μ L digital microdispenser. In addition, partly or fully automated instruments are available for the application of solutions as spots or bands in the microliter to nanoliter range. Compact bands are also produced when samples are applied manually with a micropipette as diffuse vertical streaks to plates containing a preadsorbent zone. Band application is advantageous for obtaining tighter zones, high-resolution separations, and precise quantitative results by scanning densitometry.

Chromatogram Development Techniques

Pesticide analyses have usually been carried out in paper-lined, vapor-saturated glass N-chambers using a single ascending development with the mobile phase. Increased resolution is obtained by overpressured layer chromatography (OPLC) and automated multiple development (AMD) with gradient elution. An AMD separation of a complex pesticide mixture, with multiple wavelength scanning to provide confirmation of identity, is shown in Fig. 1.

Zone Detection

Pesticides are detected after development as colored, ultraviolet (UV)-absorbing, or fluorescent zones after reaction with a more or less selective re-

agent applied to the layer by spraying or dipping. Silver nitrate with UV irradiation is an example of a chromogenic detection reagent used to visualize chlorinated pesticides, whereas arsenic trichloride-sulfuric acid has been used to detect various pesticide classes. Phenolic pesticides and metabolites are detected by use of 7-chloro-nitrobenzo-2-oxa-1,3-diazole to produce fluorescent 4-nitrobenzofuran derivatives or by means of Pauly's reagent for those compounds that can form intensely colored azo dyes. Compounds that absorb short-wavelength (254-nm) UV light, particularly those with aromatic rings and/or conjugated double bonds, can be detected by fluorescence quenching on a layer containing a fluorescent indicator (phosphor). Another important advantage of the off-line operation of TLC is the versatility achieved by use of multiple detection methods. For example, the layer can be viewed under long- and short-wave UV light, followed by one or more chromogenic, fluorogenic, or biological detection methods. Cholinesterase inhibition has been used widely for detection of certain pesticide classes, such as organophosphates, with very low detection limits.

Quantitative Analysis

Quantitative pesticide analyses are performed by measuring the areas of sample and standard zones using a slit-scanning or video densitometer. Calibration curves are prepared for each analyte, and sample amounts are interpolated from the curves. Excellent accuracy and precision can be obtained because samples and standards are chromatographed and measured in parallel under the same conditions on a single TLC plate.

Identification and Confirmation of Zones: TLC Combined with Spectrometry

The identification of unknown pesticide zones is initially based on the comparison of the migration of sample zones relative to standards developed on the same layer and colors obtained with selective chromogenic and fluorogenic detection reagents. Many densitometers can record *in situ* UV and visible absorption and fluorescence excitation spectra to confirm compound identification by the comparison of unknown spectra with stored standard spectra obtained under identical conditions or spectra of standards measured on the same plate. Additional confirmation methods include off-line and on-line combination of TLC with infrared, Raman,

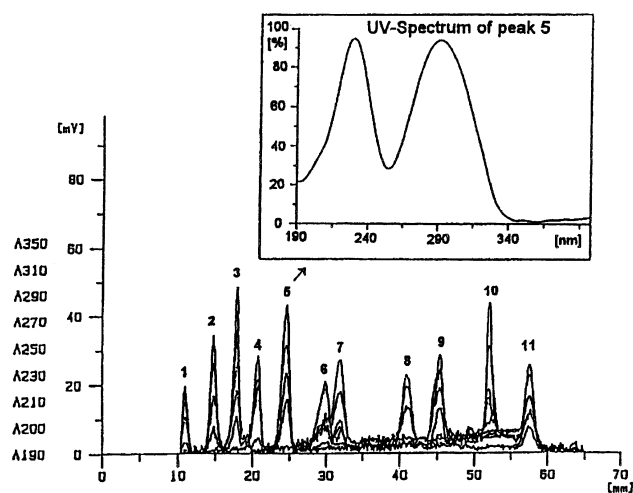


Fig. 1 Multiwave densitogram of a mixture of 11 pesticides (50 ng/compound) and *in situ* ultraviolet spectrum of peak 5. Compounds represented by peaks: 1, clopyralid acid; 2, triclopyr acid; 3, bitertanol; 4, atraton; 5, chloridazon; 6, sethoxydim; 7, atrazine; 8, iprodione; 9, desmedipham; 10, ethofumesate; 11, pendimethalin.

or mass spectrometry or with gas or column liquid chromatography. Identification of pesticides by multiwavelength UV scanning is demonstrated in Fig. 1.

Special Techniques

Thin-layer radiochromatography (radio-TLC) is widely applied for a variety of environmental studies involving radiolabeled pesticides, such as plant uptake from soil, bioaccumulation in fish, dissipation from soil, metabolism in soil, plants, and fish, and environmental fate. The determination of the lipophilicity of pesticides is important because their bioaccumulation and tendency for degradation and biotransformation are related to lipid solubility. TLC has advantages for lipophilicity studies compared to traditional partition coefficient measurement in an octanol–water system.

Examples of Pesticide TLC Analysis Applications

Determination of Carbaryl and Propoxur in Water

Sample preparation: Chloroform extraction; grain samples were also analyzed.

Layer: Silica gel G.

Mobile phase: Acetone–hexane (1:4) or butanol–acetic acid–water (3:1:6, butanol layer).

Detection: Spray with diazotized *p*-nitroaniline followed by aqueous NaOH to produce blue and purple spots, respectively.

Quantification: Colored sample and standard zones scraped and eluted with 6*M* NaOH and the solutions measured by spectrometry.

Determination of 24 Pesticides in Water

Sample preparation: One thousand-milliliter samples of ground, surface, and drinking water were extracted using a C₁₈ SPE cartridge; the cartridge was eluted with 3 mL of acetonitrile, and the eluate was used directly for TLC or cleaned up on a silica column eluted with acetonitrile.

Layer: HPTLC silica gel 60F-254; samples applied by the spray-on technique using a Linomat IV.

Mobile phase: AMD with 20-step universal gradients based on methylene chloride containing 0.1% acetic acid, methanol, and hexane (screening gradient) and *t*-butyl methyl ether containing 0.1% acetic acid, acetonitrile, and hexane (confirmatory gradient).

Detection and identification: Comparison of sample and standard chromatograms scanned at six different wavelengths with a densitometer.

Determination of Carbamate Insecticides in Water

Sample preparation: Pesticides recovered from pond water by SPE on a C₁₈ column eluted with ethyl acetate.

Layer: Channeled preadsorbent HPTLC silica gel. Mobile phase: Toluene–acetone (4:1) (for carbaryl, carbofuran, methiocarb) or hexane–acetone–chloroform (75:5:10) (propoxur).

Detection: Plate dipped into *p*-nitrobenzenediazonium fluoborate chromogenic reagent.

Quantification: Densitometric scanning of sample and standard zones at 610 nm (carbaryl), 550 nm (carbofuran, propoxur), or 510 nm (methiocarb).

Determination of Atrazine and Its Deethyl, Deisopropyl, and Hydroxy Metabolites in Surface soils and Subsoils

Sample preparation: Soil was extracted with methanol, the suspension was filtered, and the filtrate was concentrated.

Layer: HPTLC reversed-phase plates; standards and samples were applied with a Nanomat III.

Mobile phase: Methanol–water (7:3), development in a horizontal chamber.

Quantification: Zones were scanned at 222 nm with a dual-wavelength flying-spot densitometer; standard curves were prepared by quadratic regression analysis, which gave a higher correlation coefficient than linear regression.

Determination of Abate in Environmental Water

Sample preparation: Acidified water was extracted with chloroform and the extract dried by filtering through Whatman PS paper.

Layer: Channeled preadsorbent C₁₈ chemically bonded silica gel; paper-lined glass chamber, 10 cm development.

Mobile phase: Acetonitrile–water (8:2).

Detection: Spraying with 5% magnesium chloride in methanol, air-drying, spraying with 0.3% *N*,2,6-trichlorobenzoquinoneimine (TCQ) in hexane, heating for 5–10 min at 110°C; bright red-orange zone, 200 ng sensitivity.

Quantification: Scanning densitometry.



*Determination of Chlorpyrifos and Its Metabolite
3,5,6-Trichloro-2-Pyridinol in Bananas and Tap Water*

Sample preparation: Water was extracted with hexane for chlorpyrifos (a) and benzene for 3,5,6-trichloro-2-pyridinol (TCP) (b); banana samples were prepared using standard Food and Drug Administration procedures based on extraction, solvent partitioning, and silica gel or alumina column chromatography.

Layer: Channeled preadsorbent silica gel G.

Mobile phase: (a) hexane–chloroform (8:2); (b) hexane–acetone–methanol–acetic acid (60:30:10:0.2); paper-lined glass N-chamber, 10 cm development.

Detection: Dipping into silver nitrate reagent followed by exposure to UV light; dark brown spots on a white background, sensitivity 25–100 ng.

Quantification: Scanning densitometry at 440 nm.

*Determination of Cymiazole and Pentachlorophenol
in River Water and Honey*

Sample preparation: The pesticides were extracted from water and honey using C₁₈ SPE.

Layer: Channeled preadsorbent high-performance silica gel.

Mobile phase: Toluene–methanol (9:1) for pentachlorophenol (PCP); hexane–acetone–methanol–glacial acetic acid (35:10:5:0.1) for cymiazole; paper-lined twin-trough chamber.

Detection: Fluorescence quenching under 254-nm UV light; 200 ng sensitivity.

Quantification: Scanning densitometry at 215 nm for PCP and 265 nm for cymiazole.

Determination of Diflubenzuron in Water

Sample preparation: Extraction on a C₁₈ SPE column eluted with acetonitrile.

Layer: Channeled preadsorbent high-performance silica gel.

Mobile phase: Ethyl acetate–toluene (1:3); paper-lined glass HPTLC chamber.

Detection: Spraying with 6M HCl, heating for 10 min at 180°C, and spraying with Bratton–Marshall reagent [sodium nitrite and N-(1-naphthyl)ethylenediamine dihydrochloride]; purple-blue band; 100 ng sensitivity.

Quantification: Scanning densitometry at 550 nm.

Suggested Further Reading

The following references contain detailed information on the procedures and instrumentation of TLC and applications to pesticide residue analysis.

Fodor-Csorba, K., Pesticides, in *Handbook of Thin Layer Chromatography*, 1st ed. (J. Sherma and B. Fried, eds.), Marcel Dekker, Inc., New York, 1991, pp. 663–715.

Fodor-Csorba, K., Pesticides, in *Handbook of Thin Layer Chromatography*, 2nd ed. (J. Sherma and B. Fried, eds.), Marcel Dekker, Inc., New York, 1996, pp. 753–817.

Follweiler, J., and J. Sherma, *Handbook of Chromatography – Pesticides*, CRC Press, Boca Raton, FL, 1984.

Fried, B. and J. Sherma, *Practical Thin Layer Chromatography – A Multidisciplinary Approach*, CRC Press, Boca Raton, FL, 1996.

Fried, B. and J. Sherma, *Thin Layer Chromatography*, 4th ed., Marcel Dekker, Inc., New York, 1999.

Sherma, J., Pesticide analysis by thin layer chromatography, in *Analytical Methods for Pesticides and Plant Growth Regulators* (G. Zweig and J. Sherma, eds.), Academic Press, San Diego, CA, 1973, Vol. VII, pp. 3–87; 1980, Vol. XV, pp. 79–122; 1986, Vol. XIV, pp. 1–39.

Sherma, J., Thin layer chromatography of pesticides – A review of recent techniques and applications, *J. Liquid Chromatogr.* 5: 1013–1032 (1982).

Sherma, J., Thin layer chromatography of pesticides, *J. Planar Chromatogr. – Mod. TLC* 4: 7–14 (1991).

Sherma, J., Determination of pesticides by thin layer chromatography, *J. Planar Chromatogr. – Mod. TLC* 7: 265–272 (1994).

Sherma, J., Thin layer chromatography in environmental analysis, *Rev. Anal. Chem.* 14(2): 75–142 (1995).

Sherma, J., Review: Determination of pesticides by thin layer chromatography, *J. Planar Chromatogr. – Mod. TLC* 10: 80–89 (1997).

Sherma, J., Planar chromatography, *Anal. Chem.* 72: 9R–25R (2000); see also reviews of TLC each even numbered year in this journal beginning in 1970.

Sherma, J., Recent advances in thin layer chromatography of pesticides, *J. AOAC Int.* 82: 48–53 (1999).

Sherma, J. and B. Fried, *Handbook of Thin Layer Chromatography*, 2nd ed., Marcel Dekker, Inc., New York, 1996.

Singh, K. K. and M. S. Shekhawat, Thin layer chromatographic methods for analysis of pesticides residues in environmental samples, *J. Planar Chromatogr. – Mod. TLC* 11: 164–185 (1998).



pH, Effect on MEKC Separation

Koji Otsuka

Shigeru Terabe

Himeji Institute of Technology, Hyogo, Japan

Introduction

In micellar electrokinetic chromatography (MEKC), the effect of the constituents of the buffer is not significant, whereas the pH is critical, especially for ionizable analytes, as well as to the electrokinetic velocities. The change in the buffer pH, especially in the lower-pH region, causes a significant change in the velocity of the electro-osmotic flow (EOF).

Electrokinetic Velocities

When sodium dodecyl sulfate (SDS) is employed as an ionic micelle or pseudo-stationary-phase in MEKC, the relationship between the velocity of the EOF, v_{EOF} , and the migration velocity of the SDS micelle, v_{mc} , is given as

$$v_{\text{mc}} = v_{\text{EOF}} + v_{\text{ep}} \quad (1)$$

where v_{ep} is the electrophoretic velocity of the SDS micelle. The sign of each velocity is defined as plus when the migration is toward the cathode and as minus when toward the anode.

The dependence of these electrokinetic velocities on pH is shown in Fig. 1. In the case of capillary zone electrophoresis (CZE), with a bare fused-silica capillary, the pH greatly affects the EOF velocity (i.e., v_{EOF} significantly decreases with the decrease in pH from 8 to 3). In MEKC, however, the dependence of v_{EOF} on pH is different from that in CZE, especially under weakly acidic conditions (pH 7.0–5.5). In the range of pH between 7.0 and 5.5, v_{EOF} slightly decreases with the decrease in pH, due to the adsorption of the SDS molecule or monomer on the inside wall of the capillary. On the other hand, v_{EOF} rapidly decreases with the decrease in the pH below 5.5. The decrease of v_{EOF} is mainly caused by the decrease in the zeta-potential of the inside wall of the capillary, because the dissociation of silanol groups on the capillary wall is more suppressed as the solution becomes more acidic.

The electrophoretic velocity of the SDS micelle (v_{ep}) (i.e., $v_{\text{mc}} - v_{\text{EOF}}$) is almost constant over the pH

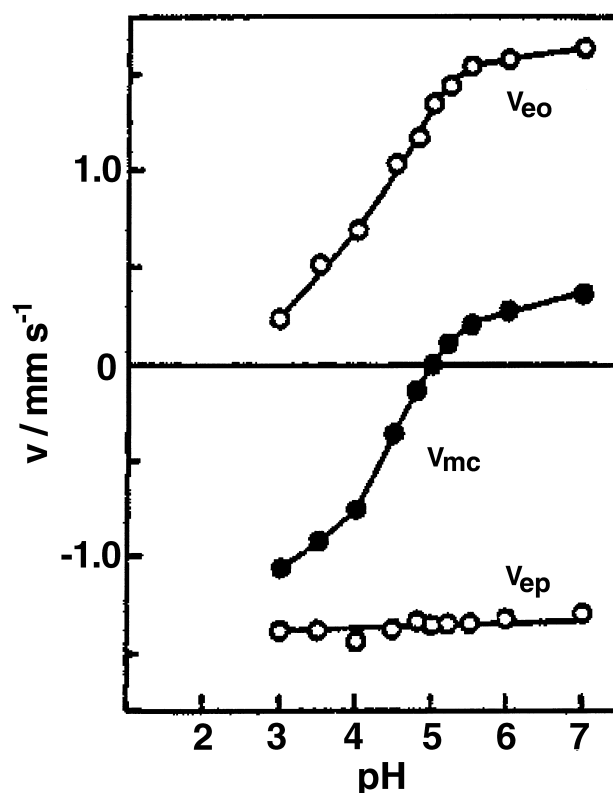


Fig. 1 Dependence of electrokinetic velocities on pH: v_{eof} = velocity of the EOF, v_{mc} = migration velocity of the micelle, v_{ep} = electrophoretic velocity of the micelle. (Reprinted from K. Otsuka and S. Terabe, *J. Microcol. Separ.*, 1989, 1, 150 with permission.)

range in Fig. 1; that is, the charge of the SDS micelle is almost constant in this pH range.

The migration velocity of the SDS micelle (v_{mc}) changes from positive to negative at a pH below 5.0, which means that the SDS micelle migrates toward the anode; thus, the migrating direction of the SDS micelle is opposite that of the EOF. One should note that the reproducibility of retention times was low in acidic solutions, especially below pH 5.0, compared with that in neutral SDS solutions.



Migration Time

The migration time, t_R , of a neutral solute in MEKC is represented by

$$t_R = \left(\frac{1 + k}{1 + (t_0/t_{mc})k} \right) t_0 \quad (2)$$

where t_0 is the migration time of an unretained solute or insolubilized solute by the micelle at all, t_{mc} is that of the micelle, and k is the retention factor of the solute. Here, we define the sign of the migration time as positive when the solute migrates toward the cathode or the velocity of the solute, v_s , is positive, and vice versa. When neutral SDS solutions are employed, the t_{mc} is positive and the t_R of any neutral solute is always positive and limited to between t_0 and t_{mc} . Under acidic condition, or typically pH below 5.0, the neutral solute totally solubilized by the SDS micelle, such as Sudan III, migrates toward the anode and, hence, t_{mc} becomes negative, whereas the solute insolubilized by the micelle (e.g., methanol) migrates toward the cathode. By considering Eq. (2), it is apparent that the migration time of the solute whose capacity factor is equal to $-(t_{mc}/t_0)$ becomes infinity when $t_{mc} < 0$ and the solute never migrates in the column, whereas the solute of $k > -(t_{mc}/t_0)$ migrates toward the same directions as the micelle.

Resolution

In MEKC, the resolution, R_s , of two peaks of which the retention factors are k_1 and k_2 is described as (see the entry Retention Factor, Effect on MEKC Separation)

$$R_s = \frac{N^{1/2}}{4} \left(\frac{\alpha - 1}{\alpha} \right) \left(\frac{k_2}{1 + k_2} \right) \left(\frac{1 - t_0/t_{mc}}{1 + (t_0/t_{mc})k_1} \right) \quad (3)$$

For the closely migrating peaks, we can assume that $k_1 = k_2 = k$. Then, the fourth term of the right-hand side of Eq. (3) will become infinity when k is equal to $-(t_{mc}/t_0)$; thus, the resolution will become maximum or infinity. The function $f(k)$, the product of the last two terms in Eq. (3), is written as

$$f(k) = \left(\frac{k_2}{1 + k_2} \right) \left(\frac{1 - t_0/t_{mc}}{1 + (t_0/t_{mc})k_1} \right) \quad (4)$$

The value of $f(k)$ approaches infinity, as in the case of t_R , as k becomes close to $-t_{mc}/t_0$, and, consequently, R_s becomes quite large. Hence, a considerably large R_s will be obtained for a solute having k close to $-t_{mc}/t_0$, although a quite long t_R is required for such a solute.

Migration Window

The parameter t_0/t_{mc} is related to the migration window. As long as t_{mc} is positive, a smaller value of t_0/t_{mc} gives a wider migration window. Some attempts to extend the migration window have been made by (a) the addition of organic modifiers (e.g., methanol, acetonitrile, and 2-propanol) to the micellar solution and (b) the use of capillaries of which the inside walls were chemically modified to reduce the silanol-group concentration. In each case, the extension was mainly achieved through decreasing the EOF owing to a decrease of the zeta-potential of capillaries. As mentioned earlier, the migration window is no longer limited when acidic micellar solutions (i.e., pH below 5.0) are employed. The value of zero for t_0/t_{mc} corresponds to the case of conventional chromatography, in which the elution range is infinity; in other words, the solute of $k = \infty$ (e.g., Sudan III) never comes out from the capillary. The case of $t_0/t_{mc} < 0$ also causes the infinite migration window.

Ionizable Solutes

If the ionized form of the solute has the same charge as the micelle, it will be incorporated into the micelle less than with its neutral form. By contrast, the ionized form of the solute will be bound to the micelle more strongly than its neutral form if the ionized solute has the opposite charge to that of the micelle. The dependence of the apparent retention factor, k_{app} , on the buffer pH for chlorinated phenols has been investigated in an SDS/MEKC, where both the ionizable solutes or chlorinated phenols and SDS have negative charge. The apparent retention factor was calculated by the usual equation for the retention factor in MEKC:

$$k_{app} = \frac{t_R - t_0}{[1 - (t_R/t_{mc})]t_0} \quad (5)$$

regardless of whether the solutes were ionized or not. For acidic compounds, the increase in pH will promote ionization; then, the distribution coefficient to the SDS or an anionic micelle will be decreased. For example, the apparent retention factor for 2,3,4,5-tetrachlorophenol ($pK_a = 5.6$) was dramatically changed from ~ 100 at pH 6.0 to 4 at pH 9.0.

It is often essential to find the optimum pH for the separation of ionizable solutes, where closely spaced peaks are obtained.



Suggested Further Reading

- Foret, F., L. Kriváková, and P. Bocek, *Capillary Zone Electrophoresis*, VCH, Weinheim, 1993, pp. 67–74.
- Lukacs, K. D. and J. W. Jorgenson, Capillary zone electrophoresis: Effect of physical parameters on separation efficiency and quantitation, *J. High Resolut. Chromatogr. Chromatogr. Commun.* 8: 405–411 (1985).
- Otsuka, K. and S. Terabe, Effects of pH on electrokinetic velocities in micellar electrokinetic chromatography, *J. Microcol. Separ. I*: 150–154 (1989).
- Otsuka, K. and S. Terabe, Micellar electrokinetic chromatography, *Bull. Chem. Soc. Jpn.* 71: 2465–2481 (1998).
- Otsuka, K., S. Terabe, and T. Ando, Electrokinetic chromatography with micellar solutions: Retention behaviour and separation of chlorinated phenols, *J. Chromatogr.* 348: 39–47 (1985).



pH-Peak-Focusing and pH-Zone-Refining Countercurrent Chromatography

Yoichiro Ito

National Heart, Lung, and Blood Institute, National Institutes of Health, Bethesda, Maryland, U.S.A.

Introduction

These two countercurrent chromatography (CCC) techniques are mutually related: pH-peak-focusing CCC is for analytical-scale separations and pH-zone-refining CCC is for preparative-scale separations.

Discussion

The pH-peak-focusing CCC technique was developed from an accidental finding that a thyroxine analog produced an unusually sharp elution peak [1,2]. The cause was found that an acid present in the sample solution affected the retention time of the analyte (Fig. 1a). The mechanism of this peak-sharpening effect is shown in Fig. 1b, where a portion of the separation column contains the organic stationary phase in the upper half and the aqueous mobile phase in the lower half. Because of its nonlinear isotherm, the acid in the sample solution forms a sharp trailing border which traps the analyte in the following manner: When the analyte molecule is present in the mobile phase (position 1), it is protonated by low pH and transferred into the organic stationary phase (position 2). As the sharp acid border moves forward, the analyte molecule is exposed to high pH (position 3), deprotonated, and transferred back to the aqueous mobile phase (position 4), where it quickly migrates through the acid border to repeat the above cycle. Consequently, the analyte molecules are trapped with the sharp acid border and eluted as a sharp peak, together with the acid border.

A similar effect can be produced by introducing an organic acid in the stationary phase. Figure 2a shows the separation of DNP-amino acids using three spacer acids (i.e., acetic acid, propionic acid, and *n*-butyric acid) in the stationary phase [2]. Hydrophilic DNP-glutamic acid is eluted between acetic and propionic acids; DNP-alanine between propionic and *n*-butyric acids, and hydrophobic DNP-leucine after *n*-butyric acid. The method can be effectively applied for the separation and concentration of a small amount of organic ions present in a large volume of the sample solution. However, the most useful application has been

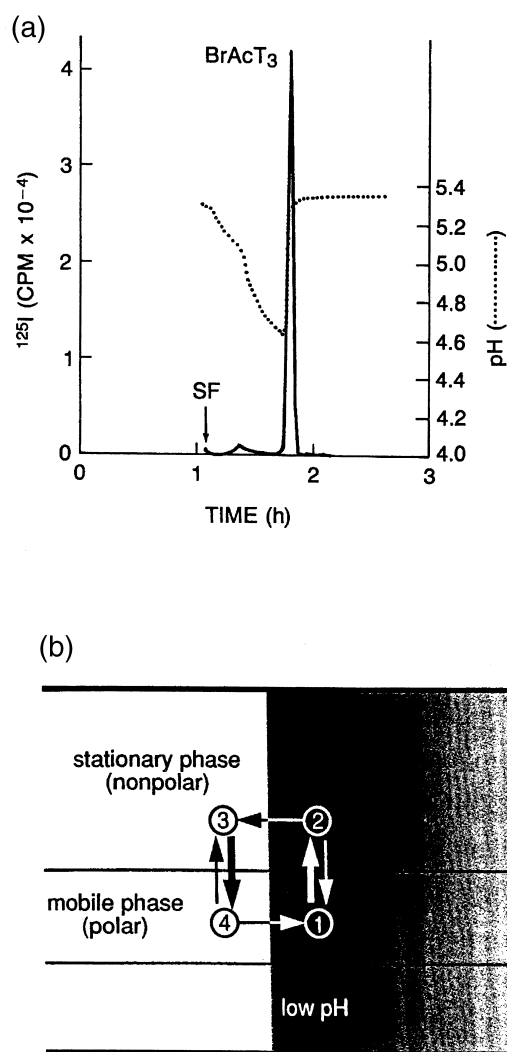


Fig. 1 (a) Sharp analyte peak produced by an acid in the sample solution; (b) mechanism of sharp peak formation.

found in the preparative-scale separation. When the sample size of the above DNP-amino acids is increased each from 6 mg to 600 mg, a strange chromatogram was produced as shown in Fig. 2b, where all peaks became rectangular in shape, each associated with its own



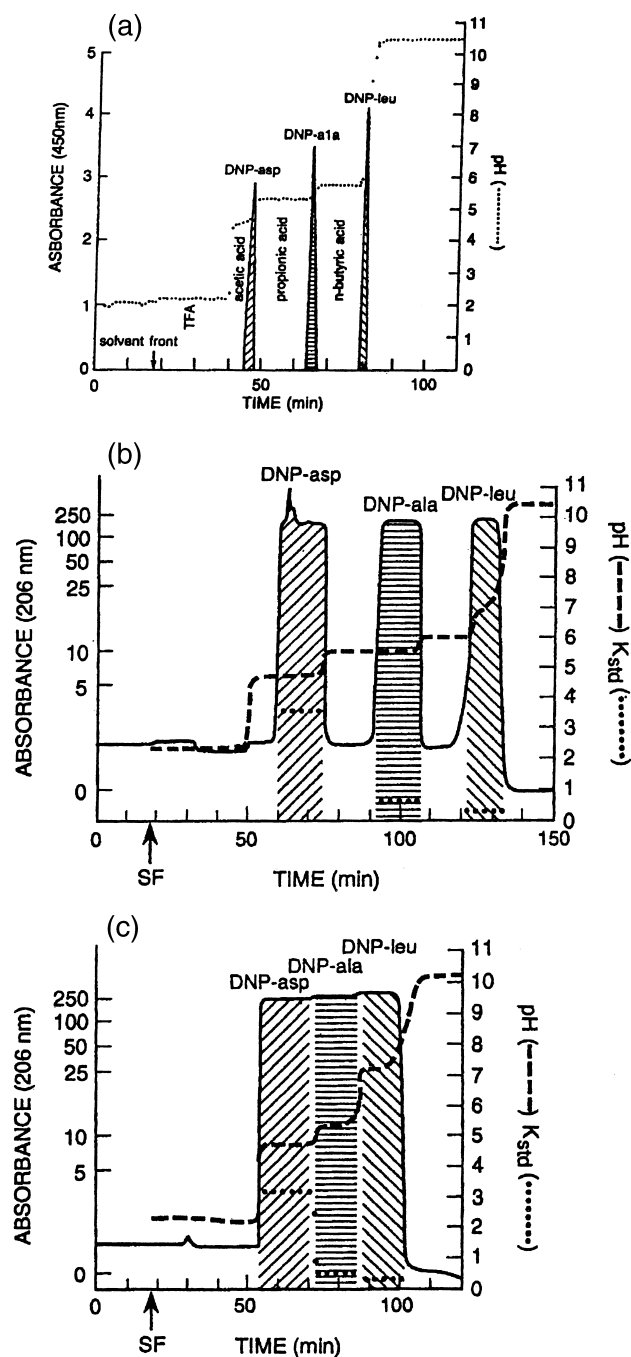


Fig. 2 Separation of three DNP-amino acids showing a transition from pH-peak-focusing CCC to pH-zone-refining CCC. (a) Analytical separation by pH-peak-focusing CCC (6 mg each component); (b) formation of rectangular peaks by increasing sample size (600 mg each component); (c) elimination of three spacer acids to form fused rectangular peaks.

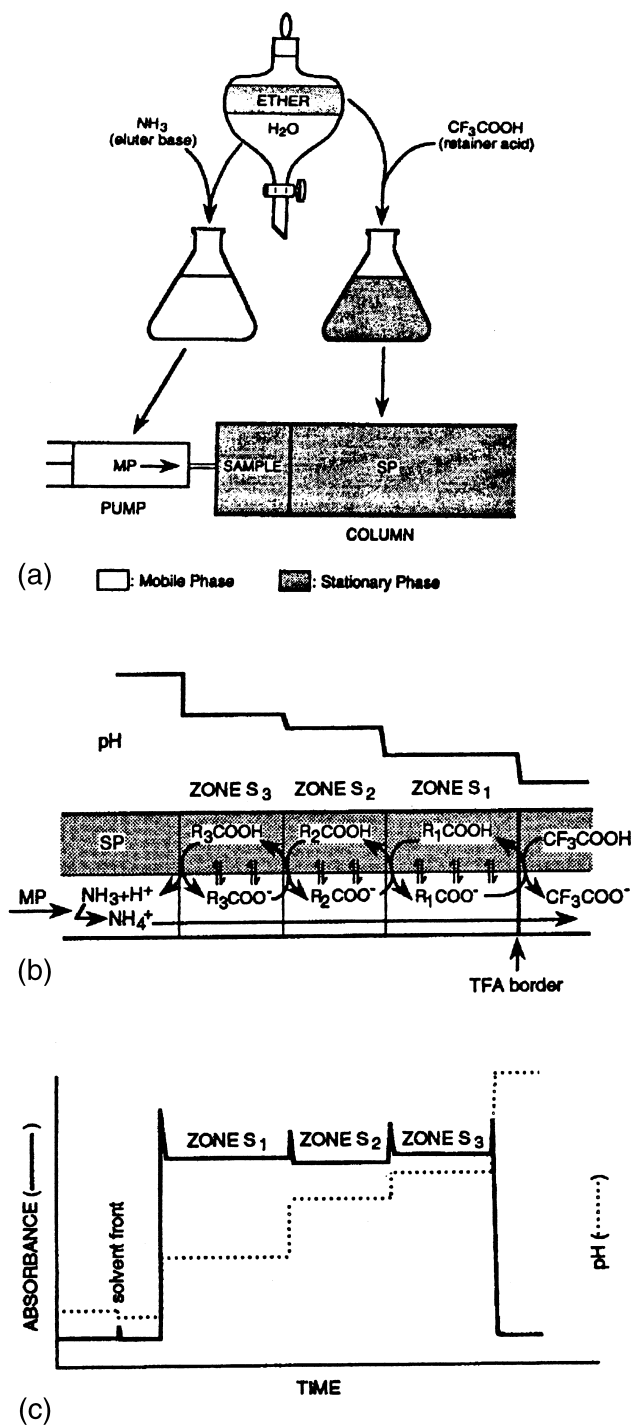


Fig. 3 Mechanism of pH-zone-refining CCC. (a) Preparation for the model experiment; (b) chemohydrodynamic equilibrium in the separation column; (c) elution profile of three major analytes.

specific pH. The elimination of the spacer acids resulted in the fusion of these peaks while maintaining their own pH, suggesting that the rectangular shape of each peak is well preserved (Fig. 2c) [2–4].

The mechanism of this pH-zone-refining CCC (for the separation of acidic compounds) is illustrated by the following model experiment [2,4,5]. Figure 3a shows the preparation of the solvent phases. Ether and water are equilibrated in a separatory funnel and separated. A suitable amount (usually 10–40 mM) of TFA (trifluoro-

acetic acid) (“retainer”) is added to the lighter organic phase, which is then used as the stationary phase. Ammonia (10–40 mM) (“eluter”) is added to the heavier aqueous phase, which is used as the mobile phase. The experiment is initiated by filling the entire column with the stationary phase, followed by injection of a sample solution containing three major acidic analytes (S_1 , S_2 , and S_3). Then, the column is eluted with the mobile phase while the apparatus is rotated at a desired g-force. Figure 3b shows steady-state chemohydrodynamic equi-

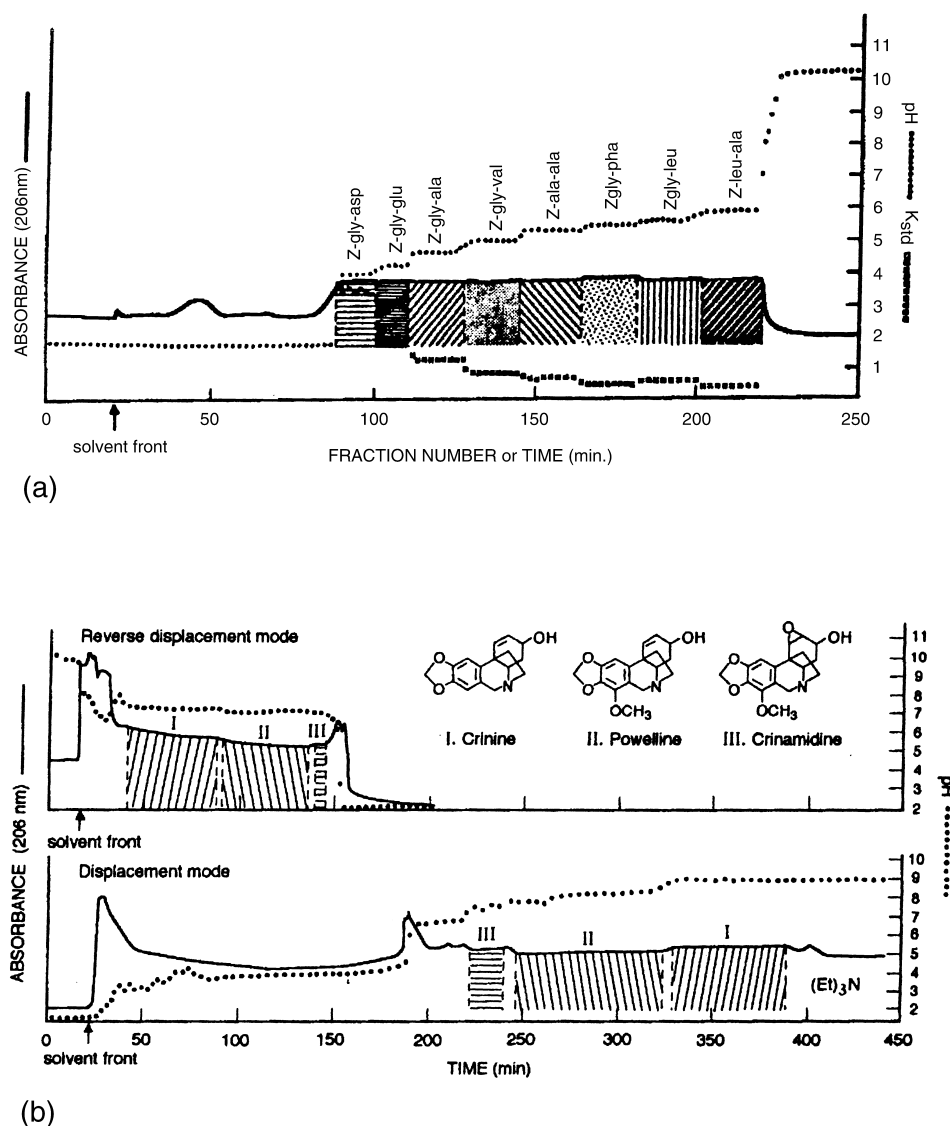


Fig. 4 Some applications of pH-zone-refining CCC. (a) Separation of eight CBZ dipeptides (see Table 1) [4,8]; (b) separation of amaryllis alkaloids using both the lower phase (upper chromatogram) and upper phase (lower chromatogram) as the mobile phase (see Table 1) [4,9]; (c) separation of catecholamines using a ligand (see Table 2) [4,12]; (d) separation of two groups of dipeptide each using an affinity ligand [4, 13] (see Table 2). (*Continued*)



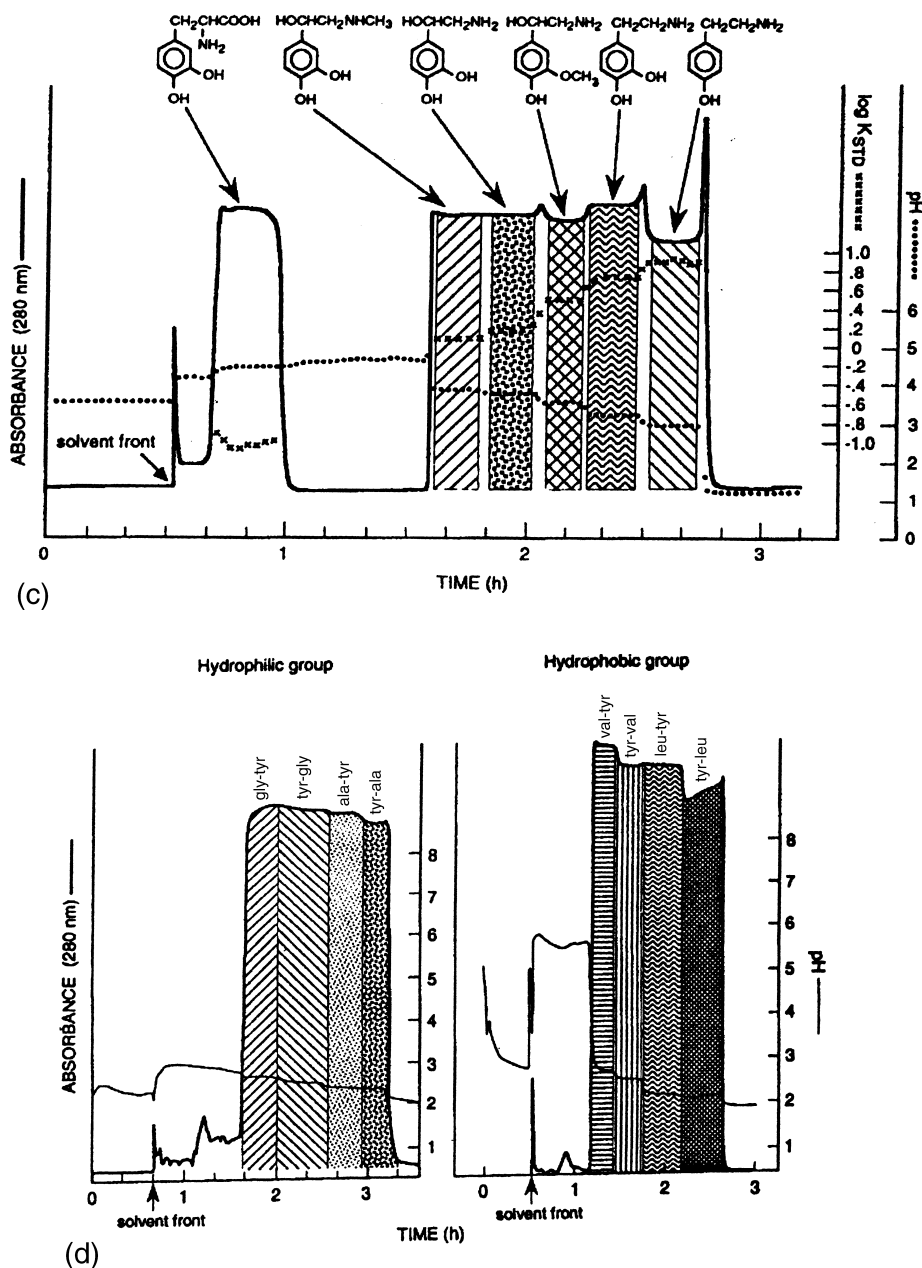


Fig. 4 (Continued)

librium established in the separation column. The retainer acid TFA forms a sharp trailing border which travels through the column at a constant rate substantially lower than that of the mobile phase.

Three analytes S_1 , S_2 , and S_3 each form a discrete pH zone behind the sharp retainer border in the order of their pK_a 's and hydrophobicities. The proton transfer takes place at each zone boundary according to the difference in pH between the neighboring zones,

causing solute exchange between the two phases, as indicated by curved arrows. Once the equilibrium is established, all solute zones move at a same rate determined by that of the sharp retainer border. Charged impurities present in each zone are eliminated either forward or backward according to their pK_a 's and hydrophobicities, and accumulated at the zone boundaries. Consequently, the analytes are eluted as fused rectangular peaks with minimum

Table 1 Samples and Solvent Systems Applied to Standard pH-Zone-Refining CCC

Sample ^a	Solvent system ^b (vol. ratio)	Pair of acid–base reagents ^c	
		Retainer	Eluter
DNP-Amino acids	MBE/AcN/H ₂ O (4:1:5)	TFA (200 μ L/SS)	NH ₃ (0.1%/MP)
Proline (OBzl) (1 g)	MBE/H ₂ O	TEA (10 mM/SP)	HCl (10 mM/MP)
Amino acid (OBzl) (0.7 g)	MBE/H ₂ O	TEA (10 mM/SP)	HCl (10 mM/MP)
Amino acid (OBzl) (10 g)	MBE/H ₂ O	TEA (5 mM/SP)	HCl (20 mM/MP)
CBZ dipeptides (0.8 g)	MBE/AcN/H ₂ O (2:2:3)	TFA (16 mM/SP)	NH ₃ (5.5 mM/MP)
CBZ dipeptides (3 g)	MBE/AcN/H ₂ O (2:2:3)	TFA (16 mM/SP)	NH ₃ (5.5 mM/MP)
CBZ tripeptides (0.8 g)	BuOH/MBE/AcN/H ₂ O (2:2:1:5)	TFA (16 mM/SP)	NH ₃ (2.7 mM/MP)
Dipeptide- β NA (0.3 g)	MBE/AcN/H ₂ O (2:2:3)	TEA (5 mM/SP)	HCl (5 mM/MP)
Indole auxins (1.6 g)	MBE/H ₂ O	TFA (0.04%/SP)	NH ₃ (0.1%/MP)
TCF (0.01–1 g)	DEE/AcN/10 mM AcONH ₄ (4:1:5)	TFA (200 μ L/SS)	MP
Red #3 (0.5 g)	DEE/AcN/10 mM AcONH ₄ (4:1:5)	TFA (200 μ L/SS)	MP
Orange #5 (0.01–5 g)	DEE/AcN/10 mM AcONH ₄ (4:1:5)	TFA (200 μ L/SS)	MP
Orange #10 (0.35 g)	DEE/AcN/10 mM AcONH ₄ (4:1:5)	TFA (200 μ L/SS)	MP
Red #28 (0.1–6 g)	DEE/AcN/10 mM AcONH ₄ (4:1:5)	TFA (200 μ L/SS)	MP
Eosin YS (0.3 g)	DEE/AcN/10 mM AcONH ₄ (4:1:5)	TFA (200 μ L/SS)	MP
Amaryllis alkaloids (3 g)	MBE/H ₂ O	TEA (5 mM/SP)	HCl (5 mM/MP)
	MBE/H ₂ O (DPCCC)	HCl (10 mM/SP)	TEA (10 mM/MP)
Vinca alkaloids (0.3 g)	MBE/H ₂ O (DPCCC)	HCl (5 mM/SP)	TEA (5 mM/MP)
Structural isomers (15 g)	MBE/AcN/H ₂ O (4:1:5)	TFA (0.32%/SP)	NH ₃ (0.8%/MP)
Stereoisomers (0.4 g)	Hex/EtOAc/MeOH/H ₂ O (1:1:1:1)	TFA, octanoic acid	NH ₃ (0.025%/MP)
Fish oil (0.5 g)	Hex/EtOH/H ₂ O (4:1:5)	TFA (10 mM/SP)	NH ₃ (0.1%/MP)
NDGA derivatives (10 g)	MBE/H ₂ O	TFA (25 mM/SP)	NaOH (100 mM/MP)

^aDNP: dinitrophenyl; CBZ: carbobenzoxy; OBzl: benzylesters; β NA: naphthyl amide; TCF: tetrachlorofluorescein; amaryllis alkaloids: crinine, powelline, and crinamidine; vinca alkaloids: vincamine and vincine; structural isomers: 2- and 6-nitro-3-acetamido-4-chlorobenzoic acid; stereoisomers: 4-methoxymethyl-1-methyl-cyclohexane carboxylic acid; fish oil: mixture of docosahexaenoic acid and eicosapentaenoic acid; NDGA: nordihydroguaiaretic acid.

^bThe upper organic phase was used as the stationary phase (SP) and the lower aqueous phase as the mobile phase (MP), except in DPCCC, where the relationship is reversed. MBE: methyl-*t*-butyl ether; AcN: acetonitrile; BuOH: *n*-butanol; Hex: hexane; EtOAc: ethyl acetate; MeOH: methanol; AcONH₄ ammonium acetate; DEE: diethyl ether; DPCCC: displacement mode.

^cTFA: trifluoroacetic acid; AcOH: acetic acid; SP: in stationary phase; MP: in mobile phase; SS: in sample solution; TEA: triethylamine.

overlap associated with sharp impurity peaks at their boundaries (Fig. 3c).

The relationship between the zone pH (pH_{zone}) and $\text{p}K_a$ /hydrophobicity in the present method is given by the following equation [2,4,5]:

$$\text{pH}_{\text{zone}} = \text{p}K_a + \log\left(\frac{K_D}{K} - 1\right) \quad (1)$$

where K_D and K indicate the distribution coefficient (an indicator for hydrophobicity) and distribution ratio of the analytes, respectively. When the $\text{p}K_a$ and K_D of the analyte are known, the zone pH can be computed from the K value.

The pH-zone-refining CCC technique shares many unique features with displacement chromatography [6] and has several important advantages over the standard CCC technique such as (a) large sample-

loading capacity, (b) highly concentrated fractions, (c) concentration and detection of minor impurities, and (d) monitoring the effluent by pH. The method has been successfully applied to the separation of various organic acids and bases, including the derivatives of amino acids [4,7] and peptides [8], alkaloids [4,9], hydroxyxanthene dyes [3,4,10], anti-human immunodeficiency virus lignans [11], indole auxins [4], structural and stereoisomers [4], and so forth. (Table 1). By being analogous to affinity chromatography, the method allows the use of an affinity ligand dissolved in the liquid stationary phase for separations of special analytes, including highly polar compounds such as catecholamines [4,12] and sulfonated dyes [4], enantiomers [4], and zwitterions such as free peptides [4,13] (Table 2). Figures 4a–4d illustrate a few examples of these applications.



Table 2 Samples and Solvent Systems Applied to Affinity pH-Zone-Refining CCC

Sample ^a	Solvent systems ^b (vol. ratio)	Set of key reagents ^c		
		Retainer	Eluter	Ligand
(±)-DNB-leucine (2 g)	MBE/H ₂ O	TFA (40 mM/SP)	NH ₃ (20 mM/MP)	DPA (40 mM/SP)
(±)-DNB-valine (2 g)	MBE/H ₂ O	TFA (40 mM/SP)	NH ₃ (20 mM/MP)	DPA (40 mM/SP)
Catecholamines (3 g)	MBE/H ₂ O	NH ₄ OAc (200 mM/SP)	HCl (50 mM/MP)	DEHPA (20%/SP)
Dipeptides (1 g) (hydrophobic)	MBE/AcN/50 mM HCl 4:1:5 (SP)	TEA (20 mM/SP)		DEHPA (10%/SP)
Dipeptides (1 g) (hydrophilic)	MBE/AcN/H ₂ O (4:1:5) (MP)		HCl (20 mM/MP)	
	MBE/BuOH/AcN/50 mM HCl (2:2:1:5) (SP)	TEA (20 mM/SP)		DEHPA (30%/SP)
	MBE/BuOH/AcN/H ₂ O (2:2:1:5) (MP)		HCl (20 mM/MP)	
Bacitracins (5 g)	MBE/50 mM HCl (1:1) (SP)	TEA (40 mM/SP)		DEHPA (10%/SP)
	MBE/H ₂ O (MP)		HCl (20 mM/MP)	
FD&C Yellow #6 (2 g)	MBE/AcN/H ₂ O (2:2:3)	H ₂ SO ₄ (0.2%/SP)	NH ₃ (0.4%/MP)	TDA (5%/SP)

^aDNB: dinitrobenzoyl.^bMBE: methyl *t*-butyl ether; AcN: acetonitrile; BuOH: *n*-butanol^cTFA: trifluoroacetic acid; NH₄OAc: ammonium acetate; TEA: triethylamine; DPA: *N*-dodecanoyl-L-proline-3,5-dimethylanilide; DEHPA: di-(2-ethylhexyl) phosphoric acid; TDA: tridodecylamine; SP: organic stationary phase; MP: aqueous mobile phase.

References

1. Y. Ito, Y. Shibusawa, H. M. Fales, and H. J. Cahnmann, *J. Chromatogr.* 625: 177–181 (1992).
2. Y. Ito, pH-Peak-focusing and pH-zone-refining countercurrent chromatography, in *High-Speed Countercurrent Chromatography* (Y. Ito and W. D. Conway, eds.), Chemical Analysis Series Vol. 132, Wiley–Interscience, New York, 1996, pp. 121–175.
3. A. Weisz, A. L. Scher, K. Shinomiya, H. M. Fales, and Y. Ito, *J. Am. Chem. Soc.* 116: 704–708 (1994).
4. Y. Ito and Y. Ma, *J. Chromatogr. A* 753: 1–36 (1996).
5. Y. Ito, K. Shinomiya, H. M. Fales, A. Weisz, and A. L. Scher, *pH-Zone-Refining Countercurrent Chromatography: A New Technique for Preparative Separation*, (W. D. Conway and R. J. Petroski, eds.), ACS Monograph on Modern Countercurrent Chromatography, 1995, pp. 154–183.
6. C. Horvath, A. Nahum, and J. H. Frens, *J. Chromatogr.* 218: 365 (1981).
7. Y. Ma and Y. Ito, *J. Chromatogr. A* 678: 233–240 (1994).
8. Y. Ma and Y. Ito, *J. Chromatogr. A* 702: 197–206 (1995).
9. Y. Ma and Y. Ito, E. Sokoloski, and H. M. Fales, *J. Chromatogr. A* 685: 259–262 (1994).
10. A. Weisz, Separation and purification of dyes by conventional countercurrent chromatography and pH-zone-refining countercurrent chromatography, in *Countercurrent Chromatography* (Y. Ito and W. D. Conway, eds.), Chemical Analysis Series Vol. 132, Wiley–Interscience, New York, 1996, pp. 337–384.
11. Y. Ma, L. Qi, J. N. Gnabre, R. C. C. Huang, F. E. Chou, and Y. Ito, *J. Liquid Chromatogr.* 21: 171–181 (1998).
12. Y. Ma, E. Sokoloski, and Y. Ito, *J. Chromatogr. A* 724: 348–353 (1996).
13. Y. Ma and Y. Ito, *J. Chromatogr. A* 771: 81–88 (1997).



Pharmaceuticals: Analysis by TLC

Philippe J. Berny

Ecole Nationale Veterinaire de Lyon, Marcy l'Etoile, France

Introduction

The pharmaceutical industry has been producing hundreds of new compounds on the market during the last decades. This evolution would certainly not have been possible without the potentialities of analytical techniques. Indeed, analysis appears necessary in at least three fields of the pharmaceutical area:

1. In the development of new drugs, for the identification of interesting compounds and their metabolites or derivatives.
2. In the whole manufacturing process, where it is essential to guarantee that the product obtained is both efficient and safe. Part of this process relies on the analytical determination of the purity and quality of the active ingredient(s), their by-products, and the excipients.
3. In human beings, as well as in other animals, analytical methods may be useful to confirm a poisoning case or to monitor undesired residues in edible tissues of food-producing animals.

In this entry, we will briefly overview these fields and see how thin-layer chromatography (TLC) or high-performance thin-layer chromatography (HPTLC) can be of value.

Research and Development of New Drugs

In the development of new drugs, HPTLC may offer very interesting features. Contrary to other chromatographic techniques, all the constituents of a mixture are spotted on the plate and can be analyzed, even if they are not identified easily. Therefore, it is possible to determine if and how a given product is broken down or metabolized. For example, nimesulide, a common nonsteroidal anti-inflammatory drug (NSAID), was detected in equine blood and urine samples following a race [1]. An unidentified spot was also detected on the same plate. This spot was further identified as a nitro derivative of the active compound. This derivative appeared to be unique to horses. Other published data mention the use of HPTLC alone or in combination with other analytical

techniques such as high-performance liquid chromatography (HPLC) or gas chromatography–mass spectrometry (GC–MS), to determine the presence and amount of new metabolites of drugs in various biological fluids and tissues. The use of TLC–HPTLC offers numerous advantages over other techniques (e.g., its simplicity and rapidity, and the potential for convenient repeated analysis), which is interesting when several tissues have to be analyzed in order to identify an unknown metabolite. Kinetic studies may also be performed with the help of TLC.

Indeed, after appropriate sample preparation, standards and samples can be spotted or sprayed onto the same plate, thereby providing a rapid and cost-effective analytical procedure to evaluate all sampling times. If an ultraviolet (UV) scanner is used, it is also possible to determine the amount of substance for each sample. Furthermore, the UV scanner sensitivity may be adapted specifically to analyze highly concentrated samples and poorly concentrated ones on the same plate, provided the calibration curve includes the values. As an example, Fig. 1 presents some kinetic data obtained for vitamin K₁, which is used as an antidote in dogs suffering from anti-coagulant rodenticide poisoning [2]. The method was developed on C₁₈-coated silica gel plates. Elution was based

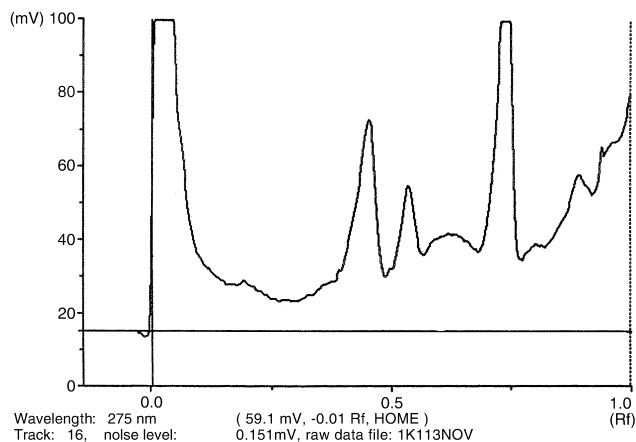


Fig. 1 Analysis of vitamin K₁ administered in dogs by the intravenous or intrarectal route (P. Berny, S. Viallet, F. Buronfosse, and G. Lorgue, European Association of Veterinary Pharmacology and Toxicology, Madrid 6–10 July, 1997).



on acetone–acetonitrile–chloroform (4:5:1) and took about 15 min for each plate. Detection was performed by UV scanning at 275 nm, followed by integration and solid-phase UV spectrum evaluation. Under such conditions, vitamin K₁ has an R_F value of 0. There were no interferences from plasma and limit of detection was 0.23 $\mu\text{g/mL}$, which was consistent with the therapeutic values obtained. The results also indicated that vitamin K₁ had a bioavailability of 82% by this route.

Standard approaches with HPTLC in research and development are usually based on the former TLC methods developed for older products. Unfortunately, these official methods (pharmacopoeias or associations of analytical chemistry) were based on TLC plates and material. The development of HPTLC material (100- or 200- μm -thick plates, microspheres of 5 μm , etc.) should improve many of these methods as far as duration of elution, resolution, and quantification are concerned. Therefore, older methods may have to be completely reviewed before being fully adapted to newer techniques.

A new step has been implemented with the development of automatic developing chambers and polarity gradients. With these techniques, development of a plate over 5–7 cm may be sufficient to separate up to 50 compounds and identify them. Universal gradient systems based on methanol, dichloromethane, and hexane, for instance (see *Camag Bibliography Service* for more information), have been developed as starting points for method development.

An example of the use of gradient techniques is given with plant extracts of the *Artemisia* genus [3]. In this entry, four related plant extracts were analyzed by isocratic and gradient techniques; the authors concluded that the gradient technique offered greater resolution and enabled the separation of more active ingredients in these plant extracts.

Drug Manufacturing Processes

Many methods have been published, based on TLC–HPTLC, for the qualitative analysis of drug or medical products. Numerous examples of quality control procedures could be presented here. It is interesting to look at quality control procedures for medicinal plants. Indeed, in this case, the only way to control the quality of a medicinal product is to make sure that the raw materials are correct (i.e., that they contain the desired active ingredients and the other constituents at the “usual” standard concentrations). The reader should refer to a review article such as in Ref. 4. HPTLC offers unbeatable characteristics for such uses: its simplicity, rapidity, and the

possibility of analyzing several samples over a very brief period of time. Identification of the active ingredients and by-products is achieved, as well as the quantitative analysis of the crude extract or the final product. Densitometry may prove to be a useful tool to establish calibration curves, but quantitation may be achieved by means of derivatization and further densitometry.

A good example of the use of TLC in quality control procedures is given by Dhanezar [5]. The author used reversed-phase HPTLC (C_{18} -coated silica gel) to quantify ceftriaxone, a novel cephalosporin-derived antibiotic. In this example, direct spotting and quantitation was used based on UV densitometry, as there was no need for separation. Using such a technique, quantitative evaluation of the product was easy and rapid. As the author concluded, neither GC nor HPLC could be used that way. Results reported by another group of researchers [6] also indicated that HPTLC analysis for cephalexin and cefaclor gave satisfactory results with regards to the limit of detection and the limit of quantitation, with precision around 3% and recovery close to 100%. Even before final products are quantified, the fermentation processes in antibiotic production can be monitored by means of HPTLC. Indeed, there is no need for extraction and a mere dilution of the fermentation matrix with methanol provides rapid and reliable results to check that the fermentation process is functioning properly. The high polarity of the silica gel plate used retains many of the matrix components and the specificity of the chromatographic procedure may be increased by the use of postderivatization techniques [7].

Many derivatization techniques, based on chemical reactions or even heat and chemical reactions, can be applied to TLC or HPTLC to specifically determine some compounds or groups of compounds; this is specific to TLC techniques. For instance, exposure to fluorecamine in acetone will convert sulfonamide antibiotics into fluorescent derivatives which can be visualized under UV radiation [8]. Other techniques are reported and, as suggested earlier, the reader should refer to the latest edition of the *Official Methods of Analysis* published by the Association of Official Analytical Chemists (Arlington VA, U.S.A.) for complete details about all the available techniques for the routine analysis of drugs.

Detection of Residues and Monitoring of Poisoning Cases

More and more often, animal products are checked for the presence of undesirable residues of veterinary drugs. This is an important issue in public health, because resi-



dues may prove either toxic or allergenic and must be kept below their maximum residual limit (MRL). For this kind of analysis, it is necessary to analyze many types of biological samples [tissues (e.g., meat) or fluids (e.g., milk)]. The analytical techniques applied need to be very sensitive (some residues are monitored below the nanogram per gram threshold) and robust to give similar results when applied in different laboratories. It may also be of interest to analyze several compounds with only a single technique. For instance, several sulfonamide residues can be determined simultaneously in eggs by TLC with fluorecamine and densitometric analysis of the fluorescent derivatives. The limit of detection was 3 $\mu\text{g/kg}$, which is compatible with most MRLs. A similar technique, with a solid-phase extraction technique, was applied to milk samples to determine residues of these drugs as well [8]. In both cases, the techniques were validated and had mean percent recoveries as well as linearity and coefficients of variation compatible with recommended values of official agencies (Committee of Veterinary Medicinal Products in the European Union, or Food and Drug Administration in the United States). This regulatory requirement has to be carefully considered when a method is developed for analyzing residues in food. The analytical techniques developed for antibiotics appear to be valuable, but they are usually applied after microbiological evaluation of biological samples.

Other products can only be determined by chromatographic or other analytical methods. A major area of investigation concerns growth promoters (anabolic steroids or β -agonists). The use of these hormones is restricted in many parts of the world, or even prohibited (European Union). Some compounds are of special interest because they may have carcinogenic effects. This is true for diethylstilbestrol, a synthetic estrogen. Several methods have been published to detect these products [9]. Although we cannot offer any specific reference here, TLC techniques would appear suitable to control doping in sports. However, many sports authorities usually require mass spectrometry to identify the potential doping agents. It is our opinion, however, considering their sensitivity and selectivity, that HPTLC techniques would certainly provide a quick and cost-effective way of screening samples.

Our final comment concerns clinical toxicology. Thin-layer chromatographic procedures can be especially useful to screen samples for the presence of various drugs and chemicals involved in poisoning cases in human beings and in animals as well. A recent review article considered using TLC on biological samples to look for benzodiazepines [10], which are commonly involved in suicidal attempts. Another example involves meprobamate. This product is a common antiepileptic drug, and it is difficult

to detect with standard HPLC–UV methods. A screening method with TLC and visualization with Erlich's reagent results in yellow spots, typical of meprobamate. This screening technique for neutral drugs appears fairly simple and is suggested prior to HPLC analysis [11]. Finally, a method has been developed for salicylates and their metabolites in urine samples. This method [12] involves acidic extraction of urine samples and analysis on silica gel plates with ferric chloride added as a chromogen. This technique allows for the determination of salicylic acid, methyl salicylate, and *p*-aminosalicylate at the same time, with detection limits below 1 $\mu\text{g/mL}$ for each compound. Analysis of the parent drug, together with its metabolites, is interesting for diagnostic purposes, because it might give some hints as to when the product was taken (approximately) or what prognosis should be expected.

Conclusion

This entry is a brief introduction to the world of TLC in pharmaceutical research and should be considered merely as such. TLC and HPTLC techniques are numerous and have been developed for several specific needs. With the introduction of gradient development, newer techniques can be expected, which should be able to detect more compounds on a single plate than commonly performed today.

References

1. P. Sarkar, J. M. McIntosh, R. Leavitt, and H. J. Gouthro, *Anal. Toxicol.* 21: 197–202 (1997).
2. P. Berny, S. Viallet, F. Bironfosse, and G. Lorgue, *J. Vet. Pharmacol. Therapeu.*, 20 (Suppl. 1): 270–271 (1997).
3. N. K. Olah, L. Muresan, G. Compan, and S. Gocan, *J. Planar Chromatogr.* 11: 361–364 (1998).
4. F. Li, S. Sun, J. Wang, and D. Wang, *Biomed. Chromatogr.* 12: 78–85 (1998).
5. S. C. Dhanesar, *J. Planar Chromatogr.* 11: 258–262 (1998).
6. D. Agbaba, S. Eric, D. Zivanov, S. Stakic, and S. Vladimirov, *Biomed. Chromatogr.* 12: 133–135 (1998).
7. Anon., *Camag Bibliography Service* 81: 10–13 (1998).
8. J. Unruh, E. Piotrovski, D. Schwartz, and R. Barford, *J. Chromatogr.* 519: 179–187 (1990).
9. G. Garcia, R. Saelzer, and M. Vega, *J. Planar Chromatogr.* 4: 223–225 (1991).
10. O. H. Drummer, *J. Chromatogr. B* 713: 201–225 (1998).
11. W. E. Lambert, *Clin. Toxicol.* 30: 683–684 (1992).
12. R. L. Kincaid, M. M. McMullin, D. Sanders, and F. Rieders, *J. Anal. Toxicol.* 15: 270–271 (1991).





Phenolic Acids in Natural Plants: Analysis by HPLC

E. Brandšteterová
A. Žiaková-Čaniová

Slovak Technical University, Bratislava, Slovakia

INTRODUCTION

Many medicinal and food plants contain large amounts of antioxidants other than vitamin C, vitamin E, and carotenoids. The antioxidative effects are mainly due to phenolic compounds: phenolic acids, flavonoids, and phenolic diterpenes. These natural antioxidants can exert considerable protection, in humans, against aging and cancer caused by free radicals, and can replace synthetic antioxidants such as butylated hydroxyanisole (BHA) and butylated hydroxytoluene (BHT), which are suspected to have toxic and carcinogenic effects on humans.

Phenolic acids constitute a large group of naturally occurring organic compounds with a broad spectrum of pharmacological activities. It was found that they possess not only antioxidant but also antiviral and antibacterial properties. The antioxidant activity of phenolics is generally combined with hydroxyl groups on their molecules. Phenolic acids are widely distributed in natural plants, e.g., fruits, vegetables, various medicinal and other plants. Phenolic acids occur in plants in different concentrations and, of course, each plant sample could be specific enough for the presence of different phenolic acids and their derivatives in combination with the other groups of phenolic compounds. Very often, all important phenolics present in plant samples are analyzed simultaneously.

Phenolic acids include the benzoic acids (C_6-C_1), e.g., gallic, vanillic, syringic, protocatechuic, *p*-hydroxybenzoic acid, as well as cinnamic acids (C_6-C_3), e.g., caffeic, *p*-coumaric, ferulic, sinapic acids, and their dep-sides and derivatives, e.g., rosmarinic acid and lithospermic acid (Fig. 1).^[1] Phenolic acids and flavonoids in plants may occur in the free form, but they are often glycosylated with various sugars, especially glucose. Phenolic acids may also be present in the esterified as well as bound forms. Free phenolic acids are found especially in herbs and spices and, very often, in compounds responsible for antioxidant activity (benzoic and cinnamic acids and some of their derivatives). The bound forms are more common for the fruits, vegetables, and other plant materials. Therefore, in some cases, it is necessary to combine the analysis of their free and bound forms.

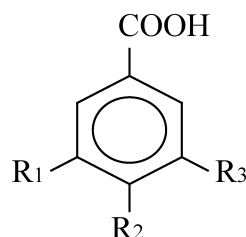
HPLC OF PHENOLIC ACIDS

The content of various phenolic acids in plants can be determined using various analytical instrumental methods (GC, TLC, CE), but high-performance liquid chromatography (HPLC), with a broad range of detection possibilities, is the best method of choice for routine analysis. HPLC techniques offer a real chance to separate simultaneously all analyzed components together with their possible derivatives or degradation products. In many cases, this method enables the determination of low concentrations of analytes in the presence of many other interfering and coeluting components. There are many advantages influencing the increased popularity of the HPLC technique in plant material analysis, such as the large choice of commercially available columns with very desirable properties; the application of all chromatographic separation principles, including the use of new generation sorbents; and the possibility of combining two or more columns in a switching mode.^[2]

HPLC Columns

The columns used for the separation of phenolic acids are mainly reversed phase (RP), other silica-based chemically bound phases, and non-silica polymers or mixed inorganic-organic phases. Special silica sorbents with reduced metallic residue contents and minimum residual silanol groups on the surface could positively influence peak symmetry without the strict demands for the successful separation of acidic analytes. Almost exclusively, RP C_{18} phases ranging from 100 to 250 mm in length and usually with an internal diameter of 3.9 to 4.6 mm are recommended. Particle sizes are in the range of 3–10 μ m. Short 50–100-mm columns with 3- μ m particles have also been tested for fast phenolic acid separations. Narrow bore columns (internal diameter 2 mm) are recommended especially for HPLC-MS applications.^[3,4] Some problems could arise with the applications of narrow or microbore columns in the direct injections of plant extracts; there is the possibility of plugging the column after repeated injections. In these cases, an additional clean-up step has to be applied instead of just the simple extraction

Benzoic acid derivatives:



Gallic acid, $R_1 = R_2 = R_3 = \text{OH}$

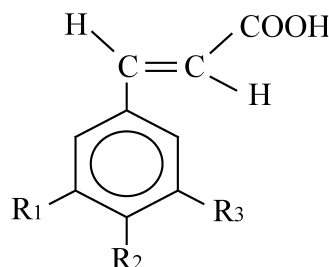
p-Hydroxybenzoic acid, $R_1 = R_3 = \text{H}$, $R_2 = \text{OH}$

Protocatechuic acid, $R_1 = R_2 = \text{OH}$, $R_3 = \text{H}$

Vanillic acid, $R_1 = \text{OMe}$, $R_2 = \text{OH}$, $R_3 = \text{H}$

Syringic acid, $R_1 = R_3 = \text{OMe}$, $R_2 = \text{OH}$

Cinnamic acid derivatives:

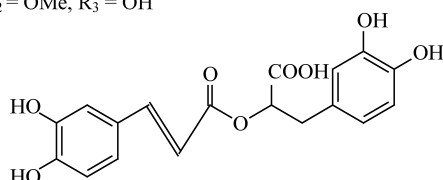


Caffeic acid, $R_1 = R_2 = R_3 = \text{OH}$

p-Coumaric acid, $R_1 = R_3 = \text{H}$, $R_2 = \text{OH}$

Ferulic acid, $R_1 = \text{OMe}$, $R_2 = \text{OH}$, $R_3 = \text{H}$

Sinapic acid, $R_1 = R_3 = \text{OMe}$, $R_2 = \text{OH}$



rosmarinic acid

Fig. 1 Structures of phenolic acids. (From Ref. [1].)

assay. Moreover, in the case when columns with lower diameters and particle sizes are used, the adaptation of HPLC equipment is often necessary, e.g., UV detection cells with reduced volume, low injection volumes, pumps with well-controlled low flow-rate, and low diameter capillary connections.^[1]

Some published results have confirmed the fact that the quality of sorbent (purity, end-capping) and the particle size does not have a very significant influence on the peak symmetry of the analyzed phenolic acids,^[5] but the chromatographic resolution and the efficiency of the column (number of theoretical plates) are better for columns with very good free silanol group covering, end-capping, or embedding. Maybe, it is the main reason for the use of good quality commercially available columns for most phenolic acid analyses in plant materials during the last years.^[6] Especially, if a great number of analytes are required to be separated simultaneously, the column with

the best separation properties is applied. The choice of columns depends also on the developed sample preparation technique, because the less clean extracts could decrease the lifetime of or cause damage to the column.

Most HPLC analyses of phenolic acids are performed at ambient column temperature, but moderately higher temperatures between 30° and 40°C have also been recommended in the analysis of fruits, vegetables, and other plants.

HPLC Mobile Phases

Both isocratic and gradient elution are applied for phenolic acid analyses. The choice depends on the number and type of analytes and the nature of plant matrix. Methanol, acetonitrile, and tetrahydrofuran are the most commonly used organic modifiers, as well as aqueous acidified solvents such as aqueous acetic acid, formic acid, phosphoric acid, or perchloric acid. In some cases, acetonitrile leads to better resolution in a shorter analysis time than methanol and, generally, acetonitrile gives sharper peak shapes, resulting in a higher plate number. However, methanol is often preferable to acetonitrile because of its nontoxic properties and the possibility of using higher percentages in the mobile phase (lower solvent elution strength) which could protect the HPLC column. Also, tetrahydrofuran, with its high elution strength, could be applied to phenolic acid separations.^[1]

As most phenolic acids have *pK*s of about 4, the recommended pH range for the HPLC assay is pH = 2–4. It is important to avoid the ionization of analytes during analysis to improve the resolution and reproducibility of the retention characteristics. The most available columns allow the application of mobile phases with pH of about 2. The pH value is controlled by adding small amounts of acids to the water–organic mixture. Some authors also recommend the use of aqueous buffers (citrate buffer, phosphate buffer, ammonium acetate buffer) instead of the addition of acid. The buffer concentration can vary from 5 to 50 mM. The next alternative for controlling analyte retention may be the application of ion-pairing reagents, added to the aqueous mobile phases. However, the new generation of sorbents recommended for simultaneous separation of acids and bases can be applied without ion-pairing agents. An additional advantage of these new sorbents is the possibility of working with aqueous mobile phases with very low organic solvent content or without any organic modifier at all. The isocratic mode has been recommended for extracts containing components with very similar properties, especially with similar polarities in the purified extracts, with a small number of impurities or for coeluting compounds. Free phenolic acids (chlorogenic, protocatechuic, *p*-hydroxybenzoic, caffeic, vanillic, syringic, *p*-coumaric, and

ferulic) could be isolated from some samples of medicinal plants or pharmaceutical preparations using a simple isocratic mobile phase (methanol–water–acetic acid).^[7,8] Simple isocratic elutions have also been used for the analysis of phenolic acids in fruit products.^[9] The same isocratic mobile phases were applied in the HPLC separations of simple phenolic acids using two columns of different properties. Chromatograms are illustrated in Fig. 2A and B. It is obvious from both chromatograms that the quality of the column, e.g., good end-capping of free silanol groups on the silica surface and low content of metal ions in silica material, can significantly influence the separation of analytes. Chromatographic resolution values are better for the SymmetryTM column, which makes quantitative analysis much simpler and reproducible. In the case when phenolic acids of different chemical structures and different polarities have to be analyzed simultaneously, gradient elution is necessary. Of course, in this case also, the choice of column is

also a very important consideration. HPLC separation of phenolic acids of different polarities (e.g., protocatechuic, caffeic, rosmarinic acids) using different quality columns often requires gradient elution.^[5,10] This separation is illustrated in Fig. 3A and B. It can be seen from the chromatograms that there is no significant difference in the asymmetry values for all analytes, but the efficiencies of the two columns and the possibility of more compounds being separated at the same time are much higher for the SymmetryTM column. The same situation occurs if phenolic acids of different polarities, as well as other groups of phenolic compounds (flavonoids, diterpenes), have to be determined in a single analytical run. In this case, the separation of more analytes of different chemical structures has not been realized using a column without special properties. The simultaneous HPLC separation of different phenolic acids and flavonoids that could be present in some medicinal plants is demonstrated in Fig. 4.^[10] The Symmetry C₁₈ column

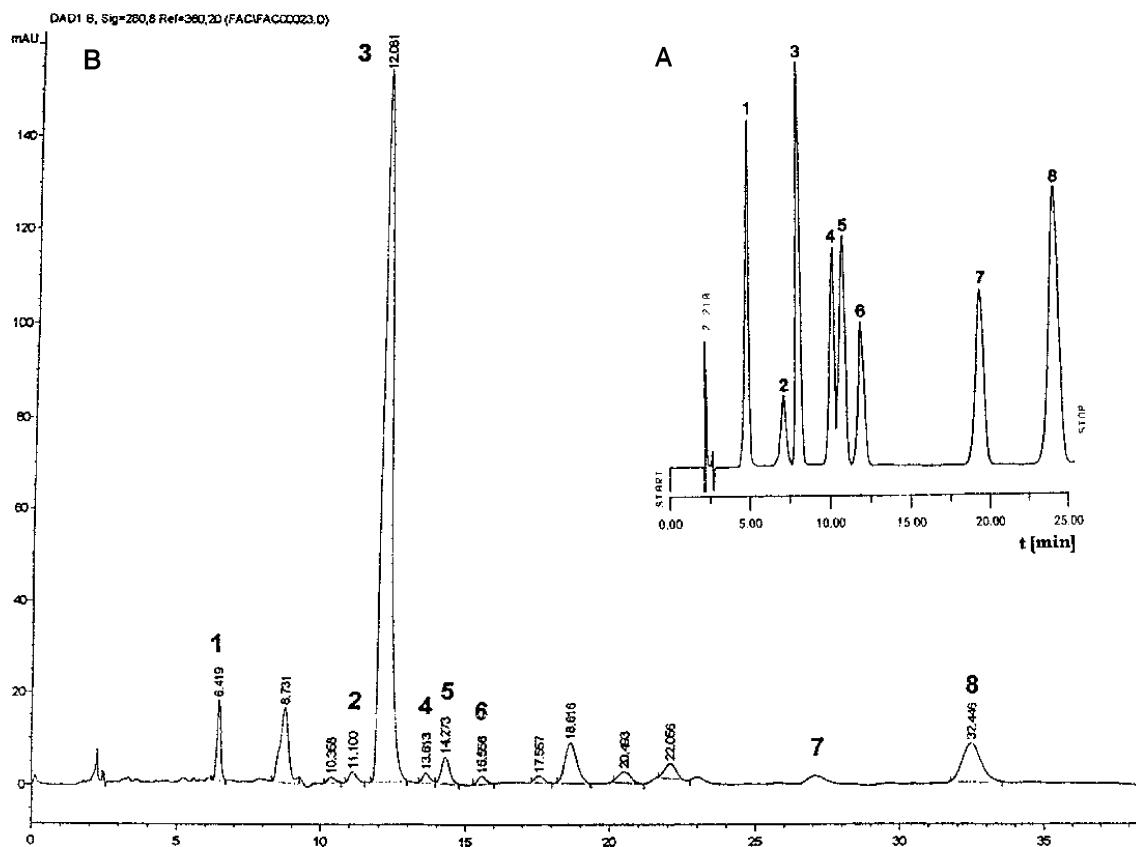


Fig. 2 HPLC chromatogram of phenolic acids using (A) ODS Hypersil column, (B) Symmetry C₁₈ column and isocratic elution. Conditions: (A) column: ODS Hypersil (200 × 4.6 mm, 5 μm), mobile phase: methanol–water–acetic acid (25:75:1), flow-rate 1 mL/min; (B) column: Symmetry C₁₈ (250 × 4.6 mm, 5 μm), mobile phase: methanol–0.001 M phosphoric acid (23:77), flow-rate 1 mL/min. Peaks: 1) protocatechuic acid; 2) chlorogenic acid; 3) *p*-hydroxybenzoic acid; 4) vanillic acid; 5) caffeic acid; 6) syringic acid; 7) *p*-coumaric acid; 8) ferulic acid. (From Refs. [7] (A) and [8] (A).)

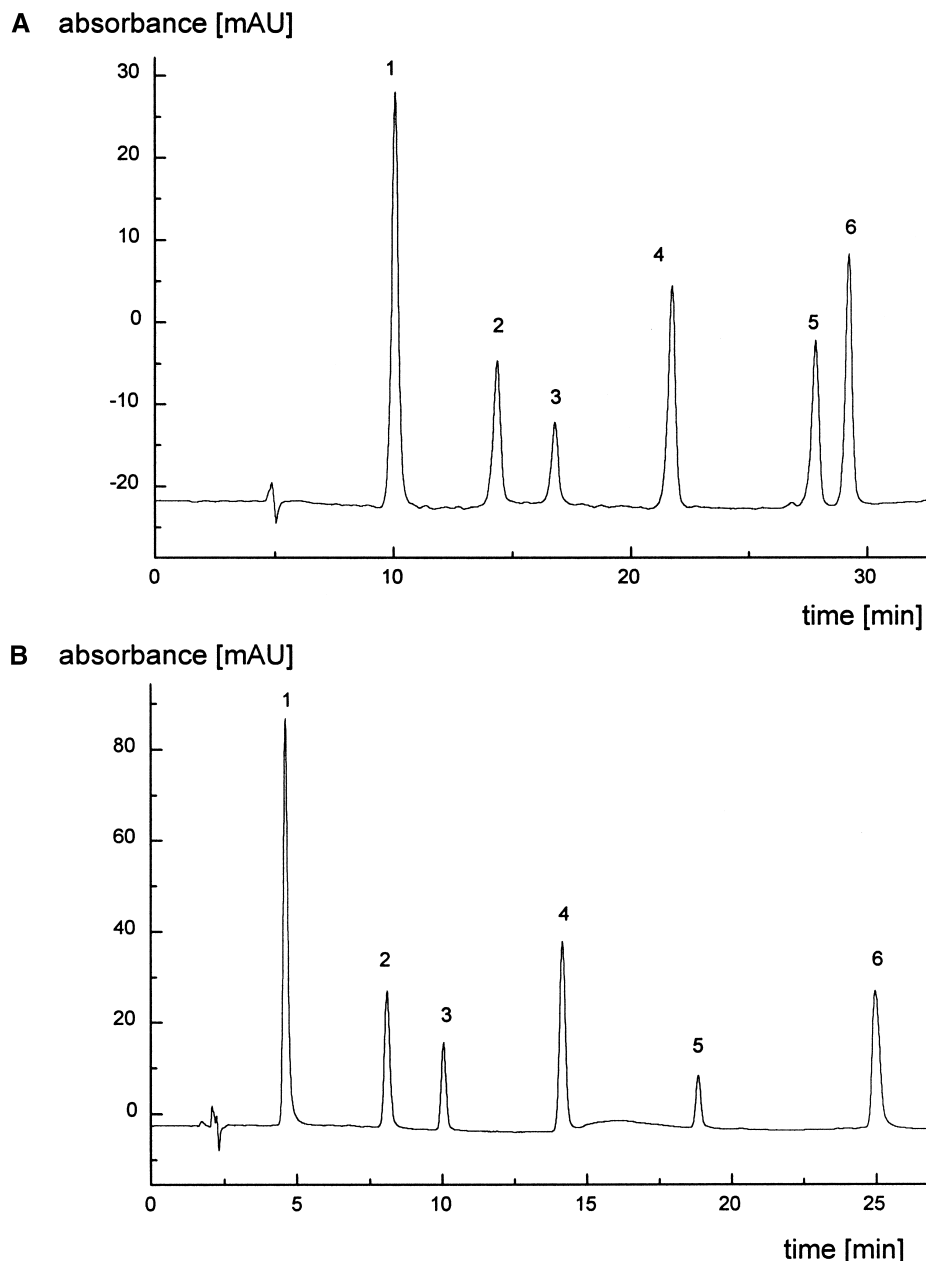


Fig. 3 HPLC analysis of phenolic acids using (a) Separon SGX C₁₈ column and (b) Symmetry C₁₈ column and gradient elution. Conditions: (A) column: Separon SGX C₁₈ (250 × 4.6 mm, 7 μm), mobile phase: methanol–water (pH = 2.5, adjusted with formic acid), linear gradient from 15% methanol to 75% methanol in 40 min, flow-rate 0.5 mL/min; (B) column: Symmetry C₁₈ (150 × 3.9 mm, 5 μm), mobile phase and flow-rate same as in (a). Peaks: 1) gallic acid, 2) protocatechuic acid, 3) catechin, 4) caffeic acid, 5) sinapic acid, 6) rosmarinic acid.

and gradient elution were used. All analytes were separated in about 30 min, with the sufficient resolution. The same choice of mobile phase components is used for the gradient mode as was mentioned for the isocratic elution. This means using organic–water mixtures with controlled pH, or organic–buffer compositions. The binary linear or step gradients are mostly used. Concerning

the elution order of separated phenolic acids, it is obvious that individual compound retention depends on their polarities and, of course, on the character of the stationary phase that is used. Generally, phenolic acids are eluted from RP columns according to decreasing polarities. Loss of polar hydroxy groups and the presence of the methoxy groups or ethylenic side chains

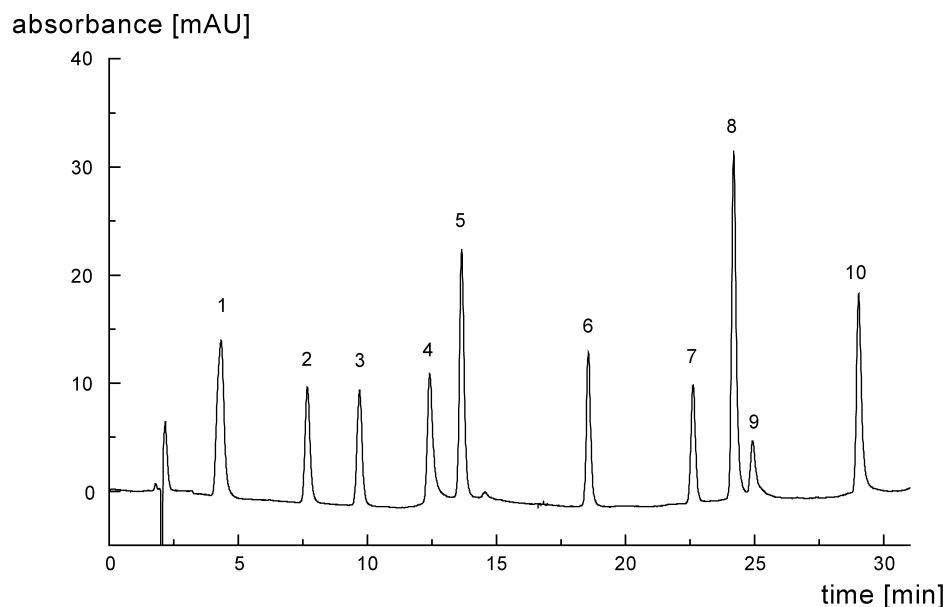


Fig. 4 HPLC analysis of phenolic acids and flavonoids using Symmetry C₁₈ column and gradient elution. Conditions: column: Symmetry C₁₈ (150 × 3.9 nm, 5 μm), mobile phase the same as in Fig. 3B, flow-rate 0.6 mL/min. Peaks: 1) gallic acid, 2) protocatechic acid, 3) catechin, 4) epigallocatechin gallate, 5) caffeic acid, 6) ferulic acid, 7) rutin, 8) rosmarinic acid, 9) myricetin, 10) quercetin.

could decrease the polarity and increase the retention time. Of course, the derivatives of common phenolic acids with two or more aromatic rings are less polar and are eluted much later than others. So, the gradient scheme has to be managed individually, according to the number and chemical properties of the analyzed compounds. Some phenolic acids could be present in natural plants as geometric isomers. Their simultaneous separation is usually possible using RP stationary phases. The greatest number of phenolic acids occurs in nature as *trans*-isomers, but on exposure to UV radiation or daylight they are gradually transformed to *cis*-isomers, which elute, usually, before *trans*-isomers.^[1,5] For this reason, the stability studies of analyzed compounds are valuable and the results have to be taken into consideration during the sample preparation method development. UV radiation and elevated temperature could decrease the extraction recoveries and lower the reproducibility of the assay.

HPLC Detection

Phenolic acids absorb well in the UV range, but no single wavelength is sufficient for their simultaneous monitoring in extracts of various natural plant extracts. Therefore, variable-wavelength UV or diode-array (DA) detectors are the most commonly used in the HPLC analyses of phenolic acids. Most of the benzoic acid derivatives have

absorption maxima at 246–262 nm, with a shoulder at 290–315 nm, except for gallic and syringic acids with absorption maxima at 271 and 275 nm, respectively. The cinnamic acids absorb in two ranges: 225–235 and 290–330 nm. As was mentioned previously, the maxima of the UV spectra differ significantly for the individual phenolic acids; the range of wavelengths for their detection is wide (210–370 nm). Systematic studies of the absorbance spectra recommended for their simultaneous separation require the following single wavelengths: 254, 280, and 320 nm; for dual monitoring: 254 and 280 nm, or 280 and 320 nm. However, detection at 280 nm is the most generally used wavelength for the simultaneous separation of mixtures of phenolic acids.^[1] Of course, DAD is the best detection choice, as it enables scanning of the UV spectra of all solutes passing through the detector; it could help in the identification of individual compounds in the extracts of complex mixtures, such as extracts of natural plants. Moreover, DAD also gives important information about the purities of all analytes.

Fluorescence detection is not very often used in phenolic acid analysis, but, in cases when very low concentrations of some analytes or many interfering compounds are present in extracts, the combination of UV and DAD with fluorescence detector could be valuable. However, the same problems could arise as in the UV detection, i.e., establishing the correct excitation and emission wavelengths, as large differences for several phenolic acids were observed. In this case, the rapid scanning

fluorescence detector, in combination with DAD, is available for applying multiple excitation and emission wavelengths.^[8]

Electrochemical detection is very sensitive for the compounds that can be oxidized or reduced at low-voltage potentials. Therefore, it could also be applied in the HPLC analysis of phenolic acids that are present in natural samples at very low concentrations. With the recent advances in electrochemical detection, multi-electrode array detection is becoming a powerful tool for detecting phenolic acids and flavonoids in a wide range of samples. The multi-channel coulometric detection system may serve as a highly sensitive way for the overall characterization of antioxidants; the coulometric efficiency of each element of the array allows a complete voltametric resolution of analytes as a function of their reaction (redox) potential. Some peaks may be resolved by the detector, even if they are unresolved when they leave the HPLC column.^[11]

The detection and identification of phenolic compounds, including phenolic acids, have also been simplified using mass spectrometry (MS) techniques on-line, coupled to the HPLC equipment. The electrospray ionization (ESI) and atmospheric pressure chemical ionization (APCI) interfaces dominate the analysis of phenolics in herbs, fruits, vegetables, peels, seeds, and other plants. In some cases, HPLC, with different sensitivity detectors (UV, electrochemical, fluorescence), and HPLC-MS are simultaneously used for the identification and determination of phenolic acids in natural plants and related food products.^[4,12,13] In some papers, other spectroscopic instrumental techniques (IR, ¹H NMR, and ¹³C NMR) have also been applied for the identification of isolated phenolic compounds.^[3]

SAMPLE PREPARATION

Sample handling is a very important part of the method development for HPLC determination of phenolic acids in natural plants. Because of the great variability of phenolic acids (different polarity, acidity, number of hydroxyl groups, and aromatic rings), the various concentration levels of individual analytes, and the very complex natural matrix with many interfering components, the choice of the technique for their isolation and quantification differs from one described HPLC assay to the next. In some cases, only a one-step extraction and simple clean-up procedure are sufficient before the HPLC analysis, but the most often described HPLC assays include two or more steps of sample preparation, especially in the case of fruits and vegetable samples. It is obvious that each step contributes, on one hand, to the higher sensitivity and selectivity, but, on the other hand, it could increase the number of errors and decrease the recovery of the method.

Therefore, it is very important to choose the optimal preparation of plant material according to the chemical structures and properties of analyzed compounds.

Liquid Extraction (LE)

Liquid extraction is the most commonly used procedure prior to HPLC analysis of phenolic acids in natural plants. Most of these samples are not of liquid consistency, and they cannot be injected directly into the HPLC column. Therefore, the analytes have to be isolated from the matrices in which they exist naturally before HPLC analysis. Of course, as the first steps of the preparation procedure, there are sample handling, milling, grinding, and homogenization. These steps can also influence the results of the complete HPLC assay. In many cases, the analyst has the possibility to control all preparation steps and to evaluate their influence on the analytical results. Commonly used extraction solvents are alcohols (methanol, ethanol), acetone, diethyl-ether, and ethyl acetate. However, very polar phenolic acids (benzoic, cinnamic acids) could not be extracted completely with pure organic solvents, and the mixtures of alcohol-water or acetone-water are recommended. On the other hand, the less polar analytes (phenolic acid derivatives) are not isolated quantitatively from plant matrices using only pure water as the extraction solvent. Less polar solvents (dichloromethane, chloroform, hexane, benzene) are suitable for the extraction of nonpolar extraneous compounds (waxes, oils, sterols, chlorophyll) from the plant matrix. Of course, other factors (e.g., the choice of pH, temperature, sample-to-solvent volume ratio, and the number and time intervals of individual extraction steps) also play an important role in the extraction procedure. All these factors influence recovery values and, of course, the validation parameters of the complete assay. Therefore, it is necessary to optimize the extraction conditions.^[5] The analysis of free phenolic acids, especially in fruits and vegetables, also often requires a hydrolysis step, as the phenolic acids could be found, in these sources, in the conjugated form and rarely in the free state. The assays could employ either acidic, alkaline, or enzymatic hydrolysis. An alkaline hydrolysis is used to break ester complexes (the most common form of phenolic acids) and acidic hydrolysis is used to disrupt glycoside linkages. Alkaline hydrolysis can be accomplished using 2N NaOH for some hours, at ambient or lower temperatures, often under nitrogen stream. Acidic hydrolysis is performed often at higher temperatures (100°C) with 2N HCl for some hours. But not all extracts are clean enough to be injected directly into the HPLC column. So, it is necessary sometimes to use additional clean-up step(s).

Extraction and clean-up procedures also apply column liquid chromatography (LC), solid phase extraction



Phenolic Acids in Natural Plants: Analysis by HPLC

(SPE), super critical fluid extraction (SFE), or matrix solid-phase dispersion (MSPD). The preferred approach is determined according to the nature of the plant matrix and the number and chemical properties of analyzed phenolic acids.

Solid-Phase Extraction

SPE is a good choice for the clean-up procedure for crude plant extracts. This technique, which applies all separation principles, has become very popular in the past decade. The advantage of SPE over LE is that SPE is faster and more reproducible, and fairly clean extracts are obtainable, emulsion creation is avoided, and smaller volumes are applied. From the environmental point of view, a lower consumption of toxic solvents is the reality of this technique. In some cases, more than one single-functional group SPE cartridge is used, or two or more SPE cartridges with different sorbents could be combined.^[7-9] New generation sorbents are now also commercially available with hydrophilic-lipophilic properties which enable the simultaneous separation of both polar and less polar compounds. Very simple SPE assay is required for all acidic and basic analyte isolation from the "crude" plant extract and high recoveries are common for this simple procedure. The great advantage of SPE is the possibility of combining the SPE procedure, on-line, with the HPLC equipment and realizing the so-called direct sample analysis (DSA). This means that the "crude" extract of plant material is injected directly into this SPE-HPLC system.

Matrix Solid-Phase Dispersion

MSPD is the next alternative for sample preparation of fruits, vegetables, herbs, cereals, and other plants. It is convenient for liquid and semi-liquid samples. This technique is a multi-residual assay which consists of matrix homogenization with a solid silica phase placed into a short column, as in SPE. Analytes and matrix interferences are retained on the mixed solid-phase material with completely new separation characteristics. Specific elution allows one to obtain analytes after the elimination of matrix compounds via washing steps. This technique combines homogenization, cellular disruption, extraction, fractionation, and purification in a single process. MSPD has many advantages: the sample is dispersed over a large surface area, the volumes of extraction solvents are low in comparison with liquid extraction, and so, as is the case with SPE, it can be automated. The application of MSPD as the preparation step before HPLC analysis of various analytes in plants, fruits, and vegetables has been reviewed.^[14] This technique has also been tested for phenolic acids in herb materials.^[10]

Supercritical Fluid Extraction

Supercritical fluids are attractive extraction agents, as the solvent power (density) can be manipulated over a wide range of temperatures and pressures. The solvating power of a supercritical fluid is varied by controlling the pressure or by adding organic modifiers such as methanol. SFE provides relatively clean extracts because the degradation of certain compounds by lengthy exposure to high temperatures and oxygen is avoided, and chlorophyll and other nonpolar compounds are insoluble in supercritical CO₂. This technique is amenable to medicinal or other plant samples^[15] and it can be combined also with other preparation techniques such as LE or SPE. Some problems could arise if SFE is used for some fruit and vegetable samples with high percentages of water. All samples are usually dried before the SFE assay. For some phenolic compounds, the extraction recoveries are not very high, as the content of organic modifier is, in many cases, not sufficient for their complete isolation, especially in the case of very polar phenolic acids.

APPLICATIONS

Herbs and Other Plants

Most papers dealing with phenolic acid HPLC analysis in herbs describe only simple liquid extraction without the hydrolysis step. Acetone, methanol, or alcoholic-water or acetone-water mixtures are applied.^[16] Very rarely, pure water is used as the extraction solvent.^[11] It was found that the extraction recoveries for water extracts are often lower in comparison to alcoholic-water mixtures, especially when the simultaneous separation of polar and less polar phenolic acids has been performed. Sometimes, the control of pH can improve the recovery.^[5] If necessary, *n*-hexane, chloroform, diethyl ether, benzene-acetone, petroleum ether, or other less polar solvents are recommended for removing interfering compounds. The extraction is usually performed by refluxing the samples for a specific time in a Soxhlet apparatus, with simple mechanical or magnetic stirring of the sample with the extraction solvent, or by plant sample maceration. The application of an ultrasonic bath for the liquid extraction has also become popular in recent years. The hydrolysis steps have also been recommended for medicinal species preparation, especially when other phenolic compounds are also analyzed simultaneously with phenolic acids in herbs.^[17]

Other plants (cereals, seeds, rye, nuts, barley, malt) can also be extracted with organic solvents or their mixtures with water, but, in many cases, less polar solvents



are also used for the elimination of pigments, oils, nonpolar and macromolecular compounds. Many of these assays have also included acidic and/or alkaline hydrolysis steps, column liquid clean-up procedures, or SPE. The simultaneous separation of phenolic acids and other phenolic compounds in these samples also complicates the preparation step. Very often, multi-step liquid extraction and sample clean-up assays are recommended. It is necessary to select extraction solvents according to the polarities of the analytes and the form of their bonding to the sample matrix. Very often, both free and bound phenolic acids are separated in plant samples, and hydrolyzed and nonhydrolyzed materials are analyzed separately. In some cases, two or more hydrolysis methods are applied for the analyses of cereals and nuts.^[18,19]

Fruits and Vegetables

In the sample preparation step for fruits and vegetables, liquid extraction is performed combined with optimized hydrolysis before the HPLC analysis of phenolic acids.^[20,21] A high quality column (e.g., Symmetry C₁₈) with simple gradient elution was used for the HPLC separation of phenolics expected to be present in vegetable samples before and after the hydrolysis steps.^[21] In the cases when not only phenolic acids but also other phenolic compounds are determined in these samples, the extraction procedure consists, in many cases, of multi-step extractions and clean-up procedures. Column liquid chromatography or SPE is also recommended.^[4] But sometimes the simple water extraction assay has been recommended for more fruits (strawberry, orange, grape, apple, banana, pear, etc.) and vegetable samples (carrot, potato, tomato, cucumber, leaf lettuce, eggplant, cauliflower, cabbage, garlic, onion, spinach).^[11] It depends on the character of the sample matrix and the detection mode of the HPLC assay. The use of fluorescence, EC, or MS detectors also makes the sample preparation procedure much simpler by comparison with the common generally used detectors (e.g., UV), where more interfering components could be eluted simultaneously with phenolic acids and, for this reason, they have to be removed effectively in the preparation step.

More knowledge about the separation conditions for the HPLC analysis of phenolic acids in plant materials is available in the cited references. Some of them represent chapters in books with abundant additional information about the above topic,^[1,2] or review article,^[6] with details from more than 60 papers published in the last 5 years, dealing with the choice of stationary phases, mobile phases, detection, sample preparation of plants prior to phenolic acid HPLC analyses, etc.

CONCLUSION

HPLC is a preferred technique for routine monitoring of phenolic acids in natural plants. With various detection possibilities, or their combinations, and completed with effective sample preparation procedures, HPLC enables the determination of phenolic acids occurring in herbs, fruits, vegetables, and other plants, in both free and bound forms; very often, phenolic acids are analyzed simultaneously with the other phenolics. Chromatographic conditions for these analyses are not complicated when efficient, commercially available, reversed-phase columns are applied. A new generation of sorbents can improve the separation parameters and, with their high separation power, can influence the number of analyzed compounds within a given relatively short separation time. The mobile phases used are also very simple (organic–water mixtures with controlled pH) and both isocratic and gradient modes are recommended. In the case of the simultaneous separation of many phenolic compounds, gradient elution is more suitable. Because of the complexity of some natural plant samples, the sample preparation procedure is the most important step of the entire assay. But today, many techniques offer the real possibility of preparing the sample before the HPLC analysis with sufficient specificity. Liquid extraction has to be, in many cases, the first step of the preparation stage. SFE or MSPD could also be suitable alternatives. Attention should be devoted to effective clean-up methods for plant extracts, such as simple column chromatography or SPE in off-line or on-line modes. The combined techniques, such as HPLC–MS, are very valuable for the possible identification of all analyzed compounds. The column-switching technique, with on-line connected columns (one as preparation and the second as the analytical column), enables the direct injection of the crude plant extract into the HPLC system, without special complicated clean-up procedures.^[10] It is obvious that all these prospective methods, which today are commonly applied in the HPLC analyses of other analytes, will also find importance and practical use in the analysis of phenolic acids in plant materials.

REFERENCES

1. Lee, H.S. HPLC Analysis of Phenolic Compounds. In *Food Analysis by HPLC*, 2nd Ed.; Nollet, L.M.L., Ed.; Marcel Dekker, Inc.: New York, 2000; 775–824.
2. Brandšteterova, E.; Kubalec, P.; Bovanova, L. HPLC Determination of Antimicrobial Residues in Edible Animal Products. In *Food Analysis by HPLC*, 2nd Ed.; Nollet, L.M.L., Ed.; Marcel Dekker, Inc.: New York, 2000; 621–691.



3. Nawwar, M.A.M.; Marzouk, M.S.; Nigge, W.; Linscheid, M. High-performance liquid chromatographic/electrospray ionization mass spectrometric screening for polyphenolic compounds of *Epilobium hirsutum*—The structure of the unique ellagitannin epilobamide. *Mass Spectrom.* **1997**, *32*, 645–654.
4. Ryan, D.; Robards, K.; Lavee, S. Determination of phenolic compounds in olives by reversed-phase chromatography and mass spectrometry. *J. Chromatogr., A* **1999**, *832*, 87–96.
5. Caniova, A.; Brandsteterova, E. HPLC analysis of phenolic acids in *Melissa officinalis*. *J. Liq. Chromatogr. Relat. Technol.* **2001**, *24* (17), 2647–2659.
6. Caniova, A.; Brandsteterova, E. HPLC analysis of phenolic acids in plant material. *Chem. Anal. (Warsaw)* **2001**, *46*, 757–780.
7. Glowniak, K.; Zgorka, G.; Kozyra, M. Solid-phase extraction and reversed-phase high-performance liquid chromatography of free phenolic acids in some *Echinacea* species. *J. Chromatogr., A* **1996**, *730*, 25–29.
8. Zgorka, G.; Kawka, S. Application of conventional UV, photodiode array (PDA) and fluorescence (FL) detection to analysis of phenolic acids in plant material and pharmaceutical preparations. *J. Pharm. Biomed. Anal.* **2001**, *24*, 1065–1072.
9. Amakura, Y.; Okada, M.; Tsuji, S.; Tonogai, Y. Determination of phenolic acids in fruit juices by isocratic column liquid chromatography. *J. Chromatogr., A* **2000**, *891*, 183–188.
10. Brandsteterova, E.; Ziakova, A., unpublished results.
11. Guo, Ch.; Cao, G.; Sofic, E.; Prior, R.L. High-performance liquid chromatography coupled with coulometric array detection of electroactive components in fruits and vegetables: Relationship to oxygen radical absorbance capacity. *J. Agric. Food Chem.* **1997**, *45* (5), 1787–1796.
12. Mailard, M.N.; Giampaoli, P.; Cuvelier, M.E. Atmospheric pressure chemical ionization (APCI) liquid chromatography-mass spectrometry: Characterization of natural antioxidants. *Talanta* **1996**, *43*, 339–347.
13. Whittle, N.; Eldridge, H.; Bartley, J. Identification of the polyphenols in barley and beer by HPLC/MS and HPLC/electrochemical detection. *J. Inst. Brew.* **1998**, *105* (2), 89–99.
14. Barker, S.A. Matrix solid-phase dispersion. *J. Chromatogr., A* **2000**, *885*, 115–127.
15. Palma, M.; Taylor, L.T. Extraction of polyphenolic compounds from grape seeds with near critical carbon dioxide. *J. Chromatogr., A* **1999**, *849*, 117–124.
16. Yuan, J.P.; Chen, H.; Chen, F. Simultaneous determination of rosmarinic acid, lithospermic acid B and related phenolics in *Salvia miltiorrhiza* by HPLC. *J. Agric. Food Chem.* **1998**, *46*, 2651–2654.
17. Andrade, P.B.; Seabra, R.M.; Valentao, P.; Areias, F. Simultaneous determination of flavonoids, phenolic acids, and coumarins in seven medicinal species by HPLC/diode-array detector. *J. Liq. Chromatogr. Relat. Technol.* **1998**, *21* (18), 2813–2820.
18. Weidner, S.; Amarowicz, R.; Karamac, M.; Dabrowski, G. Phenolic acids in caryopses of two cultivars of wheat, rye and triticale that display different resistance to pre-harvest sprouting. *Eur. Food Res. Technol.* **1999**, *210*, 109–113.
19. Yurttas, H.C.; Schader, H.W.; Warthesen, J.J. Antioxidant activity of non-tocopherol hazelnut (*Corylus spp.*) phenolics. *J. Food Sci.* **2000**, *65* (2), 276–280.
20. Bocco, A.; Cuvelier, M.E.; Richard, H.; Berset, C. Antioxidant activity and phenolic composition of citrus peel and seed extracts. *J. Agric. Food Chem.* **1998**, *46*, 2123–2129.
21. Nuutila, A.A.; Kammiovirta, K.; Oksman-Caldentey, K.M. Comparison of methods for the hydrolysis of flavonoids and phenolic acids from onion and spinach for HPLC analysis. *Food Chem.* **2002**, *76*, 519–525.

Phenolic Compounds, Analysis by HPLC

P. B. Andrade

R. M. Seabra

Faculdade de Farmácia da Universidade do Porto, Porto, Portugal

INTRODUCTION

Phenolic compounds are secondary metabolites that are quite widespread in nature. They play several physiological roles in plants where they occur, but many of them are also favorable to human health because of their antioxidant activity.^[1]

Although very widespread, some of them can work as useful markers for the botanical and geographical origin of several plant products (wine, honey, coffee beans, and jams). These reasons led scientists to develop methods of analysis that are more and more reliable, sensitive, and informative.

The characteristics of high performance liquid chromatography (HPLC) make it the method of choice for the separation of these compounds. Many improvements have been made in this field; however, it was in the area of devices for detection and identification coupled to HPLC that more advances were made in recent years. These methods avoid the tedious and time-consuming isolation of compounds for the subsequent individual identification of each compound. In this paper, an overview of the analysis of phenolics by HPLC is provided.

CHEMISTRY

Phenolics can exhibit simple structures such as arbutin, or complex ones such as those characteristic of the tannin class. They are most frequently linked to sugars, which render themselves polar compounds, or they can be permethylated or methoxylated, becoming nonpolar compounds as what happens with flavonoids found in cuticular waxes.

In a simplistic way, phenolics can be classified according to the number of constitutive carbon atoms in the basic skeleton. With a basic skeleton of C_6 , there are simple phenols and benzoquinones; with C_6-C_1 , there are hydroxybenzoic acids such as gallic acid; with C_6-C_2 , there are the phenylacetic acids; and with C_6-C_3 , there is a larger class including hydroxycinnamic acids, coumarines, and chromones. Sometimes, these structures

appear duplicated, giving rise to lignoids. Naphthoquinones have a C_6-C_4 structure, while xanthenes exhibit a $C_6-C_1-C_6$ structure. Stilbenes and anthraquinones are $C_6-C_2-C_6$ compounds. Flavonoids are most probably the largest group of phenolic compounds—subdivided into several groups—and have a $C_6-C_3-C_6$ structure. For more complete information, see Ref. [2]. If we consider a phenolic compound in a *lato sensu*, then other compounds should be considered here, e.g., the phenolic alkaloids and the phenolic terpenoids, such as the compounds of the carnosic type, found, for example, in Lamiaceae. Although their analysis is not strictly different, these compounds will not be considered here. Fig. 1 represents some structures of common phenolic compounds.

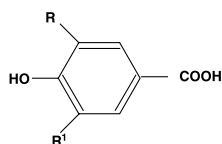
EXTRACTION AND PURIFICATION

The suitable procedure of extraction of phenolics from a plant material depends on the nature of the sample (and particularly its physical state) and the type of phenols to be extracted.^[3] The conditions employed should be as mild as possible to avoid the presence of artifacts in the extracts, resulting in oxidation, thermal degradation, and other chemical and biochemical changes in the sample.^[4]

Phenolic compounds are generally extracted using various mixtures of water and alcohol. Anthocyanins are traditionally extracted in the flavylium cation form, with methanol-containing hydrochloric acid. For the acylated anthocyanins, it is necessary to replace the hydrochloric acid with a weaker acid, either formic or acetic acid.^[3] Lipids, carotenoids, and chlorophyll are removed from the water-alcohol extracts with hexane, chloroform, or petroleum ether. The defatted extracts may be analyzed directly or after a partitioning of the phenolics into ethyl acetate.^[5]

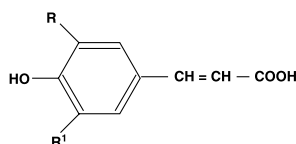
In recent years, solid-phase extraction (SPE), an adsorption-desorption technique, has become the most powerful procedure for purification, trace enrichment, and class fractionation of phenolics. The SPE extraction of phenolics is usually performed on C_{18} -bonded silica





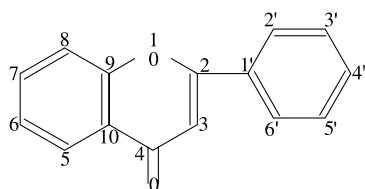
Hydroxybenzoic acids

R = R' = H; *p*-Hydroxybenzoic acid
 R = OH, R' = H; Protocatechuic acid
 R = OCH₃, R' = H; Vanillic acid
 R = R' = OH; Gallic acid
 R = R' = OCH₃; Syringic acid

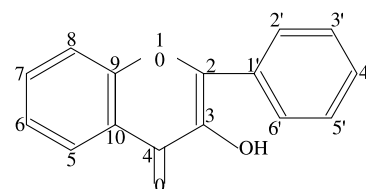


Hydroxycinnamic acids

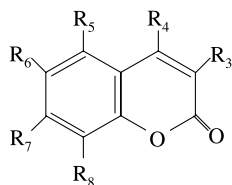
R = R' = H; *p*-Coumaric acid
 R = OH, R' = H; Caffeic acid
 R = OCH₃, R' = H; Ferulic acid
 R = R' = OCH₃; Sinapic acid



Flavone



Flavonol



Coumarines

R₇ = OH; Umbelliferone
 R₆ = R₇ = OH; Aesculetin
 R₆ = OMe, R₇ = OH; Scopoletin
 R₇ = R₈ = OH; Daphnetin

Fig. 1 Structures of commonly occurring phenolic compounds.

reversed-phase (RP) sorbents, styrene-divinylbenzene copolymers, or graphitized carbon black, but other new polymeric sorbents are successfully used in phenolic acid separation and preconcentration, such as RP105 and Oasis HLB.^[6]

In C₁₈-bonded silica RP sorbents, the number of free silanol groups is very important in the attainment of phenolic separations. Silva et al.^[7] showed that C₁₈ non-end-capped columns are more suitable for the recovery of several phenolic acids and flavonoids than the C₁₈ end-capped ones. An enhanced recovery was obtained when 1% of methanol was added to the samples.

The main problem in the analysis of phenolics in plant-derived food, such as honey, fruit juices, and jam, is the high content of sugars and other polar compounds, which cause interphasing when the liquid-liquid partitions are chosen as a method of extraction. The use of the nonionic

polymeric resin Amberlite XAD, by an adsorption-desorption technique, solved this problem. Tomás-Barbérán et al.^[8] have demonstrated that the polystyrene resins (XAD-2, XAD-4, and XAD-16) were more useful for the fractionation of flavonoids (between aglycones and glycosides) compared to polyacrylic resins (XAD-7 and XAD-8). Amberlite XAD-2 was the more suitable nonionic polymeric resin for the recovery and further fractionation of flavonoids from sugar-rich foods.

Sometimes, for solid and semisolid samples, the above-referenced methods were not suitable; the extraction times were very long, with consequent chemical modifications and appearance of artifacts. Supercritical fluid extraction provides a good recovery of phenolics. The extraction behavior of phenolics has been delineated, using supercritical carbon dioxide and either sand or an inert support as sample matrix.^[4]

SEPARATION OF THE COMPOUNDS BY HIGH PERFORMANCE LIQUID CHROMATOGRAPHY

Stationary Phases

The theory related to HPLC separation of compounds^[9] is the same as in thin layer chromatography (TLC) and column chromatography (CC), but the particle size of the adsorbent is much more reduced. These days, analytical HPLC is nearly always performed with microparticulate column packing, which is composed of small spherical or irregular silica, with nominal diameters of usually 3, 5, or 10 μm . These small particles generate a large surface area, which means that the solvents have to be pumped through the column under high pressure.

If these small silica particles are used, then the chromatography is called "normal phase," and the polarity of the stationary phase is higher than that of the mobile phase; this is what happens, for example, when silica is used in adsorption chromatography. However, almost all the work in analytical HPLC is now carried out with chemically modified silica, which is the "bonded phase." In a bonded phase, the highly polar surface of silica is modified by the chemical attachment of various functional groups. Bonded-phase chromatography is experimentally much easier, more versatile, and quicker; it also has better reproducibility than the older modes. When a nonpolar-bonded phase is used, the operation is performed in an RP mode, which means that the polarity of the stationary phase is less than that of the mobile phase. These columns, contrary to normal silica columns, elute polar compounds more rapidly than nonpolar compounds.

Almost all of the analytical work on phenols is performed in an RP mode nowadays; as phenolic compounds are usually polar compounds, they are better analyzed by RP because there is no danger that those highly polar substances may be irreversibly retained in the column, gradually changing the separation characteristics of the column.

To analyze phenolic compounds, the bonded phases most often used are octadecylsilane (ODS, or simply C_{18}) or, less frequently, C_8 stationary phases.

It is not possible to bond all the surface silanol groups of a silica packing. Untreated silanols are capable of adsorbing polar molecules, which will affect the chromatographic properties of the bonded phase. Usually, these untreated silanols produce undesirable effects, such as tailing and excessive retention in RP separations, although there have been cases reported where the untreated silanols improve such separations. The concentration of the unbonded silanols in nonpolar bonded phases is normally reduced by the process of "end

capping," in which most of the remaining silanols are reacted with a small silylating agent, such as trimethylchlorosilane. Through this method, the residual adsorptive properties of the silica are considerably reduced.

Even if we restrict ourselves to the ODS type of packing, there is a large selection available, and although they are all designed to do essentially the same job, there are differences between the C_{18} packings from different manufacturers, depending on the size, shape, and the pore size of the silica particles, and the extent of end-capping. Each of these different columns may have its own advantages for performing a specific task.

Columns are usually expensive and, with fairly crude plant extracts, they can rapidly deteriorate. Protection of the main column by adding, in line, a small guard column containing the same adsorbent as in the column is always worthwhile and can increase the effective life of a column many times over.

The columns used in analytical work can vary from 5 to 25 cm in length and 4 to 6 mm in inner diameter; these columns work with a typical flow rate of about of 1 to 2 mL/min.

Eluents

As previously mentioned, the RP-HPLC of phenolic compounds is carried out with polar eluents. Simple HPLC systems use one pump that pumps a single solvent or, more frequently, a solvent mixture through the column. This is known as isocratic HPLC. More complex gradient systems use more than one pump governed by a computer and pump changing mobile phases that can involve several solvents. Water is usually one of the components in the mixture; the other components most frequently include methanol, acetonitrile, and, more rarely, tetrahydrofuran, etc. The pH of the eluent is always acidic, and this acidity can be attained by the addition of acids such as acetic, formic, phosphoric, trifluoroacetic, and others. The selection of the acid used is dependent on the specific separation problems that need to be solved.

On using a LiChrosorb RP-18 column and a 5% aqueous formic acid and methanol, Casteel et al.^[10] were able to separate 141 flavonoids, ranging from triglycosides to aglycones.

DETECTION AND IDENTIFICATION

After the duly separated compounds elute from the column, it is necessary to proceed to their detection and identification. To achieve this objective, it is necessary to use some property that is characteristic of the analyte but not of the eluent.



Some phenols are readily oxidized or reduced, which allows detection by electrochemical detectors (ECD). However, when using single-electrode ECD, the peak identification is only based on retention times (RT). To enhance the selectivity of this technique, it is essential to use dual electrode or electrochemical array detectors, both of which would give more information based on the shape of the voltammograms of the eluting compounds.^[11]

Because every phenol exhibits a higher or lower absorption in ultraviolet (UV) or UV-visible (UV-VIS) light, given the intrinsic existence of conjugated double and aromatic bonds, UV detection is the ideal method to localize a phenol in the effluent of a column. When a UV

detector works at a fixed wavelength, the obtained information is still very limited. In this case, to identify a compound, it is necessary to perform co-chromatography (using different experimental conditions) with authentic reference compounds. On working at various wavelengths—which implies several analyses, one for each wavelength—it is possible to obtain more information (Fig. 2). In this case, chromatograms with different aspects are obtained as a result of differential UV absorption of the compounds at the wavelengths used.

Diode-array detectors (DAD) are much more useful, because they yield the full record of the UV-VIS spectrum of each compound. Because each class of

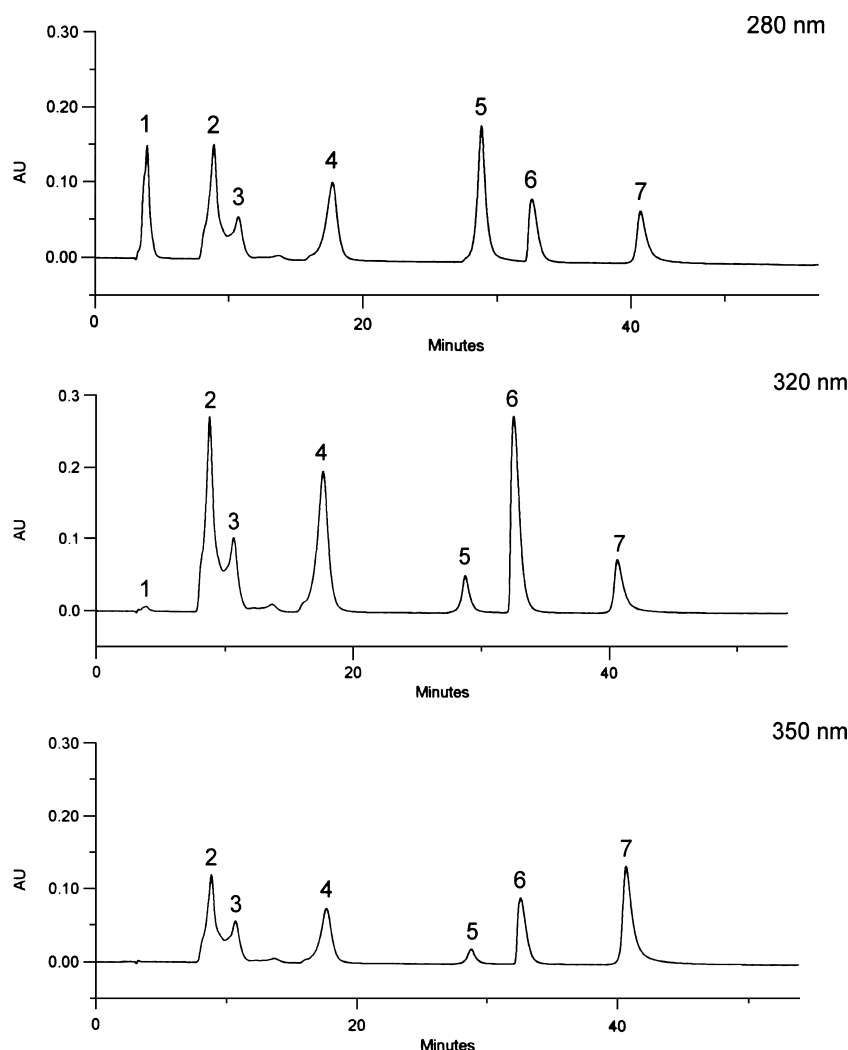


Fig. 2 High-performance liquid chromatographic profile of a standard solution at 280, 320, and 350 nm. Separation was achieved with an analytical HPLC unit (Gilson), using a reversed-phase Shepherisorb ODS2 (25.0 × 0.46 cm; 5 μm particle size) column. The solvent system used was a gradient of water/formic acid (19:1) (A) and methanol (B). The gradient was as follows: 0 min, 30% B; 15 min, 30% B; 20 min, 40% B; 30 min, 45% B; 50 min, 60% B; 53 min, 100% B; and 55 min, 100% B. Detection was accomplished with a DAD. 1—Gallic acid (hydroxybenzoic acid); 2—caffeic acid (hydroxycinnamic acid); 3—mangiferin (xanthone); 4—ferulic acid (hydroxycinnamic acid); 5—eriodictiol (flavanone); 6—herniarin (coumarine); and 7—quercetin (flavonol).

phenolic compounds has a characteristic spectrum, identification is more readily facilitated, although a safe identification still requires a standard with which to compare RT and UV spectra (Fig. 3).

When two compounds with very close, or even superimposable, RT and identical UV spectra appear in a chromatogram, it is necessary to use more sophisticated detectors that can yield much more structural information without requiring the isolation of the compounds. One often uses HPLC–mass spectrometry (HPLC–MS) and HPLC–nuclear magnetic resonance (HPLC–NMR).

Thirty years ago, the linkage of HPLC to MS seemed a physical impossibility because of two main hindrances. The first problem was how to get rid of the eluent without losing the compounds to be analyzed. Secondly, we must realize that, to obtain the mass spectrum of a compound, it is necessary to have it in the vapor state and in an ionized form. We must also remember that many phenols, especially those linked to sugars, are not volatile and are thermolabile.

The resolution of this latter problem passed through the development of the so-called soft ionization methods, in which ions are directly produced from the solid or liquid state. Field ionization (FI) and field desorption (FD) were two of the first alternative ionization methods. A few years later, other techniques were developed. Examples of these include desorption/chemical ionization (D/CI), secondary ion mass spectrometry (SI-MS), and fast atom bombardment (FAB).

However, the great improvement to solve the possibility of coupling HPLC to MS was the development of interfaces that allow the elimination of the solvent and the vaporization of the solute before this can be analyzed in the mass spectrometer. Several interfaces are now available, such as continuous flow FAB (CF-FAB), thermospray (TSP), moving belt (MB), direct liquid introduction (LDI), and atmospheric pressure ionization (API); in the field of API, three different, but fundamentally similar, techniques are available: ion evaporation, electrospray, and ion spray. In each case, the removal of

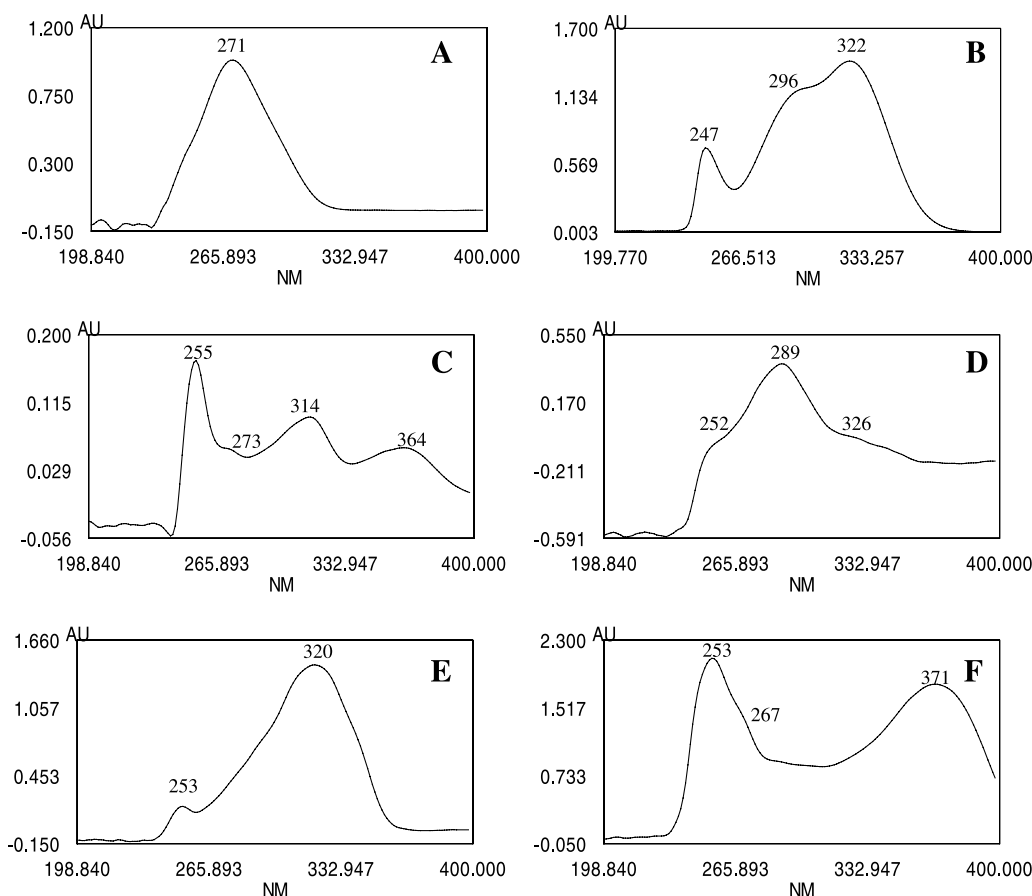


Fig. 3 UV–VIS spectra of several phenolic compounds: A—gallic acid; B—caffeic acid; C—mangiferin; D—eriodictiol; E—herniarin; F—quercetin.



Table 1 Modern HPLC methods for the determination of phenolics

Matrix	Phenolics	Sample preparation	Stationary phase	Mobile phase	Detection	References
Leaves, galls, stems, and roots of <i>Guiera senegalensis</i>	Galloylquinic tannins	Isolation methods using solvent gradient in Sephadex LH-20 column. Further purification by semipreparative HPLC	Superspher RP-18E (125 × 4 mm i.d., 4 µm particle size)	Isocratic/water/tetrahydrofuran/2-propanol (90:10:5:1). Flow 1 mL/min	DAD	[16]
Leaves and flowers of <i>Crataegus</i> spp.	Procyanidins	Liquid-liquid extraction and SPE	LiChrosorb RP-18 (250 × 4 mm i.d., 5 µm particle size)	A: methanol; B: 0.5% <i>ortho</i> -phosphoric acid (v/v). Flow 1 mL/min A: methanol/water/ acetic acid (24.5:75.0:0.5); B: methanol/water/ acetic acid (44.5:55.0:0.5); C: methanol/ acetic acid (99.5:0.5). Flow 0.2 mL/min	ECD connected in series with DAD APCI ^a -MS ESP ^b -MS	[11] [17]
Flowering tops of <i>Crataegus</i> spp.	Procyanidins	Liquid-liquid extraction and SPE	LiChrosorb-100 RP-18 (250 × 4 mm i.d., 5 µm particle size)			
Leaves of <i>Ocimum gratissimum</i> var. <i>Gratissimum</i>	Flavonoids	Extraction with 95% ethanol. Concentration, redissolution in 50% methanol Fractionation of extracts in PVP column	LiChrosorb-100 RP-18 (250 × 4 mm i.d., 5 µm particle size)	A: 2% aqueous acetic acid; B: methanol/ acetic acid/water (18:1:1)	DAD	[18]
Leaves of <i>Maytenus aquifolium</i>	Flavonoids	The sample was boiled with water. The infusion was filtered and evaporated. The residue was redissolved in methanol	C30-RP (250 × 4.6 mm i.d., 5 µm particle size)	A: 2% aqueous acetic acid; B: methanol	APCI-MS NMR	[19]

the solvent is performed in different ways, and ionization is most frequently carried out by solvent-mediated chemical ionization. In any case, LC-MS interfaces always involve complex technology, and the performance obtained depends on various parameters. For further information, consult Refs. [12–14]. In any case, these technologies have been increasingly used during the last two decades, and are obviously very helpful, not only in obtaining the molecular weight of a compound being analyzed, but also in elucidating the structural features through the study of the design of the fragments obtained.

Unquestionably, NMR is the technique that generates more information about a molecule. The problems posed by LC-NMR coupling are essentially different from those cited for LC-MS because, to obtain NMR spectra, the molecule to be analyzed is in solution. In the case of LC-NMR, the two main problems to be solved are the elimination of the signals of the eluent coming from the column and the low sensitivity of NMR detection. Because of these problems, the coupling LC-NMR is not recent and has been difficult to achieve. The use of deuterated eluents during HPLC could, theoretically, solve the first problem, but, except for D₂O, they are too expensive to make the technique routinely feasible. This problem has been overcome by the development of "solvent-suppression techniques," with which the signals of the solvents are removed, making it possible to obtain high-quality spectra.

Direct, on-line coupling of an NMR spectrometer to an HPLC has required the development of special interfaces called flow probes. These systems can basically work in two ways. One is through an "on-flow" mode (the solute passes through the system as it passes out of the column and is analyzed), but this process has a low sensitivity even when the HPLC column is overloaded. In another way, which is much more used nowadays, the HPLC control unit is equipped with a valve that invokes a stop flow of the effluent when a compound (detected by a UV detector that is always used in connection with these systems) leaves the column; in this case, the flow is stopped in order to have enough time for the acquisition of the NMR spectrum.

A more practical way to perform LC-NMR is to use a loop collector, which automatically collects the peaks of interest without stopping the LC flow. Off-line post-chromatographic analysis of the content of the loops is then automatically performed.^[15]

Table 1 lists some examples of HPLC methods of phenolic compounds collected from literature published during 2000–2001.

In conclusion, we can say that if HPLC was already indispensable for the separation of phenols (as well as other classes of compounds), the possibility of coupling it

to several detection devices has turned it into an even more valuable tool.

REFERENCES

1. Merken, H.M.; Beecher, G.R. Measurement of food flavonoids by high-performance liquid chromatography: A review. *J. Agric. Food Chem.* **2000**, *48* (3), 577–599.
2. Harborne, J.B. General Procedures and Measurement of Total Phenolics. In *Methods in Plant Biochemistry*. Vol. 1, *Plant Phenolics*; Dey, P.M., Harborne, J.B., Eds.; Academic Press: London, 1989; 1–27.
3. Macheix, J.J.; Fleuriet, A.; Billot, J. *Fruit Phenolics*; CRC Press: Boca Raton, FL, USA, 1990.
4. Antolovich, M.; Prenzler, P.; Robards, K.; Ryan, D. Sample preparation in the determination of phenolic compounds in fruits. *Analyst* **2000**, *125*, 989–1009.
5. Ryan, D.; Robards, K. Phenolic compounds in olives. *Analyst* **1998**, *123*, 31–44.
6. Kledjus, B.; Kubán, V. High performance liquid chromatographic determination of phenolic compounds in seed exudates of *Festuca arundinacea* and *F. pratense*. *Phytochem. Anal.* **2000**, *11*, 375–379.
7. Silva, B.M.; Andrade, P.B.; Seabra, R.; Ferreira, M.A. Determination of selected phenolic compounds in quince jams by solid-phase extraction and HPLC. *J. Liq. Chromatogr. Relat. Technol.* **2001**, *24* (18), 2861–2872.
8. Tomás-Barbéran, F.A.; Blázquez, M.A.; García-Viguera, C.; Ferreres, F.; Tomás-Lorente, F. A comparative study of different Amberlite XAD resins in flavonoid analysis. *Phytochem. Anal.* **1992**, *3*, 178–181.
9. Lindsay, S. *High Performance Liquid Chromatography*; Kealey, D., Ed.; John Wiley & Sons: Great Britain, 1987.
10. Castele, K.V.; Geiger, H.; Van Summer, F. Separation of flavonoids by reversed-phase high-performance liquid chromatography. *J. Chromatogr.* **1982**, *240*, 81–94.
11. Rohr, G.E.; Meier, B.; Sticher, O. Evaluation of different detection modes for the analysis of procyanidins in leaves and flowers of *Crataegus* spp.: Part I. Diode array and electrochemical detection. *Phytochem. Anal.* **2000**, *11*, 106–112.
12. Wolfender, J.L.; Maillard, M.; Marston, A.; Hostettmann, K. Mass spectrometry of underivatized naturally occurring glycosides. *Phytochem. Anal.* **1992**, *3*, 193–214.
13. Verpoorte, R.; Niessen, W.M.A. Liquid chromatography coupled with mass spectrometry in the analysis of alkaloids. *Phytochem. Anal.* **1994**, *5*, 217–232.
14. Wolfender, J.L.; Maillard, M.; Hostettmann, K. Thermospray liquid chromatography-mass spectrometry in phytochemical analysis. *Phytochem. Anal.* **1994**, *5*, 153–182.
15. Wolfender, J.L.; Ndjoko, K.; Hostettmann, K. The potential of LC-NMR in phytochemical analysis. *Phytochem. Anal.* **2002**, *12*, 2–22.

16. Bouchet, N.; Lévesque, J.; Pousset, J.L. HPLC isolation, identification and quantification of tannins from *Guiera senegalensis*. *Phytochem. Anal.* **2000**, *11*, 52–56.
17. Rohr, G.E.; Riggio, G.; Meier, B.; Sticher, O. Evaluation of different modes for the analysis of procyanidins in leaves and flowers of *Crataegus* spp.: Part II. Liquid chromatography–mass spectrometry. *Phytochem. Anal.* **2000**, *11*, 113–120.
18. Grayer, R.J.; Kite, G.C.; Zaid, M.A.; Archer, L.J. The application of atmospheric pressure chemical ionisation liquid chromatography–mass spectrometry in the chemotaxonomic study of flavonoids: Characterization of flavonoids from *Ocimum gratissimum* var. *gratissimum*. *Phytochem. Anal.* **2000**, *11*, 257–267.
19. Vilegas, W.; Villegas, J.H.Y.; Dachtler, M.; Glaser, T.; Laus, K. Application of on-line C30 RP-HPLC-NMR for the analysis of flavonoids from leaf extract of *Maytenus aquifolium*. *Phytochem. Anal.* **2000**, *11*, 317–321.
20. Huck, C.W.; Bonn, G.K. Evaluation of detection methods for the reversed-phase HPLC determination of 3',4',5'-trimethoxyflavone in different phytopharmaceutical products and in human serum. *Phytochem. Anal.* **2001**, *12*, 104–109.
21. Subagio, A.; Sari, P.; Morita, N. Simultaneous determination of (+)-catechin and (–)-epicatechin in cacao and its products by high-performance liquid chromatography with electrochemical detection. *Phytochem. Anal.* **2001**, *12*, 104–109.
22. Midorikawa, K.; Banskota, A.H.; Tezuka, Y.; Nagaoka, T.; Katsumichi, M.; Message, D.; Huertas, A.A.G.; Kadota, S. Liquid chromatography–mass spectrometry analysis of propolis. *Phytochem. Anal.* **2001**, *12*, 366–373.
23. Gu, L.-W.; Gu, W.-Y. Characterisation of soy isoflavones and screening for novel malonyl glycosides using high performance liquid chromatography–electrospray ionisation–mass spectrometry. *Phytochem. Anal.* **2001**, *12*, 377–382.



Phenolic Drugs, New Visualizing Reagents for Detection in TLC

Alina Pyka

Silesian Academy of Medicine, Sosnowiec, Poland

INTRODUCTION

Currently, the most important fields of application of thin-layer chromatography are pharmacy (30%), biochemistry, forensic chemistry, and clinical chemistry (25%), environmental (15%), food analysis and cosmetology (10%), inorganic substances (5%), and various other fields (15%). The number of publications in the field of pharmacy steadily increases.^[1]

Many phenolic derivatives have definite pharmacological and biological properties.^[2–5] The drugs that command special attention are drugs acting on the peripheral nervous system (adrenaline, dopamine, phenylephrine, metaraminol, fenoterol, bamethane, terbutaline, methyl-dopa, norepinephrine), drugs acting on the central nervous system (ethamivan), drugs applied in taeniasis (bithionol, niclosamide), analgesic drugs (pentazocine), and fungicidal and bacteriostatic drugs (hexachlorophene, salicylanilide, pyrocatechin, thymol, phloroglucinol, eugenol, as well as *o*-, *m*-, and *p*-cresol). However, α -naphthol is often applied as a component of some dermatological ointments.

There are good analytical and physicochemical reasons for describing new visualizing reagents; these reasons and the most important reagents and techniques for different types of organic compounds, including phenols, have been described elsewhere.^[1,6–13] For example, Barton's reagent was used to detect dopamine; chloramine T–sodium hydroxide, sucrose–hydrochloric acid, and Pauly's reagents for the detection of phloroglucinol; Emerson reagent to detect thymol and eugenol; fast black salt K–sodium hydroxide reagent to detect terbutaline; potassium hexaiodoplatinate reagent to detect pentazocine; and potassium hexacyanoferrate (III)–ethylenediamine reagent to detect dopamine, noradrenaline, and adrenaline.^[1,7] This paper describes applications of indicators as new visualizing reagents for detection of selected phenolic drugs in TLC.

NEW VISUALIZING REAGENTS

Pyka et al.^[9] detected the following phenolic drugs on silica gel 60 (E. Merck, #1.05721): bamethane (BM),

ethamivan (EM), hexachlorophene (HP), salicylanilide (SA), pyrocatechin (PC), thymol (TM), pentazocine (PZ), phloroglucinol (PG), eugenol (EG), niclosamide (NS), terbutaline (TB), methyl-dopa (MD), and norepinephrine (NP). Plates with methyl-dopa, norepinephrine, terbutaline, bamethane, and ethamivan were developed with a mixture containing glacial acetic acid–*n*-butanol–water (1:4:1, v/v) as mobile phase. Plates with phloroglucinol, pentazocine, hexachlorophene, pyrocatechin, niclosamide, salicylanilide, and thymol were developed with a mixture of chloroform–methanol (9:1, v/v). The plate with eugenol was developed with benzene as mobile phase. Thirteen new visualizing reagents were used to detect the above-mentioned phenolic drugs. Alkaline blue (A), aniline blue (B), neutral red (C), and brilliant green (D) were used as 50 mg/100 mL solutions in water. Bromophenol blue (E), bromothymol blue (F), brilliant cresyl blue (G), thymol blue (H), phenol red (I), bromocresol green (J), and helasol green (K) were used as 50 mg/100 mL solutions in 2% aqueous sodium hydroxide solution. Bromophenol blue (E) solution was prepared directly before use. Additionally, brilliant cresyl blue (L) and bromocresol green (M) were used as 50 mg/100 mL aqueous solutions. The chromatograms were also sprayed with 2% aqueous solutions of CuSO₄, and then aniline blue (B) or brilliant green (D). Plates were evaluated 5 min after spraying (variant 1). They were then heated at 100°C for 15 min and reexamined (variant 2).

By means of these visualizing reagents—alkaline blue (A), aniline blue (B), bromophenol blue (E), bromothymol blue (F), alkaline solution of brilliant cresyl blue (G), bromocresol green (J), thymol blue (H), and an aqueous solution of brilliant cresyl blue (L)—it is possible to detect all of the drugs investigated at levels of 100 μ g. By use of the remaining visualizing systems (C, D, I, K, and M), it is also possible to detect 100 μ g of the drugs investigated except methyl-dopa, terbutaline, norepinephrine, and ethamivan. These could not be detected by means of neutral red (C); ethamivan could not be detected by means of helasol green (D), thymol blue (H), and aqueous solution of bromocresol green (M); bamethane and salicylanilide could not be detected with phenol red (I). Limits of detection (detectability), detectability index, and broadening index are used to describe visualizing effects

Table 1 Detectability (μg), detectability index (I_{detec}) ($\mu\text{g}/\text{mm}^2$),^a and R_F values for selected phenolic drugs^b and visualized with reagents^b investigated on silica gel 60 (E. Merck, #1.05721)

Visualizing agents ^b	Drugs (symbols) ^b												
	MD	NP	TB	BM	EM	PG	PZ	HP	PC	NS	SA	TM	EG
A Detectability ^c	—	10	30	15	—	—	10	10	0.3	20	20	30	5
I_{detec} ^d	4/37	10/36	30/25	15/39	100/39	5/25	5/31	10/75	0.3/10	20/33	20/58	30/19	5/62
B Detectability ^c	—	2	20	10	50	—	0.5	3	0.4	7	7	5	5
I_{detec} ^d	4/43	2/25	10/31	10/25	50/18	5/27	0.5/68	3/26	0.3/10	7/15	7/39	5/62	5/103
C Detectability ^c	—	—	—	—	—	30	10	10	2	30	40	50	—
I_{detec} ^d	—	—	—	100/117	—	30/33	5/21	10/86	2/77	30/65	40/51	50/38	—
D Detectability ^c	—	4	20	—	—	5	10	10	1	0.8	0.8	2	5
I_{detec} ^d	4/26	2/22	20/52	30/9	—	5/20	7/39	5/61	0.3/17	0.8/18	0.8/16	2/42	5/58
E Detectability ^c	4	3	5	40	50	5	5	10	2	15	—	30	10
I_{detec} ^d	4/19	3/10	5/10	40/52	40/83	5/18	5/25	10/43	2/26	5/15	100/68	10/22	10/56
F Detectability ^c	4.8	0.6	—	—	50	20	4	5	5	10	30	20	5
I_{detec} ^d	4.8/8	0.6/28	3/11	40/46	50/41	20/32	4/59	5/45	5/21	10/24	30/34	20/24	5/37
G Detectability ^c	4.8	2	2	—	100	2	2	5	5	7	10	100	5
I_{detec} ^d	4.8/14	2/18	2/17	40/30	50/27	2/23	2/60	5/66	1/28	7/39	10/28	100/199	5/76
H Detectability ^c	3.2	10	—	—	—	8	5	10	4	50	100	20	10
I_{detec} ^d	3.2/7	10/35	20/26	25/28	—	8/25	5/116	5/37	4/64	10/23	50/23	20/24	10/35
I Detectability ^c	4	0.5	—	—	100	10	100	30	0.5	15	—	100	5
I_{detec} ^d	4/27	0.7/5	1/16	—	50/16	3/21	100/200	10/85	0.5/10	15/67	—	100/152	5/97
J Detectability ^c	4	1	20	40	50	8	5	10	2	5	60	100	5
I_{detec} ^d	4/42	1/17	10/48	40/33	40/32	8/31	5/13	10/117	1/24	5/14	60/39	100/94	5/83
K Detectability ^c	3.2	1	—	—	50	8	100	20	0.3	5	100	100	10
I_{detec} ^d	3.2/9	1/20	2/26	30/35	50/34	8/25	100/219	10/71	0.3/11	5/15	80/84	100/78	5/127
L Detectability ^c	—	—	—	—	100	5	100	20	2	50	70	100	5
I_{detec} ^d	1.2/15	100/258	20/47	50/14	100/56	5/31	100/258	10/40	2/42	20/57	70/35	100/103	5/62
M Detectability ^c	—	2	—	—	—	10	4	25	0.7	15	25	30	5
I_{detec} ^d	1.2/18	2/27	10/25	50/15	—	10/24	2/84	25/44	0.7/19	15/30	25/19	30/25	5/58
R_F values	0.52	0.56	0.69	0.78	0.87	0.26	0.30	0.68	0.72	0.81	0.92	0.96	0.36

^aAverage, $n=5$.

^bCodes as indicated in text.

^cInitial evaluation.

^dEvaluation after heating at 120°C for 30 min.

Source: Ref. [9].

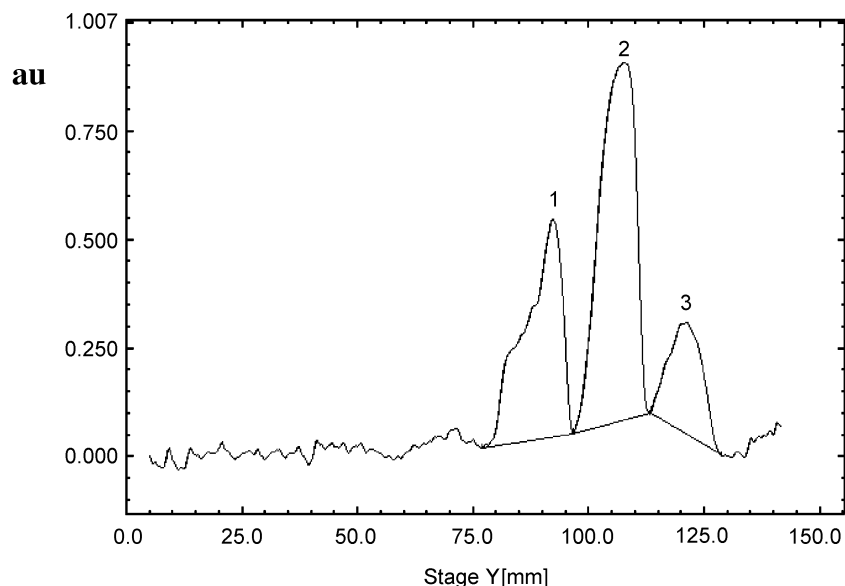


Fig. 1 Densitogram of methyl dopa (1), terbutaline (2), and bamethane (3) after spraying with brilliant green (D). (From Ref. [9].)

for phenolic drugs, which are detected by particular visualizing reagents. The broadening index is defined as

$$I_{\text{broad}} = \frac{100}{p_2} \times 100 \quad (\mu\text{g mm}^{-2}) \quad (1)$$

where 100 μg of the analyzed substance in 10 μL of solution is applied to a chromatographic plate, and p_2 is the spot area of 100 μg of analyzed substance after the

plate has been sprayed with visualizing reagents and heated at 120°C for 30 min. The detectability index is defined as:

$$I_{\text{det}} = \frac{m_1}{p_1} \quad (\mu\text{g mm}^2) \quad (2)$$

where m_1 is the smallest quantity of substance detected (μg) with the visualizing reagent (limit of detection), and

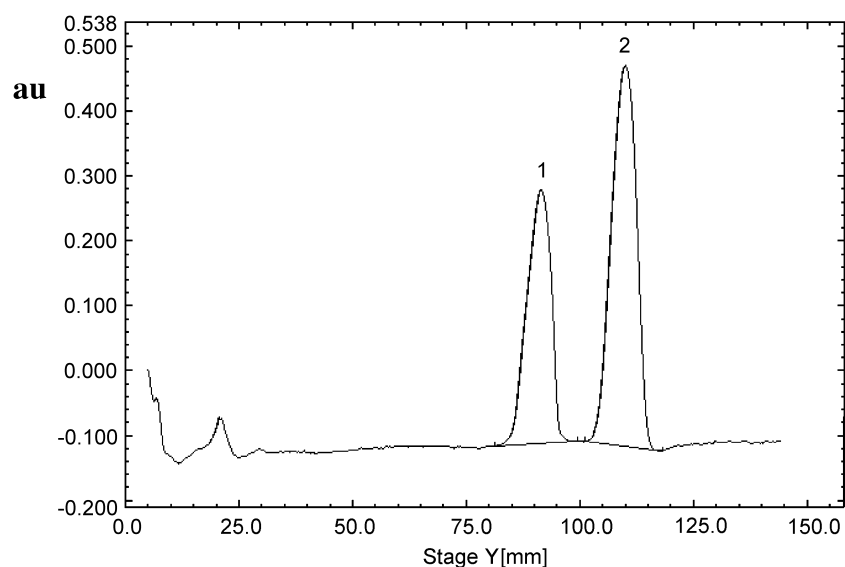


Fig. 2 Densitogram of norepinephrine (1) and bamethane (2) after spraying with aniline blue (B). (From Ref. [9].)

p_1 is the spot area of the substance (mm^2) at the limit of detection of the substance.

A good visualizing reagent has a relatively large numerical value of broadening index for a particular detected substance (small spot area, which refers to 100 μg of substance detected). The broadening indices for the drugs investigated, along with the best visualizing reagents, are (in $\mu\text{g}/\text{mm}^2$) 67 for methyl dopa with brilliant cresyl blue (G), 99 for norepinephrine with alkaline blue (A), 270 for terbutaline with aniline blue (B), 455 for bamethane with brilliant green (D), 345 for ethamivan with aniline blue (B), 152 for phloroglucinol with bromocresol green (M), 84 for pentazocine with bromophenol blue (E), 71 for hexachlorophene with brilliant green (D), 62 for pyrocatechin with bromocresol green (M), 278 for niclosamide with bromothymol blue (F), 217 for salicylanilide with alkaline solution of bromocresol green (J), 135 for thymol with bromocresol green (M), and 68 for eugenol with bromothymol blue (F).

The limits of detection of the phenolic drugs investigated with the visualizing reagents tested, directly after spraying (variant 1), or after 30 min heating at 120°C (variant 2), as well as the detection indices are presented in Table 1. For the limits of detection of the investigated drugs shown, only in some cases is the detection better after the plates were heated. Levels of detection of the phenolic drugs are in the following ranges (in μg): for pyrocatechin 0.3–5.0, pentazocine 0.5–100, norepinephrine 0.6–100, niclosamide 0.8–50, salicylanilide 0.8–100, methyl dopa 1.2–4.8, terbutaline 2.0–30, thymol 2.0–100, hexachlorophene 3.0–25, phloroglucinol 3.0–30, bamethane 10.0–100, for eugenol 5.0–10, and ethamivan 40.0–100. The most sensitive detections are obtained for pyrocatechin with alkaline blue (A), brilliant green (D), helasol green (K) (300 ng); pentazocine with aniline blue (B) (50 ng); norepinephrine with bromothymol blue (F) (600 ng); niclosamide and salicylanilide with brilliant green (D) (800 ng); and methyl dopa with aqueous solution of bromocresol green (M) (1.2 μg). The best detection reagents for the drugs investigated (being phenol derivatives) are brilliant green (D) and aniline blue (B). These two visualizing reagents were used for densitometric research. Bamethane, terbutaline, and methyl dopa were detected with brilliant green (D) and then the densitometric analysis of chromatograms was determined. Terbutaline and norepinephrine were detected with aniline blue (B). Bamethane (100 μg), terbutaline (100 μg) and methyl dopa (50 μg) were detected by means of brilliant green (D); as optimum wavelength, $\lambda=380.5$ nm was selected. Densitograms for these three drugs are presented in Fig. 1. The peak, derived from methyl dopa, has an irregular

shape, suggesting that methyl dopa contains impurities that (using the given mobile phase) could not be completely separated. For terbutaline (15.0 μg) and norepinephrine (5.0 μg), detected by means of aniline blue (B), an optimum wavelength for densitometric analysis, $\lambda=371$ nm, was chosen. Densitograms obtained for terbutaline and norepinephrine are presented in Fig. 2. The densitograms show that both aniline blue (B) and brilliant green (D) have good properties as visualizing reagents with respect to the substances detected. However, brilliant green (D), because of its properties, causes heterogeneity of the adsorbent surface, observed as noise. This effect is not observed for aniline blue (B).

Some of the visualizing reagents reported here can be used as new detection reagents for the qualitative determination of phenolic drugs. The colors of the chromatographic spots for phenolic drugs investigated, obtained with selected reagents [including the best reagents—aniline blue (B) and brilliant green (D)], are presented in Table 2. These reagents can be used to identify compounds analyzed by TLC, based on R_F values and on the different colors of the chromatographic spots. Further investigations show that guaiacol cannot be detected by use of the above-mentioned visualizing reagents.^[14]

Pyka et al.^[10] also applied various visualizing systems, always including a saturated aqueous solution of variamine blue hydroxide and another reagent, for example, 0.1% aqueous HCl, 1% aqueous $\text{Ni}(\text{NO}_3)_2$, 2% aqueous CuSO_4 , 0.1% aqueous Na_2CO_3 , 1% dithizone in methanol, and 1% aqueous EDTA. These visualizing reagents can be used for qualitative identification of eugenol and thymol. Yet, guaiacol cannot be detected by use of these visualizing reagents.^[10]

The best visualizing reagents for detection of α -naphthol on silica gel are titan yellow, eosin, and helasol green in aqueous sodium hydroxide (50 mg/100 mL of 5% NaOH).^[13] Detectability limit of α -naphthol using these visualizing reagents is 0.14 μg . Titan yellow and eosin yellow are the best visualizing reagents for detection of α -naphthol chromatographed on a mixture of silica gel and kieselguhr F₂₅₄ (detectability 0.15 μg). However, for detection of α -naphthol on polyamid 11 F₂₅₄, titan yellow as well as thymolphthalein (detectability 7.2 μg) are best. Titan yellow detects the smallest quantity of α -naphthol on all the above-mentioned chromatographic adsorbents.^[13] Titan yellow is also the best visualizing reagent for detection of *m*-cresol on silica gel 60 F₂₅₄ (detectability 1.08 μg).^[12]

Wardas et al.^[11] examined indicators for detection of adrenaline, dopamine, phenylephrine, metaraminol, fenoterol, and bithionol after TLC fractionation on silica gel,



Table 2 Description of the chromatographic spots with selected visualizing reagents based on the detection of 100 µg of the phenolic drugs

Drugs ^a	Visualizing agents ^a							
	B2 ^b	D2	E1 ^c	F2	G2	H2	J1	M2
MD	Light yellow	Light yellow	Brown	Brown	Brown	Brown/black	Brown	Light brown
NP	Yellow/brown	Orange/red/yellow	Brown/black	Yellow brown	Light brown	Light brown	Light orange/red	Brown
TB	Yellow green	Green	Light green	Green	Light brown	Yellow	White/gray	Light yellow
BM	Light blue	White	Light blue	Light pink	Light pink	Light blue	White/blue	White/blue
EM	White/blue	—	Celadon	White/blue	Light yellow	—	Light yellow	—
PG	Yellow	Yellow green	Orange/red	Light yellow	Light brown	Gray	Orange	Orange
PZ	White	Celadon	Light yellow	Light violet	White/gray	White/yellow	White/blue	Light violet
HP	Light blue	Green	White/violet	Blue	White/blue	Beige	Blue	Light yellow
PC	Light brown	Light orange /red	Dark brown	Light brown	Brown	Brown	Brown/black	Brown
NS	Light blue	Green	Orange/red/brown	Light brown	Light yellow	Light yellow	Light brown	Light yellow
SA	White/blue	Green	—	Light blue	Light gray	Light beige	Light blue	White
TM	Blue	Yellow green	Light violet	Blue	White blue	Pink blue	White/gray	White/blue with white border
EG	Light blue	Green	Light pink	Light yellow	Light yellow	Light brown	Brown	Light blue with white border
Background	Light blue	Light green	Dark violet	Light blue	Light blue	Beige	Light gray	Light celadon

Abbreviations as in Table 1.

^aCode as indicated in text.

^b(2) Evaluation after heating at 120°C for 30 min.

^c(1) Initial evaluation.

Source: Ref. [9].

Table 3 Characteristics of the visualizing effect for adrenaline, dopamine, phenylephrine, metaraminol, fenoterol, and bithionol investigated on Kieselgel 60 F₂₅₄, Kieselgel 60/Kieselguhr F₂₅₄, and polyamid 11 F₂₅₄

Sorbent	Compound	Adrenaline	Dopamine	Phenylephrine	Metaraminol	Fenoterol	Bithionol
Kieselgel 60 F ₂₅₄	Visualizing agents	Brilliant cresyl blue in 5% NaOH	Bromocresol green in 5% NaOH	Bromocresol green in 5% NaOH	Bromocresol green in 5% NaOH	Bromocresol green in 5% NaOH	Brilliant cresyl blue in 5% NaOH
	Detectability (µg)	0.1	0.1	0.25	0.5	0.1	0.5
	Detectability index (µg/mm ²)	0.1/10	0.1/15	0.25/21	0.5/15	0.1/13	0.1/77
	Color of spot	Brown	Orange	Lemon	Lemon	Brown/orange	Brown
	Description of spot	Compact, fast	Compact, fast	Compact, fast	Compact, fast	Compact, fast	Broadened, fast
Kieselgel 60/Kieselguhr F ₂₅₄	Background color	Light violet	Light blue	Light blue	Light blue	Light blue	Light violet
	R _F	0.38	0.51	0.47	0.62	0.82	0.92
	Visualizing agents	Bromocresol green in 5% NaOH	Bromocresol green in 5% NaOH	Eriochrome black T in 5% NaOH	Eriochrome black T in 5% NaOH	Eriochrome black T in 5% NaOH	Brilliant cresyl blue in 5% NaOH
	Detectability (µg)	0.25	0.25	0.5	0.5	0.5	2.5
	Detectability index [µg/mm ²]	0.25/47	0.25/25	0.5/41	0.5/35	0.5/38	2.5/68
Polyamid 11F ₂₅₄	Color of spot	Light brown	Brown/orange	Brown	Brown	Brown	Brown
	Description of spot	Broadened, fast	Compact, fast	Compact, fast	Compact, fast	Compact, fast	Broadened, fast
	Background color	Sea/green	Sea/green	Light brown	Light brown	Light brown	Light brown
	R _F	0.45	0.53	0.56	0.65	0.78	0.88
	Visualizing agents	Eosin yellow in 5% NaOH	Eosin yellow in 5% NaOH	—	Aniline blue in water	Eosin yellow in 5% NaOH	—
Kieselgel 60/Kieselguhr F ₂₅₄	Detectability (µg)	2.5	0.75	—	50	5	—
	Detectability index (µg/mm ²)	2.5/30	0.75/17	—	50/42	5/15	—
	Color of spot	Light brown	Light brown	—	Light yellow	Yellow	—
	Description of spot	Compact, instability	Compact, instability	—	Compact, fast	Compact, fast	—
	Background color	Light yellow	Light yellow	—	Blue	Light yellow	—
	R _F	0.75	0.79	0.89	0.82	0.89	0.90

Source: Ref. [12].

polyamide 11 F₂₅₄, and a mixture of silica gel and kieselguhr by use of glacial acetic acid–n-butanol–water (1:4:1, v/v) as mobile phase. They investigated the following indicators as visualizing reagents: phenol red, thymol blue, bromothymol blue, bromophenol blue, cresol green, erythrosine B, eriochrome black T, brilliant cresyl blue, eosin yellow, titan yellow, helasol green dissolved in 5% NaOH, as well as bromocresol green, aniline blue, alkaline blue, brilliant cresyl blue, and brilliant green dissolved in water. Additionally, dimethyl yellow and thymolphthalein dissolved in methanol were applied, but before being used, the chromatographic plate was sprayed with 5% NaOH. In each case, the concentration of the solutions was 0.5 mg/mL. Most reagents give positive visualizing effects on silica gel 60 F₂₅₄, a bit less on a mixture of silica gel and kieselguhr F₂₅₄, and the least on polyamide 11 F₂₅₄. Levels of detection of these phenolic drugs on silica gel are in the following ranges (in µg): for adrenaline 0.1–10.0; dopamine 0.1–10; phenylephrine 0.25–20; metaraminol 0.5–20; fenoterol 0.1–15; and for bithionol 0.5–50. Levels of detection of these phenolic drugs on a mixture of silica gel and kieselguhr are in the following ranges (in µg): for adrenaline 0.25–15.0; dopamine 0.25–7.5; phenylephrine 0.5–15; metaraminol 0.5–15; fenoterol 0.5–12.5; and for bithionol 2.5–10. Levels of detection of these phenolic drugs on polyamide are in the following ranges (in µg): for adrenaline 2.5–100; dopamine 0.75–100; metaraminol 50–100; and for fenoterol 5–100. The best detectability, equal to 100 ng, is obtained on silica gel, in the case of adrenaline with brilliant cresyl blue dissolved in water, as well as dopamine and fenoterol with bromocresol green and brilliant cresyl blue dissolved in 5% NaOH. The best detectability on a mixture of silica gel and kieselguhr F₂₅₄ is 250 ng for adrenaline and dopamine with bromocresol green in 5% NaOH, on the polyamide 750 ng for dopamine with eosin yellow. However, phenylephrine and bithionol are not detected on polyamide 11 F₂₅₄ with the studied visualizing reagents. Characteristics of the visualizing effect for adrenaline, dopamine, phenylephrine, metaraminol, fenoterol, and bithionol with the best visualizing reagents investigated on Kieselgel 60 F₂₅₄, Kieselgel 60/Kieselguhr F₂₅₄, and Polyamid 11 F₂₅₄ are listed in Table 3.

CONCLUSIONS

- In this review, indicators described as the visualizing reagents should serve as a supplement to those previously used for the detection of phenolic drugs.

- The visualizing effect depends on the chemical structure of the visualizing reagent, the structure of the substance detected, as well as the chromatographic adsorbent applied.
- Particular applications will have these visualizing reagents, which, with substances present in analyzed mixtures, will give diversified colors of chromatographic spots.
- The best and most universal visualizing reagents for detection of bamethane, ethamivan, hexachlorophene, salicylanilide, pyrocatechin, thymol, pentazocine, phloroglucinol, eugenol, niclosamide, terbutaline, methyl dopa, and norepinephrine investigated on silica gel 60 are aniline blue and brilliant green dissolved in water. These visualizing reagents have relatively good properties for quantitative research of investigated phenolic drugs.^[9]
- Eugenol and thymol can also be qualitatively detected on silica gel by use of visualizing reagents based on a saturated aqueous solution of varamine blue hydrochloride.^[10]
- The best visualizing reagents for detection of α -naphthol are the following: on silica gel: titan yellow, eosin, and helasol green in aqueous sodium hydroxide (50 mg/100 mL of 5% NaOH); on a mixture of silica gel and kieselguhr F₂₅₄: titan yellow and eosin yellow; and on polyamide 11 F₂₅₄: titan yellow and thymolphthalein. Titan yellow detects the lowest level of α -naphthol on all the above-mentioned chromatographic adsorbents.^[13]
- Titan yellow is also the best visualizing reagent for detection of *m*-cresol on silica gel 60 F₂₅₄ (detectability 1.08 µg).^[12]
- The most universal visualizing reagents for adrenaline, dopamine, phenylephrine, metaraminol, fenoterol, and bithionol are the following: on silica gel 60 F₂₅₄: bromocresol green and brilliant cresyl blue dissolved in 5% NaOH; on a mixture of silica gel and kieselguhr F₂₅₄: bromocresol green, brilliant cresyl blue, and eriochrome black T dissolved in 5% NaOH; on polyamide 11 F₂₅₄: eosin yellow dissolved in 5% NaOH.^[11]

REFERENCES

1. Jork, H.; Funk, W.; Fischer, W.; Wimmer, H. Specific Detection Methods. In *Thin-Layer Chromatography: Reagents and Detection Methods, Physical and Chemical Detection Methods: Activation Reactions, Reagents Sequences, Reagents II*; VCH: Weinheim, Germany, 1994; Vol. 1b, 11–140.
2. Floren, C.H.; Kjellstrom, T.; Bauer, C.A. Bambuterol



- raises high-density lipoprotein levels with hyperlipidaemia. *J. Int. Med.* **1997**, *242*, 167–171.
3. Grosset, J. Current problems with tuberculosis treatment. *Res. Microbiol.* **1996**, *147*, 10–16.
4. Huang, F.Y.; Chen, C.M.; Yan, S.K. Control of staphylococcal skin infections in a nursery. *Acta Paediatr.* **1991**, *32*, 165–170.
5. Meier-Hellmann, A.; Bredle, D.R.; Specht, M.; Spies, C.; Hannemann, L.; Reinhart, K. The effects of low-dose dopamine on splanchnic blood flow and oxygen uptake in patients with septic shock. *Intensive Care Med.* **1997**, *23*, 31–37.
6. Merck, E.E. *Firmenbroschüre Anfärbereagenzien für Dünnschicht- and Paper Chromatographie*; E. Merck: Darmstadt, Germany, 1980; 1–100.
7. Jork, H.; Funk, W.; Fischer, W.; Wimmer, H. *Dünnschicht-Chromatographie, Reagenzien und Nachweismethoden, Physicalische und Chemische Nachweismethoden: Grundlagen, Reagenzien I*; VCH: Weinheim, Germany, 1989; Vol. 1a, 9–118.
8. Randerath, K. *Dünnschicht-Chromatographie*, 2nd Ed.; Verlag Chemie: Weinheim, Germany, 1965; 52–55.
9. Pyka, A.; Gurak, D.; Bober, K. New visualizing reagents for selected phenolic drugs investigated by thin layer chromatography. *J. Liq. Chromatogr. Relat. Technol.* **2002**, *25*, 1483–1495.
10. Pyka, A.; Gurak, D.; Bober, K.; Niestrój, A. Application of new visualizing agents for selected essential oil components in TLC. *Chem. Anal. (Warsaw)* **2002**, *47*, 691–699.
11. Wardas, W.; Lipska, I.; Bober, K. TLC fractionation and visualization of selected phenolic compounds applied as drugs. *Acta Pol. Pharm. Drug Res.* **2002**, *57*, 15–22.
12. Wardas, W.; Pyka, A. Visualizing agents for phenols in thin layer chromatography. *J. Planar Chromatogr. Mod. TLC* **1991**, *4*, 334–336.
13. Wardas, W.; Pyka, A. Visualizing agents for phenols and naphthols in thin layer chromatography. *J. Planar Chromatogr. Mod. TLC* **1992**, *5*, 471–474.
14. Pyka, A. Unpublished data.



Phenols and Acids: Analysis by TLC

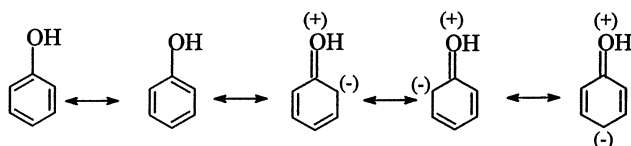
Luciano Lepri

Alessandra Cincinelli

Università degli Studi di Firenze, Firenze, Italy

Introduction

Phenols are stronger acids than alcohols, because the oxygen atom acquires a positive charge by resonance and, thus, proton release is facilitated:



Phenol is a weak acid ($pK_a = 9.98$) and the effect of a ring substituent on the acid strength depends on whether the group is electron withdrawing or releasing, its position, and its ability to give resonating structures (i.e., the methyl group is electron releasing and decreases the acid strength from all ring positions).

The phenolic group occurs in a large number of natural and industrial products, extending from phenolic resins, herbicides, surfactants, alkaloids, steroids, and glycosides to numerous other groups.

A comprehensive review of phenolic compounds in biochemical, environmental, industrial, and consumer products, as well as of sample preparation prior to thin-layer chromatography (TLC) has been effected by Tyman [1].

Chromatographic Behavior of Phenols

Substituted monocyclic phenols have been widely studied on several stationary phases (alumina, silica gel, cellulose, polyamide, silanized silica gel) and also on chemically modified adsorbents (cyano- and amino-silica plates), ion-exchange layers, and impregnated plates.

Phenols can be detected with diazotized orthonilic acid or dianisidine by spraying an ammoniacal silver nitrate solution, followed by exposure to ultraviolet light, or with a modified ferric ferricyanide reagent, and also by exposing the wet layer successively to nitrogen dioxide and ammonia vapors.

Silica Gel, Alumina, Cellulose, and Polyamide

Layers of silica gel and alumina have been employed for the separation and identification of 126 monocyclic phenols eluted with 3 solvents of increasing polarity (benzene, diisopropylether, and ethanol) [2]. Alumina is more basic than silica gel and strongly retains phenolic compounds, particularly those with more acidic properties such as chlorophenols and nitrophenols, even when eluting with a medium-polarity solvent.

Table 1 reports the retention data relative to some substituted monocyclic phenols examined on silica gel in benzene and diisopropylether.

The presence of a 2-substituent or 2,6-substituents results in an increase in the R_f value; this is likely due to hydrogen-bonding or steric effects. However, 2,6-dinitrophenol is more retained in benzene than the 2,4 and 2,5 isomers. The sequence of their R_f values ($R_{f2,6} = 0.04 < R_{f2,4} = 0.07 < R_{f2,5} = 0.38$) is in agreement with that of the corresponding pK_a values ($pK_{a2,6} = 3.71 < pK_{a2,4} = 4.09 < pK_{a2,5} = 5.22$) and, therefore, these two facts can be closely bound up with one another.

Diisopropyl ether allows the separation of nitrophenol isomers and of several nitroalkyl and nitrochlorophenols, as well as of dihydroxy and trihydroxybenzenes. On alumina plates, dimethyl and trimethylphenols are better resolved than on silica gel when eluting with the above-mentioned solvent, as shown by the following R_f value sequences:

Dimethylphenols

$$R_{f3,4} = 0.22 < R_{f3,5} = 0.26 < R_{f2,4} = 0.28 < R_{f2,3} = 0.39 < R_{f2,5} = 0.44 < R_{f2,6} = 0.52.$$

Trimethylphenols

$$R_{f3,4,5} = 0.16 < R_{f2,4,5} = 0.23 < R_{f2,3,5} = 0.46 < R_{f2,4,6} = 0.51$$

Hydrogen-bonding, steric effects, and acid-base properties of phenols are involved in their retention on silica gel and alumina with benzene and isopropylether as eluents.



Table 1 R_f Values of Substituted Phenols in Different Chromatographic Conditions

Compound	Silica gel		Cellulose + ethyl oleate ^a	Silanized silica + 4% DBS ^b		RP-18 + 4% HDBS ^c		pK_a (25°C)
	A	B	C	D	E	F	G	
Phenol	16	74	79	35	62	—	—	10.02
2-Methylphenol	24	78	62	20	35	—	—	10.32
3-Methylphenol	16	75	67	20	40	—	—	10.09
4-Methylphenol	15	74	66	19	36	—	—	10.27
2,3-Dimethylphenol	25	80	45	11	20	—	—	10.54
2,4-Dimethylphenol	28	83	42	11	19	—	—	10.60
2,5-Dimethylphenol	25	77	47	11	21	—	—	10.41
2,6-Dimethylphenol	40	76	40	12	20	—	—	10.63
3,4-Dimethylphenol	15	75	53	12	24	—	—	10.36
3,5-Dimethylphenol	15	73	51	12	25	—	—	10.19
2-Ethylphenol	27	77	40	10	21	—	—	10.2*
3-Ethylphenol	17	72	48	11	28	—	—	9.9*
4-Ethylphenol	15	69	45	11	24	—	—	10.0*
2-Chlorophenol	42	75	53	24	89	48	77	8.48
3-Chlorophenol	20	74	43	14	64	34	50	9.02
4-Chlorophenol	16	69	46	14	50	34	37	9.38
2,3-Dichlorophenol	38	63	28	22	85	35	78	7.45**
2,4-Dichlorophenol	38	65	22	16	78	27	69	7.75**
2,5-Dichlorophenol	41	77	20	28	85	41	81	7.35**
2,6-Dichlorophenol	56	83	31	55	88	59	86	6.79**
3,4-Dichlorophenol	15	63	21	7	57	18	48	8.39**
3,5-Dichlorophenol	—	—	14	9	64	16	55	7.93**
2,3,4-Trichlorophenol	—	—	—	18	68	29	66	7.59
2,3,5-Trichlorophenol	—	—	—	25	69	36	63	7.23
2,3,6-Trichlorophenol	49	76	—	45	82	52	74	6.12
2,4,5-Trichlorophenol	32	67	7	22	70	42	63	7.33
2,4,6-Trichlorophenol	49	76	15	37	73	43	63	6.42
3,4,5-Trichlorophenol	—	—	—	9	52	16	50	7.74
2,3,4,5-Tetrachlorophenol	—	—	—	14	46	35	44	6.96
2,3,4,6-Tetrachlorophenol	36	50	4	—	—	—	—	—
2,3,5,6-Tetrachlorophenol	—	—	—	25	50	38	43	5.44
Pentachlorophenol	20	21	2	13	33	—	—	5.26
2-Nitrophenol	69	79	—	61	92	—	—	7.23
3-Nitrophenol	7	62	—	29	92	—	—	8.40
4-Nitrophenol	4	46	—	66	92	—	—	7.15
Catechol (1,2)	2	49	—	—	—	—	—	—
Resorcinol (1,3)	0	39	—	56	87	—	—	9.81
Hydroquinone	0	43	—	67	e.s.	—	—	10.35

Eluents: A = benzene; B = isopropylether; C = 25% aqueous ethanol; D = 0.1 M NH_3 + 0.1 M NH_4Cl in 30% methanol (pH = 9.02); E = 1 M NH_3 in 30% methanol (pH = 11.30); F = 0.1 M NH_3 + 0.1 M NH_4Cl in 60% methanol; G = 1 M NH_3 in 40% methanol.

^a15 g cellulose impregnated with a solution of ethyl oleate in ether (70 ml of a 0.75% v/v solution);

^b20 g silanized silica gel 60 HF (C_2) mixed with a 4% triethanolamine dodecylbenzenesulphonate (DBS) solution in 95% ethanol;

^cRP-18 ready-to-use plates dipped in a 4% dodecylbenzenesulphonic acid solution in 95% ethanol;

* pK_a values at 28°C;

** pK_a values at 29°C.

Only a limited number of researches have been focused on cellulose plates, microcrystalline cellulose being the most used stationary phase with solvents such as ethylacetate-*n*-propanol-25% ammonia (3:5:2), water-formic acid (98:2), *n*-amyl alcohol-acetic acid-water (10:6:5), and benzene-propionic acid-water (4:9:3).

Polyamide is an especially useful adsorbent for the separation of phenols owing to the formation of hydrogen bonds between the phenolic compounds and the amide group of the polymer. Organic solvents of increasing polarity and aqueous-organic solutions have been used as eluents: benzene, chloroform, ethylacetate, water-methanol, water-acetone, water-acetic acid, and cyclohexane-acetic acid (93:7) mixtures.

Water-propanol-27% ammonia (1:8:1), *n*-butanol-5*M* ammonia (100:33), and *n*-butanol-ethanol-ammonia (5:1:1) have also been employed for nitrophenols.

Ion-Exchange Resins and Impregnated Plates

A wide study of the chromatographic behavior of alkyl, halogenated phenols, and phenols containing alkyl and halogeno groups by reversed-phase TLC has been performed by Bork and Graham [3] on cellulose impregnated with ethyl oleate eluting with aqueous ethanol (see Table 1).

The phenols can be removed by the stationary phase as a result of solvation of the phenolic group by the proton acceptor eluent (water or ethanol), which may be influenced by steric factors and by altering the polarity of the phenolic grouping.

Long-chain alkylphenols present in natural cashew nut shell liquid have been chromatographed on argentated silica gel G [10% (w/w) silver nitrate] with diethylether-light petroleum-formic acid (30:70:1) as eluent for the separation of unsaturated constituents.

Alkylphenols, nitrophenols, halogenophenols and polyhydroxybenzenes have been extensively studied on a thin layer of anion and cation exchangers with cellulose, paraffin, and polystyrene matrices and on silanized silica gel impregnated with anionic and cationic surfactants. The best results have been obtained by using cation exchangers and anionic surfactants as impregnating agents [4,5].

The parameters that determine the retention of phenols on layers of silanized silica gel, untreated and impregnated with anionic surfactants, are the same that affect retention on cation exchangers (i.e., the organic modifier percentage, the ionic strength, and, particularly, the pH of the eluent).

With regard to the influence of pH, the protonated form of the phenols exhibits a higher affinity toward the stationary phase than the deprotonated form. From the relationship

$$K_d = \frac{[\text{HA}]_R + [\text{A}^-]_R V}{[\text{HA}]_S + [\text{A}^-]_S W} \quad (1)$$

(where K_d is the distribution coefficient, $[\text{HA}]_R$, $[\text{A}^-]_R$, $[\text{HA}]_S$, and $[\text{A}^-]_S$ are the concentrations of the protonated and deprotonated form of the phenol in the resin and in the solution, V is the volume of the solution, and W is the weight of the resin) and introducing the K_a value into Eq. (1), combined with the Martin-Syngé equation for partition thin-layer chromatography, Lepri et al. [4] obtained the following relationship:

$$\left(\frac{1}{R_f} - 1\right) = \left(\frac{1}{R_{fac}} - 1\right) \frac{[\text{H}^+]}{K_a + [\text{H}^+]} + \left(\frac{1}{R_{falk}} - 1\right) \frac{K_a}{K_a + [\text{H}^+]} \quad (2)$$

where R_{fac} and R_{falk} are the R_f values of the protonated and deprotonated form of the phenol achieved by eluting with strong acidic and alkaline solutions, respectively.

Although the major change in $(1/R_f) - 1$ with pH occurs at $\text{pH} = \text{p}K_a$, differentiating R_f twice with respect to $\log[\text{H}^+]$ and equating to zero, the following relation is obtained:

$$[\text{H}^+] = K_a \frac{R_{fac}}{R_{falk}} \quad (3)$$

On the basis of Eq. (3), we can predict that the mean R_f value of R_{fac} and R_{falk} will be shifted

more with respect to the $\text{pH} = \text{p}K_a$ value the lower the R_{fac}/R_{falk} ratio is. Many nitrophenols, chlorophenols, and bromophenols can be easily separated by this technique eluting with aqueous-organic solutions at different pH values (see Table 1).

Chromatographic Behavior of Phenolic Acids and Their Derivatives

In general, silica gel has been more widely used than cellulose, polyamide, and silanized silica gel for the separation of phenolic acids and their derivatives.



Selected eluents for silica gel are chloroform–ethylacetate–formic acid (5:4:1), *n*-hexane–ethylacetate–formic acid (15:9:2), chloroform–acetic acid–water (2:1:1), toluene–dichloromethane–formic acid (40:50:10), and dichloromethane–acetic acid–water (100:50:50, lower phase).

Recently, two-dimensional TLC on cellulose plates has been used for the separation of 14 phenolic acids eluting with methanol–acetonitrile–benzene–acetic acid mixtures in the first direction and sodium formate–formic acid–water (10:1:200, v/v/v) in the second direction.

Phenolic aldehydes and ketones have been chromatographed on silica gel G and cellulose plates as their phenylhydrazones formed *in situ*. Toluene–chloroform–acetone (5:3:2), chloroform–acetone (8:2), anisole–methanol (8:2), and anisole–chloroform–acetone (5:3:2) are the eluents used for silica gel, whereas the layers of cellulose have been eluted with 2% formic acid, 20% potassium chloride, 10% acetic acid, or isopropanol–ammonia–water (8:1:1).

Long-chain alkylphenolic acids and their derivatives have been separated on silica gel G eluting with light petroleum (60–80°C)–ethylether–dimethylformamide–acetic acid (75:85:5:1).

Reversed-phase TLC on silanized silica gel layers (OPTI-UPC₁₂, SilC₁₈-50 and RP-18), untreated and impregnated with anionic and cationic surfactants, has been used for the separation of catecholamines, phenolic acids, and glycols excreted in the urine. Many interesting separations have been achieved on OPTI-UPC₁₂ plates eluting with 1M hydrochloric acid +3% KCl in water (biogenic amines) and with 1M sodium acetate in water (urinary phenolic acids and glycols).

Quantitative Determinations

Phenols occurring in water have been quantified by *in situ* densitometry after coupling with diazotized *p*-

nitroaniline or by using vanadium pentoxide and dichlorofluorescein.

A recent article reported the analysis of phenols included in the list of priority pollutants of the Environmental Protection Agency on silica gel G F₂₅₄ HPTLC plates and polyamide plates after solid-phase extraction from water [6].

In situ quantitation has been performed by absorptiometric ultraviolet or visible light measurements of the color developed with Würsters salts.

Planar chromatography has also been used to separate and quantify several common phenols in contaminated land leachates after derivatization with 3-methyl-2-benzothiazolinone hydrazone (MBTH) and extraction of the resulting azo dyes.

References

1. J. H. P. Tyman, Phenols, aromatic carboxylic acids, and indoles, in *Handbook of Thin-Layer Chromatography* (J. Sherma and B. Fried, eds.), Marcel Dekker, Inc., New York, 1996, pp. 877–920.
2. F. Dietz, J. Trandy, P. Koppe, and C. Rubelt, Detection and photometric determination of 126 phenolic compounds in water using group-specific reagents, *Chromatographia* 9: 380–396 (1976).
3. L. S. Bark and J. T. Graham, Studies in the relationship between molecular structure and chromatographic behaviour, *J. Chromatogr.* 23: 417–442 (1966); *J. Chromatogr.* 25: 357–366 (1966).
4. L. Lepri, P. G. Desideri, M. Landini, and G. Tanturli, Chromatographic behaviour of phenols on thin-layers of cation and anion exchangers, *J. Chromatogr.* 109: 365–376 (1975); *J. Chromatogr.* 129: 239–248 (1976).
5. L. Lepri, P. G. Desideri, and D. Heimler, Reversed-phase and soap thin-layer chromatography of phenols, *J. Chromatogr.* 195: 339–348 (1980).
6. J. Bladec, A. Rostkowschi, and S. Neffe, The application of TLC to the determination of phenol residues in water, *J. Planar Chromatogr.—Mod. TLC* 11: 330–335 (1998).



Photodiode-Array Detection

Hassan Y. Aboul-Enein

Vince Serignese

King Faisal Specialist Hospital and Research Centre, Riyadh, Saudi Arabia

Introduction

Analysis is an integral part of research, clinical, and industrial laboratory methodology. The determination of the components of a substance or the sample in question can be qualitative, quantitative, or both. Techniques that are available to the analyst for such determinations are abundant. In absorption spectroscopy, the molecular absorption properties of the analyte are measured with laboratory instruments that function as detectors. Those that provide absorbance readings over the ultraviolet-visible (UV-vis) light spectrum are commonly used in high-performance liquid chromatography (HPLC). The above method is sufficiently sensitive for quantitative analysis and it has a broader application than other modes of detection.

Discussion

The most advanced UV-vis detector that is used in HPLC is the diode array. Compared to its predecessors, the diode array generates a large amount of spectral information without compromising sensitivity or wavelength resolution. In order to discuss the properties of the diode-array detector, a brief historical description of its technological development is presented.

Historical Background and Schematics

Early on, UV-vis detectors produced data at one wavelength only (fixed-wavelength detector, FWD). Because compounds of interest do not absorb light at a fixed wavelength with equal efficiencies, the next step was to develop a detector with an adjustable wavelength range. Modifications were required in the light source. The high-energy-emitting mercury lamp in the FWD was replaced with a deuterium and/or tungsten lamp. The latter light source gave detectable energies over a wider wavelength range. The addition of a wavelength selector (monochromator) provided accurate wavelength adjustments from 190 to 800 (UV-vis) nm.

Hence, the variable-wavelength detector (VWD) was established.

At this point, single-wavelength data acquisition remained a bottleneck, restricting the analyst to one basic characteristic tool to identify the analyte: the amount of time the analyte is retained on the chromatographic column (i.e., the retention time). If there are four compounds in the sample to be analyzed, this would require a minimum of four injections to identify them. Additional work would be needed for cross-identification and so on. The concept of multiple-wavelength detection was introduced.

The diode-array detector collects data with a maximum wavelength bandwidth of 190–800 nm. All wavelengths in that range are accounted for simultaneously. As shown in Fig. 1, the upper portion represents a single detector element with three components: the photodiode, a capacitor, and a FET switch known as the field effect transistor switch. Shining light onto a single detector element produces a signal which is processed and then expressed as a digital absorbance reading. This response is for one wavelength only. The FWDs and VWDs are equipped with a single detector element. The bottom portion of Fig. 1 displays the schematics of a linear diode-array detector. Many detector elements, all of the same composition as described above, are in a linear arrangement. Each detector element is dedicated to a particular wavelength bandwidth such that there are enough of them to cover the UV-vis light spectrum. This unit produces signals that cover the entire UV-vis light spectrum. Simultaneous wavelength detection was now possible with the diode array.

Figure 2 displays the optical components of the diode-array detector. A deuterium lamp will emit light onto the flow cell, which has liquid continuously flowing through it. A shutter is provided between the light source and the flow cell, which can either be fully open or closed. The beam of light will then travel to the diffraction grating, where it will be separated into wavelengths ranging from 190 to 800 nm. The separated light will finally reach the diode array and a signal will be produced that is proportional to the amount of light



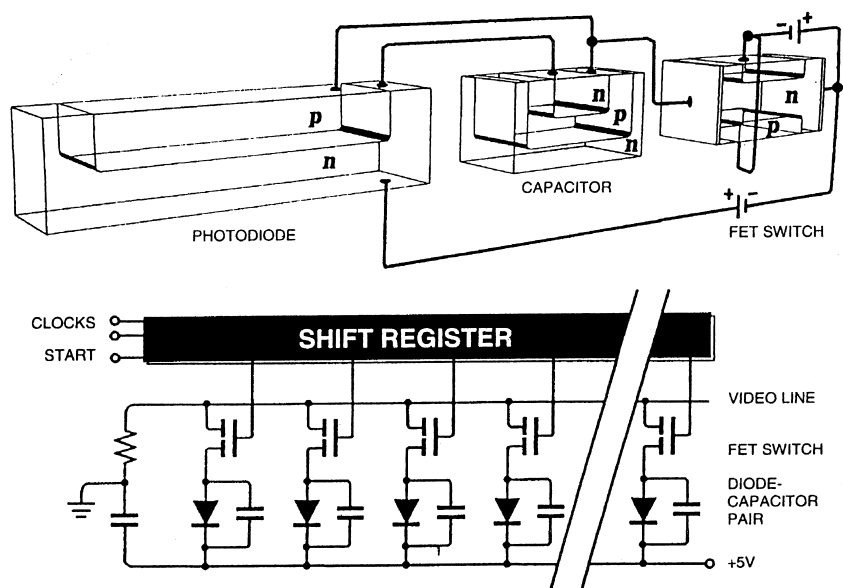


Fig. 1 Diagram of a single photodiode-capacitor switch (top) and an electronic schematic of the linear array (bottom).

received. For a detailed account of this topic, the reader is referred to the selected references cited.

Applications

Thus far, we have given a brief account on the technological development of the diode-array detector. Its applications offer several advantages to the user, which have been made possible primarily by the current computer hardware and software that are available on the market. Data acquisition and analysis are computer driven. The information acquired from the diode array can be analyzed to tailor the user's preferences. This area represents an emerging field and further advancements in analytical software tools will ultimately determine the true potential of diode-array detection.

As stated previously, a major improvement achieved with the diode array is that fewer attempts are required to identify the components of a sample mixture. A single injection can be sufficient for sample identification when spectral information in addition to peak retention time is part of the collected data. Through software capabilities, spectra can be extracted from the chromatogram of each individual peak. The spectral information combined with the retention times can be used to identify the chromatographic peaks. Furthermore, the spectra can be compared to spectral libraries compiled from the literature for purposes of spectral matching. Many proprietary

software programs have been developed for the diode-array instrument. It is up to the user's discretion to determine how he can best utilize these resources.

At first, one may show skepticism at the usefulness of diode-array detection because other analytical systems are more sensitive and offer similar features such as peak identification and purity checks. For these alternatives, one would have to refer to gas chromatography-mass spectrometry (GC-MS), liquid chromatography-mass spectrometry (LC-MS), and tandem mass spectrometry (MS-MS). However, one must keep in mind the significantly higher costs as a trade-off for enhanced sensitivity.

When assessing the merits of the diode array, the user should consider the various steps that are involved in methods development. It will become clear that for every hurdle one encounters, diode-array detection renders the task less laborious. It is most often than not that in developing new procedures you are confronted with drawbacks such as contaminants, peak overlap, artifacts, sample cleanup, and baseline noise. For instance, the presence of a shoulder on a major chromatographic peak raises questions as to its origin. With the aid of the diode array, a spectral profile of the shoulder peak will quickly determine its existence. A flat line of low absorbance throughout its spectra indicates that it is an artifact. The user can then go back to his procedure and ascertain if the root of the problem is systematic. The direction problem-solving takes is crucial and if gone astray, vast amounts of time are wasted. The

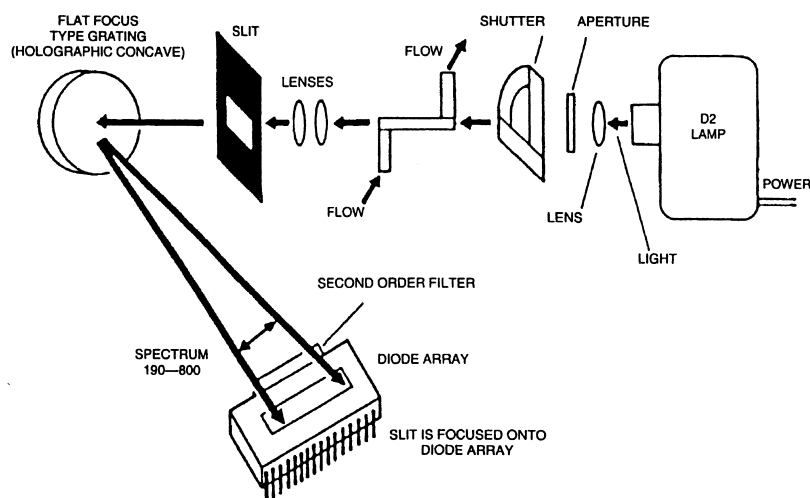


Fig. 2 Optics unit components. (Reprinted from *Waters 990+ Photodiode Array Detector Operator's Manual 1989*; courtesy of Waters Corporation, Milford, MA.)

same shoulder obtained with a FWD could have led the user to perform a time-dependent study. In this case, it was incorrectly assumed that the shoulder peak was a degradation product and additional injections at increased time intervals would show the shoulder peak increasing in size, indicating the compound of interest was degrading. Even though the analyst would eventually achieve the same result in the latter situation, the former approach is less time-consuming.

Diode-array detection has found its way into the pharmaceutical industry and the clinical laboratory. The widespread use of HPLC analysis in the product development cycle of pharmaceuticals provided an open door for the diode array. Throughout the different phases of drug development, the identification of a peak and its homogeneity must be established. The diode array confirms peak identity and compound purity by spectral analysis. Peak spectra are overlaid with spectra from standards (that are stored on the computer hard drive) for identification and spectra from the upslope, apex, and downslope of a chromatographic peak are overlaid to test for purity. Because the diode array performs continuous-flow spectral acquisition in the HPLC mode, the method can be automated to screen for thousands of compounds where only one will have the desired pharmacological action. Drug screening is common in drug development procedures, which goes hand-in-hand with drug metabolism and quantitative analysis. Diode-array detection is effective in all of these areas.

Peak purity is of utmost importance in the quality control of pharmaceutical products. The contents of

the product must be known with great certainty before it is sold to the consumer. Adjunct laboratories test the stability of the product in order to determine its expiry date. All by-products are accounted for and the amount of active ingredient is referenced. The diode array in HPLC analysis is used to determine all of the above information.

In the clinical laboratory setting, methods of analysis are used to diagnose disease and for therapeutic drug monitoring. Diode array-HPLC techniques will determine the drug concentrations and its metabolite levels in biological matrices. From these results, dosing regimens can be outlined that are specifically tailored to patients with respect to therapeutic drug concentration and drug dose, thereby avoiding drug toxicity. These procedures will ensure the safety and efficacy of clinically administered drugs.

Conclusion

The photodiode-array detector is a powerful analytical instrument that has provided enhanced detection capabilities with the addition of detailed spectral information via its multisignal detection technology. Its applications are HPLC based and can be found in basic research, automated analysis, pharmaceutical product development, and the clinical laboratory environment. Through spectral acquisition and analysis, a wealth of information can be obtained about the identity and purity of a compound. Combined with high selectivity and sensitivity, this mode of de-



tection is essential for qualitative and quantitative HPLC analysis.

Selected Further Reading

Green, R. B., Absorption detectors for high-performance liquid chromatography, in *Detectors for Liquid Chromatography* (E. S. Yeung, ed.), John Wiley & Sons, New York, 1986, pp. 42–46.

Huber, L. and S. A. George (eds.), *Diode Array Detection in HPLC*, Marcel Dekker, Inc., New York, 1993.

Lloyd, D. K., Instrumentation: detectors and integrators, in *High Performance Liquid Chromatography* (W. J. Lough and I. W. Wainer, eds.), Blackie Academic & Professional/Chapman & Hall, London, 1996, pp. 120–125.

McMaster, M. C., Hardware specifics, in *HPLC: A Practical User's Guide*, VCH, Weinheim, 1994, pp. 112–114.

Scott, R. P. W., Liquid chromatography detectors, in *Techniques and Practice of Chromatography*, Marcel Dekker, Inc., New York, 1995, pp. 284–287.



Photophoretic Effects in FFF of Particles

Vadim L. Kononenko

Institute of Biochemical Physics, Russian Academy of Sciences, Moscow, Russia

Introduction

High versatility and remarkable instrumental power of the field-flow fractionation (FFF) family of techniques are based substantially on the large variety of driving forces used [1]. Thus, the further development of FFF is associated, considerably, with the search for new types and combinations of physical and physicochemical agents suitable for the particles' and molecules' redistribution across the flow. Among the possible new force agents, light interaction with particles leading to their motion (photophoresis) deserves special attention. This is due both to the universal character of this interaction and to a large variety of particular interaction mechanisms. These mechanisms form two families: direct photophoretic and indirect photophoretic mechanisms.

Discussion

The "direct photophoretic" mechanisms include light pressure and gradient force, both associated with the direct momentum transfer from the incident light to a particle or a molecule during the absorption or scattering of photons (see Refs. 2–4 for details). The "gradient force" [3] arises from the spatial nonhomogeneity of electromagnetic field (if any) and has the same nature as the force moving electric dipoles in a static divergent field. It is characteristic of the focused light beams, evanescent waves near the refractive index boundaries, and so forth.

The "indirect photophoretic" mechanisms involve, as a primary light action, either nonuniform heating of particles or establishing a temperature gradient across the channel due to the light absorption in the carrier fluid. Such heating leads to conventional thermophoresis of particles due to tangential gradients of interfacial energy arising near the particle surface. The whole phenomenon can be referred to as photothermophoresis [5].

From the physical picture, it is evident that photophoretic effects in FFF are influenced by a remarkable diversity of particles material properties, including geo-

metrical, optical, and thermophysical characteristics. The use of these effects offers a unique possibility of including the optical properties of particles and molecules into the nomenclature of separation parameters. It promises to exploit the high spectral selectivity, in particular, the resonant character of light pressure exerted upon some solid-state and molecular structures [6,7], to separate the species identical in their density and geometry parameters.

Such selectivity can be achieved in several ways; first, by exploiting the intrinsic optical properties of the species and, second, using special preparative procedures, such as selective staining of species, or their binding to special carrier particles (molecules), having appropriately designed optical characteristics and serving as a kind of light tugs.

Let us consider, briefly, the basic theoretical principles underlying the photophoretic effects and their possible use in FFF. For further reading, see Ref. 5 and the references therein. The calculations of the direct photophoretic force, as well as of the spatial distribution of absorbed energy in the case of indirect mechanisms, require the solution of the optical problem of light scattering by a particle. This can be done using either the wave optics theory [4] or the geometrical (ray) optics description [3,5], depending on the particle size parameter $\rho = 2\pi a/\lambda$. Here, λ is the wavelength of light and a is the characteristic particle dimension (radius for the spherical particles). In practice, the boundary between the "geometrically small" and "large" particles is $a \sim 10 \mu\text{m}$ for the visible light.

The direct photophoretic force F_{ph} for "geometrically small" particles can be written as a sum of the radiation pressure force F_{pr} and the gradient force F_{∇} :

$$\begin{aligned}\vec{F}_{\text{ph}} &= \vec{F}_{\text{pr}} + \vec{F}_{\nabla} \\ \vec{F}_{\text{pr}} &= \varepsilon_m \frac{\pi a^2}{c} Q_{\text{pr}}(\varepsilon, \rho) \cdot \vec{J}_0, \\ \vec{F}_{\nabla} &= \varepsilon_m \frac{2\pi a^3}{c} \left(\frac{\varepsilon' - 1}{\varepsilon' + 2} \right) \cdot \nabla J_0\end{aligned}\quad (1)$$

Here J_0 is the incident light irradiance (measured in units of energy per unit time per unit area), c is the light velocity, Q_{pr} is the dimensionless efficiency fac-



tor of the radiation pressure [4], $\varepsilon = \varepsilon' - i\varepsilon''$ is the complex dielectric permittivity of particle material related to the permittivity ε_m of surrounding medium. In general, the efficiency factor can be calculated numerically using the electromagnetic theory [4]. It can be obtained analytically as an instructive example of a spherical particle placed in a wide slightly divergent light beam with effective radius $w_0 \gg a$ and angular divergence $|\Delta\theta| \ll 1$, $|\Delta\theta| \geq a/w_0$ [5]. Taking $\Delta\theta > 0$ for divergent beam, $\Delta\theta < 0$ for convergent beam, considering the transverse and the longitudinal gradients of beam irradiance to be $\nabla_{\perp}(J_0) \approx J_0/w_0$, $\nabla_{\parallel}(J_0) \approx -\Delta\theta(J_0/w_0)$, and regarding $\varepsilon' + 2 \approx 3$ because $|\varepsilon - 1| \ll 1$, we get [5]

$$F_{\text{ph}\parallel} \equiv F_{\text{pr}} + F_{\nabla\parallel} \approx \varepsilon_m \frac{\lambda^2 \rho^2}{4\pi c} \cdot \left(\frac{1}{4}(\varepsilon' - 1)I_1(\rho) + \frac{4}{3}\varepsilon''\rho \right) J_0 - \Delta\theta F_{\nabla\perp} \quad (2)$$

$$F_{\text{ph}\perp} \equiv F_{\nabla\perp} \approx \varepsilon_m \frac{\lambda^3 \rho^3}{12\pi^2 c w_0} (\varepsilon' - 1) J_0$$

Here $I_1(\rho)$ is an increasing function of ρ , with the small-amplitude oscillations superimposed [5]. For small particles ($\rho \ll 1$), $I_1(\rho) \approx (32/27)\rho^4$, whereas for large ones ($\rho \gg 1$), $I_1(\rho) \approx 2[\ln(4\rho) + 0.5772] - 3$. The analysis [5] of Eq. (2) shows that the longitudinal component $F_{\text{ph}\parallel}$ of direct photophoretic force can be dominated both by the light pressure term and by the gradient term, depending on the particle optical parameters and the beam nonhomogeneity: $|F_{\nabla\parallel}| > |F_{\text{pr}}|$ if $w_0 < \lambda|\Delta\theta| |\varepsilon' - 1|/4\pi\varepsilon''$. The direction of $F_{\nabla\parallel}$ is determined by the sign of $\Delta\theta$ (beam's convergence or divergence). Hence, in general, both the positive (away from the light source) and the negative photophoresis are possible. The direction of $F_{\nabla\perp}$ depends on the sign of $\varepsilon' - 1$. The particles with $\varepsilon' > 1$ are pulled into the maximum of the radial distribution of field intensity, whereas the particles with $\varepsilon' < 1$ are pushed either out of the beam or into the minimum of the field intensity. The direct photophoretic force F_{ph} has a strong dependence on the particle size: the term $F_{\text{pr}} \propto a^6$ for small particles and $F_{\text{pr}} \propto a^2$ for large particles. It depends also on their optical properties: $F_{\text{pr}} \propto |\varepsilon' - 1|^2$ for weakly absorbing particles and $F_{\text{pr}} \propto \varepsilon''$ for particles with a strong light absorption. The direct photophoretic force acting on very large particles ($\rho \gg 1$) is better for calculations using the geometrical optics picture of reflected and refracted light rays, which exert the pressure on the particle surface at their points of incidence. The total force is obtained by the integration of this pressure over the particle surface [3].

Turning to the indirect photophoretic mechanisms, or photothermophoresis, consider the problem of light-absorbing particle surrounded by transparent liquid. The opposite extreme, a transparent particle placed into a channel flow of light-absorbing fluid, reduces to an ordinary thermophoresis, however, with unusual temperature profile in the channel. The photothermophoresis problem consists of three independent stages [5]. The first is the calculations of the optical field inside the particle, in order to obtain the source function $B(\vec{r}) = E_i^2(\vec{r})/E_0^2$, which describes the heat production due to the light absorption. Here, $E_i(\vec{r})$ is the electric field strength at the point \vec{r} inside the particle and E_0 is the incident wave amplitude. The second stage is the determination of the temperature field inside and outside the particle generated by the known distribution of heat sources. The third is the calculation of the photothermophoretic velocity u_{pth} of a particle in the temperature field thus obtained on the basis of specific physicochemical models for the particle, surrounding medium, and their interfacial region. The result has the form [5]

$$u_{\text{pth}} = b_{\text{th}} g_{\text{an}}(n_r, \kappa\rho) \frac{T_0}{a} \quad (3)$$

$$\frac{T_0}{a} = 2\kappa\rho \frac{n_r J_0}{m_0 k_i}$$

$$g_{\text{an}}(n_r, \kappa\rho) = -\frac{1}{4} \left(2 + \frac{k_i}{k_e} \right) \int_0^\pi \frac{d\tau(a, \theta)}{d\theta} \sin^2\theta d\theta$$

Here, b_{th} is the ordinary thermophoretic mobility of a particle, k_i and k_e are the thermal conductivity of a particle and fluid, respectively, T_0 is the characteristic temperature of particle heating due to the light absorption, T_0/a is the characteristic temperature gradient across the particle, $\tau(a, \theta)$ is the dimensionless temperature distribution over the particle surface in units of T_0 , the polar angle θ is measured from the shadow pole of illuminated particle, $n(\lambda)$ is the refractive index, $\kappa(\lambda)$ is the absorption index of particle material, m_0 is the refractive index of fluid, and $n_r = n(\lambda)/m_0$. The function $g_{\text{an}}(n_r, \kappa\rho)$ describes the anisotropy of particle heating by light. Together with b_{th} , it defines the magnitude and sign of photothermophoretic velocity. The analysis for a solid particle in electrolyte solution shows that u_{pth} is negative for $\kappa\rho \ll 1$, goes through the zero in the range $\kappa\rho \sim 0.1-0.3$, then stays positive and increases monotonically for $\kappa\rho > 0.5$, saturating at very high $\kappa\rho$ values (~ 40) [5].

The practical implementation of photophoretic FFF encounters two major difficulties. First, the generation of substantial photophoretic force over the full length

of separation channel requires very powerful light sources and special optical delivery systems, including transparent channel walls. Second, the transparency of the channel wall should not degrade substantially with time despite the permanent contact with suspension flow. The feasibility studies of photophoretic effects in FFF were made with the focused Ar^+ -ion laser beam propagating along the axis of the round metallic capillary along the flow of water suspension of carbon-black particles [5]. Their results evidence that the practical transverse geometry Photophoretic FFF technique can be developed also. The most promising schemes are highly convergent light sheet normal to the channel wall and enabling the gradient trapping of particles, and the use of photophoretic forces in combination with some counterbalancing force, such as the gravity force.

References

1. J. C. Giddings, *Chem. Eng. News* 66: 34–45 (1988).
2. A. Askin, *Science* 210: 1081–1088 (1980).
3. A. Askin, *Biophys. J.* 61: 569–582 (1992).
4. C. F. Bohren and D. R. Huffman, *Absorption and Scattering of Light by Small Particles*, Interscience, New York, 1983.
5. V. L. Kononenko, J. K. Shimkus, J. C. Giddings, and M. N. Myers, *J. Liquid Chromatogr. Related Technol.* 20: 2907–2929 (1997).
6. S. Arnold, Spectroscopy of single levitated micron sized particles, in *Optical Effects Associated with Small Particles* (P. W Barber and R. K. Chang, eds.), World Scientific, Singapore, 1988, pp. 65–137.
7. V. G. Minogin and V. S. Letokhov, *Laser Light Pressure on Atoms*, Gordon & Breach, New York, 1987.



Plant Extracts: Analysis by TLC

Gabriela Cimpan

"Babes-Bolyai" University, Cluj-Napoca, Romania

Introduction

Thin-layer chromatography (TLC) is a powerful method for separating mixtures of compounds of very different polarity. Plant extracts are usually hydroalcoholic solutions, containing complex mixtures of compounds, many of them being still unidentified. Although plant extracts are widely used in homeopathic medicine, for the treatment of different diseases, the control of these drugs is often performed by qualitative analysis. TLC can provide a chromatographic "fingerprint" of a plant extract, very useful for identification purposes, and usually a photograph is attached to the analysis certificate [1]. The colors of the separated spots and their positions relative to standard substances are important characteristics for the plant extract identification. Quantitative analysis is seldom applied in this field, and it is usually performed by spectrophotometry, which is included in pharmacopoeias.

Discussion

TLC Analysis of Plant Extracts in Pharmacopoeias

The TLC separation of plant extracts is described as a method of analysis in different pharmacopoeias [2–5] and is usually performed on silica layers and sometimes on a silica hydrocarbon (C_8 , C_{18}) bonded phase. However, alumina or other stationary phases are not excluded.

The plant extract samples can be applied directly onto the plate, or a specific class of compounds is extracted in a suitable solvent before TLC. The polarity of the solvent used for extraction should be similar to that of the desired compounds. The samples can be applied onto the plates manually, by using calibrated micropipettes or automated applicators. The applied samples can be spots or bands, and the mobile-phase migration distances vary between 8 and 15 cm.

Normal presaturated chambers are used for development. The mobile phases used for the TLC development are characteristic of different classes of compounds. The classification of medicinal plants takes

into account the presence of different classes of compounds which are separated by using the so-called TLC fingerprint method. The analyzed compounds can be alkaloids, anthracene derivatives, bitter drugs, cardiac glycoside drugs, coumarin drugs, drugs containing essential oils, flavonoids, saponin drugs, drugs containing triterpenes, and so forth. For example, mixtures containing chloroform and diethylamine are used for the TLC separation of plant extracts containing alkaloids and toluene–ethyl acetate is used for drugs containing essential oils [1].

After development, the plates are dried in a gentle airstream, at room temperature, and are examined in ultraviolet or visible light, with or without a derivatization, depending on the chemical nature of the separated compounds. The examination in ultraviolet light is performed at 254 nm by quenching the thin-layer fluorescence or at 366 nm when the natural fluorescence of compounds is observed. Several alkaloids (quinine, quinidine, cinchonine, cinchonidine, noscapine, berberine), anthraglycosides, coumarins derivatives (scopoletin, aesculetin), or flavonoids (chlorogenic acid, rutin) have natural fluorescence and can be visualized at 366 nm. The natural fluorescence of compounds can be enhanced by spraying with different reagents, leading to low detection limits. Flavonoids show a yellow–green fluorescence after consecutively spraying with alcoholic solutions of diphenylboryloxyethylamine and poly(ethylene glycol) 4000.

The compounds which cannot be derivatized for fluorescence at 366 nm are sprayed with specific reagents and examined in visible light. The derivatization reactions can take place at room temperature or the TLC plate should be heated on a thermostated plate, at a specific temperature, for approximately 10 min. In both situations, the chromatographic plate should be examined immediately and eventually photographed. Ninhydrine is a good detecting reagent for amino acids and other biocompounds containing the primary amino group, and the compounds can be observed as blue–violet spots after heating at 100°C. Terpenoids, bitter principles, or saponins can be visualized as red–violet spots by spraying the plate with an acidic solution of anisaldehyde and heating at 100°C.



The pharmacopoeias describe the obtained colored spots after a TLC separation, taking into account their color, order, and position on the plate in the presence of reference substances. The description should match the TLC separation of the studied plant extract. The correspondence of the spots is important for the qualitative analysis of the medicinal plant. The chosen reference substances mentioned in pharmacopoeias can also be present in the analyzed plant extract or can be used for a comparison with the R_F values of the separated compounds in the plant extract.

Actual Trends in the TLC Analysis of Plant Extracts

The exact chemical composition of a plant extract is not always completely known. Many articles published in recent years attempt to identify the compounds structure by coupling chromatography with spectrometric methods. Modern densitometers are able to record the *in situ* ultraviolet-visible (UV-vis) spectra of a separated substance on a TLC plate [6]. Thin-layer chromatography can be also coupled with other methods in order to enhance the identification of compounds, such as mass spectrometry (MS) or nuclear magnetic resonance (NMR). There are devices able to record the *in situ* spectra on the TLC plate, or the separated substance is removed from the plate together with the layer, then extracted in a small volume of an adequate solvent, and the sample can be used for obtaining the spectra [6,7].

It is well known that the concentration of active substances in medicinal plants can vary widely in different parts of the plant, and it depends on the harvesting time. The quantitative determination of active substances is then very useful for a plant extracts analysis. Densitometry is the method for the evaluation of the separated substances on a TLC plate. The quantitative determination can use a calibration curve of a reference substance or the internal or external standard method. Figure 1 shows the densitograms of two medicinal plant extracts, *Uva ursi* and *Vaccinium vitis-idaea*, both containing arbutin as one of the bioactive substances. The TLC plates are scanned in UV or vis light, usually in the reflectance mode, linear or zigzag. In the zigzag mode, the absorbance of a band around the separated sample is measured and it is useful for the samples that do not migrate in a straight line due to the layer imperfections.

Automated multiple development (AMD) has been successfully applied for the separation of compounds from plant extracts. AMD is a technique using the concentration gradient to separate substances differing

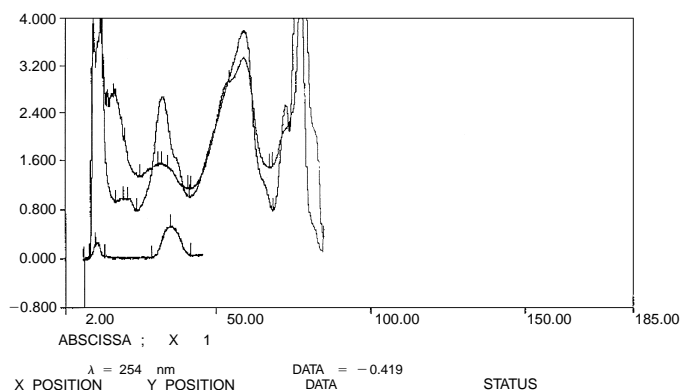


Fig. 1 The densitometry of *Uva ursi* and *Vaccinium vitis-idaea*, two alcoholic plant extracts containing arbutin. Arbutin (reference substance) is the last one, and *Vaccinium vitis-idaea* contains less arbutin than *Uva ursi*; silica gel plate, $\lambda = 254$ nm.

widely in polarity. Usually, the gradient is started from a polar composition decreasing in steps to a medium polar mobile phase and ending with a nonpolar mixtures of solvents or to a single nonpolar solvent. In this way, all the compounds from a plant extract can be separated, from very polar to nonpolar, between the start and the front line. Usually, the migration distance is 8 cm, and the number of steps can be a maximum of 25 in order to achieve a reasonable development time. The development distances increase as the solvent polarity is decreased. As the total number of compounds in a plant extract is very difficult to estimate, the AMD technique always yields a greater number of separated spots than a monodimensional or a two-dimensional isocratic TLC development [8]. Most of the reference substances used in plant extract analysis have a natural origin. As a consequence, they are not always very pure or can lead to decomposition compounds. The separation power of an AMD method can show a greater number of compounds in a reference substance than an isocratic TLC method.

Glycerinic plant extracts have various application in the naturist medicine, but they cannot be analyzed directly by TLC due to the presence of glycerin which should be removed first from the sample [9]. Solid-phase extraction (SPE) is a fast and convenient method for the separation of glycerin. The organic compounds from the analyzed plant extract are retained in the SPE cartridge on a nonpolar stationary phase (usually silica- C_{18}); the glycerin and the nonselectively retained compounds are eluted with a polar mobile phase (can be a diluted solution of methanol in water). The retained compounds are eluted from the

cartridge with a stronger mobile phase, usually acidified with a mineral acid, and the obtained solution can be analyzed by TLC directly or after concentration. The SPE recovery is very good, around 100%, and the method is successfully applied for the plant extracts cleanup before TLC.

References

1. H. Wagner and S. Bladt, *Plant Drug Analysis*, Springer-Verlag, Berlin, 1996.
2. *Homöopathisches Arzneibuch*, Deutscher Apotheker Verlag, Stuttgart/Govi-Verlag, Frankfurt, 1978 (Vol. 1) and 1991 (Vol. 2).
3. *La Pharmacopée Française, X^e Édition*, Association pour la Recherche Appliquée à la Pharmacopée, Paris, 1989.
4. *DAB 10, Deutsches Arzneibuch 10, Ausgabe 1991*, Deutscher Apotheker Verlag, Stuttgart, 1991.
5. *The United States Pharmacopoeia, XXIII Revision*, United States Pharmacopoeial Convention, Rockville, MD, 1995.
6. S. Gocan and G. Cimpan, *Rev. Anal. Chem.* 16: 1–24 (1997).
7. V. Ossipov, K. Nurmi, J. Loponen, E. Haukioja, and K. Pihlaja, *J. Chromatogr. A* 721: 59–68 (1996).
8. N.-K. Olah, L. Muresan, G. Cimpan, and S. Gocan, *J. Planar Chromatogr.-Mod. TLC* 11: 361–364 (1998).
9. S. Cobzac, G. Cimpan, N. Olah, and S. Gocan, *J. Planar Chromatogr. — Mod. TLC* 12: 26–29 (1999).



Plate Number, Effective

Raymond P.W. Scott

Scientific Detectors Ltd., Banbury, Oxfordshire, England

Introduction

The concept of the effective plate number was introduced in the late 1950s by Purnell and Bohemen [1] and Desty and Golup [2]. Its introduction arose directly as a result of the development of the capillary column. It was noted that the very high efficiencies were only realized from open-tubular columns for solutes eluted close to the column dead volume (i.e., for solutes eluted at very low k' values). In addition, the high efficiencies in no way reflected the increase in resolving power that would be expected from a packed column with much higher stationary-phase loading.

This poor performance, relative to the high efficiencies produced, results from the high phase ratio inherent with open-tubular columns. The high phase ratio is due to there being very little stationary phase in the capillary column (the film is very thin). The corrected retention volume of a solute is directly proportional to the amount of stationary phase in the column, and solutes, in general, are eluted from a capillary column at relatively low k' values relative to the magnitude of their distribution coefficient.

Discussion

To compensate for what appeared to be very misleading efficiency values, the *effective plate number* was introduced. The effective plate number uses the *corrected retention distance*, as opposed to the *total retention distance* to calculate the efficiency. Thus, the effective plate number is significantly smaller than the true plate number for solutes eluted at low k' values. At high k' values, the two measures of efficiency converge. In this way, the effective plate number appears to more nearly correspond to the column resolving power. The efficiency of the column (n) in number of theoretical plates has been shown to be given by

$$n = 4 \frac{y^2}{x^2}$$

where y is the retention distance, and x is the peak width.

Now, the number of “effective plates” (N), by definition, is given by

$$N = 4 \frac{(y - y_0)^2}{x^2} \quad (1)$$

where y_0 is the retention distance of an unretained solute (the position of the dead point). Now, from the plate theory,

$$\frac{y}{x} = \frac{n(v_m + Kv_s)}{2\sqrt{n}(v_m + Kv_s)}$$

thus,

$$\frac{y - y_0}{x} = \frac{n(v_m + Kv_s) - nv_m}{2\sqrt{n}(v_m + Kv_s)}$$

By dividing through by v_m and noting that

$$\frac{Kv_s}{v_m} = k'$$

then,

$$\frac{y - y_0}{x} = \frac{\sqrt{n}k'}{2(1 + k')}$$

Consequently,

$$4 \left(\frac{y - y_0}{x} \right)^2 = n \left(\frac{k'}{1 + k'} \right)^2 = N \quad (2)$$

Equation (2) describes the relationship between the efficiency of a column in theoretical plates and the efficiency given in “effective plates.” It is also seen that the calculation of the number of “effective plates” in a column does not provide an arbitrary measure of the column performance, but is directly related to the number of theoretical plates in the column as defined by the plate theory. It should be noted that as k' becomes large, n and N converge to the same value.

The effective plate number has an interesting relationship to the function for the resolution of a column that was suggested by Giddings [3]. Giddings proposed that the function $k'/\Delta k'$ could be a means of defining the resolving power R of a column. He employed this function in an analogous manner to the function used in spectroscopy to define resolution (i.e., $\lambda/\Delta\lambda$, where $\Delta\lambda$ is the minimum wavelength increment that can be



differentiated at a wavelength λ). The value taken by Giddings for $\Delta k'$ was the bandwidth at the base of the eluted peak which is equivalent to twice the peak width or 4σ . Thus, from the plate theory,

$$R = \frac{k'}{\Delta k'} = \frac{nk v_s}{4\sqrt{n}(v_m + K v_s)}$$

Again, dividing through by v_m and noting that

$$\frac{K v_s}{v_m} = k'$$

then,

$$R = \frac{\sqrt{n}k'}{4(1 + k')} = \frac{\sqrt{N}}{4} \quad (3)$$

It is seen from Eq. (3) that the resolving power of the column, as defined by Giddings, will be directly proportional to the square root of the number of effective plates. As a consequence, R can be used by the chromatographer to directly compare the resolving

power of columns of any size or type. However, the value of R will vary with the value of k' for the solute, and so comparison between columns must be made using solutes that have the same k' value.

References

1. J. H. Purnell and J. Bohemen, *J. Chem. Soc.* 2030 (1961).
2. D. H. Desty and A. Goldup, *Gas Chromatography 1960* (R. P. W. Scott, ed.), Butterworths, London, 1960, p. 162.
3. J. C. Giddings, *The Dynamics of Chromatography*, Marcel Dekker, Inc., New York, 1965, p. 265.

Suggested Further Reading

- Scott, R. P. W., *Liquid Chromatography Column Theory*, John Wiley & Sons, Chichester, 1992, p. 19.
- Scott, R. P. W., *Introduction to Analytical Gas Chromatography*, Marcel Dekker, Inc., New York, 1998.



Plate Theory

Raymond P.W. Scott

Scientific Detectors Ltd., Banbury, Oxfordshire, England

Introduction

Originally derived by Martin and Singh [1] and extended by Said [2], the plate theory provides an equation that describes the elution curve (the chromatogram) of a solute. By differentiating the elution curve equation and equating to zero, an expression for the retention volume of a solute can be obtained. By equating the second differential to zero, an equation for the variance and standard deviation (the peak width) can be obtained, and from these equations, methods for calculating the column efficiency can be derived, together with the numerous equations that describe resolution.

Discussion

The plate theory assumes that the solute is in equilibrium with the mobile and stationary phases. Due to the continuous exchange of solute between the two phases as it progresses down the column, equilibrium between the phases can *never* actually be achieved. To accommodate this nonequilibrium condition, a technique originally introduced in distillation theory is adopted, where the column is considered to be divided into a number of cells or plates. Each cell is allotted a finite length and, thus, the solute spends a finite time in each cell. The size of the cell is such that the solute is considered to have sufficient residence time to achieve equilibrium with the two phases. Thus, the smaller the plate, the more efficient the solute exchange between the two phases and, consequently, the more plates there are in the column. As a result, the number of theoretical plates contained by a column has been termed the *column efficiency*. The *plate theory* shows that the peak width (the dispersion or peak spreading) is inversely proportional to the square root of the efficiency and, thus, the higher the efficiency, the narrower the peak. Consider the equilibrium that is assumed to exist in each plate; then

$$X_s = KX_m \quad (1)$$

where X_m is the concentration of solute in the mobile phase, X_s is the concentration of solute in the station-

ary phase, and K is the distribution coefficient of the solute between the two phases.

It should be noted that K is defined with reference to the stationary phase (i.e., $K = X_s/X_m$), thus the larger the distribution coefficient, the more the solute is distributed in the stationary phase. Differentiating Eq. (1),

$$dX_s = KdX_m \quad (2)$$

Consider three consecutive plates in a column, the $p - 1$, the p , and the $p + 1$ plates and let there be a total of n plates in the column. The three plates are depicted in Fig. 1.

Let the volumes of mobile phase and stationary phase in each plate be v_m and v_s , respectively, and the concentrations of solute in the mobile and stationary phase in each plate be $X_{m(p-1)}$, $X_{s(p-1)}$, $X_{m(p)}$, $X_{s(p)}$, $X_{m(p+1)}$, and $X_{s(p+1)}$, respectively. Let a volume of mobile phase, dV , pass from plate $p - 1$ into plate p , at the same time, displacing the same volume of mobile phase from plate p to plate $p + 1$. In doing so, there will be a change of mass (dm) of solute in plate p that will be equal to the difference in the mass entering plate p from plate $p - 1$ and the mass of solute leaving plate p and entering plate $p + 1$. A simple mass balance procedure can be applied to plate p . Thus, bearing in mind that mass is the product of concentration and volume, the change of mass of solute in plate p will be

$$dm = (X_{m(p-1)} - X_{m(p)}) dV \quad (3)$$

Now, if equilibrium is to be maintained in the plate p , the mass (dm) will distribute itself between the two phases, which will result in a change of solute concentration in the mobile phase of $dX_{m(p)}$ and in the stationary phase of $dX_{s(p)}$. Then,

$$dm = v_s dX_{s(p)} + v_m dX_{m(p)} \quad (4)$$

Substituting for $dX_{s(p)}$ from Eq. (2),

$$dm = (v_m + Kv_s) dX_{m(p)} \quad (5)$$

Equating Eqs. (3) and (5) and rearranging,

$$\frac{dX_{m(p)}}{dV} = \frac{X_{m(p-1)} - X_{m(p)}}{v_m + Kv_s} \quad (6)$$



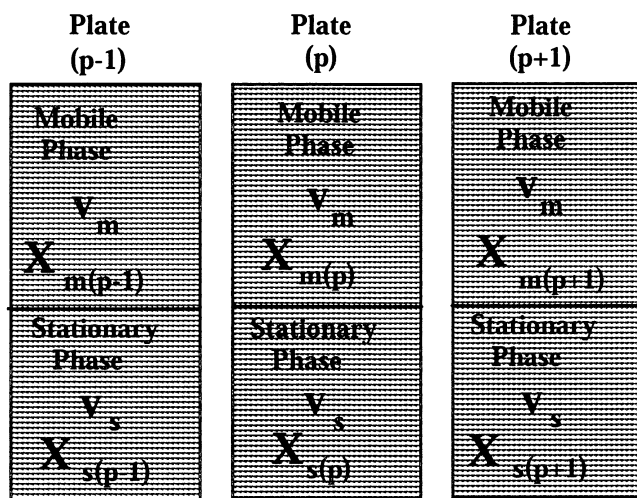


Fig. 1 The three consecutive plates in a column.

The volume flow of the mobile phase will now be measured in units of $v_m + Kv_s$, instead of milliliters. Thus, the new variable (v) can be defined as

$$v = \frac{V}{v_m + Kv_s} \quad (7)$$

The function $v_m + Kv_s$ is termed the "plate volume" and, thus, the flow of mobile phase will be measured in "plate volumes" instead of milliliters. The "plate volume" can be defined as that volume of mobile phase that would contain all the solute that is in the plate at the equilibrium concentration of the solute in the mobile phase.

Differentiating Eq. (7),

$$dv = \frac{dV}{v_m + Kv_s} \quad (8)$$

Substituting for dV from Eq. (8) in Eq. (6),

$$\frac{dX_{m(p)}}{dV} = X_{m(p-1)} - X_{m(p)} \quad (9)$$

Equation (9) is the basic differential equation that describes the rate of change of concentration of solute in the mobile phase in plate p with the volume flow of mobile phase through it. Thus, the integration of Eq. (9) will provide the equation for the elution curve of a solute eluted from any plate in the column. A simple algebraic solution to Eq. (9) is given in Ref. 3 and the resulting elution curve equation for plate n of a column of n plates is shown to be

$$X_{m(n)} = \frac{X_0 e^{-v} v^n}{n!} \quad (10)$$

Equation (10) is the basic elution curve equation; it is a Poisson function, but when n is large, the function approximates to a normal error function or Gaussian function. In practical chromatography systems, n is always greater than 100 and, thus, all chromatographic peaks will be Gaussian or nearly Gaussian in shape.

The Retention Volume of a Solute

The retention volume of a solute is that volume of mobile phase that passes through the column between the injection point and the peak maximum. It is, therefore, now possible to determine that volume by differentiating Eq. (10) and equating to zero and solving for v . Re-stating Eq. (10),

$$\begin{aligned} X_{m(n)} &= X_0 \frac{e^{-v} v^n}{n!} \\ \frac{dX_{m(n)}}{dv} &= X_0 \frac{-e^{-v} v^n + e^{-v} n v^{n-1}}{n!} \\ &= X_0 \frac{-e^{-v} v^{n-1}}{n!} (n - v) \end{aligned}$$

Equating to zero and solving for v ,

$$n - v = 0 \quad \text{or} \quad v = n$$

Thus, n plate volumes of mobile phase have passed through the column (remembering that the volume flow is measured in "plate volumes" and not in milliliters). Thus, the volume passed through the column (in ml) will be

$$\begin{aligned} V_r &= n(v_m + Kv_s) \\ &= nv_m + nKV_s \end{aligned} \quad (11)$$

Now, the total volume of mobile phase and stationary phase in the column (V_m and V_s , respectively) will be the volume of mobile phase and stationary phase per plate multiplied by the number of plates (i.e., nv_m and nv_s). Thus,

$$V_r = V_m + KV_s \quad (12)$$

Returning to Eq. (13), it is also possible to derive an equation for the adjusted retention volume, V'_r . Now,

$$V'_r = V_r - V_m \quad (13)$$

Plate Theory

Thus, from Eqs. (11) and (13),

$$V'_r = V_m + KV_s - V_m = KV_s \quad (14)$$

For the use of the plate theory to determine peak widths and column efficiency, see the entry Resolution.

References

1. A. J. P. Martin and R. L. M. Synge, *Biochem. J.* 35: 1358 (1941).

2. A. S. Said, *Am. Inst. Chem. Eng. J.* 2: 477 (1956).
3. R. P. W. Scott, *Liquid Chromatography Column Theory*, John Wiley & Sons, Chichester, 1992, p. 19.

Suggested Further Reading

Scott, R. P. W., *Techniques and Practice of Chromatography*, Marcel Dekker, Inc., New York, 1996.

Scott, R. P. W., *Introduction to Analytical Gas Chromatography*, Marcel Dekker, Inc., New York, 1998.



Pollutant–Colloid Association by Field-Flow Fractionation

Ronald Beckett

Bailin Chen

Niem Tri

Monash University, Melbourne, Australia

Introduction

The association of pollutants such as trace metals, nutrients, and toxic organic molecules to colloids is intimately connected to the health of natural waters. Colloids, with their large specific surface area, play a dominant role in the transportation and eventual deposition of these pollutants. Of particular interest is the size speciation data. It is important to know not only the total amount of pollutant present but also where it is distributed. It has been inherently difficult to study pollutant–colloid interactions because of the lack of methods for particle size determination and fractionation as well as the low concentrations of pollutants present in many systems. This entry outlines a new approach using field-flow fractionation (FFF).

Discussion

Field-flow fractionation is a separation and elution technique similar to chromatography [1]. It is based on the application of a field perpendicular to the flow of the axis of a thin (100–500 μm) channel. An externally applied field drives unlike particles to different positions across the thin channel, where they are caught up in different flow velocities. For small particles, typically less than 1 μm , the elution time depends on the particle's interaction with the field and its diffusivity. Separations in this mode, termed the *normal* mode, have the smaller particles eluting ahead of the larger particles. Larger particles tend to stay near the channel wall and move through the channel with the lower flow velocities. An alternate mode, termed the *steric* or *hyperlayer* mode, is for particles greater than about 1 μm . A reversal of the elution order is observed because they necessarily protrude into the higher flow velocities (due to their physical size). Utilizing these two modes, it is possible to probe a mass range spanning 15 orders of magnitude, starting from molecules of 1000 Da molecular weight up to particles 50 μm in diameter.

Further, it is possible to utilize different fields to yield the various FFF subtechniques. The two most common fields are centrifugal and fluid cross-flow, which give rise to the sedimentation and flow FFF subtechniques. Other fields currently in use include thermal, electrical, and magnetic fields. In the normal mode, it is possible to extract physical parameters from retention data. For example, sedimentation FFF using a centrifugal force gives information about the buoyant mass, and flow FFF gives information about the sample's diffusivity or hydrodynamic diameter.

Environmental samples often have a broad size distribution and are often heterogenous in density and chemical composition, and to add to the complexity, natural particles often have an irregular shape [2]. Thus, it is easy to appreciate that FFF with its wide and flexible range of operating parameters is the ideal tool to divide these broad distributions into discrete, roughly monodisperse fractions for subsequent analysis. Sedimentation and flow FFF, in particular, have been used to measure the size distribution of environmental samples. Karaiskakis et al. first demonstrated that it is possible to correlate chemical content (major elements such as Al, Ca, Fe, Si, and S found in bulk minerals) with particle size using sedimentation FFF with energy dispersive x-ray analysis (EDXA) [3]. However, due to the low sensitivity and long analysis time of FFF–EDXA, the technique was abandoned for the analysis of pollutants.

Much more sensitive and less time-consuming techniques such as mass spectrometry, atomic emission, and atomic absorption are needed for the analysis of pollutants. Detectors such as graphite furnace–atomic absorption spectrometer (GF–AAS), inductively coupled plasma–mass spectrometer (ICP–MS), or inductively coupled plasma–atomic emission spectrometer (ICP–AES) seem to be ideal candidates for the analysis of trace metals because of their very low detection limits. The high temperatures used avoid the need for tedious digestions in many samples. FFF–gas chromatography–mass spectrometry could perhaps be used in the analysis of particular organic molecules.



Another extremely sensitive technique applied in the study of adsorption behavior of pollutants is to add radiolabeled adsorbates (such as $^{33}\text{PO}_4^{3-}$, ^{14}C -atrazine, and ^{14}C -glyphosate) to study the distribution of the pollutant as a function of size.

Contaminant Speciation Data

In recent years, the direct coupling of the FFF channel to GF–AAS, high-resolution ICP–MS, and ICP–AES has been implemented. It has enabled high resolution size-based speciation data for pollutants to be collected. In the first instance, the data acquired by these methods is a fractogram [an instrumental signal, usually but not necessarily from an ultraviolet (UV) detector, representing the mass of eluted sample as a function of the retention time]. The retention time is rigorously but not linearly related to the particle size (i.e., diameter) and may be easily calculated from FFF theory. Suitable algorithms can be used to generate a mass-based size distribution. Figures 1a and 1b show an example of recent work conducted in our laboratory demonstrating the distribution of copper in con-

taminated soils represented as a fractogram and a size distribution.

Element concentrations in the eluent are also recorded if a suitable detector is used. This can be processed in a similar fashion to the UV signal to yield an eluent-based size distribution. If the element detector signal is divided by the mass detector signal, we obtain a quantity which is proportional to the concentration in the sample particles. When this quantity is plotted against particle diameter, we obtain the element concentration particle distribution for the sample (Fig. 1c). It is often useful to plot the element atomic ratio distributions for elements of interest. This graph is particularly useful for deducing size-based speciation data for trace elements.

The main feature of this experiment is that although the copper content in the soil roughly follows the fractogram (Fig. 1a) and the size distribution (Fig. 1b), the concentration of copper is higher for the smaller particles (Fig. 1c). However, a comparison of the copper/aluminium ratio shows that there is no change across the size distribution for this sample. Figure 1d shows that the surface-coating density of

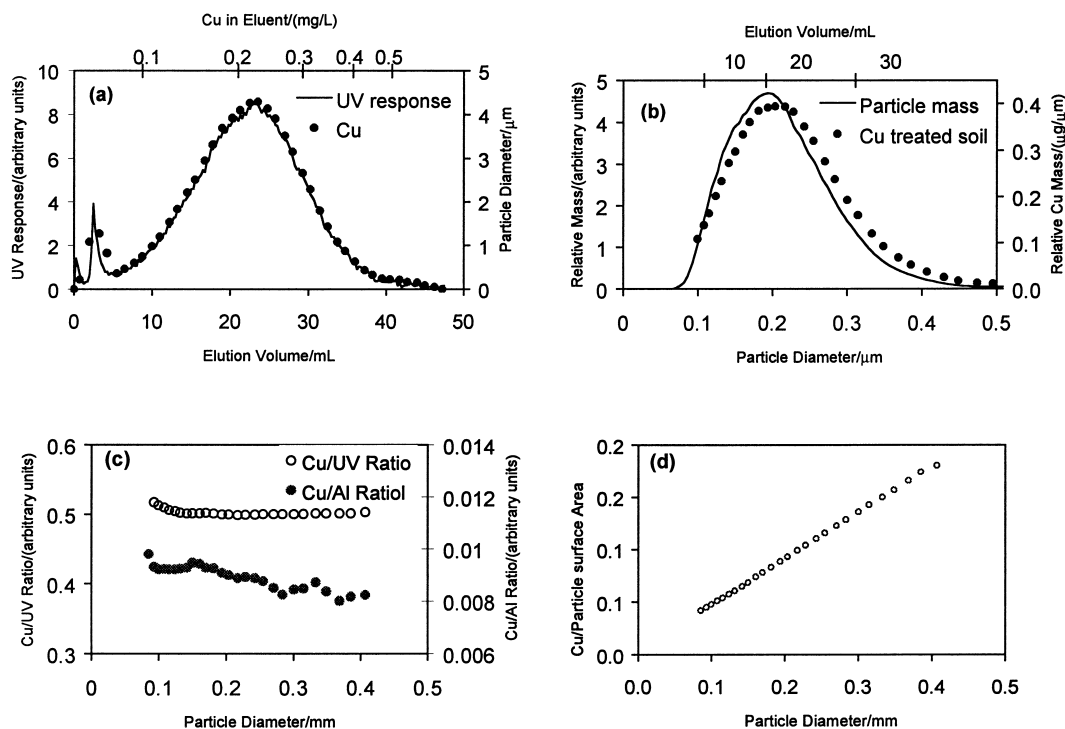


Fig. 1 Graphs showing (a) fractogram and copper concentration in eluent, (b) corresponding size distribution, (c) copper concentration distribution and element ratio distribution of copper in soil sample, and (d) copper per unit surface area distribution.

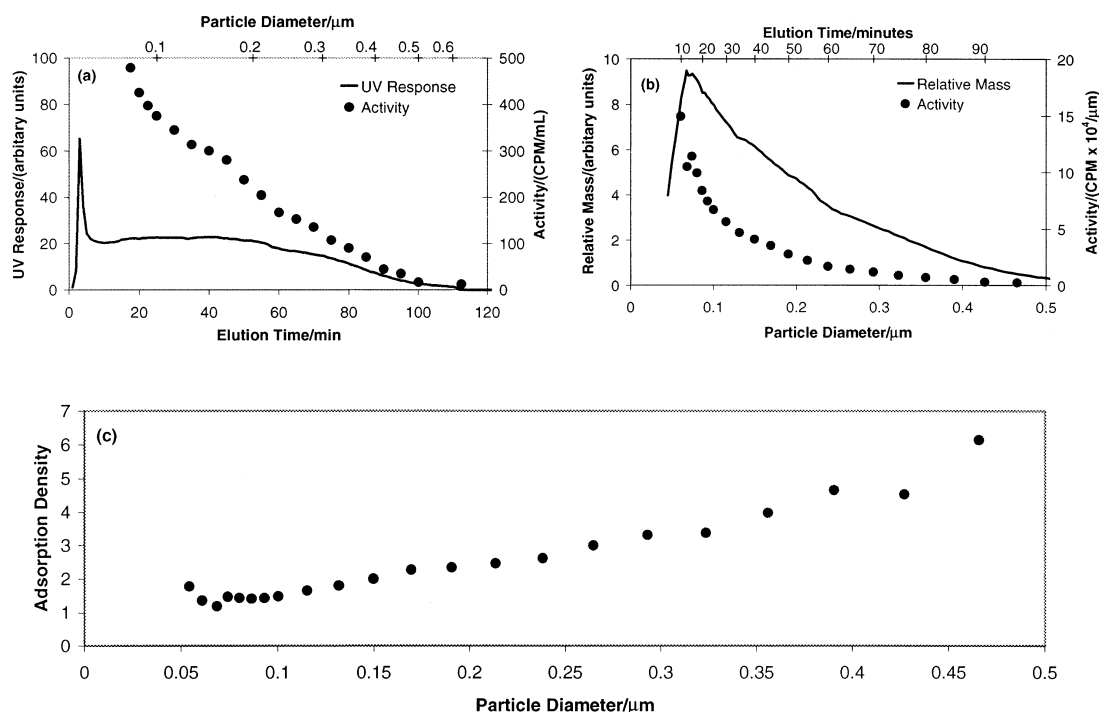


Fig. 2 Graphs showing ^{14}C -glyphosate on river suspended-particulate matter. (a) Particle mass and adsorbate fractograms; (b) particle size distribution and pollutant adsorption distribution; (c) surface-adsorption density distribution.

copper is increasing with particle size, suggesting a denser or thicker coating of copper as the particle size increases.

Contado et al. [4] coupled sedimentation FFF indirectly to GF–AAS as well as directly to ICP–MS to produce element composition data across the size distribution. The high levels of Cu, Pb, Cr, and Cd found were associated with colloidal particles taken from a river situated in a highly industrialized site. The two methods give comparable results, with on-line coupling of ICP–MS having a higher resolution, but ICP–AES yields data for some elements (such as potassium and calcium) where ICP–MS produces interferences.

Adsorption Behavior of Pollutants

The adsorption behavior of colloidal material onto river particles can play a vital role in the transport and fate of pollutants. FFF methods provide a means to evaluate the relative importance of different fractions in adsorption of contaminants in soils and sediments.

One particularly sensitive method employs the adsorption of radioactive material to natural par-

ticles [5]. Radiolabeled ^{32}P (as H_3PO_4) and ^{14}C (as glyphosate and atrazine) were adsorbed onto the river water colloid samples for several hours, then separated using sedimentation FFF and specific size fractions were collected. The fractions were subsequently analyzed for their β -activity. These data yield adsorbate (activity)-based fractograms and size distribution (Fig. 2a and b).

Dividing the adsorbate size distribution by the mass size distribution gives an adsorbate concentration (i.e., the amount adsorbed per mass of particles) distribution as outlined previously. Figure 2b shows that the smaller particles contain the highest pollution content. This is consistent with the concept that smaller particles have a higher specific surface area, but changes in geochemistry of the particle with size could also be involved.

If the adsorption were uniform, we would expect the adsorbate concentration to increase with decreasing size. This effect can be eliminated if the amount of adsorbate per unit area of particles is estimated. Assuming that the particles are spherical and have constant density, it is possible to calculate the relative amount adsorbed per unit surface area as a function of



particle diameter. This plot is known as a surface adsorption density distribution (SADD). Figure 2c shows the SADD plot for ^{14}C -glyphosate adsorbed onto a river suspended-colloid sample. This trend could be attributed to changes of particle size (as these calculations are based on a spherical particle), changes in mineralogy, and coating density across the size range.

The method outlined is also applicable to trace metal data collected by ICP–MS and ICP–AES. Recently, Hasselov et al. demonstrated that it is possible to measure major elements as well as a range of trace metals, including Cs, Cd, Cu, Pb, Zn, and La [6]. Further, they showed that it was possible to obtain speciation data across the size range.

Field-flow fractionation separations combined with other high-sensitivity analytical techniques are capable of yielding more detailed information than has been possible with existing methods. Although, at this stage,

there are still many uncertainties to the interpretation of the trends observed, this method is certain to provide further insights into the nature of pollutant–colloid interactions in natural waters.

References

1. J. C. Giddings, F. J. Yang, and M. N. Myers, *Science* 193: 1244–1245 (1976).
2. R. Beckett, *Environ. Tech. Lett.* 8: 339–354 (1987).
3. G. Karaiskakis, K. A. Graff, K. D. Caldwell, and J. C. Giddings, *Int. J. Environ. Anal. Chem.* 12: 1–15 (1982).
4. C. Contado, G. Blo, F. Fagioli, F. Dondi, and R. Beckett, *Colloids Surf. A: Physicochem. Eng. Aspects* 120: 47–59 (1997).
5. R. Beckett, D. M. Hotchin, and B. T. Hart, *J. Chromatogr.* 517: 435–447 (1990).
6. M. Hasselov, B. Lyven, and R. Beckett, *Environ. Sci. Technol.* 33: 4528–4531 (1999).



Pollutants in Water by HPLC

Silvia Lacorte

Damià Barceló

IIQAB-CSIC, Barcelona, Spain

Introduction

Over the last decade, the problem of diffuse pollution caused by industry, agricultural, and human activities, accidental spills, and waste discharges has resulted in directives to control the sources of pollution with the aim of protecting the water quality, contribute to the protection of human salubrity, and guarantee the utilization of natural resources. The European Union 76/464/CEE directive and the Environmental Protection Agency of the United States (US EPA) have listed the more toxic and persistent pollutants, including some of their degradation products, and the maximum permissible levels in surface waters [1]. The need for water monitoring has led to the development of a substantial number of analytical procedures based on an efficient sample-treatment technique and chromatographic determination. Because pollutants of different physicochemical properties are present at extremely low concentrations in complex environmental water samples, the analytical procedure should provide both a sensitive and selective detection and should generate accurate and precise data.

Discussion

Traditionally, gas chromatography (GC) was the preferred approach for the analysis of pollutants in water, due to the high sensitivity and selectivity achieved, thanks to its selective detectors such as the nitrogen-phosphorus (NPD), the flame photometric detector (FPD), and electron-capture detector (ECD), and to the ease of coupling to mass spectrometry (MS). However, high-performance liquid chromatography (HPLC or LC) is the most powerful approach for the determination of polar, nonvolatile, and thermolabile compounds (i.e., those which are not GC amenable).

The purpose of this entry is to provide an overview of the main HPLC techniques to determine priority organic pollutants in water. The recent developments in detection techniques (including diode-array detection, fluorescence detection, electrochemical detec-

tion) and especially the ability to connect a HPLC to MS has increased substantially the use of this technique for environmental monitoring. The methods described here are group-specific and cover the analysis of polycyclic aromatic hydrocarbons, phenols, pesticides, herbicides, aniline derivatives, surfactants, and explosives.

Table 1 classifies the different types of pollutants according to their chemical structure and summarizes the main HPLC techniques used for their determination. The objective is to suggest a suitable HPLC technique for each type of organic compound and to provide information on quality parameters and applicability in real environmental problems. All methods proposed are actually being accepted by the US EPA and permit one to achieve limits of detection at the low ppb–ppt level and reproducibilities below 10%.

Pesticides

Much concern is being given to the determination of pesticides in various environmental matrices, due to the increased number of pesticides detected and to the severe rules imposed by the legislation which aims to protect natural resources. Pesticides are classified as insecticides, herbicides, fungicides, and so forth, depending on the type of organism targeted. From an analytical point of view, pesticides cannot be treated as a group due to the great number of compounds with different chemical structures and physicochemical properties [2]. Many groups of pesticides, including their degradation products, are water soluble, nonvolatile, and polar, which leads to LC as the preferred approach. LC with ultraviolet (UV) or diode-array detection (DAD) are especially used for the analysis of organophosphorus and phenoxyacid pesticides, triazines and phenylurea herbicides, and quat herbicides and, in general, for compounds presenting a suitable chromophore (e.g., an aromatic moiety).

The main advantages of LC–DAD is related to its robustness and ease of use and to the fact that it offers an absorbance spectra that can be used to iden-



Table 1 Families of Priority Pollutants, Principal Method of Analysis Proposed, and Main Sources

Compound class	Extraction	LC method	Main sources
Alcohol ethoxylates	SPE	MS	Leather, textile industry
Anilines and chloroanilines	SPE, LLE	ECD, DAD, MS	Dye industry
BS and NPS	SPE	MS	Textile, tannery industry
Benzidines	SPE, LLE	ECD, DAD, MS	Industry
Carbamates	SPE, LLE	FLD, MS	Agriculture
Chlorophenols	SPE, LLE	DAD, ECD, CD, MS	Paper, pulp, plastic industry
Glyphosate	SPE	FLD, MS	Agriculture
Linear alkylbenzenesulfonates	SPE	MS	Household, chemical industry
Nonylphenol ethoxylates	SPE	MS	Leather, textile industry
Organophosphorus pesticides	SPE, LLE	DAD, MS	Agriculture, household
Phenoxyacid pesticides	SPE, LLE	DAD, MS	Agriculture
Phenylurea compounds	SPE, LLE	DAD, MS	Agriculture
Polyaromatic hydrocarbons	SPE, LLE	FLD, DAD, MS	Natural, antropogenic sources
Quats	SPE	DAD, MS	Agriculture
Triazines	SPE, LLE	DAD, MS	Agriculture, nonagricultural

SPE = solid-phase extraction; LLE = liquid-liquid extraction; DAD = diode-array detector; EC = coulometric detector; ECD = electrochemical detector; FLD = fluorescence detector; MS = mass spectrometry.

tify pesticides through spectral comparison. UV-DAD can best be combined with acetonitrile-water mixtures because of their absorbance cutoff. Interferences caused by UV-absorbing compounds (e.g., humic and fulvic acids) can seriously affect the quantification of target analytes. LC with fluorescence detection (LC-FLD) is more selective than LC-DAD and provides better sensitivity for naturally fluorescent compounds, as well as for many other compounds, such as glyphosates or carbamates, which are precolumn or postcolumn derivatized to yield fluorescent reaction products.

An alternative to LC-FLD for the analysis of aryl *N*-methylcarbamates and *N*-phenylcarbamates is LC with electrochemical detection (LC-ECD) because these compounds can be easily oxidized at 1.1 V. However, one should be aware of the problems associated with these techniques for water monitoring. Complex water samples, such as wastewater or industrial effluents might (a) increase the detection limits, (b) inhibit analyte detectability, or (c) interfere or co-elute with the analytes. In conclusion, these detection techniques are suitable for target determination of pesticides only if combined with a preconcentration and adequate cleanup step.

The matrix effect can be avoided by using MS. This technique is characterized by being highly selective and sensitive and, in addition, it offers spectral information which permits the unequivocal identification of target compounds. LC-MS with thermospray (TSP) and particle beam (PB) interfaces have been widely

used for pesticide monitoring and produce molecular information and electron-impact mass spectra, respectively. High detection limits and poor reproducibility are the main problems related to these techniques. Modern atmospheric-pressure chemical ionization (APCI) and electrospray (ESI) sources for LC-MS coupling are currently applied for the analysis of pesticides from environmental waters and limits of detection (LODs) of a few nanograms per liter and the linear response range over two orders of magnitude have been reported [3].

Polycyclic Aromatic Hydrocarbons

Polycyclic aromatic hydrocarbons (PAHs) are considered as priority pollutants due to their mutagenic and carcinogenic properties. PAHs are introduced in the environment from natural sources [e.g., incomplete combustion of organic matter from natural processes (volcanic eruptions, fires)] or anthropogenic, such as burning of fossil fuels, waste incineration, traffic, and so forth.

Polycyclic aromatic hydrocarbons have been encountered in different environmental matrices (e.g., soil, atmosphere, water, biota, etc.). Because PAHs have natural fluorescent properties, LC-FLD is advantageous over GC-MS because of its ability to measure the different PAH isomers and comparable detection limits are obtained. LC-DAD and LC-APCI-MS can also be applied and have the advantage



that hydroxylated PAH transformation products can be identified [4].

Phenolic Compounds

Phenol and its derivatives are generated in a wide variety of industrial processes (e.g., manufacture of plastics, dyes, drugs, glues) and in the pulp industry, but can also be formed as degradation products of pesticides. Chlorophenols are toxic to aquatic organisms and to man, and even at low concentrations in water, they can be the cause of unpleasant taste and odor.

Current official analytical methods include GC with flame ionization detection (FID), ECD, or MS and involve a derivatization step. However, there is a general trend to switch to LC procedures to avoid sample manipulation and because derivatization of phenols is not straightforward [5]. Common detection techniques are UV detection at 280 nm and 310 nm for nitrophenols and pentachlorophenol. LC–DAD is recommended because spectral libraries can be used for confirmation purposes. In terms of sensitivity, LC with electrochemical (ECD) or coulometric detectors (CD) produce better response than UV or DAD. However, electrochemical detection for LC has never become so popular as its inherent sensitivity and selectivity seem to indicate due to problems of electrode fouling and poor reproducibility. Moreover, electro-active matrix components can increase the background current and make ECD less robust for water monitoring. Therefore, this technique can only be recommended for monitoring clean-water samples. An attempt to use LC with direct or indirect FLD for phenols indicated acceptable detection limits, but problems related to the derivatization step made the technique less attractive. Similar to other organic pollutants, phenolic compounds can be detected by LC–APCI–MS and LC–ESI–MS and produce, in general, the protonated molecule as the base peak.

The advantages of these techniques is that an increase of the extraction voltage enhances fragmentation via collision-induced dissociation (CID) and provide structural information, useful for confirmation and identification purposes. Moreover, phenols are good candidates for capillary electrophoresis (CE) and capillary zone electrophoresis (CZE) because they permit a fast separation of polar and ionic compounds, have a high resolution, and are compatible with most LC detectors, including MS. In addition, trace enrichment can be performed in the capillary using isota-

chophoresis, making the technique suitable for water analysis.

Aniline Derivatives

In the recent years, the occurrence of anilines, chloroanilines, and benzidines in environmental waters has started to be of concern due to their widespread use in various industrial processes. Detection of these compounds is generally carried out with LC–ECD working in the amperometric mode using a glassy-carbon electrode. Problems encountered are similar to those for phenolic compounds and, therefore, confirmation is always necessary by UV, DAD, or, preferably, MS detection [6]. These compounds are also CE amenable and this approach is really promising in the sense of sensitivity and selectivity because humic and fulvic material can be separated from the analytes due to their different migration kinetics.

Surfactants

Linear alkylbenzenesulfonates (LAS), alcohol ethoxylates (AEO), and nonylphenol ethoxylates (NPEO) are synthetic surfactants used in the formulation of detergents and other cleaning products and are widely applied in the dye and leather industry and other industrial processes. These compounds, considered as estrogenic, have aroused considerable interest due to the large quantities produced globally. Their low volatility and anionic form make LC-based methods the preferred approach [7]. Due to the presence of different positional isomers, to the biodegradation intermediates, and to the lack of reference standards, LC–MS, and in particular with ESI, is the only technique which enables their identification and quantification in environmental waters.

Aromatic Sulfonates

Benzene (BS) and naphthalene sulfonates (NPS) are commonly used in the textile industry as dye bath auxiliaries and in the tannery industry as dispersants and wetting agents. After application, these compounds are discharged into surface waters and their presence in industrial effluents was not reported due to the lack of an appropriate analytical technique. Recently, ion-pair chromatography–ESI–MS and LC–ESI–MS was developed to determine BS and NPS with the final goal of determining polar, ionic, and water-soluble pollutants in wastewater [7].



Conclusions

Many organic pollutants in water can be analyzed with HPLC techniques at trace levels. From the different HPLC methods discussed in this entry, several remarks can be made: (a) For routine water monitoring, LC–DAD is the most common detection device used to analyze polar, thermolabile, and non-volatile compounds due to its robustness, high sample throughput, and the possibility of obtaining an UV spectrum that can be used for analyte confirmation; (b) LC–FD and ECD are more selective and sensitive than DAD and are especially useful for the monitoring of PAHs, carbamates, phenols, and anilines, respectively; (c) LC–MS with API sources have become highly robust techniques and the preferred option for the identification, confirmation, and quantification of organic pollutants in water. In addition, all HPLC techniques described can be

coupled, on-line, with solid-phase extraction, so that limits of detection can be decreased and their total automation permit to achieve high precision.

References

1. D. Barceló, *J. Chromatogr.* 643: 117–143 (1993).
2. D. Barceló and M. C. Hennion, *Trace Determination of Pesticides and Their Degradation Products in Water*, Elsevier, Amsterdam, 1997.
3. J. Abián, *J. Mass Spectrom.*, 34: 157–168 (1999).
4. R. Koeber, R. Niessner, and J. M. Bayona, *Fresenius J. Anal. Chem.* 359: 267–273 (1997).
5. D. Puig and D. Barceló, *Trends Anal. Chem.* 15(8): 362–376 (1996).
6. S. Lacorte, M. C. Perrot, D. Fraisse, and D. Barceló, *J. Chromatogr. A* 833: 181–194 (1999).
7. M. Castillo, M. C. Alonso, J. Riu, and D. Barceló, *Environ. Sci. Technol.* 33: 1300–1306 (1999).



Polyamide Analysis by GPC–SEC

Tuan Q. Nguyen

Department of Materials Science, Swiss Federal Institute of Technology, Lausanne, Switzerland

Introduction

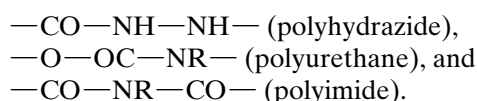
Synthetic polyamides (PA) are among the mostly widely used engineering thermoplastics, owing to their high strength and toughness, stiffness, abrasion resistance, and retention of physical and mechanical properties over wide temperature ranges. The material's outstanding properties are, to a large extent, due to their semicrystalline morphology and the cooperative intermolecular hydrogen-bonding of the amide groups. The strength of these dipolar interactions are reflected in the melting points, which are much higher in polyamides than in polyesters having comparable structures.

Proteins, including wool and silk fibers, are made up by the linkage of α -amino acids and constitute the most widespread source of natural polyamides.

Synthetic PAs are produced by polycondensation of bifunctional monomers or by cationic and anionic ring-opening polymerization of lactams. Polymers obtained with the first technique are linear, whereas chain branching may occur with anionic polymerization. Based on their chemical structure, synthetic polyamides may be classified into two categories [1]:

1. Aliphatic polyamides, also known under the generic name nylon. Industrial nylons with the general structure $[-RNHCO-]_n$, such as PA-6, PA-11, and PA-12, are called monadic; those with the general structure $[-NHR_1NHCOR_2CO-]_n$ are called dyadic (PA-4,6, PA-6,6, PA-6,9, PA-6,10, and PA-6,12).
2. Aromatic polyamides or aramids. The best known in the specialty fiber market are NomexTM (poly-*m*-phenyleneisophthalamide) and KevlarTM (poly-*p*-phenyleneterephthalamide).

A number of polymers with structures related to those of polyamides have been developed, some of which have achieved commercial importance, such as



SEC Eluants for Polyamides

High cohesive strength confers an exceptional solvent resistance to PAs, which can be dissolved only under rather drastic conditions (i.e., in highly corrosive solvents at temperatures close to the polymer melting point). This limited solubility leads to serious difficulties in the solution characterization of these polymers, such as in the determination of molecular-weight distribution (MWD). Selection of a solvent medium which is good for the polymer, chemically inert, and compatible with the stationary phase is crucial to a successful size-exclusion chromatographic (SEC) analysis [2]. These criteria are particularly demanding for many aramids, which are also rigid-rod polymers. Poly-*p*-phenyleneterephthalamide, for instance, has been analyzed in 97% sulfuric acid on silica columns.

Recently, a less corrosive room-temperature eluant consisting of methane sulfonic acid + 5% methane sulfonic anhydride + 0.1M sodium methane sulfonate has been reported for Kevlar and Technora fibers. Separation was performed on Hastelloy C columns packed with 4000 Å SAX 10- μ m particles (Polymer Laboratories), using ultraviolet (UV) detection and poly(benzoxazole) for calibration [3]. Work on the SEC characterization of aramids is extremely limited and generally lacks details of molecular-weight (MW) accuracy. In the following section, we will focus exclusively on aliphatic polyamides.

High-Temperature Solvents

The first mention of SEC analysis of PA-6 and PA-6,6 is by Goebel (1967), using *m*-cresol at 135°C with Styragel[®] columns. It was soon realized, however, that PA degrades extensively within a few hours under the above experimental conditions; alternative solvents have been proposed, most of which can be used only at elevated temperatures, due to solubility or viscosity problems [4]:

- *o*-Chlorophenol at 100°C
- Hexamethylphosphoramide (85°C)
- Dimethylacetamide + 2.5% LiCl (100–130°C)
- Benzyl alcohol (130°C).



In addition to the necessity for high-temperature SEC, each of the above solvents has its own drawbacks, such as adsorptive effects with phenol derivatives, column blocking, and carcinogenicity with hexamethylphosphoramide and corrosion of stainless steel by the dimethylacetamide-LiCl mixture.

Benzyl alcohol has been tested at 100°C on silica columns. To prevent potential solute interactions with silica stationary phase, it is recommended to prefer cross-linked PS columns with benzyl alcohol at 130°C and polytetrahydrofurans as calibration standards (polystyrene and polyethylene oxide standards interact with the stationary phase under the analytical conditions) [5].

Low-Temperature Eluants

Fluorinated Alcohols

Most solvents which dissolve nylon at room temperature are either too toxic (nitrobenzene) or too corrosive [strong acids: sulfuric, formic, dichloroacetic; concentrated alcoholic salt solutions (e.g. methanol + CaCl₂)] to be safely used as an SEC eluant. Fluorinated alcohols constitute an exception: It has been known for a long time that trifluoroethanol (TFE), tetrafluoropropanol (TFP), or hexafluoroisopropanol (HFIP), owing to the presence of strong electron-withdrawal groups ($-\text{CF}_2-$ and $-\text{CF}_3$), have the propensity to dissolve a large number of polymeric materials which possess receptive sites for H-bonding formation (proteins, stereoregular polyesters, and, more recently, polyaniline).

The application of fluoroalcohols for dissolving polyethylene terephthalate (PET) and polyamides dates back from the early 1960s. Dissolution tests show that the solubility of polyamides improves with the acidity of the fluoroalcohol and decreases with increasing steric hindrance of substituents adjacent to the hydroxyl group. The use of HFIP for the SEC of PA-6,6 and PET on porous glass and μ -Styragel columns was described by Drott in 1971. TFE was tested in the following year for the SEC separation of Nylon 6, using fractionated PMMA for calibration. Fluoroalcohols are hygroscopic and should be dried before use to avoid formation of corrosive products. Polymer adsorption was observed when the water content in the eluent is >0.03%. Moisture in TFE and HFIP can induce the formation of carboxylate end groups in nylon. Electrostatic repulsion between these groups and residual carboxyl ions present in cross-linked PS packings will lead to ion exclusion, which can be suppressed

with the addition of a salt (sodium acetate, sodium trifluoroacetate, or tetraethyl ammonium chloride) in the $10^{-2}M$ concentration range. At present, HFIP is the preferred room-temperature eluant for the SEC characterization of nylons and polyesters. TFE, although four times less expensive than HFIP, is more toxic and has limited dissolution capability for polyesters and for nylons with long alkyl sequences. In addition to high cost, the use of HFIP entails a number of difficulties, such as high volatility, health hazards, incompatibility with a PS-DVB-based stationary phase (particularly with columns of pore sizes <1000 Å), insolubility of PS standards, and the presence of non-steric exclusion effects. Most of these problems have now been largely solved: Calibration can be done with commercially available anionic poly(methyl methacrylate) (PMMA) standards or with "absolute" detection, incompatibility with the stationary phase is minimized with columns specially designed for HFIP (Polymer Laboratories, Shodex, Waters), and closed-loop distillation and the use of narrow-bore columns substantially reduces solvent consumption.

Despite this progress, SEC with HFIP remains an expensive procedure due to extra investment in fluorinated solvent and special columns. Finally, it should be noted that HFIP with a pK_a of 9.3 is sufficiently acidic to react with the nitrogen in aromatic polyimides, resulting in ring-opening solvolysis.

Mixed Eluants

In search of less expensive, less toxic, and lower viscosity eluants, a few authors have proposed diluting the active ingredient with a common SEC eluant such as toluene, dichloromethane, or chloroform. To lower the operating temperature and minimize polymer degradation, mixtures of *m*-cresol with chlorobenzene (50:50, v/v, 43°C), dichloromethane (50:50, room temperature), and chloroform have been used, with 0.25 wt% benzoic acid added to prevent adsorption. In the same vein, *o*-chlorophenol has been diluted with chloroform (25:75) and used at 20°C. The main disadvantage in this latter solvent was a small dn/dc for the polymer, which rendered refractive index measurements difficult. In addition, careful purification of the phenol is required to obtain a detection signal. Dichloroacetic acid diluted to 20 vol% with dichloromethane has been proposed as the mobile phase. However, even at this concentration, PA tends to degrade at room temperature.

Among the different solvent combinations, it appears that mixtures based on fluorinated alcohols give



the best results in terms of stability of the polymer and compatibility with the stationary phase (conventional silica or PS–DVB columns can both be used). As with pure fluoroalcohols, a salt should be added to suppress polyelectrolyte effects. Toluene, with 20 vol% HFIP, has been used for the SEC fractionation of PA-12. However, based on thermodynamic excess properties, this solvent combination should be less efficient in terms of solvation power than mixtures of HFIP with chloroalkanes.

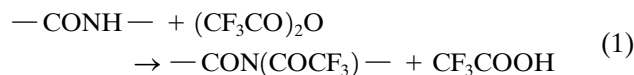
Mixtures of HFIP or TFE with CHCl_3 and CH_2Cl_2 have been successfully tested as SEC eluants. HFIP– CH_2Cl_2 mixtures have the advantage of being more stable, of low toxicity, and UV transparent up to 200 nm (an assess for UV-absorption detection) and are better solvents for PA than the other mixtures [6]. On the negative side, HFIP– CH_2Cl_2 forms a 30:70 (v/v) azeotrope at 30°C, thus limiting its use to room temperature. HFIP– CHCl_3 does not have an azeotrope, whereas TFE– CHCl_3 possesses a lower azeotrope at 55°C.

Problems Associated with Mixed Eluants

The use of mixed eluants in SEC analysis was proposed long ago to take advantage of the desirable properties of both solvent systems. Possible consequences of preferential solvation of the stationary phase and the polymer by one of the eluant components must, however, be critically evaluated: changes in mixture composition with polymer hydrodynamic volume, differences in composition of the mobile phase and of the solvent in the pores, dependence of the refractive index signal on elution volume, and the possibility of interference of the system peak with the oligomer signal in refractive index detection. Solvent recycling is more difficult and the original composition must be readjusted after distillation.

N-Trifluoroacetylation

N-Trifluoroacetylation remains a common technique to solubilize aliphatic PA for SEC analysis [7]:



With a twofold to threefold excess in trifluoroacetic anhydride, reaction (1) is quantitative within 1 day at room temperature. The N-trifluoroacetylated polyamides (NTFA–PA) are soluble in many ordinary organic solvents, such as acetone, methylene chloride, chloroform, and tetrahydrofuran. In addition to the

change in solubility, another remarkable feature of N-trifluoroacetylation is a near-two-orders-of-magnitude increase in the UV-absorption coefficient of the amide band, accompanied by a large bathochromic shift. Trifluoroacetylated polyamides have a rather small dn/dc in CH_2Cl_2 and detection was better achieved by UV absorption. Once prepared, the NTFA–PA solutions are unstable in the presence of atmospheric humidity and should be used immediately to avoid reverse hydrolysis, which converts the fluorinated polymer back into the original polyamide. It has been reported that SEC separation of NTFA–PA does not follow the universal calibration in dichloromethane, whereas better agreement was obtained in tetrahydrofuran. Comparative SEC analyses of NTFA–PA in both solvents on Styragel columns show, nevertheless, identical results [6].

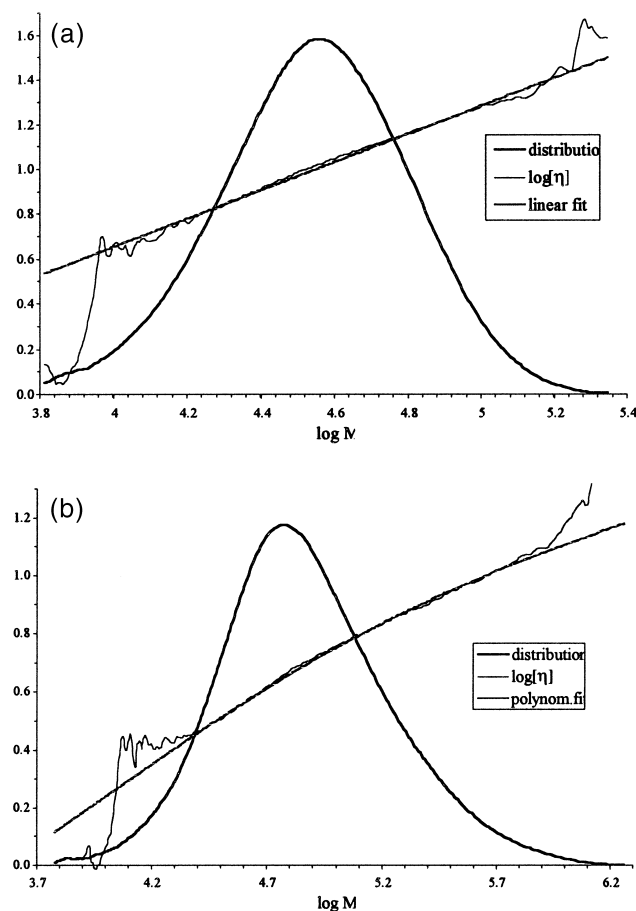


Fig. 1 SEC–viscometry characterization of a linear (a) and a branched (b) PA-12 synthesized by anionic polymerization, with different activators. Analysis conditions: mixed eluant 5:95 v/v; HFIP/ CH_2Cl_2 at 30°C; Styragel–HR2/3/4/5 columns.



Conclusions

Size-exclusion chromatography analysis of PAs remains a difficult enterprise in comparison to other amorphous thermoplastics which can be readily dissolved in common solvents at room temperature. To improve MW accuracy, calibration should be performed with absolute detection (on-line viscometer, light scattering) or with a broad MWD polymer standard of identical chemical composition to the analyzed sample. Among the high-temperature eluants, benzyl alcohol is the less corrosive and seems to give the most reliable results. In low-temperature SEC, HFIP remains the best eluant, provided the necessary extra investment is not a problem. A mixed-eluant based on HFIP is a reasonable alternative to pure HFIP for long alkyl nylons (PA-12, PA-11). For shorter alkyl sequences, the high percentage of HFIP (>10 vol%) required for dissolution of the polymer may interfere with the size-exclusion mechanism of separation [6]. *N*-Trifluoroacetylation of the PA remains an interesting alternative, provided due care is given to prevent contact of the derivatized compound with reagents

(water, alcohols, etc.) able to cause scission of the —N—COCF₃ bond.

References

1. M. S. M. Alger, *Polymer Science Dictionary*, Elsevier Applied Science, London, 1989, p. 288.
2. P. J. Wang, in *Handbook of Size Exclusion Chromatography* (C. S. Wu, ed.), Chromatography Science Series Vol. 69, Marcel Dekker, Inc., New York, 1995, p. 161.
3. R. M. Nelson and M. W. Warren, *International GPC Symposium '96*, Waters Corporation, Milford, MA, 1996, p. 453.
4. D. J. Goedhart, J. B. Hussem, and B. P. M. Smeets, in *Liquid Chromatography of Polymers and Related Materials II* (J. Cazes and X. Delamare, eds.), Chromatography Science Series 13, Marcel Dekker, Inc., New York, 1980, p. 203.
5. G. Marot and J. Lesec, *J. Liquid Chromatogr.* 11: 3305 (1988).
6. T. Q. Nguyen, *International GPC Symposium '98*, Waters Corporation, Milford, MA, 1998, p. 135.
7. E. Jacobi, H. Schuttenberg, and R.C. Schulz, *Makromol. Chem. Rapid Commun.* 1: 397 (1980).



Polycarbonates: GPC–SEC Analysis

Nikolay Vladimirov

Hercules, Inc., Wilmington, Delaware, U.S.A.

Introduction

Polycarbonate (PC) polymers are amorphous thermoplastics with excellent toughness, clarity, and high heat-deflection temperatures. They are one of the better thermoplastics where strength and elastic moduli are concerned, offering both excellent impact strength and rigidity. In general, PCs are linear aromatic polyesters of carbonic acid. Polycarbonates can be described as polymeric combinations of bifunctional phenols, or bisphenols, linked together through carbonate linkages.

Discussion

Robertson et al. used gel permeation chromatography (GPC) to examine PCs produced by different synthetic routes. They concluded that this method is superior to end-group analysis. Hoore and Hillman carried out fractionations of PCs by GPC to procure narrow molecular-weight-distribution (MWD) fractions which were used to calibrate the columns of a GPC system and an experimental “*Q* factor” of 23.8 was found. The calibration was further confirmed by membrane osmometry and light-scattering measurements [1]. The “*Q* factor” method is the simplest conversion method for molecular-weight calculations that provides data closer to the real molecular weights while still using polystyrene (PS) standards, but it lacks accuracy because it assumes the extended chain length of the polymer in solution. Most flexible polymers are not extended, but, rather, they are randomly coiled in solution. The more reliable method is to use the concept of the “hydrodynamic volume” [2]. A comprehensive listing of Mark–Houwink coefficients *K* and *a* for different solvents and temperatures are published in the *Polymer Handbook* [3]. PC standards for calibration have been commercially available for the past several years from Polymer Standard Service Co. (Mainz, Germany) and American Polymer Standards Co. (Mentor, OH, U.S.A.).

The polymerization of trimethylene carbonate (1,3-dioxan-2-one) with a complexation catalyst was studied by Kriecheldorf et al. [4]. On the basis of GPC

measurements employing a universal calibration, weight-average molecular weights up to approximately 22,000 were found. A combination of four Ultrastaygel columns was used, with nominal pore sizes of 100 Å, 500 Å, 10³ Å, and 10⁴ Å. The detector was a Waters M410 differential refractometer. The molecular weights were estimated from GPC results by means of intrinsic viscosities determined in dichloromethane at 25°C and an universal calibration curve, based on commercial PS standards.

Wang and Gonsalves [5] investigated the enzyme-catalyzed synthesis of poly(ethyl phenol) (PEP), which was modified by copolymerization with PCs. GPC was carried out on a system equipped with a differential refractive index detector (DRI) and four Ultrastaygel columns in tetrahydrofuran (THF) with a flow rate of 1 mL/min. A calibration plot, constructed with PS standards, was used to determine the molecular weights. Based on the results, a slight difference between the high- and low-temperature products was observed for the pristine PC. The copolymers PC-*co*-PEP had higher molecular weights when compared to the pristine material, due to the linkage between PC and PEP, which effectively doubled the molecular weights.

Gel permeation chromatography was used for the analysis of fullerene-functionalized polycarbonates, achieved by direct reaction of PC and fullerenes with aluminum chloride as a catalyst. THF was used as the eluent and the system was calibrated with PS standards. The working wavelength for the ultraviolet (UV) detector was 340 nm, where the starting PC was hardly detectable, but the reaction product gave two UV peaks, a strong peak in the “normal” molecular-weight (MW) region and a weak peak in the very high MW region. Because THF is a nonsolvent for fullerenes, the solubility of the polymers in THF and the GPC data served as evidence for the existence of a covalent bonding between the fullerene and PC [6].

The influence of molecular structure on the degradation mechanism of degradable polymers of poly(trimethylene carbonate), poly(trimethylene carbonate-*co*-caprolactone), and poly(adipic anhydride) was explored by Albertsson and Eklund [7]. Measuring the change of the mass and the molecular weight for the



polymeric samples during degradation is a good indication of the degradation rate and an initial measure of material deterioration. The value of the molecular weight is not absolute, but, rather, it is relative to PS standards. This is sufficient for this study, which is simply concerned with the change in molecular weight relative to the starting value in order to evaluate the degradation. While the molecular weight decreased, an increase in the polydispersity was observed for some of the samples.

Studies of the thermal decomposition of the products under a nitrogen atmosphere were carried out by combining liquid chromatography under critical conditions of adsorption (LACCC) and size-exclusion chromatographic (SEC) methods with matrix-assisted laser desorption/ionization–time-of-flight spectrometry (MALDI–TOF) and postcolumn derivatization. The critical conditions of polymer adsorption in the liquid chromatography and an optimal matrix system for MALDI–TOF are reported. The changes of molar mass distribution and chemical heterogeneity are said to be due to the simultaneous processes of degradation and recombination [8].

Branching by reactive end groups, syntheses, and thermal branching of 4-hydroxybenzocyclobutene/*p*-*tert*-butylphenol co-terminated bisphenol PC was investigated by Marks et al. [9]. Reactive end groups on bisphenol A PCs allow for significant structural changes in this condensation polymer that are not accessible by direct synthetic routes. Commercially offered branched PCs have improved melt rheological properties, compared to their linear analogues; they are manufactured by incorporation of a trifunctional comonomer in the PC polycondensation process. A GPC system, equipped with a UV detector (GPC–UV), and liquid chromatography (LC) were used for the analyses. A Hewlett-Packard 1047 DRI detector and a LALLS (CMX-100) (low-angle light scattering) photometer were connected in series. Values of dn/dc were estimated from the DRI responses and sample concentrations. Five TSK MicroPak H-series (3 GMH6, 1 G500H6, and 1 G400H8) columns were used at 30°C with THF as the eluent at 1 mL/min. Heating to 300°C for 20 min causes the BCB–OH/PTBT BA PCs to branch or cross-link. The molecular weight and polydispersity of the branched polymers increase to a value at which the onset of the gel formation is observed. GPC–LALLS (M_w 135,100 and 310,700) was performed on two of the branched samples; it shows, as expected, a significantly higher molecular weight, particularly M_w , than indicated by GPC–UV (M_w 70,600 and 64,600, respectively).

The M_w by GPC–UV of each series of BCB–OH/PTBT BA PCs increases exponentially up to the gel point. The apparent decrease in M_w after the gel point reflects the values of the soluble fraction only, which are, therefore, not representative of the entire sample. LC was applied to investigate the types and distribution of BCB reaction products formed.

Unfortunately, none of the hyperbranched polymers studied to date has demonstrated good mechanical properties. A hyperbranched PC is also expected to be a brittle material, but such a structure may prove interesting as a highly functionalized prepolymer for composites, coatings, and other applications. Hyperbranched PCs were synthesized and characterized by Bolton and Wooley [10]. The products were prepared by the polymerization of an A_2B monomer derived from 1,1,1-*tris*(4'-hydroxyphenyl)ethane. Silylation of the phenol terminated material with *tert*-butyldimethylsilyl chloride, followed by degradation of the carbonate linkages by reaction with lithium aluminum hydride and analysis of the products by high-performance liquid chromatography (HPLC) allowed for the determination of the degree of branching, which was found to be 53%. The molecular weights of the carbonyl imidazolid-, phenol-, and *tert*-butyldimethylsilyl ether-terminated hyperbranched polycarbonates were 16,000, 77,000, and 82,000, respectively, from GPC, based on polystyrene standards, 23,000, 180,000, and 83,000, respectively, from GPC with LALLS, and 24,000, 160,000, and 88,000, respectively, from GPC with SEC software. SEC was conducted on a Hewlett-Packard series 1050 HPLC with a Hewlett-Packard 1047A refractive index detector, a Wyatt MiniDawn laser-light-scattering detector, and a Viscotek Model 110 differential viscometer. Two 5- μ m Polymer Laboratories PL gel columns (300 \times 7.7 mm), connected in series, were used with THF as an eluent.

Bailly et al. investigated the separation of polycarbonate oligomers by SEC and reversed-phase LC [11]. The separation of PC oligomers was achieved by SEC with styrene–divinylbenzene microparticle gel as a stationary phase and dichloromethane as a mobile phase. Oligomers were separated up to 10 repeating monomer units. SEC is useful for the analyses of the low-molecular-weight content of commercial PC samples. Retention times are significantly influenced by the nature of end groups (O— or OH—O—) {O=phenyl}, indicating that adsorption occurs with hydroxy-terminated oligomers. Also, SEC results were compared with reversed-phase HPLC data.

Although the molecular weight of the bisphenol A polycarbonate repeat unit is relatively high, the separation of PC oligomers by SEC is difficult and has, thus,

received little attention up to now. The problem is complicated by the existence of three oligomer families resulting from the addition of chain modifiers (monofunctional phenols) during the synthesis of the polymer by the usual interfacial method. The SEC results are compared with those obtained by reversed-phase HPLC for the same systems. Adsorption of phenolic compounds is known to occur on the surface of PS–DVB gels. When several types of oligomers are simultaneously present, interpretation of chromatograms becomes difficult and should be done with caution. This is particularly true when analyzing the oligomer content of commercial PC samples. The resolution obtained by reversed-phase HPLC remains superior, but, in most cases, quantitative result cannot be obtained by this technique because of solubility problems. In contrast with previous claims, the nature of the end groups was observed to significantly influence the retention time of PC oligomers by SEC. The presence of the hydroxy terminal groups induces a reversible adsorption of the compounds onto the columns. This effect is very important for oligomers having two hydroxy end groups.

As a consequence, the precise determination of the number-average molecular weights of PC samples by SEC is possible only if the nature of the oligomers present is taken into account.

References

1. T. R. Crompton, *The Analysis of Plastics*, Pergamon Press, New York, 1984, p. 354.
2. S. Mori, HPLC application to polymer analysis, in *Handbook of HPLC* (E. Katz, R. Eksteen, P. Schoonemakers, and N. Miller, eds.), Marcel Dekker, Inc., New York, 1998, p. 836.
3. J. Brandrup and E. H. Immergut (eds.), *Polymer Handbook*, 3rd ed., John Wiley & Sons, New York, 1989, p. VII/23.
4. H. R. Kricheldorf, J. Jensen, and I. Kreiser-Saunders, *Makromol. Chem.* 192: 2391–2399.
5. J. Wang and K. E. Gonsalves, *J. Polym. Sci. Part A: Polym. Chem.* 37: 169–178 (1999).
6. B. Z. Tnag, H. Peng, M. Leung, Ch. Song, M. Takashi, Kai Su et al., *Macromolecules* 31: 103–108 (1998).
7. A.-C. Albertsson and M. Eklund, *J. Appl. Polym. Sci.* 57: 87–103 (1995).
8. O. Wachen, K. H. Reichert, R. P. Kruger, H. Much, and G. Schulz, *Polym. Degrad. Stabil.* 55(2): 225–231 (1997).
9. M. J. Marks, J. Newton, D. C. Scott, and S. E. Bales, *Macromolecules* 31: 8781–8788 (1998).
10. D. H. Bolton and K. L. Wooley, *Macromolecules* 30: 1890–1896 (1997).
11. Ch. Bailly, D. Daoust, R. Legras, and J. P. Mercier, *Polymer* 27: 776–782 (1986).



Polyester Analysis by GPC–SEC

Sam J. Ferrito

Cooper Power Systems, Franksville, Wisconsin, U.S.A.

Introduction

Gel permeation chromatography (GPC) also known as size-exclusion chromatography (SEC) has proven to be an extremely useful analytical technique for characterizing the molecular-weight distribution (MWD) of polyesters. The MWD of a polymer can provide valuable information regarding the molecular composition. For example, along with relative molecular-weight averages, polydispersity, intrinsic viscosity, and branching information can be obtained.

Discussion

Thermoplastic polyesters are popular engineering polymers because they offer excellent chemical and heat resistance, along with desirable electrical properties. When reinforced with glass or mineral fillers, they can be used to replace materials such as metals, ceramics, composites, and other less suitable plastics. In addition, thermoplastic polyesters offer excellent mechanical properties while retaining good processability [1]. Unfortunately, the polyester molecule is readily susceptible to hydrolysis. Hydrolytic degradation of the polymer causes random chain scissions to occur, normally at the ester linkages ($R-CO-O-R'$), which causes a reduction in molecular weight and, in turn, a reduction in mechanical integrity [2,3]. GPC can be used to monitor the hydrolytic process and predict product performance [4].

Aromatic polyesters, because of their crystalline structure and polar nature, require the use of aggressive solvents and/or elevated temperatures to dissolve the polymer [5]. Various solvent blends can also be incorporated to aid in the dissolution process [6,7].

Early work involving high-temperature GPC of polyesters utilized solvents such as meta-cresol and ortho-chlorophenol as mobile-phase solvents. These solvents are very viscous and require system temperatures of between 140°C and 150°C. Both solvents are also very dangerous and difficult to handle [8,9].

More recently, hexafluoroisopropanol (HFIP) has been used successfully as a mobile phase for both poly-

esters and polyamides [4,9,10]. Unfortunately, HFIP is very expensive and dangerous to handle. HFIP requires special care and attention due to its extreme corrosiveness to eyes and skin. *Handling should be conducted only by trained professionals equipped with proper splash goggles and face shield for eye/face protection, and appropriate impervious gloves, apron and other protective equipment as noted on the Material Safety Data Sheet for HFIP.* Mobile-phase distillation is necessary, due to the extreme cost of the solvent. Some laboratories have reported using blends of HFIP and methylene chloride or HFIP and chloroform successfully in an effort to reduce solvent costs [7,10–13].

Hexafluoroisopropanol is able to dissolve most polyesters and polyamides (nylons) at room temperature in about 4–8 h. Sodium trifluoroacetate (NAT-FAT) is typically added to suppress any polyelectrolyte effects that could occur in HFIP [9]. GPC columns made from cross-linked polystyrene–divinylbenzene are typically used to perform the separation [14]. Calibration is generally performed using poly(methyl methacrylate) standards instead of polystyrene standards, due to solubility constraints [5,15].

Typical polyesters characterized by GPC include polyethylene terephthalate (PET), polybutylene terephthalate (PBT), and polycyclohexylenedimethylene terephthalate (PCT). Polyphthalamides (PPA) and polyamides are also commonly analyzed.

Polyester detection is normally accomplished by using refractive index detection in conjunction with either viscometry or low-angle laser light scattering (LALLS).

The viscosity data are a quantitative gauge for monitoring the loss of high-molecular-weight chains within the polymer. Because the viscometer detector operates by measuring the pressure drop across a capillary tube, the intrinsic viscosity at a constant flow rate can be measured as follows [11,16]:

$$P = \left(\frac{8}{\pi}\right) \left(\frac{L}{r^4}\right) \eta F$$

where P is the pressure drop across the capillary, L is the capillary length, r is the internal radius of the capillary, η is the viscosity of fluid (GPC column effluent), and F is the flow rate.



Universal calibration incorporates intrinsic viscosity data with molecular-weight information provided by polymer standards of differing composition. Absolute molecular-weight determinations have proven to be inaccurate in HFIP due to non-size-exclusion interactions occurring within the process [6,17]. Typically, *relative* molecular-weight comparisons are reported when using this procedure. However, if *absolute* molecular-weight values are required, light-scattering techniques have been utilized with greater success [18–20].

Data derived from GPC analysis is commonly used to monitor the hydrolytic stability of various thermoplastic polyesters used under conditions requiring exposure to elevated temperatures and humidity. Polyester hydrolysis results in shifts in MWD toward lower molecular weight with a corresponding lowering of the intrinsic viscosity. A reduction in mechanical properties also is evident when hydrolysis occurs. Changes in mechanical properties can also be caused by moisture absorption and by weakening of the glass-fiber bond. GPC can distinguish between chemical and physical changes occurring to the material.

Figure 1 compares the changes that occur to PBT due to aging of the polymer at 60°C and 100% relative humidity for a total of 25 weeks. Samples were removed at 5-week intervals, and the molecular-weight distributions were compared. Polymer hydrolysis was evident by regular shifts in molecular-weight distribution toward lower molecular weight [4].

Gel permeation chromatographic analysis will serve as a valuable technique for evaluating the newly devel-

oped hydrolysis-resistant polyesters and for monitoring the weatherability of polyesters in outdoor applications.

References

1. E. Yokley, Thermoplastics for electrical applications, *Electrical Manuf.*, 11–13 (November 1991).
2. P. G. Kellenher, G. H. Bebbington, D. R. Falcone, J. T. Ryan, and R. P. Wentz, Thermal and hydrolytic stability of poly(butylene terephthalate), in *37th Antec SPE*, 1979, pp. 527–531.
3. R. J. Gardner and J. R. Martin, Effect of relative humidity on the mechanical properties of thermoplastic polyesters, in *37th Antec SPE*, 1979, pp. 831–834.
4. S. J. Ferrito, An analytical approach toward monitoring degradation in engineering thermoplastic materials used for electrical applications, in *International GPC Symposium Proceedings*, 1994, pp. 675–684.
5. S. Mori, Size exclusion chromatography of poly(ethylene terephthalate) using hexafluoro-2-propanol as the mobile phase, *Anal. Chem.* 61: 1321–1325 (1989).
6. A. Moroni and T. Havard, Characterization of polyesters and polyamides through SEC and light scattering using 1,1,1,3,3,3-hexafluoro-2-propanol as eluent, in *International GPC Symposium '96*, 1996, pp. 229–238.
7. C.-s. Wu (ed.), *Handbook of Size Exclusion Chromatography*, Chromatographic Science Series Vol. 69, pp. 169–172.
8. Waters Division of Millipore, Solubilizing polyester (PET) for high temperature GPC analysis, *Polym. Notes*, 3(1) (April 1988).
9. W. W. Yau, J. J. Kirkland, and D. D. Bly, *Modern Size-Exclusion Liquid Chromatography*, John Wiley & Sons, Inc., New York, 1979, pp. 390–394.
10. Q. Nguyen, GPC-viscometry characterization of polyamides and polyethylene terephthalate in HFIP/CH₂Cl₂ mixtures, *International GPC Symposium '98*, 1998, pp. 135–153.
11. R. L. Miller, R. W. Seymour, and L. W. Branscome, The application of size-exclusion chromatography to study molecular-weight changes of flame-retardant fiber-reinforced polyesters, *Polym. Eng. Sci.* 592: 31–38 (1991).
12. M. R. Milana, M. Denaro, L. Arrivabene, A. Maggio, and L. Gramiccioni, Gel permeation chromatography (GPC) of repeatedly extruded polyethylene terephthalate (PET), in *Food Addit. Contamin.* 15(3): 355–361 (1998).
13. S. Weidner, G. Kuehn, B. Werthmann, H. Schroeder, U. Just, R. Borowski, R. Decker, B. Schwarz, I. Schmuecking, and I. Seifert, *A New Approach of Characterizing the Hydrolytic Degradation of Poly(ethylene terephthalate) by MALDI-MS*, John Wiley & Sons, New York, 1997, pp. 2183–2192.
14. E. Meehan, S. Oakley, and F. Warner, *The Application of a Novel Particle Technology for GPC Using HFIP as*

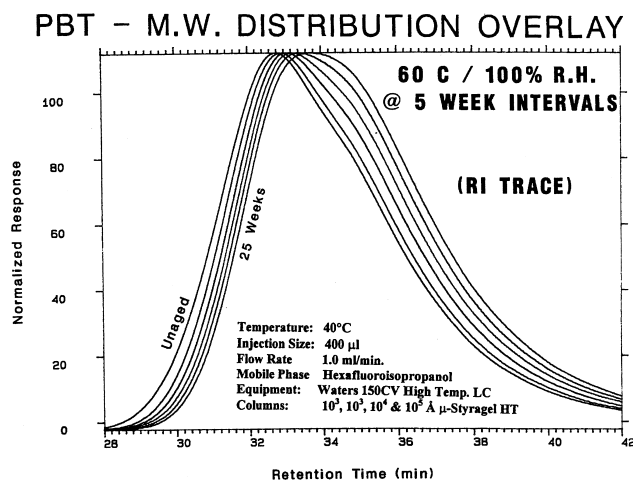


Fig. 1 Degradation of PBT at 60°C and 100% relative humidity; samples for analysis were taken at 5-week intervals.

- Eluent*, Polymer Laboratories Ltd., Shropshire, UK, pp. 353–356.
15. *The Gel Permeation Chromatography of Poly(tetramethylene terephthalate)*, John Wiley & Sons, New York, 1977, pp. 2293–2295.
 16. J. L. Ekmanis, GPC analysis of polymers with an on-line viscometer detector, in *International GPC Symposium Proceeding*, 1989.
 17. M. Szesztay, Z. S. Laszlo-Hedvig, and F. Tudos, Gel permeation chromatography identification of polyester oligomers with different endgroups, *J. Appl. Polym. Sci.* 48: 227 (1991).
 18. J. P. Sibilis (ed.), *A Guide to Materials Characterization and Chemical Analysis*, 2nd ed., VCH Publishers, Inc., New York, 1996.
 19. A. V. Pavlov, V. V. Gur'yanova, O. M. Karan'yan, A. G. Morozov, and T. N. Prudskova, Modern methods for studying the molecular characteristics of polymers, *Int. Polym. Sci. Technol.* 20(12): T/41–T/44 (1993).
 20. S. Berkowitz, Viscosity–molecular weight relationships for poly(ethylene terephthalate) in hexafluoroisopropanol–pentafluorophenol using SEC–LALLS, *J. Appl. Polym. Sci.* 29: 4353–4361 (1984).



Polymer Additives: Analysis by Chromatographic Techniques

M.L. Marín

Alfonso Jiménez Migallon

University of Alicante, Alicante, Spain

Introduction

The need for developing methods of analysis for additives in plastics materials is increasing day by day because of several aspects. First, as toxicological studies are developed, there is the presence of some substances which have been banned in specific products. Second, in production, it is necessary to carry out a quality control for additive levels. It is also necessary to determine the stability of the additives when the polymer is processed. In this case, some additional compounds, often undesirable, can be generated and their control becomes necessary. Finally, the analysis will let us know the composition of a plastic product.

It is possible to use techniques in which the additives can be determined by direct analysis of the sample, such as nuclear magnetic resonance (NMR) spectrometry, ultraviolet (UV) spectrometry, and UV desorption-mass spectrometry. These techniques are very useful when the concentrations of additives in the polymer are high. However, when additives are present in trace levels, it is necessary to carry out a preliminary extraction/concentration step before analysis. Some of the most common additives used in plastics materials are presented in Table 1.

Sample Preparation

As was previously mentioned, a preliminary extraction step is necessary for samples in which a low level of organic compounds of interest must be determined. The extraction presents advantages when compared to the direct plastics analysis solution. In this case, the polymer is dissolved directly in an organic solvent and then precipitated. This procedure is not selective and the polymer residues can affect the analysis of the additives. When an extraction is carried out, higher selectivities can be obtained when the appropriate extraction conditions are used.

Traditional methods of extraction, such as Soxhlet, have been replaced by modern techniques as supercritical fluid extraction (SFE), microwave-assisted extraction (MAE), ultrasonic extraction, and accelerated solvent extraction (ASE) during recent years. The application of specific methods to these kinds of samples has permitted the development of a great number of other extraction methods. In the following list, a brief description is given:

SFE: This method uses pressure and temperature for fluids above their critical points. Under these conditions, the density and diffusivity of a supercritical fluid are between those of liquids and gases, resulting in an increase of the solvent power.

MAE: In this case, the sample and solvent are placed in a vessel and microwave radiation is applied. The solvent is heated under pressure above its normal boiling point so it remains in the liquid state.

ASE: Common solvents are used, at elevated temperatures and pressures, to increase the speed and efficiency of the extraction process.

In general, each of these procedures presents advantages: They are faster, an extract concentration step is not necessary, a minimal amount of solvents is used, so they are environmentally friendly, and cleaner extracts are obtained. Thus, when the extract is obtained, a separation technique such as chromatography, can be applied in order to analyze the sample qualitatively and quantitatively.

There are many publications showing the applications of SFE to the determination of polymer additives. Antioxidants such as Irganox 2246, BHT and others, as well as UV stabilizers such as Tinuvin P, have been effectively extracted with supercritical CO₂. Extraction conditions varied from 15 to 25 MPa at 60°C and with a total time of 30 min [1]. If microwaves are applied to extract these compounds, a mixture of sol-



Table 1 Common Additives Used in Plastic Products

Additive type	Chemical name	Commercial name
Antioxidants	Di- <i>t</i> -butyl- <i>p</i> -cresol	Bisphenol A
	Di-octadecyl (3,5-di- <i>t</i> -butyl-4-hydroxybenzyl)phosphate	Irganox 1093
	2,2'-Methylene bis (4-methyl-6- <i>tert</i> -butylphenol)	Irganox 2246
	Tris(2-methyl-4-hydroxy-5- <i>t</i> -butylphenyl)-butane	Topanol CA
	4,4'-Thio-bis (6- <i>t</i> -butyl- <i>m</i> -cresol)	Santonox
Light stabilizers	2-(2'-hydroxy-3,3,5-di- <i>tert</i> -amylphenyl)benzotriazole	Tinuvin 328
	Bis(2,2,6,6-tetramethylpiperidin-4-yl)sebacate	Tinuvin 770
	2-(2-Hydroxy-5-methylphenyl)-2 <i>H</i> -benzotriazole	Tinuvin P
	2-Hydroxy-4- <i>n</i> -octoxybenzophenone	Chimassorb 81
Plasticizers	Di(2-ethylhexyl) phthalate	DEHP
	Disononyl phthalate	DINP
	Di(2-ethylhexyl) adipate	DOA
	Dipropylene glycol dibenzoate	Benzoflex 9-88
	Tributyl- <i>O</i> -acetyl citrate	Citroflex A
	Tris(2-ethylhexyl) phosphate	TOP
	Tri-octyl trimellitate	TOTM
	Monoazo benzimidazole pigment	
Colorants	Pigment Red 176	
	Solvent Blue 97	
	Tetrabromobisphenol A	TBBA
Flame retardants	Hexabromocyclododecane	HBBD

vents can be used (acetone–heptane, for example) and time is considerably reduced (from 3 to 6 min).

Phthalate plasticizers are extracted with the same supercritical fluid at a pressure of 48 MPa at 95°C for the same amount of time [2]. Other phthalate plasticizers, such as TOP and TOTM are extracted from poly(vinyl chloride) (PVC) by ASE with ether at 100°C for 20 min.

Characterization of Polymer Additives with Chromatographic Techniques

There are several techniques that can be used for the determination of polymer additives after extraction; for example, high-performance liquid chromatography (HPLC), supercritical fluid chromatography (SFC), and high-temperature capillary gas chromatography (GC) are the most widely used. Capillary gas chromatography is especially useful because it combines high resolution with the possibility of coupling the instrument with some sophisticated detection techniques, such as mass spectrometry (MS), Fourier transform infrared (FTIR), or atomic emission detection (AED). MS is the most suitable detector for GC; it is very easy to prepare a personal spectral library for identification of separated species. There are also commercially available spectral libraries. Apart from

the fact that the versatility of GC is due to its detectors, the injection systems provide a higher number of applications; for instance: on-column, split/splitless, and headspace techniques, among others. Today, almost every organic substance can be analyzed by gas chromatography, because of the development of high-temperature injectors. The combination of SFC with MS is also useful. In some cases, an on-line extraction is used, such as SFE–SFC [3].

The case of HPLC is quite different, because of the peak broadening or, sometimes, when the additives cannot be eluted from the stationary phase. However, it is a very useful technique when analyzing high-molecular-weight additives and, in combination with diode-array detection, provides an important tool for qualitative analysis. An important application is the determination of organic colorants in cosmetics [4]. HPLC is also applicable for the determination of linear and cyclic derivatives from poly(ethylene terephthalate), extracts of which were obtained using supercritical CO₂ [5].

Other Detection Systems

The analysis of extracts is also possible by using other techniques, such as infrared spectrometry. This kind of detector is very useful because it provides a total



spectrum for the analyte. For example, a method for analyzing poly(dimethylsiloxane) oil from polymer samples was developed by Kirschner et al. [6]. In this case, the extractor is directly coupled to the spectrometer. However, it is also possible to carry out off-line analyses with high recoveries. This combination was also used by Raynor et al. [7] in order to analyze some UV stabilizers such as Tinuvin 770, Irganox 1010, and Topanol OC. In this case, a preliminary separation was carried out by supercritical fluid chromatography.

References

1. P. J. Arpino, D. Dilettato, K. Nguyen, and A. Bruchet, Investigation of antioxidants and UV stabilizers from plastics. Part I: Comparison of HPLC and SFC; preliminary SFC/MS study, *J. High-Resolut. Chromatogr.* **13**: 5–12 (1990).
2. M. L. Marín, A. Jiménez, V. Berenguer, and J. López, Optimization of variables on the supercritical fluid extraction of phthalate plasticizers, *J. Supercrit. Fluids* **12**: 271–277 (1998).
3. H. Daimon and Y. Hirata, Directly coupled supercritical fluid extraction/capillary supercritical-fluid chromatography of polymer additives, *Chromatographia* **32**: 549–554 (1991).
4. S. C. Rastogi, V. J. Barwick, and S. V. Carter, Identification of organic colorants in cosmetics by HPLC–diode array detection, *Chromatographia* **45**: 215–228 (1997).
5. St. Küppers, The use of temperature variation in supercritical fluid extraction of polymers for the selective extraction of low molecular weight components from poly(ethylene terephthalate), *Chromatographia* **33**: 434–440 (1992).
6. C. H. Kirschner, S. L. Jordan, L. T. Taylor, and P. D. Seemuth, Feasibility of extraction and quantification of fiber finishes via on-line SFE/FT-IR, *Anal. Chem.* **66**: 882–887 (1994).
7. M. W. Raynor, K. D. Bartle, I. L. Davies, A. Williams, A. A. Clifford, J. M. Chalmers, and B. W. Cook, Polymer additive characterization by capillary supercritical fluid chromatography/Fourier transform infrared microspectrometry, *Anal. Chem.* **60**: 427–433 (1988).



Polymer Degradation in GPC–SEC Columns

Raniero Mendichi

Instituto di Chimica delle Macromolecole (CNR), Milano, Italy

Introduction

Size-exclusion chromatography (SEC) is a well-established method for the determination of the molar mass distribution (MMD) of polymers. However, the determination of the MMD by SEC substantially excludes ultrahigh-molar-mass (UHMM) polymers. Actually, it is well accepted that UHMM polymeric samples degrade, by shearing or elongational forces, in the SEC columns. The upper limit of the molar mass for a successful SEC fractionation without degradation of the sample depends on the broadness of the MMD of the sample, from the SEC columns used and, obviously, from the experimental conditions. Successful SEC fractionations of narrow MMD standards up to 1×10^7 g/mol of molar mass have been reported. Instead, when the MMD of the sample is broad, rarely does the molar mass of the polymeric samples exceed the upper limit of 1×10^6 g/mol.

Discussion

Whenever SEC fractionation has been applied to UHMM polymers, severe problems, strongly interrelated, have been invariably reported. The degradation of UHMM polystyrene during SEC fractionation in a good solvent has been often reported. The degradation of some other UHMM synthetic polymers [polyethylene, polyisoprene, polyacrylamide, polyisobutylene, poly(methyl methacrylate), etc.] has been reported. Besides, the degradation of some natural polysaccharides such as hyaluronic acid has been reported. The possible degradation of the polymeric sample is not the only problem of the SEC fractionation of UHMM polymers. The degradation of the UHMM sample in the SEC columns is often accompanied by some other important problems, such as (a) concentration effects, (b) anomalous flow, (c) poor column resolution (band broadening), and (d) very poor reproducibility.

Generally, the practical difficulties in the SEC fractionation exponentially increase with the polymer molecule's dimension, hydrodynamic volume, hence with the molar mass and the conformation, stiffness, of

the polymer. For many years, SEC has been considered inadequate for the fractionation of UHMM polymers. In the past, there have been many theoretical and experimental studies [1,2] to elucidate a better knowledge of the degradation of UHMM polymers. Furthermore, there have been notable improvements in the SEC column's performance. At this time, there are commercially available SEC columns specifically designed for the fractionation of UHMM polymers.

Evidence of the degradation of the polymeric sample may be found by using qualitative and quantitative methods. From a qualitative point of view, an accurate analysis of the chromatogram of a series of narrow MMD standards with increasing molar mass, under identical analytical conditions, would be self-evident. The resolution of the SEC columns, almost in the low-molar-mass range, generally is very good. In the high-molar-mass range, $M > 1 \times 10^6$ g/mol, the resolution of the SEC columns quickly decreases. In the presence of the degradation of the sample, the resolution of the SEC columns is poor or absent. Furthermore, the peak shapes of degraded UHMM narrow standards is abnormally broad with a severe tailing. Obviously, we assume the absence of nonsteric fractionation. To find evidence of the degradation of broad MMD samples is more difficult. The analysis of the peak shape of a broad MMD sample requires experience. Generally speaking, a chromatogram that presents too steep slopes, shoulders, excessive tailing, or multipeaks is suspect from the point of view of the degradation of the sample. Obviously, the origin of these anomalous shapes of the chromatogram could be different. Concentration effects and anomalous flow often accompany the degradation of the sample. The qualitative analysis is used only to identify the problem.

A quantitative analysis of the degradation of the sample substantially requires the use of an on-line absolute detector such as light scattering (SEC–LS). In this case, the on-line LS detector directly measures, without calibration, the molar mass of the sample. The characterization of a series of narrow MMD standards with increasing and known molar mass evidences the degradation of the sample. The simple direct comparison of the known molar mass of the standards and the



molar mass value obtained from the LS detector provides an estimate of the extent of the degradation under the experimental conditions used. Furthermore, if the dispersity D of the standards is very narrow (i.e., $D \leq 1.05$), the central part of the $M = f(V)$ plot, where M is the molar mass and V the elution volume, of each standard from the LS detector could be substantially flat. In fact, the central part of the peaks of the standards could be considered homogeneous in molar mass and the residual broadness of the peak is substantially due to the band broadening of the system. In the presence of degradation of the sample, the $M = f(V)$ plot of a narrow standards is not flat ($M = \text{constant}$) but steep. The method could be used to set up the experimental condition (columns set, flow rate, sample concentration) to avoid the degradation of the sample.

Figure 1 shows the experimental $M = f(V)$ plot of a narrow MMD polystyrene (PS) standard ($M = 1.15 \times 10^7$ g/mol, $D = 1.03$) from an on-line LS detector. The experimental conditions were as follows: one column, packed with 16- μm spherical particles of porous silica; tetrahydrofuran as the mobile phase; 0.8-mL/min flow rate; 0.1 mg/mL of sample concentration; 100- μL injection volume. Figure 1 evidences the quick decrease of the molar mass of the sample due to the degradation of the UHMM PS sample in the column. A fractionation with the identical experimental conditions, column, and concentration and a 0.2-mL/min flow rate shows a constant $M = f(V)$ plot (i.e., the absence of degradation).

The origin of the degradation of the sample could be in the SEC columns and, for UHMM polymers, also in some other critical part (detector cell, long narrow capillary tube, injector, etc.) of the fluidic system. The extent of degradation also depends on the experimen-

tal conditions, particularly the flow rate and the concentrations of the polymeric solutions. In an SEC column, there are three parameters that have to be optimized for a successful fractionation of UHMM polymers. Two parameters are related to the packing of the column: particle size and pore size. The last parameter, often incorrectly ignored, is the dimension of the pores of the inlet and outlet frits of the column. It is well accepted that for a successful fractionation of UHMM polymers, one must use SEC columns with the diameter of the particles larger than 10 μm . In organic solvents, 20- μm particle columns are customarily used. However, in aqueous solvent, there are commercially available 15- μm nominal, maximum 17- μm particle columns. Obviously, the efficiency of the column quickly decreases with the increase of particle size. As usual, one needs to find a reasonable compromise between discordant effects.

The influence of the pore size on the degradation of the sample is not generally accepted. However, to obtain a meaningful fractionation on the basis of the dimension of the macromolecules, it is necessary that the pore size be higher than the dimensions of the molecules. The maximum dimension of UHMM macromolecules could be of several hundreds of nanometers. Polymer degradation strongly decreases with the large pore size of the frits of the columns. The commercially available 20- μm -particle SEC columns commonly use 10- μm inlet and outlet frits. Finally, it is very important to remember that partially obstructed frits could cause strong polymer degradation.

Also, the experimental conditions have to be optimized to avoid the degradation of UHMM samples. Particularly, the flow rate and concentration of the sample are two critical parameters. Polymer degradation strongly increases with the increase of the flow rate. For a successful fractionation of UHMM macromolecules, it is necessary to use a very low flow rate. With UHMM macromolecules, it is not unusual to use a flow rate of 0.2 mL/min or less.

The influence of the polymer concentration is well known in SEC. Theoretically, SEC assumes independence of the elution volume with regard to the concentration of the molecular species. Practically, it is well known that a high concentration of the sample solution leads to distortion of the polymer peak and dependence of the elution volume on the concentration of the sample. The “concentration effect” [3] depends on the difference in molecular mobility between the pure solvent and the viscous polymeric solution. This difference causes nonuniform flow, often called “viscous fingering,” and, as a result, multiple peaks. In addition, it is

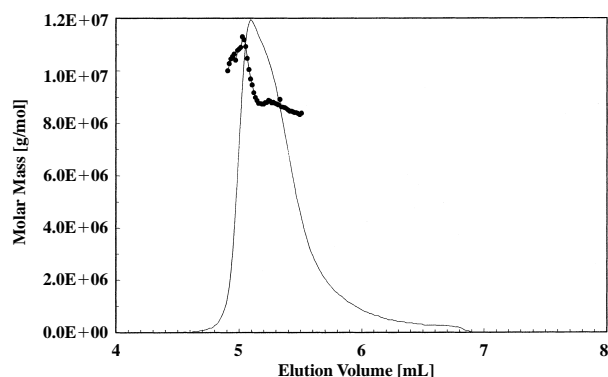


Fig. 1 Experimental $M = f(V)$ plot from an on-line LS detector.

well known that a high sample concentration decreases the hydrodynamic volume of the macromolecules. SEC fractionation is based on the hydrodynamic volume of the macromolecules; hence, this effect causes the dependence of the elution volume on the concentration, at least for high-molar-mass polymers.

The concentration, with UHMM macromolecules, also influences the degradation of the sample. Hence, in the fractionation of UHMM polymers, the concentration is very critical and has to be as low as possible. A sample concentration of 0.1 mg/mL or less is not unusual with UHMM polymers. In this case, it is necessary to use the minimal sample concentration that is consistent with the sensitivity of the concentration detector.

To avoid the degradation of the sample, some authors suggest the use of an ideal “theta” solvent as the mobile phase [4]. It is well known that the dimension of the macromolecules depends on the expansion factor α (excluded volume). For an ideal theta solvent, $\alpha = 1$ and the dimension of the macromolecules is minimal. For many polymers, an ideal theta solvent is known. For example, cyclohexane at 34.0°C is an ideal solvent for polystyrene polymers. For a polyelectrolyte polymer, ideal solvent means infinite ionic strength. Obviously, this condition is impracticable. Nevertheless, for example, the dimension of the macromolecules of an hyaluronic acid, anionic polymer, sample ($M = 7.4 \times 10^6$ g/mol) approximately decreases 20% when the solvent is changed from 0.15M to 0.5M NaCl. The use of ideal solvents to avoid the degradation of the sample is not generally accepted. In fact, using ideal solvents as the mobile phase could cause absorption of the polymer onto the column's packing. Also, some authors hypothesize that the degradation of the sample could also increase with ideal solvents.

At equilibrium conditions, at very low concentration, the elution volume of a macromolecule should be independent of the flow rate. However, with increasing molar mass in the UHMM range, in the absence of degradation, the elution volume strongly depends on the molar mass of the sample. This result does not de-

pend on the concentration of the sample. This “retardation” effect occurs also at very low concentrations below the overlapping concentration c^* . The “retardation” of UHMM macromolecules has been studied by several workers [5,6]; it is a very complex effect and substantially still not well understood. The “retardation” effect is particularly meaningful in proximity to the exclusion limit of the columns and when the pore size approximately equals or is lower than the sizes of the macromolecules. A trivial conclusion is that for a successful fractionation of UHMM macromolecules without “retardation” effects, one must use SEC columns with ultralarge pore sizes.

Degradation of the sample and related problems, such as the “concentration effect” and anomalous flow, are the more important problems in the fractionation of UHMM polymers. The critical point in the characterization of the UHMM polymers is the fractionation in the SEC columns. For a successful fractionation of UHMM macromolecules, one must use specifically designed SEC columns with large particle sizes and ultralarge pore sizes. Furthermore, many aspects of the experimental protocol, such as flow rate and sample concentration, which is not critical in the usual molar mass range, become determining with UHMM polymers. A successful characterization of UHMM polymers requires optimization of the experimental protocol. Each step of the experimental protocol should be performed methodically to achieve the absence of sample degradation and reliable results.

References

1. F. J. Bueche, *J. Appl. Polym. Sci.* 4: 101 (1960).
2. J. C. Giddings, *Adv. Chromatogr.* 20: 217 (1982).
3. A. Rudin and R. A. Wagner, *J. Appl. Polym. Sci.* 20: 1483 (1976).
4. L. Soltes, D. Berek, and D. Mikulasova, *Colloid & Polym. Sci.* 258: 702 (1980).
5. E. V. Chubarova and V. V. Nesterov, *ACS Symp. Ser.* 635: 127 (1996).
6. W. Cheng and D. J. Hollis, *J. Chromatogr.* 40: 9 (1987).



Polymerase Chain Reaction Products: Analysis Using Capillary Electrophoresis

Mark P. Richards

Growth Biology Laboratory, USDA-ARS-ANRI, Beltsville, Maryland, U.S.A.

Introduction

It is now possible to routinely analyze very small amounts of DNA using a procedure known as the polymerase chain reaction (PCR) [1]. PCR involves repeatedly subjecting a buffered salt solution containing deoxyribonucleotide triphosphates (dNTPs), two strand-specific oligonucleotide primers, a thermal-stable DNA polymerase enzyme (Taq), and a small amount of the DNA to be analyzed to a three-step temperature cycle. Using PCR, discrete regions of the source DNA molecules are copied and amplified by the repetitive cycling to readily detectable levels. It is also possible to analyze RNA sequences with PCR after an initial DNA strand (cDNA) and one complementary to it are produced from the original RNA template by the reverse transcription (RT) reaction [2]. The combined process, RT-PCR (also referred to as RNA-PCR), has been effectively used to study small amounts of RNA, such as individual messenger RNAs (mRNAs) or viral RNA, present in tissues and physiological fluids. Both PCR and RT-PCR produce double-stranded DNA (dsDNA) fragments of various sizes which are subsequently isolated and characterized by a number of qualitative and quantitative methodologies.

Discussion

The most common method of analyzing PCR and RT-PCR products involves separating a portion of the reaction mixture by agarose slab gel electrophoresis with ethidium bromide staining to detect the presence of the amplified dsDNA fragments [3]. There are several disadvantages associated with slab-gel techniques, including the following:

1. Gel casting and handling are costly, labor intensive, and not readily automated.
2. A significant portion of the PCR or RT-PCR sample is typically consumed by this mode of analysis.

3. Buffer and reagent consumption, and hazardous waste generated from the use of radioactive probes and ethidium bromide stain, can be considerable.
4. Quantitation requires additional steps and instrumentation for gel imaging and analysis.

During the past decade, capillary electrophoresis (CE)-based techniques have been developed and refined for the analysis of dsDNA products of PCR and RT-PCR [4–7]. CE has several advantages over conventional slab-gel separation techniques, including the following:

1. Capillary electrophoresis instrumentation is fully automated with respect to sample injection, separation, on-capillary detection, and post-run data analysis.
2. Because the separation is conducted in a narrow-bore capillary that facilitates Joule heat dissipation, higher field strengths can be used, resulting in enhanced resolution and shorter run times.
3. Very small amounts (nL) of sample are required for the analysis, thus preserving more of the original sample for subsequent procedures, such as cloning or sequencing.

Considering the expanding base of CE applications, it is becoming clear that the majority, if not all, of conventional slab-gel separation techniques can be readily adapted to capillary format. Analysis of PCR products by CE is becoming more routine and it will likely become one of the primary applications of CE in the area of DNA separations [6]. This entry describes the use of CE-based techniques for the analysis of dsDNA products from PCR and RT-PCR.

Table 1 summarizes selected parameters that are important for establishing a robust and reproducible technique for the separation and quantification of dsDNA products of PCR and RT-PCR using CE. Important advances have been made in a number of areas, including capillary coatings, sieving gel matrices,



Table 1 Analysis of PCR Products by CE: Selected Technique Parameters

Capillaries
Untreated (bare fused silica): not frequently used
Coated: polyacrylamide, polysiloxane (e.g., DB-1, DB-17), polyvinyl alcohol
Separation Matrix
Buffer: 89–100 mM Tris-boric acid, 2 mM EDTA, pH 8.2–8.5 (1X TBE)
Sieving gel
Chemical (fixed) gels: cross-linked polyacrylamide, bonded to capillary wall
Replaceable Gels (entangled polymer networks): linear polyacrylamide, methyl cellulose, hydroxypropylmethyl cellulose, hydroxyethylcellulose, polyethylene oxide, polyvinyl alcohol, agarose
Intercalating dyes: 9-aminoacridine (nonfluorescent), ethidium bromide, TOTO, YOYO, YO-PRO-1, TO-PRO-1, TO-PRO-3, SYBR Green I, Enhance™
Sample injection
Hydrodynamic: high reproducibility; useful for quantitative analyses; direct injection of untreated samples possible
Electrokinetic: affected by sample salt concentration (i.e., Cl^-); prior dialysis or dilution of the sample required
Detectors
Ultraviolet (UV): 254–260 nm, least sensitive
Laser-induced fluorescence (LIF): up to 1000× more sensitive than ultraviolet
Data analysis
Qualitative: optimization of PCR conditions and product characterization
Quantitative:
Relative: ratio of product (target) to “housekeeping” gene or other heterologous dsDNA internal standard
Competitive: ratio of product (target) to homologous, modified internal standard (competitor); most accurate estimate
Applications
Clinical/diagnostic: screening for genetic abnormalities and diseases
Forensic: human identity testing
Biotechnology: genetic analysis, gene expression, genotyping

and high-sensitivity detection methods. Because of a nearly identical linear negative charge density at neutral pH and above, dsDNA molecules exhibit an electrophoretic mobility in free solution that is independent of molecular size [3]. Therefore, a gel or sieving matrix is required to effect a separation based on molecular size and, for that reason, capillary gel electrophoresis (CGE) has become the specific separation mode most often used for PCR product analysis. Because of the negative charge on DNA molecules, uncoated (bare fused silica) capillaries, which above pH 7 exhibit a strong electro-osmotic flow (EOF) in the direction of the cathode, are rarely if ever used. Instead, capillaries treated with a specific interior surface coating to greatly reduce or completely eliminate EOF are routinely employed in the separation of DNA, a process that is conducted in reversed polarity mode (i.e., cathode at the capillary inlet side). Capillary surface coatings can either be covalently bound to the surface or dynamically adsorbed to the wall. Examples of typical surface coatings include polyacrylamide, polysiloxanes (dimethyl and phenyl–methyl), cellulose derivatives, and polyvinyl alcohol [4–7].

Early CGE separations of dsDNA made use of capillaries in which a polyacrylamide gel was polymerized

in and linked to the wall of the capillary, producing what has been referred to as a fixed or chemical gel [4–7]. Although such gels are capable of extremely high resolution due to a well-controlled pore size, they are not commonly used for PCR product analysis because of the problems related to air bubble formation and limited useful lifetime [5]. The development of replaceable sieving gels (also referred to as entangled polymer networks) that can be flushed from the capillary after the separation is complete has been one of the major factors in establishing CGE as a routine method for PCR product analysis. With this system of replaceable gels, a “new” gel is used for each separation. Some of the most widely used replaceable gel compounds include linear polyacrylamide, alkyl-celluloses, polyethylene oxide, agarose, and polyvinyl alcohol [4–7]. These polymer compounds are employed to produce viscous buffered solutions that enable the separation of dsDNA in a capillary based on molecular size [5]. In general, the pore size and, hence, the resolving capacity for dsDNA molecules are controlled by simply manipulating the gel concentration.

One factor that initially hampered the direct analysis of PCR samples by CGE was the presence of high levels of salt, especially chloride ions, in the samples in-

jected into the capillary. Electrokinetic injection, which is the requisite loading method when using fixed gels, is severely affected by the presence of high salt concentration because it impairs the loading of dsDNA into the capillary. Although PCR samples can be injected directly into capillaries using replaceable gels, the presence of salts adversely affects the quality of the results obtained. Also, the presence of other components in the PCR sample (dNTPs, primer oligonucleotides, etc.) not only affect the separation, but they can also obscure peaks when ultraviolet (UV) detection is employed. Fortunately, two relatively simple cleanup methods have been devised to counteract the effects of the PCR sample matrix. The two most common methods are sample microdialysis (float dialysis) and dilution of the sample (20–100-fold) with deionized water prior to CGE [6]. Both methods are effective in reducing the adverse effects of salts, but sample dilution necessitates the use of high-sensitivity detection to compensate for the reduction in the dsDNA concentration.

An important development in CE technology that has helped to promote the analysis of PCR products by CGE is the introduction of laser-induced fluorescence (LIF) detection [4–7]. Because LIF can increase the sensitivity of detection for dsDNA by more than 400-fold over UV detection, it has become the method of choice for the vast majority of dsDNA separations [5]. A practical illustration of the advantage of LIF detection is that typical separations of PCR products by slab-gel electrophoresis with ethidium bromide staining require approximately 5 ng of DNA per band for adequate detection, whereas, with CGE–LIF, subpicogram levels of DNA are readily detected [6].

In order to employ LIF detection, it is necessary to label the dsDNA molecules with a fluorescent compound prior to and/or during their separation by CGE. Two approaches have been employed. The first, and most common, involves the incorporation of an intercalating dye into the separation gel buffer (and, in some cases, into the sample loading buffer), which is highly fluorescent only when bound to dsDNA. Table 1 lists a number of commonly used intercalating dyes. Both monomeric and dimeric dyes have been developed and used to detect PCR products [8]. They offer unique advantages in that they enhance detection sensitivity two to three orders of magnitude over UV detection, and separation resolution and selectivity are often improved with their inclusion [4]. A second approach involves labeling of the primers used in PCR with a fluorophore, such as fluorescein, to produce 5'-end-labeled dsDNA products that can be separated and detected by CGE–LIF. The former approach of-

fers the highest sensitivity with the amount of intercalating dye bound proportional to the size of the dsDNA fragment (i.e., the larger the fragment, the more dye will be bound). Not only do intercalating dyes label the dsDNA for detection, but they also can enhance the selectivity and resolution of dsDNA fragments of similar size [4,6]. Intercalating dyes can also produce anomalous effects on peak shape, depending on such factors as their concentration in the separation or sample buffer and certain sequence-dependent properties of the dsDNA (e.g., %GC composition). These effects result from the binding and retention of differing amounts of dye molecules by the dsDNA fragments during CGE. Therefore, care must be taken to carefully evaluate the use of a specific intercalating dye with a particular PCR product in order to generate reproducible results.

Capillary gel electrophoresis–LIF analysis of PCR and RT–PCR products has been applied to the areas of clinical diagnostics, forensics, and biotechnology. Screening of patients for genetic and infectious diseases, human identity testing using PCR-amplified DNA fragments from specific polymorphic genomic regions (loci) defined by a variable number of tandem repeats (VNTRs) or short tandem repeats (STRs), analysis of mitochondrial DNA, genotyping, and gene expression studies are only a few examples of these applications [4–7]. The types of results that can be gained from CGE analysis of PCR products are twofold. First, CGE is useful in a qualitative evaluation of PCR by separating target DNA from nonspecific products and demonstrating that a single dsDNA fragment resulted from the amplification. CGE is also a rapid method of evaluating various PCR parameters (e.g., cycle number, temperature, $[Mg^{2+}]$, [dNTPs], etc.) for optimizing the efficiency of the reaction. Another use for CGE is to accurately determine the size of the PCR products. This approach has been applied to DNA profiling in human subjects by an assessment of PCR amplified alleles resulting from VNTRs and STRs [6].

The ability to do on-capillary detection and to calculate integrated peak areas from the collected data makes CGE–LIF very useful for the quantification of PCR- and RT–PCR-generated dsDNA products. The quantity of the amplified product can be indicative of the efficiency of PCR and this information can be used to optimize the reaction. Such information is also useful in determining the amount of a specific DNA or RNA present in the analyzed sample. Quantitation can be achieved by relative or absolute estimates. A ratio of target DNA peak area to the peak area of an added dsDNA internal standard gives an estimate of the relative amount of target DNA generated by PCR.



Internal-standard dsDNAs can derive from genes that remain at constant levels in the sample (are unaffected by experimental treatments), such as the so-called "housekeeping" genes or they can be added amounts of a known quantity of a purified and well-characterized dsDNA, such as restriction enzyme digest fragments of genomic DNA. For example, the digestion of ϕ X174 bacteriophage DNA with *Hae*III produces 11 distinct dsDNA fragments ranging in size from 72 to 1353 bp [6]. The latter type of standardization also affords the opportunity to accurately determine the size of the PCR product in addition to estimating its quantity when appropriate standards are chosen. Such standards can be obtained from commercial sources.

The most accurate means for quantitation of PCR products, especially those of low copy number, involves a method known as competitive PCR. In quantitative-competitive PCR (QC-PCR), known amounts of an internal standard (competitor) are co-amplified along with an unknown amount of target DNA. The competitor's sequence is chosen to be nearly identical to that of the target except for a small addition or deletion of sequence. The competitor is designed to use the same set of primers as the target so that a competition for them develops. Because the target and competitor are exposed to identical PCR conditions, the ratio of the two products should remain constant even after the reaction has reached its plateau phase. Thus, by plotting the different competitor/target peak area ratios against the amount of added competitor and extrapolating from the point at which the ratio is equal to 1, the amount of target DNA in the original sample can be determined in absolute terms. For RT-PCR, a competitor RNA is used to correct for variable conditions in both the RT and PCR steps [9,10].

Figure 1 depicts a scheme for the estimation of leptin mRNA (encoded by the obese gene, *ob*) contained in total RNA samples isolated from liver and adipose tissues of chickens. Using QC-RT-PCR with CGE-LIF, it was possible to derive absolute estimates (in attomoles) of leptin mRNA. Others have demonstrated a further extension of QC-RT-PCR with CGE-LIF called multiplexing, in which more than one competitor-target pair is subjected to co-amplification and subsequent analysis by CGE-LIF [9,11]. With multitarget QC-RT-PCR, it is possible to monitor PCR-amplified dsDNA corresponding to several genes simultaneously in a single sample assuming PCR conditions have been optimized for each product formed [11].

Future applications of CE to PCR product analysis will arise from improvements in CE instrumentation. Advances in miniaturization of CE devices by producing glass chips with etched channels of <1 cm in length

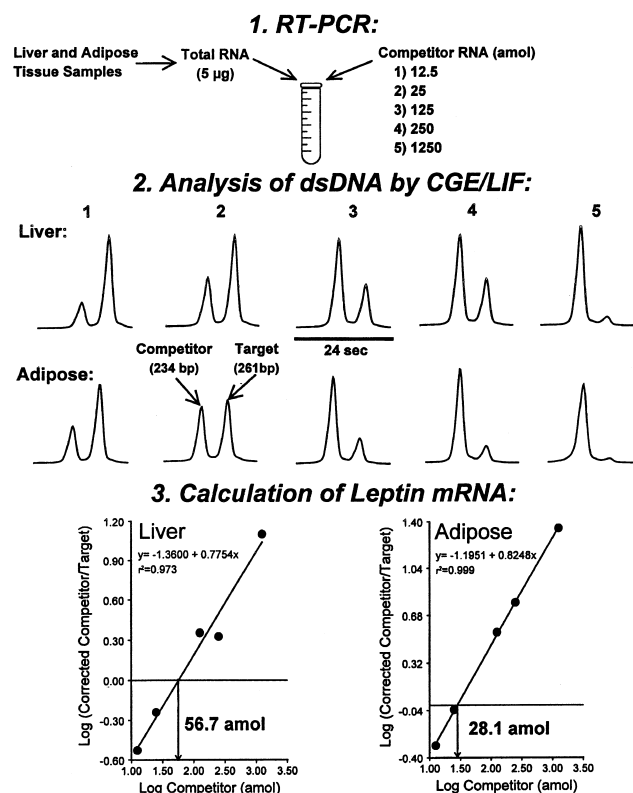


Fig. 1 Analysis of leptin gene expression in chicken liver and adipose tissue by QC-RT-PCR using capillary gel electrophoresis with laser-induced fluorescence detection (CGE-LIF). Target (261 bp) and competitor (234 bp) dsDNA amplicons were separated on a DB-1-coated capillary (27 cm \times 100 μ m inner diameter) at a field strength of 300 V/cm in a replaceable sieving matrix consisting of 0.5% HPMC in 1X TBE buffer with 0.5 μ g/mL Enhance™ intercalating dye. RT-PCR samples (1–2 μ L) were diluted 1:100 with deionized water and introduced into the capillary by electrokinetic injection. Separations were completed in under 5 min. A portion (4.4–4.8 min) of each separation shows the changes in the competitor and target peaks. CGE-LIF was more sensitive in detecting both amplicons than agarose slab gel electrophoresis with ethidium bromide staining. The integrated peak area ratio of competitor/target for a series of five individual samples (to which increasing amounts of a synthetic competitor RNA were added prior to RT-PCR) is used to calculate the amount of leptin mRNA (amol) in total RNA isolated from liver and adipose tissue by linear regression analysis.

have already been demonstrated as a feasible method for ultrafast (<45 s) separations of dsDNA [4–7]. The use of multiple capillaries or capillary arrays has proven to be useful in dedicated devices for DNA sequencing [4–7]. Recently, it has been possible to integrate PCR amplification and CE separation in a single

device using an array of eight capillaries for high sample throughput [12]. This technology will undoubtedly produce dedicated CE instruments for PCR product analysis that will feature rapid run time and high throughput. New detection methods such as mass spectrometry offer the promise of increases in selectivity, detection sensitivity, and more accurate quantification of PCR products. It is now clear that, in the future, CE-based analyses of PCR products will continue to get faster and more reliable while achieving wider acceptance by biomedical and biotechnology laboratories.

References

1. K. B. Mullis and F. A. Faloona, *Methods Enzymol.* 155: 335–350 (1987).
2. J. Chelly and A. Kahn, RT–PCR and mRNA quantitation, in *The Polymerase Chain Reaction* (K. B. Mullis, F. Ferre, and R. A. Gibbs, eds.), Birkhauser, Boston, 1994, pp. 97–109.
3. A. E. Barron and H. W. Blanch, *Separ. Purif. Methods* 24: 1–118 (1995).
4. A. Guttman and H. E. Schwartz, Separation of DNA, in *Capillary Electrophoresis Theory and Practice*, 2nd ed. (P. Camilleri, ed.), CRC Press, Boca Raton, FL, 1998, pp. 397–439.
5. K. J. Ulfelder and B. R. McCord, Separation of DNA by capillary electrophoresis, in *Handbook of Capillary Electrophoresis*, 2nd ed. (J. P. Landers, ed.), CRC Press, Boca Raton, FL, 1997, pp. 347–378.
6. J. M. Butler, Separation of DNA restriction fragments and PCR products, in *Analysis of Nucleic Acids by Capillary Electrophoresis* (C. Heller, ed.), Verlag Vieweg, Wiesbaden, 1997, pp. 195–217.
7. P. G. Righetti and C. Gelfi, Capillary electrophoresis of DNA, in *Capillary Electrophoresis in Analytical Biotechnology* (P. G. Righetti, ed.), CRC Press, Boca Raton, FL, 1996, pp. 431–476.
8. J. Skeidsvoll and M. Ueland, *Anal. Biochem.* 231: 359–365 (1995).
9. M. Fasco, C. P. Treanor, S. Spivack, H. L. Figge, and L. S. Kaminsky, *Anal. Biochem.* 224: 140–147 (1995).
10. N. D. Borson, M. A. Strausbauch, P. J. Wettstein, R. P. Oda, S. L. Johnston, and J. P. Landers, *Biotechniques* 25: 130–137 (1998).
11. W. Lu, D. S. Han, J. Yuan, and J. M. Andrieu, *Nature* 368: 269–271 (1994).
12. N. Zhang, H. Tan, and E. S. Yeung, *Anal. Chem.* 71: 1138–1145 (1999).



Polynuclear Aromatic Hydrocarbons in Environmental Materials: Extraction by Supercritical Fluid Extraction

Maria de Fatima Alpendurada

Universidade do Porto, Porto, Portugal

INTRODUCTION

Supercritical fluid extraction (SFE), usually with carbon dioxide and, often, with a modifier, has become of increasing interest in the last few years because of its selectivity, preconcentration effect, efficiency, simplicity, rapidity, cleanness, and safety, mainly concerning the extraction of organic compounds prior to separation and detection by chromatographic techniques. It has several advantages over classical solvent extractions, in comparison with recent extraction techniques. Approaches to obtain quantitative extractions, including fluid choice, extraction flow rate, modifiers, pressure, and temperature, are presented, as well as the potential for SFE to extract polynuclear aromatic hydrocarbons (PAHs) from soils, sediments, and biota. Improvements and new environmental applications are also reported.

PARAMETERS INFLUENCING THE SUPERCRITICAL FLUID EXTRACTION PROCESS AND APPLICATIONS

Since the first applications of SFE were published by Zosel in 1978, this extraction technique has developed into a key method for the separation of the contaminants from both sediment and biological matrices. Supercritical fluid extraction has a number of advantages over classical solvent extraction methods: It is faster, more selective, and less toxic, particularly when compared with techniques using solvents such as dichloromethane, thus reducing safety hazards. It has received the attention of some researchers who have reviewed and developed this technique and its suitability to the analysis of environmental matrices.^[1–3] The application of SFE to PAHs was reviewed, and new analytical strategies involving the need for modified supercritical fluids to improve extraction efficiency, restrictor prevention from blocking, collection form of the eluant, and general operation conditions, has been demonstrated. This technique is radically different from liquid–solid extraction (LSE), subcritical water extraction, microwave-assisted extraction (MAE), and accelerated solvent extraction (ASE)—also known as pressurized liquid extraction or pressurized fluid

extraction—because the main constituent of the solvent system, CO₂, separates from the extracts upon venting to the atmosphere, leaving the analytes that are trapped either on a solid phase, such as C₁₈, or in an organic solvent. The influence in the extraction process of various parameters will depend on a number of steps controlling the transport of analytes from the matrix to the bulk fluid, e.g., temperature, pressure, solvent type, and extraction time. Interested readers should consult an excellent review regarding the mechanisms controlling the binding, release, and transport in environmental materials.^[4] Supercritical fluid extraction, at low (50°C) and high (200°C) temperatures, and an 18-hr Soxhlet extraction with dichloromethane for railway soil and diesel soot samples were compared for the PAHs extraction.^[5] The samples were mixed with anhydrous Na₂SO₄. The mean recoveries for the 17 PAHs examined in the railway soil was 50% at 50°C, 81% at 200°C, and 90% at 350°C. For the diesel soot, the recovery for 13 PAHs was 51% at 50°C, 71% at 200°C, and 118% at 350°C. Although higher temperatures favored better recoveries for the higher-molecular-weight PAHs, it was also suspected that the two- to three-ring PAHs were actually generated at these elevated temperatures. So a 30-min extraction at 200°C was selected as the optimum. Temperature and organic modifiers—10% MeOH, diethylamine, and/or toluene—using a marine sediment (SRM 1941) diesel soot and air particulate matter (SRM 1649) were also examined. The best recoveries were obtained with CO₂–diethylamine at 200°C with a 15-min-static and 15-min-dynamic extraction time. Also, supercritical water at 250°C, CO₂ at 200°C, and CO₂ with 19% toluene at 80°C were compared for the extraction of PAHs from urban air. Surprisingly, the water was generally as effective as the other solvents under these conditions.^[2] However, unlike CO₂, the water had to be subsequently removed from the extract. After optimization of the SFE-CO₂ extraction method for PAHs, similar results were obtained by using the acetone with MAE, ASE with acetone/dichloromethane, or Soxhlet with dichloromethane.

The use of a binary modifier, which is added to the extraction cell at the time of the extraction, rather than continuously, in the CO₂ stream showed an almost matrix-independent SFE method for the PAHs.^[6] The



modifiers, diethylamine, trifluoroacetic acid, citric acid, isopropylamine, and tetrabutyl ammonium hydroxide, all individually at a 1% level in toluene, were tested for the extraction of CRM 392, sewage sludge, and marine sediment. The extractions were reproducible and comparatively complete and, with the correct binary modifier, did not require any prior matrix treatment, e.g., with HCl. Diethylamine at 200°C gave the highest recoveries to examine the effect on the SFE of PAHs from marine sediment, diesel soot, and air particulates. On-line coupling of an SFE system with a gas chromatography-mass spectrometry (GC-MS) instrument was performed by a homemade, suitably shaped accumulation cell,^[7] eliminating the effect of CO₂ flow on the MS detector. Moreover, it enables multistep extraction based on the direct addition of a modifier into the extraction cell. The quantitative determination of PAHs and other organic pollutants in sewage sludge was performed by using SFE as a fast extraction method, followed by a short cleanup step. The extraction step was validated with CRMs.^[8] Improving the extraction capacity of the supercritical fluid—higher temperature, higher pressure, stronger modifier effect—by using a ternary mixture of CO₂ modified with methanol/dichloromethane, 5:1, a more robust and applicable method to a larger range of matrices was obtained.^[9] Fernández et al.^[10] used an experimental design to optimize the SFE of PAHs from sediment. Under the optimum conditions, the recovery of total PAHs was ca. 15% higher with SFE than with the comparative Soxhlet extraction. A five-level factorial experimental design was used to examine the optimum conditions for the extraction of two- to six-ring PAHs from sediment with pressure, temperature, and organic modifier. Depending on the nature of the matrix and the concentration of the compounds to be determined, the SFE system can be directly connected to the detector. All of the different extraction techniques mentioned above can be used for the extraction of PAHs in very complex environmental materials. A very recently developed work

reported an extraction/cleanup procedure by SFE for biological samples (liver) and subsequent HPLC-FL determination of those compounds in the enriched extract.^[11]

COMMENTS ON THE EXTRACTION TECHNIQUES

Most recent studies on the previously discussed extraction techniques have made a direct comparison with the efficiency of Soxhlet extraction to validate the system used, effectively resulting in a benchmark method. Regarding these studies of extraction of PAHs from solid environmental samples, some overall observations can be made. With the exception of a few reports, the modern methods of extraction offer no greater efficiency than the centenary Soxhlet extraction method. Also, in terms of extraction, the extent of good agreement between data obtained by a wide range of extraction methods should suggest that there may not be any significant advantage with any particular method. Because one of the advantages of using MAE, ASE, and SFE is the use of small volumes of toxic organic solvents, in a number of cases the use of multiple extractions with a fresh change of solvent will approach the volume to the classical extraction method. Another apparent advantage of MAE, ASE, subcritical water extraction, and SFE is that the extractions are faster and, therefore, labor saving. The actual extraction cycle is short for MAE and ASE, ca. 5–10 min. However, for multiple extractions, there is little time between cycles for the analyst to undertake other tasks and also to attend the system while it is in use. The main advantage of Soxhlet extraction is that, once it has been set up, it can be left unattended for the full duration of the extraction, ca. 8–24 h. In many cases, the extent of the labor saved associated with MAE, ASE, and SFE is considerably exaggerated. Table 1 shows the conditions used to compare Soxhlet, ASE, SFE, and subcritical water

Table 1 Conditions used to compare Soxhlet, ASE, SFE, and subcritical water extractions of PAHs

Conditions	Soxhlet	ASE	SFE	Subcritical water
Sample size (g)	2	2	2	2
Extraction solvent	DCM–acetone	DCM–acetone	pure CO ₂	water
Collection solvent	–	–	DCM	toluene
Pressure (bar)	ambient	70	400	50
Temperature (°C)	b.p. of solvent	100	150	300, 250
Flow rate	15 min/cycle	1 ml/min	1 ml/min	1 ml/min
Time	18 hr	50 min	60 min	30, 60 min
Solvent volume (ml)	150	15	15	10, 20

These conditions were used for determination of PAHs in soil samples collected from an abandoned gas-manufacturing plant. (From Ref. [12].)

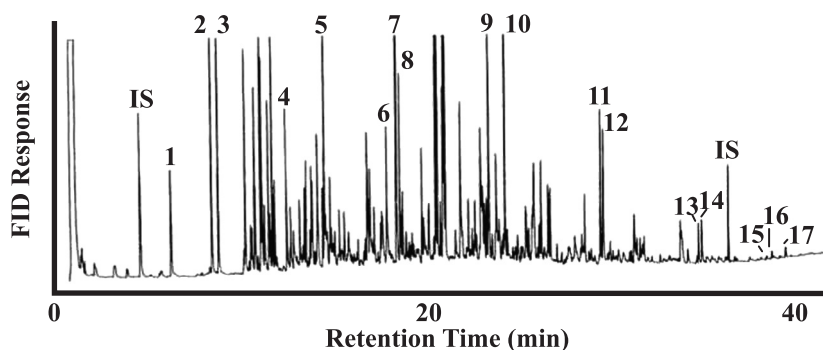


Fig. 1 Gas chromatography-flame ionization detection chromatogram of a complex mixture of PAHs extracted by SFE from a contaminated soil. (1) naphthalene; (2) 2-methylnaphthalene; (3) 1-methylnaphthalene; (4) acenaphthene; (5) fluorene; (6) dibenzothiophene; (7) phenanthrene; (8) anthracene; (9) fluoranthene; (10) pyrene; (11) benzo(a)anthracene; (12) chrysene; (13) benzo(e)pyrene; (14) benzo(a)pyrene; (15) indeno(1,2,3-cd)pyrene; (16) dibenzo(a,h)anthracene; (17) benzo(g,h,i)perylene. (From Ref. [12].)

extractions of PAHs. Also, the extraction quality greatly differed. In the case of Soxhlet and ASE, they were much darker, while extracts from subcritical water were orange, and the extracts from SFE (with CH_2Cl_2) were light yellow.^[12] The organic solvent extracts also yielded more artifact peaks in the gas chromatography-mass spectrometry and gas chromatography-flame ionization detection

chromatograms, especially when compared to supercritical CO_2 (Figs. 1 and 2). Based on elemental analysis (carbon and nitrogen) of the solid residues after each extraction, subcritical water, ASE, and Soxhlet extraction had poor selectivity for PAHs vs. soil organic matter ($\sim 25\text{--}33\%$ of the bulk solid organic matter was extracted along with PAHs), while SFE with pure CO_2

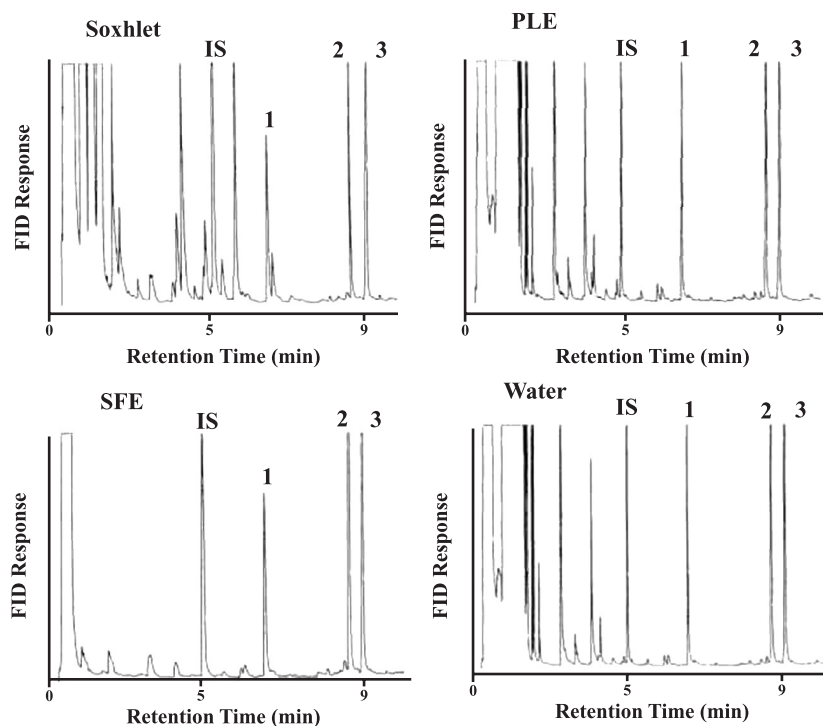


Fig. 2 Gas chromatography-flame ionization detection chromatograms containing early artifact peaks from different solvent extraction methods: Soxhlet, ASE (ple), SFE, and subcritical water extraction of a soil sample collected from a manufacturing gas plant site. The numbers refer to PAHs identified in the legend of Fig. 1. (From Ref. [12].)

Table 2 Extraction conditions for SFE of PAHs from different environmental materials

Matrix	Reference material	Extractant	Temperature (°C)	Pressure (bar)	Extraction		Solvent collection	Recovery (%)	Reference
					time (min)	Mode			
Marine sediment	NIST 1649	CO ₂ 100%	200	450	15+30	static + dynamic	DCM	–	[5]
Sediment	NRCC HS-6	CO ₂ 100% or + 3 × 20ul MeOH	70	200	15	dynamic	MeOH	80–100	[7]
Sewage sludge	CRM 088	CO ₂ 100% (step 1)	80	121	10+10	static + dynamic	toluene		[8]
		CO ₂ + 1% MeOH and 4% DCM (step 2)	120	335	10+30	static + dynamic	toluene		[8]
		CO ₂ 100% (step 3)	120	335	5+10	static + dynamic	toluene	104–122	[8]
Soil	–	CO ₂ + MeOH + DCM 5:1	95	450	15	dynamic	MeOH	90	[9]
Sediment	–	CO ₂ 100% or CO ₂ + 2 to 10% Methanol	140	340	15	dynamic	hexane	–	[10]
Soil	–	CO ₂ 100%	150	400	60	dynamic	DCM	>90%	[12]

The following abbreviations are used for organic solvents used: MeOH = methanol; DCM = dichloromethane.

removed only 8% of the bulk organic matrix. Neither MAE nor ASE is currently in a configuration that would readily lead to the automation of sample preparation. Supercritical fluid extraction can be used as on-line system that can then be connected to the chromatographic and detection systems. Connected on-line with the GC-MS, SFE was successfully used for the determination of PAHs in marine sediments. Using either CO₂ alone or modified with toluene or MeOH in the extraction, the PAHs were cryofocused in the accumulation cell of the GC and then directly chromatographed.^[7] For the study of PAHs in marine sediments, a new extraction technique, which consists of the combination of ASE (dynamic and static mode) and SFE (dynamic mode), was developed, with an extraction time longer than in ASE but shorter than in SFE, and better recoveries for five- to six-ring PAHs than in the conventional ASE and SFE.^[13] Polynuclear aromatic hydrocarbons in tap and river water were extracted by SFE, on-line, with solid-phase extraction disks.^[14] Table 2 presents the extraction conditions for SFE of PAHs from different environmental materials, as reported in the literature.

FUTURE TRENDS IN SUPERCRITICAL FLUID EXTRACTION

Supercritical fluid extraction with CO₂, whose most important benefits have already been mentioned, also

shows significant limitations that are worth studying to understand the field of application of the technique and to help in seeking alternatives in this context. The main drawbacks that SFE has to cope with are the difficulties in extracting polar analytes, the different efficiencies obtained from spiked and natural samples, and sometimes the need for a cleanup step before the analysis.^[12] To point out the future trends in this extraction technique, it is mandatory to consider the latest contributions in this area. The coupling of supercritical CO₂ with subcritical water is a very recent and promising alternative that has proven to successfully extract nonpolar analytes.^[14] The development of new analyte collection methods, with reduced solvent consumption resulting in more concentrated extracts, is also a target of current research. Another important future trend in SFE is the possibility of performing fieldwork.^[15] In this context, a single SFE method for field extraction of PAHs in soil has been developed for the U.S. Department of Defense and it is currently being tested. The approach uses dry ice (thus avoiding compressed CO₂ tanks), and works well for nonpolar analytes, but requires the use of modifiers for the extraction of polar analytes. Increased energy costs and regulatory requirements for waste reduction and site remediation have created increased interest in the benefits and application of SFE. Current research is being conducted to develop methods for application to large-scale soil remediation. Such applications will occur as the SFE knowledge base expands.^[16] Taking into account the

breakthroughs in other alternatives, such as ASE, MAE, and Soxhlet, before selecting SFE as a primary extraction method, its main benefits and limitations should be weighted. Thus considering the characteristics of the matrix and the analytes involved, the analyst must select the most appropriate alternative.

CONCLUSION

It has become clear that the environmental chemist should be more diligent in developing methods that are more environmentally friendly and provide a safer work environment. Following the Montreal Protocol, there is a gradual phasing out of the use of chlorinated solvents. While it has the major environmental impact in the dry cleaning and bulk chemical industry, it seems inappropriate to continue developing methods that require chlorinated solvents when, with a review of literature and some practice, suitable alternatives can be found. The accreditation bodies could play an important role to clearly move the existence of methodologies that use organic solvents.

In this context, SFE has a great potential for replacing older extraction methods, e.g., Soxhlet extraction. Despite important limitations described elsewhere, with the help of special strategies for the extraction of moderately polar and highly polar analytes, the SFE range of applications will dramatically increase in the near future.

REFERENCES

1. Camel, D.; Tambuté, B.; Caude, M. Analytical-scale supercritical fluid extraction: A promising technique for the determination of pollutants in environmental matrices. *J. Chromatogr., A* **1993**, *642* (1–2), 263–281.
2. Hawthorne, S.B.; Miller, D.J.; Burford, M.D.; Langenfeld, J.J.; Eckert-Tilotta, S.; Louie, P.K. Factors controlling quantitative supercritical fluid extraction of analytical samples. *J. Chromatogr., A* **1993**, *642* (1–2), 301–317.
3. Janda, V.; Bartle, D.K.; Clifford, A.A. Supercritical fluid extraction in environmental analysis. *J. Chromatogr., A* **1993**, *642* (1–2), 283–299.
4. Dean, J.R. Extraction of polycyclic aromatic hydrocarbons from environmental matrices: Practical considerations for supercritical fluid extraction. *Analyst* **1996**, *121*, 85R–89R.
5. Yang, Y.; Gharaibeh, A.; Hawthorne, B.; Miller, J.D. Combined temperature/modifier effects on supercritical CO₂ extractions efficiencies of polycyclic aromatic hydrocarbons from environmental samples. *Anal. Chem.* **1995**, *67*, 641–646.
6. Hawthorne, S.B.; Yang, Y.; Miller, J.D. Extraction of organic pollutants from environmental solids with sub- and supercritical water. *Anal. Chem.* **1994**, *66*, 2912–2920.
7. Fuoco, R.; Ceccarini, A.; Onor, M.; Lottici, S. Supercritical fluid extraction combined on-line with cold-trap gas chromatography/mass spectrometry. *Anal. Chim. Acta* **1997**, *346* (1), 81–86.
8. Berset, J.D.; Holzer, R. Quantitative determination of polycyclic aromatic hydrocarbons, polychlorinated biphenyls and organochlorine pesticides in sewage sludges using supercritical fluid extraction and mass spectrometric detection. *J. Chromatogr., A* **1999**, *852*, 545–558.
9. Gonçalves, C.; De-Rezende Pinto, M.; Alpendurada, M.F. Benefits of a binary modifier with balanced polarity for an efficient supercritical fluid extraction of PAHs from solid samples followed by HPLC. *J. Liq. Chromatogr. Relat. Technol.* **2001**, *24* (19), 2943–2959.
10. Fernández, I.; Dachs, J.; Bayona, M.J. Application of experimental design approach to the optimization of supercritical fluid extraction of polychlorinated biphenyls and polycyclic aromatic hydrocarbons. *J. Chromatogr., A* **1996**, *719* (1), 77–85.
11. Amigo, S.G.; Falcon, M.S.G.; Yusty, M.A.L.; Lozano, J.S. Supercritical liquid extraction of polycyclic aromatic hydrocarbons from liver samples and determination by HPLC-FL. *Fresenius J. Anal. Chem.* **2000**, *367* (6), 572–578.
12. Hawthorne, S.B.; Grabanski, C.B.; Martin, E.; Miller, D.J. Comparison of Soxhlet extraction, pressurized liquid extraction, supercritical fluid extraction and subcritical water extraction for environmental solids: Recovery, selectivity and effects on sample matrix. *J. Chromatogr., A* **2000**, *892*, 421–433.
13. Notar, M.; Leskovsek, H. Determination of polycyclic aromatic hydrocarbons in marine sediments using a new ASE–SFE extraction technique. *Fresenius J. Anal. Chem.* **2000**, *366* (8), 500–546.
14. Luque de Castro, D.C.; Jiménez-Carmona, M.M. Where is supercritical fluid extraction going? *Trends Anal. Chem.* **2000**, *19* (4), 223–228.
15. Bowadt, S.; Mazeas, L.; Millert, D.J.; Hawthorne, S.B. Field portable determination of polychlorinated biphenyls and polynuclear aromatic hydrocarbons in soil using supercritical fluid extraction. *J. Chromatogr., A* **1997**, *785*, 205–217.
16. Green, T.; Bonner, J.S. Environmental application of supercritical fluid extraction. *Danger. Prop. Ind. Mater. Rep.* **1991**, *11* (4), 304–310.

Porous Graphitized Carbon Columns in Liquid Chromatography

Irene Panderi

University of Athens, Athens, Greece

INTRODUCTION

Liquid chromatography is a separation technique which is used widely in many different areas of analytical chemistry and provides a powerful tool for the separation and quantification of substances in various matrices. Nowadays, the majority of the high-performance liquid chromatographic methods are carried out in reversed-phase mode using a nonpolar stationary phase and a polar mobile phase.

The most popular reversed-phase columns are manufactured from silica-based bonded phases, and, among those, the C₁₈-type bonded phase is most frequently used. These bonded phases are prepared by reacting silica with a reactive silane that carries the hydrophobic ligand after which the phase is named. However, the poor stability of silica at extreme pH values, along with the presence of underivatized silanol groups that most frequently cause secondary interactions, limits the application of silica-based supports in liquid chromatography.

POROUS GRAPHITIZED COLUMNS

Over the years, serious efforts have been devoted to the development of new reversed-phase packing materials in attempts to overcome the drawbacks of silica-based bonded phases. Thus reversed-phase separations can also be performed on polymeric columns. The great majority of these columns consist of styrene-divinylbenzene-, methacrylate-, or polyvinylalcohol-based phases and appear to be more stable over a wide pH range. Divinylbenzene packings are stable over the whole pH range, while the other two substrates (methacrylate and polyvinylalcohol) are hydrolytically stable between pH 2 and 12. Thus these polymer-based packings can be used at extreme pH values where silica-based columns degrade rapidly. However, silica-based columns are still more efficient and provide a much greater choice of different silica-based packings than polymeric columns.

The expectation that graphitized carbon-packing material would show high chemical stability over the entire pH range (pH=0–14), and ultimate hydrophobic properties, led to a number of investigations in this area.^[1] There

have been many attempts to manufacture reversed-phase carbon-based packings by the use of carbon black^[2] and led to the development of graphitized carbon black (GTCB) supports. Unfortunately, these supports were unsuitable for routine chromatographic analyses because of their extremely poor mechanical stability. Several trials have been made to overcome this limitation until the successful preparation of porous graphitized carbon (PGC) packing material.^[3]

Porous graphitized carbon packing material was developed by Knox et al.^[4–6] to provide a reversed-phase support that could have sufficient hardness to withstand high pressures, such as those encountered in high-performance liquid chromatography, and would not suffer from the disadvantages of silica-based bonded supports. This packing material was produced by the templation method using silica gel as template. Actually, a 7- μ m spherical porous silica gel template was impregnated with a phenol hexamine mixture and then heated to 150°C to form phenol-formaldehyde resin within the pores of silica gel. This polymer was further heated slowly to 900°C under a stream of oxygen-free nitrogen. The silica-carbon particles were then treated with potassium hydroxide to dissolve the silica template, and the remaining porous carbon was heated to a high temperature in the range of 2000–2800°C to anneal the surface, remove micropores, and, depending upon the temperature, produce some degree of graphitization. The particle size, shape, porosity, and pore size are determined by the choice of template material. It is thus possible to produce porous graphitized carbons with a range of pore and surface properties.^[7]

The surface characteristics of the porous graphitized carbon have been extensively investigated.^[8] X-ray diffraction provides useful information about the degree of graphitization. The Bernal structure of perfect three-dimensional graphite is one of the forms of carbon atoms to which the term graphitization can be applied and is clearly presented in Fig. 1a. However, perfect graphite is rarely formed synthetically from amorphous solid carbon because the bonding between the carbon atoms within the graphitic layers is extremely strong, while the interlayer bonding is weak. Graphitization tends to develop by the formation of graphitic layers, which are initially randomly oriented. The reorganization of

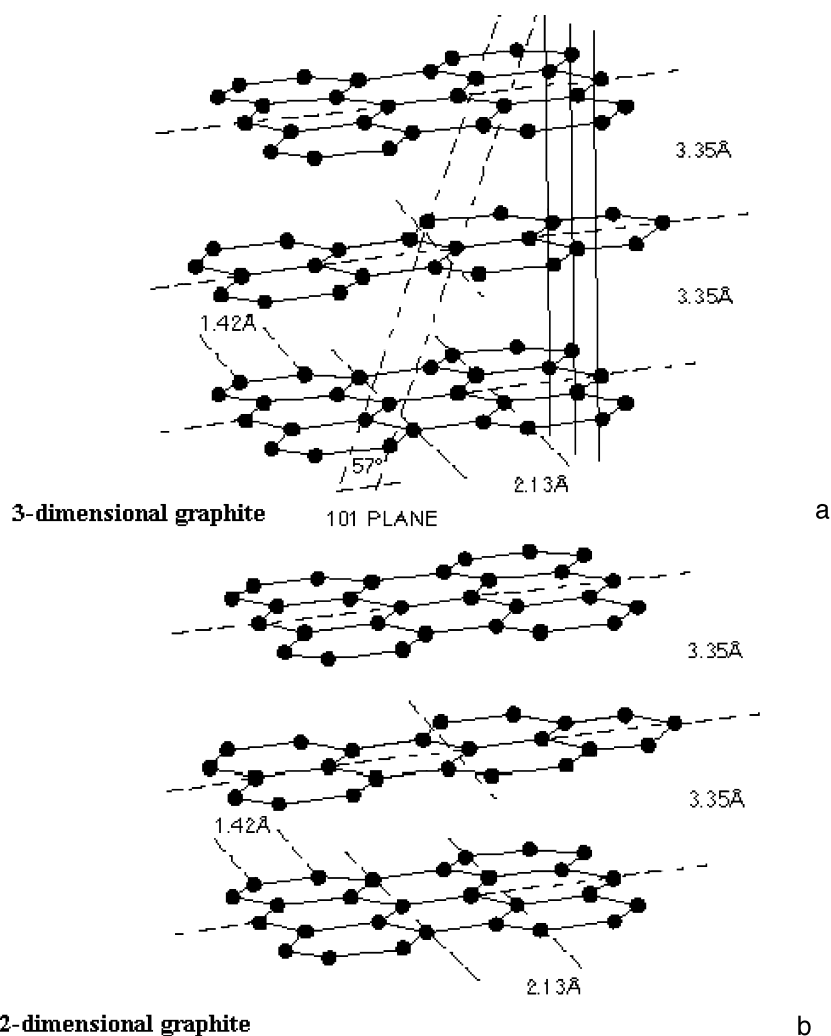


Fig. 1 Atomic structures of graphites. a) Bernal structure of perfect three-dimensional graphite. b) Warren structure of two-dimensional turbo static carbon structure. (Reproduced by kind permission of Thermo-Hypersil-Keystone.)

these layers into ordered three-dimensional graphite requires high activation energy (above 3000°C). Thus most synthetic carbons, when heated to about 3000°C, lead to a two-dimensional graphite structures. The atomic-molecular structure of PGC is clearly presented in Fig. 1b; it is a two-dimensional graphite molecular structure (Warren structure), otherwise termed turbo static carbon structure, in which graphitic layers are randomly oriented and, unlike three-dimensional graphite, there is no ordering of the atoms between layers. The high-resolution electron micrograph of PGC supports is presented in Fig. 2 and reveals a structure that is composed entirely of flat graphitic layers of hexagonally arranged carbon atoms showing sp^2 hybridization. The graphitic layers are randomly twisted and interleaved in a complex way, and, unlike silica gel, there are no surface functional groups.

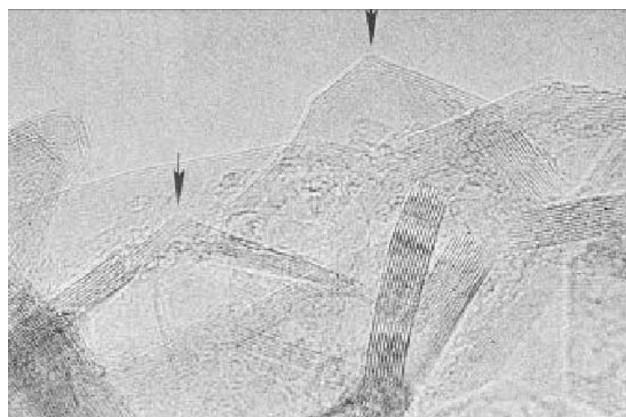


Fig. 2 High-resolution electron micrographs of porous graphitized carbon. (Reproduced by kind permission of Thermo-Hypersil-Keystone.)



It is important to mention that attempts have been made to construct porous carbon supports using entirely different carbonization procedures.^[9,10] One involved the carbonization of hydrocarbons on porous zirconia microplates.^[11] The type of chromatographic support that is obtained by this procedure is highly dependent upon the type of hydrocarbons used. In particular, when saturated hydrocarbons are used as the carbon source, the loading capacity and efficiency of the carbon supports are much greater than those obtained by unsaturated hydrocarbons. In other carbonization attempts, the three-dimensional channels of zeolites were used as templates to prepare porous carbon.^[12] The nano-spaces in zeolites are packed with carbon and then the carbon is extracted from the zeolite framework. The resultant carbons are highly porous with surface areas greater than 2000 m²/g.

Nowadays, porous graphitized carbons (PGC) are one of the most new reversed-phase packing materials with a homogenous hydrophobic surface, but they can also be used in the normal-phase mode.^[13] At the end of the 1980s, PGC packing materials were made available, the most common one under the trade name Hypercarb. This packing material exhibits a well-defined pore structure, allowing a good mass transfer of a large number of solutes and a specific surface area in the range 150–200 m²/g that gives improved retention possibilities of solutes and maintains a linear sample capacity over a large concentration range. It is totally unaffected by aggressive eluents as it exhibits high chemical stability, probably because of the lack of ordering between the graphitic layers, and can withstand high temperature. Moreover, it does not suffer from swelling or shrinking and it is hydrolytically stable across the entire pH range 0–14. Its retention and selectivity behavior is quite different from that of reversed-phase bonded phases. Porous graphitized carbon is recommended for the separation of highly polar and ionized compounds, and it gives an unrivaled stereoselective surface with unique ability to resolve isomeric and closely related compounds.^[14,15] It is thus suitable for large, fairly rigid molecules with a multitude of polar groups, such as many natural compounds and new drugs.^[16]

CHROMATOGRAPHIC CHARACTERISTICS AND RETENTION BEHAVIOR OF POROUS GRAPHITIZED CARBON COLUMNS

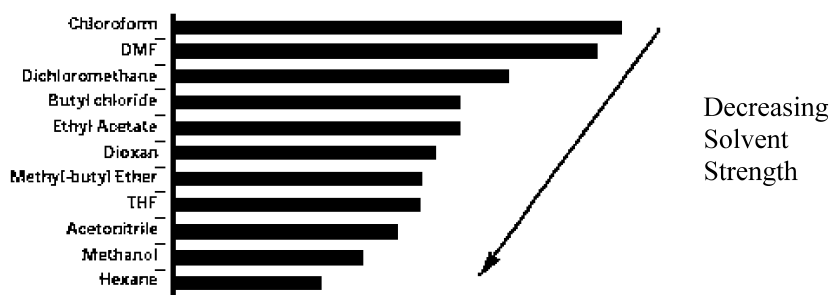
The chromatographic retention on PGC columns has been extensively investigated.^[17] Results indicate that PGC offers a unique retention mechanism that could be explained by a combination of various kinds of selective interactions between solutes, mobile phases, and PGC

packing material.^[18] These supports are not only strongly hydrophobic in comparison to the other traditional reversed-phase packing materials such as silica-based packings, but they also retain solutes through electronic (π - π) interactions. The delocalization of the π -electrons in the large graphitic layers and the high polarizability of the carbon are responsible for strong dispersion interactions. In addition, charge-induced interaction between the graphite surface and the polar substituents of the solutes, steric effects, along with hydrophobic interactions, affect the mechanism of retention onto PGC.

It was observed that, where purely hydrophobic surface-solute interactions are present, it will require higher concentrations of organic modifier to elute such solutes.^[8] Several efforts have been made to categorize solvent strength data for PGC supports into an eluotropic series using various types of solutes. Although the choice of organic modifier offers a route to modify the retention of solutes on PGC columns, the results indicated that organic modifiers did not show common eluotropic behavior and that their effects on retention are mainly dependent on the type of solutes.^[19] Thus it is possible to arrange solvents in an order of eluotropic strength for particular types of solutes. Solvent strength data for aniline, naphthalene, ethyl benzene, and phenol are presented in Fig. 3; they indicate that methanol and acetonitrile show low eluotropic strengths for aniline, naphthalene, and ethyl benzene, while for phenol, the same solvents have higher values of eluotropic strength. On the other hand, dioxane and tetrahydrofuran have higher eluotropic strengths for the majority of solutes.

A study of the retention characteristics of several aromatic hydrocarbons on PGC, using methanol as the mobile phase, showed that this graphite packing is an extremely strong adsorbent in comparison to other silica-based packing materials.^[20] Studies on the effect of eluent pH on the retention of isomers of ionizable substituted benzene compounds, including isomers with electron-donating and electron-withdrawing substituents, on PGC and ODS packings, provided valuable information on how the surface structure of the stationary phase can affect solute retention and selectivity.^[21] The retention factors of unionized solutes were generally greater on PGC than those on ODS, confirming previous observations that neutral compounds are more strongly retained on the PGC packing material. The fact that ionic interactions with ionized solutes were essentially absent on the surface of PGC implies that the retention order is probably governed by a solute molecular orientation effect induced by competing interactions of solute between the stationary phase and the mobile phase. Fig. 4 shows the effect of eluent pH and hence ionization on the retention of the zwitterionic aminobenzoic acid isomers. The greater retention is achieved where neither acid nor basic

Solvent strength data for aniline



Solvent strength data for naphthalene



Solvent strength data for ethyl benzene



Solvent strength data for phenol

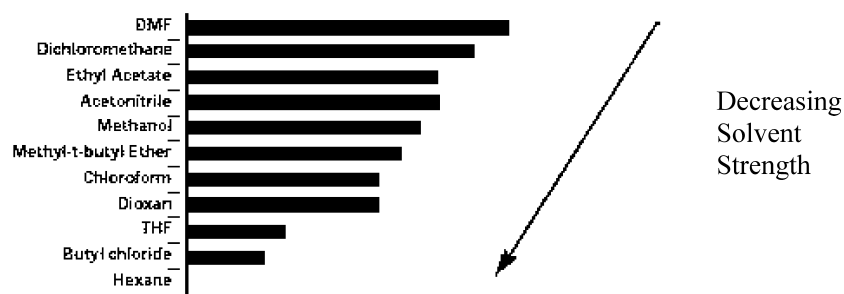


Fig. 3 Solvent strength data on porous graphitized carbon columns for the retention of aniline, naphthalene, ethyl benzene, and phenol. (Reproduced by kind permission of Thermo-Hypersil-Keystone.)

substituent is ionized. In particular, as the mobile phase pH increased, the retention factor rose initially to a peak value and then began to fall again.^[22] The homogeneous and flat crystalline surface of PGC packing is thought to be responsible for its unique selectivity toward the

discrimination of ionizable aromatic isomers compared with an ODS packing material. Thus adsorption onto a graphite surface depends on how well many of its atoms can fit onto the flat surface. Thus planar molecules and straight chain hydrocarbons can fit onto the graphite

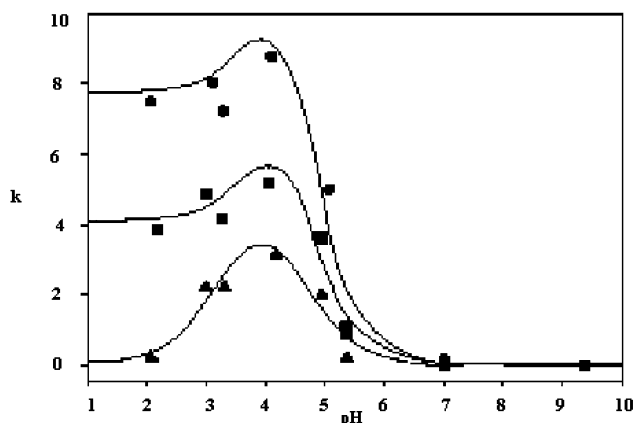


Fig. 4 Effect of the pH of the mobile phase on the retention of aminobenzoic acid isomers. (●): *o*-isomer, (▲): *m*-isomer, and (■): *p*-isomer. (Reproduced by kind permission of Thermo-Hypersil-Keystone.)

surface, whereas, as the planarity of such molecules is destroyed by the presence of nonplanar rings, the adsorption is deteriorated and a parallel decrease in retention is observed. An excellent example that reflects the unique surface properties of the graphitic carbon is the reversal of the elution order of isomeric xylenes when separated on PGC columns in comparison to the elution order of these isomers on reversed-phase silica-based packing.^[8] The methyl groups are sufficiently large that adjacent carbon atoms in the ring are just above the graphite surface and so are not as strongly retained as they would be in a totally planar molecule such as benzene. In the case of *o*-xylene and *p*-xylene, four carbon atoms contact the graphite surface (two from methyl groups and two from the ring), whereas, in the case of *m*-xylene, only three carbon atoms contact the surface (two from methyl groups and one from the ring). Therefore *m*-xylene elutes first on PGC supports, while the isomers elute later.

The retention of polar compounds (mono-, di-, and tri-substituted benzenes) on PGC, silica-based, and apolar copolymer supports^[14] was performed using unbuffered methanol water as eluent. The relationship between $\log k$ and the volume fraction of methanol was calculated separately for each solute. It was found that porous graphitic carbon retains polar compounds fairly well under reversed-phase conditions, while the retention factor increased with an increase in the number of polar substituents. In particular, the retention behavior of polar solutes on PGC supports is mainly governed by several polarity parameters (Hammett's constant, proton-donor capacity, and steric effects of substituents) and is quite different from that observed with other reversed-phase supports. Thus it was concluded that charge-induced interactions between the graphite surface as well as steric

effects force the polar groups close to the graphite surface. This type of interaction is called "polar retention effect on graphite," PREG,^[23] and proved to be more important than hydrophobic interactions in the retention mechanism of polar compounds.

Separation of various cationic and anionic compounds on PGC columns with a mobile phase containing an electronic modifier (e.g., trifluoroacetic acid) and an organic modifier (e.g., acetonitrile) in the eluent has also been demonstrated.^[24] In the same study, positively and negatively charged ions were well separated in the same chromatogram. Thus PGC seems to behave equally as an electron donor and electron acceptor and proved to be an important stationary phase for the separation of ionized solutes by a mechanism other than ion exchange. It was concluded that the retention of anionic compounds is mainly dominated by electronic interaction between the solute and the delocalized electron clouds on the graphitized carbon surface, while cationic compounds are mainly retained by ion suppression or ion pairing consistent with a reversed-phase interaction with the hydrophobic carbon surface.

Another example of electronic interaction between the graphite and ionic solutes is the retention of metal ions on PGC supports.^[25,26] Such electronic interaction, either electron donation or acceptance, is presumably between the available orbitals of metal ions and the electronic cloud of the flat graphite surface. The addition of a small concentration of oxalic acid into aqueous mobile phase tends to modify the graphite surface and to increase, through complexation, the range of metal ions retained.

It is extremely important to understand the interactions that govern retention on the graphite surface to better utilize this material and begin to predict how changes in the system will influence carbon-based separation processes.^[27] A qualitative insight into the chemical interaction that is involved in the retention process on graphite has been recently achieved through solvatochromic linear solvation energy relationships (LSERs).^[28] A variety of solute descriptors were used to correlate retention on graphite. Multiple linear regression of $\log k'$ values of 26 solutes against the LSER solute parameters indicated that all parameters were significant. Data of the fitting coefficients indicate that a combination of three solute parameters, size, dipolarity/polarizability, and hydrogen bond basicity, dictates a solute's retention. A spectral mapping technique (SPM) was also employed^[29] for the evaluation of the retention mechanism of solutes on PGC; barbiturates were chosen as probe solutes in this study, while mixtures of dioxane-water were used as eluents.^[30] Spectral mapping technique proved to be a valuable tool to separate retention strength and the selectivity of solutes and organic modifiers and thus promote a better understanding of the separation process. In particular, through



SPM, it was concluded that the retention strength of organic modifiers depends on the electronic parameter characterizing the resonance effect, suggesting that electronic interaction exerts a considerable impact on the elution strength of organic modifiers on PGC. The fact that the calculated lipophilicity of the drugs had no significant role in the chromatographic characteristics indicates, again, that the retention mechanism differs from that of octadecylsilica phase where lipophilicity is the most important parameter influencing the retention. The interaction between the graphite surface and the planar ring of the solute molecules contributes to the retention.

APPLICATION AREAS

Porous graphitized carbon columns have successfully been applied for the analysis of various compounds by high-performance liquid chromatography. As already mentioned, PGC shows a highly ordered crystalline structure with large bands of delocalized electrons, so that the retention mechanism is a mixture of hydrophobic and electronic interactions and is very different from that observed with silica-based bonded phases and apolar copolymers.^[31] Thus the following criteria must be taken into consideration during the development of a chromatographic separation on PGC columns: 1) strength of organic modifier for particular type of analytes; 2) ionization of the analytes and pH dependence as well as the effect of organic modifiers on control of ionization and pH dependence; 3) effect of the electronic modifier on analytes retention; and 4) effect of analyte shape.

Pharmaceuticals

High-performance liquid chromatography has become the most popular chromatographic technique in drug analysis. A literature survey reveals a number of papers that take advantage of the benefits of porous graphitized carbon columns for the separation and determination of several compounds of pharmaceutical interest.^[32] In particular, this material possesses several advantages, most notably its physical and chemical stability, as well as a highly stereoselective surface able to resolve diastereomers and geometric isomers; also, it is most applicable to the separation of small ionizable molecules that are not retained with octadecylsiloxane (ODS) columns.

Two different LC systems, equipped with porous graphitized carbon and silica-based RP-8 columns, respectively, were used for the assay of alprenolol and its related substances in quality control.^[33] The ability of the PGC system to separate metoprolol and closely related substances was also tested; baseline separations with high

column efficiencies were obtained. The robustness of the proposed methods was investigated using experimental design and evaluation with multivariate calculations. The results indicated that the PGC column, with its unique selectivity, excellent stability against alkaline mobile phases, and high column efficiency, is a proper complement to the traditional silica-based reversed-phase supports. Another method describes the simultaneous determination of paracetamol and its related compounds, 4-aminophenol and 4-chloroacetanilide, in pharmaceutical preparations, using PGC column.^[34] The chromatographic behavior of the three compounds under variable mobile phase compositions was thoroughly investigated, and the results indicated that retentions were dependent upon organic phase nature, concentration, and pH. Stronger eluents with dipolar properties, such as tetrahydrofuran, could be used with PGC to avoid long retention times for late eluting compounds. The retention selectivities of these compounds on PGC were compared with those on octadecylsilica (ODS) packing materials in reversed-phase liquid chromatography. Porous graphitized carbon columns showed high retention selectivity, rapid equilibrium, and a high stability during the analysis than commercially used ODS columns.

Several amines of pharmaceutical interest (e.g., alprenolol, sotalol, terbutaline, promethazine, and trimipramine) have been well separated with high enantioselectivity using, mainly, *N*-benzyloxycarbonylglycyl-L-proline (L-ZGP) and also *N*-benzyloxycarbonylglycylglycyl-L-proline (L-ZGGP) as chiral selectors on PGC column with methanol containing bases as mobile phase.^[35] The retention of the enantiomeric amines was found to increase with increasing concentration of the anionic form of L-ZGP. Previous investigation^[36] showed an improvement in peak symmetry in the presence of a mobile phase amine. Hence the addition of an alkylamine in the mobile phase in excess of L-ZGP was also investigated and led to a decrease in retention and enantioselectivity. The unique adsorption properties of porous graphitic carbon were also used for separation of racemic amines using chiral counterions dissolved in mobile phases; it was found that a column temperature below 0°C improved the enantioselective resolution.^[37] Recently, two newly synthesized chiral di-anionic ions were tested as additives for enantiomeric resolution of a set of amino alcohols on a Hypercarb porous graphitized carbon column.^[38] Z-L-Aspartyl-L-proline was used as a di-anionic counterion and resolved 9 of 12 tested racemates. One of its diastereoisomers, Z-L-Aspartyl-D-proline, was also tested, but resulted in low separation factors. The study showed the necessity to titrate the counterion with sodium hydroxide to its di-anionic form to optimize the resolution. Increased retention and enantioselectivity were observed with decreased column temperature.



Stepwise regression analysis and principal component analysis were used to examine the effect of various physicochemical parameters on the retention of 16 monoamine oxidase inhibitory drugs (propargylamine derivatives) on a PGC column, using ethanol–water mixtures as eluents.^[39] Both steric and electronic parameters were found to affect the retention of monoamine oxidase drugs on the graphite surface. An investigation was also carried out on the retention characteristics of 11 steroidal drugs on PGC using water–tetrahydrofuran mixtures as eluents.^[40] The logarithm of the capacity factor of each compound was linearly related to the percentage of tetrahydrofuran in the eluent. Principal component analysis was also used to correlate the retention characteristics and the physicochemical parameters of the steroidal. Steric conditions and electrostatic interactions were also found to be responsible for the retention of these compounds onto PGC packings. The porous graphitized carbon column proved to be suitable for the separation of the anticancer drug, taxol, a highly functionalized taxane diterpene amine, in bark and foliage of different *Taxus* species using water dioxane as eluent.^[41,42]

Bio-organic Substances

Because of the considerable importance of the analysis of bio-organic compounds in biochemical and biophysical research, many liquid chromatographic methods have been developed and applied for their separation and purity control. There is now growing evidence that PGC columns can contribute considerably to this application area. The flat graphite surface is able to differentiate between closely related compounds such as the structures of several carbohydrates found in nature.

The chromatographic behavior of oligosaccharide alditols containing two to five monosaccharides has been reported on a Hypercarb porous graphitized carbon column using gradient elution from water to acetonitrile in the presence of 0.05% trifluoroacetic acid.^[43] Elution patterns were based on size, charge, and linkage such that isomeric compounds could be separated from each other. In particular, the nature of the linkage appeared to play an important role with (1,3)-linked compounds eluting before the (1–4) linkage.

The chromatographic characteristics of 14 peptides have been determined on a PGC column, using acetonitrile–water mixtures as eluents.^[44] The majority of peptides showed irregular retention behavior; their retention decreased with increasing concentration of acetonitrile, reached a minimum, and increased again with increasing concentration of acetonitrile. For the elucidation of the relationship between the various physicochemical parameters and retention characteristics, principal component analysis (PCA) was employed. Calculations indicated that

the impact hydrophobicity, steric, and electronic parameters on the retention of peptides on a PGC column are similar, yet the steric parameters of substituents exert the highest impact on retention.

Porous graphitized carbon has also been explored for high-performance liquid chromatography of monosaccharides and disaccharides released from proteoglycans and fluorescently labeled oligosaccharide derivatives for fluorescence detection.^[45] Sulfated oligosaccharides show good retention and separation behavior on PGC columns. Gradient elution using mixtures of water with acetonitrile containing trifluoroacetic acid was used to perform the separation on a PGC column. The disadvantage of the anion exchange and reversed-phase ion-pair chromatography is that they require high salt concentrations that are not readily removed when compared with PGC which employs low concentrations of trifluoroacetic acid. Therefore PGC-based chromatography may be useful for two-dimensional sugar mapping and preparation of pure oligosaccharides, including the monitoring of derivatization efficiency with 2-aminobenzamide labels for reagent array analysis method sequencing, mass spectrometry, and NMR. In particular, liquid chromatography–electrospray mass spectrometry was used as a tool for the analysis of sulfated oligosaccharides from mucin glycoproteins prepared from pig stomach and colon.^[46] A PGC column, along with an amino-bonded column, were used and oligosaccharides were eluted with linear gradients of acetonitrile and water containing 5 mM ammonium hydrogen carbonate or formate buffers at basic pH values. Results indicated the benefits of both the amino-bonded and PGC-type chromatography in liquid chromatography–electrospray ionization–mass spectrometry (LC-ESI-MS) to achieve separations of mixtures of sulfated oligosaccharide alditols. Compounds co-eluting on one column could be separated on the other, indicated by the differing number of isomers separated in each system. The elution order of sulfated oligosaccharides does not appear to be pH-dependent on the PGC column. Various linear and branched oligosaccharides were labeled with 9-aminofluorene and further analyzed on a porous graphitized carbon column using acetonitrile water in 0.05% trifluoroacetic acid as eluent with mass spectrometric detection.^[47]

Ten guanidino compounds were analyzed in the serum of nephritic patients using a porous graphitized carbon column in combination with ion-pair LC and a post-column derivatization procedure using ninhydrin as a reagent.^[48] The retention mechanism of guanidino compounds on PGC was thoroughly investigated by computational chemical calculation using molecular mechanism (MM2). The retention mechanism of cationic compounds on PGC proved to be electrostatic interaction for cationic guanidino compounds and hydrophobic interaction for molecular-form compounds. It was found that the micelle

formation of hydrophobic ion-pair reagents reduces the retention of guanidine compounds. The successful separation of guanidino compounds was achieved by the addition of octanesulfonate in citric buffer. The authors suggest the use of a small precolumn packed with octadecyl-bonded silica to eliminate small particles and hydrophobic compounds from the analyzed samples.

Residue Analysis

The development of methods for the chromatographic separation and quantitation of trace levels of environmental pollutants is always in demand. However, these polar analytes cannot be easily retained on the most commonly used silica-based columns. It has been shown that, for some polar compounds, the retention in water can be very high using PGC columns.^[31]

An on-line technique coupling preconcentration via a precolumn packed with PGC and LC with a PGC analytical column has been applied to the trace-level determination of some polar and water-soluble organic pollutants from environmental waters.^[49] As these analytes are much more retained by the graphite surface than by silica C₁₈, preconcentration on the PGC precolumn cannot be coupled on-line with a widely used and more efficient C₁₈ silica analytical columns. In this study, applications were presented for the trace-level determination of 2-chloro-4-aminophenol, chloroanilines, aminophenols, and cyanuric acid; these organic compounds are included in the EC environmental priority pollutant list. The influence of the sample matrix was investigated with drinking and river water samples.

The environmental pollutants 3,4-dimethoxybenzaldehyde (DMB) and 3,4-dimethoxyphenylacetone (DMPA) were separated and quantitated in treated and untreated industrial wastewaters on PGC columns using HPLC and diode array detection.^[50] The effect of aerobic and anaerobic treatments on the decomposition rate of DMB and DMPA was also investigated; both techniques were found to be suitable for the decomposition of these pollutants in wastewaters. Furthermore, the chromatographic behavior of 16 environmental pollutants has been investigated on alumina and porous graphitic carbon columns using *n*-hexane as eluent.^[51] The fact that solutes were not retained on PGC surface using *n*-hexane as mobile phase indicates the greater polarity of the alumina stationary phase compared with that of PGC.

A further example for the analysis of trace levels of pollutants is the determination of polychlorinated dibenzodioxins and polychlorinated dibenzofurans in milk.^[52] The method includes gel permeation chromatography, alumina cleanup, and porous graphitized carbon chromatography, followed by analysis by gas chromatography-

high-resolution mass spectrometry. Moreover, the potential of porous graphitic carbon as an HPLC adsorbent for the isolation of halogenated aromatic compounds has been demonstrated by the fractionation of polychlorinated biphenyls (PCBs), chlorinated pesticides, polychlorinated dibenzo-*p*-dioxins (PCDDs), and polychlorinated dibenzofurans (PCDFs).^[53,54] The proposed procedures can be used in routine bases for the determination of PCDDs and PCDFs in soil extracts because of the reproducible behavior of PGC compared with activated carbons and the convenience of a single solvent elution method.

CONCLUSION

Porous graphitized carbon as a packing material meets all the requirements necessary for selective and effective stationary phases, such as rigidity of microparticles, adequate surface area, and uniformity of the surface. The development of this highly pH-stable column was motivated by the fact that the use of silica-based supports in high-performance liquid chromatography is limited by the low stability of silica at extreme pH values and by the undesirable electrostatic interactions that occur in silica-based columns between the polar substructures of solutes and the free silanol groups not covered by the hydrophobic ligand. Porous graphitic carbon is extremely hydrophobic, and the retention of ordinary compounds is quite long compared with that of the commonly used silica-based columns. Thus the high adsorption properties for polar compounds make PGC a most interesting complement to traditional silica supports. Moreover, the unique surface makes the PGC material suitable for separation of closely related structures, e.g., positional isomers and diastereomers. It has also been used to separate enantiomers using chiral mobile-phase additives.

ACKNOWLEDGMENTS

The author gratefully acknowledges Dr. Rachel Phillips, Product Manager of Thermo-Hypersil-Keystone, for the illustrations.

REFERENCES

1. Chiantore, O.; Novak, I.; Berek, D. Characterization of porous carbon for liquid chromatography. *Anal. Chem.* **1988**, *60*, 638–642.
2. Unger, K.K. Porous carbon packings for liquid chromatography. *Anal. Chem.* **1983**, *55*, 361A–375A.
3. Gilbert, M.T.; Knox, J.H.; Kaur, B. Porous glassy carbon, a



- new column packing material for gas chromatography and high-performance liquid chromatography. *Chromatographia* **1982**, *16*, 138–146.
4. Knox, J.H.; Gilbert, M.T. U.K. Patent 7939449, 1982.
 5. Knox, J.H.; Gilbert, M.T. U.S. Patent 4263268, 1982.
 6. Knox, J.H.; Gilbert, M.T. W. German Patent P 2946688-4, 1982.
 7. Matisova, E.; Skrabakova, S. Carbon sorbents and their utilization for the preconcentration of organic pollutants in environmental samples. *J. Chromatogr., A* **1995**, *707*, 145–179.
 8. Knox, J.H.; Kaur, B.; Millward, G.R. Structure and performance of porous graphitic carbon in Liquid Chromatography. *J. Chromatogr.* **1986**, *352*, 3–25.
 9. Obayashi, T.; Ozawa, M.; Kawase, T. Tonen Corporation Eur. Pat. 0458548A, 1990.
 10. Yokoyama, A.; Kawai, T.; Moriya, H.; Komiya, K.; Kato, Y.; Nippon Carbon Co. Ltd.; Tosoh Corporation. Eur. Pat. 0484176A, 1990.
 11. Forgacs, E.; Cserhati, T.; Bordas, B. Application of multivariate mathematical-statistical methods for the comparison of the retention behaviour of porous graphitized carbon and octadecylsilica columns. *Anal. Chim. Acta* **1993**, *279* (1), 115–122.
 12. Kyotashi, T.; Nagai, T.; Inoue, S.; Tomita, A. Formation of new type of porous carbon by carbonization in zeolite nanochannels. *Chem. Mater.* **1997**, *9*, 609–615.
 13. Tanaka, N.; Tanigawa, T.; Kimata, K.; Hosoya, K.; Araki, T. Selectivity of carbon packing material in comparison with octadecylsilyl- and pyrenylethylsilylsilica gels in reversed-phase liquid chromatography. *J. Chromatogr.* **1991**, *549*, 29–41.
 14. Hennion, M.C.; Coquart, V.; Guenu, S.; Sella, C. Retention behaviour of polar compounds using porous graphitic carbon with water-rich mobile phases. *J. Chromatogr., A* **1995**, *712*, 287–301.
 15. Forgacs, E.; Cserhati, T. Retention strength and selectivity of porous graphitized carbon columns. Theoretical aspects and practical applications. *Trends Anal. Chem.* **1995**, *14* (1), 23–29.
 16. Ross, P.; Knox, J.H. *Advances in Chromatography*; Brown, P., Grushca, E., Eds.; Marcel Dekker Inc.: New York, 1997; Vol. 37, 121–162.
 17. Forgacs, E. Retention characteristics and practical application of carbon sorbents. *J. Chromatogr., A* **2002**, *975*, 229–243.
 18. Weber, T.P.; Jackson, P.T.; Carr, P.W. Chromatographic evaluation of porous-carbon-clad zirconia microplates. *Anal. Chem.* **1995**, *67*, 3042–3050.
 19. Knox, J.H.; Kaur, B. Carbon in Liquid Chromatography. In *High Performance Liquid Chromatography*; Brown, P., Hartwick, R.A., Eds.; John Wiley and Sons: New York, 1989; 189–222.
 20. Kriz, J.; Adamcova, E.; Knox, J.H.; Hora, J. Characterization of adsorbents by high-performance liquid chromatography using aromatic hydrocarbons. Porous graphite and its comparison with silica gel, alumina, octadecylsilica and phenylsilica. *J. Chromatogr., A* **1994**, *663*, 151–161.
 21. Wan, Q.H.; Shaw, P.N.; Davies, M.C.; Barrett, D.A. Chromatographic behaviour of positional isomers on porous graphitic carbon. *J. Chromatogr.* **1995**, *697*, 219–227.
 22. Wan, Q.H.; Davies, M.C.; Shaw, P.N.; Barrett, D.A. Retention behaviour of ionisable isomers in reversed-phase liquid chromatography: A comparative study of porous graphitic carbon and octadecyl bonded silica. *Anal. Chem.* **1996**, *68*, 437–446.
 23. Hennion, M.C.; Coquat, V. Comparison of reversed-phase extraction sorbents for the on-line trace enrichments of polar organic compounds in environmental aqueous samples. *J. Chromatogr.* **1993**, *642* (1–2), 211–224.
 24. Gu, G.; Lim, C.K. Separation of anionic and cationic compounds of biomedical interest by high-performance liquid chromatography on porous graphitic carbon. *J. Chromatogr.* **1990**, *515*, 183–192.
 25. Merly, C.; Lynch, B.; Ross, P.; Glennon, J.D. Selective ion chromatography of metals on porous graphitic carbon. *J. Chromatogr., A* **1998**, *804* (1–2), 187–192.
 26. Elfakir, C.; Chaimbault, P.; Dreux, M. Determination of inorganic anions on porous graphitic carbon using evaporative light scattering detection—Use of carboxylic acids as electronic competitors. *J. Chromatogr., A* **1998**, *829* (1–2), 193–199.
 27. Kaliszan, R.; Osmialowski, K.; Bassler, B.J.; Hartwick, R.A. Mechanism of retention in high-performance liquid chromatography on porous graphitized carbon as revealed by principal component analysis of structural descriptor of solutes. *J. Chromatogr.* **1990**, *499*, 333–344.
 28. Jackson, P.T.; Schure, M.R.; Weber, T.P.; Carr, P.W. Intermolecular interactions involved in solute retention on carbon media in reversed-phase high-performance liquid chromatography. *Anal. Chem.* **1997**, *69*, 416–425.
 29. Forgacs, E.; Cserhati, T. Solvent strength and selectivity on porous graphitized carbon column separated by a spectral mapping technique using barbiturates as solutes. *Anal. Sci.* **2001**, *17*, 307–312.
 30. Forgacs, E.; Cserhati, T. Relationship between retention characteristics and physicochemical parameters of solutes on porous graphitized carbon column. *J. Pharm. Biomed. Anal.* **1998**, *18*, 505–510.
 31. Coquat, V.; Hennion, M.C. Trace level determination of polar phenolic compounds in aqueous samples by high-performance liquid chromatography and on-line preconcentration on porous graphitic carbon. *J. Chromatogr., A* **1992**, *600* (2), 195–201.
 32. Kaur, B. The use of porous graphitic carbon in high performance liquid chromatography. *LC-GC* **1990**, *8*, 468–474.
 33. Karlsson, A.; Berglin, M.; Charron, C. Robustness of the chromatographic separation of alprenolol and related substances using silica-based stationary phase and selective retention of metoprolol and related substances on a porous graphitic carbon stationary phase. *J. Chromatogr., A* **1998**, *797*, 75–82.
 34. Monser, L.; Darghouth, F. Simultaneous LC determination of paracetamol and related compounds in pharmaceutical

- formulations using a carbon-based column. *J. Pharm. Biomed. Anal.* **2002**, 27, 851–860.
35. Huynh, N.H.; Karlsson, A.; Pettersson, C. Enantiomeric separation of basic drugs using *N*-benzyloxycarbonylglycyl-L-proline as counter ion in methanol. *J. Chromatogr., A* **1995**, 705, 275–287.
36. Karlsson, A.; Pettersson, C. Enantiomeric separation of amines using *N*-benzyloxycarbonyl-glycyl-L-proline as chiral additive and porous graphitic carbon as solid phase. *J. Chromatogr., A* **1991**, 543, 287–297.
37. Karlsson, A.; Charron, C. Reversed-phase chiral ion-pair chromatography at a column temperature below 0°C using three generations of Hypercarb as solid-phase. *J. Chromatogr., A* **1996**, 732, 245–253.
38. Karlsson, A.; Karlsson, O. Chiral ion-pair chromatography on porous graphitized carbon using *N*-blocked dipeptides as counter ions. *J. Chromatogr., A* **2001**, 905, 329–335.
39. Forgacs, E.; Cserhati, T. Effect of physicochemical parameters on the retention of some monoamine oxidase inhibitory drugs on a porous graphitized carbon column. *J. Chromatogr., B* **1996**, 681, 197–204.
40. Forgacs, E.; Cserhati, T. Separation of steroidal drugs on porous graphitized carbon column. *J. Pharm. Biomed. Anal.* **1998**, 18, 15–20.
41. Nemeth-Kiss, V.; Forgacs, E.; Cserhati, T.; Schmidt, G. Determination of taxol in *Taxus* species grown in Hungary by high-performance liquid chromatography-diode array detection. Effect of vegetative period. *J. Chromatogr., A* **1996**, 750, 253–256.
42. Nemeth-Kiss, V.; Forgacs, E.; Cserhati, T.; Schmidt, G. Taxol content of various *Taxus* species in Hungary. *J. Pharm. Biomed. Anal.* **1996**, 14, 997–1001.
43. Davies, M.; Smith, K.D.; Harbin, A.M.; Hounsell, E.F. High-performance liquid chromatography of oligosaccharide alditols and glycopeptides on a graphitized carbon column. *J. Chromatogr., A* **1992**, 609 (1,2), 125–131.
44. Nemeth-Kiss, V.; Forgacs, E.; Cserhati, T. Anomalous retention behaviour of peptides on porous graphitized carbon column. *J. Chromatogr., A* **1997**, 776, 147–152.
45. Davies, M.J.; Hounsell, E.F. Comparison of separation models of high-performance liquid chromatography for the analysis of glycoprotein- and proteoglycan-derived oligosaccharides. *J. Chromatogr., A* **1996**, 720, 227–233.
46. Thomsson, K.A.; Karlsson, N.G.; Hansson, G.C. Liquid chromatography–electrospray mass spectrometry as a tool for the analysis of sulfated oligosaccharides from mucin glycoproteins. *J. Chromatogr., A* **1999**, 854, 131–139.
47. Franz, A.H.; Molinski, T.F.; Lebrilla, C.B. MALDI-FTMS Characterization of oligosaccharides labelled with 9-aminofluorene. *J. Am. Soc. Mass Spectrom.* **2001**, 12, 1254–1261.
48. Inamoto, Y.; Inamoto, S.; Hanai, T.; Tokuda, M.; Hatase, O.; Yoshii, K.; Sugiyama, N.; Kinoshita, T. Liquid chromatography of guanidine compounds using a porous graphite carbon column and application to their analysis in serum. *J. Chromatogr., B* **1998**, 707, 111–120.
49. Guenu, S.; Hennion, M.C. On-line sample handling of water-soluble organic pollutants in aqueous samples using porous graphitic carbon. *J. Chromatogr., A* **1994**, 665 (2), 243–251.
50. Cserhati, T.; Forgacs, E. Simultaneous determination of 3,4-dimethoxybenzaldehyde and 3,4-dimethoxyphenylacetone in industrial waste waters by high-performance liquid chromatography-diode array detection. *J. Chromatogr., A* **1996**, 750, 257–261.
51. Cserhati, T.; Forgacs, E. Relationship between the retention characteristics on an alumina column and physico-chemical parameters of some environmental pollutants. *J. Chromatogr., A* **2000**, 869, 41–48.
52. Van Rhijn, J.A.; Traag, W.A.; Kulik, W.; Tuinstra, L.G. Automated clean-up procedure for the gas chromatographic-high-resolution mass spectrometric determination of polychlorinated dibenzo-*p*-dioxins and dibenzofurans in milk. *J. Chromatogr.* **1992**, 595 (1–2), 289–299.
53. Creaser, C.S.; Al-Haddad, A. Fractionation of polychlorinated biphenyls, polychlorinated dibenzo-*p*-dioxins, and polychlorinated dibenzofurans on porous graphitic carbon. *Anal. Chem.* **1989**, 61 (11), 1300–1302.
54. Chiantore, O.; Novac, I.; Berek, D. Characterization of porous carbon for liquid chromatography. *Anal. Chem.* **1988**, 60, 638–642.



Potential Barrier Field-Flow Fractionation

George Karaiskakis

University of Patras, Patras, Greece

Introduction

Potential barrier field-flow fractionation (PBFFF), developed by Karaiskakis, is a combination of potential barrier chromatography and field-flow fractionation. It can be applied to separate colloidal particles and is based on differences in size or in any physicochemical parameters involved in the potential energy of interaction between the particles and the material of the FFF channel wall. Of the various quantities which affect the total potential energy (surface potential, Hamaker constant, and Debye–Huckel reciprocal distance), none is as accessible to empirical adjustment as the ionic strength of the suspending medium. This quantity depends on both the concentration and the cationic or anionic charge of the indifferent electrolyte added to the carrier solution. In its simplest form, the PBFFF technique consists in changing the ionic strength of the carrier solution from a high value, where only one of the colloidal components of the mixture subject to separation is totally adhered at the beginning of the FFF channel wall, to a lower value, where the total number of adhered particles is released.

The method has been applied to the separation of hematite and titanium dioxide submicron spherical particles, to the separation of submicron hematite spherical particles with different sizes, to the separation of various mixed sulfides with supramicron poly-disperse irregular particles, and to the concentration of dilute colloidal samples, in both the normal and the steric modes of operation of sedimentation FFF.

Principle of PBFFF

Field-flow fractionation is a family of high-resolution techniques capable of separating and characterizing colloids and macromolecules. In normal FFF, the particles form a Brownian-motion cloud that extends a short distance into the channel. Separation is possible because the solvent flows at different velocities at various points within the channel. The smaller particles, whose cloud protrudes out into the faster laminae, are transported more rapidly than the larger particles, so

that the two populations are soon separated. In the steric mode of operation, which happens when the protrusion of particles into the flow stream is determined by their physical bulk instead of by diffusion, the larger particles are elute earlier than the smaller ones.

In normal sedimentation FFF (SdFFF) the retention volume, V_r , of a spherical particle is immediately related to its diameter, d , via

$$V_r = \frac{\pi G w \Delta \rho V_0}{36 k T} d^3 \quad (1)$$

where G is the sedimentation field strength expressed in acceleration, w is the channel thickness, $\Delta \rho = |\rho_s - \rho|$ is the density difference between the particle (ρ_s) and the carrier liquid (ρ), V_0 is the void volume of the channel, k is Boltzmann's constant, and T is the absolute temperature.

In the sedimentation steric FFF (Sd/StFFF), the retention volume of a spherical particle is immediately related to the diameter via

$$V_r = \frac{w V_0}{3 \gamma} \frac{1}{d} \quad (2)$$

where γ is a dimensionless factor that accounts for the drag-induced reduction in velocity, as well as for the increase in velocity due to the activity of lift forces. To find γ , it is necessary to have a linear calibration curve of $\log V_r$ versus $\log d$ for standard particles of known size and nature (e.g. polystyrene latex beads). The easier way of working in the steric mode of FFF is that using the Earth's gravity as the external field (gravitational FFF = GFFF).

In the normal mode of the SdFFF operation, the potential energy, $\varphi(x)$, of a spherical particle is given by

$$\varphi(x) = \frac{\pi d^3}{6} \Delta \rho G x \quad (3)$$

where x is the coordinate position of the center of particle mass.

When the colloidal particles interact with the SdFFF channel wall, the potential energy given by Eq. (3) must be corrected, so as to include the potential en-



ergy of interaction, $\varphi(h)$. The latter can be estimated by the sum of the contributions of the van der Waals, $\varphi_6(h)$, and double-layer, $\varphi_{DL}(h)$, forces, and the total potential energy, φ_{tot} , of a spherical particle in PBSdFFF is given by the relation

$$\begin{aligned}\varphi_{tot} &= \varphi(x) + \varphi(h) \\ &= \varphi(x) + \varphi_6(h) + \varphi_{DL}(h) \\ &= \frac{4}{3}\pi a^3 \Delta \rho G x + \frac{A_{132}}{6} \left[\ln \left(\frac{h+2a}{h} \right) - \frac{2a(h+a)}{h(h+a)} \right] \\ &\quad + 16\epsilon a \left(\frac{kT}{e} \right)^2 \tan h \left(\frac{e\psi_1}{4kT} \right) \tan h \left(\frac{e\psi_2}{4kT} \right) e^{-\kappa h}\end{aligned}\quad (4)$$

where h is the separation distance between the sphere and the channel wall, a is the particle radius, A is the effective Hamaker constant, ϵ is the dielectric constant of the liquid phase, e is the electronic charge, ψ_1 and ψ_2 are the surface potentials of the particle and the wall, respectively, and κ is the reciprocal Debye length.

The last equation shows that the energy φ_{tot} in PBSdFFF is a function of the size and of the surface potential of the particle, of the Hamaker constant, and of the ionic strength of the carrier solution, as the reciprocal double-layer thickness is immediately related to the ionic strength of the suspending medium. Thus, selectivity in PBSdFFF results from differences in particle size or chemical composition of the particles and of the suspending medium, where the latter will affect the surface potential and the Hamaker constant of the particle, as well as the medium's ionic strength.

Applications of PBFFF

As model samples for the verification of the PBFFF as a separation technique, colloidal samples of hematite and titanium dioxide with submicron monodisperse spherical particles were used. In the first example, the fractionation of titanium dioxide [TiO_2 with the nominal diameter obtained by a transmission electron microscope (TEM) of $0.298 \mu\text{m}$] and hematite-I [$\alpha\text{-Fe}_2\text{O}_3(\text{I})$ with nominal diameter obtained by TEM of $0.148 \mu\text{m}$] spherical particles was succeeded by the PBSdFFF technique. Figure 1a shows the fractionation of the TiO_2 and $\alpha\text{-Fe}_2\text{O}_3(\text{I})$ particles by the normal SdFFF mode of operation, and Fig. 1b shows the fractionation of the same particles by the potential barrier mode of SdFFF. The latter is based on the difference of the total potential energy of interaction between the colloidal particles and the channel wall due to the variation of the ionic strength of the suspending medium.

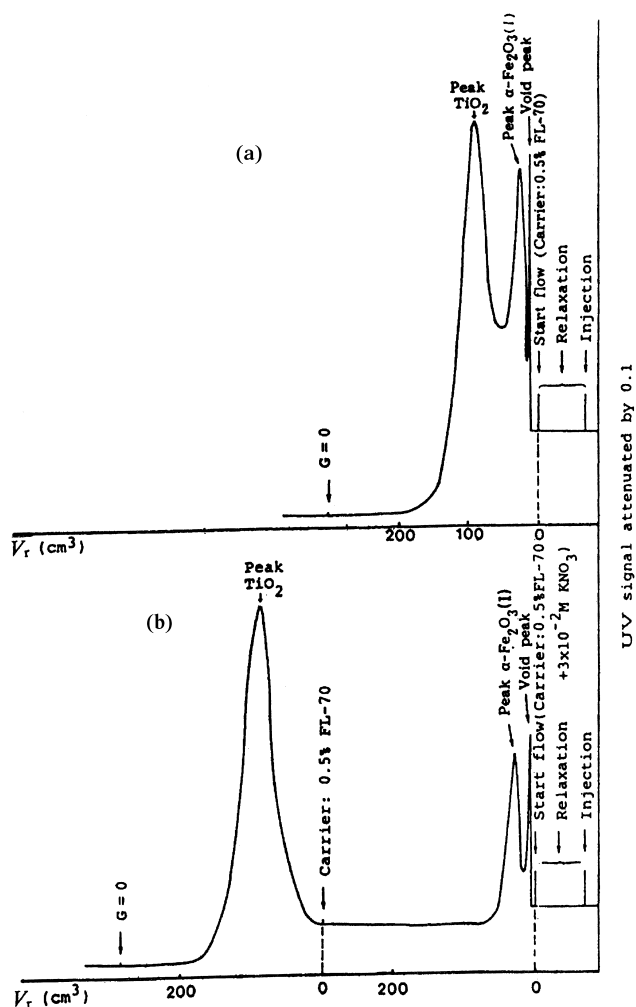


Fig. 1 Fractionation of $\alpha\text{-Fe}_2\text{O}_3(\text{I})$ (with nominal diameter $0.148 \mu\text{m}$) and TiO_2 (with nominal diameter $0.298 \mu\text{m}$) colloidal particles by (a) the normal SdFFF and (b) the PBSdFFF technique. The experimental conditions, except for those given in the scheme, were as follows: field strength = 15.5 g , flow rate = $150 \text{ cm}^3/\text{h}$, void volume of the channel = 2.06 cm^3 . [Reproduced with permission from G. Karaiskakis et al. (1990) *J. Chromatogr.* 517: 345; copyright Elsevier Science Publishers B.V.]

In the PBSdFFF technique, the mixture was introduced into the channel with a carrier solution containing 0.5% (v/v) detergent FL-70, 0.02% (w/w) NaNO_3 , and $3 \times 10^{-2} \text{ M}$ KNO_3 . At this high electrolyte concentration, all of the TiO_2 colloidal particles adhered at the beginning of the SdFFF Hastelloy-C channel wall, whereas all of the $\alpha\text{-Fe}_2\text{O}_3(\text{I})$ particles were eluted from the channel. The average diameter of the eluted $\alpha\text{-Fe}_2\text{O}_3(\text{I})$ particles determined by Eq. (1) was found

to be $0.143\ \mu\text{m}$, in good agreement with that obtained by TEM ($0.148\ \mu\text{m}$) or determined by normal SdFFF ($0.150\ \mu\text{m}$). Changing the carrier solution to one containing only 0.5% (v/v) detergent FL-70, whose ionic strength is $1 \times 10^{-3}M$, released all the adhered TiO_2 particles and gave a particle diameter ($0.302\ \mu\text{m}$) in good agreement with that obtained by TEM ($0.298\ \mu\text{m}$).

In order to show whether the size of the particles and not their nature is responsible for the variation of the total interaction energy between the colloids and the channel wall, a second example of fractionation was performed by using two samples of hematite with different particle diameters [$\alpha\text{-Fe}_2\text{O}_3(\text{I})$ with nominal diameter $0.148\ \mu\text{m}$ and $\alpha\text{-Fe}_2\text{O}_3(\text{II})$ with nominal diameter $0.248\ \mu\text{m}$]. In the present case, the separation is based only on the particle size difference, as the Hamaker constants and the surface potentials of the two samples are identical. That obtained by the PBFFF technique fractogram had the same form as that of Fig. 1b, except for the fact that the peak of $\alpha\text{-Fe}_2\text{O}_3(\text{II})$ was in the position of TiO_2 . The critical electrolyte (KNO_3) concentration for the adhesion of $\alpha\text{-Fe}_2\text{O}_3(\text{II})$ particles at the beginning of the SdFFF channel wall was found to be $3 \times 10^{-2}M$, whereas at this high concentration of KNO_3 , the whole number of $\alpha\text{-Fe}_2\text{O}_3(\text{I})$ particles are eluted from the channel. Variation of the carrier solution to one containing only 0.5% (v/v) detergent FL-70 and 0.02% (w/w) NaN_3 without any amount of KNO_3 released the total number of adherent $\alpha\text{-Fe}_2\text{O}_3(\text{II})$ particles. The particle diameters obtained by the PBFFF technique [$0.151\ \mu\text{m}$ for $\alpha\text{-Fe}_2\text{O}_3(\text{I})$ and $0.244\ \mu\text{m}$ for $\alpha\text{-Fe}_2\text{O}_3(\text{II})$] are in excellent agreement with those found by normal SdFFF [$0.145\ \mu\text{m}$ for $\alpha\text{-Fe}_2\text{O}_3(\text{I})$ and $0.237\ \mu\text{m}$ for $\alpha\text{-Fe}_2\text{O}_3(\text{II})$] or determined by TEM [$0.148\ \mu\text{m}$ for $\alpha\text{-Fe}_2\text{O}_3(\text{I})$ and $0.248\ \mu\text{m}$ for $\alpha\text{-Fe}_2\text{O}_3(\text{II})$].

In PBFFF, the variation of the potential energy of interaction between the colloidal particles and the channel wall can be succeeded, except for the variation of the ionic strength, by changing also the pH and the nature of the suspending medium. Polydisperse, irregular supramicron colloidal particles of the mixed sulfides $\text{Cu}_x\text{Zn}_{1-x}\text{S}$ ($0 < x < 1$) were used as model samples to verify the applicability of the potential barrier gravitational field-flow fractionation (PBGFFF), based on the variation of the above parameters, to fractionate colloidal particles.

A general methodology for the analysis of a colloidal mixture by PBSdFFF consists in injecting into the column the mixture with a carrier solution in which the ionic strength is too high to assure total adhesion of all the components of the mixture, except

for the one with the lower attractive force with the channel wall. Then, a programmed decrease of the ionic strength of the carrier solution is applied to release, *in time*, the adherent particles according to their size and/or surface characteristics. As the PBSdFFF technique is based on particle-wall interactions, its applications can be extended by using different from Hastelloy-C materials, such as stainless steel, Teflon, and polyimide. PBSdFFF is also a convenient and accurate method for the *concentration* and analysis of *dilute* colloidal samples. The major advantage of the proposed concentration procedure is that the method can concentrate particles even of the same size but with different surface potentials and/or Hamaker constants. The method has considerable promise for the separation and characterization, in terms of particle size, of dilute complex colloidal materials, such as those of natural water, where particles are present in low concentration.

Future Developments

Looking to the future, it is reasonable to expect continuous efforts to improve the theoretical predictions and to expand the applications of the potential barrier methodology of FFF to more complex and dilute colloidal samples. The latter can be easily succeeded by constructing FFF channels from various materials of well-defined composition.

Suggested Further Reading

- A. Athanasopoulou and G. Karaiskakis, *Chromatographia* 40: 734 (1995).
- A. Athanasopoulou and G. Karaiskakis, *Chromatographia* 43: 369 (1996).
- J. C. Giddings, *Separ. Sci.* 1: 123 (1966).
- M. E. Hansen and J. C. Giddings, *Anal. Chem.* 61: 811 (1989).
- M. E. Hansen, J. C. Giddings, and R. Beckett, *J. Colloid. Interf. Sci.* 132(2): 300 (1989).
- G. Karaiskakis and J. Cazes (eds.), *J. Liquid Chromatogr. Related Technol.* 20(16 & 17) (1997) (special issue).
- G. Karaiskakis and A. Koliadima, *Chromatographia* 28: 31 (1989).
- A. Koliadima and G. Karaiskakis, *J. Chromatogr.* 517: 345 (1990).
- A. Koliadima and G. Karaiskakis, *Chromatographia* 39: 74 (1994).
- A. Koliadima, D. Gavril, and G. Karaiskakis, *J. Liquid Chromatogr. Related Technol.* 22(18): 2779 (1999).



Preparative HPLC Optimization

Michael Breslav

R.W. Johnson Pharmaceutical Research Institute, Spring House, Pennsylvania, U.S.A.

Introduction

The approach used for preparative high-performance liquid chromatography (PHPLC) optimization depends on the goals and scale of a particular laboratory or industrial chromatographic separation. Parameters such as quantities (from milligrams to tons), required purity and recovery of the final material, cost of separation, and availability of the equipment need to be considered. The separation expenses including time, cost of solvents, stationary phase, and isolation of the product should be compared to the cost of the starting material and the value of the product being purified. Overall production cost is a function of purification costs and production rate [1]. In multiton production of a selected material, it is worthwhile to invest a substantial effort on trial experiments and mathematical modeling of the nonlinear chromatographic process. In contrast, in pharmaceutical research and development, time is the most crucial parameter for the delivery of milligram to kilogram quantities of new compounds for initial biological testing. Other applications that require fast separations on a smaller scale are the preparation of pure standards and isolation of by-products for structural determination.

Preparative HPLC optimization goals which ultimately lead to a product with a given minimum purity may include the maximum amount of the purified material per weight unit of stationary phase per time unit (g/kg/day), the maximum amount of the purified material per mobile phase unit per time unit (g/L/day), the maximum production rate (g/day), the lowest cost (\$/kg), the maximum recovery (%), and the maximum production rate with maximum recovery. Regardless of the differences in application, it is important to be aware of the following parameters that may affect the purity and recovery of the product as well as the time and cost required for the separation:

Selectivity

The separation of the material of interest and closely retained impurities is greatly affected by changes in se-

lectivity (α) when the relative distribution of the sample components between the stationary and mobile phases changes. A practical value for the selectivity (separation factor), described as $\alpha = k_2/k_1$, where k_1 and k_2 are the retention factors for adjacent peaks, is greater than 1.2. However, separation can be improved by increasing the selectivity value up to 2 or 3 whenever possible. In normal-phase chromatography, selectivity is altered by varying the organic solvents in the mobile phase. In a reversed-phase separation, changing both the type of organic solvent and water/organic ratio in the mobile phase is also used to optimize selectivity [2]. Selectivity is also dependent on the temperature and stationary phase being used, especially with enantioselective (chiral) separations. The newest addition to the stationary-phase materials designed to improve selectivity includes custom-tailored molecular-imprinted polymers [3].

Retention

It is advantageous to use the minimum retention (k) necessary for separating the product and providing the desired purity, because the cycle time is decreased and the production rate is increased. In both normal-phase and reversed-phase modes, the concentration of the product in collected fractions increases as the retention decreases. In displacement chromatography, longer sample retention provides a more concentrated product fraction. As retention increases, column efficiency increases, but the cycle time and solvent consumption are increased as well. The optimum retention is in the range of $k = 1.2$ to 2.0 for isocratic separations and $k = 3$ to 4 for gradient separations. Poorly retained impurities can be eluted from the column in the void volume. Impurities that are retained significantly longer than the product need to be washed from the column at the end of the run cycle using a step-gradient with a strong eluent; this step may include flow reversal. Although regeneration is a regular procedure in reversed-phase chromatography, in normal-phase chromatography polar impurities tend to strongly bind to the silica surface and full regeneration is difficult.



However, because of the low price of the silica, the stationary phase is often discarded after one or several runs. Methods for use with modern flash chromatography employing bare silica are easy to develop using preliminary thin-layer chromatography (TLC) results followed by scale-up with disposable cartridges. In this flash chromatography technique, an increase of the difference in column volumes of elution between the product and a closely retained impurity (ΔC_v) increases production rate of the separation:

$$\Delta C_v = \frac{1}{R_{f1}} - \frac{1}{R_{f2}}$$

where R_{f1} and R_{f2} are mobility coefficients of the separated compounds using TLC.

Stationary Phase

The high loading capacity of the stationary phase provides increased production rate. Column loadability can be increased with an increase in accessible surface area of the stationary phase by using a smaller particle size. However, this results in higher back-pressure during separation. If the stationary phase contains particles of different sizes, the fraction of larger particles controls the efficiency and the fraction of smaller particles controls the back-pressure. The use of high-quality packing with a narrow particle size distribution allows for increased production rates with less back-pressure and higher flow rates. Current average particle sizes for reversed-phase HPLC are in the range of 10–20 μm .

In preparative liquid-carbon-dioxide-based supercritical flow chromatography (SFC), smaller particles in the 5–10 μm range are used due to the decreased viscosity of the mobile phase. The pore size of the particles should be large enough to allow the molecules to readily diffuse into and out of the pores. In reversed-phase HPLC, longer alkyl chains provide better loadability because of the higher volume of interaction between the separated compounds and the stationary phase but lower resolution because of the slower kinetic rates of mass transfer [4]. The production rate (g/day) in batch chromatography increases with the increased size of the column. Columns of different length, packed with particles of different sizes of the same material, may have a similar production rate provided that the ratio of d_p^2/L is the same, where d_p is the diameter of the particles and L is the length of the column. Spherical particles have better mechanical stability and, thus, longer life than irregular particles.

Axial compression columns allow for efficient in-house packing of large columns with stationary phases. Systems utilizing radially compressed, preloaded, disposable cartridges are commercially available. In reversed-phase PHPLC, the choice between stationary phases with longer or shorter alkyl chains (C_3 , C_8 , C_{18}) depends mainly on the lipophilicities of the compounds to be separated. In order to assure that retention times are not too long for highly lipophilic compounds, a shorter alkyl chain length is preferred. This allows for faster separation to be achieved and, consequently, less organic solvent in the mobile phase, thereby cutting down on solvent costs. However, if evaporation of the collected fractions is critical, then using a longer-alkyl-chain-length stationary phase with a more volatile mobile phase may be advantageous.

Mobile Phase

The viscosity of the mobile phase influences the back-pressure and efficiency of the separation. The higher the back-pressure, the lower the flow rate that can be used and, consequently, the longer the run time. Lowering the viscosity increases mass transfer and, hence, the efficiency of the separation is improved (the peaks are narrower). Although the maximum flow rate does not provide the maximum separation, it does maximize the production rate.

The addition of nonvolatile additives to the mobile phase complicates isolation of the product after separation in reversed-phase PHPLC. The use of trifluoroacetic acid (TFA) simplifies workup due to its high volatility; it is common to add TFA to water–organic mobile phases as an ion-pairing reagent. It is important, however, to maintain a sufficient concentration of TFA, especially during loading of the sample, in order to ensure an adequate concentration of the counterion. Any residual TFA can be effectively removed from the isolated product using anion-exchange chromatography.

The solubility of the product in the mobile phase is an important parameter. Low solubility of the crude material in a mobile phase may require alterations in the method to prevent on-column precipitation of the material. If a number of different mobile-phase mixtures provides similar selectivity, the one in which the product is most soluble should be selected. For example, in normal-phase PHPLC, a mixture of 15% tetrahydrofuran in heptane may provide the same selectivity but better solubility than a mixture of 5% methanol in heptane. Separation

tion is much more reproducible when the ratio of the mobile-phase components is 50/50 rather than 99/1 because there is less chance that a small change in the mobile-phase composition will change the separation.

Some enantioselective stationary phases may be used only with a limited number of solvents. Because the cost of the mobile phase often represents more than half of the total cost of the separation (except lower cost of carbon dioxide in SFC), it is worthwhile to minimize the solvent consumption and also to increase the concentration of the product in the eluted fractions. Regeneration of the mobile phase is an economical choice at high solvent-consumption rates. Regeneration may include distillation of the used mobile phase followed by the adjustment of the mobile-phase composition if necessary. In normal-phase PHPLC, nonaqueous (nonhalogenated) solvents are easily removed from the product by evaporation and are less expensive to dispose of than water-containing mobile phases. At the same time, the use of high volumes of low-boiling flammable organic solvents may represent a safety concern. Accordingly, a less volatile solvent, heptane, for example, rather than hexane, should be used.

Flow Rate

The production rate increases at higher flow rates; however, some decrease in separation efficiency occurs. The upper limit of the flow rate depends on the ability of the stationary phase and hardware of the PHPLC system to withstand the higher back-pressure. Decreasing the flow rate may improve efficiency, and this effect is more distinctive with a reversed stationary phase containing long alkyl chains due to the more pronounced effect of the mass-transfer kinetics. Many noncovalently bonded enantioselective stationary phases may not be able to withstand higher flow rates and pressure.

Temperature

Increased temperature usually improves loadability and solubility and decreases the viscosity of the mobile phase. Consequently, the production rate increases, provided that the selectivity of separation or stability of the separated compounds and stationary phases are not compromised. However, resolution in enantioselective chromatography often improves at lower temperatures.

Gradient Program and Elution Order

Gradient elution provides a better production rate and higher recovery than using isocratic conditions if isocratic separation requires a regeneration step. The gradient profile in reversed-phase PHPLC is usually shallow, which decreases peak tailing compared to isocratic elution. After the sample injection, the gradient elution starts with a slightly weaker mobile phase (lower percentage of organic) than that required to elute the product with a desired retention, and then increases slowly in order to decrease the tailing. The gradient used is shallower when the target compound is the late-retained peak of the two peaks separated. The slope of the gradient should be steep enough to avoid dilution of the product fraction. Too shallow a gradient decreases the production rate and complicates isolation of the product. After most of the product has eluted, the gradient is raised stepwise in order to elute all late-retained impurities from the column. The column is equilibrated again with at least one column volume before the cycle is repeated.

If a compound is the major component in a mixture, the production rate increases if the impurities are eluted first. However, it is preferable for the product to be eluted prior to any closely retained impurity if a compound is not the main component in the mixture. Under self-displacement conditions, the product can actually be separated in a more concentrated solution than in a touching-band separation, especially if a later-retained impurity is in high concentration. The production rate in this case can be improved by an increase in loading, despite some decrease in recovery.

Sample Loading

Preferably, the sample is dissolved in a solvent mixture weaker than the mobile phase and introduced (concentrated) on the column in a narrow zone. Although a higher concentration of the sample contributes to a narrower zone after injection, it is not recommended to use a solution of more than twice the viscosity of the mobile phase. Column hardware should provide an even distribution of the injected solution throughout the cross section of the column.

The "dry injection" technique is often used in normal-phase flash chromatography when the solubility of the compound in a mobile phase is low. In this technique, a suspension of silica in the sample solution is concentrated to dryness and placed in a separate pre-column introduced before the actual column. In the reversed-phase mode, when there is limited sample solu-



bility, an injection of a larger volume of the less concentrated feed solution is preferable to an injection of a more concentrated material in a solution with a higher percentage of the organic solvent. Simple flash chromatographic prepurification of the crude material is always recommended for all types of PHPLC.

Direct scale-up of an analytical HPLC method at touching-band conditions is feasible only when there is a need for small (mg) amounts of the isolated material and the mobile phase does not contain nonvolatile additives. Using a touching-band optimization technique, the amount of material loaded may be increased until visible peak broadening occurs and the first sign of overlapping between the product peak and closely retained impurities is observed. The amount of product that may be loaded onto a column under touching-band conditions can be estimated as [5]

$$w \approx \frac{1}{9} w_s \left(\frac{\alpha - 1}{\alpha} \right)^2$$

where w_s is a column capacity that may be experimentally found by frontal analysis or less exactly estimated as w_s (mg) ≈ 0.4 (column surface area, m^2). The sample capacity of an analytical 25×0.46 -cm column is estimated to be 150–400 mg for small-molecule (<1000 Da) compounds.

Overloading of the column provides a much better production rate than the touching-band technique. Unlike analytical HPLC, Gaussian peak shape and baseline resolution are not a requirement in PHPLC. Overloading causes interaction between the compounds during chromatography that creates a sample self-displacement effect. This reduces peak tailing of the earlier eluting peak of the product and leads to increased purity and concentration of the eluted band. In contrast, if the concentration of the closely retained, earlier eluted compound is higher than the product, the tag-along effect compromises separation. The total capacity of the column may be found using frontal analysis [6]. A loading factor that represents the percentage of the loaded amount versus the total capacity of the column is one of the major parameters of optimization as well as efficiency (plate number) of the column. The loading factor and concentration of the product collected are usually higher in gradient and displacement chromatography than with isocratic elution.

Collection and Isolation of Separated Product

The composition of the mobile phase controls the product isolation procedure. Isolation from reversed-phase PHPLC fractions requires evaporation,

lyophilization, or dialysis of the water-containing mobile phase.

Another approach is to concentrate the fraction by diluting it with water and injecting the product on a separate column, followed by elution using a pure organic solvent. This method provides a more concentrated solution of the product in an organic phase, but it generates more waste solvents. In addition, automated collection at optimized cut points can contribute significantly to the overall optimization process.

Design of the Optimization Experiment

Nonlinearity of the Langmuir adsorption isotherms is observed even in noncompetitive chromatographic processes. Individual adsorption isotherms can be found experimentally using frontal analysis at overload conditions; however, the adsorption isotherms in the separation of mixtures are different because of the interference of other compounds in the mixture. In PHPLC method development, it is necessary to optimize separation conditions and column loading experimentally.

For optimization purposes, it is convenient to use analytical 0.46×25 -cm columns filled with the stationary phase available in bulk quantities for PHPLC. Primary evaluation and selection of the stationary and mobile phases, based on the selectivity of separation, column efficiency, and product retention, should be done initially on an analytical scale, including experiments under overload conditions on an analytical column. A particular set of chromatographic conditions includes the column, programmed mobile phase, flow rate, sample solution composition and amount injected, temperature, and collection points. These conditions are evaluated to obtain optimization of the maximum recovery of the desired material with required purity, or the maximum available purity for the required yield based on the HPLC analysis of collected fractions.

Not all of the separation parameters can be improved simultaneously and the optimization process often requires multiple experiments. In addition, separation problems, such as the sample “bleeding” through the column during loading or the product not completely eluting from the column, should be identified and corrected. Steps of the HPLC optimization experiment include (a) preliminary recording of the peak area–concentration plot for a pure product standard, (b) calculation of the amount of the target material in the solution prepared for separation, (c)



running the designed separation and collecting all fractions by time, starting after the eluted void volume and ending after the column is washed with the strong mobile phase for regeneration (*Note:* During the time in which the product and closely retained impurities elute, samples have to be taken more frequently), (d) all collected fractions should be analyzed to determine the purity (A) and the recovery of the product (C) in each fraction, and (e) the material balance of the product amount before and after separation should be measured.

Calculated product recovery $C_{\Sigma i}$ (%) if i fractions combined:

$$C_{\Sigma i} = C_1 + C_2 + \dots + C_i$$

Calculated product purity $A_{\Sigma i}$ (%) if i fractions combined:

$$A_{\Sigma i} = \frac{A_1 C_1 + A_2 C_2 + \dots + A_i C_i}{C_1 + C_2 + \dots + C_i}$$

where C_1, C_2, \dots, C_i is the product recovery (%) in fractions 1, 2, \dots, i and is calculated as a part of the total desired product presented in the injected crude material, and A_1, A_2, \dots, A_i is the product purity (%) in fractions 1, 2, \dots, i .

Comparison of the optimization results on recovery and purity assists in the selection of the optimized PHPLC conditions for scale-up. After optimum conditions are determined, a scale-up factor (Y) can be calculated, based on the results obtained on an analytical column, using the following equation:

$$Y = \frac{L_1 D_1^2}{L_2 D_2^2}$$

where L_1 and L_2 specify column lengths for the scale-up column and analytical column respectively and D_1 and D_2 are respective internal column diameters.

Continuous Process and Automation

Several techniques, such as continuous simulated moving bed (SMB) as well as closed-loop and closed-loop

steady-state recycling chromatographic techniques, are designed to improve the production rate and cost by recycling partially separated product, thus decreasing solvent consumption compared to conventional batch PHPLC. As a result, products are isolated in a more concentrated solution. These binary techniques are mostly used in the separation of pairs of stereoisomers and they require special hardware. If more than one impurity is present, the target material should be either the first or the last band to elute.

Automation allows batch chromatography to be run as a continuous process. Multiple injections using a separate pump and fraction collection provide an opportunity for continuous unattended operation. In isocratic separations, sample injection is often made before previously injected product elutes from the column, thus reducing cycle time and solvent consumption. Continuous and automated processes are always used with smaller columns and lower amounts of expensive enantioselective stationary phases. One of the future goals for modern PHPLC optimization would be the creation of software that would allow computer simulation modeling of nonlinear effects in preparative chromatography.

References

1. G. Ganetsos and P. E. Barker (eds.), *Preparative and Production Scale Chromatography*, 1993, Marcel Dekker, Inc., New York, 1993.
2. L. R. Snyder, *J. Chromatogr. B* 689: 105 (1997).
3. R. A. Bartsch and M. Maeda (eds.), *Molecular and Ionic Recognition with Imprinted Polymers*, American Chemical Society, Washington, DC, 1998.
4. D.-R. Wu and H. C. Greenblatt, *J. Chromatogr. A* 702: 157 (1995).
5. L. R. Snyder, J. J. Kirkland, and J. L. Glajch, *Practical HPLC Method Development* 2nd ed., John Wiley & Sons, New York, 1997.
6. G. Guiochon, S. G. Shirazi, and A. M. Katti, *Fundamentals of Preparative and Nonlinear Chromatography*, Academic Press, New York, 1994.



Preparative TLC

Edward Soczewinski

Teresa Wawrzynowicz

Medical University, Lublin, Poland

Introduction

Thin-layer chromatography (TLC) is mostly used as a separation technique combined with qualitative (identification) and quantitative analytical methods; the lower limit of the sample size depends on the sensitivity of detection. For ultraviolet (UV) and chemical detection, it is usually in the microgram or nanogram range. The separated spots can also be isolated for further investigations (chemical derivatization, mass spectrometry, or as chromatographic standards). To increase the scale, the dimensions and thickness of the layer are increased so that it is no longer “thin”; Nyiredy [1] proposed denoting preparative planar chromatography with the abbreviation PLC (preparative layer chromatography) (1 mg to 1 g). The flow of mobile phase during development may be due to capillary forces, pressure [forced-flow planar chromatography (FFPLC), overpressured layer chromatography (OPLC)], or centrifugal force (rotation planar chromatography, RPC).

Discussion

In analytical TLC, linear adsorption isotherms and compact spots are obtained for the loading of sample below 10^{-3} g mixture/1 g adsorbent. To increase throughput, PLC is operated under overloaded conditions, at 1 mg/1 g adsorbent or more. The overloading can be of concentration or volume type; the former is more advantageous [2].

The main goal of PLC is not the maximal peak (spot) capacity, but the maximal yield of separation.

The increased sample size is obtained by multiple spotting along the start line; when larger volumes are spotted, a series of microcircular chromatograms is obtained as the starting band; streaking from a syringe moving along the start line (e.g., as aerosol — using a programmed applicator); especially in OPLC, on-line zonal application across the plate is possible: The sample is injected into the continuous stream of eluent, distributed across the plate in a narrow channel parallel to the edge, and collected at the farther end of the

layer so that the layer acts as a flat column [1]. Similar on-line injection and collection is possible in centrifugal RPC.

The on-line application of sample, even of large volumes, is possible with certain horizontal chambers provided with distributors (Camag linear chamber, DS.-chamber [3,4]). When the mixture contains few components and the selectivity of the system is high, even large volumes of sample can be introduced from the edge of the layer so that the components are partly separated already in the application stage (frontal chromatography) and, because of mutual displacement effects, may become fully separated during development (Fig. 1), with high yield. To form a compressed starting band, the sample should be dissolved in a solvent weaker than the eluent.

Wide starting bands can also be formed by putting the edge of the plate in the sample solution. To avoid contamination of the eluent in the chamber during development, its bottom is covered by a strip of paper wetted with the eluent; more eluent is introduced when the starting band leaves the edge of the plate.

For thicker layers, the attainment of equilibrium in the gas–mobile phase–adsorbent system to avoid complicating effects (solvent demixing, preadsorption) is more difficult. The solutes migrate in a nonequibrated layer with differentiated velocity — more rapidly in the surface layer (because of the evaporation of solvent) and less rapidly closer to the carrier plate.

Two stages of PLC determine the success of separation: application of the sample and development. In the former stage, three different situations are possible: (a) sample dissolved in the eluent; (b) sample dissolved in diluted eluent; (c) sample dissolved in a solvent of different quantitative and qualitative compositions.

In case (a), minimal disturbances can be expected at the start of development; however, a wide starting band may be obtained. To obtain a narrow starting band, it is advantageous to dissolve the sample in a weaker solvent, [i.e., of lower content of modifier [case (b)]]; The solubility of the sample is the limiting factor here; the rule is to dissolve a large sample in a small volume of solvent. A good solvent of low eluent strength is chloroform or dichloromethane (e.g., for al-



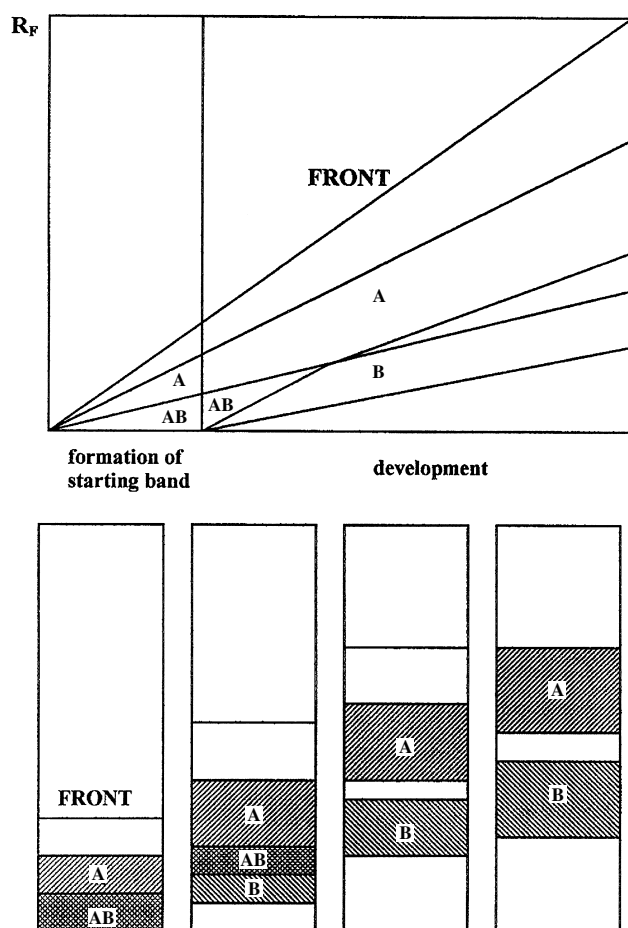


Fig. 1 Mutual displacements effects.

kaloids), toluene, or ethers. The application of sample solvent different from the eluent [case (c)] may lead to precipitation of the solutes at the beginning of development; the gradual dissolution of the precipitate in the mobile phase is reflected by comblike tailing of the starting band. It should also be taken into account that, in TLC, the ratio of volumes of the sample solvent (e.g., 0.5 mL) and eluent is greater than in analytical and preparative column chromatography and may have a more significant effect on the variation of eluent strength of the mobile phase. Evaporation of the sample solvent before development may cause precipitation of the solutes; their delayed dissolution in the mobile phase leads to tailing, which is detrimental to separation. Therefore, on-line application of the sample is advantageous.

The choice of mobile phase in PLC is also determined by the subsequent recovery of the separated solutes. Less volatile components (water, acetic acid, bu-

tanol) should be avoided, as well as nonvolatile components—buffer solutions and ion association reagents. Normal-phase chromatography and nonaqueous eluents should, therefore, be preferred. The rules of choice of eluents are otherwise similar to those for analytical chromatography (i.e., basing on elutropic and isoelutropic series) depending on the properties of the separated solutes. Usually, eluents giving R_F values in the lower range (0.1–0.5) are chosen, because the application of larger sample volumes leads to wide starting zones and increase of R_F values. For polar adsorbents, ethyl acetate belongs to the recommended modifiers, because of the good solubility of many nonpolar and moderately polar solutes, rapid equilibrium, and easy evaporation of the separated fractions.

In PLC, sorbents applied in TLC are usually used: silica, alumina, Florisil, cellulose, and silanized silica. Binding agents such as gypsum and somewhat lower amounts of water are recommended (e.g., for 1-mm silica layers, the weight ratio of water and adsorbent is 1:1.5 or 1:2). Plates with thicker layers should be dried in air in a horizontal position for a longer time (e.g., for 1-mm layers, ~ 1 h; for 2-mm layers, 2–4 h) and then dried and activated in an oven in gradually increasing temperatures. Equilibration in the chamber should also be prolonged. Because chemically bonded adsorbents are relatively expensive and, moreover, reversed phase (RP) sorbents are poorly wettable by aqueous eluents, polar adsorbents and nonaqueous eluents of low viscosity are usually applied in PLC. Special pre-coated plates of 0.5–2-mm layers are commercially available (e.g., silica gel 60 F₂₅₄₊₃₆₆). Such plates can be applied directly without activation; however, drying at 80°C for 2 h is recommended. Although the capacities of layers increase with their thickness, the separation efficiency decreases for thickness above 1.5 mm, so that optimal for PLC are layers of 0.5–1 mm thickness.

The development distance in PLC should not exceed 20 cm, because of the decreasing flow rate for longer distances and increasing diffusion of zones. A suitable system should have a resolution $R_s \geq 1.5$ in the analytical scale.

Marked improvement of separation efficiency in the separation of complex samples may be obtained by stepwise gradient elution [5] because of enhanced mutual displacement of the components in the concentrated starting band. A simple stepwise gradient of four to five steps is frequently sufficient; the generation of stepwise gradients is possible in some types of horizontal chambers [6] by consecutive delivery of eluent fractions of increasing concentrations of modifier.

Preparative layer chromatography can also be used as a pilot technique for column preparative chromatography in the same solvent–adsorbent system.

References

1. S. Nyiredy, in *Handbook of TLC*, 2nd ed. (J. Sherma and B. Fried, eds.), Marcel Dekker, Inc., New York, 1996.
2. L. R. Snyder and J. W. Dolan, *Adv. Chromatogr.* 38: 115 (1998).
3. E. Soczewinski, in *Planar Chromatography, Volume 1* (R. E. Kaiser, ed.) Hüthig, Heidelberg, 1986, pp. 79–117.
4. T. H. Dzido, G. Matysik, and E. Soczewinski, *J. Planar Chromatogr.* 4: 161 (1991).
5. E. Soczewinski, G. Matysik, and B. Polak, *Chromatographia* 39: 497 (1994).
6. E. Soczewinski, K. Czapinska, and T. Wawrzynowicz, *Sep. Sci. Technol.* 22: 2101 (1987).



Procyanidin Separation by CCC with Hydrophilic Solvent Systems

Yoichi Shibusawa

Tokyo University of Pharmacy and Life Science, Tokyo, Japan

Yoichiro Ito

National Institutes of Health, Bethesda, Maryland, U.S.A.

INTRODUCTION

Unripe apple contains polyphenols, including dihydrocalcons, phenolic acids, and others, up to 50% of the total mass of solids, whereas the rest consists of monomers, dimers, trimers, and oligomers of catechin and/or epicatechin, which are called apple procyanidins or apple condensed tannins (ACTs). Highly polymerized procyanidins have attracted attention in the fields of pharmacology and food chemistry because of their physiologic activities, such as hair-growth promotion, antiallergic, antibiotic, and inhibitory activities against enzymes and receptors. These properties of procyanidins depend on the degree of polymerization of catechin and/or epicatechin.

In order to correlate these pharmaceutical activities with their degree of polymerization, it is necessary to establish an efficient, reliable separation method. However, the application of liquid chromatography to the separation of these procyanidin oligomers is difficult because the oligomers above hexamers tend to cause irreversible adsorption onto the column packing materials.

Countercurrent chromatography (CCC)^[1] is a liquid-liquid partition technique that eliminates various complications arising from the use of solid supports. The high-speed CCC, the most advanced form in terms of partition efficiency and separation time, has been used for the separation and purification of a wide variety of natural products. The recent model of high-speed CCC, which facilitates the stationary phase retention for polar solvent systems, is particularly useful for the separation of hydrophilic, highly polymerized procyanidins.^[2,3]

APPARATUS

The CCC separation of procyanidin oligomers from apple condensed tannin was performed using a type-J high-speed CCC centrifuge (Fig. 1). The apparatus holds a multilayer coiled separation column and counterweight symmetrically at a distance of 10 cm from the central axis of the centrifuge. The separation column is fabricated by

winding a single piece of 2.0-mm-ID and 21-m-long polytetrafluoroethylene (PTFE) tubing directly onto the holder hub, making four coiled layers between a pair of flanges. The total capacity of the column is about 72 mL. The speed of the apparatus is regulated at 1000 rpm with a speed controller. The coil rotates around its axis as it simultaneously revolves around a central axis, producing an efficient mixing of the two phases while retaining a sufficient amount of the stationary phase in the column.

PREPARATION OF ACTs FOR CCC SAMPLE

The unripe apples were homogenized in potassium pyrosulfite solution, and the mixture was allowed to stand for 1 day. The supernatant was centrifuged and filtered with a glass filter funnel. The filtrate was applied to adsorption chromatography, and the ACT fraction was evaporated and lyophilized. Purified ACTs were a mixture of monomer (catechin and/or epicatechin) and oligomers from dimers to pentadecamers, as shown in Fig. 2.



Fig. 1 Photograph of the type-J multilayer coil planet centrifuge. (View this art in color at www.dekker.com.)

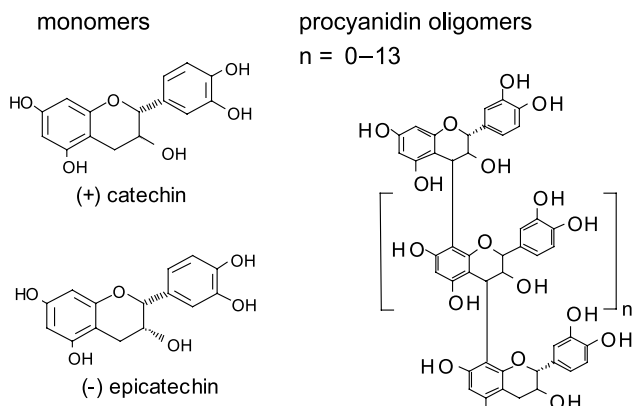


Fig. 2 Chemical structures of catechin, epicatechin, and procyanidin oligomers.

MEASUREMENT OF PARTITION COEFFICIENT OF CATECHIN AND/OR EPICATECHIN AND ACTs

CCC utilizes a pair of immiscible solvent phases that have been preequilibrated in a separatory funnel: One phase is used as the stationary phase and the other as the mobile

phase. In order to achieve efficient separation of higher polymerized, large oligomers from ACTs, the partition coefficient values (K_D) of catechin and/or epicatechin and ACTs were determined in the following four hydrophilic solvent systems:

1. *n*-butanol/water (1:1)
2. *n*-butanol/acetic acid/water (4:1:5)
3. methyl *tert*-butyl ether/acetonitrile/water (2:2:3)
4. methyl acetate/water (1:1)

As the chromatographic process in CCC is based on the partition of a solute between the mobile and stationary phases, the K_D value is the most important parameter in CCC. A K_D value of around 1.0 is most desirable in CCC, wherein a solute with $K_D=1.0$ elutes with its retention volume equivalent to the total column capacity. In the above two-phase solvent systems, the K_D values of monomers (catechin and/or epicatechin) were greater than 1.0, and those of the ACTs are always smaller than 1.0, suggesting that monomers are more hydrophobic than their oligomers present in ACTs. Among these four solvent systems, we selected a simple binary system of methyl acetate/water for the separation of procyanidin oligomers from ACTs by CCC.

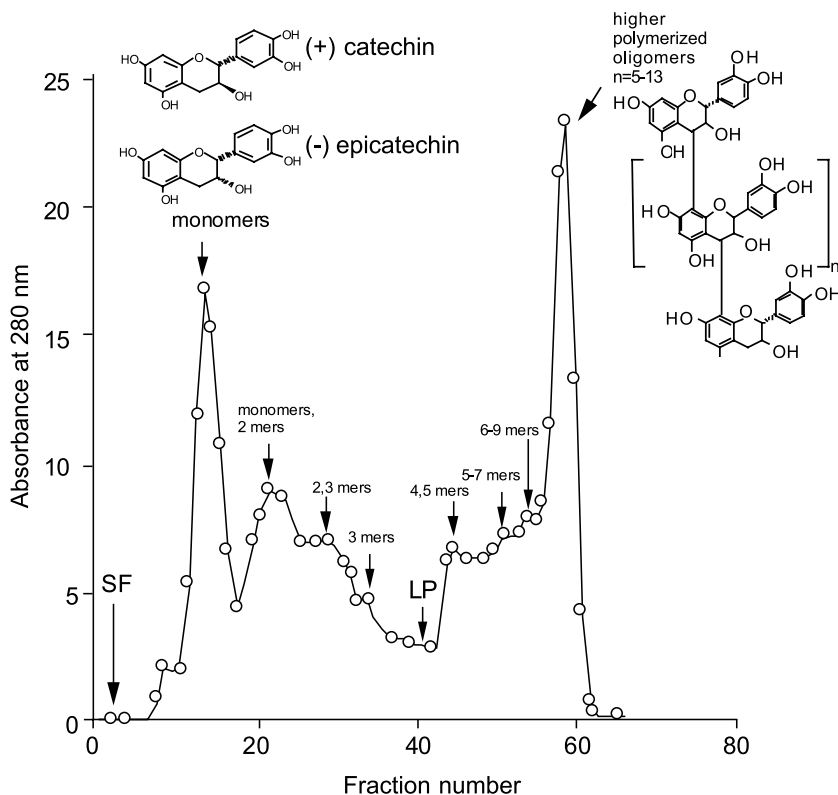


Fig. 3 Separation of procyanidins in the order of their degree of polymerization by countercurrent chromatography.

CCC SEPARATION OF ACTs BY HYDROPHILIC SOLVENT SYSTEM

Figure 3 shows a chromatogram obtained from ACTs using the two-phase solvent system composed of methyl acetate/water (1:1). After filling the multilayer coil with the lower aqueous stationary phase, 2 mL of the sample solution, containing 100 mg of ACTs, was injected into the column. The separation was performed by pumping the upper phase into the column at a flow-rate of 1.0 mL/min at 1000 rpm rotational speed. The effluent was monitored at 280 nm and fractions were collected at 3 mL per tube. The masses of the fractionated oligomers were determined by matrix-assisted laser desorption/ionization/time-of-flight mass spectrometry (MALDI-TOF-MS) analysis.

After the elution of the trimers, the lower aqueous phase was eluted through the column to facilitate a rapid elution of the oligomers still remaining in the column. The tetramers and pentamers fraction, the pentamers, hexamers, and heptamers fraction, and higher polymerized oligomers over the hexamers fraction were subsequently eluted from the column in this order. Interestingly, the elution order is also coincident with the degree of polymerization of catechin and/or epicatechin. The last large peak will contain higher polymerized oligomers (over hexamers) and was not assigned by MALDI-TOF-MS under these experimental conditions. The lower

stationary phase retained in the column was estimated as 82% of the total column capacity (72 mL) prior to the application of the elution with lower phase. The separation was completed within 3 hr.

CONCLUSION

These results indicate that the present method is capable of fractionating the apple procyanidin oligomers from ACTs according to the degree of polymerization. The highly polymerized, very hydrophilic oligomers, which tend to be adsorbed on the column packing materials by HPLC, were all recovered from the CCC column.

REFERENCES

1. Conway, W.D. *Countercurrent Chromatography: Apparatus and Applications*; VCH: New York, 1990.
2. Shibusawa, Y.; Yanagida, A.; Ito, A.; Ichihashi, K.; Shindo, H.; Ito, Y. High-speed counter-current chromatography of apple procyanidins. *J. Chromatogr., A* **2000**, *886*, 65–73.
3. Shibusawa, Y.; Yanagida, A.; Isozaki, M.; Shindo, H.; Ito, Y. Separation of apple procyanidins into different degree of polymerization by high-speed counter-current chromatography. *J. Chromatogr., A* **2001**, *915*, 253–257.



Programmed Flow Gas Chromatography

Raymond P.W. Scott

Scientific Detectors Ltd., Banbury, Oxfordshire, England

Introduction

There are three methods that can be used to accelerate the elution of strongly retained peaks during chromatographic development. Flow programming, where the flow of mobile phase is continuously increased during the development of the separation, temperature programming, and gradient elution, the latter being exclusively used in liquid chromatography. We reserve our discussion here to flow programming.

Discussion

Flow programming is not as effective in reducing the elution time of well-retained components and tends to cause increased band dispersion; it is, however, more gentle than temperature programming and would be chosen when separating thermally labile materials. The complexity of the theoretical treatment depends on whether the mobile phase is compressible or not. In gas chromatography, the mobile phase is compressible, and this must be taken into account in the first theoretical treatment.

We shall assume that under flow programming conditions, the mass flow rate will be increased linearly with time (i.e., $Q_{0(t)} = (Q_0' + \alpha t)$, where Q_0' is the initial exit flow rate, $Q_{0(t)}$ is the exit flow rate after time t and α is the program rate. These conditions are usual for modern gas flow programming devices that utilize mass flow controllers which are computer operated. Now, if ΔV_0 is an increment of exit flow, measured at atmospheric pressure, then employing the usual pressure correction factor, the corrected gas flow (ΔV_r) will be

$$\Delta V_r = \frac{3}{2} \Delta V_{r(0)} \left(\frac{\gamma^2 - 1}{\gamma^3 - 1} \right)$$

where γ is the inlet/outlet pressure ratio of the column. Then, under the above-defined programming conditions,

$$\Delta V_{r(t)} = \frac{3}{2} \left(\frac{\gamma_t^2 - 1}{\gamma_t^3 - 1} \right) (Q_0 + \alpha t) \Delta t \quad (1)$$

where (γ_t) is the inlet/outlet pressure ratio at time t and $\Delta V_{r(t)}$ is the increment of volume flow at time t .

Now, as the flow is increased, the inlet pressure will also increase and, thus, the inlet/outlet pressure ratio (γ) will change progressively during the program; the mean flow rate will be reduced according to the pressure correction function and the decrease in elution rate will not be that which would be expected. Consider an open-tubular column; from Poiseuille's equation,

$$P_0 Q_{0(t)} = \frac{(P_t^2 - P_0^2) \pi a^4}{16 \eta l}$$

or

$$P_0 (Q_0 + \alpha t) = \frac{(P_t^2 - P_0^2) \pi a^4}{16 \eta l} \quad (2)$$

where P_t is the inlet pressure at time t , P_0 is the outlet pressure (atmospheric), η is the viscosity of the gas at the column temperature, l is the length of the open-tubular column, and a is the radius of the open-tubular column.

A similar equation would be used for a packed column, except the constant $(\pi/16)$ would be replaced by the D'Arcy constant for a packed bed. Rearranging,

$$\frac{P_0 (Q_0 + \alpha t) 16 \eta l}{\pi a^4} + P_0^2 = P_t^2$$

thus,

$$\gamma_t = \frac{P_t}{P_0} = \left(\frac{(Q_0 + \alpha t) 16 \eta l}{P_0 \pi a^4} + 1 \right)^{0.5} \quad (3)$$

Assuming the column dimensions are 320 μm in inner diameter (radius $a = 0.0160 \text{ cm}$) and 30 m in length,



and it is operated at 120°C using nitrogen as the carrier gas which, at that temperature, has a viscosity of 129×10^{-6} P, then, by using Eq. (3), the change (γ) can be calculated for different flow rates. The relationship between flow rate (as measured at the column exit and at atmospheric pressure) and the column inlet/outlet pressure ratio is shown in Fig. 1. The inlet/outlet pressure ratio changes significantly during a mass flow rate program, which will attenuate the elution rate as shown by the pressure correction factor. It is seen that the curve is a close fit to a second-order polynomial function, but this relationship is fortuitous, although it might be used empirically to predict inlet/outlet pressure ratios.

It is now possible to use the values for γ_i to calculate when the solute is eluted at the retention time t_r for different flow program rates. Employing Eq. (1), when the sum of all the increments of ΔV_r is equal to the retention volume V_r , then t will be t_r , the retention time:

$$V_r = \sum_{i=0}^{t=t_r} \frac{3}{2} \left(\frac{\gamma_i^2 - 1}{\gamma_i^3 - 1} \right) (Q_0 + \alpha t)$$

With a simple computer program, the retention time t_r can be calculated for a range of different program rates (α) and for solutes having retention times of 10, 50, and 250 mL, respectively. The column was again assumed to be 320 mm in inner diameter and 30 in length and operated at 120°C using nitrogen as the

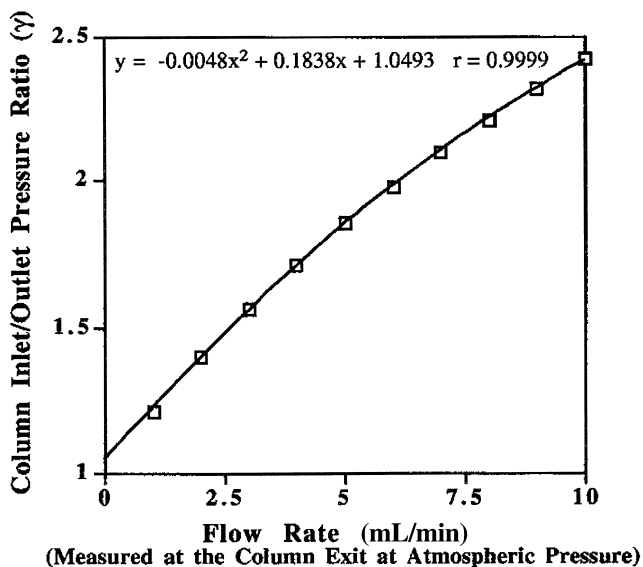


Fig. 1 The relationship between the inlet/outlet pressure ratio and exit flow rate for an open-tubular column.

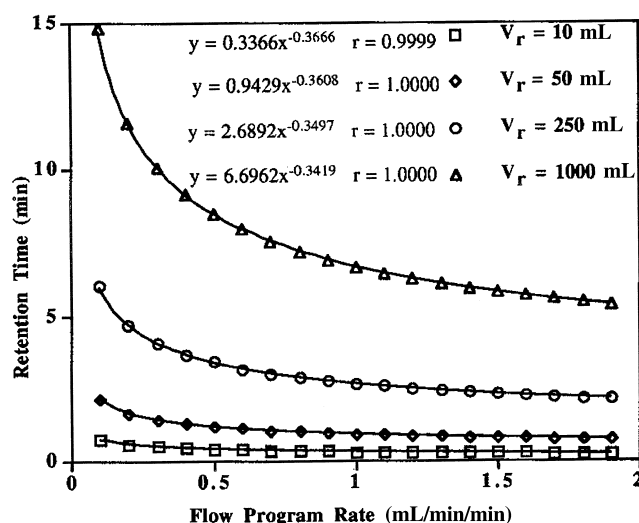


Fig. 2 Curves relating elution time to flow program rate for solutes having different retention volumes. (From Ref. 1.)

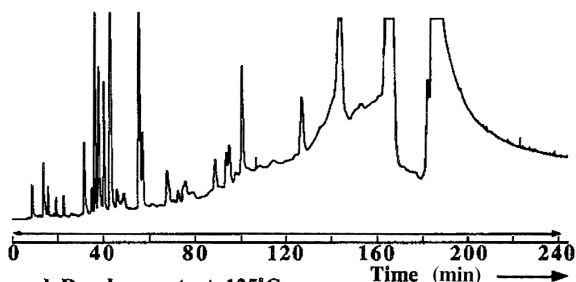
carrier gas which, at that temperature, has a viscosity of 129×10^{-6} P. The results are shown in Fig. 2.

The effect of program rate on retention time is much as would be expected. For any individual solute, the retention time is related to some power of the solute retention volume, but the indices vary significantly with the retention volume of the solute. This relationship does not have a theoretical explanation at this time but might be useful for predicting retention times from experimental data. Despite the attenuating effect of the pressure correction factor, the use of flow programming is effective in reducing the retention time of strongly retained solutes. However, unless the diffusivities of the solutes in the mobile phase are high, (i.e., mobile phases such as hydrogen or helium are employed), there will be significant peak dispersion at the higher velocities, the column efficiency will be reduced, and resolution will be lost.

An excellent example of the use of flow programming was given in a very early article describing the technique [1]. Lemon grass oil contains two substances that are very thermally labile, and these are eluted very late in the chromatogram. If temperature programming is employed, the substances decompose at the higher temperatures, producing a sloping baseline as shown in the upper chromatogram in Fig. 3. The baseline does not return to its normal level until the thermally unstable compounds have been completely

Isobaric Development at 100 psi, 60 mL/min
Temperature programmed from 125°C to 200°C
at 0.5 °C/ min

Sample Volume 2 µl



Isothermal Development at 125°C

Flow Programmed
from 40-450 mL/min

Sample Volume 2 µl

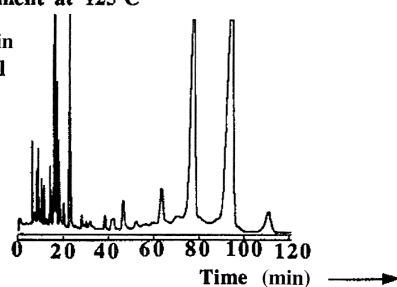


Fig. 3 The separation of lemon grass oil by temperature programming and by flow programming.

eluted. If the separation is carried out isothermally at a temperature where the decomposition is minimal, and the mixture is developed by flow programming, all the solutes are eluted on a relatively stable baseline. The elution times are high, due to long packed columns being employed, as opposed to capillary columns.

Reference

1. R. P. W. Scott, *Gas Chromatography 1964* (A. Goldup, ed.), The Institute of Petroleum, 1964, p.25.

Suggested Further Reading

Scott, R. P. W., *Introduction to Analytical Gas Chromatography*, Marcel Dekker, Inc., New York, 1998.
Scott, R. P. W., *Techniques of Chromatography*, Marcel Dekker, Inc., New York, 1995.



Programmed Temperature Gas Chromatography

Raymond P.W. Scott

Scientific Detectors Ltd., Banbury, Oxfordshire, England

Introduction

Temperature programming becomes necessary when the sample contains components that have polarities and/or molecular weights that extend over a wide range. Such samples, if separated isothermally, may well result in the less retained solutes being adequately resolved and eluted in a reasonable time. However, the more polar or higher-molecular-weight solutes may be held on the column for an inordinately long period, and the solute peaks, when they are eluted, are likely to be wide and flat and difficult to evaluate quantitatively. To avoid this situation, the column temperature can be progressively increased during development so that the late eluting peaks are accelerated through the column and are still sharp and eluted in a reasonable time. This procedure is called temperature programming.

Application

The corrected retention volume of a solute (V'_r) is given by (see the entry Rate Theory in Gas Chromatography)

$$V'_r = KV_s$$

where K is the distribution coefficient of the solute with respect to the stationary phase and V_s is the volume of stationary phase in the column.

The value of K varies with temperature in the following manner (see the entry Thermodynamics of Retention in Gas Chromatography)

$$\ln(K) = -\left(\frac{\Delta H}{RT} - \frac{\Delta S}{R}\right)$$

$$\text{or } K = \exp\left[-\left(\frac{\Delta H}{RT} - \frac{\Delta S}{R}\right)\right]$$

where ΔH is the standard enthalpy of distribution, ΔS is the standard entropy of distribution, R is the gas constant, and T is the absolute temperature. Thus,

$$V'_r = \exp\left[-\left(\frac{\Delta H}{RT} - \frac{\Delta S}{R}\right)\right]V_s$$

It is seen that as T increases, K decreases. It follows that K and, consequently, the retention volume can be progressively decreased by increasing the column temperature. In practice, this is usually achieved by situating the column in an oven, the temperature of which is controlled by appropriate electronic circuitry. Theoretically, the temperature of the oven can be increased as any function of time, but almost all program profiles are linear in form.

Consequently, programming the column from temperatures T_1 for a period of t , using a linear program (i.e., $T = T_1 + \alpha t$, where t is the elapsed time), the mean value of K will be given by the following function:

$$K = t_1^{-1} \sum_{t=0}^{t=t_1} \exp\left[-\left(\frac{\Delta H}{R(T_1 + \alpha t)} - \frac{\Delta S}{R}\right)\right]$$

where t_1 is the time period of the program. [Preferably t_1 , for maximum accuracy, should be defined in small units (e.g., seconds and not minutes)]. Similarly, the program rate α must be defined in degrees Celsius per second.

Now, when the solute is eluted, V'_r will equal the product of the mean flow rate Q_m and t_1 , which will be the retention time; that is,

$$V'_r = Q_m t_1$$

The mean flow rate through a gas chromatography column is given by [1]

$$Q_m = Q_0 \frac{3(\gamma^2 - 1)}{2(\gamma^3 - 1)}$$

where γ is the inlet/outlet pressure ratio and Q_0 is the exit flow rate.

Thus, when the solute elutes,

$$\begin{aligned} V'_r &= V_s K \sum_{t=0}^{t=t_1} \exp\left[-\left(\frac{\Delta H}{R(T_1 + \alpha t)} - \frac{\Delta S}{R}\right)\right] t_1 \\ &= Q_0 \frac{3(\gamma^2 - 1)}{2(\gamma^3 - 1)} t_1 \end{aligned}$$

where V_s is the volume of stationary phase in the column.

Solving for t in the classical manner is a cumbersome mathematical procedure and it is easier to employ a nu-



merical method to calculate t . To demonstrate the effect of temperature programming on solute elution, a computer program was used to calculate the retention time of a given solute eluted at different programming rates. The data used were that of Liao and Martire [1] for 3-methyl hexane chromatographed on n -octadecane at temperatures of 30°C, 40°C, 50°C, and 60°C.

By curve-fitting the retention data to the reciprocal of the absolute temperature, the numeric form of the distribution coefficient was found to be

$$K = \exp\left(\frac{1737.777}{T} - 2.75115\right)$$

A simple computer program provided values for the retention time, calculated for different linear program rates, and the results are shown as curves relating retention time to program rate in Fig. 1. The inlet/outlet pressure ratio (γ) was assumed to be 2 and the flow rate at the column exit was 20 mL/min (0.3333 mL/s). The logic of the program was based on a search for that value of t where the value of (V'_t) equaled the product of t and the mean column flow rate. It should be noted that the data were reported as the corrected retention volume per gram of stationary phase; thus, for simplicity, the curves are calculated on the assumption that the column contains 1 g of stationary phase. Retention times for columns containing more stationary phase would be appropriately longer. Due to the change in both the density and viscosity of a gas with temperature, the mean flow rate will change slightly during the program, but the error will be small, provided that a *mass flow controller* is employed and not a pressure controller. For the calculations, the inlet pressure was assumed to remain constant throughout the program.

This procedure is a general method for calculating the effect of the program rate on retention time. Basically, the corrected retention volume must be measured for each solute of interest at two different temperatures to provide the thermodynamic constants. The above equations will then allow the effect of different linear temperature programs on the corrected retention volume to be calculated for each solute. The effect of program rate on resolution can also be observed if some solutes elute close together. In fact, the

Programmed Temperature Gas Chromatography

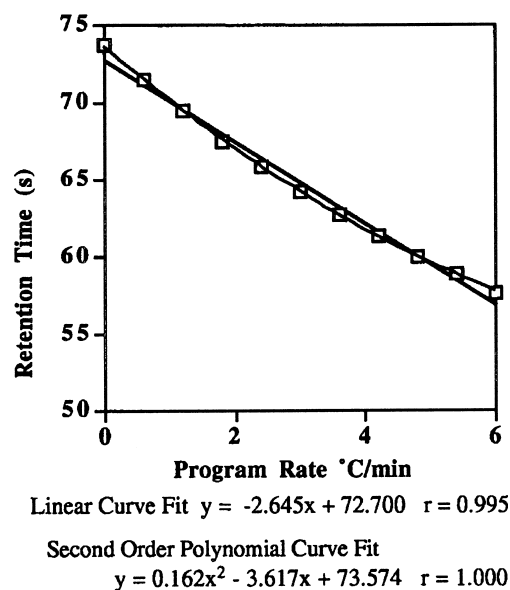


Fig. 1 Graph of retention time versus program rate.

equation can be used for program functions other than linear, but these are rarely employed. The relationship between retention time and program rate is approximately linear and can be assumed so for most practical purposes. For more accurate work, a second-order polynomial should be used to describe the retention time as a function of the program rate, which can give very accurate values.

Reference

1. H. L. Liao and D. E. Martire, *J. Am. Chem. Soc.* 94(10): 2058 (1972).

Suggested Further Reading

Scott, R. P. W., *Introduction to Analytical Gas Chromatography*, Marcel Dekker, Inc., New York, 1998.
 Scott, R. P. W., *Techniques of Chromatography*, Marcel Dekker, Inc., New York, 1995.

Prostaglandins: Analysis by HPLC

Harald John

IPF PharmaCeuticals GmbH, Hannover, Germany

Introduction

Physiology and Chemistry [1]

Prostaglandins (PG) are a class of substances representing natural metabolites of three 20 carbon fatty acids differing in their number of double bonds: arachidonic acid (AA, 5,8,11,14-eicosatetraenoic acid), 8,11,14-eicosatrienoic acid, and 5,8,11,14,17-eicosapentanoic acid. In the following, only the bisenoic PGs (produced from AA), which dominate most biological systems, will be discussed. Free AA acts as a substrate for the cyclooxygenase enzyme complex and consecutively several specific enzymes, including isomerases, reductases, and synthases, produce thromboxanes (TX) and further PGs as demonstrated in Fig. 1. Their weak ultraviolet (UV) absorption maxima are found at 192 nm and at 217 nm for PGA_2 , 228 nm for 15-oxo-PGE₂, and 278 nm for PGB₂ arising from delocalized electron systems of conjugated double bonds and oxo groups. Prostanoids are known for their high and widespread physiological potency acting as chemical messengers capable of regulating cellular behavior in mammalian tissues. The influences on platelet aggregation, contractory or dilatatory effects on muscles and vessels, mediating inflammatory diseases, and pain are only a few examples which make these compounds of great interest for diagnostic and therapeutic aims. Therefore, analytical methods are needed which allow the trace-level determination of PGs from different complex biological sources like serum, plasma, seminal fluid, urine, or culture medium.

In most cases, PGs are measured by highly specific immunoassays, although not enabling simultaneous determination of multiple components in a single experiment. Beside high-performance liquid chromatography (HPLC) techniques, GC methods are often used in combination with mass spectrometry (MS), flame ionization (FID), or electron-capture detectors (ECD). However, HPLC is still a very useful, versatile, and widespread tool for analytical or preparative separation and detection under mild conditions, allowing qualitative and quantitative measurement of oxygen-sensitive prostanoids.

Sample Preparation [2–4]

Prostanoids only occur in trace levels in complex biological samples. Therefore, the removal of substances impairing chromatographic resolution or detection and concentration of the analytes is required. Most of the samples are extracted using liquid–liquid (LLE) or solid-phase (SPE) methods without longer time of storage, thus avoiding the nonenzymatic production of isoprostanes by autoxidation of AA [5]. Due to the free carboxylic groups of prostanoids, samples are acidified to pH 3–4, usually by acetic (HOAc), formic, citric, or hydrochloric acid. Acidification to lower pH values has to be avoided due to chemical instability and degradation of some prostaglandins: PGE₂ dehydrates irreversible to PGA_2 , isomerizing to PGB₂; PGD₂ might be dehydrated to an inverted version of PGA_2 . Epimerization at C₁₅ and cis–trans isomerization may occur, as recently shown for the thromboxane synthase product 12-S-hydroxyheptadecatrienoic acid (HHT) [6]. LLE is carried out by the addition of a one-fold to fivefold volume of nonpolar solvents like diethyl ether, chloroform, or ethyl acetate, followed by shaking or stirring for a few minutes. Consecutive centrifuging enables efficient phase separation and pellets the particulate matter. Recoveries of 80–98% (dependent on the prostaglandin) are achieved.

Repetition of this procedure is seldom done and does not improve the recovery significantly. The organic layers are evaporated to dryness under reduced pressure or a gentle stream of nitrogen to concentrate the prostanoids prior to further preparations or chromatography. Extraction of biological samples using petrol ether or hexane at neutral pH values prior to extraction of acidified matrix removes nonpolar fatty acids and lipids, preventing their possible negative interferences.

Using SPE methods, adsorption of prostanoids is routinely and efficiently done by straight-phase material like silic acid or by reversed-phase C₁₈ material. Cleanup and washing steps using eluents of rising polarity for silica-based columns (e.g., increasing percentages of methanol in an ether–hexane–toluene mixture) or decreasing polarity for octadecyl columns



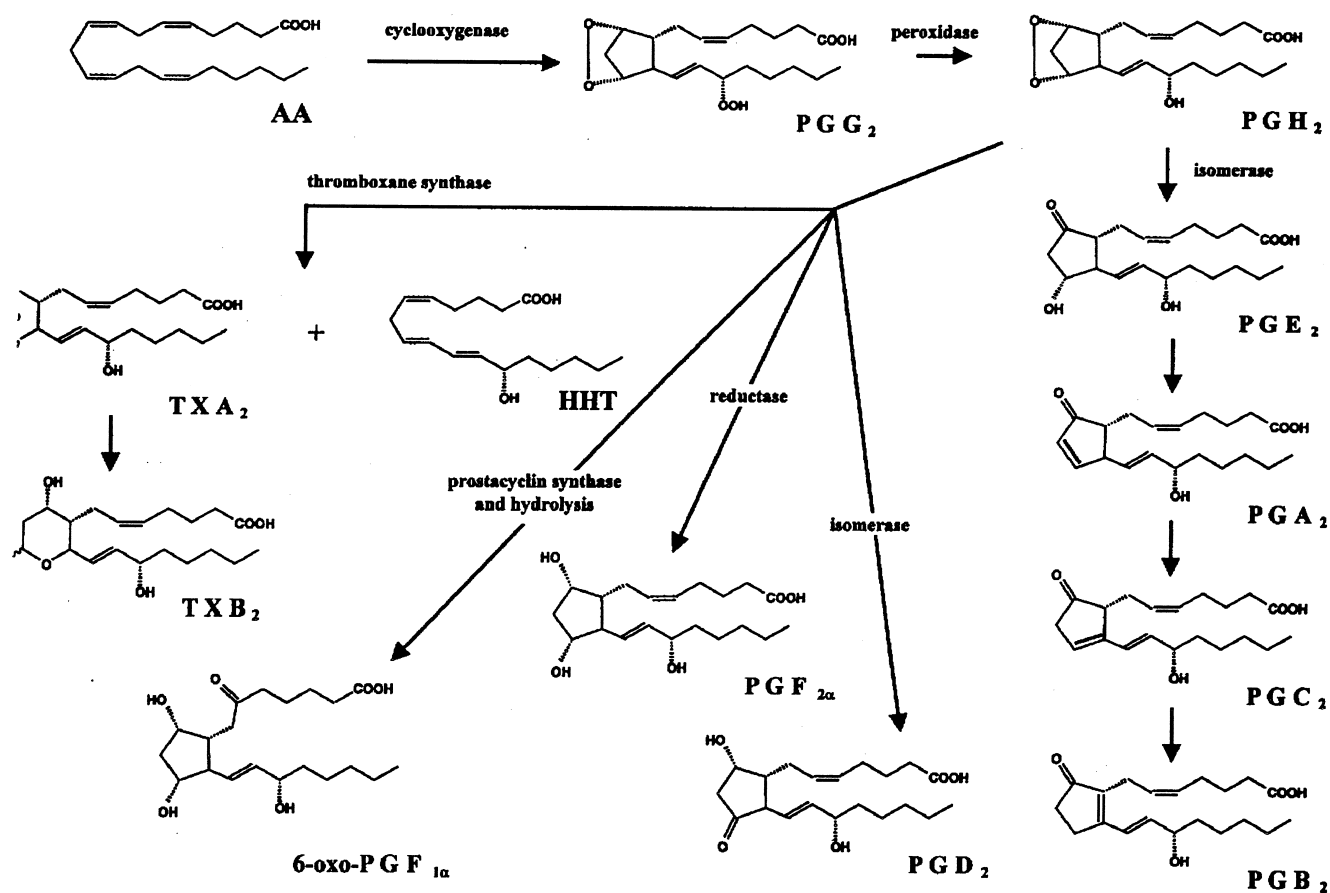


Fig. 1 Metabolism of arachidonic acid (AA) to prostaglandins (PG) and thromboxanes (TX).

[e.g., increasing percentages of acetonitrile (ACN), ethanol, or ethyl acetate in an aqueous mixture] enable sufficient extraction. These stepwise and fractionating procedures allow consecutive elution of different substance classes like polar compounds (polar lipids), fatty acids and their monohydroxy derivatives, PGs and TXs, and hydrophilic components. Recoveries for all prostanoids are in the range 90–98%. Extracts are evaporated to dryness prior to further procedure. Avoiding these manual and time-consuming extraction methods, the use of packed precolumns coupled to reversed-phase (RP)–HPLC equipped with a conventional six-port injector is a suitable alternative especially for small sample volumes.

Mobile and Stationary Phases [4,7,8]

In most cases, PGs or their derivatives are separated by partition chromatography on reversed-phase columns using gradients of organic solvents and water with in-

creasing organic content during elution. ACN enables better separation than MeOH when combined with acidified aqueous media using HOAc, trifluoric acid, or phosphoric acid. Separated by rising hydrophobicity, pure PGs are eluted typically in the following order of retention times: $6\text{-oxo-PGF}_{1\alpha} < \text{TXB}_2 < \text{PGF}_{2\alpha} < \text{PGE}_2 < \text{PGD}_2 < 13,14\text{-dihydro-15-oxo-PGF}_{2\alpha} < 13,14\text{-dihydro-15-oxo-PGE}_2 < \text{PGA}_2 < \text{PGB}_2$. Monohydroxy metabolites of AA and other fatty acids often present in PG-containing samples are eluted at much higher percentages of organic solvents, demanding a wide-range gradient.

Early PG analysis using HPLC techniques was carried out as adsorption chromatography on normal-phase (NP) columns packed with silica or alumina. The nonpolar mobile phase comprising of organic solvents (hexane, toluene, ethyl acetate, and HOAc) allows separation of PGs which are unstable in aqueous media (e.g., PGH_2 on cyano- or phenyl-bonded phases). Usually, the injection medium must be fairly polar to dissolve the PGs. This is achieved by the addition of

small volumes of isopropanol resulting in much poorer resolution of monohydroxy acids simultaneously analyzed. Furthermore, the NP chromatography enables excellent separation of geometrical isomers like PGE₂ and PGD₂. The lock–key-type steric fitting of solute molecules with the discrete adsorption sites of the silica surface is responsible for this effect. However, adsorption chromatography requires a strict temperature control influencing retention time and, therefore, reproducibility and ruggedness.

Besides the dominating NP and RP techniques, silver-ion-loaded cation- and strong-anion-exchange chromatographies have been introduced as well. The silver-ion method based on interactions between Ag⁺ and double bonds, and polar–polar attractive forces between the stationary phase and the solute is carried out using polar solvents containing low concentrations of ACN. The separation of *cis*–*trans* isomers can be achieved by this chromatographic modification. Anion-exchange chromatography has been described for underivatized PGs using tromethamine acetate–ACN mixtures at neutral pH as the mobile phase and a pellicular strong anion-exchange column as the stationary phase.

However, NP or RP methods represent the most powerful and common chromatographic techniques allowing PG analysis with very good reproducibility, sensitivity, wide linear ranges for quantitative analysis, and a broad spectrum of detectors.

Detection [4,8,9]

Investigating metabolism or stability of prostanoids, radiolabeled precursors or analytes are often used. The tritiated or ¹⁴C-labeled compounds can easily be detected without any further derivatization using on-line or off-line liquid scintillation, which is not impaired by any interferences derived from matrix components. Efficient but less sensitive PG analysis is possible by UV detection (190–210 nm) of underivatized substances demanding the remove of interfering contaminants or simple sample matrices like buffers or some cell supernatants.

Derivatization [8,10]

Due to the low physiological concentrations in the femtomolar to picomolar range and the very weak UV absorptivity of prostanoids, derivatization is often required when analyzing by HPLC procedures. Improving detection sensitivity and selectivity, many methods

have been developed allowing the quantitative and qualitative determination of these eicosanoids. Most of these techniques represent a selective and rapid pre-column derivatization of the extracted sample. Many procedures, especially for esterification of the carboxylic function, have been established. In the following, the stationary phases used for the separation of derivatized PGs are indicated in parentheses. Fluorescent derivatives with exceedingly high UV absorptivities can be obtained in almost quantitative yields by *p*-(9-anthroyloxy)-phenacyl bromide, also known as panacylbromide (LiChrosorb 100 Diol, or μ -Bondapak C18, or Radial Pak B). Panacyl esters are produced within 0.5–2 h using mild reaction temperatures between 20°C and 45°C. This reaction requires alkaline reagents like KOH or K₂CO₃ as catalysts in an organic solvent and, additionally, crown ethers as phase-transfer agents.

Ultraviolet detection is possible at 254 nm combined with fluorescence detection at about 450 nm after excitation at about 360 nm. Interferences of native fluorescent compounds are weak due to their emission wavelength range from 300 to 400 nm. Comparable phenacyl esters are synthesized with *p*-bromophenacyl bromide or *p*-nitrophenacyl bromide with a similar spectroscopic behavior (both μ -Bondapak C18). Useful derivatization by tagging the COOH — group can also be done with α -bromo-2'-acetoneaphthone resulting in well-soluble and strongly UV-absorbing (254 nm) naphthanyl esters after a reaction time of only 10 min at room temperature (LiChrosorb Si-100). Furthermore, coumarin derivatives (substituted at position 7 for higher fluorescence quantum yields) are predestinated to fluorescent ester preparation ($\lambda_{\text{ex}} \approx 330\text{--}390$ nm and $\lambda_{\text{em}} \approx 410\text{--}470$ nm) using 4-bromomethyl-7-methoxycoumarin (LiChrosorb 100 Diol or Varian CN-10 Micropak) or 4-bromomethyl-7-acetoxycoumarin (BrMAC) (LiChrosorb RP18). Luminarin-4 (a labeling reagent with a quinolizinocoumarin structure) enables chemiluminescence detection in combination with peroxyoxalate (Ultraspher ODS-2 or Spherisorb ODS-2). These reactions are carried out at more drastical conditions at about 70°C in aprotic solvents, requiring catalysis and phase-transfer agents.

When using BrMAC, postcolumn hydrolysis of separated PG esters is necessary for on-line detection of the fluorophore, resulting in detection limits of about 10 fmol. Hydrazone or amide derivatives are also suitable for fluorescence detection as well as 3-bromomethyl-6,7-dimethoxy-1-methyl-2(1*H*) quinoxalinone (YMC Pack C8) or 9-anthroyldiazomethane (ADAM) characterized by its low stability (Nucleosil ODS silica). Electrochemical detection of active com-



pounds readily reduced can be carried out with low applied potential due to low background current and noise level in the oxidative mode after COOH derivatization using compounds with aromatic structures like 2,4-dimethoxyaniline (Nucleosil C18), 2-bromo-2'-nitroacetophenone, *p*-nitrobenzyloxyamine, or 2,4-dinitrophenylhydrazine. Thermospray (TSP)-MS detection has been used after esterification with diazomethane followed by oxime synthesis using trimethylanilinium hydroxide (TMAH) and separation on Zorbax ODS.

Additional to the mentioned COOH-derivatization PGs can also be modified using their hydroxyl functions. Oxidation with pyridinium dichromate to 15-oxo-PGs enables UV detection at 230 nm due to the conjugated oxo and $C_{13}=C_{14}$ double bonds (Microbore C18). TSP-MS analysis in the positive ion mode is possible after overnight reaction at 5°C with acetic anhydride in pyridine to form acetyl derivatives capable to better chemical ionization. About 20 PGs have been determined using the selected ion monitoring (SIM) method without a gradient system in the range from 0.5 to 10 pmol (Nucleosil 100-5C18) [9]. Combined derivatization to panacyl esters prior to methoximation using methoxamine hydrochloride enables good chromatographic separations, especially for the hemiacetalic TXB₂ and PGF_{2α} (Ultraspher ODS C18 or LiChrocart Superspher 100-RP-18). Furthermore, oxo functions present in most PGs can be modified to *p*-nitrobenzyloximes at 40°C within 2 h after methyl ester formation by diazomethane allowing UV detection at 254 nm (μ -Bondapak C18).

In general, quantitative analyses are carried out as usual, using internal or external standards and calibration curves. Detection limits can be achieved in the lower picogram range dependent on the selected derivatization procedure.

Special Features of HPLC in Prostaglandin Analysis [3,4,6–8,11]

Besides quantitative determinations of endogenous PGs, HPLC techniques have been used for some special features in clinical, chemical, or pharmaceutical research, including investigations of stability, metabolism and enantiomeric purity, thermodynamic characterizations of chemical equilibria, validating im-

munological methods by matrix separations, or preparative purifications.

References

1. M. Hamberg and B. Samuelsson, Prostaglandin endoperoxides. Novel transformations of arachidonic acid in human platelets, *Proc. Natl. Acad. Sci. USA* 71: 3400–3404 (1974).
2. W. S. Powell, Rapid extraction of arachidonic acid metabolites from biological samples using octadecylsilyl silica, *Methods Enzymol.* 86: 467–477 (1982).
3. W. S. Powell and D. F. Colin, Metabolism of arachidonic acid and other polyunsaturated fatty acids by blood vessels, *Prog. Lipid Res.* 26: 183–210 (1987).
4. K. Green, M. Hamberg, B. Samuelsson, and J. C. Frölich, Extraction and chromatographic procedures for purification of prostaglandins, thromboxanes, prostacyclin, and their metabolites, in *Advances in Prostaglandin and Thromboxane Research* (J. C. Frölich, ed.), Raven Press, New York, 1978, Vol. 5, pp. 15–38.
5. J. A. Lawson, H. Li, J. Rokach, M. Adiyaman, S.-W. Hwang, S. P. Khanapures, and G. A. FitzGerald, Identification of two major F₂ isoprostanes, 8,12-iso- and 5-epi-8,12-iso-isoprostane F_{2α}-VI, in human urine, *J. Biol. Chem.* 273: 29,295–29,301 (1998).
6. H. John and W. Schlegel, Thermodynamic and structural characterization of cis-trans isomerization of 12-S-hydroxy-(5Z,8E,10E)-heptadecatrienoic acid by high-performance liquid chromatography and gaschromatography-mass spectrometry, *Chem. Phys. Lipids* 95: 181–188 (1998); 97: 195–196 (1999).
7. J. G. Hamilton and R. J. Karol, High performance liquid chromatography (HPLC) of arachidonic acid metabolites, *Prog. Lipid Res.* 21: 155–170 (1982).
8. T. Toyo'oka, Use of derivatization to improve the chromatographic properties and detection selectivity of physiologically important carboxylic acids, *J. Chromatogr. B* 671: 91–112 (1995).
9. M. Yamane and A. Abe, High-performance liquid chromatography-thermospray mass spectrometry of prostaglandin and thromboxane acetyl derivatives, *J. Chromatogr.* 568: 11–24 (1991).
10. K. Blau and J. Halket, *Handbook of Derivatives for Chromatography*, 2nd ed. John Wiley & Sons, New York, 1993.
11. H. John and W. Schlegel, Reversed-phase high-performance liquid chromatographic method for the determination of the 11-hydroxythromboxane B₂ anomers equilibrium, *J. Chromatogr. B* 698: 9–15 (1997).



Protein Analysis by HPLC

Karen M. Gooding

Eli Lilly and Company, Indianapolis, Indiana, U.S.A.

Introduction

Proteins were first separated chromatographically in the 1950s when carbohydrate gels were found to be effective as matrices for liquid chromatography. When high-performance liquid chromatography (HPLC) gained popularity, it was assumed that its higher flow rates and concomitantly higher pressures would destroy the biological activity of proteins by disrupting their three-dimensional (tertiary) structures. This was proven incorrect in the mid-1970s, when several groups, including those of Fred Regnier at Purdue university and Jiri Coupek of Czechoslovakia, demonstrated that high recoveries accompanied the high resolution of HPLC methods for protein analysis.

Modes of HPLC

The importance of tertiary structure on the biological activity of proteins implies that the most successful HPLC methods are those employing mobile and stationary phases, which cause minimal disruption of these features. Size-exclusion and ion-exchange chromatography are the gentlest methods in this regard and are generally compatible with any additives needed to enhance stability. Hydrophobic interaction and affinity chromatography have somewhat higher risk of denaturation due to either their mobile phase [high salt for hydrophobic interaction chromatography (HIC)] or stationary phase (affinity). Reversed-phase and hydrophilic interaction chromatography cause greater disruption of tertiary structure due to the presence of organic solvents, acidic pH, and/or hydrophobic stationary phases. Nonetheless, reversed-phase chromatography has shown great utility in the separation of many proteins.

Size-Exclusion Chromatography

Size-exclusion chromatography (SEC) is a method in which molecules are separated by size due to differential permeation into a porous support. This technique is especially useful for the separation of pro-

teins because they are macromolecules frequently found in the presence of smaller and larger species. The peak capacity in SEC is fairly low compared to other HPLC methods because all separation must occur in the internal volume (V_i) of the support, which is generally less than half the volume of the mobile phase in the column. Despite this deficiency, SEC is very effective for separating proteins from small molecules, polymeric forms, and other molecules which differ by size.

Supports for SEC of proteins are designed to be neutral and very hydrophilic to avoid disruption of protein structure and interaction of the solutes with the support by ionic or hydrophobic mechanisms. The base matrix can be either silica or polymer; efforts are made to totally mask its properties with a carbohydrate-like stationary phase. The pore structure is critical to successful SEC. Not only must the total pore volume (V_i) be adequate for separation, the pore diameter must be consistent and nearly homogeneous for attainment of maximum resolution between molecules with relatively small differences in molecular size (radius of gyration or molecular weight). A twofold difference in size is usually required for separation by SEC. Pore homogeneity can be assessed from the slope of the calibration curve of the logarithm of the molecular weight versus the retention time or the partition coefficient (K_D): $K_D = (V_R - V_0)/V_i$, where V_R is the retention volume and V_0 is the void or excluded volume. A less steep slope results in the separation of more closely related molecular weights. Figure 1 shows both an analysis of a protein mixture on an SEC column and its calibration curve. The second calibration curve is for a column with a smaller pore diameter, showing its effectiveness for separating smaller solutes.

The mobile phase is a critical factor in SEC because it must eliminate all solute-support interactions. This is effected by adjustment of pH (usually to neutrality), ionic strength (0.05M–0.2M), and/or addition of 5–10% organic solvent or stabilizing agents. The ionic and hydrophobic properties of proteins and their attraction to the stationary phase must be totally removed.



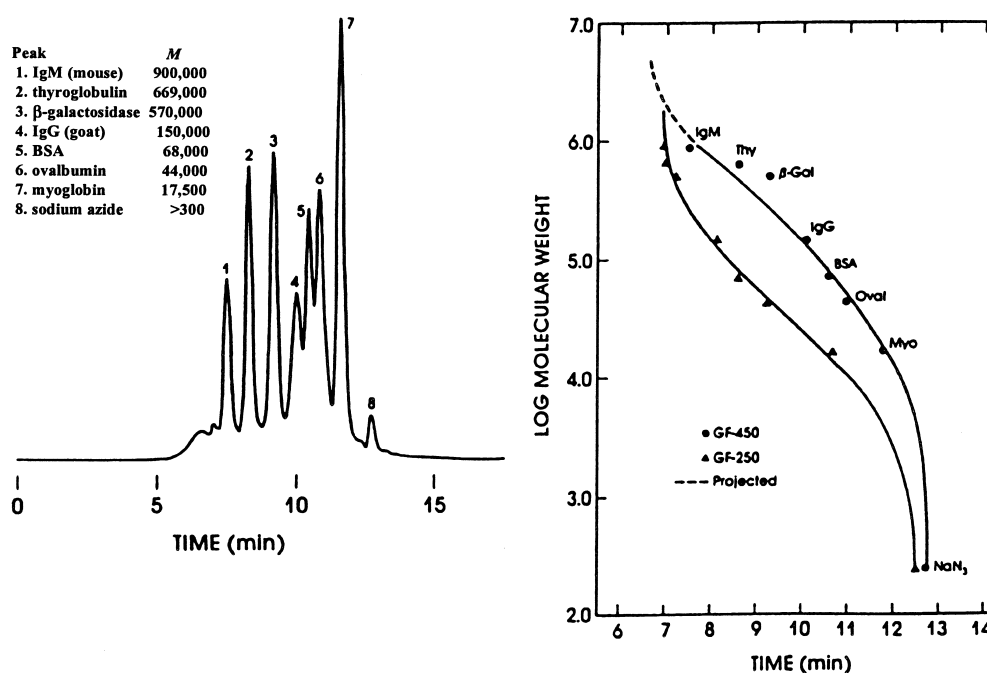


Fig. 1 Analysis of a mixture of proteins on ZORBAX® GF450. Calibration curves of proteins on ZORBAX GF250 and GF450 columns. Mobile phase: 0.2M sodium phosphate, pH 7.5; UV detection at 280 nm. (Printed with permission of Hewlett-Packard.)

Ion-Exchange Chromatography

Ion-exchange chromatography (IEC) separates proteins by ionic interaction of their surface amino acids with charges on the stationary phase. Selectivity is dependent on the number and the identity of the amino acids, as well as their spatial arrangement. A protein with charges grouped in a patch on its surface will bind differently than one whose charges are dispersed throughout the surface. IEC is so selective that it can resolve isoforms and variants differing by only one amino acid. Loading on porous IEC supports is high (100 mg/g), making IEC invaluable in purification techniques.

Supports for IEC possess either anion- or cation-exchange functionalities which are positively or negatively charged, respectively. They are also classified as weak or strong to correspond to their titration curves, similar to acid and base designations. The stationary phase totally covers the silica or polymer support matrix. The pore diameter is important in that it must be large enough to allow access of the protein. This affects not only retention but also loading capacity.

In IEC, proteins are bound in a low-ionic-strength buffer (0.02M–0.05M) at an appropriate pH (often 1–2 pH units from the *pI*). Elution occurs when the ionic

strength is increased during a concentration gradient of a salt in the same buffer. Because proteins bind via multipoint interactions, gradients are necessary for good peak shapes, resolution, and reproducibility. The pH gradients are less commonly used but can also be effective. The nature of the salt in IEC has a major effect on selectivity due to interaction of the composite ions with either the stationary phase or the solutes. Figure 2 illustrates the differences in retention of several proteins when various salts are used as the mobile phase for anion-exchange and cation-exchange chromatography. Additives which increase protein stability or improve peak shape can usually be included in the mobile phase without deleterious effects on the separation. Lower temperatures can be used to preserve biological activity, but they also result in higher retention.

Hydrophobic Interaction Chromatography

Hydrophobic interaction chromatography (HIC) is a method in which proteins in a high salt environment interact hydrophobically with nonpolar ligands. Effective salts are antichaotropic, meaning that they promote the ordering of water molecules at surfaces. Se-

lectivity is based on the hydrophobic amino acids and patches on the surface of the proteins. Many proteins, which generally remain in their native states in this technique, retain their biological activities when separated by HIC.

Supports for HIC have short alkyl chains or phenyl functionalities, the length of which is related to retention. The matrix can be either silica or polymer, as it is totally covered by the bonded phase and, thus, not ex-

posed to the solute. Pore diameters are at least 300 Å to allow access by proteins. Loading capacities are high and similar to those of ion-exchange supports.

In HIC, molecules are bound with a high concentration of salt, usually ammonium or sodium sulfate (1M–2M) in a buffer (0.02M–0.05M). Elution is attained by a gradient to a lower concentration of salt in the buffer. The pH is controlled and is usually in the range of 6–8, but it is not a critical factor in selectivity.

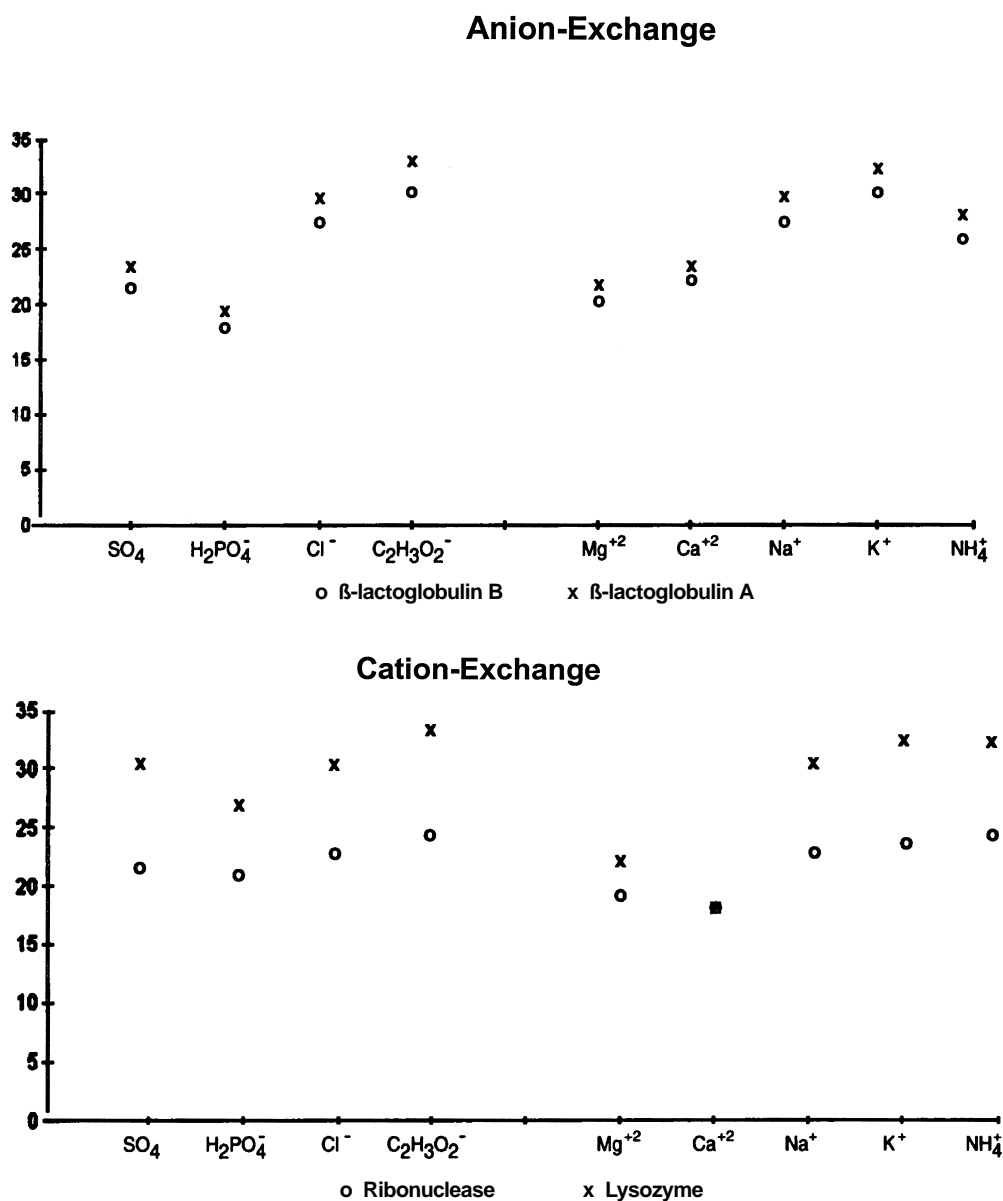


Fig. 2 Effect of salt on protein retention. Columns: SynChropak AX300 and SynChropak CM300; 30 min gradient from 0–1N salt in 0.02M Tris, pH 7. (Reprinted with permission from *Basic HPLC and CE of Biomolecules*, Bay Bioanalytical Laboratories, Richmond, VA, 1998.)



Additives to enhance protein stability are generally compatible with the process. Contrary to its effect on other modes of chromatography, reducing the temperature decreases the retention in HIC due to its being an entropy-driven technique.

Affinity Chromatography

Affinity chromatography (AFC) is a method in which biomolecules are attracted to ligands due to biospecificity. AFC is a very specific and selective technique in the aspect that many ligands are used, being customized to the analyte of interest. It is generally unlike other HPLC processes because particle diameters are larger and retention tends to be bind-release rather than partitioning, thus separating one protein or class of proteins from everything else in a mixture. Recoveries of biological activity are often high.

The variety of ligands for AFC includes proteins, cofactors, and any other molecules for which a solute has special affinity. Some common ligands are protein A, antibodies, and concanavalin A. Elution is attained by either a change in pH or ionic strength conditions or the addition of a competitor for the binding. Conditions are as varied as the number of ligands.

Reversed-Phase Chromatography

Reversed-phase chromatography (RPC) is a method in which molecules are bound hydrophobically to non-polar ligands in the presence of a polar solvent. Solutes are generally bound in an acidic mobile phase with elution occurring during a gradient to an organic solvent. The combination of acidic and organic mobile phases and a hydrophobic bonded phase usually results in tertiary structure disruption, which may or may not be reversible. Binding involves internal as well as surface amino acids depending on the extent of unfolding. The utility of RPC for protein analysis is limited by its generally denaturing characteristics; however, it can be a good method for nonpreparative techniques where preservation of biological activity is unimportant. Some enzymes, such as trypsin and chymotrypsin, can be renatured after RPC, regaining biological activity.

There are many ligands used for RPC, but the most popular for protein analysis are butyl (C_4) and octyl (C_8). Little difference in selectivity for proteins is observed with ligand-chain-length variation, but mass recovery is often enhanced on the shorter chains. Due to their higher efficiencies and wettability, silica-based supports are generally used for protein analysis. The

silica matrix is sometimes a factor in retention because reversed-phase bonded phases often do not totally eliminate silanols on the support. Pore diameters used for proteins are at least 300 Å; nonporous supports offer a high-resolution option with lower capacities. Loading capacities of RPC are at least 50% lower than those of IEC or HIC.

Many operational factors can change selectivity in RPC. The strength of the organic solvent which causes elution increases from methanol to acetonitrile to isopropanol. Acetonitrile is the most popular solvent due to its transparency at low wavelengths (<210 nm) and its tendency to yield narrow peak widths. The transparency is not critical for proteins, which can usually be detected at 254 or 280 nm. Ion-pairing agents, such as trifluoroacetic acid, can be added to the mobile phase to change the ionic or hydrophobic properties of either or both of the bonded phase or the solute. Generally, acidic pH is utilized to minimize silanol interactions; however, distinct pH conditions yield different selectivities. Increased temperatures result in shorter retention times and are especially effective in reducing the pressure generated by small-particle-diameter supports.

Hydrophilic Interaction Chromatography

Hydrophilic interaction chromatography (HILIC) is a variation of normal-phase chromatography in which solutes are retained on a polar bonded phase under high concentrations (80–90%) of organic solvent and released during a gradient to a more aqueous solvent. The organic mobile phase usually causes at least partial denaturation of proteins.

The HILIC bonded phases are hydrophilic, including amide and/or polyhydroxy functionalities. Pore diameters are at least 300 Å to allow penetration of proteins. Supports can be based on either silica or polymer because the matrix is not exposed to the solutes.

The mobile phase can offer some differences in selectivity in HILIC. A buffer is usually used to control pH. It may also serve to change the hydrophobicity of the solutes by ion-pairing; thus, it may greatly effect retention. For this reason, the pH is less important than the identity of the salt. The denaturing aspects of HILIC diminish its utility in protein analyses, particularly for preparative purification.

Conclusions

High-performance liquid chromatography provides a number of rapid and effective methods for analysis and purification of proteins and enzymes. In modes such as



SEC and IEC, quantitative yields are often obtained with full preservation of biological activity. The ability to change selectivity using the mobile phase has resulted in versatile techniques which can be rapidly optimized and implemented.

Suggested Further Reading

- Cunico, R. L., K. M. Gooding, and T. Wehr, *Basic HPLC and CE of Biomolecules*, Bay Bioanalytical Laboratories, Richmond, CA, 1998.
- Gooding, K. M. and F. E. Regnier (eds.), *HPLC of Biological Macromolecules: Methods and Applications*, Marcel Dekker, Inc., New York, 1990.
- Hancock, W. S. (ed.), *High Performance Liquid Chromatography in Biotechnology*, John Wiley & Sons, New York, 1990.
- Hearn, M. T. W. (ed.), *HPLC of Proteins, Peptides and Polynucleotides*, VCH, New York, 1991.
- Horvath, Cs. and J. G. Nikelly (eds.), *Analytical Biotechnology: Capillary Electrophoresis and Chromatography*, American Chemical Society, Washington, DC, 1990.
- Katz, E. D. (ed.), *High Performance Liquid Chromatography: Principles and Methods in Biotechnology*, John Wiley & Sons, New York, 1996.
- Mant, C. T. and R. S. Hodges (eds.), *High-Performance Liquid Chromatography of Peptides and Proteins*, CRC Press, Boca Raton, FL, 1991.



Protein Immobilization

Jamel S. Hamada

Southern Regional Research Center, USDA-ARS, New Orleans, Louisiana, U.S.A.

Introduction

Affinity chromatography is a powerful high-resolution separation technique for biomolecules. It is based on a highly specific and unique stereochemical interactions between biomolecules. Examples of these interactions are the binding of enzymes to coenzymes and inhibitors and the interactions between antigens (e.g., protein A) and antibodies. In affinity chromatography, a ligand is covalently bound to a solid matrix which is packed into a chromatography column. A mixture of components is then applied to the column. The unbound contaminants, which have no affinity for the ligand, are washed through the column, leaving the desired component (protein, peptide, etc.) bound to the matrix. Elution is accomplished by changing the pH and/or salt concentration or by applying organic solvents or a molecule which competes for the bound ligand. The purpose of this entry is to review methods for immobilization of protein ligands for affinity chromatography.

Matrix Material (Carrier)

Immobilized ligand is prepared by covalently attaching the biospecific ligand to a chromatographic bed support material, the matrix. A variety of insoluble support materials are used as matrices in affinity chromatography. These include agarose, cellulose, cross-linked dextran, polystyrene, polyacrylamide gels, and porous silica gels. The majority of matrices used in affinity chromatography are either agarose based or polyacrylamide based. The available reactive groups on these matrices are hydroxyl and amide nitrogen groups, respectively. By far the most popular support materials in use are beaded derivatives of agarose due to their ideal physical and chemical characteristics that are necessary for ligand immobilization. For instance, Sepharose, a bead-formed agarose gel manufactured by Amersham Pharmacia Biotech, has virtually all the features required of a successful matrix for immobilizing biologically active molecules. The hydroxyl groups on the sugar residues can easily

be used to covalently attach a ligand. Sepharose 4B (Amersham Pharmacia Biotech) is the most popular and widely used matrix. Its advantages include open-pore structure, molecular exclusion limit of 20×10^6 Da, easy and good binding capacities, and low non-specific attachment. A spacer arm, which is interposed between the matrix and ligand, is sometimes needed to facilitate the binding particularly when coupling small molecules (e.g., enzyme cofactors). Spacer arms are also useful for coupling ligands containing free carboxyl or amine groups and for further chemical reactions to permit the attachment of phenolic groups and diazonium derivatives to agarose matrix.

Protein Ligands

Protein ligands most commonly used in affinity chromatography are as follows: (a) protein with very high specific affinity for moieties on the desired protein; a wide range of plant lectins with a variety of sugar specificities are used as ligands to purify glycoproteins and enzymes having sugar moieties in their structures; (2) immobilized antibodies, which represent the ideal affinity separation because of the precise specificity of many antibodies, particularly monoclonal antibodies, to their specific antigens; (3) proteins or enzymes with unique affinity for other proteins or peptides, which are used as affinity ligands for the particular proteins or peptides.

Preparation of Immobilized Proteins

The immobilization of proteins and enzymes through covalent bond formation between the protein or enzyme and an activated insoluble carrier entail two processes of activation and coupling. These procedures are classified on the basis of the type of reaction that facilitates the bonding between the protein and the insoluble carrier. Mostly, with matrices containing readily available hydroxyl groups such as agarose derivatives, a variety of activation procedures are used, after which the amino groups of protein ligands are readily incorporated into the matrix (coupling reaction). After coupling of the



protein ligands to the matrix, unreacted activated coupling groups are usually hydrolyzed to inactive derivatives during washing of the coupling resin at lower pH. Alternatively, these groups can be blocked by adding an excess of an inert blocking reagent. The following methods are most commonly used for activation and coupling of protein ligands to agarose and other matrices.

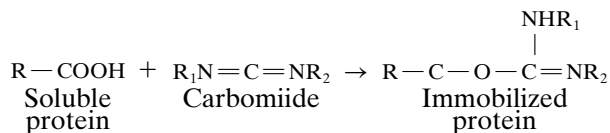
Cyanogen Bromide Activation Method

The aim of the reaction of cyanogen bromide with hydroxyl groups on agarose matrix is to produce reactive carrier to which proteins can be coupled through amino groups. Cyanogen bromide activation method is the most used method for the preparation of affinity gels because of its simplicity and its mild reaction conditions, particularly for immobilizing sensitive proteins such as enzymes and antibodies. Cyanogen bromide reacts with these hydroxyl groups and converts them to imidocarbonate groups, as shown in Fig. 1. Agarose ac-

tivated with cyanogen bromide have been used to bind a variety of proteins and enzymes. The activated groups react with primary amino groups of a protein ligand to form isourea linkages according to the reactions in Fig. 1.

Acylation Reactions

In this type of protein immobilization, reactions involve the acylation of an NH_2 group on a protein or an enzyme by pendent groups of the carrier such as azide, acid anhydride, carbodiimide, sulfonyl chloride, and hydroxysuccinimide esters. Copolymers of acrylamide and maleic anhydride have been useful for enzyme immobilization through the acid anhydride reaction with the enzyme. This system of protein immobilization involves the use of a reagent that contains an acylating or alkylating agent and a group which can form a covalent link with a carrier polymer. For instance, few protein immobilization methods are based on condensation by carbodiimides (e.g., dicyclohexylcarbodiimide). Mixing the carbodiimide reagent with the matrix and a protein ligand, stable amide bonds can be formed between an amino group on the ligand and a carboxyl group of matrix (or vice versa) in a one-step procedure of activation and coupling as follows:



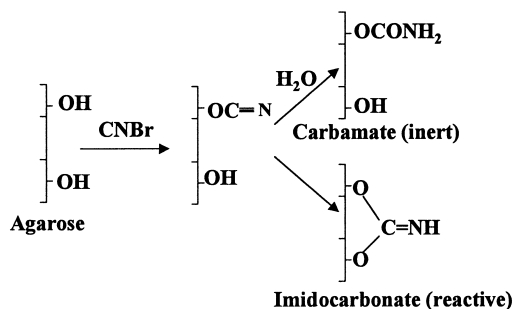
Arylation Reactions

Arylation or alkylation are used for activation of support and linking of a protein ligand. In such reactions, the functional group on the carrier combines with an NH_2 group of the protein (e.g., by 3-fluoro-4,6-dinitrophenyl group or 2-4 dichloro-*S*-triazine). In this approach, a chloro-*S*-triazine is coupled to an arylazide. The azide is converted to a nitrene, which upon activation by light reacts with a polymer carrier to form a covalent bond. The chlorotriazine then couples with the protein.

Alkylation Reactions by Bisepoxirane, Epichlorohydrin, and Divinylsulfone

Bisepoxirans activations allows the coupling of ligands containing $-\text{OH}$, $-\text{NH}_2$, and $-\text{SH}$ groups with agarose matrix. Here, the ligands are provided automatically with a hydrophilic spacer arm.

Activation



Coupling

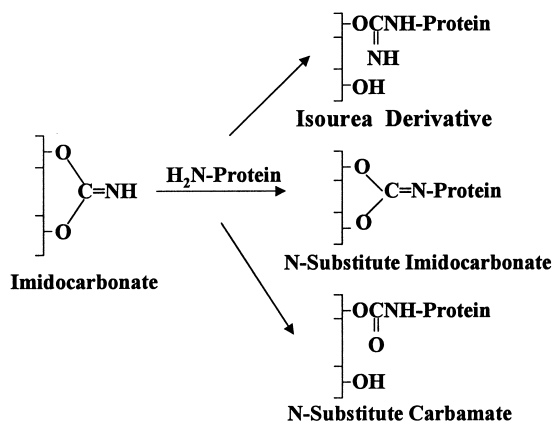


Fig. 1 Immobilization of protein ligands on agarose (activation and coupling) by cyanogen bromide.

Organic Sulfonyl Chlorides, Tosyl and Trisylchloride Methods

These methods enable the activation and the coupling of ligands containing —NH₂ and —SH groups with matrices such as agarose, cellulose, or silica derivatives.

Methods for Polyacrylamide Matrices

The glutaraldehyde and hydrazine reactions are used for matrices having amide groups such as polyacrylamide. Glutaraldehyde and hydrazine react with the polymer, and the enzyme or protein is readily bound to the treated polymer. The mechanism of the reactions involved in the activation and coupling are not well understood. In general, insoluble supports such as polyacrylamide, which tend to swell in water, form immobilized proteins or enzymes when mixed with a solution and treated with glutaraldehyde. Polyacrylamide support is activated by treatment with hydrazine (heated) followed by sodium nitrite in hydrochloric acid. The amino groups of protein ligands can then be coupled to the activated matrix via stable amide bonds.

Affinity Supports: Activated and Ready-to-Use Media

Chromatography suppliers offer affinity gels for a wide range of biomolecular applications. Availability

of activated supports allows the users to make their own affinity matrix of choice by coupling a ligand such as an antibody, enzyme, antigen, or receptor. Ready-activated supports or matrices are less expensive than the ready-to-use matrices usually offered by the same manufacturer. These activated matrices are dependable and provide flexibility and convenience in affinity chromatography. With this particular option, the chromatographer has the choice of preparing affinity matrix by activating a support, then coupling or only coupling using ready-to-use activated affinity supports. Table 1 shows the activated supports marketed by two major soft-gel chromatography suppliers that are suitable for coupling of affinity protein ligands.

On the other hand, ready-to-use matrices have a specific ligand already coupled to an affinity support. Amersham Pharmacia Biotech has developed a wide range of ready-to-use affinity gels with specific protein ligands coupled to the matrix. In specified bulletins, Amersham Pharmacia Biotech details the preparation procedures of these affinity gel columns containing immobilized proteins. Applications include monoclonal and polyclonal antibodies, fusion proteins, glycoproteins, enzymes, cells, and other proteins such as fibronectin, and membrane proteins. Likewise, Bio-Rad Laboratories offer two types of supports. One type such as Affi-Gel supports, based on agarose or polyacrylamide, are available as low-pressure gels suitable for most laboratory-scale

Table 1 Activated Affinity Matrices Marketed by Two Major Soft-Gel Chromatography Suppliers for Coupling of Protein Ligands

Matrix	Ligand specificity	Activator and functional groups	Manufacturer
CNBr-activated Sepharose 4B (or Fast Flow)	—NH ₂	CNBr	Amersham Pharmacia Biotech
EAH Sepharose 4B	—COOH	Carbodiimide coupling via 6-carbon spacer arm	Amersham Pharmacia Biotech
ECH Sepharose 4B	—NH ₂	Carbodiimide coupling via 6-carbon spacer arm	Amersham Pharmacia Biotech
Epoxy-activated Sepharose 6B	—NH ₂ , —OH, —SH	1,4-bis (2,3-epoxypropoxy-butane)	Amersham Pharmacia Biotech
Activated Thiol Sepharose 4B	—SH, —C=O, —CNH	Glutathione-2-pyridyl disulfide	Amersham Pharmacia Biotech
Affi-Gel 10 gel (or Affi-Prep 10, pressure stable)	—NH ₂	N-Hydroxysuccinimide ester via 10-atom spacer arm	Bio-Rad Laboratories
Affi-Gel 15 gel	—NH ₂	N-Hydroxysuccinimide ester via 15-atom spacer arm	Bio-Rad Laboratories
Affi-Gel 102 gel	—COOH	Carbodiimide coupling	Bio-Rad Laboratories
CM Bio Gel A	—NH ₂	Carboxymethyl, carbodiimide coupling	Bio-Rad Laboratories



affinity purification with a peristaltic pump or gravity flow elution. Affi-Prep supports, based on a pressure-stable macroporous polymer, are suitable for preparative and process scale applications. The immobilized protein ligands in these ready-prepared matrices include lectins, protein A, gelatin, avidin, and calmodulin. Affi-Gel and Affi-Prep protein A supports are used to produce highly purified immunoglobulins (IgG), to selectively remove IgG prior to analysis of other immunoglobulin classes, or to adsorb immune complexes to purify antigens. Protein A from *Staphylococcus aureus* binds to the F_c region of immunoglobulins, especially IgG from mammalian species. Affi-Prep supports offer linear flow rates up to 2000 cm/h, pressure stability up to 1000 psi (70 bar), and high chemical stability, according to the manufacturer.

Conclusion

In affinity chromatography, a ligand is covalently bound to a solid matrix by matrix activation and ligand coupling. In protein immobilization, a covalent bond is formed between the protein ligand and an insoluble solid matrix or carrier. Most of protein immobilization steps entail the formation of the insoluble immobilized proteins on cross-linked agarose gels. Most common reactions used in making immobilized proteins and enzymes are discussed. These processes are classified on the basis of the type of reaction which forms the covalent bond between the protein and the insoluble carrier. Also, a wide range of com-

mercial ready-to-use supports with specific protein ligands already coupled to a base matrix are discussed.

Suggested Further Reading

- Bell, J. E. and E. T. Bell, Protein purification: affinity chromatography, in *Proteins and Enzymes*, Prentice-Hall, Englewood Cliffs, NJ, 1988, pp. 45–63.
- Carlsson, J., J.-C. Janson, and M. Sparrma, Affinity chromatography, in *Protein Purification: Principles, High Resolution Methods, and Applications* (J. C. Janson and L. Ryden, eds.), VCH, New York, 1989, pp. 275–329.
- Dunlab, R. B., *Immobilized Biochemicals and Affinity Chromatography*, Plenum Press, New York, 1974.
- Ganttsos, G. and P. E. Barker, *Preparative and Production Scale Chromatography* (J. Cazes, ed.), Chromatographic Science Series, Marcel Dekker, Inc., New York, 1993.
- Kennedy, J. F. and C. A. White, Principle of immobilization of enzymes, in *Handbook of Enzyme Biotechnology* (A. Wiseman, ed.), Ellis Horwood, Chichester, 1986, pp. 147–207.
- Low, C. R. L., *Affinity Chromatography*, John Wiley International, London, 1974.
- Pharmacia Fine Chemicals, *Affinity Chromatography: Principles & Methods*, Pharmacia Fine Chemicals, Uppsala, 1978.
- Schott, H., *Affinity Chromatography*, Chromatographic Science Series Vol. 27, Marcel Dekker, Inc., New York, 1984.
- Scouten, W. H., *Affinity Chromatography*, John Wiley & Sons, New York, 1981.
- Sofer, G. K., *Bio/Technol.* 4: 712–715 (1987).



Protein Separations by Flow Field-Flow Fractionation

Galina Kassalainen

S. Kim Ratanathanawongs Williams

Colorado School of Mines, Golden, Colorado, U.S.A.

Introduction

Flow field-flow fractionation (flow FFF) is a separation method that is applicable to macromolecules and particles [1]. Sample species possessing hydrodynamic diameters from several nanometers to tens of microns can be analyzed using the same FFF channel, albeit by different separation mechanisms. For macromolecules and submicron particles, the normal-mode mechanism dominates and separation occurs according to differences in diffusion coefficients. Flow FFF's wide range of applicability has made it the most extensively used technique of the FFF family.

Discussion

The characteristic feature of flow FFF is the superimposition of a second stream of liquid perpendicular to the axis of separation. This cross-flow drives the injected sample plug toward a semipermeable membrane that acts as the accumulation wall. The cross-flow liquid permeates across the membrane and exits the channel, whereas the sample is retained inside the channel in the vicinity of the membrane surface. Sample displacement by the cross-flow is countered by diffusion away from the membrane wall. At equilibrium, the net flux is zero and sample clouds of various thicknesses are formed for different sample species. As with other FFF techniques, a larger diffusion coefficient D leads to a thicker equilibrium sample cloud that, on average, occupies a faster streamline of the parabolic flow profile and subsequently elutes at a shorter retention time t_r . For well-retained samples analyzed by flow FFF, t_r can be related to D and the hydrodynamic diameter d by

$$\frac{t^0}{t_r} = \frac{6D}{Uw} = \frac{2kTV^0}{\dot{V}_c w^2 \pi \eta d} \quad (1)$$

where t^0 is the void time, U is the field-induced velocity, w is the channel thickness, k is the Boltzmann constant, T is the temperature, V^0 is the channel void volume, \dot{V}_c is the cross-flow rate, and η is the viscosity of the carrier liquid. Equation (1) pertains to normal-mode separations.

It is apparent, from Eq. (1), that the primary sample property measured by flow FFF is the diffusion coefficient. Secondary information includes the hydrodynamic diameter which can be obtained via the Stokes–Einstein equation and the molecular weight if the molecule shape factor is constant. Unlike other FFF techniques, the retention time in flow FFF is determined solely by the diffusion coefficient rather than a combination of sample properties. As a consequence, flow FFF is well suited for analyses of complex sample mixtures and the transformation of the fractogram to a diffusion or size distribution is straightforward. In addition, flow FFF is applicable to a wide range of samples regardless of their charge, size, density, and so forth.

Flow FFF was first introduced as a method for protein separation and characterization by Giddings et al. in 1977 [2]. This first publication discusses the advantages of flow FFF over other protein separation methods that were used at the time (e.g., polyacrylamide gel electrophoresis and size-exclusion chromatography (SEC)). Flow FFF permits the calculation of diffusion coefficients and hydrodynamic diameter of proteins in different solution environments directly from retention data using straightforward analytical relationships. No other technique provides simultaneous separation and measurement of D and d for each sample component without the need for additional information such as charge and density. Moreover, the protein molecular weights (MWs) calculated from FFF diffusion coefficient data are on a sounder theoretical basis than that derived from electrophoretic mobility in gels or chromatographic retention data. The absence of packing material in a channel makes flow FFF suitable for the analysis of fragile high-MW proteins and protein complexes in comparison with SEC where shear forces and interfacial interactions can cause changes in the structure and activity of molecules. Flow FFF can be used to separate and characterize mixtures of proteins, protein aggregates, and protein complexes with a single FFF analysis covering a 500–1000-fold size difference. A series of SEC columns with different exclusion limits would be needed to span a similar size range. The cross-flow rate is programmed (i.e., decreased with respect to time) to maintain separation



times of 5–20 min. The open FFF channel structure permits the analysis of protein samples suspected of containing precipitated material without special pretreatment. This is not possible by SEC and gel electrophoresis.

The main disadvantage of flow FFF is the lack of commercially available membranes with flat nonadsorbing surfaces, uniform permeability, and batch-to-batch reproducibility. These features may affect

retention time, separation efficiency, and sample recovery. Numerous studies and technical improvements have been done to ensure optimum performance.

The traditional flow-FFF method, also called symmetrical flow FFF, utilizes a channel with permeable depletion and accumulation walls. The cross-flow liquid enters the channel through a microfiltration frit that acts as the depletion wall and exits through an ul-

Table 1 Examples of Flow FFF Protein Analyses

Application	Flow FFF type	Summary
Ribosomes from <i>Escherichia coli</i>	Asymmetrical	Separation of ribosomes, their subunits, and t-RNA/low-MW protein mixture in samples collected at different protein production phases and in the presence of antibiotics, specific genes, and proteins; calculation of a ribosome number per cell and a ribosome fraction using peak area [6]
Yeast acid phosphatase (APase)	Asymmetrical	Separation of APase in cultivation medium; identification of APase peak by enzymatic activity measurements [7]
Proteins from wheat flour	Asymmetrical	Fractionation of wheat proteins in the size range from 5 to 45 nm; separation of gliadins from glutenin [K.-G. Wahlund, M. Gustavson, F. MacRitchie, T. Nylander, and L. Wannerberger, <i>J. Cereal Sci.</i> 23: 113–119 (1996)]
Wheat protein fractions	Symmetrical	Size distribution of wheat protein fractions (albumins and globulins, gliadins, glutenins) prepared by extraction; influence of oxidation on size distribution of high-MW glutenin [S. G. Stevenson, T. Ueno, and K. R. Preston, <i>Anal. Chem.</i> 71: 8–14 (1999)]
Monoclonal antibodies (Mab) from hybridoma cell culture	Asymmetrical	Separation of five Mab aggregates (immunoglobulins) in half the time needed for GPC; only three partially resolved peaks were obtained by GPC; separation of samples containing precipitated material [A. Litzen, J. K. Walter, H. Krischollek, and K.-G. Wahlund, <i>Anal. Biochem.</i> 212: 469–480 (1993)]
Proteins in homogenized dairy products	Symmetrical	Separation of whey proteins from fat globules; fractionation of whey proteins and casein micelles; effect of carrier ionic strength, cross-flow rate, pH, and membrane type on retention and size distribution of micelles [M. A. Jussila, G. Yohannes, and M.-L. Riekkola, <i>J. Microcol. Separ.</i> 9: 601–609 (1997)]
Reconstituted skim milk casein	Symmetrical	Fractionation of colloidal Ca^{2+} -caseinate complexes in milk samples in size range 10–50 nm after the preliminary fractionation of 10–600-nm colloids with sedimentation FFF [P. Udabage, R. Sharma, D. Murphy, I. McKinnon, and R. Beckett, <i>J. Microbiol. Separ.</i> 9: 557–563 (1997)]
Plasma protein interactions with polymer colloids	Symmetrical	Measurement of changes in particle (PS latex) size due to aggregation and adsorption of proteins; effect of Pluronic TM surfactants on aggregation and protein adsorption [J.-T. Li and K. D. Caldwell, <i>Colloids Surf. B: Biointerfaces</i> 7: 9–22 (1996)]
Lipoproteins in human plasma	Symmetrical	Separation of low-MW proteins, HDL, LDL, and VLDL; Determination of subspecies in the lipoprotein fractions with linear programmed cross-flow rate; observation of lipoprotein profiles for different individuals [10]
Drug/plasma protein interactions	Asymmetrical	Separation of albumin, HDL, α -macroglobulin, and LDL; Determination of drug distribution in FFF fractions using a fluorimetric detector [M. Madorin, P. van Hoogevest, R. Hilfiker, B. Langwest, G.M. Kresbach, M. Ehrat, and H. Leuenberger, <i>Pharm. Res.</i> 14: 1706–1712 (1997)]
Viruses (purified)	Asymmetrical	Separation of five aggregates of the Satellite tobacco necrosis virus; isolation of the Cow pea mosaic virus [5]

trafiltration membrane that acts as the accumulation wall [1–3]. Membranes with nominal MW cutoffs in the range of 5000–30,000 Da are used to ensure that the protein sample remains in the FFF channel. Hydrophilic ultrafiltration membranes made from regenerated cellulose, cellulose acetate, and modified polyethersulfone have been used.

The sample capacity in a flow FFF channel with standard dimensions is several hundred micrograms. Sample overloading causes band broadening and a shift in retention time. The experimental procedure involves sample injection followed by a stop-flow period when the axial or channel flow is stopped and the sample is transported to equilibrium positions at the accumulation wall under action of the cross-flow. At the end of the stop-flow period, channel flow is resumed and the sample is fractionated while being swept toward the outlet. The elution of proteins is monitored with an ultraviolet (UV) spectrophotometric detector set at 280 or 210 nm wavelength. Other on-line detectors that are being used or evaluated include multiangle light scattering (MALS) which yields MW and photon correlation spectroscopy (PCS), which yields *D*. Flow FFF provides the narrow polydispersity sample fractions required for accurate MW and *D* determinations by the light-scattering detectors. These detectors provide a second independent measure of MW and *D* for comparison with values calculated from FFF retention times. In addition, MALS can be used to distinguish the polydispersity of the sample from band broadening. The main disadvantages of MALS detection for protein flow-FFF applications are the low sensitivity and particulate-free solvent requirement.

Symmetrical flow FFF has been successfully used to analyze numerous purified proteins and their dimers, protein conjugates, sodium dodecyl sulfate (SDS)–protein complexes, including precipitate [1–3] and other biological samples, as summarized in Table 1. In these applications, sample pretreatment was not required even when the proteins of interest were present in complex matrices such as plasma, dairy products, and wheat flour (in contrast to SEC and electrophoresis). Ultracentrifugation, which is commonly used to fractionate these samples, requires over 24 h in comparison with the 5–40 min for flow FFF. The short analysis time gives flow FFF an advantage in analyzing the large number of samples encountered in the medical diagnostics, pharmaceutical, and food industries. Separation efficiencies are usually of the order of several hundred theoretical plates for a typical channel length of 25–30 cm.

A later modification of flow FFF, called asymmetrical flow FFF, has generated up to 2600 theoretical plates in the separation of viruses [4]. In the asymmetrical channel, the permeable frit or depletion wall is replaced with an impermeable glass plate. The flow of carrier liquid entering the inlet of the channel is the source of both the cross-flow and channel flow. The sample is injected through an additional port located about 2–3 cm downstream from the channel inlet. For asymmetrical flow FFF, the retention mechanism is the same as for the traditional symmetrical mode. The observed higher efficiency may be based on the different relaxation procedures. In the asymmetrical channel, a so-called focusing procedure is used. The injected sample is focused to a narrow zone at the accumulation wall under action of two opposing flows (introduced simultaneously through the inlet and outlet of the channel). However, this focusing procedure has some potential drawbacks. It may promote chain entanglement of high-MW macromolecules and increase adsorption on the membrane. Lower sample capacity (several micrograms) and recovery have been observed in comparison with the symmetrical flow FFF.

Asymmetrical flow FFF has been successfully applied to several practical problems, such as the separation of monoclonal antibodies and their aggregates in downstream processing, ribosomes, and plasma protein studies (see Table 1). For example, flow FFF separations of ribosomes and their subunits have led to an alternative method of optimizing the fermentation process without having to measure protein yields [5]. Flow FFF is the technique uniquely suited for separating highly glycosylated proteins such as 10^6 Da acid phosphatase (Apase) in cultivation media [6]. Buffers commonly used in chromatographic methods cause changes in the enzymatic activity of APase.

A second variant to the traditional symmetrical flow FFF channel utilizes a hollow-fiber membrane. Even though its feasibility in separating proteins has been demonstrated [7], its development has been hindered by the lack of membranes suitable for use as an FFF channel.

Several studies involving FFF channel modifications and new experimental procedures have been aimed at increasing detectability. For example, frit-outlet flow FFF utilizes a section of the frit depletion wall near the channel outlet to remove sample-free carrier and, thus, concentrate the separated sample just prior to its reaching the detector. A 10-fold increase in the detector response of purified proteins was achieved without any effect on retention time or resolution [8]. Frit-inlet flow FFF involves a



modification at the channel inlet that enables the transport of sample to the accumulation wall without using stop-flow relaxation [8,9]. As a result, the experimental operation is simpler and the detector signal is free of fluctuations caused by stopping and resuming axial flow through the channel. Enhanced detectability can also be realized by programming the cross-flow rate during the run to accelerate elution of highly retained components [9]. Another experimental approach involves using the ultrafiltration membrane that serves as the accumulation wall to remove low-MW interferences. A nominal 30,000-Da MW cutoff membrane was used to selectively remove low-MW proteins from a blood plasma sample to allow determinations of high-, low-, and very low-density lipoproteins (HDL, LDL, and VLDL, respectively).

A fundamental study was performed to demonstrate that flow FFF is a good alternative technique for the rapid measurement of protein diffusion coefficients [10]. The results obtained for 15 proteins were in good agreement (within 4%) with the literature data based on classical methods and a group of modern methods such as photon correlation spectrometry (PCS), laminar flow analysis, a chromatographic relaxation method, and analytical split-flow thin-cell (SPLITT) fractionation. The advantages of flow FFF are the high-speed separations and the calculation of D values directly from retention data.

Protein Separations by Flow Field-Flow Fractionation

Acknowledgments

G. Kassalainen was supported by grant from ACTR/ACCELS with funds provided by the U.S. Information Agency and S. K. R. Williams by a Colorado School of Mines start-up grant.

References

1. J. C. Giddings, *Science* 260: 1456–1465 (1993).
2. J. C. Giddings, F. J. Yang, and M. N. Myers, *Anal. Biochem.* 81: 395–407 (1977).
3. J. C. Giddings, M. A. Benincasa, M.-K. Liu, and P. Li, *J. Liquid Chromatogr.* 15: 1729–1747 (1992).
4. A. Litzen and K.-G. Wahlund, *Anal. Chem.* 63: 1001–1007 (1991).
5. M. Nilsson, L. Bulow, and K.-G. Wahlund, *Biotechnol. Bioeng.* 54: 461–467 (1997).
6. A. Litzen, M. B. Garn, and H. M. Widmer, *J. Biotechnol.* 37: 291–295 (1994).
7. J. E. G. J. Wijnhoven, J.-P. Koorn, H. Poppe, and W. Th. Kok, *J. Chromatogr. A* 732: 307–315 (1996).
8. P. Li, M. Hansen, and J. C. Giddings, *J. Microcol. Separ.* 10: 7–18 (1997).
9. P. Li, M. Hansen, and J. C. Giddings, *J. Liquid Chromatogr. Related Technol.* 20: 2777–2802 (1997).
10. M.-K. Liu, P. Li, and J. C. Giddings, *Protein Sci.* 2: 1520–1531 (1993).



Proteins as Affinity Ligands

Ji-Feng Zhang

Massachusetts Institute of Technology, Cambridge, Massachusetts, U.S.A.

Introduction

Affinity chromatography using proteins as ligands explores the three-dimensional complementary molecular interactions between the ligand and its target. This noncovalent and reversible binding are the results of ionic interaction, hydrophobic interaction, hydrogen-bonding, and van der Waals–London forces. The binding constant between the immobilized ligand and the target molecule ranges from $10^4 M^{-1}$ to $10^8 M^{-1}$. The multiplicity of the interaction forces offers the superior specificity to protein-based affinity chromatography for biomolecule separation among all the chromatographic techniques.

Discussion

After the protein ligand is immobilized on a matrix support, a crude sample mixture, including the desired substance, is loaded into the affinity column under appropriate conditions. If the desired molecule forms a stable and reversible complex with the protein ligand, it will be retained and all the other contaminants are washed away. Then, the eluting buffer disrupts the binding between the desired substance and the protein ligand to recover the substance. When the interaction between the desired molecule and the ligand is too weak to form a stable complex with the ligand, it is eluted later than all the other substances in the crude sample and an eluting buffer is not required.

Protein-based affinity chromatography has found wide applications in both academic and industrial settings. The affinity chromatography using proteins as the ligand is an indispensable technique for recombinant protein purification. This review will touch the general aspects of matrix, immobilization of protein ligands, and the application of protein-based affinity chromatography. It is by no means an exhaustive review of the current technologies in protein-based affinity chromatography and only serves as an introduction to this topic. Interested readers should explore those articles listed in Suggested Further Reading for more information.

Matrix

One of the key elements for protein-based affinity chromatography is the matrix, on which the protein ligand is immobilized. The ideal matrix material should have the following characteristics (Porath, 1974): insolubility, sufficient permeability, large surface area, strong mechanical strength, zero adsorption capacity, resistance to microbial and enzyme attack, chemical reactivity for coupling protein ligand, and stability under the operating conditions. Based on their physical strength, the matrices can be divided into two categories: low pressure and high pressure. For example, agarose, dextran, polyacrylamide, and methacrylate are typical low-pressure matrices and silica and polystyrene–divinylbenzene are high-pressure matrices.

When a matrix is chosen in affinity chromatography applications, its advantages and disadvantages should be taken into account to assess its potentials and limitations. Agarose is hydrophilic and, therefore, its matrix surface has low nonspecific binding. The presence of the hydroxyl group from agarose provides a convenient way for immobilizing the protein ligand. The drawbacks of agarose are its solubility in hot water and nonaqueous solutions and its susceptibility to microbial degradation. The lack of mechanical strength for agarose limits its application only in low-pressure operation and the separation process is slow. Silica and synthetic polymers are the alternative choices of matrix support. The major advantages for those matrix supports over agarose are their rigidity, reduced diffusion rate, and well-defined pore size (i.e., 5–20 μm in diameter). The above factors decide that those matrices can be operated in fast linear flow rate under high pressure to achieve rapid separation. Nonspecific binding in silica-based matrices is a concern because of the negative-charged silanol groups and because also silica has increased solubility at alkaline pH.

Immobilization

The unique specificity of affinity chromatography is the result of the complementary interaction between the protein ligand and the target in the separation pro-



cess. It is therefore essential to maintain the structure integrity of the protein ligand during immobilization of protein ligand. It is critical to consider the following in the immobilization step: (a) The binding site in the protein ligand should be accessible after the immobilization; (b) the amino acids located at the binding site should not be modified during the immobilization step; (c) the three-dimensional structure of the binding site should be maintained after the coupling step.

Usually, the immobilization of protein ligand is a two-step process: (1) activation and functionalization of the matrix and (2) coupling of the protein ligand to the modified matrix. To avoid the possible reactions between the rest of the activated sites and the protein components from the sample, a third step is often required to quench those activated sites after the protein ligand is coupled. The most exploited function groups for coupling from the protein ligand are the C-terminal carboxyl group, the carboxyl groups of glutamic and aspartic acids, the N-terminal α -amino group, and the ϵ -amino group of lysine. Sometimes, phenolic hydroxyl groups of tyrosine, imidazole anion of histidine, or the —SH group of cysteine residues may be the candidates for coupling. The ideal linkage between the matrix and the protein ligand from Step 1 should be fairly hydrophilic and neutral to avoid the introduction of a nonspecific interaction. Carbonyldiimidazole and 2-fluoro-1-methylpyridinium toluene-4-sulfonate are two of the popular reagents for activation of the hydroxyl-containing matrix and coupling with an amine-containing protein ligand.

Because there are many options of immobilization chemistries, different immobilization strategies should be evaluated for a particular protein ligand. After immobilization, the binding site should be affected in a minimal way so that the binding function is maintained. The protein ligand could have multiple sites for coupling with the activated matrix surface. The immobilization could be a random process if those sites are located in a similar steric environment. Another undesired scenario is immobilization by multiple-site attachment, which could destroy the native structure of the protein ligand and loss of its binding ability. If feasible, site-specific immobilization is preferred because it would give better reproducibility in both surface chemistry and column performance. Carbohydrate moieties from glycoproteins (i.e., antibodies and enzymes) are often particularly taken advantage of as the coupling sites because, generally, the complementary binding site in the protein ligand is away from the oligosaccharide chains. Immunoglobins (IgG) is often immobilized through the carbohydrates on the F_c re-

gion, and, as a result, the binding sites are readily available located on the F_{ab} region of IgG.

The leaching of the protein ligand presents a significant problem for introducing contaminants into the purified product. The solvolysis of the bonds between either the matrix–activator or activator–protein is the major source of leaching. It is the reason that an extra chromatography step is often required to remove protein ligand contaminant after affinity chromatography purification.

Applications

Adsorption and desorption are involved in the operation of affinity chromatography utilizing proteins as affinity ligands. One of the major differences for protein-based affinity chromatography from other modes of chromatographic techniques (i.e., ion-exchange chromatography, reversed-phase chromatography, and hydrophobic interaction chromatography) is that the protein ligand could be denatured or attacked in other ways and lose its affinity consequently. Extreme pH, heat, and organic solvents are worrisome for protein-based affinity chromatography. If any one of them is employed, its effect on the column life should be evaluated.

For method development in protein-based affinity chromatography, the theme is to promote the specific interaction between the protein ligand and its counterpart and minimize the nonspecific interaction between the matrix and the sample components. Because ionic and hydrophobic interactions contribute to the specific binding between the ligand and its counterparts, ionic strength and pH are probably the two simple and convenient parameters to be evaluated for separation method development. The variation of pH can affect the charge distribution on both the protein ligand and its target, leading to a different binding constant between them. Changing the ionic strength of the solution could modulate the hydrophobic interaction. Another very important parameter is the binding kinetics between the immobilized protein ligand and its target. The flow rate study could provide some clue on how fast the binding reaches the equilibrium. The strategy for minimizing the nonspecific interaction depends on the surface chemistry of the matrix. For example, a running buffer of high ionic strength (0.2M) can suppress the nonspecific ionic interaction between the sample components and the negative-charged silanol group on the silica matrix.

Many proteins have been utilized as affinity ligands and there are literally thousands of references using this



technique. The following are a few samples of proteins used as affinity ligands. Antibodies or antigens are used as immunoaffinity ligand to separate the complementary counterparts. Often, only a single purification step is needed because of the superior selectivity of immunoaffinity column. Protein A and protein G are the perfect ligands for antibody purification because of their specificities and robustness.

In summary, affinity chromatography using proteins as affinity ligands provides a unique scheme for purification. Currently, a great number of matrices are available and the chemistries for immobilization of protein ligands are significantly improved. The specific three-dimensional interaction between the protein ligand and its counterpart distinguishes this technique from other chromatography methods. The key issue is maintaining the structure integrity of the binding site

in the protein ligand throughout the immobilization and column operation.

Suggested Further Reading

- Dorsey, J. G., W. T. Cooper, B. A. Siles, J. P. Foley, and H. G. Barth, *Anal. Chem.* 70: 591R–644R (1998).
Lowe, C. R., *Adv. Mol. Cell Biol.* 15B: 513–522 (1996).
Ohlson, S., M. Bergstorm, P. Pahlsson, and A. Lundblad, *J. Chromatogr.* 758: 199 (1997).
Porath, J., *Methods Enzymol.* 34: 13–30 (1974).
Pommerening, *Affinity Chromatography: Practical and Theoretical Aspects*, Marcel Dekker, Inc., New York, 1985.
Turkova, J., *Bioaffinity Chromatography*, Elsevier, Amsterdam, 1993.





Purge-Backflushing Techniques in Gas Chromatography

Silvia Lacorte

IIQAB-CSIC Barcelona, Catalonia, Spain

Anna Rigol

University of Barcelona, Barcelona, Catalonia, Spain

INTRODUCTION

Monitoring of volatile organic compounds (VOCs) in the environment has become a subject of concern because many of these compounds are toxic and persistent^[1] and, in addition, are responsible for odor and taste problems in various types of water.^[2] Their presence in water is mainly associated with industrial and urban discharges, chlorination of municipal wastewater, or on-land application of pesticides.^[3] Analysis of VOCs has been performed using various techniques involving purge and trap (P&T), headspace, liquid–liquid extraction, solid-phase microextraction (SPME), or closed loop stripping analysis (CLSA).^[4] However, P&T is the most commonly used technique because it permits the extraction of a wide range of analytes of different chemistries.

The present work is an overview of purge–trap, coupled to gas chromatography (P&T–GC) for the analysis of a wide range of VOCs. This technique has been applied to the determination, in water and solid matrices, of compounds that have sufficiently high volatility and low water solubility to be removed from water, e.g., aromatic hydrocarbons, alcohols, aldehydes, ketones, chloroaliphatic compounds, halogenated compounds, etc. In this technique, VOCs are sparged (purged) from the sample by bubbling inert gas for a fixed period of time. Purged sample components are trapped in a solid sorbent trap, generally containing Tenax[®]. Afterwards, the trap is rapidly heated and backflushed with helium to desorb the trapped sample components and introduce them directly into the gas chromatograph. Desorption can be performed with cryofocusing, which lead to better peak shapes. Chromatographic techniques are then used to identify and quantify target compounds. This article reports the optimization parameters of P&T–GC, such as sample volume, type of trap and analytical column, most widely used detectors for VOCs, and precautions that have to be taken with the sample handling and analysis of VOCs, in order to have a reliable result. Finally, the last section will be devoted to the monitoring of VOCs in environmental waters, comprising surface, groundwater, and industrial effluents.

OPTIMIZATION OF THE PURGING CONDITIONS

VOCs represent a group of contaminants of low reactivity, characterized for having low water solubility (from 0.05 to 19 g/L at 25°C), vapor pressures of 0.13–25 kPa (184 kPa for bromomethane), boiling points (bp) ranging from –13.9 to 180°C, and Henry's law constants varying, in general, from 0.1 to 3 kPa m³/mol. The Henry's law constant is used to predict the movement of VOCs in the environment, but it is also a key factor to determine the stripping process during P&T analysis. Purgable compounds must have a sufficiently high Henry's law constant to enable extraction from water or solid matrix.

P&T is a standardized method dictated by the U.S. Environmental Protection Agency (US EPA), Series 500 and 600, and is extensively used due to its wide application range, good precision, absence of solvents, ease of coupling with GC, and the possibility of automation. When a mass spectrometry (MS) detector is used, as described in US EPA Method 524.2,^[5] more than 60 compounds can be analyzed in a single run. In this method, 5–25 mL of water is purged with He at a flow rate of 30–40 mL/min for 11 min at ambient temperature. Compounds are retained in a trap which is, thereafter, heated to 180–230°C to desorb the compounds either with or without cryofocusing. Fig. 1 shows a general scheme of a P&T device. The stripping efficiency depends on the partition coefficients of the compounds, while the efficiency in trapping the stripped VOCs depends on the type of compounds and on the retention characteristics of the trap. Several purge parameters can be optimized to afford higher sensitivity and selectivity. The most relevant are:

- (i) Type of trap column.
- (ii) Purged sample volume.
- (iii) Gas flow rate and purging time.
- (iv) Desorption conditions.

Typical values are indicated in Table 1.

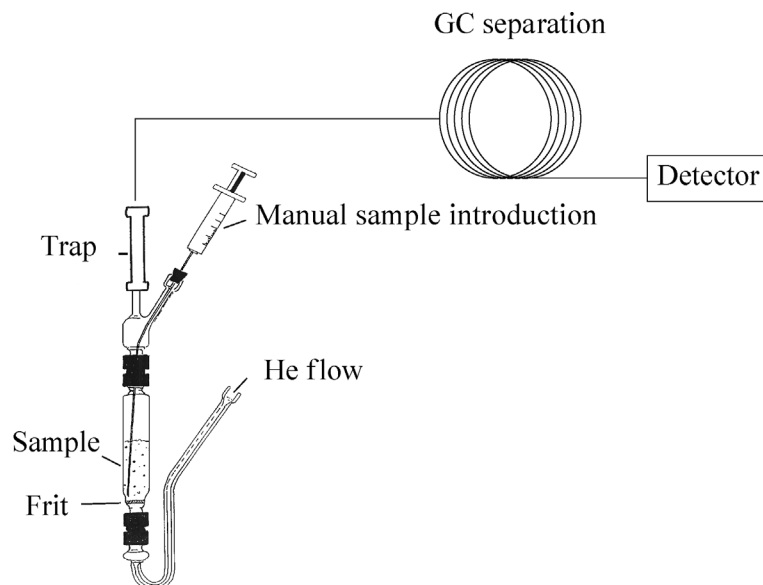


Fig. 1 Schematic of manual purge and trap gas chromatography for the analysis of volatile organic compounds in water.

The type of trap should be selected so that target analytes can be easily trapped and efficiently removed. It should provide good recoveries and good chromatographic resolution so that VOCs can be precisely quantified. Different types of trap sorbents are generally available in the market. Tenax[®] was widely adopted in 1970; it provided reliable results with high precision and detection limits at the µg/L levels.^[5] It is stable at temperatures of 180°C, and, if properly cleaned, no background contamination is observed. The main drawback is that it may lead to losses of the more volatile compounds such as vinyl chloride. This problem can be overcome by the use of mixed sorbents with Tenax[®]-SilicaGel-Charcoal or Tenax[®]-activated charcoal (Spherocharb/Carvosieve). These sorbents permit trapping of compounds with higher

molecular weights and support higher desorption temperatures, thereby enabling faster transfer of the analytes and better chromatographic separations. These combined phases also provide more reliable recoveries and allow the retention of a broader range of chemicals. The use of activated carbon and Tenax[®] is especially suitable to trap the lightest VOCs. Because the analytes are desorbed by backflushing the trap, compounds with high molecular weights are never in contact with the strong sorbent; thus, they are easily eluted. Baking of the trap is necessary to avoid memory effects between different samples. The baking temperature and time depends on the type of trap used. In general, the system is set at 230°C for 10 min, and, with these conditions, no carryover is generally observed.

Table 1 Parameters that can be optimized during P&T–GC–MS and common values used for the determination of a wide range of VOCs in waters

P&T conditions		GC–MS conditions	
Type of trap	Tenax Combined phases	Interface temperature	250°C
Sample volume	5–20 mL	Injector	Split/splitless ratio, 20:1
Purge temperature	35°C	Column	DB-624
Purge time	5–15 min	Temperature program	35°C (5 min) to 160°C at 7°C/min (1 min) and to 210°C at 5°C/min
Purge flow rate	20–50 mL/min	Carrier	He, 1 mL/min (max. 1.2)
Desorption temperature	180–250°C	MS source temperature	200°C
Desorption flow rate	3–4 mL/min	Emission current	100 µA
Desorption time	1–5 min	Detector voltage	380 V
Bake time	10–15 min	Scan range	35–300 amu
Bake temperature	230–280°C		

The sample volume that can be purged depends on the system configuration and the type of sample to be analyzed. Foaming is one of the problems that arises when purging samples with high organic content. In such cases, the sample should be diluted, or a small sample volume should be sparged. In order to have a reproducible result, a 25 mL vessel should be filled with at least 5 mL and up to 15 mL. Lower volumes may lead to high intraday variations. Higher volumes often produce problems of clogging and contamination of the trap, and, often, this may lead to long cleaning requirements for achieving stable baselines. The sample volume is also strongly related to the type of matrix involved. For “clean” water samples, such as ground or drinking water, the established purged volume is 11–13 mL, according to the EPA methods. This permits the achievement of detection limits below 0.1 µg/L for most compounds. For industrial effluents and charged waters, it is advisable to dilute the samples, e.g., to ~5–10%. This still permits detection of the analytes of interest and, at the same time, avoids interference. For soil and sediment samples, Kester^[6] has described a protocol in which 4 g of sample is dispersed in methanol. After sonication for 1 min, followed by centrifugation, an aliquot of, generally, 100 µL is added to high-performance liquid chromatography (HPLC) water which is purged as indicated above. This protocol is easy to perform, but suffers from low sensitivity, because only a small aliquot of the sample is analyzed. Increasing the volume of the extract results in a methanol peak that may overlap with some of the analytes of interest. More suitable are the specific configurations especially designed to purge solid samples, such as soils and sediments, which are provided with large bore tubes and orifices to prevent clogging and can be adapted for homogenizing the samples to provide precise extraction and delivery of analytes.

The gas flow rate and purging time must be optimized to achieve maximum sensitivity. According to EPA Method 524.2, a pre-fixed value is purged with He at 40 mL/min for 11 min. Higher purging time or flow may lead occasionally to lower limits of detection. However, precaution has to be exercised so as not to exceed the breakthrough volume, which would lead to poor recoveries.

Desorption of the analytes is accomplished by heating the trap to 180–200°C and simultaneously backflushing with an inert gas at 3–4 mL/min for around 4–5 min. If P&T is coupled to an MS system, the desorption time must be optimized to a minimum value so that it ensures the total desorption of the analytes from the trap without affecting the vacuum requirements of MS. The use of a cryogenic interface or cryofocusing is recommended to improve peak shapes. In this case, desorbed analytes are transferred to a cool trap set at –150°C. Desorption from the cool trap is performed

by heating at 250–300°C; analytes are transferred into a capillary column. At this time, the temperature program of the GC starts. The injector is then programmed in a split ratio of 20:1.

Instrumentation is available from various suppliers, and sample loading can be performed either manually or by using automated systems. Automation implies no sample manipulation and the sources of errors are minimized, being, therefore, a highly robust technique. The automated system permits a high sample throughput and is especially indicated in routine monitoring programs.^[3] Recent work related to the use of P&T for survey of VOCs in surface waters indicates the suitability and robustness of the technique for long-term monitoring studies.^[7]

SEPARATION USING VARIOUS COLUMNS

Typical columns for the analysis of VOCs are 60–75 m, 1–3 µm film thickness and high internal diameter (0.32, 0.53, or even 0.75 mm), which copes with the high flow rates often necessary to transfer the analytes from the purging device to the gas chromatograph. When a wide bore column is used, chromatography can start with the onset of thermal desorption. For narrow bore columns, cryofocusing is advisable for better peak separation. GC-MS conditions are shown in Table 1. The injector is programmed in splitless mode for 2 min, and the column flow rate is maintained constant throughout acquisition. If MS is used, the flow rate should be adjusted to 1 mL/min.

For the analysis of VOCs, the most common column is a 75 m × 0.53 mm i.d. DB-624 fused silica capillary with 3 µm film thickness. A typical DB-624 permits detection from vinyl chloride (bp = –13.9°C and solubility = 2700 g/L) up to 2-chloronaphthalene (bp = 256°C), being therefore suitable to determine a wide range of compounds of different volatilities and polarities. For specific applications, e.g., control of trihalomethanes in drinking water, a short column of 30 m can be used, and the analysis time is, of course, reduced.

DETECTION TECHNIQUES

Depending on target analytes to be determined, different detectors can be used, e.g., electron capture detector which offers high sensitivity and selectivity for halogenated compounds,^[8] MS which permits the analysis of a large number of compounds,^[9] and atomic emission detector^[10] which has been used for the analysis of environmental samples. Increasingly, however, P&T is coupled to GC with MS detection. This technique, described and vali-



dated in the EPA method 524.2,^[5] permits the analysis of a large number of analytes within a single run, gives confirmatory data according to the acquisition technique (scan mode or selected ion monitoring, registering three ions per compound for confirmatory purposes), and, finally, gives limits of detection at the 0.1 or 0.01 µg/L level, ideal for the analysis of VOCs in environmental matrices. For these reasons, it is the sole technique that avoids false positives/negatives by unequivocally assuring the presence of analytes using a single column.

Irrespective of the detection method used, the analysis of VOCs often involves the presence of interferences in the chromatogram. This is normally due to VOCs present in the atmosphere, such as normal laboratory solvents (acetone, dichloromethane, chloroform, acetonitrile, or methanol) which can be detected, especially when using a universal detector such as a mass spectrometer which operates under vacuum. This problem is eliminated when the laboratory of analysis is free of solvents and is isolated, especially from urban areas.

QUALITY CONTROL OF THE PROCESS

Due to their high volatility, the analysis of VOCs is complex and needs extreme precautions, both with the samples and with the preparation of standard solutions. The growing need to provide reliable results leads to quality control charts for a long-term guarantee of the data generated in each laboratory. Test samples and standard solutions should be kept at 4°C, but not for more than 15 days, in order to avoid sample degradation. In addition, samples should be gathered and kept without any headspace volume in order to avoid losses of the more volatile compounds. The analytical control charts involve both the analysis of reagent blanks and spiked blanks and demonstration of laboratory accuracy and precision. The analysis of reference and certified materials is highly recommended for method validation as indicated in a recent publication.^[11]

On a routine basis, the use of internal standard and surrogate is necessary to ensure an accurate measurement of all VOCs throughout an analytical experiment. In optimizing the analytical method, it is essential to use one or more surrogates that will cover the whole range of compounds studied. Depending on the equipment used, the surrogate can be automatically pumped into the purging vessel. Otherwise, the surrogate mixture can be added directly to the sample with the minimum amount of solvent possible. If an internal standard is used, a split/splitless injector is needed for direct injection. However, this option is not advisable for quantification purposes as response factors of different test compounds

may vary considerably. The most common compounds used as surrogates (or internal standard, depending on the application) are fluorobenzene, 1,2-dichlorobenzene d₄, bromochloromethane, difluorobenzene, chlorobenzene d₆, 4-bromofluorobenzene, and 1,4-dichlorobutane, among others, which elute at different intervals throughout the chromatogram. The surrogate will serve not only for method control but for analyte quantification, if properly selected.

Calibration curves should be prepared by spiking HPLC or groundwater samples with the test mixture at concentrations that permit a wide linear range. Normally, VOCs are found in environmental waters at 0.1–10 µg/L. Therefore, typical linear ranges are from 0.01 to 2–3 µg/L, with higher concentrations leading to poor linearity. “Charged” samples may have levels up to 200 µg/L and should be diluted prior to purging. In addition, a sample sequence should always include a blank sample, calibration standards or quality control standards, and samples. Blank analysis with HPLC water should be performed often (every four to five samples, depending on the matrix) to avoid carryover effects. It is crucial to have blanks which are void of interferences. Therefore, precautions must be taken in cleaning the glass material, which must be performed in an ultrasonic bath, followed by rinsing with acetone and, afterward, with distilled water. All sample preparation has to be done in a laboratory atmosphere that is free of solvents.

Quantification should be done using response factors or calibration curves. Using internal standards, variability with automated systems should not exceed 5–10%. In contrast, manual purging equipment connected to an MS can have up to 10–20% variation, depending on the compounds studied. External calibration is not recommended because a response variation of up to 50% can be detected. Limits of detection and recoveries of test compounds should be calculated in order to verify the suitability of the method for specific applications. Quality parameters of selected VOCs are indicated in Table 2. According to the US EPA, recoveries higher than 70% are acceptable. If using an internal standard for quantification, results should not be corrected by recovery. However, if external calibration is used, the percentage recovery should be indicated and used for quantification.

ENVIRONMENTAL APPLICATION

Large amounts of VOCs are generated in industrialized areas and eventually are discharged into surface waters or transported by the atmosphere. Once in the environment, VOCs can be absorbed into biota and soil, and, depending on soil characteristics, they can eventually migrate to

Table 2 Compounds studied, retention time (min), molecular weight (MW) and other two most abundant ions monitored (in bold, ion used for quantification), and calibration data obtained for spiked groundwater samples at 1 µg/L using automated P&T coupled to GC/MS

Compound	RT (min)	Monitored ions			Linearity (µg/L)	R^2	%R	STD	LD (µg/L)
		MW	Ion1	Ion2					
Vinyl chloride	2.57	62	64	–	0.04–2.20	0.9846	65	10.8	0.300
Dichloromethane	5.40	84	49	86	0.04–2.20	0.8192	105	10.2	0.062
1,1-Dichloroethane	7.58	98	63	83	0.04–2.20	0.9899	99	2.9	0.017
Chloroform	10.79	118	83	85	0.04–2.20	0.9524	93	4.2	0.002
1,1,1-Trichloroethane	11.29	132	97	61	0.04–2.20	0.9842	95	9.7	0.021
Carbon tetrachloride	11.81	152	117	119	0.04–2.20	0.9974	90	4.9	0.002
Benzene	12.45	78	77	52	0.04–2.20	0.9901	98	9.5	0.002
1,2-Dichloroethane	12.54	98	62	–	0.04–2.20	0.9813	97	7.4	0.002
Trichloroethylene	14.40	130	95	60	0.04–2.20	0.9752	97	10.5	0.010
1,2-Dichloropropane	15.02	112	63	76	0.04–2.20	0.9804	99	5.7	0.011
Dibromomethane	15.34	172	174	93	0.04–2.20	0.9964	91	3.2	0.022
1,3-Dichloropropane	17.11	110	75	–	0.04–2.20	0.9910	90	3.6	0.042
Toluene	18.01	92	91	65	0.04–2.20	0.9876	93	8.4	0.007
1,1,2-Trichloroethane	19.17	132	97	83	0.04–2.20	0.9825	92	7.5	0.023
Tetrachloroethylene	19.55	164	129	94	0.04–2.20	0.9867	91	3.5	0.014
Ethylbenzene	22.27	106	91	77	0.04–2.20	0.9901	90	5.3	0.014
1,1,1,2-Tetrachloroethane	22.28	166	83	131	0.04–2.20	0.9919	91	4.7	0.029
<i>m</i> + <i>p</i> -Xylene	22.62	106	91	77	0.04–2.20	0.9924	91	2.1	0.036
<i>o</i> -Xylene	23.73	106	91	77	0.04–2.20	0.9947	99	2.3	0.015
Bromoform	24.26	250	173	91	0.04–2.20	0.9939	98	2.1	0.027
Isopropylbenzene	24.80	120	105	77	0.04–2.20	0.9874	94	2.4	0.058
1,1,2,2-Tetrachloroethane	25.67	166	83	131	0.04–2.20	0.9388	98	2.1	0.020
1,2,3-Trichloropropane	25.76	146	75	110	0.04–2.20	0.9910	95	1.7	0.035
1,3-Dichlorobenzene	28.38	146	148	111	0.04–2.20	0.9820	96	2.3	0.014
1,4-Dichlorobenzene	28.67	146	148	111	0.04–2.20	0.9812	97	5.3	0.017
1,2-Dichlorobenzene	29.73	146	148	111	0.04–2.20	0.9802	96	4.0	0.016
Hexachloroethane	30.48	234	117	201	0.04–2.20	0.9834	97	4.3	0.115
1,2,4-Trichlorobenzene	34.84	180	145	–	0.04–2.20	0.9792	99	3.4	0.009
Hexachlorobutadiene	35.41	258	225	190	0.04–2.20	0.9916	97	4.2	0.061
1,2,4,5-Tetrachlorobenzene	39.79	216	–	–	0.04–2.20	0.9895	98	2.9	0.009
1-Chloronaphthalene	41.91	162	127	–	0.04–2.20	0.9678	74	2.6	0.014

–: No formation of additional fragment ions at 70 eV.

RT = retention time; %R = percentage of recovery; STD = standard deviation; LD = limit of detection.

groundwater by leaching.^[1,7] Compounds detected depend on the type of waters analyzed. Several directives indicate the need to regulate the use and discharge of VOCs into the environment. Some widely used and toxic VOCs are included in priority pollutant lists, and stringent regulatory requirements have resulted in routine monitoring of these compounds in different types of waters. Solvents, such as chloroform, toluene, benzene, dichloromethane, and chloroethenes, are widely used in industrial manufacturing and organic synthesis. Others, chlorobenzenes or chloropropenes, are used as solvents in the formulation of fats and in dye manufacturing. The final fate and ecotoxicological impact that they may cause depends on the type of water and their concentrations.

Surface Waters

Extensive monitoring, carried out to determine halogenated VOCs in surface water from Portugal, revealed the presence of chloroform, tetrachloroethylene, trichloroethylene, and carbon tetrachloride in 13–50% of the samples analyzed, with a median of 0.1–0.3 µg/L, except for punctual contaminated areas close to big cities where these compounds were detected up to 18 µg/L. Also, high concentrations were found in agricultural areas, where solvents are used in many pesticide formulations.^[8] In another study,^[3] in which 41 compounds of different families were studied, 37 were detected at least once at levels between 0.01 and 28 µg/L, same with that which

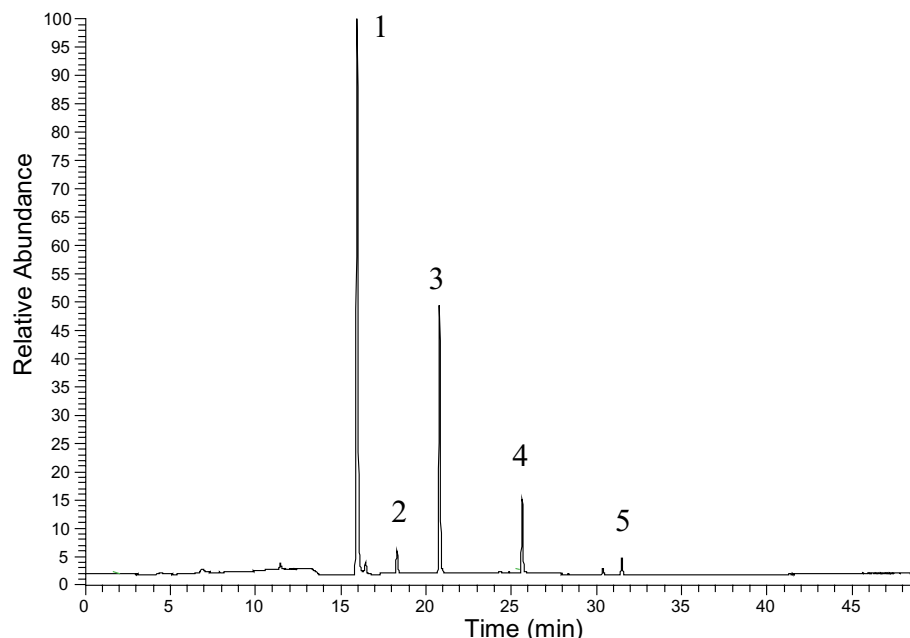


Fig. 2 P&T gas chromatography–mass spectrometry of drinking water containing: 1) chloroform; 2) 1,1,2,2-tetrachloroethene; 3) bromodichloromethane; 4) dibromochloromethane; and 5) bromoform.

was found in a monitoring survey carried out in surface waters from Greece.^[12]

Drinking Water

Other applications of P&T are related to the control of trihalomethanes in finished drinking water. Fig. 2 shows a typical profile where chloroform, bromodichloromethane, dibromochloromethane, and bromoform were detected at 80–100 µg/L. The technique, when coupled to MS, can also be applied to identify compounds responsible for taste and odor problems in water.^[13]

Groundwater Samples

Groundwater is a stable reservoir of organic pollutants. An extensive monitoring study carried out in the United States revealed that 7% of the ambient groundwater resources of the United States contain at least one VOC at levels of 0.2 µg/L and, in urban areas, 47% of the sampled wells were positive.^[7] A compound now of interest is methyl *tert*-butyl ether (MTBE), which is the most widely used ether oxygenate added to gasoline as an octane booster.^[14] MTBE enters the environment during all phases of the petroleum fuel cycle. Due to its high solubility (25–50 g/L), low K_{ow} (0.94–1.43), and Henry's law constant (55.3 Pa m³/mol), MTBE remains dissolved in surface water, where it can volatilize into the atmosphere. A small fraction can partition into soil and eventually reach

groundwater where it can persist for more than 200 days, causing odor problems at low concentrations.

Industrial Effluents

A recent study indicated that more than 50 VOCs were found in effluents from high-tech industries, leading to pollution of surrounding river waters and inducing bad atmospheric odor. Benzene, toluene, chloroform, and dichloromethane were the major contributors of industrial discharges and were detected in 30% or more of the analyzed samples.^[15]

CONCLUSIONS

The analysis of VOCs in water and solid samples is complex due to the large number of compounds to be analyzed and because precaution has to be taken to provide accurate and reliable results. The use of P&T–GC–MS is the most adequate for trace analysis of VOCs because limits of detection at the ng/L levels can be achieved and confirmatory analysis can be performed. Although P&T is a well-established technique, several analytical parameters can be optimized to obtain high sensitivity and selectivity. For the specific target analytes, method optimization and quality assurance are necessary. The main drawbacks of this technique result from the fact that high purity gases are required and that the system can



be easily polluted when charged samples are analyzed, producing carry over effects. These problems can be eliminated if precautions are taken in optimizing the analytical conditions prior to analysis.

REFERENCES

1. Heinrich-Ramm, M.; Jakubowski, B.; Heinzow, J.M.; Christensen, E.; Olson, O.; Hertel, E. Biological monitoring for exposure of volatile organic compounds. IUPAC Recommendations 2000. *Pure Appl. Chem.* **2000**, *72*, 385–436.
2. Ventura, F.; Matia, L.; Romero, J.; Boleda, R.M.; Marti, I.; Martín, J. Taste and odor events in Barcelona's water supply. *Water Sci. Technol.* **1995**, *31* (11), 63–68.
3. Martinez, E.; Llobet, I.; Lacorte, S.; Viana, P.; Barcelo, D. Fully automated purge and trap coupled to GC–MS for the low level determination of volatile organic compounds in water. *J. Chromatogr., A* **2002**, *959*, 181–190.
4. Dewulf, J.; Van Langenhoven, H. Anthropogenic volatile organic compounds in ambient air and natural waters: A review of recent developments of analytical methodology, performance and interpretation of field measurements. *J. Chromatogr., A* **1999**, *843*, 163–177.
5. Eichelberger, J.W.; Munch, J.W.; Bellar, T.A. *Measurement of Purgable Organic Compounds in Water by Capillary Column Gas Chromatography/Mass Spectrometry, Revision 4.0, EPA Method 524.2*; Environmental Monitoring Systems Laboratory, Office of Research and Development, US Environmental Protection Agency: Cincinnati, OH, 45268, 1992; 5–50.
6. Kester, P.E. *Analysis of Volatile Organic Compounds in Soils by Purge and Trap Gas Chromatography*; Tekmar Company: P.O. Box 371856, Cincinnati, OH.
7. Squillace, P.J.; Morgan, M.J.; Lapham, W.W.; Price, C.V.; Clawges, R.M.; Zogorski, J.S. Volatile organic compounds in untreated ambient groundwater of the United States, 1985–1995. *Environ. Sci. Technol.* **1999**, *33*, 4176–4187.
8. Martinez, E.; Llobet, I.; Lacorte, S.; Viana, P.; Barcelo, D. Patterns and levels of halogenated volatile compounds in Portuguese surface waters. *J. Environ. Monit.* **2002**, *4*, 1–7.
9. Lee, M.R.; Lee, J.S.; Hsiang, W.S.; Chen, C.M. Purge and trap gas chromatography–mass spectrometry in the analysis of volatile organochlorine compounds in water. *J. Chromatogr., A* **1997**, *775*, 267–274.
10. Silgonier, I.; Rosenberg, E.; Grassenbauer, M.J. Determination of volatile organic compounds in water by purge and trap gas chromatography coupled to atomic emission detector. *J. Chromatogr., A* **1997**, *768*, 259–270.
11. Huybrechts, T.; Dewulf, J.; Moerman, O.; van Langenhove, H.J. Evaluation of purge and trap–high resolution gas chromatography–mass spectrometry for the determination of 27 volatile organic compounds in marine water at ng L⁻¹ concentration level. *J. Chromatogr., A* **2000**, *893*, 367–382.
12. Kostopoulou, M.N.; Golfinopoulos, S.K.; Nikolau, A.D.; Xilourgidis, N.K.; Lekkas, T.D. Volatile organic compounds in the surface waters of Northern Greece. *Chemosphere* **2000**, *40*, 527–532.
13. Ventura, F.; Romero, J.; Pares, J. Determination of dicyclopentadiene and its derivatives as compounds causing odors in groundwater supplies. *Environ. Sci. Technol.* **1997**, *31*, 2368–2374.
14. Schmidt, T.C.; Duong, H.A.; Berg, M.; Haderlein, B. Analysis of fuel oxygenates in the environment. *Analyst* **2001**, *126*, 405–413.
15. Wu, C.H.; Lu, T.; Lo, J.G. Analysis of volatile organic compounds in wastewater during various stages of treatment for high-tech industries. *Chromatographia* **2002**, *56*, 91–98.

Purification of Cyanobacterial Hepatotoxin Microcystins by Affinity Chromatography

Fumio Kondo

Aichi Prefectural Institute of Public Health, Nagoya, Japan

INTRODUCTION

Freshwater cyanobacteria *Microcystis*, *Oscillatoria*, *Anabaena*, and *Nostoc* produce several types of toxins, among which the most commonly detected are the hepatotoxic peptides microcystins. The general structure of the microcystins is cyclo-(D-Ala¹-X²-D-MeAsp³-Z⁴-Adda⁵-D-Glu⁶-Mdha⁷), in which X and Z represent variable L-amino acids, D-MeAsp³ is D-erythro- β -methylaspartic acid, Mdha is N-methyldehydroalanine, and Adda is the unusual C₂₀ amino acid, (2S,3S,8S,9S)-3-amino-9-methoxy-2,6,8-trimethyl-10-phenyldeca-4(E),6(E)-dienoic acid (Fig. 1).^[1] The structural differences in the microcystins mainly depend on the variability of the two L-amino acids (denoted X and Z), and secondarily on the methylation or demethylation of D-MeAsp and/or Mdha.^[1] More than 60 microcystins have been isolated from bloom samples and isolated strains of cyanobacteria.^[1]

Microcystins have caused the poisoning of wild and domestic animals worldwide, and in 1996, they caused the death of 76 people in Caruaru, Brazil, which was attributed to the use of microcystin-contaminated hemodialysis water.^[2] Microcystins, like the well-documented tumor promoter, okadaic acid, strongly and specifically inhibit the protein phosphatases 1 and 2A and have a tumor-promoting activity in the rat liver.^[3] In addition to acute hepatotoxicity, microcystins pose problems to human health—which could result from low-level, chronic exposure to microcystins in drinking water, as suggested by the high incidence of primary liver cancer in the Qidong and Haimen regions of China.^[4] In 1998, the World Health Organization (WHO) proposed a provisional guideline level of 1.0 $\mu\text{g/L}$ for microcystin-LR in drinking water.^[4]

OVERVIEW

In order to achieve the rapid and precise determination of microcystins in complicated matrices, a systematic procedure is seriously required. This may include screening, sample purification, identification, and quantification processes.^[5] Screening is intended to rapidly check for the presence of microcystins in a small amount of sample,

through sensitive and simple methods. If a sample proves positive in the screening test, it will be necessary to follow through with sample purification, identification, and quantification analyses. The purpose of sample purification is to eliminate coexisting substances by a simple operation without the loss of any analyte and, considering that the microcystin concentration may be low, it also enables the enrichment of the analyte. Octadecyl silanized (ODS) silica gel has been extensively employed for this process because it retains microcystins and allows coexisting substances to pass through.^[5] A method using ODS silica gel extraction followed by a purification on silica gel has been established to effectively eliminate the coexisting substances in lake water.^[6] Although this method has been successfully applied to the analysis of microcystins in lake water samples, it had several problems. The method required a large water sample (5 L) to accumulate the low level of microcystins, resulting in a laborious and time-consuming extraction process. It was also shown that less hydrophobic coexisting substances still remained even after purification on silica gel,^[6] indicating that a more effective purification method is required.

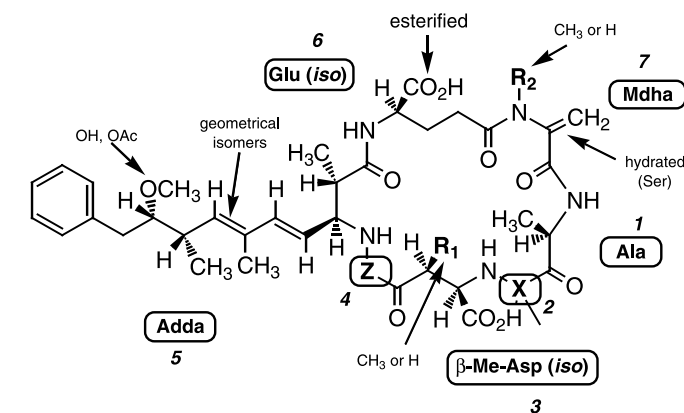
Recently, an immunoaffinity purification method using antimicrocystin-LR monoclonal antibodies (named M8H5) has been developed.^[7] This purification method was found to be remarkably effective in the removal of coexisting substances and in the enrichment of microcystins in samples.^[7–12] This work will focus on the immunoaffinity purification methods for microcystins in lake^[10] and tap water samples,^[11] and the analysis methods for microcystins and their metabolites in mouse and rat livers.^[7–9] It will also cover the reuse of the immunoaffinity column.^[12]

IMMUNOAFFINITY COLUMN

Preparation of Immunoaffinity Column

M8H5 antimicrocystin-LR monoclonal antibodies were produced by Nagata et al. as follows:^[13,14] female BALB/c mice were immunized with microcystin-LR conjugated proteins (e.g., bovine serum albumin [BSA]).





	X	Z	R ₁	R ₂	MW
Microcystin-LA	Leu	Ala	CH ₃	CH ₃	909
Microcystin-LR	Leu	Arg	CH ₃	CH ₃	994
Microcystin-YR	Tyr	Arg	CH ₃	CH ₃	1044
Microcystin-RR	Arg	Arg	CH ₃	CH ₃	1037
Microcystin-YM	Tyr	Met	CH ₃	CH ₃	1019
[D-Asp ³]microcystin LR	Leu	Arg	H	CH ₃	980
[Dha ⁷]microcystin LR	Leu	Arg	CH ₃	H	980

Fig. 1 Chemical structures of microcystins.

The spleen cells of the immunized mice and SP2/O-Ag14 cells were fused with polyethylene glycol. From the serum-free cultured supernatants of the generated hybridomas, the M8H5 monoclonal antibodies were prepared by membrane ultrafiltration, ammonium sulfate, which were then finally purified using a protein G column (Pharmacia, Sweden). This monoclonal antibody shows extensive cross-reactivity to various microcystins and nodularin (pentapeptide sharing many common features with microcystins). Based on concentrations capable of inducing 50% inhibition of antibodies in a competitive enzyme-linked immunosorbent assay (ELISA), the cross-reactivities were 100% for microcystin-LR, 109% for microcystin-RR, 51% for [D-Asp³]microcystin-LR, 48% for [Dha⁷]microcystin-LR, 44% for microcystin-YR, 26% for microcystin-LA, and 20% for nodularin.

The antimicrocystin-LR monoclonal antibody-combined gel was prepared as follows:^[7] Affi-Gel 10 (25 mL, Bio-Rad, Hercules, CA, U.S.A.) was washed with distilled ice water (250 mL) and mixed with an equal volume of 10 mg/mL of M8H5 antimicrocystin-LR monoclonal antibody in phosphate buffer saline (PBS) (pH 7.4). The gel mixture was incubated at 4°C for 24 h with gentle rocking. After the addition of 1 M ethanolamine hydrochloride (2.5 mL), the gel mixture was washed with distilled water (250 mL), followed by PBS (500 mL). The obtained gel cake was suspended in PBS containing 0.1% sodium azide (50 mL) and stored at 4°C. The gel mixture

(0.5 mL) was transferred to a polypropylene cartridge (Muromac column; Muromachi Kagaku Kogyo Kaisha, Tokyo, Japan) when used.

Protocol for Immunoaffinity Purification

The general protocol for immunoaffinity purification of the microcystins is as follows: sample extracts dissolved in PBS are loaded onto the immunoaffinity column and passed through the column. Gravity flow is usually used. After washing with PBS and distilled water, the microcystin fraction is eluted with 100% methanol.^[7,10]

Direct immunoaffinity purification of the microcystins in complicated matrices is difficult because the coexisting substances in the sample occupy the column head, so that the process ends in failure.^[10] Thus preliminary semipurification is indispensable when it comes to analyzing trace amounts of microcystins in samples containing substantial amounts of coexisting substances.

DETERMINATION OF MICROCYSTINS

Lake Water

A purification method for microcystins in lake water consists of solid-phase extraction on a Sep-Pak PS2[®]

(styrene–divinylbenzene copolymer) or Excelpak SPE-GLF[®] (polymethacrylate) cartridge, followed by immunoaffinity purification.^[10] A 1-L sample of lake water is filtered through a glass GF/C microfiber filter (Whatman, Maidstone, U.K.), and the filtrate is applied to a Sep-Pak PS-2 or Excelpak SPE-GLF cartridge at a flow rate of about 20 mL/min. The cartridge is washed with distilled water (10 mL), followed by 20% methanol–water (10 mL). Finally, the eluate from the cartridge with 100% methanol (10 mL) is collected and then evaporated to dryness under reduced pressure at 35°C. The resulting residue is dissolved in PBS containing 0.1% BSA (5 mL). Bovine serum albumin is used to prevent nonspecific binding of the microcystins with the immunoaffinity support Affi-Gel 10. The solution is subjected to an immunoaffinity column, which is preconditioned with PBS (5 mL), methanol (5 mL), distilled water (5 mL), and PBS containing 0.1% BSA (5 mL). After washing with PBS (5 mL) and distilled water (5 mL), the microcystin

fraction is eluted with 100% methanol (10 mL). The eluate is then evaporated to dryness under reduced pressure at 35°C. The residue is dissolved in 0.5 mL of 30% methanol–water and then subjected to high performance liquid chromatography (HPLC) with ultraviolet (UV) detection and liquid chromatography/mass spectrometry (LC/MS) analyses.

When an extract is prepared with a solid-phase extraction cartridge alone, the microcystins in lake water cannot be precisely detected because of the unstable baseline and many peaks on the chromatograms from coexisting substances (Fig. 2a). When this extract is further purified with the immunoaffinity column, the microcystin peaks are clearly detected (Fig. 2b) and effectively quantified because the coexisting substances are virtually eliminated. The recoveries from lake water (1 L) spiked with 100 ng each of microcystins-LR, -YR, and -RR are 92.2%, 89.2%, and 85.5%, respectively, with coefficients of variation of 3.3–7.6%. One of the

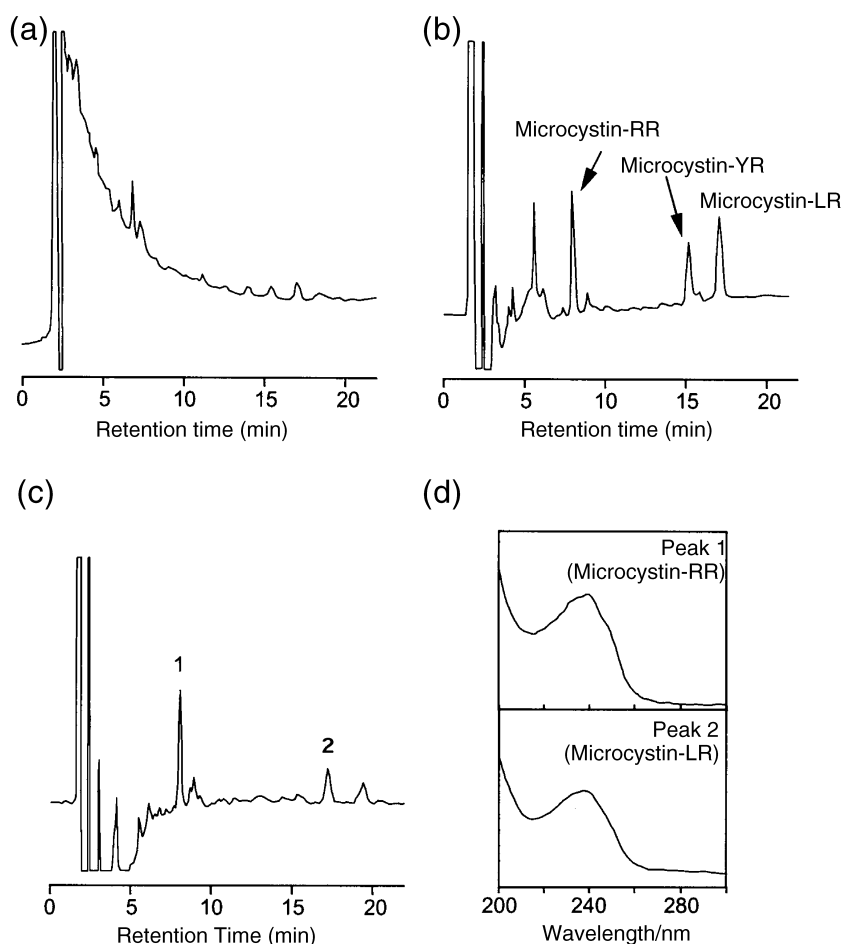


Fig. 2 HPLC analysis of lake water extracts. Microcystin-free lake water spiked with microcystins-LR, -YR, and -RR (100 ng each) was analyzed (a) before and (b) after purification with immunoaffinity column. (c) A water sample taken from Lake Suwa, Japan, in 1998 was analyzed after purification with the immunoaffinity column.

advantages of this method is its speed; it took only 3 hr to complete the entire procedure, starting from the microcystin extraction, the immunoaffinity purification, and the quantification, whereas the previous procedures (tandem use of ODS silica gel and silica gel cartridges) took a day to complete. The detection limit for all of the three microcystins in lake water is 0.005 $\mu\text{g/L}$.

Fig. 2c shows a chromatogram of a sample taken from Lake Suwa, Japan, where water blooms occurred. Two peaks with retention times of 8.0 min (peak 1) and 17.5 min (peak 2) correspond to those of microcystins-RR and -LR, respectively, and they show the typical spectra of the respective microcystins with an absorption maximum at 238 nm (Fig. 2d), affording further confirmation.

Tap Water and Cyanobacterial Cells

Direct purification of the microcystins in tap water with immunoaffinity columns can be achieved because the tap water contains relatively smaller amounts of coexisting substances.^[11] A tap water sample is filtered through glass GF/C microfiber filters, to which a 1/10 volume of 11 \times PBS is added. The sample solution is loaded onto the immunoaffinity column and passed through the column. After washing with PBS (10 mL) and distilled water (10 mL), the microcystin fraction is eluted with 100% methanol (10 mL). The eluate is evaporated to dryness and the residue is dissolved in 0.05 mL of methanol for HPLC analysis. The chromatograms of the microcystin-added tap water with immunoaffinity purification show effective elimination of the coexisting substances compared to that with the ODS cartridge (data not shown). The mean recoveries of microcystin-LR, -YR, and -RR

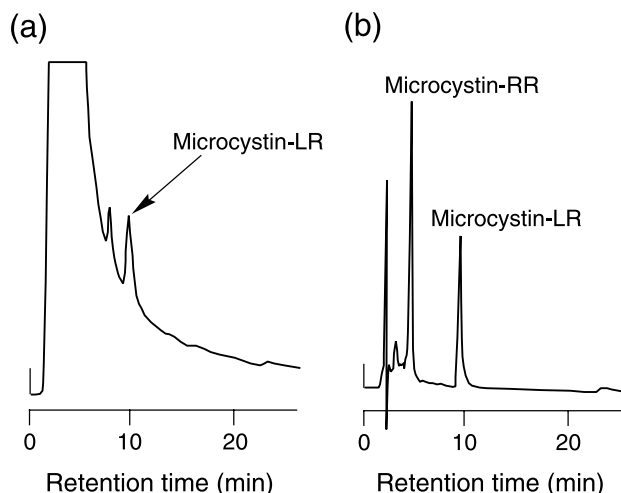


Fig. 4 HPLC analysis of a cytosolic extract from mouse liver spiked with 5 μg each of microcystins-RR and -LR. (a) Before and (b) after purification with immunoaffinity column.

added to tap water are 91.8%, 86.4%, and 77.3%, respectively, in the range 2.5–100 $\mu\text{g/L}$.

Microcystins in cyanobacterial cells can also be directly purified via immunoaffinity columns. A 1-L sample of lake water containing cyanobacterial cells is filtered through a glass GF/C microfiber filter (Whatman), and the cells on the filter are suspended in distilled water (10 mL). The cell containing suspension is freeze-thawed three times and then filtered through a glass GF/C microfiber filter. After the addition of a 1/10 volume of 11 \times PBS, the filtrate is loaded onto the immunoaffinity column and treated in a similar manner as described above. The HPLC chromatogram shows that the peaks of microcystins-LR

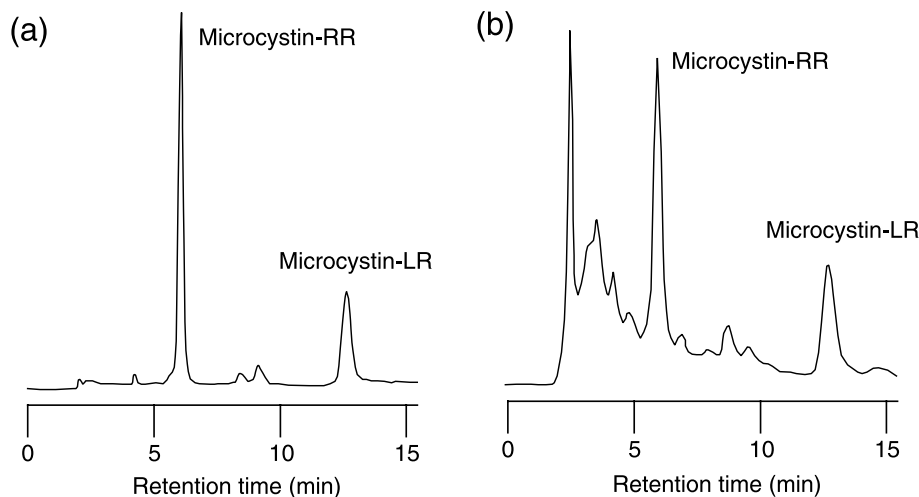


Fig. 3 HPLC analysis of cyanobacterial cells extracts. A cyanobacterial cell sample taken from Lake Suwa, Japan, in 1999 was analyzed after purification with (a) immunoaffinity column and (b) ODS silica gel cartridge.

and -RR are clearly detected and the peaks due to the coexisting substances are almost negligible (Fig. 3a). On the other hand, the chromatogram of the same sample purified with the ODS silica gel cartridge shows that the removal of less hydrophobic coexisting substances is insufficient, especially in a shorter retention time area (Fig. 3b).

Mouse and Rat Livers

The *in vivo* tissue distribution, excretion, and hepatic metabolism of microcystins have been primarily investigated using variously radiolabeled ones.^[4] The amounts of the injected microcystins were too small and the amounts of the contaminants in the tissues were too large

to investigate the metabolites by instrumental analysis, such as HPLC with UV detection and LC/MS. Fig. 4 shows the HPLC profiles of a cytosolic extract from mouse liver spiked with 5 μ g each of microcystins-LR and -RR. When the cytosolic extract is prepared by the method described by Robinson et al.,^[15] which consists of heat-denaturation, pronase digestion, and ODS silica gel treatment (Fig. 4a), the two spiked microcystins cannot be precisely analyzed because of a substantial amount of coexisting substances. When the cytosolic extract is further purified with the immunoaffinity column, the coexisting substances are effectively eliminated and the peaks of the spiked microcystins-LR and -RR are clearly detected (Fig. 4b).

The method including heat-denaturation, pronase digestion, ODS silica gel treatment, and immunoaffinity

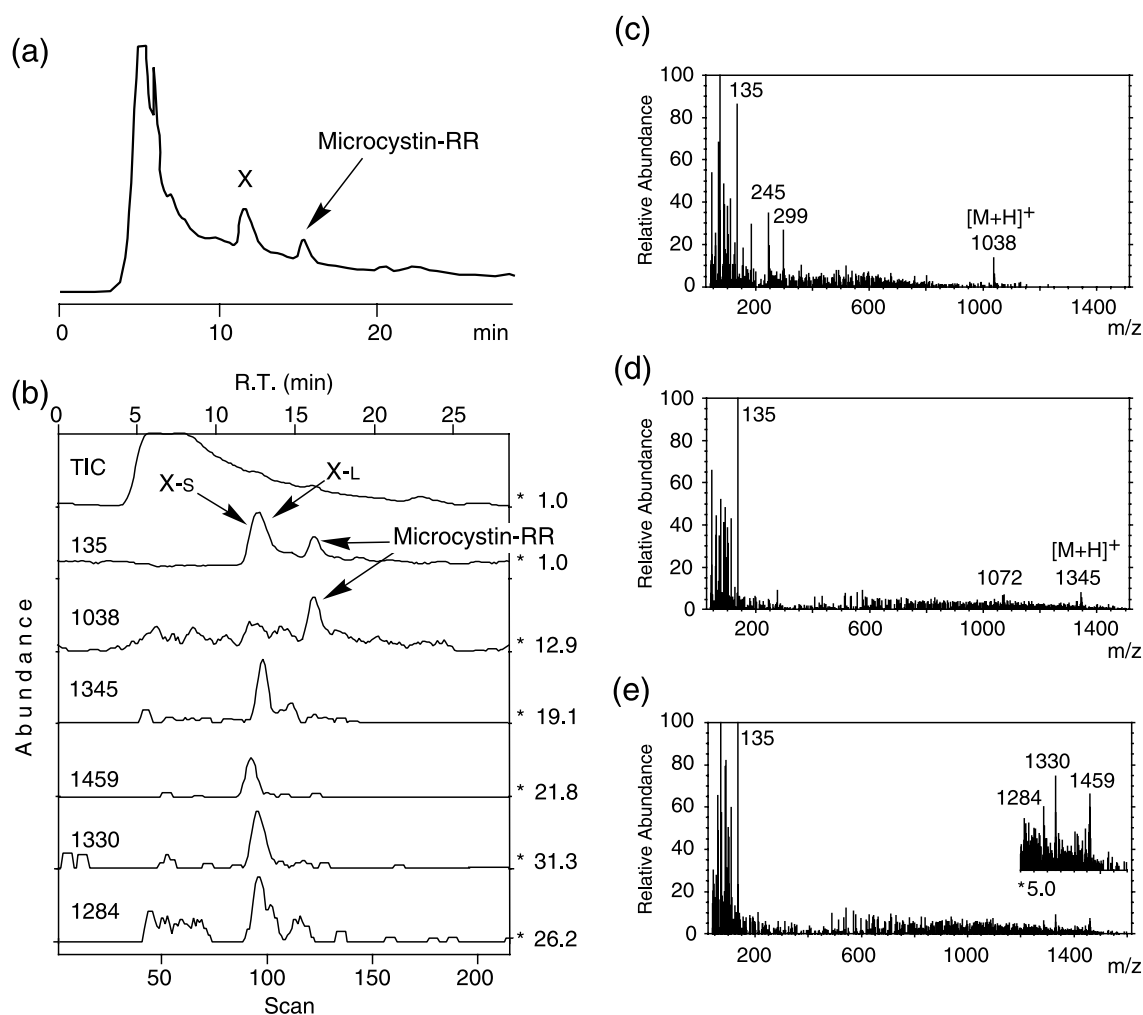


Fig. 5 Frit-FAB LC/MS analysis of a cytosolic extract from mouse liver at 3 hr postinjection of microcystin-RR. Shown are (a) simultaneously monitored UV chromatogram (238 nm), (b) total ion and mass chromatograms, (c) Frit-FAB LC/MS mass spectra of microcystin-RR, (d) longer retention time area of peak X (indicated by X-L), and (e) shorter retention time area of peak X (indicated by X-S).

purification has been applied to the analysis of microcystins and their metabolites in hepatic cytosols from mice and rats intraperitoneally administered microcystins. A purified cytosolic extract from mouse liver at 3 hr postinjection of microcystin-RR was analyzed by Frit-FAB LC/MS. The peaks of the microcystins and related compounds can be selectively detected by monitoring the mass chromatogram at m/z 135, which is the characteristic ion derived from Adda, a characteristic component of microcystins.^[16] The mass chromatogram shows the relatively broad peak X (Fig. 5a), which is confirmed to contain at least four peaks by using slightly modified HPLC analysis conditions. The mass spectrum of the longer retention time area of peak X shows an ion at m/z 1345, whose molecular weight corresponds to that of the glutathione conjugate of microcystin-RR (Fig. 5b), the thiol of GSH having been nucleophilically added to the α,β -unsaturated carbonyl of the Mdha moiety in the microcystins. The glutathione conjugate was confirmed by comparison of the retention time with that of the chemically prepared one. The mass spectrum of the shorter retention time area of peak X shows ions at m/z 1284, 1330, and 1459, with relatively low intensities (Fig. 5c). This area was considered to contain a conjugate of the oxidized Adda diene. The cysteine conjugate was identified in a cytosolic extract from mouse liver at 24 hr postinjection of microcystin-RR. Both the glutathione and cysteine conjugates were also identified in hepatic cytosols from the rat-administered microcystin-LR.

The immunoaffinity purification method, followed by LC/MS analysis, has also been used in other toxicological studies. When aged mice (32 weeks) were orally administered microcystin-LR at 500 $\mu\text{g}/\text{kg}$, 62% of the aged mice showed hepatic injury, whereas such changes in the liver were not found in young mice (5 weeks).^[81] Upon uptake of orally administered microcystin-LR at 500 $\mu\text{g}/\text{kg}$, the toxin into the liver was confirmed by Frit-FAB LC/MS after the immunoaffinity purification. When microcystin-LR was intraperitoneally injected 100 times at 20 $\mu\text{g}/\text{kg}$ into male ICR mice (5 weeks old, Charles River Japan, Atsugi, Japan) for 28 weeks, multiple hyperplastic nodules up to 5 mm in diameter were observed in every liver.^[91] Microcystin-LR and its cysteine conjugate were identified from the isolated mouse livers.

REUSABLE IMMUNOAFFINITY COLUMN

Reuse of the immunoaffinity column is apparently of great value because the immunoaffinity column requires a large amount of antibodies. The immunoaffinity column using Affi-Gel 10 as the immunoaffinity support could not be repeatedly used because the applied solutions tended

to stick owing to the massive bubbles produced. In order to overcome this disadvantage, a new immunoaffinity column using the immunoaffinity support Formyl-Cellulofine[®] has been introduced.^[12] Because of the spherical shape of the immunoaffinity support Formyl-Cellulofine, the applied solutions passed through the column smoothly even when they were used repeatedly.

The purification procedure using this immunoaffinity column has been optimized as follows: After extraction with a Sep-Pak PS2 cartridge, the extract is dissolved in 25 mM Tris-HCl buffer (pH 7.2) containing 1 mM EDTA, 0.15 M sodium chloride, and 0.1% sodium azide (Tris-HCl buffer A) with 0.1% BSA (Tris-HCl buffer B) (5 mL), and the solution is loaded onto an immunoaffinity column, which is preconditioned with Tris-HCl buffer B (10 mL). After washing with Tris-HCl buffer A (10 mL) and distilled water (10 mL), the microcystin fraction is eluted with 100% dimethylformamide (DMF) (2.5 mL). The eluate is then dried on a hot block (60 °C) under a constant stream of nitrogen. The residue is dissolved in 30% methanol-water (0.5 mL) and then subjected to HPLC-photodiode array detection (HPLC-PDA) and LC/MS analysis. The immunoaffinity column is regenerated by washing with Tris-HCl buffer B (10 mL) before each reuse.

Recoveries of the spiked microcystins to lake water from the first use of the column are 87–88%, and 83–88% was recorded from the second and third uses. Recoveries gradually drop to 63–77% from the fourth to the fifth uses. These results indicate that the column can be repeatedly used up to three times.

CONCLUSION

The immunoaffinity column using antimicrocystin-LR monoclonal antibodies has proved to be an important purification tool for microcystin analysis in lake and tap water, and cyanobacterial cells and tissue samples from mice and rats. One of the advantages of the immunoaffinity purification is specificity. It enables operators to enrich the trace amounts of the microcystins and to eliminate large amounts of coexisting substances. As a result of the substantial elimination of these coexisting substances, the microcystin peaks were successfully and reliably identified with HPLC and LC/MS by excluding a few of the nonmicrocystin peaks that appear even after the immunoaffinity purification. On the other hand, one of the disadvantages of the analytical method using the immunoaffinity column is the requirement for large amounts of antibodies. Reuse of the immunoaffinity column is one approach to overcome this limitation. Although the immunoaffinity column for microcystins is not yet com-

mercially available, it is believed that it will become more widely used within the next 2–3 years.

REFERENCES

1. Sivonen, K.; Jones, G. Cyanobacterial Toxins. In *Toxic Cyanobacteria in Water; a Guide to Their Public Health Consequences, Monitoring and Management*; Chorus, I., Bartram, J., Eds.; E & FN Spon: London, 1999; 41–111.
2. Carmichael, W.W.; Azevedo, S.M.F.O.; An, J.S.; Mollica, R.J.R.; Jochimsen, E.M.; Lau, S.; Rinehart, K.L.; Shaw, G.R.; Eaglesham, G.K. Human fatalities from cyanobacteria: Chemical and biological evidence for cyanotoxins. *Environ. Health Perspect.* **2001**, *109* (7), 663–668.
3. Falconer, I.R.; Bartram, J.; Chorus, I.; Kuiper-Goodman, T.; Utkilen, H.; Burch, M.; Codd, G.A. Safe Levels and Safe Practices. In *Toxic Cyanobacteria in Water; A Guide to Their Public Health Consequences, Monitoring and Management*; Chorus, I., Bartram, J., Eds.; E & FN Spon: London, 1999; 155–178.
4. Kuiper-Goodman, T.; Falconer, I.R.; Fitzgerald, J. Human Health Aspects. In *Toxic Cyanobacteria in Water; A Guide to Their Public Health Consequences, Monitoring and Management*; Chorus, I., Bartram, J., Eds.; E & FN Spon: London, 1999; 113–153.
5. Harada, K.-I.; Kondo, F.; Lawton, L. Laboratory Analysis of Cyanotoxins. In *Toxic Cyanobacteria in Water; A Guide to Their Public Health Consequences, Monitoring and Management*; Chorus, I., Bartram, J., Eds.; E & FN Spon: London, 1999; 999.
6. Tsuji, K.; Naito, S.; Kondo, F.; Watanabe, M.F.; Suzuki, S.; Nakazawa, H.; Suzuki, M.; Shimada, T.; Harada, K.-I. A clean-up method for analysis of trace amounts of microcystins in lake water. *Toxicon* **1994**, *32* (10), 1251–1259.
7. Kondo, F.; Matsumoto, H.; Yamada, S.; Ishikawa, N.; Ito, E.; Nagata, S.; Ueno, Y.; Suzuki, M.; Harada, K.-I. Detection and identification of metabolites of microcystins formed in vivo in mouse and rat livers. *Chem. Res. Toxicol.* **1996**, *9*, 1355–1359.
8. Ito, E.; Kondo, F.; Terao, K.; Harada, K.-I. Hepatic necrosis in aged mice by oral administration of microcystin-LR. *Toxicon* **1997**, *35*, 231–239.
9. Ito, E.; Kondo, F.; Harada, K.-I. Neoplastic nodular formation in mouse liver induced by repeated intraperitoneal injections of microcystin-LR. *Toxicon* **1997**, *35*, 1453–1457.
10. Kondo, F.; Matsumoto, H.; Yamada, S.; Tsuji, K.; Ueno, Y.; Harada, K.-I. Immunoaffinity purification method for detection and identification of microcystins in lake water. *Toxicon* **2000**, *38*, 813–823.
11. Tsutsumi, T.; Nagata, S.; Hasegawa, A.; Ueno, Y. Immunoaffinity column as clean-up tool for determination of trace amounts of microcystins in tap water. *Food Chem. Toxicol.* **2000**, *38*, 593–597.
12. Kondo, F.; Ito, Y.; Oka, H.; Yamada, S.; Tsuji, K.; Imokawa, M.; Niimi, Y.; Harada, K.-I.; Ueno, Y.; Miyazaki, Y. Determination of microcystins in lake water using reusable immunoaffinity column. *Toxicon* **2002**, *40*, 893–899.
13. Nagata, S.; Okamoto, Y.; Inoue, T.; Ueno, Y.; Kurata, T.; Chiba, J. Identification of epitopes associated with different biological activities on the glycoprotein of vesicular stomatitis virus by use of monoclonal antibodies. *Arch. Virol.* **1992**, *127*, 153–168.
14. Nagata, S.; Soutome, H.; Tsutsumi, T.; Hasegawa, A.; Sekijima, M.; Sugamata, M.; Harada, K.-I.; Suganuma, M.; Ueno, Y. Novel monoclonal antibodies against microcystin and their protective activity for hepatotoxicity. *Nat. Toxins* **1995**, *3*, 78–86.
15. Robinson, N.A.; Pace, J.G.; Matson, C.F.; Miura, G.A.; Lawrence, W.B. Tissue distribution, excretion and hepatic biotransformation of microcystin-LR in mice. *J. Pharmacol. Exp. Ther.* **1990**, *256*, 176–182.
16. Kondo, F.; Ikai, Y.; Oka, H.; Ishikawa, N.; Watanabe, M.F.; Watanabe, M.; Harada, K.; Suzuki, M. Separation and identification of microcystins in cyanobacteria by fast atom bombardment liquid chromatography/mass spectrometry. *Toxicon* **1992**, *30*, 227–237.

Purification of Peptides with Immobilized Enzymes

Jamel S. Hamada

Southern Regional Research Center, USDA-ARS, New Orleans, Louisiana, U.S.A.

Introduction

Affinity chromatography is a powerful separation technique that exploits specific binding properties among biomolecules. For protein purification, the enrichment obtainable in single-step affinity chromatography sometimes exceeds 1000-fold. This high selectivity is due to the vast variety of specific interactions that characterize the functional properties of protein molecules. Like any other affinity chromatography technique, purification of peptides by immobilized enzymes captures the unique interactions between biomolecules (see Refs. 1–3). For example, many enzymes reversibly bind to their organic cofactor molecules and inhibitors. The separation of such enzymes from other proteins can be easily achieved by using a chromatography column containing immobilized inhibitors. Inversely, the enzyme inhibitors can be isolated and purified to a high degree of purity by affinity chromatography using immobilized enzymes. Because affinity chromatography is a most selective technique, it may be used alone as a single chromatography step for peptide purification. However, as many input-material contaminants as possible must be removed prior to using affinity chromatography (e.g., before the affinity chromatography step). For instance, ultrafiltration or gel permeation chromatography is sometimes used concurrently to separate the high- and low-molecular-weight forms while exchanging buffers. In this entry, the focus will be on the use of affinity chromatography to purify peptides when the immobilized ligand is an enzyme.

General Principle of Peptide Purification by Immobilized Enzymes

The first step in this type of chromatography is the preparation of the column by enzyme immobilization on activated support. Enzymes are immobilized by covalent bonding to a packing of a chromatography column (i.e., a support solid matrix such as a cross-linked agarose bead). A mixture of components containing the peptide of interest is applied to the column. Peptides are bound with a high degree of specificity to the immobilized en-

zyme that functions as an ionic, hydrophobic, aromatic, or stoically active binding site, depending on the particular circumstances. The unbound contaminants, which have no affinity for the ligand, are washed through the column, leaving the desired peptide bound to the matrix. Bound peptides are released by manipulating the composition of the eluant buffers. Generally, the elution of the peptide is accomplished by changing the pH and/or salt concentration or by applying organic solvents or a molecule that competes for the bound ligand (Fig. 1).

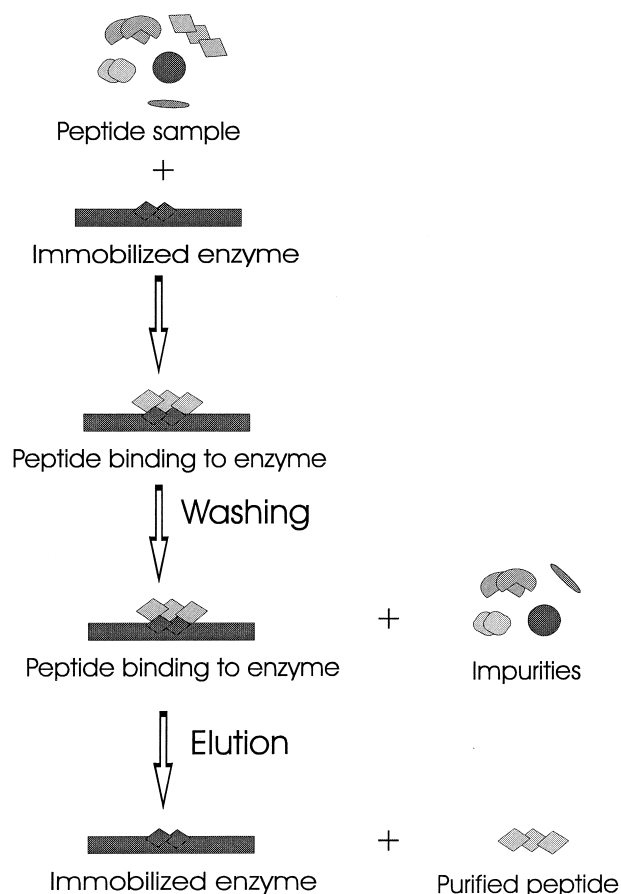


Fig. 1 Schematic illustration of purification of a peptide by affinity chromatography on an immobilized enzyme.



Examples of Purification of Peptides by Immobilized Enzymes

Purification of Protein Hydrolysates

Proteases possess special characters, including their ability to cleave at certain amino acid sites such as at the hydrophobic or neutral residues. This cleavage specificity produces protein hydrolysates that vary significantly in their molecular weights, charge characteristics, functional profiles, and, thus, their potential specific interactions. Using immobilized proteases for peptide purification is a typical application of this type of affinity chromatography. Trypsin is a serine protease; that is, it contains an essential serine at its active site and cleaves the peptide bond next to a basic amino acid residue. Anhydrotrypsin is an inert derivative of trypsin and, thus, has no catalytic activity. It contains dehydroalanine in place of the active serine residue site. The modified enzyme has 20-fold more affinity for product peptides produced by tryptic cleavage than substrate peptides. C-Terminal arginine peptides adhere more tightly than COOH-terminal lysine peptides. Accordingly, immobilized anhydrotrypsin has been used as an affinity ligand for the purification of these peptides. Because of widely varied peptide structure, further specificity may be obtained during elution, which usually involves decreasing pH gradients.

Purification of Pawpaw Glutamine Cyclotransferase

Pawpaw glutamine cyclotransferase (PQC) was purified 279-fold to near homogeneity by a combination of ion-exchange chromatography on SP-Sepharose, hydrophobic interaction chromatography on Fractogel TSK Butyl-650, and affinity chromatography on immobilized trypsin [4]. Trypsin was immobilized on Affigel-10 (Bio Rad Laboratories) according to procedures recommended by the manufacturer. After the concentration of pooled fractions from the last purification step (Fractogel column) by ultrafiltration, affinity chromatography was used. Partially purified PQC was injected into a 12.5×1.6 -cm-inner diameter column of immobilized trypsin gel preequilibrated in the eluting buffer (20 mM CaCl_2 in 50 mM Tris-HCl buffer, pH 8.2). Affinity purification was accomplished because PQC contains a unique and highly basic polypeptide chain containing covalently attached phosphate groups without any disulfide bonds.

Purification of Enzyme Inhibitors

Enzyme inhibition may be reversible or irreversible with different inhibitors. Irreversible inhibitors usually form covalent bonds and, thus, are not useful for this type of

Purification of Peptides with Immobilized Enzymes

affinity chromatography. Reversible inhibitors work by a variety of mechanisms, but usually competitive inhibitors structurally resemble the peptide substrates and bind the active center. *Trichosanthes kirilowii* trypsin inhibitor analog (Ala-6-TTI) is a trypsin inhibitor in which methionine at position 6 is replaced by alanine. Affinity chromatography was used to purify expressed fusion protein containing large proteins and (Ala-6)-TTI, with methionine as a connecting residue [5]. After cyanogen bromide cleavage and reduction of the fusion protein, followed by affinity chromatography separation on trypsin-Sepharose 4B as a matrix and on the immobilized trypsin, the fully active (Ala-6)-TTI was obtained in a high purity and high yield. The trypsin inhibitory activity and amino acid composition of the recombinant (Ala-6-TTI) were consistent with those of the natural one.

An essentially pure extracellular glycoprotein proteinase inhibitor was isolated from the latex of green fruits of papaya by a single affinity chromatography purification step [6]. An immobilized trypsin-Sepharose CL 4B column was prepared according to the manufacturer (Amersham Pharmacia Biotech), which provided elaborated bulletins for the preparation procedures and applications of these affinity gel columns. Latex extract was applied to the column after equilibration with 20 mM Tris-HCl, pH 8.0, containing 0.5M NaCl and 0.05M CaCl_2 . The column was extensively washed with the same buffer until ultraviolet (UV) absorbance became undetectible. The bound trypsin inhibitor was eluted with 0.02M HCl and recovered by lyophilization after dialysis against water.

Purification of Dipeptidyl Peptidase IV

Dipeptidyl peptidase IV (E.C. 3.4.14.5) cleaves off N-terminal dipeptides from peptides when a proline or alanine is at the penultimate position. The enzyme was purified from human seminal plasma and prostasomes by a two-step scheme of ion-exchange chromatography on DEAE-Sepharose, followed by affinity chromatography on adenosine deaminase (E.C. 3.5.4.4)-Sepharose [7]. This scheme resulted in a pure, native protein with an overall yield ranging from 35% to 55%. The preparation obtained was free of contaminating aminopeptidase activity.

Purification of Recombinant Proteins via Peptide Accession

Purification of peptides by immobilized enzymes is a relatively recent approach that may have a potential use in the purification of genetically engineered pro-



teins. Purification of recombinant proteins is often difficult and involves many purification steps for a very low yield. Smith et al. [8] found that a specific metal-chelating peptide on the NH₂ terminus of a protein can be used to purify that protein with immobilized ion affinity chromatography. The nucleotide sequence that codes for the expressed protein is extended to include codons for the chelating peptide. This concept of amino acid addition to recombinant proteins can also be beneficial in protein purification by affinity chromatography with immobilized enzymes. This will have an impact on the cloning, expression, and the purification of proteins.

Conclusion

Affinity purification of peptides by immobilized enzymes relies on the highly specific interaction of an ionic, hydrophobic, aromatic, or stoically active binding site on the desired peptide to the immobilized enzyme. The unbound contaminants are washed through and the desired peptide is released by buffer elution. This technique is beneficial in the purification of many peptides and can also be used for affinity chromatog-

raphy of recombinant proteins after cloning and expression.

References

1. J. E. Bell and E. T. Bell, Protein purification: Affinity chromatography, in *Proteins and Enzymes*, Prentice-Hall, Englewood Cliffs, NJ, 1988, pp. 45–63.
2. J. Carlsson, J.-C. Janson, and M. Sparrma, Affinity chromatography, in *Protein Purification: Principles, High Resolution Methods, and Applications* (J. C. Janson and L. Ryden, eds.), VCH, New York, 1989, pp. 275–329.
3. H. Schott, *Affinity Chromatography*, Chromatographic Science Series Vol. 27, Marcel Dekker, Inc., New York, 1984.
4. S. Zerhouni, A. Amrani, M. Nijs, N. Smolders, M. Azarkan, J. Vincentelli, and Y. Looze, *Biochem. Biophys. Acta* 1387: 275–290 (1998).
5. X. M. Chen, Y. W. Qian, C. W. Chi, K. D. Gan, M. F. Zhang, and C. Q. Chen, *J. Biochem. (Tokyo)* 112: 45–51 (1992).
6. S. Odani, Y. Yokokawa, H. Takeda, S. Abe, and S. Odani, *Eur. J. Biochem.* 241: 77–82 (1996).
7. I. De-Meester, G. Vanhoof, A. M. Lambeir, and S. Scharpe, *J. Immunol. Methods* 189: 99–105 (1996).
8. M. C. Smith, T. C. Furman, T. D. Ingolia, and C. Pidgeon, *J. Biol. Chem.* 263: 7211–7215 (1988).



Pyrolysis–Gas Chromatography–Mass Spectrometry Techniques for Polymer Degradation Studies

Alfonso Jiménez Migallon

M.L. Marín

University of Alicante, Alicante, Spain

Introduction

The characterization of relatively complex polymers is usually carried out by means of coupled techniques because sometimes a single technique is not enough to elucidate their structures. Pyrolysis of polymers is an old technique used many years ago to identify materials by their vaporized decomposition products. The coupling of this simple method with a powerful identification technique, such as infrared (IR) spectroscopy or, often, mass spectrometry (MS), has demonstrated its utility for the analysis of polymeric materials and, mainly, for the characterization of their degradation products.

The pyrolysis of a sample can be defined as the conversion of a substance into other(s) with lower molecular weights by the action of heat. In the case of organic polymers, the most interesting data we can obtain from the fragments of pyrolysis are the composition of the volatiles produced and of the nonvolatile residue, changes in molecular weight, as a function of the temperature, and evolution of the thermal decomposition process, kinetics, and activation energies of the degradation reactions.

In order to obtain these data, the most often applied approach has been coupling of gas chromatography (GC) with MS. The pyrolysis products are first separated in the column and then the separated fragments are directly analyzed in the mass spectrometer. Therefore, it is possible to obtain reliable and reproducible results with a single run and in a relatively short time of analysis.

Pyrolysis (Pyr)–GC–MS, however, presents some limitations associated with many factors, such as the complexity of the chemical reactions involved in pyrolysis, the incomplete separation of the degradation products, and, sometimes, poor peak identification and interpretation of chromatograms. However, some recent developments have permitted the application of this technique to a broader range

of samples. Those developments are principally the use of highly specific pyrolysis devices, highly efficient capillary columns, and MS libraries with a wider range of spectra. This fact has permitted the use of the technique not only for polymer identification but also for structural characterization of polymers and blends.

An important aspect of analytical pyrolysis is the production and detection of thermal fragments containing essential structural information, in order to provide insight, at least partially, into the original structures of the compounds present in the chemical matrix. Larger fragmentation products are the more informative among all fragments. Therefore, there is a current tendency in analytical Pyr–GC–MS to preserve and detect higher-molecular-weight fragments. This has led to developments in the instrumentation, such as improvement of the direct transfer of high-molecular-weight and polar products to the ion source of the mass spectrometer, the measurement of these compounds over extended mass ranges, and the use of soft ionization conditions, such as field ionization (FI) and chemical ionization (CI) instead of electron impact (EI). Methods such as FI and CI are useful due to the difficulties arising from EI, such as the variation of fragmentation depending on instrumental conditions and the fact that only low-mass ions are observed. However, one problem with the soft ionization methods is the higher cost of instrumentation.

Instrumentation

A typical Pyr–GC–MS instrument for the use in polymer analysis consists of a pyrolyzer coupled to a gas chromatograph and a mass spectrometer. A pyrolyzer, through which the carrier gas flows (usually He or N₂), is directly coupled to a gas chromatograph with a high-resolution capillary column.



Pyrolyzer

The most commonly used pyrolyzers can be classified into three groups:

1. Resistively heated electrical filaments
2. Radio-frequency induction heated wires (Curie-point pyrolyzers)
3. Microfurnace type

Each of these designs has its particular characteristics. Thus, the filament-type permits multistep pyrolysis, which enables the discriminative analysis of formulations in a compounded material. The Curie-point type offers the most precisely controlled equilibrium temperature, but the heating conditions depend greatly on the shape of the sample holder. On the other hand, a precise temperature regulation of the microfurnace type is not easy, but it is most suited for thermally labile compounds such as biopolymers.

Gas Chromatograph

The use of highly effective capillary columns is essential for high-resolution Pyr–GC–MS, because pyrolysis products of polymers are generally very complex mixtures. The bonded-phase fused-silica columns are especially effective for Pyr–GC–MS because of their low level of stationary-phase bleed at elevated column temperatures.

The split mode is usually favored for Pyr–GC–MS, because the very low velocity of the carrier gas for the splitless mode often causes undesirable secondary reactions of the degradation products in the pyrolyzer. In the split mode, however, the product composition entering the capillary column sometimes differs from the original, depending on the volatility of each component and the split temperature. This can cause problems in reproducibility and precision of results because the degradation products of polymers usually consist of complex mixtures with a broad range of volatilities. In order to overcome this problem, the splitter is modified and the dead volume is packed with an ordinary chromatographic packing material. The splitter is then maintained, independently, at the maximum temperature of the column. This arrangement permits the obtaining of reproducible results and protection of the instrument.

Mass Spectrometer

The advances in the specific determinations for peaks by GC–MS were significant for the development of the technique. In particular, a computer-controlled GC–

MS system readily leads to the rapid and accurate identification of peaks.

Methods of Analysis

A very important aspect to be controlled in Pyr–GC–MS is the reproducibility of results. This is important not only for the determination of structure but also for the reactions between fragments in the GC. In order to obtain high reproducibility, two different approaches can be used for a particular sample:

1. Isothermal (flash pyrolysis). The temperature of the sample is suddenly increased (10–100 ms) to reach the thermal decomposition level (500–800°C). This process can be carried out by means of a platinum or platinum–rhodium filament heated by an electrical current directly coupled to the injector port of the GC. Some pyrolysis fragments are obtained in a very short time and can be directly sent to the column and detector. In spite of this short time for the pyrolysis, it is possible to indicate three different phases: (a) heating (10^{-2} – 10^{-1} s), (b) stabilization of the maximum temperature, and (c) cooling. However, the main drawback of this technique is the lack of equilibrium between temperatures with the pyrolyzer.
2. Programmed temperature pyrolysis. The sample is heated at a given heating rate in a manner similar to the linear heating used in thermogravimetry or differential scanning calorimetry. The desirable conditions of this method are their uniform heating, a minimum dead volume, and a device to introduce samples. Pyrolysis fragments are then analyzed as a function of temperature.

Direct Inlet Mass Spectrometry

Pyrolysis-direct chemical ionization mass spectrometry (Pyr–DCI–MS) was recently introduced as a pyrolysis technique for the characterization of complex macromolecular samples and for the analysis of biopolymers. This technique does not require special pyrolysis equipment and can be performed with an instrument which is equipped with a chemical ionization source and a standard DCI probe, which consists of an extended wire used to introduce the sample material directly into the chemical ionization plasma. An important characteristic of this technique is the pyrolysis



in the ion plasma, using a filament that is resistively heated by a current programming device. This arrangement guarantees an optimum transfer for large and polar molecules. Moreover, temperature-resolved pyrolysis data can be obtained which can provide additional chemical information on a variety of classes of compounds with different thermal stabilities and desorption characteristics.

Direct inlet mass spectrometry (DIMS) is one of the best techniques to elucidate the structure of low-molecular-weight organic and inorganic compounds evolved from polymers. In this technique, polymer samples are introduced into the ion source of a mass spectrometer by means of a direct inlet for solid samples, and thermal degradation is carried out by a linear temperature program. The volatile products are ionized and detected immediately by repeated mass scans. This technique presents some advantages, such as the possibility to avoid manipulation of samples, because it can be used as an on-line method. Some additional advantages are the fast in-vacuum ionization, which reduces secondary reactions, the possibility of obtaining the molecular weight from the molecular ion, and the relatively low cost of the equipment.

Applications

Linear Polymers

The pyrolysis of linear polymers results in a series of fragments that are introduced into the GC–MS instrument. Polymers are completely degraded (depending on the ionization conditions) giving rise to the characteristic fragments which permit the identification of the degradation products. For instance, in Table 1, the most probable structure of the degradation of a poly(vinyl chloride) (PVC) resin is presented.

As can be observed, the maximum m/z ratio is presented at 36, which corresponds to HCl, the main degradation product of PVC. Other important products are those with m/z 35 and 38 also corresponding to HCl. Other significant peaks are those at 18 (corresponding to water) and 78 (benzene). This peak is especially important, as it can be considered as the result of a reaction between double-bond fragments leading to an aromatic product.

Analysis of Copolymers

The Pyr–GC–MS analysis of a copolymer presents a complicated fragmentation pattern, resulting in a wide variety of products and highly complicated spectra.

Table 1 Relative Intensities in the Dehydrochlorination Reaction in a PVC Resin

m/z	Intensity	m/z	Intensity
15.00	0.16	43.00	0.20
16.00	0.13	44.00	0.17
17.00	0.95	49.00	0.15
18.00	4.08	50.00	0.84
19.00	0.24	51.00	0.96
26.00	0.32	52.00	0.84
27.00	0.47	55.00	0.11
28.00	0.44	63.00	0.22
29.00	0.23	74.00	0.17
35.00	22.20	76.00	0.14
36.00	100.00	77.00	0.69
37.00	6.86	78.00	2.34
38.00	31.30	79.00	0.19
39.00	0.84	91.00	0.13
41.00	0.20	128.00	0.10

This is the case particularly when EI is used as the ionization method. CI and FI are better selections, and it is possible to obtain only the most significant peaks, corresponding to each component of the copolymer.

Analysis of Thermosets

This is a new and promising area of research and its interest is based on the possibility of identification of particular bonds or functions responsible of the scission of the chain during the first steps of the degradation. As these polymers are becoming increasingly used in industry, Pyr–GC–MS is an important technique for the analysis.

Natural Polymers

The chromatograms of natural polymers, such as proteins and polysaccharides, are so complex that they have been mostly used for general identification. The potential of Pyr–GC–MS has been greatly enhanced by the use of high-resolution capillary columns combined with computer-assisted techniques.

Suggested Further Reading

- Bate, D. M. and R. S. Lehrle, *Polym. Degrad. Stabil.* 64: 75 (1999).
 Dadvand, N., R. S. Lehrle, I. W. Parsons, M. Rollinson, I. M. Horn, and A. R. Skinner, *AR, Polym. Degrad. Stabil.* 67: 407 (2000).



- Dadvand, N., R. S. Lehrle, I. W. Parsons, and M. Rollinson, *Polym. Degrad. Stabil.* 66: 247 (1999).
- Erdogan, M., T. Yalçın, T. Tinçer, and S. Suzer, *Eur. Polym. J.* 27: 413 (1991).
- Haken, J. K., *J. Chromatogr. A* 825: 171 (1999).
- Irwin, W. J., *Analytical Pyrolysis. A Comprehensive Guide*, Chromatographic Science Series Vol. 22, Marcel Dekker, Inc., New York, 1982.
- Miranda, R., H. Pakdel, C. Roy, H. Darmstadt, and C. Vasile, *Polym. Degrad. Stabil.* 66: 107 (1999).
- Plage, R. and H. R. Schulten, *J. Anal. Appl. Pyrolysis* 19: 285 (1991).
- Pouwels, A. D., G. B. Eijkel, and J. J. Boon, *J. Anal. Appl. Pyrolysis* 14: 237 (1989).
- Statheropoulos, M., *J. Anal. Appl. Pyrolysis* 10: 89 (1986).
- Statheropoulos, M. and S. A. Kyriakou, *Anal. Chim. Acta* 409: 203 (2000).
- Tas, A. C., A. Kerkenaar, G. F. LaVos, and J. Van der Greef, *J. Anal. Appl. Pyrolysis* 15: 55 (1989).
- Wang, F. C., *J. Chromatogr. A* 833: 111 (1999).
- Wilkie, C. A., *Polym. Degrad. Stabil.* 66: 301 (1999).



Quantitation by External Standard

Tao Wang

Merck Research Laboratories, Rahway, New Jersey, U.S.A.

Introduction

An important feature of modern high-performance liquid chromatography (HPLC) is its excellent quantitation capability. HPLC can be used to quantify the major components in a purified sample, the components of a reaction mixture, and trace impurities in a complex sample matrix. The quantitation is based on the detector response with respect to the concentration or mass of the analyte. In order to perform the quantitation, a standard is usually needed to calibrate the instrument. The calibration techniques include an *external standard method*, an *internal standard method*, and a *standard addition method*. For cases in which a standard is not available, a method using normalized peak area can be used to estimate the relative amounts of small impurities in a purified sample.

In this entry, only the external standard method is discussed. Detailed discussions of other quantitation methods can be found in other entries of this encyclopedia or in Ref. 1.

Discussion

The external standard method is the most general method for determination of the concentration of an analyte in an unknown sample. It involves the construction of a calibration plot using external standards of the analyte, as shown in Fig. 1. A fixed volume of each standard solution of known concentration is injected into the HPLC and the peak response of each injection is plotted versus the concentration of the standard solution. The standards used are called “external standards” because they are prepared and analyzed separately from the unknown sample(s). After constructing the calibration plot, the unknown sample is prepared, injected, and analyzed in exactly the same manner. The concentration of the analyte in the unknown sample is then determined from the calibration plot or from the response factor of the unknown sample versus that of the standard.

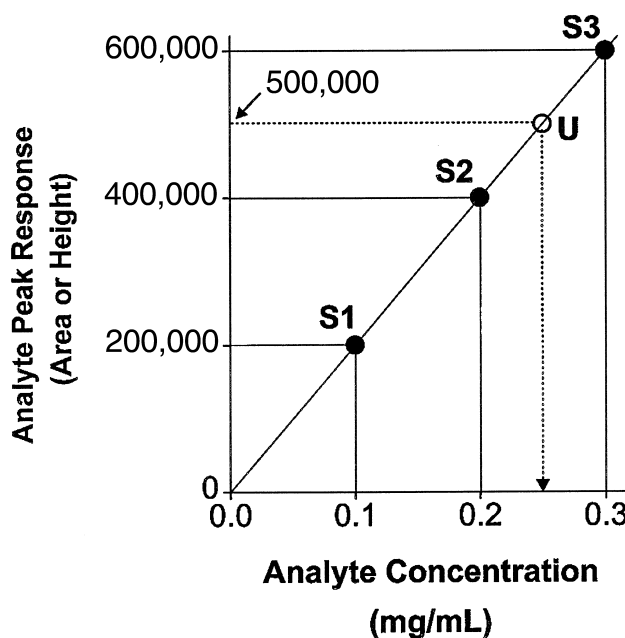


Fig. 1 Linear calibration plot for external standard method. S1, S2, and S3: external standards for calibration; U: unknown sample.

If the calibration plot is linear, the concentration of the analyte in the unknown sample can be determined based on the linear equation of the calibration plot:

$$Y = a + bX \quad (1)$$

where Y is the peak response of the analyte, X is the concentration of the analyte, a is the intercept, and b is the slope. The concentration X is

$$X = \frac{Y - a}{b} \quad (2)$$

In the example shown in Fig. 1, where $a = 0$ and $b = 2 \times 10^6$, the concentration (X) of the unknown sample (U), which shows a peak response of $Y = 500,000$, is determined to be 0.25 mg/mL using Eq. (2).

Alternatively, after the linear calibration range has been established, the concentration of an unknown sample can be determined using the *response factor*. A



response factor (RF), sometimes called a *sensitivity factor*, is determined from a standard within the linear calibration range as:

$$RF = \frac{\text{Standard peak response}}{\text{Standard concentration}} \quad (3)$$

If two or more standards of different concentrations within the linear range are measured, the RF value can be taken as the average value of the response factors for all these standards to minimize the uncertainty in determining the RF. In the example shown in Fig. 1, the RF is the slope of the calibration plot and equals 2×10^6 for all three standards because the plot is linear with a zero intercept. The concentration (X) of the analyte in the unknown sample (U) can be calculated as

$$X = \frac{\text{Sample peak response}}{RF} \quad (4)$$

which is $500,000/(2 \times 10^6) = 0.25$ mg/mL. When RF is used for quantitation, the concentration(s) of the standard(s) selected should be similar to the expected concentration of the unknown sample.

In the aforementioned techniques, it is important that the calibration plot be linear over certain concentration range and the concentration of the sample fall within this linear range (as shown in Fig. 1) so that an interpolation can provide accurate measurement of the sample concentration. If the concentration of the sample falls outside the established linear range, extrapolation of the calibration plot should be used with caution. To ensure accuracy, it is recommended that dilution be carried out to bring the concentration of the sample into the linear range prior to the analysis.

In unusual cases, where the calibration plot is not linear, the concentration of an unknown sample can be determined by interpolation of results between standards or by fitting the results of the standards into a nonlinear equation and using the nonlinear equation to calculate the concentration of the unknown sample. When interpolation is used, the concentrations of the two standards used to bracket the sample should be as close to the concentration of the sample as possible to enhance the accuracy of the result. When a nonlinear equation is used, a large enough number of standards is needed in order to more accurately determine the nonlinear equation. Obviously, quantitation in a nonlinear range involves more labor and presents a higher potential of error. Therefore, this approach is used only when there are no other alternatives.

In the external standard method, it is critical that the injections are precise. With modern instruments which employ autosamplers, adequate precision (typically \leq

0.5%) can be achieved using full-loop injection. Poorer injection precision is normally associated with manual injections or with partial-loop injections by autosamplers.

It is also critical to keep the chromatographic conditions (such as flow rate and column temperature) constant during the analysis of all standards and samples. Fluctuations of the chromatographic conditions during the analysis can cause inconsistent peak responses, which, in turn, will cause quantitation error. It is common that the HPLC system is tested using standards to ensure that the system is performing properly and reliably prior to the analysis of samples. This procedure of validating system performance is referred to as "system suitability test."

Detailed discussions on sources of error related to the external standard method, including sampling and sample preparation, chromatographic effects, and data system effects, can be found in Ref. 1. Reference 2 presented detailed discussions on the precision in HPLC.

The peak response used for quantitation can be either peak height or peak area. Peak height is usually used when incomplete resolution of the analyte peak is encountered, because the peak height measurement is subject to less interference from the adjacent overlapping peaks. On the other hand, peak area is less influenced by changes in instrumental or chromatographic parameters. The choice of peak height or peak area for quantitation requires the understanding of the effects of chromatographic parameters on the precision of each approach. The influence of certain chromatographic parameters on the precision of peak height and peak area methods, as well as the preferred method among the two when various chromatographic parameters are subject to change, are discussed in detail in Refs. 1 and 3.

More thorough discussions on external standard method can be found in Refs. 1, 3, and 4.

References

1. L. R. Snyder, J. J. Kirkland, and J. L. Glajch, *Practical HPLC Method Development*, 2nd ed., John Wiley & Sons, New York, 1997, pp. 643–684.
2. E. Grushka and I. Zamir, in *Chemical Analysis*, Vol. 98, *High Performance Liquid Chromatography*. (P. R. Brown and R. A. Hartwick, eds.), John Wiley & Sons, New York, 1989, pp. 529–561.
3. L. R. Snyder and J. J. Kirkland, *Introduction to Modern Liquid Chromatography*, 2nd ed., John Wiley & Sons, New York, 1979, pp. 541–574.
4. R. P. W. Scott, in *Quantitative Analysis using Chromatographic Techniques* (E. Katz, ed.), John Wiley & Sons, New York, 1987, pp. 63–98.



Quantitation by Internal Standard

J. Vial

A. Jardy

ESPCI, Paris, France

Introduction

The principle involved is the addition of a known quantity of a foreign substance (internal standard) to the analyzed sample, the response coefficient of which is known or arbitrarily fixed. Quantitation by the internal standard method enables one to compensate for errors in the injected volume [1].

The same quantity of constituent I (internal standard) is added both to the reference solution and to the solution to be analyzed. I is supposed to interfere with none of the constituents present in the sample. This methodology is based on the constancy of the ratios between the proportionality coefficient observed on both chromatograms (determination and calibration).

Assay Chromatogram

The assay solution includes precisely and accurately known weights of the product to be determined and of the internal standard. An injection of an approximately known volume of this solution is made. From the resulting chromatogram, areas of peaks corresponding to the internal standard and to the product(s) to be analyzed are measured. Let M_E be the weight of the sample including solute D, the assay of which τ_D is to be determined, M_I be the weight of the internal standard I, A_D be the peak area of solute D, A_I be the peak area of the internal standard, K_D be the response coefficient of the product D, and K_I be the response coefficient of the internal standard. It is possible to establish the following relationships:

$$M_E \tau_D = K_D A_D \quad (1)$$

$$M_I = K_I A_I \quad (2)$$

and

$$\tau_D = \frac{K_D}{K_I} \frac{A_D}{A_I} \frac{M_I}{M_E} \quad (3)$$

Calibration Chromatogram

The protocol is similar to the calibration solution, including accurately and precisely known weights of reference and internal standard (dilutions must be analogous to those of the assay chromatogram). An injection of an approximately known volume of this calibration solution is made. From the resulting chromatogram, areas of peaks corresponding to the internal standard and to the reference material are measured. Let M_R be the weight of the reference material, the assay of which τ_R is known, M'_I be the weight of the internal standard I, A_R be the peak area of the reference material, and A'_I be the peak area of the internal standard. Thus, it is possible to establish the following relations:

$$M_R \tau_R = K_D A_R \quad (4)$$

$$M'_I = K_I A'_I \quad (5)$$

and

$$\frac{K_D}{K_I} = \frac{M_R}{M'_I} \frac{A'_I}{A_R} \tau_R \quad (6)$$

Calculation of τ_D , the Assay of Product D in the Sample

Combining relation (3) and relation (6), it is possible to determine τ_D , the purity of the product D, by

$$\tau_D = \frac{A_D}{A_I} \frac{A'_I}{A_R} \frac{M_I}{M_E} \frac{M_R}{M'_I} \tau_R \quad (7)$$

Some conditions are required for Eq. (7) to be valid: Areas and weights must be expressed in the same unit system both for analysis and calibration; because precision and accuracy of this method only depend on the precision and accuracy of weighings, they depend neither on the precision and accuracy of the dilutions nor on the injected volume (unlike the external standard method). It requires no preliminary determination of the proportionality coefficients. However, if some points of the sample



handling are fully corrected by the use of an internal standard, other difficulties still remain [2].

Moreover, this method can quickly become laborious because an internal standard elution which is compatible with the analysis conditions must be found. Conditions that must be fulfilled by the internal standard are its purity must be known and it must be chemically inert toward solutes and mobile phase; on the one hand, its retention time must be different from those of all the constituents present in the sample and, on the other hand, it should be as close as possible as the retention time(s) of the product(s) to be determined. It has also been demonstrated that a necessary correlation was required between chromatographic behaviors of the internal standard and the product to quantify [3]. Otherwise, the use of an internal standard can even degrade the precision of the results. A comparison of the precision of internal and external standard has also been carried out through a liquid chromatography collaborative study [4].

The internal standard's coefficient of response for the detector used must be of the same order of magnitude as the one of the product to be determined; in no way can it be present as an impurity in the sample; it must be added at a concentration level that gives a peak area more or less equivalent to the one of the product to be determined. Homologues of the product to be analyzed may be used as internal standards.

The chromatogram given Fig. 1 illustrates the internal standard methodology. Here, methomyl was quantified using benzanilide as the internal standard. Using the calibration curve, the unknown methomyl assay in insecticides is deduced from the area ratio, after the addition to the sample of the same quantity of internal standard as in the calibration steps.

The internal standard method is less often used in liquid chromatography than in gas chromatography because injection of repeatable volumes has been made easier by the use of precise and reliable injection systems (loop valves). More generally, gradually, the internal standard method is being abandoned. The external standard method is, nowadays, the most common method and the use of an internal standard seems to be restricted to very specific applications; for example, when preliminary to the chromatographic analysis, the solute of interest must be extracted by means of a complex protocol.

References

1. R. Rosset, M. Caude, and A. Jardy, *Chromatographies en phases liquide et supercritique*, Masson, Paris, 1991, pp 731–733.
2. L.R. Snyder and S. Van der Wal, *Anal. Chem.* 53: 877 (1981).
3. P. Haefelfinger, *J. Chromatogr.* 218: 73 (1981).

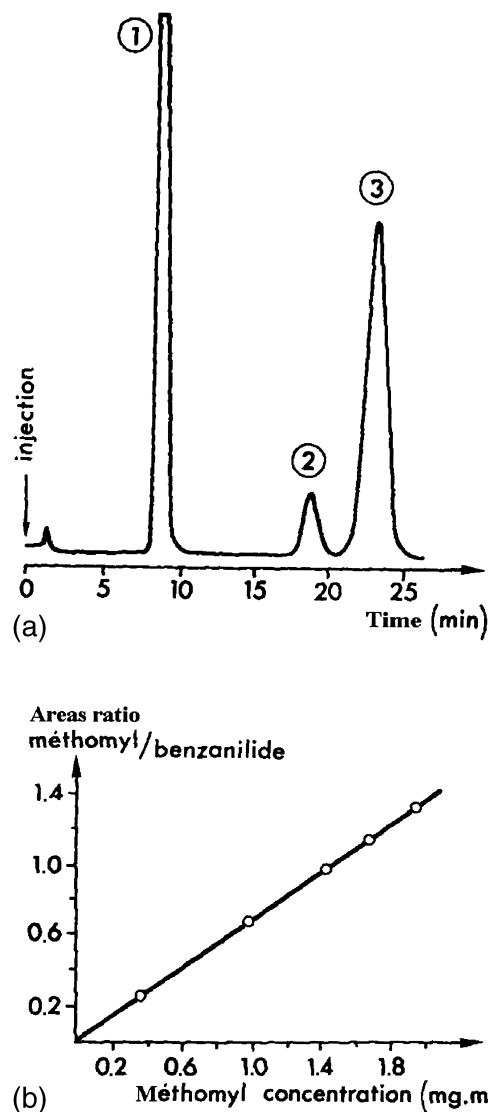


Fig. 1 Insecticide analysis by the internal standard method: (a) chromatogram; (b) calibration curve. 1: Benzanilide (internal standard); 2: methyl-*N*-hydroxythioacetimidate; 3: methomyl. (From Ref. 5.)

4. R. E. Pauls and R. W. McCoy, *J. High-Resolut. Chromatogr.* 9: 600 (1986).
5. R. E. Leitch, *J. Chromatogr. Sci.* 9: 531 (1971).

Suggested Further Reading

- Snyder, L. R. and J. J. Kirkland, *Introduction to Modern Liquid Chromatography*, 2nd ed., John Wiley & Sons, New York, 1974, pp. 552–556.
- Snyder, L. R., J. J. Kirkland, and J. L. Glajch, *Practical HPLC Method Development*, 2nd ed., John Wiley & Sons, New York, 1997, pp. 657–660.

Quantitation by Normalization

J. Vial

A. Jardy

ESPCI, Paris, France

Introduction

The principle of this method is quite simple. Provided that for each solute, i , the analytical signal lies within the linearity range, the peak area is proportional to the weight of solute having passed through the detector cell, thus, that was present in the injected volume,

$$m_i = K_i A_i \quad (1)$$

where A_i is the peak area of solute i and K_i is the response coefficient. Therefore, the percentage in weight of each analyte is given by

$$\%_i = \frac{K_i A_i}{\sum_i K_i A_i} \times 100 \quad (2)$$

Discussion

To apply this method in high-performance liquid chromatography (HPLC), several conditions have to be fulfilled: All the analytes present in the sample to be analyzed must elute from the column (no irreversible retention), with enough resolution and, furthermore, have to be detected. All the response coefficients have to be known, or at least attainable experimentally, which, in turn, implies that all the solutes are available separately in a high degree of purity. This method is unable to determine the percentage of any constituent of the mixture if a response coefficient is missing.

On the other hand, an advantage lies in the fact that there is no need to accurately know the amount of sample injected.

Practically, quantitation by the normalization method is not in as common use in HPLC as it is in GC. It is highly recommended to avoid its implementation in the case of samples for which the qualitative composition is not known exactly. It is only convenient in routine analysis, as in quality control, when the qualitative composition does not vary.

Moreover, note that, except in very particular cases, the approximation to consider all the K_i equal [Eq. (3)] is highly hazardous in HPLC, unlike in GC:

$$\%_i = \frac{A_i}{\sum_i A_i} \times 100 \quad (3)$$

A few examples of where it is possible are the following: Use of a refractive index detector, trace analysis of related substances (impurities) in pharmaceutical products, with UV detection at very low wavelength, when the accuracy of the result is of little interest [1] (e.g., when chromatography is used to monitor a chemical reaction), and when a relative value is enough. In this situation, the simplified relationship (3) is sufficient, but the analyst must not forget that the proportions found in this way are not the true proportions.

In conclusion, its efficiency and simplicity make quantitation by normalization a very attractive method that generally requires few injections. Nonetheless, it must be kept in mind that it requires the knowledge of the response coefficients for all the constituents in the mixture. The a priori hypothesis of equality for all response coefficients seldom corresponds to reality and can lead to hazardous results.

Reference

1. J. Tranchant, *Manuel pratique de chromatographie en phase gazeuse*, Masson, Paris, 1995, pp. 620–623.

Suggested Further Reading

- Parris, N. A., *Instrumental Liquid Chromatography*, Elsevier, Amsterdam, 1976, p. 243.
- Rosset, R., M. Caude, and A. Jardy, *Chromatographies en phases liquide et supercritique*, Masson, Paris, 1991, pp. 729–730.
- Snyder, L. R., J. J. Kirkland, and J. L. Glajch, *Practical HPLC Method Development*, 2nd ed., John Wiley & Sons, New York, 1997, pp. 654–655.



Quantitation by Standard Addition

J. Vial

A. Jardy

ESPCI, Paris, France

Introduction

The principle involved is that, provided the analytical signal is proportional to concentration, the initial analyte content is determined through measurement of this signal before and after the addition of a known amount of the analyte to the analyzed sample. The method of standard addition, also denoted as “spiking,” is used when an analyte is to be quantified inside a matrix, the effects of which are likely to affect the chromatographic peak behavior. In this case, the sample itself is used as the calibration matrix.

Discussion

Commonly, the unknown concentration is deduced from the increase in the peak height or the peak area resulting from the addition of known amounts of pure analyte to the sample (at least one or two additions). A comparison of peak height versus peak area for quantitation is given in Ref. 1. A more convenient protocol, which gives information both on the precision and the accuracy of the results, is the following. After each addition, the area of the chromatographic peak is measured. Then, the parameters of the regression line are computed using a least-squares regression method. The analyte quantity in the sample corresponds to the intercept-to-slope ratio, denoted x_0 . When the dilution produced by additions cannot be neglected, it is necessary to take it into account. Let A_0 be the peak area of the analyte to be determined on the chromatogram obtained with the unknown sample, A_i be the peak area of the same analyte on the chromatogram obtained after the i th addition, x_i be total quantity of analyte added after the i th addition, and f_i be the dilution factor after the i th addition. Then, a line of the areas corrected by the dilution factor versus the amount of analyte added is plotted (Fig. 1). The expression of the corrected area A_i^* is

$$A_i^* = A_0 + (A_i - f_i A_0) \quad (1)$$

If, on the chromatogram, there is another peak other than that of the analyte, well resolved, but close

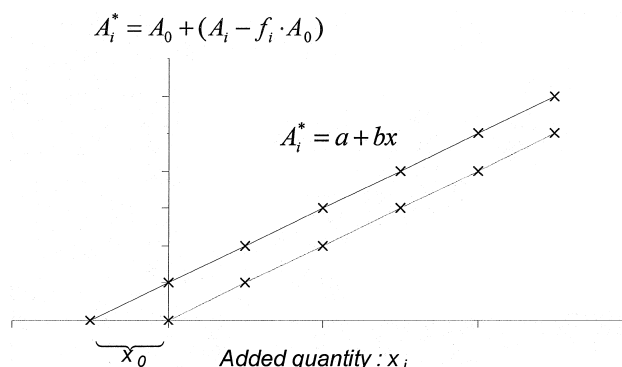


Fig. 1 Visualization of the standard addition methodology. The dotted line represents the calibration line obtained when the analyte of interest is not present in the matrix.

enough, it can be used as a tracer to evaluate f_i . Let A_t be the peak area of the tracer on the chromatogram obtained with the unknown sample and A_{ti} the peak area of tracer on the chromatogram obtained after the i th addition of pure analyte:

$$f_i = \frac{A_{ti}}{A_t} \quad (2)$$

Otherwise, the dilution factor f_i must be evaluated in another way.

Then, the parameters of the calibration curve are computed by mean of a linear least-squares regression:

$$A_i^* = a + bx \quad (3)$$

The result is given by

$$x_0 = \left(\frac{a}{b} \right) \quad (4)$$

The method of standard additions would give the true result if there were no experimental errors. Practically, this is never the case and, so, a weakness of the method appears concerning the reliability of the provided result (unknown concentration). Effectively, the use of extrapolation of a calibration curve is always less conformable and reliable than interpolation, especially concerning the errors on predicted values [2–4]. The problem is



even more explicit when the result is expressed along with its confidence interval. Confidence curves of the regression line must, thus, be used. Their expression is

$$A_i^* = a + bx \pm \hat{\sigma}_{y/x} t_{\alpha, (n-2)} \left(\frac{1}{n} + \frac{(x - \bar{x})^2}{\sum_i (x_i - \bar{x})^2} \right)^{1/2} \quad (5)$$

In Eq. (5), $\hat{\sigma}_{y/x}$ represents the estimated residual variance of the regression, $t_{\alpha, (n-2)}$ is the limit value that a Student's variable with $n - 2$ degrees of freedom has α chances out of 100 not to exceed in module, and n is the number of points used. Confidence limits of the result correspond to the zero of Eq. (5). No exact analytical solutions are available, but either it is possible to solve it numerically or approximate solutions can be used. An approximate expression of the standard deviation of the result is

$$\hat{\sigma}_{x_0} \cong \frac{\hat{\sigma}_{y/x}}{b} \left(\frac{1}{n} + \frac{\bar{y}^2}{b^2 \sum_i (x_i - \bar{x})^2} \right)^{1/2} \quad (6)$$

This leads to the following confidence interval (CI) for the unknown concentration:

$$\text{CI} = [x_0 - t_{\alpha, (n-2)} \hat{\sigma}_{x_0}, x_0 + t_{\alpha, (n-2)} \hat{\sigma}_{x_0}] \quad (7)$$

To avoid having an excessively large interval, it is strongly advised to take enough points in a relatively widespread range. A compromise must be found for the spacing out of the points. It must be maximum to decrease the error on predicted values, but all the points must, nevertheless, belong to the linear range. An example of an application describing the analysis of 5-hydroxyindolacetic acid in human cerebrospinal fluid is given in Ref. 1.

However, the method of standard addition is not only useful to quantify an analyte present in a matrix, it can also be employed to check if the matrix intro-

it can also be employed to check if the matrix introduces any proportional error. Similar additions of analyte are made to a blank matrix (the dotted line in Fig. 1) and if there is no proportional error, then the slopes of both regression lines are equal. Therefore, the slope equality has to be tested through a convenient statistical test.

To conclude, the method of standard additions is a powerful method that enables to quantify an analyte present in a matrix susceptible to modify its behavior. Nevertheless, this method is somewhat tedious, because it requires many preparations and injections to obtain enough points for a sufficient reliability.

References

1. L. R. Snyder, and J. J. Kirkland, J. L. Glajch, *Practical HPLC Method Development*, 2nd ed., John Wiley & Sons, New York, 1997. Chap. 14.
2. Commissariat à l'énergie atomique, *Statistique appliquée à l'exploitation des mesures, Tome I & Tome II*, Masson, Paris, 1978, pp. 139–141.
3. D. L. Massart, B. G. M. Vandeginste, S. N. Deming, Y. Michotte, and L. Kaufman, *Chemometrics, a Textbook*, Elsevier, Amsterdam, 1988, pp. 34, 117, 119.
4. J. C. Miller and J. N. Miller, *Statistics for Analytical Chemistry*, 2nd ed., Ellis Horwood, Chichester, 1988, pp. 103, 117–120.

Suggested Further Reading

Snyder, L. R. and J. J. Kirkland, *Introduction to Modern Liquid Chromatography*, 2nd ed., John Wiley & Sons, New York, 1974, p. 571.

Quantitative Structure–Retention Relationship in Thin-Layer Chromatography

N. Dimov

NIHFI, Sofia, Bulgaria

Introduction

The retention behavior of a compound in a chromatographic system is governed by three global factors: stationary phase–mobile phase combination, experimental conditions, and the compound's structure. In thin-layer chromatography (TLC), there is a huge choice of combinations: between stationary phases, a much greater choice of mobile-phase components, and less complex experimental conditions. It follows that an optimization strategy is necessary in order to come closer to the wanted separation. Keeping in mind that, for example, with an experimental design, 2^n experiments are necessary, where n is the number of factors, and one has to accept several factors a priori before starting the optimization. Depending on the result achieved, the separation is accepted as satisfactory or the optimization efforts continue. Once the analytical method is established (validated), it is available for application. The new problem became the reference substances necessary for system suitability verification and for identification. Although two difficult-to-separate compounds are enough for the verification, many reference materials are necessary for the identification of all compounds of interest. One of the steps helping to overcome this problem is the so-called quantitative structure–retention relationship (QSRR). It is assumed, in QSRR, that the first two global factors (stationary phase–mobile phase combination and experimental conditions) are already established and the obtained retention depends only on the compound's structure.

Discussion

There is a great number of publications on QSRR in TLC (e.g., Refs. 1–3). The protocol to be followed in QSRR calculations has, in general, the following steps: (1) composition of the experimental data set, (2) molecular structure entry, (3) structure descriptor calculation, (4) regression between experimental data and descriptors.

The compound's structure is entered using, typically, computer graphics. Each structure is optimized by molecular mechanics, which is followed by molecu-

lar orbital calculations. Topological indices, electronic parameters, physicochemical properties, indicator variables, and so forth are used as molecular structure descriptors.

The existing QSRR calculation methods are limited to the ideal case of an isolated molecule; that is, in all cases, the descriptor values are calculated at minimum molecular energy. Thus, it is accepted a priori that the structure of the analyte molecule is rigid enough to maintain its three-dimensional (3D) structure after contacts with the stationary phase. Although such assumption is disputable, this practice continues, because of the lack of knowledge of how the solute molecule is located on the stationary phase, lack of identity of chromatographic contact regions, and the impossibility of calculating the interaction forces developed between them.

To move aside from this impediment, the following have been realized:

- The interaction forces between the solute molecule and chromatographic phases during the chromatographic process release energy higher than the rotational barrier of solute bonds.
- Due to this excess of energy, the solute 3D structure undergoes changes that allow its better location on stationary phase.
- Predicting the exact 3D structure, as it is sorbed on the surface of the stationary phase, is impossible, but presuming several energetically possible structures for one and the same structure allows us to enter into Step 2 several descriptor values for one and the same analyte and use them further in Step 3. It is assumed that one of the calculated descriptor's values could give the “searched best fit” between the experimental and calculated retention values.

If the descriptors used in the most accurate predictive equation are calculated at the minimum heat of formation (CHF), then the analyte has been sorbed as a rigid molecule. If greater accuracy is achieved at higher CHF, the starting 3D structure has been changed during the chromatographic process.



This assumption will be tested first with the retention data for R_m of 9 benzene derivatives (predominantly rigid structures) and, next, for the R_f of 15 benzodiazepines (versatile structures with many σ bonds) separated on silica gel. The data for benzene derivatives were taken from the literature [4], where several mobile phases had been used. Two mobile phases with different polarities have been chosen.

In the first case, only two from all nine studied benzene derivatives have rotamers (see Fig. 1). From all tested combinations among the calculated descriptors, only one answers both to the accuracy and statistical requirements:

$$R_M = -5.50 \pm 0.22 + (24.57 \pm 0.88)DD[1] + (4.19 \pm 0.19)Q[6] + (1.26 \pm 0.19)Q[5] \quad (1)$$

for mobile phase I with correlation coefficient $r = 0.9966$, variance $v = 1.96 \times 10^{-4}$, and $F = 483$, and

$$R_M = -7.04 \pm 0.52 + (29.84 \pm 2.08)DD[1] + (4.51 \pm 0.45)Q[6] + (1.88 \pm 0.44)Q[5] \quad (2)$$

for mobile phase II with correlation coefficient $r = 0.9870$, variance $v = 1.1 \times 10^{-3}$, and $F = 127$. DD[1] stands for the donor delocalization energy of the —O— atom, and Q[5] and Q[6] stand for the charges of the fifth and sixth atoms, respectively. The increased influence of the —O— atom with the most polar mobile phase suggests checking another quantum-chemical local descriptor for the —O— atom. Equation (3) gives a statistically better prediction of the experimental values of R_M :

$$R_M = -0.93 \pm 0.09 + (10.73 \pm 0.55)AD[1] + (3.00 \pm 0.31)Q[6] + (1.65 \pm 0.29)Q[5] \quad (3)$$

with $r = 0.9913$, variance $v = 6.4 \times 10^{-4}$, and $F = 267$. AD[1] stands for the acceptor delocalization energy of

the —O— atom. The better-fitted rotamers from *o*-ethylphenol and *o*-chlorophenol are with the higher heat of formation. In the above-given final regression, only these rotamers have been included.

The calculated retention is compared with the experimental value in Table 1. From a statistical point of view, the improvement when using the rotamer with better fit is insignificant ($F_{9,9} = 1.26$ and 1.07) and the assumption could be considered as disputable. This can be explained by the small number of compounds that are able to rotate around the σ -bond in the total matrix. Independent of the reliability of the assumption, a beneficial conclusion can be drawn from Eqs. (1)–(3). They demonstrate that the retentions of the studied benzene derivatives are governed in the studied cases only by local descriptors and predominately by the local descriptors for the —O— atom in the hydroxyl group. The connectivity index used in many studies (e.g., Ref. 5) showed, in the studied case, a correlation coefficient of only 0.285.

The assumption is undoubtedly verified with the retention data for R_f of 15 benzodiazepines separated on silica. The data were taken from the literature [6] because the authors had corrected, graphically, the R_f values to those obtained with reference materials and, hence, more exact values can be expected.

Three statistically equivalent equations have been obtained. One is presented as follows:

$$R_f = -234.9 \pm 43.2 + (47.27 \pm 4.50)EN + (2918 \pm 350)DD[5] + (10.7 \pm 1.8) \ln VNH \quad (4)$$

with correlation coefficient $r = 0.949$, variance $v = 13$, and $F = 69$. EN represents the electronegativity, DD[5] is the donor delocalization energy of atom 5 (see Fig. 2), and $\ln VNH$ is an arbitrarily chosen indicator variable, accounting for the presence (value 1) or absence (value 0) of a substituent at the azepine N

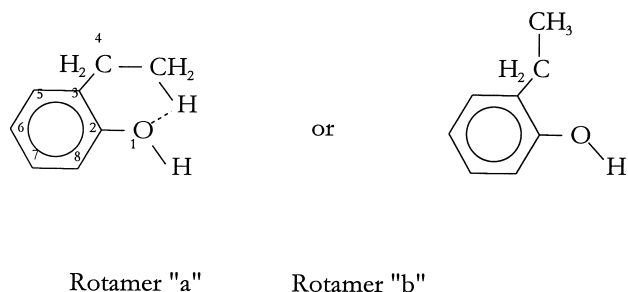


Fig. 1 Rotamer structures.

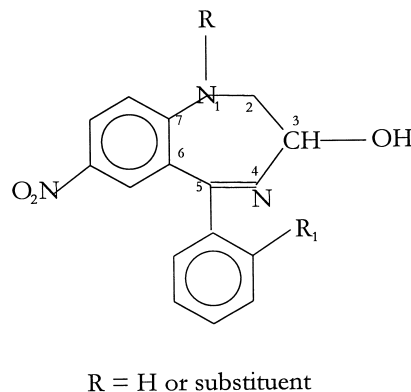


Fig. 2 Diazepine structures.

Table 1 Comparison of Experimentally Obtained Data with Two Different Mobile Phases R_M with R_M Values Calculated According to Eqs. (1) or (2), Respectively

No.	Compound	R_M exp., phase I ^a	R_M calc., Eq. (1) phase I	R_M exp., phase II ^b	R_M calc., Eq. (2) phase II	R_M calc., Eq. (3) phase II
1	<i>o</i> -Ethylphenol rotamer a	−0.31	−0.31	−0.50	−0.50	−0.48
2	<i>o</i> -Ethylphenol rotamer b	−0.31	−0.33	−0.50	−0.52	−0.47
3	<i>m</i> -Ethylphenol	−0.16	−0.18	−0.35	−0.40	−0.38
4	<i>p</i> -Ethylphenol	−0.14	−0.13	−0.31	−0.31	−0.30
5	<i>o</i> -Chlorophenol rotamer a	−0.23	−0.23	−0.43	−0.41	−0.44
6	<i>o</i> -Chlorophenol rotamer b	−0.23	−0.21	−0.43	−0.40	−0.46
7	<i>m</i> -Chlorophenol	−0.12	−0.11	−0.37	−0.32	−0.35
8	<i>p</i> -Chlorophenol	−0.07	−0.07	−0.25	−0.25	−0.25
9	<i>o</i> -Toluidine	0.07	0.07	−0.03	−0.03	−0.03
10	<i>m</i> -Toluidine	0.16	0.16	0.05	0.04	−0.05
11	<i>p</i> -Toluidine	0.27	0.26	0.16	0.17	−0.16

^aSilica gel plates 60 F_{254} with $n\text{-C}_7\text{H}_{16}\text{--C}_6\text{H}_6\text{--diethylether}$ = 1:1:1.^bSame plate with $n\text{-C}_7\text{H}_{16}\text{--C}_6\text{H}_6\text{--diethylether}$ = 1:2:2.

atom. All parameters have statistically insignificant interrelations, r_i . The R_f values calculated with Eq. (4) are given in column 4 of Table 2 and can be compared with the experimental results given in column 3. Although some of the chosen rotamers are identical to the conformers at the lowest molecular energy, the variance obtained when the descriptors were calculated for all molecules at their minimum calculated

heats of formation (CHF_{\min}) are statistically higher (32.7). Their R_f values are given in column 7 of Table 2. Taking into account the criterion relevant to acceptance of the hypothesis, it is apparent that the accuracy, if a flexible structure approach is assumed, is higher.

Another conclusion from Eq. (4) is that benzodiazepine's retention, again, is governed by local descriptors (about 65% contribution of DD[5])

Table 2 Experimental and Calculated R_f Values Obtained with Two Mobile Phases: Cyclohexane–Toluene–Diethylamine (m.ph.I) and Chloroform–Methanol (m.ph.II)

No. (1)	-azepam (2)	m.ph. I		m.ph. II		R_f m.ph. I	CHF_{\min} m.ph. II
		$R_{f\text{exp}}$ (3)	$R_{f\text{calc}}$ (4)	$R_{f\text{exp}}$ (5)	$R_{f\text{calc}}$ (6)	(7)	(8)
1	Nitra-	0	0.1	36	39.5	0.1	41.9
2	Oxa-	0	−0.7	40	40.0	−2.8	43.4
3	Lor-	1	−0.7	36	34.5	−2.7	37.8
4	Nord-	4	10.4	55	51.8	14.0	63.8
5	Lormet-	6	6.6	67	64.3	11.2	75.7
6	Tem-	8	6.2	59	63.2	13.4	67.0
7	Flunitra-	10	11.5	72	66.0	11.7	66.0
8	Nimet-	12	12.7	77	73.4	12.9	61.7
9	Cam-	13	13.2	79	80.3	10.3	74.8
10	Hal-	18	17.9	76	79.2	17.3	79.6
11	Flur-	30	34.0	48	49.8	34.6	46.2
12	Pin-	31	27.5	79	79.3	24.4	72.3
13	Tetra-	34	33.5	75	73.8	32.7	66.3
14	Pra-	36	28.5	74	69.4	26.8	79.3
15	Med-	40	42.4	74	79.1	42.8	79.1



rather than by global molecular properties (about 35% from EN). The general conclusion is that it seems possible to increase the accuracy of QSRR calculations in TLC, assuming that flexible 3D analyte structures undergo some changes during the process of adsorption onto silica gel. As a result, a better fit between the calculated and experimental retention data can be achieved if several energetically possible structures for one and the same analyte are presumed.

References

1. L. B. Kier, L. H. Hall, M. J. Murrey, and M. Randic, *J. Pharm. Sci.* 64: 19–25 (1975).
2. J. Sherma and B. Fried, *Handbook of Thin-Layer Chromatography*, Marcel Dekker, Inc., New York, 1989.
3. W. Kiridena, *J. Chromatogr.* 802: 335–347 (1998).
4. W. Wardas and A. Pyka, *J. Planar Chromatogr.* 3: 425–428 (1990).
5. A. Pyka, *J. Planar Chromatogr.* 9: 181–184 (1996).
6. M. Japp, K. Garthwaite, A. Geeson, and M. Osselton, *J. Chromatogr.* 439: 317–324 (1988).



Quinolone Antibiotics in Food, Analysis by LC

Nikolaos A. Botsoglou

Aristotle University, Thessaloniki, Greece

INTRODUCTION

With the extensive use of drugs in animal production, violative residues of the parent drugs and/or metabolites have a high potential to be present in meat, milk, eggs, and honey. The level of residues and the individual drugs they are originated from determine the public health significance of such adulteration of the food supply. Quinolones constitute an expanding group of synthetic antibiotics, which are widely used in combating various diseases in animal husbandry and aquaculture. It is estimated that oxolinic acid, one of the earliest members of this group of drugs, has been, by far, the most widely used drug in fish farming for the prophylaxis and treatment of bacterial fish disease during the last decade. Oxolinic acid, along with nalidixic acid, comprises the main members of the first-generation quinolones whose basic molecular structure includes a quinolone ring and a carboxylic acid group. Ciprofloxacin, danofloxacin, difloxacin, enrofloxacin, flumequine, marbofloxacin, norfloxacin, ofloxacin, and sarafloxacin make up the main members of the second-generation quinolones that contain a fluorine atom in their molecule and a piperazine ring, and are collectively called fluoroquinolones. Both first-generation and second-generation quinolones are analyzed in foods of animal origin mainly by liquid chromatographic methods. In this article, an overview of the analytical methodology for the determination of quinolone residues in foods is provided.

ANALYSIS OF QUINOLONES

Quinolones are amphoteric compounds that are soluble in polar organic solvents such as acetonitrile, methanol, ethanol, dimethylformamide, dichloromethane, and ethyl acetate.^[1] They are slightly soluble in water and are insoluble in nonpolar solvents such as hexane, petroleum ether, and isooctane. Most of these drugs are fluorescent and quite stable in aqueous solution and toward light, except miloxacin, which is reported to be unstable. These inherent characteristics have made quinolones difficult to analyze by chromatographic methods.

Sample Extraction

Mincing and/or homogenization of muscle, kidney, and liver samples is usually required before some type of extraction is applied. Drying of tissue samples with anhydrous sodium sulfate prior to extraction is another procedure that is often employed to enhance the recovery of analytes.^[2–5] Sample extraction and concurrent protein precipitation can be accomplished with a great variety of organic solvents, including ethyl acetate,^[2–4] acetone,^[6–8] methanol,^[9] acetonitrile,^[10,11] and ethanol.^[5] Enhancement of the extraction efficiency can be achieved by properly acidifying the sample homogenate.^[5,9] In acidic conditions, particularly at pH values lower than 3, quinolones, being zwitterions, are fully protonated; therefore, they become less bound by the matrix and more soluble in organic extraction solvents. Nevertheless, extraction of quinolones from food samples has been also accomplished by aqueous solutions, such as with water, alkaline buffers, or trichloroacetic acid.^[12]

Extract Cleanup

Various cleanup procedures, including conventional liquid–liquid partitioning, solid-phase extraction, matrix solid-phase dispersion, and on-line dialysis/trace enrichment, have all been employed to eliminate or reduce interfering compounds and to concentrate the analyte(s). In many instances, more than one of these cleanup procedures have been used in combination to enhance cleanup efficiency.^[1]

Liquid–liquid partitioning is employed to either extract the analytes from an organic sample extract into an aqueous solution, or to wash out interfering substances from the organic or aqueous sample extracts. In general, quinolones are partitioned from chloroform or ethyl acetate sample extracts into alkaline aqueous buffers, to be then backextracted into the organic solvent under acidic conditions.^[7,8] To remove lipids, sample extracts are often also partitioned with *n*-hexane^[2–4,6–8,11,12] or diethyl ether.^[10] Solid-phase extraction is also often used to remove interfering coextracted compounds.

Solid-phase extraction columns contain either nonpolar reversed-phase C_{18} sorbents, or polar sorbents such as alumina, aminopropyl, and propylsulfonic acid.^[1–5] Matrix solid-phase dispersion cleanup, using reversed-phase C_{18} material, has also been employed for the determination of oxolinic acid in catfish muscle.^[13]

On-line dialysis and subsequent trace enrichment have been further described for the extraction/cleanup of flumequine residues from fish muscle,^[12] or oxolinic acid and flumequine from chicken liver^[6] and salmon muscle.^[12] This process involves on-line use of a diphasic dialysis membrane, trapping of the analytes onto a preconcentration column filled with reversed-phase C_{18} or polymeric material, rinsing of the coextracted interfering compounds to waste, and, finally, flushing of the concentrated analytes onto the analytical column.

Liquid Chromatography Separation

Following their extraction and cleanup, residues of quinolones can be analyzed by either gas chromatography or liquid chromatography (LC). Among these chromatographic techniques, LC seems to be the method of choice because gas chromatography necessitates reduction of the analytes (oxolinic, nalidixic, and piromidic acid) by sodium tetrahydroborate prior to their determination in fish muscle.^[14] Analysis is generally carried out with nonpolar reversed-phase stationary phases that are based on octadecyl, octyl, phenyl, or polymeric sorbents. Recommended mobile phases are fairly polar, containing tetrahydrofuran, methanol, and/or acetonitrile as organic modifiers. In most applications, phosphoric acid is added to the mobile phase prior to chromatography. By acidifying the mobile phase pH to values lower than 3, the ionization of the carboxylate moiety of the analytes is suppressed. This results in increased retention and improved separation of the analytes. However, recorded chromatographic peaks generally tail. Elimination or major reduction of peak tailing can be generally achieved by addition of counter ions^[10,12] or oxalic and citric acids^[2–4] to the mobile phase.

Detection/Confirmation

Ultraviolet, fluorometric, and mass spectrometric detectors have all been successfully used for the determination of residues of quinolones in food. Quinolones exhibit remarkable ultraviolet absorption; therefore, they are ideal for direct determination by ultraviolet detection anywhere in the wavelength range from 254 to 295 nm. However, the most popular is fluorometric detection, due to the

inherent fluorescence of these drugs and the advantages in terms of selectivity and sensitivity that this detection mode offers. Confirmation of the identity of liquid chromatographic peaks in suspected samples can be obtained by means of a derivatization process in which the analytes are converted to the corresponding decarboxylated derivatives, which are then analyzed by gas chromatography mass spectrometry.^[7,8]

CONCLUSION

An analyst has a wide range of efficient extraction, cleanup, separation, and detection procedures to choose from. The choice will depend on the nature of the sample matrix (whether it is solid or liquid, or fatty or nonfatty) and the expected range and levels of quinolone residues in food.

REFERENCES

1. Botsoglou, N.A.; Fletouris, D.J. *Drug Residues in Food. Pharmacology, Food Safety, and Analysis*; Marcel Dekker, Inc.: New York, 2001.
2. Larocque, L.; Schnurr, M.; Sved, S.; Weninger, A. Determination of oxolinic acid residues in salmon muscle-tissue by liquid-chromatography with fluorescence detection. *J. Assoc. Off. Anal. Chem.* **1991**, *74*, 608–611.
3. Carignan, G.; Larocque, L.; Sved, S. Assay of oxolinic acid residues in salmon muscle by liquid chromatography with fluorescence detection—Interlaboratory study. *J. Assoc. Off. Anal. Chem.* **1991**, *74*, 906–909.
4. Degroodt, J.M.; Wyhowski de Bukanski, B.; Srebrnik, S. Oxolinic acid and flumequine in fish tissues—Validation of an HPLC method—Analysis of medicated fish and commercial fish samples. *J. Liq. Chromatogr.* **1994**, *17*, 1785–1794.
5. Roybal, J.E.; Pfenning, A.P.; Turnipseed, S.B.; Walker, C.C.; Hurlbut, J.A. Determination of 4 fluoroquinolones in milk by liquid-chromatography. *J. AOAC Int.* **1997**, *80*, 982–987.
6. Eng, G.Y.; Maxwell, R.J.; Cohen, E.; Piotrowski, E.G.; Fiddler, W. Determination of flumequine and oxolinic acid in fortified chicken tissue using online dialysis and high-performance liquid-chromatography with fluorescence detection. *J. Chromatogr.* **1998**, *799*, 349–354.
7. Pfenning, A.P.; Munns, R.K.; Turnipseed, S.B.; Roybal, J.E.; Holland, D.C.; Long, A.R.; Plakas, S.M. Determination and confirmation of identities of flumequine and nalidixic, oxolinic, and piromidic acids in salmon and shrimp. *J. AOAC Int.* **1996**, *79*, 1227–1235.



8. Munns, R.K.; Turnipseed, S.B.; Pfenning, A.P.; Roybal, J.E.; Holland, D.C.; Long, A.R.; Plakas, S.M. Determination of residues of flumequine and nalidixic, oxolinic, and piromidic acids in catfish by liquid-chromatography with fluorescence and UV detection. *J. AOAC Int.* **1995**, *78*, 343–352.
9. Pouliquen, H.; Gouelo, D.; Larhantec, M.; Pilet, N.; Pinault, L. Rapid and simple determination of oxolinic acid and oxytetracycline in the shell of the blue mussel (*Mytilus edulis*) by high-performance liquid-chromatography. *J. Chromatogr.* **1997**, *702*, 157–162.
10. Hormazabal, V.; Yndestad, M. Rapid assay for monitoring residues of enrofloxacin in milk and meat tissues by HPLC. *J. Liq. Chromatogr.* **1994**, *17*, 3775–3782.
11. Meinertz, J.R.; Dawson, V.K.; Gingerich, W.H.; Cheng, B.; Tubergen, M.M. Liquid-chromatographic determination of sarafloxacin residues in channel catfish muscle tissue. *J. AOAC Int.* **1994**, *77*, 871–875.
12. Thanh, H.H.; Andresen, A.T.; Agasoster, T.; Rasmussen, K.E. Automated column-switching high-performance liquid-chromatographic determination of flumequine and oxolinic acid in extracts from fish. *J. Chromatogr.* **1990**, *532*, 363–373.
13. Jarboe, H.H.; Kleinow, K.M. Matrix solid-phase dispersion isolation and liquid-chromatographic determination of oxolinic acid in channel catfish (*Ictalurus punctatus*) muscle tissue. *J. AOAC Int.* **1992**, *75*, 428–432.
14. Takatsuki, K. Gas-chromatographic mass-spectrometric determination of oxolinic, nalidixic, and piromidic acid in fish. *J. AOAC Int.* **1992**, *75*, 982–987.



Radiochemical Detection

Eileen Kennedy

Novartis Crop Protection, Inc., Greensboro, North Carolina, U.S.A.

Introduction

Radiochemical detectors are devices that allow the measurement of low-energy γ -rays or β particles emitted by radioisotopes. Substances called scintillators absorb the energy that is produced by the radioactive decay and transform it into light. The light from the scintillator, the intensity of which is directly proportional to the energy of the radioisotope emission, can be detected by a photomultiplier to provide an electrically countable pulse. Radiochemical detectors have been developed for various chromatographic techniques, the most common of which is high-performance liquid chromatography (HPLC). In HPLC, the detection of radioisotopes in a column eluate has allowed quantitation of discrete radiolabeled peaks in real time and in a generally nondestructive manner.

Discussion

Gamma-emitters, such as iodine-125, which give off energy in the form of photons rather than particles, are more strongly penetrating than β -emitters. A radiochemical detector for γ -rays is generally composed of a cylindrical block of specially activated sodium iodide enclosed in a thin aluminum shell. One face of the block is optically coupled to a single photomultiplier. The eluate from the HPLC column passes through a coil or U-tube, which is placed in the well of the block. As the eluate passes through the coil, γ -radiation is stopped by the very dense sodium iodide, producing light that can be measured by the photomultiplier.

Beta-emitters such as tritium (H-3) or carbon-14 (C-14) are the most commonly used radioisotopes in drug metabolism, agricultural metabolism, and toxicology studies. In HPLC, the radiochemical detector can be off-line or on-line. Off-line detection requires coupling the chromatograph to a fraction collector. The collected fractions are combined with a suitable liquid scintillation cocktail and then counted by a liquid scintillation counter. This method allows for

the control of parameters such as counting time to improve sensitivity, but it suffers from being labor and time intensive. On-line or flow-through radiochemical detectors can be homogeneous or heterogeneous. In homogeneous flow through detectors, a scintillation cocktail is added to the column eluate prior to detection in a liquid flow cell. The energy of decay from the β radionuclide is transferred to the scintillation cocktail via a solvent molecule. The liquid flow cell offers the highest sensitivity in on-line detectors but precludes recovery of the entire sample and requires an additional pump for delivery of the scintillation cocktail. In heterogeneous counting, the column eluate passes directly through a flow cell packed with a suitable solid scintillator such as yttrium silicate, calcium fluoride, or lithium glass. Use of the solid flow cell involves no additional costs for the scintillation cocktail and simplifies waste disposal. However, the solid cells have a lower counting efficiency, particularly with tritium, and can suffer from high backgrounds due to contamination. In both homogeneous and heterogeneous counting, light energy is detected by a pair of photomultiplier tubes located on either side of the flow cell, which is most often composed of a flat coil of thin-wall tubing situated in a transparent case. The photomultiplier tubes are located in fairly close proximity to each other (typically less than $\frac{1}{2}$ in. apart). Most commercially available radiochemical HPLC detectors use coincidence electronics in order to reduce noise pulses. With a coincidence counter, events are only recorded when both photomultiplier tubes are stimulated by light to give a pulse output within 20–50 ns of each other. A multichannel pulse-height analyzer sorts the outputs from the coincidence counter. A computer is then generally used to process data from the radiochemical detector as well as other on-line detectors and the results are presented either on a monitor or printer.

Unlike other chromatographic measurements such as ultraviolet (UV) absorption, the measurement and quantitation of radioactivity are based on time. Although a known percentage of a radioisotope will decay over a relatively long time, within that time pe-



riod, the instantaneous rate of decay is not known. Because radioactive decay is a statistical process, the quality of a radioactivity measurement improves as a function of time. In other words, the longer the sample is counted, the more accurate (or statistically relevant) the measurement of the radioactivity. With off-line radiochemical detection, even very small peaks can be counted for a sufficiently long time to allow for a statistically relevant measurement. With on-line detection, the total flow rate and the cell volume fix the counting time. On-line detection of low-level peaks can be improved by either a slower flow rate or by a larger flow cell. For solid flow cells, the total flow rate is equal to the mobile-phase flow rate. For liquid flow cells, the total flow rate is equal to the mobile-phase flow rate plus the flow rate of the liquid scintillator. The latter is frequently expressed as a ratio of scintillator to mobile phase. As compared to other HPLC detectors, the volume of the flow cell is relatively large in the radiochemical detector. Flow cells typically range from 250 to 500 μL for solid cells and from 1000 to 2000 μL for liquid cells. Upward limits on the size of the flow cell are governed by the possibility of more than one peak being present in the cell at any one given time. However, assuming sufficient resolution, a larger flow cell should allow for a longer counting time and, hence, a more accurate measurement of radioactivity in a given peak. The actual amount of time that the column eluate will remain in the vicinity of the photomultiplier tubes is defined as the residence time. The residence time (R), in seconds, can be calculated as follows:

$$R = \frac{V}{F} \times 60$$

where V is the cell volume in microliters and F is the total flow rate in milliliters per minute.

The counts per minute (cpm) can then be calculated for each peak in the sample as follows:

$$\text{cpm} = \frac{N}{R}$$

where N is the total net counts observed in the peak after background subtraction and R is the residence time in minutes.

Disintegrations per minute (dpm) are equal to cpm in the rare cases where the counting efficiency is 100%. Otherwise, dpm can be calculated as follows:

$$\text{dpm} = \frac{\text{cpm}}{E}$$

where E is the counting efficiency expressed as a percentage.

The efficiency of a radiochemical detector can be defined as the number of counts that are detected in the peak after background subtraction divided by the total number of radioactive events that actually occurred in the sample during the counting period. The approximate counting efficiencies that can be achieved with solid flow cells are fairly low for tritium (up to 10%) and significantly better for C-14 (up to 90%). With liquid flow cells, the counting efficiencies are greater than 55% for tritium and greater than 95% for C-14. Under isocratic conditions, the counting efficiency remains constant and can be readily determined by injecting a known amount of activity into an HPLC system, collecting the resultant peak as a single entity and counting it in a liquid scintillation counter. The number of disintegrations in the recovered peak is then compared to the calibrated activity of the standard. With gradient elution, the counting efficiency will generally change as the mobile-phase composition changes. In this situation, an efficiency calibration or quench curve can be obtained by injecting a constant known level of radioactivity during an otherwise blank gradient run. The calibration curve is then used to correct subsequent HPLC runs.

The minimum amount of radioactivity that can be detected by a flow-through radiochemical detector is a subject of continuing debate. It is generally accepted that a fairly sharp peak that contains counts that are at least twice background can be detected. One formula for calculating the minimum detectable activity (MDA) is given by

$$\text{MDA} = \frac{BW}{RE}$$

where B is the background count in cpm, W is the base width of the peak in minutes, R is the residence time in minutes, and E is the counting efficiency expressed as a percentage.

In practical terms, for a 500-dpm peak with a base width of 20 s, a counting efficiency of 70% and a residence time of 12 s, we would observe 70 counts, which would be spread out over the peak width, plus the residence time (a total of 32 s). For a detector that has a 10-cpm background, we would observe 5.3 counts over the same time period of 32 s. The ratio of the observed peak counts to background would be 13:1 and the peak should be clearly visible. However, under the same conditions, a 50-dpm peak would have a count to background ratio of only 1.3:1 and it is doubtful that this peak could be observed in on-line counting. In the latter situation, off-line radio-

chemical detection may be used to clarify the presence or absence of such a low-level peak.

Suggested Further Reading

INUS Home Page. <http://www.inus.com> (last accessed August 1999).

Parvez, H., A. R. Reich, S. Lucas-Reich, and S. Parvez (eds.), *Progress in HPLC Volume 3: Flow Through Radioactivity Detection in HPLC*. VSP, Utrecht, 1988.

Scott, R. P. W., *Chromatographic Detectors*, Marcel Dekker, Inc., New York, 1996, pp. 315–327.



Radius of Gyration Measurement by GPC–SEC

Raniero Mendichi

Instituto di Chimica delle Macromolecole (CNR), Milano, Italy

Introduction

Fundamental properties of macromolecules, such as viscoelasticity and flow behavior, primarily depend on the dimensions and the conformations of macromolecules. Primary biological functions substantially depend on the dimensions of natural macromolecules such as proteins and enzymes. Hence, a primary method to understand the physical properties of macromolecules, synthetic and natural, involves determination of the dimension as a function of the molar mass. A convenient method to fractionate macromolecules is the size-exclusion chromatography (SEC) technique. SEC fractionation is rapid and efficient and requires small amounts of the polymeric sample. A method to measure the dimension of the macromolecules as a function of the molar mass is an on-line technique to a SEC chromatographic system.

Discussion

The simplest parameter to quantify the dimension of a macromolecule is the end-to-end distance. The end-to-end distance is the spatial distance between the end groups of a linear chain. Unfortunately, there are no experimental direct methods to measure the end-to-end distance of a macromolecule. Furthermore, the end-to-end distance has no meaning for a chain without end groups (ring) and with many end groups (branched). Instead, the dimension of every type of macromolecule can be always quantified by the gyration radius $\langle s^2 \rangle^{1/2}$.

There are several experimental methods to measure $\langle s^2 \rangle^{1/2}$. Macromolecules can be represented as N segments (monomers, groups) of mass m_i and distance r_i from the center of gravity. The gyration radius $\langle s^2 \rangle^{1/2}$ is defined as the mass average of r_i :

$$\langle s^2 \rangle^{1/2} = \left(\frac{\langle \sum m_i r_i^2 \rangle}{\sum m_i} \right)^{1/2} \quad (1)$$

Actually, the term “gyration radius” is a misnomer; it originates from the kinematics, but is very popular. More correctly, it should be called “root mean square

radius.” Nonrigid macromolecules possess conformational mobility; hence, their dimension requires an additional average, $\langle \rangle$, over all the conformations. The dimension of a macromolecule also depends on its long-range interactions, excluded volume, and the polymer–solvent interactions. Therefore, $\langle s_0^2 \rangle^{1/2}$ denotes the dimension of the macromolecules in the unperturbed ideal state and $\langle s^2 \rangle^{1/2}$ denotes the expanded dimension as a consequence of the excluded volume. Finally, macromolecules are generally polydisperse and, by analogy to the molar mass, $\langle s^2 \rangle_n^{1/2}$ denotes the numeric average, $\langle s^2 \rangle_w^{1/2}$ denotes the weight average, and $\langle s^2 \rangle_z^{1/2}$ denotes the z average [1].

Size-exclusion chromatography fractionation is steric, that is, dimensional. In theory, a SEC system could be calibrated by means of some appropriate standards of known dimensions and, in this way, to measure $\langle s^2 \rangle^{1/2}$. SEC fractionation depends on the hydrodynamic radius R_H of the macromolecules: $R_H \propto M[\eta]$ where $[\eta]$ is the intrinsic viscosity. $\langle s^2 \rangle^{1/2}$ and R_H are two different parameters. $\langle s^2 \rangle^{1/2}$ is an equilibrium parameter; R_H is a dynamic parameter and depends on the method by which it is obtained. R_H becomes the Stokes radius R_D in diffusion measurements and the Einstein radius R_η in viscosity measurements. Because SEC fractionation depends on R_H , the method is not appropriate for a direct measure of $\langle s^2 \rangle^{1/2}$. Convenient experimental methods to measure $\langle s^2 \rangle^{1/2}$ are scattering techniques.

The $\langle s^2 \rangle^{1/2}$ value of macromolecules usually ranges from 2 to 3 nm (globular proteins) to several hundred nanometers (particles). The range of $\langle s^2 \rangle^{1/2}$ values determines the more appropriate scattering technique. Smaller dimensions of the molecules require shorter wavelengths of the radiation. Light-scattering (LS) wavelengths range from approximately 400 to 700 nm. The minimum $\langle s^2 \rangle^{1/2}$ value that could be measured by LS is 8–10 nm and 5–6 nm in the more favorable case (shorter wavelength). If the dimension of the molecules is small, we need to use other scattering techniques such as x-ray or neutrons.

A modern LS photometer uses coherent light (i.e., laser) with vertical polarization. In our specific case, LS concerns the interaction of the light with matter with a



solution of macromolecules. In an LS experiment, we measure the intensity of the scattering. Furthermore, to measure the $\langle s^2 \rangle^{1/2}$ value, we need the angular variation of the scattering. Because we want to measure $\langle s^2 \rangle^{1/2}$ on-line to a SEC system, after the fractionation in the columns, we need to measure the angular variation of the scattering instantaneously (i.e., simultaneously) over a wide range of angles. In this case, we need an on-line multiangle light-scattering (MALS) detector.

Following Zimm [2,3], the intensity of the scattering of a solution of macromolecules is in relation to the molar mass of the sample by

$$\frac{Kc}{\Delta R(\theta)} = \frac{1}{MP(\theta)} + 2A_2c + \dots \quad (2)$$

where $\Delta R(\theta)$ is the scattering excess (Rayleigh factor) at angle θ of the solution with regard to the pure solvent, θ is the angle between the incident light and the detector, M is the molar mass, c is the concentration, A_2 is the second virial coefficient, and K is an optical constant [$K = (4\pi^2 n_0^2 (dn/dc)^2) / (N_a \lambda_0^4)$, where n_0 is the refractive index of the solvent, dn/dc is the refractive index increment of the polymer, λ_0 is the wavelength of the light *in vacuo*, and N_a is Avogadro's number].

The parameter of interest for the measurement of $\langle s^2 \rangle^{1/2}$ is the form factor $P(\theta)$. A macromolecule may not be considered as a single point of scattering. In this case, the light scattered from two different points of the same macromolecule will not be in phase: destructive interference. The intensity of the scattering in the presence of the destructive interference is lower for large molecules. The interference depends on the angle of measure of the intensity of the scattering. The interference is absent at 0° angle and highest at 180° . The interference depends on the shape and on the dimension of the molecules. Therefore, there has been introduced a form factor $P(\theta)$ which quantifies the interference. $P(\theta)$ is defined as the ratio between the Rayleigh factor in the presence of interference ($\theta > 0^\circ$) and the Rayleigh factor in the absence of interference ($\theta = 0^\circ$). Thus, by definition,

$$P(\theta) = \frac{R(\theta)}{R(\theta = 0^\circ)} \quad (3)$$

Equation (3) states that $P(\theta) = 1$ for $\theta = 0^\circ$, independent of the dimension of the molecules, and $P(\theta) < 1$ for $\theta > 0^\circ$ when the dimension of the molecules is comparable with the wavelength λ . Fortunately, $P(\theta)$ is a useful method for measuring the dimension of the molecules $\langle s^2 \rangle^{1/2}$. Debye [4] showed that the $P(\theta)$ could be expressed independently of the shape and conformation of the macromolecules. Considering the recip-

Radius of Gyration Measurement by GPC-SEC

rocal of $P(\theta)$ [$P(\theta)^{-1}$], Debye obtained the following equation:

$$P(\theta)^{-1} = 1 + \frac{1}{3}\mu^2 \langle s^2 \rangle \quad (4)$$

where $\mu = 4\pi/\lambda \sin(\theta/2)$, $\lambda = \lambda_0/n_0$ is the wavelength of the light in the medium. Equation (4) is valid in the limit $\mu^2 \langle s^2 \rangle / 3 \ll 1$. From the initial slope of the $P(\theta)$ versus $\sin^2(\theta/2)$ plot, we can estimate the gyration radius value $\langle s^2 \rangle^{1/2}$.

To estimate M and $\langle s^2 \rangle^{1/2}$ values, Eqs. (2) and (4), we need to extrapolate to infinite dilution: $c = 0$. When the MALS detector is used as an on-line detector in a SEC system to estimate the $\langle s^2 \rangle^{1/2}$ of the molecules, we have only a concentration. In a SEC fractionation, it is generally assumed that each instant, slice, contains molecules homogeneous in molar mass and in dimension. In this case, considering the very low concentrations of the macromolecules that elute from the SEC columns, the term $2A_2c$ of Eq. (2) is ignored. However, the exact concentration of each slice has to be known. Thus, the measure of M and $\langle s^2 \rangle^{1/2}$ values by a MALS detector requires a concentration detector also, usually a differential refractometer or an ultraviolet (UV) photometer. Combining Eq. (2), deprived of the $2A_2c$ term, with Eq. (4), we obtain

$$\frac{Kc}{\Delta R(\theta)} = \frac{1}{M} + \frac{16\pi^2 \langle s^2 \rangle}{3\lambda^2 M} \sin^2\left(\frac{\theta}{2}\right) \quad (5)$$

Using an on-line dual-detector SEC system, MALS, and concentration from a linear regression of $Kc/\Delta R(\theta)$ on $\sin^2(\theta/2)$, we obtain the molar mass M from the intercept and the dimension of the molecules $\langle s^2 \rangle^{1/2}$ from the slope. If the macromolecules are polydisperse, we obtain [3] the averages M_w and $\langle s^2 \rangle_z^{1/2}$. Figure 1 shows the $Kc/\Delta R(\theta)$ versus $\sin^2(\theta/2)$ plot of a

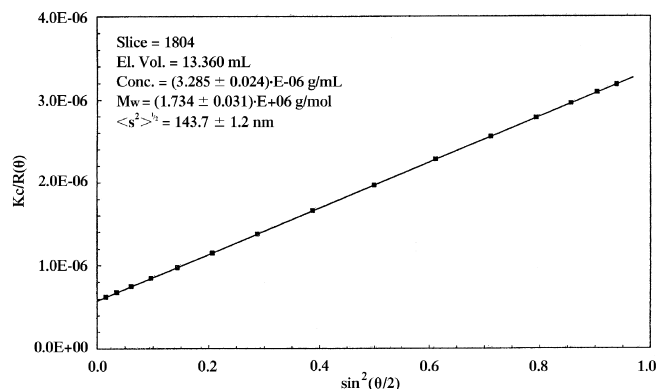


Fig. 1 $Kc/\Delta R(\theta)$ versus $\sin^2(\theta/2)$ plot of a single slice from a hyaluronic acid sample.

single slice from a polysaccharide, hyaluronic acid, sample. Figure 1 shows the classical three parameters that could be obtained at each elution volume: c_i from the concentration detector, M_i and $\langle s^2 \rangle_i^{1/2}$ from the MALS detector. An accurate measure of $\langle s^2 \rangle_i^{1/2}$ is not simple. The measurement requires a good signal-to-noise ratio, especially at low angles. In addition, if the dimension of the macromolecules is small, the measure of the slope of the $Kc/\Delta R(\theta)$ versus $\sin^2(\theta/2)$ plot is inaccurate. Conversely, if the dimension of the macromolecules is too large, the angular variation of the intensity of the scattering could be not linear. In this case, it is quite difficult to estimate an accurate value of the initial slope of the plot.

Because, for each fraction of the sample, the on-line MALS detector measures both M_i and $\langle s^2 \rangle_i^{1/2}$ from a single sample, it is possible to obtain the $\langle s^2 \rangle^{1/2} = f(M)$ power law of the polymer. The power law $\langle s^2 \rangle^{1/2} = f(M)$ is a very important function for understanding the conformation (flexible coils, compact spheres, rigid rods) of the macromolecules. In fact, if the molar mass distribution of the sample is adequately broad, it is possible, from a linear regression of $\log(\langle s^2 \rangle^{1/2})$ on $\log(M)$, to estimate the constants K and α of the power law $\langle s^2 \rangle^{1/2} = KM^\alpha$. Specifically, the slope α of the power law contains fundamental information of the conformation of the macromolecule in solution.

There are several commercially available on-line MALS detectors. Wyatt Instruments (Santa Barbara, CA, U.S.A.) commercializes two MALS detectors: Dawn-DSP (18 angles) and mini-Dawn (3 angles: 45°, 90°, and 135°). Precision Detectors (Franklin, MA, U.S.A.) commercializes a double-angle LS: 15° and 90°. SEC on-line measurement of $\langle s^2 \rangle^{1/2}$ could be performed by other techniques. Viscotek Co. (Houston, TX, U.S.A.) commercializes an alternative three-detector SEC system, the SEC³. The SEC³ system consists of (1) an on-line viscometer (VISC), (2) an on-line right-angle LS detector (RALS), and (3) a concentration detector. This three-detector SEC system also measures $\langle s^2 \rangle^{1/2}$. More exactly, $\langle s^2 \rangle^{1/2}$ is calculated, using an iterative

algorithm, from the intrinsic viscosity, by VISC, and the molar mass obtained by the RALS detector. For each instant i , the algorithm is divided into three steps:

$[\eta]_i$ is measured from VISC; the molar mass M_i is calculated by RALS using Eq. (2) and $P(\theta) = 1$.

In this first step, M is generally underestimated as a consequence of the destructive interference.

$\langle s^2 \rangle^{1/2}$ is calculated by the Flory-Fox equation [Eq. (6)]. The Ptitsyn-Eizner equation [Eq. (7)] considers the expansion of the macromolecules due to the excluded volume. In Eqs. (6) and (7), $\Phi_0 = 2.86 \times 10^{23}$ and $\varepsilon = (2a - 1)/3$, where a is the slope of the Mark-Houwink-Sakurada equation.

Finally, $P(\theta)$ is calculated by the Debye equation [Eq. (4)]:

$$\langle s^2 \rangle^{1/2} = \frac{1}{\sqrt{6}} \left(\frac{M[\eta]}{\phi(\varepsilon)} \right)^{1/3} \quad (6)$$

$$\phi(\varepsilon) = \phi_0(1 - 2.63\varepsilon + 2.86\varepsilon^2) \quad (7)$$

At this point, the algorithm restarts the first step, with $P(\theta)$ equal to the new calculated value from the previous iteration. The algorithm converges very quickly. A detailed description of the SEC³ algorithm can be found in Ref. 5.

To measure the dimension of macromolecules is a very delicate task. However, the dimension is a primary parameter needed to understand the physical properties of a macromolecule. We have described two experimental methods, MALS and SEC³, to measure $\langle s^2 \rangle^{1/2}$ on-line to a SEC system.

References

1. P. J. Wyatt, *Anal. Chim. Acta* 272: 1 (1993).
2. B. H. Zimm, *J. Chem. Phys.* 16: 1093 (1948).
3. P. Kratochvil, *Classical Light Scattering from Polymer Solutions*, Elsevier, Amsterdam, 1987.
4. P. Debye, *J. Phys. Colloid Chem.* 51: 18 (1947).
5. W. W. Yau and S. W. Rementer, *J. Liquid Chromatogr. Related Technol.* 13: 627 (1990).



Rate Theory in Gas Chromatography

Raymond P.W. Scott

Scientific Detectors Ltd., Banbury, Oxfordshire, England

Introduction

The rate theory examines the kinetics of exchange that takes place in a chromatographic system and identifies the factors that control band dispersion. The first explicit height equivalent to a theoretical plate (HETP) equation was developed by Van Deemter et al. in 1956 [1] for a packed gas chromatography (GC) column. Van Deemter et al. considered that four spreading processes were responsible for peak dispersion, namely *multi-path dispersion*, *longitudinal diffusion*, *resistance to mass transfer in the mobile phase*, and *resistance to mass transfer in the stationary phase*.

The Multipath Effect

In a packed column, the individual solute molecules will describe a tortuous path through the interstices between the particles, and some will randomly travel shorter routes than the average and some will travel longer routes. Consequently, those molecules taking the shorter paths will move ahead of the mean and those that take the longer paths lag behind the mean which will result in band dispersion. Van Deemter et al. derived the following function for the multipath variance contribution (σ_M^2) to the overall variance per unit length of the column (σ^2):

$$\sigma_M^2 = 2\lambda d_p \quad (1)$$

where d_p is the particle diameter of the packing and λ is a constant that depends on the quality of the packing.

Longitudinal Diffusion

Driven by the concentration gradient, solutes naturally diffuse when contained in a fluid. Thus, a discrete solute band will diffuse in a gas or liquid, and because the diffusion process is random, it will produce a concentration curve that is Gaussian in form. This diffusion effect occurs in the mobile phase of both packed GC and liquid chromatography (LC) columns. The longer the solute band remains in the column, the greater will

be the extent of diffusion. Because the residence time of the solute in the column is inversely proportional to the mobile-phase velocity, the dispersion will also do the same. Van Deemter et al. derived the following expression for the variance contribution by longitudinal diffusion (σ_L^2) to the overall variance per unit length of the column (σ^2):

$$\sigma_L^2 = \frac{2\gamma D_m}{u} \quad (2)$$

where D_m is the diffusivity of the solute in the mobile phase, u is the linear velocity of the mobile phase, and γ is a constant that depends on the quality of the packing.

Resistance to Mass Transfer in the Mobile Phase

During migration through the column, the solute molecules are continually transferring from the mobile phase to the stationary phase and back again. This transfer process is not instantaneous; a finite time is required for the molecules to traverse (by diffusion) through the mobile phase in order to reach the interface and enter the stationary phase. Thus, those molecules close to the stationary phase enter it immediately, whereas those molecules some distance away will find their way to it some time later. However, because the mobile phase is moving, during this time interval, those molecules that remain in the mobile phase will be swept along the column and dispersed away from those molecules that were close and entered the stationary phase immediately. This dispersion is called the resistance to mass transfer in the mobile phase.

Van Deemter derived the following expression for the variance contribution by the resistance to mass transfer in the mobile phase (σ_{RM}^2) to the overall variance per unit length of the column (σ^2):

$$\sigma_{RM}^2 = \frac{f_1(k')d_p^2}{D_m}u \quad (3)$$

where k' is the capacity ratio of the solute and the other symbols have the meaning previously ascribed to them.



Resistance to Mass Transfer in the Stationary Phase

Dispersion caused by the resistance to mass transfer in the stationary phase is exactly analogous to that in the mobile phase. Solute molecules close to the surface will leave the stationary phase and enter the mobile phase before those that have diffused further into the stationary phase and have a longer distance to diffuse back to the surface. Thus, as those molecules that were close to the surface will be swept along in the moving phase, they will be dispersed from those molecules still diffusing to the surface.

Van Deemter derived an expression for the variance from the resistance to mass transfer in the stationary phase (σ_{RS}^2), which is as follows:

$$\sigma_{RS}^2 = \frac{f_2(k')d_f^2}{D_s}u \quad (4)$$

where k' is the capacity ratio of the solute, d_f is the effective film thickness of the stationary phase, D_s is the diffusivity of the solute in the stationary phase, and the other symbols have the meaning previously ascribed to them.

As all the dispersion processes are random, the individual variances can be added to arrive at the total variance of the peak leaving the column:

$$\sigma^2 = \sigma_M^2 + \sigma_L^2 + \sigma_{RM}^2 + \sigma_{RS}^2 \quad (5)$$

where σ^2 is the total variance/unit length of the column.

Thus, substituting for σ_M^2 , σ_L^2 , σ_{RM}^2 , and σ_{RS}^2 from Eqs. (1)–(4), respectively,

$$\sigma^2 = 2\lambda d_p + \frac{2\gamma D_m}{u} + \frac{f_1(k')d_p^2}{D_m}u + \frac{f_2(k')d_f^2}{D_s}u \quad (6)$$

Now, the variance per unit length of a column is numerically equivalent to ratio of the column length to the column efficiency [2] [i.e., the height of the theoretical plate (H)]; thus,

$$H = 2\gamma d_p + \frac{2\gamma D_m}{u} + \frac{f_1(k')d_p^2}{D_m}u + \frac{f_2(k')d_f^2}{D_s}u \quad (7)$$

hence the term “HETP equation” for the equation for the variance per unit length of a column. Unfortunately, due to the compressibility of the gaseous mobile phase, neither the linear velocity nor the pressure is constant along the column, and as the diffusivity (D_m) is a function of pressure, the above form of the equation is only approximate. The Van Deemter equation was modified to take into account the compressibility of the carrier gas by Ogan and Scott [3]. The complete HETP equation for a GC column that takes into account the compressibility of the carrier gas will be

$$H = 2\lambda d_p + \frac{2\gamma D_m(o)}{u_o} + \frac{f_1(k')d_p^2}{D_m(o)}u_o + 2\frac{f_2(k')d_f^2}{D_s(\gamma + 1)}u_o \quad (8)$$

where u_o is the linear gas velocity at the column outlet, D_m is the diffusivity of the solute measured at the column outlet pressure, and γ is the inlet/outlet column ratio.

It is seen that Eq. (8) is very similar to Eq. (7) except that the velocity used is the *outlet* velocity, *not* the *average* velocity, and that the diffusivity of the solute in the gas phase is taken as that measured at the column outlet pressure (i.e., atmospheric). The shape of the H versus u curve is hyperbolic; it has a minimum value of H_{\min} at the optimum velocity u_{opt} (i.e., at the optimum velocity, the column will have a maximum efficiency). Expressions for H_{\min} and u_{opt} can be obtained by differentiating Eq. (8) with respect to u and equating to zero, solving for u_{opt} and substituting u_{opt} for u in Eq. (8) to obtain H_{\min} .

References

1. J. J. Van Deemter, F. J. Zuiderweg, and A. Klinkenberg, *Chem. Eng. Sci.* 271 (1956).
2. R. P. W. Scott, *Liquid Chromatography Column Theory*, John Wiley & Sons, Chichester, 1992, p. 97.
3. K. Ogan and R. P. W. Scott, *J. High Resolut. Chromatogr.* 7: 382 (July 1984).

Suggested Further Reading

Scott, R. P. W., *Techniques of Chromatography*, Marcel Dekker, Inc., New York, 1995.

Scott, R. P. W., *Introduction to Analytical Gas Chromatography*, Marcel Dekker, Inc., New York, 1998.



Refractive Index Detector

Raymond P.W. Scott

Scientific Detectors Ltd., Banbury, Oxfordshire, Engl;and

Introduction

The first practical refractive index detector was described by Tiselius and Claesson [1] in 1942 and, despite its limited sensitivity and its use being restricted to separations that are isocratically developed, it is still probably the fifth most popular detector in use today. Its survival has depended on its response, as it can be used to detect any substance that has a refractive index that differs from that of the mobile phase. It follows that it has value for monitoring the separation of such substances as aliphatic alcohols, acids, carbohydrates, and the many substances of biological origin that do not have ultraviolet (UV) chromophores, do not fluoresce, and are nonionic.

Discussion

When a monochromatic ray of light passes from one isotropic medium (A) to another (B), it changes its wave velocity and direction. The change in direction is called refraction and the relationship between the angle of incidence and the angle of refraction is given by Snell's law of refraction, namely

$$n'_B = \frac{n_B}{n_A} = \frac{\sin(i)}{\sin(r)}$$

where i is the angle of incident light in medium A, r is the angle of refractive light in medium B, n_A is the refractive index of medium A, n_B is the refractive index of medium B, and n'_B is the refractive index of medium B relative to that of medium A.

The refractive index of a substance is a dimensionless constant that normally decreases with increasing temperature; values are taken at 20°C or 25°C using the mean value taken for the two sodium lines of the spectrum. The optical systems that are used to exploit the refractive index for detection purposes are many and varied. One procedure is to construct a cell in the form of a hollow prism through which the mobile phase can flow. A ray of light is passed through the prism, which will be deviated from its original path, and is then focused onto a photocell. As the refractive

index of the mobile phase changes, due to the presence of a solute, the angle of deviation of the transmitted light will also alter and the amount of light falling on the photocell will change. This method of refractive index monitoring is used by many manufacturers in their refractive index detector designs.

Another method evolved from the work of Fresnel. The relationship between the reflectance from an interface between two transparent media and their respective refractive indices is given by Fresnel's equation:

$$R = \frac{1}{2} \left(\frac{\sin^2(i - r)}{\sin^2(i + r)} + \frac{\tan^2(i - r)}{\tan^2(i + r)} \right)$$

where R is the ratio of the intensity of the reflected light to that of the incident light and the other symbols have the meanings previously assigned to them.

Now,

$$\frac{\sin(i)}{\sin(r)} = \frac{n_1}{n_2}$$

where n_1 is the refractive index of medium 1, and n_2 is the refractive index of medium 2.

Consequently, if medium 2 represents the liquid eluted from the column, then any change in n_2 will result in a change in R , and, thus, the measurement of R could determine changes in n_2 resulting from the presence of a solute. An example of a refractive index detector that functions on the Fresnel principle is shown in Fig. 1. Light from a tungsten lamp is directed through an infrared (IR) filter (to prevent heating the cell) to a magnifying assembly that splits the beam into two beams. The two beams are focused through the sample and reference cells, respectively. Light refracted from the mobile-phase/prism surface passes through the prism assembly and is then focused on two photocells. The prism assembly also reflects light to a user port where the surface of the prism can be observed. The output from the two photocells is electronically processed and either passed to a potentiometric recorder or to a computer data acquisition system. The range of refractive index covered by the instrument for a given prism is limited and, consequently, three different prisms are usually made available to cover the re-



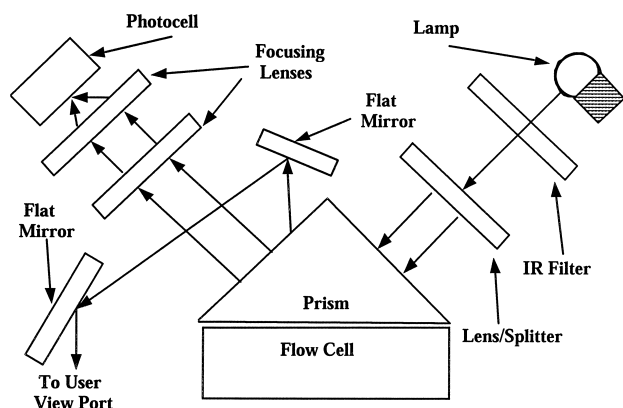


Fig. 1 A diagram of the optical system of a refractive index detector operating on the Fresnel method. (Courtesy of the Perkin Elmer Corporation.)

fractive index ranges of 1.35–1.4, 1.31–1.44, and 1.40–1.55, respectively.

Another variant on the refractive index detector arose from the work of Christiansen on crystal filters [2]. If a cell is packed with particulate material having the same refractive index as the mobile phase passing through it, light will pass through the cell with little or no refraction or scattering. If, however, the refractive index of the mobile phase changes, there will be a refractive index difference between the mobile phase and that of the packing. This difference results in light being refracted away from the incident beam, reducing the intensity of the transmitted light. If the transmitted light is focused onto a photocell and the refractive index of the packing and mobile phase initially matched, then any change in refractive index resulting from the elution of a peak will cause light scattering and a reduction in light falling on the sample photocell and, thus, provide a differential output.

In practice, because the optical dispersions of the media are likely to differ, the refractive index will only match at one particular wavelength and, thus, the fully transmitted light will be largely monochromatic. Light of other wavelengths will be proportionally dispersed depending on their difference from the wavelength at which the two media have the same optical dispersion. It follows that a change in refractive index of the mobile phase will change both the intensity of the transmitted light and its wavelength. This device has been manufactured but was not a commercial success due to its limited sensitivity and the need for different packing for different applications.

Another detector that functions on the change in refractive index of the column eluent is the interferome-

ter detector, which was first developed by Bakken and Stenberg [3] in 1971. The detector responds to the change in the effective path length of a beam of light passing through a cell when the refractive index of its contents changes due to the presence of an eluted solute. If the light transmitted through the cell is focused on a photocell coincident with a reference beam of light from the same source, interference fringes will be produced; the fringes will change as the path length of one light beam changes with reference to the other, and, consequently, as the concentration of solute increases in the sensor cell, a series of electrical pulses will be generated as each fringe passes the photocell. The effective optical path length (d) depends on the change in refractive index (Δn) and the path length (l) of the sensor cell as follows:

$$d = \Delta n l$$

Further, it is possible to calculate the number of fringes (N) (sensitivity) which move past a given point (or the number of cyclic changes of the central portion of the fringe pattern) in relation to the change in refractive index by the equation

$$N = \frac{2\Delta n l}{\lambda}$$

where λ is the wavelength of the light employed.

The larger the value of N for a given Δn , the more sensitive the detector will be. Therefore, l needs to be made as large as possible but will be limited by the dead volume of the column and the dispersion that can be tolerated before chromatographic resolution is impaired. The smallest cell ($1.4 \mu\text{L}$) (a cell volume that would be suitable for use with microbore columns) is reported to give a sensitivity of about 2×10^{-7} RI units at a signal-to-noise ratio of 2. Consequently, for benzene (RI = 1.501) sensed as a solute in *n*-heptane (RI = 1.388), this sensitivity would represent a minimum detectable concentration of 5.6×10^{-5} g/mL. The alternative $7\text{-}\mu\text{L}$ cell would decrease the minimum detectable concentration to about 1×10^{-6} g/mL, similar to that obtained for other refractive index detectors. However, the cell volume is a little large for modern high-efficiency columns. This type of RI detector has also been made commercially available but is somewhat more expensive with little gain in sensitivity over that obtained from simpler devices.

Another detector based on refractive index change is the thermal lens detector. When a laser is focused on an absorbing substance, the refractive index may be affected in such a way that the medium behaves as a lens. This effect was first reported by Gorden et al. [4]. Ther-

mal lens formation results from the absorption of laser light, which may be extremely weak. The excited-state molecules subsequently decay back to ground state and, as a result, localized temperature increases occur in the sample. Because the refractive index of the medium depends on the temperature, the resulting spatial variation of refractive index produces an effect which appears equivalent to the formation of a lens within the medium. The temperature coefficient of refractive index is, for most liquids, negative; consequently, the insertion of a liquid in the laser beam produces a concave lens that results in beam divergence.

The thermal lens effect has been used for LC detection with a small-volume sensor cell. Basically, it consists of a *heating* laser, the light from which is passed directly through the sample, and another laser which passes light through the cell in the opposite direction. When an absorbing solute arrives in the cell, a thermal lens is produced that causes the probe light to diverge and, consequently, the intensity of the light falling on a photocell is reduced. The cell can be made a few microliters in volume and would thus be suitable for use with microbore columns. A sensitivity of 10^{-6} AU is claimed with a linear dynamic range of about three orders of magnitude. The use of two lasers adds significantly to the cost of the device. Basically, as the thermal lens detector is a special form of the refractive index detector, it can be considered as a type of universal detector. However, like other RI detectors, it cannot be used with gradient elution or flow programming

and its sensitivity is no better than, if as good as, other refractive index detectors.

The refractive index detectors are very versatile in that they can detect all substances that have a different refractive index than that of the mobile phase. However, they are also one of the least sensitive detectors ($\sim 1 \times 10^{-6}$ g/mL); they have a linear dynamic range of about two to three orders of magnitude. They are extremely sensitive to flow rate, temperature, and pressure changes and cannot be used with gradient elution. Nevertheless, they are very popular for the detection of certain classes of compounds.

References

1. A. Tiselius and D. Claesson, *Ark. Kem. Mineral. Geol.* 15B(18) (1942).
2. C. Christiansen, *Ann. Phys. Chem.* 3: 298 (1884).
3. M. Bakken and V. J. Stenberg, *J. Chromatogr. Sci.* 9: 603 (1971).
4. J. P. Gorden, R. C. C. Leite, R. S. Moore, S. P. S. Posto, and J. R. Whinnery, *Bull. Am. Phys. Soc.* 9(2): 501 (1964).

Suggested Further Reading

Scott, R. P. W., *Liquid Chromatography for the Analyst*, Marcel Dekker, Inc., New York, 1994.
Scott, R. P. W., *Chromatographic Detectors*, Marcel Dekker, Inc., New York, 1996.



Resin Microspheres as Stationary Phase for Liquid Ligand Exchange Chromatography

Zhikuan Chai

Chinese Academy of Sciences, Beijing, People's Republic of China

INTRODUCTION

Among the separation modes of liquid chromatography, ligand exchange chromatography (LEC) is a particularly useful technique in many applications:

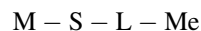
1. Chiral separation of optical isomers in chiral ligand exchange chromatography (CLEC).^[1] In this method, complexes of transition metal ions and enantiomeric molecules are formed. Chiral separation is a result of the differences between the free energies of the intermediate diastereomeric complexes formed. For the separation to be successful, the sample molecule must have two polar functional groups with the correct spacing, which can simultaneously act as ligand for the divalent transition metal ion. For this reason, the underivatized racemic amino acids with their amino and carboxyl groups and other similar compounds, such as amino alcohols, hydroxy acids, and diamines, can be resolved with CLEC. Chiral separation of racemic drugs is required by the pharmaceutical industry because different optical forms of the drugs often play different roles in their pharmacological action, metabolism, and toxicity. Chiral ligand exchange chromatography plays an important role in this respect.^[2]
2. Affinity separation of proteins in immobilized metal ion affinity chromatography (IMAC).^[3] The method is based on the fact that some protein molecules, having specific residues on the surface, can form complexes with metal ions immobilized on the sorbent matrix. Retention is determined by the coordination interactions forming the complexes. Immobilized metal ion affinity chromatography can be performed under very mild, nondenaturing conditions with extremely high selectivity; it is particularly suitable for preparative group fractionation of complex extracts and bio-fluids.
3. Separation of organic compounds capable of complexing with transition metal ions through N, S, O, and π -electrons in the molecule. The separation mechanism is similar to IMAC. With its high selectivity, the sample concentration can be low, from 10^{-7} g/mL (amino acids) to 10^{-9} g/mL (fluorides).

Ligand exchange is now routinely applied to anion chromatography by using the coordination-unsaturated complex, because such a charged complex is an anion exchange group as well. The corresponding sorbent has specific anion exchange selectivity, originating from their dual capabilities: the normal anion exchange and the ligand exchange capability.^[4]

This article discusses resin microspheres as the stationary phases for LEC. As a detailed review article on the LEC stationary phases was written in 1990,^[5] attention is given here to the publications thereafter.

STATIONARY PHASES

Chiral ligand exchange chromatography can be performed either on an achiral stationary phase with a chiral mobile phase or on a chiral stationary phase; IMAC is performed on the metal ion immobilized stationary phase. The latter two stationary phases may be symbolized by the same formula as



where M is the matrix, S the spacer, L the ligand, and Me the metal ion.

The base matrices are divided into two groups. The inorganic matrices are based on silica or zirconia, on which the transition metal ion is complexed with the ligand bonded on the matrix. The inorganic sorbents have high column efficiency but low capacity and low chemical stability. The ligand can also be coated prior to, or during, the experiment, on the octadecylated silica (ODS) reversed phase, which presents the most inexpensive but efficient and selective sorbent for CLEC.

The organic matrices are based on natural or synthetic polymers. This group of stationary phases has high capacity, high chemical stability, but low column efficiency; it is promising for preparative applications.

The spacer connects the matrix with the ligand, which plays a significant role in affinity chromatography, including IMAC. The active site of a biological substance is often located deep within the molecule and the adsorbent



prepared by coupling the small ligand directly to the matrix can exhibit low capacities because of the steric interference between the matrix and the substances binding to the ligand. In these circumstances, a spacer is interposed between the matrix and the ligand to facilitate effective binding. The length of the spacer is critical. If it is too short, the spacer is ineffective and the ligand fails to bind substances in the sample. If it is too long, nonspecific effects become pronounced and reduce the selectivity of the separation. $-\text{CH}_2\text{CH}(\text{OH})\text{CH}_2-$ and $-\text{CH}_2\text{CH}(\text{OH})\text{CH}_2-\text{O}(\text{CH}_2)_4\text{O}-\text{CH}_2\text{CH}(\text{OH})\text{CH}_2-$ are the commonly used spacers in IMAC; they are obtained from reactions with epichlorohydrin and butanediol bis(glycidyl) ether, respectively. In CLEC, introducing flexible spacers improves the column efficiency by minimizing the steric constraints for the ligand exchange reactions; introducing long hydrocarbon spacers would increase the retentions of heavy amino acids. $-\text{CH}_2-$ and $-\text{CH}_2\text{CH}(\text{OH})\text{CH}_2-$ are the commonly used spacers in CLEC. Methylene groups are introduced by chloromethylation of polystyrene or by the reaction of formaldehyde with an amide. For polyacrylamide, the short spacer of methylene is not stable under acidic and basic conditions, causing significant ligand leakage. The epoxy spacer may influence the elution order of the enantiomers by complexing of the hydroxyl group in the N-substituent of the ligand amino acid with the central metal ion in CLEC.

In CLEC, the ligand is a chiral selector. Out of 35 amino acids tested, the bidentate ligands L-proline and L-hydroxyproline were shown to be the best chiral chelating ligands: Almost all racemic amino acids could be easily and completely resolved into enantiomers on the L-hydroxyproline-modified polystyrene resin with aqueous ammonia solutions as the eluent. The tridentate ligand iminodiacetic acid (IDA) is most widely used in IMAC. The others are aminosalicylic acid, 8-hydroxyquilonine (8HQ), carboxymethylated amino acids, and ethylenediaminetetraacetic acid (EDTA). The ligand content ranges from 10^{-5} to 10^{-3} mol/g of sorbent. It was found that monomeric ligands bonded onto the matrix were less stable, while the polymeric ligands, such as L-proline grafted polystyrene, were stable, even at elevated temperatures.

Depending on the analytes, a variety of transition metal ions are adopted for LEC. For instance, Cu(II), Ni(II), Zn(II), Cd(II), Ag(I), and Hg(II) are chosen for N- and S-containing analytes, Ca(II), Mg(II), Mn(II), Fe(III), Al(III), Ti(IV), and Zr(IV) for O-containing analytes, and Ag(I) and Hg(II) for π -electron-containing analytes. For this reason, Cu(II) is commonly used in CLEC of racemic amino acids, while Cu(II), Zn(II), and Fe(III) are used in IMAC for histidine and tryptophan residues and phosphate residues containing proteins, respectively.

RESIN MICROSPHERE STATIONARY PHASES

Polystyrene

Polystyrene (PS) is of primary importance to LEC. The first LEC experiments were performed with PS beads. In 1961, the Cu(II) form of Chelex 100, a PS resin containing the strongly complexing IDA groupings, was used to selectively isolate the whole range of amino acids from sea water. In 1971, a PS resin modified with L-proline and complexed with Cu(II) was used to separate amino acid racemates. The experimental conditions (pH, ionic strength of the mobile phase, organic modifier, temperature), elution order of enantiomers, and ligands for CLEC were studied with the PS column. It was found that, on the PS- CH_2 -L-proline or L-hydroxyproline-Cu(II) column, almost all the L-amino acids eluted ahead of the D-acids, except for the tridentate amino acids histidine, allo-hydroxyproline, aspartic acid, and glutamic acid. Recently, the PS-IDA-Cu(II) particles were used for the separation of aromatic amines with methanol/ammonia as the eluent.^[6]

Macronet isoporous PS is a polymer in which pores are formed as a result of homogeneously crosslinking by rigid bridges among linear macromolecules. High ligand loading and high exchange rate are the characteristics of the sorbent. For instance, the matrix containing 11 mol% of crosslinks of diphenylmethane could have a ligand loading capacity of 2.78 mmol/g of dry resin and, as shown in Fig. 1, a glass microcolumn (100 mm \times 1 mm I.D.) filled with 5–10 μm microparticles of the polymer with ligand (*R*)-*N,N'*-dibenzyl-1,2-propanediamine could have a column efficiency of 3500 theoretical plates, enabling complete resolution of a mixture of three racemic amino acids into six components under isocratic conditions.^[7]

If PS is grafted onto the benzene ring with hydrophobic groups such as *n*- or *tert*-butyl, cyclohexyl, cyclohexylpropyl at the ortho-position of the chiral ligand, the hydrophobic interaction between the group and the enantiomeric molecule influences the stability of the intermediate diastereomeric complex. An increased enantioselectivity with respect to most amino acids was observed for the modified sorbent containing the cyclohexylpropyl group. Thus, modification of polymer skeletons may increase the enantioselectivity in racemate chromatography, as in the case with amino acids containing hydrophobic α -radicals.

The LEC experiment can be performed on ion exchange resins. Sulfonated PS beads were used to absorb the transition metal cation ions. The beads of low crosslinking (4–8% divinylbenzene) gave narrow and more symmetric chromatographic peaks. A variety of cations, from +1 to +4 valency, were loaded onto the resin; numerous compounds such as phenols, alcohols, sugars, nucleic

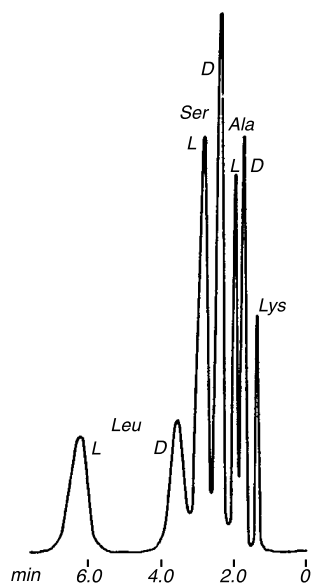


Fig. 1 Chromatogram of a mixture of racemic lysine (Lys), alanine (Ala), serine (Ser), and leucine (Leu) on a glass microcolumn (100 mm \times 1 mm I.D.) packed with the chiral diamine resin. Eluent: 0.25 M sodium acetate + 1.5×10^{-3} M copper (II) acetate, pH 5.2, flow rate 1 mL/hr, room temperature. Attention: The elution time runs from right to left and lysine is not resolved. (From Ref. [7].)

acids, aromatic acids, sulfur-containing compounds, β -diketones, amine bases, aromatic amines, pyridine derivatives, ethanolamines, aziridines, alkylhydrozines, aliphatic diamines, and unsaturated esters were separated. For instance, the Pb(II) form of Aminex HPX-87P, the Bio-Rad sulfonated PS gel, was used for qualitative and quantitative carbohydrate analysis of fermentation substrates and broths at 85°C with water as the mobile phase; glucose, xylose, galactose, arabinose, and mannose were separated.^[8] Phosphorylated PS was used in place of sulfonated PS in LEC because the cation ion exchanger gave similar results but retained metal ions more strongly.

An optically active and electroconductive polymeric sorbent was prepared by coating the PS-L-proline-Cu(II) beads with conducting polymer polypyrrole. Applying a potential difference of ± 1.5 V to the column, racemic lysine and aspartic acid were separated according to their charge characteristics and were simultaneously resolved with respect to their optical isomerism.^[9]

Polyacrylamide

Contrary to PS, polyacrylamide is a hydrophilic polymer. This may increase the ligand exchange rate, i.e., the column efficiency. Thus on the polyacrylamide-CH₂-L-proline-Cu(II) macroporous microspheres, the enan-

tiomers of valine, threonine, isoleucine, serine, phenylalanine, tyrosine, tryptophan, and asparagine were completely resolved in less than 1 hr with water as the eluent. The efficiency was markedly improved. However, the methylene bridge between the ligand and the matrix was not stable under acidic and basic conditions. The same sorbent, but with a long spacer, -CH₂CH₂OCH₂-CH(OH)CH₂-, was prepared with L-proline content 1.76 mmol/g of dry polymer.^[10] When the polymer was soaked in 0.1 M HCl, 0.1 M NaOH or 1 M NH₃, aqueous solutions, respectively, at room temperature for 1 week, the nitrogen content and Cu(II) capacity of the polymer did not change, indicating that the polymer was stable under moderately acidic and basic conditions. The new sorbent had high enantioselectivity for racemic amino acids.

Polyarylamide beads were also used for IMAC. The Biogel P200-glut-thio-Pt(II) beads were used for separation of biotin-labeled bovine serum albumin (BSA) from their unlabeled counterpart,^[11] where Biogel P200 is a commercial product of polyacrylamide, glut-glutaraldehyde, thio-thiourea. At pH 4.8, 73% of BSA-biotin was bound. A 1.0 M imidazole-HCl solution, at pH 7, was successfully used to elute the bound BSA-biotin, indicating that binding to immobilized Pt(II) was reversible.

Acrylic Polymer

Separon is a commercial product of poly(hydroxyethyl methacrylate) (PHEMA) resin microspheres. The glycidyl Separon was reacted with L-proline to obtain the chiral sorbent Separon-epoxy-L-proline-Cu(II). The copper content of the resin was 0.3 mmol/g, which probably corresponded to the content of L-proline fixed ligand. The CLEC results showed high enantioselectivities for amino acids with aqueous ammonium carbonate as the eluent and were in good qualitative agreement with the result obtained on a silica gel sorbent having similar chiral ligands. All the sorbents retained the L-enantiomers of amino acids more strongly, the only exception being proline, for which the elution of the L-isomer preceded that of the D-isomer.

Recently, PHEMA microspheres have been more and more extensively used for IMAC. Separon-IDA-Fe(III) or Cu(II) was prepared. It was found that Cu(II) interacted preferentially with histidine and tryptophan residues, while Fe(III) preferred phosphate residues, as demonstrated by the separation of lysozyme, ribonuclease A, myoglobin, and transferrin on the Cu(II) column and ovalbumin on the Fe(III) column, respectively.^[12] The PHEMA-Congo Red-Cu(II) and PHEMA-Cibacron Blue F3GA-Zn(II) microspheres were applied for adsorption of BSA.^[13] Without incorporating the metal ions, the dyed sorbents were already good stationary phases for affinity chromatography. As shown in Fig. 2, the addi-

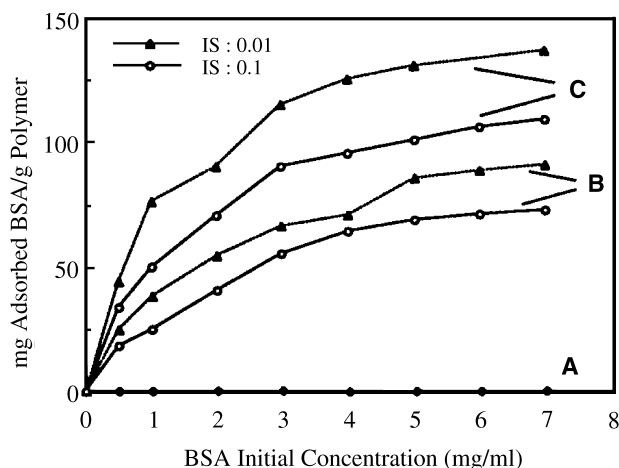


Fig. 2 Bovine serum albumin adsorption on microbeads at two different ionic strength (IS): (A) plain poly(hydroxyethyl methacrylate) (PHEMA); (B) Congo Red-derivatized PHEMA; (C) Congo Red-Cu(II)-derivatized PHEMA. (From Ref. [13].)

tional adsorption was attributed to metal–protein complexation, while the nonspecific BSA adsorption on the pure polymer was almost zero.

The weak cation exchange resin can also be used for LEC. Poly(acrylic-methacrylic acid)-type of carboxylic cation exchanger was loaded with blue-green Ni(II)–ammonia complex cations. A diamine, 1,3-diamino-2-hydroxypropane, in a dilute aqueous solution (0.001 M) which also contained a 100-fold excess of ammonia, was absorbed on the column and recovered as a sharp effluent band of high concentration (up to 40% w/v) by passing concentrated aqueous ammonia through the column. The weak ion exchanger retained the transition metals stronger and showed higher efficiency in chromatography of aromatic solutes than the sulfonated PS-type sorbent.

Hydroxylated Polyether

TSK PW is a hydrophilic polymer gel containing the group $-\text{CH}_2\text{CH}(\text{OH})\text{CH}_2\text{O}-$ as the main constituent component, which can be readily activated and chemically modified. Other features are high porosity, low specificity in adsorption, high mechanical strength, and chemical stability at pH 2–12. L-Phenylalanine, L-tryptophan, and L-histidine were grafted through epichlorohydrin onto the gel; the Cu(II) form resin was used to resolve neutral, acidic, and aromatic amino acids with fairly good column efficiency.

TSK 5PW–IDA–Cu(II) microspheres (maximum copper loading 18.5 $\mu\text{mol/mL}$ of packed gel) were used for equilibrium binding of histidine-containing cytochrome c in IMAC.^[14] TSK 5PW–IDA–Zr(IV) microspheres (IDA

content 20 $\mu\text{mol/mL}$ of packed gel) were used for the separation of phenols and carboxylic acids. The sorbent was studied as a model to obtain some insight into the retentions on zirconia.^[15]

Hydrophilic Vinyl Polymer

TSK Toyopearl is a spherical porous hydrophilic vinyl polymer; it is generally thought that the polymer is poly(vinyl alcohol). TSK Toyopearl–IDA–Zr(IV) microspheres (IDA content 33 $\mu\text{mol/mL}$ gel) were prepared for the separation and preconcentration of fluoride at ng/mL level in a flow system.^[16]

The amino-functionalized TSK Toyopearl was further modified as bis(2-pyridylmethyl)-aminated polymer (bpa-P, bpa content 0.43 mmol/g). As the bis(2-pyridylmethyl) amino (bpa) group is a tridentate ligand, and the preferable coordination number of Cu(II) is 4, the formed complex is a charged complex anion exchange group and acts not only as a simple ion exchange group but also as a ligand exchange group originating from its Lewis acidity. The sorbent, thus, showed a special anion exchange property in ion chromatography. Asahipak ODP is an octadecylated poly(vinyl alcohol) porous beads for reversed phase chromatography. When *N,N*-bis(2-pyridylmethyl)octadecylamine was coated onto the polymer (bpa-ODP, bpa content

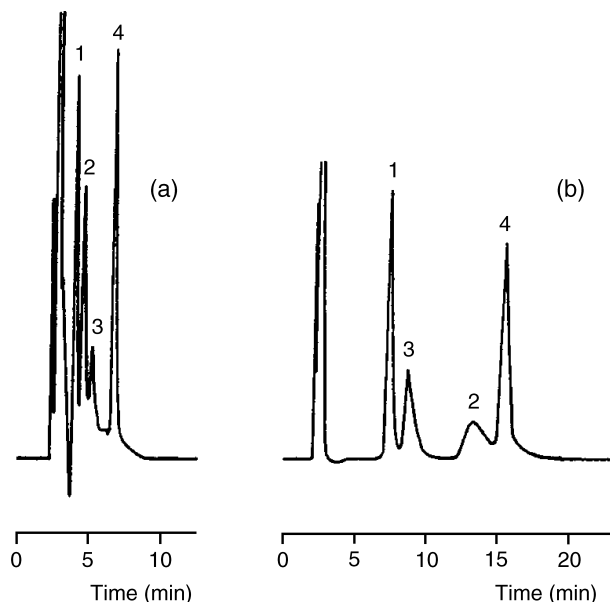


Fig. 3 Typical chromatograms of mixed sample containing (1) chloride, (2) bromide, (3) nitrate, and (4) sulfate. Anion-exchange groups (a) $\text{H}(\text{bpa-ODP})^+$ and (b) $\text{Cd}(\text{bpa-ODP})_2^{2+}$ are from the bpa-ODP, protonated, and complexed with Cd(II), respectively. Bpa-ODP is *N,N*-bis(2-pyridylmethyl)octadecylamine-coated octadecylated poly(vinyl alcohol). Eluent: 5 mmol/L benzenesulfonate (pH 5.0). (From Ref. [4].)

15.2 $\mu\text{mol/mL}$) for anion chromatography, the column efficiency was greatly improved, as shown in Fig. 3.^[4]

Polyvinylamine

L-Proline was grafted onto the hydrophilic polymer via epichlorohydrin; the Cu(II) form resin was used for the CLEC separation of racemic phenylalanine, histidine, and tryptophan.^[17]

Urea–Formaldehyde Resin

Urea–formaldehyde resin (UF) is a hydrophilic condensation polymer. The UF monosized nonporous microspheres were prepared with (+) L-2-amino-5-ureido-

pentanoic acid as the chiral ligand. The microspheres exhibited exceptional mechanical strength, chemical stability in the pH range 1–13, and low tendency toward swelling in solvents; they were used for the CLEC separation of amino acids.^[18] Later, the porous UF microspheres were also prepared and L-proline was grafted via epichlorohydrin onto the polymer (L-proline content 0.28 mmol/g). Eighteen D,L-amino acids were resolved on the sorbent with aqueous ammonia containing 30% acetoni-trile; all the D-acids eluted first, except for proline.^[19]

Polysaccharides

Polysaccharides are natural polymers including agarose, dextran, cellulose, and guaran.

Table 1 LEC on resin microspheres since 1990

Polymer matrix	Ligand	Metal ion	Analyte	Ref.
<i>1. CLEC</i>				
Polypyrrole-coated PS	L-proline	Cu(II)	Amino acids	[9]
Polyacrylamide with a long spacer	L-proline	Cu(II)	Amino acids	[10]
Polyvinylamine	L-proline	Cu(II)	Amino acids	[17]
UF	(+)L-2-amino-5-ureidopentanoic acid	Cu(II)	Amino acids	[18]
UF	L-proline	Cu(II)	Amino acids	[19]
Guaran	Borate		Mandelic acid	[22]
<i>2. IMAC</i>				
Polyacrylamide (Biogel P200)	Glut-thio	Pt(II)	Biotin labeled BSA	[11]
PHEMA (Separon)	IDA	Cu(II)	Lysozyme, ribonuclease A, myoglobin, transferrin	[12]
PHEMA (Separon)	IDA	Fe(III)	Ovalbumin	[12]
PHEMA	Congo red	Cu(II)	BSA	[13]
PHEMA	Cibacron blue F3GA	Zn(II)	BSA	[13]
Hydroxylated polyether (TSK PW)	IDA	Cu(II)	Cytochrome <i>c</i>	[14]
Sepharose	IDA	Cu(II)	Ovalbumin, lysozyme, LDH	[20]
Sepharose	OPS or 8HQ	Fe(III)	Cytochrome <i>c</i> , myoglobin	[21]
<i>3. Other LEC</i>				
PS	IDA	Cu(II)	Aromatic amines	[6]
Sulfonated PS		Pb(II)	Carbohydrate	[8]
Hydroxylated polyether (TSK PW)	IDA	Zr(IV)	Phenols, carboxylic acids	[15]
Hydrophilic vinyl polymer (TSK Toyopearl)	IDA	Zr(IV)	Fluoride	[16]
Hydrophilic vinyl polymer (TSK Toyopearl)	Bpa	Cu(II)	Anion	[4]
Bpa-coated octadecylated poly(vinyl alcohol) (Asahipak ODP-50)	Bpa	Cu(II)	Anion	[4]

PS—polystyrene; UF—urea–formaldehyde resin; glut—glutaraldehyde; thio—thiourea; BSA—bovine serum albumin; PHEMA—poly(hydroxyethyl methacrylate); IDA—iminodiacetic acid; LDH—lactate dehydrogenase; OPS—*o*-phosphoserine; 8HQ—8-hydroxyquinoline; Bpa—bis(2-pyridyl-methyl) amine.

Sephacrose, a commercial product of agarose, is widely used as a good sorbent for IMAC. This is because agarose has a high permeability to large protein molecules and there are no hydrophobic or electrostatically charged groups in the chemical structure. Sepharose-epoxy-IDA-transition metal ion is the standard structure as the sorbent for IMAC. Recently, ovalbumin, lysozyme, and lactate dehydrogenase (LDH) were purified using the Cu(II) form column. The experiments were run in displacement mode with a synthetic copolymer of vinyl imidazole and vinyl caprolactam as the displacer. Vinyl caprolactam renders the copolymer with thermo-sensitivity, i.e., a property of the copolymer to precipitate nearly quantitatively from aqueous solution on increase of the temperature to 48°C. For the first time, it was clearly demonstrated that a polymer displacer was more efficient than a monomeric displacer (imidazole) of the same chemical nature, probably because of the multipoint interaction of imidazole groups within the same macromolecule with one Cu(II) ion.^[20] Besides, Sepharose-*o*-phosphoserine (OPS, OPS content 0.40 mmol/g of dry gel) or 8-hydroxyquinoline (8HQ, 8HQ content 0.52 mmol/g) resins were prepared. The 8HQ-Fe(III) resin had a higher capacity for tuna heart cytochrome *c* than the 8HQ-Al(III) or -Yb(III) resins, while the 8HQ-Cu(II) and 8HQ-Ca(II) resins did not bind this protein. The equivalent IDA chelates showed no binding either. The OPS-Fe(III) resin bound tuna heart cytochrome *c* and horse myoglobin but did not bind hen egg white lysozyme.^[21]

Sephadex is a commercial product of dextran. The polymer in Cu(II) form was employed for group separation of amino acids and proteins. Carboxymethylated dextran gel was found useful as a sorbent for LEC of enzymes.

Carboxymethyl-, diethylaminoethyl (DEAE)-, *p*-aminobenzyl-, and phosphate-cellulose, in combination with antimony, cobalt, mercury, and silver ions, were employed in LEC for separation of amines in organic solvents.

Guaran is a polygalactomannan containing *cis*-OH groups. It is well known that the tetrahedral borate ions readily form tetrahedral complexes with the *cis*-OH groups. Thus the borate immobilized polymer (boron content 0.7 mmol/g) was used for enantioseparation of racemates such as 1,2- or 1,3-dihydroxy compounds or α -hydroxy acids.^[22] This appears to be the first example of the use of boron as a complexing ion in CLEC.

Glucosamine Polymer

Chitosan is a natural glucosamine polymer obtained from crab shells. The polymer retains Cu(II) more strongly than does cellulose. It was used in LEC of amino acids, peptides, and enzymes.

CONCLUSION

Table 1 summarizes the LEC studies since 1990. As a stationary phases for CLEC, the weakness of resin microspheres is in their low column efficiencies. The study of polypyrrole-coated polystyrene microspheres presented an effort to overcome the weakness, where a second electrokinetic interaction was added in addition to the coordination interaction. A high protein adsorption is always needed as a stationary phase for IMAC. The study of PHEMA microspheres modified with dye plus metal ion was interesting, where the protein adsorption was greatly increased by metal complexation plus dye affinity.

ACKNOWLEDGMENT

The author is grateful to NSFC for the grant 29635010.

REFERENCES

1. Davankov, V.A. 30 years of chiral ligand exchange. *Enantiomer* **2000**, *5*, 209–223.
2. Subert, J. Progress in the separation of enantiomers of chiral drugs by high performance liquid chromatography without their prior derivatization. *Pharmazie* **1994**, *49*, 3–13.
3. Porath, J. Immobilized metal ion affinity chromatography. *Protein Expr. Purif.* **1992**, *3*, 263–281.
4. Hiroshima, N.; Umehara, W.; Makizawa, H.; Honjo, T. Ion chromatography using a charged complex anion-exchange group. *Anal. Chim. Acta* **2000**, *409*, 17–26.
5. Davankov, V.A. Packings in Ligand Exchange Chromatography. In *Packings and Stationary Phases in Chromatographic Techniques*; Unger, K.K., Ed.; Marcel Dekker: New York, 1990, Chapter 9.
6. Liu, Y.; Yu, S. Copper(II)-iminodiacetic acid chelating resin as a stationary phase in the immobilized metal ion affinity chromatography of some aromatic amines. *J. Chromatogr.* **1990**, *515*, 169–173.
7. Davankov, V.A.; Kurganov, A.A. High-performance ligand chromatography of α -amino acids on a polystyrene resin with fixed ligands of the type (*R*)-*N,N'*-dibenzyl-1,2-propanediamine. *Chromatographia* **1980**, *13*, 339–341.
8. Marko-Varga, G.; Buttler, T.; Gorton, L.; Olsson, L.; Durand, G.; Barcelo, D. Qualitative and quantitative carbohydrate analysis of fermentation substrates and broths by ligand chromatographic techniques. *J. Chromatogr., A* **1994**, *665*, 317–332.
9. Lee, H.S.; Hong, J. Chiral and electrokinetic separation of amino acids using polypyrrole-coated adsorbents. *J. Chromatogr., A* **2000**, *868*, 189–196.
10. Yan, H.; Cheng, X.; Ni, A.; He, B. Resolution of amino acid enantiomers by ligand exchange chromatography on a new chiral packing. *J. Liq. Chromatogr.* **1993**, *16*, 1045–1055.
11. Miles, D.; Garcia, A.A. Separation of biotin labeled proteins

- from their counterparts using immobilized platinum(II) affinity chromatography. *J. Chromatogr., A* **1995**, *702*, 173–189.
12. Coupek, J.; Vins, I. Hydroxyethyl methacrylate-based sorbents for high performance liquid chromatography of proteins. *J. Chromatogr., A* **1994**, *658*, 391–398.
 13. Denizli, A.; Salin, B.; Piskin, E. Congo red and Cu(II) carrying poly(ethylene glycol dimethacrylate-hydroxyethyl methacrylate) microbeads as specific sorbents. Albumin adsorption/desorption. *J. Chromatogr., A* **1996**, *731*, 57–63.
 14. Todd, R.J.; Johnson, R.D.; Arnold, F.H. Multiple-site binding interactions in metal-affinity chromatography: I. Equilibrium binding of engineered histidine-containing cytochrome-*c*. *J. Chromatogr., A* **1994**, *662*, 13–26.
 15. Yuchi, A.; Mizuno, Y.; Yonemoto, T. Ligand-exchange chromatography at zirconium(IV) immobilized on iminodiacetic acid-type chelating polymer gel. *Anal. Chem.* **2000**, *72*, 3642–3646.
 16. Yuchi, A.; Matsunaga, K.; Niwa, T.; Terao, H.; Wada, H. Separation and preconcentration of fluoride at ng/ml level with a polymer complex of zirconium (IV) followed by potentiometric determination in a flow system. *Anal. Chim. Acta* **1999**, *388*, 201–208.
 17. Yuan, Z.; He, B. Preparation of polyvinylamine ligand exchange resin grafted with L-proline. *Chin. Sci. Bull.* **1991**, *36*, 903–906.
 18. Sinibaldi, M.; Castellani, L.; Federivi, F.; Messina, A.; Girrell, A.M.; Lentini, A.; Tesarova, E. New organic monosized microspheres for use in enantiomer separations by high performance liquid chromatography. *J. Liq. Chromatogr.* **1995**, *18*, 3187–3203.
 19. Chai, Z.; Zheng, X.; Sun, X. Urea–formaldehyde resin microspheres as a new packing material for liquid chromatography: Ligand exchange. *J. Liq. Chromatogr. Relat. Technol.* **2002**, *25*, 69–81.
 20. Arvidsson, P.; Ivanov, A.E.; Galaev, I.Y.; Mattiasson, B. Polymer versus monomer as displacer in immobilized metal ion affinity chromatography. *J. Chromatogr., B* **2001**, *753*, 279–285.
 21. Zacharion, M.; Traverso, I.; Hearn, M.T.W. High-performance liquid chromatography of amino acids, peptides and proteins: CXXXI. *o*-Phosphoserine as a new chelating ligand for use with hard Lewis metal ions in the immobilized-metal affinity chromatography of proteins. *J. Chromatogr.* **1993**, *646*, 107–120.
 22. Mathur, R.; Bohra, S.; Mathur, V.; Narang, C.K.; Mathur, N.K. Chiral ligand exchange chromatography on polyglactomannan (guaran). *Chromatographia* **1992**, *33*, 336–338.



Resolution in HPLC: Selectivity, Efficiency, and Capacity

J.E. Haky

Florida Atlantic University, Boca Raton, Florida, U.S.A.

Introduction

Liquid chromatography involves the analysis of mixtures. The goal of such an analysis is to achieve the greatest possible separation of the components in the mixture in the least amount of time. If performed successfully, the resulting chromatogram can be employed to obtain precise and accurate data describing the concentrations of the components in the mixture being analyzed.

Discussion

The degree of separation of components of a mixture by a liquid chromatographic method is reflected in the resulting chromatogram. For best analytical results, peaks in the chromatogram must be completely resolved from each other, with little or no overlap. The degree of separation of between adjacent chromatographic peaks is a function of the distance between peak maxima and their corresponding peak widths. For Gaussian peaks, this is adequately described by the peak resolution, R_s , defined as the ratio between the difference in the retention times t_1 and t_2 , of two peaks and the average of the widths, W_1 and W_2 , of the two peaks at their baselines, as shown by

$$R_s = \frac{t_2 - t_1}{0.5(W_1 + W_2)} \quad (1)$$

A resolution of $R_s = 1$ corresponds to about a 4% overlap of two adjacent peaks and is adequate for many chromatographic analyses. Baseline resolution occurs at R_s values of 1.5 or higher [1].

As shown by Eq. (1), the resolution of components in a liquid chromatographic separation is dependent on (1) their relative retention on a particular chromatographic system and (2) their peak widths. To optimize these parameters for maximum resolution, a clear understanding of their nature and the factors that affect them is necessary. Although the retention time of a component adequately describes the amount of time a particular solute takes to elute from a chromatographic system, a more useful parameter describ-

ing chromatographic retention is the capacity factor k . This parameter is defined as the ratio of time spent by a solute in the stationary phase to the time it spends in the mobile phase. It can be calculated by Eq. (2), where t_R is the retention time of the peak of interest and t_0 (the "dead-volume time") is the retention time of a solute that is known not to interact with the stationary phase:

$$k = \frac{t_R - t_0}{t_0} \quad (2)$$

Additionally, the relative retention of two peaks in a chromatogram may be defined by the selectivity factor, α , defined by Eq. (3), where k_1 and k_2 are capacity factors of the early- and late-eluting peaks, respectively:

$$\alpha = \frac{k_2}{k_1} \quad (3)$$

The widths of chromatographic peaks are dependent on the degree to which a band of solute molecules spreads out, over the time it spends passing through a chromatographic system. This band spreading is best defined in terms of theoretical plates, N , which can be calculated from Eq. (4), where t_R and W are the retention time and width of the peak of interest, respectively:

$$N = 16 \left(\frac{t_R}{W} \right)^2 \quad (4)$$

Higher values of N correspond to lower degrees of band broadening and narrower peaks. On this basis, theoretical plates can be described as a measure of the efficiency of a given chromatographic system [2].

Chromatographic resolution of any two components in a mixture is dependent on three factors: (1) the overall efficiency of the chromatographic system, as described by the number of theoretical plates N , (2) the inherent selectivity of the system, described by the selectivity factor α , and (3) the degree of retention of each of the components, described by their capacity factors k . For two peaks having approximately equal widths, capacity factors of k_1 and k_2 , and a mean theoretical plate number N , the following quantitative



relationship can be derived between chromatographic resolution and these parameters [3]:

$$R_s = \left(\frac{N^{1/2}}{4} \right) \left(\frac{\alpha - 1}{\alpha} \right) \left(\frac{k_2}{1 + k_2} \right) \quad (5)$$

To a first approximation, each of the terms in Eq. (5) can be treated as independent of each other. Therefore, in the development of a liquid chromatographic method for analysis or isolation of the components of any mixture, experimental conditions can be varied to modify each of these three terms to maximize resolution.

Analysis of Eq. (5) indicates that resolution increases with the square root of the number of theoretical plates in the chromatographic system. Thus, a fourfold increase in N is required to increase the resolution by a factor of 2. Experimentally, N may be increased most directly by (1) increasing the length of the column, (2) reducing the size of the particles of the stationary phase, or (3) using a mobile phase of lower viscosity. However, in modern analytical liquid chromatography, most of these options are impractical for the following reasons: (1) Increasing the length of the column can increase system back-pressures and the time required to complete the separation to unworkably high levels. (2) Stationary phases with particle sizes below $3 \mu\text{m}$ are not generally available, owing to excessively high system back-pressures they can cause and their short lifetimes. (3) Because most recommended mobile phases for liquid chromatographic separations are those with low viscosity, there are few alternative mobile phases with lower viscosity available.

For these reasons, attempting to improve resolution by increasing the number of theoretical plates in the chromatographic system is not generally recommended as a first choice in liquid chromatographic method development. Nevertheless, the effect of theoretical plates on overall resolution is important to consider in certain situations, such as in the scaling up of an analytical method to a preparative method, when stationary phases of larger particle sizes are often employed, resulting in lower values of N and poorer resolutions [1].

Adjusting the selectivity of the chromatographic system, as measured by α , is often a useful technique in improving separations in liquid chromatography. Such adjustments need to be made with consideration of the second term in Eq. (5), which is $(\alpha - 1)/\alpha$. When $\alpha = 1$, the term is equal to zero, resulting in no resolution. This indicates that the chromatographic system must exhibit some selectivity toward the components of the mixture before any separation is possible. The term

rapidly increases as α increases up to about $\alpha = 2$, beyond which only small increases are exhibited [2]. Thus, varying chromatographic conditions to obtain a selectivity factor equal or greater than 2 will often give the best resolutions.

In liquid chromatography, system selectivity can be modified by a number of techniques, including (1) changing the composition or pH of the mobile phase, (2) changing the column temperature, and (3) changing the type of stationary phase that is employed. Of these, the first method is the easiest to accomplish and is most often the first to be utilized in method development for improving selectivity.

Resolution can often be improved in liquid chromatographic separations simply by changing the retention of the components, which corresponds to changing the capacity factor k of the components to be separated. Rapid increases in the third term in Eq. (5), $k_2/(1 + k_2)$, occur as the capacity factor increases, up to $k_2 = 5$. The term increases only slowly beyond this value [2]. Therefore, in most separations by liquid chromatography, optimal resolution of mixtures occurs when each component has capacity factor values between 2 and about 10. Increasing k values to higher values results in longer analysis times with minimal improvements in resolution [2].

The effect of the capacity factor on resolution can be further exhibited by manipulation of Eq. (5) to predict the number of required theoretical plates N_{req} for a given resolution. Equation (6) enables such predictions:

$$N_{\text{req}} = 16R_s^2 \left(\frac{\alpha}{\alpha - 1} \right)^2 \left(\frac{k_2 + 1}{k_2} \right)^2 \quad (6)$$

Assuming a difficult separation of two components with $\alpha = 1.05$ and a reasonable goal of obtaining a resolution R_s of 1.0, the number of theoretical plates required at various capacity factor values can be calculated. For a capacity factor of 1.0, a minimum of 28,200 plates is required. For a capacity factor of 2.0, the required number of plates drops to 15,880. Because many liquid chromatographic systems usually do not exhibit efficiencies greater than 25,000 theoretical plates, it is evident from these calculations that developing methods for difficult separations should be performed when the capacity factors of the components to be separated are adjusted so they are all greater than 2.

In liquid chromatography, adjusting capacity factors is most often accomplished by changing the composition of the mobile phase. In reversed-phase chromatography, for example, decreasing the amount of organic component in the mobile phase (e.g., from 80% methanol, 20% water to 50% methanol, 50% water)

will generally result in lower capacity factors for all components of the mixture. Empirical models and computer software have been developed which allow the user to predict mobile-phase compositions, which will result in capacity factors of all components in a mixture to be in the optimal range of 2–10. Such programs utilize data obtained from an analysis performed using gradient elution (i.e. continuously varying mobile-phase composition throughout the separation process) [3]. In many cases, however, experimental variation of mobile-phase compositions through a trial-and-error process can be equally effective in obtaining a composition giving an optimal capacity factor range for all components.

In summary, resolution in liquid chromatography is dependent on three factors: (1) the efficiency of the chromatographic system, measured by the theoretical plate value N ; (2) the selectivity of the chromatographic system, measured by the selectivity factor α ; and (3) the degree of retention of the components on

the chromatographic system, measured by the capacity factor k . Although each of these can be independently varied to obtain acceptable separations, most method development in liquid chromatography is successfully performed through the initial choosing of the proper liquid chromatographic technique (e.g., normal phase, reversed phase, ion exchange) followed by optimizing capacity factors and system selectivity by varying the composition of the mobile phase.

References

1. L. R. Snyder and J. J. Kirkland, *Introduction to Modern Liquid Chromatography*, 2nd ed., John Wiley & Sons, New York, 1979.
2. C. F. Poole and S. K. Poole, *Chromatography Today*, Elsevier, New York, 1991, pp. 1–50.
3. L. R. Snyder, J. J. Kirkland, and J. L. Glajch, *Practical HPLC Method Development*, 2nd ed., John Wiley & Sons, New York, 1997.



Resolving Power of a Column

Raymond P.W. Scott

Scientific Detectors Ltd., Banbury, Oxfordshire, England

Introduction

Two solutes will be resolved if their peaks are moved apart in the column and maintained sufficiently narrow to permit them to be eluted as discrete peaks. Resolution is usually defined as the ratio of the distance between the peaks to the peak width at the points of inflection. It is generally accepted that a separation of 4σ is adequate for accurate quantitative analysis, particularly when employing peak heights measurements. It is, therefore, necessary to derive an expression for the peak width in order to equate to the peak separation.

Application

The plate theory gives an expression for the elution curve of a solute as

$$X_{m(n)} = \frac{X_0 e^{-v} v^n}{n!} \quad (1)$$

where $X_{m(n)}$ is the concentration of solute in the n th plate on elution, X_0 is the concentration placed on the first plate on injection, n is the number of plates in the column, and v is the flow of mobile phase in plate volumes.

By differentiating and equating Eq. (1) to zero gives the following expression for the retention volume of a solute:

$$V_r = n(v_m + Kv_s)$$

Now, by equating the second differential of the elution equation to zero and solving for v , an expression for the peak width at the points of inflexion can be obtained:

$$\begin{aligned} \frac{d^2 \left(X_0 \frac{e^{-v} v^n}{n!} \right)}{dv^2} \\ = X_0 \frac{e^{-v} v^n - e^{-v} n v^{n-1} - e^{-v} n v^{n-1} + e^{-v} n(n-1) v^{n-2}}{n!} \end{aligned}$$

Thus,

$$\frac{d^2 (X_0 (e^{-v} v^n / n!))}{dv^2} = X_0 \frac{e^{-v} v^{n-2} (v^2 - 2nv + n(n-1))}{n!} \quad (2)$$

Now, at the points of inflexion,

$$\frac{d^2 (X_0 (e^{-v} v^n / n!))}{dv^2} = 0$$

Hence,

$$v^2 - 2nv + n(n-1) = 0$$

and

$$\begin{aligned} v &= \frac{2n \pm \sqrt{4n^2 - 4n(n-1)}}{2} \\ &= \frac{2n \pm \sqrt{4n}}{2} \\ &= n \pm \sqrt{n} \end{aligned}$$

It is seen that the points of inflexion occur after $n - \sqrt{n}$ and $n + \sqrt{n}$ plate volumes of mobile phase have passed through the column. Thus, the volume of the mobile phase that has passed through the column *between* the inflexion points will be

$$n + \sqrt{n} - n + \sqrt{n} = 2\sqrt{n} \quad (3)$$

Thus, the peak width at the points of inflexion of the elution curve will be $2\sqrt{n}$ plate volumes which, in milliliters of mobile phase, will be obtained by multiplying by the *plate volume*; that is,

$$\text{Peak width} = 2\sqrt{n}(v_m + Kv_s) \quad (4)$$

The peak width at the points of inflexion of the elution curve is twice the standard deviation, and, thus, from Eq. (4), it is seen that the variance (the square of the standard deviation) is equal to n , the total number of plates in the column. Consequently, the variance of the band (σ^2) in milliliters of mobile phase is given by

$$\sigma^2 = n(v_m + Kv_s)^2$$



Now,

$$V_r = n(v_m + K v_s)$$

Thus,

$$\sigma^2 = \frac{V_r^2}{n}$$

Let the distance between the injection point and the peak maximum (the retention distance on the chromatogram) be y cm and the peak width at the points of inflexion be x cm. If the chromatographic data are computer processed, then the equivalent retention times can be used. Then, as the retention volume is $n(v_m + K v_s)$ and twice the peak standard deviation at the points of inflexion is $2\sqrt{n}(v_m + K v_s)$, then

$$\frac{\text{Ret. distance}}{\text{Peak width}} = \frac{y}{x} = \frac{n(v_m + K v_s)}{2\sqrt{n}(v_m + K v_s)} = \frac{\sqrt{n}}{2}$$

Thus,

$$n = 4\left(\frac{y}{x}\right)^2 \quad (5)$$

Equation (5) allows the efficiency of any solute peak, from any column, to be calculated from measurements taken directly from the chromatogram.

Consider the two peaks depicted in Fig. 1. The difference between the two peaks, for solutes A and B (see the entry Plate Theory), measured in volume flow of mobile phase, will be

$$n(v_m + K_B v_s) - n(v_m + K_A v_s) = n(K_B + K_A) v_s \quad (6)$$

Assuming the widths of the two peaks are the same, then the peak width in volume flow of mobile phase will be

$$2\sigma = 2\sqrt{n}(v_m + K_A v_s) \quad (7)$$

where K_A is the distribution coefficient of the first of the eluted pair of solutes between the two phases. Taking the already discussed criterion that resolution is achieved when the peak maxima of the pair of solutes are 4σ apart, then

$$4\sqrt{n}(v_m + K_A v_s) = n(K_B + K_A) v_s$$

Rearranging,

$$\sqrt{n} = \frac{4(v_m + K_A v_s)}{(K_B - K_A) v_s}$$

dividing through by v_m ,

$$\sqrt{n} = \frac{4(1 + k'_A)}{(k'_B - k'_A) v_s}$$

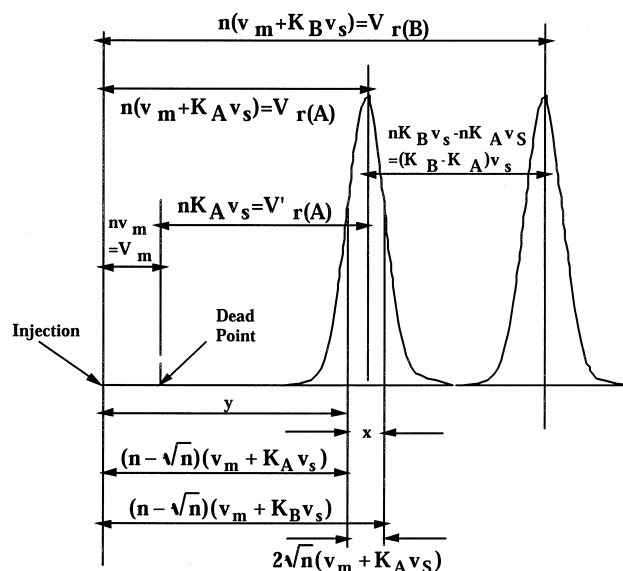


Fig. 1 A chromatogram showing two resolved solute peaks.

Now, as α , the separation ratio between the two solutes, has been defined as

$$\alpha = \frac{k'_B}{k'_A}$$

then

$$\sqrt{n} = \frac{4(1 + k'_A)}{k'_A(\alpha - 1)}$$

and

$$n = \left(\frac{4(1 + k'_A)}{k'_A(\alpha - 1)}\right)^2 = 16 \frac{(1 + k'_A)^2}{k'^2_A(\alpha - 1)^2} \quad (8)$$

Equation (8) is extremely important and was first developed by Purnell [1] in 1959. It allows the necessary efficiency to achieve a given separation to be calculated from a knowledge of the capacity factor of the first eluted peak of the pair and their separation ratio.

Reference

1. J. H. Purnell, *Nature (London)* 184 (Suppl. 26): 2009 (1959).

Suggested Further Reading

- Scott, R. P. W., *Chromatographic Detectors*, Marcel Dekker, Inc., New York, 1996.
- Scott, R. P. W., *Introduction to Analytical Gas Chromatography*, Marcel Dekker, Inc., New York, 1998.

Response Spectrum in Chromatographic Analysis

Dennis R. Jenke

Baxter Healthcare Corporation, Round Lake, Illinois, U.S.A.

INTRODUCTION

Chromatographic methods are used for a variety of purposes in real-world applications. Chromatography, in its multitude of manifestations, can be used for the purpose of scouting and discovery (i.e., to “uncover” the presence of compounds or entities in samples of unknown composition). In fact, the unique versatility of chromatography as a scouting and discovery tool is based on the almost limitless (or so it seems) combination of separation and detection strategies that can be coupled and brought to bear in investigative situations.

Once an entity has been observed to produce a chromatographic response, chromatographic procedures can be used to either characterize or identify the entity. The characterization/identification processes are facilitated by the chromatographic process, wherein both the elution and the detection properties of the entity provide information that can be useful for these purposes. The chromatographic methods may produce information that can be used to characterize the entity, which ultimately may lead to a proposal for its identity, and/or it may be used to confirm the accuracy of a proposed entity.

Although chromatography is generally considered to be an analytical tool, it also has an important role in process chemistry as a means of isolating and/or purifying substances from complex or dilute mixtures. Preparative chromatographic methods for the generation of laboratory-scale to commercial-scale quantities of pure substances are well documented in the chemical and patent literature.

OVERVIEW

As important as are the three previously mentioned applications of chromatography (Table 1), it is accurate to observe that the primary use of chromatography is for the purpose of establishing the concentration of a known entity (analyte) in a specific sample. As few chromatographic detection strategies are absolute (i.e., their response function can be derived from first scientific principles), the quantitation process includes the characterization of the response function, where the response function is the mathematical relationship that exists between the concentration of an analyte in a standard and the response that is

produced by the chromatographic system when such a standard is processed by the chromatographic method.

As shown in Fig. 1, the entire domain or spectrum of a chromatographic method's response extends from the lowest analyte concentration that can be confirmed to reliably produce a chromatographic response (limit of detection, or LOD) to the highest analyte concentration for which an increase in concentration produces an increase in response (limit of range, or LOR). Although the nature of the response function is chromatographic method-specific (although most methods have a response function similar to that shown in Fig. 2), all share, to one degree or another, the spectral characteristics shown in Fig. 1.

It is an interesting aspect of the current state of affairs in chromatographic science that although there is nearly universal agreement among practitioners with respect to the members of the chromatographic response spectrum (e.g., the concept of all methods having a LOD is universally accepted), there is significant discussion among practitioners as to the definition of, and correct method for determining, the various response spectrum members (e.g., how do you determine LOD?). Although various scientific organizations [e.g., International Union of Pure and Applied Chemistry (IUPAC), American Chemical Society (ACS), United States Environmental Protection Agency (USEPA), and International Conference on Harmonization (ICH)] have proposed standard definitions and determination procedures for some of the members of the response spectrum, it is interesting to note that the procedures are not the same, and it is fair to say that not all investigators accept such methods as being scientifically the most valid or rigorous.

The purpose of this manuscript is to provide an overview of the chromatographic response spectrum and its various members. As a general review, it will not be complete but will strive to be comprehensive and nonjudgmental.

THE CHROMATOGRAPHIC RESPONSE SPECTRUM

The chromatographic response spectrum, illustrated in Fig. 1, establishes the boundaries of the response function and breaks the response domain into appropriate

Table 1 Application of chromatographic methods

Nature	Purpose	Desirable response characteristics
Scouting/discovery	“Find” substances present in a sample of unknown composition	Sensitive, specific, with broad scope and range, “universal” response
Identification or characterization	Identify or characterize substance(s) that produce chromatographic responses	Sensitive, specific, “information-rich”
Isolation/purification	Separate a substance from all others in a complex mixture	Sufficient selectivity and specificity
Quantification	Determine the concentration at which a substance is present in a sample	Accurate, precise, specific, sensitive, “universal” response, known response function

categories and regions. The spectrum begins at the lowest analyte concentration that reproducibly produces a discernible analyte response (LOD) and ends at the highest analyte concentration that produces a response that is discernibly different from the response produced at a lower analyte concentration (LOR). Between the LOD and the LOR are the limit of identification (LOI; the lowest analyte concentration at which the identity of an analyte can be confirmed), the limit of quantitation (LOQ; the lowest analyte concentration at which assay performance meets various standards of accuracy and precision), and the limit of linear range (LOLR; the highest concentration at which the response function is best described by a linear model). Between these limits are various regions of the response spectrum, including the following:

- Not detected: Either no response or a response less than that of the LOD.
- Detected, not identified: Response between the LOD and the LOI.
- Detected, identified: Response between the LOI and the LOQ.
- Linear dynamic range: Range of analyte concentrations over which the relationship between the analyte concen-

tration and the method response can be described by a linear model of the form

$$\text{response} = \text{slope}(\text{concentration}) + \text{intercept}.$$

Dynamic range: Range of analyte concentrations over which the relationship between the analyte concentration and the method response can be described by a mathematical model of the form:

$$\text{response} = \text{function}(\text{concentration})$$

Out of range: Response is not related to the concentration of the analyte.

THE LIMIT OF DETECTION

Definition

As with many concepts in the analytical sciences, the concept of LOD suffers from the curse of intuition. That is to say that although the concept is, on an intuitive level, clear to all practitioners of the analytical sciences, if one were to ask the practitioners to define the term and

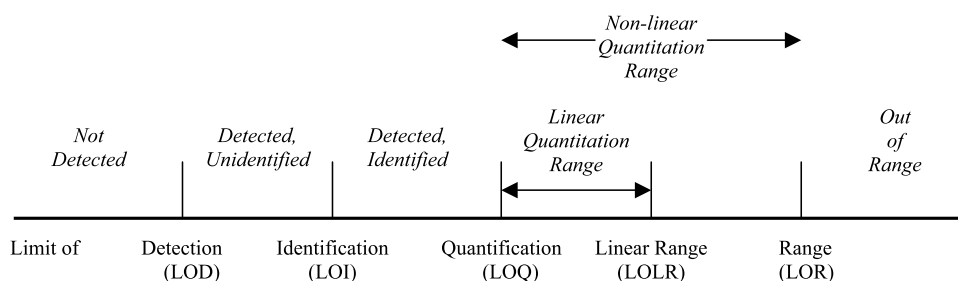


Fig. 1 The response spectrum for chromatographic analysis. The complete response spectrum extends from that analyte concentration at which a chromatographic response can be reliably confirmed to have occurred (LOD) to that concentration above which an increase in concentration no longer produces an increase in chromatographic response (LOR).



Response Spectrum in Chromatographic Analysis

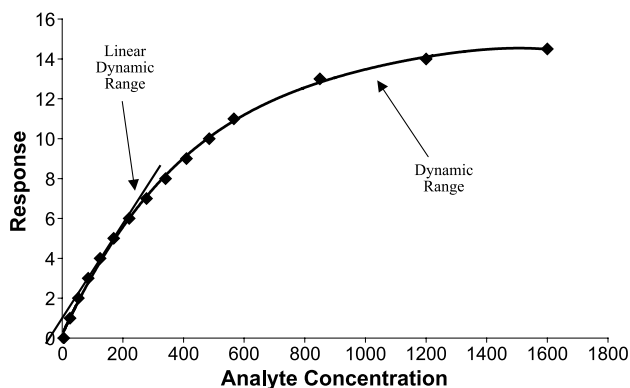


Fig. 2 Typical response function for a chromatographic method. The linear dynamic range and the dynamic range of the method are illustrated.

describe its determination, one would end up with nearly as many definitions and determination methods as there are practitioners. This is borne out in the scientific literature, which contains literally hundreds of references with the more or less general content of “my (our) definition of the LOD and how I (we) recommend you determine it” (e.g., Table 2). It is borne out by the fact that although several organizations have attempted to unify, or harmonize, the individual definitions, their own results, in fact, are not the same.

Part of the problem is that although the concept is intuitively obvious, it is sufficiently multifaceted that a concise but truly complete and rigorous definition (i.e., one that leaves all questions answered) is difficult to craft. Another part of the problem is that many definitions seek to define the term in a way that predisposes it to a certain method of determination. It is a simple statement of fact that there is a diversity of opinion on the answers to questions related to the “issues” associated with the subtle aspects of the LOD and that there are numerous mathematical methods that have been devised, which “get at” the essence of the LOD. The challenge is to draft a definition that acknowledges that these differences exist and then handles these differences not by specifying which of literally tens of candidate methods and approaches are correct but rather by requiring that the methods and approaches used be specified as part of reporting the LOD. Such a definition follows:

The LOD is the lowest concentration of a specified analyte in a sample of specified composition, determined and calculated by specified analytical and mathematical processes, that produces, with a specified consistency, a response for a specified method implemented on a specified instrument system, which one can verify, with a specified level of confidence, is different from the

response produced by a sample blank that is known not to contain the analyte.

Whether this definition is the “best” one or not, there is something “troubling” about this definition. The “problem” is that, now, it is “too complicated” to report the LOD. By this definition, it is not enough to just report a number—one must also report the context in which the number is valid. Details about the LOD required by the definition include the following:

- 1) The analyte’s identity.
- 2) Description of the test sample.
- 3) Description of the test method (e.g., mobile phase, column, flow rate, injection size, and so on).
- 4) Description of the instrumentation used.
- 5) Description of the analytical procedure used to generate the data from which the LOD was determined.
- 6) Description of the mathematical process by which the LOD was determined.

Methods of Determination

Signal to noise (graphical)

A useful characteristic of a chromatographic analysis is that it results in a pictorial record of the analysis (a chromatogram). This pictorial record can be examined and used to quantify the performance characteristics of the method (and instrument system) used. Performance characteristics useful to a determination of LOD include the magnitude of the analytical signal S for the analyte (e.g., the height of the analyte peak) and the magnitude of the variation in system response when the analyte is not eluting from the system (referred to as the system noise N). These characteristics are illustrated in Fig. 3. It is clear that a comparison of S and N provides a means of establishing detectability. Specifically, a relationship between LOD, S , N , and the analyte concentration that produced the chromatogram being examined (C) can be proposed as follows:

$$\text{LOD} = C[F(N/S)]$$

In this equation, F is a factor that literally can be interpreted as: “How much higher must the peak be than the noise in order for you to be confident that what you are calling a peak is in fact a peak and not just a manifestation of the noise?” Although several values have been proposed for F , it is generally accepted that $F=3$ is the appropriate choice. However, in the interest of clarity LOD values obtained by the signal-to-noise method must be footnoted with the value of F used.



Table 2 Various definitions for the LOD

Quantity	Definition	Calculation	Reference
MDL	MDL=minimum concentration of a substance that can be identified.	$MDL = t_{(n-1, 1-\alpha=0.99)} \times S_i^a$	[1]
Detection limit (C_L)	C_L =lowest concentration of the analyte that can be distinguished with reasonable confidence from a field blank. ^b	$C_L = k \times s_B / S^c$	[2]
Detection limit (c_L)	c_L =concentration equivalent to the smallest measure that can be detected with reasonable certainty for a given analytical procedure.	$c_L = (x_L - \mu_{b1}) / S^d$	[3]
Detection limit (c_L)	c_L =the number, expressed in units of concentration or amount, that an analyst can determine to be statistically different from an analytical blank.	$c_L = (x - \mu_{b1}) / S^{e,f}$	[4]
LOD	LOD=lowest concentration of an analyte that the analytical process can reliably detect.	$LOD = k \times s_B / S^c$	[5]
Detection limit (c_L)	c_L =lowest concentration of an analyte that can be distinguished from a field blank with reasonable statistical confidence.	$c_L = k \times s_B / S^{c,g}$	[6]
LOD	LOD=concentration of an analyte that produces a signal that exceeds the signal observed from a blank by an amount equal to three times the standard deviation for replicate measurements on the blank.	—	[7]
LOD	LOD=lowest concentration of an analyte in a sample that can be detected but not necessarily quantitated. ^h	$LOD = 3.3 \times s_B / S$ or $LOD = (F \times C \times N) / S^i$	[8]
LOD	LOD=lowest analyte concentration that can be detected but not quantified under the stated experimental conditions; LOD=lowest concentration that can be distinguished from the background noise with a certain degree of confidence.	$LOD = (F \times C \times N) / S^{i,j}$ or $LOD = F \times s_B$ or $LOD = F \times s_B / S^k$	[9]
LOD	LOD=concentration derived from the smallest measure that can be detected with a reasonable certainty for a given analytical procedure; LOD=lowest concentration of an analyte that the analytical process can reliably detect.	^l	[10]

^a S_i =standard deviation of responses obtained from seven portions of a sample (containing less than $10 \times$ the MDL of the analyte) taken through the entire analytical method.

^bA field blank is a hypothetical sample that contains zero concentration of the analyte.

^c k =A factor that should have at least a value of 3; s_B =standard deviation of the blank response (based on a minimum of 10 determinations); and S =method's sensitivity.

^d x_L =Minimum detectable response= $\mu_{b1} + (k s_{b1})$, where μ_{b1} =mean of replicate analyses of a blank (a minimum of 20 is recommended), k =a numerical factor chosen according to the confidence level desired (a value of 3 is strongly recommended); and s_{b1} =the standard deviation of the blank responses. S is the sensitivity of the method.

^eUse of a value of $k=3$ is recommended as it allows for a 99.86% level of confidence for a blank signal that follows a normal distribution and an 89% level of confidence for a non-normal distribution.

^fA more reliable value for c_L is obtained if S (typically determined as the slope of a plot of response vs. concentration) is replaced with a confidence interval [$S \pm (ts_S)$] reflecting the uncertainty of the slope.

^gThe key features of the LOD analysis are: 1) 16 replicate blank determinations; 2) a blank is devoid of the analyte; and 3) the calibration curve must be generated to calculate the sensitivity (slope).

^hThis definition is attributed to USP, section <1225>.

ⁱ C =Analyte concentration in an analyzed sample, N =peak-to-peak noise in the sample chromatogram, S =magnitude of analyte signal in the sample chromatogram (peak height), and F =statistical factor (typically 2 or 3).

^jThese authors note that F can vary from 2 to 5.

^kThese authors note that k can have a value of 3.0 or 3.3.

^lThese authors expand the basic relationship $LOD = k s_B / S$ to include: 1) the use of population statistics (vs. sample set statistics); 2) the use of the pooled standard deviation (vs. the blank standard deviation); 3) a consideration of situations where the intercept of the calibration curve is nonzero; and 4) a consideration of the errors in calibration parameters (slope and intercept).



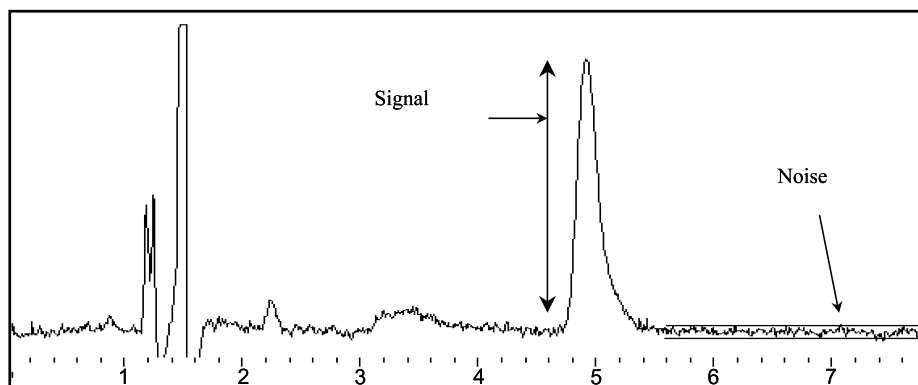


Fig. 3 Signal and noise measurements illustrated. The signal is measured from the apex of the peak to the middle of a straight-line peak base. The noise is measured as the distance between straight lines constructed from the tops and bottoms of the baseline variation. The noise should be measured in a clean portion of the chromatogram and should include a fair representation of the inherent baseline variation.

Although the signal-to-noise method for determining LOD is conceptually straightforward, its simplicity may lead to issues. Three practical issues of importance are: 1) the analyte level in the sample used to produce the chromatogram from which S and N are obtained; 2) the means of obtaining N ; and 3) the number of injections that must be used to obtain the LOD.

Considering these details in somewhat greater detail, it is clear that the calculation of LOD requires that both the signal-to-noise and the peak response be measured effectively. This can be effectively accomplished only over a relatively small range of analyte levels, which themselves are near the LOD. As a general rule of thumb, LOD should be determined from a chromatogram derived from a sample containing an amount of analyte that is from 5–15 times the LOD.

Although the concept of the noise is simple enough, its effective measurement can be quite complicated. As it is desired that the noise measured be representative of the analytical method and instrumental system, it is anticipated that N must be measured over a relatively wide portion of the chromatogram; typical recommendations suggest that a portion equal to 10–20 times the width of the analyte peak be used to measure the signal S . It is clear that the portion of the chromatogram used to measure N must be clear from analytical responses (such as those produced by other analytes, internal standards, and sample matrix components). Practically speaking, it may be difficult to “find” a chromatographic region that is sufficiently “wide” and “undisturbed” to produce an appropriately representative N .

The LOD can be calculated from S and N obtained from a single chromatogram. However, this may not be an appropriate approach given the large variation in analytical signal that occurs at analyte levels near the LOD. As

analytical signals can vary by 20% (or more) from injection to injection at analyte levels near the LOD, it is suggested that LOD be calculated from a minimum of three sample chromatograms and that the reported LOD be the mean of the individual results.

Although the previous discussion implies that the signal and noise are determined from the same chromatogram, other investigators have suggested that it is appropriate to measure the magnitude of the noise in the elution region of the analyte on a chromatogram derived from a sample blank.

Recently, Coleman et al.^[11] have observed that although S/N is a height-based determination, it is most typically the case that peak area is used for analyte quantitation. Thus these authors have proposed a procedure for setting a meaningful lower limit on peak area S/N .

One of the most common criticisms of the S/N approach is the subjective nature of the noise measurement. Although it is certainly the case that estimates for the noise may vary from one investigator to the next, such differences tend to be small, certainly well within a factor of 2.

Variation in the method blank (IUPAC/ACS)

In response to the confusion that existed regarding numerous and conflicting data on detection limits, the IUPAC adopted a model for LOD calculations in the 1970s.^[3] This standard was reaffirmed by the ACS Subcommittee on Environmental Analytical Chemistry in the early 1980s.^[5,12] The IUPAC/ACS procedure is based on two method characteristics: 1) the variation (standard deviation) of multiple blank measurements; and 2) the relationship between the response and the analyte concentration (at concentrations near the LOD). If R_B is

the mean blank responses and s_B is the standard deviation of the blank, then the LOD is calculated as:

$$\text{LOD} = R_B + ks_B$$

where k is a numerical constant whose value is chosen in accordance with the confidence level desired. As this calculation of LOD produces a result in response units, the concentration LOD is obtained using the slope S of the method's calibration curve:

$$\text{LOD} = (R_B + ks_B)/S$$

This process is illustrated in Fig. 4.

The analytical procedure used to produce the data from which the LOD is calculated is as follows:

1. A statistically significant number of blank measurements are made. Although at least 10 and as many as 20 replicates have been recommended, 16 measurements are generally selected.
2. The standard deviation of the blank measurements is calculated (in units of response, not concentration).
3. Five standard solutions of varying analyte concentrations (prepared in the blank matrix) are analyzed and a calibration curve of response vs. concentration is constructed. If the range of the standard concentrations is appropriately chosen, then the calibration curve is typically linear and its slope can be determined.
4. The LOD is calculated with the generated data per LOD equation. A value of $k=3$ is strongly recommended.

Numerous authors have proposed modifications of the IUPAC/ACS approach, typically based on a more rigorous statistical analysis of method variation and its contributing factors. Although such approaches are undoubtedly

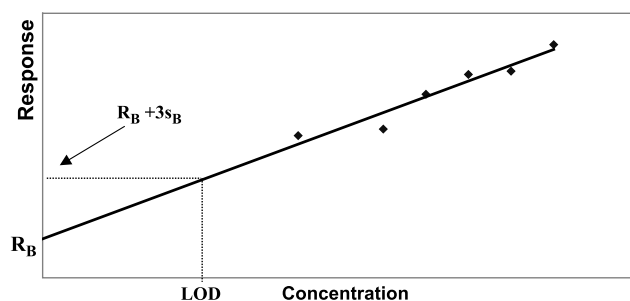


Fig. 4 Calibration graph showing the LOD. This graph illustrates the IUPAC method for determining the LOD. R_B =response of the blank; s_B =standard deviation of multiple determinations of the blank responses. (View this art in color at www.dekker.com.)

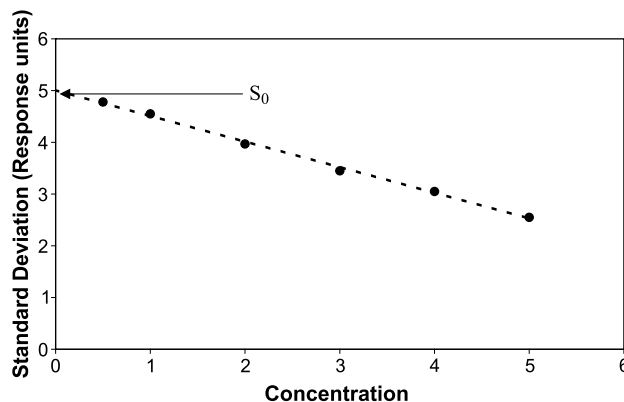


Fig. 5 Determination of LOD based on the projected standard deviation at zero concentration (S_0). The LOD is calculated as the concentration that corresponds to a response three times the value of S_0 . Although the relationship between concentration and standard deviation shown here is linear, nonlinear relationships between these two variables are likely.

scientifically more rigorous, they typically require more complex computations and their practical significance is open to question.

One significant practical problem with the IUPAC methodology occurs in the situation wherein the blank produces no analytical signal—a circumstance that is commonly encountered in chromatographic analyses. In such circumstances, it may be possible to estimate the “virtual” standard deviation at zero concentration.^[13] In this graphical technique (Fig. 5), the standard deviation (in response units) of replicate analyses of successively more dilute samples is plotted vs. the analyte concentration. The y-intercept of this plot (S_0) represents the virtual standard deviation at zero concentration. The LOD is calculated by substituting S_0 for s_B in the IUPAC LOD equation.

Another, more practical problem associated with the IUPAC methodology is the time-consuming requirement of 16 replicate analyses (injections for chromatographic analysis) of the blank. To address this issue, the ICH has devised a methodology for the calculation of LOD that is similar in concept to the IUPAC method but is different in its application.^[14] By the ICH definition, the LOD is expressed as:

$$\text{LOD} = 3.3(\sigma/S)$$

where σ is the standard deviation of the response and S is the slope of a method's calibration curve. In the ICH computation, σ can be determined based on one of three data: 1) the standard deviation of the blank; 2) the residual standard deviation of the regression line; or 3) the standard deviation of the y-intercepts of regression lines.



95% confidence intervals around the best-fit line

This graphical method, illustrated in Fig. 6, is a variation of the standard deviation-based approaches discussed previously. In this approach, the 95% confidence bounds are obtained for the best-fit, regression-based, calibration line. The upper 95% confidence bound, extrapolated to zero analyte concentration, reflects the statistical “limit” as it relates to calibration bias and imprecision, and establishes the LOD in terms of response. Mathematically, this response LOD is converted to a concentration LOD by inputting the response LOD into the lower 95% confidence bound and by solving for concentration. Graphically, this can be accomplished as shown in Fig. 6.

Lowest concentration exhibiting required performance

As an alternative to the methodologies based on standard deviation, one can define the LOD (or LOQ) to be the lowest concentration that produces an analytical response that meets predefined quality requirements. For example, one might define the LOD as the lowest analyte concentration that produces a percent relative standard deviation (%RSD) of 10%. The LOD can be determined by performing replicate analyses of successively more dilute samples. The LOD could be estimated if one plots percent relative standard deviation vs. the analyte concentration (Fig. 7).

Minimization of false conclusions

In the context of LOD, false positive and false-negative responses can be defined as follows: false positive—

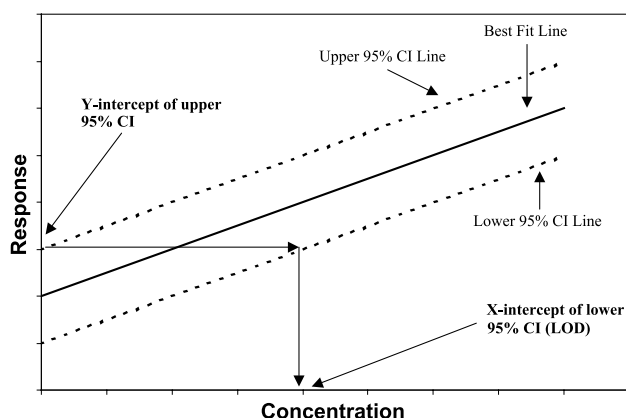


Fig. 6 Graphical determination of the LOD based on the 95% CI lines surrounding the best-fit regression model. (From Ref. [13].)

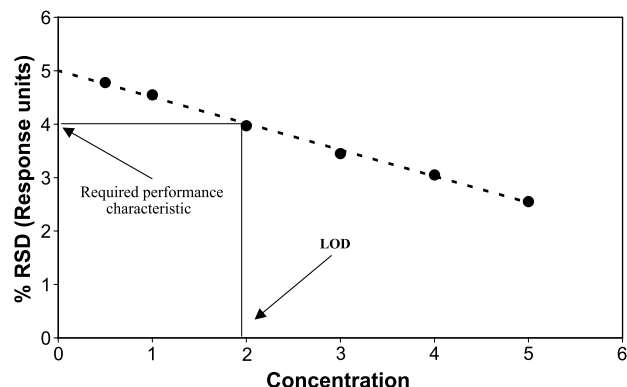


Fig. 7 Determination of LOD based on a specified performance requirement. In this example, the LOD is defined as the lowest analyte concentration with a percent relative standard deviation of not more than 4%. The interpolated value of LOD is approximately two concentration units. Although the relationship between concentration and percent relative standard deviation shown here is linear, nonlinear relationships between these two variables are likely.

a response for a blank that contains no analyte that falls above the LOD (i.e., a blank that is concluded to contain the analyte); false negative—a response for a sample that contains the analyte that falls below the LOD (therefore it is concluded that the sample does not contain the analyte at detectable levels). False-positive and false-negative responses are possible due to the assay variation (responses for a given sample are represented by a frequency distribution and not a single result). This scenario is illustrated in Fig. 8. To a certain extent, the definition and value for LOD depend on whether it is acceptable to have a false-positive or false-negative response.

Elimination of false positives is accomplished by having the LOD defined and calculated by the IUPAC procedure. With a k value of 3, the possibility of a false positive is less than 0.2% if the data are normally distributed, and less than 11% if they are not. If greater confidence is required that false positives will not occur, a larger value of k may be necessary in the LOD calculation.

Consideration of false negatives requires that one take into account two response distributions: the response distribution for the blank, and the response distribution for the sample. A false negative will occur in the region where sample and blank response distributions overlap. If the detection limit is defined as that sample concentration for which the response distributions would not overlap (i.e., the LOD is that sample concentration for which a false-negative response cannot be obtained), then clearly the LOD depends on both the standard deviation of the blank and the standard deviation of the sample. Although it is beyond the scope of this manuscript to assess this scenario

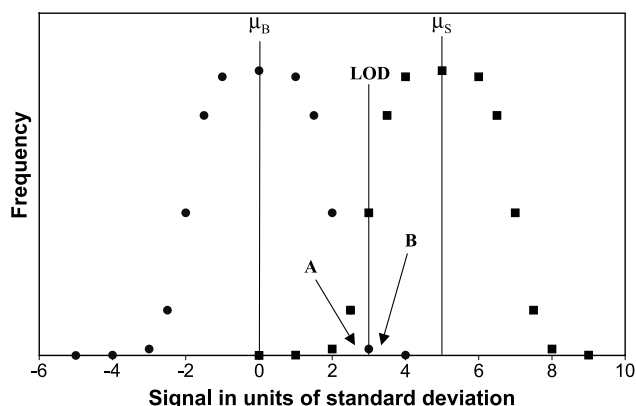


Fig. 8 Normal distribution of responses for the field blank (mean response = μ_B ; ●) and for the sample (mean response = μ_S ; ■). Although the sample has a mean analyte value above the LOD, the potential for a false-negative response (sample analyzed with signal less than the LOD obtained, therefore concluding that the analyte is not present in the sample) exists and its probability is defined by region A in the sample's response distribution. As the sample's mean signal increases, the probability of a false negative decreases. The probability for a false positive (blank producing a signal greater than the LOD, thus concluding that the blank contains the analyte) is defined by region B in the blank's response distribution. (View this art in color at www.dekker.com.)

in a statistically rigorous manner, the following example may serve to illustrate the relationship between LOD and a false negative. In this example, the response populations of the blank and the sample are normally distributed and the standard deviation of both populations is the same. If the means of the blank and the sample populations differ by six times the standard deviation, there is less than a 1% chance that a response within the sample's distribution will also fall in the blank's distribution (thereby creating a false negative). In such an example, one would be justified in calculating LOD as:

$$\text{LOD} = R_B + 6s_B$$

where R_B and s_B have been defined previously as the mean and standard deviation of the blank response respectively.

Method detection limit

Methods for determining the LOD that are based on the analysis of a field blank that does not contain the analyte of interest are problematic in many real-world applications because either such samples do not exist, or would be impossibly difficult to create. As such a circumstance is frequently encountered in environmental analysis, the USEPA adopted a detection limit procedure, termed the method detection limit (MDL), which focuses on an

operational definition of detection limit.^[15] Specifically, the MDL is defined as the minimum concentration of a substance that can be measured and reported with 99% confidence that the analyte concentration is greater than zero. The MDL is determined from a replicate analysis of a sample of a specified matrix. Specifically, at least seven aliquots of sample, spiked to contain a concentration of from one to five times the method's estimated MDL, are analyzed. The MDL calculated from these results is statistically tested to determine its "reasonableness." If the result fails the testing, this iterative process begins again with a new estimate of the MDL.

Other methods

The analytical literature abounds with additional methods for the calculation of LOD. Most of these additional methods are variations on the procedures discussed herein, where the variation involves a more rigorous statistical assessment of the various aspects of a method's response function and variation. Although such derivations are mathematically and statistically rigorous, from a practical perspective, it is open to debate whether use of such derivations: 1) clarifies the meaning of the LOD; 2) improves the utility of the LOD; or 3) has the potential to become universally accepted.

Sensitivity Vs. Detectability

A frequent error encountered in evaluating the performance of an analytical system is to confuse the concepts of sensitivity and detectability. Although both concepts address facets of a system's response, they are not identical, but rather complementary. Sensitivity relates to the ability of the system to respond to changes in analyte concentration and is most typically reflected as the slope of the method's response function. Detectability, as has been noted previously, is the ability of the method to distinguish between two responses (those responses that arise in the presence and absence of the analyte in the sample matrix of interest). It is possible to have a very sensitive method that has a relatively poor detection limit, especially if the method is very unselective or prone to high blanks. However, an insensitive method is very unlikely to exhibit a low LOD. Thus sensitivity is a necessary—but not sufficient—condition for the achievement of a low LOD.

General Comments

The following observations, relevant to LOD and its determination, are summarized from the various cited references.



A detection limit must be viewed as a temporary limit to current methodology.^[11]

The LOD is governed by both instrumental factors (e.g., capability of the analytical instrument and column) and procedural factors (e.g., recovery of the analyte from the sample). It varies with the type of sample, different batches of blank, and type and condition of instrumentation.^[16] Factors other than the analytical method itself that can influence the detection limit include the following:^[2]

- 1) The analyst.
- 2) The analytical environment.
- 3) The brand of instrumentation used.
- 4) The quality of reagents.
- 5) The nature of the samples.
- 6) The calibration protocol.
- 7) The use of blank correction.

Column efficiency can affect *S/N* measurements; therefore analysts should account for both the type and the age of the column when determining the LOD. The maintenance status of chromatographic components (e.g., detectors and injectors) will also affect the ability to measure limits.^[8] In trace analysis, the LOD is greatly influenced by the recovery of the compound; adsorption to glassware, instability or volatility, incomplete reaction (during derivatization), and poor laboratory technique are some of the causes of sample loss during analysis.^[16]

Most paradigms for the calculation of LOD are based on the following simple models of an analytical system:^[2]

- 1) The random error is normally distributed.
- 2) The population parameters are known.
- 3) The analytical method is unbiased.
- 4) The "field blank" is effectively a sample with zero analyte concentration.
- 5) The variance in the field blank measurement is essentially equal to the variance for samples with very low analyte levels.
- 6) The matrices of the field blank and samples are effectively identical, so that no unique interference effects are present.

Inherent in the model are the principles that the measured signal consists of an analytical signal (response to the analyte) and a blank signal (background, noise, or measured signal for a blank), and that both the analytical and blank signals fluctuate.^[17] Additionally, it is generally assumed that the process has a linear response function.^[18]

The calculated LOD can easily vary by an order of magnitude through the use of different statistical approaches.^[4]

A value of $k=3$ is considered minimal because it implies definite risks of 7% for false-positive (concluding

that the analyte is present when it is absent) and false-negative (the reverse) decisions.^[5]

To a certain extent, the correct calculation of LOD depends on whether greater harm is likely to be caused by false positives or false negatives.^[7]

The entire sequence of operations, from procurement of the sample through the final measurement step, ultimately determines the LOD.^[7]

Random error, reported as the coefficient of variation, ranges from about 25% to 100% at the LOD.^[18]

Numerical values that have been proposed for k in the determination of LOD are summarized in Ref. [17] and range from 1.00 to 20.

It is better to regard the LOD as a useful but approximate guide to an analytical procedure. The value of LOD should be stated with one significant figure only, and duplicate results differing by a factor of less than 2 should not normally be regarded as significantly different.^[16]

THE LIMIT OF IDENTIFICATION

As noted in the discussion of LOD, a false negative occurs when a response for a sample that is known to contain the analyte falls below the LOD. In such a case, it would be concluded (falsely) that the sample does not contain the analyte at detectable levels. At some point on the method's response spectrum between the LOD and the LOQ, there is an analyte concentration above which there is a very small chance that a false negative could occur. At this concentration, the vast majority of the responses that make up the sample's response population would fall above the LOD. This concentration is termed the LOI. Thus the LOI is defined as follows:

The LOI is that analyte concentration at which the probability of obtaining a false-negative response (i.e., a response that is below the LOD) for a sample known to contain the analyte is below a specified value defined by the required level of confidence.

If the response populations of the sample and its associated blank are both normally distributed and if the standard deviations of the populations are similar, the LOI can be calculated as:

$$\text{LOI} = R_B + 6s_B$$

where R_B and s_B have been defined previously as the mean and standard deviation of the blank response, respectively. In such a case, the probability of a false negative response is 0.13% at the 95% level of confidence. Lack of normality in either response distribution, a greater variation in the response distribution of



either the sample or the blank, or a higher required level of confidence would require that the LOI calculation have a multiplier larger than six in the s_B term.

THE LIMIT OF QUANTIFICATION

Definition

If it is an accurate observation that the LOD is a difficult concept to effectively define, the opposite is true for the LOQ. It is generally accepted that the LOQ is linked to method performance expectations including accuracy and precision. Thus a common definition of LOQ is as follows:

The LOQ is the lowest concentration of the analyte that can be measured with acceptable accuracy and precision under the stated experimental conditions.

Methods of Determination

As LOQ and LOD are related concepts, it is not surprising that the methods suitable for determining LOD are, in most cases, also suited for the determination of LOQ, at least from a conceptual standpoint. Several of the more commonly cited means of determining the LOQ are described as follows.

As a multiple of the LOD

Once a method's LOD has been determined (by any of several methods as noted earlier), the LOQ can be calculated as a simple multiple of the LOD. Although a multiple of 3.3 is commonly cited (where 3.3 is the ratio of 10:3), LOQs are routinely calculated as three to five times the LOD.

Signal to noise (graphical)

As was the case with LOD, the LOQ can be calculated from a signal-to-noise evaluation of a chromatogram arising from a field sample known to contain the analyte at a concentration approximately equal to the LOQ. The LOQ is typically calculated as the analyte concentration required to produce a signal that is 10 times larger than the peak-to-peak noise.

Based on analysis of spiked samples

This approach represents a literal interpretation of the LOQ definition. The LOQ is assessed by analyzing

replicates of a field blank spiked with a low level of the analyte (near the LOQ), along with calibration standards. The accuracy (spike recovery) and precision of the replicate analyzes are compared to prespecified performance expectations. If the expectations are met, then the spiked concentration is an estimate of the LOQ. A more accurate determination of the LOQ would involve an iterative process whereby samples containing different levels of the analyte are all repetitively analyzed. The LOQ would fall somewhere between the lowest concentration that meets the performance expectations and the highest concentration that fails to meet the expectations.

Based on standard deviation of the noise

A representative (field) blank is repetitively analyzed and the LOQ is calculated as a multiple (typically 10) of the standard deviation of the blank's responses (divided by the slope of the calibration curve). This is equivalent to the IUPAC/ACS method for determining LOD.

Based on calculated confidence intervals around the calibration curve

Calibration data, obtained at analyte concentrations near the LOQ, are fitted (by an unweighted linear regression) and the confidence intervals (CIs) are calculated. The LOQ is determined as the concentration for which the interval (at a specified level of confidence) does not overlap the CI of the matrix blank (used as a standard).

Based on background interferences and the reproducibility of the response

Responses are obtained from replicate analyses ($n=4$) of a field blank and the field blank spiked to contain a level of analyte that is close to the LOQ. The means of the obtained responses are tested statistically (with the t -test) to determine whether they are statistically different. If the difference is significant, the variability of the response in the spiked sample is evaluated by taking the ratio of its mean response to the response standard deviation. If the ratio is greater than or equal to 3, then the spiked concentration is taken as the LOQ.

Based on confidence intervals

Once again, field blanks and spiked field blanks are repetitively analyzed. The LOQ is determined as the concentration at which the lower confidence level of the mean of the spiked sample responses is at least four times greater than the upper confidence level for the mean blank response.



GENERAL DISCUSSION

It is clear from both the definition of LOQ and several of its methods of determination that a key aspect of establishing an LOQ is defining appropriate performance expectations. Although appropriate performance expectations may vary from method to method and especially from application to application, some general guidance in terms of what level of performance is reasonable to expect at the LOQ is given as follows:

For bioanalytical LC methods, the accuracy criterion is $\pm 20\%$ (80–120% of the “known” value) and the RSD should be less than 20%.^[9]

The LOQ is the lowest concentration for which RSD is less than 5%.^[13]

An *S/N* of 10 or less than 10% RSD is a good value as a rule of thumb.^[8]

A recovery of 70–130% and a precision of 10% RSD are required at the LOQ.^[19]

A survey of validation data in trace level analyses reported that the following criteria for accuracy, obtained from various references, are pertinent:^[20]

- 1) Below 100 ppb, 60–110% recovery is acceptable; above 100 ppb, 80–100% recovery is acceptable.
- 2) Below 1 ppm, 70–120% recovery is acceptable.
- 3) Impurities present at 0.1–10% should produce data within $\pm 5\%$ of actual.

The linkage of the LOQ to performance expectations clearly differentiates LOQ from LOD. LOD is a calculated result. LOQ is a calculated result compared to a performance expectation. It is the aspect of the performance expectation that makes the link between LOQ and the application more obvious than the link between LOD and the application. Although it is possible for the same method to have two different LOQ values, depending on the needs of different applications, the method will have only one LOD.

It has been previously noted that it has historically been possible to obtain widely different values for LOD and LOQ, depending on the approach used and the statistical “multiplier” applied. As the LOD and LOQ concepts have evolved and have become more standardized and harmonized, obtaining such widely varying results is no longer commonplace. A recent study^[13] examined LOD and LOQ values obtained for a multianalyte, gradient, UV-based HPLC method by four different techniques, including: 1) a performance expectation of percent relative standard deviation less than 5%; 2) a plot of standard deviation vs. concentration (ICH approach); 3) use of the 95% CI of the best-fit regression line; and

4) signal to noise (graphical). The results of this study are summarized in Table 3. In general, the results obtained via the four methods all agreed to within a factor of 2–3, and the differences between results were distributed randomly (i.e., no method gave consistently lower or higher results). Thus the authors of this study concluded that the four techniques were essentially equivalent and all were suitable for satisfying USP or ICH requirements.

Finally, the following discussion, obtained from Ref. [18], may be a useful and practical means of highlighting the meaning of, and differences between, LOD and LOQ.

Think of the LOQ as a “Beware of Dog” sign posted on the fence around a property, and the LOD as a “Beware of Dog” sign posted in the middle of the fenced yard. One may walk up and touch the first sign fairly safely. However, stay away from that second sign. Do not go into the yard.

A second example is as follows:

A driver finds himself on an apparently deserted road that extends all the way to the horizon. As a good driver should, he periodically looks to the horizon to check for oncoming traffic. For the longest time, he sees nothing. Then, suddenly, he catches a glimpse (he thinks) of

Table 3 LOD and LOQ estimated for a gradient LC/UV assay with three analytes^a

Analyte	Method 1 ^b	Method 2 ^c	Method 3 ^d	Method 4 ^e
<i>LOD (mg/mL)</i>				
A	0.06	0.05	0.02	0.04
B	0.04	0.04	0.02	0.04
C	0.04	0.10	0.05	0.10
<i>LOQ (mg/mL)</i>				
A	0.21	0.09	0.07	0.08
B	0.13	0.09	0.05	0.06
C	0.14	0.13	0.16	0.15

^aFrom Ref. [13].

^bLOQ is the lowest concentration that produces an injection to injection precision of NMT 5%. LOD = 0.3LOQ.

^cBased on the graphical extrapolation of the plot of standard deviation of replicate injections vs. analyte concentration to zero concentration (to produce S_0 , the standard deviation at zero concentration). LOD = concentration that corresponds to $3S_0$, LOQ = concentration that corresponds to $10S_0$. This is the ICH convention (Fig. 4).

^dThe 95% confidence lines are drawn around the best-fit regression plot of peak response vs. analyte concentration. A horizontal line is drawn from the y-intercept of the upper 95% CI line to the lower 95% CI line. A vertical line is drawn from the intersection point on the lower 95% CI line to the x-axis, yielding the x-intercept. The x-intercept is the LOD whereas the LOQ is 3.3LOD (Fig. 5).

^eBased on the chromatographic signal to noise. LOD = 3N/S; LOQ = 10N/S (Fig. 3).

something out there. As he keeps on checking, he is not quite sure; does he see something or not? Is it really something or just a glint off the windshield? At this point, the object is below the driver's LOD. However, as time goes on, the object appears to be there every time he looks up. He is now reasonably confident that there is an object out there. The object has reached its LOD. As the driver and the object continue to move closer, the object grows in size and is more distinguishable from the background. Finally, the driver is virtually 100% confident that the object is out there and, in fact, it appears to be a car (as opposed to a truck or motorcycle). The object has reached its LOI. As time continues and the objects move still closer (with the net result that the car gets bigger and bigger), eventually the driver is able to ascertain that the car is, in fact, a Porsche 914 roadster, containing a driver and her passenger. At this point, the LOQ has been reached.

REPORTING LOW-LEVEL RESULTS

Once the various detectability limits have been defined and established for an analytical method, the question as to the proper format for reporting low-level results arises. To address this question, it is pertinent to observe that the three detectability limits (LOD, LOI, and LOQ) clearly divide the lower end of the response spectrum into finite regions (Figs. 1 and 9). Thus the question of how to report a low-level result boils down to what region of the response spectrum does the result

fall in, and what is the appropriate reporting convention for that region.

The lowest response region in the spectrum is that which has the LOD as the upper bound. It is clear that if a response that is smaller than the response associated with the LOD is observed, the analytical result should be reported as "less than the LOD" or "not detected." In either case, the method's LOD must be reported [e.g., "<LOD (=2 ppm)."] It is also appropriate to report the method by which the LOD was determined, although this is done only infrequently.

Although the above discussion appears to be straightforward, the circumstance in which no response is observed is a bit more complex. Although there is a temptation to report such a result as a zero concentration, doing so is not correct except in the circumstance that the method's LOD is a single molecule. In all other circumstances, a nonobserved response can be produced by an analyte that is either truly not present or an analyte whose level is well below the LOD. Thus as was the case of the response below the LOD, a sample that produces no analytical response is reported as "<LOD" or "not detected," with the LOD and its method of determination being cited.

Moving to higher analyte levels in the sample, the next region in the response spectrum is that region defined by the LOD at the low end and the LOI at the high end. Responses in this region are clearly above the LOD; thus one is confident that the response is "real" (i.e., the response arises from the elution of an analyte

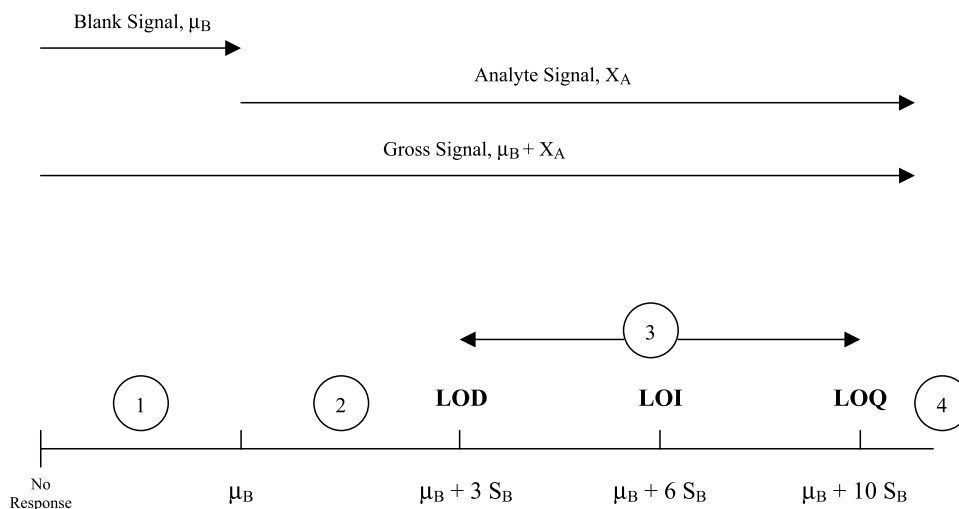


Fig. 9 Diagrammatic representation of various limits and their relationship to the mean blank response (μ_B) and the standard deviation of the blank response (s_B). The numbered regions include: 1) the region of the blank signal (reported as "not detected" and reporting the LOD); 2) the region of the blank variation (reported as "not detected" and reporting the LOD); 3) the region of detection and identification (reported as less than the LOQ and reporting the LOQ); and 4) the region of quantification (reporting the result).



from the chromatographic column and into the detector). However, the amount of analyte present is insufficient to allow for its accurate identification. In this case, it is appropriate to report the result as “detected, unidentified” and to cite the method’s LOI and its method of generation. Although it is appropriate to note that the analyte concentration in a sample producing a response that falls between the LOD and the LOI is greater than the LOD, this information may or may not be relevant to the interpretation of the result.

The next region one encounters as the response continues to increase is that region which falls between the LOI and the LOQ. As the response is above the LOI, the identity of the compound responsible for the response can be (and presumably is) identified. Thus the compound’s identity is noted and the measurement status of the analyte peak is reported as “detected, identified.” It is also appropriate to report the concentration of the analyte in such a sample as “<LOQ” and to cite the value of the LOQ and its means of determination. Although it may be tempting to “estimate” the analyte concentration in a sample whose response falls between the LOI and the LOQ, doing so is of limited value as the response function is typically poorly defined in this response region and the response is prone to a high degree of variability.

Although the above directions are clear-cut, there are circumstances where reporting a number is highly desirable (e.g., when the result is part of a data population that is undergoing statistical analysis). In such cases, it may be appropriate to report the analyte’s calculated concentration, but care must be taken to ensure that the method’s response function in the region of the analyte response is known. Such a result should be termed a concentration estimate and should be reported along with the qualifying notation “<LOQ” and the LOQ should be reported.

It goes without saying that it is appropriate to report the calculated concentration of an analyte whose response is above the LOQ. However, the reader is cautioned to remember that the response region near the LOQ is characterized by a high degree of imprecision and inaccuracy, and that good sense should be exercised in the use of significant figures in the reported value.

THE DYNAMIC RANGE

Because the primary use of chromatography is to establish the concentration of a known entity (analyte) in a specific sample and because few chromatographic detection strategies are absolute (i.e., their response function can

be derived from first scientific principles), a useful chromatographic method must have an analyte concentration region over which a response function can be established. This response function (or calibration curve) is the mathematical relationship that exists between the concentration of an analyte in a standard and the response that is produced when such a standard is processed by the chromatographic method. The dynamic range of a method is that concentration region for which a useful response function can be established. In this context, the term “useful” has three aspects. The first aspect is that the response function must be such that the sensitivity of the method is sufficient for the method’s intended application. Although a flat line response function (no change in response produced by a change in analyte concentration) can readily be described mathematically, such a response function would be useless from a quantitative perspective. The second aspect is that the response function must be unique in the sense that every response is produced by a sample containing a single amount of the analyte. Although many chromatographic detectors reach a “flat line” state at high concentration (i.e., no change in response occurs as analyte concentration changes), there are some detectors (e.g., mass spectrometers) whose response actually “bends backward” (i.e., response decreases as concentration both increases and decreases). In such a circumstance, a sample may produce a response that is linked (via the response function) to two analyte concentrations. Inputting a sample’s response into a calibration curve and obtaining multiple concentrations is clearly an outcome of limited value. The final aspect is that the response function must adequately “fit” or represent the analytical data from which it is derived. If the fit is poor (i.e., if there is a large difference between the measured response at a specific concentration vs. the response calculated from the regression model), then clearly the response function is not representative of its source data and any calculation based on the response function will be inaccurate.

The terms range and dynamic range are frequently encountered and occasionally incorrectly used interchangeably. The dynamic range is method specific and reflects the largest concentration difference for which a suitable response function can be obtained. The range of a method is application specific and does not necessarily represent the full capability of the method. Thus, for example, the range of an assay used for the purpose of quantifying an active ingredient in a finished pharmaceutical product need be only for 80–120% of the ingredient’s nominal concentration in the actual test sample.^[21] In many cases, such an application-driven range is just a small portion of the method’s true dynamic range.



A subset of the dynamic range is the linear dynamic range. The linear dynamic range is that portion of the range for which the appropriate response function is a linear one. Historically, obtaining a linear calibration model has been the desired outcome of an analytical method development activity and most guidance for analytical method validations include an assessment of linearity (along with the subtle expectation that the desired response function is, in fact, a linear one). As numerous other calibration models exist and can readily be judged in terms of their appropriateness of fit, the desire for a linear response function is truly a throwback to the days when the only regression analysis tools were a pencil and straightedge. In modern chromatographic analysis, there is no underlying need for the response function to be linear and, in fact, there are many fundamental reasons to anticipate that certain detection methods are, by their very nature, nonlinear in their response over every practically useful concentration range. It is noted in passing that the entire dynamic range may be made up of numerous smaller concentration regions whose response function is a linear one.

As a general rule of thumb, the LOQ is typically the low point of a method's dynamic range. The concentration at the high end is usually dictated by a lack of sensitivity, which leads to increased uncertainty, and is clearly method-dependent.

It is noted that the apparent dynamic range can be expanded at the high-concentration end via sample dilution provided that the dilution itself does not materially impact the response (e.g., via sample matrix effects). Additionally, a sample preparation process that accomplishes the concentration of the analyte may decrease a method's limit of detectability.

THE LIMIT OF RANGE

The LOR is that analyte concentration at which the method's response function is either no longer useful or no longer determinable. As noted previously, the LOR may reflect that concentration for which:

1. No response function that adequately fits the analytical data can be found.
2. The method exhibits inadequate sensitivity.
3. The method exhibits insufficient accuracy or precision.
4. The response function produces multiple values for a single input quantity.

Although it is typically the case that the LOR is defined by limitations in the detection portion of the

analytical system, this is not necessarily the case in chromatographic analysis. Clearly chromatographic performance (such as loss of resolution or poor peak shape) at high analyte concentrations can be the limiting factor in terms of establishing a method's LOR. Additionally, other factors, such as injection-to-injection carryover at high concentration and analyte stability issues in high concentration standard or sample solutions, may represent practical method limitations that ultimately define a method's LOR.

CONCLUSION

The response spectrum in chromatographic analysis extends from the lowest analyte concentration that consistently produces a recognizable response to the highest analyte concentration that produces a response that is uniquely different from the response produced at a different analyte concentration. In this manuscript, the response spectrum has been partitioned into several appropriately concise regions via the use of concentration limits that correspond to the functions or purposes of chromatographic analysis (detection, identification, and quantitation). Methods for calculating, using and reporting the various limits were discussed. The position at which a particular response falls on the response spectrum dictates the utility and reliability of the analyte concentration assigned to that response.

REFERENCES

1. Glaser, J.A.; Foerst, D.L.; McKee, G.D.; Quave, S.A.; Budde, W.L. Trace analyses for wastewaters. *ES&T* **1981**, *15*, 1426–1435.
2. Analytical Methods Committee. Recommendations for the definition, estimation and use of the detection limit. *Analyst* **1987**, *112*, 199–204.
3. Analytical Chemistry Division, International Union of Pure and Applied Chemistry. Nomenclature, symbols, units and their usage in spectrochemical analysis: II. Data interpretation. *Spectrochim. Acta* **1978**, *33*, 241–245.
4. Long, G.L.; Winefordner, J.D. Limit of detection, a closer look at the IUPAC definition. *Anal. Chem.* **1983**, *55*, 712A–720A.
5. ACS Committee on Environmental Improvement, Subcommittee on Environmental Analytical Chemistry. Guidelines for data acquisition and data quality evaluation in environmental chemistry. *Anal. Chem.* **1980**, *52*, 2242–2249.
6. Lindstedt, J. Limit of detection methodologies. *Plating Surf. Finish.* **1993**, *80*, 81–86.
7. Wehry, E. Quantitative Measurements. In *Handbook of*



- Instrumental Techniques for Analytical Chemistry*; Prentice Hall: Upper Saddle River, NJ, 1997. Chap. 4, 73–80.
8. Krull, I.; Swartz, M. Determining limits of detection and quantitation. *LC/GC* **1998**, *16*, 922–923.
 9. Rosing, H.; Man, W.Y.; Doyle, E.; Bult, A.; Beijnen, J.H. Bioanalytical liquid chromatographic method validation. A review of current practices and procedures. *J. Liq. Chromatogr. Relat. Technol.* **2000**, *23*, 329–354.
 10. Mocak, J.; Bond, A.M.; Mitchell, S.; Scollary, G. A statistical overview of standard (IUPAC and ACS) and new procedures for determining the limits of detection and quantification: Applied to voltammetric and stripping techniques. *Pure Appl. Chem.* **1997**, *69*, 297–328.
 11. Coleman, J.; Wrzosek, T.; Roman, R.; Peterson, J.; McAllister, P. Setting system suitability criteria for detectability in high-performance liquid chromatography methods using signal-to-noise ratio statistical tolerance intervals. *J. Chromatogr. A* **2001**, *917*, 23–27.
 12. American Chemical Society Committee Report. Principles of environmental measurement. *Anal. Chem.* **1983**, *55*, 2210–2218.
 13. Paino, T.C.; Moore, A.D. Determination of LOD and LOQ of an HPLC method using four different techniques. *Pharm. Technol.* **1999**, *23*, 86–88.
 14. Validation of Analytical Procedures: Methodology. International Conference on Harmonization of Technical Requirements for Registration of Pharmaceuticals for Human Use, Geneva, Switzerland, November, 1996; ICH-2QB.
 15. *Definition and Procedure for the Determination of the Method Detection Limit, Revision 1.12*; U.S. Environmental Protection Agency, Environmental Monitoring and Support Laboratory: Cincinnati, 1981.
 16. Mehta, A.C. Trace measurement. *Lab. Pract.* **1989**, *38*, 29–30.
 17. Oresic, L.S.; Grdinic, V. Kaiser's 3-sigma criterion: A review of the limit of detection. *Acta Pharm. Jugosl.* **1990**, *40*, 21–61.
 18. Clark, M.J.R.; Whitfield, P.H. Conflicting perspectives about detection limits and about the censoring of environmental data. *Water Resour. Bull.* **1994**, *30*, 1063–1079.
 19. Jenke, D.R.; Poss, M.; Story, J.; Odudu, A.; Zietlow, D.; Tsilpetros, T. Development and validation of liquid chromatographic methods for the identification and quantification of organic compounds leached from a laminated polyolefin material. *J. Chromatogr. Sci.* *in press*.
 20. Jenke, D.R. Chromatographic method validation: A review of current practices and procedures: Part II. Guidelines for primary validation parameters. *Instrum. Sci. Technol.* **1998**, *26*, 1–18.
 21. <1225> Validation of Compendial Methods. In *The United States Pharmacopeia, USP 26*; United States Pharmacopoeial Convention, Inc.: Rockville, MD, 2002; 2239–2242.



Retention Factor: Effect on MEKC Separation

Koji Otsuka

Shigeru Terabe

Himeji Institute of Technology, Hyogo, Japan

Introduction

In micellar electrokinetic chromatography (MEKC), an ionic surfactant micelle, such as sodium dodecyl sulfate (SDS), is used as a pseudo-stationary phase that corresponds to the stationary phase in liquid chromatography (LC). Here, the separation principle of MEKC with an anionic micelle (e.g., SDS) under a neutral condition is briefly considered. When high voltage is applied across the whole capillary, the entire solution migrates toward the cathode by electro-osmotic flow (EOF) while the SDS micelle is forced toward the anode by electrophoresis. The EOF is stronger than the electrophoretic migration of the SDS micelle and, hence, the micelle migrates toward the cathode at a more retarded velocity than the EOF.

When a neutral analyte is injected into the micellar solution at the anodic end of the capillary, it will be distributed between the micelle and the surrounding aqueous phase. The analyte, which is not incorporated into the micelle at all, migrates toward the cathode at the same velocity as the EOF. The analyte totally incorporated into the micelle migrates at the lowest velocity, or at the same velocity as the micelle, toward the cathode. The more the analyte is incorporated into the micelle, the slower the analyte will migrate. A neutral analyte always migrates at a velocity between the two extremes (i.e., the velocities of the EOF and micelle). The analytes are detected in an increasing order of the distribution coefficients by a detector located at the cathodic end of the capillary. The migration time of the electrically neutral analyte is limited between the two extremes: the migration time of a solute that is not incorporated into the micelle at all, t_0 , and that of the micelle, t_{mc} .

Under an acidic condition, however, the absolute value of the velocity of the EOF becomes lower than that of the electrophoretic velocity of the SDS micelle and, therefore, the micelle migrates toward the anode. By contrast, when a cationic surfactant is employed instead of SDS, the direction of the EOF will be reversed or toward the anode, due to the adsorption of the surfactant molecule on the inside wall of the capillary and changing the surface charges.

Retention Factor

In MEKC, the retention factor, k , for a neutral compound can be defined as n_{mc}/n_{aq} , where n_{mc} and n_{aq} are the number of the analyte incorporated into the micelle and in the surrounding aqueous solution, respectively. The retention factor can be related to the migration time of the solute, t_R , as

$$k = \frac{t_R - t_0}{t_0(1 - t_R/t_{mc})} \quad (1)$$

or

$$t_R = \left(\frac{1 + k}{1 + (t_0/t_{mc})k} \right) t_0 \quad (2)$$

The reciprocal of t_0/t_{mc} , or t_{mc}/t_0 , is a parameter representing the migration time window. One should note that when the migration time of the micelle is infinite or the micelle does not migrate in the capillary at all, the value t_0/t_{mc} will be zero; then, Eqs. (1) and (2) become identical to those for conventional LC.

In MEKC, $k = \infty$ means that t_R becomes equal to t_{mc} and the solute migrates at the same velocity as the micelle.

When $t_0 = 0$ or the EOF is completely suppressed, Eq. (2) becomes

$$t_R = \left(1 + \frac{1}{k} \right) t_{mc} \quad (3)$$

Here, the surrounding aqueous phase does not move at all in the capillary and only the micelle migrates toward the anode if an anionic micelle is employed. Note that the EOF is not essential in MEKC.

When the solute has an electrophoretic mobility Eq. (1) will be more complicated, that is, the migration of the ionic solute includes a portion generated by the micelle when the solute is incorporated into the micelle and also the other portion generated by the electrophoresis of the solute itself.



Resolution

Resolution, R_s , in MEKC is given as

$$R_s = \left(\frac{N^{1/2}}{4} \right) \left(\frac{\alpha - 1}{\alpha} \right) \left(\frac{k_2}{1 + k_2} \right) \left(\frac{1 - (t_0/t_{mc})}{1 + (t_0/t_{mc})k_1} \right) \quad (4)$$

where N is the theoretical plate number, α is the separation factor equal to k_2/k_1 , and k_1 and k_2 are the retention factors of analytes 1 and 2, respectively. When $t_0/t_{mc} = 0$, Eq. (4) will be identical to that for conventional LC.

The separation factor α is altered by the combination of the structure of the micelle as the pseudo-stationary phase and the aqueous phase as a solvent of the micelle. Because k is included in the last term of the right-hand side of Eq. (4), the effect of k on R_s in MEKC is different from that in conventional chromatography. The last two terms in Eq. (4) are defined by the function $f(k)$ as

$$f(k) = \left(\frac{k_2}{1 + k_2} \right) \left(\frac{1 - (t_0/t_{mc})}{1 + (t_0/t_{mc})k_1} \right) \quad (5)$$

Then, we can calculate the optimum value of the retention factor, k_{opt} , for accomplishing the maximum R_s by differentiating Eq. (5), that is,

$$k_{opt} = \left(\frac{t_{mc}}{t_0} \right)^{1/2} \quad (6)$$

Under a neutral condition, k_{opt} is close to 2 for SDS micelles as the pseudo-stationary phase, as shown in Fig. 1. Practically, the recommended range of k is between 0.5 and 10.

Retention Factor and Distribution Coefficient

The retention factor can be related to the distribution coefficient, K , between the micelle and aqueous phase by

$$k = K \left(\frac{V_{mc}}{V_{aq}} \right) \quad (7)$$

where V_{mc} and V_{aq} are the volumes of the micelle and aqueous phase, respectively. The value V_{mc}/V_{aq} , or the phase ratio, can be written as

$$\frac{V_{mc}}{V_{aq}} = \frac{\bar{v}(C_{sf} - CMC)}{1 - \bar{v}(C_{sf} - CMC)} \quad (8)$$

where C_{sf} , \bar{v} , and CMC are the concentration of the surfactant, partial specific volume of the micelle, and critical micelle concentration, respectively. At a low micellar concentration, we can arrange Eq. (8) as

$$k \approx K\bar{v}(C_{sf} - CMC) \quad (9)$$

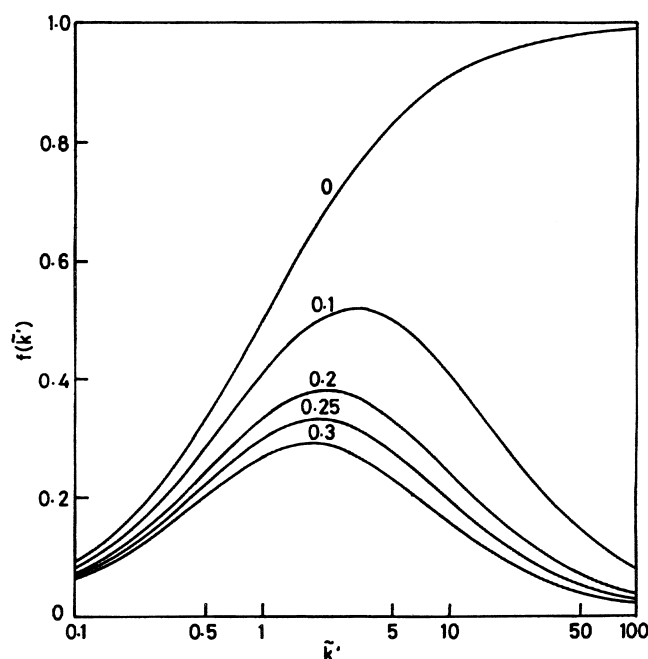


Fig. 1 Dependence of $f(k)$ on capacity factor k . The values of t_0/t_{mc} are given on each line. [Reprinted from S. Terabe, K. Otsuka, and T. Ando, *Anal. Chem.* 57: 834–841 (1985) with permission from the American Chemical Society.]

Thus, k can be adjusted by manipulating C_{sf} . Equation (9) shows that k increases linearly with C_{sf} , and we can calculate K from the slope of this relationship. Also, K remains constant regardless of C_{sf} . The applicability of Eq. (9) under various conditions and for various surfactants has been examined in a number of reports.

Suggested Further Reading

- K. Otsuka and S. Terabe, Micellar electrokinetic chromatography, *Bull. Chem. Soc. Jpn.* 71: 2465–2481 (1998).
- J. P. Quirino and S. Terabe, Electrokinetic chromatography, *J. Chromatogr. A* 856: 465–482 (1999).
- S. Terabe and Z. Deyl, Micelles as separation media in chromatography and electrophoresis, *J. Chromatogr. A* 780: (1997).
- S. Terabe, K. Otsuka, and T. Ando, Electrokinetic chromatography with micellar solution and open-tubular capillary. *Anal. Chem.* 57: 834–841 (1985).
- J. Vindevogel and P. Sandra, *Introduction to Micellar Electrokinetic Chromatography*, Hüthig, Heidelberg, 1992.

Retention Gap Injection Method

Raymond P.W. Scott

Scientific Detectors Ltd., Banbury, Oxfordshire, England

Introduction

In gas chromatographic analysis employing capillary columns, split injections are usually necessary to ensure that a very small sharp sample is placed on the column. This is important for maintaining column efficiency by not overloading the column. However, split injections generally result in an unrepresentative sample being placed on a capillary column (see the entry Split/Splitless Injector), and because of this, on-column injection is usually preferred for accurate quantitative analysis. On-column injection requires a relatively large-diameter capillary column to be used to permit the penetration of the injection syringe needle into the column. However, although this procedure ensures that a representative sample is placed onto the column, other problems can arise. On injection, the sample readily separates into droplets that act as separate, individual injections. These separate sample sources can cause widely dispersed peaks and serious loss of resolution and, in the extreme, double or multiple peaks. Grob [1] suggested a solution to this problem which he termed the *retention gap method of injection*.

Discussion

This procedure (Fig. 1) involves removing the internal coating of stationary phase from the first few centimeters of the column. This can be done by heating and volatilizing or burning off the phase. Alternatively, if the stationary phase is sufficiently soluble, it can be removed by a suitable solvent. The sample is then injected into the uncoated section of the column, and although the sample will probably split into droplets, the solvent will still vaporize in the normal way. As there is no stationary phase present, all the components of the mixture will travel at the speed of the mobile phase down the uncoated length of column until they reach a coated section. At this point, they will be absorbed into the stationary phase and all the components of the mixture will accumulate and form a compact sample at the start of the coated portion of the column.

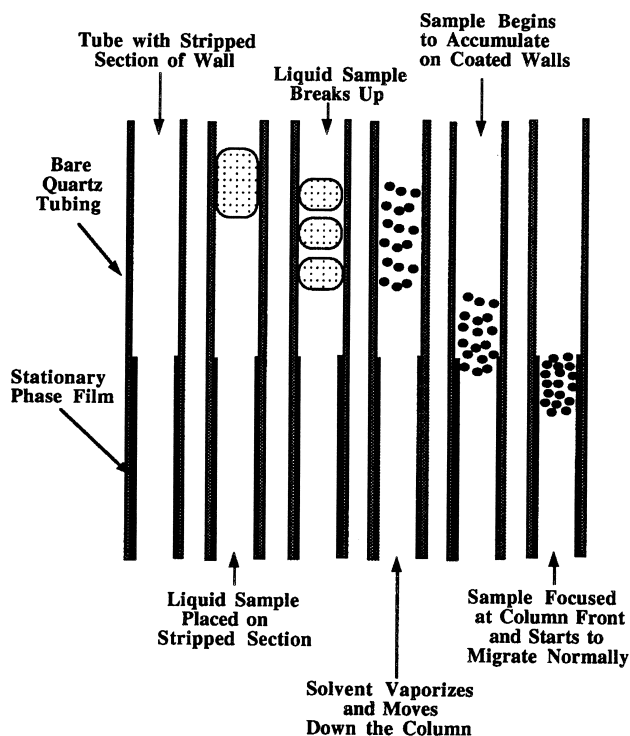


Fig. 1 The retention gap method of injection.

This technique is usually practiced in conjunction with temperature programming, the program being started at a fairly low temperature. The relatively low temperature facilitates the accumulation of all the solutes at one point in the column (i.e., where the stationary-phase coating begins). The temperature program is then started, and the solutes are eluted through the column in the normal way. The success of this method depends on there being a significant difference between the boiling points of the sample solvent and those of the components of the sample. In general, however, this procedure does significantly improve the quality of the separation and allows accurate quantitative results to be obtained.



Reference

1. K. Grob, *Classical Split and Splitless Injection in Capillary Gas Chromatography*, Huethig, Heidelberg, 1987.

Scott, R. P. W., *Techniques and Practice of Chromatography*, Marcel Dekker, Inc., New York, 1996.

Scott, R. P. W., *Introduction to Analytical Gas Chromatography*, Marcel Dekker, Inc., New York, 1998.

Suggested Further Reading

Grant, D. W., *Capillary Gas Chromatography*, John Wiley & Sons, Chichester, 1995.



Retention Time and Retention Volume

Raymond P.W. Scott

Scientific Detectors Ltd., Banbury, Oxfordshire, England

Introduction

The *retention time* of a solute is the elapsed time between the *injection point* and the peak maximum of the solute. The different properties of the chromatogram are shown in Fig. 1. The *volume of mobile phase* that passes through the column between the injection point and the peak maximum is called the *retention volume*. If the mobile phase is incompressible, as in LC, the retention volume (as so far defined) will be the simple product of the *exit flow rate* and the *retention time*.

Application

If the mobile phase is compressible, the simple product of retention time and flow rate will be incorrect, and the *retention volume* must be taken as the product of the *retention time* and the *mean flow rate*. The true *retention volume* has been shown to be given by [1]

$$V_r = V_r' \frac{3}{2} \left(\frac{\gamma^2 - 1}{\gamma^3 - 1} \right) = Q_0 t_r \frac{3}{2} \left(\frac{\gamma^2 - 1}{\gamma^3 - 1} \right)$$

where the symbols have the meanings defined in Fig. 1, and V_r' is the retention volume measured at the column exit and γ is the inlet/outlet pressure ratio.

The retention volume V_r will include the dead volume V_0 , which, in turn, will include the actual dead volume V_m and the extracolumn volume V_E .

Thus,

$$V_r = V_E + V_m + V_r'$$

The retention time can be taken as the product of the distance on the chart between the injection point and the peak maximum and the chart speed, using appropriate units. More accurately, it can be measured with a stopwatch. The most accurate method of measuring V_r for a noncompressible mobile phase, although considered antiquated, is to attach an accurate burette to the detector exit and measure the retention volume in volume units. This is an absolute method of measurement and does not depend on the accurate cal-

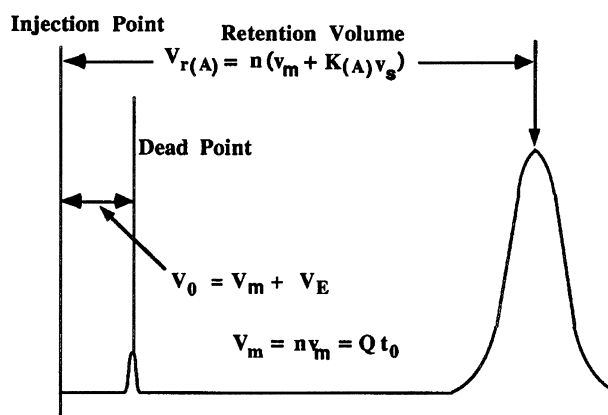


Fig. 1 Diagram depicting the dead point, dead volume, and dead time and retention volume of a chromatogram. V_0 is the total volume passed through the column between the point of injection and the peak maximum of a completely unretained peak, V_m is the total volume of mobile phase in the column, $V_{r(A)}$ is the retention volume of solute A, V_E is the extra column volume of mobile phase, v_m is the volume of the mobile phase per theoretical plate, v_s is the volume of the stationary phase per theoretical plate, K_A is the distribution coefficient of the solute between the two phases, n is the number of theoretical plates in the column, and Q is the column flow rate measured at the exit.

ibration of the pump, chart speed, or computer acquisition level and processing.

Reference

1. R. P. W. Scott, *Introduction to Analytical Gas Chromatography*, Marcel Dekker, Inc., New York, 1998, p. 77.

Suggested Further Reading

- Scott, R. P. W., *Liquid Chromatography Column Theory*, John Wiley & Sons, Chichester, 1992, p. 19.
 Scott, R. P. W., *Techniques and Practice of Chromatography*, Marcel Dekker, Inc., New York, 1996.



Reversed-Phase Chromatography: Description and Applications

Joseph J. Pesek
Maria T. Matyska

San Jose State University, San Jose, California, U.S.A.

Introduction

Classical liquid chromatography is typically practiced in what is referred to as the normal-phase mode; that is, the stationary phase is usually a polar sorbent such as silica and alumina and the mobile phase consists of a nonpolar constituent such as hexane modified with a somewhat more polar solvent such as chloroform or ethyl acetate. In this mode, the more polar compounds are preferentially retained. The reversed-phase (RP) mode utilizes the opposite approach for the separation of nonpolar analytes or compounds that have some hydrophobic character. In this case, the stationary phase must consist of sorbent that is nonpolar in nature and the mobile phase is composed of a primary polar solvent, usually water, that is modified by a more nonpolar constituent such as methanol, acetonitrile, or tetrahydrofuran.

Discussion

In order to make RP chromatography a rapid and efficient method, it is necessary to force the mobile phase through the stationary phase using high pressure. Therefore, the stationary phase must be a mechanically stable entity possessing the desired nonpolar properties for reversed-phase operation. This result is accomplished typically by using particulate silica, which is stable under high pressure, and modifying the surface with a nonpolar organic moiety. The modification takes place by reacting the silanol ($\text{Si}-\text{OH}$) groups on the silica surface with a suitable reagent, most often an organosilane compound ($\text{X}_3\text{Si}-\text{R}$ or $\text{XR}'\text{Si}-\text{R}$, where X is a reactive group such as Cl or methoxy, R' is a small organic group such as methyl, and R is another organic moiety, most often octyl (C_8) or octadecyl (C_{18}), in the RP mode. These silica modifications result in a primarily hydrophobic surface that can preferentially retain the more nonpolar compounds in a mixture. The degree of hydrophobic-

ity is controlled by both the length of the alkyl chain and the density of bonded groups on the surface, usually expressed in terms of micromoles per square meter. Due to the fact that original silica material has a high surface area (typically $100-300 \text{ m}^2/\text{g}$), the amount of hydrophobic material in the chromatographic column is considerable (from a few to as much as 20% by weight), leading to substantial interactions between solutes and the stationary phase. RP stationary phases are available with a variety of hydrophobic groups on the surface and bonding densities on silica particles of different diameters, surface areas, and pore sizes. In addition to the RP separation materials consisting of silica, some commercial products are also fabricated on other oxides such as alumina or zirconia or consist of polymeric matrices.

The second major component in modern high-performance liquid chromatography (HPLC) is the mobile phase. Since the stationary phase is a nonpolar entity, the mobile phase must be more polar to allow retention of the analytes. The most polar solvent for RP-HPLC is water, but the overall polarity of the mobile phase can be adjusted by introducing variable amounts of any of a number of organic solvents. In liquid chromatography, retention of solutes is a result of its relative affinity for the stationary and mobile phases. This can be described mathematically by the equation

$$k' = \frac{(\text{Amount of analyte})_{\text{SP}}}{(\text{Amount of analyte})_{\text{MP}}}$$

where k' is the equilibrium constant referred to as the capacity factor that relates the amounts of the analyte in the stationary phase (SP) and the mobile phase (MP). Therefore, the mobile phase exerts considerable influence on the retention and, hence, the separation of solutes. This factor makes HPLC a very powerful separation technique in that the mobile phase can be adjusted to accommodate a wide variety of solutes (from large biomolecules to small organic and inorganic compounds) having a range of chemical proper-



ties. Simultaneously, the selection of the mobile-phase composition will determine the degree of interaction between the solute and the stationary phase.

Most RP-HPLC separations are done in the isocratic mode (i.e., where the composition of the mobile phase is held constant during the analysis). This approach is suitable when the sample consists of analytes having similar properties or where their hydrophobicities encompass a small or moderate range. Under these conditions, all solutes in the sample will be eluted over a reasonable time span (i.e., not too short to prevent resolution of individual analytes and not too long to result in an inconvenient analysis period). Therefore, proper selection of the mobile-phase composition is essential in the development of any reversed-phase separation method. Fortunately, due to the decades of long practice of RP-HPLC, there exists in the literature and from commercial sources, a wealth of information on suitable mobile-phase compositions for particular types of sample, especially for the C_{18} stationary phase. In addition, the retention of solutes on hydrophobic phases has been modeled mathematically and there exist computer programs for assisting in the optimization of mobile-phase composition in the solution of various separation problems.

A single mobile composition is often not suitable for samples that contain a wide range of chemical properties or hydrophobicities. Under these conditions, an isocratic method may leave the early eluting components unresolved and the analytes having strong retention with inconveniently long elution times. The solution to this problem is to change the mobile-phase composition in a systematic way during the course of the separation. This approach is referred to as gradient elution. In gradient elution, the mobile-phase composition initially is weak (with a large percentage of the most polar component) and becomes increasingly stronger (containing greater amounts of the less polar modifier) as the separation process continues. With this approach, the retention of the less hydrophobic compounds is increased at the beginning of the separation, whereas the retention of the more hydrophobic compounds is diminished at the end of the elution period. The simplest approach to gradient elution is to vary the mobile-phase composition linearly from the beginning to the end of the analysis period. In addition to the rate of change of the mobile-phase composition, the initial and final amounts of the two solvents are also variables that can be changed to improve resolution within the shortest analysis times. Besides linear gradients, other formats have been developed to optimize separations. These gradient methods include a constant composition at the beginning and/or the end of

the analysis as well as concave, convex, or step profiles. The main disadvantage of the gradient method is the time required for the column to reequilibrate to the initial mobile-phase conditions. This reequilibration time can be from several minutes up to a half-hour or longer. However, modern instrumentation (pumps and pump controllers) has made reproducible gradients relatively easy to achieve.

Another means of controlling eluent strength is the use of ternary or quaternary solvent mixtures instead of the more common binary approach. Each solvent has its own unique properties that can be used to improve the separation of difficult-to-resolve analytes or to shorten the analysis time without sacrificing resolution. Although gradients and more complex solvent matrices are more difficult to model than binary isocratic systems, software exists for such purposes and can assist in method development.

The basic equipment for the RP mode is similar to most other types of HPLC. It consists of solvent reservoirs (one to four), a high-pressure pump, a mixing device that can create any combination of binary solvents or higher order as well as gradients (optional), an injection device, the column, and a detector connected to a data processing device. Ultraviolet (UV) detection is most often used in the reversed-phase mode, but fluorescence, refractive index, and electrochemical properties, as well as coupling to a mass spectrometer are also possible. Qualitative information is obtained by comparing the retention times of unknown compounds to those of known standards, whereas quantitative information comes from calibration curves of the peak area versus concentration. The coupling of liquid chromatographs to mass spectrometers and nuclear magnetic resonance (NMR) spectrometers is becoming more common, which makes positive identification of unknown compounds in a mixture much easier.

Applications

One of the primary factors responsible for the development of HPLC was the need to separate mixtures containing hydrophobic compounds that were not sufficiently volatile for analyzing by gas chromatography (GC) or were thermally unstable after volatilization. Although some compounds that are normally non-volatile can be made volatile by derivatization, this process adds an extra step to the analytical method. However, under any circumstances, a large majority of chemical species, perhaps as much as 70%, cannot be analyzed by GC. Among the most significant of these compounds are ionic species, both organic and inor-



ganic, as well as most biomolecules. With greater demand for the analysis of biologically related samples for medical, pharmaceutical, and biotechnological purposes, the need for reliable HPLC reversed-phase methods continues to increase. Although it is impossible to review all types of sample amenable to RP-HPLC analysis, a few examples will be given to illustrate the breadth of applications possible by this technique.

Because the mechanism of separation is primarily based on differences in hydrophobicity, a simple mixture of aromatic hydrocarbons can be used to illustrate the operation of the reversed-phase method. A chromatogram of such a separation is shown in Fig. 1, where the elution times are benzene < toluene < ethylbenzene < isopropylbenzene < *t*-butylbenzene < anthracene. When the reversed-phase mechanism is functioning, compounds are eluted in order of increasing hydrophobicity, as illustrated in Fig. 1. By increasing the degree of hydrophobicity either through longer alkyl chains [more saturated or unsaturated (aromatic) hydrocarbon groups] or more alkyl chains (higher bonding density), retention times (larger k' values) become

longer under constant mobile-phase conditions. This principle applies to a wide variety of organic compounds. The organic molecules can also have a polar functional group such as an alcohol, ether, amine, or cyano, for example, but the RP method can still be used. In this case, the polar groups may diminish the overall hydrophobicity of the compound, but there will still be some retention on a typical RP stationary phase such as octadecyl (C_{18}). A simple example is benzene and phenol. The addition of a hydroxyl group makes phenol less hydrophobic than benzene, so it will be eluted first.

The above example illustrates the principle of relative retention (i.e., that benzene is retained more strongly than phenol). In order to determine absolute retention, the k' values of each compound must be measured as follows:

$$k' = \frac{t_R - t_0}{t_0}$$

where t_R = the retention time of compound and t_0 is the time to elute an unretained compound. In HPLC, the t_0 is equivalent to measuring the elution time for air in GC. Therefore, selection of a suitable compound that will not be retained is crucial to accurate measurement of k' values. Because retention is based on hydrophobicity, the t_0 marker should be very hydrophilic (i.e., very polar or ionic). Two compounds often selected for this determination are KNO_3 and uracil. They both fulfill the requirement for hydrophilic properties and also have absorbance in the UV, which facilitates detection.

Whereas the overall hydrophobic nature of the stationary phase is the most important factor in determining retention, bonded-phase structure can also influence k' values. This effect can be observed in the separation of polycyclic aromatic hydrocarbons (PAHs). For stationary phases with a high bonding density and/or a high degree of association between adjacent bonded organic moieties, molecules that are more planar are preferentially retained. The National Institute of Standards and Technology (NIST) has developed reference mixtures to measure this effect.

In addition to a wide range of polar and nonpolar hydrocarbons that can be analyzed by RP-HPLC, it is also possible to separate ionic species. Because water is used as part of almost all mobile phases, those species which are acids and bases can be neutralized by control of pH. In cases where neutralization is not possible, then the addition of a counterion into the mobile phase so that the analyte will form a neutral complex can be used to enhance RP retention. The same principle can be applied to inorganic species by forming a neutral complex that results in reversed-phase retention.

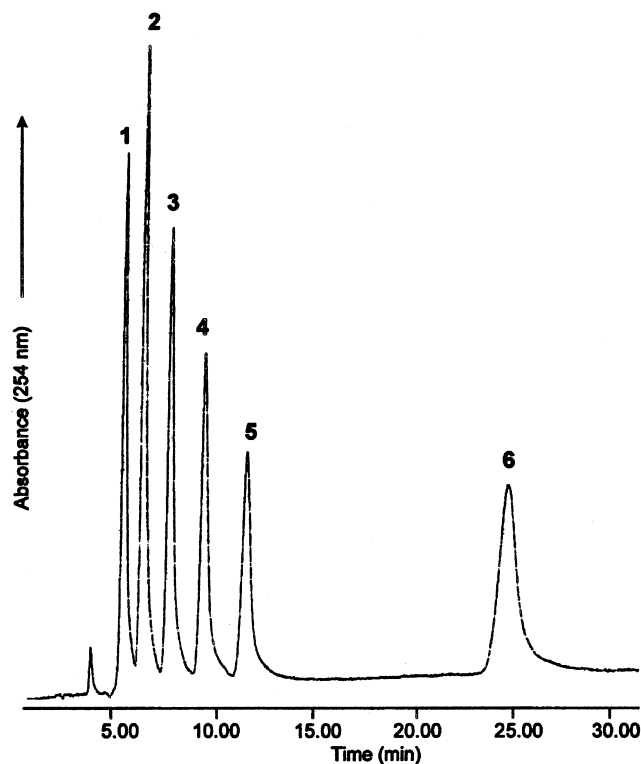


Fig. 1 Separation of reversed-phase test mixture on a C_{22} bonded phase. Mobile phase: 50:50 acetonitrile–water. Solutes: 1 = benzene; 2 = toluene; 3 = ethylbenzene; 4 = isopropylbenzene; 5 = *t*-butylbenzene; 6 = anthracene.



Large biomolecules, while being charged under most aqueous mobile-phase conditions, still have significant hydrophobic portions that interact with the

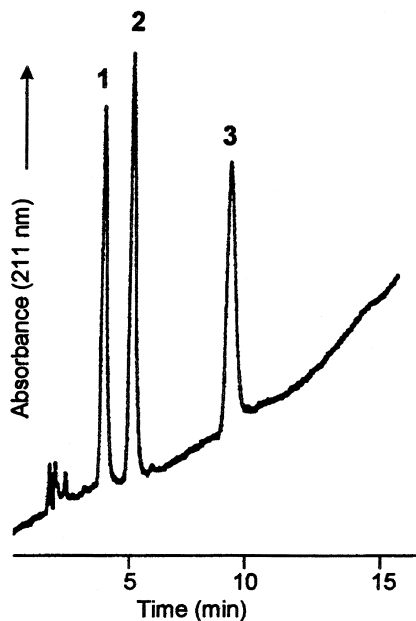


Fig. 2 Gradient separation of peptide mixture on a C_{30} bonded phase. Mobile phase, linear gradient from 25% to 45% A in 15 min. A = 0.1% trifluoroacetic acid (TFA) in 75:25 acetonitrile–water and B = 0.1% TFA in water. Solutes: 1 = bradykinin; 2 = angiotensin III; 3 = angiotensin I.

stationary phase. In many complex mixtures of proteins and peptides, the degrees of interaction with the stationary phase (k' values) vary over a broad range. Therefore, gradient elution methods are often required. An example of such a gradient method for the separation of a biochemical mixture is shown in Fig. 2. Finally, although water is used almost exclusively as the weak solvent in RP methods, a few types of sample require the use of other mobile-phase components. For example, the separation of triglycerides and fatty acids often utilize acetone as the weak solvent in the RP mode.

Suggested Further Reading

- Cunico, R. L., K. M. Gooding, and T. Wehr, *Basics HPLC and CE of Biomolecules*, Bay Bioanalytical Laboratory, Richmond, CA, 1998.
- Kirkland, J. J., *LC–GC* (May 1997).
- Mant, C. T. and R. S. Hodges (eds.), *High Performance Liquid Chromatography of Peptides and Proteins*, CRC Press, Boca Raton, FL, 1991.
- Poppe, H., Column liquid chromatography, in *Chromatography*, 5th ed. (E. Heftmann, ed.), Elsevier, Amsterdam, 1992.
- Snyder, L. R., Theory of chromatography, in *Chromatography*, 5th ed. (E. Heftmann, ed.), Elsevier, Amsterdam, 1992.
- Vansant, E. F., P. Van Der Voort, and K. C. Vrancken, *Characterization and Chemical Modification of Silica*, Elsevier, Amsterdam, 1995.

Reversed-Phase Stationary Phases

Joseph J. Pesek
Maria T. Matyska

San Jose State University, San Jose, California, U.S.A.

Introduction

The primary purpose for the development of chemically modified stationary phases was to provide a separation medium that was suited to the type(s) of solute present in the mixture to be analyzed. Historically, silica gel was the most common material used in the early development of column liquid chromatography (LC). However, silica is a polar material that contains hydroxyl groups (silanols) that are both acidic and strongly hydrogen-bonding in character. These properties make it unsuitable as a stationary phase for many typical organic molecules that are predominantly hydrophobic compounds. In addition, the silanols interact strongly with basic compounds leading to poor chromatographic results.

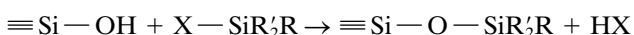
Discussion

In order to overcome these undesirable effects of silica and to have a medium more suitable for the separation of a large variety of organic compounds, modification of the surface is necessary to provide a more nonpolar (hydrophobic) material. It is advantageous to retain silica as the primary material in the column because it possesses physical and mechanical properties that make it particularly useful for modern liquid chromatography [i.e., the use of high-pressure liquid chromatography (HPLC) to force the mobile phase and sample through the system at a reasonable flow rate].

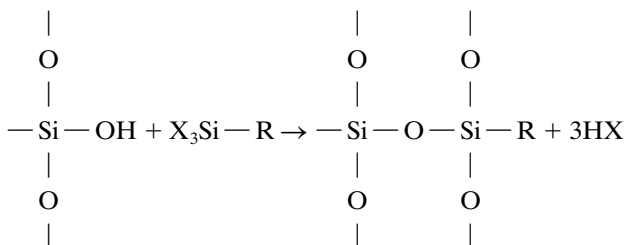
The desirable characteristics of silica are as follows: high mechanical strength, a narrow range of particle diameters, a variety of pore sizes, a broad range of surface areas, and the ability to be modified either chemically or physically by adsorption.

It is the latter property (i.e., the ability for modification) that makes silica particularly useful as a separation medium in chromatography. Although physical adsorption has been used occasionally to modify silica surfaces for chromatographic purposes, its usefulness is limited because of the nature of modern HPLC. The use of high pressure creates shear forces at the station-

ary phase–mobile phase interface so that the absorbed moiety is removed from the silica surface even though the coating may be insoluble in the liquid being pumped through the column. Therefore, chemical modification is the only practical approach to modifying the silica surface in order to create a stationary phase that is compatible with the types of solutes to be separated. The most common method for modifying silica in order to produce a hydrophobic surface is organosilanization. Two types of reaction are available by this method. The first alternative is referred to as a monomeric approach:



Here, the organosilane reagent is composed of a reactive group, X, which can be a halide, usually chloride, methoxy, or ethoxy; R' is one of two small organic groups usually methyl, and R is the main group that gives the surface its hydrophobic properties. The end result is a single point of attachment between the organosilane reagent and the surface. The second alternative shown in the following reaction is referred to as the polymeric approach for bonding.



In this case, the organosilane reagent is composed of three reactive groups; X is as described earlier and R is the main organic group that provides the hydrophobic properties to the surface. Here, the end result is that the bonded phase is attached to the surface at one point and cross-linked to neighboring bonded organosilanes through a siloxane linkage. Both of these synthetic routes are used in the production of commercially available stationary phases for HPLC. The monomeric approach generally is more repro-



ducible from batch to batch, whereas the polymeric approach leads to higher bonding densities (more R groups per unit surface area) and some additional stability due to the multiple sites of attachment.

In both types of reactions, it is the R group that determines the overall characteristics of the surface if there is a reasonable bonding density as measured in terms of micromoles per square meter. There must be a significant number of organic moieties per unit surface area so that most of the silica is covered by the R groups and relatively few of the siloxane and silanols are accessible. Under these conditions, when the organic moiety is hydrophobic, nonpolar solutes will be selectively retained by the stationary phase. Even in the case where the bonding density is reasonably high, there is still the possibility that some silanols may be accessible to solutes. This is mainly a problem when the analytes are strongly basic compounds. In order to diminish the effect of unreacted silanols on the surface or those that can be created in the polymeric reaction process when complete cross-linking does not take place, a secondary reaction involving a small reactive organosilane can be used. Typically, this reagent is trimethylchlorosilane, a compound with one reactive group and three small organic moieties. This compound is small enough to fit into the larger spaces between bonded hydrophobic groups so that access to the surface will be even more limited for typical solutes. The process of bonding a small moiety to diminish the number of accessible silanols is referred to as "end-capping." Many commercial sources will often designate whether or not a particular bonded phase has been endcapped. The presence or absence of endcapping will determine the nature of the stationary phase surface and, hence, its retention characteristics.

However, it is still the main R group that controls the overall degree of hydrophobicity of the surface. Within this context, the predominant factors in determining the hydrophobicity are the length of the alkyl chain or the total number of carbon atoms as well as the bonding density. Some examples of various alkyl groups that have been used as reversed-phase (RP) materials are shown in Table 1. The most common types of these phases are designated by C_n , where n is the number of carbon atoms for bonded linear alkyl hydrocarbon moieties. The simplest case is where $n = 1$ for the methyl-bonded phase (C_1). This material has the lowest degree of hydrophobicity and provides limited retention for most small organic molecules. However, for large biomolecules such as proteins and peptides that can have extensive hydrophobic regions as part of their three-dimensional structure, these phases can prove useful in limiting the strong interactions, leading to excessively

Table 1 Bonded Hydrophobic Groups

Methyl	$-\text{CH}_3$
Ethyl	$-\text{CH}_2\text{CH}_3$
Butyl	$-\text{CH}_2-(\text{CH}_2)_2-\text{CH}_3$
Octyl	$-\text{CH}_2-(\text{CH}_2)_6-\text{CH}_3$
Octadecyl	$-\text{CH}_2-(\text{CH}_2)_{16}-\text{CH}_3$
Triacontyl	$-\text{CH}_2-(\text{CH}_2)_{28}-\text{CH}_3$
Phenyl	$-\text{CH}_2-(\text{CH}_2)_x-\text{C}_6\text{H}_5$
Perfluoro	$-\text{CH}_2-(\text{CF}_2)_x-\text{CF}_3$

long retention times for these compounds. As the degree of hydrophobicity decreases for these large species (i.e., the macromolecule has larger hydrophilic regions or the hydrophobic areas are buried within the three-dimensional structure), the stationary phase will have to become more nonpolar. This is accomplished by extending the chain length of the bonded alkyl group. Hence, the C_2 and C_4 phases have been developed to accomplish this purpose. In general, the bonded phases C_1 , C_2 , and C_4 have been used for separations of large molecules. In order to develop more hydrophobic interactions, the next most common phase utilizes the octyl-bonded moiety (C_8). At relatively high bonding densities ($3\text{--}4\ \mu\text{mol}/\text{m}^2$), a wide range of compounds can be separated in the reversed-phase mode with this bonded moiety. Although applications involving large molecules are readily found in the literature, the predominant use involves the separation of typical small [molecular weight (MW) < 500] organic compounds. The most common reversed-phased material contains the octadecyl moiety ($n = 18$) as the bonded group. Although there are reports of phases in the literature with n values between 8 and 18, these are relatively uncommon and have not found widespread use or commercial development. The C_{18} -bonded phase was the separation material used in most of the early development of HPLC; therefore, there are several decades of applications documented in the literature. It is still by far the most often used bonded material in reversed-phase HPLC and is available in a wide variety of forms (type of silica, pore size, surface area, monomeric, polymeric, endcapped, nonendcapped, etc.) from more than 100 commercial sources. Although small organic molecules account for the majority of applications, its early commercial availability and its role in the development of HPLC has led to examples of separations involving a broad range of compounds, including ionic species, polar compounds, biomolecules, fatty acids, and diastereomers. Because most laboratories with HPLC equipment will have a C_{18}

column available, and sometimes the only one on hand, it is the first choice for initial experiments. In addition, with the broad range of applications accessible in the literature or from commercial sources, it is often easy to find a separation that is similar, allowing for selection of mobile-phase conditions that are likely to be suitable for solving a particular analytical problem.

As shown in Table 1, a number of other bonded groups have also found use in reversed-phase HPLC. Theoretically, there is no limit to the value of n for bonded alkyl groups. However, until recently, there has been little interest in phases longer than 18 carbons. Some recent studies have demonstrated interesting applications for the C_{30} phase so that its use as well as materials with alkyl chain lengths between 18 and 30 might become more common. A phenyl-bonded group (with alkyl chains attaching it to the surface of various lengths) can also function in the reversed-phase mode. The possibility of utilizing $\pi-\pi$ interactions or charge-transfer effects with the phenyl phase leads to a different selectivity than the solely hydrophobic interactions that are available from the common alkyl-bonded materials. A similar reasoning can be applied for the phases where F is substituted for H in the bonded organic group.

Although the vast majority of stationary phases for RP-HPLC are based on chemically modified silica, there are a few other supports that have been investigated and some which are available commercially. Although silica has many advantages, its main limitation is the pH range over which it is stable. Depending on the type of silica, bonding method, and surface coverage, most chemically modified silicas are useful from pH 2 to 8. Outside of this range, most materials will experience some type of accelerated degradation. One solution to this problem is to substitute an oxide with a greater pH stability than silica. Some possibilities include alumina, zirconia, and titania, which can all be fabricated in particles with properties similar to those of silica (size, porosity, and surface area) as well as having hydroxide groups on the surface that can be used for chemical modification. Another approach is to use polymeric materials as supports in RP-HPLC. Polymers can be formed into beads similar to oxide particles, can be chemically modified to contain various organic functional groups to control their chromatographic properties, and can possess pH stability in strong acids and bases. If such modification or the basic structure of the polymer is hydrophobic, then these materials can be used in the reversed-phase mode. The main disadvantage to many polymeric materials is that they often expand or contract in various mobile-phase compositions, leading to nonreproducible chromato-

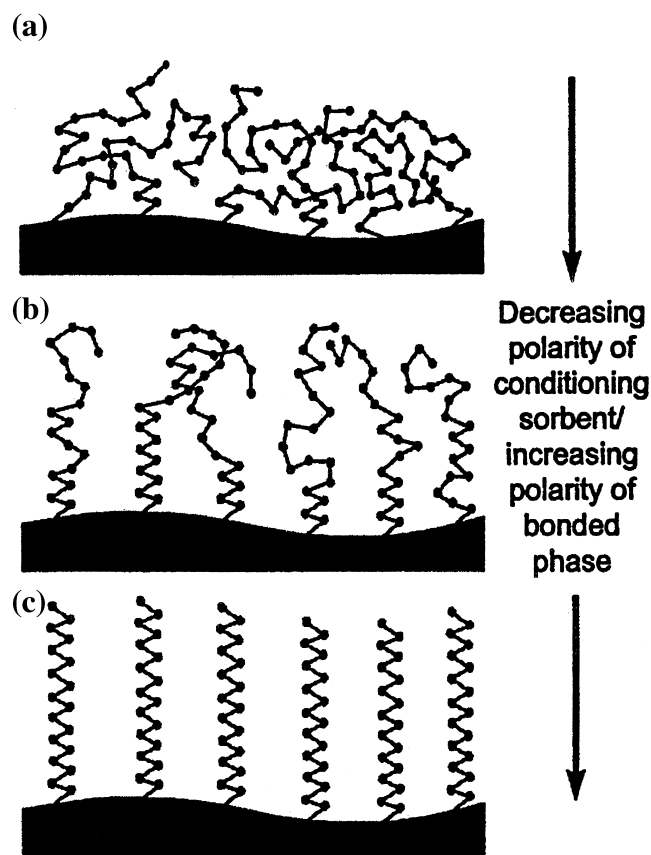


Fig. 1 Structure of a bonded phase as a function of polarity of a mobile phase: (a) highly polar mobile phase; (b) intermediate polarity mobile phase; (c) low-polarity mobile phase.

graphic performance. Despite the potential pH advantages of these alternative supports, they have not been extensively exploited because of the long-term use of silica in the development of chemically bonded stationary phases and the limited number of applications where either very acidic or basic eluents are an absolute necessity.

The structure of the alkyl-bonded moiety on the support surface has been the subject of many investigations. A variety of spectroscopic and chromatographic methods have been employed to determine the configuration of various bonded organic groups (although the vast majority of studies have been on C_{18}) in order to understand the mechanism of separation for typical solutes. There are many variables to be considered in these investigations, which include type of bonded group, bonding density, and the nature of the support surface. Some studies involve the presence of solvents to mimic the mobile phase, whereas others utilize the bonded material in the absence of any liq-



uids. Despite these differences, some generalizations can be made about the structure of typical bonded phases in the presence of water–organic solvents, as illustrated in Fig. 1. At low concentrations of an organic constituent (A), the environment around the bonded moiety is polar and the hydrophobic chains tend to collapse on each other in order to minimize their exposure to the surrounding solvent. As the percent of organic in the liquid around the bonded group increases (B \rightarrow C), the medium is less polar and the groups are no longer strongly associated with each other. Although reversed-phase bonded materials have been available for many years, there is continued development to improve their chromatographic performance and to develop new phases for specialized applications.

Suggested Further Reading

- Iler, R. K., *The Chemistry of Silica*, John Wiley & Sons, New York, 1979.
- Marciniec, B., *Comprehensive Handbook on Hydrosilylation*, Pergamon Press, Oxford, 1992.
- Nawrocki, J., *Chromatographia* 31: 177 (1991).
- Nawrocki, J., *Chromatographia* 31: 193 (1991).
- Pesek, J. J. and M. T. Matyska, *Interf. Sci.* 5: 103 (1997).
- Pesek, J. J., M. T. Matyska, J. E. Sandoval, and E. J. Williamsen, *J. Liquid Chromatogr. Related Technol.* 19: 2843 (1996).
- Unger, K. K., *Porous Silica*, Elsevier, Amsterdam, 1979.
- Vansant, E. F., P. Van Der Voort, and K. C. Vrancken, *Characterization and Chemical Modification of Silica*, Elsevier, Amsterdam, 1995.



R_f

Luciano Lepri

Alessandra Cincinelli

Università degli Studi di Firenze, Firenze, Italy

Introduction

The R_f value is the fundamental parameter in planar chromatography which describes, numerically, the position of a spot on the developed chromatogram.

The R_f Value in Linear Chromatography

The method for determining R_f values is based on the measurement of two lengths in a thin-layer chromatogram and the calculation of their ratio:

$$R_f = \frac{\text{Distance of spot center from start}}{\text{Distance of solvent front from start}}$$

where “start” is the sample application point.

R_f values are between 0 and 1 (solute remains at start or runs with the solvent front, respectively) and the maximum number of significant figures after the decimal point is currently two. R_f values are often multiplied by a factor of 100 (hR_f).

R_f values can be disturbed by side effects or demixing of the multicomponent solvent used. In order to obtain reproducible R_f values, much attention must be placed on the reproducibility of the system.

The R_f Value in Circular Chromatography

Linear R_f values can be transferred to the circular technique with the equation

$$R_{f\text{lin}} = R_{f\text{circ}}^2$$

This equation holds only if the starting line is close to the center of the layer. Circular R_f values are higher than the linear ones, with the exception of $R_f = 0$ and $R_f = 1$. The increase in the circular R_f values is greater in the lower range.

Definition of Thermodynamic R_f Value

According to the Martin–Synge model of partition chromatography [1,2], the thermodynamic R_f value (R'_f), based on the chromatographic equilibrium process of solute distribution between the mobile and

stationary phase, can be expressed as the fraction of the relative time spent by a solute molecule in the mobile phase (A) or fraction of solute molecules in the mobile phase (B):

$$R'_f = \frac{t_m}{t_m + t_s} = \frac{n_m}{n_m + n_s}$$

(A) (B)

where the subscripts m and s refer to mobile and stationary phase, respectively.

Because the fractions of solute molecules and respective mole numbers are identical, it is possible to achieve the fundamental relation (1) connecting R'_f value with the distribution coefficient $K_d = C_s/C_m$ and the phase ratio V_s/V_m :

$$R'_f = \frac{m_m}{m_m + m_s} = \frac{C_m V_m}{C_m V_m + C_s V_s} = \frac{1}{1 + K_d(V_s/V_m)} \quad (1)$$

In the Martin–Synge relationship (1), C_m and C_s are molar concentration of the solute in the mobile and stationary phase, respectively, and V_s and V_m are the volumes of these two phases. V_s/V_m is numerically equal to A_s/A_m , the ratio of the phase cross section normal to the direction of the solvent flow, which better describes the local conditions in thin-layer chromatography. The validity of the equation is limited because the amount of solvent on the layer decrease going toward the solvent front and, therefore, the phase ratio changes.

R'_f values are generally higher than R_f values and can be related to each other by the following experimental relationship

$$R'_f = \xi R_f$$

where ξ is the disturbing factor ($1 \leq \xi \leq 1.6$) [3]. This relationship usually holds in the R_f region up to 0.7 because the greatest changes of the solvent front are observed at the end of the chromatogram.

The R_{st} Number

Relative R_f values, generally called R_{st} or R_x values, can also be used but are inadequate to render R_f values in-



dependent of uncontrolled parameters, because they are dependent of the phase ratio:

$$R_{st} = \frac{(R_f)_i}{(R_f)_{st}} = \frac{\text{Migration distance of substance } i}{\text{Migration distance of reference substance, st}}$$

These values can be greater than 1.

References

1. A. J. P. Martin and R. L. M. Synge, *Biochem. J.* 35: 1358 (1941).
2. A. J. P. Martin, *Biochem. J.* 50: 679 (1952).
3. F. Geiss, *Foundamentals of Thin-Layer Chromatography (Planar Chromatography)*, Alfred Hüthig Verlag, Heidelberg, 1987, pp. 87–114.



Rotation Locular Countercurrent Chromatography

Kazufusa Shinomiya

College of Pharmacy, Nihon University, Chiba, Japan

Introduction

Rotation locular countercurrent chromatography (RLCCC) was introduced in the early 1970s [1,2] as a preparative CCC system. In general, the existing CCC systems may be classified into two groups according to the mode of solute partitioning. One is called the hydrostatic equilibrium system (HSES) and the other is called the hydrodynamic equilibrium system (HDES). RLCCC belongs to HSES as does droplet CCC, whereas the high-speed CCC is the most advanced form of HDES, which has been widely used for the separation and purification of natural products.

Although RLCCC is less efficient than high-speed CCC, in terms of resolution and separation times, it has advantages of a large-sample loading capacity and universal application of two-phase solvent systems. Retention of the stationary phase is accomplished simply by adjusting the column rotation speed and flow rate according to physical properties of the solvent system. In addition, RLCCC can be effectively performed with a short column by alternatingly eluting the col-

umn with the two solvent phases. This “alternating CCC” method [3,4] is described later in some detail.

Rotation locular countercurrent chromatography is particularly suitable for the preparative separation of natural products, and the apparatus is commercially available through Tokyo Rikakikai Co., Ltd., Tokyo, Japan.

Apparatus

Rotation locular countercurrent chromatography uses a separation column containing a series of cylindrical partition units called “locules.” This locular column is made by inserting multiple centrally perforated disks into a PTFE (polytetrafluoroethylene) or glass tubing at regular intervals. Multiple column units are connected in series with PTFE tubing and mounted in parallel around the rotary shaft of the apparatus. The column assembly is held at a constant angle from the horizontal plane and rotated at a moderate rate (60–80 rpm). Figure 1 schematically illustrates the RLCCC ap-

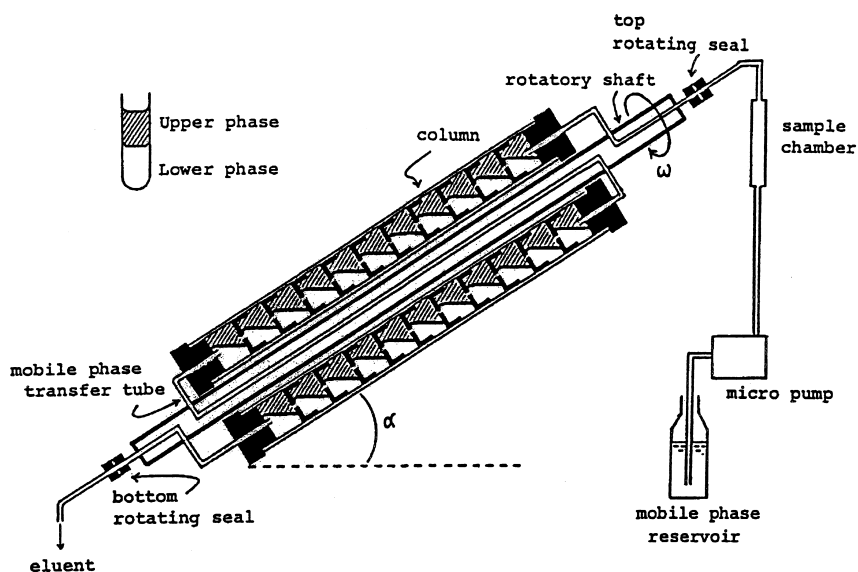


Fig. 1 Rotation locular countercurrent chromatography apparatus.



paratus. In each locule, the two phases form a horizontal interface and efficient stirring of each phase is produced by rotation of the column assembly. The system provides the choice of the mobile phase, where the upper phase is eluted in an ascending mode and the lower phase in a descending mode through the inclined column. The solutes present in the sample solution are subjected to an efficient partition process between the two phases, in each locule, and, finally, eluted according to their partition coefficients.

In the early prototype instrument [1], the columns were fabricated from relatively large-bore PTFE tubing of 4.6 mm inner diameter (i.d.) with PTFE disk inserts having 0.8-mm-diameter holes. These disks were spaced in 3-mm intervals to form 47 locules in each unit. A number of column units were connected in series to provide 5000 locules with a total capacity of 100 mL. The capability of the system was demonstrated with the separation of DNP (dinitrophenyl)-amino acids using a two-phase solvent system composed of chloroform-acetic acid-0.1M HCl at a 2:2:1 volume ratio. In this system, nine DNP-amino acids were resolved within 70 h at about 3000 theoretical plates.

A commercial RLCCC instrument is equipped with a set of 16 locular column units of 16-mm i.d. and 61 cm in length, containing 37 locules in each unit. The column assembly consists of 592 locules with an 800-mL capacity. At a flow rate of 15–25 mL/h, the system can yield 250–400 theoretical plates, which corresponds to 2.3–1.5 locules/plate [5].

Separation Procedure

Each separation is initiated by filling the column with either the upper or lower phase of an equilibrated two-phase solvent system. In order to avoid trapping air bubbles in the column, the solvent should be introduced through the bottom of each column, which is kept in a vertical position. Then, the column assembly is tilted at a desired angle (25°–30°) from the horizontal plane. After the sample solution is introduced into the column, the mobile phase is eluted from the column while the apparatus is rotated at a desired rate (60–80 rpm). In order to retain a large volume of the stationary phase, the lower phase is eluted downward from the upper terminus and the upper phase upward from the lower terminus of the column assembly. The effluent from the outlet of the column is continuously monitored with an ultraviolet (UV) monitor and collected into test tubes using a fraction collector.

Applications

Because the apparatus became commercially available in the late 1970s, RLCCC has been applied mainly to the preparative separation of natural products, due to its large sample loading capacity. As with other CCC systems, the partition efficiency of the RLCCC system highly depends on the choice of the suitable two-phase solvent system which gives a partition coefficient close to unity ($K \approx 1$) for the targeted compound. The K value can be obtained from a simple spectrophotometric measurement, thin-layer chromatography (TLC), or high-performance liquid chromatography (HPLC), whichever is appropriate.

Separation of Natural Products

Two-phase solvent systems composed of chloroform-methanol-water at various volume ratios are frequently used for the separation of moderately hydrophobic compounds, including flavone aglycones, phenylpropanoids, iridoid glycosides, and so forth [6].

The separation of more polar compounds, such as glycosides, can be achieved using a polar solvent system composed of ethyl acetate-water with a suitable modifier. Flavonoid glycosides were separated with ethyl acetate-1-propanol-water (2:1:2) and saponins with ethyl acetate-ethanol-water (2:1:2).

Chiral Separation

The separation of (\pm)-norephedrine was first performed by RLCCC using a solvent system composed of 1,2-dichloroethane and 0.5M aqueous sodium hexafluorophosphate (pH 4) containing chiral tartaric acid ester (dinon-5-yl tartrate) [7]. This method produced an efficient resolution of enantiomers at purities of over 95% from 200 mg of racemate.

Rotation locular countercurrent chromatography can be applied to the chiral separation with an aqueous-aqueous polymer phase system using bovine serum albumin (BSA) as a chiral selector. In our laboratory, the RLCCC separation of D- and L-enantiomers of kynurenine was achieved from 200 mg of D,L-kynurenine using a solvent system composed of 10% (w/w) polyethylene glycol 8000 and 5% (w/w) disodium hydrogen phosphate containing 6% (w/w) BSA [8]. Because of a long settling time of the polymer phase system under unit gravity, the method required a discontinuous operation as used in the conventional countercurrent distribution apparatus, which con-

sisted of 3 min for mixing, 10 min for settling, and 1 min for transfer of the mobile phase to the next locule at a flow rate of 1.0 mL/min. Using the lower mobile phase, L-kynurenine was eluted first, followed by D-kynurenine, and the separation was completed in 60 h.

Alternating CCC Method

In this modified method, upper and lower phases are alternately used as the mobile phase by eluting the lower phase in the descending mode and the upper phase in the ascending mode through the respective terminus of a short locular column assembly.

Each separation is initiated by filling the entire column with the upper phase of the equilibrated two-phase solvent system. Following the injection of the sample solution, the column is eluted with the lower phase while the apparatus is rotated at 60–70 rpm. After a desired period of elution, when the target compound is about to elute, the mobile phase is switched to the upper phase, which is eluted at the same flow rate but in an ascending mode in the opposite direction. This alternating elution process with the upper and the lower phases is repeated until the desired component is well resolved.

In our laboratory, this method was applied to the purification of food mono-azo dyes [3]. Amaranth, New Coccine, and Sunset Yellow FCF were purified at 99.7%, 99.5%, and 99.3%, respectively, from 1–2.5 g of commercial dyes. Continued research has led to the purification of impurities present in commercial Sunset Yellow FCF

that include RS-SA (trisodium salt of 3-hydroxy-4-[sulfophenyl]azo-2,7-naphthalene disulfonic acid), GS-SA (1-[4-sulfophenyl]azo)-2-naphthol-6,8-disulfonic acid), DONS (disodium salt of 6,6'-oxybis-2-naphthalene sulfonic acid), and 2N-SA (sodium salt of 4-[(2-hydroxy-1-naphthalenyl)azo]benzenesulfonic acid). The method successfully isolated GS-SA from Sunset Yellow FCF [4].

References

1. Y. Ito and R. L. Bowman, *J. Chromatogr. Sci.* 8: 315–323 (1970).
2. Y. Ito and R. L. Bowman, *Anal. Chem.* 43: 69A–75A (1971).
3. Y. Kabasawa, T. Tanimura, H. Nakazawa, and K. Shinomiya, *Anal. Sci.* 8: 351–353 (1992).
4. N. Ogura, Y. Nakamura, K. Shinomiya, and Y. Kabasawa, *Anal. Sci.* 11: 759–763 (1995).
J. K. Snyder, K. Nakanishi, K. Hostettmann, and M. Hostettmann, *J. Liquid Chromatogr.* 7: 243–256 (1984).
I. Kubo, G. T. Marshall, and F. J. Hanke, *Countercurrent Chromatography: Theory and Practice* (N. B. Mandava and Y. Ito, eds.), Marcel Dekker, Inc., New York, 1988, pp. 493–507.
5. W. D. Conway, *Countercurrent Chromatography: Apparatus, Theory, and Applications*, VCH, New York, 1990.
6. K. Hostettmann, M. Hostettmann, and A. Marston, *Preparative Chromatography Techniques: Applications in Natural Product Isolation*, Springer-Verlag, Berlin, 1986.
7. B. Domon, K. Hostettmann, K. Kovacevic, and V. Prelog, *J. Chromatogr.* 250: 149–151 (1982).
8. Y. Sato, K. Shinomiya, and Y. Kabasawa, *J. Chem. Soc. Japan* 1067–1071 (1994).



Sample Application in TLC

Simion Gocan

University Babeş-Bolyai, Cluj-Napoca, Romania

INTRODUCTION

It is very important to restrict the dimension of the sample initial size, in the direction of development, to a minimum to be able to utilize the excellent separation ability of thin-layer chromatography (TLC) and high-performance liquid chromatography (HPLC). Selection of solvent will affect the size of the sample zone. Good resolution will be obtained if the development chromatographic conditions are optimally selected. For TLC plates where initial spot size should be about 5 mm, this corresponds to a sample volume of 0.5 to 10 μL . For HPTLC plates where spot size is about 1.0 mm, the corresponding sample volume is from 100 to 200 nL. The sample should be dissolved in a good solvent for the sample compounds to allow quantitative transfer from the sample application device to the thin-layer plate. The sample solvent must be of low viscosity and reasonable volatility to be easily evaporated from the thin layer. It must be able to wet the sorbent layer adequately to yield good penetration of the layer. The selection of a sample application technique and the device that will be used depends primarily on the sample volume, the number of samples to be applied, the required precision, and the degree of automation.

TLC SAMPLE APPLICATION

In order to utilize separation power of the layer in TLC or HPTLC, it is very important to restrict the dimension of the sample initial size, in the direction of development, to a minimum. The choice of solvent for the sample also affects the size of the sample zone. That is, we will obtain good resolution only if the development chromatographic conditions are optimally selected. For TLC plates where the desirable initial spot size is about 5.0 mm, this corresponds to a sample volume of 0.5 to 10 μL . For HPTLC plates where starting spot size is about 1.0 mm, the corresponding sample volume is 100 to 200 nL.^[1] The sample solvent must be a good solvent for the sample compounds to allow quantitative transfer from the sample application device to the thin layer. It must be of low viscosity to be easily evaporated from the thin layer. Moreover, the sample solvent must be able to wet the sorbent layer adequately to produce good penetration to

the layer. The selection of a sample application technique and the device to be used depends primarily on the sample volume, the number of samples to be applied, the required precision, and the degree of automation, as to be discussed in detail.^[2,3]

Mode of Application of the Sample

The application of the samples can be performed as spots, bands, or rectangles (Fig. 1). In Fig. 1, the sample spot can be applied by contact transfer in a stroke or by spraying in bands and rectangles. It is often recommended that the sample should be applied in narrow bands or continuous streaks. The narrow bands of the sample ensure highest resolution even when the sample contains large numbers of components with minimal differences between their RF values. The application using zigzag spraying to produce a rectangular shape enables a large volume of the sample to be applied without washing the thin layer. This method is important for aqueous samples.

Manual Sample Application

Generally speaking, manual devices for sample application can be used for detection and are inappropriate if scanning densitometry is used. However, manual application of the samples with a spotting guide has advantages, e.g., the starting position of each spot will be known precisely. Practical experience demonstrates that to obtain good linearity and zero-intercept calibration curves, the plate should not be prepared by spotting incremental volumes from a single standard solution.

Microcapillary pipettes and microsyringes

Manual sample application employs various microcapillary pipettes and microsyringes. The microcapillary is one of the simplest and most useful methods for application of small sample volumes onto thin-layer plates. The capillary has a fixed volume of 0.5, 1, 2, or 5 μL , and accuracy is often better than 1%. The capillaries are supplied by the manufacturer in color-coded vials containing 100 pieces. The capillaries are handheld and can be positioned with a multipurpose spotting guide.

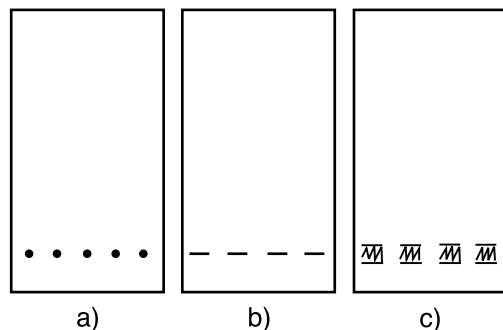


Fig. 1 Three application modes: a) spots; b) bands; c) zigzag (rectangles).

For quantitative work in HPTLC, the sample is applied to the thin layer using a fixed volume with a platinum-iridium capillary of 100- or 200-nL volume. These capillaries are sealed into glass holders.^[4] The capillary tip has a smooth planar surface of small cross-sectional area, which is brought into contact with the plate surface using a mechanical device to discharge its volume. These capillaries are unsuitable for hand spotting because they invariably cause damage to the thin layer and frequent clogging of the capillary with microparticles of sorbent from the thin layer is experienced.

Nanomat in combination with *Capillary Dispenser Camag*^[5] offers the advantage of easy application of sample onto TLC and HPTLC plates or sheets in the form of a small spot. The capillary pipettes, filled with sample solution, are loaded into the dispenser in magazines having closely controlled tolerances and inertness, and the tip of the capillary cannot damage the surface of the layer because it is lowered precisely onto the layer at a selected position. The capillary touches the thin layer with a constant pressure, which is determined solely by the friction against a permanent magnet.

The microsyringe is an alternative to the capillary pipette, which offers greater flexibility in the choice of sample volume.^[6] Hamilton microsyringes are widely used. They can be equipped with a micrometer screw for precise control of the position of the syringe plunger. The microsyringe is handheld and can be very easily positioned with the multipurpose spotting guide. For accurate application of nanoliter volumes, preselected in the range 50–230 nL, the microsyringe is controlled by a micrometer screw gauge. The repetitive application of a constant sample volume is achieved by a fixed lever mechanism. The microsyringe needle is brought only close enough to the plate surface for the convex sample solution drop of the ejected liquid to touch the layer surface. The needle does not touch the surface of the layer.

Plates with a concentrating zone

Sample may be applied as bands to TLC plates using specially prepared plates with a concentrating zone (Fig. 2).

The concentrating zone is about 2 cm wide and consists of a coating made from particles of silica that have extremely large pore diameter (ca. 5000 nm) and a relatively low surface area (ca. 0.5 m²/g) and, consequently, low retentive capacity. The concentrating band is coated closely adjacent to the normal retentive adsorbent coating which consists of particles that are 5–7 μm in diameter but with a much higher surface area and a much greater retentive capacity.^[7] The concentrating zone simplifies the process of sample application inasmuch as microliter volumes can be applied, either as spots or bands, to any position on the concentrating zone. When the plate is developed, the compounds move rapidly through the concentration zone, because of its very low retentive character, to the interface between the layers. At the interface, the compounds will have a slow migration velocity and will be focused as a sharp band at the front of the plate. Then, development will be in the usual manner.

Automatic Sample Application

Manual application of a large number of samples is time-consuming and, obviously, leads to poor reproducibility. Speed and reproducibility are often achieved by using automatic applicators. Such automatic samplers combine precision, accuracy, speed, and versatility.

A schematic diagram of an analytical syringe with mechanical control is shown in Fig. 3. The stepper motor controls the speed of movement of the syringe plunger and thus the amount of the sample per spot or band. Furthermore, a stepper motor moves the thin-layer plate on the x axis. These parameters are programmed and controlled by a microprocessor.

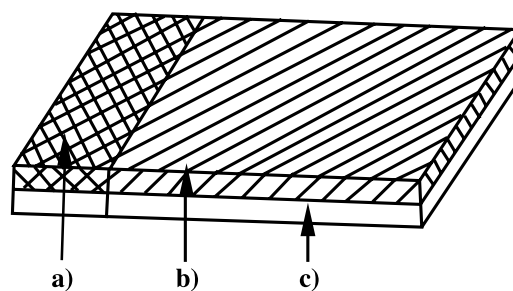


Fig. 2 TLC plate with sample concentrating zone. a) Concentrating zone; b) normal retentive adsorbent; c) glass plate.



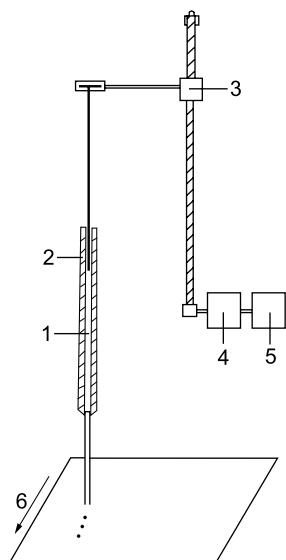


Fig. 3 Diagram of the analytical syringe with mechanical control. 1) Sample; 2) analytical syringe (Hamilton); 3) mechanical control action; 4) stepper motor; 5) stepper motor control; 6) thin-layer plate.

An automatic sample-spotting device has been developed, which uses a flexible fused silica capillary tube as the applicator and a motor-driven syringe to suck up and deposits onto the layer sample volumes in the range of 100 nL to 20 μ L as spots or bands.^[8] Controlled by a microprocessor, it can be programmed to select samples from a rack of vials and deposit fixed volumes of the samples to selected positions on the plates. The applicator can spot a whole plate with various samples and standards without operator intervention. Moreover, the applicator automatically rinses itself between two sample application sequences to eliminate carryover of samples.

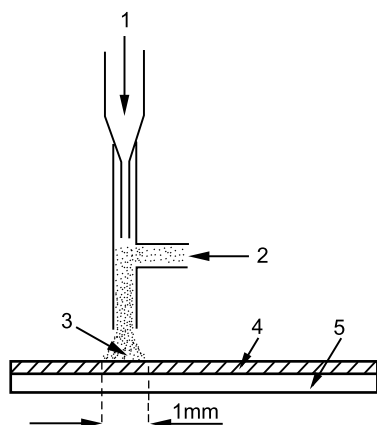


Fig. 4 Diagram of the atomizer. 1) Air or nitrogen; 2) sampling solution; 3) atomized spray; 4) adsorbent; 5) glass plate.

As an alternative to the motor-driven syringe, an atomizer device was developed (Fig. 4). The sample is atomized in a stream of air or nitrogen, depending on the nature of the sample and its tendency to become oxidized.^[3] The atomizer is mounted on a mechanical arm that can sweep from side to side while directing the atomized sample onto the surface of a TLC plate. The range and the number of sweeps are usually under microprocessor control; the speed of movement is adjusted so that the solvent can be evaporated from a given area of the sample before it receives a subsequent dose.

Linomat-5 sample applicator

The Linomat-5 is the latest development in a long line of CAMAG sample applicators, using the spray-on technique in qualitative, quantitative, and preparative TLC/HPTLC (Fig. 5). This applicator sprays samples, preferably in the form of bands of selectable length or as spots. The spray-on technique enables larger sample volumes to be applied to the layer by contact transfer. The sample dosage syringe is selectable, 100 or 500 μ L.

The instrument Linomat 5 is fully controllable by the “winCATS-Planar Chromatography Manager” software. With this system, one can select various parameters, such as number of tracks, band length, and application volume sequence, x positions on the plates, track distances, as well as application methods. The instrument applies the samples onto a thin layer automatically; however, only changing the sample, i.e., filling and rinsing the syringe, is carried out manually.^[9]

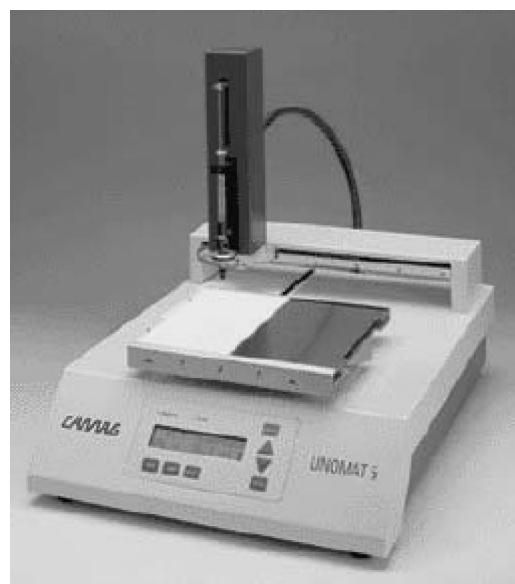


Fig. 5 Camag Linomat 5 TLC applicator. (View this art in color at www.dekker.com.)

Copyright © Marcel Dekker, Inc. All rights reserved.





Fig. 6 Camag automatic TLC sampler 4 (ATS4). (View this art in color at www.dekker.com.)

Automatic applicator AS 30 TLC

A specially modified sampler, by Desaga, converts the AS 30 TLC applicator into a fully automatic applicator system which operates according to the spray-on technique.^[10] A stream of gas carries the sample from the cannula tip onto the TLC/HPTLC plate. During the filling process, the dosing syringe is positioned over the tray, which collects rinsing and flushing solvent and excess sample. The sample is injected into the body of the syringe through a lateral opening. After the syringe has been filled, a stepping motor moves the piston downward to dose the fillport. A second stepping motor moves the tower sideways across the TLC plate. The microprocessor controls the two stepping motors and the gas valve for accurate application either as a spot or as a band. All parameters for the application of up to 30 samples are entered via a keyboard and a memory holds 10 different methods.

A specially modified sampler for Desaga expands the TLC-Applicator AS 30 into a fully automatic application system. The applicator control of the autosampler is performed by a serial interface, and it monitors the selection of sample containers, the delivery of the necessary amount of sample, and the rinsing processes. A second serial interface allows the application parameters to be documented using a printer or laboratory computer system.

Automatic TLC sampler 4 (ATS4)

Camag Automatic TLC Sampler 4 (ATS4) is a precise and fully automatic sample applicator for TLC (Fig. 6).^[9,11] This applicator is a fully automated system which can be used to apply from 10 to 30 μL of up to 96 samples.

The complete procedure for a single applied sample consists of several discrete steps: sample withdrawal, needle wipe-off, predosage application of the sample, disposal of unrequired sample, and, finally, rinse. Sample volumes of 0.1 to 5 μL per spot can be applied by contact application; however, for volumes of 0.5 to $>50 \mu\text{L}$, it uses spray-on application in the form of bands or rectangles (Fig. 6).

Sample application in the form of rectangles allows the application of large volumes or volume per unit time without disturbing or washing away the layer. This is important when aqueous sample solutions are applied.

The ATS4 program allows “over-spotting,” i.e., a sequential application from different vials onto the same position. In this way, it is possible to perform an automatic prechromatographic derivatization.

Automatic CTC TLC 100 sampler

Another sampler, the CTC-TLS 100 TLC (Leap Technologies, Chapel Hill, NC, USA), which has the capability of robotically performing plate changes of 24 ($5 \times 5 \text{ cm}$), 12 ($10 \times 10 \text{ cm}$), or 6 ($10 \times 20 \text{ plates}$ which can be loaded in a single batch (Fig. 7).^[12]

It is possible to work routinely in nano- or picogram concentrations. A wide range of different volumes can be applied by use of 1-, 10-, and 100- μL increments. This device includes the so-called “overspotting” technique and can add up to four prechromatographic derivatization reagents or standards in selectable concentrations. Up to 15-sample application methods can be stored in the on-board controller, and the methods can be sent to a printer or PC via a serial interface.^[12]

Automatic spotting lissy-TLC

Thin-layer chromatography has also been used to monitor reactions in solution phase or for screening key products

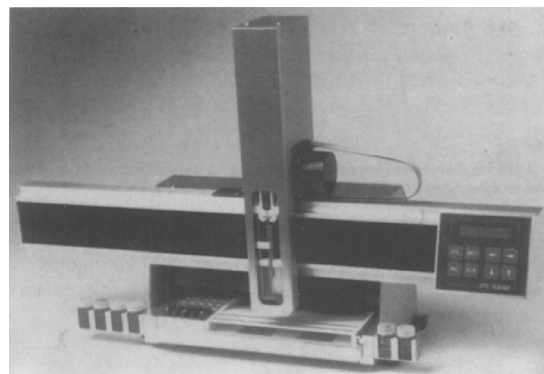


Fig. 7 CTC-TLS 100 sampler.



Sample Application in TLC

in combinatorial chemistry. It is still a well-established technology because it delivers fast and reasonable results. With TLC, it is possible to do a preselection from the products of interest. With Lissy-TLC, this technique has been successfully automated (Fig. 8).^[13] It is based on a proven pipetting robot, equipped with special dosing tips which can precisely plot the sample solution with one channel and supply nitrogen with the other channel. The thin-layer plates are positioned in stackable racks, each rack holding 6 plates of 16 spots each. This allows the 96-well format to be maintained. The system is supplied with user-friendly Windows NT software and the user can design his own protocol.

Sample application on a chromarod

The combination of TLC and flame ionization detector (FID) has been successfully brought together in the form of the Iatroscan TH10 TLC/FID instrument. Chromatographic separations are carried out on quartz rods coated with a thin layer of sintered 5- μm silica gel (the Chromarod) as the stationary phase. The chromarods are then passed through the FID to detect and quantify the separated compounds. For the sample application, a homemade device, based on a Linomat spray assembly, applies a sample as a controlled (4–15 $\mu\text{L}/\text{min}$), nebulized spray on a rotating chromarod. Sample volume can be selected from 1 to 500 μL .^[14]

Automated “4 \times 4” sample applications

Two-dimensional high-performance TLC (HPTLC) is an analytical separation method that is recommended for evaluation of trace amounts in complex matrices that are difficult to separate in a single dimension. In the horizontal chamber, the HPTLC plates are developed

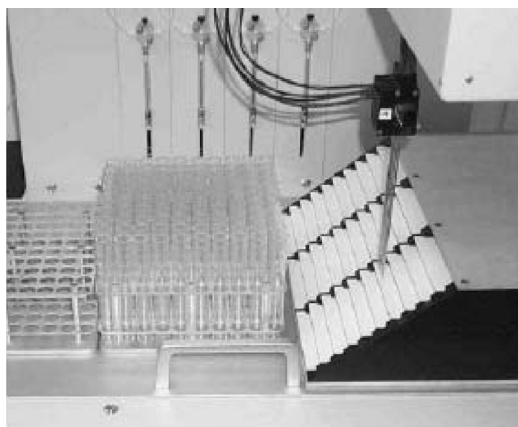


Fig. 8 Lissy-TLC automatic spotting. (View this art in color at www.dekker.com.)

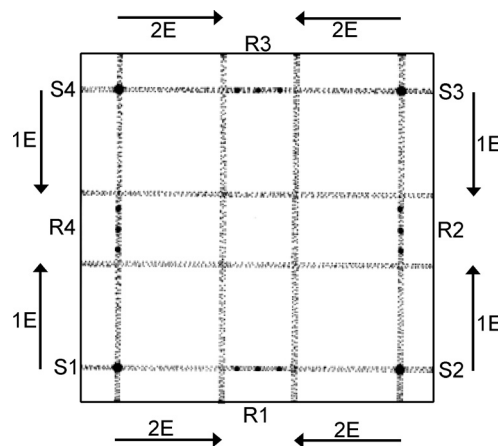


Fig. 9 Schematic diagram of the automated “4 \times 4” sample application on HPTLC plate.

from two opposing sides toward the middle, with eluent system 1E, and redeveloped in an orthogonal direction with a second mobile phase, 2E.^[15] Samples are applied to the four corners of the plate (spots S1, S2, S3, and S4) and the reference components to the four reference lines (R1, R2, R3, and R4) (Fig. 9).^[16,17] The plate’s development is performed in two runs using a linear development horizontal S chamber^[18] and in four runs in a conventional chamber.

Sample Application in Preparative TLC

The principal difference between analytical HPTLC and preparative TLC is in scale, not in principle or methodology. Preparative TLC plates range in size from 20 \times 20 to 20 \times 100 cm and are coated with a sorbent layer 0.5 to 10.0 mm thick; however, most commonly, layer thicknesses are 1.0 and 2.0 mm. Sample application is one of the most critical steps in preparative TLC.^[19,20] The sample, usually as a 5–10% solution in a volatile organic solvent, is applied as a band along one edge of the plate. The maximum sample load for a silica gel layer of 1.0-mm thickness is about 5 mg/cm. Plates with concentrating zones are useful for optimizing sample application.

The Camag automatic TLC sampler 4 (ATS4) can be used for preparative sample application. For volumes of 0.5 to >50 μL , spray-on application in the form of bands or rectangles is recommended.^[11] Alltech TLC sample streaker^[21] is a quantitative device which is especially useful for preparative TLC. This applicator has a mechanical action of forcing a syringe (250 or 500 μL) plunger downward while it travels across a sloping stainless steel bar. Furthermore, Linomat 5 and any other sampler that applies the amount of sample which is necessary for preparative chromatography can be used.^[9]

Multispotter Applicators

Manual multispotter applicator

A manual multispotter applicator was developed by Maboundou et al.^[22] for simultaneous deposition of up to 15 samples in a single operation and successively on several plates of different sizes. Manual application of a large number of samples is time-consuming and, obviously, poorly reproducible. Rapidity and reproducibility are often performed by using a manual multispotter applicator.

The manual multispotter applicator is presented in Fig. 10,^[22] and it is composed of a principal unit (1) and two modules: a carriage (2) and a removable vial rack (3). The principal unit has a nonskid working area (1a) and can hold a variable number of plates, depending on their sizes. Lateral guides (1b) ensure sample application at the desired positions when several plates have to be spotted in a series. The carriage is placed on rail (1c), which is positioned on each side of the principal unit (1). The carriage, which bears on capillary-tube rack (2a), is equipped with a lever (2b); it is designed to hold up to 15 capillary tubes (1, 2, 5, or 10 μL) positioned equidistantly, 12 mm apart. By pushing the tubes against the flat base (at the bottom) of the work area, all tubes will be adjusted to the same height. The removable vial rack (3) is placed on the bottom of the principal unit (1) and is designed to hold up to 15 vials of 1.6 mL each. By pushing the lever to rotate the carriage 90°, the capillary tubes can be inserted manually (parallel to the work area). The tube bearing (2a) is then returned to its original orientation, advanced to overlay the vial rack, and the tubes are filled by pressing on the entire lever assembly. The carriage (2) is then slid to the desired position over the thin-layer TLC plate and samples are deposited by pressing on the lever. At the finish, the tubes are then removed manually. This represents real progress, compared to the manual application of the sam-

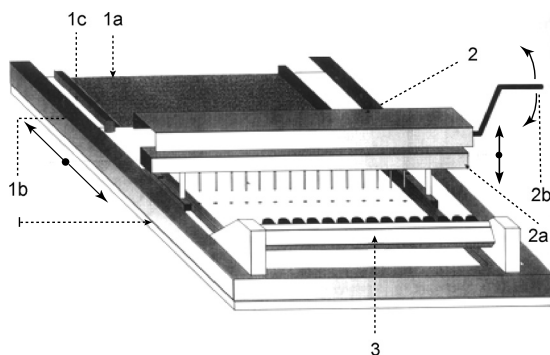


Fig. 10 Manual multispotter.



Fig. 11 Romer TLC AutoSpotter, model 10. (View this art in color at www.dekker.com.)

ples, and is also an economical option, compared to an automatic sampler.

Automatic multispotter applicator

The automatic multispotter applicator was developed for simultaneous deposition of a large number of samples on several TLC plates. This is an attractive instrument for routine practice when many samples have to be analyzed by TLC. Reproducibility and rapidity are readily achieved when using the automatic multispotter applicator.

The Romer model 10 TLC AutoSpotter has the capacity to dispense the entire contents of 18 100- μL syringes in 15 min, producing uniform sample spots (Fig. 11).^[23] The plate is heated from its rear. In this way, continuous sample enrichment is achieved. The AutoSpotter has a heater with digital readout for rapid solvent evaporation. Speed control of the syringe plunger ensures reproducibility of the spots. When the spotting process is finished, the movement of the syringe plunger will be automatically stopped. All syringes have Teflon-tipped plungers, and the needle tips have a highly polished finish, or they can be coated with Teflon to prevent sample buildup on the needle tip. Then, the syringes will be filled with samples again, for a new application after being fixed in their positions.

A similar TLC multispotter is available commercially from Alltech Associates, Inc.^[24] With this multispotter, the contents of 10, 25, 50, 100, or 250 μL syringes can be delivered at variable rates ranging from 3 to 30 min. This variable delivery rate, combined with the selection of the proper evaporation temperature, permits spotting with virtually any type of solvent. In this way, we can select the optimum delivery rate and temperature that will provide the smallest possible spots. The unit eliminates hand spotting and allows multiple spotting in minimal time. The syringe has a blunt-tipped PFTE needle for minimal sample loss during application. Use of PFTE plunger tips eliminates problems of metal to glass contamination. A user control panel can be used to select all parameters.



Solid-Phase Sample Application Method

The solid-phase method allows application of the samples, which are soluble in a nonvolatile solvent only. In this case, the sample must be dissolved in a suitable solvent and mixed with 5–10 times its weight of a deactivated adsorbent. The mixture will be carefully dried by rotary evaporation and will then be introduced into the layer that must be specifically prepared to accept it. For this reason, Botz et al.^[25] created a device that enables regular sample application in the entire cross section of the preparative layer with the advantage of in situ sample concentration and cleanup. With this device, the sample can be applied to improve the starting situation for a preparative chromatographic separation, independent of the migration of whether the mobile phase is achieved by capillary action or by forced flow.

REFERENCES

1. Pool, C.F.; Pool, S.K. *Chromatography Today*; Elsevier: Amsterdam, 1991; 710–713.
2. Omori, T. *Planar Chromatography, a Retrospective View for the Third Millennium*; Nyiredy, Sz., Ed.; Springer Scientific Publisher: Budapest, 2001; 120–136.
3. Szepesi, G. *Modern Thin-Layer Chromatography*; Grinberg, N., Ed.; Marcel Dekker, Inc.: New York, 1990; 285–292.
4. Hezel, U.B. *HPTLC, High Performance Thin-Layer Chromatography*; Zlatkis, A., Kaiser, R.E., Eds.; Elsevier: Amsterdam, 1977; 147–153.
5. Camag prospectus for Nanomat 4 and capillary dispenser; www.camag.ch.
6. Fenimore, D.C. *Instrumental HPTLC*; Bertsch, W., Hara, S., Kaiser, R.E., Zlatkis, A., Eds.; Hüthig: Heidelberg, 1980; 81–95.
7. Halpaap, H.; Krebs, K.-F. *J. Chromatogr.* **1977**, *142*, 823–853.
8. Jäenchen, D.E.; Issaq, H.J. *J. Liq. Chromatogr.* **1988**, *11*, 1941–1965.
9. Camag prospectus for Linomat 5; www.camag.ch.
10. Desaga GmbH, Postfach/P.O.B. 1280, D-69153 Wiesloch, Germany.
11. Camag prospectus for the ATS4 automatic TLC sampler; www.camag.ch.
12. Jeger, A.N.; Briellmann, T.A. *J. Planar Chromatogr.* **1994**, *7*, 157–159.
13. Zinsser Analytic, Eschborner Landstrasse 135, D-60460 Frankfurt/Main, Germany; www.zinsser-analytic.com.
14. Dewey, C.R.K.; Roberts, I.; Read, H. *Proc. 6th Int. Symp. Instrum. Planar Chromatogr., (Interlaken 1991)*; Traitlet, H., Voroshilova, O.I., Kaiser, R.E., Eds.; Institute for Chromatography: Bad Dürkheim, Germany, 1991; 81–82.
15. Gocan, S. *Encyclopedia of Chromatography*; Cazes, J., Ed.; Marcel Dekker, Inc.: New York, 2001; 533–535.
16. De Brabander, H.F.; Smets, F.; Pottie, G. *J. Planar Chromatogr.* **1988**, *1*, 369–370.
17. De Brabander, H.F.; Rasschaert, G.; Vanneste, W.H. *J. Planar Chromatogr.* **1989**, *2*, 484–485.
18. Gocan, S. *Encyclopedia of Chromatography*; Cazes, J., Ed.; Marcel Dekker, Inc.: New York, 2001; 851–854.
19. Nyiredy, Sz. *Anal. Chim. Acta* **1990**, *236*, 83–97.
20. Botz, L.; Nyiredy, Sz.; Sticher, O. *J. Planar Chromatogr.* **1990**, *3*, 10–14.
21. Alltech Associates, 2051 Waukegan Road, Deerfield, IL 60015-1899, USA; www.alltechweb.com.
22. Maboundou, C.W.; Grosse, P.-Y.; Delvordre, P.; Vermier, N. *J. Planar Chromatogr.* **1999**, *12*, 373–377.
23. Romer, 1301 Stylemaster Drive, Union, MO 63084-1156, USA; www.romerlabs.com.
24. Alltech, Data Sheet U80130, TLC Multi-Spotter; www.alltechweb.com.
25. Botz, L.; Nyiredy, Sz.; Sticher, O. *J. Planar Chromatogr.* **1990**, *3*, 10–14.



Sample Preparation

W. Jeffrey Hurst

Hershey Foods Technical Center, Hershey, Pennsylvania, U.S.A.

Introduction

Before any sample can be subjected to chromatography, some type of sample preparation is required, which can be as simple as filtration or an involved solid-phase extraction protocol. Sample preparation is that activity or those activities necessary to prepare a sample for analysis. The ultimate goal of sample preparation is to provide the component of interest in solution, free from interferences and at a concentration appropriate for detection. This entry will briefly discuss seven topic areas included in sample preparation: standard methods, solid-phase extraction (SPE), matrix solid-phase dispersion (MSPD), solid-phase microextraction (SPME), microdialysis, ultrafiltration (UF), and automated systems.

Discussion

Should the sample be solid, then the first step would involve the extraction of the sample with an appropriate solution that would solubilize the compound of interest and remove as few interfering compounds as possible. This operation is sometimes conducted using a blender or other mixer to provide as homogeneous extract as possible.

Alternatively, one could use a Soxhlet or similar apparatus to extract the sample. Other methods to prepare a sample for analysis through extraction include supercritical fluid extraction (SFE), pressurized fluid extraction, and microwave-assisted solvent extraction. There will continue to be additions to this list, as techniques evolve and modifications of the more standard techniques are made.

The standard methods that one would use in sample preparation for chromatography include filtration, sedimentation, centrifugation, liquid-liquid extraction (LLE) open-column chromatography, and concentration/evaporation. Filtration for sample preparation may be performed on numerous occasions in a sample preparation protocol, with the first filtration being used to separate large-particulate matter from solvent. The final filtration before chromatography likely uses

a 0.45- μm or smaller disposable filter unit to prevent small-particulate matter from contaminating the chromatographic system.

One of the techniques that has become increasingly used and replaced more of the traditional methods of sample preparation is SPE. SPE introduced in the early 1970s offered the possibility of, if not eliminating, at least reducing the tedium in sample preparation. SPE has been called "digital chromatography," where samples can be introduced onto a device, interferences removed, and the analyte of interest eluted in a small amount of solvent. Conversely, the SPE device can be used as a flow-through cleanup device. SPE can be used on many occasions as a substitute for LLE.

There is a wide diversity not only in SPE packing types but also SPE formats. The packing types parallel those in used in open-column chromatography and HPLC. The addition of a second-generation-type support such as the Waters OASIS and the Varian NEXUS are seen as somewhat universal supports for many sample types with other similar supports unique for SPE in continual development. Although the early SPE devices were cartridge or syringe barrel based, the formats have evolved to support the growing demands in drug discovery through the development of microtiter plate formats to support high-throughput screening (HTS) activities. In addition to columns there has also been a growth in disk-based SPE devices. Figure 1 provides an overview of SPE phase and solvent selection.

Solid-phase microextraction (SPME) was developed as an alternative to many other sample preparation methods because it uses virtually no solvents or complicated equipment. It is an adsorption/desorption device where the compounds of interest are adsorbed onto a fused-silica fiber. After a given time, the fiber is placed into a gas chromatograph (GC), where the compounds are thermally desorbed. SPME has recently been adapted for use in HPLC, where compounds that are adsorbed are desorbed using an appropriate solvent.

Matrix solid-phase dispersion (MSPD) is an SPE variant where samples are ground and mixed with a C_{18} support. This is placed in a disposable column previously packed with Florisil that traps the fat from the



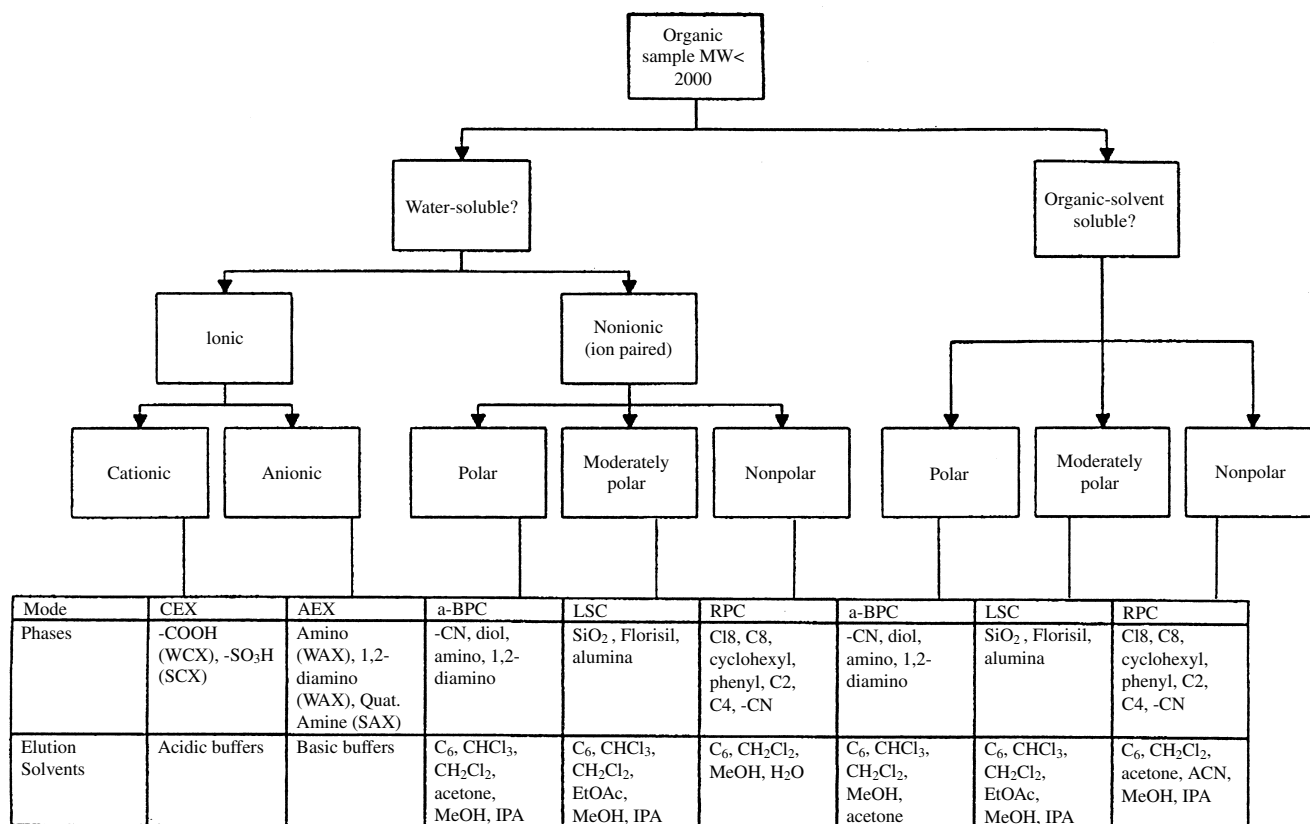


Fig. 1 Overview of SPE phase and solvent selection.

sample, allowing the compounds of interest to be eluted. This has successfully been applied to the determination of lipophilic pesticides from both fatty and nonfatty matrices.

When supercritical fluid extraction (SFE) was initially introduced, it was thought that it might be the panacea for sample extraction because it used a very innocuous solvent, CO₂. The operator varied pressure, temperature, flow rate, and extraction time, with some extraction protocols requiring the use of small amounts of polar modifiers. All of these variables affected the solvating power of the carbon dioxide. In addition to the carbon dioxide, other supercritical fluids have been used. The technique continues to evolve with increasing numbers of applications being published but has not developed as once might have been predicted.

In microwave-assisted solvent extraction (MASE), the sample and solvent are heated directly rather than in more conventional schemes where the vessel is heated to extract the sample. The sample solvents are placed into a closed vessel that does absorb microwaves. This facilitates the extraction of the samples

of interest and has been applied to a variety of sample types and matrices.

The accelerated solvent extraction (ASE) system introduced by Dionex uses standard solvents at elevated temperatures and pressures to increase extraction efficiency. Samples are placed in stainless-steel extraction vessels that are loaded into the ASE that has been programmed for the extraction protocol. The instrument allows for the unattended extraction of 24 samples. The initial units allowed for solvent blending by premixing solvents before they were placed into the ASE. Recent modifications allow solvent blending to be accomplished in-line. There has been some controversy about the use of the name ASE because it points to instrumentation from one company and other companies have introduced competing products. It has been proposed that the ASE technology be more correctly referred to as pressurized fluid extraction because ASE denotes a commercial device.

Two additional techniques that are used in sample preparation protocols are ultrafiltration and microdialysis. In ultrafiltration, pressure is applied to a membrane and those molecules smaller than the mo-

lecular-weight cutoff can pass through while molecules larger are retained. This technique can be used as a way of sample concentration or as a way to eliminate higher-molecular-weight compounds from an analytical scheme. Membranes are available with cutoffs ranging from 300 to 300,000. Microdialysis differs from the other techniques because it is in vivo sampling and has been applied to the determination of drugs and other biomolecules from tissues, organs, and biological fluids. In microdialysis, molecules can diffuse across a membrane resulting in either direct or reverse dialysis.

Finally, no discussion of this topic would be complete without the mention of automation in sample preparation and its impact on this activity. Laboratory robotics' initial focus was on the automation of sample preparation and is used in that way in many laboratories, but "islands of automation" have developed within certain organizations where certain portions of sample preparation such as SPE are automated.

Sample preparation is an extremely broad subject because there are techniques that are more likely used by those in different industry segments. This entry has provided an overview of some of the methods of sample preparation that are widely used. It likely has missed some of the more esoteric ways of sample

preparation. The reader is referred to the Suggested Further Readings for additional reading.

Suggested Further Reading

- Baker, S. A., Preparation of milk samples for immunoassay and liquid chromatographic screening using matrix solid-phase dispersion, *JAOAC Int.* 77: 848 (1994).
- Current Trends and Developments in Sample Preparation*, Supplement to *LC-GC*, Advanstar Communications Eugene, OR, 1998.
- Current Trends and Developments in Sample Preparation*, Supplement to *LC-GC*, Advanstar Communications Eugene, OR, 1999.
- Henion, J., E. Brewer, and G. Rule, Sample preparation for LC/MS/MS, *Anal. Chem.*, 70: 650A–656A (1998).
- Snyder, L. R., J. J. Kirkland, and J. L. Glajch, *Practical HPLC Method Development*, 2nd ed., John Wiley & Sons, New York, 1997.
- VanHorne, K. C., *Handbook of Sorbent Extraction Technology*, Varian Sample Preparation Products, Harbor City, CA, 1994.
- Zang Z., and J. Pawliszyn, Headspace solid phase microextraction, *Anal. Chem.* 65: 1843 (1993).



Sample Preparation and Stacking for Capillary Electrophoresis

Zak K. Shihabi

Wake Forest University, Winston-Salem, North Carolina, U.S.A.

Introduction

Unlike high-performance liquid chromatography (HPLC), the composition (matrix) of the sample itself in capillary electrophoresis (CE) affects, greatly, the separation, quantification, detection, and precision. Although the sample, in most instances, constitutes a very small portion of the overall volume in the capillary once injected (<1%), the matrix of the sample has profound effects in CE. As the sample size increases, these effects become much more important because the current conductance is affected by any change of the ionic strength along its path and, in turn, affects the sample migration.

Samples obtained from clean sources do not require much, or any, preparation, whereas samples obtained from biological fluids, food, and industrial sources often have a complex matrix, which necessitates manipulation before the CE step. This also depends on the concentration of the analytes relative to the contaminants. Complicating matters further, CE has a relatively low sensitivity, due to the short light path of the capillary, creating a need for clever manipulation of the sample to enhance the detection.

Unlike HPLC, sample preparation in CE requires careful thinking and strategy to obtain a good analysis. There is a relationship between the sample matrix and the separation buffer. Based on how the sample is prepared and how the separation buffer is selected, sample matrix effects can be both favorable and detrimental to the analysis. Matrix effects are different in capillary zone electrophoresis (CZE) from those observed in micellar electrokinetic capillary chromatography (MEKC). Understanding sample matrix effects is the first step in sample preparation in order to obtain a good separation by CE [1].

Effect of Sample Matrix in Capillary Zone Electrophoresis

Sample Ionic Strength

High ionic strength is important for solubility of many proteins. However, there is an inverse relationship be-

tween electrophoretic mobility and ionic concentration. An excess of ions in the sample, especially with large sample volumes, ruins the separation in CE. In the electrokinetic injection mode, the excess ions in the sample decreases the migration or transfer of the analytes into the capillary, leading to a diminished detector signal. Pure standards prepared in water compared to those added to serum or saline solutions show a large difference in detector signal, causing the quantification to be difficult. In the hydrodynamic injection mode, a high ionic strength in the sample leads to band broadening or multiple peaks.

Proteins

At low concentrations and under appropriate conditions, proteins have little effect on separation in CE. However, at high concentrations in the sample, the cationic proteins especially tend to adsorb preferentially to the inlet side of untreated capillary walls, changing the zeta-potential, which, in turn, affects the electroosmotic flow (EOF). Slight variations in the EOF along the capillary length cause an increase in band spreading and a decrease in peak symmetry, leading to a poor reproducibility.

pH

The ionization and net charge of the sample components are affected greatly by changes in the pH. As a result, the migration rate, the solubility, the theoretical plate number, and peak height could be all affected.

Matrix Effects in Micellar Electrokinetic Capillary Chromatography

Micellar electrokinetic capillary chromatography (MEKC) is used, often, for separating neutral and hydrophobic molecules. The surfactants in MEKC have the added advantage of solubilizing proteins. This can eliminate the need for extraction or deproteinization, allowing direct sample injection. The effect of sample matrix in MEKC is less dramatic than that in CZE. A



high SDS concentration in the running buffer causes an increase in peak height. However, at the same time, a high sodium dodecyl sulfate (SDS) concentration produces excessive current generation and long migration time.

Surfactants in the Sample

In general, a high concentration in the sample of the same surfactant used in the electrophoresis buffer decreases the peak height. Hence, a surfactant in the sample different from that of the running buffer is preferred. The peaks with higher k' are more affected by the surfactants in the buffer.

Organic Solvents in the Sample

Micelle electrokinetic capillary chromatography is often employed to separate nonpolar compounds. The addition of organic solvent to the sample, especially with large-sample injection, decreases the peak height as well as the resolution.

Sample Volume and Stacking

Because of the relatively low sensitivity of detection in CE, a high sample volume is very desirable to increase the signal [1–4]. Unfortunately, sample overloading can occur easily in CE. The theoretical plate number in CE depends greatly on the sample (volume). For example, the theoretical plate numbers dropped from 800,000 to less than 10,000 by increasing the injection time from 0.2 to 15 s [5]. A low sample volume offers very high theoretical plate numbers, but, at the same time, it yields small detector signals. The rule of thumb is to keep the sample plug, under nonstacking conditions, less than 1% of the capillary length [1].

Stacking in CZE

Sample concentration on the capillary is called stacking. Under these conditions a large sample volume is injected and the two edges of the sample are induced to migrate at different rates towards each other before entering the electrophoresis buffer. This mechanism is very useful in CE as it leads to enhanced sensitivity, higher plate numbers, and better separations. Stacking is very simple and can be brought about by several manipulations of the sample:

Low Ionic Strength in the Sample

The sample is dissolved in the same electrophoresis buffer but at a 10 times lower concentration. This causes the sample resistance and the field strength (V/cm) in the sample plug to increase. In turn, this causes the ions to migrate rapidly and stack as a sharp band at the boundary between the sample plug and the electrophoresis buffer with the positive ions lining up in front of the negative ones before entering the electrophoresis buffer. As a result of this simple manipulation, the sample can be concentrated up to 10-fold [6]. The stacking effect can be utilized with both pressure and electrokinetic injections (field amplification injection). Similar stacking can be accomplished also by injecting a very short plug of water into the capillary before injecting the sample.

pH Adjustment

Stacking based on adjusting the pH of the sample has been described. Peptides can be concentrated by dissolving the sample in a buffer 2 units above the net pI , so the peptides are negatively charged. As the potential is turned on, the peptides initially migrate toward the anode until they are stopped by the interface of the electrophoresis buffer, where they concentrate. After the short pH gradient of the sample dissipates in the electrophoresis buffer, the peptides become positively charged. Thus, they migrate toward the cathode as a sharp zone. Catecholamines can be concentrated based on the same principle at acidic conditions in the sample.

Acetonitrile–Salt Mixture

When acetonitrile is present in the sample at about 66% together with a low concentration of sodium chloride, another unique type of sample stacking occurs. In practice, biological samples (1v) are deproteinized with 2 volumes of acetonitrile and injected directly into the CE. The acetonitrile is used mainly to remove proteins; however, it has additional advantages: (1) It reverses the harmful effects of ions and allows larger volumes of sample (about one-third of the capillary volume) to be injected. The overall effect is an increased sensitivity of about 20-fold. Cationic compounds stack better in acetonitrile using a high concentration of zwitterionic buffers. The mechanism behind this stacking is not clear but it is thought to involve the low conductivity of the acetonitrile with a transient-isotacophoretic-like effect brought about by the salts [2–4].

Stacking in MEKC

Stacking in MEKC [7] is more difficult than in CZE. In general it depends on solubilizing the neutral molecules in micelles under low conductivity to accelerate their migration at a negative polarity. Another approach is using reversed-migration micelles for stacking. In a third technique, the pH of the separation buffer used is acidic so the micelles have a higher electrophoretic velocity than the EOF.

Sample Preparation

Dilution and Direct Sample Injection

One of the main advantages of CE for routine analysis in industrial and clinical settings is the simplicity of sample introduction. If the compound of interest has a strong absorptivity and/or is present in a high concentration relative to the interfering compounds, it may be injected directly without any sample treatment [1,4,8]. In order to tolerate a higher ion concentration in the sample, the ionic strength of the buffer should be as high as possible. Several drugs have been successfully analyzed with direct serum or urine injection especially by the MEKC, where the micelles solubilize the proteins.

Extraction

If the compound is present at a low concentration in the presence of many interfering compounds, cleanup and concentration steps become necessary [8]. Solvent extraction procedures are used often for sample preparation for drugs and many other small molecules in the chromatographic technique. Solid-phase methods are very popular because of the wide choice of the packing material. Sample extraction methods have two other main advantages in CE, namely sample concentration and elimination of both sample ions and proteins. Double-solvent extraction is very useful for electrokinetic injection, especially for basic compounds. It eliminates variability due to matrix effects in electrokinetic injection.

Filtration and Dialysis

Large molecules can be separated from the small ones through special dialysis and filtration membranes which are available with different molecular weight cutoff points. However, the use of small commercial dialysis cells or blocks is more suitable for CE than the

traditional bags. Both sides of the dialysis chambers can be used for CE analysis based on whether the compound of interest has a high or low molecular weight. Small volumes can also be filtered rapidly through special filtration devices in a microfuge at 15,000g. Both of these techniques can be applied to the cleanup of urine proteins for analysis by CE.

Organic Solvent Deproteinization

In HPLC, alcohols and especially acetonitrile are often added to the sample to remove serum proteins. In CE, in addition to removing proteins, the presence of acetonitrile in the sample leads to stacking and indirectly improves precision of quantification because of the ability to increase the sample volume. We have analyzed several drugs and other natural compounds by CE after acetonitrile deproteinization. Protein removal can also be accomplished by alcohols such as ethanol and by acids such as perchloric. Precipitation with acids is less desirable in CE than with organic solvents because it increases the salt load. Following precipitation, proteins could also be dissolved in the appropriate buffers and assayed by CE.

Desalting

Desalting is a difficult procedure to perform in routine assays. There are several methods for desalting, such as (1) dialysis as described earlier, (2) ion exchangers (e.g., Chelax 100 and AG 50X2), and (3) reversing the polarity during CE. Organic solvent extraction is another simple method for eliminating ions. In general, the use of high-ionic-strength running buffers enables the direct analysis of samples containing a relatively high salt concentration, eliminating the need for desalting in many instances.

References

1. Z. K. Shihabi, Effect of sample matrix on capillary electrophoresis, in *Handbook of Electrophoresis*, 2nd ed. (J. P. Landers, ed.), CRC Press, Boca Raton, FL, 1997, pp. 457–477.
2. Z. K. Shihabi, Sample stacking by acetonitrile-salt mixtures, *J. Capillary Electrophoresis* 2: 267–271 (1995).
3. M. A. Friedberg, M. Hinsdale, and Z. K. Shihabi, Effect of pH and ions in the sample on stacking in capillary electrophoresis, *J. Chromatogr. A* 781: 35–42 (1997).
4. Z. K. Shihabi, Review: Therapeutic drug monitoring by capillary electrophoresis, *J. Chromatogr. A* 807: 27–36 (1998).



5. A. Vinther and H. Soeberg, Mathematical model describing dispersion in free solution capillary electrophoresis under stacking conditions, *J. Chromatogr.* 559: 3 (1991).
6. D. S. Burgi R-L. Chien, Optimization in sample stacking for high-performance capillary electrophoresis, *Anal. Chem.* 63: 2042–2047 (1991).
7. J. P. Quirino and S. Terabe, On-line concentration of neutral analytes for micellar electrokinetic chromatography. 3. Stacking with reverse migration micelles. *Anal. Chem.* 70: 149–157 (1998).
8. J. Caslavská, S. Lienhard, and W. Thormann, Comparative use of three electrokinetic capillary methods for the determination of drugs in body fluids. Prospects for rapid determination of intoxications, *J. Chromatogr.* 638: 335–342 (1993).



Sample Preparation Prior to HPLC

Ioannis N. Papadoyannis

Aristotle University of Thessaloniki, Thessaloniki, Greece

Victoria F. Samanidou

Chemistry Department, Thessaloniki, Greece

INTRODUCTION

Among the various steps of a sample analysis, from sample collection to the final report of the results, the most tedious and time-consuming one is the *sample preparation*, which requires almost two-thirds of the total analysis time. It is also the most error-prone part of the process, as it contributes about 30% in the sources of errors, impacting on the precision and the accuracy of the overall analysis.

An effective sample preparation helps the analytical chemists to cope with today's increasing demands in the laboratory. No matter how sophisticated the available analytical equipment is, the limits of the analytes' detectability in any analytical procedure eventually depend on the effectiveness of the sample preparation.

OVERVIEW

The main objectives of sample preparation are as follows:

1. Matrix modification in order to:
 - a. Prepare the sample for introduction (injection) onto chromatographic column.
 - b. Render the solvent suitable for the analytical technique to be used.
 - c. Prolong the instrument's lifetime (e.g., column lifetime).
2. Clean-up purification in order to:
 - a. Remove impurities and obtain the required analytical performance and selectivity.
 - b. Reduce matrix interference.
3. Analyte enrichment (preconcentration) in order to improve the method sensitivity (reduction of the limits of detection and quantification).

The sample, prior to high-performance liquid chromatography (HPLC) analysis, has to be in a liquid

state. By contacting the sample with a solvent, the analytes are extracted. Then, the solvent is separated from solid residue by means of decantation, filtration, or centrifugation. Furthermore, it can be concentrated by evaporation.

Typical traditional and modern approaches of sample preparation techniques for liquid and solid samples are summarized in Table 1. These techniques are further discussed under the respective paragraphs.

SELECTION OF THE SUITABLE SAMPLE PREPARATION TECHNIQUE

The term sample preparation may refer to the various stages of the analysis procedure, as shown in Fig. 1. An ideal sample pretreatment technique should have the following characteristics:

1. Simplicity and rapidity.
2. High extraction efficiency with quantitative and reproducible analyte recoveries.
3. Specificity for the analytes.
4. High sample throughput.
5. Fewer manipulation steps to minimize the analyte losses.
6. Amenability to automation.
7. Use of the minimum amount of solvent, compatible with many analytical techniques.
8. Low cost regarding reagents and equipment.

As no ideal sample preparation technique exists, each technique has to be considered according to its own advantages and disadvantages. The analyst may choose the most suitable one, when developing a method, depending on several parameters such as sample matrix, nature, physical and chemical properties of analytes, concentration, and analytical technique that is to be applied.

Automation is one issue of paramount importance, as the biggest problem with sample preparation is time. The benefits of automation, apart from the obvious economic one, include the reduced manual operations and laboratory materials required, the increased sample throughput



Table 1 Typical sample preparation techniques for liquid and solid samples

Liquid samples	Solid samples
Dilution	Solid-liquid extraction (shake filter)
Evaporation	Forced-flow leaching
Distillation	Soxhlet extraction and automated
	Soxhlet extraction
Microdialysis	Homogenization
Lyophilization	Sonication
Liquid-liquid extraction (LLE)	Dissolution
Automated LLE	
Solid-phase extraction (SPE)	Matrix solid-phase dispersion
Automated SPE	
SPE disk technology	Accelerated solvent extraction
	Supercritical fluid extraction (SFE)
SPME	Microwave-assisted extraction
Direct analysis by column-switching techniques (on-line techniques)	
Stir bar sorptive extraction	Gas-phase extraction
	Thermal desorption

From Ref. [1].

and productivity per instrument, and the higher precision with minimal risk regarding the handling of contagious or radioactive samples.

PRELIMINARY SAMPLE PREPARATION PROCEDURES

Frequently, intermediate stages may be required prior to the extraction techniques for sample preparation. These are to minimize the analyte solubility in the matrix and to maximize the selective isolation for a quantitative, rapid extraction of the analyte of interest (e.g., changing of pH or ionic strength). Proteins must be removed prior to extraction by denaturation with organic solvents or chaotropic agents, precipitation with acid (pH modification), addition of a compound that competes for binding sites, or use of restricted-access media. Conjugated components may need to be hydrolyzed to release the free compound. Lipids may be extracted into a nonpolar organic solvent.

Once transferred into a liquid phase, the sample can either be directly injected or treated further using the steps outlined in Table 2.

TRADITIONAL LIQUID SAMPLE PREPARATION TECHNIQUES

Liquid-Liquid Extraction

Sample dilution can occasionally be applied if the analyte is present in such a high concentration that the analyte is still detectable, although this is rarely efficient. For the major part of the analyses, the analyte has to be isolated from the sample by using an extraction technique.

For many years, liquid-liquid extraction (LLE) was the classical technique for the preparation of liquid samples. In spite of several drawbacks, it was widely used in all fields of analysis. It usually involves mixing of an aqueous sample solution with an equal volume of immiscible organic solvent for a period of time, and then

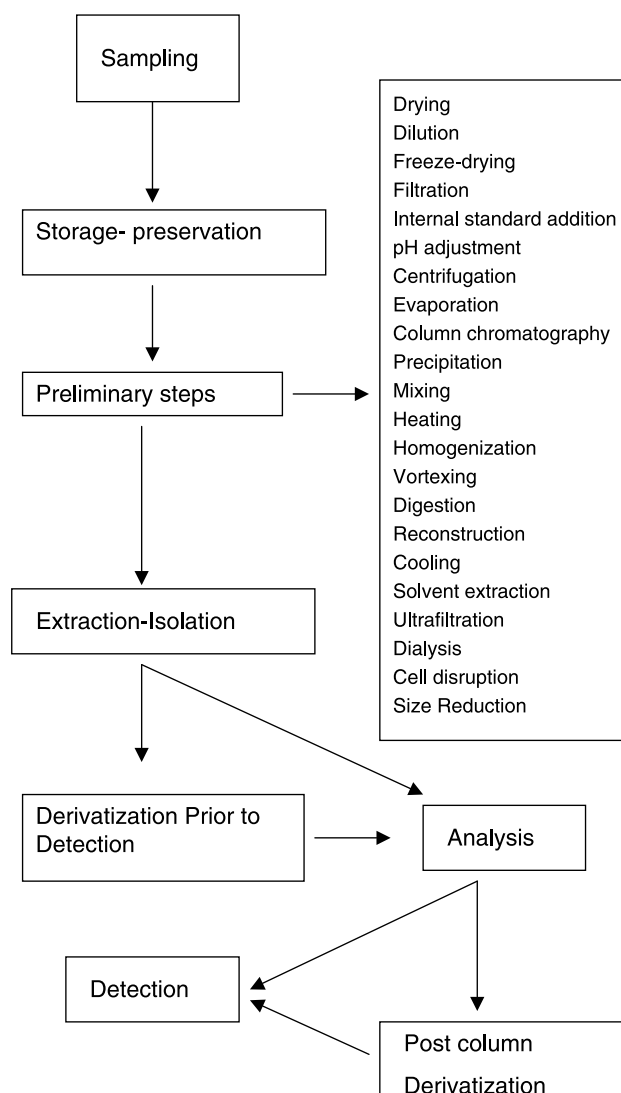
**Fig. 1** Stages of sample preparation.

Table 2 Further treatment requirements for a sample in liquid phase before analysis

-
- Dilution to the appropriate concentration ranges with a compatible solvent in case it is too concentrated.
 - Concentration by LLE, SPE, evaporation, or lyophilization.
 - Derivatization to stabilize, freeze-drying, and storage at 4°C, far from light or air exposition, in case it is reactive or thermally or hydrolytically unstable.
 - Removal of unwanted high-molecular-weight substances by size exclusion chromatography, dialysis, ultrafiltration, precipitation, and use of supported liquid membrane.
 - Removal of particulate matter by filtration, centrifugation, or sedimentation.
 - Solvent exchange if the solvent is not compatible with the analytical method.
 - Solvent can be removed by evaporation, lyophilization, or distillation, and the analytes can be reconstituted in a solvent and at a concentration suitable for the technique that will be used for analysis.
 - Addition of internal standard.
-

allowing these two liquid phases to interact so that the analytes of interest are extracted from the aqueous layer into the organic layer, as the organic solvent has a larger affinity for them. The selectivity and efficiency of the extraction process are governed by the choice of the two immiscible liquids. The more hydrophilic compounds prefer the aqueous phase, and the more hydrophobic compounds will be found in the organic solvent, as “like” dissolves “like.” Organic solvents such as methylene chloride, chloroform, ethyl acetate, and diethyl ethers are preferred as they can be easily removed by evaporation. Chelating and other complexing agents, ion pairing, and chiral reagents may also be used. After the immiscible liquids are separated, the layer containing the extracted analytes is removed, concentrated to dryness, and reconstituted in an appropriate solvent that is compatible with the analytical system (e.g., the HPLC mobile phase).

A limitation of this technique is that polar, water-miscible solvents cannot be used for the extraction. Other drawbacks of this technique are:

1. The use of large quantities of organic solvents, leading to a considerable cost for their acquisition and disposal.
2. The formation of emulsions during the mixing procedure.
3. Evaporation of the solvent is time-consuming.
4. The co-extraction of other matrix-interfering components with similar properties.
5. It is difficult to be automated in its classical form (using a separation funnel or similar apparatus), although a number of flow-system LLE approaches

have been presented, applying the principle of flow injection analysis.

In the latter approach, a chemical reaction or complexation takes place in a mixing-reaction coil, resulting in an extractable component segmented with an organic immiscible solvent stream at the phase segmenter, where small reproducible droplets of one phase are formed in the other. The phase containing the analytes of interest can be monitored by a flow-through detector, and the unwanted phase is directed to waste.

Automation in LLE has been also introduced using an instrumentation that can automate all or part of the extraction and concentration process. A number of autosamplers and workstations for HPLC and GC can perform LLE. Robotic systems can be used to handle larger-volume LLE.

Column Extraction—Liquid—Liquid Extraction

Column extraction based on the theory of LLE is a widely used technique in biochemistry, toxicology, pharmaceutical analysis, and other fields. Extrelut by Merck (Darmstadt, Germany) and Extube by Varian (Harbor City, California, USA) are commercially available preppacked columns used in these applications (Fig. 2A). Extraction is performed by fixing an aqueous solution or suspension to a supporting material (stationary phase) and allowing the other immiscible solvents (mobile phase) to pass over it. The two phases are in contact, thus permitting a continuous and multistep extraction to occur. This technique can replace the conventional LLE in a separating funnel, and thus it becomes more efficient and practical as no emulsions can be formed, less solvent volumes are used, and preparation time is reduced. Body fluids (e.g., urine) are the best example for the application of in-column LLE.

MODERN LIQUID SAMPLE PREPARATION TECHNIQUES

Solid-Phase Extraction

Solid-phase extraction (SPE) is a particularly attractive, fast, and effective technique for the isolation and pre-concentration of target analytes that avoids or eliminates the disadvantages of LLE, tending to replace it in many applications.

The principle of SPE involves a partitioning of analytes to be extracted between two phases: a solid phase, the sorbent, and a liquid phase, the matrix, which contains possible interferences. Analytes must have a greater affinity for the solid phase than for the sample matrix (retention or adsorption step), and they are



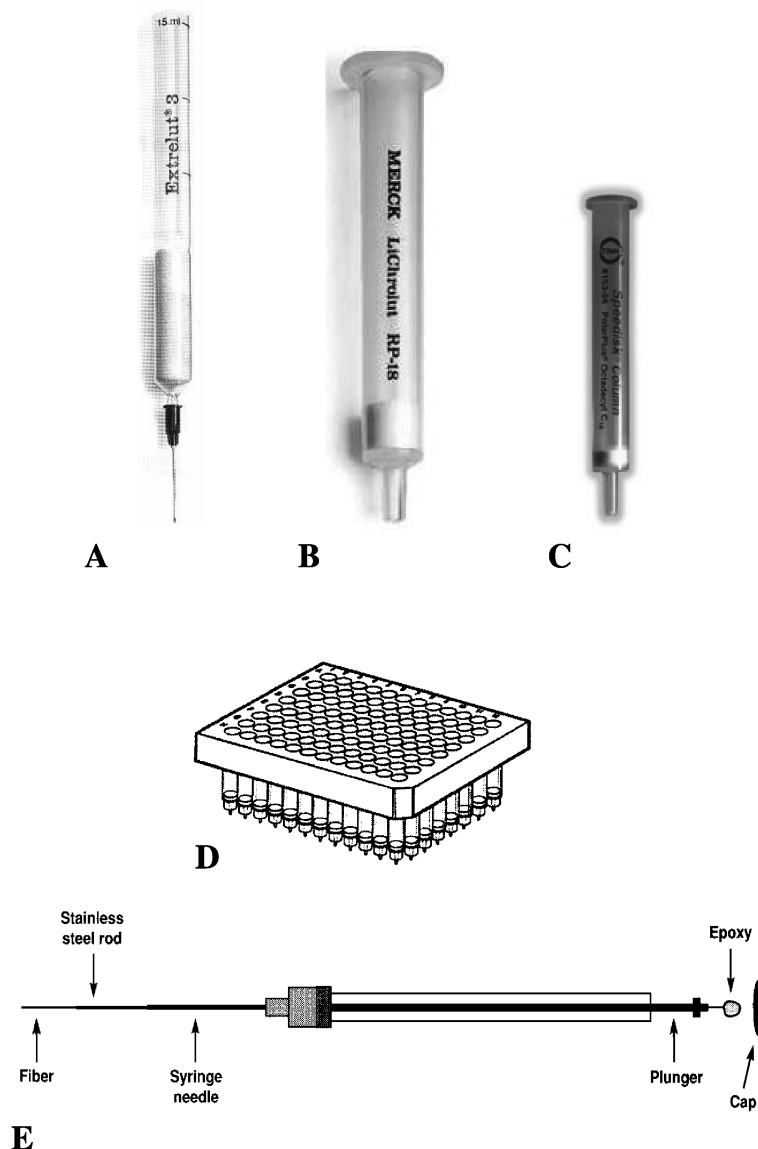


Fig. 2 (A) Extrelut column for LLE; (B) SPE cartridge; (C) SPE cartridge, disk format; (D) 96-well extraction plate; and (E) SPME device.

subsequently removed by eluting with a solvent that has a greater affinity for the analytes (elution or desorption step). The different mechanisms of retention or elution are a result of intermolecular forces among three components: the analyte, the active sites on the surface of the sorbent, and the liquid phase or matrix.

Solid-phase extraction objectives, apart from the removal of interfering compounds and the preconcentration of the sample, include:

1. The fractionation of the sample into different compounds or groups of compounds as in classical column chromatography.
2. The storage of analytes that are unstable in a liquid medium or with relatively high volatility.
3. The derivatization by reactions between the reactive groups of the analyte(s) and those on the adsorbent surface.

The major types of commercially available SPE product configurations are:

1. Syringe barrel columns.
2. Cartridges.
3. 96-Well plates.
4. Disk membranes.

5. Solid-phase extraction vacuum manifolds for simultaneous processing of 10, 12, 20, and 24 SPE tubes.

Fig. 2 illustrates the typical commercially available SPE formats.

Solid-phase extraction cartridges are available in a wide variety of sizes, with packing capacities ranging from 20 mg to 10 g and with reservoir volumes as large as 30 mL. In this configuration, extraction is carried out by a disposable cartridge of polypropylene, in a shape similar to an injection syringe without plunger and without injection needle. The column is filled with the sorbent (particle size of 40 μm) fixed between two frits (pore size of 20 μm) of polypropylene. The upper part of the barrel serves as a sample reservoir. The column can be connected to extraction systems by Luer fittings.

Although gravity can facilitate the flow of most organic solvents through the columns, samples and more viscous solvents must be drawn by vacuum applied to the column outlet, by positive pressure applied to the column inlet (gas pressure from a syringe), or by centrifugation (Fig. 3). The typical flow rate ranges between 0.2 and 1.5 mL/sec.

All sample types are amenable to SPE with suitable handling: solids, liquids, semisolids, etc. Solid-phase extraction is extensively used in sample preparation, as it offers a fast, safe, and convenient means for subsequent analysis by chromatographic techniques [HPLC, thin-layer chromatography (TLC), GC, etc.]. The major benefit is that it requires less solvent than conventional LLE methods. Impurities are removed and the analytes are

concentrated, leading to a higher sensitivity in subsequent analysis. The SPE process can be carried out either on-line or off-line.

Solid-phase extraction is performed according to the following steps:

1. Conditioning of the sorbent (i.e., solvation; activation of functional groups) and preparation of the sorbent to interact with the sample.
2. Sample loading. The sample, optionally containing the internal standard, is forced through the sorbent of the cartridge. The component of interest and some undesired compounds are adsorbed by the sorbent. In this step, the interaction between the analyte and the sorbent should be predominant. The most effective sorbent facilitates the interaction between the functional groups and the analyte. To enhance the retention of the analyte, the sample can be diluted with water, so that the polarity of the environment of the analyte is increased.
3. Washing to remove the undesired polar matrix constituents. A solvent of low elution strength is chosen as a washing solvent (water or a buffer) so that the analyte is not eluted from the sorbent. Only after the completion of this step may some air pass through the column.
4. Sorbent drying. This may be necessary to remove water if the elution solvent is immiscible with it. Drying can be performed by vacuum aspiration, nitrogen flow, or centrifugation. Analytes in a purified form are now present on the column.

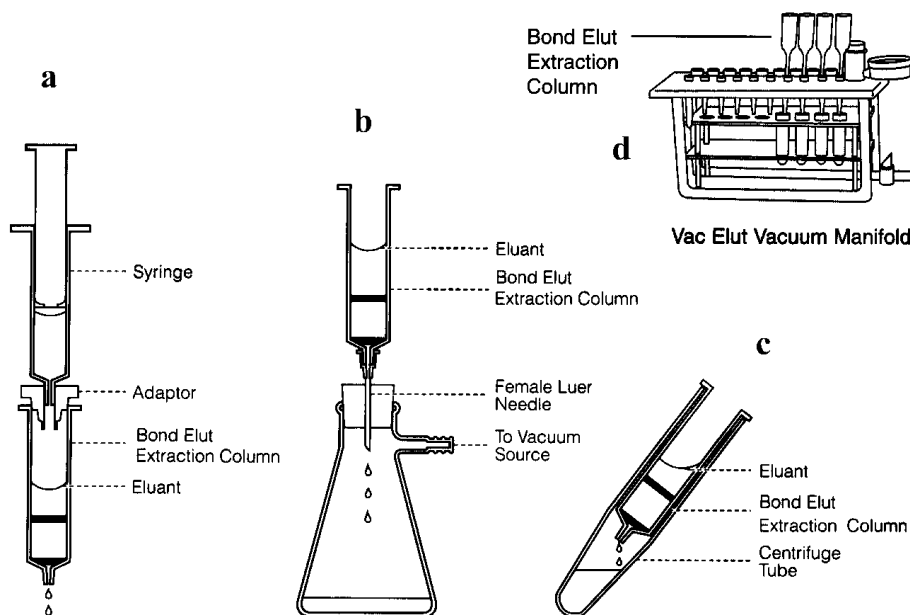


Fig. 3 Different ways of SPE process. (a) Positive pressure; (b) vacuum; (c) centrifugation; and (d) vacuum manifold.



5. Elution or extraction process. This aims for the quantitative recovery of the analyte that is achieved by selective desorption of the compounds of interest from the sorbent with a suitable solvent and collects the cartridge effluent. The interaction between the analyte and the elution solvent should be so strong that the interaction between analyte and sorbent will be overcome.
6. Solvent evaporation. The extract is directly injected or evaporated under a gentle stream of nitrogen and reconstituted in the mobile phase or after the addition of internal standard.

The optimization of SPE must be executed in each of these steps for best performance. Two different approaches can be chosen:

1. The analyte is retained on the sorbent while components pass through to waste. The analyte will be eluted later from the sorbent, with a suitable solvent, to be analyzed.
2. The matrix components are adsorbed while the analyte is evacuated.

The first approach is generally preferred as less sorbent is required and isolate preconcentration is possible. The second approach is selected when interferences are present but the concentration of analytes is not required (Fig. 4).

Solid-Phase Extraction Sorbents

Several SPE sorbents have been developed. These can be classified according to the primary interaction possibilities of the functional groups of the sorbents, mostly nonpolar, polar, or ionic. Ionic groups consist of cation exchange and anion exchange sorbents and contain functional moieties that can act as ion exchangers. Silica-based sorbents include the following: reversed phase—highly hydrophobic octadecyl (C_{18}), octadecyl (C_{18}), octyl (C_8), ethyl (C_2), cyclohexyl, and phenyl; wide-pore reversed phase—butyl (C_4); normal phase—silica modified by cyano ($-CN$), amino ($-NH_2$), and diols; adsorption, silica gel, fluorisil, and alumina; and ion exchangers, amino ($-NH_2$), quaternary amine (N^+), carboxylic acid ($-COOH$), and aromatic sulfonic acid ($ArSO_3H$). Other sorbents with a wide variety of specifications are also introduced in SPE: polymeric sorbents are polystyrene–divinylbenzene (PS–DVB) resins that overcome many of the limitations of the silica-based phases. The broader range of pH stability increases the range of method development and flexibility, providing greater analyte retention of polar compounds than C_{18} sorbents. However, a conditioning step with a wetting solvent is still required.

Hydrophilic–lipophilic polymeric sorbents have been recently introduced, claiming that no conditioning step is required as the sorbent preserves analyte retention, even if the bed dries out. Commercially available

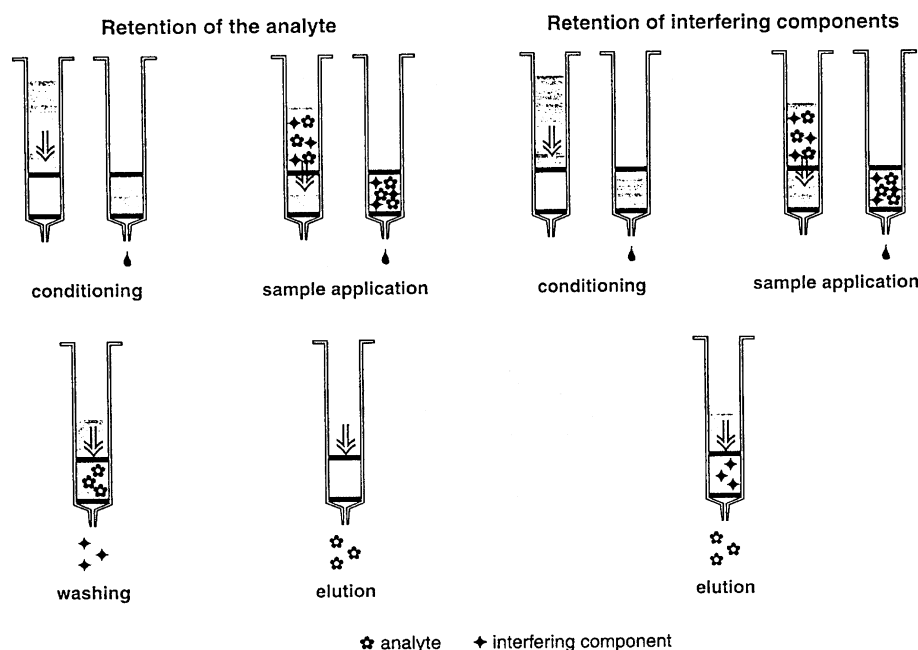


Fig. 4 The steps of solid-phase extraction technique.

products include Oasis by Waters and Absolut by Varian. These are copolymers of polyvinyl pyrrolidone (a hydrogen acceptor, which increases the water wettability of the polymer) and a cross-linked PS–DVB resin that provides the reversed-phase retention necessary to retain analytes. These are designed to extract an extensive spectrum of analytes: lipophilic, hydrophilic, acidic, basic, and neutral. They exhibit greater pH stability and enhanced retention over C₁₈-bonded silica.

Mixed-mode sorbents contain both nonpolar and strong ion (cation and/or anion) exchange functional groups, targeted for the extraction of basic drugs.

Affinity sorbents such as the *restricted-access matrix* sorbents, *immunosorbents*, or *molecularly imprinted polymers* (MIPs) have been introduced as well. These are based upon molecular recognition using antibodies with a high degree of selectivity or with molecularly imprinted polymer.

Graphitized carbon: Porous graphitic carbon, similar to the LC-grade Hypercarb, is available in SPE cartridges. This is characterized by a highly homogenous and ordered structure, made of large graphitic sheets with a specific area approximately 120 m²/g. Compounds are retained by both hydrophobic and electronic interactions so that nonpolar analytes, and also very polar analytes, can be retained from aqueous matrices. Owing to the different retention mechanism, acetonitrile and methanol can be inefficient, and it is preferable to use methylene chloride or tetrahydrofuran.

Column selection is based on the nature of the analytes, the nature of the sample matrix, the degree of purity required, the nature of the major contaminants, and the analytical technique applied.

Sorbent–Isolate Interaction

The most common chemical interactions between sorbent and isolates are nonpolar (van der Waals forces or dispersion forces), polar (hydrogen bonding, dipole–dipole, and induced dipole–dipole), ion exchange (ionic), and covalent interactions.

Nonpolar interactions are the weakest interactions, which are exerted between the C–H bonds of the analyte and those of the sorbent, usually C₁₈. Because these are facilitated by a polar solvent environment, they play a crucial role in the bioanalysis of blood, plasma, serum, and urine.

Isolated compounds include alkyl, aromatic, alicyclic, or functional groups with significant hydrocarbon structure. All isolates have a potential for nonpolar interaction (except inorganic ions and compounds with polar groups, e.g., carbohydrates). Because of this fact, the nonpolar interactions are nonselective and allow the extraction of

groups of compounds with different structures. Retention is facilitated by a polar solvent, while elution is facilitated by an organic solvent with sufficient nonpolar character (MeOH, ACN, etc.). A wash solvent should be more polar than that used for elution.

Polar interactions occur between a polar group of the sorbent and a polar group of the isolate. Silica is the typical adsorbent. Examples of groups that exhibit polar interactions are carbonyl, carboxyl, hydroxyl, sulfhydryl, and amine groups; rings with hetero atoms and with unequal electron distributions; as well as groups with π -electrons, such as aromatic rings and double or triple bonds. Hydrogen bonding is one of the most significant polar interactions. Polar interactions are stronger than nonpolar ones. Although they provide greater selectivity, they have the disadvantage of being facilitated by a nonpolar environment. Highly polar solvent facilitates elution, while wash solvent should be less polar than those used for elution.

Ionic interactions are exhibited between two groups (of analyte and sorbent) with opposite charge. These are the strongest interactions that can be seen between an analyte and a sorbent. Because few compounds possess either a cationic or an anionic group, the selectivity is high. Ionic interactions can only be effected in a polar environment. For an actual ionic interaction, it is necessary that the respective functional groups of sorbent and analyte are both ionized. Analytes can be eluted in two ways:

1. By using an elution solvent of such a pH that the respective functional groups of either the sorbent or the analyte are neutralized.
2. By using an elution buffer with a high concentration of a counterion (an ion of a charge opposite to that of the functional group of the sorbent), which will compete for the active sites of the sorbent with the analyte. Evidently, a combination of both elution ways is possible.

Applications of SPE include clinical analysis, pharmaceuticals, food analysis, environmental analysis, agrochemicals, forensic samples, etc.

Solid-Phase Extraction Disk Technology

Solid-phase extraction in disk format has been designed to overcome the limitations of the conventional packed-bed SPE columns. Disks exhibit minimal channeling, have small void volumes, do not require frits, have low capacity for interference (cleaner extracts are provided), and capture analytes of interest very effectively. They require lower solvent volumes, providing a faster sample processing and an increased throughput. Disk products

include rigid disk, flexible disk, and thin packed beds of small particles between two retained screens.

A typical extraction sequence is similar to the traditional SPE, although 500 μL of the appropriate solvent is sufficient for disk conditioning and extraction of the analytes. Several types of disk extraction media are commercially available in different dimensions depending on the application and sample volume. The most prevalent are paper-based, membrane-based, glass fiber-based, and PTFE-based products. Commercially available products are Speediscs by Baker, Empore by 3M, Novo Clean by Alltech, and SPEC by Ansys Technol.

AUTOMATED SOLID-PHASE EXTRACTION SYSTEMS

Solid-phase extraction automation is accomplished off-line and on-line. In off-line automation, SPE cartridges are not directly connected to the high-pressure flow stream of the analytical instrument. In on-line SPE, the solid-phase device is inserted into, and becomes part of, the liquid or gas flow stream. Obviously, the hardware interfacing requirements for the two approaches differ. In the manual mode, a simple vacuum is used to pull the liquids through the cartridge. However, in the automated mode, positive gas or liquid pressure is more commonly used to push liquids through the cartridge. Off-line automated SPE usually involves some form of robotic manipulation using flexible robotic arms and semiflexible modified x - y - z liquid handling devices. Most of these systems are controlled by dedicated personal computers.

The benefits of the automated solid-phase extraction are:

1. Analysts can redirect their time to other tasks.
2. Automated systems can provide a higher sample throughput with higher accuracy and precision because of minimized systematic errors than do manual systems.

Early automated systems processed individual samples *in series*. The next sample in the series was not started until the preceding sample had been completed or was on its way. However, this approach was slower than manual systems. Automated *parallel processing* SPE, where numerous samples are extracted simultaneously with significantly improved throughput, seems to be more practical. Such automated systems can achieve treatment of up to 400 samples per hour.

Autosamplers offer at some level sample preparation functions such as dilution, internal standard addition, and calibration standard preparation. In addition, some automated liquid handling devices have built-in heating,

cooling, SPE, and other functions for performing automated sample preparation. These operations are controlled by a computer system.

ON-LINE SOLID-PHASE EXTRACTION-LIQUID CHROMATOGRAPHY COLUMN-SWITCHING TECHNIQUE

On-line SPE-LC utilizes the principle of *column switching*. A typical on-line arrangement is performed using simple electrically or pneumatically driven (six-port) switching valves and commercial precolumns and holders. A fresh disposable precolumn is used for every sample, and extraction is carried out in a way similar to the off-line sequence. A solvent delivery unit provides the solvent necessary to purge, wash, and activate the precolumn, and to apply the required volume of sample. High-pressure switching valves are used to couple two or more columns that trap either defined volumes or the collected samples, usually in a loop, and direct them to a second, usually the analytical, column. Valve configuration can be used for conventional HPLC analysis, and it can perform more advanced functions such as diverting the mobile phase containing the desired solutes from the first column to the second column for defined periods of time, a process called *heart-cutting* or *on-column concentration* (trace enrichment). Additionally, it can perform "backflushing" of specific sample components from one column to waste, which leaves only the peak of interest on the second column and front-cutting and end-cutting when needed. Selecting the appropriate valve and actuating it at the correct time cause different fractions of the sample to follow different paths through the column network.

In the most common case, the pretreated biofluid is injected onto the cartridge or precolumn, which retains the target molecules. Interfering sample constituents are flushed into waste. The analytes retained on the bonded phase of the cartridge or precolumn are eluted, on-line, via the switching valve onto the analytical column. Simultaneously to the analytical separation, an exchange of the cartridge or reconditioning of the precolumn takes place (Fig. 5).

The separation of the sample occurs not only by chromatographic means, but also by physical means that are under the control of the analyst and unrelated to the chemical properties of the analyte, thus resulting in very efficient separations.

Column-switching techniques have been used to analyze a sample directly, without any pretreatment stages, with the advantage of easy automation. The increase in safety and the improved analytical speed and accuracy often make up for the initial cost of the additional

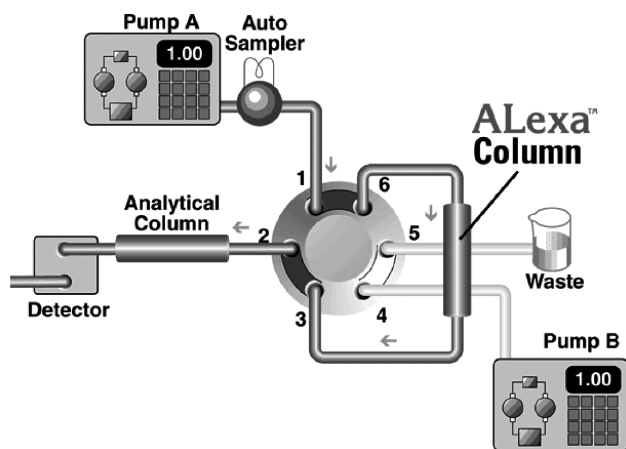


Fig. 5 On-line SPE-LC column-switching technique.

equipment that is required. Automating the column-switching systems can usually be accomplished using the timed-event tables included with HPLC instrument-control software; this enables a simpler and a more accurate control of complex column networks with minimal contamination and loss.

The limitation of column switching includes restricted sample enrichment. Another limitation is that the sample throughput using this approach probably will not be as high as for the other methods. Finally, it is considered too complicated to be practical, although modern instruments make these procedures relatively straightforward.

SOLID-PHASE MICROEXTRACTION

Solvent-free sample preparation techniques attract widespread attention to reduce the use of toxic organic solvents. Solid-phase microextraction (SPME) is a *solvent-free* technique for sample preparation that can integrate sampling, extraction, concentration, and sample introduction into single step, resulting in high sample throughput.

Generally, the term *microextraction* refers to an extraction technique where the volume of the extracting phase is very small in relation to the volume of the sample, and the extraction of the analytes is not exhaustive. The fraction of the initial analyte extracted depends on the partitioning of the analyte between the sample matrix and the extraction phase. The higher the affinity of the analyte for the extraction phase, the greater the amount of analyte is extracted. Once sufficient extraction time has been reached and equilibrium has been established, further increases in extraction time do not affect the amount of analyte extracted.

Solid-phase microextraction is an adsorption/desorption technique used to analyze the volatile and nonvolatile

compounds in both liquid and gaseous samples used as an alternative to the headspace, purge-and-trap, solid-phase extraction, or simultaneous distillation/extraction techniques. Analytes are thermally desorbed and directly introduced into any gas chromatograph or gas chromatography/mass spectroscopy (GC/MS) system. When coupled to HPLC with the proper interface, the analytes are washed out of the fiber by the mobile phase.

The SPME device, shown in Fig. 2E, consists of a 1-cm length of narrow diameter fused silica optical fiber, coated on the outer surface with a thin film of stationary phase and bonded to a stainless steel plunger, and a holder such as a modified microsyringe. The fused silica fiber can be drawn into a hollow needle by using the plunger on the fiber holder. The fiber assembly consists of an outer protective septum-piercing needle and an inner fiber attachment needle to which the fiber is epoxied. The septum flange prevents GC or HPLC mobile phase from escaping when injecting. When not in use or during transfer, the fiber retracts into the needle. The SPME processing steps include:

1. Penetration of the syringe through the septum of the sample vial.
2. Extension of the fiber into the sample or in the headspace. Organic analytes partition into the stationary phase of the fiber until equilibrium is reached.
3. Retraction of the fiber into the syringe needle and, once the equilibrium is reached, withdrawal of the syringe from the sample vial.
4. Insertion/introduction of the needle into the GC port, depression of the plunger, and thermal desorption of the analytes. Alternatively, the analytes are washed out of the fiber by the HPLC mobile phase via a modified HPLC six-port injection valve and a desorption chamber that replaces the injection loop in the HPLC system. The SPME fiber is introduced into the desorption chamber, under ambient pressure, when the injection valve is in the load position. The SPME-HPLC interface enables mobile phase to contact the SPME fiber, remove the adsorbed analytes, and deliver them to the separation column. Analytes can be removed via a stream of mobile phase (dynamic desorption) or, when the analytes are more strongly adsorbed to the fiber, the fiber can be soaked in mobile phase or another stronger solvent for a specific period of time (e.g., 1 min) before the material is injected onto the column (static desorption) (Fig. 6).
5. Removal of the syringe from the injection port. It is now ready for resampling. The thermal or solvent treatment of the coated fiber in the injection port ensures that the fiber is free from interferences or residual compounds.



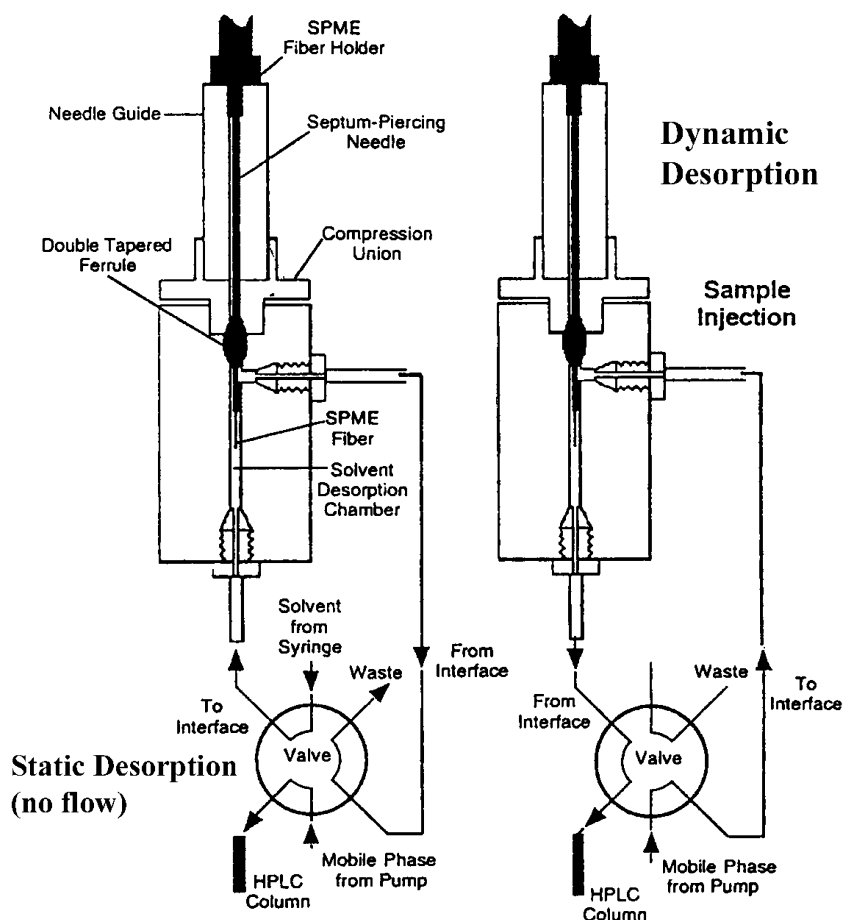


Fig. 6 SPME-HPLC interface.

With solid or dirty matrices, such as sludge and biological fluids, the technique can be operated in the headspace mode as the fiber is exposed to the gas phase above the sample. Agitation by stirring or sonication of the sample matrix improves the transport of analytes from the bulk sample phase to the vicinity of the fiber. Other parameters that influence the partition equilibrium are the sample matrix, temperature, and properties of the coating and analyte (e.g., the thickness of the coating and the distribution constant for the analyte). An equilibrium time of 30–60 min is usually enough for direct immersion SPME. Full equilibrium is not necessary for high accuracy and precision from SPME, but consistent sampling time and other sampling parameters are essential. The vial size, the sample volume, and, when using liquid samples, the depth that the fiber is immersed into the sample should be consistent. The desorption of an analyte from an SPME fiber depends on the boiling point of the analyte, the thickness of the coating on the fiber, and the temperature of the injection port. As with any other extraction/concentration technique, it is best to use

multiple internal standards, and to treat the standards and the analytes in an identical manner.

The equilibrium conditions can be described as:

$$n = K_{fs} V_f V_s C_0 / K_{fs} V_f + V_s \quad (1)$$

where n is the number of moles extracted by the coating, K_{fs} is a fiber coating/sample matrix distribution constant, V_f is the fiber coating volume, V_s is the sample volume, and C_0 is the initial concentration of a given analyte in the sample.

As indicated by Eq. 1, after equilibrium has been reached, there is a direct proportional relationship between the sample concentration and the amount of analyte extracted.

Complete extraction can be achieved for small sample volumes when distribution constants are reasonably high. When the sample volume is very large, Eq. 1 can be simplified to:

$$n = K_{fs} V_f C_0 \quad (2)$$

In this equation, the amount of extracted analyte is independent of the volume of the sample. In practice, there is no need to collect a defined sample prior to analysis, as the fiber can be exposed directly to the ambient air, water, production steam, etc.

The commercially available fibers include polydimethylsiloxane (PDMS; 100, 30, and 7 μm), PDMS-divinylbenzene (PDMS-DVB; 65 μm), polyacrylate (PA; 85 μm), carboxen-PDMS (CAR-PDMS; 75 and 85 μm), Carbowax-DVB (CW-DVB; 65 and 75 μm), Carbowax-templated resin (CW-TPR; 50 μm), and DVB-CAR-PDMS (50/30 μm). The type of fiber used affects the selectivity of extraction. In general, polar fibers are used for polar analytes, and nonpolar types are used for nonpolar analytes. Selectivity toward target analytes and interferences can be enhanced by surfaces common to affinity chromatography. Fibers can be reused up to 100 analyses or more depending on the sample matrix, on the care of the analyst, and on the applications for which used.

MEMBRANE-BASED SEPARATIONS

There are a number of different membrane techniques which have been suggested as alternatives to the SPE and LLE techniques. It is necessary to distinguish between porous and nonporous membranes, as they have different characteristics and fields of application. In porous membrane techniques, the liquids on each side of the membrane are physically connected through the pores. These membranes are used in Donnan dialysis to separate low-molecular-mass analytes from high-molecular-mass matrix components, leading to an efficient cleanup, but no discrimination between different small molecules. No enrichment of the small molecules is possible; instead, the mass transfer process is a simple concentration difference over the membrane. Nonporous membranes are used for extraction techniques.

The introduction of membranes in the field of sample preparation contributes to minimal organic solvent use, minimal contamination and exposure to toxic or dangerous samples, automation, and effective cleanup and analyte isolation.

Membranes in Sample Filtration

Membrane filters are used to remove particulates from samples and solvents prior to HPLC analysis and also for the preparation of liquid samples, where no solvent is used. Typical materials of construction for membrane filters are usually synthetic polymeric materials, although natural substances, such as cellulose, and inorganic materials, such as glass fibers, are also used: acrylic

copolymer, aluminum oxide, cellulose acetate, glass fiber, mixed cellulose esters, nitrocellulose, nylon, polycarbonate, polyester, polyether sulfone, polypropylene polysulfone, PTFE, PVC, etc. The compatibility of the polymeric material with the solvents used must be a great concern of their different chemical properties.

Membranes are available in sheet, roll, disk, capsule, cartridge, and hollow-fiber formats. For sample filtration, disk-format membranes are the most popular devices. Disks are sold in loose form or packed in disposable syringe filters or cartridges; common diameters commercially available are 3, 7, 13, 25, 47, and 96 mm, or even larger. Samples are filtered by manually applying a positive pressure or in a vacuum manifold.

DIALYSIS AND MICRODIALYSIS

Dialysis is a membrane barrier separation process in which differential concentration forces one or more sample analytes to transfer from one fluid to another through a membrane. In dialysis, the solution containing the analyte of interest (whose concentration is depleted) is called the “feed” and the fluid receiving the analyte is called the “dialysate.” Dialysis is used to remove salts and low-molecular-weight substances from solutions or to remove high-molecular-weight interferences (e.g., proteins) and to allow the measurement of small molecules.

Other variations of the porous membrane techniques include microdialysis and electrodialysis, where a membrane promotes selective transport of charged compounds.

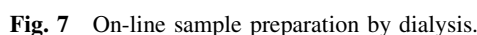
Microdialysis is a technique for *in vivo* sampling of living tissues or animals, where sampling is performed by means of a probe containing the semipermeable membrane. It is used for medical applications and for on-line monitoring of extracellular chemical events in living tissues. The membrane is placed at the end of a small piece of a small-diameter, fused silica tubing that is inserted into the tissue of an animal, being in direct contact with the interstitial space. A flowing fluid that can be void of substances of interest, or include physiologically or pharmacologically active substances, is used on the other side of the membrane. The concentration gradient across the membrane enables the diffusion of substances from the interstitial space into the dialysis probe. Usually, the probe is held in place mechanically so the animal can move freely. The outlet of the probe is connected to a collection vial or, in some cases, an HPLC microvalve that enables on-line analysis using a microbore column. Microdialysis has the advantages of easy operation, rapid isolation of components of interest from complicated and dirty matrices, and lower consumption of organic solvents. Pharmacokinetic studies can also be executed.

is a liquid or a solid (e.g., polymeric) phase that is placed between the two phases, usually liquid but sometimes gaseous. This arrangement permits the versatile chemistry of LLE to be used and extended, thus providing a highly effective cleanup as well as a high enrichment factor, and technical realizations can easily be automated. In most cases, there is no, or insignificant, use of organic solvents. The technique is known as *supported liquid membrane*. An advantage of the membrane techniques is that they are amenable to automation and connection to chromatographic instruments.

A high degree of molecular selectivity can be achieved with affinity chromatography and affinity extractions. These techniques are based on *molecular recognition* (antigen–antibody interactions). Because the antibodies are highly selective toward the analyte used to initiate the immune response, the corresponding immunosorbent may extract and isolate this analyte from complex matrices in a single step, thus eliminating matrix interference.

Membranes in Extraction

Nonporous membranes are used, as already mentioned, in membrane extraction techniques. A nonporous membrane



are easily obtained, while obtaining selective antibodies for small-size molecules is more difficult. The first step in making an immunosorbent is to develop antibodies with the ability to recognize the desired analytes. Then immunosorbents are obtained by immobilizing the antibodies on solid supports by covalent bonding, adsorption, or encapsulation. The sorbent must be chemically and biologically inert, easily activated, and hydrophilic to avoid nonspecific interactions. The common choices are activated silica, Sepharose, agarose gel, etc.

The immunoextraction procedure may be “off-line” or “on-line.” In the off-line approach, the immunosorbent is packed into a disposable cartridge. A typical SPE sequence is followed. The sorbent is first conditioned, then the sample is applied, washed to eliminate interference, and analytes of interest are desorbed by the appropriate eluent system, which may be a displacer agent, a chaotropic agent, an aqueous–organic solvent mixture, or a solution that alters pH. With the on-line approach, the immunosorbent is packed into a pre-column incorporated in a six-port switching valve, where the immunoextraction is performed at the load position, while desorption is achieved at the inject position.

MOLECULARLY IMPRINTED POLYMERS

One approach to synthesize the antibody mimics has been the development of MIP. These involve the preparation of polymers with specific recognition sites for certain molecules. The desired affinity can be introduced by adding an amount of the compound of interest to the polymerization reaction. This “pattern” (template) chemical may be removed after polymerization, leaving vacant sites of a specific size and shape, suitable for binding the same chemical again, from an unknown sample. Like immunosorbent, the recognition is a result of shape and a mixture of hydrogen, hydrophobic, and electronic interactions. Molecularly imprinted polymers have the advantage to be prepared more rapidly and easily, using well-defined methods, and to be stable at high temperatures over a large pH range and in organic solvents. They have found applications in liquid chromatography, as normal and chiral stationary phases, and in areas where they can be substitutes of natural antibodies (i.e., immunoassays, sensors, and SPE). Non-covalent imprinting protocols are the most commonly used for preparing MIPs using acrylic or methacrylic monomers—often, with methacrylic acid and ethylene glycol dimethylacrylate as cross-linkers. A problem related to the use of MIPs in SPE is the difficulty in removing all the template analytes, even after extensive washing, and the difficulty in establishing a quantitative

and rapid desorption as a result of the high greed of the MIP for the analytes.

RESTRICTED-ACCESS MATERIALS

Special sorbents possessing restricted-access properties have been developed to allow the direct injection of biological matrices into the on-line SPE–LC systems. These sorbents, the so-called *restricted-access materials*, combine the size exclusion of proteins and other high-molecular-mass matrix components that are prohibited from entering the pores of the packing, and they are not well retained by the column. Therapeutic drugs and other small molecules permeate the pores of the column packing material where they partition and are retained by conventional retention mechanics, such as hydrophobic, ionic, or affinity interactions at the inner pore surface. They are suitable for handling biological samples because they prevent the access of proteins, thus allowing on-line cleanup and trace enrichment for the determination of several drugs and their metabolites in various biological fluids in the same step.

TRADITIONAL APPROACHES OF SOLID SAMPLE PREPARATION

Solid samples such as biological tissues may be prepared for extraction by a stepwise process that begins with the disruption of the gross architecture of the sample. This modifies the physical state of the sample and provides the extracting medium with a greater surface area per unit mass. Methods reducing the sample particle size include homogenizing, cutting, milling, mincing, blending, macerating, pulverizing, chopping, grinding, sieving, and crushing. Additionally, samples may be frozen in liquid nitrogen or by exposure to dry ice, or they may be freeze-dried to produce a material that can be mechanically pulverized. The finely divided powder that is produced may then be extracted.

Dissolution is the predominant process that takes place before solid samples are injected into HPLC in order to be converted into a liquid state. This is accomplished either by dissolving the entire sample matrix, or by leaching the analytes from the solid matrix using a suitable solvent.

For many years, the *traditional sample preparation* methods, such as the Soxhlet extraction, were applied. Most of these methods have been used for more than 100 years, and they mostly require large amounts of organic solvents. These methods were tested during those times, and the analysts were familiar with the processes and protocols required. However, the trends in recent years are automation, short extraction times, and reduced



organic solvent consumption. Modern approaches in solid sample preparation include microwave-assisted solvent extraction (MASE), pressurized liquid extraction, accelerated solvent extraction (ASE), matrix solid-phase dispersion (MSPD), automated Soxhlet extraction, supercritical fluid extraction (SFE), gas-phase extraction, etc.

Solid-liquid extraction (SLE) refers to the classic extraction technology that is achieved by using the appropriate solvent that selectively dissolves the analyte of interest. The most common form of SLE is the “shake-filter” method that involves the addition of an organic solvent for organic compounds or dilute acid or base for inorganic compounds to the sample, and also agitation to allow the analytes to dissolve into the surrounding liquid until they have completely migrated. Heating or refluxing the sample in hot solvent may speed up the extraction process. The insoluble substances are subsequently removed by filtration or centrifugation. A faster and more complete extraction is achieved by *sonication*, where the sample is immersed into a solvent within a vessel that is placed in an ultrasonication bath. The ultrasonic agitation allows more intimate solid-liquid contact, and the gentle heating generated during sonication can aid the extraction process. The extract can either be directly injected, or treated further according to the procedures described under “Preliminary Sample Preparation Procedures.”

SOXHLET EXTRACTION

In this technique, the solid sample is placed in a “thimble” that is a disposable, porous container made of stiffened filter paper or Pyrex glass. The thimble is placed in the Soxhlet apparatus designed to repeatedly siphon the solvent with the extracted components, after the inner chamber that holds the thimble is filled to a specific volume with solution. The siphoned solution containing the dissolved analytes is returned to the boiling flask, and the process is repeated until the analyte is successfully removed from the solid matrix. Soxhlet extractions are usually slow, often requiring 24 hr or more. However, it requires little operator involvement after the sample is loaded, and refluxing proceeds until the termination of the extraction. Rows of Soxhlet extractors may be used usually under fume hoods, when the technique is integrated into routine analysis. In relation to modern extraction techniques, it is a low-cost method. The Soxhlet extraction glassware is rather inexpensive; however, the cost is elevated by the large solvent volumes required. Small-volume Soxhlet extractors and thimbles can accommodate sample amounts of a few milligrams. Method development involves the choice of the suitable solvent or solvent mixture (azeotrope) of

high volatility, so that it is easily removed and has a high affinity for the analyte but a low affinity toward the solid sample matrix.

A fully automated Soxhlet extraction has been patented as Soxtec by Foss Tecator (Sweden) based on a four-step solvent extraction technique. The sample is rapidly dissolved during the first step in boiling solvent. The remaining soluble matter is efficiently removed at the second step, while distilled solvent is collected at the third step. In the fourth step, the sample cup lifts off the hot plate, utilizing residual heat to predry while eliminating boil-dry risk.

FORCED-FLOW LEACHING

Forced-flow leaching is an extraction technique that can provide a nearly quantitative recovery of many organic compounds. In this technique, the sample of interest is packed into a 20 cm × 4 mm stainless steel column. An extraction solvent is pumped under a gas pressure of 2.5 kg/cm² through the column, which is heated close to the solvent's boiling point. The results are comparable to Soxhlet extraction, but the extraction time is reduced from 24 to 0.5 hr using the forced-flow technique. An advantage of this method is that the sample is subjected continuously to fresh, hot solvent, and the effluent from the column can be collected easily for further treatment.

MODERN APPROACHES OF SOLID SAMPLE PREPARATION

Supercritical Fluid Extraction

Supercritical fluid extraction is a modern sample preparation technique of great interest and utility for complex matrices, primarily considered as an alternative for Soxhlet and sonication extraction for solid and semisolid matrices.

A *supercritical fluid* is defined as a substance above its critical temperature and pressure, which means that it does not condense or evaporate to form a liquid or a gas, but is a fluid with intermediate properties. These properties change from gas-like to liquid-like as the pressure is increased.

A typical supercritical fluid extractor includes a supercritical fluid (most often CO₂ or CO₂ with an organic modifier) source, a means of pressurizing the fluid, a pumping system (for the liquid CO₂), an extraction thimble, a device to depressurize the supercritical fluid (flow restrictor), an analyte collection device, temperature-control systems for several zones, and an overall system controller.

The CO₂ remains a liquid throughout the pumping or compression zones and passes through small-diameter metal tubing as it approaches the extraction thimble itself. The fluid then passes through the extraction thimble at a flow rate and a time period predetermined at the method development stage. The supercritical fluid containing extracted analytes flows through additional capillary tubings until it reaches the restrictor zone.

Applications of SFE include the extraction of salts, proteins, carbohydrates, peptides, amino acids, and other interfering polar compounds in a biological matrix. It shows its best advantage for extracting the analytes from solids and semisolids, rather than from liquids and fluids, mainly because of the extraction thimble's design. The extraction thimbles and associated pieces are made of porous materials such as nickel, chlorofluorocarbon compounds, and stainless steel materials that are very similar to the frits used in HPLC columns. To extract a liquid sample by SFE successfully, it has to be first mixed with a solid material such as diatomaceous earth or alumina, so that the sample is no longer in a liquid state. An SPE filter bed medium may also be used while passing a liquid sample through this first.

A drawback of this technique is a clear need for SFE to be carried out on reference materials of known composition determined by an alternative technique. The advantages of SFE in comparison to LLE are:

1. Less organic solvent is used in reduced time (extraction times can be less than 0.5 hr).
2. Carbon dioxide as an extraction solvent has the advantage of low critical temperature; additionally, it is cheap, nontoxic, and nonexplosive. It is classified as a nonpolar solvent that can be modified to more polar solvent by the addition of organic solvents (modifiers) such as lower alcohols (e.g., methanol).
3. On-line and off-line analytical scale SFE can be applied. In the former, the coupling step (i.e., the transfer and collection of extracted analytes from the SFE to the chromatographic system) is of great importance.

PRESSURIZED SOLVENT EXTRACTION—ACCELERATED SOLVENT EXTRACTION

As an alternative to SFE with carbon dioxide or other supercritical fluids, it was proposed that heating the organic solvents under pressure above their boiling point, but below their supercritical point, would enhance the speed of reaction and solvent strength. This technique, known as the *pressurized solvent extraction* (PSE), provides an easy method for extraction, reducing the

amount of solvent required and speeding up the process. The system is marketed as ASE by Dionex Corporation (Sunnyvale, California, USA). Because PSE represented an extension of existing methods, it attracted attention and is often adopted by official organizations.

MATRIX SOLID-PHASE DISPERSION

Matrix solid-phase dispersion handles viscous solid, solid, or semisolid samples directly by blending with a solid-phase support, such as silica or bonded silica, similar to those used in SPE columns. This is performed by placing a small quantity (~0.5 g) of the sample into a glass mortar and blending it with a glass or agate pestle. The bonded phase acts as a lipophilic binding solvent that assists in sample factorization. The best ratio of sample-to-solid support-bonded phase is 1:4 (or other, depending on the application). The isolation of polar analytes from biological samples is assisted by the use of polar solid support phases and less polar analytes by the less polar phase. The sample components dissolve and disperse into the bound organic phase on the surface of the particle, leading to the complete disruption of the sample and its dispersion over the surface.

The conditioning of the material to be used for MSPD can greatly enhance the analyte recovery. Once the MSPD blending process is completed, the material is transferred to a column constructed from a syringe barrel or other appropriate device containing a frit that retains the entire sample, which is compressed to form column packing by using a modified syringe plunger. A second frit is placed on top of the material, which is compressed so that no channels are formed. The addition of eluting solvent to the column may be preceded by the use of some or all of the solvent to backwash the mortar and pestle. Approximately 8–10 mL of solvent is used to perform the elution. However, most target analytes are eluted in the first 4 mL.

Because the entire sample is present in the column, it is possible to perform multiple or sequential elutions, which can be conducted by gravity flow, by application of pressure to the head of the column, or by placing the columns on a vacuum manifold and applying suction.

If the eluate from an MSPD column is not adequately clean for direct injection, additional steps may be necessary to remove the co-eluted matrix components, either by using other solid-phase material packed at the bottom of the MSPD column, or by eluting the analytes from the MSPD column directly onto a second SPE column for sample cleanup and analyte concentration. Sorbents similar to SPE can be used. The ionic state of the sample components is sometimes necessary to be modified to assure that certain interactions occur



between the solid support and the eluting solvent. This may be accomplished by adding acids, bases, salts, chelating or dechelating agents, antioxidants, etc., at the time of the sample blending and/or as an additive to the eluting solvent.

Matrix solid-phase dispersion provides results equivalent to older official methods. However, it generally requires 95% less solvent and 90% less time than classical methods. Matrix solid-phase dispersion has been applied to the isolation of drugs, herbicides, pesticides, and other pollutants from animal tissue.

DERIVATIZATION IN HIGH-PERFORMANCE LIQUID CHROMATOGRAPHY

In some cases, the enhancement of detectability is required in trace analysis, when the analytes do not possess a UV-absorbing, fluorescent, or electroactive functionality; therefore derivatization is necessary. A reaction with a fluorotag will produce a highly fluorescing derivative of the compound of interest; thus very low concentrations are detectable. An improvement of UV detectability can also be obtained by a reaction with a chromotag.

The derivatization for HPLC is performed either "off-line" (pre-column) before injection into the column, or "on-line" (post-column) by mixing the reagent with the column effluent.

Precolumn derivatization offers some advantages vs. postcolumn derivatization, as it involves less reaction restrictions, simpler equipment, and no time limitation regarding kinetics, provided that all species are stable. It can be performed either manually or automated. However, there are several drawbacks such as the introduction of contaminants, a possible loss of analyte as a result of side reactions, adsorption, degradation, and incomplete reactions.

By postcolumn derivatization, the analyte is derivatized after the separation and before the detection by using a reaction detector. The simplest way is to add a reagent solution to the column effluent with an extra pump. After the mixing T-piece, a reactor with a suitable holdup volume is inserted to allow reaction to take place. The benefits of this approach are that chromatographic separation is not affected and reaction is not required to be complete.

The most common *fluorotags* (fluorescent reagents) are dansyl chloride and *o*-phthalaldehyde (OPA). *Chromotags* include *p*-bromophenacyl bromide (PBPB) for derivatization of carboxylic acids (K-salts) with a crown ether catalyst, ninhydrin for primary amines forming complexes that have their adsorption maxima at about 570 nm, and dansyl chloride for primary and secondary

amines, including amino acids, thiols, imidazoles, phenols, and aliphatic alcohols.

Chiral derivatization can be applied to improve the separation of enantiomers.

CONCLUSION

The analytical process typically consists of several discrete stages, such as sampling, preparation, instrumental analysis, quantification, data reporting, and interpretation; each step is critical in obtaining accurate and reproducible results.

A sample preparation step is often necessary to isolate the components of interest from a sample matrix, as well as to purify and to concentrate the analytes. The quality of sample preparation is pivotal in the overall quality of the analysis. Despite the advances in instrumentation and computer technology, many sample preparation practices are based on the 19th century technologies (e.g., the commonly used Soxhlet extraction that was developed more than 100 years ago).

An ideal sample preparation technique should be solvent-free, simple, inexpensive, efficient, selective, amenable to automation, and compatible with a wide range of separation methods and applications. It should also allow for the simultaneous separation and concentration of the components.

There is no universal sample preparation method, as sample preparation depends strongly on the analytical demands, as well as the size and nature of the sample. What is beyond any doubt is the continuously increasing demand for improved selectivity, sensitivity, reliability, and rapidity in the process of sample preparation.

Among the previously discussed sample preparation techniques, SPE offers a fast, safe, and convenient means for subsequent analysis by chromatographic techniques (HPLC, TLC, GC, etc.). The major benefit is that it requires less solvent than conventional LLE methods. Impurities are removed and the analytes are concentrated, leading to a higher sensitivity in subsequent analysis.

Modern techniques are currently driving out conventional approaches because of their many advantages, including speed, use of less environmentally hazardous solvents, better facilitation for the control of the extraction, as well as automation and on-line combination of the extraction with other analytical techniques. A major concern when developing techniques for sample preparation is the possibility for automating the entire analytical process, which might lead to increased sample throughput and reduced manual operations with obvious economic benefits, as well as higher accuracy and precision.

Miniaturization has become a dominant trend in analytical chemistry. The development of techniques

such as micro-LLE (in-vial extraction), ambient static headspace, disk cartridge SPE, SPME, MSPD, and MASE, which use smaller sample size, minimize solvent use, and are amenable to automation, is a positive sign for analytical science. The combination of modern sample preparation techniques may result in more cost-effective and faster analysis, higher sample throughput, lower solvent consumption, and less manpower, while maintaining, or even improving, sensitivity. Speed in sample preparation is a prerequisite in any analytical method. The future in sample preparation depends on new sorbents and new formats developed for SPE or SPME that exhibit higher selectivity and greater convenience for method development.

REFERENCE

1. Majors, R.E. Sample preparation perspectives. *LC GC Int.* **1991**, 5 (2), 12–20.

SUGGESTED ADDITIONAL READING

- Arthur, C.; Potter, D.; Buchholz, K.; Motlagh, S.; Pawliszyn, J. Solid phase microextraction for the direct analysis of water: Theory and practice. *LC GC* **1992**, 10 (9), 656–661.
- Barker, S.A. Matrix solid-phase dispersion. *J. Chromatogr., A* **2000**, 885, 115–127.
- Blevins, D.D.; Hall, D.O. Recent advances in disk format solid-phase extraction. *LC GC* **1998**, 13 (5), S16–S21.
- Eskilsson, C.S.; Bjorklund, E. Analytical-scale microwave-assisted extraction. *J. Chromatogr., A* **2000**, 902, 227–250.
- Georga, K.A.; Samanidou, V.F.; Papadoyannis, I.N. The use of novel solid phase extraction sorbent materials for HPLC quantitation of caffeine metabolism products methylxanthines and methyluric acids in samples of biological origin. *J. Chromatogr., B* **2001**, 759, 209–218.
- Hennion, M.-C. Solid-phase extraction: Method development, sorbent, and coupling with liquid chromatography. *J. Chromatogr., A* **1996**, 856, 3–54.
- Huck, W.; Bonn, G.K. Recent developments in polymer-based sorbents for solid-phase extraction. *J. Chromatogr., A* **2000**, 885, 51–72.
- Johnsson, J.A.; Mathiasson, L. Membrane based techniques for sample enrichment. *J. Chromatogr., A* **2000**, 902, 205–225.
- Jönsson, J.A.; Mathiasson, L. Membrane-based techniques for sample enrichment. *J. Chromatogr., A* **2000**, 902, 205–225.
- Lord, H.; Pawliszyn, J. Microextraction of drugs. *J. Chromatogr., A* **2000**, 902, 17–63.
- Lord, H.; Pawliszyn, J. Review. Evolution of solid-phase microextraction technology. *J. Chromatogr., A* **2000**, 885, 153–193.
- Majors, R.E. New approaches to sample preparation. *LC GC Int.* **1995**, 8 (3), 128–133.
- Majors, R.E. The changing role of extraction in preparation of solid samples. *LC GC Int.* **1996**, 9 (10), 638–648.
- Papadoyannis, I.N.; Tsioni, G.K.; Samanidou, V.F. Simultaneous determination of nine water and fat soluble vitamins after SPE separation and RP-HPLC analysis in pharmaceutical preparations and biological fluids. *J. Liq. Chromatogr.* **1997**, 20 (19), 3203–3231.
- Rossi, D.T.; Zhang, N. Automating solid-phase extraction: Current aspects and future prospects. *J. Chromatogr., A* **2000**, 885, 97–113.
- Samanidou, V.F.; Imamidou, I.P.; Papadoyannis, I.N. Evaluation of solid phase extraction protocols for isolation of analgesic compounds from biological fluids prior to HPLC determination. *J. Liq. Chromatogr. Relat. Technol.* **2001**, in press.
- Smith, R.M. Supercritical fluids in separation science—The dreams, the reality and the future. *J. Chromatogr., A* **1999**, 856, 83–115.
- Supercritical Fluid Extraction and Its Use in Chromatographic Sample Preparation*; Westwood, S.A., Ed.; Blackie Academic and Professional (an imprint of Chapman and Hall): Glasgow, UK, 1993.
- Ulrich, S. Solid-phase microextraction in biomedical analysis. *J. Chromatogr., A* **2000**, 902, 167–194.
- van de Merbel, N.C. Membrane-based preparation coupled on-line to chromatography or electrophoresis. *J. Chromatogr., A* **1999**, 856, 55–82.
- Wells, D.A. 96-Well plate products for solid-phase extraction. *LC GC Eur.* **1999**, 12 (11), 704–715.



Scale-up of Countercurrent Chromatography

Ian A. Sutherland

Brunel Institute for Bioengineering, Brunel University, Uxbridge, Middlesex, United Kingdom

Introduction

There are few processes that can be predictably scaled up from laboratory to production scale without difficulties. Preparative high-performance liquid chromatography (HPLC), for example, is not a linear scale-up; it is expensive and uses large volumes of solvents. The product can become hydrolyzed by or react with the column, which can induce chemical/steric/chiral conformation changes and often requires significant prepurification with further risk of degradation.

Countercurrent chromatography (CCC) [1,2] is a process that avoids these difficulties. It is a form of liquid–liquid chromatography without a solid support, which separates soluble natural product substances on their partition, or differential solubility, between two immiscible solvents. The principle of separation (partition) is the same in both the laboratory and the production plant and is generic in that it can be applied to an extremely broad range of purification problems in many industries. Furthermore, because there is no solid support, there is 100% sample recovery and no need for any prepurification.

Background Information

A recent review on CCC as a preparative tool [3] described an extremely useful comparison of four different CCC approaches and concluded that “the real future belongs to the new generation of centrifugal instruments.” They concluded that more reliable designs were required, that there was a need to accommodate higher loads on the 100-g to 1-kg scale, and that truly preparative instruments needed to be developed. They called for a better understanding of the mechanisms of separation in order to achieve this.

Ito's work [4] on pH zone refining makes a valuable contribution to the scale-up scenario. It offers a method of operating existing instruments preparatively when purifying ionizable compounds with the

ability of achieving sample loadings two orders of magnitude higher than normal. Sutherland et al. [5] demonstrate that preparative gram-quantity separations of crude plant extracts use one-tenth the volume of solvents compared to the equivalent prep-HPLC. Sandlin and Ito [6] have shown that CCC is feasible using a “J”-type coil planet centrifuge with tubing bore up to 5.5-mm internal diameter and have successfully demonstrated fractionations in 750-mL coils, but at relatively low flow, speed, and β value. They have also investigated the effect on resolution of increasing sample volume and sample concentration [7]. Ito and colleagues [7–9] have described unit-gravity (noncentrifugal) slowly rotating coil devices, which would be suitable for large-scale CCC separations.

Parameters Affecting Scale-up

The main parameters affecting scale-up have been analyzed in detail by Sutherland et al. [10]. For scale-up of CCC to be successful, they recommended that two measures or responses had to be maintained as the process was scaled up: retention of the stationary phase and resolution of the sample components. It was emphasized that even if it was possible to retain phases as the tubing bore increased, it was possible that the hydrodynamics of the mixing and settling zones may not work as well, as the bulk volume to surface area ratio increased.

They studied three “J”-type coil planet centrifuges with different coil sizes: analytical ($d = 0.76$ mm), lab prep ($d = 1.6$ mm), and process ($d = 3.68$ mm). By constructing the coils from stainless steel, they were able to increase flow considerably without risk of bursting the tubing or causing the tubing to work loose under the action of high cyclic forces, which can be a common problem (see later). They first showed that there was no difference in retention between coils made with stainless steel or polytetrafluoroethylene (PTFE). This was an important experiment that showed that retention was a hydrodynamic process and not governed by the surface properties of the tubing-wall material.



The Effect of These Scale-up Parameters on Retention

Figure 1 shows Sutherland et al.'s plot of retention against flow for the three CCC units with different bore sizes. It clearly shows how increasing the tubing bore not only allows higher throughput but also shows that retention with larger bores is far more tolerant or stable when flow is increased, a very important discovery for industrial scale-up. They went on to demonstrate that increasing speed allowed even higher retention and linear flows of the mobile phase and that the mean Reynold's numbers of the mobile-phase flow were still well within the laminar flow region.

They concluded that increasing two of the three major variables affecting scale-up, speed and tubing bore, actually improved retention. The third, flow, decreased retention as flow increased but less so as the bore increased. Tubing material and retention of the stationary phase therefore are no barrier to the industrial scale-up of CCC.

The Retention Behavior of Different Phase Systems

Du et al. [11] have shown that there is a linear relationship between retention and the square root of flow. The negative gradient of this line gives an indication of the stability of the retention process for a given phase system: The shallower the negative gradient, the more stable the process and the higher the flow possible for a given retention. Tables 1 and 2 give the linear regressions for the phase systems tested on the process-scale CCC [10] at 800 and 1200 rpm, respectively. In all cases, the lower phase is the mobile phase pumping from head (center) to tail (periphery). Retention was measured at four different flow rates: 10, 20, 40, and 80 mL/min, except for the butyl alcohol–acetic acid–water (4:1:5) phase system where only flows of 10 and 20 mL/min were tested before retention dropped below 50%. A range of two-phase solvent systems are listed across the polarity range. In the case of hydrophilic low interfacial tension phase systems like butyl alcohol–acetic acid–water (4:1:5), a high speed of rotation was required to achieve a reasonably high retention.

The Effect of These Scale-up Parameters on Resolution

There has not been any significant change in resolution detected [10] as the bore size increases, provided the

Scale-up of Countercurrent Chromatography

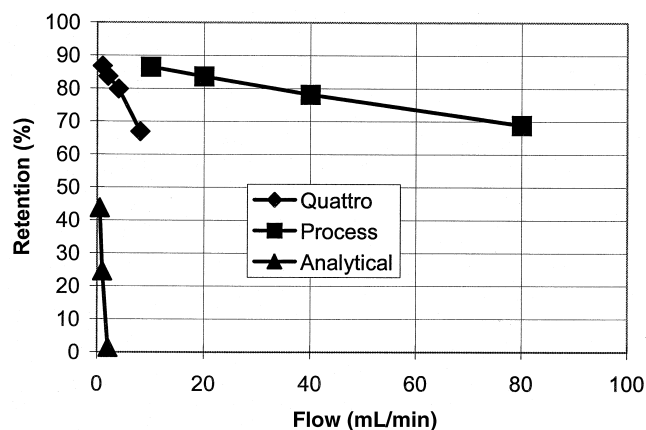


Fig. 1 Variation of retention with flow for different tubing bores: an analytical CCC (0.76 mm), a Bunel CCC (1.6 mm), and a process CCC (3.68 mm).

sample volume injected maintains the same ratio of coil volume. This is a significant finding, as in most chromatography processes, resolution reduces as the process is scaled up. Resolution was found to increase with increasing speed of rotation as would be expected due to the increased number of mixing and settling cycles per unit time.

The effect of flow on resolution is shown in Fig. 2 for the process CCC [10] running at 1200 rpm. The resolution is between benzyl alcohol and phenyl ethanol resolved using the heptane–ethyl acetate–methanol–water (1.4:0.1:0.5:1.0) phase system. Resolution drops off with increasing flow as would be expected, as the sample will have experienced fewer mixing and settling steps before it elutes and

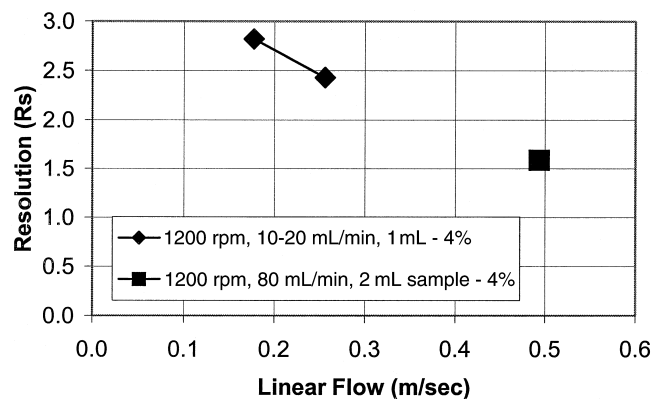


Fig. 2 Variation of resolution with flow for benzyl alcohol and phenyl ethanol in a heptane–ethyl acetate–methanol–water (1.4:0.1:0.5:1.0) phase system.

Table 1 Regression Analysis between Retention (S_f) and the Square Root of Flow (\sqrt{F}) for Phase Systems Tested on the Process CCC at 800 rpm

Solvent system	Linear regression	Correlation
Heptane–ethyl acetate–methanol–water (1.4:0.1:0.5:1.0)	$S_f = 97.27 - 3.1341\sqrt{F}$	0.9936
Heptane–ethyl acetate–methanol–water (1.4:0.6:1.0:1.0)	$S_f = 95.73 - 3.3658\sqrt{F}$	0.9988
Heptane–ethyl acetate–methanol–water (1.4:2.0:2.0:1.0)	$S_f = 102.02 - 6.0416\sqrt{F}$	0.9950
Iso-hexane–acetonitrile (1:1)	$S_f = 106.74 - 6.9389\sqrt{F}$	0.9994

Table 2 Regression Analysis between Retention (S_f) and the Square Root of Flow (\sqrt{F}) for Phase Systems Tested on the Process CCC at 1200 rpm

Solvent system	Linear regression	Correlation
Heptane–ethyl acetate–methanol–water (1.4:0.1:0.5:1.0)	$S_f = 97.724 - 2.3506\sqrt{F}$	0.9991
Heptane–ethyl acetate–methanol–water (1.4:0.6:1.0:1.0)	$S_f = 100.41 - 3.107\sqrt{F}$	0.9877
Heptane–ethyl acetate–methanol–water (1.4:2.0:2.0:1.0)	$S_f = 103.63 - 5.2379\sqrt{F}$	0.9996
Iso-hexane–acetonitrile (1:1)	$S_f = 105.84 - 5.2228\sqrt{F}$	0.9996
Butyl alcohol–acetic acid–water (4:1:5)	$S_f = 100.65 - 11.484\sqrt{F}$	1.0

the retention is lower. However, the increased flow appears to improve mixing, as it can be seen that this drop off is only gradual. Doubling flow does not halve resolution and so it would appear advantageous to increase flow as much as possible in the scale-up process.

Engineering Challenges of Scale-up

Sutherland et al. [10] and, earlier, Sandlin and Ito [6] have shown that scale-up is feasible. It can be seen that over 60% retention has been achieved for a broad range of phase systems with flows of 0.1 L/min in a 1-L capacity coil. This leads to the solvent front ($k = 0$) eluting in 4 min and the $k = 1$ point in 10 min with sample volumes of at least 0.1 L possible. All this adds up to sample process throughputs of up to 1 L/h or in weight terms as much as 1 kg/day.

However, before this can be realized, the engineering of the coil planet centrifuge will have to be made more reliable. The cyclical forces that produce the unique mixing and settling zones within the coiled tubes can cause them to shake apart and loosen. Janaway et al. [12] have solved this problem by developing new techniques for winding coils. As the scale in-

creases, the volumes of samples being pumped through become extremely high; therefore, designing flying leads that can be guaranteed to not leak becomes paramount. The coil planet centrifuge is a rotating piece of equipment and bearings can wear out. With such high cyclical forces, the reliable engineering of larger CCC units will not be trivial.

So far, Sutherland et al. [10] have only been working with 110-mm-radius coil planet centrifuge (CPC) rotors with a capacity of 1 L, which can be operated in a conventional laboratory. Sandlin and Ito [6] have gone as high as 150 mm with capacities of 0.75 L but with a lower speed and β value. The engineering challenge will be to build the next generation of process units at larger rotor radius with capacities of tens or hundreds of liters, but they would need to be installed in hazards plants using intrinsically safe manufacturing practices.

Conclusions

The chromatographic scale-up of countercurrent chromatography appears feasible, but there are engineering challenges ahead which will need to be solved before this promising new technology can be realized.



Acknowledgments

Some of the work presented was undertaken as part of a BBSRC/DTI LINK Consortium study on the "Industrial Scale up of Countercurrent Chromatography." The author would like thank both the BBSRC and the DTI for their financial support and the members of the consortium [10] who have also contributed toward progressing the scale-up of countercurrent chromatography near to reality.

References

1. W. D. Conway, *Countercurrent Chromatography: Apparatus, Theory and Applications*, VCH, New York, 1990.
2. Y. Ito, Principle, apparatus, and methodology of high-speed countercurrent chromatography, in *High Speed Countercurrent Chromatography*, (Y. Ito and W. D. Conway, eds.), Chemical Analysis Series Vol. 132, John Wiley & Sons, New York, 1996, pp. 3–44.
3. A. Marston and K. Hostettmann, Countercurrent chromatography as a preparative tool – Applications and perspectives, *J. Chromatogr.* 658: 315–341 (1994).
4. Y. Ito, pH-Peak-focusing and pH-zone-refining countercurrent chromatography, in *High Speed Countercurrent Chromatography* (Y. Ito and W. D. Conway, eds.), Chemical Analysis Series Vol. 132, John Wiley & Sons, New York, 1996, pp. 121–175.
5. I. A. Sutherland, L. Brown, S. Forbes, D. Games, D. Hawes, K. Hostettmann, E. H. McKerrell, A. Marston, D. Wheatley, and P. Wood, Countercurrent chromatography (CCC) and its versatile application as an industrial purification & production process, *J. Liquid Chromatogr.* 21(3): 279–298 (1998).
6. J. L. Sandlin and Y. Ito, Gram quantity separation of DNP (dinitrophenyl) amino acids with multi-layer coil countercurrent chromatography (CCC), *J. Liquid Chromatogr.* 7(2): 323–340 (1984).
7. J. L. Sandlin and Y. Ito, Large-scale preparative countercurrent chromatography with a coil planet centrifuge, *J. Liquid Chromatogr.* 8(12): 2153–2171 (1985).
8. Y. Ito and R. Bhatnagar, Improved scheme for preparative CCC with a rotating coil assembly, *J. Chromatogr.* 207: 171–180 (1981).
9. Q. Du, P. Wu, and Y. Ito, Low-speed rotary countercurrent chromatography using a convoluted multilayer helical tube for industrial separation, *Anal. Chem.* 72: 3363–3365 (2000).
10. I. A. Sutherland, A. Booth, L. Brown, S. Forbes, D. E. Games, A. S. Graham, D. Hawes, M. A. Hayes, S. Jackson, L. Janaway, B. Kemp, H. Kidwell, G. Lye, P. Massey, C. Preston, P. Shering, T. Shoulder, C. Strawson, F. Veraitch, R. Whiteside, H. Wolff, and P. Wood, Industrial scale-up of countercurrent chromatography, *J. Liquid Chromatogr.*, 24, in press (2001).
11. Q. Du, C. Wu, G. Qian, P. Wu, and Y. Ito, Relationship between the flow-rate of the mobile phase and retention of the stationary phase in counter-current chromatography, *J. Chromatogr. A* 835: 231–235 (1999).
12. L. Janaway, D. Hawes, I. A. Sutherland, and P. Wood, Chromatography Apparatus (coil winding process and winding tubing into a coil) UK Patent Application No 0015486.4 filed 23 June 2000.

SEC with On-Line Triple Detection: Light Scattering, Viscometry, and Refractive Index

Susan V. Greene

Ethyl Petroleum Additives Corporation, Richmond, Virginia, U.S.A.

Introduction

During the 1980s, accurate molecular weights (M) and molecular-weight distributions (MWD) could be obtained by SEC in conjunction with multiangle light scattering (LS), size-exclusion chromatography (SEC) using conventional calibration, or SEC in combination with viscometry (VISC) using universal calibration (UC). In addition to generating M and MWD, the viscometer with UC yields conformational and branching information. The impetus to combine the two advanced detector technologies of LS and VISC into a single, efficient, and accurate SEC method has been fueled by a growing interest to characterize both natural polymers and the increasing array of synthetic polymers [1,2].

New electronics and improved computer data acquisition capabilities have permitted the development of SEC with on-line triple detection using LS, VISC, and refractometry. On-line triple detection is known as size-exclusion chromatography cubed (SEC³) with the three dimensions being defined by the three detectors [3]. The use of SEC³ eliminates the requirement for column calibration, unlike conventional and universal calibration, where a premium is put on control of variables such as flow rate, temperature, and column resolution. SEC³ can offer advantages in polymer production quality control as well as in research and development of new polymers.

Theory

The schematic for one possible configuration of SEC³ hardware is shown in Fig. 1. When polymer molecules exit from the SEC column(s), they are simultaneously monitored in real time by three on-line detectors: right-angle laser LS [4], VISC, and refractive index (RI). The following simplified equations illustrate the variables that relate to the responses of the three detectors:

$$(M) \left(\frac{dn}{dc} \right)^2 (C) \rightarrow \text{LS} \quad (1)$$

$$([\eta])(C) \rightarrow \text{VISC} \quad (2)$$

$$\left(\frac{dn}{dc} \right) (C) \rightarrow \text{RI} \quad (3)$$

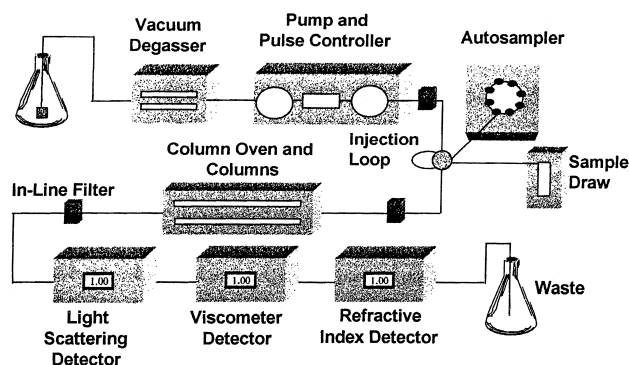


Fig. 1 Hardware schematic for a typical SEC³ triple on-line detector configuration.

The term dn/dc refers to the change in RI of a polymer relative to its concentration. The LS detector responds to M , the VISC detector responds to the intrinsic viscosity ($[\eta]$), which is inversely proportional to molecular density, and the RI detector monitors concentration (C). A single narrow standard is used to determine the offset constants related to the inter-detector volume for a given three-detector system [5]. Either C or dn/dc of a polymer sample must be known a priori in order to calculate the other variable using the RI detector [Eq. (3)]. Once both dn/dc and C are known, the LS and VISC [Eqs. (1) and (2)] can be solved to determine M and $[\eta]$, respectively, for a polymer sample [3]. Structural information, such as chain flexibility, branching, and intramolecular interactions are all related to $[\eta]$. Several key polymer properties related to $[\eta]$ are as follows:

Chain Length. As the chain length increases, $[\eta]$ increases and the density decreases. This behavior can be fitted to the well-known Mark-Houwink (M-H) equation [Eq. (4)] relating M (approximate chain length) to $[\eta]$. The M-H constant a is the slope of the double-logarithmic plot of $[\eta]$ versus M , and $\log K$ is its intercept.

$$[\eta] = KM^a \quad (4)$$



Conformation. If a polymer molecule is folded onto itself, instead of keeping the fully extended chain, the density will be higher resulting in a lower $[\eta]$. This can be induced either by strong intramolecular attractions (e.g., hydrogen-bonding) or by a poor solvent. The Flory–Fox equation [3] calculates $[\eta]$ for a linear flexible coil molecule in solution, relating $[\eta]$ to radius of gyration, R_g . Equation (5) shows this linear flexible coil example, where ϕ is the Flory–Fox constant.

$$[\eta]M = 6^{2/3}\phi R_g^3 \quad (5)$$

Chain Flexibility. If two polymers have the same M , the stiff chain one will produce a coil of lesser density and greater $[\eta]$, compared with its flexible coil counterpart.

Chain Branching. A branched molecule is more compact, having greater density and lower $[\eta]$ than its linear counterpart. The Zimm–Stockmayer theory defines the g factor for a polymer as the ratio of $[\eta]$ for the branched polymer to $[\eta]$ of the linear polymer, at the same molecular weight, with ε being the shape factor (~ 0.75).

$$g = \left(\frac{[\eta]_{\text{branched}}}{[\eta]_{\text{linear}}} \right)^{1/\varepsilon} \quad (6)$$

Once g is determined, the branching number B_n (number of branches per molecule), the branching frequency λ (number of branches per arbitrarily selected repeat unit of molecular weight), and f (number of arms for a star) can be calculated. Determinations of B_n , λ and f require equations specific to the type of branching for

that polymer [6]. (Consult the entry Long-Chain Polymer Branching: Determination by GPC–SEC an explanation of the related equations.)

Aggregation. Colloidal suspension particles are aggregates, which are formed due to poorly dissolved molecules. Aggregates are more dense and have a lower $[\eta]$ than their nonaggregated counterparts. The LS detector responds strongly to such aggregates. When a low VISC response is coupled with a high LS response, the presence of an aggregate is confirmed.

Thus, the SEC³ data obtained from its LS detector determine the MWD, whereas the VISC detector characterizes conformation and branching. The efficiency of SEC³ is a consequence of no column calibration requirement for the determination of M and MWD. The precision of the system is limited only by the signal-to-noise ratios of the LS and RI detectors, not by chromatographic variables such as flow rate and column retention. Sophisticated software is required to display the SEC³ picture of molecular structure.

Applications

Four examples of polymer characterization by SEC³ will be discussed: a dextran sample with branching transitions, a pair of brominated polystyrene (PS) samples, aggregation in chitosan, and a PS star polymer. SEC³ numerical results for dextran, chitosan, and star-branched PS are listed in the corresponding figure captions.

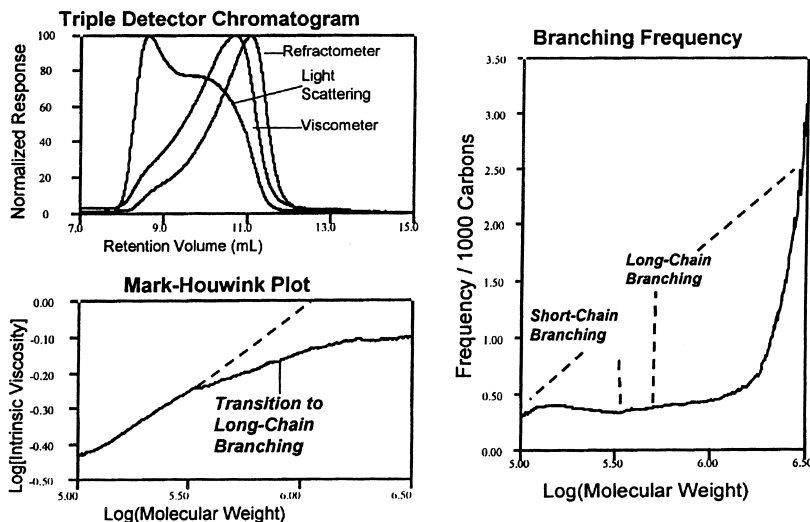


Fig. 2 In the triple-detector overlay of dextran, the shift of the LS detector toward a higher M indicates polydispersity. Both the M-H and branching frequency plots show a randomly branched polysaccharide, with both short- and long-chain branching. $M_n = 230,000$, $M_w = 540,000$, $M_z = 1,160,000$, $[\eta] = 0.54$ dL/g, $B_n = 26.6$, $\lambda = 0.43$, $dn/dc = 0.142$, $a = 0.287$, $\log K = -1.852$.

Dextran is a randomly branched polysaccharide with both long- and short-chain branching. The overlay of the traces generated by the three detectors in Fig. 2 shows a large shift toward a higher M for the LS detector, compared to the other two detectors. This indicates polydispersity within the sample, especially in the high-molecular-weight region of the MWD. Because long-chain branching decreases $[\eta]$ more than short-chain branching, the M-H plot indicates a transition from short- to long-chain branching at $\log(M) = 5.5$, where the plot deviates from linearity. The branching frequency plot is another visual presentation of the transition from short- to long-chain branching within dextran's MWD. Again, the slope of the curve change indicates a branching transition.

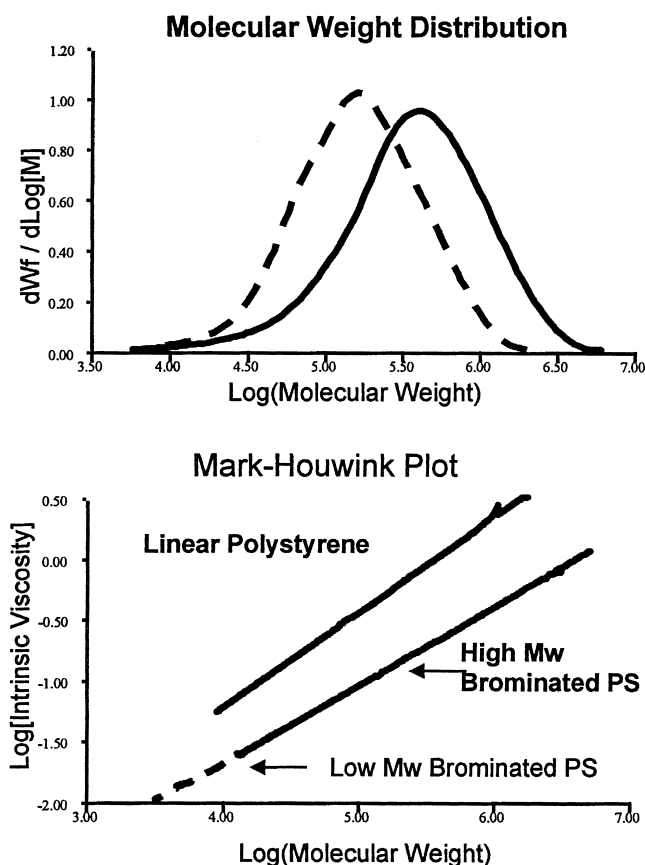


Fig. 3 Two polystyrene (PS) samples with different MWDs are compared in the upper chromatogram. In the lower graph, M-H plots of these same two samples lie on top of each other, indicating they have the same $[\eta]$ across their MWDs. It can be concluded that two PS samples of different M_w were brominated at the same level. A linear PS sample is included in the M-H plot for the purpose of comparison.

An overlay of the MWDs of two samples of brominated PS is shown in Fig. 3. From the MWD overlay, it is not clear if the MWD difference is a result of two PS samples of the same M_w brominated at different levels, or two PS samples with different M_w brominated at the same level. The M-H plot, which also includes linear PS without bromination, shows that the plots of the two samples in question lie on top of each other. The superposition of the two graphs shows that two PS samples of different M_w were brominated to the same level. The M-H plots of these two samples would be parallel to each other if PS samples of the same M_w were brominated at different levels.

Chitosan is a stiff-chain polysaccharide that has a tendency to aggregate in aqueous solution. Aggregation is indicated when a low VISC response is coupled with a high response from the LS detector. Examples of chitosan with and without aggregation are shown in Fig. 4. Note the close similarity between the nonaggregated chromatograms of the VISC and LS detectors' responses, respectively. For the aggregated sample, the LS response is much greater than that for the viscometer.

Star polymers are created when long-polymer chains are grouped covalently to a center core. The resulting polymer is denser with decreased $[\eta]$, com-

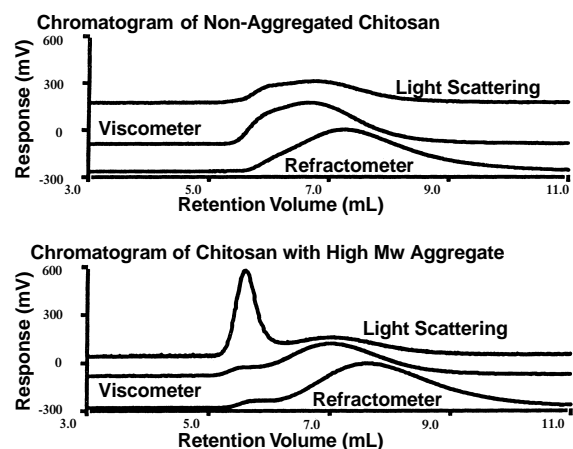


Fig. 4 Triple-detector chromatograms of nonaggregated and aggregated chitosan are compared. For the nonaggregated sample, both the LS and VISC detectors respond similarly. Aggregation in chitosan is indicated in the lower chromatogram, where the VISC response is low and the LS response is high. Nonaggregated chitosan: $M_n = 75,000$, $M_w = 260,000$, $M_z = 1,100,000$, $[\eta] = 7.9$ dL/g. Aggregated chitosan: $M_n = 90,000$, $M_w = 780,000$, $M_z = 3,000,000$, $[\eta] = 6.8$ dL/g.



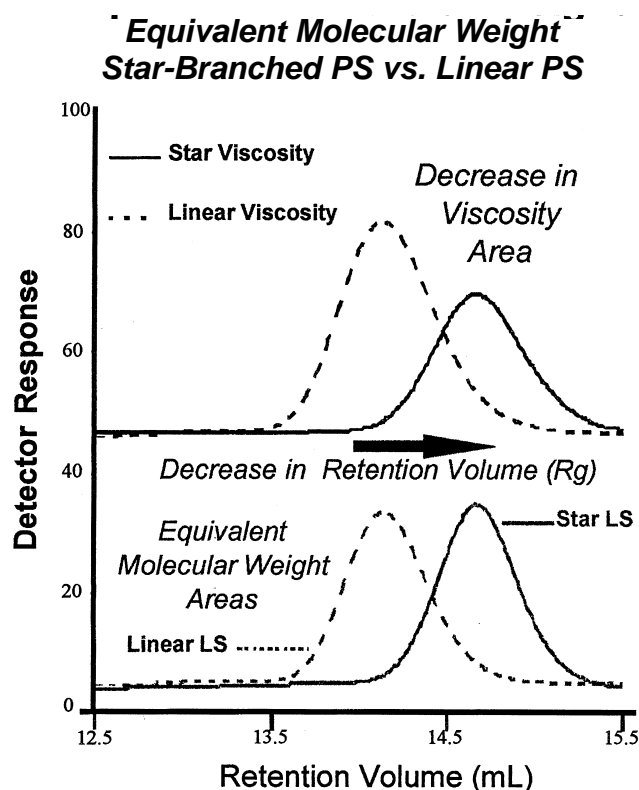


Fig. 5 The VISC traces (upper chromatogram) and the LS traces (lower chromatogram) are overlaid for a linear and a star-branched polymer with the same M . Star-branching creates a denser polymer with lower $[\eta]$ and a smaller R_g . Linear PS: $M_w = 100,000$, $[\eta] = 0.495$ dL/g, $R_g = 14$ nm. PS-star: $M_w = 100,000$, $[\eta] = 0.318$ dL/g, $R_g = 10$ nm, $f = 5$.

pared with a linear polymer of the same M . Figure 5 compares VISC and LS detector chromatograms obtained for linear and star-branched PS, both with the same M . The difference in $[\eta]$ is demonstrated by the area difference between the viscometer peaks of the two samples. The areas of the LS detector response are the same for both samples, but the delay elution of the star polymer confirms the star's increased density and smaller R_g , in accordance with Eq. (5).

Summary

The graphics associated with SEC³ capture its ability to reveal qualitative structural information in a visual format. The applications discussed show how peak displacement of the triple-detector chromatograms reflects polymer polydispersity (dex-

tran), how detector response can relate to aggregation (chitosan), and how peak area differences can indicate a change in polymer chemical composition (PS versus PS-star). The M-H plots (dextran, brominated PS) give information about polymer conformational changes, structural differences, and branching distributions [7].

The SEC³ technique has been in existence for 10 years. It is a relative newcomer to the analytical arena. The amount of information (molecular weight, conformational, and branching) produced, given the ease with which it can be generated, makes SEC³ a very attractive technique. Recently, the triple detector system has been used in conjunction with temperature rising elution fractionation (TREF) to expand fundamental understanding of polymer structure–property relationships [8].

Acknowledgments

The author thanks Dr. Max A. Haney (Viscotek Corp.) and Dr. Tze-Chi Jao (Ethyl Petroleum Additives, Inc.) for reviewing the manuscript, Dr. Wei Sen Wong (Viscotek Corp.) for contributing figures and related information, and Dr. André M. Striegel (Solutia Inc.) for helpful discussions of SEC theory.

References

1. W. W. Yau, New polymer characterization capabilities using SEC with on-line MW-specific detectors, *Chemtracts-Macromol. Chem. I*: 1–36 (1990).
2. C. Jackson, H. G. Barth, and W. W. Yau, Polymer characterization by SEC with simultaneous viscometry and laser light scattering measurements, *Waters International GPC Symposium Proceedings*, 1991, pp. 751–764 (www.waters.com).
3. M. A. Haney, T. Gillespie, and W. W. Yau, Viewing polymer structures through the triple “Lens” of SEC³, *Today's Chemist Work*, 3(11): 39–43 (December 1994).
4. M. A. Haney, C. Jackson, and W. W. Yau, SEC-viscometry–right angle light scattering, *Waters International GPC Symposium Proceedings*, 1991, pp. 49–63 (www.waters.com).
5. P. Cheung, S. T. Balke, and T. H. Mourey, Data interpretation for coupled molecular weight sensitive detectors in SEC: Interdetector transport time, *J. Liquid Chromatogr.* 15(1): 39–69 (1992).
6. D. T. Gillespie, H. K. Hammons, and S. R. Bryan, Branching and polymer modification analysis through SEC³, *MolMass International Conference Proceedings*, 1996 (www.chem.leeds.ac.uk/molmass 99).

7. L. J. Rose and F. Beer, Characterization of long chain branching in LDPE's using SEC with on-line viscosity and light scattering detectors, *MolMass International Conference Proceedings*, 1999 (www.chem.leeds.ac.uk/molmass99).
8. W. W. Yau and D. T. Gillespie, Triple-detector TREF instrument for polyolefin research, *Waters International GPC Symposium Proceedings*, 1998, pp. 252–256 (www.waters.com).

Suggested Further Reading

- Brandrup, J. and E. H. Immergut (eds). *Polymer Handbook*, 4th ed., John Wiley & Sons, New York, 1999.
- Burchard, W., Solution properties of branched macromolecules, *Adv. Polym. Sci.* 143, 113–194 (1999).
- Lovell, P. A., Dilute solution viscometry, in *Comprehensive Polymer Science* (C. Booth and C. Price, eds.), Pergamon Press, New York, 1989, pp. 173–197.



Sedimentation Field-Flow Fractionation of Living Cells

Philippe Cardot

T. Chianea

S. Battu

Université de Limoges, Limoges, France

Introduction

Living cell analysis and sorting in suspension is a major aim in life sciences. A wide panel of techniques and methodologies are available and they can be divided into three main groups. The first is based on physical criteria such as cell size, density, and shape (centrifugation or elutriation). The second group is linked to the cell surface characteristics driving to selective absorption and migration (immunodependent and electrophoretic methods). The third one corresponds to flow cytometry technologies which take advantage of cell biochemical and biophysical properties.

In their fundamental principle, field-flow fractionation (FFF) methods exploit the cell physical characteristics by means of their selective elution in a parallelepipedic channel laminarily flowed by a carrier phase under the effect of an external field applied perpendicularly to the great surface of the channel and, by consequence, perpendicularly to the flow direction. In sedimentation FFF, the external field is gravitational (G-FFF) or multigravitational (Sd-FFF).

Living cells are, in large majority, micron-sized species. Their elution mode is known to follow, roughly, the “steric-hyperlayer” model. However, the cell separation, isolation, and purification requires some specific methodological and technological features, caused by their unique multidimensional polydispersity and the necessity to preserve their viability at a reasonable rate of recovery. The objectives of this entry are, first, to drive the reader to a qualitative understanding of the FFF principle applied to micron-sized species such as living cells. Then, to focus on some specific limitations imposed by the respect of the biological interests of these separations and, finally, to monitor the reader's entrance into that exciting domain.

FFF Principle and Cell Multidimensional Polydispersity

Field-flow fractionations are chromatographlike methods, operated in the elution mode, in which the separator

(column) is a capillary ribbonlike channel whose critical dimension is its thickness. With a length/thickness ratio of over 50, the carrier phase in motion along the separator in a laminar mode creates, in the channel thickness, a parabolic flow profile. The general setup of a sedimentation FFF system is schematically described in Fig. 1a. Therefore, species focused in different positions in the channel thickness are carried out by flow streams of different velocities, creating separation. The unique feature of FFF operated in the “steric-hyperlayer” mode is that the focusing process in the channel thickness is provoked by the balance between hydrodynamic lifting forces and the external field generated ones, as schematically described in Fig. 1b(1–3). In sedimentation FFF (Sd-FFF), the force generated by the external field, applied to a single particle, is a function of the particle hydrodynamic radius and of its differential density (particle/carrier phase). The particle in motion in the channel is submitted to lifting forces of hydrodynamic nature whose origin is still under discussion (lubrification, inertia). Whatever its origin, lifting-force intensity depends on the particle size and its position into the channel thickness, as described in Fig. 1b(1) and legend. This balance drives to a flow-rate-dependent retention ratio of the eluted species. In the “steric-hyperlayer” elution mode, this balance focuses the particles into specific flow stream layers where the lifting-force module equalizes the external field generated one, as shown by the c' particle of Fig. 1b(1). The consequences are (1) that species of the same density are eluted according to their size, the bigger being eluted first, as shown in Fig. 1b(2), (2) that, at equivalent size, the denser are eluted last, as shown in Fig. 1b(3), (3) if the lifting force is overpowered by the sedimentation force, the elution mode becomes flow rate independent and only size related, the bigger particles being eluted first, as described in Fig. 1b(4). This case, described as “steric” elution mode, is often associated with very low recovery, reproducibility, and cell viability, linked to intense particles–accumulation wall interaction leading to, reversible or not, sticking of cells. It is obvious that separating cells only according to their size, at low recovery, reduces the separation power of Sd-FFF. The



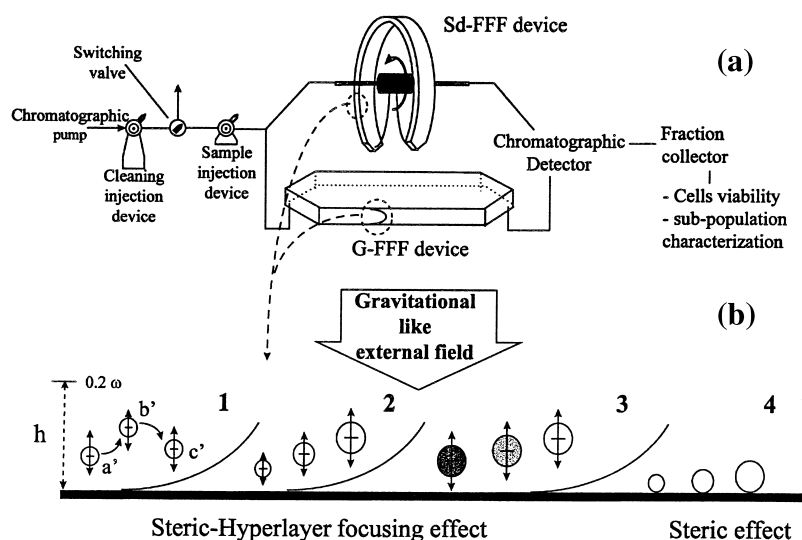


Fig. 1 (a) Schematic representation of the two sedimentation FFF systems (upper: multigravitational device or Sd-FFF; lower: gravitational device or G-FFF). Injection instrumentation is detailed with the cleaning (and decontamination) injection device (1- or 2-mL loop), the switching valve for stop-flow relaxation procedure, and the sample injection device (5–100- μ L loop). (b) The “steric-hyperlayer” mechanism: (1) Dynamics of the balance of the lifting force and of the external field created one. Under the predominant effect of the lifting force, the particle translate vertically away from the accumulation wall while in motion along the channel (a’). Under the predominant effect of the sedimentation force, the particle is driven toward the accumulation wall (b’). Finally, after a given time, an equilibrium position is reached (c’). (2) Equilibrium position and size-dependent elution order of spherical particles of identical density. (3) Equilibrium position and density-dependent elution order of spherical particles of identical size. (4) Schematic representation of the size-dependent steric elution mode.

“steric-hyperlayer” mode is, therefore, the most versatile methodology to separate particle populations according to both their size and density, among other parameters, nonformulated so far, such as shape and rigidity.

The polydispersity (P0%) concept developed for polymer analysis and characterization expressed in percentage is defined by the equation

$$P0\% = \left(\frac{\sigma}{\bar{m}} \right) \times 100 \quad (1)$$

where σ is the standard deviation of the parameter under concern and \bar{m} its mean value. In the case of micron-sized spherical particles, a size polydispersity can occur as well as a density one. In terms of cell polydispersity, this concept can be much more complex, involving numerous cell characteristics. If size expressed by the hydrodynamic radius can be evaluated as well as the density, cell shape, rigidity, and surface characteristics are more difficult to assess whatever the considerable bibliographic sources. Therefore, the cell polydispersity characteristic is a multidimensional one, described as “multipolydisperse.” It is not possible, so far, to define, precisely, the exact dimension of this multipolydispersity matrix. If the cells are considered as nonspherical particles such as red blood cells

(RBCs), for example, the multipolydispersity matrix is at least of dimension 3, with a polydispersity in size, in density, and in shape. In that case, a cell population to isolate or to purify is characterized by a 3×2 matrix of average values and polydispersity in size, density, and shape (sphericity index).

In the “steric-hyperlayer” elution condition, the cell characteristic differences will drive every subpopulation in specific flow streams of different intensity, leading to a large separation potential described in Fig. 1b(2,3) even among cell populations claimed as morphologically homogenous.

Elution Methodologies in Sd-FFF

Sedimentation FFF techniques encompass two different instrumentations; one is very simple and uses the Earth’s gravity (G-FFF), the second, much more complex, uses centrifugational field created by rotation (Sd-FFF). In any case, common features must be described.

Numerous injection procedures have been used in Sd-FFF, in two different instrumental configurations, for cell retention. In terms of instrumentation, cells can be introduced either through the upper wall or the

accumulation wall. Methodologically, cells can be injected into the flowing stream or with a time-controlled stop-flow procedure. The stop-flow procedure is known to lead to an increase of retention time of the cells, but it is often associated with (1) reduced recovery and (2) poisoning of the channel. Flow injection through the accumulation wall was demonstrated to produce an optimized response between retention loss and recovery increase. In some cases, time-controlled low flow injection is also possible. Stop-flow injection procedures are not recommended because cells are driven toward the accumulation wall in the absence of lifting forces (no flow). Particles–particles or particles–wall interactions will occur, leading to a biased retention pattern or modified viability characteristics.

To be retained, cell population retention ratio (R) (i.e., species velocity to average flow velocity ratio) must be <1 . As already described, cells should not be eluted according to a pure “steric” elution mode whose R , for a monodisperse population of size a , is

$$R_{\text{steric}} = \frac{6a}{\omega} \quad (2)$$

where a is the hydrodynamic radius of the species and ω is the channel thickness. Therefore, the R domain available for cell separation is

$$\frac{6a'}{\omega} < R < 1 \quad (3)$$

where a' is the size of the smallest micron-sized particle involved.

For a given cell population, by increasing the external field and using low flow rates, species are eluted at decreased retention ratio (i.e., closer to the accumulation wall). The eluted cells and wall proximity may drive to particles–wall interactions leading to particles sticking (reversible or not), to cell activation (biophysical and biochemical modifications), and even to cell death or destruction (decrease in recovery and viability). A price is to be paid in using a limited R domain, leading to decreased separation power. However, depending on the populations under concern, two instrumental strategies are possible, predicted by the “steric-hyperlayer” model: (1) If the population to analyze is very polydisperse, a large R domain is expected and relatively high channel thickness is chosen (250–300 μm); (2) if slight differences in cell characteristics must be emphasized, thinner channels are to be used (50–175 μm) to increase cell subpopulation separation.

The major characteristic of carrier phase in FFF is to respect the cell integrity, viability, and, if possible, an

enhanced recovery. Particle integrity is respected by means of the use of an iso-osmotic buffer of a given pH and ionic force. Most FFF studies are performed using an iso-osmotic (310 mOsm) phosphate buffer saline at pH 7.4. Particles–particles interactions are limited by means of a biocompatible surfactant such as bovine albumin (0.1% m/v) added to the buffer. In this case, a typical fractogram is obtained as shown in Fig. 2a. However, cell suspensions are complex mixtures. Some of their components (cell membrane, cytoplasmic fractions, etc.) will absorb onto the channel wall, leading to the modification of its surface characteristics, and often described as “channel poisoning,” as shown in Fig. 2b (after 47 injections). Such effect limits reproducibility, viability, and recovery and can be limited or eliminated by two complementary methodological procedures. The most described is a systematic postelution channel washing or cleaning procedure. In Sd-FFF and in the absence of external field, the carrier phase is flushed at a high flow rate to release the reversibly adsorbed cells in their integrity. Then, an osmotic shock is provoked by means of a void-volume equivalent injection of doubly-distilled water. The remaining adsorbed proteins are released by means of an equivalent large volume injection of a “protein cleaning agent.” Finally, a second distilled water flushing completes the procedure, as shown in Fig. 2c, signing reproducible elutions.

Fractograms of Figs. 2a–2c were obtained with polycarbonate channel walls and RBCs as the cell population. When more fragile nucleated cells (e.g., neuroblasts) are eluted with this procedure, no elution signal is recorded and collected fraction analysis shows a very low cell recovery ($<3\%$). By simply replacing the polycarbonate plates by polystyrene plates, the neuroblast (NB) fractogram of Fig. 2d is obtained. Such an experimental result is confirmed by the elution of an artificial mixture of neuroblast and RBCs as shown in Fig. 2e. Considerable studies on cells–material interactions, confirmed by the FFF experimentation, allowed to define empirical rules: To avoid or reduce interactions, the channel material should be as “hydrophobic” as possible if the cell surface is “hydrophilic.” However, cells–material-specific interactions could be used for specific cell subpopulation purification by depletion. If these methodological requirements, associated to soft elution conditions (“hyperlayer” mode), are fulfilled, recovery over 80 % is obtained, associated with higher reproducibility, allowing cumulated fraction collection.

Usually, Sd-FFF separator decontamination and sterilization are needed to prevent bacterial contamination; this is done by means of a 0.01% (m/v) sodium azide so-



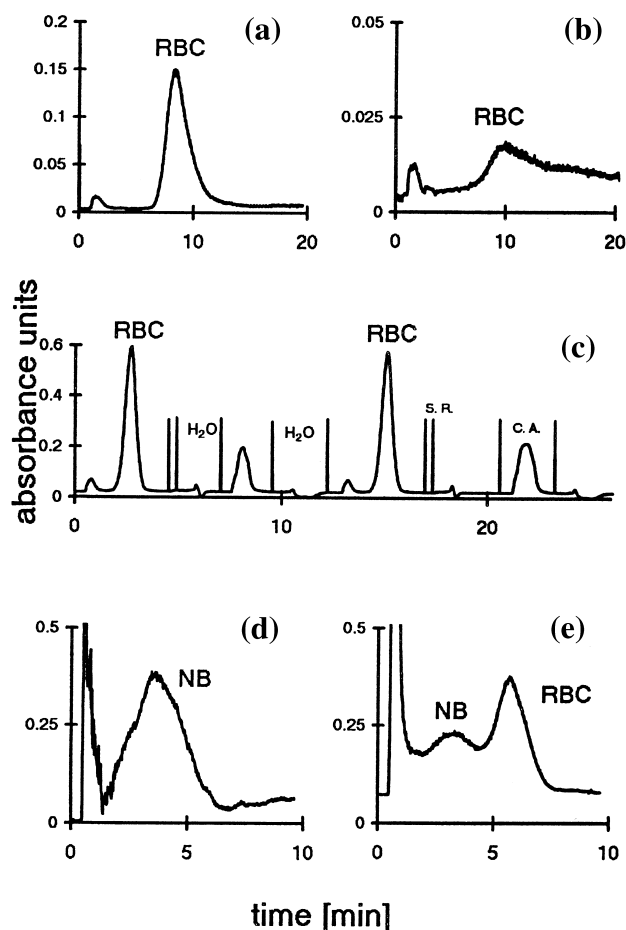


Fig. 2 Fractograms were obtained with a Sd-FFF apparatus ($77 \times 1 \times 0.0125$ cm). (a) RBC elution profile on a new or properly washed FFF channel. Elution conditions: flow injection of 5×10^6 RBCs (1/20 dilution of total blood in phosphate buffer saline pH 7.4/0.1 % of bovine albumin); external field $9.45g$ ($1g = 9.81 \text{ cm/s}^2$); flow rate: 0.7 mL/min , photometric detection at $\lambda = 313 \text{ nm}$. (b) Channel poisoning effect observed after 47 identical injections [described in (A)]. (c) Two sequences of RBC elution and channel cleaning procedure. Each sequence is RBC fractogram (flow injection of 5×10^6 RBCs (1/20 dilution of total blood in phosphate buffer saline pH 7.4), external field $25.7g$, flow rate of 1.02 mL/min , photometric detection at $\lambda = 313 \text{ nm}$), external field stopped (S.R.), hypo-osmolar shock with doubly distilled water, cleaning agent (C.A.) signal, second water washing. (d) Example of fragile nucleated cells eluted in Sd-FFF: neuroblasts (NB) case. Elution conditions: flow injection of 1.5×10^6 neuroblasts in phosphate buffer saline pH 7.4/0.1 % of bovine albumin, external field $60.0g$, flow rate of 1.25 mL/min , photometric detection at $\lambda = 254 \text{ nm}$. (e) Separation of components from an artificial mixture of neuroblasts and RBC. Elution conditions: flow injection of 1.5×10^6 neuroblasts and 5×10^6 RBC in phosphate buffer saline pH 7.4/0.1 % of bovine albumin, external field $50.0g$, flow rate of 1.25 mL/min , photometric detection at $\lambda = 254 \text{ nm}$.

Sedimentation Field-Flow Fractionation of Living Cells

lution added to the carrier phase. This compound is a cellular toxic and must absolutely avoided for cell viability and operator safety. Safe and effective decontamination process consists of an additional step to the cleaning procedure. The whole FFF system is flooded with a hypochlorite solution (3–6 Chlorometric degrees) whose volume corresponding to three to four times the Sd-FFF void volume. Prior to cell injection, the channel is flushed with ethanol and rinsed with the mobile phase. It is noted that this decontamination procedure is also a sterilization procedure if the hypochlorite solution is at least 5 Chlorometric degrees and if ethanol is over 70° . This sterilized situation is maintained by the use of sterilized mobile phase and daily bacteriological control is performed.

Cell Detection, Viability, and Recovery

Separation analysis at the outlet of the detector must respect three major conditions. The first is the cell integrity (i.e., the diagnosis of the particle). This can be operated on line, by means of classical photometric devices operated in the light-scattering mode (opacimetry) at 254 nm . Off-line methods, after fraction collection, are possible and recommended, by microscopy and granulometric analysis (Coulter[®] counting). The second objective is to analyze cell viability. Off-line methods after fraction collection are equally possible. The blue trypan exclusion test, motility measurements, or specific enzymatic activities (esterase) can be performed on an aliquot of the collected fraction.

Cell integrity and viability characteristics are of major importance for assessing the elution recovery by comparison with noneluted samples. Recovery can be described in terms of the percentage of cells in their integrity and in terms of cells alive. The third parameter under concern is the cell characteristic specificity, which signifies the biological interest of the separation. Membrane antigenic characteristics, cell surface receptor analysis, and specific protein composition and activities can be tested. In the early twenty-first century, the cell analysis and sorting reference system are flow cytometry technologies. Aliquots of FFF fractions can be characterized by means of this sophisticated method. Nevertheless, FFF separations and flow cytometry analyses are off-line techniques, and an exiting instrumental development domain is opened to realize the on-line coupling of the both techniques.

Conclusion

The number of FFF cell separation reports is increasing. Cell retention and separation rules are qualita-

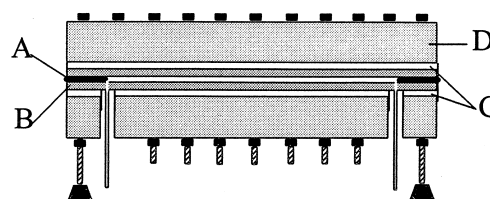
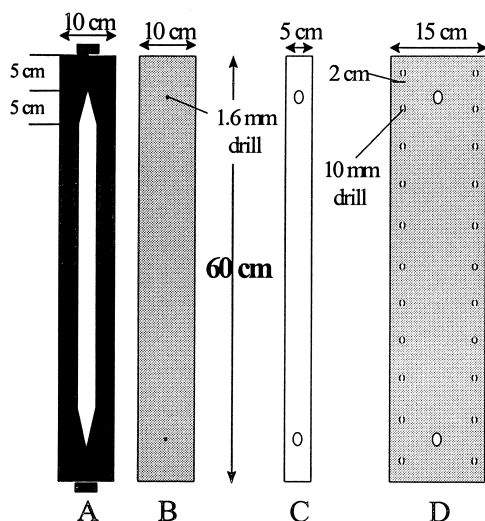
tively defined with the help of the “steric-hyperlayer” mode. Separation proofs can be assessed by an arsenal of detection and viability techniques. However, the extent of this family of methods is somehow limited by the lack of commercially available and life-science-adapted separators. This text has described instrumental and methodological basic rules to adapt FFF technologies to life science. The development of FFF in cell separation is an interfacial process between instrumental separation sciences and biological skills. Unique cell separation selectivity, unique separation speed, and unique practicability were observed with these methods, and the development of continuous FFF-based separation devices opens a field to “massive” separation opportunities whose interest in transplantation or biotechnologies will rapidly emerge.

Acknowledgment

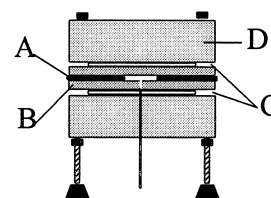
Special thanks to Frédéric Bodeau, who performed all the fractograms shown in this text.

Appendix

How to begin with FFF cell separations: gravitational separation of RBC. The general FFF setup, is analogous to classical HPLC systems. The FFF separator will simply replace the chromatographic column. To begin in cell separations with gravitational FFF, an outdated high-performance liquid chromatography (HPLC) chromatograph may be used. Basic steps are (1) construction of the separator, (2) initial filling of the FFF channel, (3) sample preparation, injection, and detection.



Longitudinal view



Transversal view

Channel construction: The channel ($50 \times 2 \times 0.025$ cm) is carefully cut in a Mylar sheet ($60 \times 10 \times 0.025$ cm, Scheme A) and sandwiched between two polycarbonate plates (Lexan) ($60 \times 10 \times 1$ cm). One of them being (1.6 mm) drilled to glue Peek® inlet and outlet tubings (scheme B). The channel is then sandwiched between two Rhodoid ($60 \times 5 \times 0.3$ cm, Scheme C and transversal view) bands whose purpose is to avoid channel shape deformation. This double-sandwich setup is sealed between two Plexiglas blocks (Scheme D) by means of a series of screw. During the sealing process special attention must be taken to fit channel tapered ends with the connection tubings. The sealing begin by the middle of the separator toward the ends with a dynamometric device, 10–20-N m forces assume complete watertightness. Special attention must be taken to ensure a complete flatness of the channel by means of equalizing stands as shown on transversal and longitudinal views.

Initial use: The channel is flowed with 100 mL methanol at 0.1 mL/min and cleaned with doubly-distilled water. Remaining bubbles are eliminated (patiently!!) with a series of surfactant solutions of decreased concentration and the mobile carrier phase finally applied. For cell separations, a simple NaCl (9 g/L) solution can be used.

Sample preparation, elution, detection: 10 μ L (injection loop volume) of 50-fold dilution of a whole-blood suspension on EDTA crystal in the carrier phase is performed at 0.1 mL/min and photometric detection recorded at 254 or 313 nm.

Additional materials: 22 (0.8×20 cm) screws with locknuts, 50-cm Peek® tubing (1/16-in. external diameter and 0.0256-cm internal diameter), Araldite® glue (low-speed polymerization quality), four adjustable stands (4×0.8 cm dimension), and dynamometric screw sealing device.



Suggested Further Reading

- Bernard, A., B. Paulet, V. Colin, and Ph. J. P. Cardot, Red blood cell separations by gravitational-field-flow fractionation: Instrumentation and applications, *Tr. A. C.* 14(6), 266–273 (1995).
- Caldwell, K. D., Z. Q. Cheng, and P. Hradecky, Separation of human and animal cells by steric field-flow fractionation, *Cell Biophys.* 6: 233–251 (1984).
- Giddings, J. C., Field-flow fractionation analysis of macromolecular, colloidal and particulate materials, *Science* 260: 1456–1465 (1993).
- Hoffstetter-Khun, S., T. Rosler, M. Ehrat, and H. M. Widmer, Characterization of yeast cultivations by steric field-flow fractionation, *Anal. Biochem.* 2: 300–308 (1992).
- Martin M. and T. S. William, Theoretical basis of field-flow fractionation, in *Theoretical Advancement in Chromatography and Related Separation Techniques* (F. Dandy and G. Guiochon, eds.), NATO ASI Series C, Vol. 383: Mathematical and Physical Sciences, Kluwer, Dordrecht, 1992, pp. 513–580.
- Metreau, J. M., S. Gallet, Ph. J. P. Cardot, V. Lemaire, F. Dumas, A. Hernvann, and S. Loric, Sedimentation field-flow fractionation of cellular species. *Anal. Biochem.* 251: 178–186 (1997).
- Yue, V., R. Kowal, L. Neargarder, L. Bond, A. Muetterties, and R. Parson, Miniature field-flow fractionation system for analysis of blood cells., *Clin. Chem.* 40(9), 1810–1814 (1994).



Selection of a Gradient HPLC System

Pavel Jandera

University of Pardubice, Pardubice, Czech Republic

INTRODUCTION

Many high-performance liquid chromatography (HPLC) analyses can be performed at constant, isocratic, operating conditions using isocratic elution. However, isocratic elution with a mobile phase of fixed composition often does not yield a successful separation of complex samples containing compounds that differ widely in retention characteristics. To keep the time of analysis within acceptable limits, the retention factors $k = (V_R/V_m - 1)$ of the most strongly retained sample components usually should be lower than 10 (V_R = retention volume, V_m = column holdup volume). For a satisfactory separation of both weakly and strongly retained sample compounds in a single run, operating conditions controlling retention, such as the composition or flow rate of the mobile phase, or the column temperature, should be varied during the chromatographic experiment. Flow programming in contemporary HPLC, using efficient small-particle columns, has only marginal effect on separation and is limited by the maximum instrumental pressure. Temperature programming is widely used in gas chromatography, but rarely in HPLC, because a large rise in temperature during the run is required to significantly reduce retention, and many columns, especially with stationary phases bonded onto a silica gel support, are not stable at temperatures higher than 60°C. Furthermore, only a few instruments that allow steep-enough temperature gradients are available because of a relatively slow response of the temperature inside the column to a change in the temperature setting in an air-heated thermostatted compartment, especially with conventional analytical columns of 2-mm inner diameter or larger.

For these reasons, solvent gradients are most frequently used in contemporary HPLC. In gradient elution, the composition of the mobile phase is changed during the chromatographic run, either stepwise or continuously, to increase the elution strength of the mobile phase, which allows to decrease the retention factors by two to three orders of magnitude in a single run. However, gradient elution requires more complicated equipment than isocratic HPLC, as two or more components of the mobile phase should be accurately mixed according to a preset time program; in addition, the selection of detectors is limited. Gradient runs generally take a longer

time than isocratic elution because the column should be reequilibrated to initial gradient conditions after each run.

PRINCIPLES OF GRADIENT ELUTION

Mobile-phase gradients can be formed outside the separation column by pumping and mixing the liquid components according to a preset time program (external gradients), or can be generated inside the column as a consequence of changing the equilibrium between the components adsorbed on the stationary phase and in the solution, induced by incoming mobile phase (internal gradients). Therefore the second approach is suitable only for a limited number of separation cases and is much less frequently used. The retention of nonionic compounds in reverse-phase (RP) and normal-phase (NP) liquid chromatography depends mainly on their polarities and the polarities of the stationary and mobile phases; hence, external polarity (solvent strength) gradients, prepared by mixing solvents of different polarities, are suitable for their separation. Solvent strength gradients are often useful for the separation of ionic compounds; however, the mobile phase should contain buffers or other ionic additives so that ionic strength or pH gradients can be also used for separations in ion exchange or ion pair gradient chromatography of ionic compounds.

Two, three, or four mobile-phase components can be mixed to create binary, ternary, or quaternary gradients, respectively. Gradient elution either consists of a few consequent isocratic steps, or the composition of the mobile phase is changed continuously according to a preset program; this can be characterized by three parameters: 1) the initial concentration; 2) the steepness (slope); and 3) the shape (curvature) of the gradient, which all affect the elution time and the spacing of the peaks in the chromatogram. A linear gradient profile is used almost exclusively in practice and can be described by Eq. 1:

$$\begin{aligned}\varphi &= A + B't = A + \frac{\Delta\varphi}{t_G}t = A + \frac{B'}{F_M}V \\ &= A + BV = A + \frac{\Delta\varphi}{V_G}V\end{aligned}\quad (1)$$

where A is the initial concentration φ of the strong solvent in the mobile phase at the start of the gradient, and B or B' is the steepness (slope) of the gradient (i.e., the increase in φ in the time unit, or in the volume unit of the mobile phase, respectively); V_G and t_G are the gradient volume and the gradient time during which the concentration φ is changed from the initial value A to the concentration $\varphi_G = A + \Delta\varphi$ at the end of the gradient; and $\Delta\varphi$ is the gradient range. Curved gradients are often substituted by multiple linear segmented gradients consisting of several subsequent linear gradient steps with different slopes B .

The theory of gradient elution chromatography allows prediction of the elution behavior of sample compounds by calculation from their isocratic retention data (or from two initial gradient experiments) in RP, NP, and ion exchange LC systems. Unlike isocratic conditions, the retention factors, change (decrease) during gradient elution and can be considered constant only in a very small (differential) volume of the mobile phase dV corresponding to migration along a differential part of the column holdup volume V_m , dV_m :

$$dV = k \cdot dV_m \quad (2)$$

The differential equation Eq. 2 can be solved after introducing the dependence of k on the volume of the eluate passed through the column from the start of the gradient run V . Any dependence of k on V can be divided into two parts: 1) a dependence of k on the concentration of a strong eluting component in the mobile phase φ controlled by the thermodynamics of the distribution process (the retention equation); and 2) the parameters of Eq. 1 describing the gradient profile, adjusted by the operator.

RP Gradient LC

RP chromatography is, by far, the most widely used LC mode for the separation of complex mixtures based on different lipophilicities of sample compounds.^[1] The effect of the volume fraction φ of the organic solvent in a binary aqueous–organic mobile phase on the retention factors k in RP chromatography can be very often described by simple equation (Eq. 3):^[1,2]

$$\log k = \log k_0 - m\varphi = a - m\varphi \quad (3)$$

Here, k_0 is the retention factor of the sample solute extrapolated to pure water as the mobile phase and m characterizes the “solvent strength” (i.e., the change in $\log k$ per concentration unit of the organic solvent). Assuming the validity of Eq. 3, the retention volume V_R in

RP gradient elution chromatography with linear gradients can be calculated from Eq. 4:^[3]

$$V_R = \frac{1}{mB} \log \{ 2.31mB[V_m 10^{(a-mA)} - V_D] + 1 \} + V_m + V_D \quad (4)$$

V_D is the so-called gradient dwell volume [i.e., the volume of the mobile phase contained in the instrument parts (mixer, filter, and tubing) between the pump and the column]. In an ideal case, linear concentration gradients in RPLC correspond to linear solvent strength (LSS) gradients according to the model developed by Snyder and Dolan;^[4] hence, Eq. 4 describes the retention data in LSS gradient elution.

NP (Adsorption) Gradient LC

In NP gradient LC on polar adsorbents, the concentration of one (or more) polar solvent(s) in a nonpolar solvent increases. A simple equation (Eq. 5) can often adequately describe the experimental dependencies of the retention factors k of sample compounds on the volume fraction φ of a polar solvent B in a binary mobile phase comprised of two organic solvents with different polarities, if the sample solute is very strongly retained in the pure, less polar solvent:

$$k = k_0 \varphi^{-m} \quad (5)$$

k_0 and m in Eq. 5 depend on the nature of the solute and on the chromatographic system, but are independent of the concentration of the strong solvent B ν in the mobile phase. Assuming the validity of Eq. 5 in NP gradient chromatography with linear concentration gradients of a polar solvent B, the elution volume V_R of a sample solute can be calculated from Eq. 6:^[5]

$$V_R = \frac{1}{B} [(m+1)B(k_0 V_m - V_D A^m) + A^{(m+1)}] \frac{1}{m+1} - \frac{A}{B} + V_m + V_D \quad (6)$$

Here, as in Eq. 4, V_m is the column holdup volume and V_D is the gradient dwell volume. In contrast to RP gradient elution, preferential adsorption of polar solvents from the mobile phase onto the surface of the polar adsorbent during a gradient run may lead to significant deviations of the actual gradient profile from the preset mobile-phase composition program and to a decrease in the reproducibility of the retention data (Fig. 1). Furthermore, because of the strong preferential adsorption of polar solvents, column reequilibration times after the end of the gradient are often long in NPLC. This has been a reason for strong bias against the use of gradient



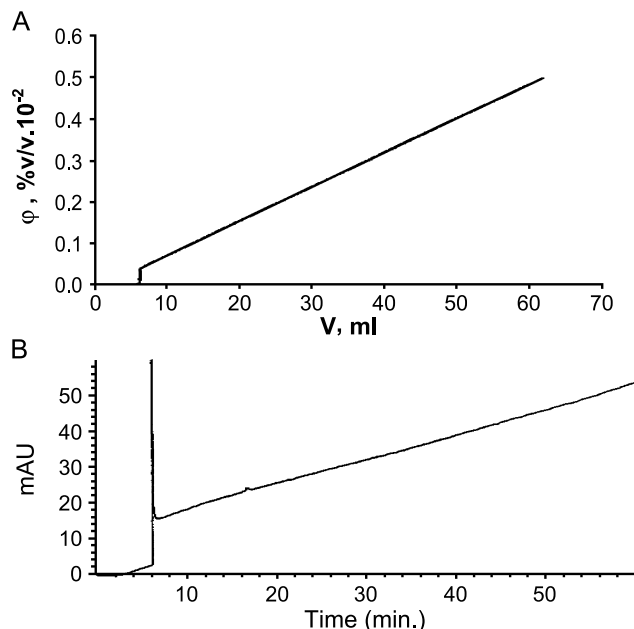


Fig. 1 (A) Calculated breakthrough curves in NP gradient elution HPLC. Simulated calculation using the experimental isotherm data and assuming $N=5000$. Gradient dwell volume = 0.50 mL. (B) Record of the blank gradient detector trace showing the breakthrough of propan-2-ol at 6 min and a "ghost peak" of impurities displaced at the breakthrough volume. Column: silica gel Separon SGX (7.5 μ m), 150 \times 3.3 mm ID, 1 mL/min, 40°C. Gradient: 0 = 50% 2-propanol in 30 min (v = concentration of propan-2-ol in the eluate; V = volume of the eluate from the start of the gradient).

elution in NP chromatography. To suppress these effects, which are most significant with gradients starting in pure nonpolar solvents, gradients should be started, rather, at 3% or more than at a zero concentration of the polar solvent, if possible, and nonlocalizing polar solvents should be used, such as dichloromethane, dioxane, or *tert*-butyl methyl ether.

Water is much more strongly adsorbed than polar organic solvents on polar adsorbents; hence, even trace water concentrations in the mobile phase decrease the adsorbent activity and very significantly affect the retention. As the distribution equilibrium of water and other polar solvents between the polar adsorbent and an organic mobile phase is strongly affected by temperature, it is very important to work with a thermostatted column. The reproducibility of the retention data in NP gradient LC can be considerably improved to the level comparable with RP gradient chromatography by keeping a constant temperature and adsorbent activity, and by controlling the water content in the mobile phase best by using dehydrated solvents kept dry over activated molecular sieves and filtered before use.^[5]

Ion Exchange Gradient LC

Because both adsorption on polar adsorbents and ion exchange are competing processes, Eqs. 5 and 6 can be used to describe, also, the effect of the ionic strength in the mobile phase on retention in isocratic and gradient ion exchange chromatography if ϕ has the meaning of the molar concentration of a salt (buffer) in the mobile phase. The dependence of the retention in gradient elution with pH gradients is less straightforward, as it is sometimes difficult to accomplish a linear change in pH during a gradient run.

EFFECTS OF GRADIENT PROFILE ON SEPARATION: COMPARISON WITH ISOCRATIC ELUTION

The gradient profile affects the retention in similar way as the concentration of the strong solvent in a binary mobile phase under isocratic conditions. This is illustrated in Fig. 2 for gradient elution RP chromatography separation of 10 homologous derivatives of *n*-alkylamines. At a constant gradient range (70%–100% methanol), the steepness of the gradient decreases as the gradient time increases from 10 to 40 min; the resolution improves, but the retention times increase (the top three chromatograms). The bottom three chromatograms show the effect of the gradient range on the separation at a constant steepness of the gradient (1% methanol/0.6 min)—as the initial concentration increases from 50% to 80% methanol, both retention and resolution decrease. The retention times of early eluting compounds are affected more significantly by the initial concentration of the strong solvent (methanol) than by the gradient steepness. The examples in Fig. 2 illustrate the importance of appropriate adjustment of both the gradient range and the initial gradient concentration to keep the analysis time short.

Equations 4 and 6 show that, for comparable retention times, a less steep gradient should be used to compensate for a higher parameter m in Eqs. 3 and 4, which usually increases with increasing size of the molecule. This behavior has the following practical consequences for gradient elution of high molecular compounds: 1) macromolecules may have so large an m that a very small change in the concentration of the strong solvent may change the retention from very strong to practically no retention, so that isocratic separation of large molecules is difficult, if possible at all; 2) shallow gradients are usually required for separations of high molecular samples, so that the selection of a suitable combination of the gradient parameters A and B is more critical than for small molecules; and 3) samples with a broad range of

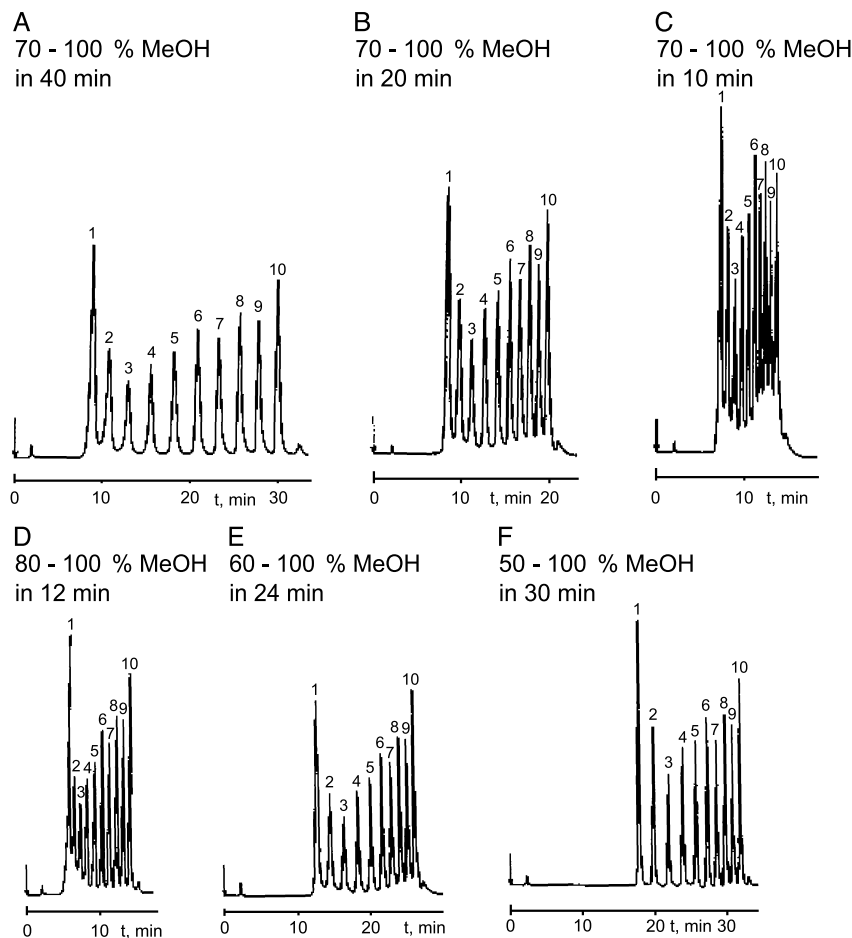


Fig. 2 RP gradient elution separation of 1,2-naphthoylebenzimidazole alkylsulphonamides. Column: Lichrosorb RP-18, 10 μ m (300 \times 4 mm id). Linear gradients of methanol in water with a constant gradient range but different gradient volumes (A–C), and with a constant gradient steepness (1.67% methanol/min) but different initial concentrations of methanol (D–F). Flow rate = 1 mL/min. The number of peaks agrees with the number of carbon atoms in alkyls.

molar masses may require a flatter gradient at the end of the chromatogram than at its start for regular band spacing (a convex gradient).

Under isocratic conditions, bandwidths increase for more strongly retained compounds, but the bandwidths in gradient elution chromatography are approximately constant for both early-eluting and late-eluting compounds. This is caused by increasing migration velocities of the bands along the column during gradient elution, so that all sample compounds eventually are eluted with very similar instantaneous retention factors k_e at the time they leave the column, which are approximately half the average retention factors (k^*) during the band migration along the column. The bandwidths decrease with steeper gradients (the three top chromatograms in Fig. 2). Because k_e values are usually significantly lower than the retention factors in isocratic LC, the peaks in gradient elution chromatography are generally narrower and higher,

improving the detector response and the sensitivity of determination. However, the beneficial effect of gradient elution on increasing sensitivity is often counterbalanced by an increased baseline drift and noise in comparison to isocratic HPLC. To avoid this inconvenience, high-purity solvents and mobile-phase additives are generally used in gradient elution HPLC.

The bandwidths w_g in gradient elution can be determined by introducing the appropriate instantaneous retention factor k_e at the elution of the peak maximum calculated using an appropriate gradient retention equation (e.g., Eq. 4 or Eq. 6):

$$w_g = \frac{4V_m(1 + k_e)}{\sqrt{N}} \quad (7)$$

Combining the appropriate equations for the retention volumes of solutes 1 and 2 with adjacent bands and Eq. 7,

for bandwidths, we can calculate the resolution in gradient HPLC as follows:

$$R_s = \frac{V_{R(2)} - V_{R(1)}}{w_g} \quad (8)$$

Here, $V_{R(1)}, V_{R(2)}$ are the retention volumes of sample compounds with adjacent peaks; N is the number of theoretical plates determined under isocratic conditions; and V_m is the holdup volume of the column. It should be noted that the correct plate number value cannot be determined directly from a gradient elution chromatogram, as the retention factors k are continuously changing during the elution. To first approximation, additional gradient band compression resulting from a faster migration of the trailing edge of the band in a mobile phase with higher elution strength with respect to a slower migration of the leading edge can be neglected.

TRANSFER OF GRADIENT METHODS BETWEEN DIFFERENT INSTRUMENTS, COLUMNS, AND SEPARATION CONDITIONS

The transfer of gradient methods between various instruments and columns with different dimensions and efficiencies is less straightforward than with isocratic HPLC, as the gradient profile should be adapted to match changing column geometry and flow rate of the mobile phase to obtain predictable results. Because, in all equations for the gradient retention data, the product of the retention volume and of the gradient steepness parameter $V_R B$ is constant as long as the product $V_m B$ is kept constant, any change of the flow rate F , column length L , or diameter d_c at a constant gradient range [i.e., with constant concentrations of the stronger solvent at the start (A) and at the end (ϕ_G) of the gradient] can be compensated by appropriate change in the gradient time t_G to keep the ratio V_m/V_G constant.

This has several important practical consequences, as follows:

1. If the flow rate of the mobile phase increases from F_1 to F_2 by a factor $f = F_2/F_1 > 1$ and the gradient time t_G is kept constant, the gradient steepness parameter B decreases by the factor f , and the gradient volume V_G increases by the same factor. Hence, the retention volumes increase, too, so that the retention times do not decrease proportionally to the increased flow rate. To keep the gradient steepness (gradient volume) constant, the gradient time should decrease by the same factor f . For example, if the flow rate is increased from 1 to 2 mL/min, the gradient time should decrease from 20 to 10 min to maintain the

same composition range of the mobile phase between the start and the end of the gradient, with the gradient volume $V_G = 20$ mL. Then, the retention times decrease proportionally to increasing flow rate, as in isocratic chromatography.

2. If a column with a larger inner diameter d_{c2} is used instead of the original column with the inner diameter d_{c1} at a constant column length (such as when upgrading an analytical method to semipreparative or preparative scale), the column holdup volume increases by the factor $f = (d_{c2}/d_{c1})^2$, but the retention volumes of the sample compounds increase less significantly and the separation may be impaired when the flow rate of the mobile phase does not change. To keep a constant product $V_m B$, the gradient steepness parameter B should decrease by increasing the flow rate by the same factor f . Then, the retention volumes increase f times, but the retention times do not change.
3. If a longer column (L_2) is used to increase the plate number with respect to the original column length (L_1) at a constant column inner diameter, flow rate of the mobile phase, and gradient time, the column holdup volume increases by the factor $f = L_2/L_1$, but the retention times and the retention volumes increase by less than f and the resolution may even decrease. This effect can be compensated by decreasing the gradient steepness (i.e., by increasing the gradient time by the factor f). The retention volumes and the retention times increase by the same factor and the expected increase in the column plate number and resolution is achieved.

TERNARY MOBILE-PHASE GRADIENTS

If the separation with binary gradients is unsatisfactory, ternary gradients can sometimes improve the selectivity by changing, simultaneously, the concentrations of two components with high elution strengths in a ternary mobile phase. For example, the early-eluting compounds show poor resolution with the gradients of methanol, but are better separated with gradients of acetonitrile in water, whereas the separation selectivity for the late-eluting compounds is better with a gradient of methanol than with gradients of acetonitrile in water. A ternary gradient with increasing concentration of methanol and simultaneously decreasing concentration of acetonitrile may improve the resolution of the sample.^[6] Two specific types of ternary gradients are probably most useful in practice, as follows:

1. The "elution strength" (or "isoselective") ternary gradients, where the concentration ratio of two strong eluents is kept constant and the sum of the



concentrations of the two eluents changes during the elution (so-called isoselective multisolvent gradient elution)

2. The “selectivity ternary gradients,” where the sum of the concentrations of two strong eluents in the mobile phase is constant, but their concentration ratio changes during the elution.

OPTIMIZATION OF GRADIENT ELUTION

Gradient elution can be optimized using strategies common in isocratic HPLC. In RP gradient elution chromatography, the Dry-Lab G commercial software is probably the most popular tool for optimization of operating parameters.^[7] Here, the retention data from two initial gradient runs are used to adjust, subsequently, the steepness and the range of the gradient, and, if necessary, other working parameters. This approach can be adapted to optimize segmented gradients. Structure-based commercial optimization software (e.g., Chromdream, Chromsword, or Eluex) predicts the retention based on additive contributions of the individual structural elements and, consequently, the optimum composition of the mobile phase is suggested. Such predictions are only approximate and do not take into account stereochemical and intramolecular interaction effects.

Some parameters may show synergistic effects on the separation. Appropriate selection of the concentration of the strong solvent in the mobile phase at the start of the gradient A is equally important as adjusting the gradient steepness B because each parameter influences, very significantly, the resolution and the time of analysis. The gradient steepness and the initial concentration of the strong solvent can be optimized simultaneously, using the simplex method,^[8] or a simple strategy employing a preset concentration of the strong solvent φ_G at the end of the gradient and gradient volume V_G . Then, the steepness parameter B of the gradient depends on the initial concentration A , and the elution volumes V_R can be calculated as a function of a single parameter A .^[6]

$$B = \frac{\varphi_G - A}{V_G} \quad (9)$$

The differences between the retention volumes of compounds with adjacent peaks or corresponding resolution R_s can be plotted vs. the initial concentration of the strong solvent A in the form of a “window diagram” to select the optimum A that provides the desired resolution for all adjacent bands in the chromatogram in the shortest time. With optimized A , the corresponding gradient steepness parameter B can be calculated for the preset gradient volume V_G and final concentration φ_G using Eq. 9. An

example of the “window diagram” for optimization of NP gradient elution chromatography is shown in Fig. 3 (Top), and the corresponding optimized separation is shown in Fig. 3 (Bottom). In addition to the gradient steepness and initial concentration, the gradient shape can be adjusted for nonlinear gradients or segmented gradients with several subsequent linear steps with different gradient steepness.

The composition of mixed mobile phases for ternary or quaternary “isoselective gradient elution” can be optimized using “overlapping resolution mapping” strategy to adjust optimum separation selectivity based on seven or more initial experiments with solvent mixtures of approximately equal elution strengths. Based on the retention data from the initial experiments, either three-dimensional diagrams or contour “resolution maps” are constructed for all adjacent bands in a selectivity triangle space as a function of the concentration ratios of three

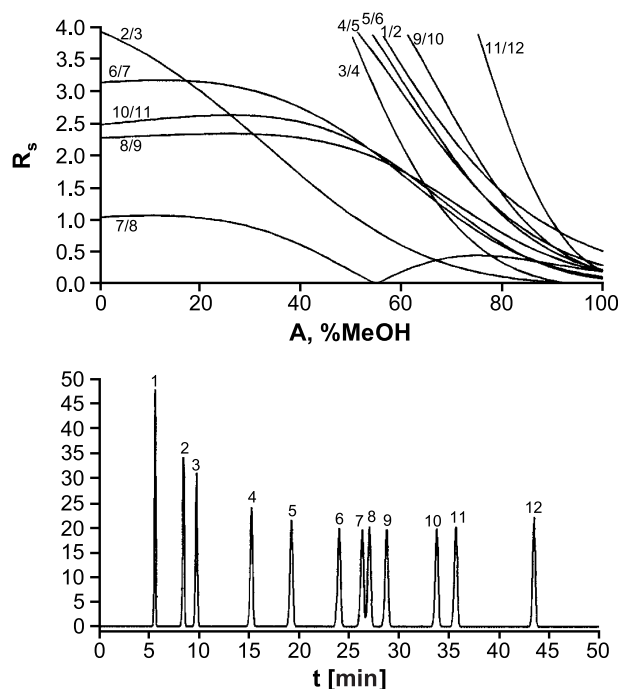


Fig. 3 Top: The resolution window diagram for RP gradient elution separation of phenylurea herbicides on a Separon SGX C18 7.5- μ m column (150 \times 3.3 mm ID) in dependence on the initial concentration of methanol in water at the start of the gradient A with optimum gradient volume $V_G = 73$ mL. Column plate number $N = 5000$; sample compounds: hydroxymetoxuron (1), desphenuron (2), phenuron (3), metoxuron (4), monuron (5), monolinuron (6), chlorotoluron (7), metobromuron (8), diuron (9), linuron (10), chlorobromuron (11), and neburon (12). Bottom: The separation with optimized binary gradient from 24% to 100% methanol in water in 73 min. Flow rate = 1 mL/min; $T = 40^\circ\text{C}$.



solvents or two solvents and the pH of the mobile phase, from which the concentration ratio of the strong solvents that provides maximum resolution is selected.^[9]

INSTRUMENTAL ASPECTS OF GRADIENT ELUTION CHROMATOGRAPHY

Even though the most common UV and fluorimetric HPLC detectors can be used without problems in gradient elution if high-purity solvents are used as the mobile-phase components, some detectors are not compatible with gradient elution, such as the universal refractometric detector, which gives a response for almost all sample compounds, but also for the mobile-phase components. However, the only universal detector that can be used for gradient elution is the evaporative light-scattering (ELS) detector, which is less sensitive for UV-absorbing compounds than the UV detector. As the ELS detector gives response to the stray light on solid particles of analytes after evaporation of the solvent from the nebulized column effluent, its use is restricted to volatile mobile phases and nonvolatile analytes. Mass spectrometric detection is ideally suited for gradient elution HPLC, as it combines the features of universality and specific detection, including possibilities of on-line mass spectral analysis of each peak.

Electrochemical detectors are generally incompatible with gradient elution, except for the multichannel coulometric CoulArray detector, which is controlled by a software compensating for the gradient baseline drift during the elution. This detector allows highly sensitive and selective detection of oxidizable or reducible compounds in gradient HPLC.

In micro-HPLC with narrow bore or capillary columns, lower flow rates should be used at comparable linear mobile-phase velocities. The flow rate should decrease in proportion to the second power of the column inner diameter, so that micro-LC columns with 1 mm ID require flow rates in the range of 30–100 $\mu\text{L}/\text{min}$, whereas capillary columns with 0.3–0.5 mm ID require flow rates between 1 and 10 $\mu\text{L}/\text{min}$, and capillary or nano-LC columns with 0.075–0.1 mm ID require flow rates in the range of hundreds of nanoliters per minute. Special miniaturized pump systems are required to accurately deliver the mobile phase at very low flow rates in isocratic LC. It is technically much more difficult to keep very low flow rates constant during a gradient run than in isocratic LC, and to simultaneously change accurately the volume proportions of the mixed solvents according to a preset time program. In contemporary micro-LC and capillary LC practice, concentration gradients can be achieved using sophisticated LC pumping systems for the delivery of microliter-per-minute gradients that are either flow-

split or sampled. High-precision microflow reciprocating pumps using precolumn flow splitting can be used for delivery of flow rates ranging down to 50 nL/min in micro-LC and capillary LC systems. If a precolumn flow splitter is used, only a small part of the mixed mobile phase from the pump flows through the column, whereas a larger part is diverted through a by-pass capillary. To avoid some problems connected with flow splitting, splitless systems with large inner volume syringe pumps for each solvent can be used, which deliver smooth flow. Mobile phase is not wasted and the systems are less affected by a change of the column backpressure in gradient runs where solvents with different viscosities are mixed.

The instrumental errors that can decrease the reproducibility of gradient elution data may originate from imperfect functioning of gradient pumps, especially when volatile or viscous solvents are mixed. These errors are usually most significant in the initial parts and the final parts of the gradient where the proportions of the solvents mixed are lower than 1:20 and rounding of the gradient is observed; this can reduce the retention times of the bands eluting near the start of the gradient and increase the retention times of bands eluting near the end of the gradient. It is usually more significant in the instruments with larger volumes between the gradient mixer and the column inlet, i.e., the “gradient dwell volume” V_D . The dwell volume may be as high as a few milliliters with some instruments and may differ from one instrument to another. It can be determined from a “blank” gradient. Much more important than contributing to the rounding of the gradient, dwell volume increases the retention times, as the sample bands migrate a certain distance along the column under isocratic conditions in a mobile phase with a low elution strength, before the front of the gradient gets to the actual position of the sample zone in the column. To avoid difficulties when a gradient HPLC method is transferred between the instruments with different V_D values and to improve the precision of predictive calculations of the gradient elution data, the correction for the gradient dwell volume should be accounted for in calculations, using appropriate equations such as Eq. 4 or Eq. 6.^[5,7] The gradient delay due to the dwell volume can be relatively very significant in microcolumn gradient operation, especially in the system using precolumn flow splitting with 0.1 mm or lower ID capillaries.

When transferring gradient methods between instruments with different dwell volumes, these differences can be compensated for experimentally by programmed delay of the sample injection after the start of the gradient elution, or by insertion of a “mixing chamber”—an additional piece of tubing or a small precolumn packed with an inert material in front of the injector to obtain equal dwell volumes with different instruments. However,

this approach contributes to the run time and may be impractical with narrow-diameter columns.

CONCLUSION

The elution with solvent gradients is the most efficient technique for improving the separation of complex samples by programmed change of retention during the HPLC separation run. An understanding of the theoretical principles of gradient elution is important for rational method development, optimization, and transfer between different instrumental systems and column geometries in RP, ion exchange, and NP modes. The gradient dwell volume of the system is the main instrumental factor complicating the method transfer and limiting rapid high-resolution in gradient micro-HPLC. The most important recent advances in the instrumentation for gradient elution HPLC have resulted in the development of sophisticated instrumentation for gradient micro-HPLC, and the availability of universal ELS detection for compounds that do not contain chromophores or fluorophores and of a sensitive multichannel coulometric detection for gradient HPLC of electroactive compounds. Gradient elution is well suited for HPLC/mass spectrometry applications.

REFERENCES

1. Snyder, L.R.; Dolan, J.W.; Gant, J.R. Gradient elution in high-performance liquid chromatography: I. Theoretical basis for reversed-phase systems. *J. Chromatogr.* **1979**, *165*, 3–30.
2. Jandera, P.; Churáček, J. Gradient elution in liquid chromatography: II. Retention characteristics (retention volume, bandwidth, resolution, plate number) in solvent-programmed chromatography—Theoretical considerations. *J. Chromatogr.* **1974**, *91*, 223–235.
3. Jandera, P.; Churáček, J. Liquid chromatography with programmed composition of the mobile phase. *Adv. Chromatogr.* **1981**, *19*, 125–260.
4. Snyder, L.R.; Dolan, J.W. The linear-solvent-strength model of gradient elution. *Adv. Chromatogr.* **1998**, *38*, 115–187.
5. Jandera, P. Gradient elution in normal-phase high-performance liquid chromatographic systems. *J. Chromatogr., A* **2002**, *965*, 239–261.
6. Jandera, P. Predictive calculation methods for optimization of gradient elution using binary and ternary gradients. *J. Chromatogr.* **1989**, *485*, 113–141.
7. Dolan, J.W.; Snyder, L.R. Maintaining fixed band spacing when changing column dimensions in gradient elution. *J. Chromatogr., A* **1998**, *799*, 21–34.
8. Schoenmakers, P.J. *Optimisation of Chromatographic Selectivity*; Elsevier: Amsterdam, 1986.
9. Glajch, J.L.; Kirkland, J.J. Method development in high-performance liquid chromatography using retention mapping and experimental design techniques. *J. Chromatogr.* **1989**, *485*, 51–63.

FURTHER READINGS

- Jandera, P.; Churáček, J. *Gradient Elution in Column Liquid Chromatography, Theory and Practice*; Elsevier: Amsterdam, 1985.
- Snyder, L.R.; Kirkland, J.J.; Glajch, J.L. *Practical HPLC Method Development*, 2nd Ed.; Wiley: New York, 1997.



Selection of an Isocratic HPLC System

Pavel Jandera

University of Pardubice, Pardubice, Czech Republic

INTRODUCTION

Any new sample type delivered for high-performance liquid chromatography (HPLC) analysis requires an adequate separation method. Previous experience with similar samples is very useful and many methods can be looked up in the literature; however, it is often necessary to modify earlier established methods to suit laboratory equipment or sample matrices, or to improve sample throughput in the laboratory. In many cases, a desired separation can be achieved with a few experiments, but some separation problems are more difficult and their solution may require considerable experimental effort. Nowadays, effects of experimental conditions on HPLC separations are well understood, and this knowledge can be used for effective method development. First, the objective of the separation should always be kept in mind. Any information available on the sample is very helpful in HPLC method development: the matrix, the approximate number of sample components, their chemical structures, concentrations, solubilities, and other properties provide clues for the selection of sample pretreatment approach (if necessary), suitable detection conditions, and a separation system. Most often, variable-wavelength or diode array ultraviolet (UV) absorbance detectors are used, but mass spectrometry (MS), coupled to HPLC, is becoming increasingly popular because it offers valuable structural information for unknown samples. Other detection techniques are used less frequently—mainly fluorimetric and electrochemical detection for sensitive and selective environmental, biological, and food analyses, or light-scattering detection for analysis of compounds that do not absorb in the UV region and neither can be oxidized nor reduced. For adequate separation, suitable chromatographic mode, stationary phase, mobile phase, flow rate, column dimension, and temperature should be selected. Many analyses can be performed at constant operating conditions using the so-called isocratic elution.

SELECTION OF A COLUMN AND PACKING MATERIAL

Many HPLC separations are performed with conventional analytical columns, which are 10–25 cm long and

3–4.6 mm in diameter. The column plate number, the pressure drop across the column, and the separation time at a constant flow rate are directly proportional to the column length. With short (2–6 mm), “high-speed” columns of the same diameter, simple separations can be accomplished in 1–3 min, so that the productivity of the laboratory is considerably increased and solvent consumption per analysis is reduced.

The flow rate and consumption of the mobile phase at a constant flow rate, and the pressure drop increase with the second power of the column diameter. Separations on “microbore” columns (15–5 cm long and 1–2 mm ID) need even less mobile phase and allow high mass sensitivity of detection, which is useful for analyses of small sample amounts with mass spectrometric detection. Separations on high-speed microbore, and especially capillary HPLC columns of 0.1–0.5 mm internal diameter, are subject to more significant extracolumn contributions of the injector, detector, and connecting tubing to band broadening in comparison to conventional analytical columns, so that miniaturized HPLC requires specially designed low-volume injectors and detectors, often at the cost of decreased sensitivity of detection. Hence, microbore and capillary HPLC columns have been, so far, more frequently used for HPLC/MS trace analysis than for other routine quantitative analytical applications.

HPLC columns contain, usually, spherical particle packings, which are carefully sorted to fractions with narrow size distribution to provide high separation efficiency. Totally porous packing materials most frequently used for separations of small molecules in contemporary HPLC have pore sizes of 7–12 nm and specific surface area of 150–400 m²/g, but wide-pore particles with pore sizes of 15–100 nm and relatively low specific surface area of 10–150 m²/g, or nonporous materials are used for separations of macromolecules. Perfusion materials, designed especially for the separation and isolation of biopolymers, contain very broad pores (400–800 nm) throughout the whole particle, which are interconnected by smaller pores. Column efficiency and flow resistance increase with small particles, and a high pressure has to be used to maintain required flow rate and to keep an acceptable time of analysis. However, the maximum operating pressure is 30–40 MPa, with common instrumentation for HPLC. Hence, short columns should

be used with small-diameter particles. Five-micrometer particles are most often used in conventional analytical columns, and particles of 3–4 μm (less often, 1–2 μm) are common in short, “high-speed” columns for rapid, simple separations.

Instead of packed columns, monolithic (continuous bed), analytical, or capillary columns in the form of a rod with flow-through pores offer high porosity and improved permeability. Silica-based monolithic columns are generally prepared by gelation of a silica sol to a continuous sol–gel network, onto which a C_{18} or another stationary phase is subsequently chemically bonded. Such columns provide comparable efficiency and sample capacity as conventional columns packed with 5- μm particle materials, but have three to five times lower flow resistance, thereby allowing higher flow rates and fast HPLC analyses. Rigid polyacrylamide, polyacrylate, polymethacrylate, or polystyrene monolithic columns are prepared by in situ polymerization.

SELECTION OF HPLC SEPARATION MODE

The first step in HPLC method development consists of selecting an appropriate separation mode. Many neutral compounds can be separated either by reverse-phase (RP) or normal-phase (NP) chromatography. An RP system is usually the best first choice because it is likely to result in a satisfactory separation of a great variety of nonpolar, polar, and even ionic compounds. Lipophilic samples often can be separated either by nonaqueous RP chromatography or NP chromatography. Weak acids or bases can be analyzed by RP chromatography with buffered mobile phases, strong acids, or strong bases by ion pair or ion exchange chromatography (IEC). Special chiral columns or chiral selector additives to the mobile phase can be used for separation of optical isomers (enantiomers).

Macromolecules are usually separated and characterized by size exclusion chromatography on columns packed with inert materials (gels) characterized by controlled pore distributions, based on different accessibilities of the pores for molecules of different sizes, with the larger molecules eluting first. For some lower polymers with molecular masses in the range 10^3 – 10^4 Da, “interactive” (i.e., RP-HPLC or NP-HPLC) modes provide better selectivity of separation than size exclusion chromatography. Many ionizable biopolymers such as peptides, proteins, oligonucleotides, and nucleic acids can be separated by IEC or RP chromatography on wide-pore packing materials, with mobile phases containing trifluoroacetic acid or triethylammonium acetate as ion pair reagents.

RPLC

The stationary phase in RP chromatography—usually an alkyl immobilized on an inorganic support—is less polar than the aqueous–organic mobile phase. Nonpolar samples are more strongly retained than the polar ones, and the retention increases with increasing polarity of the mobile phase, so that very lipophilic samples may require nonaqueous mobile phases.

Silica gel-based materials for RP chromatography with nonpolar (most often C_8 or C_{18} alkyls) or moderately polar stationary phases covalently bonded via Si–O–Si–C bonds are prepared by chemical modification of the silanol (Si–OH) groups on the silica gel surface by chloro-silane or alkoxy-silane reagents, and are relatively stable to hydrolysis. The retention in RP increases with increasing surface coverage and length of the bonded alkyl chains, so that C_{18} phases show greater retention than C_8 -bonded phases.

Monofunctional silane reagents yield efficient stationary phases with flexible “furlike” or “brushlike” structure of the chains bonded on the silica surface. When bifunctional or trifunctional silanes are used for modification, Cl or alkoxy groups are introduced into the stationary phase, which are subject to hydrolysis and react with excess molecules of reagents to form a polymerized spongelike bonded phase structure. Stationary phases prepared in that way usually show stronger retention but lower separation efficiency (plate number) than monomerically bonded stationary phases.

Bonded phases prepared by modification of silica gel, in turn prepared by gelation of soluble silicates, are not stable in mobile phases with $\text{pH} > 8$, where the silica gel slowly dissolves. However, chemically bonded groups on silica support can hydrolyze at $\text{pH} < 3$, causing stationary phase “bleeding.” The hydrolysis is enhanced at higher temperatures, so that many bonded phases are not stable at temperatures higher than 60°C . New materials prepared using high-purity silica particles made by aggregation of silica sols are stable up to pH 9–10 and do not contain metal contaminants that can form chelates, which can cause tailing of polar compounds.

Rather bulky silanization reagents can chemically modify no more than 50% of the original silanol groups. The residual silanol groups may interact with polar solutes, especially basic solutes, often causing strong and irreversible retention and poor separation with tailing or distorted peaks. Some residual silanol groups can be removed by a subsequent “end-capping” reaction with small-molecule trimethylchlorosilane or hexamethyldisilazane reagents. Another approach relies on using diisopropyl chlorosilane or diisobutyl chlorosilane reagents in a single silanization step to provide steric shielding of residual silanols.



Stationary phases prepared by modification of the silica gel surface with bidentate silanes containing C₁₈ or C₈ alkyls and two reactive groups separated by a –CH₂–CH₂– or a –CH₂–CH₂–CH₂– bridging group show high bonding density and improved stability over a broad pH range. Finally, hybrid stationary phases with methyl groups incorporated into the silica gel structure contain lower concentrations of silanol groups and show improved pH stability. Stationary phases with chemically bonded, branched hydrocarbons, perfluoroalkanes, polyethylene glycol, cholesterol, or alkylaryl groups show different separation selectivities, which can be useful for specific separations. For example, chemically bonded phenyl groups show preferential retention of aromatic compounds and increased shape selectivity for planar and rigid rodlike molecules. Incorporating amide or carbamate groups into the alkyl-bonded phases improves retention behavior in highly aqueous mobile phases.

Materials with inorganic or porous hydrophobic or (less frequently) hydrophilic organic polymer matrices and graphitized carbon are stable over a broad pH range from 0 to 12–14; hence, they are useful for separations of basic compounds. RP phases on aluminium and zirconium oxide supports exhibit hardness and mass transfer properties comparable to silica, and can be prepared by forming a cross-linked polystyrene, polybutadiene, or alkylated polymethylsiloxane layer on the support surface to which alkyls are attached. The inorganic surface, encapsulated by a nonpolar stationary phase, does not come into contact with the mobile phase or with the analyte, so these materials can be used in the pH range 1–14.

Porous graphitized carbon adsorbents with sufficient hardness, and well-defined and stable pore structures without micropores are now available with increased affinity for aromatic and polar substances, allowing difficult separations of some hydrophilic or isomeric compounds.

The mobile phase in RP chromatography contains water and one or more organic solvents, most frequently acetonitrile, methanol, tetrahydrofuran, or propanol. By the choice of the organic solvent, selective polar interactions (dipole–dipole, proton–donor, or proton–acceptor) with analytes can be either enhanced or suppressed, and the selectivity of separation can be adjusted. Binary mobile phases are usually well suited for the separation of a variety of samples, but ternary or, less often, quaternary mobile phases may offer improved selectivity for some difficult separations. The retention times t_R are controlled by the concentration of the organic solvent in the aqueous–organic mobile phase. Equation 1 is widely used to describe the effect of the volume fraction of methanol or acetonitrile ϕ on the retention factors $k = t_R/t_0 - 1$:^[1]

$$k = k_0 10^{-m\phi} \quad (1)$$

where t_0 is the column dead (holdup) time. The constants m and k_0 in Eq. 1 increase as the polarity of the solute decreases, or as its size increases. Furthermore, the constant m increases with decreasing polarity of the organic solvent.

NPLC

In NP chromatography (also called adsorption or liquid–solid chromatography), the stationary phase is more polar than the mobile phase. The retention increases as the polarity of the mobile phase decreases, and polar analytes are more strongly retained than nonpolar ones (i.e., the opposite of RP chromatography; Fig. 1). The column packing is either an inorganic adsorbent (silica gel or, less often, aluminium oxide), or a moderately polar bonded phase [cyanopropyl –(CH₂)₃–CN, diol –(CH₂)₃–O–CH₂–CHOH–CH₂–OH, or aminopropyl –(CH₂)₃–NH₂] chemically bonded onto silica gel, and the mobile phase usually is a mixture of a nonpolar solvent and one or more strongly or moderately polar solvents. NP behavior can be sometimes observed also in nonaqueous RP liquid chromatography (NARPLC), probably because of the activity of polar residual silanol groups.

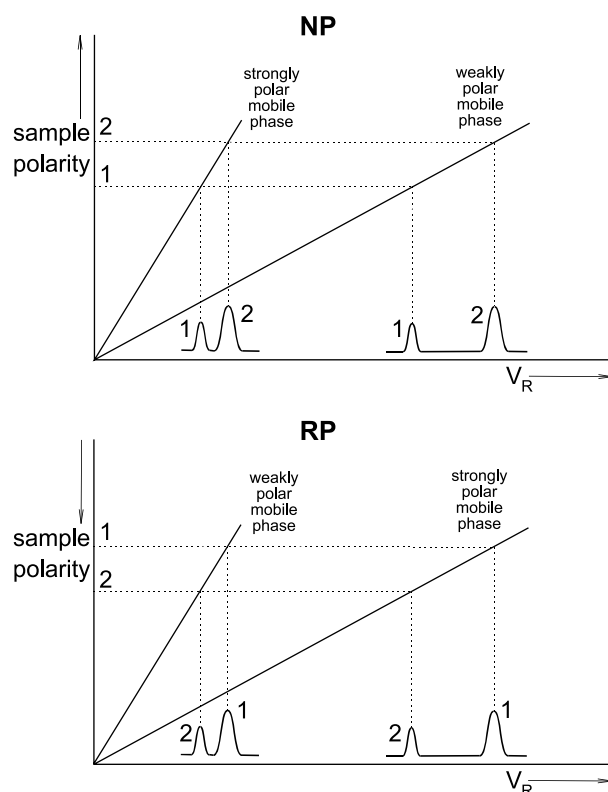


Fig. 1 Schematic diagram of the effects of sample and mobile phase polarities on retention in NPLC and RPLC. V_R = retention volume.

Copyright © Marcel Dekker, Inc. All rights reserved.



RP chromatography generally offers a better selectivity than NPLC for the separation of molecules differing in hydrophobic parts of the molecules, but there are some practical reasons for selecting NP chromatography methods in specific cases, as follows:

1. A lower organic mobile phase viscosity offers a lower pressure drop across the column than in aqueous-organic mobile phases used in RPLC at a comparable flow rate.
2. HPLC columns are usually more stable and have longer lifetimes in organic solvents than in aqueous-organic mobile phases.
3. Many samples are more soluble or less prone to decompose in organic mobile phases than in aqueous mobile phases, and do not cause injection problems in NPLC, as is occasionally observed in RPLC.
4. Unlike RP chromatography, NP chromatography enables the direct injection of samples extracted into a nonpolar solvent.
5. NPLC is usually better-suited for the separation of positional isomers or stereoisomers than RPLC.

Very large changes in separation selectivity are possible by changing either the mobile phase or the stationary phases in NPLC. Proton donor-acceptor interactions cause strong retention of basic compounds on silica gel in nonaqueous mobile phases, whereas acidic compounds show increased affinities to aminopropyl columns. The elution strength is proportional to the polarity of the mobile phase. Great changes in the selectivity of NP chromatography separations can be achieved by selecting solvents with appropriate types of selective polar interactions. With some simplification, the dependence of the retention factor k on the volume fraction φ of the polar solvent B in binary mobile phases can be described by Eq. 2:^[2]

$$k = k_0 \varphi^{-m} \quad (2)$$

The constants k_0 and m depend on the nature of the solute and on the chromatographic system, but are independent of the concentration φ , and k_0 is the retention factor in pure solvent B. The parameter m theoretically corresponds to the number of molecules of the strong solvent B necessary to displace one adsorbed sample molecule.

LC Separation of Ionic Compounds

Ionized compounds are usually much less retained than noncharged compounds; their separation in RP chromatography is usually possible only with ionic additives to the mobile phase. Basic compounds can interact with residual silanols in alkyl silica-bonded phases ionized to SiO^- anions; consequently, strong retention and tailing peaks are observed. Alkylamine additives to the mobile

phase sometimes improve peak shape by blocking the silanol groups. Repulsive interactions with the negatively charged residual $-\text{SiO}^-$ groups in the alkyl silica-bonded phases may cause ionic exclusion and poor separation of strong acids, which elute close to the column holdup time, often as asymmetrical peaks.

In mobile phases containing 10–50 mM phosphate or acetate buffers of pH 2–8.5, the ionization of weak acids (at pH <7) or bases (at pH >7) can be more or less suppressed to improve separation and peak symmetry. By adjusting the pH in the range ± 1.5 U around the pK_a , differences in the degree of ionization of the individual sample components can often be utilized to control the separation selectivity. The retention is usually adjusted by the addition of up to 30–40% acetonitrile, methanol, or tetrahydrofuran to the mobile phase.

Strong acids and strong bases are completely ionized over a broad pH range and their chromatographic behavior is usually only little affected by adding a buffer to the mobile phase. Such compounds can be separated by RP ion pair or IEC. In ion pair chromatography (IPC), ion pair reagents whose molecules contain a strongly acidic or strongly basic group and a bulky hydrocarbon part are added to the mobile phase. Basic substances can usually be separated using C_6 – C_8 alkanesulphonates, and acidic substances can be separated using tetralkylammonium salts. Ion pair additives significantly increase retention and improve peak symmetry through the formation of neutral ionic-associated species, called ion pairs, with increased affinity to a nonpolar stationary phase. The retention in IPC can be controlled by the type and concentration of the ion pair reagent or of the organic solvent in the mobile phase. Increasing the number and size of alkyls in the reagent molecules enhance retention in the reagent concentration range between 10^{-4} and 10^{-2} mol/L.

Nowadays, IEC is used mainly for the separation of small inorganic ions or ionic biopolymers such as oligonucleotides, nucleic acids, peptides, and proteins, rather than in the analysis of small organic ions, for which RP chromatography and IPC usually offer higher efficiency and better resolution. IEC columns are packed with fine particles of ion exchangers, which contain charged ion exchange groups covalently attached to a solid matrix (either an organic cross-linked styrene-divinylbenzene or ethyleneglycol-methacrylate copolymer), or inorganic support to which a functional group is chemically bonded via a spacer: a propyl, or phenylpropyl moiety. Strong cation exchangers contain $-\text{SO}_3^-$ sulphonate groups and strong anion exchangers $-\text{N}(\text{CH}_3)_3^+$ contain quaternary ammonium groups, completely ionized over a broad pH range (pH=2–12). Weak cation exchangers contain carboxylic or phosphonic acid groups, which are ionized only in alkaline solutions, and tertiary or secondary amino



groups (e.g., diethyl aminoethyl) in weak anion exchangers are ionized only in acidic mobile phases. Ion exchange separations require aqueous or aqueous–organic mobile phases containing counterions (10^{-2} – 10^{-1} mol/L salts, buffers, ionized acids, or bases), which compete with the sample ions for the ion exchange groups. The retention in IEC decreases with increasing concentration of counterions in the mobile phase and with decreasing ion exchange capacity of the column (1–5 mEq/g with organic polymer ion exchangers and 0.3–1 mEq/g with silica-based ion exchangers). Weak acids are usually separated by anion exchange chromatography at $\text{pH} > 6$ and weak bases are separated by cation exchange chromatography at $\text{pH} < 6$, and their retention increases with increasing ionization. Varying the pH of the mobile phase can adjust the separation selectivity, whereas the retention is controlled by the ionic strength.

STRATEGIES FOR SELECTING AND OPTIMIZING ISOCRATIC SEPARATION CONDITIONS

Once a suitable HPLC separation mode has been selected, experimental conditions can be adjusted using either an empirical method or a systematic method development approach. The separation of two sample compounds is conveniently characterized by resolution R_S :

$$R_S \cong \frac{\sqrt{N}}{4} (r_{1,2} - 1) \frac{k}{1 + k}$$

$$= \text{EFFICIENCY} \times \text{SELECTIVITY} \times \text{CAPACITY} \quad (3)$$

Here, N is the column efficiency expressed in terms of plate number; $r_{1,2} = k_2/k_1$ is the separation factor, which characterizes the selectivity of separation; and k is the average retention factor of the two sample compounds 1 and 2 as a measure of capacity contribution to the resolution. The three terms contributing to the resolution depend on many experimental conditions, which can be adjusted either simultaneously or in subsequent steps.

For accurate quantitative analysis, the resolution usually should be 1–1.5. However, too high a resolution may result in excessive analysis time. The chromatogram in Fig. 2A schematically illustrates adequate separation of a three-component sample. If the separation is not satisfactory, it can be improved according to the following strategy:

1. Poorly resolved peaks appearing close to the column holdup volume, such as in the example in Fig. 2B, show that the retention is too low and should be

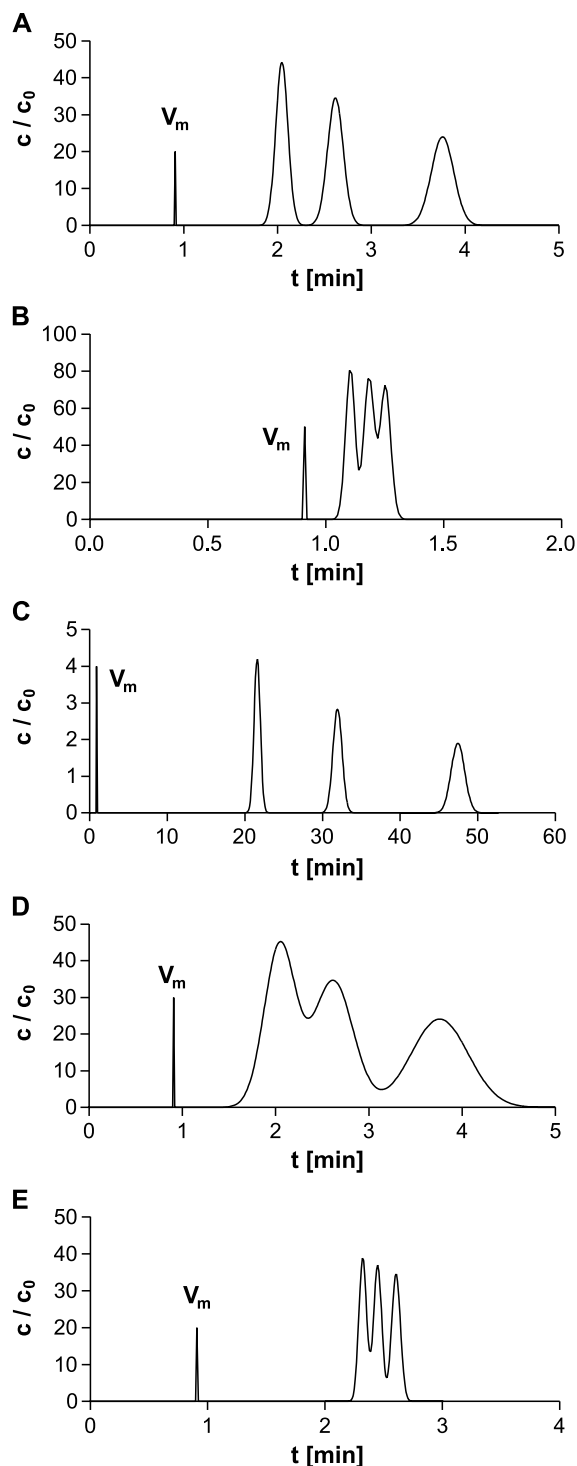


Fig. 2 Examples of chromatographic separation of a three-component sample. (A) Satisfactory separation. (B) Unsatisfactory separation, too low retention. (C) Good resolution, but too long time of separation. (D) Unsatisfactory separation, too low column efficiency. (E) Unsatisfactory separation, good retention and column efficiency, but too low separation selectivity.

Copyright © Marcel Dekker, Inc. All rights reserved.



increased; this is best done by decreasing the elution strength of the mobile phase, whereas the elution strength should be increased if the retention volumes are too large (Fig. 2C).

2. If the retention times are adequate and partial separation of the bands is apparent but the bands are relatively broad (Fig. 2D), the resolution can be possibly improved by increasing the efficiency (i.e., the plate number of the column).
3. If the bands are narrow, but are not well separated from each other, such as in Fig. 2E, the selectivity should be improved:
 - a) by changing the components of a binary mobile phase;
 - b) by using ternary or more complex mobile phases or mobile phase additives inducing specific interactions with sample components; or
 - c) by using another HPLC column with a different stationary phase.
4. If the resolution of early eluted bands is unsatisfactory and the separation time is long, the sample separation is usually improved by temperature or solvent gradients.

Control of Separation Efficiency

The efficiency contribution to the resolution (i.e., the column plate number, N) increases with decreasing particle size of the column packing, with increasing column length, and, to a lesser extent, with decreasing flow rate of the mobile phase. In this case, improved separation often is traded off for an increase in the pressure drop across the column, or for an increase in the run time. Further, column efficiency often improves as the temperature increases because of decreasing viscosity of the mobile phase and increasing diffusion coefficient and mass transfer. The chemistry of a stationary phase and the composition of the mobile phase often have only minor effects on the separation efficiency in the absence of strong interactions with adsorption centers, and when the porosity of the packing material and the viscosity of the mobile phase do not change very significantly.

Control of Retention and Separation Selectivity

The retention and the selectivity of separation depend primarily on the chemistry of the stationary phase and the mobile phase and, to a lesser extent, on temperature. The retention usually decreases by 1–2% when the column temperature increases by 1°C. A change in retention is

often accompanied by a change in separation selectivity $r_{1,2}$ so that temperature regulation can be used for optimizing the resolution. For example, increased temperature usually affects, favorably, the separation selectivity of ionic compounds. The regulation of temperature is convenient and simple, but is usually less effective for improving HPLC separations than for varying the composition of the mobile phase. Furthermore, many HPLC columns are not stable at temperatures above 60°C.

For a successful HPLC separation, the appropriate selection of the mobile phase is equally important as the correct choice of the separation column. In NPLC, the elution strength increases, whereas in RPLC, it decreases with increasing solvent polarity. Single-component mobile phases do not allow a fine adjustment of the elution strength, as there is only a limited selection of solvents compatible with UV and other common detection techniques, so that mixed mobile phases composed of solvents with different elution strengths should be used. Increasing the concentration of the strong solvent in a mixed mobile phase speeds up the elution. The retention of weak acids and weak bases in RPLC increases when the pH of the mobile phase is adjusted to suppress their ionization. A change in the retention, induced by an increase or decrease in the concentration of the strong solvent, is often accompanied by a change in the separation selectivity. The effects of the mobile phase on separation can be predicted, and the separation can be optimized using either a commercial software such as Dry Lab I, or simple predictive calculations employing, for example, Eq. 1 or Eq. 2.

Ternary and more complex mobile phases contain at least two different strong solvents with different predominant selective polar contributions (dipole–dipole, proton–donor, and proton–acceptor) in a weak solvent. Fine selectivity tuning is often possible by appropriate selection of the concentration ratios of the strong solvents.^[3] In RP chromatography, acetonitrile with dipole–dipole properties, tetrahydrofuran with proton acceptor properties, and methanol with both proton donor and proton acceptor properties are used as strong solvents in water; in NP chromatography, a nonlocalizing solvent (dichloromethane), a basic localizing solvent (methyl-*t*-butyl ether), and a nonbasic localizing solvent (acetonitrile or ethyl acetate) are mixed and diluted with hexane or heptane to adjust the elution strength. For any three-component or four-component mobile phase, the proportions of the individual selective contributions to the polarity are proportional to the concentration ratios of the three strong solvents, whereas the elution strength is controlled by the concentration of water in RPLC and alkane in NPLC.

Single-parameter optimization employs several experiments at preselected values of the optimized parameter (such as the concentration of the strong solvent in a binary



mobile phase, pH, temperature, etc.) to predict the resolution as a function of the optimized parameter using empirical or simple model-based calculations. Then, plots are constructed (the “window diagrams”)^[4] in which the range of the optimized parameter is searched for the value that provides the desired resolution for all adjacent bands in the chromatogram in the shortest time. Two examples of window diagrams (Figs. 3 and 4) illustrate the approach for optimization of binary mobile phases in NPLC and the impact of the selection of a strong solvent on the time of optimized separation.

Some parameters may show synergistic effects on the separation. In this case, simultaneous optimization of two or more parameters at a time can provide better results than their sequential optimization. Simple methods can be

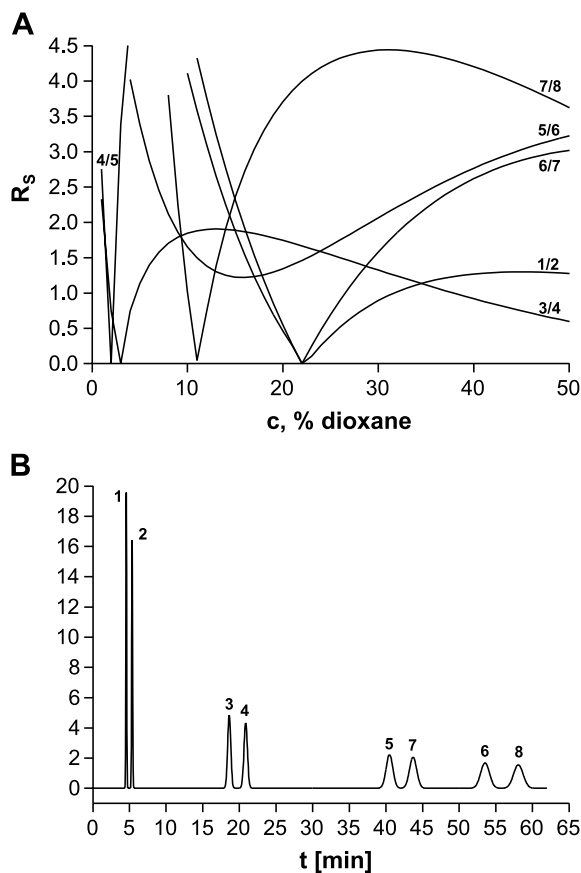


Fig. 3 (A) The window diagram (the dependence of the resolution on the concentration of dioxane in *n*-heptane as the mobile phase) for a mixture of eight phenylurea herbicides on a Separon SGX 7.5- μ m silica gel column (150 \times 3.3 mm ID). (B) The separation with an optimized concentration of 13% dioxane in the mobile phase for maximum resolution. Column plate number $N=5000$, $T=40^\circ\text{C}$, flowrate 1 mL/min. Sample compounds: neburon (1), chlorobromuron (2), 3-chloro-4-methylphenylurea (3), desphenuron (4), isoproturon (5), diuron (6), metoxuron (7), and deschlorometoxuron (8).

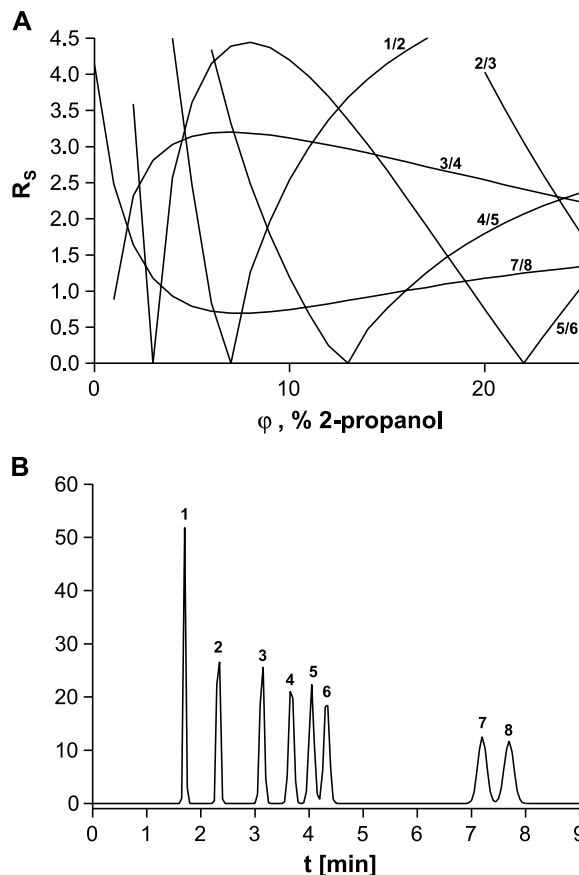


Fig. 4 (A) The window diagram (the dependence of the resolution on the concentration) of 2-propanol in *n*-heptane as the mobile phase. (B) The separation with an optimized concentration of 19% 2-propanol in the mobile phase for maximum resolution. Compounds and column are as in Fig. 3.

used for sequential multiparameter optimization in HPLC. Alternatively, the composition of mixed mobile phases can be optimized using an “overlapping resolution mapping” strategy to adjust the optimum separation selectivity based on seven or more initial experiments with solvent mixtures of approximately equal elution-strength. Based on the retention data from the initial experiments, either three-dimensional diagrams or contour “resolution maps” are constructed for all adjacent bands in the selectivity triangle space as a function of the concentration ratios of three solvents or two solvents and the pH of the mobile phase, from which the composition of the mobile phase that provides maximum resolution is selected.

Structure-based commercial optimization software (e.g., Chromdream, Chromsword, or Eluex) incorporate some features of the “expert system,” as the retention is predicted based on the additive contributions of the



individual structural elements and, consequently, the optimum composition of the mobile phase is suggested. Such predictions are only approximate and do not take into account stereochemical and intramolecular interaction effects.

CONCLUSION

Suitable detection conditions, separation mode, appropriate column dimensions, and packing materials (stationary phase) in isocratic LC should be selected, keeping in mind the objective of separation, using the information on sample properties, such as solubility, polarity, presence of specific functional groups in sample compounds, sample amount and concentration, etc. For the control of separation selectivity, resolution, and time of analysis, appropriate selection of the mobile phase is equally as important as the choice of the stationary phase, whereas the variation in flow rate and temperature usually has a lesser effect on separation. Trial-and-error optimization of separation is facilitated by a knowledge of the principles of retention mechanisms. Isocratic separations can be optimized using single-parameter or multiparameter strategies, using either commercial software or simple computer-aided predictive calculations.

REFERENCES

1. Snyder, L.R.; Dolan, J.W.; Gant, J.R. Gradient elution in high-performance liquid chromatography: I. Theoretical basis for reversed-phase systems. *J. Chromatogr.* **1979**, *165*, 3–30.
2. Jandera, P.; Churáček, J. Gradient elution in liquid chromatography: I. The influence of the composition of the mobile phase on the capacity ratio (retention volume, band width, and resolution) in isocratic elution—Theoretical considerations. *J. Chromatogr.* **1974**, *91*, 207–221.
3. Glajch, J.L.; Kirkland, J.J.; Snyder, L.R. Practical optimization of solvent selectivity in liquid–solid chromatography using a mixture–design statistical technique. *J. Chromatogr.* **1982**, *238*, 269–280.
4. Price, W.P.; Deming, S.N. Optimized separation of scopolin and umbelliferone and cis–trans isomers of ferulic and *p*-coumaric acids by reverse-phase high-performance liquid chromatography. *Anal. Chim. Acta* **1979**, *108*, 227–231.

FURTHER READINGS

- Neue, U.D. *HPLC Columns: Theory, Technology and Practice*; Wiley-VCH: New York, 1997.
- Schoenmakers, P.J. *Optimisation of Chromatographic Selectivity*; Elsevier: Amsterdam, 1986.
- Snyder, L.R.; Kirkland, J.J.; Glajch, J.L. *Practical HPLC Method Development*, 2nd Ed.; Wiley: New York, 1997.



Selectivity

Hassan Y. Aboul-Enein

Ibrahim A. Al-Duraibi

King Faisal Specialist Hospital and Research Centre, Riyadh, Saudi Arabia

Introduction

The selectivity α , also known as the relative retention, the separation factor, or chemistry factor, of a chromatographic column is a function of thermodynamic of the mass-transfer process and can be measured in terms of the relative separation of the peaks:

$$\alpha = \frac{t_{R2} - t_0}{t_{R1} - t_0} = \frac{k'_2}{k'_1} = \frac{K_2}{K_1}$$

where t_{R2} and t_{R1} are the retention times of compounds 2 and 1, respectively, t_0 is the retention time of unretained compounds, k'_2 and k'_1 are the capacity factors of compounds 2 and 1, respectively, and K_2 and K_1 correspond to the distribution coefficients of compounds 2 and 1, respectively.

So, the selectivity of the chromatographic system is a measure of the difference in retention times (or volume) between two given peaks and describes how effectively a chromatographic system can separate two compounds with slight variations in structure or molecular weight. For compounds with the same molecular weight, the structure difference may involve no more than compounds that are mirror images (i.e., optical isomers resulting from the presence of one or more asymmetric atoms). Therefore, when components interact with a column and are retained, they will be separated if their degrees of retention are not identical. Two components with identical retentions would have $\alpha = 1$, or no separation. For effective separation, an $\alpha = 1.5$ is desired.

Optimizing the Selectivity

Separation problems become substantially more difficult as the number of components increases much above 10. Such complexity is often characteristic of environmental and biological samples. Different chromatographic modes offer potentially unlimited selectivity, but the conditions for optimal selectivity are correspondingly more difficult to find. A systematic basis for the combining of independent selectivity mechanism can provide a major boost to the overall selectiv-

ity. The overall effect is multiplicative, based on the separating power, or peak capacity, of each of the steps. The serial implementation of multiple origins of selectivity is the most practical approach at present.

The net retention of a particular solute depends on all the solute-solute, solute-mobile phase, solute-stationary phase, and stationary phase-mobile phase interactions that contribute to the retention, which, consequently, affect the selectivity.

The selectivity is dependent on the temperature and the chemistry of the components that make up the chromatographic system (i.e., column, solvent, and the sample). So, it is necessary to understand the physicochemical basis of retention and the retention mechanism involved in high-performance liquid chromatography (HPLC) separation.

The Sample or Solute

The basic structure and number of functional groups in the solute molecule largely determine chromatographic retention. The functional group must be able to interact with the stationary-phase surface. Moreover, the strength of the retention is increased by the introduction of a second functional group. In addition, the type of functional group determines the elution order. Therefore, changing the chemical nature of the sample compounds or altering the functional group by chemical derivatization of an analyte should lead to compounds that can be will separated with higher α , because it will alter the chromatographic properties and the solubility of the analytes. Furthermore, the quantity of injected sample could affect k' values and column efficiency.

Stationary Phase

Selectivity enhancement through choice of stationary phase can be a simplifying approach for difficult separations, where interest is in certain critical pairs and where practical capacity is deemed important.

The nature of the stationary phase plays an important role in the improvement of the selectivity of a chro-



matographic system. Therefore, changing the chemical composition of the column from very nonpolar to a higher polarity will cause the nonpolar compounds to elute faster. Also, some phases have an affinity toward some compounds; therefore, selecting the ideal phase will improve the selectivity. For instance, the chromatographic selectivity in electron-acceptor and electron-donor stationary phase depends on the ability of the stationary phase to form complexes with solutes. The selectivity depends not only on the number and mutual position of electron-accepting substituents attached to aromatic skeleton but also on the nature of the spacer connecting the ligand with the silica surface. Also, in liquid-solid chromatography (LSQ), the sample retention is governed by adsorption to the stationary phase. For retention to occur, a sample molecule must displace one or more solvents from the stationary phase. In addition to this displacement effect, polar solvent or sample molecules can exhibit very strong interactions with particular sites on the stationary phase. The separation of enantiomers using a chiral mobile phase is possible only if transient diastomeric complexes are formed in the stationary phase. For this to happen, the stationary phase must be chiral.

Another way to improve selectivity is by using column switching, which is, in its simplest form, the use of a number, N , of different chromatographic mechanisms in sequence, which will expand the overall selectivity of a liquid chromatography system by the N th power of that obtained from a single selectivity mechanism. Column switching can create tremendous separating power, but it is a requirement that each one in the sequence of selectivity mechanism not be redundant.

Temperature

Temperature is the first of the variables affecting selectivity. Increased temperature decreases retention time on the column, sharpens peaks, and produces a change in selectivity. However, temperature is generally limited, by solvent vapor pressures, to an effective range of 20–60°C; also important is the effect temperature has on the column packing.

Temperature affects sample solubility, solute diffusion, and mobile-phase viscosity in liquid chromatography. With increasing temperature, the solute diffusion coefficient tends to increase while the mobile phase viscosity decreases, producing a favorable influence on the selectivity.

The change in selectivity with temperature appears more pronounced in ion-pair chromatography than

other HPLC methods. Therefore, temperature may be an important variable for optimizing selectivity in certain applications of ion-pair chromatography.

Mobile Phase

The most powerful approach to increase α is to change the composition of the mobile phase. If changing the concentration of the components in the mobile phase provides insufficient change, altering the chemical nature of one of the components will often be sufficient. Also, we can produce other α changes by adding mobile-phase modifiers to the mobile phase. The shifts in selectivity under certain circumstances have been attributed to the change in mobile-phase composition rather than to the stationary phase. Also, selectivity arises from the combined action of mobile phase and stationary phase.

Change in mobile phase can result in significant differences in selectivity for various sample analytes which can be obtained when the relative importance of the various intermolecular interactions between solvent and solute molecules is markedly changed. It is frequently preferable to use mixtures of solvents, rather than a single, pure solvent, as the mobile phase. However, in many cases, selecting a mobile phase is still a trial-and-error procedure. Moreover, pH has a prominence as a tool to affect the separation of some compound solutes. Likewise, an impressive separation of optically active compounds has been demonstrated through the use of chiral reagents that induce a ligand-exchange mechanism. Therefore, it should be recognized that the harnessing of liquid-phase composition to control HPLC selectivity provides a major corridor for achieving separation in an increasingly systematic manner.

The difficulty in eliminating the silanol groups from the silica substrate make it necessary to neutralize them using additives in the mobile phase. Also, solvent strength generally increases with the volume percent of organic modifier. Its effect is most important when hydrophobic mechanisms contribute significantly to retention. In this case, changing the organic modifier can be used to adjust solvent selectivity, as normally practiced in reversed-phase chromatography. Mobile-phase additives (in normal phase), which are very polar, influence the adsorption of substances strikingly, even in the very low concentration range, because they are adsorbed preferentially. On the other hand, the stationary-phase selectivity can be altered for some phases by the addition of some compounds or metallic complexes to the mobile phase.



High-performance liquid chromatography offers options to control selectivity through the mobile phase. Therefore, it is important to improve the practical understanding of liquid-phase compositions needed to achieve chemical selectivity.

Suggested Further Reading

- Ahuja, S., *Selectivity and Detectability Optimization in HPLC*, John Wiley & Sons, New York, 1989.
- Freeman, D., Advances in liquid chromatographic selectivity, in *Ultrahigh Resolution Chromatography* (S. Ahuja, ed.), American Chemical Society, Washington, DC, 1984.
- Lochmiller, C. H., Approaches to ultrahigh resolution chromatography: Interaction between relative peak (N), relative retention (α), and absolute retention (k'), in *Ultrahigh Resolution Chromatography* (S. Ahuja, ed.), American Chemical Society, Washington, DC, 1984.
- Meyer, V. R., *Practical High-Performance Liquid Chromatography*, 2nd ed., John Wiley & Sons, New York, 1993.
- Poole, C. F. and S. K. Poole, *Chromatography Today*, Elsevier Science, Amsterdam, 1991.
- Riley, C. M., Efficiency, retention, selectivity and resolution in chromatography, in *High Performance Liquid Chromatography, Fundamental Principles and Practice* (W. J. Laugh and I. W. Wainer, eds.), Blackie Academic and Professional, Glasgow, 1996, pp. 29–35.
- Snyder, L. R., J. L. Glajch, and J. J. Kirkland, *Practical HPLC Method Development*, John Wiley & Sons, New York, 1988.
- Weston, A. and P. R. Brown, *HPLC and CE Principles and Practice*, Academic Press, San Diego, CA, 1997.



Selectivity: Factors Affecting, in Supercritical Fluid Chromatography

Kenneth G. Furton

International Forensic Research Institute (IFRI), Florida International University, Miami, Florida, U.S.A.

Introduction

Retention and selectivity in supercritical fluid chromatography (SFC) are a complex function of many experimental variables and are not as easily rationalized as in the case of gas and liquid chromatography. Retention in SFC is dependent on temperature, density (and pressure drop), stationary-phase composition, and the mobile-phase composition. Many of these variables are interactive and do not change in a simple or easily predicted manner [1].

Effect of Temperature

Changes in retention at constant density are predictable from van't Hoff plots. The logarithm of the capacity factors is a linear function of the reciprocal of the column temperature, even down to subcritical conditions [1]. Analysis of the thermodynamics of the temperature-driven selectivity shifts in capillary SFC, at a constant mobile-phase fluid density, demonstrates the importance of stationary-phase polymer swelling. The other thermodynamic derivative contributing to temperature-driven selectivity shifts is the thermal pressure coefficient of the mobile-phase fluid [2]. Usually, temperature programming in SFC is done by increasing the temperature during a pressure, density, or eluent program, although negative temperature programs can also be employed to increase density. Although density conditions are the same either by decreasing temperature at constant pressure or by increasing pressure at constant temperature, the latter is preferable, as the higher diffusion coefficients at the higher constant temperature provide more favorable mass-transport properties.

Effect of Pressure Drop (Density Drop)

Selectivity is almost independent of pressure in high-performance liquid chromatography (HPLC) and gas chromatography (GC), whereas pressure (and corresponding density) is a very important parameter con-

trolling selectivity in SFC, particularly if a significant pressure or density drop occurs along the column. In general, pressure drops are low when open-tubular columns are used, but they are significantly higher with packed columns and, therefore, have a significant effect on chromatographic resolution with packed column systems [3]. The observed selectivity, α_{obs} , can be described by $\alpha_{\text{obs}} = e^{(B-mD)} \times (e^{bwL} - 1)/mwL$, where the values for the constants B , m , and b will vary depending on the compound types being separated, the mobile phase, the stationary phase, and the temperature. D is the density of the mobile phase at the head of the column, w is the rate at which the density changes along the column, and L is the total column length. Because wL is simply the density change, $\Delta\rho$, across the column, the net result is that observed SFC selectivity changes caused by a linear density change along a column are only dependent on the total density drop which occurs. Therefore, in order to maintain constant selectivity as the density drop is increased, the density at the head of the column must be increased. Alternatively, if the density at the head of the column is kept constant while $\Delta\rho$ is increased, both selectivity and retention will increase [4]. Figure 1 demonstrates the effects of the density

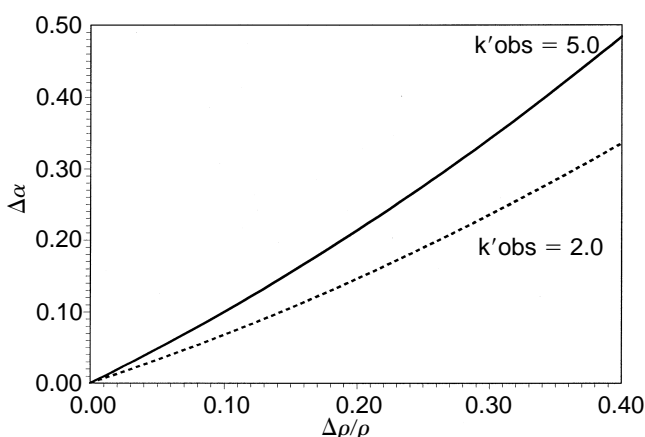


Fig. 1 Density drop effects on α at different k' s for n -alkanes in carbon dioxide.



drop across a column for *n*-alkanes in carbon dioxide (data from Ref. 4). Some general conclusions include that, on average, α_{obs} changes by 0.001 per 10% density drop up to a 30% density drop. Also, selectivity decreases more rapidly as density drops become larger and that selectivity increases at larger k' values where the mobile-phase density is lower.

Effect of Overall Density (Pressure at Constant Temperature)

The overall density of the mobile phase is one of the most important parameters used to optimize separations in SFC with density programming as common in SFC as temperature programming in GC and eluent composition in HPLC [5]. Capacity ratios, k' , decrease roughly linearly at higher densities with different slopes for different classes of compounds, thereby affording changes in selectivity [5]. A similar effect is seen for the supercritical fluid elution of analytes from octadecylsilica sorbents, as seen in Fig. 2 [6].

Effect of Stationary Phase

In SFC, both packed and capillary columns are used, each with their specific advantages and disadvantages. Packed columns in SFC are very similar to those used in HPLC, with the most often used stationary phases being modified silicas. Column selectivity follows the same rules as it does in HPLC with aromatic hydrocarbons (e.g., more retained on octadecyl silica column than on bare silica) [5]. A great variety of different selective stationary phases

have been used in packed column SFC. For example, racemic *N*-acetyl amino acid *t*-butyl esters have been resolved on chiral (*N*-formyl-L-valylamino)propylsilica using methanol-modified carbon dioxide [5]. The most often used stationary phases for open-tubular SFC are immobilized films of polymeric materials — most commonly, polysiloxanes common to GC. Selecting a suitable stationary phase follows the same rules as in GC or HPLC, bearing in mind the frequently used carbon dioxide is a relatively nonpolar eluent. For example, nonpolar substrates such as hydrocarbons are strongly retained on a dimethyl column, whereas free carboxylic acids are more retained on a cyanopropyl column.

Effect of Mobile-Phase Composition (Polarity Modifiers)

Carbon dioxide is the most commonly used mobile phase in SFC, due to its low cost, low expense, low toxicity, and low critical temperature and pressure. However, using the classification scheme of eluents by Snyder, carbon dioxide shows a polarity similar to that of hexane [5]. Therefore, the solvent power of eluents used in SFC is generally enhanced by adding small amounts of a second eluent modifier. Selection of the optimum solvents can be achieved in much the same way that selections are made for HPLC solvents, namely utilizing a solvent polarity/selectivity scheme. To be useful, a solvent characterization scheme must efficiently determine the solvent strength or polarity and the solvent selectivity. The polarity of nonelectrolytes is the capacity of the solvent for all intermolecular interactions (primarily dispersion, induction, orientation, and proton donor–acceptor interactions). Solvent selectivity is a measure of the relative capacity to enter into each specific interaction. The three primary specific interactions evaluated in all solvent characterization schemes are orientation (dipolar interaction), proton-donor (acidity), and proton-acceptor (basicity) interactions. One of the most widely used schemes is the solvent triangle introduced by Snyder and reevaluated over the years [7]. In Snyder's approach, solvent selectivity factors x_n (using nitromethane), x_e (using ethanol), and x_d (using dioxane) are used to characterize the relative importance of orientation, proton acceptor (basicity) and proton donor (acidity), respectively. When these three terms are graphed against one another for the common solvents, a so-called selectivity triangle is generated where solvents with similar selectivities are clustered into eight major selectivity "groups." Additionally, a solvent po-

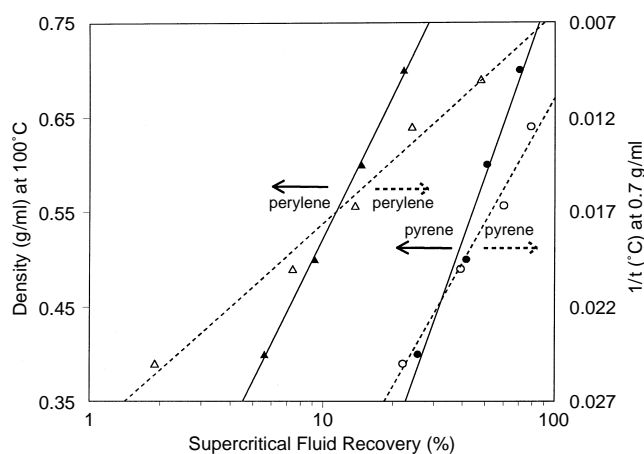


Fig. 2 Supercritical fluid recoveries of polycyclic aromatic hydrocarbons as a function of density and temperature. (From Ref. 6.)

larity index, P' , is calculated to provide a measure of the relative polarity of each solvent. Values for the various polarity/selectivity terms and critical constants are summarized in Table 1 for some common polarity/selectivity modifier solvents. (data from Refs. 7 and 8). The most recent data for Snyder's terms from Ref. 3 have been included where available. Popular alternative schemes have utilized solvatochromic parameters based on the concept of linear solvation energy relationships to quantitatively probe-specific chemical interactions such as polarizability, hydrophobicity, and hydrogen-bonding interactions.

Solvatochromic descriptors described by Abraham are summarized in Table 1, including the overall or summation hydrogen-bond acidity scale ($\Sigma \alpha_2^H$), basicity scale ($\Sigma \beta_2^H$), and dipolarity/polarizability descriptor ($\Sigma \pi_2^H$) [9]. It has been shown that solvatochromic parameters may be successfully used to predict retention near the critical point in packed column SFC and may be useful in controlling selectivity of chiral separations [10]. Supercritical fluid selectivities are comparable to subcritical selectivities with minor differences attributable to the physical nature of modifier behavior under near-critical conditions where binary mobile phases may exhibit gross compositional heterogeneity at interfaces [10]. When organic modifiers are increasingly added to the mobile phase at constant pressure (density) and temperature, the retention of analytes increases or decreases, depending on whether the supercritical analytes are more or less soluble in the modifier compared to the supercritical fluid, provided that the column activity remains the same [1].

Miscellaneous and Combined Effects

Temperature, pressure, and density may also influence SFC selectivity in other ways. For example, water solubility in supercritical fluids generally increases with temperature, causing a shift the equilibrium of the number of water-deactivated silanol groups to carbon-dioxide-deactivated groups [1]. Therefore, the solubility of analytes in the mobile phases increases but so does retention for polar analytes due to increased stationary-phase activity.

References

1. C. F. Poole and S. K. Poole, *Chromatography Today*, Elsevier, Amsterdam, 1991, pp. 601–643.
2. M. Roth, *J. Chromatogr.* 718: 147 (1995).
3. X. Lou, H.-G. Janssen, H. Snijder, and C. A. Cramers, *J. Chromatogr.* 718: 147 (1995).
4. P. A. Peadar and M. L. Lee, *J. Chromatogr.* 259: 1 (1983).
5. R. M. Smith (ed.), *Supercritical Fluid Chromatography*, Royal Society of Chemistry, London, 1988.
6. K. G. Furton and J. Rein, in *Supercritical Fluids Technology: Theoretical and Applied Approaches in Analytical Chemistry* (F. V. Bright and M. E. P. McNally, eds.), ACS Symposium Series Vol. 488, American Chemical Society, Washington, DC, 1992, pp. 237–250.
7. S. C. Rutan, P. W. Carr, W. J. Cheong, J. H. Park, and L. R. Snyder, 463: 21 (1989).
8. *Isco Tables*, 9th Edition, Isco, Inc., 1987, p. 10.
9. M. H. Abraham, G. S. Whiting, R. M. Doherty, and W. J. Shuely, *J. Chromatogr.* 587: 213 (1991).
10. G. O. Cantrell, R. W. Stringham, J. A. Blackwell, J. D.

Table 1 Critical Constants and Polarity and Selectivity Parameters for Common Organic Modifiers

Solvent	P_c (psi)	T_c (°C)	P'	χ_d	χ_e	χ_n	Group	$\Sigma \alpha_2^H$	$\Sigma \beta_2^H$	$\Sigma \pi_2^H$
Carbon dioxide	1070.4	31.1						0.00	0.10	0.42
<i>n</i> -Hexane	436.6	234.4						0.00	0.00	0.00
Triethylamine	439.5	262.0	2.19	0.08	0.66	0.26		0.00	0.79	0.15
Diethyl ether	527.9	193.7	3.15	0.13	0.53	0.34	I	0.00	0.45	0.25
Ethylene chloride	735.3	250.0	3.5	0.21	0.30	0.49	V	0.10	0.11	0.64
Isopropanol	690.4	235.3	3.92	0.17	0.57	0.26	II	0.33	0.56	0.36
Ethyl acetate	555.5	250.2	4.24	0.22	0.36	0.42	VIa	0.00	0.45	0.62
Tetrahydro-furan	752.7	267.1	4.28	0.19	0.41	0.40	III	0.00	0.48	0.52
Methylene chloride	913.7	237.0	4.29	0.33	0.27	0.40	VII	0.10	0.05	0.57
Chloroform	778.9	263.4	4.31	0.35	0.31	0.34	VIII	0.15	0.02	0.49
Acetone	681.7	235.1	5.40	0.24	0.36	0.40	VIa	0.04	0.49	0.70
Pyridine	816.6	347.0	5.53	0.22	0.42	0.36	III	0.00	0.52	0.84
Acetonitrile	700.5	272.5	5.64	0.25	0.33	0.42	VIb	0.07	0.32	0.90
Acetic acid	839.8	319.7	6.13	0.30	0.41	0.30	IV	0.61	0.44	0.65
Methanol	1173.4	239.6	6.60	0.19	0.51	0.30	II	0.43	0.47	0.44
Water	3208.2	374.3	10.2	0.37	0.37	0.25	VIII	0.82	0.35	0.45



Separation of Alkaloids by Countercurrent Chromatography

Fuquan Yang

Yoichiro Ito

National Institutes of Health, Bethesda, Maryland, U.S.A.

INTRODUCTION

Alkaloids are an important class of compounds that have pharmacological effects on various tissues and organs of humans and other animal species. More than 16,000 are known and most are derived from higher plants. Alkaloids have also been isolated from microorganisms, from marine organisms such as algae, dinoflagellates, and puffer fish, as well as from terrestrial animals, such as insects, salamanders, and toads.

Pelletier^[1] defines an alkaloid as “a cyclic compound containing nitrogen in a negative oxidation state which is of limited distribution in living organisms.” This definition includes both alkaloids with nitrogen as part of a heterocyclic system and the many exceptions with extracyclic bound nitrogen. From the viewpoint of analytical chemistry, the most important trait of alkaloids is their basicity, arising from a heterocyclic tertiary nitrogen atom. Many alkaloids are complex components which are biosynthetically derived from various amino acids, such as phenylalanine, tyrosine, tryptophan, ornithine, and lysine. The biogenesis of alkaloids is used for their classification, as this is directly linked with their molecular skeleton, e.g., the two largest groups are indole alkaloids and isoquinoline alkaloids. Other important groups are tropane alkaloids, pyridine, and pyrrolizidine alkaloids. In the past 10 years, there has been an increasing interest in the isolation and determination of alkaloids in plant materials, in pharmaceutical products, and in other samples of biological interest. Currently, much work is being carried out to discover new alkaloid molecules for different applications, such as new antiviral and antitumor treatments. So the separation and analysis of alkaloids are of great importance.^[2,3] But the problem is that extensive tailing and irreversible adsorption may occur due to the interaction between the basic alkaloids and acidic silanol groups when alkaloids are separated by conventional column chromatography with silica gel or chemically bonded C₁₈ on silica as the stationary phase.

OVERVIEW

Countercurrent chromatography (CCC), as a support-free liquid–liquid partition chromatographic separation tech-

nique, eliminates various complications such as irreversible adsorption loss, denaturation of sample, tailing of solute peaks, contamination, etc. that sometimes arise from the interaction between solute molecules and the solid support matrix present in most other chromatographic methods. Countercurrent chromatography utilizes an immiscible two-phase solvent system, one phase as the stationary phase and the other as the mobile phase. The chromatographic process in CCC is based on the partition of a solute between the stationary and mobile phases. The partition coefficient (K), being one of the most important parameters in CCC, is defined as the ratio of the concentration of a solute in the stationary phase (C_s) to that in the mobile phase (C_m). In the past, various CCC systems, such as droplet CCC, rotation locular CCC, and centrifugal partition chromatography, have been used for the final or partial separation of alkaloids from a crude sample. The high-speed CCC (HSCCC) technique developed in the early 1980s^[4] improved in both the partition efficiency and separation speed, and has been successfully applied to the separation of alkaloids.

pH-Zone-refining CCC was developed for the large-scale separation of ionizable compounds, including alkaloids and organic acids in the mid-1990s by Ito.^[5,6] It uses a retainer base (or acid) in the stationary phase to retain the solutes in the column and an eluter acid (or base) to elute the solutes according to their pK_a values and hydrophobicities, and produces a succession of highly concentrated rectangular solute peaks with minimum overlap while impurities are concentrated at the peak boundaries. This technique has been successfully used for large-scale separation of alkaloids.

SEPARATION OF ALKALOIDS BY STANDARD COUNTERCURRENT CHROMATOGRAPHY

The standard CCC separation is solely based on the difference in the partition coefficients of solutes between the two phases of a solvent system. Most alkaloids have basic properties with pK_a values ranging from 6 to 12, but usually 7 to 9. Although the free base is soluble only in organic solvents, protonation of the nitrogen in the free base usually results in a water-soluble compound. This behavior serves as the basis for the selective extraction or



isolation of alkaloids by liquid–liquid partitioning processes. On the other hand, quaternary alkaloids are poorly soluble in organic solvents, but they are soluble in water, regardless of its pH.

Generally, a systematic search for the two-phase solvent systems for CCC is focused on the hydrophobicity of the solvent system for providing a proper range of

partition coefficients of solutes. For the separation of ionizable compounds such as alkaloids, however, an additional adjustment is required with respect to the pH and ionic strength of the solvent system.

Halogen-containing organic solvents, such as chloroform and dichloromethane, have been widely used in alkaloid separation because of their relatively strong

Table 1 Separation of alkaloids by CCC

Alkaloids	Source	Two-phase solvent system	Instrument
Matrine and oxymatrine	<i>Sophora flavescens</i>	CHCl ₃ –0.07 M sodium phosphate (pH 6.4) (1:1)	HSCCC
Atropine, scopolamine, hyoscyamine	<i>Datura mete</i>	CHCl ₃ –0.07 M sodium phosphate (pH 6.5) (1:1)	HSCCC
Cephalotaxus alkaloids	<i>Cephalotaxus fortunei</i>	CHCl ₃ –0.07 M sodium phosphate–0.04 M citric acid (pH 5.0) (1:1)	HSCCC
Pyrrolizidine alkaloids	<i>Amsinckia tessellata</i> , etc.	CHCl ₃ –0.2 M potassium phosphate (pH 7.4, 6.0, 5.6, 5.0) (1:1)	HSCCC
Pentacyclic aromatic alkaloid	<i>Amphicarpa meridiana</i>	CHCl ₃ –MeOH–5% HCl (5:5:3)	HSCCC
Flavonoid alkaloids	<i>Buchenavia capitata</i>	CHCl ₃ –MeOH–0.5% HCl (5:5:3)	Sanki CPC
Isoquinoline alkaloids	<i>Ancistrocladus abbreviatus</i>	CHCl ₃ –MeOH–0.5% HBr (5:5:3)	HSCCC
Naphthyltetrahydroisoquinoline alkaloids	<i>Ancistrocladus korupensis</i>	CHCl ₃ –MeOH–0.5% HBr (5:5:3)	CPC
Aporphine alkaloids	<i>Dehaasia triandra</i>	CHCl ₃ –MeOH–0.5% HAc (5:5:3)	HSCCC
Naphthylisoquinoline alkaloids	<i>Ancistrocladus robertsoniorum</i>	CHCl ₃ –MeOH–0.1 M HCl (5:5:3)	HSCCC
Isoquinoline alkaloids	<i>Coptis chinensis</i>	CHCl ₃ –MeOH–0.2 M HCl (4:1.5:2)	HSCCC
Diterpenoid alkaloids	<i>Aconitum sinomontanum</i>	CHCl ₃ –MeOH–0.3/0.2 M HCl (4:1.5:2)	HSCCC
Pyrrolizidine alkaloids	<i>Symphytum officinale</i>	<i>n</i> -C ₆ H ₁₄ –EtOH–MeOH–0.05% TFA (5:5:5:5)	HSCCC
β-Carboline alkaloids	<i>Pachypellina</i> sp.	<i>n</i> -C ₆ H ₁₄ –MeCN–CH ₂ Cl ₂ (10:7:3)	HSCCC
Vinca alkaloids	<i>Vinca rosea</i>	<i>n</i> -C ₆ H ₁₄ –EtOH–H ₂ O (6:5:5)	HSCCC
Isoquinoline alkaloids	<i>Stephania tetrandra</i>	<i>n</i> -C ₆ H ₁₄ –EtOAc–MeOH–H ₂ O (3:7:5:5), (1:1:1:1)	HSCCC
Diterpenoid alkaloids	<i>Consolida ambigua</i>	C ₆ H ₆ –CHCl ₃ –MeOH–H ₂ O (5:5:7:2)	CPC
Pyrroloquinoline alkaloids	<i>Bazella</i> sp.	<i>n</i> -C ₆ H ₁₄ –CHCl ₃ –MeOH–H ₂ O (4:7:4:3), (2:7:6:3)	HSCCC
Pyrroloquinoline alkaloids	<i>Bazella</i> sp.	CHCl ₃ – <i>i</i> -Pr ₂ NH–MeOH–H ₂ O (7:1:6:4)	HSCCC
Pyrroloquinoline alkaloids	<i>Bazella</i> sp.	<i>n</i> -C ₇ H ₁₆ –CHCl ₃ –MeOH–H ₂ O (2:7:6:3)	HSCCC
Pyrroloquinoline alkaloids	<i>Bazella</i> sp.	<i>n</i> -C ₇ H ₁₆ –EtOAc–CHCl ₃ –MeOH–H ₂ O (4:7:4:3)	HSCCC
Acridine alkaloids	<i>Dercitus</i> sp. and <i>Stellatta</i> sp.	CH ₂ Cl ₂ –MeOH–H ₂ O (5:5:3)	HSCCC
Quinoline alkaloids	<i>Camptotheca acuminata</i>	CCl ₄ –CHCl ₃ –MeOH–H ₂ O (2:2:3:1), CH ₂ Cl ₂ –CHCl ₃ –MeOH–H ₂ O (5:3:1)	HSCCC
Ergot alkaloids	<i>Stipa robusta</i>	CHCl ₃ –MeOH–H ₂ O (5:4:3)	HSCCC
Benzylisoquinoline alkaloids	<i>Anisocycla cymosa</i>	CHCl ₃ –MeOH–H ₂ O (10:10:1)	HSCCC
Imidazole alkaloids	<i>Discodermia polydiscus</i>	CHCl ₃ –MeOH–H ₂ O (5:10:6)	HSCCC
bis-Indole alkaloid	<i>Strychnos guianensis</i>	EtOAc–MeOH–H ₂ O (4:1:3)	HSCCC
Indole alkaloids	<i>Strychnos usambarensis</i>	<i>n</i> -BuOH–0.1 M NaCl (1:1)	HSCCC
Indole alkaloids	<i>Venezuelan curare</i>	<i>n</i> -BuOH–Me ₂ CO–H ₂ O (8:1:10)	HSCCC

proton-donor character. The chloroform-containing, two-phase solvent systems (chloroform–aqueous phosphate or citrated buffer and chloroform–methanol–dilute inorganic acid) have been widely used for the separation of alkaloids by CCC (Table 1).

Cai et al. first used a chloroform–0.07 M sodium phosphate buffer (pH 6.4–6.5) solvent system for the separation of matrine and oxymatrine from *Sophora flavescens*, atropine, scopolamine, and hyoscyamine from *Datura metel* L. by HSCCC.^[7] Cooper et al. successfully used chloroform–0.2 M potassium phosphate buffer with an optimum pH value of each at 5.0, 5.6, 6.0, and 7.4 for the separation of pyrrolizidine alkaloids from various sources of *Senecio douglasii* var. *longilobus*, *Trichodesma incanum*, *Symphytum* spp. and *Amsinckia tessellata*, respectively.^[8]

A two-phase solvent system composed of chloroform–methanol–dilute inorganic acid has been used for the separation of a variety of alkaloids including isoquinoline alkaloids, naphthyl-tetrahydroisoquinoline alkaloids, flavonoid alkaloids, pentacyclic aromatic alkaloids, diterpenoid alkaloids, aporphine alkaloids, etc. The following example illustrates a typical systematic solvent selection for the separation of palmatine, berberine, epiberberine, and coptisine from the crude alkaloids of *Coptis chinensis* Franch by analytical HSCCC.^[9] In Fig. 1, nine chromatograms are arranged in such a way that the effects of the concentration of HCl (0.3–0.1 M) and the relative volumes of methanol (4:3:2–4:1.5:2, v/v) on the separation of alkaloids from *C. chinensis* Franch are each readily observed. As the concentration of HCl is reduced from 0.3 to 0.1 M in the solvent system, the retention time

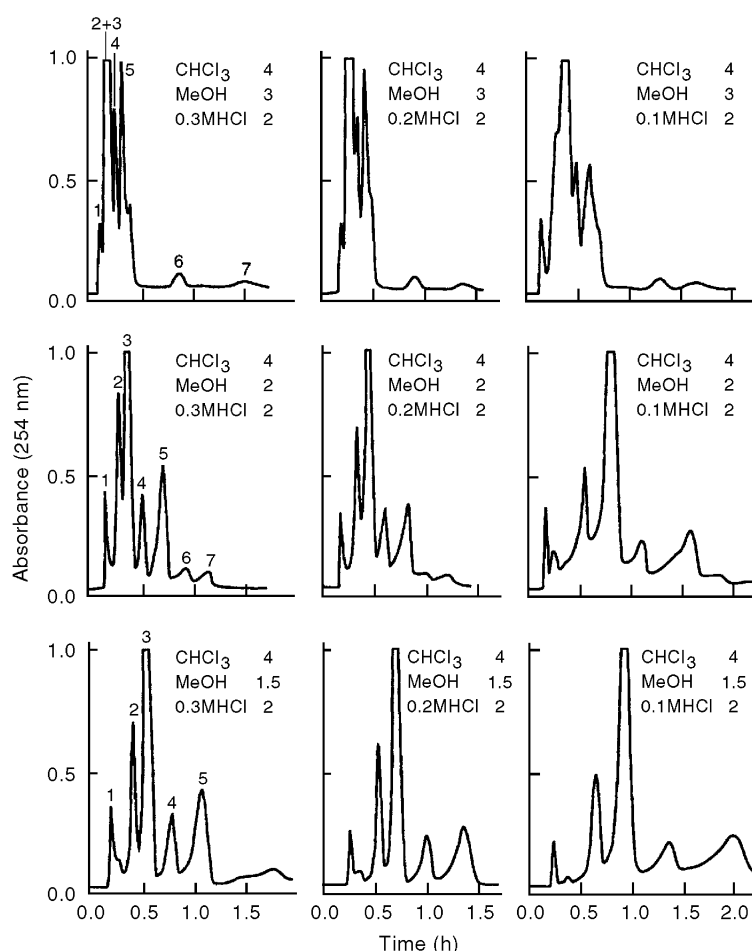


Fig. 1 Chromatograms of the crude alkaloids from *C. chinensis* Franch by analytical HSCCC. Nine chromatograms are arranged in such a way that the effects of methanol and HCl concentrations on the alkaloid separation are each clearly visualized. Experimental conditions: apparatus: analytical HSCCC instrument equipped with a multilayer coil of 0.85 mm I.D. and 30 mL capacity; sample: 2.5 mg of crude alkaloid extract of *C. chinensis* Franch; solvent system: shown above each chromatogram; mobile phase: lower organic phase; flow rate: 1 mL/min; revolution: 1500 rpm. Retention of the stationary phase was as follows: CHCl_3 –MeOH–(0.1–0.3 M HCl) (4:3:2), 77%; CHCl_3 –MeOH–(0.1–0.3 M HCl) (4:2:2), 80%; and CHCl_3 –MeOH–(0.1–0.3 M HCl) (4:1.5:2), 77%.



of alkaloids and their peak resolution are increased. A similar effect is also produced by decreasing the relative volumes of methanol in the solvent system from 4:3:2 to 4:1.5:2). Among those, the solvent system composed of CHCl_3 –MeOH–0.2 M HCl (4:1.5:2) produced the best separation of all four major alkaloids components. The optimum solvent system thus obtained led to the successful separation of alkaloids from *C. chinensis* Franch by preparative HSCCC. A similar method was also used for the separation of diterpenoid alkaloids, including lappaconitine, ranaconitine, *N*-deacetylappaconitine, and *N*-deacetylranaconitine from *Aconitum sinomontanum*.^[10]

More than 10 kinds of neutral two-phase solvent systems have been successfully used for the separation of alkaloids by CCC.^[11] Most of the alkaloids from marine sponge—including acridine, pyrroloquinoline, imidazole, β -carboline alkaloids, etc.—were separated with neutral two-phase solvent systems by HSCCC in the final or middle step of separation (Table 1).

SEPARATION OF ALKALOIDS BY pH-ZONE-REFINING COUNTERCURRENT CHROMATOGRAPHY

Fig. 2 shows a typical separation of 3 g of three alkaloids from a crude extract of *Crinum moorei* using a binary

solvent system composed of methyl-*tert*-butyl ether–water where triethylamine (5–10 mM) was added to the organic phase and HCl (5–10 mM) was added to the aqueous phase.^[12] In Fig. 2A, where the aqueous phase was used as the mobile phase and HCl as the eluter, the alkaloids were eluted as HCl salts, while in Fig. 2B, where the organic phase is used as mobile phase and triethylamine as the eluter, the alkaloids were eluted as free bases. The same binary solvent system was also used for the separation of alkaloids from the root of *S. flavescens* Ait.^[13] In order to increase the solubility of the alkaloids in methyl-*tert*-butyl ether–water solvent system, this solvent system was modified to methyl *tert*-butyl ether–tetrahydrofuran–water (2:2:3, v/v), while triethylamine (10 mM) was added to the upper organic stationary phase as a retainer and hydrochloric acid (10 mM) to the aqueous mobile phase as an eluter. This solvent system was applied to the separation of diterpenoid alkaloids from a crude prepurified sample containing lappaconitine at about 90% purity. Up to 10.5 g of the sample loading yielded 9.0 g of lappaconitine at a high purity of over 99% as determined by HPLC.^[14] As most alkaloids have a high solubility in chloroform, a binary solvent system composed of chloroform–water is suitable for a large-scale preparative separation when 18–24 mM HCl was added to the aqueous stationary phase as a retainer and 0.1% triethylamine (TEA) to the organic mobile phase as an eluter. This system was successfully used for the

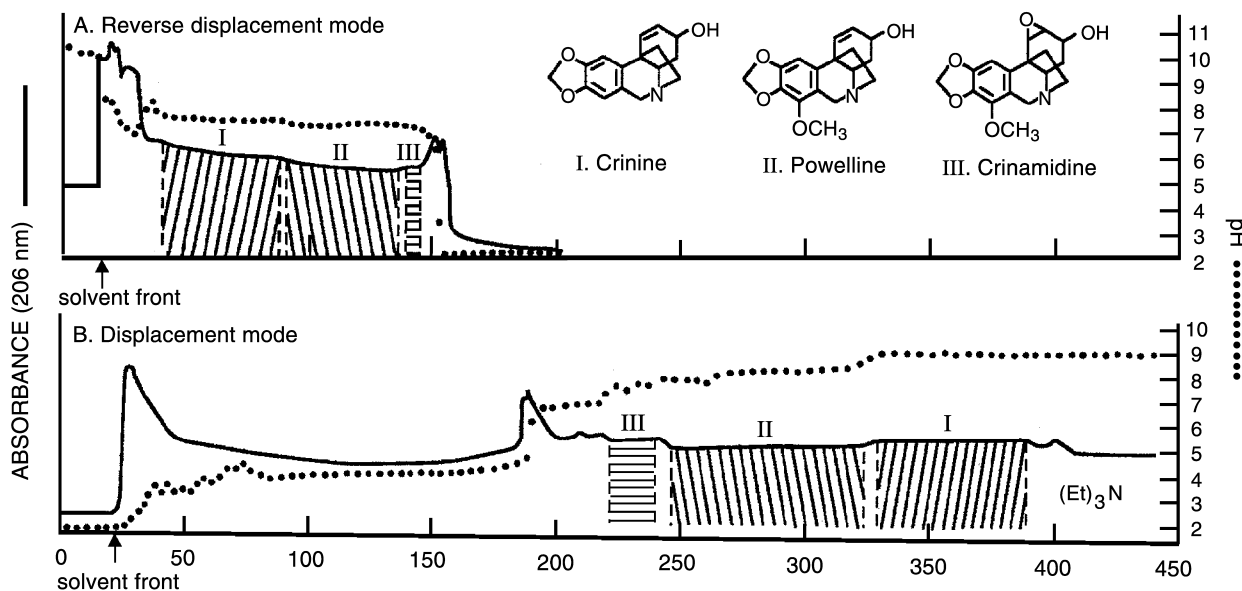


Fig. 2 Chromatograms of the crude alkaloid extract of *Crinum moorei* obtained by pH-zone-refining CCC. Experimental conditions were as follows: apparatus: high-speed CCC centrifuge equipped with a multiplayer coil of 1.6 mm I.D. and about 300 mL capacity; solvent system: methyl-*tert*-butyl ether–water; stationary phase: (A) upper phase (5 mM triethylamine) and (B) lower phase (10 mM HCl); mobile phase: (A) lower phase (5 mM HCl) and (B) upper phase (10 mM triethylamine); flow rate: 3.3 mL/min; sample: crude alkaloid extract of *C. moorei*, 3 g dissolved in 30 mL of each phase; revolution: (A) 800 rpm (600 rpm until 66 mL of mobile phase was eluted) and (B) 600 rpm throughout.

Table 2 Separation of alkaloids by pH-zone-refining CCC

Alkaloids	Source	Solvent systems ^a	Retainer ^b	Eluter ^c
Amaryllis alkaloids	<i>Crinum moorei</i>	MtBE–H ₂ O (1:1)	TEA (5 mM/SP)	HCl (5 mM/MP)
		MtBE–H ₂ O (1:1)	HCl (10 mM/SP)	TEA (10 mM/MP)
Vinca alkaloids	<i>Vinca minor</i>	MtBE–H ₂ O (1:1)	TEA (5 mM/SP)	HCl (5 mM/MP)
Matrine, sophocarpine	<i>Sophora flavescens</i>	MtBE–H ₂ O (1:1)	TEA (10 mM/SP)	HCl (5–0 mM/MP)
Diterpenoid alkaloids	<i>Aconitum sinomontanum</i>	MtBE–THF–H ₂ O (2:2:3)	TEA (10 mM/SP)	HCl (10 mM/MP)
Isoquinoline alkaloids	<i>Hydrastis canadensis rhizomes</i>	CHCl ₃ –H ₂ O (1:1)	18–24 mM HCl	TEA (0.1%/MP)

^aMtBE = methyl *tert*-butyl ether; THF = tetrahydrofuran.^bTEA = triethylamine; SP = stationary phase.^cMP = mobile phase.

separation of berberine chloride, canadine, β -hydrastine, and isocorypalmine from a methanolic extract of Goldenseal by pH-zone-refining CCC.^[15] The separation of alkaloids by pH-zone-refining CCC is summarized in Table 2.

CONCLUSION

Countercurrent chromatography overcomes all of the problems caused by solid support matrix present in most other chromatographic methods. Countercurrent chromatography can purify alkaloids with high recovery and reproducibility.

pH-Zone-refining CCC extends the preparative capacity of HSCCC and provides many important advantages over the conventional CCC method, including an over 10-fold increase in sample loading capacity, high concentration of fractions with very high purity, concentration of minor impurities, etc.

REFERENCES

- Pelletier, S.W., Ed. *Alkaloids: Chemical and Biological Perspective*; John Wiley: New York, 1983; Vol. 1–6.
- Muzquiz, M. *Alkaloids/Gas Chromatography*. In *Encyclopedia of Separation Science*; Wilson, I.D., Adlard, E.R., Cooke, M., Poole, C.F., Eds.; Academic Press: New York, 1938–1949; Vol. 5.
- Verpoorte, R. *Alkaloids/Liquid Chromatography*. In *Encyclopedia of Separation Science*; Wilson, I.D., Adlard, E.R., Cooke, M., Poole, C.F., Eds.; Academic Press: New York, 1949–1956; Vol. 5.
- Ito, Y. High-speed countercurrent chromatography. *CRC Crit. Rev. Anal. Chem.* **1986**, *17* (1), 65–143.
- Ito, Y. pH-Peak-Focusing and pH-Zone-Refining Countercurrent Chromatography. In *High-Speed Countercurrent Chromatography*; Ito, Y., Conway, W.D., Eds.; Wiley: New York, 1996; 121–175.
- Ito, Y.; Ma, Y. pH-zone-refining countercurrent chromatography. *J. Chromatogr. A* **1996**, *753* (1), 1–36.
- Cai, D.G.; Gu, M.J.; Zhang, J.D.; Zhu, G.P.; Zhang, T.Y.; Li, N.; Ito, Y. Separation of alkaloids from *Datura mete* L. and *Sophora flavescens* Ait by high-speed countercurrent chromatography. *J. Liq. Chromatogr.* **1990**, *13* (12), 2399–2408.
- Cooper, R.A.; Bowers, R.J.; Beckham, C.J.; Huxtable, R.J. Preparative separation of pyrrolizidine alkaloids by high-speed countercurrent chromatography. *J. Chromatogr. A* **1996**, *732* (1), 43–50.
- Yang, F.Q.; Zhang, T.Y.; Zhang, R.; Ito, Y. Application of analytical and preparative high-speed countercurrent chromatography for separation of alkaloids from *Coptis chinensis* Franch. *J. Chromatogr. A* **1998**, *829* (1–2), 137–141.
- Yang, F.Q.; Ito, Y. Preparative separation of lappaconitine, ranaconitine, *N*-deacetylappaconitine and *N*-deacetylranaconitine from crude alkaloids of sample *Aconitum sinomontanum* Nakai by high-speed countercurrent chromatography. *J. Chromatogr. A* **2002**, *943* (2), 219–225.
- Marston, A.; Hostettmann, K. Countercurrent chromatography as a preparative tool applications and perspectives. *J. Chromatogr. A* **1994**, *658* (2), 315–341.
- Ma, Y.; Ito, Y.; Sokoloski, E.; Fales, H.M. Separation of alkaloids by pH-zone-refining countercurrent chromatography. *J. Chromatogr. A* **1994**, *685* (2), 259–262.
- Yang, F.Q.; Quan, J.; Zhang, T.Y.; Ito, Y. Preparative separation of alkaloids from the root of *Sophora flavescens* Ait by pH-zone-refining countercurrent chromatography. *J. Chromatogr. A* **1998**, *822* (2), 316–320.
- Yang, F.Q.; Ito, Y. pH-Zone-refining countercurrent chromatography of lappaconitine from *Aconitum sinomontanum* Nakai: I. Separation of prepurified extract. *J. Chromatogr. A* **2001**, *923* (1–2), 281–285.
- Chadwick, L.R.; Wu, C.D.; Kinghorn, A.D. Isolation of alkaloids from goldenseal (*Hydrastis canadensis rhizomes*) using pH-zone-refining countercurrent chromatography. *J. Liq. Chromatogr. Relat. Technol.* **2001**, *24* (16), 2445–2453.

Separation of Antibiotics by Countercurrent Chromatography

M.-C. Rolet-Menet

UFR des Sciences Pharmacochimie et Biologie, Paris, France

Introduction

An antibiotic is a chemical compound made either by a living organism or by chemical synthesis. It has the property to inhibit, at low concentrations, some vital processes of viruses, microorganisms (such as bacteria, fungi, etc.) and some cells of a pluri-cellular individual (cancerous cells, parasites cells, etc.). The development of antibiotics made by microorganisms requires isolation and purification of a desired compound from a complicated matrix such as a fermentation broth. These bioactive microbial metabolites are often produced in very small quantities and have to be removed from other secondary metabolites and nonmetabolized media ingredients. Antibiotics are normally biosynthesized as mixtures of closely related congeners and many are labile molecules, thus requiring mild separation techniques with a high-resolution capability. Although recent advances in the HPLC technology, using sophisticated equipment and refined adsorbents, greatly facilitate the isolation of antibiotics, some drawbacks remain, which are related to various complications arising from the use of a solid support, such as adsorptive loss, deactivation of sample components, contamination, and so forth. Moreover, high-performance liquid chromatography (HPLC) purification always requires sample preparation, pre-purification, concentration, and so forth. Liquid-liquid partition techniques, particularly countercurrent chromatography (CCC), are suitable for the separation of antibiotics because it utilizes a separation column which is free of a solid support matrix and which is made of inert Teflon® channels or tubes.

Raw material can be injected into the column without any previous sample treatment, which simplifies the purification procedure. Oka et al. [1] have gathered antibiotics purification by CCC from crude extract and fermentation broth. They have shown that CCC has been successfully applied to the separation of macrolides and of various antibiotics, including various peptide antibiotics which are generally strongly adsorbed to silanol groups on silica gel used in the stationary phase in HPLC. Several CCC types are used, such as DCCC (droplet countercurrent chromatogra-

phy) [2] and the more recent, *X*-axis CCC, foam CCC, CPC (centrifugal partition chromatography), and HSCCC (high-speed countercurrent chromatography).

Antibiotics

Antibiotics have a more or less high polarity. They are synthesized by various living materials, such as bacterial strains (such as *Streptomyces* [3], *Bacillus*), marine sponges, and so forth. We will focus our discussion on the separation of macrolides and polypeptide antibiotics by CCC.

Several separations of macrolide and polypeptidic antibiotics by CCC are reported in the literature. Macrolides are heterosides of which aglycone is a cyclic macrolactone with at least 14 atoms. They act by stopping protein syntheses. Polypeptide antibiotics are frequently cyclic molecules. They act by disorganizing proteinic structure of the bacterial membrane. Figures 1–3 show the structures of several molecules whose purification will be described later. Spoviridines are produced by *Kutzneria viridigrisea*. They are very polar molecules and are water-soluble basic glycoside antibiotics (Fig. 1). They consist of six components, each having a 34-membered lactone and seven monosaccharide units, a pentasaccharide (viridopentaose), and two monosaccharides. They are active against Gram-positive bacteria, acid-fast bacteria, and trichophyton.

Ivermectins B1 are derived from the avermectines B1, the natural fermentation products of *Streptomyces avermitilis*. The avermectins B1 have double bonds between carbon atoms at 22 and 23, whereas the ivermectins B1 have single bonds in these positions (Fig. 2a). They have an intermediate polarity. The ivermectins B1 are a mixture of two major homologs, ivermectins B1a (>80%) and ivermectins B1b (<20%), but a crude ivermectin complex also contains various minor components. Ivermectins B1 are broad-spectrum antiparasitic agents used against *Onchocerca volvulus* in human medicine and for food production animals such as cattle, swine, and horses.



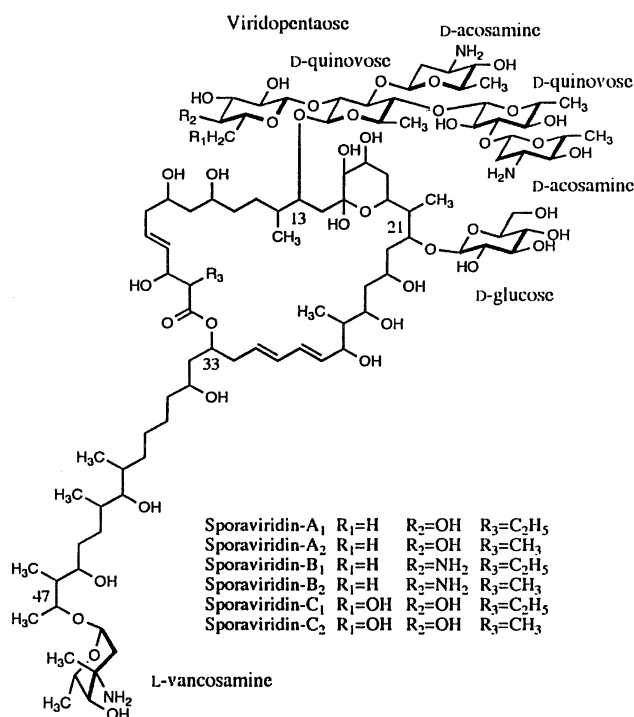


Fig. 1 Chemical structure of sporaviridins.

The bryostatins have been isolated from marine materials, bryozoan *Bugula neritina* [4] (Fig. 2b). They are macrolides with intermediate polarities. They show significant activity against lymphocytic leukemia in vitro.

Finally, bacitracins are peptide antibiotics produced by *Bacillus subtilis* and *B. licheniformis*. Over 20 components are contained in the bacitracin complex medium, among which the major active components are bacitracin A and F (Fig. 3). They exhibit an inhibitory activity against Gram-positive bacteria and are among the most commonly used antibiotics as animal feed additives.

Solvent Systems

The polarities of these molecules are, more or less, high according to the oses number contained in the chemical formula. Several procedures for choosing a solvent system are described in the literature. Usual solvent systems are biphasic and consist of three solvents, two of which are immiscible. If the polarities of the solutes are known, the classification established by Ito and co-workers [1] can be taken as a first approach. They classified the solvent systems into three groups,

according to their suitability for apolar molecules ("apolar" systems, based on *n*-hexane), for intermediate polarity molecules ("intermediary" system, based on chloroform), and for polar molecules ("polar" system, based on *n*-butanol). The molecule must have a high solubility in one of two immiscible solvents. The addition of a third solvent enables a better adjustment of the partition coefficients (*K*).

Oka et al. [5] proposed a choice of various solvent systems to purify antibiotics. They have to fulfill various criteria. The settling time of the solvent system should be shorter than 30 s to ensure the satisfactory retention of the stationary phase. The partition coefficient of the target compounds should be close to 1, and the separation factor (α) between the compounds must be larger than 1.5. Two series of solvent systems can provide an ideal range of the *K* values for a variety of samples: *n*-hexane–ethyl acetate–*n*-butanol–methanol–water and chloroform–methanol–water. These solvent series cover a wide range of hydrophobicity, continuously, from the nonpolar *n*-hexane–methanol–water system to a more polar *n*-butanol–water system.

CCC for Purification of Antibiotics

Several CCC devices are commonly used to purify antibiotics, such as rotating coil instruments particularly used in HSCCC and cartridge instruments used in CPC. An entry of this encyclopedia is entirely devoted to the various CCC devices, so that we only give some indications about performances of CCC as compared to preparative HPLC.

Menet et al. [6] have compared performances of CCC and preparative HPLC owing to a separation of two antibiotics X and Y. The CCC apparatus used was a centrifugal partition chromatograph (CPC, Sanki* LLN) of 250 mL internal volume. For this purpose, classical parameters of preparative-scale chromatography were calculated: experimental duration, including the sample preparation and the separation time, solvent consumption, including the volume of the mobile phase, the stationary phase and the injection solvent, and purity of the purest fraction in Y. The parameter "purity in Y" was chosen because Y is the solute most difficult to purify because of its physical properties (particularly hydrophobicity) which are close to those of the main impurities. The hourly yield (g/h) is defined as the ratio of the recovered quantity to the experimental duration. The volumic yield (g/L) is defined as the ratio of the recovered quantity to the solvent consumption. Table 1 summarizes the results of

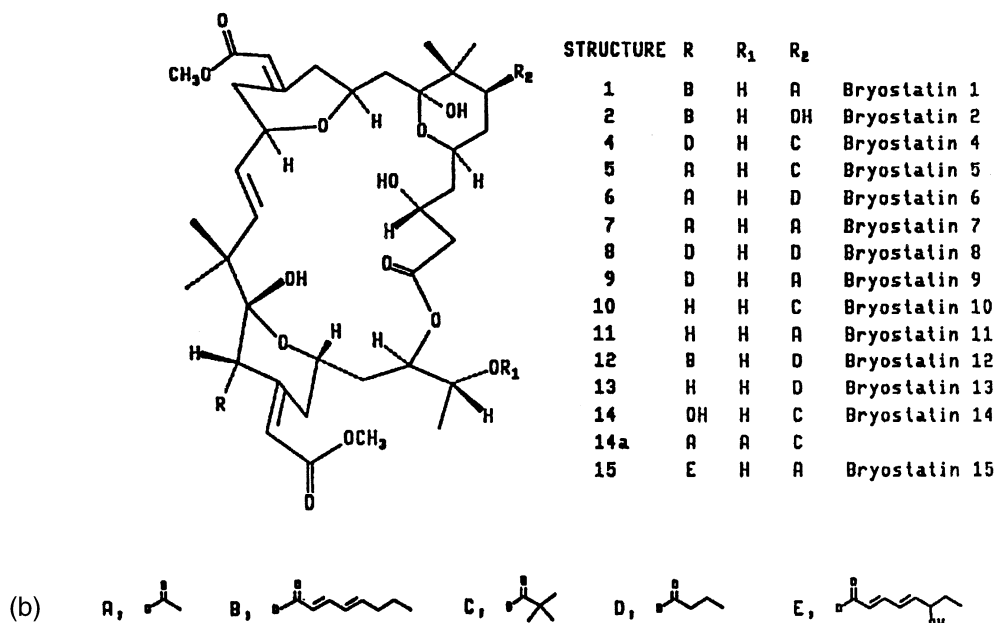
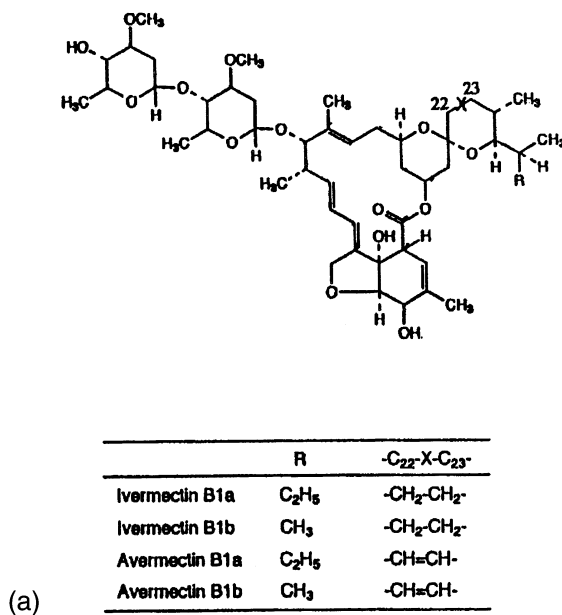


Fig. 2 Chemical structure of ivermectins (a) and bryostatins (b).



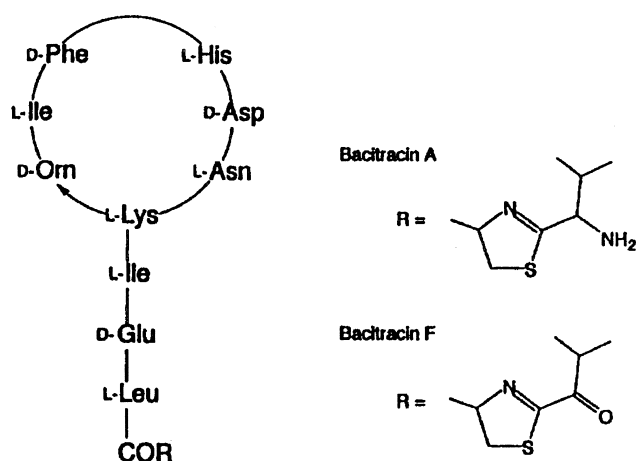


Fig. 3 Chemical structure of bacitracins.

separations of Y by CCC and preparative HPLC. The solvent volume consumption is the volume of the stationary and mobile phases in CCC or the volume of the mobile phase used in HPLC and the samples. The injected sample in CCC was not prepurified to concentrate it in Y from 7% to 25%. So the injected quantity in Y in CCC is lower (0.28 g against 1.59 g in preparative HPLC). For similar volumic yields (i.e., 0.20 g/L in CCC and 0.15 g/L in preparative HPLC), the enrichment in Y is higher with CCC than with preparative HPLC. Indeed, starting from a crude extract at 7% in Y with CCC or from a 25% in Y extract with preparative HPLC leads to the same 95% highest purity. These results demonstrate the interest of CCC in directly purifying crude extracts. Moreover, no preliminary purification of the extract is required, contrary to preparative HPLC, which requires a 1-day enrichment of the crude extract from 7% to 25% in Y.

Table 1 Comparison of CCC and HPLC Performance

	CCC	HPLC
Crude extract purity in Y (%)	7	25
Injected quantity of Y (g)	0.28	1.59
Experimental duration (h)	6.2	2.2 ^a
Solvent volume consumption (L)	1.4	10.8
Purity of the purest fraction in Y	>95%	>95%
Hourly yield (g/h)	0.035	0.72
Volumic yield (g/L)	0.20	0.15

^aOne hour for the column equilibration at the 90 mL/min flow rate + 1 h for the separation.

Examples of Purification

Sporaviridins Separation [7]

Chemical structures of sporaviridins are described in Fig. 1. They are only soluble in polar solvents such as water, methanol, and *n*-butanol. Therefore, a two-phase solvent system containing *n*-butanol was examined. A nonpolar solvent such as diethyl ether has been added to the *n*-butanol–water system to decrease the solubility of molecules in *n*-butanol and to obtain partition coefficients close to 1. The partition coefficients, *K*, are defined as the ratio of the solute concentration in the upper phase (butanol rich) to its concentration in the lower one (water rich). A two-phase solvent system of *n*-butanol–diethyl ether–water (10:4:12, v/v/v) was selected because it allows one to obtain the almost equally dispersed partition coefficients among six components (C2, B2, A2, C1, B1, A1). The preparative separation of six components from sporaviridin complex by HSCCC was performed in 3.5 h (500 mL of elution volume). The six components were eluted in the order of their partition coefficients, yielding pure components A1 (1.4 mg), A2 (0.6 mg), B1 (0.7 mg), B2 (0.5 mg), C1 (1.1 mg), and C2 (1.4 mg) from 15 mg of the sporaviridin complex.

Ivermectins Separation [8]

These molecules have an intermediary polarity (Fig. 2a). A two-phase solvent system, composed of *n*-hexane, ethyl acetate, methanol, and water, has been selected. In this case, the partition coefficients, *K*, are defined as the ratio of the solute concentration in the upper phase to its concentration in the lower one. A solvent mixture of *n*-hexane–ethyl acetate–methanol–water (19:1:10:10, v/v/v/v) yielded the best *K* values from 0–2.83. 25 mg of crude ivermectin separated in 4.0 h. This separation yielded 18.7 mg of 99.0% pure ivermectin B1a, 1.0 mg of 96.0% pure ivermectin B1b, and 0.3 mg of 98.0% pure avermectin B1a.

Bryostatins Separation [4]

By extraction from 1000 kg of *Bugula neritina* 906.5 g of lymphocytic leukemia cell line active fraction was obtained. Further purification was performed with HSCCC. Bryostatins have intermediate polarity, so that *n*-hexane–ethyl acetate–methanol–water (3:7:5:5, v/v/v/v) was employed with the upper layer as the mobile phase and the lower layer as the stationary phase. By this technique, from 300 mg to 3 mg of seven bryostatins have been isolated, including a new molecule called bryostatin 14 (Fig. 2b).

Bacitracins Separation [9]

The bacitracin complex (Fig. 3) was purified by foam CCC. The column design for foam CCC consists of a Teflon tube. Simultaneous introduction of N₂ and the liquid phase through the respective flow tube produces a countercurrent between the gas and the liquid phase through the coil. The sample mixture injected through the middle portion of the column is separated according to the foaming capability: The foam-active components travel through the coil with the gas phase and elute through the foam collection line, whereas the rest of components move with the liquid phase and elute through the liquid collection line.

After the experiment, fractions from the foam and liquid outlets are collected and analyzed. The elution curve of bacitracin components from the foam outlet shows three major peaks, and the one from the liquid outlet. The HPLC analysis of fractions clearly indicate that the bacitracin components are separated in the order of hydrophobicity of the molecule in the foam fractions and in increasing order of their hydrophilicity in the liquid fractions.

References

1. H. Oka, K.-I. Harada, Y. Ito, and Y. Ito, *J. Chromatogr.* 812: 35–52 (1998).
2. K. Hostettman, C. Appolonia, B. Domon, and M. Hostettmann, *J. Liquid Chromatogr.* 7: 231–242 (1984).
3. G. M. Brill, J. B. McAlpine, and J. E. Hochlowski, *J. Liquid Chromatogr.* 8(12): 2259–2280 (1985).
4. G. R. Pettit, F. Gao, D. Sengupta, J. C. Coll, C. L. Herald, D. L. Doubek, J. M. Schimdt, J. R. Van Camp, J. Rudloe, and R. A. Nieman, *Tetrahedron* 47(22): 3601–3610 (1991).
5. F. Oka, H. Oka, and Y. Ito, *J. Chromatogr.* 538: 99–108 (1991).
6. M.-C. Menet and D. Thiébaud, *J. Chromatogr.* 831: 203–216 (1999).
7. K.-I. Harada, I. Kimura, A. Yoshikawa, M. Suzuki, H. Nakazawa, S. Hattori, and Y. Ito, *J. Liquid Chromatogr.* 13: 2373–2388 (1990).
8. H. Oka, Y. Ikai, J. Hayakawa, K.-I. Harada, M. Suzuki, A. Shimizu, T. Hayashi, K. Takeba, H. Nakazawa, and Y. Ito, *J. Chromatogr.* 723: 61–68 (1996).
9. H. Oka, K.-I. Harada, M. Suzuki, N. Nakazawa, and Y. Ito, *J. Chromatogr.* 482: 197–205 (1989).



Separation of Chiral Compounds by CE and MEKC with Cyclodextrins

Bezhan Chankvetadze

Tbilisi State University, Tbilisi, Georgia

Introduction

Cyclodextrins (CD) and their derivatives represent a unique group of chiral selectors which can be used for enantioseparations in almost all instrumental separation techniques, such as gas chromatography (GC), high-performance liquid chromatography (HPLC), super/subcritical fluid chromatography (SFC), and capillary electrophoresis (CE). CDs are nonreducing, cyclic oligosaccharides produced enzymatically from starch. The most widely applied native α -, β -, and γ -CD are constructed from six, seven, and eight glucose units bonded through 1,4- α -linkages. The inner cavity of the CD, which is lined with hydrogen atoms and glycosidic oxygen bridges, is hydrophobic, which favors hydrophobic interactions between a guest and the CD host. The outer CD rims are formed by the secondary 2- and 3- and the primary 6-hydroxyl groups. The location of the polar hydroxyl groups on the outer rim determines the solubility of the CDs in aqueous solutions. The hydrogen-bonding between the secondary C(2) and C(3) hydroxyl groups of adjacent D-glucopyranosyl residues stabilizes the shape and structure of the CD macrocycle.

Discussion

The ability of CDs to form intermolecular complexes with other molecules was already known in the early twentieth century. Another important property of CDs is that each glucose molecule in this macrocycle contains five chiral carbon atoms, which results in a chiral recognition ability in complex formation. This property of CDs was first evidenced by Cramer [1]. The relative easy availability from regenerable natural sources, the existence in various sizes, the stable structure, the localized hydrophobic area, the solubility in the hydrophilic solvents, the ability of intermolecular complex formation and the chiral recognition ability together with their nontoxicity, ultraviolet (UV) transparency, feasibility of their modification, and so forth contributed greatly to the establishment of CDs as a

major chiral selectors in CE and CD-modified MEKC separations of enantiomers.

The first applications of CDs as chiral selectors in CE were reported in capillary isotachopheresis (CITP) [2] and capillary gel electrophoresis (CGE) [3]. Soon thereafter, Fanali described the application of CDs as chiral selectors in free-solution CE [4] and Terabe used the charged CD derivative for enantioseparations in the capillary electrokinetic chromatography (CEKC) mode [5]. It seems important to note that although the experiment in the CITP, CGE, CE, and CEKC is different, the enantiomers in all of these techniques are resolved based on the same (chromatographic) principle, which is a stereoselective distribution of enantiomers between two (pseudo) phases with different mobilities. Thus, enantioseparations in CE are commonly based on an electrophoretic migration principle and on a chromatographic separation principle [6].

Chiral separations in CE are characterized by some peculiarities compared to true electrophoretic separations based on the different charge-to-mass (size) ratios of analytes. These peculiarities need to be realized when looking at the differences between enantioseparations using charged and neutral chiral selectors, between CZE and MEKC separations, for the evaluation of the role of the electro-osmotic force (EOF) in chiral CE separations, and so forth.

The separation of enantiomers in CE means that they reach a detection window in a different period of time after their simultaneous injection at the capillary inlet. Thus, the enantiomers must migrate with a different velocity along the longitudinal axis of a separation capillary. For a species possessing a different charge-to-mass (size) ratio, this occurs automatically after the application of a voltage gradient at the ends of the separation capillary. However, enantiomers do not differ from each other in terms of their effective charge-to-mass ratio in achiral medium. Therefore, in order to achieve enantioseparations, additional chiral substances are required that are able to transform an achiral medium into a chiral one. These chiral substances are called chiral selectors. A chiral selector will



interact with enantiomers of an analyte stereoselectively and this secondary equilibrium can generate a mobility difference between enantiomers ($\Delta\mu$) that can be calculated according to the equation [7]:

$$\Delta\mu = \frac{\mu_f + \mu_{C,R}K_R[C]}{1 + K_R[C]} - \frac{\mu_f + \mu_{C,S}K_S[C]}{1 + K_S[C]} \quad (1)$$

where μ_f is the mobility of the free enantiomers and $\mu_{C,R}$ and $\mu_{C,S}$ are the mobilities of complexed *R* and *S* enantiomers. K_R and K_S are the binding constants between the chiral selector and the *R* and *S* enantiomers, and $[C]$ is the concentration of a chiral selector.

Analyzing Eq. (1), one realizes that when $\mu_{C,R} \neq \mu_{C,S}$, the requirement $K_R \neq K_S$ is not necessary for obtaining $\Delta\mu \neq 0$. This means that in CE, a chiral recognition in the classical meaning of this definition ($K_R \neq K_S$) is not always necessary for a chiral separation. This is theoretically feasible but has not been undoubtedly evidenced yet experimentally. More common is the case when $\mu_{C,R} = \mu_{C,S}$ and then $K_R \neq K_S$ is the necessary requirement for enantioseparation. A combined contribution of both a stereoselective binding of the enantiomers to a chiral selector ($K_R \neq K_S$) and a mobility difference between the transient diastereomeric complexes ($\mu_{C,R} \neq \mu_{C,S}$) is also possible.

In the case when $\mu_{C,R} = \mu_{C,S}$ (the most common case), Eq. (1) can be simplified as follows [7]:

$$\Delta\mu = \frac{C(\mu_f - \mu_c)(K_R - K_S)}{1 + C[K_R + K_S] + C^2K_RK_S} \quad (2)$$

This simplified equation allows one to calculate the optimal concentration of a chiral selector [7], a better design of chiral separation systems containing multiple chiral selectors [6], and the design of the enantiomer migration order [6,8] and indicates why micellar additives are sometimes required in chiral CE with CDs.

As shown in Eq. (2) together with the chiral recognition ($K_R \neq K_S$), the other necessary requirement for enantioseparations in CE is a mobility difference between the free and the complexed analyte ($\mu_f - \mu_c \neq 0$). Otherwise, it will be impossible to transfer a chiral recognition into a chiral separation. This requirement does not hold when neutral analytes are analyzed with neutral chiral selectors. In such a case, an additional buffer component is required that will assist in generating a difference between the mobilities of an analyte in its free and complexed forms with a chiral selector. This is achieved by an achiral micellar phase in cyclodextrin-modified micellar electrokinetic chromatography (CD-MEKC) [9]. However, a charged CD or a chiral micellar phase can combine the

above-mentioned functions of both a neutral CD and a micellar phase [5,6,8,10–12].

The EOF contributes significantly to the mobility of analytes in CE. The EOF is considered to be a nonselective mobility. However, for enantiomers, both the EOF and the electrophoretic mobility of the analyte are inherently nonenantioselective. The stereoselective analyte-selector interactions may turn both of these mobilities into a selective transport with equal success. This is the principal difference between the roles of the EOF in true electrophoretic separations and in chiral CE separations.

The principal mechanism of enantioseparations is a stereoselective interaction of enantiomers with CDs, which is the same in CE and MEKC as well as in CIP, CGE, and even in capillary isoelectric focusing (CIEF). One of the significant advantages of chiral CE compared to other instrumental enantioseparation techniques together with the extremely high peak efficiency, miniaturized size, low costs, less environmental problems, and so forth [8] is the high flexibility. The separation in different modes can be performed using the same instrumental setup and it takes just a few minutes to change from one chiral selector to another one, to combine two or more chiral selectors, to vary the concentration of a chiral selector, and so forth. All of these variations are very difficult and time-consuming in a chromatographic system.

There are much more variables that can be applied for the optimization of a separation in CE than in a pressure-driven system. These include the type and concentration of a chiral selector, the pH of the background electrolyte, the concentration and type of the buffer, the achiral buffer additives, the capillary dimensions and the nature of the inner surface, the EOF, the temperature, and so forth.

Cyclodextrins are commercially available in various sizes (α , β , γ), carrying different functionalities, charge, and so forth. At present, β -CD and its neutral and ionic derivatives are considered to be the most suitable chiral selectors in CE. However, α - and γ -CD sometimes offer a complementary chiral separation ability [8]. Among the native CDs, β -CD is characterized by the lowest solubility in aqueous solutions. Therefore, the neutral derivatives carrying alkyl and hydroxyalkyl substituents which possess a higher solubility in aqueous buffers and sometimes offer complementary chiral recognition properties are widely used as chiral selectors in CE. Among the neutral CD derivatives, single-component heptakis-(2,6-di-*O*-methyl)- β -CD and heptakis-(2,3,6-tri-*O*-methyl)- β -CD represent special interests. The latter exhibits the opposite

binding affinity toward many chiral compounds compared to native β -CD. Elucidation of the molecular mechanisms of this phenomenon can contribute markedly to a better understanding of the nature of the forces determining the binding and chiral recognition properties of CDs.

Ionic derivatives of CDs represent another group of effective chiral selectors in CE [5,6,8,10–12]. They offer the following advantages for enantioseparations: (a) enhanced solubility in the aqueous buffers; (b) self-electrophoretic mobility enabling their application also for enantioseparations of uncharged chiral compounds; (c) additional groups for more effective intermolecular interactions; (d) use as chiral carriers; (e) higher separation power toward oppositely charged enantiomers which are not only due to more tight interactions but also to the countercurrent mobility of an analyte and a selector; (f) easier on-line coupling of chiral CE with mass spectrometry (MS), nuclear magnetic resonance (NMR), and so forth [8].

Charged CD derivatives are commercially available with cationic or anionic groups. Among cationic CDs, randomly substituted 2-hydroxypropyltrimethylammonium salts of β -CD and 6-monoamino-6-deoxy- β -CD have been intensively studied [6,8,10]. Cationic CD derivatives tend to be adsorbed to the negatively charged inner surface of a fused-silica capillary and revert the direction of the EOF from the cathode to the anode. Therefore, these derivatives need to be used with capillaries having neutral or positive inner-wall coatings. CD derivatives with positively charged amino, alkylamino, and ammonium groups in a desired position can be synthesized relatively easily from a native CD. In spite of this, there are just two of these derivatives commercially available at present. This seems to be the reason for their incomplete evaluation as chiral selectors in CE [5,6,8,10].

Among anionic CDs, randomly substituted carboxyalkyl, sulfoalkyl, and sulfate derivatives are commercially available and play an important role in the development of chiral CE [6,8,10–12]. However, all randomly substituted neutral and charged derivatives of CDs suffer from the disadvantage to be a multicomponent mixture. The individual components of these mixtures may exhibit markedly different chiral-resolving properties. In rare cases, even the opposite migration order of the enantiomers has been reported depending on the degree of substitution of a charged CD [6]. Thus, it is extremely difficult to optimize and validate a chiral CE separation using randomly substituted derivatives of CD. Recently, Vigh and co-workers developed single-isomer CD polysulfates which are

currently commercially available [10]. These derivatives represent a significant interest not only for the development of reproducible, validated methods in chiral CE but also for mechanistic studies.

One important advantage of charged CD derivatives is their use as chiral carriers [5,6,8,10–12]. This enables one to mobilize a neutral analyte even in the absence of the EOF, a charged analyte in the opposite direction to its electrophoretic mobility, and to suppress a mobility of an analyte in the uncomplexed form. The last offers a significant advantage for the improvement of a separation selectivity.

Two unique advantages of chiral CE, using the selector in a double function for the enantioseparation and transport of the resolved enantiomers to the detector as well as the feasibility of a combination of two chiral selectors, are illustrated in Fig. 1. The chiral compounds are the well-known former sedative drug thalidomide (TD) and its hydroxylated metabolites recently observed in human blood plasma and liver. The drug had been withdrawn from clinical practice several decades ago due to severe toxic effects probably residing in one enantiomer, but it has been reapproved again by Food and Drug Administration in 1998 as a result of its recently discovered antileprosy, anti-HIV (human immunodeficiency virus), anti-inflammatory, and antireumatoid activity. The compounds are uncharged and, therefore, lack an electrophoretic mobility. This makes a separation difficult. In the separation system described in Fig. 1, the analytes are stereoselectively accelerated with one of the CDs (sulfobutyl- β -CD) and also stereoselectively decelerated with another CD (β -CD). In combination with an easy variation of the CD concentration, this allows one to adjust simultaneous baseline separations and enantioseparations of all components. This example also illustrates the application of chiral CE separations for solving of practical biomedical problems. This seems to be one of the major application areas of chiral CE [8,12].

Together with the high application potential of chiral CE, due to the high separation efficiency and versatility, this technique allows to study very fine nuances of binding and chiral recognition mechanisms by CDs.

Thus, native CDs and their derivatives are definitely established as a major group of chiral selectors in CE, CEKC, and MEKC. Perhaps, in the near future, the main emphasis will be directed to the use of a well-characterized, single isomer native and derivatized (neutral and charged) CDs as chiral selectors and to the use of chiral CE for solving problems in chemical, agrochemical, food, environmental, and, mainly, in



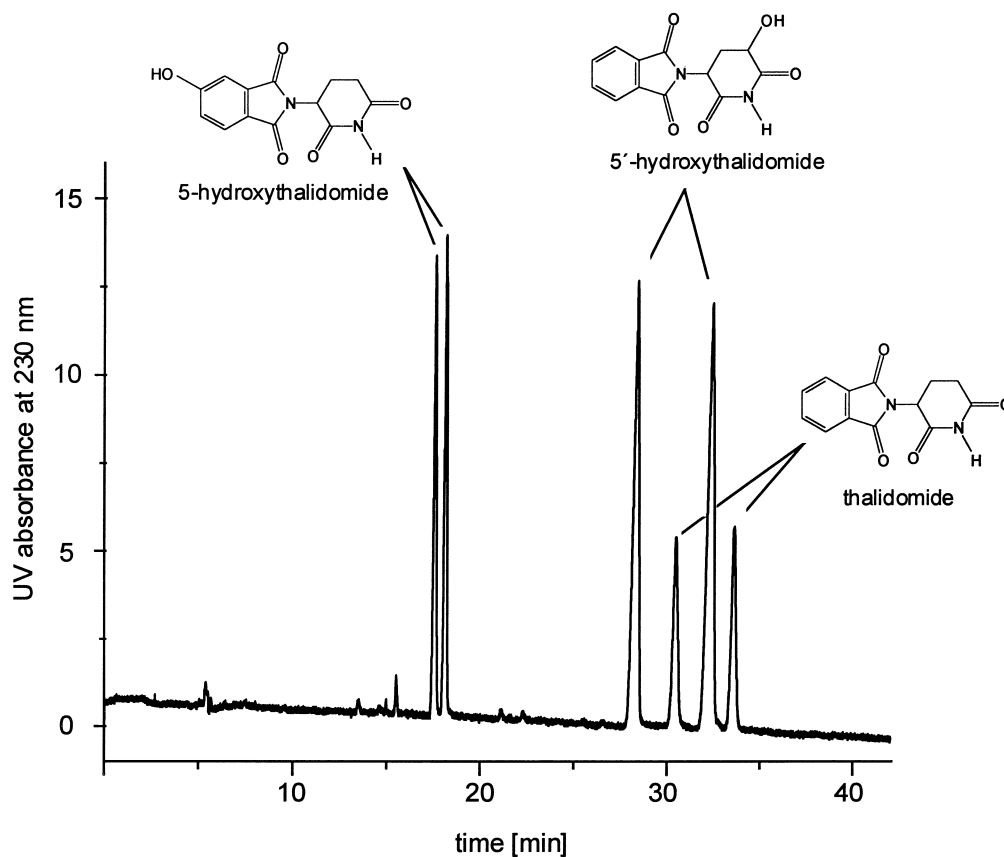


Fig. 1 Simultaneous separation and enantioseparation of thalidomide, 5-hydroxythalidomide, and 5'-hydroxythalidomide in CE using polyacrylamide-coated capillary and a mixture of 15 mg/mL sulfobutyl (4.0)- β -CD and 10 mg/mL β -CD as the chiral carrier.

biomedical fields. Mechanistic studies for a better understanding of the nature of intermolecular interactions governing the binding and chiral recognition properties of CDs seems to be an interesting topic also.

References

1. F. Cramer, *Angew. Chem.* 64: 136 (1952).
2. J. Snopek, I. Jelinek, and E. Smolkova-Keulemansova, *J. Chromatogr.* 438: 211–218 (1988).
3. A. Guttman, A. Paulus, A. S. Cohen, N. Grinberg, and B. L. Karger, *J. Chromatogr.* 448: 41–53 (1988).
4. S. Fanali, *J. Chromatogr.* 474: 441–446 (1989).
5. S. Terabe, *Trends Anal. Chem.* 8: 129–134 (1989).
6. B. Chankvetadze, *J. Chromatogr. A* 792: 269–295 (1997).
7. S. A. C. Wren and R. C. Rowe, *J. Chromatogr.* 603: 235–241 (1992).
8. B. Chankvetadze, *Capillary Electrophoresis in Chiral Analysis*, John Wiley & Sons, Chichester, 1997.
9. S. Terabe, Y. Miyashita, O. Shibata, E. R. Barnhart, L. R. Alexander, D. G. Patterson, B. L. Karger, K. Hosoya, and N. Tanaka, *J. Chromatogr.* 516: 23–31 (1990).
10. Gy. Vigh and A. D. Sokolowski, *Electrophoresis* 18: 2331–2342 (1997).
11. A. M. Stalcup and K.-H. Gahm, *Anal. Chem.* 68: 1360–1368 (1996).
12. M. Fillet and P. Hubert, *J. Crommen. Electrophoresis* 19: 2834–2840 (1998).

Separation of Flavonoids by Countercurrent Chromatography

L. M. Yuan

Yunnan Normal University, Kunming, P.R. China

INTRODUCTION

Various countercurrent chromatography (CCC) methods employ two-phase solvent systems for separation of flavonoids. $\text{CHCl}_3\text{:CH}_3\text{OH:H}_2\text{O}$ (4: x :2, for which x is between 2.5 and 4 for different samples) may be used for their prefractionation. Two-phase solvent systems can be divided into four types: $\text{CHCl}_3\text{:CH}_3\text{OH:H}_2\text{O}$, $\text{CHCl}_3\text{:CH}_3\text{OH:}n\text{-BuOH:H}_2\text{O}$, $\text{EtOAc:PrOH:H}_2\text{O}$ or $\text{BuOH:HOAc:H}_2\text{O}$, and $n\text{-C}_6\text{H}_{14}\text{:EtOAc:CH}_3\text{OH:H}_2\text{O}$, respectively. CCC fractionation permits the use of either stepwise elution or gradient elution, and analytical-scale CCC can also be carried out for separation of flavonoids.

FLAVONOIDS

Flavonoids are polyphenolic compounds and have a wide polarity range. Successful CCC depends on the appropriate choice of a solvent system. The partition of solutes between two immiscible solvent phases is an ideal method for the separation of flavonoids because the phenomenon of irreversible adsorption, tailing, sample loss, and denaturation, which plague analysts using other forms of liquid chromatography, are avoided.

SEPARATION OF FLAVONOIDS BY CCC

Flavonoids are a specific class of polyphenols. It is generally believed that flavonoids include a wide variety of phenolic compounds, such as flavones, flavonols, flavanones, flavanonols, anthocyanidins, flavan-3,4-diols, xanthenes, flavan-3-ols, isoflavones, isoflavanones, chalcones, dihydrochalcones, aurones, and homoisoflavones. Their separation poses special problems because there is often irreversible adsorption and even hydrolysis on solid supports.

The development of CCC began in the mid-1960s. Among various types of CCC modes for the separation of flavonoids, the main techniques are droplet countercurrent chromatography (DCCC), rotary locular countercurrent chromatography (RLCCC), and centrifuge partition

chromatography (CPC). Today, the cartridge and multi-layer coil CPC methods are the leading techniques.

The selection of a solvent system is the most important step in performing CCC. Selecting a solvent system for CCC means *simultaneously* choosing the column and the eluent. The chromatographic literature contains numerous examples of solvent systems used in various CCC systems for separation of flavonoids,^[1–6] and consultation of these references may give some leads as to possible systems that would be useful for a particular separation. The selection of appropriate biphasic solvent systems also may be aided by thin-layer chromatography (TLC) or high-performance liquid chromatography (HPLC) experiments.

One quite remarkable comparative separation of flavonoids by DCCC, RLCC, and cartridge and multilayer coil CPC methods, with the same solvent system (chloroform–methanol–water, 33:40:27), is shown in Fig. 1.^[7,8]

Elutions of the three peaks were similar and according to the order of increasing polarity: hesperetin, kaempferol, quercetin. The above peak effect can be seen in the various CCC methods, which have similar two-phase solvent systems, for the separation of flavonoids, but DCCC and RLCC require much more time than CPC.

A versatile two-phase solvent system for flavonoid prefractionation by high-speed CCC was introduced.^[9] The flavonoid compounds encompass a wide polarity range and exhibit good solubility in methanol. The two-phase solvent system composed of $\text{CHCl}_3\text{:CH}_3\text{OH:H}_2\text{O}=4\text{:}x\text{:}2$, in which x was between 2.5 and 4 for different samples, was selected for the separation of crude flavonoid extracts because this solvent system contains methanol and provides nearly equal volumes of the upper and lower phases with reasonably short settling times. Changing the ratio of methanol in the solvent system permitted changing, simultaneously, the selectivity of the upper and lower phases, as methanol can dissolve in chloroform and water and may change the polarity of the two phases.

The previous applications of CCC are summarized in Table 1. One may use this table to search for suitable solvent systems that have been previously used for similar compounds.

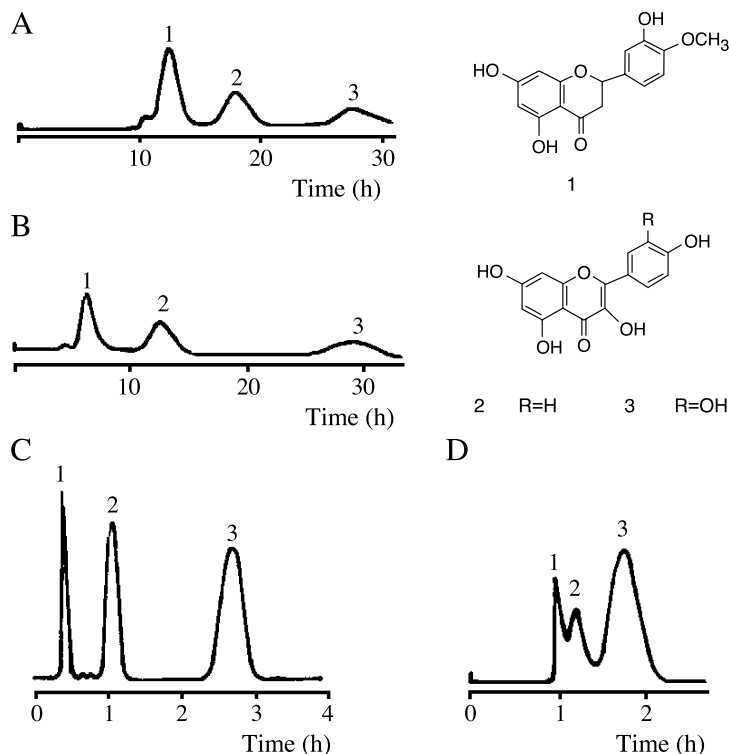


Fig. 1 Chromatograms of hesperetin (1), kaempferol (2), and quercetin (3) by different countercurrent chromatographic methods. Solvent system: chloroform–methanol–water (33:40:27). (A) DCCC; (B) RLCC; (C) multilayer coil CPC system; and (D) cartridge CPC system. (Elsevier Science Ireland, Ltd.)

In Table 1, the various two-phase solvent systems are divided into four types. It has been shown that the solvent system chloroform–methanol–water has been used for the greatest number of applications. $\text{CHCl}_3\text{:CH}_3\text{OH:H}_2\text{O}$ is a versatile CCC solvent system for flavonoid separations as well.

The second most used two-phase solvent system is $\text{CHCl}_3\text{:CH}_3\text{OH:}n\text{-BuOH}$ (*i*-PrOH or PrOH): H_2O . It is similar to $\text{CHCl}_3\text{:CH}_3\text{OH:H}_2\text{O}$, but CH_3OH is partially replaced by BuOH, *i*-PrOH, or PrOH. The desirable *K* value may be obtained by varying the ratios.

The third most used type of two-phase solvent system is EtOAc:PrOH (BuOH or EtOH): H_2O or BuOH:HOAc (or PrOH): H_2O . It is a more polar solvent system and is useful for the separation of flavonoid glycosides.

The final type of solvent system is $n\text{-C}_6\text{H}_{14}\text{:EtOAc:CH}_3\text{OH:H}_2\text{O}$. Sometimes CH_3OH also may be substituted by other solvents such as BuOH. It is a slightly more hydrophobic solvent system than $\text{CHCl}_3\text{:CH}_3\text{OH:H}_2\text{O}$.

Analogous to HPLC, CCC fractionation permits the use of either stepwise elution or gradient elution, provided that some precautions are taken. For example, in the isolation of extracts of *Ginkgo biloba*, one starts with water as a stationary phase, eluting with ethyl acetate with

increasing amounts of *i*-butanol and finally reaching the 6:4 proportion of ethyl acetate:*i*-butanol at the end of the elution.^[10]

Samples ranging in size from microgram to gram quantities can be separated with the range of available instruments. Analytical-scale CCC also was carried out for the separation of flavonoids.^[11]

CONCLUSION

The application of CCC to the separation of flavonoids has been proven to be very successful. Chloroform–methanol–water can be chosen as starting point and, by modifying the relative proportions of methanol or by replacing methanol with other solvents, it is possible finally to obtain the required distribution of sample components between the two phases. $\text{EtOAc:PrOH:H}_2\text{O}$ and $n\text{-C}_6\text{H}_{14}\text{:EtOAc:CH}_3\text{OH:H}_2\text{O}$ also are very useful solvent systems. The technique is versatile and can be employed for the initial fractionation of crude extracts for the separation of closely related flavonoids and/or the isolation of pure products.



Table 1 Separations of flavonoids by CCC

Sample	Solvent system
Flavonoids	CHCl ₃ :CH ₃ OH:H ₂ O, 4:3:2 CHCl ₃ :CH ₃ OH:H ₂ O, 7:13:8 CHCl ₃ :CH ₃ OH:H ₂ O, 33:40:27 CHCl ₃ :CH ₃ OH:H ₂ O, 5:6:4
Flavonol glycosides	CHCl ₃ :CH ₃ OH:H ₂ O, 7:13:8
Isoflavonol glycosides	CHCl ₃ :CH ₃ OH:H ₂ O, 7:13:8
<i>Baccharis trimera</i>	CHCl ₃ :CH ₃ OH:H ₂ O, 13:7:4
<i>Orthosiphon spicatus</i>	CHCl ₃ :CH ₃ OH:H ₂ O, 13:7:4
<i>Epilobium parviflorum</i>	CHCl ₃ :CH ₃ OH:H ₂ O, 7:13:8
Licorice	CHCl ₃ :CH ₃ OH:H ₂ O, 7:13:8
Sea buckthorn	CHCl ₃ :CH ₃ OH:H ₂ O, 4:3:2
<i>Daphne genkwa</i> sieb et zucc	CHCl ₃ :CH ₃ OH:H ₂ O, 4:3:2
<i>Strychnos variabilis</i>	CHCl ₃ :CH ₃ OH:H ₂ O, 5:6:4
<i>Pericarpium citri</i> reticulata	CHCl ₃ :CH ₃ OH:H ₂ O, 4:4:2
<i>Radix puerariae</i>	CHCl ₃ :CH ₃ OH:H ₂ O, 4:2.9:2
<i>Radix glycyrrhizae</i>	CHCl ₃ :CH ₃ OH:H ₂ O, 4:4:2
<i>Radix scutellariae</i>	CHCl ₃ :CH ₃ OH:H ₂ O, 4:3.8:2
<i>Flos genkwa</i>	CHCl ₃ :CH ₃ OH:H ₂ O, 4:3.6:2
Flavonoids	CHCl ₃ :CH ₃ OH:5% HCl, 5:5:3
Flavonoid glycosides	CHCl ₃ :CH ₃ OH: <i>n</i> -BuOH:H ₂ O, 10:10:1:6
Flavonol glycosides	CHCl ₃ :CH ₃ OH: <i>n</i> -BuOH:H ₂ O, 7:6:3:4 CHCl ₃ :CH ₃ OH: <i>n</i> -BuOH:H ₂ O, 10:10:1:6 CHCl ₃ :CH ₃ OH: <i>n</i> -BuOH:H ₂ O, 10:10:2:6
<i>Galipea trifoliata</i>	CHCl ₃ :CH ₃ OH: <i>n</i> -BuOH:H ₂ O, 10:10:1:6
<i>Arnica</i> species	CHCl ₃ :CH ₃ OH: <i>n</i> -BuOH:H ₂ O, 10:10:1:6
Flavonol glycosides	CHCl ₃ :CH ₃ OH: <i>i</i> -PrOH:H ₂ O, 5:6:1:4
<i>Bidens pilosa</i>	CHCl ₃ :CH ₃ OH: <i>i</i> -PrOH:H ₂ O, 5:6:1:4
<i>Picea abies</i>	CHCl ₃ :CH ₃ OH: <i>i</i> -PrOH:H ₂ O, 5:6:1:4
<i>Alangium premnifolium</i>	CHCl ₃ :CH ₃ OH: <i>i</i> -PrOH:H ₂ O, 9:12:2:8
<i>G. biloba</i>	CHCl ₃ :CH ₃ OH:PrOH:H ₂ O, 5:6:1:4
<i>Vaccinium uliginosum</i>	CHCl ₃ :CH ₃ OH:PrOH:5% HOAc, 31.2:37.5:6.25:25
<i>Oxytropis ochrocephala</i>	CHCl ₃ :CH ₃ OH:EtOH:H ₂ O, 2:5:8:5
<i>Tephrosia vogelii</i>	CHCl ₃ :CH ₃ OH:EtOH:H ₂ O, 7:3:3:4
Flavonoid glycosides	EtOA:PrOH:H ₂ O, 4:2:7
<i>Arnica montana</i>	EtOA:PrOH:H ₂ O, 4:2:7
<i>Stryphnodendron adstringens</i>	EtOA:PrOH:H ₂ O, 35:2:2
Anthocyanidins	EtOA:PrOH:H ₂ O, 140:8:80
Flavonoid glycosides	EtOA:BuOH:H ₂ O, 2:1:2
<i>Crossopteryx febrifuga</i>	EtOA:BuOH:H ₂ O, 2:1:2 EtOA:EtOH:H ₂ O, 2:1:2 EtOA:94% EtOH:H ₂ O, 2:1:2
<i>Tephrosia vogelii</i>	BuOH:HOAc:H ₂ O, 4:1:5
Flavonoid glycosides	BuOH:HOAc:H ₂ O, 4:1:5
Anthocyanidins glycosides	BuOH:HOAc:H ₂ O, 4:1:5
<i>Sambucus nigra</i>	BuOH:HOAc:H ₂ O, 4:1:5
<i>Pavetta owariensis</i>	BuOH:PrOH:H ₂ O, 4:1:5
<i>Arnica</i> species	CH ₂ Cl ₂ :PrOH:H ₂ O, 7:13:8
Biflavonoids	<i>n</i> -C ₆ H ₁₄ :EtOAc:CH ₃ OH:H ₂ O, 2:8:5:5
<i>Brackenridgea zanguebarica</i> anthocyanidins	<i>n</i> -C ₆ H ₁₄ :EtOAc:CH ₃ OH:H ₂ O, 8:8:6:6 <i>n</i> -C ₆ H ₁₄ :EtOAc:CH ₃ OH:H ₂ O, 8:6:7:10 <i>n</i> -C ₆ H ₁₄ :EtOAc:BuOH:HAc:1% HCl, 2:1:3:1:5
Gradient elution	
<i>G. biloba</i>	EtOAc→EtOAc- <i>i</i> -BuOH, 6:4
<i>Esenbeckia pumila</i>	Et ₂ O→EtOAc-PrOH-H ₂ O (10:1:2)→EtOAc-PrOH-H ₂ O (4:1:2)



ACKNOWLEDGMENTS

This work is supported by the National Natural Science Foundation, Yunnan Province Natural Science Foundation, and TRAPOYT of China.

REFERENCES

1. Ito, Y. High-speed countercurrent chromatography. *Crit. Rev. Anal. Chem.* **1986**, *17*, 65–143.
2. Marston, A.; Slacanin, I.; Hostettmann, K. Centrifugal partition chromatography in the separation of natural products. *Phytochem. Anal.* **1990**, *1*, 3–17.
3. Marston, A.; Hostettmann, K. Counter-current chromatography as a preparative tool—Applications and perspectives. *J. Chromatogr., A* **1994**, *658*, 315–341.
4. Yuan, L.M.; Fu, R.N.; Zhang, T.Y. Separation of bioactive components from medicinal plants by high-speed counter-current chromatography. *Chin. J. Med. Anal.* **1998**, *18* (1), 60–64.
5. Hostettmann, K.; Hostettmann, M.; Marston, A. Counter-current chromatography. In *Preparative Chromatography Techniques*; Springer-Verlag: Berlin, 1986; 80–126.
6. Ito, Y.; Conway, W.D. High-Speed Countercurrent Chromatography of Natural Products. In *High-Speed Countercurrent Chromatography*; Wiley-Interscience: New York, 1996; 189–251.
7. Slacanin, I.; Marston, A.; Hostettmann, K. Modifications to a high-speed counter-current chromatograph for improved separation capability. *J. Chromatogr.* **1989**, *482*, 234–239.
8. Marston, A.; Borel, C.; Hostettmann, K. Separation of natural products by centrifugal partition chromatography. *J. Chromatogr.* **1988**, *450*, 91–99.
9. Yuan, L.M.; Ai, P.; Chen, X.X.; Zi, M.; Wu, P.; Li, Z.Y.; Chen, Y.G. Versatile two-phase solvent system for flavonoid prefractionation by high-speed countercurrent chromatography. *J. Liq. Chromatogr. Relat. Technol.* **2002**, *25* (5), 10.
10. Vonhaelen, M.; Vanhaelen-Fastre, R. Counter-current chromatography for isolation of flavonol glycosides from *Ginkgo biloba* leaves. *J. Liq. Chromatogr.* **1988**, *11*, 2969–2975.
11. Zhang, T.Y.; Xiao, R.; Xiao, Z.Y.; Pannell, L.K.; Ito, Y. Rapid separation of flavonoids by analytical high-speed counter-current chromatography. *J. Chromatogr.* **1988**, *445*, 199–206.



Separation of Metal Ions by Centrifugal Partition Chromatography

S. Muralidharan

Western Michigan University, Kalamazoo, Michigan, U.S.A.

Introduction

Centrifugal partition chromatography (CPC), a multi-stage countercurrent liquid–liquid distribution technique employing discrete stages and two immiscible bulk liquid phases, is ideally suited for the detailed examination through separation factors and efficiencies, the influence of bulk aqueous and liquid–liquid interfacial equilibria and kinetics, on the separations of metal ions. This has been demonstrated by separations of transition metals, platinum group metals, and trivalent lanthanides; the significant findings are as follows: (a) Separation efficiencies are mainly limited by back-extraction kinetics which occur in the bulk aqueous phase and at the organic–aqueous interface as indicated by a direct linear correlation between the half-lives ($t_{1/2}$) of the dissociation reactions and the reduced plate height. (b) The interfacial areas calculated through this correlation are much larger in many cases than those generated in highly stirred two-phase mixtures. (c) The addition of surfactants and interfacial catalysis of the formation and dissociation of the complexes dramatically improve efficiencies. Examples of the separation of platinum group metal and trivalent lanthanides and the kinetic information that can be derived from their chromatograms are discussed.

Centrifugal Partition Chromatography

The CPC apparatus, manufactured by Sanki Engineering Company, Japan [1], consists of a series of cartridges, with each cartridge containing 40–400 channels, depending on the desired internal volume. These channels serve as stages in the separation experiment and the total number of channels is sometimes 400–4800, depending on the number of cartridges employed. The cartridges are arranged in a rotor which is rotated at 700–1200 rpm and the centrifugal force generated keeps one of the two phases (usually the organic phase) stationary while the other phase (usually the aqueous phase) is moved through it at a constant flow rate. The injected analyte mixture is carried by the aqueous mobile phase into the cartridges where they are extracted into the organic

stationary phase by simple distribution if they are organic or by complexation with a suitable ligand if they are metals. When the mobile phase is depleted of the analytes, further flow of the mobile phase of the same (isocratic elution) or different (gradient elution) composition causes the back-extraction of the analytes, which can be detected by a suitable method. If the analytes are completely separated, they appear as discrete peaks similar to conventional chromatographic methods such as high-performance liquid chromatography (HPLC), and, hence, it is called centrifugal partition chromatography. CPC has these unique features: a large number of discrete stages (400–4800 depending on the operational volume chosen); high loading capacity for extractants and analytes; negligible loss of stationary phase due to “bleeding”; flexible organic–aqueous phase volume ratios; high stationary phase to mobile phase ratio; and ready adaptability to the process scale.

The basic parameters employed in the analysis of the CPC chromatograms are the retention volume V_r , which is related to the stationary phase and mobile phase volumes V_s and V_m , respectively, and the distribution ratio of the analyte D [Eq. (1)], the chromatographic efficiency, as measured by the number of theoretical plates N , which is calculated from the retention volume V_r and the width of the chromatogram w , [Eq. (2)], the chromatographic inefficiency represented by the channel equivalent of a theoretical plate (CETP), which is analogous to reduced plate height and is the ratio of the number of channels (CH) (2400 in our experiments) to N [Eq. (3)], and the selectivity I achieved in the separation of two analytes (1 and 2), which is the ratio of their distribution ratios D_1 and D_2 [Eq. (4) [2]:

$$V_r = V_m + DV_s \quad (1)$$

$$N = 16 \left(\frac{V_r}{w} \right)^2 \quad (2)$$

$$\text{CETP}_{\text{obs}} = \frac{\text{CH}}{N} \quad (3)$$

$$\alpha = \frac{D_2}{D_1} \quad (D_2 > D_1) \quad (4)$$



Separation of Platinum Group Metals

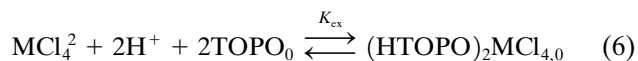
Separation, extraction, and purification of the platinum group metals (PGM) Pt, Pd, Ir, and Rh in their various oxidation states continues to be challenging and represent interesting areas of research. The separation of PGM from chloride media by solvent extraction can be achieved either by complexation with a suitable ligand or through ion-pair formation with a large cation. Complexation with a ligand is more selective but generally suffers from slow complex formation and dissociation kinetics. By contrast, ion-pair formation is diffusion controlled and not very selective, but it is necessary to separate kinetically inert species such as PtCl_6^{2-} and IrCl_6^{2-} .

Triethylphosphine oxide (TOPO) is an organophosphorus compound and is a stable and inexpensive extractant. TOPO, as we have shown [3–5], is unique in that it can function as a monodentate ligand and as a cation for ion-pair extraction when protonated and the extraction equilibrium for the neutral ligand is shown in Eq. (5), indicating the extraction of the neutral complex $\text{MCl}_2(\text{TOPO})_2$ [$\text{M} = \text{Pd(II)}, \text{Pt(II)}$; $n = 2-4$]:



The K_{ex} values for PdCl_2 , PdCl_3^- and PdCl_4^{2-} are 794.3 M^{-2} , 2.75 M^{-1} , and 0.14 respectively. A single peak was observed in the CPC chromatogram of Pd(II) at any concentration of Cl^- , as its hydrolytic equilibria are rapid. The corresponding values for the three Pt(II) chloro species are 48 M^{-2} , 0.047 M^{-1} and 0.018 , clearly indicating the better extractability of Pd(II) over Pt(II) . The difference in the K_{ex} values for the MCl_4^{2-} species can be exploited to obtain an efficient separation of Pt(II) and Pd(II) from Rh(III) and Ir(III) .

Formation of HTOPO^+ , at HCl concentrations of 0.1 M , resulted in the extraction of $(\text{HTOPO})_2\text{MCl}_4$ ($\text{M} = \text{Pt}$ or Pd):



The chromatogram of the separation of RhCl_6^{3-} , PdCl_4^{2-} , and PtCl_4^{2-} by HTOPO^+ is shown in Fig. 1. The K_{ex} values of Pd(II) and Pt(II) are 93.3 M^{-4} and 1961 M^{-4} , respectively, indicating that Pd(II) elutes ahead of Pt(II) in the ion-pair separation, whereas the opposite is true in the separation by complexation. While the chromatogram of Pt(II) involves only the formation of $(\text{HTOPO})_2\text{PtCl}_4$, the chromatogram of Pd(II)

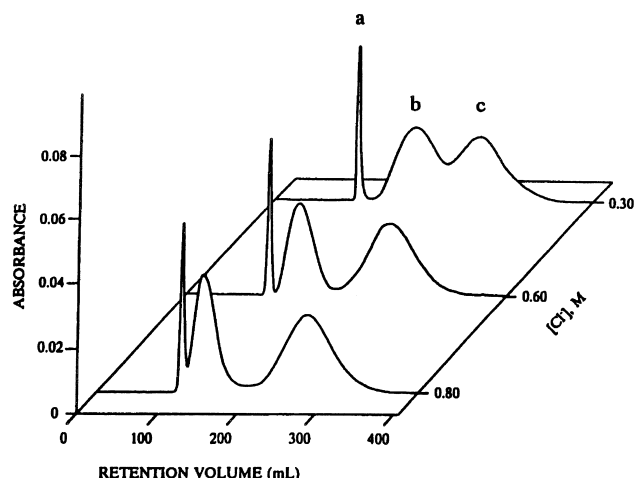


Fig. 1 Separation of $10^{-4} \text{ M IrCl}_6^{2-}$, PtCl_4^{2-} , and $10^{-3} \text{ M PdCl}_4^{2-}$ as their ion pairs with HTOPO^+ as a function of $[\text{Cl}^-]$ with 0.5 M TOPO at 0.1 M HCl and 4.0 mL/min flow rate. Eluting species are (a) IrCl_6^{2-} , (b) PdCl_4^{2-} , and (c) PtCl_4^{2-} .

also involves the formation of $(\text{HTOPO})\text{PdCl}_3$. In fact, under the experimental conditions employed in these separations, this is the major Pd ion pair that is extracted. The extraction equilibrium constant for $(\text{HTOPO})\text{PdCl}_3$ is 18.25 M^{-1} . Similarly, Pt(IV) and Ir(IV) could be separated by HTOPO^+ by ion-pair formation with their MCl_6^{2-} species. The K_{ex} values for the Pt(IV) and Ir(IV) species are 1576 M^{-4} and 8035 M^{-4} , respectively.

Separation Efficiencies of Platinum Group Metals

We observed, early on, that CETP values are significantly larger for metal-ion separations than those for simple organic analytes under the same conditions. They are far larger than could be explained in terms of mass-transfer and diffusion factors. Moreover, they increase more rapidly with increasing flow rate than those of organic analytes, indicating a chemical kinetic component affecting the CETP. The CETP values observed with metal ions, after correction for mass transport and diffusion (achieved using an organic analyte with similar distribution characteristics), reflect the half-lives of chemical reactions causing the added inefficiencies. Metal-complex formation and dissociation reactions with half-lives of milliseconds (i.e., rapid enough that in batch experiments they reach equilibrium “instantaneously”) will lower the efficiencies of CPC chromatograms. Conversely, CETP values can be used to study rapid reaction kinetics if this rela-

tionship is found to be generally valid. Thus, CPC is a useful tool not only for uncovering kinetics of metals separations but also for obtaining detailed mechanisms of those reactions responsible for inefficiencies in multistage metals separations. This demonstrates the utility of CPC for examining the kinetics of metal-complex formation and dissociation reactions in two-phase systems that are too rapid for the automated membrane extraction system (AMES).

It was evident, from the separations of PGM, that their experimental CETP values were much larger compared to that for an organic analyte at identical distribution ratios. These results indicated that factors other than mass transfer and diffusion were responsible for the additional bandwidths in the case of the metal ions. The most likely factor is the slow kinetics of back-extraction of the metal ions as the forward extraction reactions are usually rapid. To test this hypothesis, 3-picoline was used as the model compound for the determination of the CPC bandwidth due to mass transfer and diffusion (CETP_{dif}), and the CETP value due to slow chemical kinetics (CETP_{ck}) was derived by expressing the experimental CETP (CETP_{obs}) as a sum of CETP_{dif} and CETP_{ck} :

$$\text{CETP}_{\text{obs}} = \text{CETP}_{\text{dif}} + \text{CETP}_{\text{ck}} \quad (7)$$

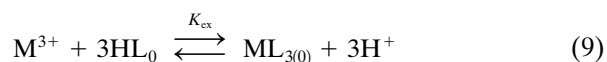
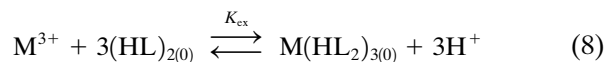
The CETP_{ck} values determined by varying the concentrations of the species in the aqueous and organic phases clearly showed that the slow back-extraction kinetics of the metal complexes were indeed responsible for the broad bands in the CPC chromatograms. On the basis of these results, a mechanism of the dissociation step could be deduced, which indicated that the dissociation of $\text{MCl}_2(\text{TOPO})$ is rate limiting in the back-extraction of $\text{MCl}_2(\text{TOPO})_2$ ($\text{M} = \text{Pd}, \text{Pt}$). A plot of the CETP_{ck} values for $\text{MCl}_2(\text{TOPO})_2$ against the $t_{1/2}$ values yielded a straight line. Further, these points and those for the $\text{Pd}(\text{II})$ system fall on a single line, indicating a general correlation for the separation of these two metals using TOPO in the heptane– H_2O phase pair.

Dissociation reactions with half-lives ranging from milliseconds to seconds can adversely affect the CPC efficiencies. It is important to realize the consequence of these findings: Extraction and back-extraction reactions that appear to be rapid in single-stage equilibrations may still be slow enough to reduce the efficiencies of multistage separations. A further significant finding of this work is that a direct linear correlation exists between CETP_{ck} and $t_{1/2}$ for the $\text{Pd}(\text{II})$ –TOPO system and several other systems. Because the CETP_{ck} values are a measure of the half-lives of the slow dissociation steps

in metal-complex dissociation reactions, CPC is a useful tool for examining the kinetic and the equilibrium aspects of such reactions.

Separation of Trivalent Lanthanides

The trivalent lanthanides have been separated using acidic organophosphorous ligands and the acylpyrazolones [6–8]. The phosphinic acid bis(2,4,4-trimethylpentyl)phosphinic acid (Cyanex 272) in the heptane–water phase pair is dimeric and provides excellent separations of the adjacent light lanthanides at a fixed pH and a mixture of light and heavy lanthanides using a pH gradient (Fig. 2). Cyanex 272 is a chelating ligand that extracts the trivalent lanthanides by chelating them in its dimeric form [Eq. (8)]. The acylpyrazolones, 1-phenyl-3-methyl-4-benzoyl-5-pyrazolone (HPMBP) and 1-phenyl-3-methyl-4-capryloyl-5-pyrazolone (HPMCP, see structure below) have also been used in the toluene– H_2O phase pair for the extraction and separation of the trivalent lanthanides. The extraction equilibrium constant for HPMBP and HPMCP are given in Eq. (9).



Significant differences are seen between Cyanex 272 and the acylpyrazolones. The extractability of the triva-

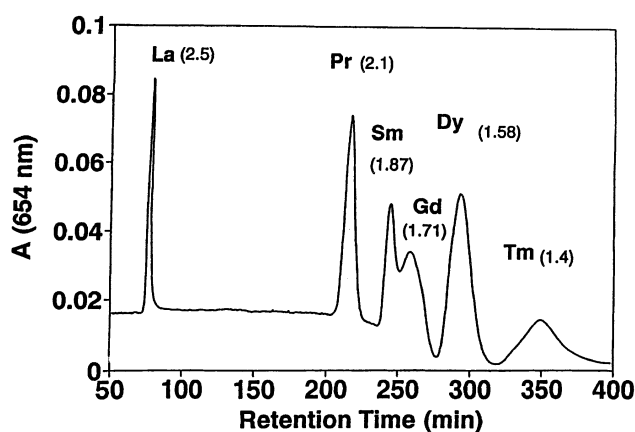


Fig. 2 Separation of lanthanides by use of a pH gradient with 0.1 M Cyanex 272 at $V_s/V_m = 0.18$ and flow rate of 1 mL/min. The concentrations and pH of elution are as follows: La (2 ppm; 2.5), Pr (6 ppm; 2.1), Sm (4 ppm; 1.87), Gd (4 ppm; 1.71), Dy (10 ppm; 1.58), and Tm (8 ppm; 1.4).



lent lanthanides is higher with Cyanex 272 than with the acylpyrazolones, where HPMBP shows better extraction than HPMCP. The stability constants of the lanthanides increases from the light to heavy, and the values for the Cyanex 272 and HPMCP complexes are larger than those of HPMBP. The separation factor (or selectivity) for a pair of lanthanides is much better with Cyanex 272 than with HPMBP or HPMCP, which have similar separation factors.

The lanthanide complexes lack distinct ultraviolet–visible spectra and, hence, kinetic information on their complex formation and dissociation reactions was obtained indirectly by the metallochromic indicator method [9]. These studies indicate that in the case of the Cyanex 272 complexes, the CPC efficiencies are mainly limited by the slow dissociation of the $M(HL_2)HL^+$ complex at the heptane– H_2O interface. In the case of the complexes of the acylpyrazolones, the CPC efficiencies are again limited by the dissociation of the lanthanide–pyrazolone complexes at the organic–aqueous interface with the rate-limiting step being the dissociation of the ML^{2+} complex. It was also shown that because the dissociation reactions are interfacial separations, efficiencies can be dramatically improved by the addition of surfactants like Triton X-100 to the organic phase and by interfacial catalysis by the addition of a aqueous soluble metallochromic indicator, which formed highly interfacially active lanthanide–indicator complex. The adsorption of this complex at the organic–aqueous interface catalyzed the metal–complex formation and dissociation reactions leading to high efficiencies in CPC separations [10].

Two significant results have emerged from the CPC separations of metals ions, namely (a) separation efficiencies are significantly reduced by slow metal–complex formation and dissociation kinetics and (b) CPC separations can be entirely interfacially driven analogous to conventional liquid chromatography.

References

1. A. P. Foucault (ed.), *Centrifugal Partition Chromatography*, Marcel Dekker, Inc., New York, 1994.
2. A. Berthod and D. W. Armstrong, Centrifugal partition chromatography II. Selectivity and efficiency, *J. Liquid Chromatogr.* 11: 567 (1988).
3. Y. Surakitbanharn, S. Muralidharan, and H. Freiser, Separation of palladium(II) from platinum(II), iridium(III) and rhodium(III) using centrifugal partition chromatography, *Solvent Extract. Ion Exchange* 9: 45 (1991).
4. Y. Surakitbanharn, S. Muralidharan, and H. Freiser, Centrifugal partition chromatography of palladium(II) and the influence of chemical kinetic factors on separation efficiency, *Anal. Chem.* 63: 2642 (1991).
5. Y. Surakitbanharn, H. Freiser, and S. Muralidharan, Centrifugal partition chromatographic separations of platinum group metals by complexation and ion pair formation, *Anal. Chem.* 68: 3934 (1996).
6. R. Cai, S. Muralidharan, and H. Freiser, Improved separation of closely related metal ions by centrifugal partition chromatography, *J. Liquid Chromatogr.* 13: 3651 (1990).
7. K. Inaba, H. Freiser, and S. Muralidharan, Effect of kinetic factors on the efficiencies of centrifugal partition chromatographic separations of tervalent lanthanides with bis(2,4,4-trimethylpentyl)phosphinic acid as extractant, *Solvent Extract. Res. Dev. Japan* 1: 13 (1994).
8. G. Ma, H. Freiser, and S. Muralidharan, Centrifugal partition chromatographic separation of tervalent lanthanides using acylpyrazolone extractants, *Anal. Chem.* 69: 2835 (1997).
9. K. Inaba, S. Muralidharan, and H. Freiser, Simultaneous characterization of extraction equilibria and back-extraction kinetics: Use of arsenazo III to characterize lanthanide–bis(2,4,4-trimethylpentyl)phosphinic acid complexes in surfactant micelles, *Anal. Chem.* 65: 1510 (1993).
10. G. Ma, H. Freiser, and S. Muralidharan, Interfacial catalysis of formation and dissociation of tervalent lanthanide complexes in two phase systems, *Anal. Chem.* 69: 827 (1977).



Separation Ratio

Raymond P.W. Scott

Scientific Detectors Ltd., Banbury, Oxfordshire, England

Introduction

The *separation ratio* between two solutes has two uses. The first is to help identify a solute or confirm its identity. The second is to help calculate the minimum efficiency required to achieve a given separation (this aspect of the separation ratio will be discussed under resolution). The first chromatographic parameter to be used for solute identification, other than the corrected retention volume, is the capacity ratio of the solute.

Discussion

The capacity ratio of a solute (k') was defined as the ratio of the distribution coefficient (K) of the solute to the phase ratio (a) of the column. In turn, the phase ratio of the column was defined as the ratio of the volume of mobile phase in the column (V_m) to the volume of stationary phase in the column (V_s); that is,

$$a = \frac{V_m}{V_s}$$

and, as

$$V'_r = KV_s$$

Thus,

$$k' = \frac{K}{a} = \frac{KV_s}{V_m} \quad \text{and} \quad k' = \frac{V'_r}{V_m}$$

where V'_r is the corrected retention volume of the solute.

As the measurement of k' does not depend on flow rate, it is unaffected by flow changes and is, thus, a more reliable measurement than corrected retention volume for solute identification.

Unfortunately, both V_m and V_s will vary between different columns and, due to the partial exclusion that

can occur with porous supports and stationary phases, may vary between different solutes. For this reason, the separation ratio (α) was introduced as an identification parameter. For two solutes, (A and B), the separation ratio is defined as

$$\alpha_{A/B} = \frac{V'_{r(A)}}{V'_{r(B)}} = \frac{K_A V_s}{K_B V_s} = \frac{K_A}{K_B}$$

It is seen that the separation ratio is independent of all column parameters and depends only on the nature of the two phases and the temperature. Thus, comparing data from two different columns, providing that the same phase system is used in each, and the columns operated at the same temperature, then any two solutes will have the same separation ratio on both systems. Thus, the separation ratio will be *independent of the phase ratios* of the two columns and the *flow rates*. It follows that the separation ratio of a solute can be used more reliably as a means of solute identification.

In practice, a standard substance is often added to a mixture and the separation ratio of the substance of interest to the standard is used for identification purposes. The separation ratio is taken as the ratio of the distances in centimeters between the dead point and the maximum of each peak, or if data processing is employed and the flow rate is constant, chart distances can be replaced by the corresponding retention times.

Suggested Further Reading

Scott, R. P. W., *Liquid Chromatography Column Theory*, John Wiley & Sons, Chichester, 1992, p. 26.

Scott, R. P. W., *Chromatographic Detectors*, Marcel Dekker, Inc., New York, 1996.

Scott, R. P. W., *Introduction to Analytical Gas Chromatography*, Marcel Dekker, Inc., New York, 1998.



Sequential Injection Analysis in HPLC

Raluca-Ioana Stefan

Jacobus F. van Staden

University of Pretoria, Pretoria, South Africa

Hassan Y. Aboul-Enein

King Faisal Specialist Hospital and Research Centre, Riyadh, Saudi Arabia

Introduction

All of the samples analyzed using a chromatographic technique need special preparation before they are introduced into the column. This process is laborious, not reliable enough, and often expensive. There are several steps involved in sample preparation: dialysis, dilution, extraction (selective extraction or concentration), and derivatization. Sometimes, the derivatization step is part of the extraction process. The expenses refer to the reagents and solvents of chromatographic purity grade. The sample preparation will become easier and not so expensive by automation.

Sequential injection analysis (SIA), introduced in 1990 [1,2], is a technique with a high potential for on-line process measurements. It is simple and convenient because sample manipulation can be automated. Furthermore, it consumes low volumes of reagents and solvents. Up to now, all the necessary steps done manually before introduction of the sample into the high-performance liquid chromatograph (HPLC) were separately introduced in SIA systems. By including SIA in sample preparation, it became faster, more accurate, and precise. Contamination is reduced substantially and the objectivity of the analysis increased. The main advantages of the coupling of SIA with HPLC are high precision of sample injection into the column, low contamination, low consumption of sample, reagents, and solvents, and the short time of preparation that decreases the time of analysis.

Dialysis

For on-line measurements, the dialysis step is very important because, through dialysis, the solid particles can be retained, the solution can be purified, and also some of the interference can be eliminated. The main disadvantages of dialysis are the slow speed involved

and the low recovery of analyte. These parameters can be improved by introducing the dialyser into the conduits of a SIA system [3].

With the incorporation of a passive, neutral, semi-permeable dialysis membrane into the conduits of the sequential injection system, the contact time of the sample zone with the membrane had much influence on the quantity of analyte that dialyzed through the membrane. It is necessary to determine, first, the time necessary to propel the entire sample zone over the membrane. After the propelling of the sample zone over the membrane, the flow direction is reversed and the sample zone is drawn back into the holding coil for fixed periods of time; usually these periods of time can vary from 2 to 60 s. By increasing of the dialysis time, the sensitivity of dialysis and, finally, the sensitivity of the analytical information are increased. A long dialysis time is also not good to consider, because this increases the dispersion of the dialyzed sample (situated below the membrane) due to a longer time delay before it is drawn in the specific holding coil for analysis.

To increase the percentage of dialysis, as well as the dialysis time, multiple flow reversals with a time of 20 s between each flow reversal is selected. Similar results are obtained by using a sequential injection system with the stopped-flow period around 150 s. The advantage of utilizing the stopped-flow mode over multiple flow reversals in the sequential injection analysis systems is that it needs less programming and, also, it reduces the strain on the pump.

Dilution

It is well known that HPLC techniques are performed at low concentration ranges. Sometimes, the sample is too concentrated in the analyte to be determined, and a dilution step is absolutely necessary. When a SIA system containing a dialyzer is utilized for sampling before a HPLC, the sample is already diluted. If the dilu-



tion is still not enough, a special step must be adopted in the program of the SIA system. The next step, when the analyte is extracted into a solvent, can also be considered a dilution.

There are two methods that can be adopted for a dilution in SIA: by using a dilution coil and by using a dilution step [4,5]. The easier dilution technique in SIA is by using a dilution step which can also be accomplished in a shorter time. There are three types of volumes that can control the dilution: the sample volume (the volume of sample or standard that is drawn into the holding coil via the sample port), the transfer volume (the volume of sample plus accompanying wash in the holding coil and tubing that is transferred into the dilution conduit from the holding coil), and the analysis volume (the volume taken from the dilution conduit to the holding coil) [4].

Concentration

The concentration step is very easy to implement in sequential injection analysis. The system is very simple and the results are reproducible. Most of the time, this step is not necessary for HPLC. When it is necessary, it can easily be done in the same time with the extraction step.

Extraction

There are two types of extraction that can be used in sampling. The first one involves a chemical reaction before the extraction, and the other one is just a simple extraction of analyte(s) from the solution. When a chemical reaction is involved, the derivatization step that may be necessary is included in the extraction step.

Extraction techniques that involve a chemical reaction can be classified as nonselective extraction or concentration, when more than one analyte is extracted from the solution by using the organic collectors (e.g., 8-hydroxyquinoline and dithizone derivatives) and selective extraction or separation. The first step in such an extraction technique is the formation of the complex by adding the reagent(s) to the solution of analyte, and after the extraction of the complex in an organic solvent. The problem that can arise in a SIA system with these types of extraction is the precipitate that is formed, and this can contaminate the other sample and also can block the tubing. To avoid these problems, it is necessary either to dilute the sample in such a way that the precipitation equilibria will not be reached and that all the complex will remain dissolved in the solution, or by derivatization of the ligands to

make the complexes soluble in the aqueous solution by introducing hydrophilic groups into their structures (e.g., in the place of 8-hydroxyquinoline, the 7-iodo, 8-hydroxyquinoline, 5-sulfonic acid can be used).

Three types of SIA system were proposed in coupling with the extraction technique: The first one is based on the introduction of bubbles into the system [6], the second system is based on wetting film that is formed on a Teflon tube wall [7], and the third one is based on solid-phase extraction [8]. The most utilized system is the one based on bubbles. The most reliable is the one based on a Teflon tube wall, and the principle of functioning of this system is as follows. The aqueous sample is propelled through the segment of organic solvent whose flow is impeded due to hydrophobic interactions with the walls of Teflon extraction coil. This wall drag allows the faster moving aqueous sample to penetrate through and ultimately separate from the organic solvent. These steps are repeated with a re-extraction into a second aqueous segment that is collected and which is going to the analyzer [9].

Derivatization

This step can be included in the extraction techniques because, in most of the cases of extraction, the analytes are being transformed. This step is only necessary for analytes that cannot be determined directly in the form that they already exist in solution. In the SIA system, the derivatization process can be assimilated with a reaction between analyte(s) and reagent with the optimum parameters for both the reaction and SIA system [8,10]; the difference is that the product of the reaction is not channeled to the detector, but is channeled to the chromatograph.

SIA-HPLC Systems

Sequential injection is the perfect vehicle for HPLC, which, in turn, enhances sequential injection by eliminating the problem of dialysis, dilution, or concentration, extraction, and mixing reactants during the loading process. HPLC can be carried out in different modes: affinity chromatography, ion chromatography, extraction chromatography, and so forth.

Most of the SIA-HPLC systems have been applied for the separation and assay of radionuclides. The reason for selecting such a system is the potential radiation and contamination of an operator during the sampling process. By using SIA-HPLC systems, all steps are automated and the contact of the operator with



them is minimal. Grate and Egorov [11] reviewed the radiometric separation and gave to SIA–HPLC systems the main place between automatic analytical separation in radiochemistry. They found that the type of chromatography suitable for coupling with SIA is extraction chromatography. For radiochemical separation, a wide-bore holding coil, in combination with air segmentation and sequential loading and delivery of solutions, instead of zone stacking in the holding coil, is proposed.

Enzymes and antibody–antigen systems have been used to measure a large number of analytes in relation to SIA–HPLC systems [12]. A very interesting application of these systems is given when the HPLC is carried out in the bead injection (BI) form [13]. As BI is presently restricted to relatively short columns, it is focused on separations based on mobile-phase changes, rather than relying on the separating power provided by a large number of theoretical plates. The SIA–BI system has also been applied with very good results for the separation of radionuclides.

An automated sequential trace enrichment dialyzer and gradient HPLC system is proposed for pharmaco-

kinetic studies of drugs and their metabolites [14]. The dialyzer is essential in the determination of pharmaceutical compounds from tablets and biological fluids (e.g., blood). By its incorporation into the conduits of a SIA system and coupling with the HPLC, the objectivity and reproducibility of the measurements were increased.

Features for SIA–HPLC Systems

The ideal system for sample preparation in a chromatographic method is that the operation of all the steps between sample dissolution and chromatography is done through a SIA technique (Fig. 1). The first part of the system will consist of a sample dialysis (unit 1) and the outlet will be channeled into the second unit consisting of concentration or dilution steps and extraction of the analyte. It is always assumed that the concentration, dilution, and derivatization steps can be done by extraction—in most cases, it is absolutely necessary.

The proposed SIA–HPLC (Fig. 1) system operates by a well-programmed computer which will be able to

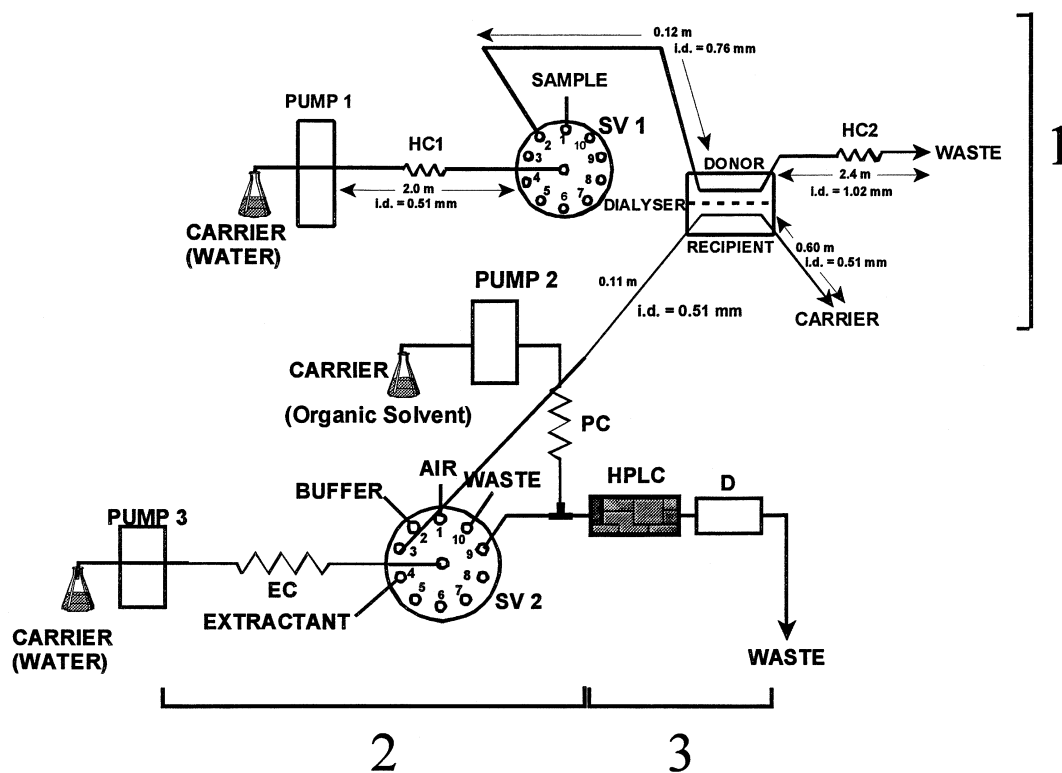


Fig. 1 Schematic representation of SIA–HPLC–detector system: 1: the dialysis unit; 2: the extraction (dilution, concentration, derivatization) unit; 3: the HPLC–D unit. SV is the selection valve; EC is the extraction coil; D is the detector.



analyze all types of sample: from environment, from the food industry, from the pharmaceutical industry, and also biological samples.

Conclusions

The utilization of sequential injection analysis coupled with HPLC systems increases the reliability of an HPLC analysis considerably because the primary factor that contributes to the increasing uncertainty is the sample preparation. It is always necessary to look to the most reliable methods for sample preparation, because only these methods will give the best results after the automation by using sequential injection analysis. The best coupling must be concerned with the selectivity and sensitivity assured by a sequential analysis system and by the selectivity and sensitivity of the HPLC technique. The introduction of bead injection considerably improves the reliability of the discussed system.

References

1. J. Růzicka and G. D. Marshall, *Anal. Chim. Acta* 237: 329 (1990).
2. J. Růzicka, G. D. Marshall, and G. D. Christian, *Anal. Chem.* 62: 1861 (1990).
3. J. F. van Staden, H. du Plessis, and R. E. Taljaard, *Anal. Chim. Acta* 357: 141 (1997).
4. M. Boron, J. Guzman, J. Růzicka, and G. D. Christian, *Analyst* 117: 1839 (1992).
5. J. F. van Staden and R. E. Taljard, *Fresenius J. Anal. Chem.* 357: 577 (1997).
6. Y. Luo, R. Al-Othman, J. Růzicka, and G. D. Christian, *Analyst* 121: 601 (1996).
7. J. W. Grate and R. H. Taylor, *Field Anal. Chem. Technol.* 1: 39 (1996).
8. J. F. van Staden and R. E. Taljard, *Anal. Chim. Acta* 344: 281 (1997).
9. R. E. Taljaard and J. F. van Staden, *S. Afr. J. Chem.* 52: 36 (1999).
10. J. F. van Staden and R. E. Taljard, *Anal. Chim. Acta* 331: 271 (1996).
11. J. W. Grate and O. B. Egorov, *Anal. Chem.* 70: 779A (1998).
12. J. Emneus and G. Marko-Varga, *J. Chromatogr. A* 703: 191 (1995).
13. J. Růzicka and L. Scampavia, *Anal. Chem.* 71: 257A (1999).
14. J. D. H. Cooper, N. J. Shearsby, J. E. Taylor, and C. T. C. Fook-Sheung, *J. Chromatogr. B: Biomed. Appl.* 702: 227 (1997).



Settling Time of Two-Phase Solvent Systems in Countercurrent Chromatography

Jean-Michel Menet

Aventis Pharma, Vitry-sur-Seine, France

Introduction

Countercurrent chromatography (CCC) is based on the use of two-phase liquid solvent systems. One of the characteristics of a two-phase system is its settling time, which is the time required for the mixture of both phases to be completely separated into two layers, usually in the Earth's gravitational field. The measurement of the settling time itself is helpful in preparing the experiment, for instance, when preparing the mobile and stationary phases in the same vessel. However, it is also intrinsically linked to the hydrodynamic behavior of the two-phase system and, therefore, to its physical parameters such as densities, viscosities, and interfacial tension. It was, therefore, used as a parameter for predicting the hydrodynamic behavior of various solvent systems in J-type CCC devices.

How to Measure the Settling Time?

The settling time depends not only on the nature of the solvent system but also on the experimental environment. As its definition is the time needed for the two phases to completely separate into two layers, the worker has to precisely choose the experimental conditions for the measurement. For instance, Ito [1] chose the following:

- Equilibrate the two-phase solvent system in a separatory funnel at room temperature.
- Separate the two phases.
- Take an aliquot of each phase.
- Put each aliquot in a graduated cylinder, which is then sealed with a glass stopper.
- Gently mix the two-phase system by inverting the cylinder five times.
- Place the cylinder immediately on a flat table in an upright position.
- Measure the time required for the two phases to settle.
- Repeat the experiment several times and take the mean time.

It is necessary to perform several experiments, as significant differences in the values are observed. A second set of tests may be performed by vigorously shaking the graduated cylinder five times and then averaging the times measured on several experiments.

The described experimental environment can be summarized as a 1:1 ratio of both phases, the choice of a graduated cylinder, room temperature, five-time inversion of the cylinder in a gentle or a vigorous manner, and the Earth's gravitational field. This should be only considered as an example of measuring the settling time, but what is important is to remain with a single definition in order to then use the resultant values in a comparative way.

Values of Settling Times for Usual CCC Solvent Systems

Ito has carried out the experiments, as described earlier, for 15 solvent systems. All mean values for gentle mixing and for vigorous mixing are gathered in Table 1 in the *T* and *T'* columns, respectively, [1].

The *T* and *T'* values are close; thus, they both can be considered as reliable measurements of the settling time for each solvent system. The values range from a few seconds (i.e., 3–5 s) to about 1 minute.

Other types of solvent system can be used in CCC. For instance, aqueous two-phase polymer systems (discussed elsewhere in this volume) are made of two aqueous liquid phases containing various polymers. Such systems are gentle toward biological materials and they can be used for the partition of biomolecules, membrane vesicles, cellular organelles, and whole cells. They are characterized by a high content of water in each phase, very close densities, very low interfacial tension, and high viscosities of the phases. Settling times are particularly long and may last up to 1 h. We refer the reader to the ATPS entry (see entry Aqueous Two-Phase Solvent Systems for Countercurrent Chromatography) for further information on these systems.



Table 1 Values of the Settling Times for 15 Solvent Systems

Two-phase solvent system	Volume ratio	Settling time	
		<i>T</i> (s)	<i>T'</i> (s)
Hexane–water	1:1	<1	8
Ethyl acetate–water	1:1	15.5	21
Chloroform–water	1:1	3.5	5.5
Hexane–methanol		5.5	6
Ethyl acetate–acetic acid–water	4:1:4	15	16
Chloroform–acetic acid–water	2:2:1	29	27.5
Butanol-1–water	1:1	18	14
Butanol-1–0.1 <i>M</i> NaCl	1:1	16	14.5
Butanol-1–1 <i>M</i> NaCl	1:1	23.5	21.5
Butanol-1–acetic acid–water	4:1:5	38.5	37.5
Butanol-1–acetic acid–0.1 <i>M</i> NaCl	4:1:5	32	30.5
Butanol-1–acetic acid–1 <i>M</i> NaCl	4:1:5	26.5	24.5
Butanol-2–water	1:1	57	58
Butanol-2–0.1 <i>M</i> NaCl	1:1	46.5	49.5
Butanol-2–1 <i>M</i> NaCl	1:1	34	33.5

Note: *T* is the average value after five gentle mixings, and *T'* stands for five vigorous mixings.
Source: Ref. 1.

Hydrodynamic Behavior and Settling Time

The true purpose of Ito’s study was to build a classification among the 15 solvent systems, based on their hydrodynamic behavior inside the column, measured through the retention of the stationary phase for various experimental conditions, on a J-type CCC device.

The first three solvent systems of Table 1 define the “hydrophobic” group, because they require the same given combination of two experimental parameters [choice of a lighter or heavier phase as stationary one, and choice of the pumping direction (i.e., from the head to the tail of the column or vice versa)] to achieve a good retention of the stationary phase and because their organic phase is hydrophobic. The last six solvent systems define the “hydrophilic” group, based on the same combination of two experimental conditions, which are reversed as compared to “hydrophobic” systems, because their organic phase can be considered as hydrophilic. There remains six solvent systems whose hydrodynamic behavior is more complicated, as it depends on the ratio of the radius of the coil on the rotation radius of the apparatus. They define the “intermediate” group.

Table 1 reveals that the classification may be defined from the values of the settling times. Indeed, the settling times of the hydrophobic solvent systems are the shortest ones, ranging from 1 to 20 s, whereas those of hydrophilic systems are in the 25–60-s range. Solvent

systems belonging to the intermediate group exhibit moderate settling times, ranging from 6 to 30 s.

Consequently, the measurement of the settling time for a solvent system which is different from the 15 studied is a simple way of roughly classifying it among the 3 groups defined by Ito and then to know the best experimental combinations to obtain the highest retention of the stationary phase on a J-type device.

Increasing the temperature or the concentration of a salt in the aqueous phase are known ways of reducing the settling time. This is interesting, as systems with low settling times are easier to handle and are characterized by a “hydrophobic” hydrodynamic behavior in J-type CCC devices, which leads to high values of the retention of the stationary phase.

Hydrodynamics and Settling Time

Three theoretical parameters were introduced by Menet et al. in order to better understand the hydrodynamic behaviors of two-phase solvent systems [2]. We will not discuss, here, the capillary wavelength, as it only enables the description of the formation of droplets of one liquid in another liquid. The two other parameters were introduced because it appeared interesting to introduce other “theoretical” parameters to better describe the dynamic phenomena occurring inside a CCC column (i.e., after the formation of the droplet described by the capillary wavelength). Two of these are presented here, namely V_{low} for the fall of a droplet of the heavier liquid phase (lower) in the continuous lighter one (upper) and V_{up} for the rise of a droplet of the lighter liquid phase in the continuous heavier one, and are defined as follows:

$$V_{\text{low}} = \gamma \left(\frac{2 + 3(\eta_{\text{low}}/\eta_{\text{up}})}{\eta_{\text{up}}3 + 3(\eta_{\text{low}}/\eta_{\text{up}})} \right)^{-1} \quad \text{and}$$

$$V_{\text{up}} = \gamma \left(\frac{2 + 3(\eta_{\text{up}}/\eta_{\text{low}})}{\eta_{\text{low}}3 + 3(\eta_{\text{up}}/\eta_{\text{low}})} \right)^{-1}$$

with γ the interfacial tension between the two liquid phases, η_{up} the dynamic viscosity of the lighter phase, and η_{low} the dynamic viscosity of the heavier phase.

It is interesting to note that as neither V_{up} nor V_{low} depend on g , these velocities do not depend on the selected angular velocity of rotation. This is because the field intensity influences in the same way the size of the capillary wavelength and the sedimentation velocity of the droplet.

Menet et al. have computed the V_{low} and V_{up} values for the 15 solvent systems studied by Ito, along with 6

not previously studied [i.e., dimethyl sulfoxide (DMSO)–heptane (1:1, v/v), dimethyl formamide (DMF)–heptane (1:1, v/v), toluene–water (1:1, v/v), *o*-xylene–water (1:1, v/v), heptane–acetic acid–methanol (1:1:1, v/v) and chloroform–ethyl acetate–water–methanol (2:2:2:3, v/v)]. All the results have allowed them to define ranges of settling velocities linked to the hydrophobic, intermediate, or hydrophilic behavior of the solvent system. They have demonstrated the most reliable scale was that based on V_{up} , which is the description of the rise of a droplet of the lighter phase in a continuous heavier one.

It was further demonstrated that this theoretical parameter was the right one to use, as Menet et al. have carried out experiments on the evolution of the hydrodynamic behavior of the butanol-1–water system with the temperature [3]. They showed that the observed change in behavior was explained by an increase in the V_{up} settling velocity with the temperature, and, thus, a decrease of the settling time, explaining the “hydrophobic” behavior of the solvent system.

As a conclusion, the research worker can use the settling time for both purposes. One is the knowledge of the solvent system, mainly its ease of use, as long settling times complicate the use of the solvent system.

The other one is to roughly predict the hydrodynamic behavior inside a J-type CCC device, in order to know the best combinations of some experimental conditions to obtain the highest retention of the stationary phase. For this purpose, the research worker may also use the theoretical settling velocity of a droplet of a lighter phase inside the heavier continuous liquid phase. It was demonstrated to be the better way of predicting the hydrodynamic behavior and, consequently, the best combination of experimental parameters for the highest retention of the stationary phase.

References

1. Y. Ito, Principles and instrumentation of CCC, in *Countercurrent Chromatography — Theory and Practice* (N. B. Mandava and Y. Ito, eds.), Marcel Dekker, Inc., New York, 1988.
2. J. M. Menet, D. Thiébaud, R. Rosset, J.-E. Wesfreid, and M. Martin, *Anal. Chem.* 66: 168–176 (1994).
3. J.-M. Menet and M. C. Rolet-Menet, Characterization of the solvent systems used in countercurrent chromatography, in *Countercurrent Chromatography*, (J. M. Menet and D. Thiébaud, eds.), Marcel Dekker, Inc., New York, 1999.



Silica Capillaries: Chemical Derivatization

Joseph J. Pesek
Maria T. Matyska

San Jose State University, San Jose, California, U.S.A.

Introduction

Capillaries for capillary electrophoresis (CE) are made of fused silica that has been drawn to precise internal and external diameters. Virtually all fused-silica capillaries used in CE, whether for home-made instruments or for commercial systems, have an external diameter of approximately 375 μm . Internal diameters vary over a wider range but generally lie between 50 and 100 μm . Smaller-diameter capillaries generally lead to detection problems, especially if spectroscopic methods are used, because the optical path length becomes too short. Larger-diameter capillaries dissipate heat inefficiently and can lead to band-broadening at higher applied voltages. All capillaries are covered externally with a polyimide coating for protection against breakage and to provide flexibility in fitting the typical column (50–100 cm) into the instrument.

Background Information

Fused silica has surface properties that are similar to the porous particulate matter used as a support material in high-performance liquid chromatography (HPLC) packings. The most important features are the presence of silanol ($\text{Si}-\text{OH}$) groups that are polar and ionizable and siloxane linkages ($\text{Si}-\text{O}-\text{Si}$) that have a hydrophobic character. It is generally recognized that the silanols are the most influential in determining the surface properties of silica. For capillary electrophoresis, the $\text{Si}-\text{OH}$ moieties contribute in at least three ways to the overall performance of the electrophoretic experiment. The presence of silanols on silica surfaces can be considered as a result of the formation of a polymer during condensation of silicic acid. When the polymer cross-links, all four bond sites on each silicon atom do not form siloxane linkages, leaving a hydroxyl group in one position. Because the silanols are acidic groups, they can dissociate in the presence of aqueous solution and behave as any weak acid. The $\text{p}K_a$ of this moiety is near 5 but can vary depending on the purity of the silica material. Therefore, when the pH of the solution in contact with the inner

wall of the capillary is approximately 3 or less, the sites will be fully protonated and the surface will be polar. If the pH is 7 or greater, then the silanols will be fully ionized. The acidic nature of the silanols leads to two of the salient features of the fused-silica surface with respect to electrophoretic experiments. Upon ionization of at least some of the silanols, a double layer is created at the surface when a voltage is applied to a capillary filled with aqueous buffer. This double layer is responsible for electro-osmotic flow (EOF), the movement of solvent toward the cathode. Because of the acidic nature of the silanols, there also is a strong tendency to adsorb basic compounds when these groups are ionized. Finally, the silanol moiety can be considered a reactive group on the surface and it functions as the site for chemical modification of the inner wall. This property will be discussed in more detail later.

Because the first two properties of the silanol, creation of EOF and strong affinity for bases, can often be regarded as undesirable, the third property, the possibility of chemical modification, is used to eliminate these unwanted effects. The presence of EOF diminishes the ability of the CE experiment to separate solutes with very similar electrophoretic mobilities. For basic solutes, the acidic nature of the silanol can result in irreversible adsorption on the surface, which leads to either a complete loss of or greatly reduced detectability. When the silanol group has been modified with an organic moiety, the EOF is greatly diminished and the strong affinity for bases is significantly reduced or eliminated. In addition to chemical derivatization of the surface through a reaction at the silanol, it is also possible to modify the inner wall by adsorption of various compounds that masks the effect of the $\text{Si}-\text{OH}$ group.

Wall Coating Through Chemical Modification

Chemical modification of the inner wall of fused-silica capillaries and the surfaces of porous silica supports for HPLC utilize the same reactions. The most common method is based on organosilanization. Within this general reaction scheme, there are two possible



approaches, as shown in Table 1. The first possibility involves the use of an organosilane reagent ($\text{RR}'\text{R}'\text{SiX}$) with only a single reactive group (X). The substituents on the silicon atom are as follows: X = halide most often Cl; R = the organic moiety giving the surface the desired properties (i.e., hydrophobic, hydrophilic, ionic, etc.); R' = a small organic group typically methyl. This reaction leads to a single siloxane bond between the reagent and the surface. Because of the single point of attachment of the reagent, the resulting bonded material is referred to as a monomeric phase. The second approach to organosilanization involves a reagent with the general formula RSiX_3 . The substituents on the silicon atom in this reagent are defined earlier. The basic difference between the approaches as shown in Table 1 is that the

reagent with three reactive groups results in bonding to the surface as well as cross-linking among adjacent bonded moieties and is referred to as a polymeric phase. This cross-linking effect provides extra stability to the bonded moiety but is less reproducible than the monomeric method. The one-step organosilanization procedure is relatively easy and the modification of the surface can be done by forcing the reagent continuously through the capillary or simply filling the capillary with the organosilane solution. The capillary is heated for about 1–2 h and then rinsed with a solvent such as toluene to remove the excess reagent. As is the case with the production of stationary phases for HPLC, organosilanization accounts for virtually all of the commercially available chemically modified capillaries.

Table 1 Types of Reactions for Modifying Capillary Walls

Reaction type	Reaction	Surface linkages
Organosilane	$\text{Si}-\text{OH} + \text{X}-\text{SiR}'_2\text{R} \rightarrow \text{Si}-\text{O}-\text{SiR}'_2\text{R} + \text{HX}$ $\begin{array}{c} \text{O} \\ \\ \text{Si}-\text{OH} + \text{X}_3\text{Si}-\text{R} \end{array} \rightarrow \begin{array}{c} \text{O} \quad \text{O} \\ \quad \\ \text{Si}-\text{O}-\text{Si}-\text{R} \end{array} + 3\text{HX}$ $\begin{array}{c} \\ \text{O} \\ \end{array} \quad \begin{array}{c} \\ \text{O} \\ \end{array} \quad \begin{array}{c} \\ \text{O} \\ \end{array}$	Si—O—Si—C
Chlorination followed by reaction of Grignard reagents or organolithium compounds	$\text{Si}-\text{OH} + \text{SOCl}_2 \xrightarrow{\text{Toluene}} \text{Si}-\text{Cl} + \text{SO}_2 + \text{HCl}$ $\text{a) Si}-\text{Cl} + \text{BrMgR} \rightarrow \text{Si}-\text{R} + \text{MgClBr}$ or $\text{b) Si}-\text{Cl} + \text{Li}-\text{R} \rightarrow \text{Si}-\text{R} + \text{LiCl}$	Si—C
TES silanization	$\begin{array}{c} \\ \text{O} \\ \\ \text{Si}-\text{OH} \end{array} \quad \begin{array}{c} \\ \text{O} \\ \\ \text{Si}-\text{O}-\text{Si}-\text{H} \end{array} \quad \begin{array}{c} \\ \text{O} \\ \\ \text{Si}-\text{H} \end{array}$ $\begin{array}{c} \\ \text{O} \\ \\ \text{Si}-\text{OH} \end{array} \rightarrow \begin{array}{c} \\ \text{O} \\ \\ \text{Si}-\text{O}-\text{Si}-\text{H} \end{array} \quad \begin{array}{c} \\ \text{O} \\ \\ \text{Si}-\text{H} \end{array}$ $\begin{array}{c} \\ \text{O} \\ \\ \text{Si}-\text{OH} \end{array} \quad \begin{array}{c} \\ \text{O} \\ \\ \text{Si}-\text{O}-\text{Si}-\text{H} \end{array} \quad \begin{array}{c} \\ \text{O} \\ \\ \text{Si}-\text{H} \end{array}$ $\begin{array}{c} \\ \text{O} \\ \end{array} \quad \begin{array}{c} \\ \text{O} \\ \end{array} \quad \begin{array}{c} \\ \text{O} \\ \end{array}$	Si—H monolayer
Hydrosilation	$\text{Si}-\text{H} + \text{CH}_2=\text{CH}-\text{R} \xrightarrow{\text{Catalyst}} \text{Si}-\text{CH}_2-\text{CH}_2-\text{R}$	Si—C

A second modification scheme that has been reported for the modification of capillaries is based on a chlorination/organometalation two-step reaction sequence. This process is also depicted in Table 1. In the first step, the silanols on the surface are converted to chlorides via a reaction with thionyl chloride. This step must be done under extremely dry conditions because the presence of any water results in the reversal of the reaction with hydroxyl replacing the chloride ($\text{Si}-\text{Cl}$), resulting in the regeneration of silanols ($\text{Si}-\text{OH}$). If the chlorinated surface can be preserved, then an organic group can be attached to the surface via a Grignard reaction or an organolithium reaction. The main advantage of this process is that it results in a very stable silicon-carbon linkage at the surface. However, the stringent reaction conditions for the first step and the possibility of forming salts as by-products in the second reaction have resulted in relatively little commercial use of this process.

The third method reported for the modification of capillary inner walls involves first silanization of the silica surface followed by attachment of the organic group through a hydrosilation reaction. The process is also depicted in Table 1. In the first step, the use of triethoxysilane under controlled conditions results in a monolayer of the cross-linked reagent being deposited on the surface. This reaction results in the replacement of hydroxides by hydrides. In the second step, an organic moiety is attached to the surface via the hydride moiety in a catalyzed hydrosilation reaction. The catalyst is usually hexachloroplatinic acid (Speier's catalyst) but can be other transition metal complexes or a free-radical initiator. This process also results in a silicon-carbon bond at the surface, does not require dry conditions (water is required as a catalyst in the first step), and is applicable to a variety of unsaturated functional groups in the hydrosilation reaction, although terminal olefins are the most common. The silanization/hydrosilation method also has seen limited commercial utilization to date.

The result of all three of the chemical modification schemes described here is to eliminate or drastically reduce EOF. In some cases, the EOF can be reversed by the attachment of a positively charged group, such as $\text{R}-\text{NH}_3^+$, to the surface. Whether the EOF is diminished, eliminated, or reversed, separation is improved because electrophoretic mobility differences are enhanced. The replacement of silanols by various organic moieties also has beneficial effects with respect to the separation of basic compounds. An example of the difference in peak shapes seen for bare and modified capillaries is shown in Fig. 1. In some cases,

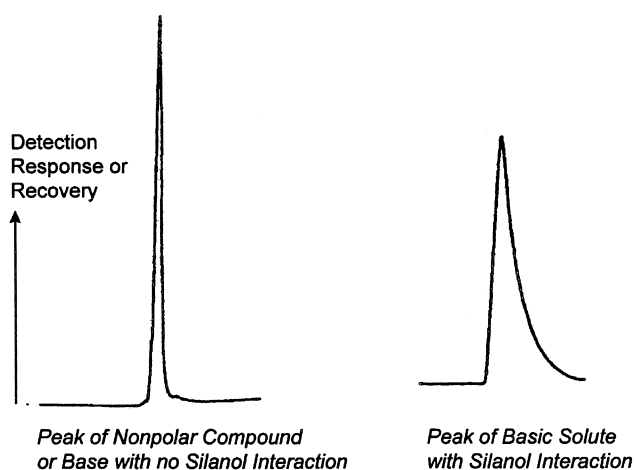


Fig. 1 Comparison of peak shapes for modified and bare capillaries.

the tailing observed for highly basic compounds is more severe than shown in the figure and in the worst cases irreversible adsorption results in the complete absence of a peak in the electropherogram.

Once a reaction scheme has been selected, then a choice must be made as to the type of surface that is suitable for a particular separation. The surface properties are controlled by the "R" group of the reactions shown in Table 1. Hydrophobic coatings can be achieved by using organic moieties that are common in reversed-phase HPLC. The most common would be either octadecyl (C_{18}) or octyl (C_8). In general, hydrophobic coatings are used for small molecule separations where the main concern is the suppression of EOF and the elimination of possible adsorption at the silanol sites. However, for the separation of proteins, peptides and DNA related species that have considerable hydrophobic character, it is more desirable to have a hydrophilic coating. The presence of any neutral bonded group will reduce or eliminate the EOF and a hydrophilic species will prevent strong interactions with the surface that would occur if the coating was hydrophobic. Because of the importance of CE in the separation of biomolecules, considerable effort has been devoted to the development of hydrophilic wall coatings. By far, the most extensively used hydrophilic coating is polyacrylamide. The surface is first modified with a linker such as 3-methacryloxypropyltriethoxysilane having a double bond available as a site for acrylamide to attach and polymerize. Derivatives of polyacrylamide have also been bonded which result in increased stability at high pH. Other polymers such as polyethylene glycol, cellulose, and poly(vinyl alcohol)



have also been used in order to achieve a hydrophilic surface. The presence of any polymer on the capillary usually results in a reasonably thick layer that shields the surface and drastically lowers or eliminates EOF. Polymers containing cationic or anionic species can also be useful in preventing adsorption of hydrophobic compounds on the surface as well as controlling EOF. The type charge on the polymer controls the direction of the EOF. For negatively charged groups (sulfonic acid), the direction is cathodic, and for positively charged groups (quaternary amine), the direction is anodic.

Wall Coating Through Buffer Additives

Another approach to reducing the EOF as well as wall adsorption is to add a compound to the running buffer that will compete with the solute for the silanol sites on the surface. These materials must have some affinity for the charged or polar sites on the inner wall and so they must, themselves, be hydrophilic or charged. Nonionic surfactants are hydrophilic to prevent solute adsorption on the wall and block the silanols in order to reduce the EOF. The use of cationic polymers in the buffer results in a reversal of EOF to the anodic direc-

tion, whereas the use of anionic polymers preserves the cationic direction but tends to stabilize the flow in comparison to a bare capillary. Other additives such as diaminoalkanes and polyvinylalcohol result in reduced EOF and less solute adsorption on the wall.

Column technology is one of the most rapidly developing areas of CE. The capillary is the key to separation, so it is likely that numerous column formats will be established to meet specific separation needs similar to stationary-phase development in HPLC.

Suggested Further Reading

- Altria, K. D., *Capillary Electrophoresis Guidebook: Principles, Operation and Applications*, Humana Press, Totowa, NJ, 1996.
- Camilleri, P., *Capillary Electrophoresis*, CRC Press, Boca Raton, FL, 1998.
- Landers, J. P., *Handbook of Capillary Electrophoresis*, 2nd ed., CRC Press, Boca Raton, FL, 1997.
- Pesek, J. J. and M. T. Matyska, *Electrophoresis* 18: 2228 (1997).
- Vansant, E. F., P. Van Der Voort, and K. C. Vrancken, *Characterization and Chemical Modification of the Silica Surface*, Elsevier, Amsterdam, 1995.



Silica Capillaries: Epoxy Coating

James J. Bao

Advanced Medicine, Inc., South San Francisco, California, U.S.A.

Introduction

Capillary electrophoresis (CE) has proven to be one of the best possible techniques available for the separation of proteins. However, CE separation of proteins is often complicated by the interaction between the analytes and the silanol groups on the inner surface of the capillary. This interaction often results in broad asymmetrical peaks, poor efficiency, altered electro-osmotic flow (EOF), reduced protein recovery, and poor reproducibility. Attempts have been made to reduce this interaction by chemically modifying the surface with a layer of chemical coating. Capillary coating has the advantage of allowing analysts to freely modify the composition of the buffer to optimize the separation. Different coatings have been made and each of them has unique characteristics. For protein separations, the most commonly used capillary coatings are hydrophilic coatings [1–6]. For example, epoxy coating is one of these hydrophilic coatings; various protein samples have been separated successfully on this coating.

Preparation of Epoxy Coating

A typical procedure for preparing epoxy coating can be found in the literature [7,8]. Basically, a fused-silica capillary is activated with 1.0M NaOH solution for 10–20 min and then washed with dilute HCl and water for another 20 min each. The washed capillary is then heated in an oven for 3 h at 120°C with N₂ slowly passing through. A γ -glycidoxypolytrimethoxysilane (GOX) in CH₂Cl₂ is pushed into the pretreated capillary and heated for 3 h. Next, a solution of ethyleneglycol diglycidyl ether (EGDE) and 1,4-diazabicyclo-[2.2.2]-octane (DABCO) is forced through the column and allowed to react at 120°C for at least 3 h. Finally, the capillary is washed with methanol at room temperature.

Separation of Proteins on the Epoxy Coating

Epoxy coating is a hydrophilic coating due to the high content of ether and hydroxyl groups. It is expected that this hydrophilic surface will reduce protein adsorption and, thus, is suited for protein separations.

Separation of Model Proteins at Neutral pH

The usefulness of this epoxy coating for protein separation can be demonstrated with the separation of various model proteins using 10–50 mM phosphate buffer near pH 7. The model proteins are lysozyme (*pI* 11), cytochrome-*c* (*pI* 10.2), ribonuclease-A (*pI* 9.3), α -chymotrypsinogen (*pI* 8.8), trypsinogen (*pI* 8.7), α -chymotrypsin (*pI* 8.4, 8.8), and myoglobin (horse heart, *pI* 7.3). They are all positively charged at pH 7 and have high tendency to adsorb onto the negatively charged walls of uncoated capillaries. Therefore, very poor separation is seen with an uncoated capillary. However, a good separation of these proteins can be achieved on the epoxy-treated surface. Figure 1 shows that all five proteins are baseline resolved with a high separation efficiency.

Coating the inner surface of capillary reduces the amount of surface silanol groups and, thus, the EOF in the capillary. The epoxy coating retains about one-third of the EOF of an uncoated capillary at pH 7. This EOF is critical for the separation and detection of samples containing neutral to slightly negatively charged proteins. For example, α -chymotrypsin, myoglobin (whale, *pI* 6.9), conalbumin (*pI* 6.3), carbonic anhydrase (*pI* 6.1), and α -amylase (*pI* 5.9) can also be separated at pH 7.

Separation of Model Proteins at Other pHs

One of the major advantages of coating the inner surface of the capillary is that it allows the buffer pH to be freely adjustable to achieve the best separation. Coat-



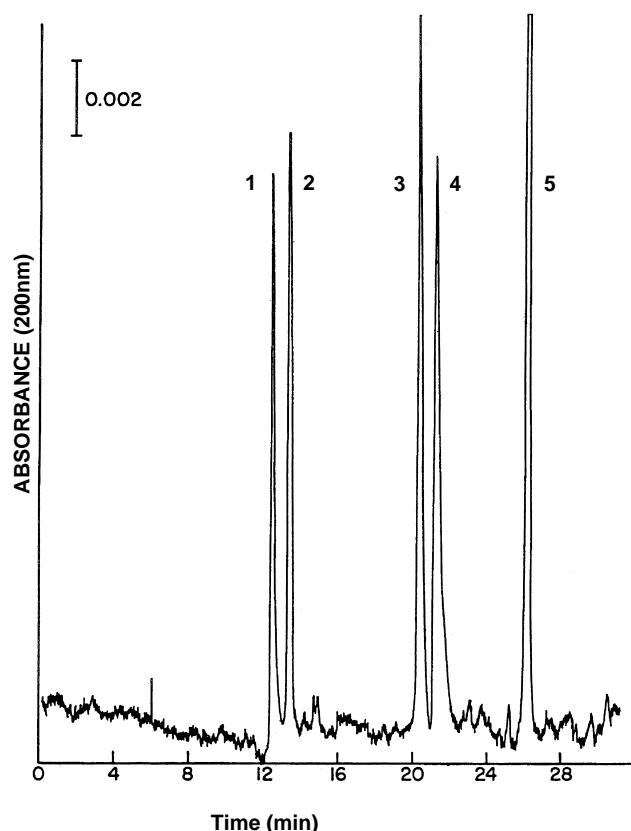


Fig. 1 Capillary electrophoretic separation of five basic model proteins in an epoxy-coated capillary. Experimental condition: 65 cm separation length, inner diameter/outer diameter 50/363 μm , 0.01M phosphate buffer, pH 7, 300 V/cm, 17 μA . Peaks: (1) lysozyme, (2) cytochrome-*c*, (3) ribonuclease A, (4) α -chymotrypsinogen, and (5) myoglobin (horse heart).

ing reduces the effect of pH on EOF, electrophoretic mobility, and protein separation. For example, the EOF in the coated capillary has less than half (from 0 to $3 \times 10^{-4} \text{ cm}^2/\text{VS}$) the variation as seen in the uncoated capillary (from 1×10^{-4} to $8 \times 10^{-4} \text{ cm}^2/\text{VS}$) between pH 3 and 11.

The five positive model proteins as shown in Fig. 1 can also be separated at various other pHs (pH 4–10) [7]. However, the migration times of these individual proteins vary with pH change differently. Although the electrophoretic mobility of these proteins changes accordingly with pH, the overall effect of pH on both EOF and electrophoretic mobility varies at different pH values. This variation provides a basis for optimizing pH for the separation of these proteins.

The theoretical plate number for the separation of these model proteins has a maximal value at pH 7. However, the peak capacity increases with pH because

the separation window between lysozyme and myoglobin increases with pH, whereas the peak width does not change significantly. The resolution between the two pairs of proteins, ribonuclease A and α -chymotrypsinogen, and α -chymotrypsinogen and myoglobin, increases with the pH. However, the resolution between lysozyme and cytochrome-*c* increases slightly from pH 5 to 7, drops to zero at pH 8 (no separation at all), and then increases again as the pH is increased.

Protein Recoveries

In general, the efficiency of protein separation in CE should be directly proportional to the separation length (i.e., $N = L/H$), where N is the theoretical plate number, L is the separation length, and H is the height-equivalent theoretical plate. Results obtained by locating two detectors at 20 and 65 cm from the injection end show that longer separation length gave much better separation. Much higher than expected separation efficiency is obtained from the 65-cm separation length segment than that from the 20-cm separation length. Therefore, a long capillary should be used when better resolution and higher efficiency are desired. However, no significant improvement in separation efficiency can be achieved when the capillary length exceeds 1 m. On the other hand, a short capillary is preferred when separation time is of major concern.

The adsorption of positive proteins onto the epoxy capillary surface can be quantitatively evaluated by using the two on-line detector design. From the responses of the two detectors, it is possible to determine the adsorption of proteins on the surface between the two detectors. Zero-percent recoveries have been reported on an uncoated capillary at pH 7 for lysozyme, cytochrome-*c*, ribonuclease A, and α -chymotrypsinogen. However, most of these proteins had recoveries between 84.4% and 95%, except for lysozyme (55.5%), on an epoxy-coated capillary. Therefore, coating does reduce protein adsorption significantly.

Reproducibility and Stability

The reproducibility of protein separation from run to run, day to day, segment to segment, column to column, and chemist to chemist is very high. From run to run, the % relative standard deviation (RSD) ($n = 5$) of migration times for neutral marker (MO) and lysozyme are 0.94 and 0.71, respectively. The %RSD in EOF for day to day ($n = 5$) and segment to segment ($n = 6$) are 2% and 3.5%, respectively. For column to

column, the EOF at pH 7 varied from 0.5×10^{-4} to 2×10^{-4} cm²/VS with an average of 1.14×10^{-4} cm²/VS for nine columns coated over a 3-month period.

The major challenge to capillary coatings, especially hydrophilic coatings, is the stability. Adding a hydrophobic moiety into the coating may increase coating stability but interfere with protein separations. Epoxy coating provides a balance between hydrophilicity and stability. Epoxy is well known for its chemical and mechanical stability. The epoxy is covalently bound to the silica surface and is cross-linked to generate a stable surface. This coating has shown to be suitable for protein separations at pH 4–10. When stored at room temperature, this column is stable for at least several months.

Separation of Cytochrome C Variants

The separation of cytochrome-*c* variants was challenging because of their similarity in structure. Each of them differs by only a few amino acids in their sequences. When five cytochrome-*c* variants were injected, only four peaks were obtained, with the horse and dog variants migrating together. Varying the experimental conditions still did not help the separation of the horse and dog variants. Very reproducible separations were obtained at pH 6–8 [8].

Separation of Recombinant Proteins

BMP-2 is a recombinant protein which has the potential to develop into a biotech drug. Previous experiments with an uncoated capillary and a commercially available hydrophilic-coated column (Celect P150) failed to separate the BMP-2 components with repro-

ducible results. By using the epoxy coating, the various BMP-2 components were separated. IL-11 is another recombinant protein under investigation. Using this epoxy coating, a CE method was developed to monitor the stability of IL-11 at different storage conditions. The results showed that there were some significant differences in the CE profiles of the three IL-11 samples stored at different temperatures for different periods of time [8].

Conclusions

Epoxy coating is well suited for the separation of proteins in CE. This coating is easy to prepare and can be used for a broad range of pHs. High recoveries of proteins prove that this epoxy modified surface has reduced the protein adsorption significantly.

References

1. S. Hjerten, *J. Chromatogr.* 347, 191 (1985).
2. R. M. McCormick, *Anal. Chem.* 60: 2322 (1988).
3. G. J. M. Bruin, R. Huisden, J. C. Kraak, and H. Poppe, *J. Chromatogr.* 480: 339 (1989).
4. W. Nashabeh and Z. El Rassi, *J. Chromatogr.* 559: 367 (1991).
5. J. T. Smith and Z. El Rassi, *J. High Resolut. Chromatogr.* 15: 573 (1992).
6. X. Ren, Y. Shen, and M. L. Lee, *J. Chromatogr. A* 741: 115 (1996).
7. J. K. Towns, J. Bao, and F. E. Regnier, *J. Chromatogr.* 599: 227 (1992).
8. J. J. Bao, *J. Liquid Chromatogr. Related Technol.* 23: 61 (2000).



Silica Capillaries: Polymeric Coating for Capillary Electrophoresis

Xi-Chun Zhou

Cambridge University, Cambridge, England

Lifeng Zhang

Environmental Technology Institute, Innovation Centre (NTU), Singapore

Introduction

The performance of capillary electrophoresis with an unmodified fused-silica capillary is dependent on the chemical properties of the silica surface. The residual Si—OH groups on the surface lead to *electro-osmotic flow* (EOF), which contributes to solute migration. For cationic solutes moving toward the negative electrode, the EOF will diminish the resolution, because it contributes toward migration in this direction and reduces the overall migration time. For anionic solutes, EOF is necessary for migration toward the negative electrode or it retards the movement toward the positive electrode and enhances resolution. Therefore, when cationic solutes are the analytes, it is often desirable to diminish the EOF in order to enhance resolution and, therefore, a bare capillary may not be the best choice for a column in this situation.

Another drawback of the unmodified capillary is that the silanols are potential sites for adsorption of certain solutes, especially high-molecular-weight proteins, which leads to poor recovery of the analyte and variable migration times due to the decrease in EOF.

Polymeric Coatings

Capillary columns modified with polymeric coatings are a desirable approach for controlling EOF and adsorption of solutes on the wall. In general, for a coating to be successful in CE, the polymers should be able to (a) modify or suppress the electro-osmotic flow, (b) be stable for a long period (many injections) in the presence of aqueous buffer solutions so that migration times remain constant and good quantitative determinations are possible, and (c) suppress strong, or even irreversible, adsorption of analyte molecules (e.g., proteins).

According to the way polymers are attached to the column surfaces, the polymeric coatings can be differentiated

between those substances that are covalently attached to the capillary surface and those coatings that are not covalently attached but are adsorbed to the surface by physical or ionic forces. Comparatively, adsorbed coatings are simpler to prepare, whereas covalently bonded coatings require elaborate chemical reactions. With regard to the mechanism by which prevention of adsorption of proteins occurs and the properties that they render to the coated surfaces, the compounds currently used as adsorbed coatings belong mainly to two categories: aminated or cationic polymers and hydroxylic or neutral polymers. Aminated polymers, such as polybrene, are adsorbed to the silica wall by Coulombic attraction.

The mechanism for which wall interactions are minimized is primarily due to the ionic repulsion of proteins and peptides at a pH below their *pI*. These polymers generate a positively charged layer at the surface of the silica wall and, therefore, lead to an anodal EOF. These polymer coatings are very stable and are useful over a wide pH range. Hydroxylic or neutral polymers are attached onto the silica wall by weaker interactions such as hydrogen-bonding. The mechanism for which wall interactions are minimized is described as a shielding of the silanol groups. Because these polymers are not charged, the EOF is, in most cases, suppressed. The working pH range is narrower and is limited to the acidic pH regime. Coating procedures may be varied to generate the coating thickness and homogeneity. Most commonly, the reagent is simply passed through the capillary in a suitable buffer. In the case of hydroxylic polymers, thermal immobilization is usually required. Prior to electrophoresis, the unbonded reagent is flushed from the capillary. The main limitation of adsorbed coatings is their instability under basic conditions.

A polymeric coating which is covalently bonded to the surface of capillary wall is the most significant approach among the surface deactivation methods. This



method provides a more flexible approach in preventing adsorption of analytes and, at the same time, permits manipulation of separation parameters to optimize selectivity and efficiency. The silanization of the silica surface is an elegant method which enables the production of a large variety of polymer coatings that are chemically bonded to the capillary column surface. In general, polymers are attached to the silica surface by an Si—O—Si linkage or Si—C linkage. Many different mono-, di-, or tri-functional silanization reagents are commercially available or can be easily synthesized. The capillary coated with polymers via Si—C linkage show better stability under alkaline conditions and improved reproducibility of the separation than that of the Si—O—Si linkage.

Among the bonded materials described in the literature, polyacrylamide is one of the most popular and successful for achieving good protein separations. Initial studies were based on the bonding of the linker 3-methacryloxypropyltriethoxysilane between the surface and the polymerized, and in some cases cross-linked, acrylamide. The main drawback of this type of wall coating is its long-term stability. In order to overcome this effect, the surface silanization agent was replaced with 7-oct-1-enyltrimethoxysilane. Improvement in stability, as well as efficiency and reproducibility of migration times, in comparison to the columns with linear polyacrylamide bonded by the conventional method, was achieved. However, at the high pH range, the amido bonds in polyacrylamide are possibly hydrolyzed, leading to degradation of the attached polymer and a loss of column performance. In order to overcome this effect, N-substituted acrylamide monomers can be used which provide steric protection to the amido bond. Poly-(acryloylaminoethoxyethanol) was shown to have dramatically improved stability over polyacrylamide at a high pH. Poly-(N-(acryloylaminoethoxy)ethyl- β -D-glucopyranose was demonstrated to be even more stable. In addition to the improved stability of the amido bond, the linkage of polymer to the capillary surface via a Si—C bond made through a silanization/hydrosilation process contributed greatly toward the length of coating's service.

Various types of polyethers and diol moieties are also effective hydrophilic coating, which often function in a manner similar to polyacrylamide. Different combinations of polyether with triethoxysilane groups or anchored poly(ethylene glycol)s have resulted in low electro-osmotic flow and low adsorptive coatings. It has also been possible to combine the characteristics of the two most common hydrophilic coatings by linking a polyvinylmethylsiloxanediol to linear polyacrylamide. As combining cellulose, functionalized polyethyleneimine

and polyether in various proportions thus allows the control of EOF that is independent of pH. The mixed phase from ethylene glycol diglycidyl ether and glycidol also exhibits low electro-osmotic flow and protein adsorption. Polysiloxanes are another type of capillary coating used in the formation of mixed materials to produce surfaces more conducive to electrophoretic conditions.

Other types of polymers have also been attached to the inner walls of fused-silica capillaries through different linking agents. A common approach involves the bonding of a methacryl group via standard organosilane chemistry. Then, bonding of another species to the linker takes place by a double-bond reaction and polymerization. For example, in the case of a cellulose coating, the species attached to the linker can be allyl methylcellulose. Other polymers include cross-linked dextrin, triblock poly(ethylene oxide)–poly(propylene oxide) and poly(vinyl alcohol).

Charged polymeric coatings are also bonded to the column surface to control the adsorption and EOF, especially in the analysis of oppositely charged species in a single run, or for fast separation of analytes with sufficient differences in electromobilities. One effective approach is the cryptand-containing polymer coating, which generates a switchable EOF depending on the pH of the running buffer. Other charged coatings can be synthesized with sulfonic acid or quaternary ammonia groups that provide more stable EOF over a fixed buffer pH range.

Capillaries with chiral polymer coatings have been applied in CE for resolution of enantiomers. Possibly because of its inclusive effect, cyclodextrin seems to be an effective chiral selective agent when bonded to a fused-silica capillary surface. In this case, the purpose of the modification is to induce interactions with the chiral material on the surface. Certainly, the cyclodextrin moiety lowers EOF like other wall modifications because it diminishes the number of silanols. The lower EOF allows for slower migration of the solute through the column and, hence, more time for interaction with the chiral selector. The diminished number of silanols also results in less nonspecific interactions with the fused-silica surface, which would tend to degrade the enantiomeric separation.

Capillaries bonded with polymeric coatings are also applied to capillary electrochromatography (CEC) for separation of neutral molecules. In this case, the polymeric coating participate to solute–bonded phases interaction in a manner similar to open-tubular LC. Most polymeric coating preparations have followed the procedures typically used in open-tubular LC and GC.

Polymer-coated columns offer advantages in the respect that the surface is generally well shielded from the



solutes as they migrate through the system. Most polymer procedures involve a multistep process that can often be time-consuming and/or experimentally difficult. Recently, it has been demonstrated that polymer coatings can be produced in a single step by mixing the polymer, a surface-derivatizing agent, and a cross-linking agent in a solvent that is then placed in the capillary. The coated capillary is then heat-treated, which removes the solvent and immobilizes the polymer film on the surface. A number of polymers were tested and higher efficiencies obtained for basic protein separation. The formation of organic-inorganic polymeric coatings by the sol-gel technique has also been reported to be a simpler way.

Further development in the preparation of polymeric coatings with more reproducible reaction con-

ditions and better reagents will make the capillary electrophoresis a more challenging separation technique.

Suggested Further Reading

Chiari, M., M. Neri, and P. G. Righetti, in *Capillary Electrophoresis in Analytical Biotechnology* (P. G. Righetti, ed.), CRC Series in Analytical Biotechnology, CRC Press, Boca Raton, FL, 1996.

Heiger, D. N. and R. E. Majors, *LC-GC 13*: 13-23 (1995).

Li, S. F. Y., Capillary electrophoresis, principles practice and applications, *J. Chromatogr. Lib.* (1993).

Schomburg, G., *Trends Anal. Chem.* 10: 163-169 (1991).



Silver Ion TLC of Fatty Acids

Boryana Nikolova-Damyanova

Bulgarian Academy of Sciences, Sofia, Bulgaria

INTRODUCTION

Fatty acids (FA) are basic structural elements of lipid molecules, determining many of their chemical and physical properties. Therefore determination of FA composition is mandatory for lipid analysis. For many years, silver ion thin-layer chromatography (Ag-TLC) has been one of the basic separation techniques employed in lipid analysis, the resolution of FA mixtures being one of the main tasks. FAs are separated according to the number, the configuration and, to some extent, the positions of the double bonds. While gas chromatography (GC) has always been the basic method in FA analysis, the specific separation features of Ag-TLC make this technique indispensable in performing certain analytical tasks. The complementary employment of gas chromatography (GC) or/and gas chromatography/mass spectrometry (GC-MS) together with Ag-TLC is probably the most powerful tool for elucidation of fatty acid composition in complex lipid samples.

SILVER ION COMPLEXATION WITH DOUBLE BONDS

The use of Ag-TLC in fatty acid analysis is based on the ability of Ag(I) to form weak, reversible charge-transfer complexes with olefinic double bonds. It is now considered that a σ -type bond is formed between the occupied $2p\pi$ orbitals of the olefinic bond, and the free $5s$ and $5p$ orbitals of Ag(I) and a weaker π -acceptor backbond is formed between the occupied $4d$ orbitals of Ag(I) and the free antibonding $2p\pi^*$ orbitals of the olefinic bond. Quantitative data on equilibrium constants exists for some short-chain mono- and diolefins only. The retention of longer-chain unsaturated compounds, such as FAs, is described on the basis of data collected by different silver ion separation techniques (mostly GC and Ag-TLC) and is supposed to depend on the strength of complexation with Ag(I). The latter, in turn, depends on the number, configuration, and the distance between double bonds. Thus the migration rules in Ag-TLC can be summarized as follows:

- The stronger FAs are held, the higher is the number of double bonds in the chain.

- FAs with *trans* double bonds are held less strongly than FA with *cis* double bonds.
- The retention of FAs with more than one double bond depends on the distance between the bonds, the order of decreasing retention being separated double bonds > methylene interrupted double bonds > conjugated double bonds.
- Longer-chain FAs are less strongly held than shorter-chain FA of the same unsaturation.
- FAs with an olefinic double bond are more strongly held than FAs with an acetylenic bond.
- Deuterated FAs are more strongly held than hydrogen analogs.

Although there is evidence that complexation with silver ions is the governing interaction in Ag-TLC, other factors should also be considered. Thus silica gel, which is the most widely used supporting material, possesses appreciable polarity and adsorption activity. Therefore, in many cases, an impact of mixed retention mechanism on migration, geometry of spots, and selectivity of resolution is to be expected. Also, the mobile-phase solvents are active elements of the chromatographic system and interactions both with the supporting material and FA is possible; this may also have a serious effect on the whole separation process.

SOME PRACTICAL CONSIDERATIONS

Both homemade and precoated glass plates are used in Ag-TLC. Silica gel G (with calcium sulfate as binder) is usually the supporting material. Layer thickness varied between 0.2–0.3 mm for analytical plates and 0.5–1.0 mm for preparative plates. Fully automated spreaders are now available, but simple spreaders are also effective. Some practice is needed to prepare the layer in the laboratory; thus precoated plates are often preferred.

The impregnation of the layer with silver ions is performed by either incorporating the silver salt into the silica gel slurry or by immersing or spraying the plate with water, ethanol, methanol, ammonia, or acetonitrile solutions of the salt. Silver nitrate is normally used. The only method that affords proper control of the Ag(I) content in the layer is to add silver nitrate to the slurry. However, this

is inconvenient and messy and is less used now. Because it is evident from analytical practice that the content of silver ions in the layer is not critical over rather broad limits, immersion and spraying are considered equally good. Immersion procedures can be sufficiently well standardized to provide satisfactory results, and can be

applied both to homemade and precoated plates. Spraying procedures are also often used in FA analysis, although they are less easily standardized and are messier. Spraying may have to be repeated from two to six times until the layer is properly wetted. This is especially important for precoated plates.

The concentrations of impregnating solutions vary depending on the purpose. Immersion or dipping is carried out most often with 0.5–20% solutions of silver nitrate, while 10–40% solutions of silver nitrate are recommended for the spraying procedure.

After impregnation, the plates are air-dried, preserved in a dark place, and activated (between 5 and 30 min at 110–120°C in an oven) before sample application.

In spite of all precautions, humidity is not easy to control and is one of the main reasons for the relatively poor overall reproducibility of separations in Ag-TLC.

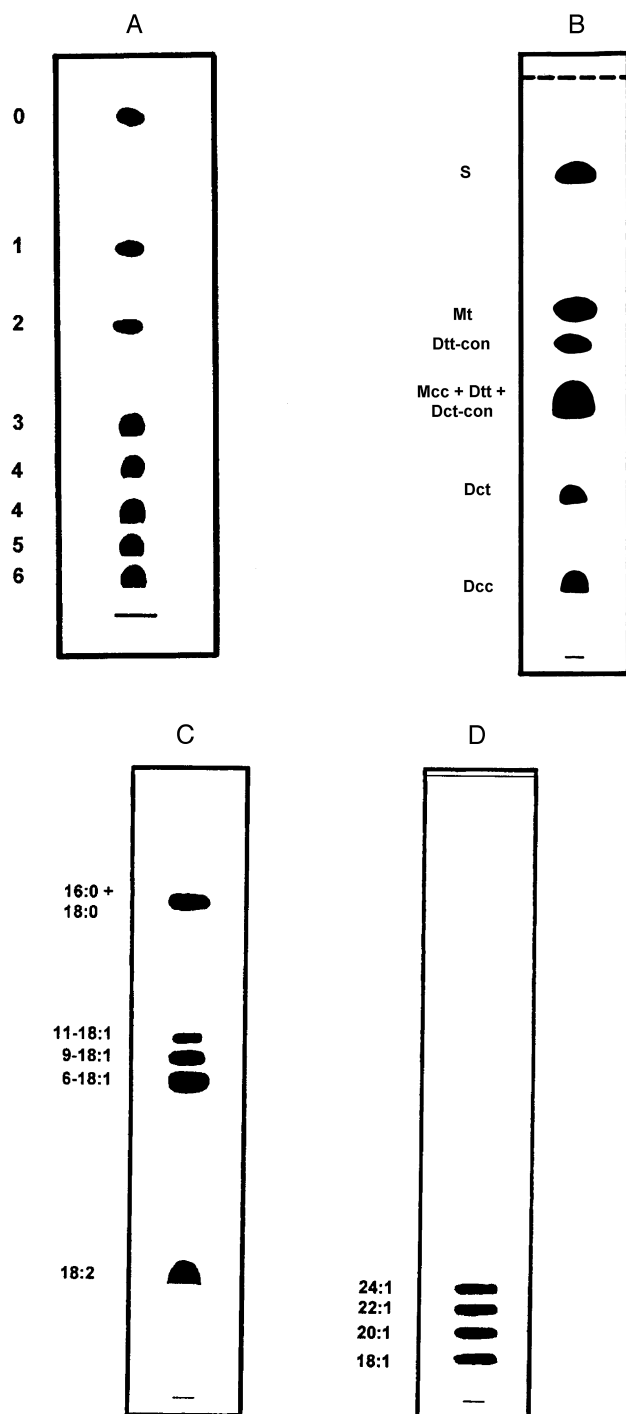


Fig. 1 (A) Separation of a reference mixture of fatty acid methyl esters by Ag-TLC according to the number of double bonds. The plate was impregnated by dipping with 0.5% methanolic silver nitrate (w/v) and developed with 5 mL of light petroleum ether–acetone–formic acid, 97:2:1 (v/v/v); spots were detected by treating the plate in sequence with bromine and sulfonyl chloride vapors, followed by heating at 180–200°C. Numbers alongside denote the number of double bonds. (From B. Nikolova-Damyanova, *Lipids by TLC*. In: *Encyclopedia of Chromatography*, (J. Cazes, ed) Marcel Dekker, New York, 2001, pp. 483–486, Fig. 1). (B) Separation of reference mixture of fatty acid methyl esters by Ag-TLC according to the configuration of the double bond. The plate was impregnated with silver nitrate as in A, and developed with 2 mL of light petroleum–acetone, 100:2 (v/v) followed by 3 mL light petroleum–acetone, 100:7 (v/v). The spots are detected as in A. S, saturated; M, monoenic; D, dienic fatty acid methyl esters; c, *cis*; t, *trans*; con, conjugated double bonds (From D. Chobanov, R. Tarandjiska, and B. Nikolova-Damyanova, Quantification of isomeric fatty acids by argentation TLC, *J. Planar Chromatogr. Mod. TLC*, 5 (1992) 157–163). (C) Separation of fatty acid phenacyl esters in *Pimpinella anisum* seed oil by Ag-TLC according to the position of the double bond in the chain. Plate was impregnated by dipping with 1% methanolic silver nitrate and was developed twice with mobile phase chloroform–acetone, 100:0.25 (v/v); a–c:n denotes the position of the double bond—the number of carbon atoms in the chain: the number of double bonds. (D) Separation of reference mixture of fatty acid methyl esters by Ag-TLC according to the chain length. The plate was sprayed with 20 mL acetonitrile containing 2 g silver nitrate until the layer was saturated. It was then activated for 30 min at 110°C and developed with toluene–hexane, 40:60 (v/v) in saturated closed standard tank. Spots were visualized by charring (the procedure was not specified). (From R. Wilson and J.R. Sargent, High-resolution separation of polyunsaturated fatty acids by argentation thin-layer chromatography, *J. Chromatogr.*, 623 (1992) 403–407).



FAs are subjected to Ag-TLC usually in the form of methyl esters. The methods for methylation and transmethylation are simple, easy to perform, and with practically 100% yield. Methyl esters are particularly suitable when Ag-TLC is used as a complementary method with GC. Butyl and isopropyl esters were employed for the fractionation of butterfat FAs by Ag-TLC because these derivatives provided better resolution in GC. Conversion of positionally isomeric 18:1 and 20:1 FAs into phenacyl esters ensured complete resolution of the components by Ag-TLC; however, this is not possible when using methyl esters.

Mobile phases generally consist of two- and, rarely, three-component mixtures. Hexane or petroleum ether (BP 40–60°C), chloroform, benzene, and toluene are most often the major components, while smaller proportions of diethyl ether, acetone, methanol, ethanol, or acetic acid may be added.

The conventional approach is to perform the development in closed standard rectangular tanks lined with filter paper to saturate the atmosphere with the mobile-phase vapors. Equal, and in many cases better, results are achieved by development in “open” cylindrical containers where a fixed volume of the mobile phase is added, passed through the plate, and permitted to evaporate from the upper edge of the plate.

Detection of separated zones depends on the analytical task. Destructive procedures are used for qualitative analysis and for quantification by photodensitometry. They consist in carbonization of the FAs by heating at 180–200°C after treating the plate with charring reagents. These can be introduced by spraying, by treatment with the respective vapors, or by incorporation of the reagent into the layer. Up to 50% ethanolic sulfuric or phosphomolybdic acids and copper acetate–phosphoric acid have been used as spraying reagents. Reliable results have been obtained by saturating the silica gel layer with vapors of sulfonyl chloride. Nondestructive procedures are used in preparative Ag-TLC. It is performed by spraying the plate with a fluorescent indicator, mostly 2,7-dichlorofluorescein in ethanol, and viewing under UV light. The bands are then scraped from the plate and extracted with diethyl ether or hexane–methanol (in appropriate proportions). The excess silver ions and indicator are removed by passing the extract through a small silica column, or by washing with bicarbonate, ammonia, or sodium chloride solutions.

Examples of the separation of fatty acid derivatives by Ag-TLC are given in Fig. 1.

CONCLUSION

Silver ion TLC is a simple but reliable approach for separation, identification, quantification, and preparative isolation of fatty acids in lipid samples, depending on the number, configuration, position, and chain length (see Refs. [1–9] for additional information).

ACKNOWLEDGMENT

The partial financial support of the Bulgarian National Science Fund, Contract No. X1009, is gratefully acknowledged.

REFERENCES

1. Morris, L.J. Separation of lipids by silver ion chromatography. *J. Lipid Res.* **1967**, 7, 717–732.
2. de Ligny, C.L. The Investigation of Complex Association by Gas Chromatography and Related Chromatographic and Electrophoretic Methods. In *Advances in Chromatography*; Grushka, E., Cazes, J., Brown, P.R., Eds.; Marcel Dekker: New York, 1976; Vol. 14, 265–304.
3. Christie, W.W. *Lipid Analysis*; Pergamon Press: Oxford, 1982.
4. Christie, W.W. *Gas Chromatography and Lipids*; The Oily Press: Ayr, 1989.
5. Nikolova-Damyanova, B. Silver Ion Chromatography and Lipids. In *Advances in Lipid Methodology—One*; Christie, W.W., Ed.; The Oily Press: Ayr, 1992; 181–237.
6. Firestone, D.; Shepperd, A. Determination of *trans* Fatty Acids. In *Advances in Lipid Methodology—One*; The Oily Press: Ayr, 1992; 273–322.
7. Nikolova-Damyanova, B. Quantitative thin-layer chromatography of triacylglycerols: Principles and application. *J. Liq. Chromatogr. Relat. Technol.* **1999**, 22, 1513–1537.
8. Fried, B.; Sherma, B. *Thin-Layer Chromatography*; Marcel Dekker: New York, 1999; 197–222.
9. Nikolova-Damyanova, B.; Momchilova, Sv. Silver ion TLC of fatty acids—A survey. *J. Liq. Chromatogr. Relat. Technol.* **2001**, 24, 1447–1466.



Size Separations by Capillary Electrophoresis

Robert Weinberger

CE Technologies, Inc., Chappaqua, New York, U.S.A.

Introduction

Electrophoretic separation based on molecular size is the predominant technique for the separation of large biomolecules [1]. Using the traditional slab-gel, a rigid anticonvective gel is required to provide mechanical stability for the separation. The gels are designed for a single use at relatively low electric field strengths.

During the early days of high-performance capillary electrophoresis (HPCE), rigid gels were polymerized *in situ* within the capillary. These gel-filled capillaries were used for multiple runs at high field strengths. The capillaries were prone to failure and proved too unreliable for routine use. It was soon discovered that low-viscosity pumpable media was capable of defining molecular pores required for a size separation. In the capillary format, the walls of the tube provide the requisite mechanical stability, so high viscosity gels are unnecessary. These solutions are known as polymer networks, entangled polymers, or physical gels. When polymer networks are used for size separations, a fresh matrix is employed for each run. Through the use of high-pressure pumping systems, polymer networks suitable for DNA sequencing can be pumped in and out of the capillary.

This technology has facilitated the development of instruments containing arrays of 96 capillaries for high-throughput applications such as DNA sequencing. Other high-throughput DNA applications that will eventually be incorporated include genetic analysis and human identification. Ultimately, microfabricated devices may be used for many of these applications.

Separation Mechanism

Several mechanisms for the migration of macromolecules through polymer networks have been described. The Ogston model considers the molecule as a nondeformable sphere. The speed of migration is based on the mobility of the solute in free solution modified by the probability of an encounter with a restricting pore.

This mechanism is operative when the radius of gyration of the macromolecule is less than or equal to the average pore size of the polymer network. Separation of sodium dodecyl sulfate (SDS)–proteins is thought to occur following this mechanism.

Large biopolymers, such as DNA and oligosaccharides, do not follow the Ogston model. These molecules can deform during transit through the porous network. Instead, a strand of DNA can move through the polymer matrix in a snakelike manner known as reptation. It is also known that fragment resolution decreases as the length of macromolecule increases. The molecules align with the electric field in a size-dependent manner. This process is known as biased reptation. The effect limits the size of DNA molecules that can be separated using conventional slab-gel techniques. The high electric field strength used in CE further limits the separation. Beyond 20,000 base pairs (bp), separations become poor and pulsed-field techniques must be employed [2]. This equipment is not available for commercial capillary electrophoresis instrumentation.

Further masking a full understanding of the separation mechanism is the interaction of the macromolecule with the polymer network reagents. Separations have been reported in polymer concentrations far below what is required to define pores [3].

Denaturation of Macromolecules

Because separations occur based on molecular size, the macromolecule must be denatured to ensure that all solutes have the same charge-to-mass ratio. DNA and RNA are denatured by heating in formamide at 90°C for a few min. This improves both the separation and sizing accuracy.

To denature proteins, the disulfide bonds must be reduced and the molecule must be unfolded. Heating to 90–95°C for a few minutes using a solution composed of 0.1% SDS and a reducing agent, β -mercaptoethanol or dithiothreitol (DTT), is sufficient to de-



nature most proteins. When the molecular weight of a protein is less than 10 kDa, the SDS binding stoichiometry may change resulting in errors when calculating molecular weight [4].

Materials for Polymer Networks

A wide variety of polymeric materials can be employed for size separations. It appears that the molecular weight and concentration of the polymer is more important than the polymer type itself. Once the polymer concentration is greater than the overlap threshold, the porous matrix is defined and reproducible. It is best if the polymer does not interact with the macromolecules being separated.

Among the materials used as polymer network reagents are linear polyacrylamide, dimethylpolacrylamide, methylcellulose derivatives, poly(ethylene oxide) and others. The appropriate molecular weight of the polymer is important. Sometimes, blends of different molecular weights are used. For example, the mixture of 2% linear polyacrylamide (LPA), molecular weight (MW) = 9 mDa and 0.5% LPA, MW = 50 kDa is used to separate DNA sequencing reaction products of up to 1000 bases in less than 1 h, as shown in Fig. 1 [5]. The viscosity of this polymer is 30,000 cps. The solution exhibits non-Newtonian properties as the viscosity drops upon the initiation of flow. The use of 2% 16 mDa LPA and 0.5% 250 kDa at 125 V/cm extends the read length to 1300 bases in 2 h [6].

Injection

Electrokinetic injection provides the highest-efficiency separations. If the salt concentration of the sample is greater than 50 mM, hydrodynamic injection gives better results. It is better to desalt the sample by dialysis, precipitation, or ultracentrifugation.

Detection

For SDS-proteins, low-ultraviolet (UV) detection at 200 nm or 220 nm is used depending on the UV transparency of the polymer network. For oligonucleotides, UV detection at 260 nm is employed. When performing DNA sequencing, short tandem repeat or genetic analysis, laser-induced fluorescence (LIF) is the method of choice. Intercalating dyes

such as YOYO or YO-PRO fluorescence when complexed in between the DNA strands are sometimes added to the background electrolyte when monitoring polymerase chain reaction (PCR) products and restriction digests and for genetic analysis. For DNA sequencing, the fluorescent tag is incorporated in the chain-terminating dideoxynucleotide reagent. When separating short tandem repeats for human identification, the PCR primers can incorporate the fluorescent tag.

When separating oligosaccharides in polymer networks with LIF detection, a good tagging reagent is 9-aminopyrene-1,4,6-trisulfonic acid (APTS). This reagent is used in conjunction with the argon-ion laser.

Applications

DNA applications, in particular DNA sequencing, human identification, and genetic analysis dominate the field. Other DNA applications including oligonucleotides, antisense DNA, restriction fragments, plasmids, PCR products, hybridization (DNA probe), and RNA have also been demonstrated [7,8].

DNA testing is rapidly becoming the predominant technique for human identification. The restriction fragment-length polymorphism (RFLP) method requires large amounts of DNA (20–100 ng) and is extremely time-consuming and labor-intensive.

A PCR method employing short tandem repeats (STR) is now the method of choice. STRs are sequences where two to seven nucleotides of DNA are constantly repeated. Unlike the DNA of a gene, STRs are prone to DNA replication errors. The lengths of these fragments vary from one person to the next, thereby providing the potential for DNA fingerprinting. The use of PCR and LIF detection provides high sensitivity, so very little DNA is required. The need for higher specificity is addressed with multiplex PCR, where several dye-labeled primers simultaneously amplify multiple locations throughout the genome.

The most widely used genetic screening technique, PCR-RFLP detects a mutation at a specific restriction endonuclease cleavage site at the mutation locus [9]. The products from other techniques such as ARMS (amplification refractory mutation system), SSCP (single-strand conformational polymorphism), HPA (heteroduplex polymorphism), and CDCE (constant denaturant capillary electrophoresis) and PCR are usually separable using polymer networks.



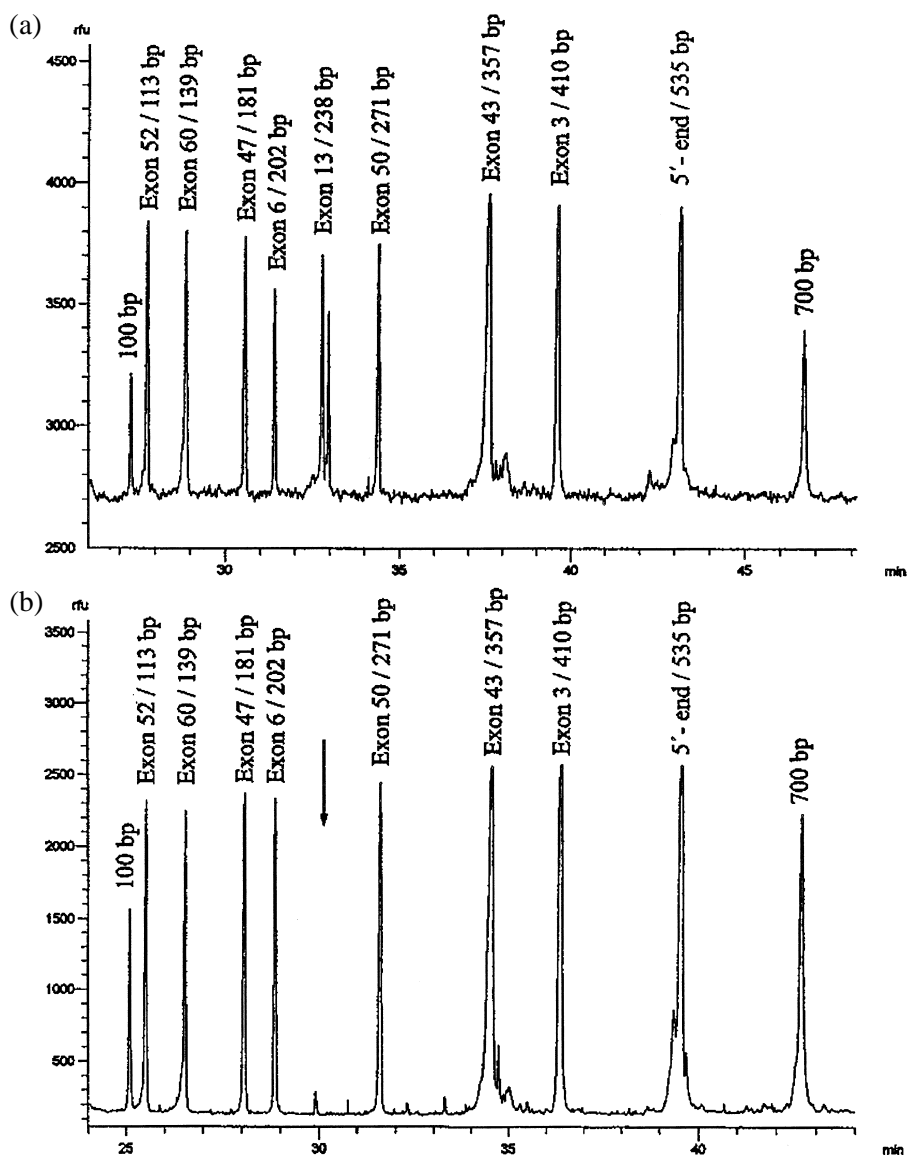


Fig. 2 Multiplex PCR profile of exons in Duchenne or Becker muscular dystrophy genes combined with two flanking standards. Capillary: 40 cm (65 cm total length) \times 75 μ m polyacrylamide coated; background electrolyte: 0.5% poly(ethylene oxide), 1 MDA in 1X Tris-borate-EDTA, 10 μ M aminoacridine, 2 nM Vistra Green; field strength: 108 V/cm; detection: LIF, 488 nm. [Reprinted with permission from *J. Chromatogr. A* 781: 295 (1997), copyright 1997, Elsevier Science Publishers.]

Polymerase chain reaction is particularly useful for genetic analysis because both amplification and primer specific isolation of gene fragments occur simultaneously. Allele-specific amplification can be employed to detect a single base-pair mutation through the use of a specially designed primer which is complementary to

the mutated DNA [10]. PCR amplification only takes place if the mutation is present. Figure 2 illustrates the separation of multiplex PCR fragments in this case, searching for specific deletions in the dystrophin gene thought to result in Duchenne muscular dystrophy. The deletion is indicated by the arrow.

References

1. R. Westheimer, N. Barnes, Gronau-Czybalka, and C. Habeck, *Electrophoresis in Practice: A Guide to Methods and Applications of DNA and Protein Separations*, 2nd ed., John Wiley & Sons, New York, 1997.
2. Y. Kim and M. D. Morris, *Anal. Chem.* 66: 3081 (1994).
3. A. E. Barron, H. W. Blanch, and D. S. Soane, *Electrophoresis* 15: 597 (1994).
4. T. Takagi, *Electrophoresis* 18: 2239 (1997).
5. O. Salas-Solano et al., *Anal. Chem.* 70: 3996 (1998).
6. A. W. Miller, Z. Sosic, B. Buckholz, A. E. Barron, L. Kotler, B. L. Karger, *Anal. Chem.* 72: 1045 (2000).
7. P. G. Righetti (ed.), *Capillary Electrophoresis in Analytical Biotechnology*, CRC Press, Boca Raton, FL, 1996.
8. C. Heller (ed.), *Analysis of Nucleic Acids by Capillary Electrophoresis*, Vieweg, Weinheim, 1997.
9. K. R. Mitchelson and J. Cheng, *J. Capillary Electrophoresis* 2: 137 (1995).
10. C. Barta, M. Sasvari-Szekely, and A. Guttman, *J. Chromatogr. A* 817: 281 (1998).



Solute Focusing Injection Method

Raymond P.W. Scott

Scientific Detectors Ltd., Banbury, Oxfordshire, England

Introduction

In capillary-column gas chromatography, split injections are necessary to ensure that a very small, compact sample is placed on the column. However, split injections generally result in an unrepresentative sample being placed on a capillary column; thus, on-column injection is usually preferred for accurate quantitative analysis.

Discussion

On-column injection demands the use of large-diameter tubes to permit the penetration of the injection syringe needle into the column. However, this procedure also causes other problems to arise. On injection, the sample readily separates into droplets which act as separate, and individual, injections that cause widely dispersed peaks and serious loss of resolution. In the extreme, double or multiple peaks are formed. Grob [1] suggested two solutions to this problem: the retention gap method of injection and the solute focusing method.

The solute focusing method is claimed to be more effective than the retention gap method, but the technique requires more complicated equipment. In the solute focusing method, the injector is designed so that there are two consecutive, independently heated and cooled column zones, located at the beginning of the column. A diagram of the solute focusing system and its mode of action is shown in Fig. 1. Initially, both zones are cooled and the sample is injected onto the first zone, where immediate sample splitting almost inevitably occurs. The carrier gas is then allowed to preferentially remove the solvent by eluting it through the column, leaving the contents of the sample dispersed along the cooled section of the tube. The selective removal of the solvent occurs because the solvent components are significantly more volatile than the components of the sample, even at the reduced temperature. The first zone is then heated and the second zone is continued to be kept cool. The solutes in

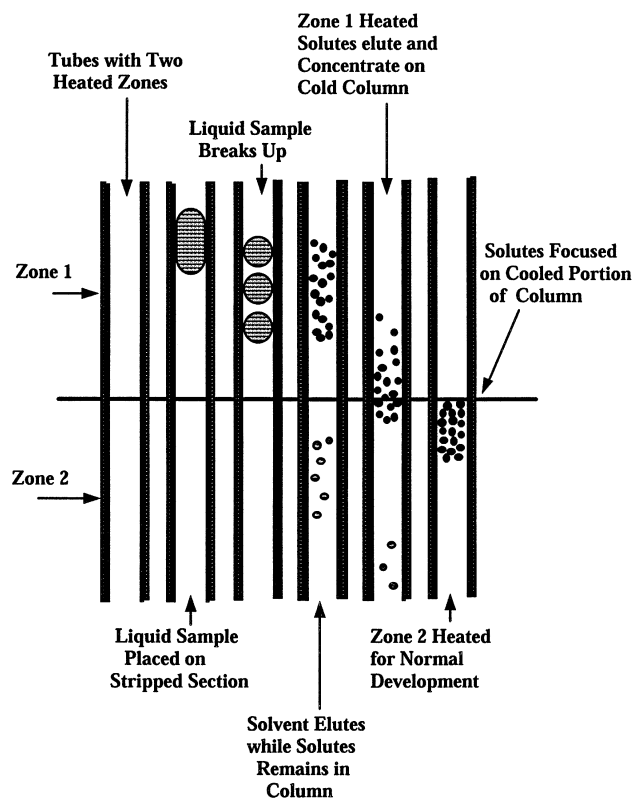


Fig. 1 The solute focusing method.

the first zone progressively elute through the zone at the higher temperature until they meet the cooled zone. The movement of all the components is now significantly slowed down and they begin to accumulate at the beginning of the cooled second zone. The net effect is that the entire sample is now focused at the beginning of the cooled portion of the column. The temperature of the second zone is now programmed to the appropriate rate and the separation developed in the usual manner. This technique has more flexibility than the retention gap method, but the apparatus and the procedure is more complex and expensive. It should be pointed out that sample splitting does not



occur in packed columns. It follows that if the sample is amenable to separation on such columns, then the packed column may be the column of choice if high accuracy and precision are required.

Reference

1. K. Grob, *Classical Split and Splitless Injection in Capillary Gas Chromatography*, Huethig, Heidelberg, 1987.

Suggested Further Reading

- Grant, D. W., *Capillary Gas Chromatography*, John Wiley & Sons, Chichester, 1995.
- Scott, R. P. W., *Techniques and Practice of Chromatography*, Marcel Dekker, Inc., New York, 1996.
- Scott, R. P. W., *Introduction to Analytical Gas Chromatography*, Marcel Dekker, Inc., New York, 1998.



Solute Identification in TLC

Gabriela Cimpan

Tonbridge, Kent, United Kingdom

INTRODUCTION

Solute identification means qualitative analysis. Various methods are used today to identify a separated substance on a thin-layer chromatographic plate. Of all chromatographic methods, thin-layer chromatography (TLC) provides a unique simultaneous separation of up to 70 samples on the same plate; therefore the reproducibility of the experimental conditions is not an issue because the experimental conditions are the same for all samples. This, together with the advantage of separating compounds with very different polarity and the possibility of using different detection methods for the same spot or for adjacent spots on the same plate, is the power of TLC.

UV-VIS DETECTION

Observing a substance in UV or visible light is the simplest way of detection and identification of the substance in TLC. If the substance is fluorescent, the identification is most reliable. However, many substances show similar behavior in UV light or have similar colors in visible light. Therefore a more accurate way of identification is required.

Often, the R_f value of the separated substances is compared with the R_f values of references. Not a long time ago, this information, together with the similar color, was usually enough to identify a substance. Today, modern densitometers are capable of measuring, more accurately, migration distances (therefore the R_f value) and to scan the in situ UV-Vis spectrum of the spot.

The majority of substances do not provide enough information based on their UV-Vis spectra; therefore a derivatization reaction should be applied to enhance the identification range. The derivatization is a chemical reaction designed to selectively improve the spectral characteristics of the separated substances and can be performed before or after the chromatographic separation. The prechromatographic derivatization can be performed during sample preparation or directly at the starting zone on the TLC plate. A preconcentration zone is recommended for the in situ prechromatographic derivatization reaction because all the formed substances will

be concentrated at the starting point before the chromatographic separation. Postchromatographic derivatization can be nondestructive or destructive, and it is performed by covering the TLC plate with a homogenous layer of reagent, either by spraying or dipping. Sometimes, heating the plate is necessary for reaction completion.

If the substance is colored, the visible spectrum of the separated substance is recorded and compared with the reference spectrum. If the substance is not colored, but is active in UV light, there are two ways of identifying it, i.e., by fluorescence quenching, when the substance quenches the layer fluorescence, or by measuring the native fluorescence of the substance (before and/or after derivatization). UV-Vis fluorescence covers more than a third of the total methods of identification used in TLC, while the derivatization technique represents a similar percentage. All derivatization reactions are specific for chemical groups. The rest of about 20% consist of other methods of identification used in TLC: IR, MS, etc.

INFRARED DETECTION

The on-line technique for coupling high-performance thin-layer chromatography (HPTLC) with Fourier transform infrared spectroscopy (FTIR) has provided a powerful tool of using IR spectra and the rich information for the compound identification in TLC. The information contained in a UV-Vis spectrum is poor compared with IR, and only the chromophores can be identified by the former method. Thin-layer chromatography was first coupled with FTIR in 1989, thereby providing a powerful tool for in situ measurement of separated compounds, with applications in the pharmaceutical, biological, environmental, and related sciences. Even the substances which do not absorb in UV have an IR spectrum; thus the method is universal. However, the strong IR absorption of the conventional stationary phases used in planar chromatography is a serious drawback of on-line coupling of HPTLC-FTIR.

The FTIR spectrometer is connected to the external unit by an interface mirror which diverts the beam to the spot on the plate. The reflected beam is then collected by using another set of mirrors and directed to a mercury

cadmium telluride (MCT) narrow-band detector. This instrument can be used even with the strong absorbing layers used in TLC.

Various classes of drugs can be identified from complex mixtures by this method. UV-Vis spectra can help to recognize different structural groups; then, FTIR can further identify the compounds. All the spectra can be included in UV-Vis or IR spectral libraries and can be used as references for further assays.

The HPTLC-FTIR on-line coupling has been used for analyzing compounds from complex biological matrices where the number of compounds can be very high and the polarities very different; gradient development often has to be applied to obtain a separation.

Further development in obtaining and interpreting the data in this method will allow the identification and quantitation of separated unknown compounds.

RAMAN SPECTROSCOPY

Raman spectroscopy is the measurement of the wavelength and intensity of inelastically scattered light from molecules. The Raman scattered light occurs at wavelengths that are shifted from the incident light by the energies of molecular vibrations. The mechanism of Raman scattering is different from that of infrared absorption, and Raman and IR spectra provide complementary information. Typical applications are in structure determination, multicomponent qualitative analysis, and quantitative analysis. The most common light source in Raman spectroscopy is an Ar-ion laser. Because Raman scattering is a weak process, a key requirement to obtain Raman spectra is that the spectrometer should provide a high rejection of scattered laser light. New methods, such as very narrow rejection filters and Fourier-transform techniques, are becoming more widespread.

Special HPTLC plates allow direct Raman spectroscopy to be run after the separation without removal from the plate. They are made of a special 3–5 μm spherical silica gel on a 10 \times 10 cm plate. The thickness is 0.1 mm to allow more of the compound to reside on the surface for this analysis.

Modern Raman spectrometers allow scanning of a surface up to A4 size, with XY translation stage and fine spatial adjustment to allow the operator to align the laser probe onto samples as small as 5 μm in diameter. Sample selection is assisted by the use of an integral video microscope with a rotating turret that can be fitted with up to four objective lenses to provide on-screen magnification of up to 500 \times .

Surface-enhanced resonance Raman scattering (SERRS) is a very sensitive technique with many applications, especially in forensic analysis. SERRS was successful in

differentiating the majority of the 26 inks examined in an experiment designed to show that the method is less invasive than TLC and can be used coupled with an HPTLC plate.

MASS SPECTROMETRIC DETECTION

The on-line coupling between TLC and mass spectrometry provides a powerful combination for the detection and identification of substances separated by a planar chromatographic method. The on-line coupling between these two methods has to overcome the problem of vaporizing and introducing the sample into the mass spectrometer. Different methods are reported in the literature, but the analytical principle is the same: the sample is ionized from the layer surface by means of a laser beam, under vacuum, and in the presence of an energy-buffering matrix. Once the ions are transferred into the mass spectrometer, more sophisticated methods can be applied for data analysis and interpretation, e.g., MS-MS.

In planar chromatography, the sample is fixed on the layer and can be found in three-dimensional space. The interface between the layer and MS must separate the compound molecules from the layer molecules and must present a way to transport them into the MS, either via a liquid or a gaseous phase. The main difference between MS and the spectroscopic methods is that MS is a destructive method, consuming the sample, while the others are nondestructive.

The samples can be removed from the layer-by-laser desorption or matrix-assisted laser-desorption ionization (MALDI) which can be coupled with a time-of-flight (TOF), ion trap, or Fourier-transform mass spectrometer. MS-MS can also be an option for further analysis. The electron or chemical ionization methods are most commonly used to break the sample molecules into fragments (ions) in the gaseous phase. The obtained spectra can be used for sample identification by comparison with a spectral library. The laser desorption ionization assisted by a matrix (MALDI and SALDI techniques) uses the ionization of the sample at the surface of the thin layer, and the matrix plays a role of energy buffer. Electrospray ionization is another method of transferring the sample to the MS by spraying organic solvents containing the molecules of the sample.

The presence of the layer material, together with the sample, raises many problems in designing an appropriate interface for TLC-MS. More details can be found in the bibliographic references.

The instrumentation for TLC-MS is not as widespread as for other chromatographic methods (e.g., GC-MS and LC-MS) mainly because of the complexity of the interface involved.



IMAGE ANALYSIS

Image analysis has brought new possibilities to compound detection, identification, and quantitation in TLC; it takes advantage of the main benefit of planar chromatography, i.e., the possibility of separating and analyzing up to 70 samples on a single plate. The image can be obtained by charge-coupled device (CCD) cameras, digital camcorders, or flatbed scanners and can be further processed with a computer. The power of image-analysis systems relies on good resolution and contrast and the capacity to minimize the distortion and the perspective errors from a lens. The settings of the factors for obtaining a good image can be different from sample to sample. Although the colored image is more similar to the real chromatographic plate, the black and white image, with shades of gray, can be interpreted better by the human eye, as it is more sensitive to small changes in black and white than are colors.

Charge-coupled devices have been used as detectors in planar chromatography, although more applications have been found in quantitative analysis. Videodensitometers have been used to measure the absorption or the fluorescence of a separated spot on a TLC plate.

The miniaturization of the TLC technique will be a challenge for image analysis, but, probably, this will be the technique for creating image libraries for compounds or for complex mixtures such as plant extracts.

PHOTOACOUSTIC DETECTION

Nonuniformity of the layer or of the sample distribution in the layer and light scattering are some of the difficulties that an on-line spectroscopic detection method has to overcome.

Photoacoustic detection measures the pressure variation caused by the heating of a gas in the vicinity of the sample. If the sample is enclosed in a photoacoustic cell equipped with a microphone, the modulated signal can be interpreted as a function of temperature, pressure, and the quantity of the sample.

Since photoacoustic spectroscopy (PAS) was first reported in 1975, the method was gradually improved, and now, nanograms to picograms of substances can be successfully detected and quantified on TLC plates. When the method was first developed, the separated spot had to be scratched from the plate and introduced into the PAS cell for the measurements; but now, the PAS cell can be fixed directly onto the layer surface. Other instruments can be laser-based densitometers with signal enhancement at a resonant frequency of the cell. The detection limit is very low in this case, and the linearity of the quantitative determination is over 3 orders of magnitude. Moreover,

FTIR can be used in combination with the PAS technique for in situ measurements. The presence of helium might be necessary to prevent high background noise, which is mainly produced by the silica-based layer.

FLAME IONIZATION DETECTION

Thin-layer chromatography coupled with on-line flame ionization detection (TLC-FID) has been developed for the analysis of organic substances which show no UV absorption and no fluorescence and which present difficulties by GC analysis.

Planar chromatography is usually performed on a quartz rod (Chromarod[®]) coated with a thin layer of silica or alumina onto which the sample is developed and separated. The rod is advanced at a constant speed through the flame of the FID, and the substances are ionized through energy obtained from the hydrogen flame. Influenced by the electric field applied to the poles of the FID, the ions generate electric current with an intensity proportional to the amount of each organic substance entering the flame. Spotting of the sample is performed with a specially designed application system; the rods are further developed in special development tanks, then the rods are scanned through the hydrogen flame.

Applications have been reported in many areas including analysis of lipids, oils, fatty acids, polymers, asphalt, and surfactants. The advantages of this method are high throughput, low cost per sample, easy quantitation using standard chromatography software, and simple method development analogous to standard TLC.

The quantitation of samples using Chromarods is not very linear, as the rods are not uniform, but nevertheless, the method remains a very useful tool for difficult samples.

DIGITAL AUTORADIOGRAPHY

Digital autoradiography (DAR) can be used in combination with TLC for the analysis of radiolabeled compounds, most frequently ³H and ¹⁴C. The method is simple and requires reasonably priced instrumentation; therefore it is widely used for biochemical and pharmacological applications. The instrumentation for TLC-DAR can scan a 20 × 20 cm area, the radioactivity bands are visualized with a digital radiograph, and the digital data are processed with a high-capacity computer.

The analysis of samples in biological matrices is extremely powerful compared with drawbacks such as narrow concentration range for quantitative measurements and long time required for spot detection. Digital autoradiography can be used in hyphenated off-line and



on-line methods. A powerful example is TLC-DAR-FABMS (-MS) with applications in in vitro and in vivo metabolism studies.

autography is an additional method for the screening of biologically active compounds and provides good selective postchromatographic detection.

BIOAUTOGRAPHY

Bioautography is a method developed for the study and analysis of biologically active substances from simple samples to complex biological matrices. Antimicrobial activity is the monitored parameter, and it can be either growth-inhibiting or growth-promoting.

The screening of biological activity can be performed by diffusion method, dilution method, and bioautography.

The diffusion method uses an agar layer impregnated with the organism being tested; a filter paper disk containing the sample is placed on top. After an appropriate incubation time, the paper disk is removed and the average diameter of each zone of growth inhibition is measured.

In the dilution method, the sample is mixed with a suitable medium which has been previously impregnated with the organism being tested. After the incubation time, the growth of microorganisms can be determined by comparing the test culture with a control culture.

Bioautographic methods involve a chromatographic layer containing the biologically active compound which migrates, by diffusion, to an inoculated agar plate. The inhibition zones can be easily visualized by specific reagents. In direct bioautography, the microorganisms grow directly on the TLC plate and further analysis steps are performed on the plate. Silica gel and cellulose plates produce good results, while polyamide and aluminum oxide are not recommended for this type of assay. Bio-

FURTHER READING

- Barman, B.N. J. Chromatogr. Sci. **1996**, 34, 219–225.
- Bhullar, A.G.; Karlson, D.A.; Backer-Owe, J.; Le Tran, K.; Skalmes, E.; Berchemmann, H.H.; Kittelsen, J.E. J. Pet. Geol. **2000**, 23, 221–244.
- Charge-Transfer Devices in Spectroscopy*; Sweedler, J.V., Ratzlaff, K.L., Denton, M.B., EdsVCH: New York, 1994.
- Filthuth, H. J. Planar Chromatogr. **1989**, 2, 198–202.
- Filthuth, H. *Planar Chromatography in the Life Sciences*; Touchstone, J.C., Ed.; John Wiley: New York, 1990; 167–183.
- Kawazumi, H.; Yeung, E.S. Appl. Spectrosc. **1988**, 42, 1228–1231.
- Kovar, K.A.; Enblin, H.K.; Frey, O.R.; Rienas, S.; Wolff, S.C. J. Planar Chromatogr. **1991**, 4, 246–250.
- Pfeifer, A.; Tolimann, G.; Ammon, H.P.T.; Kovar, K.A. J. Planar Chromatogr. **1996**, 9, 31–34.
- Planar Chromatography, A Retrospective View for the Third Millennium*; Nyiredy, Sz., Ed.; Springer Scientific Publisher: Budapest, 2001.
- Proceedings of the 1st International Meeting on Imaging Techniques in Planar Chromatography, Jezersko, Slovenia, 1999; Vovk, I., Prošek, M., Medja, A., Eds.
- Rosencwaig, A.; Hall, S.S. Anal. Chem. **1975**, 47, 548–549.
- Viger, A.J.; Robert, J.K.; Selitrennikof, C.P. Mol. Plant-Microb. Interact. **1991**, 4, 315–323.
- Wilson, I.D. J. Chromatogr., A **1999**, 856, 429–442.
- Wilson, I.D.; Morden, W. LC GC Int. **1999**, 12, 72–80.



Solvent Effects on Polymer Separation by ThFFF

Wenjie Cao

Mohan Gownder

Huntsman Polymers Corporation, Odessa, Texas, U.S.A.

Introduction

The early research of Myers et al. [1,2] shows that polymer thermal field-flow fractionation (ThFFF) retention and thermal diffusion are solvent dependent. Recently, Sisson and Giddings [3] indicated that polymer ThFFF retention could be increased by mixing solvents. Rue and Schimpf [4] extended the molecular-weight range that can be retained by ThFFF to much lower molecular weights (<10 kDa) by using solvent mixtures without using extreme experimental conditions. There are several other reports on the effect of solvents on polymer retention, selectivity, and the universal calibration in FFF in last few years [5].

Discussion

The dissolving of a polymer into a solvent is governed by the free energy of mixing [6],

$$\Delta G_m = \Delta H_m - T\Delta S_m \quad (1)$$

where ΔG_m is the free-energy change of the solution, ΔH_m is the enthalpy change of the solution, and ΔS_m is the entropy change of the solution.

The enthalpy change is given by

$$\Delta H_m = V \left(\left(\frac{\Delta E_1^v}{V_1} \right)^{1/2} - \left(\frac{\Delta E_2^v}{V_2} \right)^{1/2} \right)^2 \phi_1 \phi_2 \quad (2)$$

where V is the volume of the mixture, ΔE_i^v is the energy of vaporization for species i , V_i is the molar volume of species i , and ϕ_i is the volume fraction i in the solution.

The solubility parameter, δ_i , has been defined [6] as the square root of the cohesive energy density (CED), $\Delta E_i^v/V_i$, and describes the strength of attraction between molecules:

$$\delta_i = \left(\frac{\Delta E_i^v}{V_i} \right)^{1/2} \quad (3)$$

Equation (1) may be rewritten as

$$\Delta G_m = V(\delta_1 - \delta_2)^2 \phi_1 \phi_2 - T\Delta S_m \quad (4)$$

Because the second term, the entropy term, is always positive for the process of polymer dissolution, the deciding factor in determining the sign of the

Gibbs energy change in Eq. (4) is the first term, which contains the solubility parameters of the polymer and the solvent. In general, $(\delta_1 - \delta_2)^2$ must be small for the polymer and the solvent to be miscible. A polymer dissolves most easily in a solvent whose solubility parameter matches it or is close to its own. This is consistent with the “like dissolves like” rule.

If a polymer is easily soluble in a solvent, by convention, the solvent is called a good solvent, and the converse, it is a poor solvent [6]. Therefore, a solvent whose δ value is close to the δ value of a polymer family is a good solvent for this polymer family. As examples, the δ value of polystyrene (PS) is about 18, which is closer to the δ value of 18.6 of tetrahydrofuran (THF) than the δ value of 16.8 of cyclohexane (CH). Therefore, THF is expected to be a better solvent for PS than CH. For polyisoprene (PIP), the situation is reversed; CH is a better solvent than THF.

Polymer molecules tend to spread out to a larger hydrodynamic size in a good solvent than they do in a poor solvent, which results in a reduced diffusion coefficient D as the Stoke–Einstein equation shows:

$$D = \frac{kT}{6\pi\eta R_h} \quad (5)$$

where k is the Boltzmann constant, T is the absolute temperature, η is the solvent viscosity, and R_h is the hydrodynamic radius of the polymer molecules in a solvent.

The retention of polymer molecules in thermal field-flow fractionation is determined by the diffusion coefficient and the thermal diffusion coefficient D_T , illustrated approximately by [8]

$$\frac{t_r}{t^0} \approx \frac{1}{6\lambda} = \frac{\Delta T}{6} \frac{D_T}{D} \quad (6)$$

where λ is the reduced mean layer thickness of a sample zone in the ThFFF channel, t_r is the polymer retention time, t^0 is the elution time of the nonretained species, and ΔT is the temperature difference across the channel thickness.

From the point of view of diffusion, the reduced D , obtained by replacing a poor solvent with a good solvent, will result in smaller λ if ΔT and other experi-



mental conditions are kept unchanged. The reduced λ (sample zone is closer to the accumulation wall) will cause the polymer molecules to elute out of the ThFFF channel later because of the parabolic flow inside a ThFFF channel [8]. Higher retention, therefore, should be expected for polymers eluted by good solvents in ThFFF.

D_T for the polymer solution is not well understood. There are several theories of polymer thermal diffusion in liquids. Extensive reviews have been done by Schimpf and colleagues in several publications [4,9]. As an example, the radiation pressure theory of Gaeta and Scala shows that D_T is proportional to the cross-sectional area of the solute molecules [10]:

$$D_T = Z_A \left(\frac{\kappa_s}{U_s} - \frac{\kappa_p}{U_p} \right) \frac{\sigma}{f} \quad (7)$$

where Z_A is the acoustical impedance, a quantity related to the density and velocity of sound waves in the polymer and solvent, κ_p and κ_s are the thermal conductivity of the polymer and solvent, respectively, U_p and U_s are the corresponding velocities of sound in the two media, f ($f \propto \eta R_h$) is the frictional coefficient, and σ ($\sigma = \pi R_h^2$) is the cross-sectional area of the polymer molecules.

As discussed earlier, the sizes, or cross-sectional areas, of polymer molecules dissolved in a good solvent are larger than that in a poor solvent. Therefore, the D_T of a polymer in a good solvent is predicted to be larger than that in a poor solvent according to Eq. (7).

From the point of view of both diffusion and thermal diffusion (assuming Gaeta's theory is correct in this case), ThFFF retention of a polymer should be larger in a good solvent than in a poor solvent.

The study of Sisson and Giddings [3] shows that polymer retention in some binary solvents can be enhanced while retention is relatively unaffected or even diminished in other cases. In the case of a mixture of 30% dodecane and 70% THF, polymer retention was enhanced by 35% relative to pure THF. The low end of the molecular-weight range, which can be analyzed by ThFFF, therefore, can be expanded further down by using binary carriers.

Rue and Schimpf [4] investigated component partition of a solvent mixture under thermal gradient. It is indicated that when one solvent is a significantly better solvent for a polymer, then the gradient of this solvent will cause the polymer to migrate in the same direction as the thermophoretic motion of this solvent. This is called solubility-based migration as a partitioning effect. When the better solvent partitions to the cold wall of the ThFFF channel, polymer retention is enhanced; when the better

solvent partitions to the hot wall, retention is diminished. Five polystyrene samples, ranging in molecular weight from 2500 to 179,000, were separated in a mixture carrier containing 45 vol% THF in *n*-dodecane. This separation was the first time that polymers of molecular weight below 2500 become separated from the void peak without using extreme experimental conditions such as channel pressurization, ultrahigh ΔT , and so forth.

If the solvent effect is the same for both small and large polymer homologs, the selectivity will not be changed by switching solvents. This might not be the case, because small polymer molecules tend to be spread out to the maximum length of the flexible chain, even in a relatively poor solvent, whereas larger polymer molecules may need better solvents to spread out to their maximum. A different solvent effect might, therefore, be expected when a poor solvent is replaced by a good solvent for a homologous polymer series, and vice versa. It is possible, therefore, to manipulate the selectivity of polymer separation by ThFFF through solvent selection. Any dependence of D_T on molecular weight may be different for different solvents, and this may also contribute to changes in selectivity. Better retention and, probably, better selectivity are expected for PS in THF and PIP in CH among the possible four polymer-solvent pairs, as an example.

Figure 1 shows the overlaid fractograms of PS eluted by THF and CH under the same experimental conditions of cold-wall temperature, temperature drop, flow

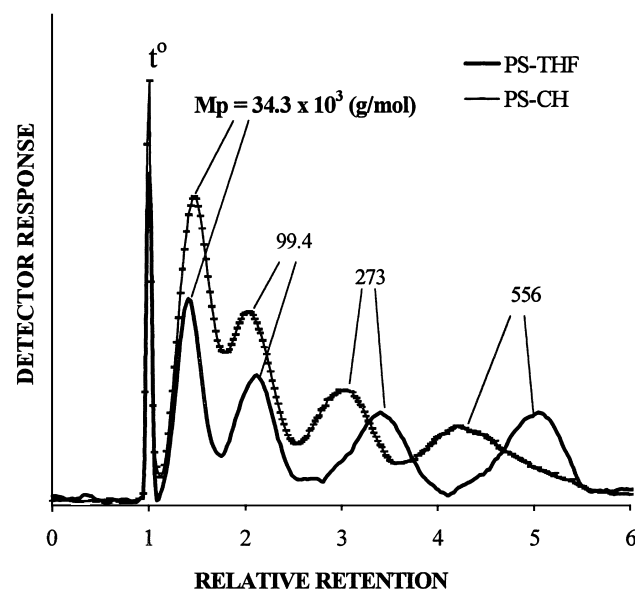


Fig. 1 Fractograms of PS in THF and CH. $\Delta T = 50^\circ\text{C}$; $T_c = 25^\circ\text{C}$. Flow rate is 0.1 mL/min and sample mass is 1 μg .

rate, and sample mass (1 μg) [5]. The fractograms show that a small PS of molecular weight 34,300 is retained approximately the same in both THF and CH, whereas the retentions of larger polymers show significant differences in the two solvents, with the larger PS retained longer in THF. This indicates that using better solvents may enhance both retention and selectivity.

References

1. M. N. Myers, K. D. Caldwell, and J. C. Giddings, *Separ. Sci. Technol.* 9: 47–70 (1974).
2. J. J. Kirkland, L. S. Boone, and W. W. Yau, *J. Chromatogr.* 517: 377–393 (1990).
3. R. M. Sisson and J. C. Giddings, *Anal. Chem.* 66: 4043–4053 (1994).
4. C. A. Rue and M. E. Schimpf, *Anal. Chem.* 66: 4054–4062 (1994).
5. W. J. Cao, P. S. Williams, and M. N. Myers, Solvent effects on polymer retention and universal calibration in ThFFF, in preparation.
6. J. Brandrup and E. H. Immergut, *Polymer Handbook*, 3rd ed., John Wiley & Sons, New York, 1989.
7. P. G. de Gennes, *Scaling Concepts in Polymer Physics*, Cornell University Press, Ithaca, NY, 1979.
8. J. C. Giddings, *Science* 260: 1456–1465 (1993).
9. M. E. Schimpf and J. C. Giddings, *J. Polym. Sci. Part B: Polym. Phys.* 27: 1317–1332 (1989).
10. F. S. Gaeta and G. Scala, *J. Polym. Sci.: Polym. Phys. Ed.* 13: 177 (1975).





Spacer Groups for Affinity Chromatography

Terry M. Phillips

National Institutes of Health, Bethesda, Maryland, U.S.A.

INTRODUCTION

A major problem arising in both affinity and immunoaffinity chromatography is the inefficiency of analyte recovery as a result of steric hindrance between the ligand (capture molecule) support and the analyte (molecule to be isolated), resulting in reduced or no recovery. This situation commonly occurs when low molecular weight ligands, such as pharmaceutical drugs, enzyme substrates, or receptor-binding ligands, are employed as the immobilized capture molecules. An accepted approach to rectify this situation is the employment of an accessory molecule or spacer arm to extend the capture molecule or ligand from the support surface.

USE OF SPACER ARMS

As a result of the popularity of affinity and immunoaffinity separation procedures, supports incorporating suitable spacer arms are commercially available (Table 1). The addition of even a short (4–6 carbon atoms) spacer arm will often ensure adequate clearance of the ligand from the support surface. This gives the analyte (molecule to be isolated) adequate access to the immobilized ligand.

A spacer molecule should be employed in cases where ligand attachment lies in close proximity to the analyte-binding site and interferes with analyte–ligand binding. In such cases, the length of the spacer arm is crucial and must be determined empirically, with six to eight carbon atoms often being the most successful. The spacer should be hydrophilic and not bind proteins nonspecifically, either because of its hydrophobicity or its charge. Some activation chemistries will automatically insert a suitable spacer between the support and the ligand, e.g., bis-oxirane, although the simplest technique for introducing a spacer arm is to directly derivatize a long carbon chain onto the surface itself. Many supports can be modified to accept a suitable carbon-based spacer arm and a convenient approach is to condense the spacer onto the support

surface using carbodiimides. During the coupling stage, the carbodiimide reacts with carboxyl groups to form *O*-cylisourea at pH 4–5. The activated carboxyl group then condenses with an amino group on the support surface to form a peptide-bond-generating urea, a by-product that has to be removed from the reaction mixture. Two water-soluble carbodiimides are commercially available: 1-ethyl-3-(3-ethylamino-propyl) carbodiimide (EDC) or 1-cyclohexyl-3-(2-morpholinoethyl) carbodiimide metho-*p*-toluene sulfonate (CMC). Both of these agents have been successfully used to couple spacer arms to any support that has free amino groups.

Spacer arms can be attached directly to the support surface by linking them to reactive side chains present on the support itself, the ligand being attached to a reactive group positioned at the end of the spacer farthest away from the support surface. Pimplikar and Reithmeier^[1] described a technique for the affinity isolation of a specific protein from solubilized erythrocyte ghosts using hydrophilic spacer arms of four or greater atoms in length. The support was prepared by reacting 4-acetamido-4'-*iso*-thiocyanostilbene-2,2'-disulfonate with Affi-Gel 102. The incorporation of the spacer arm was found to be essential for protein binding, removing steric hindrance of the support and allowing the protein to bind via its stilbene disulfonate-binding site. In a similar manner, Ivanov et al.^[2] covalently immobilized the small blood group B

Table 1 Commercially available support spacer arm molecules

Hexamethylenediamine
Aminocaproic acid
<i>N</i> -hydroxysuccinimide
Arylsulfonate
Bis-oxiran
3,3'-Diaminodipropylamine
Hydroxyalkyl
Long-chain hydrazine biotin



antigenic molecule, trisaccharide-beta-aminopropyl glycoside, to poly-*N*-(2-hydroxyethyl) acrylamide-modified porous glass. This affinity support was then used to isolate anti-blood group B monoclonal antibodies. The incorporation of a short (4–6 atom) spacer arm was found to be essential in order to project the affinity ligand away from the support surface.

REFERENCES

1. Pimplikar, S.W.; Reithmeier, R.A. Affinity Chromatography of Band 3, The Anion Transport Protein of Erythrocyte Membranes. *J. Biol. Chem.* **1986**, *261*, 9770–9778.

2. Ivanov, A.E.; Bovin, N.V.; Korchagina, E.Yu.; Zubov, V.P. Favourable biospecific reactivity of blood group B antigenic trisaccharide chemically attached to poly-*N*-(2-hydroxyethyl)acrylamide-coated porous glass. *Biomed. Chromatogr.* **1992**, *6*, 39–42.

SUGGESTED ADDITIONAL READING

- Matejtschuk, P. *Affinity Separations*; IRL Press at Oxford University Press: Oxford, U.K., 1997.
- Mohr, P.; Pommerening, K. *Affinity Chromatography: Practical and Theoretic Aspects*; Marcel Dekker, Inc.: New York, 1985.
- Phillips, T.M. *Analytical Techniques in Immunochemistry*; Marcel Dekker, Inc.: New York, 1992; 40–74, Chapter 3.

Spiral Disk Assembly: An Improved Column Design for High-Speed Countercurrent Chromatography (HSCCC)

Yoichiro Ito

Fuquan Yang

National Institutes of Health, Bethesda, Maryland, U.S.A.

INTRODUCTION

The high-speed countercurrent chromatography (HSCCC) centrifuge uses a multilayer coil as a separation column which produces high-efficiency separation with good retention of the stationary phase with a variety of two-phase solvent systems.^[1,2] However, the method often fails to retain a satisfactory amount of the stationary phase for highly viscous, low interfacial solvent systems such as polymer phase systems, which are useful for the separation of macromolecules and particulates. A new column design called "spiral disk assembly," described below, provides a universal application of solvent systems, including the polymer phase systems for HSCCC.

PRINCIPLE

Retention of the stationary phase in the coiled column of the HSCCC system totally relies on the Archimedean screw force generated by the planetary motion of the column. However, this force is often too weak to retain the stationary phase for some polar solvent systems, such as aqueous–aqueous polymer phase systems, resulting in carryover of the stationary phase from the column.

The new spiral column design improves the retention of the stationary phase by modifying the configuration of the column from a coil to a spiral, so that the centrifugal force gradient produced by the spiral pitch helps to distribute the heavier phase in the periphery and the lighter phase in the proximal portion of the column. This effect can be enhanced by increasing the pitch of the spiral. Although a spiral column can be prepared simply by winding the tubing into a flat spiral configuration,^[3,4] it can provide a limited spiral pitch (outer diameter [O.D.] of the tubing), and, additionally, the connection between the neighboring spiral columns is rather difficult.

These problems can be solved by making a single or plural spiral channel(s) in a solid disk. In the first model, a single spiral channel is made in a plastic disk, which can be serially connected by stacking multiple disks

sandwiched with Teflon sheet septa. In the second model, four spiral channels are incorporated in a single disk, symmetrically around the center, so that the spiral pitch is increased by four times that of the above single spiral channel without losing the column space. Connection between the neighboring spiral channels is formed by a short straight channel situated radially on the other side of the disk. A set of these disks can be serially connected by spacing a Teflon sheet between the neighboring disks, so that the column provides a large capacity that is somewhat comparable to that of the multilayer coil. The separation disk with a single spiral will serve as a control to evaluate the effect of the pitch on the partition efficiency.

DESIGN OF THE SPIRAL DISK

The design of the spiral column assembly is shown in Fig. 1. Fig. 1A shows a full view of the column assembly, which can be mounted on the type-J multilayer coil planet centrifuge (P.C., Inc., Potomac, MD, USA). The column components are illustrated in Fig. 1B. The column consists of a pair of flanges (one equipped with a gear), nine disks with spiral grooves, and ten Teflon sheet septa. The drawing, and dimensions for each component are illustrated in Fig. 2A–E.

The design of the individual separation disk with one spiral channel (diameter: 17.5 cm, thickness: 3 mm, with a 1.25-cm diameter center hole) is shown in Fig. 2A. The dimensions of the channel are 2.6 mm wide, 2 mm deep, with 1 mm ridge width, which gives a spiral pitch of 4 mm. The total channel length is about 4 m, comprising 12 spiral turns, with a total capacity of ca. 23 mL. The channel starts at the internal inlet (23 mm from the center) and extends to the external outlet (75 mm from the center), which is connected to the radial channel on the other side through a hole of ca. 1 mm diameter. The performance of this single spiral column may be compared to that of the following four-channel spiral column, by using a polar butanol solvent system and polymer phase systems.



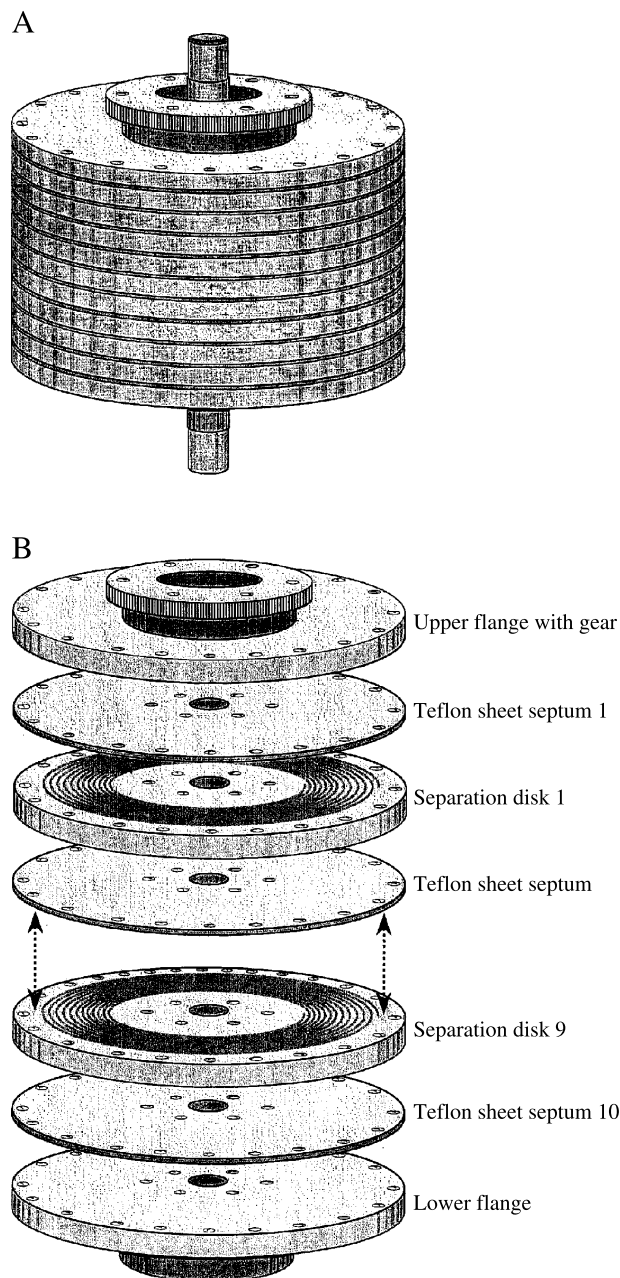


Fig. 1 Schematic illustration of the spiral disk assembly. A. Whole view, B. Exploded view showing each component.

Design of the individual separation disk for four separate spiral channels is shown in Fig. 2B. A plastic disk (17.5-cm diameter and 4 mm thick, high-density polyethylene) has four spiral channels (grooves), each 2.6 mm wide, 2 mm deep, and ca. 1 m long, with a capacity of about 6 mL. The ridge between each groove is 1 mm and, therefore, the pitch of each spiral becomes as large as 16 mm (four times that of the single spiral channel). Each

channel starts at the inner end (I_1 , I_2 , I_3 , and I_4) to reach the outer end (O_1 , O_2 , O_3 , and O_4 , respectively). As shown in the diagram, each channel forms 3.25 spiral turns so that the outer end of channel 1 (O_1) radially coincides with the inner end of channel 2 (I_2), and those of channels 2, 3, and 4 ($O_{2,3,4}$) similarly coincide with the inner ends of channels 3, 4, and 1 ($I_{3,4,1}$), respectively. Each end of the channel (except for O_1) has a hole (ca. 1 mm diameter) through the disk to reach the other side, where a radial channel (dotted line) leads to the next spiral channel through another hole. The outer end of channel 4 (O_4) is connected to a similar radial channel which leads to channel 1 (I_1) of the next disk, or the column outlet, through an opening in the Teflon septum (Fig. 2C).

All disks have screw holes (clearing an 8-32 screw) at both inner and outer edges, at regular intervals (10° for the outer edge and 45° for the inner edge). Similar holes are also made in both the Teflon sheets and the flanges.

The design of the flanges is shown in Fig. 2D and E. The upper flange (Fig. 2D) is equipped with a plastic gear (9 mm thick, 10-cm pitch diameter), which engages with an identical stationary gear on the high-speed CCC centrifuge. Fig. 2E shows the lower flange, which has two screw holes (90° apart), for tightly fixing the column assembly against the column holder shaft (0.9-in. diameter). Both upper and lower flanges each have an inlet hole which fits into an adapter with a 1/4-28 screw thread. They also have a set of screw holes (clearing an 8-32 screw) around the outer and inner edges as in the separation disks and Teflon septa. The column assembly is mounted on the rotary frame of the multilayer coil centrifuge and counterbalanced with brass blocks. A pair of flow tubes from the column assembly is led downward through the center hole of the column holder shaft and passed through the hollow central pipe to exit the centrifuge at the center hole of the top plate, where it is tightly fixed with a pair of clamps. These tubes are protected with a sheath of Tygon tubing to prevent direct contact with metal parts.

EXPERIMENTAL PROCEDURE

Each two-phase solvent system is thoroughly equilibrated in a separatory funnel at room temperature and the two phases are separated before use. The sample solution is prepared by dissolving the sample in an appropriate volume (1–5 mL) of the upper and/or lower phase of the solvent system. In each experiment, the column is first entirely filled with the stationary phase (upper or lower phase), followed by sample injection through the sample

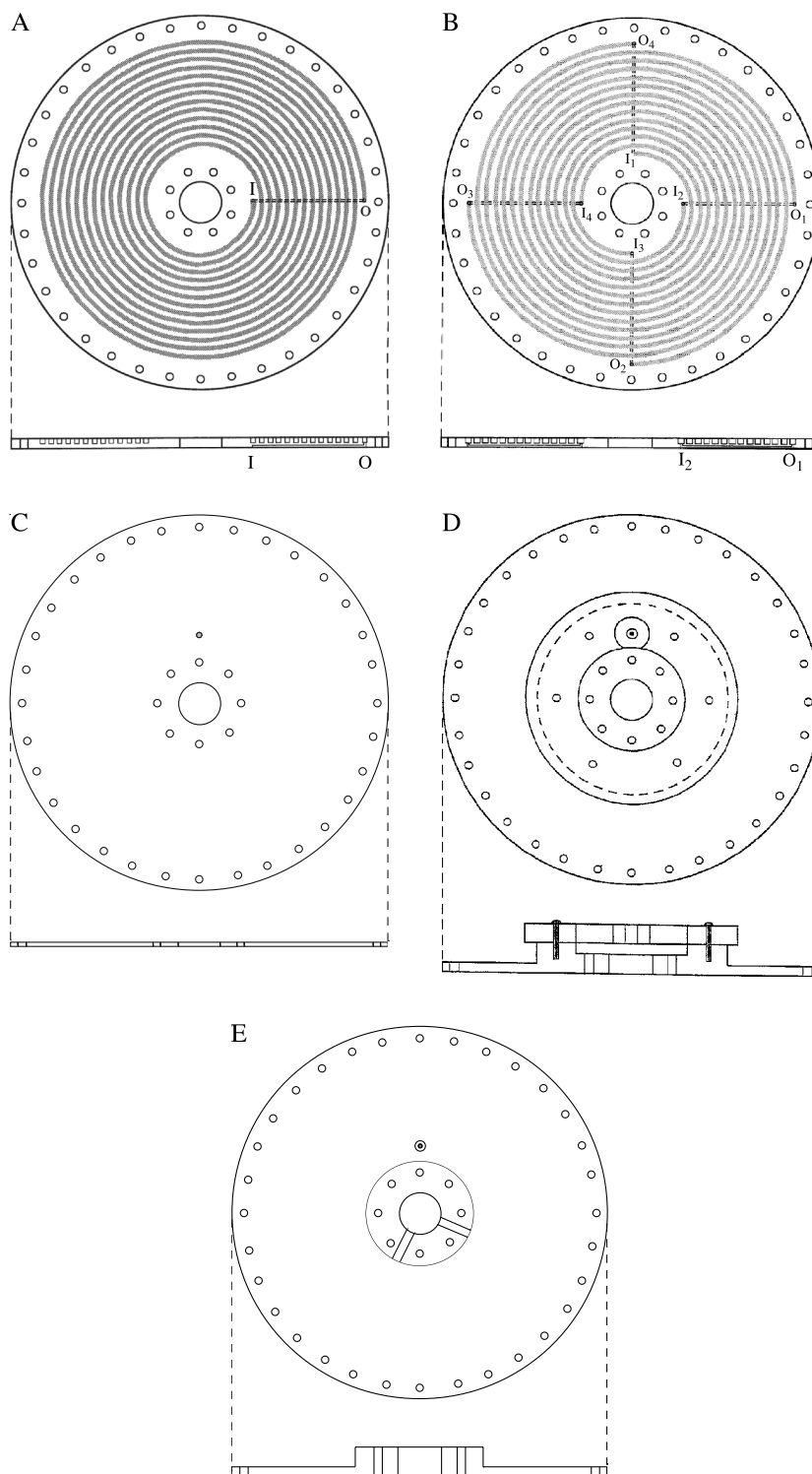


Fig. 2 Drawing of each component of the spiral disk assembly. A. Disk with a single spiral, B. Disk with four spirals, C. Teflon sheet septum, D. Upper flange equipped with a plastic gear, E. Lower flange.



Table 1 Dimensions of four spiral channels used in the present studies

Disk no.	Number of spiral	Width ^a (mm)	Depth ^a (mm)	Pitch (mm)	Capacity (mL)
Column I	1	2.6	2.0	4	23
Column II	1	1.5	3.7	4	21
Column III	4	2.6	2.0	16	23
Column IV	4	1.5	3.7	16	21

^aThe width of the spiral groove becomes the depth of the channel and the depth becomes the width of the channel when assembled.

port. Next, the apparatus is rotated at 800 rpm, while the mobile phase is eluted through the column at the desired flow rate. The separation may be repeated by changing the direction of the revolutions and/or elution mode (head to tail and tail to head), although it is expected that

the best result would be obtained by eluting either the lower phase from the internal terminal toward the external terminal of the spiral channel, in a tail-to-head elution mode, or the upper phase in the opposite direction in a head-to-tail mode. The effluent from the

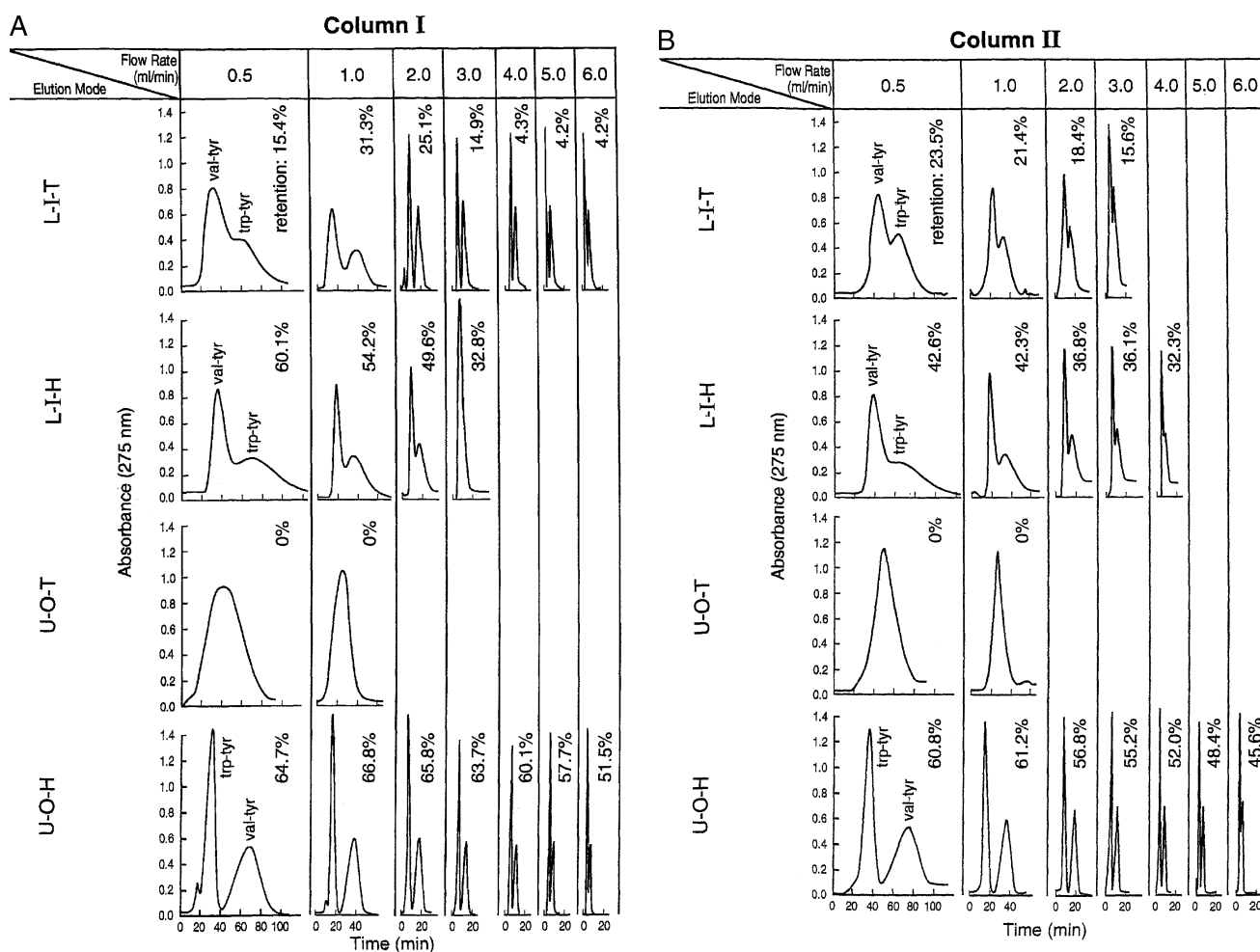


Fig. 3 Separation of peptides with a set of four single disks. Experimental conditions: apparatus, type-J coil planet centrifuge with 10-cm revolution radius; A. Column I, B. Column II, C. Column III, and D. Column IV (dimensions of channels are listed in Table 1); sample: trp-tyr (0.5 mg) + val-tyr (2 mg) in 1 mL of upper phase; solvent system: 1-butanol-acetic acid/water (4:1:5); elution modes: L-I-T, lower phase from the inner terminal at tail, L-I-H, lower phase from the inner terminal at head, U-O-T, upper phase from the outer terminal at tail, and U-O-H, upper phase from the outer terminal at head; flow rate: 0.5–10 mL/min as indicated; rpm: 800, stationary phase retention: indicated in the figure.

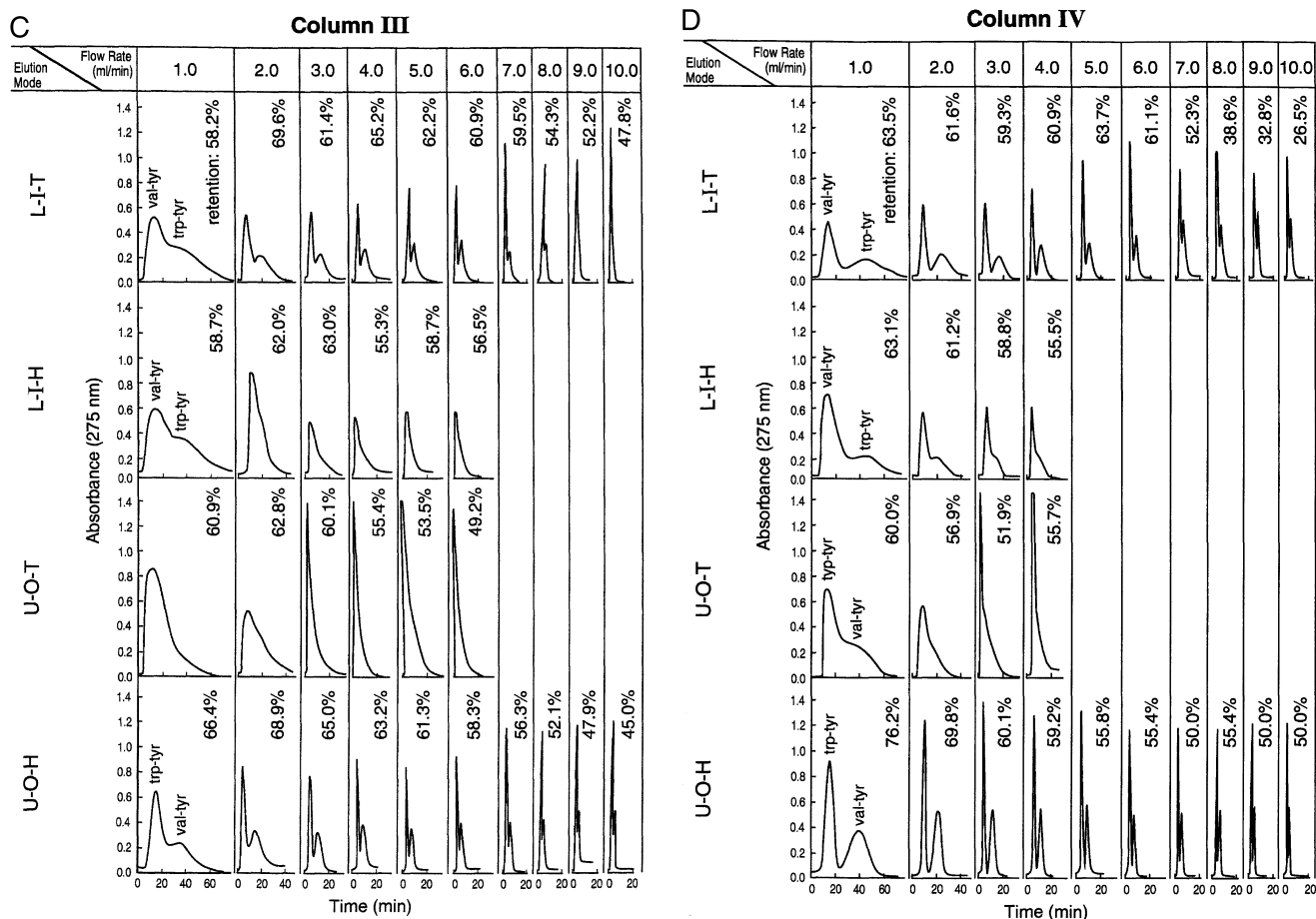


Fig. 3 (Continued).

outlet of the column is continuously monitored through an ultraviolet (UV) detector.

BASIC STUDIES WITH SINGLE DISKS

Using a single disk with each channel design, a series of experiments was performed to evaluate the performance of the disk in terms of partition efficiency and retention of the stationary phase, by using three different types of two-phase solvent systems: 1-butanol/acetic acid/water (4:1:5, v/v/v) for separation of dipeptides; 12.5% (w/w) polyethylene glycol (PEG)-1000, 12.5% (w/w) dibasic potassium phosphate in water for protein separations; and 4% (w/w) PEG-8000, 5% (w/w) dextran T500 in water for measuring the retention of the stationary phase. The experiments were performed at various flow rates of the mobile phase, using four different elution modes, i.e., L-I-T (lower phase eluted from the inner terminal at the tail); L-I-H (lower phase eluted from the inter terminal at the head); U-O-T (upper phase eluted from the outer terminal

at the tail); U-O-H (upper phase eluted from the outer terminal at the head). Four other reversed elution modes, including L-O-T, L-O-H, U-I-T, and U-I-H, showed considerably less retention of the stationary phase, compared with their counterparts, because of the adverse effect of the radial centrifugal force gradient. The dimensions of these four spiral channels are given in Table 1.

1-Butanol/Acetic Acid/Water (4:1:5) System

Fig. 3A–D shows the separation of a standard sample mixture of trp-tyr (0.5 mg) and val-tyr (2 mg) with a two-phase solvent system composed of 1-butanol/acetic acid/water (4:1:5), by using a set of four different spiral columns (columns I–IV in Table 1).

In each chromatogram, the UV absorbance (280 nm) was plotted against the elution time, together with the % retention volume of the stationary phase relative to the total column capacity. In each group, a set of chromatograms is arranged according to the four different elution modes, i.e., L-I-T, L-I-H, U-O-T, and U-O-H,

where L and U indicate the lower phase mobile and upper phase mobile; I and O denote eluting from internal terminal and external terminal of the spiral; and T and H represent "tail-to-head" and "head-to-tail" elution mode, each under various flow rates of the mobile phase.

In column I (Fig. 3A), the elution with upper phase from the head of the spiral (U-O-H) produces the best peak resolution and the highest % retention of the stationary phase. The elution with the lower phase from the head of the spiral (L-I-T) also shows a good peak resolution up to the flow rate of 6 mL/min, in spite of its low retention of the stationary phase. Elution of the lower

phase from the head (L-I-H) retains a satisfactory amount of the stationary phase under the flow rate of 0.5–2 mL/min, while the peak resolution is much lower than those of its counterpart (L-I-T). The elution of the upper phase from the tail (U-O-T) shows no retention of the stationary phase, even at a low flow rate of 0.5 mL/min. These elution trends are also found in column II (Fig. 3B), except that the peak resolution is much reduced in the elution of the lower phase from the tail (L-I-T), under a similar retention level of the stationary phase.

Fig. 3C and D shows the chromatograms obtained from the four-spiral disks under otherwise identical

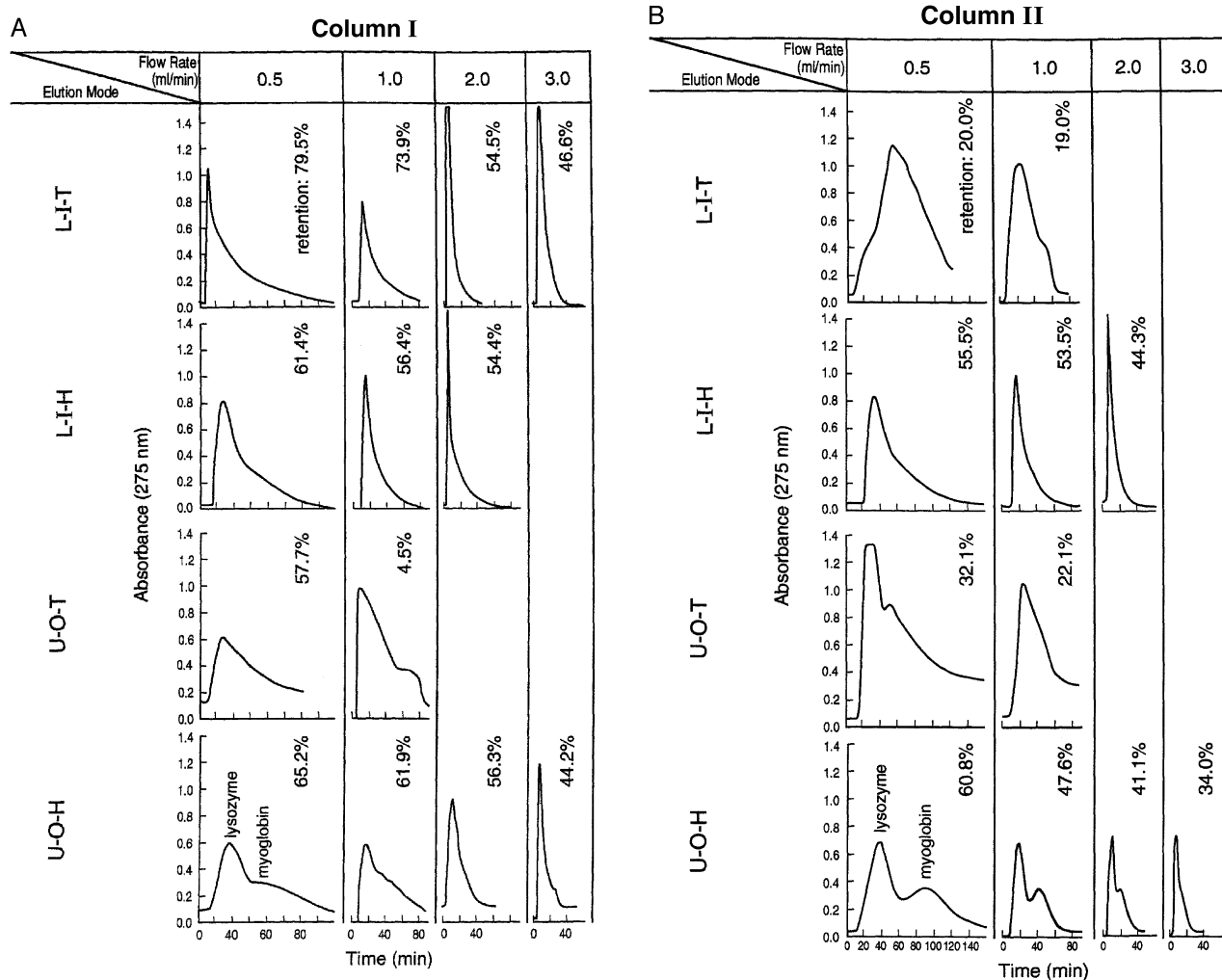


Fig. 4 Separation of proteins with a set of four single disks. Experimental conditions: apparatus, type-J coil planet centrifuge with 10-cm revolution radius; A. Column I, B. Column II, C. Column III, and D. Column IV (dimensions of channels are listed in Table 1); sample: lysozyme and myoglobin each 5 mg in 1 mL of upper phase; solvent system: 12.5% (w/w) PEG1000 and 12.5% (w/w) potassium diphosphate in water; elution modes: L-I-T, lower phase from the inner terminal at tail, L-I-H, lower phase from the inner terminal at head, U-O-T, upper phase from the outer terminal at tail, and U-O-H, upper phase from the outer terminal at head; flow rate: 0.5–5 mL/min as indicated; rpm: 800, stationary phase retention: indicated in the figure.

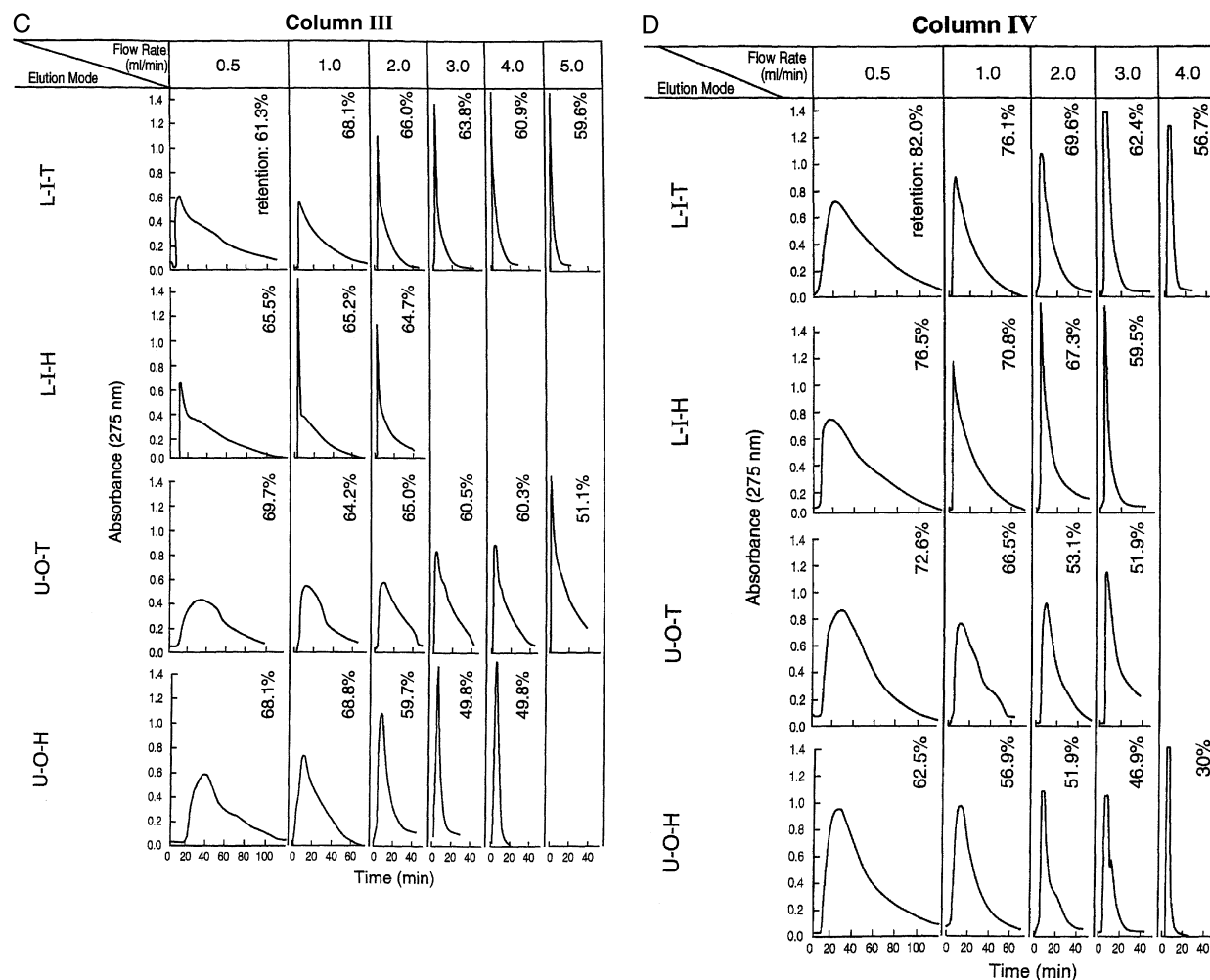


Fig. 4 (Continued).

experimental conditions. It clearly indicates that the retention of the stationary phase is much improved in all elution modes. Although the peak resolution of the two dipeptides was substantially reduced, the flow rate could be increased up to 10 mL/min to yield a moderate degree of peak resolution as emphasized by column IV (Fig. 3D).

This suggests that, if one used a multichannel spiral disk with a large pitch, the separation of peptides might be achieved in a very short elution time.

PEG 1000-Dibasic Potassium Phosphate Polymer Phase System

Fig. 4A–D similarly illustrates the peak resolution between two protein samples (lysozyme and myoglobin, 10 mg each) in the PEG–phosphate system obtained from

the four different spiral disks. In the single-spiral disks (Fig. 4A and B), the best results were obtained by eluting the upper PEG-rich mobile phase from the head end of the outer terminal (U–O–H); other modes resulted in low resolution. Except for L–I–T and I–O–T in column II, all groups show a satisfactory level of stationary phase retention with a flow rate of 0.5 mL/min, indicating that mixing of two phases in the spiral column is inefficient. This tendency is more pronounced in the four-spiral disks (Fig. 4C and D), which show much higher retention of the stationary phase (over 60%), but without any peak resolution. Comparing columns in Fig. 4A and B shows the latter to yield somewhat higher peak resolution, which is probably a result of the shallow channel which facilitates mass transfer between the two phases. This suggests that the separation might be further improved by reducing the width of the spiral groove.



Table 2 % Retention of 4% PEG8000–5% dextran T 500 in 10 mM Na₂HPO₄ system

	Column			
	I	II	III	IV
Flow rate (mL/min)	0.5–1	0.5–1	0.5–1–2	0.5–1.0–2.0
L–I–T	40.0–14.8	14.3–3.3	61.1–50.0–14.3	55.6–33.3–4.0
L–I–H	37.1–2.0	10.9–6.5	53.9–47.8–17.4	52.0–33.3–9.6
U–O–T	71.8–32.3	31.0–17.4	67.8–65.7–50.0	64.4–56.0–42.7
U–O–H	61.9–28.0	15.1–10.1	59.8–46.8–45.1	58.5–54.5–44.0

PEG 8000–Dextran 500 Polymer Phase System

A series of experiments was performed to examine the retention of the PEG–dextran polymer phase system without samples. Results are shown in Table 2, where % retention of the stationary phase is indicated at the flow rates of 0.5–1 or 2 mL/min for each spiral column. The results indicate that, among the single-spiral disks (I and II), column I with a deep channel retained over 60% of the lower dextran-rich stationary phase (U–O–H and U–O–T), at a low flow rate of 0.5 mL/min while, under other conditions, the retention was substantially less than 50% of the total column capacity. In contrast, the four-spiral disks (columns III and IV) attained remarkably im-

proved retention of over 50% for all elution modes, at 0.5 mL/min flow rate. Again, the results indicate the effect of the greater spiral pitch, which favors the retention of the stationary phase.

PRELIMINARY SEPARATION WITH A SPIRAL DISK ASSEMBLY

The performance of the present column design was examined by using a spiral disk assembly consisting of eight units of column I, with a total capacity of 165 mL. Results are shown in Fig. 5A and B. In Fig. 5A, a mixture of five dipeptides was well resolved and was completely eluted in 2 hr. The upper organic phase of the 1-butanol

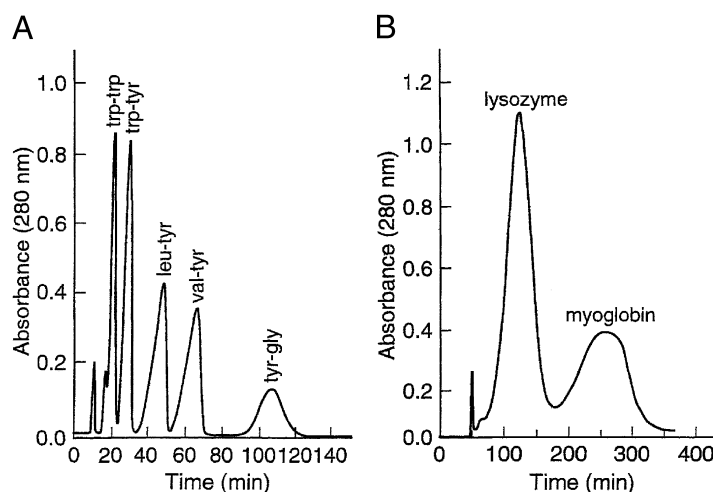


Fig. 5 Preliminary separation of peptides and proteins by a spiral disk assembly. A. Separation of a set of dipeptides. B. Lysozyme and myoglobin. Experimental conditions are as follows: apparatus: type-J coil planet centrifuge with 10-cm revolution radius; column: spiral disk assembly consisting of eight disks (column I) with a total capacity of about 200 mL; sample: A. trp–trp (1.25 mg), trp–tyr (2.5 mg), leu–tyr (10 mg), val–tyr (10 mg), tyr–gly (10 mg) in 5-mL upper phase, B. lysozyme and myoglobin each 50 mg in 5 mL lower phase; solvent system: A. 1-Butanol/acetic acid/water (4:5:1), B. 12.5% (w/w) PEG1000, 12.5% (w/w) K₂HPO₄ in water; mobile phase: A. Upper organic phase, B. Upper PEG-rich phase; flow rate: A. 4 mL/min, B. 0.5 mL/min, elution mode: A. U–O–H, B. U–O–H, revolution: 800 rpm, retention of stationary phase: A. 60%, B. 77.4%.

solvent system was eluted at a flow rate of 4 mL/min. Similar separations were shown with the standard multi-layer coils in HSCCC, but only with more stable butanol solvent systems.^[1]

Fig. 5B shows the separation of two stable proteins (lysozyme and myoglobin) by using a PEG 1000/K₂HPO₄ polymer phase system at a flow rate of 1 mL/min, where they were well resolved in slightly over 5 hr. As suggested by the basic studies, the separation may be substantially improved by using the column II disk assembly, which provides a shallower channel to facilitate mass transfer in viscous polymer phases.

CONSIDERATION OF VARIOUS PARAMETERS GOVERNING PERFORMANCE OF THE SPIRAL COLUMN

Depth and Width of the Spiral Channel

Differing from the ordinary coiled column prepared from Teflon tubing, the channel of the spiral column has a rectangular cross-section. Because the centrifugal force acts along the radius of the disk, the width of the groove on the disk becomes the depth of the channel, and the depth of the groove becomes the width of the channel. Here it is reasonable to consider that a greater depth of the channel favors the retention of the stationary phase, while it provides a less efficient mass transfer rate. In the present studies, we used two different dimensions of the spiral channel: columns I and III are 2.6 mm in depth (or width of the groove) and 2.0 mm in width (or depth of the groove), while columns II and IV are 1.5 mm in depth and 3.7 mm in width. The experimental data clearly indicate that, with few exceptions, the deeper column (columns I and III) produces a better retention of the stationary phase. This trend is most clearly observed in the viscous PEG-dextran system in the single-channel spiral disks (columns I and II).

The effects of channel geometry on partition efficiency in terms of peak resolution gives a more complex picture: in the dipeptide separation with the butanol solvent system, the deeper channel of the single spiral disk (column I) produced a substantially better peak resolution, especially in the lower phase mobile mode (L-I-T), whereas the shallower channel in the four-spiral disks (column IV) produced a somewhat better separation than its counterpart. We do not understand the reason why higher peak resolution is obtained in the deeper channel of column I in L-I-T, despite the low retention of the stationary phase. In protein separation, with the PEG-phosphate system, the shallower spiral channel of the single-spiral disk displayed

the best separation in the upper PEG-rich mobile phase, whereas both four-spiral disks (columns III and IV) showed less efficient separations.

The overall results suggest that the shallower channel shows better separation of proteins by using the PEG-phosphate polymer phase system and the deeper channel favors the retention of viscous PEG-dextran solvent systems.

Spiral Pitch

The effects of the spiral pitch on the present studies are observed by comparing the chromatograms between columns I and III for the deep channel and between columns II and IV for the shallow channel. It is clearly observed that, in the dipeptide separation with the 1-butanol solvent system, the greater pitch results in lower peak resolution at a given flow rate, while it provides higher retention of the stationary phase, thereby allowing a higher flow rate of the mobile phase to reduce the separation time. Similar effects are also observed in the protein separation with the PEG-potassium phosphate solvent system. In the PEG-dextran system, a greater pitch provides a substantial increase in retention of the stationary phase, some exceeding 50% retention at a flow rate of 1 mL/min.

Flow Rate of the Mobile Phase

The flow rate of the mobile phase is an important parameter which determines the elution time. In the dipeptide separation, the optimum flow rate producing the best peak resolution is present in all spiral disks. In the four-spiral disk systems (columns III and IV), which retain a large volume of the stationary phase, the application of a high flow rate of up to 10 mL/min is possible to reduce the separation time, without substantial loss of peak resolution. In the separation of proteins with PEG-phosphate, the low flow rate produced the best peak resolution with higher retention of the stationary phase.

EFFECTS OF VARIOUS INSERTS PLACED INTO THE CHANNEL SPACE

One of the advantages of the spiral disk over the spiral tubing is that the spiral channel can be modified in various ways to improve the partition efficiency. Early trials to place fine Teflon tubing (end closed) or small glass beads (less than 1.5 mm diameter) into the channel resulted in continuous carryover of the stationary phase, apparently a result of vigorous mixing (turbulence) caused by the rotating centrifugal force field. However, inserting short segments of Teflon tubing (ca. 2 mm O.D., 2–3 mm in

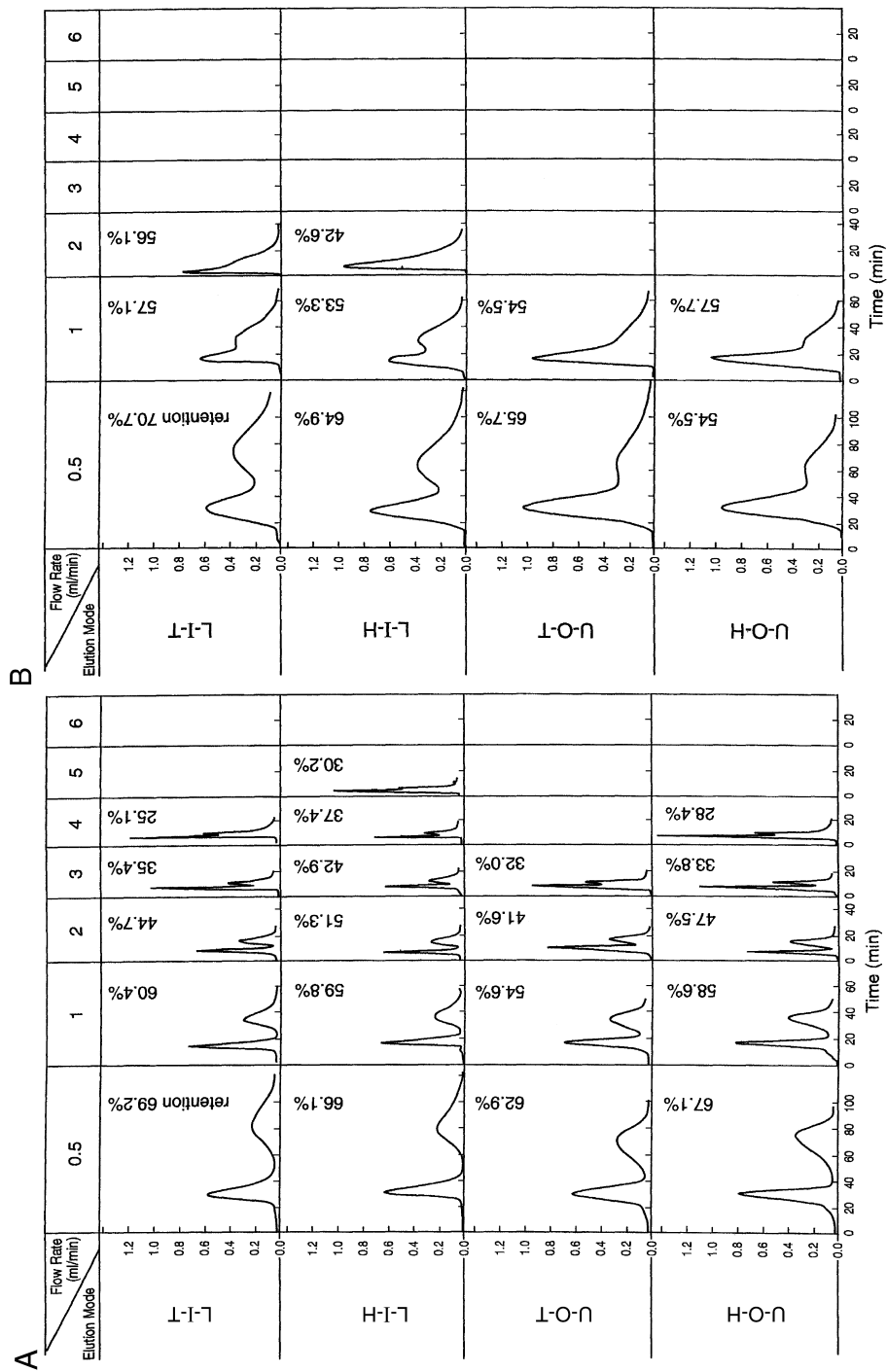


Fig. 6 Locular column IV. Four spiral channels: 1.5 mm (width) \times 3.7 mm (depth), each 1 m long, locule: 1 cm \times 310. (a) 1-Butanol/acetic acid/water (4:1:5). (b) (PEG 1000-dibasic potassium phosphate (each 12.5%, w/w).



length) into the channel at regular intervals (1 cm) produced substantial improvement of the peak resolution, especially in column IV with high-pitch four spiral channels (Table 1). These findings suggest that the shape of the spiral groove can be modified into a locular configuration to improve the partition efficiency (Fig. 6).

CONCLUSION

The rectangular spiral channel embedded in a solid plastic disk, applied to the J-type HSCCC centrifuge, enhances the retention of stationary phase for viscous, low interfacial tension, two-phase solvent systems. Its main advantages are as follows:

1. Use of polymer phase systems for separation of biopolymers (proteins, deoxyribonucleic acid [DNA] and ribonucleic acid [RNA], and polysaccharides).
2. Reliable retention of the stationary phase for polar or low interfacial tension solvent systems (e.g., 1-butanol/water), which are useful for separation of bioactive compounds such as peptides.

3. Improved stationary phase retention against emulsification.
4. Application of the large column for industrial-scale separations by mounting the column assembly on the slowly rotating horizontal shaft.
5. The system allows further modification of the shape of spiral channels to improve the partition efficiency.

REFERENCES

1. Ito, Y. *High-Speed Countercurrent Chromatography*; Ito, Y., Conway, W.D., Eds.; Wiley-Interscience: New York, 1996.
2. Ito, Y. Test to evaluate countercurrent chromatographs. Liquid stationary phase retention and chromatographic resolution. *CRC Crit. Rev. Anal. Chem.* **1986**, *17*, 65–143.
3. Berthod, A.; Billardello, B. J. *Chromatogr., A* **2000**, *902*, 323–335.
4. Shinomiya, K.; Kabasawa, Y.; Ito, Y. Protein separation by cross-axis coil planet centrifuge with spiral coil assemblies. *J. Liq. Chromatogr. Relat. Technol.* **2002**, *25* (17), 2665–2678.

Split/Splitless Injector

Raymond P.W. Scott

Scientific Detectors Ltd., Banbury, Oxfordshire, England

Introduction

The split/splitless detector has been designed for use with open-tubular columns or solid-coated open-tubular (SCOT) columns. Due to the small dimensions of such columns, they have very limited sample load capacity and, thus, for their effective use, require sample sizes that are practically impossible to inject directly. The split injector allows a relatively large sample (a sample size that is practical to inject with modern injection syringes) to be volatilized, and by means of a split-flow arrangement, a proportion of the sample is passed to the column while the remainder is passed to waste. A diagram of a split/splitless injector is shown in Fig. 1.

Discussion

The body of the injector is heated to ensure the sample is volatilized and inside is an inert glass liner. This glass liner helps minimize any sample decomposition that might occur when thermally labile materials come in contact with hot-metal surfaces. The carrier gas enters behind the glass liner and is thus preheated. The sample is injected into the stream of carrier gas that passes down the center of the tube, a portion passes down the capillary column,

and the remainder passes out of the system through a needle valve. The needle valve is used to adjust the relative flow rates to the column and to waste and, thus, controls the amount of sample that is placed on the column.

This process of sample injection has certain disadvantages. Due to the range of solute types present in most mixtures for analysis, the components will have different volatilities and their vapors will have different diffusivities in the carrier gas. Differential volatilization and diffusion rates will result in the sample that enters the capillary tube, being unrepresentative of the original mixture. For example, the more rapidly diffusing solutes will be more dispersed and, consequently, more diluted in the carrier gas than those of lesser diffusivity. This results in the slower-diffusing substances having a higher concentration in the sample entering the column than those of higher diffusivity. As a consequence, the sample will be proportionally unrepresentative of the original mixture. The differential sampling that results from split injection systems can become a serious problem in quantitative analysis with capillary columns.

An alternative approach is to use a splitless injection system. If the valve in Fig. 1 is closed, then all the sample passes into the column and there is no split; *ipso facto*, the device is a *splitless* injector. When used in the splitless mode, however, it is usual to employ a somewhat wider capillary column, which will allow the penetration of a small-diameter injection syringe and thus permit *on-column* injection. Under these circumstances, there can be no differential sampling of the form described. This procedure, however, introduces other injection problems that can affect both resolution and quantitative accuracy that need to be addressed (See the entries Retention Gap Injection Method and Solute Focusing Injector Method).

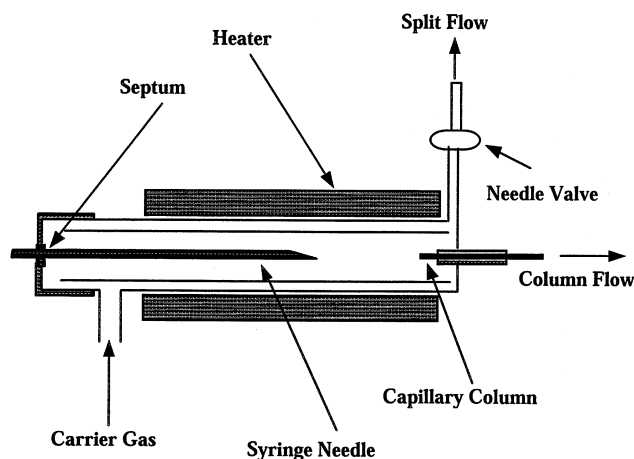


Fig. 1 Split/splitless injector.

Suggested Further Reading

Grant, D. W., *Capillary Gas Chromatography*, John Wiley & Sons, Chichester, 1995.

Scott, R. P. W., *Techniques and Practice of Chromatography*, Marcel Dekker, Inc., New York, 1996.

Scott, R. P. W., *Introduction to Analytical Gas Chromatography*, Marcel Dekker, Inc., New York, 1998.



Stationary Phases for Packed Column Supercritical Fluid Chromatography

Stephen L. Secreast

Pharmaceutical Sciences, Pharmacia Corporation, Kalamazoo, Michigan, U.S.A.

Introduction

The name, packed column supercritical fluid chromatography (pSFC), has been applied to separations performed on particulate stationary phases, using mobile phases pressurized to supercritical, near-critical, or subcritical conditions [1,2]. Typically, the stationary phases used for pSFC are commercially available high-performance liquid chromatography (HPLC) columns, consisting of a porous solid support, usually with a covalently linked bonded phase to provide desired chromatographic interactions. Various column configurations have been used. Separate consideration of supercritical, near-critical, and subcritical pSFC applications provides a convenient, although arbitrary, means of subgrouping a discussion of the types of stationary phase used. More specific information on the stationary phases discussed in this overview can be found in Refs. 1–4.

Supercritical Applications

Supercritical pSFC applications can be defined as those in which the mobile phase is a single substance heated and pressurized above its critical point. Carbon dioxide has overwhelmingly been the compound of choice for these mobile phases. Stationary phases typically used for these applications have been polymeric materials or polymer-coated porous silica. Chromatography on uncoated silica-based stationary phases with CO₂ has, in general, been unsuccessful.

Polystyrene–divinyl benzene beads are the most common polymer material phases reported. The successful use of these phases has been mainly limited, however, to relatively hydrophobic compounds. Also, problems associated with bead physical instability, such as shrinking and swelling, affecting chromatographic reproducibility, have also been encountered. Stationary phases consisting of porous silica coated with a covalently bonded polysiloxane layer, containing cyano, phenyl, or alkyl functional groups, have been used with more success. The polymer coating is applied to the silica to mask excessive analyte–station-

ary phase polar interactions that generate poor peak shapes and yield incomplete analyte recovery with the neat CO₂ mobile phase. As with the polymer materials, these phases work best for hydrophobic compounds such as petroleum-based compounds, lipids, and plastics additives. The apparent degree of silica deactivation obtained with the polymer coating is insufficient to provide quality CO₂ chromatography for polar compounds. An example of plastic additives chromatography obtained with CO₂ on a polymer-coated stationary phase is shown in Fig. 1 [5].

Recently, interest in polymer-coated silica phases has been renewed, with investigators (Chen and Lee [2]) exploring the use of more efficient deactivation techniques and more polar polymers to coat silica particles for neat CO₂ chromatography. Polyethyleneimine-coated silica and amino-terminated polyethylene oxide-coated silica appear promising for pSFC of moderately polar basic compounds. Similarly, hydroxy-terminated polyethylene-oxide-coated silica has been used successfully for pSFC of alcohols and acids. Optimization and commercial production of these stationary phases could significantly extend the polarity range of compounds that can be chromatographed with neat supercritical CO₂.

Near-Critical Applications

Near-critical pSFC applications can be described as those where the mobile phase is solvent-modified CO₂, pressurized only enough to maintain a single phase, with temperatures near (typically less than) the critical temperature. Many commercially available HPLC bonded silica phases have been used with modified-CO₂ mobile phases to achieve normal-phase separations, the choice of stationary phase being dictated by sample polarity. The modifiers added to CO₂ acceptably overcome the unwanted analyte–silica interactions observed with neat CO₂ mobile phases. For structural separation of polar compounds such as pharmaceuticals [typically weak acids or bases of molecular weight (MW) <1000], polar phases such as diol-, amino-, and cyano-bonded silica (or bare silica)



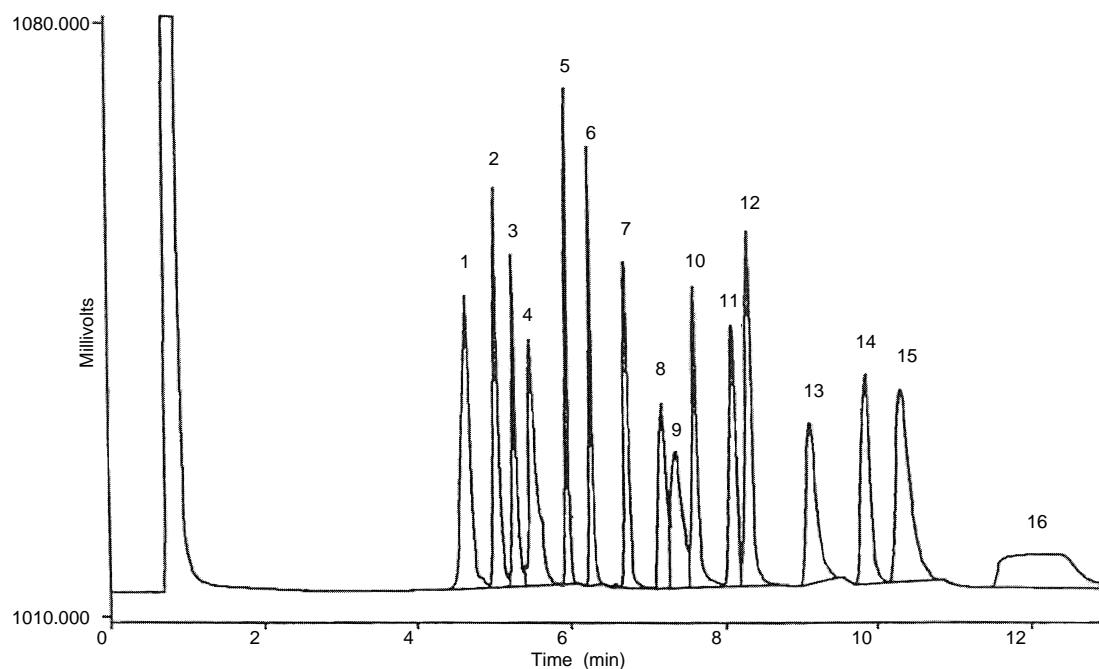


Fig. 1 Use of polymer-coated silica stationary phase with a neat carbon dioxide mobile phase. Column: Deltabond SFC Methyl (150×2.0 mm); mobile phase: CO_2 ; pressure gradient: 75 bar initial for 2 min, then 50 bar/min ramp to 180 bar, then 15 bar/min ramp to 300 bar; flow: 0.5 mL/min; temperature: 100°C ; injection: $5 \mu\text{L}$; detection: flame ionization detector; sample solvent: methylene chloride. Peak key: 1: BHT; 2: dimethyl azelate; 3: triethyl citrate; 4: tributyl phosphate; 5: methyl palmitate; 6: methyl stearate; 7: diethylhexyl phthalate; 8: Tinuvin 327; 9: Spectra-Sorb UV531; 10: tri(2-ethylhexyl) trimellitate; 11: dilauryl thiodipropionate; 12: Irganox 1076; 13: 1,3-diolein; 14: distearyl thiodipropionate; 15: Ionox 330; 16: Irganox 1010.

are used. Numerous applications for pharmaceutical, natural product, environmental and other compound classes have been reported in the recent literature (reviewed in Refs. 1 and 2). For structural separation of higher-molecular-weight, less polar compounds, octyl- or octadecyl silane (ODS)-bonded phases are used (Berger [1], Lesellier and Tchaplal [2]). The reported applications include stationary-phase columns obtained from many different commercial manufacturers, covering almost the complete range of packing particle size and pore size.

Modified- CO_2 mobile phases excel at stereochemical separations, more often than not outperforming traditional HPLC mobile phases. For the separation of diastereomers, silica, diol-bonded silica, graphitic carbon, and chiral stationary phases have all been successfully employed. For enantiomer separations, the derivatized polysaccharide, silica-based Chiralcel and Chiralpak chiral stationary phases (CSPs) have been most used, with many applications, particularly in pharmaceutical analysis, readily found in the recent literature (reviewed in Refs. 1 and 2). To a lesser extent, applications employing Pirkle brush-type, cyclodextrin and antibiotic CSPs have also been described. In addition,

the use of silica and graphitic carbon stationary phases with chiral modifiers added to the CO_2 mobile phase has been reported.

A major advantage of modified- CO_2 pSFC is that due to the low pressure and similarity of the mobile phases used for structural and stereochemical separations, multiple stationary-phase columns can be connected in series, generating separations not achievable by other chromatographic methods. Multiple columns of the same phase have been serially connected to provide significantly amplified chromatographic efficiencies [1]. A recent example chromatogram obtained by connecting four 250×4.6 -mm Chiralpak AD columns in series is shown in Fig. 2 [6]. With the four columns in series, concurrent separation of the four stereoisomers of each of two structurally different compounds was achieved.

Serial connection of different stationary phases provides some very interesting separations. The combination of different CSPs provides systems capable of resolving a wide range of enantiomers (Sandra et al. [2], Gyllenhaal [2]). Recent applications combining normal-phase bonded-silica (diol, cyano, amino) columns with CSPs in series, to provide concurrent structural

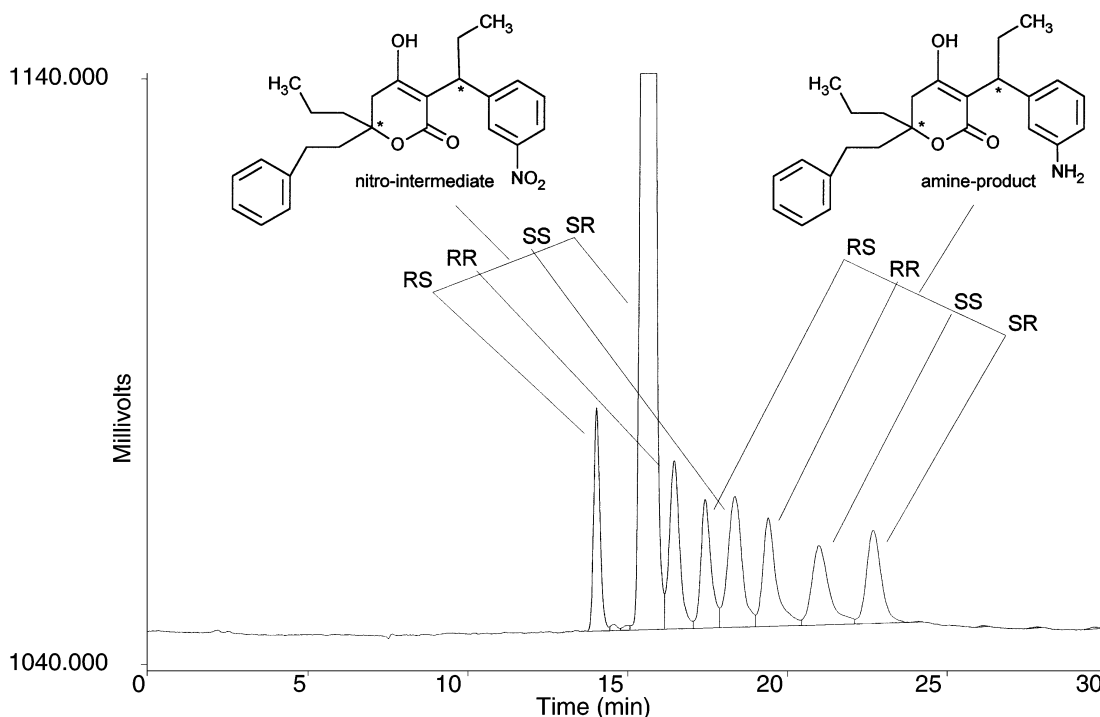


Fig. 2 Use of multiple columns (same stationary phase) in series to improve chromatographic efficiency. Columns: four Chiralpak AD (5 μ m, 250 \times 4.6 mm) in series; mobile phase: CO₂ with modifier gradient; modifier: ethanol–methanol–isopropylamine (50:50:0.5); gradient: 20% modifier for 2 min, then 1%/min ramp to 35%; flow: 2.0 mL/min; pressure: 150 bar; temperature: 35°C; injection: 5 μ L; detection: UV 210 nm; sample solvent: methanol.

and stereochemical separations, have been described (Phinney [4], Kline and Matuszewski [4], Williams et al. [4]). An example of chromatography obtained for a pharmaceutical compound and its degradants by connecting a Zorbax SB cyano column and three Chiralpak AD columns in series is shown in Fig. 3 [7]. The cyano column provides the structural separation of the parent compound and the two degradants, and the Chiralpak columns provide concurrent enantiomer separations for the two degradants. The ability to combine different or multiple traditional HPLC stationary phases to generate unique separations is a hallmark of modified-CO₂ pSFC.

Subcritical Applications

Recent work describing the use of subcritical water as a chromatographic mobile phase has been reported. Water heated to 100–200°C, pressurized to 20–50 bar, can be used as a reversed-phase chromatography eluant. This application exists somewhere in the boundary region between pSFC and HPLC. Stationary phases that have been used successfully for subcritical

(or superheated) water chromatography include polystyrene–divinyl benzene beads [8,9], ODS silica [8,10], porous graphitic carbon [11], and polybutadiene-coated zirconia [11]. Of these phases, relatively rapid performance deterioration was reported for the ODS silica materials [11], presumably due to silica solubility. As research in this area increases, undoubtedly so will the number of identified suitable stationary phases.

Conclusions

Packed column SFC stationary phases are very similar or identical to those used for HPLC. With neat CO₂ mobile phases, polymer or polymer-coated silica stationary phases have typically been used. With modified-CO₂ mobile phases, bonded-phase silica columns are typically used. For structural separations, diol, amino, or cyano stationary phases are most often used. For stereochemical separations, derivatized polysaccharide-bonded silica columns are most often the stationary phases of choice. A powerful feature of modified-CO₂ pSFC is the ability to serially connect different stationary phases to obtain enhanced or mul-



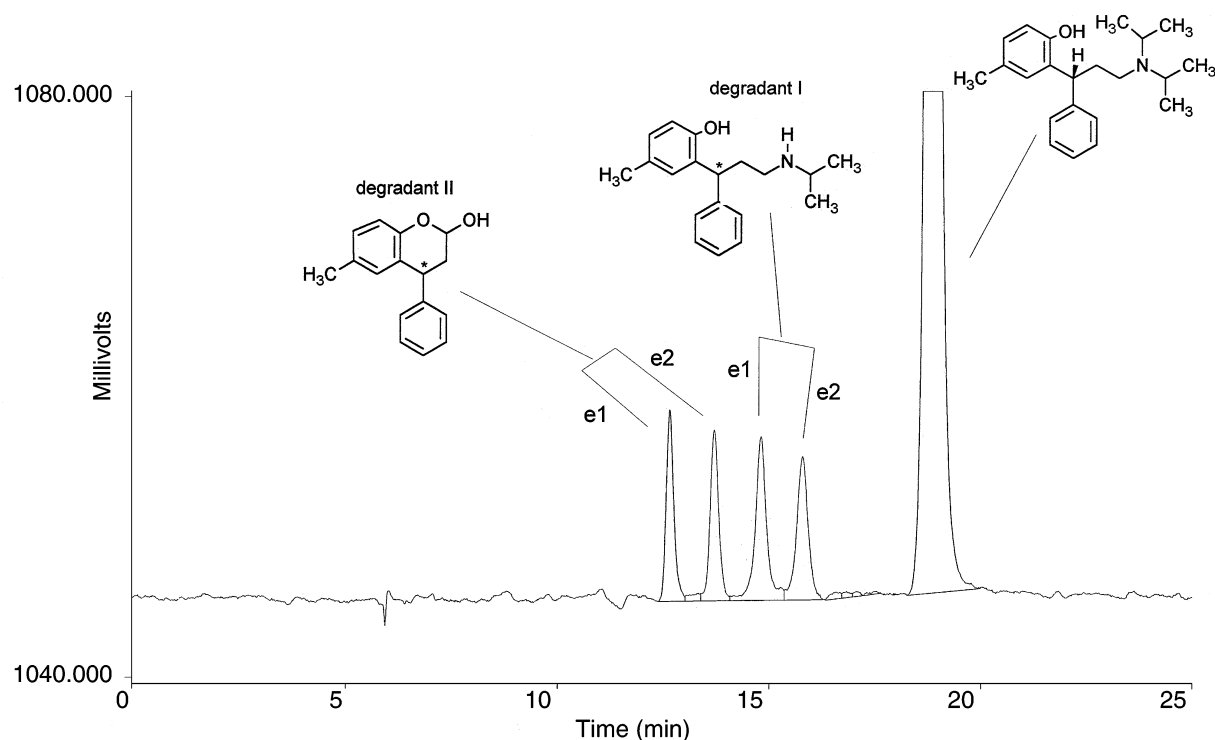


Fig. 3 Use of multiple columns in series (achiral and chiral stationary phases) to provide mixed-mode selectivity. Columns: Zorbax SB CN ($5\ \mu\text{m}$, $250 \times 4.6\ \text{mm}$) plus three Chiralpak AD ($5\ \mu\text{m}$, $250 \times 4.6\ \text{mm}$) in series; mobile phase: CO_2 -methanol (containing 0.5% isopropylamine) (85:15); flow: 2.0 mL/min; pressure: 150 bar; temperature: 35°C ; injection: $5\ \mu\text{L}$; detection: UV 220 nm; sample solvent: methanol.

multiple mechanism separations. With subcritical (superheated) water mobile phases, the use of polymer, porous graphitic carbon, and polymer-coated zirconia stationary phases has been described.

References

1. T. A. Berger, *Packed Column SFC*, Royal Society of Chemistry, Cambridge, 1995.
2. K. Anton and C. Berger (eds.), *Supercritical Fluid Chromatography with Packed Columns*, Marcel Dekker, Inc., New York, 1998.
3. 7th International Symposium on Supercritical Fluid Chromatography and Extraction, 1996.
4. 8th International Symposium on Supercritical Fluid Chromatography and Extraction, 1998.
5. S. L. Secreast, unpublished application. Packed-column supercritical fluid chromatography of plastics additives. Pharmacia Study Report, 1996.
6. S. L. Secreast and L. K. Wade, 8th International Symposium on Supercritical Fluid Chromatography and Extraction, 1998.
7. S. L. Secreast, American Association of Pharmaceutical Scientists Annual Meeting, 1999.
8. R. M. Smith and R. J. Burgess, *J. Chromatogr. A* 785: 49–55 (1997).
9. D. J. Miller and S. B. Hawthorne, *Anal. Chem.* 69: 623–627 (1997).
10. Y. Yang, M. Belghazi, A. Lagadec, D. J. Miller, and S. B. Hawthorne, *J. Chromatogr. A* 810: 149–159 (1998).
11. R. M. Smith, R. J. Burgess, O. Chienthavorn, and J. Rose, *LC-GC* 17(10): 938–945 (1999).

Stationary-Phase Retention in Countercurrent Chromatography

Jean-Michel Menet

Aventis Pharma, Vitry-sur-Seine, France

Introduction

The retention of the stationary phase is a key parameter for countercurrent chromatography (CCC), as it influences all the chromatographic parameters describing a separation. First, it is important to closely monitor its value, commonly named SF; we give the reader three methods to determine this value. Then, the best conditions for obtaining the highest SF value are described for the three main CCC devices, which include (a) a Sanki centrifugal partition chromatograph, (b) a type J high-speed countercurrent chromatograph, and (c) a cross-axis countercurrent chromatograph. Finally, some theoretical approaches are introduced in order to estimate the value before any experimental work is performed.

How to Measure SF?

Figure 1 indicates the principle of use of any CCC device for the equilibrium of two liquid, nonmiscible phases. In this case, the stationary phase which is chosen is the lighter phase of the solvent system (dark gray in Fig. 1), whereas the mobile phase is indicated in white. For simplification, the coil is considered as an empty cylinder and the phenomena which occur inside the column are highly schematized as a stack of disks of mobile and stationary phases. This allows us to visualize the progression of the mobile phase inside the column. After the solvent system has reached equilibrium (complete settling of the two phases), the phase chosen as the stationary phase is pumped into the apparatus. The latter is considered as filled as soon as droplets of this stationary phase are expelled out of the column; this is Step 1 of Fig. 1.

The apparatus is then started, and when the desired rotational speed is reached, the mobile phase is pumped into the apparatus. A graduated cylinder is then put at the outlet of the apparatus. The two phases undergo a hydrodynamic or hydrostatic equilibrium inside the column while the mobile phase progresses toward the outlet of the column; this is Step 2. After a certain time, the mobile phase has reached the end of the column and then the first droplet of the mobile phase falls into the graduated cylinder; this Step 3. The experimenter then reads the

volume, V_1 , of the stationary phase which has been expelled from the column. The experiment is continued until the desired total volume is reached in the graduated cylinder. The experimenter can read the respective volumes of the stationary phase, named V_2 , and the mobile one; this is Step 4. Finally, the apparatus can be emptied (for instance, by pushing with nitrogen gas) and the liquids collected in another graduated cylinder; the volume of the stationary phase is V_3 . For simplification purposes, the extracolumn volumes are neglected. Three measurements of the stationary phase retention are available:

- One just after the equilibrium inside the column: $SF_1 = (V_{\text{column}} - V_1)/V_{\text{column}}$
- One after a certain amount of time: $SF_2 = (V_{\text{column}} - V_2)/V_{\text{column}}$
- One by emptying the apparatus: $SF_3 = V_3/V_{\text{column}}$

If the equilibrium of the two phases was stable and not disturbed by any external event (change in rotational speed, flow rate, etc.), the three values of SF should be similar by a few percent of precision.

Best Conditions for SF for the Three Main CCC Devices

The best combinations of experimental parameters (e.g., choice of lighter or heavier phase, choice of the inlet to pump the mobile phase into, etc.) in order to retain the maximum amount of stationary phase inside the column are related to complex hydrodynamic phenomena which are based on the behavior of the solvent system inside the column of a given CCC apparatus. Many experiments have been carried out on the three main types of CCC devices by varying the experimental parameters and the solvent systems, in order to gather solvent systems by groups characterized by a combination of experimental parameters.

Sanki-Type Apparatus

The principle of this instrument has been precisely described in the entry (see entry Centrifugal Partition



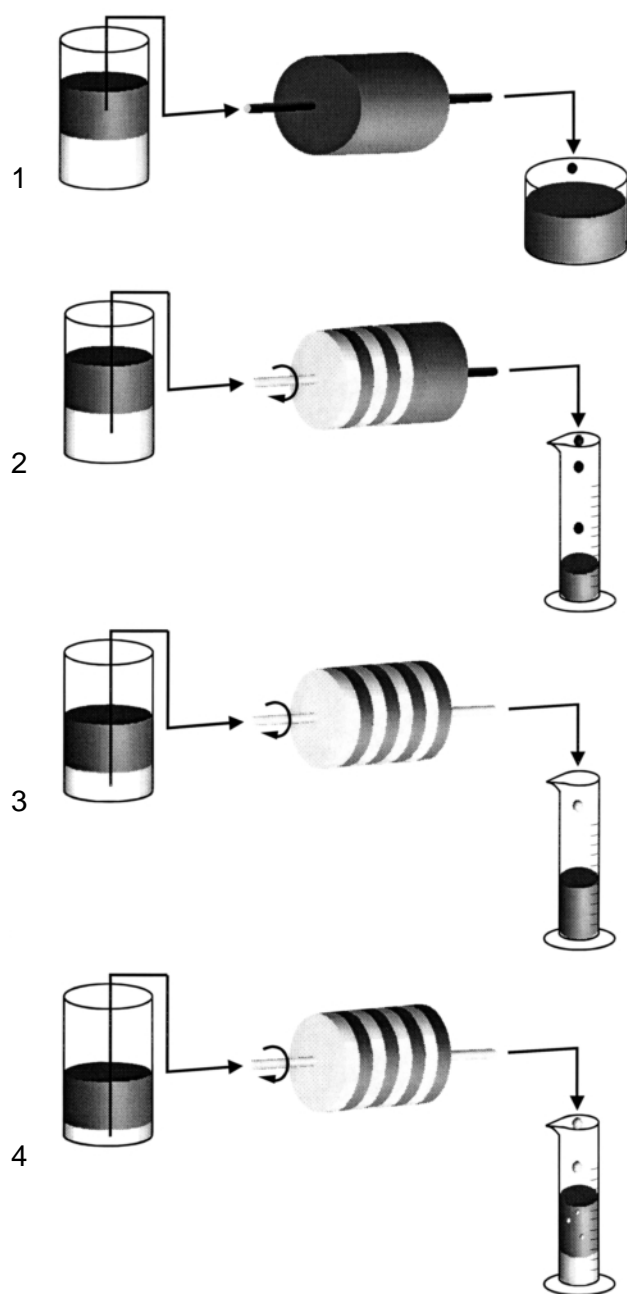


Fig. 1 Principle of the two-phase equilibrium inside a CCC column.

Chromatography: An Overview) devoted to this topic in this volume. The apparatus is a centrifuge, in which cartridges or plates are installed. Two rotating seals are required to allow the flow of the liquid phase: One stays at the top of the centrifuge, the other one at the bottom (solvent inlet and outlet).

Whatever the solvent system may be, the optimization for the best retention of the stationary phase is quite simple. Among the four possibilities, only two of them lead to a good retention of the stationary phase inside the cartridges or the plates; they are based on the combination of the lighter mobile phase pumped from the bottom to the top seal, also called the “ascending” mode, and the heavier mobile phase pumped from the top to the bottom seal, also called the “descending” mode.

Type J Apparatus

The principle of this apparatus has been precisely described in an entry (see entry Dual Countercurrent Chromatography) devoted to this topic in this volume. Two main parameters for using a two-phase solvent system with this apparatus are the choice of the heavier or the lighter mobile phase and the pumping mode [i.e., from the tail to the head or the head to the tail of the column (as a rotating coil defines a tail and a head, carrying, for instance, a small solid from the tail to the head)].

The designer of this type of device [Dr. Yoichiro Ito (National Institutes of Health, Washington, DC)], has tried various solvent systems in order to ascertain the best combinations of the two main parameters [1]. He observed that, among the four possibilities, only two led to the best retention of the stationary phase. However, the two optimal conditions were dependent on the nature of the solvent system and, for some solvent systems, on the geometrical dimension of the apparatus.

Ito has, consequently, decided to carry out a systematic study with 15 solvents [1]. His first conclusion was that only one condition was optimal among the two pumping modes for a given phase (i.e., lighter or heavier phase). The second conclusion was that the pumping modes to be used are reversed if the liquid phase is chosen as lighter instead of heavier, or vice versa.

Two groups of solvent systems have, consequently, been defined. One gathers solvent systems for which the two best combinations are the pumping of the lighter phase from the tail to the head of the column and the pumping of the heavier phase from the head to the tail of the column. The organic phases of such solvent systems are hydrophobic; thus, this group is called “hydrophobic” (e.g., hexane–water). The other group gathers solvent systems for which the two best combinations are the pumping of the lighter phase from the head to the tail of the column and of the heavier phase from the tail to the head of the column. The organic

phases of such solvent systems are quite hydrophilic; thus, this group is called “hydrophilic” (e.g., butanol-2–water). The best combinations are reversed between the two groups.

However, there was a need to define a third group to take into account the behaviors of some solvent systems for which optimal combinations depend on the geometric dimensions of the apparatus. The discriminating parameter was found to be the β ratio of the coil radius on the distance between the two axis of rotation. For β values smaller than 0.3, solvent systems belonging to this third group behave like the solvent systems of the “hydrophilic” group. Conversely, for β values greater than 0.3, they behave like solvent systems of the “hydrophobic” group. The group was named “intermediate,” which was also consistent with the mild hydrophobic (or hydrophilic) character of the organic phase (e.g., chloroform–methanol–water).

The main drawback of this classification comes from the experimental determination of the three groups. For a solvent system not previously studied, either by Ito or cited in the literature, the experimenter has to carry out four experiments in order to determine the two best combinations and, consequently, the group to which it belongs.

Cross-Axis-Type Apparatus

The general principle of this type of apparatus is described in the corresponding entry (see entry Cross-Axis Coil Planet Centrifuge for the Separation of Proteins) of this volume. Contrary to the two previous CCC devices, four main parameters have to be considered here. Two of them are common to the other types of CCC units (i.e., choice of a lighter or a heavier phase and pumping mode from tail to head or from head to tail). Two additional parameters intervene: the pumping direction, from the inside to the outside of the core or reverse, and the rotation direction, clockwise or counterclockwise.

The same designer of this type of apparatus as for type J device, Ito, has applied the same procedure to classify various solvent systems by varying the main running parameters [2,3]. However, it has proven difficult to draw clear and precise conclusions from the results, because of the number of operating parameters. The methodology of experimental design has, consequently, emerged as the rational method to use for this purpose; it is easy to use and it elucidates the effects of the parameters and their interactions. A thorough, but global, analysis based on the experimental design methodology applied to the cross-axis-type

device, was reported by Goupy et al. [4]. The overall analysis carried out by the use of experimental design with a coil mounted in the L position simplifies the operation of the cross-axis apparatus, as the best combination does not depend on the solvent system. Indeed, the retention of the stationary phase is mainly related to the choice of the mobile phase and of the elution direction. A heavier mobile phase requires the outward elution direction, whereas a lighter mobile phase requires an inward elution direction.

Consequently, no classification among solvent systems may be built from their behaviors inside a cross-axis device.

Theoretical Approaches to Correlate Physical Parameters and Observed Behavior Inside a CCC Column

The capillary wavelength and settling velocities have been retained as interesting parameters to step forward the description of the behavior of solvent system inside a CCC column. Moreover, they have also enabled a simple prediction of the effect of the temperature on the behavior of solvent systems, thus, on “Ito’s classification.”

The “theoretical” parameter capillary wavelength, λ_{cap} , has been precisely described by Menet et al. [4,5]. The capillary wavelength is a means of describing the microscopic behavior at the interface between two immiscible liquids. It stands for the wavelength of the deformations which may occur at the interface of the two liquids or represents the mean diameter of drops of a liquid in another one. For common liquids, its average value is 1 cm in the Earth’s gravitational field. For CCC devices, it is in the order of 1 mm, because of the generated centrifugal force field.

As the capillary wavelength only enables the description of the formation of droplets of one liquid in another one, it seemed interesting to introduce other “theoretical” parameters to better describe the dynamic phenomena occurring inside a CCC column. Two of these are presented here, namely V_{low} for the fall of a droplet of the heavier liquid phase (lower) in the continuous lighter one (upper) and V_{up} for the rise of a droplet of the lighter liquid phase in the continuous heavier one.

In order to determine if a correlation exists between “Ito’s classification” and the values of the previous “theoretical” parameters, the 15 solvent systems used for the design of the classification have been studied. The values of interfacial tension, of densities, and of dynamic viscosities of the solvent systems were used to



compute the values of the capillary wavelength and the settling velocities. The values of the three theoretical parameters have allowed to set ranges within which a solvent system is named “hydrophobic,” “intermediate,” or “hydrophilic.” The main interest is that the knowledge of some physical parameters of the solvent systems allows one to know, before any experiments, the best combinations for the greatest stationary-phase retention.

The values of the capillary wavelengths are smaller for “hydrophilic” solvent systems than those for “hydrophobic” ones: The first family of solvent systems tends to form small droplets of one phase in the other one, hence leading to a more stable emulsion. Their stationary phase is consequently less retained in the CCC column than the one of “hydrophobic” solvent systems; this phenomenon is well known in CCC [1].

From additional studies of six new solvent systems and by studying the influence of the temperature,

Menet et al. have shown the best classification is that based on V_{up} [4].

References

1. N. B. Mandava and Y. Ito, *Countercurrent Chromatography — Theory and Practice*, Marcel Dekker, Inc., New York, 1988.
2. Y. Ito and T.-Y. Zhang, *J. Chromatogr.* 449: 135–151 (1988).
3. Y. Ito, *J. Chromatogr.* 538: 67 (1991).
4. J. Goupy, J. M. Menet, and D. Thiébaud, Experimental designs applied to countercurrent chromatography: Definitions, concepts and applications, in *Countercurrent Chromatography* (J. M. Menet and D. Thiébaud, eds.), Marcel Dekker, Inc., New York, 1999.
5. J. M. Menet, D. Thiébaud, R. Rosset, J.-E. Wesfreid, and M. Martin, *Anal. Chem.* 66: 168–176 (1994).



Steroid Analysis by Gas Chromatography

Gunawan Indrayanto
Mochammad Yuwono

Airlangga University, Surabaya, Indonesia

INTRODUCTION

Steroids are a class of compounds that have a cyclopentanoperhydrophenanthrene skeleton, which occurs in nature and in synthetic products, and which can be classified into six groups according to the number of C-atoms: gonane (C-17), estrane (C-18), androstane (C-19), pregnane (C-21), cholane (C-24), and cholestane (C-27). These compounds are natural hormones or hormone precursors, except for cholane. In the naturally occurring steroids, the fusion of rings B and C is always *trans* and of the rings C and D usually *trans* (*cis* in the cardenolides and bufadienolides). Rings A and B are fused in *cis* and *trans* configurations with about equal frequency. Natural steroids possess either one or, more usually, two methyl groups at angular positions at which two rings meet. According to their function, steroid hormones can be divided into estrogen, androgen, glucocorticoids, and mineralocorticoids.

The other steroids, such as bile acids (cholane), vitamin D, saponin steroids, steroid alkaloids, cardiac glycosides, and brassinosteroids, also have biologically important activities. Due to the metabolic versatility of steroid molecules, extremely complex mixtures are often encountered, necessitating the use of chromatographic methods (HPLC, TLC, GC) for their analyses.

The application of gas chromatography (GC) to steroid analysis seems to have many difficulties due to their insufficient volatility and thermolability. The development of high-resolution gas chromatography (HRGC) and various derivatization procedures enables the efficient separation of complex steroid mixtures for application in clinical, forensic toxicology, and natural products analysis. The development of low-cost MS detectors, in recent years, has also promoted the application of GC-MS systems for the analysis of the complex mixtures.

THERMAL STABILITIES OF STEROIDS

According to their thermal stability, steroids can be divided into three groups.^[1] The first group of steroids can be analyzed by GC without any difficulties. This

includes steroids that possess Δ^5 -3-hydroxy, Δ^4 -3-keto, $\Delta^{1,4}$ -3 keto, 11-hydroxy, 17-hydroxy groups, and phenolic ring A in free, ether, or ester form. The steroids of the second group are those that, at high temperatures, undergo a certain decomposition, but this decomposition could be suppressed by careful selection of the GC experimental procedures. The steroids that belong to this second group are steroids that possess tertiary hydroxy groups (e.g., 17 α -methyl-17-hydroxy steroids) and deethynylation of 17 α -ethynyl-17-hydroxy steroids to 17-ketone. The third group of steroids contains those that decompose during analysis by GC; hence their direct chromatographic determination by GC cannot be carried out. The steroids belonging to this group are corticosteroids and Δ^4 -3-hydroxy or acyloxy derivatives. Another source of instability is the possible decomposition of steroids and their derivatives by metals; so, using all-glass systems, including glass-line vaporizer of the GC equipment, is essential.^[2]

DERIVATIZATION OF STEROIDS FOR GAS CHROMATOGRAPHY ANALYSIS

The main reasons for derivatization of steroids are to decrease heat sensitivity of steroids; to avoid irreversible adsorption of steroids onto the stationary phase; to increase volatility of steroids; to increase the separation efficiency; to achieve enhanced selectivity of the separations, and to improve the sensitivity of the detectors.^[2] Segura et al.^[3] described some important general requirements for derivatization reactions, i.e., a single derivative should be formed for each analyte; the reaction should be simple and rapid, and they should occur under mild conditions; the derivate should be stable, reproducible, and produced with high yield; in quantitative analyses, the calibration curve should be linear. The main derivatization method for steroids is silylation, but other derivatization methods using, for example, acetic acid anhydride, trifluoroacetic anhydride (TFA), pentafluoropropionic acid (PFPA), or heptafluoroabutyric anhydride (HFBA) could also be used.^[3,4] For anabolic steroids



and metabolites containing nitrogen, the use of acyl derivatives is also interesting.^[3] The primary factor in the choice of a suitable derivative will also be dependent upon the type of detector used. For the application of the very sensitive electron capture detector (ECD), it is quite favorable to prepare derivatives that show a high affinity for electrons, so, in this case, chloroacetate and heptafluorobutirate derivatives are mostly used. For analysis of steroids using GC-ID-MS (isotope dilution GC-MS) applications, silylation is not recommended due to the fairly high abundance of ²⁹Si and ³⁰Si in natural silicon,^[4] so derivatization using TFA, PFPA, and HFBA is preferred. Enzymatic hydrolysis is required before performing derivatization of glucono- or sulfo-conjugated steroids in urine.^[5,6] Derivatization of steroids using solid-phase micro extraction (SPME) and head space methods was also described previously.^[7] Detailed discussions of the derivatization methods for steroids were provided in an earlier topic in this encyclopedia^[8] and in Ref. [3].

STATIONARY PHASES

In the analysis of steroids by GC, silicone oils (SE-30, OV-1, OV-101) are most often used. These phases are suitable for the analysis of steroids on the basis of their molecular weight or on the shapes of the molecules. These silicone phases are considered as nonselective stationary phases. For separating stereoisomers or structural isomers, saturated or unsaturated derivatives, selective stationary phase such as methyltrifluoropropyl (QF-1, OV-210), methylphenylcyanopropyl (OV-225), and methyl-β-cyanoethyl (XE-60, AN-600) can be used.^[2] For packed column application of solid supports such as Gas-Chrom Q, Gas-Chrom S, Chromosorb AW or DMCS, and Chromosorb W HP DMCS, with 3% concentration of the stationary phase, have been generally used.^[1,9] For separating complex steroid mixtures, application of a glass or fused silica column is recommended. The length of the column ranges between 17 and 30 m, diameter of 0.2 to 32 mm, film thickness from 0.1 to 0.33 μm. The stationary phase consists mostly of polydimethylsiloxane, with 0–50% diphenyl groups.^[4]

DETECTORS

The flame ionization detector (FID) is mostly used as detector in steroid analyses. For very low concentrations of steroids, the application of electron capture detection (ECD) is needed. Thermal conductivity detectors (TCD)

cannot be used in the analysis of steroids, due to their very low sensitivity.^[1,2] For steroidal alkaloids, a nitrogen specific detector (NPD) has also been used. By the use of dual detector systems (FID and NPD, for example), closely related nitrogen- and nonnitrogen-containing steroids can be easily differentiated. The application of mass spectrometry (MS) as detector was already discussed in a previous chapter on this encyclopedia.^[10] By using a GC-MS system, the identity of the peak(s) can be determined in an undisputed manner.^[3]

GAS CHROMATOGRAPHY PARAMETERS FOR STEROID IDENTIFICATION

The identification of steroids in an unknown sample can be based on GC or GC-MS parameters, such as relative retention times, retention indices, steroid number, mass spectra, and/or important ion fragments.

Relative retention time (RR_t) is defined as the ratio of the analyte and the reference compound's retentions. The RR_t of sterols relative to cholesterol and cholestane, stearyl acetates to cholesteryl acetate, estrogen derivatives to cholestane, estrogen TMS ether to cholestane on various packed columns was described by Heftman.^[9] The RR_t of some estrane, androstane, and pregnane derivatives was also reported.^[2]

The concept of retention index (RI) was first published by E. Kovats in 1961. Detailed discussion of RI was already described previously in this encyclopedia.^[11] Van Gelder^[13] described the RI of various steroid alkaloids and saponins.

Steroid number (SN) is the sum of quantities characteristic of the skeleton and the functional groups in a molecule.^[1,7]

$$SN = S + F_1 + F_2 + \dots F_N$$

where *S* is the number of C atoms, *F*₁...*F*_{*N*} are values that are characteristic of the functional groups. The values of SN and *F* of some steroids, determined in packed columns, were already described in previous works.^[1,9]

Gas chromatography-mass spectrometry parameters for anabolic steroid metabolites,^[5,14,15] steroid alkaloids and saponins,^[13] and their MS data were published previously.

SELECTED APPLICATIONS

Anabolic Steroids

Anabolic steroids, which are related in structure and activity to testosterone, are used to improve muscle

mass and to accelerate recovery times from exercises. The use of anabolic steroids by athletes during competition and training was forbidden by the IOC. For doping control in sports, urine samples are mostly used. It is not easy to detect parent compounds, except for oxandrolone and testosterone, because the steroids are extensively metabolized.^[16] Before derivatization, urine samples are passed through a pasteur pipette containing Serdolit AD-2 slurry^[16,17] or extracted using SPE.^[5,6] For conjugated steroids, hydrolysis is performed (at pH 8.5) prior to derivatization.^[6] For analysis of anabolic steroids, Choi et al.^[16] used an Ultra-2 crosslinked capillary column of 5% phenylmethylpolysiloxane (30 m \times 0.2 mm; film thickness 0.33 μ m), with an oven temperature of 150°C (2 min) to 300°C (2 min) with a step rate of 20°C/min, injection temperature of 300°C, detection using MS (negative chemical ionization using methane), and tandem MS (MS/MS with collision energy for collision-induced dissociation of 1.0). Yoon and Lee^[6] used a glass capillary column (17 \times 2 mm), with an oven temperature of 180°C (6 min), then increased to 224°C (4°C/min), and finally 300°C at 15°C/min, detection using MS (negative chemical ionization using methane). Interested readers can consult Refs. [3,6,16–18] for details.

Brassinosteroids

Brassinosteroids are steroidal plant hormones which are required for normal growth and development. About 40 brassinosteroids have been characterized from the plant kingdom.^[19] For analysis of brassinosteroids, Park et al.^[19,20] used an HP-5 fused silica column (30 m \times 0.25 mm, film thickness 0.25 μ m) with an oven temperature of 175°C (2 min) then elevated to 280°C (40°C/min). Prior to injection, the samples were treated with methanouronic acid in pyridine (70°C for 30 min) to produce bismethaneburonate. For analyzing typhasterol, testosterone, 6-deoxytyphasterol, and 6-deoxoteassterone, Nomura et al.^[21] silylated the methaneburonate to MB-TMS derivatives before being injected into the GC (capillary DB-1 column 25 m \times 0.25 mm, 0.25 mm film thickness; oven temperature 170°C for 1.5 min, then increased to 280°C at 37°C/min).

Corticoids

Corticoids or corticosteroids are divided into mineralocorticoids that act in the metabolism of electrolytes, and glucocorticoids that act in saccharometabolism.^[18] Due to the instability of their dihydroxy acetone side chain at C-17, direct analysis using GC is impossible. Methoximation, followed by trimethylsilylation (TMS) derivatiza-

tion, is the most widely used approach.^[3] Interested readers should consult previous publications.^[4,18]

Estrogens

Estrogens are regarded as typical female hormones, which differ in a characteristic way from all other steroids by the presence of an aromatic A ring and the lack of a methyl group at C-10. Fritsche^[22] analyzed 17 β -estradiol and estrone and the estrogenic metabolites estriol and 17 β -estradiol in foodstuffs using a DB-5 fused silica column (30 m \times 0.25 mm, film thickness 0.25 μ m), detection using MS (EI, electron energy: 60 eV, ion source temperature: 180°C). The steroids were previously derivatized with *N*-methyl-*N*-trimethylsilyltrifluoroacetamide/trimethyliodosilane/dithioerythritol (1000:2:2) at 60°C for 15 min. Roy et al.^[23] developed a GC method with a ⁵³Ni pulsed electron-capture detector for measuring the rate of formation of 2-hydroxyestradiol and 4-hydroxyestradiol from estradiol from microsomal preparations. The steroids were converted to heptafluorobutyl esters and separated with a DB-5 fused silica capillary column (30 m \times 0.25 mm). The GC conditions were splitless injection, 280°C injection temperature, and a temperature gradient of 30°C/min from 100 to 245°C was followed by a 5-min isothermal period at 245°C and a second temperature gradient of 1°C/min from 245 to 265°C. Gas chromatography analysis of the pentafluorobenzyl derivatives of estrogen in river water and effluents was also developed by Xiao et al.^[24]

Neurosteroids

Neurosteroids are steroids that are synthesized de novo in the central nervous system (androsterone, dihydrotestosterone, testosterone, allopregnanolone, isopregnanolone, and pregnanole). After extraction of plasma and cerebrospinal fluids, using solid-phase extraction (SPE), and derivatization with carboxymethoxime, pentafluorobenzyl, and trimethylsilyl, the derivatized samples were injected into a GC-MS system for quantitative evaluation with a selected ion monitoring (SIM) method. Details of the method have been described in Ref. [25].

Sterols

Various TMS derivatives of sterols in tuna olive oil could be separated using CP-Sil 8 CB fused silica column (15 m \times 0.22 mm i.d.; 240°C isothermal; FID). Plant sterols (brassicasterol, campesterol, stigmasterol, and sitosterol) were analyzed using a fused silica column



(15 m × 0.25 mm i.d., 260°C isothermal; FID).^[26] Using a glass packed column (0.125 in. × 6 ft; 3 % SE-30 on Gas Chrom Q, 220–270°, 4°C/min; FID) the analysis of campesterol, sitosterol, and diosgenin was described.^[27] The separation of plant sterols (cholesterol, campesterol, stigmasterol, and sitosterol), squalene, and some lupane triterpenes was reported using a glass packed column (2 m × 2 mm i.d.; 3 % OV-1 on Gas Chrom Q; 200–280°, 4°C/min; FID).^[28] Analysis of plant sterols in food and vegetable oils has been reviewed by Abidi.^[29] Kalo and Kuranne^[30] described the GC analysis and electrospray tandem mass spectrometry of free sterols in fats and oils.

Steroid Saponins and Steroid Alkaloids

The separation of diosgenin and solasodine was reported using a glass packed column (0.125 in. × 6 ft; 3 % SE-30 on Gas Chrom Q, 220–270°, 4°C/min; FID). Diosgenin and its 5 α -derivative (tigogenin) can be well separated after derivatization using TFA and analyzed using a glass packed column (0.125 in. × 10 ft; 3 % QF-1 on Gas Chrom Q; 220°C isothermal; FID).^[27] Solanidine, demissidine (5- α -derivative of solanidine), and solasodine, which could not be separated using a glass packed column (1 m × 2 mm; 10 % SE-30 on Chromosorb W-HP, 260–300°C, 5°C/min, FID), were well separated using a fused silica (50 m × 0.22 mm; CP-Sil 5, film thickness 0.12 μ m; 290°C isothermal; FID) (13). Using fused silica (50 m × 0.22 mm; CP-Sil 5 CB, film thickness 0.12 μ m; 270°C isothermal; FID), various steroids, 5- α -cholestane, solanthrene, cholesterol, solanidine, demissidine, solasodine, stigmasterol, diosgenin, tigogenin, solasodine, and tomatidine could be separated without derivatization.^[13] Some methods of analysis of solasodine using GC were described in a previous publication.^[31]

REFERENCES

- Görög, S.; Szász, G. *Analysis of Steroid Hormone Drugs*; Elsevier Scientific Publishing Company: Amsterdam, Oxford, New York, 1985; 137–169.
- Görög, S. *Steroid Analysis in the Pharmaceutical Industry*; Ellis Horwood Limited: Chichester, 1989; 114–125.
- Segura, J.; Ventura, R.; Jurado, C. Derivatization procedure for gas chromatography-mass spectrometric determination of xenobiotics in biological samples, with special attention to drug abuse and doping agents. *J. Chromatogr., B* **1998**, *713*, 61–90.
- Wolthers, B.G.; Kraan, G.P.B. Clinical application of gas chromatography-mass spectrometry of steroids. *J. Chromatogr., A* **1999**, *843*, 247–274.
- Ayotte, C.; Goudreault, A.; Charlebois, A. Testing for natural and synthetic anabolic agents in human urine. *J. Chromatogr., B* **1996**, *687*, 3–25.
- Yoon, J.M.; Lee, H.K. Gas chromatography and mass spectrometric analysis of conjugated steroids in urine. *J. Biosci.* **2001**, *26*, 627–634.
- Okeyo, P.; Rentz, S.M.; Snow, N.H. Analysis of steroids for human serum by SPME with headspace derivatization. *J. High Resolut. Chromatogr.* **1999**, *20*, 171.
- Scott, R.P.W. Derivatization of Steroids for GC-Analysis. In *Encyclopedia of Chromatography*; Cazes, J., Ed.; Marcel Dekker, Inc.: New York, Basel, 2001; 240–241.
- Heftmann, E. *Chromatography of Steroids*; Elsevier Scientific Publishing Company: Amsterdam, Oxford, New York, 1976.
- Scott, R.P.W. Gas Chromatography-Mass Spectrometry Systems. In *Encyclopedia of Chromatography*; Cazes, J., Ed.; Marcel Dekker, Inc.: New York, Basel, 2001; 365–371.
- Moffat, A.C.; Jackson, J.V.; Moss, M.S.; Widdop, B. *Clarke's Isolation and Identification of Drugs*; The Pharmaceutical Press: London, 1986; 190.
- Zenkevich, I.G. Kovats Retention Index System. In *Encyclopedia of Chromatography*; Cazes, J., Ed.; Marcel Dekker, Inc.: New York, Basel, 2001; 466–470.
- Van Gelder, W.M.J. Ph.D. Thesis; University of Wageningen: Holland, 1989.
- Bowers, L.D.; Borts, D.J. Separation and confirmation of anabolic steroids with quadrupole ion trap tandem mass spectrometry. *J. Chromatogr., B* **1996**, *687*, 69.
- Schänzer, W.; Delahaut, P.; Geyer, H.; Machnik, M.; Horning, S. Long term detection and identification of methandienone and stanozolol abuse in athletes by GC-high resolution mass spectrometry. *J. Chromatogr. B* **1996**, *687*, 93–108.
- Choi, M.H.; Chung, B.C.; Kim, M.; Choi, J.; Kim, Y. Determination of 4 anabolic steroid metabolites by gas chromatography/mass spectrometry with negative ion chemical ionization and tandem mass spectrometry. *Rapid Commun. Mass. Spectrom.* **1998**, *12*, 1749–1755.
- Choi, M.H.; Chung, B.C.; Lee, W.; Lee, U.C.; Kim, Y. Determination of anabolic steroid metabolites by gas chromatography/mass spectrometry with negative ion chemical ionization and tandem mass spectrometry. *Rapid Commun. Mass. Spectrom.* **1999**, *13*, 376–380.
- Shimada, K.; Mitamura, K.; Higashi, T. Gas chromatography and high performance liquid chromatography of natural steroids. *J. Chromatogr., A* **2001**, *935*, 141–172.
- Park, S.C.; Kim, T.W.; Kim, S.K. Identification of brassinosteroids with 24-*R*-methyl in immature seeds of *Phaseolus vulgaris*. *Bull. Korean Chem. Soc.* **2000**, *21*, 1274–1276.
- Kim, T.S.; Park, S.H.; Joo, S.H.; Kim, Y.S.; Choo, J.; Kim,

- S.K. Metabolism of typhasterol in suspension cultured cells of *Marchantia polymorpha*. Bull. Korean Chem. Soc. **2001**, 22, 651–654.
21. Nomura, T.; Kitasaka, Y.; Tokatsuto, S.; Reid, J.B.; Fukami, M.; Yoko, T. Brassinosteroid/sterol synthesis and plant growth affected by lka and lkb mutation of pea. Plant Physiol. **1999**, 119, 1517–1526.
22. Fritsche, S. Ph.D. Thesis; University of Hamburg: Germany, 1998.
23. Roy, D.; Hachey, D.L.; Liehr, J.G. Determination of estradiol 2- and 4-hydroxylase activities by gas chromatography with electron-capture detection. J. Chromatogr. **1991**, 567, 309–318.
24. Xiao, X.-Y.; McCalley, D.V.; McEvoy, J. Analysis of estrogen in river water and effluents using solid-phase extraction and gas chromatography-negative chemical ionisation mass spectrometry of the pentafluorobenzyl derivatives. J. Chromatogr., A **2001**, 923, 195–204.
25. Kim, Y.S.; Zhang, H.; Kim, H.Y. Profiling neurosteroids in cerebrospinal fluids and plasma by gas chromatography/electron capture negative chemical ionization mass spectrometry. Anal. Biochem. **2000**, 277, 187–195.
26. *Chromatography Illustrated*; Preston Publication: Niles, IL; 33–34.
27. Carle, R. Ph.D. Thesis; University of Tübingen: Germany, 1979.
28. Indrayanto, G. Ph.D. Thesis; University of Tübingen: Germany, 1983.
29. Abidi, S. Chromatographic analysis of plant sterols in food and vegetable oils. J. Chromatogr., A **2001**, 935, 173–201.
30. Kalo, P.; Kuranne, T. Analysis of free sterols in fats and oils by flash chromatography, gas chromatography and electrospray tandem mass spectrometry. J. Chromatogr., A **2001**, 935, 237–248.
31. Indrayanto, G. Solasodine. In *Analytical Profile of Drugs and Excipients*; Brittain, H.G., Ed.; Academic Press: San Diego, 1996; Vol. 24, 487–522.



Steroid Analysis by TLC

Muhammad Mulja
Gunawan Indrayanto

Airlangga State University, Surabaya, Indonesia

Introduction

Steroids, which are a class of compounds that occur in nature and in synthetic products, have a cyclopentanoperhydrophenanthrene skeleton. The carbon atoms and rings are labeled according to the scheme shown in Fig. 1. The following classes of compounds belongs to steroids: sterols, bile acids, cardenolides, androgens, estrogens, corticosteroids, steroid saponinins, steroid alkaloids, ecdysteroids, and vitamin D.

In the naturally occurring steroids, the fusion of ring B and C is always trans and that of the ring C and D is usually trans (cis in the cardenolides and bufadienolides). Rings A and B are fused in cis and trans configurations with about equal frequency. The configuration of the substituents is referred to that of the 19-methyl group on C₁₀. Every substituent that is in a configuration identical to the methyl group is indicated by the β -position; substituents of opposite configuration are termed α -substituents (dotted lines). If the substituents lie in the planes of the rings, they are termed equatorial (e), and if perpendicular to the rings, they are called axial (a). Thus, for example, in an A/B *cis*-steroid, a 3 β -hydroxy group is axial and equatorial in an A/B *trans*-steroid (see Fig. 1). In general, equatorial substituents are more stable than axial substituents. In various reactions, the formation of the former is favored.

In the field of steroid analysis, thin-layer chromatography (TLC) is still the method of choice, especially when many simultaneous analyses have to be carried out; hundreds of analyses can be performed in a short time and with small demands on equipment and space. Samples can be analyzed with minimal cleanup, and analyzing a sample by the use of multiple separation steps and static postchromatographic detection procedure is also possible because all sample components are stored on the layer without the chance of loss. The time required in TLC analysis is about 10–60 min. As little as 0.01 μ g of steroids/spot can be detected by TLC. Using a TLC plate with thicker adsorbent layers (0.5–2 mm), several grams of substance can be isolated (preparative TLC).

Sorbents

The TLC of steroids has been tried on a great variety of sorbents, but various forms of silica gels are most frequently used. In order to achieve adequate stability, adhesion, and resistance to abrasion of the (precoated) layers, the sorbents usually contain a binder. Either they do not contain any additive at all, designated by “H” in the article designation, or gypsum (“G”) as binder. The sorbents designated by “P” are suitable for preparative purposes. An “F” designates the addition of fluorescent indicators and, if applicable, the number that follows gives the excitation wavelength and an “s” following this indicates the acid stability of the indicators. A number placed immediately after the name of the sorbent indicates the pore diameter of the sorbents (in Å). In high-performance thin-layer chromatography (HPTLC), the particle diameter is about 3–10 μ m, whereas in TLC, it is about 4–25 μ m. The plates can be easily prepared in the laboratory or readily purchased from commercial sources as precoated plates or sheets, but it is recommended to use ready-made (precoated) plates or sheets because they are more convenient and more uniform than those manually prepared in the laboratory.

An addition of 3–10% of silver nitrate to silica gel or kieselguhr is considerably helpful in the separation of sterols and steroids that differ only through an unconjugated double bond. For C₂₇ steroid saponinins and alkaloids, it was recommended to use a higher concentration of silver nitrate (15%). Precoated TLC–HPTLC plates can be dipped in a 20% silver nitrate solution for 15–20 min, then, in the absence of light, drying the plate in air. Finally, it is activated in a drying oven. Impregnating silica gel with 10–25% formamide in acetone can be used for separating digitalis glycosides, estrogens, and equilin. Impregnation with boric acid could be used, also, for the delicate separation of cardiac glycosides on silica gel layers. The silica gel can also be modified into nonpolar reversed phases (RP) such as C₁₈ (octadecyl function), C₈ (octyl function), CN (cyanopropyl function), NH₂ (aminopropyl function), and diol (vicinal hydroxyl function on C chains). Progesterone steroids can be well separated using CN



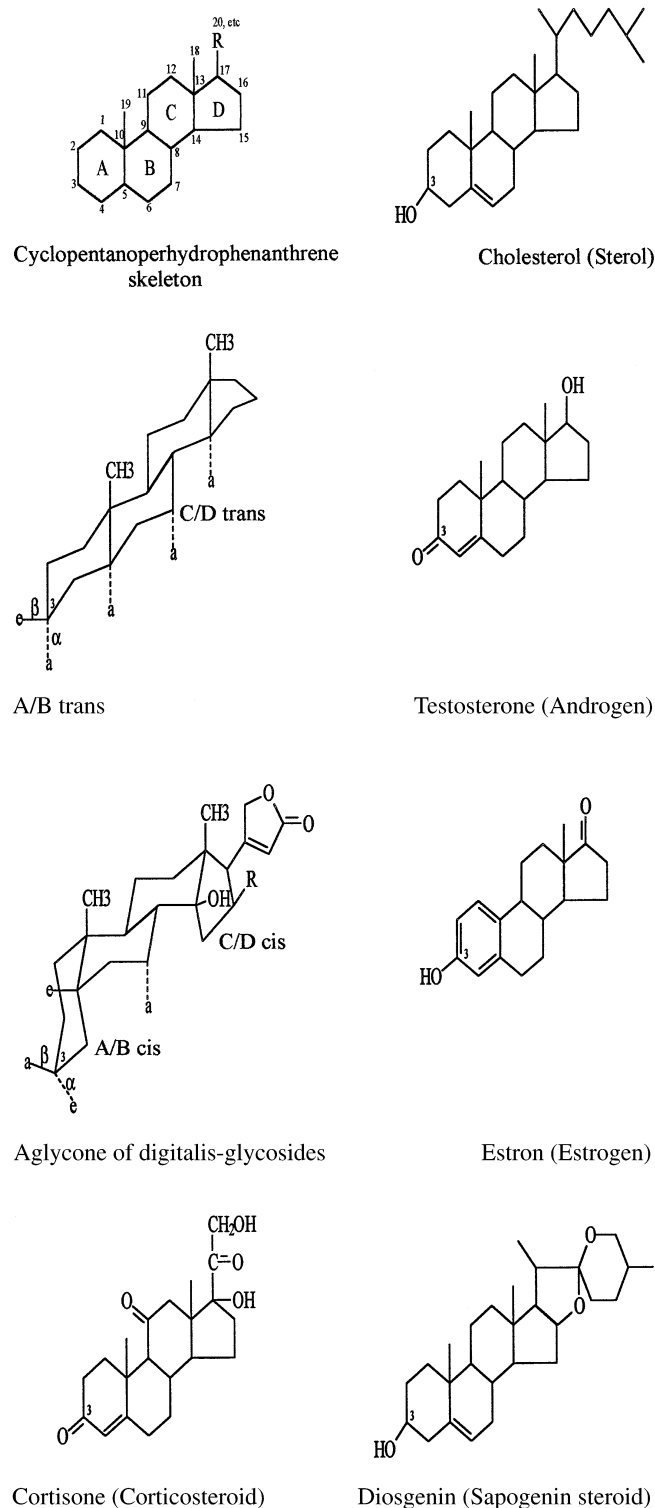


Fig. 1 The structure of some important steroids.

F₂₅₄ and RP plates. Reversed phases C₁₈, C₈, and C₂ could be used for analyzing the ecdysone steroids and RP C₁₈ for estrogen conjugates.

Other sorbents that have also been used for separating steroids in TLC are cellulose, kieselguhr, alumina, polyamide, magnesium oxide, and celite. Androstanes can be analyzed using cellulose layers impregnated with 1,2 propanediol. Layers consisting of alumina and magnesium oxide can be used to separate some sterols and sterol acetates.

Layers of alumina that are deactivated with 2.5% acetic acid could be employed for separating some corticosteroids. An advantage of using alumina rather than silica gel in TLC of Δ^4 -3-ketosteroids is that they form fluorescent oxidation products when the plate is heated to 150–180°C. As little as a nanogram of steroids can be detected by this method. By using a layer that consists of a mixture of MgO–Al₂O₃–CaSO₄ (15:5:1), complex mixtures of sterols as their 3,5 dinitrobenzoate derivatives can be resolved using hexane–ethyl acetate (9:1, v/v) as the mobile phase.

Although most steroids are stable on the silica gel layers, some steroids (e.g., estrogens and vitamin D) can decomposed readily. To avoid the decomposition, a preliminary treatment of the sorbent with a solution of ascorbic acid (antioxidants) in ethanol is recommended.

Development

Simple development will usually be enough for the TLC of steroids. In some cases, multidevelopment in the same or different solvent system or a two-dimensional technique is required to achieve better separation. For ensuring reproducibility of the R_f value, Nether [1] recommended the use of the same number of plates and always using fresh solvent for each run. A system containing a similar volatility maintains a more stable composition and, thus, has more reproducible R_f values during several runs. Our experiences shown that, by weighing the solvent components, the R_f values of testosterone (0.37) and estradiol (0.52) on silica gel plates were unchanged after four runs by using cyclohexane–ethyl acetate (1:1, w/w) as the mobile phase.

Detection

Destructive Detection Methods

Most of the reagents used for detecting steroid spots by *in situ* reactions (destructive reagents) contain sulfuric acid. Sulfuric acid, without any additive, can also

produce characteristic colors and fluorescence response, as well as permanent black zones after heating. The initial color, the color after heating for 10 min, and the color in ultraviolet (UV) (366 nm) of various classes of steroids (141 compounds) were presented by Heftmann [2]. Other destructive reagents that are most generally applicable are antimony trichloride (Carr–Price's reaction; for vitamin D, cardenolides, bufadienolides, triterpenoids), aromatic aldehyde–acids (for sapogenin steroids, steroid alkaloids, ketosteroids), molybdophosphoric acid (reducing and unsaturated steroids, cholesterol ester, bile acids; blue on yellow background), chlorosulphonic acid–acetic acid (cardenolides, green, blue violet fluorescence), and phosphoric acid (color similar to sulfuric acid).

For the detection of ketosteroids, an *m*-dinitrobenzene solution can be used (17-keto-steroids, violet; 3-keto- Δ^4 groups, blue). Δ^4 -3-Oxo steroids and $\Delta^{4,6}$ -3-oxo steroids can be distinguished using a phthalic acid–*p*-phenylenediamine reagent, which gives yellow and orange-brown colors, respectively. Detailed discussion of the destructive detection methods of steroid spots is described in the books of Macek [3] and Touchstone [4]. Thus, by spraying and heating the plates, various class compounds of steroids can be deduced; to confirm this, cochromatography with authentic standards is needed. If the standard is unavailable, isolating the substance and then identification by spectroscopic analysis is recommended.

Nondestructive Detection Methods

Steroids containing an α,β -unsaturated structure, such as Δ^4 -3-oxo, Δ^7 -6-oxo, Δ^5 -7-oxo and Δ^{16} -20-oxo groups, can be visualized under UV light (254 nm). For this purpose, the samples should be spotted on plates that contain a fluorescent indicator (GF₂₅₄ or F₂₅₄). The steroid spots will appear as dark zones on the layer. Sorbent layers without the indicator must be sprayed with a dilute solution of fluorescein or morin before exposure to UV light. This method has a great advantage over the destructive methods because the unchanged steroids can be eluted or isolated from the sorbents for further analysis.

Other nondestructive detection methods use iodine vapors or iodine–potassium iodide reagents (Mylius's reaction). Yellow, orange, or brown zones will appear on the layer. The zones will have to be marked, because the iodine will eventually evaporate. The sensitivity of the iodine test can be greatly increased by the use of layers containing rhodamine 6G. Most of the steroids are recovered unchanged af-

ter exposure for 30 min with iodine vapor, except for estrogen and Vitamin D.

Formation of Derivatives (Microreaction)

It is well known that steroid derivatives such as acetates, benzoates, propionates, and trifluoroacetates can be better separated in TLC–HPTLC than the free substances themselves. These derivatization reactions can be performed directly on the TLC layers. Acetylation can be accomplished by treating 10–100 μ g of steroids with 0.1 mL acetic anhydride and 0.1 mL pyridine for 8–16 h at room temperature. Following the reaction, blowing with nitrogen at 60°C can remove the reagent. Benzoylation is carried out in the same way, but by using 0.1 mL benzoyl chloride. Propionylation is performed by dissolving the steroids in 0.3 mL of warm propionyl chloride and allowing the mixture to stand 10 min at 20°C. Extraction with hexane and washing with water and sodium carbonate solution can purify the ester. Trifluoroacetylation is performed by mixing the steroids with a small excess of trifluoroacetic anhydride in hexane.

The steroid critical pairs (such as saturated or unsaturated with one double bond) can be separated better by spotting with 0.1% bromine solution in chloroform directly at the starting spot. A similar differentiation is accomplished by spotting with a solution of *m*-chlorperbenzoic acid in chloroform; but, by this method, epoxidation of the double bond occurs.

Quantitative Analysis

Spot Elution Technique

After elution from the chromatoplates, the separated steroids can be analyzed by using various methods such as UV–vis spectroscopy or fluorometry. Although this method is very simple, at the present time its application is significantly diminished due to some disadvantages (e.g., it is difficult to locate the spot position accurately, nearly quantitative elution of the spots is required, the loss originating from irreversible adsorption during chromatography must be minimized, etc.). When the UV method is used, special care should be taken because the eluate of silica gel with some semipolar solvents (e.g., ethanol, methanol) exhibit absorption in the UV region. It is recommended to use a blank containing the same amount of adsorbents from an empty part of the plate.



In Situ TLC Technique (Densitometry)

In situ quantification of steroids on the chromatoplate can be performed by using UV (for UV-active steroids), vis (usually using destructive reagents), and fluorometric methods. For UV-active steroids, such as corticosteroids, it is common to scan the steroid spots on the basis of fluorescence quenching at 254 nm using F₂₅₄ precoated layers. For steroids that use destructive reagents for their visualization, a reflectance–absorbance method in the vis range (370–700 nm) is used. The steroid sapogenins (diosgenin, hecogenin, manogenin, etc.), steroid alkaloids (solasodine, tomatidine), and total sterols may be assayed using an absorbance–reflectance densitometry method (in the vis region) after treatment of the steroid spots with anisaldehyde–sulfuric acid reagent. It was found that this densitometric method was faster, simpler, and less expensive when compared to HPLC or gas liquid chromatography (GLC). Three methods are available for *in situ* fluorometric measurement. The first is to produce active derivatives on the layer by spraying with a suitable reagent. The second is to induce fluorescence on the plate, and the third is to prepare fluorescent derivatives prior to the analysis. The DL (detection limit) of the fluorometric method is much lower compared to the UV and vis evaluation methods.

Validation of the Method

Before the assay methods can be used for routine application (e.g., in a quality control laboratory), it must first be validated. The parameters for the validation methods are specificity, linearity, accuracy, precision (repeatability and intermediate precision), detection limit (DL), quantitation limit (QL), and applicable range. A detailed discussion is provided in Ref. 5.

Applications

Many publications dealing with TLC–HPTLC steroid analysis have appeared every year. The publications can be summarized into categories as follows: analytical control of steroid formulations (drug preparations), determination of steroids in biological media and natural resources, and analytical control of the production of steroids (including raw material, syntheses, and biotransformation). A cumulative database of thousands of TLC methods (including steroids) is provided in compact-disk (CD) format by Camag [6].

References

1. R. Neher, *TLC of Steroids and Related Compounds*, in *Thin Layer Chromatography* (E. Stahl, ed.), Springer International Student Edition, Springer-Verlag, Berlin, 1969, pp. 311–357.
2. E. Heftmann, *Chromatography of Steroids*, Journal of Chromatography Library Vol. 8, Elsevier Scientific, Amsterdam, 1976, pp. 14–27.
3. K. Macek, *Pharmaceutical Application of Thin-Layer and Paper Chromatography*, Elsevier, Amsterdam, 1972, pp. 275–348.
4. J. C. Touchstone, *CRC Handbook of Chromatography of Steroids*, CRC Press, Boca Raton, FL, 1986, pp. 27–40.
5. B. Renger, H. Jehle, M. Fisher, and W. Funk, *J. Planar Chromatogr.* 8: 269–278 (1995).
6. Camag Bibliography Service, *Thin-Layer Chromatography, Cumulative CD version 1.00*, Camag, Muttenz, 1997.
7. S. Görög and G. Szasz, *Analysis of Steroid Hormone Drugs*, Elsevier Scientific, Amsterdam, 1978.
8. S. Görög, *Steroid Analysis in the Pharmaceutical Industry*, Ellis Horwood, Chichester, 1989.



Supercritical Fluid Chromatography with Evaporative Light-Scattering Detection

Christine M. Aurigemma

William P. Farrell

Pfizer Global Research and Development, La Jolla, California, U.S.A.

Introduction

The evaporative light-scattering detector (ELSD) was originally developed for use with high-performance liquid chromatography (HPLC) to detect nonvolatile compounds by mass rather than ultraviolet (UV) absorbance detection [1]. The response is dependent on the light scattered from particles of the solute remaining after the mobile phase has evaporated and is proportional to the total amount of the solute. Because no chromophore is necessary, a response can be measured for any solute less volatile than the mobile phase.

Discussion

Although ELSD is considered a universal detector for HPLC [2], there are additional advantages obtained from coupling ELSD to packed column supercritical fluid chromatography (SFC). SFC provides better selectivity and faster analysis times over HPLC as a result of the low-viscosity and high solute diffusion coefficients characteristic of supercritical fluids [3]. Detection limits for some solutes are improved using ELSD with SFC relative to HPLC [4]. In order to increase solvating power and improve peak shape, CO₂ is often modified with a polar organic solvent such as methanol [5,6]. Using this binary fluid allows for improved separation efficiency of compounds having a wide range of polarities that may otherwise require a buffer.

When compared to other mass-sensitive detectors such as flame ionization (FID), refractive index (RI), and mass spectrometry (MS), the ELSD can detect analytes without interference from organic modifiers and additives. The use of organic solvents in FID limits usefulness due to an increase in baseline noise, and FID cannot be used with HPLC. RI detectors, in general, are less sensitive than other detectors and are incompatible with gradient elution. Although the MS can be used with modifier gradients, ionization efficiencies

can vary over orders of magnitude depending on the solute and mode of ionization. The ELSD is more practical than conventional UV detectors because solutes lacking in UV-absorbing chromophores can be directly detected without any sample derivatization or pretreatment. Baseline disturbances due to absorption of the mobile-phase solvents are not observed with ELSD. However, solvents containing trace levels of impurities and columns with low bleed characteristics must be employed for high-sensitivity work. The ELSD can be optimized to generate a narrow range of response factors to components within a structural class, and the use of appropriate standards would allow for quantitative analysis of these compounds.

Because organic solvent gradients do not interfere with ELSD, the detector is an ideal choice for coupling with SFC. A wide range of SFC–ELSD biomedical and pharmaceutical applications have demonstrated higher sensitivity, shorter analysis times, and better separation efficiencies with SFC than HPLC. Compounds without UV chromophores, such as carbohydrates and ginkgolide extracts, have been reported by Lafosse et al. [2], Carraud et al. [4], and Strode et al. [7] using SFC modifier gradients. More efficient baseline separations of these compounds were achieved by SFC–ELSD than with HPLC, and no time-consuming derivatization steps were necessary. The analysis of triglycerides using SFC–ELSD, which required a polar organic modifier to elute, yielded a significant increase in sensitivity over HPLC–ELSD [4]. Underivatized amino acids were also effectively separated by SFC–ELSD [3]. A more complete review of the various SFC–ELSD interfaces and applications was recently published by Lafosse [2].

Evaporative light-scattering detection response was found to have an exponential relationship to the mass of the solute by the equation:

$$A = am^b \quad (1)$$

where A is the peak area of the ELSD signal, m is the solute mass, and a and b are constants which depend



on the nature of the mobile phase and of the solutes [8]. Because the peak area response is proportional to the amount of solute, a linear response would be more desirable if quantitation of sample components is required. Linearity can be achieved by plotting calibration curves on a log-log scale as in Eq. (2):

$$\log A = b \log m + \log a \quad (2)$$

The ELSD detector response is influenced by the functions of its three main units: the nebulizer, drift tube, and light-scattering cell. As the mobile phase passes through the nebulizer, it becomes dispersed by a flow of carrier gas such as nitrogen and forms an aerosol. The resultant droplets vary in size depending on factors including the flow rate of the nebulizer gas and the geometry of the nebulizer [6]. The droplets then travel through a heated drift tube where the mobile phase is evaporated, leaving behind only unsolvated particles. Upon exiting the drift tube, the solute particles enter a detection chamber and pass through a beam of light from either a polychromatic (tungsten lamp) or a monochromatic (laser) source. The light is scattered and a photomultiplier or photodiode detector, which measures the light intensity, produces a chromatographic signal. Refer to Ref. 1 for a more detailed discussion of the principles of light scattering.

When coupling a low-pressure detector such as the ELSD with SFC, detection takes place at atmospheric pressure, usually downstream of the back-pressure regulator [2]. Figure 1a shows a common SFC-ELSD interface with downstream pressure control. Factors affecting ELSD response in this configuration include nebulizer design, evaporation conditions, carrier gas flow rate, and the use of makeup fluid.

Most commercial ELSDs employ a standard or modified HPLC nebulizer (Venturi flow type). It was believed that this nebulizer was not necessary for SFC because nebulization of the SFC mobile phase is accomplished by gas expansion in a restrictor which controls pressure and mobile-phase flow rates. To counter the cooling effects of CO₂ decompression in the linear fused-silica restrictor and improve heat transfer, Nizery et al., using a Cuno Clichy Model DDL 10 detector, placed the restrictor tip into a heated brass ring and applied heat to a small section of tubing between the restrictor and the drift tube [9]. They found that baseline noise resulting from the formation of ice crystals decreased and the performance of the ELSD was unaffected.

The droplet sizes formed and the flow rate of the particles in the drift tube are influenced by the design of the nebulizer. In order to maintain a constant nebulization, droplet sizes should not be too large making them difficult to evaporate or too small where solute

vaporization could occur. This requires sufficient liquid and a carrier gas (usually nitrogen). Carraud et al. replaced a conventional ELSD nebulizer (Cuno Clichy Model DDL 10) with a short fused-silica restrictor and determined that the ELSD signal response was dependent on the CO₂ flow rate, although this was later disproved [4].

Larger particle sizes produce higher intensities of scattered light. In order to obtain maximal ELSD sensitivity, evaporator temperatures must be sufficient to allow for the formation of appropriately sized particles. A loss in sensitivity is observed if temperatures are too high because smaller particles may result from sublimation of some compounds. Upmooor and Bruner [10] studied the effects of varying evaporator temperature on ELSD sensitivity and found that the optimal range of temperatures was between 40°C and 70°C. At lower temperatures, longer residence times required in the drift tube produced peak broadening as well as an increase in baseline noise.

The flow rate of the carrier gas (usually N₂) influences the residence time of the sample in the light-scattering chamber. Low gas flows may allow solute bands to broaden as they travel in the drift tube to the detector. Strode and Taylor [11] observed a decrease in ELSD signal with an increase in the carrier gas flow rate. However, the increase in gas flow improved peak width compared to that observed with the UV detector. It was later found that the total flow of gas (carrier gas plus the decompressed CO₂) through the detector influenced the signal response and the peak width [11].

Most SFC-ELSD instruments employ a direct connection of the outlet of a back-pressure regulator to the detector inlet, as outlined in Fig. 1a. By operating in this manner, peak broadening in the transfer line between the back-pressure regulator and the detector may occur. Additionally, the pressure decrease in the transfer line may affect the strength of the mobile phase and, thus, the ability of the solutes to become completely solubilized. Pinkston bypassed the back-pressure regulator with a postcolumn tee that introduced a makeup fluid such as methanol from a high-pressure syringe pump under pressure control [12]. A fused-silica linear restrictor at the ELSD inlet maintained the pressure and was regulated by the flow of the makeup fluid, as shown in Fig. 1b. Pinkston theorized that this method of pressure control would prevent mass-transfer problems that diminish detector sensitivity and decrease the dependence of the ELSD response on mobile-phase composition [12]. The flow of makeup solvent enhanced the solubility of the analytes in the mobile phase. Additionally, the efficiency of forming appropriately sized particles in the ELSD was



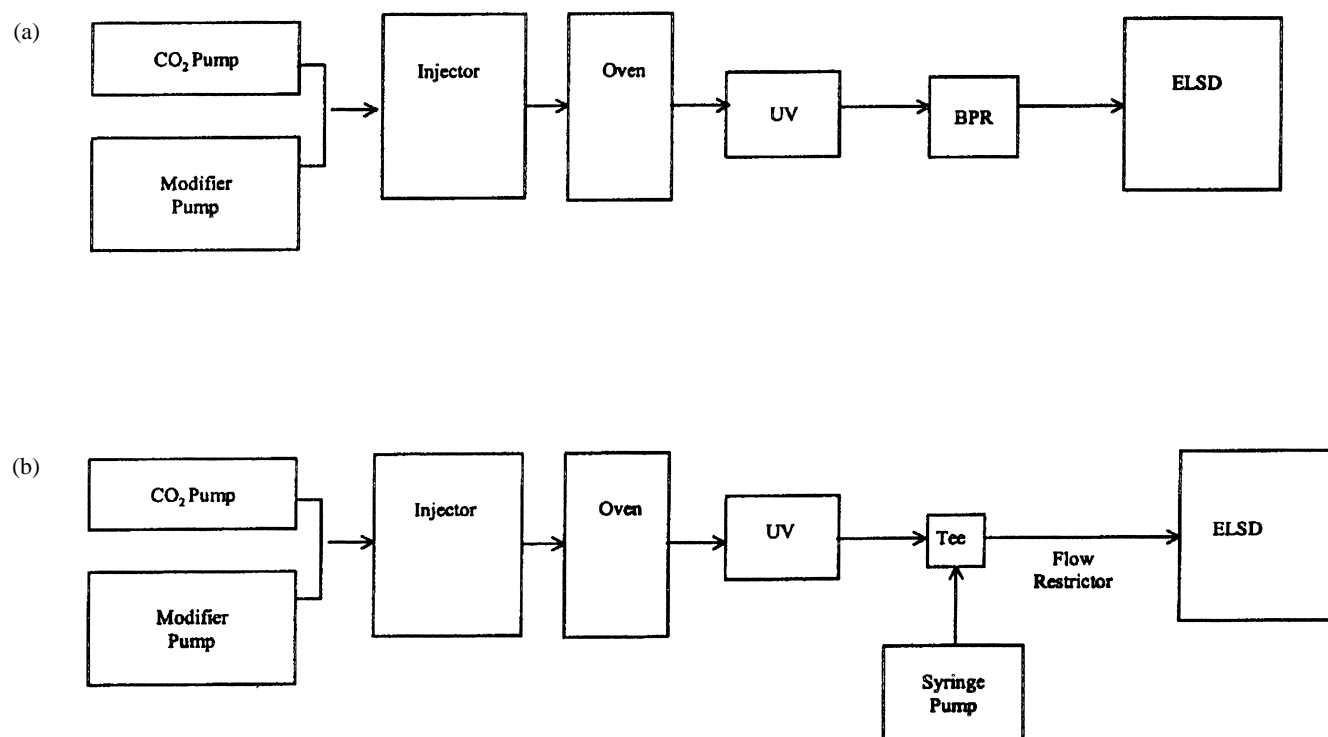


Fig. 1 Two common arrangements for SFC-ELSD coupling: (a) shows pressure control by a back-pressure regulator (BPR), and in (b), the pressure is regulated by a makeup fluid delivered by a pressure-controlled syringe pump. (From Ref. 12.)

improved, generating better peak shapes and higher signal-to-noise ratios.

In conclusion, an ELSD with SFC provides a sensitive analytical tool for qualitative and quantitative analysis of solutes. Detection depends only on the solute being less volatile than the least volatile mobile-phase component. Detection is independent of the basicity or presence of a chromophore for a given solute. The detector response is a logarithmic function of the mass of the solute. The SFC-ELSD combination should be considered whenever a universal high-throughput analysis is needed.

References

1. J. T. B. Strode, L. T. Taylor, K. Anton, M. Bach, and N. Pericles, *Supercritical Fluid Chromatography with Packed Columns: Techniques and Applications*, Marcel Dekker, Inc., New York, 1997, pp. 97-123.
2. M. Lafosse, Evaporative light scattering detection in SFC, *Chromatogr. Princ. Pract.* 201-218 (1999).
3. M. Lafosse, C. Elfakir, L. Morin-Allory, and M. Dreux, *J. High Resolut. Chromatogr.* 15: 312-318 (1992).
4. P. Carraud, D. Thiebaut, M. Caude, R. Rosset, M. Lafosse, and M. Dreux, *J. Chromatogr. Sci.* 25: 395-398 (1987).
5. T. A. Berger, *Packed Column SFC*, The Royal Society of Chemistry, Cambridge, 1995.
6. M. Dreux and M. Lafosse, *LC-GC Int.* 10: 382-390 (1997).
7. J. T. B. Strode, L. T. Taylor, and T. A. van Beek, *J. Chromatogr. A* 738: 115-122 (1996).
8. M. Dreux, M. Lafosse, and L. Morin-Allory, *LC-GC Int.* 9: 148-153 (1996).
9. D. Nizery, D. Thiebaut, M. Caude, R. Rosset, M. Lafosse, and M. Dreux, *J. Chromatogr.* 467: 49-60 (1989).
10. D. Upmooor and G. Brunner, *Chromatographia* 33: 255-260 (1992).
11. J. T. B. Strode III and L. T. Taylor, *J. Chromatogr. Sci.* 54: 261-270 (1996).
12. T. L. Chester and J. D. Pinkston, *J. Chromatogr. A* 807:



Supercritical Fluid Chromatography with Mass Spectrometric Detection

Manuel C. Ventura

Pfizer Global Research and Development, La Jolla, California, U.S.A.

Introduction

In recent years, supercritical fluid chromatography (SFC) has been exploited as an alternative to high-performance liquid chromatography (HPLC) because of its superior speed and enhanced selectivity for most organic compounds, with the exception of highly polar species. The higher diffusion coefficient and lower viscosity of the SFC mobile phase, primarily consisting of condensed CO₂, permit faster run times than HPLC with longer columns and, thus, higher plate counts. These properties, combined with the advantages of mass spectrometry (MS) instrumentation used as chromatographic detectors, give rise to interest in coupling SFC with MS. When one considers the chromatographic and mass spectrometric advantages inherent with such an interface, SFC–MS is an attractive alternative to LC–MS for many applications.

Discussion

Considerations of primary importance in developing an interface for SFC–MS are (a) preserving performance of the ionization source and mass spectrometer, (b) preserving integrity of the chromatography, (c) minimizing thermal degradation, and (d) a rugged, simple design. The “guiding hand” behind the design of the interface is the type of mass spectrometer ionization source employed.

Vacuum ionization sources such as electron-impact (EI) or chemical ionization (CI), commonly used for gas chromatography–mass spectrometry (GC–MS), were initially used when the first SFC–MS interfaces were assembled. By EI, a high degree fragmentation occurs, usually obscuring the analyte molecular ion, but potentially elucidating some structural information. EI spectra for many compounds are well known and are stored in the National Bureau of Standards library. In CI, a gas-phase charge transfer with a reagent gas in the source ionizes solutes in a softer fashion than EI, usually producing significant levels of

MH⁺, MH⁺, or M⁺ charged adduct ions. In either EI or CI, more than a minimal gas load on the source is not tolerable. For SFC–MS with EI or CI, low source pressure is maintained using a low flow rate or split-flow direct fluid introduction (DFI), sometimes termed DLI (direct liquid introduction) [1]. Alternatively, differential pumping of the effluent from a restrictive nozzle is feasible as used with the molecular beam interface employed in some early SFC–MS experiments [2]. The DFI interface includes an isothermal union of a transfer line and column, attached to a heated fixed restrictor to counteract cooling from the adiabatic expansion of CO₂ prior to introduction of the effluent into the ionization source. Performance of such systems is compromised by adverse effects of gradient conditions on ionization and ion transmission. Increased pressure in the ion source resulting from high flow rates reduces ionization efficiency by EI and CI, thus limiting such experiments to low-polarity species, which do not require high levels of polar organic modifier to elute by SFC.

Complex interfaces were also designed to eliminate the gas load on the mass spectrometer from the SFC effluent. Particle beam and moving-belt interfaces originally used for LC–MS were employed with some success, due to their capacity to limit the effect of the mobile-phase on the MS analysis. The particle beam interface generally employs two momentum separators to remove volatilized mobile-phase molecules from the solute beam entering the EI or CI source [3]. Although spectral interferences and chemical noise levels are reduced, the interface suffers from reduced efficiency due to losses of more volatile components in the momentum separator and nonlinear response factors, especially for more nonvolatile compounds. The high-flow-rate moving-belt interface functions by transporting adsorbed solutes on the belt while eliminating more volatile mobile-phase molecules that do not adhere or thermally desorb from the belt prior to introduction to the ionization region [4]. Problems associated with moving-belt interfaces include losses of volatile or thermally labile solutes, and for some sol-



utes, poor sensitivity and carryover due to inefficient desorption from the belt. In both cases, sensitivity is compromised due to inefficient mass transport and thermal degradation.

Thermospray interfaces, originally designed for constant vapor pressure conditions, have nonetheless been utilized for SFC–MS by several researchers [5]. The column effluent is vaporized in a heated fixed restrictor probe in which solutes are ionized by mobile-phase-mediated chemical ionization (e.g., with ammonium acetate), producing CI-like spectra (prevalent in MH^+ or MH^- ions). The ionization process is sometimes assisted by an electron current beam across the probe outlet into the source vacuum region, producing EI-like spectra. The resulting beam of ions is then deflected by an electric potential into the mass analyzer region. Recently, thermospray usage for SFC–MS has declined in prominence due to low sensitivity from mass-transport inefficiency to the analyzer or thermal degradation, and it suffers from poor reproducibility in general. The recent alternative of atmospheric pressure ionization (API) sources has slowed further improvements to the thermospray interface.

The recent success of SFC–MS using API sources have contributed to a general decline in the use of many interface designs described earlier. API sources include electrospray ionization (ESI) and atmospheric pressure chemical ionization (APCI). A general schematic illustrates the basic form of the interface of SFC to an API source (Fig. 1). Along with providing usually unambiguous mass spectral identification (MH^+ or MH^- signals predominate), API sources for

SFC–MS provide attractive advantages for the analytical chemist. Many commercially available interfaces originally designed for LC–MS require minimal modification to effectively couple an SFC to API–MS systems. Another advantage of such interfaces is the “self-volatilizing effect” provided by CO_2 in nebulization of the mobile-phase solutes.

Electrospray ionization occurs in the solution phase prior to vaporization at atmospheric pressure in the mass spectrometer source. Ions are desolvated in the strong electric potential gradient from the needle tip to the inlet of the mass analyzer. In the early period of SFC–ESI–MS development, Sadoun et al. [6] constructed an interface using a 25–30-cm-long fused-silica restrictor [25 or 60 μm inner diameter (i.d.)] with one end attached to the outlet of a packed column and the other end to the source (see Fig. 1a). The last 10 cm of silica was coated with a layer of conductive nickel paint to simulate an electrospray needle. Employing a gradient with methanol–water as the polar modifier, detection limits in the low picogram range were reported; however, ionization efficiency was significantly affected by the mobile-phase composition and severe tailing for low-volatility compounds was observed. Some of these deficiencies were addressed by Pinkston and Baker [7] using a sheath liquid of methanol–water–ammonium acetate with an ion spray (or pneumatically assisted electrospray) interface for open-tubular or packed column SFC–MS. In the latter application, a syringe pump supplied methanol through a tee between the mobile-phase outlet and the transfer line to provide back-pressure regulation without a variable restrictor valve (Fig. 1a). Advantages of this interface included reduced tailing and lowered modifier composition requirements in the gradient, allowing for higher flow rates and shorter retention times. Sjöberg and Markides described a similar sheath liquid-type ESI interface also convertible to an APCI interface [8].

Atmospheric pressure chemical ionization is similar to ESI in that both ionization processes occur at atmospheric pressure. Ionization by APCI is fundamentally different, however, in that nebulized solute molecules encounter a plasma of protons, ions, and electrons generated by the corona discharge ionization of background N_2 , H_2O , or methanol, and ionize either by proton transfer or charge exchange. The proton-transfer agents, usually water or methanol, are supplied by saturating the N_2 nebulizing gas or using the SFC mobile-phase polar modifier, again usually methanol. The first report of packed column SFC with APCI by Huang et al. [9] described an interface in which the back-pressure regulator was bypassed and the restrictor was a

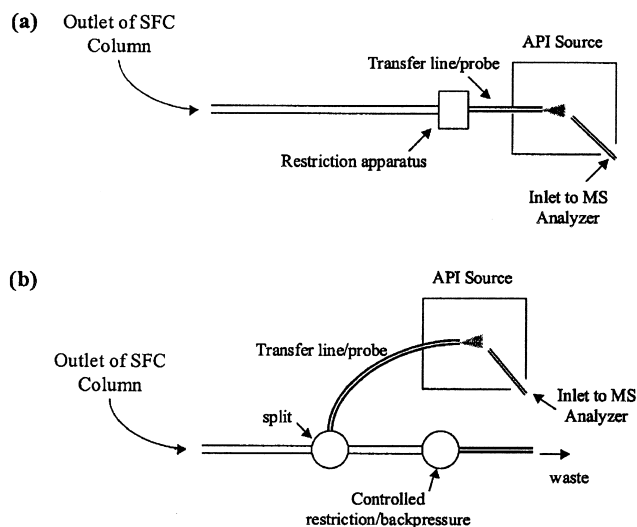


Fig. 1 SFC–MS interfaces.

20- μm -i.d. stainless-steel pinhole diaphragm. The effectiveness of this interface was limited by inadequate heating in the nebulization region, resulting in chromatographic tailing for more involatile substances. This problem was addressed by the interface designed by Tyrefors et al. [10]. This interface was constructed to maintain the temperature of the mobile phase in the column up to the tip of the restrictor and provide consistent intense vaporization conditions somewhat independent of flow rate. The outer tube was actively insulated with a heating coil while a coaxial nebulizing gas flowed around the restrictor tube into which a fine heating wire was inserted.

An SFC-APCI interface style employed by Morgan et al. [11] was constructed and tested independently on three commercial mass spectrometers equipped with API inlet systems. Comparison studies were performed to test the ideal dimensions (length and i.d.) of the PEEKTM transfer tube as well as the fused-silica used in the APCI source inlet. Significantly, neither the PEEK tubing length nor its diameter below 1 mm had any chromatographic implications. The fused-silica diameter impacted chromatographic integrity as diameters above 100 μm gave rise to extreme peak deformation and tailing. The optimal dimensions of the tubing were shown to be independent of the MS source on test. Another APCI interface design reported by Ventura et al. [12] employs a postcolumn (post-UV detector) split upstream of the variable restrictor in the style of some DFI interfaces (Fig. 1b). A 50- μm -i.d. fused-silica capillary carries the split flow from the tee to the exit tip of the APCI needle housing, whereupon expansion and nebulization occur. This method reduces delay between UV and MS signal detection while maintaining chromatographic integrity for MS peaks. An orthogonal analyzer inlet allows flow rates up to 6 mL/min to be used routinely with methanol modifier compositions as high as 60%. The interface is effective for applications in which trace detection is not required.

Further information may be obtained from reviews on SFC-MS, including those by Pinkston and Chester [13], Arpino and Haas [14], and Combs et al. [15].

Two general styles for interfacing SFC to API sources are depicted in Fig. 1. In Fig. 1a, the SFC column effluent is directed entirely into the API source.

In some systems, the restriction apparatus is a simple transfer tube restriction used for low-flow experiments. In others, a variable restrictor or back-pressure regulator is used between the outlet and the source. In the configuration used by Pinkston and Baker [7], the restriction apparatus is a series of tees to add a coaxial flow of nebulizing gas, electrospray buffer sheath flow, and another to introduce liquid from a syringe pump to regulate mobile-phase pressure. In Fig. 1b, a direct interface is shown in which a split directs a fraction of the effluent flow toward the API source while the remainder is sent to waste through a back-pressure regulator or some controlled restriction to maintain system pressure.

References

1. L. G. Randall and A. L. Wahrahaftig, *Anal. Chem.* 50: 1703 (1978).
2. L. G. Randall and A. L. Wahrahaftig, *Rev. Sci. Instrum.* 52: 1283 (1981).
3. P. O. Edlund and J. D. Henion, *J. Chromatogr. Sci.* 27: 274 (1989).
4. A. J. Berry, D. E. Games, and J. R. Perkins, *J. Chromatogr.* 363: 147 (1986).
5. J. Via and L. T. Taylor, *Anal. Chem.* 66: 1385 (1994).
6. F. Sadoun, H. Virelizier, and P. J. Arpino, *J. Chromatogr.* 647: 351 (1993).
7. J. D. Pinkston and T. R. Baker, *J. Am. Soc. Mass Spectrom.* 9: 498 (1998).
8. P. J. R. Sjöberg and K. E. Markides, *J. Chromatogr. A* 785: 101 (1997).
9. E. Huang, J. D. Henion, and T. R. Covey, *J. Chromatogr.* 511: 257 (1990).
10. L. N. Tyrefors, R. X. Moulder, and K. E. Markides, *Anal. Chem.* 65: 2835 (1993).
11. D. G. Morgan, K. L. Harbol, and N. P. Kitrinis, Jr., *J. Chromatogr. A* 800: 39 (1998).
12. M. C. Ventura, W. P. Farrell, C. M. Aurigemma, and M. J. Greig, *Anal. Chem.* 71: 4223 (1999).
13. J. D. Pinkston and T. L. Chester, *Anal. Chem.* 67: 650A (1995).
14. P. J. Arpino and P. Haas, *J. Chromatogr. A* 703: 479 (1995).
15. M. T. Combs, M. Ashraf-Khorassani, and L. T. Taylor, *J. Chromatogr. A* 785: 85 (1997).

PEEKTM is a trademark of Victrex plc.



Supercritical Fluid Chromatography with Nitrogen Chemiluminescence Detection

William P. Farrell

Pfizer Global Research and Development, La Jolla, California, U.S.A.

Introduction

Supercritical fluid chromatography (SFC) with nitrogen chemiluminescence detection (NCD or CLND) is a chromatographic technique that can be used to obtain quantitative results for nitrogen-containing analytes without the use of matching standards. For industries where sample throughput is an issue, such as combinatorial chemistry, SFC–NCD could reduce the need to isolate large numbers of standards and improve the speed of chromatographic characterization of synthetic reaction products. This entry will discuss the fundamental parameters that need to be considered to make SFC and NCD interfacing successful. Two other forms of nitrogen detection used with SFC will also be mentioned, but they fall outside the scope of this entry.

Discussion

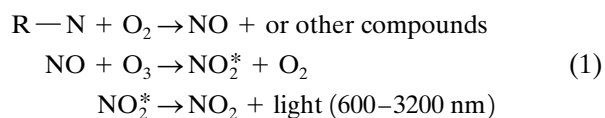
Supercritical fluid chromatography utilizes a compressed or dense gas as a mobile phase (i.e., carbon dioxide) and has been shown to be a powerful separation technique. The low viscosity and high diffusivity of supercritical fluids allow for the use of longer columns than in high pressure liquid chromatography (HPLC) without increasing runtimes. The increased number of theoretical plates available, combined with optimum linear velocities (μ_0) three to five times greater than in LC, can provide more separations per unit time. Berger has written a more detailed description of the functionality of packed column SFC [1].

Supercritical fluid chromatography has some of the same characteristics of both HPLC and gas chromatography (GC). Packed column SFC uses the same column technology as HPLC, and when used with binary or tertiary solvents, has a broad range of applicability [1]. This range is much broader than GC, because compounds need not be volatile or thermally stable. As in GC, SFC can be coupled to most modern chromatographic detectors, such as element-specific detectors. These detectors are often very selective for

the element under study, with detection limits below parts per billion [1]. Coupled to an SFC, an element-specific detector can become a powerful tool that offers selectivity, sensitivity, and speed.

Two other types of element-specific detector for nitrogen currently in use coupled to SFCs are the nitrogen phosphorus detector (NPD) and the thermal energy analyzer (TEA). The NPD uses a hot, catalytically active solid surface immersed in a layer of dissociated H_2 and O_2 to form electronegative N and P ions which are detected on a nearby electrode [2]. NPD has been shown to have broad application in SFC, especially in the agrochemical industry [3]. The TEA, as described by Fine et al. [4], uses low-temperature pyrolysis, followed by ozone-induced chemiluminescence, for the detection of compounds containing NO_2 groups. The TEA has been used for the determination of tobacco-specific nitrosamines and explosives [5]. Both of these detectors require specific standards of the analytes of interest for quantitation.

The use of NCD, especially in pharmaceutical applications, have focused on exploiting the chemiluminescence properties of nitrogen dioxide (NO_2) formed from the high-temperature combustion of nitrogenous compounds [6–8]. This type of detector, originally developed for GC by Parks and Marietta [9], forms nitric oxide followed by ozone-induced chemiluminescence. The reaction is characterized as follows:



Excited-state nitrogen-dioxide-mediated chemiluminescence occurs on a 1:1 molar ratio with solute nitrogen, provided that the combustion products form NO (and not N_2). With complete combustion of the solute, the NCD can directly provide a quantitative measure of the amount of nitrogen in a chromatographic peak. This means that a single calibration curve using a stable nitrogen-containing compound can be used to quantify nitrogen content of any un-



known peak in a chromatogram [6]. With a linear range of at least three orders of magnitude and picogram detection limits, SFC–CLND can provide an efficient technique for the quantification of nitrogen-containing compounds [6].

The basic setup of a NCD system is shown in Fig. 1. In almost all cases, only a portion of the entire SFC mobile phase is diverted to the CLND detector using a fused-silica capillary or restrictor [6–8,10,11]. Use of a restrictor minimizes the effects of the SFC decompressed carbon dioxide (CO_2) and solvent composition on the pyrolysis reaction and chemiluminescence. The CO_2 flow rate, dictated largely by the SFC outlet pressure, can affect the residence time of the solute in the pyrolysis chamber and the efficiency of the ozone reaction. The addition of modifiers to the SFC mobile phase (e.g., methanol) can compete for the available pyrolysis oxygen and can reduce signal response. High concentrations of modifier can dramatically affect the detection limits of some compounds [7]. Moreover, the sample concentration also appears to be limited by competition for oxygen, resulting in incomplete combustion.

The parameters that need special consideration for the successful coupling on an SFC to a CLND are restrictor position, ozone generation, combustion efficiency (temperature and oxygen flow rate), and quenching. Each of these will be discussed in detail.

Restrictor Position

An important aspect for maintaining peak integrity using any split flow into a detector is the position of the restrictor tip relative to the detector source. Because SFC utilizes a gas under pressure, the rapid release of that pressure causes localized adiabatic cooling at the restrictor tip. On the other hand, at high temperatures,

the mobile phase expands while the fluid density drops dramatically, resulting in precipitation of solutes at the end of the restrictor [1]. Careful attention to the restrictor placement should eliminate solute precipitation, maintain peak integrity, and provide sufficient mixing with oxygen for combustion. Several articles have discussed optimized placement of the restrictor for the Antek 705D CLND [6, 7,10]. Inserting the restrictor beyond the inlet oxygen port to the pyrolysis chamber appears to provide both adequate solute nebulization and mixing prior to introduction into the furnace [7].

Ozone Generation

Because ozone is very expensive to obtain in pure form and is quite unstable over long periods of time, CLND detectors utilize an ozone generator. Some of the oxygen flow is diverted over an electric arc to form ozone, which is then fed directly into the reaction cell. Because chemiluminescence occurs on a 1:1 molar ratio with NO, as described in Eq. (1), there must be excess ozone for chemiluminescence of NO independent of the other combustion products. Inlet oxygen flows of 5–10 mL/min appear to be adequate for most of the SFC–CLND experiments reported [6,10,12].

Combustion Efficiency

Because detection is based on the formation of NO, the combustion conditions must be sufficient to completely convert the nitrogenous analytes to NO in the presence of mobile-phase modifiers. Temperatures ranging from 1050°C to 1100°C appear to provide the best environment for combustion. The amount of available oxygen for combustion is also highly dependent on the application. Table 1 outlines some of the conditions that have been reported. These conditions cover a wide range of mobile-phase flow rates (as decompressed CO_2) and modifier percentages. Shi et al. reported that too high an oxygen flow may reduce the residence time of the solute in the pyrolysis chamber and can negate any increase in combustion efficiency [7].

Quenching

Nitrogen chemiluminescence takes place in a reaction cell, under vacuum, where the emitted light is measured using a photomultiplier tube. The primary combustion products from a methanol-modified SFC mo-

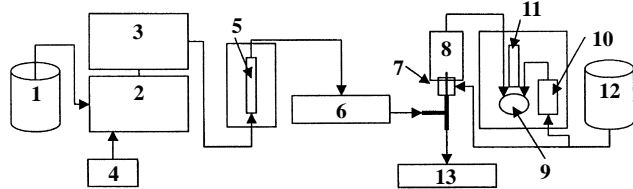


Fig. 1 Schematic diagram of SFC–CLND system: (1) CO_2 tank, (2) SFC pumping system, (3) autosampler, (4) modifier pump, (5) column, (6) UV detector, (7) pyrolysis inlet with linear restrictor, (8) pyrolysis chamber, (9) reaction cell, (10) ozone generator, (11) photomultiplier tube, (12) O_2 tank, (13) back-pressure regulator.

Table 1 Reported Oxygen Flow Rates for Several SFC–CLND Applications

CO ₂ flow rate (mL/min)	Restrictor inner diameter (mm)	Modifier (%)	Oxygen flow (mL/min)	Ref.
3	0.025 ^a	0	48	5
1200	0.025	8	185–200	11
600	0.075	10	50	3
150	0.075	15	50	4

^aOpen-tubular SFC.

bile phase are CO₂ and H₂O. Excessive CO₂ and water can increase the total number of colliding molecules in the reaction cell and reduce the signal. The addition of a membrane drier to selectively remove water has been shown to increase the detection limit of sulfamet-hazine by an order of magnitude [11].

Careful attention to the above-described parameters should allow for the successful interfacing of a CLND detector to an SFC system. Combining the separation efficiency of SFC with the specificity and sensitivity of CLND results in a powerful analytical technique for the quantification of nitrogenous solutes.

References

1. T. A. Berger, *Packed Column SFC*, Royal Society of Chemistry, Cambridge, 1995.
2. P. Patterson, *Detectors for Capillary Chromatography*, John Wiley & Sons, New York, 1992, Chap. 7.
3. T. A. Berger, *Chromatographia* 41(7/8), (October 1995).
4. D. H. Fine, F. Rufe, and B. Gunther, *Anal. Lett.* 6: 731 (1973).
5. E. S. Francis, D. J. Eatough, and M. L. Lee, *J. Microcol. Separ.* 6: 395 (1994).
6. H. Shi, J. T. B. Strode III, L. T. Taylor, and E. M. Fujinari, *J. Chromatography A* 757: 183–191 (1997).
7. H. Shi, J. T. B. Strode III, L. T. Taylor, and E. M. Fujinari, *J. Chromatography A* 734: 303–310 (1996).
8. H. Shi, J. T. B. Strode III, L. T. Taylor, and E. M. Fujinari, *Instrumental Methods in Food and Beverage Analysis*, Elsevier, Amsterdam, 1998.
9. R. E. Parks and R. L. Marietta, U.S. Patent 4,018,562 (24 October 1975).
10. J. T. B. Strode III, T. P. Loughlin, T. M. Dowling, and G. R. Bicker, *J. Chromatogr. Sci.* 36: 511–515 (1998).
11. M. T. Combs, M. Ashraf-Khorassani, and L. T. Taylor, *Anal. Chem.* 69: 3044–3048 (1997).
12. H. Shi and L. T. Taylor, *J. High Resolut. Chromatogr.* 19: 213–216 (1996).



Supercritical Fluid Chromatography: An Overview

Fernando M. Lanças

M.C.H. Tavares

Instituto de Química de São Carlos, Universidade de São Paulo, São Carlos/SP, Brazil

Introduction

A phase diagram, as shown in Fig. 1, can describe the physical stage of a substance of fixed composition. In this pressure–temperature diagram for CO₂, there are three lines describing the sublimation, melting, and boiling processes. These lines also define the regions corresponding to the gas, liquid, and solid states. Points along the lines (between the phases) define the equilibrium between two of the phases. The vapor pressure (boiling) starts at the triple point (Tp) and ends at the critical point (Cp). The critical region has its origin at the critical point. At this point, we can define a supercritical fluid (SF) as any substance that is above its critical temperature (T_c) and critical pressure (P_c). The critical temperature is, therefore, the highest temperature at which a gas can be converted to a liquid by an increase in pressure. The critical pressure is the highest pressure at which a liquid can be converted to a traditional gas by an increase in the liquid temperature. In the so-called critical region, there is only one phase and it possesses some of the properties of both a gas and liquid. Subcritical (liquid) CO₂ is found in the triangular region formed by the melting curve, the boiling curve, and the line that defines the critical pressure [1].

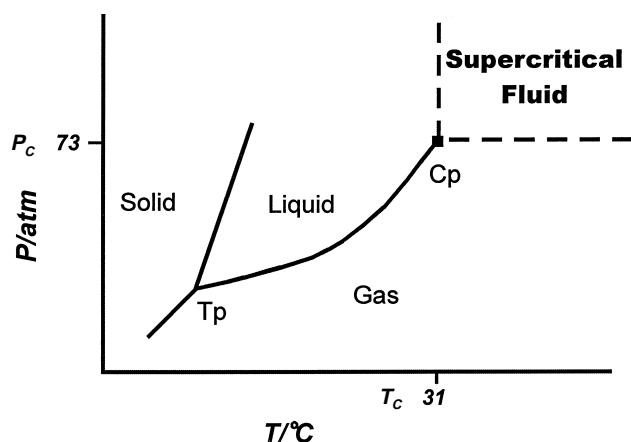


Fig. 1 Phase diagram for CO₂. P_c = critical pressure; T_c = critical temperature; Cp = critical point; Tp = triple point.

Discussion

Supercritical fluids begin to exhibit significant solvent strength when they are compressed to liquidlike densities. This makes physical sense intuitively because it is known that gases are not considered as good solvents.

The density of a pure solvent changes in the region of its critical point. For a reduced temperature ($T_r = T/T_c$) in the range 0.9–1.2°C, the reduced solvent density ($\rho_r = \rho/\rho_c$) can increase from gaslike values of 0.1 to liquidlike values of 2.5 as the reduced pressure ($P_r = P/P_c$) is increased to values higher than ~ 1.0 atm. However, as T_r is increased to 1.55, the supercritical fluid becomes more expanded and reduced pressures greater than 10 are needed to obtain liquidlike densities. By operating in the critical region, the pressure and the temperature can be used to regulate density, which regulates the solvent power of a supercritical fluid [2].

The viscosity changes rapidly in the critical region; even at the high-pressure levels of 300–400 bar, it is only about 0.09 cP, an order of magnitude below typical viscosities of liquid organic solvents.

The properties of gaslike diffusivity and viscosity, zero surface tension, coupled with liquidlike density, combined with the pressure-dependent solvating power of SF have provided the impetus for applying SF technology to analytical separation problems.

Supercritical Fluid Chromatography: An Introduction

The first reported observation of the occurrence of a supercritical phase was made by Baron Cagniard de la Tour in 1822 [3]. He noted visually that the gas/liquid boundary disappeared when heating each of them in a closed glass container increased the temperature of certain materials. From these early experiments, the critical point of a substance was first discovered. The first workers to demonstrate the solvating power of supercritical fluids for solids were Hannay and Hogarth in 1879 [4]. They studied the solubility of cobalt(II) chloride, iron(III) chloride, potassium bromide, and



potassium iodide in supercritical ethanol ($T_c = 243^\circ\text{C}$, $P_c = 63\text{ atm}$).

Klesper et al. first demonstrated, in 1962, SFC by the separation of nickel porphyrins using supercritical chlorofluoromethanes as mobile phases [5]. Sie and Rijniers [6] and Giddings [7], in 1966, developed the technique further, both practically and theoretically, as well as many applications. A few years later, Gouw and Jentof reviewed the general aspects of SFC, including different mobile phases, solute retention, selectivity, and applications [8].

Until the beginning of the 1980s, SFC was characterized by the utilization of packed columns, in the so-called "LC-like SFC" [9]. The introduction in 1981 of capillary open columns with small internal diameters and immobilized stationary phases has opened perspectives to the "GC-like SFC," or c-SFC (capillary supercritical fluid chromatography), with the great advantage of the high-resolution power of capillary columns. The combination of these columns with detectors traditionally utilized in gas chromatography (GC) allows the analysis of compounds with lower volatility and/or higher molecular weight than those in GC [10].

Instrumentation in SFC

A schematic drawing of the main parts of the SFC system is shown in Fig. 2. It consists of a high-pressure pump for pressurizing and delivering the solvent, usually CO_2 , connected to an oven, generally a modified gas chromatograph used as the temperature controller for the SFC column. The injector should introduce small sample volumes into the column and a restrictor is placed between the end of the column and the detector to maintain the mobile phase in the supercritical state. A detailed description of each part of the system follows.

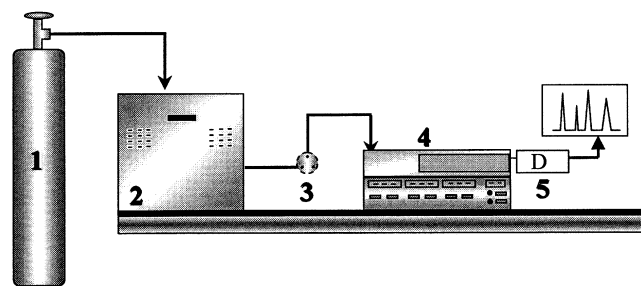


Fig. 2 Schematic drawing of a SFC apparatus. 1: CO_2 tank, 2: high-pressure pump, 3: injection valve, 4: oven (containing the column and restrictor), 5: detector (D).

Mobile Phase

Pure CO_2 has been the preferred solvent due to its favorable properties. The CO_2 is used in siphoned cylinders to assist the transference of the solvent to the pump. CO_2 passes through a cooling system to increase its density before being inserted in the heating system. When required, a vessel containing a modifier can be added to the system in a way similar to that already well known in supercritical fluid extraction (SFE).

Pump

Although several high-pressure pumps have been used in SFC, the syringe-type pump has been the preferred to deliver CO_2 into the system. This choice is made due to the absence of pulses of syringe pumps and the possibility of flow rate and pressure control.

Sample Introduction

Samples are usually injected through a high-pressure injection valve fitted with a small internal loop.

Temperature Control

To control and maintain the critical temperature of the mobile phase (CO_2), the column is installed in an oven, similar to those used for GC or high-performance liquid chromatography (HPLC), depending on the type of column used (Fig. 2).

Columns

Two types of columns are used in SFC: packed columns containing solid particles of small inner diameter or wall-coated open-tubular columns (WCOT), usually called just capillary columns. Packed columns have been preferred when capacity is the most relevant issue; capillary columns are selected when efficiency is the goal.

Restrictor

In order to maintain the desired SF mobile-phase conditions, the end of the column is connected to a restrictor. Although several types of restrictor are available [11], the most popular is the linear restrictor, which consists of a small piece ($\sim 10\text{ cm}$) of a fused silica or metal tube of small inner diameter ($50\text{ }\mu\text{m}$ or less).

Detectors

One of the attractions of SFC is that it can use both GC- and LC-like detectors, including the almost universal flame ionization detector (FID) for non-volatile and volatile analytes after separation on either capillary or packed columns. Selective responses could be also obtained from a number of detectors as NPD, ECD, FPD, ultraviolet, Fourier transform infrared, nuclear magnetic resonance, and mass spectrometry.

Application

An important field of application of analytical chemistry involves the isolation, identification, and quantification of components in complex samples. Chromatography is one of the most used techniques, because modern chromatographic methods have an excellent separation power, are versatile, and can be used with several detection techniques.

During the last 15 years, the applications of supercritical fluids (SFC and SFE) have shown a fast advance; among others, from a historical perspective, SFC was developed after GC was well established and when HPLC was starting. The interest for SFC has grown with the GC and HPLC development and technological innovations that had occurred independently of SFC research, but surely allowed that commercial SFC instruments could be introduced in the 1980s.

Supercritical fluid chromatography has been applied to environmental analyses, chemical foods, polymers, pharmaceutical, and agro-industry research. This process generates quite complex products, which has been analyzed by different chromatographic approaches, including SFC. Considering the complexity of these samples, a high-resolution technique is required. Even considering that packed column SFC has some advantages in certain cases, capillary columns coated with polymeric phases presents more efficiency (*N*) per column, being more adequate for complex samples.

As an example, in natural product analysis, SFC offers perspectives in the analysis of several classes of compounds that present difficulties in either conventional LC or GC. In this area, it is very common that the analytes do not have chromophore groups, thus making difficult the detection through UV-vis, the most popular HPLC detector. At the same time,

several of them are not volatile enough to be analyzed by GC. In this case, the use of SFC with capillary columns and FID detection is a valuable tool. Figure 3 shows a chromatogram of a mixture of triterpenes containing a —COOH functional group (betulinic acid, oleanolic acid, ursolic acid, and polpunonic acid) [12]. These compounds are a good example of a class of compounds that presents biological activities and are difficult to be analyzed by either GC or HPLC without an additional derivatization step.

Conclusion

Supercritical fluid chromatography is a very important chromatographic technique still underestimated and underutilized. It presents characteristics similar to both GC and HPLC, although having its own characteristics. Whereas the column temperature control is the way to achieve a good separation in GC and the solvating power of the mobile phase is controlling factor in HPLC, in SFC the density of the fluid is the major factor to be optimized. Both packed (LC-like) and capillary (GC-like) columns have been used in this technique, which has found applications in practically all areas in which GC or HPLC has shown to be the selected separation technique.

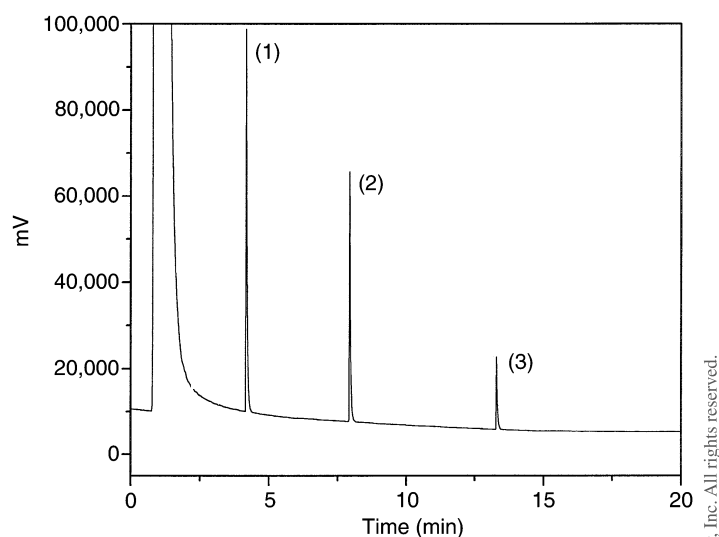


Fig. 3 c-SFC chromatogram of a mixture of triterpenic acids: (1) oleanolic acid, (2) ursolic acid, (3) polpunonic acid. Column: 20 m \times 100 μ m \times 0.20 μ m (5% phenyl, 95% methyl polysiloxane cross-linked); *T* = 80°C; *P* = 120 atm.



References

1. L. T. Taylor, *Supercritical Fluid Extraction*, John Wiley & Sons, New York, 1996, pp. 1–30.
2. M. A. McHugh and V. J. Kruponis, *Supercritical Fluid Extraction. Principles and Practice*, 2nd ed., Butterworth–Heinemann, Boston, 1994, pp. 1–26.
3. C. Cagniard de la Tour, *Ann. Chim. Phys.* 21(2): 127, 178 (1822).
4. J. B. Hannay and J. Hogarth, *Proc. Roy. Soc. (London)*, 29: 324–326 (1879).
5. E. Klesper, A. H. Corwin, and D. A. Turner, *J. Org. Chem.* 27: 700–701 (1962).
6. S. T. Sie and G. W. A. Rijnders, *Separ. Sci.* 1: 459–490 (1966); 2: 699–727, 729–753, 755–777 (1967).
7. J. C. Giddings, *Separ. Sci.* 13: 73–80 (1966).
8. T. H. Gouw and R. E. Jentoft, *J. Chromatogr.* 68: 303–323 (1972).
9. D. R. Gere, R. Board, and D. McManigill, *Anal. Chem.* 54: 736–740 (1982).
10. M. Novotny, S. R. Springston, P. A. Peaden, J. C. Fjeldted, and M. L. Lee, *Anal. Chem.* 53: 407A–414A (1981).
11. R. D. Smith, J. L. Fulton, R. C. Petersen, A. J. Kopriva, and B. W. Wright, *Anal. Chem.* 58: 2057–2064 (1986).
12. M. C. H. Tavares, J. H. Y. Vilegas, and F. M. Lanças, *Phytochem. Anal.* (in press).



Supercritical Fluid Extraction

Christopher E. Bunker

Air Force Research Laboratory, Wright-Patterson Air Force Base, Ohio, U.S.A.

INTRODUCTION

Supercritical fluid extraction (SFE) was originally proposed as a process for compound separation or purification as early as 1879 by Hannay and Hogarth.^[1,2] A rebirth of the field in the 1940s, and again in the 1970s, was brought about by significant advances in technology and a drive toward more energy-efficient and environmentally friendly processes.^[1,2] Today, SFE is widely applied in various industries for purification of high-value chemicals or materials, for environmental remediation, and for incorporation into larger green processes that employ supercritical fluids as reaction solvents. Currently, its most widely known application is associated with the decaffeination process used in the treatment of coffee beans. Within the petroleum field, the application of SFE technology varies widely from cleanup procedures to high-value materials production.^[3–5] In this article, first we will discuss the properties of a supercritical fluid that make SFE an attractive alternative to normal liquid–solvent processes; next, we will describe the equipment and function of a typical SFE process; and, finally, current areas of interest in petroleum research will be reviewed briefly.

SUPERCRITICAL FLUID PROPERTIES

To understand the properties of a supercritical fluid, one must first understand what is meant by the term “supercritical.” In this case, “supercritical” refers to that region of the phase diagram (Fig. 1) defined by temperatures greater than the critical temperature ($T > T_c$) and pressures greater than the critical pressure ($P > P_c$). In this region, the substance exists as a single phase, regardless of temperature or pressure. In most industrial applications, supercritical fluids are used in this region; however, it is important to note that a single phase exists for a substance at any pressure when the system is above T_c . Researchers investigating the properties of supercritical fluids have found it necessary to include the pressure region below P_c to obtain a full understanding of the nature of a supercritical fluid.^[6–8] For this reason, the loose definition of a supercritical fluid is: any substance at a temperature greater than its critical temperature.

The most important properties of a supercritical fluid are the low densities between those of a gas and those of a liquid, which are easily tunable with a change in pressure at constant temperature, and the local density effects. The latter are termed solute–solvent and solute–solute clustering and are best understood as local concentrations of a solvent or solute, respectively, that are greater than the bulk concentration. These phenomena are attributed to the unique nature of a supercritical fluid (i.e., a supercritical fluid is macroscopically homogeneous but microscopically inhomogeneous, consisting of solvent clusters and free volumes). An experimentally observable effect related to this unique structure is critical opalescence, where a fluid viewed through an optical port is observed to become opaque as it transitions through the critical region. This phenomenon is attributed to the efficient scattering of light by the unique structure of a supercritical fluid in the near-critical region.

In SFE processing, the low and tunable fluid densities are of the greatest importance. For a constant temperature greater than T_c , low pressures yield gaslike densities, and high pressures yield liquidlike densities (Fig. 1). Increasing the pressure from low to high moves the fluid density through the near-critical region, where small changes in pressure result in large changes in fluid density (see Fig. 4 of Ref. [2] for an idealized density-vs.-pressure diagram). Because solubility is, to a first approximation, proportional to fluid density, the solubility of an analyte can be dramatically affected by small changes in pressure in the near-critical density region.

For many supercritical fluids, the solubilities of the compounds of interest, even in the high-density region, may be too low for practical application. This limitation can be overcome through the use of a cosolvent. Early on, researchers discovered that the addition of small amounts of a cosolvent could dramatically enhance the solubility of various analytes.^[6–8] In many cases, the enhancement exceeded that predicted based on the bulk concentration of the cosolvent in the supercritical fluid. The results suggested an enhancement of solvent strength under supercritical conditions. The phenomenon, termed the entrainer effect, is related to solute–solute clustering; the entrainer effect served as preliminary evidence of unusual behaviors and pointed researchers toward solute–solute clustering.

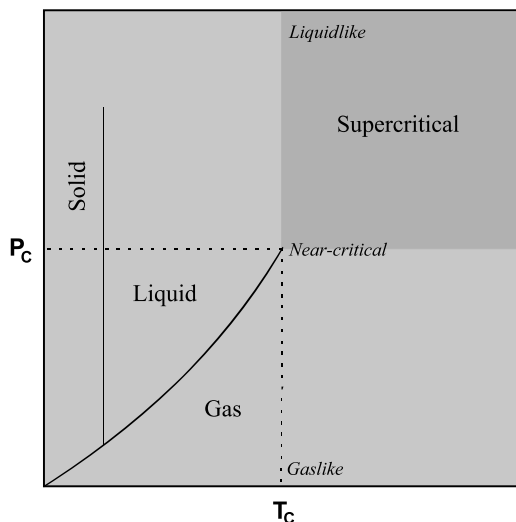


Fig. 1 Idealized phase diagram depicting the supercritical region. T_c and P_c are the critical temperature and pressure, respectively. (View this art in color at www.dekker.com.)

Thus, taken as a whole, the tunable densities and tunable solubilities, the availability of cosolvents as property modifiers, the ability to utilize fluids that are gases under ambient conditions, and the possibility of employing fluids that are environmentally friendly (e.g., CO_2 or water) (the unique properties of supercritical fluids) make SFE a valuable alternative to normal liquid extraction processes.

SFE SYSTEM

The design of any SFE system will be a function of the application, and the details will vary depending on the size and the mode of the process (batch or continuous), the nature of the extracted material and the substrate (corrosive, toxic, and benign), and the fluid employed. The only guaranteed commonality with all such systems is the necessity to ensure safe operation. Proper safety precautions must be observed in the handling and maintenance of the required high-pressure equipment; the consequences of a failure can be severe.

A simple laboratory-scale SFE system is shown in Fig. 2. The system consists of a fluid supply, a pump/delivery device, an extraction vessel, a temperature-controlled zone, a collection vessel (including restrictor), and numerous valves, pressure gauges, and temperature sensors (although not shown, pressure-relief valves are highly recommended). Such systems embodying these components and offering many variations in operation (e.g., programmable control, recirculation, and multistage extraction) are readily available. In a typical extraction, the

extraction vessel is loaded with the substrate to be extracted. In the configuration shown in Fig. 2, this would involve disassembly of the extraction vessel and manual loading of the material. In many industrial processes, this step is automated. Once loaded, the extraction vessel is equilibrated at the desired temperature ($T > T_c$), and fluid is introduced. For a static process, the system is brought to the desired pressure and sealed; for a continuous process, backpressure regulators or restrictors are used to maintain the pressure while the fluid is continuously flowed. In the recovery of the extracted material, it is important to recall that small changes in pressure in the vicinity of the critical region result in large changes in density and solubility. To avoid precipitation of the extracted material within the extraction system, additional fluid must flow to maintain the system pressure. Several collection vessel designs facilitate collection of the extracted material. The simplest ones involve expansion of the fluid into a low-pressure region, thus inducing nucleation and precipitation of the extracted material [rapid expansion of a supercritical solution (RESS)], expansion of the fluid into a collection liquid where the extracted material has good solubility (applicable to somewhat volatile species), or expansion of the fluid onto a solid absorbent. Other possibilities include recovery and recirculation of the supercritical fluid, secondary extraction with modification of the fluid, and reaction of the extracted material using the fluid as an alternative reaction solvent. The reader is referred to Refs. [1] and [2] for additional information.

CURRENT AREAS OF INTEREST IN PETROLEUM RESEARCH

With respect to the petroleum industry, research into supercritical fluids and SFE can be roughly divided into product-oriented research, property investigations, and

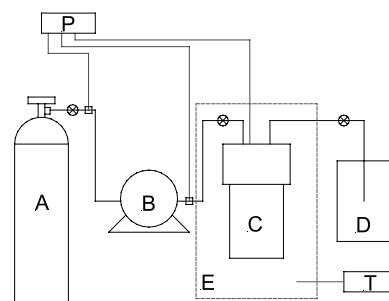


Fig. 2 Schematic for a typical laboratory-scale supercritical fluid extraction system: (A) fluid supply; (B) pump/delivery device; (C) extraction vessel; (D) collection vessel; (E) heated zone; (P) pressure measurement device; (T) temperature controller. (View this art in color at www.dekker.com.)

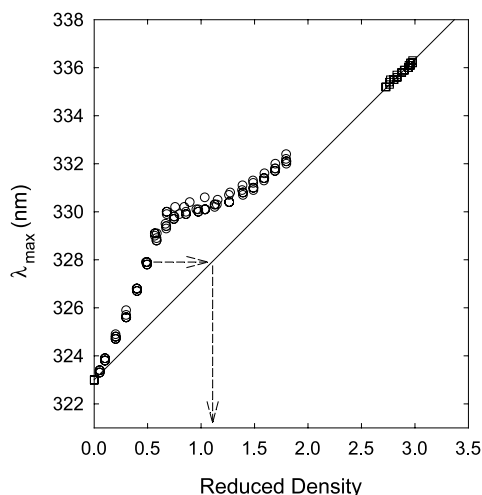


Fig. 3 Experimental data obtained for the spectral maximum of the pyrene excitation spectrum in supercritical toluene at 335°C as a function of reduced density: (—) normal liquid behavior; (○) supercritical fluid data; (◐) liquid data. (From Ref. [7].)

environmental remediation efforts.^[3–5] In a recent review, Rudzinski and Aminabhavi^[3] noted that researchers have been investigating the application of SFE technology to the processing of coal, bitumen, oil shale, crude oil, and coal tar pitch. The fluids utilized included pure CO₂, modified CO₂, organic fluids such as propane and toluene, and water. Concerning property investigations, research is ongoing to understand the fundamental properties of high-temperature supercritical fluids because these fluids can serve as models for supercritical aviation fuel.^[7] Figure 3 demonstrates the unusual nature of supercritical toluene. Reduced density (density divided by the critical density) is plotted as a function of the solvation strength of toluene (λ_{\max} is the solvatochromic shift of the excitation spectrum of the molecular probe, pyrene). The solid line represents the normal liquid behavior of toluene—a trend that

is proportional to fluid density. The data obtained in supercritical toluene (circles) clearly deviate from that line. The dashed arrows demonstrate that, at any given point, the observed density is greater than the measured bulk density—a direct result of solute–solvent clustering—the implication being possible discrepancies between predicted properties based on bulk densities and observed properties influenced by local densities (the properties being solubility, viscosity, polarity, heat transfer characteristics, etc.). The goal of such research is to develop quantitative models capable of determining the local (as opposed the bulk) properties of a supercritical fluid. The significance of the discrepancies shown in Fig. 3 will be determined in future efforts to design and operate supercritical fluid fuel systems.

REFERENCES

1. McHugh, M.; Krukonis, V. *Supercritical Fluid Extraction*, 2nd Ed.; Butterworth-Heinemann: Newton, MA, 1994.
2. Taylor, L.T. *Supercritical Fluid Extraction; Techniques in Analytical Chemistry*; John Wiley and Sons: New York, 1996.
3. Rudzinski, W.E.; Aminabhavi, T.M. A review on extraction and identification of crude oil and related products using supercritical fluid technology. *Energy Fuels* **2000**, *14*, 464–475.
4. Levy, J.M.J. *High Res. Chromatogr.* **1994**, *17*, 212–216.
5. Kershaw, J.R.J. *J. Supercrit. Fluids* **1989**, *2*, 35–45.
6. *Supercritical Fluid Science and Technology*; Johnston, K.P., Penninger, J.M.L., Eds.; ACS Symposium Series, American Chemical Society: Washington, DC, 1989; Vol. 406.
7. Bunker, C.E.; Rollins, H.W.; Sun, Y.-P. Fundamental Properties of Supercritical Fluids. In *Supercritical Fluid Technology in Materials Science and Engineering*; Sun, Y.-P., Ed.; Marcel Dekker: New York, 2002; 1–57.
8. *Supercritical Fluid Technology. Reviews in Modern Theory and Applications*; Bruno, T.J., Ely, J.F., Eds.; CRC Press: Boca Raton, FL, 1991.



Surface Phenomena in Sedimentation FFF

S.N. Semenov

Institute of Biochemical Physics RAS, Moscow, Russia

Introduction

Field-flow fractionation (FFF) presents a unique method where particles move in a liquid flow, maintaining a quasi-equilibrium Boltzmann transverse concentration distribution in an FFF channel [1]. It allows one to obtain, from experiments, the transverse Peclet number Pe defining the thickness of the layer, where particles are accumulated, and the retention of the FFF process Ret :

$$Pe = \frac{bW}{D} \quad (1)$$

where b is the generalized mobility of a particle, a droplet, or a macromolecule (the velocity in the unit gradient of the transverse potential), W is half of the potential drop across the FFF channel (assuming that the transverse particle velocity over the FFF channel is constant), and D is the particle diffusion coefficient. If the transverse Peclet number is higher than about 5, we can write [1]

$$Ret = \frac{1}{3}Pe \quad (2)$$

One can predict the parameter Pe by measurement of the diffusion coefficient D or by deriving it from the Stokes expression [2–4] (for the spherical or ellipsoidal particles), derivation of the b value, and measure or calculate the transverse potential drop. In sedimentation FFF (SdFFF), the common way to derive the transverse Peclet number Pe is the substitution of the gravity or sedimentation force acting on the particle,

$$F = \Delta\rho vG \quad (3)$$

where $\Delta\rho$ is the density difference between the particle and the carrier liquid, v is the particle volume, and G is the acceleration of the centrifugal or gravitational force, into the standard expression for the transverse Peclet number. However, for small particles being the objects of SdFFF with sizes ranging from 10^{-6} to 10^{-4} cm [1], this approach may fail, because it does not take into account phenomena occurring in the surface layer of the particle and causing a liquid flow there. In electrolytes, a so-called sedimentation electrostatic potential arises as a consequence of these surface phenom-

ena [2]. To have the complete picture of the particle sedimentation, one should to derive the particle mobility in a force field, accounting for the phenomena near the particle surface.

How Surface Effects Affect the Particle Sedimentation

As the actual theory shows, the “surface-driven” movement may be caused by the flow of a carrier liquid in the surface layer, where the surfactant ions or molecules are accumulated due to action of the surface potential. The surfactant accumulation leads to an increase of the osmotic pressure in the surface layer. If the gradient of such an osmotic pressure arises, it causes a liquid flow in the surface layer. This “slipping” flow in a surface layer can cause either phoretic (surface-driven) movement of a particle or the osmotic flow of a liquid (when the solid surface is fixed) [2,3]. Gradients of the osmotic pressure in the particle surface layer may be due to the macroscopic gradients of surfactant concentration or temperature established in the FFF channel. If the particle movement is due to the “body” force, similar to the centrifugal one, a gradient of the osmotic pressure also may arise. This may be caused by the intensive transport of surfactant molecules or ions along the particle surface, which is due to its sedimentation movement and should be compensated by the exchange of these molecules or ions between the surface layer and the outer liquid. As a consequence, the longitudinal gradient of the concentration may arise, which leads to the osmotic pressure gradient and, in turn, to the “slipping” of the liquid in the surface layer. This mechanism may add surface-driven movement to the “body-driven” sedimentation movement of the particle.

Slip-Flow Velocity in the Surface Layer

The theory of the surface kinetic phenomena is based on the Navier–Stokes equations for the liquid in the surface layer [2,3]:



$$\eta \frac{\partial^2 u_z}{\partial y^2} = \frac{\partial p_0}{\partial z} + \frac{\partial p_{\text{osm}}}{\partial z} \quad (4)$$

where $u_z(y)$ is the tangential flow velocity profile in the surface layer at a distance y from the particle surface, η is the liquid viscosity, p_0 is the pressure excess due to sedimentation movement of particle and the corresponding hydrodynamic viscous stresses, p_{osm} is the osmotic pressure, and z is the longitudinal coordinate on the particle surface. For a spherical particle $z = R\vartheta$, where ϑ is the angle between the direction of the vector \vec{F} given by Eq. (3) and the radius vector \vec{r} , and R is the particle radius. On the outer surface of the surface layer, the surfactant concentration is $c_{\text{os}}(y, z)$, which may differ from the surfactant concentration in a liquid far from the particle c_0 due to concentration polarization. The surfactant concentration distribution in the surface layer is the Boltzmann distribution, which allows us to write the pressure distribution in the surface layer as

$$p = p_0 + kTc_{\text{os}} \left[\exp\left(-\frac{\Phi}{kT}\right) - 1 \right] \quad (5)$$

The first boundary condition to Eq. (4) is the absence of the liquid slipping on the particle surface:

$$u_z = 0 \quad \text{at } y = 0 \quad (6)$$

The second boundary condition is related to the transformation of the flow profile in the surface layer into the flow profile for the Stokes problem on the flow around a sphere outside the thin surface layer near the particle surface [4] and can be written as

$$\left. \frac{\partial u_z}{\partial y} \right|_{r=\infty} = \left. \frac{\partial u_\varphi^e}{\partial r} \right|_{r=R} \quad (7)$$

where u_φ^e is the tangential flow velocity in the conventional Stokes problem. Using Eqs. (5)–(7) and the standard expression for the outer pressure p_0 [4], one can solve Eq. (4) and have the boundary conditions for the “outer” Stokes problem, where surface phenomena are accounted for:

$$u_\varphi^e(r = R) = u_s \quad (8)$$

$$u_r^e(r = R) = 0 \quad (9)$$

where u_r^e is the radial flow velocity in the standard Stokes problem and

$$u_s = \frac{kT}{\eta R} \frac{\partial c_{\text{os}}(R, \varphi)}{\partial \varphi} \int_0^\infty dy \int_\infty^y dy' \left[\exp\left(-\frac{\Phi(y')}{kT}\right) - 1 \right] \quad (10)$$

is the slip flow velocity in the surface layer.

Equations (8)–(10) allow the determination of the velocity U of the particle, which is driven by a “body”

force compensated by the hydrodynamic friction force established in consequence [5].

Concentration Polarization of Moving Particle

Surface phenomena affect the particle sedimentation when a tangential surfactant concentration gradient exists near the particle surface. This situation is described by the stationary diffusion equation for the surfactant concentration outside the surface layer in the form $\Delta c_{\text{os}} = 0$ [2,3], where the boundary condition, which reflects the substance conservation in a very thin surface layer, may be written as

$$-D_s \left. \frac{\partial c_{\text{os}}}{\partial r} \right|_{r=R} = \int_0^\infty \left[c_0 u_z(y, z) - D_s \left. \frac{\partial c_{\text{os}}}{\partial z} \right|_{r=R} \right] \cdot \left[\exp\left(-\frac{\Phi(y)}{kT}\right) - 1 \right] dy \quad (11)$$

where D_s is the diffusion coefficient of the surfactant [2]. This diffusion equation is solved using the assumption on the dipole form of the surfactant concentration distribution [2]. For the deep surface potential well ($\varepsilon_0 \geq 5$, where ε_0 is the depth of the surface potential well in kT units), the concentration polarization should be most significant, due to the intensive transport of the surfactant which is highly accumulated in such a well. In this case, we can assume that

$$\frac{\Phi}{kT} \approx -\varepsilon_0 \left(1 - \frac{y}{h} \right) \quad (12)$$

where h is the characteristic width of this well. The physicochemical nature of these parameters is discussed in the next section. The general expression for the slip velocity can be written compactly as

$$u_s = \left(\frac{a'}{R} - \frac{3b'}{R^3} \right) \frac{h}{\varepsilon_0 R} f(\delta, \varphi, \text{Rel}) \quad (13)$$

where φ is the volume fraction of the surfactant, $\delta = hR/\varepsilon_0 d^2$ is the reduced parameter characterizing the relationship between the parameters of the surface potential well, the particle, and the surfactant (d is the surfactant molecule diameter), the criterion $\text{Rel} = h e^{\varepsilon_0}/\varepsilon_0 R$ characterizes the degree of the concentration polarization, and

$$f(\delta, \varphi, \text{Rel}) = 4\varphi\delta\text{Rel}^2/(2 + \text{Rel} + 4\varphi\delta\text{Rel}^2) \quad (14)$$

is the function characterizing the concentration polarization. The parameters a and b are unknown constants of the Stokes problem [4,5]. This function ranges from zero (at $\text{Rel} = 0$) to one (at very large Rel values). Us-

Table 1

Surface potential	Analytical expressions for $\Phi(y)$, ε_0 and h			Ranges of values for ε_0 and h	
	$\Phi(y)$	ε_0	h	ε_0	h
van der Waals forces	$-Ad^3/y^3$	A/kT	$d/3$	5–50 ^a	$\approx 10^{-8}$ cm (low-molecular surfactant)
Coulomb electrostatic forces	$-q\zeta e^{y/\lambda}$	$q\zeta/kT$	λ	0–10	$10^{-7} \div 10^{-4}$ cm (aqueous electrolytes) ^b
Adsorption forces	None	None	None	0–10	$\approx 10^{-7}$ cm
Structure forces	None	None	None	0–10	$\approx 10^{-5}$ cm

^aThe maximum values of Hamaker constant are characteristic for metals.

^bThe maximum value of the Debye length is reached in the pure water, where only H^+ and OH^- ions exist.

ing Eq. (14) and boundary conditions [Eqs. (8) and (9)], we have, for the particle sedimentation velocity,

$$U = U_0 \left(1 - h \frac{f}{\varepsilon_0 R} \right) \quad (15)$$

where $U_0 = F/6\pi\eta R$ is the standard value of the sedimentation velocity. The maximum relative change of the particle sedimentation velocity at very large criterion Rel values is

$$\frac{U - U_0}{U_0} = -\frac{h}{\varepsilon_0 R} \quad (16)$$

Parameters of the Surface Potential Well and Criterion Rel

There are several main mechanisms to accumulate the ions or molecules near the surface [5]: dispersion or van der Waals interaction with the potential $\Phi(y) = -Ad^3/y^3$, where A is the Hamaker constant; Coulomb electrostatic interaction in electrolytes with the potential $\Phi(y) = -q\zeta \exp(-y/\lambda)$, where q is the electric charge of the surfactant ion, ζ is the particle electrokinetic potential, and λ is the Debye length [2]; and the adsorption and structure forces due to structural changes in the surface layer, which have no analytical dependence of the surface potential on the distance but have the parameters ε_0 and h derived from the experimental data (see Table 1).

Thus, Eq. (16), together with the data from Table 1, predict an observable contribution of surface phenomena to the particles' sedimentation velocity for all the types of surface interaction, except the van der Waals interaction. The possible values of criterion Rel range from about 1000 ($h \approx 10^{-6}$ cm and $\varepsilon_0 = 5$) to about 2000 ($h \approx 10^{-6}$ cm and $\varepsilon_0 = 10$).

The volume fraction of surfactant φ may be estimated, taking into account that the molar concentration of surfactant is usually about 10^{-3} – 10^{-2} m/L; that

is, the numeric concentration of the surfactant molecules c_0 is about 10^{18} – 10^{19} cm³. For a typical surfactant molecule radius $d = 3 \times 10^{-8}$ cm, we have $\varphi \approx 10^{-4}$ – 10^{-3} . The values of parameter δ at $\varepsilon_0 = 10$ range from 10 (at $h = 10^{-7}$ cm and $R = 10^{-6}$ cm) to 10^4 (at $h = 10^{-6}$ cm and $R = 10^{-4}$ cm). As the data of Table 1 show, the most of the particles that are the object of FFF should have an apparent degree of polarization. The small particles seem to be strongly polarized, and Eq. (16) should describe, adequately, the contribution of the surface phenomena in the particle sedimentation. For the smaller particles, where the saturation may be reached even at $\varepsilon_0 = 5$, the related velocity change may reach 0.2. Such a change of the sedimentation velocity must be measurable in the real FFF conditions. This difference can be useful in the determination of the role of surface phenomena in sedimentation, and the decrease of the sedimentation velocity with the surfactant concentration also may indicate the significant role of the surface phenomena at moderate values of the criterion Rel.

References

1. M. Martin and P. S. Williams, Theoretical basis of fieldflow fractionation, in *Theoretical Advancement in Chromatography and Related Separation Techniques* (F. Dondi and G. Guiochon, eds.), Kluwer, Dordrecht, 1992, pp. 513–580.
2. V. G. Levich, *Physicochemical Hydrodynamics*, Prentice-Hall, Englewood Cliffs, NJ, 1962.
3. J. L. Anderson, *Anal. Rev. Fluid Mech.* 21: 61–97 (1989).
4. L. D. Landau and E. M. Lifshits, *Mechanics of Continuous Media*, State Publishing of Technical and Theoretical Literature, Moscow, 1954 (in Russian).
5. S. N. Semenov, *J. Liquid Chromatogr. Related Technol.* 20: 2669–2685 (1997).
6. B. V. Derjagin, *Theory of Stability of Colloids and Thin Films*, Nauka, Moscow, 1986 (in Russian).



Surfactants: Analysis by HPLC

Juan G. Alvarez

Beth Israel Deaconess Medical Center, Harvard Medical School, Boston, Massachusetts, U.S.A.

Introduction

Surfactants are widely used for a variety of reasons, including surface wetting agents, detergents, emulsifiers, lubricants, gasoline additives, and enhanced oil-recovery agents. The type of surfactants selected for a particular application often depends on the chemical and physical properties required and on economics or other considerations such as environmental concerns. To meet these requirements, a typical surfactant formulation may contain blends of a variety of commercial products, which could include ionic and nonionic ethoxylated surfactants, alkylsulfonates, and alkylaryl-sulfonates, and petroleum sulfonates.

Commercial surfactants contain mixtures of isomers and homologs and may also contain variable amounts of unreacted starting material or extraneous oil that is added as a diluent or thinning agent. Variable amounts of water and inorganic salts are usually present in these products. In order to maintain quality assurance, considerable effort must be put in the development of accurate quantitative techniques for the characterization of components present in these surfactants. Several publications and reviews are available that describe techniques developed for surfactant analysis [1–6].

Problems are often found in many analytical methods due to the complex nature of the mixture and the lack of adequate detection means, thus leading to poor quantitation techniques. For the routine separation of a broad range of surfactants, high-performance liquid chromatography (HPLC) appears to be the most cost-effective [7–18]. Ultraviolet (UV) and fluorescence detectors are commonly used in HPLC analysis of surfactants because of their compatibility with separation techniques requiring gradient elution. However, these detectors have two inherent limitations: (a) the detector response is dependent on molecular structure (i.e., degree of aromaticity and type of substitution) and (b) only species with a chromophore can be detected. To overcome those limitations, postcolumn reaction detectors, based on extraction of fluorescent ion pairs, were introduced for on-line detection of alkylsul-

fonates in HPLC [19–22]. However, the ion-pair formation and extraction efficiency were still dependent on the molecular structure and could not easily be used for quantitation.

The recent introduction of evaporative light-scattering (ELS) detectors, also known as a mass detector and as a universal detector for nonvolatile compounds, has significantly changed the landscape in the analysis of surfactants. The ELS detector measures light refracted by the nonvolatile particles after the effluent from the HPLC column is nebulized and the carrier solvent is evaporated. The amount of refracted light is proportional to the concentration of the analyte species. Based on the above, this entry will focus on the separation and quantitation of different surfactants by HPLC by means of the ELS detector for universal detection based on the experience of the author, thus enough details can be provided concerning the methodology used.

Methodology

High-performance liquid chromatography is performed using a Hewlett-Packard 1090 chromatograph equipped with a ternary-solvent delivery system, an autoinjector with a 0–20- μ L injection loop, an oven compartment, and a diode-array UV detector. An ELS detector (Alltech Associates, Deerfield, IL) is connected in series to the UV detector. Hexane, 2-propanol, and water were used for the analysis of nonionic surfactants. Water and tetrahydrofuran (THF) are used for the analysis of anionic surfactants. No preliminary sample preparation is used other than dilution. The nonionic surfactants are diluted 1:40 (v/v) with hexane. The anionic surfactants (alkyl ether sulfates and synthetic and petroleum sulfonates) are diluted 1:20 (v/v) with water–THF (50:50). The calcium sulfonate surfactants were diluted 1:20 (v/v) with a THF–38% hydrochloric acid solution of pH 1. Hydrochloric acid is required to prevent salt precipitation by converting any excess water-insoluble calcium carbonate into water-soluble calcium chloride. All diluted samples are



filtered through a 0.2- μm filter (Gelman Acrodisc CR) directly into the injector vials.

The nonionic ethoxylates are separated according to the number of ethylene oxide (EO) groups (n) using normal-phase chromatography. The separation is achieved on an amino column [DuPont Zorbax NH2, 25 cm \times 4.6 cm inner diameter (i.d.), 5 μm particle size]. A precolumn (Zorbax BP NH2, 2.5 cm \times 0.2 cm i.d.) is connected to the analytical column. The solvent system is a gradient of hexane, 2-propanol, and water as follows: 100% hexane at time 0, and 37% hexane, 60% 2-propanol, and 3% water at 55 min. Components of the alkyl ether sulfate surfactants are separated into inorganic salt, sulfates, and unreacted alcohol using reversed-phase chromatography. The column used for this separation is a 2.5-cm \times 0.2-cm-i.d. column packed with 10 μm C₁₈. The solvent system consists of a 4-min gradient program of water and THF, as summarized in Table 1. The synthetic and petroleum sulfonate components are separated into inorganic salt, sulfonates, and unreacted oil by the same reversed-phase chromatographic method.

The diode-array UV and ELS detectors are connected in series. The UV signals are monitored at 230 and 254 nm. The operating conditions of the ELS detector are optimized for maximum detector response and stable baseline. Surfactants with UV absorbance are detected by both detectors, whereas the UV-transparent surfactants could only be detected by the ELS detector.

Separation of Surfactants by HPLC

Analysis of Nonionic Ethoxylates

Aliphatic and aromatic nonionic ethoxylated surfactants, RO(CH₂CH₂O) _{n} H, were used in order to determine the distribution of the ethoxylate oligomers.

Table 1 Gradient Elution Program for Reversed-Phase HPLC of Alkyl Ether Sulfate Synthetic and Petroleum Sulfonate Surfactants

Time (min)	Water (%)	THF (%)	Mode of operation
0.0	90	10	Normal flow
0.5	90	10	Normal flow
1.0	40	60	Normal flow
2.5	40	60	Normal flow
2.6	0	100	Backflush
4.0	90	10	Backflush

Oligomers with different numbers of EO groups are separated by normal-phase HPLC, as summarized in Table 2. The separated components are monitored by both the ELS and UV detectors. Table 2 shows the high resolution of components in a nonylphenolethoxylated alcohol, NP11, revealing a range of oligomers from $n = 3$ to 20.

Analysis of Alkyl Ether Sulfates

Anionic alkyl ether sulfate surfactants are produced by sulfating nonionic alcohol polyalkyloxylates such as the ethoxylated surfactants discussed earlier. The sulfated products generally contain variable amounts of unconverted alcohols and inorganic salts as reaction by-products. Determination of the ratio of anionic to nonionic components in surfactant mixtures is desired for quality control and performance evaluation. Separation of the ionic sulfate and nonionic alcohol components is achieved by reversed-phase chromatography. The separation of four alkyl ether sulfate surfactants is shown in Table 3.

The first component is inorganic salt and it is eluted with 90% water and 10% THF. As the THF concentration increases to 60%, the ionic sulfate surfactant components are eluted. After elution of these ionics, the nonionic components are backflushed with 100% THF. The analysis time is 4 min per sample.

Table 2 Quantitative Analysis of NP11 Oligomers Using UV and ELS Detection

No. of EO	UV (%)	ELS (%)	Elution time (min)
3	0.83	0.01	10.0
4	2.30	0.71	12.3
5	4.16	2.16	14.6
6	6.24	4.25	16.9
7	8.54	7.27	19.2
8	10.51	10.65	20.5
9	11.76	12.78	23.0
10	11.91	13.72	24.4
11	11.05	13.07	26.4
12	9.46	11.30	27.7
13	7.66	8.95	29.2
14	5.84	6.19	30.8
15	4.02	3.92	31.9
16	2.60	2.39	34.6
17	1.60	1.38	35.7
18	0.95	0.80	37.6
19	0.56	0.40	40.0



Table 3 HPLC Analysis of Inorganic Salt, Sulfated Surfactant, and Unreacted Alcohol in Alkyl Ether Sulfate Surfactants

Surfactant	Retention time (min)		
	Inorganic salt	Sulfated surfactant	Unreacted alcohol
BU-6B2ECOS	9.2	10.0	12.5

Analysis of Synthetic and Petroleum Sulfonates

Synthetic and petroleum sulfonates are analyzed by the same reversed-phase chromatographic system used for the analysis of alkyl ether sulfate surfactants. Similar to alkyl ether sulfates, the sulfonate mixtures are separated into three fractions: inorganic salt, sulfonates, and unreacted oil. The analysis of two petroleum sulfonates, NaPS-1 and NaPS-2, is shown in Table 4. Good separation was obtained between the inorganic salt and the sulfonated components. The oil present in NaPS-1 and NaPS-2 surfactants consisted of low-molecular-weight components, which were totally volatile under the detector operating conditions and, therefore, could not be detected. These two sulfonates are considerably different in molecular structure distribution. However, their elution characteristics were the same as those observed for the synthetic single-component sulfonates.

References

1. D. Hummel, *Identification and Analysis of Surface-Active Agents*, Interscience, New York, 1962.
2. M. J. Rosen and H. A. Goldsmith, *Systematic Analysis of Surface-Active Agents*, Wiley-Interscience, New York, 1972.
3. G. F. Longman, *The Analysis of Detergents and Detergent Products*, John Wiley & Sons, New York, 1976.
4. M. Kuo and H. A. Mottola, *CRC Crit. Rev. Anal. Chem.* 9: 297 (1980).

Table 4 HPLC Analysis of Inorganic Salt, Sulfated Surfactant, and Unreacted Alcohol in Alkyl Ether Sulfate Surfactants

Surfactant	Retention time (min)	
	Inorganic salt	Sulfated surfactant
NaPS-1	3.0	4.0
NaPS-2	2.5	3.5

5. R. A. Llenado and R. A. Jamieson, *Anal. Chem.* 55: 174R (1981).
6. R. A. Llenado and T. A. Neubecker, *Anal. Chem.* 55: 93R (1983).
7. P. Jandera and J. Churacek, *J. Chromatogr.* 197: 181 (1980).
8. A. Nakae, K. Tsuji, and M. Yamanaka, *Anal. Chem.* 53: 1818 (1981).
9. G. R. Bear, C. W. Lawley, and R. M. Riddle, *J. Chromatogr.* 302: 65 (1984).
10. M. Ahel and W. Giger, *Anal. Chem.* 57: 2584 (1985).
11. K. Levsen, W. Wagner-Redeker, K. H. Shafer, and P. Dobberstein, *J. Chromatogr.* 323: 135 (1985).
12. I. Zeman, *J. Chromatogr.* 363: 223 (1986).
13. M. S. Holt, E. H. McKerrell, J. Perry, and R. J. Watkinson, *J. Chromatogr.* 362: 419 (1986).
14. G. R. Bear, *J. Chromatogr.* 371: 387 (1986).
15. A. Marcomini, S. Capri, and W. Giger, *J. Chromatogr.* 403: 243 (1987).
16. A. Marcomini and W. Giger, *Anal. Chem.* 59: 1709 (1987).
17. J. A. Pilc and P. A. Sermon, *J. Chromatogr.* 398: 375 (1987).
18. R. H. Schreuder and A. Martijn, *J. Chromatogr.* 435: 73 (1988).
19. J. F. Lawrence, U. A. Th. Brinkman, and R. W. Frei, *J. Chromatogr.* 185: 473 (1979).
20. W. M. A. Niessen, J. F. Lawrence, C. F. Werkhoven-Goewie, U. A. Th. Brinkman, and R. W. Frei, *Int. J. Environ. Anal. Chem.* 9: 45 (1981).
21. F. Smedes, J. C. Kraak, C. F. Werkhoven-Goewie, U. A. Th. Brinkman, and R. W. Frei, *J. Chromatogr.* 247: 123 (1982).
22. Y. Hirai and K. Tomokumi, *Anal. Chim. Acta* 167: 409 (1985).



Synergistic Effects of Mixed Stationary Phases in Gas Chromatography

L. M. Yuan

Yunnan Normal University, Kunming, People's Republic of China

INTRODUCTION

It is generally believed that multicomponent stationary phases, or mixed stationary phases, show the average effect of individual pure phases in gas chromatography (GC). Investigations have shown the existence of a synergistic effect in some mixed GC stationary phases and about 18 articles have been published since 1996.^[1,2] Some chromatographic properties of the mixtures, such as separation factor (α), retention factor (k'), elution order of Grob test reagent, and McReynolds constants, are not the simple addition of the chromatographic properties of the two pure phases. These values of mixed stationary phases may be greater or less than either of the pure stationary phases. It is different from general experimental results. The positive synergistic effect is very useful in the separation of some substance pairs.

SYNERGISTIC EFFECT

The synergistic effect was first discovered in 1957 by Blake in the study of extraction of U(VI).^[3] It has been widely studied in the extraction of inorganic and organic compounds. Generally, mixed stationary phases prepared from polar or nonpolar stationary phases show the average effect of the corresponding individual pure phases. But for a few isomers, the separation factor (α) obtained by the use of the capillary columns coated with side-chain crown ether polysiloxane (PDB-14-C4) + heptakis(2,3,6-tri-*O*-ethyl)- β -cyclodextrin (PE- β -CD) was greater or smaller than those obtained from the individual columns coated with either PDB-14-C4 or PE- β -CD; a new term, the "coordination effect" was suggested to describe this unexpected and puzzling phenomenon.^[1] Yuan et al. studied it carefully and used the "synergistic effect" to describe it because gas-liquid chromatography is actually partition chromatography and its principle is similar to solvent extraction.^[4] The purpose of the present paper is to investigate this phenomenon using packed columns containing heptakis(2,3,6-tri-*O*-pentyl)- β -cyclodextrin + AgNO₃, heptakis(2,3,6-tri-*O*-pentyl)- β -cyclodextrin + TiNO₃, and xylene isomers as sample compounds.^[3] They have positive synergistic effects for the separation

of *m*- and *p*-xylene isomers, but negative synergistic effects for the *m*- and *o*-isomers (see Figs. 1 and 2).

The packed column gas chromatographic separations of some other aromatic compounds using special selectivity mixed stationary phase consisting of heptakis(2,3,6-tri-*O*-pentyl)- β -cyclo-dextrin + AgNO₃, heptakis(2,3,6-tri-*O*-pentyl)- β -cyclodextrin + TiNO₃, bentone + AgNO₃, and heptakis(2,3,6-tri-*O*-pentyl)- β -cyclodextrin + *o*-methyl-*p*-phenylene-bis-(*p*-heptoxy benzoate) liquid crystalline (BPBHPB) were investigated too. Most of the separations deviated from the additivity, and the synergistic effect was observed.^[5] The synergistic effects of packed columns, by mixing the stationary phases before coating the support, were more pronounced than those from columns mixing the two packings.

A great deal of research about the synergistic effect of gas chromatography was reported using capillary column gas chromatography. Based on the experiences developed in Ref. [3], ethylhexylresorcarene + heptakis(2,6-di-*O*-pentyl-3-*O*-trifluoroacetyl)- β -CD mixed stationary phase was used for isomer separation.^[6] Heptakis(2,3,6-tri-*O*-butyl)- β -cyclodextrin + AgNO₃ was used for some enantiomer and isomer separations.^[7] Synergistic effects were observed on those phases. By investigating the chromatographic properties of the mixed stationary phase containing heptakis(2,3,6-tri-*O*-pentyl)- β -cyclodextrin + PEG-20M, the synergistic effect was observed in this mixed stationary phase.^[8] Several similar synergistic effects were shown for the phases mixed with heptakis(2,3,6-tri-*O*-pentyl)- β -cyclodextrin + MPBHPB,^[9] BPBHPB + heptakis(2,6-di-*O*-pentyl-3-allyl)- β -cyclodextrin, heptakis(2,3,6-tri-*O*-pentyl)- β -cyclodextrin + Dibenzo-18-crown-6, heptakis(2,3,6-tri-*O*-pentyl)- β -cyclodextrin + resorcarene derivative, and 25,27-dibutoxy-5,11,17, 23-tetra-tert-butyl-26,28-diundecenyloxy calix[4]arene + permethyl- β -cyclodextrin.^[9,10] Mixed cyclodextrin derivatives such as permethylated β -CD + heptakis(2,6-di-*O*-butyl-3-*O*-butyryl)- β -CD and permethylated β -CD + heptakis(2,6-di-*O*-nonyl-3-*O*-trifluoroacetyl)- β -CD had synergistic effects in the separation of enantiomers.^[11] Our recent investigation has also shown the existence of a synergistic effect in mixed perpentylated- β -CD + permethylated β -CD stationary phase for the separation of enantiomers.



Besides cyclodextrin derivatives, other mixed special selectivity stationary phases also had synergistic effects in the separation of isomers. Those reported include dibenzo-18-crown-6 + MPBHpB,^[12] dibenzo-18-crown-6 and resorcarene derivative,^[2] MPBHpB + resorcarene derivative,^[13] and 25,27-dibutoxy-5,11,17,23-tetra-*tert*-butyl-26,28-diundecenyl-oxy cali[4]arene + ω -undecylomethyl-18-crown-6 polysiloxane.^[10]

The effects of temperature, linear velocity of carrier gas, and relative amounts of the individual phases in the mixed stationary phase were also examined.^[2,4,5,8,9,12,13] These facts show that the synergistic effect is dependent upon the above three factors.

The synergistic effect was only found in mixed stationary phases that have a special selectivity. Those stationary phases were CD, crown ether, liquid crystalline, resorcarene, calixarene, AgNO₃, and others. Crown ether, CD, calixarene, and resorcarene possess cyclic moieties with cavity-like structures that are able to form inclusion complexes with metal ions and organic molecules. Liquid crystalline stationary phases have temperature-dependent ordered structures and the retention is governed by the solute's length-to-breadth ratio. AgNO₃ retards olefins by the formation of loose adducts. Together with the above special selectivity stationary phases, they have already been the focal point of supramolecular chemistry.

CONCLUSION

A synergistic effect of mixed stationary phases that have special selectivity exists in gas chromatography. It is based on the "steric fit" and on the probability of simul-

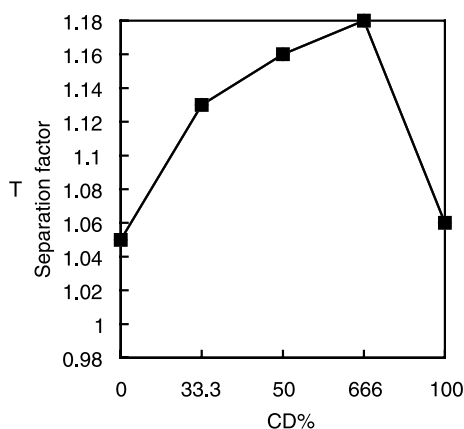


Fig. 1 Plot of $\alpha_{p,m}$ vs. CD% on mixed stationary phases. (From Ref. [3].)

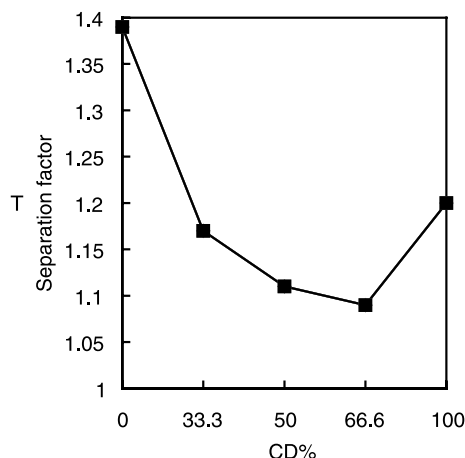


Fig. 2 Plot of $\alpha_{o,m}$ vs. CD% on mixed stationary phases. (From Ref. [3].)

taneous interaction of mixed stationary phases with the solute pair. It can be assumed that the largest synergistic effect is attained with maximum steric fit and simultaneous interaction probability. This probability may depend on temperature, mixing ratio, linear velocity of carrier gas, and how mixing is accomplished.

ACKNOWLEDGMENT

The work is supported by the National Natural Science Foundation, Yunnan Province's Natural Science Foundation, and TRAPOYT of China.

REFERENCES

1. Jing, P.; Fu, R.N.; Dai, R.J.; Gu, J.L.; Huan, Z.; Chen, Y. Consequence of diluting modified β -cyclodextrins in a side-chain crown ether polysiloxane and in a side-chain liquid-crystalline polysiloxane-containing crown ether as stationary phases in capillary gas chromatography. *Chromatographia* **1996**, *43*, 546–550.
2. Yuan, L.M.; Lin, Y.; Fu, R.N. Synergistic effect of dibenzo-18-crown-6 and resorcarene derivative mixed stationary phase in gas chromatography. *Chem. J. Chin. Univ.* **2000**, *21* (2), 213–215.
3. Blake, C.A.; Crouse, D.J.; Coleman, C.F.; Brown, K.B.; and Kelmers, A.D. U.S. Atomic Energy Commission, ORNL- 2172 (1957), CA. 51: 8391e (1957).
4. Yuan, L.M.; Fu, R.N.; Gui, S.H.; Xie, X.T.; Dai, R.J.; Chen, X.X.; Xu, Q.H. Synergistic effect in mixed gas chromatographic stationary phases containing Hepta-

- kis(2,3,6-tri-*O*-pentyl)- β -cyclodextrin and AgNO₃ or TiNO₃ in the separation of xylene isomers. *Chromatographia* **1997**, *46* (5/6), 291–294.
5. Yuan, L.M.; Fu, R.N.; Gui, S.H.; Chen, X.X.; Dai, R.J. Synergistic effect in special selectivity mixed gas chromatographic stationary phase in the separation of aromatic compounds. *Chin. Chem. Lett.* **1998**, *9* (2), 151–155.
 6. Xiao, D.Q.; Lin, Y.; Wen, Y.X.; Fu, R.N.; Gu, J.L.; Dai, R.J.; Luo, A.Q. Synergistic effect of resorcarene and cyclodextrin mixed stationary phase in gas chromatography. *Chromatographia* **1997**, *46* (3/4), 183–188.
 7. Chen, F.; Mo, W.M. Study of pebutylated- β -CD and AgNO₃ mixed stationary phase in capillary gas chromatography. *Chin. J. Chromatogr.* **2000**, *18* (3), 247–251.
 8. Yuan, L.M.; Fu, R.N.; Chen, X.X.; Gui, S.H.; Dai, R.J. Synergistic effect of PEG-20M and Heptakis(2,3,6-tri-*O*-pentyl)- β -cyclodextrin mixed stationary phase in gas chromatography. *Chem. Lett.* **1998**, 141, 142.
 9. Yuan, L.M.; Ai, P.; Zi, M.; Fu, R.N.; Gui, S.H.; Chen, X.X.; Dai, R.J. Synergistic effect of heptakis(2,3,6-tri-*O*-pentyl)- β -cyclodextrin and *o*-methyl-*p*-phenylene-bis-(*p*-heptoxy benzoate) mixed stationary phase in capillary gas chromatography. *J. Chromatogr. Sci.* **1999**, *37*, 395–399.
 10. Yu, X.D.; Lin, L.; Wu, C.Y. Synergistic effect of mixed stationary phase in gas chromatography. *Chromatographia* **1999**, *49* (9/10), 567–571.
 11. Nie, M.Y.; Zhou, L.M.; Wang, Q.H.; Zhu, D.Q. Gas chromatographic enantiomer separation on single and mixed cyclodextrin derivative chiral stationary phases. *Chromatographia* **2000**, *51* (11/12), 736–740.
 12. Yuan, L.M.; Fu, R.N.; Chen, X.X.; Gui, S.H. Synergistic effects in mixed gas chromatographic stationary phases consisting of dibenzo-18-crown-6 and MPBHpB. *Chromatographia* **1998**, *47* (9/10), 575–578.
 13. Yuan, L.M.; Lin, Y.; Fu, R.N. Synergistic effect of liquid crystalline and resorcarene mixed stationary phase. *Chin. J. Chem.* **1999**, (2), 52–54.

Systematic Selection of Solvent Systems for High Speed Countercurrent Chromatography

Hisao Oka

Aichi Prefectural Institute of Public Health, Nagoya, Japan

Yoichiro Ito

National Institutes of Health, Bethesda, Maryland, U.S.A.

INTRODUCTION

High speed countercurrent chromatography (HSCCC) produces highly efficient chromatographic separations of solutes without the use of solid supports.^[1-3] Thus the method eliminates all complications caused by the solid support, such as adsorptive loss and deactivation of samples, tailing of solute peaks, contamination, etc. As with other CCC schemes, HSCCC utilizes two immiscible solvent phases, one as a stationary phase and the other as a mobile phase, and the separation is highly dependent on the partition coefficient values of the solutes, i.e., the ratio of the solute concentration between the mobile and stationary phases. Therefore the successful separation necessitates a careful search for the suitable two-phase solvent system that provides an ideal range of the partition coefficient values for the applied sample.

In the past, the search for suitable two-phase solvent systems entirely relied on a laborious and time-consuming trial-and-error method that has often discouraged the users of HSCCC, while the method for systematic solvent search has not been reported. In this article, we introduce a method for the systematic selection of suitable two-phase solvent systems for HSCCC and its application to the separation of antibiotics and dyes.

HOW TO SELECT SUITABLE SOLVENT SYSTEM

In addition to the basic requirements of stability and solubility of the sample, the two-phase solvent system should satisfy the following.

- 1) For ensuring the satisfactory retention of the stationary phase, the settling time of the solvent system should be considerably shorter than 30 sec. Using the equilibrated two-phase solvent system, the settling time is measured as follows: A 2-mL volume of each phase (the total volume is 4 mL) is delivered

into a 5-mL-capacity graduated glass cylinder, which is then sealed with a glass stopper. The solvent in the cylinder is gently mixed by inverting the cylinder five times and the cylinder is immediately placed on a flat table in an upright position. Then, the time required for the solvent mixture to settle into two clear layers is measured. The experiment is repeated several times to obtain the mean value.

- 2) For efficient separation, the partition coefficient (K) of the target compound(s) should be close to 1, and the separation factor (α) between the components should be greater than 1.5. If $K \ll 1$, the solutes are eluted close together near the solvent front, resulting in a loss of peak resolution, and, if $K \gg 1$, the solutes are eluted in excessively broad peaks and require a long elution time. The minimum α value of 1.5 is required for the baseline separation in a semipreparative CCC equipment providing a moderate partition efficiency of around 800 theoretical plates. The K value is determined simply by measuring the ultraviolet (UV) absorbance of the solute in each of the two phases after partitioning in the equilibrated two-phase solvent system and dividing the solute concentration in the upper phase by that in the lower phase. However, when the sample is a mixture of various components, the precise K values of each component cannot be determined by this method. In such a case, a mixture is partitioned with a two-phase solvent system as described above and the resulting upper and lower phases are analyzed by high performance liquid chromatography (HPLC). Each K value is determined by dividing the corresponding peak area of the upper phase by that of the lower phase.
- 3) In addition to the above two major requirements, it is desirable that the solvent system provides nearly equal volumes of each phase to avoid excessive waste of the solvent.
- 4) It is also convenient to use a volatile solvent system: The pure compound is obtained simply by evaporating the collected fractions.



Table 1 *n*-Hexane/ethyl acetate/*n*-butanol/methanol/water system

<i>n</i> -Hexane	Ethyl acetate	<i>n</i> -Butanol	Methanol	Water
10	0	0	5	5 (hydrophobic)
9	1	0	5	5
8	2	0	5	5
7	3	0	5	5
6	4	0	5	5
5	5	0	5	5
4	5	0	4	5
3	5	0	3	5
2	5	0	2	5
1	5	0	1	5
0	5	0	0	5
0	4	1	0	5
0	3	2	0	5
0	2	3	0	5
0	1	4	0	5
0	0	5	0	5 (hydrophilic)

By keeping the above in mind, the following three series of solvent systems can provide an ideal range of the *K* values for a variety of samples: *n*-hexane/ethyl acetate/*n*-butanol/methanol/water, chloroform/methanol/water, and *tert*-butyl methyl ether/butanol/acetonitrile/water.

In each solvent series,^[4] the partition coefficient of the sample can be finely adjusted by modifying the volume ratio of the components. The first series covers a broad range in both hydrophobicity and polarity continuously from *n*-hexane/methanol/water to *n*-butanol/water. The second series of chloroform/methanol/water provides moderate hydrophobicity and the third series of *tert*-butyl methyl ether/*n*-butanol/acetonitrile/water is suitable for hydrophilic compounds. Most of these two-phase solvent systems provide near 1:1 volume ratios of the upper/lower phases, together with the reasonable range of settling times in 30 sec or less, so that they can be efficiently applied to HSCCC and other centrifugal CCC schemes.

Table 2 Chloroform/methanol/water system

Chloroform	Methanol	Water
10	0	10 (hydrophobic)
10	1	9
10	2	8
10	3	7
10	4	6
10	5	5
10	6	4
10	7	3 (hydrophilic)

Table 3 *tert*-Butyl methyl ether/*n*-butanol/acetonitrile/water system

<i>tert</i> -Butyl methyl ether	<i>n</i> -Butanol	Acetonitrile	Water
1	0	0	1 (hydrophobic)
4	0	1	5
6	0	3	8
2	0	2	3
4	2	3	8
2	2	1	5 (hydrophilic)

For the sample mixture with an unknown composition, the search for the suitable two-phase solvent system may be initiated with the partition coefficient measurement with *n*-hexane/ethyl acetate/*n*-butanol/methanol/water (5:5:0:5:5) (Table 1), chloroform/methanol/water (10:3:7) (Table 2) or *tert*-butyl methyl ether/butanol/acetonitrile/water (6:0:3:8) (Table 3). If the $K_{(org/aq)}$ value is too large, the search should be directed toward the more hydrophobic solvent systems and, if the *K* value is too small, the search should be directed toward the more hydrophilic solvent systems until the proper *K* values are obtained.

If the above solvent search reaches the solvent system of *n*-hexane/methanol/water (2:1:1), which is suitable for the most hydrophobic compounds, and a more hydrophobic solvent system is required, one may reduce the amount of water from the above solvent system and/or replace methanol with ethanol. Some useful solvent systems for the extremely hydrophobic compounds are *n*-hexane/ethanol/water (6:5:2) and *n*-hexane/methanol (2:1). On the other hand, if the solvent search reaches the solvent systems of *n*-butanol/water or *tert*-butyl methyl ether/butanol/acetonitrile/water (2:2:1:5), which are suitable for the most hydrophilic compounds, and a still more hydrophilic solvent system is required, the above solvent system may be modified by the addition of acid or salt; trifluoroacetic acid (TFA) or ammonium acetate has been successfully used.

APPLICATION TO THE SEPARATION OF ANTIBIOTICS AND DYES

Separation of Bacitracin Components

Bacitracins (BCs) are peptide antibiotics produced by *Bacillus subtilis* and *Bacillus licheniformis*.^[5] They exhibit an inhibitory activity against Gram-positive bacteria and are most commonly used as animal feed additives for domestic animals, such as calf and swine, for preventing bacterial infection and/or improving feed

conversion efficiency. Over 20 components are contained in the bacitracin complex, among which BC-A is the major antimicrobial component and BC-F is a degradation product having nephrotoxicity.

We tested three groups of two-phase solvent systems containing *n*-butanol, ethyl acetate, or chloroform as a major organic solvent, and ethanol and/or methanol as a modifier against water in each group. The most promising *K* values were obtained from the chloroform, ethanol, and/or methanol, water system. Among all combinations for the solvent volume ratio, chloroform/ethanol/methanol/water (5:3:3:4) yielded the most desirable *K* values, and the α values between the adjacent components are all greater than 1.5.

Fig. 1 shows a countercurrent chromatogram of bacitracin components using the chloroform/ethanol/methanol/water (5:3:3:4) system. A 50-mg amount of the bacitracin complex was loaded into the HSCCC column. The retention of the stationary phase was 72.7% and the elution time was about 3 hr. All components were eluted in an increasing order of their partition coefficients, yielding 5.5 mg of pure BC-A and 1.5 mg of pure BC-F.

Separation of Colistin Components

Colistin (CL) is a peptide antibiotic produced by *Bacillus polymyxa* var. *Colistinus*; it inhibits the growth of Gram-negative organisms. Colistin is a mixture of many components, among which the two main components are colistin A (CL-A) and colistin B (CL-B).^[6] As in the case of bacitracin, CL is used as a feed additive.

CL is soluble in water, slightly soluble in alcohols, but insoluble in nonpolar solvents such as hexane and chloroform. Based on these properties, we selected *n*-butanol and water as a basic solvent system. However, this combination was not suitable by itself, because the CL components were entirely partitioned into the lower aqueous phase. In order to partition the CL components partly into the *n*-butanol phase, various salts (sodium chloride and sodium sulfate) or acids (hydrochloric acid, sulfuric acid and TFA) were added as a modifier. A desirable effect was obtained by the addition of TFA, where the partition coefficients of CL components rose as the concentration of TFA in the solvent system was increased. As TFA forms an ion pair with amino groups in the molecule of CL, the hydrophobicity of CL components

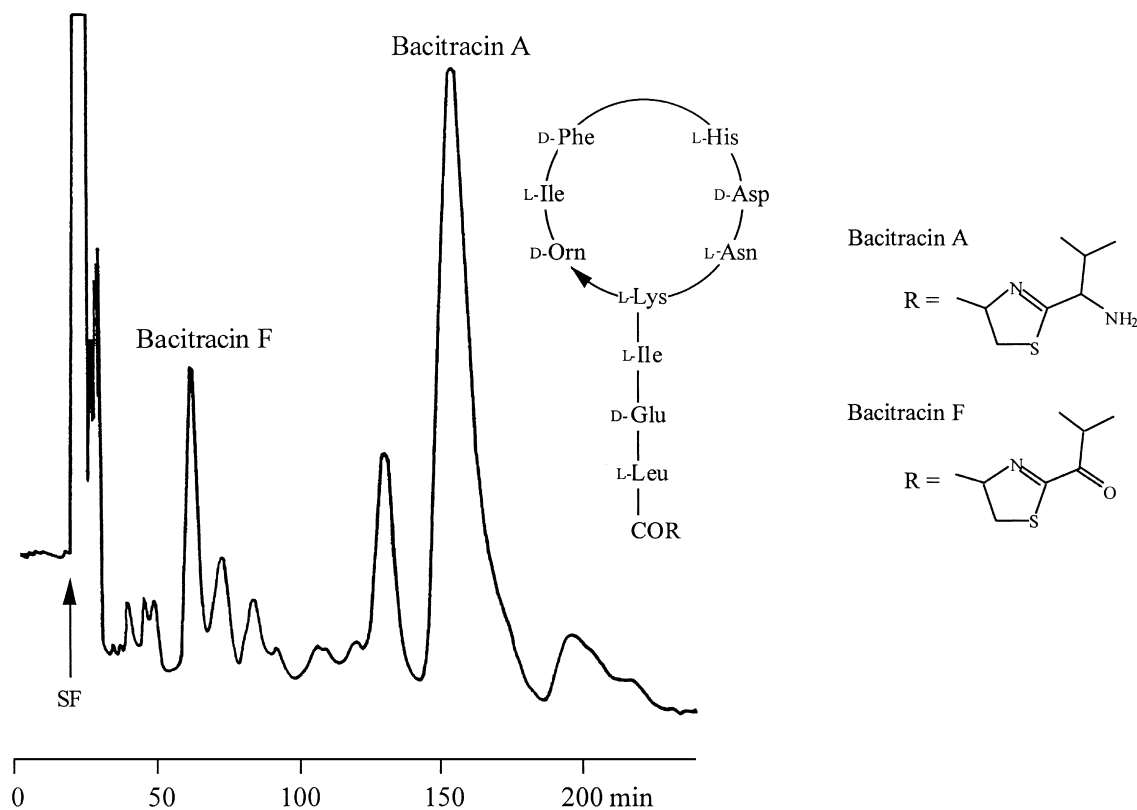


Fig. 1 HSCCC separation of bacitracin components. Solvent system: chloroform/ethanol/methanol/water (5:3:3:4); mobile phase: lower phase; flow rate: 3 mL/min; detection: 254 nm.



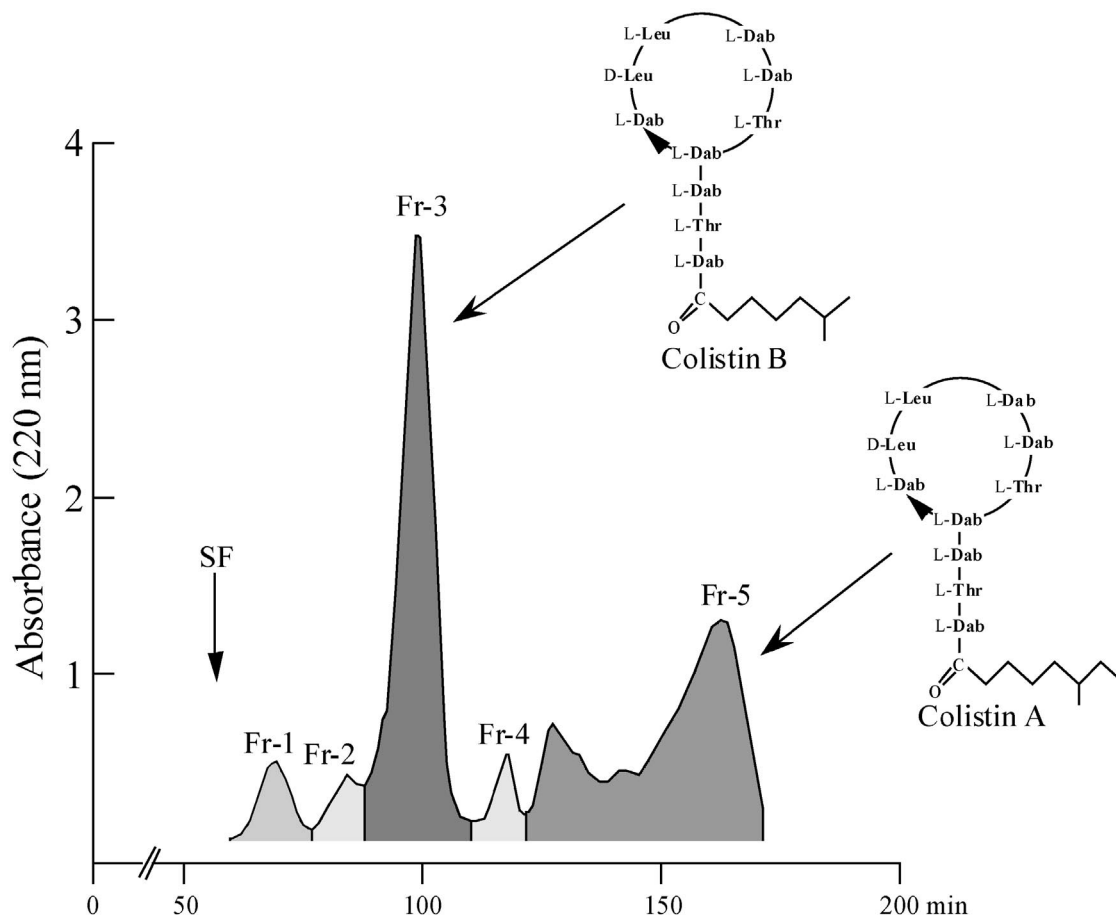


Fig. 2 HSCCC separation of colistin components. Solvent system: *n*-butanol/0.04 M trifluoroacetic acid (1:1); mobile phase: lower phase; flow rate: 2 mL/min; detection: 220 nm.

increases with the concentration of TFA, resulting in the partition of components toward the organic phase. In order to determine the optimal concentration of TFA in the solvent system, *K* values were measured at various TFA concentrations. The *K* value of each component increases with the TFA concentration and, at 40 mM TFA concentration, the *K* values of CL-A and CL-B reach 1.5 and 0.6, respectively. At this TFA concentration, the α values between the adjacent peaks are all greater than 1.5, promising a good separation for all components. The settling time of the solvent system was 28 sec, which is within an acceptable range. Therefore we selected a solvent system of *n*-butanol/40 mM TFA aqueous solution (1:1) for the HSCCC separation of CL components.

Using the above solvent system, a 20-mg portion of commercial CL was separated by HSCCC. The retention of the stationary phase was 45%. The elution curve, monitored at 220 nm, is shown in Fig. 2. The yields of CL-A and CL-B were 9 mg each, and those of the other minor components were 0.5–1.0 mg. From HPLC

analysis, the fractions of CL-A and CL-B each produced almost a single peak with a high purity of over 90%.

Separation of Ivermectin Components

Ivermectins B1 are broad-spectrum antiparasitic agents widely used for food-producing animals such as cattle, swine, and horse.^[7] They are derived from avermectins B1, the natural fermentation products of *Streptomyces avermitilis*.

We have selected a two-phase solvent system composed of *n*-hexane, ethyl acetate, methanol, and water. As described above, this solvent system is conveniently used for the separation of components with a broad range of hydrophobicity by modifying the volume ratio between the four solvents. In the *n*-hexane/ethyl acetate/methanol/water (8:2:5:5) system first examined, the *K* values of the components were 0, 0.46, 0.61 (ivermectin B1a); ∞ , 1.86 (ivermectin B1b); 3.06 (ivermectin B1a); and 4.38,

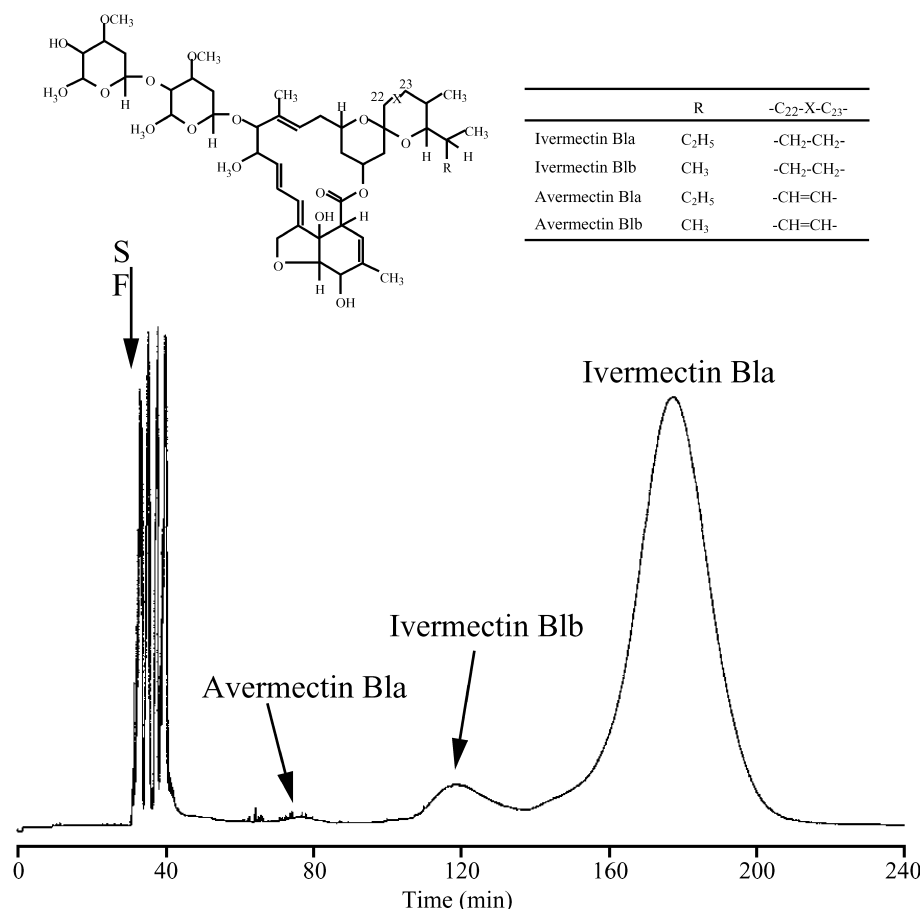


Fig. 3 HSCCC separation of ivermectin components. Solvent system: *n*-hexane/ethyl acetate/methanol/water (19:1:10:10); mobile phase: lower phase; flow rate: 2 mL/min; detection: 245 nm.

respectively. This indicates that the component corresponding to ivermectin B1a is mostly partitioned in the upper organic phase. Although the *n*-hexane/ethyl acetate/methanol/water (9:1:5:5) system somewhat improved the *K* value of ivermectin B1b to 2.31, it was still too large. Finally, a slightly less polar solvent mixture at the volume ratio of 19:1:10:10 yielded the best *K* values: 0, 0, 0.18 (avermectin B1a); 0.48, 0.79 (ivermectin B1b); 1.36 (ivermectin B1a); and 2.83, with desirable α values of over 1.5 for all components. The settling time of this solvent system was 7 sec, promising excellent retention of the stationary phase. In addition, the volume ratio between the two phases is nearly 1, indicating that either phase can be used as the mobile phase without wasting the solvents. Therefore the above solvent system was selected for the separation of ivermectin components.

A 25-mg quantity of crude ivermectin was separated using the above solvent system at a flow rate of 2 mL/min. The retention of the stationary phase was 67.6% and the total separation time was 4.0 hr. The HSCCC elution curve of the ivermectin components, monitored at 245

nm, is shown in Fig. 3, where all components are separated into three peaks. This separation yielded 18.7 mg of 99.0% pure ivermectin B1a (Fig. 3), 1.0 mg of 96.0% pure ivermectin B1b (Fig. 3), and 0.3 mg of 98.0% pure avermectin B1a.

Separation of Lac Dye Components

Lac dye is a natural food additive extracted from a stick lac, which is a secretion of the insect *Coccus laccae* (*Laccifer lacca* Kerr), and is widely used for coloring food.^[8] It is known that its red color is derived from water-soluble pigments including laccaic acids A, B, C, and E.

Laccaic acids have two or three carboxyl groups, five or six hydroxyl groups, and/or one amino group, and are freely soluble in water, but only slightly soluble in organic solvents such as chloroform and ethyl acetate. Based on these physicochemical properties of laccaic acids, we selected a two-phase solvent system composed



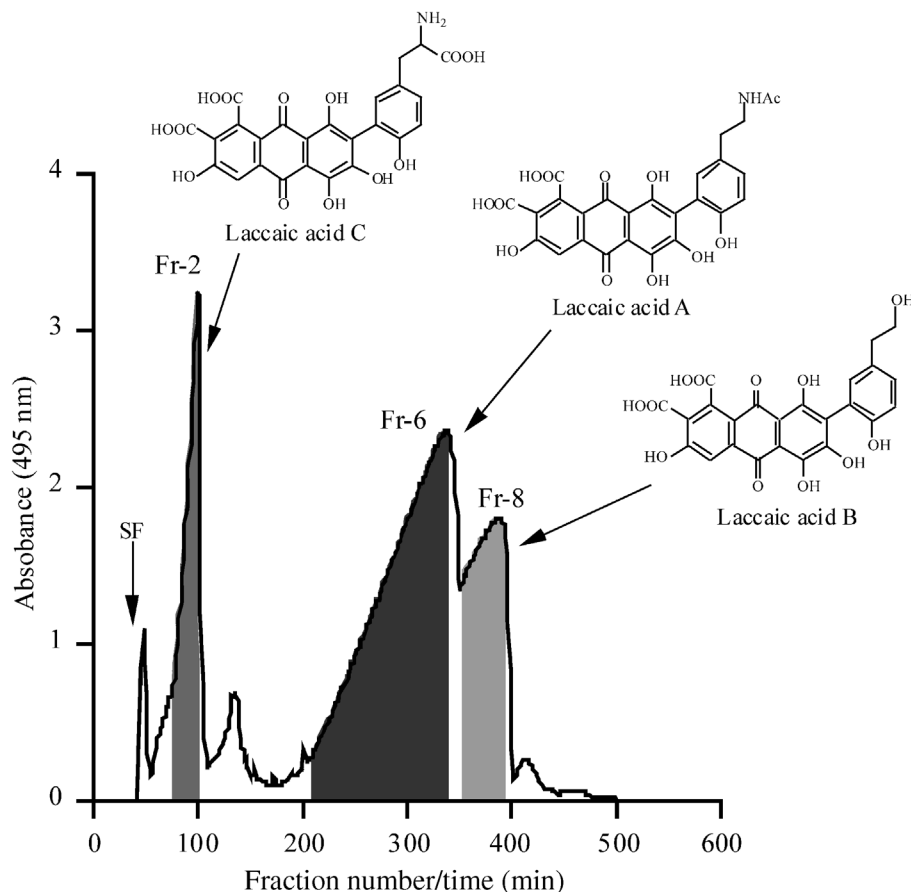


Fig. 4 HSCCC separation of lac dye components. Solvent system: *tert*-butyl methyl ether/*n*-butanol/acetonitrile/water (2:2:1:5); mobile phase: lower phase; flow rate: 1 mL/min; detection: 495 nm.

of *tert*-butyl methyl ether/*n*-butanol/acetonitrile/water, which has been frequently used as the solvent system for the separation of hydrophilic compounds as described earlier. In the *tert*-butyl methyl ether/*n*-butanol/acetonitrile/water (4:2:3:8) system first examined, the *K* values of the components were 0.08, 0.10 (laccacid acid C), 0.19, 2.00, 0.84 (laccacid acid B), and 0.60 (laccacid acid A), respectively. This indicates that the first component (*K* value: 0.08) and laccacid acid C (*K* value: 0.10) would be eluted together near the solvent front because of their small *K* values. A more polar solvent composition of *tert*-butyl methyl ether/*n*-butanol/acetonitrile/water (2:2:1:5) yielded the best *K* values, with desirable α values of over 1.5 for all components. The settling time of this solvent system is less than 30 sec, which ensures a satisfactory retention of the stationary phase in HSCCC as described before. Therefore we selected this solvent system for the separation of the lac dye components.

A 25-mg quantity of lac dye was separated using the above solvent system at a flow rate of 1 mL/min. The retention of the stationary phase was 83.6%. The total

separation time was 8.3 hr. The absorbance of effluents in every tube was measured at 495 nm to draw the elution curve (Fig. 4). In the HPLC analysis of the original sample, laccacid acids A, B, and C constituted about 37.1%, 18.0%, and 35.5% of the total peak area at 280 nm, respectively. After only one-step operation by HSCCC, the purities of the above three components were increased to 98.1% (laccacid acid A), 98.2% (laccacid acid B), and 97.2% (laccacid acid C), respectively. These results demonstrate the high resolving power of HSCCC achieved by the careful selection of the proper solvent system.

CONCLUSION

Because of a support-free partition system, HSCCC provides an important advantage over other chromatographic methods by eliminating various complications, such as adsorptive loss and deactivation of samples, as well as contamination from the solid support. As shown

by our examples, HSCCC can isolate various components from a complex mixture of natural products by carefully selecting the two-phase solvent system to optimize the partition coefficient (K) of the target component(s). The HSCCC system can also be applied to microanalytical-scale separations without excessive dilution of samples. We believe that HSCCC is an ideal method for the separation and purification of natural products.

REFERENCES

1. Mandava, N.B.; Ito, Y. *Countercurrent Chromatography—Theory and Practice*; Chromatographic Science Series, Marcel Dekker Inc.: New York, 1988; Vol. 44.
2. Conway, W.D. *Countercurrent Chromatography—Apparatus, Theory, and Applications*; VCH: New York, 1990.
3. Ito, Y.; Conway, W.D. *High Speed Countercurrent Chromatography*; John Wiley & Interscience: New York, 1996.
4. Oka, F.; Oka, H.; Ito, Y. Systematic search for suitable two-phase solvent systems for high-speed counter-current chromatography. *J. Chromatogr.* **1991**, 538, 99–108.
5. Harada, K.-I.; Ikai, Y.; Yamazaki, Y.; Oka, H.; Suzuki, M.; Nakazawa, H.; Ito, Y. Isolation of bacitracins A and F by high-speed counter-current chromatography. *J. Chromatogr.* **1991**, 538, 203–212.
6. Ikai, Y.; Oka, H.; Harada, K.-I.; Suzuki, M.; Hayakawa, J.; Kawamura, N.; Nakazawa, H.; Ito, Y. Isolation of colistin A and B using high-speed countercurrent chromatography. *J. Liq. Chromatogr.* **1998**, 21, 143–155.
7. Oka, H.; Ikai, Y.; Hayakawa, J.; Shimizu, A.; Hayashi, T.; Harada, K.-I.; Suzuki, M.; Takeba, K.; Nakazawa, H.; Ito, Y. Separation of ivermectin components by high-speed counter-current chromatography. *J. Chromatogr., A* **1996**, 723, 61–68.
8. Oka, H.; Ito, Y.; Yamada, S.; Kagami, T.; Hayakawa, J.; Harada, K.-I.; Atsumi, E.; Suzuki, M.; Odani, H.; Akahori, S.; Maeda, K.; Nakazawa, H.; Ito, Y. Separation of lac dye components by high-speed countercurrent chromatography. *J. Chromatogr., A* **1998**, 813, 71–77.



Taxanes Analysis by HPLC

Georgios A. Theodoridis

Aristotle University of Thessaloniki, Thessaloniki, Greece

INTRODUCTION

Taxanes have gained wide interest due to the pharmacological properties of paclitaxel (TaxolTM), the most well-known member of this large family of natural products. Paclitaxel is a complex diterpene amide originally derived from the pacific yew tree. The drug has been characterized by the National Cancer Institute (NCI) as “the most important anticancer agent for the past 15 years.” The interest in paclitaxel dates back to 1962, when crude extracts of *Taxus brevifolia* bark were tested in a large-scale exploratory plant-screening program of the NCI. Paclitaxel was identified as the active constituent of the bark extracts by Wani et al.^[1] However, the clinical development of paclitaxel was delayed due to high toxicity, difficulties in formulation, and mainly its scarcity, which hampered a reliable supply for clinical use.

PACLITAXEL AND TAXANES

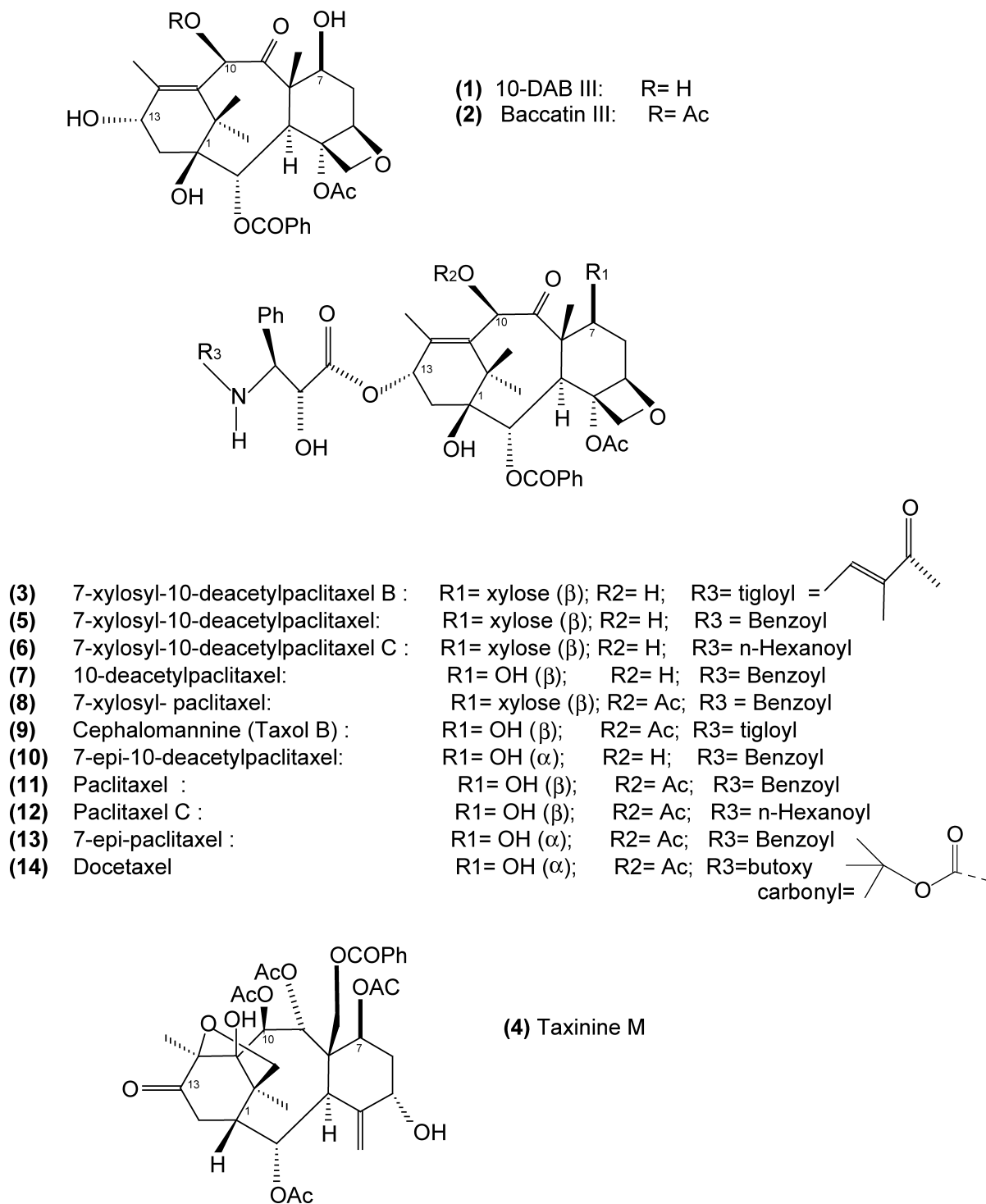
Awareness about paclitaxel increased dramatically in the late 1970s, when scientists at Albert Einstein Medical College (New York) described the unique mechanism of its cytotoxic action as a promoter of microtubule assembly. In contrast to most of the conventional anticancer drugs, paclitaxel inhibits mitosis through the enhancement of tubulin's polymerization and the consequent stabilization of microtubules. In 1983, the NCI commenced Phase I clinical trials. Six years later, the John Hopkins Oncology Center (Baltimore) reported exceptional clinical results for the treatment of ovarian cancer. The same year, Bristol-Myers Squibb was selected by the NCI as its partner to commercialize the drug under the trademark TaxolTM. Since then, numerous other pharmaceutical companies focused on the development of novel anticancer agents of *Taxus* origin. Hence, a number of taxane pharmaceuticals were launched: Yewtaxan[®] (paclitaxel from Yew Tree Pharmaceuticals), paclitaxel (Napros; Australia). Researchers at the French CNRS, in cooperation with Rhone Poulenc (now Aventis), developed a semisynthetic derivative, starting from 10-deacetyl baccatin III (Fig. 1). The drug was called Taxotere and it exhibited attractive features compared to paclitaxel

itself: better water solubility, potency, and the particular way of its production from a renewable source. Taxotere has received Food and Drug Administration (FDA) approval for the treatment of locally advanced or metastatic breast cancer and nonsmall cell lung cancer (NSCLC). Taxanes, in general, are used as a second-line cytostatic agent, meaning that they are often administered in cases where cancer recurs after chemotherapy with platinum drugs.

Paclitaxel is one of the best performers in the pharmaceutical market, with sales increasing by 62% in 1995 and reaching \$941 million in 1997. Paclitaxel and taxotere have shown promising results in patients with advanced squamous cell carcinoma of the head and the neck, malignant melanoma, advanced NSCLC, small cell lung cancer (SCLC), germ cell cancer, urothelial cancer, esophageal cancer, non-Hodgkins lymphoma, and multiple myeloma. Furthermore, they have been tested in HIV and multiple sclerosis patients. Taxanes were also successfully combined with cisplatin, carboplatin, and/or etoposide in the treatment of patients with NSCLC, SCLC, or advanced squamous cell carcinoma of the head and neck.

The drugs are now considered a prototype for a new class of chemotherapeutic agents and research has been proceeding at record pace for years. The publication of five books on the chemistry, pharmacology, and medical therapy stands as a witness of the excitement that the compound has raised.^[2-6]

Despite its low content (100 mg/kg of dry bark) and its notoriously slow growth, *T. brevifolia* was, until recently, the sole source of paclitaxel. Supply shortage and increasing demands for clinical use necessitated the investigation for alternative sources. Hence, plant species, tree parts, cell culture, fungi, and (semi)synthesis have been sought to solve the tremendous supply crisis in the mid-1990s. Nowadays, remaining problems include the compound's inherent toxicity, poor solubility in water, and difficulty encountered during formulation. Hence, optimization of the drug delivery, improvement of its molecular properties, and production of paclitaxel analogues (more potent, less toxic, and easier to formulate) are still a matter of considerable research and development efforts.

**Fig. 1** Molecular structures of the most common taxanes.



ANALYTICAL CHALLENGES AND METHODS

In general, the analysis of taxanes is driven by the following:

1. The need for the determination of paclitaxel (or docetaxel to a lesser extent) and their metabolites in biological samples.
2. The need for the purification or/and determination of taxanes in plant material, cell culture, or synthetic mixtures.

The starting point presides over the choice of the final analytical protocol. Analysis in biological samples for pharmacokinetic purposes poses limited difficulties because the determination of paclitaxel in human blood is rather straightforward. In contrast, analysis of plant samples deals with samples containing lesser quantities of a complex mixture of several taxanes. Separation and identification is thus a real challenge for the chromatographer.

Analysis of taxanes is performed almost exclusively by high-performance liquid chromatography (HPLC). Immunological techniques [enzyme-linked immunosorbent assay (ELISA), radioimmunoassay (RIA)] have found minimal use in screening human plasma and plant extracts. Such biological methods suffer from cross reactivity of several taxanes with paclitaxel and their use is thus limited in semiquantitative aspects.

Mass spectrometry (MS), employing most of the ionization techniques, has been used either independently, or in combination with HPLC, for the determination of the dissociation scheme of paclitaxel or for the identification of taxanes and paclitaxel metabolites. Tandem MS has enhanced identification and structure elucidation capabilities in the analysis of either biological or plant samples.

A few research groups utilized other chromatographic techniques for the purification of taxanes from natural sources or synthetic organic mixtures. Techniques such as thin-layer chromatography (TLC), flash chromatography, high-speed countercurrent chromatography (HS-CCC), micellar electrokinetic chromatography (MEKC), and supercritical fluid chromatography (SFC) and extraction (SFE) have been used for either sample purification and/or analysis. TLC on silica gel has been used for the isolation and, together with NMR and MS, for the identification of new taxanes from several *Taxus* species. Visualization was accomplished by spraying the plates with anisaldehyde solution and heating. HS-CCC provides an elegant method for fast and efficient processing of large sample quantities, a parameter of great importance for scale-up purposes. HS-CCC is not based in adsorption chromatographic mechanisms, in contrast to the established taxane purification methods (including the FDA-approved official method), which employ column

chromatography. A two-phase system of light petroleum–ethyl acetate–methanol–water purified plant samples of up to 400 mg, achieving purity of up to 97% for paclitaxel. MEKC performed on uncoated fused silica capillaries proved suitable for the analysis of paclitaxel, cephalomannine, and baccatin III in needle extracts. Finally, SFC has been carried out in both capillary and packed C_{18} or cyano columns. The packed cyano column gave the best performance for the analysis of taxanes after SFE of *Taxus baccata* clippings.

HPLC OF TAXANES

HPLC analysis of taxanes is achieved almost exclusively in reversed phase mode on various stationary phases. The normal-phase HPLC mode has been applied in very limited cases and resulted in broad peaks and long analysis times (retention times of 45 min for paclitaxel and 38 min for cephalomannine). The nature of the sample is the main criterion for the choice of the stationary phase. Analysis of plant material is performed mostly on phenyl, biphenyl, and pentafluorophenyl materials, but silica-based cyano, C_{18} , and C_8 materials have been used as well. C_{18} phases are the most common material utilized in pharmacokinetic studies. Mobile phases typically consist of mixtures of methanol, acetonitrile, and water or buffer (mostly ammonium acetate). Detection is performed by UV, mostly in the low region of 225–230 nm. Taxanes give similar UV spectra with a minimum at 210–215 nm and a maximum at 225–232 nm. Therefore, detection is performed, preferably at 227–228 nm. Dual/multiple UV detection is performed in both low and upper regions, e.g. 227 and 273 nm; 230 and 280 nm; 227, 254, and 270 nm, etc. (Fig. 2).

In the reported LC-MS schemes, both positive and negative ionization modes have been used; however, positive ionization is the dominant mode. Thermospray and electrospray interfaces have been utilized for the coupling of reversed phase mobile phases to the MS. In tandem MS, fragments are obtained from the taxane ring (ions with m/z 268 and 286) and the C-13 side ester chain (ions with m/z 569, 551, and 509).

Detailed description of the analytical separation systems for the analysis of paclitaxel by HPLC (stationary and mobile phases, sample type, sample pretreatment) can be found in a review that appeared recently.^[7]

HPLC Analysis of Plant Material and Cell Culture

Analysis of paclitaxel in plant material bids a challenge for the separation scientist for many reasons:

1. The taxanes are present in low quantities in the original samples (either plant or cell culture).

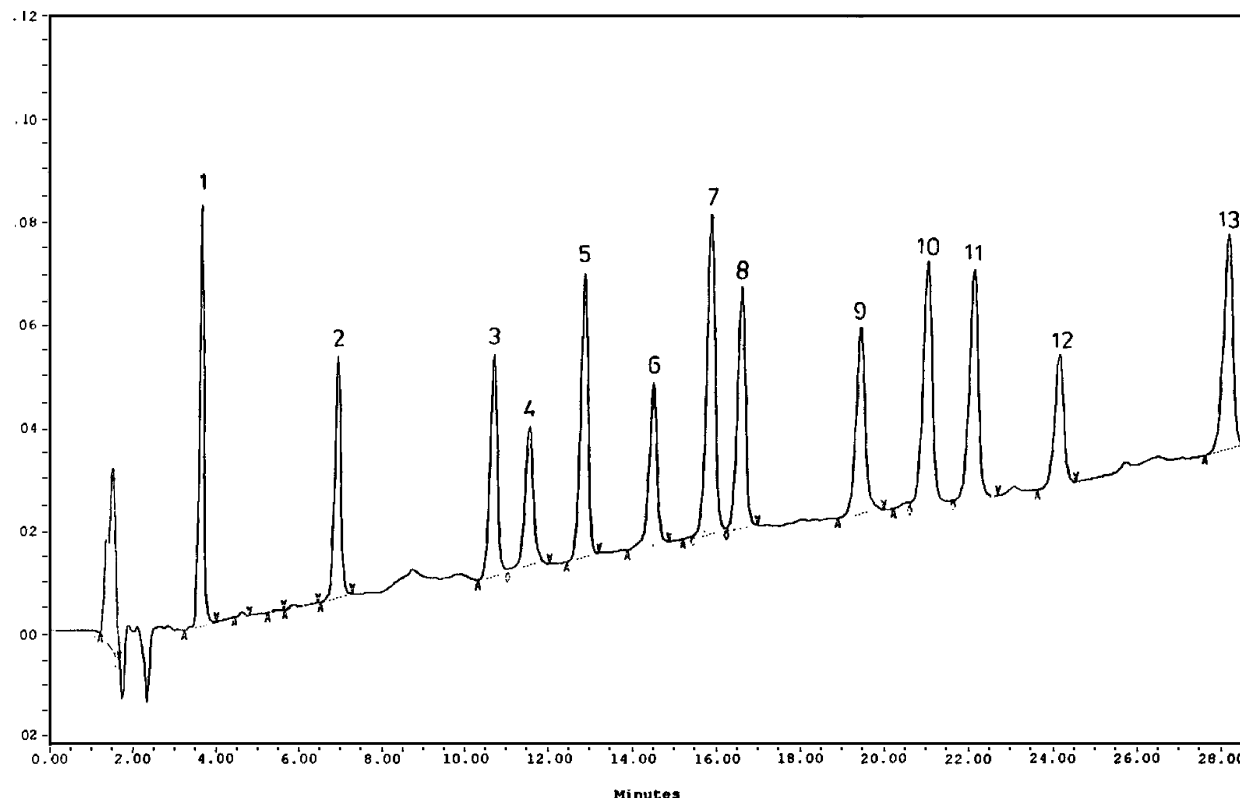


Fig. 2 UV spectra obtained by HPLC analysis of a *Taxus* cell culture extract. Detection with a photodiode array detector. 1 = Paclitaxel, 2 = cephalomannine, 3, 4, and 5 correspond to unknown interferences from the sample.

2. The differences between the molecular structure of different taxanes are small (Fig. 1).
3. Plant extracts encompass a diversifying range of endogenous compounds. These problems can be easily perceived in the reported chromatograms: broad peaks, long analysis times, and poor resolution from endogenous interferences.

Initially, researchers focused on the separation of paclitaxel from cephalomannine, a paclitaxel analogue that shares the C-13 ester side-chain and, therefore, exhibits cytotoxic activity. Cephalomannine was found to elute close to paclitaxel and caused interferences for determination and purification purposes. Lately, the main taxane targets are baccatin III and 10-deacetyl-baccatin III (10-DAB III). Both compounds lack the C-13 side-chain (Fig. 1); thus, they do not show antitumour activity. Both baccatins, especially 10-DAB III, serve as synthons for the synthesis of paclitaxel or analogues. 7-Epi-paclitaxel differs from paclitaxel only in the stereochemistry of the hydroxy group in the C-7 position. 7-Epi-paclitaxel, a product of paclitaxel epimerization, shows cytotoxic activity and difficulty in separation from paclitaxel. The deacetyl derivatives of paclitaxel, 7-epi-paclitaxel, baccatin III, and cephalomannine, are also quite often the

subject of analysis. The problems mentioned above designated a market for HPLC column manufacturers, which did not take long to fill with “tailor made” or “specialty” columns. Taxanes are probably the sole group of compounds that labeled so many HPLC columns: Phenomenex has produced three Curosil™ columns (silica-based reversed phase packing material), Metachem Technologies also manufactured three Taxil™ columns, Zorbax made the SW-Taxane column (bonded silica), and Whatman the TAC 1 column. It should be pointed out that such columns are usually developed in order to solve special problems. According to their manufacturers, the chemical and physical properties of the packing material (which are often proprietary) are designed with appropriate characteristics for a specific analyte or group of analytes. However, it is often observed by many researchers (the author included) that the best results are actually obtained by utilizing a low-cost conventional material.^[9] An example is illustrated in Fig. 3, which shows a UV chromatogram of a reference taxane mixture obtained by gradient elution on a generic phenyl column. The same chromatographic analysis performed on electrospray MS provided mass spectral data that were used for the identification of unknown peaks in *Taxus* bark extracts. Results are depicted in Table 1.

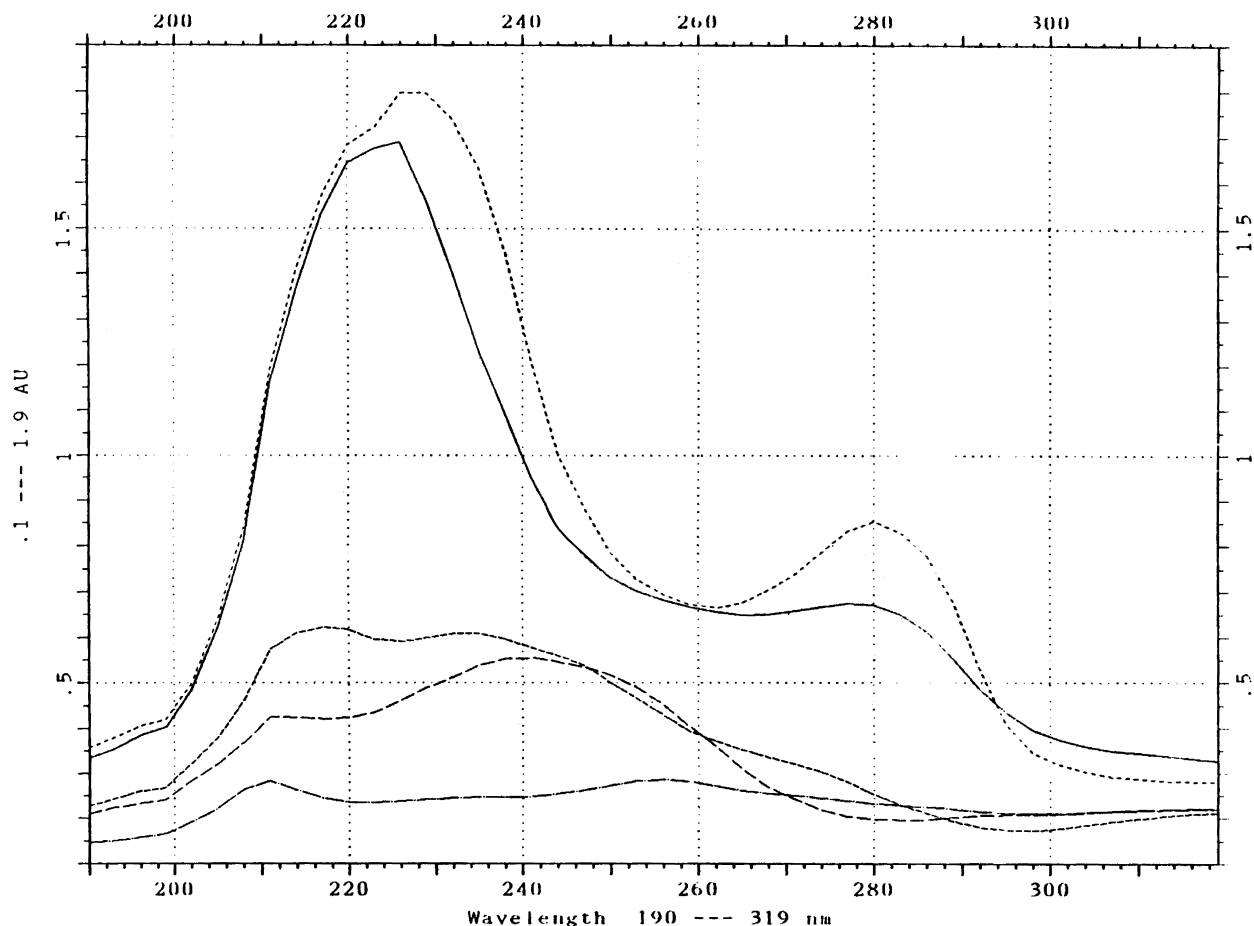


Fig. 3 Analysis of a taxane standard mixture. Chromatographic conditions: Column Novapak Phenyl column (Waters); eluted with the gradient program: Initially 100% A–0% B, linearly 56% A–34% B at 30 min and then back to 100% A–0% B at 32 min. A = 0.05 M $\text{CH}_3\text{COONH}_4$: CH_3CN 7:3 v/v, B = 0.05 M $\text{CH}_3\text{COONH}_4$: CH_3CN 1:9 v/v. Flow rate 0.8 mL/min and detection at 227 nm. Peak identities as in Fig. 1. (From Ref. [9].)

Sample Pretreatment of Plant Material and Cell Culture

Optimization of the extraction and purification of taxanes from plant material, tissue culture, or biological fluids has been the subject of extensive research. As mentioned already, taxanes are present in small quantities in a very complex matrix, thus making extraction and purification complicated. Simple extraction schemes do not cope with straightforward HPLC analysis because they are subject to column plugging and deterioration, low recovery, and poor chromatographic resolution. On the other hand, tedious and complex procedures that have been developed to overcome such problems require large amounts of solvent and long extraction times (surpassing even 48 hr).

A typical strategy takes advantage of the limited water solubility of taxanes to partition the compounds between water, and an apolar organic solvent (often a chloro-

methane). Hence, a plant material in the form of a crude methanolic plant extract is partitioned between water and dichloromethane; the dichloromethane fraction is evaporated to dryness, reconstituted in methanol, and analyzed by HPLC. Initially, such simple extraction procedures were used for the determination of taxanes in plant extracts, but they resulted in high back pressure and the need for frequent column flushing. Furthermore, as *Taxus* phytochemistry consolidated, analytical methods of higher resolving power became necessary. Additional extraction steps for the removal of nonpolar components (especially from samples such as needles) utilized hexane or similar apolar solvents. The plant material is first extracted with hexane for the removal of waxes and other lipophilic substances. Alternative protocols employed techniques such as column chromatography, HS-CCC, SFE, and semipreparative HPLC.

Recently, solid phase extraction (SPE) on several stationary phases has been extensively used in the pre-

Table 1 Results of the LC-MS analysis of a taxane standard mixture and a *T. baccata* bark extract

Compound	m/z	Peak	MW	t _R (min)	Bark
(1) 10-DAB III	562	[M + NH ₄] ⁺	544	3.95	+
(2) Baccatin III	604	[M + NH ₄] ⁺	586	6.88	+
(3) 7-Xylosyl-10-deacetyltaxol B	922	[M + H] ⁺	921	10.78	+
(4) Taxinine M	704	[M + H] ⁺	703	11.50	+
(5) 7-Xylosyl-10-deacetyltaxol	944	[M + H] ⁺	943	13.10	—
(6) 7-Xylosyl-10-deacetyltaxol C	938	[M + H] ⁺	937	14.60	+
(7) 10-Deacetyltaxol	812	[M + H] ⁺	811	15.65	+
(8) 7-Xylosyl-taxol	986	[M + H] ⁺	985	16.40	+
(9) Cephalomannine	832	[M + H] ⁺	831	19.65	+
(10) 7-Epi-10-deacetyltaxol	812	[M + H] ⁺	811	21.20	—
(11) Paclitaxel	854	[M + H] ⁺	853	22.15	+
(12) Taxol C	848	[M + H] ⁺	847	24.20	+
(13) 7-Epi-taxol	854	[M + H] ⁺	853	28.15	—

Chromatographic conditions are as in Fig. 2. t_R = retention time; (+) = detection of the compound; (—) = no detection. (From Ref. [9].)

treatment of both plant and biological samples. Typically, crude extracts are mixed with appropriate solvents (methanol or ethanol) and the resulting solutions are applied onto the SPE cartridges. The cartridges are next washed with appropriate solvents to take out impurities and, finally, the taxanes are eluted in an optimized “recovery solvent.” The obtained taxane fraction is evaporated to dryness and, after reconstitution to solution, an aliquot is analyzed by HPLC.

The author has studied the SPE of taxanes at length.^[10] SPE offers an attractive alternative to the long and tedious liquid–liquid extraction schemes. The author’s work on HPLC determination of taxanes^[9] and SPE for the pretreatment of *Taxus* plant and cell culture samples^[10] resulted in fast and robust schemes for either screening or accurate determination of taxanes in plant and cell cultures. In this work, problems were observed in liquid–liquid extraction of the cell suspension medium as a result of the formation of emulsions. Such formations are difficult to break and require time-consuming and laborious centrifugation. Therefore, the major goal of the developed SPE protocols was the straightforward application of aqueous medium on the SPE column. As a result, consumption of time and organic solvents was lowered significantly. Washing the cartridge with water and aqueous MeOH (up to 50% in water) facilitated the removal of many interfering matrix constituents. Taxanes were recovered from the SPE cartridge with the elution fraction of 80% MeOH.^[10]

HPLC Analysis of Biological Material

Interest for the analysis of taxanes in biological fluids deals, in most cases, with the determination of the two pharmaceuticals, paclitaxel, and docetaxel, and their metabolites in blood plasma. The complexity of this matrix and the interference of endogenous compounds are, in

principle, decreased, compared to plant material; therefore, extensive sample pretreatment and high chromatographic resolution are not essential. Thus, fast and simple separation systems with the use of a C₈ or a C₁₈ column are often preferred. SPE is extensively used for sample pretreatment (especially in recent reports) because of its advantages over liquid extraction: limited organic solvent consumption, higher reproducibility and extraction efficiency, and cleaner extracts. Furthermore, sophisticated on-line SPE schemes that employ column switching or automated SPE increase sample throughput.

Paclitaxel and docetaxel are very lipophilic pharmaceuticals; thus, they bind to plasma proteins rapidly and to a great extent (>95%). Small quantities are excreted in urine because most of the drug is removed from the plasma metabolized in the liver and subsequently excreted into the bile.^[2] Paclitaxel pharmacokinetics follow a bimodal distribution. Usually, such studies are modeled with a two-compartment system: a central administration compartment (plasma–liver) and a second peripheral compartment (tissue where the drug is transported by secondary mechanisms). It should be pointed out that the lipophilicity of taxane pharmaceuticals causes tremendous problems in formulation and clinical administration. Paclitaxel’s vesicle is a mixture of 50% polyethoxylated castor oil (a surfactant labeled Cremophor EL), and 50% ethanol. This mixture causes serious adverse effects to patients. Cremophor is also subject to interferences in chemical analysis of pharmaceutical preparations of the drug. The drug is infused intravenously for varying time periods. Depending on the length of infusion, the concentration maximum in plasma varies from 3–4 μM (short infusion of 6 hr) to 0.7–0.9 μM (long infusion of 24 hr). Following HPLC, detection of paclitaxel by UV (227 nm) is sufficient; however, MS offers much higher sensitivity and identification capabilities.

Separation systems are rather simple and they employ solvents such as methanol or acetonitrile and buffers such as sodium acetate, ammonium acetate, or phosphate buffers. Isocratic elution suffices in most cases because the polarity of the drug is far different than most endogenous compounds, thereby enabling an easy chromatographic separation.

The sample that draws the greatest interest is human plasma, but other physiological human fluids, such as urine and bile, have also been the subject of analysis. To cover the needs of in vivo preclinical studies, many researchers developed methods for the determination of paclitaxel/docetaxel and their metabolites in samples from animal models such as rat and mouse.

Coupling of HPLC analysis to MS (either on-line or off-line) provided the means for structure elucidation and identification of taxane metabolites. Utilizing tandem MS (MS-MS), both aspects were significantly enhanced. Hydroxylation, epimerization, and hydrolysis are considered to be the main routes of metabolism of taxane pharmaceuticals.^[3] The principal metabolites of both paclitaxel and docetaxel result from hydroxylation. Hydroxylation of paclitaxel was initially observed in rat and mouse, but the finding was later extended to human subjects. Nine metabolites of paclitaxel (mono or dihydro derivatives) have been identified in rat by HPLC, NMR, and LC-MS. With regard to docetaxel, 18 derivatives have been identified in the rat bile. Hydrolytic derivatives result from cleavage of the side C-13 chain, and include baccatin III and 10-DAB III. Epimerization of taxanes is mainly focused on the C-7 and C-10 atoms, and occurs in solution. Epimerization has also been detected in cell culture in both the medium and inside the cell. It should be stressed that epimers are not naturally occurring taxanes; thus, they are not found in plants.^[2,3,8,9]

A detailed tabulated list of HPLC methods (columns, mobile phases, applications, and detection modes) can be found in Ref. [8].

CONCLUDING REMARKS

Analysis of taxanes in biological samples and plant extracts is performed, mainly by reversed phase HPLC. Separation of paclitaxel from cephalomannine, baccatin III, and other taxanes is often performed with phenyl columns (especially for plant material analysis). For less complex biological samples, C₁₈ columns are preferred because they give shorter analysis times. Extraction of plant material or cell cultures is often performed by water-dichloromethane partitioning, but lately, the application of SPE has become a basic step in order to obtain cleaner samples, higher extraction recovery, better chromatographic resolution, and longer column lifetime. Detection of taxanes is performed, in most cases, at 227–228 nm.

REFERENCES

1. Wani, M.C.; Taylor, H.L.; Wall, M.E.; Coggon, P.; McPhail, A.T. Plant antitumor agents: VI. The isolation, and structure of taxol, a novel antileukemic and antitumor agent from *Taxus brevifolia* trees. *J. Am. Chem. Soc.* **1971**, *93*, 2325–2327.
2. Suffnes, M. *Taxol Science and Applications*; CRC Press: Boca Raton, 1995.
3. Farina, V. *The Chemistry and Pharmacology of Taxol*; Elsevier: Amsterdam, 1995.
4. McGuire, W.P.; Rowinski, E.K. *Paclitaxel in Cancer Treatment*; Marcel Dekker, Inc.: New York, 1995.
5. Georg, G. *Taxane Anticancer Agents*; Developed from a Symposium Sponsored by the Divisions of Chemical Health, and Safety, American Chemical Society: Washington, 1995.
6. Goodman, J.; Walsh, V. *The Story of Taxol: Nature, and Politics in the Pursuit of an Anti Cancer Drug*; Cambridge Univ. Press: Cambridge, 2001.
7. VanHaelen-Fastre, R.; Diallo, B.; Jaziri, M.; Faes, M.-L.; Homes VanHaelen, M. High-speed countercurrent chromatography separation of taxol and related diterpenoids from *Taxus baccata*. *J. Liq. Chromatogr.* **1992**, *15*, 697–706.
8. Theodoridis, G.; Verpoorte, R. Taxol analysis by HPLC. A review. *Phytochem. Anal.* **1996**, *7*, 169–184.
9. Theodoridis, G.; Laskaris, G.; de Jong, C.; Hofte, A.J.P.; Verpoorte, R. Determination of paclitaxel and related diterpenoids in plant extracts by high performance liquid chromatography with UV detection in high performance liquid chromatography-mass spectrometry. *J. Chromatogr., A* **1998**, *802*, 297–305.
10. Theodoridis, G.; de Jong, C.; Laskaris, G.; Verpoorte, R. Application of SPE for the HPLC analysis of taxanes from *Taxus* cell cultures. *Chromatographia* **1998**, *47*, 25–34.

FURTHER READINGS

- Fang, W.; Wu, Y.; Zhou, J.; Chen, W.; Fang, Q. Qualitative, and quantitative determination of taxol and related taxanes in *Taxus cuspidata* Sied et Zucc. *Phytochem. Anal.* **1993**, *4*, 115–119.
- Monsarrat, B.; Mariel, E.; Cros, S.; Gares, M.; Guenard, D.; Gueritte, V.; Wright, M. Taxol metabolism. Isolation and identification of three major metabolites of taxol in rat bile. *Drug Metab. Dispos.* **1990**, *18*, 895–901.
- Rosing, H.; Lustig, V.; Koopman, F.P.; ten Bokkel Huinink, W.W.; Beijnen, J.H. Bio-analysis of docetaxel and hydroxylated metabolites in human plasma by high-performance liquid chromatography and automated solid-phase extraction. *J. Chromatogr., B, Biomed. Sci. Appl.* **1997**, *696*, 89–98.
- Theodoridis, G.; Laskaris, G.; Verpoorte, R. HPLC analysis of taxoids in plant and plant cell tissue culture. *Am. Biotechnol. Lab.* **1999**, *17*, 40–44.
- Vergniol, J.C.; Bruno, R.; Montay, G.; Frydman, A. Determination of taxotere in human plasma by a semi-automated high-performance liquid chromatographic method. *J. Chromatogr.* **1992**, *582*, 273–278.



Taxines Analysis by HPLC

Georgios Theodoridis

Aristotle University of Thessaloniki, Thessaloniki, Greece

INTRODUCTION

The toxicity of *Taxus* plants has been known for a long time (reports date as far back as the time of Julius Caesar).^[13] In the 19th century, phytochemical work attributed *Taxus* toxicity to an alkaloid that was called taxine. This alkaloid was a complex mixture, isolated from leaves. Taxine was later shown to be a mixture of more than seven alkaloids, with taxine A and taxine B as main constituents. Taxines are very strong cardiotoxic agents; they cause convulsions, fall in blood pressure, and stopping of the heart in diastole. Phytochemical work on *Taxus* during the 1940s and 1950s was focused on taxines and their cinnamate analogues, taxinines. The discovery of the potent cytostatic agent paclitaxel in *Taxus* bark in the late 1960s overshadowed any interest in taxines. Paclitaxel and the semisynthetic derivative docetaxel attracted unprecedented interest and remained the major research topic for scientists on diverse areas as follows: phytochemistry, pharmacognosy, molecular pharmacology, synthetic chemistry, analytical chemistry, and, most of all, clinical medicine.

TAXINES

A chief problem in the early development of taxane pharmaceuticals was the establishment of a steady and dependable supply. Taxanes are present in low quantities in plants. In contrast, taxines are relatively abundant in plants (especially in *Taxus baccata* and *Taxus cuspidate*); they can serve as an alternative starting material for semisynthetic production of paclitaxel derivatives. The major taxines are taxine A and taxine B.^[1,2] There is a significant structural resemblance between taxine B and taxanes (Fig. 1). Both groups share the main taxane ring; moreover, the C-5 side chain of the taxines has a close spatial position to the C-13 side chain of the taxanes (the latter is essential for antitumor activity). A biosynthetic hypothesis involved the intermediacy of a C-5 to a C-13 ester transfer; it was also demonstrated that taxine B can be converted into a baccatin V derivative. Taxines do not show antitumor activity, whereas the cardiotoxicity of taxol is lower compared to taxines but is undesirable for

clinical administration. Hence, it was assumed that the structural features necessary for cardiotoxicity are different from the features necessary for antitumor activity. Understanding the factors responsible for the toxicity of taxines could lead to the design of taxol analogues with diminished cardiotoxicity. However, taxines do not show intrinsic antitumor activity, whereas the cardiotoxicity of paclitaxel is lower compared to taxines but is undesirable for clinical administration. Hence, it was assumed that the structural features necessary for cardiotoxicity are different from the features necessary for antitumor activity. Understanding the factors responsible for the toxicity of taxines could lead to the design of paclitaxel analogues with diminished cardiotoxicity. Sophisticated analytical methods are therefore necessary for their analysis and determination in plant or biological samples.

Unfortunately, research work on taxines was hampered by their instability and the loss of activity upon storage because of the loss of dimethylamino moiety from the C-3' atom (Fig. 1) and the formation of corresponding cinnamates. Isolation of taxines is accomplished by alkaline/base extraction but it is difficult to obtain them in a purified form because of rapid acetate isomerization and/or decomposition to taxinines. To the author's knowledge, there are no taxine/taxinine reference compounds commercially available. It is no surprise therefore that there are limited works that report on the high-performance liquid chromatography (HPLC) of taxines. Taxines were found in plant extracts interfering in extraction, isolation, and analysis of paclitaxel from plant material.^[1-4,7]

HPLC ANALYSIS OF TAXINES

Workers of the phytochemical group at the University of Wageningen identified and isolated six taxine alkaloids from the needles of *T. baccata*. Acidic extraction with 0.5% (v/v) H₂SO₄ was followed by an extraction with Et₂O and basic extraction with 25% aq. NH₃. Taxines were recovered with CHCl₃ with a yield of 0.5–1% for the total crude taxine fraction. This report comprises the first analytical methodology for the determination of taxines. HPLC analysis employed a C₁₈ column, eluted by a linear gradient of acetonitrile over methanol and 0.05 M sodium dihydrogen phosphate buffer.^[5]

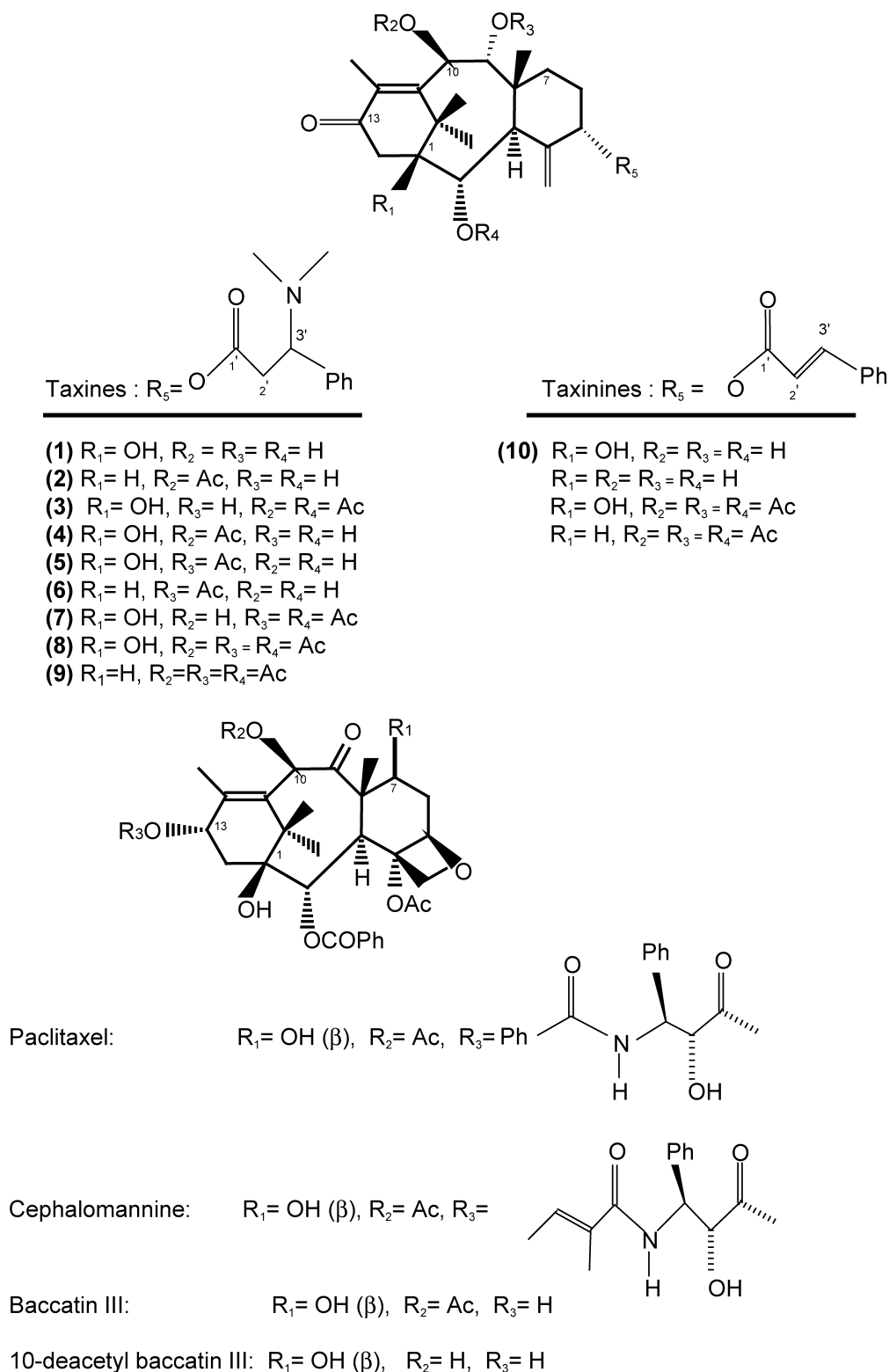


Fig. 1 Molecular structures of taxines, taxinines, and taxanes.

The research group of P. Potier, a group that has long been engaged in research activity on *Taxus*, studied the analysis of four taxines and 10-DAB III in *Taxus* needles in investigations for highly productive plants. The authors developed a normal phase separation system (silica eluted with chloroform/methanol/triethylamine, 99.4:0.5:0.1) for the evaluation of the total taxine content in *Taxus* needles. To separate the taxines, they used reversed phase (C_{18} eluted with acetonitrile/water/tetrahydrofuran, 23:77:0.5). The method, although it suffered from peak asymmetry and tailing, was useful for preparative objectives because it avoids the use of buffers.^[6] Taxines have also been determined by gas chromatography-mass spectrometry (GC-MS) in a search of *Taxus* poisoning in cattle and horses. Even though taxines are molecules that are too large to be analyzed by GC, the authors actually measured an ion at $134\ m/z^+$, which was attributed to a specific fragment at the 2' atom of the taxine side chain (Fig. 1).

The author's work on the HPLC analysis of taxines was a follow-up of previous research work on the HPLC of taxanes.^[9,10] Unknown peaks present in the analysis of plant and cell culture extracts were suspected to be taxines. In previous works, several other researchers have reported the detection of impurity peaks in the extracts of *Taxus x media* (Hicksii) needles during the determination of taxanes. These uncharacterized impurities showed a UV maximum at 280 nm, with a A_{280}/A_{228} ratio of approximately 3.5. Using absorbance ratio with these two or similar wavelengths, the researchers managed to overcome quantitation problems.^[8] Taxines and taxinines were also reported to cause problems in the HPLC analysis of taxanes, coeluting with the peak of paclitaxel.

In our work at Leiden University, apart from HPLC-photodiode array (PDA) detection, HPLC-electrospray mass spectrometry was used as characterization and identification tools. A semipurified taxine extract obtained with acid/base extraction of *T. baccata* needles was ana-

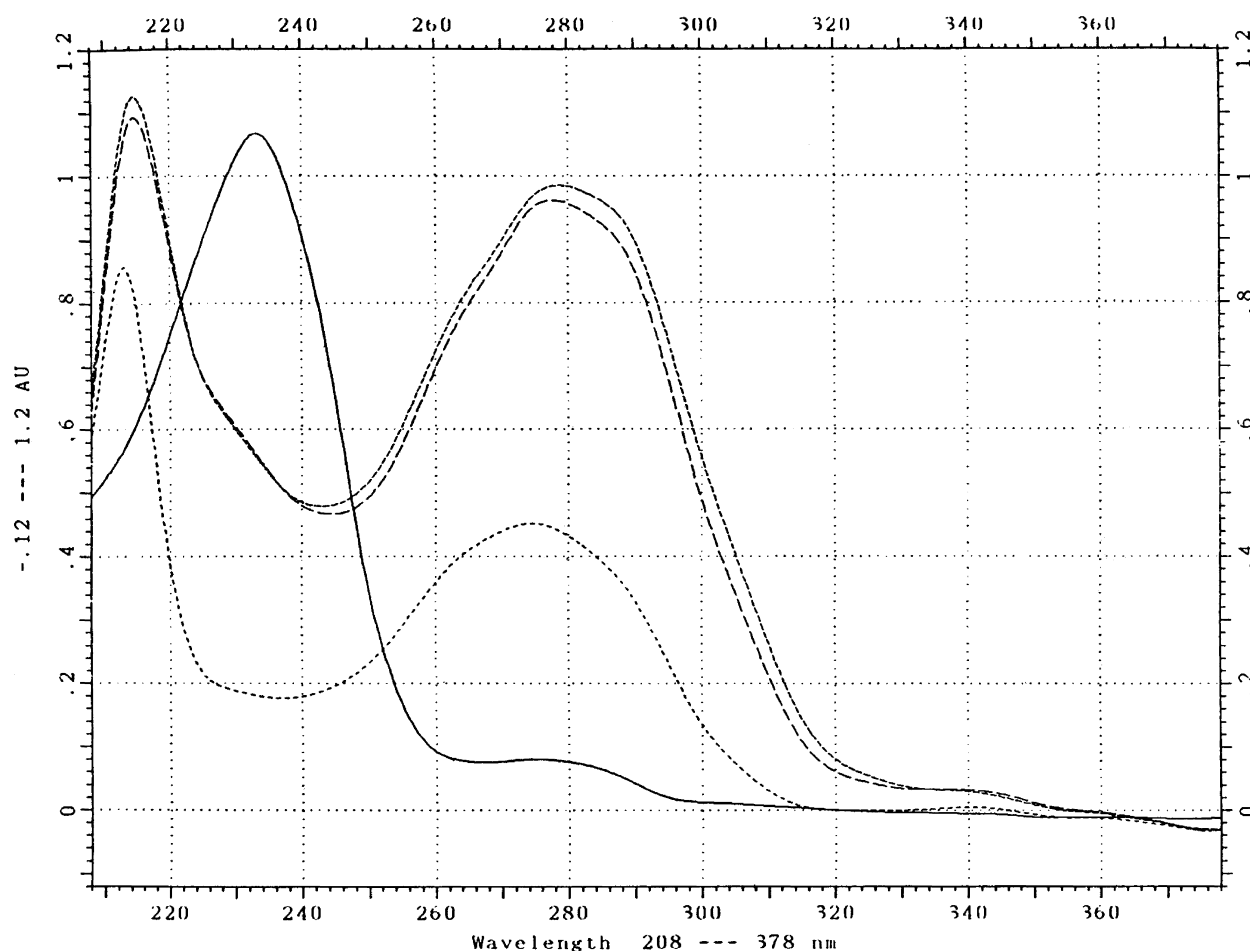


Fig. 2 UV spectra of a taxane (1), a taxine (2), and two taxinines (3). (From Ref. [11].)

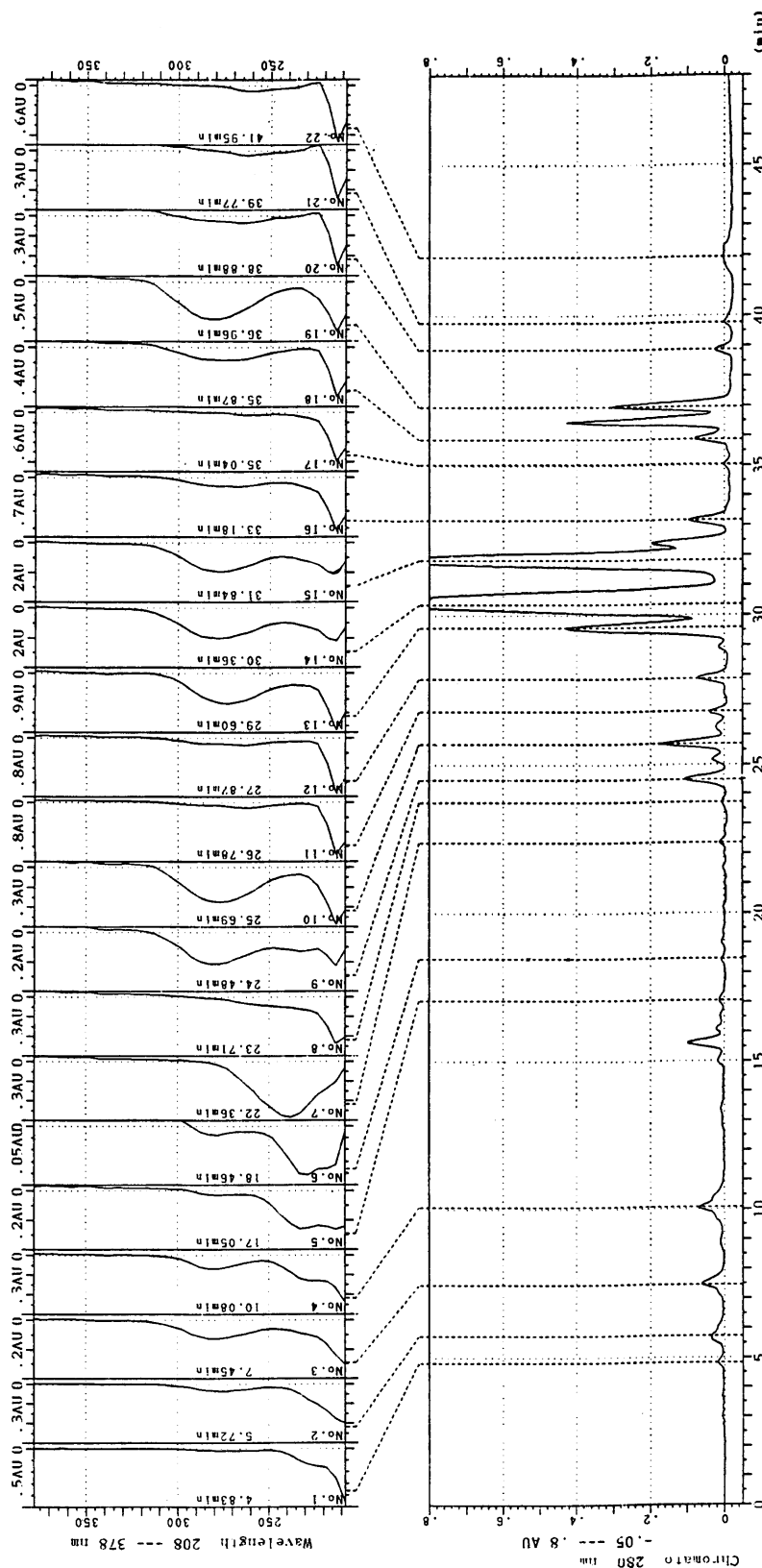


Fig. 3 HPLC analysis of the semipurified taxine extract. Conditions: Luna C₁₈ Column (Phenomenex) eluted with a gradient program of methanol (B) over 0.05 M CH₃COONH₄ (A). Initially A:B 65:35 v/v, linearly to A:B 25:75 v/v (38 min), then to A:B 0:100 v/v (38.1 min), stable at A:B 0:100 v/v till 44.5 min, then back to A:B 65:35 v/v at 45 min. Flow rate: 0.8 mL/min. Peak identities in Table 1. (From Ref. [11].)

Taxines Analysis by HPLC

5

Table 1 Chromatographic data obtained after the LC-PDA and LC-MS analysis of the purified taxine mixture on the Luna column

Compound	t_R (min)	$A_{227}/$ A_{249}	$A_{227}/$ A_{280}	$A_{249}/$ A_{280}	m/z
Taxane	13.5	3.57	10.66	2.96	N/Dt
10-DAB III	15.5	2.53	10.44	4.12	545
Taxane	17	3.8	10.12	2.78	N/Dt
Taxane	18.5	4.17	24.2	5.8	N/Dt
Ut	18.8	N/Dn	N/Dn	N/Dn	612
U	19.2	3.26	N/Dn	N/Dn	604
Taxane	20.3	3.22	15.1	4.72	584
U	22.4	1.16	13.1	11.36	584
2	24.5	2.03	0.93	0.46	568
1	25.4	1.62	1.08	0.66	542
3	25.8	1.21	1.10	0.92	626
Ut	25.8	N/Dn	N/Dn	N/Dn	642
5	26.8	1.60	1.12	0.66	568
Ut	27.4	N/Dn	N/Dn	N/Dn	628
Ut	27.7	1.97	0.94	0.48	584
Ut	29.6	1.30	2.25	1.73	628
4	30.4	1.16	1.13	0.98	584
5	31.8	1.28	1.23	0.96	584
7	32	1.85	0.93	0.47	626
Ut	32.3	3.83	N/Dn	N/Dn	610
U	32.6	5.63	3.25	0.57	784
8	33.1	1.75	0.88	0.51	668
Ut	33.6	1.75	0.90	0.50	612
Ut	36.5	1.44	0.32	0.45	668
Ut	37	1.90	0.45	0.32	610
Ut	38.9	3.77	1.19	0.31	654
Ut	39.5	2.18	1.02	0.47	610
9	41.4	1.88	1.50	0.80	652
Ut	41.9	N/Dn	N/Dn	N/Dn	668

Conditions as in Fig. 3.

U = unknown; Ut = unknown "taxine"; N/Dt = not detected; N/Dn = not determined.

(From Ref. [11].)

lyzed in reversed phase; nine taxines, one taxinine, and six taxanes were found present in the sample. Furthermore, 10-deacetyl baccatin III (paclitaxel's main precursor) and other taxanes were also found in the extract. Identification of the peaks was made with online LC-MS and offline NMR following fraction collection at the end of the HPLC. Retention and spectral data of the identified peaks were used as tool to screen for taxines and taxinines in plant and cell culture extracts. Several members of both groups of compounds were found in samples of various origin. LC-MS verified the presence of some of the known taxines and taxinines in extracts of *Taxus* needles, pollen, and seeds.^[9,10]

HPLC-PDA detection offers an alternative for the cost-effective separation of taxanes and taxines in complex

plant extracts. The spectrum index plots in Fig. 2 depict the chromatographic analysis of the taxine-purified extract on a C₁₈ column with gradient elution. The UV spectra of the detected peaks are illustrated in the upper part of the chromatogram. A clearer prospect of the corresponding spectra is given in Fig. 3. It can be seen that 227 nm represents the maximum for the UV spectrum of taxanes, whereas 280 nm is the λ_{\max} of taxinines and taxines. Hence, 280 nm can be used as a "selective" wavelength for the detection of taxines and taxinines. Use of absorbance ratios between three (or more) wavelengths can also provide a means of identification.^[12] The absorbance ratios obtained after the analysis of reference mixtures were as follows:

For 10-DAB III: $A_{227}/A_{215} = 1.67$, $A_{227}/A_{249} = 2.99$,
 $A_{215}/A_{249} = 1.78$.

For taxol: $A_{227}/A_{215} = 1.35$, $A_{227}/A_{249} = 3.51$, $A_{215}/A_{249} = 2.55$.

Comparison of these values with the ones calculated from peaks eluting at similar retention times in the analysis of extracts could be a fast way to verify the identity and to check the peak purity. Analysis of the semipurified taxine mixture by gradient HPLC-DAD revealed the presence of seven taxanes with 10-deacetyl baccatin III (10-DAB III) among them. All the nine expected taxines were positively identified (Table 1).

CONCLUDING REMARKS

Taxines were the subject of very few reported works over the last two decades although, until the 1960s, they were in the heart of phytochemical work on *Taxus*. The major reason for this is the instability of taxines and the unavailability of reference compounds. It can be concluded that HPLC seems to be the best method for the analysis of taxines because all the publications reporting on the analysis of taxines employ HPLC. Since taxines are abundant in plants, they could offer an attractive alternative for the supply of high-value taxanes by semisynthesis.

REFERENCES

1. Kingston, D.G.I. Natural Taxoids: Structure and Chemistry. In *Paclitaxel Science and Application*; Suffness, M., Ed.; CRC Press: Boca Raton, 1995; 287–315.
2. Appendino, G. Naturally Occurring Taxanes. In *The Chemistry and Pharmacology of Paclitaxel and Its Derivatives*; Farina, V., Ed.; Elsevier: Amsterdam, 1995; 7–53.



3. Baxter, J.N.; Lythgoe, B.; Scales, B.; Scrowston, R.M.; Trippet, S. Taxine: Part I. Isolation studies and the functional group of *O*-cinnamoytaxicin-I. *J. Chem. Soc.* **1962**, 2964–2971.
4. Ettouati, L.; Ahond, A.; Poupat, C.; Potier, P. Revision structurale de la Taxine B, alcaloïde majoritaire des feuilles de l'if Europe, *Taxus baccata*. *J. Nat. Prod.* **1991**, *54*, 1455–1458.
5. Jenniskens, L.H.D.; van Rozendaal, E.L.M.; van Beek, T.A.; Wiegerinck, P.H.G.; Scheeren, H.W. Identification of six taxine alkaloids from *Taxus baccata* needles. *J. Nat. Prod.* **1996**, *59*, 117–123.
6. Adeline, M.T.; Wang, X.P.; Poupat, C.; Ahod, A.; Potier, P. Evaluation of taxoids from *Taxus* sp. crude extracts by high performance liquid chromatography. *J. Liq. Chromatogr. Relat. Technol.* **1997**, *20*, 3135–3145.
7. VanHaelen-Fastre, R.; Diallo, B.; Jaziri, M.; Faes, M.-L.; Homes VanHaelen, M. High speed countercurrent chromatography separation of taxol and related diterpenoids from *Taxus baccata*. *J. Liq. Chromatogr.* **1992**, *15*, 697–706.
8. Theodoridis, G.; Verpoorte, R. Taxol analysis by HPLC. A review. *Phytochem. Anal.* **1996**, *7*, 169–184.
9. Theodoridis, G.; Laskaris, G.; Verpoorte, R. HPLC analysis of taxoids in plant and plant cell tissue culture. *Am. Biotechnol. Lab.* **1999**, *17*, 40–44.
10. Theodoridis, G.; Laskaris, G.; de Jong, C.; Hofte, A.J.P.; Verpoorte, R. Determination of paclitaxel and related diterpenoids in plant extracts by high performance liquid chromatography with UV detection in high performance liquid chromatography-mass spectrometry. *J. Chromatogr., A* **1998**, *802*, 297–305.
11. Theodoridis, G.; Laskaris, G.; van Rozendaal, E.L.M.; Verpoorte, R. Analysis of taxines in *Taxus* seeds, needles and cell culture by HPLC-PDA and HPLC-ESI-MS. *J. Liq. Chromatogr.* **2001**, *24*, 2267–2282.
12. Castor, T.P.; Tyler, T.A. Determination of taxol in *Taxus x media* needles in the presence of interfering components. *J. Liq. Chromatogr.* **1993**, *16*, 723–731.
13. Wilson, C.R.; Sauer, J.-M.; Hooser, S.B. Taxines: A review of the mechanism and toxicity of yew (*Taxus* spp.) alkaloids. *Toxicon* **2001**, *39*, 175–185.

Taxoids Analysis by TLC

Tomasz Mroczek

Kazimierz Głowniak

Medical University, Lublin, Poland

Introduction

Taxoids are diterpenoid compounds isolated from different yew species and possessing strong anticancer activity [1]. There are different chemical groups of natural taxoids, but among the most important taxoids is a group derived from 10-deacetylbaccatin III (10-DAB III), a diterpenoid compound occurring in high concentration in the European yew, *Taxus baccata* L. It possesses a scheme of structure of four skeletons (6/8/6/4-membered) which was named taxan and 10-DAB III is a derivative of hexahydroxy-11-taxen-9-one. Baccatin III, which is another compound from this group, has, additionally, an acetyl group estrified with the β -OH group at position C-10. Paclitaxel and cephalomannine are less polar taxoids because they possess amide-acid side chains at position C-13. In the case of paclitaxel, this is (2*R*,3*S*)-*N*-benzoyl-3-phenylserine and cephalomannine (2*R*,3*S*)-*N*-tigloyl-3-phenylserine side chains. There are also compounds in this group which have an epimer OH group at position C-7 and other substituents are also met [1]. Thus, there are many compounds usually with similar polarity and small differences in structure which are, thus, difficult to separate.

Discussion

Thin-layer chromatography (TLC) is mainly applied in micropreparative taxoids separation [2–4]. Silica gel 60F₂₅₄ preparative plates are usually applied for this purpose. The problem of taxoids separation involves not only their similar chemical structure (e.g., paclitaxel versus cephalomannine) but also, due to different coextracted compounds usually encountered in crude yew extracts (polar compounds such as phenolics and nonpolar ones such as chlorophylls and biflavones), the separation is very difficult. The common band of paclitaxel and cephalomannine was satisfactorily resolved from an extraneous fraction in isocratic elution with ethyl acetate as a polar modifier [4] and *n*-heptane–dichloromethane as the solvent mixture and it was of suitable purity for high-performance liquid chromatography (HPLC) quantitative determination.

The combination of micropreparative TLC separation of callus extract of *Taxus baccata* with *n*-hexane–ethyl acetate (2:3) mobile phase and preparative HPLC on a Lichrosorb RP-18 column enabled 10-deacetylbaccatin III isolation [3].

Systematic studies on the selection of the best mobile phases to assure the best micropreparative separation of analyzed taxoids, especially of 10-DAB III, as well as its less polar derivatives: baccatin III, paclitaxel, and cephalomannine obtained from the extracts of fresh and dried needles and stems of *Taxus baccata* L. by Głowniak and Mroczek have been undertaken [2]. The TLC investigation on silica gel included solvent systems with one and two polar modifiers, multicomponent mobile phases, as well as some multiple development techniques and gradient elution. As polar modifiers, methanol, acetone, dioxane, ethyl acetate and ethylmethylketone, as well as their mixtures, have been reinvestigated, but dichloromethane, chloroform, benzene, toluene, heptane, and their mixtures were used as solvents.

Using binary mobile phases containing 25–30% of one polar electron-donor modifier (acetone, dioxane) in dichloromethane or chloroform, high values of separation factor α (10-DAB III/paclitaxel) are observed as well as low elution of polar extraneous compounds. Such chromatographic systems can be applied to separation by column chromatography of polar from less polar taxoids and their polar coextracted compounds in preliminary CC investigations on taxoids before further detailed studies.

The addition (already about 15%) of a small amount of π -electron solvents such as benzene improves the separation of the band of less polar taxoids (paclitaxel, cephalomannine) and closely eluted chlorophylls.

The mobile phases with two polar modifiers (acetone–methanol, ethylmethylketone–methanol) assure relatively high values of the α factor and the separation in the area of less polar taxoids is better in comparison with the separation obtained by single electron-donor mobile phases.

Because of the complexity of the composition of yew extracts, different gradient elution programs can



be considered as further steps of detailed CC or TLC separations of different taxoids on silica gel.

The multicomponent solvent system consisted of benzene–chloroform–acetone–methanol (20:92.5:15:7.5), developed over a distance of 15 cm (2x; in some cases, a third development was necessary) enabled very good separation of coextracted compounds, both with 10-DAB III and paclitaxel as well as the separation of the whole yew extract (*Taxus baccata*), which was also very good. The separation of taxoids was better in the extracts obtained from fresh needles and stems than from the dried plant material. The extracts from the dried needles contained the highest concentrations of extraneous compounds which interfered with the bands of analyzed taxoids. The common band of paclitaxel, cephalomannine, and baccatin III was satisfactorily purified from coextractives; the 10-DAB III band could be easily isolated and further HPLC determination in two isocratic mobile phases have been applied. The investigated taxoids eluted in the following order: paclitaxel + cephalomannine, baccatin III, and 10-DAB III. Interesting was the considerable slope of baccatin III retention on silica gel in comparison with retention of its 10-deacetyl derivative (10-DAB III) (the separation factor α of 10-DAB III/baccatin III amounted to 2.8) [2]. This indicates an increase of hydrophobic properties in the molecule of baccatin III. Such chromatographic behavior of baccatin III can be explained, first, by the absence of a free OH group at position C-10, capable of effectively competing with free OH groups on the surface of silica gel (hydrogen-bonding interactions) but, on the other hand, the presence of an acetyl (ester) group at position C-10 can impede adsorption of baccatin III on silica gel caused by hydrogen-bonding interactions between the carbonyl group at position C-9 and OH groups on the surface of silica gel (a type of spherical hindrance, observed in computer modeling of spatial structures of taxoids by HYPERCHEM) because a role of this carbonyl group in polar properties of taxoids was confirmed by analysis of ¹H-NMR (nuclear magnetic resonance) spectra. This can be responsible for the decrease of baccatin III retention on silica gel, which is similar to the retention of paclitaxel and cephalomannine; both possess the acetyl group at position C-10 and low-polarity side chain at position C-13. Because of a very slight difference in the structure of the amide substituent of the acyl side chain at position C-13 (*N*-benzoyl versus *N*-tigloyl) and low polarities, these two compounds have the same retention on silica gel.

Similar solvent systems can be applied for analytical TLC of taxoids in screening of, for example, callus cultures for taxoids presence [5].

The reversed-phase TLC system [stationary phase: RP-18F254s; mobile phase: water–methanol–tetrahydrofuran 5:2:3 (v/v/v) applied two times] was used in analysis of taxoids fractions obtained after high-speed countercurrent chromatography isolation and was suitable for paclitaxel and cephalomannine qualitative determination [6].

The TLC–densitometric paclitaxel determination in different yew samples with two-stage gradient development has been also attempted [7], but, due to the high concentration of coextractives, it is difficult to estimate the precision of this method.

Stasko et al. [8] elaborated two interesting procedures of multimodal TLC for the separation of taxol and related compounds from *Taxus brevifolia*. For the first procedure, a cyano-modified silica gel plate was developed, in the first dimension, in dichloromethane–hexane–acetic acid (9:10:1) and, in the second dimension, in water–acetonitrile–methanol–tetrahydrofuran (8:5:7:0.1). For the second procedure, a diphenyl-modified silica gel plate was developed, in the first dimension, in hexane–isopropanol–acetone (15:2:3) and, in the second dimension, in methanol–water (7:3). These two methods enabled paclitaxel resolution from cephalomannine, which is impossible on silica gel plates, and at least another 20 compounds.

Besides typical ultraviolet detection on plates with a fluorescent agent (F_{254}), different visualization methods can be applied:

1. Anisaldehyde spray reagent [8] (76% methanol, 19% *o*-phosphoric acid, and 5% *p*-anisaldehyde followed by heating at 110°C for 5 min. Paclitaxel appeared as a gray–brown spot.
2. A 3% sulfuric acid methanolic solution followed by heating at 115°C for 5 min (visualization: UV at 366 nm and VIS) [6].
3. A 3% sulfuric acid ethanolic solution, then a 1.5% solution of vanillin in ethanol, followed by heating at 105°C for 10 min [5]. DAB III appeared as a gray spot.

Summing up this entry, it should be stated that because of differences in taxoids' and other compounds' compositions in different yew and yew-derived materials, a suitable approach for TLC taxoids separation ought to include problems involving both taxoids separation and appropriate separation of coextracted compounds from taxoids which usually are in higher concentration. The separation method should also be elaborated precisely for each type of extract.

References

1. M. Suffness and G. A. Cordell, *Taxus* alkaloids, in *The Alkaloids (Chemistry and Pharmacology)* (A. Brossi, eds.), Academic Press, New York, 1985, Vol. 25, pp. 6–18.
2. K. Głowniak and T. Mroczek, *J. Liquid Chromatogr.* 22(16): 2483 (1999).
3. Zhiri, M. Jaziri, Y. Guo, R. Vanhaelen-Fastre, M. Vanhaelen, J. Homes, K. Yoshimatsu, and K. Shimomura, *Biol. Chem. Hoppe–Seyler* 376: 583–586 (1995).
4. K. Głowniak, G. Zgórk, A. Józefczyk, and M. Furmanowa, *J. Pharm. Biomed. Anal.* 14: 1215 (1996).
5. Y. Gou, M. Jaziri, B. Diallo, R. Vanhaelen-Fastre, A. Zhiri, M. Vanhaelen, J. Homes, and E. Bombardelli, *Biol. Chem. Hoppe–Seyler* 375: 281 (1994).
6. R. Vanhaelen-Fastre, B. Diallo, M. Jaziri, M. L. Faes, J. Homes, and M. Vanhaelen, *J. Liquid Chromatogr.* 15(4): 697 (1992).
7. G. Matysik, K. Głowniak, A. Józefczyk, and M. Furmanowa, *Chromatographia* 78(41): 485 (1995).
8. M. W. Stasko, K. M. Witherup, T. J. Ghiorzi, T. G. Mc Cloud, S. Look, G. M. Muschik, and H. J. Issaq, *J. Liquid Chromatogr.* 12(11): 2133 (1989).



Temperature Program: Anatomy

Raymond P.W. Scott

Scientific Detectors Ltd., Banbury, Oxfordshire, England

Introduction

The principle of temperature programming in gas chromatography (GC) is based on the thermodynamic explanation of retention and is employed for samples that have components that cover a wide range of polarities and/or molecular weights. Its purpose is to accelerate the late eluting peaks through the column to reduce the analysis time and, at the same time, to maintain symmetrical elution profiles that are amenable to accurate quantitative assessment. As the temperature is increased, the magnitude of the distribution coefficient with respect to the stationary phase is reduced and, as a consequence, the retention volume and retention time is reduced. The programming rate must be chosen such that the integrity of the separation is maintained and the peak shapes are not distorted.

Discussion

The programming procedure usually involves three stages. An initial isocratic period is introduced to efficiently separate the early eluting peaks with adequate resolution. The isocratic period is followed by a linear increase in column temperature with time, which accelerates the well-retained peaks so that they also elute in a reasonable time and are adequately resolved. The effect of linear programming can be calculated employing appropriate equations and the retention times of each solute predicted for different flow rates (see the entry Programmed Temperature Gas Chromatography). To do this, some basic retention data must be measured at two temperatures and the results are then employed in the retention calculations. The tempera-

ture program often ends with a final isothermal period. This is usually introduced either because the upper temperature limit of the stationary phase has been reached and so a higher temperature will damage the column, or to purge any remaining, strongly retained solutes from the column. The upper temperature limit of the stationary phase should not be exceeded, as not only will the column be spoiled but the performance of the detector is often impaired and deposits are formed that can permanently increase the detector noise.

Temperature programming is employed in most GC separations and the optimum programming conditions are usually easy to identify from a few preliminary separations using different gradients. If, however, there is a pair of solutes that elute close together (e.g., a pair of enantiomers) and there is a temperature of coelution, then some considerable effort may be necessary to identify the optimum temperature program [1] to achieve a satisfactory separation in a reasonable time. Such situations, however, are not common, unless the applications involves complex samples such as multicomponent chiral mixtures.

Reference

1. T. E. Beesley and R. P. W. Scott, *Chiral Chromatography*, John Wiley & Sons, Chichester, 1998, p. 39.

Suggested Further Reading

Scott, R. P. W., *Techniques of Chromatography*, Marcel Dekker, Inc., New York, 1995.

Scott, R. P. W., *Introduction to Analytical Gas Chromatography*, Marcel Dekker, Inc., New York, 1998.



Temperature: Effect on MEKC Separation

Koji Otsuka

Shigeru Terabe

Himeji Institute of Technology, Hyogo, Japan

Introduction

The distribution coefficient, K , of a solute for an equilibrium between the aqueous phase and micelle, or the micellar solubilization, depends on temperature; generally, the distribution coefficient decreases with an increase in temperature. This means that the migration time of a solute, t_R , will be reduced when the temperature is elevated under typical micellar electrokinetic chromatography (MEKC) conditions, where, for example, sodium dodecyl sulfate (SDS) is employed as a pseudo-stationary phase at a neutral condition (i.e., pH 7). Also, the velocity of the electro-osmotic flow (EOF), u_{EOF} , and the electrophoretic velocity of the micelle, u_{ep} (mc), will be increased by an increase in temperature because of a reduced viscosity of the micellar solution employed in a MEKC system.

Discussion

The increase in temperature during a separation is observed to be due to Joule heating: Ideally, the retention factor, k , should be independent of the applied voltage or current, but, actually, k does depend on the applied voltage. Although the temperature of the separation capillary is controlled with a liquid coolant or a circulating airstream in most commercially available capillary electrophoresis (CE) instruments, the retention factor usually decreases, almost linearly, with an increase in the velocity of the EOF or an increase in the current. However, the dependence is much less than that observed in a CE system without forced-cooling apparatus.

The critical micelle concentration (CMC) and the partial specific volume, \bar{v} , depend on the temperature. The relationship between k and K is represented as

$$k = K \left(\frac{V_{mc}}{V_{aq}} \right) \quad (1)$$

where V_{mc} and V_{aq} are the volumes of the micelle and the remaining aqueous phase, respectively. The phase ratio, V_{mc}/V_{aq} , is described as

$$\frac{V_{mc}}{V_{aq}} = \frac{\bar{v}(C_{sf} - CMC)}{1 - \bar{v}(C_{sf} - CMC)} \quad (2)$$

where C_{sf} is the surfactant concentration. Approximately, the volume of the micelle is negligible and, hence, Eq. (1) can be rewritten as

$$k = K\bar{v}(C_{sf} - CMC) \quad (3)$$

For example, the CMC of SDS and \bar{v} of the SDS micelle depend on temperature as presented in Table 1, where a 100-mM borate–50-mM phosphate buffer (pH 7.0) was used to prepare SDS solutions. It should be noted that the CMC value observed in a buffer solution or electrolyte solution is smaller than that in pure water (e.g., 8.1 mM at 20°C).

In MEKC, an ionic surfactant is used as a pseudo-stationary phase, and the Krafft point is also an important temperature. At a temperatures lower than the Krafft point, C_{sf} does not exceed the CMC, due to reduced solubility and, therefore, no micelle is formed. At the Krafft point, C_{sf} reaches the CMC and then the formation of the micelle is begun. The Krafft point of SDS is $\sim 16^\circ\text{C}$ in a pure water, whereas it is $\sim 31^\circ\text{C}$ for potassium dodecyl sulfate in pure water. Thus, a potassium salt is not an adequate buffer component for the SDS–MEKC system.

Table 1 CMC of SDS and \bar{v} of SDS Micelle Dependence on Temperature

Temp. (°C)	CMC (mM)	\bar{v} (mL/g)
20	—	0.8562
22	2.8	—
25	2.9	0.8610
30	2.5	0.8686
35	2.6	0.8710
40	3.0	0.8758



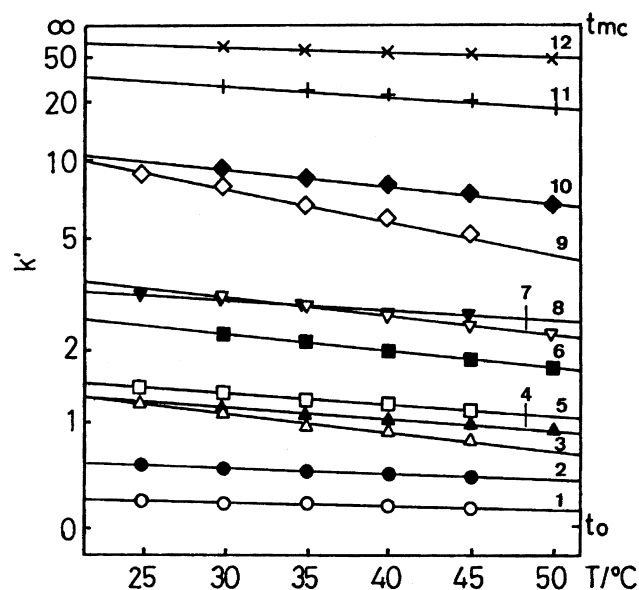


Fig. 1 Dependence of the retention factor, k' , on temperature, T . The solutes are (1) resorcinol, (2) phenol, (3) *p*-nitroaniline, (4) *o*-cresol, (5) nitrobenzene, (6) 2,6-xylenol, (7) 2,4-xylenol, (8) toluene, (9) 2-naphthol, (10) *p*-propylphenol, (11) *p*-butylphenol, and (12) *p*-amylphenol. Capillary: 50 μ m inner diameter \times 570 mm (effective length, 500 mm); separation solution: 50 mM SDS in 100 mM borate–50 mM phosphate buffer (pH 7.0); applied voltage: 15 kV; detection wavelength: 214 nm. Reprinted from Ref. 3, with permission.

Figure 1 shows the dependence of the distribution coefficients on temperature for several solutes in MEKC, where SDS is employed as a pseudo-stationary phase. Different dependencies are observed among the solutes; that is, temperature affects the selectivity.

As mentioned, temperature seriously affects the migration time, whereas its effect on selectivity is not remarkable. It is important to maintain temperature precisely to obtain reproducible results.

References

1. S. Terabe, K. Otsuka, and T. Ando, Electrokinetic chromatography with micellar solution and open-tubular capillary, *Anal. Chem.* 57: 834 (1985).
2. S. Terabe, T. Katsura, Y. Okada, Y. Ishihama, and K. Otsuka, Measurement of thermodynamic quantities of micellar solubilization by micellar electrokinetic chromatography with sodium dodecyl sulfate, *J. Microcol. Separ.* 5: 23 (1993).
3. S. Terabe, Micellar electrokinetic chromatography, in *Capillary Electrophoresis Technology* (N. A. Guzman, ed.), Chromatographic Science Series Vol. 64, Marcel Dekker, Inc., New York, 1993; Chap. 2.
4. K. Otsuka and S. Terabe, Micellar electrokinetic chromatography, *Bull. Chem. Soc. Jpn.* 71: 2465 (1998).

Temperature: Effects on Mobility, Selectivity, and Resolution in Capillary Electrophoresis

Jetse C. Reijenga

Eindhoven University of Technology, Eindhoven, The Netherlands

Introduction

Although not a major separation parameter, as in gas chromatography, the operating temperature clearly affects migration behavior in capillary electrophoresis (CE). This alone should be reason to work under uniform, well-thermostated conditions. The temperature affects bulk viscosity, electro-osmotic flow, ionic mobilities, even pK values and buffer pH.

Buffer Behavior

A buffer for electrophoresis is usually prepared at room temperature by adding ingredients and measuring the final pH. When this buffer is used for CE at a different temperature, a different pH might result. For example, when a buffer consists of Tris-acetate at pH 5, Tris is fully charged and the temperature dependence of pK of acetic acid is the one involved. This value is small so that the pH of the buffer is virtually inde-

pendent of temperature. This is not the case if the same buffer ingredients are used to prepare a buffer around pH 8; in that case, acetate is fully ionized and the pK of Tris is involved. This pK has a temperature coefficient of -0.031 per degree; a 10°C increase leads to a 0.31 decrease in buffer pH (Table 1).

In case of single-buffering background electrolyte solutions, the temperature coefficient of the buffer pH equals the temperature coefficient of the pK of the buffering ion. In case of a double-buffering system, pK 's of both buffer anion and buffer cation are involved, which obviously makes the situation potentially more complicated.

In some situations, the pH of the buffer can be very critical. An example of such a critical pair of components is given in Fig. 1; a mixture of benzoic and 2,3-dimethoxy benzoic acid, analyzed around pH 4.67. A

Table 1 pK Values and Their Temperature Dependence of Some Buffer Components

Name	pK (20°C)	dpK/dT
Phosphoric acid, pK_1	2.12	
Citric acid, pK_1	3.13	
Formic acid	3.75	-0.000
Glycine, pK_1	3.75	-0.000
Acetic acid	4.76	-0.000
Histidine	6.12	-0.045
MES	6.15	-0.011
ACES	6.90	-0.020
Imidazole	6.95	-0.018
MOPS	7.20	-0.006
HEPES	7.55	-0.014
Tris	8.30	-0.031
Boric acid	9.24	-0.007
CHES	9.50	-0.009
Glycine, pK_2	9.77	
CAPS	10.40	-0.009

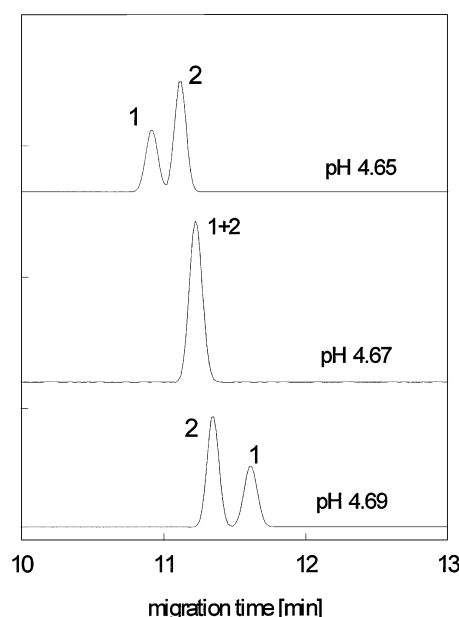


Fig. 1 Separation of benzoic acid (1) and 2,3-methoxy benzoic acid in 10 mM Tris-acetic acid buffer of three different pH values.



pH change of as little as 0.04 pH units will change the migration order.

Another aspect involved is buffer conductivity; on average, ionic conductivities have a temperature coefficient of around 2.5%/degree. A higher temperature, therefore (at constant voltage), leads to a higher current. This can have a significant effect on power dissipation and, through the corresponding plate-height terms, on separation efficiency (see the entry Band Broadening in Capillary Electrophoresis).

Sample Ion Behavior

Ionic mobilities generally have a temperature coefficient of around +2.5%/degree, but it is not exactly the same for all ions. Incidentally, water viscosity has a temperature coefficient of approximately -2.5%/degree. This sometimes leads to the erroneous conclusion that ionic mobility is, by definition, inversely proportional to liquid viscosity, which is an oversimplification, originating also from the following relationship:

$$\mu = \frac{q}{6\pi\eta r}$$

in which q is the effective charge, η is the liquid viscosity, and r is the radius. The misunderstanding is that, in

reality, the above relationship is valid only for rigid spherical particles, not necessarily for individual solvated ions.

For the electro-osmotic flow, temperature-induced viscosity change at the plane of shear for the electric double layer is more straightforward. Analysis times will generally shorten with increasing temperature.

Suggested Further Reading

- Boček, P., M. Deml, P. Gebauer, and V. Dolník, *Analytical Isotachophoresis*, VCH, Weinheim, 1988.
- Everaerts, F. M., J. L. Beckers, and Th. P. E. M. Verheggen, *Isotachophoresis: Theory, Instrumentation and Applications*, Elsevier, Amsterdam, 1976.
- Friedl, W., J. C. Reijenga, and E. Kenndler, *J. Chromatogr. A* 709: 163 (1995).
- Mohan, C., Buffers, in *A Guide for the Preparation and Use of Buffers in Biological Systems*, Calbiochem, San Diego, CA, 1997.
- Reijenga, J. C. and E. Kenndler, *J. Chromatogr. A* 659: 403 (1994).
- Reijenga, J. C. and E. Kenndler, *J. Chromatogr. A* 659: 417 (1994).
- Reijenga, J. C., Th. P. E. M. Verheggen, J. H. P. A. Martens, and F. M. Everaerts, *J. Chromatogr. A* 744: 147 (1996).



Terpenoids, Separation by HPLC

Gabriela Cimpan

Tonbridge, Kent, United Kingdom

INTRODUCTION

Terpenoids are C_{10} and C_{15} , usually volatile, organic compounds derived from plants; they are generally associated with characteristic fragrances. Some terpenes are alcohols (e.g., menthol from peppermint oil), and some terpenes are aldehydes (e.g., citronellal). Terpenes are made up of isoprene (C_5) units. Because terpenoids occur in complex mixtures in natural products or in plants, chromatography is a powerful method for their separation and further analysis. Gas chromatography provides good separations and low detection limits for the volatile compounds. This was the reason for the delay in the development of high-performance liquid chromatography (HPLC) methods for terpenoids and has become the method of choice for the nonvolatile, thermolabile, or polar compounds.

OVERVIEW

High-performance liquid chromatography can be used as a separation method of volatile compounds, followed by GC or GC-MS for further separation and analysis. The most common assay is performed by reversed-phase HPLC, usually on C_{18} , when the separation of the compounds is according to their hydrophobicity, i.e., according to chain length and polar groups.

Sonication and liquid chromatography are a rapid pair of techniques for extraction and fractionation of plant material. The method combines extraction by sonication with a mixture of nonmiscible solvents, rapid preseparation of the crude extract by vacuum-liquid chromatography (silica gel 60H), and separation by preparative, reversed-phase HPLC or classical liquid chromatography with polyvinylpyrrolidone.

High-performance liquid chromatography can be also used as an analytical method for the separation, identification, and quantification of terpenoids.

TERPENOID ANALYSIS

The use of diode-array detection is limited because many of the terpenoids do not have chromophores for the UV

region. Refractive index, evaporative light scattering detectors (ELSD), or low-UV detectors can overcome, to a certain extent, this problem. However, the refractive index detector has a lower sensitivity compared with the spectrophotometric detectors, and it will not be useful for trace analysis. The organic solvents used for the mobile phase composition absorb the low UV radiation, and this is another problem for the terpenoids analysis by HPLC.

Temperature influences dramatically the separations; in the literature, assays can be found performed at -15°C , with pentane as mobile phase on LiChrosorb Si60.

The stationary phase is usually C_8 or C_{18} , but the use of Spherisorb CN or Nucleosil columns was also reported. The mobile phase for reversed-phase chromatography is aqueous, while, for normal-phase chromatography, it generally contains pentane or hexane. The elution can be isocratic or with a gradient. The detection is usually UV in the range 116–254 nm.

One of the most studied plants is *Ginkgo biloba* because of its medical applications. *Ginkgolides* are a group of unique terpene lactones with properties of improving cardiovascular and cerebrovascular activities. Ginkgo terpene lactones have very weak absorption below 220 nm; therefore HPLC cannot be coupled with UV detection methods. Infrared was proposed as an alternative, but HPLC-MS and HPLC-NMR have produced the best results in terms of simplicity, sensitivity, and selectivity. High-performance liquid chromatography-evaporative light scattering detection (HPLC-ELSD) is an economic option for this type of measurements.

Ginkgolide A, B, C, and bilobalide in *G. biloba* leaves were determined simultaneously by RP-HPLC-ELSD. Methanolic extracts (10%) of the leaves were cleaned up by solid phase extraction via polyamide cartridge and silica gel cartridge, successively. RP-HPLC was carried out on a C_{18} column with MeOH– H_2O as mobile phase, eluted in gradient mode, and detected by ELSD. The poor linear response of ELSD could be compensated by multilevel calibration and logarithmic calculation. Methanol–water–orthophosphoric acid mobile phase was used in conjunction with refractive index (RI) detection.

Terpenes in *G. biloba* L. extracts were analyzed on a column packed with C_8 Nucleosil 300, and ProOH–THF– H_2O was used as the mobile phase with detection at 220 nm.

High-performance liquid chromatography was the first method of choice for the nonvolatile terpenes as terpene trilactones. The analysis is performed by RP-HPLC on C₁₈ with isocratic development either in methanol–water or methanol–water–THF. Detection can be carried out by UV (taking into consideration poor UV absorption of the compounds), RI, ELSD, or MS.

Sesquiterpenes

Sesquiterpenes are C-15 terpenoids which can be found in natural products as hydrocarbons, oxygenated forms (aldehydes, ketones, etc.), or lactones. Sesquiterpene lactones can be found in a limited number of plant species and often have therapeutic properties.

The major constituents of the plant *Ambrosia maritima* L. were isolated using TLC and identified by IR and GC-MS. From HPLC screening, ambrosin and damsine were detected at high levels in the leaves and flowers, while stems and seeds contained only traces. Sesquiterpenes from *Aucklandia lappa* (Decne.) were determined by HPLC. A Shim-pack CLC-ODS column (6.0 × 150 mm) was used as separation column, MeOH–H₂O (65:35) as mobile phase, and the detection wavelength was 225 nm.

The GC-MS and HPLC analyses of oils from *Salvia sclarea* provided a comparative analysis profile of different plant materials. Sesquiterpene hydrocarbons (e.g., germacrene D and β-caryophyllene), monoterpene alcohols (e.g., α-terpineol), diterpenoids (mainly sclareol), monoterpene hydrocarbons (e.g., myrcene, limonene, and the two ocimene isomers), and the principal components (linalyl acetate and linalool) were analyzed.

Two comparable procedures of reverse-phase HPLC with spectrophotometric detection at 254 nm, with mobile phases of MeOH–0.05 M acetate buffer (70:30) or THF–0.01 M phosphate buffer (55:45), were used to resolve leukomisin, matricarin, austrocin, anhydroaustrocin, and potential antiarteriosclerotic sesquiterpene lactones from aerial parts of *Artemisia leucodes*.

A new HPLC technique has been developed for the rapid analysis of sesquiterpene phytoalexins such as capsidiol, rishitin, luminin, and phytuberol. This method employs a cyanopropyl-bonded phase column with an isocratic mixture of hexane and isopropanol. Flame ionization and UV detection were used for the analysis of capsidiol, rishitin, lubimin, phytuberol, and debneyol. Although both detectors proved to be useful, the signal response with the flame ionization detector was proportional to the mass of each of the phytoalexins, while the signal with the UV detector was proportional to the number of carbon–carbon bonds in each of the compounds.

The antifungal sesquiterpene dialdehydes polygodial and warburganal, from *Polygonum hydropiper*, were determined by HPLC on an ODS column using methanol–

H₂O as a mobile phase. These sesquiterpene dialdehydes were accumulated in young leaves and shoots and possessed antifungal activity.

Fourteen sesquiterpenes of *Petasites hybridus* (L.) G.M. et Sch. were separated on a normal-phase Nucleosil 100-3 column with hexane-diisopropyl ether-acetonitrile mixtures as eluents and photodiode array detection.

Sesquiterpenes were also separated by chiral chromatography on a Chiracel OD column.

Sometimes, the analyzed compounds absorb significantly only below 220 nm. In this case, postcolumn derivatization was used for a better UV detection.

Terpenes

A liquid chromatography-tandem mass spectrometry (LC-MS-MS) method was developed to detect tumor-promoting diterpene esters of the tiglane and ingenane types within plant extracts. Fractionation on a C₁₈ HPLC column was followed by MS-MS-multiple reaction monitoring (MRM).

Liquid chromatographic-thermospray mass spectrometry was used for the analysis of crude plant extracts containing phenolic and terpene glycosides. In crude plant extracts, constituents of biological or pharmaceutical interest often exist in the form of glycosides. Mass spectral investigations of these metabolites require soft ionization techniques such as desorption chemical ionization (D/CI) or fast atom bombardment if information on molecular mass or sugar sequence is desired. Thermospray (TSP) provides mass spectra similar to those obtained with positive-ion D/CI-MS using NH₃ and thus is potentially applicable to on-line analyses for these compounds and can be applied to plant extract analysis. Extracts of Gentianaceae, Polygalaceae, and Leguminosae species have been screened by LC-TSP-MS. High-performance liquid chromatography was performed on reversed-phase columns using methanol–water or acetonitrile–water gradients. Good optimization of the temperature of the source and the vaporizer was crucial for the observation of pseudomolecular ions of glycosides.

Triterpenes

Bisdesmosidic triterpene saponins were isolated from the aquatic plant *Ranunculus fluitans* L. (Ranunculaceae) in the Rhine river. The saponin structures were established by the identification of the aglycon and sugar moieties by HPLC and chiral capillary zone electrophoresis (CZE), ion-spray LC/MS, and extensive 1-D and 2-D homonuclear and heteronuclear NMR spectroscopy.

Many triterpene derivatives (some of them being new compounds) were isolated from the AcOEt fraction of Brazilian medicinal plant *Caruca*, *Cordia multispicata*



(Boraginaceae). The separation was performed on silica gel and reversed-phase HPLC columns, and the structures were elucidated by means of spectral methods, especially with 2-D NMR.

Several ginsenosides, previously obtained from *Panax ginseng* and *Panax notoginseng*, were analyzed by HPLC.

A new HPLC method permitted the separation of 13 triterpene glycosides isolated from different *Astragalus* species within 40 min. A water/acetonitrile gradient was used as eluent, RP-18 was used as stationary phase, and evaporative light scattering detection was used. The method facilitated differentiation of different *Astragalus* species.

Preparative High-Performance Liquid Chromatography

Successful preparative separations were obtained for pure compounds by RP-HPLC. When normal-phase chromatography was used, better results were obtained if the silica-based stationary phase was treated with silver ions.

Preparative HPLC was used to separate sterols and triterpene alcohols from the unsaponifiable matter in plant oils from *Camellia weiningensis* L., *Brassica juncea* L., and *Microula sikkimensis*. The isolated compounds were acetylated and further purified by AgNO₃-impregnated silica gel preparative thin layer chromatography (TLC). The identification was done by IR and MS.

Oryzanols are mixtures of ferulic acid esters of triterpene alcohols and plant sterols. Oryzanols were extracted from crude rice by column chromatography on a silica gel column using different volumes and ratios of hexane and di-Et ether. The fraction containing 18% oryzanol was further enriched by rechromatography, then 98% pure oryzanol was crystallized.

Coupled Methods with High-Performance Liquid Chromatography

High-performance liquid chromatography can be coupled, on-line, with high-resolution gas chromatography (HRGC) and MS. Gas chromatography allows the separation of chemically similar compounds from the previous separation provided by HPLC between the compounds with different polarities.

When thermolabile compounds are present, GC cannot be used, so MS can be coupled directly with HPLC. Care should be taken when using ionization methods, as MS does not provide a characteristic fragment pattern and the molecule cannot be identified precisely.

Natural products are often sources for drugs. When screening a natural compound extract, many of the analyzed compounds have been analyzed previously; therefore a method capable of selecting the new compounds such as HPLC-NMR-MS is very useful. Many plant extracts were analyzed by this method. Alternatively, HPLC-UV-MS can be used to obtain rich spectral information [application on *Tanacetum parthenium* (L.) Schultz Bip., Asteraceae].

FURTHER READING

- Li, W.; Fitzloff, J.F. J. Pharm. Biomed. Anal. **2002**, 30, 67–75.
- Merfort, I. J. Chromatogr., A **2002**, 967, 115–130.
- Nishii, Y.; Yoshida, T.; Tanabe, Y. Biosci. Biotechnol. Biochem. **1997**, 61, 547.
- van Beek, T.A. J. Chromatogr., A **2002**, 967, 21–55.
- Vogg, G.; Achatz, A.; Kettrup, A.; Sandermann, A., Jr. J. Chromatogr., A **1999**, 855, 563–573.
- Wilson, I.D. J. Chromatogr., A **2000**, 892, 315–327.



Theory and Mechanism of Thin-Layer Chromatography

Teresa Kowalska

Institute of Chemistry, Silesian University, Katowice, Poland

Wojciech Prus

Technical University of Łódź, Bielsko-Biała, Poland

Introduction

General classification of the modes of thin-layer chromatography (TLC) is based on the chemical nature of the stationary and mobile phases. The following three types of thin-layer chromatography given are widely recognized as different modes:

Adsorption TLC

In this mode, active inorganic adsorbents (e.g., silica, alumina, or Florisil) are usually employed as stationary phases and, hence, the overall mechanism of retention is governed predominantly by the specific intermolecular interactions between the functionalities of the solutes, on the one hand, and active sites on the adsorbent surface, on the other. In adsorption TLC, aqueous mobile phases are never used, and stationary-phase activity prevails over the polarity of the mobile phase employed.

Normal-Phase TLC

This mode of chromatography usually involves organic chemically bonded stationary phases with polar (e.g., 3-cyanopropyl) ligands. This particular mode is characterized by a mixed mechanism of solute retention: Solute molecules interact specifically with the polar functionalities of the organic ligand and with the residual active sites of the silica matrix, whereas their interactions with the hydrocarbon moiety of the organic ligands are entirely nonspecific in nature. Again, aqueous mobile phases are never employed in normal-phase (NP) TLC, and stationary phase activity prevails over the polarity of the mobile phase employed.

Reversed-Phase TLC

This chromatographic mode usually involves aliphatic chemically bonded stationary phases with,

for example, octyl, octadecyl, or phenyl ligands. The mode of chromatography also is characterized by a mixed mechanism of solute retention: Solute molecules interact specifically with the residual active sites of the silica matrix, whereas their interactions with the aliphatic ligands are nonspecific (and predominantly hydrophobic) in nature. Reversed-phase (RP) TLC is usually performed with aqueous mobile phases containing organic modifiers [such as, e.g., methanol, acetonitrile (ACN), tetrahydrofuran (THF), etc.], and in this case, the activity of the stationary phase — as an exception — is less than that of the high-polarity mobile phase employed.

TLC Parameters of Solute Retention

The parameter R_f is the quantity most commonly used to express the position of a solute in the developed chromatogram. It is calculated as a ratio:

$$R_f = \frac{\text{Distance of chromatographic spot center from origin}}{\text{Distance of solvent front from origin}} \quad (1)$$

Using symbols from Fig. 1, R_f can be given as

$$R_f = \frac{z}{l} \quad (2)$$

R_f values vary between 0 (solute remains at the origin) and 0.999 (solute migrates with the mobile-phase front). From a practical standpoint, the most reliable analytical results are achieved when the parameter R_f ranges from 0.20 to 0.80.

In the theory and practice of chromatography, another parameter of solute retention is also employed, the so-called R_M value. This quantity was defined by Bate-Smith and Westall [1] as

$$R_M = \log\left(\frac{1 - R_f}{R_f}\right) \quad (3)$$



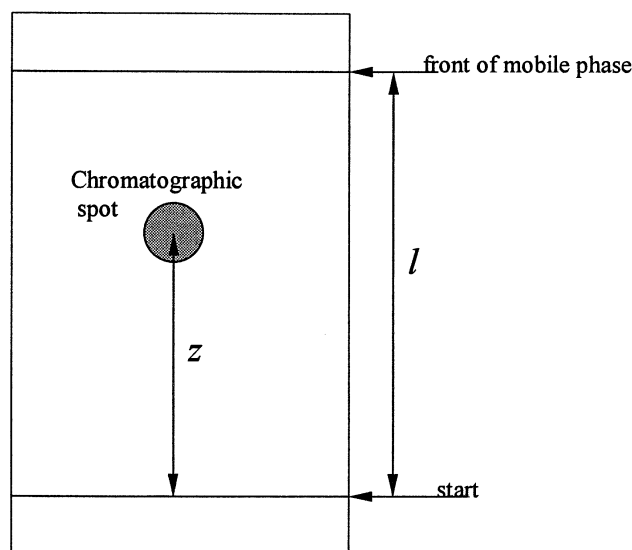


Fig. 1 The thin-layer parameters used to calculate the retention parameter R_f .

Selected Models of the Chromatographic Process

The adsorption and partition mechanisms of solute retention are the two most universal mechanisms of chromatographic separation, both operating on a physical principle. In fact, almost all solutes can be adsorbed on a microporous solid surface or be partitioned between two immiscible liquids. It is the main aim of semiempirical chromatographic models to couple the empirical parameters of retention with the established thermodynamic quantities generally used in physical chemistry. The validity of these models in chromatographic practice can hardly be overestimated, because when incorporated in separation selectivity-oriented optimization strategies, they often successfully help overcome the old trial-and-error approach used to optimize analyses. In the forthcoming sections, we will discuss a selection of the most popular and best-performing models and concepts of solute retention.

Martin and Synge Model of Partition Chromatography

Partition chromatography was the first chromatographic technique to be given a thermodynamic foundation, by the pioneering work of Martin and Synge [2], the 1952 Nobel Prize winners for chemistry. The

Theory and Mechanism of Thin-Layer Chromatography

Martin and Synge model describes the idealized parameter R_f (i.e., the parameter R'_f) as

$$R'_f = \frac{t_m}{t_m + t_s} = \frac{n_m}{n_m + n_s} = \frac{m_m}{m_m + m_s} \quad (4)$$

(I) (II) (III)

where t_m and t_s denote the time spent by a solute molecule in the mobile and stationary phases, respectively, n_m and n_s are numbers of solute molecules present in the mobile and stationary phases at equilibrium, and m_m and m_s are the respective numbers of moles.

Equation (4) can be further transformed as follows:

$$R'_f = \frac{m_m}{m_m + m_s} = \frac{c_m V_m}{c_m V_m + c_s V_s} = \frac{1}{1 + c_s V_s / c_m V_m} \quad (5)$$

where c_m and c_s are the molar concentrations of the solute in the mobile and stationary phases, respectively, and V_m and V_s are volumes of these phases, respectively.

Assuming that

$$K = \frac{c_s}{c_m} \quad (6)$$

where K is the thermodynamic equilibrium constant for solute partitioning, we obtain

$$R_f = \frac{1}{1 + K\Phi} \quad (7)$$

where Φ is the so-called phase ratio (i.e., $\Phi = V_s/V_m$).

Equation (7) unites the empirical retention parameter of the solute, R'_f , with the established thermodynamic (i.e., theoretical) quantity K , expressed as

$$\ln K = \frac{\Delta\mu_p^0}{RT} \quad (8)$$

where $\Delta\mu_p^0$ is the standard chemical potential for partition. Hence, the retention model given by Eq. (8) can rightfully be called semiempirical.

Snyder and Soczewinski Model of Adsorption Chromatography

The semiempirical model of adsorption chromatography, analogous to that of Martin and Synge, was established only in the late 1960s by Snyder [3] and Soczewinski [4] independently, and it is often referred to as the displacement model of solute retention. The crucial assumption of this model is that the mechanism of retention consists in competition among the solute and solvent molecules for the active sites of the adsorbent and, hence, in a virtually

endless process of the solvent molecules displacing those of the solute from the solid surface (and vice versa). Further, the authors assumed that some of the mobile phase remains adsorbed and stagnant on an adsorbent surface. This adsorbed mobile phase formally resembles the liquid stationary phase in partition chromatography. Thus—utilizing with imagination the main concept of the Martin and Synge model of partition chromatography—Snyder and Soczewinski managed to define the R_f' parameter valid for adsorption chromatography as

$$R_f' = \frac{t_m}{t_m + t_a} \equiv \frac{n_m}{n_m + n_a} = \frac{m_m}{m_m + m_a} \quad (9)$$

$$= \frac{c_m(V_m - V_a W_a)}{c_m(V_m - V_a W_a) + c_a V_a W_a}$$

where t_m and t_a denote the time spent by a solute molecule in the mobile phase and on the adsorbent surface, respectively, n_m and n_a are numbers of solute molecules contained in the mobile phase and on the adsorbent surface at equilibrium, respectively, m_m and m_a are the numbers of moles of solute molecules contained in the nonadsorbed and adsorbed moieties of the mobile phase, respectively, c_m and c_a are molar concentrations of solute in the nonadsorbed and the adsorbed moieties of mobile phase, respectively, V_m is the total volume of mobile phase, V_a is the volume of the adsorbed mobile phase per unit mass of adsorbent, and W_a is the mass of adsorbent considered.

Transformation of Eq. (9) results in the relationship

$$R_f' = \frac{1}{1 + K_{th}[V_a W_a / (V_m - V_a W_a)]} \quad (10)$$

where $K_{th} = c_a/c_m$, K_{th} being the thermodynamic equilibrium constant of adsorption, and $\Phi = V_a W_a / (V_m - V_a W_a)$.

Simplified Relationships Derived from the Snyder and Soczewinski Model

Two very simple relationships have been derived from the general framework of the Snyder and Soczewinski model of adsorption chromatography; these have proved useful for rapid prediction of solute retention in chromatographic systems employing binary mobile phases. One (known as the Soczewinski equation) proved successful for adsorption and normal-phase TLC; the other (known as the Snyder equation) proved similarly successful in reversed-phase TLC.

Soczewinski Equation

The Soczewinski equation [5] [Eq. (11)] is a simple linear relationship with respect to $\log X_s$, linking the retention parameter (i.e., R_m) of a given solute with the quantitative composition of the binary mobile phase used:

$$R_M = C - n \log X_s \quad (11)$$

where C is, in the first instance, the equation constant (although with clear physicochemical significance), X_s is the molar fraction of the stronger solvent in the non-aqueous mobile phase, and n is the number of active sites on the surface of the adsorbent.

Apart from enabling rapid prediction of solute retention, the Soczewinski equation enables molecular-level scrutiny of solute–stationary phase interactions. Thus, a numeric value of the parameter n of Eq. (11) of approximately unity ($n \approx 1$) implies one-point attachment of the solute molecule to the stationary-phase surface. Numerical values of n higher than unity indicate that in a given chromatographic system, solute molecules interact with the stationary phase at more than one point (so-called multipoint attachment).

Snyder Equation

The Snyder equation [6] [Eq. (12)] is another simple linear relationship with respect to φ , which links the retention parameter (i.e., $\ln k$) of a given solute with the volume fraction of the organic modifier in the aqueous binary mobile phase (φ):

$$\ln k = \ln k_w - S\varphi \quad (12)$$

where k is the retention coefficient of the solute [$k = (1 - R_f)/R_f$], k_w is the retention coefficient extrapolated for pure water as the mobile phase, and S is a constant characteristic of a given stationary phase.

Chromatographic Activity of Adsorbents and Elution Strength of Solvents [7–9]

Consequences of the Snyder and Soczewinski model are manifold, and they are of significant practical importance. The most spectacular conclusions of this model are (a) the possibility of quantifying the activity of an adsorbent and (b) the possibility of defining and quantifying the “chromatographic polarity” of solvents (known as their elution strength). These two conclusions could be drawn only upon the assumption of the displacement mechanism of solute retention. An obvi-



ous necessity in this model was to quantify the effect of displacement, which resulted in the relationship given by Eq. (13) for the thermodynamic equilibrium constant of adsorption, K_{th} , for an active chromatographic adsorbent and a monocomponent mobile phase:

$$\log K_{th} = \log V_a + \alpha(S^0 - A_s \varepsilon^0) \quad (13)$$

where α is a function of the adsorbent surface energy and is independent of the properties of the solute (it is known as the activity coefficient of the adsorbent; practical determination of its numerical values can be regarded as quantification of adsorbent activity), S^0 is the adsorption energy of a solute chromatographed on an active adsorbent with *n*-pentane as the mono-component mobile phase, A_s is the surface area of the adsorbent occupied by an adsorbed solute molecule, and ε^0 is the parameter usually referred to as the solvent elution strength, or simply solvent strength (it is the energy of adsorption of solvent per unit surface area of adsorbent).

Assuming that the adsorbent surface occupied by an adsorbed solute molecule (A_s) and that occupied by a stronger solvent (n_B) are equal, the eluent strength of a binary mobile phase, ε_{AB} , has the following dependence on its quantitative composition:

$$\varepsilon_{AB} = \varepsilon_A + \frac{\log(x_B \times 10^{\alpha n_B(\varepsilon_B - \varepsilon_A)} + 1 - x_B)}{\alpha n_B} \quad (14)$$

where ε_A is the eluent strength of the weaker component (A) of a given binary mobile phase, ε_B is the eluent strength of the stronger component (B) of the same mobile phase, and x_B is the molar volume of the component B.

Combining Eqs. (13) and (14) gives the following relationship, which expresses the dependence of the retention parameter of a solute, $R_M (= \log k)$, on the quantitative composition of a given binary mobile phase:

$$\log k = \log V_a + \alpha[S^0 - A_s \varepsilon_A] - \frac{A_s \log(x_B \times 10^{\alpha n_B(\varepsilon_B - \varepsilon_A)} + 1 - x_B)}{n_B} \quad (15)$$

Schoenmakers Model of Reversed-Phase Chromatography

In this particular model, it is assumed that Hildebrand's concept of the solubility parameter (δ), origi-

Theory and Mechanism of Thin-Layer Chromatography

nally formulated for liquid nonideal solutions, can also be applied to the solute and to the stationary and mobile phases of chromatographic systems.

The solubility parameter of any given substance (δ) is defined as

$$\delta = \sqrt{\frac{-E}{V}} \quad (16)$$

where E denotes its heat of vaporization at zero pressure, $-E$ is the energy of cohesion needed for transportation of one mole of an ideal gas phase to liquid phase, and V is the molar volume of the liquid.

One of the basic retention parameters (i.e., the solute's retention coefficient k) can be expressed as a function of the solubility parameters, δ :

$$\ln k_i = \frac{v_i}{RT}(\delta_m + \delta_s - 2\delta_i)(\delta_m - \delta_s) + \ln\left(\frac{n_s}{n_m}\right) \quad (17)$$

where v_i is the molar volume of the i th solute, δ_i , δ_s , and δ_m are respectively the solubility parameters of this solute and of the stationary and mobile phases employed, and n_s and n_m are respectively the numbers of moles of the stationary and mobile phases.

Finally, the principal equation of the Schoenmakers model [10] of solute retention in reversed-phase chromatography employing a binary aqueous mobile phase takes the parabolic form

$$\ln k = A\varphi^2 + B\varphi + C \quad (18)$$

where the equation constants A , B , and C have a clear physicochemical significance:

$$A = \frac{v_i}{RT}(\delta_a - \delta_w)^2 \quad (19)$$

$$B = 2\frac{v_i}{RT}(\delta_a - \delta_w)(\delta_a - \delta_i) \quad (20)$$

$$C = \frac{v_i}{RT}(\delta_w + \delta_s - 2\delta_i)(\delta_w - \delta_s) + \ln\left(\frac{n_s}{n_m}\right) \quad (21)$$

where δ_w and δ_a denote respectively the solubility parameters of water and of the organic modifier as the constituents of a given aqueous mobile phase.

References

1. E. C. Bate-Smith and R. G. Westall, *Biochim. Biophys. Acta* 4: 427 (1950).
2. A. J. P. Martin and R. L. M. Synge, *Biochem. J.* 35: 1358 (1941).



3. L. R. Snyder, *Principles of Adsorption Chromatography*, Marcel Dekker, Inc., New York, 1968.
4. E. Soczewinski, *Anal. Chem.* 41: 179 (1969).
5. L. R. Snyder, *Anal. Chem.* 46: 1384 (1974).
6. L. R. Snyder, J. W. Dolan, and J. R. Gant, *J. Chromatogr.* 165: 3 (1979).
7. L. R. Snyder and J. L. Glajch, *J. Chromatogr.* 214: 1 (1981).
8. J. L. Glajch and L. R. Snyder, *J. Chromatogr.* 214: 21 (1981).
9. L. R. Snyder and J. J. Kirkland, *Introduction to Modern Liquid Chromatography*, 2nd ed., John Wiley & Sons, New York, 1979.
10. P. J. Schoenmakers, H. A. H. Billiet, and L. De Galan, *J. Chromatogr.* 185: 179 (1979).



Thermal FFF of Polymers and Particles

Martin E. Schimpf

Boise State University, Boise, Idaho, U.S.A.

Introduction

Thermal field-flow fractionation (FFF) can be applied to virtually any polymer that can be dissolved in an organic solvent (subject to low-molecular-weight limitations discussed here) [1]. Water-soluble polymers are more difficult to separate because thermodiffusion, and therefore retention, is weak in water and other protic solvents. Still, certain nonionic polymers can be separated, and with the use of mobile-phase additives, even charged materials have been retained. For example, poly(ethylene oxide) and poly(ethylene glycol) show strong retention in a range of aqueous solvents, including deionized water, whereas poly(styrene sulfonate) is moderately retained in 5 mM Tris- Na_2SO_4 buffer [2]. Proteins, on the other hand, have not been successfully separated by thermal FFF.

Other hydrophilic polymers that could not be retained in water have been separated in aprotic solvents. For example, a variety of polysaccharides have been separated in dimethyl sulfoxide (DMSO), including pullulans, dextrans, various starches, and FicollTM. The latter material is a highly branched copolymer of sucrose and epichlorohydrin. Dextrans have been separated in mixtures of water and DMSO.

Discussion

The major limitation of thermal FFF occurs in the separation of low-molecular-weight materials. Thus, the technique is not widely applicable to molecular weights below about 10^4 g/mol. This limit can be reduced somewhat by the use of solvent mixtures. For example, polystyrene components as small as 2500 g/mol were resolved in a mixture of tetrahydrofuran and dodecane [4]. Even lower molecular weights than 2500 g/mol have been retained, but only through the use of special channels, which were highly pressurized in order to increase the temperature gradient without boiling the solvent.

Thermal FFF has virtually no upper limit to the molecular weights that can be resolved. The channel is not packed with a stationary phase, and the flow of carrier

liquid through the channel is laminar. As a result, large materials can be eluted without plugging the channel, and fragile materials are eluted without being damaged. In a comparison of thermal FFF and size-exclusion chromatography (SEC) [5], for example, it was found that SEC consistently underestimates the molecular weight of ultrahigh-molecular-weight polymers, even when extremely low flow rates are employed and a multiangle light-scattering detector is used to directly measure the molecular weight of the eluting components. In addition to the problem of shear-induced damage, SEC suffers from anomalous retention effects due to adsorptive interactions between high-molecular-weight polymers and the stationary phase. Although not completely absent, surface interactions are minimized in thermal FFF because there is no packing material. Finally, the resolution of thermal FFF for ultrahigh-molecular-weight polymers is vastly superior to that of SEC. As a result, thermal FFF enjoys a unique niche in the separation of these materials.

Another application in which thermal FFF enjoys an advantage over SEC is the analysis of high-temperature polymers. The operating temperature is limited only by the degradation temperature of the spacer used to form the channel, which for polyimides can be as high as 600 K. In the analysis of high-molecular-weight polyethylene, for example, temperatures in excess of 400 K are required for the samples to be soluble. Under these conditions, column stability and separation efficiency limit the application of SEC. By contrast, such samples can be routinely analyzed with commercially available thermal FFF channels.

Retention times in FFF are affected by the magnitude of the applied field, which can therefore be optimized for a particular molecular-weight range. For extremely broad molecular-weight distributions, the field can be programmed. Figure 1 illustrates the separation of polystyrene standards ranging in molecular weight from 9×10^3 to 5.5×10^6 g/mol in a single run. Note that the elution order is from low to high molecular weight. The field, which is expressed in Fig. 1 by the temperature difference (ΔT) between hot and cold walls, was programmed to decay exponentially from 80 to 10 K over the course of the 25-min separation.



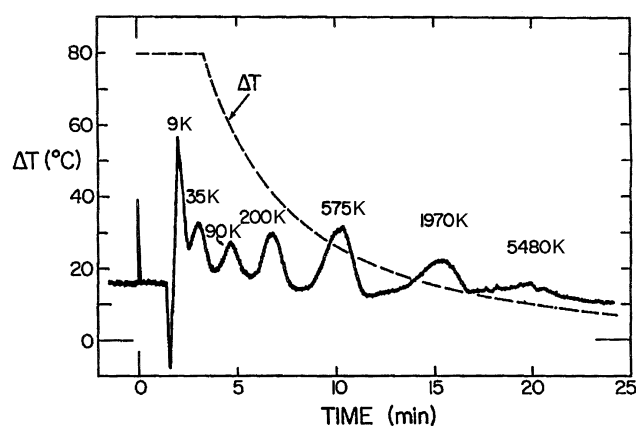


Fig. 1 Separation of seven polymers of indicated molecular weights by programmed thermal FFF. (Reproduced, with permission, from Ref. 7.)

Polymer Gels

Thermal FFF is also unique in its ability to handle gel-containing polymers. To analyze such materials by SEC, the sample solution must first be filtered to prevent damage in the form of contamination or even blockage in the column. With thermal FFF, such samples can be injected directly into the channel, and the gel content can even be characterized. The advantage of thermal FFF for analyzing samples in which the gel contains information that is critical to the analysis has been demonstrated with acrylate elastomers [5]. Thermal FFF was used to correlate the gel content of such elastomers to mechanical properties after SEC combined with viscometry and light scattering failed to elucidate any difference among the samples. In a related application, thermal FFF also proved superior in the analysis of natural rubber [8], where the ability to analyze unfiltered samples is a clear advantage.

Polymer Blends and Copolymers

The driving force for polymer retention in thermal FFF is thermodiffusion, which varies with polymer composition. As a result, polymer blends and copolymers can be separated even when the molecular weights or diffusion coefficients are identical. Furthermore, because thermodiffusion can be measured quantitatively by thermal FFF through the thermodiffusion coefficient (D_T), the compositional distribution can, in principle, be obtained directly from elution profiles, provided the dependence of D_T on composition is known. In practice, there are several complications.

First, retention does not yield D_T directly, but rather the Soret coefficient, which is the ratio of D_T to the ordinary diffusion coefficient (D). Because compositional information is contained in D_T alone, an independent measure of D must be available. Second, a general model for the dependence of D_T on composition has not been established; therefore, the dependence must be determined empirically for each polymer-solvent system. Fortunately, D_T is independent of molecular weight, and for certain copolymers, the dependence of D_T on chemical composition has been established. With random copolymers, for example, D_T is a weighted average of the D_T values for the corresponding homopolymers, where the weighting factors are the mole fractions of each component in the copolymers [9]. As a result, the composition of random copolymers can be determined by combining thermal FFF with any technique that measures D .

Several techniques for measuring D have been combined with thermal FFF to obtain values of D_T and, subsequently, the composition of separated polymer and copolymer components. Besides dynamic light scattering, SEC can be used by establishing calibration curves that relate $\log D$ to retention volume. The validity of such calibration curves are based on the same arguments used for universal calibration in SEC [10]. The method was demonstrated in the characterization of both the molecular weight and composition of a styrene-isoprene copolymer [10]. Even more powerful is the combination of thermal FFF and SEC to produce two-dimensional separations, as demonstrated on a four-component blend of homopolymers and block copolymers of styrene and ethylene oxide [11]. In two-dimensional separations, the components are first separated by SEC [12]. Fractions from the SEC elution profile, which are homogeneous in D , are further separated according to chemical composition by thermal FFF. The SEC retention volume can be combined with information from mass and viscosity detectors to calculate the viscosity-average molecular weight of the components. The thermal FFF retention volume can be combined with the D value obtained from SEC to calculate D_T values and, subsequently, the composition of the separated polymer components.

With block copolymers, compositional analysis by thermal FFF is complicated by the fact that thermal diffusion is dominated by the composition of monomer units in the outer free-draining region of the polymer-solvent sphere. When block copolymers are dissolved in a selective solvent, which is a solvent that solvates certain blocks better than others, the more soluble blocks tend to segregate to the outer regions of the

polymer–solvent sphere. In the extreme case of such segregation effects, the thermal diffusion of the block copolymer will mimic that of a homopolymer composed of the better-solvated component. As a result, the compositional characterization of block copolymers by thermal FFF requires the use of a nonselective solvent. In the styrene–ethylene oxide work discussed earlier [11], two solvents were combined in the proper proportion to yield a nonselective mixture and, therefore, a linear dependence of D_T on composition.

Colloids and Particles

Historically, the application of FFF to colloids and particles has been limited to flow and sedimentation FFF. However, the thermal FFF channel is not only capable of separating these materials, it is simpler in design and can be used with both aqueous and organic solvents. Furthermore, the dependence of retention on chemical composition presents unique opportunities for the separation of such materials.

The application of thermal FFF to a variety of colloids and particles has been demonstrated in both aqueous and organic carrier liquids. Figure 2 illustrates the dependence of retention on the surface composition of polystyrene particles. The three particles are similar in size, but the surface of one of the samples has been carboxylated, whereas another has been aminated. The relative elution order of the three particles can be changed by modifying the carrier liquid [13].

Experimental Considerations

One of the most common mistakes made in the analysis of polymers by thermal FFF and SEC is the injection of too much sample; this is often referred to as overloading. It is important to understand that D , and therefore retention volume (V_r), varies with polymer concentration. The effect of concentration is especially large near the so-called critical concentration (c^*), where polymer solutions undergo an abrupt transition from “dilute to semidilute” behavior. In the semidilute regime, polymer coils tangle with one another and the magnitude of D drops dramatically. Therefore, it is important to keep the polymer concentration below c^* in order to avoid overloading effects, which are manifested as peak “fronting” and an increase in V_r . With excessive overloading, additional peaks occur in thermal FFF due to the formation and separation of aggregates.

Although experienced users of SEC are aware of overloading effects, they are not always aware that

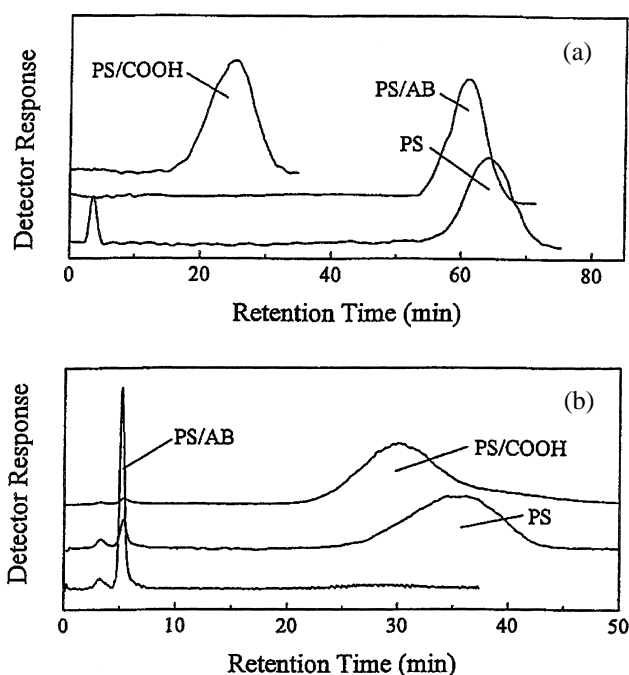


Fig. 2 A comparison of thermal FFF elution profiles for 0.2 μm particles of polystyrene (PS), carboxylated PS (PS/COOH), and aminated PS (PS/AB) in (a) an aqueous solution containing 9 mM NaN_3 and 0.05 wt% FL-70 surfactant (pH 8.5); (b) 10 mM phosphate buffer (pH 4.7). Differences in retention are due to differences in thermodiffusion, which is governed by the surface composition of the particle.

overloading occurs with a smaller sample load in thermal FFF. First, the channel has a relatively small volume (1–2 mL); therefore, injection volumes are smaller (3–30 μL) compared to SEC. More importantly, the sample is initially concentrated against one wall by the field. The extent of concentration varies with the sample and the magnitude of the applied field. A general rule that should be used to avoid overloading when a new method is being developed is to prepare the sample with a concentration that is one-tenth of the expected critical concentration. Of course, the critical concentration varies with molecular weight and other factors. For the experienced SEC user, a sample concentration of one-tenth that used in SEC should suffice. Sample concentrations between 0.01 and 1 mg/mL are typical. When one is uncertain of the critical concentration, the injected concentration should be varied and the elution profiles examined for indications of sample overloading. Otherwise, peak shape and reproducibility will be compromised. With recent advances in the sensitivity of detectors used for polymer analysis, sample overloading is less of a prob-



lem because more dilute samples can be analyzed, but overloading can still occur if the user is not aware of the potential.

References

1. M. E. Schimpf, *TRIP I*: 74 (1993).
2. J. J. Kirkland and W. W. Yau, *J. Chromatogr.* 353: 95 (1986).
3. J. Lou, M. N. Myers, and J. C. Giddings, *J. Liquid Chromatogr.* 17: 3239 (1994).
4. C. A. Rue and M. E. Schimpf, *Anal. Chem.* 66: 4054 (1994).
5. S. Lee, in *Chromatography of Polymers: Characterization by SEC and FFF* (T. Provder, ed.), ACS Symposium Series Vol. 521, American Chemical Society, Washington, DC, 1993, pp. 77–88.
6. L. Pasti, S. Roccasalvo, F. Dondi, and P. Reschiglian, *J. Polym. Sci. B* 33: 1225 (1995).
7. J. C. Giddings, V. Kumar, P. S. Williams, and M. N. Myers, in *Polymer Characterization by Interdisciplinary Methods* (C. D. Craver and T. Provder, eds.), ACS Symposium Series Vol. 227, American Chemical Society, Washington, DC, 1990.
8. S. Lee and A. Molnar, *Macromolecules* 28: 6354 (1995).
9. M. E. Schimpf, L. M. Wheeler, and P. F. Romeo, in *Chromatography of Polymers: Characterization by SEC and FFF* (T. Provder, ed.), ACS Symposium Series Vol. 521, American Chemical Society, Washington, DC, 1993, pp. 63–76.
10. M. E. Schimpf, in *Chromatographic Characterization of Polymers* (T. Provder, H. G. Barth, and W. Urban, eds.), ACS Symposium Series Vol. 247, American Chemical Society, Washington, DC, 1995, pp. 183–196.
11. S. J. Jeon, and M. E. Schimpf, in *Chromatography of Polymers: Characterization by SEC, FFF, and Related Methods for Polymer Analysis* (T. Provder, ed.), American Chemical Society, Washington, DC, 2000.
12. A. C. van Asten, R. J. van Dam, W. Th. Kok, R. Tijssen, and H. Poppe, *J. Chromatogr. A* 703: 245 (1995).
13. S. J. Jeon, A. Nyborg, and M. E. Schimpf, *Anal. Chem.* 67: 3442 (1997).



Thermal FFF of Polystyrene

Seungho Lee

Hannam University, Taejeon, Korea

Introduction

Thermal FFF (thermal field-flow fractionation) is an elution-type separation technique applicable to the characterization of various synthetic organic polymers with molecular weights higher than about 10^4 [1]. In thermal FFF, a dilute solution of polymer sample is injected into a thin ribbon-shaped flow channel across which an external “field” (in the form of a temperature gradient) is applied. Under the influence of the temperature gradient, different components of the sample are carried down the channel at different velocities, leading to the elution of different components at different times and separation is achieved.

Molecular-Weight-Based Separation

In thermal FFF, retention time t_r is given by

$$t_r = \frac{t^0 \Delta T}{6} \left(\frac{D_T}{D} \right) \quad (1)$$

for well-retained components. Here t^0 is the channel void time (a constant for a given channel dimension), ΔT is the temperature drop across the channel, D_T is the thermal diffusion coefficient, and D is the mass diffusion coefficient. For most polymeric materials, D is related to the molecular weight M by

$$D = \frac{A}{M^b} \quad (2)$$

Combining Eqs. (1) and (2) yields

$$t_r = \frac{t^0 \Delta T D_T}{6A} M^b \quad (3)$$

It has been shown that D_T is independent of branching configuration and molecular weight for homopolymers (such as polystyrene) in a given solvent [3]. Thus, under a fixed experimental condition, the retention time of polystyrene depends only on the molecular weight, resulting in a molecular-weight-based separation (i.e., the retention time increases as the molecular weight increases).

Effect of ΔT in Polystyrene Separation

It is seen, from Eq. (3), that dt_r/dM (difference in retention time for the same molecular-weight difference) increases with ΔT , indicating the separation (and thus the resolution) between two polystyrene components increases with ΔT . However, the gain in the resolution comes at the cost of time, as the use of higher ΔT requires longer analysis times. An optimum condition for ΔT must be determined for each sample by observing the time and the profile of the elution at various ΔT values.

Finding the optimum ΔT is relatively easy for samples having narrow molecular-weight distributions. However, for samples having broad distributions, finding that the optimum ΔT may not be trivial. Field programming may be required for samples having very broad molecular-weight distributions, where ΔT starts at a high level and is gradually decreased during a run to prevent excess retention of high-molecular-weight components [4]. Figure 1 shows a separation of four polystyrene standards having nominal molecular weights ranging from 4.7×10^4 to about 1×10^6 Da.

Determination of Physicochemical Properties

The simplicity of both retention mechanism and the channel geometry of thermal FFF allows one to theoretically predict the degree of retention of a sample, once certain physicochemical properties of the sample are known. Conversely, one may determine the physicochemical properties of a sample by measuring its retention.

Determination of Diffusion Coefficients

As seen in Eq. (1), the retention time in thermal FFF is a function of the ratio between two diffusion coefficients, D_T/D . If one of the two diffusion coefficients is known, the other can be determined directly from the retention time using Eq. (1). It is noted that the values of the diffusion coefficients may vary in various solvents.



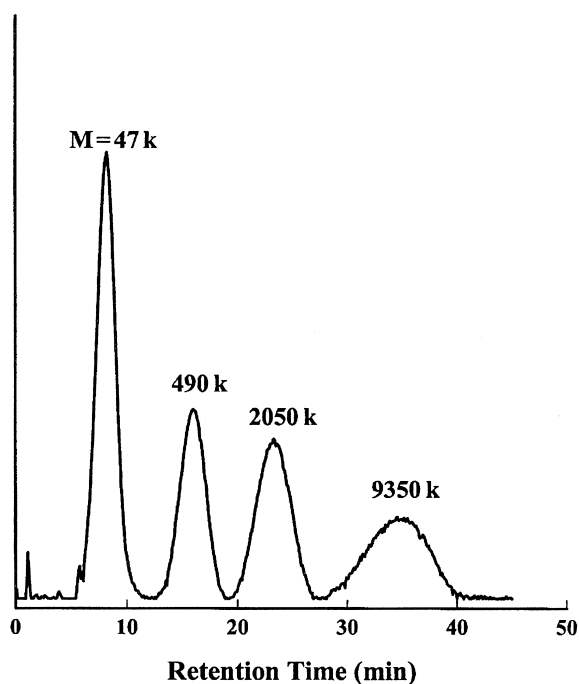


Fig. 1 Thermal FFF separation of polystyrene standards having nominal molecular weights as indicated. A power programming was used with initial $\Delta T = 80^\circ\text{C}$, predecay time $t_i = 3$, $t_a = -6$, and the hold $\Delta T = 10^\circ\text{C}$. The solvent/carrier was tetrahydrofuran and the flow rate was fixed at 0.2 mL/min.

Determination of Molecular Weight

If the values of A , b , and D_T are available, the molecular weight of a polymer can be directly determined from its retention time using Eq. (3). If D_T is not available, one may use a calibration curve [$\log(D/D_T)$ versus $\log M$] constructed with a series of narrow polystyrene standards of known molecular weights. For the molecular-weight analysis of an unknown, the D/D_T value of the sample is first calculated from its measured retention time, and then the molecular weight is determined from the calibration curve.

Use of molecular-weight-sensitive detectors (e.g., differential viscometer or light-scattering detector) eliminates the need for calibration. With a differential viscometer used as a detector for thermal FFF, the intrinsic viscosity is first measured for each retention time and is then converted to molecular weight using the Mark–Houwink constants [5]. The use of accurate

values of Mark–Houwink constants is essential in this method. Unlike the viscometer, the light-scattering detector measures the absolute molecular weight of the polymers directly. In multiangle light scattering, the scattered-light intensity is measured over a broad range of the scattering angles, allowing the determination of molecular size (radius of gyration) as well as the molecular weight [6].

Analysis of High-Molecular-Weight Polystyrene

Thermal FFF is often compared with size-exclusion chromatography (SEC), as both can be used for the same application (i.e., the molecular-weight determination of polymers). In SEC, the elution volume of the sample in a column (or in a column set) is limited to values between the interstitial volume of the column (“total exclusion limit”) and the total liquid volume (“total permeation limit”). The resolving power of SEC quickly drops as the elution volume approaches these limits. By contrast, there is no theoretical limit in thermal FFF, and the applicable molecular weight is virtually unlimited to the high-molecular-weight region. Also, the openness of the channel minimizes the shear degradation and adsorption of polymers sometimes observed with SEC. Thus, thermal FFF is useful for characterizing high-molecular-weight polymers that are difficult to analyze using SEC.

It is noted, however, that for polymers of molecular weight below about 1×10^4 Da, SEC may be more useful than thermal FFF. Analysis of such low-molecular-weight samples using thermal FFF requires the application of a very high ΔT that may require the use of a pressurized system to avoid boiling of the solvent.

References

1. J. C. Giddings, *Science* 260: 1456 (1993).
2. P. M. Shiundu, E. E. Remsen, and J. C. Giddings, *J. Appl. Polym. Sci.* 60: 1695 (1996).
3. M. E. Schimpf and J. C. Giddings, *Polym. Sci. Part B: Polym. Phys.* 27: 1317 (1989).
4. P. S. Williams and J. C. Giddings, *Anal. Chem.* 59: 2038 (1987).
5. J. J. Kirkland and S. W. Rementer, *Anal. Chem.* 64: 904 (1992).
6. S. Lee and O.-S. Kwon, *Polym. Mater. Sci. Eng.* 65: 408 (1993).

Thermal FFF: Basic Introduction and Overview

Martin E. Schimpf

Boise State University, Boise, Idaho, U.S.A.

Introduction

Thermal field-flow fractionation (FFF) is a subtechnique of the FFF family that employs a temperature gradient as the applied field [1]. For the reasons to be outlined, thermal FFF is applied primarily to industrial polymers that are soluble in organic liquids. The molecular-weight range of thermal FFF complements that of size-exclusion chromatography (SEC). Thus, oligomers and polymers with molecular weights below about 10^4 g/mol are not generally well separated by thermal FFF unless extraordinary measures are taken. On the other hand, the resolving power of thermal FFF for polymers with molecular weights above 10^5 g/mol is generally several times that of SEC [2]. For molecular weights above 10^6 g/mol, SEC is limited by shear-induced fragmentation of the chains as they travel through the packed bed under high pressure [3]. By contrast, shear forces in the FFF channel are extremely low, therefore ultrahigh-molecular-weight polymers, gels, and particles can be separated without degradation or sample pretreatment.

Thermal FFF Retention

Like other FFF subtechniques, materials are retained in thermal FFF as a result of their field-induced concentration at one wall of the channel. In thermal FFF, that field is a temperature gradient. Several terms are used to express the movement of material in response to a temperature gradient, including thermal diffusion, thermodiffusion, thermophoresis, and the Soret effect. The term thermodiffusion is used here, as it has been adopted by the scientific committee for The International Symposium on Thermodiffusion, which is devoted to the scientific study of this phenomenon.

Like other transport processes, thermodiffusion is typically quantified by a phenomenological coefficient that defines the dependence of a mass or energy movement on a potential energy gradient. Thus, the thermodiffusion coefficient (D_T) relates the velocity (U_x) induced in a material by a temperature gradient: $U_x = D_T(dT/dx)$, where T is temperature and x represents

the dimension in which the gradient is applied. This definition of thermodiffusion can be substituted into the general model of FFF retention to yield the following equation, which approximates the retention volume (V_r) of an analyte component in a thermal FFF channel:

$$\frac{V_r}{V^0} \cong \frac{\Delta T}{6} \frac{D_T}{D} \quad (1)$$

Here, ΔT is the temperature drop across the channel, which is set by the user, and D is the ordinary (mass) diffusion coefficient. The parameter V^0 is the geometric volume of the channel, which is constant for a given instrument. Note that V_r is the same parameter used to define retention in SEC and that the ratio on the left side of Eq. (1) is the number of channel volumes required to flush a sample component through the thermal FFF channel. Although Eq. (1) is an approximation, it becomes accurate to within 3% when $V_r/V^0 > 10$. More important for this discussion, Eq. (1) characterizes the influence of analyte parameters D and D_T on retention in thermal FFF.

According to Eq. (1), the retention of an analyte component is governed by the two transport coefficients D and D_T . The coefficient D scales directly with hydrodynamic volume and is the same parameter that differentiates retention in SEC. Thus, thermal FFF, like SEC, separates material according to differences in their hydrodynamic volume, which is related to molecular weight. However, V_r increases with D in SEC and decreases with D in thermal FFF, so the elution orders are opposite in the two techniques; low-molecular-weight components elute ahead of higher-molecular-weight components in thermal FFF.

Although V_r scales with the log of D in SEC, it scales directly with D in thermal FFF. As a result, molecular-weight components are distributed across a wider range of retention volumes in thermal FFF compared to SEC. Although resolving power benefits from this spread in molecular weight over V_r , thermal FFF has fewer theoretical plates than SEC. As a result, the resolving power of thermal FFF exceeds that of SEC only for molecular weights above about 10^5 g/mol,



where the compression of M (due to the log scale) leads to a rapid decline in the resolving power of SEC.

The dependence of retention on thermodiffusion imparts an additional dimension to the thermal FFF separation that is not present in SEC. Although our understanding of thermodiffusion in solids and liquids is incomplete, certain aspects are clear. For example, thermodiffusion is very sensitive to the chemical composition of the polymer. As a result, thermal FFF is capable of separating components that differ in composition, even though they may have the same molecular-weight or diffusion coefficient. An example [4] of the separation of polystyrene and poly(methyl methacrylate) standards by thermal FFF is illustrated in Fig. 1. This separation cannot be accomplished with SEC because the diffusion coefficients (or hydrodynamic volumes) of the two materials are virtually identical. The ability of thermal FFF to separate materials by chemical composition has spurred additional research designed to increase our understanding of thermodiffusion [5], which, in turn, has led to the application of thermal FFF to polymer blends and copolymers [6].

Although D_T varies with the polymer-solvent system, it is independent of molecular weight in a given system, at least for random coil homopolymers. The separation of differing molecular-weight components is therefore based solely on differences in D , which means that the principles of universal calibration that are relevant to SEC are also applicable to thermal FFF. Thus, a calibration curve made with one polymer-solvent system can be applied to other systems, provided the two D_T values associated with each polymer-solvent system are available. Fortunately, accurate values

of D_T can be obtained from the combination of thermal FFF with any technique that measures D , such as dynamic light scattering or even SEC (the latter is a secondary method that relies on calibration curves). Values of D_T for many polymer-solvent systems are available in the thermal FFF literature.

Compared to SEC, a broader concept of universal calibration is possible with thermal FFF because thermal FFF channels do not contain the inherent variability associated with SEC packing materials. As a result, calibration curves are universal to all thermal FFF channels that use the same cold-wall temperature. A common cold-wall temperature is important because both D and D_T vary with temperature.

Retention in thermal FFF is directly proportional to the temperature drop (ΔT) across the channel [see Eq. (1)]. The linear relationship between V_r and ΔT holds even for moderate levels of retention ($V_r/V^0 > 3$). Having a predictable dependence of retention on ΔT means that ΔT can be efficiently tuned in order to optimize the trade-off between resolution and analysis time for each application. ΔT can also be varied over the course of a separation in order to resolve samples of extreme polydispersity in the most efficient manner. Decreasing ΔT over the course of a separation is analogous to temperature programming in gas chromatography or solvent programming in reversed-phase high-performance liquid chromatography (HPLC).

Applications of Thermal FFF

Historically, thermal FFF has been applied primarily to lipophilic polymers. The technique has not found wide applicability to hydrophilic polymers because thermodiffusion, and therefore retention, is very weak in water. Although a few hydrophilic polymers have been separated by thermal FFF, they generally must have a high molecular weight ($>10^7$ g/mol) in order to be adequately retained for characterization by thermal FFF. Alternatively, an aprotic solvent such as dimethyl sulfoxide can be used to separate hydrophilic polymers with lower molecular weights. However, flow FFF is more suited to the characterization of hydrophilic polymers.

The open FFF channel is especially suited to fragile materials, and thermal FFF has found a definite niche in its application to ultrahigh-molecular-weight polymers. Furthermore, because samples need not be filtered, thermal FFF is the technique of choice for analyzing gels, rubbers, and other materials that tend to plug SEC columns [7]. Even particles can be analyzed

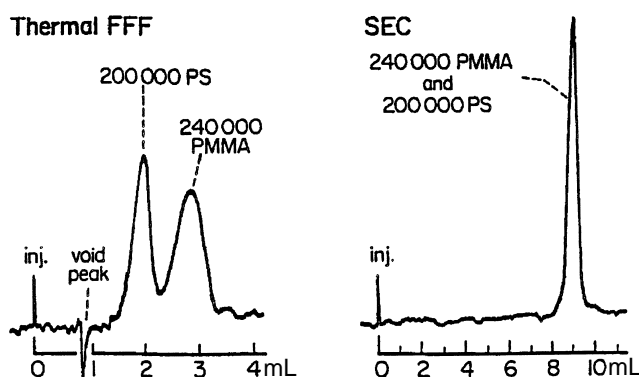


Fig. 1 Elution of similarly sized polystyrene (PS) and poly-(methyl methacrylate) (PMMA) polymers by thermal FFF and SEC, illustrating the dependence of thermal FFF retention on polymer composition. (Adapted, with permission, from Ref. 2.)

by thermal FFF [8], although flow and sedimentation FFF are more commonly used. Still, thermal FFF has the unique ability to separate particles by their composition [9], and as we increase our understanding of the thermodiffusion of particles, new applications are sure to emerge.

Advances in our understanding of thermodiffusion in polymer solutions have led to the application of thermal FFF to copolymers. With random copolymers, for example, the dependence of D_T on chemical composition is now predictable [6], so that compositional information can be obtained from retention measurements. With block copolymers, thermal FFF can still be used to separate components according to molecular weight, branching, and composition, but independent measurements on the separated fractions must be made in order to get quantitative information, except when "special" solvents are used. Special solvents yield a predictable dependence of D_T on composition even for block copolymers [6]. Different solvents are "special" for different copolymer systems.

As with SEC, the combination of thermal FFF with information-rich detectors is a powerful one. Detectors that yield information on the intrinsic viscosity, molecular weight, or chemical composition of eluting fractions allow detailed information on the distribution of such parameters in a complex sample. Thermal FFF can also be combined with SEC or hydrodynamic chromatography to achieve two-dimensional separations. The combination of SEC and thermal FFF is a particularly powerful one and has been used to characterize variations in chemical composition with the molecular weight of copolymers [10].

The Price of Versatility

The ability of a single thermal FFF channel to be used for the separation of lipophilic polymers, gels, rubbers, and particles makes it a very useful tool for polymer and colloid analysis. The versatility, however, comes with a price. Because all of the various applications cannot be implemented with a single field strength or carrier liquid, the user must have more than just a basic familiarity with the technique. To use thermal FFF efficiently, while taking advantage of its versatility, the user must understand the fundamentals behind the separation mechanism and assimilate a certain amount of experience.

Perhaps the most common difficulty encountered by new users arises from their tendency to use high field

strengths and high sample concentrations. Unlike SEC, the elution volume is, in principle, without limit, and the application of a high field can easily lead to an elution time of hours. Thus, it is best to begin with a small temperature gradient ($\Delta T = 10\text{--}20\text{ K}$) in the development of a new application, then increase it as necessary to achieve the desired resolution.

For a detailed discussion of appropriate sample concentrations, see the entry Thermal FFF of Polymers and Particles. In general, much lower sample concentrations are used in thermal FFF compared to SEC because the sample is initially concentrated at one wall by the field. Due to the viscous nature of flow in the thin FFF channel, sample concentrations that are too high lead to poor resolution and reproducibility. On the other hand, whereas samples are initially concentrated by the field, extremely polydisperse samples are eventually diluted over a wide range of retention volumes due to the high resolving power of the technique. As a result, such samples require highly sensitive detectors. Although this requirement once posed a significant problem, the availability of highly sensitive and universal detectors, such as the evaporative mass detector, has virtually eliminated the issue of sensitivity in thermal FFF.

References

1. M. E. Schimpf, *TRIP* 4: 114 (1996).
2. J. J. Gunderson and J. C. Giddings, *Anal. Chim. Acta* 189: 1 (1986).
3. S. Lee, in *Chromatographic Characterization of Polymers: Hyphenated and Multidimensional Techniques* (T. Provder, H. Barth, and M. Urban, eds.), American Chemical Society, Washington, DC, 1995, pp. 93–107.
4. J. J. Gunderson and J. C. Giddings, in *Comprehensive Polymer Science, Vol. I, Polymer Characterizations* (C. Booth and C. Price, eds.), Pergamon Press, Oxford, 1989, pp. 279–291.
5. M. E. Schimpf, *Entropie* (in press).
6. M. E. Schimpf, C. A. Rue, G. Mercer, L. M. Wheeler, and P. F. Romeo, *J. Coat. Technol.* 65: 51 (1993).
7. S. Lee, *J. Microcol. Separ.* 9: 281 (1997).
8. P. M. Shiundu and J. C. Giddings, *Anal. Chem.* 67: 2705 (1995).
9. S. J. Jeon, A. Nyborg, and M. E. Schimpf, *Anal. Chem.* 69: 3442 (1997).
10. A. van Asten, R. J. van Dam, W. T. Kok, R. Tijssen, and H. Poppe, *J. Chromatogr.* 703: 245 (1995).



Thermodynamics of GPC–SEC Separation

Iwao Teraoka

Polytechnic University, Brooklyn, New York, U.S.A.

Introduction

As with most other chromatographic separation methods, gel permeation chromatography–size-exclusion chromatography (GPC–SEC) is based on partitioning of analyte polymer molecules between the stationary phase (which, in the case of GPC–SEC, is contained within the pores of a porous stationary-phase support) and the mobile phase. Ideally, the mobile phase establishes a concentration equilibrium with the stationary phase at each plate in the column before being transferred to the next plate. The concentration equilibrium is dictated by an equal chemical potential of the polymer chain between the two phases [1,2]. In normal conditions of GPC–SEC, the polymer concentration c_M in the mobile phase is sufficiently low, and the solution behaves ideally dilute. Its chemical potential μ_M per molecule in the mobile phase is then given as

$$\mu_M = \mu^0 + k_B T \ln\left(\frac{c_M}{c^0}\right) \quad (1)$$

where μ^0 and c^0 are the chemical potential and the concentration, respectively, at an appropriate reference state, k_B is the Boltzmann constant, and T is the temperature. In the stationary phase, the chemical potential μ_S has additional terms due to changes in the entropy and the enthalpy upon bringing the polymer chain into the stationary phase:

$$\mu_S = \mu_0 + k_B T \ln\left(\frac{c_S}{c^0}\right) - T\Delta S + \Delta H \quad (2)$$

where c_S is the polymer concentration in the stationary phase, and ΔS and ΔH refer to the changes per chain. The partition coefficient K , defined as the ratio of the two concentrations, is then given as

$$K \equiv \frac{c_S}{c_M} = \exp\left(\frac{\Delta S}{k_B} - \frac{\Delta H}{k_B T}\right) \quad (3)$$

The primary purpose of GPC–SEC is to obtain a retention curve that represents the molecular weight (MW) distribution of the analyte. Because the retention volume is a linear function of the partition

coefficient, the coefficient must be a monotonically decreasing or increasing function of MW.

In GPC–SEC, porous beads of various pore sizes are used as separating media. The solution in the pore channels is the stationary phase, and the volume of liquid between the beads constitutes the mobile phase. A linear polymer chain can take different conformations in the unrestricted mobile phase. The number of conformations, W , increases in a power law of N , with N being the degree of polymerization. In the stationary phase, however, all of the monomers on a single chain have to reside within the pore space. Thus, W does not increase as rapidly with N as in the mobile phase. Because the conformational entropy of the polymer chain is calculated as $k_B \ln W$, the geometrical confinement of the pore makes $\Delta S < 0$. The way $|\Delta S|$ increases with N is determined by the geometry of the polymer chain (whether the chain is linear or branched, whether the chain is swollen or not, whether the chain is stiff or not, etc.) and the pore geometry, but $|\Delta S|$ is roughly a function of the chain dimension to the pore size, as shown below. The detailed atomic sequence in each polymer is rather of second importance. This feature is responsible for the universality of GPC–SEC.

Columns used in GPC–SEC are supposed to provide negligible ΔH regardless of MW for a given polymer. Otherwise, the dependence of ΔH on MW, different from that of ΔS , will complicate the analysis of the retention curve. Furthermore, ΔH would exhibit widely different characteristics determined by the interactions among the polymer, the pore surface, and the solvent, and thus negate the universality of GPC–SEC. With negligible ΔH , the partition coefficient is determined solely by the decrease in the conformational entropy:

$$K = \exp\left(\frac{\Delta S}{k_B}\right) \quad (4)$$

Equivalently, K is the ratio of the probability to place the polymer chain in the pore without touching the pore walls, averaged over different conformations.

As MW increases, K decreases from 1 to 0. To have a high resolution in GPC–SEC, the dependence of K on MW needs to be sharp. Users of GPC–SEC also



want the range of MW analysis in a single run to be as broad as possible, typically three to five decades. The finite range of K , however, makes the two requirements mutually exclusive, a severe restriction on the resolution. The resolution can be improved by increasing the number of theoretical plates, typically employing smaller porous beads and connecting a multiple columns in series. In normal-phase and reversed-phase high-performance liquid chromatography (HPLC), by contrast, a stationary phase that gives a large value of K , in excess of unity, offers high resolution and a broad range of analyte composition in a relatively short column.

Partition Coefficient

Examples for the plots of the partition coefficient as a function of the chain dimension are shown for some of the geometries of polymer molecules in a cylindrical pore of radius R_p . The simplest geometry is a sphere. The center of a spherical molecule of radius R_s is not allowed to get closer to the pore wall beyond the distance equal to the sphere radius. The ratio of the volume accessible to the sphere center to the total pore volume gives the partition coefficient. In Fig. 1, the two volumes are indicated by the interior and the exterior cylinders, respectively. Then,

$$K = \left(1 - \frac{R_s}{R_p}\right)^2 \quad (5)$$

The partition coefficient of a Gaussian chain of radius of gyration R_g was calculated by Casassa [3] and the partition coefficient of a rodlike molecule was obtained by Giddings et al. [4]. The results are compared in Fig. 2. When plotted as a function of R_g/R_p , the three polymer geometries show only a small difference, except that, at large R_g/R_p , the rodlike molecule has a larger K than the other two geometries of the molecule. The plots were converted to functions of N , in Fig. 3, for the monomer size a equal to $R_p/100$. The par-

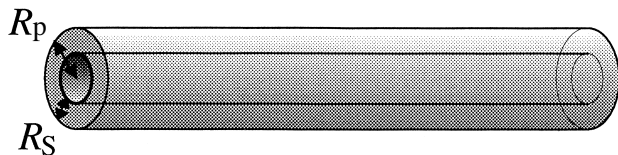


Fig. 1 The volume accessible to the center of a spherical molecule of radius R_s within a cylindrical pore of radius R_p is the interior cylinder of radius $R_s - R_p$.

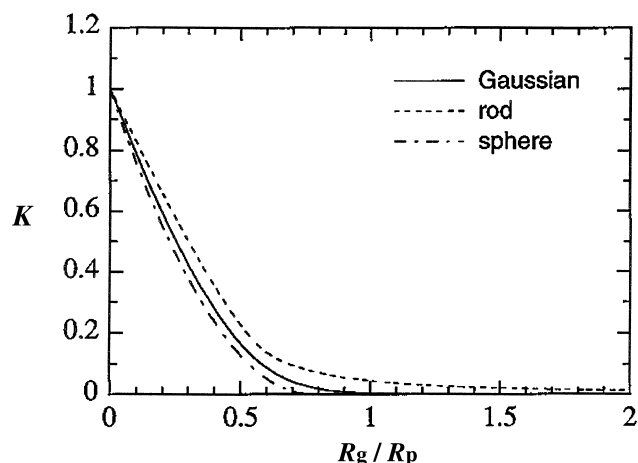


Fig. 2 Partition coefficient K plotted as a function of the radius of gyration R_g relative to the pore radius R_p for a spherical molecule, Gaussian chain, and a rodlike molecule.

tition coefficient of a star-branched polymer, in which each arm takes a Gaussian conformation, was calculated by Casassa and Tagami [5].

The partition coefficient for a real chain (excluded volume chain) has not been obtained except by the scaling theory [6]. The theory gives only a qualitative relationship between K and N for chains sufficiently longer than the pore size ($R_g \gg R_p$):

$$\frac{\Delta S}{k_B} \equiv -N \left(\frac{a}{R_p} \right)^{1/\nu} \approx - \left(\frac{R_g}{R_p} \right)^{1/\nu} \quad (6)$$

where $\nu \approx 0.588$. A computer simulation result shows that, compared at the same R_g , the real chain has a slightly larger K than the ideal chain that allows monomer overlap [7]. It is common to both models for sufficiently long chains that $K \sim \exp(-\beta M)$, where β is a numerical coefficient and M is the MW.

All of the currently used porous packing materials have a three-dimensional network structure, effectively giving rise to a pore size distribution. In these separating media, the dependence of K on N will be less sharp compared with the one in Fig. 3. It is desired by chromatographers that the retention time is a linear function of $\log M$. Because the retention time is a linear function of K , the plot of K needs to be a linear function of $\log M$ in as broad a range of MWs as possible. A naturally occurring pore size distribution is not sufficient to cause the desired linearity. Therefore, mixed-bed columns, packed with porous materials of different pore-size-distribution ranges, have been developed and used broadly as “linear” columns.

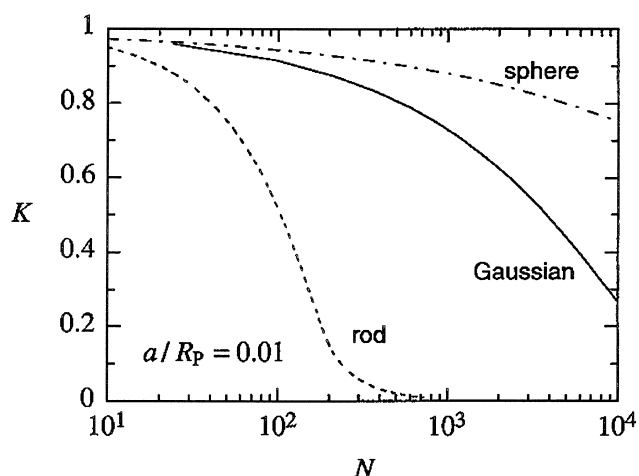


Fig. 3 Partition coefficient K plotted as a function of degree of polymerization, N , for a spherical molecule, Gaussian chain, and a rodlike molecule. The monomer size a is set to be $R_p/100$.

Effect of Intermolecular Interactions

It is often observed that, as the concentration of the polymer solution injected increases at a constant injection volume, the retention curve shifts toward a longer time [8]. This effect, called “overloading,” is manifested universally when the mobile phase is a good solvent for the polymer being analyzed and is more significant for a polymer of a higher MW. Simple thermodynamics explains this effect [2]: As c_M increases, the solution starts to deviate from the ideally dilute solution, and it becomes difficult to neglect the second virial coefficient A_2 . For a solution in a good solvent, a positive A_2 makes μ_M larger than the one in the ideally dilute solution of the same concentration, as given by

Eq. (1). The same change applies to μ_S . Since $c_S < c_M$, the increase in μ_M is greater than the increase in μ_S , resulting in an increase in K . At higher concentrations, the analyte polymer is retained longer, thereby delaying the retention curve. The concentration at which the effect of A_2 becomes not negligible is around the overlap concentration c^* which can be defined as $c^*[\eta] = 1$, where $[\eta]$ is the intrinsic viscosity. The actual concentration of c^* is low, especially for high-MW polymer. This is why a concentration as low as 0.1 wt% sometimes exhibits a concentration-dependent chromatogram.

Another mechanism that causes a change in the retention curve with concentration is intermolecular association. In a solution in which A_2 is negative, such as a solution in a poor solvent, a polymer chain tends to associate with other chains at higher concentrations. In effect, the pore in the GPC–SEC column senses the presence of suspensions of a larger dimension, causing the retention curve to shift to a shorter time.

References

1. J. C. Giddings, *Unified Separation Science*, John Wiley & Sons, New York, 1991.
2. I. Teraoka, *Progr. Polym. Sci.* 21: 89 (1996).
3. E. F. Casassa, *J. Polym. Sci. Polym. Lett. Ed.* 5: 773 (1967).
4. J. C. Giddings, E. Kucera, C. P. Russell, and M. N. Myers, *J. Phys. Chem.* 72: 4397 (1968).
5. E. F. Casassa and Y. Tagami, *Macromolecules* 2: 14 (1969).
6. P. G. de Gennes, *Scaling Concepts in Polymer Physics*, Cornell University Press, Ithaca, NY, 1979.
7. Y. Wang and I. Teraoka, *Macromolecules* 30: 8473 (1997).
8. R. E. Boehm, D. E. Martire, D. W. Armstrong, and K. H. Bui, *Macromolecules* 17: 400 (1984).



Thermodynamics of Retention in Gas Chromatography

Raymond P.W. Scott

Scientific Detectors Ltd., Banbury, Oxfordshire, England

Introduction

The Plate Theory shows that retention volume of a solute is directly proportional to its distribution coefficient between the two phases. Classical thermodynamics provides an expression that relates the *equilibrium constant* which, in the case of chromatographic retention, will be the distribution coefficient to the change in *standard free energy* of the solute, when transferring from one phase to the other.

Application

The expression is

$$RT \ln K = -\Delta G_0$$

where R is the gas constant, T is the absolute temperature, and ΔG_0 is the standard free-energy change.

Now,

$$\Delta G_0 = \Delta H_0 - T\Delta S_0$$

where (ΔH_0) is the standard enthalpy change and ΔS_0 is the standard entropy change.

Thus,

$$\ln K = -\left(\frac{\Delta H_0}{RT} - \frac{\Delta S_0}{R}\right)$$

or

$$K = \exp \left[-\left(\frac{\Delta H_0}{RT} - \frac{\Delta S_0}{R}\right) \right] \quad (1)$$

Equation (1) can also be used to identify the type of retention mechanism that is taking place in a particular separation by measuring the retention volume of the solute over a range of temperatures. Rearranging Eq. (1),

$$\log K = -\frac{\Delta H_0}{RT} + \frac{\Delta S_0}{R}$$

Bearing in mind that

$$V' = KV_s$$
$$\log V' = -\frac{\Delta H_0}{RT} + \frac{\Delta S_0}{R} - \log V_s$$

It is seen that a curve relating $\log(V')$ to $1/T$ should give a straight line, the slope of which will be proportional to the *enthalpy* change during solute transfer. In a similar way, the intercept will be related to the *entropy* change and, thus, the dominant effects in any distribution system can be identified from such curves. Curves relating $\log(V')$ to $1/T$ are called van't Hoff curves, which can be used to identify the mechanism of retention and elucidate the role played by temperature in a separation (see the entries van't Hoff Curves and Chiral Separations by GC).

In the majority of distribution systems encountered in gas chromatography, the slopes of the van't Hoff curves are positive and the intercept negative. The negative value of the intercept means that the standard entropy change of the solute has resulted from the production of a less random and more orderly system during the process of distribution. More important, this entropy change *reduces* the magnitude of the distribution coefficient. This means that the greater the forces between the molecules, the greater the energy (enthalpy) contribution, the larger the distribution coefficient, and the greater the retention. In contrast, any reduction in the random nature of the molecules or an increased amount of order in the system reduces the distribution coefficient and *attenuates* the retention. Thus, in the majority of distribution systems in chromatography, the enthalpy and entropy changes oppose one another in their effect on solute retention, although one will generally dominate over the other.

Suggested Further Reading

Scott, R. P. W., *Techniques of Chromatography*, Marcel Dekker, Inc., New York, 1995.

Scott, R. P. W., *Introduction to Analytical Gas Chromatography*, Marcel Dekker, Inc., New York, 1998.



Thin-Layer Chromatographic Study of Quantitative Structure–Retention Relationships

L. Zhang

Qin-Sun Wang

National Key Laboratory of Elemento-Organic Chemistry, Nankai University, Tianjin, People's Republic of China

Introduction

The study of quantitative structure–retention relationships (QSRRs) is one of the most important theoretical fields of chromatography; it has become a new investigation branch of chromatographic science.

Quantitative structure–retention relationships studies are widely investigated in high-performance liquid chromatography (HPLC), gas chromatography (GC), and thin-layer chromatography (TLC). Recently, QSRR studies in TLC have attracted more and more researchers [1]. It is known that TLC has some advantages: It is rapid, relatively simple, low cost, and easy to operation, there is a wide choice of adsorbents and solvents, and very small amounts of substance are needed. In this entry, the establishment and application of QSRR studies are reviewed.

Establishment of QSRR Equations

Nonspecific parameters, physicochemical parameters, and topological indices are the main parameters used in QSRR studies in TLC. The establishment of QSRR equations in TLC are reviewed according to these parameters.

Based on Nonspecific Parameters

Nonspecific parameters include the number of carbon atoms in a molecule, molecular volume, solvent-accessible surface, and so forth. This is relatively simple, and the most commonly used nonspecific parameter is the number of carbon atoms in the compound.

There is a relationship between the number of carbon atoms and the retention data in HPLC and GC; a similar relationship was also found in TLC. Boyce and Milborrow [2] found that there was a linear relationship between the R_m values and the number of carbon atoms in the R group of *N*-*n*-alkyltritylamines (ph_3CNHR). Janjic et al. [3] carried out a series of stud-

ies on the relationship between transition metal complexes and the number of carbon atoms in the complexes.

Because of their simplicity, nonspecific parameters can be obtained relatively conveniently, but it is not very well correlated for complex molecules.

Based on Physicochemical Parameters

Physicochemical parameters are widely used in QSRR studies. Among the many physicochemical parameters, lipophilicity is one of the most widely used parameters in TLC QSRR studies. As is well known, there is a linear relationship between the R_m [$R_m = \log(1/R_f - 1)$] values and the connection of organic modifier in mobile phase:

$$R_m = R_{m0} + bc$$

where c is the concentration of organic modifier in mobile phase and b is the slope, which is the decrease of R_m values when the concentration of organic modifier in the mobile phase increases 1%. R_{m0} is the intercept of the TLC equation which represents the extrapolated R_m value (i.e., the theoretical R_m value at 0% organic solvent). This linear relationship has been verified by many workers [2,4].

Pliska and Schmidt [5] first described the theoretical relationship between R_f and P values and presented the details of the computational procedure. At the same time, the relationship between the intercept R_{m0} and the slope b in the TLC equation was also studied by many other researchers. Biagi et al. [4] performed extensive work in this field. They found that R_{m0} values were not dependent on the nature of the organic solvent and that it does not make much difference whether the organic solvent is acetone, methanol, or acetonitrile. In addition, there is a linear relationship between the intercept (R_{m0}) and the slope (b). Biagi et al. considered that the existence of the linear relationship is a reason why the chromatographic method can be used to determine lipophilicity. The intercept of



the TLC equation can be considered as a measure of the partitioning of the compounds between a polar mobile phase and a nonpolar stationary phase (i.e., as the result of the balance between the interactions with the nonpolar phase and the interactions with the polar phase), whereas the slope of the TLC equation indicates the rate at which the solubility of the compound increases in the mobile phase [4]. There are many studies dealing with this aspect.

Based on Topological Indices

Based on the plot of the suppressed hydrogens of the molecular under study, the calculation methods of molecular connectivity indices was developed. It has been used in many fields, such as the studies of correlation between structure and physicochemical and pharmacological properties, especially the relationship between structure and retention behavior, and the evaluation of the hydrophobicities of organic compounds by chromatographic methods.

The relationship between the retention behavior of benzodiazepine, sulfamides, substituted anilines, barbiturates, a group of natural phenolic derivatives, diethanolamine isomers, amino acids, sulfoether, thioalcohol, 2,4-dinitrophenylhydrazones, and their molecular connectivity indices were studied. All of the results indicate that the R_f or R_m values are highly correlated with molecular connectivity indices.

Pyka [6–8] performed a series of experiments applying topological indices to QSRR studies in TLC. Topological indices, such as Gutman, Randic, and Wiener indices as well as other indices were used. A new optical index (I_{opt}) was proposed [6], which enables distinction between isomers of D- and L-configuration. Pyka also established a new stereoisomeric topological index (I_{STI}), which enables distinction between stereoisomers with hydroxyl groups in axial and equatorial positions. Using this index, the retention behavior of stereoisomeric menthols and thujyols have been studied.

Introducing topological indices to QSRR studies widens the possibility of correlation analysis. Molecular connectivity indices are calculated according to molecular structure; it is relatively objective. Topological indices can be calculated without synthesizing the compound. In addition, using topological indices, the molecular structure can be described by some parameters which have physicochemical significance. However, there is also a limitation in the range of application of topological indices. They can be applied as the sole parameter only when they have been correlated with other features of molecular structure, such as vol-

ume, ring size, carbon chain length, and so forth. Generally, they are combined with other parameters that characterize other properties of the compounds of interest.

Combination of Several Kinds of Parameters

As we can see, every kind of parameters have limitations; thus, the combination of several kinds of parameters is advantageous. The combination of several kinds of parameters can often completely reflect the properties of compounds. Wang et al. [9] conducted some studies in this field. They introduced several structural parameters to study the correlation between the molecular structures of *O*-ethyl-*O*-aryl-*N*-isopropyl phosphoroamidothioates, *O*-ethyl, *O*-isopropyl phosphoro(thioureido) thioates, and their retention factors in high-performance TLC (HPTLC), respectively.

Application of QSRR Studies in TLC

Prediction of Retention and Separation

From the discussion earlier, it can be seen that all the QSRR equations established in the previous part can be used to predict R_f or R_m values of compounds. This goal of QSRR is very easy to comprehend.

Determination of Lipophilicity

Many works [5] have illustrated that there is a linear relationship between R_m values and $\log P$. R_{m0} values also can be used to measure the lipophilicities of chemical substances. In general, the chromatographic method is an excellent alternative to the traditional flask-shaking method for lipophilicity determination. It avoids the difficulties that one may encounter in the flask-shaking method. It is simple and rapid and requires only minute amounts of substances (which need not necessarily be very pure); it does not need quantitative analysis; the nature of the organic modifier does not affect the measurement of the lipophilic character, as the R_{m0} value is not affected by the organic modifier.

Evaluation of Some Physicochemical Parameters of Chemicals

The research on the evaluation physicochemical parameters using the TLC QSRR equation is very limited. Until now, only the $\log E_{T(30)}$ values of some organic solvents [10] and the pK_a values of some substituted phenols [8] have been predicted using this



method. In addition, topological indices are introduced to evaluate the pK_a values.

Evaluation of Biological Activities of Compounds

Although, as early as 1965, Boyce and Milborrow [2] studied the relationship between R_m values of N - n -alkyltritylamines (ph_3CNHR) and their LD_{50} values, the research on this aspect is limited. When only the R_m values is considered, the activity [$\log(1/C)$ or LD_{50}] is correlated with the square of R_m .

Topological indices were also introduced to study the biological activities of compounds. Pyka [7] studied the relationship among R_m values, topological indices, and biological activity [$\log(1/C)$]. All of the equations he obtained show good correlation. There is a good agreement between predicted $\log(1/C)$ values and experimental $\log(1/C)$ values.

Explanation of Separation Mechanism

Theoretically speaking, a good QSRR equation can reflect the most characteristic parameters that influence the retention behavior of compounds. Thus, it can explain the retention mechanism quantitatively and qualitatively, but research on this aspect has made only poor progress until now.

Cserhati and Forgacs [11,12] did some work on this field which illustrates the high impact of steric interactions on retention. However, until now, some of his hypotheses [12] need further experimental verification to support them.

Prospects

Quantitative structure–retention relationships play a vital role in chromatographic research. The research and application fields of QSRR studies are becoming increasingly broad. Up to now, compounds used in

QSRR studied are homologous series. How to establish QSRR equations that fit different kinds of compounds requires much more experimental effort.

From the viewpoint of application, QSRR equations in TLC are mainly used for retention prediction. The explanation of the separation mechanism awaits further investigation. With the application of various statistical methods, it is possible to select the primary retention-effect factors from many solute related factors which will offer explanations of separation mechanisms.

In conclusion, QSRR studies are making excellent progress in recent years, due to increased interest in this field of study. We can anticipate that QSRR studies will become more and more important in the future.

References

1. Q. S. Wang and L. Zhang, *J. Liquid Chromatogr. Related Technol.* 22: 1 (1999).
2. C. B. Boyce and B. V. Milborrow, *Nature* 208: 537 (1965).
3. T. J. Janic, G. Vuckovic, and M. B. Celap, *Chromatographia* 42: 675 (1996).
4. G. L. Biagi, A. M. Barbaro, A. Sapone, and M. Recanatini, *J. Chromatogr. A* 662: 341 (1994).
5. V. Pliska, M. Schmidt, and J.-L. Fauchere, *J. Chromatogr.* 216: 79 (1981).
6. A. Pyka, *J. Planar Chromatogr. — Mod. TLC* 4: 316 (1991).
7. A. Pyka, *J. Planar Chromatogr. — Mod. TLC* 7: 108 (1994).
8. A. Pyka, *J. Planar Chromatogr. — Mod. TLC* 9: 52 (1996).
9. Q. S. Wang, B.-W. Yan, and H.-Z. Yang, *J. Planar Chromatogr. — Mod. TLC* 10: 118 (1997).
10. A. Ahmad, Q. S. Muzaffar, A. Andrabi, and P. M. Qureshi, *J. Chromatogr. Sci.* 34: 376 (1996).
11. T. Cserhati, E. Forgacs, *J. Liquid Chromatogr.* 18: 2783 (1995).
12. T. Cserhati, *Anal. Chim. Acta* 292: 17 (1994).



Thin-Layer Chromatography of Natural Pigments

Tibor Cserhádi
Esther Forgács

Institute of Chemistry, Chemical Research Center, Hungarian Academy of Sciences, Budapest, Hungary

Introduction

Various natural pigment classes, such as flavonoids, anthocyanins, carotenoids, chlorophylls and chlorophyll derivatives, porphyrins, quinones, anthraquinones, betalains, and so forth are abundant in many families of the vegetable and animal kingdoms. As consumers generally dislike the color of synthetic dyes, the concentration and composition of pigments in foods and food products exert a considerable impact on the consumer acceptance and, consequently, on the commercial value of the products. It has been proven many times that one of the main properties employed for the commercial evaluation of the quality of products is their color; that is, an adequate color is an important requirement of marketability.

Discussion

Spectroscopic methods for measuring the absorbance of pigment solutions or the adsorbance of the color of product surfaces on one or more wavelengths in the visible range are excellent tools for the accurate determination of the quantity of pigments; however, they do not contain any useful information on the concentration of the individual pigment fractions.

As the stability of the various pigments against hydrolysis, oxidation, and other environmental conditions shows marked differences, the assessment of the pigment composition may help for the prediction of the shelf life of products and the elucidation of the impact of various technological steps on the individual pigment fractions resulting in more consumer-friendly processing methods. Moreover, the exact knowledge of the pigment composition may facilitate the identification of the origin of the product. The advantageous characteristics of thin-layer chromatography (TLC) (easy to use, low operating costs, no need for complicated instrumentation, manifold possibilities of detection, etc.) make it a method of preference for the separation and, to a lesser extent, for the quantitative analysis of natural pigments.

The earlier results in the application of TLC for the analysis of natural color pigments, in general [1], and especially in plants [2], have been reviewed. Pigments are more or less strongly bonded to cellulose, protein, cell-wall components, and so forth in both plant and animal issues; therefore, the efficacious extraction sometimes is difficult and time-consuming with the traditional extraction methods, and the recoveries sometimes are inadequate. Depending on the character of the accompanying matrix and the solubility of the pigment, a considerable number of extraction solvents or solvent mixtures were proposed and used in the TLC analysis of natural pigments.

Thus, ethanol–water (7:3 v/v) and methanol–water in various ratios for flavonoids, methanol–25% HCl (9:1 v/v), methanol–acetic acid (5%), methanol–trifluoroacetic acid (3%) for unstable anthocyanins, acetone, methanol–acetone mixtures for carotenoids, acetone and petroleum ether for chlorophylls, and so forth. The pigments are fairly stable in their natural environment, but they generally become unstable in extracts; this has to be taken into consideration in the development of new, more efficacious extraction procedures.

The impact of the extraction conditions using various solvents on the recoveries has never been studied in detail, and the results have never been compared. The introduction of modern extraction methods, such as microwave-assisted extraction, supercritical fluid extraction, and solid-phase extraction, probably will improve the efficiency of extraction, even in the instance of unstable pigments and pigment mixtures. The majority of TLC separations were carried out on traditional silica layers. As the chemical structures and, consequently, the retention characteristics of pigments are highly different, a wide variety of eluent systems has been employed for their separation, consisting of light petroleum, ethyl formate, ethyl acetate, benzene, toluene, chloroform, methanol, *n*-butanol, formic or acetic acid, and so forth.

Besides silica, other direct phase supports such as alumina, diatomaceous earth, cellulose, MgO–diatomaceous earth, and sucrose layers were employed for the separation of various pigment mixtures. Mixed-



mode supports (cyano, diol, and aminosilica layers) were also employed in both the direct and reversed-phase elution modes for the separation of natural pigments, but their performance was markedly lower than those of traditional silica layers. Reversed-phase supports (polyamide, octadecylsilica, alumina, silica, and diatomaceous earth impregnated with paraffin oil) were also applied for the separation of color pigments (carotenoids from *Capsicum annuum*, anthocyanins from red wines) and it was found that their separation capacity was commensurate with those of direct phase layers. The separation of 22 pigment fractions extracted from paprika powders on diatomaceous layers impregnated with paraffin oil, using mixtures of acetone–water, was reported and it was established that baseline separation of each fraction cannot be achieved in one run and at a single mobile-phase composition [3].

Unconventional layers have also been employed in the TLC analysis of pigments of sour cherry and blueberry. Baseline separations were carried out on corn and rice starch layers in the *n*-butanol–glacial acetic acid–water–benzene (30:20:10:0.5, v/v) mobile phase [4]. A considerable number of carotenoid standards can be separated in one run as demonstrated in Table 1, showing the R_f values of carotenoids in various eluent systems [5].

Pigment extracts either derived from one plant or one part of a plant generally contain a considerable number of fractions with highly different retention characteristics. The separation of these extracts cannot be successfully achieved by the traditional TLC techniques. Elution methods similar to gradient elution in high-performance liquid chromatography were developed to overcome this difficulty. Stepwise gradient elution can be carried out by introducing eluent fractions with increasing eluent strength to the layer without interrupting the separation process. In programmed multiple-gradient development, the plate is developed to different distances with mobile phases of decreasing elution strength.

The plate is first developed for a given distance with the eluent having the highest elution strength and then the plates are dried. Pigments with the lowest mobility are separated. Then, a new eluent with a lower elution strength is applied for the separation of pigments with a higher mobility. The procedure can be repeatedly employed up to 25 times using eluents with decreasing elution strength. The advantages of programmed multiple development were exploited in the separation of complex plant extracts of *Radix rhei* and *Cortex frangulae* [6]. Due to the considerable number of pigment

Table 1 The R_f Values Obtained for Carotenoids by Use of Different Mobile Phases

No.	Carotenoid	R_f value in mobile phase		
		1	2	3
1	β -Carotene	0.93	0.92	0.93
2	α -Cryptoxanthin	0.76	0.83	0.80
3	β -Cryptoxanthin	0.75	0.83	0.80
4	Zeaxanthin	0.46	0.72	0.51
5	Lutein	0.46	0.73	0.52
6	Nigroxanthin	0.52	0.78	0.63
7	α -Carotene monoepoxide	0.92	0.92	0.91
8	β -Carotene monoepoxide	0.92	0.90	0.91
9	β -Carotene diepoxide	0.91	0.90	0.91
10	Lutein epoxide	0.46	0.58	0.47
11	Antheraxanthin	0.45	0.55	0.47
12	Violaxanthin	0.41	0.46	0.44
13	Cycloviolaxanthin	0.58	0.74	0.77
14	Cucurbitaxanthin A	0.50	0.72	0.63
15	Capsanthin 3,6-epoxide	0.43	0.61	0.55
16	Capsanthin	0.38	0.60	0.44
17	Capsanthin 5,6-epoxide	0.35	0.47	0.39
18	Capsorubin	0.32	0.42	0.38
19	Capsanthol (6'R)	0.25	0.26	0.23
20	Capsanthol (6'S)	0.38	0.68	0.49
21	5,6-Diepikarpoxanthin	0.35	0.36	0.39
22	6-Epikarpoxanthin	0.26	0.38	0.24
23	5,6-Diepilatoxanthin	0.36	0.45	0.33
24	5,6-Diepicapsokarpoxanthin	0.28	0.30	0.30

Note: Mobile phase 1: petroleum ether–acetone (6:4, v/v). Mobile phase 2: petroleum ether–*tert*-butanol (8:2, v/v). Mobile phase 3: methanol–benzene–ethyl acetate (5:75:25, v/v/v).

Source: Reprinted with permission from Ref. 5.

fractions in an extract, the identification of the individual pigments separated by TLC is extremely difficult. Pigments can be identified by spotting an authentic standard on the neighboring track; however, in the instance of natural pigment mixtures, authentic standards are generally not available.

Coupled spectroscopic methods such as TLC–UV (ultraviolet) and visible spectroscopy, TLC–mass spectrometry, and TLC–FTIR (Fourier transform infrared) have been developed to overcome this difficulty [7]. Their future application in the TLC analysis of natural pigments will markedly increase the information content of this simple and interesting separation technique. The automation of the various steps of TLC analysis (sample application, automated developing chambers, TLC scanners, etc.) greatly increased the reliability of the method, making it suitable for official control and legislative purposes [8].

References

1. O. M. Andersen and G. W. Francis, in *Handbook of Thin-Layer Chromatography* (J. Sherma and B. Fried, eds.), Marcel Dekker, Inc., New York, 1996, pp. 715–752.
2. J. Pothier, in *Practical Thin-Layer Chromatography*, CRC Press, Boca Raton, FL, 1996, pp. 33–49.
3. T. Cerháti, E. Forgács, and J. Holló, *J. Planar Chromatogr. — Mod. TLC* 6: 472 (1998).
4. N. Perisic-Janjic and B. Vujicic, *J. Planar Chromatogr. — Mod. TLC* 10: 447 (1998).
5. J. Deli, *J. Planar Chromatogr. — Mod. TLC* 11: 311 (1998).
6. G. Matysik, *Chromatographia* 43: 39 (1996).
7. E. Pastene, M. Montes, and M. Vega, *J. Planar Chromatogr. — Mod. TLC* 10: 362 (1997).
8. R. Brockmann, *Fleischwirtschaft* 78: 143 (1998).



Thin-Layer Chromatography of Synthetic Dyes

Tibor Cserhádi
Esther Forgács

Institute of Chemistry, Chemical Research Center, Hungarian Academy of Sciences, Budapest, Hungary

Introduction

Synthetic dyes are extensively used in many up-to-date industrial processes and research, mainly in the preparation of textile, food, and leather products, as well as in cosmetics and medicine. The widespread application of synthetic dyes has resulted in serious environmental pollution: Their occurrence in ground water and wastewater and the accumulation in sediment, soil, and various biological tissues has often been observed and reported. Dyes and intermediates can cause abnormal reproductive function in males and show marked toxic effects toward bacteria. The rate of biodegradation of the majority of synthetic dyes is very low, enhancing the toxicological hazard and environmental impact.

Discussion

Commercial synthetic dyes generally contain more than one color product. As the knowledge of the exact composition of dye mixtures is prerequisite for their successful application in many fields of industry and research, many efforts have been devoted for the development of various chromatographic techniques suitable for their separation and quantitative determination. Moreover, the exact determination of the composition and quantity of synthetic dye is required in the control of industrial processes, in the following of efficacy of wastewater treatment, in environmental protection studies, and in forensic science.

The chemical structures of synthetic dyes show considerable variety. They generally contain more than one aromatic group, condensed aromatic substructures or heterocyclic rings (pyrazolone, thiazole, acridine, thiazine, oxazine) which are mainly hydrophobic, and, frequently, a polar basic or cationic group which is strongly hydrophilic. Due to these structural characteristics, they readily bind both to polar adsorptive and apolar reversed-phase chromatographic supports, making their successful separation difficult. As the synthetic dyes are not volatile and volatile derivatives are not known, gas chromatographic (GC) methods cannot be employed for their analysis. Thin-layer chromatography (TLC),

high-performance liquid chromatography (HPLC) and, to a lesser extent, capillary zone electrophoresis (CZE) have been equally applied for this purpose. Due to its inherent advantages (simplicity, low cost, rapidity, etc.), a large number of TLC methods have been developed and successfully applied for the analysis of synthetic dyes. Previous results obtained in the application of TLC for the separation of synthetic dyes were reviewed earlier [1]. The planar chromatography of dyes used in the leather [2] and cosmetic industries [3] was reviewed separately. The majority of TLC separations have been performed on the traditional silica layers using many solvents and solvent mixtures (chloroform, various alcohols, pyridine, *n*-hexane, toluene, ethyl acetate, etc.). The polar character of some substructures in the dyes frequently made necessary the addition of acidic (formic and acetic acid) or basic additives (ammonia, diethylamine) to the mobile phase to suppress the dissociation of these hydrophilic groups in order to increase, in this manner, the efficiency of separation and to improve spot shape. However, other than silica layers, various eluent additives have also been employed for the enhancement of the efficacy of TLC. Thus, microcrystalline cellulose thin layers were employed for the study of the retention behavior of some synthetic dyes such as methyl orange (4-[[4-(dimethylamino)phenyl]azo]benzene acid sodium salt), methyl red (2-[[4-(dimethylamino)phenyl]azo]benzoic acid), methyl yellow (*N,N*-dimethyl-4-(phenylazo)benzeneamine), ethyl orange (4-[[4-(diethylamino)phenyl]azo]benzene acid sodium salt), ethyl red (2-[[4-(diethylamino)phenyl]azo]benzoic acid), alizarin yellow R (2-hydroxy-5-[(4-nitrophenyl)azo]benzoic acid) and alizarin yellow 2G (2-hydroxy-5-[(3-nitrophenyl)azo]benzoic acid monosodium salt) [4]. The R_f values of dyes obtained in the presence of various eluent additives are compiled in Table 1. The data clearly show that eluent additives can be successfully used for the modification of the retention behavior of azo dyes, improving the separation capacity of TLC.

The separation characteristics of a considerable variety of other TLC supports were also tested using different dye mixtures (magnesia, polyamide, silylated silica, octadecyl-bonded silica, carboxymethyl cellulose, zeolite, etc.); however, these supports have not



Table 1 R_f Values of Azo Dyes on Microcrystalline Cellulose Thin Layers (Merck 557) with Various Eluent Additives at Room Temperature (CD = cyclodextrin)

Azo dye	0.5 M HCl		1 M Na ₂ CO ₃		Control	1 M NaCl		
	α -Cd polymer 1%	α -CD 1%	α -CD polymer 1%	α -CD 1%		α -CD polymer 0.5%	β -CD polymer 0.5%	γ -CD polymer 0.5%
Methyl orange	1.00	0.77	0.89	0.72	0.10	1.00	0.80	0.79
Methyl red	0.38	0.17	0.30	0.14	0.08	0.13	0.24	0.23
Methyl yellow	0.92	0.73	0.69	0.40	0.00	0.88	0.55	0.54
Ethyl orange	1.00	0.97	0.91	0.73	0.44	1.00	0.97	1.00
Ethyl red	0.66	0.35	0.68	0.23	0.12	0.28	0.50	0.48
Alizarin yellow R	0.71	0.22	0.70	0.43	0.00	0.52	0.43	0.41
Alizarin yellow 2G	0.80	0.00	0.70	0.51	0.03	0.55	0.48	0.61

Source: Reprinted with permission from Ref. 4.

been frequently applied in practical TLC of this class of compounds. Optimization procedures such as the prisma and the simplex methods have also found application in the TLC analysis of synthetic dyes [5]. It was established that six red synthetic dyes (C.I. 15580; C.I. 15585; C.I. 15630; C.I. 15800; C.I. 15880; C.I. 15865) can be fully separated on silica high-performance TLC (HPTLC) layers in a three-solvent system calculated by the optimization models. The theoretical plate number and the consequent separation capacity of traditional TLC can be considerably enhanced by using supports of lower particle size (about 5 μ m) and a narrower particle size distribution. The application of these HPTLC layers for the analysis of basic and cationic synthetic dyes has also been reviewed [6]. The advantages of overpressured (or forced flow) TLC include improved separation efficiency, lower detection limit, and lower solvent consumption, and they have also been exploited in the analysis of synthetic dyes.

The detection of synthetic dyes on any type of TLC or HPTLC support is very easy; they contain chromophore groups and can be seen without using an ultraviolet (UV) lamp or detection reagents.

The quantitative evaluation of the amount of dyes in a spot can be carried by the traditional method of scrapping the spot from the plate, dissolving the dyes in a solvent and measure the extinction of the solution. This method is time-consuming and the reproducibility is fairly poor. To date, quantitative evaluation methods such as videodensitometry and scanning densitometry have also found application in the TLC analysis of dyes. The reproducibility of these evaluation methods is higher and commensurate with those obtained by high-performance liquid chromatography; the time consumption is significantly lower than that of the tradi-

tional "scrapping-dissolving" method. The separation and quantitative determination of the impurities of the dye Phloxim B (2',4',5',7'-tetrabromo-4,5,6,7-tetrachloro-3',6'-dihydroxyspiro[isobenzofuran-1(3H),9'-[9H]xanthen-3-one-sodium salt) was performed on silica HPTLC layers [7]. A lower-halogenated impurity (2',4',5'-tribromo derivative) was separated by the mobile-phase acetone-chloroform-*n*-butylamine (66:24:4.5 v/v). Ethyl ester impurity was separated from the main fraction of Phloxim B with chloroform-glacial acetic acid (4:1 v/v). The concentration of impurities was determined *in situ* by videodensitometry. It was established that HPTLC-videodensitometry is rapid and reliable and can be successfully used for the measurement of impurities in Phloxim B. Although the TLC analysis of synthetic dyes is well established, the number of theoretical articles dealing with the quantitative relationship between retention characteristics, molecular structure, and physicochemical parameters of solutes is surprisingly low. The retention behavior of seven monotetrazolium and nine ditetrazolium salts on alumina and reversed-phase alumina was recently studied and the relationship between retention and physicochemical parameters of this class of synthetic dyes was elucidated by canonical correlation analysis [8].

Calculations indicated that the retention on both TLC supports is of mixed character, including hydrophobic, electronic and steric parameters.

It can be concluded from the present state of the art of TLC analysis of synthetic dyes that the methods are mainly limited to the application of traditional TLC technique. Due to the rapidly developing instrumentation and automation of the various steps of TLC analysis and the introduction of coupled methods (TLC-

mass spectrometry, TLC–Fourier transfer infrared spectrometry, etc.), their acceptance and successful application in the analysis of synthetic dyes can be expected in the near future. The use of new TLC techniques not only increases the separation capacity of the method but also considerably decreases the detection limit of solutes and may contribute to their identification.

References

1. V. K. Gupta, in *Handbook of Thin-Layer Chromatography* (J. Sherma and B. Fried, eds.), Marcel Dekker, Inc. New York, 1996, pp. 1001–1032.
2. D. Muralidharan and V. S. Sundara, *J. Soc. Leather Technol. Chem.* 79: 178 (1995).
3. L. Gagliardi, D. De Orsi, and O. Cozzoli, *Cosmet. Toiletries Ed. Ital.* 16: 34 (1995).
4. M. Lederer and H. K. H. Nguyen, *J. Chromatogr. A* 723: 405 (1996).
5. K. Morita, S. Koike, and T. Aishima, *J. Planar Chromatogr. — Mod. TLC* 11: 94 (1998).
6. A. B. Gharpure, *Text. Dyer Printer* 29: 13 (1996).
7. P. Wright, N. Richfield-Fratz, A. Rasooly, and A. Weisz, *J. Planar Chromatogr. — Mod. TLC* 10: 157 (1997).
8. T. Cserháti, A. Kósa, and S. Balogh, *J. Biochem. Biophys. Methods* 36: 131 (1998).



Thin-Layer Chromatography–Mass Spectrometry

Jan K. Różyło

Marie Curie-Skłodowska University, Lublin, Poland

Introduction

There are many methods of detection of substances following separation of mixtures by thin-layer chromatography (TLC) or, in wider aspect, planar chromatography (PC). Some of the methods have been continuously used since the beginnings of TLC. These are described in other sections of this volume. The newest method in this field is mass spectrometry (MS) coupled with planar chromatography. The concept of using MS as a detection method for samples separated by TLC is not new; it dates almost to the beginning of organic mass spectrometry itself. It was Kaiser who suggested the possibility of using a coupled TLC–MS method in his review 30 years ago. Despite a long and successful history of application as a detector in gas chromatography (GC) and liquid–liquid chromatography (LLC), mass spectrometry has been underutilized as a detector for TLC. The need for application of this combined analytical method (i.e., mass spectrometric detection with separation by TLC) was evident by the late 1980s. The success of the method depended, above all, on the elaboration of suitable experimental means, devices, and solutions to the challenge of transfer of substances from TLC plates to the mass spectrometer.

Basic Principle of Mass Spectrometry and Its Application to TLC

In a mass spectrometer, instead of an optical spectrum in the spectrometer, we have a mass spectrum of matter radiation. The necessary condition for using a mass spectrometry detection is ionization of components of the analyzed sample. Thus, we can say that mass spectrometry is a destructive method of analysis. There are many techniques and systems for mass spectrometry, but they all have the same three elements: source of ions, ion analyzer, and ion detector (Fig. 1).

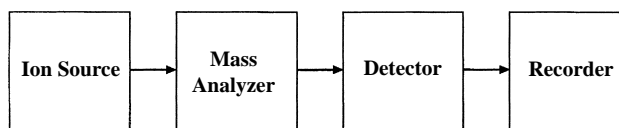


Fig. 1 Scheme of the mass spectrometry procedure.

The Source of Ions

Positive ions can appear by simple removal of one electron. This process can be demonstrated by means of the equation



The M^{+} ion is called a *molecular ion*. It is characterized by means of mass (m) and charge (z). In order to produce a molecular ion, there must be supplied energy at least equal to the energetic potential of the molecule. The first ionization potential for most organic molecules is between 8 and 15 eV. The studied sample is transferred to a vessel under vacuum, in which there is an anode and a cathode. The potential difference between anode and cathode is over 20 kV. With such a large potential difference and small distance between anode and cathode, there appear electrical discharges which cause the ionization of sample molecules. The positive ions are pushed away by repellent electrodes and directed toward an *acceleration gap*. Of course, it is possible that the electron would be captured by the analyzed molecule and produce a negative ion, but the probability of such a process is small. However, fragmentation of a negatively charged molecule is much easier than fragmentation of a positively charged molecule. The higher the ionization energy used, the greater will be the probability of fragmentation of a molecule.



Analysis of Ions

Magnetic fields affect charged molecules if these molecules are in motion. The direction of this action is perpendicular to the direction of the field and perpendicular to the direction of movement of the investigated ion. The strength of the force acting on an ion in a magnetic field depends on the ion charge and its velocity. The effects of the action of this force depends on mass and velocity. Finally, the ions move along arcs of circles and the deviation from their original direction of movement depends on their m/z ratio.

The most popular mass spectrometers used in chromatography are sector magnetic spectrometers. They are large, expensive, and relatively slow spectrometers. Their primary advantage is their high resolution. A constant, strong electrical field within the acceleration gap speeds the ions up to their terminal velocities. The ion beam goes into the analyzer, *in vacuum* (10^{-7} – 10^{-8} Tr), and placed in the magnetic field. In order to obtain a spectrum, either the magnetic field in which the analyzer is located or the accelerating voltage between the electrodes in the acceleration gap is changed. The ion beam leads into a collector, whereas the signal is amplified by means of an electron multiplier.

Quadrupole Spectrometer

The resolution of this spectrometer is not high, but the spectrometer are of relatively low cost and fast; they collect a full spectrum of the investigated substance in about 0.3 s. In the spectrometer (also called *quadrupole filter*), there appears an electromagnetic field which causes the oscillation of ions. At given voltages, the oscillation amplitude of ions under a certain mass is larger than the distance between one of the pairs of electrodes; such ions are thrown out of the filter. Through the filter to the detector, there arrive only the ions of a determined mass.

Ion Trap

In an ion trap, in contrast to other mass spectrometers, ionization and analysis occur in the same location but at different times. A chromatographic sample is introduced directly into the space between the electrodes, where ionization takes place. An appropriate voltage across the electrodes causes appearance of an electrical field within the trap. This field keeps the ions pro-

Thin-Layer Chromatography–Mass Spectrometry

duced during ionization inside the trap and does not allow them to leave. When ionization is completed, the voltage of the electrodes is constantly changed so that the ions leave the trap in the order of increasing m/z ratio.

Soon after the advent of fast-atom bombardment (FAB) ionization, it was realized that there is an ionization technique which is ideally suited for analyzing compounds resolved on a TLC plate. There are several early examples of the direct analysis of spots from TLC plates (without prior extraction of the adsorbed material). Detection limits of these TLC–FAB–MS measurements depend on the sample, but they are typically in the 0.1–10- μ g range.

The coupled TLC–FAB–MS, without the prior recovery of analyte from the TLC plate, provides a powerful tool for the unambiguous identification of sample components. The use of tandem MS–MS represents a further refinement of this approach, enabling identification to be performed even when the separated components are incompletely resolved from each other or are subject to background interference.

General Approaches to Sample Preparation for the Coupled TLC–MS

The following are combinations to these approaches:

1. The compound is eluted from the chromatographic plate, collected, and introduced into the mass spectrometer as a discrete sample. In this method, samples collected from a TLC spot, identified with an independent method of visualization, must be sufficiently volatile to evaporate into the source of the mass spectrometer.
2. The sample and support are not separated, but both are introduced simultaneously into the source of the mass spectrometer. The spot is scraped from the support and placed on the direct insertion probe of the mass spectrometer. As the probe is heated, the more volatile sample is evaporated into the source, whereas the fairly nonvolatile chromatographic matrix remains in the probe.
3. The entire intact chromatogram is placed within the source of the mass spectrometer and analyzed.

For the last two methods, there is the assumption that extraneous material from the chromatogram does not unduly and adversely affect the quality of the mass spectrum which is recorded. The chromatogram is placed, intact, within a source housing and a spatially



resolved map of organic or bio-organic compounds distributed across the surface is measured.

At the present time, the most up-to-date methods of ionization in TLC–MS are FAB and secondary ionization mass spectrometry (SIMS) in which organic molecules are sputtered from surface by impact of a stream of high-energy molecules, and laser desorption (LD), in which sputtering of organic molecules from surface of a support is due to the influence of high thermal energy produced by a laser beam onto plate surface. The ions produced this way are usually even-electron ($M^+ + H$)⁺ and appear by means of chemical ionization, and the interpretation of spectrum follows the same lines.

Bush designed an excellent instrument which can be used for analyses of TLC chromatograms by FAB–MS which provides spatially discrete mass spectra directly from the surface layer.

Some Practical Problems

The use of MS as a detector for TLC concerns identification of substances in a mixture, as well their

separation. A necessary condition in this approach is the purity of a sample within a spot on the chromatogram. A special problem is the large quantity of support and, sometimes, also a binding material, and mobile-phase residues. Some other factors which hinder TLC–MS might potentially be water, which is physically bound to the support, as well as, in some cases, the organic modifier of the support. A factor which complicates the detection process in TLC–MS may also be the presence of derivatives in a sample peak displayed on a chromatogram. That is why the analyzed sample should be as free of contamination with other additives as possible and the support matrix should be carefully removed before MS analysis. These indications refer, to a lesser degree, to other methods of detection which are performed after total extraction of sample molecules from sample matrix. It is a widely known fact that most of the analyses using a TLC–MS method are performed after exhaustive extraction of the sample from the matrix.

There are also some practical problems connected with the instrumental issues of MS. Most of the sources used in mass spectrometers are so small that it is pos-

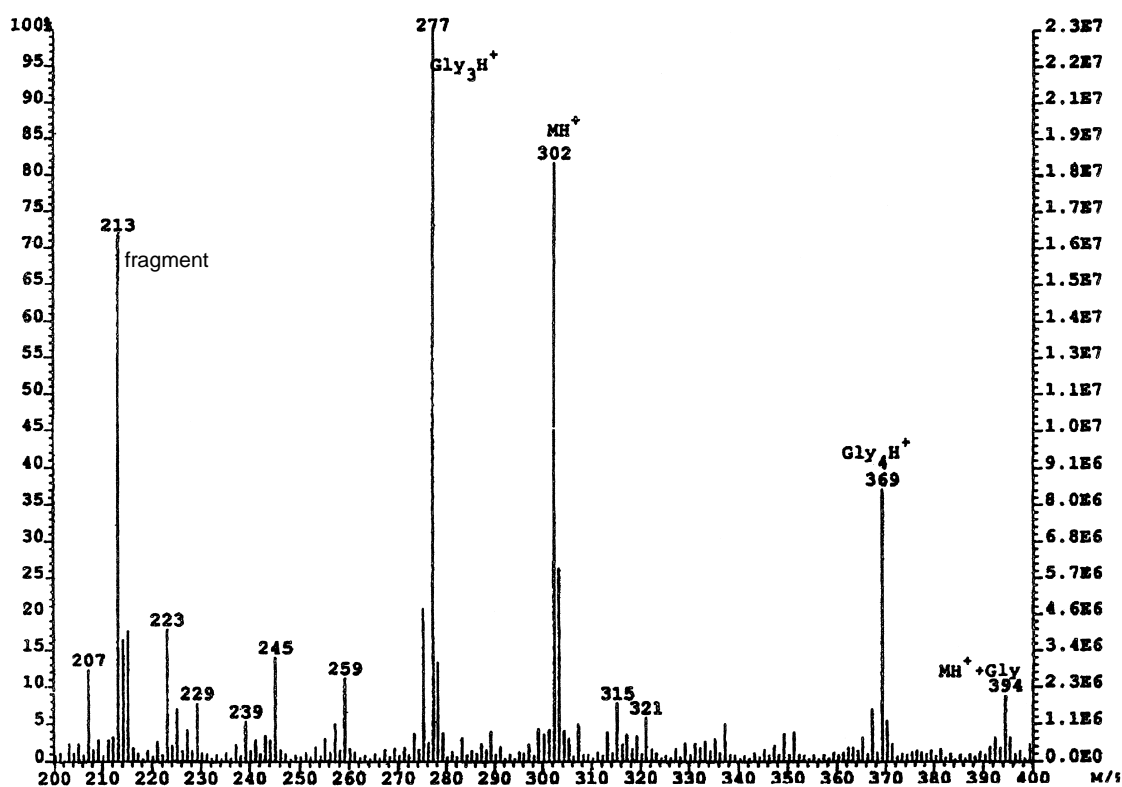


Fig. 2 TLC–FAB–MS spectrum obtained after of 1 μ g deramciclane standard with an acidic mobile phase. Gly indicates glycerol clusters. (Permission of *J. Planar Chromatogr.* 10: 90–96 (1997).)



sible to also have, for example, a very small inlet for the gas or liquid. In this case, such TLC–MS methods may only be used if they are based on the introduction of samples via a stream of gas. The matrix, together with sample material, may be introduced directly into the MS source. Some types of instruments even allow for the insertion of a whole chromatographic plate into the MS source.

Applications

Expansion in the field of analytical mass spectrometry has taken place in recent years; in particular, the applicability of TLC–MS in the field of chemical and biochemical science has been significantly broadened. This technique can now be used for the analysis of macromolecules such as peptides, proteins, oligosaccharides, and oligonucleotides, etc. (Refer to Fig. 2.)

The combination of TLC and MS is well established and may be used for on- and off-line analysis. The increase in popularity of this combined technology also resulted from the improvements in the separating power of TLC and the widespread availability of suit-

Thin-Layer Chromatography–Mass Spectrometry

able MS techniques for difficult-to-analyze molecules. The TLC–MS is, at present, a simple and readily implemented means of combining a separation with mass spectrometric identification of substances. With the development of MS suited to direct TLC analysis, it seems clear that the application of TLC–MS will grow in the next decade.

Suggested Further Reading

- S. M. Brown and K. L. Bush, *J. Planar Chromatogr.* 4: 198 (1991).
- K. L. Bush, in *Handbook of Thin-Layer Chromatography* (J. Sherma and B. Fried, eds.), Marcel Dekker, Inc., New York, 1966, p. 183.
- K. L. Bush and R. G. Cooks, *Science* 218: 247 (1982).
- K. L. Bush, J. O. Mullis, and J. A. Chakel, *J. Planar Chromatogr.* 5: 9 (1992).
- R. J. Day, S. E. Unger, and R. G. Cooks, *Anal. Chem.* 52: 557A (1980).
- R. E. Kaiser, *Chem. Britain* 5: 54 (1969).
- P. Martin, W. Morden, P. Wall, and I. Wilson, *J. Planar Chromatogr.* 5: 255 (1992).
- Y. Nakagawa, *Iyo Masu Kenkyukai Koenshu* 9: 39 (1984).



Three-Dimensional Effects in Field-Flow Fractionation: Theory

Victor P. Andreev

Institute for Analytical Instrumentation, Russian Academy of Sciences, St. Petersburg, Russia

Introduction

A field-flow fractionation (FFF) channel is normally ribbonlike. The ratio of its breadth b to width w is usually larger than 40. This was the reason to consider the 2D models adequate for the description of hydrodynamic and mass-transfer processes in FFF channels. The longitudinal flow was approximated by the equation for the flow between infinite parallel plates, and the influence of the side walls on mass-transfer of solute was neglected in the most of FFF models, starting with standard theory of Giddings and more complicated models based on the generalized dispersion theory [1]. The authors of Ref. 1 were probably the first to assume that the difference in the experimental peak widths and predictions of the theory may be due to the influence of the side walls.

Discussion

The essence of the side walls effect follows. The flow velocity turns to zero at the side walls as well as at the main (accumulation and depletion) walls of the FFF channel. Therefore, the flow profile is nonuniform, not only along the width of the channel but also along its breadth. The size of the regions near the side walls where the flow is substantially nonuniform is of the same order as w . The nonuniformity of the flow in both directions, combined with diffusion of solute particles, leads to Taylor dispersion and peak broadening that could be different from the one predicted by the 2D models.

The first 3D model of FFF was developed in Ref. 2. The 3D diffusion–convection equation was solved with the help of generalized dispersion theory, resulting in the equations for the cross-sectional average concentration of the solute and dispersion coefficients K_1 and K_2 , representing the normalized solute zone velocity and the velocity of the corresponding peak width growth, respectively. Unfortunately, only the steady-state asymptotic values of dispersion coefficients $K_1(\infty)$ and $K_2(\infty)$ were determined in Ref. 2, leading to the prediction of the solute peaks much wider than the experimental ones.

The incorrectness of the steady-state approach was noted by the authors of Ref. 3 and can be explained as follows. There are two characteristic diffusion times in an FFF channel: $t_{D1} = w^2/4D$ and $t_{D2} = b^2/4D$, where D is the diffusion coefficient of solute molecules. As the ratio $b/w > 40$, then $t_{D1}/t_{D2} > 1600$. Experimental values of retention time are usually equal to several t_{D1} , but are never as large as $1600t_{D1}$. Thus, the steady-state values of K_1 and K_2 corresponding to $t \gg t_{D2}$ are never reached during the experiment. (For the channel with $w = 200 \mu\text{m}$, $b = 1 \text{ cm}$, and solute with $D = 10^{-6} \text{ cm}^2/\text{s}$, $t_{D1} = 100 \text{ s}$ and $t_{D2} = 2.5 \times 10^5 \text{ s}$.)

In Ref. 3, the nonstationary solution was produced for $K_1(\tau)$ and $K_2(\tau)$, where $\tau = t/t_{D1}$, leading to much better correspondence with experimental peak widths. Similar to Ref. 2 not the exact equation for the flow profile in the rectangular channel but its approximation was used:

$$V_x(y, z) = V_{\max} \left(1 - \frac{4y^2}{w^2} \right) \left(1 - \frac{\cosh(2\sqrt{3}z/w)}{\cosh(\sqrt{3}b/w)} \right) \quad (1)$$

Only the case of uniform initial distribution of solute in the channel cross section was studied in Ref. 3.

A more general case was studied in Refs. 4 and 5, where different initial solute distributions were examined, including the distributions describing the syringe inlet with and without the stop-flow relaxation. The 3D generalized dispersion theory was used to solve the 3D diffusion–convection equation. Unlike Refs. 2 and 3, the exact equation for flow profile in the rectangular channel was used:

$$V_x(y, z) = 4V_{\max} \sum_{n=0}^{\infty} (-1)^n \left(1 - \frac{\cosh(2\varphi_n z/w)}{\cosh(\varphi_n b/w)} \right) \frac{\cos(2\varphi_n y/w)}{\varphi_n^3} \quad (2)$$

where $\varphi_n = (2n + 1)\pi/2$, $|z| \leq b/2$, and $|y| \leq w/2$, transversal coordinates (the zero of coordinates being at the axis of FFF channel).

The exact equation for the flow profile was chosen because, although approximation (1) gives very similar results for $K_1(\tau)$, the deviation for $K_2(\tau)$ could be very significant. Figure 1 presents dependences of $K_2(\tau)$ for



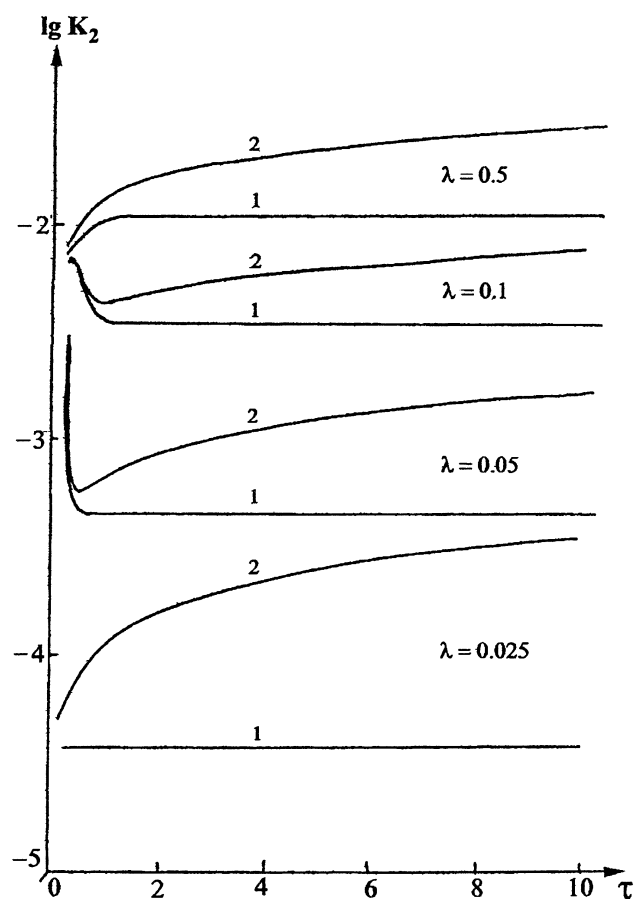


Fig. 1 Time dependences of the dispersion coefficient $K_2(\tau)$. Curve 1: 2D model; curve 2: 3D model. The solute was initially uniformly distributed in the channel cross section.

different values of the FFF parameter λ , calculated with the help of 3D [4] and 2D [1] models. It can be seen that the difference between 2D and 3D results is growing with time τ and is larger for smaller values of λ . The growth of $K_2(\tau)$ with time leads to the nonlinear growth of the peak variance with time:

$$\sigma^2(t) = 2Dt + \frac{V_{\max}^2 W^4}{8D^2} \int_0^{4Dt/W^2} K_2(\gamma) d\gamma \quad (3)$$

If K_2 is constant for the typical experimental values of retention time, as predicted by the 2D theory, then $\sigma^2 \sim t$ and resolution $R_s \sim \sqrt{t}$, where $R_s = \Delta X/4\sigma$ and ΔX is the distance between peak maximums for two types of solute molecule. According to the 3D model, $K_2(\tau)$ grows with time, so $\sigma^2 \sim \alpha t + \beta t^2 + \dots$, and there exists some value of retention time for each λ , when resolution stops growing with time.

This effect is even more pronounced for the case of a syringe inlet. At the beginning of the process, the solute is distributed in the region close to $z = 0$, so it does not feel the influence of the side walls and, only after the period of time commensurate with the second diffusion time t_{D2} , the solute particles diffuse to the side walls. That is why, at the beginning of the process, the value of K_2 is close to the 2D value of K_2 and is growing toward its asymptotic 3D value slower than for the case of the solute initially distributed uniformly in the channel's cross section (presented in Fig. 1).

In Ref. 5, the time needed to separate two types of solute molecule with resolution $R_s = 1$ was studied for the cases of different initial solute distributions. It was shown, for example, that for solute molecules with $\lambda = 0.1$ and $\lambda = 0.125$, the time needed to separate them, predicted by the 3D model for uniform initial solute distribution, is 5% larger than predicted by the 2D theory, whereas, for the case of the syringe inlet, the value predicted by the 3D model is much closer to the 2D value (only 0.5% difference). The difference in 2D and 3D predictions can be more significant for closer values of λ , when the retention time needed to fractionate the solute is larger.

More complicated 3D effects were studied in Refs. 6 and 7 with the help of 3D Monte Carlo digital simulation performed with a rather powerful computer (RISK System/6000). Sedimentation FFF with different breadth-to-width channel ratios and both codirected and counterdirected rotation and flow were studied. Secondary flow forming vortices in the y - z plane is generated in the sedimentation FFF channel, both due to its curvature, and the Coriolis force caused by the centrifuge rotation. The exact structure of the secondary flow was calculated by the numerical solution of the Navier-Stokes equations and was used in the Monte Carlo simulation of the movement of solute molecules.

It was shown that when rotation and flow are codirected, there is a considerable amount of molecules eluted prematurely before the main peak, because they are caught by the vortex of the secondary flow. This effect is practically negligible when the flow and rotation are counterdirected. So, the counterdirected mode is always preferable in sedimentation FFF. Note that this important practical finding of Ref. 7 is of pure 3D nature and cannot be done with the 2D theory.

The contribution of the channel endpieces to the peak broadening is certainly a 3D effect and should be mentioned here, although the theory used in Ref. 8 to analyze this effect was a 2D, not a 3D, one. In FFF instruments, the inlet and outlet tubes are connected with the rectangular FFF channel by triangular end-

pieces. So, if the solute is introduced to the channel with the flow, then “the fanning out process between the inlet and the main rectangular section of the FFF channel leads to crescent-shaped bands, a type of distortion that persists down the channel and is responsible for some incremental band broadening” [8]. The 2D (in the x - z plane) model was developed. The flow was considered to be ideal and described by the stream function, satisfying the Laplace equation. The streamlines calculated were used to simulate the solute band profile and to estimate the contribution of the endpieces effect to the theoretical plate height:

$$H_e = \frac{b^2 \beta^2 \tan^2(\theta/2)}{4L} \quad (4)$$

where L is the total FFF channel length, θ is the angle of the triangular endpiece, and β is a function of θ , determined from the calculated band profiles. It was shown that $\beta^2 \tan^2(\theta/2)$ grows dramatically with θ , and is equal to 0.0226 for $\theta = 30^\circ$ and to 0.389 for $\theta = 120^\circ$. The role of the end effects must not be overestimated, as even for the channel with unusually large breadth $b = 6$ cm ($\theta = 75^\circ$), the absolute value of H_e was 0.0586 cm, much smaller than the typical FFF HETP values (~ 1 cm). Naturally, this type of contribution to peak width is absent if the solute is introduced by the syringe into the main rectangular section of the channel.

Finally, it must be said that in most of the practical cases, retention ratio and peak width are satisfactorily predicted by the 2D models. The role of the 3D models was to estimate the contributions of the 3D effects and to determine the optimal conditions when these

contributions are negligible. As it was shown, to minimize the 3D effects, one must use FFF channels with a larger breadth-to-width ratio, use the syringe inlet, and/or use the longer endpieces with the sharper angle; in the case of sedimentation FFF, one is to avoid codirected flow and rotation mode.

References

1. S. Krishnamurthy and R. S. Subramanian, Exact analysis of FFF, *Separat. Sci. Technol.* 12: 347 (1977).
2. T. Takahashi and W. N. Gill, Hydrodynamic chromatography: Three dimensional laminar dispersion in rectangular conduits with transverse flow, *Chem. Eng. Sci.* 5: 367 (1980).
3. E. K. Kim and I. J. Chung, Transient convective mass transfer in rectangular FFF channels, *Chem. Eng. Commun.* 42: 349 (1986).
4. V. P. Andreev and M. I. Khidekel, Field-flow fractionation in a rectangular channel. Three dimensional model, *Nauchn. Appar.* 4: 123 (1989) (in Russian).
5. V. P. Andreev and M. I. Khidekel, On the influence of the channel side walls on the resolution time in FFF, *Zh. Phys. Chim.* 65: 2619 (1991).
6. M. R. Shure, Digital simulation of sedimentation FFF, *Anal. Chem.* 60: 1109 (1988).
7. M. R. Shure and S. K. Weeratunga, Coriolis-induced secondary flow in sedimentation FFF, *Anal. Chem.* 63: 2614 (1991).
8. P. S. Williams, S. B. Giddings, and J. C. Giddings, Calculation of flow properties and end effects in FFF channels by a conformal mapping procedure, *Anal. Chem.* 58: 2397 (1986).



TLC Immunostaining of Steroidal Alkaloid Glycosides

Waraporn Putalun

Hiroyuki Tanaka

Yukihiro Shoyama

Graduate School of Pharmaceutical Sciences, Kyushu University, Fukuoka, Japan

Introduction

The immunoassay system using monoclonal antibodies (MAbs) is indispensable to biological investigations. However, because this was rare for naturally occurring bioactive compounds having small molecular weights, we have prepared the MAbs and established assay systems using enzyme-linked immunosorbent assay (ELISA) for forskolin [1], marijuana compound [2], opium alkaloids [3], solamargine [4], ginsenoside Rb1 [5], crocin [6], and glycyrrhizin [7]. Furthermore, the Western blotting method against ginseng saponins [8] and glycyrrhizin [9] have been established for the search of natural resources and for the breeding project of medicinal plants.

The natural resources of adrenocortical and sex hormones, which have been mainly supplied by diosgenin, are becoming rare in the world. The most important feature of solasodine is that it can be converted to dehydropregnenolone. Therefore, the steroidal alkaloid glycosides of solasodine type, such as solamargine, have become important as a starting material for the production of steroidal hormones. Rapid, simple, highly sensitive and reproducible assay systems are required for a large number of plants and a limited, small amount of samples, in order to select the strain of higher yielding steroidal alkaloid glycosides.

We present, here, a simple determination method for solasodine glycosides by using thin-layer chromatography (TLC)–immunostaining.

Materials and Methods

Chemicals and Immunochemicals

Bovine serum albumin (BSA) and human serum albumin (HSA) were provided by Pierce (Rockford, IL, U.S.A.). Peroxidase-labeled anti-mouse IgG was provided from Organon Teknika Cappel Products (West Chester, PA, U.S.A.). Polyvinylidene difluoride (PVDF) membranes (Immobilon-N) were purchased from Millipore Corporation (Bedford, MA, U.S.A.). A

glass microfiber filter sheet (GF/A) was purchased from Whatman International Ltd. (Maidstone, England). All other chemicals were standard commercial products of analytical grade.

Solamargine and solasonine were isolated from fresh fruits of *S. khasianum* as previously described [10]. Solasodine was obtained from solamargine by acid hydrolysis as previously described [10]. Solamargine (1 mg) was dissolved in MeOH containing 1M HCl (1 mL). The mixture was heated at 70°C for 10, 20, 30, 60, and 90 min, respectively. Individual hydrolysates were evaporated *in vacuo* and applied to TLC. Spots developed on TLC were determined by H₂SO₄ and Dragendorff reagent.

TLC

Solasodine glycosides were applied to TLC plates and developed with chloroform–methanol–ammonia solution (7:2.5:1). A developed TLC plate was dried and then sprayed with blotting solution mixture of isopropanol–methanol–water (5:20:40, by volume). It was placed on a stainless-steel plate, then covered with a PVDF membrane sheet. After covering with a glass microfiber filter sheet, the whole plate was pressed evenly for 45 s with a 130°C iron, as previously described [11], but with a modification. The PVDF membrane was separated from the plate and dried.

Immunostaining of Solasodine Glycosides on PVDF Membrane

The blotted PVDF membrane was dipped in water containing NaIO₄ (10 mg/mL) under stirring at room temperature for 1 h. After washing with water, 50 mM carbonate buffer solution (pH 9.6) containing BSA (1%) was added and stirred at room temperature for 3 h. The PVDF membrane was washed twice with phosphate buffer solution containing 0.05% of Tween 20 for 5 min, and then washed with water. The PVDF membrane was immersed in anti-solamargine MAb



and stirred at room temperature for 1 h. After washing the PVDF membrane twice with TPBS and water, a 1000 times dilution of peroxidase-labeled goat anti-mouse IgG in phosphate buffer solution containing 0.2% gelatin (GPBS) was added and stirred at room temperature for 1 h. The PVDF membrane was washed twice with TPBS and water, then exposed to 1 mg/mL 4-chloro-1-naphthol–0.03% H_2O_2 in PBS solution which was freshly prepared before use for 10 min at room temperature, and the reaction was stopped by washing with water. The immunostained PVDF membrane was allowed to dry.

Results and Discussion

After solasodine glycosides were transferred to the PVDF membrane sheet from the TLC plate by heating as previously reported [11], the PVDF membrane was treated with NaIO_4 solution, followed by conjugation with BSA, because solasodine glycosides on PVDF membrane are washed out by buffer solution or water without the formation of conjugate with carrier protein. The PVDF membrane was immersed in anti-solamargine MAb and then peroxidase-labeled secondary MAb. When the substrate and H_2O_2 were added, clear blue spots appeared.

Figure 1 shows the immunostaining of acid hydrolysis products of solamargine hydrolyzed by 1M HCl for 10, 20, 30, and 60 min, respectively. Individual hydrolysates were applied to three TLC plates, then developed with a CHCl_3 –MeOH– NH_4OH solvent system. Two plates were sprayed and colored with H_2SO_4 . Figure 1 shows the immunostaining (a) and stainings by H_2SO_4 (b) and Dragendorff reagent (c). When the staining

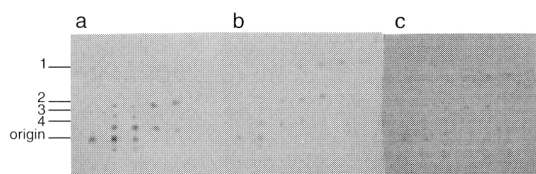


Fig. 1 Hydrolyzed products of solamargine by HCl. (a), (b), and (c) show TLC–immunostaining and the stainings with sulfuric acid and with Dragendorff reagent, respectively. Solamargine was hydrolyzed by 1M HCl for 10, 20, 30, 60, and 90 min, respectively. Spots 1–4 were identified with solasodine, 3-*O*- β -D-glucopyranosyl solasodine, L-rhamnosyl-(1 \rightarrow 4)-*O*-3- β -D-glucopyranosyl solasodine, L-rhamnosyl-(1 \rightarrow 2)-3- β -*O*-D-glucopyranosyl solasodine, respectively.

TLC Immunostaining of Steroidal Alkaloid Glycosides

sensitivities of the three methods were compared, the immunostaining was the highest, followed by the H_2SO_4 , then Dragendorff reagent. It is easily suggested that product 1 may be aglycone of solamargine, solasodine and products 2–4 might be solasodine monoglycosides and diglycosides. Therefore, products 1–4 were identified as solasodine, 3-*O*- β -D-glucopyranosyl-solasodine, *O*- α -L-rhamnosyl-(1 \rightarrow 4)-3-*O*- β -D-glucopyranosyl-solasodine and *O*- α -L-rhamnosyl-(1 \rightarrow 2)-3-*O*- β -D-glucopyranosyl-solasodine, respectively, by direct comparison with authentic samples. Compared with two stainings between immunostaining (Fig. 1a) and H_2SO_4 staining (Fig. 1b), solasodine was not detected by immunostaining despite 44% of cross-reactivity [4]; the sugar moiety was necessary in this staining process. Thus, we separated two functions, the sugar moiety of solasodine glycosides conjugates to the membrane via Schiff base and an aglycone part which is stained by MAb.

Figure 2 shows the immunostaining and H_2SO_4 staining of the crude extracts of *Solanum* species fruits which contain the higher solasodine glycosides [10]. Although the H_2SO_4 staining (Fig. 2B) detected many spots, including, probably, sugars and different types of saponins in various *Solanum* species, the immunostaining (Fig. 2A) detected only limited solasodine glycosides. Bands 1, 2, and 3 were identified to be khasianine, solamargine, and solasonine, respectively, by comparison with authentic samples. Different sensitivities between solamargine and solasonine were observed, and the sensitivity of solasonine was somewhat higher compared to that of solamargine. The detectable limit was 1.6 ng of solasonine, as previously reported.

This is the first report in which the TLC–immunostaining for solasodine glycosides is described. This

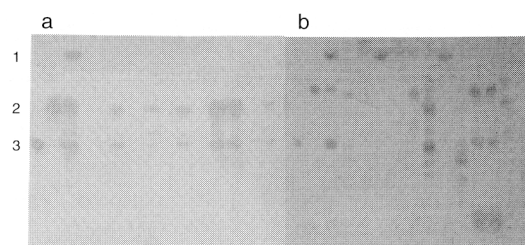


Fig. 2 TLC–immunostainings of steroidal alkaloid glycosides in the crude extracts of *Solanum* species fruits. Crude extracts were developed by a CHCl_3 –MeOH– NH_4OH solvent system on silica gel TLC plate. After being transferred to a PVDF membrane, the membrane was treated with NaIO_4 and stained by MAb. Spots 1–3 were identified with khasianine, solamargine, and solasonine, respectively.

assay method can be routinely used for survey of natural resources of solasodine glycosides as a simple and rapid analysis. Moreover, this methodology may be available for the assay in vitro *Solanum* plantlets; therefore, it makes it possible to study a large number of cultured plantlets, and a limited small amount of sample in vitro for the breeding of *Solanum* species containing a higher amounts of steroidal alkaloids. Furthermore, this system may be useful for the analysis of animal plasma samples of glycoside or glucuronide not limited to solasodine glycosides and/or distributions in organs or tissues, because very low concentrations are expected. Although it is difficult to detect a low-molecular-weight compound by the Western blotting method, the approach described here will be particularly attractive in a wide variety of comparable situations as indicated in the distribution of solasodine glycosides in the fruit of *S. khasianum*. In the expanding studies of this result, naturally occurring pharmacologically active glycosides such as ginsenosides Rb₁, [8] and glycyrrhizin [9] have been investigated.

References

1. R. Sakata, Y. Shoyama, and H. Murakami, *Cytotechnology* 16: 101 (1994).
2. H. Tanaka, Y. Goto, and Y. Shoyama, *J. Immunoassay* 17: 321 (1996).
3. Y. Shoyama, T. Fukada, and H. Murakami, *Cytotechnology* 19: 55 (1996).
4. M. Ishiyama, Y. Shoyama, H. Murakami, and H. Shinohara, *Cytotechnology* 18: 153 (1996).
5. H. Tanaka, N. Fukuda, and Y. Shoyama, *Cytotechnology* 29: 115 (1999).
6. L. Xuan, H. Tanaka, Y. Xu, and Y. Shoyama, *Cytotechnology* 29: 65 (1999).
7. H. Tanaka and Y. Shoyama, *Biol. Pharm. Bull.* 21: 1391 (1998).
8. N. Fukuda, H. Tanaka, and Y. Shoyama, *Biol. Pharm. Bull.* 22: 219 (1999).
9. S. J. Shan, H. Tanaka, and Y. Shoyama, *Biol. Pharm. Bull.* 22: 221 (1999).
10. S. B. Mahato, N. P. Sahu, A. X. Ganguly, R. Kasai, and O. Tanaka, *Phytochemistry* 19: 2018 (1980).
11. H. Tanaka, W. Putalun, C. Tsuzaki, and Y. Shoyama, *FEBS Lett.* 404: 279 (1997).



TLC Sandwich Chamber

Simion Gocan

"Babes-Bolyai" University, Cluj-Napoca, Romania

Introduction

In column chromatography, the stationary phase exists in a closed column that is adequately packed with a suitable sorbent. The stationary phase is preequilibrated with the mobile phase before the first sample is introduced. In this case, the stationary phase cannot be in contact with vapors of the mobile phase during the chromatographic process.

Column chromatography is different from thin-layer chromatography (TLC) because, in planar chromatography, and, therefore, in TLC, development generally starts with a dry stationary phase. Therefore, the mobile-phase front moves forward in the dry stationary phase. This process takes place in the limited, confined volume of the chromatographic chamber.

The kinetics of eluent migration will depend on the degree of saturation of the chamber. The eluent front runs faster in a saturated chamber than in an unsaturated one. The problem of the reproducibility of R_f values can be seriously affected by an unsaturated chamber.

The chromatographic chamber commonly used in TLC can be divided into two categories. A normal chamber (N chamber) is a chromatographic chamber of a large volume with a distance of gas phase in front of a thin-layer greater than about 3 mm. Conversely, a sandwich chamber (S chamber) is a small chromatographic chamber having a small volume and a distance of gas space in front of the thin layer plate less than 3 mm.

The equilibration of the sorbent thin layer with the vapor phase is easily achieved in the compact S chamber. A threefold larger variation of the R_f values for experiments in unsaturated atmosphere has been observed. Also, it has been proved that, in an unsaturated chamber, the so-called "edge effect" appears, owing to the more intense evaporation at the edge of the plate. This effect may be avoided by complete saturation of an N chamber with eluent vapor or by using an S chamber.

There are two methods for development, taking into account the position of the thin-layer plate (i.e., ascending, or vertical, and horizontal).

S Chamber

The S chamber (Fig. 1a) is limited to a small volume by using a thin-layer plate as a near wall (1) to the tank. The opposite wall is a cover plate (2) of small size. This is a frame plate, which has glass strips (5 mm wide and 3 mm thick) sintered along three edges. The two plates are held together by two clamps fixed at the vertical edges of the S chamber (3). This S chamber is placed in a trough which consists of a double jacket (4) of stainless steel filled with solvent (5). The other jacket can be turned to obtain slits at varying distances, which enables plates of different widths to be introduced and ensures a tight seal for the S chamber. The S chamber has a support (6) which permits a vertical position. Only 15 mL of mobile phase are needed for the thin-layer plate (20 × 20 cm). Before application, a 10-mm strip of adsorbent should be removed from three sides of the TLC plate.

There is another type of S chamber which permits prior saturation of the chamber atmosphere, simultaneously with the preconditioning of the adsorbent, before starting the chromatographic process (Fig. 1b). For this purpose, the adsorbent is removed (a 1 cm width) from all the sides of the plate (1). The opposite frame plate (2) contains, on all of its surface, a thin layer of sorbent. The two plates are fixed by two clamps (3). The chamber is introduced into the trough (4) through a slit. At the beginning, the level of the eluent (5) does not touch the bottom of adsorbent on the thin-layer plate (1). When saturation of the atmosphere is achieved, a volume of eluent is added to the eluent in the trough until the adsorbent is wetted. At this moment, the separation can be started.

Method of Operation

A template is indispensable for ensuring proper spacing of the starting spots during manual sample application. The sample is applied to the layer using a glass capillary or a micropipette of appropriate size (1–10 μ L). Sample may be applied as bands to the TLC plates using a band applicator such as the Camag automatic TLC sampler. The automatic TLC



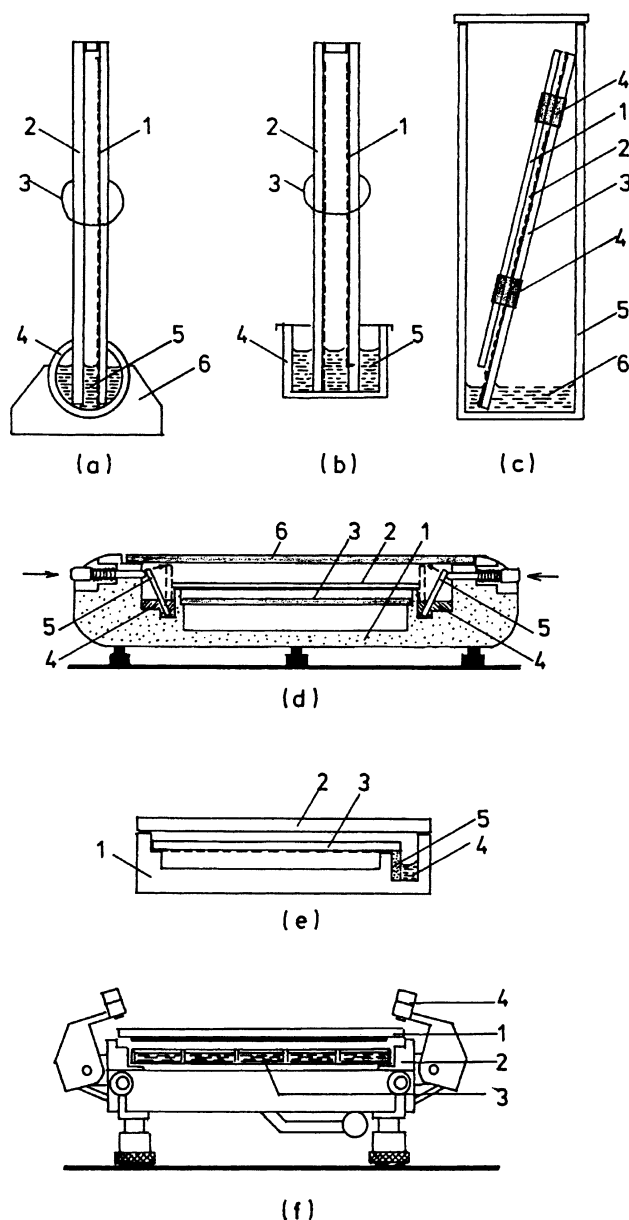


Fig. 1 Different TLC sandwich chambers: (a) diagram of the S chamber; (b) diagram of the saturation S chamber; (c) diagram of the Camag sandwich cover plate; (d) diagram of the Camag horizontal developing S chamber; (e) diagram of the Desaga H-separation chamber; (f) diagram of the Camag Vario-KS chamber.

sampler works by mechanically moving the plate. This applies the sample automatically by a controlled nitrogen spray from the syringe, forming narrow bands or spots on the plate surface. Programming, operation, and documentation are performed under a Windows-programmed environment.

When the samples have been applied, the frame plate is placed on the top of the TLC plate and fastened by two wide clamps at the right and left edges. In this way, the S chamber is ready to be placed into the trough filled with eluent. The S chamber is kept upright by a fork-shaped holding arm fixed to the trough. Then, the trough slit is sealed by gentle rotation of the outer jacket.

The separation process can be considered finished when the eluent front touches the upper edge of the thin-layer plate.

Camag Sandwich Cover Plate

This type of S chamber has the purpose of reducing the volume of the gas phase, which is in front of the thin layer by a counterplate placed at a small distance (Fig. 1c). The cover glass (1) has two fixed glass spacers (2) located on two sides. The cover plate (1) is 2 cm shorter than the TLC plate (3) and is fixed so that it does not sit deeply into the eluent. The thin-layer plate and cover plate are held together by four stainless-steel clamps (4). The S chamber is not closed at the top edge. In this configuration, there is no need to scrape off the sorbent layer at the edges. With the Camag sandwich cover plate, the TLC plate can be developed into an N chamber (5) which contains, on the flat bottom, the eluent (6). The N chamber is used only as eluent holder. This system permits simultaneous development of two plates.

Horizontal S Chamber

The horizontal developing chamber is a sandwich-type chamber (Fig. 1d). The horizontal S chamber for TLC consists of a flat body of the chamber made from polytetrafluoroethylene (PTFE) (1) so that it is resistant to all liquids. The TLC or high-performance TLC (HPTLC) plate (2) lies on the supports with the thin layer facing downward. The glass plate (3) is used for development in the sandwich configuration (not presented with saturation configuration). A narrow trough (4) holds the eluent. Development is started by shifting the glass strips (5) to the chromatographic plate. In this way, a capillary slit is formed between glass strip and the trough wall, so that a vertical meniscus of the eluent is formed and rises instantaneously. It enters the layer evenly from its front. The glass strip (5) is tilted inward by pushing the rods (arrows). The chamber is kept covered with the glass plate (6) during both preequilibration and development.

Method of Operation

In the horizontal chamber, the HPTLC plate is developed from both opposing sides toward the middle. This permits the number of samples to be doubled, as compared with development in an N chamber. The horizontal S chamber is available for plate sizes 10×10 cm and 20×10 cm. The optimum separation distance for HPTLC silica gel, 45 mm, is still available.

The mobile phase is transported from the trough to the sorbent layer by surface tension and capillary forces and will continue to travel through the sorbent layer by capillary action. When a plate is developed from both edges simultaneously, the chamber must be kept in a perfectly horizontal position to allow the two solvent fronts the same rate of migration and to meet precisely in the middle. At this point, the capillary forces balance out and the chromatographic development ceases.

The chromatographic process takes less than 10 min per plate and the amount of solvent used is much smaller than in an N chamber. On a 20×20 cm HPTLC plate, it is possible to simultaneously develop, from both ends to the centers, up to 70 samples, or 35 samples in a single direction, from one end to the other.

The horizontal S chamber can be used in saturation configuration (N type) when the counter glass plate (3) is not inserted. In this way, the horizontal S chamber permits the conditioning of the adsorbent layer with the different solvent vapors by introducing several drops of the eluent or another solvent on the bottom of the chamber before placing the chromatographic plate face down.

H-Separation Chamber

The H-separation chamber (DESAGA), a mini horizontal development chamber (Fig. 1e), is made of solvent resistant PTFE (1) covered with a sheet of glass (2) 4 mm thick. The HPTLC plate (5×5 cm) is laid down for development with the thin layer underneath (3). The mobile phase from the trough (4) is led by a glass frit rod (5) to the thin layer of sorbent. The groove in which the frit rod sits ensures

even distribution. The maximum eluent consumption is 2 mL on the plates.

Method of Operation

The sample is applied to the starting line on the layer using a capillary of appropriate size. The applied spots have to be dried completely before the plate is introduced into the separation chamber. The effective migration distance on a plate of 5×5 cm is only 3 cm and the migration time is 3 min.

Vario-KS Chamber

The Vario-KS chamber (Camag, Fig. 1f) is used for optimization of developing conditions for 10×10 cm plates by simultaneously testing of up to six different mobile phases and vapor equilibration conditions with N or S chamber conditions. Also, the Vario-KS chamber may be used for optimization of developing conditions for 20×20 cm TLC plates. The thin-layer plate (1) is laid down on the support (2). The eluent in the reservoir is connected to the thin layer of adsorbent by means of a filter paper strip. Under the thin-layer plate, there are many troughs (3) filled with solvents for preconditioning of the adsorbent layer. The chamber is tightly sealed by two clamps (4).

Suggested Further Reading

- F. Geiss, *Fundamental of Thin-Layer Chromatography*, Hüthig, Heilbelberg, 1987.
- N. Griberg (ed.), *Modern Thin-Layer Chromatography*, Marcel Dekker, Inc., New York, 1990.
- J. G. Kirchner, *Thin-Layer Chromatography*, 2nd ed., John Wiley & Sons, New York, 1978.
- J. Sherma and B. Fried (eds.), *Handbook of Thin-Layer Chromatography*, 4th ed., Marcel Dekker, Inc., New York, 1999.
- E. Stahl (ed.), *Thin-Layer Chromatography*, Springer-Verlag, New York, 1969.
- J. C. Touchstone, *Practice of Thin-Layer Chromatography*, 3rd ed., John Wiley & Sons, New York, 1992.
- A. Zalatki and R. E. Kaiser (eds.), *HPTLC : High Performance Thin-Layer Chromatography*, Elsevier, Amsterdam, 1977.



TLC Sorbents

Luciano Lepri

Alessandra Cincinelli

Università degli Studi di Firenze, Firenze, Italy

Introduction

Since the introduction of commercial precoated plates in the mid-1960s, continual developments with regard to the increase of selectivity and improvement of separation efficiency were pursued [i.e., ready-to-use layers suitable for high-performance thin-layer chromatography (HPTLC), polar and hydrophobic bonded phases, plates with concentrating zones].

A wide variety of TLC and HPTLC precoated plates, which give reproducible results, are commercially available today, even though it is also possible to prepare these plates in the laboratory. Home-made plates can allow access to stationary phases which are not otherwise available.

On HPTLC layers, the average particle size and the range of particle sizes are smaller than on TLC (e.g., 2–10 μm and 5–17 μm respectively for Macherey–Nagel HPTLC and TLC silica plates) and a marked fall in theoretical plate heights is observed (about one order of magnitude smaller than on standard silica layers). Consequently, smaller plate sizes (from 20 \times 20 to 10 \times 10 cm) and small sample volumes (from 1–3 to 0.1–0.2 μL or even less) and shorter migration distances (from 10–16 to 3–8 cm) can be employed.

A rational classification system of commonly used sorbents in thin-layer chromatography is shown in Table 1.

Hydrophilic Unmodified Sorbents

Silica, Silica Gel, or Silicic Acid

This product is by far the most frequently used sorbent in TLC and is prepared by dehydration of aqueous silicic acid generated by addition of a strong acid to a silicate solution.

Chemically, each silicon atom is surrounded by four oxygen atoms in the form of a tetrahedron. The surface of silica contains (a) siloxane groups ($\text{Si} - \text{O} - \text{Si}$), (b) silanol groups ($\text{Si} - \text{OH}$), (c) water hydrogen-bonded to the silanol groups, and (d) nonsorbed “capillary” or bulk water. The silanol groups (about 8 $\mu\text{mol}/\text{m}^2$) represent adsorption-active surface centers

that are able to interact with solvent and solute molecules during the separation process.

Surface energy and surface extension together characterize the activity of silica (“activity” is the surface property of the adsorbent), and the size of the surface is reduced when covered with molecules such as water and glycol, which deactivate the surface of the sorbent. An increase in surface activity results in lower R_f values which, therefore, depend on silica porosity and humidity changes. The surface pore diameter can vary over a wide range; TLC sorbents have pores of 40, 60, 80, and 100 Å. The specific surface area of silica gel ranges from 200 to 800 m^2/g .

Activation by heating at 150–200°C removes the physically bound water. The assumption that one silica is most suitable for adsorption and another for liquid–liquid partition chromatography is questionable and, beyond that, irrelevant because pure adsorption or partition retention mechanisms generally do not occur.

Thin-layer chromatographic silica gels have specific pore volumes ranging from 0.5 to 2.0 mL/g ; sorbents with the highest values are preferred for partition chromatography. Typical applications of silica gel in TLC separation of classes of organic compounds are listed in Table 2.

Alumina

The sorbents for TLC are obtained by thermal removal of water from hydrated aluminum hydroxide preparations, at low temperature (200–600°C), and the specific surface area of these aluminas ranges from 50 to 250 m^2/g . Hydroxyl groups and oxide ions are present on the surface and the latter are responsible for the basic properties of the sorbent. The use of gypsum (calcium sulfate hemihydrate) as a binder is said to neutralize the alumina surface. Aluminas with pH values of 9–10, 7–8, and 4–4.5 are designated basic, neutral, and acidic in character, respectively. Owing to the high density of hydroxyl groups (about 13 $\mu\text{mol}/\text{m}^2$), alumina tends to adsorb water and become deactivated. For this reason, it is recommended to activate aluminum oxide precoated layers, before use, by heating 10 min at 120°C.



Table 1 Classification of the Most Used TLC Sorbents

General class	Sorbents
Polar inorganics (hydrophilic)	Silica gel or silicic acid, alumina, diatomaceous earth (Kieselguhr), magnesium silicate (Florisil)
Polar organics	Cellulose, starch, chitine, polyamide 6 or 11
Polar bonded phases	Aminopropyl-, cyanopropyl-, and diol-modified silica
Hydrophobic bonded phases	C ₂ -, C ₈ -, C ₁₈ -, and phenyl-modified silica; cellulose triacetate and triphenylcarbamate
Ion exchangers	
Inorganic	Zirconium phosphate, tungstate and molybdate, ammonium molybdophosphate and tungstophosphate, hydrous oxides
Organic	Polystyrene-based anion and cation exchangers, polymethacrylic acid; cellulose-based anion and cation exchangers; substance-specific complexing ligands
Impregnated layers	Silica impregnated with saturated and unsaturated hydrocarbons (squalene, paraffin oil), silicone and plant oils, complexing agents (silver ions, boric acid and borates, unsaturated and aromatic compounds), ligands (EDTA, digitonin), and transition metal salts; silanized silica gel impregnated with anionic and cationic surfactants
Gel filtration media	Cross-linked, polymeric dextran gels (Sephadex)
Chiral phases	Cellulose, cellulose triacetate, silanized silica gel impregnated with the copper(II) complex of (2 <i>S</i> , 4 <i>R</i> , 2' <i>RS</i>)- <i>N</i> -(2'-hydroxydodecyl)-4-hydroxyproline (CHIRALPLATE, HPTLC CHIR)

Table 2 Application in Normal- and Reversed-Phase TLC

Sorbent	Substance class
Silica gel	Aflatoxins, alkaloids, anabolic compounds, barbiturates, benzodiazepines, bile acid, carbohydrates, etheric oil components, fatty acids, flavanoids, glycosides, lipids, mycotoxins, nitroanilines, nucleotides, peptides, pesticides, steroids, sulfonamides, surfactants, sweeteners, tetracyclines, vitamins
Alumina	Aromatic hydrocarbons, herbicides, hydrazines, insecticides, metal ions, fat-soluble vitamins, lipids, lipophilic dyes, PAHs
Cellulose	Amines, amino acids, antibiotics, artificial sweeteners, carbohydrates, catechols, flavanoids, PAHs, peptides
Alkyl- and aryl-bonded phases	Alkaloids, amides, amines, amino acids, amino phenols, antibiotics, antioxidants, barbiturates, drugs, fatty acids, indole derivatives, nucleobases, oligopeptides, optical brighteners, PAHs, peptides, pharmaceuticals, phenols, phthalates, porphyrins, preservatives, steroids, surfactants, tetracyclines
Amino-modified silica gel	Nucleosides, nucleotides, pesticides, phenols, purine derivatives, steroids, vitamins
Cyano-modified silica gel	Analgesics, antibiotics, benzodiazepines, carboxylic acids, carotenoids, pesticides, phenols, steroids
Diol-modified silica gel	Nucleosides, pesticides, pharmaceuticals, phospholipids
Cellulose-based ion exchangers	DNA adducts, DNA and RNA fragments, dyes for food, inorganic ions, steroids
Polystyrene-based ion exchangers	Amines, amino acid, inorganic ions, peptides, purine and pyrimidine derivatives
Ammonium tungstophosphate	Amines, amino acids, indole derivatives, oligopeptides, polyamines, sulfonamides
Silica gel impregnated with paraffin, silicon, and plant oils	Barbiturates, carboxylic esters, fatty acid derivatives, nitrophenols, PCBs, peptides, pesticides, phenols, steroids, surfactants, triazines
Silanized silica gel impregnated with anionic and cationic surfactants	Aliphatic and aromatic amines, alkaloids, amino acids, amino sugars, carboxylic and sulfanilic acids, drugs, indole derivatives, nucleobases, nucleosides, nucleotides, peptides, dipeptides, polypeptides, phenols, phenothiazine bases, steroids, sulfonamides, water-soluble food dyes
Silver-impregnated silica gel	<i>cis</i> -Monoenoic esters, <i>cis/trans</i> - and <i>trans/trans</i> -Dienoic esters, fatty acid cholesteryl esters, positional and geometric isomers of fatty acid methyl esters, terpenoids, prostaglandins

Aluminas are of notable selectivity in adsorption chromatography of aromatic hydrocarbons; examples of separations of organic and inorganic compounds by adsorption and partition chromatography on layers of alumina are reported in Table 2.

Cellulose

Cellulose is formed by long chains of β -glucopyranose units connected one to another at the 1–4 positions. TLC sorbents are native fibrous cellulose and microcrystalline cellulose AVICEL.

The polymerization degree of native cellulose ranges from 400 to 500 glucose units and the fibers are shorter (2–20 μm) than those in paper chromatography, preventing the instantaneous spreading of solutes. The specific surface area is about 2 m^2/g .

High-purity fibrous cellulose, obtained by washing under very mild acidic conditions and, successively, with organic solvents, is also used in TLC. AVICEL is formed by dissolving the amorphous part of native cellulose by hydrolysis with hydrochloric acid.

Partition chromatographic mechanisms operate on cellulose thin layers even if adsorption effects cannot be excluded (for separation of substance classes, see Table 2).

Polyamide

Synthetic organic resins used in TLC are polyamide 6 (Nylon 6) and polyamide 11, which consist of polymeric caprolactam and undecanamide, respectively. Therefore, polyamide 6 is more hydrophilic than polyamide 11, owing to the shorter hydrophobic chain of its monomeric unit.

Polyamide precoated plates are currently used for the separation of phenols and phenolic compounds (i.e., anthocyanins, anthoxanthines, anthroquinone derivatives, and flavones) using solvents of different elution strength (DMF > formamide > acetone > methanol > water). Such eluents and solutes compete for the hydrogen bonds with the peptide groups of the polyamide.

Due to the medium polarity of polyamide 6, the sorbent can be made more or less hydrophobic than the mobile phase selecting appropriate polar and nonpolar eluents; therefore, normal- and reversed-phase chromatography and also two-dimensional technique can be developed.

Polar and Hydrophobic Bonded Phases

A variation of chromatographic selectivity in TLC has been obtained using surface-modified silica gel or cellulose.

Alkyl- and Aryl-Bonded Silica Plates

These materials are suitable for reversed-phase thin-layer chromatography owing to their lipophilic properties. Reversed phase (RP) means that the stationary phase is less polar than the mobile phase.

Although unbonded silica is still the sorbent preferred by most workers, there is an increasing demand for nonpolar plates, because they broaden the applicability of TLC.

The commonly used RP layers consist of dimethyl- (RP-2), octyl- (RP-8), octadecyl- (RP-18), and phenyl-bonded silica gel, type 60, with different mean particle sizes and particle size distributions.

The lipophilic character of the sorbent increases from RP-2 to RP-18, but it is also determined by the surface density of hydrophobic residues. Consequently, silicas are reacted to a different degree, either totally (100%) or partially (i.e., 50% of the reactive silanol groups) in order to obtain materials of various hydrophobicity and wettability.

Because aqueous–organic mixtures are commonly used as eluents, it should be noted that RP-18 plates can be developed with solvents containing a maximum water content of approximately 60% (v/v), whereas on 50% modified silica layers, water percentages as high as 80% can be employed. Wettable RP-18W plates for normal- and reversed-phase chromatography can be eluted with purely organic and aqueous–organic solvents as well with purely aqueous eluents.

Typical applications of reversed-phase chromatography are shown in Table 2. Beyond analytical applications, RP-TLC on bonded phases is also a tool for physicochemical measurements, particularly for molecular lipophilicity determination of biologically active compounds. Hydrophobicity can be measured by partition between an immiscible polar and nonpolar solvent pair, particularly in the reference system *n*-octanol–water. The partition coefficient, *P*, is frequently used to interpret quantitative structure–activity relationships (QSAR studies).

Boyce and Milborrow [1] showed that the R_M values [$R_M = \log(1/R_f - 1)$] can be used as hydrophobic parameters.



These sorbents possess, as functional groups, cyano, amino, and diol residues, bonded by short-chain hydrophobic spacers to the silica matrix. With respect to polarity, hydrophilic-modified silicas range between nonmodified silica and the nonpolar alkyl- or aryl-bonded phases:

In the case of NH_2 and CN plates, the functional groups are bonded through a trimethylene chain to the silica gel. The hydrophilic-modified layers are wetted by all solvents, including water, and are useful for the separation of polar substances which can cause problems with silica or alumina (see Table 2). The NH_2 ready-to-use plates can act as a weak basic ion exchanger.

Several functional groups have been used to obtain cellulose anion exchangers [aminoethyl (AE), diethylaminoethyl (DEAE)], or cation exchangers [carboxymethyl (CM), phosphate (P)] for thin-layer chromatography. PEI cellulose is not a chemically modified cellulose, but a complex of cellulose with polyethyleneimine. These cellulose exchangers are particularly useful for the separation of proteins, aminoacids, enzymes, nucleobases, nucleosides, nucleotides, and nucleic acids.

The large surface area of cellulose exchangers causes a large number of functional groups to be close to the surface. The distances of the active groups are longer than on exchange resins (about 50 Å and 10 Å, respectively), but cellulose ion exchangers, despite their smaller exchange capacity with respect to polystyrene-based exchangers, can be easily penetrated by large hydrophilic molecules, such as proteins, enzymes, and nucleic acids, which, therefore, interact with all the active groups.

On the contrary, the majority of ionic substituents of exchange resins do not participate in the reaction,

because they are located inside the synthetic resin matrix which hydrophilic molecules cannot penetrate.

The selectivity of sorbents can be easily improved by their impregnation with suitable organic and inorganic substances. The impregnating agent can be added to the sorbent suspension before plate preparation or, alternatively, the precoated layers may be dipped into an appropriate solution containing the impregnating agent.

Ready-to-use impregnated plates are also commercially available (i.e., caffeine- or ammonium-sulfate-impregnated silica for the separation of polynuclear aromatic hydrocarbons and surfactants, respectively).

A large number of impregnating agents have been tested, the most frequently used in TLC are silver nitrate, metal ions, cationic and anionic surfactants, silicone, and paraffin oil. Boric-acid-impregnated silica gel layers are suitable for the resolution of carbohydrates and lipids.

Argentation chromatography, in which silver is used as a π complexing metal on a silica gel support, is usually employed for the separation of organic compounds with electron-donor properties due to the presence of unsaturated groups in the molecule of the analytes (see Table 2).

Thin-layer chromatography is particularly appropriate for applying silver complexation techniques because the instability of silver causes severe limitations to column lifetime and, therefore, to HPLC methods.

The first investigation on alkyl-bonded silica layers impregnated with anionic and cationic surfactants was carried out by Lepri and co-workers [2]. The optimal concentration of the alcoholic solution of the impregnating agent was found to be 4%.

As regards the layers, ready-to-use alkyl-bonded silica plates were found to have many advantages over the previously employed home-made plates. An appropriate term proposed for this chromatographic technique is surely "dynamic ion-exchange chromatography." The method can be applied to separation of a wide variety of ionic compounds and classes of compounds (see Table 2).

Polymeric, cross-linked dextran gels, called Sephadex[®], are used in size-exclusion TLC. Sephadex[®] gels, which are available in coarse (100–300 μm), medium (50–150 μm), fine (20–80 μm), and superfine (10–40 μm) par-

ticle size distributions, must be applied in a total swollen condition as chromatographic sorbents and eluted with the aid of continuous development techniques.

A typical application in TLC is the determination of the molecular weight of proteins [3].

Layers for Chiral Chromatography

Only cellulose, cellulose triacetate, and silanized silica gel impregnated with the copper(II) salt of derivatized L-hydroxyproline have been used as chiral stationary phases for the separation of enantiomeric solutes.

Detailed information on the topic can be drawn from the entry Enantiomer Separations by TLC.

References

1. C. B. C. Boyce and B. V. Milborrow, A simple assessment of partition data for correlating structure and biological activity using thin-layer chromatography, *Nature (London)* 208: 537 (1965).

2. L. Lepri, P. G. Desideri, and D. Heimler, Soap thin layer chromatography of some primary aliphatic amines, *J. Chromatogr.* 153: 77 (1978).
3. P. Fasella, A. Giartosio, and C. Turano, Applications of thin-layer chromatography on Sephadex to the study of proteins, in *Thin-Layer Chromatography* (G. B. Marini-Bettolo, ed.), Elsevier, Amsterdam, 1964, pp. 205–211.

Suggested Further Reading

- Geiss, F., *Fundamentals of Thin Layer Chromatography (Planar Chromatography)*, Alfred Hüthling Verlag, Heidelberg.
- Grassini-Strazza, G., V. Carunchio, and A. M. Girelli, Flat-bed chromatography on impregnated layers, *J. Chromatogr.* 466: 1 (1989).
- Hauck, H. E., and M. Mark, Sorbents and precoated layers in thin layer chromatography, in *Handbook of Thin Layer Chromatography* (J. Sherma and B. Fried, eds.), Marcel Dekker, Inc., New York, 1996, pp. 101–128.



Topological Indices, Use in HPLC

Alina Pyka

Silesian Academy of Medicine, Sosnowiec, Poland

INTRODUCTION

A tendency in chemical investigations is for the prediction of physicochemical and biological properties of chemical compounds from their structural parameters. The fundamental establishment of these investigations is based on the fact that the structure of a molecule determines its properties. The prediction of physicochemical and toxicological properties of organic compounds with selected topological indices has been reviewed in monographs and dedicated articles. The first topological indices used for the prediction of selected physicochemical properties (boiling point, heat of formation, heat of vaporization, molar volume, and molar refraction) were the Wiener index, polarity number, and Platt's index. The Wiener index has been continuously modified.

MOLECULAR STRUCTURE AND PROPERTIES

Only quantum mechanics completely describes the structure of a molecule, characterizing its geometric and electronic structures. In many cases, the structural description of a molecule is shown by type and order of the connections of atoms, and by the form and size of a molecule. The topological indices, which are derived from graph theory, are the simplest means of describing the structure of a molecule. The topological indices encode the structural information of a molecule. The topological index characterizes a molecule by a single number.^[1–3]

The applications of the topological indices in investigations—quantitative structure–activity relationship (QSAR), quantitative structure–property relationship (QSPR), and quantitative structure–retention relationship (QSRR)—for organic compounds have been described in the scientific literature. The compounds investigated were homologous series or mixtures of compounds from different classes of organic compounds. The topological indices have been applied in chromatographic investigations. The short distance traveled by a solute on a chromatographic column is the reason for the limited application of topological indices in high-performance liquid chromatography (HPLC).

The range and field of application of topological indices are limited.^[1,2] The topological indices can be applied as a descriptor only, when the correlated property is primarily dependent on the structure of a molecule. Often, the monoparametric and multiparametric equations have low values for correlation coefficients. In such circumstances, the authors introduce the correlation or modification in the way of the topological indices calculation. Such procedures lead to correlation equations with high values of correlation coefficients.^[1–3]

The application of the topological indices is an important field in theoretical chromatography. Topological indices open a new field of investigation in chromatographic science. Many scientists have reported the application of topological indices for the prediction of the retention data for different groups of organic compounds. The extent of this application in recent years has been unexpectedly large and includes the application of the topological indices in liquid chromatography [thin-layer chromatography (TLC) and HPLC].

In previous work, Pyka^[3] described the possibility of using topological indices in TLC. The objectives of this review are to describe the use of topological indices in HPLC investigations reported in the scientific literature, and to discuss the significance of such works.

PRESENTATION AND DISCUSSION

The investigation of chromatographic retention is one of the most active areas for QSRR studies using various topological indices. Many papers have been written for this important area of analytical chemistry.^[1–25] The first topological indices used for the prediction of retention parameters or lipophilic parameters were: Randi's indices (molecular connectivity indices), the Wiener index, and the Balaban (I_B) index. Selected applications of topological indices for the prediction of retention parameters of compounds separated by HPLC are covered later in this work.

Jinno and Kawasaki^[4] correlated $\log k'$ with the connectivity index χ of 26 polycyclic aromatic hydrocarbons (PAHs) separated on phenyl ($r=0.9926$), ethyl ($r=0.9905$), octyl ($r=0.9944$), and octadecyl ($r=0.9912$)

columns. Hurtubise et al.^[5] separated 34 PAHs by reversed-phase (RP) HPLC and correlated their $\log k'$ with connectivity index χ :

$$\log k' = -0.55\chi + 0.30 \quad r = 0.97 \quad (1)$$

Jinno and Kawasaki^[6] also obtained the best correlations between $\log k'$ and topological index χ , van der Waals volume (V_w), and hydrophobic parameter ($\log P$) for alkylbenzenes separated on reversed-phase C₂, C₈, and C₁₈ columns by HPLC ($r > 0.94$). In addition, Smith^[7] presented relationships between $\log k'$ and connectivity index χ for alkylbenzenes and *n*-alkylbenzenes separated by RP-HPLC on SAS-Hypersil and ODS-Hypersil columns ($r > 0.97$).

Burda et al.^[8] separated 54 alkanes (C₅–C₁₁), with different degrees of branching, by RP-HPLC on an octadecyl-silica Lichrosorb R18 column, by using a mixture of methanol and water (80:20) as mobile phase. The connectivity index χ was employed to correlate the structures of investigated alkanes with their obtained retention parameter, $\log k'$.

Wells et al.^[9] investigated 16 C₁–C₅ *n*-alkylbenzamides by RP-HPLC on a Partisil ODS column using methanol and water, as well as acetonitrile and water, in different volume compositions as mobile phases. $\log k'$ and $\log k'_w$ values were correlated with topological indices ${}^m\chi_t$ and ${}^m\chi_t^v$ values. The highest correlations were obtained with connectivity data that describe molecular bulk, branching in the hydrocarbon portion of the molecule. For example, for $\log k'_w$ values for 0% acetonitrile in mobile phase on Partisil ODS-2 and Ultrasphere ODS, the following correlation equations were obtained:

1) For Partisil ODS-2:

$$\begin{aligned} \log k'_w &= 0.070(\pm 0.013)[{}^5\chi_{PC}]^2 \\ &+ 20.930(\pm 0.917)[{}^6\chi_p^v]^2 \\ &+ 2.154(\pm 0.082) \\ r &= 0.9885 \end{aligned} \quad (2)$$

2) For Ultrasphere ODS:

$$\begin{aligned} \log k'_w &= 0.834(\pm 0.026)[{}^0\chi^v] \\ &+ 0.326(\pm 0.031)[{}^6\chi_{PC}^v]^{-1} \\ &- 3.991(\pm 0.267) \\ r &= 0.995 \end{aligned} \quad (3)$$

Adler et al.^[10] applied the Wiener index for calculating HPLC parameters for polycyclic hydrocarbons. Reten-

tion index (I) was correlated with the Wiener index for 10 PAHs:

$$\log I = 0.225(\pm 0.026)W^{(0.460 \pm 0.019)} \quad (4)$$

Siwek and Sliwiok^[11] applied connectivity, Wiener index, and Balaban index to evaluate hydrophobicities ($\log k'_w$) of selected isomer ketones, by using an RP-HPLC technique. Topological indices do not correlate well with $\log k'_w$ for a large group of compounds:^[11]

$$\begin{aligned} \log k'_w &= 0.015W + 0.50 \\ n &= 10, \quad r = 0.804 \end{aligned} \quad (5)$$

$$\begin{aligned} \log k'_w &= 1.62\chi + 1.0 \\ n &= 10, \quad r = 0.787 \end{aligned} \quad (6)$$

$$\begin{aligned} \log k'_w &= -0.28I_B + 3.41 \\ n &= 10, \quad r = 0.616 \end{aligned} \quad (7)$$

However, they can be used successfully for qualitative comparisons of hydrophobicity within the field of isomer pairs.

Kakoulidou and Rekker^[12] predicted capacity factors (k') for 14 selected *alkyl-substituted* benzophenones and four *halogen-substituted* benzophenones (separated by RP-HPLC) based on connectivity indices ${}^0\chi^v$, ${}^4\chi_{PC}^v$:

For *alkyl-substituted* benzophenones:

$$\begin{aligned} \log k' &= 0.215(\pm 0.022) \cdot {}^0\chi^v \\ &- 0.223(\pm 0.091) \cdot {}^4\chi_{PC}^v \\ &- 1.458(\pm 0.143) \\ n &= 14, \quad r = 0.9939, \\ s &= 0.037, \quad F = 483 \end{aligned} \quad (8)$$

For *halogen-substituted* benzophenones:

$$\begin{aligned} \log k' &= 0.491(\pm 0.085) \cdot {}^0\chi^v \\ &- 0.695(\pm 0.231) \\ n &= 4, \quad r = 0.9965, \\ s &= 0.051, \quad F = 281 \end{aligned} \quad (9)$$

Wells et al.^[13] investigated a series of twenty-three 5,5-dialkylbarbituric acid derivatives by RP-HPLC on Partisil ODS and Partisil ODS-2 columns using mixtures of methanol and water in volume compositions 30:70 and 50:50. The same three molecular connectivity indices were selected: ${}^1\chi$, ${}^3\chi_p$, and ${}^3\chi_p^v$ in the chromatographic



process at both 30% and 50% vol/vol methanol in water and on two different columns:

For Partisil ODS:

$$\begin{aligned}\log k'_{30\% \text{ MeOH}} &= 0.033(\pm 0.002) \cdot ({}^1\chi)^2 \\ &\quad - 0.059(\pm 0.004) \cdot ({}^3\chi_p)^2 \\ &\quad + 0.708(\pm 0.040)({}^3\chi_p^v) \\ &\quad + 1.294(\pm 0.085) \\ r &= 0.990\end{aligned}\quad (10)$$

$$\begin{aligned}\log k'_{50\% \text{ MeOH}} &= 0.018(\pm 0.001) \cdot ({}^1\chi)^2 \\ &\quad - 0.036(\pm 0.002) \cdot ({}^3\chi_p)^2 \\ &\quad + 0.431(\pm 0.020)({}^3\chi_p^v) \\ &\quad - 0.886(\pm 0.042) \\ r &= 0.991\end{aligned}\quad (11)$$

For Partisil ODS-2:

$$\begin{aligned}\log k'_{50\% \text{ MeOH}} &= 0.034(\pm 0.002) \cdot ({}^1\chi)^2 \\ &\quad - 0.064(\pm 0.004) \cdot ({}^3\chi_p)^2 \\ &\quad + 0.773(\pm 0.035)({}^3\chi_p^v) \\ &\quad + 1.526(\pm 0.075) \\ r &= 0.992\end{aligned}\quad (12)$$

This implies that the topological indices ${}^1\chi$, ${}^3\chi_p$, and ${}^3\chi_p^v$ define those molecular features that govern the RP-HPLC retention of barbiturates. The topological index ${}^1\chi$ decreased with increased branching of an alkyl group. The topological indices ${}^3\chi_p$ and ${}^3\chi_p^v$ described the exact position of branching for the investigated barbiturates.^[13]

Wells et al.^[14] also used the combination of topological indices ${}^0\chi$, ${}^0\chi^v$, ${}^4\chi_{pc}$, and ${}^4\chi_{pc}^v$ to predict retention of the hydrocarbons on various C_{18} stationary phases in aqueous methanol and acetonitrile.

Lehtonen^[15–17] used molecular connectivity indices to correlate chromatographic parameters with molecular structure for *n*-ethylbenzamides, amines, and dansylamines separated by HPLC. The best regression equation for 22 isolated amines from wines is:^[15]

$$\begin{aligned}\log k' &= -22.1({}^1\chi^v)^{-2} - 5.08({}^4\chi_{pc}^v)^{-2} \\ &\quad - 0.049({}^6\chi_{pc}) + 2.61 \\ r &= 0.991\end{aligned}\quad (13)$$

For example, the regression equation for 16 dansyl derivatives of amines (dansylamides) separated on a

Nucleosil 5 C_{18} column using the mobile phase at 39% of propanol in water is:^[16]

$$\begin{aligned}\log k' &= 0.00894({}^1\chi^v)^2 + 0.604({}^0\chi^v)^2 \\ &\quad - 2.138 \\ r &= 0.9910\end{aligned}\quad (14)$$

Lehtonen^[17] also calculated molecular connectivity indices to the third order, and a high degree of correlation was observed between the measured $\log k'$ and topological indices for 16 *n*-ethylbenzamides:

For Spherisorb S5 ODS-2 column:

$$\begin{aligned}\log k' &= 1.207(\pm 0.039) \cdot {}^1\chi^v \\ &\quad - 0.550(\pm 0.066) \cdot {}^1\chi \\ &\quad - 1.406(\pm 0.072) \\ r &= 0.9935\end{aligned}\quad (15)$$

For μ Bondapak C_{18} column:

$$\begin{aligned}\log k' &= 1.074(\pm 0.086) \cdot {}^1\chi^v \\ &\quad - 0.482(\pm 0.059) \cdot {}^1\chi \\ &\quad - 1.173(\pm 0.064) \\ r &= 0.9937\end{aligned}\quad (16)$$

The selected pesticides, monolinuron, chlortoluron, diuron, isoproturon, linuron, dimefuron, diflubenzuron, teflubenzuron, and lufenuron were separated by an isocratic RP-HPLC technique using methanol and water as mobile phase, in which the proportional content of methanol was from 45% to 90%. *n*-Hexane was selected for the determination of the retention time of an unretained compound. The topological indices based on connectivity: Gutman (M, M^v) and Randić (${}^0\chi, {}^1\chi, {}^2\chi, {}^0\chi^v, {}^1\chi^v, {}^2\chi^v$) were calculated for the investigated compounds. The $\log k$ values obtained for the all investigated urea pesticides were extrapolated to pure water (to 0% vol/vol of methanol in mobile phase) according to the equations of Soczewiński and Wachtmeister. Obtained parameters of lipophilicity $\log k_w$ and $\varphi_{o(\text{HPLC})}$ were correlated with topological indices. Only the Gutman index M^v from among all topological indices was useful in the QSAR analysis of studied urea pesticides:^[18]

$$\begin{aligned}\log k_w &= 1.0383(\pm 0.3290) \\ &\quad + 0.005267(\pm 0.000750)M^v \\ n &= 9, \quad r = 0.9358, \quad s = 0.463, \\ F &= 49.33, \quad p < 0.0005\end{aligned}\quad (17)$$

The Gutman index M^v correlates worse with $\varphi_{o(\text{HPLC})}$ ($r=0.8861$) in comparison with $\log k_w$.

The relationship between $\log k_w$ values and Gutman M^v index according to Eq. 17 is presented in Fig. 1.

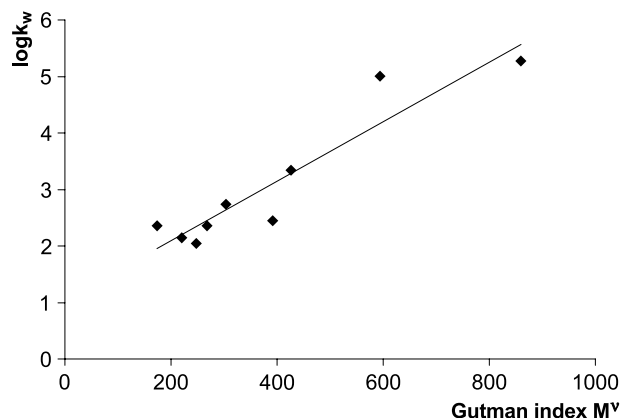


Fig. 1 Relationship between the log k_w values of selected pesticides and Gutman index M^v according to Eq. 17. (From Ref. [18].)

Amić et al.^[19] developed a simple relationship between experimental retention time by HPLC and the Wiener index (W), polarity number (p), and number of OH groups (n_{OH}) in flavyliums:

$$t_R = a[W/(pn_{OH})] + b \quad (18)$$

where a and b are statistical parameters to be determined by least squares regression. Three groups of flavyliums were investigated and three correlation equations were obtained:

For anthocyanidins:

$$\begin{aligned} t_R &= 7.1794(\pm 0.1870)[W/(pn_{OH})] \\ &\quad - 17.7954(\pm 0.7309) \\ n &= 6, \quad r = 0.9986, \\ F &= 1474.6, \quad s = 0.32 \end{aligned} \quad (19)$$

For anthocyanin 3-glucosides:

$$\begin{aligned} t_R &= 19.1354(\pm 0.7039)[W/(pn_{OH})] \\ &\quad - 41.7504(\pm 4.6820) \\ n &= 10, \quad r = 0.9946, \\ F &= 739.1, \quad s = 4.25 \end{aligned} \quad (20)$$

For anthocyanin 3,5-diglucosides:

$$\begin{aligned} t_R &= 13.6883(\pm 0.5346)[W/(pn_{OH})] \\ &\quad - 41.6262(\pm 3.7626) \\ n &= 10, \quad r = 0.9940, \\ F &= 655.6, \quad s = 2.66 \end{aligned} \quad (21)$$

Amić et al.^[19] also correlated the Schultz index MTI for anthocyanins. They suggest that the QSRR with MTI index should be identical to those with the Wiener index.

Martorell et al.^[20] separated a series of twenty-two 6-fluoroquinolones by ion pair RP-HPLC. The multi-

ple linear correlation that best fits the experimental data is:

$$\begin{aligned} \log k' &= 6.8448(\pm 1.3184)QX_{24} \\ &\quad - 0.2249(\pm 0.0933)DM \\ &\quad - 4.0366(\pm 2.1135)DIF^3\chi_c \\ &\quad + 5.0421 \\ n &= 22, \quad r = 0.8543 \end{aligned} \quad (22)$$

where QX_{24} is the negative net charge associated with the heteroatom X situated at position 4 of the heterocyclic aliphatic ring that functionalizes position C₇, DM is the dipolar moment, and $DIF^3\chi_c$ is the difference between the molecular connectivity index of valency and nonvalency of the order 3 cluster.

In recent years, topological indices have become prominent on several different fronts. Many new topological indices were described after 1990.^[1,21] Some from among them were also applied in QSRR analyses of compounds investigated by the HPLC technique.^[1,18,19,21–25]

De Julian-Ortiz et al.^[21] calculated connectivity indices to the fourth order and proposed charge indices (G_k, J_k) for racemic hydantoins, racemic α -amino acids, and racemic arylamides. The best correlation equation for racemic hydantoins separated on β -cyclodextrin column using 10% methanol as a mobile phase is:^[21]

$$\begin{aligned} \log k' &= -1.314 + 1.280 \cdot {}^4\chi_p^v - 0.185G_3^v \\ n &= 17, \quad r = 0.9426, \quad F = 55.76, \\ p &< 0.001 \end{aligned} \quad (23)$$

The best correlation equation for racemic α -amino acids separated on α -cyclodextrin column using 1% triethylamine acetate (pH=5.1) as a mobile phase is:^[21]

$$\begin{aligned} k' &= -8.262 + 0.2935G_2 - 12.187G_4 + 13.701G_4^v \\ n &= 15, \quad r = 0.9702, \quad s = 0.62, \\ F &= 58.70, \quad p < 0.001 \end{aligned} \quad (24)$$

The best correlation equation for racemic arylamides separated on 1-(α -naphthyl)ethylamine column using n -hexane-tetrahydrofuran (75:25, vol/vol) as a mobile phase is:^[21]

$$\begin{aligned} \log k' &= 3.264 - 0.209Pr_0 \\ &\quad + 1.289({}^1\chi - {}^1\chi^v) \\ &\quad - 1.943 \cdot {}^4\chi_{pc}/{}^4\chi_{pc}^v \\ n &= 14, \quad r = 0.9554, \quad s = 0.12, \\ F &= 38.3, \quad p < 0.001 \end{aligned} \quad (25)$$

where Pr_0 is the number of vertices showing topological valence equal to 4.

Pyka^[22] separated six selected steroids (corticosterone acetate, 11-dehydrocorticosterone acetate, corticosterone, 11-dehydrocorticosterone, hydrocortisone, and cortisone

by RP-HPLC on Separon Six C₁₈ column. Column void time was determined using the peak derived from a solution of sodium nitrite in methanol. The mobile phase was prepared from analytical-grade methanol and redistilled water (3:2, vol/vol). The Randić (⁰χ, ⁰χ^v, ¹χ, ¹χ^v), Wiener (W), Balaban (*I*_B), and Pyka (*A*, ⁰*B*) indices were calculated for the investigated compounds. The chromatographic data, log *k'* and partition coefficient log *P* values, of the compounds have been correlated with the numerical values of topological indices. The most accurate predictions of the log *k'* and log *P* values of the selected steroids were achieved by using monoparametric equations employing the topological indices ⁰*B*:

$$\begin{aligned} \log k' &= 18.5859(\pm 2.2622) \\ &\quad - 7.0362(\pm 0.8882) \cdot {}^0B \\ n &= 6, \quad r = -0.9696, \quad s = 0.053, \\ F &= 62.75, \quad p = 0.0014 \end{aligned} \quad (26)$$

$$\begin{aligned} \log P &= 106.454(\pm 3.332) \\ &\quad - 41.464(\pm 1.308) {}^0B \\ n &= 6, \quad r = -0.9980, \quad s = 0.078, \\ F &= 1004.23, \quad p = 0.0000 \end{aligned} \quad (27)$$

Pyka and Sliwiok^[23] separated six esters of nicotinic acids: methyl nicotinate, ethyl nicotinate, isopropyl nicotinate, butyl nicotinate, hexyl nicotinate, and benzyl nicotinate by adsorption HPLC on a LiChrospher Si 60 column. The mixtures containing benzene and methanol in volume proportions (0+10, 1+9, 2+8, 3+7, 4+6, and 5+5) were used as the mobile phases. The *t*_R (min) values of esters investigated have been correlated with the dipole moments (*μ*_{mph}) of the mobile phases applied, with numerical values of one topological index from among those based on the distance matrix (*A*, *W*, ⁰*B*, ¹*B*, ²*B*) or the adjacency matrix (⁰χ^v, ¹χ^v, ²χ^v), with electrotopological states SaaCH, aaN, aasC, dO, ssO, and dssC, and structural descriptors based on information theory (*I*_{SA} and *I*_{SA}). Dipole moments were used to characterize mobile phases. The correlation equations that enable the calculation of *t*_R values were obtained with topological indices based on adjacency matrices ⁰χ^v and ¹χ^v, with indices based on distance matrices ¹*B* and ²*B*, with index based on information theory (*I*_{SA}, *I*_{SA}), and with electrotopological state aaN. All the equations are characterized by determination coefficients *R*² > 90%. The best correlation equations were obtained with topological indices based on information theory *I*_{SA} and *I*_{SA}, as well as based on distance matrices ¹*B* and ²*B*. For example:

$$\begin{aligned} t_R &= -0.766(\pm 0.165) + 0.546(\pm 0.043) \mu_{\text{mph}} \\ &\quad + 2.179(\pm 0.100) \bar{I}_{\text{SA}} \\ n &= 36, \quad R^2 = 95.08\%, \quad F = 318.6, \\ s &= 0.046, \quad p < 0.0001 \end{aligned} \quad (28)$$

$$\begin{aligned} t_R &= 1.838(\pm 0.082) + 0.546(\pm 0.050) \mu_{\text{mph}} \\ &\quad + 1.600(\pm 0.087) {}^1B \\ n &= 36, \quad R^2 = 93.30\%, \quad F = 230.0, \\ s &= 0.053, \quad p < 0.0001 \end{aligned} \quad (29)$$

The correlation equations (Eqs. 28 and 29) can be used to calculate *t*_R values of investigated esters. For example, the relationship between *t*_R (min) values measured experimentally and values calculated using Eq. 29 is shown in Fig. 2.

Equations 28 and 29 can also be used to predict the *t*_R values of the esters of nicotinic acid, whose measurement points have not been taken into consideration in the equation. A test was performed on Eqs. 28 and 29 to determine how well they predict *t*_R values of points not included in the training set. Three values were removed from the training sets (Eqs. 28 and 29). Isopropyl nicotinate (separated in benzene:methanol, 5:5, vol/vol) and ethyl nicotinate (separated in benzene:methanol, 4:6, and 0:10, vol/vol) from Eqs. 28 and 29 were removed. This subset of two parametric equations was recalculated as:

$$\begin{aligned} t_R &= -0.753(\pm 0.175) + 0.533(\pm 0.048) \mu_{\text{mph}} \\ &\quad + 2.183(\pm 0.105) \bar{I}_{\text{SA}} \\ n &= 33, \quad R^2 = 94.85\%, \quad F = 276.2, \\ s &= 0.047, \quad p < 0.0001 \end{aligned} \quad (30)$$

$$\begin{aligned} t_R &= 1.872(\pm 0.090) \\ &\quad + 0.522(\pm 0.056) \mu_{\text{mph}} \\ &\quad + 1.604(\pm 0.090) {}^1B \\ n &= 33, \quad R^2 = 93.07\%, \quad F = 201.6, \\ s &= 0.055, \quad p < 0.0001 \end{aligned} \quad (31)$$

The *t*_R values for esters of nicotinic acids, omitted during the derivation of Eqs. 30 and 31 and subsequently predicted using these equations, are listed in Table 1.

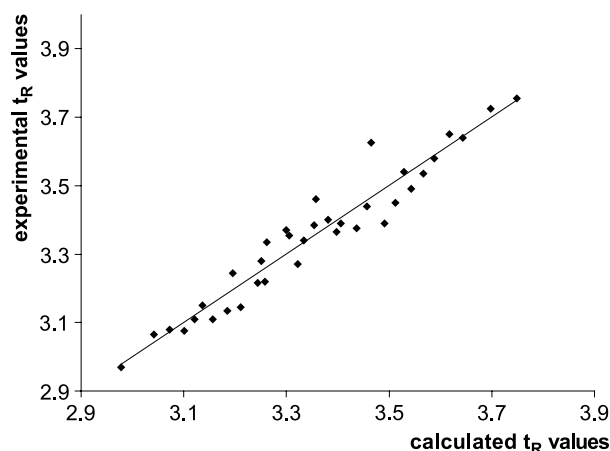


Fig. 2 Relationship between the experimental *t*_R (min) values of nicotinic acid esters and the *t*_R values calculated using Eq. 29. (From Ref. [23].)

Table 1 The t_R values (min) of nicotinic acid esters omitted from Eqs. 30 and 31, and predicted by these equations

Omitted point	t_R				
	Experimental	Predicted by Eq. 30	$ \Delta t_R $	Predicted by Eq. 31	$ \Delta t_R $
Isopropyl nicotinate (benzene:methanol, 5:5, vol/vol)	3.220	3.226	0.006	3.266	0.046
Ethyl nicotinate (benzene:methanol, 4:6, vol/vol)	3.365	3.406	0.041	3.402	0.037
Ethyl nicotinate (benzene:methanol, 0:10, vol/vol)	3.650	3.621	0.029	3.614	0.036

Source: Ref. [23].

These equations are statistically significant and can be used for a reasonably good prediction of the t_R values of the investigated esters of nicotinic acid. The high compatibility between experimental and predicted t_R values for esters omitted in the considered correlation equations was stated.

Djaković-Sekulić et al.^[24] separated eight anilides of 2,2-dimethylpropanoic acid, nine anilides of benzoic acid, and nine anilides of α -phenyl acetic acid by RP-18 HPLC using mixtures containing methanol and water in volume proportions 6+4, 6.5+3.5, and 7+3 as the mobile phases. The $\log k$ values of investigated anilides have been correlated with the dipole moments (μ_{mph}) or permittivities (ϵ_{mph}) of the mobile phases applied, with numerical values of one topological index from among those based on the distance matrix ($R, W, A, {}^0B, {}^1B, {}^2B$) or on the adjacency matrix ($M, M^v, {}^0\chi, {}^1\chi, {}^2\chi, {}^0\chi^v, {}^1\chi^v, {}^2\chi^v$), with partition coefficient by Rekker ($\log P_{\text{Rek}}$), or with the number of hydrogen acceptors (HA), or with the solubility ($\log S$), or with the molecular weight (M_w). Authors found 77 multiparametric equations with $R^2 > 90\%$. The best equations for these groups of investigated anilides are as follows:

For anilides of 2,2-dimethyl propanoic acid:

$$\begin{aligned} \log k_p = & -46.7031(\pm 2.5201) \\ & + 25.7452(\pm 1.4278)\mu_{\text{mph}} \\ & + 0.002877(\pm 0.000467)M_w \\ & + 0.2711(\pm 0.0230)\log P_{\text{Rek}} \\ n = 24, \quad R^2 = 97.31\%, \\ F = 240.8, \quad s = 0.0471, \quad p < 0.0001 \end{aligned} \quad (32)$$

For anilides of benzoic acid:

$$\begin{aligned} \log k_b = & -6.7551(\pm 0.5235) \\ & + 0.09581(\pm 0.00874)\epsilon_{\text{mph}} \\ & + 0.007500(\pm 0.00164)M \\ & + 0.4211(\pm 0.0344)\log P_{\text{Rek}} \\ n = 27, \quad R^2 = 92.16\%, \\ F = 90.1, \quad s = 0.0848, \quad p < 0.0001 \end{aligned} \quad (33)$$

For anilides of α -phenyl acetic acid:

$$\begin{aligned} \log k_{\text{ph}} = & -46.9896(\pm 2.2419) \\ & + 25.6156(\pm 1.2646)\mu_{\text{mph}} \\ & + 0.004629(\pm 0.001086)M \\ & + 0.3965(\pm 0.0208)\log P_{\text{Rek}} \\ n = 27, \quad R^2 = 97.36\%, \\ F = 283.1, \quad s = 0.0443, \quad p < 0.0001 \end{aligned} \quad (34)$$

For all anilides investigated:

$$\begin{aligned} \log k_{\text{all}} = & -52.7102(\pm 1.8869) \\ & + 25.9835(\pm 1.0372)\mu_{\text{mph}} \\ & + 0.07725(\pm 0.01892){}^2\chi^v \\ & + 2.2767(\pm 0.1816){}^0B \\ & + 0.002736(\pm 0.000360)M \\ & + 0.3222(\pm 0.0142)\log P_{\text{Rek}} \\ n = 78, \quad R^2 = 95.06\%, \\ F = 277.6, \quad s = 0.0671, \quad p < 0.0001 \end{aligned} \quad (35)$$

Equations 32–35 can also be used for $\log k$ value prediction of anilides investigated, whose measurement points have not been taken into consideration in the equation. Four of the tests of predictive equations, such as Eqs. 32–35, show how well they predict values of points not included in the training set.

From Eq. 32, $\log k$ for $(\text{CH}_3)_3\text{C}-\text{CO}-\text{NH}-\text{C}_6\text{H}_4-\text{CF}_3$ [separated with methanol and water, 7+3 (vol/vol)] was omitted, and the best subset equation using three parameters was recalculated as follows:

$$\begin{aligned} \log k_p = & -46.3329(\pm 2.6616) \\ & + 25.5281(\pm 1.5118)\mu_{\text{mph}} \\ & + 0.002907(\pm 0.000480)M_w \\ & + 0.2738(\pm 0.0240)\log P_{\text{Rek}} \\ n = 23, \quad R^2 = 97.34\%, \\ F = 231.4, \quad s = 0.0480, \quad p < 0.0001 \end{aligned} \quad (36)$$

From Eq. 33, $\log k$ for $\text{C}_6\text{H}_5-\text{CO}-\text{NH}-\text{C}_6\text{H}_4-\text{F}$ [separated with methanol and water, 6+4 (vol/vol)] was omitted, and



Table 2 The log k values of anilides omitted (experimental) from Eqs. 36–38, and predicted by these equations

Anilide	Log k_p			Log k_b			Log k_{ph}		
	Experimental (methanol + water, 7 + 3, vol/vol)	Predicted by Eq. 36	$ \Delta \text{Log } k_p $	Experimental (methanol + water, 6 + 4, vol/vol)	Predicted by Eq. 37	$ \Delta \text{Log } k_b $	Experimental (methanol + water, 7 + 3, vol/vol)	Predicted by Eq. 38	$ \Delta \text{Log } k_{ph} $
$(\text{CH}_3)_3\text{C-CO-NH-C}_6\text{H}_4\text{-CF}_3$	0.176	0.206	0.030	—	—	—	—	—	—
$\text{C}_6\text{H}_5\text{-CO-NH-C}_6\text{H}_4\text{-F}$	—	—	—	0.288	0.329	0.041	—	—	—
$\text{C}_6\text{H}_5\text{-CH}_2\text{-CO-NH-C}_6\text{H}_4\text{-F}$	—	—	—	—	—	—	−0.112	−0.088	0.024

Source: Ref. [24].

Table 3 The log k_{all} values of anilides omitted from Eq. 39 and predicted by this equation

Anilides	Log k_{all}		
	Experimental	Predicted by Eq. 39	$ \Delta \log k_{all} $
$C_6H_5-CH_2-CO-NH-C_6H_4-CH_3$	-0.002 ^a	-0.003	0.001
$C_6H_5-CH_2-CO-NH-C_6H_4-CN$	-0.208 ^a	-0.207	0.001
$C_6H_5-CO-NH-C_6H_4-Cl$	0.358 ^b	0.334	0.024
$(CH_3)_3C-CO-NH-C_6H_4-CF_3$	0.689 ^c	0.705	0.016
$(CH_3)_3C-CO-NH-C_6H_4-Br$	0.406 ^b	0.397	0.009
$(CH_3)_3C-CO-NH-C_6H_4-COCH_3$	-0.292 ^a	-0.287	0.005

^aWith methanol + water, 7+3, vol/vol as mobile phase.

^bWith methanol + water, 6.5+3.5, vol/vol as mobile phase.

^cWith methanol + water, 6+4, vol/vol as mobile phase.

Source: Ref. [24].

the best subset equation using three parameters was recalculated as follows:

$$\begin{aligned} \log k_b = & -6.7834(\pm 0.5360) \\ & + 0.09685(\pm 0.00917)\epsilon_{\text{mph}} \\ & + 0.007390(\pm 0.00169)M \\ & + 0.4199(\pm 0.0351)\log P_{\text{Rek}} \\ n = 26, \quad R^2 = 92.19\%, \\ F = 86.5, \quad s = 0.086, \quad p < 0.0001 \end{aligned} \quad (37)$$

From Eq. 34, log k for $C_6H_5-CH_2-CO-NH-C_6H_4-F$ [separated with methanol and water, 7+3 (vol/vol)] was omitted, and the best subset equation using three parameters was recalculated as follows:

$$\begin{aligned} \log k_{ph} = & -46.6855(\pm 2.3584) \\ & + 25.4532(\pm 1.3258)\mu_{\text{mph}} \\ & + 0.004548(\pm 0.001116)M \\ & + 0.3954(\pm 0.0213)\log P_{\text{Rek}} \\ n = 26, \quad R^2 = 97.26\%, \\ F = 260.5, \quad s = 0.0450, \quad p < 0.0001 \end{aligned} \quad (38)$$

Table 4 Relationships between retention time (t_r ; sec) and selected topological indices for 16 PAHs separated by HPLC

Correlation equation	Statistical parameters ^a		
	r	F	s
Eq. 40	0.9868	520	78.0
Eq. 41	0.9850	455	83.3
Eq. 42	0.9816	370	92.0
Eq. 43	0.9730	248.9	111.2
Eq. 44	0.9686	212.5	111.9
Eq. 45	0.9717	236.8	113.9
Eq. 46	0.9697	220.7	117.8
Eq. 47	0.9807	351.5	94.4
Eq. 48	0.9841	428.9	85.7

^aFor Eqs. 40–48: $n=16$ and $p<0.0001$.

Source: Ref. [18].

From Eq. 35, log k values for $C_6H_5-CH_2-CO-NH-C_6H_4-CH_3$, $C_6H_5-CH_2-CO-NH-C_6H_4-CN$, $(CH_3)_3C-CO-NH-C_6H_4-COCH_3$ [separated with methanol and water, 7+3 (vol/vol)], $C_6H_5-CO-NH-C_6H_4-Cl$, $(CH_3)_3C-CO-NH-C_6H_4-Br$ [separated with methanol and water, 6.5+3.5 (vol/vol)], and $(CH_3)_3C-CO-NH-C_6H_4-CF_3$ [separated with methanol and water, 6+4 (vol/vol)] were omitted, and the best subset equation using five parameters was recalculated as follows:

$$\begin{aligned} \log k_p = & -52.6507(\pm 2.0879) \\ & + 25.9692(\pm 1.1317)\mu_{\text{mph}} \\ & + 0.07771(\pm 0.02096)^2\chi^v \\ & + 2.2620(\pm 0.2002)^0B \\ & + 0.002742(\pm 0.000385)M \\ & + 0.3213(\pm 0.0156)\log P_{\text{Rek}} \\ n = 72, \quad R^2 = 94.32\%, \\ F = 219.1, \quad s = 0.0644, \quad p < 0.0001 \end{aligned} \quad (39)$$

The experimental and predicted log k values calculated by Eqs. 36–39 are presented in Tables 2 and 3. The differences between experimental and predicted values $|\Delta \log k|$ were small.

Pyka^[18] separated 16 PAHs (naphthalene, acenaphthylene, acenaphthene, fluorene, phenanthrene, anthracene, fluoranthene, pyrene, benzo[*a*]anthracene, chrysene, benzo[*b*]fluoranthene, benzo[*k*]fluoranthene, benzo[*a*]pyrene, dibenzo[*a,h*]anthracene, benzo[*g,h,i*]perylene, and indeno[1,2,3-*cd*]pyrene) according to the Environmental Protection Agency (EPA) by gradient HPLC on a LiChrospher[®] PAH column using acetonitrile and water as mobile phases. Retention times t_r (sec) of investigated PAHs were correlated with topological indices based on the adjacency matrix (M , ${}^0\chi^v$, ${}^1\chi^v$, ${}^2\chi^v$, χ_{012}) and the distance matrix (W , A , C , D), and correlation equations were obtained, as follows (Table 4):

$$t_R = -564.65(\pm 75.78) + 8.649(\pm 0.379) \cdot M^v \quad (40)$$



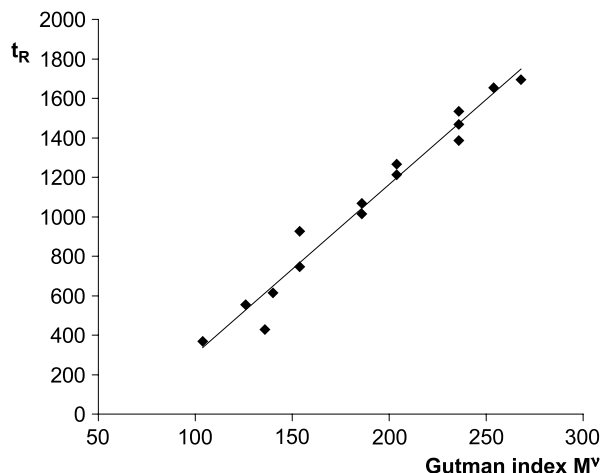


Fig. 3 Relationship between the t_R (sec) values and Gutman index M^V for 16 PAHs according to Eq. 40. (From Ref. [18].)

$$t_R = -822.91(\pm 92.82) + 209.86(\pm 9.84) \cdot {}^0\chi^v \quad (41)$$

$$t_R = -866.18(\pm 105.10) + 335.35(\pm 17.43) \cdot {}^1\chi^v \quad (42)$$

$$t_R = -660.57(\pm 115.41) + 391.63(\pm 24.82) \cdot {}^2\chi^v \quad (43)$$

$$t_R = 308.08(\pm 62.44) + 2.413(\pm 0.166) \cdot W \quad (44)$$

$$t_R = 155.71(\pm 68.04) + 6.074(\pm 0.395) \cdot A \quad (45)$$

$$t_R = -400.5(\pm 105.6) + 116.03(\pm 7.81) \cdot C \quad (46)$$

$$t_R = 16.497(\pm 62.750) + 28.61(\pm 1.53) \cdot D \quad (47)$$

$$t_R = -792.9(\pm 97.2) + 304.1(\pm 14.7) \cdot \chi_{012} \quad (48)$$

The equations with the highest statistical parameters were obtained with topological indices based on the adjacency matrix. The relationship between t_R values and Gutman M^V index according to Eq. 40 is presented in Fig. 3.

Pyka and Sliwiok^[25] separated α -tocopherols, β -tocopherols, γ -tocopherols, and δ -tocopherols by normal-phase high-performance liquid chromatography (NP-HPLC) and RP-C₁₈-HPLC. The selected topological indices based on connectivity (M^V , ${}^1\chi^v$), distance matrix (W , 0B , MTI), and information theory (I_{AC} , \bar{I}_{AC}) were

calculated for these tocopherols. As presented in Table 5, the topological indices clearly show that β -tocopherols and γ -tocopherols, as positional isomers, possess the same numerical values of topological indices ${}^1\chi^v$, M , I_{AC} , and \bar{I}_{AC} . In addition, the retention times have the same values for β -tocopherols and γ -tocopherols investigated by RP-C₁₈-HPLC. Instead, the numerical values of the topological indices W and MTI for α -tocopherols, γ -tocopherols, β -tocopherols, and δ -tocopherols in the given sequence grow smaller (decrease). Only the numerical values of the topological indices 0B grow smaller (decrease) in the following order: α -tocopherols, β -tocopherols, γ -tocopherols, and δ -tocopherols. But the difference between the numerical values of the topological index 0B is very small for β -tocopherols and γ -tocopherols. The definite dependence between the numerical values of topological index 0B and the chromatographic separation of the investigated tocopherols was obtained. In the given sequence, grow retention times of tocopherols were investigated by NP-HPLC.^[25]

CONCLUSION

Topological index is indirectly connected with the structures of chemical compounds. Topological indices, as well as retention parameters, are most important for physicochemical characteristics of organic compounds. Chromatography is applied to the separation of chemical compounds both for analytical and preparative aims. Correlation of retention parameters of organic compounds with selected topological indices (with structures of compounds studied) permits assignment of definite rules, which enable the prediction of chromatographic separations.

This work is an assessment of the possibility of using topological indices with the HPLC technique. Every quoted work is a new aspect of the use of topological indices. Data from the scientific literature indicate that the discussed topological indices can be used to predict and describe retention and lipophilic parameters obtained by HPLC for the different classes of organic compounds.

Table 5 Retention times (t_r) obtained by NP-HPLC and RP-HPLC and numerical values of topological indices for the tocopherols investigated

Compound	Retention time (t_R) (min) obtained		Topological indices						
	NP-HPLC	RP-HPLC	${}^1\chi^v$	M	W	0B	MTI	I_{AC} (bit)	\bar{I}_{AC} (bit)
α -Tocopherol	2.80	17.66	13.0432	252	3165.14	2.2070	15,433.13	88.45	1.092
β -Tocopherol	3.86	13.98	12.6205	244	2944.79	2.1769	14,554.13	85.58	1.097
γ -Tocopherol	4.88	13.98	12.6205	244	2945.96	2.1764	14,560.14	85.58	1.097
δ -Tocopherol	5.60	10.80	12.1979	236	2728.94	2.1479	13,692.47	82.70	1.103

Source: Ref. [25].



The results of the studies presented here indicate that the topological indices have significance in analytical and physicochemical investigations of organic compounds. These results indicate the capacity of molecular topology to identify and predict different structural features that determine HPLC data for a variety of organic compounds. The application of topological indices in the physicochemical investigation of organic compounds is constantly increasing. One reason for this is, among others, the use of computer programs to calculate topological indices.^[1]

This review indicates that further investigations on the application of topological indices in HPLC are warranted.

REFERENCES

1. Devillers, J.; Balaban, A.T. *Topological Indices and Related Descriptors in QSAR and QSPR*; Gordon and Breach Science Publishers: The Netherlands, 1999.
2. Pyka, A. Topological indices and their significance in chromatographic investigations, Part II. *Wiad. Chem.* **1998**, *52*, 727–754. (in Polish).
3. Pyka, A. The application of topological indexes in TLC. *JPC, J. Planar Chromatogr. Mod. TLC* **2001**, *14* (3), 152–159.
4. Jinno, K.; Kawasaki, K. Correlations between the retention data of polycyclic aromatic hydrocarbons and several descriptors in reversed-phase HPLC. *Chromatographia* **1983**, *17* (8), 445–449.
5. Hurtubise, R.J.; Allen, T.W.; Silver, H.F. Comparison of molecular connectivity and a chromatographic correlation factor in reversed-phase high-performance liquid chromatography for polycyclic aromatic hydrocarbons. *J. Chromatogr.* **1982**, *235*, 517–522.
6. Jinno, K.; Kawasaki, K. Correlations between retention data of isomeric alkylbenzenes and physical parameters in reversed-phase micro high-performance liquid chromatography. *Chromatographia* **1983**, *17* (6), 337–340.
7. Smith, R.M. Reversed-phase liquid chromatography of isomeric alkylbenzenes. *J. Chromatogr.* **1981**, *209*, 1–6.
8. Burda, J.; Kuraš, M.; Křiž, J.; Vodička, L. Relationship between retention behaviour and molecular structure of alkanes in reversed-phase high-performance liquid chromatography. *Fresenius Z. Anal. Chem.* **1985**, *321*, 549–552.
9. Wells, M.J.; Clark, C.R.; Patterson, R.M. Investigation of *n*-alkylbenzamides by reversed-phase liquid chromatography: III. Correlation of chromatographic parameters with molecular connectivity indices for the C₁–C₅ *n*-alkylbenzamides. *J. Chromatogr.* **1982**, *235*, 61–74.
10. Adler, N.; Babić, D.; Trinajstić, N. On the calculation of the HPLC parameters for polycyclic aromatic hydrocarbons. *Fresenius Z. Anal. Chem.* **1985**, *322*, 426–429.
11. Siwek, A.; Sliwiok, J. Reversed-phase high-performance liquid chromatography in the investigation of the hydrophobicity of selected ketones. *J. Chromatogr.* **1990**, *506*, 109–118.
12. Kakoulidou, A.; Rekker, R.F. A critical appraisal of log *P* fragmental procedures and connectivity indexing for reversed-phase thin-layer chromatographic and high-performance liquid chromatographic data obtained for a series of benzophenones. *J. Chromatogr.* **1984**, *295*, 341–353.
13. Wells, M.J.M.; Clark, C.R.; Patterson, R.M. Correlation of reversed-phase capacity factors for barbiturates with biological activities, partition coefficients, and molecular connectivity indices. *J. Chromatogr. Sci.* **1981**, *19*, 573–582.
14. Wells, M.J.; Clark, C.R.; Patterson, R.M. Structure-retention relationship analysis for some mono- and polycyclic aromatic hydrocarbons in reversed-phase liquid chromatography using molecular connectivity. *Anal. Chem.* **1986**, *58*, 1625–1633.
15. Lehtonen, P. Isolation and HPLC determination of amines in wine. *Z. Lebensm.-Unters. Forsch.* **1986**, *183*, 177–181.
16. Lehtonen, P. Use of molecular connectivity indices to predict LC retention of dansylamides in six different eluent systems. *Chromatographia* **1984**, *19*, 316–321.
17. Lehtonen, P. Reversed-phase liquid chromatographic elution characteristics of substituted *n*-ethylbenzamides. *J. Chromatogr., A* **1983**, *267*, 277–284.
18. Pyka, A. Unpublished data.
19. Amiđ, D.; Davidović-Amiđ, D.; Trinajstić, N. Application of topological indices to chromatographic data. Calculation of the retention indices of anthocyanins. *J. Chromatogr., A* **1993**, *653*, 115–121.
20. Martorell, C.; Calpena, A.C.; Escibano, E.; Poblet, J.M.; Freixas, J. Influence of the chromatographic capacity factor (log *k'*) as an index of lipophilicity in the antibacterial activity of a series of 6-fluoroquinolones. Relationship between physico-chemical and structural properties and their hydrophobicity. *J. Chromatogr., A* **1993**, *655*, 177–184.
21. De Julian-Ortiz, J.V.; Garcia-Domenech, R.; Galvez-Alvarez, J.; Soler-Roca, R.; Garcia-March, F.J.; Anton-Fos, G.M. Use of topological descriptors in chromatographic chiral separations. *J. Chromatogr., A* **1996**, *719*, 37–44.
22. Pyka, A. Chromatographic data-topological index dependence for selected steroids. *J. Liq. Chromatogr. Relat. Technol.* **2001**, *24* (4), 453–460.
23. Pyka, A.; Sliwiok, J. Use of traditional structural descriptors in QSRR analysis of nicotinic acid esters. *J. Liq. Chromatogr. Relat. Technol.* **2004**, *27* (5), 785–798.
24. Djaković-Sekulic, T.; Perišić-Janjić, N.; Pyka, A. Correlation or retention of anilides and some molecular descriptors. Application of topological indexes for prediction of log *k* values. *Chromatographia* **2003**, *58* (1/2), 47–51.
25. Pyka, A.; Sliwiok, J. Chromatographic separation of tocopherols. *J. Chromatogr., A* **2001**, *935*, 71–76.



Trace Enrichment

Fred M. Rabel

EM Science, Gibbstown, New Jersey, U.S.A.

Introduction

Trace enrichment is a sample precleaning procedure which is performed prior to a sample analysis. The purpose of any sample preparation procedure is twofold. First, such a procedure must selectively collect and concentrate the components of interest. Second, the method should eliminate any other components that would either interfere with the analysis or would contaminate an analytical gas chromatography (GC) or high-performance liquid chromatography (HPLC) column to shorten its useful analytical life.

Discussion

There are many sample preparation techniques listed in texts, from a simple filtration or centrifugation to many other kinds of extraction procedures, including both liquid-liquid and solid-phase extraction. When any type of sample preparation is used, it often is done manually if only a few samples are involved. If a large number of samples are to be analyzed, the entire procedure should lend itself to automation. Regardless of the number of samples, most sample preparation is done off-line; that is, the samples are prepared first with one of the methods listed, then placed into an automated sample injection system for sequential analysis of all samples.

Trace enrichment is the sample preparation procedure which is performed by passing a crude sample through a special "collection" column, but with a couple of added features. It is often done on-line, one at a time, just prior to the analytical procedure. It usually involves a minicolumn very similar to an off-line device, like a solid-phase extraction tube, but packed into a stainless-steel column and attached to the injection valve. This is called a "trace enrichment" column in many published procedures. Another name that is often given to this technique is "column switching" in the title or key words of published articles. This is because this technique involves valves that must be switched from one solvent flow stream to another. The valve, in its initial position, allows the "crude" sample

to be passed through the trace enrichment column, whereas the mobile phase is being passed only through the analytical column. After the trace enrichment column has collected the sample components of interest, these components are backflushed onto the analytical column by switching the valve to its alternate position. (See Fig. 1.)

The complete procedure for using a trace enrichment (TE) column is as follows:

1. The TE column is equilibrated with a minimum of two solvent combinations. The first solvent is strong, to wash the TE column free of impurities it may have accumulated from a previous sample (remember, this column is used over and over, so this step is critical so there is no sample carryover). This solvent is probably pure methanol or acetonitrile if using a reversed-phase filled TE column. The second solvent is not strong; it is used to bring the TE column to equilibrium to accept the sample components of in-

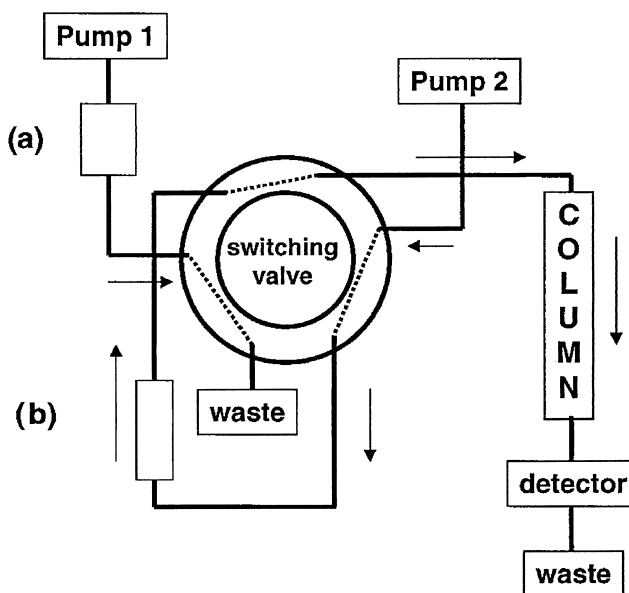


Fig. 1 Switching device.



terest. Again if a reversed-phase filled TE column is used, this could even be pure water.

2. The "crude" sample is injected or pumped onto the TE column. [Note: Even a "crude" sample requires membrane filtration and/or centrifugation to prevent shortened column life of the trace enrichment column.] The TE column will attract the components of interest, depending on the nature bonded phase in the TE column, the solvent in which the sample is dissolved, and the solvent in which the TE column has been equilibrated. The TE column, most likely, will remove more than just the components of interest and, thus, might need an additional solvent wash sequence to remove other collected impurities.
3. Finally, when sufficient sample has been passed through the TE column, the valve is switched so that the final solvent mixture is passed, with a *reversed* flow direction, through the TE column. This is usually a stronger eluting solvent combination that elutes the collected components to be chromatographed from the TE column. It is often the chromatographic mobile phase, which will also perform the actual analysis on the HPLC analytical column. Once the components are on the analytical column, the separation begins.

While the actual analytical separation is taking place, a second sample can be prepared with the same TE column. Again, a strong solvent wash, then the equilibration solvent wash precede injection of the second sample. The actual TE process on the minicolumn is usually accomplished within a few minutes, perhaps 2–3 min, and the actual separation might take 10 min. Thus, the time-limiting factor is the actual analysis, not the TE process itself. Shortening the analysis time with a shorter, more efficient column would lead to greater productivity as long as the actual analysis time is at least 1 min longer than the TE step.

The TE column ideally collects only the components of interest, permitting all unwanted impurities to pass through it. This is seldom completely true in practice, so the details of the entire trace enrichment have to be experimentally determined. These details involve determining which minicolumn packing to use and, perhaps, up to three solvent combinations. The first of these combinations is a solvent(s) which will dissolve the sample so that it carries the sample onto the TE column and simultaneously allows capture of the desired components. With experience, this first

solvent combination may also remove (elute) some unwanted components.

A second solvent combination will be used to wash more of the remaining impurities out of the minicolumn. Finally, the third solvent combination is used to backflush the captured components from the TE column onto the analytical column. This latter solvent often is the mobile phase that will also perform the actual separation.

Because about 80% of the separations being performed by HPLC are done using a reversed-phase column, this is also the most used type of minicolumn used for TE columns. It could, however, be any type, because it only has to have some degree of affinity for the components of interest in the solvents chosen for the work, based on their solubility and the chemistry of the TE packing.

When beginning the development of a TE column procedure, an excellent source of solid-phase extraction (SPE) information may be found in SPE device manufacturers' literature (or on their websites). Most manufacturers offer at least 25 years of literature references on their products. Their procedures will often provide useful information about compound types and the SPE chemistries used and solvents for cleanup and elution. The same packing material may be used in the TE column, either the same size (usually 40–63 μm for SPE tubes) or it can be a 5- or 10- μm version of it. Buying the TE packing material from the same company that makes the SPE tubes will allow the solvent information to be used with the on-line work.

Other bonded-phase chemistries will give different capture capacities and efficiencies, so the solvent to capture or elute would be completely different. If in doubt about the equivalency of the chemistries, again, manufacturers are a good source of information.

One of the most difficult types of samples to cleanup are those derived from serum, plasma, urine, or other plant or animal matrices. Proteins or other high-molecular-weight biopolymers will quickly contaminate a HPLC column if they are not removed from samples. Such off-line procedures might involve multiple steps. However, another type of packing with special bonding has been used for of this type of sample cleanup. It is called the RAM or *restricted access material*. This packing material has an outer diol-bonded phase and an internal bonded reversed phase. Biopolymers cannot penetrate the smaller pores and are repelled by the diol phase and, thus, pass completely through the column. However, the components of interest, which are usually much lower-molecular-weight drug substances, are able to pass into the pores and attach themselves to

the reversed phase. As mentioned earlier, it is still necessary to filter and centrifuge the samples before they are introduced onto the TE column, but these columns can often handle up to 2000, 50- μ L injections before having to be replaced.

If biological samples are being purified, studies should also be conducted to see under what conditions any compounds of interest are released from the proteins being eluted from the typical RAM column mentioned earlier. This is due to the strong binding experienced with many compounds onto proteins. If 50% remain bound to the protein as it is washed away, then there is 50% less compound collected for making a measurement. One might never achieve 100% release, but an extra 10–20% might be helpful in trace work.

The size of the TE column can be as small as 2–3 mm \times 10–25 mm. It simply has to have sufficient capacity to capture all, or a major percentage, of the components of interest. It should be remembered that a TE column usually captures structurally related compounds and, perhaps, some impurities; hence, it might be assumed that only 15–25% of the capacity is taken up by the compound(s) of interest. Because a relatively strong mobile phase is used for backflushing, band

broadening is not generally a problem, regardless of the size of the column.

The way most of them are used with a valve–loop injector is that the sample first flows in one direction for capture, then is backflushed onto the analytical column. This process of backflushing could also push particulates resting on the inlet frit back to the inlet of the analytical column; therefore, this is another good reason for filtration/centrifugation of samples before introducing them onto the TE column. An in-line filter can also prevent particulates from migrating to places where they can cause problems.

Suggested Further Reading

Majors, R., K.-S. Boos, C.-H. Grimm, and D. Lubda, Practical guidelines for integrated sample preparation using column switching, *LC/GC Mag.* 14: 554 (1996).

Yu, Z., D. Westerlund, and K.-S. Boos, Evaluation of LC behavior of RAM precolumns in the course of direct injection of large volumes of plasma samples in column switching systems, *J. Chromatogr.* 704: 53 (1997).



Troubleshooting HPLC Instrumentation

I. N. Papadoyannis

V. F. Samanidou

Aristotle University of Thessaloniki, Thessaloniki, Greece

INTRODUCTION

Despite the advances in technology and instrumentation, problems still arise when practicing high-performance liquid chromatography (HPLC), which cause headaches to chromatographers. During several stages of analysis, such as method development or routine operation, a variety of separation artifacts may be noticed. Pressure abnormalities, sample recovery, poor reproducibility, loss of resolution, instability, leaks, etc. are common problems.

General problems can be detected by smell, sight, or sound, although major symptoms in the LC system show up as changes in the chromatogram, such as irregular peak shapes, extra peaks, negative peaks, varying retention times, and many others. It is well known that, if a picture is worth a thousand words, then a chromatogram, to a chromatographer, is equally valuable. Any chromatographer who has injected many samples into an LC system has occasionally confronted more than one of the above-mentioned problems. Some problems can be corrected by changes in the equipment, whereas others require modification of the assay procedure. However, many of the common LC problems can be prevented with routine preventive maintenance.

Guides for troubleshooting HPLC instrumentation provide analysts and laboratory technicians with a readily available, very useful aid for solving operational problems of equipment and techniques. In order that the chromatographer effectively solves an arising problem in HPLC, he/she should be aware of the role of operating parameters, as these are indicators of system performance. Step-by-step troubleshooting protocols for each system component should be followed to isolate the problem and its cause.

OVERVIEW

This article covers problem identification and procedures for solving them, as well as practices to maintain HPLC systems in good operating condition. It also guides users of HPLC equipment to investigate the source of a malfunction through each system component, from sample preparation to detection and integration.

PROBLEMS: CAUSES AND SOLUTIONS

In an HPLC system, problems can arise from many sources. Malfunction can be allocated to various points. Chromatographers should use not only their experience to locate problems but also all their senses (obviously, except taste) to identify LC problems. For example, a leak can be noticed by smell before it is actually seen. A strange noise indicates some kind of malfunction and a "hot" smell indicates an overheating module. Most problems, however, are identified by sight, and they can mainly be observed as changes in the chromatogram. As soon as the problem has been defined, actions should be taken to correct the malfunctioning component. The incident should be recorded, in a log book kept for this purpose, to help with further failure problems at a later time.

The HPLC user should know or learn what to look for and what to do to prevent HPLC problems and, finally, what can and should be done before calling a service technician. User's manuals, manufacturer's advice, books, articles in scientific journals, computer programs, and network sites can be used as resources for troubleshooting. A general rule is that one can know that a problem exists only when one knows how the system operates when it is working well. This means that keeping detailed records of system performance (log book) is very helpful.

Dolan (refer to "Suggested Additional Reading") has very effectually set forth five rules of thumb for HPLC troubleshooting.

1. Do not change more than one thing at a time.
2. A problem is considered as problem when it occurs more than once.
3. A questionable system component should be substituted/replaced with one that is known to be working properly. Known good parts should be put back into service while all failed parts should be thrown away.
4. An experienced chromatographer should try to anticipate what will fail next.
5. Good records of maintenance and troubleshooting actions should be kept.



Table 1 Peak shape problems and remedies**Peak shape***A. Fronting*

1. Column overloaded → Decrease sample amount or dilute sample.
2. Sample solvent incompatible with mobile phase. → Adjust solvent
3. Nonresolved peak from another component. → Improve resolution by altering mobile or stationary phase.
4. Wrong pH value of mobile phase. → Adjust pH.
5. Channeling in column. → Replace or repack column.

B. Tailing

1. Secondary retention effects; residual silanol interactions. → Use ion pair reagent, or competing base or acid modifier. Triethylamine for basic compounds, acetate for acidic compounds.
2. Wrong pH value of mobile phase. → Adjust pH. For basic compounds lower pH usually provides more symmetric peaks.
3. Wrong stationary phase. → Change column.
4. Void at column inlet. → Repack top of column with stationary phase.
5. Wrong injection solvent. → Dissolve sample in mobile phase.
6. Interference in sample. → Check column performance with standards. Change mobile phase or stationary phase. Check selectivity.
7. Chelating solutes—trace metals in base silica. → Use high purity silica-based column with low trace-metal content, add EDTA or chelating compound to mobile phase; use polymeric column.
8. Unswept dead volume. → Minimize number of connections; ensure injector rotor seal is tight; ensure all compression fittings are correctly scaled.
9. Silica-based column-degradation at high temperature. → Reduce temperature to less than 50°C

Double (split) peaks

1. Column voided. → Repack top of column with stationary phase; replace column.
2. Partially blocked frit. → Clean or replace the plugged frit. Install an in-line filter between pump and injector to remove solids from mobile phase or between injector and column to filter particulates from sample.
3. If only one peak is split co-eluting interfering components. → Use sample clean up.
4. Sample solvent incompatible with mobile phase. → Inject samples in mobile phase.
5. Blocked frit. → Replace or clean frit, install 0.5-um porosity in-line filter between pump and injector to eliminate mobile-phase contaminants or between injector and column to eliminate sample contaminants.
6. Co-elution of interfering compound from previous injection. → Use sample cleanup; adjust selectivity by changing mobile or stationary phase. Flush column with strong solvent at end of run; end gradient at higher solvent concentration.
7. Column overloaded. Sample volume too large → Use higher-capacity stationary phase, increase column diameter, decrease sample amount.
8. Column void or channeling → Replace column, or, if possible, open top endfitting and clean and fill void with glass beads or same column packing; repack column.

Table 1 Peak shape problems and remedies**Peak shape**

9. Injection solvent too strong → Use weaker injection solvent or stronger mobile phase.

Broad peaks (all)

1. Large injection volume; detector operating outside linear dynamic range. → Injection of smaller sample volume or diluted sample (1:10).
2. High viscosity of mobile phase → Change mobile phase, or increase column temperature. Change to lower viscosity solvent.
3. Poor column efficiency due to column void or column contaminated/worn out. → Repack top of column; replace column.
4. Incorrect detector settings. → Check settings and adjust.
5. Low mobile phase flow rate. → Increase flow rate.
6. Tubing too long or too wide; large extra column volume → Use right tubing, shorten path. Use low- or zero-dead-volume endfittings and connectors; use smallest possible diameter of connecting tubing (< 0.10 in. i.d.); connect tubing with matched fittings.
7. Leaks between column and detector. → Check for leaks.
8. Guard column contaminated/worn out. → Replace guard column.
9. Retention times too long. → Use gradient elution or a stronger mobile phase for isocratic elution.
10. Too large volume of detector cell. → Use smaller cell volume.
11. Slow detector time constant → Adjust time constant to match peak width.

Broad peaks (some)

1. Late eluted peak from previous run. → Flush the column with a strong eluent after each run or end gradient at a higher concentration of strong solvent.
2. High molecular weight sample. → Optimize sample clean up.

Negative peaks

1. Highly UV absorbing mobile phase. → Change detection wavelength taking into account the UV cutoff of mobile phase solvents.
2. Refractive index of mobile phase is very different from RI of sample. → Change eluent.
3. Recorder connections. → Check polarity

Ghost peaks

1. Dirty mobile phase. → Use HPLC grade solvents.
2. Carryover. Retained compound from previous injection. → Flush column with strong solvent to remove late eluting compounds. End gradient at higher solvent concentration.
3. Contamination of injector. → Flush injector.
4. Contamination of column. → Flush column with strong solvent.
5. Unknown interferences in sample → Use sample cleanup or prefractionation before injection.

Spikes

1. Bubbles in mobile phase. → Degas mobile phase. Sparge it with helium (3–5 psi) during use; ensure that all fittings are tight; store column tightly capped.

(Continued)

Table 1 Peak shape problems and remedies (*Continued*)**Peak shape**

2. Bubbles in detector. → Use back-pressure regulator at detector outlet.

Extra column dispersion

1. Wrong tubing dimensions. → Use short, small internal diameter (narrower) tubing between injector and column and between column and detector.

2. Detector overloaded. Outside linear dynamic range. → Use a low volume detector cell.

3. Large sample volume. → Inject small sample volumes.

No peaks

1. Detector off. → Check detector.

2. No flow. Pump off. → Start pump.

3. No sample. Sample deteriorated. → Check injector. Check sample stability.

4. Wrong settings on recorder or detector. → Check attenuation, gain, and detector wavelength.

5. Flow interrupted. → Check reservoirs, loop, degassing of mobile phase, and compatibility of mobile phase components.

6. Leaks. → Check fittings and pump for leaks and pump seals.

7. Air trapped in the system. → Prime pump.

In HPLC instrumentation troubleshooting, problems can be classified as follows. Major HPLC problems are discussed under this paragraph, while an extended summary of problem causes and remedy actions are tabulated in the respective tables.

Problems with the Chromatogram**Peak shape**

Broad peaks, ghost peaks, pseudo peaks, negative peaks, peak doubling, peak fronting, peak tailing, spikes, no peaks. The major causes and their solutions are tabulated in Table 1.

Variable retention times

Retention time inconsistency (changing, increasing, decreasing), change in separation (loss of resolution). Table 2 summarizes their causes and solutions.

Baseline

Short-term noise, long-term noise, and drift. The causes of the baseline problems and their remedies are discussed in Table 3.

Pressure abnormalities

These include increased pressure, decreased pressure, unstable/fluctuating pressure, and high backpressure. Table 4 lists the major causes and their solutions.

Leaks

Leaks at various points, such as the column, fittings, the detector, the injection valve, or the pump. Table 5 summarizes their causes and solutions.

Change in quantitation

Including imprecision, change in selectivity, change in peak height—lack of sensitivity, poor sample recovery. Table 6 summarizes their causes and solutions.

Fig. 1 illustrates some of the changes that appear in the chromatogram as a result of the various problems.

Table 2 Retention time inconsistency*Variable retention times*

1. Leaks. → Check for loose fittings, pump leaks, seals.

2. Change in mobile phase composition. → Prepare new. Ensure that gradient system is delivering correct composition. Prevent evaporation.

3. Air trapped in pump. → Prime pump. Degas mobile phase—Spurge it with helium (3–5 psi) during use.

4. Overloading. → Dilute sample.

5. Sample dissolved in a solvent that is incompatible with the mobile phase. → Dissolve sample in the mobile phase.

6. Temperature fluctuations. → Use column oven.

7. Isocratic elution: Insufficient equilibration time. → Pass 10–15 column volumes of mobile phase through column for equilibration.

8. Gradient elution: Insufficient column regeneration time. → Increase equilibrating time.

Loss of resolution

1. Leak. Pump flow problems. → Check for leaks.

2. Obstructed guard or analytical column. → Replace guardcolumn. Reverse analytical column and flush disconnected from the detector. Change inlet frit. Replace the column.

3. Improperly prepared mobile phase; contaminated mobile phase. → Prepare fresh mobile phase. Check pump-proportioning valve for malfunction.

4. Sample overloaded. → Dilute sample and reinject.

5. Extra column dead volume. → Check system plumbing and all connections for dead volume.

6. Injector problem. → Leaking injection valve or a damaged or blocked needle has to be corrected.

7. Temperature fluctuations. → Use column oven.



Table 3 Baseline**Baseline***Regular noise*

1. Air bubbles. → Prime pump. Degas solvent. Sparge mobile phase with helium during use.
2. Pump pulsations → Use a pulse dampener.
3. Incomplete mixing. Malfunctioning proportioning valves → Ensure complete mixing. Clean or replace the proportioning valve; partially remix solvents.
4. Other electronic equipment on the same line. → Check electronic equipment in line. Correct as necessary.
5. Leaks → Check pump for leaks, salt build-up. Check fittings and pump seals.
6. Continuous-detector lamp problem or dirty flow cell → Replace UV lamp (each should last 2000 hr); clean and flush flow-cell

Irregular noise

1. Leaks. → Check fittings, pump seals, and pump for leaks.
2. Electronics. → Locate problem. Get servicing. Isolate detector and recorder electronically. Use a voltage stabilizer for the LC system or use an independent electrical circuit for the chromatography equipment.
3. Insufficient grounding → Establish sufficient grounding.
4. Flow cell contamination. → Clean detector cell.
5. Detector lamp failing. → Replace detector lamp.
6. Mobile phase mixer inadequate or malfunctioning. → Repair or replace the mixer or mix off-line in case of isocratic elution.
7. Air bubbles in detector. → Install backpressure regulator after detector.
8. Occasional sharp spikes—external electrical interference → Use voltage stabilizer for LC system; use independent electrical circuit.
9. Periodic-pump pulses → Service or replace pulse damper; purge air from pump; clean or replace check valves.
10. Random-contamination buildup → Flush column with strong solvent; clean up sample; use HPLC grade solvent.

Drift

1. Strongly retained materials. → Flush column with strong solvent.
2. Default mixing. → Check mixer. Check flow rate and composition.
3. Air in the detector cell. → Clean cell. Use backpressure regulator at detector outlet.
4. Contamination of mobile phase. → Flush column with strong solvent; use HPLC grade solvents; clean-up sample.
5. Fluctuation of column temperature. → Use column oven.
6. Gradient elution. a. Positive direction. Absorbance of mobile phase B. → Add UV absorbing compound to mobile phase A. b. Negative direction. Absorbance of mobile phase A. → Add UV absorbing compound to mobile phase B.
7. Temperature at RI detector unstable. → Control changes in room temperature. Insulate column, use column oven, cover RI detector keeping it out of air currents.
8. Mobile phase not in equilibrium with column. → Allow more time for column equilibration.

Table 4 Pressure abnormalities*Increased pressure*

1. Blocked flow lines: Pump. Injector. Tubing. → Locate obstruction, by systematic disconnection of system components. Replace or clean blocked components.
2. Obstructed column or guard column, from particulate buildup at top of column. → Replace guard column. Reverse analytical column and flush disconnected from the detector. Change inlet frit. Replace the column. Filter sample.
3. Salt precipitation. → Ensure mobile phase compatibility with buffer concentration.
4. High viscosity of mobile phase. → Use solvent of lower viscosity or increase temperature.
5. Microbial growth in the column. → Store column with at least 25% organic solvent. Add 0.02% sodium azide to aqueous mobile phases, or use a mobile phase with at least 10% organic solvent.

Decreased pressure

1. Leaks in the system: Fittings not tight. → Check all connection for leaks. Tighten or replace fittings. Replace or clean check valves.
2. Piston seal(s) worn. → Replace piston seal(s).
3. Air trapped in pump. → Prime pump.
4. Mobile phase interrupted. Insufficient flow from pump. → Check reservoirs, loop, degassing of mobile phase, and compatibility of mobile phase components.

Unstable-fluctuating pressure

1. Air bubbles in pump. → Degas mobile phase—Sparge it with helium (3–5 psi) during use. Prime pump.
2. Leaks in pump check valve or seals. → Replace or clean check valves; replace pump seals.

High backpressure

1. Plugged frit, pre-filter, guard column; plugged inlet frit → Backflush column/cartridge. Replace frit, pre-filter, guard column; replace endfitting or frit assembly.
2. Irreversibly retained contaminants on the column head. → Column cleaning/regeneration.
3. Precipitation of buffer. → Flush with water at low flow rate.
4. Precipitation or aggregation of proteins in column, particulate matter trapped by the top and/or bottom filter build-up of lipids, DNA, or other macromolecules nonspecifically bound to the column microbial contamination → Clean column, following column instructions with appropriate solvents, change top and/or bottom filter.
5. Column blocked with irreversibly adsorbed sample → Improve sample cleanup; use guard column; reverse-flush column with strong solvent to dissolve blockage.
6. Column particle size too small (for example, 3 μm) → Use larger particle size (for example, 5 μm).
7. Microbial growth on column → Use at least 10% organic modifier in mobile phase; use fresh buffer daily; add 0.02% sodium azide to aqueous mobile phase: store column in at least 25% organic solvent without buffer.
8. Mobile phase viscosity too high → Use lower viscosity solvents or higher temperature. Replace frit or guard column.

(Continued)

Table 4 Pressure abnormalities (*Continued*)*High backpressure*

9. Plugged frit in in-line filter or guard column; plugged inlet frit → Replace end-fitting or frit assembly.
10. Polymeric columns—solvent change causes swelling of packing → Use correct solvent with column; change to proper solvent composition! Consult manufacturer's solvent-compatibility chart; use a column with a higher percentage of cross-linking.
11. Salt precipitation (especially in reversed-phase chromatography with high concentration of organic solvent in mobile phase) → Ensure mobile phase compatibility with buffer concentration; decrease ionic strength and water-organic solvent ratio; premix mobile phase.
12. When injector disconnected from column—blockage in injector → Clean injector or replace rotor.

Changes in the Chromatogram**Baseline**

Baselines in chromatograms are not always smooth. On the contrary, a baseline may have spikes, noise, and other disturbances, indicating existing problems. Indeed, by magnifying the baseline, chromatographers can obtain information to recognize the problem and correct it. For example, trace contaminants in water, buffer, and reagents may cause peaks when using gradient elution.

Very often baseline problems are related to detector problems. Many detectors are available for HPLC systems. The most common are fixed and variable wavelength ultraviolet spectrophotometers, refractive index, and conductivity detectors. Electrochemical and fluorescence detectors are less frequently used, as they are more selective. Detector problems fall into two categories: electrical and mechanical/optical. The instrument manufacturer should correct electrical problems. Mechanical or optical problems can usually be traced to the flow cell; however, improvements in detector cell technology have made them more durable and easier to use. Detector-related problems include leaks, air bubbles, and cell contamination. These usually produce spikes or baseline noise on the chromatograms or decreased sensitivity. Some cells, especially those used in refractive index detectors, are sensitive to flow and pressure variations. Flow rates or backpressures that exceed the manufacturer's recommendation will break the cell window. Old or defective source lamps, as well as incorrect detector rise time, gain, or attenuation settings will reduce sensitivity and peak height. Faulty or reversed cable connections can also be the source of problems.

Electronic noise from fluorescent lights and other common sources is often called 60-cycle noise because it

coincides with the 60-Hz frequency of the alternating current servicing the laboratory.

To isolate the origin of the problem due to the detector, the chromatographer may perform the "dry cell test": by disconnecting the detector from the column and then blowing the cell dry with dry nitrogen. Under these conditions no drift should be observed.

Ghost peaks

These peaks appear in a chromatogram due to contamination of mobile phase, injector, column, or strongly retained compounds from previous sample injections. When an autosampler is used, the problem is often referred to as "carryover." Flushing the injector and the column with strong solvent will remove interfering or late eluting compounds. To correct carryover problems, the chromatographer should change injection size, check

Table 5 Leaks**Leaks****Injector leaks**

- Rotor seal failure → Replace rotor seal.
- Blocked loop → Clean or replace loop.
- Loose injection-port seal → Tighten.
- Waste line siphoning → Keep waste line above surface waste.
- Waste line blockage → Replace waste line.
- Column leaks.
- Loose endfitting. → Tighten endfitting.
- Improper frit thickness. → Use proper frit.

Detector leaks

- Cell gasket failure → Prevent excessive backpressure; replace gasket.
- Cracked cell window → Replace window.
- Leaky fittings → Tighten or replace.
- Blocked waste line → Replace waste line.
- Leaky fittings
- Loose fitting → Tighten.
- Stripped fitting → Replace.
- Overtightened fitting → Loosen and retighten; replace.
- Dirty fitting → Disassemble and clean; replace.
- Mismatched parts → Use parts from the same brand so that they match.

Leaks at pump

- Loose check valves or fittings → Tighten.
- Mixer seal failure → Replace mixer seal; replace mixer.
- Pump seal failure → Repair or replace.
- Pressure transducer failure → Repair or replace.
- Pulse damper failure → Replace pulse damper.
- Proportioning valve failure → Check diaphragms, replace if leaky; check for fitting damage, replace.
- Purge valve → Tighten valve; replace purge valve.



Table 6 Imprecision*Change in selectivity*

1. Not enough sample is injected. → Increase amount of injected sample.
2. Sample loop of injector is underfilled. → Overfill loop with sample.
3. Sample is lost during sample preparation. → Optimize sample preparation.
4. Autosampler line is blocked. → Clean blockage.
5. Detector attenuation is set too high. → Reduce detector attenuation.
6. Peaks are outside detector's linear range. → Dilute or enrich sample to reach linear range of detector.
7. Column is worn out. → Replace column.
8. Column temperature is altered. → Use column oven to maintain constant temperature.

Change in height—lack of sensitivity

1. Sample deterioration → Use fresh sample.
2. Leak. → Check for pump leaks and fittings.
3. Nonreproducible sample volume. → Ensure loop is completely filled. Check autosampler. Check flow and clear any blockages.
4. Low detector response. → Check detector settings and operating conditions.
5. Detector attenuation is set too high. → Reduce detector attenuation.
6. Sample is lost during preparation. → Optimize sample preparation. Use internal standard during sample preparation.
7. Peaks are outside the linear range of the detector. → Dilute or enrich the sample until concentration is within the linear range of the detector.
8. First few sample injections—sample adsorption in injector sample loop or column → Condition loop and column with concentrated sample.
9. Injector sample loop is underfilled → Overfill loop with sample.
10. Not enough sample is injected → Increase amount of sample injected.
11. Peaks are outside detector's linear range → Dilute or concentrate sample to bring detector response into linear range.

Imprecision

1. Operator dependence during sample processing and clean-up. → Check all steps for errors.
2. Sample injection. → Check autosampler; fill loop completely.
3. Detection. → Clean flow-cell. Improve signal-to-noise ratio.
4. Separation. → Improve resolution.
5. Data processing and calibration. → Use internal standard. Calibrate frequently.

Poor sample recovery

1. Absorption or adsorption of proteins. → Reduce nonspecific interactions by changing HPLC mode; add protein-solubilizing agent, strong acid or base (with polymeric columns only), or detergent such as SDS to mobile phase.
2. Adsorption or chemisorption on column packing or on different hardware components. → Increase mobile phase strength; add competing base (for basic compounds) or use base-deactivated packing; ensure no reactive groups are present; use inert tubing and flow-path components, e.g., PEEK.

Table 6 Imprecision*Poor sample recovery*

3. Irreversible adsorption on active-sites (less than 90% yield) → For basic compounds use end-capped, base-deactivated, sterically protected, high coverage, or polymeric reversed-phase; → for acidic compounds use endcapped or polymeric packing; acidify mobile phase.

wash solvent, increase wash solvent volume, adjust its pH value, use a portion of organic solvent, change a needle seal, injection loop, and check fitting assembly.

Ghost peaks in gradient runs can be avoided by increasing the equilibration time between analyses.

No peaks and negative peaks

If no peaks are observed, then the chromatographer should check the detector, the connections, the flow (leaks, pump function, air bubbles), the sample (for its stability), and settings on the detector (e.g., wrong wavelength), or integration.

Negative peaks are due to wrong polarity of recorder, or absorbance or refractive index of mobile phase higher than that of solute.

Peak tailing and peak fronting

Peak Tailing (Peak Asymmetry Factor > 1.2). This is attributed to the wrong pH value, wrong column, wrong sample solvent (mobile phase is better to be used), void volumes at column inlet (the column may need repacking), as well as to active sites within the column which can be solved with the use of a competing basic or acidic modifier.

If only some of the peaks tail, secondary retention effects, such as residual silanol interactions, may take place. Another possibility is that a small peak is eluting on the tail of a larger peak. If all peaks tail, this may be due to a bad column or build up of contamination on the column inlet frit.

Peak Fronting (Peak Asymmetry Factor < 0.9). This indicates that a small band is eluting before a large band, a wrong pH value of the mobile phase is used, an overloaded column, a void volume at the inlet, or that the sample solvent is incompatible with the mobile phase.

Double peaks, rounded peaks, and broad peaks

A void volume in the column, or a partially blocked frit can possibly cause double or split peaks. In case that only one peak is a doublet, then co-eluting compounds may be present.

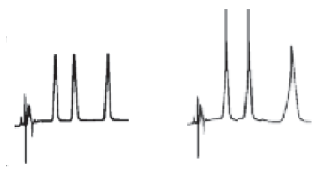


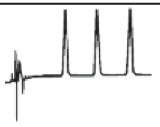
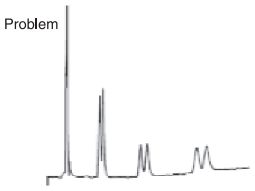

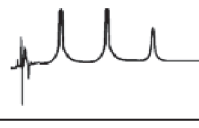
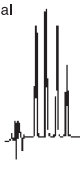


Problem	Diagnostic Symptom
Peak Fronting	
Peak Tailing	<div>Normal</div>  <div>Problem</div> 
Double (split) Peaks	 <div>Problem</div> 
Broad peaks	 
Negative Peak	<div>Normal</div>  
Spikes	

Fig. 1 Typical changes that appear in the chromatogram as a result of various problems in HPLC. Reprinted with permission of Supelco, Bellefonte, PA, from Bulletin 826D (1999) (Continued).

Rounded peaks are attributed to high concentrations (the detector response being outside the linear dynamic range), wrong sample solvent, or too high a setting of the detector or integrator time constant.

Additionally, these peak-related problems may be attributed to column overload, too long or too wide tubing, column contamination, low flow rate, etc.

If all peaks are broadened, possible causes include a large sample volume injected, or a viscous mobile phase, or a column that has lost its efficiency, possibly due to the

presence of a column void. If only some peaks are broadened, then a peak from a previous run may be eluted late, or a high molecular mass sample, e.g., a protein or a polymer is present.

System peaks

A system peak is a peak that originates from the chromatographic system itself, i.e., mobile phase and column,



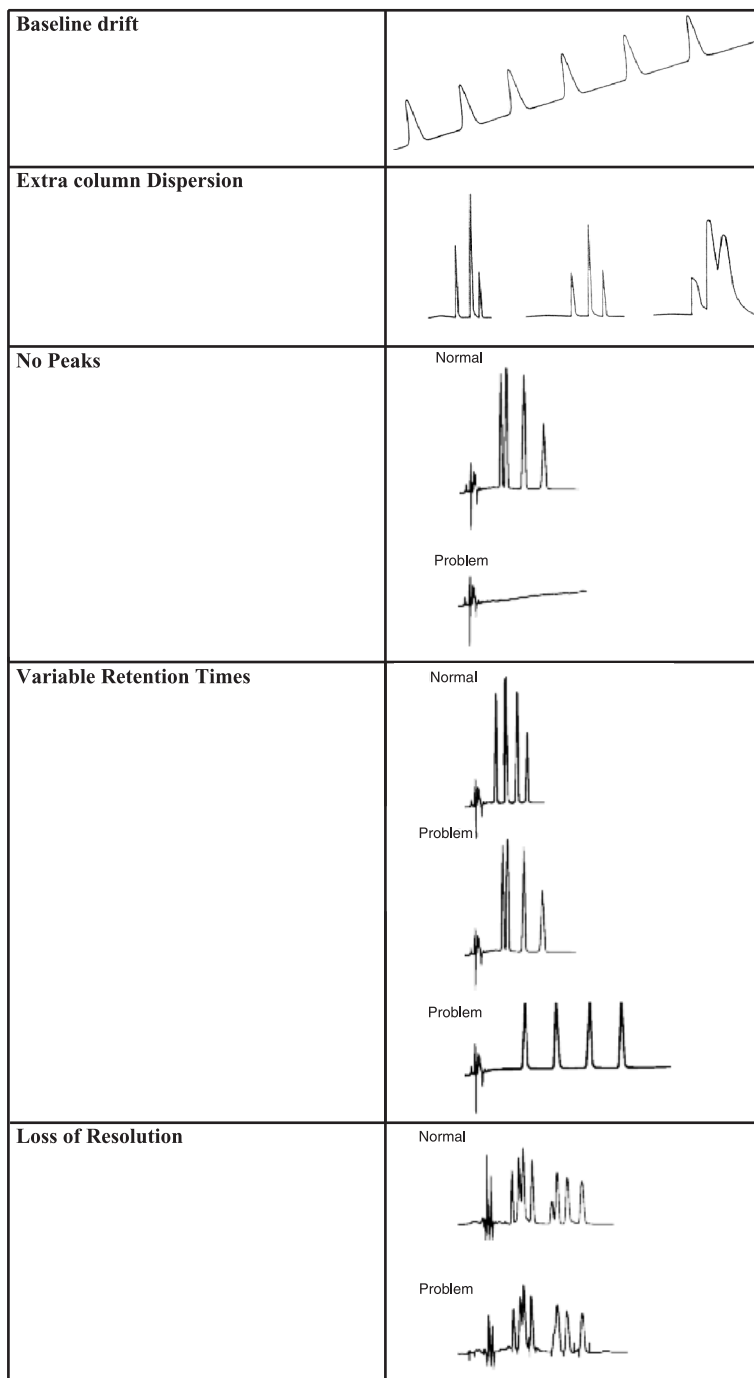


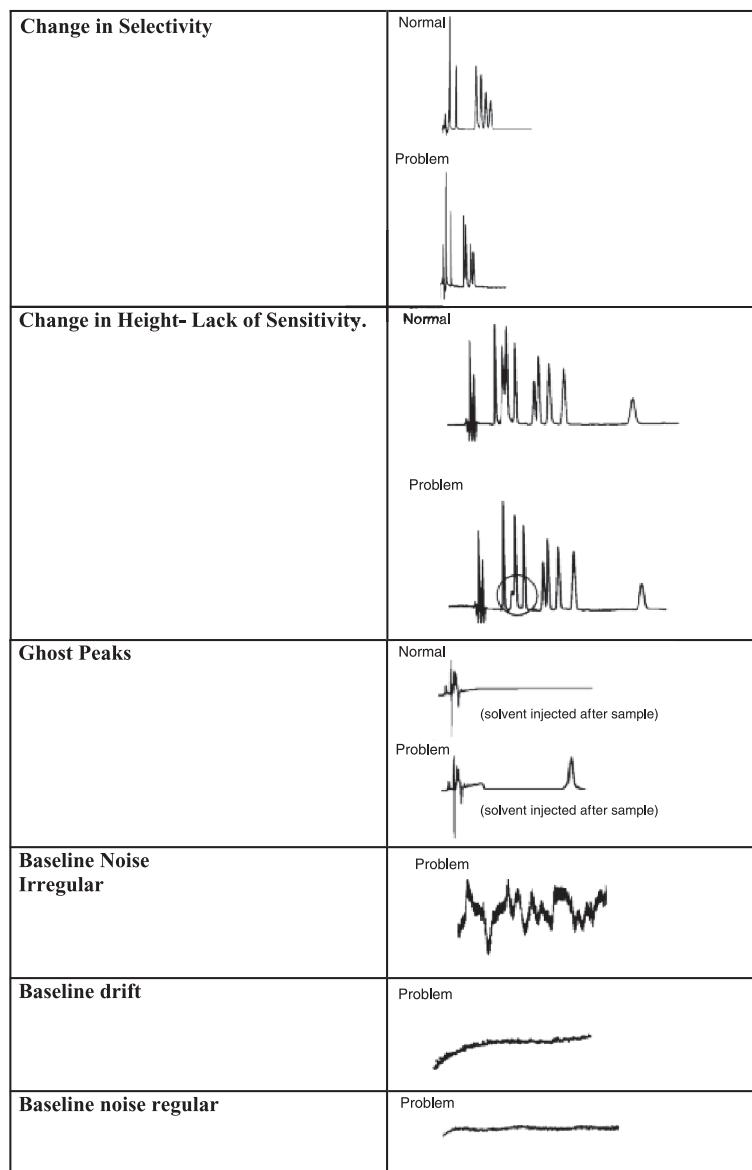
Fig. 1 Typical changes that appear in the chromatogram as a result of various problems in HPLC (*Continued*).

and not from the sample. Its appearance and size are sensitive to the sample composition, but its origins are generally the mobile phase components.

When a mobile phase is introduced to a column, its components undergo distribution until equilibrium is attained. Injection of a sample different from the mobile phase causes a small equilibrium perturbation at the column head. The equilibrium of each component of the mobile phase can be disturbed and, thereby, manifested

by one system peak for each mobile phase additive, using the appropriate detection conditions.

System peaks are most often recognized as a pair of peaks, one positive and the other negative, which represent enrichment and depletion zones eluted from the column. They may vary in retention time and size, depending on the sample matrix, injection volume, mobile phase composition, and the stationary phase. Dissolving samples in the mobile phase is the best way to minimize

**Fig. 1** (Continued).

system peak effects. System peaks are especially important in ion-pairing chromatography and in ion chromatography. In the latter, they are pH dependent and they often interfere with sample components.

Pressure abnormalities

Lower pressure than anticipated is observed due to leaks, insufficient flow from the pump, air bubbles, and worn pump seals. Fluctuating pressure is attributed to air trapped in the pump, or leaking pump check valves or seals. Higher pressure than anticipated is due to blocked flow lines, particulate build up at the head of the column, or buffer salt precipitation. To locate blockage, components should be systematically disconnected,

starting from the detector-end to column-end. Once the blocked component is located, it must be either cleaned or replaced. Back flushing of column will help to remove particulates at the top of column, thus reducing pressure. If buffers are used, their compatibility with the mobile phase should be checked to avoid precipitation within the system.

Change on separation (loss of resolution) and changes in height

Changes in separation, implying a loss of resolution, are attributed to leaks or an obstructed column. Change in height originates from sample deterioration, leaks, non-reproducible sample volumes, and low detector response.



A fresh sample should be checked, as well as detector settings and operating conditions.

Leaks

Leaks can be detected visually or by smell before even a pressure decrease is noticed. They can take place in different positions in the LC system, such as the column, the pump, the injection valve, or the detector. In case of leaks at the column or fittings, a leaky fitting should be tightened or replaced. The detector seal should be replaced if there is a leak at the detector.

A worn or scratched valve rotor in the injection valve should be replaced to prevent leaks in the injection valve.

In case of pump seal failure, pump seals should be replaced, or the piston should be checked for scratches and should be replaced if necessary.

Sample introduction

Problems with the sample introduction may arise both in manual injection and during autosampling. Table 7 summarizes the problems related to sample introduction.

In the case of autosamplers, although they are considered as time saving devices, their function is associated with some common problems. For example, needle depth adjustment is very critical when there is not enough sample available; a needle blockage may occur from a septum. Another common problem related to the autosampler is carryover that causes the appearance of a peak in a blank injection following injection of a high concentration of sample. Sample stability is a figure of merit that certainly has to be evaluated to avoid imprecision and lack of sensitivity.

PREVENTIVE MAINTENANCE

Many of the problems that the chromatographer encounters can be avoided if preventive maintenance is performed in routine operation, in every step of chromatographic analysis, from sample preparation to the final step of an analysis.

Precautions regarding the use of the analytical columns, as well as the operation of each module, e.g., the pump, the detector, etc., may help keep away or postpone most of the abovementioned problems related to HPLC instrumentation.

Preventive Maintenance During Sample Preparation

As already mentioned, many problems concerning increased pressure and backpressure are due to plugged frits or system clogging from a sample matrix particulates or salt precipitation.

Table 7 Problems related to sample introduction

Manual injector problems

Damaged rotor seal → Rebuild or replace valve.

Rotor too tight → Adjust rotor tension.

Valve misaligned → Adjust alignment.

Blocked loop → Replace loop.

Dirty syringe → Clean or replace syringe.

Blocked lines → Clean or replace lines.

Autoinjector problems

No air pressure → Supply proper pressure.

Rotor too tight → Adjust.

Valve misaligned → Adjust alignment.

Blockage → Clean or replace blocked portion.

Jammed mechanism → See service manual.

Faulty controller → Repair or replace controller.

Carryover problems →

1. Replace blank
2. Change injection size.
3. Check fitting assembly and washing mechanism.
4. Use fresh wash solvent.
5. Increase wash volume.
6. Use more organic solvent in wash.
7. Adjust wash pH.
8. Change injection solvent.
9. Change needle seal, injection loop.
10. Replace valve.

Preventive actions include the following:

1. Sample filtration to ensure it contains no solids.
2. Sample dissolution in the mobile phase or solvent weaker than the mobile phase.
3. Use of reduced sample volumes, whenever possible.

Mobile phase inlet filters, pre-injector and pre-column filters, saturator columns, and guard columns greatly reduce problems associated with complex separations.

Moreover, all solvents should be filtered through 0.2- μ m filters, while particulates from samples can be removed by filtration through 0.45- or 0.2- μ m syringe filters.

Bacterial Growth Precautions

Bacteria that grow in water reservoirs can yield by-products such as metabolites and dead bacteria, thus producing ghost peaks. Adding organic solvent to the aqueous part of the mobile phase, at a percentage of >20% or sodium azide 0.04% will prevent bacterial growth.

Sources of Contamination

Numerous sources of contamination should be taken into account: air particles from the laboratory environment,

phthalates from plastic stoppers, plasticizers from plastic containers, detergents and cleaning agents from sample containers and glassware, stabilizing agents and additives from solvents, reagents and chemicals solvent impurities, purified water, and microorganisms. The use of reagent blanks (sample matrix is water in this case) and matrix blanks may help to monitor an analysis on a day-to-day basis.

The compatibility of an organic solvent with a buffer in the mobile phase must be checked as the buffer salts can be easily precipitated when using on-line mixing, thus causing frit blockage, check valve malfunction, and other problems.

Good Column Practice: Column Protection

The most common problem associated with analytical columns is column deterioration. Deterioration may appear as poor peak shapes, split peaks, shoulders, loss of resolution, decreased retention times, and high backpressure. These symptoms indicate contaminants that have accumulated on the frit or column inlet, or there are voids, channels, or a depression in the packing bed. Deterioration is more evident in higher efficiency columns. For example, a column with 3- μm packing is more susceptible to plugging than one with 5- or 10- μm packing. Proper column protection and sample preparation are essential to prolong a column's life and obtain its best performance.

Filters and guard columns prevent particles and strongly retained compounds from accumulating on the analytical column. Silica particles in a saturator column dissolve in high pH mobile phases, protecting the silica-based packing in the analytical column. The useful life of these disposable products depends on mobile phase composition, sample purity, pH value within the recommended range, etc. As these devices become contaminated or plugged with particles, pressure increases and peaks broaden or split.

Keeping records of column backpressure and important chromatographic parameters [number of theoretical plates (N), peak asymmetry factor (A_s), retention factor (k'), resolution factor (R_s)] helps to monitor the required column performance, while storage in the appropriate organic solvent extends column lifetime. Table 8 presents the preventive actions for column protection.

Lamp Failure

Many detectors track the number of hours the lamp is ignited. Although the lamp life may vary, the detector's meter reading can be a helpful guide for troubleshooting. Lamps can sometimes operate for more than 2000 h. To distinguish a lamp problem from air bubbles, one should stop the mobile phase flow. A lamp problem will persist when the flow is stopped, whereas, if the problem is due

to the presence of a bubble, the baseline remains steady on- or off-scale. If the bubble stops in the flow cell, it causes a dramatic baseline shift, usually off-scale.

Solvent degassing and backpressure regulators after the detector minimize bubble formation. It is a helpful practice to perform blank runs every day to provide reference data that can be consulted at a later date.

Spikes in chromatograms can come from many sources, such as aging detector lamps or bubbles in the flow cell; both can be easily corrected. External electrical noise sources, such as ovens, refrigerators, cellular telephones, and fluorescent lights, and other possible noise sources such as system electronics or from external electronic sources, and laboratory power feed may be beyond a chromatographer's control.

Having an unused spare detector lamp available makes checking the problems attributed to the lamp performance an easy task.

Preventing and Solving Common Hardware Problems

Special care can be taken to avoid high backpressure in the LC system. Preventive actions to this end, as well as general preventive maintenance practices that can generally help reduce the failure rate, are summarized in Table 8.

Preventing leaks

Leaks are a common problem in HPLC analysis. Their occurrence can be minimized by avoiding interchanging hardware and fittings from different manufacturers. Incompatible fittings can be forced to fit initially, but repeated connections may eventually leak. If interchanging is unavoidable, the appropriate adapters should be used and all connections should be checked for leaks before proceeding.

Highly concentrated salts ($> 0.2 \text{ M}$) and caustic mobile phases can reduce pump seal efficiency. The lifetime of injector rotor seals also depends on mobile phase conditions, e.g., operation at high pH. In some cases, prolonged use of ion pair reagents has a lubricating effect on pump pistons that may produce small leaks at the piston seal. Some seals do not perform well with certain solvents.

Instrument manufacturers' specifications should be consulted before using a pump under adverse conditions. To replace seals, refer to the maintenance section of the manufacturer's pump manual.

Unclogging the Column Frit

A clogged column frit is another common HPLC problem. To minimize this problem from the start, the

Table 8 Preventive maintenance for HPLC instrumentation

Preventive maintenance for HPLC columns	Preventive maintenance to avoid high backpressures	General preventive maintenance
Filter solvents before use.	Use HPLC or analytical grade buffers, freshly prepared, filtered and degassed before use.	Filtering mobile phase prevents often replacing inlet frits and check valves.
Use in-line filters for all columns, and guard columns for dirty samples; pre-treat dirty samples, remove particulates.	Filter or centrifuge the sample to remove particulate matter. Turbid samples should not be injected onto column.	Degassing mobile phase prevents bubble formation.
Check samples for compatibility with mobile phase.	Set the maximum backpressure of the pumps at or slightly below the value suggested in the column instructions so that in case of increased pressure, the system will turn off before any damage occurs.	Inlet frits prevent check valve failure.
Avoid extreme column temperatures. Keep column temperature below 60°C	Use the recommended flow rates for the column.	Rotor seal wear should not be over-tightened.
Flush column frequently/daily with strong solvent. Use stronger solvent protocol for dirty samples.	Ethanol, glycerol, high salt, urea, and cause increases in back pressure—reduce flow rate accordingly.	Sample filtration prevents injector function, frit blockage.
Keep the mobile phase pH between 3 and 7. If operating outside of this pH range use a precolumn.	When performing the separation at low temperatures e.g. at 4°C, the recommended flow rate should be reduced by 50%.	In line filters or guard column prevent frit blockage.
Use fresh buffer solutions and aqueous mobile phases or treat them with sodium azide.	Wash the chromatography column thoroughly at the end of each separation.	Use of guard column or pre-column help avoiding void at top of column.
To prepare column for storage purge column of buffers and leave in appropriate solvent. Cap tightly.	Clean columns when needed, following the column instructions.	The use of restrictor after cell prevents bubble formation in cell.
Prevent microbial growth when storing columns by using 50–100 % organic/ water mixtures or adding azide to gel filtration columns.	Maintain a log of each chromatographic run, including buffer composition, flow rate, observed back-pressure (before and after sample application), sample composition, binding, and elution conditions.	Flushing buffer from LC prevents corrosive abrasive damage.
Avoid physically mishandling columns: banging, dropping, or over-tightening fittings.	Monitor column efficiency via regular column testing (i.e., acetone tests, function tests).	Keeping spare parts in lab can reduce waiting time intervals.

use of a pre-column filter and/or guard column is recommended. To clean the clogged inlet frit, the column must be disconnected and reversed. Then it should be connected to the pump (but not to the detector), and solvent should be pumped through it at twice the standard flow rate. About 5–10 column volumes of solvent should be sufficient to remove small amounts of particulate material from the inlet frit. The performance of the cleaned column has to be evaluated by using a standard test mixture. It should be noted, however, that some columns are designated by the manufacturer as not to be used in a reverse flow mode. Of course, if the plugging prevents the column from being used anyway, then reverse flow treatment is an acceptable action.

Filling a Void/Replacing a Frit at the Column Inlet

Sometimes, neither solvent flushing nor restoration procedures restore a column's performance. If the column is proved to be the problem source, a void in the packing or a persistent obstruction on the inlet frit may exist. In this case, replacing the frit and/or topping the column with slurry of the sorbent material in a volatile solvent, e.g., acetone, to fill the void, may help.

Mobile Phase

Contamination of mobile phase reservoirs can often become a possible source of problems such as blocked



frits, irregular pump performance, extra peaks, or noise in the chromatogram. Mobile phase degassing by helium sparging, sonication, and vacuum or heating (mostly in case of electrochemical detection) prior to, or during, use prevents air bubble formation.

Manually mixed mobile phases can be adequately degassed before pumping. However, if mixing takes place in the LC equipment, solvents must be simultaneously degassed. Besides bubble formation, oxygen is the primary problem interfering with detector response. In UV detectors, oxygen can cause a significant baseline rise. In fluorescence detectors, oxygen can adversely affect sensitivity by quenching sample fluorescence. Also, oxygen-free mobile phase is required for electrochemical detectors in the reductive mode.

Degassing is not required only in some cases of normal phase LC or nonaqueous SEC due to not significantly different solubility of air in the solvents used (e.g., hexane, toluene, dichloromethane, etc.).

Another case where degassing is not necessary is when high-pressure mixing is performed, where mobile phase components are mixed after the pump, at the high pressure side of the pump, so that gas is kept dissolved in solution by the high pressure.

Keeping Accurate Records

Most problems do not occur suddenly; rather, they usually develop gradually. Accurate record keeping, then, is of paramount importance in detecting and solving many gradually developing problems. When using a new column for the first time, it should be evaluated initially and at regular intervals thereafter. By keeping a written history of column efficiency, mobile phases used, lamp current, pump performance, etc., the chromatographer can monitor a system's performance.

Records also help prevent mistakes, such as introducing water into a silica column, or precipitating buffer in the system by adding too much organic solvent. Many analysts occasionally modify their HPLC systems for a variety of reasons. Reliable records are the best way to ensure that a modification does not introduce problems. For problems relating to pumps, detectors, automatic samplers, and data systems, instrument manuals provide suitable troubleshooting guides.

Referring to the maintenance and troubleshooting sections of an instrument's manual is highly recommended. Many individuals consult manuals only after a catastrophic failure and then only when all other problem-solving approaches have been exhausted. Modern HPLC systems often have self-diagnostic capabilities that help isolate the problem area within the instrument.

CONCLUSION

The common problems in HPLC concern pressure (high, low, or unstable, or none), leaks, quantitation (detection problems, injection problems, sample problems or data-system problems), chromatogram (peak shape), and hardware.

Troubleshooting HPLC instrumentation guides provide a systematic approach to isolating and correcting common HPLC problems. Referring to the maintenance and troubleshooting sections of instrument manuals is strongly recommended. Modern HPLC systems often have simple self-diagnostic capabilities that help isolate the problem area within the instrument.

It is good practice to run quality control samples (samples spiked at known levels) randomly among samples of unknown assay levels.

Performing a system suitability test each day provides a good assay reference.

Preventive maintenance helps the chromatographer to reduce instrument downtime, allowing for more efficiency and cost effectiveness in the HPLC laboratory.

SUGGESTED ADDITIONAL READING

- Cooley, L.; Dolan, J. Reproducibility and carryover-A case study. *LC GC Eur.* **2001**, *11*, 209–214.
- Dolan, J. Communicating with baseline. *LC GC Eur.* **2001**, *9*, 530–534.
- Dolan, J. Attacking carryover problems. *LC GC Eur.* **2001**, *11*, 664–668.
- Dolan, J. *Merck LC Troubleshooting Chrombook*; Merck: Rahway, NJ, USA.
- Dolan, J. Problem isolation: three more things. *LCGC Int.* **1993**, *6* (1), 14–17.
- Dolan, J.; Snyder, L.R. *Troubleshooting LC Systems*; Humana Press: Clifton, NJ, USA.
- Frasca, V. Troubleshooting high back pressure. *Sci. Tools Pharm. Biotech.* **1997**, *2*, 3.
- HPLC Troubleshooting Technical Notes*, 1st Ed.; Phenomenex Corp.: Torrance, CA, USA. 2 Feb 1993.
- <http://kerouac.pharm.uky.edu/asrg/hplc/troubleshooting.html>.
- McDowall, R.D. Where did that peak come from? *LC GC Int.* **1997**, *6*, 358–359.
- Nelson, M.; Dolan, J. UV detection noise. *LC GC Int.* **1995**, 64–70.
- Supelco HPLC troubleshooting guide. *Bulletin* **1999**, 826D.
- <http://www.chromatography.co.uk/TECHNIQS/HPLC/trouble1.html>.
- <http://www.chromtech.com>.
- <http://www.dq.fct.unl.pt/QOF/hplcts.html>.
- <http://www.fortunecity.de/lindenpark/lilienthal/8/trouble.html>.
- <http://www.hplc1.com/shodex/english/dd.htm>.
- <http://www.metachem.com/tech/troubleshoot>.
- <http://www.rheodyne.com/tsguide/tsg.html>.

Two-Dimensional Thin-Layer Chromatography

Simion Gocan

"Babeş-Bolyai" University, Cluj-Napoca, Romania

INTRODUCTION

The two-dimensional (2-D) thin-layer chromatography (TLC) technique is one of the more versatile methods of TLC development. The first application of the 2-D chromatographic method to paper chromatography was reported in 1944 by Consden, Gordon, and Martin.^[1] Since that time, this method has been mostly used for the separation of a large number of compounds that cannot be separated in a one-dimensional (1-D) TLC experiment. In 2-D TLC, separation is on one surface spread along the entire area of the plate. The resolving power of the 2-D TLC method has great application, especially in the areas of biochemistry, biology, natural products, pharmaceuticals, and environmental analysis.

TWO-DIMENSIONAL DEVELOPMENT

Two-dimensional TLC is performed by spotting the sample in one corner of a square thin-layer plate and developing in the usual manner with the first eluent. The chromatographic plate is then removed from the developing chamber and the solvent is allowed to evaporate from the layer. Then, the plate is placed in the second eluent so that development can take place in a second direction which is perpendicular to that of the first direction of development. In 2-D TLC, usually, the layer is of continuous composition, but two different eluents must be employed to obtain a better separation of a mixture. The success of the separation will depend on the ability to modify the selectivity of the second eluent compared to the selectivity of the first eluent. Fig. 1 shows the scheme of spot distribution on a 2-D TLC plate, following two developments for a theoretical case. In 2-D TLC, any spot can be identified by a pair of x_i and y_i coordinates or $R_{f,i1}$ and $R_{f,i2}$, respectively, where x_i divided by $Z_{f,1}$ is equal to $R_{f,i1}$ for the first eluent and $y_i/Z_{f,2}$ is equal to $R_{f,i2}$ for the second eluent. The final position of the spot can be determined by the coordinates (x_i, y_i) , in which $R_{f,i2-D}$ can be expressed as $(R_{f,i1}, R_{f,i2})$.

A very good method for selection of the appropriate mobile phase for 2-D TLC separations is with the use of the "Prisma" system.^[2]

The indole group of compounds is conveniently divided into the so-called "simple" indole derivatives and the indole alkaloids, which often have complicated structures, and indole dyes. Thus it was demonstrated that not all compounds are completely separated by either the basic eluent, methyl acetate–isopropanol–25% ammonia (45:35:20, v/v), or the acidic eluent, chloroform–96% acetic acid (95:5, v/v). Therefore one combines the effects of both of these eluent systems in the 2-D TLC method; in this way, 14 simple indole derivatives and anthranilic acid can be separated. Compounds are separated into groups according to their polarities.^[3]

The 2-D TLC was successfully applied to the separation of amino acids as early as the beginning of thin-layer chromatography. Separation efficiency is, by far, best with chloroform–methanol–17% ammonium hydroxide (40:40:20, v/v), *n*-butanol–glacial acetic acid–water (80:20:20, v/v) in combination with phenol–water (75:25, g/g).^[4] A novel 2-D TLC method has been elaborated and found suitable for the chromatographic identification of 52 amino acids. This method is based on three 2-D TLC developments on cellulose (CMN 300; 50 μ) using the same solvent system I for the first dimension and three different systems (II–IV) of suitable properties for the second dimension. System I: *n*-butanol–acetone–diethylamine–water (10:10:2:5, v/v); system II: 2-propanol–formic acid–water (40:2:10, v/v); system III: *sec*-butanol–methyl ethyl ketone–dicyclohexylamine–water (10:10:2:5, v/v); and system IV: phenol–water (75:25, g/g) (+ 7.5 mg Na-cyanide) with 3% ammonia. With this technique, all amino acids can be differentiated and characterized by their fixed positions and also by some color reactions. Moreover, the relative merits of cellulose and silica gel are discussed in relation to separation efficiency, reproducibility, and detection sensitivity.^[5] Two-dimensional TLC separation of a performic acid oxidized mixture of 20 protein amino acids plus β -alanine and γ -amino-*n*-butyric acid was performed in the first direction with chloroform–methanol–ammonia (17%) (40:40:20, v/v) and in the second direction with phenol–water (75:25, g/g). Detection was performed via ninhydrin reagent spray.^[6]

The thin-layer chromatographic method was developed for amino acids; therefore, in principle, it is equally applicable to peptides. Peptides, such as amino acids, are



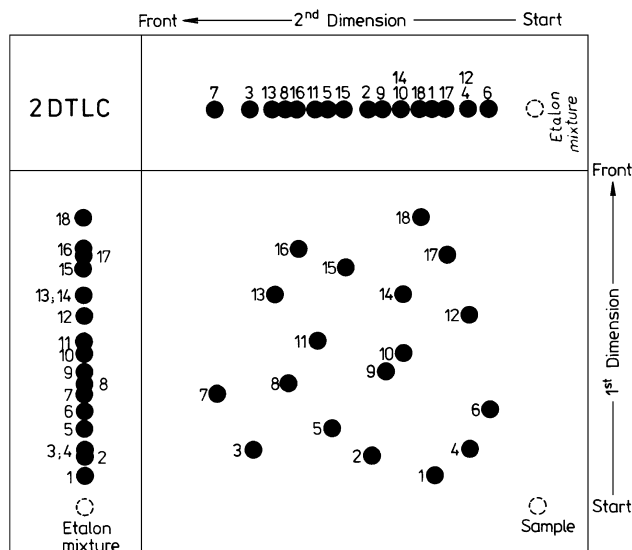


Fig. 1 Scheme of spot distribution on a 2-D TLC plate.

generally hydrophilic. There are, however, limits to this analogy. Dinitrophenylamino acid derivatives (DNP amino acids) and phenylthiohydantoin derivatives (PTH amino acids) are obtained when reaction of peptides or proteins with dinitrofluorobenzene or phenyl mustards are properly degraded.^[7,8] Their separation from reaction mixtures and their identification are considerable practical importance because they constitute essential steps in the process of sequential analysis of peptide and protein structures. Generally, the run in the first direction is carried out in a toluene system. For the run in the second direction, there are many eluent systems that may be selected. Two-dimensional TLC was used to perform separation of DNP amino acids, using toluene as eluent for first direction and chloroform–benzylalcohol–glacial acetic acid (70:30:3, v/v),^[9] chloroform–methanol–glacial acetic acid (95:5:1, v/v), or benzene–pyridine–glacial acetic acid (80:20:2, v/v) as eluent for the second direction.^[10] The majority of DNP amino acids are colored yellow.

The 2-D TLC separation of PTH amino acids may be performed with chloroform–methanol (90:10, v/v) and with chloroform–formic acid (100:5, v/v) as eluents in the first and the second developments, respectively.^[11] There are many other systems of eluents that can be used to obtain good resolution. The chlorine/tolidine reagent is very useful for detection of PTH amino acids. An alternative is offered by fluorescence quenching.

A very complex mononucleotide mixture can be separated by 2-D TLC on poly(ethyleneimine)-cellulose anionexchange thin layers. After applying the nucleotide solution at the starting point, the chromatogram is developed in a closed rectangular jar by stepwise elution with LiCl solution of 0.2, 1.0, and, finally, 1.6 M. In

order to remove LiCl, the plate is placed in a flat dish filled with anhydrous methanol. Then, the chromatogram is developed in the second direction with formic acid–sodium formate buffers, pH 3–4, by a stepwise elution with buffers of 0.5, 2.0, and 4.0 M. The complete resolution of a model mixture containing DPA, TPN, six nucleotide sugars, and 14 common nucleoside-5'-mono-, di-, and triphosphates takes less than 3 hr.^[12]

The separation and identification of plant phospholipids and glycolipids was performed by 2-D TLC silica gel using chloroform–methanol–water (65:25:4, v/v) and diisobutyl ketone–acetic acid–water (80:50:10, v/v) as eluents for the first and the second dimensions, respectively.^[13]

Amino-modified high-performance TLC (HPTLC) silica gel layers (NH_2 F_{254s} HPTLC) was used for identification of 13 amphetamine derivatives by unidimensional multiple development (UDM) in the 2-D TLC mode. The mobile phases used were ethanol–triethylamine–*n*-hexane (15:9:76, v/v) and acetone–triethylamine–*n*-hexane (23:9:68, v/v) in the first and the second directions, respectively. Because 1-D HP-TLC was not effective, UDM with the same solvent system and development distance and with two development steps was investigated. The resolution of separation was higher in the low hR_f compared to that predicted by the UDM theory.^[14]

In the first direction, the development is isocratic; in the second direction, it is automated multiple development (AMD). The instrumental chromatographic method, AMD, provides a mean of normal-phase gradient developed in HPTLC. A maximum of 25 steps can be used to form an AMD gradient. The development distances increase as the solvent polarity is reduced. The plates are dried by vacuum between consecutive steps. The bands on the plate will be compressed by repeated developments, resulting in increased sensitivity and resolution. For the functional principle of the AMD device, one should consult Ref. [15]. The developed distance was 8 cm. Isocratic TLC was performed with one typical eluent as the mobile phase in normal chambers previously equilibrated with the mobile phase. The AMD system was performed in a Camag device (Muttenez, Switzerland), but the gradient systems must have a different selectivity compared to isocratic development. The number of compounds separated by this method was greater than with isocratic TLC or with 1-D AMD.^[16] The use of 2-D AMD with two gradients of different selectivities is a powerful method that can improve the separation of samples containing an unknown number of constituents in hydroalcoholic plant extracts.^[17] The plant extract “fingerprint” is better for authenticity certification of the respective extract.

Two-dimensional TLC is a simple method that makes possible the rapid recognition of changes in individual components of a mixture. For this purpose, separations

must be carried out in both directions, under exactly identical conditions. In such circumstances, a slight increase in resolution might occur because of an increase by a significant factor of the distance of migration of the zone which is a diagonal line ($Z_{f,2}$). However, this method of development indicates alterations of compounds during chromatography if the resulting spots do not lie on a diagonal line bisecting the plate. Between the first and the second developments, the compounds that suffer several structural transformations under physical agent (action of radiation) or from chemical reaction can be detected. This method can be used in photochemistry and stability control.^[4]

TWO-DIMENSIONAL DEVELOPMENT ON BILAYERS

There are many reports concerning the placement of two adsorbents on the same plate.

An apparatus for simultaneously coating a plate with two adjacent layers of different adsorbents was accomplished by placing a plastic insert into a commercial spreader, thus forming two independent chambers. For this reason, combinations of two adsorbents, such as cellulose, silica gel, alumina, charcoal, silicic acid, magnesium silicate, etc., as a function of the sample were used. Then, the two eluents systems were optimized for the two development directions, e.g., 2-D separation of some ketones on a bilayer (charcoal/silicic acid) with benzene–ether–acetic acid (82:9:9, v/v) in the first direction (on charcoal) and with benzene–ether (85:15, v/v) in the second direction (on silicic acid).^[18] In another paper,^[19] the first adsorbent was silica gel (air-dried) and the second adsorbent was deactivated aluminum oxide. The same solvent system, toluene–ethyl acetate (3:1, v/v), was used in the two directions. In this condition, a mixture of 2,4-dinitrophenylhydrazine derivatives of hydroxycarbonyl compounds was resolved.

Silver nitrate-impregnated silica gel has also been used successfully in the separation of some classes of compounds that contain double bonds in their structures. Thus it was used in the separation of glycerides and isomers of unsaturated fatty acid esters. The 2-D TLC on adjacent layers of silica gel G and silica G impregnated with 5% of silver nitrate was used for development. The silica gel G layer covered a surface of 3×20 cm and the difference of the surface of 17×20 cm was covered with silica gel G impregnated with 5% AgNO_3 . The first direction was performed on silica gel G with petroleum ether–diethyl ether (9:1, v/v) as eluent. The second direction was carried out on the impregnated silica gel G and developed twice with the same eluent as in the first direction. After the first direction, the mixture was

fractionated into four groups of compounds (trialkyl glyceryl ethers, dialkoxo glycerides, alkoxy diglycerides, and triglycerides). After the second direction, each group was fractionated for another period into three or four compounds.^[20] Thus the efficiency of the impregnated layer was demonstrated.

A method for the complete structural analysis of complex mixtures of methyl esters of saturated and unsaturated fatty acids has been performed by 2-D TLC. Adsorbent silica gel impregnated with a 10% solution of dodecane was used for the first direction with acetonitrile–acetone (1:1, v/v) as eluent. The silica gel for the second direction was impregnated with a 20% AgNO_3 and dipropyl ether–hexane (2:3, v/v) was used as eluent. In this way, complete separation of a standard mixture of the methyl esters of six saturated, nine monoethylenic, and three polyenic esters were achieved.^[21]

The 2-D TLC on bilayers, silica gel for normal phase (NP) and reversed phase (RP), offer the special possibility to carry out two different separation processes on the same plate. Normal-phase chromatography can be performed in the first direction on silica gel; after the evaporation of the solvent, the plate was impregnated with paraffin oil dissolved in petroleum ether. After removal of the excess solvent, the plate was reversed phase developed in the second direction.

Another approach may also be performed by transferring the spots from one plate to another plate.^[18] In such circumstances, the development in the first direction was carried out on a narrow 2-cm strip. After drying, it was clipped face to face to a 20×20 or 10×10 cm plate for development in the second direction. Close contact has to be maintained between the two layers for a proper development. In this case, the first plate can be used with a silica gel layer and the second plate can be used with a silica gel RP- C_{18} or vice versa.^[22] In this way, the analysis of saponins in *Silene vulgaris* Gracke was carried out in the first direction on RP-18W HPTLC plates with 1.0% aqueous formic acid–methanol (30:70, v/v) as mobile phase and in the second, perpendicular, direction on silica gel Si 60 HPTLC with chloroform–methanol–formic acid–water (100:40:10:10, v/v) as mobile phase. With the use of 2-D TLC bilayers, the saponin mixture could be separated into 18 components, while conventional TLC could separate the mixture into nine components only.^[23]

TWO-DIMENSIONAL SEPARATION BY THIN-LAYER CHROMATOGRAPHY/ELECTROPHORESIS

Peptide maps of the tryptic digest of myosin have been performed on thin-layer plates (20×20 cm) by successive TLC and electrophoresis. In the first-dimension TLC



with chloroform–methanol–ammonium hydroxide 34% (40:40:20, v/v) as eluent, the time was as long as 60 min. The second-dimension electrophoresis with pyridine–glacial acetic acid–water (1:10:489, v/v) buffer and 980 V, 30 mA current, the time was 1 hr. The peptide mixture is applied in amounts of 0.05 to 0.5 mg per peptide map.^[24] In another paper,^[25] electrophoresis was applied in one direction on buffered adsorbents, followed by chromatography in the second dimension. Here, phosphate esters were separated by TLC development twice with *n*-propanol–ammonium hydroxide–water (60:30:1, v/v), and electrophoresis was carried out in 0.28 M acetate buffer (pH 3.6), 1000 V, 35 mA, and 16 min.

CHROMATOGRAM EVALUATION

The best 2-D TLC separation is when all the components are separated and distributed on the entire surface of the chromatographic plate. The estimation of this separation can be made by an objective function. Generally, a good agreement between visual evaluation of a chromatogram and computer evaluation using these objective functions was noticed.^[26] On the other hand, a function is needed which can predict R_f value of the one-component function of the composition from the mobile phase.

There are programs for simulated chromatograms which are comparable to that obtained with experimental chromatograms.^[26] Other details concerning the strategy of optimization of the mobile phase can be found in Ref. [22].

CONCLUSION

In conclusion, for difficulty separation problems the application of 2-D TLC is necessary because the power of 1-D TLC is often inadequate for complete separation of the complex samples with a high number of compounds. The main advantage of 2-D TLC separation process is that compounds are distributed widely over two-dimensional space with high zone (peak) capacity (ca. 1500). The separation efficiency of 2-D TLC can be substantially increased in the future by a combination of the stationary

and mobile phases of different polarity with automated multiple development.

REFERENCES

1. Consden, R.; Gordon, A.H.; Martin, A.J.P. *Biochem. J.* **1944**, *38*, 224.
2. Nyiredy, Sz.; Dallenbach-Tölke, K.; Sticher, O. *J. Planar Chromatogr.* **1988**, *1*, 336.
3. Stahl, E.; Kaldewey, H. Hoppe-Seyler's. *Z. Physiol. Chem.* **1961**, *323*, 182.
4. Stahl, E. *Thin-Layer Chromatography*; Springer-Verlag: Berlin, 1965; 36, 403.
5. von Arx, E.; Neher, R. *J. Chromatogr.* **1963**, *12*, 329.
6. Hirs, C.H.W. *J. Biol. Chem.* **1956**, *219*, 611.
7. Biserte, G.; Holleman, J.W.; Holleman-Dehove, J.; Sautière, P. *J. Chromatogr.* **1959**, *2*, 225.
8. Biserte, G.; Holleman, J.W.; Holleman-Dehove, J.; Sautière, P. *J. Chromatogr.* **1960**, *3*, 85.
9. Brenner, M.; Pataki, G. *Experientia* **1961**, *17*, 145.
10. Brenner, M.; Niederwieser, A. *Experientia* **1961**, *17*, 237.
11. Pataki, G. Thesis; Basel University: Basel, Switzerland, 1962.
12. Randerath, E.; Randerath, K. *J. Chromatogr.* **1964**, *16*, 126.
13. Lepage, M. *J. Chromatogr.* **1964**, *13*, 99.
14. Fatér, Z.S.; Tasi, G.; Szabady, B.; Nyiredy, Sz. *J. Planar Chromatogr.* **1998**, *11*, 225.
15. *Encyclopedia of Chromatography*; Cazes, J., Ed.; Marcel Dekker, Inc.: New York, 2001; 533.
16. Muresan, L. Thesis; Babeş-Bolyai University: Cluj-Napoca, 1998.
17. Olah, N.-K.; Muresan, L.; Cîmpan, G.; Gocan, S. *J. Planar Chromatogr.* **1998**, *11*, 361.
18. Kirchner, J.G. *Thin-Layer Chromatography*, 2nd Ed.; John Wiley & Sons: New York, 1978; 136–137.
19. Anet, E.F.L.J. *J. Chromatogr.* **1962**, *9*, 291.
20. Schmid, H.H.O.; Baumann, W.J.; Cubero, J.M.; Mangold, H.K. *Biochim. Biophys. Acta* **1966**, *125*, 189.
21. Bergelson, D.; Dyatlovskaya, E.V.; Voronkova, V.V. *J. Chromatogr.* **1964**, *15*, 191.
22. *Planar Chromatography. A Retrospective View for the Third Millennium*; Nyredy, Sz., Ed.; Springer: Budapest, 2001; 103–119.
23. Glensk, M.; Cisowski, W. *J. Planar Chromatogr.* **2000**, *13*, 9.
24. Ritschard, W.J. *J. Chromatogr.* **1964**, *16*, 327.
25. Bielecki, R.L. *Anal. Biochem.* **1965**, *12*, 230.
26. *Modern Thin-Layer Chromatography*; Grinberg, N., Ed.; Marcel Dekker, Inc.: New York, 1990; 361–368.

Ultrathin-Layer Gel Electrophoresis

András Guttman

Torrey Mesa Research Institute, La Jolla, California, U.S.A.

Csaba Barta

Árpád Gerstner

Institute of Medical Chemistry, Molecular Biology, and Pathobiochemistry, Semmelweis University, Budapest, Hungary

Huba Kalász

Department of Pharmacology and Pharmacotherapy, Semmelweis University, Budapest, Hungary

Mária Sasvári-Székely

Institute of Medical Chemistry, Molecular Biology, and Pathobiochemistry, Semmelweis University, Budapest, Hungary

Introduction

Electrophoretic separation of double-stranded DNA (dsDNA) molecules, such as RFLP fragments or polymerase chain reaction (PCR) products, is usually accomplished in agarose, polyacrylamide, or composite agarose–polyacrylamide gels [1]. Agarose gels are extensively used to analyze DNA fragments from hundreds of base pairs (bp) to tens of thousands of base pairs, and polyacrylamide gels are regularly used for high-resolution DNA fragment analysis from several base pairs up to a thousand base pairs. In spite of numerous refinements in electrophoresis techniques during the past decade, agarose gel electrophoresis is still not efficient enough. The existing methodology requires multiple steps, such as gel casting, sample loading, staining, and imaging/documentation/data evaluation, making it very tedious and time-consuming because these tasks are not readily integrated and automated for high-throughput applications. Although several attempts have been made for automation, dsDNA fragment analysis in most laboratories is still done in a very conventional way: using submarine format agarose gel electrophoresis separation with ethidium bromide staining [2]. Some of the large, automated DNA sequencing systems are recently reported to be used for genotyping and STR profiling using cross-linked polyacrylamide gels and fluorescently labeled primers, and the configuration of these devices does not accommodate the use of agarose gels as separation medium.

Discussion

Attempts to discover higher-resolution and faster electrophoresis separation techniques and media started

in the 1960s, when miniaturized methods [3] were described as microelectrophoresis, but imaging technologies were not yet quite as adequate to be able to capture separations on such a minute scale. Later, polyacrylamide gels contained in glass capillaries were employed in order to separate both DNA and RNA molecules, but this progress was ultimately hampered by the inability to control extra-Joule heat. Recently emerging capillary-electrophoresis-based methods are much less susceptible to the effects of Joule heat, due to the ability to dissipate heat via the large surface-to-volume ratios typical of narrow-bore capillary columns. Obtaining similarly high surface-to-volume ratios in planar-format electrophoretic systems require very thin layers, preferably reaching thickness in the capillary dimension (i.e., no greater than 0.25 mm).

The most recent advances in the electrophoretic separation of nucleic acids come from exploration of new separation matrices. Linear, non-cross-linked polymers, such as polyacrylamide, derivatized celluloses, and polyethylene oxides, have all been demonstrated to be effective in the size separation of biopolymers [4]. The advantages of these non-cross-linked polymers were proven almost entirely in high-performance capillary electrophoresis applications [5]; however, it has been shown that very high-concentration non-cross-linked polymers can also be used in planar slab–gel format [6] for the separation of dsDNA molecules. Chemically modified agarose gels or composite agarose–non-cross-linked polymer gels capable of resolving differences of merely a few bases in DNA fragments of several hundreds of bases in length have also been developed [7]. The use of highly concentrated non-cross-linked polymers for DNA fragment analysis applications may be advantageous in several respects. First, it has been shown that non-cross-linked poly-



mers may be supplied in a dessicated, dry form, providing a long shelf life [8]. Second, planar-form non-cross-linked polymer gels can be rehydrated to any of the range of final gel concentrations, buffer compositions, and/or ionic strengths. In addition to that, lower viscosity non-cross-linked polymers can be easily replaced in the separation platform; therefore, cassettes supporting repetitive work with non-cross-linked polymers can be readily used with these matrices.

Visualization by covalent labeling of nucleic acids with fluorescent tags, such as fluorescein, tetramethylrhodamine, Texas Red, and so forth, has been practiced for years [9]. This approach can be used for high-sensitivity DNA fragment analysis provided that the analyte is labeled by the appropriate fluorophore prior to the separation step. The approach reported in this work uses affinity binding (e.g., intercalation) dyes for *in migratio* labeling of the dsDNA fragments during the course of their electrophoretic separation. This method is beneficial in two aspects. First, unlabeled DNA fragments can be readily analyzed, because they become labeled during the separation process. Second, the complexation phenomenon usually increases the separation selectivity, resulting in a higher resolution [10].

Large-scale, high-resolution DNA fragment analysis (e.g., mapping) requires an affordable, fully automated high-throughput agarose gel-electrophoresis-based separation device that enables rapid, high-performance separations in a wide molecular-weight range. Here, we describe a system that greatly enhances the productivity of DNA fragment analysis by automating the current manual procedure and also reducing the separation time and human intervention from sample loading to data analysis.

Separation Platform

Figure 1 shows the block diagram of the automated ultrathin-layer agarose gel electrophoresis system consisting of a high-voltage power supply (1); platinum electrodes (2 and 3); ultrathin layer separation platform with built-in buffer reservoirs (4), and a fiber-optic-bundle-based detection system (5). A lens set (7) connected to the illumination/detection system via the fiber-optic bundle, scans across the gel by means of a translation stage (6). A 532-nm frequency doubled Nd:YAG laser excitation source (8) and an avalanche photodiode detector (9) are connected to the central excitation fiber and the surrounding collecting fibers of the fiber-optic bundle, respectively.

Interface electronics (10) is used to digitize the analog output of the detector and to connect the system to a personal computer. The separation platform also includes a positional heat sink holding the gel-filled cassette in horizontal position. This heat sink also eliminates local heat-spot-generated separation irregularities by means of homogenous dissipation of any extra heat over the gel surface during the separation. Three heating cartridges and a high-speed fan control the temperature (above ambient) of the separation platform at a preprogrammed level. The preheated (40–45°C) separation cassettes (18 cm × 7.5 cm × 190 μm) are filled with melted 2% agarose. After a few minutes of cooling/solidification, the gel-filled cartridge is ready to be used. The effective separation length of the agarose-gel-filled ultrathin-layer cartridge is 6 cm. The applied separation voltage is 750 V, generating 5–7 mA of current.

Reusable Gel Cassettes and Membrane-Mediated Sample Loading

The reusable separation cassette has a flat bottom and top plate joined and secured in parallel, spaced 190 μm apart, with buffer reservoirs permanently fixed to both ends. Two spacers run along the inner-face edges of the plates to assure consistent distance between the glass plates (see the cassette in Fig. 1). For filling the cassette, a pump (e.g., large syringe) is used with a sealing applicator nozzle that matches to the top of the buffer reservoirs. To introduce the melted agarose gel into the cassette, the gel nozzle is placed at the top of one of the reservoirs, and the gel is pumped into the platform. The cassette should be preheated to approximately 40–45°C prior to the introduction of the melted agarose gel, in order to prevent premature solidification of the separation matrix. An appropriate amount of DNA staining dye [e.g., ethidium bromide (10–50 nM)] should be added to the melted agarose solution just before filling into the cassette.

Membrane-mediated sample loading provides a rugged, easy loading mechanism for ultrathin-layer electrophoresis gels, conveniently applicable for both vertical and horizontal formats [11]. The samples are spotted manually or automatically (robots) onto the surface of the loading membrane tabs, outside of the separation platform. The sample spotted membrane is then placed into the injection (cathode) side of the separation cassette, in intimate contact with the gel edge. By the application of the electric field, the sample components migrate into the gel. There is no need to



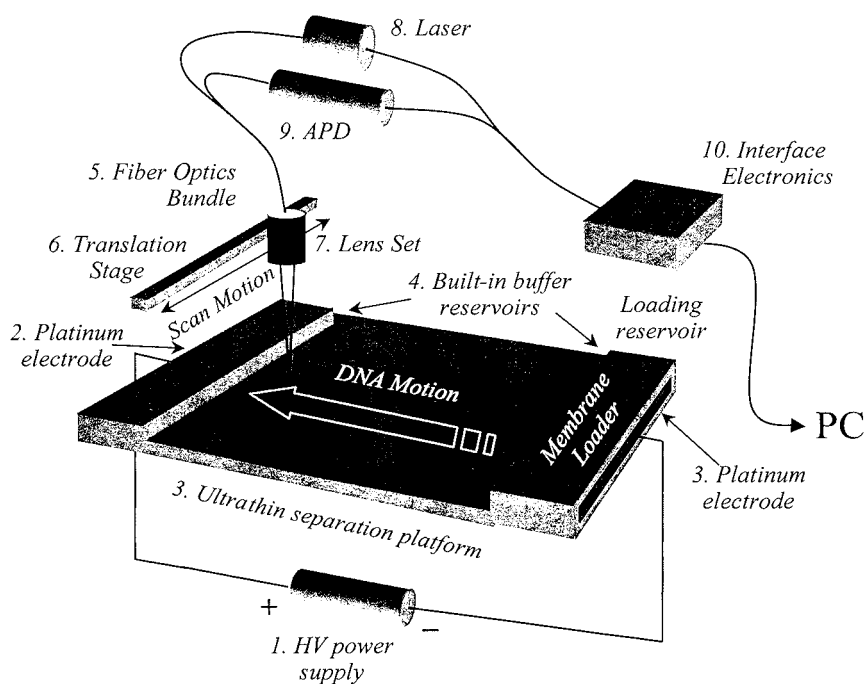


Fig. 1 Block diagram of the automated ultrathin-layer agarose gel electrophoresis system.

form individual injection wells in the separation gel and loading is accomplished easily on the bench top. This novel sample injection method could be readily applied to most high-throughput gel electrophoresis based DNA analysis applications.

***In Migratio* Fluorescent Labeling**

The use of fluorophore labeling of DNA fragments in gel electrophoresis expands the detection sensitivity and separation potential. Complex formation with fluorophores enables *in migratio* labeling [i.e., the migrating DNA fragments (negatively charged) complex with the countermigrating fluorophore intercalator dye (positively charged) which is dissolved in the separation matrix]. Using this method, high-sensitivity detection of the migrating DNA fragments as well as the high resolution of closely migrating components can be simultaneously obtained in a broad molecular-weight range. The appropriate concentration and type of the fluorophore complexing dye should be optimized for the wavelength of the excitation laser used in the illumination/detection system. For a 532-nm laser, ethidium bromide provides a good match ($EX_{\max} = 512 \text{ nm}$), but other high sensitivity dyes can also be used [12].

Agarose-Based Replaceable Separation Matrix

In the ultrathin-layer slab-gel format described in this entry, dsDNA fragment analysis was accomplished using 2% agarose gel, filled into the separation cassette at 60°C and used for electrophoresis separation at room temperature. The advantage of employing liquefied agarose above its gelling temperature is that the gel can be easily replaced in the separation platform by simply pumping fresh melted gel into the cassette (i.e., it can be easily filled, rinsed, and refilled). The inner surface of the separation platform was coated with linear polyacrylamide in order to avoid the formation of an electric double layer and concomitant electro-osmotic-flow generation [13].

Mutation Screening by Ultrathin-Layer Agarose Electrophoresis

Screening of 10 patients for the dopamine D₄ receptor (D4DR) gene polymorphism was used as a model system to demonstrate the capability of this device [14]. D4DR is the major receptor type in the limbic system. Its gene contains a 48-base-pair sequence repeat in exon 3 with a variable (twofold to eightfold) repeat number in individuals. This polymorphism is believed



to be associated with personality characteristics, such as novelty seeking and extravertation/introvertation. The fragment containing the polymorphic site was amplified by PCR using two primers that anneal upstream and downstream of this region, resulting in products different in length (359 and 475 bp) which were then separated by ultrathin-layer agarose gel electrophoresis (Fig. 2).

Conclusion

In this entry, we reported the use of an automated, high-performance DNA fragment analyzer for high-throughput applications, employing replaceable agarose gels in conjunction with a reusable ultrathin-layer separation cassette format in horizontal configuration. Sample loading onto the ultrathin separation platform was accomplished by membrane-mediated loading technology, which also enabled robotic spotting of multiple samples [15]. The sample loading membranes also allow bar coding for identification and cataloging purposes and can be stored for several days between spotting and analysis. The analyte DNA fragments were stained during the separation process by *in migratio* complexation with appropriate fluorophore intercalator dyes and detected by a scanning fiber-optic-bundle-based integrated laser-induced fluorescence-avalanche photodiode imaging system.

Cost-effectiveness for high-throughput applications was assured by simple replacement of the separation matrix by pumping fresh melted gel composition into

the cassette for each consequent analysis. After a few minutes of solidification, the gel-filled cassette was ready to be used again. When compared to regular submarine agarose gel electrophoresis, the separation performance and detection sensitivity of this new method utilizing the ultrathin-layer electrophoresis platform were found to be far superior, allowing significantly faster and higher-resolution analysis (more than 10-fold). With full system integration and automation, a high-throughput automated dsDNA analysis system can be developed by simply coupling DNA sample preparation, PCR amplification, restriction digestion, sample loading, electrophoresis separation, data analysis, and map construction.

Acknowledgments

The authors gratefully acknowledge the technical help of Doug Evans, Loi Nguyen, Swarna Ramanjulu, Nick Wilder, and Greg Theriault. This work was supported by the U.S.–Hungarian Joint Fund (J.F.No.654/96) and by the Hungarian funds FKFP 0658/1999, OTKA T022608.

References

1. A. Chrambach, *Practice of Quantitative Gel Electrophoresis*, VCH, Deerfield Beach, FL, 1985.
2. F. Sambrook, E. F. Fritsch, and T. Maniatis, *Molecular Cloning*, 2nd ed., Cold Spring Harbor Laboratory Press, Plainview, NY, 1987.
3. T. Andrews, *Electrophoresis*, 2nd ed., Clarendon Press, Oxford, 1986.
4. P. Shieh, N. Cooke and A. Guttman, in *High Performance Capillary Electrophoresis* (M. G. Khaledi, ed.), John Wiley and Sons, New York, 1998, Chap. 5.
5. A. Guttman, in *Handbook of Capillary Electrophoresis* (J. P. Landers, ed.), CRC Press, Boca Raton, FL, 1994.
6. H. J. Bode, *Electrophoresis '79*, Walter de Gruyter & Co., New York, 1980, p. 39.
7. D. Soto and S. Sukumar, *PCR Methods Applic* 2: 96 (1992).
8. H. Schwartz and A. Guttman, *Separation of DNA by Capillary Electrophoresis*, Beckman Instruments, Fullerton, CA, 1995.
9. L. M. Smith, J. Z. Sanders, R. J. Kaiser, P. Hughes, C. Dodd, C. R. Connell, C. Heiner, S. B. H. Kent, and L. E. Hood, *Nature* 321: 674 (1986).
10. A. Guttman and N. Cooke, *Anal. Chem.* 63: 2038 (1991).
11. S. Cassel and A. Guttman, *Electrophoresis* 19: 1341 (1998).

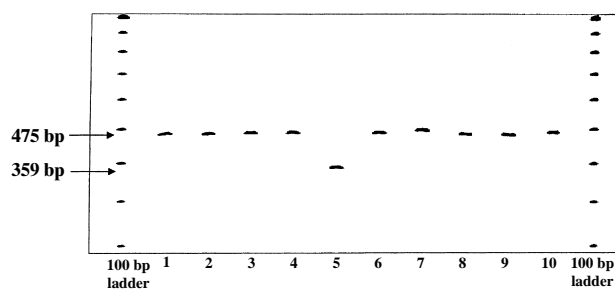


Fig. 2 Real-time electrophoretic image of the screening of 10 patients for the dopamine D_4 receptor (D_4DR) gene polymorphism. Lanes 1–4 and 6–10 exhibit the 475-bp PCR product representing the common fourfold repeat allele in homozygous form, whereas lane 5 shows a 359-bp fragment representing a patient homozygous for the twofold repeat polymorphism. [PCR was done in 35 cycles ($95^\circ\text{C}/\text{min}$, $60^\circ\text{C}/\text{min}$, $72^\circ\text{C}/\text{min}$) using primers P1: 5'-GCG ACT ACG TGG TCT ACT CG-3' and P2: 5'-AGG ACC CTC ATG GCC TTG-3'].

12. R. P. H. Haugland, *Handbook of Fluorescent Probes and Research Chemicals* (M. T. Z. Spence, ed.), Molecular Probes, Inc., Eugene, OR, 1996, Chap. 8.
13. S. Hjerten, *J. Chromatogr.* 347: 191 (1985).
14. M. Szoke, M. Sasvari-Szekely, Cs. Barta, and A. Guttman, *Electrophoresis* 20: 497, 1999.
15. J. E. Stanchfield and D. W. Batey, in *Genome Mapping and Sequencing Symposium*, 1998, p. 214.



Unified Chromatography

Fernando M. Lanças

Laboratório de Cromatografia, Instituto de Química de São Carlos, Universidade de São Paulo, São Carlos/SP, Brazil

Introduction

Gas chromatography (GC) was the first instrumental chromatographic mode to be demonstrated, back in the beginning of the 1950s [1]. Shortly after, Golay [2] proposed, in the same decade, the miniaturization of the technique by introducing the so-called capillary gas chromatography (CGC). It took almost two decades (1960s and 1970s) to spread out worldwide, particularly due to the problems in handling fragile glass columns, however in the 1980s and 1990s CGC became the preferred gas chromatographic mode using wall-coated open-tubular (WCOT) columns.

Supercritical fluid chromatography (SFC) was first demonstrated in the 1960s [3], but became popular only after the 1980s. Two different approaches were developed: one using packed columns of large inner diameter (i.d.) similar to those used in liquid chromatography, and the other one using nonpacked or open-tubular capillary columns similar to those used in CGC. Although open-tubular columns offer the same advantages over packed columns already perceived in CGC, packed columns are still, by far, used more than open-tubular columns in SFC.

Liquid chromatography (LC) was the first chromatographic mode to be developed almost one century ago [4]. Its instrumental version [usually referred as high-performance liquid chromatography (HPLC)] was developed during the end of the 1960s. Although its miniaturization has been discussed since then, its development has not followed the same successful route as CGC. The first step in the miniaturization of LC was the development of 1.0-mm-i.d. columns [5], nowadays usually termed “microbore columns.” The next attempt to follow this direction was the introduction of capillary LC with columns of inner diameter smaller than 0.5 mm [6]. This approach is still far from being developed to a satisfactory extension in order to become a widely accepted routine technique as its GC counterpart (CGC). Although being developed slower than it should be, the miniaturization of the chromatographic techniques is mandatory for the development of unified chromatography.

The Concept of Unified Chromatography

Although the chromatographic techniques namely GC, LC, and supercritical fluid chromatography (SFC) have been developed in a completely independent way, there are no theoretical boundaries between these techniques, as pointed out by Giddings in 1965 [7]. Based on this concept Ishii later proposed and demonstrated in practice the idea of unified chromatography [8]. According to him [8], it is possible to demonstrate different-mode separations (viz. LC, SFC, and GC separation) using a single chromatographic system. According to the same author, the separation mode could be selected, changing the column temperature and pressure [8]. Shortly after the early experiments on unified chromatography by Ishii and co-workers, Yang proposed that the practice of GC, SFC, and microcolumn HPLC become more similar as the column diameter becomes smaller [9]. He also proposed that in this case, the injector, column, and detector may all be the same. In the same year, Bartle and co-workers pointed out that unified microcolumn chromatography allows high-resolution separations that make use of the same chromatographic components (injector, column, and detector) for capillary GC, microcolumn SFC, and HPLC [10].

A few reviews on unified chromatography have been published since its initial development [11–13]. To those readers interested in these techniques, it is highly recommended to consult the pioneer work described in these reviews because there is also, in the literature, some confusion about unified chromatography and multidimensional chromatography, as will be discussed next.

Unified Chromatography or Multidimensional Chromatography?

As discussed in the previous section, the concept of unified chromatography as agreed upon by the pioneers of this technique includes the use of the same chromatographic components (injector, column, and detector) performing GC, SFC, and LC separations. Because it is very common from the beginning, unified chromatography allows several combinations of chromatographic



techniques, such as GC combined with LC, GC combined with SFC, SFC combined with GC, and so on. In this case, the separation is performed in such a way that the sample is introduced into the column and a fraction of it is eluted using one of the chromatographic modes (for instance, GC). After that, the conditions (in the single-substance mobile-phase mode) or the chemical nature (in the multisubstance mobile-phase mode) of the mobile phase is changed in order to perform another chromatographic mode to elute the analytes still retained in the column (for instance, using SFC).

In this example, the first step will allow the elution of the more volatile compounds in the GC mode while the less volatile will be eluted in the SFC mode. If these two modes were not enough to elute all analytes, it would have been possible to later perform a LC separation using the same instrument with a fraction of the sample still in the column. This is the original concept of unified chromatography. This concept has been confused with multidimensional chromatography that uses different columns to perform the separation. In this case, several publications deal with techniques such as GC–GC, LC–LC, SFC–SFC, GC–SFC, LC–GC, and so on. In this approach, either the total or a fraction of the analytes leaving a chromatographic column is transferred to a second column in order to obtain another dimension of analysis (thus the name “multidimensional chromatography”). In unified chromatography, there is no column transfer (switch) and the second dimension of the separation is provided by the change in the mobile-phase characteristics.

Terminology of Unified Chromatography

Several terms have been used to identify this technique. Some of them include the following:

- Unified Approach to Chromatography
- Unified Capillary Chromatography
- Unified Microcolumn Chromatography
- Unified GC and SFC
- Unified Chromatography for GC, SFC, and LC
- Unified Chromatography

The last term is more general and appropriate to the actual stage of the technique.

Instrumentation

The instrumentation used in unified chromatography is based on the ones used for GC, LC, and SFC with minor modifications.

Single-Substance Mobile-Phase Approach

Using a single substance as the mobile phase makes the instrumentation much easier than a multisubstance approach. In this case, the instrument could be a simple modification of HPLC equipment to also deal with a supercritical fluid, as used originally by Ishii. In this case, simply adjusting the mobile-phase pressure and temperature in order to be either in the SFC or LC mode can make the selection of the chromatographic mode (LC or SFC). This is the easiest way to perform unified chromatography but also the more limited one because it is difficult to find a single substance that presents good behavior as a chromatographic mobile phase in the GC mode as well as in the HPLC mode.

Multisubstance Mobile-Phase Approach

In this approach, the mobile-phase chemical nature is changed during the analysis when going from one chromatographic mode to the other. The elution of the sample components can start in the GC mode by introducing the mobile phase (usually a gas) into the column and providing the elution of the volatile compounds. After finishing this step the mobile-phase supply is interrupted and a second eluent (for instance, a supercritical fluid or a liquid) is introduced into the column in order to perform the second separation step. If a third mode is intended, the second eluent is interrupted and the third one is introduced into the column. As a consequence of this approach, a more complex and expensive instrument will have to be built, but also results will be more interesting because each one of the modes will have the mobile phase optimized independently. Whereas for simple samples, the first approach can be used, the multisubstance mobile phase approach might be necessary for more demanding and complex ones.

Selected Applications

Although unified chromatography still has to find its own applications niche, it has been already used for the analysis of a wide variety of samples from aromatic hydrocarbons, styrene, esters, phthalates, crude oil, amines, household wax, pesticides in vegetable oils and many others [11,14–16]. Its major application in the near future will certainly be centered in the analysis of complex samples such as environmental samples, biological fluids, forensic chemistry, and so forth. In this case, there is a need for more than one separation mode because the sample might contain volatile, semi-



volatile, and nonvolatile compounds of interest, thus requiring different chromatographic conditions.

Projected Enlargement of the Unified Chromatography Concept

When unified chromatography was first proposed, the chromatographic techniques were divided into GC, SFC, and LC. Nowadays, there has been a general acceptance that GC and LC are extreme mobile-phase conditions and that several intermediate conditions are possible. This includes solvated gas chromatography, enhanced liquid chromatography, and subcritical fluid chromatography, among other possibilities. Considering this fact, we can expect that in the near future, all these modes will be performed in the same instrument designed for unified chromatography. This will not only enlarge the theoretical concept of this technique but will also broaden its application range.

Limitations

The major limitation of unified chromatography is that there is no commercial instrument available up to this moment available to those interested in the techniques. The few existing instruments are basically located in universities and are built in-house to attend to the purpose of the investigator. Another considerable limitation of the techniques is the difficulty in making columns that can show good performance in more than two chromatographic modes. WCOT columns made for SFC can usually operate well in the capillary GC mode; packed columns for SFC can operate in the LC modes. However, a column, which operates in an optimized way in the GC and LC mode, is still to be developed. Although some attempts have been made in research laboratories, they are not commercially available. Another difficulty is related to the identification mode. Nowadays, mass spectrometry is the most powerful detector for all chromatographic modes. However, the interfaces for GC-MS and LC-MS (the extreme modes used in unified chromatography) are completely different. More research has to be developed in this field in order to fulfill this gap in the identification of the peaks eluted in unified chromatography.

Conclusion

Unified chromatography is an infant technique that combines all chromatographic modes in just one in-

strument. Although it is a fascinating task from the theoretical point of view, in practice it still presents several limitations. A severe one is the absence of commercial instruments, which hinders the development of further applications. It is expected that in the near future, the technique will be fully developed and the frontiers between the chromatographic world will be removed.

Acknowledgments

Professor Lanças wishes to acknowledge FAPESP (Fundação de Apoio à Pesquisa do Estado de São Paulo) and CNPq (Conselho Nacional de Desenvolvimento Científico e Tecnológico) for the financial support to his laboratory.

References

1. A. T. James and A. J. P. Martin, *Biochem. J.* 50: 679 (1952).
2. M. E. Golay, "Brief Report on Gas Chromatography Theory," in *Gas Chromatography* (1960 Eidinburg Symposium), R. P. Scott (ed.), Butterworths, London, 1960, p. 139.
3. E. Klesper, A. H. Corwin, and D. A. Turner, *J. Org. Chem.* 27: 700 (1962).
4. M. Tsett, *Ber. Deut. Botan. Soc.* 24: 316 (1906).
5. C. G. Horváth, B. A. Preiss, and S. R. Lipsky, *Anal. Chem.* 39: 1422 (1967).
6. D. Ishii, K. Asai, K. Hibi, T. Jonokuchi, and M. Nagaya, *J. Chromatogr.* 144: 157 (1977).
7. J. C. Giddings, "Dynamics of Chromatography," Marcel Dekker, Inc., New York, 1965.
8. D. Ishii, T. Niwa, K. Ohta, and T. Takeuchi, *J. High Resolut. Chromatogr.* 11: 800 (1988).
9. F. J. Yang, "Microbore Column Chromatography. A Unified Approach to Chromatography," Marcel Dekker, Inc., New York, 1989.
10. K. D. Bartle, I. L. Davies, M. W. Raynor, A. A. Clifford, and J. P. Kithinji, *J. Microcol. Separ.* 1: 63 (1989).
11. D. Tong, K. D. Bartle, and A. A. Clifford, *J. Chromatogr.* 703: 17 (1995).
12. T. L. Chester, *Anal. Chem.* 69: 165A (1997).
13. F. M. Lanças, "GC \times SFC \times LC: Towards Unified Chromatography," Proc. VIth Latin American Congress on Chromatography, COLACRO VI, Caracas, Venezuela, Intevp (ed.), 25-P1 (1996).
14. Y. Liu, F. Y. Yang, *Anal. Chem.* 63: 926 (1991).
15. I. L. Davies and F. J. Yang, *Anal. Chem.* 63: 1242 (1991).
16. D. Tong, K. Bartle, A. A. Clifford, and R. Robinson, *Analyst* 120: 2461 (1995).



Uremic Toxins in Biofluids, Analysis by HPLC

Ioannis N. Papadoyannis

Victoria F. Samanidou

Aristotle University of Thessaloniki, Thessaloniki, Greece

INTRODUCTION

During the 1960s, target substances for removal in the blood of uremic patients were *small molecules*, such as urea, creatinine, and guanidine compounds. In the 1970s, “middle molecular substances,” i.e., substances with molecular weights ranging from 300 to 5000 Da, were also included in the list of substances that have to be removed. Hemodiafiltration was developed as a more efficient method for removing middle molecular toxins, and separation and identification of such substances in uremic serum were actively attempted by many researchers worldwide.

UREMIA

The term “uremia” was initially proposed by Piorry and L’Heritier in 1840 to mean “urine in the blood.” *Uremia*, or azotemia, is a condition resulting from advanced stages of kidney failure, in which urea and other nitrogen-containing wastes are found in the blood. Lethargy, mental depression, loss of appetite, and edema are some of the early signs of uremia, while subsequent symptoms include diarrhea, anemia, convulsions, coma, and a gray-brown coloration.

Treatment of uremia is usually performed with dialysis and/or renal transplantation. Since 1840, more than 2000 toxic substances were reported in uremic blood.^[1,2]

UREMIC TOXINS

Uremic toxins are chemicals and waste products normally excreted by the kidneys; they are responsible for many of the signs of kidney disease. Blood urea nitrogen (BUN) is one of those substances, but it is not the only one. Early definitions (in 1978) proposed the following as minimal for the identification of uremic toxins:

1. They should be chemically identifiable and quantifiable in biological fluids
2. The concentration in uremic subjects should exceed that in nonuremic subjects.
3. The concentration should correlate with specific uremic symptoms that disappear at the normal concentration.
4. Toxic effects in a test system should be demonstrable at the concentration found in uremic subjects.

Nowadays, this definition can be considered as classical. Because all of these criteria are rarely met simultaneously, the concept of uremic toxins has changed. In the new concept, substances that damage normal physiological functions, or interfere with physiological defense mechanisms in renal failure, have also been recognized as “uremic toxins.” Some may play a role in the progression of renal disease, inducing uremic symptoms, and may contribute to dialysis-related complications.

As already mentioned, one way to treat uremia is through dialysis. Uremic toxins and excess fluid are removed by hemodialysis, which is accomplished by using a dialyzer. This is a convenient configuration, incorporating a semipermeable dialysis membrane with provisions for the flow of blood and dialysate on either side of the membrane. Blood is removed for purification from the patient’s body via the blood access, pumped by the blood pump through blood tubing into the dialyzer, and is then pumped back to the patient. Dialysate of the desired chemical composition is prepared through the dialysate delivery system, by mixing water and concentrate in the appropriate ratio. Dialysate is pumped through the dialyzer to remove toxins and fluid crossing over from blood. An anticoagulant, such as heparin, is infused into the extracorporeal blood circuit to prevent blood clotting by a pump. Patients usually receive hemodialysis three times weekly for 4 hr each time.

Table 1 summarizes substances considered as possible uremic toxins. Fig. 1 illustrates the chemical structures of some of the most important uremic toxins that are determined by high-performance liquid chromatography (HPLC). In this paper, some of the most important uremic toxins are discussed (concerning their chromatographic determination).

Table 1 Possible uremic toxins

Small water-soluble compounds

Guanidines
Asymmetric dimethylarginine
Creatinine
Purines
Oxalate
Phosphorus
Urea

Middle, large molecules

Advanced glycosylated end products
Parathyroid hormone
Oxidation products
Peptides (beta-endorphin, methionine-enkephalin, beta-lipotropin, granulocyte inhibiting proteins I and II, degranulation-inhibiting protein, adrenomedullin)
Beta 2-microglobulin
Complement factor D

Protein-bound compounds

Indoles
3-Carboxy-4-methyl-5-propyl-2-furanpropionic acid
Hippuric acid
Homocysteine
Indoxyl sulfate
p-cresol
Polyamines

DETERMINATION BY HPLC

Creatine–Creatinine

Molecules serving as effective biomarkers in clinical fluids are often low-molecular-mass metabolic end products. These small molecules can often be directly determined in urine; however, their determination in plasma or serum often requires some form of protein removal. Creatinine is the most widely used clinical marker to assess renal function.

The reliable determination of uremic toxins, creatine, and creatinine in biofluids is a matter of great importance in clinical chemistry.

Creatine is present in muscle, brain, and blood and, although not present in large amounts in normal urine from adults, it is abundantly present in the urine of adults who have recently ingested creatine supplements. Ingestion of a creatine supplement has been shown to increase the level of phosphocreatine, and this has become extremely popular in recent years with many athletes who want to increase muscular power and to enhance their performance. Because of this, analysis for creatine has become more important in the clinical setting. Additionally, elevated serum concentrations of creatine can be observed in some cases of muscle catabolism such as

primary myopathy, myositis, and muskeltrophie, as well as in the case of hyperthyroidism.

Creatinine is the end product of creatine catabolism. It is found in muscle tissue, blood, and urine as it is formed from the breakdown of muscle creatinine, and is proportional to the muscle mass. It results from the irreversible nonenzymatic dehydration and loss of phosphate from phosphocreatine, as shown in Fig. 2. Creatinine concentrations are very useful indices for evaluating glomerular filtration rate and, in general, are an important clinical marker of renal function.

Although creatinine concentration should be stable from day to day, it is a function of the amount of creatinine entering the blood from muscle, its volume of distribution, and its rate of excretion. Because the first two are usually constant, changes in the serum creatinine level would usually be a result of a change in the glomerular filtration rate (GFR). Abrupt cessation of glomerular filtration causes the serum creatinine to rise by 1–3 mg/dL daily. The blood urea nitrogen also rises with renal dysfunction, but is influenced by extrarenal factors as well.

Urine creatinine is used to adjust the values of urinary biological indicators; for example, creatinine measurements are necessary for correction of vanilmandelic and homovanillic acids, which indicate neuroblastoma and pheochromocytoma, when excreted in urine in abnormally increased concentrations. Ratios of vanilmandelic and homovanillic acids to creatinine have been utilized as a diagnostic index of these diseases.

Measurement of creatinine in serum and urine is routinely performed by photometric methods such as the Jaffé reaction, which is widely accepted and involves the formation of an adduct of creatinine with picric acid in alkaline solution, whose absorbance is measured at 500 nm. However, this method is unspecific and subject to perturbation by many interfering substances from endogenous and exogenous origins.

Therefore great efforts were undertaken to improve existing methods or to develop new measurement principles, using enzymatic and HPLC-based methods. Chromatographic techniques are attractive for clinical analysis because of their inherent ability to analyze multiple component biofluids and determine the analytes of interest with minimal interference from other species. Chemical methods give higher values because of the presence of endogenous and exogenous substances. HPLC methods for the determination of creatinine that can be found in literature involve ion exchange, ion-pairing, and reversed phase. Most of these require deproteinization before analysis, but direct analysis of serum creatinine can also be achieved by column switching liquid chromatography. Liquid–liquid extraction for isolation of creatinine among other compounds has been reported. Capillary electro-



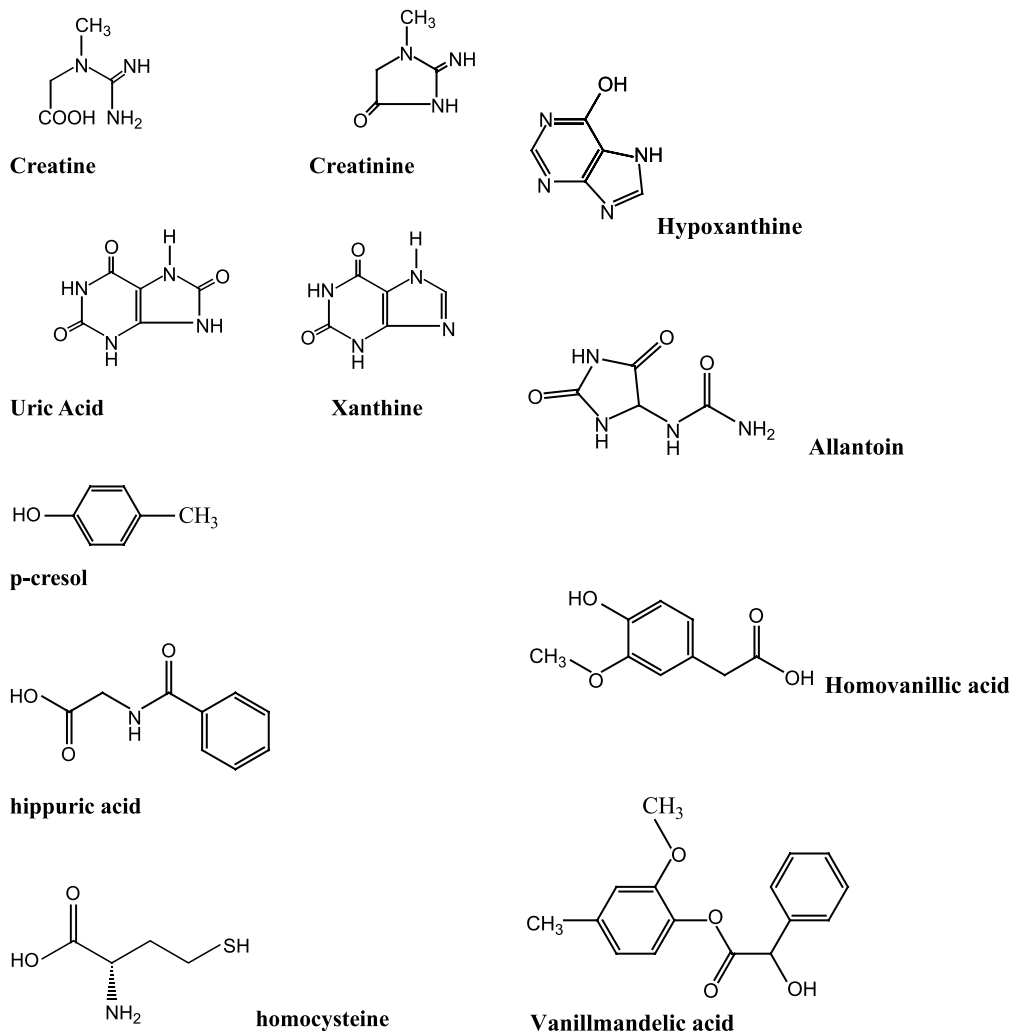


Fig. 1 Chemical structures of possible uremic toxins that are determined by HPLC.

phoretic methods are also reported for the determination of creatine and creatinine.^[3-9]

PURINE METABOLITES

Oxypurines: Allantoin, Uric Acid, Hypoxanthine, and Xanthine

Purines are metabolized in a series of reactions involving hypoxanthine, xanthine, uric acid, and allantoin as end products that are subsequently excreted in urine. Fig. 3 shows the metabolic pathways for xanthine. Measurement of urinary excretion of purine metabolites, primarily allantoin or, additionally, uric acid, xanthine, and hypoxanthine, has been proposed as a marker for microbial

protein synthesis. The problem of nonspecificity of the colorimetric assay for purine metabolites can be overcome by using a multitude of methods, with or without derivatization. HPLC determination of these compounds can be performed in urine samples directly after dilution.

Uric acid is a primary end product of urine metabolism in the kidney. Uric acid levels in human urine are like creatinine as an important parameter of renal function and a marker for renal failure as well as toxicity. As shown in Fig. 3, uric acid is the final product of catabolization of the purine nucleosides, adenosine, and guanosine.^[10]

Xanthines, e.g., hypoxanthine and xanthine, are intermediates of the metabolism of adenine and guanine to uric acid and are, therefore, important analytes for diagnosis of certain types of metabolic disease.

Uric acid and xanthines are markers for metabolic disorders such as gout, Lesch-Nyman syndrome, and



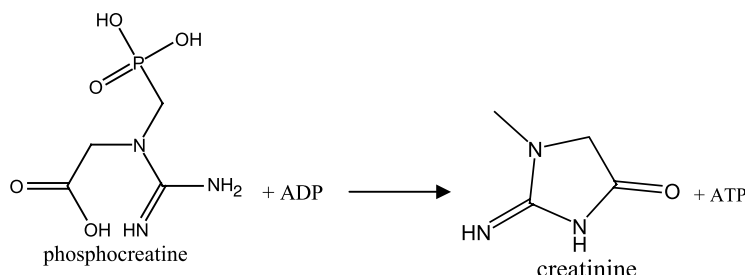


Fig. 2 Phosphocreatine metabolism.

xanthinuria. Measurements of urinary excretion of purine metabolites, among them uric acid and xanthine, have been proposed as a marker for microbial protein synthesis. Their simultaneous determination is useful for diagnosis and treatment of hyperuricemia. In addition to xanthine and hypoxanthine, notable members of the xanthine class include caffeine, theophylline, and theobromine.^[11–15]

Clearly, the determination of such compounds is crucial for diagnosis and monitoring of renal disease and metabolic disorders. The concentration of oxypurines in blood serum is among the most important parameters in biochemistry and clinical chemistry. Determination of uric acid is performed by enzymatic methods or colorimetrically by reduction of phosphotungstate.

The combination of HPLC reversed-phase C₈ columns with monitoring of the effluent at 205 nm provides an acceptable analytical tool for quantification of purine metabolites in the urine. Detection at short ultraviolet

(UV) wavelengths up to 215 nm results in compromised method selectivity and, therefore, longer and more specific detection wavelengths were applied in recent methods. The combination of the direct separation and determination using a reversed-phase HPLC system, coupled with photodiode array detection, is found to be accurate and more precise and selective than previously published methods for the determination of purine metabolites in urine.

HPLC methods for the determination of uric acid found in literature include ion exchange, ion-pairing, reversed phase, and size exclusion. Most of these require deproteinization before analysis, but direct analysis of serum uric acid was also successful by column switching liquid chromatography.

In recent years, a number of methods based on HPLC, isocratic or gradient, have been reported for the quantification of allantoin and purine metabolites in biological fluids.

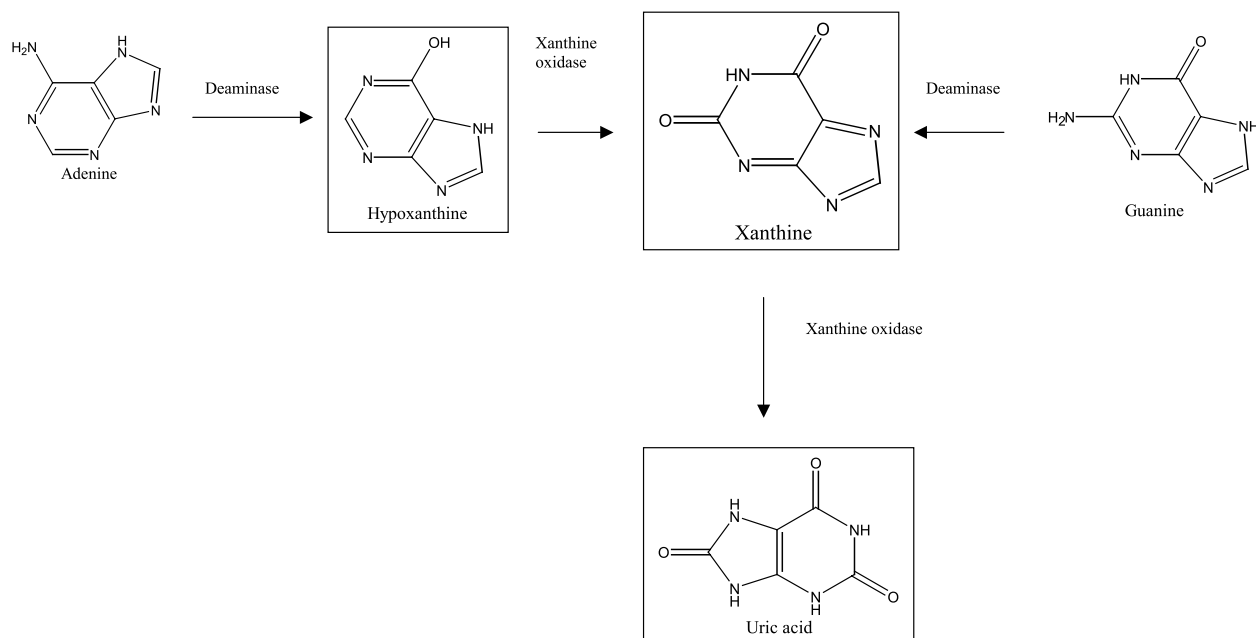


Fig. 3 Xanthine metabolic pathways.

Various analytical methods for determining purine metabolites in biological samples, such as urine or blood plasma, have been described. These procedures are based mainly on separation by HPLC methods using reversed-phase C_{18} columns and monitoring at wavelengths ranging from 200 to 218 nm, or at 254 nm for compounds other than allantoin. The main advantage of these methods is that urine samples are analyzed directly, while the plasma samples only need acid deproteinization. Unfortunately, UV detection at short wavelengths (i.e., up to 218 nm) is not selective enough. Because allantoin is poorly retained on a C_8 column and has a very low molar absorptivity at wavelengths above 220 nm, allantoin may be converted to a derivative containing a chromophore group (Rimini-Schryver reaction). Some research groups removed the uric acid prior to the derivatization of allantoin; however, these methods are time-consuming and labor-intensive.

Simultaneous Determination of Creatine, Creatinine, Uric Acid, and Xanthine

Although several papers can be found in the literature dealing with the determination of single analytes or simultaneous determination of creatinine and uric acid, only a few have reported on the simultaneous determina-

Table 2 Chromatographic and sample preparation conditions for the simultaneous determination of creatine, creatinine uric acid and xanthine

Chromatographic conditions

Mobile phase: 10 mmol/L KH_2PO_4
Analytical column: Kromasil C_8 , 250×4 mm (ID), 5 μ m
Pressure: 110–120 kg/cm²
Flow rate: 0.8 mL/min
Detection: 200 nm

Sample preparation

Serum samples

- 1) 500 μ L serum sample + 1 mL acetonitrile to precipitate proteins
- 2) Centrifugation at 3500 rpm for 15 min
- 3) Evaporation of acetonitrile
- 4) Dilution of residual 10–20 times with deionized water
- 5) Direct analysis or spiking with stock solutions to apply standard addition technique

Human urine samples

- 1) Collection from healthy volunteers and storage at $-20^\circ C$ until analysis
- 2) Filtration through 0.2- μ m membrane filters to remove cells and other particulate matter
- 3) Dilution, 400–500 times with deionized water
- 4) Direct analysis or spiking with stock solutions to apply standard addition technique

(From Ref. [1].)

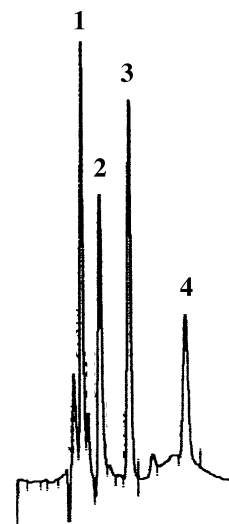


Fig. 4 High-performance liquid chromatogram of standard solution containing: 1) creatine, 2.631 min; 2) creatinine, 3.400 min; 3) uric acid, 4.645 min; and 4) xanthine, 7.014 min. Chromatographic conditions are described in Table 2. (From Ref. [1].)

tion of creatine, creatinine, uric acid, and xanthine in human biofluids. One of them reports about an HPLC method with UV detection permitting the analysis of human serum and urine for the determination of these substances in a single run. Low-wavelength UV detection is achieved at 200 nm using 10 mmol/L KH_2PO_4 , as mobile phase, at a flow rate 0.8 mL/min and a Kromasil C_8 , 250×4 mm, analytical column. Analysis is completed within approximately 8 min. Table 2 summarizes the chromatography and the sample preparation conditions. Fig. 4 shows a typical chromatogram obtained under the described chromatographic conditions.^[16]

The limits of detection obtained by this method are 4 pg for creatine and creatinine, 20 pg for uric acid, and 6 pg for xanthine, while the limits of quantitation are 10 pg for creatine and creatinine, 60 pg for uric acid, and 20 pg for xanthine, when 20 μ L are injected onto the column. A rectilinear relationship is observed up to 2 ng/ μ L for creatine and creatinine, 12 ng/ μ L for uric acid and 5 ng/ μ L for xanthine.

The statistical evaluation of the method was examined by performing day-to-day ($n = 8$) and within-day ($n = 8$) calibration and was found to be satisfactory with high accuracy and precision results. Relative standard deviation (RSD) values were in the range of 0.4–4.3% for within-day measurements and 3.5–7.4% for day-to-day precision measurements.

This method was applied to serum and urine, simply after dilution. A typical chromatogram of creatine, creatinine, uric acid, and xanthine in serum and urine are shown in Figs. 5 and 6, respectively. The sensitivity of this

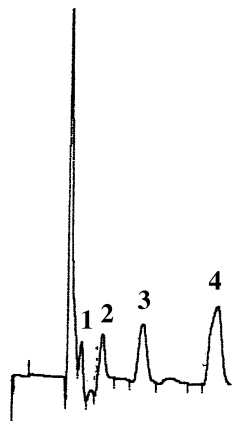


Fig. 5 High-performance liquid chromatogram of spiked human blood serum sample (after 20-fold dilution) containing: 1) creatine, 2.760 min; 2) creatinine, 3.615 min; 3) uric acid, 5.232 min; and 4) xanthine, 7.488 min. Chromatographic conditions are described in Table 2. (From Ref. [1].)

method was high enough to determine the concentration of creatinine and uric acid in diluted serum (10- to 20-fold dilution) and urine (400- to 500-fold dilution) samples. Percentage recovery of analytes in spiked samples was in the range 91–105%. No interference was observed from endogenous compounds of human serum and urine. Correlation of analyzed samples using the developed method and conventional routine methods for creatinine and uric acid gave significantly similar results. The method appears to be a very useful tool for routine analysis of clinical samples, for simultaneous determination of creatinine, creatine, uric acid, and xanthine levels in serum and urine.

Phenol and Cresols

Urinary phenol, cresols, *p*-nitrophenol, and *p*-aminophenol are biological indicators of human exposure to aromatic hydrocarbons. Fig. 7 illustrates the scheme of phase 1 and phase 2 metabolism of inhaled benzene and toluene vapors, while Fig. 8 shows the metabolism of inhaled xylene and ethyl benzene vapors.

The determination of urinary cresols, particularly *o*-cresol, has been proposed as a biological monitoring method for toluene, as a fraction of the inhaled vapor is oxidized at the aromatic ring with the production of cresols.^[17–19]

p-Cresol and hippuric acid are included among uremic toxins. *p*-Cresol (4-methylphenol) is a volatile, low-molecular-weight phenolic compound that is largely protein-bound, mainly to albumin, with partial lipophilic properties. It is related to several biochemical, biological, and physiological functions at concentrations currently observed in uremia.

p-Cresol can be considered as a prototype of protein-bound uremic retention solutes, with a protein binding of >99% in healthy subjects and approximately 90% in uremic patients. Several recent studies suggest that *p*-cresol interferes with various biochemical and physiological functions at concentrations currently observed in uremia. Concentrations of phenol and *p*-cresol in uremic serum are significantly higher than those in normal serum.

The present concept of dialysis focuses mainly on the removal of small water-soluble compounds, and the currently applied kinetic parameters of dialysis adequacy are also based on the behavior of water-soluble compounds. Nevertheless, many of the currently known biological effects in uremia are attributable to compounds with different physicochemical characteristics and, among these, protein-bound solutes may play an important role. Hippuric acid, homocysteine, and *p*-cresol are considered.^[20]

Phenol and *p*-cresol noticeably accumulate in the serum of undialyzed and dialyzed uremic patients; they play a role in the development of uremic coma and defective platelet aggregation. They are synthesized in the small intestine from phenylalanine and tyrosine through

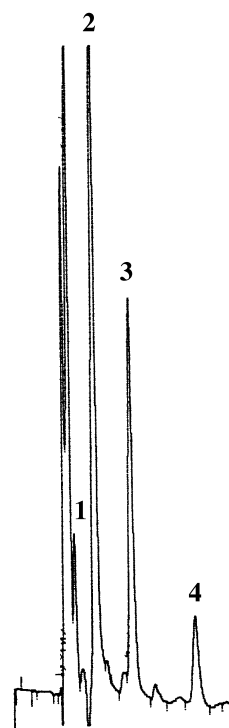


Fig. 6 High-performance liquid chromatogram of urine sample (after 400-fold dilution) containing: 1) creatine, 2.774 min; 2) creatinine, 3.675 min; 3) uric acid, 5.365 min; and 4) xanthine, 7.494 min. Chromatographic conditions are described in Table 2. (From Ref. [1].)



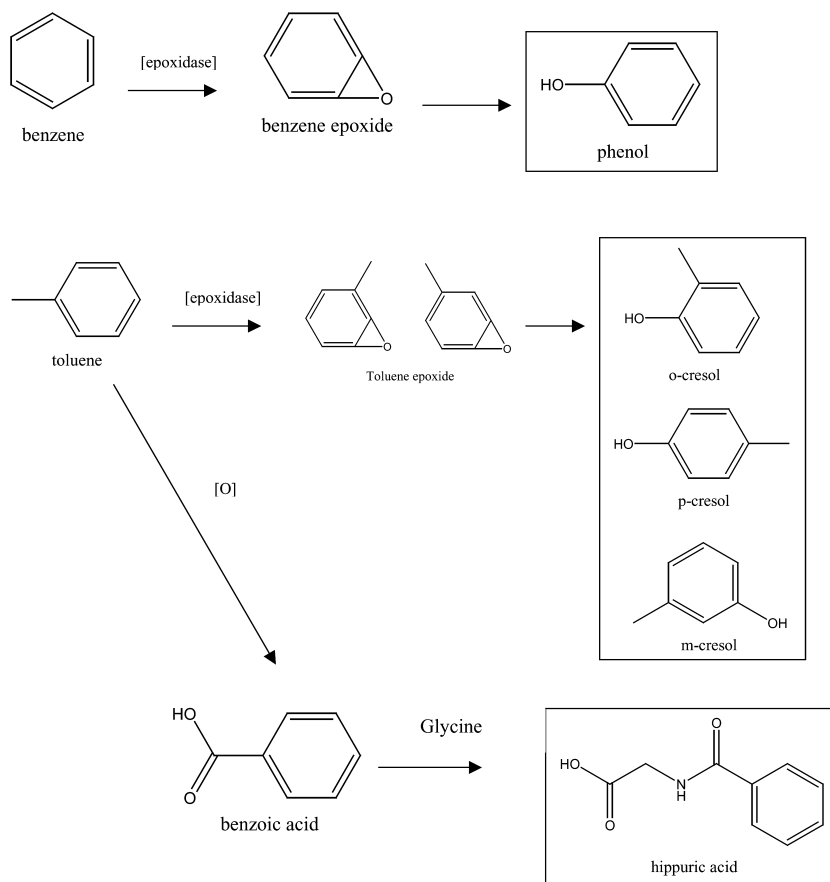


Fig. 7 Scheme of phase 1 and phase 2 metabolism of inhaled benzene and toluene vapors.

4-hydroxybenzoic acid and 4-hydroxyphenylacetic acid, respectively, by intestinal bacteria, as shown in Fig. 9. Aerobic bacteria tend to produce phenol from tyrosine, whereas anaerobic bacteria produce *p*-cresol. These phenols are absorbed from intestine and normally excreted into urine. In uremia, renal clearance of the phenols is impaired, leading to accumulation of the phenols in the blood. Compared to healthy controls, the serum *p*-cresol levels are 7–10 times higher in continuous ambulatory peritoneal dialysis patients, uremic outpatients, and hemodialysis patients.^[21]

Only a few methods are available for the determination of *p*-cresol concentration in serum. In addition, these methods have only been used for the determination of total *p*-cresol. In particular, the evolution of free (nonprotein-bound) *p*-cresol is of concern because, conceivably, this is the biologically active fraction. However, the concentration of free *p*-cresol is markedly lower than that of total *p*-cresol, in view of its important protein binding. Methods enabling the measurement of total and free *p*-cresol concentration in the serum of healthy controls and uremic patients are also reported in literature.

Deproteinization, extraction, and HPLC procedures are efficient, without interference of other protein bound ligands and/or precursors of *p*-cresol or phenol, via spiking experiments, and measurement of the UV absorbance over the 200–400 nm wavelength range.

HPLC methods can use fluorescence as a detector for quantifying serum phenol and *p*-cresol in uremic patients on hemodialysis.

Fluorescence detection at 284/310 nm (extinction/emission wavelengths) leads to a detection limit of 1.3 mmol/L (0.14 mg/mL for *p*-cresol). Identification of phenol and *p*-cresol may be confirmed by liquid chromatography/mass spectrometry. Because HPLC methods require only simple extraction, e.g., by ethyl acetate, and do not require further steps such as derivatization, they are simple and rapid compared with gas chromatography or gas chromatography/mass spectrometry. Such methods are useful for monitoring serum phenols in dialyzed patients as an index of hemodialysis adequacy. However, the separation of the three isomers of cresol can only be performed by adding β -cyclodextrin to the liquid phase.



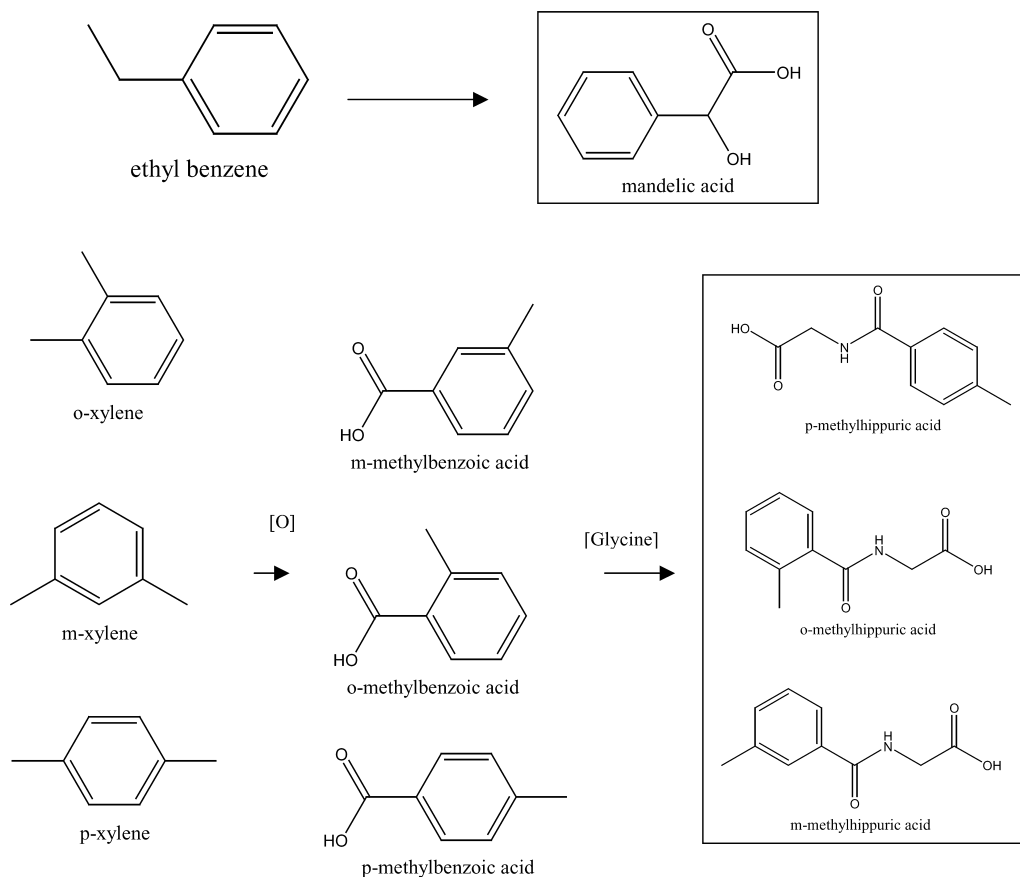


Fig. 8 Scheme of phase 1 and phase 2 metabolism of inhaled xylene and ethylbenzene vapors.

Hippuric Acid

Toluene and *o*-, *m*-, and *p*-xylene have been widely used, separately and as mixtures, as organic solvents, ingredients of thinners, and in the synthesis of chemicals.

Toluene is widely used in industry as a replacement for the carcinogenic benzene, but toluene also exhibits considerable toxicity. In vivo, toluene is oxidized; the main metabolite in man is benzoic acid, which is then conjugated with glycine and excreted in urine as hippuric

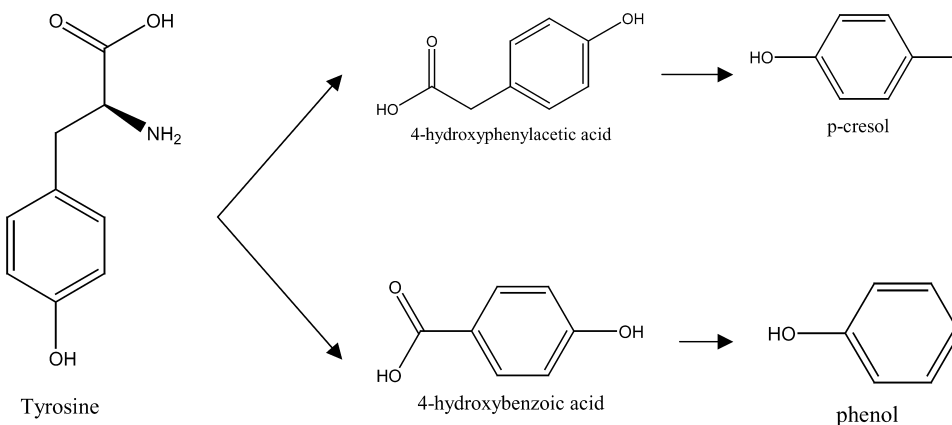


Fig. 9 Tyrosine metabolism.

acid. Although hippuric acid is an endogenous metabolite commonly found in human urine, on exposure to toluene, the level is enhanced.^[19–21] The three isomers of xylene in a mixture are commonly called “xylol.” In vivo, these isomers are oxidized to isomeric toluic acids, then conjugated with glycine and excreted in urine as *o*-, *m*-, and *p*-methylhippuric acid.

Hippuric acid has been recognized as a potential marker of uremic toxicity in chronic renal failure. Additionally, hippuric acid and *o*-, *m*-, and *p*-methylhippuric acids are used as biological markers in studies of occupational exposure to diesel industrial solvents, because they show a good correlation with the level of exposure to toluene and xylenes. In urinary biological monitoring, expressing the amount of urinary metabolite per gram of creatinine has been used for spot samples of urine. This correction is thought to be particularly applicable for very concentrated and dilute samples. Therefore the biological exposure indices of urinary hippuric acid in toluene exposure, methylhippuric acid in xylene exposure, and mandelic acid in styrene exposure are expressed as metabolite concentrations in urine, corrected for creatinine.

For the simultaneous determination of metabolite concentrations in the urine of workers exposed to aromatic solvents, high-performance liquid chromatography has been widely used to obtain accurate and reliable results. Also, gas chromatography has been used for the determination of metabolite concentrations.

HPLC methods are considered by the National Institute for Occupational Safety and Health (NIOSH) to be the reference methods (e.g., NIOSH #8301). However, these methods cannot separately quantify each isomer of hippuric acid and methylhippuric acids.

Gas chromatographic methods are considered to be specific for determination of hippuric acid and methylhippuric acid, although they require a derivatization procedure with various reagents; for example, several investigators have used diazomethane; others have used trimethyl-silyl derivatives.

Reversed-phase high-performance liquid chromatography has been used without derivatization with ultraviolet or electrochemical detection. Liquid-liquid extraction can be performed, as well as solid phase extraction (SPE), for sample preparation after acidification with HCl 1mol/L (pH 1). Removal of the homovanillic acid from the variable salt concentration of the sample enhances the control of the ion exchange step. This is accomplished by SPE using a C₈ cartridge. This first stage also helps to reduce the number of anionic compounds from the matrix that will be loaded onto the strong anion exchange cartridge.^[22] Recently, high-performance capillary electrophoresis (HPCE) has developed into a powerful analytical technique in diverse fields, and shows a high separation power with a short analysis time. In the field

of occupational health, there are not many HPCE methods for the determination of metabolites in the urine of workers exposed to aromatic solvents, although HPCE methods have been used for hippuric acid (HA) in human urine and human serum, and for creatinine and uric acid.

Protein-bound uremic solutes play a role in the inhibition of drug protein binding. Substantial changes in protein binding of drugs occur during the progression of renal insufficiency. It has been suggested that hippuric acid in uremic ultrafiltrate is an inhibitor of theophylline protein binding. The inhibitory effect on theophylline protein binding of the deproteinized uremic serum has been shown to be higher than with ultrafiltrate ($p < 0.05$).^[23]

Dose-response curves with the characterized compounds revealed that the most important role in binding inhibition could be attributed to hippuric acid. The identified uremic compounds are not entirely representative for the decreased protein binding of theophylline, indicating that additional factors than those identified in this study affect the protein binding as well.

Homocysteine

The absence of a chromophore for sensitive detection is a problem which is met with HPLC determination of these thiol analytes. However, two approaches are possible to resolve this point: 1) direct detection using electrochemistry, either amperometry on gold/mercury amalgamated electrodes or coulometry on porous graphite electrodes; 2) derivatization coupled with UV or spectrofluorometric detection. The derivatization reactions, either precolumn or postcolumn, involve different thiol selective reagents: ammonium 7-fluorobenzo-2-oxa-1,3-diazole-4-sulphonate (SBD-F), *ortho*-phthalaldehyde (OPA), etc.

Reversed-phase HPLC with fluorescence detection, after derivatization of plasma thiols with ammonium 7-fluorobenzo-2-oxa-1,3-diazole-4-sulphonate (SBD-F), is the most widely used method to determine total plasma amino thiols (cysteine, cysteinylglycine, and homocysteine). The time required for sample preparation (thiolic reduction, deproteinization, and precolumn derivatization with SBD-F) and for thiol derivatives separation is nearly 2 h per sample.

Catecholamine Metabolites: Homovanillic and Vanillylmandelic Acid

Homovanillic and vanillylmandelic acids, the major metabolites of catecholamines, are often tested in urine for neurological diagnosis and for monitoring the



response to therapy in diseases such as pheochromocytoma and neuroblastoma.

Various high-performance liquid chromatography methods have been described, mainly employing ion-pair reversed-phase chromatography, with electrochemical or fluorimetric detection, most of them including sample pretreatment with solid-phase or liquid extraction.

The determination of catecholamines requires a highly sensitive and selective assay procedure capable of measuring very low levels of catecholamines that may be present. In past years, a number of methods have been reported for measurement of catecholamines in both plasma and body tissues. A few of these papers have reported simultaneous measurement of more than two catecholamine analytes. One of them utilized lised UV for end-point detection and the samples were chromatographed on a reversed-phase phenyl analytical column. The procedure was slow and cumbersome because of due to the use of a complicated liquid-liquid extraction and each chromatographic run lasted more than 25 min with a detection limit of 5–10 ng on-column. Other sensitive HPLC methods reported in the literature use electrochemical detection with detection limits 12, 6, 12, 18, and 12 pg for noradrenaline, dopamine, serotonin, 5-hydroxyindoleacetic acid, and homovanillic acid, respectively. The method used very a complicated mobile phase in terms of its composition while whilst the low pH of 3.1 used might jeopardize the chemical stability of the column. Analysis time was approximately 30 min. Recently reported HPLC methods utilize amperometric end-point detection.^[22,24]

CONCLUSION

Uremic toxins are chemicals and waste products normally excreted by the kidneys and are responsible for many of the signs of kidney disease. Since 1840, more than 2000 toxic substances were reported in uremic blood. Obviously, the determination of such compounds is crucial for diagnosis and monitoring of renal disease and metabolic disorders. The concentrations of several uremic toxins in blood serum and urine are among the most important parameters in biochemistry and clinical chemistry.

REFERENCES

1. <http://www.embbs.com/cr/rf/rf3.htm>.
2. <http://www.outlinemed.com/demo/nephrol/11244.htm>.
3. Shingfield, K.J.; Offer, N.W. Simultaneous determination of purine metabolites, creatinine and pseudouridine in ruminant urine by reversed phase HPLC. *J. Chromatogr., B* **1999**, *723*, 81–94.
4. Kochansky, C.; Strein, T. Determination of uremic toxins in biofluids: Creatinine, creatine, uric acid and xanthines. *J. Chromatogr., B* **2000**, *747*, 217–227.
5. Czauderna, M.; Kowalczyk, J. Simultaneous measurement of allantoin, uric acid, xanthine and hypoxanthine in blood by high-performance liquid chromatography. *J. Chromatogr., B* **1997**, *704*, 89–98.
6. Seki, T.; Orita, Y.; Yamaji, K.; Shinoda, A. Simultaneous determination of uric acid and creatinine in biological fluids by column-switching liquid chromatography with ultraviolet detection. *J. Pharm. Biomed. Anal.* **1997**, *15*, 1621–1626.
7. Eiteman, M.A.; Gordillo Cabrera, M.L. Analysis of oxonic acid, uric acid, creatine, allantoin, xanthine and hypoxanthine in poultry litter by reverse phase HPLC. *Fresenius J. Anal. Chem.* **1994**, *348*, 680–683.
8. Shirao, M.; Suzuki, S.; Kobayashi, J.; Nakazawa, H.; Mochizuki, E. Analysis of creatinine, vanilmandelic acid, homovanillic acid and uric acid by micellar electrokinetic chromatography. *J. Chromatogr., B* **1997**, *693*, 463–467.
9. Resines, J.A.; Arin, M.J.; Diez, M.T.; Garcia del Moral, P. Ion-pair reversed HPLC determination of creatine in urine. *J. Liq. Chromatogr. Relat. Technol.* **1999**, *22* (16), 2503–2510.
10. Seki, T.; Yamaji, K.; Orita, Y.; Moriguchi, S.; Shinoda, A. Simultaneous determination of uric acid and creatinine in biological fluids by column-switching liquid chromatography with ultraviolet detection. *J. Chromatogr., A* **1996**, *730*, 139–145.
11. Czauderna, M.; Kowalczyk, J. Quantification of allantoin, uric acid, xanthine and hypoxanthine in ovine urine by high-performance liquid chromatography and photodiode array detection. *J. Chromatogr., B* **2000**, *744*, 129–138.
12. Schoots, A.C.; Homan, H.R.; Gladdines, M.M.; Cramers, C.A.; de Smet, R.; Ringoir, S.M. Screening of UV absorbing solutes in uremic serum by reversed phase HPLC change of blood levels in different therapies. *Clin. Chim. Acta, Int. J. Clin. Chem.* **1985**, *146* (1), 37–51.
13. de Smet, R.; Vogeleere, P.; van Kaer, J.; Lameire, N.; Vanholder, R. Study by means of high-performance liquid chromatography of solutes that decrease theophylline/protein binding in the serum of uremic patients. *J. Chromatogr., A* **1999**, *847*, 141–153.
14. Georga, K.A.; Samanidou, V.F.; Papadoyannis, I.N. Improved micro-method for the HPLC analysis of caffeine and its demethylated metabolites in human biological fluids after SPE. *J. Liq. Chromatogr. Relat. Technol.* **2000**, *23* (10), 2975–2990.
15. Georga, K.A.; Samanidou, V.F.; Papadoyannis, I.N. Use of novel solid-phase extraction sorbent materials for high-performance liquid chromatography quantitation of caffeine metabolism products methylxanthines and methyluric acids in samples of biological origin. *J. Chromatogr., B* **2001**, *759*, 209–218.
16. Samanidou, V.F.; Metaxa, A.S.; Papadoyannis, I.N. Direct simultaneous determination of uremic toxins: Creatine, creatinine, uric acid, and xanthine in human biofluids by HPLC. *J. Liq. Chromatogr. Relat. Technol.* **2002**, *25* (1), 43–57.



17. Abreo, K.; Gautreaux, S.; de Smet, R.; Vogeleere, P.; Ringoir, S.; van Holdre, R. *p*-Cresol, a urinary compound, enhances the uptake of aluminum in hepatocytes. *J. Am. Soc. Nephrol.* **1997**, *8* (6), 935–942.
18. DeSmet, R.; David, F.; Sandra, P.; VanKaer, J.; Lesaffer, G.; Dhondt, A.; Lameire, N.; van Holder, R. A sensitive HPLC method for the quantitation of free and total *p*-cresol in patients with chronic renal failure. *Clin. Chim. Acta* **1998**, *278*, 1–21.
19. Fujii, T.; Kawabe, S.; Horike, T.; Taguchi, T.; Ogata, M. Simultaneous determination of the urinary metabolites of toluene, xylenes and styrene using high-performance capillary electrophoresis. Comparison with high-performance liquid chromatography. *J. Chromatogr., B* **1999**, *730*, 41–47.
20. Garcia, A.J.; Apitz-Castro, R. Plasma total homocysteine quantitation: An improvement of the classical high-performance liquid chromatographic method with fluorescence detection of the thiol-SBD derivatives. *J. Chromatogr., B* **2002**, *779*, 359–363.
21. Laurens, J.B.; Mbianda, X.Y.; Spies, J.H.; Ubbink, J.B.; Vermaak, W.J.H. Validated method for quantitation of biomarkers for benzene and its alkylated analogues in urine. *J. Chromatogr., B* **2002**, *774*, 173–185.
22. Garcia, A.; Heinanen, M.; Jimenez, L.M.; Barbas, C. Direct measurement of homovanillic, vanillylmandelic and 5-hydroxyindole acetic acids in urine by capillary electrophoresis. *J. Chromatogr., A* **2000**, *871*, 341–350.
23. Vanholder, R.; de Smet, R.; Lameire, N. Protein bound uremic solutes: The forgotten toxins. *Kidney Inter., Suppl.* **2001**, *78*, S266–S270.
24. Chi, J.D.; Odontiadis, J.; Franklin, M. Simultaneous determination of catecholamines in rat brain tissue by HPLC. *J. Chromatogr., B* **1999**, *731*, 361–367.



Validation of HPLC Instrumentation

Ioannis N. Papadoyannis

Victoria F. Samanidou

Aristotle University of Thessaloniki, Thessaloniki, Greece

INTRODUCTION

Validation is the process of providing documented evidence that an instrument, a system, a method, a product, or a procedure performs as expected within specified design parameters and requirements so that the obtained results are reliable. Validation efforts should be broken down into separate components addressing the equipment—both the instrument and the computer controlling it—and the analytical method run on that equipment. After these have been separately verified, they should be checked together to confirm the expected performance limits of the system (system suitability testing, SST). Fig. 1 illustrates the basic validation steps with regard to computerized high-performance liquid chromatography (HPLC) equipment.

The need for validation in analytical laboratories may originate from regulations such as current Good Manufacturing Practices (cGMP), Good Laboratory Practice (GLP), and Good Clinical Practices (GCP); or quality and accreditation standards such as the International Standardization Organization (ISO) 9000 series, ISO 17025, and the European Norm (EN 45001), United States Pharmacopoeia (USP), Food and Drug Administration (FDA), and Environmental Protection Agency (EPA). All regulations require instruments to be calibrated, well maintained, and suitable for their intended use. However, validation of equipment and analytical methods is necessary not only because of the regulations and accreditation standards, but also as a prerequisite in terms of any *good analytical practice*.

OVERVIEW

Validation is a regular process that starts before an instrument is placed on-line and continues long after method development and transfer. It consists of at least three stages, each being critical to the overall description of the process:

Phase 1. Instrument or equipment qualification, including computer qualification. Individual modules of equipment (hardware and firmware) have to be separately

validated, as well as the entire system. Validation of computer systems includes the evaluation of hardware and software.

Phase 2. Analytical method validation prior to routine use and after changing method parameters.

Phase 3. Analytical system suitability testing, which combines instrument, computer, and method. When the equipment and a particular method have been selected and validated, the equipment for that method goes through an SST prior to, and within, sample analyses, or practically on a day-to-day basis.

Information about validation procedures concerning HPLC instrumentation and guidelines are discussed in the following sections.

EQUIPMENT VALIDATION OR QUALIFICATION

Validation of HPLC instrumentation, also called “qualification,” is the procedure that ensures that the instrument is qualified; that is, that its performance complies with the method’s predetermined requirements, providing reliable and valid results. Modern HPLC systems are computerized, generally consisting of analytical hardware, computer hardware, peripherals, and software.

Validation of instrument hardware includes testing according to documented specifications. If HPLC instruments consist of several modules, individual modules (modular validation), as well as the entire system (holistic validation), should be validated. However, the latter is preferred, as individual module tests should be performed as part of the diagnosis if the system fails.

The equipment used in a study should be tested on site before it is used the first time, within certain time intervals, and after repairs. It should be periodically inspected, cleaned, maintained, and calibrated according to the Standard Operating Procedures (SOPs). Records of these activities should be maintained.

Qualification of HPLC equipment (Equipment Qualification, EQ) begins at the vendor’s site. During this stage, the instrument and software are developed, designed, and produced in a validated environment according to



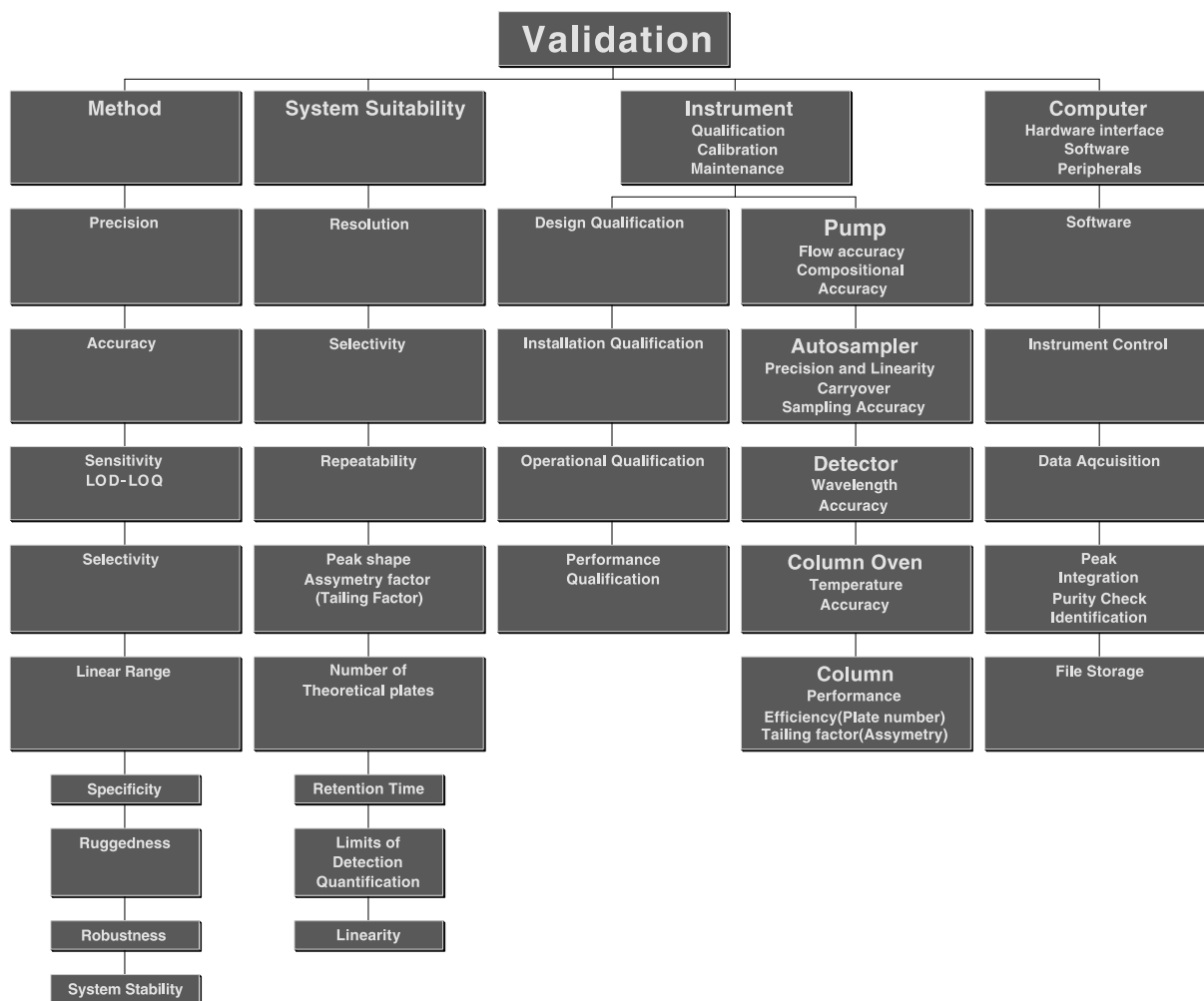


Fig. 1 Basic validation steps in an analytical laboratory.

GLP, cGMP, and/or ISO 9000 standards, preferably ISO 9001; ISO 9002 or 9003 are insufficient because they do not cover development.

Qualification can be subdivided into four stages: 1) Design qualification (DQ); 2) installation qualification (IQ); 3) operation qualification (OQ); and 4) performance qualification (PQ).

Design Qualification

Design qualification (DQ) covers setting of user requirements, as well as functional and performance specifications. Design qualification should ensure that the instrument has all the necessary functions and performance criteria that will enable it to be successfully used for the intended application. Design qualification includes: 1) Description of the intended use of the equipment; 2) se-

lection of the analysis technique, selection of the technical, environmental, and safety specifications, and final selection of the supplier and equipment; and 3) development and documentation of final functional and operational specifications.

Installation Qualification

Installation qualification establishes that the instrument is received as designed and specified, that it is properly installed in the selected environment, and that this environment is suitable for the operation and use of the instrument. During installation, one should: 1) Compare the equipment, as received, with the purchase order; 2) check documentation for completeness or for any damage; 3) install hardware (computer, equipment, fittings and tubings for fluid connections, columns in HPLC,

power cables, and instrument control cables); 4) install software on the computer following the manufacturer's recommendation, and verify correct software installation; 5) make a backup copy of the software; 6) configure peripherals, e.g., equipment modules; 7) switch on the instrument and check for any error messages; 8) identify all hardwares and make a list with a description of each; 9) list equipment manuals and SOPs; 10) inject and qualitatively evaluate a standard; and 11) prepare an installation report describing how and by whom the instrument was installed.

Operational Qualification

Operational qualification, or acceptance testing, is the process of demonstrating that the whole instrument or its modules will function according to its operational specification, in the selected environment, according to previously defined functional and performance specifications ("acceptance criteria"). This procedure can be performed to the extent of the self-diagnostics routine test or to a more detailed procedure regarding flow-rate, injector precision, or wavelength accuracy. It can be carried out by the user or the vendor on behalf of the user.

Performance Qualification

Performance qualification (PQ) is the process of testing and calibrating the instrument before and during routine use to verify system performance. This test is repeatedly executed to ensure that the entire system generates valid results and performs as intended, throughout representative or anticipated operating ranges. The criteria of PQ should also be used for revalidation later. After the instrument is placed on-line in the laboratory, and after a period of use, regulations require maintenance, followed by calibration and standardization. Each laboratory should have SOPs that define the period of use (usually a reasonable time interval in which the instrument properly operates). Records should be kept to track instrument maintenance.

The frequency of PQ depends on the type of instrument, on the stability of the performance parameters, on the specified acceptance criteria, and on the use of the equipment. The test frequency for PQ is much higher than for OQ. Performance qualification is always performed under similar conditions to establish a routine sample analysis; that is, using the same column, the same analysis conditions, and the same test compounds. PQ should be performed on a daily basis or whenever the instrument is used. For a liquid chromatograph, the most important unit

may be the chromatographic column or the detector's lamp condition. The test criteria and frequency should be determined during the development and validation of the analytical method. In practice, PQ can mean SST, where critical system performance characteristics are measured and compared with documented, preset limits. An example sequence for PQ includes: 1) Definition of the performance criteria and test procedures; 2) selection of critical parameters: Precision of the peak area/height, precision of retention times, resolution between two peaks, peak width at half height or peak tailing, limit of detection (LOD), and limit of quantitation (LOQ), wavelength accuracy of a UV/Visible detector; 3) definition of the frequency, e.g., every day, every time the system is used, before, between, and after a series of runs; 4) specification of corrective actions in case the system does not meet the criteria.

Design qualification should always be performed by the user, whereas installation qualification for large, complex, and high-cost instruments should be performed by the vendor. In some cases, warranty is lost if the user installs the system. Operation qualification can be performed by either the user or the vendor. The decision mainly depends on the available resources at the user's site, and on the vendor's capability to offer such a service with high quality. Performance qualification should always be performed by the user because it is very application-specific and the vendor may not be familiar with the method. As PQ should be performed on a daily basis, this practically limits this task to the user anyway. On completion of equipment qualification, detailed documentation should be available, considering qualification checklist, procedures for testing, qualification test reports with signatures and dates, PQ test procedures, and representative results.

Computer Validation or Qualification

Computer validation/qualification refers to computer hardware, peripherals, and software validation, the latter including operating software, e.g., Microsoft Windows, MS-DOS, and the application HPLC software. In the hardware, the most important unit to validate is the analog-to-digital converter (ADC) because it converts input voltage into numeric data. Software, however, is very difficult to validate because of its complex structure. For this reason, the vendor should check, validate, and document software according to Computer-Aided Software Engineering (CASE) principles. After installation, software validation can be performed with regard to the integrity of program code and data, as well as the data security, with special software packages; this can be automatically checked at power on. On the other hand,



comprehensive validation of a data system is beyond the capability expected from many chromatography laboratories. The only parts of the software package that is created after installation are user-written programs (macros); they should be tested, ensuring security of data with restricted access to data and regular backup copies, documenting every change made either on the data acquisition system computer or software. Computer systems should be validated during, and at the end of, the development process and after software updates.

Equipment validated under a specified set of conditions must be revalidated whenever there is a change in those conditions. For example, changes in application software may influence the correct functioning of the computer system. Revalidation refers to those items of the system that are affected by the change.

HIGH-PERFORMANCE LIQUID CHROMATOGRAPHY INSTRUMENTATION QUALIFICATION

Instrument hardware should be validated for its intended use before and during its operation as part of the overall validation process; that is, prior to routine use, after repair, and at regular time intervals.

The main qualification tests applied to HPLC instrumentation concern:

The injection system (usually an autosampler). The parameters that have to be checked are precision and accuracy.

The pump. The parameters that have to be checked are flow-rate precision, flow-rate accuracy, and stability regarding an isocratic pump. Gradient delay volume and gradient mixing volume, repeatability of the gradient, and mixing and proportioning accuracy are important when a gradient pump is used.

The detector. The parameters that have to be checked are wavelength accuracy detection, refractive index sensitivity, linearity, spectral quality (PDAD) short-term or long-term noise, drift, and flow sensitivity.

Column efficiency.

Within-day and between-day reproducibility of the whole chromatographic system.

The first step is to establish internal specifications; then, compare the obtained results with the manufacturer's specifications; and, finally, interpret the differences. Within-day and interday reproducibility is the minimum test for routine use. Chromatographic systems should be tested for suitability to the performance criteria of the method on a daily basis before and during routine application. An HPLC system should be tested before

each single sample analysis, or, if a series of samples are analyzed within a sequence, before each sequence.

Retention time, peak height or area, resolution, and peak shape are the data used to monitor the performance of the HPLC system. Peak shape is one of the first things that experienced chromatographers notice when looking at a chromatogram. Ideal chromatographic peaks are Gaussian-shaped; however, in practice, most peaks show some peak tailing, which is measured by using the asymmetry factor or the USP tailing factor as described in Fig. 2A. Column plate number, N , is the most common parameter to describe the shape of the peak. Resolution R_s , as described in Fig. 2B, is the measure of separation of two peaks, as well as of the efficiency of the column.

The frequency of the control sample analysis depends on the nature of the analysis. Successful analysis of the control samples assures that the system is performing as expected under the SOP. Validation of HPLC equipment assures that valid measurements are obtained. The quality of the analytical data can be maintained by keeping, in a safe place, records of the actual instrument conditions at the time the measurements were made. Backups should also be maintained.

The tests can be performed by using a typical C_{18} analytical column, 250×4 or 250×4.6 mm, and a mobile phase consisting of water–methanol or water–acetonitrile mixture. The analysis should concern compounds similar to those used for testing the performance of C_{18} columns (e.g., phenol) or compounds used for routine analysis in the laboratory. New columns must be checked for performance. Records of its chromatographic parameters must be kept.

Modular Calibration: Detector Performance

The refractive index sensitivity affects gradient analysis and should be checked by measuring the absorbance when the cell is filled with methanol ($n = 1.329$) and cyclohexane ($n = 1.427$) at 270 nm.

Noise and drift are measured in static (dry detector cell) and in dynamic mode at different wavelengths, e.g., 200, 254, and 390 nm. The change in the absorbance as a function of flow rate at the same wavelengths reflects flow sensitivity. Noise is expressed in AU/cm, drift in AU/hr, and flow sensitivity in AU min/mL. Some equipment units can automatically perform calibration for accuracy. For example, some HPLC–UV/Visible detectors include holmium oxide filters for measurement and calibration of the wavelength accuracy.

The characteristics of an equipment may change over time, e.g., UV detector lamps lose intensity, or pump piston seals abrade, or short-term noise affecting the LOD is increased because of flow cell contamination. These changes will have a direct impact on the performance of

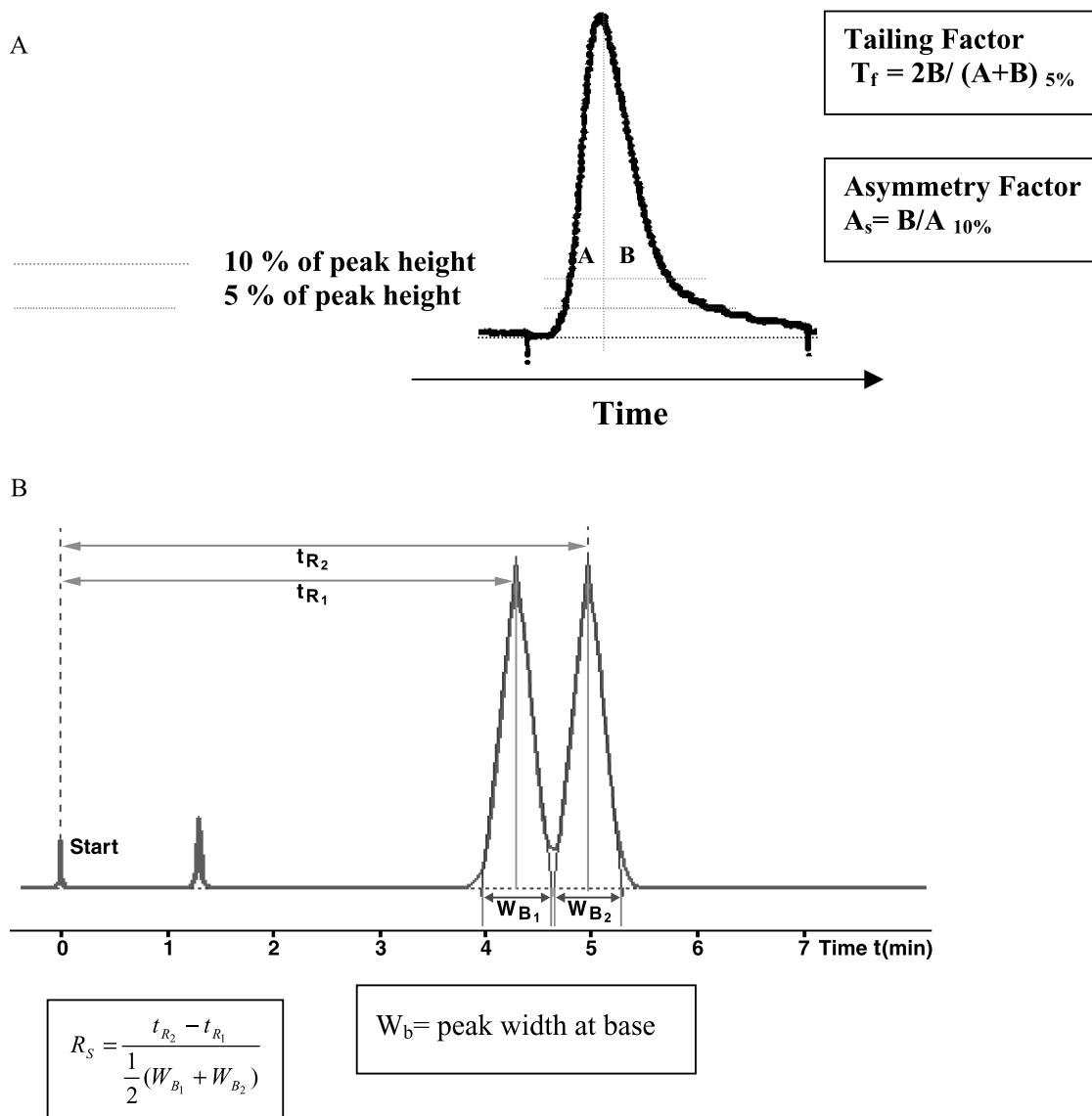


Fig. 2 (A) Measurement of peak tailing using USP tailing factor and peak asymmetry factor. (B) Peak resolution. (From Merck HPLC Tutorial.)

the HPLC instrument. The frequency of performance tests will be determined by experience and is based on need, type, and history of equipment performance. Intervals between the checks should be shorter than the time the instrument drifts outside acceptable limits. New instruments need to be checked more frequently, and, if the instrument meets the performance specifications, the time interval can be increased.

Long-term noise can be erroneously considered as late-eluting peaks, while drift affects the obtained data when the instrument is running over a long time period. Flow sensitivity affects flow rate and gradient programs using constant pressure pumps.

Photodiode array (PDA) or variable ultraviolet/visible detector

A number of reference chemicals with well-defined UV spectra have been used for detector wavelength calibration, e.g., uracil, erbium perchlorate, holmium oxide, caffeine, etc.

Pump

The accuracy and stability of the pump flow rate can be checked at 1 mL/min, with the column in place, by measuring the time required to fill a 10-mL volumetric flask

at the detector outlet. Other flow rates can be tested if analyses with narrow bore or fast LC are routinely performed. An acceptance criterion is 1.00 ± 0.05 mL/min. Flow-rate variations affect retention times.

Gradient pumps

Gradient delay volume, gradient mixing volume, and mixing and proportioning accuracy should be evaluated. These tests are executed by replacing the column with short tubing and filling the reservoirs with water and aqueous phenol solution. Increasing and decreasing steps must be used. The abovementioned parameters affect R_t and the selectivity of the separation. This is especially important when the gradient method has to be transferred from one system to another. Repeatability of the gradient analysis, important for the precision of the gradient method, is assessed by calculating the RSD of the peak area and retention times for replicate analysis of a control compound solution. Compositional accuracy is determined by making 5-min step gradients from water in one solvent line to 0.1% acetone in water in a second solvent line. The absorbance of each step against that of the 100% step is measured. A higher flow rate of 2 mL/min can be used to sharpen the step definition and increase test robustness. All four solvent lines are checked in a 1-h solvent program.

Gradient methods in HPLC depend on the dwell volume, V_d , i.e., the volume between the point of mixing eluents A and B and the column inlet, including the loop of the injector. This volume differs from instrument to instrument, so that a method can be transferred only if this volume is well defined. When there is a significant difference in dwell volume between the two systems, retention times and resolution are dramatically different. So one must be state in which range of V_d the method is still valid.

Autosampler

Autosampler precision can be checked by replicate injections of a control sample, with wash injection intervals between every two sample injections. The repeatability of peak areas, mathematically expressed as RSD, is used as a criterion for autosampler precision. For example, when 10 consecutive injections of 10 μ L of a solution are performed, the expected RSD for peak area precision ranges from 0.5% to 1.0%. Single injections of different volumes, such as 5, 10, 50, or 80 μ L, can also be used, simultaneously checking the linearity of the injector, the detector, and the data system. Another approach to qualify the autosampler involves the gravimetric determination of the average volume of water per injection withdrawn from a tared vial after six 50- μ L injections. The procedure

takes less than 10 min and has an acceptance criterion of 50 ± 2 μ L.

The same experiment can be used for the assessment of flow-rate precision by evaluating the repeatability of retention times for the examined compounds, expressed again as RSD. Both terms, flow-rate and injection volume precision, affect the precision of the results of the analysis. Carryover problems can be identified in the wash chromatograms at maximum detector sensitivity. They can be checked by multiple analyses of high-concentration samples followed by blank injections.

Column oven

A temperature accuracy test of the column oven, using a calibrated thermal probe, is used with an acceptance criterion of $35 \pm 2^\circ\text{C}$.

Column

Two peaks are considered resolved if the R_s value is > 1.5 . For multicomponent mixtures, a number of R_s values may have to be considered. The resolution between the most critical peaks may solely be considered as an indicator of the quality of the separation. Typical values for R_s range from 1.5 to 2.0 for critical resolution.

Computer

A computer associated with an HPLC equipment may control the instrument or part of it, e.g., the photodiode array detector, or acquire data generated by the instrument, such as the peak area of analytes.

Software functions: For an automated HPLC analysis, required software functions include instrument control, data acquisition, peak integration, peak purity checks, compound identification through spectral libraries, quantitation, file storage and retrieval, and a printout of methods and data.

Hardware interface: Determining the true performance of an electronic interface of a chromatography data system requires special instrumentation that is not generally found in a chromatographic laboratory. Testing procedure is similar to that of calibrating any electronic instrument.

The equipment hardware and computer software should be developed and validated according to a documented procedure, e.g., according to a product life cycle. The vendor should have a documented and certified quality system, e.g., ISO 9001. Quality must be designed and programmed into software prior to, and during, its development phases by following written develop-

ment standards, including the use of appropriate test plans and methods.

Correct functioning of software and computer systems should be verified after installation and before routine use. Operational qualification for software and computer systems is more difficult than for hardware, as 1) it is more difficult to define specifications, test procedures, and acceptance criteria; and 2) there are hardly any guidelines available on OQ of software and computer systems. Because of these problems, there is even more uncertainty for software and computer systems than for equipment hardware.

The type of testing required for the qualification of software and computer systems depends very much on the type and complexity of software, i.e., if the software and computer hardware are supplied by one vendor, or computer systems that are interconnected and/or interfaced to analytical systems, or if the software are developed in the user's laboratory in addition to a vendor-supplied package (e.g., a macro).

ANALYTICAL METHOD VALIDATION

After equipment validation, the next step is analytical method validation, which covers testing of significant method characteristics according to good analytical practice guidelines. The validation of an HPLC method is the procedure that gives the chromatographer information to determine whether the system is operating as it should, providing accurate, precise, and reliable analytical data in a specific situation, meeting the preestablished specifications.

The validity of a specific method should be demonstrated in laboratory experiments by using samples or standards that are similar to the unknown samples that will be routinely analyzed. Chromatographic methods need to be validated before the first routine use. To obtain the most accurate results, all of the variables of the method should be considered, such as sampling, sample preparation, chromatographic separation, detection, and data evaluation, using the same matrix as that of the intended sample. The proposed procedure must go through a rigorous process of validation. All validation experiments should be documented in a formal report.

Although the need to validate analytical methods is clear, the procedure for performing the validation is not clearly defined in terms of the validation parameters to be used, the specific procedures to be used in evaluating a particular parameter, and the appropriate acceptance criteria for a particular parameter.

Successful completion of the validation results in a method that can reliably be used to characterize "real samples." Ongoing validation activities may also be

necessary during the routine utilization of an analytical procedure, as well as the revalidation of the analytical procedure, as certain operational aspects of the method are changed during its routine and continuous application.

Validation Parameter Guidelines for Method Validation

After the method has been developed, its performance must be validated with respect to different performance parameters. To determine which operational parameters should be included in a formal validation protocol, the chemical literature may be used to assess the practical state of the art among the practitioners of the desired methodology. Alternatively, existing guidelines published by organizations with recognized authority may be examined. Regulatory agencies and published literature provide the criteria for what constitutes a validated chromatographic method. The USP, for example, has published specific guidelines for method validation regarding pharmaceuticals. However, there are no official guidelines referring to biological fluids.

An attempt for harmonization was made at the International Conference on Harmonization (ICH) in 1995 and 1996 by representatives from the industry and regulatory agencies from the United States, Europe, and Japan, who defined parameters, requirements, and, to some extent, also methodology, for analytical methods validation.

In 1990, the USP 22 guideline listed eight individual parameters that must be investigated and documented in order to validate a method: 1) Accuracy; 2) precision; 3) limit of detection; 4) limit of quantification; 5) selectivity; 6) range; 7) linearity; and 8) ruggedness.

In 1995, USP 23 changed these parameters to some extent. Selectivity is now explicitly referred to as specificity, linearity and range were combined, and robustness was broken out of ruggedness. Ruggedness retains its original definition of day-to-day, instrument-to-instrument, operator-to-operator, etc., reproducibility. The robustness of an HPLC method is defined as a measure of its capacity to remain unaffected by small but deliberate variations in method parameters and provides an indication of its reliability during normal usage. So USP 23 includes: 1) Accuracy; 2) precision; 3) limit of detection; 4) limit of quantification; 5) specificity; 6) linearity and range; 7) ruggedness(*); 8) robustness(*). The asterisk is indicating that the terminology is included in an ICH publication, but they are not part of required parameters.

The definitions of these parameters and the indicative acceptance criteria are discussed in the following paragraphs. Each of the above-listed parameters is evaluated in terms of validating an HPLC method. The procedures for performing the validation must be presented in a complete, well-defined, practical, and understandable



format. Once the validation is complete, an investigator must be able to interpret the results. The acceptance criteria allow the researcher to definitely determine, by comparing method performance data to the criteria, whether the method under evaluation is performing in a valid manner. These criteria should be universally applicable, numerically and mathematically explicit, complete, and achievable.

Accuracy and Recovery

The accuracy of an analytical method is the degree of agreement of results generated by the method to the true value or a conventional true value. Accuracy can be assessed by applying the analytical method to samples or mixtures of sample matrix components to which known amounts of the analyte have been added, above and below the normal levels expected in the samples. Method accuracy is the agreement between the difference in the measured analyte concentrations of the fortified (spiked) and unfortified samples and the known amount of analyte added to the fortified sample.

Comparison of the method's results can be performed by using an established reference method, assuming that the latter is free from systematic errors. Second, accuracy can be measured by analyzing a certified reference material, and comparing the measured value with the true value as supplied with the material. If such reference material is not available, a blank sample matrix can be spiked with a known concentration that should cover the range of concern, including one concentration close to the quantitation limit. The expected recovery depends on the sample matrix, on the sample processing procedure, and on the analyte concentration. Recoveries can be determined by either external or internal standard methods. Although it is desirable to attain a recovery close to 100%, other values such as not less than 50%, 80%, and 90% have been used as limits. Quantification by external standard is the most straightforward approach because the peak response of the standard is compared to the peak response of the sample. The standard solution concentration should be close to that expected in the sample solution. Precise control of the injection volume is mandatory because it influences the accuracy. Peak response is measured as either peak height or peak area.

For the internal standard method, a substance is added at the earliest possible point in the analytical scheme to compensate for sample losses during extraction, cleanup, and final chromatographic analysis. The internal standard must be completely resolved from all other peaks in the chromatogram, having chemical and physical properties as similar as possible to those of the analyte of interest, so that the detector response is similar to the solute to be quantified. However, it is sometimes difficult to find

the proper internal standard, as this must be stable over the time of the measurement period, absent from real samples, not reactive with the analytes, and eluted within a reasonable retention time. Analogs, homologs, and isomers are usually preferred. In the presence of analytes with different chemical or physical properties, two or more internal standards representing these analytes should be used.

Reagent blank, internal standard blank, solvent blank, and compound blank samples must also be analyzed for accurate qualitative and quantitative results.

Procedural guidelines for accuracy determination include replicate analysis, e.g., three to six assays, at five levels, over the range from 80% of the lowest expected assay value to 120% of the highest expected assay value, or from 75% to 125% of label claim, six samples of drug in the matrix spanning 50% to 150% of the expected content. At minimum, three concentrations must be used within the analytical range (extremes and midpoint of expected or near quantitation limit, center of range, and upper bound of standard curve).

For trace level analyses, acceptance criteria include 60–110% recovery for concentrations below 100 ppb, 80–100% recovery for concentrations above 100 ppb, and 70–120% for concentrations below 1 ppm. In biological samples, method accuracy for discovery phase investigations should be $\pm 20\%$ of actual, with recoveries of $\pm 10\%$ being necessary in preclinical and clinical studies. Alternatively, it is recommended that the mean recovery value should be within $\pm 15\%$ of actual, except at the quantitation limit where $\pm 20\%$ is acceptable.

Precision and Reproducibility

The precision of a method is the extent of agreement among individual test results, when the procedure is repeatedly applied to multiple samplings. Precision can be divided into three categories: 1) Repeatability; 2) intermediate precision; and 3) reproducibility.

Repeatability (intra-assay or within-day precision) is obtained when the analysis is carried out in one laboratory by one operator, using one piece of equipment over a relatively short time span. It reflects the variation in replicate procedures performed within a short time period, with the same operational conditions.

At least five or six determinations of three different matrices at two to three concentrations should be performed and expressed by the RSD. The acceptance criteria for precision depend on the type of analysis. While a precision of better than 1% RSD is easily achieved for compound analysis in pharmaceutical quality control, the precision may be at levels of 10–15% for biological samples. For environmental and food samples, the precision is very much dependent on the sample

matrix, the analyte concentration, and the analysis technique, varying between 2% and 20%.

Intermediate precision is defined by ICH as “the long-term variability” of the measurement process, and is determined by comparing the results of a method run within a single laboratory over a number of weeks. A method’s intermediate precision may reflect disagreement in results obtained by different operators, from different instruments, with standards and reagents from different suppliers, with columns from different batches, or a combination of these. The objective of intermediate precision validation is to verify that, in the same laboratory, the method will provide the same results after finishing the method development.

Reproducibility, as defined by ICH, represents the precision obtained between laboratories with the objective of verifying if the method will provide the same results in different laboratories. The reproducibility of an analytical method is determined by analyzing aliquots from homogeneous lots in different laboratories with different analysts, and by using operational and environmental conditions that may differ from, but are still within the specified, parameters of the method (interlaboratory tests). Various parameters affect reproducibility. These include differences in room environment (temperature and humidity), operators with different experience, equipment with different characteristics (e.g., delay volume of an HPLC system), variations in material and instrument conditions (e.g., in HPLC), mobile phases composition, pH, flow rate of mobile phase, columns from different suppliers or different batches, solvents, reagents, and other material with different quality.

Reproducibility is defined as the long-term variability of the measurement process, which may be determined for a method run, within a single laboratory, but on different days. Reproducibility also applies to a method, either run by different operators, different instruments, or a combination of the above. The reproducibility standard deviation is typically twofold to threefold larger than that for repeatability. Precision is often expressed relative to 1 day as intraday (within-day) precision or relative to a period of days, as interday (between days) precision. Reproducibility, in the sense of intralaboratory precision, is related to the procedure being performed at two or more laboratories as in, e.g., a collaborative study.

Precision in retention times and peak area or height is a major criterion of a separation system. Retention-time precision is important because R_t is the primary means for peak identification. It is also an important performance criterion and diagnostic for an LC pump and a column.

Precision of peak areas or heights is important because they are used for calculating amounts during quantification. It is also the most important performance criterion for an LC injection system. Precision should be deter-

mined using a minimum of five replicate chromatograms. For bioanalytical samples, precision is studied at least at low, medium, and high concentrations. This is repeated on separate days to calculate intraday and interday precision.

Precision reflects a procedure’s ability to reproduce the same, but not necessarily the correct or expected, result each time it is correctly performed. Precision is assessed by repetitively injecting a number of samples and statistically evaluating the resulting data. Important issues related to the precision determination include the number of replicates required and the type of sample to be tested. For the determination of repeatability, recommendations include: 1) Five to ten replicates for release or stability assays; 2) duplicate measurements made on 10 samples at each of three different analyte levels; 3) five replicates at three levels (limit of quantitation, midrange, and upper calibration bound); 4) replicate samples at analyte levels of 80–120% of expected for dosage forms and drug substance tests.

For intermediate precision, the repeatability experiments should be performed on 2, 3–5, or at least 10 separate days. To assess reproducibility, the experiments have to be performed in at least two laboratories.

System precision should be $\leq 1\text{--}2\%$ RSD (or higher for low-level impurities). The repeatability is generally 1/2 to 1/3 of the reproducibility. However, for biological samples, an RSD of 10–15% should be acceptable as the minimum precision.

Systematic errors result from sources traced to the methodology, the instrument, or the operator. These affect both the accuracy and the precision of the measurement. Random errors affect the precision and are difficult to eliminate as they result from random fluctuations in the measured signal because of noise and other factors. The imprecision of the entire procedure is often dominated by the random errors of the most imprecise step. The difference between an accurate and a precise method is illustrated in Fig. 3.

Selectivity–Specificity

The terms selectivity and specificity are often interchangeably used. The term specificity generally refers to a method that produces a response for a single analyte only, while the term selective refers to a method that provides responses for a number of chemical entities that may or may not be distinguished from each other. Because there are very few methods that respond to only one analyte, the term selectivity is usually more appropriate. The USP defines selectivity of an analytical method as its ability to accurately measure an analyte in the presence of interferences, such as synthetic precursors, excipients, enantiomers, and known (or likely) degradation products that may be expected to be present in the sample matrix.



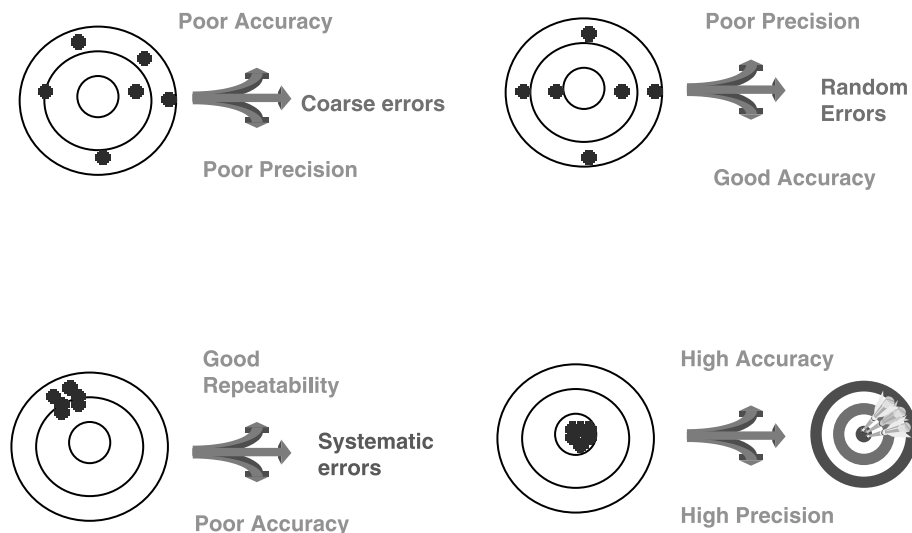


Fig. 3 Comparison of precision and accuracy parameters of an analytical method.

Selectivity in HPLC is obtained by setting optimal chromatographic conditions, such as mobile phase composition, column temperature, and detector wavelength. There are a variety of ways to validate selectivity. One approach is to demonstrate a lack of response in the blank biological matrix. A second approach is to check whether the intercept of the calibration curve is significantly different from zero.

Peak purity is one important parameter in chromatography to determine whether the peaks within a sample chromatogram are pure or if it consists of more than one compound. To determine the homogeneity of a chromatographic analyte response, the use of UV/Visible photodiode-array detector (PDAD) and mass spectrometers is recommended, acquiring spectra during the entire chromatogram. The acquired spectra are normalized and overlaid for graphical presentation; if they are different, then the peak consists of at least two compounds. Usually, the simplest and most frequently used peak purity algorithm compares three spectra across a peak: On the upslope, at the peak apex, and on the downslope.

Specificity relates to the ability of a method to measure only what it is intended to be measured with a requisite level of accuracy and precision, although the sample may contain other related compounds. The most commonly cited specificity evaluation procedure is the analysis of a placebo, wherein the sample matrix without the analyte is analyzed and the resulting system response is examined for the presence of responses, which interfere or overlap with that of the analyte of interest. Other procedures for specificity include: 1) Peak reanalysis, wherein the peak of interest is collected and reanalyzed by different chromatographic conditions or with methods that are sensitive

to analyte structure; 2) collaboration, in which the sample is quantitatively analyzed using two or more detection or separation strategies, and the results compared; 3) use of detectors (e.g., MS or PDAD to assess peak purity).

Linearity and Range

The linearity of an analytical method is its ability to extract test results that are directly, or by means of well-defined mathematical transformations, proportional to the concentration of analytes in samples within a given range. In chromatography, peak parameters are related to analyte concentration via standardization procedures. This relationship is then used to convert a sample's peak parameter to its analyte concentration. Linearity is determined by a series of three to six injections of five or more standards, whose concentrations span over the range of expected concentrations, or 80% of the lowest expected level to 120% of the highest expected level, or 50–150% or 10–200% of the expected working range, or 25–125% of the target range specified. The response should be directly or, by means of a well-defined mathematical calculation, proportional to the concentrations of the analytes. A linear regression equation applied to the results should have an intercept not significantly different from zero; otherwise, it should be demonstrated that there is no effect on the accuracy of the method. Frequently, the linearity is graphically evaluated in addition to, or alternatively to, mathematical evaluation.

The correlation coefficient of the best linear least squares regression model should be between 0.98 and 1.00 or greater than 0.999 with the slope and intercept reported. However, there is no rule stating that the

relationship between instrumental response and analyte concentration must be directly linear for a procedure to be valid. The desire to have a linear relationship reflects the practical consideration that a linear relationship can be accurately described with fewer standards than a non-linear relationship, and the subjective expectation that a linear relationship is more rugged than a more complicated, nonlinear relationship.

A method's range is linked to its linearity. The range is the interval between the lower and upper analyte concentration, for which it has been demonstrated that the analytical procedure has a suitable level of accuracy, precision, and linearity. The range is expressed in the same units as the analytical method's results (e.g., ng/ μ L, ppb, %, etc).

Limits of Sensitivity: Limit of Detection and Limit of Quantitation

Sensitivity is the ability of a method to reliably respond in a consistently recognizable manner to decreasingly smaller amounts of analyte. Frequently utilized measures of sensitivity are the limit of detection (LOD) and the limit of quantitation (LOQ). For chromatographic procedures, LOD is the lowest concentration of analyte that can be detected above the baseline detector noise at the most sensitive instrument setting, but not necessarily quantified. In chromatographic practice, the detection limit is the injected amount that results in a peak with a height twice or three times as high as the baseline noise.

The LOD can be determined either directly or from other validation data. Its direct measurement involves an analysis of the method's peak-to-peak baseline noise or an analysis of the variation in the method's blank response. In either case, LOD is calculated as either 2 or 3 times the variation in measured response, where the factors are associated with the 95% and 99% confidence intervals for a normal distribution. Practically, LOD can be measured by the serial dilution of samples until the peak can no longer be observed. LOD can be estimated as the value of the linear calibration curve's y intercept.

The LOQ is the minimum injected amount that gives precise measurements in chromatography, typically requiring peak heights 10 to 20 times higher than baseline noise. Another approach is the EURACHEM: A number of samples with decreasing amounts of the analyte are injected six times. The calculated RSD% of the precision is plotted against the analyte amount. The amount that corresponds to the previously defined required precision is equal to the LOQ. Alternatively, LOQ is the lowest injected amount of analyte, which results in a reproducible measurement of peak areas and can be reproducibly quantitated above the baseline noise. Peak heights are typically required to be about 10 to 20 times higher

than baseline noise. Quantitation implies that the measurement possess a specified accuracy and precision. In some applications, LOQ is defined as the smallest concentration included in the standard curve.

The baseline response method for estimating LOQ involves the following procedure: The chromatogram resulting from a blank injection is examined over a range of 20 peak widths and the noise is measured as either the largest peak-to-peak fluctuation or as the largest deviation (positive or negative) from the mean response. The LOQ is then calculated as the product of 10 times the measured deviation and the calibration curve slope. The LOQ can also be determined as the lowest analyte concentration for which duplicate injections result in a %RSD $\leq 2\%$. In routine applications, it has been recommended that LOQ should be within the working linear concentration range and that a specification limit should be no lower than twice the LOQ. For clinical applications, the LOQ should be at least 10% of the minimum effective concentration.

Ruggedness

It is generally expected that an analytical method will perform in an acceptable manner each time it is used. While a consideration of method ruggedness is a necessary part of any method's validation, it is a critical issue for compendial methods because of their widespread use in many different laboratories.

Ruggedness establishes a method's ability to effectively perform in the face of variations on operational and environmental conditions, which can reasonably be expected to occur whenever the method is applied. More specifically, ruggedness is the reproducibility of test results obtained by the analysis of samples under a variety of normal test conditions such as different laboratories, analysts, instruments, reagent lots, elapsed assay times, temperatures, etc. Thus, ruggedness addresses unintentional variation in the method introduced by its application, at different times, by different people, at different locations, using different instrumentation and materials. A rugged method will be able to withstand minor operating or performance changes and has built-in buffers against typical procedural abuses, such as differences in care, technique, equipment, and conditions.

For the determination of the method's ruggedness within a laboratory, a number of chromatographic parameters, e.g., flow rate, column temperature, detection wavelength, or mobile phase composition is varied within a realistic range, and the quantitative influence of the variables is determined. If the influence of the parameter is within a previously specified tolerance range, the parameter is said to be within the method's ruggedness range. Clearly, ruggedness is assessed by analyzing aliquots from homogeneous sample lots using operational



and environmental conditions that differ, but are still within the method's specified operating range. The ruggedness test should be performed at several values of each operational parameter that affects method performance, e.g., mobile phase flow rate and composition, (pH, buffer concentration, ion pairing reagent concentration, percent organic phase, column temperature, injection volume, gradient dwell time, column lots or column manufacturers, different room temperature and humidity in separate laboratories, detection wavelength, analysts with different experience, instruments from various vendors, reagents from different suppliers, columns from different batches, sample and standard preparation procedures, and operating temperature. For operator-related ruggedness, a number of analysts, e.g., three to five, perform one assay per day for 3 days. The utilization of statistically designed experiments (e.g., nested ANOVA) to establish the ruggedness of an assay is recommended.

In ruggedness assessment regarding the column, the specificity (selectivity) of at least three columns, from three different batches, supplied by one column manufacturer must be checked. A similar column from another manufacturer should also be evaluated. Variability also arises from the degradation of the column over its lifetime. Even columns with the same material and dimensions may vary in performance and selectivity. If columns are packed in the laboratory, they should be tested before they are first used. Columns purchased from vendors should be supplied with test certificates.

The quantitative measure of a method's ruggedness is the precision behavior it exhibits over the course of the various operational scenarios, examined during the validation exercise. Generally, a rugged method's reproducibility is 2 to 3 times greater than the method's repeatability (inherent method precision under "normal" controlled operating conditions).

Robustness

Robustness tests examine the effect operational parameters have on the analysis results. For the determination of a method's robustness, a number of chromatographic parameters (e.g., flow rate, column temperature, injection volume, detection wavelength, or mobile phase composition) are varied within a realistic range and the quantitative influence of the variables is determined. If the influence of the parameter is within a previously specified tolerance, the parameter is said to be within the method's robustness range. Obtaining data on these effects will allow one to judge whether a method needs to be revalidated when one or more of parameters are changed, for example, to compensate for column performance over time.

The difference between ruggedness and robustness is that the former is related to unintentional variation in a method because of its use in varying analytical situations, although the latter is the procedure's capacity to remain unaffected by small but deliberate variations in method parameters. Thus, robustness is a measure of the procedure's reliability during normal usage. Although it is time-consuming, thorough robustness studies will help to avoid unexpected results in subsequent applications of the method. While data for robustness is not usually submitted in regulatory product applications, a robustness evaluation is recommended. Clearly, a robust method is one that is operationally immune to commonly encountered but relatively minor variations in its critical operating parameters.

It has been suggested that, in order to determine robustness, a method's critical operational variables should be identified by breaking the testing process into unit operations and then assessing the potential variability of each operation. Unit operations might include: 1) Analytical solution preparation—amount of material used, volumes of solvent used, dissolution times and conditions, and solvent used; 2) variation in the tested product (inhomogeneity, aging); 3) instrumental analysis—detection wavelength, mobile phase composition and flow rate, and column use history.

Stability

Many solutes readily decompose prior to chromatographic investigations, e.g., during the preparation of the sample solutions, during extraction, cleanup, phase transfer, and during storage of prepared vials (in refrigerators or in an automatic sampler). Under these circumstances, method development should investigate the stability of the analytes.

The term "system stability" is a measure of the bias in assay results generated during a preselected time interval, e.g., every hour up to 10 h, using a single solution. Stability should be determined by replicate analysis of the sample solution and the relative standard deviation calculated. The assay results obtained in different time intervals should not exceed more than 20% of the corresponding value of the system precision. If the value is higher on plotting the assay results as a function of time, the maximum duration of the usability of the sample solution can be calculated.

The effect of long-term storage and freeze–thaw cycles can be investigated by analyzing a spiked sample immediately upon preparation and on subsequent days of the anticipated storage period. A minimum of two cycles at two concentrations should be studied in duplicate. If the integrity of the drug is affected by freezing and

thawing, spiked samples should be stored in individual containers and appropriate caution should be employed for study samples.

In most routine applications, solutions are not immediately used after preparation, but may be stored under specified conditions prior to use. Verifying solution stability is an important aspect of method validation; specifically, a valid method is one for which all related and analytical solutions are stable over the period typically required for their utilization or analysis. To address stability, the analytical solutions should be prepared, assayed, allowed to stand (in accordance with the method's protocol or specification) for a length of time equal to the anticipated maximum analysis time, and then reassayed. For analytical procedures involving overnight runs, up to three to four sample solutions over the working concentration range should be repetitively analyzed over the course of at least 16 hr. In such evaluations, the analytical solution is stable if all concentration values obtained before and after storage agree to within three times the system precision. Additionally, no new peaks should appear, nor should existing peaks be lost, from the chromatograms of the first and last sample injection. The stability of a solution must be checked for at least 16 hr, especially when an autosampler is used.

Table 1 Parameters to be included in a validation report

1. Objective and scope of the method (applicability, type).
2. Type of compounds and matrix.
3. Detailed chemicals, reagents, reference standards, and control sample preparations.
4. Procedures for quality checks of standards and chemicals used.
5. Safety considerations.
6. Method parameters.
7. Critical parameters indicated from robustness testing.
8. Listing of equipment and its functional and performance requirements, e.g., cell dimensions, baseline noise, and column temperature range.
9. Detailed conditions on how the experiments were conducted, including sample preparation.
10. Statistical procedures and representative calculations.
11. Procedures for quality control in the routine (e.g., system suitability tests).
12. Representative plots, e.g., chromatograms, spectra, and calibration curves.
13. Method acceptance limit performance data.
14. The expected uncertainty of measurement results.
15. Criteria for revalidation.
16. Analyst who developed and initially validated the method.
17. Summary and conclusions.

(From Ref. [1].)

The preparation and execution should follow a validation protocol, preferably written in a step-by-step instructional format. Once the validation protocol is completed, the validation report should be prepared, including data listed in Table 1.

There are no official guidelines on the sequence of validation experiments and the optimal sequence can depend on the method itself. A potentially useful sequence for a liquid chromatographic method is: 1) Selectivity of standards (optimizing separation and detection of standard mixtures); 2) precision of retention times and peak areas; 3) linearity, limit of quantitation, limit of detection, range; 4) selectivity with real samples; 5) trueness or accuracy, at different concentrations; 6) ruggedness.

The more time-consuming experiments, such as accuracy and ruggedness, are put toward the end. Some of the parameters can be measured in combined experiments. For example, when the precision of peak areas is measured over the full concentration range, the data can be used to validate the linearity.

Revalidation

Once the method is validated, any modification requires revalidation to demonstrate that it still works as defined. If the new parameter is within the tolerance range of the method as specified during the ruggedness test of method validation, the method does not need to be revalidated. In other cases, it should go through revalidation. With the system suitability software frequently offered by analytical equipment vendors, methods can be automatically revalidated with little operator interaction. The validation can be performed overnight.

Operating ranges should be defined for each method based on experience with similar methods, or they should be investigated during robustness studies. Availability of such operating ranges makes it easier to decide when a method should be revalidated. Part or full revalidation may also be considered if SST or the results of quality control sample analysis are out of preset acceptance criteria and the source of the error cannot be tracked back to instruments or anything else.

For HPLC methods, significant changes could occur, and the recommended parameters for revalidation are summarized in Table 2. For bioanalytical methods, precision, accuracy, and limit of quantitation are considered to be the minimum revalidation tests.

SYSTEM SUITABILITY TESTING

Daily, prior to the sample analyses, the analyst must establish that the HPLC system and procedure are capable of providing data of acceptable quality. The validation



Table 2 Method changes and revalidation tests required

Method characteristics changed	Performance parameters to revalidate
Instrument changes	Linearity (working range), LOD, LOQ, system precision.
Product changes	Selectivity, accuracy, precision.
Sample preparation procedure (same solvent, same concentration range)	Accuracy, recovery, precision, ruggedness
Sample preparation procedure (different solvent, different concentration range)	Complete reassessment of all previously used validation parameters.
Analyst changes	Qualification testing (perform retests, side-by-side collaborative studies).
Chromatographic change (e.g., column, mobile phase)	Selectivity, linearity, LOD/LOQ, system precision.
Extraction solvent, buffer, back extraction, matrix or injection solvent	Linearity, recovery, LOQ, intrabatch precision and accuracy, in-process solution stability. Additionally, if injection solvent is changed, processed sample stability should be checked, but recovery or in-process stability checks are not necessary.
Chromatographic conditions [column, mobile phase composition, detector type or monitoring condition (e.g., wavelength) change]	Linearity, selectivity, and intrabatch precision and accuracy (recovery not necessary).
Extending the upper end or reducing calibration curve range	Linearity, LOQ (if reduced), lower end of the intrabatch precision and accuracy at revised upper or lower levels.
Internal standard.	Selectivity, intrabatch precision and accuracy, recovery.

(From Ref. [2].)

procedure of an analytical system combining the analytical method and instrument performance is referred to as system suitability testing. The objective of an SST is to assess if the chromatograph or its modules, i.e., the column, the mobile phase, the detector lamp, etc., perform as required for a particular analytical run and can generate results of acceptable accuracy and precision or should be replaced before samples are committed for analysis. System suitability testing provides the analyst with diagnostic information by warning that part of the process is likely to be out of control. It typically represents a subset of the method validation procedure.

The requirements for SST are usually developed after method development and validation have been completed, giving information about acceptable system operation by comparing observed performance versus previously established criteria or guidelines.

Critical issues of concern include the identification of performance characteristics that need to be monitored and the frequency of test execution. In general, intervals be-

tween tests should be shorter than the observed time in which the system drifts outside of acceptable levels: In most cases, at the beginning and at the end of a run, or in a more thorough approach, a quality control sample is run for every 10 samples. Additionally, an SST evaluation is performed each time an instrument malfunction has been observed during the course of a run. The final decision is based on the experience of the analyst depending on need, as well as previous performance of the equipment. In case the system is in continuous use for the same analysis, it may be sufficient to perform an abbreviated SST check each day. Full SST should be performed each time the system is assembled for the assay.

Quality control samples at three concentrations (low, middle, and high) around the expected range can be used to assess accuracy by two to five injections. The acceptance criteria established for the SST evaluation must balance the need to ensure adequate performance with the practical reality of performing chemical analyses. This means that they must be sufficiently tight, but not so

Table 3 Recommended system suitability testing acceptance criteria

Parameter	Assay type	Acceptance criterion
Capacity factor	General	2–8
	Trace	1–3
	Stability indicating	>4
Selectivity	General	1.05–2.0
Retention time	General	<0.1 min
Resolution	General	>2.0
	Quantitative analysis	>1.5
	Biologicals	>1.2
Plate count (<i>N</i>)	General	>2000
Precision	General	%RSD <1.5%
	Biologicals	%RSD <5%
	Trace	%RSD 5–15%
Tailing factor	General	1.5–2.0

(From Ref. [2].)

restrictive that acceptable systems fail to pass. Some examples of the acceptance criteria are summarized in Table 3.

System suitability testing parameters regarding HPLC methods reflect problems associated with the performance of chromatographic procedures, e.g., flow irregularity, injection irreproducibility, system plumbing problems, detector misalignment or malfunction, wavelength accuracy, oven temperature, column malfunction, and mispreparation of analytical solutions regarding mobile phase, standard solutions, or samples. Detailed records of maintenance and changes must be kept. Documentation can be accomplished by using software especially designed for the task. The same software can be used to troubleshoot the method.

To obtain a good and acceptable analytical result, two requirements must be met: 1) The method has to be adequate; and 2) the execution has to be adequate.

The simplest form of an HPLC SST involves comparison of the chromatogram with a standard one, allowing comparison of the peak shape and the peak width baseline resolution. Additional parameters that can be experimentally calculated to provide quantitative SST report include the number of theoretical plates, separation factor, resolution, tailing or peak asymmetry factor, accuracy, and precision (RSD of six measurements). Resolution may also be combined with a selectivity test to check the resolution of the analytes from components present in the sample matrix. If matrix components interfere with a method, a matrix blank may be included in the SST. Peak shape and asymmetry, or tailing factor, can

have a major impact on the performance of a quantitative method, especially at low amounts or concentrations, and may vary over the lifetime of a column.

The number of theoretical plates can provide the historical data needed to determine if the column needs to be replaced, based on scientific reasoning, and not simply a by a judgment that the column does not work.

Retention times tend to vary over time because of a number of causes, e.g., differences between batches of mobile phase, column performance and different columns, and ambient temperatures of laboratories. The RSD of retention time, especially important because it is used for peak identification, is influenced by: 1) Pump flow; 2) composition precision; 3) mobile phase composition of solvent delivery systems; and 4) column temperature. Imprecise retention time indicates problems within the HPLC system such as piston seals, check valves, etc.

Signal-to-noise (S/N) ratio may become important when measuring analytes at low concentrations. Related to this measurement may be the limits of detection (LOD) or quantification (LOQ), which may be of particular importance in trace analysis. For methods determining analytes over a large concentration range, a linearity test can be incorporated into the SST.

The RSD of the peak area is influenced by: 1) Injection mode and volume; 2) pump flow and pulsation; 3) detector noise, drift, and response; and 4) sampling rate and integration parameters of the data system.

Additional checks should be performed in some cases; this could be a routine check of the wavelength accuracy, the baseline noise, and the intensity of the UV lamp.

Automation of the System Suitability Testing

Modern data-acquisition systems can offer SSTs with the basic software, leaving the analyst to fill in the required parameters. Storing chromatograms and multiple plotting of chromatograms over time provides a chromatographer with the ability to see the historical performance of the analytical column for the past week, month, or even the column's lifetime.

CONCLUSION

A successful chromatographic analysis depends on the precise performance of the HPLC instrumentation, i.e., control of pressure, the composition of mobile phase, the performance of the analytical column, the detector, the injector or autosampler, and the electronic data handling system.

Validation is the process of confirming that the analytical equipment, method, or system for a specific test is suitable for its intended use. Methods need to be validated



before their introduction into routine use and revalidated whenever there is a change (outside the original scope of the method) in any parameter of the method.

In accordance with GLP, a chromatographic procedure must 1) exactly follow a protocol; 2) be conducted by a qualified personnel; 3) be controlled by standard operating procedures (SOPs); 4) use proper and adequate facilities; 5) use calibrated and well maintained equipment; and 6) provide fully retrievable raw data.

Satisfactory results for a method can only be obtained with properly performing equipment that is periodically inspected, cleaned, maintained, and calibrated according to SOPs. Records of those activities should be maintained.

A laboratory applying a specific method should have documentary evidence that the method has been appropriately validated; this holds for methods developed in-house as well as for standard methods, to demonstrate the validity of the method in the laboratory environment.

For routine use, relevant tests should be selected, depending on the use of the equipment, in order to verify that the instrument is performing in a regulated, controlled manner.

Instrument hardware should be validated prior to routine use, after repair, and at regular time intervals. Computer systems should be validated during, and at the end of, the development process and after software updates. Computer systems with complex software are frequently gradually developed over many years. It is critical to note that quality cannot be tested into a product or system at the final testing stages. To ensure quality during the development process, the life cycle concept has been developed.

Analytical methods should be validated prior to routine use and after changing method parameters.

Analytical systems should be tested for system suitability prior to, and during, routine use, practically on a day-to-day basis.

However, validation and verification of an HPLC equipment are not one-time events. They are on-going processes, covering the entire life of the instrument.

revalidation and system suitability. *J. Liq. Chromatogr.* **1996**, *19* (12), 1873–1891.

SUGGESTED ADDITIONAL READING

- Currie, L. Nomenclature in evaluation of analytical methods including detection and quantification capabilities (IUPAC recommendations 1995). *Anal. Chim. Acta* **1999**, *391*, 105–126.
- Dong, M.; Paul, R.; Roos, D. Committeeing to calibrate HPLC. *Today's Chem. Work* **2001**, 42–48. (February).
- Hearn G.M. *A Guide to Validation in HPLC*; Perkin Elmer: England, 1991; 1–20.
- Hokanson, G.C. A life cycle approach to the validation of analytical methods during pharmaceutical product development. Part I: The initial validation process. *Pharm. Technol.* **1994**, *9*, 118–130. (September).
- Huber, L. *Good Laboratory Practice and Current Good Manufacturing Practice*; Hewlett-Packard Germany, 1994; 152.
- Huber, L. Laboratory accreditation. Part 3: Validation and calibration of equipment. *Int. Lab.* **1995**, *25*, (9), 8–12.
- Huber, L. Validation of computerized analytical systems. Part I: Overview, regulations and terminology. *LC GC Int.* **1996**, *9* (9), 564–572.
- Huber, L. Validation of computerized analytical systems, Part 3: Installation and operational qualification. *LC GC* **1996**, *14* (9), 806–812.
- <http://www.labcompliance.com/index.htm>.
- Jenke, J.R. Chromatographic method validation: A review of current practices and procedures. Part I. General concepts and guidelines. *J. Liq. Chromatogr.* **1996**, *19* (4), 719–736.
- Jenke, J.R. Chromatographic method validation: A review of current practices and procedures. Part II. Guidelines for primary validation parameters. *J. Liq. Chromatogr.* **1996**, *19* (5), 737–757.
- McDowall, R.D. A suitable system for chromatography? *LC GC Int.* **1995**, *8* (4), 196–206.
- Molnar, I. Validation of robust chromatography methods using computer-assisted method development for quality control. *LC GC Int.* **1996**, *9* (12), 800–808.
- Ouchi, G.I. Data file monitoring chromatography system performance. *LC GC Int.* **1993**, *6* (6), 356–360.
- Snyder, L.R.; Kirkland, J.J.; Glajch, J.L. *Practical Method Development*, 2nd Ed.; John Wiley & Sons, Inc.: New York, 1997; 685–713. Chapter 15.
- Swartz, M.E.; Krull, I.S. *Analytical Method Development and Validation*; Marcel Dekker, Inc.: New York, 1997; 92 pp.
- van der Voet, H.; van Rhijn, J.A.; van de Wiel, H.J. Inter-laboratory, time, and fitness-for-purpose aspects of effective validation. *Anal. Chim. Acta* **1999**, *391*, 159–171.

REFERENCES

1. Huber, L. Validation of analytical methods: Review and strategy. *LC GC Int.* **1998**, *11* (2), 96–105.
2. Jenke, J.R. Chromatographic method validation: A review of current practices and procedures. Part III. Ruggedness,

Validation of TLC Analyses

Gunawan Indrayanto
Mochammad Yuwono

Airlangga University, Surabaya, Indonesia

INTRODUCTION

According to USP 25–NF 20,^[1] validation of an analytical method is the process by which it is established, by laboratories studies, that the performance characteristics of the method meet the requirements for the intended analytical applications. Therefore, validation is an important step in determining the reliability and reproducibility of the method because it could confirm that the method is suitable to be conducted on a particular system. The performance parameters that should be determined in validation studies include specificity, linearity, accuracy, precision, detection limit (DL), quantitation limit (QL), range, ruggedness, and robustness.^[1,2] The parameters that require to be validated depend on the type of the analyses; thus, different test methods require different validation schemes. The most common types of analyses are identification, quantitative determination of impurities, limit value determination of impurities, and quantitative determination of active ingredients.^[3] Besides the general validation parameters mentioned above, the software and hardware of instrument for thin-layer chromatography (TLC) densitometry, such as scanning, application, and chromatography methods, should also be validated first.^[3,4]

SPECIFICITY/SELECTIVITY

The terms specificity and selectivity are often interchangeably used. A method is said to be specific if it provides a response for only a single analyte. If the response in question is distinguished from all other responses, the method is said to be selective.^[5] The International Conference on Harmonization (ICH)-2 does not differentiate both terms and defines specificity or selectivity as “the ability to unambiguously determine the analyte in the presence of other components whose presence is to be expected.” This includes typical impurities, decomposition products, and matrix components.^[3] The specificity of the method for TLC analyses was proved by identification and purity checks of the analyte spots. This can be done by measuring in situ the ultraviolet and visible spectroscopy (UV–VIS) spectra of

the analyte(s) and the authentic reference standard(s), those eluted on the same plate, and then by calculating their correlations (the r value should be ≥ 0.999). This correlation should be calculated on the upslope, the apex, and the downslope of the peaks. Other parameters should ideally be in the following range: R_f ($0.1 \leq R_f \leq 0.9$); tailing factor, T ($0.9 \leq T \leq 1.1$); resolution, R_s (≥ 1.0).^[6]

LINEARITY

The linearity of a method is its ability to provide measurement results that are directly proportional to the concentration of the analyte or are directly proportional after mathematical transformation. The linearity is usually documented as the linear regression curve of the measured responses as a function of increasing analyte concentrations.^[3] To perform the linearity testing, it is recommended to use 5–10 concentrations with range equivalent to 80–120%,^[6] 25–200%,^[7] or 50–150%^[8] of the expected content of the analyte. For the determination of degradant and preservative in the stability study, ranges of 0–40% and 50–110%, respectively, were recommended.^[2] It is also essential that the basic calibration is performed by using independent samples and not by samples that have been prepared by dilution and spotted on one TLC plate. For the evaluation of basic calibration line, several parameters can be used, e.g., the relative process standard deviation value (V_{xo}), the Mandel's test, the X_p value,^[9] the plot of response factor vs. concentration, the residual test, the analysis of variance (ANOVA), etc. It is recommended that the correlation coefficient (r) alone is not used anymore. The correlation coefficient does not indicate the linearity or lack thereof.^[10] Readers should refer to previous works for further discussion.^[9,11] The variance homogeneity over the whole range of the basic calibration line should also be proved using the F test.^[6,9]

ACCURACY

Accuracy or trueness of an analytical method is given by the extent by which the value obtained deviates from the



true value.^[3] Firstly, accuracy can be determined by analyzing a sample with known concentration and then by comparing the results between the measured and the true value. The second approach is by comparing the test results obtained from the new method to the results from the existing method that is known to be accurate. The third and fourth approaches are based on the percent recovery of known analyte spiked into blank matrices or products. The last technique is known as the standard addition method.^[8] For spiked samples into blank matrices, it is recommended to prepare the sample in five different concentrations at the level of 80–120% of the target concentration. On the other hand, for the standard addition method, the spiking concentrations are 30–60% of the label-claimed value. To prove whether systematic errors will not occur, a linear regression of recovery curve of \mathbf{X}_f (concentration of the analyte measured by the propose method) against \mathbf{X}_c (nominal concentration of the analyte) should be constructed, and the confidence range of the intercept $\{VB(a_f)\}$ and slope $\{VB(b_f)\}$ from the recovery curves are calculated for $p = 0.05$.^[9]

PRECISION

The realistic standard deviation in TLC analyses are ca. 0.2% on multiple scanning of one spot, 0.8–1.5% on multiple spotting and analysis of the same sample solution, and 1.5–2.0% on multiple analysis of the same sample.^[6] As a general rule, the standard deviation of a method should be lower than 1/6 of the specification range,^[12] or the relative standard deviation (RSD) value should be not more than 2%.^[7] For validation purposes, precision is determined by multiple application of the complete analytical procedure on one homogenous real sample. According to ICH, both repeatability and intermediate precision should be tested.^[6] Repeatability is defined as precision under the same conditions, i.e., same analyst, equipment, reagents, time, and TLC plate. Intermediate precision was performed by repeatability testing on the different combinations of analyst, equipment, reagents, and time within one laboratory. It is recommended to do 6–10 measurements on each repeatability study.^[6,7] A detailed discussion on the maximum of standard deviation for assay determination was recently published.^[12]

RANGE

The range of measurement is the interval for which linearity, accuracy, and precision have been tested. Analysis outside the range is not permitted.^[3]

DETECTION LIMIT AND QUANTITATION LIMIT

Detection limit is defined as the lowest concentration of an analyte that can be detected under the analytical condition to be used. However, it cannot be quantitatively measured. Quantitation limit is the lowest concentration that can be determined with acceptable accuracy and precision under the analytical conditions.^[3] Generally, QL can be estimated as three times of DL.^[11] DL and QL for instrumental (chromatographic) analytical methods can be defined in terms of the signal-to-noise ratio (2:1 to 3:1 for DL and 10:1 for QL),^[6] or in terms of the ratio of the standard deviation of the blank response, the residual standard deviation of the calibration line, or the standard deviation of intercept (σ) and slope (S) ($DL = 3.3\sigma/S$ and $QL = 10\sigma/S$).^[12] By constructing a linear regression of relatively low concentrations of analyte, accurate values of DL can be calculated; in this case, $DL = X_p$.^[9] The authors recommend using 5–10 relatively low concentrations of analyte spotted on a TLC plate. DL can be increased by using pre- or postchromatographic derivatization.^[3]

ROBUSTNESS/RUGGEDNESS

Robustness can be defined as a measure of the capability of the method to remain unaffected by small, but deliberate, variations in method parameters. It provides an indication of its reliability during normal usage.^[1,13] Ruggedness of a method is the degree of reproducibility of test results obtained by the analysis of same samples under a variety of conditions such as different laboratories, analysts, and instruments; different lot of reagents; different days; etc.^[1] Some important parameters for testing of TLC methods are the following: the stability of analyte in the solution being analyzed and on the plate before and after development; the influence of temperature and humidity; the method of application, scanning, and evaluation; the spot shape and size, eluent composition, and pH; the batch of TLC plate; the sample volume; and the drying conditions of the plate.^[3,13] A detailed guidance for robustness/ruggedness testing has been recently published.^[13]

CONCLUSION

The important performance characteristics for TLC validation procedures have been described in brief in this paper to provide guidance to the analytical chemists. For obtaining reliable and reproducible analysis results, it is

essential to validate the TLC method first, before using it for routine works in a Quality Control Laboratory.

ACKNOWLEDGMENT

We thank Mrs. Mangestuti Agil (Faculty of Pharmacy, Airlangga University) for her excellent technical assistance.

REFERENCES

1. *The United States Pharmacopoeia 25—The National Formulary 20, Asian Edition*; The United States Pharmacopoeial Convention, Inc.: Rockville, MD, 2001; 2256–2258.
2. Carr, G.P.; Wahlich, J.C. A Practical approach to method validation in pharmaceutical analysis. *J. Pharm. Biomed. Anal.* **1990**, *8* (8), 613–618.
3. Hahn-Deinstrop, E. *Applied Thin-Layer Chromatography*; Wiley-VCH Verlag GmbH: Weinheim, 2000; 201–205.
4. Prosek, M.; Puki, M.; Miksa, L.; Golc-Wondra, A. Quantitative thin-layer chromatography: Part 12. Quality assessment in QTLC. *J. Planar Chromatogr.* **1993**, *6* (1), 62–65.
5. Karnes, H.T.; Shiu, G.; Shah, V.P. Validation of bioanalytical methods. *Pharm. Res.* **1991**, *8* (4), 421–426.
6. Renger, B.; Jehle, H.; Fischer, M.; Funk, W. Validation of analytical procedure in pharmaceutical analytical chem-

- istry; HPTLC assay of theophylline in an effervescent tablet. *J. Planar Chromatogr.* **1995**, *8* (4), 269–278.
7. Edwardson, P.A.D.; Bhaskar, G.; Fairbrother, J.E. Method validation in pharmaceutical analysis. *J. Pharm. Biomed. Anal.* **1990**, *8* (8), 929–933.
8. Green, J.M. A practical guide to analytical validation. *Anal. Chem.* **1996**, *68*, 305A–309A.
9. Funk, W.; Dammann, V.; Donnevert, G. *Qualitätssicherung in der Analytischen Chemie*; VCH Verlagsgesellschaft mbH: Weinheim, 1992; 10–44.
10. Analytical method committee. Uses (proper and improper) of correlation coefficient. *Analyst* **1988**, *113* (9), 1469–1471.
11. Ebel, S. Validerung in der DC/HPTLC. In *WSA Würzburger Skripten zur Analytik. Reihe Validerung, Teil 6.3*; Bayerische Julius-Maximilians Universität, Institut für Pharmazie und Lebensmittelchemie: Würzburg, 1992; 41–58.
12. Ermer, J. Validation in pharmaceutical analysis: Part 1. An integrated approach. *J. Pharm. Biomed. Anal.* **2001**, *24*, 755–767.
13. Van der Hyden, Y.; Nijhuis, A.; Smayers-Verbeke, J.; Vandeginste, B.G.M.; Massart, D.L. Guidance for robustness/ruggedness test in method validation. *J. Pharm. Biomed. Anal.* **2001**, *24*, 723–753.

FURTHER READING

Eurachem. *The Fitness for Purpose of Analytical Methods: A Laboratory Guide to Method Validation and Related Topics*; LGC (Teddington) Ltd: Middlesex, 1998.

van't Hoff Curves

Raymond P.W. Scott

Scientific Detectors Ltd., Banbury, Oxfordshire, England

Introduction

van't Hoff curves are strictly graphs of $\log[\text{distribution coefficient } (K)]$ against the reciprocal of the absolute temperature, but, in practice, $\log[\text{capacity factor } (k')]$ or $\log[\text{corrected retention volume } (V')]$ are used as alternatives (see the entry Plate Theory). van't Hoff curves can be very informative and explain both the nature of the separation and the importance of temperature in achieving an adequate resolution. An example of two van't Hoff curves relating $\log(V')$ against $1/T$ for two different types of distribution system are shown in Fig. 1. The two curves are highly exaggerated for the sake of emphasis and clarity.

Discussion

It is seen that distribution system A has a large enthalpy value $(\Delta H_0/RT)_A$ and a low-entropy contribution $[(\Delta S_0/R) - V_s]_A$. The large value of $(\Delta H_0/RT)_A$ means that the distribution is *predominantly controlled by molecular forces*. The solute is preferentially distributed in the stationary phase as a result of the interactive forces between the solute molecules and those of the stationary phase being much greater than the interactive forces between the solute molecules and those of the mobile phase. Because the change in enthalpy is the major contribution to the change in free energy, *the distribution, in thermodynamic terms, is said to be "energy driven."*

In contrast, it is seen that for distribution system B, there is only a small enthalpy change $(\Delta H_0/RT)_B$, but in this case, a high-entropy contribution $[(\Delta S_0/R) - V_s]_B$. This means that the distribution is *not* predominantly controlled by molecular forces. The entropy change reflects the degree of randomness that a solute molecule experiences in a particular phase. The more random and "more free" the solute molecule is to move in a particular phase, the greater its entropy. A large entropy change means that the solute molecules are more restricted or less random in the stationary phase in system B. This loss of freedom is responsible for the greater distribution of the solute in the stationary

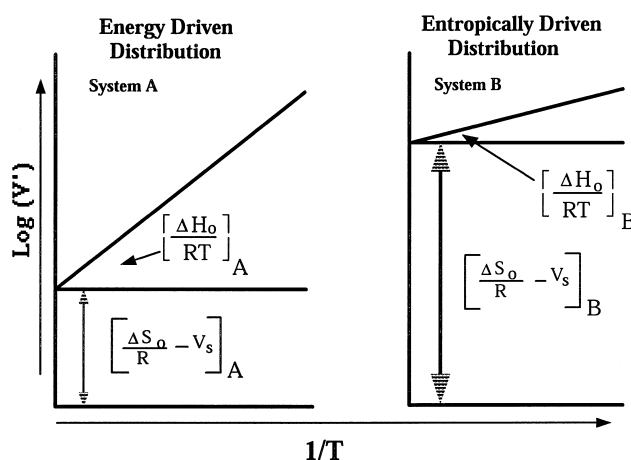


Fig. 1 van't Hoff curves for two distribution systems.

phase and, thus, greater solute retention. Because the change in entropy in system B is the major contribution to the change in free energy, *the distribution, in thermodynamic terms, is said to be "entropically driven."*

Separations dominated by size exclusion are examples of entropically driven systems. Chromatographic separation need not be exclusively "energetically driven" or "entropically driven"; in fact, very few are. In most cases, retention has both "energetic" and "entropic" components, which, by careful adjustment, can be made to achieve very difficult and subtle separations.

It is very rare, if at all, in gas chromatography (GC) that two solutes have identical standard free energies. Even when considering enantiomeric pairs, they will have differing standard free enthalpies and standard free entropies and, consequently, differing standard free energies. Accepting these facts, the van't Hoff curve provides critical information for the chromatographer. If two solutes (e.g., a pair of enantiomers) have different standard free enthalpies, then the linear van't Hoff curves must have different slopes and, therefore, they must intersect. As a consequence, there must be a temperature where the two curves intersect and there



will be a specific temperature at which the two solutes must coelute. The coelution temperature may, or may not, be in the practical operating range of the chromatographic system, but it is clear that temperature is an essential operating variable. Temperature does not merely control the elution rate and allow the analysis to be achieved more rapidly, but also critically determines the column selectivity for closely eluting peaks. In fact, this is also true for liquid chromatography.

There are some examples in the literature that purport to show nonlinear van't Hoff curves. Taking an example from liquid chromatography (LC), a graph relating $\log(V'_r)$ against $1/T$ for solutes eluted by a mixed solvent from a reverse bonded phase will often be nonlinear. However, it must be emphasized that graphs relating $\log(V'_r)$ against $1/T$ can only be termed van't Hoff curves, and be treated as such if they apply to an *established distribution system*, where the nature of *both* phases does not change with *temperature*. If a mixed-solvent system is employed as the mobile phase, the *solvents themselves* are distributed between the two phases *as well* as the solute. Depending on the actual concentration of solvent, as the temperature changes, so may the relative amount of solvent adsorbed on the stationary-phase surface, and so the nature of the distribution system will also change. Consequently, the curves relating $\log(V'_r)$ against $1/T$ may not be linear and, as the distribution system is varying, will not constitute van't Hoff curves. This effect has been known for many years and an early example is afforded in some early work carried out by Scott and Lawrence [1], who investigated the effect of water vapor as a moderator on the surface of alumina in some gas-solid separations of some *n*-alkanes. Examples of the results obtained by those authors are shown in Fig. 2. The alumina column was moderated by a constant concentration of water vapor in the carrier gas. As the temperature of the distribution system was increased, less of the water moderator was adsorbed on the surface. As a consequence, the alumina became more active and the distribution system changed. Thus, initially, as

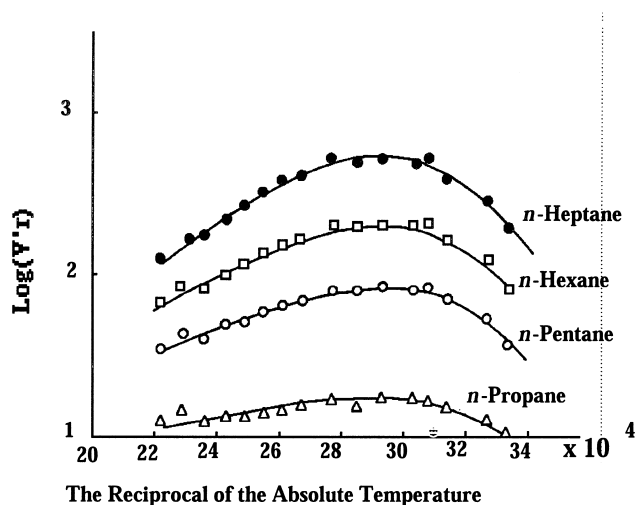


Fig. 2 Graphs of $\log(V'_r)$ against $1/T$ for some *n*-alkanes separated on water-vapor-moderated alumina.

the temperature was raised, the retention volume of each solute increased. When all the water was desorbed and the alumina surface assumed a constant interactive character and the distribution system also remained the same, the retention volume began to fall again in the expected manner and this part of the curve would then be a van't Hoff curve.

Reference

1. R. P. W. Scott and J. G. Lawrence, *J. Chromatogr. Sci.* 7: 65 (1969).

Suggested Further Reading

- Scott, R. P. W., *Techniques of Chromatography*, Marcel Dekker, Inc., New York, 1995.
 Scott, R. P. W., *Introduction to Analytical Gas Chromatography*, Marcel Dekker, Inc., New York, 1998.

Vinyl Pyrrolidone Homopolymer and Copolymers: SEC Analysis

Chi-san Wu
Larry Senak
James Curry
Edward Malawer

International Specialty Products, Wayne, New Jersey, U.S.A.

Introduction

Polyvinylpyrrolidone (PVP) is a synthetic polymer derived from the Reppe chemistry and is widely used in the pharmaceutical, personal care, cosmetic, agriculture, beverage, and many industrial applications. PVP is a polar and amorphous polymer which is soluble in water and some organic solvents, such as alcohols, chlorinated hydrocarbons, dimethyl formamide, dimethyl acetamide, and *N*-methyl pyrrolidone.

Nonionic, anionic, and cationic VP copolymers are all available commercially to enhance the hydrophilic, hydrophobic, and ionic properties of PVP for specific applications. Important comonomers include vinyl acetate (VA), acrylic acid (AA), vinyl alcohol, dimethylaminoethylmethacrylate (DMAEMA), styrene, maleic anhydride, acrylamide, methyl methacrylate, lauryl methacrylate (LM), α -olefins, methacrylamidopropyltrimethyl ammonium chloride (MAPTAC), vinyl caprolactam (VCL), and dimethylaminopropylmethacrylamide (DMPMA).

Molecular Weight and Molecular Distribution of PVP by Size-Exclusion Chromatography

Commercial PVP are available in five grades, K-15, K-30, K-60, K-90, and K-120 with the respective range of M_w 7000–12,000, 40,000–65,000, 350,000–450,000, 900,000–1,500,000 and 2,000,000–3,000,000. Interactions between PVP and columns, such as adsorption, partition, and electrostatic interactions, have to be eliminated by prudent choice of column and mobile phase in order to obtain true separation by size and 100% recovery.

Belenkii et al. reported in 1975 [1] the size-exclusion chromatography (SEC) of PVP using Pharmacia Sephadex G-75 and G-100 columns and 0.3% sodium chloride solution as the mobile phase. Hashimoto et al. reported in 1978 [2] the SEC of PVP K-30 and K-90 us-

ing TSK-PW 3000 and two 5000 columns and 0.08M Tris-HCl buffer (pH = 7.94) as the mobile phase.

By using an E. Merck LiChrospher SI300 column, modified with an amide group ($-\text{NH}-\text{CO}-\text{CH}_3$) chemically bonded to the surface, Englehardt and Matheson reported in 1979 [3] the SEC of PVP. Herman et al. synthesized monomeric diol onto E. Merck LiChrospher SI-500 and reported in 1981 [4] the SEC of PVP. Mori reported in 1983 [5] the SEC of PVP K-15 to K-90 using two Shodex AD-80M/S columns with DMF and 0.01M LiBr as the eluent at 60°C. Domard and Rinaudo grafted quaternized ammonium groups onto silica gels with pore diameters of 150, 300, 600, 1250, and 2000 Å and reported in 1984 [6] the SEC of PVP.

Malawer et al. [7] reported in 1984 the SEC of PVP K-15, K-30, K-60, and K-90 using diol-derivatized silica gel column sets and aqueous mobile phase modified with various polar organic solvents. Senak et al. reported in 1987 [8] the determination of the absolute molecular weight and molecular-weight distribution of PVP by SEC-LALLS and SEC with universal calibration. The column set used consists of TSK-PW 6000, 5000, 3000, and 2000 columns and a mobile phase of water-methanol (50:50, v/v) with 0.1M LiNO₃. One hundred percent recovery was reported. The results showed good agreement in M_w from SEC-LALLS and from SEC with universal calibration for PVP K-30, K-60, and K-90.

Size-exclusion chromatography of PVP K-15, K-30, K-60, K-90, and K-120 using linear aqueous columns such as the Showa Denko Shodex OH pack, Toyo Soda TSK-PW, and Waters Ultrahydrogel has been reported in 1995 by Wu et al. [9]. Using single linear columns also greatly reduces analysis time and solvent consumption, making SEC a practical method for quality assurance. A comparison of four commercial linear aqueous columns and four sets of commercial PEO standards for SEC of PVP K-15, K-



30, K-60, K-90, and K-120 was reported by Wu et al. in 1999 [10]. In recent years, SEC-MALLS has also been applied in this laboratory to PVP. Figure 1 shows an overlay of SEC-MALLS chromatograms of all commercial grades of PVP using a linear aqueous column. The excellent overlap of absolute M_w versus retention volume plots for all commercial grades of PVP in Fig. 1 demonstrates that there is no significant difference in branching among all commercial grades of PVP, despite the different methods used to make them.

Finally, the following SEC columns, which have been introduced in recent years, have been demonstrated by the vendors to be successful with PVP: Jordi DVB Glucose BR linear column [in dimethyl sulfoxide (DMSO)], PL aquagel-OH column (in 0.1M–0.3M salt-buffer with 20% methanol); PSS Suprema column (in 0.1M Tris pH 7 buffer), and PSS SDV column (in DMAC, 0.1% LiBr) [11–13].

Molecular Weights and Molecular-Weight Distributions of VP-Based Copolymers by SEC

Wu et al. reported in 1991 [14] the SEC of a nonionic copolymer, such as copolymers of vinyl pyrrolidone and vinyl acetate (VP-VA) with different mole ratios and molecular weights, and a terpolymer of vinyl pyrrolidone, dimethylaminoethyl methacrylate and vinyl caprolactam (VP-DMAEMA-VC) in both aqueous and nonaqueous systems. For the aqueous system the column set used consisted of four Waters Ultrahydrogel columns of pore sizes 120, 500, 1000, and 2000 Å, and the mobile phase

was water–methanol (1:1, v/v) with 0.1M LiNO₃. For the nonaqueous system, the column sets were Shodex KD-80M plus Ultrahydrogel 120 Å, Shodex KD-80M plus PL gel 100 Å, and PL gel 10⁴ Å plus 500 Å and the mobile phase was DMF with 0.1M LiNO₃. However, it is the aqueous system that showed the best separation at the low-molecular-weight end. Figure 2 shows the overlay of SEC chromatograms of VP-based copolymers in water–methanol (50:50) with 0.1M lithium nitrate and a linear Shodex OH-PAK column.

Wu and Senak reported in 1990 [15] absolute molecular-weights and molecular-weight distributions of a quaternized copolymer of vinyl pyrrolidone and dimethylaminoethylmethacrylate (PVP-DMAEMA) by SEC-LALLS and SEC with universal calibration using Waters Ultrahydrogel 120, 500, 1000, and 2000 Å columns and a 0.1M Tris, pH 7 buffer with 0.5M LiNO₃ as the mobile phase. Due to the cationic charges on the molecules, a much higher salt content (0.5M LiNO₃) is needed in the SEC mobile phase to improve the separation and recovery of the polymer. The water–methanol (1:1, v/v) mobile phase with 0.4M lithium nitrate has also been used in this laboratory for SEC of this cationic copolymers with the Shodex OH pak or Ultrahydrogel linear columns with good results. Figure 3 shows the overlay of SEC chromatograms of this cationic copolymers in a pH 7 buffer and a linear Shodex OH-PAK column.

Wu et al. reported in 1991 [14] the SEC of anionic copolymers, vinyl pyrrolidone and acrylic acid (VP-AA) with different mole ratios and molecular weights, using a 0.1M pH 9 Tris-buffer with 0.2M LiNO₃ as the mobile phase and the Ultrahydrogel 120, 500, 1000,

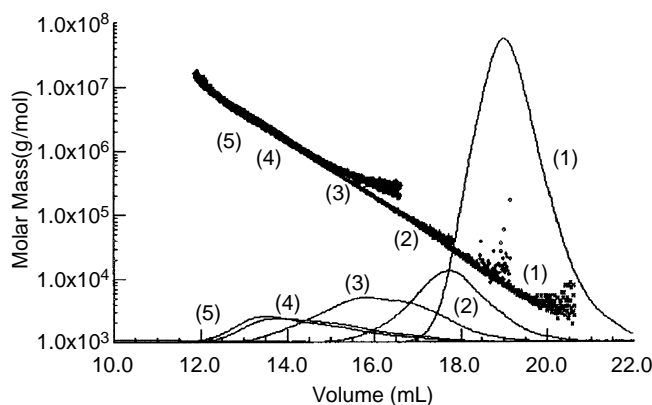


Fig. 1 Overlay of SEC chromatograms and M_w versus retention volume plots by MALLS for PVP grades: (1) K-15; (2) K-30; (3) K-60; (4) K-90; (5) K-120.

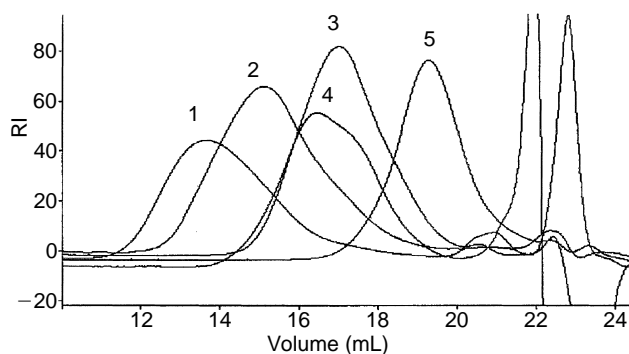


Fig. 2 Overlay of SEC chromatograms of VP-based copolymers in water–methanol (50:50) with 0.1M lithium nitrate: 1: VP-DMAPMA; 2: VP-DMAPMA-AA-LM; 3: VP-VCL-DMAPMA; 4: VP-AA-LM; 5: VP-VA.

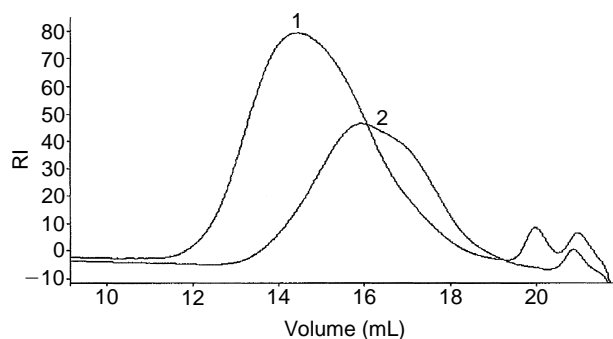


Fig. 3 Overlay of SEC chromatograms of VP-based copolymers in a pH 7 buffer: 1: high-MW VP-DMAEMA cationic copolymer; 2: medium MW VP-DMAEMA cationic copolymer.

and 2000 Å column set. Figure 4 shows overlay of SEC chromatograms of anionic copolymers in a pH 9 buffer and a linear Shodex OH-PAK column.

Copolymers and grafted copolymers of vinyl pyrrolidone and α -olefins, with α -olefins' contents higher than 60%, are not soluble in water or the water-methanol mixture. They should be analyzed in tetrahydrofuran using cross-linked polystyrene columns. However, copolymers and grafted copolymers of vinylpyrrolidone and α -olefins, with only 10% α -olefins, can be analyzed in the water-methanol mixture (50:50) with 0.1M lithium nitrate.

Summary

With a proper choice of mobile phase (aqueous or nonaqueous), many commercially columns are available for SEC of PVP and VP-based copolymers. Mobile-phase modifiers (such as methanol, salt, and buffer) are normally required to eliminate interactions with columns. A single linear or mixed-bed column has been found to provide good separation of PVP and VP-based copolymers with a molecular weight range of from a few thousands to several millions. In general, the aqueous SEC system has better long-term stability and provides better separation than the nonaqueous SEC system, especially at the low-molecular-weight end. Hydroxylated methyl-methacrylate-type columns and water-methanol mobile phase (50:50, with salt) is a good first choice for SEC of PVP and many VP-based copolymers. New columns have been introduced to the marketplace in recent years; hopefully, they will offer better separation, solvent compatibility, stability, and minimal interactions.

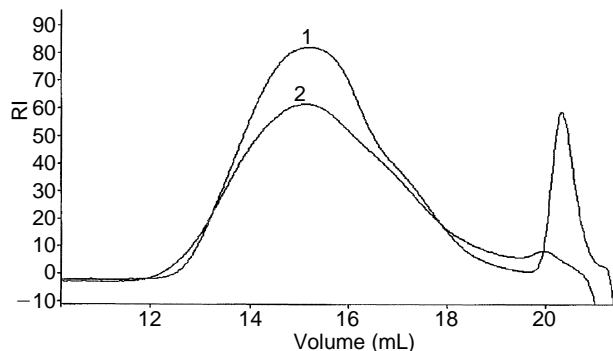


Fig. 4 Overlay of SEC chromatograms of VP-based copolymers in a pH 9 buffer: 1: VP-AA anionic copolymer; 2: VP-AA-LM anionic copolymer.

References

1. B. G. Belenkii, L. Z. Vilenchik, V. V. Nesterov, V. J. Kolegov, and S. Y. A. Frenkel, *J. Liquid Chromatogr.* 109: 223 (1975).
2. T. Hashimoto, H. Sasaki, M. Aiura, and Y. Kato, *J. Polym. Sci. Polym. Phys. Ed.* 16: 1789 (1978).
3. H. Engelhardt and D. Mathes, *J. Chromatogr.* 185: 305 (1979).
4. D. P. Herman and L. R. Field, *J. Chromatogr. Sci.* 19: 470 (1981).
5. S. Mori, *Anal. Chem.* 55: 2414 (1983).
6. A. Domard and M. Rinaudo, *Polym. Commun.* 25: 55 (1984).
7. E. G. Malawer, J. K. DeVasto, and S. P. Frankoski, *J. Liquid Chromatogr.* 7(3): 441 (1984).
8. L. Senak, C. S. Wu, and E. G. Malawer, *J. Liquid Chromatogr.* 10(6): 1127 (1987).
9. C. Wu, J. F. Curry, E. G. Malawer, and L. Senak, in *Handbook of Size Exclusion Chromatography* (C. Wu, ed.), Marcel Dekker, Inc., New York, 1995, pp. 311–330.
10. C. Wu, L. Senak, D. Osborne, and T. Cheng, in *Column Handbook for Size Exclusion Chromatography* (C. Wu, ed.), Academic Press, New York, 1999, pp. 499–529.
11. H. Jordi, in *Column Handbook for Size Exclusion Chromatography* (C. Wu, ed.), Academic Press, New York, 1999, pp. 367–425.
12. E. Meehan, in *Column Handbook for Size Exclusion Chromatography* (C. Wu, ed.), Academic Press, New York, 1999, Chap. 12.
13. P. Kilz, in *Column Handbook for Size Exclusion Chromatography* (C. Wu, ed.), Academic Press, New York, 1999, Chap. 9.
14. C. S. Wu, J. Curry, and L. Senak, *J. Liquid Chromatogr.* 14(18): 3331 (1991).
15. C. S. Wu and L. Senak, *J. Liquid Chromatogr.* 13(5): 851 (1990).



Viscometric Detection in GPC–SEC

James Lesec

Laboratoire Physique et Chimie Macromoléculaire, CNRS-ESPCI, Paris, France

Introduction

At the beginning of gel permeation chromatography (GPC), in the early 1960s, there was only one detector at the outlet of GPC columns, generally a differential refractometer, to continuously measure the concentration of eluents. This detection provided a chromatographic peak corresponding, roughly, to the mass distribution. In addition, it was possible to build a calibration curve corresponding to the response of the column set $\log(M) = F(V_e)$ (M being the molecular weight and V_e being the elution volume), which was roughly linear, by multiple injections of narrow standards with known molecular weights and very narrow molecular-weight distributions. At each increment of elution volume, the slice concentration C_i was calculated using the polymer peak intensity and the slice molecular weight M_i , using the calibration curve. Then, it was possible to calculate, by integration

$$\begin{aligned}\frac{\sum C_i}{\sum (C_i/M_i)} &= M_n \\ \frac{\sum C_i M_i}{\sum C_i} &= M_w \\ \left(\frac{\sum C_i M_i^a}{\sum C_i} \right)^{1/a} &= M_v \\ \frac{\sum C_i M_i^2}{\sum C_i M_i} &= M_z\end{aligned}$$

[a being the viscosity-law (Mark–Houwink) exponent], the different average molecular weights (in number, M_n ; in viscosity, M_v ; in weight, M_w ; in z , M_z), in a single experiment.

The use of the GPC technique spread very quickly but, very soon, it became obvious that this method was imperfect. Every polymer has its own calibration curve which differs from one polymer to another. Moreover, for copolymers or branched polymers, the molecular weight calibration curve does not work correctly.

In 1966, the “universal calibration” method was established at the University of Strasbourg, France [1]. It used, as a parameter, not molecular weight M , but the hydrodynamic volume represented by the product $[\eta]M$,

$[\eta]$ being the intrinsic viscosity. This universal calibration curve $\log([\eta]M) = F(V_e)$ was supposed to be applied to every polymer and copolymer, linear or branched, as a unique calibration curve; it worked very well.

From that point, the necessity of continuously measuring viscosity, in addition to polymer concentration, became obvious. Several attempts were made to adapt existing viscometers as GPC detectors, but the problem of internal volume was critical. Ouano [2] published the first design of a single-capillary viscometer which was based on pressure measurement. Several similar designs [3–6] were published and a commercially available instrument, the Waters Model 150CV (Waters Associates, Milford, MA, U.S.A.), based on a design described in Ref. 4, became commercially available.

Single-Capillary Viscometer

The single-capillary viscometer (SCV) is represented in Fig. 1a. Its design is a direct extrapolation of classical viscometry measurement. It is composed of a small capillary, through which the solvent flows at a constant flow rate, and a differential pressure transducer (DPT), which measures the pressure drop across the capillary. SCV obeys Poiseuille’s law and the pressure drop ΔP across the capillary depends on the geometry of the capillary, on flow rate Q , and on viscosity of the fluid η according to

$$\Delta P = \left(\frac{8}{\pi} \right) \left(\frac{l}{r^4} \right) \eta Q$$

where l and r are the length and radius of the capillary, respectively.

Classical viscometers maintain ΔP constant and calculate η by measuring the variations of flow rate Q . By contrast, the SCV uses the advantage of GPC, which already has a constant flow rate Q and allows the calculation of η by measuring the pressure drop variations ΔP across the capillary. At constant flow rate Q , the pressure drop is proportional to viscosity η , and at constant viscosity η , the pressure drop is proportional to flow rate Q . Consequently, in order to use the SCV as an accurate viscometer, the flow rate must be main-



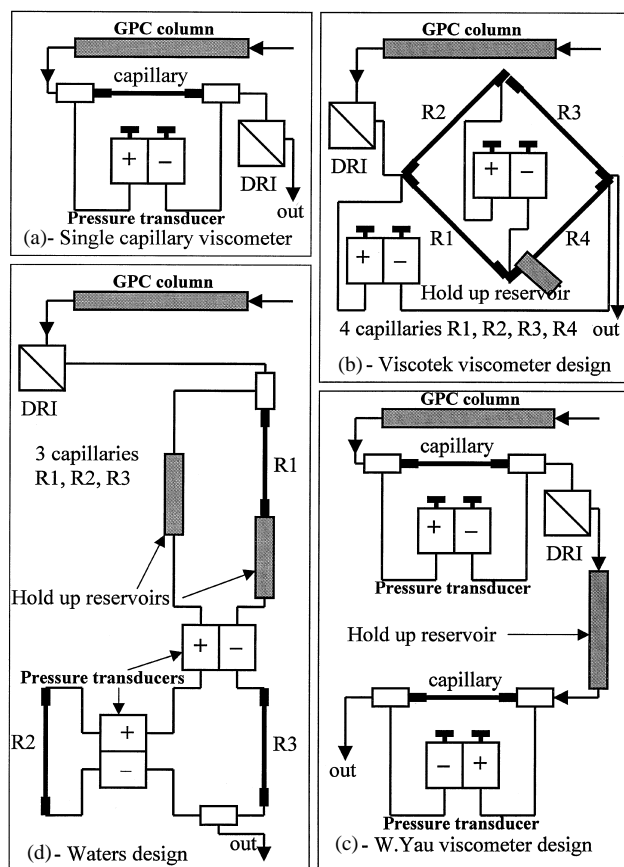


Fig. 1 Various designs of viscometric detection.

tained absolutely constant during the GPC experiment. Conversely, SCV allows perfect control of flow rate and can also be used as a very accurate flow meter when only pure solvent comes out of columns. At the outlet of the GPC columns, the polymer concentration is very small and the increase of solvent viscosity η is very small as well. When measuring ΔP proportional to ηQ , Q should be maintained extremely constant; this requires pulse dampeners in the flow system to smooth small flow variations due the pumping system design.

For that reason, some other, more complicated, viscometers, which are insensitive to small flow variations, were designed using multiple capillaries and pressure transducers.

Multiple-Capillary Viscometers

The general purpose of multiple-capillary viscometers is to simultaneously measure the polymer solution in one part of the detector and pure solvent in a second

part of the detector. In order to have these two parts at the same time, it is necessary to include a holdup reservoir to delay the polymer passing through the second part of the detector. One needs to wait until the delayed polymer comes out of the detector before re-injecting another sample. The basic principle is that one part of the detector measures polymer plus flow and the other part measures only flow. By obtaining the difference, the result is a signal which is proportional to polymer viscosity and insensitive to flow rate variations.

The first multiple-capillary viscometer was designed by the Viscotek Company (Houston, TX, U.S.A.) [7]. It is represented in Fig. 1b. It is composed of four identical capillaries, assembled as a bridge. Here, the difference is generated by the bridge itself as a differential viscometer. The central DPT provides a differential viscosity signal DP and the second, DPT, provides inlet pressure IP . The intrinsic viscosity $[\eta]$ can be calculated by the formula

$$[\eta] = \frac{1}{C} \left(\frac{4DP}{IP - 2DP} \right)$$

Another design was described by the Dupont Company [8]. It is represented in Fig. 1c. It is composed of two single-capillary viscometers. The first one (measure) is located as a normal SCV (Fig. 1a) and measures polymer plus flow. The second one (reference), identical to the first one, is located after a holdup reservoir which is connected after the refractometer and measures only the flow with pure solvent. It is just necessary to obtain the difference between the two signals to obtain the polymer signal with no flow contribution.

The last differential viscometer design is the Waters Corporation detector [9], which is in the Alliance GPCV2000 high-temperature instrument. It is composed of three capillaries, two differential pressure transducers, and two holdup reservoirs; it is represented in Fig. 1d. The pressure transducers are connected flow-through; this eliminates the need for frequent purges. This detector provides, at the same time, "relative viscosity information" and "relative flow information." This design does not require a perfect matching of the capillaries.

The Use of Viscometric Detection

The first purpose of viscometric detection in GPC is to use a "universal calibration curve." At every slice, the concentration C_i is obtained through refractometric data, intrinsic viscosity $[\eta]_i$ is obtained through refractometric and viscometric data, and hydrodynamic vol-

ume $[\eta]M_i$ is obtained from the universal calibration curve. It is just necessary to divide $[\eta]M_i$ by $[\eta]_i$ to get M_i and obtain the couple C_iM_i that is necessary to calculate the various average molecular weights, as shown at the beginning of this entry, independently of the chemical nature of the sample and the standards used for calibration.

The secondary use of viscometric detection is for the determination of long-chain branching. At the same molecular weight, a long-chain branched polymer has a more compact molecular structure than the linear one; consequently, it also has a smaller intrinsic viscosity. Therefore, it is eluted at a higher elution volume with a linear polymer of smaller molecular weight. That means that at a given elution volume, there is a mixture of

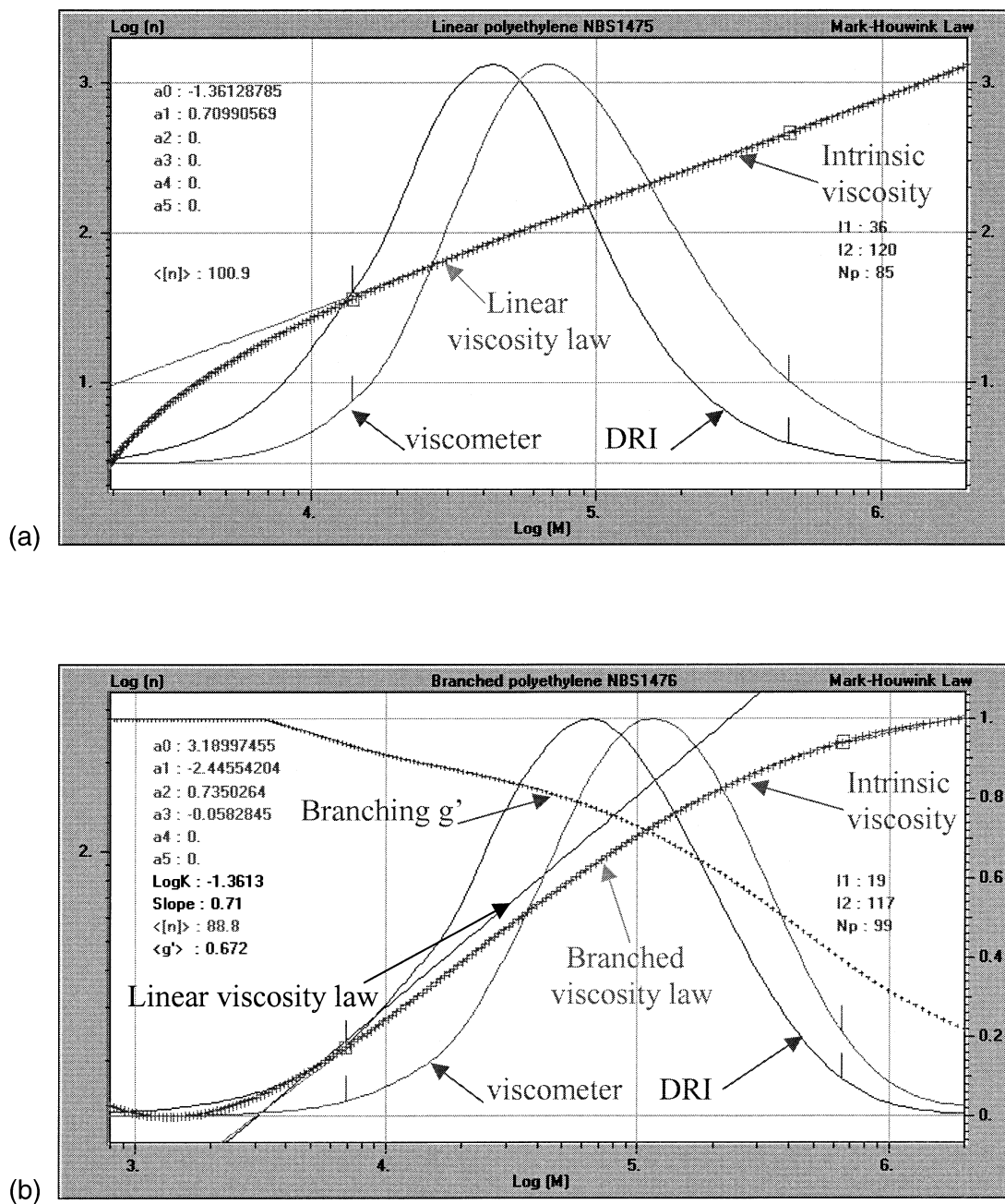


Fig. 2 Mark-Houwink plot for linear polyethylene NBS1475. (b) Mark-Houwink plot for branched polyethylene NBS1476.

polymers with different molecular weights and different degrees of branching eluting from the GPC column.

As intrinsic viscosity is affected by long-chain branching, viscometric detection provides branching information, just by comparing polymer viscosity laws. Figure 2a represents the viscosity-law plot of a linear polymer, polyethylene (NBS1475), with a linear viscosity law and an exponent of 0.71. Conversely, Fig. 2b represents the viscosity-law plot of a branched polymer, polyethylene (NBS1476), with a curved viscosity law, under the linear polymer law (linear viscosity law). At every molecular weight, the branching distribution g'_i is calculated by

$$g'_i = \frac{[\eta]_{br_i}}{[\eta]_{lin_i}}$$

where $[\eta]_{br_i}$ and $[\eta]_{lin_i}$ are the slice intrinsic viscosities of the branched and the linear polymer, respectively.

Conclusion

Viscometric detection in GPC-SEC is extremely useful. It allows continuous viscosity measurements, which, in turn, permits the use of a unique calibration curve for all polymers (universal calibration). In addition,

the viscosity law is determined for linear polymers and long-chain-branching information can be obtained for branched polymers.

References

1. H. Benoit, Z. Grubisic, P. Rempp, D. Dekker, and G. Zilliox, *J. Chim. Phys.* 63: 1507 (1966).
2. A. C. Ouano, *J. Polym. Sci. A1* 10: 2169 (1972).
3. J. Lesec and C. Quivoron, *Analysis* 4: 399 (1976); L. Letot, J. Lesec and C. Quivoron, *J. Liquid Chromatogr.* 3: 407 (1982).
4. D. Lecacheux, J. Lesec, and C. Quivoron, *J. Appl. Polym. Sci.* 27: 4867 (1982); D. Lecacheux, J. Lesec, and R. Prechner, French Patent 82402324.6 (1982); U.S. patent 4478071 (1984).
5. F. B. Malihi, C. Kuo, M. E. Kohler, T. Provder, and A. F. Kah, *ACS Symp. Ser.* 245: 281 (1984); C. Kuo, T. Provder, M. E. Kohler, and A. F. Kah, *ACS Symp. Ser.* 352: 130 (1987).
6. J. Lesec, D. Lecacheux, and G. Marot, *J. Liquid Chromatogr.* 11: 2571 (1988); J. Lesec and G. Marot, *J. Liquid Chromatogr.* 11: 3305 (1988).
7. M. A. Haney, *J. Appl. Polym. Sci.* 30: 3037 (1985).
8. S. D. Abbot and W. W. Yau (to Dupont), U.S. Patents 4478990 and 4627271 (1986).
9. J. L. de Corral (to Waters Corp.), U.S. Patent 5637790 (1997).



Vitamin B₁₂ and Related Compounds in Food, Analysis by TLC

Fumio Watanabe

Emi Miyamoto

Kochi Women's University, Kochi, Japan

INTRODUCTION

Vitamin B₁₂ (B₁₂ or CN-B₁₂) is synthesized only in certain bacteria. Usual dietary sources of B₁₂ are animal food products (meat, milk, eggs, and shellfish), but not generally plant food products. However, some plant foods (e.g., edible algae) contain large amounts of B₁₂. Various B₁₂ compounds with different upper (L) and/or lower (R) ligands naturally occur (Fig. 1), especially MeB₁₂ and AdoB₁₂, which function as coenzyme forms of B₁₂. Some food products contain unidentified or inactive B₁₂-related compounds, which may not be bioavailable in humans. Appreciable loss of B₁₂ also occurs in foods during cooking and/or other food processing.

This article summarizes the purification and characterization of B₁₂ compounds found in various food products and of B₁₂ degradation compounds formed by cooking and/or food processing, using thin-layer chromatography (TLC) as a powerful separation and analytical tool.

PURIFICATION AND CHARACTERIZATION OF VITAMIN B₁₂ AND RELATED COMPOUNDS BY TLC

Commercially Available Reagents

Some commercially available B₁₂ reagents, especially OH-B₁₂ and dicyanocobinamide, contain small amounts of impurities (Fig. 2). Each B₁₂ reagent should be purified with silica gel 60 TLC and then used for experiments as an authentic "standard" material. The authentic OH-B₁₂, purified by TLC on silica gel, has been used in the experiments conducted in the authors' laboratory.^[1]

Vitamin B₁₂ Degradation Products by Cooking and/or Food Processing

To determine whether the loss of B₁₂ in microwave-treated foods is derived from the conversion of B₁₂ to some inactive B₁₂ degradation products, the OH-B₁₂ that predominates in food is treated by microwave heating for 6 min and then analyzed by TLC on silica gel 60 with

1-butanol–2-propanol–water (10:7:10 vol/vol) as the solvent. The treated OH-B₁₂ is separated into three red spots [major compound I with an R_f of 0.03, identical R_f of intact OH-B₁₂, and minor compound II (about 18.2%) with an R_f of 0.16 and compound III (4.2%) with an R_f of 0.27].^[2] Although a novel OH-B₁₂ degradation product with an R_f of 0.12 has not been separable from intact OH-B₁₂ by the TLC system, it can be completely separated by silica gel 60 column chromatography.^[1]

The OH-B₁₂ degradation products with R_f values of 0.12 and 0.16 are further purified to homogeneity by the use of silica gel 60 TLC and reversed-phase high-performance liquid chromatography (HPLC).^[1,2] The ¹H nuclear magnetic resonance (NMR) spectra of the OH-B₁₂ degradation products show that the degradation product with an R_f of 0.12 is a B₁₂ compound with the lower ligand structure changed slightly, but that with an R_f of 0.16 is a B₁₂ compound without the base portion in the lower ligand.^[1,2] Structural information on the degradation compound with an R_f of 0.27 is not available because a purified sample was not obtained for NMR study. Although the degradation product with an R_f of 0.12 has about 13% and 23% biological activity of authentic B₁₂ in hog intrinsic factor (IF; the most specific mammalian B₁₂-binding protein) and *Lactobacillus delbrueckii* ATCC 7830 (a microorganism for B₁₂ bioassay), respectively, the product with an R_f of 0.16 does not show any biological activity.^[1,2] Intravenous administration of both purified degradation products to rats indicates that the compounds are not toxic.^[1,2] These results indicate that the conversion of B₁₂ to these inactive B₁₂ degradation products occurs in food during microwave heating.

Appreciable loss of B₁₂ occurs in the multivitamin–mineral food supplements containing B₁₂ because B₁₂ is converted to inactive B₁₂ compounds by the addition of substantial amounts of vitamin C in the presence of copper.^[3] The destruction of B₁₂ is probably concerned with radicals generated by vitamin C in the presence of copper. Although vitamin C alone or metal ion (Cu²⁺) alone does not decompose B₁₂, B₁₂ is destroyed significantly by mixing vitamin C and Cu²⁺ together (vitamin C–Cu²⁺ system).^[4] Many B₁₂ degradation compounds (ladderlike red-colored spots) are separated from the

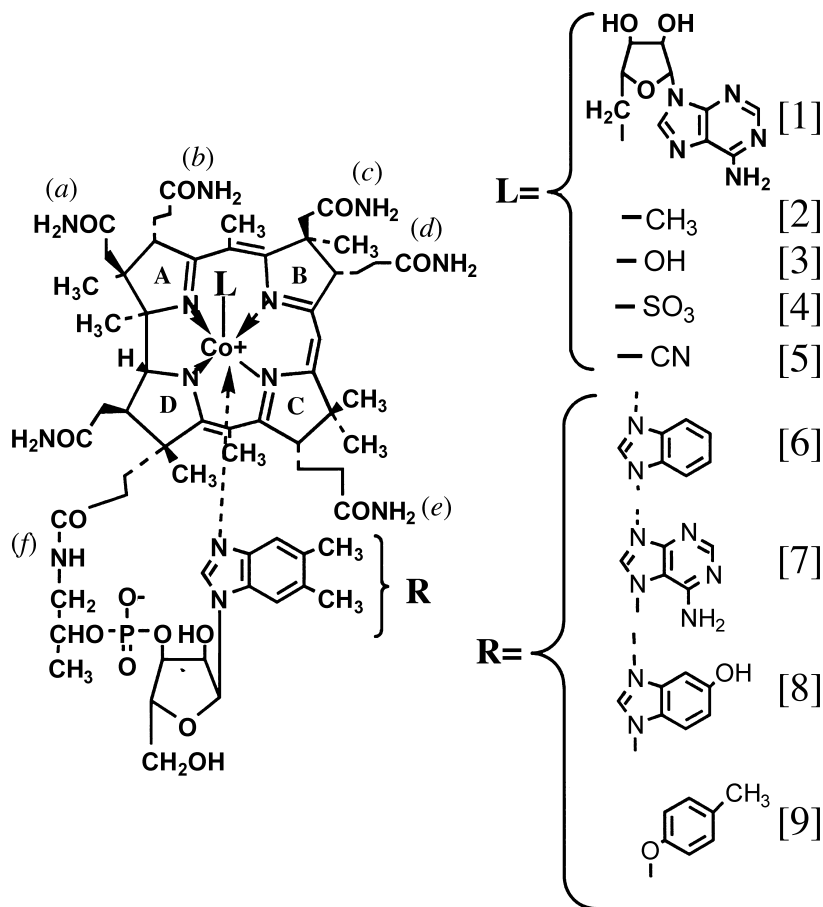


Fig. 1 Structural formulae of B₁₂ compounds. The partial structures of B₁₂ compounds show only those portions of the molecule that differ from B₁₂. (1) AdoB₁₂; (2) MeB₁₂; (3) OH-B₁₂; (4) SO₃-B₁₂; (5) CN-B₁₂ or B₁₂; (6) benzimidazolyl cyanocobamide; (7) pseudovitamin B₁₂; (8) 5-hydroxybenzimidazolyl cyanocobamide; (9) *p*-cresolyl cyanocobamide.

B₁₂ treated with the vitamin C–Cu²⁺ system by TLC on silica gel 60.^[4] Some of the B₁₂ compounds formed appear to block B₁₂ metabolism in mammalian cells.^[3]

Vitamin B₁₂ Compounds From Foods

Shellfish

The shellfish that siphon large quantities of B₁₂-synthesizing microorganisms from the sea are known to be excellent sources of B₁₂. These microorganisms can synthesize various B₁₂ compounds (including inactive B₁₂ compounds for humans). B₁₂ contents of various edible shellfish were determined by both *L. delbrueckii* ATCC 7830 microbiological and IF chemiluminescence methods. The values determined by the microbiological method were 1.2-fold to 19.8-fold greater in the shellfish than the values determined by the IF chemiluminescence method.^[5] To clarify why such differences in the B₁₂ contents determined by the two methods occur, some B₁₂

compounds have been purified from edible shellfish (oyster, mussel, and short-necked clam) using silica gel 60 TLC and a reversed-phased HPLC method, and subsequently characterized.^[5]

The *R_f* values (0.18 and 0.59) of the red-colored B₁₂ compounds purified from these shellfish are identical to those of authentic B₁₂, but not to those of benzimidazolyl cyanocobamide (*R_f* values: 0.15 and 0.55), 5-hydroxybenzimidazolyl cyanocobamide (*R_f* values: 0.16 and 0.47), pseudo-B₁₂ (*R_f* values: 0.14 and 0.46), and *p*-cresolyl cyanocobamide (*R_f* values: 0.27 and 0.64) in two solvent systems [1-butanol–2-propanol–water (10:7:10) and 2-propanol–NH₄OH (28%)–water (7:1:2), respectively] by TLC on silica gel.^[5] Although the higher values in the determination of B₁₂ by the microbiological method may be because of the occurrence of B₁₂ substitution compounds (probably deoxyribosides and/or deoxynucleotides), the edible shellfish would be excellent B₁₂ sources, judging from the values (6 µg/100 g) determined by the IF chemiluminescence method.



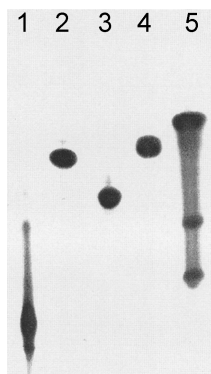


Fig. 2 Silica gel 60 TLC pattern of commercially available B₁₂ reagents. The concentrated solution (4 μ L) was spotted on the silica gel TLC sheet and developed with 2-propanol–NH₄OH (28%)–water (7:1:2 vol/vol) at room temperature in the dark. (1) OH-B₁₂; (2) CN-B₁₂; (3) AdoB₁₂; (4) MeB₁₂; (5) dicyanocobinamide.

Edible algae

Edible algae are known to be rich in vitamins and minerals, as well as being good dietary fibers. Dried lavers (nori) appear to be the most widely eaten edible alga worldwide, and they have been reported to contain substantial amounts of B₁₂.^[6] As the bioavailability of the laver B₁₂ in mammals is not well understood, B₁₂ compounds have been purified from the dried purple (*Porphyra yezoensis*) and green (*Enteromorpha prolifera*) lavers using silica gel 60 TLC and a reversed-phase HPLC method and subsequently characterized.^[7,8]

The silica gel 60 TLC and reversed-phase HPLC patterns of the pink-colored compound purified from each laver are identical to those of authentic B₁₂, but not to those of B₁₂ compounds inactive for humans.^[7,8]

Algal health food

A health food fad involves tablets of *Spirulina* sp. (blue-green algae). When the B₁₂ concentration of algal health food (*Spirulina* tablets) has been determined by both *L. delbrueckii* ATCC 7830 microbiological and IF chemiluminescence methods, the values determined by the microbiological method are about sixfold to ninefold greater in the *Spirulina* tablets than the values determined by the IF chemiluminescence method.^[9] To evaluate whether the B₁₂ found in the *Spirulina* tablets is true B₁₂ or inactive B₁₂-related compound, B₁₂ compounds have been purified from the *Spirulina* tablets using silica gel 60 TLC and a reversed-phased HPLC, and then characterized.^[9]

The major (83%) and minor (17%) B₁₂ compounds purified from the *Spirulina* tablets are identified as

pseudo-B₁₂ and B₁₂, respectively, judging from TLC, HPLC, ¹H NMR spectroscopy, ultraviolet–visible spectroscopy, and biological activity data.^[9] The *Spirulina* tablets are not suitable for use as a B₁₂ source, especially for vegetarians, because pseudo-B₁₂ appears to be inactive for humans.

In the case of other algal health foods (e.g., *Chlorella* tablets^[10] and a coccolithophorid alga^[11]), some B₁₂ compounds have also been purified using TLC on silica gel 60 and then characterized. They contain substantial amounts of true active B₁₂.

VITAMIN B₁₂ BIOASSAY AFTER TLC SEPARATION

To evaluate whether foods contain true B₁₂ or not, B₁₂ compounds can be separated by TLC and then assayed. Various kinds of fish sauces, traditional food supplements in the diet, are widely used in the world as condiments, and sometimes substituted for soybean sauces. Although a fish sauce (Nam-pla) appears to contribute a major source of B₁₂ in Thailand, B₁₂ compounds found in the nine selected fish sauces were separated by TLC on silica gel 60 and then determined with the *Lactobacillus* microbiological method, indicating that most B₁₂ is

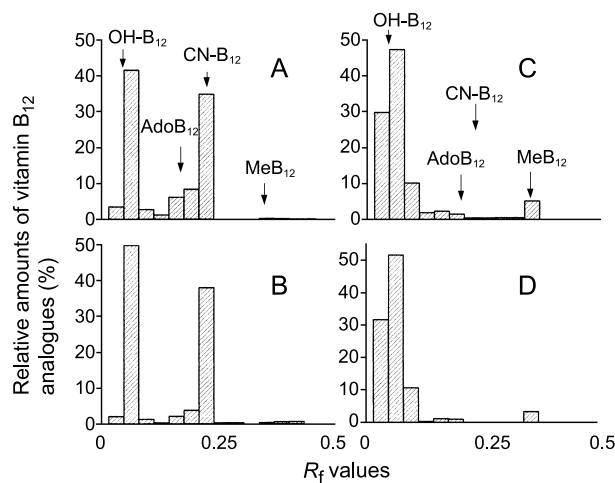


Fig. 3 Silica gel 60 TLC analysis of B₁₂ compounds of dried green and purple lavers. The green laver B₁₂ compounds were determined according to the chemiluminescence B₁₂ assay (A) and microbiological B₁₂ assay (B) methods. The purple laver B₁₂ compounds were determined according to the chemiluminescence B₁₂ assay (C) and microbiological B₁₂ assay (D) methods. The R_f values of authentic OH-B₁₂, AdoB₁₂, CN-B₁₂, and MeB₁₂ on this TLC system [1-butanol–2-propanol–water (10:7:10 vol/vol) as a solvent] were 0.03, 0.20, 0.22, and 0.36, respectively. (From Ref. [3]. © American Chemical Society, 1999.)

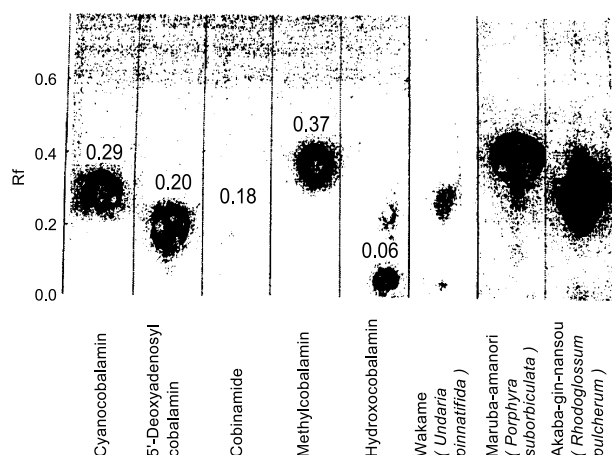


Fig. 4 Bioautogram of B₁₂ and related compounds in the edible algae. A TLC plate was prepared from a slurry mixture of three weights of powdered cellulose (Whatman, Microgranular Cellulose, and CC41) and one weight of silica gel (Silica gel G, Type 60; Merck). Extracts of the edible algae, solutions of authentic B₁₂ compounds, and cobinamide were applied at one of the plate, and developed with 2-butanol-NH₄OH (28%)–water (75:2:25 vol/vol). After drying the cellulose–silica gel plate, agar containing basal medium and *E. coli* 215 was overlaid and then incubated at 30°C for 20 hr. After spraying methanol solution of 2,3,5-triphenyltetrazolium salt on the gel plate, the position of B₁₂ was visualized as red color by *E. coli* growth. (From Ref. [2]. © Center for Academic Publications Japan, 1996.)

derived from unidentified B₁₂ compounds^[12] and suggesting that fish sauce may not be suitable for use as a B₁₂ source.

Coenzyme forms of B₁₂ are also separated by TLC and then assayed. Occurrence of B₁₂ coenzymes in the dried purple and green lavers is shown by the use of silica gel 60 TLC (Fig. 3).^[13] The dried green laver contains four known types of biologically active B₁₂ compounds (approximately OH-B₁₂, 45%; CN-B₁₂, 35%; AdoB₁₂, 6%; and MeB₁₂, 0.2%), and the noncoenzyme forms (OH and CN forms) of B₁₂ predominated. Most B₁₂ (about 80%) found in the dried purple laver are recovered in the OH-B₁₂ fraction.

ONE-DIMENSIONAL AND TWO-DIMENSIONAL BIOAUTOGRAPHY

Because levels of B₁₂ are very low in foods, tissues, and body fluids, bioautography is used before densitometry. A selected strain of *Escherichia coli* is used as the micro-organism for the bioautography. Growth spots are enhanced by the addition of 2,3,5-triphenyltetrazolium

chloride, which is converted to the red-colored formazan by *E. coli* growth.

The one-dimensional bioautography of authentic B₁₂ compounds, cobinamide, and extracts of three edible algae, using TLC on mixture of silica gel and cellulose, is shown in Fig. 4.^[14] The R_f value of a dominant red color spot found in the extract of Maruba-amanori is identical to that of authentic MeB₁₂. A single spot corresponding to CN-B₁₂ is found in the extract of Wakame.

A sensitive two-dimensional bioautography has also been developed to investigate B₁₂ metabolism in health and a wide range of diseases,^[15] but it has hardly been used for food B₁₂ analysis.

CONCLUSION

To evaluate whether food products contain true B₁₂ or inactive (or unidentified) B₁₂-related compounds, B₁₂ compounds were purified and analyzed by TLC on silica gel 60. Sensitive one-dimensional or two-dimensional bioautography was also available in samples with lower levels of B₁₂.

The results presented here indicate that TLC offers great advantages (simplicity, flexibility, speed, and relatively low cost) for the separation and analysis of B₁₂ compounds in foods.

ABBREVIATIONS

AdoB ₁₂	Deoxyadenosylcobalamin or adenosyl-vitamin B ₁₂
B ₁₂ or CN-B ₁₂	Cyanocobalamin or vitamin B ₁₂
MeB ₁₂	Methylcobalamin or methyl-vitamin B ₁₂
OH-B ₁₂	Hydroxocobalamin or hydroxo-vitamin B ₁₂

REFERENCES

1. Watanabe, F.; Abe, K.; Katsura, H.; Takenaka, S.; Mazumder, S.A.M.Z.H.; Yamaji, R.; Ebara, S.; Fujita, T.; Tanimori, S.; Kirihaata, M.; Nakano, Y. Biological activity of hydroxo-vitamin B₁₂ degradation product formed during microwave heating. *J. Agric. Food Chem.* **1998**, *46* (12), 5177–5180.
2. Watanabe, F.; Abe, K.; Fujita, T.; Goto, T.; Hiemori, M.; Nakano, Y. Effects of microwave heating on the loss of vitamin B₁₂ in foods. *J. Agric. Food Chem.* **1998**, *46* (1), 206–210.
3. Herbert, V. Vitamin B₁₂. *Present Knowledge in Nutrition*; Brown, M.L., Ed.; International Life Science: Washington, DC, **1990**, 170–179.
4. Takenaka, S.; Sugiyama, S.; Watanabe, F.; Abe, K.;

- Tamura, Y.; Nakano, Y. Effects of carnosine and anserine on the destruction of vitamin B₁₂ with vitamin C in the presence of copper. *Biosci. Biotechnol. Biochem.* **1997**, *61* (12), 2137–2139.
5. Watanabe, F.; Katsura, H.; Takenaka, S.; Enomoto, T.; Miyamoto, E.; Nakatsuka, T.; Nakano, Y. Characterization of vitamin B₁₂ compounds from edible shellfish, clam, oyster, and mussel. *Int. J. Food Sci. Nutr.* **2001**, *52*, 263–268.
6. Watanabe, F.; Takenaka, S.; Kittaka-Katsura, H.; Ebara, S.; Miyamoto, E. Characterization of bioavailability of vitamin B₁₂-compounds from edible algae. *J. Nutr. Sci. Vitaminol.* **2002**, *48* (5), 325–331.
7. Watanabe, F.; Takenaka, S.; Katsura, H.; Miyamoto, E.; Abe, K.; Tamura, Y.; Nakatsuka, T.; Nakano, Y. Characterization of a vitamin B₁₂ compound in the edible purple laver, *Porphyra yezoensis*. *Biosci. Biotechnol. Biochem.* **2000**, *64* (12), 2712–2715.
8. Watanabe, F.; Katsura, H.; Miyamoto, E.; Takenaka, S.; Abe, K.; Yamazaki, Y.; Nakano, Y. Characterization of vitamin B₁₂ in an edible green laver (*Entromopha prolifera*). *Appl. Biol. Sci.* **1999**, *5*, 99–107.
9. Watanabe, F.; Katsura, H.; Takenaka, S.; Fujita, T.; Abe, K.; Tamura, Y.; Nakatsuka, T.; Nakano, Y. Pseudovitamin B₁₂ is the predominant cobamide of an algal health food, *Spirulina* tablets. *J. Agric. Food Chem.* **1999**, *47* (11), 4736–4741.
10. Kittaka-Katsura, H.; Fujita, T.; Watanabe, F.; Nakano, Y. Purification and characterization of a corrinoid compound from *Chlorella* tablets as an algal health food. *J. Agric. Food Chem.* **2002**, *50* (17), 4994–4997.
11. Miyamoto, E.; Watanabe, F.; Ebara, S.; Takenaka, S.; Takenaka, H.; Yamaguchi, Y.; Tanaka, N.; Inui, H.; Nakano, Y. Characterization of a vitamin B₁₂ compound from unicellular coccolithophorid alga (*Pleurochrysis carterae*). *J. Agric. Food Chem.* **2001**, *49* (7), 3486–3489.
12. Takenaka, S.; Enomoto, T.; Tsuyama, S.; Watanabe, F. TLC analysis of corrinoid compounds in fish sauce. *J. Liq. Chromatogr. Relat. Technol.* **2003**, *26* (16), 2703–2707.
13. Watanabe, F.; Takenaka, S.; Katsura, H.; Mazumder, S.A.M.Z.H.; Abe, K.; Tamura, Y.; Nakano, Y. Dried green and purple lavers (nori) contain substantial amounts of biologically active vitamin B₁₂ but less of dietary iodine relative to other edible seaweeds. *J. Agric. Food Chem.* **1999**, *47* (6), 2341–2343.
14. Yamada, S.; Shibata, Y.; Takayama, M.; Narita, Y.; Sugawara, K.; Fukuda, K. Content and characteristics of vitamin B₁₂ in some seaweeds. *J. Nutr. Sci. Vitaminol.* **1996**, *42* (6), 497–505.
15. Linnell, J.C. Hydrophilic Vitamins. In *Handbook of Thin-Layer Chromatography: Second Edition, Revised and Expanded*; Sherma, J., Fried, B., Eds.; Marcel Dekker, Inc.: New York, 1996; 1047–1054.



Void Volume in Liquid Chromatography

Kiyokatsu Jinno

School of Materials Science, Toyohashi University of Technology, Toyohashi, Japan

Introduction

The column dead volume can be defined as the space in the column which is not working for the chromatographic separations (i.e., not occupied by the stationary phase and its support). Its value is generally determined by an elution time or elution volume of a nonretained solute in the chromatographic system. If the column dead volume is measured by a retention time of a nonretained solute, one can refer to this as a *column dead time* t_0 .

Discussion

The accurate determination of the column void time, t_0 , is of fundamental importance in chromatography [1]. This is explained by the fact that a reliable estimation of this quantity is essential for the correct calculation of the retention factors (some refer to this as the *capacity factor*), k , which serves as the fundamental parameter for the comparison of retention data and for the interpretation of the physicochemical phenomena taking place within a chromatographic column. However, the determination of this parameter is very sensitive to the estimated value of the column void time, as can be seen from the equation

$$k = \frac{t_r - t_0}{t_0} \quad (1)$$

where t_r is the solute retention time and t_0 is the column dead time (Fig. 1). A precise knowledge of t_0 is also essential for the proper optimization of the chromatographic system [2]. In contrast to gas chromatography (GC), where the problem of column dead-time determination has been satisfactorily solved [3], determination of the true column void time in liquid chromatography (LC) presents both theoretical and practical difficulties and still remains an open question.

Controversial opinions exist among scientists regarding the meaning of “column dead time” in LC [4]. In its broad sense, the term “column dead time” refers to the elution volume of an unretained and unexcluded

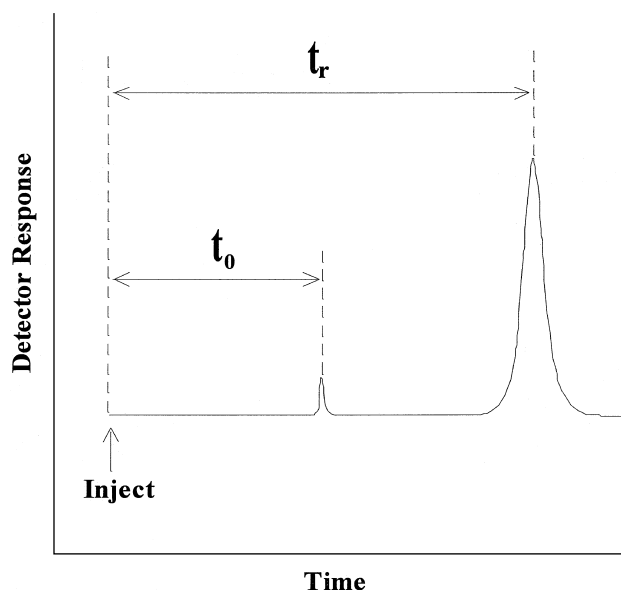


Fig. 1 Void volume determination.

solute, but it is not easy to establish which solute (if any) can be treated as both unretained and unexcluded. In LC practice, quite a large number of solutes [5] (e.g., mobile-phase components, isotopically labeled mobile-phase components, ionic and nonionic species) had been used as void time markers. The most popular method used in reversed-phase LC is to use sodium nitrate or sodium nitrite as the probe, but the use of such compounds as the marker was termed clearly dangerous by Berendsen et al. [6]. Use of small ionic species such as sodium nitrate as a void time marker was found to have the drawback that there exists a possibility of exclusion of the ionic species and, when used in small concentrations, they serve as the marker for ionic exclusion volume instead of column dead volume (Donan exclusion). Even to use higher concentrations of ionic species is now rarely utilized due to obvious shortcomings by the Donan exclusion effect. Other existing experimental methods for the determination of LC column dead time also represent a serious contradiction of opinions among scientists



and, at this moment, there are no definitive methods to determine column t_0 .

One promising approach to experimentally determine t_0 is the linearization method [6], although there are opinions against this method as "undesirable," pointing out some shortcomings. The linearization approach uses the homolog series of compounds, which have various alkyl chains; their retention times are plotted against their chain lengths. Then, the resultant linear curve is extrapolated to zero chain length for the t_0 value. Some people proposed various solutes in homolog series for this purpose, but there is no confirmation concerning the accuracy of the measured t_0 value and, therefore, the opinions against on this method have also appeared in many publications. On the other hand, static methods [7] have been found to represent the upper limit of column porosity, and not the column dead volume proper.

Although the above discussions have appeared numerous times in many publications, workers always need to determine the retention factor, k , in LC separations. In order to determine t_0 experimentally, one

has to state what kind of method was used to determine t_0 in his experiments. This is the only best way at this moment to recommend to all chromatographers concerning column void time, although, in the near future, the "best, reliable, theoretically well-interpreted" methods will be adopted.

References

1. A. M. Krstulovic, H. Colin, and G. Guiochon, *Anal. Chem.* 54: 2438 (1982).
2. A. Alhedai, D. E. Martire, R. P. W. Scott: *Analyst* 114: 869 (1989).
3. L. S. Ettre, *Chromatographia* 13: 73 (1980).
4. J. H. Knox and R. Kaliszan, *J. Chromatogr.* 349: 211 (1985).
5. A. Malik and K. Jinno, *Chromatographia* 30: 135 (1990).
6. G. E. Berendsen, P. J. Schoenmakers, L. de Galan, G. Vigh, Z. Varga-Puchnoy, and J. Inczedy, *J. Liquid Chromatogr.* 3: 1669 (1980).
7. E. H. Slaats, J. C. Kraak, W. J. T. Brugman, and H. Poppe, *J. Chromatogr.* 149: 255 (1978).



Weak Affinity Chromatography

David S. Hage

University of Nebraska, Lincoln, Nebraska, U.S.A.

INTRODUCTION

Weak affinity chromatography (WAC) is a subset of affinity chromatography that makes use of weak interactions for the separation or analysis of chemicals. This method is also referred to as *dynamic affinity chromatography*. Like traditional affinity chromatography, this is a liquid chromatographic technique that uses a selective binding agent as the stationary phase. This agent, which is known as the affinity ligand, might be a biological substance such as a protein, nucleic acid, or carbohydrate. The affinity ligand might also be a substance that mimics a biological system or uses specific interactions for retention, such as is found for certain dyes, biomimetic ligands, and boronates.

Traditional affinity chromatography generally makes use of the on/off mode of elution. In this mode, a ligand with strong binding for the solute of interest is placed within the column. A sample containing this solute is then injected onto this column in the presence of a mobile phase, known as the *application buffer*, which has a pH, ionic strength, and solvent composition that provides for strong and essentially irreversible solute–ligand binding. After nonretained sample components have been washed from the column in this buffer, a second solvent is applied for elution of the retained compounds. This second solvent is known as the *elution buffer* and acts to dissociate the retained substances from the affinity ligand by either disrupting their interactions with this stationary phase or displacing them with another chemical that binds to the ligand or analyte. This is usually performed with a step gradient, but other types of gradient elution schemes can also be used.

However, a different elution approach is used in weak affinity chromatography. In this case, a ligand is used within the column that has only weak-to-moderate binding to the target solutes. This involves the use of a system that has an association equilibrium constant of 10^5 to 10^6 M^{-1} or lower, as well as relatively fast association and dissociation kinetics. Under these conditions, a solute can take part in many binding and dissociation events with the ligand as it passes through the column. This also makes it possible for a solute to elute in the presence of the original application buffer, eliminating the need for a separate

elution buffer. This process is usually performed under isocratic conditions rather than with gradient elution.

THEORY OF WEAK AFFINITY CHROMATOGRAPHY

For a simple 1:1 interaction between an injected analyte (A) and an immobilized affinity ligand (L), the following equations can be used to describe the binding that occurs between A and L within an affinity column.



$$K_a = k_a/k_d = \{\text{A} - \text{L}\}/[\text{A}]\{\text{L}\} \quad (2)$$

In this equation, K_a is the association equilibrium constant for the binding of A with L, k_a is the association rate constant for this reaction, and k_d is the corresponding dissociation rate constant. The terms $[\text{A}]$, $\{\text{L}\}$ and $\{\text{A} - \text{L}\}$ represent the concentration of the analyte in solution at equilibrium and the surface concentrations of the ligand and analyte–ligand complex under these same conditions.

The reaction between the analyte and ligand in this system can also be related to the retention of A on the affinity column in terms of its retention factor (k). As in any other chromatographic method, the value of this retention factor can be determined by using the retention time (or retention volume) for the analyte. Eq. 3 shows the relationship that is used for this purpose with an affinity column that is operated under linear elution conditions (i.e., when a small amount of analyte is injected).

$$k = (t_R - t_M)/t_M \quad (3)$$

In this relationship, t_R is the average retention time measured for the analyte in the mobile phase and t_M is the void time of the system (i.e., the observed elution time for a totally nonretained solute).

The retention factor for an analyte can also be related to its association equilibrium constant with the immobilized ligand in the affinity column. This is shown by Eq. 4,

$$k = K_a m_L / V_M \quad (4)$$

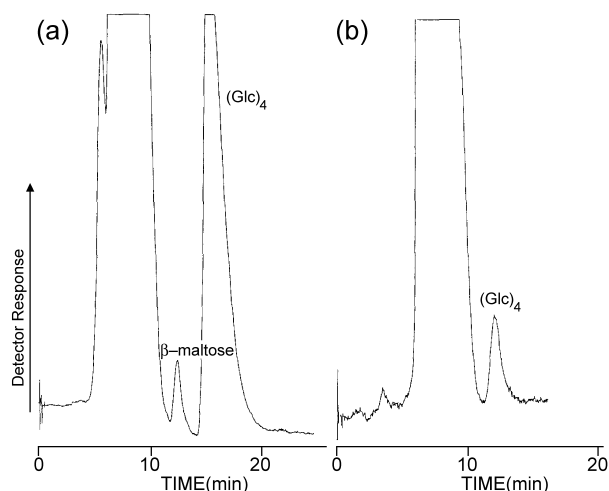


Fig. 1 Analysis of the oligosaccharide (Glc)₄ in (a) human urine and (b) serum by weak affinity chromatography. The affinity column was 5 mm I.D. × 100 mm and contained immobilized monoclonal antibodies against (Glc)₄. Elution was carried out under isocratic conditions at a flow rate of 0.2 mL/min using a pH 7.5, 0.02 M phosphate buffer that contained 0.1 M sodium sulfate. (From Ref. [1].)

where m_L is the moles of active ligand in column, V_M is the column void volume, and the combined term m_L/V_M is the phase ratio (i.e., the relative amount of stationary phase vs. mobile phase in the column). According to Eq. 4, the retention factor for an analyte on an affinity column will depend on two factors. The first of these is the strength of analyte–ligand binding in the mobile phase, as represented by the association equilibrium constant. The second is the relative concentration of active ligand within the column, as represented by the binding capacity or phase ratio (m_L/V_M). An increase in either of these two factors will cause a proportional increase in a solute's retention factor, as well as in its retention time and retention volume.

Many biological ligands have moderate to large equilibrium constants for their target solutes under physiological conditions. This gives these ligands strong retention and long elution times when they are used in affinity columns under normal sample application conditions. For instance, a typical polyclonal antibody with an association equilibrium constant of 10^8 to 10^{10} M^{-1} for a target compound will give a retention factor of 100–10,000 when this antibody is present at a concentration of 10^{-6} M in an affinity column. This level of retention is much higher than the optimum range of $k=1$ –20 that should ideally be present for work under isocratic conditions. This is the reason why step changes in the mobile phase or gradients are usually required for elution

with such columns. However, with a weaker ligand it is possible to use isocratic elution. As an example, a ligand with an association constant of 10^6 M^{-1} for an analyte will give a retention factor of $k=1$ when this ligand is present at an effective concentration of 10^{-6} M within an affinity column, or $k=10$ when the ligand is present at a concentration of 10^{-5} M .

APPLICATIONS OF WEAK AFFINITY CHROMATOGRAPHY

All binding agents used in affinity chromatography can be placed into one of two categories. These are 1) high-specificity ligands and 2) general, or group-specific, ligands. High-specificity ligands bind to only one or a few closely related molecules. These tend to be biological compounds (e.g., antibodies) with large association equilibrium constants and high retention for their solutes. Consequently, they are usually not used in weak affinity chromatography, since they require step or gradient elution to dissociate their adsorbed solutes.

General ligands are agents that bind to a family or class of related molecules. These ligands can be of either biological or nonbiological origin. Examples include lectins, cyclodextrins, serum proteins, boronates, and triazine dyes. These ligands tend to have lower association constants than high-specificity ligands, making them more useful for work in weak affinity chromatography. However, there are exceptions to this. Two examples are protein A and protein G, which are general ligands commonly used in antibody isolation and which have association equilibrium constants of 10^7 to 10^8 M^{-1} for some types of antibodies. It is further possible to select or design some types of high-specificity ligands (e.g., monoclonal antibodies) to have sufficiently weak binding for work with isocratic elution. For instance, monoclonal antibodies with association equilibrium constants of 10^2 to 10^4 M^{-1} for carbohydrates have been used in several studies examining the theory and behavior of weak affinity chromatography (Fig. 1).

Two other types of biological ligands that can be used in weak affinity chromatography are enzymes and lectins. As an example, the enzyme α -chymotrypsin has weak interactions with many of its inhibitors, which has allowed the separation of these inhibitors under isocratic conditions on an immobilized α -chymotrypsin column. Lectins are nonimmune system proteins that bind carbohydrates with low to moderate association constants, allowing these agents to be used as affinity ligands under isocratic conditions. For instance, wheat germ agglutinin has been used in an affinity column under such conditions



for separating the *N*-acetyl derivatives of mono-, di-, tri-, and tetrasaccharides.

Additional biological ligands that have been used in weak affinity separations include human serum albumin, bovine serum albumin, α_1 -acid glycoprotein, and β -cyclodextrin. These ligands have been particularly useful as chiral stationary phases for the separation of drugs and other agents, with each of these ligands being able to bind to a fairly broad range of solutes. It is common with these immobilized ligands to use a mobile phase that contains a small amount of an organic modifier or displacing agent to reduce analyte retention times and improve peak shapes. However, these can also be used under physiological conditions as tools for studying the interactions of drugs with such ligands in the body.

Several nonbiological ligands can be utilized in weak affinity chromatography, such as those employed in dye-ligand affinity chromatography. In this method, a synthetic triazine or triphenylmethane dye acts as the immobilized ligand. Biomimetic affinity chromatography is a closely related method that can also be used in weak affinity chromatography. This uses ligands that have been designed or selected to mimic the binding of a substance to a natural ligand. Synthetic dyes produced by combinatorial techniques might be utilized for this purpose, as well as binding agents that have been created through phage display or ribosome libraries.

Boronic acid and its derivatives are another class of nonbiological ligands that have weak binding and are often used under isocratic conditions. These are employed in the method of boronate affinity chromatography, which makes use of the ability of such ligands to form covalent

bonds with compounds that contain *cis*-diol groups. Such a property has made boronate ligands useful for the purification and analysis of many compounds that contain sugar residues, such as polysaccharides, glycoproteins, ribonucleic acids, and catecholamines.

REFERENCES

1. Ohlson, S.; Zopf, D. *Handbook of Affinity Chromatography*; Kline, T., Ed.; Marcel Dekker: New York, 1993. Chap. 11.

FURTHER READINGS

- Benes, M.J.; Stambergova, A.; Scouten, H. *Molecular Interactions in Bioseparations*; Ngo, T.T., Ed.; Plenum Press: New York, 1993; 313.
- Hage, D.S. *Clin. Chem.* **1999**, *45*, 593.
- Hage, D.S. *J. Chromatogr., A* **2001**, *906*, 459.
- Labrou, N.E.; Clonis, Y.D. *Theory and Practice of Biochromatography*; Vijayalakshmi, M.A., Ed.; Taylor & Francis: London, 2002; 335.
- Ohlson, S.; Bergstrom, M.; Leickt, L.; Zopf, D. *Bioseparation* **1998**, *7*, 101.
- Ohlson, S.; Lundblad, A.; Zopf, D. *Anal. Biochem.* **1988**, *169*, 204.
- Strandh, M.; Andersson, H.S.; Ohlson, S. *Methods in Molecular Biology*; Bailon, P., Ehrlich, G.K., Fung, W.-J., Berthold, W., Eds.; Humana Press: Totowa, NJ, 2000; Chap. 2.
- Wikstroem, M.; Ohlson, S. *J. Chromatogr.* **1992**, *597*, 83.
- Zopf, D.; Ohlson, S. *Nature* **1990**, *346*, 87.



Wheat Protein by Field-Flow Fractionation

S.G. Stevenson

K.R. Preston

Canadian Grain Commission, Winnipeg, Canada

Introduction

The storage proteins of wheat, collectively referred to as gluten, cover a wide molecular-size range and include some of the largest known naturally occurring biological proteins [1]. The monomeric storage proteins (gliadins), as well as the salt-soluble albumins and globulins, normally have molecular weights of less than 100,000. The polymeric storage proteins (glutenin) have molecular weights that extend into the millions. The size distribution of the gluten proteins and, in particular, the polymeric wheat proteins are closely related to the dough processing characteristics and quality of wheat-based products [2]. Size-fractionation techniques such as size-exclusion-high-performance liquid chromatography (SE-HPLC), gel filtration, and sodium dodecyl sulfate-polyacrylamide gel electrophoresis (SDS-PAGE) are commonly used to characterize these proteins. These methods normally provide fractionation ranges up to molecular weights of $(0.5-1) \times 10^6$ or slightly higher. However, the larger polymeric glutenin proteins appear in the void volume with SE-HPLC and gel filtration and are not resolved [3]. Flow field-flow fractionation (FFF) provides a new tool with which to examine the polymeric wheat proteins, especially those constituting the high-molecular-weight glutenin fraction, because its resolution is not impeded by an exclusion limit [3].

Discussion

Flow FFF is one of a family of techniques which allows the fractionation of macromolecules based on size-related parameters. A detailed explanation of the mechanism and theory appears elsewhere in this encyclopedia. Fractionation is achieved by the application of a field (cross-flow) perpendicular to the channel flow [4]. Components showing greater response to the force exerted by the field are displaced further from the center of channel flow and toward the channel wall. Because the laminar flow through the channel produces a parabolic flow profile, the elution order of components is determined by their relative displacement. The size-

fractionation range, resolution, and run time can be adjusted by manipulating both the channel flow and the strength of the field. In symmetrical flow FFF, the eluent cross-flow is introduced through a porous frit on one side of the channel (depletion) wall and exits through a semipermeable membrane and frit which form the other (accumulation) wall. In conventional-mode flow FFF, the separation of macromolecules up to approximately $1 \mu\text{m}$ is based on their diffusion coefficient. Diffusion coefficients and the related Stokes diameters of separated species can be directly calculated based on elution time and channel characteristics [4].

The first two reports of the use of flow FFF for separating wheat proteins appeared in the literature in 1996. Researchers from two independent laboratories reported the characterization of wheat proteins from different varieties, extracted by different methods, and analyzed on two different types of flow FFF apparatus. Wahlund and co-workers [5] used asymmetrical flow FFF to examine proteins extracted from two bread wheat varieties of different protein content using sequential extraction with increasing concentrations of dilute hydrochloric acid (HCl). FFF fractograms showed an increase in the molecular size of the protein extracts concomitant with an increase in HCl concentration. Fractions extracted with lower concentrations of HCl showed peaks indicative of the presence of components corresponding in size to gliadins (about 8 nm) [5]. Fractions extracted with high concentrations of HCl showed the presence of very large components with hydrodynamic diameters in the range 15–35 nm. The calculation of molecular weights in these fractions based on hydrodynamic diameter transformations (lower limit defined by flexible random coil and upper limit by spherical protein) resulted in values consistent with those reported in the literature for glutenins (440,000 to 11 million).

Stevenson and Preston [3] used symmetrical stop-flow flow FFF to examine proteins extracted from Katepwa, a high-quality bread wheat variety, using a modification of the traditional Osborne extraction procedure. Fractions isolated by this sequential extraction procedure included wheat proteins ex-

Encyclopedia of Chromatography

DOI: 10.1081/E-Echr 120005355

Copyright © 2002 by Marcel Dekker, Inc. All rights reserved.



tractable in 0.5M sodium chloride (albumins and globulins), 70% ethanol (gliadins), and 0.05M acetic acid (HAc extractable glutenins). Proteins remaining in the residue were disbursed in either 0.5M HAc or 0.001M HCl with 30-s sonication (sonicated acid extractable proteins). The albumin and globulin and the gliadin fractions showed major peaks of less than 10 nm, indicative of monomeric proteins. Analysis of the HAc extractable glutenin fraction showed a large peak at about 10 nm, representing smaller polymeric proteins and a smaller peak at 17 nm representing larger polymeric proteins. The bulk of the very large polymeric glutenin proteins were detected in the fractions extracted with sonication (broad distribution range from 11 to 36 nm with a peak at 18 nm). In both studies, the reduction of the polymeric glutenin fractions with dithiothreitol [3] or 2-mercaptoethanol [5] produced shifts in peak positions to less than 10 nm, indicating the release of their interchain disulfide-bonded constituent subunits.

A more widespread use of conventional FFF for the study of proteins has been impeded by the difficulty in obtaining reproducible fractograms which can be accurately integrated for quantification and by the lack of automation. During operation, pressure fluctuation due to the open nature of the system can result in baseline instability. This is further exacerbated by the requirement for stop-flow relaxation, where channel flow is briefly stopped/interrupted (directed via a two-way valve around the channel) when the protein enters the channel to allow equilibrium against the cross-flow. To reduce the impact of pressure fluctuations, pressure balance is maintained by manual adjustment of back-pressure valves on the channel and cross-flow outlets. The requirement for very small sample size (normally $<2\ \mu\text{g}$) to prevent overloading and the dilution effect incurred with the relatively large channel flow necessitates the use of very sensitive detector settings resulting in low signal-to-noise ratios which negatively influence baseline resolution and reproducibility.

A number of innovations in FFF design have been introduced recently which have improved resolution and sensitivity and reduced the major obstacles to automation. The introduction of cross-flow recirculation has resulted in better control of system pressures, thereby reducing baseline fluctuation and improving reproducibility [6]. The incorporation of a frit inlet (FI) into the flow FFF channel has permitted the use of hydrodynamic relaxation as a replacement for stop-flow relaxation, thus eliminating pressure fluctuations associated with the latter [7]. FI also reduces sample adhesion to the membrane on the accumulation wall, thereby reducing the likelihood of baseline drift and artifacts [7].

For the FI technique, a small piece of permeable frit material equipped with a separate frit inlet is embedded in the depletion wall of the channel just past the sample inlet. As the sample enters the channel, buffer entering through the frit inlet displaces the sample toward the accumulation wall, allowing hydrodynamic relaxation to occur [7]. Optimum results with this technique are obtained when the flow through the frit inlet is set at about 7–10 times the flow rate through the sample inlet. The incorporation of a frit outlet (FO) located at the depletion wall of the channel just before the channel outlet has facilitated the removal/recirculation of a high proportion of eluent buffer. The remaining eluent buffer containing the sample components is eluted in the channel outlet flow at much higher (up to 10 times) [6,7] effective concentrations, resulting in much higher detector signal-to-noise ratios, thereby eliminating the need for extremely sensitive detection methods.

Development and application of an automated frit inlet/frit outlet (FI/FO) flow FFF channel with recirculating frit and cross-flows to wheat protein fractionation, characterization, and quantification was described for the first time by Stevenson and co-workers [8] in 1999. Analysis of wheat protein fractions produced by the same fractionation method and from the same flour as used for previous stop-flow studies [3] showed improved separation with more well-resolved peaks, particularly with the two polymeric glutenin protein fractions (HAc extractable and sonicated HAc extractable). As can be seen in Figs. 1a and 1b, the major peaks for albumins and globulins and for gliadins indicate molecular sizes less than 10 nm. The HAc extractable proteins (Fig. 1c) show major peaks at 8 and 11 nm plus significant tailing in the 20–35-nm area, indicating the presence of larger polymeric glutenin. From these fractograms, it is evident that the bulk of the large polymeric material is extracted with sonication (Fig. 1d) and that the molecular size distribution in the sonicated fraction covers a very broad range (12–50+ nm). Using the automated FI/FO system, the average coefficient of variability for peak area and/or size ranges was less than 2% for six standard molecular-size marker proteins and less than 5% for wheat protein, thus permitting accurate quantification of results.

Field-flow fractionation has shown to be useful for systematically monitoring physicochemical changes in wheat proteins caused by addition of substances such as oxidants or reductants [8]. Recent studies in our laboratory [9] using automated FI/FO FFF have shown strong relationships between the size distribution of very large polymeric glutenin proteins determined by flow FFF and quality characteristics related to dough strength properties and have permitted the size frac-



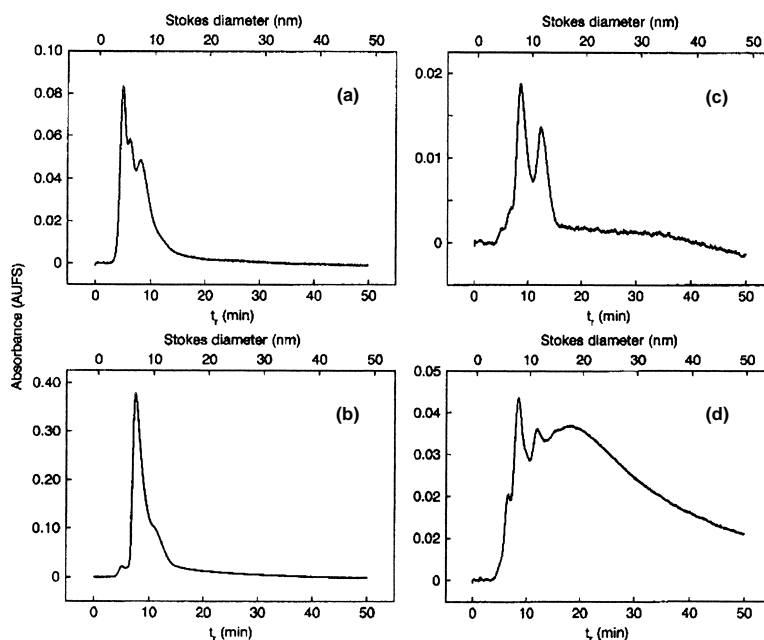


Fig. 1 Elution profiles for (a) albumin and globulin, (b) gliadin, (c) glutenin, and (d) sonicated acetic acid extractable fractions run on a FI/FO automated FFF channel. Normal operating conditions are $V_s = 0.2$, $V_f = 1.4$, and $V_c = 5$ mL/min.

tionation of subfractions collected from the void volume peak in SE-HPLC.

References

1. C. W. Wrigley, *Nature* 381: 738 (1996).
2. F. MacRitchie, *Adv. Food Nutr. Res.* 36: 1 (1992).
3. S. G. Stevenson and K. R. Preston, *J. Cereal Sci.* 23: 121 (1996).
4. J. C. Giddings, *Science* 260: 1456 (1993).
5. K.-G. Wahlund, M. Gustavsson, F. MacRitchie, T. Nylander, and L. Wannerberger, *J. Cereal Sci.* 23: 113 (1996).
6. P. Li, M. Hansen, and J. C. Giddings, *J. Microcol. Separ.* 10: 7 (1998).
7. J. C. Giddings, *Anal. Chem.* 62: 2306 (1990).
8. S. G. Stevenson, T. Ueno, and K. R. Preston, *Anal. Chem.* 71: 8 (1999).
9. T. Ueno, S.G. Stevenson, K.R. Preston, M.J. Nightingale, and B.M. Marchylo, *Cereal Chem.* 79: 155 (2002).



Whey Proteins, Anion-Exchange Separation

Kyung Ho Row

Du Young Choi

Inha University, Incheon, South Korea

INTRODUCTION

Three strong anion exchange membranes (CIM QA, Q100, and HiTrap Q) and reversed-phase high-performance liquid chromatography (RP-HPLC; 15- μ m particle with a pore size of 300 μ m) were investigated for the separation of major proteins, which are contained in whey, such as α -lactalbumin, bovine serum albumin (BSA), and β -lactoglobulin. Experiments were performed to determine the optimum mobile phase composition for separating the whey proteins using standard reagents for the proteins. For strong anion exchange membranes, the mobile phases were buffer A (20 mM piperazine-HCl, pH 6.4) and buffer B (buffer A + 1 M NaCl), with a linear gradient elution change of salt concentration applied. For RP-HPLC, the mobile phase consisted of a linear gradient of the two mixtures of 0.1% trifluoroacetic acid (TFA) in water and 0.1% TFA in acetonitrile (ACN). Standard protein reagents were used to investigate optimal mobile phase compositions with the three anion exchange membranes. From the experimental results, it was found that HiTrap Q was the most effective in separating whey proteins.

SEPARATION OF WHEY PROTEINS

Milk proteins are the most important source of bioactive peptides. The primary components of bovine milk are water, fat, lactose, and minerals; up to 6% of the mass consists of proteins and peptides, among them a number of high-value substances.^[1] Particularly, milk contains two major protein groups (i.e., caseins and whey proteins), which differ greatly with respect to their physicochemical and biological properties. Normal milk contains 30–35 g/L proteins, approximately 80% of which are caseins, with the remainder being whey proteins.^[2] Whey proteins can be acquired as a by-product in cheese manufacturing. The required long-term stability in functional performance of these proteins is often lacking. Although the two major proteins are scientifically significant materials, the study of the functional properties of whey proteins has attracted scientific interest for more than 20 years.^[3] In general, whey is a dilute liquid composed of lactose, and a variety

of proteins, minerals, vitamins, and fat. Whey contains about 6% solids, of which 70% or more is lactose and about 0.7% is proteins.^[4] Whey protein components are α -lactalbumin, β -lactoglobulin, immunoglobulin A (IgA), immunoglobulin M (IgM), immunoglobulin G (IgG), BSA, lactoferrin, and lactoperoxidase. β -Lactoglobulin is the major whey protein in bovine milk. β -Lactoglobulin has a molecular mass of 18.4 kDa, possesses 162 amino acid residues, and has a concentration of 2–4 g/L. α -Lactalbumin is an albumin that has 123 amino acid residues. It possesses a molecular mass of 14.2 kDa and its concentration in milk is 0.6–1.7 g/L.^[5] Bovine whey proteins have potential applications in veterinary medicine, food industries, and as supplements for cell culture media. IgG, IgA, lactoferrin, and lactoperoxidase, present in bovine whey, have high pharmaceutical value.^[6] α -Lactalbumin can be used in infant formula and as a nutraceutical because of its high tryptophan content. β -Lactoglobulin is used in the production of confections.^[7] Oral administration of bovine IgG is known to be an effective treatment of various infections of newborn infants.^[8] Lactoferrin and lactoperoxidase are known to act as antimicrobial factors.^[9] Therefore the whey proteins are used to replace other proteins, or to improve the functional properties of baby food, luncheon meat, soft drinks and milk-based drinks, ice cream, bakery, and convenience products.^[10]

Traditionally, separation and purification are frequently achieved by RP-HPLC, although other HPLC methods such as ion exchange chromatography (IEC), hydrophobic interaction chromatography (HIC), size exclusion chromatography (SEC), and various types of affinity chromatography (AC) have also been used.^[11] With the development of DNA recombinant techniques, HPLC has become an important tool in both quality control and process control in the production of recombinant proteins of pharmacological interest. This has contributed significantly to the development of RP-HPLC methods that can be used to carry out very rapid analyses for proteins with minimum complexity in both instrumentation and operating conditions.^[12] Given the low diffusivity of biopolymers, the need to achieve fast separation of proteins by RP-HPLC has led to the development of different types of packing materials, such as nonporous microparticles ($dp < 5 \mu$ m) or wide-pore materials^[13,14] that solve mass transfer problems in the stationary phase, allowing good

separations within a reasonable time. The particles used in RP-HPLC have a porous structure of 300 μm .

Separation of whey proteins using ion exchange membranes has been investigated by many researchers and several methods have been reported.^[15,16] Ion exchange separations take advantage of electrostatic interaction between surface charges of biomolecules, such as amino acids or proteins, and clusters of charged groups on a membrane. Adsorbing biomolecules displace counterions associated with the surface, discharging a complementary buffer salt in the process. Adequate buffering is required to shield native protein structures from changes in pH adjacent to exchange surfaces (Donnan effect) and pH effects induced by sorption. Selection of an appropriate buffer is critical to the success of ion exchange membranes.^[17] Large molecules ($>1,000,000 M_w$) such as plasmid DNA are able to access charged groups, which envelope large pores of membrane adsorbers, although they would commonly be excluded from cellulose-based ion exchangers. Mobile phases and buffers employed in ion exchange bioseparations are non-denaturing to hydrophilic proteins. Elution and recovery of biologicals using ion exchange on performance are considered, as well as effects of additives and flow rate. The mobile phase composition is adjusted in the linear gradient along with NaCl concentration.

This work focused on the comparison of the separation characteristics of whey proteins using three strong anion exchange membranes (CIM QA, Q100, and HiTrap Q). In an analytical column ($3.9 \times 300 \text{ mm}$), the experiments were performed at a particle size of 15 μm with large pore sizes of 300 μm . The mobile phase was a binary system of water with 0.1% of TFA and ACN with 0.1% of TFA.

EXPERIMENTAL

Chemicals

The whey powder (from bovine milk) used in this experiment was purchased from Sigma Chemical Co. (St. Louis, MO, USA). The chemical composition of whey protein is shown in Table 1. Samples were prepared by diluting the appropriate amount of whey powder with water. The concentration of the samples remained at approximately 200,000 ppm. The standard chemicals of α -lactalbumin (Type III: deplete, from bovine milk, approximately 85%), β -lactoglobulin (from bovine milk, approximately 90%), and BSA were purchased from Sigma Chemical Co. Standard protein solutions were prepared in water. Standard solutions were made for each protein of 10 mg dissolved in 1 L with water. The water was filtered with HA 0.5- μm membranes (Division

Table 1 Molecular masses and isoelectric points for whey proteins

Protein	Molecular weights	Isoelectric points (pI)
α -Lactalbumin	14,000	4.2–4.5
β -Lactoglobulin	18,300	5.35–5.49
BSA	69,000	5.13

of Millipore, Waters Co., Milford, MA, USA) and deionized prior to use. The extra pure grade solvent of ACN was purchased from Duksan Pure Chemicals Company (Incheon, Korea). TFA was purchased from Sigma Chemical Co. The sample for injection was filtered with 0.45- μm polyvinylidene fluoride (PVDF) (Waters Co.). Sodium chloride and hydrochloric acid were purchased from Duksan Pure Chemicals Company. Piperazine was purchased from Sigma Chemical Co. For the anion exchange membrane, buffer A was 20 mM piperazine-HCl, pH 6.4, and buffer B was made by addition of 1 M NaCl to buffer A. The mobile phases for RP-HPLC were as follows: buffer A, 0.1% TFA in water; and buffer B, 0.1% TFA in ACN.

Equipment

The analytical column was a stainless steel μ -BondapakTM C₁₈. The size of the analytical column was $3.9 \times 300 \text{ mm}$, and it was packed in-house with RP-C₁₈ (15 μm Merck Co.) by high-pressure pumping with solvent. The strong anion exchange membranes used in this experiment were CIM QA (BIA Separation Co.), Q100 (Sartorius), and HiTrap Q (Pharmacia). The Monolithic Convective Interaction Media (CIM) QA disk has a diameter of 16 mm and a thickness of 3 μm . The base material of CIM QA is a macroporous glycidyl methacrylate-co-ethylene dimethacrylate (GMA-EDMA) polymer matrix and the CIM QA disk bears a quaternary amine. The membrane material of Q100 is cellulose. The adsorption area of Q100 is 100 cm^2 and the binding capacity of protein is 100 $\mu\text{g}/\text{Q100 unit}$. The ion exchange media packed in HiTrap ion exchange columns are based on Sepharose high-performance material. The column volume of HiTrap Q is 1 mL. In RP-HPLC, the sample solution was passed through an Amicon 8400 (USA; maximum pressure, 75 psi) as an ultrafiltration kit and the UF membrane of cellulose discs [30,000 molecular weight cutoff (MWCO)] was utilized to extract lactose.

The analytical HPLC system was a Waters Model 600S liquid chromatography system (Waters Associates, Milford, MA, USA) equipped with a Waters 515 Multisolvant Delivery System with a 486 Tunable Absorbance



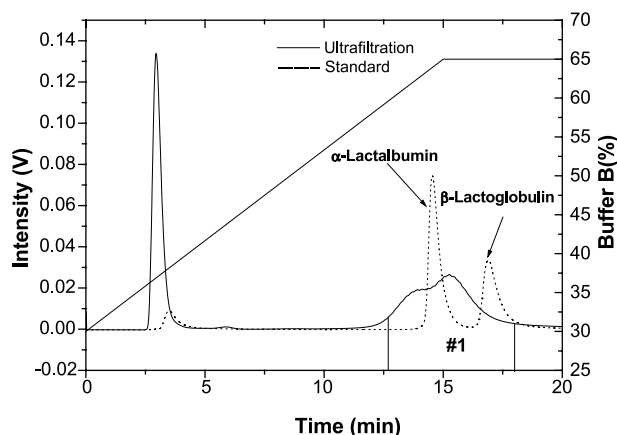


Fig. 1 Comparison of the two standard chemicals of α -lactalbumin and β -lactoglobulin and whey proteins after ultrafiltration (MWCO 30,000) by RP-HPLC (buffer A/buffer B = 70/30–35/65 vol.%, gradient time of 15 min).

Analytical Detector, and a Rheodyne injector (50- μ L sample loop). The data acquisition system was a Chromate (Ver. 3.0; Interface Engineering, South Korea) installed in a PC. The flow rate of mobile phase was fixed at 4, 2, and 1 mL/min with CIM QA, Q100, and HiTrap Q, respectively. The wavelength was fixed at 260 and 280 nm and the injection volume was fixed at 20 μ L. The experiment was performed at room temperature.

RESULTS AND DISCUSSION

Linear change or step change in mobile phase composition may produce differential migration of concentrated solutes. The average velocity of each desorbed solute is proportional to its fractional equilibrium mobile phase concentration. Therefore gradient elution has been normally used to remove adsorbed components from membranes. Gradient elution is convenient because it is difficult to determine, a priori, the modifier concentration required to selectively elute just the desired species.

The whey proteins α -lactalbumin and β -lactoglobulin from bovine milk were separated by RP-HPLC at room temperature using a silica-based, wide-pore C_{18} (300 μ m) column and a linear binary gradient of ACN/water/0.1% TFA. However, it was observed that because of the small structural differences between α -lactalbumin and β -lactoglobulin, the desirable resolution of these proteins at the baseline was difficult to achieve. Several gradients of water–ACN, containing TFA (0.1%), were used. Figure 1 shows the comparison of separation of the two standards of α -lactalbumin and β -lactoglobulin (dotted line) and the real whey proteins (solid line) after ultrafiltration (MWCO 30,000). The gradient condition consisted of a two-step

linear binary gradient: buffer A/buffer B = 70/30–35/65 (vol.%), gradient time of 15 min.

For the anion exchanger experiment, a gradient mode with change in NaCl concentration was used to separate whey proteins of α -lactalbumin, β -lactoglobulin, and BSA. The protein standards were used and the strong anion exchange membranes used in this experiment were CIM QA (BIA Separation Co.), Q100 (Sartorius), and HiTrap Q (Pharmacia). The mobile phases were buffer A (20 mM piperazine–HCl, pH 6.4) and buffer B (buffer A + 1 M NaCl). In this experiment, the sample of whey was injected only with filtered 0.45- μ m PVDF, without further pretreatment by ultrafiltration. Generally, the retention times of proteins were shorter with increasing amounts of NaCl in buffer B. The elution order of the proteins was α -lactalbumin, BSA, β -lactoglobulin B, and β -lactoglobulin A. β -Lactoglobulin was composed of β -lactoglobulin A and β -lactoglobulin B. In Fig. 2, CIM QA was used to separate whey proteins. In this case, the ratio of the volume of buffer A to the volume of buffer B in the mobile phase (buffer A/buffer B) was changed as follows: 100/0–95/5 (0–10 min), 95/5–80/20 (10–30 min), and 80/20–10/90 (30–31 min), and the flow rate of mobile phase was 4 mL/min. Although only α -lactalbumin was resolved from the other proteins, the resolution was not very good. The coeluted peak of BSA and β -lactoglobulin followed.

Figure 3 shows the separation of whey proteins by Q100. The buffer A/buffer B ratio was changed as follows: 100/0–85/15 (0–30 min), 85/15 (30–40 min), 85/15–75/25 (40–60 min), and 75/25–10/90 (60–61 min), and the flow rate was 2 mL/min. The resolution of α -lactalbumin was better than that using CIM QA;

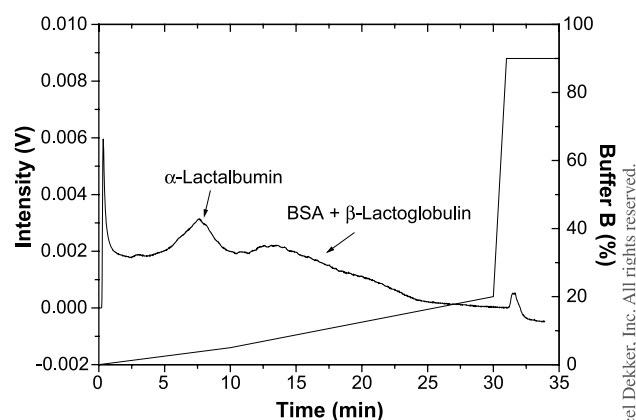


Fig. 2 Separation of standard chemicals of whey proteins using CIM QA [buffer A/buffer B: 100/0–95/5 (0–10 min), 95/5–80/20 (10–30 min), and 80/20–10/90 (30–31 min), CIM QA (BIA Separation Co.), 4 mL/min, 20 μ m, 260 nm].

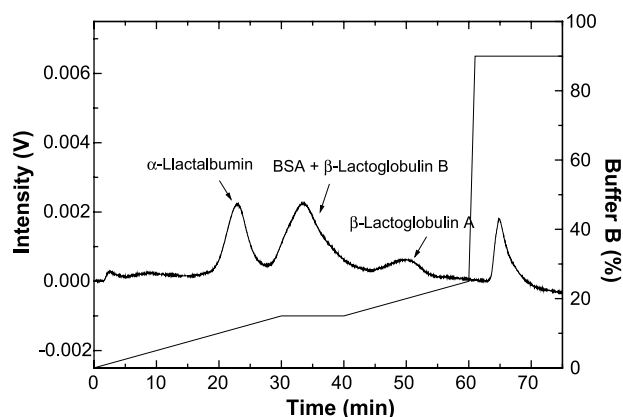


Fig. 3 Separation of standard chemicals of whey proteins using Q 100 [buffer A/buffer B: 100/0–85/15 (0–30 min), 85/15 (30–40 min), 85/15–75/25 (40–60 min), and 75/25–10/90 (60–61 min), Q100 (Sartorius), 2 mL/min].

β -lactoglobulin A was also resolved, but BSA and β -lactoglobulin B coeluted.

The separation of whey proteins by HiTrap Q is shown in Fig. 4. The buffer A/buffer B ratio was changed as follows: 95/5–90/10 (0–5 min), 90/10 (5–10 min), 90/10–87/13 (10–20 min), 87/13–70/30 (20–40 min), and 70/30–10/90 (40–45 min), and the flow rate was 1 mL/min. The resolutions for whey proteins were quite excellent.

Real whey proteins were separated by the change of mobile phase composition obtained from Fig. 5. The injection volume was increased to 50 μ L and the change of mobile phase composition was slightly modified to accommodate the larger injection volume and to improve the resolution of whey proteins. This result is shown Fig. 5.

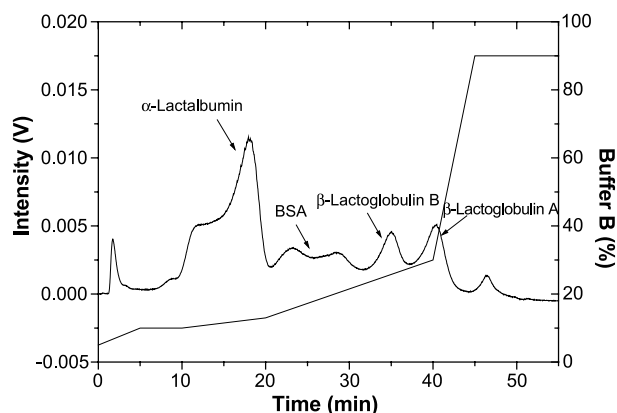


Fig. 4 Separation of standard chemicals of whey proteins using HiTrap Q [buffer A/buffer B: 95/5–90/10 (0–5 min), 90/10 (5–10 min), 90/10–87/13 (10–20 min), 87/13–70/30 (20–40 min), and 70/30–10/90 (40–45 min), HiTrap Q (Pharmacia), 1 mL/min].

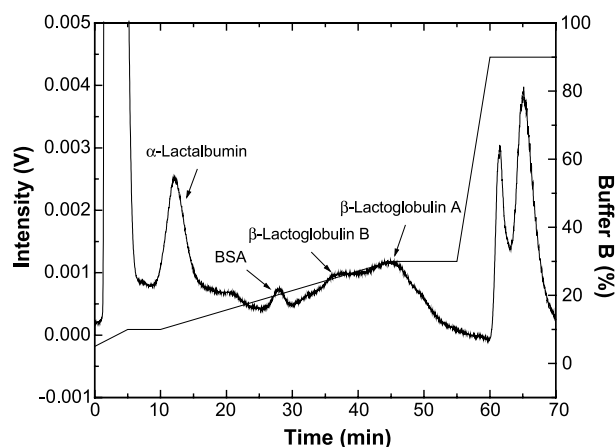


Fig. 5 Separation of the proteins contained in whey using HiTrap Q [buffer A/buffer B: 95/5–90/10 (0–5 min), 90/10 (5–10 min), 90/10–87/13 (10–20 min), 87/13–70/30 (20–40 min), and 70/30–10/90 (40–45 min), HiTrap Q (Pharmacia), 50 μ L, 1 mL/min].

Although β -lactoglobulin A and β -lactoglobulin B were not satisfactorily separated, the other whey proteins were well resolved. The buffer A/buffer B ratio was changed as follows: 95/5–90/10 (0–5 min), 90/10 (5–10 min), 90/10–70/30 (10–45 min), 70/30 (45–55 min), and 70/30–10/90 (55–60 min).

In this work, three strong anion exchange membranes and RP-HPLC were used to separate whey proteins. From the result, it was found that anion exchanger and RP-HPLC were of similar separation efficiencies; in addition, HiTrap Q (Pharmacia) was the most effective anion exchange membrane for separation of whey proteins.

CONCLUSION

The separation characteristics of whey proteins of α -lactalbumin, BSA, and β -lactoglobulin were investigated with strong anion exchange membranes and RP-HPLC in a gradient mode. In RP-HPLC, the optimum experimental conditions of the mobile phase compositions and gradient conditions were experimentally determined to separate α -lactalbumin and β -lactoglobulins A and B contained in whey. The concentration of NaCl and the numbers of linear gradient steps were adjusted to find the optimum mobile phase with the commercially available anion exchange membranes. It was experimentally confirmed that HiTrap Q was the most effective in resolving the whey proteins. The described RP-HPLC method may be applicable to the wide application in the routine analysis of whey, fractionated whey streams, and whey protein powders produced by dairy industries.



ACKNOWLEDGMENTS

The authors gratefully acknowledge the financial support of the Center for Advanced Bioseparation Technology. This work was performed in the High-Purity Separation Laboratory of Inha University (Incheon, Korea).

REFERENCES

1. Amigo, L.; Recio, I.; Ramos, M. Genetic polymorphism of bovine milk proteins: Its influence on technological properties of milk—A review. *Int. Dairy J.* **2000**, *10* (3), 135–149.
2. Korhonen, H.; Pihlanto-Leppäla, A.; Rantamäki, P.; Tupasela, T. Impact of processing on bioactive proteins and peptides. *Trends Food Sci. Technol.* **1998**, *9* (8–9), 307–319.
3. Lieske, B.; Konrad, G. Physico-chemical and functional properties of whey protein as affected by limited papain proteolysis and selective ultrafiltration. *Int. Dairy J.* **1996**, *6* (1), 13–31.
4. Gerberding, S.J.; Byers, C.H. Preparative ion-exchange chromatography of proteins from dairy whey. *J. Chromatogr., A* **1998**, *808* (1–2), 141–151.
5. Choi, D.Y.; Row, K.H. Separation of proteins in whey by strong anion-exchange membrane of Q Sepharose. *Hwahak Konghak* **2002**, *40* (4), 461–466.
6. Hahn, R.; Schulz, P.M.; Schaupp, C.; Jungbauer, A. Bovine whey fractionation based on cation-exchange chromatography. *J. Chromatogr., A* **1998**, *795* (2), 277–287.
7. Zydney, A.L. Protein separations using membrane filtration: New opportunities for whey fractionation. *Int. Dairy J.* **1998**, *8* (3), 243–250.
8. Hutchens, T.W.; Magnuson, J.S.; Yip, T.T. Secretory IgA, IgG, and IgM immunoglobulins isolated simultaneously from colostral whey by selective thiophilic adsorption. *J. Immunol. Methods* **1990**, *128* (1), 89–99.
9. Strange, E.D.; Malin, E.L.; Van Hekken, D.L.; Basch, J.J. Chromatographic and electrophoretic methods used for analysis of milk proteins. *J. Chromatogr., A* **1992**, *624* (1–2), 81–102.
10. Kim, J.I.; Choi, D.Y.; Row, K.H. Separation of whey proteins by anion-exchange membranes. *Korean J. Chem. Eng.* **2003**, *20* (3), 538–541.
11. Torre, M.; Cohen, M.E.; Corzo, N.; Rodriguez, M.A.; Diez-Masa, J.C. Perfusion liquid chromatography of whey proteins. *J. Chromatogr., A* **1996**, *729* (1–2), 99–111.
12. Nadler, T.K.; Paliwal, S.K.; Regnier, F.E. Rapid, automated, two-dimensional high-performance liquid chromatographic analysis of immunoglobulin G and its multimers. *J. Chromatogr., A* **1994**, *676* (2), 331–335.
13. Kalghatgi, K.; Horvath, C. Rapid peptide mapping by high-performance liquid chromatography. *J. Chromatogr., A* **1988**, *443* (29), 343–354.
14. Lloyd, L.L.; Warner, F.P. Preparative high-performance liquid chromatography on a unique high-speed macroporous resin. *J. Chromatogr., A* **1990**, *512* (20), 365–376.
15. Gerberding, S.J.; Byers, C.H. Preparative ion-exchange chromatography of proteins from dairy whey. *J. Chromatogr., A* **1998**, *808* (1–2), 141–151.
16. Hong, S.B.; Row, K.H. Separation characteristics of whey protein by high performance membrane chromatography. *Korean J. Chem. Eng.* **2001**, *16* (6), 314–337.
17. Keith, D.R.; Edwin, N.L. Separation of biomolecules using adsorptive membranes. *J. Chromatogr., A* **1995**, *702* (1–2), 3–26.



Zeta-Potential

Jetse C. Reijenga

Eindhoven University of Technology, Eindhoven, The Netherlands

Introduction

When an insulator is in contact with an aqueous solution of buffer components, the solid surface has a nonzero electric potential that decreases exponentially as a function of distance from that surface, to become zero at infinity.

Discussion

Taking silica (bulk composition silicon oxide, SiO_2), from which capillary material in capillary electrophoresis (CE) is manufactured, as an example, one can readily understand this when taking into account that on the silica surface, there are silicon hydroxide groups that are subject to an acid–base equilibrium according to



indicating that the negative surface charge of the silica wall is pH dependent and becomes more negative as the buffer pH increases. At pH 2 or lower, the zeta-potential is virtually zero, as the above equilibrium is largely forced to the left due to an abundance of hydrogen ions. As the magnitude of the zeta-potential directly determines the electro-osmotic mobility, it is of importance to understand the effect of different buffer constituents on the zeta-potential and, hence, on the electro-osmotic flow (EOF). The electro-osmotic mobility μ_{EOF} is defined as

$$\mu_{\text{EOF}} = -\frac{\zeta\epsilon}{\eta}$$

in which ζ is the zeta-potential, ϵ is the dielectric constant of the liquid, and η is the viscosity of the liquid at the plane of shear. The electro-osmotic velocity v_{EOF} is now

$$v_{\text{EOF}} = \mu_{\text{EOF}}E = -\frac{\zeta\epsilon E}{\eta}$$

in which E is the electric field strength. Taking a more detailed look at the zeta-potential, one must realize that this potential is not really the value on the negatively charged silica surface, but rather the value on the plane of shear (i.e., at the interface between the stagnant layer

of solvent molecules directly at the silica surface and the volume element that is subject to flow, caused by, for example, a longitudinal pressure drop). The combination of these is called the electric double layer.

There are several ways to dynamically change the zeta-potential and, thus, electro-osmosis. Adding a surfactant at a low concentration [generally smaller than the critical micelle concentration (CMC)] will alter the wall charge and zeta-potential due to selective adsorption on the capillary surface: sodium dodecyl sulfate (SDS) will make the zeta-potential more negative (and EOF more pronounced) and may even mask the pH dependence mentioned earlier. Cetyltrimethyl ammonium bromide (CTAB) can neutralize the wall charge, making the zeta-potential close to zero and, thus, eliminating EOF at a concentration of $5 \times 10^{-5}M$. A higher CTAB concentration will make the zeta-potential positive and reverse the EOF. Other additives merely decrease the zeta-potential exponentially to zero or to a small negative value; they include polymers such as poly(vinyl alcohol), hydroxypropylmethylcellulose, and others. Changing the liquid viscosity near the electric double layer is a usual side effect of these additives, another cause of EOF suppression. Polymers like those mentioned and many others have also been used successfully for chemical modification of the capillary surface, so that addition to the buffer (so-called dynamic coating) is not necessary.

Effect on Migration Time

In uncoated fused-silica capillaries, surface charge and zeta-potential (and, consequently, EOF) can have a significant effect on migration time of anions, especially at higher pH values. As anions and EOF move in opposite directions, longer migration times are more sensitive to zeta-potential changes. This can be seen from the equation for migration time t_m :

$$t_m = \frac{L_d L_t}{(\mu_{\text{eff}} + \mu_{\text{EOF}})V}$$

where, because of opposite signs for μ_{eff} and μ_{EOF} , the denominator can be quite small. Consequently, migration time can be sensitive to slight EOF changes.



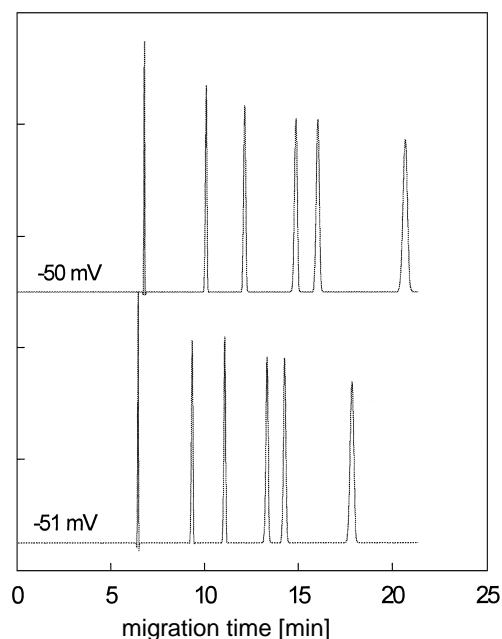


Fig. 1 Effect of capillary zeta-potential on the analysis of a mixture of anions in an uncoated fused-silica capillary in a 10 mM Tris-acetate buffer of pH 8. Normal zeta-potentials are around 50 mV at this pH.

In the example in Fig. 1, a mixture of anions is analyzed in a Tris-acetate buffer of pH 8. A 2% change in zeta-potential, from -50 to -51 mV, results in a dramatic shift in migration time of peaks with longer migration times.

Suggested Further Reading

- Beckers, J. L., *Isotachophoresis, some fundamental aspects*, Thesis, Eindhoven University of Technology, 1973.
- Boček, P., M. Deml, P. Gebauer, and V. Dolník, *Analytical Isotachophoresis*, VCH, Weinheim, 1988.
- Everaerts, F. M., J. L. Beckers, and Th. P. E. M. Verheggen, *Isotachophoresis: Theory, Instrumentation and Applications*, Elsevier, Amsterdam, 1976.
- Hjertén, S. *Chromatogr. Rev.* 9: 122 (1967).
- Jorgenson, J. W. and K. D. Lucaks, *Science* 222: 266 (1983).
- Kenndler, E., *J. Capillary Electrophoresis* 3(4): 191 (1996).
- Li, S. F. Y., *Capillary Electrophoresis — Principles, Practice and Applications*, Elsevier, Amsterdam, 1992.
- VanOrman, B. B., G. G. Liversidge, G. L. McIntire, T. M. Olefirowicz, and A. G. Ewing, *J. Microcol. Separ.* 2: 176 (1990).



Zirconia–Silica Stationary Phases for HPLC: Overview and Applications

R. Andrew Shalliker

Sindy Kayillo

University of Western Sydney, Sydney, New South Wales, Australia

INTRODUCTION

This review details the development of zirconia–silica stationary phases in liquid chromatography. Zirconia–silica stationary phases are just one member of a group of mixed oxide materials that have recently been studied in liquid chromatography. Other members of this group include alumina–silica, magnesia–silica, and titania–silica.^[1,2] Each of these mixed oxide composites contains silica, which is the most widely employed stationary phase material in modern high-performance liquid chromatography (HPLC). The dominance of silica in the chromatographic industry reflects the many desirable properties that silica affords the chromatographer. Silica can be prepared in a wide variety of pore size and particle size materials, and can be easily modified to yield stationary phases with a wide range of differing selectivities. For instance, the C₁₈ column displays vastly different retention behavior to that of native silica and is the most widely employed reversed phase chromatography column. Other types of modified silica stationary phases include, but are not limited to, the C₈ column for intermediate retention of nonpolar compounds in reversed phase LC, the C₄ column for protein work, and the phenyl, nitrile, and amino columns. Silica also has a high mechanical strength, making it suitable for the preparation of columns under high pressure; when operated under suitable conditions, these columns have a long life span. Collectively, each of these attributes has made silica the material of choice as a stationary phase or stationary phase support. In many respects, the high efficiency of today's chromatography column owes much to the properties of silica. However, as a chromatographic stationary phase, silica has some limitations. The siloxane linkage is the Achilles heel in any silica-based material, being easily hydrolyzed at low pH. Furthermore, silica has a high solubility in an alkaline environment, especially at higher temperatures, leading to a loss in column bed integrity. This, in general, limits the use of silica and modified silica to pH regions between 2 and 8. Another limitation of silica is the strong and often irreversible adsorption of basic species, occurring as a consequence of

the hydrogen bonding between the solute and the surface silanol groups. This belies one of the most desirable features of a stationary phase; that being good adsorption and good desorption characteristics. Many modified silica-based stationary phases are consequently subjected to rigorous procedures that attempt to protect the solute from the residual hydroxyl groups through processes such as end capping.

Resolution (R_s) in a chromatographic system is a function of three essentially independent variables: the capacity factor (k') (defined generally by the solvent strength), the number of theoretical plates (N), and the selectivity (α) according to the well-known equation given below:

$$R_s = \frac{1}{4} \sqrt{N} \left(\frac{k'}{1+k'} \right) (\alpha - 1)$$

Of these three variables, changes in the selectivity very often yield the most substantial gain in resolution, albeit with results that are often unpredictable. One of the driving forces in the development of new stationary phases is the change in selectivity to yield improvements in separation. A second driving force is developing materials that overcome the limitations of silica as noted above. One of the more successful stationary phase materials that have been developed is that of zirconia and zirconia-based stationary phases, which are now commercially available as a high-grade chromatographic product. As a stationary phase, zirconia has several important attributes. Zirconia is a highly rigid support able to withstand the rigors of conventional column-packing processes. Zirconia is temperature-stable and is insoluble in alkaline and acidic solvents, allowing mobile phases with pHs between 1 and 14 to be employed as eluents. This is particularly useful for protein work, allowing “dirty” columns to be cleaned with strong base such as NaOH. The surface of zirconia is, however, heterogeneous, containing Lewis acid, Bronsted acid, and Bronsted base sites, which leads to a multitude of retention mechanisms that may complicate the elution process.^[3] However, because zirconia is highly resistant to solvent attack, virtually any

mobile phase modifying agent can be employed to control any unwanted interactions. Consequently, the highly functionalized zirconia surface can be fully utilized to maximize selectivity. Zirconia can also be synthesized in a variety of particle size and pore size materials, in much the same manner as silica. Furthermore, zirconia can be modified to yield a variety of stationary phases with different selectivities. Nawrocki et al.^[3] published an excellent review on zirconia for chromatographic use, and hence a detailed discussion on zirconia is not warranted in this text.

Recent studies in stationary phase development have lead chromatographers to explore the concept of mixed oxide chromatographic supports and materials for use in liquid chromatography. These include alumina–silica, magnesia–silica, titania–silica, and zirconia–silica.^[1,2] The driving force behind the development of these mixed oxide supports comes from the possibility of attaining a surface with properties that exploit the best attributes of both components in the mixed oxide. For example, the band tailing of basic species on magnesia–silica columns is substantially reduced compared to silica columns due to the reduced concentration of acid sites on the surface of the magnesia–silica composite.^[1] In the current text, we present an overview on the development of zirconia–silica composites as stationary phase supports and then detail some applications for which this support has been employed.

PREPARATION OF ZIRCONIA–SILICA MIXED OXIDE SUPPORTS

The demand for mixed oxide chromatographic-quality stationary phase materials is small and only a few methods that detail their preparation are available in the literature. There are, however, numerous examples of the preparation of zircon powders and Ref. [4] is an example of such a process. In general, these types of powders are unsuitable for chromatographic stationary phases because their particle sizes are in the submicron range with very broad distributions. The synthesis of mixed oxide supports for chromatographic applications can essentially be divided into two types: coprecipitation methods and coating methods.

Coprecipitation Methods

Kaneko et al.^[1,2] employed a coprecipitation method, which involved a base-catalyzed procedure that precipitated irregular particles of zirconia–silica mixed oxides. Specifically, a zirconium salt (zirconyl chloride octahydrate) was added to an acidified solution of sodium metasilicate ennehydrate. The solution was made alkaline

(pH 7–9) to allow the precipitation of the mixed oxide gel. The gel was aged for 10 hr, collected by filtration and washed to remove residual chloride ions. The gel was dried at 110°C and then ground to an appropriate mesh size. The resulting precipitate was regarded as an intimate mixture of silica and metal oxide gel (in this case, zirconia). The silica framework was partly occupied with a widely spread metal oxide, hence decreasing the surface area of the silica gel itself.^[1,2] In this procedure, the gel was not subjected to thermal treatment above 110°C.

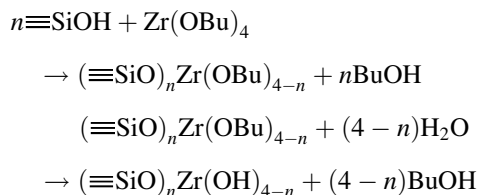
Zhang, Feng, and Da^[5] improved on the method of Kaneko et al.^[1,2] by employing an oil emulsion sol–gel procedure, resulting in the formation of mixed oxide spherical particles (spherical particles being a desirable property of a modern LC packing). In their method, sodium metasilicate pentahydrate was hydrolyzed in an acidic aqueous solution and zirconyl chloride octahydrate was added with stirring. The resulting mixture was suspended in a surfactant-stabilized oil and homogenized for 10 min at a speed calibrated to yield 5- μ m spherical particles. Precipitation of the gel was initiated by the slow addition of base. The resulting hydrogel was collected and washed to remove residual solvent and dried at 120°C for 2 hr, after which the material was calcined at 600°C for 1 hr.

Coating Processes

Coating processes have been used by a number of researchers. Chicz, Shi, and Regnier^[6] coated commercially available 15–20 μ m Vydac silica particles with zirconia. The surface coating was obtained by reacting a combination of 2,4-pentanedione, zirconium isopropoxide, and toluene (1:3:3) (v/w/v) with silica for 1 hr. The zirconyl-clad silica was then vacuum-dried overnight and calcined at 500°C for 8 hr, after which the material was washed with 2-propanol and then vacuum-dried. The zirconyl-clad silica was further modified with polyethyleneimine (PEI) to produce an ion-exchange surface that was tested for retention of proteins. The pore diameter of the resulting zirconyl-clad silica (22.6 nm) was approximately 75% of the original Vydac silica (300 nm), while the surface area decreased marginally (~10%).

Peixoto, Gushiken, and Baccan^[7] employed a similar coating process to prepare zirconized silica. Silica particles were added to a solution of $ZrCl_4$ in anhydrous ethanol. The mixture was refluxed for 8 hr under a nitrogen atmosphere. The zirconized silica was then collected and dried at approximately 125°C, before being hydrolyzed and washed in water to remove the residual chloride ions. The final product was dried at 120°C for 5 hr. The resulting zirconized silica had a 3.25% ZrO_2 surface coverage. Melo et al.^[8,9] modified the method of Peixoto et al. and coated 10- μ m silica particles with

zirconia by reacting the silica with zirconium(IV) butoxide in toluene according to the following reaction process:^[8]



where $\equiv\text{SiOH}$ stands for silanol groups on the silica surface. Following hydrolysis, the zirconized silica contained 15.3% Zr on the surface.

More recently, a similar procedure for the preparation of zirconia-coated silica microspheres was employed by Tsurita and Nogami,^[10] who coated 3- μm silica spheres with zirconia derived from zirconyl chloride octahydrate. The resulting zirconia–silica spheres were subjected to thermal treatment in order to bring about crystallization and the subsequent development of the porous structure within the material.

A coating process was also employed by Shalliker et al.^[11] where zirconia–silica mixed oxide supports were prepared by coating preformed zirconia microspheres with silica, the reverse process to the methods of Chicz et al.,^[6] Peixoto et al.,^[7] Melo et al.,^[8,9] and Tsurita and Nogami.^[10] In this method,^[11] zirconia microspheres were first formed using a sol–gel method. The resulting spherical zirconia hydrogels were suspended in water and a solution of hydrolyzed sodium metasilicate pentahydrate was added. The quantity of sodium metasilicate pentahydrate varied depending upon the desired Zr/Si ratio in the final composite. The solution (~ 200 mL) containing the zirconia microspheres and the hydrolyzed sodium metasilicate pentahydrate was heated to 60°C , allowing the slow evaporation of water to a final volume of 15% of the original amount. The microspheres were collected by filtration and then washed. Calcination of the material followed, which influenced the crystallization and resulting surface properties of the support.^[11–15] Extended calcination at 1300°C resulted in the complete homogenization of the support, yielding zircon.^[11]

PROPERTIES OF ZIRCONIA–SILICA MIXED OXIDE SUPPORTS

Crystallization

The crystalline nature of zirconia microspheres prepared for chromatographic purposes is dependent upon the thermal history of the zirconia. A detailed discussion on the porous nature of zirconia and silica is not warranted in this text but is covered in detail in a review by Nawrocki

et al.^[3] It is perhaps important to note that zirconia is amorphous until subjected to temperatures that exceed the phase transition temperature required to form the tetragonal phase (usually between 440 and 470°C depending on the procedure used to prepare the zirconia). Once thermal treatment exceeds this phase transition temperature, a metastable tetragonal phase predominates—where, after cooling, zirconia slowly transforms to the stable monoclinic form. As thermal treatment of the zirconia is required to obtain a suitable pore-structured stationary phase, most zirconias prepared for chromatographic purposes are predominantly monoclinic, or perhaps more correctly polymorphous.^[3] Complete conversion from the amorphous phase to the monoclinic phase requires a substantial degree of thermal treatment and then time to allow the tetragonal phase to form the monoclinic phase. In contrast, the most common form of silica as a stationary phase material is usually the amorphous form,^[16] but, on occasion, Cristobalite has been reported.^[10] Silica doping of the zirconia, however, has been shown to have a marked effect on the crystallization of the zirconia phase.^[4,5,11–15] As the concentration of silica increased, the phase transition temperature from the amorphous phase to the metastable tetragonal phase increased.^[12] This was independent of whether the material was prepared through a coprecipitation process^[5] or by a coating process.^[11] For example, the relationship between the phase transition temperature and the percentage weight of silica in the zirconia–silica composite is shown in Fig. 1. As the concentration of silica doping increased, the phase transition temperature increased monotonically and was linear until 700°C .^[11] Furthermore, the addition of the silica stabilized the metastable

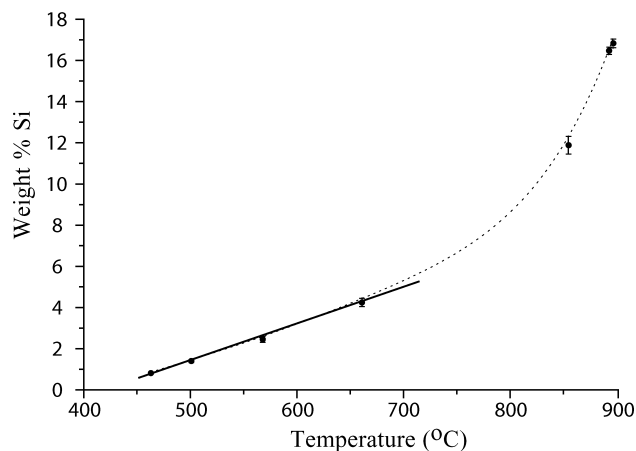


Fig. 1 Plot showing the relationship between the phase transition temperature from the amorphous to the tetragonal state and the composition of silica in the composite material. (From Ref. [12].)

tetragonal phase, which delayed the transformation to the monoclinic phase.^[11] In general, increased silica content decreased the apparent crystallinity. Studies by Tsurita and Nogami^[10] on zirconia-coated silica microspheres support the findings described above. In their work, as the concentration of Zr doping increased (or, in other words, the relative concentration of Si decreased), there was a corresponding increase in the concentration of tetragonal zirconia. Furthermore, increasing concentrations of ZrO_2 suppressed the crystallization of silica gel.

Pore Structures

Many of the most important properties of a chromatographic stationary phase relate to the pore structure, which provides a high surface area and pore volume for solute interaction for the chromatographic retention process to occur. As such, the pores should be of a suitable size to allow the solutes of interest to have unimpeded entry and exit to and from the pores. Microporous materials are of little interest in the chromatographic industry. They provide a high surface area, but one that is inaccessible to the vast majority of solutes. Mesoporous materials are the most sought after, with pore sizes between 2 and 50 nm, although macroporous materials find specialized use in the separation of macromolecules, e.g., Ref. [16], but at the cost of a reduced surface area. Ideally, the pore shape should represent that of a cylinder and should be described by a type IV nitrogen sorption isotherm^[17] as

depicted in Fig. 2(a). These types of isotherms are common in many industrial adsorbents with mesoporous structures. The hysteresis loop in the type IV isotherm is usually associated with capillary condensation in a mesoporous structure. These hysteresis loops can form several shapes; however, from a chromatographic aspect, the most important type of hysteresis loop is the type H1 (Fig. 2(b)), which represents pores that are uniform in shape and with a narrow size distribution. Many chromatographic surfaces display type H2 or intermediate H1–H2 hysteresis loops, which in a simplified form represents surfaces that have pore structures with wide bellies and narrow necks (“ink bottle” pores).^[17]

In general, the pore size and subsequent surface area of zirconia-containing supports is a function of the thermal history, i.e., the crystalline nature. Calcination of the material at high temperatures leads to an increase in the pore size and a reduction in the surface area, as a consequence of particle sintering and crystallization.^[3] Kaneko et al.^[1] measured the physical properties (pore size distributions, specific surface areas, and pore volumes) of their stationary phases using nitrogen adsorption isotherms. The surface area and pore diameter of their stationary phase material reflected the absence of calcination at temperatures high enough to induce crystallization. Their stationary phase material was predominantly microporous, with a high surface area ($122 \text{ m}^2/\text{g}$). No mention was made with regard to the pore shape.

In comparison, the stationary phases prepared using the coprecipitation process of Zhang, Feng, and Da^[5] with

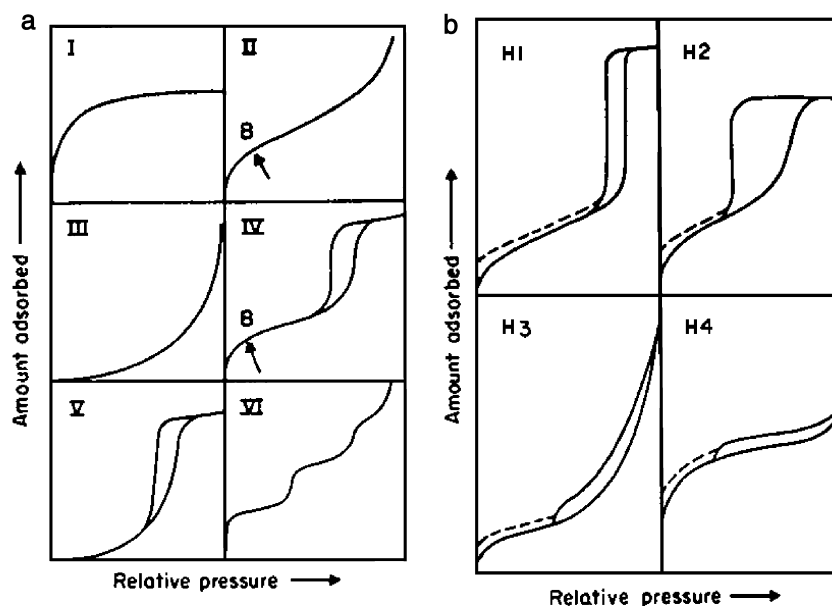


Fig. 2 (a) Types of physisorption isotherms. (b) Types of hysteresis loops. (From Ref. [17].)

thermal treatment at 600°C were mesoporous. The mean pore diameters were 8.6 nm for a composite containing 3.4% Si and 5.9 nm for a composite containing 15.8% Si. These stationary phase materials had surface areas of 29 and 76 m²/g, respectively. It is of interest to note that the surface area for the composite containing the higher silica content was greater than the surface area for the composite with the lower silica content. The average pore diameter of the material with the low silica content was greater than the average pore diameter of the composite with higher silica content. This reflects the decrease in crystallinity associated with an increase in the concentration of silica doping,^[5] and the change in density due to the different zirconia concentrations. The composite materials prepared by Zhang, Feng, and Da^[5] were reported as being type IV isotherms with H1 hysteresis loops, making them ideally suited as chromatographic adsorbents.

The pore structures of zirconia–silica composites prepared by Shalliker et al.^[11–15] via a coating procedure were substantially different to those reported by Zhang, Feng, and Da.^[5] In studies by Shalliker et al.,^[13–15] the pore characteristics were determined using inverse size exclusion chromatography and nitrogen sorption. The inverse size exclusion technique was employed to measure the chromatographically available pore surface, while the nitrogen sorption measurements were carried out for comparative purposes with information already available in the literature. A range of composites were prepared with either 5 or 10 mol% silicon.^[14,15] These composites were calcined for 1 hr at either 700 or 810°C. Calcination of these materials at 810 or 700°C yielded composites that were either predominantly amorphous or tetragonal depending on the concentration of the silicon doping. The increase in the phase transition temperature compared to that of native zirconia was consistent with the degree of silicon doping. For a composite material containing 10 mol% Si and calcined for 1 hr at 810°C, a type IV nitrogen sorption isotherm with an H3 hysteresis loop was obtained.^[15] The type H3 hysteresis loop extended from the high relative pressure region to P/P_0 approximately 0.42, indicating that the surface had a broad pore size distribution. The close proximity of the adsorption and desorption branches indicated that the entrances of the pores offered little restriction to the pore body. This type of hysteresis loop was consistent with a surface containing slit-like pores. The BET-specific surface area of the composite was 2.7 m²/g and the pore size distribution was very broad and skewed significantly to the macroporous region, with a maximum at 3.4 nm.^[15] The specific pore volume of this material was very low (0.0056 mL/g), consistent with a macroporous material. In comparison, the specific pore volume of the stationary phases prepared by Zhang, Feng, and Da^[5] were 0.062

and 0.112 mL/g for the 3.4% Si and 15.8% Si composites, respectively. The specific pore volume of the stationary phase prepared by Kaneko et al.^[11] was 0.17 mL/g.

The size exclusion curve for polystyrenes that eluted from a column prepared from the 10 mol% silicon composite of Shalliker et al.^[14] also indicated that the material had a broad pore size distribution that extended well into the macroporous region. No exclusion limit was determined despite the elution of polymers with molecular weights in excess of 1.8 million Da. The mean pore diameter determined from the inverse size exclusion method was 56.2 nm (essentially a macroporous support) and the specific surface area agreed remarkably well with the BET-specific surface area (2.75 compared to 2.7 m²/g). Reducing the calcination temperature from 810 to 700°C, which was below the phase crystallization temperature for the same 10 mol% silicon phase, yielded an amorphous material. The mean pore diameter was 8.9 nm and there was a significant microporous contribution. Because of the microporous nature of this amorphous material, the surface area was almost 20-fold greater with a pore volume almost threefold higher than the predominantly tetragonal phase material obtained following calcination at 810°C.^[14] Reducing the concentration of silicon to 5 mol% and calcining at 700°C yielded a very similar material to the one containing 10 mol% silicon, which was also calcined at 700°C. However, there was a significant concentration of the tetragonal phase in the 5 mol% silicon material, which was not the case for the 10 mol% silicon phase calcined at 700°C. The phase transition temperature of 5 mol% silicon support was approximately 700°C, hence the presence of the tetragonal phase. Fig. 3 illustrates the cumulative pore volumes of these three supports. This figure depicts the change in porosity as a function of the silica doping

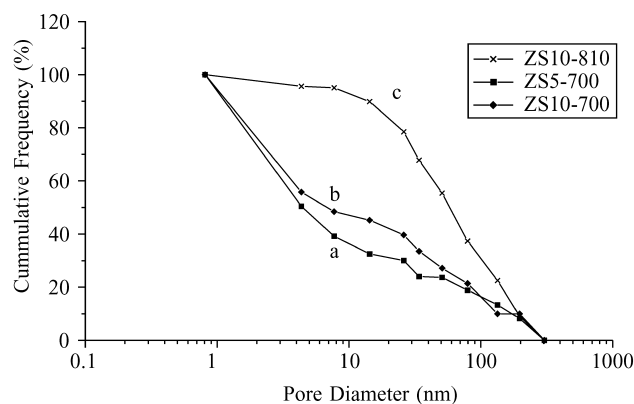


Fig. 3 Cumulative pore frequency plots of composite zirconia–silica stationary phases. (a) ZS5-700, (b) ZS10-700, and (c) ZS10-810. (From Ref. [14].)

concentration and the thermal treatment of the support. For instance, for both phases calcined at 700°C, approximately 50% of the pores were less than 4 nm in diameter, whereas there were essentially no pores of this diameter for the material calcined at 810°C. The authors concluded in their study that because of the unfavorable pore shape, such supports would be unsuitable for chromatographic purposes.

Several researchers have investigated the inclusion of high melting point salts during the calcination processes in the synthesis of silica,^[10,18] zirconia,^[19] and zirconia–silica composites.^[10,13–15] The function of the salt is to improve the pore structure of the material. The pores are homogeneously filled with a salt solution (typically sodium chloride), which is allowed to evaporate to dryness leaving behind salt deposited in the pores. Upon sufficient heating, both the salt and the stationary phase material partially liquefy and phase separation occurs.^[18] The size and shape of the pores depend on the nature of the salt and on the calcination conditions. The stationary phase and salt solidify when cooled, and residual salt can be removed by washing, leaving behind widened pores. In the case of silica, this procedure has been used to prepare wide pore (>1000 nm) materials designed for bioseparations.^[18] The surface structure of a LiChrosphere Si100 stationary phase that has been subjected to pore widening using a salt impregnation process is illustrated in Fig. 4. Salt impregnation during calcination

transformed mesoporous zirconia with surfaces that had type IV nitrogen isotherms with H1–H2 hysteresis loops to surfaces with type H1 hysteresis loops. No substantial increase in the overall pore diameter was observed although the salt transformed “ink bottle”-shaped pores to cylindrical-shaped pores.^[19] Salt impregnation of zirconia–silica composites resulted in materials that had type H3 hysteresis loops being transformed to materials with intermediate type H1–H2 hysteresis loops.^[15] The addition of salt resulted in a more than 15-fold increase in the pore volume and a greater than sixfold increase in the surface area (measured by the BET method).^[15] The pore size distribution changed from being a very broad distribution for a zirconia–silica composite calcined without salt to one being mesoporous when calcined with salt. Even with the aid of salt impregnation, evaluation of the nitrogen sorption isotherms showed evidence of pores with hindered access. The mean pore radius was 21.0 nm when measured from the adsorption branch and 10.0-nm mean pore radius when measured from the desorption branch of a nitrogen sorption isotherm. The difference between the two mean pore radii determined from the adsorption and desorption branches indicated that the pores contain wider bellies with some degree of restriction near the pore entrance. Hence, the authors’ concluded that these surfaces contained a significant degree of type H2 hysteresis and the hindered pore access limited their chromatographic suitability.^[15]

Surface Acidity

The surface of zirconia is known to be basic, with a pK_a of between 10.5 and 12.8. The acidity of silica is dependent upon the state of hydrolysis, typically imparting a slight acidic nature to the surface.^[3] Very little information has been published with respect to the acid/base properties of zirconia–silica composites and this is not surprising given the limited experience chromatographers have with these types of stationary phases. Zhang, Feng, and Da^[5] determined that the acidity of their zirconia–silica composite increased as the concentration of silica increased. This finding was consistent with an increase in the concentration of acidic hydroxyl groups associated with the increase in silica content. In contrast, Kaneko et al. measured the acid/base properties of zirconia–silica mixed oxide supports via an amine titration method.^[1] They found that in a comparison between the acidity of the four mixed oxides (alumina–silica, titania–silica, magnesia–silica, and zirconia–silica), only the zirconia–silica composite contained strong acid sites—despite the fact that both alumina and silica are more acidic than zirconia.^[3] All four mixed oxides exhibited stronger acidity than native silica, which is somewhat surprising given the findings of Zhang, Feng, and Da.^[5] This may indicate that routine preparation of these mixed oxide supports is sen-

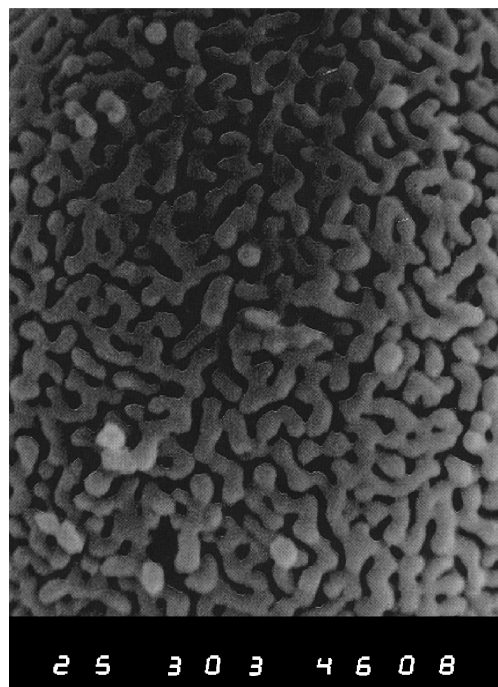


Fig. 4 Scanning electron micrograph of LiChrosphere Si100 soaked in NaCl solution and dried, heated to 800°C for 1 hr, washed out with water, and dried. (From Ref. [18].)

sitive to the process employed including thermal treatment, dehydroxylation, and rehydroxylation.

Surface Modification

Two excellent reviews that detail procedures for the preparation of bonded phase supports have recently been published by Leonard^[16] and Buchmeiser.^[20] One of the most popular methods of surface chemical modification involves the use of organosilanes. These organosilanes react with the surface metal hydroxyl groups and form a surface, which may be represented as M–O–R, where R represents an alkyl chain and M represents the metal (i.e., silica, zirconia, titania, etc.). One important factor that must be stated, however, is that the order of stability of M–O–R bonds increases in the order of M=Si > Zr > Ti > Al.^[16] Improvements in the hydrolytic stability can be achieved by shielding the siloxane bond with, for instance, polymeric phases or an intensive multivalent attachment of the bonded layer.^[16]

As zirconia–silica composites are relatively new surfaces in chromatography, few studies have detailed methods that modify the surface. One research group, however, has reported the preparation of reversed phase zirconia–silica stationary phases.^[8,9] In studies by Melo et al.,^[8,9] a C₈ stationary phase material was prepared by grafting poly(methyloctasiloxane) (PMOS) to the zirconia–silica composite followed by a gamma irradiation immobilization procedure. Surface modification was achieved by drying the zirconia–silica particles in air at 120°C for 24 hr. PMOS was dissolved in dichloromethane at a concentration to yield 1 g PMOS + support per 12 mL dichloromethane, resulting in a packing material with 50% w/w PMOS. The mixture (PMOS + zirconia–silica particles + dichloromethane) was stirred for 3 hr at room temperature after which the solvent was allowed to evaporate. The PMOS-sorbed zirconia–silica microspheres were then subjected to gamma irradiation at either 80 or 120 kGy using a Co-60 source. Columns prepared from the grafted and gamma-immobilized PMOS were tested for performance and compared to PMOS-sorbed silica and PMOS-sorbed zirconia–silica stationary phases that were not subjected to gamma irradiation. The authors concluded that the gamma irradiation of the PMOS-sorbed zirconia–silica composite improved the chromatographic performance for neutral and basic species. Furthermore, the gamma-irradiated PMOS-sorbed zirconia–silica stationary phase was shown to have superior chromatographic performance following alkaline stability trials when compared to PMOS-sorbed silica or zirconia–silica stationary phases that were not subjected to gamma irradiation. This was despite there being an apparent loss in sorbed PMOS (as indicated by a reduction in the capacity factor) following washing in very basic (pH 10) solvents. No retention information was presented on the performance of gamma-irradiated

PMOS-sorbed silica in comparison to gamma-irradiated PMOS-sorbed zirconia–silica.

An inorganic anion-exchange resin based on a zirconia–silica support was prepared by Chiciz, Shi, and Regnier.^[6] The Lewis acid sites were employed as adsorption sites that permanently retained a PEI coating which then acted as an anion-exchange ligand. In this study, a continuous film of cross-linked PEI was achieved. These surfaces were then tested for the analysis of ovalbumin and bovine serum albumin.

Through chance discovery, Shalliker et al.^[13,21] prepared a surface-modified normal phase zirconia–silica composite. In studies designed to optimize the pore structure of zirconia–silica composites, sodium iodide was used as a salt for pore widening experiments. However, following calcination and subsequent washing to remove residual salt, the stationary phase was left with a permanent brown-yellow discoloration, indicating the presence of iodide remaining on the surface. Elemental analysis confirmed this to be so. Consequently, the authors considered that the presence of iodide may protect the solute from the Lewis acid sites on the surface of the support.^[21] Normal phase retention studies showed a reduction in the degree of retention of basic solutes together with an improvement in the peak shape of basic compounds such as pyridine and aniline.

Alkaline Stability

One of the advantages of zirconia–silica composite stationary phases is supposedly a reduction in the solubility of the surface in alkaline solvents. However, only a limited amount of information detailing the alkaline stability of the surface is currently available. Chiciz, Shi, and Regnier^[6] demonstrated that a zirconia–silica composite that was coated with a PEI coating was stable in boiling alkaline solvent (1 M KOH) for 24 hr with no visual change in the stationary phase material. In contrast, a silica phase coated with PEI dissolved within 30 min in boiling 1 M KOH. As mentioned above, Melo et al.^[8,9] also observed stability in their reversed phase modified support following passage of 5000 column volumes of mobile phase (NH₄⁺/NH₃ buffer) at pH 10. A reduction in retention was observed, but the column efficiency and resolution remained essentially constant.

APPLICATIONS

Commercially, zirconia–silica composites have, at present, found limited use in liquid chromatography due to the popularity and dominance of silica and silica-based supports. The highly competitive market and the drive to satisfy consumer demand has ensured manufacturers of silica-based supports to investigate methods that overcome or limit the shortfalls of the surface, particularly

with respect to the solubility of silica in aqueous and basic solvents. The synthesis of the new generation hybrid silica (XTerra) is an example of these developments.^[20] Surface protection of the silica surface, with appropriate care being taken during the dehydroxylation and rehydroxylation of the surface also improves the behavior of basic solutes. There is, at present, very limited commercial interest in developing zirconia–silica composites and, consequently, applications on these surfaces are limited to researchers who prepare their own packing materials. Nevertheless, studies that have been published so far detail differences in selectivities between silica or zirconia and zirconia–silica composites. The employment of basic test substances such as pyridine and aniline in normal phase chromatography serves as a useful indicator of selectivity and secondary adsorption effects. This is particularly true for surfaces such as zirconia as these basic compounds display strong affinity toward Lewis acid sites and are also sensitive to the presence of hydroxyl groups. With that in mind, Kaneko et al.^[11] used a mixture of benzene, dimethyl phthalate, and pyridine to observe the retention characteristics of four mixed oxide supports in a hexane (99%)/methanol (1%) mobile phase. Pyridine was not observed to elute from either the column packed with silica or from the column packed with the zirconia–silica composite. The column prepared from a silica–magnesia stationary phase gave the best separation, while extreme band tailing of the pyridine was observed on columns prepared from silica–alumina and silica–titania. Fig. 5 illustrates the results that were

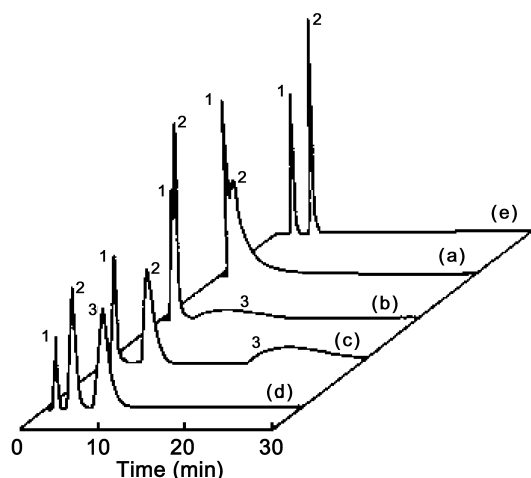


Fig. 5 Chromatograms obtained on four mixed oxide packing materials. Solute: 1 = benzene; 2 = dimethyl phthalate; 3 = pyridine. Column packing material: (a) silica–zirconia; (b) silica–alumina; (c) silica–titania; (d) silica–magnesia; (e) silica gel. Mobile phase, *n*-hexane containing 1% methanol; flow rate, 1 mL/min; column temperature, ambient; detection, UV 254 nm. (From Ref. [1].)

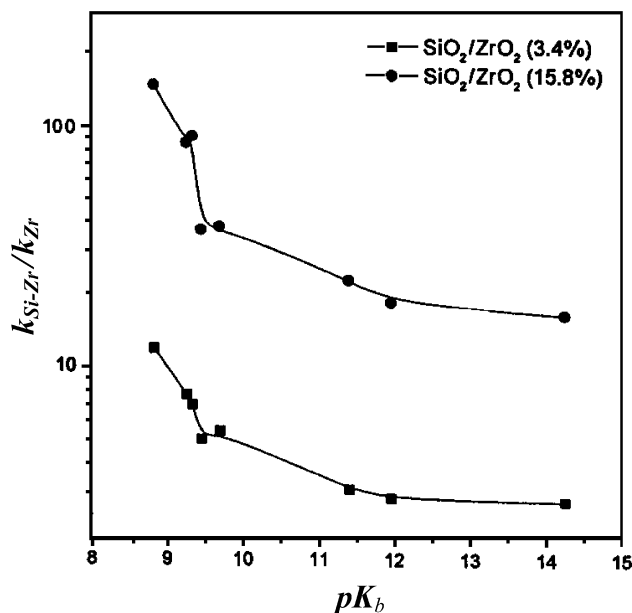


Fig. 6 Relationship between the $k'_{\text{Si-Zr}}/k'_{\text{Zr}}$ and the $\text{p}K_{\text{b}}$ of basic compounds. (From Ref. [14].)

obtained. The authors concluded that because their zirconia–silica composite contained the highest concentration of strong acid sites, pyridine could not be eluted, whereas a broad tailing pyridine band was observed for the silica–titania and silica–alumina columns, both of which had a slightly lower concentration of strong acid sites than the zirconia–silica stationary phase. The silica–magnesia stationary phase with only weak acid sites gave the best separation and a symmetrical peak for pyridine.

In contrast, pyridine and other basic test solutes in normal phase conditions were observed to elute from zirconia–silica composites prepared by Zhang, Feng, and Da.^[5] The retention of the basic solutes was greater on the zirconia–silica composite stationary phase than on a native zirconia stationary phase. The ratio $k'_{\text{Si-Zr}}/k'_{\text{Zr}}$, where $k'_{\text{Si-Zr}}$ and k'_{Zr} are measures of the capacity factor on the zirconia–silica stationary phase and the zirconia phase, respectively, decreased with an increase in the $\text{p}K_{\text{b}}$ of the test solute, as illustrated in Fig. 6. Retention was also greater on the stationary phase containing the greater concentration of zirconia. However, the elution order of the aniline and *p*-nitroaniline was reversed when the surface concentration of zirconia increased from 3.4% to 15.3% and this was attributed to the stronger acid properties of the 15.8% zirconia–silica composite. Neutral compounds (PAHs) were also shown to be retained on the surface of the zirconia–silica composites and zirconia, and this was attributed to interactions between π electrons and Lewis acid sites.^[5] The retention of acidic compounds was also studied by Zhang, Feng, and Da^[5] and they

Zirconia–Silica Stationary Phases for HPLC: Overview and Applications

9

Table 1 Capacity factor and asymmetry factors for pyridine in a normal phase separation on various silica and zirconia stationary phases

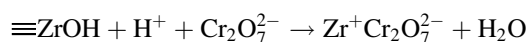
Stationary phase	Capacity factor	Asymmetry factor
Silica	9.50	2.450
Zirconia	0.99	1.840
Zirconia–silica	0.86	1.795
NaI impregnated zirconia–silica	0.24	1.330

(From Ref. [21].)

suggested that the crystal structure of the support may be a factor in determining the extent of retention. In their study, retention of acidic compounds increased in the order of zirconia–silica (3.4% Zr) < zirconia < zirconia–silica (15.8%). The addition of silica to the zirconia improved the peak asymmetry.

Shalliker et al.^[21] used pyridine and aniline as test solutes in normal phase chromatography. Strong retention of pyridine was observed on a native silica column ($k' = 9.5$), while the sample was only weakly retained on a native zirconia column ($k' \sim 1$). Even less retention was observed for pyridine on a zirconia–silica column ($k' = 0.86$). All pyridine bands were severely tailed with asymmetry factors as high as 2.4 for pyridine eluting from the silica column. However, elution of pyridine from a sodium iodide impregnated zirconia–silica column occurred with a capacity factor of 0.26, but most importantly, the peak tailing decreased substantially, as shown in Table 1. Similar results were observed for the elution of aniline. However, selectivity differences resulted in the elution order of pyridine and aniline being reversed between the sodium iodide impregnated zirconia–silica column and the unmodified zirconia–silica column. In general, iodide impregnation decreased retention, and improved peak shape.

The ion-exchange properties of zirconia–silica surfaces were utilized in a study by Peixoto, Gushiken, and Baccan.^[7] In this study, zirconia–silica microcolumns were employed for the selective extraction and enrichment of chromium(VI) in a flow injection system. The hydrated zirconia–silica surface adsorbed cations or anions depending on the pH. At low pH, the surface behaved as anion exchanger by a mechanism in which OH^- was displaced from the surface according to:^[7]



They showed that the method was suitable for the analysis of Cr(VI) in natural waters with little interference from common ions normally found in these water samples.

The ion-exchange properties of zirconia–silica surfaces were also evaluated by Chiczy, Shi, and Regnier;^[6] however, their study was conducted on surfaces modified with a layer of PEI. A number of different stationary phase base support materials were employed in their study including zirconia–silica. They found that retention was dependent on the amount of PEI bound to the surface, leading them to suggest that base materials with similar

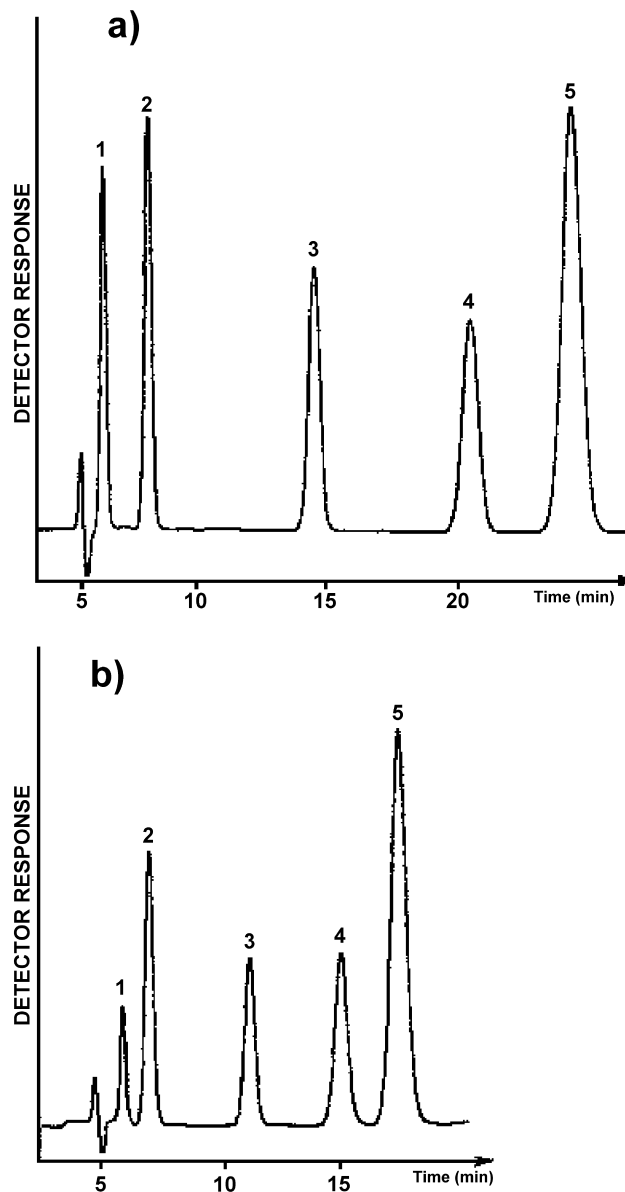


Fig. 7 Chromatograms of a mixture of acetone (1), benzonitrile (2), benzene (3), toluene (4), and naphthalene (5), obtained from a zirconized silica column with a radiation-immobilized PMOS coating (a) before initiating the stability test and (b) after completing the stability test with 5000 column volumes each of neutral and alkaline (pH 10) mobile phases. (From Ref. [8].)

charge density, surface area, and pore diameter (in other words, materials with the same capacity to adsorb the PEI coating) should behave in much the same manner. The advantage of the zirconia–silica base support over silica was that the zirconia–silica phase was stable in alkaline solvents whereas the silica phase rapidly dissolved.

Only one research group has illustrated the reversed phase retention behavior of solutes on zirconia–silica modified surfaces. In the study by Melo et al.^[8,9] on PMOS gamma-irradiated modified surfaces, the reversed phase retention behavior of a test mixture containing acetone, benzonitrile, benzene, toluene, and naphthalene was evaluated. The authors illustrated good resolution of the five-component test mixture as shown in Fig. 7. Retention, however, decreased after the stationary phase was washed with 5000 column volumes of base (pH 10). Despite the base washing, uniform peak shape was maintained, with only a slight reduction in resolution as discussed in “Alkaline Stability” above.

CONCLUDING REMARKS

In searching for new separation processes, the chromatographer develops new types of stationary phase materials in order to gain improvements in selectivity. The development of zirconia–silica composites is an example which—although, at present, applications on these surfaces are limited to their development—typifies the ongoing search. Whether the separations achieved on the zirconia–silica composites are better or worse than those achieved on either zirconia or silica is immaterial to the fundamental process of discovery. The important factor is that the separation is different and, therefore, an alternative separation strategy may be employed. In addition to the differences in selectivity that may be found when new surfaces are developed, beneficial surface properties may also be realized. These may be related to aspects such as the pore structure, the acidic or basic properties, or the solubility of the support.

In the specific case of zirconia–silica composites, the stationary phase could be prepared through relatively simple processes using either coprecipitation or coating methods. The addition of silica to the zirconia matrix increases the phase transition temperature from the amorphous phase to the tetragonal phase, which in turn stabilizes the tetragonal phase. The pore structure can be controlled through processes similar to those employed in the preparation of zirconia. However, the type of pore structure obtained appears to be dependent on the method of preparation. Calcination in the presence of salts improves the pore shapes. Zirconia–silica phases can also be surface-modified and C₈ and ion-exchange media have been prepared. Composite zirconia–silica stationary

phases coated with PEI were shown to have a lower solubility in alkaline solvents than silica modified in the same manner. The ion-exchange properties of zirconia–silica stationary phases were utilized in the analysis of natural waters, where the concentration of chromium(VI) was enriched in a flow injection system that incorporated a microcolumn packed with zirconia–silica stationary phase. Several studies have shown the elution behavior of basic solutes on these composites, and one study illustrated that modifying the surface with a Lewis base could minimize peak tailing.

Future work in stationary phase design will probably continue to include studies on mixed oxide composites although these will continue to constitute only a small fraction of the stationary phase materials made for general purpose use. Many of the mixed oxide supports will be custom-made for specific applications, and at least in the short term, these types of stationary phases will be made by individual research groups.

REFERENCES

1. Kaneko, S.; Mitsuzawa, T.; Ohmori, S.; Nakamura, M.; Nobuhara, K.; Masatani, M. Separation behaviour of silica-containing mixed oxides as column packing materials for liquid chromatography. *J. Chromatogr., A* **1994**, *669*, 1–7.
2. Kaneko, S.; Mitsuzawa, T.; Ohmori, S.; Nakamura, M.; Nobuhara, K.; Masatani, M. Silica-containing mixed oxides gels prepared by a coprecipitation method as novel packing materials for liquid chromatography. *Chem. Lett.* **1993**, 1275–1278, and references cited therein.
3. Nawrocki, J.; Rigney, M.P.; McCormick, A.; Carr, P.W. Chemistry of zirconia and its use in chromatography. *J. Chromatogr., A* **1993**, *657*, 229–282.
4. Kanno, Y. Thermodynamic and crystallographic discussion of the formation and dissociation of zircon. *J. Mater. Sci.* **1989**, *24*, 2415–2420.
5. Zhang, Q.-H.; Feng, Y.-Q.; Da, S.-L. Preparation and characterization of silica–zirconia supports for normal phase liquid chromatography. *J. Liq. Chromatogr. Relat. Technol.* **2000**, *23* (10), 1461–1475.
6. Chicz, R.M.; Shi, Z.; Regnier, F.E. Preparation and evaluation of inorganic anion-exchange sorbents not based on silica. *J. Chromatogr.* **1986**, *359*, 121–130.
7. Peixoto, C.R.M.; Gushiken, Y.; Baccan, N. Selective spectrophotometric determination of trace amounts of chromium(VI) using a flow injection system with a microcolumn of zirconium(IV) oxide modified silica gel. *Analyst* **1992**, *117*, 1029–1032.
8. Melo, L.F.C.; Collins, C.H.; Collins, K.E.; Jardim, I.C.S.F. Stability of high performance liquid chromatography columns packed with poly(methyloctylsiloxane) sorbed and radiation-immobilized onto porous silica and zirconized silica. *J. Chromatogr., A* **2000**, *869*, 129–135.
9. Melo, L.F.C.; Jardim, I.C.S.F. Development of C₈ station-



- ary phases immobilized by γ -radiation on zirconized silica for high-performance liquid chromatographic applications. *J. Chromatogr., A* **2000**, 845, 423–431.
10. Tsurita, Y.; Nogami, M. Preparation of porous supports in the SiO_2 – ZrO_2 – Na_2O system from microspherical silica gels. *J. Mater. Sci.* **2001**, 36, 4365–4375.
 11. Shalliker, R.A.; Rintoul, L.; Douglas, G.K.; Russell, S.C. A sol–gel preparation of silica coated zirconia microspheres as chromatographic support materials. *J. Mater. Sci.* **1997**, 32, 2949–2955.
 12. Shalliker, R.A.; Douglas, G.K.; Rintoul, L.; Russell, S.C. The analysis of zirconia–silica composites using differential thermal analysis, Fourier transform–Raman spectroscopy and X-ray scattering/scanning electron microscopy. *Powder Technol.* **1998**, 98, 109–112.
 13. Shalliker, R.A.; Douglas, G.K.; Rintoul, L.; Comino, P.R.; Kavanagh, P.E. The measurement of pore size distributions, surface areas, and pore volumes of zirconia and zirconia–silica mixed oxide stationary phases using size exclusion chromatography. *J. Liq. Chromatogr. Relat. Technol.* **1997**, 20 (10), 1471–1488.
 14. Shalliker, R.A.; Douglas, G.K. The development of stationary phase supports for liquid chromatography: I. Examination of the pore structure of zirconia–silica composites using size exclusion chromatography. *J. Liq. Chromatogr. Relat. Technol.* **1998**, 21 (12), 1749–1765.
 15. Shalliker, R.A.; Douglas, G.K.; Elms, F.M. The development of stationary phase supports for liquid chromatography: II. Examination of the pore structure of zirconia–silica composites using nitrogen sorption. *J. Liq. Chromatogr. Relat. Technol.* **1998**, 21 (12), 1767–1781.
 16. Leonard, M. New packing materials for protein chromatography. *J. Chromatogr., B, Biomed. Sci. Appl.* **1997**, 669, 3–27, and references cited therein.
 17. Sing, K.S.W.; Everett, D.H.; Haul, R.A.W.; Moscou, L.; Pierotti, R.A.; Rouquerol, J.; Siemieniewska, T. Reporting physisorption data for gas/solid systems with special reference to the determination of surface area and porosity. *Pure Appl. Chem.* **1985**, 57, 603–619.
 18. Novak, I.; Berek, D. Structural inhomogeneities in wide-pore silica gels. *J. Chromatogr., A* **1994**, 665, 33–36, and references cited therein.
 19. Shalliker, R.A.; Douglas, G.K.; Comino, P.R.; Kavanagh, P.E. Examination of various size zirconias for potential chromatographic applications. *Powder Technol.* **1997**, 91, 17–23.
 20. Buchmeiser, M.R. New synthetic ways for the preparation of high performance liquid chromatography supports. *J. Chromatogr., A* **2001**, 918, 233–266.
 21. Shalliker, R.A.; Rizk, M.; Stocksiek, C.; Sweeney, A.P. Retention behaviour of basic solutes on zirconia–silica composite stationary phase supports in normal phase liquid chromatography. *J. Liq. Chromatogr. Relat. Technol.* **2002**, 25 (4), 561–572.

Zone Dispersion in Field-Flow Fractionation

Josef Janča

Université de La Rochelle, La Rochelle, France

Introduction

All separation processes are inherently accompanied by zone broadening, which is due to the dynamic spreading processes dispersing the concentration distribution achieved by the separation [1]. As long as the relative contributions of these dispersive processes decrease, the efficiency of the separation increases. A conventional empirical parameter describing, quantitatively, the efficiency of any separation system is the number of theoretical plates per separation unit, N , or the height equivalent to a theoretical plate (the theoretical plate height) H defined by

$$N = \left(\frac{V_R}{\sigma_V} \right)^2, \quad H = \frac{L}{N} \quad (1)$$

where V_R is the retention volume, σ_V is the standard deviation of the elution curve (fractogram) of a uniform retained sample, expressed at the same retention volume units, and L is the length of the separation unit; in the case of the field-flow fractionation (FFF), it is the length of the fractionation channel. Figure 1a shows a model fractogram and the method of graphical determination of the efficiency of the involved separation system. A more accurate procedure for the determination of the efficiency of the separation system from the experimental fractogram consists in the numerical calculation of the statistical moments of the fractogram (viz. of the first statistical moment, which corresponds to the maximum of the fractogram and, thus, to the retention volume):

$$V_R = \frac{\sum V_i h_i}{\sum h_i} \quad (2)$$

where h_i are the heights of the fractogram at the corresponding retention volumes V_i . The square root of the second central moment corresponds to the standard deviation of the fractogram and, thus, to its width:

$$\sigma_V = \left(\frac{\sum (V_i - V_R)^2 h_i}{\sum h_i} \right)^{1/2} \quad (3)$$

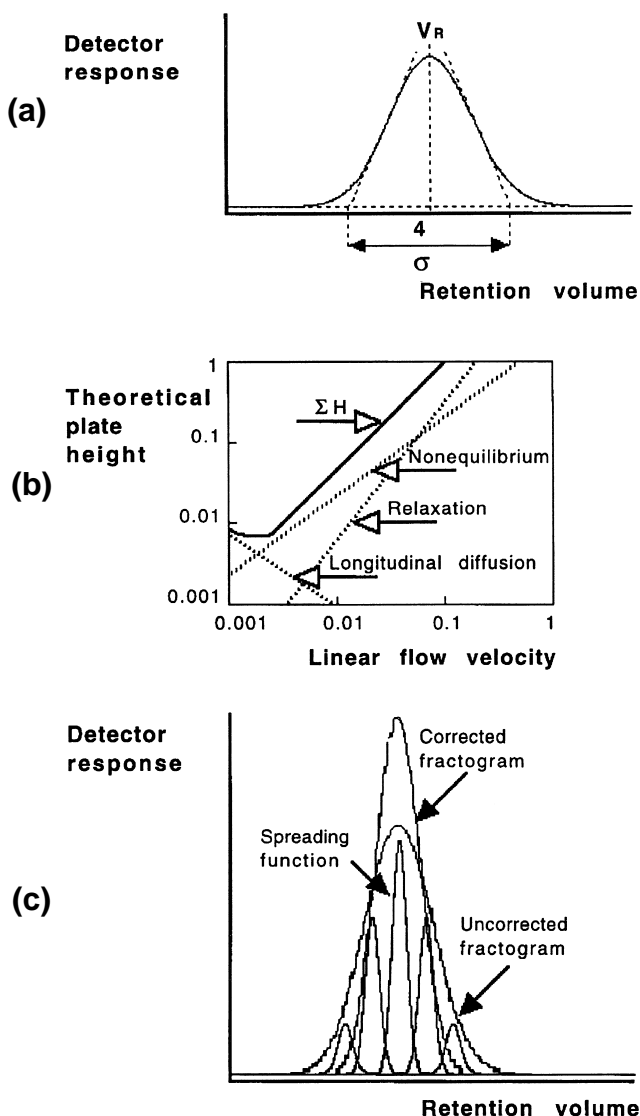


Fig. 1 Zone broadening and its correction. (a) Schematic demonstration of the evaluation of the efficiency of the separation system of FFF; (b) dependence of the theoretical plate height on the linear flow velocity; (c) schematic demonstration of the application of the correction for the zone broadening on a model fractogram.



It must be stressed that the terms band or zone broadening, spreading, and dispersion used here are equivalent from the viewpoint of their physical meanings.

Processes Contributing to Zone Broadening

Several dispersive processes contribute to zone broadening: longitudinal diffusion, nonequilibrium and relaxation processes, spreading due to the external parts of the whole separation system, such as the injector, detector, connecting capillaries, and so forth. It has theoretically been found [2] that the resulting efficiency of the FFF, characterized by the height equivalent to a theoretical plate, can very accurately be described by

$$H = \frac{2D}{R\langle v(x) \rangle} + \frac{\chi w^2 \langle v(x) \rangle}{D} + \sum H_{\text{ext}} \quad (4)$$

where D is the diffusion coefficient of the retained species, R is the retention ratio, $\langle v(x) \rangle$ is the average linear velocity of the carrier liquid, w is the thickness of the fractionation channel, χ is the dimensionless parameter defined later, and $\sum H_{\text{ext}}$ is the sum of all contributions to the zone broadening from the external parts of the separation channel (injector, detector cell, and connecting capillaries).

The retention ratio R is defined as

$$R = \frac{V_0}{V_R} \quad (5)$$

where V_0 and V_R are the retention volumes of the unretained and retained species, respectively. Graphical representation of the particular spreading processes, as a function of the average linear velocity of the carrier liquid and of their sum, which results in a curve exhibiting a minimum, are shown in Fig. 1b. At very low linear velocities of the carrier liquid, the longitudinal diffusion, represented by the first term on the right-hand side of the Eq. (4), plays a dominant role of all zone-spreading processes. The relaxation and nonequilibrium processes, represented by the second term on the right-hand side of the Eq. (4), become more important when increasing the velocity. The result is that H passes through the above-mentioned minimum. As the diffusion coefficients of the macromolecules and particles are relatively low, the contribution of the longitudinal diffusion is almost negligible and the optimal efficiency (the minimum on the resulting curve) appears at a very low flow velocity. The zone spreading due to the external elements of the fractionation channel can be minimized by reducing their volume.

The dimensionless parameter χ is a complex function of the retention parameter λ which, itself, can be approximated by the relationship

$$\lim_{\lambda \rightarrow 0} R = 6\lambda \quad (6)$$

Another approximate relationship holds between χ and λ :

$$\lim_{\lambda \rightarrow 0} \chi = 24\lambda^3 \quad (7)$$

Equation (7) is a very important relationship because, with respect to Eq. (4), it indicates that in the most practical range of the linear flow velocities, above the optimal flow, the efficiency of the separation in FFF increases very rapidly with the retention ratio. This is rather an exceptional case among separation methods and the importance of this behavior has to be regarded with respect to the fact that the FFF methods and techniques are especially convenient for the fractionation of large and polydisperse species, such as macromolecules and particles. As the retention usually increases with the molar mass or particle size in polarization FFF, the efficiency is higher in the high molar mass or large particle size domain. This is one of the reasons why the FFF methods are particularly competitive in this field of application.

Nevertheless, the difficulty to separate the large polydisperse species enough, independently of the method or technique used, impose the necessity to introduce, and apply the powerful numerical methods, which are able to evaluate the amplitude of the zone-broadening contribution to the apparent molar mass distribution (MMD) or particle size distribution (PSD), calculated by a simple data treatment of the experimental fractograms, and to correct, casually, the MMD and PSD data for zone broadening. Whenever the zone spreading attains a level not acceptable from the point of view of the analytical results obtained by a simple data treatment of the raw fractograms, a correction for the zone broadening must be applied.

Relaxation

Relaxation represents an important contribution to the zone broadening and merits mention in particular, especially because it can be reduced by an appropriate experimental procedure [3]. The concentration distribution of the fractionated sample across the channel established immediately after the injection is far from the steady state, which is formed progressively during the elution. This leads to additional zone broadening. However, if the flow is stopped after the injection for a

time necessary to achieve a steady state, the shift of the retention volume and the zone spreading can substantially be reduced. So-called secondary relaxation broadening can occur when the intensity of the field varies rapidly during the elution (e.g., by programming).

Correction for the Zone Broadening

The fractogram of a polydisperse sample is a superposition of the separation and of the zone broadening. This is shown in Fig. 1c, where the spread zones of the discrete species are overlapped and the fractogram is, in fact, a convolution of all individual zones. Whenever the zone spreading is important, the accurate MMD or PSD can be calculated from the experimental fractograms only by using a correction procedure. An efficient correction method applicable in FFF [4] was derived from well-known correction procedures used in size-exclusion chromatography [5].

A raw fractogram $h(V)$ is a convolution of the fractogram corrected for the zone broadening $g(Y)$ and the spreading function $G(V, Y)$ which is a detector response to a uniform species having the elution volume Y :

$$h(V) = \int_0^\infty g(Y)G(V - Y) dY \quad (8)$$

The spreading function can be approximated by

$$G(V, Y) = \left(\frac{1}{2\pi\sigma_s^2} \right)^{1/2} \exp\left(-\frac{(V - Y)^2}{2\sigma_s^2} \right) \quad (9)$$

where the standard deviation σ_s should be independent of the elution volume. This independence is valid in FFF only within a not very wide range of the elution volumes. Equation (9) can correctly be applied to the fractograms of the samples with a narrow MMD or

PSD only. On the other hand, whenever a nonuniform spreading function with the σ_s dependent on the retention has to be used, the correction to be applied is

$$h(V) = \int_0^\infty g(Y) \left[\frac{1}{[2\pi(\sigma_s(Y))^2]} \right]^{1/2} \exp\left(-\frac{(V - Y)^2}{[2(\sigma_s(Y))^2]} \right) dY \quad (10)$$

which is convenient for samples exhibiting wide MMD or PSD. Equation (10) can be numerically solved. The graphical representation of a model result of the application of the described correction procedure is shown in Fig. 1c.

Practical utility of the described correction procedure of the experimental fractograms was demonstrated first by applying it to the real fractograms of a polymer latex obtained from sedimentation FFF [4] and was subsequently confirmed [6–8].

References

1. J. C. Giddings, *Dynamics of Chromatography*, Marcel Dekker, Inc., New York, 1965.
2. M. E. Hovingh, G. H. Thompson, and J. C. Giddings, *Anal. Chem.* 42:195 (1970).
3. J. Janča, *Field-Flow Fractionation: Analysis of Macromolecules and Particles*, Marcel Dekker, Inc., New York, 1988.
4. V. Jáhlová, F. Matulík, and J. Janča, *Anal. Chem.* 59: 1039 (1987).
5. A. E. Hamielec, in *Steric Exclusion Chromatography of Polymers* (J. Janča, ed.), Marcel Dekker, Inc., New York, 1984.
6. M. R. Schure, B. N. Barman, and J. C. Giddings, *Anal. Chem.* 61: 2735 (1989).
7. Y. Mori, K. Kimura, and M. Tanigaki, *Spec. Publ. Roy. Soc. Chem.* 102: 290 (1992).
8. J.-C. Vauthier and P. S. Williams, *J. Chromatogr.* 805: 149 (1998).

